PIGMENT BIOSYNTHESIS

nature

Volume 285 No.5759   1 May 1980

NEWS

NEWS AND VIEWS

REVIEW ARTICLE

ARTICLE

LETTERS

Cover. When frozen, polysilicic acid forms parallel fibres, as
shown in this scanning electron micrograph. See p.27. The
biosynthesis of pigments essential to living organisms is reviewed
on p.17.

M

LETTERS

BOOK REVIEWS

OBITUARY

MISCELLANY

GUIDE TO AUTHORS

● Review articles should be aimed at a relatively wide readership. Many reviews are invited, but submitted articles may also be accepted; it is advisable to consult us before writing a review article.
● Articles may be up to 3,000 words long with at most six displayed items (figures and tables); they are reports of major research developments.
● Letters are brief reports of original research of unusual and wide interest, not in general longer than 1,000 words; they have at most three or four displayed items.
● 'Matters Arising' permits short discussion (up to 300 words) of papers that have recently appeared in *Nature*.
Articles should be accompanied by an abstract of not more than fifty words. Letters should begin with a paragraph giving the background and main conclusion in terms intelligible to as wide a readership as possible.
 Manuscripts may be submitted either to London or New York. Three typed copies should be submitted, each including lettered copies of figures. Typing (including references) should be double spaced. The title should be brief and informative. Pages should be numbered. References, tables and figure legends should start on separate pages. Experimental detail vital to the paper yet which would interrupt the narrative is best placed in the figure legends. Units should be identified in the margin on their first appearance. Equations should occupy single lines if possible: exp(*a*) is preferred to e^*a* if '*a*' is more than one character.

References are indicated by superscripts in the text. See any contemporary *Nature* for style, but note:
(i) only one reference number need be used if the reference is to several papers by identical authors.
(ii) first and last pages of references should be cited.
 Abbreviations should follow the *World List of Scientific Periodicals*, fourth edn (Butterworth, 1963-65). Symposia are often difficult to refer to and only published or soon-to-be-published volumes should be mentioned in references. Their publisher and place of publication should be clearly indicated 'Personal communication' and 'unpublished' should be incorporated in text.
 Artwork should be sent with the manuscript and clearly marked with author's name and the figure number. Line drawings should be either photographic prints or in Indian ink on heavy cartridge paper, tracing paper or similar materials. Most figures are reduced to one column width so originals should be about as wide as a page of *Nature*. To enable figures, particularly maps, to be edited in the same style as the text, they should contain only essential material. Ideally, an unlettered original and three lettered copies should be provided; labelling on halftones should, if possible, be avoided entirely. Magnifications quoted should be for the figures as submitted. We are always glad to see artwork for possible use on the cover, but cannot guarantee its return.
 In order to save on postal expenses we return only the top copy and artwork of manuscripts that we cannot publish.
 Nature's publishing policy is outlined in **258**, 1 (1975) and **264**, v, 11 Nov. (1976).

nature

Volume 285 No.5760   8 May 1980

NEWS

NEWS AND VIEWS

REVIEW ARTICLE

ARTICLES

LETTERS

iv

LETTERS

MATTERS ARISING

BOOK REVIEWS

MISCELLANY

This issue of *Nature* contains fewer Articles and Letters than usual because of an industrial dispute which has affected the typesetting of manuscripts accepted for publication.

GUIDE TO AUTHORS

Getting down to the finer details of microelectronics

As a leading manufacturer, and user, of micro-electronic technology, Philips is constantly searching for techniques that will improve the production process, or the product, or – ideally – both. This objective has now been achieved with the development of the 'Beamwriter' vector scan lithography system. In fact, it's the only production-oriented vector scan electron beam writing system available in the world.

Compared to conventional optical lithography techniques, vector scanning produces significant savings in the time taken to produce a set of masks or reticles; hours instead of days. It is also much more efficient than the raster scan E-beam method because the writing beam is directed only to points where exposure is required. The Beamwriter also generates an exposure dosage twenty times greater than other

Circle No. 18 on Reader Enquiry Card.

PHILIPS

NEWS

NEWS AND VIEWS

ARTICLES

LETTERS

Cover. Early Tertiary fossil angiosperm leaf from King George Island, Antarctic peninsula. New evidence for a more complicted volcanic history of the area is presented on p.157. Also this week Mrs Gandhi talks to Anil Agarwal on p.127.

BOOK REVIEWS

OBITUARY

MISCELLANY

GUIDE TO AUTHORS

● Review articles should be aimed at a relatively wide readership. Many reviews are invited, but submitted articles may also be accepted; it is advisable to consult us before writing a review article.

● Articles may be up to 3,000 words long with at most six displayed items (figures and tables); they are reports of major research developments.

● Letters are brief reports of original research of unusual and wide interest, not in general longer than 1,000 words; they have at most three or four displayed items.

● 'Matters Arising' permits short discussion (up to 300 words) of papers that have recently appeared in *Nature*.

Articles should be accompanied by an abstract of not more than fifty words. Letters should begin with a paragraph giving the background and main conclusion in terms intelligible to as wide a readership as possible.

Manuscripts may be submitted either to London or New York. Three typed copies should be submitted, each including lettered copies of figures. Typing (including references) should be double spaced. The title should be brief and informative. Pages should be numbered. References, tables and figure legends should start on separate pages. Experimental detail vital to the paper yet which would interrupt the narrative is best placed in the figure legends. Units should be identified in the margin on their first appearance. Equations should occupy single lines if possible: exp(*a*) is preferred to e^*a* if '*a*' is more than one character.

References are indicated by superscripts in the text. See any contemporary *Nature* for style, but note:

(i) only one reference number need be used if the reference is to several papers by identical authors.

(ii) first and last pages of references should be cited.

Abbreviations should follow the *World List of Scientific Periodicals*, fourth edn (Butterworth, 1963-65). Symposia are often difficult to refer to and only published or soon-to-be-published volumes should be mentioned in references. Their publisher and place of publication should be clearly indicated 'Personal communication' and 'unpublished' should be incorporated in text.

Artwork should be sent with the manuscript and clearly marked with author's name and the figure number. Line drawings should be either photographic prints or in Indian ink on heavy cartridge paper, tracing paper or similar materials. Most figures are reduced to one column width so originals should be about as wide as a page of *Nature*. To enable figures, particularly maps, to be edited in the same style as the text, they should contain only essential material. Ideally, an unlettered original and three lettered copies should be provided; labelling on halftones should, if possible, be avoided entirely. Magnifications quoted should be for the figures as submitted. We are always glad to see artwork for possible use on the cover, but cannot guarantee its return.

In order to save on postal expenses we return only the top copy and artwork of manuscripts that we cannot publish.

Nature's publishing policy is outlined in **258**, 1 (1975) and **264**, v, 11 Nov. (1976).

nature

Volume 285 No.5762   22 May 1980

NEWS

NEWS AND VIEWS

ARTICLES

LETTERS

Cover. Vertical sections through rain and cloud using conventional radar (top) and dual-polarization radar (bottom). The vertical scale spans 0–6 km and the horizontal range is about 30 km. The first two-dimensional distribution of drop sizes and rain drop concentrations using dual-polarization radar are described on p.195.

LETTERS

BOOK REVIEWS

MISCELLANY

nature

Volume 285 No.5763   29 May 1980

NEWS

NEWS AND VIEWS

ARTICLES

LETTERS

Contents continued overleaf

Cover. The striking polymorphism of *Cepaea* is depicted here from a painting by Gordon Riley. Evolutionary mechanisms affecting shell polymorphism was an important topic at a conference reported on p.283. The painting, reproduced by courtesy of A.J. Cain, was presented to him by M. Lamotte.

LETTERS

BOOK REVIEWS

MISCELLANY

GUIDE TO AUTHORS

● Review articles should be aimed at a relatively wide readership. Many reviews are invited, but submitted articles may also be accepted; it is advisable to consult us before writing a review article.
● Articles may be up to 3,000 words long with at most six displayed items (figures and tables); they are reports of major research developments.
● Letters are brief reports of original research of unusual and wide interest, not in general longer than 1,000 words; they have at most three or four displayed items.
● 'Matters Arising' permits short discussion (up to 300 words) of papers that have recently appeared in *Nature*.

Articles should be accompanied by an abstract of not more than fifty words. Letters should begin with a paragraph giving the background and main conclusion in terms intelligible to as wide a readership as possible.

 Manuscripts may be submitted either to London or New York. Three typed copies should be submitted, each including lettered copies of figures. Typing (including references) should be double spaced. The title should be brief and informative. Pages should be numbered. References, tables and figure legends should start on separate pages. Experimental detail vital to the paper yet which would interrupt the narrative is best placed in the figure legends. Units should be identified in the margin on their first appearance. Equations should occupy single lines if possible: exp(*a*) is preferred to e^a if '*a*' is more than one character.

References are indicated by superscripts in the text. See any contemporary *Nature* for style, but note:
 (i) only one reference number need be used if the reference is to several papers by identical authors.
 (ii) first and last pages of references should be cited.
 Abbreviations should follow the *World List of Scientific Periodicals*, fourth edn (Butterworth, 1963-65). Symposia are often difficult to refer to and only published or soon-to-be-published volumes should be mentioned in references. Their publisher and place of publication should be clearly indicated 'Personal communication' and 'unpublished' should be incorporated in text.

Artwork should be sent with the manuscript and clearly marked with author's name and the figure number. Line drawings should be either photographic prints or in Indian ink on heavy cartridge paper, tracing paper or similar materials. Most figures are reduced to one column width so originals should be about as wide as a page of *Nature*. To enable figures, particularly maps, to be edited in the same style as the text, they should contain only essential material. Ideally, an unlettered original and three lettered copies should be provided; labelling on halftones should, if possible, be avoided entirely. Magnifications quoted should be for the figures as submitted. We are always glad to see artwork for possible use on the cover, but cannot guarantee its return.

 In order to save on postal expenses we return only the top copy and artwork of manuscripts that we cannot publish.

 Nature's publishing policy is outlined in **258**, 1 (1975) and **264**, v, 11 Nov. (1976).

nature

Volume 285 No.5764 5 June 1980

NEWS

NEWS AND VIEWS

REVIEW ARTICLE

ARTICLES

LETTERS

Cover. The *Drosophila melanogaster* imaginal disk shown has been stained with fluorescein-conjugated monoclonal antibody specific for an antigen that seems to be present only on diploid epithelial cells of the insect. The production of the antibody and the tissue distribution of the antigen are described on p.403. Changes in the ecosystem of the English Channel off Plymouth and ecosystem stability are reviewed on p.361.

LETTERS

BOOK REVIEWS

MISCELLANY

GUIDE TO AUTHORS

• Review articles should be aimed at a relatively wide readership. Many reviews are invited, but submitted articles may also be accepted; it is advisable to consult us before writing a review article.

• Articles may be up to 3,000 words long with at most six displayed items (figures and tables); they are reports of major research developments.

• Letters are brief reports of original research of unusual and wide interest, not in general longer than 1,000 words; they have at most three or four displayed items.

• 'Matters Arising' permits short discussion (up to 300 words) of papers that have recently appeared in *Nature*.

Articles should be accompanied by an abstract of not more than fifty words. Letters should begin with a paragraph giving the background and main conclusion in terms intelligible to as wide a readership as possible.

Manuscripts may be submitted either to London or New York. Three typed copies should be submitted, each including lettered copies of figures. Typing (including references) should be double spaced. The title should be brief and informative. Pages should be numbered. References, tables and figure legends should start on separate pages. Experimental detail vital to the paper yet which would interrupt the narrative is best placed in the figure legends. Units should be identified in the margin on their first appearance. Equations should occupy single lines if possible: exp (*a*) is preferred to e^a if '*a*' is more than one character.

References are indicated by superscripts in the text. See any contemporary *Nature* for style, but note:

(i) only one reference number need be used if the reference is to several papers by identical authors.

(ii) first and last pages of references should be cited.

Abbreviations should follow the *World List of Scientific Periodicals*, fourth edn (Butterworth, 1963-65). Symposia are often difficult to refer to and only published or soon-to-be-published volumes should be mentioned in references. Their publisher and place of publication should be clearly indicated 'Personal communication' and 'unpublished' should be incorporated in text.

Artwork should be sent with the manuscript and clearly marked with author's name and the figure number. Line drawings should be either photographic prints or in Indian ink on heavy cartridge paper, tracing paper or similar materials. Most figures are reduced to one column width so originals should be about as wide as a page of *Nature*. To enable figures, particularly maps, to be edited in the same style as the text, they should contain only essential material, ideally, an unlettered original and three lettered copies should be provided; labelling on halftones should, if possible, be avoided entirely. Magnifications quoted should be for the figures as submitted. We are always glad to see artwork for possible use on the cover, but cannot guarantee its return.

In order to save on postal expenses we return only the top copy and artwork of manuscripts that we cannot publish.

Nature's publishing policy is outlined in **258**, 1 (1975) and **264**, v, 11 Nov. (1976).

nature

Volume 285 No.5765   12 June 1980

Cover. Pattern of actin in the eye lens of a calf is demonstrated here using immunofluorescence staining. The distribution of actin in the eye lens is described on p.506 and the possible role of actin in visual accommodation is discussed.
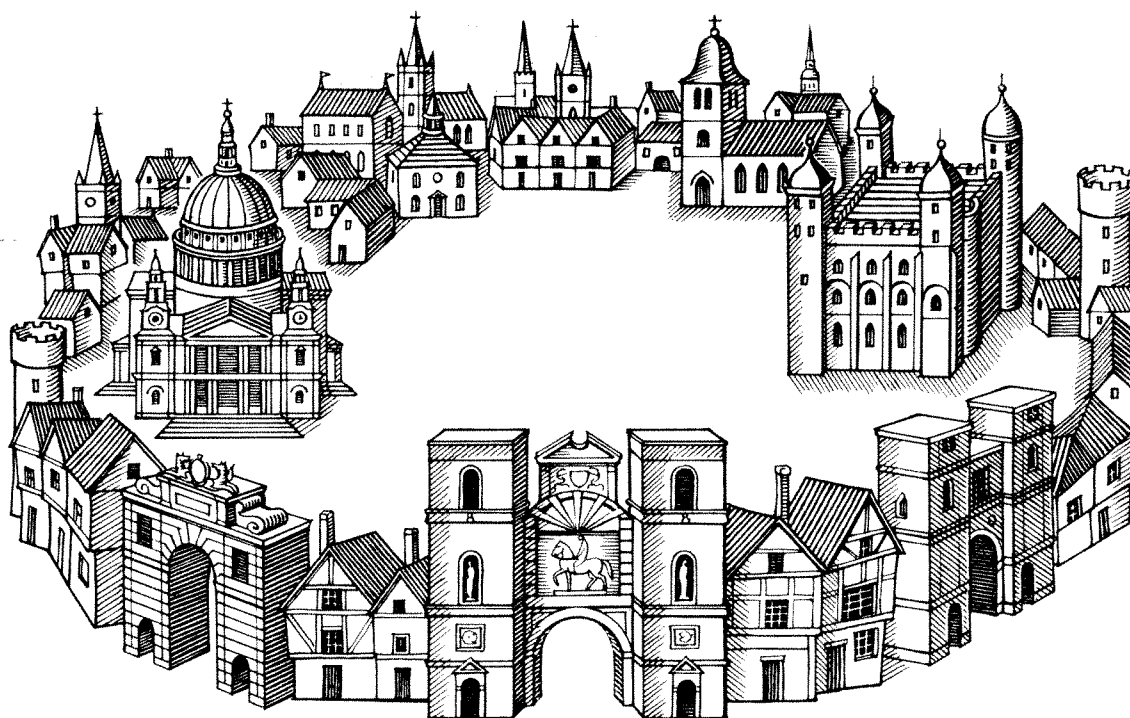
When in London do as the Romans did—
settle on the Barbican.
(It's the perfect place for a conference.)

It's a long time since the Romans left. (About 1,500 years, in fact.) But you can still see traces of their occupation – including remains of the original Roman city wall.

The Barbican Centre is located in the heart of the City of London. So it's surrounded by centuries of history and culture plus the bustle and excitement of one of the world's leading financial communities.

The Barbican Centre itself, however, will be among the most modern and well equipped conference centres available.

There's a spacious conference hall. A variety of lecture theatres, seminar and committee rooms. A Film Theatre – with the most advanced audio-visual equipment. The Barbican Theatre. Interpretation facilities for six languages. A display and exhibition area. Plus a plentiful supply of bars and restaurants.

The Barbican caters for cultural appetites, too. The Royal Shakespeare Company will have its permanent home there. So will the London Symphony Orchestra. And the Guildhall School of Music and Drama. There's an Art Gallery. A Sculpture Court.

In other words, it's as civilised a forum for a conference as even the Romans could have dreamed of.

We're already taking bookings from 1981 onwards.

So, if there's anything more you'd like to know about the Barbican, just contact our Conference Sales Director.

And don't worry. She speaks English. Not Latin.

Barbican Centre
11 Cromwell Tower, Barbican, London EC2Y 8DD, England. Telephone: 01-638 4141.
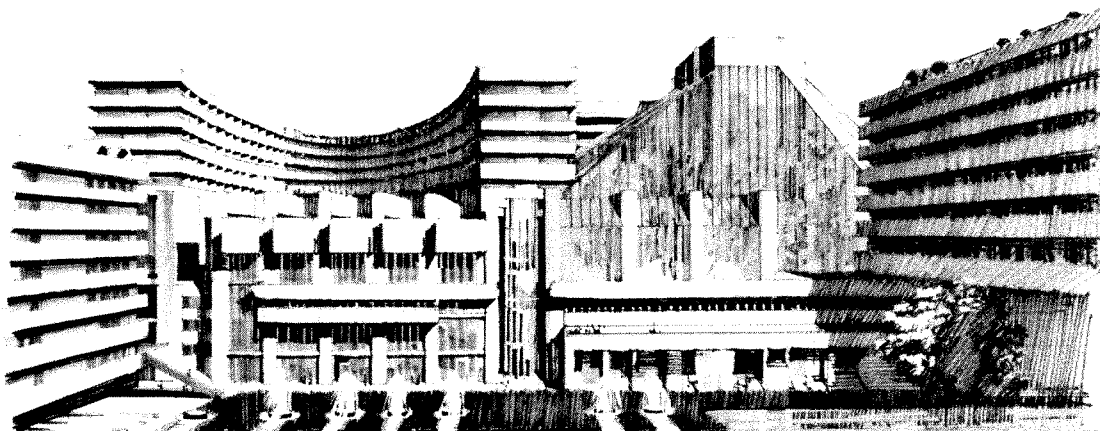
A display and exhibition area totalling 8,000 square metres gross (86,000 square feet).

The Barbican Hall comfortably seats 2,000 delegates.

A variety of lecture theatres, seminar and committee rooms to take anything from 5 to 265 people.

The Film Theatre seats 275 people.

The Barbican Theatre seats 1,150.

LETTERS

BOOK REVIEWS

MISCELLANY

nature

Volume 285 No.5766   19 June 1980

NEWS

NEWS AND VIEWS

ARTICLES

LETTERS

LETTERS

MATTERS ARISING

BOOK REVIEWS

MISCELLANY

SCIENTIFIC & MEDICAL DIVISION
MACMILLAN PUBLISHERS

THE ECOLOGY & CONSERVATION OF LARGE AFRICAN MAMMALS

S. K. ELTRINGHAM

DEPARTMENT OF APPLIED BIOLOGY, UNIVERSITY OF CAMBRIDGE.

£15.00; 288pp; ISBN 0 333 23580 0.

"Keith Eltringham has produced a valuable book which treats the ecology of large African mammals in the widest context. In a compact volume he considers their social behaviour, population, biology, and feeding in an ecological framework. Perhaps the most important sections are the last three chapters which deal with conservation, wild life management, and man and national parks".
BIOLOGIST, APRIL 1980.

"Eltringham's book is written as a textbook for undergraduates but he also had in mind the value of making the book of interest to those with a more cusory contact with African habitats. Accordingly, it is written with a pleasant directness, lack of jargon, and wry humour".
TIMES HIGHER EDUCATION SUPPLEMENT, MARCH 1980.

"The appearance of this book is timely. Many talk about conservation without doing anything about it. Keith Eltringham has done an excellent job by providing much needed information. He has obviously drawn from his vast experience as a wildlife biologist in East Africa for many years. Writing about a subject he knows so well makes the account vivid and very much alive".
AFRICAN JOURNAL OF ECOLOGY, MARCH 1980.

"This immensely readable book will be essential for any undergraduate studying mammals and ecology but it will also be attractive to a wider audience – not only those who have been fortunate enough to visit Africa. Many people are now familiar with these animals through films, television, zoos and safari parks, and this book will interest all those who wish to know how they are living together and surviving in the world.
BRITISH BOOK NEWS, APRIL 1980.

Macmillan books are available from all leading booksellers.

In case of difficulty write to Frances Roach, Macmillan Retail Ltd., Houndmills, Basingstoke, Hampshire, England, enclosing remittance plus 70 pence (p&p).

nature

Volume 285 No.5767   26 June 1980

NEWS AND VIEWS

How Selfish is DNA?

ARTICLES

LETTERS

Cover. The Palomar Sky Survey. The triple QSO PG1115 + 08 as seen on the TV guiding screen of the Steward Observatory's 2.3 – m telescope; the brightest component is masked by the circular aperture. The background star field is from a Palomar Sky Survey photograph. See p.641 for more details of this object.

LETTERS

BOOK REVIEWS

MISCELLANY

GUIDE TO AUTHORS

● Review articles should be aimed at a relatively wide readership. Many reviews are invited, but submitted articles may also be accepted; it is advisable to consult us before writing a review article.

● Articles may be up to 3,000 words long with at most six displayed items (figures and tables); they are reports of major research developments.

● Letters are brief reports of original research of unusual and wide interest, not in general longer than 1,000 words; they have at most three or four displayed items.

● 'Matters Arising' permits short discussion (up to 300 words) of papers that have recently appeared in *Nature*.

Articles should be accompanied by an abstract of not more than fifty words. Letters should begin with a paragraph giving the background and main conclusion in terms intelligible to as wide a readership as possible.

Manuscripts may be submitted either to London or New York. Three typed copies should be submitted, each including lettered copies of figures. Typing (including references) should be double spaced. The title should be brief and informative. Pages should be numbered. References, tables and figure legends should start on separate pages. Experimental detail vital to the paper yet which would interrupt the narrative is best placed in the figure legends. Units should be identified in the margin on their first appearance. Equations should occupy single lines if possible: $\exp(a)$ is preferred to e^a if 'a' is more than one character.

References are indicated by superscripts in the text. See any contemporary *Nature* for style, but note:

(i) only one reference number need be used if the reference is to several papers by identical authors.

(ii) first and last pages of references should be cited.

Abbreviations should follow the *World List of Scientific Periodicals*, fourth edn (Butterworth, 1963-65). Symposia are often difficult to refer to and only published or soon-to-be-published volumes should be mentioned in references. Their publisher and place of publication should be clearly indicated 'Personal communication' and 'unpublished' should be incorporated in text.

Artwork should be sent with the manuscript and clearly marked with author's name and the figure number. Line drawings should be either photographic prints or in Indian ink on heavy cartridge paper, tracing paper or similar materials. Most figures are reduced to one column width so originals should be about as wide as a page of *Nature*. To enable figures, particularly maps, to be edited in the same style as the text, they should contain only essential material. Ideally, an unlettered original and three lettered copies should be provided; labelling on halftones should, if possible, be avoided entirely. Magnifications quoted should be for the figures as submitted. We are always glad to see artwork for possible use on the cover, but cannot guarantee its return.
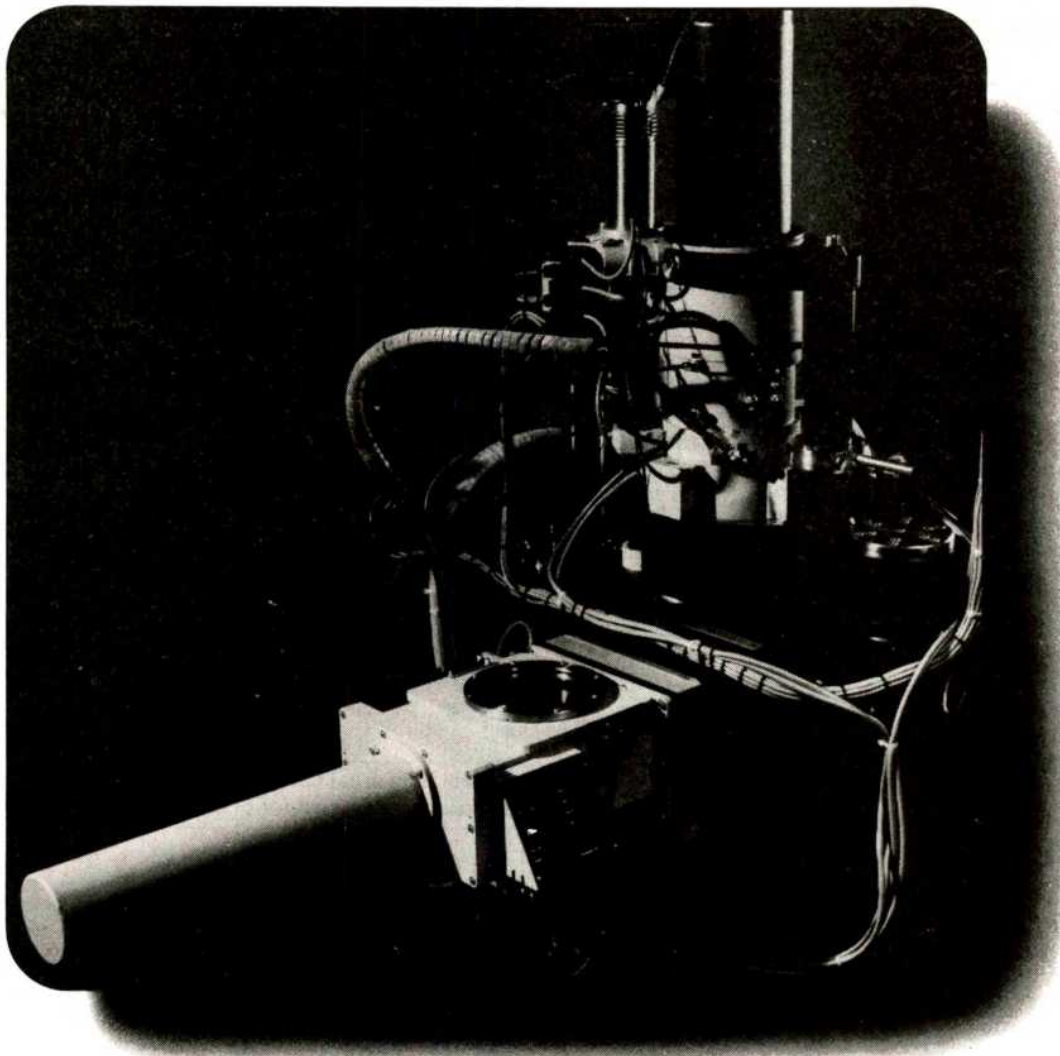
In order to save on postal expenses we return only the top copy and artwork of manuscripts that we cannot publish.

Nature's publishing policy is outlined in **258**, 1 (1975) and **264**, v, 11 Nov. (1976).

nature

1 May 1980

Does science need a tax-break?

SHOULD President Carter introduce generous new tax incentives — in particular increased deductions for money spent on research and development — to help reverse the productivity decline widely claimed as a major source of the nation's economic problems? American business is convinced that he should: the Committee for Economic Development, for example, synthesising the views of many large corporations, said earlier this year that 'top priority' should be given to appropriate tax changes as a means of stimulating technological innovation.

The administration itself is less certain. While accepting the argument that tax relief for R and D could help increase the rate of innovation (and even this is yet to be supported by hard data) administration officials also point to the cost of such measures in terms of reduced federal revenues. Revisions to the tax law have long been promised, and many expected them to be included in the package of measures to spur innovation which the President presented to Congress last autumn. But such moves have since been overshadowed by attempts to balance the budget.

At present, although private companies can deduct R and D expenditures as running expenses, no special incentives exist for investment in R and D equipment. This is in contrast to France, for example, where accelerated depreciation is allowed on all investments in research. Or Germany, where a 7.5 per cent tax-free cash subsidy is granted on money spent on R and D facilities.

Current demands to reduce the tax burden represent the intersection of two trends. The first is a general political thrust to reduce taxes on both individuals and corporations, represented most vividly by a proposal before Congress for an immediate 30 per cent cut in personal income tax. The other is a more detailed argument that, in order to encourage more private R and D, it should be made more attractive than other possible investments — with the tax system being used to this end.

In general the two trends reinforce each other. But there are ways in which they could conflict. For example, political enthusiasm for tax relief to major corporations has produced broad-based support for a bill introduced by representatives James R Jones and Barber B Conable which would shorten the time over which companies could write off capital investments. Rather than using a 'useful life' formula which differs from industry to industry, the bill proposes fixed depreciation times of ten years for buildings, five for machinery and equipment, and three for light vehicles (hence referred to as the 10-5-3 proposal).

Supporters of the bill, which has more than 300 co-sponsors in the House of Representatives and would include R and D equipment, argue that it would free capital for more lucrative investment, and is thus precisely the type of measure needed to raise the general level of economic activity. Critics, however, have suggested that the benefits of such a bill would be skewed in favour of capital-intensive industries, and not necessarily high technology firms with large R and D costs, where the 'write-off' time may already be short. It is also argued that the Jones-Conable bill would cost $5 billion in the first year, and $25 billion after five years — and that the resultant inflationary pressures could outweight any benefits.

In the light of such objections, a separate proposal has been made by representative Charles Vanik of Ohio. He has proposed a Basic Research Revitalisation Act which would offer tax incentives to companies supporting university research. In particular, companies would be given a 25 per cent tax credit on money deposited in a special research reserve (up to five per cent of the company's business income). And any money taken from this reserve to fund basic or 'exploratory' research in universities could be claimed as a tax deduction, providing it was spent within four years.

Research universities are understandably enthusiastic about the Vanik bill, which has been co-sponsored by over half the members of the House Committee of Science and Technology. As funds for federal support for basic research grow tighter, universities are increasingly looking to industry as a source of financing. A typical example is the announcement expected this week from the Massachusetts Institute of Technology that it is to receive a large grant from the Exxon Company to support fundamental combustion research. Exxon officials have already spoken in support of tax relief for such moves, claiming it would encourage other companies to follow their example.

But the question hanging over the Vanik proposals is whether they would make any significant impact on the problem they are intended to address, namely the nation's declining productivity and the consequent slowdown in economic growth. Most analysts agree that it is not support for R and D itself which is missing, but adequate mechanisms for translating knowledge into useful and acceptable products. A report published last week by the National Science Foundation, for example, shows industrial R and D to be in a surprisingly healthy state, experiencing a five per cent real growth between 1976 and 1977, with a 22 per cent increase in the number of qualified scientists and engineers employed between 1972 and 1977.

Demands for tax incentives to stimulate research, particularly made at a time when the overall level of R and D effort would appear adequate, reflect a desire to short the control of research funds from the public to the private sector. Such a move has obvious attractions to those who would benefit most directly; but whether it is the best solution is a political, not a technical, judgement. The success of Japanese industry in fields from motorcycles to digital watches has been achieved in active partnership with government. In Britain the Spinks report on biotechnology endorses a similar marriage. In the US, the key to rekindling innovation should be better government — not less. □

United States

An excess of doctors...

David Dickson reports from Washington on the levels of manpower in medicine, and womanpower in science.

AFTER fifteen years' rapid expansion, US medical schools are beginning to produce more doctors than the country needs. Earlier this month the Department of Health, Education and Welfare (DHEW) predicted that the surplus could be between 4,000 and 40,000 by 1990; and other estimates make it considerably higher.

Numbers alone, however, hide the fact that not all medical graduates go where they are required. In particular, the more lucrative fields of surgery continue to exert higher attraction than primary health care, especially on those who may leave medical school with outstanding loans of $40,000 to $50,000.

Ironically the current situation is largely the result of the success of the government's previous efforts to fit medical education to social needs. These were initiated in the late 1960s, when a national shortage of doctors led the government to offer generous grants to medical schools willing to increase their enrollments.

With the encouragement of 'capitation' grants (based on the number of students) and funds for the creation of new medical schools, the number of places for medical students has doubled, from about 8,000 to 16,000. And although the rate of expansion has slackened off, there is no indication that it is likely to fall, particularly given the continued excess of applicants over available places.

The consequence of a growing domestic supply plus the influx of foreign doctors during the period of shortage is that, according to figures prepared by DHEW's Bureau of Health Manpower, there will be 600,000 doctors in the US by 1990 — but the need will only be for between 553,000 and 596,000.

Congress' Office of Technology Assessment (OTA) predicts an even wider gap. In a report on the bureau's statistical methodology published last week, it agrees with the supply figure but points out that the projected need is based on a linear extrapolation of an observed increase in the per capita demand for physicians over the period 1968 to 1976.

The OTA report also points out, however, that since 1971 the per capita demand has been falling. And that if this trend is combined with expected demographic changes, the need for doctors by 1990 could be as low as 415,000.

No-one is particularly worried about the surplus itself. Despite the growing signs of a shift away from surgery into general practice, there are still likely to reamin — as

both the DHEW and the OTA report emphasise — fields in need of more doctors, for example, for work among imigrant and minority populations.

The dilemma is over the appropriate response of both the federal government and the medical schools. The Carter Administration is using the over-supply figures to support its proposal that all direct federal aid to medical schools should now be dropped, confining assistance to student grants and loans.

The schools, in contrast, feel that relying on tuition fees alone would place unacceptable pressures on students. And that some form of additional support, not tied to providing health services or to funding research which are both tightly regulated, would now be welcome.

So far the administration's attempt to eliminate capitation grants has met limited success. Although omitted from DHEW's budget request for 1980 last year, they were put back by Congress reacting to pressure from the medical schools. In January the President asked that the capitation grants be withdrawn from the 1980 budget, but again Congress disagreed. A further attempt to cut the money out was made in the President's revised budget request last month among the revisions for 1980. And the issue remains unresolved.

However congressional attitudes are changing, reflecting the schools' acceptance of the current illogic of measures to increase doctor supply. Last week a House subcommittee proposed that, in renewing the health education support legislation which runs out this year, capitation grants should be 'phased-down' by steps of 25% over the next three years. And although remaining agnostic over whether the nation faces an oversupply of doctors, the subcommittee agreed that no new medical schools should receive federal funding.

The main problem facing the schools is the implication of the growth in tuition fees, which can now go as high as $8,000 a year. One approach has been to seek new forms of outside assistance; thirteen private medical schools announced last week that they are to divide $1.3 million next year awarded by the Henry J. Kaiser Foundation to assist students with more forthcoming later to those able to raise matching grant from alumni or elsewhere.

Others are seeking new forms of federal support for teaching. "One way would be to develop a two-part system. All schools would get a certain base amount, and you could then pick and choose programmes which might qualify for additional funding" says Dr Richard Ross, Dean of the Medical Faculty and Johns Hopkins Medical School.

Without some such support, fears are growing that many of the trends which federal funding has encouraged — such as the growing recruitment of students from minority or low-income groups — could be reversed. And that current mismatches between the supply of physicians and health needs may only be exacerbated. □

...and a dearth of women

A political struggle appears to be looming on the Washington horizon over the steps that the US government should take to encourage the participation of women in science.

In passing the National Science Foundation's budget for 1981 last Thursday, the Senate Subcommittee on Health and Scientific Research included a provision for $23 million to be allocated to a new 'women in science' programme within the foundation.

The elements of the programme are broadly similar to those included in a bill introduced last year by Senator Edward Kennedy. They include a new centre for women in science, a special committee within the foundation to examine the position of women scientists, the creation of appropriate university positions, and the appointment of a special assistant to the NSF director.

Subcommittee members say the need for such a programme is shown by the fact that the number of women in science remains

disproportionately low. But to make room for the programme while remaining under the revised ceiling for the NSF's budget proposed by President Carter earlier this month, the committee is recommending a *pro rata* 9% cut on all items listed in the original January budget request.

Although the impact on basic research programmes would be mitigated by the transfer of money that would have been spent on upgrading research facilities, this would cut back their increase from 11% to 7%. Funds for mathematical and physical sciences, for example, would fall from a proposed $260 million to $244 million.

The corresponding House Sub-committee, in voting on the NSF budget last week, kept closer to the administration's revised request for $1,074 million. However, it added applied research and science education items, and cut back the proposed government /industry ocean margin drilling project from $5 million to a $500,000 study by the National Academy of Sciences. □
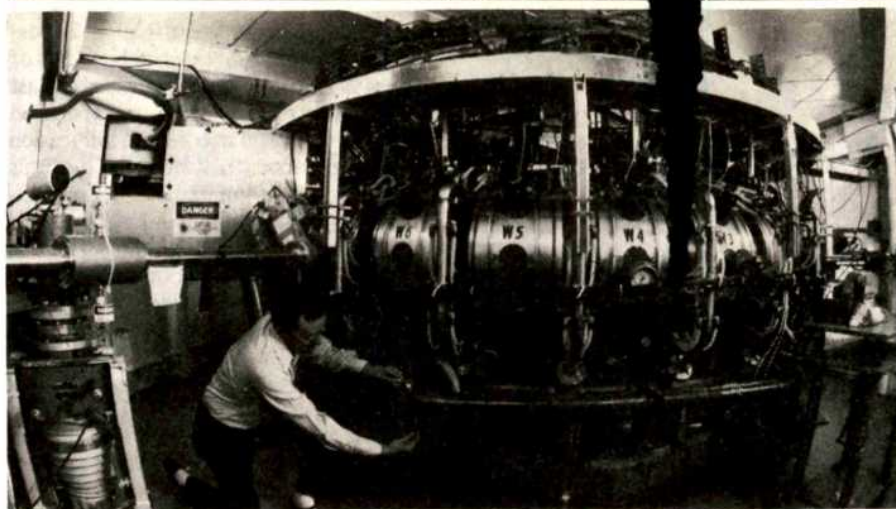
ELMO Bumpy Torus: dark horse of fusion

To most nuclear engineers, magnetic confinement fusion technology tends to be identified with the familiar doughnut shape of the Russian-designed Tokamak, which gained acceptance over US designs in the early 1960s, and of which 40 are now in experimental operation world wide.

But both Tokamak technology and the less familiar mirror confinement techniques still face many unanswered questions. And two years ago an *ad hoc* review committee appointed by the US Department of Energy recommended that, in the light of such uncertainties, increased support be given to alternative designs.

Two contenders emerged from a further review. One was the reversed field pinch, an adaptation of the Tokamak design; the other was a device that had been worked on at the Oak Ridge National Laboratory since the 1960s, known as the ELMO Bumpy Torus (EBT). A hybrid between the Tokamak and mirror designs, the EBT was subsequently selected for development to a point where it can be compared directly to the operation of existing Tokamaks.

Last Autumn, four industrial consortia — headed by Westinghouse, Grumman, McDonnell-Douglas and Ebasco — produced separate plans for a 'proof-of-principle' EBT. These were amalgamated into a single design. And earlier this month the four consortia were asked to bid competitively for what has become known as the EBT-P.

The Bumpy Torus is based on a discovery made by a team headed by Dr Ray Dandl at Oak Ridge in the 1960s. When magnetic 'mirrors' produced by current-carrying coils are used at either end of a cylindrical cavity to keep plasma particles from escaping, and the plasma is heated by radio waves at the electron cyclotron frequency, a ring of electrons is found to form around the plasma at the mid-point between the two end coils.

This ring is of sufficiently high energy to keep the plasma away from the walls of the cylinder, necessary because of its high temperature. And the ring remains in place even when the end coils are inclined at an angle of 15 degrees to each other.

Putting 24 such cylindrical modules together end-to-end results in a torus. It is called 'bumpy' because the magnetic field is narrower between the mirrors than in the centre of each segment. No-one except Ray Dandl knows why it is called ELMO and he is not saying.

So far two experimental EBTs have been built at Oak Ridge (and one in Japan), and both have operated successfully according to theoretical predictions.

Operationally the EBT has two important advantages over the Tokamak, according to Dr John Sheffield, head of the Experimental Confinement Section at Oak Ridge. The first is that it operates in a steady state, rather than the pulsed mode of the Tokamak.

The second is that, without the complexity of the interlocking coils required by the Tokamak design — and the engineering difficulties caused by their magnetic interaction — construction problems could be considerably less.

Whether these advantages are sufficient to overcome the relative lack of knowledge about the EBT compared to the extensive amount already known about the behaviour of Tokamaks remains to be seen. At present EBT technology is about ten years behind; and with Congress pushing the DOE hard for the construction of an engineering test facility (ETF) for the Tokamak, it will be difficult to catch up.

Furthermore, promising results are being reported from tests with mirror confinement devices at the Lawrence Livermore Laboratory, three to five years behind the Tokamak but still ahead of the EBT. DOE officials are considering putting a request for $100 million to construct a new mirror test facility in the 1982 budget.   □

Senate approves patent changes

HOPES are high among US research universities that, following a six-year campaign, the US Congress will soon pass legislation boosting their rights to benefit directly from the results of research carried out with federal funds.

Last week the Senate passed a bill which would allow universities and small businesses, under certain defined conditions, to license any patents arising from such research. Similar measures are already under active consideration in the House of Representatives. And given the large majority that voted for the Senate measure, university lobbyists in Washington are confident that they will have a new law on the books by the end of the year.

Revision to the patent law has been a cornerstone of attempts both in Congress and by the Administration to tackle the recent drop in industrial productivity and an apparent decline in the rate of technological innovation. Both are claimed to contribute to the nation's economic problems. And both, it is argued, could be reversed by assisting the flow of research results into the market-place.

A variety of bills has been introduced into both legislative bodies over the past year. Some, such as a bill passed by a subcommittee of the House Science and Technology Committee three weeks ago, have recommended that patent rights be awarded to anyone carrying out federally-sponsored research.

The universities, however, fearful that too broad an approach might fail to win sufficient support, have put their efforts behind a more limited bill introduced by senators Birch Bayh and Robert Dole which gives patent rights to universities and small businesses, but excludes large businesses.

Six weeks ago, when the bill reached the floor of the Senate, it was threatened with a filibuster by Senator Russell Long, who claimed that liberalising the patent laws would encourage monopoly practices and discourage competition. The bill was subsequently withdrawn from debate.

When offered last Thursday, Senator Long spoke strongly against the bill. But he did not offer any amendments that might have killed the measure, and the final vote was 91 to 4 in favour, an indication of the depth of support.

Under the Senate Bill, a university will have the exclusive rights to a 17-year patent on federally sponsored research results, providing it illustrates that it has the institutional means to license the patent. The bill contains a provision that if the patent proves commercially successful, the government should be paid back for the costs of the research.   **David Dickson**

United States

Asbestos: reductions urged

SCIENTISTS from the Occupational Safety and Health Administration and the National Institute for Occupational Safety and Health have urged further stringent reductions in the permitted exposure limits to asbestos fibres in the air.

Since 1972, the maximum permitted concentration in the work-place has been two million fibres per cubic metre in air. The scientists have now issued a report recommending that this exposure level be reduced to 100,000 fibres per cubic metre — the lowest level that can be accurately measured — and have urged a ban on all non-essential uses of asbestos.

At a news conference in Washington last week, Dr Eula Bingham, Assistant Secretary of Labour for Occupational Safety and Health, said that the agency intended to push shortly for reduced exposure limits — but refused to say whether it would endorse the study group's recommendation or a higher one.

Mind the spores!

THE US Defense Department published details last week of experiments carried out in the mid-1960s to test the New York subway system as a method for dispersing bacterial weapons.

According to the defence scientists who carried out the tests, commuters using the subway system paid little attention when they were sprayed with harmless strain of the bacterium *Bacillus subtilis* through gratings in the sidewalk, even though the aerosol clouds were clearly visible.

This lead the research workers to the conclusion that the subway system, where the draughts caused by trains would disperse the biological agents over a wide area, could prove an effective way of inflicting severe casualties on civilian populations.

Particularly effective were light-bulbs containing the test bacilli which were dropped from moving trains within the subway system. According to the Defense Department report, released after a Freedom of Information request from the Church of Scientology, the bacteria "aerosolised and dispersed rapidly by the movement of trains, penetrating stations and trains in the area and persisting there for one hour or longer."

The report says that information about the effectiveness of subway dispersion had both defensive and offensive value.

"*Forget the heroin business, Bugsy! I've something more profitable lined up!*"

Interferon sales $2 billion-plus?

ACCORDING to a report prepared by the US brokerage and investment firm Bache Halsey Stuart Shields, interferon sales could have a world wide market of $2 billion a year within three to five years. The report, summarised in *European Chemical News*, specifies three major health areas — cancer, chronic inflammations and viral diseases — in which interferon could have widespread application.

Bache estimates that in the US 5.4 million cancer patients a year could receive interferon treatment. Assuming a five-injection course of therapy at a factory price of $10 per dose, this produces a $270 million-a-year market. Subtracting $100 million a year for competing drug therapies leaves an interferon market of $170 million a year from cancer treatment.

For chronic inflammatory diseases such as arthritis, Bache estimates that interferon could capture half the market now occupied by steroid treatment. At 11.5 million patients and a course of five $10 injections the market would be around $300 million. Viral diseases are estimated to plague nine million people a year in the US. With a shorter course of three injections per treatment course sales would be worth $270 million a year. Total US sales would then be around $750 million.

Bache then estimates world wide sales on the basis of current pharmaceutical sales. In 1979, the US market accounted for 20% of the world market. Since new drugs take longer to penetrate non-US markets, Bache estimates non-US sales for interferon to be three times the US total.

The author of the report, Ronald Norman, formerly of Warner Lambert and Bache's specialist on the pharmaceutical industry, admits that some of the estimates are only guesses. In particular, the factory price of a dose could end up falling anywhere between $1 and $100 dollars a dose. "We create a rough guideline and leave it to our clients to make their own educated guesses" says Norman. (G.D. Searle in the UK has estimated that their fibroblast technique could bring the factory price down to around $2 a dose.)

Joe Schwartz

United Kingdom

Coalite health survey talks

WORKERS exposed to the toxic chemical 2,3,7,8-tetrachlorodibenzo-p-dioxin (dioxin) at Coalite and Chemical Products Ltd between 1968-1971 are to be told today the results of three surveys of their state of health (*Nature*, 6 March, page 2). But because of the make-up of the control group surveyed, interpretation of results is difficult, and the investigation may have to be repeated.

Officials of the Health and Safety Executive (HSE) are to meet the workers, and management, to give them the Executive's assessment of the surveys; but the Executive is expected to say that it is not possible to draw any firm conclusion from results so far.

Two of the studies — those on the blood chemistry and immunology — detected differences between the dioxin-exposed men and the control group; but the third study on chromosome changes reported no differences between the two. The study of blood chemistry showed changes in total blood cholesterol and high density lipoprotein cholesterol levels in the exposed workers. And the immunology study reported reduced levels of two immunoglobulins, IgD and IgE in a significant proportion of them.

However, the control group used was not properly matched with the exposed group, making comparison between the two difficult. The control group included management staff undergoing lipid screening at the time.

One HSE official hinted that something might be salvaged from the studies when the raw data had been examined but admitted that the investigation may have to be repeated.

Even though the HSE persuaded Coalite to arrange the studies two years ago, it did not receive the results until a few weeks ago. This delay was due in part to a belief within the HSE that it lacked the necessary powers to compel Coalite to disclose the findings.

An Executive spokesman has now said that the HSE does have the legal powers under Section 27 of the 1974 Health and Safety at Work Act to serve a notice on any individual to disclose information which the Executive requires. **Alastair Hay**

France

Cap la Hague restarted

THE accident at the reprocessing plant at Cap la Hague which resulted in the total loss of electric power a fortnight ago (*Nature,* 24 April, page 653) may have been the result of circuit overloading according to the CFDT, the main union representing nuclear workers at the plant. A spokesman for the union told *Nature* that some of the power supply equipment was 15 years old and had been initially designed for the reprocessing of low activity spent fuel only. However, high activity fuel was now reprocessed there although the plant had not been fully upgraded to cope with the increased current this demanded.

According to reports in the *Guardian*, Cogema decided to restart operations last week after receiving clearance from the Ministry of Industry. A spokesman for Cogema had said that radiation levels were acceptable. Workers at the plant, however, were worried that several parts of the plant were still highly contaminated. According to the CFDT spokesman, an expert who had visited the plant had recommended that it should not be restarted. The director however, decided to go ahead.

The union met at the end of last week to discuss how to react to Cogema's decision to restart operations even though full repairs have not been carried out. In the absence of any detailed technical report, no agreement on what action to take was reached except that the union's concern over the decision should be expressed.

Cogema's desire to restart only eight days after the accident is seen as a move to reprocess spent fuel already stored at the plant to make room in the storage ponds for a consignment of Japanese spent fuel awaiting shipment in the UK. Workers believe that as soon as this backlog is cleared, the plant will be closed in two to three weeks time for full repairs.   □

Mozambique

The politics of African archaeology

THE opening of a new museum at Manyikeni in Mozambique marks a change in the presentation of archaeology in Southern Africa.

At issue are the "Zimbabwes" — a chain of 150 ancient settlements characterised by central stone-walled enclosures spread across Mozambique and what is now called Zimbabwe. White settlers in Rhodesia argued that the stone walls were Egyptian temples built by the Queen of Sheba, while the Portuguese in Mozambique opted for their construction by mythical Lusitanians.

As early as 1905, the British Egyptologist, Randal McIver, established that not only were the ruins not Egyptian, but that they were built in the past 1000 years, and thus necessarily by local, black, people. Later all other archaeologists agreed. But that answer was totally unacceptable to the white settlers, who stuck by the Queen of Sheba.

The advent of scientific archaeology made this position increasingly untenable. The first carbon tests in the 1950s suggested that Great Zimbabwe, after which the country Zimbabwe has taken its name, was built around 1000 years ago. (Great Zimbabwe was the most striking of these settlements and with a population of 10,000, must have been the largest city in southern Africa at its peak in 1400.)

A guidebook to Great Zimbabwe published in the early 1960s contained the carbon dates and dismissed the Queen of Sheba explanations. In the late 1960s and early 1970s much better carbon dates were

Manyi Keni . . . first exhibition on basic data

produced for Great Zimbabwe, but the then Rhodesian government not only refused to permit them to be displayed, but ordered the removal of all dates from the Zimbabwe displays in museums. And the guidebook was allowed to go out of print. In 1975, when a new guidebook was being written, the government ruled that carbon dates could not be included.

In Mozambique the attitude was different. The Portuguese simply never excavated the Zimbabwes, so there was no data to contradict the Lusatanians.

In 1975, however, after independence in Mozambique one of the Zimbabwes — Manyikeni, 50 km west of Vilanculos was excavated. The work has been done by a Mozambican archaeologist, Joao Morais, and two British archaeologists, Peter Garlake and Paul Sinclair. Both Garlake and Sinclair had worked at Great Zimbabwe, and both quit over the supression of scientific data.

Carbon dating, done free of charge by the University of Rome, shows that Manyikeni was occupied from 1250 to 1750, and that the walls were built around 1450. The stone walls, about two metres high, and similar to English dry stone walling, made an enclosure inside which about five families lived. The new museum displays show carbon dates and detail the

recent excavations and scientific stories.

Several scientific techniques have been brought to bear on the site, some for the first time. One is stratified sampling, in which the site was first divided into 20 metre by 20 metre squares, and then four randomly selected one metre by one metre trenches excavated within each of the larger squares. This gives a better overall picture of life in the settlement than just by digging at "likely looking" spots. Until the early 1970s, all the excavation was done inside the walls. But then it was realised that the bulk of the settlement was actually outside. The area outside is too large to excavate completely and stratified sampling is the only sensible way. Manyikeni is the first Zimbabwe to be extensively excavated outside the walls.

The excavation of this site represents one of Mozambique's first efforts to illuminate its history before the colonists arrived. It also reflects Mozambique's attempt to popularise science. The excavation was done by local people, under the supervision of the professional archaeologists. And the musuem is primarily intended to teach local people their own history. Yet it also represents the first exhibition in Mozambique or Zimbabwe of some basic scientific data.

Joseph Hanlon

NEWS IN BRIEF

Three Mile Island health effects

HEALTH officials in Pennsylvania have discounted recent claims that increased infant mortality in the area around the Three Mile Island nuclear power plant was due to the accident at the plant last March. They point out that the area also experienced an increase in total births, and that the mortality rate therefore remained constant.

However, they have also reported a "surprising" degree of anxiety among residents living near the reactor, with significant increases in the use of tranquillisers and sleeping pills. Nearly half of 1,000 people interviewed in January who live within 10 miles of the plant reported physical symptoms of stress, ranging from headaches and diarrahoea to a loss of appetite and the appearance of rashes.

The survey, conducted by behavioural scientists at the Hershey Medical Center of Pennsylvania State University, also found that nearly 13% of those living within five miles of the Three Mile Island plant had become anti-nuclear activists. Dr. H. Arnold Muller, the State Secretary of Health, called this figure "very significant."

Drilling Project faces big cut

THE US House of Representatives Science and Technology committee has proposed that federal support for the first year of a massive Ocean Margin Drilling Project, to be sponsored jointly by the National Science Foundation and private oil companies, be reduced from $5 million to $500,000.

The $5 million recommended by the Carter Administration in its revised budget proposals last month had already been reduced from $10 million included in the original NSF budget proposal in January. However, the Senate Health and Human Resources Committee, voting last week on the NSF appropriations request for the fiscal year 1981, is proposing restoring funding for the project to about $9 million — which provides room for an appropriate compromise.

MIT raises $250 million

THE Massachusetts Institute of Technology announced last week that it has successfully raised $250.2 million — $25 million above its target figure — in a five-year fund raising campaign.

About a quarter of the total will go to endowing new faculty positions, and an equivalent amount to new teaching and research facilities, including the construction of the new Whittaker College of Health Sciences. The remaining funds will go to supporting new programmes and other uses.

MIT is also expected to announce this week a major agreement with the Exxon oil company to support basic combustion research at the institute.

Chojecki held

MIROSLAV Chojecki (above), a young Polish physicist and human rights activist, was recently arrested under a "procurator's sanction", which empowers the police to hold him up to 90 days without charge or trial.

Chojecki was formerly a research assistant working for his PhD at the Warsaw Nuclear Research Institute. During 1976, he was a frequent observer at the trials in Radom of workers who had taken part in the June demonstrations against food price rises. In October 1976 he was dismissed from his post and has not since been able to find professional employment. He has recently been active in "Nowa", the "independent" (i.e. underground) dissident publishing group.

In an "open letter" written shortly before his arrest, Chojecki stated that since his first arrest on 30 September 1976, he has spent about five months in detention (equivalent to one day a week). His flat has been searched 15 times ("once a quarter") and his person 80 times ("once a fortnight"). On only three occasions was a search warrent issued.

Items confiscated from him range from a text book of Fortran programming to a jar of curry powder (thought by the police to be radioactive isotopes), cuttings from the official Polish press, three tins of imported meat and the contents of his waste-paper basket. He has been fined on a number of occasions for petty offences a total of 19,000 zl. (£350).

It is understood that he is likely to be charged in the near future with being in unlawful possession of printing equipment.

Burbridge to head astrophysics unit

DR Margaret Brubridge has been appointed to direct the new Centre for Astrophysics and Space Sciences at the University of California in San Diego. The centre has been organised to coordinate the scientific activities of several groups which carry out research in astrophysics and space science in three university departments — physics, electrical engineering and computer science. Also included in the regrouping of space science disciplines is the cosmochemistry group in the chemistry department. The centre will house under one roof high energy astrophysics, solar physics, optical and infrared astronomy, the Faint Object Spectrograph (Space Telescope) team, magnetospheric physics and radio astronomy. Laurence E. Peterson and Elden C. Whipple will be associate directors of the centre.

CND marches again

The UK Campaign for Nuclear Disarmament (CND) has organised a major demonstration to protest the installation of the Cruise missile on British soil. The demonstration will begin in Oxford and participants will march 18 miles to the US Air Force base in Upper Heyford, an expected site for the Cruise missile.

An internationally known organisation for the expression of grass roots opposition to nuclear war in the early 1960s, CND is undergoing a revival in the UK at the present time. "Judging from our mail and our discussions with the large number of volunteers that have come forward, people now are concerned about the international situation, particularly Carter's irresponsibility in Iran, the government's attempt to revive civil defence, and the increasing cost of the military budget at the expense of social services," says Caroline Coles of CND.

Monkey business

The Indian Commerce Minister, Z. R. Ansari, recently told Parliament that there was no proposal to lift the export-ban on rhesus monkeys, though several representations had been received from importing countries. The ban was imposed two years ago by the Janta Government following revelations that rhesus were being used in neutron bomb testing. The US drug industry is trying to convince the Indian government that the ban has adversely affected the introduction of several new drugs and even caused shortage of polio vaccine, which is sold in large quantities in India.

FEATURES

A social worker makes a health call on a Brazilian family . . . but will the bureaucratic machine get in her way?

Brazilian paralysis: the real disease

AFTER being invited to work in Brazil by the country's Minister of Health in January, received with official honours by the President of the Republic, and feted as a Nobel prize-winner (which he is not), Dr Albert Sabin, developer of the oral anti-polio vaccine, has left the country a disillusioned man. The muddle, inefficiency and sheer obstructiveness of the Brazilian Health Ministry proved too frustrating for Sabin to bear, and he has returned to his Charleston, Carolina, laboratory without taking leave of Health Minister Valdir Arcoverde.

"In truth," he commented, "it is difficult to take leave of a man who does not let himself be approached."

By Sabin's account, the history of Brazil's approach to its regular epidemics of polio is one of garbled statistics and

---

Health care in Brazil is not simply a matter of science and sound management. It is a matter of politics. **Maurice Bazin** reports on a case history — the 'Sabin episode'

---

official indifference to the plight of the thousands of children who still contract the disease. And he has said as much in a letter to President Figuereido.

"Bureaucratic problems of various types do not permit that this work be properly developed," he complained. "I must emphasise to your Excellency that this

same bureaucracy was responsible for the failures in combating poliomyelitis in the past, and, as for the present, I have strong reasons to doubt that the next attempts will be successful."

The President has not replied.

The first major problem Sabin encountered during his two-month stay in Brazil was the impossibility he found in obtaining an estimate, however approximate, of the scale of the polio problem over the preceding ten years.

He pointed out to the Health Ministry that statistics published during that period by the Institute of Geography and Statistics (IBGE) on the one hand and the Health Ministry on the other differed by factors "at times as high as 60 and 170". Brazil's reports to the World Health Organization showed 15,000 cases of polio per year from
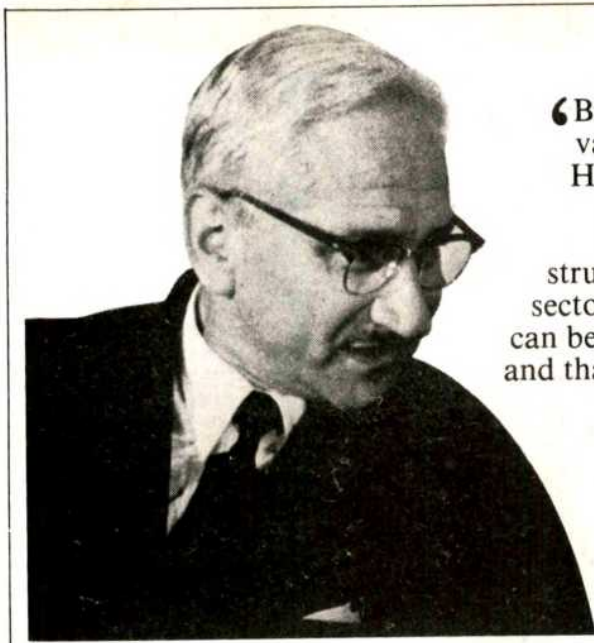
> ❛Brazil needs a national vaccination campaign. However, this task will continue to come up against bureaucratic structures and unreliable sectors. There is a lot that can be done, must be done, and that is not being done❜
> — Albert Sabin

1969 to 1972 followed by an abrupt decline to 2,100 cases per year from 1973 up to the present. Could this effect be the reflection of a national immunization campaign carried out in 1971? Looking through the records, Sabin found out that the high figure came from the IBGE whose data was transmitted to WHO up to 1972, while the low figure came from the Health Ministry's own statistics. The apparent drop corresponded to no more than the switch in data sets. Furthermore, since 1975, IBGE had been forbidden to supply any more statistics about polio.

"Nobody lied or manipulated the data," he said, "but the whole truth was not told. The officials of the Health Ministry are guilty of breach of duty because they did not inform the public about the change from one set of statistics to another. And still now they continue to give out improper information to WHO."

While working with a local vaccination campaign Sabin heard that his proposal for obtaining realistic statistics about polio incidence from a survey of school children was considered by the ministry to be "of dubious statistical value", although it had been approved by the minister six weeks earlier. But he organized a local statistical evaluation of the incidence of polio for 1969-72 and 1973-76 by looking for sequels of paralysis in children 10 to 11 years of age and six to seven years of age respectively in the Federal District around Brasilia today.

He enlisted the participation of local doctors and school personnel and found 57 cases of clear paralytic sequels in a sample of 25,000 children. From the detailed data, which represents a minimum evaluation, he could conclude that the IBGE statistics for these periods were closer to reality than those of the Health Ministry, which were at least five times below the true level.

Sabin's own data, however, are certainly still very much below a realistic estimate of the number of polio cases because they rely upon a sample of children presently in schools. In the poor districts around Brasilia many children do not go to school, and physically maimed children are often beggars in the streets and not registered school children. The only technical comment that minister Arcoverde made after Sabin made his results public at the end of March was:

"Dr Sabin is an excellent epidemiologist, however, he is no a statistician." To which Sabin replied publicly: "The Minister says that the ministry's statistics are satisfactory; I say it's completely untrue."

In the course of his investigation in the Federal District, Sabin found out that 88% of the children had contracted polio before two years of age and 45% before reaching one year, and that parents only knew of it when they noticed that their child had difficulty in starting to walk. As he went to the slum satellite cities of the Federal District and around Brasilia, diagnosing the origin of children's physical deformities, he could remember that official statistics reported no polio cases outside the capital proper during 1976, 1977 and 1978. Today, he noted, the industrial suburbs of the city of Sao Paulo have a polio incidence five times higher than the city proper.

Using the weekly reports of polio cases for different states of Brazil, Sabin found that epidemics appeared to last much longer than in European countries, at times up to six months or more. However, looking with care at the geographical origin of the reported cases, he could prove that an epidemic propagates across a state and lasts the customary three to four weeks in each locality. He therefore proposed a plan of action to stop the ongoing epidemics in the state of Santa Catarina in the south of Brazil, which he had been called to help control in January. The state's health secretary mobilized thousands of school teachers, policemen and community members to carry out a massive vaccination in one day in the communities immediately in front of the wave of contamination.

"We learnt that we could not do a vaccination in one day because the statistics about the number of children in the community were wrong. In some places we had vaccinated 110% of the children! But by the second day we reached almost all children, with teachers going door to door all day in the hot sun." Three weeks later the last hospital admittance for polio was registered in Florianopolis, the state capital.

Open conflict between the scientist and the minister never occurred. Health bureaucrats, comfortably installed in their futuristic buildings in Brasilia, continued smiling to the scientist, but stopped answering his memoranda. In a mixture of efficiency and idealism, Sabin would announce in a memo that there were no steel lungs available to save children with affected respiratory muscles outside the cities of Rio and Sao Paulo, indicate how to recover the huge lungs which were used in the US before vaccination existed, and where to acquire new plastic models. He included in the memo the telephone numbers of the manufacturers.

"Unfortunately, these recommendations dissolved away in bureaucratic side tracts" he wrote in his open letter to the President of the Republic.

At the same time, the Society of Pediatrics of Brasilia declared that "vaccination campaigns are never executed adequately for administrative reasons mixed with politics."

Sabin's letter to the President added: "Brazil needs a national vaccination campaign, organised in a highly efficient way and conducted every year. However, this task will continue to come up against bureaucratic structures and unreliable sectors. Just like in military operations, inexact information about enemy forces can bring about disasters; the same occurs when you face an epidemic disease . . . I have met in Brazil dedicated and competent men and women, capable of carrying through this task. I accompanied them in Goiás, Santa Catarina, Paraná and the Federal District, and I personally observed the contrast between their work and that of the official bureaucracy . . . There is a lot that can be done, must be done, and that is not being done."

Despite Sabin's efforts the fundamental social problem remains of how to protect a whole population through a lasting organized effort of routine vaccination. To contribute to this effort was part of Sabin's plans for 1980. It is now very doubtful that anything will come of it.

For saying aloud what officials in power were not interested in hearing, Sabin is now back home, and his data on polio in Brazil will be published in English-speaking professional magazines only. The president of the Society of Medicine and Surgery of Rio has compared the "Sabin episode" to the case of Galileo. □

CORRESPONDENCE

Expanding on Parkinson's Law

SIR, — Parkinson summarised his large experience of administration in the law that Work Expands So As To Fill The Time Available For Its Completion (C.N. Parkinson, *Parkinson's Law*, 1958). A corollary of this law, that the proportion of administrators within a public organization tends to increase with the size of that organization, has been confirmed by empirical observation (R. Moss, *Nature*, 273, page 184, 1978). Schumacher in *Small is Beautiful* (1974), challenged conventional wisdom by showing that large, centralized organizations are often less efficient than small ones, and Moss made observations on the staffing structure of the Natural Environment Research Council (NERC) which showed that component bodies of NERC in which the administration was dispersed amongst many addresses have fewer administrators and other support staff than other, more centralized bodies of comparable size. Further, J. Flux's detailed study of the Ecology Division of the New Zealand Department of Scientific and Industrial Research (in *Focus on Social Responsibility in Science,* 1979), showed that the production of scientific papers per man decreased as the organization increased in size.

These scientific observations have not been followed by a reorganization in the administration of scientific research. Colleagues have suggested that this is partly because the original empirical observations were not accompanied by a theoretical model. Such a model is therefore presented.

Consider the situation in which we have a number W (W = 4 in the example of the figure) of individuals or groups of individuals doing a certain amount of work such as making scientific discoveries or collecting tax. The simplest possible situation is that each individual worker gets on with his job, pausing occasionally to speak with colleagues, answer letters and arrange for the office windows to be cleaned. As W increases, such primitive liaison techniques may become less effective and an administrator may be appointed.

In the model, the administrative workload of an individual is a function of the number of people with whom he communicates. This is the number of lines of communication l, as may be seen in the figure and, for brevity, is subsequently referred to as 'workload'. In stage one of the model each speaks with each of his colleagues and also with the outside world

$$l_{wi} = W$$

where l_{wi} is the workload of worker i.

In stage two of the model, when the administrator is newly appointed, each worker continued to speak with other workers, but also communicates with the administrator. Of course a 'worker' in this model could as easily be a constituent organization within an 'umbrella' organization such as the Agricultural Research Council (ARC), the Medical Research Council (MRC) or NERC. In stage two

$$l_{ai} = W + 1$$

and, as before

$$l_{wi} = W$$

where l_{ai} is the workload of administrator i (of course the suffix $_i$ is redundant at this stage, but it becomes useful later).

When the excitement of reorganization has settled into the humdrum of routine, the administrator has an idea which many readers will recognise. "It is grossly inefficient for all of you (W) to be wasting time liaising both with each other and with me (a$_i$). Let us re-organize our lines of communication so that you all communicate through me". This is
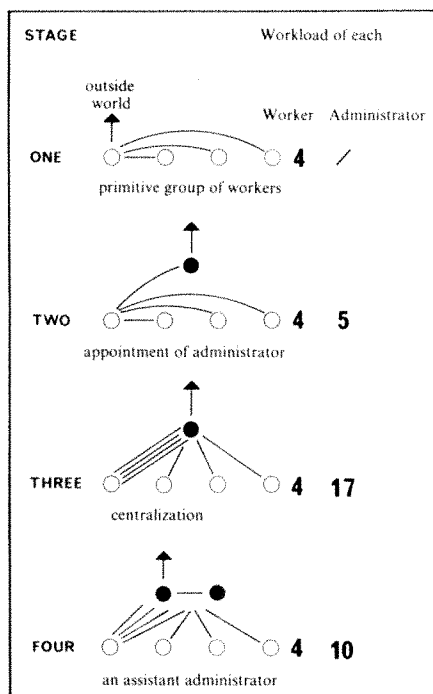
Figure. Illustrating the number of lines of communication (administrative workload) between members of an organization containing four workers, as it passes through the four stages of Parkinson's Progression.

Note. For clarity, lines of communication for one worker only are shown — lines of communication for the others follow an identical pattern.

stage three in the figure. "That will be much more efficient". Efficiency, of course, is only one objective of this course of action. Lust for power is an important motivation and the concept of 'accountability' is often pressed into use at this stage.

In stage three the workload of each worker remains the same, although cooperation amongst them is slowed down by the length of time that their messages lie on the administrator's desk. But the workload of the hard-pressed administrator now rises sharply as he grapples with all the matters that had previously been the subject of direct communication between workers. As well as communicating directly with W and the outside world, he now passes minutes to and from all the W.

$$l_{ai} = W^2 + 1$$

and, as before

$$l_{wi} = W$$

This situation is intolerable: in our example it can be seen that the administrator's workload has increased by more than three times, without any increase in the number of workers. This is the effect of centralization. In desperation our administrator applies for assistance. This is stage four where efficient co-operation amongst administrators gives

$$l_{ai} = \frac{W^2}{A} + A$$

and, as before

$$l_{wi} = W^2 + A$$

A being the number of administrators. Our exemplary administrator in the figure has thriftily indented for only one assistant and so the number of administrators has now doubled, but the workload of each is

nonetheless double what it was in stage two. Both administrators are working very hard, as evidenced by the large number of minutes processed since stage four came into operation. More assistants may well be needed to cope with the increased workload.

Our two administrators may well assume that the more colleagues they have, the smaller will be their individual workload. This is true up to a point, the point being four administrators to four workers in our example Beyond that number, however, l_{ai} increases again as the administrators spend an increasing proportion of their time sending minutes to each other. In general, the minimum workload per administrator $l_{ai_{min}}$ is attained when A = W, that is when the proportion of administrators in the organization is 50%. This may well be the 'maximum ratio' referred to by Parkinson, beyond which the proportion of administrators is unlikely to increase. It is notable that the maximum percentage of non-scientific staff in any of the component bodies of NERC is exactly 50%.

At this point, let us turn our attention to the next rank up in the hierarchy, the chief administrator c_i who appointed our administrators in the first place and to whom they are responsible. His workload will increase as A increases. Initially, his workload will bear the same relation to A as that of A did to W. But, as A increases, he may decide that further centralization is called for in pursuit of increased efficiency . . . with the inevitable consequence that stages three and four repeat themselves at this and possibly higher levels in the hierarchy.

Parkinson's Law has long been regarded as a joke by administrators who know that they work very hard. But what do they work hard at? The writer's experience is that questions such as this, pursued in the course of objective scientific analysis, are sometimes resented by administrators of scientific organizations. The model presented here shows simply and not unrealistically that the effects of centralization are to increase the amount of information that an administrator processes, whilst decreasing the proportion of workers in the organization. Had this model been available and accepted by those in authority some years ago, the re-organization of, for example, local government and the National Health Service, accompanied by decreased standards of service and increased administrative staffs, might not have occurred.

A problem with the model is the simplified assumption that all lines of communication are equivalent in the amount or work that they represent. A logical step next is to test the robustness of this approximation by making measurements of the amount of work per line of communication in the field, factory, office or laboratory.

The principles that the number of administrators tends to increase irrespective of the amount of external work done by an organization, due to Parkinson, and that increased centralization is accompanied by decreased effectiveness, pointed out by Schumacher[2], were empirical and inductive observations made by wise and experienced men. I provide a deductive and quantitative basis for these classic observations, a step towards management by reason rather than intuition.

Yours faithfully,

ROBERT MOSS

Station House, Crathes,
by Banchory Kincardineshire,
Scotland.

NEWS AND VIEWS

The third category of extraterrestrial material

from A.E. Fallick and C.T. Pillinger.

OVER the past ten years two new sources of extraterrestrial material have led to rapid advances in our understanding of the chemistry of the cosmos. The first, of course, was the return of samples from the Moon by the Apollo and Luna spacecraft. The second was the discovery of early condensate-type inclusions in the Allende meteorite, which were found to have anomalous isotopic abundances of various elements and are believed by some workers (see *Nature* 283, 813; 1980) to be older than the Solar System itself.

Now a third class of extraterrestrial material, consisting of the "Brownlee particles" collected in the stratosphere by specially adapted U-2 aircraft, and meteor ablation debris scavenged from the ocean floor (see *Nature* 279, 20; 1979), may be added to the above. As common meteors have orbital parameters indicative of a cometary origin, the new material is of particular interest because it is generally held that comets represent the most primitive sample of the Solar System. Some arguments (for example Napier & Clube *Nature* 282, 455; 1979) have been presented that comets may even be planetesimals temporarily captured during passage of the solar system through the spiral arms of the Galaxy. If this view is correct cometary material becomes of immense importance, for it is then possible that it may be rapidly cooled, explosive debris from highly evolved, massive stars.

Last year, Ganapathy and Brownlee (*Science* 206, 1075; 1979) definitely identified two stratospheric particles as micrometeorites by comparing volatile and nonvolatile trace element concentrations with those of CI chondrites, reckoned also to be primitive solar system material. Studies on single grains less than about 40μm in diameter are not easy but results reported at the recent Lunar and Planetary Science Conference* show studies of stratospheric and deep sea material have great potential. Don Brownlee and colleagues (Seattle and Caltech) have recognised unmelted carbonaceous chondrite, CI and CM materials in deep-sea sediments, and P. Fraundorf and co-workers (St. Louis) have demonstrated the presence of the "cosmic" 10μm feature in the optical absorption spectrum of

*The XI Lunar and Planetary Science Conference was held at the NASA Johnson Space Centre, Houston, Texas, March 17-21, 1980.

stratospheric particles. B. Hudson and co-workers also of St. Louis, succeeded in refining experimental techniques to allow them to determine He, Ne and Ar concentrations in a sample of thirteen Brownlee particles, each typically 10μm across and with estimated total weight of around 10^{-8} g. They found a $^{20}Ne/^{36}Ar$ ratio of 9 ± 3, which resembles the ratio for lunar soil fines (~7) more than it does the terrestrial ratio (~0.5). Assuming the gases to be solar in origin, the time taken to accumulate the Ne and Ar could be the surprisingly low figure of 10-100 years, based on current estimates of solar wind fluxes. As microparticle analysis seems likely to become more efficient and with proposals for a European Space Agency mission to the comet Halley in 1985-6 still active, perhaps the 1980's will be the decade of cometary science.

Work on the first two categories of extraterrestrial materials continues to become much more refined. New studies of solar noble gases in lunar regolith minerals were unveiled by Peter Signer (Zurich). His group have measured ^4He or ^{36}Ar and ^{38}Ar in some 90 individual plagioclase grains and failed to find evidence for whole grain saturation in either ^4He or ^{36}Ar. A search for microscopic saturation is under way using track density studies; the absence of such saturation as a common feature would allow mean noble gas abundances in the ancient solar wind to be inferred from minerals exposed at the appropriate time. M. Thiemans and R. N. Clayton (Chicago) are studying $^{15}N/^{14}N$ in the Apollo 17 deep drill core in an attempt to reconstruct the history of the supposed solar wind nitrogen isotope variations. "Nitrogen is the newest member of the family of noble gases" quipped Clayton.

Dieter Heymann (Rice, Texas) attempted to develop a plausible Xe isotope stratigraphy for a massive star immediately prior to, and after, the supernova explosion. Because of the paucity of observational constraints such a model is difficult to assess, but Heymann pointed out the remarkable agreement between the Xe isotopic profile of the explosive products and the well-defined Xe components in carbonaceous chondrites. More stringent testing will come from the application of the model to isotope profiles of other elements.

Sam Epstein (Caltech) has devised a technique whereby $\delta^{17}O$ may be estimated to $\pm 0.5\%$ from $\delta^{18}O$ and $\delta^{13}C$ determinations on CO_2. This obviates the necessity for running O_2 in the mass spectrometer. The procedure was checked by analysing three inclusions from the Allende meteorite and then applied to investigating reactions involving excited species of oxygen compounds. G. Arrhenius and others have suggested that similar reactions may produce strongly nonlinear kinetic isotope fractionations (see *Nature* 279, 20; 1979); however, in his preliminary experiments, Epstein found no evidence of this, despite a spread of 100% in $\delta^{18}O$. An important step forward in understanding the stable isotopes of H, C and N in extracts from meteorites was reported by F. Robert and colleagues, also from Epstein's laboratory at Caltech. Using a combination of solvent extraction, HF hydrolysis and stepwise heating techniques, they detected isotopic differences in C and N between different organic components in CM chondrites. Deuterium associated with insoluble organic fractions is enriched by 90% (sic) compared to inorganic nitrogen, and decoupling from ^{13}C and ^{15}N enrichment is suggested. Interest now centres on whether equilibrium-type mechanisms of Fischer-Tropsch-type reactions will be successful in accounting for such observations, or if (as seems more likely) different source materials for the various components are required.

Nature still continues to spring surprises on those investigating the host phases of rare gases in meteorites. The Chicago-Berkeley controversy over the identification of the various carriers took a new twist with the report by Roy Lewis and co-workers (Chicago) of no fewer than five different forms of carbyne in Murchison and Allende. Carbynes are a series of linear polymorphs of carbon with alternating single and triple bonds; they are the stable low pressure forms above 2600°K and have recently been suggested by Webster (*Mon. Not. Roy. Astron. Soc.* in press) as candidates for interstellar dust and stellar

A.E. Fallick and C.T. Pillinger are in the Planetary Sciences Unit, Department of Mineralogy and Petrology, University of Cambridge.

condensates. U. Ott (Berkeley) has made a detailed study of colloidal separates from an Allende acid residue with the aim of unravelling more clues to the enigmatic phase Q (defined operationally as a residue fraction soluble in oxidising acids). His results are consistent with Q being carbonaceous rather than an inorganic mineral. Several years ago, Srinivasan *et al.* (*J. geophys. Res.* **82**, 762; 1977) compared Reynolds' first measurements on xenon in meteorites to the opening of Pandora's box: perhaps the pace of advance now encourages us to believe that before long the reluctant Hope will be coaxed out of the box also.   □

Discrete Σ-hypernuclear states

from R. H Dalitz

LAST summer, an experimental group headed by B. Povh, Max-Planck- Institut für Kernphysik, Heidelberg and working at CERN, reported to a conference 'held at Vancouver, the observation of well-defined peaks in the pion spectra following the $K^- \to \pi^{\pm}$ reactions at $0°$, for K^- mesons of momentum 720 MeV/c incident on ^{7}Li, ^{9}Be and ^{12}C targets. These peaks are in the part of the spectrum which corresponds to the production of a Σ-hyperon, and the widths reported for these discrete states are of order 10 MeV. These narrow Σ-hypernuclear states were not anticipated by theoreticians but turned up in the course of a study of the highly-excited Λ-hypernuclear states produced in the $K^- \to \pi^-$ reaction.

The hyperons Λ and $(Σ^-, Σ^0, Σ^+)$ are well-known. The Σ-hyperons are about 75 MeV heavier than the Λ hyperon and have the same strangeness quantum number, $s = -1$. $Σ \to Λ$ reactions, of the type $Σ^- + p \to Λ + n$, are exothermic and allowed by all the selection rules governing strong nuclear interaction processes. This led to the general expectation that a Σ-hyperon in contact with a nucleus would transform to a Λ-hyperon in a time of order 10^{-24}s. Since this is less than one-tenth of the time taken by a hyperon to travel across a nucleus, it appeared most unlikely that discrete quantum states could exist for a Σ-hyperon within a nucleus. All of our experience of Σ-hyperon processes observed in nuclear emulsion and in bubble chambers was consistent with this view. For example, the study of X-rays emitted by $Σ^-$-hyperons in atomic orbits around nuclei showed that $Σ^-$-hyperons coming to rest in condensed matter are captured by the nucleus predominantly from high-lying orbits. As the $Σ^-$-nucleus system cascades down through its atomic levels (which are due to their Coulomb attraction), emitting a photoelectron or X-ray at each step, the capture reaction $ΣN \to ΛN$ occurs as soon as there is any appreciable overlap of the $Σ^-$ wavefunction with that of the outer nucleons of the nucleus. Thus, the nuclear capture processes take place on the extreme periphery of the nucleus, and the yield of X-rays due to transitions between the inner atomic orbits is low relative to those for

R.H. Dalitz is Royal Society Research Professor in the Department of Theoretical Physics, Oxford University.

the outer orbitals since few $Σ^-$ hyperons escape nuclear capture and reach the inner levels.

The $K^- \to \pi^{\pm}$ reactions studied in these CERN experiments are termed "strangeness exchange reactions". The strangeness of the meson increases by $\Delta s = +1$, and the strangeness of the target nucleus (initially $s = 0$) becomes -1, since total strangeness is conserved by the strong interactions. Thus the final nuclear system reached includes one hyperon. These reactions have a special feature, due to the fact that the mass difference $(m_K - m_{\pi}) \simeq 355$ MeV is greater than the mass difference $(M_Σ - M_N) \simeq 255$ MeV. In this case, the $N \to Σ$ strangeness exchange reaction can take place for a K^- meson at rest and in contact with nuclear matter. For non-zero incident momentum $p_{\bar{K}}$, we confine attention here to pions emitted at $0°$ to the K^- momentum since this configuration gives the least momentum transfer q to the target nuclear system. As $p_{\bar{K}}$ increases from zero, this momentum transfer falls until a "magic momentum" p_0 is reached at which the momentum transfer q is zero. As $p_{\bar{K}}$ rises further, the momentum transfer q increases from zero, but it rises only to 290 MeV/c, even in the limit of infinite incident momentum.

For the $0°$ reaction, the strangeness exchange process allows no spin flip for the target nucleons. At the magic momentum $p_0 \simeq 280$ MeV/c, the orbital states in the initial nucleus are preserved in the final hypernuclear state, since the momentum transfer $q = 0$. The reaction then consists of replacing a nucleon by a Σ particle, with precisely the same wavefunction; the amplitude for this replacement receives coherent contributions from all the nucleons of the target and the cross section is correspondingly enhanced. There has already been much experience with these coherent transitions for the case $N \to Λ$, where $p_0 \simeq 530$ MeV/c (Povh *Ann. Revs. Nucl. Phys.* **28**, 1; 1978). In practice, it has become evident that this coherence extends only to the nucleons in a given shell, but the coherent transitions leading to final Λ-hypernuclear states with the same spin-parity J^P as the target nucleus do stand out clearly in the $0°$ pion spectrum, even for incident K^- momentum $p_{\bar{K}} = 720$ MeV/c, for which we have $q \simeq 40$ MeV/c. For p-shell nuclei, which have had the most

detailed study, the Λ-hypernuclear states reached in this way are necessarily excited states. Substitution of a 1s neutron by a Λ hyperon leaves a hole in the 1s neutron shell; substitution of a 1p neutron by a 1p Λ hyperon leaves the V particle far above its 1s ground state. These remarks also apply to the Σ-hypernuclear states coherently produced by the strangness exchange transition $N \to Σ$. The important difference was the expectation that the strong absorptive reaction $ΣN \to ΛN$ would cause these states to be so broad as to be unobservable in the pion spectrum. The CERN experiments have now shown that this expectation does not hold for all Σ-hypernuclear levels; some discrete levels do exist, even if only for a time of order 10^{-22}sec.

First, it is useful to remark that some particular Σ-hypernuclear states are expected to be semi-stable, i.e. to have lifetimes of order 10^{-11} sec., comparable with the lifetime for free $Σ^-$ hyperons, if they exist as bound states. The clearest examples are the systems ($Σ^-$ + neutrons); charge conservation does not allow any transition $Σ^- \to Λ$ on a neutron since there is no nucleon state with negative charge. Despite much searching, no empirical evidence has been found for any bound states of this type, nor for the charge-symmetric systems ($Σ^+$ + protons).

Gal and Dover (*Phys. Rev. Lett.* **44**, 379; 1980) have now made calculations intended to demonstrate that the existence of some discrete Σ-hypernuclear states is compatible with our other knowledge of hyperon-nucleon interactions, and to identify the structure of these states. The strength of $ΣN \to ΛN$ absorption is taken from experimental data, as interpreted in terms of theoretical hyperon-nucleon potentials. The rate used is $(v\sigma_{abs}) \simeq 19$ mb, the average being over the nucleon momentum distribution in a nucleus, v denoting the Σ-N relative velocity. The Σ-nucleus interaction can also be viewed as a "cloudy crystal ball", i.e. a potential with the nuclear shape ϱ (r) and a complex strength $(U + iV)$. Then V is proportional to $(v\sigma_{abs})$ and therefore known. U has to be left as a free parameter, whose value can be determined later from the energy observed for an identified Σ-hypernuclear level, but it is not of importance for the total absorption rate. The solution of the Schrodinger equation for the Σ-hyperon in this potential will give a complex energy value $E = (\varepsilon - i \Gamma/2)$ for each orbital (n,l), the imaginary part Γ (n,l) being the width for this orbital.

For heavy nuclei, the Σ hyperon sees "nuclear matter" and the width Γ does not depend strongly on the orbital (n,l), when this lies dominantly within the nucleus. Typical values for Γ are then in the range 20-30 MeV, a width large relative to the spacing of the energy levels so that the individual levels cannot be distinguished.

For light nuclei (^{12}C and lighter, say), it is

important to take into account the isospin- and spin-dependence of the ΣN interaction. For ΣN isospin 3/2, there is no absorption possible, since the ΛN state has isospin 1/2; the absence of nuclear absorption in a state $(\Sigma^- + \text{neutrons})$ is a particular example of this situation. Also, we believe that, for low ΣN energies, the $\Sigma N \rightarrow \Lambda N$ absorption rate is much less in the singlet spin state than in the triplet spin state. Hence the observation of a narrow Σ-hypernuclear width calls for a configuration where (i) the nucleon density is small where the Λ-particle is, (ii) the isospin-3/2 ΣN interactions have a high relative weighting, and (iii) the singlet ΣN interactions have a high relative weighting, and (iv) its formation is coherent. For ^{12}C target, this state is identified by Dover and Gal to be the isospin-3/2 particle-hole state with structure $((1p)_N^{-1}(1p)_\Sigma)_{J=0}+$, its calculated width due to absorption being about 5 MeV. The isospin 3/2 state can be formed in both reactions $K^- \rightarrow \pi^\pm$, and this is also the case empirically. No other state considered has width much less than 20 MeV and no others are claimed empirically, at present. The isospin-1/2 state with the same structure has a calculated absorption width of about 18 MeV.

Two Σ-hypernuclear peaks were seen for ^9Be target. The lower state has only one possible interpretation, with a calculated absorptive width of about 7 MeV, consisting of the Σ-hyperon attached to the low-lying spinless isospin-0 states of ^8Be. The outstanding candidate for the upper peak is the isospin-2 configuration built on the isospin-1 ^3P core occurring at about 17 MeV in ^8Be, for which the calculations give $\Gamma = 6$ MeV, but there are a number of other $A=9$ Σ-hypernuclear states with predicted widths of less than 12 MeV.

When these interpretations have been tested in more detail and verified, the properties of these exceptional states will give us information about the ΣN interactions otherwise difficult to obtain. First, their absolute location will determine the mean Σ well depth U. The spacing between the two ^9Be peaks will give another measure of this real part of the ΣN potential. The most interesting situation will be that for target ^{16}O, which contains both $p_{3/2}$ and $p_{1/2}$ nucleons. Two particle-hole states exist, which can both be produced coherently; their wave-functions are linear superpositions of the two configurations $((1p_j)_N^{-1}(1p_j)_\Sigma)_{J=0}+$, for $j=3/2$ and 1/2. The measurement of their spacing will give us a measure of the ΣN spin-orbit interaction, just as we have recently learned the strength of the ΛN spin-orbit interaction from the spacing between the corresponding $^{16}_\Lambda O^*$ states (Brückner et al., *Phys. Lett,* **79B**, 157; 1978). With data having less background, it may be possible to see the Σ-hypernuclear spectrum in more detail and to learn empirically about the spin-spin and isospin-isospin components of the hyperon-nucleon forces. An improved K^- beam is now being installed at CERN to allow these Σ-hypernuclear experiments to be carried out for lower incident momenta $p_{\bar{K}}$, closer to the magic momentum $p_0(\Sigma) \simeq 280$ MeV/c, so that the coherent states with narrow width will stand out more strongly in the data. We may expect more information on the Σ-nucleus interaction from this experimental program during 1981. □
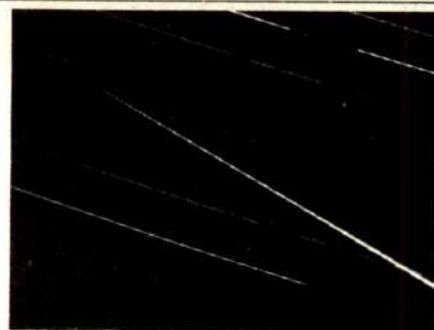
The Pribram fireball. A rotating shutter cut off the light ten times a second. The number of breaks in the trail shows the meteor took seven seconds to cross the photograph. (Ondrejov Observatory, Czechoslovakia)

The problem becomes much more difficult in the case of the large meteorites. These lose the majority of their mass in the lower atmosphere where the mean free path of the air molecules is very much smaller than the size of the incoming object. So a large aircap is formed around the meteorite, shock waves occur in the region between this aircap and the atmosphere it is moving into and the meteorite is followed by an active, turbulent wake. Visual radiation is usually emitted from all these regions as well as from the meteorite itself. There is also another complication. Observations of meteors using Super Schmidt cameras have shown that the small meteoroids do not decelerate appreciably in the atmosphere. The loss of energy they suffer is exhibited by a mass loss rather than a velocity loss. The observed radiation also comes in the main from the ablated meteoroid atoms. The large meteorites however do decelerate. In many cases they are retarded to the free fall velocity and the remnants of the meteorite drops to the Earth's surface. Radiation also comes from many sources.

The luminous efficiency of meteoritic fireballs has been discussed in detail in a recent paper (*J. geophys. Res.* **84**, 6255; 1979) by Douglas ReVelle of Northern Arizona University and R. S. Rajan of the Carnegie Institution of Washington.

The authors stress the fact that the majority of the radiation from the fireball, when it is low down in the atmosphere, is in the ultraviolet region of the spectrum. They also take into account the deceleration term for the first time. Their theoretical work can unfortunately only be checked by reference to three meteorite entries. The first is the Pribram meteorite which fell in Czechoslovakia in 1959. The fall was photographed by a series of all sky camera's and the authors estimate that about 53 kg of meteorite eventually hit the earth even though outside the atmosphere the meteorite had a mass of around 1300 kg. — a loss of 96% of the mass. The other two meteorites, Lost City and Innisfree fell and were photographed in North America. In both cases about 70% of the initial mass was lost as the object came through the atmosphere. These mass loss figures are supported by an analysis of the cosmic ray tracks in the recovered meteorites. The

Meteoritic fireballs and luminous efficiency

from David W. Hughes

LUMINOUS streaks of light flashing across the sky are caused by cosmic dust particles burning out in our atmosphere. They are a common enough phenomena and have been seen ever since man looked up to the heavens, but even to-day they still present problems. One of the more pressing ones is the discovery of the exact relationship between the light intensity of the trail and the mass and velocity of the incident object. Things are relatively simple if the incident particle is less than about 1 cm in radius. These small meteoroids burn out at heights between about 80 and 110 km, in an atmospheric region where the mean free paths of the molecules are much larger than the meteoroid dimensions. The atoms that ablate from the particle leave without serious mutual interference. They have

David W. Hughes is in the Department of Physics, University of Sheffield.

kinetic energies of a few tens to some hundreds of electron volts and are thus excited and ionized. Also they can excite and ionize the molecules they collide with. Excited atoms and molecules emit radiation and the luminous power so produced has been found to be proportional to the rate of loss of kinetic energy of the ablated atoms. The constant of proportionality, known as the luminous efficiency factor, depends on the velocity of the incident meteorite, its composition (stone, iron, stoney iron) and its physical structure (i.e. whether it is a solid body or a dust ball).

Most of the early work in this field was done by Öpik and he prepared an indispensable series of tables which enabled the initial masses of small meteoroids to be estimated from measurements of the meteor luminosity and the meteoroid velocity.

bombardment of the meteorite in space by cosmic rays produces a network of radiation damaged material. The density of this network shows appreciable depth dependence and a measurement of this density in the recovered meteorite leads to an estimate of how much material overlayed that region when it was in space.

The photographic records of these meteorites are of paramount importance because from them the velocity of the meteorite and the luminosity of the fireballs may be calculated as a function of height. ReVelle and Rajan applied their theoretical model to the observed light and velocity profiles and, after introducing a few assumptions (such as that the radiation field was isotropic and that the mass of the main body at any specific moment is much larger than the mass of the associated fragments), they obtained a curve which showed how the luminous efficiency varies as a function of height in the atmosphere and as a function of meteorite velocity.

The authors compared their results with a low velocity laboratory simulation experiment carried out by Givens and Page (*J. geophys. Res.* **76**, 1039; 1971). Here artificial meteors were produced by firing 0.6 mm stainless steel spheres with a light gas gun into a column of still air at 0.052 atmospheres of pressure. The resulting 'meteor' train was observed using a series of broad band multiplier phototube radiometers. The velocities of the spheres were about 8 km s^{-1} in comparison to the Pribram meteorite which initially had a velocity of 21 km s^{-1} and Lost City and Innisfree meteorites which had velocities about 14 km s^{-1}. When corrections were made for the velocity effect the results agreed very well.

The main conclusion of ReVelle and Rajan is that there is a phase lag between the ablation of meteoritic material and the emission of luminosity. The luminous efficiency was found to be a rather complicated function of the meteorite velocity. Also when the meteorites Lost City and Innisfree were losing mass at the maximum rate, the luminous efficiency in the visible wavelength region of the spectrum was about 0.3%. For the faster Pribram meteorite the value was about 0.04%. The authors adding the proviso that the Pribram results are regarded as being less reliable.

It is important to note that the 0.3% result is a factor of between 5 and 10 higher than the empirical luminous efficiency assumed by Ceplecha and McCrosky (*J. geophys. Res.* **81**, 6257; 1976) in their analysis of fireball trails. This means that even though only 3 parts in 1000 of the energy lost by a meteorite goes into visual radiation this is considerably more than was estimated previously. So, bright fireballs are now thought to be produced by smaller incident meteoroids and the total mass of cosmic material hitting the Earth in the fireball size range has to be revised downwards by a factor of 5 to 10. □

100 years ago
METEOR SHOWERS
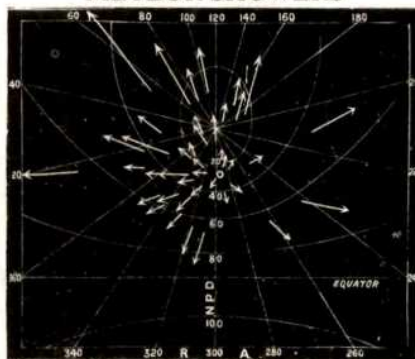
Shower of Aquariads July 27–30th.

SEVERAL of the meteor streams observed at Bristol within the last two years appear to be of such marked intensity as to merit special description, and the following notes in connection with them may possess some interest to observers.

My observations in July, 1878, led me to recognise a large number of slow meteors with long paths (averaging 17°) and occasionally leaving faint trails of sparks, ascending amongst the stars of Pegasus, Andromeda, &c., which, by their parallelism of motion, obviously proceeded from a common radiant point south of Pegasus. I watched them narrowly, and determined the position with fair precision as near δ Aquarii.

A succession of clear nights occurred from July 26 to August 2 in 1878, and I obtained some lengthy observations. In about twenty-two hours of watching more than 400 shooting stars were seen in the eastern sky, chiefly amongst the constellations of Perseus, Cassiopeia, and Andromeda. I saw many swift meteors leaving short streaks and otherwise exhibiting much uniformity in their appearances and directions. The radiant point was not reconcilable with that of the well-known annual shower of Perseïds. It was sharply defined about 3°S. of the group χ Persei, and the maximum of the shower was witnessed on July 31, when 21 meteors were noted diverging from the point described.

Shower of Perseids II July 28–August 1st.

From *Nature* **21**, 29 April, 621; 1880.

The Uninvited Guests

from Graham Darby

MOST people are no doubt unaware that they are accompanied through life by several herpes viruses lying dormant in the tissues of their bodies. The human herpes viruses have the characteristic of establishing long-term relationships with their hosts, emerging only infrequently to cause disease.

Since these viruses are ubiquitous in the population the first encounter between the infectious agent and its human host usually occurs early in life and results in an in-apparent infection or rather mild disease. In the developed countries of the world this initial encounter often occurs later in life and, paradoxically, this delay may result in a more serious primary disease. Subsequently the viruses remain with us for life. There is little evidence that cytomegalovirus (CMV) or Epstein-Barr virus (EBV) usually cause further problems but both herpes simplex (HSV) and varicella-zoster (VSV) which establish latent infections in the peripheral nervous system may re-emerge to cause recurrent episodes of disease. HSV type 1 causes periodic eruptions of cold sores around the mouth but these generally heal quickly and leave no scars. However, a closely related virus, HSV type 2, is more damaging as it usually infects the genital regions where it causes a painful and often socially embarrassing disease. Indeed, in some areas of the world it is emerging as the most common problem seen in V.D. clinics. VZV can remain latent for many years after childhood chicken pox but it too many reactivate, usually late in life, to cause shingles.

An overall view of our understanding of these agents and the diseases caused by them was provided by a meeting in Atlanta this Spring*. Both virologists and clinicians attended the meeting and the growing clinical importance of molecular biology was nicely demonstrated by B. Roizman

Deep sea diving

from M. J. Halsey

A new record was recently set at Duke University when three men successfully underwent conditions simulating a dive to a depth of 650m of sea water. This achievement set the background for a recent workshop* on the problems of very deep dives, in the range 460-760m (1500-2500ft).

Fifty years ago men dived using only compressed air but nitrogen narcosis, which increases with increasing partial pressure of the gas, effectively prevented this technique from being used at depth. The subsequent development of helium/oxygen mixtures allowed safe diving to depths beyond 50m, but problems develop when the 450-550m range is reached. At these depths the high pressure neurological syndrome (HPNS), characterised by muscular tremor, disorientation, and short sleep-like periods of loss of attention develops; in animal experiments even higher pressures have been shown to cause convulsions. However, a breakthrough has now been achieved by the discovery that HPNS can be overcome by the use of low partial pressures of anaesthetics. It is this that has lead to new techniques and to new records in deep diving. In experiments with animals, gases with anaesthetic action such as nitrogen or nitrous oxide and low doses of intravenous anaesthetics such as ketamine or althesin have been found effective. Nitrogen deliberately introduced in small quantities into the helium/oxygen breathing mixture was the basis of the trimix which was used in the record chamber dive. This has also been used in the successful open sea dive to 460 m by Comex, S.A. Marseille, which has set a new standard for deep

water work.

Current work on a wider pharmacological approach to the problem suggests that selective drugs for HPNS may exist. Structural isomers of some steroid anaesthetics, such as althesin, have been found in animals to continue their action against HPNS even though they no longer have anaesthetic effect.

Additional problems in deep diving include those of temperature control, respiration and decompression. Temperature control is of great concern in working dives because high pressure seems to affect the body's thermoregulatory capacity. Not only is there a narrowing of the limits within which the body can make corrections to mantain a stable temperature but also the subjective experience of heat and cold may become divorced from actual conditions.

Respiration in chamber dives is not a general problem but dyspnoea, exacerbated by exercise, is present. This could become a limitation in future deep dives. The phenomenon appears to be unrelated to gas density but is an aspect of HPNS that is not alleviated by nitrogen. Decompression from deep depths is proving possible although recompression or a change of gas breathing mixture may prove difficult.

Although diving beyond 460 m has now certainly been made possible, and both naval and commercial interests agree there will be a definite need for such dives, it must be remembered that the principles underlying the effects described above are not at all understood. The number of men who have been beyond 300m remains very small; only an understanding of the basic mechanisms involved can ensure that such deep dives can continue in safety.   □

M.J. Halsey is in the HPNS group at the Clinical Research Centre, Harrow, U.K.

---

extremely strong, but much less certain is the connection between HSV type 2 and cervical cancer. R.P. Eglin and his colleagues (Institute of Virology, Glasgow) reported some very careful *in situ* hybridization experiments which showed low level expression of HSV-specific RNA sequences in pre-invasive and invasive carcinoma tissues, while two groups reported the induction of cervical carcinomas in animal model systems, W.B. Wentz and colleagues (Case Western Reserve University, Cleveland) using inactivated HSV type 2, and C. Minhui and associates (Hupei Medical College, Wuhan, China) using live virus. A very large prospective study to determine the risks associated with HSV type 2 infections in women is currently underway in Czechoslovakia (V. Vonka and colleagues, Institute of Sera and Vaccines, Prague) involving colposcopy, cytological smears and blood tests on 10,000 women selected at random.

One of the tantalizing questions about herpes viruses is how latent infections are maintained for long periods. What factors are important in the suppression of the infection? This is an area in which very little real progress has been made although it is generally accepted that specific antibodies are important in maintaining HSV latency. However some elegant experiments described by H. Openshaw (University of California, Sacramento) using a mouse model throw considerable doubt on this idea. Latent infections were established in mice which were protected during the primary infection by administration of immune antibody so that their own immune systems were not primed. It was shown in the majority of animals that as the passive antibodies faded the latent infections were maintained.

From the clinical point of view there are two areas which require urgent attention. The clinician would like to be in a position to offer some protection to a patient (e.g. a prospective organ recipient) who he knows will be at risk from these viruses in the immediate future. Such protection could be generated by a suitable vaccine. Secondly he needs effective drugs to control the more serious diseases associated with these viruses. There appear to be encouraging developments in both areas.

The problems associated with assessing the safety of attenuated herpesvirus vaccines are considerable since we have to take into account not only the primary infection but also recurrent disease and the oncogenic potential of these viruses. Attenuated VZV vaccine strains have been developed and are in use in some countries although the prevailing view, expressed by P.A. Brunnel (University of Texas), was that these vaccines should be used only in cases where patients are exposed to serious risk. An attenuated CMV vaccine has also

---

(University of Chicago). Over a brief period there were 8 cases of HSV encephalitis at Massachusetts General Hospital, and since this is an extremely rare disease it was inevitably thought that the epidemic was caused by a particularly neurovirulent strain of virus. However, restriction enzyme analyses were made on the genome DNA of viruses isolated from all 8 patients and as the patterns were distinct from each other it was proven that the cases were caused by different virus strains.

The viruses may be particularly dangerous in two situations; infections of the newborn and of the immunosuppressed. CMV may cross the placenta and infect the fetus sometimes causing severe brain damage. HSV may be contracted from the infected genital tract of the

mother leaving the fetus with only a 50/50 chance of survival (A.J. Nahmias, Emory University, Atlanta). HSV, CMV and VZV are all common infections of immunosuppressed patients such as those under-going cancer therapy or organ transplantation. The diseases in these patients are often very severe and they are a significant cause of death. There were also suggestions that such diverse conditions as hardening of the arteries and psychotic depression (S. Sprecher, Institut Pasteur du Brabant) and even gastric ulcers (B.F. Vestergaard, Institute of Medical Microbiology, Copenhagen) might be initiated by recurrent HSV infections.

It has long been debated whether herpes viruses are involved in the induction of human cancers. Certainly the association between EBV and Burkitt's Lymphoma is

Graham Darby is in the Department of Pathology, University of Cambridge.

been developed and is undergoing clinical trials for renal transplant patients (S.C. Marker and H.H. Balfour, Jr., University of Minnesota). In the case of HSV and EBV where the oncogenic potentials are more clearly defined the development of attenuated strains has apparently been ruled out. Attention with HSV has been focused on nucleic acid-free subunit vaccines. The use of monoclonal antibodies in animal model systems has the potential to tell us which antigens are likely to elicit a protective response (R. Dix and colleagues, Veterans Administration Medical Center, San Francisco). These vaccines may also have problems associated with them since they are unlikely to generate long term immunity and there may be dangers in delaying primary infection.

Chemotherapy of herpes virus infections has been hampered by the toxicity of the antiviral compounds available, so that treatment has been limited to topical application or desperate situations. However excitement is now running high as we appear to be entering a new era with the appearance of several low toxicity nucleoside analogues which are extremely effective against HSV. The most exciting of these compounds, Acyclovir, has generated very encouraging results in animals and the results of trials in humans are eagerly awaited.   □

Free-electron lasers

from J.N. Elgin

IN conventional laser systems, gain is obtained as a consequence of electronic transitions between bound states of the host substance. As a result, the gain band width of the laser is limited by the line width of the relevant bound-bound transition. In free-electron laser systems the electrons are free and gain is produced by the interaction of these free electrons, with the static magnetic field, as discussed below. Thus, these systems have the attractive advantage that their gain band width is, at least in principle, infinite.

Much interest has been generated in free-electron lasers since the recent experiments of Madey and coworkers at Stanford (*Phys. Rev. Lett.* **38**, 717; 1976; ibid **38**, 892; 1977). In their first experiment, the system was operated as a single pass amplifier and gain was demonstrated at 10.6μ, and in their second the system operated as a laser oscillator with output at 3.4μ.

For each case, the basic experimental arrangement can be represented schematically by the full outline in the figure. Here, a relativistic electron beam traverses a periodic magnetic structure and, in so doing, emits synchrotron radiation into the forward direction. Stimulated emission of this radiation can occur in the vicinity of the resonance frequency (J.D. Lawson, *Nature* **277**, 262; 1979)

$$\omega_r = ck_T = \frac{c\beta}{1-\beta k_o}$$

where $c\beta$ is the component of the electron velocity along the symmetry axis, and $k_o = 2\pi/\lambda_o$ is the wave number of the static "wiggler" field. The gain curve for stimulated emission is markedly different from that encountered in conventional laser systems, being asymmetric about the resonance frequency ω_r (resembling somewhat an anomalous dispersion curve with resonance at ω_r). Only frequencies to one side of resonance are amplified, while those in the complementary region are strongly absorbed.

In each of the above experiments, electrons were passed only once through the apparatus, then discarded. In the experiment demonstrating gain at 10.6μ, it was found that about 0.2% of the electron's energy was converted to radiation without any evidence of saturation. It would appear at first sight that this efficiency could be vastly improved simply by recirculating the electrons in a storage ring in which an r.f. cavity makes good all energy losses to radiation (i.e. in both the laser cavity and the ring), as indicated by the remaining part of the figure. In this way, efficiencies of, say, 20% or greater may be possible.

Unfortunately, energy spread of the input electron beam during transit through the laser cavity raises a nontrivial objection to the above scheme. Normally, the electrons enter the laser cavity with random optical phase so that $v_1\varepsilon$ — where v_1 is the transverse component of the electrons velocity and ε is the electric field strength of the laser radiation — is just as likely to be positive as it is negative. In other words, just as many electrons are extracting energy from the radiation field as are contributing energy to the field. The energy spectrum of the electrons therefore broadens (laser heating) and this effect is in general much larger than the (second-order) shift of the energy mean, which determines the net energy loss to the radiation field. Unless the recycling scheme can counteract this spread, it will become progressively larger with each transit, with a corresponding decrease in gain, until eventually the laser system ceases to function.

The simplest way in which the storage ring might be used to eliminate spread is quite simply to use radiation losses in the ring to damp out the spread. The radiative energy loss by a particle moving round the ring increases with increasing values of energy of the particle, and so a broad energy distribution necessarily narrows. The r.f. cavity makes good all radiative losses and the cycle is repeated, converging ultimately to the point where the spread has a constant value at input to the laser cavity. Of course, if this steady state distribution is too broad, the gain may become negligibly small and the laser will cease to function.

A more detailed study of the combined storage-ring laser system has recently been published by Deacon and Madey (*Phys. Rev. Lett.* **44**, 449; 1980). The object here is to determine whether there are any possible conditions under which the electrons have isochronous orbits for transits through the complete system; that is, where the period for the complete orbit (laser plus storage ring) is independent of the initial conditions of the electron. Such a system necessarily has the required property of reversing the spread. The assumption is first made that the laser is operating in the Compton (or single particle) regime — which is the case for the experiments at Stanford — and the motion of the electrons through the laser cavity is accordingly modelled by the pendulum equation (Colson, *Phys. Lett.* **64A**, 190; 1977)

$$\frac{\delta^2\theta}{\delta t^2} = -\Omega^2 \sin\theta$$

Here, $\theta = k_r\delta Z(t)$, where k_r is the wave number for the radiation field inside the

Magnetic Wiggler

laser +
e-beam

Storage Ring

R.F. Generator
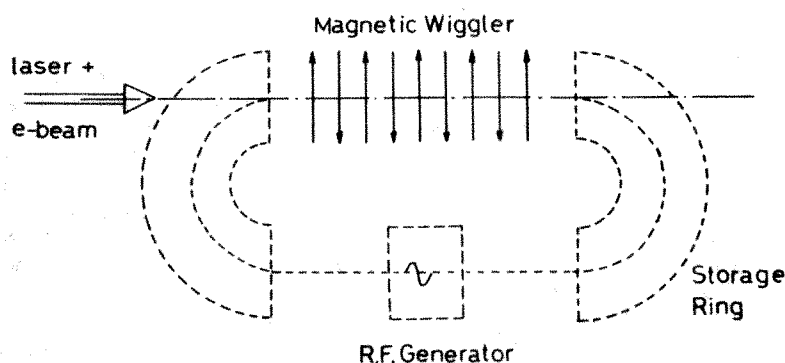
IN a recent paper in Astrophysical Journal (**235**, 625; 1980) H. Yoshimura has presented new results from computational simulations of non-linear astrophysical dynamos; in particular he has reproduced magnetic Field reversals. This represents a contribution to the theory of field generation (i.e. dynamo action) in a sphere of electrically conducting fluid, the object of such investigations being to explain the observed features of the magnetic fields of the Earth and the Sun. In the terrestrial context, it is necessary to explain why the magnetic field of the Earth survives in a quasi-steady state over geological time scales much longer than the natural decay time of the field (of order 10^4 years). In the solar context, it is necessary to explain why the general magnetic field of the Sun evolves in an approximately periodic manner (with the same period as that of the sunspot cycle i.e. about 22 years) when the natural (ohmic) time scale for the Sun is of the order of 10^9 years.

Traditional dynamo theory starts from coupled equations for the velocity field **u** and the magnetic field **B** in the fluid region

$$\left. \begin{array}{c} \dfrac{\delta \mathbf{B}}{\delta t} - \lambda \nabla^2 \mathbf{B} = L\{\mathbf{u}, \mathbf{B}\} \\[2ex] \dfrac{\delta \mathbf{u}}{\delta t} - \nu \nabla^2 \mathbf{u} = N\{\mathbf{u}, \mathbf{B}\} + \mathbf{F} \end{array} \right\} \quad (1)$$

In these equations L represents a differential operator that is linear in each of **u** and **B**, N represents a nonlinear integral-differential operator, and **F** represents the force distribution, whatever this may be, which maintains the motion. Much controversy surrounds the nature of this force field in the terrestrial context, but in the solar

H.K. Moffat is in the School of Mathematics, University of Bristol.

Non-linear astrophysical dynamos

from H.K. Moffat

context it is certainly of thermal origin.

For a given force field, one would like to solve these equations, and demonstrate the existence of solutions for **B** which have the observed property in either context. Unfortunately, this task is far beyond either analytical solution, or the power of present computers. Approximate techniques must be adopted in order to reduce the problem to a level that will yield to the computer. A first dramatic stage has been achieved over the last 20 years, with the realisation that when the velocity field **u** is turbulent, the mean magnetic field <**B**> satisfies a simpler equation

$$\left(\frac{\delta}{\delta t} - \lambda \nabla^2 \right) <\mathbf{B}> = <L><\mathbf{B}> \quad (2)$$

where <L> is an averaged differential operator which is in principle determinate in terms of the statistical properties of the turbulence. For different forms of this averaged operator, solutions of equation (2) are known of types that capture the main features either of the Earth's quasi-steady field, or of the Sun's quasi-periodic field.

The magnetic field itself influences the structure of the turbulence, through the second of Equations (1), and it is this "back reaction" effect that more recent theories are attempting to incorporate. First attempts in this direction were those of Stix (*Astron. Astrophys.* **20**, 9; 1972) and Jepps (*J. Fluid Mech.* **67**, 417; 1975), both of whom incorporated a fairly simple cut-off in the "regenerative" part of <L> when the magnetic field exceeded

a level at which the back reaction effect was assumed to become significant. Yoshimura has developed this approach in a series of papers, in which he has considered increasingly sophisticated forms of the operator <L>, incorporating in particular a time-lag between the generation of a magnetic field and the (later) manifestation of its dynamic effects. This increasing sophistication in his models has enabled him to compute solutions of Equation (2) which resemble the observed fields of Earth and Sun in remarkable detail. As might perhaps be anticipated the more disposable parameters that are introduced in the assumed form of <L>, the more freedom there is at the end of the calculation to choose these parameters in a way that achieves agreement with observation. In particular, Yoshimura has now found solutions exhibiting reversals, like the well-documented occasional reversal of the Earth's field.

While Yoshimura's approach does not increase physical insight at the fundamental level, it does lead to the accumulation of an interesting catalogue of possible behaviours of solutions of equations of the form (2), when time delay is incorporated in the operator <L>. The approach however is open to criticism in that all the subtleties of the dynamical equation (1b) are parametrized in what many would regard as an unacceptably crude manner. Alternative approaches (e.g. that advocated by Malkus & Proctor (*J. Fluid Mech.* **67**, 417; 1975) treat the dynamics in a less brutal manner, and although such approaches have not yet been pushed as far (in terms of results) as Yoshimura's, they hold more promise in the longer term for providing a convincing theory of dynamo action including proper recognition of the role of dynamic effects. □

---

cavity and δZ is the longitudinal deviation from resonance, and $\Omega^2 \alpha B_0 \varepsilon$, the product of the wiggler field strength and the electric field amplitude of the generated radiation. The physics of electron bunches moving round storage rings is in general very complicated. However, as a first approximation, the ring system can also be modelled by a pendulum equation of the above type, where θ is now proportional to τ, the time displacement of a test particle from the nominal position, and $\Omega^2 \alpha V$, the amplitude of the applied r.f. field.

For either system (laser or ring) taken in isolation, the above equation predicts trapped particle solutions, where the particles oscillate backwards and forwards in the potential wells determined by Ω — a phenomenon well known in plasma physics. The length scale of the potential wells (or 'buckets') will of course be different in the two systems, being very much shorter in the laser cavity where they

are of the order of the optical wavelength. If the two systems are now coupled, as shown in the figure, we have a very complicated system indeed comprising as it does two coupled highly nonlinear differential equations. Clearly, such a system can only be properly studied using numerical techniques.

In their preliminary study of the problem, Deacon and Madey proceed by linearising the above system and, in so doing, are able to establish that isochronous orbits *will* occur provided the operating parameters of the system fall within defined limits. Within these limits, the large operating efficiencies (> 20%) referred to earlier should be realised. It will be interesting to see whether a more complete (numerical) study of the problem confirms these preliminary results.

J.N. Elgin is in the Department of Physics, Imperial College, London.

It is perhaps worth while mentioning two alternative schemes to the laser-ring system discussed above, both of which have received some theoretical study. In the first of these, an attempt is again made to reverse the energy spread of the electrons, but this time using echo techniques. Here, the effect is similar to one obtained in nonlinear optics where a randomising process can be reversed by a suitable coherent interaction of an optical pulse with the system. The second alternative uses a tapered wiggler magnet to slow down the electron bunches trapped in the optical potential wells referred to earlier, with the loss in energy of the bunches going into the radiation field. This latter method would of course be single pass only. Each possible method has its advantages and disadvantages and, at the time of writing, it is not yet clear which (if any) will provide the means of obtaining high efficiencies in free-electron laser systems. □

REVIEW ARTICLE

Biosynthesis of the pigments of life: formation of the macrocycle

Alan R. Battersby, Christopher J. R. Fookes, George W. J. Matcham & Edward McDonald

University Chemical Laboratory, Lensfield Road, Cambridge CB2 1EW, UK

The organic nuclei of chlorophylls, haems, cytochromes and vitamin B_{12} are biosynthesised from a single tetrapyrrolic intermediate which has an unexpected, rearranged structure. The mechanism of biosynthesis of this key intermediate has now been characterised in detail. Some of the information thereby obtained is also of use in the investigation of human diseases such as the porphyrias.

MANY vitally important functions in living systems are carried out by metal ions held as complexes within tetrapyrrolic macrocycles. Photosynthesis depends on chlorophylls (Mg^{2+} complexes), whilst the oxygen-carrying properties of haemoglobin and myoglobin are based on the Fe^{2+} complex (protohaem) of the macrocycle protoporphyrin-IX (compound 6). Electron transport, reduction of oxygen and hydroxylation reactions are mediated by a family of cytochromes which similarly depend on Fe^{2+} complexes (haems). Also, vitamin B_{12} is a related complex of Co^{3+}. Thus the entire group of macrocyclic pigments can fairly be called the pigments of life. This review outlines the highlights from 10 years of work aimed at discovering the biosynthetic pathways by which the organic macrocycles of these pigments are built. Only by having a full understanding of the normal biosynthetic processes can one pinpoint the failures which lead to disease.

Living systems tend to synthesise many complex molecules by assembling and/or modifying a relatively small number of starting materials[1]. This is certainly true for the macrocyclic pigments. Indeed, all the natural pigments mentioned above are biosynthetically derived from a single intermediate, uroporphyrinogen-III (3) (uro'gen-III). In plants, animals and most bacteria, the major forward pathway then involves decarboxylation of uro'gen-III (3) to yield coproporphyrinogen-III (copro'gen-III) (4), which by oxidative decarboxylation produces protoporphyrinogen-IX (proto'gen-IX) (5). Aromatisation of proto'gen-IX (5) gives protoporphyrin-IX (6) from which one set of pigments is built, as shown in Fig. 1. A second branch from uro'gen-III (3) leads via cobyrinic acid (7) to vitamin B_{12}; here, the key modifying process is not oxidation but methylation on carbon.

This central position for uro'gen-III (3) in a family of pigments of immense biological importance, emphasises the value of understanding its biosynthesis.

Building blocks and enzymes

Shemin, Granick, Bogorad, Neuberger and Rimmington had shown in pioneering work[2] that two enzymes are required to catalyse the conversion of four molecules of the monopyrrole porphobilinogen (PBG) (1) into uro'gen-III (3) and ammonia (Fig. 1). The names of these enzymes 'PBG-deaminase' and 'uro'gen-III cosynthetase' will be shortened here to deaminase and cosynthetase. In the absence of cosynthetase, deaminase catalyses the conversion of PBG into uro'gen-I (2), an unnatural isomer but the one expected from simple head-to-tail combina-

tion of four PBG units. However, uro'gen-I (2) is not converted into uro'gen-III (3) by cosynthetase nor by the complete deaminase–cosynthetase system. It is fascinating that living systems have developed during evolution a highly specific method of catalysing a rearrangement process which produces the unexpected type-III isomer (3), having adjacent propionate groups on rings C and D. How do the two enzymes work together to achieve the synthesis and what are the intermediates? These problems have a special fascination because four identical building blocks (PBG) are used for uro'gen-III (3); because they are identical new approaches had to be devised to solve this riddle.

Nature of the rearrangement

To produce uro'gen-III (3) from PBG (1), deaminase–cosynthetase must be capable at some stage of breaking the bond linking the C-11 methylene group to its pyrrole nucleus for one or more of the four PBG units. Obviously, there are many ways in which four pyrrole rings and the four methylene groups can be shuffled to produce uro'gen-III (3). It is a measure of the intense interest in this problem that at least 25 hypothetical schemes have been proposed for the biosynthetic process.

The various possible ways of building uro'gen-III (3) from PBG (1) differ in which of the four bridge carbons (C-5, 10, 15 and 20) are still attached to the same carbons at the same pyrrole nuclei as they were in the original PBG units. Methods had therefore to be found to study processes which break established C—C bonds and make new ones. ^{13}C-NMR proved to be a suitable method. The principle of this approach is simple; the ^{13}C-NMR signal from a ^{13}C-atom is affected by another ^{13}C-atom only if both are in the same molecule. Parallel synthetic work showed[3,4] that two directly bonded ^{13}C-atoms (●—●, Fig. 1, structure (6)) give characteristic ^{13}C-NMR signals, easily distinguishable from those given by ^{13}C-atoms separated by three bonds (for example, ▲—C—N—▲, structure (6)). These in turn were clearly different from the signals given by two ^{13}C-atoms in different molecules.

PBG (1a, Fig. 2) was synthesised carrying 90 atom% ^{13}C at both C-2 and C-11; thus 81% of the PBG molecules carried two ^{13}C-atoms. This product (one part) was diluted with unenriched PBG (four parts) in which a negligible proportion of molecules carry two ^{13}C-atoms at C-2 and C-11. Incubation of the resultant PBG sample with an enzyme system rich in deaminase–cosynthetase from *Euglena gracilis* first produced uro'gen-III (3a). However, because the biological system contained all the
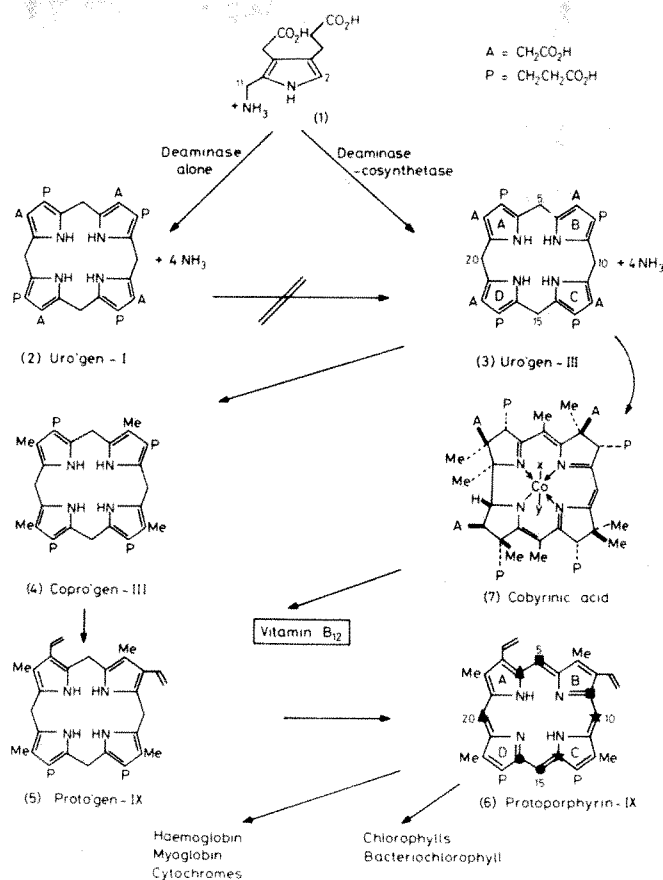
Fig. 1

enzymes necessary to convert uro'gen-III, as it was formed, into protoporphyrin-IX (6) by the steps shown in Fig. 1, it was this porphyrin which was isolated.

^{13}C-NMR then proved[5,6] that the ^{13}C-pattern of the labelled protoporphyrin-IX was as shown in structure (6). The geometrical shapes each represent a ^{13}C-atom and those given the same shape were proved to be present in the same molecule. As protoporphyrin-IX is formed from uro'gen-III without disruption of the macrocycle (Fig. 1) the results for the former also hold good for the latter (3a, Fig. 2). Exactly the same pattern was found[5,6] when the experiment was repeated: (i) with an enzyme preparation from chicken's blood; and (ii) using *Propionibacterium shermanii*. It follows that the deaminase–cosynthetase system assembles four PBG molecules to form uro'gen-III in exactly the same manner in a photosynthetic alga, in avian blood and in a bacterium, and the mode of assembly, not considering the mechanism at this stage, is that illustrated in Fig. 2.

Timing of the rearrangement step

Thus three PBG units are built intact into uro'gen-III (3) together with one intramolecularly rearranged unit corresponding to ring D and C-15. In principle, the single rearrangement could occur at any stage in the overall process, at the monopyrrole, dipyrrole, tripyrrole or tetrapyrrole levels. In fact, many experiments with mono- and dipyrroles pointed strongly to rearrangement at the tetrapyrrole level[7-9], in contrast to other claims[10-12].

Proof that this is the case came from synthesis of the bilane (Fig. 3, 9a) corresponding to straightforward, head-to-tail joining of four PBG units. It was first made in unlabelled form[13] but later carrying two ^{13}C-atoms[14]. One sample was labelled with 90 atom% ^{13}C at ● (9b) and the other at ▲ (9c) and both were diluted with unlabelled material before use (compare with the earlier work with PBG[14]).

To determine what happens non-enzymatically to the bilane samples (9b and 9c), they were allowed to ring-close at pH 7, and the product in each case was shown to be almost pure uro'gen-I (2b and 2c), with only traces of other isomers[13,14]. Thus no significant chemical rearrangement occurred and the foundation was established for the key enzymatic experiments. These involved separate incubation of each of these diluted samples (9b and 9c) with deaminase-cosynthetase. Strikingly, the product in each case now contained 80% uro'gen-III (3b and 3c) and only 20% of uro'gen-I (2b and 2c). The same bilane in the unlabelled form was prepared by a different method[15] and deaminase-cosynthetase from *P. shermanii* partly transformed it into uro'gen-III (type-III: type-I ratio 16:84). ^{13}C-NMR of the type-III isomer isolated from one experiment showed that the two ^{13}C-atoms, shown as ● in Fig. 3, 3b, had become bonded intramolecularly. The same was true in the other experiment for the two ^{13}C-atoms marked ▲ (Fig. 3, 3c). The ^{13}C-spectra were run on the derived coproporphyrin-III tetramethyl ester (10b and 10c), obtained by aromatisation of uro'gen-III with iodine, decarboxylation of the acetic acid side chains and esterification. The ▲ labels in the second experiment above lie at the two ends of the bilane (9b) so the further important conclusion could be drawn that the entire bilane (9c) was converted intact into uro'gen-III (3c).

The above studies depended on quantitative determinations of the amounts of uro'gen-III (3) and uro-gen-I (2) (and also the type-II and type-IV isomers) present in a mixture of these macrocycles. In carefully selected conditions, separation of the four coproporphyrin methyl esters derived from the uro'gens was achieved in a single HPLC run, a method which could be adapted to the analysis of porphyrin isomers from porphyric patients.

It is now firmly established that the deaminase–cosynthetase system brings about head-to-tail assembly of four PBG units to form an unrearranged bilane (8). A group X is shown in Fig. 3 because it was clear that the $^+$NH$_3$-group of PBG (1) (and similarly the $^+$NH$_3$-group of the $^+$NH$_3$CH$_2$-bilane (9a)) might be enzymatically replaced before the final ring-closure with rearrangement[14,16]. It was envisaged that the group X could be some nucleophilic group on the enzyme or an external nucleophile. The unrearranged bilane (8) is then enzymatically transformed intact into uro'gen-III (3) with intramolecular inversion solely of ring D, exactly as found earlier for PBG (1). Rings A, B, C and D of the bilane (8) correspond respectively to rings A, B, C and D of uro'gen-III.

Order of assembly of the four pyrrole rings

Is there an obligatory order of assembly of the bilane (8)? If so, does the first PBG unit enzymatically bound eventually become ring A of bilane (8), and so ring A of uro'gen-III, followed by sequential addition of ring B, ring C and finally ring D, or vice versa?

Answers came only after isolation of a relatively large quantity of enzyme. Approximately 0.25 μmol of deaminase-cosyn-
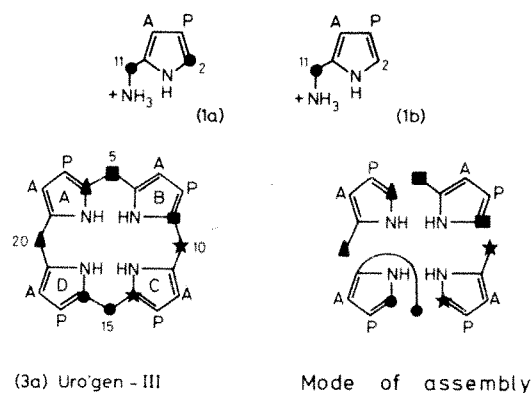
Fig. 2

thetase was treated with a deficiency (~0.5 μmol) of unlabelled PBG (1). This was designed to produce the greatest 'loading' on to the enzymatic site to which the first PBG binds. The corresponding 'loadings' at the other sites should decrease in a stepwise way so that the last site to be filled should carry least. The loading referred to covers pyrrolic material on that site whether it be monopyrrole (for example Fig. 4, 12) or part of a di- (for example, 13), tri- (14) or tetrapyrrole (8). An excess of 90 atom% [11-^{13}C]PBG (Fig. 2, 1b) was then added to chase through the bound pyrrolic species to form uro'gen-III (3) which as earlier was converted into coproporphyrin-III methyl ester (11) for NMR study.
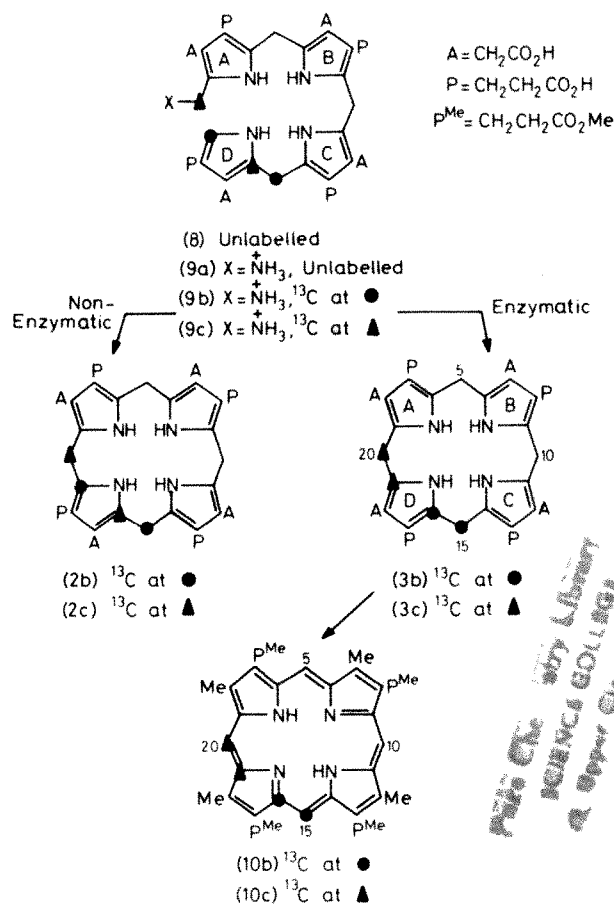
Fig. 3

The ^{1}H-NMR signal from a ^{1}H-atom attached to, for example, C-20 of compound (11) will give a singlet if C-20 is a ^{12}C-atom but a widely split doublet will appear if C-20 is a ^{13}C-atom. Thus the size of the central ^{1}H-singlet is a measure of the ^{12}C content at that 'bridge' position. It can now be seen clearly from Fig. 5 that the ^{12}C-content is greatest at C-20 and that the ^{12}C-levels at the other bridge carbons fall in the order C-5 > C-10 > C-15. Thus[17] the first PBG unit to bind becomes ring A (with C-20), the second ring B (with C-5), the third ring C (with C-10) and the last ring D (and C-15). The same conclusion is reached independently in a recent study based on ^{14}C-labelling[18].

The intermediate hydroxymethylbilane

The studies so far made use of the complete deaminase–cosynthetase system but further progress demanded the individual enzymes; they had not been separated previously from *Euglena gracilis*. Classical work[19,20] showed that cosynthetase from other sources is thermally less stable than deaminase, and this holds true for the *Euglena* enzymes. However, both enzymes from *Euglena* are sufficiently stable to be cleanly separated chroma-

tographically and handled with workable levels of activity (ref. 21 and G.W.J.M., E.McD. and A.R.B., in preparation).

When deaminase–cosynthetase acted on the $^+$NH$_3$CH$_2$-bilane (9a), as outlined above, there was enzymatic acceleration of the ring-closure, relative to the non-enzymatic rate, and the formation of uro'gen-III (3) showed no lag phase. However, when the $^+$NH$_3$CH$_2$-bilane (9a) was incubated with deaminase (free of cosynthetase), there was an initial lag before acceleration of the formation of uro'gen-I (2). An even more striking lag was observed[22] in the production of uro'gen-I (2) by deaminase from PBG (see Fig. 6); there was no lag in formation of uro'gen-III (3) from PBG when the deaminase–cosynthetase system was used.

Clearly, an intermediate substance is released into the medium when deaminase alone acts on PBG (1) or on the $^+$NH$_3$CH$_2$-bilane (9a); proof will be given later that the same intermediate is formed from both. What is its structure?

The intermediate was first generated from PBG (1) using deaminase to point A in Fig. 6 and it was then allowed to ring-close. The product was more than 99% uro'gen-I (2), showing that four PBG units had been joined head-to-tail without rearrangement. The intermediate was then generated as before but from [11-^{13}C]PBG (Fig. 2, 1b) and, after the enzymatic reaction was quenched, ^{13}C-NMR of the intermediate showed it to contain one HO^{13}CH$_2$-pyrrole residue and three methylene groups in the environment pyrrole-^{13}CH$_2$-pyrrole. These results proved[22] that the intermediate produced from PBG (1) by deaminase alone is the unrearranged hydroxymethylbilane (Fig. 4, 15), abbreviated below to HOCH$_2$-bilane. Similar ^{13}C-NMR studies showed[17] that deaminase converts the $^+$NH$_3$CH$_2$-bilane (9a) into this same HOCH$_2$-bilane (15).
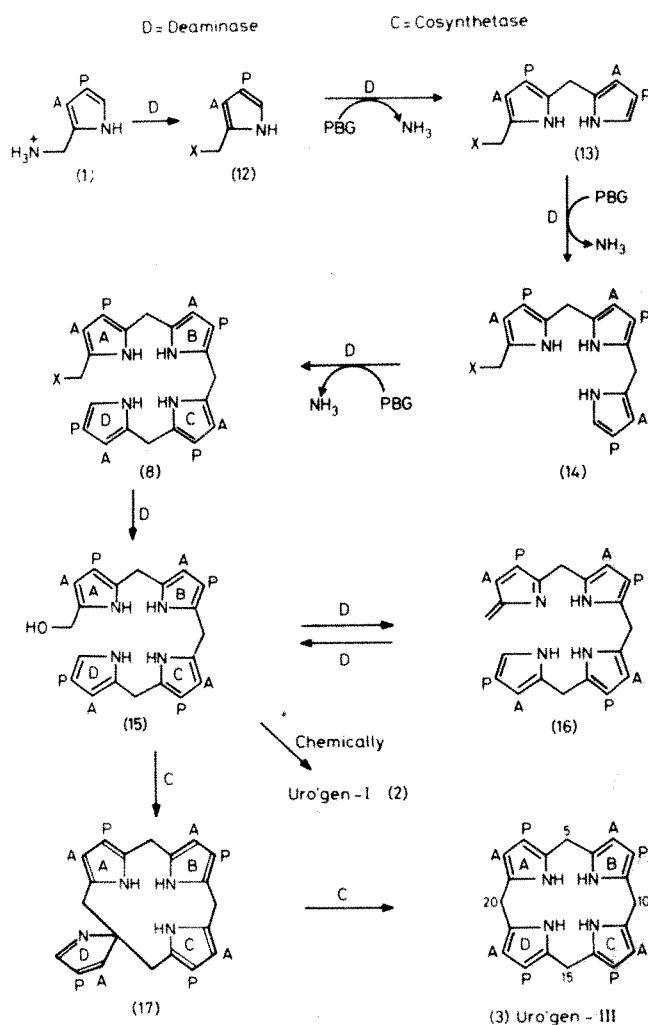
Fig. 4

We can look back at the comments made earlier concerning the group X in Fig. 3; it is now clear that when deaminase acts alone on PBG, the final nucleophile is water and X = OH.

Rigorous confirmation of the HOCH$_2$-bilane structure (15) for the intermediate came from its synthesis. This presented more than the usual challenge since the half life of the HOCH$_2$-bilane in physiological conditions is only a few minutes. Synthesis was achieved[23] by generating the labile HOCH$_2$-pyrrole residue only at the penultimate stage. This synthetic HOCH$_2$-bilane (15) was chemically and spectroscopically identical with the natural intermediate. The stage was thus set for enzymatic comparisons of the natural and synthetic HOCH$_2$-bilane (15).

The roles of deaminase and cosynthetase

Deaminase. The HOCH$_2$-bilane (15) was shown to be the endproduct of deaminase action on PBG by generating the bilane as earlier to point A, Fig. 6, and allowing it to ring-close chemically. A second equivalent portion of (15) was treated at point B, Fig. 6, with additional deaminase. The two rates, from A and B, of uro'gen-I (2) formation were essentially the same. So deaminase is not an enzyme for ring-closure and, in the absence of cosynthetase, its product is the unrearranged HOCH$_2$-bilane (15)[22].

This product does not react chemically at an appreciable rate with added nitrogenous nucleophiles such as $^+NH_4$ or NH$_2$OH, but when the HOCH$_2$-bilane (15) is treated with these nucleophiles in the presence of deaminase there is essentially complete conversion into $^+NH_3CH_2$-bilane (9a) and HONHCH$_2$-bilane

(8, X = HONH), respectively. The nucleophiles are thus trapping a substance, probably enzyme-bound, which is more reactive than the HOCH$_2$-bilane (15) and can be derived enzymatically from it[22]. The properties of this species suggest that it is the enzyme-stabilised methylenepyrrolenine (16). The earlier important observations of such nucleophilic trapping[24,25] fall into place on this view.

These trapping experiments have valuable mechanistic implications but the major point is this: with the unrearranged tetrapyrrole system (15) having been built, deaminase has done its job ready for cosynthetase to play its part.

Cosynthetase. The HOCH$_2$-bilane (15) generated enzymatically to point C, Fig. 6, was treated initially with deaminase-cosynthetase and the result was dramatic[22]. Virtually instantaneous ring-closure occurred with rearrangement to produce uro'gen-III (3), Fig. 6.

Fig. 6 Formation of hydroxymethylbilane (15) from PBG by deaminase followed by ring-closure from points A, B and C: *a*, without additional deaminase; *b*, with additional deaminase; *c*, with added deaminase–cosynthetase.
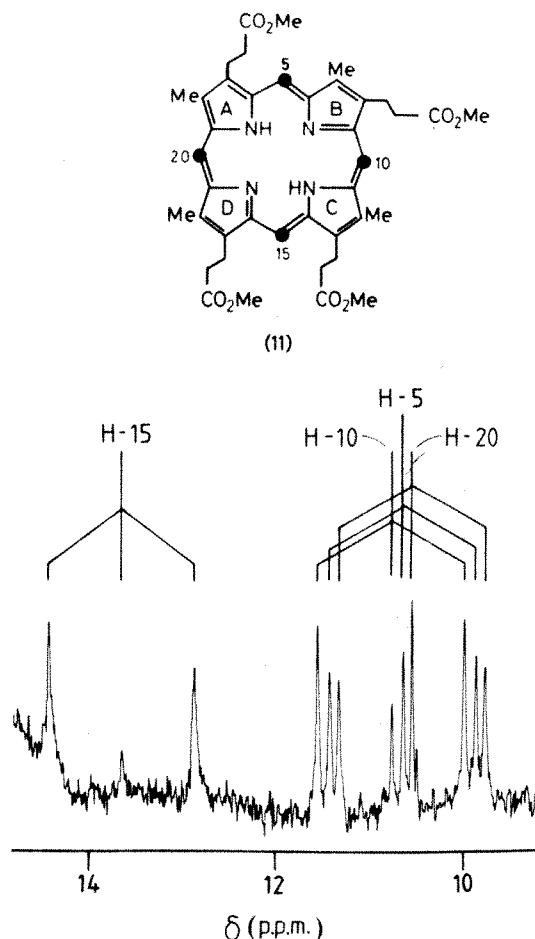
It was satisfying to find that cosynthetase alone acted in the same very rapid way on the HOCH$_2$-bilane (15) to form >98% isomerically pure uro'gen-III (3); the same result was obtained whether the HOCH$_2$-bilane (15) had been enzymatically generated or chemically synthesised[23]. Table 1 gives a comparison of the two preparations and particular attention is drawn to the quantitative agreement of the kinetic data. Cosynthetase is thus the ring-closing and rearranging enzyme; its substrate is now known and is available synthetically.

Assay for cosynthetase. The foregoing results are of relevance to medical studies of certain porphyrias. In the past, no direct assay was available for cosynthetase; its presence or absence in an enzyme preparation could be crudely checked by combining it with deaminase and determining the proportion of uro'gen-III (3) in the macrocyclic products formed from PBG. The availability of synthetic HOCH$_2$-bilane (15) allows rapid, direct and quantitative assay for cosynthetase and so should allow identification of porphyria patients deficient in this enzyme.

Deaminase–cosynthetase. Bearing in mind knowledge summarised so far, there are two ways in which deaminase and cosynthetase could operate in forming uro'gen-III (3). (i) They could be completely independent enzymes such that in their natural state the HOCH$_2$-bilane (15) from deaminase is released into the medium to be picked up by cosynthetase; the two enzymes can certainly function quite independently *in vitro*. (ii) Deaminase and cosynthetase, each with its independent active site, may be closely associated by physical binding and uro'gen-III could be formed by transfer of the HOCH$_2$-bilane within the complex. The experimental distinction between (i) and (ii) is important and requires more work. It is known[21,26] that

(11)

δ (p.p.m.)

Fig. 5 ^{1}H-NMR signals from positions 5, 10, 15 and 20 of coproporphyrin-III tetramethyl ester (11) from experiment on order of assembly of the pyrrole rings; the relative positions of the signals, spread by added shift reagent, had previously been assigned[14].

deaminase and cosynthetase can bind to each other but it remains to be seen whether evolutionary pressures have selected what would be expected to be the more efficient possibility (ii); we hope that time, on our human scale, will allow the distinction to become evident.

Valuable enzymatic work in this area has been reported independently by Scott's group[27] but their chemistry and conclusions are completely different from ours; evidence from many angles[23] does not favour their view.

Table 1 Comparison of synthetic and natural $HOCH_2$-bilane (15)

	$t_{\frac{1}{2}}$ (pH 8.25 at 37 °C)	% Uro'gen-III formed by cosynthetase alone	V_{max} for cosynthetase*
Synthetic	4.0 min	>98	151
Natural	4.2 min	98	148

* μmol uro'gen produced at pH 8.25 at 25 °C per hour, per ml of cosynthetase preparation.

Present knowledge and prospects

The biosynthetic pathway which has emerged from the work outlined here is illustrated in Fig. 4. Four units of PBG (1) are assembled head-to-tail by deaminase, starting with ring A and building round to ring D to form the unrearranged bilane (8). In the absence of cosynthetase, the bilane is released into the medium as hydroxymethylbilane (15). Deaminase has then done its job; it is not an enzyme for ring-closure, although it does equilibrate the $HOCH_2$-bilane (15) with a more reactive species (probably enzyme stabilised) which has properties expected of the methylenepyrrolenine (16).

Cosynthetase then takes charge by ring-closing the $HOCH_2$-bilane (15) at high speed to form uro'gen-III (3). This involves an intramolecular rearrangement which affects only ring D and the atoms which become C-15 and C-20 of uro'gen-III (3) (see Fig. 3 for what joins to what). The most probable intermediate in this rearrangement is the spiro-system (17).

We are now seeking direct evidence for the intermediate(s) between the $HOCH_2$-bilane (15) and uro'gen-III (3) and also information about the nature of group X (Fig. 4). The recently acquired knowledge reviewed here opens the way to fascinating opportunities in the medical and enzymatic areas where exciting advances should be possible.

1. Battersby, A. R. *Ciba Fdn Symp.* **53**, 25–51 (1978).
2. Battersby, A. R. & McDonald, E. *Porphyrins and Metalloporphyrins* (ed. Smith, K. M.) 61–122 (Elsevier, Amsterdam, 1975).
3. Battersby, A. R., Hodgson, G. L., Ihara, M., McDonald, E. & Saunders, J. *J. chem. Soc. Chem. Commun.* 441–442 (1973); *J. chem. Soc. Perkin Trans.* I, 2923–2935 (1973).
4. Battersby, A. R., Ihara, M., McDonald, E., Saunders, J. & Wells, R. J. *J. chem. Soc. Perkin Trans.* I., 283–291 (1976).
5. Battersby, A. R., Hunt, E. & McDonald, E. *J. chem. Soc. Chem. Commun.* 442–443 (1973).
6. Battersby, A. R., Hodgson, G. L., Hunt, E., McDonald, E. & Saunders, J. *J. chem. Soc. Perkin Trans.* I, 273–282 (1976).
7. Battersby, A. R. *et al. J. chem. Soc. Chem. Commun.* 768–770 (1973).
8. Battersby, A. R., Buckley, D. G., McDonald, E. & Williams, D. C. *J. chem. Soc. Chem. Commun.* 115–117 (1977).
9. Battersby, A. R., Johnson, D. W., McDonald, E. & Williams, D. C. *J. chem. Soc. Chem. Commun.* 117–118 (1977).
10. Frydman, R. B., Valasinas, A., Rapoport, H. & Frydman, B. *FEBS Lett.* **25**, 309–312 (1972).
11. Frydman, R. B., Valasinas, A. & Frydman, B. *Biochemistry* **12**, 80–85 (1973).
12. Scott, A. I., Ho, K. S., Kajiwara, M. & Takahashi, T. *J. Am. chem. Soc.* **98**, 1589–1591 (1976).
13. Battersby, A. R., McDonald, E., Williams, D. C. & Würziger, H. K. W. *J. chem. Soc. Chem. Commun.* 113–115 (1977).
14. Battersby, A. R., Fookes, C. J. R., McDonald, E. & Meegan, M. J. *J. chem. Soc. Chem. Commun.* 185–186 (1978).
15. Dauner, H.-O., Gunzer, G., Heger, I. & Müller, G. *Z. physiol. Chem.* **357**, 147–152 (1976).
16. Battersby, A. R., Fookes, C. J. R., Matcham, G. W. J. & McDonald, E. *J. chem. Soc. Chem. Commun.* 1064–1066 (1978).
17. Battersby, A. R., Fookes, C. J. R., Matcham, G. W. J. & McDonald, E. *J. chem. Soc. Chem. Commun.* 539–541 (1979).
18. Jordan, P. M. & Seehra, J. S. *FEBS Lett.* **104**, 364–366 (1979).
19. Bogorad, L. & Granick, S. *Proc. natn. Acad. Sci. U.S.A.* **39**, 1176–1188 (1953).
20. Bogorad, L. *J. biol. Chem.* **233**, 501–509; 510–515 (1958).
21. Frydman, R. B. & Feinstein, G. *Biochim. biophys. Acta* **350**, 358–373 (1974).
22. Battersby, A. R., Fookes, C. J. R., Matcham, G. W. J., McDonald, E. & Gustafson-Potter, K. E. *J. chem. Soc. Chem. Commun.* 316–319 (1979).
23. Battersby, A. R., Fookes, C. J. R., Gustafson-Potter, K. E., Matcham, G. W. J. & McDonald, E. *J. chem. Soc. Chem. Commun.* (1979).
24. Radmer, R. & Bogorad, L. *Biochemistry* **11**, 904–910 (1972).
25. Davies, R. C. & Neuberger, A. *Biochem. J.* **133**, 471–492 (1973).
26. Higuchi, M. & Bogorad, L. *Ann. N.Y. Acad. Sci.* **244**, 401–418 (1975).
27. Burton, G. *et al. J. Am. chem. Soc.* **101**, 3114–3116 (1979).

ARTICLE

Inverted terminal repetition in vaccinia virus DNA encodes early mRNAs

Riccardo Wittek, Ernest Barbosa, Jonathan A. Cooper, Claude F. Garon, Hardy Chan & Bernard Moss

National Institute of Allergy and Infectious Diseases, National Institutes of Health, Bethesda, Maryland 20205

Vaccinia virus DNA contains a long inverted terminal repetition of MW ~6.8 × 10⁶. A fragment of MW 6.3 × 10⁶ from this repetition has been cloned in coliphage λ and used to isolate RNA from virus-infected cells. Electron microscopy indicates that early RNAs are transcribed from the repeated sequence and cell-free translation shows that the RNAs code for polypeptides.

IDENTICAL sequences are present at the two ends of the genome of many viruses, presumably to fulfil an essential function in DNA replication[1–7]. However, the long ($\sim7 \times 10^6$ dalton) inverted terminal repetition in vaccinia virus[6,7] appears to be transcribed[7], suggesting that the region may also encode viral proteins. To investigate this interesting possibility, we have used coliphage λ to clone a fragment of molecular weight (MW) 6.3×10^6 from the end of the 122×10^6 MW vaccinia virus

genome and have used the recombinant DNA to isolate RNA from virus-infected cells. Electron microscopy indicates that early RNAs are transcribed from the repeated sequence, and cell-free translation shows that these RNAs code for polypeptides.

Length of the terminal repetition

Restriction endonuclease analyses were undertaken both to confirm the length of the inverted terminal repetition, which was estimated by electron microscopy to be of MW 6.8×10^6 daltons for the WR strain of vaccinia virus[7], and to select suitable DNA fragments for cloning. *Hin*dIII digestion of vaccinia virus DNA produces two end fragments of MW approximately 17.8 and 13.4×10^6 (ref. 7). When these were further digested with *Hin*cII and analysed by agarose gel electrophoresis, 8 of the 15 bands from the larger (*Hin*dIII B) end fragment co-migrated with 8 of the 14 bands from the smaller (*Hin*dIII C) end fragment (Table 1). Similarly, 8 common bands were detected by *Hpa*II digestion of the two *Hin*dIII end fragments (Table 1). The sums of the common *Hin*cII and *Hpa*II fragments were 6.6×10^6 and 6.2×10^6 daltons, respectively, which is consistent with their deriva-

Fig. 2 Ethidium bromide-stained agarose gel showing fragment patterns produced by cleavage of the recombinant phage DNA (track 1) and by cleavage of vaccinia virus DNA *Hin*dIII fragments B (track 2) and C (track 3) with *Eco*RI. A mixture of the two *Hin*dIII end fragments B and C was isolated from sucrose gradients[7] and the cross-links were removed by treatment with a single-strand specific DNase isolated from vaccinia virions as described previously[7,9]. One μg of octameric *Eco*RI linker (Collaborative Research) was phosphorylated with polynucleotide kinase and ligated to approximately 5 μg of *Hin*dIII fragments as described[15] except that ligation was performed at 11.5°C for 17.5 h. After ligation, linker oligomers were removed by chromatography on a Sepharose 6B column. The DNA was recovered in the void volume, extracted with phenol and precipitated with ethanol. The DNA was then cleaved with *Eco*RI and the fragments were ligated to the arms of λgt WES·λB (ref. 16) which had been purified by chromatography on RPC5. Recombinant DNA molecules were encapsidated by '*in vitro* packaging'[17] and the resulting phage were used to infect *E. coli* K12 DP50/supF (ref. 16) under P2-EK2 conditions in line with NIH guidelines for recombinant DNA experiments. Phage containing the *Eco*RI end-fragment were detected by the plaque-hybridisation technique[18] using ^{32}P-labelled *Sal*I end-fragment (MW 2.35×10^6) of vaccinia virus DNA as a probe. Positive phage plaques were picked and used to infect a 5 ml culture of DP50/supF cells. The phage were partially purified[19], after which the DNA was extracted, cleaved with *Eco*RI, and analysed on a 15 cm long 0.8% agarose gel. *Eco*RI digests of *Hin*dIII end fragments B and C, which were isolated from 0.6% agarose gels and purified by binding to glass-powder[20], were analysed on the same gel. The smallest *Eco*RI fragments of *Hin*dIII fragment B (MW ~0.52×10^6) and *Hin*dIII fragment C (MW ~0.7×10^6) have both run off the gel.

Fig. 1 Autoradiograph showing agarose gel electrophoresis of end fragments obtained by partial *Hin*cII digestion of *Hin*dIII fragments B and C. Approximately 1 μg of purified *Hin*dIII fragments B and C were digested separately with 1 unit of *Hin*cII. At 1 to 30 min after addition of enzyme, portions of the incubation mixture were removed and digestion was stopped by addition of EDTA. Samples were combined and electrophoresed on a 0.8% agarose gel. DNA fragments were transferred to nitrocellulose[8] and probed with the *Sal*I end-fragment (MW 2.35×10^6) labelled with ^{32}P by nick-translation[14]. Molecular weights of the partial digestion products were determined by comparison of their electrophoretic mobilities with those of λ and adenovirus DNA fragments of known size. B, Partial products from *Hin*dIII fragment B; C, partial products from *Hin*dIII fragment C.

tion from a 6.8×10^6 dalton terminal repetition. This was confirmed by showing that the sizes of 8 partial *Hin*cII digestion products derived from the two ends of the genome were identical. After partial *Hin*cII digestion of *Hin*dIII fragments B and C and agarose gel electrophoresis, the terminal 2.35×10^6 dalton *Hin*cII fragment and all partial digestion products containing this sequence were identified by hydridisation to a ^{32}P-labelled 2.35×10^6 dalton end fragment probe. Figure 1 reveals that the first eight *Hin*cII sites occur in the same locations in *Hin*dIII fragments B and C, thereby generating eight common bands. From this point on, the partial digestion products from *Hin*dIII fragments B and C diverged (Fig. 1). The largest common partial end fragment is 6.6×10^6 daltons in agreement with the sum of the eight co-migrating *Hin*cII fragments (Table 1). The partial digestion method was also used to show eight

Fig. 3 Ethidium bromide-stained agarose gel showing the fragment patterns produced by cleavage of the cloned DNA insert and of authentic vaccinia virus DNA with *Hpa*II. *Hind*III fragments B (track 1) and C (track 2) were isolated from 0.6% agarose gels by binding to glass powder[20] and cleaved with *Hpa*II. Recombinant phage DNA was cleaved with *Eco*RI and the 'insert' was purified and cleaved with *Hpa*II (track 3). Authentic *Eco*RI end fragment was obtained by cleavage of isolated *Hind*III fragment C from vaccinia virus DNA with *Eco*RI and isolation of the *Eco*RI end fragment. The purified fragment was further digested with *Hpa*II (lane 4). Electrophoresis was carried out in 1.4% agarose gels.
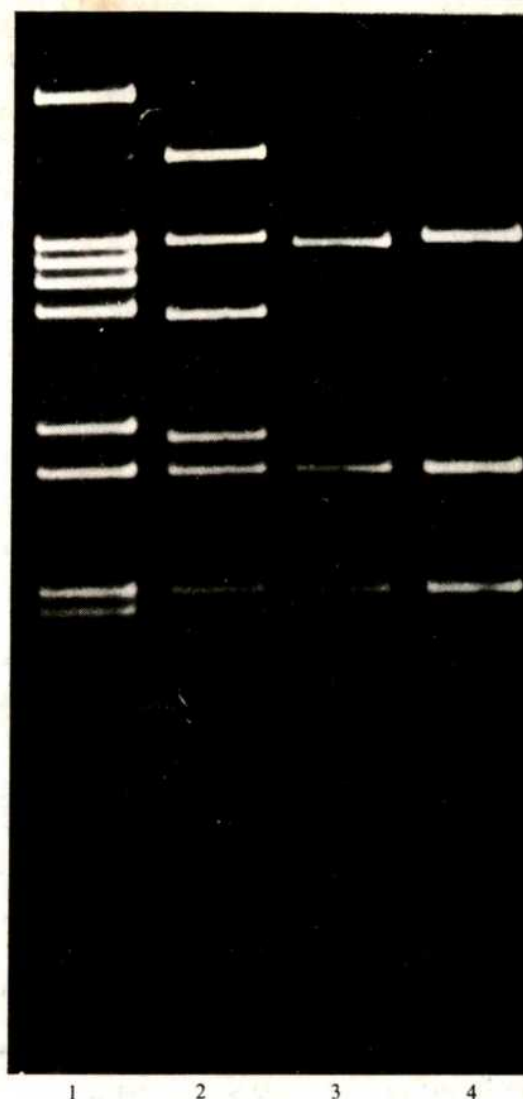
identical *Hpa*II sites at both ends of the vaccinia virus genome (not shown). Thus restriction endonuclease analyses indicated that the inverted terminal repetition is greater than 6.6×10^6 daltons.

Cloning the terminal repetition

*Hinc*II and *Hpa*II were useful for determining the minimum length of the terminal repetition because they make a large number of cuts in that region. However, to obtain a fragment for cloning, we required a restriction endonuclease that made its first cut just before the junction of the repeated and unique sequences. Screening for such an enzyme was simplified by an unusual feature of vaccinia virus DNA. Because the two strands of DNA are covalently linked at their ends[9], terminal fragments produced by restriction endonucleases can be identified by their ability to renature rapidly[10]. As anticipated, agarose gel electrophoresis showed a single rapidly renaturing end fragment when the first cut occurred within the terminal repetition whereas two end fragments were found when the first cut was beyond the 6.8×10^6 dalton repetition. From this survey, we noted that *Eco*RI produced a single 6.3×10^6 dalton rapidly renaturing end fragment from whole vaccinia virus DNA and the same size fragment on sub-digestion of either of the two large *Hind*III end fragments (Table 1; tracks 2 and 3, Fig. 2). Accordingly, the *Eco*RI end fragment was selected for cloning.

The strategy used to insert the *Eco*RI end fragment of vaccinia virus DNA into coliphage λ, detailed in Fig. 2 legend, involved cleavage of the covalently linked termini of isolated vaccinia *Hind*III end fragments with a single-strand specific DNase;

Table 1 Molecular weights $\times 10^{-6}$ of *Hinc*II, *Hpa*II and *Eco*RI restriction fragments produced by subdigestion of *Hind*III fragments B and C

Restriction endonuclease *Hind*III fragment	*Hinc*II		*Hpa*II		*Eco*RI	
	B	C	B	C	B	C
	2.80		3.80		6.30*	6.30*
	2.43			3.00	5.15	
	2.35*	2.35*	2.30*	2.30*		4.41
	2.24		2.15		3.30	
		2.20	2.05			3.10
	1.48		1.92		2.86	
		1.32		1.90	1.70	
	1.28		1.50			0.70
	1.00			1.45	0.57	
	0.97	0.97†	1.40	1.40		
	0.93	0.93	1.10	1.10		
	0.85	0.85†	0.98			
		0.73		0.85		
		0.68	0.66	0.66		
	0.63	0.63		0.55		
		0.58	0.43			
	0.47†	0.47	0.40			
		0.25†		0.38		
	0.20	0.20	0.25	0.25		
	0.17	0.17	0.20	0.20		
	0.15		0.17	0.17		
			0.15	0.15		
Sum of total	18.4	14.4	19.5	14.4	19.9	14.5
Sum of common	6.6		6.2		6.3	

* Fragments identified by agarose gel electrophoresis after rapid renaturation as containing cross-links.

† Intense ethidium bromide-staining bands suggesting two fragments of similar molecular weight.

blunt-end ligation of an octameric linker containing the *Eco*RI site to the terminus; *Eco*RI digestion of the product and ligation of the vaccinia DNA fragment to λ 'arms'. After *in vitro* packaging of the recombinant DNA, *Escherichia coli* were infected and plaques were identified by hybridisation using the 2.35×10^6 dalton ^{32}P-labelled *Sal*I end fragment of vaccinia virus DNA as a probe. For further identification, the recombinant phage DNA was purified and digested with *Eco*RI. Four
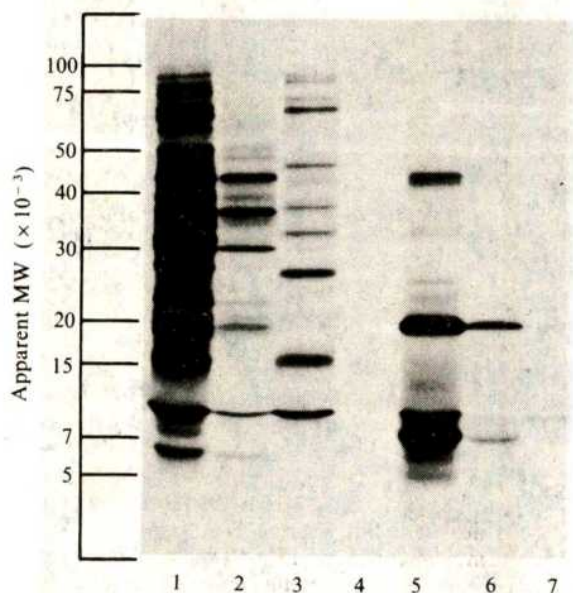
Fig. 4 Autoradiograph of a polyacrylamide gel showing the polypeptides synthesised in a reticulocyte cell-free system programmed with RNA selected by hybridisation to the cloned terminal repetition of vaccinia virus DNA. Cytoplasmic RNA was purified from HeLa cells which had been infected with approximately 30 plaque-forming units of purified vaccinia virus per cell[11]. Immediate early, early and late RNA were prepared from cells infected for 4 h in the presence of $100 \mu g \, ml^{-1}$ cycloheximide, $40 \mu g \, ml^{-1}$ cytosine arabinoside or for 6 h without inhibitors, respectively. Approximately $210 \mu g$ of each RNA preparation was hybridised to 0.2 pmol of recombinant DNA immobilised on nitrocellulose filters in $300 \mu l$ of 80% formamide, 0.4 M NaCl, 40 mM PIPES pH 6.4, 1 mM EDTA and 0.1% SDS at 37°C in a shaking water bath for 18 h. At the end of the hybridisation, the filters were stringently washed to remove unhybridised RNA[21]. This consisted of three washes at room temperature with 4 ml of 10 mM Tris-HCl pH 7.5, 1 mM EDTA, 0.1% SDS, then three washes with 10 mM Tris-HCl pH 7.5, 1 mM EDTA. The filters were then washed twice using 0.4 ml of hybridisation solution lacking SDS at 37°C for 15 min and finally in 0.4 ml of 80% formamide, 40 mM PIPES pH 6.4, 1 mM EDTA at 37°C for 15 min. Hybridised RNA was eluted in 0.2 ml of water at 100°C for 2 min, and then alcohol precipitated with $20 \mu g$ of calf liver tRNA (Boehringer Mannheim). The precipitate was washed twice with 70% ethanol and dried *in vacuo*. This RNA was used to programme cell-free protein synthesis in 10-μl reactions containing message-dependent reticulocyte lysate[12,22]. Samples of each reaction (2 μl) were prepared for electrophoresis and analysed on a 9 cm long, SDS polyacrylamide (20% T, 0.33% C) gel[11,12]. An 8-h fluorographic exposure is shown. The reticulocyte lysate was programmed with tRNA only (track 4), with tRNA and 1 μg of unpurified immediate early, early or late RNA (tracks 1, 2 and 3, respectively), or with the immediate early, early or late RNA purified by hybridisation to recombinant DNA sequences (tracks 5, 6 and 7, respectively). The apparent space at ~15,000 daltons, and the compression just below it, are due to large amounts of unlabelled globin from the reticulocyte lysate. Similar polypeptides were detected when RNA, purified by solution hybridisation and isolation of the hybridised RNA on potassium iodide density gradients[23], was translated.
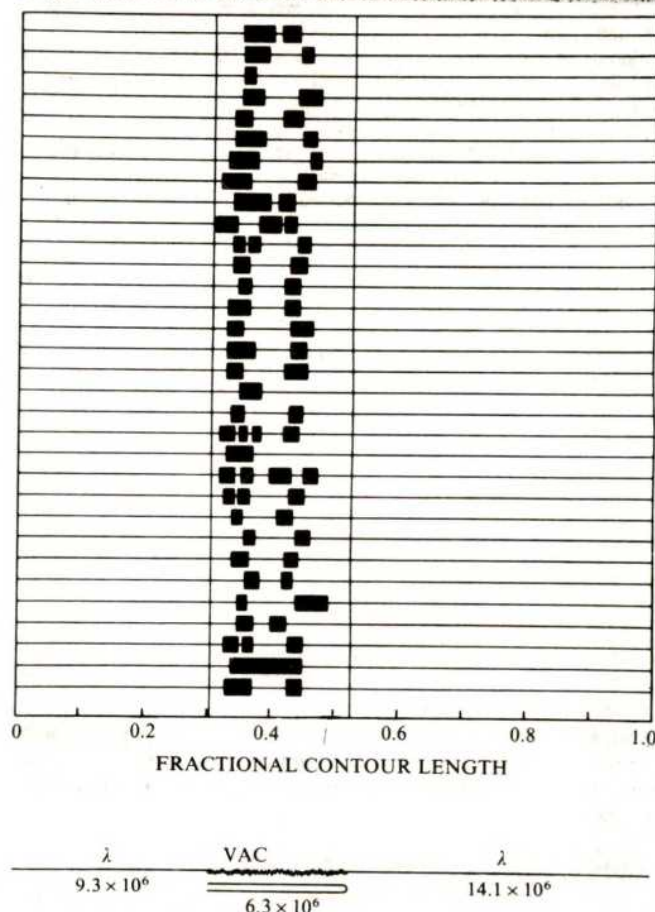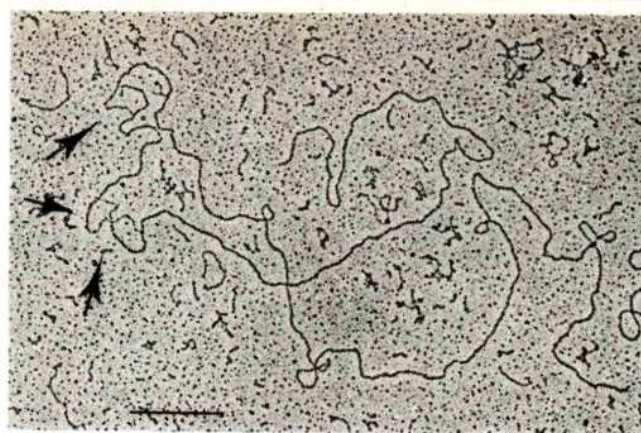
Fig. 5 Electron microscopic analysis of R-loop structures formed between intact recombinant DNA and early viral RNA. Recombinant DNA ($8 \mu g \, ml^{-1}$) and cytoplasmic RNA ($300 \mu g \, ml^{-1}$) from cells infected in the presence of cytosine arabinoside were incubated at 42°C for 20 h in a solution containing 70% formamide, 0.1 M Tricine buffer pH 8.0, 0.25 M NaCl and 0.01 M EDTA. Samples were mounted for electron microscopy by spreading the above mixture with no additions other than cytochrome *c* over a distilled water hypophase. Grids were rotory shadowed with platinum–palladium and examined in a Siemens Elmiskop 101 microscope at 40 kV accelerating voltage. Electron micrographs were taken on Kodak electron image plates at magnifications of 6,000. Magnification was calibrated with a grating replica (E. F. Fullam., cat. no. 1000), and contour lengths were measured with a Numonics digitiser interfaced to a Wang 2200 computer. R-loops are indicated by arrows, scale bar, 0.5 μm. In this molecule, the possibilities that there are two R-loops, one of which is twisted, or three R-loops, two of which are adjacent, could not be distinguished. A schematic representation of the map positions of hybridised RNA is also presented. VAC indicates the position of the vaccinia virus DNA insert with the orientation of the original cross-linked end.

bands were resolved by agarose gel electrophoresis (track 1, Fig. 2). Starting at the top of the gel, the first three correspond to the reannealed λ arms and the individual large and small λ arms, respectively. Significantly, the fourth band co-migrated with authentic EcoRI end fragment obtained by EcoRI digestion of the larger (track 2, Fig. 2) or smaller (track 3, Fig. 2) HindIII end fragments of total vaccinia virus DNA.

To prove that the cloned DNA is identical to authentic EcoRI end fragment from vaccinia virus DNA, the insert was separated from the λ arms and cleaved with HpaII. The HpaII fragments obtained from the cloned insert (track 3, Fig. 3) co-migrated with common HpaII fragments obtained by sub-digestion of the two HindIII end fragments from vaccinia virus DNA (tracks 1 and 2, Fig. 3) as well as with HpaII fragments obtained by digestion of authentic EcoRI end fragment also isolated from vaccinia virus DNA (track 4, Fig. 3). In addition, since the largest HpaII fragment obtained from the insert is derived from the originally cross-linked end of the genome and since the mobility of this fragment is similar to that of the HpaII fragment containing the cross-link, relatively little DNA was lost by single-strand nuclease treatment prior to cloning. The orientation of the inserted vaccinia DNA was determined by mapping the single XhoI restriction site of the EcoRI end fragment of vaccinia virus DNA within the recombinant molecule. The recombinant used in these studies has the originally cross-linked end of the vaccinia virus genome attached to the large arm of the λ vector. However, a recombinant with the opposite orientation was also identified.

Expression of inverted terminal repetition

Preliminary results[7] indicated that some sequences contained within the inverted terminal repetition are transcribed in vaccinia virus infected cells and further evidence for this was obtained by hydridisation of ^{32}P-labelled RNA to HpaII and HincII digests of HindIII fragments B and C from vaccinia virus DNA (E. B., unpublished). The cloned EcoRI fragment, however, provided a tool for isolating sufficient RNA to extend these studies. In particular, we wished to know whether RNA isolated by hybridisation to the cloned terminal repetition could serve as a messenger. Previously the message-dependent reticulocyte lysate, supplemented with calf liver tRNA, was shown to faithfully translate early and late vaccinia virus mRNA[11,12]. In those studies we found that RNA made in the presence of an inhibitor of protein synthesis (referred to as immediate early RNA) and RNA made in the presence of an inhibitor of DNA synthesis (referred to as early RNA) programmed synthesis of similar sets of polypeptides although some differences were also noted. When translating RNA extracted from cells late after infection, a new set of polypeptides was made in addition to continued synthesis of some early polypeptides.

Figure 4 shows the virtually blank endogenous incorporation of the reticulocyte lysate (track 4) whereas tracks 1, 2 and 3 show polypeptides synthesised when the cell-free system was programmed with total immediate early, early and late mRNAs. Tracks 5, 6 and 7 show polypeptides synthesised when the cell-free system was programmed with mRNAs selected by hybridisation to the recombinant DNA immobilised on nitrocellulose membranes. In contrast to the large number of total

immediate early polypeptides, only three prominent polypeptides of MWs 42,000, 19,000 and 7,500 as well as several minor polypeptides were detected using selected immediate early mRNA (track 5). Similar polypeptides, but in lesser amounts, were also made with selected early mRNA (track 6). Longer periods of fluorography revealed synthesis of small amounts of the same three prominent early polypeptides using selected late RNA (track 7); however, no unique late polypeptides were detected.

Electron microscopy was used to visualise the early RNA species. Cytoplasmic RNA, from cells infected with vaccinia virus in the presence of cytosine arabinoside, was annealed to the recombinant DNA in conditions of high formamide concentration which favours RNA·DNA over DNA·DNA hybridisation[13]. Nearly all molecules contained at least one 'R-loop' formed by partial displacement of a DNA strand; most molecules contained two or three R-loops. From contour length measurements of the recombinant DNA, it was apparent that all R-loops were located within the vaccinia virus DNA insert. A photograph of one DNA molecule containing R-loops and schematic representations of the R-loop locations on 32 separate DNA molecules are shown in Fig. 5. To confirm the orientation of the R-loops within the vaccinia virus DNA insert, HindIII was used to cleave recombinant molecules within the short λ arm. A similar distribution of R-loops was observed in an additional 40 molecules. The R-loop (mean 0.28 ± 0.07 μm) nearest to the large λ arm (that is, the end of the vaccinia genome) was clearly observed to contain a short single-strand extension in 28 of 160 molecules. In each case the single-strand projection, presumably a poly (A) tail, was located on the side of the R-loop nearer to the long λ arm. As represented in Fig. 5, the R-loops nearer to the short λ arm were variable in size (0.19–0.79 μm; mean 0.45 ± 0.17 μm) and in apparent poly (A) tail position. However, in molecules where one large R-loop was visible, the appearance suggested that two adjacent mRNAs had been transcribed from opposite strands. Direct evidence for strand switching has recently been obtained (R. W. and J. C., unpublished) by hybridisation of RNA to separated recombinant DNA strands. Of some interest was the absence of any R-loops within the 2.08 (± 0.06) × 10[6] daltons corresponding to the very end of the viral genome. A similar conclusion was also reached by failure of ^{32}P-labelled early RNA to hybridise to HpaII and HincII terminal restriction fragments from virion DNA (E. B., unpublished). Accordingly, this region of the genome appears to be transcriptionally inactive. Another point of interest was our inability to visualise R-loop structures containing intervening DNA, suggestive of split genes, such as have been found for other DNA viruses.

Conclusion

We have shown that the inverted terminal repetition in vaccinia virus DNA is divided into transcriptionally active and inactive regions and thus appears to have more than one function. Besides a putative role in DNA replication, a portion of the terminal repetition codes for several early mRNA species. Although the genome organisation of herpesvirus is quite different from that of poxviruses, evidence for transcription of repetitive sequences in that system has also been found[24].

1. Garon, C. F., Berry, K. W. & Rose, J. A. Proc. natn. Acad. Sci. U.S.A. 69, 2391–2395 (1972).
2. Wolfson, J. & Dressler, D. Proc. natn. Acad. Sci. U.S.A. 69, 3054–3057 (1972).
3. Koczot, F. J., Carter, B. J., Garon, C. F. & Rose, J. A. Proc. natn. Acad. Sci. U.S.A. 70, 215–219 (1973).
4. Berns, K. I. & Kelley, T. J. Jr J. molec. Biol. 82, 267–271 (1974).
5. Sheldrick, P. & Berthelot, N. Cold Spring Harb. Symp. quant. Biol. 39, 667–668 (1974).
6. Wittek, R. et al. J. Virol. 28, 171–181 (1978).
7. Garon, C. F., Barbosa, E. & Moss, B. Proc. natn. Acad. Sci. U.S.A. 75, 4863–4867 (1978).
8. Southern, E. M. J. molec. Biol. 98, 503–518 (1975).
9. Geshelin, P. & Berns, K. I. J. molec. Biol. 88, 785–796 (1974).
10. DeFilippes, F. M. J. Virol. 17, 227–238 (1976).
11. Cooper, J. A. & Moss, B. Virology 88, 149–165 (1978).
12. Cooper, J. A. & Moss, B. Virology 96, 368–380 (1979).
13. Thomas, M., White, R. L. & Davis, R. W. Proc. natn. Acad. Sci. U.S.A. 73, 2294–2298 (1976).
14. Rigby, P. W. J., Dieckmann, M., Rhodes, C. & Berg, P. J. molec. Biol. 113, 237–251 (1977).
15. Maniatis, T. et al. Cell 15, 687–701 (1978).
16. Leder, P., Tiemeier, D. & Enquist, L. Science 196, 175–177 (1977).
17. Sternberg, N., Tiemier, D. & Enquist, L. Gene 1, 255–280 (1977).
18. Benton, W. D. & Davis, R. W. Science 196, 180–182 (1977).
19. Tiemeier, D. C., Tilghman, S. M. & Leder, P. Gene 2, 173–191 (1977).
20. Vogelstein, B. & Gillespie, D. Proc. natn. Acad. Sci. U.S.A. 76, 615–619 (1979).
21. McGrogan, M., Spector, D. J., Goldenberg, C. J., Halbert, D. & Raskas, H. J. Nucleic Acids Res. 6, 593–607 (1979).
22. Pelham, H. R. B. & Jackson, R. J. Eur. J. Biochem. 67, 247–256 (1976).
23. Cooper, J. A. & Moss, B. Nucleic Acids Res. 6, 3599–3612 (1979).
24. Clement, J. B., Watson, R. J. & Wilkie, N. M. Cell 12, 275–285 (1977).

LETTERS

Improved position and new optical candidate for A0538 − 66

M. D. Johnston*, R. E. Griffiths† & M. J. Ward‡

* Center for Space Research, Department of Physics, Massachusetts Institute of Technology, Cambridge, Massachusetts 02139
† Harvard-Smithsonian Center for Astrophysics, 60 Garden Street, Cambridge, Massachusetts 02138
‡ Institute of Astronomy, Cambridge, UK

Among X-ray transients, A0538 − 66 is unique: between June and December 1977 it was observed to undergo seven outbursts[1-3], characterized by different durations (from ~12 h to ~15 days) and peak intensities (from ~0.03 to 0·1 Crab). Most remarkably, the outbursts were all separated by an interval of either 16.7 days or a small multiple thereof. The source may be a member of the Large Magellanic Cloud (LMC) and thus one of the most luminous stellar X-ray sources known [$(L_x(2-17\,\mathrm{keV}) \simeq 8 \times 10^{38}\,\mathrm{erg\,s^{-1}})$]. No steady counterpart to the flaring source has yet been detected. We report here a reanalysis of the HEAO 1 modulation collimator (MC) data which has led to the detection of the five outbursts which occurred between August and December 1977. A uniquely precise (25 arc s) position has been obtained which excludes the previously suggested optical candidate. We have searched archive plates of the LMC and find that one of the stars in the refined error region shows variability in the B band by ~1 mag.

The first two outbursts of A0538 − 66 were observed with the Ariel 5 satellite[1], leading to a position accurate to ~0.5°, and, for one of the outbursts, a spectrum best characterized by a thermal bremsstrahlung model with $kT = 6.5$ keV and no detectable low-energy absorption ($N_H < 2 \times 10^{22}$ cm^{-2}). Both of these outbursts lasted ≤ 1 day. After the launch of HEAO 1, the LMC was under nearly constant scanning surveillance due to its location at the south ecliptic pole. Two more brief (~1 day) outbursts were detected with the HEAO 1 MC in October and November 1977, resulting in three possible source locations within or near the Ariel 5 error region[2]. Based on these four events, it was suggested that the outbursts showed a regularity in their onset that could be described by:

$$T_0 = (2443323.96 \pm 0.03) + (16.662 \pm 0.006)n$$

where T_0 is the Julian date of the onset time of the nth outburst[2]. The Ariel 5 events correspond to $n = 0$ and 1, and the HEAO 1 MC observations to $n = 6$ and 8. A search for other brief outbursts in the HEAO 1 MC data was unsuccessful, and an upper limit of 0.9 μJy was placed on the (1.5–13.5 keV) flux density of a steady component. A subsequent analysis of the HEAO 1 Large Area Sky Survey (LASS) data revealed that outbursts corresponding to $n = 3, 4$ and 11 did occur at the expected times[3]. The events at $n = 3$ and 4 lasted significantly longer than the other five; the flare at $n = 11$ occurred while LMC X − 3 was unusually bright[4].

The MC data for A0538 − 66, taken at maximum brightness according to the LASS light curve[3], were superimposed about the centre of the previous most likely error region. (For a description of the instrument and data analysis technique, see ref. 5). For this optimum set of data, significant detections of all five outbursts were obtained (Table 1), yielding five pairs of lines of position spanning 150° in position angle. These lines have only one common intersection within ~2° of the Ariel 5 error region, thus confirming that all five outbursts, in spite of their different durations and peak intensities, originate from the same

source. The five pairs of lines were combined[6,7] to yield the most likely source position:

$$\alpha(1950.0)\ 5\,\mathrm{h}\ 35\,\mathrm{min}\ 42.7\,\mathrm{s}, \qquad \delta -66° 53' 44''$$

with a 90% confidence error circle radius of 25 arc s. A finding chart of the region is presented in Fig. 1a. The northern half of the previous most likely error region (region A of ref. 2), including the suggested optical candidate[2] (star 19 of Fig. 1a), is excluded by the refined position reported here.

We have made a crude search for X-ray spectral variability by computing the hardness ratio R for each detected outburst. This is defined as the ratio of the counting rates in the 5.4–13.3 keV to 0.9–5.4 keV energy bands. This ratio is not well determined for the flare at $n = 11$ due to the low statistical significance of the detection and to confusion with LMC X − 3 in the lowest energy channel (0.9–2.6 keV). Three of the remaining four outbursts ($n = 3, 4$, and 6) are consistent with a constant hardness ratio, ($R = 0.51 \pm 0.05$; $\chi^2 = 1.8$ for 2 d.f.) and with the Ariel 5 spectral parameters. The outburst at $n = 8$ was significantly harder than the others: $R = 1.42 \pm 0.25$. Assuming negligible low-energy absorption, this corresponds to a change in the logarithmic slope of a power-law (energy) spectrum from −0.5 to +0.7. The data are, however, not sufficient to distinguish between a flattening of the source spectrum and an increase in the low-energy absorption. We note that the observed spectral change may complicate intensity comparisons between different instruments.

A search for optical variability or proper motion of the stars in the refined error region has been carried out with archival plate material at the Harvard College Observatory. The plates, taken with the 24″ Bruce doublet at Bloemfontein, South Africa, were examined with a blink comparator, and the two showing the strongest evidence for variability were subsequently measured with an iris photometer. Nine nearby stars from the photometric sequence of Dachs[8] were used for calibration. Star Q (Fig. 1a) is observed to be variable between extremes of $B \sim 14.5$ (12 November 1945; Plate no. A25156) and $B \sim 15.5$ (19 November 1941; Plate no. A22993), although the plates are not of sufficient quality for a detailed light curve to be compiled. Figure 1b shows the range of variability observed. Astrometry for stars C, D, Q and R has been carried out on plates taken 13 November 1896 (stars Q and R) and 19 November 1941 (stars C and D) and compared with the positions of the same stars on the ESO Quick Blue Survey plate (21 November 1973). Upper limits (3σ) of 0.28 arc s yr^{-1} (stars C and D) and 0.15 arc s yr^{-1} (stars Q and R) are placed on their proper motion, indicating that they are not very local objects[9].

Spectra of stars Q and R were obtained 31 July 1979 (~5 days before the extrapolated flare onset time) with the RGO spectrograph and IPCS at the 3.8m Anglo-Australian telescope. Star R shows H and He absorption lines typical of a normal O star: we estimate $V = 13.8$, $B - V = -0.2$. Star Q shows the absorption spectrum of a B-type star: we estimate $V = 15.7$,

Table 1 Dates of observations used for position measurements

Outburst no. (n)	Dates (JD − 2443000)	Detection Significance MC1 (σ)	Detection Significance MC2 (σ)	Average flux density* (μJy)
3	375.107–380.032	11.6	17.4	25
4	390.997–392.339	5.1	5.9	20
6	423.935–424.274	8.3	7.5	45
8	457.149–457.440	9.9	6.8	25
11	507.119–507.264	5.4	4.9	17

* For an assumed Crab-like spectrum averaged over 1.5–13.5 KeV; $1\mu\mathrm{Jy} = 0.242 \times 10^{-11}$ erg cm^{-2} s^{-1} keV^{-1}.
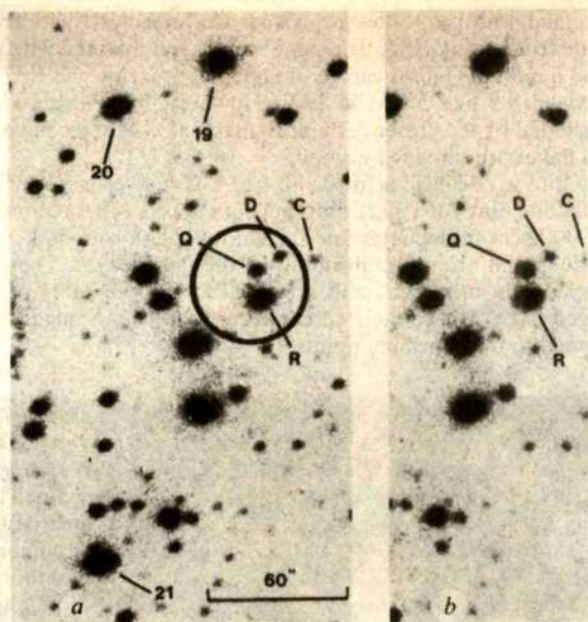
Fig. 1 Finding chart for A0538−66 prepared from Harvard College Observatory Plate no. A22993, taken 19 November 1941 with the 24-inch Bruce doublet in Bloemfontein, South Africa. (*b*), taken from Plate no. A25156 made with the same instrument on 12 November 1945, illustrates the variability of star Q by ~1 mag in the *B* band. The celestial location (±2 arc s) of star Q is:

$$\alpha (1950.0)\ 5\ h\ 35\ min\ 42.4\ s, \qquad \delta −66° 53' 39''$$

Star numbers are from the photometric sequence of Dachs[8].

$B − V = 0.0$, and conclude that it is a probable LMC member ($M_v = −3.8$ for an assumed distance modulus[10] of 18.6 and foreground extinction $A_v = 0.2$ mag). We note the similarity of this star to the optical candidate for LMC X−3 ($V = 16.9$, $B − V = −0.06$, weak Hβ emission, variable by 0.1 mag; see ref. 4 and refs therein).

Transient X-ray phenomena on time scales of seconds (for example X-ray bursts; see review in ref. 11) and months (for example classical X-ray transients; see review in ref. 12) have led to optical identifications and extensive studies of the stellar counterparts. In contrast, sources with characteristic outburst times of hours to days have been observed[13-17] but none have been positioned with sufficient accuracy for a convincing optical identification to be made (with the possible exception of H0449−55; ref. 17). Among sources exhibiting fast-transient behaviour, A0538−66 is of particular interest as its outbursts may have either hard or soft spectra, and may last hours or days. It thus spans the range of behaviour observed in other fast-transient sources, which, while possibly recurrent, are not located in a region of the sky subject to as continuous a surveillance as the LMC during the HEAO 1 mission. Several possible explanations for the behaviour of this source were considered in ref. 2, but present data do not significantly constrain possible source models. Optical and radio monitoring of star Q, especially near the expected times of X-ray outbursts, will be important in establishing variability commensurate with the X-ray periodicity and in elucidating the nature of this unusual system.

1. White, N. E. & Carpenter, G. F. *Mon. Nat. R. astr. Soc.* **183**, 11P (1978).
2. Johnston, M. *et al. Astrophys. J. Lett.* **230**, L11 (1979).
3. Skinner, G. *et al. Astrophys. J.* (submitted).
4. Johnston, M., Bradt, H. & Doxsey, R. *Astrophys. J.* **233**, 514 (1979).
5. Gursky, H. *et al. Astrophys. J.* **223**, 973 (1978).
6. Johnston, M. thesis MIT (1978).
7. Avni, Y. *Astr. Astrophys.* **66**, 307 (1978).
8. Dachs, J. *Astr. Astrophys.* **223**, 730 (1972).
9. Johnson, H. *Astrophys. J.* **223**, 282 (1978).
10. Crampton, *Astrophys. J.* (in the press).
11. Lewin, W. H. G. in *X-ray Astronomy* (eds Baity, W. A. & Peterson, L. E.) 133 (Pergamon, Oxford, 1979).
12. Cominsky, L., Jones, C., Forman, W. & Tananbaum, H. *Astrophys. J.* **224**, 46 (1978).
13. Rappaport, S., *et al. Astrophys. J. Lett* **206**, L139 (1976).
14. Cooke, B. A. *Nature* **261**, 564 (1976).
15. Ricketts, M. J., Cooke, B. A. & Pye, J. P. *Bull. Am. astr. Soc.* **10**, 516 (1978).
16. Schrijver, J. *et al. Astr. Astrophys.* **69**, L1 (1978).
17. Griffiths, R. E. *et al.* in *X-ray Astronomy* (eds Baity, W. A. & Peterson, L. E.) 93, (Pergamon, Oxford, 1979).

Freeze-formed silica fibres

Walter Mahler & Max F. Bechtold

Central Research and Development Department, E. I. du Pont de Nemours & Company, Wilmington, Delaware 19898

Phase separation during directional freezing of liquid systems leads to a variety of microstructures of the components due to the interplay of heat transfer, diffusion kinetics, and interfacial surface energy[1-6]. One of the more dramatic effects is the *in situ* formation of parallel fibres in directionally solidified eutectic superalloy. We report here similar morphological consequences of freezing aqueous polysilicic acid. This system is unique not only because it has an amorphous component, polysilicic acid, but this substance undergoes accelerated, concentration-dependent polymerization immediately after phase separation. As a result, it becomes insoluble, and after thawing, preserves the structure that had been conferred on it by the surrounding ice. We have explored the relationships of polymerization, composition, and freezing conditions with the morphology of the products, in particular with regard to fibre formation.

A solution of silicic acid in water (100 ml, 1 M in SiO_2) was prepared by ion exchange[7], adjusted to pH 5 with 0.3 ml 1 M NH_4OH, and placed in a 24×2.7 cm polypropylene cylinder. The silicic acid, which gelled 15 min after adjusting the pH, was allowed to age for another 30 min and was then directionally frozen by lowering the plastic cylinder into a −70 °C cold bath at 4 cm h^{-1}. After thawing, all the silica was in the form of insoluble parallel fibres with polygonal cross-section, ~0.005 cm in diameter and 15 cm long (Figs 1, 2). Fibres have been obtained from gels of this type with freezing rates from 0.3 to 150 cm h^{-1} and bath temperatures from −10° to −196 °C (ref. 8). Average fibre diameter decreases with lower silicic acid concentration, colder freezing baths, or with faster freezing rates in agreement with theoretical treatments of eutectic alloys[1-6].

Although each fibre has a unique cross-sectional geometry, the cross-section is invariant along the length of the entire fibre when freeze-formed in uniform conditions. When a cylinder of gelled silicic acid is frozen statically by cooling one end, both the thermal gradient and the freezing rate decrease as the ice-gel interface advances[9]. In these conditions, the resulting fibres are tapered (for example, 0.004 cm diameter at one end, and 0.026 cm at the other end of an 11-cm long fibre).

After drying in air at 150 °C, the composition of the fibres corresponds to $Si_3O_5(OH)_2$. The fibres are amorphous (X ray) and porous; surface area is about 900 m^2 g^{-1}, and the density measured by flotation in carbon tetrachloride–bromoform is 1.99 g cm^{-3}. The tensile strength is 86 ± 35 MPa. After heating at 925 °C for 8 h, the composition corresponds to SiO_2; surface area is decreased, the density is 2.20 g cm^{-3}, and the tensile strength is 510 ± 216 MPa. After 8 h at 1,000 °C, the average tensile strength drops to 253 MPa, and incipient crystallization can be detected; except for shrinkage, the fibre geometry remains unchanged.

Fig. 1 Scanning electron micrograph of a bundle of silica fibres bound with twine and cut with scissors. Scale bar, 100 μm. Magnification ×20.

The slower polymerization rate of 1 M silicic acid at *p*H 3 (gel time is 24 h at 25 °C) permits a wider range of product morphologies to be prepared. Fresh silicic acid, frozen and thawed promptly, reforms soluble silicic acid[10]. After ageing 1 M silicic acid 1 day at 25 °C, freezing and thawing gives insoluble imbricated flakes, roughly 0.1 cm across with parallel ridges 0.001–0.002 cm apart on one side (Fig. 3). The same morphology is observed when fresh silicic acid is frozen, aged 1 day at −10 °C, and then thawed. After 3 days' ageing at 25 °C before freezing, flakes are obtained that are accompanied by honeycomb structures and 6 days' ageing before freezing gives polygonally cross-sectioned fibres having about 550 m^2 g^{-1} surface area after drying. After ageing for about 20 days, fibres are
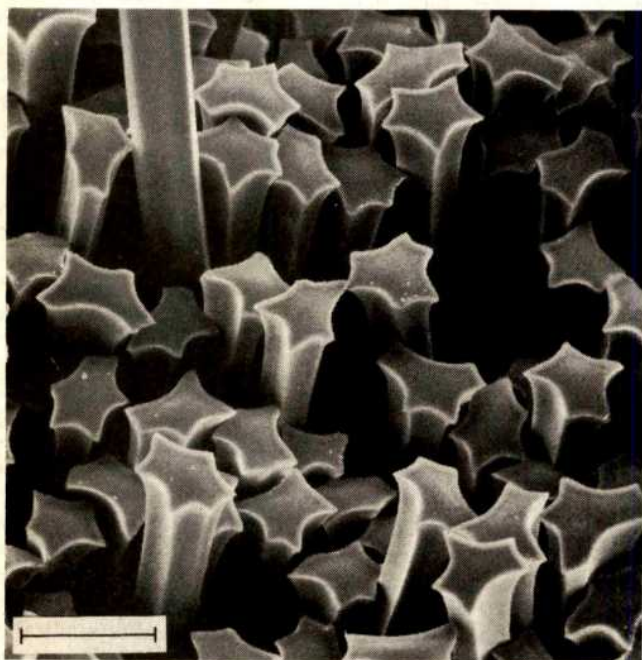
Fig. 2 Silica fibres. Scale bar, 100 μm. Magnification ×200.

obtained with properties equivalent to those described above made from gel at *p*H 5. The same results are obtained with gels aged 6 months. Fibres can be obtained by freezing gels that are between 0.5 and 5.0 M in SiO$_2$. However, fibre formation is precluded by the presence of more than 0.025 M salts. Featureless flakes are obtained instead.

Dilute aged silicic acid (0.1–0.5 M SiO$_2$) gives a mixture of flakes and fibres of a quite different appearance. These fibres are ~0.0002 cm in diameter and 0.2 cm long with rounded cross-sections that are not uniform along the fibre length. They are occasionally branched, and seem to be the remnants of the ridged flakes where the interconnections between ridges have thinned to the vanishing point.
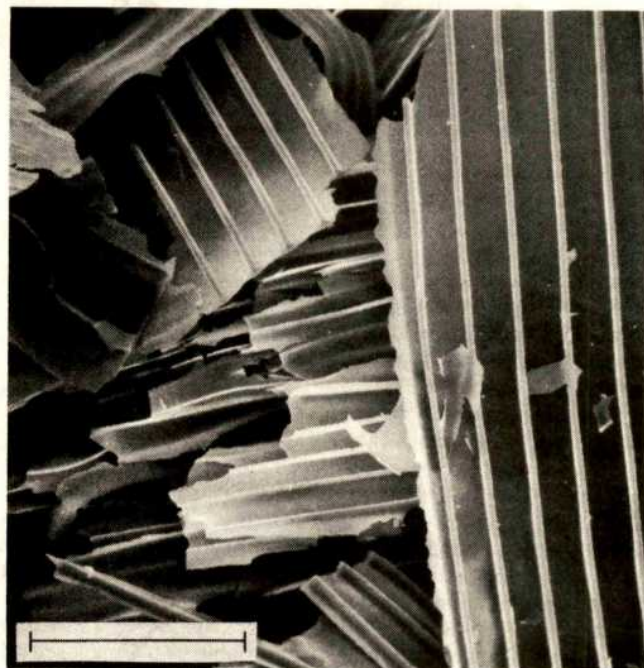
Fig. 3 Ribbed flakes. Scale bar, 100 μm. Magnification ×300.

Freezing of silicic acid and other colloids has been widely discussed, but all morphological descriptions of the products have been of small particulates, specifically powders[11], flakes[12,13], ribbed flakes[14], interconnected cells[15], and granules[16,17]. Our finding that high gel strength, low electrolyte concentration, and unidirectional freezing seem to be essential for obtaining polygonally cross-sectioned fibres may have some generality. Zirconia gels prepared by dialysis have responded similarly.

1. Tiller, W. A., Jackson, K. A., Rutter, J. W. & Chalmers, B. *Acta metall.* **1**, 428–437 (1953).
2. Tiller, W. A. in *The Art and Science of Growing Crystals* (ed. Gilman, J. J.) 276–312 (Wiley, New York, 1963).
3. Mullins, W. W. & Sekerka, R. F. *J. appl. Phys.* **34**, 323–329 (1963).
4. Kraft, R. W. *J. Metals, N.Y.* **18**, 192–200 (1966).
5. Hunt, J. D. & Jackson, K. A. *Trans metall. Soc. AIME* **236**, 843–852 (1966).
6. Double, D. D. *Krist. Technol.* **9**, 569–586 (1974).
7. Bird, P. G. US Patent 2,244,325 (1941).
8. Mahler, W. US Patent 4,122,041 (1978).
9. Carslaw, H. S. & Jaeger, J. C. *Conduction of Heat in Solids* 282–293 (Clarendon, Oxford, 1959).
10. Hazel, J. F. & Schipper, E. *J. Colloid Sci.* **5**, 532–540 (1950).
11. Kolosentsev, S. D., Belotserkovskii, G. M. & Plachenov, T. G. *J. appl. Chem. USSR* **48**, 253–254 (1975).
12. Lottermoser, A. *Chem. Ber.* **41**, 3976–3979 (1908).
13. Kautsky, H. & Irnich, R. *Z. anorg. allg. Chem.* **295**, 192–217 (1958).
14. Hinz, W., Ruttloff, H. & Täufel, A. *Silikattechnik* **10**, 378–381 (1962).
15. Halberstadt, E. S., Henisch, H. K., Nickl, J. & White, E. W. *J. Colloid Interface Sci.* **29**, 469–471 (1969).
16. Schorger, A.W. US Patent 1,949,360 (1934).
17. Vol'khin, V. V., Ponomarev, E. I. & Zolotavin, V. L. *Inorg. Mater. USSR* **1**, 1435–1438 (1965).

A thin-film polycrystalline photoelectrochemical cell with 8% solar conversion efficiency

Gary Hodes

Department of Plastics Research, The Weizmann Institute of Science, Rehovot, Israel

Photoelectrochemical solar cells (PECs) may become an economic method for conversion of light to electricity, due largely to the simplicity of formation, and quality, of the polycrystalline semiconductor–electrolyte junction. Within the past few years, conversion efficiencies of thin-layer polycrystalline-based cells have increased from ~1% to a recently reported 7.3% for the n-GaAs/Se$_x^{2-}$ system[1]. PECs based on the CdSe-polysulphide system have been studied extensively recently. CdTe, with a band-gap, E_g, ~1.45 eV is better matched to the solar spectrum than CdSe (E_g ~ 1·75 eV), but is unstable in polysulphide solutions as a photoanode at the current densities to be expected under normal solar irradiation (>10 mA cm^{-2}). A polysulphide-based PEC is described here which uses polycrystalline layers of CdSe$_{0.65}$Te$_{0.35}$, electrodes of which are prepared by painting a slurry of the semiconductor onto a Ti substrate, and sintering. Subsequent surface treatments of these layers lead to a solar-to-electrical conversion efficiency of up to 8%, with stability comparable to the thin-layer polycrystalline CdSe/polysulphide system[2].

CdSe and CdTe form solid solutions over the entire composition range. The electrical, optical and thermoelectrical properties of these alloys have been studied, and a minimum in the band gap of ~1.35–1.45 eV (depending on crystal structure) has been found[3]. To use these alloys as photoelectrodes in liquid junction photovoltaic cells layers of the alloys were prepared by a process similar to screen printing, whereby a CdSe$_{0.65}$Te$_{0.35}$ powder (prepared by sintering CdSe and CdTe powders

Fig. 2 Spectral response of a polycrystalline CdSe$_{0.65}$Te$_{0.35}$ photoanode in polysulphide solution (1 M each KOH, Na$_2$S, S). The photocurrent is corrected for photon density (that is the spectrum compares the relative quantum efficiency with the wavelength). The shape of this response, together with X-ray diffraction data, which shows that these electrodes are of a single composition, and with lattice parameters to be expected from this composition (compared with those of ref. 6), proves that the semiconductor is indeed a homogeneous alloy.

together with a CdCl$_2$ flux) was made into a smooth aqueous paint together with CdCl$_2$, painted onto a Ti substrate and then annealed in an inert atmosphere. The resulting electrodes were etched, and tested in an aqueous electrolyte containing 1 M each of KOH, Na$_2$S and S, with a counter electrode of sulphide brass gauze[4]. The light source was either solar illumination, or a tungsten source calibrated for the CdSe$_{0.65}$Te$_{0.35}$ cells against solar illumination.

The performance of the photoelectrodes depends strongly on the etching treatment used. Figure 1 shows examples of the output characteristics for three different treatments. The dotted line represents output characteristics obtained after a HCl:HNO$_3$ etch (the usual etch for CdSe photoelectrodes). Solar efficiencies up to 5.0% have been obtained after this treatment. Etching in dilute aqeous CrO$_3$ leads to an improved open circuit voltage and solar efficiencies up to 5.5%. The same increase of the OCV can be obtained after the HCl:HNO$_3$ etch by treating the electrode surface with a solution containing CrO$_4^{2-}$ ions before immersion in the polysulphide electrolyte.

A major increase in both short circuit current and fill factor (FF) was obtained by a subsequent photoetch, whereby the photoelectrode, shorted to a carbon counter electrode, was illuminated in a dilute aqueous mineral acid solution, for example, 0.1 M H$_2$SO$_4$. After treatment with an aqueous K$_2$CrO$_4$ solution, solar efficiencies up to 8.0% were obtained (the solid line in Fig. 1 shows the performance of a CdSe$_{0.65}$Te$_{0.35}$ photoelectrode after such a treatment).

Figure 2 shows the spectral response for a CdSe$_{0.65}$Te$_{0.35}$ photoelectrode in 1 M each of KOH, Na$_2$S and S. The short wavelength cutoff can be attributed to absorption by the polysulphide electrolyte. As the photocurrent loss due to this absorption is the same for CdSe and the CdSe$_x$Te$_{1-x}$ system, the fractional loss in the case of CdSe (E_G ~ 1.75 eV) is considerably greater than for the smaller band-gap mixed compounds. This explains the much greater photocurrents obtained for CdSe$_{0.65}$Te$_{0.35}$ than for CdSe (~60% increase was typically found), compared with what would be expected from the difference in band gaps, calculated on the basis of photon intensity of the relevant sections of the solar spectrum (<40% increase). The plateau region is surprisingly flat, and the long

Fig. 1 Photocurrent–photovoltage characteristics for polycrystalline CdSe$_{0.65}$Te$_{0.35}$ electrodes in polysulphide solution (1 M each KOH, Na$_2$S, S) under 0.85 X AMI simulated sunlight. ·····, after HCl:HNO$_3$ etch, electrode area 0.22 cm^2; ---, after CrO$_3$ etch or K$_2$CrO$_4$ treatment; ——, after photoetch + K$_2$CrO$_4$ treatment, electrode area 0.55 cm^2.

wavelength cutoff is fairly sharp (considering the polycrystalline nature of the electrode), and shows an effective band gap of ~1.45 eV, similar to that of CdTe.

The output stability of the photoelectrodes in polysulphide electrolyte has been measured in various conditions. In an electrolyte 3 M each in KOH and Na_2S and 4 M in S, and at 35 °C, the photocurrent remained stable for 21 h at 20 mA cm^{-2}. After 21 h the illumination intensity was increased to give a photocurrent density of 28 mA cm^{-2}. The photocurrent decreased 3.6% (to 27 mA cm^{-2}) after a further 20 h. Another electrode, illuminated to give an initial photocurrent density of 42 mA cm^{-2}, dropped 16.8% in current output after 49 h. Note that the normal operating currents of such photoelectrodes would be less than 20 mA cm^{-2}. It has been shown that for CdSe operating in a polysulphide electrolyte, complete stability may be obtained for a certain amount of charge passed at low photocurrent densities, while at higher current densities, a large degree of instability may be manifested for the same amount of charge passed[5]. This is a consequence of the exchange between solution sulphide and selenium from the CdSe, which depends on the relative rates of the competing S^{2-} oxidation and CdSe photodecomposition reactions[2,5]. The same mechanism is to be expected at the mixed $CdSe_xTe_{1-x}$ electrodes. Therefore the actual stability of these electrodes in normal (solar) operating conditions will be considerably better than suggested by the above 'worst case' conditions.

The effect of the photoetching treatment has been found to be general for many semiconductors besides $CdSe_{0.65}Te_{0.35}$. Scanning electron micrographs of the semiconductor surface show extensive pitting of the surface by the photoetch, which therefore seems to act as a selective etch. The increased surface area resulting is clearly visible to the eye as a change from a dull grey surface to a velvet matt black one. Part of the increase in photocurrent after photoetching is probably due to a lowered reflectivity of the surface, but this cannot explain it completely, as the original surface was itself not very reflecting (~10% reflectivity). Also, the increase in the fill factor, typically by ~10%, remains to be explained. The photoetching effect and the effect of the composition of the $CdSe_xTe_{1-x}$ electrodes on their output stability will be discussed in detail elsewhere.

1. Heller, A., Miller, B., Chu, S. S. & Lee, Y. T. *J. Am. chem. Soc.* **101**, 7633–7634 (1979).
2. Cahen, D., Hodes, G. & Manassen, J. *J. electrochem. Soc.* **125**, 1623–1628 (1978).
3. Tai, H., Nakashima, S. & Hori, S. *Phys. Status Solidi* **30**, K115–119 (1975).
4. Hodes, G., Manassen, J. & Cahen, D. *J. electrochem. Soc.* **127**, 544–549 (1980).
5. Heller, A., Schwartz, G. P., Vadimsky, R. G., Menezes, S. & Miller, B. *J. electrochem. Soc.* **125**, 1156–1160 (1978).
6. Stuckes, A. D. & Farrell, G. *J. phys. Chem. Solids* **25**, 477–482 (1964).

NH_4^+-tetraalkyl ammonium systems in the synthesis of zeolites

D. M. Bibby, N. B. Milestone & L. P. Aldridge

Chemistry Division, DSIR, Private bag, Petone, New Zealand

ZSM-5 (ref. 1) and ZSM-11 (ref. 2) are silica-rich aluminosilicate zeolites with similar two-dimensional intersecting channel structures. They are conventionally synthesised from Na^+-tetraalkylammonium (Na^+-TAA) systems at high *p*H and temperatures around 160 °C (refs 3–6). We report here what we believe to be the first use of systems free of alkali metal ions in the synthesis of the zeolites ZSM-5 and ZSM-11.

In the conventional synthesis other alkali metal ions can be used but we have found that the rate of reaction is highest with Na^+. Tetraethyl ammonium (TEA) or tetrapropyl ammonium (TPA) give ZSM-5, while tetrabutyl ammonium (TBA) forms ZSM-11. The TAA ions probably act as templates[7] and are
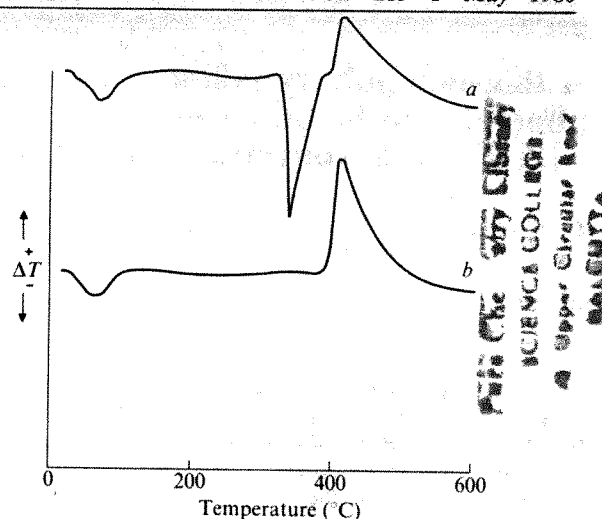
Fig. 1 Differential thermal analysis in one atmosphere oxygen of: *a*, precursor to ZSM-5 prepared from the NH_4^+-TPA system; *b*, precursor to ZSM-5 prepared from the Na^+-TPA system. The small endotherm at ~100 °C is due to the loss of absorbed water. The endotherm at ~340 °C and exotherm at ~410 °C are due to the decomposition of the NH_4^+ ion and the oxidation of TPA decomposition products respectively.

occluded into the structure to give precursors to the zeolites. Because of the channel size the organic ions can be removed only by thermal degradation, giving the zeolites. When the precursors are synthesised from the Na^+-TAA system, Na^+ ions remain in the zeolite for charge compensation. These must be exchanged by conventional ion exchange procedures if the H-form of the zeolite is required. This form has considerable potential for catalysing the conversion of oxygen-containing organic compounds, particularly methyl alcohol, to hydrocarbons[8,9].

For our present experiments we used NH_4^+-TAA systems which produce precursors containing NH_4^+ ions for charge compensation. When the precursors are heated to remove the occluded organic ions the NH_4^+ ions also decompose, giving a direct route to the H-form of the zeolite. This is shown by differential thermal analysis (Fig. 1). As the temperature is increased, the initial reaction is the decomposition of the NH_4^+ ion to give NH_3 and H^+. This is followed by decomposition of the TAA to give the H-form of the zeolite directly. A further advantage of NH_4^+-TAA systems is that the reaction stops with the formation of the zeolite, whereas in Na^+-TAA systems the zeolite is only an intermediate and the final reaction product is α-quartz. Crystals produced in the NH_4^+-TAA systems differ slightly in morphology from those produced using Na^+-TAA systems[1,2]. The ZSM-5 crystals are often twinned. The ZSM-11 crystals are the same ovate shape as those produced in the Na^+-TAA system, but are about five times longer, being up to 10 μm long.

A typical preparation for H-ZSM-5 is: SiO_2, 0.0655 M; Al_2O_3, 0.000205 M; TPA hydroxide, 0.008 M; NH_4OH, 0.15 M; H_2O, 1.0 M; heated at 160 °C under autogeneous pressure for 3 days. The SiO_2 has to be in an active form, such as silicic acid or colloidal SiO_2, and Al_2O_3 can be supplied as $Al(OH)_3$. When low Na-content reagents are used in the NH_4^+-TAA system, H-ZSM-5 and H-ZSM-11 can be prepared containing 1 p.p.m. Na. We have found approximately the same reaction rates and product yields in these Na^+-free NH_4^+-TAA systems and in the Na^+-TAA systems, and do not believe that Na^+ plays an essential part in the NH_4^+-TAA systems.

Other zeolites which have been synthesised in single-base systems free of alkali metal ions are analcite, faujasite, type A and harmotome in systems containing NH_4OH only or tetramethyl ammonium (TMA) only[10], and sodalite[11] and gismondine[12] in systems containing TMA only. However, the Na^+

contents of these systems were not reported, and may have been of significance as it has been found[13] that 'trace' amounts of Na are necessary to initiate crystallisation of some zeolites.

Silicalite-1[14] and silicalite-2[15], the aluminium-free analogues of ZSM-5 and ZSM-11 respectively, differ from the zeolites in that no charge compensating cations are incorporated into the structure. Their syntheses differ in some minor respects from those of the zeolites. We find that the silicalites can be prepared using TAAs only, although the reaction proceeds very slowly. However, we have had no success in preparing the zeolites in the presence of TAAs only. Silicalite-2 cannot be prepared in the presence of any alkali metal ion, although it is claimed that the corresponding zeolites can be synthesised using the Na^+-TBA system[5].

Note that ZSM-5 can also be produced using the Na^+–primary amine system[16]. However, when the Na^+ is replaced with NH_4^+ the rate of reaction is very much less and it is possible that trace amounts of Na^+ ($\sim0.01\%$) are catalysing the reaction.

1. Kokotailo, G. T., Lawton, S. L., Olson, D. H. & Meier, W. M. *Nature* **272**, 437–438 (1978).
2. Kokotailo, G. T., Chu, P., Lawton, S. L. & Meier, W. M. *Nature* **275**, 119–120 (1978).
3. US Patent 3 702 886.
4. US Patent 3 728 408.
5. US Patent 3 709 979.
6. UK Patent 1 161 974.
7. Rollman, L. D. in *Inorganic Compounds with Unusual Properties* Vol. II (ed. King, R. B.) 387–395 (American Chemical Society, New York, 1979).
8. Meisel, S. L., McCullough, J. P., Lechthaler, C. H. & Weisz, P. B. *Chem. Technol.* **6**, 86 (1976).
9. Chang, C. D. & Silvestri, A. J. *J. Catal.* **47**, 249–259 (1977).
10. Barrer, R. M. & Denny, P. J. *J. chem. Soc.* 971–982 (1961).
11. Baerlocher, Ch. & Meier, W. M. *Helv. chim. Acta* **52**, 1853–1860 (1969).
12. Baerlocher, Ch. & Meier, W. M. *Helv. chim. Acta* **53**, 1285–1293 (1970).
13. US Patent 3 306 922.
14. Flanigen, E. M. *et al. Nature* **271**, 512–516 (1978).
15. Bibby, D. M., Milestone, N. B. & Aldridge, L. P. *Nature* **280**, 664–665 (1979).
16. Australian Patent 70481/74.

Clinoenstatite in boninites from the Bonin Islands, Japan

Keiichi Shiraki*, Naoshi Kuroda†, Hayaomi Urano‡ & Shigenori Maruyama§

* Department of Earth Sciences, Nagoya University, Nagoya 464, Japan
† Institute of Geoscience, Shizuoka University, Shizuoka 422, Japan
‡ Department of Earth Sciences, Aichi University of Education, Kariya 448, Japan
§ Department of Earth Sciences, Toyama University, Toyama 930, Japan

Highly magnesian andesitic lavas were considered a rare and unusual rock type, before boninites proved to be so extensive among the Tertiary volcanic rocks in the Bonin–Mariana region[1–5] and some ophiolitic basalts[6,7]. Protoenstatite is also a rare mineral and its terrestrial occurrence has been confined to the high-Mg andesites from Cape Vogel, eastern Papua[8], and the Mariana Trench[3]. Some boninites from the Bonin Islands were found to contain abundant multiply-twinned clinoenstatite (inverted protoenstatite) with or without olivine. The clinoenstatite, coexisting with olivine with a similar forsterite content to that in the mantle, shows that protoenstatite crystallized later than the olivine, whereas in the olivine-free, clinoenstatite-bearing rock which has more SiO_2 than the clinoenstatite-bearing or -free boninites with olivine, the protoenstatite may have been the liquidus mineral. We show here that the presence of inverted protoenstatite in the Bonin Islands confirms our earlier suggestion[1,9,10] that boninites may have been formed by extensive partial melting of hydrous peridotite at relatively low pressures and rapid quenching from high temperatures at shallow depths.

The Bonin or Ogasawara Islands, which form the outer arc of the Idu–Mariana island arc in the Western Pacific, comprise three island groups: Chichi, Haha and Muko, which consist predominantly of volcanic rocks of Eocene to Oligocene age. The central Chichi-jima group is composed of a sequence of lower boninite pillow lavas and upper andesite or dacite breccias, on which late Oligocene limestone rests unconformably. The Haha-jima group, lying some 50 km south of Chich-jima, has a basalt–andesite–dacite suite with tholeiitic affinities of Eocene age, but boninite has never been found[2]. We have shown[11] that Muko-jima, ~70 km north of Chichi-jima, is made up largely of boninite pillow lavas and breccias containing occasional clinoenstatite. We found pillow lavas having more than 5 modal % clinoenstatite from Uguisu-hama, Muko-jima; Yoake-daira, Chichi-jima; and Kasa-yama, Chichi-jima. Komatsu also reported[12] some clinoenstatite-bearing boninites from Chichi-jima and Muko-jima.

The pillow lava from Uguisu-hama of Muko-jima contains abundant, large, dull white phenocrysts of clinoenstatite up to 10 cm long in the central part of the pillow, together with bright green bronzite phenocrysts up to 3 cm long. Olivine is very rarely present, having completely altered to pale brown or green products and carbonates. The rim is glass-rich and fine-grained; most phenocrysts are <1 mm in size. Its mineral proportions are: (modal %) clinoenstatite phenocrysts 1, orthopyroxene phenocrysts and microlites 16, clinopyroxene (augite and pigeonite) microlites 35, and glass 48. The whole rock analysis (Table 1, column 1) shows high SiO_2 content relative to clinoenstatite-free boninites (Table 1, columns 3 and 4). Electron probe analyses of the clinoenstatite phenocrysts ($\alpha_{min} = 1.660$; $2V_z = 38$–$48°$) reveal the highest Mg/Fe ratio and the lowest CaO, Al_2O_3 and Cr_2O_3 content in those from the boninites, whereas the orthopyroxene phenocrysts ($2V_x = 71$–$94°$) have nearly the same composition as other boninite orthopyroxenes (Table 2 and Fig. 1). CaO, Al_2O_3 and Cr_2O_3 contents in the clinoenstatite increase with decreasing Mg/Fe ratio.

Table 1 Wet chemical analyses (wt %) of clinoenstatite-bearing and -free boninites from Bonin Islands (recalculated anhydrous)

	1	2	3	4
SiO_2	59.04	56.65	56.70	55.99
TiO_2	0.20	0.20	0.25	0.23
Al_2O_3	11.47	11.54	13.22	10.47
Fe_2O_3	1.65	2.36	0.66	2.65
FeO	7.21	6.57	6.83	6.66
MnO	0.30	0.22	0.17	0.17
MgO	11.18	14.33	12.58	15.64
CaO	6.99	6.99	6.79	6.77
Na_2O	1.38	0.85	2.00	1.16
K_2O	0.56	0.27	0.72	0.24
P_2O_5	0.01	0.01	0.06	0.01
Cr (p.p.m.)	600	1150	840	1240
Ni (p.p.m.)		320		
Rb (p.p.m.)		10	8	0.5
F (p.p.m.)	120		110	140

1, Clinoenstatite-bearing rock, rim of pillow, Uguisu-hama, Muko-jima.
2, Clinoenstatite-bearing boninite, pillow breccia, Kasa-yama, Chichi-jima.
3, Clinoenstatite-free boninite, centre of pillow, Tsuri-hama, Chichi-jima.
4, Olivine-bronzite andesite, centre of dyke, Hatsune-ura, Chichi-jima.

The boninites from Yoake-daira and Kasa-yama of Chichi-jima have similar general petrographic characteristics. Both rocks contain prominent phenocrysts of both olivine and clinoenstatite together with orthopyroxene phenocrysts. The phenocrysts are set in a groundmass composed of ortho- and clino-pyroxene microlites and glass.

The clinoenstatite-bearing boninite from Yoake-daira is the most olivine- and clinoenstatite-enriched so far observed, consisting of 10% olivine, 11% clinoenstatite, 29% orthopyroxene, 25% clinopyroxene and 25% glass and others. The olivine phenocrysts of 0.5–3 mm across are consistently more magnesian ($Fo_{90–91.5}$) than those from the clinoenstatite-free boninites ($Fo_{87–89.5}$) (ref. 13); their $2V_x$ values are high, ranging

Table 2 Representative electron probe analyses for clinoenstatite, bronzite and olivine in clinoenstatite-bearing boninites from Bonin Islands

	1	2	3C	3M	4C	4M	5E	5B	6E	6B
SiO_2	58.10	58.31	57.79	56.81	40.46	40.49	58.05	57.51	56.78	55.88
TiO_2	0.00	0.00	0.01	0.01	0.00	0.00	0.02	0.01	0.01	0.00
Al_2O_3	0.12	0.17	0.36	0.56	0.04	0.01	0.42	0.57	0.52	0.84
Cr_2O_3	0.29	0.22	0.32	0.37	0.12	0.08	0.41	0.68	0.35	0.59
FeO	5.25	5.29	5.95	7.40	9.29	9.63	5.96	6.89	7.96	9.19
MnO	0.12	0.07	0.14	0.16	0.15	0.18	0.18	0.22	0.19	0.22
NiO	0.02	0.02	0.06	0.05	0.34	0.27	0.06	0.03	0.15	0.02
MgO	35.75	35.82	35.10	34.16	49.50	49.36	34.84	33.60	32.71	31.27
CaO	0.19	0.22	0.32	0.42	0.09	0.14	0.33	0.95	0.67	1.54
Na_2O	0.01	0.03	0.00	0.01	0.02	0.00	0.01	0.01	0.02	0.08
K_2O	—	0.01	—	—	—	—	—	—	—	—
Total	99.85	100.16	100.05	99.95	100.01	100.16	100.28	100.47	99.36	99.63
Mg/(Mg+Fe)	0.924	0.924	0.913	0.892	0.905	0.902	0.912	0.897	0.880	0.858
Mg	92.1	92.0	90.8	88.4	90.4	90.0	90.7	88.1	86.9	83.3
Fe	7.6	7.6	8.6	10.8	9.5	9.8	8.7	10.1	11.9	13.7
Ca	0.3	0.4	0.6	0.8	0.1	0.2	0.6	1.8	1.3	2.9

1, Large clinoenstatite phenocryst, centre of pillow, Muko-jima. 2, Clinoenstatite phenocryst, rim of pillow, Muko-jima. 3C, M, Core and margin of rim clinoenstatite around olivine (analysis 4), Yoake-daira. 4C, M, Core and margin of olivine adjacent to clinoenstatite (analysis 3), Yoake-daira. 5E, B, Clinoenstatite and bronzite of composite crystal, Yoake-daira. 6E, B, Clinoenstatite and bronzite of composite crystal, Kasa-yama. Mineral analyses were done on a JXA-5A electron microprobe at Nagoya University.

from 89 to 97°, compared with other boninite olivines ($2V_x$ = 86–93°) (ref. 10). Clinoenstatite occurs as: (1) discrete phenocrysts usually 0.5–3 mm long, rarely reaching 1 cm; (2) rims around the olivine phenocrysts; and (3) composite crystals with bronzite. Some of the phenocryst clinoenstatites have higher Mg/Fe ratio than the coexisting olivine phenocrysts, although the rim clinoenstatites are generally lower in Mg/Fe than the olivine. Note that the Mg/Fe ratio is higher in a core (Table 2, column 3C) of a large rim clinoenstatite (0.5 mm across) than in the adjacent olivine (Table 2, column 4), whereas it is lower at the margin (Table 2, column 3M) immediately adjacent to the olivine. In the composite crystals clinoenstatite is richer in Mg and Si, and poorer in Fe, Mn, Ca, Al, and Cr than bronzite, as already shown[8,14]. The rock includes the most magnesian orthopyroxene ($2V_x$ = 101°; Fig. 1) analysed in the boninites.

The clinoenstatite-bearing boninite from Kasa-yama is less olivine- and clinoenstatite-enriched, having 4% olivine and 7% clinoenstatite. The size of those phenocrysts is small, mostly <0.5 mm. No fresh olivine was observed. The clinoenstatite

Fig. 1 Compositions of phenocryst clinoenstatites (○), rim clinoenstatites (◎), composite crystals (●), orthopyroxenes (◦), and olivines (+) in clinoenstatite-bearing boninites plotted on the pyroxene quadrilateral. Adjacent grains are connected by lines.

(α_{min} = 1.661) is the least magnesian among the three clinoenstatite-bearing rocks. The whole rock chemical composition (Table 1, column 2) is not very different from that of the clinoenstatite-free typical boninite, although it may be slightly higher in SiO_2 at a given MgO content.

In the clinoenstatite-bearing boninites of Chichi-jima the distribution of Mg and Fe between the olivine and rim clinoenstatite suggests that the latter formed by reaction of olivine and magma, although some of the phenocryst clinoenstatite may have crystallized almost simultaneously with olivine. On the other hand, for the clinoenstatite-bearing rock of Muko-jima in which olivine is virtually absent, the large clinoenstatite phenocrysts richest in Mg seem to have been the liquidus phase instead of olivine. The crystallization of the clinoenstatite (protoenstatite) may have been promoted by the high SiO_2 content in the magma and/or the release of water from the water-saturated magma at a shallow depth. The clinoenstatite-bearing boninites would be generated at higher temperatures than the clinoenstatite-free boninites.

All the clinoenstatite-bearing rocks from the Bonin Islands, Cape Vogel and the Mariana Trench have high MgO contents, >11 wt%. Judged by the experimental studies[15,16], high temperatures at least 1,200 °C at relatively low pressures (< 15 kbar) would be required to produce such highly magnesian and siliceous liquids even in water-saturated conditions. In many island arcs it seems unlikely that temperatures above or near the descending slab are high enough to generate the clinoenstatite-bearing rocks. A possible site may be a spreading ridge or an island arc with a steep geothermal gradient by previous magma generation where water liberated from the underlying subducted oceanic crust can be introduced.

1. Kuroda, N. & Shiraki, K. *Rep. Fac. Sci., Shizuoka Univ.* 10, 145–155 (1975).
2. Shiraki, K., Kuroda, N., Maruyama, S. & Urano, H. *Bull. volcan.* (in the press).
3. Dietrich, V., Emmermann, R., Oberhänsli, R. & Puchelt, H. *Earth planet. Sci. Lett.* 39, 127–144 (1978).
4. Meijer, A. & Shipboard Scientific Party IPOD Leg 60 *EOS* 59, 1182 (1978).
5. Bloomer, S., Melchior, J., Poreda, R. & Hawkins, J. *EOS* 60, 965 (1979).
6. Sun, S.-S. & Nesbitt, R. W. *Geology* 6, 689–693 (1978).
7. Cameron, W. E., Nisbet, E. G. & Dietrich, V. J. *Nature* 280, 550–553 (1979).
8. Dallwitz, W. B., Green, D. H. & Thompson, J. E. *J. Petrol.* 7, 375–403 (1966).
9. Shiraki, K. & Kuroda, N. *J. Geogr. (Tokyo)* 86, 174–190 (1977).
10. Kuroda, N., Shiraki, K. & Urano, H. *Bull. volcan.* (in the press).
11. Shiraki, K., Kuroda, N. & Urano, H. *J. geol. Soc. Jap.* 85, 591–594 (1979).
12. Komatsu, M. *Rep. Studies for Rock-forming Minerals (Sendai)* 47–58 (1979).
13. Shiraki, K., Kuroda, N. & Urano, H. *Bull. volcan. Soc. Japan* 22, 257–261 (1977).
14. Nakamura, Y. *Miner. J.* 6, 264–276 (1971).
15. Kushiro, I. *Earth planet. Sci. Lett.* 22, 294–299 (1974).
16. Green, D. H. *Can. Miner.* 14, 255–268 (1976).
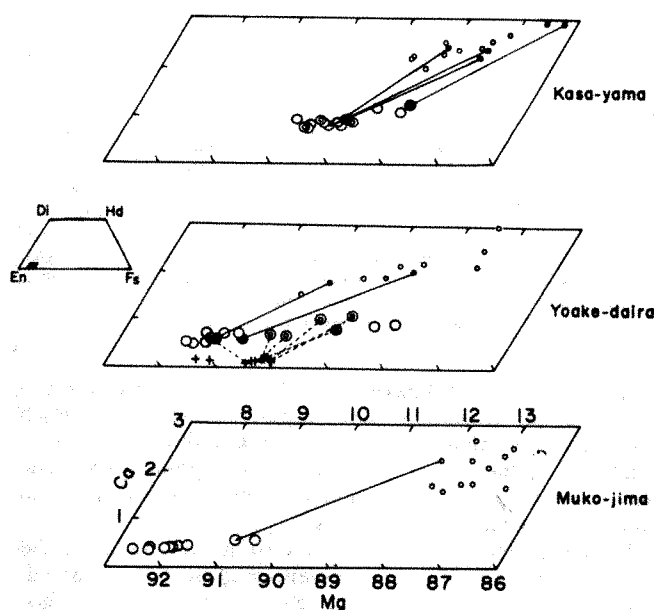
Palaeozoic plants from Saudi Arabia

A. A. El-Khayal*, W. G. Chaloner† & C. R. Hill‡

* Geology Department, Faculty of Science, Riyadh University,
Saudi Arabia
† Botany Department, Bedford College, Regent's Park,
London NW1 4NS, UK
‡ Palaeontology Department, British Museum (Natural History),
Cromwell Road, London SW7 5BD, UK

A fossil flora recently discovered in the central part of Saudi Arabia is reported here. This represents the first assemblage of plants of Permo-Carboniferous age in the Arabian peninsula. The assemblage is of interest in showing affinity with contemporaneous northern Euramerian floras rather than those of Cathaysia or Gondwanaland to the east and south of Arabia.

More than 1,000 specimens were collected from an exposure alongside the Unayzah to Buraydah road, in the town of Unayzah (Fig. 1). The plants are preserved as impressions in a 5–20-cm limonitic shale band within a sequence of beds of alternating sand and shale, close to the base of the Khuff Formation. The Khuff has been tentatively assigned to the Upper Permian on faunal evidence; the Lower Khuff fauna was collected between 40 and 72 m above the base of the Khuff and that of the Upper Khuff, collected from 2 to 28 m below the top of the formation[1].

No rocks of Carboniferous or early Permian age have yet been recognized as occurring in outcrops in the Arabian peninsula, although strata dated as Carboniferous on palynological evidence have been recognized[2] in sub-surface occurrence. Powers et al.[1] reported Lepidodendron and Dadoxylon as having been recorded from outcrop of the Khuff Formation, but no documentation for these records or other details are given. Carboniferous beds with plant fossils are known from Syria[3] and Iran[4].

The most abundant plant in the assemblage from Unayzah (occurring on approximately two-thirds of the rock specimens seen) is a species of Pecopteris (Fig. 2f). Some of this material bears sporangia (Fig. 2c) and these indicate an affinity with the Dizeugotheca–Acitheca complex. Fronds of similar aspect (Pecopteris hemiteloides, P. unitus) are widely known from European and Cathaysian late Carboniferous and Permian floras, but also occur in some of the so-called mixed floras of Gondwanaland (for example, that at Wankie, Rhodesia[5]).

Of similar abundance to the Pecopteris are strap-shaped leaf fragments up to 5 cm broad, with fine parallel venation, resembling Cordaites principalis (Fig. 2a). This species occurs widely in the Northern Hemisphere late Carboniferous and early Permian. The third most abundant species is Annularia stellata (Fig. 2b). This species of calamite foliage is reported widely in North America and Europe, and also from the Cathaysian flora[6,7]. The leaves are evenly spaced in their whorls, unlike the characteristically Cathaysian genus Lobatannularia, which has a distinct segregation of leaves of each whorl into two opposed groups. The Arabian leaves show features of structural detail which uniquely characterize this species; a broad strip of longitudinal striations overlies the midrib, and is flanked by broad zones of transverse striations[8].

In addition, there are other fern-like leaves, such as Validopteris, with pinnae about 20 mm broad. Other pinnae of similar dimensions are determined, as cf. Marattiopsis (Fig. 2d,e). Attempts to extract spores from the Unayzah matrix and attached sporangia have failed.

The plants from Unayzah suggest an age not greater than Westphalian (late Carboniferous), particularly on the association of Annularia, Cordaites and the abundant Pecopteris, and the occurrence of Annularia stellata further suggests that the flora is not younger than early Permian. Marattiopsis, however, has recently been described from the late Permian of eastern

USSR[9] and this genus is otherwise only recorded from Triassic and younger Mesozoic rocks in which it is a characteristic element of northern floras. The plant assemblage described here, taken as a whole, favours an age between late Carboniferous and early Permian; if this age is sustained by further evidence, this Arabian Marattiopsis will constitute the oldest record of the genus.
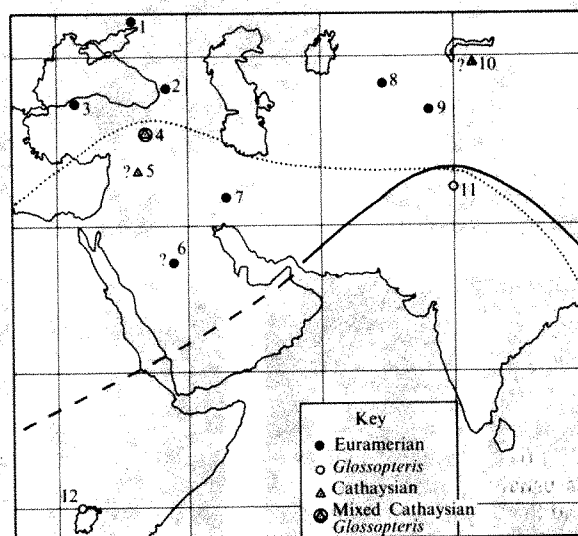
Fig. 1 Fossil plant occurrences relevant to the Unayzah flora, of Carboniferous to Permian age. 1, Donbass, USSR (Carboniferous)[10]; 2, Caucasus Mts (Carboniferous)[10]; 3, Zonguldak, Turkey (Carboniferous)[10]; 4, Hazro, Turkey (late Permian)[13]; 5, Ga'ara, Iraq (late Permian)[12]; 6, Unayzah, Saudi Arabia (late Carboniferous–early Permian); 7, Chal-i-Sheh, Iran (Carboniferous)[4]; 8, Uzbekistan, USSR (Carboniferous)[10]; 9, Fergana region, USSR (Carboniferous and early Permian)[10]; 10, Malajsary, USSR (Permian)[10]; 11, Kashmir (Carboniferous and early Permian)[10]; 12, Entebbe, Uganda (Permo-Carboniferous)[11]. The two boundary lines indicate the northernmost limits of the Glossopteris flora according to Wagner[13] (· · · ·) and W.G.C. and Lacey[11] (- - - - - and ——). The question marks beside localities 5, 6 and 10 relate in each case to uncertainty in the assignment to the floral province indicated by the symbol.

Saudi Arabia has hitherto represented a blank area on palaeogeographic maps of Palaeozoic floras[10,11]. The nearest records of more or less contemporaneous floras are those of Iraq[12] (late Permian, Fig. 1:5), Iran[4] (Carboniferous, Fig. 1:7) and Turkey[13] (late Permian, Fig. 1:4) to the north, the Glossopteris floras at Entebbe (Permo-Carboniferous, Fig. 1:12) 3,000 km to the south, and Kashmir (Permo-Carboniferous, Fig. 1:11) at a similar distance to the north-east. Palaeogeographic reconstructions of Permo-Carboniferous land masses based on palaeomagnetic evidence generally show the Arabian peninsula in juxtaposition with the African block, much as in its present configuration, but lying to the south of the Tethyan Gulf, and hence contiguous with the land mass occupied by the Glossopteris flora of Gondwanaland to the south and west. The Unayzah flora comes from a region which has hitherto been considered[11] to include the boundary of northern and Gondwana floras. The outlying record of Glossopteris at Hazro (Fig. 1:4) is made the basis for the northern boundary of the Glossopteris flora by Wagner[13] (dotted line, Fig. 1), but W.G.C. and Lacey[11] query the validity of this record and show a more southerly position for this boundary (solid and broken lines, Fig. 1). The geographical significance of the Saudi Arabian flora therefore lies in the extent to which it shows clear affinity with the major floral provinces around it, and particularly in the
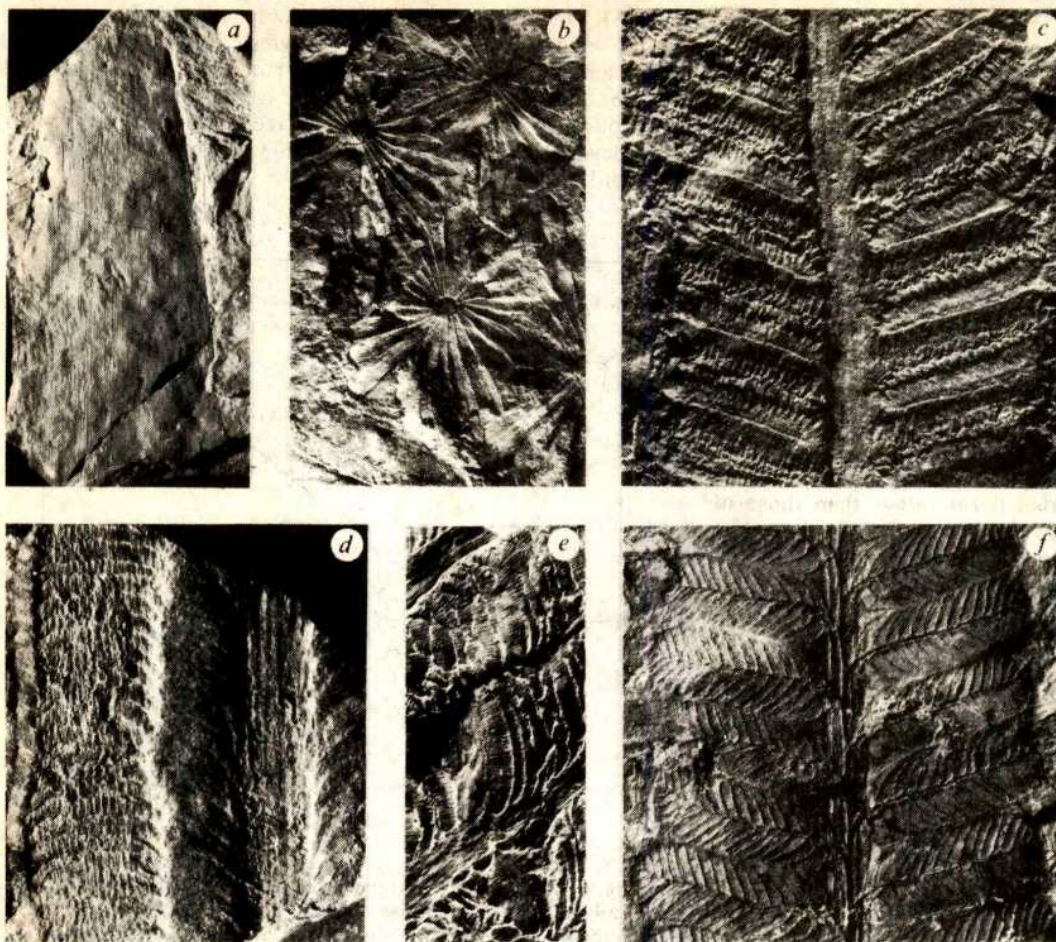
Fig. 2 Plant fossils from the base of the Khuff Formation, Unayzah. *a*, *Cordaites* cf. *principalis* (Germar), ×0.5; *b*, *Annularia stellata* (Schlotheim) ×0.9; *c*, Fertile *Pecopteris* ×4.7; *d*, *Marattiopsis* sp. ×5.4; pinna midrib at right, band of synangia at left, with intervening lamina between; *e*, the same, showing details of synangia on two adjacent pinnae, ×2.2; *f*, *Pecopteris* cf. *hemiteloides* (Brgt.) Stur., ×3.1. These specimens are deposited in the Geology Department of Riyadh University.

extent to which it may help clarify the northern boundary of the Gondwana province. Based on the present flora, it is clear that the most abundant and securely determined genera *Annularia*, *Pecopteris* and *Cordaites* are widespread throughout the Euramerian and Cathaysian provinces, whereas the *Marattiopsis*, if correctly determined, is known from more or less contemporaneous rocks only in eastern USSR. Apart from this taxon, the assemblage would conform with those of the Euramerian province within this period of time. In relation to the neighbouring floras of comparable diversity and age in Iraq[12] (Fig. 1:5) and at Hazro in Turkey[13] (Fig. 1:4), the lack of genera characteristic of Gondwana and Cathaysian floras is significant because the neighbouring, although probably younger, Permian floras seem to contain these elements, but occur well to the north of Unayzah. Taken at face value, the plants from Unayzah would otherwise suggest that the northern boundary of the Gondwana flora lies somewhere to the south of the central part of the Arabian peninsula at that time.

1. Powers, R. W., Ramirez, L. F., Redmond, C. D. & Elberg, E. L. Jr *Prof. Pap. U.S. geol. Surv.* **560**D, D1-D147 (1966).
2. Hemer, D. O. *5th Arab Petroleum Congress*, Cairo (1965).
3. Wolfart, R. in *Beiträge zur Regionalen Geologie der Erde* (ed. Martini, H. J.) 1–326 (Gebrüder Borntraeger, Berlin-Nikolassee, 1967).
4. Seward, A. C. *Phil. Trans. R. Soc.* **221**B, 377–390 (1932).
5. Walton, J. *Bull. geol. Surv. Sth Rhod.* **15**(2), 62–76 (1929).
6. Halle, T. G. *Palaeont. sin.* A**2**, 1–316 (1927).
7. Lee, H.-H. *Palaeont. sin.* A**6**, 1–185 (1963).
8. Walton, J. *Phil. Trans. R. Soc.* **226**B, 219–237 (1936).
9. Burago, V. I. in *Palaeobotany in the Far East* (ed. Krassilov, V. A.) 45–51 (USSR Academy of Sciences, Vladivostock, 1977).
10. Vakhrameev, V. A., Dobruskina, I. A., Meyen, S. V. & Zaklinskaja, E. D. *Paläozoische und mesozoische Floren Eurasiens und die Phytogeographie dieser Zeit* (Fischer, Jena, 1978).
11. Chaloner, W. G. & Lacey, W. S. *Spec. Pap. Palaeont.* **12**, 271–289 (1973).
12. Ctyroky, P. *Neues Jb. Geol. Paläont. Mh.* **7**, 383–388 (1973).
13. Wagner, R. C. r. *4me Congr. Avanc. Étud. Stratigr. Géol. Carb.*, Heerlen **3**, 745–752 (1962).

Cytotoxic T-cell response to H–Y in 'non-responder' CBA mice

Arno Müllbacher & Mary Brenan

Transplantation Biology Section, Clinical Research Centre, Watford Road, Harrow, Middx HA1 3UJ, UK

Murine cytotoxic T-cell (T_c cell) responses to various antigens are controlled by immune response genes (Ir) mapping in the major histocompatibility complex (H–2). Both helper T cells, controlled by I region-coded genes, and T_c cells, controlled by K/D antigens, are necessary for a positive response. An H–2-restricted T_c-cell response to the male specific minor transplantation antigen (H–Y) can be elicited in B10 (H–2^b) female mice primed with syngeneic male spleen cells intraperitoneally (i.p.) or intravenously (i.v.), or by skin grafting followed by restimulation *in vitro* in mixed lymphocyte culture (MLR) with male cells[1]. CBA (H–2^k) mice do not respond by these routes of *in vivo* priming, and this was thought to be due to a lack of permissible Ir genes for helper function[2]. However, we now report that subcutaneous hind-footpad (fp) immunisation of 'non-responder' CBA mice with syngeneic male cells changes them to responders, a result which argues against a generalised Ir gene-controlled helper defect.

We tested B10 female and (CBA × B10)F_1 (k × b) female spleen cells for their ability to mount an H–2-restricted T_c-cell response to H–Y *in vitro* after priming with male cells *in vivo*. B10 females were primed with 10^7–2×10^7 non-irradiated or irradiated male spleen cells, administered i.v. or i.p.; (k × b) female mice were primed with either 2×10^7 CBA male or
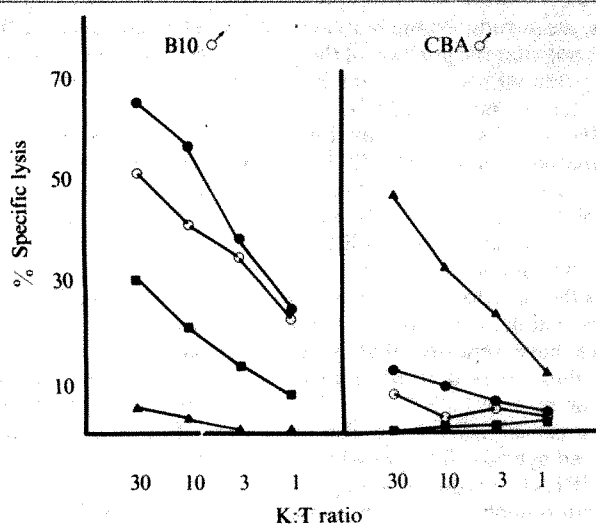
Fig. 1 Cytotoxicity of B10 and $(k \times b)F_1$ H–Y immune T_c cells. B10 female mice were given 1–2×10^7 unirradiated B10 male cells i.v. (●) or i.p. (○). $(k \times b)F_1$ mice were given either 2×10^7 2,000R irradiated CBA (▲) or B10 (■) male spleen cells i.v. Spleens of individual animals were removed at least 2 weeks after immunisation and cell suspensions prepared in RPMI supplemented with 10% heat-inactivated fetal calf serum (FCS), 2×10^{-5} M 2-mercaptoethanol and penicillin/streptomycin, and cultured at 2×10^6 cells ml^{-1} for 5 d at 37 °C and 10% CO_2 with equal numbers of 2,000R-irradiated male stimulator cells homologous to the immunising cells. Thereafter, graded numbers of spleen cells were tested for cytotoxic activity against 2×10^4 ^{51}Cr-labelled concanavalin A (Con A)-stimulated B10 male and CBA male lymphoblasts. (Spleen cells cultured for 24 h in RPMI supplemented with 10% FCS plus Con A at a concentration of 4 μg ml^{-1}, cell concentration 5×10^6 per ml.) The cytotoxicity assay was carried out in triplicate in microtitre plates over a 3-h period with s.e.m. < 3%. The range of spontaneous ^{51}Cr release was 8–20%. % Specific lysis was calculated according to the formula: % specific lysis = (experimental release – medium release/maximum release – medium release) × 100. K:T ratio, ratio of killer to target cells.

2×10^7 B10 male spleen cells irradiated with 2,000R to avoid a possible allogeneic effect and boosted *in vitro* with the same antigen as used for priming. As can be seen in Fig. 1, $(k \times b)$ H–Y immune T_c cells can lyse B10 male targets specifically when primed and boosted with B10 male cells and lyse CBA male targets when primed and boosted with CBA male spleen cells; these results show that H–2^k plus H–Y can be recognised by T_c cells in an immunogenic fashion, a result also shown by others[1,3]. No differences could be detected in the B10 response when priming was carried out by different routes of immunisation, i.v. or i.p.
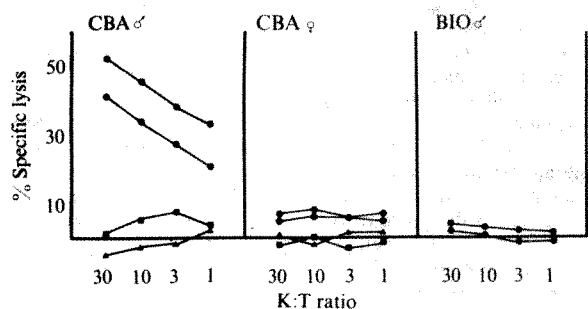
Fig. 2 Cytotoxicity of CBA H–Y immune T_c cells. CBA female mice were given 1–2×10^7 syngeneic non-irradiated male spleen cells i.v. (■), i.p. (▲) or fp (●). Spleen cells were boosted *in vitro* 5 weeks after priming, and assayed for cytotoxicity on CBA female, CBA male and B10 male targets as described in Fig. 1 legend.

The evidence for H–2^k plus H–Y association led us to investigate the possibility that H–2^k female mice can respond to H–Y when primed with CBA male cells. The two approaches taken were various doses of cells and different routes of administering cells. The results of the latter studies are shown in Fig. 2. CBA female mice primed i.p. or i.v. with syngeneic male spleen cells could not be boosted *in vitro* to generate an anti-H–Y response. This occurred over a dose range of 10^5–10^8 male spleen cells per mouse for priming and is in contrast to the results obtained with B10 and $(k \times b)$ mice. On the other hand, fp inoculation of 1×10^7–2×10^7 CBA non-irradiated male spleen cells into CBA female mice resulted in the generation of a secondary *in vitro* T_c-cell response of equal strength to that obtained with B10 mice after i.v. or i.p. priming. The response is H–2 restricted and H–Y specific.

From the large number of CBA mice tested which gave a good H–Y-specific response, only one also caused significant cross-reactive lysis of male and female B10 targets. It is not known whether this reflects true cross-reactivity by one population of T_c cells or whether different populations are responsible for the result.

Neither spleen cells of CBA female mice primed with $(k \times b)F_1$ male cells i.v. (to generate possible help *in vivo* through an allogeneic effect) nor spleen cells from lethally irradiated CBA male mice reconstituted with CBA female spleen cells for more
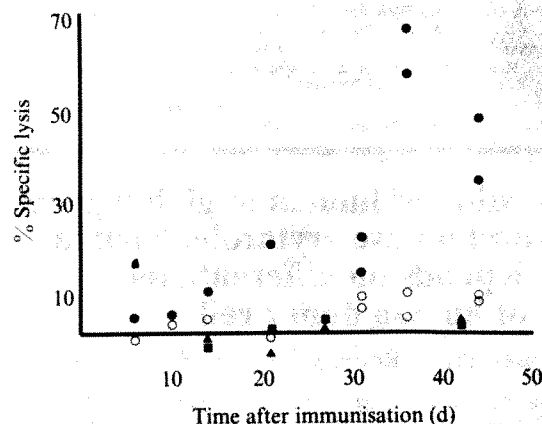
Fig. 3 Kinetics of anti-H–Y response in CBA mice. CBA mice primed as described in Fig. 2 legend were boosted *in vitro* 6–44 d post-priming and tested for cytotoxic activity on male (closed symbols) and female (open symbols) CBA lymphoblast targets. Values of 10:1 killer to target ratios from titration curves were used (details as in Fig. 1 legend).

than 2 weeks, could be boosted *in vitro* to generate an H–Y-specific T_c-cell response. Thus, only fp immunisation could generate a memory T_c-cell population specific for H–Y in H–2^k mice. A further difference between the response of B10 mice and CBA mice to the H–Y antigen lies in the time of appearance of the 'memory' T_c-cell pool in the spleens of primed animals.

Optimal or near-optimal responses in B10 can be obtained 2 weeks after priming, whereas with CBA mice, optimal results are only obtained 4–5 weeks after fp priming, although significant lysis is apparent after 2 weeks (Fig. 3). No responses were obtained at any time following i.v. or i.p. priming of CBA mice.

Our studies thus demonstrated that CBA mice are responders to H–Y antigen if they are immunised through the footpad and tested more than 4 weeks after immunisation.

These results are at variance with the interpretation of data obtained with H–2^k mice in chimaeric studies[2,4,5], in which it was suggested that H–2^k mice genetically lack the ability to generate H–Y-specific helper cells necessary for a T_c-cell response to H–Y, due to non-permissive Ir helper genes. This is in contrast to H–2^b mice, which apparently possess a permissive Ir helper gene.

As we have shown that mice of H–2^k haplotype can respond clearly to H–Y with a T$_c$-cell response, it must be postulated that T-helper cells are not necessary for the generation of a T$_c$-cell response to H–Y, at least, not after fp immunisation, or that i.v. and i.p. immunisation provides inadequate antigen presentation or induces a suppressor mechanism in H–2^k mice. We consider a lack of helper cell requirement unlikely, as helper T cells have been demonstrated both in H–2-restricted responses to viral antigens[6] and in alloresponses[7]. Evidence for a suppressor mechanism in the antibody response to hen egg lysozyme has recently been shown, where a B10 non-responder after i.p. immunisation becomes a responder after fp immunisation[8]. Footpad immunisation may be physiologically a more natural route of priming and may be a very effective mechanism of antigen presentation, involving lymph node T-cell subsets, such as the T-initiator cells described by Cohen and Livnat[9] capable of recruiting T$_c$-cell precursors or helper precursors. The difference in kinetics of the CBA fp response to the (k × b) i.v. response suggests a different mechanism is involved in eliciting a T$_c$-cell response to H–2^k plus H–Y.

1. Simpson, E. & Gordon, R. D. *Immun. Rev.* **35**, 59 (1977).
2. von Boehmer, H., Hass, W. & Jerne, N. K. *Proc. natn. Acad. Sci. U.S.A.* **75**, 2439 (1978).
3. von Boehmer, H., Haas, W. & Pohlit, H. *J. exp. Med.* **147**, 1291 (1978).
4. Matsunaga, T. & Simpson, E. *Proc. natn. Acad. Sci. U.S.A.* **75**, 6207 (1978).
5. von Boehmer, H. & Haas, W. *J. exp. Med.* **150**, 1134 (1979).
6. Ashman, R. B. & Müllbacher, A. *J. exp. Med.* **150**, 1277 (1979).
7. Pilarski, L. M. *J. exp. Med.* **145**, 709 (1977).
8. Araneo, B. A., Yowell, R. L. & Sercarz, E. E. *J. Immun.* **123**, 961 (1979).
9. Cohen, I. R. & Livnat, S. *Transplantn Rev.* **29**, 24 (1976).

Expression of human α-globin genes in hybrid mouse erythroleukaemia cells depends on differentiated state of human donor cell

A. Deisseroth, U. Bode, J. Fontana & D. Hendrick

Experimental Hematology Section, Pediatric Oncology Branch, National Cancer Institute, National Institutes of Health, Bethesda, Maryland 20205

We have developed a system which can be used to study the mechanisms that may govern the expression of human α-globin genes in human erythroid and non-erythroid haematopoietic cells[1,2]. Human chromosome 16, which has been shown to bear the human α-globin genes[3], is introduced by cell fusion into mouse erythroleukaemia (MEL) cells to generate continuously proliferating cell lines that retain permanently the human α-globin genes. We have shown that hybrid diploid MEL cells with human α-globin genes from erythroid donor cells express these genes fully through globin chain synthesis, while hybrid diploid MEL cells containing human α-globin genes from non-erythroid human haematopoietic donor cells contain very low levels of human α-globin mRNA and no detectable human α-globin chains. The levels of human α-globin mRNA in these hybrid cells were found to depend on factors present in the MEL recipient cell as well as on the differentiated state of the human donor cell, suggesting that this system may be suitable for characterisation of mechanisms governing haematopoietic differentiation in man.

We used normal fresh human haematopoietic cells as donor cells rather than established or transformed cell lines of fibroblasts or leukaemia cells. The Friend MEL cell was chosen as the recipient cell because it is committed to the expression of mouse globin genes; incubation of these cells in dimethyl sulphoxide (DMSO) increases cytoplasmic levels of mouse globin mRNA 50-100-fold (refs 4–6).

To ensure that the expression of the human globin genes in the hybrid MEL cells reflected the differentiated state of the donor

cells, we introduced the human genes by cell fusion because this does not alter the position of the genes in the donor genome, and the potential for alterations in the structure of the genes can therefore be minimised.

Hybrid cells derived by fusion of MEL cells and human haematopoietic donor cells lose human chromosomes during continuous culture. The biased loss of human chromosomes coupled with selection, based on the marker adenine phosphoribosyl transferase (APRT), for human chromosome 16 (refs 7, 8) which contains the human α-globin gene in man[3], facilitates the isolation of cloned hybrid MEL cells which differ only in the cellular origin of this human chromosome.

We have reported that hybrid MEL cells bearing human α-globin genes derived from erythroid cells (populations of human marrow cells dominated by erythroid cells) fully express those genes[1,2]. We have also shown that four independently derived hybrid cell clones which retain a tetraploid complement of MEL chromosomes ($\sim$80 mouse chromosomes) as well as human α-globin genes on human chromosome 16 from non-erythroid human haematopoietic donor cells, contain detectable levels of human α-globin chains[7]. Because these latter hybrid cells contained human chromosome 16 in the absence of all other human chromosomes, these studies showed that the only human chromosome which must be present in hybrid MEL cells
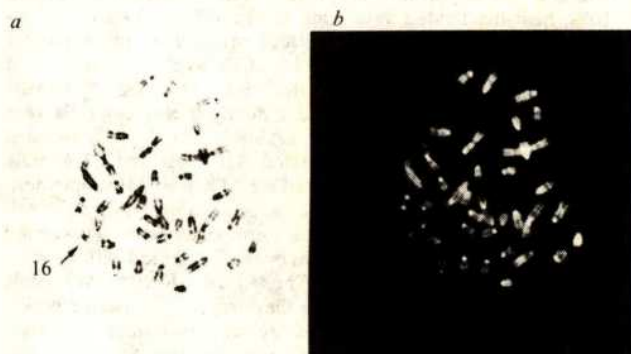
Fig. 1 Metaphase spread of hybrid cell derived by fusion of diploid MEL cells with non-erythroid human haematopoietic cells stained by Glemsa–trypsin banding (*a*) and Hoechst 33258 (*b*). Hybrid cells were isolated in alanosine-adenine medium which is lethal to unfused APRT-deficient MEL cells and promotes the growth of hybrid cells which have retained human chromosome 16[2,7]. Human cells used for fusion were isolated from peripheral blood of donors by Ficoll–Hypaque centrifugation[9]. These cells contained less than 1/50,000 cells which stained positive for haemoglobin with benzidine[7], and are known to contain less than 1/5,000 erythroid committed precursor cells[10]. Neither we[7] nor others[11,12] have detected human α-globin mRNA in such populations of mononuclear human cells or in leukaemia cell lines of human origin with markers of myeloid or lymphoid differentiation. Thus our population of donor cells had no detectable haemoglobin or human α-globin mRNA, and was dominated by at least a 3–4-log excess of non-erythroid human haematopoietic cells. Thirty-five metaphase spreads of hybrid diploid MEL cells with non-erythroid human α-globin genes were analysed by incubating log phase cells in colchicine, exposing successively to hypotonic and fixing media and spreading on washed glass slides as before[3,7]. Such slides were then exposed to trypsin and Giemsa stain so as to generate banding patterns specific for each of the human and mouse chromosomes[7,13,14]. Each of the 35 metaphase spreads was photographed, destained in fixative, and exposed to the fluorescent dye Hoechst 33258, which generates a uniform light fluorescence in human chromosomes, but an uneven fluorescent pattern in most mouse chromosomes, being very intense in the region of the centromere. An example of such a sequentially stained metaphase spread of hybrid cell no. 3 is shown here. Human chromosome 16 is indicated by the arrow. Although this hybrid MEL cell contains a near diploid complement of MEL chromosomes and human chromosome 16, it has lost most of the other human chromosomes, as is the case for most hybrid cells derived by fusion of MEL cells with human haematopoietic cells.

Table 1 Chromosomal constitution of hybrid MEL cells

Property measured	Hybrid cell no. 1 (human erythroid × diploid MEL)	Hybrid cell no. 2 (human non-erythroid × diploid MEL)	Hybrid cell no. 3 (human non-erythroid × diploid MEL)	Hybrid cell no. 4 (human non-erythroid × tetraploid MEL)
(A) No. mouse chromosomes	37	39	39	81
(B) Human chromosomes				
4	20	0	0	0
5	50	0	0	0
6	60	0	0	0
16	80	100	100	100
21	0	0	11	0
22	0	0	22	0
(expressed as % of metaphase spreads analysed)				
(C) poly ($A+$) cytoplasmic RNA / Human α-globin cDNA	1,050	ND	3,000	3,999
(D) Relative level of human α globin mRNA	1/350	ND	1/1,000	1/1,333
(E) Relative level of mouse globin mRNA	1/175	ND	1/22	1/100
(F) Human α globin mRNA / Mouse globin mRNA (ratio of previous 2 ratios)	0.5	ND	0.02	0.08
(G) Ratio of $\frac{\text{human } \alpha}{\text{mouse } \alpha}$ globin genes	1/2	1/2	1/2	1/4
(H) Human α globin mRNA / Mouse globin mRNA (corrected to the ratio of $\frac{\text{human } \alpha}{\text{mouse } \alpha}$ globin genes found in a diploid hybrid MEL cell)	0.5	ND	0.02	0.16
(I) Human α globin chains	Present	Undetectable	Undetectable	Present

APRT, chromosomes and globin chains of hybrid populations no. 1 and no. 4 were analysed as before[2,7]. In all cases, chromosomal analysis is based on more than 25 metaphase spreads per cell line, analysed by a combination of banding and Hoechst 33258 staining as outlined in Fig. 1. All human chromosomes found are listed above. Hybrid populations no. 1 and no. 3 were uncloned, while no. 2 and no. 4 were clonal. APRT was assayed as before[2,8]. Human α-globin mRNA was determined in induced hybrid MEL cells after 72 h of exposure to DMSO by RNA-cDNA hybridisation. Cytoplasmic extracts of those cells[7] were fractionated on columns of oligo (dT) as before[16]. Human α-globin mRNA, obtained from the reticulocytes of a nonthalassemic donor was purified from human β-globin mRNA first by electrophoresis on 5% polyacrylamide gels in 100% formamide[7,17]. Human globin cDNA was generated using the more rapidly migrating band (predominantly human α-globin mRNA) as a template for avian myeloblastosis reverse transcriptase as before[7]. Preparative hybridisation was used as before[7] to remove the 8–10% of this human α-globin cDNA that was complementary to non-α-globin mRNA. The human α-globin cDNA used was greater than 99% pure, and had a specific activity of 42,000 d.p.m. ng^{-1}. It migrated on 5% polyacrylamide gels as a single peak with a molecular weight of 230,000. Hybridisation was carried out as before[2,7] in 50% formamide and 0.5 M NaCl at 66°C for 90 h; each 2-μl reaction mixture contained 0.1 ng of cDNA in addition to the RNA from the hybrid cell. Hybrids were identified by resistance to S_1 nuclease[2,17]. Because the hybrid cells contained no non-α-globin genes and the hybridisation conditions prevented cross hybridisation of mouse globin mRNA with human globin cDNA (Fig. 3, ref. 7), the percentage hybridisation of the human α-globin cDNA was a measure of the amount of human α-globin mRNA present. To obtain the data shown in row H of Table 1, we added various amounts of poly ($A+$) RNA from hybrid cells or human reticulocytes to a fixed amount (0.1 ng) of human α-globin cDNA and incubated in 2-μl mixtures as described above. The percentage of human α-globin cDNA protected in each case was plotted against the ratio of poly ($A+$) RNA/human α-globin cDNA. The lowest ratio at which maximal protection of human α-globin cDNA was observed is given in row C. We then divided the ratios for each cell type given in row C into that for human reticulocytes (which was determined to be 3 in the same experiments), to generate an estimate of the relative level of human α-globin mRNA in each hybrid cell (shown in row D). We then conducted the same analysis using mouse reticulocytes and mouse globin cDNA to estimate the relative level of mouse mRNA in each hybrid cell, the results of which are shown in row E. The final levels of mouse globin mRNA in MEL cells vary as a function of induction and are not affected by the presence or absence of human chromosome 16 from either erythroid or non-erythroid donor cells; similar amounts of mouse α and β-globin chains were present in both these hybrid populations. We then divided the human α-globin mRNA levels (row D) by the mouse globin mRNA levels (row E) for each hybrid cell to normalise the human α-globin mRNA levels for the induction process variables. These normalised estimates of human α-globin mRNA generated for hybrid cells with human α-globin genes derived from donor cells of different types (given in row F) can then be compared to determine if the potential for human α-globin gene expression varies in different types of donor cells. These ratios following correction for the ratio of human α/mouse α-globin genes found in a hybrid MEL cell with a diploid complement of mouse chromosomes and a single human chromosome 16, are given in row H. ND, not done.

for full expression of human α-globin genes is chromosome 16.

In the study reported here, we isolated two different populations of hybrid cells (Table 1) derived by fusion of diploid APRT-deficient MEL cells with non-erythroid human haematopoietic cells in conditions outlined in Fig. 1. Neither human donor exhibited any abnormalities of globin gene expression in peripheral blood or marrow erythroid cells. Analysis of these hybrids by staining of metaphase spreads showed that an intact human chromosome 16 was retained in more than 80% of the cells studied while most of the other human chromosomes had been lost (as shown in Table 1 and Fig. 1). The presence of human APRT in these hybrid cells also confirmed the presence of human chromosome 16 (Table 1). As Fig. 2 and Table 1 (row I) show, there were no detectable human α-globin chains in either of the diploid MEL hybrid cells containing non-erythroid human α-globin genes, in spite of the presence of normal levels of mouse α- and β-globin chains.

Table 1 shows that the cloned hybrid MEL population no. 2 (devoid of human α-globin chains) and no. 4 (positive for human α-globin chains), both of which retained human α-globin genes from non-erythroid haematopoietic cells, differed only with respect to the presence of a diploid (no. 2) or a tetraploid (no. 4) complement of MEL chromosomes. We therefore compared the levels of human α-globin mRNA in these cells, by the methods outlined in Table 1. The relative level of human α-globin mRNA in the hybrid tetraploid MEL cells (no. 4) which contain non-erythroid human α-globin genes was 0.16 (Table 1, row H), eight times higher than that found in diploid MEL cells, suggesting that the MEL cell contained some factor or process which depended on the dosage of MEL chromosomes in the hybrid cell, and which resulted in higher steady state levels of human α-globin mRNA.

We next compared the relative levels of human α-globin mRNA in the DMSO-induced hybrid MEL cells no. 1 and no. 3,
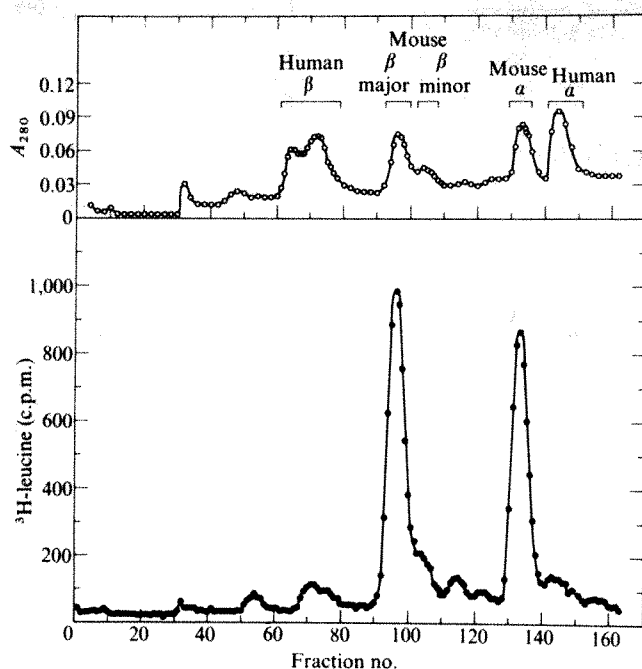
Fig. 2 Pattern of globin chain synthesis in hybrid cells derived by fusion of non-erythroid human haematopoietic cells with diploid MEL cells. 5×10^6 cells from the hybrid cell population were collected after incubation for 5 d in 1.25% DMSO. Cells were then incubated for 6 h in 0.5 mCi of ^{3}H-leucine specific activity 50 mCi mmol^{-1}) dissolved in 25 ml of Ham's F-12 medium supplemented with 10% fetal calf serum. Fractionation of haemoglobin from other labelled cytoplasmic proteins was carried out on a 2-ml bed volume carboxymethyl cellulose column in 0.01 M phosphate buffer as discussed previously[4,7]. After extraction of haem, globin chains were fractionated in 8M urea–0.01 M phosphate at pH 6.9 on columns of carboxymethyl cellulose[15]. The solid circles define the elution profile of ^{3}H-leucine-globin chains from hybrid cell population no. 3, using a 2-ml fraction volume. Open circles define the elution profile of unlabelled globin chains added as markers.

both of which contained a diploid complement of MEL chromosomes as well as human α-globin genes from erythroid and non-erythroid haematopoietic cells respectively (Table 1). The ratio of human α-globin mRNA to mouse globin mRNA in hybrid population no. 1, the hybrid MEL cell which contains a single human chromosome 16 derived from erythroid donor cells, is 0.5, as shown in Table 1, row *F*. This ratio corresponds to an average of 3,000 copies of human α-globin mRNA per cell. In contrast, in the hybrid diploid MEL cell no. 3 which contained human α-globin genes on human chromosome 16 from non-erythroid haematopoietic cells, this ratio was only 0.02 (Table 1, row *F*), which is one-twenty-fifth (120 copies of human α-globin mRNA per cell) of that found when human α-globin genes come from an erythroid donor cell. Because hybrid no. 3 contains human chromosome 16 in the absence of all other human chromosomes, the data suggest that the mechanism which mediates the decreased potential of human α-globin genes in non-erythroid human haematopoietic donor cells is *cis*-effective and the pattern of expression of human α-globin genes in the hybrid diploid MEL cells is dependent on the differentiated state of the human donor. Whether these differences in human α-globin gene expression arise from differences in the DNA itself or from some other fixed chromosomal state which stabilises the expression of human α-globin genes cannot be concluded. The data suggest that at least one mechanism limiting expression of human α-globin genes in non-erythroid haematopoietic cells is *cis*-effective. Further studies in this system of the pattern of expression of human α-globin genes in mouse erythroleukaemia cells may help to clarify which regions of the gene or its neighbouring sequences are important in the regulation of globin gene expression in differentiated and undifferentiated cells.

1. Deisseroth, A., & Hendrick, D. in *Cellular and Molecular Regulation of Hemoglobin Switching* (ed. Stammatoyannopoulos, G. & Nienhuis, A.) 761–777 (Grune and Stratton, New York, 1978).
2. Deisseroth, A. & Hendrick, D. *Cell* **15**, 55–63 (1978).
3. Deisseroth, A. *et al. Cell* **12**, 202–218 (1977).
4. Friend, C., Scher, W., Holland, J. & Sato, T. *Proc. natn. Acad. Sci. U.S.A.* **68**, 378–382 (1971).
5. Gilmour, R. S., Harrison, P. R., Windass, J. D., Affara, N. A. & Paul, J. *Cell Diff.* **3**, 9–22, (1974).
6. Birnie, G. D., MacPhail, E., Young, B. D., Getz, M. J. & Paul, J. *Cell Diff.* **3**, 221–232 (1974).
7. Deisseroth, A. & Hendrick, D. *Proc. natn. Acad. Sci. U.S.A.* **76**, 2185–2189 (1979).
8. Tischfield, & Ruddle, F. *Proc. natn. Acad. Sci. U.S.A.* **76**, 45–49 (1974).
9. Boyum, A. *Scand. J. clin. Lab. Invest.* **21**, Suppl. 97, 97–99 (1968).
10. Clarke, B. J. & Housman, D. *Proc. natn. Acad. Sci. U.S.A.* **74**, 1105–1109 (1977).
11. Gianni, A. M. *et al. Nature* **274**, 610–611 (1978).
12. Miller, D. N., Turner, P., Nienhuis, A., Axelrad, D. C. & Gopalkrishnan, T. V. *Cell* **15**, 511–521 (1978).
13. Kozak, C., Lawrence, J. & Ruddle, F. *Expl Cell. Res.* **105**, 109–117 (1977).
14. Yoshida, M. C., Ikeuchi, R. & Sasake, M. *Proc. Jap. Acad.* **51**, 184–187 (1975).
15. Clegg, J. B., Naughton, M. A. & Weatherall, D. F. *J. molec. Biol.* **19**, 91–108 (1966).
16. Aviv, H. & Leder, P. *Proc. natn Acad. Sci. U.S.A.* **69**, 1408–1412 (1972).
17. Forget, B. G., Housman, D., Benz, E. & MaCaffrey, R. P. *Proc. natn. Acad. Sci. U.S.A.* **72**, 984–988 (1975).

Molecular consequences of deletion formation mediated by the transposon Tn9

Michèle P. Calos*

Biological Laboratories, Harvard University, Cambridge, Massachusetts 02138

Jeffrey H. Miller

Département de Biologie Moléculaire, Université de Genève, Genève, Switzerland

Insertion elements and transposons stimulate deletion formation, mediating the elimination of neighbouring host sequences at a high rate compared to the background of deletions occurring in their absence. The (non-lethal) deletions generated by a variety of transposable elements end at or near the terminus of the element[1] (for reviews see refs 2–4). The finding that transposable elements generate the repetition of a short segment of host DNA on either side of the integrated element[5,6] raises new questions about deletion formation at the sequence level. Do the deletions terminate at the precise endpoint of the element and remove the repeated sequence, or do they end within it or leave it intact? Is deletion formation linked to the transposition process? To study the above questions we have used the transposon Tn9, which carries the genetic determinants for chloramphenicol resistance flanked on either side by the insertion sequence IS1[7,8] (in the same orientation), and which like IS1 generates a nine base pair repeat upon integration[5,6,9]. Starting with a Tn9 integrated into the lacI gene of Escherichia coli, we examined deletions extending into the neighbouring lacZ and lacY genes. Sequence analysis, reported below, shows that after deletion formation the ends of the transposon remain intact, although one copy of the repeated 9 base pairs is removed by the deletion, fusing the end of Tn9 to host sequences several thousand base pairs away (in these cases). (Studies with Tn3[10], IS1[11] and IS2[12] are consistent with these results.) We also find that the Tn9-distal end of the deletions terminate preferentially within the same region of DNA in which Tn9 insertion points cluster, suggesting that the processes of deletion formation and transposition share a common pathway.

*Present address: Département de Biologie Moléculaire, Université de Genève, Sciences II, Genève, Switzerland.
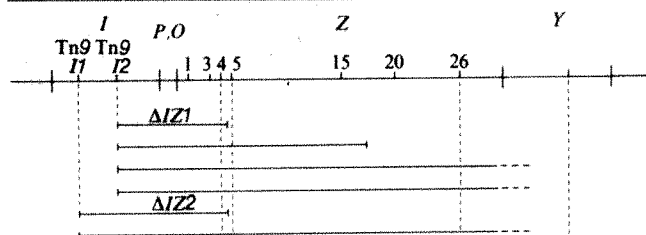
Fig. 1 The map position of several Tn9 mediated deletions is shown. The starting strain, X7733, used for the generation of deletions has been described previously[23]. It carries Tn9 in the I gene of an F'lacproB episome and a galE⁻ mutation and a lacproB deletion on the chromosome. Although deletions can extend in either direction, only those causing the Z⁻ phenotype could be scored easily. The insertions lacI1::Tn9 and lacI2::Tn9 were used[9]. The map position of several Tn9-mediated deletions is shown. Cultures from single colonies were grown at 34 °C and streaked onto glucose minimal plates containing phenyl-β,D-galactoside[24] and the indicator dye 5-bromo-4-chloro-3-indoxyl-β,D-galactoside (Xgal)[25]. The starting strain cannot grow on this medium, although Z⁻ survivors form white colonies. From each culture four to eight colonies were picked and the Z⁻ mutations mapped against the Y⁻ point mutation YA7047 contained in strain CSH7[25]. Z⁻ colonies were present between 10⁻³ and 10⁻⁴ of the population, and ~15% of these gave Lac⁺ recombinants with CSH7. The respective mutations were mapped against other point mutations in Z (CSH1–6, CSH8–11)[25]. Only one deletion mutation derived from the same original culture was analysed. The Z⁻ point mutations shown in the above figure are in one of 27 intervals in the gene[25], indicated by the figures above the line. The deletion mutations ΔI-Z1 and ΔI-Z2 were chosen for subsequent sequence analysis.

The starting strains for this work carried a Tn9 insertion in the *lacI* gene of an F'*lacproB* episome (see legend to Fig. 1). Deletions can extend in either direction from the integrated element, although only those deletions which prevent Z expression can be easily detected in this system. We examined independently occurring Z⁻ derivatives from two different *lacI*::Tn9 insertions and mapped them against different point mutations in the *lac* region. Figure 1 shows the map position of several deletions detected in this manner.

The two deletions *lacI1*::Tn9ΔIZ1 and *lacI2*::Tn9ΔIZ2 were crossed genetically onto a plasmid derived from pMB9, pMC4[5], which contains *lacI* and most of *lacZ*, using techniques described previously[5,9]. Figure 2 depicts the restriction mapping and sequencing of the deletion endpoints. In each case, while the left juncture of Tn9 in the *I* gene is intact, the right end of Tn9 is now fused to sequences in the interior of *Z*. The element is now flanked by unrelated sequences of nine base pairs (Fig. 3). The exact ends of Tn9 are preserved. This includes 10 base pairs of the right arm and 50 base pairs of the left arm (as drawn in Figs 2 and 3) for Tn9 in ΔIZ2, and 65 base pairs of the right arm of Tn9 in ΔIZ1. Moreover, the *Hae*III restriction pattern is indistinguishable from the starting Tn9 in both cases.

As Fig. 3 shows, the derivatives of Tn9 resulting from deletions extending into the *Z* gene are no longer flanked by repeated sequences of nine base pairs. We determined the frequency of transposition of these Tn9 derivatives, as well as the starting Tn9 elements. Tables 1 and 2 show that the frequency of transposition is unaffected by the removal of the nine base pair repeat.

Table 1 Cointegrate formation mediated by Tn9 derivatives

pMC4 donor plasmid	Frequency of Camʳ colonies
lacI2::Tn9	4.7 ± 0.7 × 10⁻⁶
lacI2::TnΔIZ2	4.5 ± 0.5 × 10⁻⁶

An F factor carrying a non-transposable *kan'* marker (courtesy of Dr F. Heffron) was used to detect transposition of Tn9 from the pMC4 plasmid. The donor strain (R90C) background was recAΔ(lacproB) rif nalA. The F⁺ factor was transferred to a Strʳ recipient (Q90C) and the approximate frequency of transposition calculated by monitoring the proportion of Camʳ Kanʳ Strʳ colonies among the Kanʳ Strʳ colonies, averaged for 20 experiments in each case. (The error given in the Table represents the standard deviation.) Most of the colonies are Tetʳ, since the plasmid was transferred due to a presumed cointegrate intermediate in the transposition process, although 0.2% of the colonies were Tetˢ in each case. That the transfer of the plasmid is mediated by Tn9 was shown by the fact that almost no transfer (1.5 × 10⁻⁸) of Tetʳ is found when the pMC4 plasmid does not contain Tn9.

We examined the distribution of deletion endpoints in the *lac* region by characterising independently-occurring deletions generated by *lacI1*::Tn9. Only the Z⁻ phenotype was selected for initially, so any deletion extending into or past the Z promoter could be detected. We tested the *lacZ* mutations for recombination with the late Y⁻ amber mutation MAB19[13]. We subsequently mapped 65 of these deletions against a series of mutations in the Z gene and the Y gene. As Fig. 4 shows, most of the deletions (~80%) end within a region consisting of the very end of the Z gene and most of the Y gene, even though this region is only about one third of the size of the Z gene (assuming that Z and Y are not separated by a very large region). However, the deletion endpoints are distributed in many different places both in Z and Y.

We have examined the sequence alteration produced by two different Tn9-mediated deletions extending from the *lacI* gene into the *lacZ* gene. In both cases the deletions end at the exact
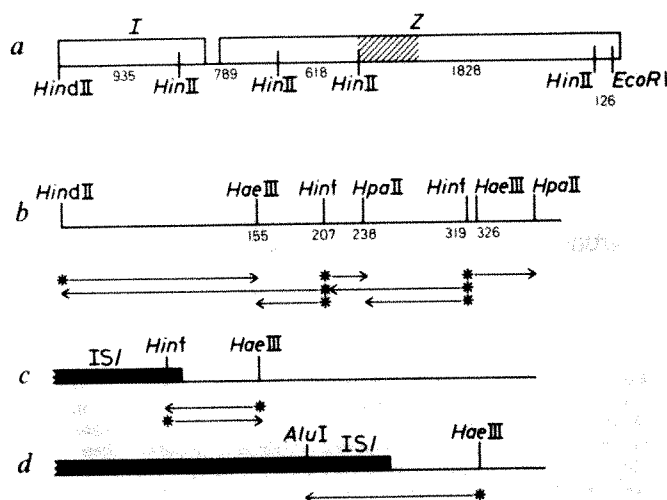
Fig. 2 Restriction mapping and sequencing deletion endpoints. *a*, The *Hind*II cuts in the *lacI* and Z genes. Distance between cuts is given in base pairs (bp). The single R1 cut in the region occurs 126 bp beyond the final *Hin* cut and 53 bp from the end of Z. The two Tn9-mediated deletions were crossed to pMC4, which contains this region up to the R1 cut. In a plasmid containing Tn9 in *I*, the 935 bp *Hin* fragment is replaced by a fragment 3,600 bp long (the 2,700 bp Tn9 has no *Hin* cuts). In plasmids carrying the deletions, the corresponding band is now 4,600 bp and comprises the first part of the 935 bp fragment of *I*, Tn9 and most of the 1,828 bp fragment of Z. The 789 and 618 bp *Hin* fragments are missing. A comparison of the restriction map of the 4,600 bp *Hin* fragment with the restriction map obtained from the wild-type *Hin* 1,828 bp fragment indicates that both deletions end within the first few hundred bases of the 1,828 bp fragment. Therefore, this wild-type region, in the centre of the Z gene (indicated by shading), was sequenced. *b*, Restriction map of the first 400 bp of the *Hin* 1,828 bp fragment. Distances are given in bp from the *Hin* cut. Fragments sequenced are indicated by arrows. *, Indicates ³²P. Sequencing was done by the method of Maxam and Gilbert[26]. Sequences on the upper strand were obtained by cutting a *Hin-Hpa* 238 bp fragment labelled with ³²P with *Hae*III, yielding the 155 bp fragment sequenced. A labelled *Hinf-Hinf* 112 bp fragment was recut with *Hpa* and the resulting 31 bp fragment was sequenced. A labelled *Hinf-Hinf* fragment approximately 800 bp long was recut with *Hpa* and a fragment approximately 70 bp long was sequenced. On the lower strand, labelled *Hind-Hinf* 207 bp and *Hinf-Hinf* 112 bp fragments were strand separated and sequenced. Also, the 207 bp fragment was recut with *Hae* and a 52 bp fragment was sequenced, and the 112 bp fragment was recut with *Hpa* and an 81 bp fragment was sequenced. *c*, Juncture of Tn9 and Z in *lacI2*::Tn9ΔIZ2. Starting with the 4,600 bp *Hin* fragment, a 365 bp *Hae* fragment extending from 210 bp inside Tn9 (IS1) to the *Hae* cut 155 bp from the *Hin* cut was isolated, labelled with ³²P, and recut with *Hinf*, yielding a 73 bp fragment which gave the juncture sequence on the lower strand. The upper strand of the same juncture was sequenced by labelling a 105 bp *Hinf* fragment extending from 10 bp inside IS1 to the *Hinf* cut 207 bp from the *Hin* cut, recutting with *Hae*, and sequencing 73 bp junction fragment. *d*, The sequence of the juncture of Tn9 and Z for *lacI1*::Tn9ΔIZ1 was obtained by isolating and labelling the 281 bp *Hae* fragment extending from the *Hae* cut 210 bp inside IS1 to the *Hae* cut 326 bp from the *Hin* cut. This fragment was recut with *Alu* and the 136 bp fragment giving the lower strand junction was sequenced. For both deletions the left juncture (in the *I* gene) was shown to remain intact by restriction mapping. In *lacI2*::Tn9ΔIZ2 the left juncture was also sequenced, using the *Hae-Hpa* junction fragment described[9] for *lacI2*::Tn9 and is identical to the juncture sequence reported there.

```
353          360                        370                              a
AsnArgHisGluHisHisProLeuHisGlyGlnValMetAspGluGlnThrMetValGlnAspIleLeuLeuMet

AACCGTCACGAGCATCATCCTCTGCATGGTCAGGTCATGGATG GCAGACGATGGTGCAGGATATCCTGCTGATG
TTGGCAGTGCTCGTAGTAGGAGACGTACCAGTCCAGTACCTACT CGTCTGCTACCACGTCCTATAGGACGACTAC
HindII

380                  390                           400
LysGlnAsnAsnPheAsnAlaValArgCysSerHisTyrProAsnHisProLeuTrpTyrThrLeuCysAspArg

AAGCAGAACAACTTTAACGCCGTGCCGCTGTTCGCATTATCCGAACCATCCGCTGTGGTACACGCTGTGCGACCGC
TTCGTCTTGTTGAAATTGCGGCACGCGACAAGCGTAATAGGCTTGGTAGGCGACACCATGTGCGACACGCTGGCG
         AGTCATTACCCGCCGTG
Tn9...TCAGTAATGGCGCGGCAC..etc.   lacI2::Tn9 ΔIZ2

410                        420
TyrGlyLeuTyrValValAspGluAlaAsnIleGluThrHisGlyMetValProMetAsnArgLeuThrAspAsp

TACGGCCTGTATGTGGTGGATGAAGCCAATATTGAAACCCACGGCATGGTGCCAATGAATCGTCTGACCGATGAT
ATGCCGGACATACACCACCTACTTCGGTTATAACTTTGGGTGCCGTACCACGGTTACTTAGCAGACTGGCTACTA

430                  440                         450
ProArgTrpLeuProAlaMetSerGluArgValThrArgMetValGlnArgAspArgAsnHisProSerValIle

CCGCGCTGGCTACCGGCGATGAGCGAACGCTAACGCGAATGGTGCAGCGCGATCGTAATCACCCGAGTGTGATC
GGCGCGACCGATGGCCG CTACTCGCTTGCGCATTGCGCTTACCACGTCGCGCTAGCATTAGTGGGCTCACACTAG
         AGTCATTACCGTAACGC
Tn9.....TCAGTAATGGCATTGCG..etc.   lacI1::Tn9 ΔIZ1

460                        470
IleTrpSerLeuGlyAsnGluSerGlyHisGlyAlaAsnHisAspAlaLeuTyrArgTrpIle

ATCTGGTCGCTGGGGAATGAATCAGGCCACGGCGCTAATCACGACGCGCTGTATCGCTGGATC
TAGACCAGCGACCCCTTACTTAGTCCGGT GCCGCGATTAGTGCTGCGCGACATAGCGACCTAG
```

```
lacI1::Tn9 ΔIZ1      CATCAACAG____Tn9____GTAACGCGA        b
                     GTAGTTGTC                CATTGCGCT

lacI2::Tn9 ΔIZ2      GTGGAAGCG____Tn9____CGCCGTGCG
                     CACCTTCGC                GCGGCACGC
```

Fig. 3 *a*, The sequence of 360 base pairs starting from the *Hin*dII cut at the end of the 1,828 base pair fragment, as determined as shown in Fig. 2. Numbers refer to amino acids in the β-galactosidase sequence[27]. There are two minor differences from the reported protein sequence at positions 356 (Gln to Glu) and 412 (Asp to Asn). They are indicated by *. The position of the deletion endpoints of *lacI*::Tn9ΔIZI and *lacI2*::Tn9ΔIZ2 are shown; only the last 10 base pairs of Tn9 and the first few bases to which it is fused are shown. *b*, The nine base pair sequences now flanking Tn9 in the two deletions. Each Tn9 insertion was flanked by a direct repeat of the sequence shown on the left. After deletion formation it is flanked by unrelated sequences of 9 base pairs.

terminus of the element, eliminating one copy of the nine base pairs of *I* gene DNA which were repeated during the integration of Tn9. This result extends the genetic and biochemical work of other authors, which indicated that such deletions end within 50 base pairs or less of the respective terminus of the element[1-4]. Sequence studies with IS*1*, IS*2* and Tn*3*-mediated deletions are also consistent with the results reported here[10-12].

Tn9 derivatives which are no longer flanked by repeated sequences of 9 base pairs (Tables 1 and 2), transpose with normal frequencies (Tables 1 and 2), strengthening arguments that Tn9 transposition does not involve homologous pairing by this flanking sequence, but rather generates the repeated sequence during the process of insertion itself[9]. (Experiments with Tn*10* also argue that the flanking repeated sequences are not necessary for transposition[14].)

Genetic mapping of deletion endpoints in *Z* and *Y* shows that 80% of the endpoints fall within a region extending from the extreme distal end of *Z* to the end of *Y* (see Fig. 4), a region one third of the size of the remainder of *Z*; within this preferred region deletion endpoints occur at many different positions. Transpositions of Tn9 into *Z* and *Y* show a similar strong preference for *Y* and the end of *Z*, as ~98% of Tn9 transpositions into *Z* and *Y* occur in this region, and like the deletion endpoints the transpositions fall at many positions within it (ref. 9 and J.H.M, M.P.C. and D. Galas, unpublished results). Coincident specificities of both deletion endpoints and transposition integration points have also been reported for Tn*3*[15], Tn*1*[16] and Tn*10*[17], and argue for a common step in the mechanism of both events.

Table 2 Transposition of Tn9 derivatives to F⁺*kan*

Tn9 derivative (on chromosome of CSH51)	Frequency of Cam^r, Kan^r colonies (R90C background)
lacI1::Tn9	3.8 × 10⁻⁵
lacI1::Tn9ΔIZ1	4.0 × 10⁻⁵
lacI2::Tn9	3.8 × 10⁻⁵
lacI2::Tn9ΔIZ2	3.5 × 10⁻⁵

The Tn9 insertions were crossed by genetic recombination into the *lac* region of strain CSH51[24], which harbours a *lacproB* deletion and carries a φ80*dlac* prophage. (In order to determine that the recombinant carried the original insertion mutation, backcrosses were used, in which the insertion was re-crossed into an F*lacproB* episome and subsequently mapped and characterised.) After introduction of an F⁺*kan* factor these strains were used as donors in a cross against R90C (see legend to Table 1). The frequency of Cam^r, Kan^r, Rif^r colonies among the Kan^r, Rif^r colonies was determined in several experiments. The Cam^r, Kan^r colonies, when cured of the *kan^r* episome, also lost the Cam^r character, demonstrating that the Cam^r was carried by the F⁺ episome.

How does a transposable element cause a deletion in its vicinity? These sequence results show that, as in transposition, the exact end of the transposable element must be an active participant. Moreover, studies with bacteriophage Mu, a transposable element, show a structural requirement for both ends of Mu in deletion formation[18]; if one can generalise from this result then, presumably, both ends of Tn9 are involved in deletion formation. These findings and the coincident specificity of deletion endpoints and transposition integration sites indicate a close relationship between transposition and deletion formation. Models giving a specific mechanism linking deletion formation to transposition have been proposed[19,20]. Shapiro[20] has outlined a mechanism for transposition in which a copy of the transposable element is replicated into the target site. When this mechanism is applied to transposition to a nearby site within the same replicon, in one orientation a deletion will result generating a fusion of the end of the transposable element to a new sequence, having the structure that we found, plus another copy of the transposable element fused to the deleted material. In the opposite orientation a second copy of the transposable element occurs in inverted orientation, along with inversion of the intervening material. (We have not examined inversions in our study of *Z⁻* mutations.) Thus, a deletion may be the result of a transposition event, when the target for transposition is an adjacent region on the same chromosome. In this regard it would be interesting to examine the effect on deletion formation of host mutations affecting transposition frequencies, and vice
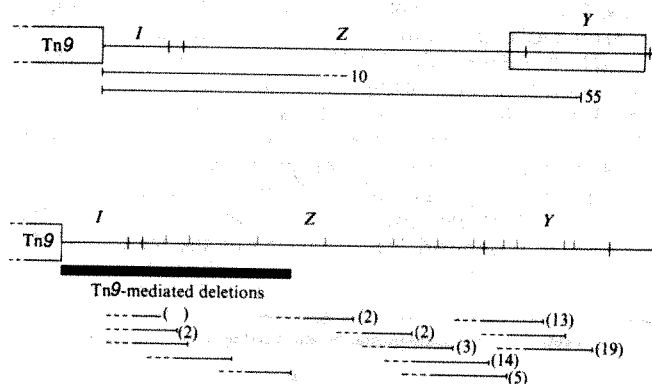
Fig. 4 The distribution of deletion endpoints generated by Tn9. The Tn9 insertion *lacI1*::Tn9 was used to generated deletions in *Z* and *Y*. The top part of the figure shows that 10 of 65 deletions terminate within the major portion of *Z*, whereas 55 deletions end in *Y* or at the very end of *Z*. As can be seen in the lower part of the diagram, many different endpoints are involved. The deletions were mapped against point mutations in *Z*[25] and *Y*[13] whose positions are indicated by the vertical lines along the lower part of the figure. The values in parentheses indicate the number of deletions with endpoints in this interval. Experimental details were the same as those given in the legend to Fig. 1, except that 32 °C was used, and the late *Y⁻* mutation *MAB19*[13] mapping at the far end of the *Y* gene was used for initial screening. Approximately 25% of the *Z⁻* mutations were deletions ending before *MAB19*.

versa. One mutation that apparently decreases the rate of IS*1*-mediated deletions has been reported[21].

The structure of *int*-mediated deletions from the *att* site of phage λ is analogous to the structure of deletions mediated by transposable elements and has been interpreted in a similar fashion; that is, as integration events into adjacent regions of the λ chromosome instead of into the normal bacterial *att* site[22].

1. Reif, H.-J. & Saedler, H. *Molec. gen. Genet.* **137**, 17–28 (1975).
2. Starlinger, P. & Saedler, H. *Curr. Topics Microbiol. Immun.* **75**, 111–152 (1976).
3. Kleckner, N. *Cell* **11**, 11–23 (1977).
4. Bukhari, A., Shapiro, J. & Adhya, S. (eds) *DNA Insertion Elements, Plasmids, and Episomes* (Cold Spring Harbor Laboratory, New York, 1977).
5. Calos, M., Johnsrud, L. & Miller, J. H. *Cell*, **13**, 411–418 (1978).
6. Grindley, N. *Cell* **13**, 419–426 (1978).
7. Gottesman, M. M. & Rosner, L. *Proc. natn. Acad. Sci. U.S.A.* **72**, 5041–5045 (1975).
8. Mac Hattie, L. & Jackowski, J. in *DNA Insertion Elements, Plasmids, & Episomes* (eds Bukhari, A., Shapiro, J. & Adhya, S.) 219–228 (Cold Spring Harbor Laboratory, New York, 1977).
9. Johnsrud, L., Calos, M. & Miller, J. H. *Cell* **15**, 1209–1219 (1978).
10. Ohtsubo, H., Ohmori, H. & Ohtsubo, E. *Cold Spring Harb. Symp. quant. Biol.* **43**, 1269–1277 (1979).
11. Ohtsubo, H. & Ohtsubo, E. *Proc. natn. Acad. Sci. U.S.A.* **75**, 615–619 (1978).
12. Peterson, P., Ghosal, D., Sommer, H. & Saedler, H. *Molec. gen. Genet.* **173**, 15–21 (1979).
13. Hobson, A., Gho, D. & Müller–Hill, B. *J. Bact.* **131**, 830–838 (1977).
14. Kleckner, N. *Cell* **16**, 711–720 (1979).
15. Nisen, P., Kopecko, D., Chou, J. & Cohen, S. *J. molec. Biol.* **117**, 975–998 (1977).
16. Weinstock, G. & Botstein, D. *Cold Spring Harb. Syp. quant. Biol.* **43**, 1209–1215 (1979).
17. Noel, K. & Ames, G. *Molec. gen. Genet.* **166**, 217–223 (1978).
18. Faelen, M. & Toussaint, A. *J. Bact.* **136**, 477–483 (1978).
19. Grindley, N. & Sheratt, D. *Cold Spring Harb. Symp. quant. Biol.* **43**, 1257–1261 (1979).
20. Shapiro, J. *Proc. natn. Acad. Sci. U.S.A.* **76**, 1933–1937 (1979).
21. Nevers, P. & Saedler, H. *Molec. gen. Genet.* **160**, 209–214 (1978).
22. Landy, A., Hoess, R., Bidwell, K. & Ross, W. *Cold Spring Harb. Symp. quant. Biol.* **43**, 1089–1097 (1979).
23. Farabaugh, P. J., Schmeissner, U., Hofer, M. & Miller, J. H. *J. molec. Biol.* **126**, 847–857 (1978).
24. Schmeissner, U., Ganem, D. & Miller, J. H. *J. molec. Biol.* **109**, 303–326 (1977).
25. Miller, J. H. *Experiments in Molecular Genetics* (Cold Spring Harbor Laboratory, New York, 1972).
26. Maxam, A. & Gilbert, W. *Proc. natn. Acad. Sci. U.S.A.* **74**, 560–564 (1977).
27. Fowler, A. & Zabin, I. *J. biol. Chem.* **253**, 5521–5525 (1978).

Migration of capillary endothelial cells is stimulated by tumour-derived factors

Bruce R. Zetter

Department of Surgery, Children's Hospital Medical Center and the Department of Microbiology and Molecular Genetics, Harvard Medical School, Boston, Massachusetts 02115

Angiogenesis, the growth of new blood vessels, occurs normally during osteogenesis, luteinisation and the development of the embryo, and in pathological states such as chronic inflammation, certain immune reactions and neoplasia[1]. Furthermore, solid tumours have been reported to secrete a diffusible factor which promotes the directional growth of new capillaries towards a growing tumour[2]. Two events required for the formation of a new capillary in response to an angiogenesis factor *in vivo* are the migration and subsequent proliferation of capillary endo- thelial cells[3]. Progress in purifying angiogenesis factors and studying their action has been hindered, however, by the lack of quantitative *in vitro* assays for capillary cell migration and proliferation. Recently, we have been able to isolate clonal cell lines of bovine capillary endothelial cells that can be maintained in long-term culture using tumour-conditioned growth medium[4]. I now report a quantitative *in vitro* assay for endo- thelial cell migration based on the phagokinetic track assay of Albrecht-Buehler[5]. The evidence presented here demonstrates that tumour-derived factors stimulate the migration of capillary endothelial cells whereas the same factors have no effect on the migration of aortic endothelial cells.

In the elegant system devised by Albrecht-Buehler to analyse the movement of cultured cells, the cells are first plated onto glass coverslips that have been previously coated with gold particles[5]. The cells ingest the gold and, as they move, leave bare areas or tracks that serve as a record of their movement. Figure 1 demonstrates the phagokinetic tracks made by bovine capillary endothelial (BCE) cells during an 18-h period. In normal growth medium containing 10% calf serum, little phagokinetic move- ment takes place (Fig. 1*a*). In contrast, when the assay is carried out in medium conditioned by mouse sarcoma 180 cells, phagokinetic movement increases and the size of the tracks is significantly larger than for cells incubated in non-conditioned medium (Fig. 1*b*).
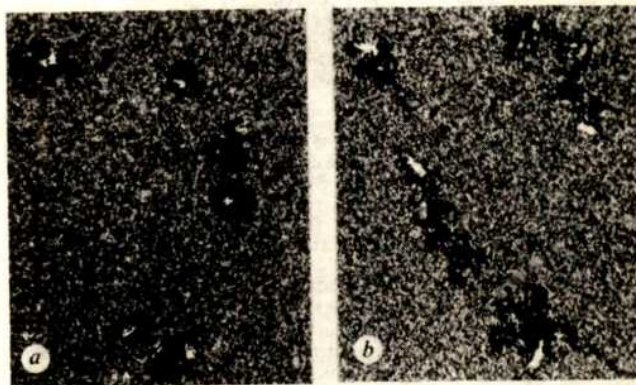
Fig. 1 Tumour-stimulated migration of bovine capillary endothelial cells. Bovine capillary endothelial cells (3,000) were seeded on gold-coated 22 × 22 mm glass coverslips prepared according to the method of Albrecht- Buehler. The cultures were incubated at 37 °C in Dulbecco's modified Eagle's medium containing 10% calf serum (DME-CS) until the cells had attached to the coverslips (~4 h). The coverslips were then transferred to 35-mm culture dishes containing either DME–CS alone (*a*) or mixed 1:1 with sarcoma-conditioned medium prepared as described in ref. 4 (*b*). After an additional 18 h, the medium was removed and replaced with 2.5 ml of 10% buffered formalin phosphate (Fisher Scientific) to terminate the experiment. The phagokinetic tracks were observed under incident light with a Nikon MS inverted microscope and photographed using a Wild MKa4 photoautomat camera. ×20.

It has been noted that an increased rate of cell movement will be reflected by an increased phagokinetic track size[6], but there have previously been no reports of a quantitative migration assay based on this technique. In the experiments reported here, the precise dimensions of endothelial cell phagokinetic tracks were measured with the aid of a MOP-3 digital image analyser (Carl Zeiss) as described in Fig. 2 legend. For each experimental point, the outlines of 100 tracks were traced and analysed to determine the perimeter length, maximum diameter and area. Because an increase in cell locomotion does not always correlate with an increase in directionality of movement[7], the pattern of the tracks is highly irregular and therefore an increase in phagokinetic movement can best be detected as an increase in the mean area of the tracks rather than by their absolute lengths. Therefore, in all figures, migration is expressed in units of area of the phagokinetic tracks (μm^2).

Quantitative measurement of BCE cell phagokinetic tracks reveals that there is a linear increase in track size as the concentration of tumour-conditioned medium is increased between 0 and 100% (Fig. 2). Whereas the capillary endothelial cells move slowly in the absence of tumour-conditioned medium and rapidly in its presence, aortic endothelial cells move rapidly regardless of the presence or absence of tumour-conditioned medium (Fig. 2). These results are consistent with our previously published observations on endothelial cell proliferation. Capil- lary endothelial cells grew slowly in normal growth medium but rapidly in tumour-conditioned medium whereas aortic endo- thelial cells grew rapidly in either[4].

To determine whether medium conditioned by other cell
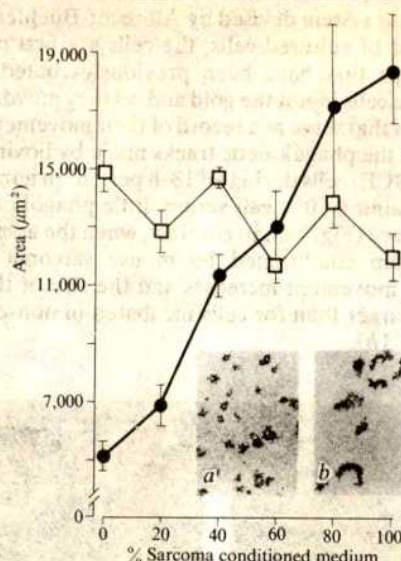
Fig. 2 Effect of sarcoma-conditioned medium on migration of bovine capillary and aortic endothelial cells. Bovine capillary endothelial cells (3,000) (●) or bovine aortic endothelial cells (□) were seeded on gold-coated coverslips as described in Fig. 1 legend and incubated for 18 h in DME-CS supplemented with the indicated concentration of sarcoma-conditioned medium. At the end of the experiment, the images of the phagokinetic tracks were transferred from the inverted microscope (×4 objective) to the screen of a Setchell–Carson 10M915 television by means of an RCA TC1005 video camera. The images were then traced from the television screen onto sheets of transparent plastic which were subsequently placed onto the magnetic tablet of a Zeiss MOP-3 digital image analyser. The tracings of the phagokinetic tracks were then retraced using the magnetic stylus of the MOP-3 and automatically processed for dimensions of area (shown above) as well as maximum diameter and length of perimeter. To eliminate consideration of cell division or cell collisions, only tracks formed by a single cell were analysed. Each point represents the mean area of 100 samples ± s.e.m. The inset shows the phagokinetic tracks of capillary (*a*) and aortic (*b*) endothelial cells in non-conditioned medium.

types might also stimulate endothelial cell migration, harvest fluid was collected from rapidly growing cultures of bovine aortic endothelial cells, bovine smooth muscle cells, BCE cells and mouse sarcoma 180 cells. When these media were tested for their ability to stimulate BCE cell phagokinetic movement (Fig. 3), the smooth muscle and aortic endothelial cell-conditioned media were completely inactive. Medium conditioned by the capillary endothelial cells themselves induced a 20% increase in the size of the phagokinetic tracks whereas the sarcoma cell-conditioned medium brought about a 90% increase. Once again, aortic endothelial cell tracks were large in the absence of any conditioning factors. None of the conditioned media caused an increase in the size of the aortic cell tracks to greater than 10% beyond control values (Fig. 3). In a second series of experiments, conditioned media from several other normal cell types had no effect on the migration of either capillary or aortic endothelial cells. The cell types tested included Swiss mouse 3T3 cells, F2408 Fisher rat embryo fibroblasts, early-passage human

Table 1 Growth of capillary endothelial cells in medium conditioned by sarcoma 180 cells or aortic endothelial cells

Growth medium	Cell no. after 5 days
Non-conditioned medium (10% calf serum)	2.14×10^4
Sarcoma 180-conditioned medium	8.4×10^4
Aortic endothelial cell-conditioned medium	6.8×10^4

10^4 cells were seeded in gelatin-coated 16-mm tissue culture wells containing 1 ml of non-conditioned medium. After 18 h to allow plating, the medium was aspirated and replaced with test medium prepared as described in Fig. 3 legend. All test media contained a final concentration of 10% calf serum. Fresh test medium was added on day 3. On day 5, the cells were removed from the wells with 0.25% trypsin and counted with a Coulter Model Zf particle counter.

diploid skin fibroblasts, MDCK canine kidney epithelial cells and primary C57 mouse bladder epithelial cells. In contrast to these normal cells, medium conditioned by benzpyrene-transformed C57 mouse bladder epithelial cells had significant migration-stimulating activity (data not shown).

It could be argued that if migration were an obligatory response to any growth stimulus, the migration assay would simply be an indirect measure of mitogenic activity. However, aortic endothelial cell-conditioned medium stimulates the growth of BCE cells to a level nearly equivalent to the sarcoma conditioned medium (Table 1), but has no effect on the BCE cell migration as shown in Fig. 3. This indicates that BCE cell growth and migration are independent events and might therefore be mediated by separate factors.

In a preliminary attempt to determine whether a quantitative assay could be devised to detect angiogenesis factors based on their ability to stimulate endothelial cell movement, increasing concentrations of an extract of human hepatoma cells were tested for their ability to increase the size of BCE cell phagokinetic tracks. This same extract shows angiogenic activity in the rabbit cornea and the chick chorioallantoic membrane (data not shown). Figure 4 shows that an increase in track size can be detected with 0.1 μg ml^{-1} and reaches a peak at 100 μg ml^{-1}. As neovascularisation is a complex phenomenon involving basement membrane hydrolysis, cell proliferation, cell junction formation and lumen formation in addition to cell migration[3], it is unlikely that any single *in vitro* assay could totally replace the *in vivo* bioassays that have been developed to study angiogenesis[1]. Nevertheless, the migration assay described here should provide a sensitive, rapid (18 h), quantitative assay for one critical component of angiogenesis.

The quantitative assay described above has already proved useful in demonstrating the effect of tumour-derived factors on
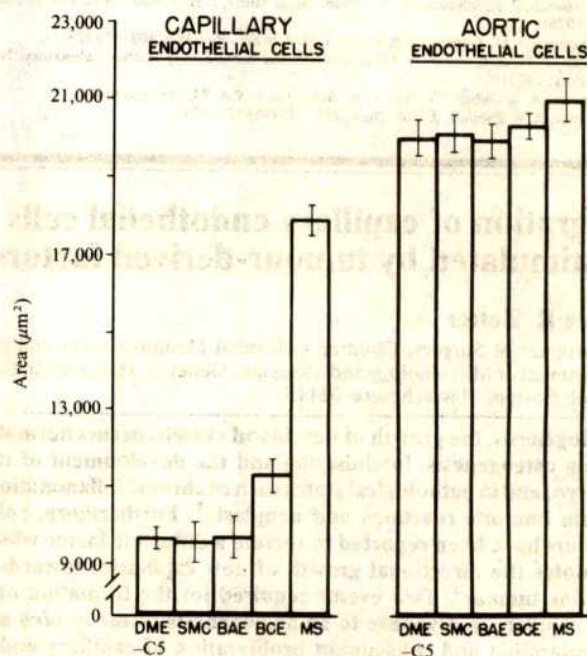
Fig. 3 Effect of conditioned medium from several different cell lines on the migration of bovine capillary and aortic endothelial cells. Bovine capillary endothelial cells (3,000) (left panel) or bovine aortic endothelial cells (right panel) were seeded on gold-coated coverslips as described in Fig. 1 legend and allowed to migrate for 18 h at 37 °C in DME-CS that had been mixed 1:1 with conditioned medium prepared by 48 h incubation with subconfluent cultures (6.6 × 10^4 cells cm^{-2}) of bovine aortic smooth muscle cells (SMC), bovine aortic endothelial cells (BAE), bovine capillary endothelial cells (BCE) and mouse sarcoma 180 cells (MS). For each sample, 100 phagokinetic tracks were traced from the television screen and retraced on the magnetic tablet of the Zeiss MOP-3 image analyser for determination of mean track area ± s.e.m.

Fig. 4 Effect of human tumour extracts on capillary endothelial cell migration. Human hepatoma cell extracts provided by Dr B. Wildi were prepared by incubating suspensions of cultured hepatoma cells (5×10^7 cells ml^{-1}) in phosphate-buffered saline for 4 h at 4 °C. The cells were removed by centrifugation and the resulting supernatant was concentrated and diluted in phosphate buffer (0.1 M NaH$_2$PO$_4$–0.02% NaN$_3$) four times to remove the saline. The final concentrate was applied to a CM-Sephadex C-50 column equilibrated with the 0.1 M phosphate buffer. The material that eluted with the starting buffer was collected, pooled, dialysed and lyophilised. Increasing concentrations of this material were added to 35-mm culture dishes containing 2 ml DME-CS. Gold-coated coverslips onto which 3,000 bovine capillary endothelial cells had been plated were transferred into these culture dishes and incubated 18 h at 37 °C. Areas of the phagokinetic tracks were determined as described in Fig. 2 legend. Each point represents the mean area of 100 samples ±s.e.m.

capillary cell migration and in so doing has pointed out a fundamental difference between capillary endothelial cells and endothelial cells from larger vessels. Furthermore, it may lead to a new understanding of certain biological agents such as interferon, which we have recently found can act as a reversible inhibitor of cell migration[8]. The application of this method is not limited to endothelial cells. Phagokinesis can be studied with virtually any motile cell that adheres to a substratum[5,6]. Thus, many cellular movements that were previously amenable to study only by time-lapse microcinematography may now be quantified by measurement of cell tracks. Possible uses could include the study of migration of neural cells, leukocytes and embryonic cells, the migration patterns of invasive and metastatic cells and the screening of cancer chemotherapeutic agents for anti-migratory activity.

1. Folkman, J. & Cotran, R. *Int. Rev. exp. Path.* **16**, 207–248 (1976).
2. Folkman, J., Merler, E., Abernathy, C. & Williams, G. *J. exp. Med.* **133**, 275–288 (1971).
3. Ausprunk, D. H. & Folkman, J. *Microvascular Res.* **14**, 53–65 (1977).
4. Folkman, J., Haudenschild, C. & Zetter, B. R. *Proc. natn. Acad. Sci. U.S.A.* **76**, 5217–5221 (1979).
5. Albrecht–Buehler, G. *Cell* **11**, 395–404 (1977); *J. Cell Biol.* **72**, 595–603 (1977).
6. Ali, I. U. & Hynes, R. O. *Cell* **14**, 439–446 (1978).
7. Pouyssegur, J. & Pastan, I. *Expl Cell Res.* **121**, 373–382 (1979).
8. Brouty-Boyé, D. & Zetter, B. R. *Science* (in the press).

Histone H1⁰ accumulates in growth-inhibited cultured cells

John Pehrson & R. David Cole

Department of Biochemistry, University of California, Berkeley, California 94720

The H1 class of histones contains several molecular species, even within a single organism [1]. The combination of these subfractions varies according to the state of terminal differentiation[2,3], embryonic development[4] and hormonal induction[5]. One of the subfractions, H1⁰, occurs at levels that are inversely correlated with the rate of cell division in mammalian tissues[6]. Although H1⁰ might be functionally or even structurally distinct from the usual H1 histone, Panyim and Chalkley[6] established that its size and amino acid composition resembled other H1 histones. The quantitative studies of its relationship to mitotic index were greatly extended by Marks *et al.*[7], and others[8-12] have measured H1⁰ contents during processes such as tissue regeneration and selective tissue destruction. All these observations were consistent with the notion that histone H1⁰ suppresses gene replication. One limitation in these demonstrations of the inverse correlation between H1⁰ and cell division is that there are many variable parameters, other than mitotic index, when comparing one tissue to another. This problem is largely overcome by comparing regenerating tissues to their normal counterparts[8-11]. In the latter situation, it is possible that cell types which always have low H1⁰ contents are preferentially replaced early in the regeneration process, while different cell types with high H1⁰ levels build up in the tissue later. If it could be demonstrated that H1⁰ accumulated along with the arrest of cell division in a single cell type, these ambiguities would be removed. We report here such a demonstration using cultured cells.

Comparisons were made between the H1⁰ content of rapidly growing HeLa cells and that of cells whose growth had been inhibited by high cell density (after 10 days culture on a plate). Another comparison was made between H1⁰ levels in rapidly growing mouse neuroblastoma cells, and the same cells whose growth was inhibited by serum deprivation (4 days without serum). In both cases there were substantially higher amounts of H1⁰ (relative to other H1 histone) in the more slowly dividing cells. H1 histones were selectively extracted using perchloric acid (PCA) and submitted to polyacrylamide gel electrophoresis (Fig. 1). An electrophoretic band, assumed to be H1⁰ because of its mobility[6], was clearly more pronounced in preparations from growth-inhibited HeLa cells, than in those from rapidly growing cells, and it was clearly present in higher amounts in extracts of serum-deprived neuroblastoma cells than it was in their rapidly

Table 1 Levels of histone H1⁰ in rapidly growing and growth-inhibited cells

Cell	Growth state	Relative H1⁰ content
Neuroblastoma	rapid growth	0.08 ± 0.01
	serum deprived	0.30 ± 0.06
HeLa	rapid growth	0.05 ± 0.01
	density inhibited	0.20 ± 0.02

Polyacrylamide gels were stained in aqueous 0.03% (w/v) Coomassie blue R-250, 24% (v/v) isopropanol, 10% (v/v) acetic acid; and destained in 0.003% Coomassie blue, 10% isopropanol, 10% acetic acid followed by washing in 10% acetic acid. The gels were scanned at 610 nm. H1⁰ content is given as the ratio of H1⁰ to the ordinary H1 which is essentially constant in all chromatin[15]. Each ratio is the average of 5 to 14 observations with the standard deviations shown.
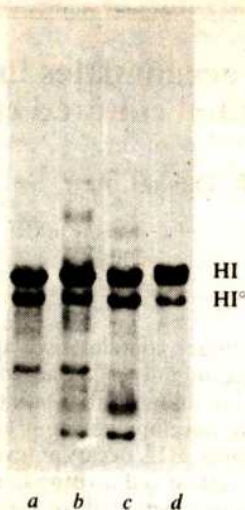
Fig. 1 Gel electrophoresis of perchloric acid (PCA) extracts of rapidly dividing and growth-inhibited cells. HeLa cells were grown on tissue culture flasks at 37 °C, 5% CO_2, in Dulbecco's modified Eagles medium (DMEM) with 5% calf serum. Mouse neuroblastoma cells N-115 (from Marc Kirschner) were grown on flasks at 37 °C, 10% CO_2, in DMEM supplemented with glutamine (2 mmol per 1 of DME), and 10% fetal calf serum except as indicated. Whole cells were extracted twice with 0.74 M PCA: the extracts were combined and trichloroacetic acid was added to 20% to precipitate the proteins. The precipitate was washed twice with ethanol, dried and electrophoresed in polyacrylamide, acetic acid, urea gels according to Panyim and Chalkley[16], except that the acrylamide was reduced to 7.5%. *a*, High density HeLa; *b*, rapidly growing HeLa; *c*, serum-deprived mouse neuroblastoma; *d*, rapidly growing mouse neuroblastoma.

growing counterparts. A quantitative analysis of several such experiments is presented in Table 1. The increase of H1⁰ in both types of cells was about three- to fourfold when cell division was inhibited.

To prove the identity of the putative H1⁰, we purified it from PCA extracts of serum-deprived mouse neuroblastoma cells and submitted it to amino acid analysis. For this purpose we used chromatography on Bio-gel P100 (ref. 13), which was more rapid than the previously used Biorex 70 chromatography[6]. A representative chromatogram is shown in Fig. 2 along with electrophoretic analyses of the two peaks. The amino acid composition of the purified H1⁰ listed in Table 2 is like that of the H1⁰ reported by Panyim and Chalkley[6].

Table 2 Amino acid composition of H1⁰

Amino acid	Mol %
Asp	3.9
Thr	5.4
Ser	9.1
Glu	6.1
Pro	8.2
Gly	4.3
Ala	16.6
Val	6.5
Met	0.7
Ile	2.4
Leu	2.1
Tyr	0.8
Phe	0.9
Lys	28.8
His	0.5
Arg	3.3

H1⁰ was hydrolysed in 6M HCl, 0.1% phenol for 20 h at 110°C. The figures are averages from two determinations using a Beckman amino acid analyser.

These results make it clear that histone H1⁰ content is not just a static characteristic of certain cells that become enriched in mitotically inactive tissues, but that H1⁰ levels are associated with a functional change in individual cells. Moreover, they suggest the possibility that H1⁰ is synthesised at times other than the S phase. In this regard it might be asked if H1⁰ ought to be compared to histone H5, whose synthesis is also not dependent on S phase[14]. The fact that both of these histones suppress chromatin activity adds interest to the comparison of H1⁰ and H5, metabolically, structurally and functionally. Such studies are under way.

Fig. 2 Bio-Gel P-100 chromatography of PCA extracts. The 0.74 M PCA extract of serum-deprived mouse neuroblastoma cells was dissolved in 8 M urea, 0.01 M HCl and applied to a 2 × 150 cm Bio-Gel P-100 column equilibrated in 0.01 M HCl. The column was eluted with 0.01 M HCl at a flow rate of 6 ml h⁻¹. Fractions (1.2 ml) were collected, peaks were pooled, lyophilised and subjected to polyacrylamide electrophoresis, as shown inset. The left hand lane represents the earlier chromatographic peak, while the right hand lane corresponds to the other peak.

1. Kinkade, J. M. Jr & Cole, R. D. *J. biol. Chem.* **241**, 5790–5797 (1966).
2. Bustin, M. & Cole, R. D. *J. biol. Chem.* **243**, 4500–4505 (1968).
3. Kinkade, J. M. Jr *J. biol. Chem.* **244**, 3375–3386 (1969).
4. Ruderman, J. V. & Gross, P. R. *Devl Biol.* **36**, 286–298 (1974).
5. Hohmann, P. & Cole, R. D. *J. molec. Biol.* **58**, 533–540 (1971).
6. Panyim, S. & Chalkley, R. *Biochem. biophys. Res. Commun.* **37**, 1042–1049 (1969).
7. Marks, D. B., Kanefsky, T., Keller, B. J. & Marks, A. D. *Cancer Res.* **35**, 886–889 (1975).
8. Marsh, W. H. & Fitzgerald, P. J. *Fedn Proc.* **32**, 2119–2123 (1973).
9. Varricchio, F., Mabogunje, O., Kim, D., Fortner, J. G. & Fitzgerald, P. J. *Cancer Res.* **37**, 3964–3969 (1977).
10. Benjamin, W. B. *Nature new Biol.* **234**, 18–20 (1971).
11. Garrard, W. T. & Bonner, J. *J. biol. Chem.* **249**, 5570–5579 (1974).
12. Seyedin, S. M. & Kistler, W. S. *J. biol. Chem.* **254**, 11264–11272 (1979).
13. Medvedev, A. Z., Medvedeva, M. N. & Robson, L. *Gerontology* **24**, 286–292 (1978).
14. Appels, R. & Wells, J. R. E. *J. molec Biol.* **70**, 425–434 (1972).
15. Kornberg, R. D. *Science* **184**, 868–871 (1974).
16. Panyim, S. & Chalkley, R. *Archs Biochem. Biophys.* **130**, 337–346 (1969).

Continuous synthesis of long DNA chains by chick embryo DNA polymerase γ

Masamitsu Yamaguchi*, Akio Matsukage†
& Taijo Takahashi

Laboratory of Biochemistry, Aichi Cancer Center Research Institute, Chikusa-ku, Nagoya 464, Japan

There is evidence for at least two mechanisms of DNA replication in eukaryotic cells. One is nuclear DNA replication in which DNA strands are synthesised in relatively short pieces (4–5S) that are later elongated and joined together[1–6]. These short DNA intermediates are also observed in the replication of viral DNA such as polyoma virus[7,8] and simian virus (SV40)[11,12], but not in adenovirus DNA[13,19] and mitochondrial DNA[15], where longer DNA chains are synthesised continuously. Studies of the subcellular localisation and the inhibitors of DNA polymerases[16,17] suggest that DNA polymerase α, β and γ are involved in nuclear DNA replication, DNA repair and mitochondrial DNA replication, respectively. And it is suggested that DNA polymerase α and γ are involved in the replication of SV40 DNA[18] and adenovirus DNA[19], respectively. Does the difference between the two types of replication depend on the difference in the reaction property of DNA polymerases α and γ? DNA polymerase α from human KB cells incorporated about 11 nucleotides per binding event[20]. Using mouse enzymes we found that one DNA polymerase β molecule polymerises dTMP on the multiple oligo(dT) primers with poly(rA) templates in a highly discontinuous fashion, while DNA polymerase γ may synthesise rather long poly(dT) chains in a one enzyme–one product fashion. We report here that using nearly homogeneous chick embryo DNA polymerase γ, the results clearly indicating that one DNA polymerase γ molecule synthesises one long DNA in a highly progressive fashion.

DNA polymerase γ was purified from an extract of 11-day chick embryos by phosphocellulose column chromatography, ammonium sulphate fractionation, gel filtration on Sephadex G-200, hydroxylapatite column chromatography and native DNA–cellulose column chromatography. The final preparation has a specific activity of 570,000 units (nmol ³H-dTMP incorporated per h at 37 °C) per mg protein with poly(rA) · oligo(dT) as a template · primer. A typical result of SDS-polyacrylamide gel electrophoresis is shown in Fig. 1. The major polypeptide which accounts for 86% of total protein is the polypeptide with a molecular weight (MW) of 47,000. This was the only polypeptide whose amount varied in proportion with the DNA polymerase activity during DNA–cellulose column chromatography, indicating that the 47,000-MW polypeptide was the only component of DNA polymerase γ. Purified DNA polymerase γ (149.4 U) was applied to SDS-polyacrylamide gel and the amount of the 47,000-MW polypeptide was determined as 0.224 μg (Fig. 1). Therefore, the specific activity with respect to the 47,000-MW polypeptide is 660,000 U per mg protein. The result of gel filtration and the sedimentation coefficient (7.5S in the presence of 1 M KCl and 0.5% Triton X-100) indicate that the molecular weight of this enzyme is about 180,000 (data not shown), assuming that this enzyme is spherical (as our preliminary electron-microscopic observation suggests). Therefore, it is comprised of four identical 47,000-MW polypeptides. From the specific activity and the molecular weight of this enzyme, the turnover number is calculated as 1,980 nucleotides per min per enzyme molecule.

The size of poly(dT) products synthesised by the highly purified chick embryo DNA polymerase γ on poly(rA) · oligo(dT) was analysed by alkaline sucrose gradient centrifugation. Polymerisation of ³H-dTMP continued almost linearly for at least 2 h (Fig. 3a). The sizes of products synthesised in the reaction for 0.4, 0.9, 1.5, 2 and 3 min were 7.0S, 11.9S, 13.0S and 13.9S, respectively (Fig. 2). After 3 min, the rate of chain elongation levelled off and the size of products synthesised in a reaction lasting 10 min or longer was always 14.6S. Molecular weights of the products were calculated from sedimentation coefficients according to Abelson and Thomas[22], and represented in nucleotide number (Fig. 3b). The initial chain elongation rate was about 1,900 nucleotides per min. The final length (average about 4,100 nucleotides) was reached at about 4 min—after that the size did not change but the number of products at the final length increased. Further studies are necessary to clarify how the final length is determined.

The coincidence of turnover number and DNA chain elongation rate indicates that one DNA polymerase γ molecule completes synthesis of one long poly(dT) chain before it starts with the other primer. The number of the products (equal to the number of dTMP molecules incorporated per average number of nucleotides per product) per enzyme molecule (number of enzyme molecules was calculated from the specific activity of the 'pure' enzyme, the molecular weight and the amount of enzyme

MW × 10⁻³

Top 160 150   90   68   47 45 40   23   Dye
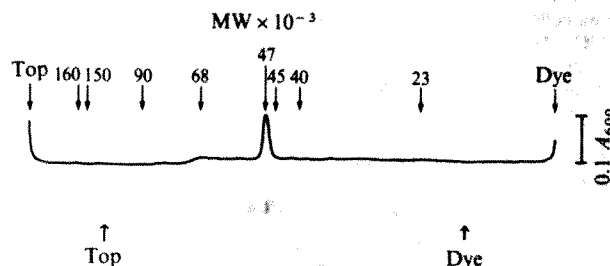
Fig. 1 SDS-polyacrylamide gel electrophoresis of the purified DNA polymerase γ. The detailed procedure for the purification of DNA polymerase γ from chick embryo will be published elsewhere. Extract was made by homogenisation, ultrasonication and centrifugation in the presence of 0.5 M KCl and 0.5% Triton X-100. Purification steps were: phosphocellulose column chromatography with stepwise elution; ammonium sulphate fractionation (0–55% saturation); a second phosphocellulose column chromatography with the elution in a linear salt gradient; gel filtration on a Sephadex G-200 column, hydroxylapatite column chromatography and native DNA–cellulose column chromatography. The preparation in the most purified fraction of DNA–cellulose column chromatography was used as the electrophoresis sample. DNA polymerase activity was determined in Fig. 2 legend DNA polymerase γ (149.4 units) eluted from a native-DNA cellulose column, which has a high specific activity of 570,000 U per mg protein, was precipitated with 15% trichloroacetic acid, redissolved in 20 μl sample buffer containing 0.0625 M Tris-HCl (pH 6.8)/2% SDS/10% (v/v) glycerol/5% (v/v) 2-mercaptoethanol/0.001% bromphenol blue, then electrophoresed essentially as described by Laemmli[25], in which 10% acrylamide slab gel of 1 mm thickness with 5% condensation gel was used. After electrophoresis (8 h at 60 V), the gel was fixed and stained with 0.1% Coomassie brilliant blue in 10% acetic acid/25% isopropanol and was destained with 10% acetic acid/10% isopropanol. The gel was photographed (bottom) and scanned at 600 nm by a Fujiox scanning densitometer (top). The molecular weight of the polypeptide band was estimated by comparison of its mobility to those of marker proteins: *Escherichia coli* RNA polymerase containing subunits of β' (MW160,000), β (MW150,000), σ (MW90,000), and α (MW40,000); bovine serum albumin (MW68,000); ovalbumin (MW45,000); bovine α-chymotrypsinogen (MW23,000). The protein amount in the gel was determined by comparing with the intensity of stained standard proteins of the known variable amounts (0.1–2 μg). Standard proteins were electrophoresed and stained in the same conditions as DNA polymerase γ. The average value of dye-intensity of three proteins; bovine serum albumin, ovalbumin and α-chymotrypsinogen, was used as the calibration standard.

* Permanent address: Research Institute for Microbial Diseases, Osaka University, Yamada-kami, Suita, Osaka 565, Japan.
† To whom all correspondence should be addressed.

used) was one for the initial 3 min of the reaction, and then increased in proportion to reaction time (Fig. 3c and inset). One enzyme molecule synthesised 35 products in 120 min, indicating that the average time required to complete one product is 3.4 min, agreeing very well with the time of termination of chain elongation (Fig. 3b). Thus, the mechanism of DNA chain elongation of chick embryo DNA polymerase γ is highly progressive.

In contrast, a mouse DNA polymerase β molecule synthesises poly(dT) chains on many primers in a highly discontinuous way[21]. The number of products per DNA polymerase β molecule was always about 30 for the long reaction time, and the average size of all products increased slowly and consistently for at least 30 min[21]. The processive nature of DNA polymerase α is not so great as that of DNA polymerase γ (refs 20, 23). Furthermore, our unpublished data indicate that the DNA products synthesised by DNA polymerase α are short (about 3-4S), using mouse enzyme and single-stranded calf thymus DNA-3'-(dT)_n with oligo (rA) as a template · primer. Thus, the reaction properties of DNA polymerases α, β and γ are different from each other.

The behaviour of DNA polymerase γ in DNA chain elongation makes it suitable for the replication of mitochondrial DNA and adenovirus DNA which are synthesised continuously
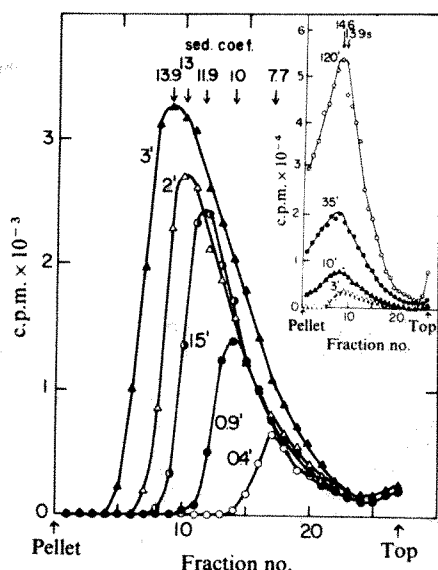
Fig. 2 Alkaline sucrose gradient centrifugation of poly(dT) products synthesised by DNA polymerase γ. The products were synthesised by highly purified DNA polymerase γ in optimal conditions. Reaction mixtures were incubated at 37 °C for 0.4, 0.9, 1.5, 2, 3, 10, 35 and 120 min in a final volume of 100 μl contained the following components: 50 mM Tris-HCl (pH 8.5), 0.5 mM MnCl₂, 1 mM dithiothreitol, 110 mM KCl, 20 mM potassium phosphate, 400 μg per ml bovine serum albumin, 14% glycerol, 80 μg per ml (rA)_m, 16 μg per ml (dT)_{12-18}, 12.7 μM ³H-dTTP (1837 c.p.m. pmol⁻¹), and 0.65 U DNA polymerase γ. After incubation, a 5-μl portion of each reaction was withdrawn to measure the amount of ³H-dTMP incorporated into poly(dT) as described previously[21]. The other portion (95 μl) was mixed with an equal volume of a 2×denaturing solution containing 2 M NaCl, 0.6 M NaOH, 1.5% Sarcosyl and 30 mM EDTA, then incubated at 37 °C for 20 min. 100 μl aliquots of the resulting solutions were layered over 4.8 ml 5-20% sucrose gradients made in the solution containing 1 M NaCl, 0.3 M NaOH and 5 mM EDTA, and then centrifugation was carried out for 15 h at 38,000 r.p.m. at 5 °C in an RPS 42T2 rotor of a Hitachi ultracentrifuge. The gradient was fractionated into 27 fractions from the bottom and a 100-μl portion was placed on a DEAE-cellulose paper disk and washed as described elsewhere[21]. Radioactivity in poly(dT) retained to the disk was measured using a Beckman liquid scintillation counter. Authentic poly(dA) (8.5S) was centrifuged in an accompanying tube as a sedimentation marker, and the position was determined by measuring the absorbance at 260 nm.
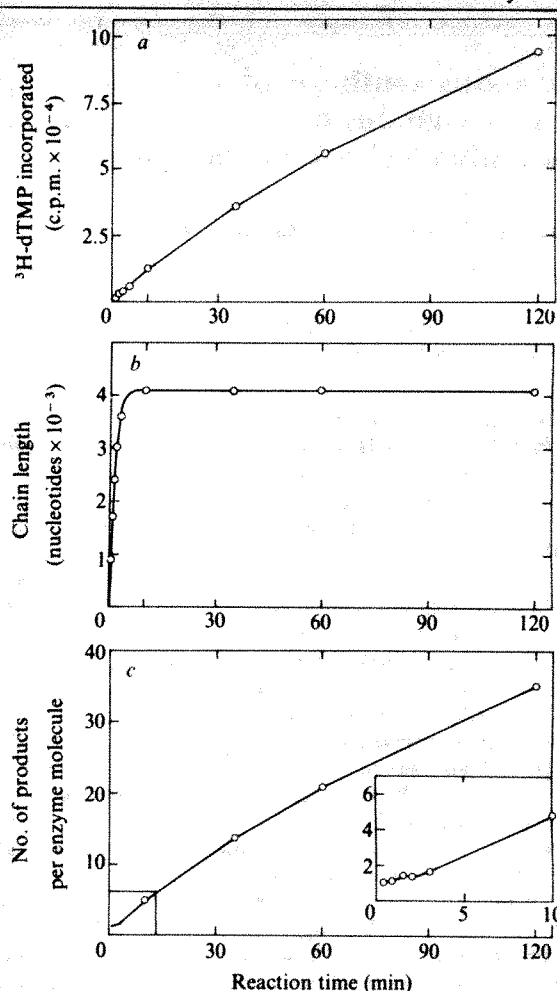
Fig. 3 The time course of incorporation of ³H-dTMP into poly(dT) (a), elongation of poly(dT) chains (b) and the number of products per DNA polymerase γ molecule (c). Incorporation of ³H-dTMP was measured as described in Fig. 2 legend. The chain length of poly(dT) products was calculated from the sedimentation coefficients as described previously[21] and represented as the number of dTMP residues. The mole number of products was calculated by dividing the mole number of incorporated ³H-dTMP by the chain length. The mole number of DNA polymerase γ was calculated from the unit of enzyme used, the molecular weight and the specific activity of the homogenous enzyme as described in the text.

without short intermediates. This is in good agreement with observations[13,24] that have suggested that DNA polymerase γ is involved in the replication of mitochondrial and adenovirus DNA.

We thank Miss M. Nishizawa for assistance. This work was supported in part by a Grant-in-Aid for Cancer Research from the Ministry of Education, Science and Culture, Japan and by a grant from the Research Foundation for Cancer and Cardiovascular Diseases, Osaka, Japan.

1. Taylor, J. H. *J. molec. Biol.* **31**, 579-594 (1968).
2. Lavine, A. J., Kang, H. S. & Bilheimer, F. E. *J. molec. Biol.* **50**, 549-568 (1970).
3. Tsukada, K., Moriyama, T., Lynch, W. E. & Lieberman, I. *Nature* **220**, 162-164 (1968).
4. Fareed, G. C. & Salzman, N. P. *Nature new Biol.* **238**, 277-279 (1972).
5. Fox, R. M., Mendelsohn, J., Barbosa, E. & Goulian, M. *Nature new Biol.* **245**, 234-237 (1973).
6. Tseng, B. Y. & Goulian, M. *J. molec. Biol.* **99**, 339-346 (1975).
7. Magnusson, G., Pigiet, V., Winnacker, E. L., Abrams, R. & Reichard, P. *Proc. natn. Acad. Sci. U.S.A.* **70**, 412-415 (1973).
8. Fliasson, R. & Reichard, P. *Nature* **272**, 184-185 (1978).
9. Hunter, T. & Franke, B. *J. molec. Biol.* **83**, 123-130 (1974).
10. Waqur, M. A. & Huberman, J. A. *Biochem. biophys. Res. Commun.* **51**, 174-180 (1973).
11. Qasba, P. K. *Biochem. biophys. Res. Commun.* **60**, 1338-1344 (1974).

12. Su, R. T. & DePamphilis, M. L. *J. Virol.* **28**, 53–65 (1978).
13. Yamashita, T., Arens, M. & Green, M. *J. biol. Chem.* **250**, 3273–3279 (1975); *J. biol. Chem.* **252**, 7940–7946 (1977).
14. Kaplan, L. M., Kleinman, R. E. & Horwitz, M. *Proc. natn. Acad. Sci. U.S.A.* **74**, 4425–4429 (1977).
15. Kasamatsu, H., Grassman, L. I., Robberson, D. L., Watson, R. & Vinograd, V. *Cold Spring Harb. Symp. quant. Biol.* **38**, 281–288 (1973).
16. Hübscher, U., Kuenzle, C. C. & Spadari, S. *Proc. natn. Acad. Sci. U.S.A.* **76**, 2316–2320 (1979).
17. Waqar, M. A., Evans, M. J. & Huberman, J. A. *Nucleic Acids Res.* **5**, 1933–1946 (1978).
18. Edenberg, H. J., Anderson, S. & DePamphilis, M. L. *J. biol. Chem.* **253**, 3273–3280 (1978).
19. Arens, M., Yamashita, T., Padmanabhan, R., Tsuruo, T. & Green, M. *J. biol. Chem.* **252**, 7949–7954 (1977).
20. Korn, D., Fisher, P. A., Battey, J. & Wang, T. S.-F. *Cold Spring Harb. Symp. quant. Biol.* **43**, 613–624 (1979).
21. Matsukage, A., Nishizawa, M. & Takahashi, T. *J. Biochem.* **85**, 1551–1554 (1979).
22. Abelson, J. & Thomas, C. A., Jr. *J. molec. Biol.* **18**, 262–291 (1966).
23. McKune, K. & Holmes, A. M. *Biochem. biophys. Res. Commun.* **90**, 869–870 (1979).
24. van der Vliet, P. C. & Kwant, M. M. *Nature* **276**, 532–534 (1978).
25. Laemmli, V. K. *Nature* **227**, 680–685 (1970).

Conservation of segmental variants of satellite DNA of *Mus musculus* in a related species: *Mus spretus*

S. D. M. Brown & G. A. Dover

Department of Genetics, University of Cambridge, Downing Street, Cambridge CB2 3EH, UK

Fig. 1 Analytical UV absorbance profiles of Hoechst 33258–CsCl gradients after sedimentation to equilibrium for 18 h at 44,000 r.p.m. at 25 °C on a Centriscan 75 analytical centrifuge: *a*, *Mus musculus*; *b*, *Mus spretus*. 10 μg of DNA were bound to 10 μg Hoechst 33258 in the presence of 1% Sarkosyl[21]. CsCl was added to an initial density of 1.64 g cm⁻³. Arrow indicates *M. musculus* satellite band. H and L indicate heavy and light sides of the gradient respectively.

There has been much recent discussion on the biological function of the highly-repetitive DNAs (satellite DNAs) of higher organisms[1–9], that have several curious features of sequence organization. First, some satellite sequences show a high degree of conservation between related species[10–15]. Second, there is independent evolution of 'type B' segments (sequence variants) within a block of tandem repeats[16]. The majority of the *Mus musculus* satellite DNA can be cut to produce a type A pattern with either *Eco*RII or *Ava*II (ref. 8). However, digestion of *M. musculus* satellite with other enzymes produces a limit series of fragments from only part of the total satellite (type B segment)[16]. To understand the significance of the segmental sequence variants, it is necessary to characterize their distribution between individual chromosomes of a genome[18] and between closely related genomes. We report here the distribution of type A and B patterns in the two closely related species, *Mus musculus* and *Mus spretus*[19,20]. The data show that the genome of *M. spretus* contains homologous sequences that are organized into the same type B segments as *M. musculus*, except for one type B segment that is underrepresented in *M. spretus*. From a knowledge of the genetic distance and hybrid fertility between these species[19,20], we are able to exclude one of the proposed biological roles for these particular genomic components.

Analytical equilibrium sedimentation in neutral CsCl of total DNA of *M. spretus* that is bound to the dye Hoechst 33258 does not reveal a satellite DNA component (Fig. 1*b*) equivalent to that resolved from the total DNA of *M. musculus* sedimented in the same conditions (Fig. 1*a*). Hoechst 33258–CsCl density gradient centrifugation is a method that is particularly sensitive for the resolution of small amounts of AT-rich satellites[17,21].

To detect any '*musculus*' type A or B patterns in *M. spretus* it is necessary to use a sample of pure total satellite DNA of *M. musculus*, that contains all sequence variants, in 'Southern' hybridizations[23] against *M. spretus* DNA after digestion with type A or B enzymes. In order to obtain a probe of high purity, total *musculus* DNA was resolved into satellite and main-band components after repeated fractionation in Hoechst 33258–CsCl gradients. The final purity of the satellite was monitored by restriction with a type A enzyme to produce the expected complete pattern of fragments (Fig. 2*a*) and by analytical centrifugation. On this basis we are confident that the *musculus*

type A and type B variants detected by the probe in *M. spretus* are unlikely to be due to the presence of other contaminating components. A type B pattern of the probe is shown in Fig. 2*b*.

The majority of the *M. spretus* sequences that are homologous to the *M. musculus* satellite were susceptible to *Ava*II in that little homologous material remained at the origin (Fig. 3*a*). The amount of homologous '*musculus*' sequences in *M. spretus* has been estimated as ~1% (at this stringency of hybridization) both
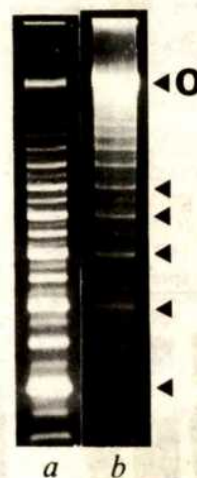
Fig. 2 Type A and type B patterns in *M. musculus*. Ethidium bromide stained agarose gel after *Ava*II digestion (*a*) and *Hinf* digestion (*b*) of *M. musculus* satellite DNA. Arrows indicate an ascending series of multimers based on a monomer length of approximately 240 base pairs (lowest arrow). O indicates undigested material left near the track origin. Purified satellite was prepared as described previously[17] and 5 μg digested for 2 h with 2 units *Ava*II in 80 mM tris-HCl (pH 7.4), 10 mM MgCl₂, 30 mM NaCl at 37 °C, or, digested for 2 h with 2 units *Hinf* in 6 mM tris-HCl (pH 7.5), 6 mM MgCl₂, 100 mM NaCl, 6 mM 2-mercaptoethanol at 37 °C. Digests were fractionated on a 1.6% agarose gel (15 × 15 × 0.3 cm) using a Tris-borate buffer (Tris 89 mM, boric acid 89 mM, Na₂EDTA 2.5 mM). Current loading was at 20 mA for 30 min and then increased to 40 mA (10 V cm⁻¹) for 3 h. Gels were stained with ethidium bromide and visualised on a short wave UV transilluminator and photographed.

from the exposure times needed to produce in *M. spretus* patterns of equivalent intensity to the *M. musculus* control and by the amount of radioactivity (detected by scintillation counting) on the *M. musculus* and *M. spretus* filters.

Southern hybridisations using *Taq*I, *Alu*I, *Hinf*, *Mbo*I and *Eco*RI produced bype B patterns similar to *M. musculus* in that only a portion of the homologous sequences were cut into bands and the rest remained as a dense band close to the origin (Fig. 3*b–l*). All enzymes, apart from *Alu*I, cut a similar proportion of 'musculus' sequences in *M. spretus* to that cut in total *M. musculus* satellite: *Taq*I, ~35%; *Hinf*, ~10%; *Mbo*I and *Eco*RI, ~3% (as estimated from microdensitometer tracings). The results clearly indicate that the sites for *Alu*I are under-represented in *M. spretus*: *Hinf* and *Alu*I cut very similar proportions of *M. musculus* satellite but in *M. spretus* the bands produced from *Alu*I cuts 2–3% of the *M. spretus* sequences and *Eco*RI 1–2% approximately. With the use of double enzyme digestions (Fig. 3*c, e, h, k*) we have investigated the overlap of some of the type B segments in *M. musculus* and *M. spretus*. The data provides no evidence for a substantial overlap of the type B segments in either of the two species. In all double digests no new prominent bands were observed. Overlapping type B segments would give rise to new bands due to the presence of different type B restriction sites lying at different positions within the basic 240-base pair repeat. Furthermore, the double digest bands are of greater intensity than the single digests,

indicating that the two respective enzymes cut largely non-overlapping portions of the total population of repeats.

Our failure to detect a satellite DNA in analytical Hoechst 33258—CsCl gradients of *M. spretus* (Fig. 1*b*) suggests that although similar distributions of restriction sites have been maintained in the two sets of homologous sequences, there has also been sequence modification that now renders the two sets differentially susceptible to Hoechst 33258.

Our results suggest that there are considerable differences in amounts of satellite DNA and some differences in organization and sequence composition between the genomes of *M. spretus* and *M. musculus*. It is possible that the presence of *musculus* type B patterns in *M. spretus* indicates the earlier evolutionary introduction of these patterns in a progenitor genome. The differences in amounts would be the result of independent evolution of the homologous sequences within each of the genomes subsequent to divergence. Given the broad similarity of the relative amounts of the type B segments in *M. spretus* to those in *M. musculus*, it may be that there has been a corresponding and equivalent reduction in satellite sequences at every centromere in *M. spretus*; or, alternatively, an amplification in *M. musculus*. However, the under-representation of *Alu*I sites in *M. spretus* suggests that some chromosomal specificity may underly the overall changes. Differences in abundance of the type B segments and some differences in the frequencies of type A multimers between an
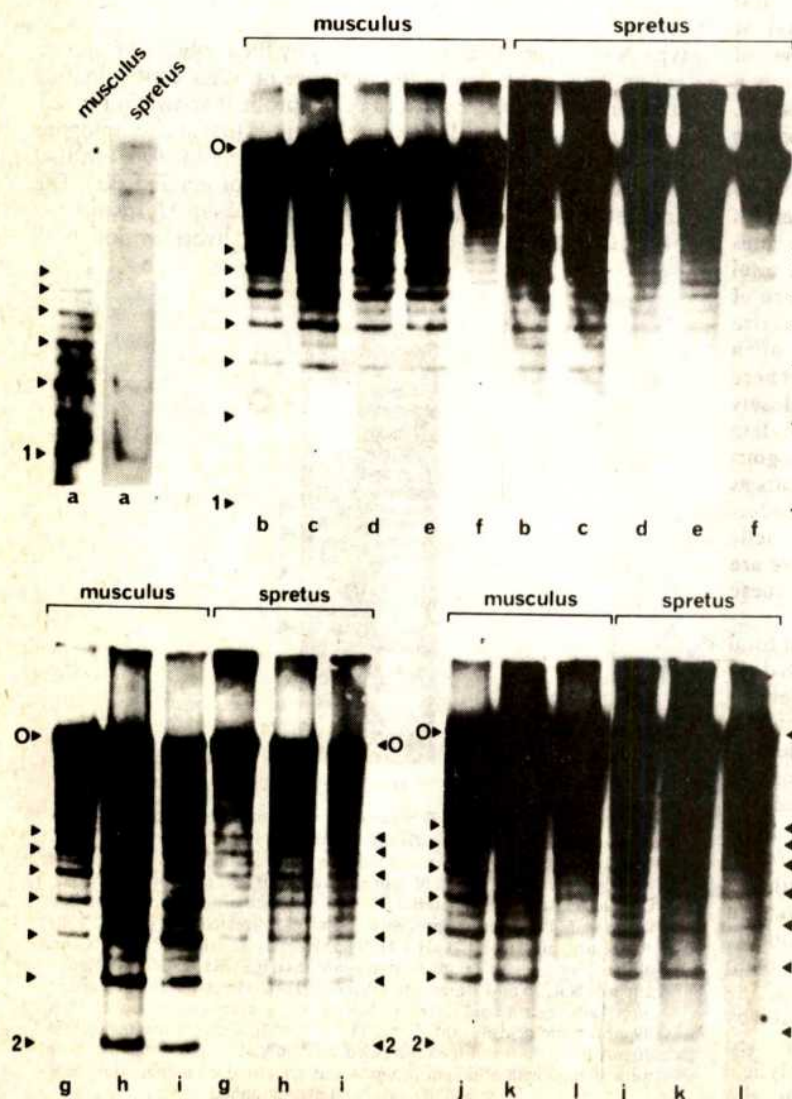
Fig. 3 Type A and type B patterns in *M. musculus* and *M. spretus*. Autoradiographs of digests of total DNA that have been fractionated on agarose gels, transferred to nitrocellulose and hybridised to ^{32}P-labelled *M. musculus* satellite. *M. spretus* lanes have been exposed 5–10 times longer than *M. musculus* to achieve a similar intensity. For clarity, different blocks of filters from the same species have been exposed for different times. Thus, for example, *M, spretus g–i* is a relatively shorter exposure than *M. spretus j–l*. All tracks have been exposed sufficiently to reveal the full arrays of bands of lower molecular weight. This has entailed a degree of overexposure of the high molecular weight material. Arrows indicate an ascending series of fragments based on multiples of a monomer length of ~240 base pairs. The multiple of the lowest arrow is indicated. Hybridization at the monomer position was barely detectable in all autoradiographs due to; first, the inefficient retention of fragments of this size during the hybridization reaction and, second, the small percentage of these fragments produced in a type B pattern (see Fig. 2*b*). Where there has been barely detectable hybridization at the monomer position this region of the autoradiograph has been omitted from some of the lanes (g–l). O indicates undigested material left near origin. a, *Ava*II; b, *Hinf*; c, *Hinf* + *Alu*I; d, *Alu*I; e, *Alu*I + *Eco*RI; f, *Eco*RI; g, *Hinf* + *Taq*I; i, *Taq*I; j, *Hinf*; k, *Hinf* + *Mbo*I; l, *Mbo*I. Purified *musculus* satellite was nick-translated^{22} with [α-^{32}P]-labelled dATP and dCTP (350 Ci mmol^{-1}; Amersham) to a specific activity of 10^8 c.p.m. μg^{-1}. Digests of total DNA (6 μg) were run on 1.6% gels with a Tris-borate buffer (see above): conditions of digestion were *Ava*II (as above); *Hinf* (as above); *Mbo*I, 6 mm Tris-HCl (pH 7.9) 6 mM MgCl$_2$, 6 mM 2-mercaptoethanol; *Taq*I, 6 mM Tris-HCl (pH 7.4), 6 mM MgCl$_2$, 1 mM dithiothreitol at 50 °C; *Alu*I, 6 mM Tris-HCl (pH 7.7), 6 mM MgCl$_2$, 50 mM NaCl, 6 mM 2-mercaptoethanol, 100 μg ml^{-1} bovine serum albumin at 37 °C; *Eco*RI, 100 mM Tris-HCl (pH 7.5), 10 mM MgCl$_2$, 50 mM NaCl at 37 °C. Digestion was with 5 units of enzyme, for 2 h. Gels were denatured and neutralized according to Southern^{23} and transferred overnight at room temperature to nitrocellulose paper (Schleicher and Schull, BA 85). Filters were baked *in vacuo* at 80 °C for 2 h. Whole filters representing 10 gel slots were hybridized with 12 ml of hybridization mixture containing 2×10^7 c.p.m. of ^{32}P-labelled *M. musculus* satellite DNA after it had been denatured at 100 °C for 10 min. Conditions of hybridization were $5 \times$ SSC, 50% formamide, 0.5% SDS at 37 °C overnight with gentle agitation. Filters were washed extensively in 3 mM Tris base (unneutralized), dried and autoradiographed using preflashed Fuji X-ray film backed by Fuji MachII intensifying screen.

isolated X-chromosome cell line and the total genome of *M. musculus* suggests that independent evolution of sequences is occurring, not only within each species genome, but also between chromosomes of a species[18].

The surprising finding, however, is that all recent sequence amplifications in either single chromosomes or in whole genomes address themselves to patterns that are already present within the genome and do not randomly generate new ones. In similar manner, recent data on the detailed organization of sequences that are shared between groups of species of Old World primates[15] and between chromosomes and species of Gramineae[24] show that there are related sets of conserved sequences, with more recent amplifications of particular sequence patterns occurring within each species or species group.

1. Jones, K. *Nature* **255**, 912–915 (1970).
2. John, B., Miklos, G. L. G. *Int. Rev. Cyt.* **58**, 1–114 (1979).
3. Peacock, W. J. *et al. Cold Spring Harb. Symp. quant. Biol.* **42**, 1121–1136 (1978).
4. Beauchamp, R. S., Mitchell, A. R., Buckland, R. A. & Bostock, C. J. *Chromosoma* **71**, 153–166 (1979).
5. Yamamoto, M. & Miklos, G. L. G. *Chromosoma* **66**, 71–98 (1978).
6. Singh, L., Purdom, I. F. & Jones, K. W. *Chromosoma* **71**, 167–181 (1979).
7. Smith, G. P. *Science* **191**, 528–535 (1976).
8. Southern, E. M. *J. molec. Biol.* **94**, 51–69 (1975).
9. Musich, P. R., Maio, J. J. & Brown, F. L. *J. molec. Biol.* **117**, 657–677 (1977).
10. Fry, K. & Salser, W. *Cell* **12**, 1069–1084 (1977).
11. Barnes, S. R., Webb, D. A. & Dover, G. A. *Chromosoma* **67**, 341–363 (1978).
12. Gall, J. G. & Atherton, D. D. *J. molec. Biol.* **85**, 633–664 (1975).
13. Manuelidis, L. & Wu, J. C. *Nature* **276**, 92–94 (1978).
14. Gosden, J. R., Mitchell, A. R., Seuanez, H. N. & Gosden, C. M. *Chromosoma* **63**, 253–271 (1977).
15. Donehower, L. & Gillespie, D. *J. molec. Biol.* **134**, 805–834 (1979).
16. Horz, W. & Zachau, H. G. *Eur. J. Biochem.* **73**, 383–392 (1977).
17. Brown, S. D. M. & Dover, G. A. *Nucleic Acids Res.* **6**, 2423–2434 (1979).
18. Brown, S. D. M. & Dover, G. A. *Nucleic Acids Res.* **8**, 781–792 (1980).
19. Bonhomme, F., Martin, S. & Thaler, L. *Experientia* **34**, 1140 (1978).
20. Britton, J. & Thaler, L. *Biochem. Genet.* **16**, 213–225 (1978).
21. Manuelidis, L. *Analyt. Biochem.* **78**, 561–568 (1977).
22. Rigby, P. W. J., Dieckmann, M., Rhodes, C. & Berg, P. *J. molec. Biol.* **113**, 237–251 (1977).
23. Southern, E. M. *J. molec. Biol.* **98**, 503–517 (1975).
24. Bedbrook, J. R., Jones, J., O'Dell, M., Thompson, R. D. & Flavell, R. B. *Cell* **19**, 545–560 (1980).

It is too early to specify the reasons for such evolutionary conservation and periodic amplifications (although speculation abounds), in our ignorance of the biological consequences of variation in types, amounts and distribution of sequence patterns. However, it seems unlikely that the differences in amount of satellite DNA in *Mus* are directly involved with the determination of chromosome homology during meiosis. These two species hybridize in the laboratory to produce fully fertile females and the species status of these two sympatric species is probably due to the evolution of premating isolation mechanisms[19].

We thank Dr Bonhomme for providing *M. spretus* livers and introducing us to his studies. S.D.M.B. acknowledges the receipt of a NI SRC postgraduate studentship.

Raman difference spectroscopy of tertiary and quaternary structure changes in methaemoglobins

D. L. Rousseau*, J. A. Shelnutt*§, E. R. Henry†
& S. R. Simon‡

*Bell Laboratories, Murray Hill, New Jersey 07974
† Department of Physics, Princeton University, Princeton, New Jersey 08544
‡ Department of Biochemistry, State University of New York at Stony Brook, Stony Brook, New York 11790

There have been several resonance Raman scattering investigations of the effect of inositol hexaphosphate (IHP) on methaemoglobins[1-5]. In those studies the sensitivity for detecting frequency differences was limited to 1–2 cm^{-1}, and consequently frequency differences were not detected although spectral intensity differences due to changes in spin equilibria were. Shelnutt *et al.* recently reported on the observation of frequency differences induced by changes in the quaternary structure of chemically modified deoxyhaemoglobins[6]. An improved Raman difference spectroscopic technique[7] with 0.1 cm^{-1} sensitivity allowed the detection of these differences. We report here the application of this technique to a series of methaemoglobins with and without the addition of IHP. In addition to the intensity changes resulting from changes in the spin equilibria, we have observed frequency differences. In all liganded methaemo-globins that we examined a decrease in frequency of the mode in the 1,370 cm^{-1} region was observed on addition of IHP. In those in which a quaternary structure change is known to occur the frequency difference is greater than 0.5 cm^{-1}. In those in which no quaternary structure change occurs [metHbA(CN$^-$) and methHbA(N$_3^-$)] the frequency difference is smaller ($\sim$0.15 cm^{-1}).

Human adult haemoglobin (HbA) was isolated and purified by standard procedures[8]. The ferric form was made by oxidation with NO$_2^-$ followed by extensive dialysis or column chromato-

§ Present address: Sandia Laboratories, D5114, Albuquerque, New Mexico 87185

graphy to isolate the purified methaemoglobin. This stock solution was stored at 4 °C until ready for use when it was diluted in 0.1 M bis-Tris buffer to yield a haem concentration of between 50 and 100 μM. When IHP was added its concentration was between 4 and 10 times the haem concentration. The ligands were added so as to attain 0.1 M levels. Resonance Raman data were obtained on previously described instrumentation designed to have a high sensitivity for detection of small differences by simultaneous data gathering from two samples and subsequent analysis on a minicomputer[6,7]. Data were obtained with 4,131 Å excitation from a krypton ion laser.

The Raman line of the porphyrin macrocycle in the 1,350–1,380 cm^{-1} region has been well characterised as an indicator of oxidation state[9], and, for low-spin ferrous porphyrins, to display a correlation with the degree of back-donation from the iron atom[10]. Shelnutt *et al.* recently reported that in deoxy-haemoglobins this Raman line is an indicator of quaternary structure[6]. They also found that in liganded proteins the line can serve as a measure of conformational stabilisation[6]. Because of these results the frequency of the line also might be expected to be sensitive to the quaternary structure change in methaemo-globins. We have examined several liganded methaemoglobins and found this to be the case.

In Fig. 1 the behaviour of the $\sim$1,370 cm^{-1} line is displayed for several methaemoglobins on addition of IHP. MetHbA(H$_2$O) and metHbA(F$^-$), both of which have a well characterized quaternary structure change on addition of IHP[11,12], show clear frequency differences of 0.73 and 0.63 cm^{-1} respectively (Table 1). The additional broad line in metHbA(H$_2$O) at $\sim$1,355 cm^{-1} in the difference spectrum results from deoxyhaemoglobin preferentially formed in the presence of IHP by photoreduction[13]. In both metHbA(H$_2$O) and metHbA(F$^-$) the addition of IHP does not result in a linewidth change but instead the entire line shifts to lower frequency. The metHbA(H$_2$O) data are displayed to demonstrate this fact by superposition of the two spectra thereby allowing visual observation that both lines have the same width and that the Raman line in the sample containing IHP has the lower frequency.

For some of the other liganded methaemoglobins, complex line-shape changes occur on addition of IHP. For metHbA(Im$^-$) there is a broadening of the line at 1,374.4 cm^{-1} when IHP is present. From optical, circular dichroism, and additional Raman
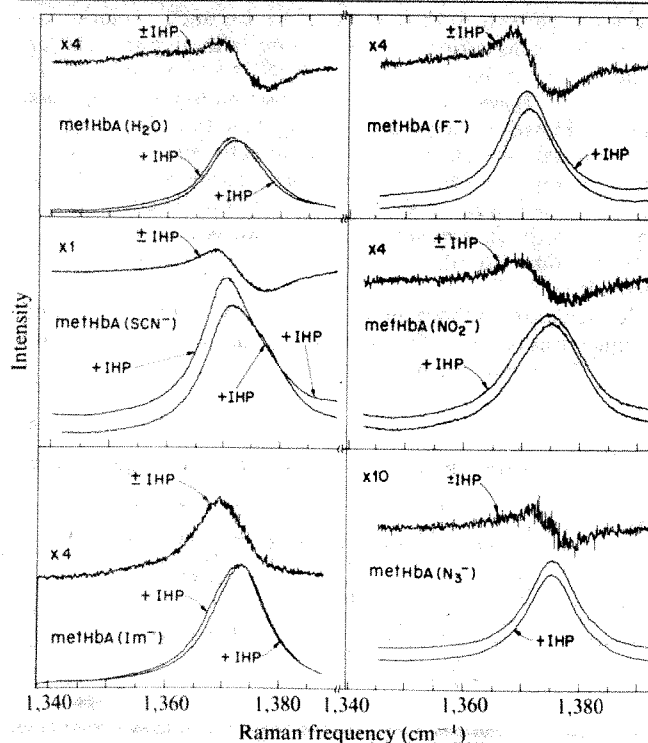
Fig. 1 Raman spectra and Raman difference spectra of the line in the 1,370–1,380 cm^{-1} region for a series of methaemoglobins with and without IHP. The line at 1,355 cm^{-1} present in the difference spectrum of metHbA(H$_2$O) results from photoreduction in the presence of IHP. The metHbA(Im$^-$) difference spectrum was balanced so as to cancel the unchanged components of the lines.

measurements it has recently been found[14] that this broadening results from a change in equilibrium in which additional metHbA(H$_2$O) is formed when IHP is added. This conclusion is supported by the difference spectrum in Fig. 1 in which a line appears at about the metHbA(H$_2$O) frequency. Because of this change in equilibrium we are unable to determine if there is a small change in frequency of the low-spin metHbA(Im$^-$) component. MetHbA(SCN$^-$) (see Fig. 1) and metHbA(OCN$^-$) are both of mixed spin character[15] and have very asymmetrical lines in the 1,370 cm^{-1} region consisting of major peaks at 1,371.7 and 1,370.7 cm^{-1} respectively, and high frequency shoulders near 1,377 cm^{-1}. As seen from Fig. 1 in metHbA(SCN$^-$) a substantial change in shape and shift in frequency (-1.5 cm^{-1}) occurs on addition of IHP. The effect of IHP on metHbA(OCN$^-$) could not be determined because carbamylation at the N-terminus inhibits IHP binding. The influence on these data of changes in spin equilibrium, changes in the relative ligand/H$_2$O binding equilibrium, and changes in binding to either the N-end or the S/O-end remains to be determined. MetHbA(NO$_2^-$) which is also mixed spin[15] and in which it is not known whether binding occurs to one of the O atoms or to the N atom gives an increased broadening on addition of IHP and a change in frequency of -0.5 cm^{-1}. On addition of IHP to metHbA(N$_3^-$) (see Fig. 1) and metHbA(CN$^-$) the frequency decreased by 0.15 and 0.18 cm^{-1} respectively.

In a preliminary experiment on the ferrous protein, HbA(NO), we found that the addition of IHP also resulted in a lowered frequency (~ 1 cm^{-1}) of the 1,375.8 cm^{-1} line and a broadening as well. A complex change of shape in this case is expected because the coordination of the iron is known to change on addition of IHP[16,17]. In a recent study by J. M. Friedman and K. B. Lyons[18] the T structure of HbA(CO) was formed by partial photolysis of HbA(CO) in conditions of low CO partial pressure. In these experiments[18] a 1–2 cm^{-1} shift to lower frequency of the 1,373 cm^{-1} line was detected.

To determine if frequency differences occurred in other Raman modes, we have examined the higher frequency region

of the spectrum of metHbA(F$^-$) and metHbA(H$_2$O) (Fig. 2). MetHbA(F$^-$) has a fully high spin ground state and metHbA(H$_2$O) has mixed spin character with a sufficiently small energy separation between the low and high spin states that the two states are populated according to their spin degeneracies at room temperature[19]. From magnetic susceptibility measurements determined by NMR[15] addition of IHP does not alter the spin distribution of either of these liganded species. With F$^-$ as the ligand, when IHP is added there is a decrease in intensity of the line at 1,478 cm^{-1}, an increase in intensity at $\sim 1,490$ cm^{-1} and a shift to higher frequency of the line at 1,564 cm^{-1}. Note, when considering the relative intensities of the 1,478 cm^{-1} line in metHbA(F$^-$) and metHbA(H$_2$O), the IHP-induced decrease in intensity of this line in metHbA(F$^-$) is consistent with a partial dissociation of the fluoride ligand and the consequent formation of metHbA(H$_2$O). Low frequency data (not shown here) on the line assigned[4] as the Fe–F$^-$ stretching mode also suggests such an interpretation. The behaviour of metHbA(H$_2$O) on addition of IHP is very different. For this case the intensities of the lines at 1,480 and 1,563 cm^{-1} increase on addition of IHP while the intensities of the lines at 1,505, 1,582 and 1,639 cm^{-1} decrease. The former frequencies correspond to the 'high spin' lines seen for example in metHbA(F$^-$) and the latter correspond to the 'low spin' lines seen for example in metHbA(CN$^-$). In spite of the qualitative difference in behaviour of these high frequency lines for metHbA(H$_2$O) and metHbA(F$^-$), the line in the 1,370 cm^{-1} region shifts to lower frequency in both cases.

The interpretation of the IHP-induced differences in the high frequency region of metHbA(H$_2$O) and metHbA(F$^-$) is intri-
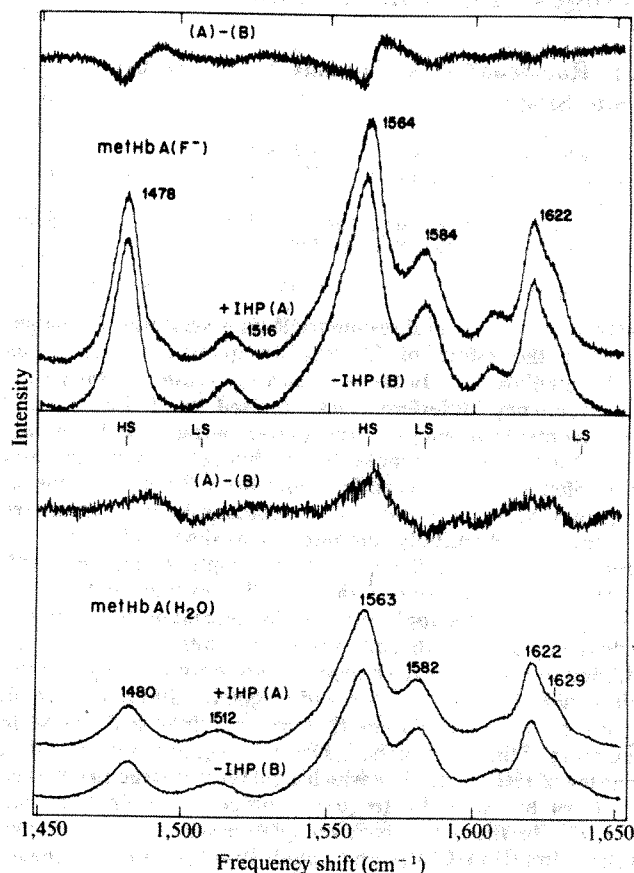
Fig. 2 Raman spectra and Raman difference spectra of the high frequency (1,450–1,650 cm^{-1}) regions of metHbA(F$^-$) and metHbA(H$_2$O) with and without IHP. The frequencies labelled HS and LS are those of high spin and low spin marker lines respectively. The scale of the difference spectrum for metHbA(F$^-$) is the same as that of the Raman spectra and for metHbA(H$_2$O) it is four times that of the corresponding Raman spectra.

Table 1 Properties of the structure dependent Raman line for several liganded haemoglobins

Ligand	Frequency	Width	IHP-induced difference
OCN^-	1,370.7	14.5	—
F^-	1,371.4	11.4	−0.63
SCN^-	1,371.7	14.5	−1.5
H_2O	1,372.0	12.5	−0.73
Im^-	1,374.4	11.5	—
CN^-	1,374.5	9.9	−0.18
NO_2^-	1,375.4	13.7	−0.54
N_3^-	1,376.1	10.6	−0.15
$NO(Fe^{2+})$	1,375.8	13.1	−1.0

The frequencies were determined from the peak positions of the lines in the absence of IHP. The widths are the full width at half height. The IHP induced differences were all determined from the intensities in the difference spectrum. No difference is reported for OCN^- because carbamylation of the N-terminal residue blocks IHP binding. No difference is reported for imidazole (Im^-) because IHP modifies the relative Im^-/H_2O to haemoglobin binding constants.

guing. The crystallographically observed structural changes at the iron in $metHbA(F^-)^{20}$ could account for the differences observed for this species. However an origin due to changes in the non-bonded interactions between the porphyrin macrocycle and the protein cannot be excluded. Observed spectral changes in deoxyhaemoglobins have been interpreted as originating from such an effect[6]. From NMR magnetic susceptibility measurements on $metHbA(H_2O)$, it was found[15] that the susceptibility is unaffected by the addition of IHP. On the other hand, from the Raman data reported here by using the $1,372 \text{ cm}^{-1}$ line as a reference we calculate a 10% increase in the intensities of the high spin marker lines when IHP is added to $metHbA(H_2O)$. Such behaviour could result from changes in iron d-level energies, but these changes might be expected to modify the spin equilibria as well, and this would be reflected in the susceptibility measurements. It seems more likely that these changes result from a direct interaction between the protein and the porphyrin macrocycle. Such an origin for the changes we observe in $metHbA(H_2O)$ also might account for the related observations in the visible absorption spectrum in which the transition in the quaternary structure from R to T produces an increase in the 'high spin' bands and a decrease in the 'low spin' bands[15]. Solvent-induced changes in the absorption spectrum originally thought to be signatures of spin state differences also have been observed in model haem compounds in the absence of spin state changes[21].

It was previously observed in deoxyhaemoglobins that the Raman line in the $1,370 \text{ cm}^{-1}$ region was sensitive to changes in protein conformation[6]. The experiments reported here demonstrate that in methaemoglobins as well this Raman line is sensitive to tertiary and quaternary structural changes. In $metHbA(N_3^-)$ and $metHbA(CN^-)$ in which quaternary structure changes do occur, we observed IHP-induced frequency differences of about 30% of the differences in $metHbA(F^-)$ and $metHbA(H_2O)$ in which quaternary structure changes do occur. This is approximately the same ratio as is observed for the UV difference spectra of these materials[11]. In those methaemoglobins in which quaternary structure changes may be brought about by the addition of organic phosphate we observe differences of greater than 0.5 cm^{-1}. The Raman difference spectra may therefore be used as a quantitative indicator of quaternary structure change.

1. Szabo, A. & Barron, L. D. *J. Am. chem. Soc.* **97**, 660–662 (1975).
2. Ferrone, F. A. & Topp, W. C. *Biochem. biophys. Res. Commun.* **66**, 444–450 (1975).
3. Scholler, D. M., Hoffman, B. M. & Shriver, D. F. *J. Am. chem. Soc.* **98**, 7866–7868 (1976).
4. Asher, S. A., Vickery, L. E., Schuster, T. M. & Sauer, K. *Biochemistry*, **16**, 5849–5856 (1977).
5. Scholler, D. M. & Hoffman, B. M. *J. Am. chem. Soc.* **101**, 1655–1662 (1979).
6. Shelnutt, J. A., Rousseau, D. L., Friedman, J. M. & Simon, S. R. *Proc. natn. Acad. Sci. U.S.A.* **76**, 4409–4413 (1979).
7. Shelnutt, J. A., Rousseau, D. L., Dethmers, J. K. & Margoliash, E. *Proc. natn. Acad. Sci. U.S.A.* **76**, 3865–3869 (1979).
8. Allen, D. W., Schroder, W. A. & Balog, J. *J. Am. chem. Soc.* **80**, 1628–1636 (1958).
9. Spiro, T. G. & Strekas, T. C. *J. Am. chem. Soc.* **96**, 338–345 (1974).
10. Spiro, T. G. & Burke, J. M. *J. Am. chem. Soc.* **98**, 5482–5489 (1976).
11. Perutz, M. F., Fersht, A. R., Simon, S. R. & Roberts, G. K. *Biochemistry* **13**, 2174–2176 (1974).
12. Perutz, M. F. *A. Rev. biochem.* **48**, 327–386 (1979).
13. Kitagawa, T. & Nagai, K. *Nature* **281**, 503–504 (1979).
14. Rousseau, D. L., Shelnutt, J. A. & Simon, S. R. *FEBS Lett.* (in the press).
15. Perutz, M. F. *et al. Biochemistry* **17**, 3640–3652 (1978).
16. Perutz, M. F., Kilmartin, J. V., Nagai, K., Szabo, A. & Simon, S. R. *Biochemistry* **15**, 378–387 (1976).
17. Maxwell, J. C. & Caughey, W. S. *Biochemistry* **15**, 388–396 (1976).
18. Friedman, J. M. & Lyons, K. B. (in preparation).
19. Messana, C. *et al. Biochemistry* **17**, 3652–3662 (1978).
20. Fermi, G. & Perutz, M. F. *J. molec. Biol.* **114**, 421–431 (1977).
21. Brault, D. & Rougee, M. *Biochemistry* **13**, 4598–4602 (1974).

Inhibition of photosynthesis by ethylene

S. J. Kays

University of Georgia, Athens, Georgia 30602

J. E. Pallas Jr

USDA-SEA-AR, Watkinsville, Georgia 30677

Little is known about how the plant hormone ethylene influences plant growth, except that it probably affects a fundamental control system. Research with inhibitors of ethylene binding and action has significantly expanded the level of understanding of the hormone. While CO_2, an inhibitor of ethylene binding, has been studied extensively[1,2] the effect of ethylene on CO_2 metabolism in photosynthesis has been virtually ignored. An initial communication indicated no photosynthetic response to ethylene by either *Pisum sativum* L. or *Zea mays* L.[3], but the exposure and the number of species tested were extremely limited. We therefore made a more extensive examination of the relationship between photosynthesis and ethylene. We report here a pronounced and reversible effect of hormonally significant levels of ethylene on the photosynthesis of the peanut.

Net photosynthesis, dark respiration and CO_2 compensation were measured on fully expanded leaves of 3-week-old plants of *Arachis hypogaea* L. cultivar Florunner. We used a semiclosed compensating system in which the amount of carbon dioxide supplied to maintain CO_2 at a given concentration was measured. Air circulated constantly through the plant chamber at 25 m min^{-1}. Chamber air temperature (25 °C) and vapour pressure deficit were controlled by the dewpoint principle, whereby humidified circulating air was brought to the desired dewpoint temperature and then reheated before entering the plant chamber. Light was provided from VHO cool-white fluorescent lamps supplemented with incandescent lamps giving $340 \mu Em^{-2} s^{-1}$ photosynthetically active radiation (PAR). The CO_2 content of the chamber was monitored by a Model 215 A-S Beckman infrared CO_2 analyser and held at a constant $300 \pm 2 \mu l \ CO_2$ per l of air by the compensating system. Carbon dioxide compensation was measured with the same system, however, without adjusting the CO_2 in the chamber.

The effects of light intensity were examined at both 1.5% and 21% O_2. We combined three sources of light: (1) the standard fluorescent–incandescent light banks used for routine plant growth; (2) 625 and 1,500 W quartz-iodine lamps; (3) a carbon arc, burning high-intensity photo 88 rods, which simulate the spectral composition of sunlight. The lowest light intensity was obtained by placing plastic shade cloth between the light bank and the plant chamber. This provided light levels of 180, 340,
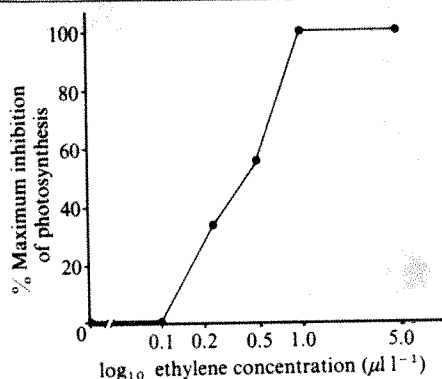
Fig. 1 Effect of a 2-h exposure to various levels of ethylene on the percentage maximum inhibition of photosynthesis of peanut leaves (25 °C, 300 μl CO_2 per 1 of air).

570, 920, 1,150 and 1,400 $\mu Em^{-2} s^{-1}$ PAR, all below saturation of photosynthesis for this cultivar[6]. At any light intensity other than 340 $\mu Em^{-2} s^{-1}$, the radiant energy was applied for 15 min. Light was increased in five steps from lowest to highest. (For a more detailed description of the methods and apparatus (see ref. 4).

A measured amount of ethylene (research purity, 99.9%) was introduced into the system using a hypodermic syringe with the internal level measured chromatographically (Perkin Elmer 881, FID) every 10 min. Samples of 1 ml of air from the chamber were separated at 110 °C on a column of activated alumina (1.83 m × 3.2 mm), with flow rates of 35, 30 and 550 $cm^3 min^{-1}$ of nitrogen, hydrogen and air, respectively. During an experiment the ethylene metabolised by the plant and/or partitioned into aqueous phase was replaced.

Exposure of peanut leaves for 2 h to concentrations of ethylene (0.25, 0.50, 1.0 and 5.0 μl ethylene per 1 of air) resulted in a substantially reduced rate of photosynthesis (Fig. 1). The concentration of ethylene required to induce a decrease in photosynthesis was small and compared favourably with the concentration dependency kinetics of many ethylene-mediated growth responses[5]. A 2-h exposure of peanut leaves to 0.25 μl ethylene per 1 of air resulted in 33% of the maximum inhibition of photosynthesis, while 0.50 μl ethylene per 1 of air represented 56% of the maximum inhibition of photosynthesis.

The decrease in photosynthesis did not occur until 2.0–2.5 h after exposure and increased with length of exposure to ethylene (for example, 0.50 μl ethylene per 1 of air for 6 h resulted in a 39% inhibition in photosynthesis). The rate of photosynthesis returned to near normal with short periods of exposure (0.5–2 h) within 5 h of the initial exposure to the hormone.

Propylene, a structurally similar unsaturated hydrocarbon gas which can induce ethylene-like responses in some plants similar to that of ethylene[1], did not inhibit photosynthesis of the peanut
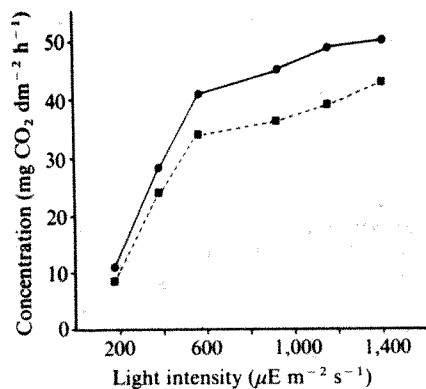
Fig. 2 Effect of light intensity on the inhibition of photosynthesis of peanut leaves by ethylene (1.0 μl l^{-1}) at 1.5% O_2 (25 °C, 300 μl CO_2 per 1 of air). ■, Ethylene; ●, control.

at a concentration (100 μl) propylene per 1 of air) 100 times that required to produce maximum inhibition by ethylene.

Photosynthesis was inhibited by ethylene (1.0 μl per 1) at all light intensities tested (Fig. 2); however, the percentage of total inhibition of photosynthesis remained constant at each light intensity (~18%). These data (Fig. 2) represent photosynthetic rates at 1.5% O_2, showing that the decreased rate of photosynthesis cannot be accounted for by increased photorespiration. Similar curves, at lower rates of photosynthesis, were obtained at 21% O_2.

There was a significant change in the photosynthetic compensation point (Fig. 3). Exposure of peanut leaves to 1.0 μl ethylene per 1 of air increased the compensation point from 48 μl CO_2 per 1 of air to around 60 μl CO_2 per 1 of air. Because the stomata would be open at this level of CO_2, the inhibition of photosynthesis by ethylene did not seem to involve a stomatally controlled mechanism.

A decrease of photosynthesis in *Helianthus annuus* L. was also detected, whereas neither *Pisum sativum* L. nor *Phaseolus vulgaris* L. were effected by hormonal concentrations of ethylene. From past work[5], the peanut would be expected to be the least susceptible of the three to such an effect. It has the least number of known responses to ethylene—inhibition of hypocotyl elongation and stimulation of hypocotyl diameter at 0.34 and 0.35 μl ethylene per 1 of air for 50% response saturation, respectively. The effect of ethylene on the photosynthetic rate of peanut and sunflower may be associated with their unusually high photosynthetic capacities[6,7] and is being investigated.
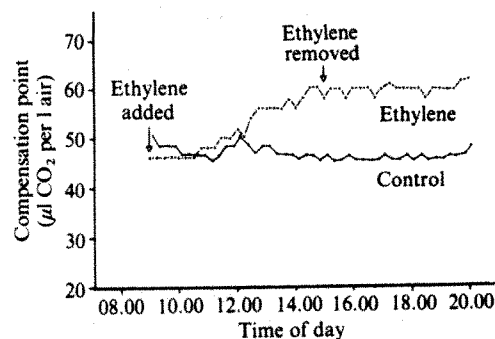
Fig. 3 Alteration of the photosynthetic compensation point of peanut leaves by 1.0 μl ethylene per 1 of air (25 °C).

An effect of ethylene on chlorophyll degradation has been reported at pharmacologically high concentrations[8] (>10.0 μl per 1 of air). However, based on the relatively short exposure time for the induction of inhibition of photosynthesis by ethylene (2.0–2.5 h) and subsequent recovery, it is doubtful that an alteration in the rate of chlorophyll degradation and/or synthesis could account for the response we measured. This is supported by the work of Aharoni and Lieberman[9] in which 3–4 d of exposure to 10.0 μl ethylene per 1 of air was required before a significant decrease in chlorophyll was detected in excised tobacco leaf disks. Alteration of chlorophyll degradation and/or synthesis, if it occurs in the peanut in these conditions, probably represents a secondary response which occurs substantially later than the initial molecular action of ethylene. In view of the diverse physiological responses of plants to ethylene, a more plausible explanation of the effect on photosynthesis would involve an effect on membrane permeability.

We thank D. Maxey and W. Turnbull for technical assistance.

1. Burg, S. P. & Burg, E. A. *Pl. Physiol.* **42**, 144–152 (1967).
2. Abeles, F. B. *Ethylene in Plant Biology* 220–236 (Academic, New York, 1973).
3. Pallaghy, C. K. & Raschke, K. *Pl. Physiol.* **49**, 275–276 (1972).
4. Samish, Y. B. & Pallas, Jr., J. E. *Photosynthica* **7**, 345–350 (1973).
5. Goeschl, J. P. & Kays, S. J. *Pl. Physiol.* **55**, 670–677 (1975).
6. Pallas, J. E. Jr. & Samish, Y. B. *Crop Sci.* **14**, 478–482 (1974).
7. Hesketh, J. D. *Crop. Sci.* **3**, 493–496 (1963).
8. Frenkel, C., Klein, I. & Dilley, D. R. *Pl. Physiol.* **43**, 1146–1153 (1968).
9. Aharoni, N. & Lieberman, M. *Pl. Physiol.* **64**, 796–800 (1979).

BOOK REVIEWS

The chilling story

H. M. Rosenberg

THE application of cold impinges on modern living in many ways and in this book David Wilson, the well-known radio and television science correspondent, describes the history and current developments of many aspects of refrigeration and cryogenic technology. The book is intended for the reader who has no specialized scientific background and the presentation is indeed clear and instructive.

After the introductory chapter which describes man's success in making fire as well as using cold, we are led into the seventeenth and eighteenth centuries — the world of Fahrenheit, Réamur and Celsius. The measurement of temperatures and early methods of cooling below room temperature are described. This then leads on to a discussion on what is really meant by temperature and heat, and to the concept of an absolute zero of temperature. The third chapter is a fascinating account of the history of food preservation. The description of the development of the North American ice trade is particularly interesting. Ice was shipped not only from the northern to the southern states of the USA, but ice cargoes were even sent to India and Australia. With the increasing reliability of refrigeration machinery the ice trade declined, although natural ice was still harvested for food preservation until well into the present century. The saga of the development of refrigerated ships and the rise of the New Zealand meat industry is yet another part of the story that is extremely well told. The next stage was the mass production and distribution of frozen food to the general public. This started on a large scale with Thomas Wall's "Stop me and buy one" tricycles — 8500 of them — for selling ice cream to a mass market. But at that time few people had refrigerators and the gradual setting-up of the complete 'cold chain' from the freezing of fresh or prepared food to distribution via cold stores to the supermarket cabinet and then to the domestic freezer took another 40 to 50 years.

But nowadays we need temperatures even below that of frozen fish fingers, and the story of the liquefaction of the 'permanent gases' — nitrogen, oxygen and later on hydrogen and helium — is told with a keen sense of historical detail. It is sad to learn that Dewar, who was the first

---

Supercold: An Introduction to Low Temperature Technology. By D. Wilson. Pp.272. (Faber and Faber: London and Boston, 1979.) £8.50.

---

person to liquefy hydrogen, never really had an opportunity to score a double by liquefying helium, because of the row which developed between him and the man who had the only large supplies of helium gas in this country — Ramsay. And so credit for the first liquefaction of helium went to the great Dutch physicist, Kamerlingh Onnes of the University of Leiden, and on that date, 10 July 1908, the science of low temperature physics really began.

Although the extremely low temperatures now attainable with the liquefied 'permanent gases' catch the imagination, it is important to realize that the most widespread application of cryogenic engineering techniques is in the production and transport of gases. Gone are the heavy cylinders of compressed gas which are nearly as heavy when they are empty as when they are full. Nowadays oxygen and nitrogen are carried in bulk as liquids. Every large steel works has its liquefaction and fractionation plant in order to extract oxygen from the air — but the cold is wasted. Indeed, one of the problems of the gas producers is the surfeit of liquid nitrogen which is necessarily produced with the liquid oxygen. It is now being used as a refrigerant in the frozen food industry, in plants which shred old car tyres and as a cold bath for frozen bull semen. But by far the largest refrigeration enterprises are the plants which liquefy natural petroleum gas so that it may be stored and shipped from one country to another. The problems of liquefying and transporting such enormous quantities of potentially explosive liquid are extremely great and they have not yet been entirely overcome.

Another chapter is devoted to the problems of freezing biological material. Can we freeze living things solid, so that they revive when thawed out? There is no simple answer. Some fairly simple celled structures seem to survive freezing if they are first treated with glycerol, but whole animals, including humans, seem to be out. However it is possible to store animal embryos, thereby enabling us to ship a herd

of pedigree cattle to a far-off land in a Dewar flask of liquid nitrogen. But the storage of blood and of bull semen are the most successful products so far.

The final few chapters in the book deal with the properties of materials at liquid helium temperatures — within a few degrees of the absolute zero of temperature. From the technological angle the most exciting phenomenon is that of superconductivity — the complete vanishing of the electrical resistance in some metals and alloys. Superconductivity implies that we can pass electric currents through superconducting wires without any energy loss and this, in our conservationist world, is a very attractive idea. But although small prototypes of superconducting generators and motors have operated satisfactorily we are still some way from seeing a large superconducting generator in a power station. The prospect of a superconducting motor in a ship is intriguing — let us hope that sufficient funds will be made available to try it out! By far the most successful application of superconductivity up to now has been in the construction of extremely powerful electromagnets — magnets which produce fields which were almost unrealizable about 10 years ago are now available at a very reasonable cost. One exotic application of superconductivity which is not described and which should have been mentioned is the Japanese magnetically-levitated train using superconducting coils. A small prototype has been operated successfully. Computers with a very high packing of elements made from superconducting junctions seem to be promising but with these, as with any other application outside the scientific laboratory, the need for utter reliability is paramount, and it is far harder to make things foolproof at the temperature of liquid helium than at room temperature.

How low a temperature can we reach? To a certain extent it depends on what is meant by temperature. The lowest temperature to which a complete system in thermal equilibrium has been cooled is probably just below a thousandth of a degree, but a sub-system of nuclear spins can be magnetically aligned so that the effective temperature is only about a millionth of a degree above absolute zero.

Besides superconductivity other remarkable things happen at low

temperatures. There is the analogous effect in liquid helium which becomes superfluid at 2.17 K and for which we still do not have a completely satisfactory explanation. And, still colder, we have the remarkable series of changes which occurs in the light isotope of helium — liquid helium three.

This is a book which whets the appetite. The treatment is simple and yet the explanations are not so oversimplified that they would worry a scientist. Occasionally the broadcasting voice of the author comes through a little too strongly so that the excitation and marvelling at new phenomena or techniques, which is very necessary via the microphone, is perhaps a little bit too enthusiastic in print. But this is only a minor point. David Wilson has done a good job and it is evident that he enjoyed doing it.　　　　　　　　□

H. M. Rosenberg is University Reader in Physics at the Clarendon Laboratory and a Fellow of St Catherine's College, University of Oxford, UK.

Molecular optical activity

S.F. Mason

FOR Louis Pasteur, the non-superposability of mirror-image molecular structures was the primary characteristic of natural products, as opposed to synthetic substances, and the distinctive physical property of handed molecules, their optical activity, provided him with a demarcation criterion between chemistry and life. The investigation of the optical rotatory power of chiral molecules, fundamentally, their differential interaction with left- and right-circularly polarized light, played a central role in the development of stereochemistry during the nineteenth and early twentieth centuries. From the 1950s, however, the chiroptical methods became increasingly overshadowed by more sophisticated physical techniques in structural chemistry, and their particular value in problems concerned with chiral recognition and discrimination was sometimes overlooked. The thalidomide tragedy, for example, could have been averted if this synthetic racemate had been separated into its optical isomers, for only the left-handed (S)-(–)-isomer has teratogenic properties. While occupying a subsidiary place in mainstream chemistry from the 1950s, the study of the electronic and structural basis of optical activity has proliferated at the periphery, in biophysics, biochemistry and chemical physics. The present book was written from the Laboratory of Chemical Physics, NIH, Bethesda, and the majority of the current theories of optical activity reviewed were first published in the *Journal of Chemical Physics,* rather than the orthodox physical chemistry journals.

The author's primary aim, which has been largely achieved, is the systematic development of the fundamental principles underlying the modern theory of the optical properties of chiral molecular structures, and of the derived semi-empirical models employed in the stereo-chemical and other applications of chiroptical spectroscopy. After an introductory historical survey, the classical and the quantum theory of the interaction of an assembly of molecules with electro-magentic radiation is discussed, with the extension beyond the standard treatment required to account for optical activity, namely, the explicit consideration of terms dependent upon the ratio of the molecular dimensions to the wavelength of the radiation. The particular approximate models covered are those of the 'symmetric chromophore', or light-absorbing group, bonded to a dissymmetric array of substituent groups in a chiral molecule, the 'coupled chromophore pair' of a chiral dimer, and the general but more miscellaneous case of the 'inherently dissymmetric chromophore'. A group-theoretical treatment of chirality follows, with applications to the sector rules connecting the stereochemical configuration of an enantiomer with its rotary strength in a given electronic transition. There is a minor confusion in this section. The second of the three classes of point group symmetries listed (p.152) should be partitioned between the first and the third, since there are but two classes, chiral molecules with pure rotation symmetry and achiral structures with rotation–reflection symmetry, which implies the super-posability of the mirror-image forms. Subsequent chapters are devoted to individual chromophore systems, the optical activity of polymers and of orientated molecule assemblies, and to recent developments. The latter include luminescence- and fluorescence-detected optical activity, and, more particularly, vibrational optical activity in both infrared absorption and Raman scattering spectroscopy.

The book is well illustrated, with a good selection of relevant absorption and circular dichroism spectra, and contains useful appendices of technical terms and of the unit systems in current use. It is recommended to all research workers concerned with chiroptical spectroscopy, as well as for general library reference.　□

S.F. Mason is Professor in the Department of Chemistry, King's College, University of London, UK.

Insight into disorder

Praveen Chaudhari

IN THIS book, Professor Ziman presents the first comprehensive and systematic review of the theoretical literature on the major forms of disorder. It is a remarkable book, both because of the subjects covered and because of the insight that the author brings to bear in explaining the generality and limitations of theoretical models.

The various forms of disorder are reviewed in the first three chapters. Chapter 1 is concerned with disorder where an underlying lattice can define the spatial arrangement of atoms. For example, compositional disorder in an alloy or spin disorder in an Ising model. This chapter contains a theme that is often repeated in the book — that of showing how the same mathematical model can be used to describe a number of situations which initially appear to be unrelated. In this instance the simple Ising model Hamiltonian is shown to apply to atomic interactions in a binary alloy. Its applicability to ferroelectric solids is briefly narrated. Chapter 2 deals with topological disorder characteristics of amorphous solids and liquids. Following a review of how the nature of disorder is described and modelled, there is a section on the analytical theories of the liquid state. In a natural progression, Chapter 3 contains a review of the statistical properties of random fields in continuous approximation. Chapter 4 has a brief and compact description of diffraction theory used in the study of disorder by experimental techniques. This is not a chapter that one can read and perform an experiment but rather one which contains the underlying physics and limitations on the information that can be extracted.

Chapter 5 has a detailed discussion of substitutional disorder. The success and limitations of the mean field approximations, the quasi-chemical approximation, the Bethe lattice and the pseudo-assembly method of Kikuchi are described. From these approximate solutions the author moves towards exact solutions of the one- and two-dimensional Ising model. The difficulties with obtaining a solution of the three-dimensional Ising model are touched upon and graphical methods are introduced. The chapter concludes with a succinct review of scaling and renormalization developments of the last few years. Chapter 6 deals with the thermodynamics of topological disorder. As in the preceding chapter, Professor Ziman begins with one-dimensional topological order and shows how genuine topological order cannot be

present in such models. He then proceeds to analyse the various approximations (for example, the van der Waal or the Percus-Yevick) used in coping with the difficult three-dimensional topological disorder. The role of computer simulation techniques in melting and the liquid state is emphasized, and the chapter concludes with a short discussion of the configurational and communal entropy and free volume.

Chapter 7 summarizes the statistical properties of polymers in solution. Branching, gel formation, rubber elasticity and random walks are some of the topics covered. The statistical treatments of the gels are connected to the Bethe lattice and the percolation problem. Chapters 8, 9 and 11 are concerned with excitations — magnons and phonons — in disordered solids. Chapter 8 develops the notion of localization or gaps in the spectral density using a linear chain model, and in Chapter 9 the discussion is extended to the three-dimensional case. Here the tight bonding and coherent potential approximation are discussed in some depth. Anderson localization and percolation theory and their significance in our understanding of disordered solids are presented. Chapter 11 contains a review of the dynamics of liquids and glasses.

Chapter 10 has a derivation of the resistivity equation (the Ziman formula) frequently used by experimentalists to explain the resistivity data on glasses and liquids. The generality and applicability of this deceptively simple formula is discussed. The remaining part of this chapter is concerned with scattering theories and their application to disordered solids. Chapter 12 contains a rather brief description of spin and ferromagnetic glasses. There is no mention made in this chapter of recent theoretical developments in spin glasses using topological notions. The final chapter contains the theory of metal–insulator transition and hopping conductivity.

Professor Ziman's book is primarily aimed at theoretical physicists. For readers with such a background or interest the book provides excellent reading of the current status of the field of disorder. The limitations of theoretical approaches, which are frequently assumed in the original sources, are clearly stated.

There are, however, a few areas which are either not adequately covered or are omitted entirely. Superconductivity and optical properties of disordered solids are not discussed. The theory of structural defects is barely mentioned. Considering the amount that has been covered these omissions are, perhaps, understandable. Overall, this book should be a very useful acquisition to anyone who is interested in the field of disorder.   □

Praveen Chaudhari is a Research Staff Member at the IBM Thomas J. Watson Research Center, Yorktown Heights, New York.

Nuclear theory

Norman K. Glendenning

Nuclear Physics with Heavy Ions and Mesons. Edited by R. Balian, M. Rho and G. Ripka. Vol. I, pp.432; Vol. II, pp.548. (North-Holland: Amsterdam and New York, 1978.) Vol. I £66.75, Dfl.150; Vol. II $80, Dfl.180; two volume set $133.25, Dfl.300.

IN THE last half dozen years or so, the subject matter of nuclear theory has expanded remarkably, and no volumes that I know of chronicle this better than do these. The modern theoretical nuclear physicist becomes more and more a theoretical physicist as the techniques and concepts that he develops or borrows from other disciplines to understand nuclear behaviour under unusual conditions make intimate connections with other branches of physics. The articles are all excellent.

Volume I deals with collisions between heavy nuclei from low to relativistic energies. Semi-classical theory for peripheral low-energy collisions is developed in several powerful approaches. The richness in behaviour of nuclear material under the stress of more intimate reactions or rapid rotation, or under the impact of relativistic collision, is the main subject.

For me, Vol. II is more exciting, perhaps only because the material is less familiar, but I think also because it indicates a new frontier of nuclear physics, where it blends with particle physics and with astrophysics. By now my copy is well worn. Most of this volume treats nuclear matter in the framework of a relativistic field theory for the light mesons and baryons, as is appropriate for studying new phases of matter at densities higher than normal such as exist in neutron stars or fleetingly at the site of a collision between nuclei at relativistic energy. This volume will be difficult going for the traditional nuclear physicist, but it opens the door to a new world.

The editors and authors are all to be congratulated for a fine work.   □

Norman K. Glendenning is Head of the Nuclear Theory Group at the Lawrence Berkeley Laboratory, University of California.

Three on food and land use

Joseph Hutchinson

The Growth of Hunger. By R. Dumont and N. Cohen. Pp.229. (Marion Boyars: London, 1980.) Paperback £3.50. *Green and Pleasant Land?: Social Change in Rural England.* By H. Newby. Pp.301. (Penguin: Harmondsworth, UK, 1980.) Paperback £2.50. *Farmland, Food and the Future.* Edited by M. Schnepf. Pp.214. (Soil Conservation Society of America: Ankeny, Iowa, 1980.) $8.

I THOUGHT *The Growth of Hunger* was about hunger in the world getting worse. It is not. Repeatedly this is assumed, but nowhere is there any documentation of the extent of hunger, or any hard evidence given that it is more widespread now than it used to be. The book is, in fact, an attack on landlords, colonialism, the market economy, the Green Revolution, agrochemicals, multinational corporations, and poverty and injustice in society. There is already an extensive literature in this vein, and *The Growth of Hunger* does not add usefully to it.

In *Green and Pleasant Land?*, Howard Newby, after a decade of research into social change in rural East Anglia, writes perceptively, cogently, and with sympathy but not emotion. After an introductory chapter there are chapters on land and land ownership, the farming industry and the rise of agribusiness, and the farm worker and the drift from the land.

There follow two chapters on the new influences that threaten the dominance of the agricultural interest in rural affairs. First is an account of the migration of urban-based families to rural domiciles, and second a discussion of the growth of environmentalism and its challenge to the privileged position of farming in planning legislation.

Newby probes deeply into the rural situation, and exposes the impotence and the growing isolation of the rural poor. The in-migration of urban people has generated a new affluent component in the rural population, and increased the polarization between rich and poor. With their cars and their town associations, the incomers have no difficulty in avoiding the isolation of the countryside, and they offer little support for rural services.

The incompatibility between the needs of the underprivileged and what it is economic to provide, is matched by the inconsistency between what the environmentalists regard as good and the agribusinessmen find is profitable. And having lucidly described these dilemmas, Newby leaves us. He has written a very good book, but now will he please write another. The conclusion I draw from *Green and Pleasant Land?* is that the social scientist — if he is as good as Newby — should advise us on what we should do, and the economist should then tell us what it would cost, and how we should pay for it.

Farmland, Food and the Future has nothing of the unity and coherence of *Green and Pleasant Land*. It is a series of essays sponsored by the Soil Conservation

Society of America on the loss of farm land to other uses. It was planned to draw attention to the facts of the loss of farm land, chiefly for urban uses, to consider whether they constituted a serious problem, and to report on what is being done about it. The essays are timely, since it is clear that the loss of farm land has only recently become a topic of concern in America, and there is not yet an agreed evaluation of the situation.

It is interesting and significant to compare the situation in the USA with that in England described by Newby. Many factors are similar. In both countries the erosion of farm land to meet the demands of urban users is very great, and losses are heaviest from the best land categories. Both have experienced a long-continued drain of the rural population to the towns, and equally they now have to accept a reverse migration. Indeed, they are also alike in the propensity of the urban migrants to become defenders of the sanctity of the countryside. To quote: "Oregon is the victim of tremendous in-migration, yet the newest immigrant is the first to want to slam the gate".

There are also fundamental differences. The underprivileged farm workers are the historical consequence of the 'Master and Man' structure of English farming, which has no counterpart in the 'Family Farming' tradition of America. The American urban sprawl has been largely forestalled in England by planning legislation that would in America be an infringement of rights of property.

These essays will help to crystallize what is at present a rather amorphous debate.

Sir Joseph Hutchinson is Drapers' Professor of Agriculture Emeritus at the University of Cambridge, UK.

Flood adjustment

Malcolm D. Newson

Human Adjustment to the Flood Hazard. By K. Smith and G.A. Tobin. Pp.130. (Longman: Harlow, UK, 1979.) Paperback £3.95.

THE reviewer has just spent 48 hours monitoring the silt load of a Welsh river in high flood but, along with others who study the purely physical properties of flooded rivers, he is almost ashamed of the satisfaction such studies provide; to the general public and especially to those who suffer from disruption, damage or even bereavement from floods, they are nothing more nor less than a hazard to life. The authors' premise for this book is that the physical approach to floods, which has its eventual utility in incorporation by engineers into flood protection schemes, is divorced entirely in this country from the behavioural approach.

They begin their book by describing the flood as a hazard, adding financial figures in pounds or dollars lost by flood damage — as we all do these days to point to an economic justification for research! However, the striking thing is not that floods comprise 30% of all natural disasters, nor that they may be increasing in frequency, but that Man courts disaster so assiduously by developing floodplain sites for housing and industry. The book divides the remedies society provides into structural (mainly engineering solutions, but including land-use control upstream of the floodable area) and non-structural (insurance, flood-zoning and the fast-developing field of flood forecasting are included). By the middle of the book the largely review material is dispensed with in favour of a statement of the ideal form of comprehensive floodplain development, one in which hydrological technology is matched, not only with cost-benefit analysis, but also with studies of social feasibility and the whole operated on a planned basis. The original material, researched along the River Eden in Cumbria, describes how both Appleby (a loss-bearing upland case) and Carlisle (a case of muddled floodplain adjustment) treat the threat of flooding from the Eden. The date of the most recent damaging flood is important in both local and regional studies (on the Eden it was 1968) and this makes the reviewer very anxious about how flood adjustment studies can ever become more widespread.

Other doubts about ever attaining the authors' ideals come from questionnaire survey results, illustrating just what an unmanageable lot we all are when confronted by hazard! Just as planner will never get all the people in one road to have grey front-doors they are unlikely to standardize the response to hazard. Here the authors' use of the word 'authoritarian' response to describe 'official' response to floods produces a shudder that the cure might be worse than the ailment!

Admitting the bias of the reviewer, it is of great interest to read that advances in hydrology and in technology have now given Britain something of a lead in flood warning; after the Lynmouth disaster in 1952 no-one in the water industry believed we would ever be in a position to give an hour's warning of flooding; but now we could.

The book is well illustrated, copiously referenced and shows that, whilst the engineer and sociologist do not seem to be talking, the geographer holds a substantial key; will it be used to open doors outside Eden? □

Malcolm D. Newson is Resident Hydrologist at the Institute of Hydrology, Plynlimon, UK.

Protologic

Peter Bryant

The Origins of Logic (Six to Twelve Months). By Jonas Langer, Pp.437. (Academic: New York and London,1979.) $26.50, £15.

QUITE a common move in psychological research with babies these days is to look for what are called 'precursors'. The idea, most frequently applied to language acquisition, is that the things babies have to do and particularly the social routines which develop between them and their parents are sufficiently complex for them to pick up certain abstract rules which will help them a year or so later on when they begin to learn grammar. Analogies are made between the rules of the earlier social habits and grammatical rules, and it is argued that the one lays the basis for the other. This argument is often used in attacks on Chomsky's idea of an innate language acquisition device. The rules are learned not innately, it said, but they are learned before. The argument is attractive, but it has the flaw that it is very difficult to support empirically. How do you establish a causal link between the earlier and the later events? Simply to appeal to an analogy between the two is glib.

The same unsolved problem, as well as several others, stalks the pages of Professor Langer's book, which is an attempt to discover the precursors of logic. He gives babies in their first year sets of objects to play with. If they put two things together here is said to be the precursor of addition — protoaddition it is called. Protosubtraction, protomultiplication, proto one-to-one correspondence, protoinference follow thick and fast. When a six-month-old baby puts a brick in his mouth, takes it out, but leaves his mouth open we are told that this is protosymbolic behaviour, because the gesture is detached from the object. The author hardly considers the possibility that what the babies are doing has nothing to do with logic, and he never questions his often-repeated assertion that the experiences they have playing with objects lays the basis for their later understanding of logic. Yet he gives no evidence, because no evidence is possible, for this central assumption. The observations are often acute, but the assumptions behind them, hedged though they are with impressive terms and often impenetrable prose, are very insecure. □

Peter Bryant is in the Department of Experimental Psychology, University of Oxford, UK.

OBITUARY

Roy Markham

THE DEATH of Professor Roy Markham, Director of the John Innes Institute, on 16 November 1979 has deprived us of a scientist who made outstanding contributions to research in several quite different experimental fields. He was born in London on 29 January 1916, the son of A.C.C. Markham, and educated at St Paul's School. In 1935 he entered Christ's College, Cambridge and read biochemistry for Part II of the tripos. After graduation in 1938 he decided on a research career, joining N.W. Pirie in the biochemistry department. In 1940 he joined Kenneth M. Smith at the Plant Virus Research Station which was then under the auspices of the Ministry of Agriculture.

By modern laboratory standards the available facilities at the Plant Virus Research Station were very primitive. They consisted of a few glasshouses and part of a wooden potato storage shed which had neither heating nor running water. However, they were fortunate enough to be allowed to continue making use of a room as a laboratory at the top of the Molteno Institute, previously allocated to Professor David Keilin. In this room, together with some additional facilities made available on the Downing site, Roy Markham laid the foundations for his later achievements. By 1942 he had already developed a steam distillation apparatus suitable for micro-Kjeldahl analysis which was subsequently listed under the British Standards Institute B.S.1428.

In 1940 Kenneth Smith was working with a new plant virus (turnip yellow mosaic) which was shown to have several interesting properties. Roy Markham became particularly interested in the physico-chemical properties of this and other small plant virus particles which stimulated his interest in the problem of high speed centrifugation. He had a genius for improvising and was highly skilled in making his own apparatus from bits and pieces found in the laboratory. An air driven high speed centrifuge was one of the devices he constructed to isolate virus particles.

It was soon realised that highly concentrated virus suspensions could be produced with a high speed centrifuge, and it was relatively easy to purify the virus with ethanol and half saturated ammonium sulphate. These highly concentrated suspensions led to the formation of octagonal crystals and this virus was one of the first (if not the first) insect-transmitted (flea beetle) viruses to be crystallised.

A number of important results emerged

from these early experiments; it was shown that turnip yellow mosaic virus could be separated into two fractions which were named "top" and "bottom" components. At the time there was considerable controversy concerning the presence of nucleic acid and its significance in virus particles, but Roy Markham clarified the issue by establishing that the "bottom" component containing the RNA was highly infectious whereas the "top" component devoid of the nucleic acid was non-infectious.

In 1945 the research came under the aegis of the Agricultural Research Council and the Plant Virus Research Unit was established. Roy Markham became increasingly involved with the physiocochemical properties of plant viruses. Kenneth Smith concentrated more on the biology, ultrastructure and transmission of plant and insect viruses. However, Roy Markham, together with Ellis Cosslett were among the first investigators to record electron micrographs of plant virus microcrystals.

He will be particularly remembered for his work on viruses when he was joined by J.D. Smith and R.E.F. Matthews. They formed a most fruitful collaboration, producing a series of important publications which established the composition and properties of several plant viruses. He was elected Fellow of the Royal Society at the early age of forty.

His interest in electron microscopy started when examining air-dried and unstained samples of viruses in an early RCA machine which was installed in the Cavendish Laboratory. Although many biologists were highly critical of the images produced from early studies in electron microscopy, Roy Markham quickly realised the powerful potential of applying these instruments to the structure and measurement of virus particles. When the Plant Virus Research Unit was fully established at the University Farm in Huntingdon Road, Cambridge, the laboratory possessed one of the first production electron microscopes. In addition, extensive research facilities were made available with the aid of various grants Roy Markham had obtained in support of the expanding virus research programme.

Kenneth Smith retired in 1959 and Roy Markham became Director of the Plant Virus Research Unit. The work continued to expand and a regular flow of visiting scientists came to his laboratory. His interest and enthusiasm for developing and building apparatus gathered momentum as war surplus equipment continued to

provide an ideal source of materials. The symmetry associated with the architecture of virus particles together with their repeating features stimulated him to construct a device which allowed the regular structural features of viruses recorded in electron micrographs to be averaged and subsequently reinforced. The technique was established as the "Markham averaging method". In addition he investigated the potential of image analysis by building a simple ultra-violet light optical diffractometer for recording the diffraction spectra from electron micrographs and making accurate measurements.

There will be very many visitors to the Plant Virus Research Unit at Cambridge who will remember the warm welcome and hospitality they received from Roy and Margaret (née Mullen whom he married in 1940), who enjoyed entertaining their guests in a most elegant style. Roy Markham had a lighted-hearted approach to research, coupled with an infectious sense of humour which visitors from abroad found difficult to appreciate on first impression, and it must be said led to some misunderstanding on more than one occasion.

In 1967 the Directorship of the John Innes Institute fell vacant at a time when a decision had been made to move the institute from Bayfordbury in Hertfordshire to Norwich. Roy Markham was invited to fill the post, and saw an opportunity to create an unique centre for research by proposing that an institute could be established by moving the Plant Virus Research Unit in Cambridge to form part of the John Innes Institute at Norwich. This resulted in a considerable undertaking, as Roy Markham became involved in the planning of a large complex of laboratories and ancilliary services. The John Innes Institute brought together under Roy Markham's Directorship and guidance during a period of just over ten years, has been re-established as a centre of international standing.

It is characteristic of Roy Markham that he left little record of his life, apart from his collection of scientific and administrative material. Although he had relatively few interests outside the laboratory, he devoted a great deal of his spare time at home to designing and constructing experimental apparatus for people within the institute. During his long illness he persisted until the end in working on a second and more advanced device for the processing of electron microscope images with the aid of computers.

R.W. Horne

T. L. McMeekin

THOMAS LEROY MCMEEKIN, commonly known as "Mac" to his friends, died in Columbia, South Carolina on 11 November 1979. He did notable work in protein chemistry over more than three decades, first in academic research and later as the head of an important government laboratory.

Born on 8 May 1900 in Monticello, South Carolina, he took his PhD at the University of Chicago in 1925, under the direction of Professor F. C. Koch, his thesis dealing with the purification of pepsin. In 1928, he joined the Department of Physical Chemistry at Harvard Medical School, headed by Professor Edwin J. Cohn. Cohn, whose primary concern was with the physical chemistry of proteins, was then engaged in purifying the substance in liver that was active in the treatment of pernicious anemia. This program achieved a clinically effective liver extract, though it failed to overcome the formidable problem of isolating what was much later to be known as vitamin B_{12}. McMeekin played a central part in this work, but his major contribution came in studies on the physical chemistry of amino acids, peptides, and a wide variety of related molecules.

This cooperative enterprise involved Cohn, J. P. Greenstein, myself and other members of the laboratory, together with George Scatchard and John G. Kirkwood at MIT, and Jeffries Wyman at the Harvard Biological Laboratories. McMeekin's role was primarily in the choice and synthesis of a wide variety of organic compounds, chosen to define the relations between structure and relative solubility in water and organic solvents, and other properties such as partial molal volumes. The aim was to provide a basis for interpreting the unusual properties of amino acids and peptides, and (by implication) of proteins, in terms of their content and arrangement of polar, non-polar, and electrically charged groups. McMeekin's work was essential to all this; in particular his studies on the influence of non-polar groups on solubility in various media provided fundamental data and systematic relations for the understanding of what later came to be called hydrophobic interactions. In studies on proteins, he achieved the crystallization of two forms of albumin from horse serum.

In 1940 he joined the Eastern Regional Laboratory of the U.S. Department of Agriculture in Philadelphia, and later became director of its Protein Division. With R. C. Warner in 1942 he carried out a fundamental study on the hydration of ß-lactoglobulin crystals, showing for the first time that it was possible to study protein crystals by direct analysis of water, salt, and protein, and to relate the composition of the crystal to that of the surrounding medium. His studies on milk proteins — notably on β-lactoglobulins and on the separation and characterization of several components of casein — led to his receiving the Borden Award in 1950. Other important contributions from his laboratory involved the preparation of new types of protein fibers and study of partial specific volumes of proteins in relation to their structure.

On retiring from the Protein Division in 1965 he became Research Professor of Biology at the University of South Carolina in Columbia until 1972. He spent his last years near by, in Monticello, his birthplace, remaining active and alert until his final brief illness.

He was twice married, first to the late Vera Crockatt, and subsequently to Crystal Stribling, who survives him. He had two daughters and a son by his first marriage. One daughter, Dorothy McMeekin, is Professor in the Department of Natural Science in Michigan State University at East Lansing.

McMeekin was modest and gentle in manner; but his strength of character was obvious to those who knew him. He was ever helpful to his colleagues and to younger co-workers. He had an excellent quiet sense of humour, and a shrewd eye for the strengths and weaknesses of other human beings. Above all he was a man of complete integrity, who will be remembered with admiration and affection, especially by that band of protein chemists of which he was a distinguished member.

John T. Edsall

H. H. Plaskett

WITH THE DEATH of Professor H. H. Plaskett on 26th January 1980, Britain has lost one of its most distinguished astronomers.

Harry Hemley Plaskett was born in 1893, the elder son of Dr J. S. Plaskett, who later became Director of the Dominion Astrophysical Observatory in Victoria, B.C. After service in France during the First World War, Plaskett joined his father's observatory as a staff member, where he remained for eight years until he became Professor of Astrophysics at Harvard in 1928. He was appointed Savilian Professor of Astronomy in Oxford in 1932, but his productive years were again interrupted by war service between 1939 and 1944. Part of the later years of the war were spent by him in developing a new type of sextant for the Ministry of Aircraft Production, which was in constant use until quite recently.

Almost the whole of Plaskett's working life was spent in astronomical spectroscopy, beginning during his years in Canada with stellar spectroscopy and his pioneering work on the emission spectra of gaseous nebulae. He had always recognised the importance of solar studies as a basis for understanding stellar atmospheres, and remarked in 1931 that "spectroscopic investigations of the sun seem likely to yield more information about stellar physics than spectroscopic studies of the stars themselves". In this year he published his classical observations of the variation of the profiles of the Mgb lines across the solar disk. This was an important step forward in astrophysics which involved the development and application of new and accurate techniques of spectrophotometry, many of them devised by Plaskett himself especially for this study. It also came at an appropriate time because of parallel work on the theory of line formation in stellar atmospheres being conducted by Eddington and Milne, following earlier work by Schuster. Plaskett's comparison of theory and observation led to a first good understanding of the mechanisms by which stellar spectrum lines are formed.

On his appointment at Oxford, Plaskett decided to devote himself wholly to solar studies. To this end he built an advanced solar telescope with a high dispersion spectrograph at the observatory. With it he planned a series of observations of photospheric mass motion through the Doppler displacements of special lines. Although this work was soon stopped by the Second World War, he felt so much encouraged by its progress after the war that he built a second solar telescope of aperture 20 in and focal length 35 m, complete with a fine spectrograph. With this he resumed his work on solar mass motions, the results of which, and their interpretation, were presented in a well known series of papers. During his 28 years in Oxford, Plaskett built up a small but distinguished group of solar astronomers, which was strengthened through close contacts with mathematicians and theoretical astronomers in other departments of the university. Over the years, many astronomers became indebted to him for the great help they received, and many owed the start of their careers to him.

Plaskett had a considerable influence on the development of astronomy in Britain. In a celebrated Presidential Address to the Royal Astronomical Society in 1946, he proposed the building of a large optical telescope in Britain. This resulted in the construction in 1968 of the 98 in Isaac Newton telescope at Herstmonceux, which is now soon to be moved to the new Northern Hemisphere Observatory in the Canary Islands.

After his retirement, Plaskett continued to work in the Department of Astrophysics and he worked regularly with the 20 in telescope until the age of 84 years. He was elected a Fellow of the Royal Society in 1936 and was awarded the Gold Medal of the Royal Astronomical Society in 1963. He is survived by his wife Edith, and his son and daughter.

D.E. Blackwell

Banking DNA sequences

MOUNT Everest, as we all know, was first climbed "because it was there". The Everest of those scientists who are devoted to the sequencing of DNA is the complete human genome, a peak that cannot yet be conquered. Nevertheless it seems not out of the question, even now, to attempt to sequence a single chromosome from man or Drosophila; or at least to tackle a substantial fragment of one such chromosome. And certainly some of the more ambitious sequencers would no longer consider the complete genome of the bacterium *Escherichia coli* to be a sufficient challenge to their skills.

The reasons why grandiose sequencing can now be contemplated are technical. In the early 1960s when Walter Fiers embarked upon the, then, highly ambitious project of sequencing the first complete genome, that of the bacterial virus MS2, it was not possible to sequence fragments of longer than eight nucleotides at one time. The complete structure of the 3,569 nucleotide genome of MS2 was published in 1976. Now, thanks largely to techniques developed by Alan Maxam and Walter Gilbert in Harvard and by Fred Sanger and his colleagues in Cambridge, one can sequence stretches of up to 250 nucleotides at a time. The sequencing of MS2 would now be no more than a single PhD project in a laboratory where the necessary techniques were already in operation.

Rapid sequencing, however, is only half the trick. One needs also relatively large amounts of pure DNA to be sequenced. For that, the techniques of cloning recombinant DNA in bacteria have been invaluable.

The combination of rapid sequencing and cloning has made it feasible to tackle larger and larger genomes. Following MS2, there came the bacterial virus ΦX174 and the mammalian SV40, polyoma and hepatitis viruses. In the offing is the complete sequence of several more viruses, led by adenovirus, and that of the genome of mammalian and yeast mitochondria. In quantitative terms this is progress from the 3.6 kilobases (one thousand nucleotides) of MS2 to the 5.4 kilobases of ΦX174, through the 35 kilobases of adenovirus to the 50 kilobases of yeast mitochondria.

By contrast the complete genome of *Escherichia coli* is about 10,000 kilobases, the Drosophila genome an order of magnitude greater and a single human chromosome some 500,000 kilobases of DNA. With a realistic outlook the *Escherichia coli* sequence could be completed by a team of ten in less than five years; with an optimistic one, a tenth of a human chromosome would not take as long because the very thought of devoting a lifetime to the task would force an order of magnitude increase in the speed of sequencing!

The dilemma for sequencers deciding what to tackle next is that, whereas a new graduate in the right laboratory might immediately stumble upon an iconoclastic stretch of DNA, so might a bevy of experts take several years to reveal nothing more than another 1,000 kilobases of uninteresting sequence.

Not that it is possible to overestimate the astonishing discoveries that have emerged, unsuspected, from sequencing: overlapping genes, split genes, degenerate genes and the bizarre features of the mitochondrial genome, including a genetic code that breaks the rule that the code is universal.

As with so much in science, hunches may be the only way to make decisions, be they by project leaders or grant givers.

From any large scale sequencing there now arises a series of irritating problems. The first is in what quanta to report the sequence; gene by gene or only when the sequence of the whole genome is essentially complete? In theory the latter approach is preferable, unless any particularly interesting feature is revealed along the way. But can the pressure to milk a sequence for as many papers as possible, or even just one for each collaborator, be resisted?

Then there is the problem, faced by journals, of printing screeds of ATCG permutations, less appetising to those who have not acquired the taste, than even the stock exchange page of a newspaper. The temptation — perhaps to be resisted — is to photo-reduce them to near-illegibility. Worse only is the suggestion, sometimes voiced, that sequences should be available from the author, but not be published at all. That would serve the thinking reader about as well as does television's The Forsyte Saga act as a guide to Galsworthy's literary style.

Finally, one major problem arises from the quantity of sequencing that has already been amassed — of the order of 100 kilobases — let alone that which the next few years will bring. The problem is how best to collate as much data as possible so as to bring out salient features. Although number, or rather letter, crunching is no substitute for thought, nevertheless computers are an essential aid to sequence collation. Already they are needed in any large scale sequencing simply to piece together the data obtained from the sequencing of random fragments of large genetic units. What does not yet exist is any central data bank in which all sequences could be deposited and made freely available to the whole scientific community. There are good precedents for such a service in the Brookhaven Protein Data Bank and the Cambridge Crystallographic Data Centre. The need for a DNA sequence bank is becoming urgent. At its best it would operate on a computer network system and offer search programme facilities. At its most meagre it would be no more than a depository, run by a keyboard operator, which sent out tapes for a nominal fee. Proposals to start some kind of bank in the US have been in the air for at least a year, and last week the European Molecular Biology Laboratory veered towards a decision to start one. It matters little by whom, or where, a bank is started. What is important is that it should start soon. □

United States

More tests required on new chemicals

THE Environmental Protection Agency has for the first time used its powers to block the introduction of new chemicals, which have not been tested sufficiently for safety.
David Dickson reports

EVER since the Toxic Substances Control Act (TSCA) was passed by Congress in 1976, it has remained the centre of fierce controversy. The chemical industry has claimed that many of its rules on new and existing chemicals impose an unduly harsh economic burden; environmentalist groups argue that the Environmental Protection Agency has been dragging its feet in enforcing the Act.

Now the Agency has decided to bare its teeth. Under a section of the Act requiring all companies to provide pre-manufacturing notices (PMNs) containing data on safety tests before a new chemical is introduced, the EPA last week announced that it was blocking the manufacture of six chemicals for which it felt that data submitted were inadequate.

The name of the company is being withheld at its request. However the EPA said that the chemicals are six phthalate esters, members of a group of so-called plasticisers which are added to polyvinyl chloride products to make them flexible, and that proposed production levels would involve 300 to 400 production workers, and up to 10,000 plastic goods workers.

The EPA's actions are based partly on the results of a study being carried out by the National Cancer Institute which seems to be proving that DEHP, a widely-used plasticiser with a similar chemical structure, can cause liver cancer in mice and rats.

According to the agency, the company proposing to manufacture the new phthalate esters had not been aware of the NCI studies. And in submitting the PMN, it provided no reports on safety studies, leading the EPA to assume that none had been carried out.

EPA Deputy Administrator Barbara Blum said last week that, before manufacture is allowed to proceed, the company must provide information about the potential carcinogenicity of the new chemicals.

The action is the strongest so far to have been taken by the Agency under the TSCA. This reflects feeling among officials that some chemical companies are being excessively reluctant to provide data.

In a recent letter to a Congressional Sub-committee, for example, Dr Stephen Jellinek, Assistant Administrator for Toxic Substances, wrote that the lack of adequate test information was contrary to congressional intent in passing the Act, and "contradicts industry's oft-expressed view

of how it conducts its premanufacture activities".

Under the provisions of TSCA, companies must submit all existing test data about the safety of a new chemical, but are not required to carry out any additional tests unless the EPA determines that the production of the chemical could pose an "unreasonable risk" or would be in particularly large quantities. Environmental groups have criticised the flexibility of this arrangement. They argue that the EPA could have been more aggressive.

"The EPA says that the Act does not give them authority to promulgate rules for tests. But we feel that the Act does give it the power to gather any information they feel is necessary," says Dr Karim Ahmed of the Natural Resources Defense Council (NRDC).

The NRDC has already successfully sued the EPA over delays in implementing another section of the Act, which requires it to take action on a priority list of potentially dangerous chemicals drawn up by an interagency committee.

The Agency had argued that a 12-month time limit set by the Act required it merely to publish a progress report. However, three months ago a district judge in New York upheld the NRDC's contention that the actions themselves had to be carried out within this time. He said the 28 months which had elapsed since the priority list was published, and during which the EPA had taken no action against any of the listed chemicals, did not fulfil the congressional requirement.

NRDC members claim that the court victory strengthens their argument that the EPA could be moving more firmly to implement the provisions of the TSCA. In particular, it is arguing that the Agency has the power to set guidelines for the type of safety test data required to be submitted with PMNs.

This would bring the US more in line with actions recommended by the European Economic Commission that before starting production of a new chemical, a company would have to provide a certain amount of data on its potential environmental and health effects, in this case the amount of data depending on the proposed level of production.

The NRDC is proposing a 'tiered' scale of tests, with short term tests — for example for mutagenicity or chronic toxicity — required for all chemicals, and additional tests for those which are more

likely to be dangerous.

This approach, however, is being resisted by the chemical industry. "You have to consider how each chemical is going to be used. To have a laundry list of tests is too simplistic", says Dr Geraldine Cox, Technical Director of the Chemical Manufacturers' Association, who says that the current arrangement allows companies to talk to the EPA on a "scientist to scientist" basis.

Last week's actions indicate that the agency intends to "prosecute vigorously" the PMN provisions, according to one official. Its apparent commitment to a more aggressive stance on chemical testing was illustrated two days after the phthalate esters announcement, when Ms Blum told several leading chemical manufacturers that new safety tests would have to be carried out on the herbicide 2,4-D.

Unlike 2,4,5-T, 2,4-D does not contain dioxin contaminants, and there is no direct evidence that it is a health hazard. However, because of the structural similarity between the two substances, the EPA is demanding that new studies be carried out to eliminate any suspicion that it might be dangerous. □

Record rise in federal R&D backing

FEDERAL support for university-based research and development increased by $610 million to a total of $3,958 million between 1977 and 1978, the largest net growth since records were started in the early 1960s and the largest percentage growth since 1972, according to figures released by the National Science Foundation. The largest part of this increase came from the National Institutes of Health, whose support for university research increased by $262 million. The 1978 figures represented an 8% real growth in funding over 1977.

The NSF statistics indicate that the majority of research support is concentrated in relatively few institutions. In 1963, when records were first compiled, 90% of federal R & D support went to the top 100 research universities. In 1978, the top 100 universities received 84% of all R & D funds, compared to only 56% of total federal funds to universities.

Top recipient was Johns Hopkins University, whose $196 million of federal support — largely the result of incorporating for the first time the Defense Department-sponsored Applied Physics Laboratory — put the university far ahead of the previous leader, the Massachusetts Institute of Technology. □

CO₂ could increase global tensions

A strong warning that, since the global build-up of atmospheric carbon dioxide will have varying climatic effects on different parts of the world, it could lead to increased tension between rich and poor nations, has come from a special committee of the Academy of Sciences.

In a report prepared for President Carter's Science Adviser, Dr Frank Press, the committee says that such a build-up will only be minimised by international agreement to reduce the use of fossil fuels and develop alternative energy sources. And in view of the potential divisiveness of the CO₂ issue, it recommends that "in the near term emphasis should be on research, with as low a political profile as possible."

The committee, which was chaired by Dr Thomas C Schelling, professor of political economy at Harvard University, was asked by Dr Press to look at the social and economic consequences of increased concentrations of atmospheric CO₂. Accepting the scientific consensus that such an increase is likely to take place, the committee concentrates on what it considers the most serious consequences, namely the relative distribution of the resultant gains and losses throughout the world.

It points out, for example, that developed countries with temperate climates are not only the largest consumers of fossil fuels, but may also benefit from the climatic effects, with raised temperatures and rates of photosynthesis leading to increased agricultural yields. Both the US and the USSR could benefit in this way.

In contrast, countries in subtropical arid zones could suffer a decline in rainfall and possible droughts with decreased food production and resultant shifts in population distribution — as well as potential demands for international compensation.

"It seems that climate change might well tend to make the already poor still poorer and increase the difference between North and South, rich and poor, developed and developing" says the committee.

Research on adaptive and preventive measures are, it says, "apparent and urgent" to help mitigate the consequences. For example it recommends efforts to improve the resilience of agriculture to climatic change. And in particular suggests that ways should begin to be explored of protecting low-lying land areas from the possible elevation of ocean levels due to the disintegration of the West Antarctic ice sheet.

Finally, responding to two recent reports in the scientific literature which suggest that the rate of carbon dioxide build-up may be an order of magnitude less than most scientists now fear — reports which have become the centre of fierce controversy in the climate research community — the committee says it agrees with the views of experts it consulted that "these are based on incomplete assessments that unrealistically omit important feedback processes." □

Exxon supports MIT research

BREAKING away from more conventional patterns of research funding, the Massachusetts Institute of Technology and Exxon Research and Engineering Company announced last week a ten-year agreement under which the company will provide up to $8 million to support basic research at the institute into combustion processes.

In return, the company — the research arm of Exxon Corporation — will receive royalty-free, non-exclusive licenses to any patents which MIT obtains on technology arising from the research and will share any royalties on technology licensed to third parties.

Areas of research to be supported by Exxon include the burning of coal, coal liquids, shale oil and heavy crude petroleum. According to Dr Ed David, President of ER&E, a prime objective of the agreement is to "help generate the scientific base for more efficient and more environmentally acceptable burning of high sulphur, high nitrogen, hydrogen deficient fossil fuels" of particular interest to utilities and industrial companies.

Under the terms of the agreement, all results of the research can be published openly. ER&E will select the research projects it is prepared to finance from a list proposed by MIT. And in addition to this, an additional 20% of the total will be made available by Exxon to MIT scientists to pursue their own combustion science research projects.

The two principal investigators at MIT will be Professor John P. Longwell, who joined the institute faculty in 1977 after a long research career with Exxon, and Professor Adel F. Sarofim. Initial research projects to be carried out under the agreement include studies of the relationship of flame hydrocarbon intermediates to surface deposits and hydrocarbon emissions; and the interaction of mineral matter with sulphur during coal combustion.

The agreement is, according to the university, "one of the largest and longest of its kind" and is the result of protracted negotiations between the two sides over terms. It cannot be terminated without two years notice from either side, and in the words of MIT president Dr Jerome Wiesner "provides the university with the certainty that these long-range research programmes will have the financial continuity and stability to ensure effective performance".

The novelty of the agreement lies in the

MIT: receiving industrial support for basic research

fact that whereas industrial support of applied research on university campuses is a common phenomenon, it is relatively unusual for a private company to sponsor more long-term, basic research.

This role has, at least in the post-war period, been conventionally assumed by the federal government, on the grounds that basic research is a common good. However, in recent months a number of industry executives — among which Ed David and other Exxon officials have been some of the more outspoken — have argued that the private sector should take on more responsibility for supporting 'goal-oriented' basic research carried out in universities, arguing that because of changing political, social and economic factors, government may not have the staying power or the style of management to meet industry's long-term needs.

Recently one Exxon official suggested that industry's share of support for basic university research should increase to 15% from its current level of about 3%. The MIT-Exxon agreement is one of the first steps in this direction.

David Dickson

Smallpox

Gone for good?

TODAY in Geneva, the World Health Organisation will officially declare smallpox eradicated from the Earth. It will be the culmination of an astonishingly successful 22-year programme by the WHO, which included, in the two years since the last endemic case was reported in Somalia, the unclaimed $1,000 reward offered for new cases reported (*below*). But could smallpox ever recur? **Peter Newmark** examines the evidence.

Only five years ago . . . a WHO worker interviewing a child with smallpox in Ethiopia.

THE WHO campaign to eradicate smallpox was launched in 1958, a year in which 250,000 cases of the disease were recorded. At first success was slow to come by. Even vaccination of 90% of the population of a country was sometimes found to leave a sufficient residuum of the virus for it to bounce back with a vengenance.

By 1967 the disease was still endemic, or in serious danger of being so, in 50 countries. The WHO therefore hatched and launched an intensified campaign of eradication.

By any reckoning, the success of that campaign was remarkable. Ten years and $300 million later the last case of endemic smallpox was recorded.

Two and a half years later, the WHO is convinced that smallpox has gone for ever. In coming to that conclusion the WHO has considered three possible routes of re-infection but deemed them to be most unlikely, if not impossible.

The first would be if the virus could lie dormant in smallpox scabs that have survived this long. But the WHO is satisfied that the virus quickly becomes harmless in scabs.

The second possible source of re-infection comes from the smallpox virus stocks that are being held in the seven WHO-approved and inspected laboratories. That possibility last became a reality in Birmingham, UK, in 1978 when one worker died and another became mildly ill. Since these were not endemic cases they did not count within the WHO's definition of the 'last' cases. They did however, lead the WHO to increase its biosafety requirements and inspections, and to speed up its policy of closing down as many smallpox laboratories as possible. In two years, it is hoped, there will be only four, but some will have to be maintained indefinitely because of the possibility, however remote, that the virus could reappear from some other source, necessitating a new programme of diagnosis and vaccination. WHO plans to keep in reserve sufficient freeze-dried vaccine for 200 million people.

Meanwhile research is continuing on the third conceivable route of reemergence, by mutation from monkeypox virus. That possibility was raised in 1978 by the publication in *Nature* of experiments carried out in the WHO-sponsored Research Institute of Virus Preparations in Moscow, under the direction of Dr S S Marennikova. These showed that both in the course of passage of monkeypox virus through hamsters, and in the pock appearing on chorioallantoic membranes infected with monkeypox, there sometimes emerged a virus that was indistinguishable from smallpox virus in laboratory tests.

That conclusion was controversial from the start because of the considerable differences between the smallpox and monkeypox virus; although both are members of the orthopoxvirus family, as is vaccinia virus from which smallpox vaccine is produced, monkeypox very rarely infects man and, when it does, appears not to be transmitted from person to person; in the laboratory every test, from its molecular characteristics to the colour of the pocks it produces, distinguishes it from smallpox. Whereas that does not preclude the possibility of mutation of monkeypox to smallpox virus, recent, as yet unpublished restriction enzyme analysis of the genome of twenty-one mutants newly derived from monkeypox show that, despite instances of major deletions and rearrangements of genes, all of the mutants were still recognizable as monkeypox virus, and none closely resembled smallpox virus. The laboratories responsible for this work (those of Prof. K R Dumbell, in St Mary's Hospital Medical School, London, and Dr J H Nakano at the Center for Disease Control, Atlanta, USA) have also analysed the genome of six of the mutants obtained from monkeypox in Moscow in 1978, and the two monkeypox stocks from which they were derived. And at the molecular level, restriction enzyme maps of the two viruses show that the differences between them are so considerable that as Dr Nakano told *Nature*: "it seems highly improbable that the smallpox virus could ever be derived from the monkeypox virus by mutation".

However, Dr Nakano's laboratory has also analysed the four smallpox-like viruses isolated in Moscow from white pock on chorioallantoic membranes infected with monkeypox. Each of these mutants was indistinguishable from smallpox virus, confirming Dr Marennikova's identification of them.

The current position therefore seems to be that whereas it has not been possible to reproduce Dr. Marennikova's derivation of smallpox virus from monkeypox virus, and the genomic differences between the two viruses make such an event highly improbable, yet the evidence is clear that the Russian mutants are indistinguishable from smallpox.

There are two possible explanations, both unpalatable in their own way. The first is that Dr. Marennikova's results were the result of contamination. Obviously that can never be ruled out, and one of her two original monkeypox virus strains does appear to show signs of contamination with smallpox virus; however, the other does not.

The other possible explanation, and much the more worrying one, is that, despite the improbability, monkeypox virus *can* mutate to smallpox virus. That possibility is described by WHO as "highly unlikely, but impossible to disprove". All it can do is to continue to sponsor research — and hope that today's declaration of smallpox eradication is the very last one. □
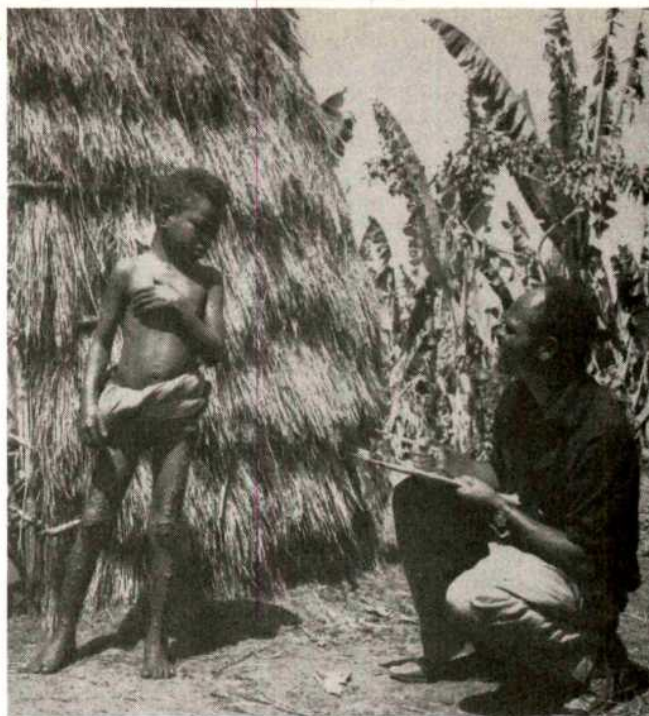
Cell culture

Fetal calf serum drought hits cell culture laboratories

CELL culture laboratories throughout the world have been hit by their own fuel crisis — a shortage of fetal calf serum, the magic component of the media in which many biologists grow their cells. Supply has become uncertain, and the price has escalated; in the UK it has doubled in the past year and is now pushing £100 a litre.

Scientists are now exploring alternative ways of growing cells. At the very least they are in for a lot of trial and error, and time consuming work, as cells are weaned off fetal calf serum. Some projects will have to be abandoned.

Changes in world agricultural policies and practices lie behind the shortage, says Mr Tom Coutts, the managing director of Gibco Europe Ltd., which with Flow Laboratories, is the main distributor of fetal calf serum in Europe. He believes the overall supply will be bad for one or two years but may ease in the long term.

Flow was unable to supply any fetal calf serum at the end of April, and the company described the shortage as "very, very serious". In late April Gibco wrote to customers saying "severe shortages" would affect supply "for the foreseeable future . . . it is in our customers' interest to take every possible step to reduce their dependence on this product". Both companies hope the short term situation will be boosted by the start in April of the serum collection season in Australia and New Zealand, Europe's main sources of supply.

Fetal calf serum is a by-product of the beef industry. It is extracted by cardiac puncture when a cow brought to market for slaughter is found to be pregnant. Mr Coutts traces the current shortage back three years when beef prices were low, cattle were slaughtered rather than raised for the meat market, and calves, which would have become today's breeding stock, were lost. Now beef prices have risen and calves are being reared. Also, the US has lifted beef import quotas against Australia, making it even more profitable for Australian farmers to keep their calves.

Fetal calf serum is widely used by research institutes, hospitals, and universities for medical research, and by pharmaceutical companies in drug production. Its application includes use in diagnostic procedures, cancer research, and virology.

In the past the serum has been freely available, with just the occasional minor problem of supply. It has also been relatively inexpensive and extremely effective, curiously for reasons not yet understood. Its widespread introduction during the 1960s meant an end to the practice of scientists undergoing a self-imposed 24-hour starvation and obtaining a pint of their own blood for use in the medium.

Dr John Birch of Searle Research and Development says that "a great mythology" surrounds fetal calf serum. Dr Eric Hall, an English scientist at Columbia University in New York, says: "Tissue culture work using fetal calf serum has got a bit out of hand. We have sloshed it around because it was cheap and available. Some work has been done just for fun. We need to rethink our priorities." Now many laboratories will have to stop using it.

The Imperial Cancer Research Fund (ICRF) in London, which has about 70 people in tissue culture work, replenishes its supplies monthly and is now receiving about half the fetal calf serum (75 litres a month) it needs to meet its planned research programme. ICRF scientists have been asked to halve the amount of serum they use in media, to 5%.

University departments simply do not have the money to keep paying for the serum. Small laboratories are faced with a dilemma: either they pay high prices with the knowledge that they can successfully grow their cells, or they gamble with cheaper sera which may not give the desired results.

Professor Sydney Shall of the Biochemistry Department at Sussex University suggests that the number of places able to do tissue culture work will decrease. "It's a grave issue," he says. His cell lines are sensitive human cultures such as brain cells and they need 10% fetal calf serum. His department is rethinking its research programme.

Dr Colin Arlett of the Medical Research Council's Cell Mutation Unit, at Sussex, can provide an example. He is growing fibroblasts from patients suffering from ataxia telangectasia, a genetic disease. These cells are difficult to grow even on fetal calf serum and "if it becomes completely unavailable, or the price prohibitive, work on these cells will have to cease."

Cell biologists in Europe are no longer given the luxury of testing batches of fetal calf serum before purchase. They have been told by distributors to take what they are given or look for another source. Without testing, there is no guarantee that a particular batch of serum will support adequate growth of the cells being used.

"At least we have a buffer compared with smaller laboratories," Mr William House, manager of research services at ICRF, said. "If a particular batch of fetal calf serum doesn't suit one person's cell lines, it can be used by someone else."

The attitudes and methods of biologists themselves may be contributing to the problem. Panic buying has occurred over the last 12 months says Mr Coutts. The demand is artificially high, fed by the rumours of the impending short supply. Unwillingness to try alternatives and over dependence on fetal calf serum may also be factors.

In searching for alternatives, the most popular solution is likely to be weaning the cells onto other sera. Indeed, some scientists claim that they predicted problems of supply of fetal calf serum and have successfully changed to other sera. Alternative sera are less costly and more readily available. However, there may also be some problems.

New born calf serum, asceptic calf serum, and horse serum will support the growth of some cells, although usually with poorer growth rates; and some primary cell lines may have an absolute requirement for fetal calf serum.

Another complicating factor is whether or not the properties of the cells will change. Once the cells are growing on other sera, partially completed projects face the possibility of a change in the cellular response to the treatment — such as irradiation or drugs — under investigation. Earlier experiments which used fetal calf serum may have to be repeated. Dr Hall has already reported such cellular changes in response to chemotherapeutic drugs.

Many scientists believe that the ideal solution to the dual problems of the supply of serum and the variability it causes in the growth of cells can be solved by the use of a totally defined or synthetic medium. Attempts over the last 20 years to identify the magic ingredient(s) in fetal calf serum have not been successful; the latest shortage may revive this work. Several cell lines already grow on a totally defined medium and the popularity of these cells is sure to increase.

A further question arising from the shortage is the effect it will have on the anti-vivisectionist movement which believes that biologists should turn to tissue culture in preference to research using animals. Legislation to encourage this development has been proposed in the UK and elsewhere in Europe. But biologists working with animals are unlikely to change to tissue culture if they see such problems with the supply of serum.   **Ian Anderson**

Ian Anderson is a freelance journalist

NEWS IN BRIEF

EEC funds 10 new solar energy projects

THE Commission of the European Communities approved last week grants to 10 new solar energy projects totalling 3 million EUA (1 EUA = £.665). The projects include an award of 53,000 EUA to K.U. Leuven of Belgium for an electric car using solar energy and nine awards to solar heating projects which include block central heating by solar power for 250 houses in Alpes-Maritime in France, solar heating of greenhouses in Italy, a West German project to study solar heating of swimming pools and a project for solar energy heating of phosphorising vats at a refrigerator production plant in Pordenone, Italy.

UK locates geothermal energy source

AN exploratory borehole at Marchwood, near Southampton has located a large deposit of water at a temperature of 70°C the Secretary of State announced in Parliament last week. The water was found at a depth of 5,600 feet and can be brought to the surface at a temperature of 65°C a drop of only 5°C. There is sufficient water in the well to heat about 1000 houses over a period of several decades. Pumps will be installed late this summer to bring the water to the surface and its mineral content is being assessed.

Geothermal energy has been in use in Hungary since the beginning of the 20th century and has found increasing uses in France to heat apartment blocks in the Paris suburbs. France plans to have half a million geothermally heated buildings by 1990 which will produce a 15% saving in running costs. The UK's £1.8 million

Midland Valley of Scotland

Weardale granite

East Yorks-Lincs. Basin

Cheshire Basin

▨ Igneous rocks

■ Sedimentary basins

Worcester Basin

Bath/Bristol

Hampshire Basin

borehole project is part of a £11 million yearly programme to explore alternative energy sources including wave, wind, tidal and solar energy.

UK Seveso report issued

AN English translation of the 1978 Italian Parliamentary Commission report on the Seveso accident was published by the UK Health and Safety Executive last week. The Executive clearly feels that the Seveso accident involving the discharge from a chemical factory of some 250-500 grams of 2, 3, 7, 8-tetrachlorodibenzo-p-dioxin (dioxin) over a populated area was serious enough to warrant a report of the causes and consequences of the incident being made more widely available. But central to the concern over the health of the Seveso residents was the two week delay in ordering their evacuation from the dioxin-contaiminated area: on this point the report has been criticised as inaccurate. For a detailed discussion see *Nature* 22 February 1979, page 588.

Seveso: A translation by the Health and Safety Executive of the official report of the (Italian) Parliamentary Commission of Enquiry. £25.00

Queen's Award to new, safe insecticide

A GROUP of UK scientists received a Queen's Award last week for their development of a class of highly active insecticides that have low mammalian toxicity. Chemists and biologists at the Rothamsted Experimental Station solved the problem of making synthetic pyrethroid compounds, known from the group's previous research to attack insect but not mammalian nervous systems, stable against exposure to sunlight. According to Paul Needham of the Rothamsted Station the compounds break-down rapidly in soil and residues are unlikely to accumulate to contaminate the environment. Three compounds of the new class of insecticides, permethrin, cypermethrin, and decamethrin, are sufficiently active to be used at dosages of an oder of magnitude less (10-200 g/ha) than that of most other insecticides (500-1500 g/ha). The pyrethroids are effective against lepidopterous larvae in cotton, timber, wool and stored products.

Collection of Yeast Cultures finds home

THE UK National Collection of Yeast Cultures, threatened by withdrawal of funds by two of its sponsors last January (*Nature*, 24 January page 325) will be moved to the Agricultural Research Council's Food Research Institute in Norwich before the end of the year. The Collection, consisting of 1,500 yeast strains widely

used throughout Europe was saved by a decision of the Advisory Board for the Research Councils to provide the money to move and maintain the collection. The ABRC will provide about £24,000 annually so that the Collection can carry out its central functions of maintaining and supplying fully characterised yeast cultures to industry, universities and schools as well as acting as a reference and information centre for identification and deposit of yeast cultures. The collection will continue to be housed in its present quarters, the Brewery Research Foundation, until the transfer is effected during the summer.

Research could help industry: Canadian report

INCREASED support for basic research in areas such as materials science and processing, vehicle control systems and battery electrochemistry could provide a long-term boost to the Canadian car industry, according to a report prepared by Arthur D Little of Canada Ltd for the Ministry of State for Science and Technology.

The report, prepared on parallel lines to an initiative (already under way) of the US government to stimulate research through projects jointly supported by federal and industry funding, lists a number of areas of "directed basic research opportunities" relevant to automotive technology which might be performed in universities or research institutes. "This kind of research is not directly intended to result in the design of new vehicles, engines, or components; it is meant to focus on achieving a fuller understanding of the physical and chemical processes underlying vehicle technology," the report says. But it adds that programmes of this nature, with a time horizon for commercialisation primarily in the 10 to 20 year range, must receive adequate government funding in order to be successful. "There are a large number of government sponsored research programmes in Canadian universities and government research centres that we believe are underfunded," the report says.

Errata

IN the leader of 17 April, page 583 David Howell was erroneously referred to as the UK opposition spokesman on energy. This should have been David Owen.

The letter from John Goddier in 24 April, page 658 was written in his capacity as Branch secretary of the Agricultural Research Council Branch Institution of Professional Civil Servants. It does not represent an official ARC view.
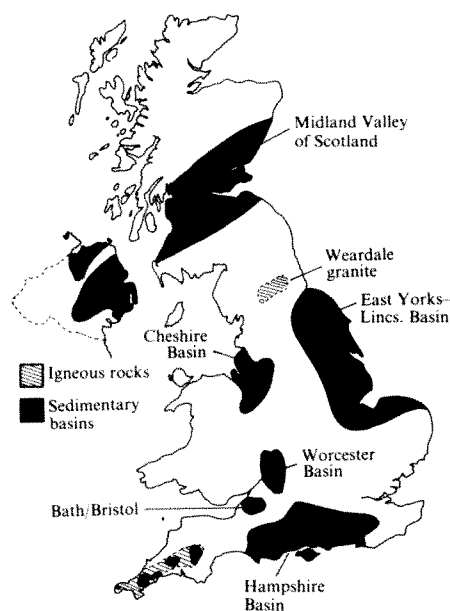
A birthday party with real rockets

Bulgaria is celebrating 1,300 years of nationhood next year, and scientific events are among the festivities. But as **Vera Rich** reports, the best birthday present the country could have would be a pollution-free water supply

LATER this month, Bulgaria will hold its second national conference on molecular biology — the first scientific event of the jubilee.

Dedicating a scientific congress to an event in the remote past may seem novel to western eyes, but it is merely one of a whole series of scientific events associated with the anniversary. In spite of its relatively small size and low science budget (about 1.3% of the GNP) Bulgaria is doing work at an international level in a number of fields, molecular biology included.

According to Dr Rumen Tsanev, of the Institute of Molecular Biology of the Bulgarian Academy of Sciences, work in molecular biology began some 10 years ago — before the Soviet decrees of 1974 which assigned priority to catching up in molecular biology and genetics. Lysenkoism, however, never really took hold in Bulgaria; there was some theoretical discussion of it in the 1950s but this was quickly over and, said Professor Tsanev, there was no persecution of people who did not accept it.

Bulgarian work on molecular biology has included: the discovery that the nucleosome consists of two sub-units; the formulation of mathematical models of cell differentiation; study of the role of histones in DNA transcription; and, most recently, two-dimensional electrophoresis studies of differences in the primary structure of nucleosomes. As for genetic engineering, "We feel it can only be developed as part of general molecular biology", Tsanev explained. "We started only last year, and at present we are simply trying to introduce methods of handling and mastering the techniques". Preparing too for genetic engineering, is Dr Basil Staikov of Bulgaria's unique "Rose Institute" at Kazanlak, a research station devoted to every aspect (from biochemistry to the mechanics of harvesting) of the Kasanlak roses whose essential oils play so significant a role in the Bulgarian economy. For the moment, however, Dr Staikov explained, Kazanlak has not the equipment for genetic engineering, and new varieties are still obtained by traditional cross-breeding methods; γ-irradiation experiments begun some four years ago, said Staikov, have so far given no definite results, although the general indications seem "promising".

Bulgaria is extremely proud of the scientific traditions it has established during the last century or so. The Academy of Sciences was founded in 1869. Bulgarian

Citizen-cosmonaut Ivanov. His space mission failed last year — but the scientific side of the programme was carried through.

scientists have been particularly active in solid state physics; but last year, according to Dr Milko Borisov, Director of the Academy's Joint Centre for Physics, the best results in Bulgarian physics came from work on liquid crystals, dielectric and flexielectric properties. Specialists from the Centre are cooperating with Polish and Italian teams on an "Atlas of liquid crystals" to be published by the Bulgarian Academy, probably in 1981.

International projects, naturally, cannot be dedicated to the Bulgarian jubilee. Nor, it seems, can the new astronomical observatory at Roehen, with its 200cm hyperbolic mirror with a Richey-Chretien-Coudé focus system. Much of the optical equipment came from Karl Zeiss (JENA) and when the observatory is formally opened later this year, it seems likely that it will be dedicated to DDR-Bulgarian friendship.

However, Bulgarian statehood will be celebrated in astrophysics. A special satellite Bulgaria–1300 will be launched by a Soviet rocket towards the end of the year. The experiments it will carry are, for the moment, a secret, but, according to Dr Kiril Serafimov, head of space research, Bulgaria is an active participant in all five sections of the "Interkosmos" programme — space physics, meteorology, communications, space biology/medicine, and remote geophysical sensing. Even before "Interkosmos" was set up as the official organisation for Comecon joint research, Bulgarian physicists assisted their Soviet colleagues in evaluating data from the "Elektron" probe — and later, from US satellites.

The Bulgarian public is still hopeful that their "space" celebrations might include the launch of a second Bulgarian cosmonaut, and with greater success than Georgi Ivanov, who with a Soviet crewmate, failed last year to link up with Salyut-6. But 20 of his scheduled experiments were carried out by the Soviet team on board including work with the Bulgarian Spektr-15 remote sensing camera (which weighs only 15.2kg but has 15 channels), the casting of an aluminium-hydrogen foam, work on epitaxial surfaces and crystal growth, and electrophoto-magnetic experiments on the aurora. Only the seven medical experiments scheduled for Ivanov had to be abandoned.

Perhaps the biggest scientific contribution to the jubilee will be the publication of Bulgaria's "Red Book" of endangered species. According to Professor Simeon Nedyalkov, of the Institute for the Coordination of Research for Environmental Conservation Bulgaria is, from a geobotanical point of view, a "melange" of boreal, mediterranean, pontic and Asia-minor species. Since the "technical revolution", especially around the country's new metallurgical plants, many species are threatened. There has been over-cutting of valuable timber; snowdrops have been depleted by the demands of the medical profession (they yield nivalin — an alkaloid used in the treatment of polio); and a well-intentioned attempt to step up trout production by introducing American varieties proved disastrous, for the newcomers failed to adapt to local plankton and became predators on the native trout.

Now, however, said Professor Nedyalkov, Bulgaria has a well established national monitoring system for all forms of air and water pollution, and in especially menaced areas, soil pollution also; and work is going forward on the resistance of plants to toxic elements.

Bulgaria's concern for the environment extends to the international level — not surprisingly, since its only sizeable river, the Danube, arrives too polluted even for irrigation. The existing Danube Commission covers only pollution from ships, and Bulgaria has been one of the most active of the riparian states in pressing for a Danube Convention to cover all aspects of monitoring and research into water quality and ecology. The preliminary text for a Convention has already been drafted and, said Dr Veselin Petrov of the Committee of Environmental Protection of the Council of Ministers, it is hoped that a final text will be signed this year. That would be the best 1300th birthday present Bulgaria could receive from the up-stream Danube countries. □

CORRESPONDENCE

Tumour surveillance in beige mice

SIR, — Since beige mice have been shown to have defective natural killer (NK) cells[1], several groups have reported recently in *Nature* on the presumed consequences — *viz.* poor immuno-surveillance for spontaneous tumours in mice[3,4] and men[4]. Padgett[5] reviewing Chediak-Higashi-syndrome of man, mink and cattle noted raised incidence of lymphoma. Beige mice are the murine equivalent. The gene, *bg^J*, was long ago obtained from the Jackson Laboratory on its C57 BL background and in this laboratory crossed onto a $(C_3H \times 101)F_1$ background and maintained thus. Neither of these Harwell strains nor the F_1 is noted for natural lymphoma. After the reported NK defect in C57 BL *bg bg*, 40 Harwell beige mice were set aside for life-time study. Others had been used for determining the origin of the osteoclast from the haematopoietic stem cell[6,7] during which electron microscopy studies of their bones had revealed C type virus, often in substantial numbers, in young mice. Of the 40 mice, now aged 15-18 months, 11 (27%) have died or been killed with a variety of disseminated lymphomas. The remainder suffer from ataxia noted around the age of one year and currently under investigation.

Yours faithfully,
J.F. LOUTIT
K.M.S. TOWNSEND
J.F. KNOWLES

MRC Radiobiology Unit, Harwell, Didcot, Oxon., UK

1 Roder J. and Duwe A., *Nature* 278, 451-453; 1979
2 Talmadge J.E., Meyers K.M., Prieur D.J. and Starkey J.R. *Nature* 284, 622-624; 1980
3 Kärre K., Klein G.O., Kiessling R., Klein G. and Roder J.C. *Nature* 284, 624-626; 1980
4 Roder J., Haliotis T., Klein M., Korec S., Jett J.R., Ortaldo J., Heberman R.B., Katz P. and Fauci A.S. *Nature* 284, 553; 1980
5 Padgett G.A. *Adv. vet. Sci.* 12, 240-284; 1968
6 Ash P., Loutit J.F., and Townsend K.M.S. *J. Path* (In press).
7 Ash P., Loutit J.F., and Townsend K.M.S. *Nature* 283, 669-670; 1980

What should be called a lectin?

SIR, — During the past decade, interest in lectins (also referred to as agglutinins, phytohemagglutinins, phytoagglutinins and protectins) has increased enormously. The term lectin has frequently been used to describe substances which differ markedly from those classically considered lectins, that is plant seed carbohydrate binding proteins. Nevertheless, the discovery of lectin-like substances in widely diverse sources (bacteria, fungi, fish sera, snails, *etc*) appears to warrant an expansion of the term. For the sake of clarity we would suggest the following definition of "lectin".

A lectin[1] (from the Latin *legere*: to chose) is a sugar-binding protein or glycoprotein of non-immune origin which agglutinates cells and/or precipitates glycoconjugates.
● Lectins bear at least two sugar-binding sites, agglutinate animal and plant cells (most commonly erythrocytes, unmodified or enzyme-treated) and/or precipitate polysaccharides, glycoproteins and glycolipids.
● The specificity of a lectin is usuallly defined in terms of the mono-saccharide(s) or simple oligosaccharides that inhibit lectin-induced agglutination (or precipitation or aggregation) reactions.

● Although first discovered in plants, lectins also have been found in many organisms from bacteria to mammals. A lectin may be soluble in biological fluids (eg concanavalin A) or membrane-bound (eg rabbit or rat liver lectins).
● There are several other types of sugar-binding proteins including sugar specific enzymes (glycosidases, glycosyltransferases, glycosylkinases, glycosylpermeases, glycosylepimerases . . .), transport proteins, hormones (thyroid-stimulating hormone, follicle-stimulating hormone, . . .) and toxins (ricin, abrin, modeccin . . .), etc.

Under some conditions, sugar-specific enzymes with multiple combining sites agglutinate cells (and/or precipitate glycoconjugates) and so act as a lectin.

In spite of similarities to true lectins from the same source, toxins — which bear only one sugar-binding site — should not be called lectins since they do not agglutinate cells or precipitate glycoconjugates.

Yours faithfully,
IRWIN J. GOLDSTEIN
University of Michigan, Ann Arbor, Michigan, US
R. COLIN HUGHES
National Institute for Medical Research, Mill Hill, London, UK
MICHEL MONSIGNY
Centre de Biophysique Moleculaire, Universitie d'Orleans, France
TOSHIAKI OSAWA
Faculty of Pharmaceutical Sciences, University of Tokyo, Japan
NATHAN SHARON
The Weizmann Institute of Sciences, Rehovot, Israel

1. Boyd, W.C. and Slapeigh, E., Specific precipitating activity of plant agglutinins (lectins), *Science* 119, 419; 1954.

Thought for lowly locusts

SIR, — We were surprised, nay disappointed by the conclusion to your article (24 April, page 659) entitled 'Pores for thought', namely "There is every reason to believe . . . and will be followed by those of channels induced by a variety of neurotransmitters'. May we remind you that *Nature* published a paper last year entitled 'Single glutamate activated channels on locust muscle' (**278**, 643; 1979). Are we to believe that glutamate is not a serious contender as a transmitter? Perhaps the lowly status of locusts precludes them from serious consideration by Acting Editors of eminent journals.

Yours faithfully,
P.N.R. USHERWOOD   K.A.F. GRATION
The University of Nottingham, UK

Amanda and the scientists: a verse on syntax

SIR, — The following verses are intended to both amuse and instruct your readers, many of whom, judged by their contributions to your pages, are guilty of faults of syntax:

"Papa," said Amanda, "I want to know what
These scientists mean when they write:
'The dye was identified using a plot
Of *E* against wavelength of light.'

"Or here: 'The bacilli were easily seen
When using high magnification

And judging by leucocytes found in the spleen
They had caused an acute inflammation.'

"And in *Astronom. Rev.* I read: 'Bearing in mind
The value ascribed to log *g*
Circinus X-1 is now better defined
As a neutron low-mass binary.'

"But can germs use a microscope, dyestuffs a plot?
Are bacilli with judgement endowed?
Is it logs on the mind that makes neutron stars hot?
I protest that my mind's in a cloud."

Said Papa, "Your confusion is natural enough
But in time you will find it amusing
To know you can always spot scientists' stuff
By this typical misuse of using.

"Misattached participles are constantly seen
In scientists' journals today
For scientists rarely can say what they mean
Or, in consequence, mean what they say.

"They treat with derision linguistic precision,
Their syntactical errors are massive
And chiefly because of the quaint superstition
That the Voice of true Science is passive.

"Still, think of the blessings by Science bestowed:
The quasars and antibiotics;
The strontium-90, the helical code,
Carcinogens, quarks and narcotics!"

"Oh I do!" said Amanda, "Yet since you've explained
That their writings need mental translation
To be understood, I conclude that, though trained,
Most scientists lack education."

"That remark," said Papa, "though quite frequently heard
No iota of difference will make:
They language and logic abuse undeterred
With a confidence nothing can shake.

"To a study of leptons or nebulous Crabs
Ne'ertheless you may one day aspire.
For a start go and visit the Veterinary labs
And admire what there is to admire."

"Yes I will!" said Amanda, and seizing her coat
Ran off to that innocent band
Who were busy improving Rebecca the goat
By transplanting her mammary gland.

Yours faithfully,
R.F. GLASCOCK
With acknowledgements to Belloc.
Reading, UK

Taxi illusion — explained

SIR, — Surely the explanation of the "taxi illusion" (24 April, page 658) is as follows:—

Suppose the taxi is travelling at speed *V*. The passenger, looking back through the rear windscreen sees objects along the road receding at speed *V* relative to the taxi.

Looking forward, he sees the reflected images of those objects, apparently moving forward at speed *V* relative to the taxi.

He sees the images against a background of real objects seen through the front windscreen moving towards the taxi at speed *V*.

The reflected images therefore appear to be passing the real objects at a speed 2*V*.

Yours faithfully,
J.P. FREEMAN
8, Vicarage Close, Ravensden, Bedford, UK

NEWS AND VIEWS

Icebergs: technology for the future

from Herbert E. Huppert

EVERY year some 5000 icebergs, totalling 10^{12} m^3 of ice, are calved from Antarctic glaciers and ice shelves. Each iceberg consists of approximately 10^8 tons of pure fresh water. It drifts for a number of years under the influence of the currents and the winds, gradually breaking up and melting into the Southern Ocean. Occasionally, icebergs drift as far as 30°S, and may influence regional climate as well as local weather. At the time of calving each iceberg has a flat top and vertical sides which plunge some 200m into the water. After several years they may be worn into very convoluted shapes as can be seen in the cover illustration.

A recent conference on The Use of Icebergs* was mainly devoted to discussions of the physical characteristics of icebergs, including the way they break and roll over, their melt-rate, and the feasibility of capturing icebergs and towing them to Australia, South Africa, California or Saudi Arabia, where they could be used as a supply of fresh water.

Icebergs break due to the flexural strains induced by ocean swell and differential melting. Breaking can be enormously enhanced by the presence of flaws such as the cracks and deep crevasses that are frequently found in ice shelves. P. Wadhams (Cambridge University) presented calculations for the elastic response of a perfect, two-dimensional ice sheet to a given swell-induced pressure distribution at the base of the ice. The results yielded the maximum strain as a function of the amplitude of swell and size of the ice, the ice fracturing when the strain exceeds a postulated breaking strain. His calculations suggest that large ice sheets will not be broken up in seas which can destroy smaller sheets. Only very large icebergs would thus be expected to remain intact as they drift into regions far from the Antarctic coast. This fits well with the

observations that few medium-sized icebergs are seen in these areas. O. Orheim (Norsk Polarinstitutt, Oslo) reported that the 1978/9 Norwegian Antarctic Research Expedition found very few crevasses at the base of the 24 tabular icebergs on which they landed. If this is generally true, it suggests that icebergs are calved from the ice shelf along every basal crevasse, although it is possible that the ice around each crevasse had melted since calving.

The processes of iceberg melting were surveyed by H. E. Huppert (Cambridge University), who argued that the base of an iceberg was likely to melt less than the vertical sides. Melting at the sides of an iceberg into an ocean of uniform density leads to a turbulent, entraining plume containing upwardly moving melt water mixed with oceanic salty water. In regions where the ocean is vertically stratified, the melt water largely flows out in a horizontal series of layers (Huppert & Turner, *Nature*, **271**, 46; 1978 and *J. Fluid Mech.*, in press). There was evidence of both forms of convection in measurements taken around a grounded iceberg in Conception Bay, Newfoundland by E. G. Josberger (Oregon State University). An experiment in which a block of ice 1m × 0.5m × 0.25m was melted into water at approximately 20°C and 35°/oo was described by D. S. Russell-Head (University of Melbourne). Under these conditions it appeared that the basal melt rate was comparable to that for the vertical walls. This is possibly due to melt water formed at the base being able to flow up the sides.

Calculations for the frequencies of oscillation of an iceberg of given shape, and the shapes which lead to instability and hence roll-over, were the subject of a number of presentations. J. F. Nye (University of Bristol) presented an analysis based on catastrophe theory. From Nye's results it can be inferred that if the melt-rate increases with increasing depth the iceberg remains stable and is unlikely to roll over. This melting pattern was noted in the experiments above but in the Antarctic the melt-rate may be sufficiently influenced by local variations

in temperature and current speed to alter the resultant geometrical shape. All the calculations neglected the induced motion in the water, although this has been found by naval architects to be important (J. N. Newman, *Marine Hydrodynamics*, M.I.T. Press).

A number of results are already available from the 1978/9 Norwegian Antarctic Research Expedition. This was one of the first expeditions to obtain field data from Antarctic icebergs rather than just ice shelves. South of about 66°S, the measured annual melting was less than a few centimeters. Measurements of the temperature of the upper 10m of the bergs indicated that the temperature rose above that of the –20°C of the ice shelf to –5°C and higher. The expedition employed a sidescanning sonar to determine the underwater shapes of icebergs and ice shelves. The most exciting result, reported by B. A Fossum (Continental Shelf Institute, Trondheim), is the discovery of an underwater ram of ice protruding more than 180m at a depth of 100m from the ice wall at Kapp Norvegia. This contrasts with the completely vertical face mapped at Blåenga which is less than 100km away.

Iceberg Transport International have carried out a number of scaled towing tests and some of the results were reported by F. Mauviel (Iceberg Transport International, Paris). The tests consisted of towing a wooden 1/100 scaled model of a tabular iceberg in Brienz Lake, Switzerland, and a steel 1/60 model in St. Malo Harbour, France. Propulsion was provided by outboard motors, or by sails, or by hauling on lines attached to a very large parachute drogue ahead of the model. The last means of propulsion appears to be the most efficient. Extrapolating from the test results, Mauviel estimated that a reasonable efficiency could be achieved by using two drogues of 10^5 m^2 to propel an

Herbert E. Huppert is in the Department of Applied Mathematics and Theoretical Physics, University of Cambridge.

iceberg through the water at a speed of 0.5 knots. The two drogues would be pulled alternately, operating, in principle, like the hands of a swimmer doing the Australian crawl. The drag acting on the models was noted to be a fairly strong function of shape and to be least for an "iceberg" whose maximum girth is amidships and whose vertical walls are tapered so that the bow and stern width are approximately 3/5 of the central width. It is envisaged that the next series of tests will involve an actual Arctic iceberg that is roughly 1/10 the size of an Antarctic berg.

A study by D. J. DeMarle (Rochester Institute of Technology, New York) focused on the feasibility of processing icebergs in Saldanha Bay, on the west coast of South Africa. The region has been listed as a future metropolitan growth area by the South African Department of

Environmental Planning. Instead of melting the iceberg on arrival, DeMarle proposed that it be mined using existing technology. A slurry of ice fragments and water would then be pumped ashore via an ocean pipeline. The operation might be powered by the waste heat of a nearby industrial complex, for which a large cold sink could help to increase efficiency.

M. W. Holdgate (Department of the Environment, UK) highlighted the audacious simplicity and social benefits of using icebergs as an inexhaustible source of water. However, such a scheme is not without dangers, not only because of accidents which could result from a stream of broken off icebergs being abandoned in shipping lanes but also because we have little idea of the environmental effects of moving icebergs around the world. □

of available SRS, so described because the bulk of the research over this period concentrated on material chemically released with the ionophore A23189, rather than the immunologically generated SRS-A.

In May 1979, at the international prostaglandin conference in Washington, Bengt Samuelsson of the Karakinska Institute in Stockholm, in collaboration with Borgeat, Hammarstrom and Murphy described the work which led to the characterization of the leukotriene (LT) structures LTA, LTB and LTC from a murine mastocytoma cell line and from rabbit polymorpho-nuclear leukocytes. LTA was shown to be 5.6 epoxyarachidonic acid, LTB a dihydroxy-arachidonic acid and LTC as 5 hydroxy 6 cysteinyl arachidonic acid. His suggested name derived from the leucocytes which release the material and the conjugated triene system of double bonds in the structure. These double bonds were also responsible for the chromophore at around 280 nm, an observation made by both Piper's and Parker's groups.

A relationship was suggested between this chemically released SRS, now to be known as leukotriene C, and SRS-A but the picture was not yet complete. At the end of 1979, and in early 1980 Samuelsson, in collaboration with the chemical group of Corey at Harvard, described LTC as glutathionyl hydroxy arachidonate. Comparison of the biological activities of the natural with totally synthesized material showed them to be identical. It should be stressed, however, that this natural material was chemically released and so could not be correctly called SRS-A. Also, early in 1980, Piper and Morris characterized an SRS chemically released from guinea pig lung as glycly-cysteinyl hydroxy arachidonate, differing from the LTC described by Corey and Samuelsson by a glutamic acid residue.

SRS-A and the leukotrienes

from W. Dawson

THE discovery of a new class of biologically active compounds is always exciting, even at the present time when knowledge is advancing so rapidly.

The leukotrienes are a new structural class deriving from arachidonic acid, a precursor which has already given us the prostaglandins, thromboxanes, prostacyclin and various hydroxy fatty acids. The systems from which the leukotrienes have been released and characterized are closely related to immediate hyper-sensitivity reactions and it has been proposed that SRS-A, slow reacting substance of anaphylaxis is a member of the leukotriene family.

Slow reacting substances (SRS) are so-called because of the characteristic slow contractile response they induce in smooth muscle preparations *in vitro*. The original SRS from lung tissue was described by Kellaway and Trethewie in 1940, being released from guinea pig lung by snake venom. In a series of papers in the early 1950's Brocklehurst isolated and characterized a similar substance released from guinea pig lung following anaphylactic challenge and named it SRS-A. He later identified a similar product released *in vitro* from human lung, derived from an asthmatic person in response to the specific allergen. This work clearly linked SRS-A with the long lasting bronchoconstriction experienced by asthmatics.

For the next 25 years many research groups attempted to identify the chemical structure of SRS-A, notably those of Brocklehurst himself in England and Austen with the late Robert Orange in the USA. Although advances were made, the structure remained elusive. Undoubtedly the extreme potency of SRS-A, the relatively small amounts of material available, and its unusual physico-chemical properties were the major causing slow progres of this research.

During the 1960's and early 1970's the prostaglandin (PG) family of structures were identified and their pharmacology described. It seemed natural that the analytical challenge of SRS-A should attract workers in the PG field and within a relatively short period of time publications from many research groups appeared in the literature. The independent work of Parker, Piper and Bach all suggested incorporation of radiolabelled arachidonate into SRS-A-like biological activity whilst two groups, at St. Louis and Lilly, showed incorporation of 35 sulphur. The Harvard group identified sulphur by spark emission spectroscopy in their SRS-A preparation and it seemed clear that it was only a matter of time before the structure was revealed.

During 1978 and early 1979, both Parker and Jakschik in St. Louis and Piper and Morris in London suggested various functional groupings which they felt were present in the molecule. In particular, the chromophore at 278-280 nm seemed a key to the purification of the minute amounts

In this issue of *Nature* (p. 104) Piper and Morris describe the first characterization of immunologically released SRS-A from guinea pig lung, achieved with a novel mass spectrometric procedure, and show that it is identical with the chemically released material released from this tissue.

Developments in this field are so rapid, however, that Samuelsson described the same compound at the Winter Prostaglandin Conference in Snowbird, Utah this April and showed that it was formed from leukotriene C by the enzyme A-glutamyltranspeptidase. He named it leukotriene D and described, in collaboration with a number of his colleagues, various aspects of the pharmacology of the leukotriene compounds: A, B, C and D.

It is pertinent to note that the majority of the data presented by the various groups is chemical in nature and the biological activity of these compounds will need to be clearly defined. No doubt in the ensuing months biological flesh will be put on these exciting chemical bones. □

W. Dawson is in the Lilly Research Centre Ltd., Windlesham, UK.

Is the homing pigeon's map geomagnetic?

from Bruce R. Moore

RACING pigeons released six hundred miles from home often return within the day. Their remarkable performance reflects true navigation, not piloting or random search. The animals are known to obtain directional information from the sun, and appear to possess, in addition, a magnetic compass. Although the precise mechanism of magnetic detection remains unknown, two possible receptors have now been identified (see Presti & Pettigrew, this issue of *Nature*, p. 99). Moreover, there is evidence that the earth's field may provide not merely directional, but also positional, information: a compass, but also a map.

The pigeon's use of a solar compass has been shown in several ways but most dramatically in a demonstration in which the birds were made to fly, essentially, north, south, east or west by phase-shifting their diurnal rhythms (Schmidt-Koenig, *Cold Spr. Hrbr. Symp. Quant. Biol.* **25**, 389; 1960). Normal animals treat the direction of the noon sun as south and, when released, "home" properly. If, however, their diurnal rhythms have been advanced by six hours, they treat the sun's noon azimuth as west, and if retarded by six hours, as east; such animals fly 90° left or right of home. Others, phase-shifted by a full 12 hours, err by 180°. In each case the birds are seen to correct for the sun's apparent movement at an average rate near 15°/hour.

"Clock-shift" experiments such as these work, and should work, only when the sun is visible. When the sky is heavily overcast, experienced birds are still able to home, whatever the phase of their rhythms (Keeton, *Science* **165**, 922; 1969). Obviously, then, there is an another mechanism besides the solar compass. This alternative appears to be magnetic.

The seminal paper on magnetic effects was that of Keeton (*Proc. natn. Acad. Sci. U.S.A.* **68**, 102; 1971) which showed that fastening strong magnets to the backs of experienced birds interfered with their orientation on sunless days. Three years later, Keeton *et al.* (*J. comp. Physiol. A.* **95**, 95; 1974) found that pigeons' bearings were affected by even minor fluctuations in the geomagnetic field. Changes of less than one milligauss — a five-hundredth of the natural field — were accompanied by appreciable anti-clockwise deflections of the birds' initial flight bearings. This was confirmed by Larkin and Keeton (*J. comp. Physiol. A.* **110**, 227; 1976); and again by Richardson (*Ibis* **118**, 309; 1976) in observation of diurnal migrants. Again with migrants, Wiltschko and Wiltschko (*Science* **176**, 62; 1972) appeared to show that the magnetic receptor, whatever and wherever it might be, reacted not simply to

the horizontal component of the earth's field but, rather, to its direction of inclination; Walcott and Green (*Science* **184**, 180; 1974) reported consonant findings with pigeons.

The nature and location of the magnetic receptor remained a mystery, but the literature provided several clues: the experiments of Keeton and of Walcott and Green suggested that the organ should first be sought in the animals' heads or necks; additionally, it was known that organisms as diverse as bacteria (Blakemore, *Science* **190**, 377; 1975), molluscs (Lowenstam, *Science* **156**, 1373; 1967) and arthropods (Gould *et al.*, *Science* **201**, 1026; 1978) are able to synthesize particles of lodestone — or, more properly, magnetite.

The same substance has now been detected in the heads and necks of homing pigeons (Walcott *et al.*, *Science* **205**, 1027; 1979; Presti & Pettigrew, this issue of *Nature*, p. 99).

Walcott *et al.* analysed more than twenty pigeon specimens and found, in each, a single small pocket of magnetic material, just beneath the skull. Electron-probe and X-ray analysis, colour, and a Curie point near 580°C, collectively revealed the material as Fe_3O_4, magnetite. Electron-microscopic analysis showed numerous small elongated particles, of a size and shape which would act as elemental magnets, i.e., as single domains (Butler & Banerjee, *J. geophys. Res.* **80**, 4049; 1975). The tissue contained perhaps 10^7 such particles. It also contained nerve fibres, although of unspecified origin.

Presti and Pettigrew did not encounter this structure in any of nineteen pigeon specimens which they examined. The reasons for the discrepancy are not entirely clear, but it should be noted that both groups of investigators were obliged to work with cumbersome glass dissecting tools, and that, perhaps as a consequence of this, the anatomic location of the structure had not been specified.

Presti and Pettigrew did, however, discover other deposits of magnetite. These were in neck muscle and surrounding tissue in both homing and feral pigeons, and various species of migrants. The authors suggest a functional connection with sensitive stretch detectors.

The physical basis of the suggested mechanism is quite straightforward. Magnetite is composed of ferrous (FeO) and ferric (Fe_2O_3) oxides, and thus contains three Fe ions. The electron spin of one of

these is characteristically opposite to the others, giving a net magnetic effect. Magnetic poles exist in pairs, and in the Earth's weak, locally-uniform field, dipoles twist toward alignment. Whether the resultant torque could be detected, even by spindle receptors, in the *Sturm-und-Drang* of flight might perhaps be debated. But, as with the subcranial structures of Walcott *et al.*, the ultimate test of the proposed receptor will be electrophysiological.

When the avian magnetic receptor is finally and unequivocally demonstrated, a fundamental functional question may remain. Does the receptor supply a compass alone, or also, perhaps, a "map"? This possibility was touched upon by a number of speakers at a recent symposium*.

The Earth's field contains positional, as well as directional, information. Between the magnetic pole and equator, the field's strength and inclination, and therefore the strengths of its horizontal and vertical components, change systematically. Any two of these measures, or any one of them plus declination, could be used to form a bicoordinate map — an imperfect map in many ways, marred by anomalies and ambiguities, and subject to distortion by magnetic storms, but nonetheless, perhaps, serviceable (Talkington, *A.A.A.S.*, 1964).

In fact, birds released near magnetic anomalies do behave as if their "maps" have been affected (Walcott in *Animal migration, navigation, and homing*, Springer-Verlag, 1978). The related effects of magnetic storms have been known for decades (Thauzies, *Arch. de Psychol.* **9**, 66; 1910), but have not received sufficient attention. The most informative data here are those of Keeton *et al.* (op. cit.) showing anti-clockwise deflection of pigeons' initial flight bearings. Storms of apparent magnitude (K_{FR}) 3-5 caused deflections of 13° at one release site and 36° at another. One might suppose that the birds' compasses had been deflected, but field rotations in magnetic storms do not reach 36°, or 13°, or even 1°. The effect on the birds was clearly magnetic (see Larkin & Keeton, *J. comp. physiol. A.* **110**, 227; 1976), but could not have involved any obvious sort of compass.

A more plausible explanation would be that the storms had somehow affected the animals' sense of location. One release site was north and slightly west of the home loft, the other west and slightly south. In each case the animals reoriented as if they had been transported several tens of kilometers southwest of their true locations. At the times of release, and throughout the

preceding nights, the magnetic storms had changed local field strengths by, at most, a few parts per thousand. The birds' sensitivity to these small changes was astonishing. The scale factors cannot be determined precisely from published data, but were of the order of 10°-40° rotation per milligauss. The birds reoriented as if the storms had produced magnetic fields (or

Bruce R. Moore is in the Department of Psychology, Dalhousie University, Halifax.

perceived fields) like those normally prevailing southwest of the actual release sites.

Many other "maps" have been proposed, based upon solar position or movement, stars, sounds, odours, coriolis forces, landmarks and inertial guidance. The data have not, to date, supported even the most plausible of these hypotheses. I think that, perhaps, the time has come to take seriously an earlier suggestion (Viguier, *Rev. Phil.* **14**, 1; 1882) that the pigeon's map is geomagnetic. ☐

Superfluorescence: macroscopic quantum fluctuations in the time domain

from Q.H.F. Vrehen, M.F.H. Schuurmans and D. Polder

THE process of spontaneous emission of radiation from a collection of excited atoms is commonly called superfluorescence. Superfluorescence produces radiation pulses which have much larger amplitudes than those which one would obtain in normal incoherent atomic radiation processes. The phenomenon is intrinsically quantum mechanical because the decay of the entire excited system is initiated by a single spontaneous emission due to quantum fluctuations.

Spontaneous emission by excited atoms has been commonly viewed as a random process in which the stored energy is released in the natural life time τ_n of the excited state. However, in 1954 Dicke[1] predicted that under certain conditions the energy is released cooperatively and in a much shorter time $\tau_R \sim \tau_n/N$, where N is the number of excited atoms. Correspondingly, the emission intensity is proportional to N^2 instead of N as expected for random individual emission. Of course, such an N^2 intensity behavior is well-known from the coherent emission of driven electric dipoles. However, excited atoms have no dipole moment; classically the atoms would not even radiate. Nevertheless, the prediction is that cooperative behaviour develops in this system and leads to an emission intensity proportional to N^2 and an emission time proportional to τ_R/N — the phenomenon of superfluorescence (SF).

The first experimental observation of SF was made by Feld and collaborators [2] in 1973. Since then SF has been observed on a number of near-infrared, infrared and optical transitions (Ref. 3 and references therein). SF from a pencil shaped volume of active atoms has been studied systematically [3] in atomic cesium. The SF emission from the pencil goes mainly

Q.H.F. Vrehen, M.F.H. Schuurmans and D. Polder are in the Philips Research Laboratories, Eindhoven, Netherlands.

through its end-faces into two narrow solid angles $\Delta\Omega$. The emitted light pulse reaches a peak intensity proportional to N^2 at the so-called delay time $\tau_D \sim (\tau_R/4) (\ln N)^2$ where $\tau_R \equiv \tau_n/(N\Delta\Omega/4\pi)$. The emitted field behaves as a classical coherent field. It has a well-defined amplitude and phase: SF emission pulses from two different samples with slightly different SF transition frequencies produce beats [3]. When the atomic system is repeatedly raised to the same excited state by single shot pulse excitation, the emitted SF pulses show macroscopic fluctuations from shot to shot in properties such as delay time and shape. These fluctuations are of quantum-mechanical origin. Such experiments provide a unique opportunity to study macroscopic quantum fluctuations in the time domain. This phenomenon has recently attracted the attention of theorists and experimentalists [3-9].

The fluctuation behavior observed here may be compared with that of a needle initially placed upright in the gravitational field. In a gaseous atmosphere atoms will collide with the needle, providing a stochastic force which turns the needle away from its upright position. With increasing polar angle θ, gravity will contribute more and more and eventually the trajectory of the needle becomes deterministic with a fixed azimuthal angle φ. When the needle is repeatedly put upright its trajectory is unpredictable as regards φ. The time it takes the needle to reach the horizontal position fluctuates from experiment to experiment. The fate of the needle is mainly determined by the unpredictable events in the early stage of the experiment.

The unpredictability of the path of the needle from one experiment to the other results from the incomplete knowledge of the system as regards the positions and velocities of the colliding atoms. In quantum mechanics a different kind of

incomplete knowledge arises. It is related to the Heisenberg uncertainty in the results of measurements on two non-commuting observables. Often this uncertainty may be accounted for classically by introducing fluctuations in the various quantities. SF is initiated by such quantum fluctuations. The initially excited atoms are in an energy eigenstate. The energy does not commute with the electric dipole moment and consequently the dipole moment is uncertain. The electromagnetic field is initially in the vacuum state, with no photons present, and in that state the electric field is uncertain. The initiation of SF requires a quantum-mechanical description. Early important contributions of this nature are due to Bonifacio and Lugiato[4]. Recently, Glauber and Haake[5] (GH) and the present authors[6] (PSV) have obtained analytical solutions for the early stage of SF evolution by linearizing the equations of motion and decoupling the forward and backward emission. In the GH work the SF starts from the quantum fluctuations describing the uncertainty in the initial dipole moment; such a description is particularly suited to the calculation of the electric field variables. In the PSV work the SF starts from the quantum fluctuations of the electro-magnetic field in vacuum; such a description is particularly useful for the calculation of the atomic variables. The two approaches have also been combined in one complete linear quantum theory[7]. Haake and collaborators[8] have extended the linear theory into the non-linear regime by assuming that the system evolution becomes already classical in the linear regime. They have numerically calculated single shot outputs.

In the above theories the various fluctuating quantities are expanded in plane wave modes passing through the pencil in all directions. The dominant gain of the modes in the solid angles $\Delta\Omega$ is used to describe the formation of two collective plane-wave-like dipole modes along the pencil axis. This collective, antenna type, behavior in the forward and the backward direction leads to the N^2 peak emission intensity and the characteristic emission time $\tau_R = \tau_n/(N\Delta\Omega/4\pi)$.

The collective behavior of the atomic system is very similar to the behavior of the needle mentioned earlier. Different single shot SF outputs correspond to different trajectories of the needle after it has been put upright. The eventually deterministic behavior of the needle corresponds to the classical behavior of the SF single shot emission field; collective field and dipole modes eventually outgrow the noise in strength. The SF pulse has a fixed but unpredictable phase and its delay time fluctuates from shot to shot.

SF is particularly interesting because the quantum fluctuations reveal themselves in the time domain. The strength of the initiating quantum noise determines the average delay time. The stochastic properties are manifest in the delay time

fluctuations. Experiment[9] confirms the prediction of the linear theory[5-7] that the strength of the initiating quantum noise is such that, on average, SF is set off by the first photon emitted spontaneously in the solid angle $\Delta\Omega$. The relative standard deviation in the delay time of 12% at $N = 10^8$ atoms, as predicted by both the linear and the more complete nonlinear[8] theory, is in good agreement with preliminary measurements by one of us[3].

It is amazing indeed that such large fluctuations, quantum mechanical in origin, can be observed in nearly classical coherent pulses containing as many as 10^8 photons. □

1. Dicke, R.H., *Phys. Rev.* 93, 99 (1954).
2. Skribanowitz N., *et al. Phys. Rev. Lett.* 30, 309 (1973); MacGillivray, J.C. & Feld, M.S., *Phys. Rev.* A14, 1169 (1976).
3. Vrehen, Q.H.F., *Laser Spectroscopy IV, Proceedings of the Fourth Int. Conf. Rottach-Egern, Fed. Rep. Germany, June 11-15, 1979,* ed. Walther, H. & Rothe K.W., Springer-Verlag, Heidelberg (1979).
4. Bonifacio, R. & Lugiato, L.A., *Phys. Rev.* A11, 1507 (1975); A12, 587 (1975).
5. Glauber, R. & Haake, F., *Phys. Lett.* 68A, 29 (1978).
6. Polder, D. *et al. Phys. Rev.* A19, 1192 (1979).
7. Schuurmans, M.F.H. & Polder, D., *Laser Spectroscopy IV, Proceedings of the Fourth Int. Conf. Rottach-Egern, Fed. Rep. Germany, 1979,* ed. Walther, H. & Rothe, K.W., Springer-Verlag, Heidelberg (1979).
8. Haake, F. *et al., Phys. Rev. Lett.* 42, 1740 (1979).
9. Vrehen, Q.H.F. & Schuurmans, M.F.H., *Phys. Rev. Lett.* 42, 224 (1979).

Sun-weather effects

from R. Gareth Williams

IN a recent paper, Nastrom and Belmont (*J. geophys. Res.*, **85** C1, 443; 1980) have found an interesting correlation between the 11-year sunspot cycle and the upper troposphere and lower stratosphere. They have thoroughly and carefully analysed data from the Northern Hemisphere for a period covering 1949 to 1973, i.e., just over two solar cycles. Their results indicate that during the winters of this period, the average position and, to a lesser extent, the strength of the jet stream and the intensity of features such as the Siberian upper level trough, have a strong correlation with solar activity. It is not so much the statistical significance of the results which is surprising, but rather that in certain areas of the hemisphere 50% of the interannual variance is explained.

In order to consider the significance of these new findings, it is necessary first to review the general state of sun-weather effects. Despite almost 180 years of study, we have little evidence to support the hypothesis that solar activity significantly effects the troposphere. There is a plethora of statistical correlations, but many of these have been produced by over-filtering and selecting the data and the remainder have nearly all failed where the data sets have been extended in time. Also, there are no thoroughly evaluated mechanisms which explain how solar activity may affect either the climate or day-to-day weather. Indeed, there is a good reason why it is difficult to establish such a causal link; the energies associated with solar activity are very small when compared with tropospheric values (see, for example, Willis, *J. Atmos. Terr. Phys.*, **40**, 513; 1974). This means that any proposed mechanism will necessarily be indirect and complicated, and also that any statistical correlations, on their own, must be viewed with caution.

So, with this particular study by Nastrom and Belmont, although there is no doubt that the correlations are real (question marks raised by the authors over spatial coverage and the number of independent stations should only alter the details of the conclusions) the crucial, unanswered question is: 'Are the correlations caused by the changes in solar activity?'. The authors suggest that their findings may eventually be explained in terms of a direct solar effect on the stratosphere/mesosphere which, in turn, could modulate the upward propagation of tropospheric energy. There is clear theoretical and experimental evidence for the August 4th, 1972 solar proton event affecting stratospheric ozone. However, relationships between the solar cycle and ozone are somewhat controversial and thought at best to be small (< 1%) (Dutsch *J. Atmos. Terr. Phys.* **41**, 771; 1979). Correlations between other stratospheric parameters and the solar cycle are similarly not yet fully accepted and are generally based on short time series. The authors refer to the atmospheric model of Bates (*Quart. J. R. Met. Soc.*, **103**, 397; 1977)

R. Gareth Williams is in the Atmospheric Physics Group, Imperial College of Science and Technology, London.

which had a troposphere that was very responsive to changes in the stratosphere. More recent work by Shutts (*Quart. J. R. Met. Soc.*, **104**, 331; 1978) shows that this sensitivity is model dependent. Both studies use linearised equations. Nastrom and Belmont cannot indicate which aspect of the solar output is thought to be causing their correlations, so we do not know where in the atmosphere any proposed mechanism should start.

If we jump the gun (by quite probably at least a decade) and assume that these correlations are solar induced, well understood physically and that these upper tropospheric effects manifest themselves at the surface, then it is appropriate to consider what their impact on climate forecasting might be. Since 11-year trends in seasonal averages have been analysed, there will be no effect on day-to-day weather forecasts, nor on the 'long range' forecasts produced a month or so in advance. However, in localised regions of the globe it might become possible, for example, to forecast a run of 2 or 3 years with, on the average, cold winters. Such forecasts could, of course, have enormous economic impact. The drawback is that it is also necessary to be able to predict solar activity!

In conclusion, it seems unlikely that this present study will, on its own, alter the opinions of most meteorologists who view sun-weather effects with extreme scepticism. Only some very solid physics will do that and much theoretical work, coupled with further data analysis, will be needed to provide such firm footing. Even though it is free of the criticisms levelled at so many previous studies in this field, this paper will undoubtedly suffer, rightly or wrongly, from so many past correlations which were later found to be invalid. □

---

100 years ago

A Parisian speculator has inaugurated the aëronautical season by a private ascent on April 25 at La Villette gasworks. The baloon, of only 300 cubic meters capacity, bore one aëronaut, with 30 kilograms of handbills, which were distributed all over Paris. The wind being slight, with a favourable direction, thousands of these prospectuses were picked up by street passengers and largely read. The whole expense of the aërial expedition, gas and everything, did not exceed 10*l*. sterling.

The French Minister of Fine Arts has entered into an agreement with the Jablochkoff Electric Light Company to light the palace during the whole of the two months devoted to the exhibition. The number of lights fed by the machinery is about 400, and the motive power regarded at about 320 horses. The inauguration was to take place on May 1, and a large crowd had congregated to witness the process. But the crank of one of the principal engines broke, and it was necessary to postpone the opening for a few days. In spite of the growing opposition of the friends of the gas company, M. Garnier, the architect of the Paris Opera, will establish a trial of the principal electrical burners, to decide which is the more really fit for use in the house.

We learn from Catania, under date April 26, that the inhabitants were apprehending an eruption of Etna. An immense cloud of smoke has been observed.

A contemporary gives the following method of illustrating the indestructibility of matter: — Two sealed glass tubes of equal weight, one of them containing oxygen and a little powdered charcoal, are prepared. The charcoal may be caused to burn away completely by heating it by means of a small flame. On placing the two tubes on a balance it will be seen that there has been no variation in weight.

from *Nature* 22; May 6, 17&18; 1880.

The emergence of Man

from Glyn Issac

ON March 12th the Royal Society and the British Academy convened a two day meeting to consider "The Emergence of Man". The central problem, presented by the chairman J. Z. Young, was to identify the kinds and timing of changes that led to human characteristics and the evolutionary pressures that produced them. The conference was characterized by the diversity of the methods being used to tackle these problems, contributions coming not only from paleontologists and anatomists but also from biochemists, immunologists, archaeologists and social psychologists.

Garniss Curtis (University of California, Berkeley) summarised geochronological information on the dates of important anatomical changes. In particular, evidence from fossils and footprints now demonstrates that bipedal locomotion was adopted between 3 and 4 million years ago. The age of the oldest fossils that show significant brain enlargement and which are classified into a species of the genus *Homo* has been the subject of controversy. A large series of new potassium-argon and fission track dates now all show that Koobi Fora early *Homo* specimens, including skull 1470, are close in age to the Olduvai Bed I *Homo habilis* fossils, that is between 1.7 and 2.0 million years in age. (*Nature* **283**: 368; 1980).

Elwin Simons (Duke University) reviewed information from fossils of the forerunners of bipedal hominids. Formerly the *Ramapithecus* specimens from the Siwaliks and from Kenya have seemed the most likely fossil ancestors of man. Simons showed that while this is still possible a spate of discoveries of fossils of *Ramapithecus*-like creatures in different parts of Eurasia complicates interpretations. These new finds from Greece, Hungary, Turkey and China indicate wider geographic range and more diversity than had been expected. Further study and the recovery of more associated postcranial material is needed before the phylogenetic relationships of the various forms can be regarded as settled. The oldest securely dated, substantial sample of early hominid skeletal reamins are the 3 to 3½ million year old fossils from the Afar in Ethiopia. Russel Tuttle (University of Chicago) reported briefly on features of the Afar hand and foot bones. He indicated that in spite of numerous primitive and ape-like characteristics there was evidence of

Glyn Isaac is in the Department of Anthropology, University of California, Berkeley.

anatomical shifts in the human direction. He was confident that the hands could have made and used tools and he showed that even ape hands have considerable ability in this regard.

J. Lowenstein (University of California, San Francisco) reported on some entirely new research which could have far reaching effects in the testing of phylogenetic hypotheses. He succeeded in extracting small samples of collagen, albumin and transferrin from fossils, and using the techniques of radio-immuno-assay he has succeeded in measuring immunological differences between the fossil proteins and living organisms. A series of tests, including on forms such as fossil mammoths, fossil bison and various marsupials have indicated the taxonomic reliability of the method. Clearly, when determinations have been made for *Ramapithecus* the results could help to settle the long-standing controversy over the date of divergence between apes and hominids.

The meeting circled rather warily round its central challenge — the evolution of the human brain and its relation to human abilities. R. E. Passingham (Oxford University) reported on new experimental work that explored the function of Broca's area. It seems likely that the area does not control sound production itself but rather the way in which sounds are assembled into sequences. Chimpanzees may have no need for such an area because their natural calls are not made up by varying the sequential order of elementary units. It was suggested that the development of such centres, where intricate sequences of motor control impulses are sent to a central organ, is accompanied by the development of dominance by one of the cerebral hemispheres. The localisation of motor control over human language in one hemisphere is paralleled by similar neural mechanisms in song birds and Passingham predicted that lateralisation might also be found in 'singing' cetaceans. The reason for lateralisation may be simply be to avoid interference from two controlling centres.

Ralph Holloway (Columbia University, New York) reported on the development of new techniques for establishing quantitative models of the shapes of human and hominid cranial endocasts. Not only have several hominid taxa turned out to be distinguishable from each other but some brain regions where differences are strongly represented; notably the lower parietal lobule, the anterior occipital zone and the dorsoanterior region of the frontal lobe, have been identified. The integration of this kind of research with information on brain function is clearly of importance.

Tool making and archaeology were also explored as sources of evidence regarding developments in brain function. Tobias pointed out that the transition to bipedal locomotion and the acquisition of enhanced manipulative abilities occurred long before the fossil record gave any indications of major changes in brain form

and size. Previously he had advocated tools as the crucial innovation, now he suggests instead that about 2 million years ago a situation arose in which biological and cultural evolution were in a positive reciprocal feedback relationship. In this "autocatalytic system", speech, along with tools, was a crucial component.

A somewhat different view was presented by Glyn Isaac (University of California, Berkeley). He suggested that the early representatives of the genus *Homo*, who between 1-1/2 to 2 million years ago formed the oldest known archaeological sites at the Omo, Olduvai, Koobi Fora and elsewhere, were non-taking, non-human hominids. The formation at that time of clusters of artefacts and of broken up bones does, however, encourage the hypothesis that the hominids had a social system involving food-sharing. This system could in turn have created novel selection pressures towards the development of language.

Further archaeological evidence was reported by Peter Jones (Oxford University). In experiments at Olduvai he made stone tools similar to those found at various Acheulian sites, in each case using the correct local raw material. The raw material has a strong influence on the finished form of the tool; this may well raise problems for our understanding of the development of tool making.

A new approach which may allow us to determine the diet and nutrition of early man was described by Alan Walker (John Hopkins University, Baltimore). Scanning electron microscopy of the occlusal surfaces of cheek teeth allows us, at least, to clearly state what early man was not eating. The early hominid species were not feeding either on grass (including grass seed heads) nor were they crunching bones in their jaws. The wear and polish found on early hominid teeth is comparable to that found on primates and other forms which feed on fruits and soft leaves. Biochemical studies also suggest that the robust australopithecines were not eating foods that required a different pattern of mastication from that of the gracile forms but simply had to process more food per jaw movement.

A dramatic find was described by Mary Leakey. A trail of footprints discovered at Laetoli in Tanzania has been shown to date to between 3-1/2 and 4 million years ago. Leakey believes that the trail belongs to a phase when human ancestors had become upright bipeds with their hands free of locomotor function but when involvement in stone tool making had not yet begun.

The meeting clearly brought out a variety of new approaches. However, such important problems as the circumstances surrounding the adoption of bipedal locomotion, the possible role of dietary shifts in guiding human evolution and the nature of selection pressures favouring brain development, all remain to be resolved. □

REVIEW ARTICLE

Calmodulin—an intracellular calcium receptor

Anthony R. Means & John R. Dedman

Department of Cell Biology, Baylor College of Medicine, Houston, Texas 77030

Calmodulin, a protein that binds calcium with high affinity and specificity, is structurally conserved and functionally preserved throughout the animal and plant kingdoms. It serves as an intracellular Ca^{2+}-receptor and mediates the Ca^{2+} regulation of cyclic nucleotide and glycogen metabolism, secretion, motility and Ca^{2+} transport. Calmodulin is also a dynamic component of the mitotic apparatus.

CALCIUM is involved in regulating a variety of cellular enzyme systems and in most types of cell motility[1-3]. The possibility that Ca^{2+} might not act in its free ionic form but rather requires the presence of a binding protein was first suggested by Meyer *et al.*[4] who reported that Ca^{2+} was necessary for the activity of muscle phosphorylase kinase. Bradham *et al.*[5] demonstrated the inhibition of bovine brain adenylate cyclase by EGTA and its reversal by Ca^{2+}. Kakiuchi *et al.*[6] and Cheung[7] independently discovered a heat-stable protein activator of brain cyclic nucleotide phosphodiesterase and 2 years later, Wolff and Siegel[8] purified a Ca^{2+}-binding protein from bovine brain. Weisenberg[9] found that neurotubules were destabilised in micromolar Ca^{2+} and Bond and Clough[10] found that a soluble protein fraction from haemolysates stimulated the activity of red blood cell Ca^{2+}-Mg^{2+}-ATPase. Pires *et al.*[11] discovered that a specific skeletal muscle myosin light chain kinase was dependent on Ca^{2+} for optimal activity.

It is now known that the same Ca^{2+}-binding protein acts as a mediator of Ca^{2+} regulation in each of these systems. Because it modulates enzyme activities in a Ca^{2+}-dependent manner, this Ca^{2+}-binding protein is now commonly known as calmodulin. As shown in Table 1, calmodulin regulates a number of fundamental cellular activities such as cyclic nucleotide and glycogen metabolism, intracellular motility (microtubules and microfilaments), and calcium transport as well as less defined Ca^{2+}-dependent protein kinases. Since we have been particularly interested in correlating the cellular and subcellular localisation of the protein with mechanistic studies carried out in defined biochemical systems, it has been necessary to determine the major physicochemical properties of the protein, to produce monospecific calmodulin antibodies, and to use these antibodies to answer a number of specific biological questions. In this review we will summarise our findings and how they integrate with the many other studies on calmodulin.

Physicochemical properties of calmodulin

Calmodulin exists as a monomer of molecular weight (MW) 17,000 and in the presence of Ca^{2+} resists denaturation (boiling, 8 M urea, 1% SDS)[12]. It is well established that calmodulin contains four calcium binding sites although reported affinity and specificity of the sites vary considerably. Binding of Ca^{2+} to any one of the four equivalent sites results in a conformational change. In this state over 50% of the molecule exists in an α-helical configuration. This conformational change is required in order for calmodulin to regulate any of the enzyme systems listed in Table 1. Data from our laboratory reveal that whereas phosphodiesterase activation can occur maximally with only one Ca^{2+} bound, the effect on microtubule depolymerisation requires all four sites to be filled. Thus it is possible that the

fractional occupancy of the Ca^{2+} binding sites may dictate the systems regulated by calmodulin and help to explain how this protein can be involved in such diverse biological processes.

Calmodulin from rat[13], cow[14] and the marine coelenterate *Renilla reniformis*[15] has been sequenced. It has 148 amino acid residues with no more than six conservative amino acid substitutions and only one of these in a calcium-binding domain. The protein is devoid of cysteine and tryptophan and contains a single histidine. The high ratio of phenylalanine to tyrosine (8:2) is reflected in the distinctive ultraviolet absorption profile and low molar extinction coefficient[12]; the high ratio of acidic to basic residues (2.7) accounts for the low isoelectric point (3.9)[12]. The most distinctive feature of the protein molecule is that the epsilon amino group of lysine 115 is post-transcriptionally trimethylated[16]. This modification preserves the positive charge and may influence the interaction of calmodulin with its multiple binding proteins, by analogy with the claim that trimethylation of yeast cytochrome *c* enhances its interaction with cytochrome oxidase[17].

Homology with troponin C

Many similarities exist between calmodulin and skeletal muscle troponin-C (TnC). These proteins cross-react in their respective biological systems[18-21]. Indeed, Kuo and Coffee[22] characterised a TnC-like protein from adrenal medulla that was subsequently shown to be calmodulin. The most obvious sequence difference between calmodulin and troponin C from rabbit skeletal muscle (STnC) or bovine cardiac muscle (CTnC) is that calmodulin is 7 or 8 amino acids shorter at the amino terminal region. This region is evolutionarily variable in the troponin C family[23,24], suggesting limited functional importance. In addition, TnC has three extra amino acids between positions 78 and 79 of calmodulin, and a single extra residue at the C-terminus. There is 45% direct homology between the two proteins, increasing to 78% for conservative replacements (substitution by functionally similar amino acids). The region of greatest homology is in the interior portion of the molecules (amino acids 30–77) where over 70% of the residues have exact identities. Other interesting features are the fact that all eight calmodulin phenylalanines and tyrosine-99 are invariant and the remaining tyrosine (residue 138) aligns with either a tyrosine or phenylalanine. Furthermore, 8 of the 11 calmodulin glycines seem to be invariant. It can be predicted that these glycines are located at sharp turns of the α-helical chain as is true for cytochrome *c*. Calmodulin, like the troponin C's[13,14,24] and parvalbumin[25], displays significant internal homology in and around the Ca^{2+}-binding sites. Sites I and III, and II and IV, contain high degrees of homology. These data would suggest that the Ca^{2+}-binding proteins evolved from a smaller ancestral precursor (which bound a single Ca^{2+}) by

gene duplication. Gene duplication is further suggested by the three residue deletion in calmodulin which occurs between binding domains II and III.

Antibody production

Calmodulin has proven to be a poor antigen, presumably because it is small, very acidic, and highly conserved in eukaryotic cells and tissues from diverse species. We have shown, however, that inoculation of animals (goat or sheep) with large quantities of homogenous calmodulin elicited a highly specific antibody[26,27]. Andersen *et al.*[28] also produced calmodulin antibody using alum-precipitated protein. More recently, Wallace and Cheung[29] elicited antibody to dinitrophenylated calmodulin.

Our antibody, purified by calmodulin-affinity chromatography specifically inhibits the activation of cyclic nucleotide phosphodiesterase by calmodulin[26] and specifically precipitates ^{125}I-labelled or ^{35}S-labelled calmodulin from a complex mixture of labelled protein[27].

The availability of antibody led to the development of a radioimmuno-assay (RIA) for calmodulin[27]. The immunoactivity of calmodulin in all tissues and cells is considerably greater than the activity determined by phosphodiesterase activation assay. This could be because calmodulin binding proteins in cell extracts compete with phosphodiesterase for Ca^{2+}-dependent binding, whereas the RIA is routinely performed in the presence of EGTA to prevent interference with calmodulin binding proteins. Alternatively there may be structural modifications (such as TML?) of calmodulin which prevent its interaction with some enzymes but allow association with others.

Regulation of calmodulin levels

The rate of synthesis and degradation of calmodulin in tissue culture or in tissue treated *in vivo* can be determined with an antibody precipitation technique[27]. Using this we have re-evaluated claims that there is more calmodulin in virally transformed cells than in normal counterparts not expressing the viral genome[30,31].

In both SV-3T3 and S-NRK cells, calmodulin levels were 2–3 times higher than in non-transformed counterparts and the rate of protein synthesis, including that of calmodulin, was also increased. However, whereas the rate of total protein degradation was markedly enhanced in the transformed cells, calmodulin degradation was only slightly altered. Since the doubling time of each cell type was reflected by the rate of total protein degradation, our results suggest that the degradation of calmodulin may be constitutive. Thus the elevated calmodulin levels in transformed cells are due to a general increase in protein synthesis that accompanies the transformed state.

Further evidence of the constitutive expression of calmodulin comes from experiments in which follicle-stimulating hormone (FSH) is injected into immature or hypophysectomised rats or added to culture media containing a homogeneous population of Sertoli cells[32]. Although FSH stimulates RNA and protein synthesis in Sertoli cells[33], calmodulin levels are unaltered. Similarly, although the expression of every other measured protein or enzyme in the chicken oviduct has been shown to be dependent on steroid hormones, calmodulin levels per cell remain constant regardless of the hormone environment. Collectively these data suggest that regulation of calmodulin-mediated enzymes is due to alterations in the net flux or distribution of Ca^{2+} rather than to changes in the cellular content of calmodulin.

Location of calmodulin in interphase cells

The purified, monospecific antibody has been used to localise calmodulin in a variety of animal cells by adopting the indirect immunofluorescence procedure described by Fuller *et al.*[34]. The cells were grown on sterile glass coverslips, fixed in formaldehyde and acetone, and then treated with the primary antibody: goat anti-calmodulin. After washing, the cells were exposed to a second antibody, rabbit anti-goat globulin tagged with fluorescein. Specificity of the immunofluorescence was tested by performing four controls: (1) use of preimmune goat γ-globulin fraction as the primary antibody; (2) use of the nonabsorbed affinity column material as the primary antibody; (3) pre-absorbance of the purified anti-calmodulin with a fivefold excess of homogeneous testis calmodulin; and (4) incubation of the second antibody without the primary (anti-calmodulin) antibody. The background fluorescence of the controls was quite low with only traces of nonspecific fluorescence. In interphase PtK_2 cells calmodulin was present throughout the cytoplasm yet appeared to be excluded from the nucleus[26,35]. Immunofluorescence also was observed in actin containing filaments extending, in some cases, across the entire length of the cell. A similar pattern of anti-calmodulin fluorescence was found in fibroblasts from humans, chick and *Xenopus* as well as rat Sertoli cells which are of epithelial origin[26].

The association of calmodulin with the actin containing filaments is presumably related to its role in the regulation of actomyosin ATPase activity in nonmuscle cells. Perry and associates[11] first described a calcium-dependent protein kinase in striated muscle that specifically phosphorylated the 20,000-MW light-chain (LC_{20}) of myosin. Subsequently, Yazawa and Yagi[36] purified this enzyme and discovered that it was composed of a catalytic subunit (MW ~100,000) and a calcium binding regulatory subunit (MW 20,000). This regulatory subunit was later identified by Yagi *et al.*[37] as calmodulin. Independently, Waisman *et al.*[38] described a similar skeletal muscle kinase that was regulated by calmodulin. Chick gizzard, as a form of smooth muscle, was subsequently studied with regard to the regulation of myosin ATPase activity. Again Dabrowska *et al.*[39] found that the myosin light chain kinase consisted of a catalytic and regulatory component, the latter being calmodulin. Even the myosin light chain kinase present in nonmuscle cells has been shown to be a calmodulin-dependent enzyme. This has been most carefully examined in blood platelets[39,40] and baby hamster kidney cells[18] in tissue culture. Taken together, these observations argue that calcium binds calmodulin and this complex activates the kinase to phosphorylate myosin (LC_{20}). This results in a conformational change to allow actin to come into contact with the myosin head group thus stimulating myosin ATPase activity. It has been demonstrated that such interaction results in increased tension development and presumably motility.

Localisation of calmodulin during mitosis

In mitotic cells, anti-calmodulin fluorescence was associated with the mitotic apparatus of 3T3 and PtK_2 cells[26] in all phases of mitosis (Fig. 1). Fluorescence was most intense at the spindle pole and projected towards the chromosome in a distribution
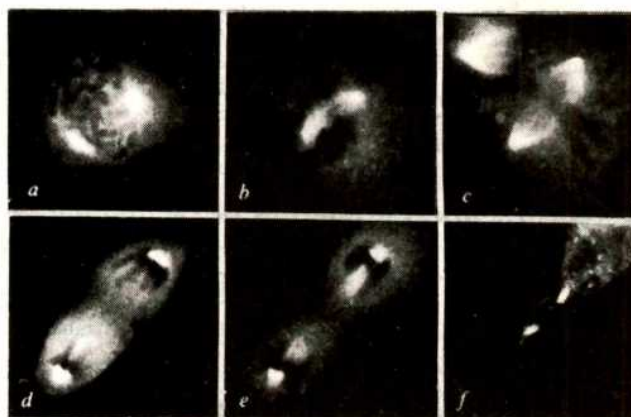
Fig. 1 Distribution of calmodulin during mitosis visualised by indirect immunofluorescence microscopy. Monolayers of rat kangaroo PtK_2 cells were plated on glass coverslips and prepared for immunofluorescent localisation of calmodulin as described by Welsh *et al.*[41]. Calmodulin antibody was raised in sheep and purified by affinity chromatography on calmodulin-Sepharose[26]. The fluorescein-labelled second antibody was rabbit anti-sheep. *a*, Prophase; *b*, prometaphase; *c*, metaphase; *d*, anaphase; *e*, late anaphase; *f*, telophase.

that gave the appearance of fibres. However, the pattern of calmodulin-specific fluorescence did not traverse the metaphase plate but instead terminated on or before reaching the chromosomes. Only in very late anaphase was calmodulin-specific fluorescence demonstrated transiently in the intrazonal region but again extremely close to the chromosomes. These data were independently confirmed by Andersen et al.[28] using an anti-calmodulin prepared in rabbits.

The distribution of calmodulin and tubulin was similar but not identical during mitosis[41]. Treatment of cells with colcemid disrupted the mitotic apparatus and caused a disappearance of specific fluorescence both for tubulin and for calmodulin. On the other hand, cytochalasin B, which under some circumstances dissociates microfilaments, had no effect on the mitotic apparatus. Similarly, no effect was noted on specific fluorescence patterns of tubulin or calmodulin. Nitrous oxide treatment causes the disorganisation of the mitotic spindle but does not result in disassembly of spindle microtubules. Treatment of Chinese hamster ovary cells with nitrous oxide disrupted spindle structure as seen with either tubulin or calmodulin specific fluorescence.

Finally, exposure of cells to low temperatures has been shown to effectively disrupt certain populations of microtubules in tissue culture. Intrazonal microtubules depolymerise when mitotic cells are incubated at 4 °C whereas the kinetochore-to-pole microtubule bundles are unaffected[42]. Experiments performed with anti-tubulin fluorescence confirmed previous studies in that the pole-to-pole microtubules were disrupted leaving only the cold stable pole-to-chromosome microtubules. On the other hand, such treatment did not affect the localisation of calmodulin. These results suggest that calmodulin might be preferentially associated with the chromosome-to-pole microtubules and thus, might be involved in the assembly/disassembly of microtubules that occurs during the movement of chromosomes from the metaphase plate to the spindle poles.

Brinkley and Cartwright[43] utilised electron microscopy to quantitate the number of microtubules present in serial sections of mitotic cells. When these data were compared to the localisation data for calmodulin, it was found that in all instances and in all phases of mitosis, the high concentrations of calmodulin were associated with low or nonexistent numbers of microtubules. Not only did this hold true in metaphase and early anaphase, but at very late anaphase, corresponding to the transient association with calmodulin on either side of the separating chromosomes, no microtubules were found in this region but were restricted to the portion of the cell corresponding to the developing cleavage furrow.

A role for calmodulin in assembly/disassembly of microtubules

It has long been known that microtubules are sensitive to calcium, although the concentration of calcium required for depolymerisation of microtubules has been somewhat controversial[9,44]. To determine whether calmodulin had any effect on microtubule polymerisation and might represent a protein involved in the assembly/disassembly processes, microtubule protein was isolated from rat brain by a modification of the temperature-dependent assembly/disassembly method described by Borisy et al.[45]. In order to control calcium concentrations, the calcium/EGTA buffer system described by Perrin and Sayce[46] and modified by Potter and Gergley[47] was used. Calmodulin alone (at 0.4 μM free calcium) or 11 μM of calcium alone caused only a slight reduction in the rate or degree of microtubule protein polymerisation[48]. However, the addition of 11 μM calcium combined with calmodulin abolished microtubule assembly. Thus, the calcium–calmodulin complex prevented the in vitro assembly of microtubule protein. In a complementary series of experiments, the calcium–calmodulin complex promoted complete disassembly of microtubules. Similar data have been reported by Kumagai and Nishida[49] using slightly different conditions and monitoring microtubule assembly/disassembly by viscometry.
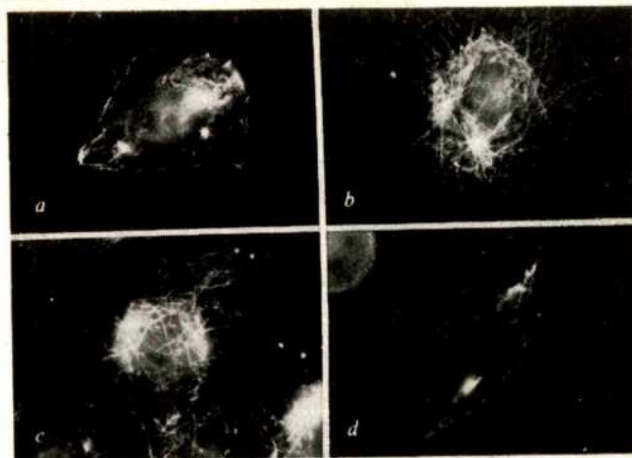
Fig. 2 Effect of Ca^{2+}-calmodulin on microtubule assembly in lysed interphase 3T3 cells. Swiss mouse 3T3 cells were treated with colcemid to disrupt the cytoplasmic microtubule network and lysed with 0.05% Triton X-100. Phosphocellulose purified 6S tubulin was added to the lysed cells and allowed to incubate for 15 min at 37°C. Microtubules were visualised by indirect immunofluorescence microscopy using rabbit anti-tubulin[34]. This system was developed by B. R. Brinkley et al.[85]. a, Colcemid-treated cells. A few short microtubules can be seen at the cell periphery. Note the highly fluorescent spots that correspond to the centrosomal regions of the cell. b, Colcemid-treated cells following addition of 6S tubulin. Numerous long microtubules can be seen which have nucleated from the organising centres seen in (a). c, Colcemid-treated cells following incubation with 6S tubulin and 11 μM free Ca^{2+}. Again numerous long microtubules are evident. d, Colcemid-treated cells incubated with 6S tubulin, 11 μM Ca^{2+} and calmodulin. Microtubule assembly from the centrosomes has been prevented.

Collectively these immunofluorescence, biochemical and ultrastructural observations have led us to propose that calmodulin functions in mitosis to depolymerise the microtubules in the polar region, shortening the kinetochore-to-pole microtubules and allowing movement of chromosomes to the poles. However, it was unclear from our studies whether calmodulin acted directly on 6S tubulin, capped the assembly end of microtubules or interacted with the microtubule associated proteins. Therefore, we have established another system to investigate the potential role of calmodulin in polymerisation of microtubules.

In the interphase cell, microtubules arise from a single organising centre associated with the centrosome[50]. It seems likely, therefore, that if the cytoplasmic microtubule network could be dissociated, and the depolymerised tubulin removed from the cell, this organising centre could be used to nucleate assembly of microtubules. If cells were incubated in the absence of tubulin a fluorescent organising centre could be seen, but no microtubules could be found emanating from the centre (Fig. 2). Addition of 6S tubulin resulted in a large number of microtubules arising from each organising centre and lengths reached up to 35 μm. If calmodulin, in the absence of calcium alone or 11 μM was added, microtubule assembly proceeded without change (Fig. 2). However, if calcium and calmodulin were added together, microtubule assembly was completely prevented. Thus, this additional procedure also demonstrated a role for calmodulin in microtubule assembly/disassembly. Microtubules examined by electron microscopy were shown not to contain high molecular weight microtubule-associated proteins. This meant that if microtubule-associated proteins were important for assembly, they would have to have been present in the lysed cell system.

Immuno-electron microscopy using horseradish peroxidase-coupled Fab fragments of anti-calmodulin showed a specific reaction product in close proximity to the centrioles and to the kinetochores (Fig. 3). In addition, calmodulin was localised in smooth endoplasmic reticulum that was parallel to the microtubule bundles in the half spindle, and also in association with membrane vesicles and mitochondrial membranes. No calmodulin was found in direct association with the pole-to-pole
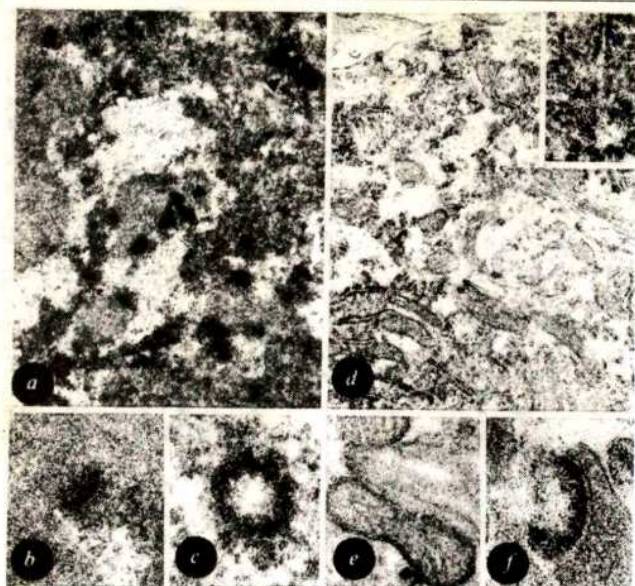
Fig. 3 Immunoelectron microscopic localisation of calmodulin. Calmodulin was localised in mitotic 3T3 cells and in rat cerebellar Purkinje cells using a calmodulin-specific Fab fragment coupled to horseradish peroxidase. The procedure was identical to that described by Lin *et al.*[86] and the experiments were performed in collaboration with Thomas Lin and B. R. Brinkley. *a*, A mitotic cell showing calmodulin reaction product around centrioles (triangle in upper left), kinetochores (triangle in middle), and some spindle microtubule bundles (×11,500). *b*, A cross-section of a centriole from another mitotic cell showing heavy deposition of reaction product around the microtubule areas. The microtubules are not evident since the sections were not counterstained. The centre of the centriole is unstained (×44,400). *d*, One Purkinje cell body from rat cerebellum showing calmodulin reaction product on free and bound ribosomes, plasma membrane, smooth endoplasmic reticulum and mitochondrial membranes (×11,000). Insert: high magnification from another area of the same cell. Dense reaction product is seen on membrane bound ribosomes and free polysomes (×25,000). *e*, High magnification of mitochondria from a neuronal dentrite. Calmodulin reaction product can be seen to decorate both outer and inner mitochondrial membranes (×30,000). *f*, A synapse from the cerebellar cortex showing heavy deposition of reaction product on a postsynaptic membrane (×46,000).

microtubules. These data support the information gained from the lysed cell system and suggest at least three possibilities for the role of calmodulin in the mitotic apparatus. First, calmodulin might directly regulate microtubule assembly/disassembly in the centrosomal regions. Second, calmodulin may regulate actomyosin. Herman and Pollard[51] have clearly demonstrated by immunofluorescence microscopy that the pattern of actin in the mitotic apparatus is very similar to what we have found for calmodulin. Unfortunately, the presence of myosin in the mitotic spindle is somewhat less clear. Nevertheless, because of the role of calmodulin in the regulation of actomyosin ATPase activity in interphase cells[18,26,35,37,39,40,52], this must be considered and is clearly a testable hypothesis. The third possibility is that calmodulin may be regulating membraneous calcium pumps. In almost all instances calmodulin was associated with various types of membranes in the mitotic cell. Since this protein, in association with calcium, has been shown to regulate the red cell calcium pump[53], the sarcoplasmic reticulum calcium pump[54] and the endoplasmic reticulum calcium pump, it is possible that one of the major roles of calmodulin in the mitotic apparatus is to regulate the concentration of calcium in the microenvironment of the spindle.

Additional roles for calmodulin

Multiple roles for calmodulin are suggested by its multiple localisation in all tissues, best illustrated in the rat cerebellum (Fig. 3). Calmodulin was concentrated in Purkinje and glial cell bodies where it was predominantly associated with free and bound ribosomes, the nuclear envelope, coated membranes of smooth and rough endoplasmic reticulum, mitochondrial and

plasma membranes[55]. Calmodulin was also found in the neuronal dendrites of the Purkinje cells, in which it coated the surface of smooth endoplasmic reticulum, small vesicles, and inner and outer mitochondrial membranes. In addition, granular calmodulin could be found in the central portion of the neuronal process. However, the neurotubules showed no specific association with calmodulin. The localisation in the neuronal process is in keeping with the suggestion by Iqbal and Ochs[56] that calmodulin may be important in mediating fast axonal transport. Calmodulin was also found by us, by Grab *et al.*[57] and by Wood *et al.*[58] on the inner surface of the postsynaptic membrane present in a variety of nervous system structures. Together these observations suggest that calmodulin is synthesised on both free and bound ribosomes and discharged into the cytosol. A large portion of this protein becomes associated with intracellular membranes. In addition, some calmodulin seems to be transported along the neuronal process to the postsynaptic membrane. At the postsynaptic membrane calmodulin may mediate the calcium effects on synaptic transmission and thus have a role in the release of neurotransmitters[59].

Satir and colleagues, in collaboration with our laboratory have revealed the presence of calmodulin in the basal bodies of cilia from *Paramecium*, *Tetrahymena* and the freshwater mussel *Elliptio*, and Jamieson *et al.* have shown that calmodulin is a constituent of the axonemal complex of cilia[60]. These data suggest that the effect of calcium on ciliary arrest might involve calmodulin. This possibility is supported by the localisation of calmodulin in mammalian sperm to the acrosome, in the midpiece associated with the fertilisation ridge and on both ends of the axonemal complex in the tail[61]. Since it seems that assembly of the axoneme can be controlled at both ends, calmodulin may have a role similar to that which it has in the mitotic apparatus during karyokinesis. In addition, the dynein of mammalian spermatozoa is similar to myosin in that it contains a Ca^{2+}-dependent ATPase[62]. It is, therefore, possible that calmodulin may modulate the dynein ATPase activity. In brief, calmodulin may be involved in promoting the attenuation of motility.

It has also been found to be associated with coated vesicles involved in receptor-mediated endocytosis. In collaboration with Linden and Roth[63], we have discovered that Ca^{2+}-calmodulin specifically binds to isolated coated vesicles with a dissociation constant of 10^{-8} M. The binding is calcium-dependent. In fact, half-maximal binding occurs at 2.4 μM free Ca^{2+} which is identical to the K_d of calmodulin for Ca^{2+} (ref. 12). The predominant calmodulin binding protein is clathrin. The biological function of calmodulin present in coated vesicles is unknown, but it is reasonable to suppose that it modulates the vesicle's calcium-dependent ATPase.

Table 1 Calmodulin-mediated processes

Process	Selected refs
Cyclic nucleotide metabolism	
Phosphodiesterase	6, 7, 71
Adenyl cyclase	71
Protein phosphorylation	
Membrane proteins	72, 73
Cytoplasmic proteins	74
Myosin light chain kinase	
Skeletal muscle	37
Smooth muscle	52
Non-muscle	18, 39, 40
Stress fibre localisation	22, 23
Microtubule assembly/disassembly	35, 41, 48
Glycogen metabolism	
Phosphorylase kinase	67, 75, 28, 29, 76, 77
Calcium flux	
Ca^{2+}-Mg^{2+} ATPase	78, 79, 80
Ca^{2+} transport	53, 54, 56
Secretion	
Intestinal ion secretion	81
Neurotransmitter release	57
Other enzyme systems	
NAD$^+$ kinase	82
Tryptophan 5'-monooxygenase	83
Phospholipase A_2	84

Receptor-mediated calcium regulation

The mechanism of action of Ca^{2+} is different from that of other metal ions. Indeed, the role of Ca^{2+} seems to be more similar to the regulatory actions of cyclic nucleotides which produce multiple metabolic effects by binding to the regulatory subunits of cyclic AMP-dependent protein kinase and thereby activating the enzyme. The specificity of the cyclic nucleotide system of any cell is determined at two levels. The first is by the receptors (for hormones and so on, that elevate the intracellular content of cyclic AMP) the membrane is endowed with. The second is which substrate(s) for the protein kinase that the cell possesses. By analogy to cyclic AMP, it has been proposed that Ca^{2+} is an intracellular second messenger[1]. Continuing this analogy, calmodulin may be considered an intracellular receptor for Ca^{2+}. Evidence consistent with this is that (1) in non-muscle cells it represents the major high affinity Ca^{2+}-binding protein; the affinity for Ca^{2+} is approximately equal to the estimated intracellular free-Ca^{2+} concentration, suggesting that physiologically active cellular Ca^{2+} is calmodulin bound; (2) no alternate function (that is, enzymatic or structural) has been demonstrated; (3) it has been structurally conserved and functionally preserved throughout both animal and plant kingdoms, suggesting that it is involved in numerous cellular activities which require an invariant mediator; (4) it would be predicted that, in order to account for its many cellular activities, calmodulin would have multiple 'acceptor' proteins and a number of the major forms have been identified (Table 1). Many more probably exist. Studies by Grand and Perry have shown that each mammalian tissue possesses a distinct set of these proteins[64], through which the specificity of Ca^{2+} action is presumably determined. Amplification of a Ca^{2+} signal, like a cyclic AMP signal, can be accomplished through the activation of specific protein kinases which in turn may affect a number of additional enzyme activities. It is likely that the discovery of calmodulin and the developing understanding of how this protein is involved in the regulation of numerous calcium mediated events will provide a link in our understanding of the interaction of calcium and cyclic nucleotides in the control of cellular metabolism.

At the moment most of the data concerning calmodulin regulation must be considered as phenomenological. What is now required is a concerted effort to understand the chemical basis for each of calmodulin's actions. This will require isolation and purification of the enzyme systems regulated by this protein. Indeed, some success has already been achieved along these lines. Phosphodiesterase[65,66], myosin light chain kinase[37,52], phosphorylase kinase[67] and ATPase[68,69] have all been purified and calmodulin stimulated adenyl cyclase[70] is reported to have been partially purified. Even when one understands the interaction of calmodulin with these enzyme systems, it will be necessary to discover how hormones regulate the activity of calmodulin. Since this protein seems to be constituently synthesised it is likely that the activity is regulated by the concentration of available calcium.

1. Rasmussen, H., Goodman, D. B. P., Freidmann, N., Allen, J. A. & Kurokawa, K. in Handbook of Physiology, Endocrinology, Section VII (ed. Aurbach, G. D.) 225–264 (Williams and Wilkins, Baltimore, 1976).
2. Rubin, R. P. Calcium and the Secretory Process (Plenum, New York, 1974).
3. Dedman, J. R., Brinkley, B. R. & Means, A. R. Adv. Cyclic Nucleotide Res. 11, 131–174 (1979).
4. Meyer, W. L., Fischer, W. H. & Krebs, E. G. Biochemistry 3, 1033–1039 (1964).
5. Bradham, L. S., Holt, D. A. & Samo, M. Biochim. biophys. Acta 201, 250–160 (1969).
6. Kakiuchi, S., Yamazaki, R. & Nakajima, H. Proc. Jap. Acad. 46, 587–591 (1970).
7. Cheung, W. Y. Biochem. biophys. Res. Commun. 33, 533–538 (1970).
8. Wolff, D. J. & Siegel, F. J. biol. Chem. 247, 4180–4185 (1972).
9. Weisenberg, R. C. Science 177, 1104–1105 (1972).
10. Bond, G. H. & Clough, D. L. Biochim. biophys. Acta 232, 592–599 (1973).
11. Pires, E., Perry, S. V. & Thomas, M. A. W. FEBS Lett. 41, 292–296 (1974).
12. Dedman, J. R., Potter, J. D., Jackson, R. L., Johnson, J. D. & Means, A. R. J. biol. Chem. 252, 8415–8522 (1977).
13. Dedman, J. R., Jackson, R. L., Schreiber, W. E. & Means, A. R. J. biol. Chem. 253, 343–346 (1977).
14. Vanaman, T. C., Sharief, F. & Watterson, D. M. in Calcium-Binding Proteins & Calcium Function (eds Wasserman, R. H. et al.) 106–116 (North-Holland, New York, 1977).
15. Vanaman, T. C. & Sharief, F. Fedn Proc. 38, 788 (1979).
16. Jackson, R. L. et al. Biochem. biophys. Res. Commun. 77, 723–729 (1977).
17. Uy, R. & Wold, F. Science 198, 890–896 (1977).
18. Yerna, M. J., Hartshorne, D. J. & Goldman, R. D. Biochemistry 18, 673–678 (1979).
19. Amphlett, G., Vanaman, T. & Perry, S. FEBS Lett. 72, 163–168 (1976).
20. Dedman, J. R., Potter, J. D. & Means, A. R. J. biol. Chem. 252, 2537–2440 (1977).
21. Cohen, P., Picton, C. & Klee, C. B. FEBS Lett. 104, 25–30 (1979).
22. Kuo, I. C. Y. & Coffee, C. J. J. biol. Chem. 251, 1603–1609 (1976).
23. Van Eerd, J.-P. & Takahashi, K. Biochemistry 15, 1171–1180 (1976).
24. Collins, J. H., Greaser, M. L., Potter, J. D. & Horn, M. J. J. biol. Chem. 252, 6356–6362 (1977).
25. Kretsinger, R. H. & Nockolds, C. E. J. biol. Chem. 248, 3313–3326 (1973).
26. Dedman, J. R., Welsh, M. J. & Means, A. R. J. biol. Chem. 253, 7515–7521 (1978).
27. Chafouleas, J. G., Dedman, J. R., Munjaal, R. P. & Means, A. R. J. biol. Chem. 254, 10262–10267 (1979).
28. Andersen, B., Osborn, M. & Weber, K. Cytobiologie 17, 354–364 (1978).
29. Wallace, R. W. & Cheung, W. Y. J. biol. Chem. 254, 6564–6571 (1979).
30. Watterson, D. M., van Eldik, J. J., Smith, R. E. & Vanaman, T. C. Proc. natn. Acad. Sci. U.S.A. 73, 2711–2715 (1976).
31. LaPorte, D. C., Gidwitz, S., Wever, M. J. & Storm, D. R. Biochem. biophys. Res. Commun. 86, 1169–1177 (1979).
32. Beale, E. G., Dedman, J. R. & Means, A. R. Endocrinology 101, 1621–1634 (1977).
33. Means, A. R., Fakunding, J. L., Huckins, C., Tindall, D. J. & Vitale, R. Rec. Prog. Horm. Res. 32, 477–527 (1976).
34. Fuller, G. M., Brinkley, B. R. & Boughter, J. M. Science 187, 948–950 (1975).
35. Welsh, M. J., Dedman, J. R., Brinkley, B. R. & Means, A. R. Proc. natn. Acad. Sci. U.S.A. 75, 1867–1871 (1978).
36. Yazawa, M. & Yagi, K. J. Biochem. 82, 287–289 (1977).
37. Yagi, K., Yazawa, M., Kakiuchi, S., Ohshima, M. & Uenishi, K. J. biol. Chem. 253, 1338–1340 (1978).
38. Waisman, D., Stevens, F. & Wang, J. J. biol. Chem. 253, 1106–1113 (1977).
39. Dabrowska, R. & Hartshorne, D. J. Biochem. biophys. Res. Commun. 85, 1352–1359 (1978).
40. Hathaway, D. R. & Adelstein, R. S. Proc. natn. Acad. Sci. U.S.A. 76, 1653–1657 (1979).
41. Welsh, M. J., Dedman, J. R., Brinkley, B. R. & Means, A. R. J. Cell Biol. 81, 624–634 (1979).
42. Brinkley, B. R. & Cartwright, J. Ann. N.Y. Acad. Sci. 253, 428–439 (1975).
43. Brinkley, B. R. & Cartwright, J. J. Cell Biol. 50, 416–431 (1971).
44. Olmstead, J. B. & Borisy, G. G. Biochemistry 14, 2996–3005 (1975).
45. Borisy, G. G., Marcum, J. M., Olmstead, J. B., Murphy, D. B. & Johnson, K. A. Ann. N.Y. Acad. Sci. 253, 107–132 (1975).
46. Perrin, D. D. & Sayce, I. G. Talanta 14, 833–842 (1967).
47. Potter, J. D. & Gergely, J. J. biol. Chem. 250, 4628–4633 (1975).
48. Marcum, J. M., Dedman, J. R., Brinkley, B. R. & Means, A. R. Proc. natn. Acad. Sci. U.S.A. 75, 3771–3775 (1978).
49. Kumagai, H. & Nishida, E. J. Biochem. 85, 1267–1274 (1979).
50. Brinkley, B. R., Fuller, G. M. & Highfield, D. P. in Cell Motility (eds Goldman, R., Pollard, T. & Rosenbaum, J.) 435–456 (Cold Spring Harbor Laboratory, New York, 1976).
51. Herman, I. M. & Pollard, T. D. J. Cell Biol. 80, 509–520 (1979).
52. Dabrowska, R., Aromatorio, D., Sherry, J. M. F. & Hartshorne, D. J. Biochemistry 17, 253–258 (1978).
53. Hinds, T. R., Larsen, F. L. & Vincenzi, F. F. Biochem. biophys. Res. Commun. 81, 455–461 (1978).
54. LePeuch, C. J., Haiech, J. & Demaille, J. G. Biochemistry 18, 5150–5157 (1979).
55. Lin, C. T., Dedman, J. R., Brinkley, B. R. & Means, A. R. J. Cell Biol. (in the press).
56. Iqbal, Z. & Ochs, S. J. Neurochemistry 31, 409–418 (1978).
57. Grab, D. J., Berzins, K., Cohen, R. S. & Siekevitz, P. J. biol. Chem. 254, 8690–8696 (1979).
58. Wood, J. G., Wallace, R. W., Whitaker, J. N. & Cheung, W. Y. J. Cell Biol. 84, 66–76 (1980).
59. DeLorenzo, R. J., Freedman, S. D., Yohe, W. B. & Maurer, S. C. Proc. natn. Acad. Sci. U.S.A. 76, 1838–1842 (1979).
60. Jamieson, G. A. Jr, Vanaman, T. C. & Blum, J. J. Proc. natn. Acad. Sci. U.S.A. 76, 6471–6475 (1979).
61. Lenz, R. W., Jones, H. P., Palevitz, B. A. & Cormier, M. J. Proc. natn. Acad. Sci. U.S.A. (in the press).
62. Voglmayr, J. K., Quinn, P. J. & White, I. G. Biol. Reprod. 1, 215–222 (1969).
63. Linden, C. D., Dedman, J. R., Chafouleas, J. G., Means, A. R. & Roth, T. F. Proc. natn. Acad. Sci. U.S.A. (in the press).
64. Grand, R. J. & Perry, S. V. Biochem. J. 183, 285–295 (1979).
65. Klee, C. B., Crouch, T. H. & Krinks, M. H. Biochemistry 18, 722–729 (1979).
66. Kincaid, R. L. & Vaughan, M. Proc. natn. Acad. Sci. U.S.A. 76, 4903–4907 (1979).
67. Cohen, P. et al. FEBS Lett. 92, 287–293 (1978).
68. Haaker, H. & Racker, E. J. biol. Chem. 254, 6598–6602 (1979).
69. Niggli, V., Penniston, J. T. & Carafoli, E. J. biol. Chem. 254, 9955–9958 (1979).
70. Westcott, K. R., LaPorte, D. C. & Storm, D. R. Proc. natn. Acad. Sci. U.S.A. 76, 204–208 (1979).
71. Bromstrom, C. O., Huang, Y. C., Breckenridge, B. N. & Wolff, D. J. Proc. natn. Acad. Sci. U.S.A. 72, 64–68 (1975).
72. Schulman, H. & Greengard, P. Nature 271, 478–479 (1978).
73. Schulman, H. & Greengard, P. Proc. natn. Acad. Sci. U.S.A. 75, 5432–5436 (1978).
74. Yamauchi, T. & Fujisawa, H. Biochem. biophys. Res. Commun. 90, 1172–1178 (1979).
75. Soderling, T. R., Srivastava, A. K., Bass, M. A. & Khatra, B. S. Proc. natn. Acad. Sci. U.S.A. 76, 2536–2540 (1970).
76. DePaoli-Roach, A. A., Roach, P. J. & Larner, J. J. biol. Chem. 254, 4212–4219 (1979).
77. Walsh, K. X., Millikin, D. M., Schlender, K. K. & Reimann, E. M. J. biol. Chem. 254, 6611–6616 (1979).
78. Gopinath, R. M. & Vincenzi, F. F. Biochem. biophys. Res. Commun. 77, 1203–1209 (1977).
79. Jarrett, H. W. & Penniston, J. T. Biochem. biophys. Res. Commun. 77, 1210–1216 (1977).
80. Sobue, K., Ichida, S., Yoshida, H., Yamazaki, R. & Kakoicjo, S. FEBS Lett. 99, 199–202 (1979).
81. Ilundian, A. & Naftalin, R. J. Nature 279, 466–468 (1979).
82. Anderson, J. M. & Cormier, M. J. Biochem. biophys. Res. Commun. 84, 595–602 (1978).
83. Yamauchi, T. & Fujisawa, H. Biochem. biophys. Res. Commun. 90, 28–35 (1979).
84. Wong, P. Y. K. & Cheung, W. Y. Biochem. biophys. Res. Commun. 90, 473–480 (1979).
85. Brinkley, B. R. et al. 37th Ann. Proc. Electron Microscop. Soc. Am. 14–17 (1979).
86. Lin, T. et al. J. Histochem. Cytochem. 23, 624–630 (1975).

ARTICLES

Mutations which alter the function of the signal sequence of the maltose binding protein of *Escherichia coli*

Huges Bedouelle*§, Philip J. Bassford Jr†, Audree V. Fowler‡, Irving Zabin‡, Jon Beckwith† & Maurice Hofnung*§

* Unité de Génie Génétique, Institut Pasteur, 75015 Paris, France
† Department of Microbiology and Molecular Genetics, Harvard Medical School, Boston, Massachusetts 02115
‡ Department of Biological Chemistry, UCLA School of Medicine and Molecular Biology Institute, University of California, Los Angeles, California 90024

The maltose binding protein of Escherichia coli *is secreted into the external periplasmic compartment of the cell by virtue of an amino-terminal signal sequence. Using DNA sequencing, we have determined the precise nature of mutations in the signal sequence which prevent the export of the maltose binding protein, causing it to accumulate in the cytoplasm in its precursor form. In most cases, the change of a single hydrophobic or uncharged amino acid to a charged amino acid within the signal sequence is sufficient to block the secretion process.*

MOST secreted proteins in both prokaryotic and eukaryotic cells are initially synthesised with an amino-terminal extension of some 15 to 30 amino acids which is subsequently excised. It has been proposed that this 'signal sequence' is responsible for initiating passage of the polypeptide through the membrane while it is still a nascent chain attached to the ribosome[1-3]. The exact mechanism by which this is accomplished, and the nature of the putative receptor in the membrane, are unknown. Among the different signal sequences thus far determined, there seems to be no significant primary sequence homology[4]. However, one feature common to all signal sequences is a central core of 9–24 predominantly hydrophobic amino acids. In most cases, this is preceded by one or more charged residues, usually lysine and/or arginine. One approach to defining those features of the signal sequence which are essential for initiating protein export is to generate mutations which alter the signal sequence of a secreted protein, resulting in the failure of the cell to export the protein from the cytoplasm.

The Gram-negative bacterium *Escherichia coli* provides a convenient system for isolating mutants which affect secretion, as genetic manipulations of it are relatively easy and many of its proteins are localised in the cell envelope, and, therefore, must be secreted through the cytoplasmic membrane. Evidence exists that signal sequences are involved in the export of proteins to at least two of the bacterial envelope compartments[5]. These compartments are the outer membrane and an aqueous layer located between the two membranes, called the periplasmic space.

One of the proteins found in the periplasmic space of *E. coli* is the maltose binding protein (MBP), a key component of the maltose transport system[6]. We recently described a selection procedure which enabled us to isolate mutants of *E. coli* which fail to secrete the MBP into the periplasm[7]. In the mutants we obtained, the MBP accumulates in the cytoplasm in its higher molecular weight precursor form. From the genetic data, we suggested that the mutations in these strains resulted in single amino acid substitutions in the MBP signal sequence. We now report the DNA sequence coding for the first 50 amino acids of

the wild-type MBP precursor, the identification of the signal sequence which was done through partial amino acid sequence determination, and the DNA sequence changes for several MBP export-defective mutants.

Partial determination of the MBP signal sequence using a *malE–lacZ* hybrid protein

Because the MBP precursor does not accumulate to appreciable amounts in wild-type cells, material for determining the MBP signal sequence was obtained from another source. We had previously isolated *E. coli* strains in which the *malE* gene encoding the MBP is genetically fused to the *lacZ* gene encoding the enzyme β-galactosidase[8]. The resultant hybrid gene codes for a hybrid protein which has at its amino-terminus an amino-terminal portion of the *malE* gene product and, at its carboxy-terminus, enzymatically active β-galactosidase. One such strain, PB4-81, synthesises a hybrid protein which is cytoplasmic and which seems, from the genetic and biochemical data, to include only a very small, amino-terminal portion of the *malE* gene product. Consequently, we suspected that this protein contained only a portion of the MBP signal sequence. Thus, this protein should provide material for a partial signal sequence determination.

The determination of the PB4-81 hybrid protein sequence was made possible by techniques developed for the sequence analysis of a hybrid protein between β-galactosidase and the *lac* repressor[9]. A partial signal sequence for alkaline phosphatase had been determined previously in this way[10]. The procedure used to generate hybrid proteins must result in the removal of at least the first 17 amino acids of wild-type β-galactosidase, thus eliminating the first methionine residue. If the amino acid sequence which replaces the normal β-galactosidase amino-terminus does not contain any methionine (other than the initiating methionine), only one new cyanogen bromide fragment (CNBr2*) should result from treatment of the hybrid protein. This proved to be the case with the hybrid β-galactosidase from strain PB4-81. Sequence analysis of the CNBr2* indicated that the first 14 residues are not derived from β-galactosidase (Table 1). These residues are derived from the

Table 1 Sequencer analysis of the *malE–lacZ* hybrid protein from strain PB4-81

Residue no.*	Amino acid identified			Residue no.*	Amino acid identified		
	Intact protein†	CNBr2*‡	CNBr2* T4§		Intact protein†	CNBr2*‡	CNBr2* T4§
1 Met	+			*16 Pro	+	+	
2 Lys	+	+		*17 Gly	+	+	
3 Ile	+	+		*18 Val	+	+	
4 Lys	+	+		*19 Thr	+	+	
5 Thr		+		*20 Gln		+	
6 Gly	+	+		*21 Leu	+	+	
7 Ala	+	+		*22 Asn		+	
8 Arg		+		*23 Arg			
9 Ile	+	+	+	*24 Leu		+	
10 Leu	+	+	+	*25 Ala		+	
11 Ala	+	+	+	*26 Ala		+	
12 Leu	+	+	+	*27 His		+	
13 Ser		+		*28 Pro			
14 Ala	+	+	+	*29 Pro		+	
15 Ser		+		*30 Phe		+	
				31 Ala		+	

All sequencing was done using 0.1 M Quadrol in a Beckman 890C sequencer. The peptides were sequenced using a dual wash program . The intact carboxymethylated protein was sequenced with a program similar to that of Hunkapiller and Hood . All other procedures were as described previously , except that recently identification was also carried out with HPLC. + Indicates that the amino acid indicated was detected. A blank indicates either an ambiguous result or that it was not possible to detect the amino acid by this technique.

* Amino acids identified with an asterisk correspond to residues 19–34 of native *E. coli* β-galactosidase.

†The hybrid β-galactosidase was purified by the same procedure as for the *lac* repressor–β-galactosidase hybrid . Strain PB4-81 was grown in a 150-l New Brunswick fermentor at 30°C in medium 63 containing 1% glycerol and 0·2% maltose. The hybrid protein was purified 40-fold with a yield of 36% based on β-galactosidase activity. It was greater than 90% pure on SDS gels[22] and migrated with a mobility close to that of wild-type β-galactosidase.

‡ The hybrid protein was carboxymethylated and digested with cyanogen bromide as described elsewhere[21]. The CNBr2* peptide was purified using CM-cellulose and SP-Sephadex ion-exchange chromatography in 8 M urea and gel filtration on Sephadex G-50 in 30% acetic acid[21]. The radioimmunoassay used to monitor purification on CNBr2* has been described previously[9]. The yield of CNBr2* from purified hybrid protein was 25%. The elution volume on Sephadex G-50 suggested a size of about 90 residues. Amino acid composition data indicated that the PB4-81 CNBr2* contains lysine whereas wild-type CNBr2 has no lysine.

§ To confirm the presence of serine at residue 14 of CNBr2*, the peptide was cleaved with trypsin and the resulting peptides purified. Amino acid analysis of CNBr2* (corresponding to residues 9–23 of the intact protein) indicated two residues of serine and three residues of leucine. Details of the protein and peptide purifications and sequence analysis will be presented elsewhere (A.V.F., I.Z., P.J.B. Jr and J.B. in preparation).

amino-terminus of the protein to which β-galactosidase has been fused, in this case, the *malE* gene product. Two factors suggested that these 14 residues, along with the amino-terminal methionine from the hybrid protein, corresponded to the first 15 amino acids of the MBP precursor. First, this 15-residue sequence, with three basic residues among the first eight followed by several predominantly hydrophobic amino acids, is similar to other signal sequences. Second, none of this sequence was encountered when the protein sequence of the amino-terminal 25 amino acids of the mature MBP was determined (data not shown, see Fig. 1 legend).

DNA sequence of the wild-type *malE* signal sequence region

Cleavage of plasmid pHC5, which carries the *malB* operon (see Fig. 2), with the restriction endonuclease *Eco*RI, generates a fragment of 1,227 base pairs, comprised of 850 base pairs from the *malB* region of the *E. coli* chromosome and 377 base pairs derived from the vector (plasmid pBR322) (Fig. 2). This *Eco*RI–*Eco*RI hybrid fragment includes the promoter-proximal portion of the *malE* gene which codes for the MBP signal sequence region. Beginning with this fragment, a region of 600 nucleotides extending from the *Eco*RI cleavage site in the *malK* (ref. 11) gene in the direction of the *malE* gene has been sequenced on both strands, using the dideoxy/nick-translation technique of Maat and Smith[12]. This region includes the entire regulatory interval between the two *malB* operons and will be described elsewhere (H.B., in preparation).

We have taken the *Eco*RI cleavage site in *malK* on the strand encoding the MBP as the origin for numbering purposes. Starting from this point and examining the sequence towards the *malE* gene, the first ATG initiation triplet which is not soon followed in phase by a nonsense triplet is at nucleotides 457–459. Just before this point, at nucleotides 443–447, there is a 5-nucleotide sequence complementary to the 3'-OH end of the 16S rRNA (Shine and Dalgarno sequence[13]). This sequence suggests the existence of a translation start which is used *in vivo*. In fact, nucleotides 457–498 correspond to the first 14 amino acids of the MBP precursor, as determined from the protein sequence of the PB4-81 *malE–lacZ* hybrid protein described

above. Nucleotides 535–600 correspond to the first 22 amino acids of the mature MBP. Consequently, we deduce that the complete MBP signal sequence, that part of the MBP precursor which is excised to yield the mature protein, must be 26 amino acids long and encoded by nucleotides 457–534 (summarised in Fig. 1 legend).

Note that the serine at residue 15 of the PB4-81 hybrid protein (Table 1) is not derived from either the *malE* or the *lacZ* gene; neither can it arise from a simple fusion of the *malE* and *lacZ* genes within a codon. This serine residue may have been generated during the *in vivo* gene fusion technique which used bacteriophage Mu to obtain the *malE–lacZ* hybrid gene[8].

Sequencing the DNA of the *malB* region of MBP export-defective mutants

From the DNA sequence of the regulatory interval between the two *malB* operons, we identified a cleavage site for endonuclease *Hinf*I at nucleotide 406, and a cleavage site for *Ava*II at nucleotide 445. Restriction analysis revealed that the enzymes *Hinf*I and *Ava*II cleaved the *Eco*RI–*Eco*RI hybrid fragment of plasmid pHC5 at only one site each, this being the one identified from the sequence (Fig. 2). Simultaneous digestion of the hybrid fragment with *Hinf*I and *Ava*II yields two large fragments, as well as one small 39-base pair fragment corresponding to nucleotides 407–445 on the numbered strand.

To determine the sequence of the putative *malE* signal sequence mutations we had previously isolated, we used the technique developed by Sanger and co-workers[14] with the 39-base pair *Hinf*I–*Ava*II fragment serving as a primer. The advantages of this technique were as follows. (1) The genetic data on these mutations indicated that they were located early in the *malE* gene[7]. (2) These mutations were isolated directly on a transducing phage carrying the region of interest. Thus, phage DNA for each of the mutants could be used as template for the sequencing procedure after strand separation. (3) The *Ava*II end of the *Hinf*I–*Ava*II fragment is located 11 nucleotides from the beginning of the *malE* gene. This allowed us to read approximately 150 nucleotides into the *malE* gene in a single experiment.

Using this procedure, we have verified the wild-type DNA

```
                                        (18-1)
           (10-1)            (14-1) (16-1)
                                         (19-1)
            Pro               Glu    Lys    ArgArg

            CCC               GAA    AAG    AGGAGG
             ↑                 ↑      ↑      ↑  ↑

ATGAAAATAAAAACAGGTGCACGCATCCTCGCATTATCCGCATTAACGACGATGATGTTTTCCGCCTCGGCTCTC

MetLysIleLysThrGlyAlaArgIleLeuAlaLeuSerAlaLeuThrThrMetMetPheSerAlaSerAlaLeu

         5            10              15             20             25


GCCAAAATCGAAGAAGGTAAACTGGTAATCTGGATTAACGGCGATAAAGGCTATAACGGTCTCGCTGAA

AlaLysIleGluGluGlyGlyLysLeuValIleTrpIleAsnGlyAspLysGlyTyrAsnGlyLeuAlaGlu
  ↑         30              35             40             45
```

Fig. 1 The DNA sequence of the first 144 nucleotides of the *malE* gene, corresponding to the first 48 amino acids of the MBP precursor. Only one strand, that with the same polarity as the *malE* message, is shown. Those amino acids underlined represent residues which were also determined from protein sequencing. The sequence beginning at residue 26 was determined on the mature MBP protein (A.V.F. and I.Z., unpublished). On the basis of protein sequencing, the evidence for glutamic acid at residue 3 of the mature MBP is tentative only. The arrow after residue 26 indicates the position at which the precursor is cleaved to yield the mature MBP. The five codon changes corresponding to the different signal sequence mutations are indicated above the position in the sequence where they occur, along with the predicted changes for the amino acid sequence.

sequence for the first 144 nucleotides of the *malE* gene which had previously been obtained by the dideoxy/nick-translation technique (Figs 1, 3).

Phenotype of MBP export-defective mutants

The mutations thought to result in MBP signal sequence alterations were initially obtained in a *malE–lacZ* hybrid gene carried on the λ transducing phage, λp72–47 (ref. 7). In this case, the hybrid gene encodes a hybrid protein that includes a substantial portion of the MBP, including the entire MBP signal sequence[8]. The mutations, which were located in the *malE* portion of the hybrid gene, were subsequently recombined into a wild-type *malE* gene on the bacterial chromosome. The resulting recombinants are Mal⁻ when scored on maltose tetrazolium agar, indicating that their ability to utilise maltose as a carbon source has been impaired. When they are induced for the expression of the *malEFG* operon, they accumulate the MBP precursor in the cytoplasm. However, these strains are not absolutely defective, for they grow slowly on maltose minimum medium and export a small amount of native MBP to the periplasm (see ref. 7). Furthermore, the mutants vary in their ability to utilise maltose, indicating that they may each affect the secretion of MBP to different extents (Table 2).

DNA sequence alterations in MBP export-defective mutants

Using the same sequencing procedure described above, we determined the DNA sequence of the promoter-proximal 144 nucleotides of the *malE* gene for nine spontaneous, independently isolated MBP export-defective mutants. The DNA used as template was obtained from the λ transducing phage on which the mutations were initially isolated (derivatives of λp72–47).

Each of the nine mutants sequenced exhibited an alteration in the region of the *malE* gene corresponding to the MBP signal sequence. Five different alterations were recognised (Fig. 7). The transition CTC (Leu) to CCC (Pro), resulting in a change in residue 10 of the MBP precursor, occurred in one mutant. The transversions GCA (Ala) to GAA (Glu) at position 14, ACG (Thr) to AAG (Lys) at position 16, and ATG (Met) to AAG (Arg) at positions 18 and 19 were encountered 3, 1, 2 and 2 times, respectively.

Discussion

We have presented here the DNA sequence of the MBP signal sequence and of mutant signal sequences which result in defective export of the maltose binding protein. The MBP signal sequence is similar to signal sequences which have been determined for other exported proteins in both prokaryotic and eukaryotic systems. Of the 26 amino acids comprising the MBP signal sequence, almost two-thirds are hydrophobic residues. Furthermore, all three charged residues present (two lysines and an arginine) are clustered in the first eight residues. Following

the arginine at residue 8, only the neutral amino acids serine and threonine interrupt the hydrophobic nature of the MBP signal. The amino acid just before the cleavage site in the MBP precursor is alanine. This is consistent with other signal sequences, where the residue here usually has a side chain with no more than one carbon moiety[4].

```
    malG      malF       malF   Pmal    malK      lamB
                                          ↑
                                         SalI

   (pBR322)                      Pmal


 EcoRI        ⎡BglII⎤   AvaII HinfI              EcoRI
              ⎣BamHI⎦
```
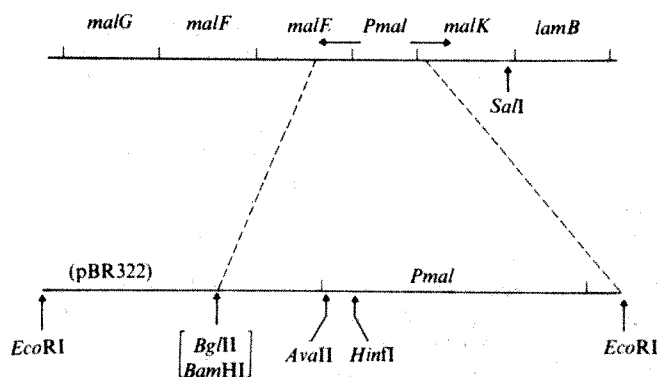
Fig. 2 The *malB* region of *E. coli* includes the *malE* gene and four other genes whose products are also components of the maltose transport system[23]. These are organised into two operons orientated in opposite directions and which diverge from the promotor region designated here as *Pmal* (ref. 24). The 1,227-base pair *Eco*RI–*Eco* RI hybrid fragment shown above is obtained by *Eco*RI digestion of plasmid pHC6. This plasmid carries a bacterial fragment of 1,750 base pairs which extends between cleavage sites in the *malB* region for restriction endonucleases *Sal*I (in *malK*) and *Bgl*II (in *malE*)[25]. This fragment was inserted between cleavage sites for *Sal*I and *Bam*HI in pBR322[26]. Details on the construction and characterisation of plasmid pHC6 will be presented elsewhere (J. M. Clement, D. Perrin and J. Hedgpeth, in preparation). Sites for cleavage of the hybrid fragment by *Ava*II and *Hinf*I are also indicated (see text).

The isolation of mutants with well defined alterations in the signal sequence of a secreted protein and in an outer membrane protein (see accompanying paper[15]) which result in the failure of the cell to secrete these proteins, provides the first genetic proof for the role of the signal sequence in the initial steps of protein secretion. Other workers on bacterial systems have suggested that the basic residues early in the signal sequence are responsible for the initial interaction of the precursor with the negatively charged inner surface of the cytoplasmic membrane[16,17]. Subsequently, according to this model, the hydrophobic portion of the signal begins to penetrate the membrane as the first step in the translocation process. Four of the five mutations we have characterised introduce a single charged residue into the hydrophobic core of the MBP signal sequence. Three of these mutations were found at least twice in independently isolated mutants. This strongly supports the notion that the hydrophobicity of the signal sequence has a key role in initiating protein export through the membrane. In the remaining case,

Fig. 3 Composite figure comparing autoradiograms of sequencing gels for the wild-type *malE* gene and the *malE* signal sequence mutations. Only the relevant parts of the gels are shown. *a*, The wild-type sequence. Points along the sequence where mutations were encountered are indicated on the left. The enlarged letter indicates the exact nucleotide that is altered in the mutants. *b–f* Represent the five classes of signal sequence mutations which we obtained in this analysis. The mutations shown in *e* and *f* correspond to those present in *E. coli* strains PB1101 and PB1102, respectively, as described in ref. 7.
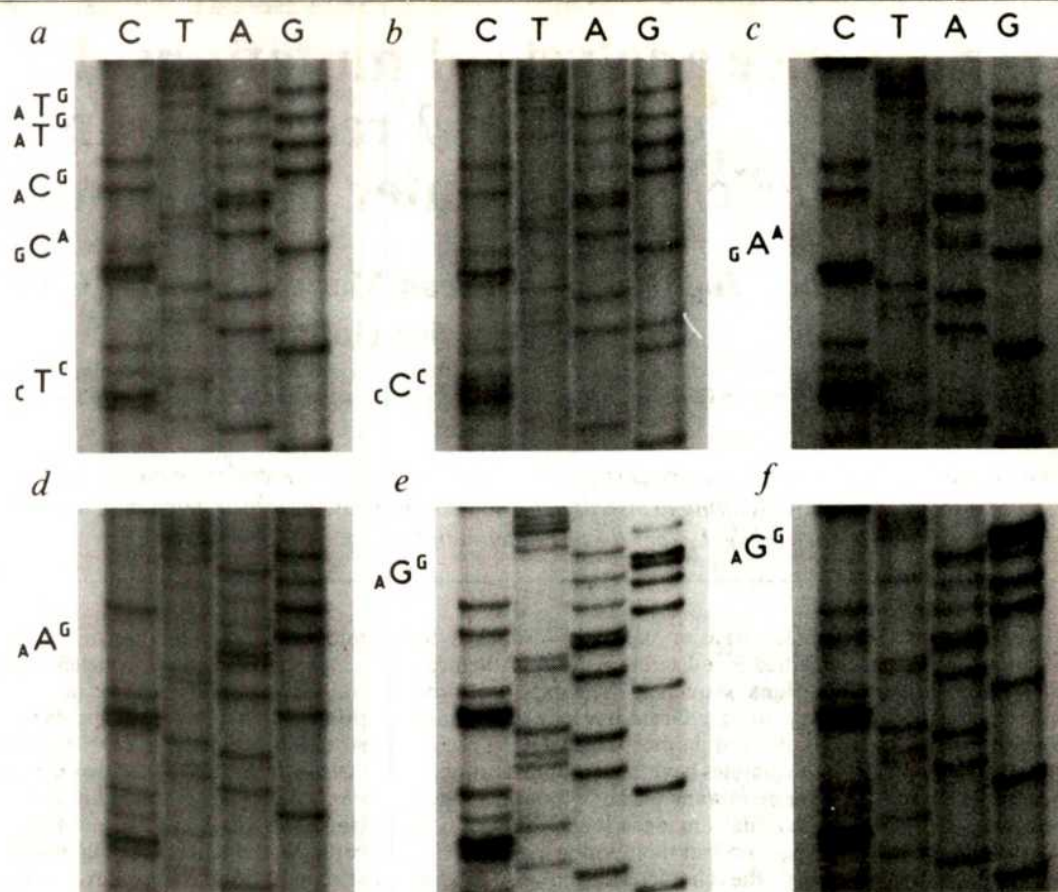
the substitution of proline for leucine at residue 10 represents an exchange of hydrophobic residues. Proline does have the property of interrupting α-helices in polypeptide chains[18], so it is conceivable that secondary structure of the signal sequence plays a part in the initial steps of secretion.

The changes observed have differing effects on MBP secretion (Table 2). The two mutations with the strongest effects are 18-1 and 19-1, which change a hydrophobic to a charged amino acid. The three remaining mutations, which do not cause such a dramatic reduction in growth on maltose, involve a hydrophobic to hydrophobic amino acid change (10-1) and an uncharged to a charged amino acid change (14-1 and 16-1). These results are also consistent with the notion that the overall hydrophobic nature of this region is the most important feature for the secretion process.

All of the mutations we have obtained in the MBP signal sequence are point mutations which readily revert[7]. We hope to obtain additional information on the important structural features of the MBP signal sequence through a sequence analysis of such revertants.

Table 2 Growth properties of *malE* signal sequence mutants

Mutant no.	Growth on maltose minimal medium
Wild-type	+ + + +
10-1	+ +
14-1	+ +
16-1	+ + +
18-1	±
19-1	+

The mutants examined here are given numbers according to the amino acid position in the protein. Mutants 18-1 and 19-1 correspond to mutants 1101 and 1102, respectively, as described in ref. 7. The growth phenotype was determined by observing colony size on maltose minimal agar at 37 °C after 1 day. The hierarchy of growth rates corresponded exactly to the gradient of colours seen on maltose tetrazolium agar. For example, the wild-type parent forms white colonies, whereas mutant 18-1 formed the darkest red colonies on this agar. Mutant 16-1 forms a pink colony on the same agar, but apparently secretes enough MBP to the periplasm to allow near normal growth on maltose minimal media.

1. Blobel, G. & Dobberstein, B. *J. Cell Biol.* **67**, 835–851 (1975).
2. Inouye, H. & Beckwith, J. *Proc. natn. Acad. Sci. U.S.A.* **74**, 1440–1444 (1977).
3. Randall, L. L., Hardy, S. J. S. & Josefsson, L.-G. *Proc. natn. Acad. Sci. U.S.A.* **75**, 361–365 (1978).
4. Austen, B. M. *FEBS Lett.* **103**, 308–313 (1979).
5. Silhavy, T. J., Bassford, P. J. & Beckwith, J. R. in *Bacterial Outer Membrane: Biosynthesis, Assembly and Functions* (ed. Inouye, M.) 203–254 (Wiley, New York, 1980).
6. Kellermann, O. & Szmelcman, S. *Eur. J. Biochem.* **47**, 139–149 (1974).
7. Bassford, P. & Beckwith, J. *Nature* **277**, 538–541 (1979).
8. Bassford, P. Jr., Silhavy, T. J. & Beckwith, J. *J. Bact.* **139**, 19–31 (1979).
9. Brake, A. J., Fowler, A. V., Zabin, I., Kania, J. & Müller-Hill, B. *Proc. natn. Acad. Sci. U.S.A.* **75**, 4824–4827 (1978).
10. Sarthy, A., Fowler, A., Zabin, I. & Beckwith, J. *J. Bact.* **139**, 932–939 (1979).
11. Raibaud, O., Clement, J. M. & Hofnung, M. *Molec. gen. Genet.* **174**, 261–267 (1979).
12. Maat, J. & Smith, A. J. H. *Nucleic Acids Res.* **5**, 4537–4545 (1974).
13. Shine, J. & Dalgarno, L. *Proc. natn. Acad. Sci. U.S.A.* **71**, 1342–1346 (1974).
14. Sanger, F., Nicklen, S. & Coulsen, A. R. *Proc. natn. Acad. Sci. U.S.A.* **74**, 5463–6467 (1977).
15. Emr, S.D., Hedgpeth, J., Clément, J.-M., Silhavy, T.J. & Hofnung, M. *Nature* **285**, 82–85 (1980).
16. DiRienzo, J. M., Nakamura, K. & Inouye, M. *A. Rev. Biochem.* **47**, 481–532 (1978).
17. Halegoua, S. & Inouye, M. *J. molec. Biol.* **130**, 39–61 (1979).
18. Chou, P. Y. & Fasman, G. D. *A. Rev. Biochem.* **47**, 251–276 (1978).
19. Brauer, A. W., Margolis, M. N. & Haber, E. *Biochemistry* **14**, 3029–3035 (1975).
20. Hunkapiller, M. W. & Hood, L. E. *Biochemistry* **17**, 2124–2144 (1978).
21. Fowler, A. V. & Zabin, I. *J. biol. Chem.* **253**, 5499–5504 (1978).
22. Laemmli, U. K. *Nature* **227**, 680–685 (1970).
23. Silhavy, T. J. *et al. Molec. gen. Genet.* **174**, 249–259 (1979).
24. Hofnung, M. *Genetics* **76**, 169–184 (1974).
25. Marchal, C., Greenblatt, J. & Hofnung, M. *J. Bact.* **136**, 1109–1119 (1978).
26. Sutcliffe, J. G. *Nucleic Acids Res.* **5**, 2721–2728 (1978).

Sequence analysis of mutations that prevent export of λ receptor, an *Escherichia coli* outer membrane protein

Scott D. Emr[*‡], Joe Hedgpeth[†§], Jean-Marie Clément[†§], Thomas J. Silhavy[*‡] & Maurice Hofnung[†§‖]

* Department of Microbiology and Molecular Genetics, Harvard Medical School, Boston, Massachusetts 02115
† Unité de Génie Génétique, Institut Pasteur, 28 rue du Docteur Roux, 75015 Paris, France

The amino-terminal signal sequence is required for initiation of transmembrane protein transfer of the Escherichia coli λ *receptor protein. Mutations leading to insertion of charged amino acids into or deletion of amino acids from the hydrophobic segment of this sequence prevent export of this outer membrane protein.*

TRANSMEMBRANE protein transfer has been proposed to require information contained in a discrete portion of the protein molecule, called the signal sequence[1]. The export of proteins to the cell envelope of the Gram-negative bacterium *Escherichia coli* seems to proceed, in most cases, by the use of signal sequences[2]. Several examples have been found of proteins localised to either the outer membrane or the periplasmic space of this bacterium which are initially made as longer polypeptide chains containing signal sequences at their amino-termini. The preceding paper described the characterisation of mutants which prevent the secretion to the *E. coli* periplasm of the maltose binding protein[3]. In this paper, we focus on the transfer and localisation of an outer membrane protein, the bacteriophage λ receptor. This protein acts as the receptor on the cell surface for bacteriophage (ref. 4) and is also involved in the transport of maltose and maltodextrins[5,6].

The λ receptor protein is preferentially synthesised on membrane-bound polysomes[7]. In addition, it is initially synthesised in a larger precursor form[7,8]. Recent studies involving DNA sequencing of the early part of the *lamB* gene (which codes for the λ receptor protein) and amino acid analysis of the λ receptor precursor synthesised *in vitro* have revealed that this protein has a 25-amino acid signal sequence at its amino-terminal end[9].

We have devised a technique which has allowed us to select for mutations that prevent export of the λ receptor protein to the outer membrane[10–12]. In such mutant strains, the unprocessed precursor form of this protein accumulates in the cytoplasm. We describe here the sequence analysis of the DNA of 15 of these mutants cloned into a bacteriophage λ vector. These mutants and those described in the preceding paper[3] provide information concerning the role of the signal sequence in protein export.

DNA sequence of *lamB* gene in λ receptor export-defective mutants

The coding region for the amino-terminal 25-amino acid receptor signal sequence has been shown to be present on a 750-base pair *Sal*I DNA restriction fragment[9] (Fig. 1). The signal sequence is encoded by an early segment of this fragment. We have shown that 27 genetically and physically well characterised *lamB* mutations, which prevent export of the λ receptor pro-

tein, also map in this region[12].

We used the DNA sequencing method of Sanger *et al.*[13]. The well defined location of the mutations enabled us to select DNA primers that allowed sequencing of these mutations on both strands of the template DNA to ensure accuracy of the results. As shown in Fig. 1, the two primers chosen include a 67-base pair *Hpa*II–*Hin*fI fragment and a 51-base pair *Hpa*II–*Hpa*II fragment. The 115-base pair region between these two primers contains the entire coding region for the λ receptor signal sequence[9]. Separated DNA strands of the λ*apmalB*13*h*80 phage containing these mutations were used as templates[12,14] (see Fig. 1).

As previously described[12], the 27 *lamB* mutations affecting λ receptor export have been characterised as 14 point mutations and 13 deletion mutations. Detailed mapping of these independently isolated mutations has revealed that several of them are apparently repeats of the same mutational event. For this reason, only 15 of the 27 mutations were chosen for DNA sequencing. Eight point mutations and seven deletion mutations were sequenced.

The results (Fig. 2) of the sequences are: (1) all 15 mutations lead to alterations in the λ receptor signal sequence; (2) the eight point mutations represent single base changes in four distinct base pairs of the DNA. Three lead to a change in amino acid residue 15 (Ala to Glu), three in residue 19 (Met to Arg), one in residue 14 (Val to Asp) and one in residue 16 (Ala to Glu); (3) all the point mutations are transversions in the second position of each of four codons; (4) three of the deletions are internal to the portion of the DNA encoding the signal sequence. The remaining four deletions delete into this region of the DNA but are not confined to it.

Analysis of sequenced prokaryotic signal sequences

The DNA sequence of 15 mutations in the portion of the *lamB* gene encoding the λ receptor signal sequence has been determined. These mutations prevent export of the λ receptor protein to the outer membrane of *E. coli*, and instead, cause the accumulation of the precursor form of the λ receptor protein in the cytoplasm. These mutations and those described in the previous paper[3] represent the first genetic proof of the functional role of the signal sequence in protein export or secretion. The nature of the amino acid alterations caused by these mutations indicates components of the signal sequence that are critical for the initiation of transmembrane protein transfer.

A comparison between known prokaryotic as well as eukaryotic signal sequences indicates that they share several similar characteristics[15]. The seven known sequenced prokary-

Fig. 1 The λap*malB*13*h*80 phage contains the maltose transport genes, *malK,E,F,G* and approximately two-thirds of the *lamB* gene[14]. The putative λ receptor signal sequence mutations were recombined from the *lamB-lacZ* hybrid gene in which they were isolated into the portion of the *lamB* gene contained on this phage. The two critical *Sal*I sites used in the physical mapping of these mutations are shown[12]. To make template DNA for sequencing, phage DNA strands were separated on caesium chloride density gradients after heat denaturation in the presence of poly (U, G)[9,25]. The two primers used in the sequencing were derived from plasmid pHC5 (ref. 9). This plasmid carries a fragment of bacterial DNA which contains the entire *lamB* gene[9]. Plasmid DNA restriction fragments were separated on 4% polyacrylamide gels and were then electroeluted from the gel[26]. The two primers, *Hpa*II-*Hin*fI and *Hpa*II-*Hpa*II, were used to prime on the separated *l* and *r* phage DNA strands, respectively.
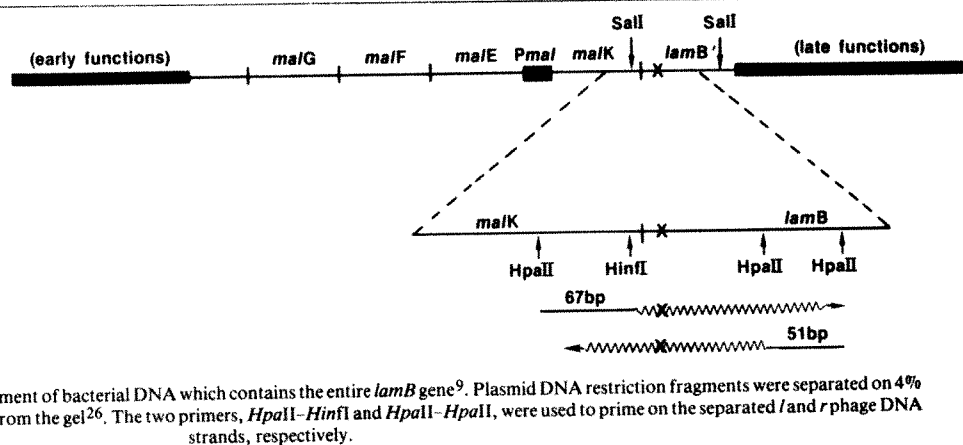
otic signal sequences (Fig. 3) can all be broken down into two principal segments, a short amino-terminal hydrophilic basic segment followed by a predominantly hydrophobic segment of amino acids that extends up to the site of processing. There are from one to three basic amino acids (Arg and/or Lys) in the basic portion of the signal sequence. These positively charged residues have been suggested to play a part in initial attachment of the polysomes to the negatively charged inner surface of the cytoplasmic membrane[15,16]. The hydrophobic segment directly follows the last basic residue in this initial segment. Charged amino acids, basic or acidic, are completely absent from this portion of the signal sequence. It has been suggested that this hydrophobic region loops into the membrane lipid bilayer or becomes associated with specific membrane protein(s), thereby initiating the transmembrane transfer of the polypeptide[1,15–17].

Possible mechanisms for the initiation of transport

The mutations described here for the λ receptor signal sequence and those described for the maltose binding protein (MBP)

signal sequence in the previous paper[3] argue strongly for a critical role of the hydrophobic segment of the signal sequence in the initiation of the export process. The four different single amino acid changes in the λ receptor signal sequence and four of the five amino acid changes in the MBP signal sequence are all changes from hydrophobic (Leu, Met, Val, Ala) or weakly hydrophilic (Thr) amino acids to very hydrophilic charged amino acids (Arg, Lys, Glu, Asp), and all these changes occurred in the hydrophobic segment of the signal sequence. These mutations, therefore, strongly support the requirement of the hydrophobicity of this segment.

Note that a similar alteration in the lipoprotein (another outer membrane protein) signal sequence at amino acid position 14 also affects this hydrophobic segment[33]. This mutation, which changes a glycine residue to an aspartic acid, does not have a dramatic effect on lipoprotein export, but does prevent processing of the lipoprotein precursor. The reason for this is not clear.

It is interesting that, in both the λ receptor and MBP systems, multiple copies of the same mutational events were isolated. In the λ receptor, at least, 17 of the 18 amino acid residues in the
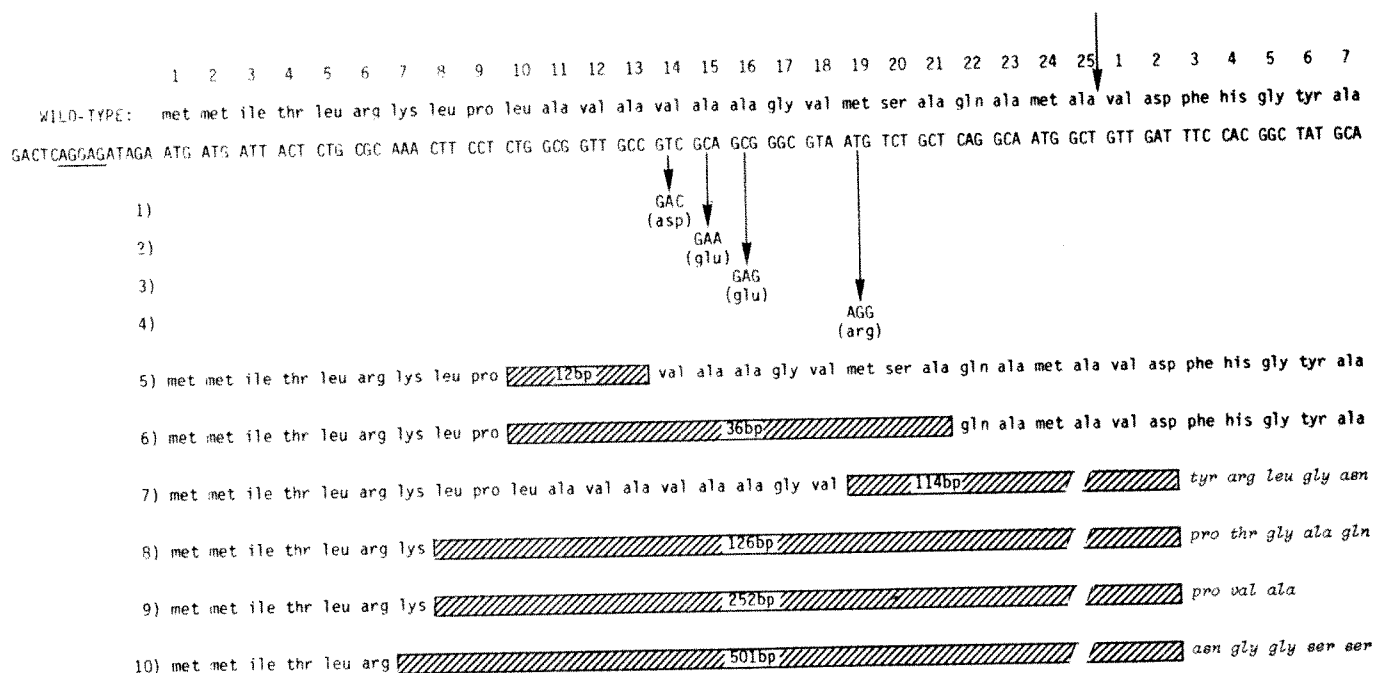
Fig. 2 Sequences shown were determined using the chain termination procedure[13]. Sequence reactions were run on thin 8% polyacrylamide gels[27]. Gels were autoradiographed (Kodak No-screen X-ray film) for 12–24 h at −20 °C before reading off the above sequences. The signal sequence of wild-type λ receptor (top) and that of 15 *lamB* signal sequence mutations are shown. These mutations correspond to those present in the following *E. coli* strains: (1) SE2071; (2) SE2070, SE2079 and SE2105; (3) SE2099; (4) SE2069, SE2088 and SE2100; (5) SE2078; (6) SE2060 and SE2084; (7) SE2087; (8) SE2068; (9) SE2089; (10) SE2106. These strains are all described in detail in ref. 12. The amino acids to the right of deletions 7–10 above have not been confirmed by wild-type DNA sequencing. For this reason they are shown in italics. In (8), (9) and (10) above, the deletion end points are within codons. The amino acid directly following each of these deletions is, therefore, the result of a fused codon which may encode an amino acid not normally found at this position in the wild-type sequence.

λ RECEPTOR:
met met ile thr leu arg lys leu pro leu ala val ala val ala ala gly val met ser ala gln ala met ala val asp phe

asp glu glu   arg

MALTOSE BINDING PROTEIN:
met lys ile lys thr gly ala arg ile leu ala leu ser ala leu thr thr met met phe ser ala ser ala leu ala lys ile glu

pro   glu   lys   arg arg

LIPOPROTEIN:
met lys ala thr lys leu val leu gly ala val ile leu gly ser thr leu leu ala gly cys ser ser

asp

β-LACTAMASE:
met ser ile gln his phe arg val ala leu ile pro phe phe ala ala phe cys leu pro val phe ala his pro glu

fd MAJOR PHAGE COAT PROTEIN:
met lys lys ser leu val leu lys ala ser val ala val ala thr leu val pro met leu ser phe ala ala glu gly

fd MINOR PHAGE COAT PROTEIN:
met lys lys leu leu phe ala ile pro leu val val pro phe tyr ser his ser ala

BACTERIAL ALKALINE PHOSPHATASE:
met lys gln ser thr

|◄─────────────────►|◄──────────────── ─ ─ ─ ─►|
HYDROPHILIC SEGMENT   HYDROPHOBIC SEGMENT

Fig. 3 The amino acid sequence of seven known prokaryotic signal sequences. These include λ receptor[9], MBP[3], lipoprotein[28], β-lactamase[29], fd major phage coat protein[30], fd minor phage coat protein[31] and alkaline phosphatase[32]. Mutational alterations in the λ receptor signal sequence, the MBP signal sequence[3] and the lipoprotein signal sequence[33] are indicated below their corresponding wild-type sequences. The site of processing for these signal sequences is indicated above each sequence by an arrow.

hydrophobic portion of the signal sequence can be changed to charged amino acids by single base changes in the DNA. Despite this fact, of 14 independently isolated point mutations only 4 separate amino acids were changed. This suggests that only changes in a defined subset of the signal sequence amino acids will drastically affect export. (Although the *lamB* signal sequence mutants result in a λ-resistant phenotype, they are not totally defective in λ-receptor export, as small amounts are found in the outer membrane.) It may be that the lipoprotein mutation mentioned above has not affected such a critical amino acid. A more extensive mutant search will be necessary to confirm such a contention.

Export-defective mutations were not found in the amino-terminal basic segment of the signal sequence in either λ receptor or MBP. This might indicate that this portion of the signal sequence is not critical for protein export. Alternatively, the stringency of the selection for these mutations may not have allowed for detection of such mutants. The deletion and point mutations do, however, clearly demonstrate that this hydrophilic segment of the signal sequence is not sufficient for protein export.

The secondary structure of signal sequences has also been suggested to be important for the initiation of the secretion process[16]. Using available techniques for predicting polypeptide secondary structure[18,19], the structure of the λ receptor signal sequence and that of the mutants was determined. The results indicate that these mutations do not significantly alter the secondary structure of this signal sequence. Furthermore, the secondary structures of two signal sequences (for λ receptor and lipoprotein) seem to be quite different (unpublished results). However, the accuracy of these predictive techniques is questionable when considering such short peptides.

The fact that all the export-defective mutations studied lead to alterations in the signal sequence and not elsewhere in the proteins suggests that for these bacterial proteins the signal sequence is the only component of the protein required in the initial stages of translocation. Thus, the attachment of ribosomes to the cytoplasmic membrane and the initiation of the passage of such proteins through the membrane depend on an intact signal sequence. This agrees with synchronous translation experiments with the vesicular stomatitis virus glycoprotein which have shown that polysome binding to the membrane occurs at a time during translation when the signal sequence and little else of the polypeptide has been extruded from the ribosome[20]. However, it seems likely that other components of the exported proteins

are essential in subsequent steps of the secretion process which ensure that such proteins arrive at their proper final destination. That this is the case is supported by recent studies on the export of certain hybrid proteins[21,22].

The results of the DNA sequencing have also indicated how at least some of the *lamB* deletions may have occurred. The 36-base pair deletions present in SE2060 and SE2084 represent two of six deletions that are genetically and physically identical[12]. It is very likely that they are all the result of the same deletion event. Analysis of the DNA sequence in the region of the end points of this deletion reveals a segment of homology in direct repeat on either side of the deletion. There is evidence that limited homology of this type can promote specific deletion formation[23].

In genetic crosses of the λ receptor signal sequence mutants against *lamB*::Mu insertions, we found a very high percentage (18%) of the Mu insertions mapped under the 12-base pair deletion present in mutant SE2078[12]. DNA sequencing of this deletion reveals no obvious reason for the apparent preference of Mu for this site. However, several of the sequences known to flank Mu insertions are present within the 12 deleted base pairs, including the most commonly occurring sequence, CAG[24]. One can also detect DNA homologies in this region that would allow certain secondary structures in the DNA to form. The exact role these might have in Mu insertion is not clear. Continued analysis of new and other classes of apparent λ receptor signal sequence mutations should yield further insight into the mechanism of the important process of protein localisation.

1. Blobel, G. & Dobberstein, G. *J. Cell Biol.* **67**, 835–851 (1975).
2. Silhavy, T., Bassford, P. J. Jr & Beckwith, J. R. in *Bacterial Outer Membrane: Biosynthesis, Assembly and Functions* (ed. Inouye, M.) 203–254 (Wiley, New York, 1980).
3. Bedouelle, H. *et al. Nature* **285**, 78–81 (1980).
4. Randall-Hazelbauer, L. L. & Schwartz, M. *J. Bact.* **116**, 1436–1446 (1973).
5. Szmelcman, S., Schwartz, M., Silhavy, T. J. & Boos, W. *Eur. J. Biochem.* **65**, 13–19 (1976).

6. Szmelcman, S. & Hofnung, M. *J. Bact.* **124**, 112–118 (1975).
7. Randall, L.L., Hardy, S.J.S. & Josefsson, L.-G. *Proc. natn. Acad. Sci. U.S.A.* **75**, 361–365 (1978).
8. Marchal, C., Perrin, D., Hedgpeth, J. & Hofnung, M. *Proc. natn. Acad. Sci. U.S.A.* (in the press).
9. Hedgpeth, J., Clément, J. M., Marchal, C., Perrin, D. & Hofnung, M. *Proc. natn. Acad. Sci. U.S.A.* (submitted).
10. Silhavy, T. J., Shuman, H. A., Beckwith, J. & Schwartz, M. *Proc. natn. Acad. Sci. U.S.A.* **74**, 5411–5415 (1977).
11. Emr, S. D., Schwartz, M. & Silhavy, T. J. *Proc. natn. Acad. Sci. U.S.A.* **75**, 5802–5806 (1978).
12. Emr, S. D. & Silhavy, T. J. *J. molec. Biol.* (submitted).
13. Sanger, F., Nicklen, S. & Coulson, A. R. *Proc. natn. Acad. Sci. U.S.A.* **74**, 5463–5467 (1977).
14. Raibaud, O., Clément, J. M. & Hofnung, M. *Molec. gen. Genet.* **174**, 261–267 (1979).
15. DiRienzo, J. M., Nakamura, K. & Inouye, M. *A. Rev. Biochem.* **47**, 481–532 (1978).
16. Chan, S. J. *et al.* in *From Gene to Protein: Information Transfer in Normal and Abnormal Cells* (ed. Russell, T. R.) (Academic, New York, in the press).
17. Kreibich, G., Ulrich, B. L. & Sabatini, D. D. *J. Cell Biol.* **77**, 464–487 (1978).
18. Chou, P. Y. & Fasman, G. D. *A. Rev. Biochem.* **47**, 251–276 (1978).
19. Garnier, J., Osguthorpe, D. J. & Robson, B. *J. molec. Biol.* **120**, 97–120 (1978).
20. Rothman, J. E. & Lodish, H. F. *Nature* **269**, 775–780 (1977).
21. Bassford, P. J. Jr, Silhavy, T. J. & Beckwith, J. R. *J. Bact.* **139**, 19–31 (1979).
22. Moreno, P., Fowler, A., Hall, M., Silhavy, T. J., Zabin, I. & Schwartz, M. *Nature* (submitted).
23. Miller, J. H. in *The Operon* (eds Miller, J. H. & Reznikoff, W. S.) 31–88 (Cold Spring Harbor Laboratory, New York, 1978).
24. Kahmann, R. & Kamp, D. *Nature* **280**, 247–250 (1979).
25. Szybalski, W., Kubinski, H., Hradecna, Z. & Summers, W. C. *Meth. Enzym.* **21**, 383–413 (1971).
26. Wu, A. M. & Platt, T. *Proc. natn. Acad. Sci. U.S.A.* **75**, 5442–5466 (1978).
27. Sanger, F. & Coulson, R. *FEBS Lett.* **87**, 107–110 (1978).
28. Inouye, S., Wang, S., Sekizowa, J., Halegoua, S. & Inouye, M. *Proc. natn. Acad. Sci. U.S.A.* **74**, 1004–1008 (1977).
29. Sutcliffe, J. G. *Proc. natn. Acad. Sci. U.S.A.* **75**, 3737–3741 (1978).
30. Sugimoto, K., Sugisaki, H., Okamoto, T. & Takanami, M. *J. J. molec. Biol.* **111**, 487–507 (1977).
31. Schaller, H., Beck, E. & Takanami, M. in *The Single Stranded DNA Phages* (eds Denhardt, D., Dressler, D. & Ray, D.) 139–153 (Cold Spring Harbor Laboratory, New York, 1978).
32. Sarthy, A., Fowler, A. V., Zabin, I. & Beckwith, J. *J. Bact.* **139**, 932–939 (1979).
33. Lin, J. J. C., Kanazawa, H. & Wu, H. C. *Proc. natn. Acad. Sci. U.S.A.* **75**, 4891–4895 (1978).

The λ phage *att* site: functional limits and interaction with Int protein

Pei-Ling Hsu, Wilma Ross & Arthur Landy*

Section of Microbiology and Molecular Biology, Division of Biology and Medicine, Brown University, Providence, Rhode Island 02912

Site-specific integrative recombination of bacteriophage λ *involves unequal partners. The minimal phage* att *site is composed of approximately 240-base pairs and four distinct binding sites for Int protein, at least three of which are crucial for function. This 'donor site' recombines efficiently with a smaller 'recipient site' that lacks the extensive interactions with* Int *protein.*

THE integration/excision pathway of bacteriophage λ is a particularly favourable system for studying site-specific recombination at the molecular level (for reviews see refs 1, 2). Integration of the phage genome into the chromosome of the host occurs by a reciprocal recombination between the phage *att* site (POP') and the bacterial *att* site (BOB'). The products are two prophage *att* sites which comprise the left (BOP') and right (POB') junctures between bacterial DNA and the integrated prophage (the formal equivalent of this recombination is shown in Fig. 1*b*). Both the integration and excision reactions require the phage-encoded protein Int as well as the products of several host *Escherichia coli* genes[3]. An additional requirement for the excision reaction is the phage-encoded protein Xis. The Int and Xis proteins are 356 and 72 amino acids respectively, as determined from their encoding DNA sequences[4]. Recent *in vivo* experiments suggest that in some situations, Xis can partially replace, or be replaced by, the host factors[5]. Highly purified Int protein forms specific stable complexes with *att* DNA, has an enzymatic activity for cutting and resealing DNA strands, and is functional in an *in vitro* intermolecular recombination system[6–11].

A structural feature of integrative recombination, both *in vivo* and *in vitro*, is that the phage *att* site must be on a negatively supercoiled DNA molecule[8,11,12]. The cross-over event of Int-dependent recombination must take place within, or at the boundaries of, a 15-base pair core sequence that is common to all four *att* sites and is designated 'O' in the *att* site nomenclature[13]. DNA sequences of the four arms of the *att* sites, designated P, P', B and B', are all different from each other. The four *att* sites can also be distinguished from each other genetically by their distinctive behaviour in pairwise crosses[14–16].

The results reported here define the functional limits of the phage *att* site. We have also extended our studies of the interaction between Int protein and *att* sites[9]. The minimal phage *att* site is quite large (approximately 240 base pairs) and has several

widely spaced Int binding sites that differ in size and in response to heparin challenge. In contrast, the minimal sequence required for a phage *att* site partner (such as the bacterial *att* site) may not be much larger than the 15-base pair common core. We suggest a model in which integrative recombination involves two unequal partners; accordingly the phage *att* site is denoted the 'donor' and the bacterial *att* site or its analogue the 'recipient'.

Generating resected *att* sites

The λ phage *att* site is in the centre of a 492-base pair *Hind*III–*Bam*HI restriction fragment that extends from positions −251 to +242. (For numbering DNA sequences in this region of the λ chromosome, the centre of the common core region is taken as 0; positive numbers extend to the right, through the *int* and *xis* genes, and negative numbers extend to the left[13].) This *att*-containing restriction fragment was cloned into pBR322 in place of the *Hind*III–*Bam*HI fragment from the *tet* gene. The resulting plasmid, pWR1, carries all of the information necessary to specify a functional phage *att* site as determined by its competence for Int-dependent recombination with a bacterial *att* site *in vitro* (see below). This plasmid was used as the starting point for defining the functional limits of the phage *att* site. The question is then, how much DNA can be removed from around the phage *att* site without impairing its function?

When comparing different plasmids for relative amounts of phage *att* site function it is desirable that only one of the two phage *att* site arms should be altered at a time, and that non-*att* sequences (that is, plasmid DNA) adjacent to the different shortened termini should all be the same. We therefore generated phage *att* sites with incremental lengths of one arm as summarised in Fig. 1. The first procedure involved exonucleolytic digestion of the terminal nucleotides and cloning of the shortened *att* sites. An additional procedure involved reassortment of shortened arms between two *att* sites by Int-dependent recombination and recovery of the products.

Protocols were designed so that the final *att*-containing restriction fragments always have one *Hind*III and one *Bam*HI

---

* To whom request for reprints should be addressed.

terminus, thus facilitating subsequent cloning, restriction analysis and sequencing. The details for the construction of each plasmid will be described elsewhere.

Function of resected phage *att* sites

Competence for phage *att* site function was tested in an *in vitro* Int-dependent recombination system[10,11]. In the assay conditions used the phage *att* site must be on a supercoiled molecule[11] and the bacterial *att* site functions best when it is on a linear molecule (K. Mizuuchi, personal communication). Control experiments established that this assay registers only phage *att* site function on the supercoiled parent, and not prophage *att* site function (Fig. 3, right panel).

All plasmids carrying a P arm equal to or longer than that of pPH54 (−160) recombined efficiently with the bacterial *att* site, but none of those carrying a shorter arm (−115 or less) did so (Fig. 2 and Table 1). Thus some DNA between positions −160 and −115 is essential for the proper functioning of the P arm in a phage *att* site.

A family of P' arm-shortened plasmids generated as outlined in Fig. 1*a*, had a constant left terminus at -115. Because this did not include all the information required for a functional P arm (see above and Fig. 2), a longer P arm was restored to each plasmid as outlined in Fig. 1*b*. All *att* sites with P' arms equal to or greater than that of pPH307 (+82) were efficient recom-

bination partners, whereas those with shorter P' arms (+64 or less) failed to recombine efficiently (Table 1). The shortest P' arm that functions as a phage *att* site contains essentially all the DNA identified as forming heparin-resistant complexes with purified Int protein[9]. The longest P' arm which fails to function as a phage *att* site contains only half of this sequence.

To test whether the combination of a minimal P arm and a minimal P' arm is sufficient for full function, a phage *att* site carrying both minimal arms was constructed. A *Hind*III–*Hinf*I fragment from −160 to −115 (from pPH54) and a *Hinf*I–*Bam*HI fragment from −115 to +82 (from pPH307) were cloned together into the *Hind*III–*Bam*HI sites of pBR322. The resultant plasmid, pPH507 (−160 to +82), thus contains all the elements of a minimal P arm and a minimal P' arm, as defined by the experiments described above.

The function of this plasmid was compared with that of pPH7 (−115 to +82), pPH10 (−115 to +46) and pPH510 (−160 to +46). In recombination with the bacterial *att* site pPH507 recombined as well (60–100%) as the control plasmid pWR1, whereas the other three gave no detectable recombination (Fig. 3). In these assay conditions, supercoiled plasmid DNAs carrying the bacterial *att* site or the left or right prophage *att* sites all failed to recombine efficiently with the linear bacterial *att* site (Fig. 3). Therefore, the competence of pPH507 must reflect phage *att* site function (and not prophage or bacterial *att* site
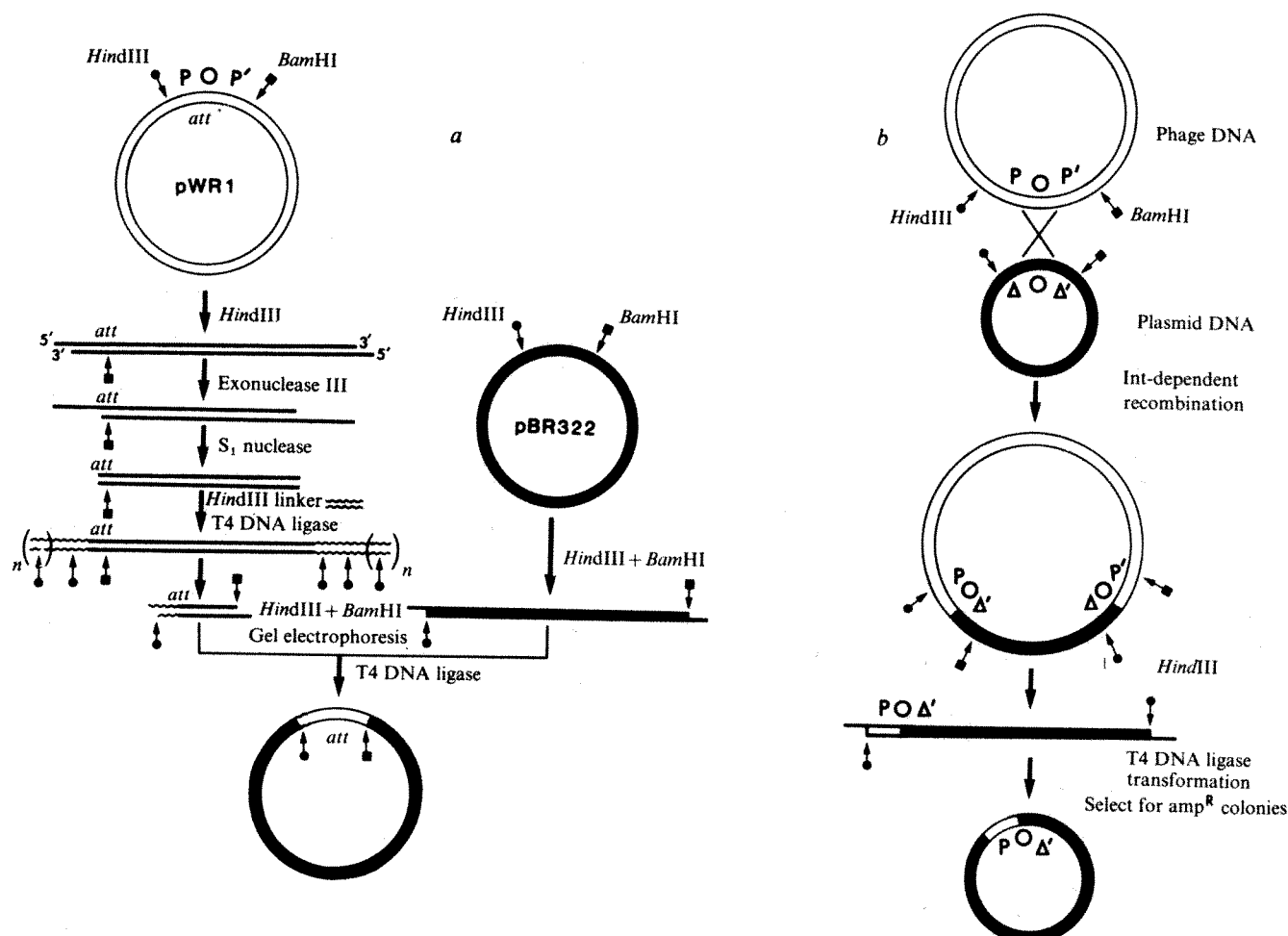
Fig. 1 Construction of plasmids carrying resected *att* sites. *a*, Plasmid pWR1 was first linearised, for example with *Hind*III for shortening the P arm. Digestion of the linear DNA with a combination of exonuclease III from *E. coli* (New England Biolabs) and nuclease S₁ (Miles) generates a series of shortened plasmids carrying flush base-paired termini. A chemically synthesised decamer *Hind*III linker (Collaborative Research) was ligated to the blunt end by T4 DNA ligase. Digestion with *Hind*III and *Bam*HI generates a family of fragments with unaltered P' arms and P arms shortened to different extents. These were fractionated by gel electrophoresis and regions corresponding to the desired size were excised and eluted. Finally, the size selected fragments were recloned between the *Hind*III and *Bam*HI sites of pBR322 and the plasmid carried in each clone characterised by restriction fragment analysis. In an analogous fashion, shortening of the P' arm would be carried out by using *Bam*HI in the place of *Hind*III to linearise the plasmid and using a *Bam*HI linker in place of the *Hind*III linker. *b*, Cells harbouring a plasmid with a shortened *att* site arm were infected with λ phage carrying a wild-type *att* site. As a result, some of the infecting phage underwent Int-dependent recombination with the *att* site on the plasmid and thus acquired the ability to transduce amp^R (D. Kamp and K. Mizuuchi, personal communication). The *att* site at each phage–plasmid junction has one arm derived from the plasmid and the other arm derived from the phage. Recovery of the recombinant *att* site on a self-replicating plasmid was accomplished by digesting the plasmid–phage hybrid DNA with *Hind*III, recircularising the DNA (by means of the *Hind*III ends) and selecting ampicillin-resistant transformants. These procedures will be described in detail elsewhere (P.-L. H. and A.L., in preparation). /

Fig. 2 Integrative recombination of plasmids with resected P arms. Each reaction mixture contained ~1 µg supercoiled plasmid DNA with an intact, or P arm-resected, phage *att* site and 1µg of linear DNA with a bacterial *att* site (*Eco*RI–*Bam*HI fragment; 1,600-base pairs) at a molar ratio of 1:3. The recombination was carried out in a 20-µl mixture containing 50 mM Tris-HCl (*p*H 7.4), 5 mM EDTA, 40 mM KCl, 12.5 mM spermidine, 4 µl of sonicated bacterial extract and 1.5 µl of Int fraction I (refs 8, 10) After incubation at 25 °C for 40 min, 30µl of a buffer containing 0.3 M NaCl, 10 mM Tris-HCl (*p*H 7.4) was added and the samples were extracted with phenol-CHCl₃ before being loaded onto a 1% agarose slab gel and electrophoresed at 35 V for 16 h in E buffer (40 mM Tris, 20 mM Na-acetate, 2 mM EDTA, 18 mM NaCl, adjusted to *p*H 7.9 with acetic acid). The gel was strained with EtBr(1 µg ml⁻¹) for 15 min and then photographed under UV light. For quantitation the fragment containing the bacterial *att* site was first end-labelled with ³²P by T4 polynucleotide kinase[9]. After recombination and gel electrophoresis, portions of the gels corresponding to the unreacted linear DNA and the recombination product were excised and counted individually for ³²P radioactivities. The percentage of phage *att* site molecules that recombined with labelled bacterial *att* site DNA (present in threefold molar excess) was calculated as follows:

$$\% \text{ phage } att \text{ sites recombined} = \frac{^{32}\text{P radioactivity in the product band}}{\text{total } ^{32}\text{P radioactivity}} \times 3$$

The P arm end point of each resected plasmid, as determined by restriction enzyme analysis or by DNA sequencing is shown at the bottom (also see Table 1). All plasmids contain a P′ arm extending to the *Bam*HI site at position +242. Positions on the electropherogram are indicated for the ³²P-labelled linear DNA containing the bacterial *att* site (*att*B), the unlabelled circular plasmid DNA containing the intact or resected phage *att* sites and migrating as supercoils (s.c.) or nicked circles (n.c.), and the linear ³²P-labelled products of recombination (arrows). Binding sites for Int protein (■) (see legends to Figs 4 and 5), and the 15-base pair common core sequence (hatched) are indicated on the linear map of the *att* site region.
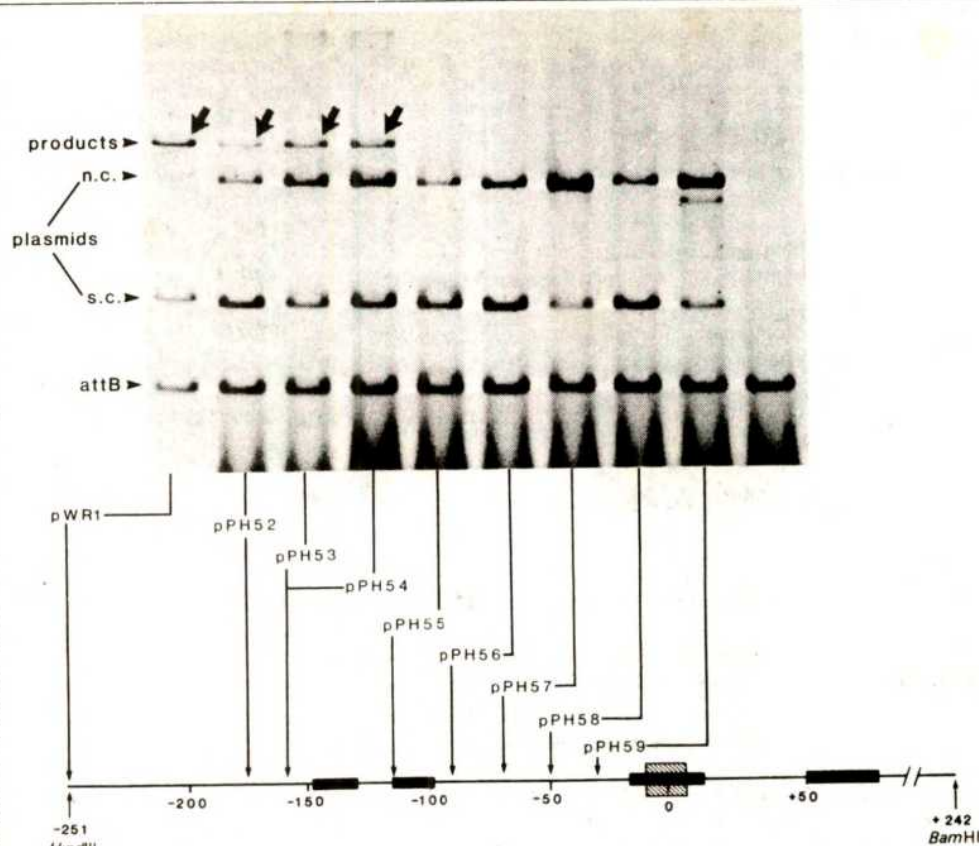
function). We conclude that the sequences delimited by the minimal P and P′ arms (−160 to +82) are both necessary and sufficient for phage *att* site function.

Sequence and Int binding of minimal phage *att* site

Most of the DNA comprising the minimal region required for phage *att* site function was included in our reported sequence extending from −114 to +203 (ref. 13), within which two specific sites of Int interaction were detected[9] (see below). One of these 30–35-base pair binding sites has at its centre the 15-base pair common core sequence where the cross-over occurs in recombination. The second site is in the P′ arm (+50 to +86) and the sequence protected by Int extends to the right boundary of (3 to 4 bases beyond) the minimal length P′ arm. Clones lacking part or all of this P′ arm Int binding site failed to function as phage *att* sites (Fig. 3 and Table 1), indicating a requirement for this Int interaction for phage *att* site function (see below).

We now report the sequence for the remaining DNA in the P arm that is required for phage *att* site function as well as sequence extending further to the left (Fig. 4). The sequence from −250 to −200 is 47% A+T, in contrast to a relatively uniform distribution of 62% A+T from −200 to −115. When combined with the previously determined sequence[13] this yields an average base composition of 71% A+T for the minimal phage *att* site.

The newly sequenced P arm region was examined for additional Int binding sites using the technique of DNase footprinting[17]. In the presence or absence of Int protein a singly end-labelled restriction fragment was digested with a nonspecific

nuclease in conditions where each molecule was cut approximately once. On a DNA sequencing gel the end-labelled fragments form a ladder, with gaps at those positions protected by Int. Using a restriction fragment that extends in both directions beyond the minimal phage *att* site, we observed that Int protects four regions from digestion by the AT-specific antitumour agent neocarzinostatin (Fig. 5*a*). Two of these regions correspond to

Table 1 Integrative recombination of plasmids with resected P arms or resected P′ arms

Plasmid	End point		% Relative recombination†	
	P arm	P′ arm	Expt 1	Expt 2
pWR1	−251	+242	100 (41)	100 (30)
pPH52*	−174	+242	48	100
pPH53	−160	+242	95	75
pPH54	−160	+242	99	106
pPH55	−115	+242	<0.5	<0.5
pPH56	−90	+242	<0.5	<0.5
pPH57*	−70	+242	<0.5	<0.5
pPH58*	−50	+242	<0.5	<0.5
pPH59*	−30	+242	<0.5	<0.5
pWR1	−251	+242	100 (32)	100 (20)
pPH303	−251	+124	113	80
pPH304*	−251	+100	95	75
pPH307	−251	+82	69	90
pPH308	−251	+64	<0.5	<0.5
pPH310	−251	+46	<0.5	<0.5

* The end points of these plasmids were determined by restriction fragment analysis. All other end points were determined by DNA sequencing.
† See Fig. 2 for quantitation. The results are normalised to 100% for pWR1. The absolute value for pWR1 in each experiment is shown in parentheses.
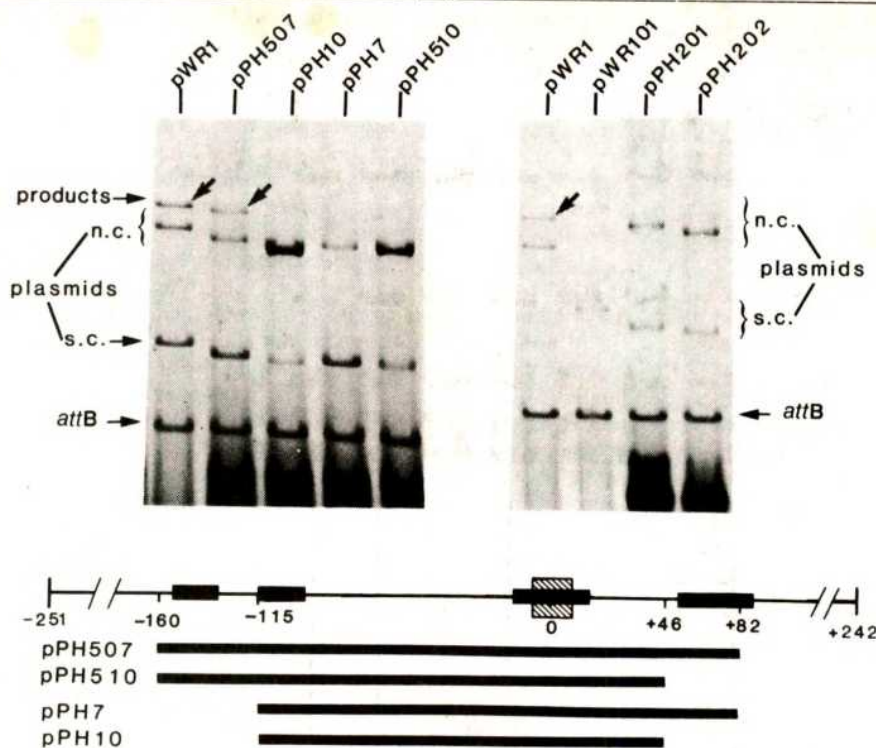
Fig. 3 Integrative recombination of the minimal phage *att* site. The *in vitro* recombination reaction and gel electrophoresis were carried out as described in Fig. 2 legend. The structure and boundaries of the cloned fragments used in the left panel were confirmed by restriction fragment analysis and by DNA sequencing. The extent of each cloned fragment is indicated by a long bar beneath the map of the *att* site region. The *att* sites carried by plasmids in the right panel are: pWR1-phage *att* site (*Hind*III-*Bam*HI-492), pWR101-bacterial *att* site (*Eco*RI-*Bam*HI-1,600), pPH201-left prophage *att* site (*Eco*RI-*Bam*HI-1,300) and pPH202-right prophage *att* site (*Hind*III-*Bam*HI-800). Positions on the electropherogram are indicated for the 'recipient' linear DNA containing the bacterial *att* site (*att*B), the 'donor' circular plasmid DNA containing truncated or intact phage *att* site and migrating as supercoils (s.c.) or nicked circles (n.c.) and the linear products of recombination (arrows). Binding sites for Int protein (■) (see legends to Figs 4 and 5), and the 15-base pair common core sequence (hatched) are indicated on the linear map of the *att* site region.

the common core and P′ arm binding sites[9]. The two others are located in the P arm, within the minimal phage *att* site; P arm site 1 extends from −148 to −129, and P arm site 2 from −116 to −98 (see also Fig. 4). Good agreement with these results was obtained by monitoring DNase I digestion of the complementary (bottom) strand (Figs 4 and 5*b*). These two binding sites are most probably the basis for nitrocellulose filter retention of Int complexed with P arm-containing restriction fragments[18].

The importance of P arm site 1 is indicated by the fact that its removal abolished phage *att* site function (Figs 2, 3). However, it cannot be determined from exonuclease resection experiments whether P arm site 2 is also necessary. Base changes or deletions within P arm site 2 will be required to clarify this point.

An additional feature of Int–DNA interaction was visualised by DNase I, but not neocarzinostatin digestion. With Int concentrations higher than the minimum required to observe specific protection there was a series of strongly enhanced bands at 10-base pair intervals (Fig. 5*b*, lane 1, positions −75, −85,

−95, −117 and −128). Similar patterns of enhanced DNase I cutting were also observed to varying extents on other restriction fragments in regions surrounding the common core and P′ arm binding sites (data not shown), but not to the left of P arm site 1 (Fig. 5*b*). These results are to be distinguished from the possibly related observation that exonuclease digestion produced a 10-base pair pattern within the Int-protected sequence of the P′ arm[18].

Structural relations between Int binding sites

The P arm Int binding sites (15–20 base pairs) are each shorter than either the common core or the P′ arm sites, but are comparable in size to the 15-base pair protected region in the *att*B common core[9] (Fig. 6). However, the P arm sequences do not share homology with the common core sequence or with the core–arm juncture sequences[9].

The common core and P′ arm Int binding sites show very little sequence homology with each other, possibly suggesting their

Fig. 4 Sequence of the left portion of the P arm and location of Int binding sites P arm 1 and P arm 2. P arm sequence is given negative numbers proceeding leftward from the centre of the common core region (0). We have previously reported the sequence from −114 to +203 (ref. 13). DNA sequence was determined for both strands (with the exception of −252 to −237) by the method of Maxam and Gilbert[27] using 5′ termini labelled with ³²P by polynucleotide kinase[9]: top strand sequence from −241 to −90 was obtained from the *Hind*III end of the *Hind*III (−251)–*Alu*(−6) fragment (see ref. 13); top strand sequence from −252 to −241 was determined using the *Eco*RI site of pBR322 in the plasmid carrying the *Hind*III(−251)–*Bam*HI(+242) *att* fragment (pWR1, see text). Complementary

sequence, from −116 to −237, was obtained from the *Hinf*I end of fragment *Hinf*I(−115)-*Mnl* I (recognition site at −231). The left boundaries of the shortest functional P arm (−160, pPH54) and the longest nonfunctional P arm (−115, pPH55) obtained in these experiments are indicated (⌐→). The locations of Int-binding sites P arm 1 and P arm 2 were determined by the method of DNase I footprinting[17] with modifications described previously[9] (see also Fig. 5). Int protection of sequences in the top strand from neocarzinostatin[28,29] digestion (■) was carried out using two different fragments, each labelled at the *Hind*III end: *Hind*III(−251)–*Alu*(−6), carrying only P arm sequences, and *Hind*III(−251)–*Hpa*II(+305), carrying the entire minimal phage *att* site sequence (shown in Fig. 5*a*). Int protection of the bottom strand from neocarzinostatin (■) or DNase I (□) digestion was carried out on a fragment from plasmid pPH310 containing *att* sequence from +46 to −251 (*Hind*III), labelled at the *Bam*HI linker adjacent to position +46. Partially protected bases are designated ▨▨▨ . Ambiguities in the precise boundaries of the protected regions are due to the failure of neocarzinostatin (●) or DNase I (○) to cut certain bases in the control digests. An inverted repeat structure (→ ←) which includes sequence from each of the two Int-binding sites plus additional sequence between the two sites is indicated.
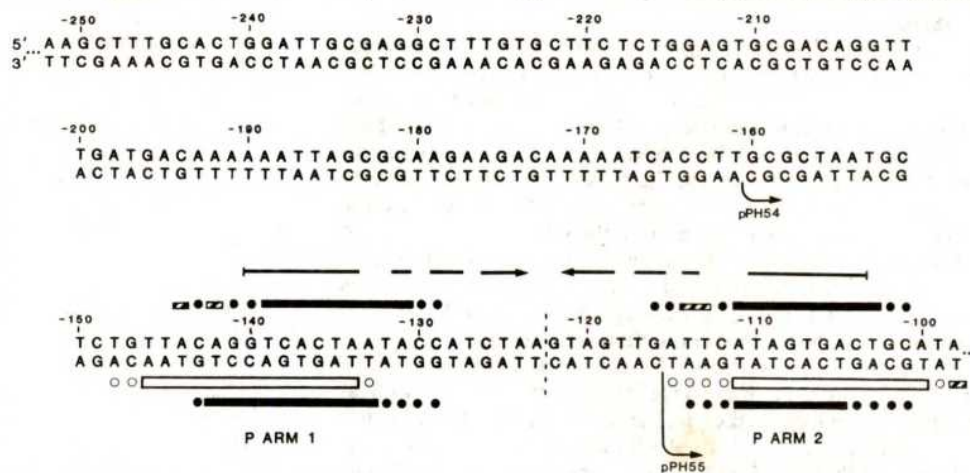
interactions with different domains of the Int protein. In contrast, however, each of the P arm sites shares a considerable uninterrupted homology (11-base pairs in P arm 1 and 8-base pairs in P arm 2) with the left portion of the P' arm site. The two P arm sites also share this homologous sequence but with an inverted orientation, such that P arm 1 is a direct repeat and P arm 2 is an inverted repeat of the P' homology. A number of bases in the sequence shared among the P' and P arm protected regions have been identified as 'contact' sites in the Int–DNA interaction, as defined by methylation-protection experiments with the P' site (data not shown). Included within the left half of the P' site is the 7-base pair sequence, TCACTAT, which, in addition to being part of the homology with the two P arm sites, is found (with one mismatch) in the right half of the P' site.

Int binding in the P' arm has the unique property of resistance to challenge by the polyanion heparin (Fig. 5a and ref. 9). Furthermore, in studies with DNA carrying only the P' arm site (data not shown) we have established that the heparin-resistant binding is not dependent on the presence of the other binding sites. Thus, Int binding and resistance to heparin challenge are intrinsic features of the P' arm sequence. As Int binding at sequences homologous to the left half of the P' arm site (P arm sites 1 and 2) did not show the property of heparin resistance (Fig. 5a), the right half of this site, which is essential for recombination (Table 1), might be responsible for heparin resistance.

We have also used the footprinting assay to examine restriction fragments carrying other combinations of one to three Int binding sites (data not shown). The P arm 1 site was capable of binding Int when present singly. The common core region, when tested using a fragment containing *att* sequence from −115 to +46, bound Int independently of the P arm 1 and P' sites. Quantitative measurements to determine whether there are subtle differences in binding affinities as a function of the simultaneous presence of two or more binding sites have not yet been carried out.

Efficient partners for phage *att* site

From *in vivo* Int-dependent crosses it was found that the phage *att* site recombines most efficiently with the bacterial *att* site and less efficiently with itself or either of the prophage *att* sites[14–16]. Similarly, in the *in vitro* conditions used here the phage *att* site recombined most efficiently with the bacterial *att* site. (Both *in vivo* and *in vitro* relative recombination values are strongly affected by reaction conditions and it is therefore difficult to make quantitative comparisons between them[16,19–21]).

In our *in vitro* experiments the supercoiled phage *att* site recombined with the linear bacterial *att* site at a level of approximately 50% and with the linear right prophage *att* site (*att*R) at a level of approximately 5–10% (Fig. 7). With the linear left prophage *att* site (*att*L) the level of recombination was just above background in this experiment (not visible in the reproduced photograph), and recombination with the linear phage *att* site was not detectable. The relative recombination efficiencies were affected significantly by factors such as Int concentration, and this aspect of the reaction is being investigated. Nevertheless, we always found that a linear bacterial *att* site gave very high values and a linear phage *att* site gave very low values in their respective recombination patterns with supercoiled phage *att* site. Is this difference due to the presence of unique features that confer competence on the linear bacterial *att* site, or is it due to certain features on the linear phage *att* site (and linear *att*L) that inhibit recombination with a supercoiled phage *att* site?

Four plasmids containing the common core and different combinations of P or P' arm Int binding sites (as described in Fig. 3) were used as linear partners for a supercoiled phage *att* site (Fig. 7). It is clear from the fact that linear pPH10 recombines

Fig. 5 Footprints of Int binding on restriction fragments containing: *a*, the entire minimal phage *att* site (using neocarzinostatin); or *b*, the P arm and common core regions (using DNase I). *a*, In lanes 1–3 the restriction fragment *Hin*dIII(−251)–*Hpa*II(+305), ^{32}P-labelled at the 5′ end of the top strand (*Hin*dIII), was partially digested with neocarzinostatin[28,29] in the absence (lane 3) or presence of purified Int protein at 10 μg ml⁻¹ (lane 2) or 20 μg ml⁻¹ (lane 1). The Int–DNA complex in lane 1 was challenged with heparin before neocarzinostatin digestion. Sequence markers for this restriction fragment, A+G (lane 4), and C+T (lane 5), were prepared according to the method of Maxam and Gilbert[27]. Details of these methods and electrophoresis conditions have been described previously[9]. A linear map of the minimal phage *att* site region depicts the relative sizes and positions of the four Int protected sequences (■) seen in the neocarzinostatin footprint. Also indicated are the boundaries (−160 and +82) of the smallest functional *att*P region obtained in these experiments (see Fig. 3) and the 15-base pair common core sequence (hatched). *b*, In lanes 1–3 a restriction fragment from plasmid pPH310, containing *att* sequence from +46 to −251(*Hin*dIII) (labelled at the 5′ end of the bottom strand at the *Bam*HI linker adjacent to position +46), was partially digested with DNase I in the absence (lane 3) or presence of purified Int protein at 2.5 μg ml⁻¹ (lane 2) or 5 μg ml⁻¹ (lane 1). The footprinting and electrophoresis conditions were as described previously[9]. The common core region has been run off this gel. Positions of enhanced cutting by DNase I (→) at ~ 10-base pair intervals (−75, −85, −95, −117, −128) are indicated in lane 1.

```
                              -10          0
att B. CORE    5'..T G A A G C C T G C T T T T T T A T A C ...
               3'..A C T T C G G A C G A A A A A A T A T G ...
```

```
                        -10              0                +10
att P CORE   5'...T T C T C G T T C A G C T T T T T T A T A C T A A G T T G G C A T T ...
             3'...A A G A G C A A G T C G A A A A A A T A T G A T T C A A C C G T A A ...
```

```
                     -140                    -130
P ARM 1    5'..T G T T A C A G G T C A C T A A T A C C ...
           3'..A C A A T G T C C A G T G A T T A T G G ...
```

```
                +50              +60              +70              +80
P' ARM   5'..A C G A A C A G G T C A C T A T C A G T C A A A A T A A A A T C A T T A T T T G A ...
         3'..T G C T T G T C C A G T G A T A G T C A G T T T T A T T T T A G T A A T A A A C T ...
```

```
                  -100            -110
P ARM 2    5'..T A T G C A G T C A C T A T G A A T C ...
           3'..A T A C G T C A G T G A T A C T T A G ...
```

Fig. 6 Comparison of Int-protected sequences in the bacterial and phage *att* sites. The sequence shown for each binding site is the maximum length of DNA protected by Int from either neocarzinostatin or DNase I digestion (see Figs 4 and 5 and ref. 9). The sequence of the P arm 2 site has been inverted (compare Fig. 4) to facilitate comparison of sequence homologies. A 6-base pair homology between the two common core sites and the P' arm site is indicated by a line between the two strands of sequence (——). Homologies between the left portion of the P' arm site and each of the two P arm sites are indicated (—)(see text). A 7-base pair sequence in the left half of the P' arm protected region, found within the sequence shared with the two P arm sites, is also found, with one mismatch, in the right half of the P' arm site (●).

efficiently with supercoiled *att*P that an efficient partner for the phage *att* site requires neither the P arm 1 nor the P' binding sites. In this test of integrative recombination the bacterial *att* site does not possess any unique features that cannot be provided or mimicked by a phage *att* site lacking the P arm 1 and P' Int binding sites (compare lanes 2 and 6, Fig. 7).

The only difference between the two *att* sites that recombined efficiently with *att*P and the two that failed to recombine significantly was the presence of the P' arm Int binding site. Thus, the presence of the P' arm site on the linear partner was unnecessary, and actually interfered with its ability to recombine with a supercoiled phage *att* site. The P arm 1 binding site did not contribute as much interference (Fig. 7, compare pPH10 and pPH510). The interfering effect did not seem to be due to titration by the P' arm binding site as it was not abolished by higher concentrations of Int.

Discussion

Our results reveal the involvement in recombination function of approximately 240-base pairs of DNA adjoining the cross-over locus. Similar experiments, using a different method for obtaining shortened *att* sites, have been carried out by Mizuuchi and Mizuuchi[22]. In addition, they found function for an *att* site in which bacterial DNA is substituted for phage DNA up to position −152 (8-base pairs less than our shortest functional P arm, pPH54 and pPH507). Therefore, it is probable that a clone carrying phage *att* site DNA from positions −152 to +82 (235-base pairs) would also be functional.

The diversity of the Int binding regions, both in sequence and in size (Fig. 6) is surprising. Considerable sequence homology is found among the three sites in the P and P' arms, but the sequence in the common core binding region does not share this homology. Sequence differences are almost certainly respon-

sible for the unique heparin-resistant character of binding in the P' arm site. The lack of homology between the core and the other sites could reflect more than one DNA-binding domain within the Int protein, or a single domain responding differently to the respective sequences. It is clear, however, that Int has at least two distinct capabilities. In addition to the 'structural' or DNA-binding properties involving sequences quite distant from the cross-over site of recombination, Int also has a nicking-closing (topoisomerase) activity[10]. Although no specificity for the phage *att* site has yet been demonstrated in the topoisomerase assays, it is clear from our results that Int does interact specifically with the normal substrate for this enzymatic activity[9].

The nature of the role of the distant Int binding sites in the P and P' arms is much less apparent. Int binding seems to be an intrinsic feature of the individual DNA sequences since protection was seen for the P arm 1 and P' sites when present singly and for the common core in the absence of the P arm 1 and P' sites. The kinetics has not yet been studied, however, and it is possible that there is facilitation of binding at one site by Int bound at another site.

The two size classes of Int binding sites, approximately 30–35-base pairs and 15-base pairs, could reflect differences in the number of bound Int monomers. Similarities between the two P arm sites and each half of the larger P' site also suggest the possibility of higher order Int complexes. The linear distance between the P arm 1 and P' Int binding sites, or between the common core and either of these sites, is not incompatible with a three-dimensional structure in which a loop of DNA would bring any of these sites together in the same Int complex. For example, the distance between non-contiguous sequences which are in close proximity in the three-dimensional structure of the nucleosome is estimated to be approximately 80-base pairs[23]. By analogy with studies on nucleosomes[24,25] and DNA gyrase

Fig. 7 The efficiency of different *att* sites as linear recombination partners. The *in vitro* recombination reactions and gel electrophoresis were performed as described in Fig. 2 legend. Each reaction mixture contained supercoiled pWR1 (1.5 μg) and linear recipient DNA in a three to one molar ratio. The linear plasmids were generated by *Pst*I digestion of pPH7, 10, 507, 510 or by *Eco*RI digestion of pWR1, pWR101, pPH201 and pPH202. The origin and boundaries of the restriction fragments carried by each plasmid are described in Fig. 3 legend. Positions are indicated on the electropherogram for DNA containing different 'recipient' *att* sites (linear plasmid), the 'donor' circular plasmid DNA (pWR1) containing the phage *att* site and migrating as supercoils (s.c.) or nicked circles (n.c.) and the linear product of recombination (arrows).
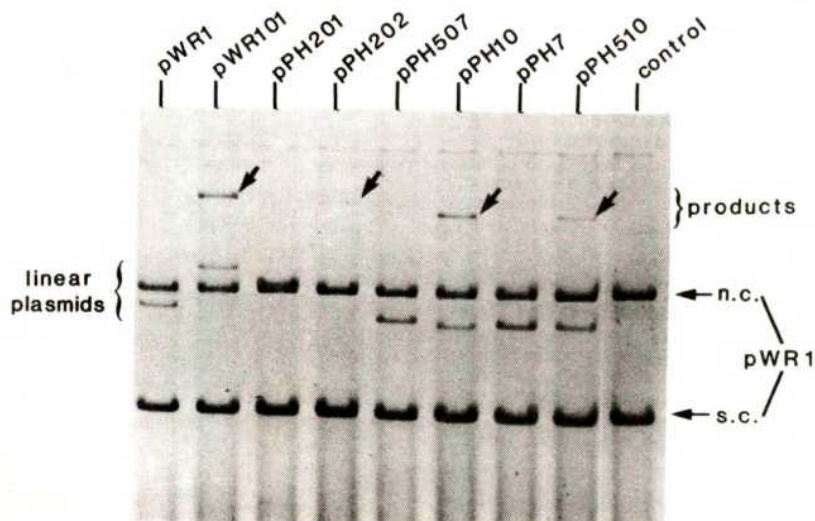
complexes[26] the 10-base pair pattern of enhanced cutting around the binding sites (Fig. 5b) is suggestive of DNA wrapping around, or lying on, the surface of a higher order oligomer of Int. This idea is consistent with the electron microscope observation of Int complexes (8–10 monomers) interacting with the phage *att* site (Bob Yuan, personal communication).

Although their specific functions have not yet been defined, it is clear that the P arm 1 and P′ Int binding sites have critical roles in recombination. Further experiments will be necessary to ascertain whether the P arm 2 binding site is also critical and whether the observed Int–DNA interactions are influenced by host factor proteins or by negatively supercoiled DNA substrate.

Our results suggest a model for integrative recombination that involves two unequal partners. The large size and complexity of the phage *att* site contrasts with the smaller size and simplicity of its partner. We refer to the phage *att* site, which must be supercoiled and which provides most of the structural information and specificity for the reaction, as the 'donor' molecule. A 'donor' *att* site recombines efficiently with an appropriate 'recipient' *att* site, such as the bacterial *att* site. Although we have yet to define the minimal requirements for 'recipient' *att* sites, several properties are known. We have shown previously that Int binding to the bacterial *att* site results in the protection

of a short (approximately 15-base pairs) DNA sequence at the left core–arm juncture[9]. The present results (and additional data, not shown) establish that a 'recipient' *att* site does not require the presence of the P arm 1 or P′ arm binding sites. Furthermore, the absence of the P′ site is necessary for a good 'recipient' *att* site. The sequence homology between the shortened phage *att* site (pPH10) and the bacterial *att* site, together with their respective Int protection patterns, suggests that an efficient 'recipient' site may not be much larger than the common core and partially homologous core–arm junctures[13]. Additional experiments will be necessary to confirm, and possibly extend, the applicability of this 'donor–recipient' model for integrative recombination.

1. Gottesman, M. E. & Weisberg, R. A. in *The Bacteriophage Lambda* (ed. Hershey, A. D.) 113–138 (Cold Spring Harbor Laboratory, New York, 1971).
2. Nash, H. A. *Curr. Topics Microbiol. Immun.* **78**, 171–199 (1978).
3. Miller, H. I., Kikuchi, A., Nash, H. A., Weisberg, R. A. & Friedman, D. I. *Cold Spring Harb. Symp. quant. Biol.* **43**, 1121–1126 (1979).
4. Hoess, R., Foeller, C., Bidwell, K. & Landy, A. *Proc. natn. Acad. Sci. U.S.A.* (in the press).
5. Gottesman, S. & Abremski, K. *J. molec. Biol.* **138** (in the press).
6. Kotewicz, M., Chung, S., Takeda, Y. & Echols, H. *Proc. natn. Acad. Sci. U.S.A.* **74**, 1511–1515 (1977).
7. Kikuchi, Y. & Nash, H. A. *J. biol. Chem.* **253**, 7149–7157 (1978).
8. Kikuchi, Y. & Nash, H. A. *Cold Spring Harb. Symp. quant. Biol.* **43**, 1099–1109 (1979).
9. Ross, W., Landy, A., Kikuchi, Y. & Nash, H. A. *Cell* **18**, 297–307 (1979).
10. Kikuchi, A. & Nash, H. A. *Proc. natn. Acad. Sci. U.S.A.* **76**, 3760–3764 (1979).
11. Mizuuchi, K. & Mizuuchi, M. *Cold Spring Harb. Symp. quant. Biol.* **43**, 1111–1114 (1979).
12. Mizuuchi, K., Gellert, M. & Nash, H. A. *J. molec. Biol.* **121**, 375–392 (1978).
13. Landy, A. & Ross, W. *Science* **197**, 1147–1160 (1977).
14. Guerrini, F. *J. molec. Biol.* **46**, 523–542 (1969).
15. Echols, H. *J. molec. Biol.* **47**, 575–583 (1970).
16. Guarneros, G. & Echols, H. *Virology* **52**, 30–38 (1973).
17. Galas, D. J. & Schmitz, A. *Nucleic Acids Res.* **5**, 3157–3170 (1978).
18. Davies, R. W., Schreier, P. H., Kotewicz, M. L. & Echols, H. *Nucleic Acids Res.* **7**, 2255–2273 (1979).
19. Pollock, T. J. & Abremski, K. *J. molec. Biol.* **131**, 651–654 (1979).
20. Nash, H. A. *Proc. natn. Acad. Sci. U.S.A.* **72**, 1072–1076 (1975).
21. Gottesman, S. & Gottesman, M. E. *J. molec. Biol.* **91**, 489–499 (1975).
22. Mizuuchi, M. & Mizuuchi, K. *Proc. natn. Acad. Sci. U.S.A.* in the press.
23. Finch, J. T. *et al. Nature* **269**, 29–36 (1977).
24. Noll, M. *Nucleic Acids Res.* **1**, 1573–1578 (1974).
25. Lutter, L. C. *Nucleic Acids Res.* **6**, 41–56 (1979).
26. Liu, L. F. & Wang, J. C. *Cell* **15**, 979–984 (1978).
27. Maxam, A. & Gilbert, W. *Proc. natn. Acad. Sci. U.S.A.* **74**, 560–564 (1977).
28. D'Andrea, A. D. & Haseltine, W. *Proc. natn. Acad. Sci. U.S.A.* **75**, 3608–3612 (1978).
29. Hatayama, T., Goldberg, I., Takeshita, M. & Grollman, A. *Proc. natn. Acad. Sci. U.S.A.* **75**, 3603–3607 (1978).

LETTERS

IR observations of the double quasar 0957 + 561 A, B and the intervening galaxy

**B. T. Soifer*, G. Neugebauer*, K. Matthews*,
E.E. Becklin†, C.G. Wynn-Williams† & R. Capps†**

* Palomar Observatory, California Institute of Technology, Pasadena, California 91125
† Institute for Astronomy, University of Hawaii, Honolulu, Hawaii 96822

The properties of the remarkable double quasar 0957 + 561 were first described by Walsh et al.[1]. Recently Young et al.[2] have described CCD observations of a distant galaxy associated with the quasar pair, and have identified this galaxy as a gravitational lens forming a double image of a single quasar. We report here 1.2–2.2-μm observations of the system that support the conclusion that the twin quasars are a pair of images of a single object; the quasar has an energy distribution that is unusual. The intervening galaxy is shown to be highly luminous with a bolometric luminosity of about $2 \times 10^{11} L$.

As described by Walsh et al.[1] the system consists of two 17th magnitude visual objects with redshift $z = 1.4$; they refer to these as A and B, object A lying 5.7 arc s north of B. The galaxy
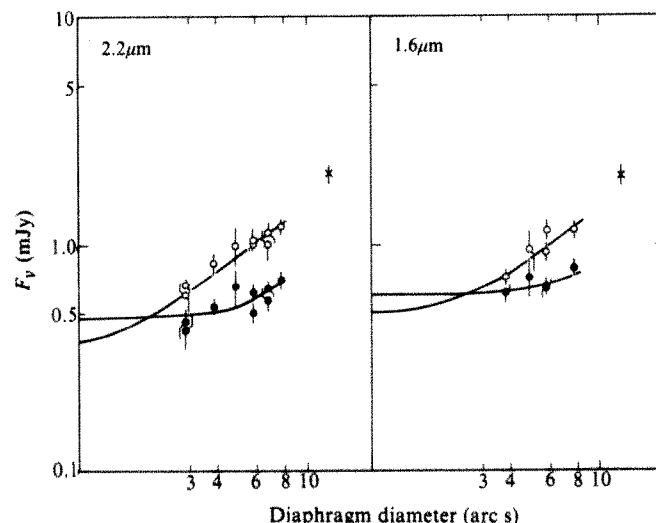
Fig. 1 The flux density plotted versus observing diaphragm for 1.6 and 2.2 μm. ●, Observations centred on 0957 + 561A; ○, observations centred on 0957 + 561B. × indicates an observation made with a 12.5 arc s diaphragm centred between the two quasars. The solid lines are fits of a point source plus galaxy contribution in diaphragms centred on the quasars. The change in flux with diaphragm diameter for the galaxy is scaled from the visual observations of Young, et al.[2].

Table 1 Observed flux density of 0957 + 561 A, B

Diaphragm (arc s)	Date (UT) 1979	Flux density (mJy) 1.2 μm A	B	1.6 μm A	B	2.2 μm A	B
2.9	17 December					0.45 ± 0.07	0.60 ± 0.09
	18 December					0.42 ± 0.08	0.66 ± 0.05
3.8	18 December			0.60±0.05	0.71±0.05	0.53 ± 0.05	0.89±0.06
5.0	26 November*	0.6 ± 0.1	0.8 ± 0.1	0.72±0.14	0.95±0.19	0.66 ± 0.12	0.99±0.18
5.8	18 December			0.65 ± 0.06	0.94 ± 0.08	0.62 ± 0.06	1.01 ± 0.08
	2 November			0.64 ± 0.06	1.16 ± 0.12	0.51 ± 0.05	1.06 ± 0.11
6.7	17 December					0.57 ± 0.08	1.00 ± 0.15
						0.64 ± 0.05	1.13 ± 0.11
7.7	18 December			0.79 ± 0.06	1.17 ± 0.08	0.70 ± 0.07	1.21 ± 0.09
12.5	17 December	1.2 ± 0.3		2.1±0.2		2.1 ± 0.2	

* At 5-m Hale telescope.

found by Young et al.[2] lies 0.8 arc s north of B; it has a redshift of 0.4 and has angular dimensions of the order of 5 arc s.

The observations reported here consist of IR photometry of the twin quasars at 1.6 and 2.2 μm through a series of diaphragms. These observations were obtained using the 3-m telescope of the NASA IR Telescope Facility at the Mauna Kea Observatory and the 5-m Hale telescope on Palomar Mountain. The most extensive observations were obtained on the nights of December 16 and 17 1979 at Mount Kea in conditions when the seeking disk was ≤1 arc s. Variations in seeing during the multiple-diaphragm observations were accounted for by observing the star ϕ Ursae Majoris as a secondary standard before each observation of the quasar pair. This sequence was repeated for each wavelength and each diaphragm used. In addition to the multiple diaphragm observations on each quasar, observations were obtained at 1.2, 1.6 and 2.2 μm with a 12.5 arc s diaphragm centred between the two quasars.

Table 1 and Fig. 1 show the observed flux densities within various diaphragms centred on quasars A and B. The 1.6- and 2.2-μm observations of quasar B show a strong dependence of flux on observing diaphragm, the observed 2.2-μm flux doubling between the 3 and 8 arc s diaphragms. This observation clearly shows the presence of extended IR emission in the vicinity of quasar B. A similar, but much smaller, effect is also seen in the observations of quasar A.
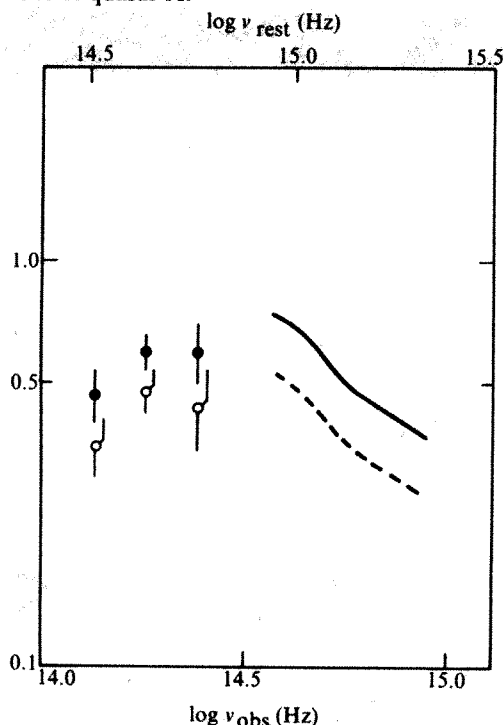
Fig. 2 The energy distributions of the quasars 0957 + 561A (●) and B (○) from 0.35 to 2.2 μm. The data have been corrected for the contribution of the underlying galaxy and represent only the quasar contributions. At visual wavelengths, the flux densities for quasar B are taken as 0.72 of quasar A, as per Young et al.[2].

We interpret the extended emission as being due to the galaxy identified by Young et al.[2]. To separate the contributions to the multiple-diaphragm observations from the galaxy and from the quasars the light distribution for the galaxy, as reported by Young et al.[2], has been numerically integrated for various diaphragms centred on quasars A and B. The IR observations centred on quasar B were first fitted as the sum of a quasar component which is constant with diaphragm plus a galaxy component for which the IR flux density was assumed to follow the visual light distribution as measured by Young et al.[2]. The best fit to the observations centred on B is included in Fig. 1 and listed in Table 2; for this fit, 42% of the 2.2-μm flux density in a 3-arc s diameter diaphragm arises in the intervening galaxy. To determine the flux densities of quasar A, the galaxy contribution to the observations centred on A was determined from the fit to the observations centred on B. The best fit to these observations is also shown in Fig. 1.

The ratio of fluxes of the B and A quasars are $F_\nu(B)/F_\nu(A) = 0.80 \pm 0.15$ and 0.74 ± 0.15 at 1.65 μm and 2.2 μm respectively. These ratios are consistent with the ratio of B/A found visually by Young et al.[2] of 0.75 ± 0.04 and at radio wavelengths of 0.80 ± 0.05 (refs 3, 4). Thus, in all observed wavelength ranges, the two quasars have a constant flux ratio, consistent with the achromatic imaging predicted by the gravitational lens model. This conclusion is valid if there is no significant difference in the extinction along the two separate light paths through the intervening galaxy.

The 0.35–2.2-μm continuum distribution of the quasars shown in Fig. 2 is unusual. The increase in flux density from $10^{14.5}$ to 10^{15} Hz in the quasar rest frame is rare; of the 39 quasars observed by G.N. et al.[5] all but one show a negative spectral index at these wavelengths. The similar energy distribution of quasars A and B make them far more similar to each other than to any other known quasar. This again strongly suggests the idea that these objects are two images of a single physical object, rather than two quasars in the same cluster.

Because the light emitted from the galaxy dominates the flux longward of 1 μm, the properties of the galaxy can be inferred from a fit to the IR observations. Figure 3 shows the energy distribution of the galaxy in a 7-arc s diaphragm; Table 2 gives the flux densities of the whole galaxy at 1.2, 1.6 and 2.2 μm. Young et al.[2] find an R magnitude for the entire galaxy of $R \sim 18.5 \pm 0.2$ mag; thus $(R-[2.2])_{galaxy} = 4.3 \pm 0.3$ mag and $([1.6]-[2.2])_{galaxy} = 0.8 \pm 0.3$ mag. These colours are consistent with those found for luminous galaxies at a redshift of around 0.4 by S. E. Persson, K.M. and G.N. (unpublished results).

Table 2 Derived flux densities

	1.2 μm*	1.65 μm	2.2 μm
0957 + 561 A	0.6 ± 0.1	0.60 ± 0.06	0.47 ± 0.07
0957 + 561 B	0.4 ± 0.1	0.48 ± 0.06	0.35 ± 0.06
Galaxy (12.5 arc s)	0.6 ± 0.3	0.95 ± 0.15	1.23 ± 0.15

* The flux densities derived at 1.2 μm are based on extrapolations and have unknown systematic uncertainties.
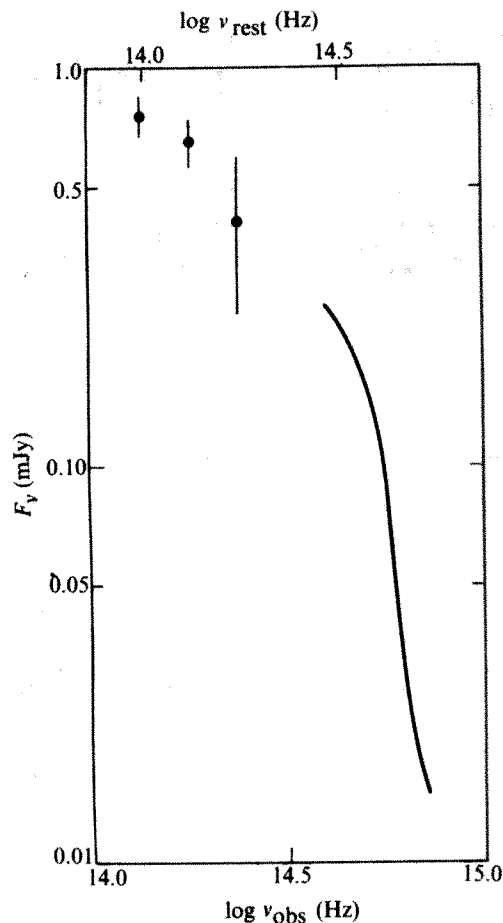
Fig. 3 The energy distribution from 0.35 to 2.2 μm of the galaxy associated with the quasars 0957+561A, B as derived from observations in a 7 arc s diaphragm centred on the B quasar. At all wavelengths, the contribution from the quasars have been subtracted from the observed flux to yield this energy distribution. At 1.2 μm the equivalent flux density in a 7 arc s diaphragm has been derived from observations in a 5 arc s diaphragm. The visual observations are from Young *et al.*[2].

If the Hubble constant $H_0 = 60$ km s^{-1} Mpc^{-1} and the deceleration parameter $q_0 = 1$, the luminosity of the galaxy in the observed wavelength range 0.4–2.2 μm is $2 \times 10^{11} L_\odot$, establishing it as a highly luminous galaxy. If the energy distribution of this galaxy resembles that of the giant elliptical galaxy M87, which has a bolometric luminosity of $1.3 \times 10^{11} L_\odot$ (ref. 6), then the bolometric luminosity of the lens galaxy in the double quasar system is $2.4 \times 10^{11} L_\odot$.

In conclusion, IR observations of the double quasar 0957+561 A,B support the gravitational lens model of these objects in two significant ways.

(1) The ratio of the IR flux densities of the two components is the same as found in the visual and at radio wavelengths. Furthermore, the derived energy distributions for the two components are the same and extremely unusual. This strongly supports the suggestion that quasars A and B are indeed two images of the same physical object.

(2) The IR properties of the lens galaxy are entirely consistent with it being a giant elliptical galaxy at a redshift of ~0.40.

We thank J. Gunn, J. Oke, S. Persson, A. Stockton, D. Walsh, G. Rieke, and P. Young for discussions and for letting us see their data before publication. We also thank our telescope operators J. Carrasco, R. Koehler and B. Shaeffer. This work was supported by NASA grants NGL 05-002-207 and NASW-3159 and NSF grants AST 77-20516 and AST 78-26028. B.T.S., G.N. and C.G.W-W. are visiting astronomers at the NASA IR Telescope Facility of Mauna Kea, Hawaii.

1. Walsh, D., Carswell, R. F. & Weymann, R. J. *Nature* **279**, 381 (1979).
2. Young, P., Gunn, J. E., Kristian, J., Oke, J. B. & Westphal, J. A. Preprint (1980).
3. Pooley, G. G. *et al. Nature* **280**, 477 (1979).
4. Roberts, D. H., Greenfield, P. E. & Burke, B. F. *Science* **205**, 894 (1979).
5. Neugebauer, G., Oke, J. B., Becklin, E. E., & Matthews, K. *Astrophys. J.* **230**, 79 (1979).
6. Frogel, J. A., Persson, S. E., Aaronson, M. & Matthews, K. *Astrophys. J.* **220**, 75 (1978).

Spectra of interplanetary scintillation

T. W. Cole & O. B. Slee

Division of Radiophysics, CSIRO, Sydney, Australia

A new type of radio spectrograph is described here which has been used to observe the interplanetary scintillation of a radio source over a two-to-one frequency range. Simultaneous observations over this range provide a direct insight into the time variations of intensity and the physical form of the interplanetary irregularities producing them. A specific example shows the direct way in which the spectral record can indicate the physical details of the electron density variations of the interplanetary medium.

The scintillation of small-diameter radio sources[1] due to scattering in the outer layers of the solar corona has been analysed statistically[2,3] and the observations fit the theory of diffraction at a thin screen reasonably well[4]. The corona is subject to strong day-to-day variations, and some of the inconsistencies would be due to the non-simultaneous observations at the specific frequencies used in these comparisons. However, the theories are not complete and particular problem areas include[3,5] the actual form of the irregularities, and an excess of enhanced emission occurring as the scattering moves from being weak to strong—the r.m.s. phase deviation on the wavefront emerging from the screen increases to 1 rad and beyond. It is in these areas that the spectral observations are particularly illuminating.

The observations are made with a new and unique form of radio spectrum analyser, the acousto–optical radio spectrograph. The broadband radio signal from the radio telescope is converted to a travelling ultrasonic wave in a solid medium. A Bragg interaction between the travelling ultrasonic beam and a transverse, collimated beam from a helium–neon laser produces diffracted light whose angular intensity distribution can be shown to be the power spectrum of the applied radio signal [8,9]. In the observations discussed here, the Parkes 64-m radio telescope was used with a broadband feed and amplifier in such a way that the frequency range 280–520 MHz was analysed by the spectrograph. The optical output was detected by a self-scanned array of photodiodes and digitized [6,7]. The 240 MHz bandwidth was resolved into 256 simultaneous channels and complete spectra were recorded on magnetic tape 25 times per second.

Source 3C273 was observed on 10 and 11 October 1978, when its line of sight was 13° (0.23 AU) from the Sun's centre. At this position the current theory[4] predicts that the mean r.m.s. phase deviation, ϕ_0, varies from ~0.65 to ~0.35 rad over 280–520 MHz respectively and that the scale size, a_0, of irregularities, assumed to have a correlation distribution $\exp(-r^2/2a_0^2)$, is ~55 km. If one defines a Fresnel distance z_0 as $2\pi a^2/\lambda$, these values of a_0 correspond to z_0 varying between 0.12 and 0.25 AU over 280–520 MHz respectively. On an average day one would be well into the 'far-field' of the diffraction. A sample of the data obtained on 11 October is shown in Fig. 1 with a 40-ms time resolution and smoothed to 53 frequency channels over the range 280–520 MHz. Without resorting to statistical analysis one can see that the variations are highly correlated over the frequency range and are dominated by both weak and strong curved ridges of emission which take about 1 s to sweep across the frequency range.
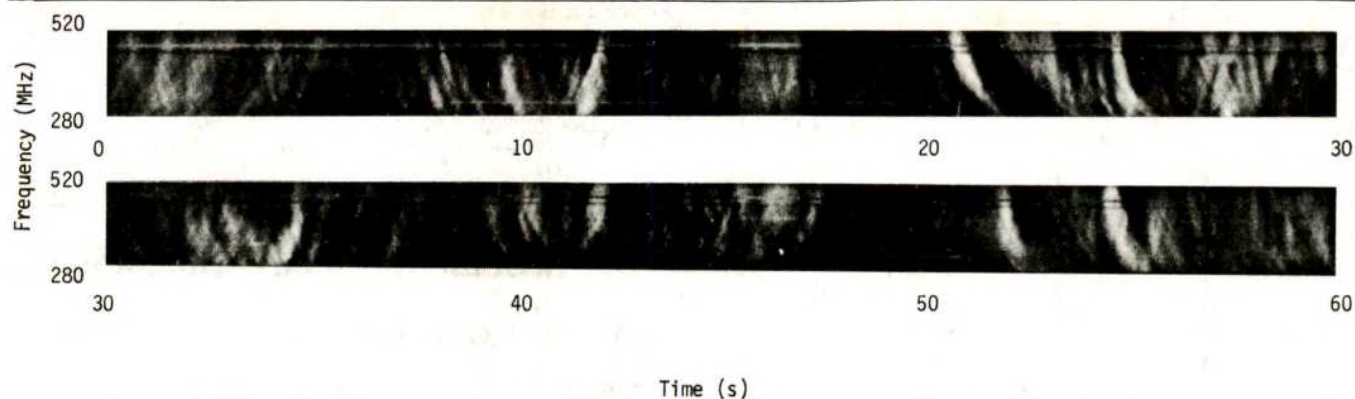
Fig. 1   An example of the intensity variations of source 3C273 due to interplanetary scintillation. Systematic structure on the frequency–time plane is evident. The figure is plotted with a frequency resolution of 4 MHz, time resolution of 40 ms, and white represents increased intensity.

As suggested by Hewish, the simplest explanation for the curved bands in Fig. 1 is that a normal, random diffraction pattern has been refracted by large wedge-shaped irregularities which are themselves too large to produce intensity variations. This would account for the increasing curvature at lower frequencies, where the refractive index of the plasma is also higher.

However, the dynamic spectrum reveals details which cast doubt on such an explanation. It can be seen that Fig. 1 contains bands of a characteristic shape. That is, the curvature at any frequency is always of essentially the same magnitude although the sign of the curvature can vary. The refracting wedges would need to be of constant wedge angle. The wedge would also need to change sharply from this angle to the negative value of the same angle within 1 s to explain sections of Fig. 1 such as at 10 s and 41 s. An even greater difficulty is illustrated by Fig. 2, where the section of Fig. 1 at around 45 s is shown in greater contrast. As at other parts of the record, bands of opposite sign are observed superimposed. Multiple refracting wedges in the line of sight would simply add the refracting angles algebraically and one could not expect to maintain the characteristic curvatures observed.

Further details are revealed in the more intense bands, one of which is displayed in higher contrast in Fig. 3. The peak intensity takes about 1 s to sweep across the frequency range. At an assumed solar wind speed of 400 km s^{-1}, this represents an angular displacement of 400 km in 1 AU or 0.55″. If the refractive index (and hence refracting angle) of the plasma varies as f^{-2}, then it is 3.5 times greater at 280 than at 520 MHz. The 0.55″ then represents the difference in refraction angles or 2.5 times the refraction angle at 520 MHz. The increasing curvature to the band indicates a typical refraction angle of 0.22″ at 520 MHz and 0.77″ at 280 MHz.

Figure 3 also indicates a feature visible on all the stronger bands of Fig. 1. At the higher-frequency end and always on the

inside of the curvature is a region of intensity which is reduced below the mean intensity level. This is also indicative of refraction if the figure is interpreted as interference between a plane wave and a wave impinging at an angle. The strong band is a region of constructive interference and the reduced intensity is where a half-wavelength phase difference produces destructive interference. These successive interference fringes are seen to be about 0.6 s apart in time at 520 MHz or 240 km for an assumed solar wind speed of 400 km s^{-1}. The corresponding angle at 520 MHz is a half-wavelength in 240 km or 0.25″. Both the curvature and fringes indicate the origin for the band as
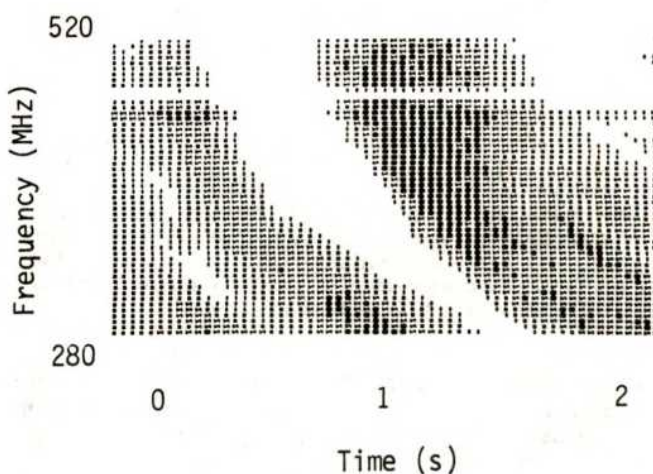
Fig. 3   A high-contrast picture of a strong band reveals the characteristic increasing curvature and the successive bright and dark interference fringes at the higher frequencies.

being due to refraction. The interference fringes are, however, also incompatible with the refraction being due to a large wedge. With a large wedge the background wave would also be refracted and the interference would not be observed.

An alternative explanation is that the bands are the result of individual refracting elements in the interplanetary medium. That is, at least for this solar elongation, there are insufficient irregularities in the line of sight to produce a random diffraction pattern. A picture emerges of irregularities in the form of comparatively sharp gradients in the plasma density. This picture is quite different from that usually assumed and certainly different from the 'weakly scattering' assumptions at the basis of work such as that of Uscinski[3]. The observed fact that strong, individual bands or 'spikes' are seen only at the smaller solar elongations[5] is also consistent with one seeing fewer irregularities in the line of sight and, at least for the stronger cases, the effects of individual irregularities.

Fig. 2   A section of Fig. 1 is reproduced with increased contrast to illustrate the superposition of bands of opposite curvature.

More observations, analysis and modelling are to be done, but even these preliminary results suggest the value of dynamic spectral observations in the analysis of interplanetary scintillations. Just as spectral observations of scintillations from the ionosphere gave greater insight[8] than single-frequency studies, so the spectral observations reported here extend single-frequency interplanetary studies. The fact that single-frequency observations of interplanetary scintillations might obey Rayleigh statistics is not always sufficient proof that a random scattering medium is actually involved. One possibility suggested here is of systematic diffraction from sharp density gradients.

We thank Itek Corporation for the spectometer's modulator and Professor A. Hewish for help in our understanding of the scintillation process.

1. Hewish, A., Scott, P. F. & Wills, D. *Nature* **203**, 1214 (1964).
2. Salpeter, E. E. *Astrophys. J.* **147**, 433 (1967).
3. Uscinski, B. J. *The Elements of Wave Propagation in Random Media* (McGraw-Hill, New York, 1977).
4. Readhead, A. C. S., Kemp, M. C. & Hewish, A. *Mon. Not. R. astr. Soc.* **185**, 207 (1978).
5. Cohen, M. H. & Gundermann, E. J. *Astrophys. J.* **155**, 645 (1969).
6. Cole, T. W., Stewart, R. T. & Milne, D. K. *Astr. Astrophys.* **67**, 277 (1978).
7. Cole, T. W. & Milne, D. K. *Proc. astr. Soc. Aust.* **3**, 108 (1977).
8. Wild, J. P. & Roberts, J. A. *J. atmos. terr. Phys.* **8**, 55 (1956).
9. Lambert, L. E. *IRE Intl. Conv. Rec.* Pt 6, **10**, 69 (1962).
10. Milne, D. K. & Cole, T. W. *Proc. Inst. Radio Electron. Eng. Aust.* **40**, 43 (1979).

An alternative interpretation by A. Hewish*

Cole and Slee have suggested that their beautiful observations of interplanetary scintillation cannot be explained by conventional models of the solar plasma. I do not share their view and now outline my reasons for believing that the new data reinforce the standard theory.

On conventional models, derived from spacecraft and radioastronomical data, the solar plasma contains density irregularities having a three-dimensional wavenumber power spectrum $P(K)$ which approximates to a Kolmogorov spectrum $P(K) \propto K^{-11/3}$ for irregularities on a scale $10^6 \text{km} > 2\pi K^{-1} > 10^3\text{km}$. Evidence for a flattening of the spectrum for $2\pi K^{-1} < 10^3\text{km}$ has been reviewed elsewhere[1,2]. At a solar elongation of 13°, and at 400 MHz, Readhead *et al.*[1] predict intensity fluctuations on a time scale of about 0.7s, with a scintillation index of about 0.75, and which correlate over a band of about 200 MHz. These features are in good agreement with Fig. 1.

It is well known that irregularities on a scale larger than about 10^3km (at this elongation) give reduced intensity fluctuations at 400 MHz because the Earth is then within the near-field zone. The larger irregularities, therefore, introduce phase gradients across the incident wavefront. I have shown elsewhere[3], in connection with the interstellar scintillation of pulsars, that scintillation due to small-scale irregularities combined with phase gradients due to large-scale irregularities produces characteristic frequency drifts similar to those observed by Cole and Slee. The drift rate is

$$\frac{\text{d}\nu}{\text{d}t} = \pm \frac{V\nu}{2Z\theta_r}$$

where V is the drift velocity of the diffraction pattern, Z the distance to the irregularities, and θ_r the angular refraction corresponding to the phase-gradient. This phenomenon was originally discussed by Shishov[4].

The observations of Cole and Slee show frequency drifts which change sign in about 5 s, corresponding to a periodicity of roughly 10 s. This requires irregularities of scale $2\pi K^{-1} \sim 4 \times 10^3\text{km}$ assuming a solar wind speed of 400 km s^{-1}. The model of Readhead *et al.*[1] indicates a phase modulation $\phi \sim 0.53$ rad at 400 MHz for small-scale irregularities which produce scintillation on a time scale of about 0.7 s. Assuming $P(K) \propto K^{-11/3}$

we derive $\phi \sim 0.53(10/0.7)^{5/6} \simeq 5$ rad for the integrated phase modulation on scales up to 4×10^3 km. Putting $\theta_r \sim \phi K \lambda/2\pi \approx 0.2$ arc s we obtain $\text{d}\nu/\text{d}t \sim \pm 390 \text{ MHzs}^{-1}$ for $Z = 1$ AU and $\nu = 400$ MHz. This drift rate is typical of many features seen in Fig. 1. The question of simultaneous drifts with opposite sign mentioned by Cole and Slee raises no problems. The magnitude of θ_r ensures that wave fronts refracted convergently at a distance of 1 AU must, on arrival at the Earth, be overlapping for $\sim 10\%$ of the total time, leading to the superposition of patterns having drifts in opposite directions. The convergence and divergence of wave fronts suggest that overlap regions should be flanked by bands of negative slope on the preceding side, and positive slope on the following side, which is certainly true for the feature at 45 s discussed by Cole and Slee. They should also be associated with a higher mean intensity which can again be seen.

Finally it should be mentioned that the 'spiky' nature of the intensity variations is typical of diffraction patterns at distances not too far from the 'focusing' distance of the random irregularities. This property has been reviewed by Uscinski[5]. I conclude that the standard theory, involving the integrated effect of many 'weak' irregularities along the line of sight, is in excellent agreement with the present observations. I believe that more extended data of this kind could add considerably to our knowledge of $P(K)$.

1. Readhead, A. C. S., Kemp, M. C. & Hewish, A. *Mon. Not. R. astr. Soc.* **185**, 207 (1978).
2. Coles, W. A. & Harmon, J. K. *J. geophys. Res.* **83**, 1413 (1978).
3. Hewish, A. *Mon. Not. R. astr. Soc.* (in the press).
4. Shishov, V. I. *Astr. Zh.* **50**, 941 (1973).
5. Uscinski, B. J. *The Elements of Wave Propagation in Random Media* (McGraw-Hill, New York, 1977).

Crystal structure of Ag · TCNQ

N. Uyeda, T. Kobayashi, K. Ishizuka & Y. Fujiyoshi

Institute for Chemical Research,
Kyoto University,
Uji, Kyoto 611, Japan

High resolution electron microscopy (HREM) has been used for the direct imaging of complex crystal structures. High resolution at an atomic level cannot be expected from most organic crystals due to their high sensitivity to electron radiation damage, although we [1] have previously considered the conspicuous images of chlorine and copper atoms in chlorinated copper phthalocyanine molecules as a special case dependent on the very radiation-resistant property of the compound. In practice, however, some organic crystals may be able to withstand the dosage necessary for the image recording itself but could not tolerate the extra dosage necessary for searching the proper image field and for successive careful focusing. In this respect, the principle of the minimum exposure proposed by Williams and Fisher[2] is attractive as it might reduce the unnecessary damage which takes place before the actual image recording. We describe here the structure images of a metal complex of 7 7', 8, 8'-tetra-cyanoquinodimethane (TCNQ) with the resolution of an atomic level obtained by developing an automated device which is basically similar to that by Unwin and Henderson[3]. The electron microscope equipped with the low dosage device was JEM-200CX, which gives the instrumental resolution of 0.24 nm.

The various metal salts of TCNQ behave as the charge transfer complexes which show interesting electronic and magnetic properties. A thin crystalline film of complex salt forms by solid state diffusion when a thin film is prepared in the form of a double layer by the successive vacuum condensation of TCNQ and metal on a suitable substrate[4]. If the metal film is deposited on TCNQ crystallites which have been epitaxially grown in advance on a KCl cleavage face, the reaction leads to a

*Department of Physics, University of Cambridge, Cavendish Laboratory, Madingley Road, Cambridge CB3 OHE, UK
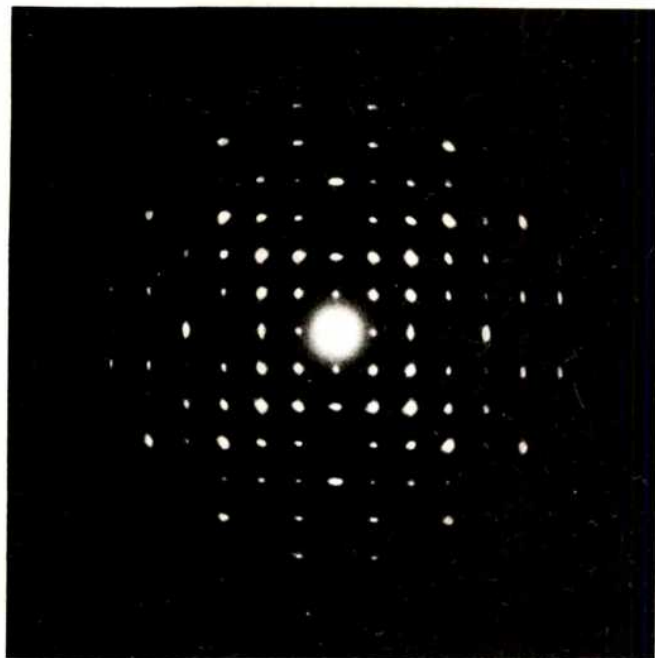
Fig. 1   SAD pattern from a crystallite of Ag.TCNQ salt taken with the incident electron beam parallel to the c-axis of a tetragonal unit cell.

topotactic formation of the complex crystallites which eventually assume characteristic orientations. This type of solid state formation of complex salts was found to be possible in general with many metals such as Al, Ag, Au, Co, Cs, Cu, Fe, Li, Mn, Ni, Ti and Zn. In the present work, we used very thin crystallites of Ag · TCNQ because the medium heavy ions such as silver were expected to give sufficient contrast for the clear recognition of their individual images. The selected area diffraction (SAD) indicated that the crystal assumes a tetragonal unit cell the dimensions of which are $a = 1.25$ nm and $c = 0.70$ nm. With the electron beam incident normal to the specimen habit face, the single crystal pattern presents a characteristic tetragonal symmetry as shown in Fig. 1 and the reflections are expected to contribute to the formation of high resolution images. To avoid the confusing effect of the dynamical electron scattering on the image formation, the crystal thickness was carefully controlled to be as thin as 3nm by monitoring it with a quartz crystal microbalance.

The images of Ag · TCNQ complex salt were recorded on Fuji FG films for 0.7 s at the electron optical magnification of 170,000 with the electron dosage of ~0.2 C cm^{-2}. The optical density of the film developed with Kodak D-19 was <0.5, causing a considerable amount of photographic noise which was enhanced by the quantum fluctuations in the images. To increase the signal-to-noise ratio the final images were translationally averaged over the crystal periodicities along the two tetragonal axes by applying the photographic multiple exposure technique. An enlarged photomicrograph of the structure image thus obtained is reproduced in Fig. 2a.

The characteristic features of the structure image are the square net pattern composed of the obtuse zigzag lines and the rod-like figures of roughly 0.3 nm in width all located in the middle of the elemental squares. As each rod is orientated to be normal to those in the neighbouring squares, the two dimensional unit cell is assigned as the large square indicated in Fig. 2, showing a good agreement with that expected from the diffraction data. Note the high contrast dots at every knot of the net structure. Both ends of the individual rods are related to the square sides at their re–entrant tips.

The structure of this crystal had been analysed using the modified multislice calculation of the electron diffraction
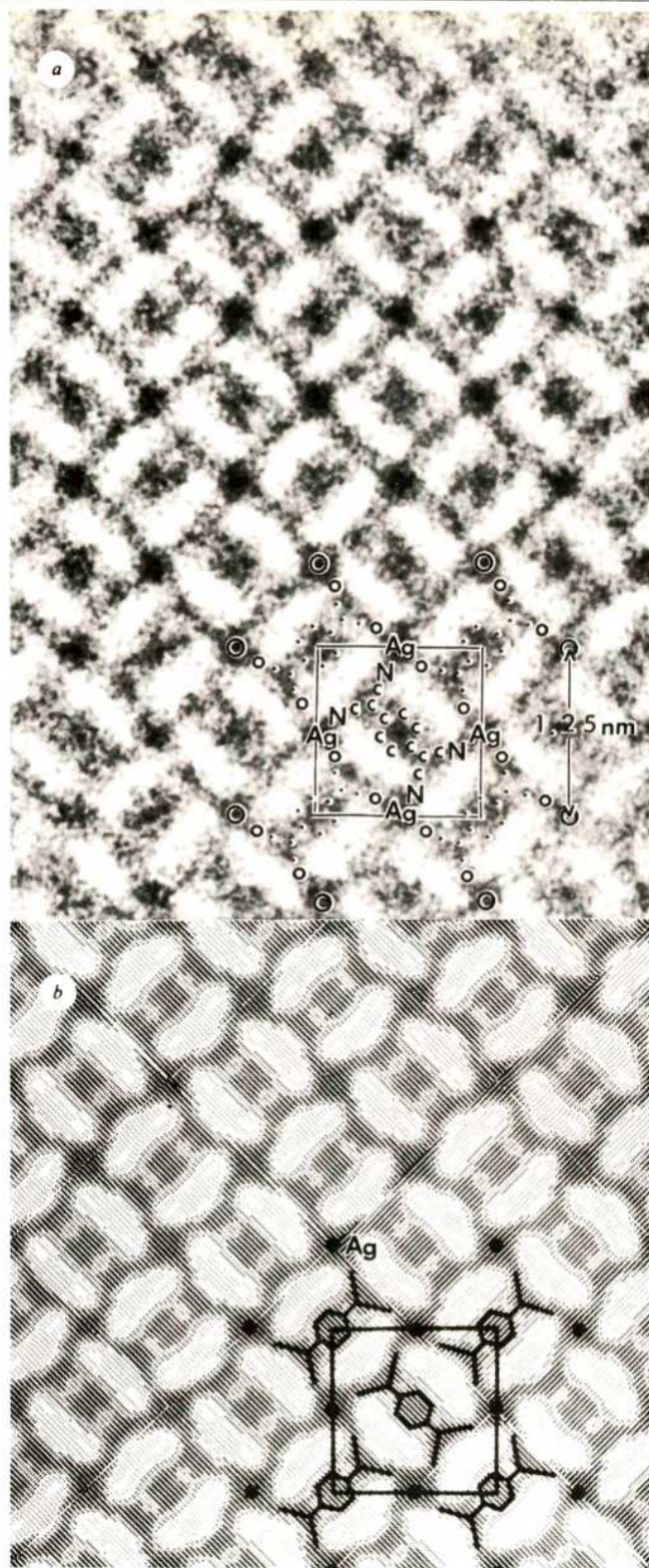
Fig. 2   *a*, Enlarged electron photomicrograph of Ag · TCNQ crystallite showing the images of Ag ions and TCNQ anions as indicated by the inserted molecular diagram. *b*, Computer-simulated images of the structure based on the projection as indicated by the schematic diagram. The imaging conditions of JEM-200CX are: the defocus spread, 15 nm, the illuminating angle, 0.1 mrad; and the Δf for the Scherzer focus, 55 nm.

intensities, although the details are not presented here. The molecular arrangement obtained as the preliminary result is shown in Fig. 2b which presents the theoretical images computer-simulated with the atomic parameters and the actual imaging conditions taken into account. Comparison of these two images clearly shows that the contrast distribution in the real images can be interpreted in terms of the molecular and ionic arrangements as indicated by Fig. 2a. The re-entrant side of each square corresponds to the chain of N–C–C–C–N, and the oblong rod can be regarded as the benzole ring, although they are all the columnar projections of 7–10 identical species. On the basis of this remarkable coincidence, the dark dot which is visible at every knot of the net structure can be regarded as the image of Ag ions superimposed in the direction of the column axis.

As far as the projection along a proper axis is concerned, this type of molecular and metal ionic arrangements show remarkable similarities to those of K, Na and Rb salts of TCNQ determined by Richard et al.[5], Konno and Saito[6], and Hoekstra et al.[7], respectively. In particular, the K salt seems to show the closest resemblance as its projection along the a-axis of a monoclinic unit cell almost produces a tetragonal symmetry in the molecular and ionic arrangements. The TCNQ complexes of

other metals such as Al, Au, Cs, Cu, Li and Ni were found by SAD to assume structures which are all isomorphic to the present Ag salt when prepared by the solid state topotaxy. In fact, Hoekstra et al.[7] has found by X-ray diffraction that the Li salt has a tetragonal unit cell although no detailed structure analysis has been performed.

The critical radiation dose($\sim$0.3 C cm^{-2}) of the present complex is measured by applying 100-kV electrons to the fading time method. This dose is less than those for some aromatic compounds which are known to be rather radiation-resistant. However, the atomic resolution is attainable only if the minimum exposure technique is applied to those organic crystals which are radiation-resistant to this extent.

1. Uyeda, N., Kobayashi, T., Ishizuka, K. & Fujiyoshi, Y. *Chem. Scr.* **14**, 47–61 (1979).
2. Williams, R. C. & Fisher, H. W. *J. molec. Biol.* **52**, 121–123 (1970).
3. Unwin, P. T. N. & Henderson, R. *J. molec. Biol.* **94**, 425–440 (1975).
4. Uyeda, N., Kobayashi, T. & Suito, E. *Microscopie Electronique 1970* Vol. 1 (ed. P. Favard) 443–444 (Societé Française de Microscopie Electronique, Paris, 1970).
5. Richard, P., Zanghi, J.-C. & Guédon, J.-F. *Acta crystallogr.* **B34**, 788–792 (1978).
6. Konno, M. & Saito, Y. *Acta crystallogr.* **B30**, 1294–1299 (1974).
7. Hoekstra, A., Spolder, T. & Vos, A. *Acta crystallogr.* **B28**, 14–25 (1972).

Inelastic electron tunnelling spectroscopic study of lubrication

A. Bayman & P. K. Hansma

Department of Physics, University of California, Santa Barbara, California 93106

Inelastic electron tunnelling spectroscopy reveals the vibrational spectrum of organic molecules on the oxide of a metal-oxide–metal junction[1-3]. A vibrational mode of frequency ν appears in the tunnelling spectrum as a peak in the second derivative of voltage with respect to current, d^2V/dI^2, at a voltage $V = h\nu/e$ (where h is the Planck's constant, and e is the electron charge). Both IR and Raman active modes can be observed. Tunnelling spectroscopy[4,5] has been used as an effective surface probe in the studies of adhesion[6-8], biochemistry[9,10], water pollution[11], damage due to electron beam irradiation[12], or UV irradiation[13], surface chemistry and catalysis[14-18]. We report here a new application of tunnelling spectroscopy—to lubrication—and present spectra of 1,2 hexadecanediol, hexadecanol and hexadecanoic acid and relate the results to their properties as boundary lubricants for aluminium. Because diols give the best results in both friction measurements and tunnelling spectra, we studied the adsorbtion of the smallest diol, ethylene glycol, and found that both OH groups react with the alumina surface.

As the experimental details are described elsewhere[2], we only give an outline here. We evaporated an aluminium strip 700-Å thick onto a clean 1×3 inch glass slide and oxidized the aluminium strip by venting the chamber to pure O_2. When a thicker alumina layer was needed to produce a junction of the desired resistance we thermally oxidized the strip in air at 200 °C. We doped the oxidized aluminum strip either with a liquid solution of the molecules of interest or a vapour. Before vapour doping the alumina was cleaned in an argon glow discharge[19]. We completed the junction with a 3,500 Å thick evaporated lead cross strip.

We checked the electrical resistance of each junction with a low-power ohmmeter. Doped junctions with resistances in the range 100–1,000 Ω were acceptable. For the spectra to be taken the slide was mounted on the sample holder with small screw clamps which made the electrical connections to the evaporated electrodes. The junction assembly was then immersed into liquid helium at 4.2 K and tested for the proper current–voltage tunnelling characteristics to ensure that all the current flow was
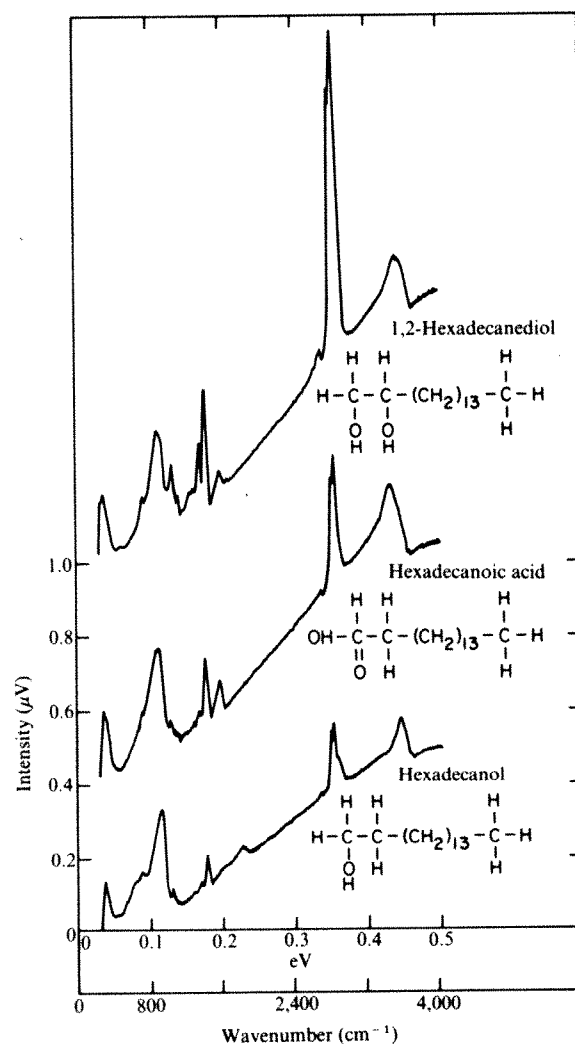
Fig. 1 Tunnelling spectra of C_{16} molecules with different attachment groups. The compounds are doped at the same concentration, 0.05%, from an emulsion of 90% D_2O and 10% hexane.

due to tunnelling. Second derivative spectra were then obtained by detecting the second harmonic voltage due to a small modulation current with a lock-in amplifier as a function of voltage.

Figure 1 shows the inelastic electron tunnelling spectrum of hexadecanol, hexadecanoic acid and 1,2-hexadecanediol. The compounds were doped from an emulsion of 90% D_2O and 10% hexane at a concentration of 0.05%. Among the three spectra 1,2-hexadecanediol has the most intense peaks. It also gave the most reproducible results. The second harmonic intensity, plotted on the y axis, is an intensive quantity independent of junction area and resistance[20]. The peak highs are a measure of surface coverage[21]. The acid was the most difficult to work with. It often gave shorted junctions indicating damage to the junction's oxide layer. The alcohol adsorbed least, as indicated by the relatively small peaks. From these observations, we guess that the diol would be the best lubricant: it had strong, reproducible adsorbtion without damaging the oxide.

Hotten's measurements of the load-carrying and wear-reducing properties of emulsions containing long-chain alcohols and diols show that the failure load is higher and aluminium
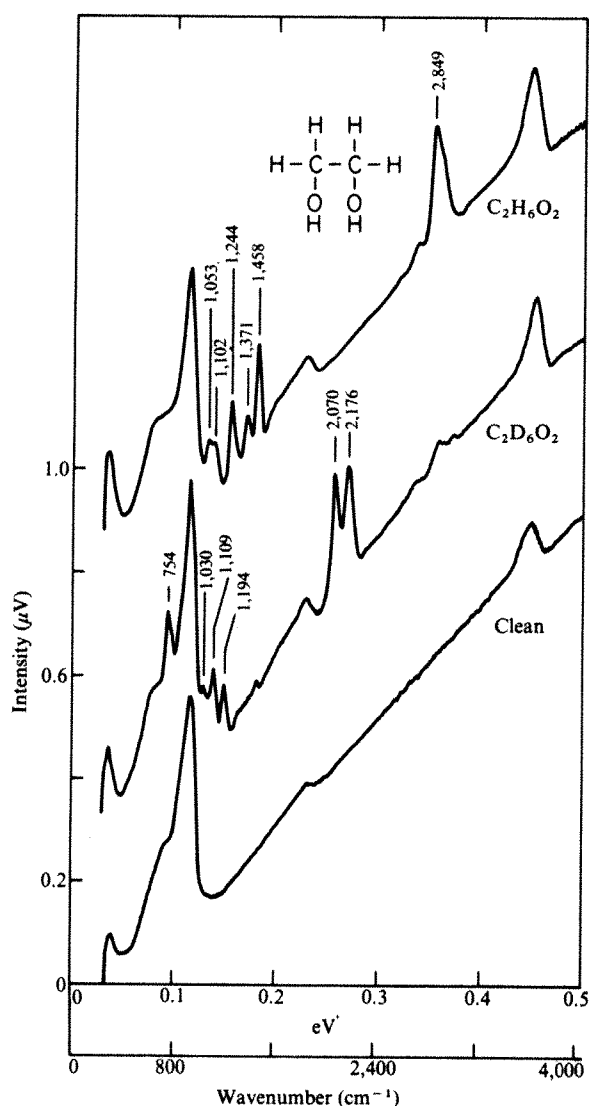
Fig. 2 Tunnelling spectra of ethylene glycol, deuterated ethylene glycol and a clean junction. The ethylene glycol and the deuterated ethylene glycol were doped at 1×10^{-3} torr and 3×10^{-3} torr for 1 min and 4 min respectively. The OH or OD vibrations of the diols are not present in the spectra implying that the hydroxyl groups lose their protons and attach to the oxidized aluminium surface through their oxygens.
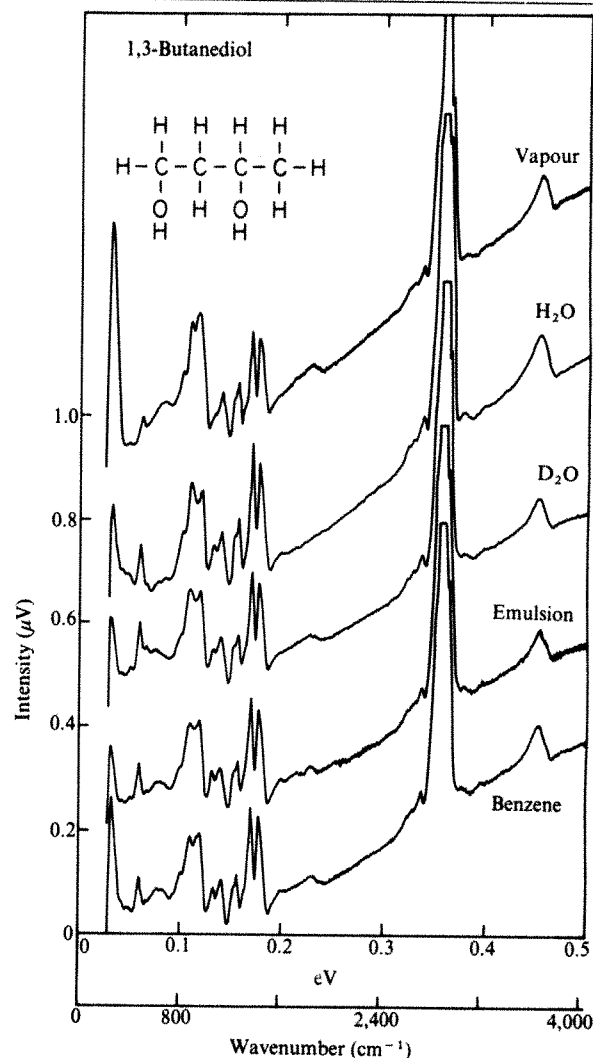
Fig. 3 Tunnelling spectra of 1,3-butanediol. The same surface species results from vapour doping or liquid doping from different solutions. The vapour doping was at 1×10^{-3} torr for 100s. The liquid doping concentrations were 25%, 50%, 12% and 20% by volume for the H_2O, the D_2O, the emulsion of 80% D_2O and 8% hexane, and the benzene respectively.

wear is lower (by a factor of ~ 3) for 1,2 and 1,3 diols compared with the corresponding alcohols[22]. Although there have been experiments to determine the lubrication properties of long chain acids on aluminium[23], no direct comparison is possible with the diols.

The emulsion that was used was meant to model the emulsions typically used in the lubrication of aluminium during rolling and cutting operations. An important difference is that D_2O was substituted for H_2O. This D_2O should have exchanged the two protons on the hydroxyl groups of the diol, the one on the carboxylate group of the acid; and the one on the hydroxyl group of the alcohol. Note, however, that there are no OD bands in the spectra. (They would be expected between 2,400 and 2,700 cm^{-1}.) This indicates that all these exchangeable protons are lost during bonding of the compounds. This was anticipated in the case of the alcohol and the acid. Greenler[24], Evans and Weinberg[15], and Evans *et al.*[16] showed that alcohols absorb as alcoxides on alumina, losing the proton of their hydroxyl group. Klein *et al.*[25], Hall and Hansma[26], Brown *et al.*[27], Lewis *et al.*[28] and others showed that acids adsorb as carboxylate ions on alumina, losing the proton of their carboxylate group. Figures 1–3 show that diols lose protons from both hydroxyl groups.

Figure 2 shows the spectra of ethylene glycol, totally deuterated ethylene glycol and a clean junction. Ethylene glycol is the smallest molecule that has the same attachment group as 1,2-hexadecanediol. There are no peaks in the tunnelling spectra where the O–H and O–D vibrations for ethylene glycol should occur[29,30] which shows again that the molecule loses its protons from both hydroxyl groups during bonding to the aluminium oxide surface. Unfortunately there are no IR or Raman spectra available for metal salts of ethylene glycol with which we can make a direct comparison of our spectra. The most we can say is that there is a good comparison between our observed peak positions and those of model compounds such as p-dioxane[31] and glycol nitrate[32] which contain the X–O–CH_2–CH_2–O–X structure.

Does the vapour doping technique that is useful for these small molecules give the same surface species as would be deposited from a lubricant solution? Figure 3 shows the tunnelling spectra of 1,3-butanediol vapour doped and liquid doped from various solvents. Every peak in the vapour-doped spectrum is present in the other four spectra which shows that the surface species formed is independent of the doping technique and solvent used. The similarity of spectra doped from both aqueous solutions to the others also suggests that the water is not chemically modifying the oxide layer: not converting the oxide layer to a hydroxide. Note that deuteration of the OH groups by the use of D_2O as a solvent gives the same spectrum as with H_2O. This is consistent with the results for ethylene glycol and 1,2-hexadecanediol.

Inelastic electron tunnelling spectroscopy can reveal the surface adsorbed species from model lubricant solutions. Long chain 1,2- and 1,3-diols which are effective boundary lubricants chemisorb to the aluminium oxide surface more readily than the corresponding alcohols or acids and they are less destructive to the oxide layer than acids. In diols both hydroxyl groups react with the alumina surface. The same surface species is formed from both vapour doping and liquid doping from polar and non-polar solvents and emulsions.

1. Weinberg, W. H. *A. Rev. phys. Chem.* **29**, 115–139 (1978).
2. Hansma, P. K. *Phys. Rep.* **30**, 145–206 (1977).
3. Kirtley, J. & Hansma, P. K. *Accounts Chem. Res.* **11**, 440–445 (1978).
4. Jaklevic, R. C. & Lambe, J. *Phys. Rev. Lett.* **17**, 1139–1140 (1966).
5. Lambe, J. & Jaklevic, R. C. *Phys. Rev.* **165**, 821–832 (1968).
6. White, H. W., Godwin, L. M. & Wolfram, T. *J. Adhes.* **9**, 237–249 (1978).
7. Diaz, A. F., Hetzler, U. & Kay, E., *J. Am. chem. Soc.* **99**, 6780–6781 (1977).
8. Henrickson, P. N., Chu, H. T., Eib, N. K. & Gent, A. N. *Advances in Chemistry Series* No. 174, 87–98 (1979).
9. Hansma, P. K. & Coleman, R. V. *Science* **184**, 1369–1371 (1974).
10. Cass, P. A., Strauss, H. L. & Hansma, P. K. *Science* **192**, 1128–1130 (1976).
11. Skarlatos, Y., Barker, R. C. & Haller, G. L. *Surf. Sci.* **43**, 353–368 (1974).
12. Hall, J. T., Hansma, P. K. & Parikh, M. *Surf. Sci.* **65**, 552–562 (1977).
13. Clark, J. M. & Coleman, R. V., Preprint (University of Virginia).
14. Kroeker, R. M., Kaska, W. C. & Hansma, P. K. *J. Catal.* **57**, 72–79 (1979).
15. Evans, H. E. & Weinberg, W. H. *J. chem. Phys.* **71**, 1537–1542 (1979).
16. Evans, H. E., Bowser, W. M. & Weinberg, W. H. *Surf. Sci.* **85**, L497–L502 (1979).
17. Kroeker, R. M., Kaska, W. C. & Hansma, P. K. *J. Catal.* (in the press).
18. Korman, C. S., Lau, J. C., Johnson, A. M. & Coleman, R. V. *Phys. Rev.* **B19**, 994–1014 (1978).
19. Mango, R. & Adler, J. G. *Phys. Rev.* **B13**, 2262–2269 (1976).
20. Keil, R. G., Graham, T. P. & Roenker, K. D. *Appl. Spectrosc.* **30**, 1–18 (1976).
21. Langan, J. D. & Hansma, P. K. *Surf. Sci.* **52**, 211–216 (1975).
22. Hotten, B. W. *Paper presented at ASLE/ASME Lubrication Conf.* Atlanta, Georgia, October 16–18, 1973.
23. Buckley, D. H. *Lewis Research Center Rep.*, (NASA TND-4994, 1968).
24. Greenler, R. G. *J. chem. Phys.* **37**, 2094–2100 (1962).
25. Klein, J., Leger, A., Belin, M., Defourneau, D. & Sangster, M. J. L. *Phys. Rev.* **B7**, 2336–2348 (1973).
26. Hall, J. T. & Hansma, P. K. *Surf. Sci.* **71**, 1–14 (1978).
27. Brown, N. M. D., Nelson, W. J. & Walmsley, D. G. *JCS Faraday Trans. II* **75**, 17–31, 31–37, 261–270 (1978).
28. Lewis, B. F., Moseman, M. & Weinberg, W. H. *Surf. Sci.* **41**, 142–164 (1974).
29. Buckely, P. & Giguere, P. A. *Can. J. Chem.* **45**, 397–407 (1967).
30. Sarirsry, W., Wiederzu, K. & Dawson, J. W. *Spectrochim. Acta* **23A**, 799–806 (1967).
31. Ward, W. R. *Spectrochim. Acta* **21**, 1311–1331 (1965).
32. Rossmy, G. *Chem. Ber.* **88**, 1969–1974 (1955).

Ferromagnetic coupling to muscle receptors as a basis for geomagnetic field sensitivity in animals

David Presti* & John D. Pettigrew

Beckman Laboratories of Behavioral Biology, California Institute of Technology, Pasadena, California 91125

Over the past decade several investigators have provided convincing evidence that the orientation of pigeons and other birds during homing and migrational activities is significantly affected by Earth-strength (<0.5 G) magnetic fields[1-8]. The presumed mediator of such effects would be a highly sensitive magnetoreceptor which the birds would normally use to extract navigational information from the geomagnetic field. The recently reported measurement of magnetic remanence in honeybees[9] and in homing pigeons[10] has stimulated interest in the possibility that the magnetically sensitive structure may be constructed from permanently magnetic material. Here we report the detection of permanently magnetic material in the neck musculature of pigeons (*Columba livia*) and migratory white-crowned sparrows (*Zonotrichia leucophrys*). We propose that a magnetic field detector might involve the coupling of magnetic particles to a sensitive muscle receptor such as a spindle. A detection mechanism of this kind could account for the difficulties encountered in conditioning immobile homing pigeons to magnetic field changes[11,12] and for the puzzling requirement of movement in other behavioural experiments involving pigeons and magnetic fields[13,14].

As behavioural experiments suggest that the magnetically sensitive structure in the homing pigeon might be located in the head or neck[1,2], we concentrated on this region. We tested for the presence of permanently magnetic material by measuring specimens in a SQUID (Superconducting Quantum Interference Device) magnetometer, an instrument used extensively by geologists to measure palaeomagnetic remanence in rocks[15] and also used in earlier studies of honeybees[9] and pigeons[10]. Birds were freshly perfused with phosphate-buffered formaldehyde (4%, pH 7.4), as the acid pH of unbuffered fixative might attack magnetic iron oxides. All dissections were conducted with clean glass microtome knives to prevent possible contamination from metallic instruments. To maximize the signal from any permanently magnetic material present, specimens were exposed to a 1,000-G field from a small cobalt-samarium magnet immediately before being measured in the magnetometer. This exposure has the effect of increasing the alignment of any permanently magnetic moments; the resulting measurement is termed inducible magnetic remanence.

Eleven homing pigeons from our Caltech loft (eight of local stock; three of an Oregon stock specifically chosen for their ability to orientate in overcast conditions; aged from 12 days to 12 years) and eight local feral pigeons were tested using the SQUID magnetometer. Inducible remanence of magnitude 1.0×10^{-6} to 1.5×10^{-5} e.m.u. was found in the head and neck area of all 19 pigeons tested (Table 1). Within the head, reproducible remanence was found to be associated with the skull. This remanence was diffuse, being spread rather uniformly throughout the entire skull; we could find no visible magnetic structures in the skull. This is in contrast to the results of Walcott *et al.*[10] who found permanently magnetic material in the pigeon head to be concentrated in a small, unilateral, innervated piece of tissue between the dura and the skull. We also found reproducible inducible magnetic remanence in the neck musculature of the pigeon, especially in the complexus muscle and associated fascia (Table 1).

* To whom correspondence should be addressed.

Seven migratory white-crowned sparrows (all adults at least one season old) were also tested for inducible magnetic remanence in the head and neck (Table 1).

In addition to pigeons and white-crowned sparrows, frozen specimens of approximately 40 other species of birds were tested for inducible magnetic remanence in the head and neck. Widely varying results from $<10^{-6}$ to $>10^{-5}$ e.m.u. were found; however, all cases of appreciable remanence were associated with migratory birds (for example, tree swallow [*Iridoprocne bicolor*], 5×10^{-6} e.m.u.; western grebe [*Aechmophorus occidentalis*], 9×10^{-6} e.m.u.; pintail duck [*Anas acuta*], 6×10^{-6} e.m.u.).

We were able to visualize magnetic material imbedded in the neck musculature of three homing pigeons (aged 3, 11 and 12 years) and two white-crowned sparrows. This material had the form of diffuse patches of black magnetic material in fascia or muscle (Fig. 1) or particles of black magnetic material embedded in muscle fibres. The black magnetic material was sometimes found together with transparent orange crystals possibly similar to those associated with magnetic material in chiton teeth [17,18] and also reported by Walcott *et al.* [10] in pigeons. Electron probe X-ray analysis (MAC-5-SA3 electron microprobe) of magnetic material from the neck musculature of pigeons and white-crowned sparrows indicated that iron was the major elemental component. This, together with the black colour and appreciable permanent magnetism, suggests that the material is probably composed largely of magnetite (Fe_3O_4), in agreement with the conclusions of previous reports of magnetic remanence in honeybees[9] and in pigeons[10]. Remanence of 1.0×10^{-6} e.m.u. could be produced by approximately 6×10^9 0.07-μm cubic single domain particles of magnetite[16] (amounting to 10^{-8}g), provided their magnetic moments were all aligned. If the magnetic domains interact, adjacent moments would tend to cancel and a larger amount of magnetite would be required to produce the same remanence.

Geomagnetic field sensitivity in animals may arise from the coupling of small permanent magnets to sensory structures which originally evolved to serve other functions. Animal skeletal muscle is richly innervated with sensory fibres which supply receptors sensitive to pressure and stretch. One such receptor type, the muscle spindle, is acutely sensitive to stretch and has a major role in the regulation and perception of muscle movement, both at the spinal and supraspinal levels[19-21]. We propose that permanently magnetic grains, coupled to such a muscle receptor so that the torque exerted on the grain ensemble in the geomagnetic field is sufficient to stimulate the muscle receptor, might form an effective basis for magnetic field sensitivity. This proposal is, of course, motivated by our finding of significant reproducible magnetic remanence and visualizable iron-rich magnetic material in the neck musculature, although we think it unlikely that the large visualizable deposits in the older birds are more than epiphenomenal.

One important implication of a muscle spindle-based magnetic field sensor is that natural motion of the muscle may be requisite for the perception of magnetic stimuli. This suggestion is based on the findings of several experiments with humans which indicate that perception of muscle spindle discharge is
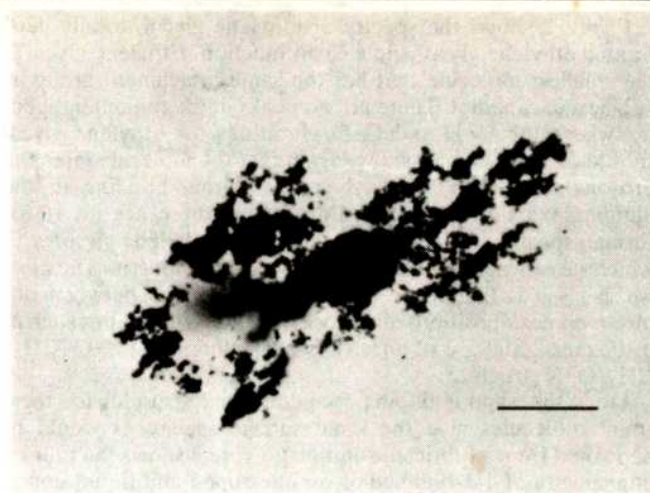
Fig. 1 Highly magnetic black particles (induced remanence of approximately 15×10^{-6} e.m.u.) found between the surface of the complexus muscle and the superficial fascia of a 3-yr-old homing pigeon. The particles are imbedded in a sheet of fascia. Unstained whole mount. Scale bar, 25 μm.

indirect, and seems to be possible only with reference to movements initiated by the subject[22-24]. This might account for one slightly puzzling aspect of geomagnetic field sensitivity in homing pigeons; namely, the failure of several investigators to condition a cardiac response to magnetic stimuli in the laboratory[11,12]. In these experiments the pigeon is held immobile in the centre of coils with which the ambient magnetic field can be altered. Also intriguing are the results of laboratory experiments by Bookman[13,14]. He found that homing pigeons could be trained to discriminate between the presence and absence of an Earth-strength (0.5 G) magnetic field and that successful discrimination was accompanied by fluttering (hovering, short flights) of the birds during the testing. If muscle activity of the sort normally executed by the bird during flight is required for the detection of magnetic stimuli, then the rather enigmatic results of Bookman's experiments would be readily explained.

It has not escaped our notice that our proposed mechanism may be relevant to the claim that positive dowsing responses in humans, indicated by the sudden flicking of a forked stick or the swinging of a pair of L-shaped rods, are correlated with relatively small changes in the local magnetic field[25-28]. As the dowsing instruments are held in such a way that the slightest movement of the wrists or forearms will be amplified into an appreciable movement of the stick or rods, a magnetically sensitive muscle receptor could conceivably give rise to muscular movement sufficient to produce the classic dowsing responses.

Table 1 Inducible magnetic remanence in the head and neck musculature of pigeons and white-crowned sparrows

	Head (e.m.u.)	Neck musculature (e.m.u.)
Pigeon	$1-7 \times 10^{-6}$ (19)	$1-15 \times 10^{-6}$ (19)
White-crowned sparrow	$2-4 \times 10^{-6}$ (2) 6×10^{-7} (5)	$1-8 \times 10^{-6}$ (7)

The numbers of birds which were found to have the various remanence values are shown in parentheses. For comparison with neck muscle specimens, comparably sized specimens of pectoral muscle and associated fascia from both pigeons and white-crowned sparrows had inducible magnetic remanences of less than 6×10^{-7} e.m.u. The noise level of the magnetometer was about 5×10^{-8} e.m.u.

1. Keeton, W. T. *Proc. natn. Acad. Sci. U.S.A.* **68**, 102–106 (1971).
2. Walcott, C. & Green, R. P. *Science* **184**, 180–182 (1974).
3. Keeton, W. T., Larkin, T. S. & WIndsor, D. M. *J. comp. Physiol.* **95**, 95–103 (1974).
4. Walcott, C. *J. exp. Biol.* **70**, 105–123 (1977).
5. Walcott, C. in *Animal Migration, Navigation, and Homing* (eds Schmidt-Koenig, K. & Keeton, W. T.) 143–151 (Springer, Berlin, 1978).
6. Wiltschko, W. & Wiltschko, R. *Science* **176**, 62–64 (1972).
7. Emlen, S. T., Wiltschko, W., Demong, N. J., Wiltschko, R. & Bergman, S. *Science* **193**, 505–508 (1976).
8. Viehmann, W. *Behaviour* **68**, 24–30 (1979).
9. Gould, J. L., Kirschvink, J. L. & Deffeyes, K. S. *Science* **201**, 1026–1028 (1978).
10. Walcott, C., Gould, J. L. & Kirschvink, J. L. *Science* **205**, 1027–1028 (1979).
11. Kreithen, M. L. & Keeton, W. T. *J. comp. Physiol.* **91**, 355–362 (1974).
12. Beaugrand, J. P. *J. comp. Physiol.* **110**, 343–355 (1976).
13. Bookman, M. A. *Nature* **267**, 340–342 (1977).
14. Bookman, M. A. in *Animal Migration, Navigation, and Homing* (eds Schmidt-Koenig, K. & Keeton, W. T.) 127–134 (Springer-Berlin, 1978).

15. Goree, W. S. & Fuller, M. *Rev. Geophys. Space Phys.* **14**, 591–608 (1976).
16. Butler, R. F. & Banerjee, S. K. *J. geophys. Res.* **80**, 4049–4058 (1975).
17. Towe, K. M., Lowenstam, H. A. & Nesson, M. H. *Science* **142**, 63-64 (1963).
18. Lowenstam, H.A. *Science* **156**, 1373-1375 (1967).
19. Matthews, P. B. C. *Physiol. Rev.* **44**, 219–288 (1964).
20. Barker, D. in *Muscle Receptors, Handbook of Sensory Physiology* Vol. III Part 2 (ed. Hunt, C. C.) 1–190 (Springer-Berlin, 1974).
21. Hunt, C. D. in *Muscle Receptors, Handbook of Sensory Physiology* Vol. III Part 2 (ed. Hunt, C. C.) 191–234 (Springer-Berlin, 1974).
22. Merton, D. A. *Symp. Soc. exp. Biol.* **18**, 287–400 (1964).
23. Gelfan, S. & Carter, S. *Exp. Neurol.* **18**, 469–473 (1967).
24. Goodwin, G. M., McCloskey, D. I. & Matthews, P. B. C. *Science* **175**, 1382–1384 (1972).
25. Rocard, Y. in *Biological Effects of Magnetic Fields* (ed. Barnothy, M. F.) 279–286 (Plenum, New York, 1964).
26. Chadwick, D. G. & Jensen, L. *Utah Water Res. Lab. Prog. Rep.* 78-1 (1978).
27. Harvalik, Z. V. *Physiol. Chem. Phys.* **10**, 525–534 (1978).
28. Williamson, T. *New Scient.* **81**, 371-373 (1979).

Evidence for fixed charge in the nexus

Peter R. Brink & Maynard M. Dewey

Department of Anatomical Sciences, School of Basic Health Sciences,
Health Sciences Center, State University of New York at Stony Brook,
New York 11794

The nexus or gap junction has been characterized as a low-resistance junction as well as a highly permeable junctional membrane to many molecules[1-6]. The transfer of electrical current from one cell interior to another, the aqueous solubility of dyes used to trace cell to cell communication and the fact that these molecules move across the nexus more rapidly than the plasma membrane[4-10] have led to the hypothesis of an aqueous channel in the junction. Both Ca^{2+} (ref. 11) and H^+ (ref. 12) are thought to alter nexal membrane conductance, and a voltage-sensitive gate has been demonstrated within the junction[13]. Recently, Flagg–Newton *et al.*[14] have concluded that mammalian junctions may contain fixed charge or be of smaller diameter than arthropod junctions. Here, we have investigated these alternatives by examining the permeability of nexuses of septa of the median giant axon of *Lumbricus terrestris*[1,15] with various derivatives of fluorescein. Both carboxyfluorescein and aminofluorescein were found to have depressed permeabilities relative to their predicted permeabilities based on molecular size and weight (MW). Fluorescein diffusion was significantly suppressed in axons pre-injected with aminofluorescein but carboxyfluorescein had no such effect (Table 1). These data suggest the existence of fixed anionic charge within the nexal channel which may have affinity for amino groups.

Figure 1*a* and *b* illustrate the propagation of action potentials at the septa. The microelectrodes were 500 μm from the septum on either side; the position of the septum was delineated by a fluorescein injection. The action potential propagated across the septum at 8.0 m s^{-1}. Figure 1*c* shows the conduction of an action potential along the same axon in the absence of a septum. Here the conduction velocity was 25 m s^{-1}. The microelectrode separation was 1 mm. The velocity of the propagated action potential across the septum is reduced to 32% of the velocity measured along the axon. Note the slight loss in amplitude of the action potential after it has traversed the septum. Propagation of an action potential in either direction showed the same loss in amplitude. In Fig. 1*c* no loss in amplitude is observed when the action potential is conducted along the axon. The introduction of carboxyfluorescein, aminofluorescein or any of the halogen derivatives did not increase the time delay at the septum. Nexal membrane conductance was measured in the presence of carboxyfluorescein and aminofluorescein, and no statistically significant alteration in conductance was observed over controls[4].

Figure 2 illustrates the nexal permeabilities of various molecules plotted as a function of their widest dimension. With increasing size, molecules have more difficulty traversing the

junction. However, in the case of carboxyfluorescein and aminofluorescein this relationship does not hold. One possible conclusion is that the extra carboxyl and amino groups are interacting electrostatically with fixed charge in the nexal pore, resulting in decreased junctional permeability for those molecules. The hydration radius of the two molecules would be expected to be greater than that of fluorescein by virtue of their greater polarity[16] and this may in part explain their suppressed permeabilities. It must be remembered that all the probes to a greater or lesser degree are also hydrated. In contrast to carboxyfluorescein and aminofluorescein, tetrachlorofluorescein permeability on the basis of size (1.0 nm) and MW (471) would have a predicted permeability similar to those of dibromofluorescein or diiodofluorescein. Data given here show the permeability to be between those of dibromofluorescein and diiodofluorescein. The data in Fig. 2 also suggest a functional channel diameter of 1.2 nm.

Aminofluorescein binds to cytoplasmic proteins[1], and affinity for cytoplasmic proteins in part explains the suppressed permeability of aminofluorescein. It may also have an affinity for membrane proteins. However, carboxyfluorescein has little binding affinity for cytoplasmic proteins (Table 1). For

Aminofluorescein
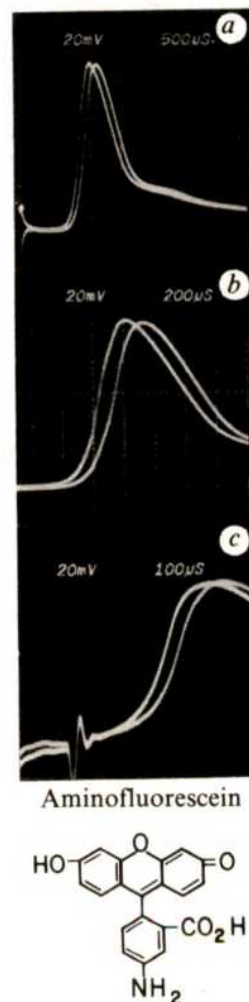
Fig. 1*a* An action potential recorded by two microelectrodes 1 mm apart with a septum between. The amplitude of the action potential is decreased slightly on the 'postsynaptic side' of the septum. The time delay across the septum was the same regardless of the direction of action potential propagation. Microelectrode resistance varied from 20 to 40 M Ω. Dye injections were done to confirm septum position. Dye was injected by applying hyperpolarizing current pulses for 15–30 min. *b*, As in *a* except 100 μs cm^{-1}. The conduction velocity in the region of the septum was 8 m s^{-1}. *c*, An action potential recorded between two microelectrodes 1 mm apart with no septum between. Note that the action potential shows no alteration in amplitude. The conduction velocity in the septum-free region was 25 m s^{-1}. Aminofluorescein contains an amine group in the γ position relative to the primary carboxyl group. Carboxyfluorescein substitutes a carboxyl group for the amine.

carboxyfluorescein, its extra electronegativity can be hypothesized to cause the molecule to experience increased repulsive forces in the region of the nexal channel, hindering its flux across the nexus. It can be speculated that aminofluorescein has a suppressed flux because the amine group is interacting with an anionic site in the junctional channel itself, but its size does not allow complete blocking of the channel.

Aminofluorescein or carboxyfluorescein was pre-injected into an axon using the method reported by us[1]. Because both molecules diffuse across the septa slowly, within an hour only small or trace amounts of dye had traversed the septum into adjacent cells. Within that hour, fluorescein was injected (15 min) and post-injection photographs were made at 5-min intervals for 15 min after fluorescein injection. A photograph of the pre-injection of aminofluorescein or carboxyfluorescein was made immediately after its injection. The densitometric tracing of the pre-injection was subtracted from subsequent densitometric tracings made following fluorescein injection[1]. Aminofluorescein significantly reduces fluorescein permeability whereas carboxyfluorescein has no such effect (Table 1). If there was significant diffusion of aminofluorescein or carboxyfluorescein into adjacent cells, it would result in an apparent elevation of the permeability, not a suppression of it.

No rectification is seen across the septum with propagated action potentials or with applied current pulses[4]. Likewise, no preferred diffusion or polarity was observed for any of the dyes. The nexal pores discriminate on the basis of charge and size but not with respect to the direction from which the molecule approaches and crosses the junction. If the nexal membrane is assumed to have a transnexal potential of 0, then the fixed charge could be placed near the cytoplasmic openings or anywhere along the interior of the channel and no rectification would be observed[17].

The resistance for the earthworm septal membrane is $4 \times 10^4\,\Omega$ (ref. 4). Electron microscopic data have revealed that the septa contain nexuses over 4–5% of their surfaces[1], with a total of 3×10^6 particles per septum. Assuming that all the nexal channels are in parallel and similar in size, the resistance of each channel is $1.2 \times 10^{11}\,\Omega$ or 8 pS. However, assuming the channel is 1.5 nm in diameter and filled with axoplasm having a resistivity of $200\,\Omega$ cm (r_a), the channel resistance (R_p) would be $2.3 \times 10^{10}\,\Omega$ or 43 pS using the equation

$$R_p = r_a L / A \qquad (1)$$

where L and A symbolize length and cross-sectional area of the channel, respectively. The conductance of a single potassium

Fig. 2 Nexal membrane permeability plotted against the widest dimension of the molecules. Carboxyfluorescein (□) and aminofluorescein (▽) are the only molecules that do not fit the general relationship of decreasing P_n with dimension or as MW increases for anionic molecules[1]. The permeabilities of fluorescein (△), dichlorofluorescein (▲), dibromofluorescein (●), diiodofluorescein (○) and tetrabromofluorescein (■) were taken from ref. 1. The permeabilities of carboxyfluorescein, aminofluorescein and tetrachlorofluorescein (▼) were computed using the same methods as in ref. 1. Carboxyfluorescein contains an extra negative charge at physiological pH whereas aminofluorescein exists as a zwitterion. Even with these additional groups the widest dimension of the derivatives is the same as fluorescein (9.5 Å), assuming no hydration radius. The carboxyl group of fluorescein has a $pK = 3$–4 (ref. 20). Tetrabromofluorescein has a $pK = 5$ (ref. 21). Aminofluorescein would have a $pK = 3$–4 while the amine group would be assumed to have a $pK = 10$. The conductance of the junction in the presence of the halogen derivatives fell within the range of junctional conductance with none of the fluorescent probes present. Permeabilities not listed in Table 1 are given in ref. 1.

channel was estimated by Cole[18] from $1/f$ noise of hyperpolarized node membranes to be 0.5 pS. The sodium channel conductance has been given a similar value[19]. The diameter of the potassium channel is thought to be 0.3–0.4 nm. Using equation (1), where $r_a = 200\,\Omega$ cm and $L = 10.0$ nm, the single channel conductance is 2.5 pS. The lower conductance value can be attributed to electrostatic forces acting over molecular distances in the potassium channel and nexal membrane channel. The data presented here therefore suggest the existence of an anionic site within the nexal membrane channel.

Table 1 The influence of aminofluorescein on nexal membrane permeability

Dye	Permeability (cm s⁻¹)	Standard deviation (n)	Cytoplasmic binding
Fluorescein	5.4×10^{-5}	2.1×10^{-5} (10)*	
Aminofluorescein + fluorescein	2.2×10^{-5}	1.8×10^{-5} (11)*	
Carboxyfluorescein + fluorescein†	4.6×10^{-5}	1.3×10^{-5} (4)	
Aminofluorescein	6.0×10^{-7}	3.0×10^{-7} (8)	
Carboxyfluorescein	5.6×10^{-6}	3.0×10^{-6} (6)	6.8%
Tetrachlorofluorescein	2.1×10^{-5}	1.5×10^{-5} (4)	4.0%

Cytoplasmic binding was measured by the method given in ref. 1. The ratio of protein (cytosol) to dye was 10 to 1 assuming the average protein/MW was 10^4–10^5. The control permeability value for fluorescein in the absence of other dyes was taken from ref. 1. Aminofluorescein was injected into an axon followed by a fluorescein injection. The aminofluorescein injection was accomplished by applying a hyperpolarizing pulse of 20 nA amplitude, 100 ms duration, every 150 ms for 20 min. The fluorescein injection followed immediately with the same conditions. The pH of the electrode solutions was 8.2. Permeability was calculated by the method reported by us[1]. Aminofluorescein diffuses at such a slow rate that only trace amounts appear in the adjacent cell over an hour, allowing fluorescein to be injected (15 min) and photographs of subsequent fluorescein diffusion to be made at 5-min intervals for 15 min. Densitometric tracings were made of negatives and permeability calculated. Each photographic exposure was 40 s.
* Student's t-test comparison between fluorescein permeability and fluorescein permeability with a pre-injection of aminofluorescein. $P > 0.01$.
† Carboxyfluorescein was pre-injected using the same conditions as aminofluorescein followed by fluorescein injection. Fluorescein permeability and fluorescein permeability of carboxyfluorescein-injected axons were statistically insignificant.

1. Brink, P. & Dewey, M. M. *J. gen. Physiol.* **72**, 67–86 (1978).
2. Dewey, M. M. & Barr, L. *J. Cell Biol.* **23**, 553–585 (1964).
3. Barr, L., Dewey, M. M. & Berger, W. *J. gen. Physiol.* **48**, 797–823 (1965).
4. Brink, P. & Barr, L. *J. gen. Physiol.* **69**, 517–536 (1977).
5. Weidmann, S. *J. Physiol., Lond.* **187**, 323–342 (1966).
6. Weingart, R. *J. Physiol., Lond.* **240**, 741–762 (1974).
7. Goodenough, D. A. *Cold Spring Harb. Symp. quant. Biol.* **40**, 37–44 (1975).
8. McNutt, W. S. & Weinstein, R. S. *Prog. molec. Biol.* **26**, 45–101 (1973).
9. Caspar, D. L. D., Goodenough, D. A., Makowski, L. & Phillips, W. C. *J. Cell Biol.* **74**, 605–628 (1977).
10. Makowski, L., Caspar, D. L. D., Phillips, W. C. & Goodenough, A. *J. Cell Biol.* **74**, 629–648 (1977).
11. Olivera-Castro, G. M. & Loewenstein, W. R. *J. Membrane Biol.* **5**, 51–77 (1971).
12. Turin, L. & Warner, A. *Nature* **270**, 56–57 (1977).
13. Harris, A. L., Spray, D. C. & Bennett, M. V. L. *Biophys. J.* **25**, 80a (1979).
14. Flagg-Newton, J., Simpson, I. & Loewenstein, W. R. *Science* **205**, 404–407 (1979).
15. Kensler, R. W., Brink, P. & Dewey, M. M. *J. Neurocytol.* **8**, 565–590 (1979).
16. Markin, R. B. *Introduction to Biophysical Chemistry* (McGraw-Hill, New York, 1964).
17. Finkelstein, A. & Mauro, A. in *The Nervous System*, Section 1 (ed. Kandell, E. 161–214 (1977).
18. Cole, K. S. in *Membranes, Ions and Impulses*, 535 (University of California Press, 1972).
19. Almers, W. & Levinson, S. R. *J. Physiol., Lond.* **247**, 483–509 (1975).
20. Zwicker, E. F. & Grossweiner, L. I. *J. phys. Chem.* **67**, 549–555 (1963).
21. Levitan, H. *Proc. natn. Acad. Sci. U.S.A.* **74**, 2914–2918 (1977).

Allergic encephalomyelitis induced in guinea pigs by a peptide from the NH₂-terminus of bovine P₂ protein

Steven W. Brostoff, James M. Powers & Michael J. Weise

Departments of Neurology and Pathology, Medical University of South Carolina, Charleston, South Carolina 29403

Experimental allergic neuritis (EAN) is an inflammatory demyelinating disease of the peripheral nervous system (PNS) first described by Waksman and Adams[1,2] in rabbit, guinea pig and mouse after injection of PNS antigen in Freund's complete adjuvant. In rabbit and mouse, the histological lesions were confined to the PNS but the guinea pig reacted curiously to PNS antigens by developing lesions in the central nervous system (CNS) as well as the PNS. Experimental allergic encephalomyelitis (EAE), the CNS counterpart of EAN, is known to be a response to CNS myelin basic protein. In early experiments[3,4], basic proteins from PNS myelin also produced a disease in guinea pigs characterised by CNS lesions. Characterisation of the proteins of PNS myelin demonstrated the presence of a basic protein (P₁) which was similar to the encephalitogenic basic protein of CNS myelin[5]. At first it seemed that the CNS lesions were being caused by this (P₁) protein. However, immunological studies from our laboratories suggested that when guinea pigs were sensitised to PNS myelin, the resulting lesions were a response to the small PNS myelin basic protein (P₂) and not to the P₁ protein[6]. In a preliminary report[7], we indicated that a peptide fraction derived from the P₂ protein could produce a disease in guinea pigs characterised by CNS lesions. Sequence studies under way in our laboratory now enable us to report that this response is being caused by a tryptophan-containing 20-residue peptide (CN3) derived from the NH₂-terminal segment of the bovine P₂ protein.

Bovine P₂ protein prepared from spinal nerve roots[8] has three methionine residues. Treatment of P₂ protein with CNBr results in four peptide chains, two of which remain covalently linked by an interchain disulphide bond. These chains consist of a peptide of 20 amino acids from the NH₂-terminus (CN3), a peptide of approximately 88 residues located internally (CN1), and the disulphide-linked dipeptide (CN2) representing the COOH-terminal 18 amino acids[9]. The sequence of the NH₂-terminal 65 residues which include CN3 has been reported[10].

In early experiments[11], P₂ protein (55 mg) was digested with CNBr (in 3.0 ml 70% formic acid) and the resulting peptides were separated by chromatography on a column (1.5 × 69 cm) of

Encephalitogenic determinant

Residues 114–122 of bovine CNS MBP

PHE–SER–TRP–GLY–ALA–GLU–GLY–GLN–LYS
114   122

Peptide CN3

Residues 1–20 of PNS P₂ protein

N–AC–SER–ASN–LYS–PHE–LEU–GLY–THR–TRP–LYS–LEU–
1
VAL–SER–SER–GLN–ASN–PHE–ASP–GLU–TYR–MET
                                           20

Fig. 1 Sequences of the encephalitogenic determinant of bovine CNS myelin basic protein and peptide CN3 of bovine PNS myelin P₂ basic protein.

Sephadex G-50. The column was equilibrated and eluted with 0.1 M acetic acid at 35 ml h⁻¹; 3.0-ml fractions were collected. Only two main peptide-containing peaks were isolated. The peak appearing in the void volume (fractions 10–35) was designated fraction I and contained only the large internal peptide CN1. The second peak (fractions 38–43) was designated fraction II and was later shown to be a mixture of peptides CN2 and CN3. Each of these fractions was tested for its ability to produce disease in guinea pigs (Table 1). Of the two, fraction II clearly contained a disease-inducing site for guinea pigs, and produced a response characterised by strong clinical symptoms (at 75 μg dose) and histological lesions in the CNS characterised by unusually large numbers of plasma cells in the infiltrates as compared with either EAE or EAN.

In later experiments[9], the peptides resulting from CNBr digestion of the P₂ protein were separated by chromatography on G-25, which allowed isolation of CN2 and CN3. To establish which of the two contained the disease-inducing site, both were tested at two doses in guinea pigs. The data in Table 1 suggest that the determinant for disease induction in the guinea pig resides in the NH₂-terminal 20 amino acids of P₂ protein that comprises peptide CN3. The response in one of the three guinea pigs sensitised with CN3 also resulted in histological lesions in the CNS characterised by infiltrates containing unusually high numbers of plasma cells.

Because P₁ is encephalitogenic[12], the question of contamination of peptides derived from P₂ with the encephalitogenic determinant of P₁ must be considered. Our P₂ preparation is

Table 1 Disease-inducing properties in guinea pigs of CNBr peptides derived from the basic P₂ protein

Antigen	Dose (μg)	No. of animals tested	No. with clinical signs (day of onset)	No. with perivascular infiltration (severity) CNS	Histology PNS	No. with demyelination CNS	PNS
Fraction I (CN1)	50	3	0	2 (+/−)	0	0	0
Fraction II	75	4	4 (12, 12, 14, 19)	4 (++)*	0	4	0
	50	4	1 (15)	4 (+/− to +)*	0	2	0
CN2	75	2	0	0	0	0	0
	25	3	0	0	0	0	0
CN3	75	3	1 (15)	3 (+/− to +)	0	1	0
	25	3	0	2 (+/− to +)	0†	2	0

Each animal was injected into each hind footpad with 0.1 ml (0.2 ml per animal) of an emulsion containing equal volumes of antigen dissolved in saline and Freund's complete adjuvant (Difco, H37 ra). Clinical signs and histology were evaluated as described previously[11]. Perivascular infiltration was graded in severity according to the system of Alvord and Kies[15].
* Plasma cells were unusually prominent in the mixed cellular infiltrates.
† A small focus of perivascular lymphocytes was observed in the nerve root of one animal.

assessed to be free of contamination with the encephalitogenic P_1 protein by its failure to produce allergic encephalomyelitis when injected into rabbits, even at 5 mg doses[8]. It is even more unlikely that CN3 is contaminated with the encephalitogenic determinant from P_1 because, after cyanogen bromide cleavage of P_1, this determinant would remain in a large (146 residue) peptide which would easily separate from the small (20 residue) CN3 during subsequent purification by column chromatography and paper electrophoresis. There is no evidence that CN3 contains additional peptides even after tryptic digestion[9].

CN3 apparently contains the antigenic determinant in bovine P_2 responsible for producing a neurological disease in guinea pigs characterised by perivascular infiltration and demyelination in the CNS. The encephalitogenic determinant for EAE in the guinea pig has been shown[13] to be a peptide (residues 114–122) of the bovine CNS myelin basic protein containing that molecule's only tryptophan residue (see Fig. 1). Tryptophan is essen-

tial for disease induction in conjunction with a Gln-Lys (or Gln-Arg sequence)[14]. By way of comparison, peptide CN3 (residues 1–20 of the bovine PNS myelin basic protein) also contains a single tryptophan, an Asn-Lys sequence and produces an EAE-like disease in guinea pigs. One might speculate that the chemical requirements of a determinant for EAE are not exact and that the presence of tryptophan, asparagine and lysine in CN3 may be sufficient for its disease induction. One might further speculate that the reason for the required large dose of this peptide and resultant milder disease (compared with the encephalitogenic peptide of CNS myelin basic protein) is that the relative locations of tryptophan and lysine residues are different.

1. Waksman, B. H. & Adams, R. D. *J. exp. Med.* **102**, 213–235 (1955).
2. Waksman, B. H. & Adams, R. D. *J. Neuropath. exp. Neurol.* **15**, 293–314 (1956).
3. Bencina, B., Carnegie, P. R., McPherson, T. A. & Robson, G. *FEBS Lett.* **4**, 9–12 (1969).
4. Brostoff, S., Burnett, P., Lampert, P. & Eylar, E. H. *Nature* **235**, 210–212 (1972).
5. Brostoff, S. W. & Eylar, E. H. *Archs Biochem. Biophys.* **153**, 590–598 (1972).
6. Carlo, D. J., Karkhanis, Y. D., Bailey, P. J., Wisniewski, H. M. & Brostoff, S. W. *Brain Res.* **88**, 580–584 (1975).
7. Brostoff, S. W., Levit, S. & Powers, J. *Trans. Am. Soc. Neurochem.* **8**, 205 (1977).

8. Brostoff, S. W. *et al. J. Neurochem.* **23**, 1037–1043 (1974).
9. Weise, M. J., Hsieh, D. L., Hoffman, P. M., Powers, J. M. & Brostoff, S. W. *J. Neurochem.* (in the press).
10. Weise, M. J., Hsieh, D. L., Levit, S. & Brostoff, S. W. *J. Neurochem.* (in the press).
11. Brostoff, S. W., Levit, S. & Powers, J. M. *Nature* **268**, 752–753 (1977).
12. Brostoff, S. W., Karkhanis, Y. D., Carlo, D. J., Reuter, W. & Eylar, E. H. *Brain Res.* **86**, 449–458 (1975).
13. Eylar, E. H. & Hashim, G. A. *Proc. natn. Acad. Sci. U.S.A.* **61**, 644–650 (1968).
14. Westall, F. C., Robinson, A. B., Caccam, J., Jackson, J. & Eylar, E. H. *Nature* **229**, 22–24 (1971).
15. Alvord, E. C. & Kies, M. W. *J. Neuropath. exp. Neurol.* **18**, 447–457 (1959).

Structure of slow-reacting substance of anaphylaxis from guinea-pig lung

Howard R. Morris*, Graham W. Taylor*, Priscilla J. Piper† & John R. Tippins†

* Department of Biochemistry, Imperial College, South Kensington, London SW7, UK
† Department of Pharmacology, Institute of Basic Medical Sciences, Royal College of Surgeons, Lincolns Inn Fields, London WC2, UK

Slow-reacting substance of anaphylaxis (SRS-A) is a primary mediator of immediate-type hypersensitivity reactions, probably having a major bronchoconstrictor role in asthma. Although it was discovered some 40 years ago[1] the structure has remained unknown. Major advances in purification technology[2,3] have resulted in the preparation of chemically pure material, and the demonstration that SRS-A has a characteristic UV spectrum[2] has enabled a correlation to be made between biological activity and a structural moiety in the molecule. Previous studies have indicated that SRS-A from guinea pig lung is derived from arachidonic acid[4]; data, based on the chemical and enzymatic destruction of biological activity, have indicated the presence of α-amino, carboxyl and thioether functions[3]. We now report the first spectroscopic (mass spectrometric) and analytical protein chemical data on intact SRS-A which allows us to define unequivocally the complete covalent structure of this immunologically generated material as the novel peptidolipid 5-hydroxy-6-cysteinyl glycinyl-7, 9, 11, 14-eicosatetraenoic acid. The structure determined is identical to that which we have assigned to the major non-immunologically generated slow-reacting substance (SRS) obtained from rat basophil leukaemia (RBL-1) cells[5], but different from that of a recently synthesized chemical with SRS-like activity[6] whose structure was modified from an earlier, incorrect structure of the natural product[7].

SRS-A was prepared from immunologically challenged lungs of guinea pigs sensitized to ovalbumin[8] and purified to homogeneity by our previously published methods[2,3] (Fig. 1); the difficulties associated with the purification of vanishingly small amounts of SRS-A were overcome by use of the procedures shown in Fig. 1, including the introduction of reverse-phase HPLC[2,8], with its attendant high resolution separative capabil-

ity. It was shown that the essentially homogeneous material prepared, had a characteristic UV spectrum[2] (Fig. 2) (λ_{max}^{MeOH} 280 nm) and this discovery has been very useful in locating SRSs[8,9] and providing a cross-correlation between biological activity on the guinea pig ileum and a chemical entity, the conjugated triene attributed to this chromophore[8].

In the final purification (Fig. 1) the active SRS-A fraction from HPLC-1 separated[3] into four UV-absorbing compounds (Fig. 2); compound I (λ_{max} 280 nm) fulfills all the criteria for SRS-A[8]; compound II has a similar UV spectrum, but is shifted hypsochromically by 2–3 nm (λ_{max} 278 nm). This material has apparently reduced biological activity, probably corresponding to a *cis-trans* isomerization of one of the double bonds in SRS-A; compound III (λ_{max} 270 nm) does not contract the guinea pig ileum and we have previously shown this to be 5, 12 dihydroxy-6, 8, 10, 14 eicosatetraenoic acid[3], compound IV is probably related to compound III by a similar isomerization to that observed for compounds I and II.

The precursor role of arachidonic acid has been indicated by data on the potentiation of SRS-A from guinea pig chopped lung[4]. Destruction of biological activity by soya bean lipoxygenase (w6 specificity) has shown the presence of a 1—4 *cis* pentadiene unit in the SRS-A molecule[10].

Lung effluent collected on ice

↓

Charcoal absorption,
elution with 80% ethanol,
rotary evaporation

↓

Gel filtration on Sephadex G-15

↓

Ether extraction from pH 3
acetic acid (5 °C)

↓

HPLC-1, methanol : water

↓

HPLC-2, propanol : acetic acid : water
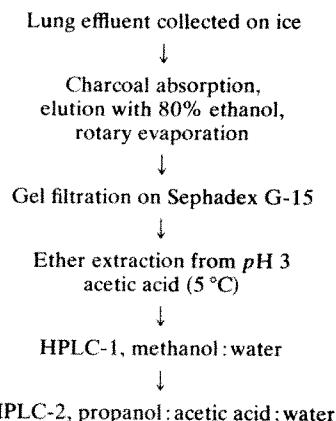
Fig. 1 The extraction and purification of SRS-A from guinea pig lung[3,8]. At all stages of purification SRS-A was monitored by bioassay on guinea pig ileum (in the presence of mepyramine and hyoscine).
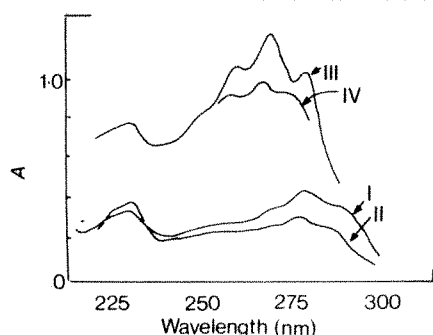
Fig. 2 The full UV spectra of compounds 1–IV isolated by purification of the active fraction from immunologically challenged guinea pig lung.

Chemical inactivation data studied by monitoring the loss of biological activity after brief exposure of SRS-A to various reagents indicates the presence of certain functional groups[3]— α-amino (short acetylation), thioether (cyanogen bromide) and carboxyl (methylation). The presence of the α-amino group thus postulated in SRS-A, was used to provide a marker label in the mass spectrometric work (see below), thus enabling location of the relevant SRS-A signals and differentiation from those signals arising from background contribution.

Amino acid analysis of the peak tubes of biological activity showed the presence of the amino acids, glycine and cysteine. Tubes corresponding to compound III were devoid of amino acids above background level. To determine the sequence of the two amino acids, the active sample was dansylated, hydrolysed and the dansyl derivative examined by TLC[11]. The results showed a fluorescent spot arising from a single N-terminus, moving more slowly than dansyl glycine in all dimensions; dansyl cysteine prepared as a standard in the presence of arachidonic acid gave a spot with identical mobility.

Derivatives for mass spectrometry were chosen to improve the volatility of SRS-A in a manner which would not affect the basic structural units, (1) by using reactions previously well studied in protein chemistry[12], and (2) by rejecting those reactions which caused changes in either UV absorbance or λ_{max} of the triene chromophore.

To monitor the variables of absorption phenomena, reagents and reaction conditions used in the final stages of the structure elucidation, a slow reacting substance (SRS), whose structure we have previously defined[5], was prepared from rat basophil leuk-aemia cells (RBL-1).

The RBL-1 SRS had a similar elution position in the HPLC-2 step (Fig. 1), and identical pharmacological and physicochemical properties to SRS-A. The full UV spectrum of the SRS-A used for the mass spectrometric experiments was determined, (600 U, A = 1.3), and a deliberately smaller amount of RBL-1 SRS was taken for the control experiments, corresponding to 0.75 of the SRS-A UV absorbance. RBL-1 SRS was derivatized using acetic anhydride in the acetylation step, whereas the guinea pig lung SRS-A was acetylated using a 1:1 mixture of acetic anhydride and d_6 acetic anhydride to provide the mass spectrometric marker. The other derivative-forming steps were identical, being esterification in ethereal diazomethane (30 min) and trimethylsilylation in pyridine/bis (trimethylsilyl) trifluoroacetamide/trimethylchlorosilane (1:6:1 30 min).

Figure 3 shows the mass spectrum produced at 240 °C from guinea pig SRS-A (Fig. 3a) compared with that produced from the RBL-1 control (Fig. 3b) and with our previously reported spectrum of RBL-1 SRS, from which its structure was deduced[5] (Fig. 3c). The spectra unequivocally show that SRS-A from guinea pig lung is identical to that of RBL-1 SRS in covalent structure, as the same fragment ions are observed in the same relative abundance ratios at an identical ion source temperature.

Figure 3 also illustrates the considerable difficulty of determining structure on the small quantity of SRS-A available from lung, for, in contrast to our previous work on RBL-1 SRS, at this lower level the molecular ion was not observed for either SRS-A or the RBL-SRS control. The absence of the molecular ion does not in any way affect the interpretation, as the full structure is found by combining the information from the fragment ions formed. For example, in Fig. 3a, m/e 607 corresponds to $M^+ - OCH_3$ (containing both the peptide and lipid moieties), m/e 548 corresponds to $M^+ - TMSOH$ (showing the presence of a hydroxyl group), m/e 404/405 and m/e 314/315 (−TMSOH) define the lipid portion of the molecule and m/e 203 defines the substitution of the hydroxyl at C-5. Confirmatory experiments on the signals shown in Fig. 3, involving further isotopic labelling (for example, d_9 TMS), and high resolution mass measurements enable us to define rigorously the structure of SRS-A from guinea pig lung as the novel peptidolipid 5-hydroxy-6-cysteinyl glycinyl-7, 9, 11, 14-eicosatetraenoic acid (Fig. 4).

Using the same arguments as previously described in the structure elucidation of RBL-1 SRS[5], we can position the double bonds in SRS-A and define the substitutions of the tetraene (C_{20}: 4-eicosatetraenoic acid) at C-5 (hydroxyl) and C-6 (thioether). Importantly, the mass spectrum also shows what is not present in the structure; for example, we can say that the SRS-A does not contain a glycine-amide which would be difficult to discount by chemical or enzymatic methods. Similarly, we can say that SRS-A does not contain a sulphate moiety, widely expected from the results of destruction of biological activity by aryl sulphatase, reported in the literature[8,13]. It is of some interest that the structure we propose here for SRS-A derived from immunologically stimulated lung is identical to that which we have previously described for SRS released by non-immunological stimulation from malignant basophils. Furthermore, this structure could be biosynthetically derived by an intriguing combination of the lipoxygenase metabolism of arachidonic acid[14] with the glutathione detoxification pathway[15] involving nucleophilic attack of the
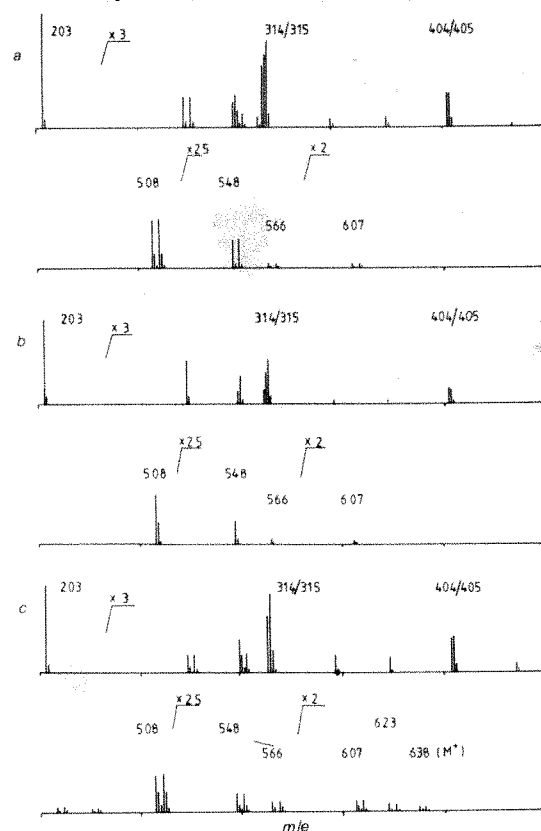
Fig. 3 (a), The electron impact mass spectrum of the trimethylsilyl (TMS) ether of the N-acetyl (CH_3CO/CD_3CO 1:1) methyl ester of SRS-A from guinea pig lung. Source temperature 240 °C. b, The mass spectrum of the same derivative (excluding isotopic labelling on the acetyl group) of the control sample of RBL-1 SRS. c, The mass spectrum of the same derivative of RBL-1 SRS[5].
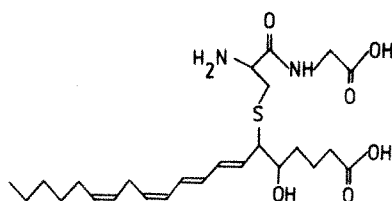
Fig. 4 The full covalent structure of SRS-A from guinea pig lung. Synthesis will be required to determine the full stereochemistry[6]. The detailed interpretation of the mass spectrum will be reported elsewhere.

cysteinyl sulphur on a 5,6-oxido-eicosatetraenoic acid. Interestingly, we find no evidence in either the natural SRS-A reported here or our previous SRS preparations[5], for a glutathionyl structure such as that recently described for a synthetic substance possessing SRS-like pharmacological and chromatographic properties[6]. The cysteinyl glycine structure reported here (Fig. 4) is rigorously defined for both SRS-A and SRS[5] from the mass spectrum (Fig. 3). We discount the possibility of having lost a major component of any putative glutathionyl SRS-(A) during purification, because (1) all fractions from the various column eluates were screened for biological activity, and (2) where partitioning took place (that is, at the charcoal absorption and ether extraction steps) no biological activity was found in the aqueous fractions. Despite yields of > 75% at these stages, this does not preclude either a minor component having adsorbed to charcoal (unlikely for a more polar substance) or enzymatic processing (either physiologically significant or otherwise) of compounds in the perfusate. In any event, the structure identified here for lung SRS-A is the major biologically active compound studied by pharmacologists and while the detailed enzymatic steps in the biosynthesis of SRSs are under investigation, it is, however, possible that SRSs of different cellular origins may have different structures or metabolism.

The first demonstration, given here, that a mass spectrum can be produced from undegraded SRS-A, taken together with our previous work on SRS[5], forms the basis for future precise identifications of all these substances, using the readily formed derivatives suggested; the mass spectrum can also be used in quantitative studies.

This definition of the structure of guinea pig lung SRS-A and the likelihood that human SRS-A has the same structure[8], open the way towards new and enlightened study into the pathology and therapy of asthma and other allergic diseases. It will also lead to exploration of the physiological roles of SRS-A, 5,12-dihydroxyeicosatetraenoic acid and the other UV absorbing lipoxygenase products.

1. Kellaway, C. H. Trethewie, E. R. Q. J. exp. Physiol. **30**, 121—145 (1940).
2. Morris, H. R., Taylor, G. W., Piper, P. J., Sirois, P. & Tippins, J. R. FEBS Lett. **87**, 203–206 (1978).
3. Morris, H. R., Taylor, G. W., Piper, P. J. & Tippins, J. R. Ag. Actions Suppl. **6**, 27–36 (1979).
4. Piper, P. J., Tippins, J. R., Morris, H. R. & Taylor, G. W. Ag. Actions Suppl. **4**, 37–48 (1979).
5. Morris, H. R., Taylor, G. W., Piper, P. J., Samhoun, M. N. & Tippins, J. R. Prostaglandins **19**, 185–201 (1980).
6. Corey, E. J. et al. J. Am. chem. Soc. **102**, 1436–1438 (1980).
7. Hammarstrom, S. et al. Biochem. biophys. Res. Commun. **91**, 1266–1272 (1979).
8. Morris, H. R., Piper, P. J., Taylor, G. W. & Tippins, J. R. Br. J. Pharmac. **67**, 179–184 (1979).
9. Murphy, R. C., Hammarstrom, S. & Samuelsson, B. Proc. natn. Acad. Sci. U.S.A. **76**, 4275–4279 (1979).
10. Engineer, D. M., Morris, H. R., Piper, P. J. & Sirois, P. Br. J. Pharmac. **64**, 211–218 (1978).
11. Hartley, B. S. Biochem. J. **119**, 805–822 (1970).
12. Morris, H. R. Biochem. Soc. Trans. **3**, 465–467 (1975).
13. Orange, R. P., Murphy, R. C. & Austen, K. F. J. Immun. **113**, 316–322 (1974).
14. Borgeat, P., Hamberg, M. & Samuelsson, B. J. biol. Chem. **251**, 7816–7820 (1976).
15. Chasseaud, L. Adv. Cancer Res. **29**, 175–274 (1979).

Chemical inducers of differentiation in Friend leukaemia cells inhibit lymphocyte mitogenesis

K. H. Stenzel, R. Schwartz, A. L. Rubin & A. Novogrodsky

Rogosin Kidney Center, Departments of Biochemistry, Medicine and Surgery, Cornell University Medical College, New York, New York 10021

Several phorbol esters, the potent tumour-promoting agents[1] isolated from croton oil, induce proliferation of human lymphoctyes[2,3] and enhance the mitogenic effect of lectins on bovine lymphocytes[4]. While studying the mitogenic properties of one of these agents, phorbol myristate acetate (PMA), we found that dimethyl sulphoxide (DMSO), frequently used as a solvent for PMA, markedly inhibits PMA-induced mitogenesis at DMSO concentrations that have little effect on phytohaemagglutinin (PHA)-induced responses. DMSO, as well as a variety of other organic compounds, induce erythroid differentiation in Friend leukaemia (FL) cells[5-9]. Phorbol esters, on the other hand, are potent inhibitors of both spontaneous and induced cellular differentiation[10-13]. We therefore investigated the relationship between the potency of compounds to induce erythroid differentiation in FL cells and their potency to inhibit lymphocyte proliferation induced by PMA and other mitogens. We report here that many of the compounds that induce erythroid differentiation in FL cells are similar to DMSO in selectively suppressing PMA-induced lymphocyte mitogenesis.

The effect of a variety of organic solvents on the proliferation of human lymphocytes stimulated with either PMA or PHA is shown in Table 1 and compared with their reported effects on the differentiation of FL cells. Compounds that induce erythroid differentiation in FL cells inhibit lymphocyte mitogenesis, whereas compounds inactive in inducing erythroid differentiation in FL cells do not inhibit lymphocyte mitogenesis. The concentrations of those compounds which suppress lymphocyte proliferation are in the same range as those reported to induce differentiation. Among the compounds outlined in Table 1, butyric acid, previously reported to inhibit lymphocyte activation[14], is the most potent inducer of erythroid differentiation[6] and is also the most active inhibitor of PMA-induced mitogenesis. However, compounds which are structurally related to butyric acid, but which do not induce erythroid differentiation,
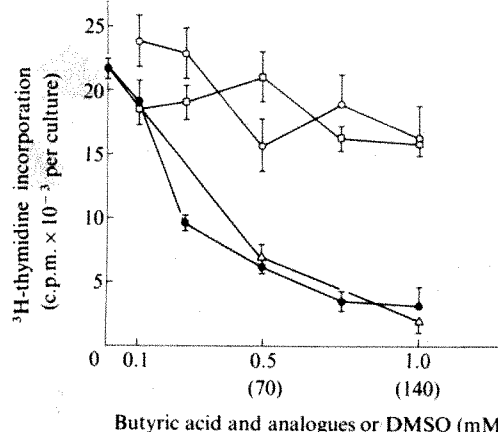
Fig. 1 Effect of butyric acid (●), DMSO (△), isobutyric acid (○) and α-aminobutyric acid (□) on the proliferative response of a human one-way mixed lymphocyte culture. The culture was done as previously described[26]. This experiment is typical of three additional studies. Results are presented as the mean ±s.e.m. of quadruplicate cultures.

Table 1 Inhibition of lymphocyte mitogenesis by compounds which induce erythroid differentiation in FL cells

Compound tested	Concentration range (mM) resulting in 50% inhibition of ^{3}H-thymidine incorporation		Concentrations (mM) reported to induce maximum erythroid differentiation in FL cells
	PMA-induced responses	PHA-induced responses	
Polar organic solvents			
Dimethyl sulphoxide	60	>210	280(7)*, 280(9), 70–300(6)
Dimethylformamide	75	120	60(11), 150(7)
N,N-dimethylacetamide	5–10	25	20(9), 30(7)
Short-chain fatty acids			
Propionic acid	1–1.5	10	2(6)
n-Butyric acid	0.1–0.4	1.4	1–2(6), 1(9)
n-Valeric acid	1.6	>4.0	2(6)
Caproic acid	>10	>10	Inactive(6)
Butyric acid analogues			
Isobutyric acid	4–5	>10	30(24)
β-OH-butyric acid	>10	>10	Inactive(6)
γ-OH-butyric acid	>10	>10	
α-Amino-butyric acid	>10	>10	
β-Amino-butyric acid	>10	>10	
γ-Amino-butyric acid	>10	>10	Inactive(6)
Purine analogues			
Hypoxanthine	1–2	>5.0	3.7(15)
1-Methylhypoxanthine	0.5–1.0	3–5.0	3.3(15)
Xanthine	>5.0	>5.0	Inactive(15)
Allantoin	>5.0	>5.0	Inactive(15)

Human peripheral blood mononuclear cells were obtained from normal subjects as previously described[25]. Final cell preparations (10^6 cells ml^{-1}) were suspended in RPMI-1640 medium containing 5% heat-inactivated fetal calf serum and supplemented with penicillin (100 U ml^{-1}) and streptomycin (100 μg ml^{-1}). Cells were distributed (0.2-ml aliquots) in flat-bottom microwells, the mitogens (PMA 10 ng ml^{-1} or PHA 2 μg ml^{-1}) and compounds to be tested were added, and the cells were then incubated at 37 °C in a 95% air, 5% CO_2 atmosphere for 72 h. ^{3}H-thymidine incorporation (2 μCi per well) into DNA was determined during the final 52–72 h of incubation. The extent of proliferation as determined by ^{3}H-thymidine incorporation in the absence of the test compounds was: PMA (n = 76) 91,169 c.p.m. (s.e.m. = ±2,312), PHA (n = 78) 133,260 c.p.m. (s.e.m. = ±4,012). *Numbers in parenthesis indicate reference from which data were obtained.

do not inhibit lymphocyte proliferation (Table 1). DMSO and butyric acid inhibit PMA-induced morphological transformation and ^{3}H-leucine, ^{3}H-uridine and ^{3}H-thymidine incorporation.

The organic compounds do not inhibit lymphocyte mitogenesis by nonspecific effects on cell viability as directly assessed by the trypan blue exclusion assay. Moreover, following a 2-day incubation with 0.5–1.0 mM butyric acid or 70–140 mM DMSO, lymphocytes are capable of responding to mitogens when the organic solvents are removed by washing the cells. We also found that the organic solvents are most inhibitory when added early in blastogenesis and are much less effective when added 24 h after the mitogenic stimulus. Lymphocyte responses induced by other mitogens (concanavalin A, soybean agglutinin, peanut agglutinin and treatment with neuraminidase and galactose oxidase) have the same resistance to inhibition by DMSO and butyric acid as responses induced by PHA. Lymphocyte activation induced by allogeneic cells in one-way mixed lymphocyte cultures, on the other hand, are as sensitive to suppression by DMSO and butyric acid as are responses to PMA (Fig. 1).

Hypoxanthine and 1-methylhypoxanthine, both known to induce FL cell differentiation[15], inhibit mitogenic responses to PMA and, to a lesser degree, responses to PHA. Xanthine and allantoin, on the other hand, are inactive in both assays (Table 1). Haemin, another known inducer of FL cells[16], differs from the polar organic compounds in that it seems primarily to induce early events in differentiation[17] and does not inhibit FL cell division[18]. We found that haemin alone induces modest increases in ^{3}H-thymidine incorporation in human peripheral blood lymphocytes (Fig. 2). When cells are stimulated with PMA or PHA, haemin inhibits mitogenesis at approximately the same concentrations reported to induce FL cell differentiation (0.75–0.1 mM) (Fig. 2).
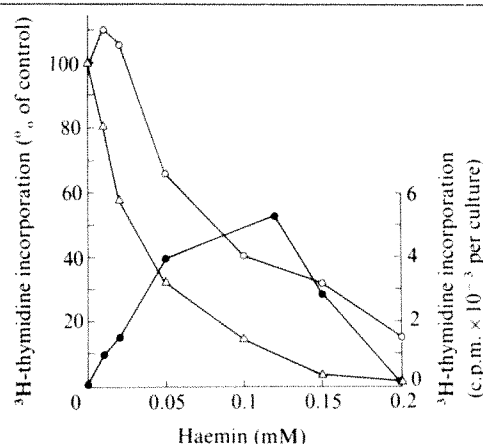
Fig. 2 Effect of haemin on the proliferative response of human peripheral blood lymphocytes (●), ^{3}H-thymidine incorporation (c.p.m. × 10^{-3} per culture), and on PMA (△) and PHA (○) induced ^{3}H-thymidine incorporation (% of control = % of ^{3}H-thymidine incorporation in cultures stimulated with the mitogen in the absence of haemin). Results are presented as the mean of duplicate cultures. Three additional experiments gave similar results.

These studies indicate that there is a remarkable parallelism between the potency of compounds to induce erythroid differentiation in FL cells and their potency to inhibit lymphocyte mitogenesis. Inducers of erythroid differentiation have multiple effects on FL cells[19] and it is unknown which of these effects are relevant to inhibition of mitogenesis. A prominent effect of the polar organic solvents is to decrease the fluidity of lipid membranes[20]. The phorbol esters, on the other hand, increase the fluidity of cell membranes[21], as do other mitogens[22]. It is possible, then, that the inducers of FL cell differentiation inhibit lymphocyte mitogenesis by interfering with the mitogenic signal at the membrane level. The selective inhibitory effect of the various inducers on lymphocyte responses to different stimuli might be due to different triggering signals induced by the different stimulatory agents, or to different subpopulations of lymphocytes responding to the different stimuli. An indication that PMA-responsive lymphocytes are distinct from those responding to PHA and concanavalin A was previously reported[23].

The chemical inducers of differentiation in FL cells constitute a new class of inhibitor of lymphocyte mitogenesis. Their potential use as immunosuppressive agents is now under investigation. A critical evaluation of the relationship between inhibition of lymphocyte mitogenesis and induction of differentiation should provide new insights into the mechanisms of these processes.

1. Van Duuren, B. L. & Orris, L. Cancer Res. 25, 1871–1875 (1965).
2. Estensen, R. D. et al. in Control of Proliferation in Animal Cells (eds Clarkson, B. & Baserga, R.) 627–634 (Cold Spring Harbor Laboratory, New York, 1973).
3. Abb, J., Bayliss, G. J. & Deinherdt, F. J. Immun. 122, 1639–1642 (1979).
4. Mastro, A. M. & Muella, C. G. Expl Cell Res. 88, 40–46 (1974).
5. Friend, C. W., Scher, W., Holland, J. G. & Sato, T. Proc. natn. Acad. Sci. U.S.A. 68, 378–382 (1971).
6. Leder, A. & Leder, P. Cell 5, 319–322 (1975).
7. Tanaka, M. et al. Proc. natn. Acad. Sci. U.S.A. 72, 1003–1006 (1975).
8. Scher, W., Preisler, H. D. & Friend, C. J. cell. Physiol. 81, 63–70 (1973).
9. Reuben, R. C., Wife, R. L., Breslow, R., Rifkind, R. A. & Marks, P. A. Proc. natn. Acad. Sci. U.S.A. 73, 862–866 (1976).
10. Yamasaki, H. et al. Proc. natn. Acad. Sci. U.S.A. 74, 3451–3455 (1977).
11. Rovera, G., O'Brien, T. G. & Diamond, L. Proc. natn. Acad. Sci. U.S.A. 74, 2894–2898 (1977).
12. Cohen, R., Pacifici, M., Rubenstein, N., Biehl, J. & Holtzer, H. Nature 266, 538–540 (1977).
13. Ishi, D. N., Fibach, E., Yamasaki, H. & Weinstein, E. B. Science 200, 556–559 (1978).
14. Kyner, D., Zabos, P., Christian, J. & Acs, G. J. exp. Med. 144, 1674–1678 (1976).
15. Gusella, J. F. & Housman, D. Cell 8, 263–269 (1976).
16. Ross, J. & Sautner, D. Cell 8, 513–520 (1976).
17. Lowenhaupt, K. & Lingrel, J. B. Proc. natn. Acad. Sci. U.S.A. 76, 5173–5177 (1979).
18. Housman, D. et al. in Differentiation of Normal and Neoplastic Hematopoietic Cells (eds Clarkson, B., Gill, J. E. & Marks, P.) 193–207 (Cold Spring Harbor Laboratory, New York, 1978).

19. Friend, C. & Freedman, H. A. *Biochem. Pharmac.* **27**, 1309–1313 (1978).
20. Lyman, G. H., Preisler, H. D. & Paphadjopoulos, D. *Nature* **262**, 360–363 (1976).
21. Castagna, M., Rochette-Egly, C., Rosenfeld, C. & Mishal, Z. *FEBS Lett.* **100**, 62–64 (1979).
22. Inbar, M. & Shinitzky, M. *Eur. J. Immun.* **5**, 166–170 (1975).
23. Touraine, J. L. *J. exp. Med.* **145**, 460–465 (1977).
24. Freidman, E. & Schildkraut, C. L. *Proc. natn. Acad. Sci. U.S.A.* **75**, 3813–3817 (1978).
25. Novogrodsky, A., Stenzel, K. H. & Rubin, A. L. *J. Immun.* **118**, 852–857 (1977).
26. Suthanthiran, M., Stenzel, K. H., Rubin, A. L. & Novogrodsky, A. *Transplantn Proc.* **10**, 923–925 (1978).

Levels of 2,3-diphosphoglycerate in Friend leukaemic cells

G. C. T. Yeoh

Department of Physiology, University of Western Australia, Nedlands, Western Australia 6009, Australia

Most cells are thought to contain trace amounts of 2,3-diphosphoglycerate (DPG), as it acts as a cofactor in the interconversion of 2-phosphoglycerate and 3-phosphoglycerate by the glycolytic enzyme phosphoglyceromutase. DPG is synthesized from 1,3-diphosphoglycerate by the action of diphosphoglycerate mutase. Lowry *et al.*[1] reported levels of 29 µmol DPG per kg wet weight brain tissue which is approximately 3 pmol per 10^8 cells, assuming that 1 g of brain tissue contains 10^9 cells. In contrast, erythroid cells contain 50–100 nmol DPG per 10^8 cells, depending on the species and the stage of development[2]. This is of the order of a 1,000-fold more DPG compared with non-erythroid cells. In red cells DPG concentration modulates the binding of oxygen to haemoglobin[3,4]. I show here that erythroid precurser cells also contain markedly raised levels of DPG.

The terminal stage of erythropoiesis is accompanied by the appearance of haem, globin, spectrin and carbonic anhydrase. There is evidence that the genes associated with these markers are expressed by virtue of a mitotic division[5]. Using Friend leukaemic cells (FLC) as a model of erythropoiesis[6], this laboratory has attempted to obtain markers which characterize early cells in the erythroid lineage by studying the uninduced FLC. This cell seems to be arrested at about the proerythroblast stage of red cell differentiation[7] unless it is induced to proceed further by a variety of polar compounds, generally dimethyl-sulphoxide (DMSO)[8].

Anticipating that these erythroid precursor cells would develop mechanisms for accumulating iron before haemoglobin synthesis, the level of transferrin receptors in uninduced FLC was measured. These receptors bind transferrin specifically and facilitate its internalization together with two atoms of iron per molecule of transferrin. Our study[9], and those of other laboratories[10,11], have shown that transferrin receptors are indeed present in uninduced FLC.

How iron is released from transferrin intracellularly is unclear. However, *in vitro* experiments using cell-free extracts have shown that DPG is able to mediate the release of iron from transferrin[12]. Therefore, it is possible that this process takes place in the intact cell. If so, it would be expected that, in addition to red cells and induced FLC, erythroid precursor cells and uninduced FLC would display levels of DPG significantly higher than that found in non-erythroid cells. The level of DPG measured fluormetrically[1] in uninduced FLC is 4.3 nmol per 10^8 cells (Table 1). This increases by about twofold after the cells are induced to differentiate by DMSO. In comparison, mouse red cells contain 81 nmol DPG per 10^8 cells. DPG in cultured embryonic mouse fibroblasts could not be detected using the standard assay, even after increasing the sensitivity of the assay 100-fold, that is, to the 10–50-pmol range. Similar results were obtained with cultured epithelial cells derived from embryonic rat hepatocyte cultures[13] and cultured human lymphocytes of the IM-9 line[14]. It is concluded that these cells contain < 10 pmol DPG per 10^8 cells. This is less than reported for brain tissue[1], but in those experiments no precautions were taken to

Table 1 DPG levels in Friend leukaemic cells

Cell type	DPG (nmol per 10^8 cells)	% Hb cells
FLC (0)	4.3 ± 0.5	0.3
FLC (3)	5.2 ± 0.4	29
FLC (6)	6.1 ± 0.3	90
FLC (9)	8.7 ± 0.2	82
Mouse RBC	81.1 ± 3.2	100
Mouse fibroblast	ND	0
Rat epithelial cells	ND	0
Human lymphoid cells (IM-9)	ND	0

FLC were cultured as previously described[9] in the presence of 1.86% DMSO for days indicated in parentheses. Duplicate estimations of DPG were performed on three cultures for each group and four samples for mouse RBC. Per cent haemoglobinized cells was determined by benzidine staining[19]. Between 5×10^7 and 10^8 cells were used for each sample. Cells were pelleted then washed twice with ice-cold balanced salts solution by centrifugation at 1,000g. The final pellet was sonicated in 100µl 0.5 N HClO$_4$, centrifuged at 4,000g for 10 min and the supernatant removed and neutralized with 100µl 0.5 M NaOH. Aliquots of between 10 and 40 µl were taken for DPG determination by the enzyme-coupled fluorometric method of Lowry *et al.*[1]. Each assay contained 5.2 nmol of NADH and the decrease in absorbance at 340 nm was measured in a Perkin Elmer fluorescence spectrophotometer model 240-A. DPG and NADH standards were incorporated in each set of determinations. Results are expressed as means ± s.e.m. DPG could not be detected (ND) in extracts of cultured embryonic mouse fibroblasts, rat epithelial cells of human lymphoid cells in spite of 100-fold increase in sensitivity over the standard assay. Therefore, these cells are estimated to contain less than 0.01 nmol DPG per 10^8 cells.

exclude possible contamination of samples with blood, whereas this is avoided in cultured cells. Reddy and Burns[15] have attempted to measure DPG levels in myocytes, hepatocytes and adipocytes of the rat and conclude that levels were undetectable. They were also unable to demonstrate the presence of 2,3-diphosphoglycerate mutase, the enzyme responsible for DPG synthesis.

These results indicate that erythroid precursor cells, as judged by the levels found in uninduced FLC, have at least a 1,000-fold more DPG than non-erythroid cells; for example, rat epithelial cells, human lymphoid cells or mouse fibroblasts. The small percentage (0.3%) of haemoglobinized cells in the uninduced culture cannot account for the relatively high levels of DPG found in the control culture. This result differs from those of Kabat *et al.*[16] and Scher *et al.*[17], who were unable to detect DPG in uninduced or induced FLC using the method of Maeda *et al.*[18] This may be explained by the greater than 100-fold increase in sensitivity of the method used in this study achieved by fluorometric measurement of NADH oxidation by enzyme-coupled assay in contrast to the spectrophotometric determination of inorganic phosphate liberated from DPG used in previous studies. After induction, when most of the FLC are haemoglobinized, there is only a small increase in DPG. The presence of DPG in uninduced non-haemoglobinized FLC suggests it is not one of the group of erythroid markers which appear at the terminal stage of erythropoiesis, as would be predicted if its only role in the red cell was to modulate the affinity of oxygen for haemoglobin. Its early appearance is consistent with the proposal that it may have a role in iron accumulation by the developing red cell and that it continues to accumulate during erythroid maturation.

1. Lowry, O. H., Passonneau, J. V., Hasselburger, F. X. & Schulz, D. W. *J. biol. Chem.* **239**, 18 (1964).
2. Bartlett, G. R. *Comp. Biochem. Physiol.* **61A**, 191 (1978).
3. Oski, F. A. & Gottleib, A. J. *Prog. Hemat.* **7**, 33 (1971).

4. Finch, C. A. & Lenfant, C. *New Engl. J. Med.* **286**, 407 (1972).
5. Campbell, G. M., Weintraub, H., Mayall, H. & Holtzer, H. *J. Cell Biol.* **50**, 669 (1971).
6. Friend, C., Scher, W., Holland, J. G. & Sato, T. *Proc. natn. Acad. Sci. U.S.A.* **68**, 378 (1971).
7. Harrison, P. R. *Nature* **262**, 353 (1976).
8. Tanaka, M. *et al. Proc. natn. Acad. Sci. U.S.A.* **72**, 1003 (1975).
9. Yeoh, G. C. T. & Morgan, E. H. *Cell Differentiation* **8**, 331 (1979).
10. Hu, H. Y., Gardner, J., Aisen, P. & Skoultchi, A. I. *Science* **197**, 559 (1977).
11. Glass, J., Nunez, M. T., Fisher, S. & Robinson, H. *Biochim. biophys. Acta* **542**, 154 (1978).
12. Morgan, E. H. in *Proteins of Iron Metabolism* (ed. Brown, E. B.) 227 (Grune & Stratton, New York, 1977).
13. Yeoh, G. C. T., Bennett, F. A. & Oliver, I. T. *Biochem. J.* **180**, 153 (1979).
14. Fahey, J. L., Buell, D. N. & Sox, H. C. *Ann. N.Y. Acad. Sci.* **190**, 221 (1971).
15. Reddy, W. J. & Burns, A. H. *Biochim. biophys. Acta* **428**, 476 (1976).
16. Kabat, D., Sherton, C. C., Evans, L. H., Bigley, R. & Koler, R. D. *Cell* **5**, 331 (1975).
17. Scher, W., Parkes, J. & Friend, C. *Cell Differentiation* **6**, 285 (1977).
18. Maeda, N., Chang, H., Benesch, R. & Benesch, R. E. *New Engl. J. Med.* **284**, 1239 (1971).
19. Cooper, M. C., Levy, J., Cantor, L. N., Marks, P. A. & Rifkind, R. A. *Proc. natn. Acad. Sci. U.S.A.* **71**, 1672 (1974).

Saccharin may act as a tumour promoter by inhibiting metabolic cooperation between cells

J. E. Trosko, B. Dawson, L. P. Yotti & C. C. Chang

Department of Pediatrics and Human Development, College of Human Medicine, Michigan State University, East Lansing, Michigan 48823

The possible role of saccharin in the carcinogenic process is, at present, still unclear. Carcinogenesis is a complex process involving, in many test systems, initiation and promotion phases[1]. Current evidence favours the hypothesis that initiation is due to a mutagenic event, while promotion (at least the early portion) is the result of epigenetic changes[2]. Although saccharin has been reported to be a weak mutagen in various *in vitro* test systems and a weak initiator in mouse skin[3-7], there is increasing evidence from *in vitro*, as well as *in vivo*, studies that it might act as a tumour promoter[8-13], rather than as a mutagen[14-19]. Recently, L.P.Y. *et al.*[20] and J.E.T. *et al.*[21] developed an *in vitro* assay to detect tumour promoters, which has been independently reported by Murray and Fitzgerald[22]. The assay is based on the principle that phorbol ester-type tumour promoters block 'metabolic cooperation' or a type of cell–cell communication between cells. We report here a series of experiments demonstrating the elimination of metabolic cooperation in the hypoxanthine guanine phosphoribosyltransferase (HGPRT) system in Chinese hamster V79 cells, indicating that saccharin shares properties similar to those of other known promoters.

In an attempt to examine the potential biological effects of saccharin in intercellular communication, we seeded a small number of HG-PRT$^-$ (6-thioguanine resistant) V79 cells in the presence of a large number of HG-PRT$^+$ (6-thioguanine sensitive) cells sufficient to reduce the recovery of the resistant cells via the mechanism of metabolic cooperation[23]. If the same experiment is conducted with the addition of 12-tetradecanoyl-13-phorbol-acetate (TPA) or a chemical with promoting properties, the reduction in the recovery of 6-thioguanine resistant cells is significantly prevented. Figure 1 depics the result of adding various concentrations of saccharin (Sigma, Lot 65C-0129) to this metabolic-cooperation assay. With saccharin levels

Table 1 Recovery of 6-thioguanine resistant cells in the presence of TPA, pure saccharin, impure saccharin and Sweet'N Low

No. of V79 cells (HG-PRT$^+$)	No. of 6-TG^r cells (HG-PRT$^-$)	Drug	Concentration	% Recovery
—	100	—	—	79.1
7×10^5	100	—	—	18.9
7×10^5	100	TPA	0.1 µg ml^{-1}	96.4*
7×10^5	100	Pure saccharin	3 mg ml^{-1}	40.2*
7×10^5	100	Impure saccharin	3 mg ml^{-1}	42.0*
7×10^5	100	Sweet'N Low	3 mg ml^{-1}	22.2
7×10^5	100	Sweet'N Low	5 mg ml^{-1}	23.6

* Treatment significantly increased recovery ($P < 0.01$) according to SNK test.

Fig. 1 Dose–response curve for the effect of saccharin on the inhibition of metabolic cooperation between 6-thioguanine sensitive and resistant Chinese hamster V79 cells. The shaded areas correspond to the mean recovery of 6-TG cells for the control and TPA-treated groups ±s.d. Wild-type s-TG^s cells and X-ray-induced 6-TG^r cells were grown in modified Eagle's medium supplemented with a 100% increase of non-essential amino acids, 1 mM sodium pyruvate and 5% fetal calf serum. Both cell lines were plated in 100-mm plates at the same time (7×10^5 6-TG^s and 100 6-TG^r), allowed to attach, and then treated with the TPA (0.1 µg ml^{-1}) or saccharin and 6-thioguanine (10 µg ml^{-1}). The medium was replaced after 3 days and 5 days with medium containing 6-thioguanine. After 7 days the colonies were fixed, stained with Giemsa and scored. The results are expressed as the percentage of plated 6-TG^r cells (determined by control plates containing 100 6-TG^r cells for each treatment) that formed colonies in the presence of the 6-TG^s cells. None of the saccharin doses decreased the colony-forming ability. All of these *in vitro* promotion assays are done with non-toxic concentrations of presumptive promoters.

above 2 mg ml^{-1}, there is a linear 'rescue' of 6-thioguanine resistant cells. Compared with TPA, the effect of saccharin on the inhibition of metabolic cooperation is weak. Whereas 0.1 µg ml^{-1} of TPA resulted in a four- to fivefold increase in the recovery of 6-thioguanine resistant cells, 5 mg ml^{-1} of saccharin caused only a twofold increase.

Since Wolff and Rodin[4] showed that both impure (lot S1022, Maumee process, Sherwin-Williams) and pure samples of saccharin induced sister chromatid exchanges, we performed an experiment to find whether this same impure saccharin and a commercial preparation (Sweet'N Low) would affect metabolic cooperation. Table 1 shows that both the impure and pure saccharin worked to block metabolic cooperation. Sweet'N Low failed to block metabolic cooperation, probably because only 4% of the mixture was saccharin (the maximum concentration of saccharin was 0.2 mg ml^{-1}).

The demonstration that the saccharin preparation seems to be a weak promoter of certain cancers and to block metabolic cooperation. Table 1 shows that both the impure and pure to other promoters suggests that, at least for rodents, it can influence tumorigenesis at a high concentration by affecting cell–cell communication rather than by mutating cells. The observation that sister chromatid exchanges are induced not only by known DNA damaging agents/mutagens[24], but also by a tumour promoter (TPA)[25] and anti-promoters raises some new and interesting problems related to both the mechanism of action of tumour promoters and the assays used to detect them.

1. Slaga, T. J., Sivak, A. & Boutwell, R. K. *Carcinogenesis: Mechanisms of Tumor Promotion and Cocarcinogenesis*, Vol. 2 (Raven, New York, 1978).
2. Trosko, J. E. & Chang, C.C. in *Chemical Carcinogens and DNA* (ed. Grover, P. L.) (CRC Press, Cleveland, 1979).
3. Batzinger, P. P., Ou, S. L. & Bueding, E. *Science* **198**, 944–946 (1977).
4. Wolff, S. & Rodin, B. *Science* **200**, 543–545 (1978).
5. Moore, C. & Schmick, A. *Mutat. Res.* **67**, 215–219 (1979).
6. Moore, C. & Schmick, A. *Science* **205**, 1007–1010 (1979).
7. Renner, H. W. *Experientia* **35**, 1364 (1979).
8. Reuber, M. D. *Environmental Health Perspectives* **25**, 173–200 (1978).
9. Boyland, E. *Nature* **278**, 123–124 (1979).
10. Hicks, R. M., Wakefield, J. St. J. & Chowaniec, J. *Nature* **243**, 347–349 (1973).
11. Hicks, R. M. & Chowaniec, J. *Cancer Res.* **37**, 2943–2949 (1977).
12. Mondal, S., Brankow, D. W. & Heidelberger, C. *Science* **201**, 1141–1142 (1978).
13. Cohen, S. M., Arai, M., Jacobs, J. B. & Friedell, G. H. *Cancer Res.* **39**, 1207–1217 (1979).
14. Kramer, P. G. N. *Mutat. Res.* **32**, 81–92 (1975).
15. Lutz, W. K. & Schlatter, C. *Chem. biol. Int.* **19**, 253–257 (1977).
16. Brogger, A., Ardito, G. & Waksvik, H. *Hereditas* **91**, 135–138 (1979).
17. Poncelet, F., Roberfroid, M., Mercier, M. & Lederer, J. *Fd Cosmet. Tox.* **17**, 229–232 (1979).
18. Sweetman, T. W. & Renwick, A. G. *Science* **205**, 1019–1020 (1979).
19. Leonard, A. & Leonard, R. D. *J. envir. path. Tox.* **17**, 229–232 (1979).
20. Yotti, L. P., Chang, C. C. & Trosko, J. E. *Science* **206**, 1089–1091 (1979).
21. Trosko, J. E., Yotti, L. P., Dawson, B. & Chang, C. C. in *Short Term Tests for Chemical Carcinogens* (ed. Stich, H.) (Springer Berlin, in the press).
22. Murray, A. W. & Fitzgerald, D. J. *Biochem. biophys. Res. Commun.* **91**, 395–401 (1979).
23. van Zeeland, A. A., Van Digglin, M. C. E. & Simons, J. W. I. M. *Mutat. Res.* **14**, 355–363 (1972).
24. Wolff, S. A. *Rev. Genet.* **11**, 183–201 (1977).
25. Kinsella, A. R. & Radman, M. *Proc. natn. Acad. Sci. U.S.A.* **75**, 6149–6153 (1978).

Embryonal carcinoma stem cells lack a function required for virus replication

James W. Gautsch

Department of Cellular and Developmental Immunology, Research Institute of Scripps Clinic, 10666 N. Torrey Pines Road, La Jolla, California 92037

Embryonal carcinoma (EC) stem cells are thought to be equivalent to the ectoderm of the preimplantation mouse embryo because they share morphological, biochemical and antigenic properties[1,2]. These near diploid EC cells can be induced to differentiate into cell types of all three germ layers[1,2]. They also can take part in normal differentiation and contribute cells to many tissues in chimaeric mice derived from preimplantation mouse embryos injected with them[3]. The ability to restrict the growth of certain viruses is a distinguishing characteristic of EC cells[4–8], but it is intriguing that this restriction disappears after differentiation. The ability of EC cells to block totally productive infection by the highly infectious and oncogenic Moloney strain of murine leukaemia virus (M-MuLV) is remarkable, as virtually all other murine cells are permissive to the growth of this virus. Teich et al.[7] suggested that replication of M-MuLV in EC cells is blocked at some point after integration of proviral DNA into the cell's genome. Here I enquire into the dominant or recessive nature of the restriction, that is, do EC cells show transdominant inhibition of virus replication analogous to that imposed by interferon or the mouse Fv-I locus, or is the block to MuLV replication due to the lack of something in the EC cell? This report shows that the restriction of M-MuLV in EC cells can be overcome by fusion with permissive cells. The resulting complemented growth of M-MuLV in EC/permissive cell heterokaryons indicates that the restriction over M-MuLV is a recessive trait of EC cells and, therefore, defines a hitherto unknown host function that is vital to virus growth but missing in EC cells.

Virtually all permissive mouse cells (SC-1 and 129/Sv mouse embryo fibroblasts (MEF)) infected with M-MuLV formed syncytial plaques in an infectious-centre XC assay (Table 1a). Infected EC-A cells did not form plaques, indicating that pro-

geny virus was not produced. However, when EC-A cells were infected with M-MuLV and then fused with uninfected permissive cells, XC plaque formation was evident (Table 1b). This complementation of M-MuLV growth in infected EC-A cells was provided by fusion with uninfected SC-1 cells, 129/Sv secondary MEF, mink lung cells or rabbit epithelial cells. The latter two types complement M-MuLV growth although these mink and rabbit cells are themselves resistant to infection by M-MuL V (either because they lack surface membrane receptors[9] or because the virus cannot penetrate their plasma membranes). In the control, fusion of infected EC-A cells with uninfected EC-A cells did not result in XC plaque formation. The appearance of XC plaques did not result from free or EC-bound infectious virus because the addition of permissive cells to infected EC-A cells, without fusion, resulted in little, if any, plaque formation. Also, culture supernatants collected at various times before and after polyethylene glycol (PEG) fusion, and used to 'infect' SC-1 cells, were consistently negative for infectious plaque-forming virus. This was done to eliminate the

Table 1 Complementation of M-MuLV growth in EC-A cells

M-MuLV-infected cells*	Uninfected complementing cells	$\log_{10}$ ICPFU $ml^{-1\dagger}$ fused[‡]	not fused
a			
EC	—	<0.3	(<0.3)
SC-1	—	4.1	(5.4)
129/Sv MEF	—	3.6	(4.9)
RLE	—	<0.3	(0.6)
MLC	—	<0.3	(<0.3)
b		$\log_{10}$ ICPFU per plate	
EC	EC	<0.3	(<0.3)
EC	SC-1	3.1	(1.4)
EC	129/Sv MEF	2.6	(0.6)
EC	RLE	1.9	(<0.3)
EC	MLC	1.7	(<0.3)

*EC-A cells were supplied by Dr W. C. Speers as a subclone[25] of the PCC4azal embryonal carcinoma cell line derived from a teratocarcinoma of the 129/Sv mouse, as first described by Jakob et al.[19]. When grown as monolayers *in vitro* without feeder cells, less than 0.1% of these cells spontaneously differentiate without specific stimulation; PCC4azal and most other subclones spontaneously differentiate at higher frequencies. EC-A cells were grown in Eagle's minimal essential medium (EMEM) containing 10% fetal calf serum and antibiotics. The SC-1 murine cell line is highly permissive to type-C murine retrovirus infection[20]. 129/Sv MEF were secondary cells derived from 14-day embryos of a 129/Sv mouse. Rabbit lung epithelial (RLE) and mink lung cells (MLC)[21] are permissive for xenotropic and amphotropic viruses and non-permissive to ecotropic MuLV. M-MuLV is the exogenous Moloney strain of MuLV; the plaque-forming M-MuLV-148 subclone used in these studies has a ecotropic host range and grows well in mouse cells but very little, if at all, in cells from other species.

† Virus production was assayed by a quantitative infectious-centre XC plaque assay, SXC, that requires only a single cycle of infection in mouse cells[22]. Therefore, a single virus-producing mouse cell caused an XC syncytial-plaque expressed as an infectious-centre plaque forming unit (ICPFU). Cells were treated with DEAE dextran (25 μg ml⁻¹ for 30 min) before infection with M-MuLV at a multiplicity of 1–20 plaque forming units per cell. EC cells infected in this manner were allowed to adsorb virus for 1 h at 37 °C. The cells were then washed twice with EMEM and incubated for an additional 1–2 h to allow penetration of the cells by the adsorbed virus. The infected cells were lifted and washed extensively to ensure the elimination of any free M-MuLV that did not adsorb to the cells. These infected EC cells, as a single cell suspension, were plated on 35-mm diameter tissue culture plates at 2 × 10⁵ cells per plate, and an equal number of complementing cells was added. The cells were allowed to attach to the surface of the dishes for at least 2 h before fusion.

‡ Cells were fused with 47.5% polyethylene glycol (PEG) as described previously[23]. The efficiency of cell fusion and the toxicity of PEG to cells is difficult to estimate as these factors vary from one cell type to another and are highly dependent on PEG concentration, which can vary throughout an exposed plate due to the presence of residual media[23]. Cultures that were observed 3 h or more after PEG exposure had areas of non-viable cells, areas of large multinucleated heterokaryons, and areas of single cells and small heterokaryons. Viable cells (trypan blue exclusion) at 16 h after infection normally contained approximately 10% bi- and multinucleated heterokaryons. Multinucleated heterokaryons were lost from cultures that were carried for several generations. Similar results were obtained when cells were fused with inactivated Sendai virus, although there were fewer multinucleated heterokaryons formed and little if any toxicity. Fused or unfused infected cells were lifted 16 h after infection, before progeny virus-induced secondary infections could occur, counted, and dilutions of the single cell suspensions were cocultivated with XC cells and dexamethasone, as described[24]. Heterokaryons that produced progeny virus caused infection and fusion of surrounding XC cells resulting in syncytial plaques that were small relative to M-MuLV infected permissive mouse cells, suggesting that fewer progeny virus were produced by the fused cells.
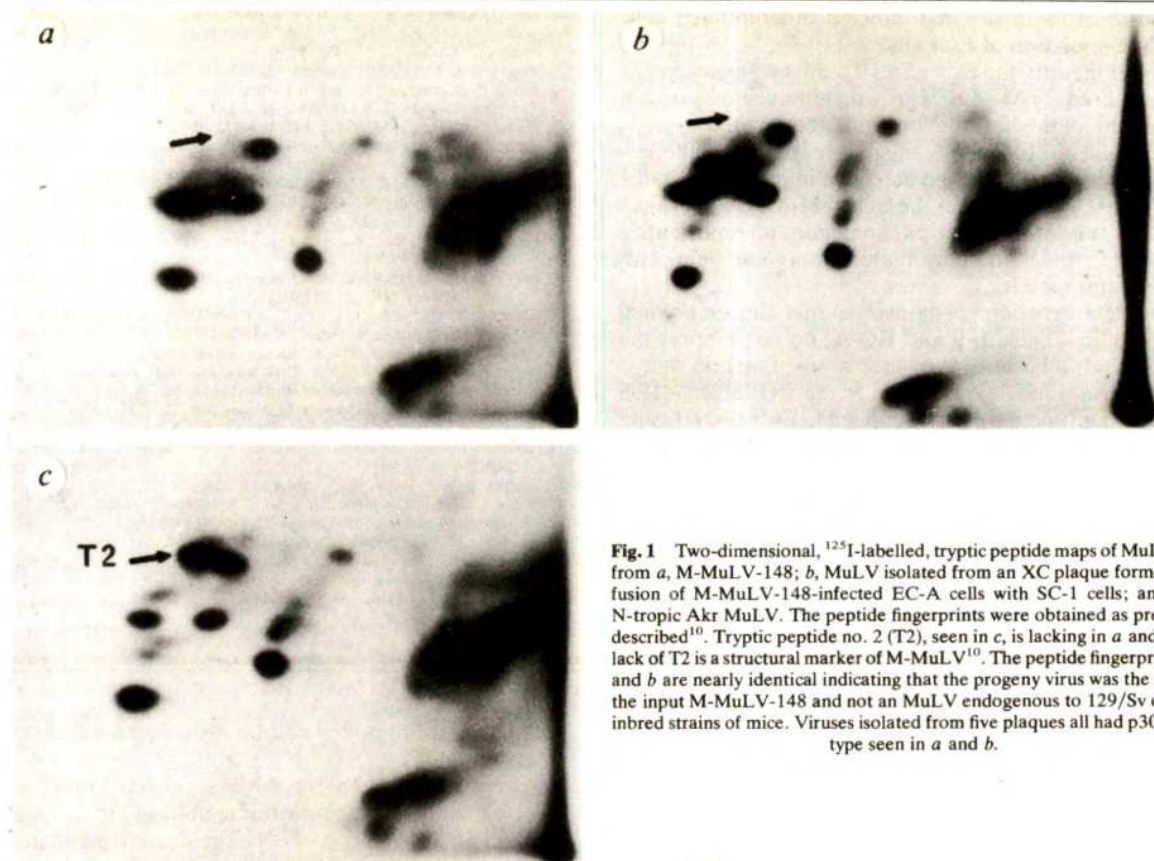
Fig. 1 Two-dimensional, ^{125}I-labelled, tryptic peptide maps of MuLV p30s from *a*, M-MuLV-148; *b*, MuLV isolated from an XC plaque formed after fusion of M-MuLV-148-infected EC-A cells with SC-1 cells; and *c*, an N-tropic Akr MuLV. The peptide fingerprints were obtained as previously described[10]. Tryptic peptide no. 2 (T2), seen in *c*, is lacking in *a* and *b*. This lack of T2 is a structural marker of M-MuLV[10]. The peptide fingerprints of *a* and *b* are nearly identical indicating that the progeny virus was the same as the input M-MuLV-148 and not an MuLV endogenous to 129/Sv or other inbred strains of mice. Viruses isolated from five plaques all had p30s of the type seen in *a* and *b*.

possibility that plaques were caused by secondary infections of SC-1 cells by input M-MuLV liberated from EC cells after exposure to PEG.

Viruses were isolated from individual XC plaques and grown in SC-1 cells, after which peptide maps of the viral p30 core protein were obtained, as described previously[10]. Figure 1 shows that the p30 peptide maps contained markers specific for M-MuLV, indicating that the plaques were caused by progeny of the input M-MuLV, as opposed to a possible fusion-induced production of virus endogenous to the EC-A[11,12] or permissive cells. Therefore, heterokaryons formed between infected EC-A cells and uninfected permissive cells produced infectious progeny M-MuLV, whereas infected EC-A cells alone did not.

The efficiency of permissive cell complementation of M-MuLV growth in EC cells was dependent on the time of heterokaryon formation. M-MuLV-infected EC-A or F-9 cells were fused with uninfected SC-1 cells at various times after infection and assayed for infectious centres. As seen in Table 2, complementation of M-MuLV growth in EC cells was much more frequent when heterokaryons were formed 8–12 h after infection. Unexpectedly, before this time, and even after, fusion yielded little complementation of M-MuLV growth. These results suggest: (1) that the virus requires the host cell function only during a discrete period of its replication cycle, that is 8–12 h after infection; and (2) as heterokaryon formation before 8 h postinfection was not efficient in complementing M-MuLV growth, the host function must itself be labile and not replenished in the heterokaryon. Since the entire contents of the EC and permissive cells are present initially in heterokaryons, a dominant regulatory component of the EC cell apparently represses production of the required function that permissive cells express. This is not surprising when one considers the ability of EC cells to confer pluripotency to somatic cell hybrids between EC cells and thymocytes[13] or Friend erythroid cells[8] and suggests a generalized dominant nature of undifferentiated embryonic stem cells.

A separate, third, consideration is that complementation of M-MuLV production in infected EC-A and F-9 cells, by fusion

with uninfected SC-1 cells, decreases rapidly 12 h or more after infection (Table 2). After this interval, virus apparently cannot use the host component that complements M-MuLV growth in EC/permissive cell heterokaryons. This suggests that the virus has changed or is under different control after the period of complementation passes (8–12 h postinfection). We have isolated subclones of infected EC cells that are known to be non-productively infected with M-MuLV[14]. These cells cannot be induced to produce M-MuLV by fusion with permissive cells. This latter point is consistent with related studies with M-MuLV[7] and SV40[15], in which EC/permissive cell heterokaryons, formed several days after infection of EC cells, did not replicate virus, whereas fusion soon after polyoma virus infection did result in viral antigen expression[16]. Also, as complementation decreased when fusion occurred later than 12 h postinfection, it is unlikely that fusion simply allowed

Table 2 Temporal effect of SC-1 cell complementation of M-MuLV growth in EC-A and F-9 cells

			ICPFU per plate*					
		No	PEG fusion (h after infection)					
Expt	EC cell	PEG	4	8	12	16	20	24
1	EC-A	2	86	162	248	12	ND	0
2	EC-A	1	20	98	124	ND	3	ND
3	EC-A	0	0	14	40	12	ND	0
4	EC-A	8	70	860	787	86	12	ND
5	EC-A	26	112	690	1274	ND	118	ND
6	EC-A	1	30	110	114	ND	5	ND
6	F-9	0	37	180	228	ND	20	ND

*Subconfluent EC-A and F-9 monolayer cells were infected with M-MuLV, co-cultivated with SC-1 cells, fused with PEG, and assayed for XC plaque formation as described in Table 1. F-9 cells, a 'nullipotent' EC cell line that does not spontaneously differentiate in monolayer culture[26] were from Dr F. Dutko. F-9 cells were grown in monolayers on plastic tissue culture flasks or plates that had been previously treated with 0.1% gelatin at 4 °C for 2 h to enhance attachment. PEG fusion was timed from the first exposure of EC cells to M-MuLV. Numbers represent the average ICPFU for duplicate or triplicate plates at each time point. ND, Not determined.

amplification of virus in the few infected differentiated cells present in the population of EC cells.

These studies identify the existence of a missing factor in EC cells that is required for M-MuLV growth, although they do not specify the nature of the host function, possibly an enzyme(s) or organelle(s). Recent studies[17,18] suggest that the undifferentiated F-9 line of EC cells may be defective in producing stable SV40 RNA transcripts. Whether the lack of M-MuLV growth in F-9 and EC-A cells is a similar phenomenon, or represents a general characteristic of undifferentiated embryonic stem cells, has yet to be determined.

The data presented here demonstrate that the embryonal carcinoma stem cell lines, F-9 and EC-A, do not support the growth of M-MuLV because they lack a host function that is required for virus replication and must be available 8–12 h postinfection. This function can be supplied to EC cells by fusion with differentiated mouse, rabbit or mink cells. If this fusion-induced complementation of M-MuLV growth can be used to purify the responsible factor from permissive cells, the related function should become clear.

I thank W. C. Speers, R. M. Liskay, F. Dutko and R. A. Lerner for helpful criticisms.

1. Martin, G. R. *Cell* **5**, 229–243 (1975).
2. Hogan, B. L. M. *Int. Rev. Biochem.* **15**, 333–376 (1977).
3. Mintz, B. & Illmensee, K. *Proc. natn. Acad. Sci. U.S.A.* **72**, 3585–3589 (1975).
4. Swartzendruber, D. E. & Lehman, J. M. *J. cell. Physiol.* **85**, 179–188 (1975).
5. Kelly, F. & Boccara, M. *Nature* **262**, 409–411 (1976).
6. Peries, J., Alves-Cardoso, E., Canivet, M., Debons-Guillemin, M. C. & Lasneret, J. *J. natn. Cancer Inst.* **59**, 463–465 (1977).
7. Teich, N. M., Weiss, R., Martin, G. R. & Lowy, D. R. *Cell* **12**, 973–982 (1977).
8. Miller, R. A., Ward, D. C. & Ruddle, F. H. *J. cell. Physiol.* **91**, 393–402 (1977).
9. Schnitzer *et al. J. Virol.* **23**, 449–454 (1977).
10. Gautsch, J.W., Elder, J.H., Schindler, J., Jensen, F.C. & Lerner, R.A. *Proc. natn. Acad. Sci. U.S.A.* **75**, 4170-4174 (1978).
11. Emanoil-Ravicovitch, R., Robert, J., Cavinet, M., d'Auriol, L. & Peries, J. *C.r. Séanc. hebd. Acad. Sci., Paris* **286**, 1277–1280 (1978).
12. Huebner, K., Tsuchida, N., Green, C. & Croce, C. *J. exp. Med.* **150**, 392–405 (1979).
13. Miller, R. A. & Ruddle, F. H. *Cell* **9**, 45–55 (1976).
14. Speers, W. C., Gautsch, J. W. & Dixon, F. (in preparation).
15. Swartzendruber, D. E., Friedrich, T. D. & Lehman, J. M. *J. cell. Physiol.* **93**, 25–30 (1977).
16. Boccara, M. & Kelly, F. *Virology* **90**, 147–150 (1978).
17. Segal, S., Levine, A. J. & Khoury, G. *Nature* **280**, 335–338 (1979).
18. Segal, S. & Khoury, G. *Proc. natn. Acad. Sci. U.S.A.* **76**, 5611–5615 (1979).
19. Jakob, H., Boon, T., Gaillard, J., Nicolas, J. F. & Jacob, F. *Ann. Microbiol. Inst. Pasteur* **124B**, 269-282 (1973).
20. Hartley, J. W. & Rowe, W. P. *Virology* **65**, 128–134 (1975).
21. Elder, J. H. *et al. Proc. natn. Acad. Sci. U.S.A.* **74**, 4676–4680 (1977).
22. Gautsch, J. W. & Meier, H. *Virology* **72**, 509–513 (1976).
23. Davidson, R. L. & Gerald, P. S. *Somat. Cell Genet.* **2**, 165–176 (1976).
24. Gautsch, J. W., Bedigian H. G. & Meier, H. *Virology* **83**, 462–466 (1977).
25. Speers, W.C., Birdwell, C.R. & Dixon, F.J. *Am. J. Path.* **97**, 563-578 (1979).
26. Bernstine, E.G., Hooper, M.L., Grandchamp, S. & Ephrussi, B. *Proc. natn. Acad. Sci. U.S.A.* **70**, 3899-3903 (1973).

Encephalomyocarditis virus infection of cultured murine pancreatic β-cells

G. L. Wilson, B. J. D'Andrea, S. C. Bellomo & J. E. Craighead

Department of Pathology, University of Vermont, College of Medicine, Burlington, Vermont 05405

Encephalomyocarditis virus (EMC) possesses many of the biological and pathogenetic features of the human Group B coxsackieviruses which have been implicated in the aetiology of insulin-dependent diabetes mellitus[1,2]. The M variant of EMC produces a diabetes-like disease when inoculated into some strains of mice. In these animals, cytolysis of β-cells is prominent, and there is an accompanying mononuclear inflammatory cell response (insulitis). Hyperglycaemia is observed during the acute stages of infection followed by varying degrees of carbohydrate intolerance[3–5]. In other mouse strains, β-cell lesions are less prominent and insulitis fails to occur, even though the animals develop a systemic infection. In these animals diabetes is observed either infrequently or not at all. Although the susceptibility of mice to the diabetogenic effect of the virus is believed to be influenced by one or more recessive genes, the pathogenetic basis for differences between the strains has not been defined[6,7]. The basis for the unique tropism of the M variant for β-cells also is uncertain because other serotypically similar strains of this virus cause pancreatic acinar cell necrosis, but lack a diabetogenic effect[3,5]. We have studied mouse pancreatic β-cells in tissue culture to determine whether or not these cells are uniquely susceptible to the M variant of EMC. Additionally, we examined the viral susceptibility of cultured β-cells derived from mouse strains that varied in their resistance to the diabetogenic effects of the M variant. The results show that cultured mouse β-cells can be infected by a variety of EMC viruses, and β-cells from different strains of mice are susceptible to infection by the M variant of EMC.

The majority of cells in our monolayer cultures stained positively by an immunoperoxidase technique[8,9] using anti-bovine insulin serum. The cultures secreted insulin into the medium at a gradually increasing rate for periods of longer than 1 month[10,11]. However, because the monolayers were prepared from fresh pancreata, the number of cells and the absolute amount of

insulin released into the culture dishes varied from experiment to experiment.

After maintenance for 9 days *in vitro*, monolayers were infected with 10^4 plaque-forming units of virus at an estimated multiplicity of infection of ~1. The deviation and properties of the M variant and the non-diabetogenic E (ref. 12), r^+ (ref. 13), and Mengo[14] strains have been reported[15]. The viruses were
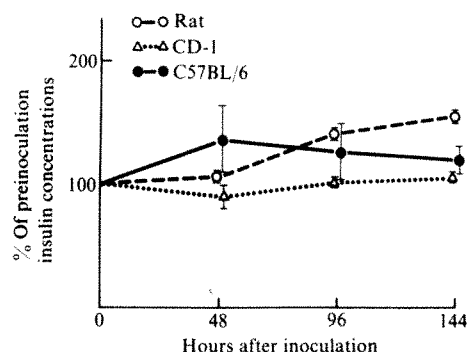
Fig. 1 Monolayer cultures of mouse β-cells were prepared from the pancreatic tissue of 4- to 6-week-old mice. The isolated pancreata were dissociated in a phosphate-buffered saline solution containing 0.04% collagenase, 0.02% α-chymotrypsin, 0.03% DNase and 4% fetal calf serum. Rat β-cells were prepared by the method of Chick *et al.*[11]. β-Cell preparations were enriched using discontinuous Ficoll gradients and purified by differential adhesion and treatment with cysteine-free culture medium[24]. Cells were plated into multiwell plates (24 wells per plate, Co-Star) and maintained with Medium 199 (Gibco) containing 10% fetal calf serum, glucose (300 mg dl^{-1}) and gentamicin (1 mg dl^{-1}). The culture medium was replenished at 48-h intervals. Insulin in the culture medium was determined by the method of Wright *et al.*[25] using I^{125}-labelled porcine insulin (Cambridge Nuclear) diluted with cold porcine insulin (Dr Ronald Change, Eli Lilly), and guinea pig anti-bovine insulin serum (Linco) with purified mouse insulin (Novo) serving as a standard. Using this method insulin concentrations as low as 50 μU per ml of culture medium can be detected. Insulin release by β-cells in control cultures is displayed. The cultures were prepared from the pancreata of CD-1 and C57BL/6 mice and CD rats (Charles River). Data are expressed as a percentage of the insulin released during days 7 to 9 of culture. The 100% insulin concentrations averaged 1.5 ± 0.3 mU per culture for the CD-1 cultures, 0.5 ± 0.03 mU per culture for the C57BL/6 cultures and 10.6 ± 0.4 mU per culture for the CD rat cultures.

grown and titred in a continuous line of mouse fibroblasts (L-929) maintained in this laboratory.

Culture medium was collected at 48-h intervals after infection and assayed for insulin. Control cultures released insulin at a steady rate (Fig. 1). The results of insulin radioimmunoassays on the medium of infected β-cell cultures prepared from CD-1 mice are summarised in Fig. 2. Studies with the diabetogenic M and the non-diabetogenic E, r[+] and Mengo strains were conducted in a similar fashion. In replicate experiments insulin in the culture medium was reduced appreciably at 48 h after inoculation and was not detectable after 96 h. During this time cultures were monitored daily by phase contrast microscopy, and extensive cytolysis was observed. Thus, morphological evidence of cell death clearly supported the insulin data. The effects noted above were not influenced substantially by virus dosage. To exclude nonspecific cytotoxic effects of the viral inoculum and subtle changes in culture conditions, parallel studies were carried out with β-cell cultures prepared from neonatal rats. Insulin release by these cells was unchanged during the course of the experiments, and morphological alterations were not observed. Although it is possible that the procedure for the preparation of cultures altered mouse, but not rat, β-cells in such a way as to unmask hidden virus receptors, we feel this is unlikely. The 9-day culture period before infection should be of sufficient duration to permit repair of membrane components[16].

The results of experiments using β-cell cultures prepared from diabetes-prone CD-1 and resistant C57Bl/6 mice are shown in Fig. 3. Radioimmunoassays on the medium from these cultures demonstrated a comparable decline in insulin release, and similar cytopathology was observed.

It has been contended in other studies that genetic factors code for the presence of viral receptor density on the β-cell surface and thus determine susceptibility to the virus[17,18]. The morphological methods used by these investigators to identify β-cells are questionable, however, due to nonspecific staining[9,19]. If the cell cultures in their studies comprised a mixture of fibroblasts and pancreatic cells (acinar and insular), it seems likely that the assays could not assess definitively the receptor density of β-cells. Using insulin release as a measure of

Fig. 3 Insulin release by β-cells in culture after inoculation with EMC M variant virus. The cultures were prepared from the pancreata of CD rats, CD-1 mice and C57BL/6 mice. Data are expressed as a percentage of the insulin released in each culture during the 48-h period immediately preceding inoculation (mean ± s.e.m. of four observations). The average 100% pre-inoculation insulin concentrations are: 10.2 ± 0.3 mU per culture (CD rat); 1.5 ± 0.1 mU per culture (CD-1 mouse); and 0.5 ± 0.02 mU per culture (C57BL/6 mouse).

viral induced cell injury, we found no difference between β-cells from mice resistant and susceptible to the diabetogenic effect of the virus. Moreover, several antigenically similar, but non-diabetogenic, EMC virus strains infected β-cells in culture. Thus, β-cells *in vitro* fail to exhibit unique susceptibility for the M variant.

Recent *in vivo* studies in our laboratory indicate that the islets of resistant mice sustain significant cytological injury. Although pancreata are depleted of insulin during the acute stages of infection, hyperglycaemia fails to develop. We have also found that alterations in the metabolic state of mice affect the severity of β-cell damage and the expression of diabetes (refs 20, 21 and B.J.D'A., G.L.W. and J.E.C., unpublished data). Similarly, culture conditions could affect susceptibility of β-cells to this virus[22,23]. Our observations do not exclude the possibility that viral susceptibility of β-cells in the intact animal is a consequence of the presence of specific receptors. We suggest, however, that other factors such as metabolic influences also are critical determinants affecting viral susceptibility and injury to β-cells.

Fig. 2 Insulin release by β-cells in culture after inoculation with various strains of EMC virus. The cultures were prepared from the pancreata of CD rats and CD-1 mice. Data are expressed as a percentage of the insulin released in each culture during the 48-h period immediately preceding inoculation (mean ± s.e.m. of four observations). The average 100% pre-inoculation insulin concentrations for the CD rat and CD-1 mouse cultures, respectively, are: 8.6 ± 0.6 mU per culture and 1.5 ± 0.1 mU per culture (E variant); 10.2 ± 0.3 mU per culture and 1.5 ± 0.1 mU per culture (M variant); 9.5 ± 0.3 mU per culture and 1.3 ± 0.07 mU per culture (Mengo); and 7.9 ± 1.5 mU per culture and 1.4 ± 0.03 mU per culture (r[+]).

1. Gamble, D. R., Taylor, K. W. & Cumming, H. *Br. med. J.* **4**, 260–262 (1973).
2. Yoon, J. W., Austin, M., Onodera, T. & Notkins, A. L. *New Engl. J. Med.* **300**, 1173–1179 (1979).
3. Craighead, J. E. & McLane, M. F. *Science* **162**, 913–914 (1968).
4. Craighead, J. E., Kanich, R. E. & Kessler, J. B. *Am. J. Path.* **74**, 287–300 (1974).
5. Craighead, J. E. *New Engl. J. Med.* **299**, 1439–1445 (1978).
6. Craighead, J. E. & Higgins, D. A. *J. exp. Med.* **139**, 414–425 (1974).
7. Boucher, D. W., Hayashi, K., Rosenthal, J. & Notkins, A. L. *J. infect. Dis.* **131**, 463–466 (1975).
8. Sternberger, L. A., Hardy, P. H., Cuculis, J. J. & Meyer, H. G. *J. Histochem. Cytochem.* **18**, 315–333 (1970).
9. Wilson, G. L., Chick, W. L. & Appel, M. C. *TCA Manual* (in the press).
10. Wilson, G. L. & Craighead, J. E. (in preparation).
11. Chick, W. L., Lauris, V., Flewelling, J. E., Andrews, K. A. & Woodruff, J. M. *Endocrinology* **92**, 212–218 (1973).
12. Craighead, J. E. *Am. J. Path.* **48**, 333–345 (1966).
13. Takemoto, K. K. & Leibhaber, H. *Virology* **14**, 455–562 (1961).
14. Dick, G. W. A., Smithburn, K. E. & Haddow, A. J. *Br. J. exp. Path.* **29**, 547–588 (1948).
15. Craighead, J. E. *Proc. Soc. exp. Biol. Med.* **119**, 408–412 (1965).
16. Macchi, A., Zeytinoglu, F. & Beaser, S. B. *Proc. Soc. exp. Biol. Med.* **145**, 500–503 (1974).
17. Yoon, J. W. & Notkins, A. L. *J. exp. Med.* **143**, 1170–1185 (1976).
18. Chairez, K., Yoon, J. W. & Notkins, A. L. *Virology* **85**, 606–611 (1978).
19. Leiter, E. H., Coleman, D. L. & Eppig, J. J. *In Vitro* **15**, 507–521 (1979).
20. Craighead, J. E. & Steinke, J. *Am. J. Path.* **63**, 109–130 (1971).
21. Craighead, J. E. in *Proceedings of the Franqui Foundation Colloquia* (ed. Bastenie, P. A) 227–232 (Excerpta Medica, Amsterdam, 1974).
22. Kunin, C. M. *Bact. Rev.* **28**, 382–390 (1964).
23. Smith, H. in *Virus Infection and the Cell Surface* (eds Poste, G. & Nicolson, G. L.) 1–34 (North-Holland, Amsterdam, 1977).
24. Chick, W. L., Like, A. A. & Lauris, V. *Endocrinology* **96**, 637–643 (1975).
25. Wright, P. J., Makulu, D. R., Vichick, D. & Sussman, K. E. *Diabetes* **20**, 33–45 (1971).

Non-mendelian mutation affecting ribulose-1, 5-bisphosphate carboxylase structure and activity

R. J. Spreitzer & L. J. Mets

Department of Biology, Case Western Reserve University, Cleveland, Ohio 44106

Chlamydomonas reinhardii, **a haploid unicellular green alga, is the only organism in which the non-mendelian (uniparental) genes thought to reside in chloroplast DNA have been observed to recombine. Thus, genetic mapping by recombination analysis is possible, and a single linkage group with a large number of markers has been characterized[1,2]. Although circumstantial evidence is consistent with the hypothesis that this uniparental linkage group is located in the chloroplast,[1,2] there is no direct evidence associating any of the known markers with chloroplast DNA. As the gene for the large subunit (LS) of ribulose-1, 5-bisphosphate carboxylase (RubPCase) has been located on the physical map of *C. reinhardii* chloroplast DNA,[3,4] a genetic marker in this same gene would help to prove the relationship between the uniparental linkage group and chloroplast DNA. We have now succeeded in isolating a mutation in a *C. reinhardii* gene which controls the structure and function of the LS of RubPCase. This new genetic marker will serve as the first reference point in our efforts to correlate the physical and genetic maps for the chloroplast genome. At the same time, the fact that we have obtained this mutant should encourage further attempts to produce genetic modifications of this key photosynthetic enzyme with the goal of improving plant productivity[5].**

RubPCase is an oligomeric enzyme which has two important enzymatic activities. The holoenzyme has eight copies of the 55,000 molecular weight MW LS and eight copies of a 12–20,000 MW small subunit (SS) which is a nuclear gene product[6]. Net CO_2 fixation during photosynthesis depends on the RubPCase-catalysed carboxylation of ribulose-1, 5-bisphosphate in the Calvin cycle[7]. On the other hand, the enzyme also catalyses the reaction of O_2 with the same substrate. This reaction, which is the first step in photorespiration, leads ultimately to CO_2 evolution and an apparently wasteful consumption of Calvin cycle intermediates which might otherwise be used for CO_2 fixation[7]. The catalytic site, which seems to be the same for both the carboxylase and oxygenase activities[8], is located on the LS [7].

Non-photosynthetic mutants of *C. reinhardii*, including presumptive LS mutants, can be maintained on medium containing acetate. Many such mendelian [9] and also uniparental [10] acetate-requiring mutants have been isolated, but only one has been found with a specific defect in a Calvin cycle enzyme (phosphoribulokinase) [11]. We reasoned that a Calvin cycle mutant, in addition to having an acetate-requiring phenotype, might be photosensitive as a result of the build-up of unused reductant generated by an active photosynthetic electron transport system. A light-sensitive phenotype would also account for the apparent rarity of RubPCase mutants, and Calvin cycle mutants in general, because selection experiments have usually been carried out at high light intensities. Taking this into account, we adopted a mutant selection protocol which would allow the recovery of light-sensitive, acetate-requiring mutants.

Independent cultures of wild-type *C. reinhardii*, strain 2137 mt[+] (ref. 12), were grown in 10 mM sodium acetate medium in the dark at 25°C until they reached stationary phase. To enhance uniparental mutant recovery, 1 mM 5-fluorodeoxyuridine was included in these cultures[13]. Cells were then collected, washed by centrifugation and mutagenised with ethyl methanesulphonate[14]. Washed cells were grown in the dark in acetate medium to allow expression of mutant phenotypes. Cells from each of these cultures were plated at 100–500

cells per plate onto acetate medium in the dark. Colonies were replica plated to medium without acetate and placed in 4,000 lx cool white fluorescent light. Colonies unable to grow on this minimal medium were recovered at a frequency of one per 10^3 cells plated, and included both mendelian and uniparental acetate requirers, as determined by standard tetrad analysis[15]. All the uniparental mutants were light sensitive, growing better in the dark with acetate than in the light (2,000 lx) with acetate.

RubPCase was purified from all the uniparental mutants by sucrose gradient centrifugation[16] and subjected to isoelectric focusing (IEF) in 8 M urea[17]. Molecular weights were determined by two-dimensional SDS-polyacrylamide gel electrophoresis[17] and used to verify the identity of the RubCase LS and SS bands observed on the first-dimension IEF gels[12,18].
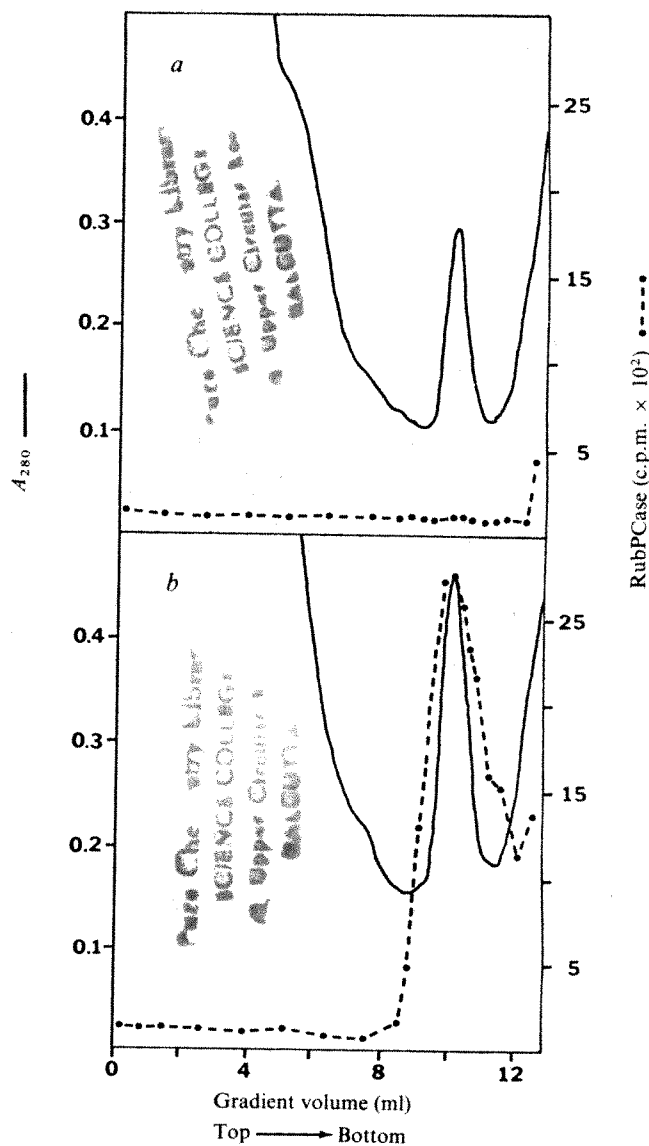
Fig. 1 Sucrose gradient centrifugation and assay of RubPCase from *rcl-u-1* and wild type. *a*, *rcl-u*1-10-6C; *b*, wild type. Cultures were grown in acetate medium in the dark. Approximately 6×10^8 cells were sonicated at 0 °C in 1.5 ml of sonication buffer: 1 mM dithiothreitol (DTT), 5 mM $MgCl_2$, 10 mM $NaHCO_3$ and 50 mM Tris base, *p*H 7.5. Following centrifugation at 27,000*g* for 15 min, 1 ml of the supernatant was layered onto a 12-ml linear sucrose gradient (10–30% sucrose in sonication buffer), which was run in an SW-40 rotor at 37,000 r.p.m. for 20 h at 4 °C. The gradient was fractionated into 0.3-ml fractions and scanned at 280 nm. RubPCase was assayed[16] by mixing 0.1 ml of a sucrose gradient fraction with 0.1 ml of reaction mix: 1 mM DTT, 15 mM $MgCl_2$, and 90 mM NaH $^{14}CO_3$ (0.22 μCi μmol^{-1}). After 15 min at 25 °C, the reaction was terminated with the addition of concentrated HCl/acetic acid (4:1) and the samples were then processed for liquid scintillation counting.

Fig. 2 IEF of RubPCase from reciprocal crosses between rcl-u-1 and wild type. *a*, rcl-u-1 mt⁺X wild-type mt⁻: (1) rcl-u-1 mt⁺; (2) wild-type mt⁺; (3) mixture of (1) and (2); (4)–(7) progeny from a single tetrad. *b*, Wild-type mt⁺ X rcl-u-1 mt⁻: (1) wild type mt⁺; (2) rcl-u-1 mt⁻; (3) mixture of (1) and (2); (4)–(7) progeny from a tetrad. Mendelian markers present in the crosses segregated 2:2 among the progeny. The SS on gels B5 and B7 did not reproduce well in the photograph. All parents and progeny were grown in acetate medium in the dark. RubPCase was purified by sucrose gradient centrifugation (Fig. 1). Samples obtained from the gradient were prepared by adding solid urea to 9M, and applied to 13.5×0.4 cm gels as 50-μl aliquots (5–50 μg RubPCase). IEF was carried out[17] with pH 5—7 ampholines and 8M urea in polyacrylamide gels for 12 h at 400 V and 1 h at 800 V constant voltage at 25 °C. The gels were stained in bromphenol blue and Coomassie blue. The pH gradient was measured with stab pH and reference electrodes on fresh gels. This showed that the isoelectric point of the SS was 7.4 and that of the wild type LS was 6.3.
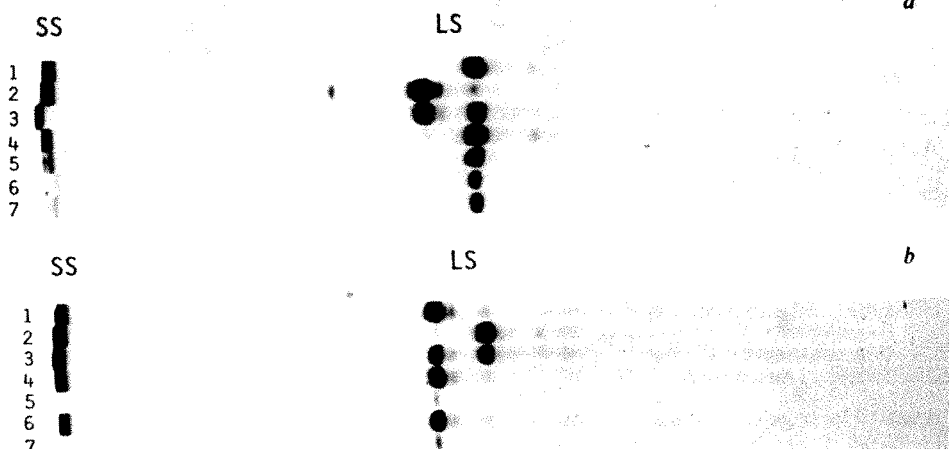
One mutant was found to have a lower isoelectric point for the LS. This mutant, named rcl-u-1-10-6C (rcl-u-1 referring to its genetic locus), was a stringent acetate requirer that could not be maintained on acetate medium above 2,000 lx, but grew as well as wild type in the dark. Although rcl-u-1-10-6C maintained normal levels of RubPCase holoenzyme (Table 1), RubPCase activity was absent (Fig. 1). Further biochemical analysis (Table 1) showed that the mutant had normal levels of photosystem II (PSII) activity and chlorophylls, but lacked the ability to fix CO_2. The mutant was indistinguishable from wild type in holoenzyme sedimentation value (Fig. 1) and in LS and SS MW (data not shown). Reciprocal crosses indicated that the altered LS was inherited in a uniparental pattern (Fig. 2), along with the light-sensitive, acetate-requiring phenotype.

The evidence presented suggests that rcl-u-1-10-6C is a mutation in the chloroplast structural gene of the LS. Unlike other presumptive RubPCase mutants[19,20], the mutant phenotype is inherited in a uniparental pattern, which is the pattern expected for a mutation in a chloroplast gene[21,22]. Because the mutant maintains normal PSII activity, amount of chlorophyll, and amount of RubPCase protein, defects in chloroplast protein synthesis or other defects which exert pleiotropic effects can be

ruled out. This is not the case for several maternally inherited mutants of *Oenothera* which have been presumed to be LS structural gene mutants[23]. In contrast to other presumptive RubPCase mutants[19,20,23,24] rcl-u-1-10-6C is the first mutant in which a change in LS structure is evident. Because apparently normal holoenzyme structure exists in the mutant, major processing errors are probably not responsible for the LS alteration. The difference in IEF properties between the mutant and wild-type LS could be due to a difference in primary amino acid sequences, or a difference in secondary modification. The critical discrimination between these two possibilities requires comparative sequence analysis of the two proteins. In either case, rcl-u-1 is a uniparental gene which controls the apparent charge and activity of the RubPCase LS. We are now determining whether this gene is linked to the other uniparental genes in *C. reinhardii*.

The photosensitivity of rcl-u-1-10-6C must be considered in designing protocols for obtaining additional mutants. Light intensities in excess of 2,000 lx, as have been used by other workers[10], would not allow this mutant to survive. We have not investigated the mechanism of photosensitivity in this mutant, but we know that light-sensitive phenotypes are not confined to mutants with Calvin cycle defects. We have recovered many light-sensitive, non-photosynthetic mutants with specific defects either in PSI or in PSII. Each group includes both mendelian and uniparental mutants, which will be discussed in detail elsewhere.

This work was supported by a grant from the NSF.

Table 1 Biochemical comparison of rcl-u-1-10-6C and wild type

	rcl-u-1-10-6C	Wild type
CO₂ fixation (μmol per h per mg Chl)	12	640
PSII activity (DCPIP) (μmol per h per mg Chl)	135	144
Chlorophyll $a + b$(Chl) (mg per 1×10^9 cells)	1.11	1.30
RubPCase protein (mg per 1×10^{10} cells)	4.39	4.36

Cultures were grown in acetate medium in the dark. CO_2 fixation was assayed by adding 0.2 ml of 50 mM NaH $^{14}CO_3$ (0.5μCi μmol^{-1}) to 2×10^7 cells in 2 ml of minimal medium at 25 °C and 60,000 lx (ref. 12). For PSII activity, cells were sonicated at 4 °C in reaction buffer: 2.5 mM $MgCl_2$, 20 mM KCl, 1 mM K phosphate buffer (pH 7.0)[25]. The lysate was centrifuged at 480g for 5 min and the supernatant was diluted 10× with 0.1 mM dichlorophenol indophenol (DCPIP) in reaction buffer. The red light-dependent (180 μE m^{-2} s^{-1} between 640 and 740 nm) reduction of DCPIP was measured spectrophotometrically at 25 °C. Chlorophyll (Chl) was measured spectrophotometrically in 80% acetone extracts of whole cells[26]. RubPCase protein was estimated from the absorbance at 280 nm of the RubPCase peak on sucrose gradients[16].

1. Sager, R. *Cytoplasmic Genes and Organelles* (Academic, New York, 1972).
2. Gillham, N. W. *Organelle Heredity* (Raven, New York, 1978).
3. Gelvin, S., Heizmann, P. & Howell, S.H. *Proc. natn. Acad. Sci U.S.A.* **74**, 3193-3197 (1977).
4. Rochaix, J. D. & Malnoe, P. in *Chloroplast Development* (ed. Akoyunoglou, G.) 581–586 (Elsevier, Amsterdam, 1979).
5. Ogren, W. L. in *CO₂ Metabolism and Plant Productivity* (eds Burris, R. H. & Black, C. C.) 19–29 (University Park Press, Baltimore, 1976).
6. Kung, S. *Science* **191**, 429–434 (1976).
7. Jensen, R. G. & Bahr, J. T. *A. Rev. Pl. Physiol.* **28**, 379–400 (1977).
8. Lorimer, G. H. & Andrews, T. J. *Nature* **243**, 359–360 (1973).
9. Levine, R. P. *Bot. Monogr.* **10**, 424–433 (1974).
10. Shepherd, H. S., Boynton, J. E. & Gillham, N. W. *Proc. natn. Acad. Sci. U.S.A.* **76**, 1353–1357 (1979).
11. Moll, B. & Levine, R. P. *Pl. Physiol.* **46**, 576–580 (1970).
12. Spreitzer, R. J. thesis, Case Western Reserve Univ. (1979).
13. Wurtz, E. A., Boynton, J. E. & Gillham, N. W. *Proc. natn. Acad. Sci. U.S.A.* **74**, 4552–4556 (1977).
14. Loppes, R. *Molec. gen. Genet.* **102**, 229–231 (1968).
15. Levine, R. P. & Ebersold, W. T. *A. Rev. Microbiol.* **14**, 197–216 (1960).
16. Goldthwaite, J. J. & Bogorad, L. *Analyt. Biochem.* **41**, 57–66 (1971).
17. O'Farrell, P. H. *J. biol. Chem.* **250**, 4007–4021 (1975).
18. Spreitzer, R. J. & Mets, L. *J. Cell Biol.* **79**, 319a (1978).
19. Nelson, P. E. & Surzycki, S. J. *Eur. J. Biochem.* **61**, 465–474 (1976).
20. Kung, S. D. & Marsho, T. V. *Nature* **259**, 325–326 (1976).
21. Mets, L. J. *J. supramolec. Struct. Suppl.* **3**, 144 (1979).
22. Grant, D., Boynton, J. E. & Gillham, N. W. *J. Cell Biol.* **83**, 365a (1979).
23. Hallier, U. W., Schmitt, J. M., Heber, U., Chaianova, S. S. & Volodarsky, A. D. *Biochim. biophys. Acta* **504**, 67–83 (1978).
24. Andersen, K. *Biochim. biophys. Acta* **585**, 1–11 (1979).
25. Bennoun, P. & Levine, R. P. *Pl. Physiol.* **42**, 1284–1287 (1967).
26. Arnon, D. I. *Pl. Physiol.* **24**, 1–15 (1949).

MATTERS ARISING

A 'random transition' in the cell cycle?

EVIDENCE is presented by Shields[1], partly mathematical and partly from real and simulated experiments, that the cell cycle contains an exponentially distributed phase. Unfortunately, there are flaws in his probabilistic argument at two points. His conclusions are probably not invalidated, but it seems appropriate to point out the errors in the hope that they will not be repeated elsewhere.

We are concerned with the probability distribution of cell cycle times, and with the distribution of the difference in cycle time of sister cells. It seems that sister cycle times T_1, T_2, say, may be well represented in terms of three independent random variables T_B, U_1, U_2 as

$$T_1 = T_B + U_1$$
$$T_2 = T_B + U_2 \qquad (1)$$

Here, U_1 and U_2 are identically distributed, whereas T_B is common to the two sisters and must be a non-constant random variable for T_1 and T_2 to be correlated. Shields himself mentions that the T_i values are correlated, quoting a typical value for the correlation coefficient of 0.78; according to representation (1) above, the correlation is in general

$$\rho(T_1, T_2) = \frac{\mathrm{Var}(T_B)}{\mathrm{Var}(T_B) + \mathrm{Var}(U_i)} \qquad (2)$$

In contradiction to this, Shields then assumes that T_1 and T_2 are independent, in order to derive an expression for $\beta(t)$, the survivor function of $|T_1 - T_2|$, in terms of $Q(t)$, that of T_i. In fact, this argument may be rescued: in view of representation (1), $|T_1 - T_2| = |U_1 - U_2|$. On the basis of empirical α curves, we might assume the model

$$Q^*(t) = Pr\{T_i > t + T_B\}$$
$$= Pr\{U_i > t\}$$
$$= \exp(-kt), \qquad t \geqslant 0, i = 1, 2 \qquad (3)$$

from which it is true that

$$\beta(t) = Pr\{|T_1 - T_2| > t\}$$
$$= Pr\{|U_1 - U_2| > t\}$$
$$= \exp(-kt), \qquad t \geqslant 0 \qquad (4)$$

This approach is tantamount to redefining Shields' function $Q(t)$ as a conditional survivor function.

The second flaw concerns Shields' claim at the end of paragraph 5 that representation (4) implies representation (3). This
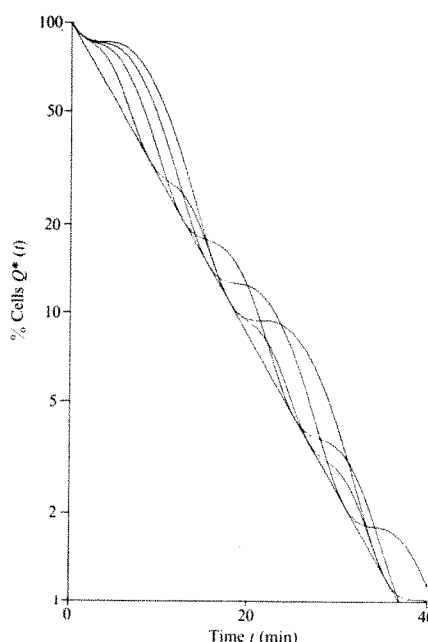
Fig. 1 Semi-logarithmic plot of $Q^*(t) = \left(1 + 2d^2 \sin^2\left(\frac{kt}{d}\right)\right) e^{-kt}$ against t for $k = \frac{1}{8}$ and $d^2 = 0, \frac{1}{8}, \frac{1}{4}, \frac{3}{8}$ and $\frac{1}{2}$.

is not the case, and many other forms of $Q^*(t)$ give the same expression for $\beta(t)$: for example, the whole family

$$Q^*(t) = \left(1 + 2d^2 \sin^2\left(\frac{kt}{d}\right)\right) \times$$
$$\times \exp(-kt), \qquad t \geqslant 0 \qquad (5)$$

as d varies from 0 (corresponding to representation (3)) to $1/2^{1/2}$. These solutions are illustrated in Fig. 1; presumably, however, they are rather unlikely to represent correctly the biological reality. Further, Shields' observation that exponential β curves are obtainable irrespective of the age of the younger of a sister pair is, of course, conclusive evidence that representation (3) is the correct solution, as such curves completely determine the joint distribution of (T_1, T_2).

I thank Russell Smith for finding the counter-example (5) above.

PETER J. GREEN

Department of Mathematics,
Science Laboratories,
South Road,
Durham DH1 3LE, UK

1. Shields, R. *Nature* **273**, 755–758 (1978).

SHIELDS REPLIES—Green is quite right to point out that the cell cycle times of sister cells are frequently correlated and that my equation for the distribution of differences of sister cell cycle times is not valid without qualification. We have argued that correlations in the cycle times of sister cells arise because the cell cycle consists of two parts, one of which (the B phase) is common to the sisters, whereas the other (A state) is independently and identically distributed. According to this model, the correlation of cell cycle times of sister cells arises from the identity of the B phase, the differences from the A state. If these assumptions are correct, what does an exponential distribution of differences in cell cycle time (the β curve) tell us? Green points out that many A state distributions will give exponential curves (an example is given in his paper); this is why I added the condition that exponential β curves were obtained irrespective of the cell cycle times of the younger cell in the cell pair when curves are calculated from cohorted data.

If this condition is met, then, as Green pointed out, the A state must be exponentially distributed. However, if A states are not independently and identically distributed, other cell cycle models can be devised which give exponential β curves (D. Rigney, personal communication). What I had intended to do was to focus attention on the statistic $|T_1 - T_2|$, which has been largely ignored in cell cycle analysis. It should not be forgotten that any proposed cell cycle model should explain the exponential nature of $|T_1 - T_2|$ as well as give a description of the overall distribution of cell cycle times in a cell population. A modified version of the original transition probability hypothesis seems to do this successfully[1].

ROBERT SHIELDS

Unilever Research,
Colworth House,
Sharnbrook, Bedford MK44 1LQ, UK

1. Brooks, R. F., Bennett, D. C. & Smith, J. A. *Cell* **19** (in the press).

BOOK REVIEWS

The road to equality

Eric Ashby

THE fear that Western civilization will collapse from exhaustion of resources was the Great Red Herring of the 1970s, deflecting our attention from a more likely cause of collapse: the unequal distribution of resources. In the 1980s we shall, I hope, get back to the problems that really matter, namely how to persuade — and, if we fail to persuade, compel — affluent nations to share their resources of food, stored energy and mineral wealth, with nations that lack one or other of these resources. If America and Canada cut down their acreage of grain crops, if the Arabs decide to keep their oil in the ground, if South Africa and Zimbabwe stop the export of chromium, the prime danger will not be privation; it will be war. The way ahead, in the short term at any rate, is now becoming clearer. It is not to pursue the mirage of zero growth, nor is it to let the market economy rip in a frenzy of free competition; it is to continue growth with prudence, cutting down waste, protecting the environment, and to distribute the products of growth with greater equity than nations have ever shown in the past.

This is the theme in what (to my mind) is the most important statement about the human condition that has been made in the last decade: the book of essays entitled *World Futures* produced from the Science Policy Research Unit in the University of Sussex (reviewed in *Nature* **276**, 144-146; 1978). *World Futures* is a symposium by several authors. It does not ram a message down the reader's throat; it offers him the facts and leads him (with skilful encouragement by Marie Jahoda in the concluding chapter) to a choice among four options: high growth, high equality (a big cake fairly shared); high growth, low equality (a big cake hogged by the rich); low growth, high equality (a small cake fairly shared); and low growth, low equality (a small cake hogged by the rich). Marie Jahoda's choice is for the big cake fairly shared.

John Gribbin has written an epitome of *World Futures*. It is about half the length of the original book. One reason he gives for having written it is that *World Futures*

Future Worlds. By John Gribbin. Pp.225. (Sphere:London, 1979.) Paperback £1.75.

---

is "inevitably intimidating to the more casual reader". I'm afraid I don't like this reason. There are some issues — and this surely is one of them — on which people can't afford to be casual. If they will not take the trouble to read 390 pages of closely argued, but non-technical essays about the future, they have no right to hold opinions about the future.

But there are other reasons, and good ones, why John Gribbin wrote this book. First, he was associated with the team — though not a member of it — so his book is not just a rehash of *World Futures* with the title reversed: it is an observer's reflections on the work at Sussex. Second, he is an experienced journalist, skilled in the art of turning casual readers into serious readers. Third, he has picked out the preferred option — a big cake fairly shared — and concentrated on that, adding opinions of his own. So although the book is an epitome of *World Futures* it is a judiciously selected epitome.

If you put your faith in the possibilities of a high-growth, high-equality option, you have to be persuaded that the potential for high growth is present. Gribbin believes that it is, in the short term at any rate; and in this view he is supported by the recently published report sponsored by OECD, known as *Interfutures* and summarized in the *OECD Observer* last September. Enough food is already grown in the world to provide the estimated world population with a diet of over 2,000 kilocalories a day, if only the food was "available in the right place, at the right time, at a price they can afford". Millions of people live at starvation-level because they can't buy food, not because there is no food to buy. For energy the position is more complicated and more dangerous. Gribbin makes the point that reserves of recoverable coal are very large and that the really ominous problem is to ensure supplies of energy in the forms we need.

With a rigorous insistence on economies, the demand for electrical energy may reach a peak; for it can't be efficiently stored and already a power station has to be built to cope with peak loads, leaving the station (a slight exaggeration, perhaps) "twiddling its thumbs while waiting for a frosty day". An all-electric world is not a likely scenario for the future. So Gribbin gives the (now) conventional answer: we must plan for a mix of energy sources, anticipating the exhaustion of natural gas, which in 1974 provided some 21% of the Western world's supplies of energy; and the perpetual threat of a strangulation in oil supplies, which in 1974 provided 45% of the energy; and a return to coal (the proportion of which, in the energy balance sheet, dropped from 90% in 1900 to 32% in 1974), supplemented by nuclear energy and energy from sun, wind and vegetable products. Over the third prerequisite for high growth — raw materials — Gribbin is optimistic, indeed more so than is justified by such data as we have. It is true that aluminium replaces copper for some purposes, and glass fibres may replace some metals; but there are awkward problems about finding substitutes for some raw materials, mercury and lead, for example. It is here that 'use less' is likely to be the only practicable policy.

Gribbin's conclusion from this analysis is that the high-growth option, in the short term, is a practicable option. What about the other term in the equation: more equality? Here Gribbin, and indeed all analysts of the future, are obliged to speculate in the murky waters of political science. Put crudely, and in a vastly simplified form, the position is as follows. Without a massive transfer of material wealth from North to South, from 'haves' to 'have nots', there will be (1) insufficient markets for the 'haves' to establish high growth, and (2) mounting geopolitical tensions leading to conflict. But, in order to make a massive transfer of material wealth from North to South, the 'haves' in the North will have to make sacrifices. How is a nation persuaded to make sacrifices? Only (if history is any guide) for

fear of something worse than the sacrifices they are asked to make. Under a threat from outside, as in time of war, people will endure severe privation. But when the threat is from within, caused by strains upon the economic and social system, we just do not know what privations people will be prepared to accept. The danger is that we shall find ourselves on the brink of internecine conflict before we realize that problems about the equitable distribution of food and energy are — as President Carter has fruitlessly reminded the American people — "the moral equivalent of war".

An outstanding feature of *World Futures* is a discussion of the four options, ranging from 'big-cake-fairly-shared' to 'small-cake-hogged-by-the-rich', as regarded by people of different political persuasions: conservatives, reformists and radicals. Gribbin gives a good summary of the interaction of these three political attitudes toward his preferred option. He sets out what it might be like to live in a high-growth, high-equality world under

one or other of these three styles of government. The radicals would reach this kind of world through revolution and a phase of dictatorship. Conservatives would see it evolving naturally as more and more people find satisfaction in the share of the cake they get. Reformists would hope to make the transition by a technocratic managed economy which somehow (but how?) would preserve the traditional freedoms of Western democracy. Under all styles of government there would be an alarming increase of unemployment which would euphemistically be called leisure. And this is the sixty-four dollar question for all studies about the future: how to replace the work-ethic of the nineteenth century by a leisure-ethic for the twenty-first century. One of the essays in *World Futures* does ask the question. No one yet has provided a credible answer. ☐

Lord Ashby is Chancellor of Queen's University, Belfast, and a Fellow of Clare College, Cambridge, UK.

Catalysis at work

V. Gold

Enzymic and Non-Enzymic Catalysis. Edited by P. Dunnill, A. Wiseman and N. Blakebrough. Pp.250. (Ellis Horwood: Chichester, UK. Distributed by Wiley: Chichester, UK, and New York, 1979.) £19.75, $50.

IN April 1978 the Microbiology, Fermentation and Enzyme Technology Group of the Society of Chemical Industry initiated an international gathering of biochemists, chemists and chemical engineers. The purpose of the meeting was a discussion of topics of common interest in the general field of catalysis by enzymes and enzyme-like materials, especially the status and industrial potential of stereoselective catalysis. The volume under review contains a full account of the proceedings, including a verbatim record of about 20 pages of more or less ephemeral discussion remarks. Its nine chapters can be clearly divided into two groups. The first group is devoted to biochemical and chemical studies, and the second to the design and performance of catalytic reactors. One hopes that the meeting produced much mutual education of and by the two groups of participants. The industrial exploitation of the remarkable effects of enzymes and the simulation of enzyme-like catalysis by synthetic materials represent tremendous challenges of potential industrial importance. This message is rather well conveyed by the volume. Of course, things have not stood still in the period since the meeting, and fuller or more up-to-date reviews of some of the topics are available elsewhere. The publication of the book will nevertheless have been justified if it succeeds in creating a greater appreciation, in universities and industry, of the promising possibilities in this area of endeavour.

The scope of the book is by no means comprehensive, and its content is fairly well reflected by the following, sometimes paraphrased, chapter headings: present knowledge of enzyme catalysis (A.R. Fersht, 12 pages); current status of enzyme technology (P. Dunnill, 22 pages); enzymes in organic synthesis (J.B. Jones, 27 pages); enzyme analogues, mostly of the crown ether type (J.F. Stoddart, 25 pages); micellar catalysis (J.M. Brown *et al.*, 17 pages); performance of non-biological catalyst reactors (R.E. Goddard, 42 pages), and of enzymic reactors (J.-M. Engasser, 26 pages); asymmetric homogeneous catalysis (D.J. Thompson, 17 pages); polymer-attached homogeneous catalysis (R.H. Grubbs and S.-C. H. Su, 12 pages). Most of the chapters in this very attractively produced volume include informative lists of references. ☐

V. Gold is Professor of Chemistry at King's College, University of London, UK.

Advice on techniques in IR spectroscopy

M.A. Ford

Applied Infrared Spectroscopy. By A. Lee Smith. Pp.336. (Wiley: New York and Chichester, UK, 1979.) $38.30, £17.40.

THE concept of this book can best be described by using the author's own words: "It is a volume based on practical experience, stressing the fundamental concepts and limitations of analytical IR spectroscopy for the chemist". Reference to "the chemist" is important, as a reasonable knowledge of chemistry is assumed. And the "practical experience" is very apparent, as there is wealth of advice on good spectroscopic techniques and the avoidance of pitfalls.

The main chapters cover instrumentation, sampling techniques, qualitative applications and quantitative applications with — rightly — by far the greatest emphasis on qualitative aspects. There is also a short chapter entitled "Spectroscopic Literature" concerned with collections of reference spectra and retrieval systems.

Instrumentation is described very adequately without going into excessive detail and the chapter includes descriptions of all the less common types of spectrometer, for example, Hadamard transform, as well as 'conventional' ones. Very useful advice is given on "optimising the spectrometer variables" and "performance tests and spectrometer calibration". There are two small points on

which I would take issue with the author; blazing a grating increases the intensity at a certain angle of incidence rather than "in a certain order", and noise and signal: noise ratio are more conventionally spoken of in terms of a notional peak to peak noise rather than the RMS value.

In the chapter on sampling techniques, the extent of the author's practical experience is very obvious and even a well experienced spectroscopist is likely to pick up some useful tips. Some techniques are, of necessity, covered only briefly but the reader is always referred to the relevant publications in the excellent bibliography.

A large part of the chapter on qualitative applications is devoted to a good general introduction to the theory of IR absorptions and the concept and use of group frequencies. Interpretation of spectra is covered relatively briefly but, again, there are full references to the available literature and there is much good advice. In addition, extensive correlation charts and lists of characteristic group frequencies are given in appendices. There is also a short description of typical applications.

The final chapter on quantitative applications emphasizes the need for good experimental technique — and very good advice is given — and the need to know "how precise the determination must be". There is good coverage of all commonly, and most less-commonly, used methods and again a full bibliography is given.

Overall, this is an excellent book which can be strongly recommended to both new and experienced IR spectroscopists. ☐

M.A. Ford is Technical Director of Perkin-Elmer Limited, Beaconsfield, UK.

Comparative decomposition

P.W. Flanagan

Decomposition in Terrestrial Ecosystems.
By M. Swift, O. Heal and J. Anderson.
Pp.400. (Blackwell: Oxford, 1979.)
£22.50.

IN AN ecosystem sense, decomposition simply means the disassociation of the constituent elements of organic matter with concomitant release of energy and increase in entropy. This volume is a documented synthesis of the study of decomposition in varying organic residues across different terrestrial ecosystems. It goes to a crucial additional step by attempting to relate decomposition processes to the functioning of the entire ecosystem and succeeds more than any other volume presently available. It is both specific in detail and comprehensive in scope.

The first two chapters review ecosystem-level perspectives on decomposition processes so that they may serve as the basis for an analysis in depth of the decomposer organisms and their activities (Chapter 3). In Chapters 4, 5 and 6, respectively, the influences of substrate quality, soil chemistry and climate on decomposition are examined and compared within and between ecosystems. The last chapter returns the reader again to the wider view and correlates all the fundamental biological, climatic and chemical factors to show how they operate together to produce

the process of decomposition to varied degrees in latitudinally separated ecosystems.

It is an extremely well documented account of the perspectives and accomplishments of those scientists working within and alongside the International Biological Programmes' committees of 'Dirty Rotters', i.e. the microbiology and decomposition working groups. In large part, it pre-empts the necessity for an interbiome synthesis of decomposition data and is consistent with the modern principles of microbial ecologists, soil biologists and students of decomposition in ecosystems.

The authors are to be complimented for explicating the reservations felt by many concerning the use of the *K* constant in studies of decomposition.

In a book of this scope there are sure to be aspects where coverage is insufficient to satisfy individual readers. I would like to have seen more emphasis given to the measurement of microbial and microfaunal biomass and to the tentative estimates of turnover in microbial subsystems. Other reservations about this volume include the fact that there was insufficient reference to work done in the Southern Hemisphere, New Zealand, Australia and South America, and proportionally too much to that done in the Northern Hemisphere, particularly to data from North America.

Figure 7.4 on p.279 caused me concern when it first appeared in another volume. It implies that in order for decomposition processes to increase in rate, the rate of primary productivity must decline. This inference could be very misleading.

Sometimes the generalizations are too broad — for example, referring to the taiga forest ecosystem: "Water is in excess all year around . . .". This is certainly not the case. Most decomposition processes in organic layers of taiga forests suffer from water deficiency throughout the summer season. Also, in tundra biological activity goes on throughout the year, though microbial processes do cease for 5–7 months.

Still, these are small imperfections in an otherwise first-rate volume. I feel that this book will become the standard reference text for students of decomposition in the 1980s. It is one of the most exciting books produced in this field since 1881 and Charles Darwin's *The Formation of Vegetable Mould through the Action of Worms with Observations on their Habitats* . . . . I am sure it will provide stimulus for students of microbial ecology, decomposition, agriculture, forestry and general ecology, as well as for anyone who just wants to know more about vital processes in natural environments.

The names of the authors guaranteed that the treatment exhibited substantial hybrid vigour. Meshing the intuition and experience of field-seasoned mycologists, soil zoologists and the experience of interbiome (IBP) synthesis has resulted in an excellent book for teaching and research reference in microbial ecology and decomposition. □

P.W. Flanagan is Professor of Microbiology at the Institute of Arctic Biology, University of Alaska, Fairbanks, Alaska, and represented the US (IBP) Tundra Biome on International Decomposition and Microbiology Working Committees.

Seeing the wood for the phylogenetic trees

Barry Cox

Phylogenetic Analysis and Paleontology.
Edited by Joel Cracraft and Niles Eldredge. Pp.233. (Columbia University Press: New York and Guildford, UK, 1979.) Hardback $28.10; paperback $11.25.

IT is unlikely that, in the days following his vision on the road to Damascus, St Paul was widely famed for the variety of his after-dinner conversations, or that Moses found it easy to say anything nice about the Golden Calf. Missionaries, and especially the recently converted, tend to be obsessional, and also simplistic in their wholesale condemnations of the "old ways". Similarly, the advent of what is now commonly called "cladistic systematics" was accompanied by a

polarization of many systematists into one of two camps — cladists or traditionalists. The errors of any partisan, once identified, were then hailed as the inevitable faults of his whole ideology, and used as sticks to belabour all his supporters. The voice of reasoned debate all too quickly rose to the shrill shriek of the pedlar of magic potions. Not surprisingly, many systematists invoked a curse on both their houses, and went about their business until the dust had settled, and better tempers had returned. It looks as though that time has arrived.

This volume is based on a symposium on "Phylogenetic Models" which took place during the North American Paleontological Convention in 1977, and contains seven essays debating the values of the cladistic and of the traditional methods.

There are four papers by supporters of cladistic methods. The first, introductory, paper is by Cracraft, who points out the similarity between cladistic systematics (in which no taxon is ever considered as ancestral to another) and the model of speciation by punctuated equilibria (in

which it is predicted that ancestors will rarely be identifiable, because a new species arises by rapid change in a peripheral, isolated population). Gaffney and Eldredge give accounts of the methods of the cladistic approach, with examples from their own fields of work. Here I preferred Eldredge's clear distinction between cladograms (showing the pattern of character-distribution), phylogenetic trees (showing the hypothesized relationships of the taxa) and "scenarios" (in which an attempt is made to explain the reasons for what appears to have taken place). Though asked to write a pro-cladist commentary on the symposium as a whole, Wiley instead devotes most of his space to an account of what he calls the "evolutionary species concept".

Appearing for the traditionalists are Gingerich and Bretsky, who argue that species have a considerable range in time and space, and that the range of variation within a species is also so wide that a method which totally rejects any possibility that an ancestor–descendant relationship can be recognized is unnecessarily narrow.

Bretsky also points out that the vicariance model of speciation implies that much speciation will be gradualist within one of the newly separated areas, so that preservation of ancestor–descendant lineages may not be so rare, and that the palaeontological record may in some cases be far more complete than is generally thought. In his commentary on the symposium on behalf of the traditionalists,

Boucot acknowledges that the cladists have made an important contribution to systematic taxonomic procedures in insisting on methodically constructed diagnoses; he also gives useful critiques of the other contributions.

There is inevitably some overlap in the various pro-cladistic expositions of the methods and merits of the technique of phylogenetic analysis by the evaluation of

the patterns of distribution of novel characters amongst the taxa. But the papers are on the whole stimulatingly written, with useful examples of the use of the different methods, and with a more balanced, less chauvinist attitude to the views of the opposition than had previously been common. □

Barry Cox is Professor of Zoology at King's College, University of London, UK.

Problems in carbon-13 NMR

Elizabeth A. Williams

Carbon-13 NMR Based Organic Spectral Problems. By Philip L. Fuchs and Charles B. Bunnell. Pp.316. (Wiley: New York and Chichester, UK, 1979.) Paperback $14.97, £7.55.

THE use of carbon-13 NMR spectroscopy as a routine analytical tool for organic chemists is now widespread. This book originated with a perceived need to incorporate this technique into the teaching of modern organic structure determination using the problem solving approach. The text is intended to be used in conjunction with several suggested references which provide compilations of standard mass spectral, infrared, proton NMR and carbon NMR data. It does not contain any introduction to the various techniques and is intended for those already familiar with the basic principles involved.

The book contains 125 unknowns which are comprised of the more common functional groups as well as some more unusual structures. Each unknown is allotted two pages containing its elemental analysis, infrared, 90 MHz proton NMR, 20 MHz carbon NMR and mass spectrum. Special proton NMR experiments such as D_2O addition or homonuclear spin decoupling and carbon-13 off-resonance decoupling experiments are included as inserts in the appropriate spectra. The unknowns are arranged on two facing pages so that all of the data for one compound may be examined without turning the page. The problems are arranged in order of increasing complexity of the molecular formula in a reasonably successful attempt to save the more difficult unknowns for later in the book. Isomeric structures are presented together to enable them to be worked on simultaneously. Immediately following the unknowns is an appendix containing a general approach to the solution of these problems followed by a detailed analysis of this approach as applied to ten selected problems of varying difficulty.

This book is a very useful text to incorporate into any course on organic spectroscopy. Although the authors state that it has evolved over a five-year period in a course taken by juniors, seniors and beginning graduate students, some of the problems are quite difficult and seem more appropriate for the latter two groups of students. Although concisely written, the discussion of the general protocol for solving organic spectral problems and the solutions to the ten selected problems are sufficiently detailed to take the student very clearly through the thought processes involved in deducing the structure from analytical data. Of particular note is the care taken by the authors to provide a feeling for which data are unambiguous and which data can be misleading. For example, they point out the dangers in assuming analytical "additivity" parameters are valid without the use of the appropriate model compounds. Similarly, they make note of alternative structures

where possible and suggest experiments to eliminate or confirm these.

Although the title of the book suggests that it is primarily concerned with carbon-13 NMR, in fact, equal attention is given to all of the techniques included in the problems. It is worthwhile remembering that the unknowns included in this text have already been "student tested" and found to be successful as a teaching aid. As a companion to one of the standard texts on organic spectroscopy this book is highly recommended. The answers are given to only ten of the problems which limits its value for independent study. If, however, the answers are obtained from the publisher, it would be very useful as a refresher to individuals already familiar with the analytical methods presented. □

Elizabeth A. Williams is an Organic Chemist in charge of the Nuclear Magnetic Resonance Facility at General Electric Corporate Research and Development, Schenectady, New York.

Stimulating sex hormones

R.J.B. King

Female Sex Steroids. By J.H. Clark and E.J. Peck. Pp.245. (Springer: Berlin, Heidelberg and New York, 1979.) DM 78, $43.70.

BOOKS can be categorized according to combinations of the four words useful, useless, boring, stimulating. The useful and stimulating category is all too small but this monograph decidedly falls into that group. It is the latest addition to a series that, with a few lapses, has maintained a high standard. The book is divided into 10 chapters dealing with the three aspects of oestrogen and progestogen receptors — namely methods of measurement (36 pages), intracellular characterization (99 pages) and physiological relevance (67 pages). The methodological section contains a series of recipes which, taken with the lucidity which graces the rest of the book, makes it eminently suitable for both

students and people wishing to initiate work in this area. On the other hand, the discussion of type I and II binding sites and the questioning of the basic dogma that steroids carry receptors from cytoplasm to nucleus make essential reading for *aficionados* of this area of endocrinology. It has been a feature of this series of monographs that the authors have communicated their own experiences within the given topic. The present volume continues this style with data, both published and unpublished, from their own laboratory blended with that of other workers. This is complemented by a catholic survey of the literature that makes the discussions and conclusions more formidable. I found this feature of the book particularly good because so many articles written about receptors for steroid hormones have taken a more parochial attitude. The main conclusions have been itemized at the end of the book. My own conclusion is that this is one of the best books yet written about the cellular endocrinology of the female sex hormones. □

R.J.B. King is Head of the Hormone Biochemistry Department at the Imperial Cancer Research Fund, London, UK.

nature

15 May 1980

European subnuclear physics goes American

THE news (page 122) that American subnuclear physicists wish to spend increasing sums on design studies for a new generation of accelerators — for fear of European competition — was aptly paralleled last week by an announcement from CERN, the European Centre for Subnuclear Physics near Geneva. It made official an earlier understanding that Professor Herwig Schopper, a Czechoslovak-born (but now German) physicist who is presently director of the German national accelerator laboratory, DESY, is to be CERN's next director-general. This should send a shiver up every American subnuclear spine.

Why? Because Schopper's reputation rests on transferring the 'American', pragmatic style of accelerator design to Europe, and specifically to DESY, the Deutsches Elecktronen Synchrotron laboratory near Hamburg. Moreover, DESY is an electron laboratory, specialising in accelerating electrons and their antiparticles (positrons) and colliding them with one another and with protons. CERN has been exclusively a proton accelerating laboratory, but has plans for building a giant electron-positron collider, LEP. To CERN, Schopper will bring not only his Americanism, but also his expertise in electron machine design — a problem quite different from proton machine design because of the low mass of the electron (1837 times less than the proton).

In the past America has taken a firm lead in subnuclear physics, starting with Lawrence's cyclotron (which created the pion) and the Berkeley Bevatron of the early 1950s, (which found the antiproton). At that time Europe was recovering from the Second World War, and it was a great feat of political will to create CERN just seven years after the war's end. It was initially a theoretical institute; ultimately accelerators were built, at CERN and in European nations, but always the US was in the lead. The first close race was in the early sixties, for the 'omega minus' predicted by Gell-Mann and Ne'eman's SU3 theory (which lead to the concept of quarks). The Brookhaven laboratory on Long Island won. Of the more recent fundamental discoveries — scaling in electron proton scattering (evidence for point-like quarks), of the J/psi and charmed quarks, of the neutral current weak interaction, of the 'upsilon' containing 'bottom' quarks — only one (neutral currents) was European, despite roughly equal spending on both sides of the Atlantic.

DESY, under Schopper's guidance, was the first to break this potential barrier, with the construction of PETRA, a 19 GeV on 19 GeV electron-positron collider, more than a year ahead of the American equivalent PEP. Unfortunately nature was not kind: there has been only one (contended) discovery, evidence for the decay of the 'gluon', the photon of the inter-quark force. The 'top' quark, possibly the last quark, is probably accessible to PETRA but it is still hiding. More significant was the way PETRA

was built — very fast, cutting all corners, finding money from all sources (including a federal budget for propping up an ailing civil construction industry). Schopper's objective was clearly to produce PETRA physics as fast as possible — not, as has arguably been the case with CERN, to produce beautiful accelerators that turn on at the switch of a button.

The interesting questions now are whether HERA, DESY's effort at a very high energy electron proton collider (to probe proton and quark structure), will go ahead so well without Schopper's guidance, and whether the 4000-staff, 12-nation CERN establishment at Geneva will respond as well as DESY to the Schopper shake-up. It is also interesting to see that Schopper's mentor in the US, ex-Fermilab director Robert Wilson, is also flexing his muscle again (he created Fermilab at breakneck speed and low cost and beat CERN to 400 GeV), and is talking of attaching electron rings to existing or planned American proton machines in a bid to beat HERA to its 1989 target. The game may be more even now than it was over the 400 GeV race (where there was a long European squabble over siting) because the sites for HERA and LEP are already agreed; and government money in the US and Europe for subnuclear physics is probably equally tight.

Schopper's plans for CERN involve an absolute minimum version of LEP, sparer even than the 'minimum LEP' defined by CERN design teams. His budget-LEP would just reach the predicted intermediate vector boson (a keystone of modern theories), but be capable of upgrading when the money is available. He also wants to bring the physicists and the accelerator design teams closer together, by encouraging more flexible arrangements for exchange of posts for limited periods. In CERN, the two groups have long been suspicious of one another. There is also a very active staff union, which may prove conservative; and there is the problem of 12-nation politics on CERN Council. It will be very interesting to see what Professor Schopper, who takes up his post on 1 January 1981, can do. We wish him well. □

Editor of Nature

Dr Peter Newmark, Acting Editor of Nature since the beginning of the year, hands over to John Maddox from the next issue. Dr Newmark remains Deputy Editor. Mr Maddox, Editor of Nature between 1966-1973 and lately Director of The Nuffield Foundation, resumed the post of Editor on 13 May.

United States

Physicists urge greater efforts on long-range acclerator research

HAVE US physicists become so engrossed in the short and medium-term challenges of the design of particle accelerators that they have neglected to give adequate attention to more long-term research needs?

The question is raised empirically by current delays in the production schedules of new accelerators at Fermilab and Brookhaven National Laboratories, at both of which the development of superconducting magnets is presenting more difficulties than originally anticipated.

And it is answered in the affirmative by the Department of Energy's High Energy Physics Advisory Panel (HEPAP) which is about to publish a 'call to arms' to the physics community warning that longrange research is ignored at its peril.

Currently such research consumes less than 1.5% of the total operating budget of the high energy physics programme. The panel is recommending that this be increased to about 4% — roughly $10 million at current levels — although aware that general budget stringencies make it unlikely that this figure will be realised in the near future.

The report has been prepared by a subpanel of HEPAP. It points out that impressive developments in accelerator technology — frequently based on ideas originating in Europe or the USSR but with their application refined in the US — have produced significant savings in the cost per unit of beam energy. But it also emphasises that the energy demands of physicists have been increasing even faster, roughly by an order of magnitude every seven years.

The net result is that the overall costs of new accelerators continues to rise. Any particular technological advance, such as beam focusing techniques or superconducting magnets, only have a limited effect on reducing costs. "Redoubled efforts" it says are therefore an "essential investment" if further technical breakthroughs are to be found which make the costs of new machines politically acceptable.

The total sums devoted to accelerator R & D are not large. But the money tends to be concentrated on specific projects, with even theoretical work dominated by shortterm goals. 60% of funds, for example, now go on research on the super-conducting magnets at Fermilab and Brookhaven.

Nor is there necessarily a manpower problem. Of about 1100 high energy physicists in the US, 200 are working fulltime on accelerator research. The report says that the supply of accelerator scientists, although marginal, is not critical.

"We are saying that the mechanisms for accelerator R & D funding are adequate. What is not adequate is the perception of need in the physics community," Dr Maury Tigner of Cornell University, chairman of the subpanel which produced the report, told HEPAP last week.

"This report is a call-to-arms to the field in general, pointing out that all of us have a problem. Sitting where we are today we can see the beginning of the end of the line of the current generation of accelerators; we want to encourage the community to start thinking about what happens next."

The report emphasises that international comparisons show western Europe and the USSR put more theoretical and experimental effort into long-range accelerator research. "The number of physicists available for this work is larger than in the US, and they are well supported," it says.

Among the areas that it suggests might benefit from increased funding are research on very high field superconducting magnets, on radio-frequency superconducting cavities, and on fundamental characteristics such as performance limiting phenomena.

It also recommends a substantial increase in funds for studies of new accelerator concepts. Among, these it lists laser-driven accelerators, and the possible use of linear accelerators with very high beam currents, currently being investigated for their potential use as particle beam weapons, but which have so far received little attention as tools for experimental physicists.

In the near future, however, the chances of increased funding for accelerator R & D look bleak. The operation of the three national accelerators is already being held back to meet construction commitments on Fermilab's energy saver/doubler and Brookhaven's Isabelle. And the Congress has high energy physics in view as one area to absorb a 'pause' in funding with no shortterm impact on the national economy.

Furthermore the Office of Management and Budget has always been reluctant to consider long-range research proposals, looking on them as, in the words of one energy department official, "the way in which we get pregnant with expensive accelerators". But even some politicians are becoming piqued at the US's loss of leadership to Europe. And this combined with the arguments that accelerator technology can have valuable spin-offs, may provide a counter-balance to budgeteer's fears.

David Dickson

Laying the foundations for ISABELLE: has the US lost its initiative?

New plans to catch the vector boson

EUROPEAN and American physicists continue to play cat and mouse with their plans for new particle accelerators. First it was over who will get first crack at the Z^0 particle, the neutral intermediate vector boson predicted by the Weinberg-Salam unified field theory.

Investigating the characteristics of the Z^0 — if it exists — is a prime goal of the Large Electron Position ring (LEP), proposed for construction at the European Centre for Nuclear Research (CERN) with earliest possible completion planned for 1986.

Rising to the challenge, physicists at the Stanford Linear Accelerator Center worked out a way they could adapt their machine to produce single collisions beteen bunches of electrons and positrons at the 90 GeV range where the Z^0 is expected to be found, thus beating the Europeans to the mark.

CERN, under strong prompting from its director-general elect Dr Herwig Shopper, responded by pushing forward plans for LEP so that it could become partly operational by 1986, thereby closing and possibly eliminating the gap with the US.

Now US physicists are suggesting another tack, proposing that if the Z^0 race is conceded to Europe, it might make more sense to try competing in a different area, namely by constructing a machine to examine electron-proton interactions.

In Europe, where theoretical physicists have been supporting the study of electronproton interactions for some time, such experiments will be carried out on Germany's proposed HERA accelerator in Hamburg. The construction schedule for HERA, however, which has still to be approved by the German government, would start with electron-electron interactions, not bringing the proton ring into operation until 1988 or 1989.

Some US physicists are arguing that, if an electron storage ring can be attached to one of the existing proton accelerators, they could get there considerably sooner, perhaps even by 1983.

Specific proposals about how this might be achieved using either Fermilab's Tevatron or Brookhaven's Isabelle have been drawn up at Columbia University under the enthusiastic guidance of Dr Robert Wilson, ex-director of Fermilab.

According to Dr Wilson, the physics possibilities, which include the study of interactions with polarised electron beams, are 'substantial'. He also argues that an electron-proton collider is "competitive with more expensive projects" — a crack at the SLAC proposal which is likely to cost two or three times the $30 million he says the electron-proton project needs for "a modest experiment at low energy".

Fermilab scientists, initially sceptical about the practicality of adding an intersecting electron ring, have carried out their own calculations and found the technical aspects relatively straightforward.

Scientists at Columbia are enthusiastic about the idea. They suggest that although considerable uncertainty exists about what might be found, electron-proton interactions could help elucidate the structure of quarks. They might even, according to Dr W Lee, provide under certain conditions a quark 'factory'.

Enthusiasm for such a project has also come from Canada, where physicists have independently been working on their own proposal to add an electron ring at Fermilab.

A steering committee has been set up for what is known as the Canadian High Energy Electron Ring (CHEER), and it is intended to present a feasibility study for a project costing about $50 million to the Canadian government in September.

There could even be scope for Japanese participation. Japan already has provisional plans for its own electron-proton machine. But this would not be built for some time; and meanwhile some physicists are arguing that there is scope for a multilateral project drawing on the resources of all three nations.

Physicists less directly involved are more ambivalent about the proposal. They accept the argument that if Stanford's experiment only precedes the broader-based European experiments by a year or two, there may be little advantage in duplicating efforts. However, many feel that recent advances in high energy physics indicate that electron-positron scattering could prove a more fruitsul direction that stabbing in the dark with electron-proton collisions.

The picture is further clouded by the informally-announced intentions of Cornell University to develop a rival proposal to SLAC for raising the energy of its electron storage ring (CESR) to the range where the Z^0 particle is expected to be found. So, if funds for a new construction somehow materialise in next year's HEP budget — at present a rather faint possibility — intense competition can be expected for the direction in which they will be allocated. □

Academy to examine US links with European and Japanese scientists

FINANCIAL stringencies have reduced the contact of US scientists — particularly those at an early stage of their careers — with colleagues in other western countries precisely when these countries are beginning to catch up and occasionally surpass the US in scientific capability. This trend is worrying some US scientists. The National Academy of Sciences is therefore setting up a new committee on international human resource issues to look at the obstacles to closer links between US scientists and their colleagues in western Europe and Japan.

Academy officials say that the need for such a study comes more from a general impression of declining contacts than from any body of hard data. But they point, for example, to a recent NAS study which showed that there was a 55% drop between 1971 and 1977 in the number of new PhDs in science and engineering — indicating a firm commitment to postdoctoral study abroad.

The numbers involved are not large; in 1971 the total number was 409, and by 1977 this had fallen to 147, a decline from 2.4% to 1.2% of the total PhDs. But the trend this indicates is confirmed by more anecdotal evidence of the low number of US scientists to be found in most European laboratories, and the decreasing tendency to request foreign travel funds as a component of applications for research grants.

Academy President Dr Philip Handler warned the academy's members at their annual meeting in Washington last month that although small science in Europe seemed to be suffering the same financial pressures as in the US, cooperation in big science was proceeding rapidly, with potential implications for trans-Atlantic scientific relations.

"As their common strategic planning waxes, the strength of their scientific relations with this country will undoubtedly wane unless we exert special efforts," Dr Handler said. "That makes particularly ironic the decline in the number of young American scientists who can arrange meaningful experiences in European laboratories — where the benefits of such experience are now larger than ever."

Dr Handler said that he had asked the academy's foreign secretary, Dr Thomas Malone, to take a closer look at the changing relationships and "to ascertain whether we are losing touch with European science and whether any important trends may be discerned."

The chairman of the new committee is Dr Walter Rosenblith, Provost of the Massachusetts Institute of Technology, and funding for the committee's work is currently being sought from a number of government agencies and private foundations.

If appropriate funds are forthcoming, the committee will initially set up a number of working groups to examine issues such as the funding of foreign travel by US scientists, and the effects of national taxation, employment and immigration policies on scientific exchange. The focus of the committee's work xill be on links with western Europe and Japan, possibly including other western industrialised nations such as Australia, but omitting either the USSR or the Third World.

Dr Rosenblith said last week that a proper study could not be carried out by the US alone, but would benefit from the active participation of other nations, either individually or through organisations such as the European Science Foundation. "It is a question of the general rationalising of resources" Dr Rosenblith said. "We want to be sure that science as an international activity does not become too fragmented."

David Dickson

US signs scientific cooperation agreement with Japan

PRESIDENT Carter and Japanese Prime Minister Masayoshi Ohira last week signed a five-year agreement covering cooperation in scientific and technological research between the US and Japan.

In addition to encouraging more conventional forms of scientific exchange, the agreement provides a framework for the development of joint research projects between the two countries, and follows an earlier agreement on energy research which was signed in Washington last May.

Officials from both sides have identified 40 projects on which possible collaboration is now being investigated. These include the use of recombinant DNA techniques,

particle accelerator research, and studies of the detoxification and disposal of hazardous wastes and the climatic impact of increased carbon dioxide concentrations in the atmosphere.

One area in which plans for bilateral co-operation are already well advanced is in space research, where agreement in principle has already been reached for collaboration on 17 projects, and has formally been signed on nine. Areas of joint collaboration include the study of plasmas close to the Earth, and projects for a possible mission to rendezvous with the Comet Halley, and to send a joint orbiter and probe to Saturn. □

France

Biotechnology company planned

A French banking consortium intends to create a company called Transgène to develop commercial applications of genetic engineering. Although plans have not yet been finalised, the consortium, known as Paribas, is expecting initially to invest about £8 million in a five year programme of research.

In addition to its own laboratories, Transgène is likely to have close links with universities and government research institutes. Paribas are negotiating the financial and legal aspects of such links and are said to favour a scheme in which collaborating laboratories and institutes would be rewarded with shares in the company.

Negotiations appear to be complicated by the involvement of many of the French scientists with relevant expertise in a public sector organisation, G-3, set up over a year ago because of the lack of private investment in biotechnology. G-3 is financed and run chiefly by the Institut Pasteur and the Centre National de la Recherche Scientifique, with minor contributions from the Institut National de la Santé et de la Recherche Médicale and the Institut National de la Recherche Agronomique. It has a laboratory and about five scientific staff at the Institut Pasteur and will be spending about £0.3 million this year, much of it on the development of a vaccine against hepatitis B.

A further complication may arise from the possible role of Institut Pasteur Production (IPP), the commercial arm of the institute. At first IPP had preferential rights on any successful G-3 project, but that arrangement no longer exists. The future of IPP is currently unclear, following the breakdown of long and complex negotiations over a merger with two French pharmaceutical companies, l'Institut Merieux and Rhone-Poulenc; a possible merger with Sanofi, a subsidiary of the oil company Elf, is now being negotiated. To close the circle of negotiations, a report in *Le Monde* suggests that Sanofi is also considering joining Transgène.

Given the limited number and prior involvement in G-3 of French scientists with expertise in genetic techniques it is likely that Transgène will recruit internationally. It remains to be seen whether they will be able to attract such a large number of good candidates as has the Geneva-based company of Biogen, which has just appointed the first director of its scientific laboratory (*see below*).

Meanwhile the UK National Enterprise Board continues to contemplate the creation of a publicly-owned biotechnology company. Although enthusiasm for the idea is said to be high within the NEB, hopes for an early decision have abated probably because of pressure to involve private industry in the proposed company.

● Julian Davies, Professor of Biochemistry at the University of Wisconsin, is to be the first director of Biogen's laboratory in Geneva. A British-born and -trained biochemist, Professor Davies is best known for his work on the mechanisms of bacterial resistance to antibiotics.

Peter Newmark

United States

Solar Polar Mission threatened

EUROPEAN space officials travelled hastily to Washington last week in an attempt to prevent the US Congress from killing the International Solar Polar Mission, a joint effort by US and European scientists to send two spacecraft in complementary orbits around the Sun.

The mission was originally scheduled for launch in 1983, jointly funded by the National Aeronautics and Space Administration and the European Space Agency. Last month, reflecting moves to balance the federal budget and find additional funds for the much-delayed space shuttle, NASA announced that the launch would be delayed until 1985.

Now a Congressional Committee is recommending that the mission be abandoned. In passing NASA's request for further support for the space shuttle in the current financial year, a House Appropriations Subcommittee has suggested that $15 million be cut from the ISPM's budget of $47 million — and that the mission should be terminated.

It was the same subcommittee, chaired by Edward Boland of Massachusetts, which three years ago almost succeeded in killing the Galileo mission to Jupiter. No comparable move to cut the ISPM is likely in the equivalent Senate Subcommittee, which has a number of ardent space supporters, including ex-astronaut Jack Schmitt. But a fierce fight seems likely when House and Senate meet to resolve their diferences over NASA's budget.

Current plans for the solar polar mission are that the two spacecraft will be launched simultaneously to fly over the sun's poles in opposite directions. It would be Europe's first deep-space mission, and contracts for $56 million were awarded last year for spacecraft development and manufacture to Dornier, chief contractor for the multi-national STAR consortium.

The ISPM has been allocated 20% of the ESA's current science budget. European officials have pointed out that it is now too late to allocate the funds to other projects. □

Canada

33 percent boost for research

CANADA'S new liberal government has, as expected, endorsed the substantial growth in support for basic research promised by the previous conservative government shortly before it was defeated in the general election last February.

Mr John Roberts, the Minister of State for Science and Technology, announced last week that the Natural Sciences and Engineering Research Council (NSERC), the largest of the three research councils, will receive a 35% increase in its 1980/81 budget over the current year. This will bring the research council's total budget to $162.6 million.

The NSERC increase is precisely the figure announced by Mr Robert's predecessor, Mr Howard Grafftey, in January, and is based on a five-year plan which the research council submitted to the government last year. The Medical Research Council will have its budget increased by 17% to $8.2.2 million, and the Social Science and Humanities Research Council by 16% to $41.7 million.

In announcing these budget increases to the Canadian Association of University Research Administrators, Mr Roberts also said that the liberal government remained committed to its goal of raising the amount of the gross national product devoted to R&D from 0.9% to 1.5% by the mid 1980s. However to keep in line with this will, he said, require the government to find an extra $30 million for R & D in 1980/81 over and above the total increases of $155 million already announced.

Canadian scientists, who have criticised the decision of Prime Minister Pierre Trudeau not to emulate the conservatives by appointing a minister with special responsibility for science — Mr Roberts also holds the portfolio for mines and energy — have nevertheless been cheered by the announcement that promised that funding increases will be honoured.

The Canadian government is also expected to announce shortly that it is setting up a high-level committee to examine how Canada should pursue its involvement in the field of biotechnology.

A study that has been prepared by the Ministry of State for Science and Technology shows that although various research programmes are currently underway — ranging from research on the cloning of insulin genes to studies of nitrogen fixation — they are widely dispersed and often lacking in depth.

For example, although about 100 university scientists are currently involved in biotechnology research, they are divided between 22 universities. Similarly of over 33 firms in the field, only ten have more than one or two research workers involved.

David Dickson

The Netherlands

Tilting back to windmills

The old Dutch windmill . . .

THE windmill is a traditional feature of the Netherlands landscape; but now there is a new turn for it as an energy source. The Netherlands government is carrying out a multi-disciplinary study, and a plan has been put forward for a large wind-and-water power scheme for electricity generation in the unreclaimed part of the Zuiderzee.

The plan comes from hydraulic engineer L W Lievense, and would not reclaim the 40,000 hectare Markerwaard area, but convert it into a huge storage reservoir behind 15-metre dykes, on which would be mounted 400 wind turbines generating 1 to 1.5 MW. The turbines would pump up to 30 cm of water a day into the lake, from which water would fall 12.5 metres at four points in the dyke to drive 160 water turbines, generating 10MW each. At night, a third of the water turbines would themselves pump water into the reservoir, doubling the inflow to 60cm a day. Mr Lievense claims the scheme would generate 10% of national electricity demand at a
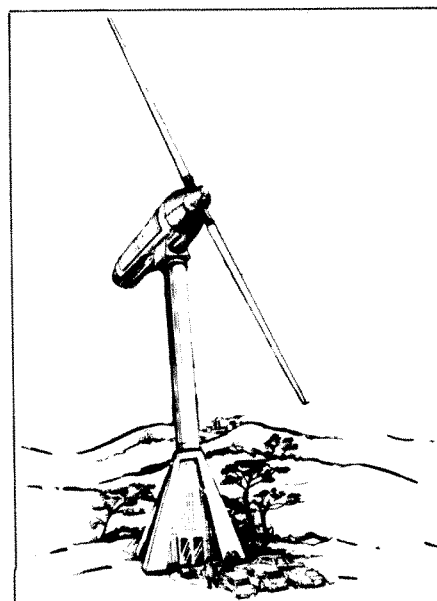
. . . and the new: a wind turbine due to come into use this year

capital cost of 3,000 million guilders.

Six government departments are involved in preparing the Lievense scheme, and the first detailed study is expected in August. There are ecological objections to it: lack of sunlight in the deep water would kill organisms on which fish life now depends, and fewer fish, together with the strong currents caused by the overflow points would threaten bird life.

Wind energy is generating great interest in the Netherlands: a private study has calculated that small private 10kW turbines could supply half the electricity needs of groups of 20 houses.

The government's own wind energy research programme is mainly directed to large-scale application. When the programme was started in 1976 it was thought that 5,000 windmills could generate up to 15% of national electricity. Now estimates have been cut back, due to the cost and difficulty particularly of building the offshore windmills envisaged earlier. But the government still believes that 500 turbines could generate up to 2,500MW a year, saving a million tonnes of oil equivalent. **Caspar Schuuring**

Australia

Probe into A-bomb test deaths

THE South Australian Health Service has sent a team to check on reported deaths and blindness suffered as a result of two British atomic bomb tests in October 1953. Members of the Yankunyatjara ethnic group of Australian Aborigines claimed that several of their people became ill or died when a "rolling black mist" enveloped their homes in Willatinna, 45 miles north of the Emu atomic bomb test field. Witnesses claimed the tests resulted in the blindness of 45 people, including many otherwise healthy children, as well as uncontrollable diarrhoea, vomiting and skin rashes. It is also claimed that older members of the group started dying within five days of the tests.

A former sheep station owner in South

Australia, has confirmed the report; she says she saw the cloud, which left an oily dusty residue on buildings and fruit trees, which later died. Her husband died from liver cancer in 1964.

The investigation comes on the heels of public protest about cancer deaths among workers and soldiers at nuclear test sites. The South Australian Campaign against Nuclear Power says that a large amount of low level nuclear waste was left behind at the test site and has only recently been fenced in, with warning signs in English which the Yankunyatjara cannot read. The Australian Veterans' Association has demanded immediate government action to clean up the site and compensate the victims of the exposure. □

United Kingdom

Scientists' union says nuclear inspectors are under-staffed

THE Institution of Professional Civil Servants, the trade union for government-employed scientists, released a document last week criticising the government for allowing staffing levels in the Nuclear Installations Inspectorate to fall 22 members short of its complement of 104. The NII no longer has a fracture mechanic specialist to assess the potential for fast fractures in pressurised water reactor vessels, an important aspect of PWR safety (*Nature,* 28 February, page 804). In addition, a single nuclear inspector has covered two power stations, Calder Hall and Chapel Cross, since December. In spite

of heavy advertising over the last two years, only two suitable candidates have been found for the 22 vacant posts.

An official with the Health and Safety Executive conceded that the shortages were serious, but said that adequate safety levels were baing maintained on a short-term basis. On the question of fast fracture analysis, the Executive says that it has the capacity to make the analysis, but that it may have to subcontract the work to the Safety and Reliability Directorate of the Atomic Energy Authority in the case of "unforeseen occurrences". Mr F R Mullin of IPCS said this would compromise an

independent analysis of PWR safety, and IPCS members in both the NII and the AEA would not cooperate with a sub-contracting policy.

The UK Secretary of State for Employment has revealed that of the six Health and Safety inspectorates (agriculture, alkalis and clean air, factory, mines and quarries, and nuclear installations) only the NII has been permitted to decline in strength. Since 1977, overall HSE, staffing levels have increased by 6%, while in the NII they have declined by 21%.

Joe Schwartz

NEWS IN BRIEF

Stanford's success with colliding beams

PHYSICISTS at the Stanford Linear Accelerator Center California, US, have reported that they have successfully generated collisions between beams of electrons and positrons on the new Positron-Electron Project (PEP), now nearing completion at a total cost of $78 million.

The initial collisions were carried out at an energy of 16 billion electron volts. Eventually PEP will be producing collisions at 36 billion electron volts, and at this energy it is hoped that it may have more success than the German PETRA machine, which came into operation last year, in seeking the sixth quark.

Although plagued by both political and construction delays — and by the shortage of qualified technicians on the West Coast — operation of the colliding beams occured only a few months behind schedule. However the delays have meant that European scientists are about a year ahead in operating colliding beam machines.

NSF to investigate handling of MIT patent

THE National Science Foundation is to investigate whether the Massachusetts Institute of Technology has properly exercised its responsibilitites in licensing the results of research into magnetic filters supported by NSF funds.

MIT has offered Magnetics International of Ohio a non-exclusive license on the high gradient magnetic separator. However, the company wants better terms; and it has asked the NSF to judge whether the arrangement proposed by MIT is "reasonable under the circumstances".

Under the terms of the current institutional patent agreements between the NSF and universities, the Foundation has "march-in" rights to determine whether a university is doing its best to ensure that the results of the research are reaching the market-place.

The Foundation has published a notice in the *Federal Register* announcing its intention to exert these rights, and to evaluate whether current patent law allows MIT to retain exclusive rights to the patent. A public hearing will be held next month.

US backs off non-proliferation stance

THE US State Department made it known last week that President Carter had decided to support the export of 38 tons of enriched uranium to India, even though Prime Minister Indira Ghandi has refused to make any commitment to halt further nuclear tests.

A request for an export license for the uranium, to fuel the power station at Tarapur, is being considered by the Nuclear Regulatory Commission. Under the terms of the Nuclear Non-Proliferation Act of 1978 — largely drawn up as a result of earlier nuclear tests by India — the NRC cannot grant a license if the recipient country has not signed the Non-Proliferation Treaty, or agreed to accept international inspection of its nuclear facilities.

Despite India's continued refusal to observe either of these conditions on the grounds that they represent interference in the country's internal affairs, State Department officials say President Carter is likely to overrule the NRC's expected rejection of the license application. They argue that the political stability of the near East is more likely to be maintained by keeping on good terms with India.

In a separate decision taken last week, the NRC has agreed to permit the export of a 625 MW nuclear power station to the Philippines, despite objections that the reactor is to be built on the slope of a non-active volcano and in a known earthquake zone. Three of the five commissioners found that the Westinghouse reactor did not pose an unacceptable risk to the "global commons" of the oceans or the atmosphere. Considering earthquake risks did not come under their mandate, the commissioners decided.

"Ten to one the reactor goes first!"

UK unions to make independent dioxin study

Two of the UK's largest unions are to make independent assessments of the effects of dioxin exposure on their members employed at Coalite and Chemical Products Ltd in Bolsover, Derbyshire. The unions have questioned a report prepared by the Health and Safety Executive that found no long-term differences between workers exposed to dioxin as a result of an explosion in 1968, and a control group of management personnel (*Nature,* 6 March and 1 May 1980). The Association of Scientific, Technical and Managerial Staffs has screened 21 of its 300 members at the plant for liver and heart conditions, and the Transport and General Workers Union will check a sample of 35 members for dioxin effects.

In the meantime, the EEC Commission is to conduct an enquiry into 2,4,5-T, the dioxin-containing weedkiller. The Commission, which has the power to ban the use of dangerous substances, was pressed into the investigation by Mr Ken Collins, a UK member of the Labour group in the European Parliament after he received a dossier on the chemical from the UK National Union of Agricultural and Allied Workers, which was instrumental in getting the chemical banned by the Trades Union Congress early this year.

Soedjatmoko to head UN University

MR K. Soedjatmoko has been appointed Rector of the United Nations University in Tokyo. A specialist in Southeast Asian and Indonesian social, political and cultural development, Mr Soedjatmoko, aged 58, is currently adviser to the National Development Planning Agency for Social and Cultural Affairs of Indonesia. He was Indonesia's ambassador to the US from 1968-1971. Mr Soedjatmoko is involved with a number of international development research organisations, including the Ford Foundation and the Club of Rome.

Bondi to chair environment research council

SIR Herman Bondi has been named the first full-time chairman of the British Natural Environment Research Council (NERC). The appointment, announced last week by Mark Carlisle, Secretary of State for Education and Science, will be for four years starting 1 October 1980. Under a major administrative rearrangment, Bodi will replace the present part-time chairman, Sir James Beament, as a full time executive and accounting officer. The change, and the appointment of Bondi, presently Chief Scientist at the Department of Energy, is expected to make the NERC more effective in carrying out its programme of investigation of nuclear waste disposal problems, one of its primary tasks. Bondi will continue to hold his job as Chairman of the Advisory Council on Energy Conservation.

Taking an 'all round attitude' to science

Indian Prime Minister Indira Gandhi (right) takes a keen interest in the development of her country's science and technology. Here, she talks to **Anil Agarwal**

DISCUSSIONS at the United Nations Conference on Science and Technology for Development held in Vienna last year revealed that few Third World leaders take an active interest in the scientific and technological development of their nations, and this is a constant complaint of their scientists. Prime Minister Indira Gandhi of India is an exception. She holds direct charge of the Indian government science and technology, atomic energy and space and electronics departments, and is also President of the Council of Scientific and Industrial Research (CSIR). In effect she is India's minister of science and technology. Why with all her other duties as the chief executive of a state, should Mrs Gandhi take on this role? Her reply is simple: "Because the scientists think that it's important. They think that they are then much freer of the bureaucratic stranglehold." This direct access to the top has made Indian scientists the envy of their counterparts in many Third World countries.

Prime Minister Indira Gandhi recently called a meeting of selected heads of scientific institutions to discuss problems faced by India scientists. The government may soon issue a statement to scientists emphasizing their role in national development. Mrs Gandhi herself has suggested that science and technology planning should be extended beyond central government. She would like committees such as the National Committee on Science and Technology — the existing policy-making institution of the central government's Department of Science and Technology — to operate at state government and, if possible, district level. Young scientists with suggestions for new uses of science and technology for development could be included on these committees.

Environmental problems

As well as her interest in the role of scientists in development, Mrs Gandhi also takes a keen interest in the related issue of the environment. She recently released the World Conservation Strategy prepared by the International Union of Conservation of Nature and Natural Resources, and called a private meeting of Indian ecologists to discuss environment. It is a concern she says she was born with. "I happen to deeply love the earth, and I have

from childhood been concerned about the cutting of trees. I sympathise with Bernard Shaw when people asked him why don't you keep flowers, and he said that I love children but I don't chop off their heads and keep them in my drawing room. So that's the sort of outlook I have always had. The aesthetic point of view is very much there. Most urban life is an uglification. To me personally this is the more serious aspect.

"Now we find that progress itself and the use of science and technology is creating its own pollution, which is very much worse. Just yesterday I read in *Time* magazine of this chemical that was sprayed in Vietnam and now all the children have been born deformed, apart from the fathers being diseased. Now that is all part of pollution. We are completely dependent for our very survival on at least air and water. And if those are going to be dirty or polluted, then mankind can't survive. Now I said somewhere that I don't know if it is important for it to survive or not. Presumably most people want it to survive, so I suppose they should pay greater attention to it."

In India there has been considerable interest in the extensive deforestation that has taken place in the Himalayas. There are two philosophies about its causes; one is that pressure of growing population is leading to deforestation; the other is that a wrong development strategy, which has failed to attack poverty, has led also to environmental problems.

According to Mrs Gandhi "it is much easier to cut trees than to grow them. This

process started in a very, very big way during the Second World War, and people did get the mentality of thinking of forests only either for timber or for industry, paper industry or something else. All of which is destructive. Whereas you can have what is called forest farming or social forestry, and so on. But it is true that when you make plans you don't think of every aspect of it. You think these people are poor, they need jobs and you need such and such goods, and you then have a proposal which will try and do both things. Until a decade or so ago, nobody thought about the environment or other aspects. I was just reading in a health magazine that even the effect of a very good programme such as bringing water to an arid area can bring disease to which the local people are not immune if you are not careful about it. So it means that you have to be all the time on your toes and keep looking at the problem from all around." Indian scientists have sometimes failed to display this "all round attitude", she complained.

In the Himalayan region of the State of Uttar Pradesh, local villagers have launched a unique movement against the state government sponsored auctions of vast tracts of forests. For several years they have prevented felling by hugging the trees — hence, the movement's name: Chipko Andolan, the hugging movement. To what extent does Mrs Gandhi appreciate such a popular movement? "Well, frankly, I don't know all the aims of the movement," she replied diplomatically. "But if it is that the trees should not be cut, I'm all with it." But the movement is also concerned about

A new improved camel cart with rubber tyres

the poverty in the region. "Naturally, anybody who lives in an economically backward country has to be concerned with that," she argued. But emphasizing the importance of trees in themselves, she added; "the cutting of trees has immediately brought havoc because it has increased our drought, it has increased our floods. And it has made vast areas much more difficult to live in."

What about the energy needs of the very poor who subsist on fire wood? "We are taking up a massive tree plantation programme," she says. "In it, we have also said that all aspects should be considered; food, for instance. Where fruit trees could grow we should try and emphasize that. And quick growing trees which could finance the programme (and be used for fuel), and longer growing trees which you need for other purposes. But, of course, you can use other things for fuel. Even in forests you can use various things which can be dried and used."

She believes a more imaginative approach is needed for this problem. The Planning Commission is considering setting up a National Ecodevelopment Corporation to assist local communities to take up extensive tree planting.

Oil and alternative energy

The energy problem is "very serious just now for us", says Mrs Gandhi. An overwhelming proportion of India's export earnings are being used to import fuel and fertiliser, because of the increased price of oil. Future rises could make matters worse. "Although we have oil," explains the Indian Prime Minister, "it is only lately that we have started trying to get it out, and even that is a very expensive process. (Most recent oil discoveries in India have been offshore.) Now we are experimenting with solar energy, we are experimenting with wind energy; in some parts, it has been successful, but we haven't tried it on a big

scale. So we are trying everything possible, any new idea that comes."

But wouldn't the further spread of the energy-intensive 'green revolution' exacerbate the energy crisis? Indian farmers last year suffered a crippling diesel famine and their irrigation pumps remained dry just at a time when the country was witnessing its worst drought of this century. India had no choice but to initiate the green-revolution-type of agriculture, believes Mrs Gandhi. "It was a time of acute grain shortage, and the point was how do we immediately double the production of wheat. And so we went all out, and that is how we have been able to survive all this time, even through other droughts. It's true we went a big way into diesel because we even transformed our railways. So now we have to see other forms of energy."

Commercially viable solar energy may soon be a reality which could make a big difference to India, believes Mrs Gandhi. But there have been arguments over imports of solar technology. The scientists at the state-owned Central Electronic Ltd who have been coordinating India's R&D on solar cells have strongly protested against the efforts of a private Indian company to manufacture solar-powered pumps with imported solar cells in collaboration with a US company. "We are never allergic to importing anything that we really need," Mrs Gandhi says. "What we have to ensure is that it doesn't hit our national interest in any way. And if we are making that thing in India, obviously it is better to have that even if it is a little inferior. But if we don't have it and it is going to help the people, then we have never hesitated."

The US federal budget alone for solar research in 1979 was more than the entire R&D budget of India in that year, I pointed out. The gap between the size of the two efforts was so big that it was certainly very

difficult for Third World scientists to keep up with R&D in the West. "It is very difficult to keep up, and yet our scientists are doing a very good job," she replied. "No, I don't think that the gap matters much. We are not competing with R&D in the West. It is much more important to have a solid base than to just have a very sophisticated top, which is, for instance, what Iran did. So from that point of view, even to be able to digest the knowledge that other countries are producing, you have to have a base. You can't have a base unless your scientists have the opportunity at every level of experimenting and of trying out these things. So it has to be a mixture. If you feel there is something that will help your scientists if you take it from outside, then you should take it from outside, providing that country is not going to use that as a foothold to influence other policies."

The Indian Prime Minister believes in the need to conserve energy and respect old, culturally-accepted energy-saving technologies. "All the new houses," she points out, "are built for energy consumption. They are hot in summer and cold in winter, whereas our old houses are not. The ancient house in which I was born and lived contained no cement, so probably it was cheaper to build. It never leaked in my memory. But when this house came under the purview of the Jain Fund, they said Oh! the ceiling might fall on the children because it was a children's home. So then they got engineers and they found it was only made out of bran and lime and various things like that, and it was at least 100 years old then. But it has never fallen yet. So we have not only to have new technology, but look a bit to the old technology. There is much sense in what people have evolved over the years to suit their climate, their environment their way of living. You can't keep all of it, because our way of life has changed, but I think a lot of it can be adapted and made more efficient."

Appropriate technology is important

But in contrast to the previous administration, Mrs Gandhi has been described as a critic of small-scale, village-oriented "appropriate technology". Did she think it was important? "I think it is very important," she immediately replied. But added a note of caution! "I don't think it excludes the other. I think that we have to have a mixture of cottage industry, village industry, small-scale industry, medium industry and heavy industry. Without heavy industry we cannot keep our freedom because we would be completely dependent on other countries. But we certainly can't survive only with heavy industry. So it is a question of encouraging things all along the line. For instance, take a bullock cart. Now you would like the farmer to advance from the bullock cart, but until we can advance, I would rather

that he had tyres on the bullock cart than we ignored it altogether.''

India is attaching a lot of importance to bio-gas plants, pointed out Mrs Gandhi. She admits, however, that they are acquired by rich farmers only. ''I'm sorry to say this happens in every field, no matter what you do. The people who are more powerful — even at the lowest level — are the ones who somehow grab the advantage. And with biogas what has happened is that the poor person who was getting the cowdung free, no longer gets it (after the introduction of bio-gas plants) as it becomes a commercial item. And, its the same with wood. We find the same thing happening with our fishing. We introduced deep-sea fishing, and here I must say that at least I was aware from the very first discussion on buying trawlers. I said well what are we going to do about the existing fishermen. The others assured me that they would be assimilated, they would be trained and so on, and that all the area closer to the shore would be theirs. But, in fact, it has not happened and they have suffered.''

What then can be done to ensure that the introduction of new science and technology does not worsen the lot of the poor? ''There is nothing much you can do about it,'' answered Mrs Gandhi, ''except where you find this happening you do something to help those who are being neglected.''

How can a developing country like India respond to the rapid advances in electronics which are bound to have an enormous impact? ''In India I would say that if you found that a computer made a lot of difference to efficiency you should get it. Where there is greater efficiency and greater production, that automatically makes for more employment. Even in farming where the agricultural production has gone up, it has not made for less people working. They need more labourers and they are able to pay them higher wages. I don't think that in any of these modern technologies there is a basic conflict provided you are all the time seeing what harm it can do either to health or employment or the poor or whatever it could be. You should be all the time willing to change if you find that it is not functioning as it should.

The bureaucracy in Mrs Gandhi's scheme has to play a major role in protecting the poor from the vagaries of modern technology. Now this is where we come up with a difficulty with government action. Somehow the bureaucracy — and even the brightest of them — likes to go along a set path and they feel that if there is a little deviation somehow heavens would fall or something.''

North-South and South-South relations

The recent Brandt Commission report on North-South issues has voiced some of the beliefs of Third World leaders like Mrs

Gandhi: that the economic development of the South is in the interest of the North and that part of aid should be in the form of an international tax. But she says she hasn't yet read the report carefully. ''I have just flipped over pages. Most of it depends on the Group B countries (UN language for western countries) and this is the trouble — the difficulty rather — that these are the countries that don't want to move. So where do we go from there?''

Can the developing countries get together to increase their bargaining position with the North? There is much talk in the UN, for instance, about technical cooperation amongst developing countries. ''This is what we are trying to do. This was our effort in the non-aligned movement,'' she says. ''In each of them — Lusaka, Algiers, Colombo — we had to go further along in that direction. The trouble is that we are very bad propagandists, we just don't know how to sell ourselves and what we are able to do in this country. When most people come to India they would rather go and see the Taj, so that even when they come here they don't return with very much more knowledge.''

There were a number of examples, said Mrs Gandhi, where India had obtained a contract from another developing country

only after it had been broken with a western country. Third World countries still look mainly towards the West. However, the developing country, she said, remarked: ''how much better it was, and how satisfied they were and they hadn't realised that (a) we could do the job and (b) because we ourselves came from a similar economy we would know and understand their difficulties and what they wanted to do much better.''

Now that Indian companies have started operating in various Third World countries, did the Indian Prime Minister think there was any way by which countries like Tanzania or Zambia could ensure that the commercial operations of Third World companies led to increased self-reliance of the host countries instead of increased dependence as happens with the operations of multinational corporations? ''Obviously, I would like them to grow keeping the national interest in view,'' she replied. ''The tendency as you saw in the report on ITT is that the multinationals think of profits first and everything else second and third. For the developing countries, joint ventures are a useful way of cooperation.''

As the Indian government restricts Indian companies from investing capital

Baking wood to make charcoal (above): tree denuded of its branches (below) which are removed for firewood.

abroad, many operations abroad are indeed joint ventures gained on the strength of Indian know-how.

What will her own administration's policy be towards the multinationals? Contrary to some suggestions in the Indian press that her government may be more receptive to multinational investment, Mrs Gandhi replied: "Generally, we are not for multinationals. It depends, however. If by multinationals, you mean only the very big concerns, then we would rather steer clear of them. But there are areas where you can't like oil drilling. Or there are areas where it doesn't matter. Suppose they made Coca-Cola here — I have never even tasted it — I don't think it matters much because it is controllable. You have to look at these things individually, but generally speaking we would rather not get involved with them." Coca Cola and IBM were the two leading western companies that had to wind up their operations in India during former Prime Minister Desai's administration.

Nuclear energy

Finally, a word about nuclear technology. Did she in any way share the growing concern in the West about the feasibility and safety of nuclear technology? "On the other hand," she countered, "in Sweden they voted for it."

Mrs Gandhi has been a strong supporter of India's nuclear programme and its objective of achieving self-reliance. But she says she "can't prophesy anything at this stage" about whether India could achieve that self-reliance in the face of difficulties and delays in its nuclear programme. She did feel that India should put some, if not all, effort in achieving this aim. "We are using it for agriculture and various other things".

Mrs Gandhi did not know when India would receive deliveries of enriched uranium fuel from the US for the Tarapur Atomic Power Station. India has maintained that the US has to supply nuclear fuel under an agreement that came into force in 1963 which cannot be changed unilaterally. She is still extremely critical of western efforts to restrict the spread of nuclear technology. "It is the whole attitude of not allowing the developing to develop more. Once somebody has atom bombs, they are willing to accept it, they don't mind," she says, probably referring to western acquiescence over China's acquisition of the bomb. "They don't want us even to have peaceful explosions, when we have made it very clear that we are not going to make bombs or stockpile any kind of nuclear armaments."

The US administration last week announced that they were asking the US Nuclear Regulatory Commission to send two further shipments of nuclear fuel to India even though it has not signed the Non-Proliferation Treaty. The political sensitivity of the region because of Afghanistan was cited as the reason. □

Two by two

THE teaching of evolution in American schools has long been slowed by a successful campaign that demands "equal time" for an alternative theory of origins. The leading organization in this effort (advertised in *Nature* p.vi 21 February, 1980) is the Creation Research Society (CRS). In 1972, all members subscribed to the Statement of Belief, the first three paragraphs of which are:

● The Bible is the written Word of God, and because it is inspired throughout, all its assertions are historically and scientifically true in all the original autographs.

● All basic types of living things, including man, were made by direct creative acts of God during the Creation Week described in Genesis. Whatever biological changes have occurred since Creation Week have accomplished only changes within the original created kinds.

● The great Flood described in Genesis, commonly referred to as the Noachian Flood, was a historic event worldwide in its extent and effect.

The Creation Research Society does not promote alternatives to evolutionary theory in other religions. Many readers of the first chapter of Genesis have interpreted allegorically the sweep of the story of creation, but the account of the Noachian flood, in contrast, is precise with measurements, including the dimensions of the ark and the duration of the flood.

On 7 February, 1973, John D. Morris, field director of the Creation Research Institute's Ararat Expedition spoke in Pinole, California, and showed slides of the search for the remains of Noah's ark. His organization is currently taking legal action to challenge the teaching of evolution. Its speakers assert that isotopic dating is erroneous, that evolutionary theory contravenes the second law of thermodynamics and that the fossil record shows an absence of "transitional forms", and is based on bones of animals that were drowned in the Noachian flood.

The Creation Research Society has demanded that, in school textbooks "both the theory of special creation and the theory of evolution are fully and fairly treated". We should therefore examine the details of the flood as explicitly set forth in Genesis 6-8. Genesis 6 specifies the dimensions of the three-story ark as having a volume of about 43,800 cubic metres (one cubit = 0.46 metre). Noah and his family, totalling eight, cared for all living terrestrial animal species for one year and ten days in the ark. This included gathering and loading the necessary food supply.

During the flood, the mountains were covered with water* "and every living
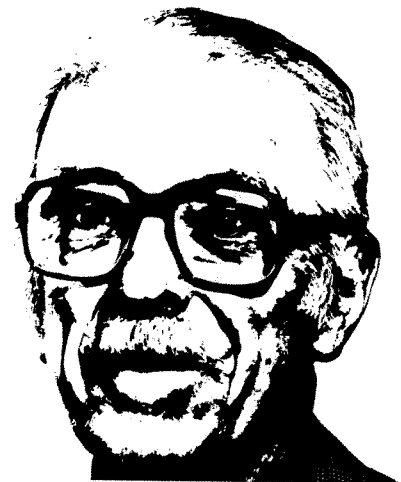
THOMAS H. JUKES

substance was destroyed which was upon the face of the ground . . . and Noah only remained alive, and they that were with him in the ark, and the waters prevailed on the earth 150 days".

The care of all living terrestrial species of animals would include the maintenance of an insectary containing about a million species, many of which are obligate predators or parasites upon others, and some upon vertebrates, an aviary with 25,000 species of birds and an animal colony containing, in addition to 2,500 species of amphibians and 6,000 species of reptiles, 15,000 pairs of mammals. The volume of the ark provided an average of less than 1 cubic metre for a pair of vertebrates plus their food supply. The mechanics of the "disposal problem" are not mentioned in any discussion I have seen. Another unmentioned problem was that of colonizing and preserving a culture collection of tens of thousands of species of bacteria and protozoa, including specialized parasites, before the existence of the microscope. Early explanations of such microbiology relied on the theory of spontaneous generation that was later ruled out by Pasteur's discoveries, and in any case is excluded by the Statement of Belief. The botanical problem is apparent, but is usually not mentioned.

If rain fell to a depth of 10,000 ft (a conservative estimate, insufficient to cover the mountains; actually "all the high hills that were under the whole heaven were covered" and Mt Ararat is 17,000 feet high), the volume of precipitation would have been 393,000,000 cubic miles, which is 1.4 times that of all the water presently on the earth. This rainfall occurred in 960 hours, at a daily rate of 104 ft. Its "drying up" took 167 days. Where did the water go? If it had rapidly entered the interior of the Earth, one would have expected numerous Krakatoa-like explosions. If it had escaped into outer space, why was not all the hydrosphere simultaneously dissipated?

NEWS AND VIEWS

Peptide pathology . . . of mice and men

from T. M. Jessell and J. S. Kelly

ANY examination of the significance of brain peptides in neuroendocrinology and neurology is assured of variety and diversity since more than 20 different peptide species have now been identified within the CNS (Hökfelt *et al. Nature* **284**, 515; 1980). Inevitably it is a little difficult to take an overall view in so novel a field. One objective of a recent meeting* was to explore, in particular, the clinical implications of recent research into neuropeptide function.

Encouraged by earlier work showing Parkinson's disease and Huntington's chorea to be associated with changes in transmitter levels, a number of laboratories have begun to map the distribution of neuropeptides in human tissue. It is, however, becoming clear from animal studies that the distribution of peptides in the brain is not necessarily the same as that of peptide receptors. For instance, the enkephalin concentration in the rat globus pallidus is extremely high, while the density of opiate receptors is only moderate. Similarly, bovine cerebellum is rich in angiotensin binding sites, but apparently devoid of angiotensin. Mapping the distribution of peptide receptors in human tissue may, then, provide clues to potential sites of peptide action that are not revealed by examining the distribution of the peptide itself.

A method applicable to human tissue was described by Pert and Herkenham (N.I.M.H. Bethesda) for opioid peptide receptors. The visualization of these receptors was achieved by labelling unfixed, slide-mounted sections of the brain, *in vitro,* with an opiate antagonist, ^{3}H-naloxone, fixing the label by lyophilization and exposure to hot paraformaldehyde vapours, followed by traditional autoradiographic processing. A similar method, developed by Young and Kuhar (*Nature* **280**, 393; 1979) has already been used to locate benzodiazepine receptors (for which one of the endogenous ligands may well be a peptide) within human cerebral and cerebellar cortex. It may, then, soon be possible to determine the precise distribution of peptide receptors within the normal and diseased human brain.

Some indication of the consequences of abnormalities in central peptide receptor

function might be obtained by studying similar disturbances in the periphery. J. Flier (Beth Israel Hospital, Boston) summarized evidence that a variety of disease states in man are produced by autoantibodies directed against cell membrane receptors. There is now substantial evidence that autoantibodies to the nicotinic acetylcholine receptor play a role in the aetiology of myasthenia gravis (Patrick *et al. Proc. natn. Acad. Sci. U.S.A.* **70**, 334; 1973, Almon *et al. Science* **189**, 55; 1974). More recently, Venter *et al. (Science* **207**, 1361; 1980) have reported the presence of autoantibodies to $ß_2$-adrenergic receptors in patients suffering from allergic rhinitis and asthma. Autoantibodies against peptide hormone receptors have also been found. The sera of some patients with Graves' disease contain two classes of thyroid stimulating immunoglobulins (Smith & Hall *Lancet* **ii**, 427; 1974; Manley *et al. J. Endocrinol.* **61**, 437; 1974). These immunoglobulins inhibit the binding of TSH to thyroid membranes and also stimulate thyroid adenylate cyclase activity leading to a clinical state of hormone excess. Similarly, the binding of insulin to its receptor is inhibited by circulating anti-insulin receptor antibodies in some obese patients with insulin resistance and numerous diabetic symptoms (Flier *et al. Science* **190**, 63; 1975). Almost exactly the same syndrome can be found in the genetically obese (NZO) mouse (Harrison & Itin *Nature* **279**, 334; 1979) which also has circulating autoantibodies that inhibit insulin receptor binding. Other inbred strains of laboratory animals may then provide models for as yet unreported disturbances in human peptide-receptor interactions. Could the low levels of opiate receptor binding and opiate resistance exhibited by the CXBK mouse (Baran *et al. Life Sci.* **17**, 633; 1975; Peets & Pomeranz *Nature* **273**, 675; 1978) for instance, be due to circulating antibodies to the opiate receptor? With so many peptide receptors to choose from, further examples of abnormalities in receptor function seem certain.

Of course, in the short term, it is more impressive when a single injection of a peptide produces a dramatic amelioration of symptoms. Sobue *et al.* (*Lancet* **i**, 418; 1980) have reported that a single, intravenous injection of thyrotropin releasing hormone (TRH) can bring about an immediate improvement in the major symptomatology of spino-cerebellar

degeneration. How TRH reduces body sway and nystagmus is unclear. Sobue suggests it may be related to the TRH-mediated improvement in abnormal noradrenaline metabolism in the cerebellum and brainstem seen in the mutant 'Rolling Mouse Nagoya'.

Another, more generally applicable therapeutic advance that may follow better understanding of the role of neuropeptides was reported by Holaday and Faden, (Walter Reed Medical Center, Washington D.C.) who found that a single, intravenous injection of the opiate antagonist naloxone could protect rats from otherwise lethal hypotension. The protective effects of naloxone are accompanied by an early restoration of blood pressure and appear to be equally effective in endotoxic, hypovolaemic and neurogenic shock (*Brain Research* **189**, 295; 1980). That the release of endorphins may be involved in the pathogenesis of shock is supported by Rossier *et al.* (*Nature* **270**, 618; 1977; *Science* **197**; 1368; 1979) who showed that ß-endorphin and ACTH are secreted concommitantly in response to stress. Since the stress-induced release of ß-endorphin has been confirmed in man, it is significant that ß-endorphin release is also induced in animals by the injection of morphine (Rossier *et al. Proc. natn. Acad. Sci. U.S.A.* **77**, 666; 1980). Morphine also inhibits the secretion of neurohypophyseal hormones (Clarke *et al. Nature* **282**, 746; 1979; Iversen *et al. Nature* **284**, 350; 1980) that may be involved in homeostatic responses to stress. Although these results may not support the introduction of naloxone in the treatment of the hypotensive, respiratory and hypothermic consequences of shock, they certainly draw attention to the possible adverse consequences of the use of opiates in patients bordering on shock.

Another attractive possibility for peptide therapy could be in the treatment of obesity. Although the precise role played by gastrointestinal peptides in the control of food intake is still far from clear, the release of cholecystokinin (CCK) or a shorter C-terminal fragment, such as CCK-8, may play a peripheral or central role in satiety (Gibbs *et al. Nature* **245**, 232; 1973; Straus & Yalow *Science* **203**, 68; 1979). Smith (Cornell University) reported that the suppression of food intake is

T.M. Jessell and J.S. Kelly are at St George's Hospital Medical School, London.

produced only by CCK and bombesin (Gibbs *et al. Nature* **282**, 208; 1979) and that the effects of CCK on satiety are decreased by gastric vagotomy (Smith *et al. Soc. Neurosci. Abstr.* **5**, 224; 1979). The central perception of satiety is, therefore, probably mediated through the vagus, rather than through circulating peptides passing the blood-brain barrier.

It seems clear that, with almost 30 neuropeptides and 300 diseases (Pliny; *Natural History* 7, Chapter 11, AD77) any summary of their relationship is premature. For the future direction of clinical research into neuropeptides, one need, as usual, go no further than to consult Robert Burton's treatise (*Anatomy of Melancholy*, Oxford, 1621) on diseases of the mind "that pertain to the substance of the brain itself, in which are conceived frenzy, lethargy, melancholy, madness, weak memory, coma and sleeplessness". □

Did Flamsteed see the Cassiopeia A supernova?

from David W. Hughes

CASSIOPEIA A is the brightest radio source in the sky and has been identified optically with a rapidly expanding emission nebulosity. Astronomers soon realised that Cassiopeia A was a supernova remnant and immediately started to question whether the supernova had been seen from Earth. Unfortunately there are snags. Firstly the source appears from Earth to be in the Milky Way. Calculations also show that it is 2,800 pc away (about a third the distance between us and the nucleus of our galaxy). So absorption along the path between the supernova and Earth will be considerable. Secondly an analysis of the rate of expansion of the nebulosity shows that the supernova would have been seen from Earth in about AD 1667 ± 8, assuming, of course, that it was visible at all.

Supernovae as a rule are difficult to overlook. The currently accepted production rate in our Galaxy is around two or three per century. They have a maximum brightness equivalent to an absolute magnitude of about −15. Without absorption the Cassiopeia supernova would have had, for a time, an apparent magnitude of about −3, similar to that of Jupiter or Venus. With absorption van den Bergh and Dodd (*Astrophys. J.* **162**, 485; 1970) suggested that a magnitude of +2 is more realistic. Even so, some astronomers have used the lack of a seventeenth century observation as a means of relegating Cassiopeia A to a class of abnormal supernovae. Maybe this is not necessary.

One of those interesting anomalies in science has occurred in which people have not only had similar ideas but have also published papers on the subject in the same month. William B. Ashworth Jr of the University of Missouri and Karl W. Kamper of the David Dunlap Observatory have both questioned whether Flamsteed recorded the supernova. Their papers appear respectively in the February editions of the *Journal of the History of Astronomy* (**11**, 1; 1980) and *The Observatory* (**100**, 3; 1980). The third worker, Peter Broughton, unknown to both Kamper and Ashworth recently read a paper on the subject to the Royal Astronomical Society of Canada.

John Flamsteed, the first Astronomer Royal, was actively cataloguing the sky during the period when the supernova could have been seen. Did he see it? Well Flamsteed recorded a star of sixth magnitude known as 3 Cassiopeia, close to the position of Cas A and there is no naked eye star visible in that position today. Certain possibilities arise. Flamsteed's catalogue appeared posthumously in 1725 under the title of *Historia coelestis Britannica.* unfortunately it contained numerous errors of observation, transcription, computation and publication. Francis Baily detected and corrected the great majority of these but the case of 3 Cas left him perplexed. He could not discover when Flamsteed had observed the star or how he could have seen a star which is no longer present. Baily concluded that the affair was 'singular'.

Caroline Herschel resolved the problem by stating that Flamsteed's 3 Cas was actually a faint 5th magnitude variable star AR Cas and that Flamsteed had made an error in calculating its position. Baily, however, found that Flamsteed has seen AR Cas as well as 3 Cas and rejected Herschel's solution.

William Ashworth investigated why Cas A has not been identified with 3 Cas before. He concludes that there were two main reasons. 3 Cas hasn't appeared in any star catalogue for more than 140 years, people believing it to be a mistake. Also, even if you went back to Flamsteed's catalogue, the reader would have been deterred by the statement that the original observations from which the position of 3 Cas was reduced cannot be found. Ashworth and Kramer, however, did find them, among the early sextant observations printed in Halley's 1712 edition. Flamsteed had apparently recorded the distance of 3 Cas from two brighter stars, Beta Pegasi and Beta Persei. The observations were made on 16 August 1680.

At this point the two authors start to diverge. Ashworth notes that the positions of Cas A and 3 Cas differ by 12.1′ in right ascension and 8.6′ in declination. Considering that Flamsteed insufficiently accounted for atmospheric refraction in one of his determining stars and that the sextant observations suffered from errors Ashworth concludes that the actual

Flamsteed's 3 Cassiopeia lies at the tip of the sceptre of Cepheé. From Atlas Céleste de Flamstéed, L'Académie Royale des Sciences, Paris, 1776; by courtesy of the Royal Astronomical Society, Burlington House, London.
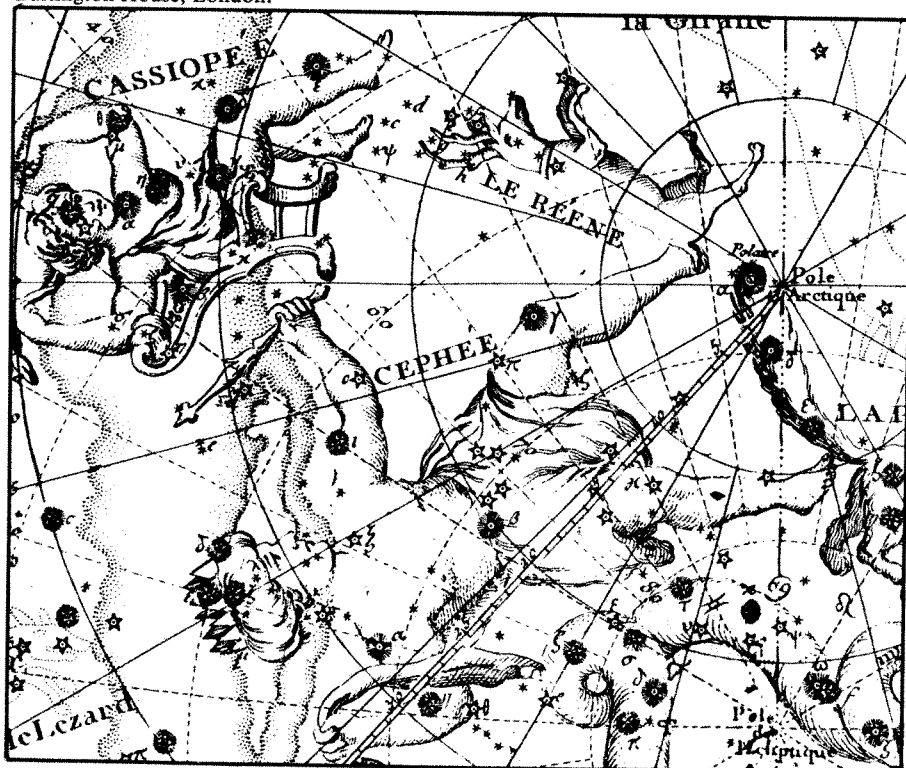
David W. Hughes is in the Department of Physics, University of Sheffield.

observing error was approximately 6′. Flamsteed regularly made errors of 1′ and discrepancies of 4′ are not infrequent so an error of 6′ is not unprecedented. To quote Ashworth "It seems almost certain that John Flamsteed did indeed observe the Cassiopeia A supernova in 1680". According to David H. Clark and F. Richard Stephenson (*The Historical Supernovae*, Pergamon) there have been four certain, two probable and two possible historical observations of supernovae in the Galaxy. Flamsteed's would be the ninth and latest.

Kamper is much more cautious. He suggests that the two sextant observations recorded by Flamsteed on 16 August 1680 were not of one star but of two different ones which still exist and are close to Cas A. The arc from Beta Pegasi agrees with the position of the 5th magnitude variable AR Cas to within an error of 32″. The arc from Beta Persei agrees with the 7th magnitude star BD + 56° 2999 to within an error of 64″. Both these errors are comparable with the errors of other arcs measured on that night. Kamper concludes that he can make no case for Flamsteed's supernova.

But does the story end here. Instead of asking Flamsteed to make a 6′ error in a sextant measurement we are now asking him to overlook the fact that the star he was observing that night had mysteriously dropped in brightness by two magnitudes. I think the least we can say is that the question is still open. □

An X-ray image of Kepler's supernova remnant obtained with the High Resolution Imager aboard the Einstein Observatory.

X-ray images of supernova remnants

from David J. Helfand

THAT the Crab Nebula is object number 1 in the eighteenth century Messier Catalogue of diffuse celestial objects testifies to the long-standing importance of optical imaging in the study of supernova remnants (SNR). Excluding the Crab, however, the optical radiation from the debris of these massive stellar explosions is primarily limited to the relatively dense cool regions in the swept up interstellar matter or, in the case of the youngest remnant Cas A, to knots of ejected material. With the advent of interferometers, SNR were among the first objects imaged by radio astronomers. The radio emission is thought to be more closely associated with the expanding shock wave from the explosion, arising as it does from the acceleration of high energy particles in regions of turbulent gas and compressed magnetic fields. However, the total flux emitted in the radio regime is but a tiny fraction of the overall energy budget of the remnant.

It is the X-ray emission that traces out the boundary of the expanding shock and dominates the radiative energy losses of the remnant for the first 20,000 yr. It is X-ray emission that can provide information on the possible collapsed remnants of the explosion (neutron stars or black holes), and it is the X-ray emission which allows us to use the SN shock to probe the structure of the interstellar medium (ISM). As a result of this rich potential, many rocket payloads and much observing time on satellite modulation colimator experiments have been dedicated over the past decade to producing X-ray images of large, nearby SNR such as Vela, Puppis A, the Cygnus Loop, and, through lunar occultation, the Crab Nebula. The best spatial resolution obtained was typically a few arc minutes. Recently published results of such experiments are a map of the northeast region of the Cygnus Loop which shows evidence for X-ray emission outside the boundary of the optical filaments (Tuohy

et al. Astrophys. J. Lett. **L101**; 1979) and a HEAO-1 modulation collimator image of Tycho's remnant indicating a roughly spherical shell with enhanced emission from the western limb (Fabbiano *et al. Astrophys. J.* **235**, 163; 1980).

As in the rest of X-ray astronomy, however, the launch of the Einstein Observatory a year and a half ago has provided a quantum leap in our abilities to produce X-ray images of SNR (*Nature* **279**, 371; 1979). With vastly increased sensitivity and arc second spatial resolution, these new pictures are surpassing our expectations of what is to be learned in each of the areas noted above: SNR dynamics and evolution, the physics of collapsed remnants, and the structure of the ISM. The only picture published to date is that of Cas A (Murray *et al. Astrophys. J.* **234**, 169; 1979). It shows a generally spherical shell outlining the blast wave's progress studded with bright knots of emission, some associated with the fast moving ejecta and others overlying optical filaments linked to the interstellar or circumstellar material heated by the passage of the shock. No central point source, expected if a hot neutron star had been a product of the explosion, is present.

Images of nearly 50 other remnants have already been collected and preliminary results for many of these were discussed in contributed talks and an invited review at the recent meeting of the High Energy Astrophysics Division of the AAS in Cambridge, Massachusetts. Most remnants of the historical supernovae show well-defined, circular, limb-brightened shells, although, large brightness variations around the rim are a common feature. The enhanced emission near the shock front begins to fade as the remnant ages: several remnants thought to be more than 10–20,000 years old no longer

David J. Helfand is in the Department of Astronomy, Columbia University, New York.

show a clearly defined boundary between remnant and ISM, and only an amorphous volume of cooling gas belies the presence of the recent explosion. The detection of more than 20 remnants in the Large Magellanic Cloud (where distances are determined to better than 10%), offers an excellent sample of objects for use in the study of remnant evolution.

Another type of X-ray morphology is exemplified by the distinct class of remnants for which the Crab is the archetype. Emitting synchrotron rather than thermal photons and powered by the rapidly spinning central pulsar rather than by an expanding shock, the Crab-like remnants show X-ray surface brightness distributions which are sharply peaked toward the central source. Several prospective members of this class, first suggested by radio studies, are being examined with Einstein, and at least two have already been detected, although a search for X-ray pulsations from them has not yet been effected.

One of the questions to be addressed with these high resolution images is that of the prevalence of neutron stars in SNR (Helfand *et al. Nature* **283**, 337; 1980). Theoretical work prior to last year led to the expectation that a neutron star, formed at a temperature of 10^{11} K, would remain hot (> few million degrees) long enough to be observed in any of the remnants less than a few thousand years old. In fact, point sources have been found in only three objects: the Crab and Vela remnants which were already known to contain radio pulsars, and the young southern remnant RCW 103 (Garmire & Tuohy *BAAS* **11**, 791; 1980). In the case of the Crab, most of the emission is pulsed (and, presumably, nonthermal), although a recent result indicates that there may be an unpulsed component, (< 1% of the total) which represents thermal emission from the stellar surface at a temperature of 2×10^6 K (Harnden *et al. BAAS* **11**, 789; 1980). In Vela, an arc second resolution image shows that there is an extended X-ray nebula surrounding the pulsar (a scaled down version of the Crab Nebula), making separation of the surface neutron star radiation difficult (Harnden *et al. BAAS* **11**, 424; 1979). For RCW 103, the flux from the weak point source at the remnant centre also yields a temperature of $\sim 2 \times 10^6$ K for

a 15 km neutron star. Limits for most of the other young remnants lie in the range of 0.5 — 2 × 10⁶ K and, while a burst of activity on the part of theorists has pushed the predictions to lower values, our current understanding of neutron star physics will probably not admit the possibility of cooling a remnant in SN1006 to half a million degrees in less than a thousand years. Thus, we must conclude either that the standard cooling theory is incorrect (presenting an important fundamental lesson in the physics of matter at supranuclear densities), or, that the majority of SN do not leave pulsars behind (driving the discrepancy between the pulsar birthrate and the galactic SN rate into such violent disagreement that a new method of producing neutron stars need be found).

Yet another important facet of the X-ray SNR images is the information they can provide on the nature of the ISM. Our ideas about the distribution of diffuse matter in the galaxy have changed dramatically in the last five years. The once rather homogeneous picture has been supplanted by observations which show ranges in temperature from 10^1 to 10^6 K and ranges

in density of from 10^8 to 10^{-3} cm^{-3}. While circularly symmetric expansion shells and correlations of X-ray enhancements with optical filaments recall the largely (> 90%) diffuse medium and evaporating cloudlets suggested by McKee and Ostriker (*Astrophys. J.* **218**, 148; 1977), the large scale brightness changes around the limb of many remnants suggest a large scale (~ 10pc) structure to the ISM reminiscent of the interstellar tunnels of Cox and Smith (*Astrophys. J. Lett.* **189**, L105; 1974). Comparison of the morphology of the LMC remnants with their local galactic environment and the detailed correlation of X-ray, optical, and radio maps with ~ 10^3 AU spatial resolution for nearby remnants such as the Cygnus Loop will clearly have a major impact on this problem in the future.

Detailed work in many of the areas outlined has only just begun. The preliminary results assure us, however, that from the structure and evolution of the remnants themselves, to the physics of neutron stars and the study of the energy balance and structure of the ISM, the contribution to be made by X-ray imaging of SNR is large indeed. □

are shown in the lower part of Fig. 1. In this case the residues of the projectile and the target remain distinct and they are kicked apart by the highly compressed head shock zone. The uranium nucleus moves slowly at right angles to the initial projectile direction and its large deformation and angular momentum makes it likely that it will fission, while the projectile is deflected through about 30°.

Figure 2 shows how these two types of collision are distingushed by the characteristic dependence of the energy and angular distributions of the fragments on the impact parameter. As the impact parameter increases, the angular distributions broaden and the peak angle for the projectile fragments moves to smaller angles. The high-energy tail of the spectra increases with the impact parameter due to the deflected projectile residue and to the matter from the exploding headshock wave. For large impact parameters there are two distinct contributions to the matter distribution, one from the bounced-off projectile-like fragments at large transverse and forward momenta and the other from the residue of the target at low parallel and perpendicular momenta.

Many of these features of energetic nuclear collisions have been found experimentally. Studies of neon-gold interactions at Berkeley by Meyer and collaborators show heavy-target residues moving at right angles to the incident beam in coincidence with correlated jets of fast light particles in the opposite azimuthal direction, just as in the lower part of Fig.

Hydrodynamical analysis of energetic nuclear collisions

from Peter Hodgson

WHEN two nuclei collide at energies of several hundred MeV. per nucleon all the nucleons are involved in a violent interaction that is too complicated to analyse in terms of their individual motions. Instead a good overall understanding of the interaction can be obtained by using the methods of classical hydrodynamics.

A calculation of this type has recently been made by Stöcker, Maruhn and Greiner (*Phys. Rev. Lett.* **44**, 725; 1980) and the results show how the character of the interaction depends on the classical impact parameter.

They made their calculations for the collisions of 400MeV. per nucleon neon nuclei with uranium nuclei. The nuclei were treated as fluid systems described by the Euler equations, and these were integrated numerically in three dimensions. This automatically ensures the conservation of particle number, momentum and energy. The nuclear characteristics were included through the equation of state, which gives the dependence of the internal energy and pressure on the local density and temperature. The internal energy comprises the compression energy and the thermal energy. For the compression energy they used a parabolic expansion around the ground state density with a

Peter Hodgson is in the Department of Nuclear Physics, University of Oxford.

compression constant of 200MeV. and for the thermal energy a Fermi gas expression. The Coulomb and Yukawa potentials were included, thus giving a realistic account of the binding and surface energies of the nuclei.

These calculations give the time evolution of the collision process, and they were continued until the nucleons were so far apart that they could no longer be considered to be in thermal contact. Calculations were made for various values of the impact parameter b, the distance of closest approach in the absence of interactions, and some of the results are shown in Fig. 1. The upper picture shows the density and temperature contours and the velocity field (arrows) in the scattering plane at a late stage of a head-on collision ($b = 0$). It is notable that a strongly compressed, highly excited head shock is formed, and this pushes matter sideways giving a strong sideward compression wave. The particle velocities are everywhere small and no projectile-like fragments are observed, showing that all the forward momentum of the projectile has been transferred to the combined system. The angular distribution of the emitted fragments is given in Fig. 2, and shows a sideways peak at the Mach shock angle of about 70°. Most of the particles in the peak have quite small kinetic energies around 20 MeV.

The results of calculations for an intermediate impact parameter ($b = 6$ fm)

Figure 1 Nuclear density and temperature contours and velocity field (arrows) in the scattering flow at a late stage of the collision of a 400MeV. per nucleon neon nucleus with uranium. The upper picture is for a head-on collision and the lower for an impact parameter of 6 fm.

Figure 2 Variation with impact parameter of (a) the angular distribution (inset: position of maximum) and (b) the energy spectrum of the reaction products.

1. Studies of nearly central collisions of neon with uranium at Darmstadt by Stock gave a broad distribution peaked around 90° for the low-energy particles, and this becomes narrower and shifts to forward angles with increasing kinetic energy, in qualitative agreement with the hydrodynamical calculations.

These calculations show that many of the features of energetic collisions between nuclei can be understood using classical hydrodynamical concepts. Such collisions subject nuclear matter to very high pressures, and thus provide a way of testing the nuclear equation of state that is employed in the calculations. An additional possibility is the discovery of abnormal super-dense states of matter from irregularities in the excitation function of the Mach shock-wave angle and in other measurable quantities like the pion production rate and the nuclear temperature. □

Bio-Energy '80*

from D. O. Hall

WHEN over 1800 people and large official delegations from Brazil, China, France, Sweden and the US get together for discussions and to display equipment for biomass-for-energy systems then something serious must be happening in the field — such a meeting was inconceivable even two years ago. That something, of course, is the belated realization that the world's oil production has already peaked (not for technical reasons) and that future oil price increases

will be maintained above the inflation rate. In addition it is recognized that biomass already supplies about 15% of the world's energy but because this use occurs mainly in the rural areas of the developing world it has not been given due attention. Even in the developed world the US currently derives 2% and Sweden 10% of its energy from biomass.

The Bio-Energy Council of Washington, D.C. — a foundation and subscription funded organization — has only been established for some three years and has already made a significant impact in the biomass-for-energy field. Their main aim is to serve as an international information centre and to this end they have already published the third edition of the *Bioenergy Directory 1980* — it contains over 650 one-page summaries of bio-energy activities in 34 countries and also abstracts 250 additional reports from the 1979 Directory.

The Congress was so large that only a partial view can be given. The 'hottest' topic was undoubtedly the alcohol programmes of Brazil and the US. Brazil leads the world as it started its programme in 1975 and now spends about $700m a year. About 4 billion litres of ethanol will be produced in 1980 and about 10 billion litres in 1985. The alcohol is blended to 20% in petrol but a quarter of a million cars will be produced this year alone to run on 100% alcohol. The Government is controlling the rate of use of alcohol to try to prevent shortages or surpluses.

The main source of alcohol is sugar cane but cassava, sweet sorghum and babussu palm are being rapidly developed as crops with wider land potential and less stringent agronomic requirements. Brazilian companies can now sell turn-key plants to the rest of the world. A Brazilian speaker made it clear that the decision to implement the programme was a political one and that economic and technical factors played secondary roles. The discussion of energy ratios was, according to him, totally irrelevant. Energy independence and foreign currency savings were the key factors. This point was well taken by the US Congressmen from the Iowa cornbelt who is one of those pushing the US gasohol programme in Washington. The Americans blend alcohol to 10% in gasoline and it is now being sold in thousands of stations in the US. It has received tax credits from Federal and State governments and is very popular with the public who perceive it as one way of 'helping America'. Current biological alcohol production in the US is about 80m gallons per year; it is hoped to expand this to 500m gallons per year within 2 or 3 years by massive federal aid — about $1 billion per year for up to 10 years.

D.O. Hall is a Professor of Biology of King's College, London and past-chairman of the UK Section of the International Solar Energy Society.

Surplus corn is the primary source of feedstock now, but other grains, sweet sorghum, sugarbeet, sugar cane and other crops are being examined. Small-scale ethanol producing facilities on farms are being rapidly implemented and encouraged. Local self-sufficiency is the prime aim. Surplus sugar production from sugarbeet in Europe and from sugar cane in tropical countries was also widely discussed as a potential source of alcohol.

Direct combustion of wood, residues from agriculture and forestry, and wastes from cities and industry is already commercially viable in many parts of the States — especially in the north east where energy costs are high and organic matter is abundant. This use of biomass and the construction of biogas generators seemed the next most popular topics of discussion. The Chinese delegation described how they have constructed 7 million biogas digestors over the past few years and are currently building them at the rate of 1 million a year. Attention is also being given to the production of methanol from woody material — especially since such technology is compatible with coal-based systems. This was certainly stressed by the Europeans and Canadians — and would find echoes in Australia and Brazil.

There seems little doubt that biomass-for-energy systems are here to stay and their implementation must certainly be encouraged. Like any energy systems there are disadvantages in using biomass, e.g. land use competition, requirements for fertilizer and water, soil erosion problems, uncertain costs at this early stage, lack of infrastructure, and so on. The one most controversial topic right now is that of food versus fuel — should we divert plant material to fuel and away from its use as a food, or is there a rational way of providing both, e.g. by feeding corn to make ethanol and use the stillage as cattle feed. These discussions will inevitably intensify. In developing countries decisions on reforestation and rehabilitation of semi-arid regions must be made quickly if energy (mostly in the form of woodfuel and residues) is to be available on a continous basis.

To those of us who have been advocating careful, continued and increasing use of biomass as a source of fuel this Congress and Exhibition was a dream come true. Even two or three years ago such an event may have been fortunate to attract a few hundred dedicated persons. Now the field is recognized to be of worldwide importance and will probably continue to be so as long as the 'energy problem' continues. This is likely to be for at least the next 15 to 20 years as the world pays the price of decisions made in the 1950s and 1960s which locked us in to an oil economy. The decision cannot be reversed quickly and we are belatedly realizing this fact. Biomass will be only one component in a future energy mix but it can provide liquid, gaseous or solid fuels as required. □

Biotechnology and the production of proteins

from A.J. MacLeod

THE idea of using recombinant DNA techniques to construct bacterial strains capable of synthesizing therapeutic proteins is currently being widely promoted. It is not, though, the only possibility for large scale production of proteins and the advantages and disadvantages of different methods need to be considered. Particularly for proteins intended for therapeutic use there are severe constraints on the precise nature and purity of the products.

Bacterial methods would seem to have the advantage of almost limitless production with recovery from a relatively simple mixture. However, apart from albumin, virtually all of the protein species in plasma are glycoproteins or lipoproteins. Modulation of the antigenicity or pharmacokinetics of the proteins is likely to be important *in vivo* and the ability of bacteria to reproduce these features faithfully is doubtful. This problem may be reduced by *in vitro* modification (Marshall & Humphreys, *J. appl. biochem.* **1**, 88; 1979). As bacteria degrade abnormal proteins efficiently (Goldberg & St John *Ann. Rev. Biochem.* **45**, 747; 1976) it is probable that partial digestion of the product will occur with effects on biological activity, even if antigenic loci remain intact.

Should synthesis of significant quantities of biologically active protein be achieved in a bacterial system, its recovery will still present major difficulties. In systems where secretion of human proteins, with or without a bacterial protein carrier, has been attempted, secretion has occurred into the periplasmic layer and the products have not successfully passed into the culture supernatant. (Villa-Komaroff *et al. Proc. natn. Acad. Sci. U.S.A.* **75**, 3727; 1978. Fraser & Bruce *Proc. natn. Acad. Sci. U.S.A.* **75**, 5936; 1978). Protoplasts have to be prepared to release the proteins but this has the disadvantage of releasing a mass of other bacterial products and debris into the crude preparation. If the cells have to be lysed to release accumulated protein this problem will be much more severe. Even if secretion into the culture supernatant can be achieved bacterial products and debris will still be present as contaminants.

Bacterial proteins are intensely antigenic in mammals and cell debris is pyrogenic. Even trace levels of bacterial contamination repeatedly administered over a long period, as in the control of haemophillia or in cancer therapy, may be dangerous. Products from bacterial cultures will have to approach absolute

A.J. MacLeod is the Protein Fractionation Centre, Scottish National Blood Transfusion Service, Edinburgh.

purity. However, as greater purity is sought with large-volume processes costs rise exponentially and consequently the processing cost may offset the initial production cost advantage of bacterial systems. A particular difficulty in this case, as opposed to the production of antibiotics or viral vaccines, is that some of the impurities will be very similar, chemically and physically, to the product.

Rather than using bacterial systems for human protein production it might be better to manipulate human cells so that they can be cultured more easily and be more productive. The plasminogen activator urokinase produced by normal human kidney cells *in vitro* is already available for clinical use (Lewis *Thrombos. Haemostas.* **42**; 895; 1979). Transformation of mammalian cells with genes from prokaryotes and eukaryotes has been demonstrated (Wigler *et al. Cell* **16**, 777; 1979). A more direct route to a satisfactory cell line might be to construct cell hybrids as has been done with leukocyte-lymphoblastoid hybridomas (Galfre *et al. Nature* **266**, 550; 1977). A step in this direction was the recent announcement by Widman *et al.* (*J. Cell. Phys.* **100**, 391; 1979) of the immortalization of a normal differentiated liver function in a hepatoma cell hybrid. The liver is the site of production of many of the plasma proteins. Systems capable of supporting very large-scale cultures of animal cells have been developed and are being introduced in association with established fermentation technology (*Eur. Soc. Anim. Cell Technol.* 3rd Meeting, *Develop. biol. Stand* **46**; 1980).

The advantages of human cell systems are that the products are likely to be correctly modified, they should be secreted into the medium, and antigenicity and pyrogenicity will be much reduced. Cell lines have the advantage that the cultures will not age as do normal cells and it may even be possible to construct lines that will grow and function in suspension. The disadvantages with cell lines include the incorporation of tumour cells that could release oncogenic material. However, methods of overcoming this problem have been suggested (Hillman *Advances Exp. Med. Bio.* **118**, 47; 1978).

The absolute homogeneity of the products from cloned systems may cause considerable complications in their use. Genetic polymorphism of plasma proteins resulting in multiple allelic forms is now well established with more than 20 variants of human albumin identified to date. Administration of such products over a prolonged period, if they do not match the recipients serum type, could induce the production of antibodies. Avoiding this could require production from several cell strains, each producing material of a

different serum protein-type. The plasma proteins currently available minimize this complication because they are prepared from pooled donation and thus contain a variety of serum protein types. Even so the development of antibodies to factor VIII in haemophiliacs receiving therapy can occur (Shapiro *Clinics in Haematology* **8**, 207; 1979).

Human protein has already been in use for some 30 years from products of the industrial fractionation of plasma from routine blood donations. Improvements in process control, fluid handling and separation techniques applied to the established cold-ethanol precipitation process have facilitated the design of a continuous, sequential precipitation process that yields defined fractions from large volumes of plasma. The products currently available include the albuminoid stable plasma protein solution, various immunoglobulin preparations and coagulation factor concentrates (Watt & Dickson *Proc. Int. Workshop on Technology for Protein Separation and Improvement of Blood Plasma Fractionation, U.S.D.H.E.W.* Publ. No. (NIH) 78 — 1422, 245; 1978). These products are widely used but their quality is affected by damage to the proteins during processing and by contamination. The latter include both exogenous material such as hepatitis B virus and bacterial pyrogens, and redundant plasma proteins which may be biologically active, provoking, for instance, thrombogenic or hypotensive side-effects. These problems can largely be attributed to the inherent difficulty of recovering a substantial proportion of a particular component from a milieu as complex as plasma.

An attractive possibility might be to exploit the well established techniques of plasma fractionation along with developments in human cell culture. Currently, substantial quantities of human protein pastes are produced as by-products of plasma fractionation. These byproducts consist largely of α and β globulins, and low molecular weight proteins and have already been shown to contain many of the specific components required for serum-free culture of animal cells *in vitro* (MacLeod & Drummond *Develop. Biol. Stand.* **46**, 17; 1980) The preparation of a nutrient culture medium for human cells based on human plasma proteins would avoid exposure of the cells to heterologous proteins which could subsequently contaminate the product (Bonin *et al. J. Biol. Stand.* **1**, 187; 1973). Thus it is possible to envisage a situation where human plasma would be collected and processed to yield albumin and possibly some immunoglobulins. The remainder would be processed to support the synthesis of a wide range of products by human cells *in vitro*, the whole constituting an integrated unit based on technology of which much is already well developed. □

ARTICLES

Mapping radio sources with uncalibrated visibility data

A. C. S. Readhead, R. C. Walker, T. J. Pearson & M. H. Cohen

Owens Valley Radio Observatory, California Institute of Technology, Pasadena, California 91125

There are many situations in which it is possible to detect interference fringes, but with large systematic errors in amplitudes. A new method is described for mapping objects from such data. In principle this method is applicable to any system which can produce detectable fringes, and is not limited to radio frequencies.

IN very long baseline interferometry (VLBI) radio astronomers are faced with making maps from visibility data with large systematic phase and amplitude errors. At frequencies below 10 GHz it is usually possible to calibrate amplitudes to 5%, but the phases cannot be calibrated except in a few special cases. Jennison[1,2] showed that it is possible to derive a good observable from the observed phases by forming the algebraic sum of these phases around a closed loop of three, or more, baselines. Rogers *et al.*[3] called this the "closure phase", and used it to derive structure from VLBI observations.

Hybrid mapping, incorporating the use of the closure phase, has now become a standard method of producing maps from VLBI data[4-6]. A limitation of this method is that it relies on well calibrated amplitude data, which are difficult or impossible to obtain at high frequencies ($\geqslant 10$ GHz). Thus, few reliable continuum maps have yet been made at or above 23 GHz, although several telescopes now operate at this frequency.

Twiss *et al.*[7] showed that it is possible to derive a good observable from uncalibrated amplitudes by forming ratios of the amplitudes observed on four or more baselines. We shall refer to such amplitude ratios as 'closure amplitudes'. They considered the limited case in which there are two or more equal spacings, but we shall show that closure amplitudes can also be used in non-redundant situations, such as obtain in VLBI or at the Very Large Array (VLA) in New Mexico. We present examples which show that the closure amplitude is a good observable, with errors determined by the random noise at the individual telescopes. Most of the systematic amplitude errors due to a particular telescope cancel exactly. These include amplitude errors due to atmospheric absorption and emission, to telescope gain errors, and to receiver temperature and gain variations. If the object is much smaller than the primary beam width of the individual telescopes, the pointing errors also cancel.

We describe here an extension of the hybrid mapping procedure which uses the closure amplitudes instead of the observed amplitudes. We have conducted some blind tests which confirm that reliable maps can be made from the closure amplitude and phase.

The closure amplitude

The complex visibility function of a source of brightness distribution $I(\sigma)$ is

$$V(\mathbf{b}) = \int_{-\infty}^{\infty} d\sigma \, I(\sigma) \exp(2\pi i \mathbf{b} \cdot \sigma) \qquad (1)$$

(ref. 8). An interferometer composed of two telescopes p, q measures the complex correlation coefficient, ξ_{pq}, between the electric fields at the two antennas. The relationship between the observed ξ and V may be written

$$\xi_{pq} = K_{pq}(G_p G_q)^{1/2} \exp\{2\pi i (\psi_p - \psi_q)\} V(\mathbf{b}_{pq})$$

where $\mathbf{b}_{pq}$ is the vector separation of the telescopes in wavelengths; K_{pq} depends on the correlator; the constants G_p and G_q represent the effects of the gain of the telescopes and the absorption in the atmosphere; and ψ_p and ψ_q represent the phase errors associated with the two telescopes, including propagation effects, oscillator drifts, clock errors and errors due to uncertainties in the positions of the source and the telescopes. Thus errors introduced in propagation from the source to the telescope and from the telescope to the correlator are included in G and ψ, while errors introduced during or after correlation are included in K. In many interferometer systems the observed correlation coefficient also depends on the system temperature at each telescope. This effect can also be included in G.

If measurements of the visibility are made on a sufficient number of different baselines $\mathbf{b}$, the brightness distribution of the source can be reconstructed by Fourier inversion of equation (1). This is the principle of aperture synthesis. If the constants G_p, ψ_p and so on are subject to large uncertainties, however, this is not possible; but all is not lost if simultaneous observations are made with a network of four or more telescopes.

When observations are made with four telescopes p, q, r, s the closure visibility A_{pqrs} can be calculated:

$$A_{pqrs} = \frac{\xi_{pq}\xi_{rs}^*}{\xi_{pr}\xi_{qs}^*}$$

It can be seen that in this ratio the G and ψ factors cancel and

$$A_{pqrs} = \frac{V(\mathbf{b}_{pq})V^*(\mathbf{b}_{rs})}{V(\mathbf{b}_{pr})V^*(\mathbf{b}_{qs})}$$

is simply the corresponding ratio of the four complex visibility functions, assuming the factors K are all equal, which is the case if all the interferometer pairs are correlated in the same way. The closure amplitude is defined as the modulus of the closure visibility $|A_{pqrs}|$. The argument of the closure visibility is the closure phase defined around a quadrilateral.

Table 1 The fraction of visibility information in closure amplitudes and phases

No. of telescopes	No. of baselines	Fraction of amplitudes	Fraction of phases
3	3	0	0.33
4	6	0.33	0.50
5	10	0.50	0.60
7	21	0.67	0.71
10	45	0.78	0.80
15	105	0.86	0.87
20	190	0.89	0.90
27	351	0.92	0.92
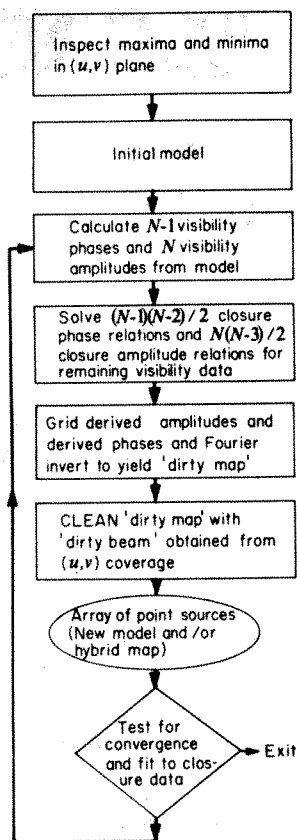
Fig. 1 Flow diagram of hybrid mapping procedure using closure phases and closure amplitudes.

If all six of the interferometer pairs formed by the four telescopes are available, three independent closure visibilities can be calculated: A_{pqrs}, A_{pqsr} and A_{psrq}. However, there are only two independent closure amplitudes.

For N telescopes there are $N(N-1)/2$ pairs, and there are N values of G at each instant. There are also N values of ψ, but the origin of the phase is arbitrary, and can be set to zero for one telescope. The values of ψ are then the phase errors relative to this telescope, and there are $N-1$ independent values. In an array with no redundant spacings the number of independent closure phases is thus $N(N-1)/2 - (N-1) = (N-1)(N-2)/2$, and the number of independent closure amplitudes is $N(N-1)/2 - N = N(N-3)/2$. In a non-redundant array, therefore, the fraction of the total visibility information in these two good observables is $(N-2)/N$ in closure phases, and $(N-3)/(N-1)$ in closure amplitudes. Table 1 shows these fractions for different numbers of telescopes, and demonstrates that the improvement achieved by adding an extra station is significant up to $N = 10$, by which stage nearly 80% of the visibility information is contained in the closure data.

This analysis assumes no redundancy. However, in a redundant array the number of free parameters is further restricted, and this can be an advantage in some situations. Rogers[9] has considered this point in the case of closure phases.

Observational test

Systematic errors due to a given telescope cancel exactly in the closure amplitude, but systematic errors can also arise if the K-factors are not equal for all the interferometer pairs. Such effects could be caused, for example, by a correlator bias. Table 2 shows an example of the observed closure amplitudes on a four telescope network, at 5,011 MHz on the BL-Lacertae object AO0235. AO0235 has long been used as a calibration source at this frequency on US baselines, and is thought to be slightly resolved on transcontinental baselines. Note that the closure amplitude $|\xi_{BH}\xi_{ON}^*/\xi_{BO}\xi_{HN}^*|$ is consistent with unity. This is expected for a

Table 2 Observed closure amplitudes on AO0235 at 5,011 MHz

Greenwich Sidereal time	$\left\|\dfrac{\xi_{BN}\xi_{OH}^*}{\xi_{BO}\xi_{NH}^*}\right\|$	$\left\|\dfrac{\xi_{BN}\xi_{HO}^*}{\xi_{BH}\xi_{NO}^*}\right\|$	$\left\|\dfrac{\xi_{BH}\xi_{ON}^*}{\xi_{BO}\xi_{HN}^*}\right\|$
05 h 3 min	1.094 ± 0.02	1.093 ± 0.03	1.003 ± 0.01
05 33	1.139 ± 0.02	1.103 ± 0.02	1.033 ± 0.02
05 59	1.125 ± 0.01	1.105 ± 0.02	1.019 ± 0.02
06 19	1.153 ± 0.02	1.119 ± 0.02	1.030 ± 0.01
06 45	1.186 ± 0.02	1.165 ± 0.02	1.020 ± 0.02
07 05	1.202 ± 0.02	1.207 ± 0.02	0.995 ± 0.01
07 25	1.294 ± 0.04	1.278 ± 0.08	1.028 ± 0.03
08 11	1.321 ± 0.03	1.319 ± 0.04	1.000 ± 0.01
		Mean =	1.016 ± 0.008

B, Bonn 100-m telescope, FRG; N, NRAO 41-m telescope, US; O, OVRO 40-m telescope, US; H, Hat Creek 26-m telescope, US. The maximum projected baseline lengths perpendicular to the line of sight to AO0235 are: BN—106, BO—137, NO—56, BH—135, NH—59 and OH—8, in units of $10^6 \lambda$. In forming the closure amplitudes we have taken the values of the raw correlation coefficients observed in 2-min coherent integrations, formed the closure amplitudes, and then averaged over 20 min. The errors are the s.e.m. for each 20 min interval.

source which is only slightly resolved, as the distance between Hat Creek and the Owens Valley is so small compared with other distances, thus $\gamma_{BH} \approx \gamma_{BO}$ and $\gamma_{NH} \approx \gamma_{NO}$ (γ_{BH} is the amplitude of the visibility, $|V(\mathbf{b}_{BH})|$). This demonstrates that, to within the level of accuracy of these measurements ($\leqslant 2\%$) the systematic amplitude errors cancel, as expected. This is a good test of the interferometer network. The other two closure amplitudes are the same, within the errors, in each interval, and they show the same trend over this 3-h period—they both increase from 1.09 at 05 h 13 min to 1.32 at 08 h 11 min. This is because $\gamma_{BO} \approx \gamma_{BH}$ and $\gamma_{NO} \approx \gamma_{NH}$ for this object. Note also that these closure amplitudes are always above unity. This is to be expected because γ_{BO} and γ_{BH} are less than γ_{BN}, and γ_{NO} and γ_{NH} are less than γ_{OH}.

Hybrid mapping with the closure amplitude

Although the closure amplitude is a good observable, it is difficult to interpret because it involves visibility amplitudes at four different points in the (u, v) plane. A similar problem arises with the closure phase, involving three points in the (u, v) plane. This problem is overcome in the hybrid mapping procedure[5], by assuming a model brightness distribution, and using the model
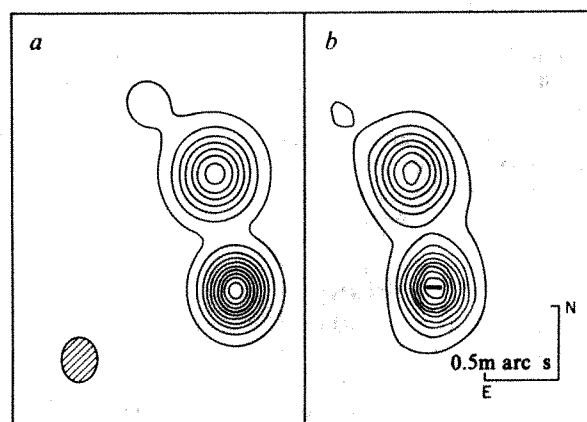
Fig. 2 Test 1: *a*, the test object, convolved with the gaussian beam with FWHM shown by the hatched ellipse. Contour levels, 5, 15, 25, ...95% of peak intensity. The object is assumed to be at $\delta = 50°$. *b*, Hybrid map derived from closure amplitudes and phases. The raw data have been badly corrupted by systematic and random errors (see text). There are no negative contours $\leqslant -5\%$.

Fig.3 As for Fig, but for Test 2. Contour levels, 5, 15, 25....95% of peak intensity. There are no negative contours ≤—%. Component A has 10 contours to the peak.
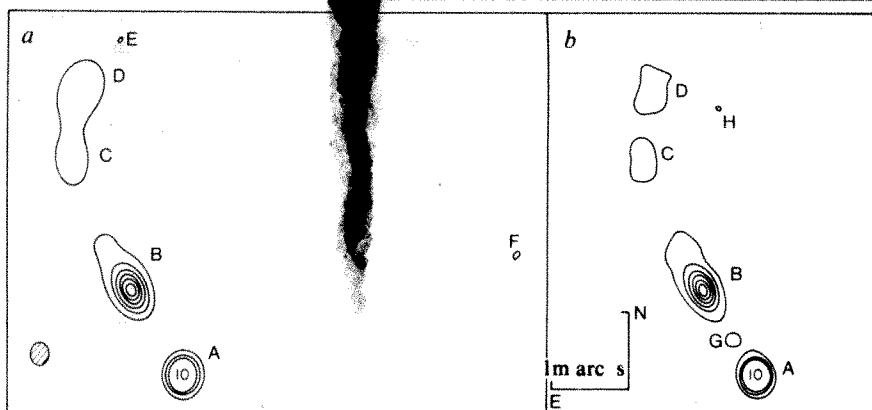
phases on $(N-1)$ baselines and the closure phase relationships to solve for the phases on the remaining baselines. This enables us to make a map, which is then used as the model, and we iterate until a stable solution is reached. To make use of the closure amplitudes we have extended this procedure. We now use the model to set the amplitudes on N baselines and the phases on $N-1$ baselines, and solve all the closure relations, both amplitude and phase, to obtain the amplitudes and phases on the remaining baselines. A flow diagram of the procedure is given in Fig. 1.

If there are data missing on some baselines, the maximum number of closure amplitudes which might have to be searched for a solution is $3\binom{N}{4}$, which rises rapidly with N, but this does not pose a serious computing problem. The computer time required for the phase and amplitude calculations is less than that required to Fourier-transform the data and clean the resulting map even for a 27 station array such as the VLA.

There are other ways to use the closure amplitudes. For example, a procedure is being developed at NRAO by Schwab[10], which attempts to ascribe phase and amplitude errors to specific telescopes by comparing the observed quantities with quantities derived from a model of the source. An iterative procedure is then used to obtain a self-consistent solution. This self-consistent solution is simply that in which the closure relations are satisfied, and thus this procedure is equivalent to hybrid mapping.

In the full hybrid mapping procedure, using closure amplitudes as well as closure phases, the absolute flux density and the position of the source are lost. However, the flux density can be recovered if a single baseline can be calibrated. The position of the source is more difficult to recover, and requires a properly phase stable interferometer to provide good phase information on a single baseline.

Blind tests

We have tested the usefulness of the closure amplitudes by performing blind tests in which sources were invented by one of us, and solved by another. In each case the solution was not revealed until a final map had been decided on, and a short description of the source had been written.

To simulate the real situation, gaussian noise was added vectorially to the simulated data to produce errors in both amplitude and phase. In addition, random factors were applied to the amplitudes to simulate the effects of bad weather, mispointing of antennas and gain errors at each telescope. The main effect of these errors was to decrease the amplitudes, as happens in practice. The random gain variations altered the amplitudes by factors of up to 3, making it impossible to map the sources by conventional means. The only effect on the closure amplitudes is to increase the noise. This increase is substantial in cases where the amplitude is severely reduced. The mapper was given the corrupted amplitude data, and the closure amplitude and closure phase data.

The first two tests simulated observations at 23 GHz with a network of six telescopes at Bonn, West Germany; Haystack,

Massachusetts; Green Bank, West Virginia; Algonquin, Ontario; the VLA, and Owens Valley Radio Observatory, California. These telescopes were chosen because they have both 23 GHz receivers and VLBI capability. Elevation limits of 80° were assumed for all telescopes except those at Bonn and OVRO, for which limits of 78° were used.

The objects set as blind tests are shown in Figs 2a, 3a and 4a. These have been convolved with a two dimensional gaussian beam which has the same FWHM as the central peak of the point source response of the array. The hybrid mapping solutions are shown in Figs 2b, 3b and 4b. In comparing these maps note that the correct solutions represent the maps which would be made with a perfect instrument, that is, with no random or systematic errors, and with complete (u, v) coverage.
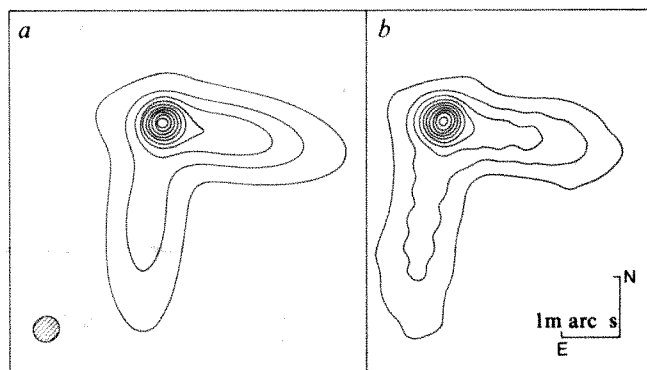
Fig. 4 As for Fig. 2, but for Test 3. Contour levels, 5, 15, 25, ... 95% of peak intensity. There are no negative contours ≤ −5%.

The first test is shown in Fig. 2. The conclusions of the mapper, before the solution was revealed to him, were: "The object is a simple double, with no structure outside this double above the 5% level in a field 6 m arc s square. The southern component is slightly brighter than the northern component. The northern component is slightly resolved, with size in the range 0.15–0.3 m arc s, the southern component is barely resolved, or unresolved. The separation of the double is 0.8 ± 0.03 m arc s, in PA $10.5° \pm 1.0°$".

These conclusions are largely correct, the only error being the statement that there is no structure outside the 5% contour of the double. There is a weak component to the north-east, which is in fact reproduced in the hybrid map, but the mapper believed this to be an artefact introduced by the hybrid mapping procedure, that is, he felt that a dynamic range of slightly less than 20 : 1 had been achieved, whereas in fact it is slightly better than this.

The second test is shown in Fig. 3. In this case the conclusions

of the mapper were: "The source consists [...] o bright components (A, B) and two components (C, [...] hich have brightest contours ~5% of the peak of A when c [...] ved with a 0.3 × 0.25 m arc s beam. Component A is unres [...] , although there is some evidence of an intervening compon [...] G) linking it to B. Component G is just picked up at the 5 [...] vel, and is probably real, however, more observations woul [...] needed to confirm this. Component B is unresolved along [...] 122° and resolved along PA 32°. Components C and D are [...] eved to be real. These show up more clearly when convolve [...] ith a larger beam. There is a small possibility that a very we [...] component (H) is real, but this just shows up at the 5% level—more telescopes are needed to give a bigger dynamic range to test this possibility".

In this case the two components about which the mapper expresses doubts (G, H) are not real, and there are two very weak components (E, F) which have been missed altogether. The dynamic range is slightly less than 20.

The final test is shown in Fig. 4. This was a more difficult test than the others because there were no strong features, such as deep minima, in the visibility data, and the area contained within the 5% contour covers a large number of beam areas. This test proved to be too difficult to map with the above six stations, because it is very highly resolved on the long baselines, with only 1/40th of the flux remaining, and as a result the signal-to-noise ratio is very low. The mapper realized that there was very little information on these baselines and attempted to map the object with the five North American stations only. He obtained a fairly good fit to the data in this way, but he concluded that more stations were needed to make a reliable map. A new set of data was produced from seven stations which included the above five North American stations and two additional hypothetical stations at Boulder, Colorado, and Fairbanks, Alaska. The information provided by these seven stations was sufficient to map the object (Fig. 4b). The conclusions of the mapper were:

"The object consists of a bright resolved core about 0.2–0.3 m arc s in size, with extensions to the west in PA 260° ± 1°, 3 m arc s long to the 5% contour, and to the south in PA 170° ± 1°, 3.5 m arc s long to the 5% contour. Both extensions are well resolved perpendicular to their long axes, with half-power widths of ~0.7 m arc s. There are no other components above the 5% contour level".

In each of these blind tests the hybrid map is a good representation of the object, and if these were real objects, most of the interesting astrophysics would be correctly inferred from the hybrid maps. The procedure did not fail in any case, that is, produce a final map with substantial errors.

Conclusion

The blind tests show that it is possible to make maps from completely uncalibrated visibility data in which both the amplitudes and the phases have substantial systematic errors and realistic random noise. A dynamic range of 20 can be obtained using an array of six or seven telescopes.

This procedure should prove invaluable for both VLBI and aperture synthesis mapping at high frequencies, where the effects of the atmosphere on both the phase and the amplitude can be severe. It opens up the wavelength range available for VLBI mapping through 1 cm into the millimetre region, where the most severe problems are atmospheric absorption and telescope pointing. The procedure is not limited to radio frequencies. The only limitation is that fringes of sufficiently high signal-to-noise ratio must be detectable in a time which is short compared with the time for phase and amplitude changes.

1. Jennison, R. C. thesis, Univ. Manchester (1953).
2. Jennison, R. C. *Mon. Not. R. astr. Soc.* **118**, 276 (1958).
3. Rogers, A. E. E. *et al. Astrophys. J.* **193**, 293 (1974).
4. Wilkinson, P. N., Readhead, A. C. S., Purcell, G. H. & Anderson, B. *Nature* **269**, 764 (1977).
5. Readhead, A. C. S. & Wilkinson, P. N. *Astrophys. J.* **223**, 25 (1978).
6. Readhead, A. C. S. in *IAU Symp.* No. 92 (1980).
7. Twiss, R. Q., Carter, A. W. L. & Little, A. G. *Observatory* **80**, 153 (1960).
8. Fomalont, E. B. & Wright, M. C. H. in *Galactic and Extragalactic Radio Astronomy* (eds Verschuur, G. L. & Kellermann, K. I.) (Springer, New York, 1974).
9. Rogers, A. E. E. in *Proc. 1980 int. Optical Computing Conf.* (in the press).
10. Schwab, F. R. in *Proc. 1980 int. Optical Computing Conf.* (in the press).

Single channel recordings of K⁺ currents in squid axons

Franco Conti

Laboratorio di Cibernetica e Biofisica, CNR I-16032 Camogli, Italy

Erwin Neher

Max-Planck-Institut für biophysikalische Chemie, D-3400 Göttingen, FRG

Ionic currents from individual K⁺ channels in squid axon membrane have been recorded. At hyperpolarizing membrane voltages, unit events occur as widely spaced rectangular pulses with short interruptions. The frequency of occurrence of the units increases strongly when the membrane is depolarized.

ELECTRICAL excitability is conferred on the nerve membrane through the voltage-dependent opening and closing of ion-specific membrane pores or channels[1,2]. Their existence has been established, on the basis of toxin binding[3] and by noise analysis[4–7]. Recently, it has become possible to record electrical signals directly from individual chemically activated channels[8]. These measurements confirmed many of the conclusions drawn from noise analysis and provided a very detailed kinetic

description of channel gating in acetylcholine-activated channels. Here, we report the measurement of discrete contributions to the ionic current in squid axons, displaying the kinetics of opening and closing of single K^+ channels. Some of the known properties of K^+ channels are illustrated on the single channel level, and some more detailed features of the elementary current contribution are indicated.

Experimental arrangement

Short sections (3–4 cm long) of large axons (diameter > 500 μm) were internally perfused with a technique similar to that developed by Tasaki et al.[9] as illustrated in Fig. 1. During preliminary perfusion with a standard K^+-rich solution, the axon was internally treated with pronase (Calbiochem grade B) at a concentration of 1 mg ml^{-1} until the inactivation of voltage-clamp Na^+ currents was reduced to about one-half[10]. This procedure usually took 10–15 min. The internal perfusion was then switched to a low ionic strength medium with the following composition (mEquiv. l^{-1}): 20 Na^+, 1 K^+, 2.15 phosphates, 15.8 F^-, 1 Cl^-, pH 7.8–8. The external medium was also changed to a high K^+ solution with the composition (mM): 460 KCl, 50 $CaCl_2$, 1 Tris-HCl, pH 8. Tetrodotoxin at 3×10^{-7} M was added
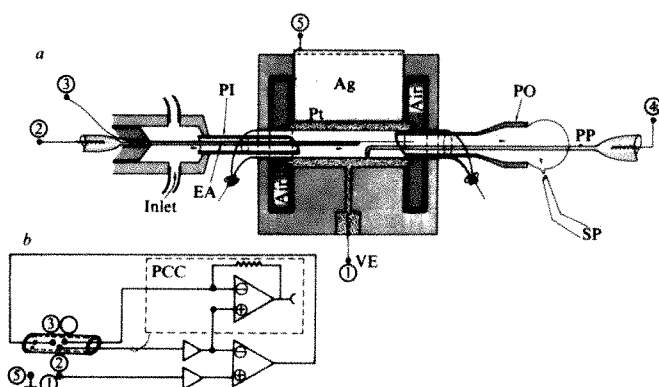
Fig. 1 Experimental set-up. *a*, Mechanical arrangement built onto a Perspex block with airgaps (Air), a platinum-coated silver block (Ag) for cooling and electrical grounding, a Ag–AgCl electrode for external voltage recording (VE), perfusion inlet cannula (PI) with a sliding internal electrode assembly (EA), perfusion outlet cannula (PO) and patch pipette (PP). The sliding electrode assembly (EA) consists of a 80-μm platinized wire for internal current injection and a 80-μm o.d. glass capillary with floating Pt wire for internal voltage recording. It is kept inside the PI cannula in the early stage of perfusion. Perfusion is started with the aid of a long outlet cannula (not shown) inserted through PO over the length of the axon until it overlaps with PI. During perfusion, constant hydrostatic pressure is maintained in the axon by maintaining a drop of constant diameter at the outlet through a suction pipette (SP). After longitudinal insertion, the patch pipette (PP) is laterally advanced towards the membrane by means of a motor-driven micromanipulator. The airgaps are 2 mm wide; the immersed part of the axon is ~10 mm long. *b*, Schematic diagram of standard voltage clamp and patch clamp circuit (PCC). The numbers refer to equivalent points in *a*.

to the external medium to suppress Na^+ currents. The chamber and the inflowing external solution were cooled to 5 °C using a Peltier cooler. An L-shaped pipette for patch recording was introduced longitudinally through a specially designed perfusion-outlet cannula (for details see Fig. 1). The patch pipette and the electrical circuit connected to it were similar to those described previously[8] except for the following modifications. The pipette had a 90° bend 100–200 μm from its end and a

prolonged shank ~15 mm long and 100–200 μm in diameter. This required the insertion of a 50-μm floating platinum wire for its whole length, to reduce the internal resistance. The pipette contained low ionic strength internal perfusion medium; its resistance was 50–100 MΩ. The virtual ground circuit and a shield to the pipette holder were driven by the output of the voltage follower to the internal (clamp) potential recording. Thus, the pipette interior followed changes of potential inside the axon. A compensation circuit was included to remove slow drifts in d.c.

The arrangement outlined above was dictated by considerations on the resolution of the measurement. A high driving force for K^+ ions is required in the voltage range of interest, where voltage-dependent gating occurs (−10 to −40 mV); thus, a positive equilibrium potential is indicated. To achieve low background noise, a good seal must be established between pipette and membrane and this rules out any approach from the outside, where the Schwann cell layer obstructs easy access, and suggests the use of low ionic strength internal solutions. In this way, seal resistances as large as 300 MΩ could be obtained.

On the other hand, the arrangement chosen has two serious disadvantages: low ionic strength implies large series resistance in the axon interior, and consequently, a strong spillover from the whole cell clamp arrangement into the patch measurement unless the internal voltage recording electrode is carefully positioned very close to the patch. Longitudinal insertion of the patch electrode brings with it a large stray capacitance between pipette interior and the axon, which increases the background noise at higher frequencies. Therefore, recordings are probably not meaningful above 500 Hz bandwidth and responses to jumps in membrane voltage are contaminated by large and long-lasting artefacts.

Effects of varying membrane potential

In the conditions chosen, reversal potentials for K^+ currents were between +70 and +100 mV as estimated from potential measurements after removal of K^+ inactivation. For a macroscopic characterization, the axon was normally kept at its steady-state resting potential, which ranged between +50 and +70 mV. It was intermittently clamped for short periods (≈1 s) to −50 mV, to which depolarizing steps of 30–120 mV amplitude were added. K^+ inward currents developed during the pulses and were followed by large, long-lasting inward tail currents on return to −50 mV. In Fig. 2c, the amplitudes of the macroscopically measured tails are plotted against the membrane voltage during the preceding pulse. This yields, basically, the steady-state activation curve of the K^+ system. The curve is shifted along the voltage axis, as compared with the standard Hodgkin–Huxley axon[1]. This shift is probably the effect of the low internal ionic strength (in analogy to ref. 11).

On the patch records, dramatic changes can be observed when the membrane voltage is shifted across the range of channel activation. Starting from a very strongly depolarizing voltage, that is, one close to the K^+ equilibrium potential, small, slow fluctuations are observed. They increase in size as the membrane voltage is slowly made more negative (Fig. 2a, traces at +34, +17 and −8 mV). However, within a narrow voltage range, fluctuations decrease very rapidly (Fig. 2a, traces at −19 mV and below). They appear as discrete waveforms at voltages lower than −10 mV, and become progressively more rare as membrane voltage is further lowered. We interpret these discrete, one-sided (inwardly directed) fluctuations as contributions from individual K^+ channels, which cannot be seen easily at more depolarizing voltages because there are many channels on the patch which are open simultaneously. Their openings and closings overlap to give large fluctuations. However, at hyperpolarizing voltages most channels are closed. The rare event of channel opening can be observed above a quiet background.

Figure 2b shows the variance, σ^2, of traces, like those in Fig. 2a plotted against voltage V, together with the expectation of a very simple model: given that there are N active, independently
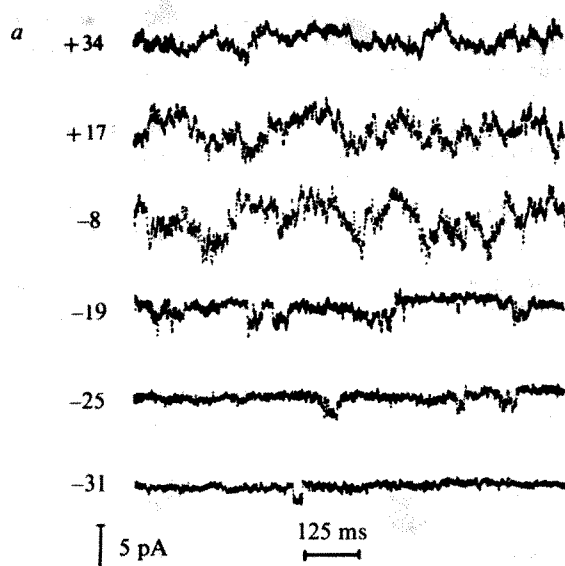
Fig. 2 *a*, Recordings of patch current at different membrane potentials (as indicated in mV). Temperature, 5.5 °C, pipette resistance before approaching the membrane, 100 MΩ, after approach, 280 MΩ. *b*, Variance of segments like those in *a* (bandwidth, 250 Hz) plotted against membrane potential. Membrane voltage was changed in irregular steps several times across the whole voltage range in both directions. Different symbols refer to different sweeps. *c*, Tail currents at −50 mV holding potential as a function of membrane potential during the preceding test pulse, which was 30 ms in duration. A small correction was applied to the three lowermost points to account for incomplete settling of the current response during the test pulses. The curve in *c* was drawn by eye through the experimental points and was used to represent $P(V)$ for the calculation of variance (equation (1)) in *b*. Only one free parameter could be adjusted to fit the data in *b*, which was the product $N\gamma^2$ of equation (1). It was given a value of 2×10^{-21}. This, together with $\gamma = 17$ pS (see below), yields an N of 7. Thus, there were about seven active channels under the pipette.
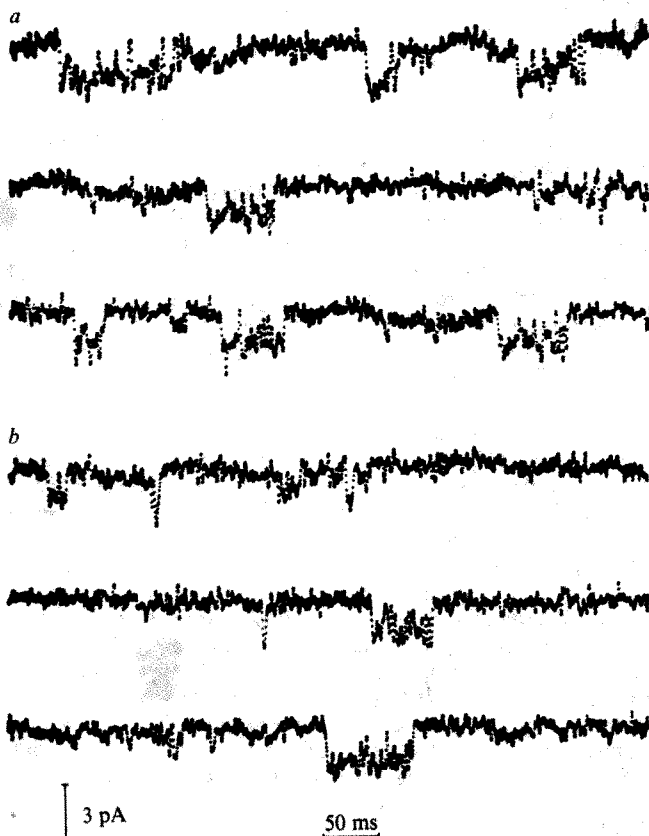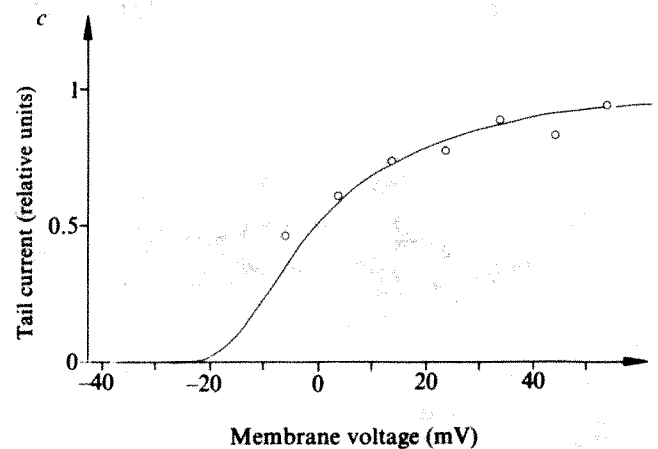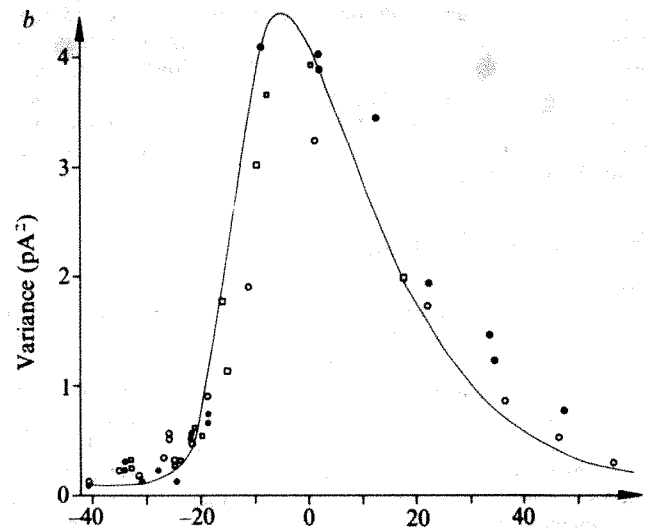
Fig. 3 Several traces of patch recordings at higher time resolution. *a* was taken at −25 mV membrane potential, *b* at −35 mV. The elementary events seem to be bursts of closely spaced pulses. Histograms of open times and closed times of this and nine similar records (a total of 270 bursts) were calculated. The open times were distributed approximately exponentially with a mean open time of 6.1 ms. The closed times had a bimodal distribution: short intervals corresponding to interruptions within a burst were superimposed on an approximately exponential distribution of long intervals corresponding to intervals between bursts. The two classes of intervals could be well separated. There were, on average, 0.65 short intervals per long interval. However, the mean duration of the short intervals was close to the time resolution limit of the measurement. Therefore, a great number of short intervals had probably been missed in the analysis. Their number was estimated by extrapolation of the closed time histogram, assuming that the short intervals are distributed exponentially. This gave a corrected number of 1.8 interruptions per burst. For consistency, this correction necessitated a further correction regarding the mean open time of the short pulses, because a given burst was then assumed to be divided into more pulses. The corrected value for the mean open time was 3.5 ms.

operating channels, each with a probability $P(V)$ of being in its open state with conductance γ, the variance of the current record should be

$$\sigma^2 = \sigma_b^2 + N(1 - P(V))P(V)\gamma^2(V - V_K)^2 \qquad (1)$$

where V_K is the K^+-equilibrium potential, and σ_b^2 the background noise in the absence of any channel openings. The solid line in Fig. 2b is calculated according to equation (1) with $P(V)$ derived from Fig. 2c (see Fig. 2 legend) assuming V_K to be $+90$ mV and σ_b to be constant. Various factors can make the prediction of equation (1) inaccurate: (1) σ_b is probably not a constant; (2) the macroscopic activation curve was obtained in conditions of roughly constant K^+ inactivation[12], whereas changes in K^+ inactivation, although expected to be small in the voltage range covered, may have occurred during the long-lasting polarizations of Fig. 2a; (3) a constant value of γ is not appropriate for characterizing the current–voltage relationship of K^+ channels for strongly asymmetric transmembrane ionic concentrations such as those used in the present study. The fit of the data of Fig. 2b with the solid line is therefore as good as it can be and is evidence that the fluctuations of Fig. 2a are indeed derived from the random open–close transitions of K^+ channels.

Properties of single channel fluctuations

Regarding the shape of the elementary event, one can see waveforms resembling square pulses at hyperpolarizing voltages (see, for instance, Fig. 2a, lowermost trace). Their mean amplitude is approximately 1.6 pA (range 1.4–2.0 pA). At closer inspection, however, the majority of the waveforms show short interruptions and appear as bursts of short pulses. Examples are seen in Fig. 2a (trace at -25 mV), and, at better resolution, in Fig. 3. Statistical analysis of time intervals in the records[13], correcting for limited time resolution (see Fig. 3 legend), shows that there are on average 2.8 short pulses per burst, each with a mean open time of about 3.5 ms. The mean duration of the interruptions is 1.3 ms. Thus, a burst lasts, on average, 12 ms. These numbers are obtained from pooled data at membrane potentials between -20 and -35 mV. In this range, elementary events are rare enough to be well separated in time. The probability of any channel being in the open state is >0.03 (see Fig. 2c). The frequency of appearance of bursts increases strongly with voltage. The other parameters given above, however, do not change significantly in the narrow voltage range studied. At more strongly depolarizing potentials, whenever elementary events overlap, it is virtually impossible to reach any conclusion about the waveform, due to the flickering nature of the elementary event and limited resolution.

The records shown above come from one of the patches with the highest activity that we have encountered. Generally, the degree of activity varied widely, even on patches (≈ 1 μm diameter) which were immediately adjacent. A good fraction of patches did not, indeed, show any activity at all. This inhomogeneity enabled us also occasionally to observe discrete fluctuations at more strongly depolarized potentials. However, these were chance observations and were not further analysed.

Analysis of results

The examples given clearly show that it is possible to resolve single channel currents of the squid axon K^+ system, although, compared with other single channel measurements, such as

endplate channels, it is much harder to obtain adequate resolution due to: (1) difficulty in obtaining good contact between the glass pipette and the inner membrane surface, (2) high current density in squid axon membrane and numerous associated artefacts, and (3) uniform activation of channels over both the seal and patch area, producing excess background noise and non-uniformity in single channel amplitude.

Unit current values were as large as 2 pA at about -25 mV. Thus, assuming ohmic behaviour and a reversal potential of $+90$ mV, a single channel conductance of 17.5 pS is obtained. This value cannot be considered adequate to describe K^+ channel conductances in normal physiological solutions because our measurements were done in very unphysiological and asymmetric ionic conditions. Assuming that the IV characteristic of open channels obeys the constant field equation, one can calculate from the current value above a single channel K^+ permeability of $p = 2.85 \times 10^{-14}$ cm^3 s^{-1}. With this value, the chord conductance at -50 mV, which is expected to describe physiological conditions, is 9–11 pS, assuming p_{Na}/p_K values of 0.01 or 0.05, respectively[14], and an intracellular K^+ concentration of 400 mM (ref. 15). This is very close to that obtained from noise analysis[4].

The mean channel open time (burst duration) of 12 ms seems rather long. However, it has also been observed in macroscopic measurements that K^+ tail currents are prolonged in conditions of high extracellular K^+ (ref. 16). For instance, at -50 mV, we observed exponentially decaying tail currents with $\tau = 8$ ms after depolarizing pulses. Thus, the duration of the elementary events is in the time range expected from macroscopic currents.

The short interruptions within a burst are indicative of some closed channel state which is in relatively fast equilibrium with the open state. For a tentative interpretation, a sequential reaction scheme is assumed:

$$\cdots \underset{k_{-2}}{\overset{k_2}{\rightleftharpoons}} C_2 \underset{k_{-2}}{\overset{k_2}{\rightleftharpoons}} C_1 \underset{k_{-1}}{\overset{k_1}{\rightleftharpoons}} O \qquad (2)$$
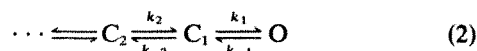
where C_2 and possible other states to its left are closed states, C_1 is a temporarily or transiently closed state, and O is the open state. Bursts of activity are predicted if k_2 is much smaller than all the other rates. These, then, can be calculated easily from our data. The mean number, n, of interruptions within a burst is k_1/k_{-2} (ref. 17) and the mean time of the short interruptions within a burst is $1/(k_{-2} + k_1)$, which is the mean lifetime of state C_1 (refs 13, 17). With the numbers given above, we obtain $k_{-2} = 274$ s^{-1}, $k_1 = 493$ s^{-1} and $k_{-1} = 285$ s^{-1}. The Hodgkin–Huxley model for the K^+ currents can be considered a special case of a sequential model[18] like scheme (2). As such, it predicts a grouped appearance of pulses. However, quantitatively, the predictions are very different from what is observed. For instance, the mean number, $\bar{n}$, of interruptions within a group would be $\bar{n} = k_1/k_{-2} = \alpha_n/3\beta_n = n_\infty/3(1 - n_\infty)$, where α_n, β_n and n_∞ are the Hodgkin–Huxley variables. For $n_\infty \leq 0.03^4 \approx 0.4$, this is smaller than 0.25. The number measured, in contrast, is 1.8. Thus, a Hodgkin–Huxley type mechanism cannot be invoked to explain the single channel measurements.

1. Hodgkin, A. L. & Huxley, A. F. *J. Physiol., Lond.* **117**, 500–544 (1952).
2. Hille, B. in *Membranes: Lipid Bilayers and Biological Membranes: Dynamic Properties* Vol. 3 (ed. Eisenman, G., 255–323 (Dekker, New York, 1975).
3. Ritchie, J. M. & Rogart, R. B. *Rev. Physiol. biochem. Pharmac.* **79**, 1–50 (1977).
4. Conti, F., De Felice, L. J. & Wanke, E. *J. Physiol., Lond.* **248**, 45–82 (1975).
5. Begenisich, T. & Stevens, C. F. *Biophys. J.* **15**, 843–846 (1975).
6. Conti, F., Hille, B., Neumcke, B., Nonner, W. & Staempfli, R. *J. Physiol., Lond.* **262**, 699–727 (1976).
7. Sigworth, F. J. *Nature* **270**, 265–267 (1977).
8. Neher, E., Sakmann, B. & Steinbach, J. H. *Pflügers Arch. ges. Physiol.* **375**, 219–228 (1978).
9. Tasaki, I., Watanabe, A. & Takenaka, T. *Proc. natn. Acad. Sci. U.S.A.* **48**, 117–1184 (1962).
10. Armstrong, C. M., Bezanilla, F. & Rojas, E. *J. gen. Physiol.* **62**, 375–391 (1973).
11. Chandler, W. K., Hodgkin, A. L. & Meves, H. *J. Physiol., Lond.* **180**, 821–836 (1965).
12. Ehrenstein, G. & Gilbert, D. L. *Biophys. J.* **6**, 553–566 (1966).
13. Neher, E. & Steinbach, J. H. *J. Physiol., Lond.* **227**, 153–176 (1978).
14. Bezanilla, F. & Armstrong, C. M. *J. gen. Physiol.* **60**, 558–608 (1972).
15. Keynes, R. D. & Lewis, P. R. *J. Physiol., Lond.* **114**, 151–182 (1951).
16. Stuehmer, W. & Conti, F., in preparation.
17. Colquhoun, D. & Hawkes, A. G. *Proc. R. Soc.* **B199**, 231–262 (1977).
18. Armstrong, C. M. *J. gen. Physiol.* **58**, 413–437 (1971).

Model for antenatal diagnosis of β-thalassaemia and other monogenic disorders by molecular analysis of linked DNA polymorphisms

P. F. R. Little*, G. Annison, S. Darling & R. Williamson

Biochemistry Department, St Mary's Hospital Medical School, University of London, London W2 1PG, UK

L. Camba & B. Modell

Departments of Paediatrics and Obstetrics, University College Hospital Medical School, London WC1, UK

Polymorphisms of DNA restriction sites within the human fetal globin genes have been used to identify chromosomes that carry β-thalassaemia genes in individuals heterozygous for this disease. This has allowed an antenatal diagnosis for β-thalassaemia to be carried out by observation of the pattern of the inherited polymorphism of a linked DNA sequence not involved in the genetic pathogenesis of the disease. In the populations we have investigated there is no constant pattern of polymorphism that segregates with the β-thalassaemia gene. The use of linked polymorphisms should, therefore, be applicable to antenatal diagnosis both of β-thalassaemia and of any other single-gene defect for which there is a DNA probe specific for a sequence linked to the affected locus.

GENETICALLY determined human diseases are becoming increasingly important in modern medical practice. The incidence of monogenic disorders is geographically variable, but in Europe approximately 1 in 100 of the newborn population is affected[1]. There are now two clinical approaches to such disorders: treatment of symptoms of the disease or prevention of the disease by antenatal diagnosis and therapeutic abortion.

Antenatal diagnosis of a monogenic disorder is generally attempted by obtaining fetal cells which express the protein abnormality. For many enzyme defects, antenatal diagnosis is by analysis of enzyme activity in fetal fibroblasts. These may be isolated from the amniotic fluid by the relatively simple procedure of amniocentesis. This strategy is possible for about 60 of more than 1,000 known single-gene disorders[2,3]. However, it is not possible for β-thalassaemia as fibroblasts do not synthesize haemoglobin. For the haemoglobinopathies it is necessary to obtain fetal red blood cells, a technically difficult procedure which carries a 7% risk of abortion[4]. A sample of fetal blood is obtained from a placental vessel and its ability to synthesize β-globin estimated *in vitro*[5]. The β-thalassaemias are characterized by low or absent synthesis of β-globin chains.

The thalassaemias also provide an example of an alternative approach to antenatal diagnosis—the direct analysis of genes in DNA isolated from fetal fibroblasts obtained by amniocentesis. This analysis is most straightforward when the disease is caused by a gene deletion, as for α-thalassaemia[6-11] or δβ°-thalassaemia[12], but such an approach is not possible for the common forms of β-thalassaemia, as the β-globin gene is present[13,14].

Kan and Dozy used a different approach for the antenatal diagnosis of sickle-cell disease[15,16]. They demonstrated linkage between the sickle-cell globin mutation in the β-globin gene and a restriction site polymorphism approximately 5 kilobases to the 3' side of the gene, using a plasmid containing the β-globin gene sequence as a probe.

We show here that it is possible to perform an antenatal diagnosis for β-thalassaemia by detecting restriction enzyme site polymorphisms that are shown to be segregating within the family at risk. The polymorphism is detected as variation in the band pattern obtained in a Southern blot after digestion with the

appropriate restriction enzyme[17-19]. We have used a probe, not for the affected gene (β-globin) but for a neighbouring gene, γ-globin. In principle this could allow the antenatal diagnosis of any disease caused by a single-gene defect for which there exists a DNA probe specific for the affected locus, or for a locus close enough to be linked genetically.

Results

Jeffrys[20] and Tuan *et al.*[21] have used Southern blot hybridization to show that the two human fetal globin genes are polymorphic for a restriction site for the enzyme HindIII (and thus HsuI, which recognizes the same AAGCTT sites)[22]. Either the ^{G}γ- or ^{A}γ-globin gene, or both, may contain a cleavage site, at the same position within the large intron (Fig. 1)[23].

We have studied families and individuals from Cypriot, Italian and Indian thalassaemic populations. γ-Gene polymorphisms were identified on the chromosomes carrying the thalassaemia genes in a given family, and antenatal diagnosis was then performed by detecting the pattern of chromosome-specific polymorphism inherited by the fetus. Diagnosis of thalassaemics was by familial
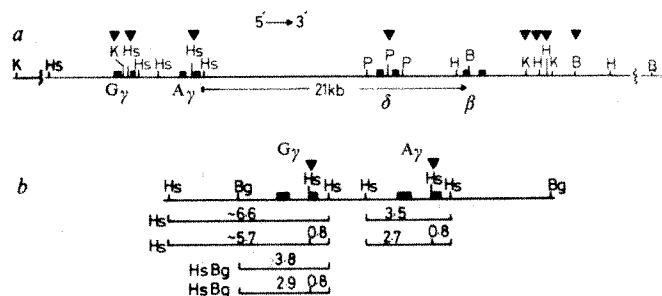
Fig. 1 *a*, The structure of the human ^{G}γ-^{A}γ-δ-β-globin gene loci[26-30]. The positions of polymorphic restriction sites marked are taken from refs 20, 21 and 29 for *Pst*I and *Hsu*I (*Hin*dIII), from ref. 16 for *Hpa*I, from ref. 31 and R. A. Flavell (unpublished data) for *Kpn*I and from Y. W. Kan (unpublished data) for *Bam*HI. Only a single intron is shown within each structural gene; the position of the smaller intron is now shown. Hs, *Hsu*I (*Hin*dIII); K, *Kpn*I; P, *Pst*I; B, *Bam*HI; H, *Hpa*I. Sites marked ▼ are polymorphic. Sizes are in kilobase pairs. *b*, Sizes of fragments generated by *Hsu*I and *Bgl*II sites around and within the ^{G}γ- and ^{A}γ-globin genes. Hs, *Hsu*I (*Hin*dIII); Bg, *Bgl*II.

* Present address: Division of Biology, California Institute of Technology, Pasadena, California 91125.
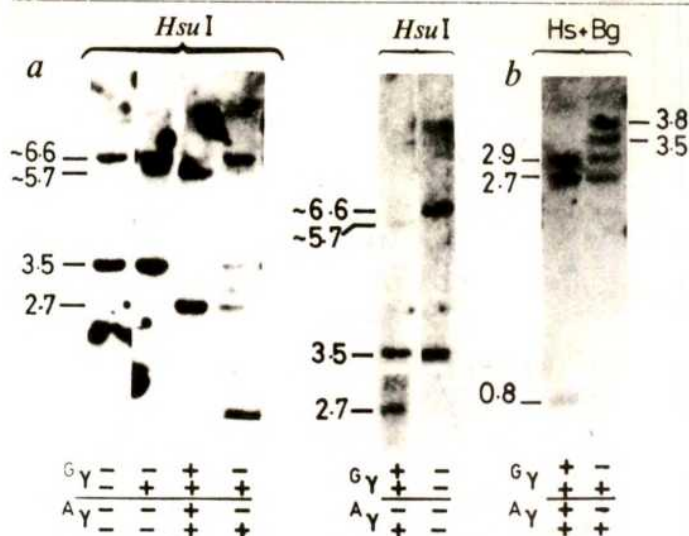
Fig. 2 Autoradiographs of Southern blots demonstrating polymorphism of *Hsu*I sites associated with the $^G\gamma$- and $^A\gamma$-globin genes. *Hsu*I digests of DNA from people with restriction patterns G−−/A−−, G+−/A−−, G++/A++, G+−/A+− and G++/A+− (where G+− indicates that one $^G\gamma$-globin gene has the *Hsu*I site and one does not, and so on) are shown (*a*) as well as *Hsu*I/*Bgl*II double digests of the G++/A++ and G+−/A+− persons (*b*). 10 μg of each human DNA was digested to completion and run on a 1% agarose gel. Slot dimensions were 0.75×0.2 cm, voltage gradient was 2 V cm^{-1}, run time was 17 h and the running buffer was 10 mM Tris, 0.25 M NaAc, 1 mM EDTA, pH 7.7 supplemented with 0.5 μg ml^{-1} ethidium bromide. After running gels were denatured, neutralized, transferred and filters hybridized to radioactive *p*H γGl, a pCRI recombinant plasmid containing 500 base pairs of DNA was made on a template of mRNAγ (ref. 32). All methods are as described in refs 17, 26, 27. Growth and preparation of the plasmid was at Category I* as recommended by the UK Genetic Manipulation Advisory Group.

history, in particular the existence of a homozygous thalassaemic child, and also by red cell indices and HbA₂ levels. No attempt was made to classify the β-thalassaemia further.

The fragment patterns generated by the presence or absence of particular *Hsu*I sites associated with the γ-globin genes are shown in Fig. 2. To confirm that the pattern of $^G\gamma$-fragments has been correctly interpreted, we have also analysed double digests with *Hsu*I plus *Bg*/II. Figure 1*b* shows the location of the *Bg*/II site within the larger ($^G\gamma$)*Hsu*I fragment. The double digest fragment pattern for persons identified by *Hsu*I digest as having restriction sites G+− and G++ is precisely as predicted (Fig. 2).

We have examined individual families with thalassaemia to determine the familial pattern of *Hsu*I polymorphisms linked to the β-thalassaemia genes. Restriction sites of two families are illustrated in Fig. 3. Family A, of Cypriot origin, consists of a β-thalassaemia carrier mother (pattern G+−/A−−), a carrier father (G+−/A+−), a carrier daughter (G+−/A+−) and a homozygote β-thalassaemic son (G−−/A−−). Genotypes may be assigned as follows: the son can only be $\dfrac{-\,-}{-\,-}$, which indicates both parents must contain a haplotype $-\,-$. Hence the mother can only be $\dfrac{+\,-}{-\,-}$, the father $\dfrac{+\,+}{-\,-}$ and the daughter $\dfrac{+\,+}{-\,-}$. As the son is a homozygous β-thalassaemic his genotype can only be $\dfrac{-\,-\ thal}{-\,-\ thal}$ and the mother $\dfrac{+\,-}{-\,-\ thal}$, the father $\dfrac{+\,+}{-\,-\ thal}$ and the daughter $\dfrac{+\,+}{-\,-\ thal}$.

Family B consists of a β-thalassaemia carrier mother (G+−−/A−−−) of Italian origin, a carrier father (G+−−/A+−−), a homozygous β-thalassaemic daughter (G++/A+−) and a carrier son (G+−

/A−−). The daughter can only have a genotype $\dfrac{+\,-}{+\,+}$, the son $\dfrac{+\,-}{-\,-}$ and the mother $\dfrac{+\,-}{-\,-}$. The father could be either $\dfrac{+\,+}{-\,-}$ or $\dfrac{+\,-}{-\,+}$. The former genotype must be correct as this is the only genotype that contains the haplotype $+\,+$ that is inherited by the daughter. Thalassaemia genes are assigned as follows. The daughter can only be $\dfrac{+\,-\ thal}{+\,+\ thal}$. Thus the father must be $\dfrac{-\,-}{+\,+\ thal}$. The mother must have donated the $+\,-$ chromosome and therefore must be $\dfrac{-\,-}{+\,-\ thal}$. The son has therefore inherited $\dfrac{-\,-}{+\,-\ thal}$.

From these data it is clear that it is possible to follow a β-thalassaemia gene through some families by identifying the *Hsu*I γ-globin gene polymorphisms.

We studied an Asian Indian family requesting antenatal diagnosis. The family comprised the mother and father, both of whom are β-thalassaemia carriers with restriction patterns G+−/A−−, and a homozygous β-thalassaemic child who is also G+−/A−− (Fig. 4). Amniocentesis and fetal blood sampling were carried out on the mother. DNA from 20 ml of amniotic fluid was analysed and found to be G−−/A−−. As we know that the homozygous thalassaemic child has a restriction pattern G+−/A−−, and therefore a genotype $\dfrac{+\,-\ thal}{-\,-\ thal}$, we can conclude that the fetus must be β-thalassaemic carrier, genotype $\dfrac{-\,-\ thal}{-\,-}$. It is not possible to determine the thalassaemic genotypes of the parents: the son has the genotype $\dfrac{+\,-\ thal}{-\,-\ thal}$, but as both parents have the same genotype, $\dfrac{+\,-}{-\,-}$, it is impossible to determine the parental origin of the β-thalassaemia chromosomes. One parent must be $\dfrac{+\,-\ thal}{-\,-}$, the other $\dfrac{+\,-}{-\,-\ thal}$.
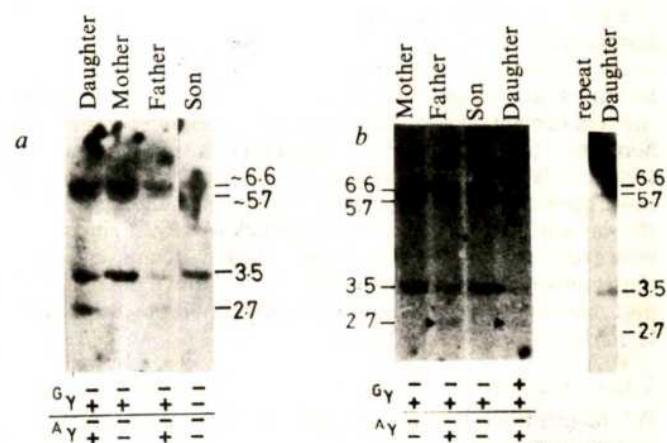
Fig. 3 Inheritance of *Hsu*I polymorphisms. DNA samples from families A and B respectively were analysed for intragenic *Hsu*I sites as described in Fig. 2 legend. Restriction patterns observed are detailed. Sizes are in kilobase pairs.

Analysis of the fetal blood sample carried out in parallel showed that the diagnosis obtained using direct gene linkage analysis is correct (Fig. 5). The fetus was synthesizing β-globin at a level appropriate to a β-thalassaemia carrier, with a β/γ synthetic ratio of 0.039. In our laboratory the β/γ ratio for homozygous β-thalassaemia is generally not greater than 0.017, the β-thalassaemia carrier β/γ ratio is in the range 0.022–0.05 and the normal range is between 0.045 and 0.10 (unpublished data). The fetus has not yet come to term.
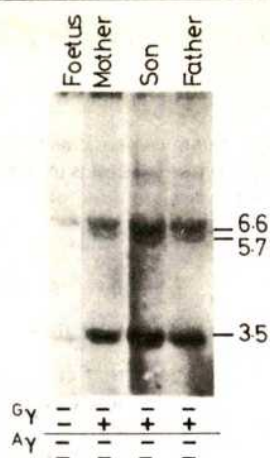
Fig. 4 Antenatal diagnosis of a case of β-thalassaemia. DNA from an Indian family and their unborn child was analysed for γ-globin intragenic *Hsu*I sites. DNA from fetal cells was obtained as follows. Amniotic fluid (20 ml) was centrifuged at 10,000*g* for 10 min. The pellet of cells was taken up in 200 μl 0.15M NaCl, 0.1M EDTA, *p*H 10.5. The cells were lysed by adding SDS to 0.1% (w/v). Proteinase K was added to 10 μg ml⁻¹ and the suspension incubated at 37 °C for 4 h. The DNA was extracted with an equal volume of phenol (redistilled under N₂ gas and equilibrated with 0.15M NaCl, 0.1M EDTA *p*H 10.5), and then with an equal volume of chloroform/octan-2-ol (24 : 1 v/v). DNA was precipitated with two volumes of ethanol. The whole of the DNA sample (estimated at between 2–5 μg) was digested with *Hsu*I and run on the transfer gel and analysed as described in Fig. 2 legend.

Population considerations

Human populations differ in frequencies of polymorphic sites[24]. Should this be the case for the *Hsu*I polymorphisms studied here, and if populations exist that have low frequencies of these polymorphisms, then this would limit their general usefulness for diagnosis.

We have analysed the *Hsu*I restriction sites of 21 Cypriots, 31 Italians and 14 Indians (Table 1). All are thalassaemia carriers. It is not possible to assign genotypes to all restriction patterns, nor is it possible in every case to identify the chromosomes carrying the thalassaemic gene. Therefore, we cannot draw conclusions about the frequency of polymorphisms on the normal compared to the thalassaemic chromosomes. The data are too sparse for more general conclusions to be made regarding the frequency of the various genotypes, and whether linkage disequilibria exist. However, it is likely that the greater degree of heterogeneity of the Italian thalassaemic population would make the diagnostic approach we have used more commonly applicable than with the Indian or Cypriot populations.

Conclusions

We have shown that it is possible to use two specific linked polymorphisms that are present in a particular family to perform an antenatal diagnosis by DNA restriction fragment analysis. The method described here may be applied to any defective gene for which a probe exists, or where a probe for an adjacent gene exists, as in this case. The only condition must be that either a homozygote or a normal child must have been born to the family at risk, or that the disease be diagnosable in a heterozygous state to allow identification of the affected chromosome by family analysis. There are certain couples without appropriate restriction sites, for whom chromosomal assignments are not possible.

Most genetic diseases do not have a high incidence, and it will be difficult to establish the existence of the linkage disequilibria seen for thalassaemia and sickle cell anaemia. Therefore, it seems likely that antenatal diagnosis of most gene defects will not be possible using a single linked polymorphism. The estimate of Jeffrys[21] that 1 base in 100 is different between any two

Table 1 Frequency of occurrence of *Hsu*I polymorphisms in the γ-globin genes in various thalassaemia carrier populations

Restriction pattern	Cypriot	Italian	Indian
G++/A++	—	4	—
G++/A+−	—	2	1
G++/A−−	—	1	—
G−−/A−−	13	6	2
G+−/A−−	7	6	7
G+−/A+−	1	12	4
Frequency A+	0.023	0.35	0.18
G+	0.19	0.52	0.46
Total (individuals)	21	31	14

Frequency of occurrence of the *Hsu*I site in the ᴬγ- and ᴳγ-globin genes were calculated from restriction digest patterns shown in Fig. 2.

healthy humans who are not related suggests that any coding gene, defective or normal, will be surrounded by a unique set of DNA polymorphisms. The technique we have described here should be generally applicable for monogenic human genetic diseases.

Two questions remain. First, how closely linked do polymorphisms have to be to reduce the risk of misdiagnosis due to meiotic recombination? There is no specific information on the rate of crossing over that would be expected over the 20-kilobase section spanning the ᴬγ- to β-globin gene distance. It has been estimated that meiotic recombination occurs with a frequency of 1 per 10⁸ base pairs per generation[25]. From this it is clear that the chance of misdiagnosis due to crossing over in a single generation is extremely small. It is not yet possible to estimate the effect of mitotic recombination.

Second, how common are DNA polymorphisms in the human genome? The positions of eight polymorphisms which have been detected using DNA probes specific for the γ- or β-, δ-globin genes are shown in Fig. 1. The low frequency of recombination should allow large pieces of DNA to be scanned for useful polymorphisms. The human β-like globin locus is about 50 kilobases long. Distances greater than 1,000 kilobases could in principle be scanned for linked polymorphisms using cloned genomic DNAs or cDNAs as probes.
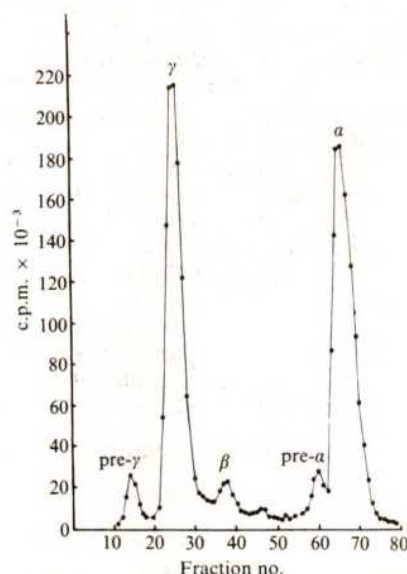
Fig. 5 CM-Cellulose elution pattern of globin proteins from fetus diagnosed in Fig. 4. Red cells obtained by fetoscopic fetal blood sampling were labelled with ³H-leucine, lysed, globin prepared and co-chromatographed with cold cord blood carrier globin on CM32 columns in 8M urea and a phosphate gradient according to ref. 33. The γ-, β- and α-globin peaks were located by optical density (not shown) and by their radioactivity. Ratios were determined as described elsewhere. (Ref. 5 and Matsakis *et al.* in preparation.)

Note added in proof: Kan et al. have recently shown[36] that β^0—thalassaemia in Sardinia may be diagnosed by the presence of BamHI site 9.3 kilobases to the 3' side of the β-globin gene. Unaffected Sardinians normally have a BamHI site at 22 kilobases from the β-globin gene.

1. Carter, C. O. J. med. Genet. 14, 316–320 (1977).
2. Siggers, D. C. in Prenatal Diagnosis of Genetic Disease, 20–22 (Blackwell, Oxford, 1978).
3. McKusick, V. A. Mendelian Inheritance in Man. Catalogues of Autosomal Dominant, Autosomal Recessive and X-Linked Phenotypes 4th edn (Johns Hopkins Hospital University Press, Baltimore, 1974).
4. Fairweather, D. V. I. et al. Br. med. J. 1, 350 (1978).
5. Alter, B. P. et al. New Engl. J. Med. 295, 1437–1443 (1976).
6. Ottolenghi, S. et al. Nature 251, 389–392 (1974); Taylor, J. M. et al. Nature 251, 392–393 (1974).
7. Orkin, S. H. et al. Cell 17, 33–42 (1979).
8. Embrey, S. et al J. clin. Invest. 63, 1307–1310 (1979).
9. Dozy, A. M. et al. Nature 250, 605–607 (1979).
10. Kan, Y. W. et al. New Engl. J. Med. 295, 1165–1167 (1976).
11. Dozy, A. M. et al. J. Am. med. Ass. 241, 1610–1612 (1979).
12. Orkin, S. H. et al. New Engl. J. Med. 299, 166–172 (1978).
13. Orkin, S. H. et al. Proc. natn. Acad. Sci. U.S.A. 76, 2400–2404 (1979).
14. Flavell, R. A. et al. Nucleic Acids Res. 6, 2749–2760 (1979).
15. Kan, Y. W. & Dozy, A. M. Lancet ii, 910–912 (1978).
16. Kan, Y. W. & Dozy, A. M. Proc. natn. Acad. Sci. U.S.A. 75, 5631–5635 (1978).
17. Southern, E. M. J. molec. Biol. 98, 503–517 (1975).
18. Botchan, M., Topp, W. & Sambrook, J. Cell 9, 269–287 (1976).
19. Jeffrys A. J. & Flavell, R. A. Cell 12, 429–439 (1977).
20. Jeffrys, A. J. Cell 18, 1–10 (1979).
21. Tuan, D. et al. Nucleic Acids Res. 6, 2519–2544 (1979).
22. Roberts, R. J. CRC crit. Rev. Biochem. 123–164 (1976).
23. Gilbert, W. Nature 271, 501 (1978).
26. Flavell, R. A. et al. Cell 15, 25–41 (1978).
27. Little, P. F. R. et al. Nature 278, 227–231 (1979).
28. Fritsch, E. F., Lawn, R. M. & Maniatis, T. Nature 279, 598–603 (1979).
29. Lawn, R. M. et al. Cell 15, 1157–1174 (1978).
30. Bernards, R. et al. Proc. natn. Acad. Sci. U.S.A. 76, 4827–4831 (1979).
31. Ramirez, F. et al. Nucleic Acids Res. 1147–1162 (1979).
32. Little, P. F. R. et al. Nature 273, 640–643 (1978).
33. Weatherall, D. J., Clegg, J. B. & Naughton, M. A. Nature 208, 1061–1065 (1965).
34. Bodmer, W. F. & Cavalli-Sforza, L. L. in Genetics, Evolution and Man (W. H. Freeman, San Francisco, 1976).
35. Kurnit, D. M. Lancet i, 104 (1979).
36. Kan, Y. W. et al. New Engl. J. Med. 302, 185–188 (1980).

Sea urchin histone mRNA termini are located in gene regions downstream from putative regulatory sequences

Christopher Hentschel, Jean-Claude Irminger, Philipp Bucher & Max L. Birnstiel

Institut fur Molekularbiologie II der Universität Zürich, Hönggerberg, 8093 Zürich, Switzerland

S_1 *nuclease mapping of the Psammechinus miliaris embryonic histone mRNAs locates the 5' termini in or adjacent to a short sequence homology (5'pyCATTCpu3') downstream from the putative RNA polymerase II regulatory sequence (5'TATAAATA3') or related sequences. The 3' termini map just after a sequence containing GC-rich hyphenated dyad symmetry, a feature of most known terminator sequences.*

THE rapid growth in recombinant DNA technology has led to the isolation of an increasing number of cloned eukaryotic genes, and in many cases the DNA sequences of substantial areas of the genes have been determined. The mode of action of functional elements of the sequence remains unclear. Analogy with prokaryotic systems, however, leads us to expect that several non-coding regulatory sequences are involved in such functions as transcription, RNA maturation, translation and DNA replication. In eukaryotes, one might also expect to find a set of more complex regulatory sequences involved in nucleo-cytoplasmic transport, topological segregation of RNA species in the cell, and even in the ontogenic regulation of genes in specific cells of the fertilized egg.

We have described several available approaches towards the identification of putative regulatory sequences using the sea urchin histone gene clusters. Because they are repeated and hence probably comprise a complete functional unit, these provide a particularly opportune starting material[1,2]. Two prerequisite sequential analytical steps are envisaged: (1) RNA mapping coupled with comparative sequence analysis to help identify sequence elements which are conserved in equivalent topological locations of the genes, and hence are presumably important in some way to their expression, and (2) functional testing of the proposed regulatory sequence and their mutant counterparts in a surrogate genetic system which operationally recognizes the sequence[3,4].

We describe here results relating to the first of these prerequisites for the cloned and almost fully sequenced 6-kilobase histone repeat from *Psammechinus miliaris* (h22)[5,6]. The h22 repeat was previously predicted as being part of an embryonic programme due to both its high reiteration frequency and the homology of its deduced histone products with genuine embryonic-type histones from other sea urchins[6]. This view has been confirmed at the RNA level by the finding that h22 hybridizable RNA derived from early embryonic stages produces hybrids completely resistant to excess S_1 nuclease activity (see below). We were therefore prompted to determine where these mRNAs mapped on the h22 sequences relative to several conserved sequence elements flanking the histone-coding regions of the genes[7–9]. The most ubiquitous of these, the 'Hogness box' (ref. 10), is found upstream from several histone- and other polymerase II-transcribed genes and comprises a sequence related to the consensus form 5'TATAAATA3'. About 20 nucleotides downstream from this sequence, there is a sequence related to 5'pyCATTCpu3' (ref. 8). A second pair of homology blocks is found downstream from sea urchin histone gene-coding sequences, including the five h22 genes (see below); they comprise a large block closer to the protein termination codon, and are characterized by a 16-nucleotide GC-rich hyphenated dyad symmetry element separated by a short, relatively AT-rich stretch from a smaller homology with a consensus sequence 5'CAAGAAAAGAA3' (ref. 9).
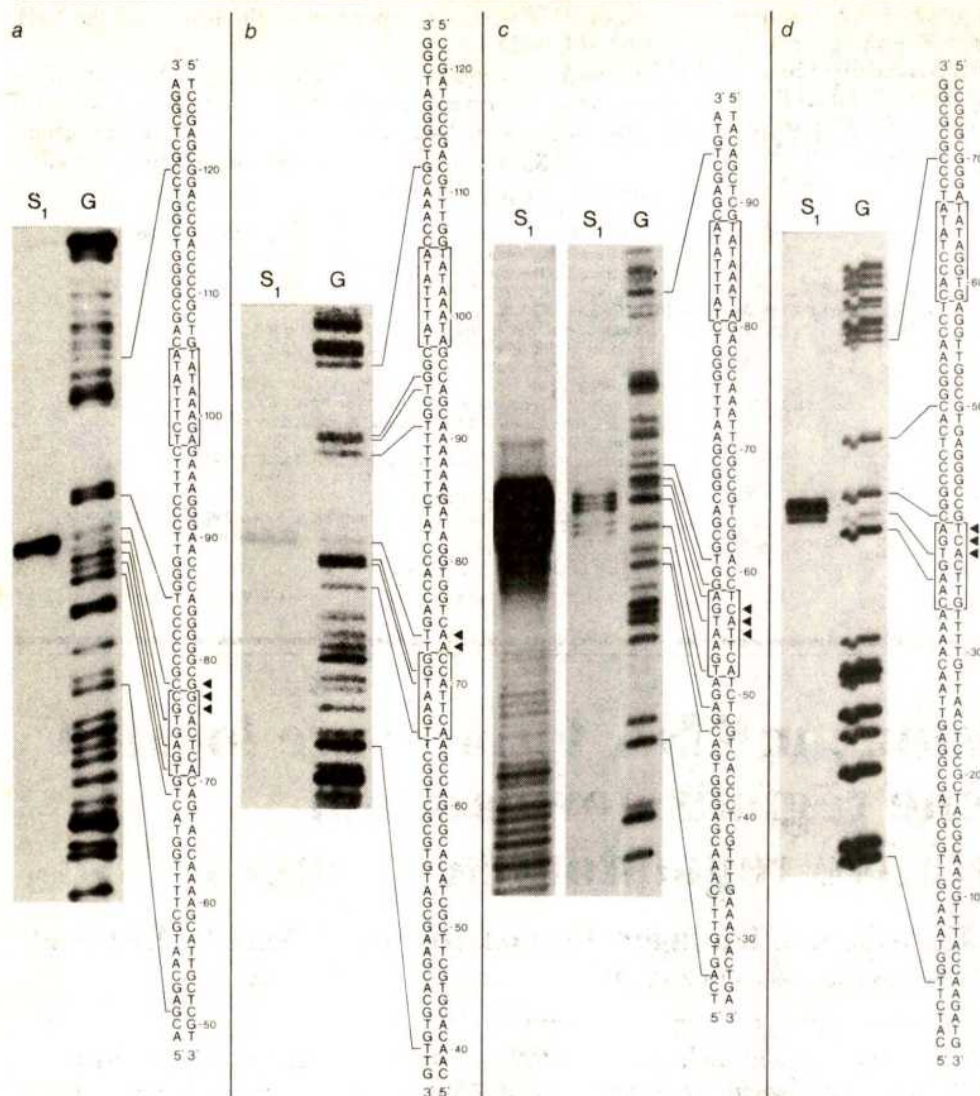
Fig. 1 Autoradiogram of S_1 mapping of the H2B (*a*) H2A (*b*). H3 (*c*) and H1 (*d*) mRNA 5′ termini. Mapping was essentially as described by Berk and Sharp[11] with the following modifications[13]. Approximately 1.5 pmol of, respectively, *Hinf*/*Hpa*II, *Hae*II/*Xho*I, *Hae*III/*Hpa*II and *Hinf*/*Hpa*II restriction fragments of h22 insert DNA[6], which span the mRNA 5′ termini from within the coding sequence and 5′ ^{32}P-labelled at the internal sites were used. These were hybridized for 3 h at 48 °C and 250 μg of RNA obtained by phenol/chloroform extraction of *P. miliaris* embryos at the 128-cell stage of development in 50 μl of formamide 80%, 0.4M NaCl, 40 mM MOPS, *p*H 6.7, and 1 mM EDTA. After dilution with 9 volS_1 nuclease buffer (0.25 M NaCl, 0.03 M sodium acetate, *p*H 4.6, 1 mM ZnSO$_4$), hybrids were digested with 10 units of S_1 nuclease purified as described by Vogt[33] at either 37 °C for 1 h (*a*,*b*,*d*) or 45 °C for 2 h (*c*). Protected DNA was precipitated with 2 vol ethanol, washed with 70% ethanol, vacuum dried and dissolved in formamide 80% (v/v), 0.05% bromphenol blue/ xylene cyanol and 1 mM EDTA. Samples were electrophoresed at 30 V cm^{-1} on 8% acrylamide, 8 M urea, thin sequencing gels[16], in parallel with G cleavage fragments [15], of the end-labelled restriction fragment and *Hpa*II-cut 5′ end-labelled pBR322 (ref. 29) for size orientation (not shown). Autoradiography of the gel was with prefogged Kodak XR-5 film and intensifying screen at — 70 °C (ref. 34). The region of the autogradiogram shown has been aligned in part with the sequence of the protected coding strand. Note that the G cleavage fragments represent a set of fragments shorter by one nucleotide than a G in the sequence. Indicated sequence positions are from the initiator codon with conserved sequences boxed (see text). Nucleotides corresponding to the 3′ termini of protected DNA are indicated with triangles. In the case of the H3 mapping experiment (*c*), the effect of the more stringent S_1 digestion is illustrated in the overexposed tract.

A knowledge of the location of the histone mRNA termini to these homology blocks is required before we can evaluate their significance in the processes involved in mRNA production.

Mapping of mRNA 5′ termini

Several methods for mapping RNA onto DNA sequences have recently become available. We have studied variants of the Berk/Sharp S_1 nuclease protection methodology[11-14]. The advantages of this technique are due not only to its sensitivity and specificity but also to the fact that both 5′ and 3′ termini can be mapped in heterogeneous RNA preparations. Additionally, we already had good reason to believe that at least in the case of the H4, H2B, H3 and H2A genes no introns existed which might complicate the analysis[6]. In preliminary experiments, the ability of the mRNAs to form completely uninterrupted S_1-resistant hybrids with H22 sequences was tested. These results, and those described below, confirmed this view for all the genes, including the H1.

The H2B and H2A genes were initially selected for mapping experiments. In each case, uniquely 5′-end-labelled restriction fragments were prepared that overlapped the 5′-mRNA termini from the labelled ends which lay within the protein coding region. Hybrids formed between the labelled coding DNA and the homologous mRNAs present in RNA preparations derived

from *Psammechinus* embryos at the 128-cell stage of development were trimmed using S_1. The protected DNA was then analysed on thin sequencing gels using as size markers the respective G cleavage fragments of the unhybridized DNAs[15,16]. Autoradiograms of these gels are shown in Fig. 1(*a*, *b*). As the DNA sequences are known (ref. 8 and unpublished results), the G cleavage fragments provide sufficient information for alignment of the S_1-resistant DNA with the corresponding sequence. Note that only a selected subset of the G cleavage markers are actually aligned in Fig. 1 and that each one comprises a 5′-end labelled fragment up to but not including the G in the sequence, as this is eliminated by the cleavage reaction[15]. The mobility of the 3′-OH-terminated S_1 fragments is very slightly slower than that of their 3′-P-terminated counterparts produced by chemical cleavage. This usually has little effect on alignment as it results in a difference of less than one-half nucleotide spacing[17,18] and would therefore produce a small error compared with the indeterminacy of the ragged 3′ ends of the S_1-resistant DNA [13]. S_1-resistant DNA which had lost even a single 5′ nucleotide would, of course, not be displayed.

Interpretation of the results shown in Fig. 1 requires a knowledge of the exact behaviour of S_1 nuclease at the junction between single strand and hybrid DNA. From preliminary trials, we concluded that the degree of S_1 trimming could vary over a

few nucleotides depending on the severity of the S_1 digestion conditions used, and similar results have been reported by others[14,18]. The variability usually results from a 3'-ragged DNA overhang of one to five nucleotides[12,14,18], and digestion into the hybrid can only be detected in high yield in circumstances which allow selective 'breathing' of the 3' DNA end of the hybrid. In addition to this inherent heterogeneity of the S_1-resistant DNA, it has recently become clear that mRNA 5' termini can, at least in some cases, themselves exhibit microheterogeneity (see, for example, ref. 19) which, if present, would also cause further heterogeneity in the S_1-resistant DNA. The detection of heterogeneous mRNA termini by the S_1 technique is clearly only possible if abundant species are further apart than the spread of the DNA ragged ends, and would need to be confirmed by direct analysis of the capped sequences. The results of the H2A and H2B mapping (Fig. 1 *a, b*) can therefore only locate the region of the mRNA 5' termini to within two or three nucleotides. Even with this limitation, however, it is clear that the 5' ends of these RNAs are adjacent to or within a heptameric region of the high sequence homology found in front of sea urchin histone genes[8], with a consensus sequence 5'pyCATTCPu3'. In the case of the core histones (H4, H2B, H3, H2A) of the variant gene repeats, h19 and h22 of *Psammechinus*, only three mismatches are found to this sequence, two of which occur in the H2B gene of h22 (Fig. 1*a*). Although the exact location of the 5' termini of the H2A and H2B genes cannot be determined from these results, the fact that histone mRNA cap structures are predominantly of the form $7mGpppA^m$ (refs 20, 21) suggests that the most abundant termini will end in an A. In the case of the H2B this constraint suggests that the A of the homology box (at −75) is the pre-dominant terminus. In addition, this location is 23 nucleotides downstream from a Hogness box and it has been suggested that this is, to within a nucleotide, a rule for mRNA 5' termini[10]. In the case of the H2A mRNA (Fig. 2*b*), there are three As (−70, −73, −74) which could fall within the resolution of the S_1 mapping, one of which is (as for the H2B) the highly conserved A of the homology box at −70. However, only the A at −74 fits with the 23 ± 1 rule relative to its Hogness box, so that either the rule is too stringent or the homology box does not define the exact 5' nucleotide.

No evidence for abundant 5'-RNA microheterogeneous species can be discerned from these mapping results for the H2A and H2B mRNAs; at least, not with a range greater than two or three nucleotides, as the protected DNA bands are about this wide. No significant decrease in the size of the main protected bands is obtained by increasing the amount of S_1 nuclease used in the digestion beyond that used for the results in Fig. 1 (*a, b*), suggesting that these are essentially limit digests. Heavy exposure of these highly digested samples, however, revealed that low levels of digestion within the hybrids occurred in these samples at non-random sites, possibly due to breathing of the hybrids and 'nibbling in' at the termini. Such nibbling was clearly observed in a previous study, when very large amounts of S_1 were used[18], and we have observed similar effects when more stringent S_1 digestion conditions were used, particularly at higher digestion temperatures. An example is shown in the overexposed tract in Fig. 1*c*, which maps the H3 5' terminus. In this case, the principal protected DNA bands were a few nucleotides shorter relative to the homology box than in the H2A and H2B mapping experiments. We cautiously interpret this result as being consistent with the A at −56 being the most abundant 5'-coded nucleotide of the H3 mRNA. This location also lies appropriately downstream from a Hogness box.

Although the exact locations of the 5' termini of the H2A, H2B and H3 mRNAs are not defined by these S_1 mapping results, it seems clear that the termini are topologically related to conserved sequence boxes in front of the genes, suggesting that these sequences are in some way related to the generation of the termini. In the case of the remaining two genes of the h22 repeat (H1 and H4), the degree of homology to the 'consensus' form of the homology boxes is poorer than for the H2A, H2B and H3

genes. Nevertheless, the same general location is observed for the 5' termini of these mRNAs relative to their somewhat deformed homology boxes. Figure 1*d* shows the S_1 mapping of the H1 5' terminus. The cap box in the case of this gene (5'pyCACTTpu3') shows a five out of seven fit to the consensus 5'pyCATTCpu3' sequence, whereas the region considered to be the Hogness box for this gene fits in five out of eight positions. In the case of the H4 mRNA, the region of 5' terminus had already been tentatively located by comparison with its location in the *S. purpuratus* histone repeat[6,22]. We have confirmed this location with a further S_1 mapping experiment (Fig. 2). For this experiment, the DNA probe was labelled by nick-translation, as the *Hae*II site which forms the internal protected end of the hybrid with the H4 mRNA could not be conveniently 5'-end labelled. Thus, in this experiment the protected DNA is compared with a heterologous size marker which can only be approximately related to the sequence. Even with this limitation, it is clear that the result shown in Fig. 2 places the H4 5' terminus adjacent to or within its cap box.

3' Termini

The sequence conservation in the homology blocks downstream from sea urchin histone genes is so great that their informational content cannot be doubted[9]. The relevant sequences for the h22 clone histone genes have now been determined and, as shown in Fig. 3, each gene fits with the pattern predicted by Busslinger *et al.*[9]. It was therefore of particular interest to determine the location of the 3'-mRNA termini in relation to these sequences. The location of the H3 3'-mRNA terminus was first mapped using S_1 nuclease and, as shown in Fig. 4, is about 169 nucleotides downstream from an internal *Hae*III site (at −113), which by comparison with the sequence (Fig. 3), places it within a few
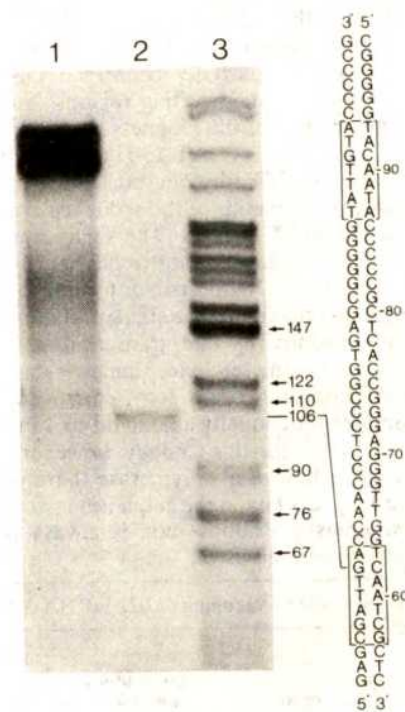
Fig. 2 Autoradiogram of S_1 mapping of the H4 mRNA 5' terminus. A *Hind*III/*Hae*II fragment spanning the H4 5' terminus from 44 base pairs within the coding region[6] was labelled by a nick-translation procedure producing largely full-length DNA[35], as shown in lane 1. S_1 nuclease mapping was carried out as in Fig. 1*a* but using approximately 0.5 pmol of DNA probe. The protected DNA (lane 2) is about 106 nucleotides long by comparison with pBR322/*Hpa*II size markers[29] (lane 3), and this position is indicated on the sequence by an arrow. The regions of the cap box and Hogness box are indicated.

HaeIII−25/HinfI +219   TAAGTGAAGCAGACTTGGCTAGAATAACGGCTCTTTTCAGAGCCACCAAATATTCAAGAAAGATTGGTTTTATATTACT   Post H4

HinfI −97/BamHI +197   TAAACGGTTACACCCTAGTCCCTTCGGACTGACAACGGCCCTTTTCAGGGCCACCAAACATCCAAGAAAGAATTGTGTCATAAATCA   Post H2B

HaeIII−113   TAGATCCCATCCGTGCACGCCATATGATTTACAAACGGCTCTTTTCAGAGCCACCACACCCCCAAGAAAGATTCTCGTTAAATAGTT   Post H3

HaeIII +37/HaeIII +50   TAAATTTGTTTGCTACCTCTTGCAACCTCAACAACGGCCCTTATCAGGGCCACCAAATATTCAAGAAAGATAAAAGTCTCTGTAAT   Post H2A

TaqI−5/AluI +167   TGATGTTGCACGTCCTACTCGTGTCACCACAACACAACGGCTCTTTTCAGAGCCACCACATTTCCACGAAAGACCAATGCCTTATTTTG   Post HI

3′ termini

Fig. 3 Sequences downstream from histone gene termination codons of h22. Sequencing was carried out by chemical cleavage [9,15] from the indicated restriction sites. Sequences for the H1 and part of the H2A and H2B 3′ non-coding regions are in refs. 6 and 9. The approximate locations of the mRNA 3′ termini are indicated.

nucleotides downstream from the dyad symmetry element. The DNA probe in this and subsequent 3′-mapping experiments was labelled by nick-translation and, as in Fig. 4, compared with size markers which could then be related to the sequence (see Table 1 and Fig. 3). Although this procedure is liable to greater error than the direct sequence comparison used for the 5′ termini, all the 3′ mRNA termini map in a similar relative position just after the dyad symmetry. The region of these termini indicated in Fig. 3 is uncorrected for possible DNA overhangs. It is, however, no more than two nucleotides downstream from the corresponding location for the last detectable 3′ nucleotides in the *S. purpuratus* H3 and H2A mRNase determined by RNA sequencing (I. Sures, personal communication). The very last 3 nucleotides may, however, be the highly conserved sequence ACCA-OH as this also seems to be the sequence of the 3′-terminal oligonucleotide of the *L. pictus* H4 mRNA[36].

Discussion

We have shown that the mRNA termini coded by the principal embryonic histone repeat of *Psammechinus miliaris* are topologically related to partially conserved DNA sequence elements flanking the protein coding regions. The first in the direction of transcription is the Hogness box[10]; this is found in the consensus form (5′TATAAATA3′) in front of the H2A and H3 genes and only modified by one nucleotide in front of the H2B gene. Deformed versions of the sequence are also present in front of the H4 and H1 genes. The significance previously attached to this degenerate homology relies heavily on its rather constant proximity to mRNA precursor termini[10,12,14,23] and, in particular, to the fact that it lies in a similar relationship to the 5′ terminus of the adenovirus late transcription unit[24]. These observations, as well as the sequence similarity, have previously led to the suggestion that it may form part of an RNA polymerase II promoter functionally analogous to a Pribnow box in prokaryotes. The basis for this analogy, however, has recently proved rather limited. Several polymerase II-transcribed genes exist without a Hogness box in the sequence upstream from the cap sites[19], whereas a Pribnow box is always discernible in prokaryotic promoter regions[25].

Recent work in this laboratory has shown that deletion of the TATAAATA as well as some flanking sequences in front of the H2A reduces the level of H2A mRNA production only about fivefold when the mutated DNA is expressed following microinjection into *Xenopus* oocyte nuclei, whereas the deletion of a Pribnow box abolishes prokaryotic promoter function[4]. A potentially more revealing observation is that the absence of the 5′TATAAATA3′, whether natural[19] or of artificial[4] origin, leads to multiple cap sites, suggesting that the sequence may be a 'selector' instrumental in specifying a unique, or at least predominant cap site[4]. Although we have no direct evidence that this occurs as part of the initiation of a primary transcript in the histone system, there is mounting evidence for a 'cap-promoter' hypothesis[24,26]. Note also that prokaryotic as well as eukaryotic transcripts generally begin with a purine preceded and followed by a purine, with CAT being a favoured combination[27,29]; thus, there may be some selectivity at this level which is reflected in the 5′pyCATTCpu3′ homology near or at the *Psammechinus* histone mRNA 5′ termini. Moreover, Levy et al. have recently shown that an identical cap box lies close to the *S. purpuratus* H2B mRNA 5′ terminus[30].

The exact function of the conserved sequence blocks downstream from the sea urchin histone coding sequences is unknown. However, they share several features with typical prokaryotic terminator or attentuator sequences[25,31,32] as well as

Fig. 4 Autoradiogram of S₁ mapping of the H3 3′ terminus. The *Hae*III fragment used for sequencing the H3 3′ non-coding region (Fig. 3) was nick-translated and used for S₁ nuclease mapping of the H3 3′ terminus as in Fig. 2. The protected DNA (lane 1) is about 169 nucleotides long compared with known partial A cleavage fragments[15] (lane 2), and, therefore, maps the 3′terminus about 56 nucleotides downstream from the termination codon.

Table 1 S₁ nuclease mapping of h22 mRNA 3′ termini

mRNA	Location of 3′ end of DNA probe		Approximate length of protected DNA	Deduced location of 3′ mRNA terminus (see Fig. 3)
H4	*Hae*II	−25	71	46
H2B	*Mbo*II	−83	138	55
H3	*Hae*III	−113	169	56
H2A	*Xho*I	−184	240	56
H1	*Hae*III	−23	79	56

Restriction cut sites are as in ref. 5 and locations indicated are upstream from termination codons. Probes were labelled by nick-translation and mapping was carried out essentially as in Fig. 2 using either pBR322/*Hpa*II size markers (H4, H2B, H2A, H1) or a partial known sequence ladder (H3, Fig. 4).

with polymerase III terminator sequences[27]. Most striking is the GC-rich hyphenated dyad symmetry followed by a relatively AT-rich region. We do not know the mode of production of the mRNA 3' termini, but the fact that they map within or a few nucleotides downstream from this feature is consistent with a termination model.

If the sea urchin histone mRNA termini do normally arise through promotion of termination, one would not expect that RNA from spacer regions of the genes would be present in cells actively transcribing the h22-like genes, and so far we have failed to detect such RNA using spacer-specific cloned DNA probes. However, it is conceivable that the proposed termina-tion is regulated so that a normally negligible level of read-through could, in certain circumstances, become significant,. as is the case in prokaryotes[25,31,32]. This possibility could reconcile some of the conflicting evidence on the mode of transcription of these genes[7].

1. Birnstiel, M. L. & Chipchase, M. Trends biochem. Sci. 2, 149–152 (1977).
2. Hentschel, C. C. & Birnstiel, M. L. in Proc. FEBS Symp. DNA, Prague (eds Zadrazil, S. & Sponar, J.) (Pergamon, Oxford, 1980).
3. Probst, E., Kressmann, A. & Birnstiel, M. L. J. molec. Biol. 135, 709–732 (1979).
4. Grosschedl, R. & Birnstiel, M. L. Proc. natn. Acad. Sci. U.S.A. 77, 1432–1436 (1980).
5. Clarkson, S. G., Smith, H. O., Schaffner, W., Gross, K. W. & Birnstiel, M. L. Nucleic Acids Res. 3, 2617–2632 (1976).
6. Schaffner, W. et al. Cell 14, 655–671 (1978).
7. Kedes, L. H. A. Rev. Biochem. 48, 837–870 (1979).
8. Busslinger, M., Portmann, R., Irminger, J. C. & Birnstiel, M. L. Nucleic Acids Res. 8, 957–977 (1980).
9. Busslinger, M., Portmann, R. & Birnstiel, M. L. Nucleic Acids Res. 9, 2997–3008 (1979).
10. Gannon, F. et al. Nature 278, 428–434 (1979).
11. Berk, A. J. & Sharp, P. A. Proc. natn. Acad. Sci. U.S.A. 75, 1274–1278 (1978).
12. Tsujimoto, Y. & Suzuki, Y. Cell 16, 425–436 (1979).
13. Moss, T. & Birnstiel, M. L. Nucleic Acids Res. 6, 3733–3743 (1979).
14. Weaver, R. F. & Weissmann, C. Nucleic Acids Res. 7, 1175–1195 (1979).
15. Maxam, A. M. & Gilbert, W. Proc. natn. Acad. Sci. U.S.A. 74, 560–564 (1974).
16. Sanger, F. & Coulson, A. R. FEBS Lett. 87, 107–110 (1977).
17. McConnell, D. J., Searcy, D. G. & Sutcliffe, J. G. Nucleic Acids Res. 5, 1729–1739 (1978).
18. Sollner-Webb, B. & Reeder, B. Cell 18, 485–499 (1979).
19. Baker, C. C. Herisse, J., Courtois, G., Galibert, F. & Ziff, E. Cell 18, 569–581 (1979).
20. Surrey, S. & Nemer, M. Cell 9, 589–595 (1976).
21. Faust,M., Millward, S., Duchastel, A. & Fromson, D. Cell 7, 597–604 (1976).
22. Grunstein, M. & Grunstein, J. E. Cold Spring Harb. Symp. quant. Biol. 42, 1083–1092 (1977).
23. Tsuda, M., Ohshima, Y. & Suzuki, Y. Proc. natn. Acad. Sci. U.S.A. 76, 4872–4876 (1979).
24. Ziff, E. B. & Evans, R. M. Cell 15, 1463–1475 (1978).
25. Rosenberg, M. & Court, D. A. Rev. Genet. 13, 319–353 (1979).
26. Salditt-Georgieff, M., Harpold, M., Chen-Kiang, S. & Darnell, J. E. Cell 19, 69–78 (1980).
27. Korn, L. & Brown, D. Cell 15, 1145–1156 (1978).
28. Scherer, G. E. F., Walkinshaw, N. D. & Arnott, S. Nucleic Acids Res. 5, 3759–3773 (1978).
29. Sutcliffe, J. G. Nucleic Acids Res. 5, 2721–2728 (1978).
30. Levy, S., Sures, I. & Kedes, L. H. Nature 279, 737–739 (1979).
31. Pribnow, D. in Biological Regulation and Development Vol. 1 (ed. Goldberger, R. F.) 250–277 (Plenum, New York, 1979).
32. Adhya, S. & Gottesman, M. A. Rev. Biochem. 47, 967–997 (1978).
33. Vogt, V. M. Eur. J. Biochem. 33, 192–200 (1973).
34. Laskey, R. A. & Mills, A. D. FEBS Lett. 82, 314–316 (1977).
35. Maniatis, T., Jeffrey, A. & Kleid, D. G. Proc. natn. Acad. Sci. U.S.A. 72, 1184–1188 (1975).
36. Gurmstbein, M. & Schedl, P. J. molec. Biol. 104, 325–349 (1976).

LETTERS

Search for radio emission from the young supernova remnants in NGC6946

M. P. Ulmer*, Patrick C. Crane†, Robert L. Brown† & J. M. van der Hulst‡

*Department of Physics and Astronomy Northwestern University, Evanston, Illinois 60201
†National Radio Astronomy Observatory
‡Department of Astronomy, University of Minnesota

Although recent supernovae in our own Galaxy are among the brightest radio sources in the sky—particularly Cas A and the Crab Nebula (500-1,000 yr post-outburst)—the evolution of their radio emission from outburst to the present is, of course, unknown. Unless and until we have the opportunity to study a new galactic supernova, our information on the immediate post-outburst radio properties of supernova remnants must come from studies of identified supernovae in external galaxies. NGC6946 is one galaxy in which such a study is particularly favourable both because supernovae occur frequently in this galaxy—four supernovae have been identified since 1917—and because of its relative proximity. Two previous searches have failed to detect radio emission from these remnants[1,2]. However, the greater sensitivity presently available at radio wavelengths allows us not only to conduct a more sensitive search for these remnants but also to determine whether the radio emission has brightened since the last surveys ~ 5 yr ago.

In March 1979 we mapped NGC6946 with the VLA at 6 and 20 cm. For these observations we used 14 antennas which provided 91 baselines ranging in length from 50 m to 18 km; the resulting resolution was as high as 0.3 arc s at 6 cm and 0.8 arc s at 20 cm. We restricted the instrumental bandwidth to 12 MHz so as to obtain fields of view $\geqslant 10$ arc min at both wavelengths (FWHM). We first made a large but low resolution (4 arc s per cell) map of the entire region centred on the nucleus of NGC6946 to identify possible confusing field sources. From this map we subtracted the best fit to the central component and then made high resolution maps centred on the positions of each of the four supernova remnants[3]. We did not detect radio emission at any of these positions; our observational limits are summarised in Table 1. Excluded from this tabulation is a tentative 1969 supernova identification which was not confirmed; it does not appear on a list of recent extragalactic supernovae compiled by Sargent et al.[3].

Although no radio emission from the supernova remnants (SNRs) in NGC6946 was detected, our limits are, nevertheless, a factor ~5 lower than those obtained in 1971 at 20 cm with the WSRT[1] and they are a factor of more than 10 lower than the limit obtained at 11 and 3.7 cm in the 1975 NRAO inter-ferometer survey[2]. Moreover, if we adopt 7 Mpc as the distance to NGC6946 (ref. 4) (note that estimates of this distance range between 4.2 (ref. 5) and 10.5 Mpc (ref. 6)) we find that our limits on the 20 cm (1,400 MHz) monochromatic luminosity of the SNRs in NGC6946 are comparable with the present mono-chromatic luminosity of Cas A at this frequency (2.5×10^{18} W Hz^{-1}). To the extent, therefore, that Cas A is suitably representative of evolving Type II SNRs, we conclude that the peak radio luminosity must occur between 50 and 300 yr after the outburst.

That the flux density is not greatest at outburst is not surpris-ing in view of the large free-free optical depth of the remnant at early times ($\leqslant 10$ yr)[7]. However, a reliable determination of precisely when the radio emission should reach maximum intensity depends not only on the nebular parameters but also on the density of the ambient medium[7] and whether or not a pulsar contributes to the supply of relativistic particles within the remnant[8]. Hence, a full interpretation of our results depends critically on ancillary information particular to the supernova and its environment about which we have no specific knowledge. A few general remarks are necessary, however.

Assuming that the temperature in the expanding SNR envelope is ~10^4 K at the typical age of the historical remnants in NGC6946, $t \sim 10^9$ s, then the nebular envelope will still be

Table 1 Upper limits (3σ) to the radio emission from recent supernovae in NGC6946

				Flux density (mJy)		Luminosity $(10^{18}\text{W Hz}^{-1})$*	
Supernova	Type	α(1950)	δ(1950)	20 cm	6 cm	20 cm	6 cm
1917a	(I)	20 h 33 min 44.5 s	59° 57′ 07″	<0.6	<0.7	<3.5	<4.1
1939c	II	20 33 20.7	59 59 16	<0.6	<0.8	<3.5	<4.7
1948b	(II)	20 34 19.0	59 59 52	<0.6	<0.9	<3.5	<5.3
1968d	II	20 33 55.4	59 59 12	<0.6	<0.6	<3.5	<3.5

*Monochromatic luminosity.

optically thick to free–free absorption if

$$\left(\frac{M}{10M_0}\right)^2\left(\frac{v}{5{,}000\text{ km s}^{-1}}\right)^{-5} \geqslant 0.5$$

Adopting $M = 10M_0$ we can thus distinguish two cases: rapidly expanding remnants $v > 5{,}000$ m s^{-1}, and slowly expanding remnants, $v \leqslant 5{,}000$ km s^{-1}; the former will (now) be optically thin whereas the latter are still thick. Consider first the optically thick nebulae. In this case the expected radio flux density is $S = (\varepsilon_s/\kappa_{th})\Omega$ where ε_s is the synchrotron emissivity and κ_{th} is the thermal absorption coefficient. For a typical power law spectrum of relativistic electrons $N(E)\,dE = N_0 E^{-2.5}\,dE$ in the remnant which extends to energies as low as 10 meV, our 5-GHz observations impose the following constraint on a SNR expanding at 5,000 km s^{-1},

$$E_e < 1.0 \times 10^{43} B^{-7/4}\text{ erg}$$

where E_e is the total energy in relativistic electrons in the SNR and B(G) is the magnetic field. This inequality is illustrated in Fig. 1. Further, the synchrotron emission will be suppressed at 5 GHz by the Razin–Tsytovich effect unless $B > 9.2 \times 10^{-5}$ G; this limit is imposed by the condition that $\nu_R > 5$ GHz is also shown on Fig. 1.

Hence we conclude that if the historical SNRs in NGC6946 are slowly expanding at $v \leqslant 5{,}000$ km s^{-1}, then our observational limits require either (1) that the magnetic field in the remnants is $B < 9.2 \times 10^{-5}$ G, or (2) that the total energy in relativistic electrons in the remnants $E_e < 1.2 \times 10^{50}$ erg (that is less than 4% of the SNR kinetic energy).

Similar results are obtained for rapidly expanding, optically thin remnants. For example, if we adopt $v = 10{,}000$ km s^{-1} as an expansion velocity and carry out the same calculations as described above, the corresponding limits on E_e and B are

$$E_e < 5.5 \times 10^{42} B^{-7/4}\text{ erg}$$
$$B > 1.1 \times 10^{-5}\text{ G}$$

These results, while specific, are representative of the results obtained with any other reasonable choice of remnant parameters.

Of the two possible explanations for the low radio luminosity of the SNRs in NGC6946—that the total energy in relativistic electrons is $\leqslant 10\%$ of the SNR kinetic energy or the magnetic field is sufficiently low to cause the 5-GHz radio emission to suffer Razin–Tsytovich suppression—the weak magnetic field seems less likely to be correct because this requires such large departures from equipartition: the total magnetic field energy $< 10^{-9}$ of the SNR kinetic energy. Thus it seems that the young (<50 yr) SNRs in NGC6946 are not (yet) radio sources as luminous even as Cas A because they have not acquired (or generated) enough relativistic electrons. This in turn means either that newly formed pulsars require $\geqslant 50$ yr to begin producing copious quantities of energetic particles, or that relativistic electrons are accelerated in the expanding SNRs at a rate $\leqslant 10^{41}$ erg s^{-1}. Eventually, the way to distinguish between these latter two possibilities is to follow the detailed radio evolution of a historical extragalactic supernova remnant; at present, however, it seems far more profitable to direct efforts to a thorough elucidation of the energetics of the youngest galactic remnants[7,9].

1. de Bruyn, A. G. *Astr. Astrophys.* **26**, 105–112 (1973).
2. Brown, R. L. & Marscher, A. P. *Astrophys. J.* **220**, 467–473 (1978).
3. Sargent, W. L. W., Searle, L. & Kowal, C. T. in *Supernovae and Supernova Remnants*, 33 (ed. Cosmovicj, C. B.) (Dordrecht, Reidel, 1974).
4. de Vaucouleurs, *Astrophys. J.* **224**, 710–717 (1978).
5. Roberts, M. S. *Astr. J.* **74**, 859–876 (1969).
6. Sandage, A. & Tamman, G. A. *Astrophys. J.* **194**, 559–568 (1974).
7. Gull, S. F. *Mon. Not. R. astr. Soc.* **161**, 47–69 (1973).
8. Marscher, A. P. & Brown, R. L. *Astrophys. J.* **220**, 474–483 (1978).
9. Chevalier, R. *Astrophys. J.* **188**, 501–516 (1974).

Fig. 1 Limits on the magnetic field B and the total energy in relativistic electrons E_e of a $10 M_0$ SNR expanding at 5,000 km s^{-1}, 10^9 s after outburst. If Razin–Tsytovich suppression is not important (see text), then the observational limits require the SNR to lie in the unshaded portion of this figure.

Possible existence and chemistry of ClO·O₂ in the stratosphere

Sheo S. Prasad

Jet Propulsion Laboratory, California Institute of Technology, 4800 Oak Grove Drive, Pasadena, California 91103

The possible existence and chemistry of asymmetric ClO·O₂ in the stratosphere could resolve the current apparent discrepancy between the observed steep but theoretically predicted much slower decrease of ClO mixing ratio with altitude below the peak. This conjecture follows from the recent finding[1] that possible formation of ClO·O₂ from ClO and O₂ may be the physical mechanism by which O₂ suppresses the quantum yields in chlorine photosensitized decomposition of ozone (refs 2, 3 and C. S. Lin, S. Jaffe and W. DeMore, unpublished results). In this letter it is suggested that introduction of ClO·O₂ in current photochemical models of the stratosphere could make the observed variability of ClO more understandable. It could also provide a possible mitigating influence on the present estimates of O₃ destruction from CFM consumption.

Formation of an asymmetric $ClO \cdot O_2$ complex might explain[1] the observed suppression of the quantum yield in chlorine photosensitized decomposition of ozone when O_2 is present (refs 2, 3 and Lin *et al.* unpublished results). An equilibrium constant $K_1 = k_{1f}/k_{1r} = 3.7 \times 10^{-19}$ cm^3 molecule^{-1} at 298 K was derived for the assumed reaction:

$$ClO + O_2 + M \underset{k_{1r}}{\overset{k_{1f}}{\rightleftharpoons}} ClO \cdot O_2 + M \qquad (1)$$
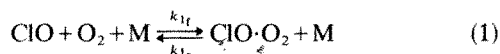
It was also shown that the potential reaction:

$$ClO \cdot O_2 + Cl \to Cl_2O + O_2 \qquad (2)$$
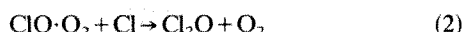
provided a viable explanation for the very low quantum yield (<2) observed by Wongdontri-Stuper *et al.*[3] when the ozone partial pressure was very small (a few millitorr) in their experiments. We conjecture that $ClO \cdot O_2$ complex may exist in significant quantities in the stratosphere, and that the following reactions of $ClO \cdot O_2$ with O, NO, and NO_2 can be hypothesized:

$$ClO \cdot O_2 + O \to ClOO + O_2 \qquad (3a)$$

$$ClO \cdot O_2 + NO \to ClONO + O_2 \qquad (4)$$

$$ClO \cdot O_2 + NO_2 \to ClONO_2 + O_2 \qquad (5)$$
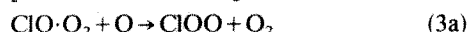
Switching reactions similar to reactions (2), (4) and (5) are common with cluster ions[4], and it may be that neutral clusters (such as $ClO \cdot O_2$) share with their ionic analogue a tendency to undergo these reactions. The possible existence of $ClO \cdot O_2$ in the stratosphere provides a potential explanation for the current discrepancy between *in situ* measurements[5,6] and theoretical predictions[7] of the stratospheric ClO mixing ratio at lower altitudes.

Figure 1 illustrates the present discrepancy between observed and calculated profiles of ClO mixing ratios. Observed and theoretical values of ClO mixing ratios can be matched in the 35–40 km region by suitable choices of ClX and H$_2$O ratios. The values of ClX needed for this match result in satisfactory concentrations for most other related species—Cl for instance. This agreement in the 35–40 km altitude region is not matched at altitudes below about 35 km. The rapid decrease with altitude in the observed n(ClO) mixing ratio is a problem which has been attributed to experimental errors and/or some omission in the theoretical chemical model.

To appreciate the possibility of resolving this problem by invoking our $ClO \cdot O_2$ hypothesis, note that diurnally averaged models may be almost completely insensitive to the presence of $ClO \cdot O_2$. This is a result of the following reactions:

$$ClO \cdot O_2 \overset{O}{\to} ClOO \overset{M}{\to} Cl + O_2 \qquad (6)$$

$$ClO \cdot O_2 \overset{NO}{\longrightarrow} ClONO \begin{cases} \overset{h\nu}{\longrightarrow} Cl + NO_2 & (7) \\ \overset{h\nu}{\longrightarrow} ClO \overset{NO}{\longrightarrow} Cl + NO_2 & (8) \\ \overset{h\nu}{\longrightarrow} NOCl \overset{h\nu}{\longrightarrow} Cl + NO & (9) \end{cases}$$
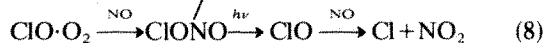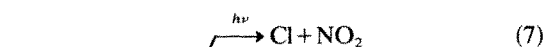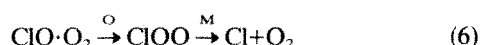
in which the end products of the possible reactions of $ClO \cdot O_2$ with O and NO in sunlight are the same as those of reactions between ClO and O and NO. Because of the possible occurrence
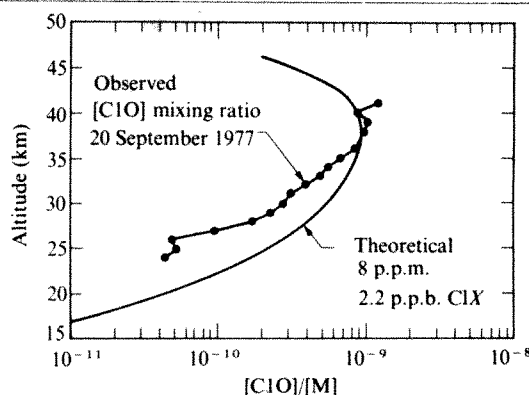
Fig. 1 Comparison between *in situ* measurements of stratospheric ClO mixing ratio and theoretical model predictions. Experimental data (●) are from Anderson *et al.*[6]. Theoretical profile, due to Logan *et al.*[7] (solid line) corresponds to spring/autumn conditions at 30°N. The rapid decline of measured ClO mixing ratio with decreasing altitude seen here is also evident in additional examples of *in situ* measurements and theoretical calculations presented by Anderson *et al.*[6].

of reaction (5), the predicted n(ClONO$_2$) profile may also remain virtually unaffected. Thus, diurnally averaged models with and without $ClO \cdot O_2$ would be almost identical, except that n(ClO)+n(ClO·O$_2$) in the former case would equal n(ClO) in the latter case. The measurements of Anderson *et al.*[5,6], however, would discriminate between ClO and $ClO \cdot O_2$ because atomic chlorine may not be produced in reactions of $ClO \cdot O_2$ with NO. Thus, while ClO is measured by Anderson *et al.*[5,6], $ClO \cdot O_2$ would be undetected. In other words, the difference between n(ClO) observed by Anderson *et al.*[5,6], and that calculated on the basis of current photochemical models (see ref. 7) may possibly be equal to the amount of n(ClO·O$_2$) present in the stratosphere. Possible stratospheric n(ClO·O$_2$)/n(ClO) ratios estimated on the basis of above considerations and data presented in Fig. 1 are shown in Table 1.

Assuming that stratospheric $ClO \cdot O_2$ is quite loosely bound, collisional dissociation of $ClO \cdot O_2$, that is, $ClO \cdot O_2 + M \to ClO + O_2 + M$, is likely to be faster than photodissociation, so that

$$n(ClO \cdot O_2)/n(ClO) = K_1 n(O_2) \qquad (10)$$

should be a good first-order approximation. Values of K_1 calculated on this basis are also given in Table 1. A plot of $\ln K_1$ against $1/T$ is shown in Fig. 2. Error bars attached to the stratospheric data points were determined by considering: (1) ±35% uncertainty in the measured ClO mixing ratios; (2) ClO measurements on 11/78, 12/77, 10/77, 9/77 and 12/76 and corresponding theoretical calculations of Logan *et al.* using only 5.5 p.p.m. of H$_2$O as shown in Fig. 8 of ref. 6; (3) uncertainties in the assumed background model atmosphere; and (4) uncertainties in stratospheric n(OH) due to possible pressure dependence of the rate coefficient for the reaction $HO_2 + OH \to H_2O + O_2$ as recently discussed by Turco *et al.*[8]. Uncertainty in $\ln K_1$ obtained from a previous analysis[1] of the laboratory data of

Table 1 Estimated n(ClO·O$_2$)/n(ClO) ratio in the stratosphere and the associated equilibrium constant for reaction (1)

Altitude (km)	T(K)*	$n(O_2)$* ($\times 10^{16}$ cm^{-3})	Observed ClO† mixing ratio ($\times 10^{-10}$)	Theoretical ClO† mixing ratio ($\times 10^{-10}$)	Estimated n(ClO·O$_2$)/n(ClO)	K_1 ($\times 10^{-18}$)
25	221.6	16.7	0.53	2.2	3.13	18.7
30	226.5	7.66	2.8	5.7	1.04	13.7
35	236.5	3.52	6.7	9.0	0.343	9.75

* Data from US Standard Atmosphere Supplements, 1966 and correspond to mid-latitude spring/autumn conditions.
† Data from Fig. 1.
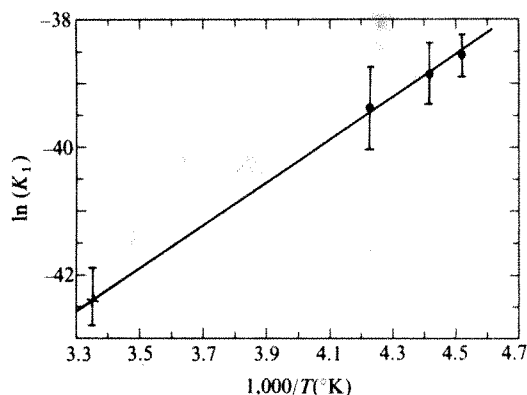
Fig. 2 A $\ln(K_1)$ plotted against $1,000/T$. The point marked X is from an analysis of the experimental data of Wongdontri-Stuper *et al.* Remaining data points (●) are from an analysis of stratospheric measurements as explained in the text. The straight line represents a least square fit to the data points.

Wongdontri-Stuper *et al.* arises from the uncertainty in the rate coefficient of the overall reaction of $ClO \cdot O_2$ with ClO. The error bar attached to this $\ln K_1$ reflects an arbitrary, but reasonable, conjecture that the abovementioned rate coefficient may be either a factor of two larger or smaller than the nominal value used previously[1]. A least square analysis yields $K_1(T) = 3.28 \times 10^{-24} \exp(3,470/T)$ cm^3 molecule^{-1}, with $K_1(T) = 7.28 \times 10^{-24} \exp(3,464/T)$ and $1.16 \times 10^{-24} \exp(3,549/T)$ cm^3 molecule^{-1} as the upper and lower bounds. The main points are: (1) K_1 obtained from two entirely independent considerations— analysis of laboratory data and stratospheric measurements—lie very close on a single plot, and (2) the slope of this $\ln K$ against $1/T$ plot is as expected by analogy with other loosely bound species, such as $ClOO$. These are not unlikely to be chance coincidences. These two points suggest that the possible existence of $ClO \cdot O_2$ complex in laboratory experimental situations can be extrapolated to a possible existence of $ClO \cdot O_2$ in the stratosphere; in quantities sufficient to resolve the current discrepancy between the measurements of Anderson *et al.*[5,6] and current theoretical models of stratospheric ClO mixing ratios.

As pointed out by Logan *et al.*[7], "The observed variability of ClO is puzzling, and raises the possibility of a major gap in our description of the chlorine cycle". Our conjecture is that the potential existence of $ClO \cdot O_2$ in the stratosphere bridges this gap. We have already seen how $ClO \cdot O_2$ complex may possibly explain the current discrepancy between observed and theoretically predicted altitude profiles of the ClO mixing ratio. Rocket measurements[9] of stratospheric T and n indicate that local changes in these quantities tend to reinforce each other's effect on the ratio $n(ClO \cdot O_2)/n(ClO)$ via equation (10), and a day-to-day variability of this ratio by as much as 50–60% is quite possible even at 30 km from this cause alone. Thus, the introduction of $ClO \cdot O_2$ could make the observed variability of ClO more understandable. In addition, it is possible that the reaction:

$$ClO \cdot O_2 + O \rightarrow OClO + O_2 \qquad (3b)$$
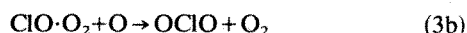
occurs. Photodissociation of $OClO$, that is, $OClO + h\nu \rightarrow O + ClO$, results in regeneration of odd oxygen. The fraction of $ClO \cdot O_2$ which reacts with O via reaction (3b) to produce $OClO$ does not immediately destroy odd oxygen. Consequently, $ClO \cdot O_2$ in the stratosphere and reaction (3b) together may have a mitigating influence on the present estimates of ozone reduction due to chlorofluoromethane consumption. Finally, a direct experimental verification of possible $ClO \cdot O_2$ formation from ClO and O_2 would be very useful.

1. Prasad, S. S. & Adams, W. M. *J. Photochem.* (in the press).
2. Norrish, R. G. W. & Neville, G. H. *J. chem. Soc.* 1864 (1934).
3. Wongdontri-Stuper, W., Jayanti, R. K. M., Simonaitis, R. & Heicklen, J. *J. Photochem.* **10**, 163 (1979).
4. Ferguson, E. E. *Atomic Data and Nuclear Data Tables* **12**, 159 (1973).
5. Anderson, J. G., Margitan, J. J. & Stedman, D. H. *Science* **198**, 501 (1977).
6. Anderson, J. G., Grassl, H. J., Shetter, R. E. & Margitan, J. J. *J. geophys. Res.* (in the press).
7. Logan, J. A., Prather, M. J., Wofsy, S. C. & McElroy, M. B. *Phil. Trans. R. Soc.* **290**, 187 (1978).
8. Turco, R. P., Whitten, R. C., Toon, O. B., Inn, E. C. Y. & Hamill, P. Preprint (1980).
9. Smith, W., Theon, J., Katchen, L. & Swartz, P. *NASA Tech. Rep. TR R-245* (NASA, Washington, DC, 1966).

Observation of static electromagnetic angular momentum *in vacuo*

G. M. Graham & D. G. Lahoz

Department of Physics, University of Toronto,
Toronto, Canada M5S 1A7

Our programme of measurement of forces related to electromagnetic momentum at low frequencies in matter has culminated in the first direct observation of free electromagnetic angular momentum created by quasistatic and independent electromagnetic fields E and B in the vacuum gap of a cylindrical capacitor. A resonant suspension is used to detect its motion. The observed changes in angular momentum agree with the classical theory within the error of ~20%. This implies that the vacuum is the seat of something in motion whenever static fields are set up with non-vanishing Poynting vector, as Maxwell and Poynting foresaw.

In establishing the electromagnetic nature of light, Maxwell[1] opposed Weber's "action at a distance" with his "dynamical" model of a vacuum with hidden matter in motion. His ideas were expanded by Poynting through the energy-flux theorem, but relativity theory initially dealt them a blow. However, despite Einstein's explicit reconciliation with the aether[2] there is currently some doubt about Maxwell's medium. It was in a relativistic context that Minkowski[3] found, as a purely mathematical consequence of Maxwell's equations, that the Lorentz force density could be exactly expressed as the divergence of Maxwell's tensor *in vacuo*, T_{vac}, decreased by the rate of change of Poynting's vector:

$$\rho \, \mathbf{E} + \mu_0 \mathbf{J} \times \mathbf{H} = \nabla \cdot T_{vac} - \frac{\partial}{\partial t} \, \varepsilon_0 \mu_0 \mathbf{E} \times \mathbf{H} \qquad (1)$$

According to Maxwell–Poynting ideas, the last (Minkowski's) term in equation (1) can be interpreted as a local reaction force acting on charges and currents when the vacuum surrounding them is loaded with electromagnetic momentum. Einstein and Laub[4] observed that if equation (1) is integrated to all space, the term $\nabla \cdot T_{vac}$ generates a vanishing surface integral and therefore the system of all Lorentz forces in the Universe needs to be supplemented with the quantity $\int_\infty \varepsilon_0 \mu_0 \, \partial/\partial t \mathbf{E} \times \mathbf{H} \, dv$ to preserve Newton's third law. The opposite of this last vector is usually interpreted as the net unlocalized reaction on charges and currents due to radiation fields but, classically at least, it also represents a real reaction force even with induction fields.

We have made, to our knowledge, the first direct observation of the Minkowski term with induction fields $\mathbf{E}$ and $\mathbf{B}$, which are confined to a small volume so that the local nature of the vacuum reaction term has also been demonstrated. The experiment consists of measurement of the axial torque on a cylindrical capacitor and its radial leads, located in an axial magnetic field. Thus $\mathbf{E} \times \mathbf{H}$ is azimuthal inside the vacuum gap of the capacitor. The details of the capacitor and its mounting on a torsion oscillator are shown in Fig. 1. The capacitor and its leads form a rigid and nearly closed electrical loop. The magnetic field and the capacitor voltage are time varied so that one Fourier component of their product is locked to the resonant frequency

of the mechanical system, which is of sufficiently high $Q(>10^5)$ to yield a measurable oscillation amplitude when viewed by a μ-radian sensitive optical lever. Knowledge of the resonant amplitude and frequency, moment of inertia and free decay time (with $\mathbf{E} = 0$) yield the driving torque. The suspension system is located in the vacuum interspace of a liquid helium Dewar. The magnetic field, uniform to $\sim 2\%$, is supplied by a superconducting solenoid.

This technique is an extension of our previous work[5] on electromagnetic forces in material media, with dielectric or magnetic material in the capacitor. In those experiments, the magnetic field was held fixed and the voltage was impressed at the resonant frequency. This resulted in a large resonant noise due to elestrostatic forces (at the second harmonic) which coupled back in some degree at the resonant frequency. The present experiment was made possible by detuning the voltage from resonance by ~ 1 Hz, using as a source the output of a high stability oscillator. This signal ($\nu = 243.31$ Hz) was electronically multiplied by the signal ($\nu = 242.18$ Hz) from the slave oscillator phase locked to the resonant system by the optical lever, so that sum and difference frequencies were generated. After low pass filtering, the difference signal was used to drive the magnet. In this way, one component of the product $\mathbf{EH}$ was at the resonance but $(\mathbf{E}^2)^{1/2}$ was not. The various phase shifts in the circuitry were carefully nulled. A calibrated pick-up coil provided absolute measurement of $\mathbf{H}$. The apparatus permitted reasonable measurements of torque over a range of about a factor of 3 in both $\mathbf{E}$ and $\mu_0\mathbf{H}$, up to maximum amplitudes of 2×10^6 V m^{-1} and 0.3 T respectively.

Measured torques are compared in Table 1 with calculated torques acting on the suspension which arise entirely from the net Lorentz force on the current I in the radial leads which charges the vacuum component of the suspended capacitor, that is, a torque $I\mu_0 H(a^2 - b^2)/2$, where a and b are the outer and inner radii of the capacitor cylinders (~ 5.5 and 4.5 mm). Here I has been corrected for the known stray capacitance to earth

Table 1 Calculated and observed torque amplitude for typical field amplitudes (the electric field is given at the inner electrode)

E_0 (MV m^{-1})	B_0 (T)	$T_{0,\text{calc}}$ (pN m)	$T_{0,\text{obs}}$ (pN m)
0.58	0.13	2.0	1.8
0.64	0.22	3.5	4.4
1.3	0.22	7.1	8.5
1.7	0.19	7.9	8.7
2.3	0.22	12.4	17.0

external to the suspension (~ 1 pF effective) and for the fraction of conduction current which corresponds to polarization current in the dielectric end plates, as that part corresponds to a closed loop of current contributing no torque. Thus I corresponds to charging a pure vacuum capacitance C_0 only. C_0 was calculated from the geometry (4.7 pF) and also estimated by measuring the effect of removing one end plate (4.9 pF). The error in the calculated torque is mainly due to the uncertainty in the corrections for stray capacitance. It is estimated to be $\sim 10\%$. The systematic trend in the ratio of T_{calc} to T_{obs} can be understood in terms of a small, amplitude dependent, non-linearity in the equation of motion, due to magnetic field dependence of the damping, which results in imperfect cancellation of the resonant noise[5] at high fields. Consequently, the tabulated discrepancies are within an estimated total error of $\sim 20\%$.

Although this result is to be expected by classical electromagnetism, it leads inexorably to the acceptance of the physical reality of the Poynting vector, even though $\mathbf{E}$ and $\mathbf{H}$ arise from independent sources. This can be seen by seeking the system on which the third law reaction torque must act. It can be neither the external electrical circuit, as the loop is essentially closed within the suspension, nor in the magnet, which, as a coil, cannot receive an axial torque (force parallel to its own current). For angular momentum conservation, the loop is an isolated system and the reaction torque can only be considered as a change in electromagnetic angular momentum carried by the fields themselves in the region of their co-existence, that is, within the vacuum gap of the capacitor. As $I = C_0 dV/dt$, the calculated torque is exactly equal to the volume integral of $\mathbf{r} \times \partial(\mathbf{E} \times \mathbf{H})/\partial t c^2$, so that the complete reaction is accounted for by the assignment of a real angular momentum density to $\mathbf{r} \times (\mathbf{E} \times \mathbf{H})c^2$ (ref. 5).

It is remarkable that no known 'particle' can be identified as the agent of the observed electromagnetic angular momentum in exchange with the mechanical detector. However, this does not imply that a new entity has to be introduced, because the concept of energy-momentum carried by macroscopically quasistatic electromagnetic field is already contained in Maxwell's equations. According to these, and as directly implied by our experimental result, permanent magnets and electrets can be used to build a flywheel of electromagnetic energy steadily flowing in circles in the vacuum gap of a capacitor as if Maxwell's medium were endowed with a property corresponding to superfluidity. The certainly new insight is that the quasistatic Maxwell's field is not merely an unobservable medium of interaction between matter and matter: it has in fact the mechanical properties postulated by Maxwell, in contradistinction to any "action at a distance" theory.

This experiment is continuing and a complete report will be published elsewhere.

Fig. 1 (*a*). Scale views of the capacitor and its rigid leads. The capacitor is formed from two stainless steel cylinders, the rigid leads run radially to the electrodes from near the axis, where they are fixed to 0.03 mm copper fibres. (*b*), The capacitor clamped to the suspension system with polyurethane end plates (the clamping details are schematic only). M, Mirror for optical lever; C, end plates; P, capacitor electrodes; L, radial leads; F, fibres; W, stiff feed wires; T, torsion shaft; B base.

1. Maxwell, J. C. *Phil. Trans. R. Soc.* **155**, 459–512 (1865).
2. Einstein, A. *Aether und Relativitaetstheorie* (Springer, Berlin, 1920).
3. Minkowski, H. *Gesamm. Abhand.* Pap. 30 (Chelsea, 1967).
4. Einstein, A. & Laub, J. *Annls Phys. (Leipzig)* **26**, 541–550 (1908).
5. Lahoz, D. G. & Graham, G. M. *Can. J. Phys.* **57**, 667–676 (1979); *Phys. Rev. Lett.* **42**, 1137–1140 (1979).

Diphosphine is an intermediate in the photolysis of phosphine to phosphorus and hydrogen

James P. Ferris & Robert Benson

Department of Chemistry, Rensselaer Polytechnic Institute, Troy, New York 12181

Phosphine (PH_3) has recently been identified as a constituent of the atmospheres of Jupiter and Saturn[1-3]. It is probably formed in the hot depths of the atmospheres of these planets and is carried to the upper levels by atmospheric turbulence. The red colorations in the atmosphere and Great Red Spot of Jupiter may be due to the photolysis of the PH_3 in the upper atmosphere to red phosphorus (P_4) (ref. 4). We initiated an investigation of PH_3 photolysis because of its potential significance in the atmospheric chemistry of Jupiter[4-6]. We report here that P_2H_4 is the initial product of PH_3 photolysis and that it is the principal intermediate in the formation of red phosphorus. These findings require substantial revision of the previously accepted mechanism for PH_3 photolysis[6-8].

Photolysis of PH_3 (87 torr) at room temperature with a 206.2 nm light source[9] gave a product with UV absorption extending from 270 nm to below 200 nm (Fig. 1). This compound was identified as P_2H_4 by comparison of its IR[10] and UV spectra and gas chromatographic retention time (on a 6 ft OV-1 column operating at 30 °C) with that of an authentic sample[11]. No products, other than hydrogen and PH_3, were detected by gas chromatography. The yield of P_2H_4 as a function of illumination time increases to a maximum and then decreases to about 20% of its maximum value (Fig. 2). (We cannot explain the maximum in the formation of P_2H_4. This reproducible finding is not due to P_2H_4 photolysis because PH_3 absorbs more than 97% of the light at 206.2 nm when the concentration of P_2H_4 reaches a maximum. Consequently little if any P_2H_4 photolysis will be occurring. This same variation in N_2H_4 yield is

observed when NH_3 is photolysed. The yield of N_2H_4 first increases and then decreases with irradiation time[12]. The yield of P_4 levels off with time in Fig. 2 because the 206.2 nm light intensity is attenuated by the formation of a P_4 layer on the cell window.) This is due in part to the build-up of P_4 on the window of the reaction cell which reduces the intensity of the 206 nm light. P_2H_4 may not have been discovered previously as a photoproduct because product analysis was performed after prolonged irradiation[7].
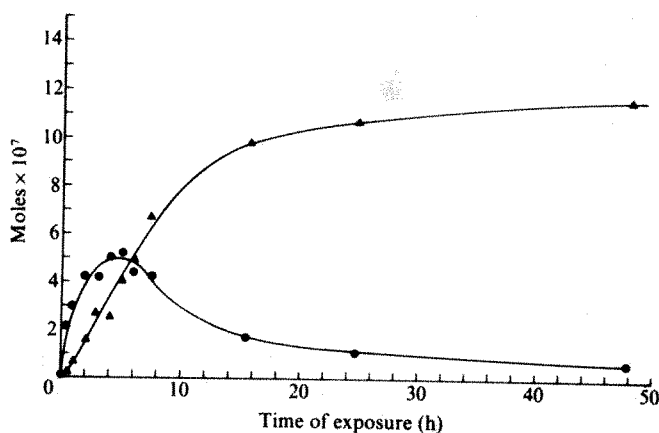
Fig. 2 Yields of P_4 (▲) and P_2H_4 (●) as a function of time of irradiation. Photolysis of 87 torr PH_3 at room temperature in a 10 cm quartz cell (capacity ~75 cm^3) using an iodine lamp with principal emission at 206.2nm. Shorter wavelengths were removed with a 1cm quartz cell containing distilled water.

In the previous mechanisms for the photolysis of PH_3 to P_4 (reactions (1)–(6)) a reaction sequence involving disproportionation of the initially formed PH_2 was proposed (reaction (2))[7,8]. Our discovery of P_2H_4 as a photoproduct suggests an alternative mechanism which includes the formation of P_2H_4 from PH_2 (reaction (8)).

$$PH_3 \xrightarrow{h\nu} PH_2 + H \tag{1}$$

$$2PH_2 \rightarrow PH_3 + PH \tag{2}$$

$$2PH \rightarrow P_2 + H_2 \tag{3}$$

$$2P_2 \rightarrow P_4 \tag{4}$$

$$H + PH_2 \xrightarrow{wall} PH_3 \tag{5}$$

$$H + H \xrightarrow{wall} H_2 \tag{6}$$

$$PH_3 + H \rightarrow PH_2 + H_2 \tag{7}$$

$$PH_2 + PH_2 + M \rightarrow P_2H_4 \tag{8}$$

$$P_2H_4 + H \rightarrow P_2H_3 + H_2 \tag{9}$$

$$P_2H_4 + PH_2 \rightarrow P_2H_3 + PH_3 \tag{10}$$

$$P_2H_3 + H \rightarrow P_2H_2 + H_2 \tag{11}$$

$$2P_2H_3 \rightarrow P_2H_2 + P_2H_4 \tag{12}$$

$$P_2H_3 + PH_2 \rightarrow P_2H_2 + PH_3 \tag{13}$$

$$P_2H_2 \rightarrow P_2 + H_2 \tag{14}$$

Fig. 1 UV spectrum of P_2H_4 measured in a 10 cm cell with Cary 219 spectrophotometer.
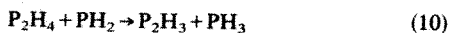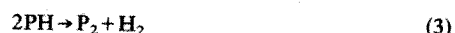
If disproportionation of PH_2 (reaction (2)) is an important pathway in P_4 formation then P_4 will be formed along with P_2H_4 (reaction (8)) at very short irradiation times while in the absence of disproportionation P_4 formation will be negligible. It can be shown that $k_2/k_8 = \lim_{t \to 0}(4n_{P_4}/n_{P_2H_4})$ and a plot of $n_{P_4}/n_{P_2H_4}$ against time of irradiation will go through the origin if there is no
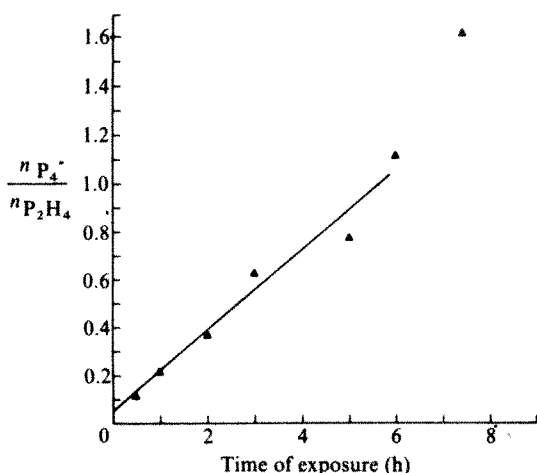
Fig. 3 Ratio $n_{P_4}/n_{P_2H_4}$ versus time of irradiation.

disproportionation of PH_2. (This expression is derived from equations (1)–(8) assuming PH, PH_2 and P_2 are formed in small steady state amounts. Equations (9)–(14) are not included because they apply only at longer irradiation times.) The data of Fig. 3 prove that disproportionation is a minor reaction pathway, a finding which establishes that P_2H_4 is the principal intermediate in the photoconversion of PH_3 to P_4.

The quantum yield for PH_3 (ϕPH_3) loss was determined by both the sum of $4\phi P_4$ and $2 \phi P_2H_4$ and the sum of the $2/3 \phi H_2$ and $4/3 \phi P_2H_4$. (P_2H_4 was determined by its UV absorbance at 235 or 250 nm; H_2 was determined using a thermal conductivity gas chromatograph on a 6 ft molecular sieve 5 Å column with Ar as carrier gas; P_4 was determined colorimetrically as described in ref. 13; actinometry was performed by photolysis of 100 torr of NH_3 in a 10 cm cell ($\phi = 0.31^{14}$). ϕPH_3 is ~ 0.7 by both methods for long irradiation times as reported previously[7] but is greater than 1 at short irradiation times. That the ϕPH_3 is >1 suggests that hydrogen abstraction from PH_3 (reaction (7)) is significant in the conversion of PH_3 to PH_2 (ref. 15). The conversion of P_2H_4 to P_4 may proceed by several pathways (equations (9)–(14), (4)) suggested by analogy with conversion of NH_2NH_2 to N_2 (refs 16, 17). The data presented here establish that P_2H_4 is formed from PH_3, using light of 160–210 nm (ref. 18), by reactions (1), (7) and (8). The detection of P_2H_4 in these studies suggests that it is a likely consitituent of the atmospheres of the jovian planets which may be detected by Earth-based IR spectroscopy or during NASA's Galileo mission to Jupiter.

1. Ridgway, S. T., Wallace, L. & Smith, G. R. *Astrophys. J.* **207**, 1002–1006 (1976).
2. Ridgway, S. T., Larson, H. P. & Fink, U. *Jupiter* (ed. Gehrels, T.) 384–417 (University of Arizona Press, Tucson, 1976).
3. Bregman, J. D., Lester, D. F. & Rank, D. M. *Astrophys. J.* **202**, L55–L56 (1975).
4. Prinn, R. G. & Lewis, J. S. *Science* **190**, 274–276 (1975).
5. Strobel, D. F. *Astrophys. J.* **214**, L97–L99 (1977).
6. Ruiz, H. G. V. & Rowland, F. S. *Geophys. Res. Lett.* **5**, 407–410 (1978).
7. Melville, H. W. *Proc. R. Soc.* **A138**, 374–394 (1932); **139**, 541–557 (1933).
8. Norrish, R. G. & Oldershaw, G. A. *Proc. R. Soc.* **A262**, 1–9 (1961).
9. Harteck, P., Reeves, R. R. Jr. & Thompson, B. A. *Z. Naturforsch.* **19A**, 2 (1964).
10. Nixon, E. R. *J. phys. Chem.* **60**, 1054–1059 (1956).
11. Evers, E. C. & Street, E. H. Jr *J. Am. chem. Soc.* **78**, 5726–5730 (1956).
12. Groth, W. E., Schurath, W. & Schindler, R. N. *J. phys. Chem.* **72**, 3914–3920 (1968).
13. Halmann, M.(ed.) *Analytical Chemistry of Phosphorous Compounds*, 30 (Wiley, New York, 1972).
14. Noyes, W. A. Jr & Leighton, P. A. *The Photochemistry of Gases* 374 (Dover, New York, 1966).
15. Lee, J. H., Michael, J. V., Payne, W.A., Whytock, D. A., Stief, L. J. *J. chem. Phys.* **65**, 3280–3283 (1976).
16. Peterson, D. B. *The Radiation Chemistry of Ammonia* (NSRDS-NBS44, U.S. Department of Commerce, National Bureau of Standards, 1964).
17. Stief, L. J. & Payne, W. A. *J. chem. Phys.* **64**, 4892–4896 (1976).
18. DiStefano, G., Lenzi, M., Margani, A., Mele, A. & Xuan, C. N. *J. Photochem.* **7**, 335–344 (1977).

Angiosperm fossils in supposed Jurassic volcanogenic shales, Antarctica

T. H. Jefferson

Department of Geology, Downing Street, University of Cambridge, Cambridge CB2 3EQ, UK
and
British Antarctic Survey, Natural Environment Research Council, Madingley Road, Cambridge CB3 0ET, UK

During palaeobotanical studies in the Antarctic Peninsula in February 1979, late Cretaceous or younger fossil angiosperm leaves were found within volcaniclastic rocks widely believed to be of late Jurassic age[1]. Although poorly preserved, these fossils are of great stratigraphical importance. They occur at Cape Alexandra, Adelaide Island (Fig. 1), in rocks correlated with the lowest part of the exposed succession (Sloman Glacier succession[1]). The fossils were found less than 10 km from the type locality for this succession at the head of Sloman Glacier (Fig. 1). However, towards the northern end of the island at Mount Bouvier (Fig. 1), ammonites and bivalves indicate that supposedly equivalent rocks[1] are of Upper Jurassic age[2]. This intensive study of a very small part of the succession indicates that the volcanic history of Adelaide Island is much more complicated than was previously suggested by reconnaissance mapping.

The leaves were found 10 m above the lowest stratigraphical horizon exposed at Cape Alexandra, in a succession of volcanic and volcaniclastic rocks which are at least 1,050 m thick. Nineteen specimens of pyritized impressions in a highly indurated black shale were collected. The leaves are open veined, without clearly defined margins. In several specimens there is a marginal zone of intensely pyritized material which
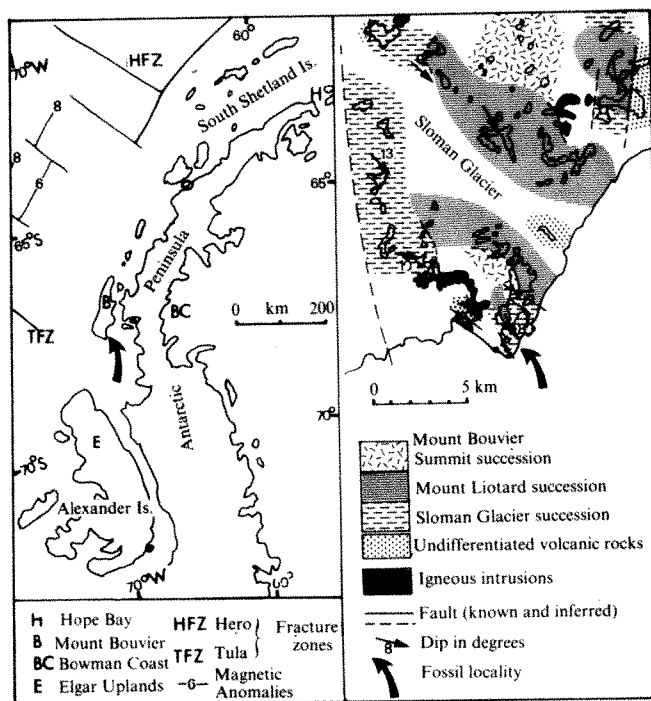
Fig. 1 *a*, A map of the Antarctic Peninsula showing the position of localities mentioned in the text. *b*, Geological map of the Cape Alexandra area, southeastern Adelaide Island (after Dewar[1], Fig. 5).

probably represents the decayed lamina edge. Two nearly whole, narrow ovate[3] leaves were recovered, the smaller of which is 7.6 × 4.2 cm (Fig. 2a), and the larger 8.0 × 4.1 cm (Fig. 2b). Mid-veins are straight, up to 1.3 mm in width (Fig. 2c) and taper towards the apex. Secondary veins are opposite to sub-opposite, arising at intervals of 7–9.5 mm near leaf bases and 6–7.5 mm at apices. They arise at 25°–45° from the mid-vein, angles at apices being up to 7° less than at bases. In two cases the basal secondary veins bifurcate (Fig. 2a, b). No tertiary veins or cuticles are preserved.

Preservation of the leaves is too poor to permit certain identification. However, the leaves bear a close resemblance to those found in volcanic rocks in the Elgar Uplands of Alexander Island[4], and to beech-like leaves in the Tertiary plant beds of the South Shetland Islands[5]. The leaves from the Elgar Uplands occur in rocks correlated lithologically with tuffs dated by K–Ar methods at 70 Myr (ref. 6). However, more extensive work on lavas interbedded with these tuffs gives K–Ar dates ranging from 41 to 63 Myr (R. J. Pankhurst, personal communication). Only one of the fossil floras from the South Shetland Islands has been described. Its age was assessed as Miocene[5], but preliminary K–Ar dating of associated lavas, by Pankhurst, suggests that an early Tertiary age is more likely.

Very few palynomorphs have been recovered using bulk HF techniques on two separate samples. Those found are highly carbonized, most are fragmentary and numbers are insufficient for positive identification. However, the recovered pollen grains which are complete have smooth exines. Two possess six colpi and are probably related to the form-genus *Psilastephanocol-pites*[7] (Fig. 3a, b). One has three colpi and is probably related to the form-genus *Psilatricolpites*[8] (Fig. 3c). Pollen grain fragments with a reticulate sculpture were also recovered (Fig. 3d). These forms are undoubtedly angiospermid. Further work is planned both on existing samples and on material to be collected during the 1979–80 field season.

Also found at Cape Alexandra were numerous compressed tree trunks and/or branches. These are all highly carbonized and no cellular details remain. Their size (up to 3 m in length) indicates that the arborescent vegetation was not in a dwarf or shrub form. Furthermore, the size of the leaves, and of those
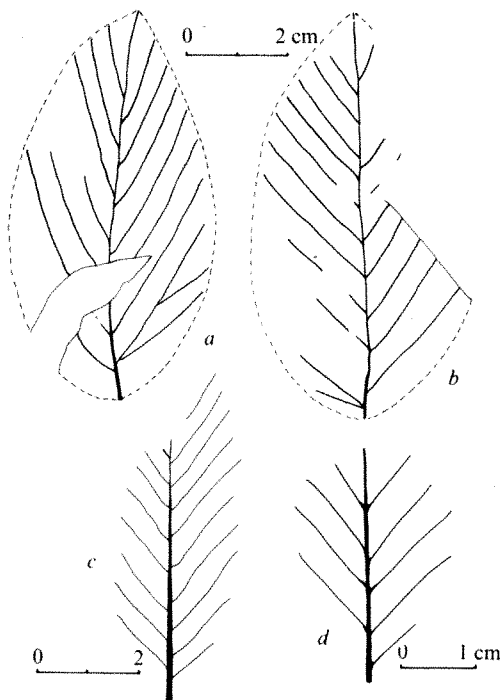
from the Elgar Uplands[4], suggests a temperate climate for the southern Antarctic Peninsula at this time.

Although Cretaceous and Tertiary calc-alkaline volcanic rocks occur in the northern Antarctic Peninsula area, principally the South Shetland Islands[9,10], and in Alexander Island[11], evidence for post-Jurassic volcanism in the central part of the peninsula is at present very tenuous. Altered volcanic and volcaniclastic rocks throughout the Antarctic Peninsula have almost always been assigned an Upper Jurassic age[12], or referred to the 'Upper Jurassic Volcanic Group'[13,14]. This is on the basis of lithological similarity to rocks at Hope Bay (Fig. 1) overlying plant beds of supposed Middle Jurassic age[15]. The extension of the volcanic history of the Antarctic Peninsula through Upper Cretaceous and into Middle Tertiary time has been suggested previously. Taylor *et al.*[3], considered that rocks within the 'Upper Jurassic Volcanic Group' probably represent a much greater time period and Thomson[16] redefined the group as the Antarctic Peninsula Volcanic Group, a name which avoids time constraints. The discovery of the fossil leaves is the first direct evidence from the central Antarctic Peninsula area to demonstrate conclusively that volcanism continued well beyond the late Jurassic into Cretaceous and probably Tertiary times.
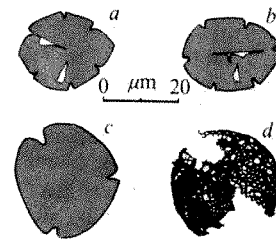
Fig. 3 Carbonized palynomorphs from Cape Alexandra, Adelaide Island.

Magnetic anomalies[17] indicate that subduction of the south-east Pacific plate under the Antarctic Peninsula between the Hero and Tula fracture zones (Fig. 1) continued until at least the Oligocene. This would be compatible with the probable continuous igneous activity on the Bowman Coast from early Jurassic to middle Tertiary times[18] and with the occurrence of angiosperm fossils within a volcaniclastic sequence on southern Adelaide Island.

Fig. 2 Fossil angiosperm leaves from Cape Alexandra, Adelaide Island.

1. Dewar, G. J. *Scient. Rep. Br. Antarct. Surv.* 57 (1970).
2. Hickey, L. J. *Am. J. Bot.* 60, 17–33 (1973).
3. Taylor, B. J., Thomson, M. R. A. & Willey, L. E. *Scient. Rep. Br. Antarct. Surv.* 82 (1979).
4. Thomson, M. R. A. & Burn, R. W. *Nature* 269, 139–41 (1977).
5. Orlando, H. A. in *Antarctic Geology* (ed. Adie, R. J.) 629–36 (North-Holland, Amsterdam, 1964).
6. Grikurov, G. E., Krylov, A. Ya. & Silin, Yu. I. *Dokl. Akad. Nauk. SSSR, Geol.* 172, 168–71 (1967).
7. Leidelmeyer, P. *Leid. geol. Meded.* 38, 53 (1966).
8. Pierce, R. L. *Minnesota geol. Surv. Bull.* 42, 24–49 (1961).
9. Barton, C. M. *Scient. Rep. Br. Antarct. Surv.* 44 (1965).
10. Davies, R. E. S. *Bull. Br. Antarct. Surv.* (in the press).
11. Bell, C. M. *Bull. Br. Antarct. Surv.* 39, 35–44 (1974).
12. Adie, R. J. in *Antarctic Geology and Geophysics* (ed. Adie, R. J.) 137–42 (Universitets-forlaget, Oslo, 1972).
13. Fleet, M. *Scient. Rep. Br. Antarct. Surv.* 59 (1968).
14. Adie, R. J. in *Antarctic Research* (eds Wexler, H., Rubin, M. J. & Caskey, J. E.) 26–39 (American Geophysical Union, Geophysical Monograph 7, 1962).
15. Halle, T. G. *Wiss. Ergebn. schwed. Sudpolarexped.* 3, 14 (1913).
16. Thomson, M. R. A. *3rd Symp. Antarctic Geology and Geophysics* (ed. Craddock, C.) (in the press).
17. Fraser, A. G. & Grimley, P. H. *Scient. Rep. Br. Antarct. Surv.* 67 (1972).
18. Herron, E. M. & Tucholke, B. E. *Init. Rep. DSDP* Leg 35, 263–78 (1976).

Biotin and the sudden infant death syndrome

A. R. Johnson & R. L. Hood

CSIRO Division of Food Research, PO Box 52, North Ryde 2113, Sydney, Australia

J. L. Emery

Children's Hospital, Sheffield, UK

A diet which is marginally deficient in the vitamin biotin may cause sudden unexpected death of young broiler chickens when they are exposed to stress[1,2]. Chickens affected with this disorder have low levels of biotin in their livers. In conditions of biotin insufficiency, we postulate that a similar disorder, triggered by mild stress, may occur in the human infant. We have now used a radiochemical technique to measure the biotin content of 204 livers obtained from infants at autopsy. The levels of biotin in the livers of infants who had died of sudden infant death syndrome (SIDS; cot death) were significantly lower than those in livers of infants of similar age, who had died of explicable causes. These findings support an association of biotin with SIDS.

The stress, which precipitates death in chickens, need only be very mild; for example, disturbance and removal of their food at 2.30 a.m. resulted in chickens being dead, or almost dead by 8.00 a.m. Death occurred quietly with no signs of a struggle. This disorder is known as the fatty liver and kidney syndrome and often affects the largest chickens in a flock. When the birds' diet was supplemented with biotin the disorder was eliminated. In this disorder there are no symptoms of classical biotin deficiency, such as poor conversion of feed, dermatitis or other skin disorders. The birds were hypoglycaemic and death results from hypoglycaemic coma due to a reduction in the activity of the biotin-dependent enzyme pyruvate carboxylase[2]. This is a key enzyme in the gluconeogenic pathway which is responsible for the maintenance of blood glucose levels. When dietary biotin levels are marginal the pathway can synthesise sufficient glucose for the normal needs of a chicken but is unable to supply the amount required when the bird is challenged by a stress. We have suggested that stress-induced deaths may occur in animals of other species[2,3] including human infants[4] when their diets are marginally deficient in biotin. In a preliminary communication it was reported that biotin levels in the livers of infants who had died of SIDS were statistically lower than those in the livers of infants who had died of explicable causes[4].

In studies of SIDS it is essential to have a valid and consistent classification of the cause of death in infants[5]. In the present study, the classification of the cause of death was made (by J.L.E.) with no prior knowledge of the biotin content of the livers. The system of classification[6] is:

(A) Children with gross congenital deformities.

(B) Children with definite and severe disease such as would normally claim hospital admission and from which they could have died.

(C) Children with a mild disease which is of itself insufficient to explain death adequately.

(D) Children with no definite diagnosable disease to account for death, even though there may be evidence that the child may have been unwell at the time of death.

Infants whose cause of death was classified in group C or D are deemed to have died of SIDS.

In the adult, biotin can be derived from both the diet and synthesis by bacteria in the gastrointestinal tract. The contribution, if any, of intestinally synthesised biotin to the overall biotin supply is not known and as a result there are no definite recommended dietary allowances for biotin[7]. In the infant some weeks are required for a mixed population of gut microflora to develop and the increased biotin levels in infants over 1 week of age are probably derived from the diet alone until the mixed population becomes established. The biotin levels in the livers of stillborn infants or infants who died within 1 week post-partum were significantly ($P<0.001$) lower than those in livers of infants surviving more than 1 week (Table 1). The low levels in the newborn infants reflect the transfer of biotin from the mother through the placenta to the fetus.

The peak incidence of SIDS occurs at 3–4 months post-partum. In this study infants who had died between 1 and 52 weeks of life were treated as one group (Table 1). It was interesting to note that there was only one infant whose death was classified as group D. The remainder of SIDS victims were in category C; that is, there was some evidence of a disease which under normal circumstances would not cause death but would almost certainly impose an additional stress on an infant.

The median biotin levels in the livers of infants who died from SIDS between 1 and 52 weeks of life were significantly ($P<0.02$) lower than those of infants who died from explicable causes. The infants in groups A and B cannot be considered as normal controls. However, the impossibility of obtaining biotin levels from healthy infants makes this comparison the only one possible. Intermediate levels of biotin were found in the livers of infants who had died after 52 weeks of life. No conclusions can be drawn from this as the majority of infants had diseases of long standing.

It has been reported[8] in the UK that "cot death is commoner among bottle-fed babies even when the measure is only taken from records of feeding in the first few days[9]: breast feeding gives some protection". It was difficult to obtain reliable and objective information on the duration of breast feeding, but the majority of SIDS cases investigated in this study had been fed infant formulations at the time of death. If biotin is involved in SIDS it may be related to a difference between the available biotin content of breast milk and of infant formulations. A related paper[10] demonstrates that a considerable loss of biotin occurs during the manufacture of certain infant formulations.

There are three observations that indicate that biotin deficiency may be implicated in SIDS. First, there is unequivocal evidence of stress-induced sudden death in young chickens whose diet is marginally deficient in biotin. Second, the biotin levels in the livers of SIDS victims are lower than those in the livers of infants whose deaths were explicable. Third, biotin is

Table 1 Median values of the biotin content of infant livers

Age at death and SIDS classification	n	Liver biotin ($ng\, g^{-1}$)	95% Confidence limits of the median lower	upper
Stillborn and less than 1 week	69	249	222	307
1–52 weeks; groups A and B	57	419	368	462
1–52 weeks; groups C and D	35	336	277	356
>52 weeks	43	344	321	399

The biotin contents of the infant livers were assayed using the radiochemical method of Hood[11,12], with no prior knowledge of the cause of death at the time of analysis. Livers obtained at autopsy were supplied by the Children's Hospital, Sheffield. Following autopsy, the samples were frozen and flown to Sydney while still frozen. A test of skewness on the data for groups A and B and groups C and D indicated that the distribution of biotin levels were skewed ($P<0.05$). Therefore, a statistical test was used that did not assume the distributions were normal. It is a test of the null hypothesis that within each experiment the median of each group is the same. The levels of biotin were replaced by ranks and then the ranks of those observations in one treatment group were summed within each experiment. This provided a Wilcoxan rank sum statistic separately for each experiment. These values were then added. The sampling distribution for this sum was generated from 10,000 simulated experiments.

lost during the processing of some infant formulations[10], thus some bottle-fed infants may be receiving a diet marginally deficient in biotin.

The findings do not suggest that SIDS results from biotin deficiency alone, but, by analogy with chickens, we postulate that biotin insufficiency may leave the infant in a condition in which SIDS can be triggered by mild stress, for example infection, a missed meal, excessive heat or cold, or a changed environment. The evidence to date is circumstantial and it would be difficult to provide 'unequivocal proof' linking biotin, or for that matter any nutrient, with SIDS because of the difficulties in undertaking biochemical studies with experimental and control subjects.

Epidemiological techniques will have to be used and if our recommendation to supplement infant formulas with biotin[10] is implemented, the subsequent trends in the incidence of SIDS may enable the existence of any association to be evaluated more effectively.

1. Pearson, J. A., Johnson, A. R., Hood, R. L. & Fogerty, A. C. *Aust. J. biol. Sci.* 29, 419–428 (1976).
2. Hood, R. L., Johnson, A. R., Fogerty, A. C. & Pearson, J. A. *Aust. J. biol. Sci.* 29, 429–441 (1976).
3. Johnson, A. R., Hood, R. L., Pearson, J. A. & Fogerty, A. C. *Proc. Nutr. Soc.* 35, 130A–131A (1976).
4. Johnson, A. R., Hood, R. L., Cullen, J. A. & Emery, J. L. *Proc. Nutr. Soc. Aust.* 3, 101 (1978).
5. Wigglesworth, E. C. *Med. J. Aust.* 2, 389–390 (1976).
6. Emery, J. L. & Carpenter, R. G. in *Sudden Infant Death Syndrome* (ed. Robinson, R. R.) 7–19 (Foundation for the Study of Infant Death, London and Toronto, 1974).
7. *Recommended Dietary Allowances* 8th edn, 80–81 (National Academy of Sciences, Washington, DC, 1974).
8. Gunther, M. *Lancet* i, 441–442 (1975).
9. Carpenter, R. G. & Emery, J. L. *Nature* 250, 729 (1974).
10. Hood, R. L. & Johnson, A. R. *Nutr. Rep. Int.* (in the press).
11. Hood, R. L. *J. Sci. Fd Agric.* 26, 1847–1852 (1975).
12. Hood, R. L. *Analyt. Biochem.* 79, 635–638 (1977).

The role of gastropod pedal mucus in locomotion

Mark Denny

Department of Zoology, University of British Columbia, Vancouver, B.C., Canada V6T 1W5

Gastropods move using a single appendage—the foot. For many gastropods the power for locomotion is provided by muscular waves moving along the ventral surface of the foot[1-3], the force of these waves being coupled to the substratum by a thin layer of pedal mucus. This mucus acts as a glue, allowing the animal to adhere to the substratum on which it crawls[2,3]. This adhesive ability is advantageous, particularly to animals (such as limpets and certain snails) which live in intertidal or arboreal habitats where the forces of waves and gravity must be resisted while the animal forages. However, the adhesiveness of the pedal mucus presents the animal with a problem. How can an animal with only one foot walk on glue? This question was studied using as an example the terrestrial pulmonate slug, *Ariolimax columbianus*, and locomotion is found to depend on the unusual mechanical properties of the pedal mucus.

The pedal mucus of *A. columbianus* is 96–97% water and dissolved salts[4]. The relevant mechanical properties of the material are determined by the remaining 3–4% which is a high molecular weight glycoprotein. The glycoprotein, a polyelectrolyte, is highly expanded in water, and individual molecules are crosslinked to form a gel network[4]. The presence of this

* Present address: Department of Zoology, University of Washington, Seattle, Washington 98195
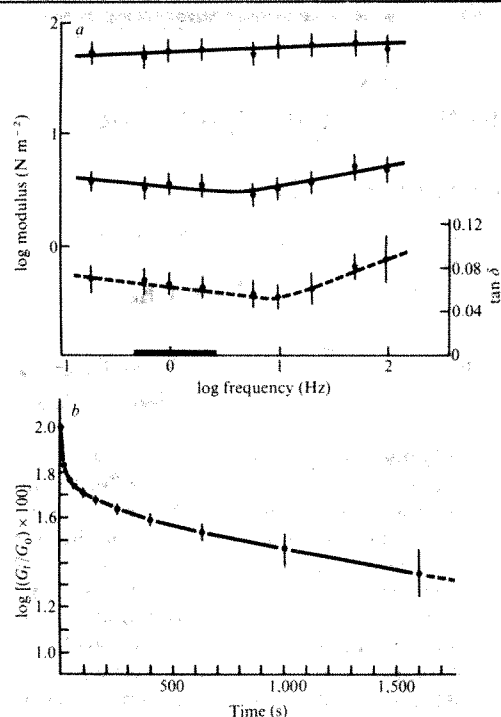
Fig. 1 Network properties of pedal mucus. [Stress is force divided by area (Nm^{-2}); shear strain is shear deformation divided by sample thickness[6].] *a*, The dynamic stiffness of *A. columbianus* pedal mucus at small strains. Results shown are the average from six samples tested in air at 100% relative humidity, 22–23 °C. The bars are 95% confidence intervals. Tests are performed by applying a sinusoidal strain ($\gamma = 0.2$ to 0.5) and measuring the resulting stress. Stress amplitude/strain amplitude is G^*, the complex modulus, a measure of the material's stiffness at a given frequency[6]. The phase shift between strain and stress (δ) is a measure of the relative viscous and elastic contribution to G^*: G', the storage modulus, $=G^* \cos \delta$, and is a measure of elastic stiffness. G'', the loss modulus, $=G^* \sin \delta$, and is a measure of viscous stiffness. The ratio G''/G' is $\tan \delta$. The parallel plate dynamic apparatus (from ref. 8), was modified to test samples in shear rather than in tension. The bar on the abscissa shows the approximate range of frequencies at which the mucus is deformed under a crawling slug. *b*, The stress relaxation behaviour of *A. columbianus* pedal mucus. In the relaxation tests a sample is quickly deformed to a set strain and the force required to maintain that strain is followed with time. The curve shown is the average of 10 tests carried out in air at high relative humidities, 21–23 °C. The bars are 95% confidence intervals. Values on the ordinate are the ratio of the shear modulus at time $t(G_t)$ to the shear modulus at the start of the test (G_0), plotted as the logarithm. No small set of relaxation times adequately describes this relaxation behaviour.

crosslinked network accounts for any elasticity shown by the mucus[5,6]. The nature of the crosslinks was determined by examining the material's solubility. The glycoprotein network is not readily soluble in water, but is soluble in 1% 2-mercaptoethanol and in 8 M urea or 8 M guanidine HCl. Solubility in 1% 2-mercaptoethanol indicates the presence of disulphide bonds as network crosslinks[7], formed between the cysteine molecules which comprise 3% of the amino acids of the protein chains. Solubility in 8 M urea or 8 M guanidine HCl is evidence of the presence of a second form of network crosslink—hydrogen bonds and/or hydrophobic interactions between carbodydrate chains[7].

The mechanical properties of the mucus at small shear strains, γ, (Fig. 1 legend) were measured in a parallel plate dynamic testing apparatus (modified from Gosline[8]). This apparatus allows the elastic (G') and viscous (G'') components of the material's dynamic stiffness (G^*) to be measured as a function of the frequency of deformation. At small deformations ($\gamma < 5$) the pedal mucus shows the properties of a soft, primarily elastic solid (Fig. 1a). G' is 100 N m^{-2} (10^{-4} times the stiffness of rubber) and G'' is about 8 Nm^{-2}. Both values are virtually constant from 0.1

to 100 Hz. The stress relaxation properties of the mucus were measured at small strains ($\gamma < 5$) with a cone and plate apparatus in which the mucus is held between a small angle acrylic plastic cone and a coaxial aluminium plate. Rotation of the plate by an electric motor shears the mucus, and the consequent force is measured by monitoring (with a linearly variable differential transformer) the torsion of the bar supporting the cone. The theory of this apparatus is described by Ferry[6]. The gel stress relaxes without reaching equilibrium (Fig. 1b), indicating[6] that the network crosslinks, while stable over short times encountered during dynamic testing (milliseconds to seconds), are labile under stresses applied for long periods (minutes to hours).

These mechanical properties, although representative of the mucus at small strains, will not necessarily apply if higher strains are encountered during locomotion. The thickness of the mucus layer (measured by a method similar to that used by Lissman[9] for slugs crawling on aluminium foil) is typically 10–20 μm. The surface of the foot of *A. columbianus* moves forward about 1 mm with each wave; and the strain is thus 50–100, considerably higher than that used in the tests described above.

The properties of the pedal mucus at large strains were measured with the cone and plate apparatus. At $\gamma = 5$ to 6 the mucus network is disrupted and the material yields (Fig. 2a). With further extension the mucus shows the properties of a viscous liquid. The magnitudes of the yield stress (σ_y) and the

flow stress (σ_f) increase with increasing strain rate (Fig. 2b), while the yield strain does not vary with strain rate. If, after the mucus has yielded, the material is allowed to stand unstressed, the mucus will 'heal' that is, as the mucus stands the gel network reforms, and the material again shows the properties of an elastic solid. The mucus can be shown[4] to regain appreciable solidity in times as short as 0.1 s. This 'yield–heal' cycle can be repeated 20 to 30 times without change in either σ_y or σ_f. The precise mechanism of the healing process is not known, though it seems likely that it involves the easily reformed hydrogen and/or hydrophobic bonds of the gel network rather than the covalent disulphide bonds.

The yield–heal characteristics of this mucus are ideally suited to the locomotion of *A. columbianus*. During locomotion 12 to 17 muscular waves are present on the slug's foot; each wave being an area of forward motion, initiated at the posterior end of the animal as the tail is pulled forward. A wave is translated anteriorly until it reaches the head of the animal where it is dissipated as the head moves forward. In a small area (50–100 μm long anterio-posteriorly) at the leading edge of a wave the mucus is stressed to yielding; consequently most of the wave area moves over mucus in its liquid form. This liquid offers little resistance to movement. The waves alternate with interwaves, these being stationary relative to the ground. The mucus beneath the leading edge of the interwave quickly heals, and most of the interwave rests on mucus in its solid form. If the shear strength of the solid mucus (σ_y) is sufficient to resist the forces produced by the movement of the waves, the animal will be able to crawl forward. The mechanical properties reported here can be combined with precise measurements (from video tapes) of foot movements and areas to produce a model of the forces operating under a moving slug. The model predicts that the mucus beneath the interwaves is indeed capable of resisting wave forces, and these predictions prove accurate when compared to those forces actually measured under *A. columbianus* crawling horizontally[10]. Thus the yield–heal cycle of the pedal mucus allows it to act as a material ratchet, facilitating forward movement, but resisting backward movement. The result is effective adhesive locomotion.

I thank J. M. Gosline and S. K. Denny for discussions. This research was funded by NRC grant 67–6934 to J.M.G.

1. Jones, H. D. in *Pulmonates* (eds Fretter, V. & Peake, J.) Vol. 1, 1–32 (Academic, New York, 1975).
2. Lissman, H. W. *J. exp. Biol.* **21**, 58–69 (1945).
3. Miller, S. L. *J. exp. mar. Biol. Ecol.* **14**, 96–156 (1974).
4. Denny, M. W. & J. M. Gosline (in preparation).
5. Flory, P. J. *Principles of Polymer Chemistry* (Cornell University Press, Ithaca, 1953).
6. Ferry, J. D. *Viscoelastic Properties of Polymers* (Wiley, New York, 1970).
7. Creeth, J. M. *Br. med. J.* **34**, 17–24 (1978).
8. Gosline, J. M. *Biopolymers* **18**, 2091–2103 (1979).
9. Lissman, H. W. *Nature* **156**, 391 (1945).
10. Denny, M. W. (in preparation).
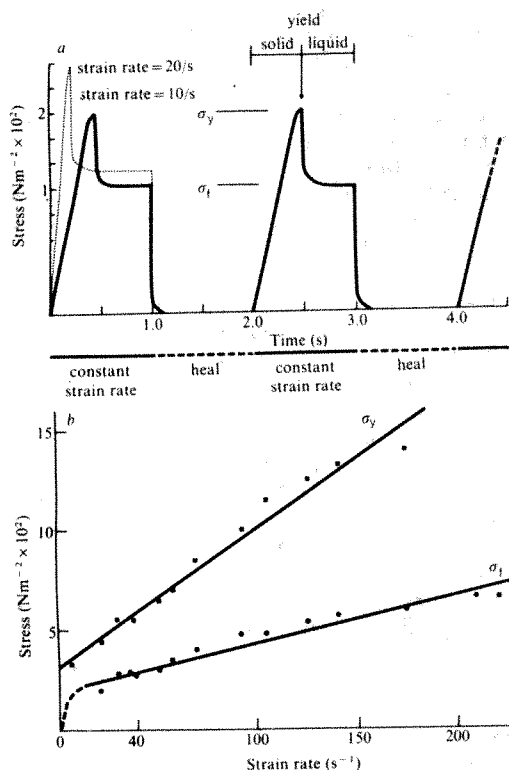
Fig. 2 Properties of pedal mucus under simulated natural conditions. *a*, Mechanical properties of *A. columbianus* pedal mucus at high strains. The abscissa is calibrated in seconds, where for alternate periods the mucus is sheared at a constant strain rate and held stationary. The mucus is thus exposed to conditions analogous to those found under a crawling slug. When first sheared, stress is proportional to strain, indicating that the mucus is an elastic solid. At a strain of 5–6 (stress = σ_y) the mucus yields. With further strain stress is proportional to strain rate, that is, the mucus behaves as a liquid. When shearing is stopped the mucus begins to heal. The healing period of 1 s represents the time the mucus is unsheared beneath an interwave during locomotion. Yield stress and flow stress both increase with increasing strain rate; yield strain is constant. *b*, A representative plot of yield stress (σ_y) and flow stress (σ_f) as a function of strain rate. The range of strain rates is approximately that found under crawling slugs. While σ_f is linearly related to strain rate at the rates measured, it is assumed to have a nonlinear behaviour (shown by the dashed line) at strain rates below those measured in these tests. [σ_y:$y = 6.9x + 313$; $r = 0.986$. σ_f:$y = 2.3x + 199$; $r = 0.971$]

Inhibitory effect of prolactin on ovulation in the *in vitro* perfused rabbit ovary

Yasuo Hamada, Sheldon Schlaff, Yoshimune Kobayashi, Rosie Santulli, Karen H. Wright & Edward E. Wallach

Department of Obstetrics and Gynecology, Pennsylvania Hospital and The University of Pennsylvania School of Medicine, Philadelphia, Pennsylvania 19107

Prolactin is best known for its effects on the breast, promoting mammary growth and lactation. In some species, including rat, mouse, hamster, sheep and rabbit, prolactin is necessary for the maintenance of the corpus luteum[1-5]. Further, a relationship has

been recognised between hyperprolactinaemia and ovulatory failure in the human. The site of action is thought to be the hypothalamus and or adenohypophysis[6]. McNatty *et al.*[7] have postulated a direct ovarian effect of prolactin, reporting that low prolactin levels were essential for progesterone production by preovulatory human granulosa cells cultured *in vitro*. However, high levels of prolactin decreased progesterone production. The present investigation sought to determine the effect of prolactin on ovulation using the *in vitro* perfused rabbit ovary preparation. We report that its effects are inhibitory.

The technique for cannulating the rabbit ovarian artery and details of the *in vitro* perfused ovary system have been described previously[8,9]. Using this system, ovulation can be achieved following the direct addition of human chorionic gonadotropin (HCG) to the perfusion medium[9,10]. The ovaries are continually observed for 12 h to determine the state of follicular development and ovulation. Follicles are considered ruptured when an extruded cumulus oophorus is observed on the ovarian surface.

Two series of experiments were carried out. In the first, the dose of prolactin was kept constant, while the amount of HCG was varied. In the second series, a standard amount of HCG was used, while the dose of prolactin was varied. Five groups of five rabbits each were used in the first series. Both ovaries were removed from an isolated, untreated, sexually mature New Zealand white rabbit and placed in the perfusion chamber. Ovaries were perfused at a rate of 1.5 ml min^{-1}. Ovine prolactin (100 μg) was dissolved in 1 ml of saline, 1 ml of the prolactin solution was added to the perfusate of one ovary (final concentration in the perfusate 100 μg per 150 ml) and 1 ml saline was added to the contralateral ovary, which served as a control. Ten minutes later, HCG (15, 25, 50, 75 or 100 IU per 150 ml) was added to the perfusate of each pair of ovaries.

In the second series of experiments (three groups of five rabbits), varying amounts of prolactin (5, 15 or 45 μg prolactin per 150 ml) were added to the perfusate of the experimental ovary. A standard dose of HCG (50 IU per 150 ml) was added to the perfusate of both ovaries 10 min after the addition of prolactin. The contralateral ovary was perfused with HCG only and served as a control.

The total number of mature follicles observed at the onset of the experiment did not differ significantly among the groups, suggesting that the pool of follicles available for ovulation was similar in all ovaries. In the control ovaries, a relationship was demonstrated between the number of ovulations per ovary and the dose of HCG, with maximal effectiveness attained at a level of 50 IU per 150 ml (1.55×10^{-9} M). The number of ovaries which demonstrated ovulation did not differ significantly among the five control groups. Inclusion of 100 μg prolactin (2.67×10^{-8} M) significantly reduced the following parameters: the

number of ovulations per ovulating ovary in response to 25 or 50 ($P < 0.05$) units of HCG (Student's *t*-test), and the number of mature follicles proceeding to rupture in response to 15 ($P < 0.01$), 25 ($P < 0.005$), 50 ($P < 0.005$) or 100 ($P < 0.05$) units of HCG (χ^2, Yate's correction). All data are included in Table 1. In those experiments in which the dose of HCG was maintained at 50 IU and the amount of prolactin varied, the number of ovulating ovaries was not significantly reduced regardless of the dose of prolactin.

Endogenous luteinising hormone (LH), evoked by mating or by the administration of HCG, promotes follicular development and ultimate rupture within 12 h in the intact rabbit and in the *in vitro* perfused rabbit ovary. HCG was effective at various dose levels, as low as 15 IU per 150 ml, in promoting ovulation. The addition of prolactin to the perfusate reduced the occurrence of ovulation. This effect seemed to be dose related and was observed with 100 μg per 150 ml; lower doses were ineffective. Prolactin at 100μg uniformly inhibited ovulation regardless of the dose of HCG.

Prolactin exerts a dual effect on ovarian function. It is required for maintenance of the corpus luteum in certain species, and elevated levels of prolactin have been associated with attenuated corpus luteum function[11]. McNatty *et al.*[7] demonstrated that prolactin at 100 ng ml^{-1} inhibited progesterone production in cultured human granulosa cells whereas a low level of prolactin was necessary in the culture medium to promote progesterone production. The dose-dependent relationship encountered in the present experiments also suggests that at certain levels prolactin interferes with follicular rupture.

Several explanations may be proposed for the inhibitory effect of prolactin on ovulation observed in these experiments. Prolactin may act directly at the level of the ovary, independent of HCG, to inhibit final stages of follicular maturation, follicular rupture or ovum maturation. Nolin[12], using immunohistochemical techniques, has indicated the presence of prolactin in luteal cells and in dictyate oocytes of primordial and maturing ovarian follicles, in the rat, and speculates that prolactin may act to provide nutritive support for the developing oocyte. Prolactin may also influence the number of LH receptors in the follicular cells; an interaction may exist between LH and prolactin and their respective receptors at the ovarian level. In the rat, LH acts on granulosa cells of mature follicles to increase prolactin receptors[13], whereas increased prolactin leads to an increase in basal ovarian LH receptors[14]. Rolland *et al.*[15] have demonstrated an inhibitory effect of prolactin on the restoration of normal cycling levels of LH in postpartum women, suggesting that this effect of prolactin is exerted at the level of the ovary itself. Only when prolactin levels were low did ovulation and LH return to normal. Prolactin may also act as a competitive inhibi-

Table 1 The effect of prolactin (PRL) on ovulation in the *in vitro* perfused rabbit ovary

Treatment	No. of ovaries ovulating ($N = 5$)	No. of ovulations per ovulating ovary (mean ± s.e.)	No. of ovulations per no. of mature follicles
HCG 15 IU	3	4.00 ± 1.00	$12/35$ $P < 0.01$
HCG 15 IU + PRL 100 μg	1	2.00 ± 0	$2/35$
HCG 25 IU	4	4.75 ± 0.94 $P < 0.05$	$19/31$ $P < 0.005$
HCG 25 IU + PRL 100 μg	3	2.00 ± 0.57	$6/31$
HCG 50 IU	5	5.40 ± 1.21 $P < 0.05$	$27/32$ $P < 0.005$
HCG 50 IU + PRL 100 μg	5	1.80 ± 0.20	$9/32$
HCG 75 IU	4	3.50 ± 0.64	$14/36$
HCG 75 IU + PRL 100 μg	2	3.50 ± 1.50	$7/38$
HCG 100 IU	5	3.60 ± 0.40	$18/33$ $P < 0.05$
HCG 100 IU + PRL 100 μg	3	3.00 ± 0.58	$9/33$
HCG 50 IU	5	3.40 ± 0.75	$17/34$
HCG 50 IU + PRL 45 μg		2.50 ± 0.65	$8/31$
HCG 50 IU	4	2.75 ± 0.48	$11/31$
HCG 50 IU + PRL 15 μg	2	2.50 ± 0.50	$5/29$
HCG 50 IU	5	3.00 ± 0.55	$15/32$
HCG 50 IU + PRL 5 μg	4	2.75 ± 0.85	$11/32$

tor of the action of HCG on the ovarian receptor.

The precise point at which prolactin interferes with ovulation is difficult to identify. Prolactin may act by interfering with final critical stages of follicular development which ultimately lead to ovulation or with mechanical events within the ovary that are required for rupture of a mature graafian follicle. In any event, these data provide additional support for the concept that prolactin acts directly on the ovary to influence the process of ovulation. This effect seems to be dose related.

1. Evans, H. M., Simpson, M. E., Lyons, W. R. & Turpeinen, K. *Endocrinology* **28**, 933–945 (1941).
2. Kovacić, N. *J. Reprod. Fert.* **8**, 165–186 (1964).
3. McNatty, K. P., Neal, P. & Baker, T. G. *J. Reprod. Fertil.* **47**, 155–156 (1976).
4. Denamur, R. J. & Short, R. V. *J. Reprod. Fert.* **132**, 207–220 (1973).
5. Spies, H. G., Hillard,J. & Sawyer, C. H. *Endocrinology* **83**, 354–367 (1968).
6. Archer, D. F. *Fert. Steril.* **28**, 125–134 (1977).
7. McNatty, K. P., Sawers, R. S. & McNeilly, A. S. *Nature* **250**, 653–655 (1974).
8. Lambertsen, C. J., Greenbaum, D. F., Wright, K. H. & Wallach, E. E. *Fert. Steril.* **27**, 178–187 (1976).
9. Wallach, E. E., Wright, K. H. & Hamada, Y. *Am. J. Obstet. Gynecol.* **132**, 728–738 (1978).
10. Hamada, Y., Wright, K. H. & Wallach, E. E. *Fert. Steril.* **32**, 335–339 (1979).
11. Andrews, W. C. *Fert. Steril.* **32**, 501–509 (1979).
12. Nolin, J. M. *Endocrinology* **102**, 402–406 (1978); *J. Cell Biol.* **79**, 177a (1978).
13. Richards, J. S. & Midgley, A. R. *Biol. Reprod.* **14**, 82–94 (1976).
14. Seguin, C. & Kelly, P. A. *Biol. Reprod.* **20**, Suppl. 1, 86A (1979).
15. Rolland, R., DeJong, F. H., Schellekens, L. A. & Lequin, R. M. *Clin. Endocr.* **4**, 27–38 (1975).

Direct evidence for a two-signal mechanism of cytotoxic T-lymphocyte activation

Hung-Sia Teh & Soo-Jeet Teh

Department of Microbiology, University of British Columbia, Vancouver, British Columbia, Canada V6T 1W5

The cellular requirements for the activation of cytotoxic T lymphocytes to alloantigens are complex. In addition to cytotoxic precursors (CLPs), metabolically active stimulator cells[1], adherent accessory (A) cells[2,3] and antigen-specific helper T cells[4] are also required. However, the requirement for A cells[5,6], metabolically active stimulator cells[7,8] or helper T cells[9] can be replaced by soluble factors or co-stimulator (CoS)[10], a lymphokine obtained by stimulation of murine spleen cells with concanavalin A (Con A). We show here that in the presence of CoS, cultures containing on average one lymph node lymphocyte (LNL) and Con A can be activated to produce single cytotoxic clones. This observation strongly suggests that one of the target cells of CoS is the CLP and provides more direct evidence for a two-signal mechanism for cytotoxic T lymphocyte activation.

Culture conditions limiting for CLPs can be achieved by supplementing limiting numbers of responder cells with nu/nu spleen cells syngeneic to the responder[11]. The efficacy of CoS in rendering culture conditions limiting for CLP was therefore compared with that of nu/nu spleen cells (Table 1). It is clear that in the conditions specified in Table 1, CoS is more effective than nu/nu spleen cells in promoting a cytotoxic response to alloantigens. The frequency of CLPs in C57BL/6J(B6) (H-2[b]) mice to DBA/2(D2)(H-2[d]) alloantigens in CoS-supplemented cultures was 2,844 per 10^6 H-2[b] LNLs and 1,642 per 10^6 H-2[b] LNLs in H-2[b]-nu/nu spleen cell-supplemented cultures. H-2[b] LNLs cultured with CoS alone in similar conditions did not give

Table 1 CoS can substitute for nu/nu spleen cells in limiting dilution assays

B6 LNLs	D2 spleen (2,000R)	CoS*	% Specific lysis per culture (mean ± s.e.)	No. of responding cultures
0	1×10^5	10 units ml^{-1}	0.0 ± 0.2	0/12
200	1×10^5	10 units ml^{-1}	1.0 ± 0.1	6/12
400	1×10^5	10 units ml^{-1}	5.4 ± 2.4	6/12
800	1×10^5	10 units ml^{-1}	39.8 ± 6.1	12/12
1,600	1×10^5	10 units ml^{-1}	66.6 ± 3.6	12/12
CLPs per 10^6 cells†				2,844
95% confidence limits				1,782–4,539
χ^2				3.02

B6 LNLs	D2 spleen (2,000R)	B6-nu/nu spleen		
0	2×10^5	2×10^5	0.0 ± 0.2	0/24
200	2×10^5	2×10^5	2.4 ± 2.3	6/24
400	2×10^5	2×10^5	4.9 ± 3.2	9/24
800	2×10^5	2×10^5	17.4 ± 5.6	20/24
CLPs per 10^6 cells				1,642
95% confidence limits				1,160–2,325
χ^2				2.39

Microcultures were set up in V-bottom microtitre trays (Cat. No. 76-024-05, Linbro) as previously described[11]. Each culture contained the indicated additions in a volume of 0.20 ml and was incubated for 5 days at 37 °C in 5% CO_2 in air. The culture medium used was RPMI-1640 supplemented with 10% fetal bovine serum (batch no. C791224, Gibco), 5×10^{-5} M 2-mercaptoethanol, 10 mM HEPES buffer and 50 μg ml^{-1} gentamycin sulphate (Sigma). B6 LNLs were taken from the brachial, auxillary and inguninal nodes. After 5 days, each culture was assayed for cytotoxic activity against 2×10^3 ^{51}Cr-labelled P815 (H-2[d]) target cells as detailed previously[14]. Briefly, 0.10 ml of supernatant was removed from each culture and 2×10^3 ^{51}Cr-labelled P815 target cells in 0.10 ml were then added to each culture with a 100-μl Eppendorf pipette, suspending the cell pellet in the process. The microtitre trays were then centrifuged at 120g for 5 min before being incubated for a further 4–6 h at 37 °C. Spontaneous release was determined by taking the mean of the ^{51}Cr release from 12 cultures that had received all other additions except B6 LNLs. The spontaneous release of ^{51}Cr-labelled P815 targets in all experiments was 10–20% of the maximum releasable counts; this was determined by freezing and thawing the target cells three times. Test cultures were scored as positive if their counts exceeded the 95% confidence limits of the spontaneous counts. The results remained unchanged if the responding cultures were taken as those that exceed the 99% confidence limits of the spontaneous counts.

Per cent specific lysis

$$= \frac{\text{Test counts} - \text{Spontaneous release}}{\text{Maximum releasable counts} - \text{Spontaneous release}} \times 100\%$$

*Fraction II co-stimulator was prepared according to the method of Shaw *et al.*[32]. A concentration of 1 unit ml^{-1} of CoS was defined as the amount that produced 37% of the maximal stimulation of DNA synthesis of murine thymocytes cultured at 5×10^5 per ml and mitogenic concentrations of Con A for 3 days[32]. Maximal DNA synthetic responses were usually obtained with about 5 units ml^{-1} CoS.

† This was calculated according to the method of Porter and Berry[33]. All the data reported here gave satisfactory fits to the zero order term of the Poisson distribution ($P < 0.05$) according to χ^2 statistics.

rise to any detectable cytotoxic response to H-2[d] (data not shown); this suggests that CoS does not exert its action by acting as a T-cell mitogen[10]. Supernatants from secondary mixed lymphocyte reactions (MLR) also contain factor(s) that renders culture conditions limiting for CLPs[12].

The above observation is consistent with a two-signal mechanism for the activation of CLPs[13,14]. According to this model, a CLP is first stimulated by antigen (signal 1). The antigen-stimulated CLP is then activated to cell proliferation and differentiation by a non-antigen-specific inductive factor (signal 2). The definitive experiment to test this hypothesis will require the isolation of a CLP and the demonstration that when it is stimulated with the specific H-2 alloantigen and CoS, it will form a cytotoxic clone specific for that H-2 alloantigen. Because the frequency of CLPs to H-2[d] alloantigens in H-2[b] mice is about 2,844 per 10^6 LNLs, only about 1 in 350 cultures containing single LNLs can form a cytotoxic clone to H-2[d] when stimulated with CoS and H-2[d] alloantigens. This approach is unfeasible, as thousands of cultures would have to be set up to obtain a statistically reliable number of responders. However, about 1 in 40 H-2[k] LNLs can be activated by Con A to form a

cytotoxic clone in nu/nu spleen cell-supplemented cultures[15]. Rather similar results were observed for CoS-supplemented cultures; the frequency of CLPs in $H-2^b$ LNLs able to give rise to a cytotoxic clone is about 31,804 per 10^6 LNLs and about 11% of these clones are specific for $H-2^d$ alloantigens (Table 2). Cytotoxic clones of all H-2 specificities were assayed for by adding phytohaemagglutinin (PHA) to the cytotoxic assay and cytotoxic clones specific for $H-2^d$ assayed for by adding α-methylmannoside to the cytotoxic assay. PHA reveals nonspecific cytotoxicity by agglutinating cytotoxic T lymphocytes to target cells[16] whereas the addition of α-methylmannoside allows the detection of specific cytotoxic lymphocytes by preventing any nonspecific, Con A-mediated interactions between cytotoxic lymphocytes and targets[17]. About 1 in 30 cultures containing single $H-2^b$ LNLs can be stimulated by Con A and CoS to form a cytotoxic clone; it is therefore feasible to test whether Con A and CoS can activate cultures containing as few as one LNL per culture. Cultures were set up such that on average each culture would contain 1, 3 or 10 $H-2^b$ LNLs, CoS and Con A. After 5 days, these cultures were assayed for cytotoxic activity against $H-2^d$ targets in the presence of PHA. The results from three experiments showed that out of 240 cultures containing an average of 1 $H-2^b$ LNL, the numbers of cultures giving rise to detectable cytotoxic clones were 7, 11 and 6, respectively (Table 3). In all three experiments, the observed numbers of responders for cultures containing 1, 3 or 10 $H-2^b$ LNLs were within those predicted by Poisson statistics; the mean CLP frequency for these three determinations is $30,876 \pm 5,369$ per 10^6 B6 LNLs. A log–log plot of lytic activity per culture against cell dose was linear and gave a slope of 1.06 (Fig. 1), further suggesting that the only limiting cell type in these cultures is the CLP[18]. These findings provide relatively direct evidence that the minimal conditions for the activation of CLPs are mitogenic concentrations of Con A and
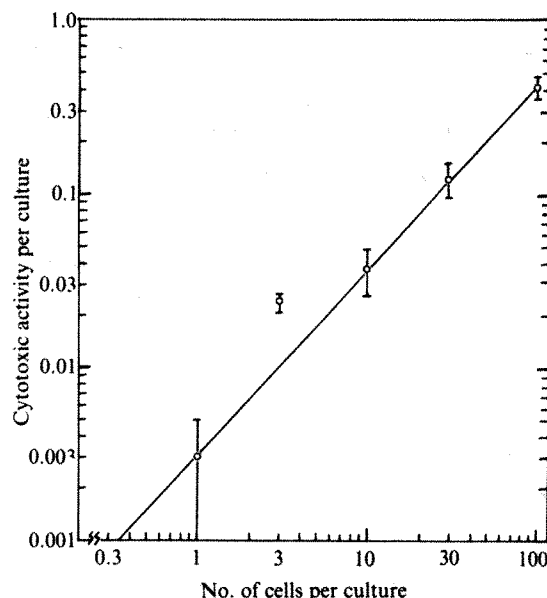
Fig. 1 Log plot of cytotoxic activity per culture against responder cell dose, Cultures containing the indicated number of B6 LNLa were stimulated with $2.5\ \mu g\ ml^{-1}$ Con A and $7.5\ units\ ml^{-1}$ CoS in V-bottom trays for 5 days; total volume 0.10 ml. On day 5 each culture was assayed for cytotoxic activity against 2×10^3 ^{51}Cr-labelled P815 target cells in the presence of $10\ \mu g\ ml^{-1}$ PHA. The number of responding cultures for each cell dose is given in the last column of Table 3. Cytotoxic activity was calculated according to the method of Miller and Dunkley[34] and is defined as $-\ln(1-f)$, where $f =$ fraction of target cells damaged. At low f values, $f = p =$ fractional specific ^{51}Cr release. This method of expressing the data yields a number proportional to the number of effector cells present rather than the number of target cells destroyed. A value of 0.10 corresponds to 10% specific ^{51}Cr release and a value of 0.30 corresponds to 26%. The vertical bars represent the standard errors.

Table 2 Activation of CLPs by Con A and CoS

B6 LNLs	CoS (units ml^{-1})	Con A ($\mu g\ ml^{-1}$)	% Specific lysis (mean ± s.e.)	No. of responding cultures	CLPs per 10^6 LNLs
0	7.5	2.5	0.0 ± 0.4	0.12	
40	7.5	2.5	12.2 ± 5.4	7/12	31,804*
80	7.5	2.5	29.7 ± 4.8	12/12	19,670–51,424
160	7.5	2.5	41.9 ± 4.3	12/12	$\chi^2 = 2.00$
0	7.5	2.5	0.0 ± 0.3	0/12	
400	7.5	2.5	5.4 ± 1.4	8/12	3,617†
800	7.5	2.5	18.4 ± 6.7	12/12	2,185–5,989
1,600	7.5	2.5	23.6 ± 4.7	12/12	$\chi^2 = 1.31$

Culture and assay conditions were similar to those described in Table 1 legend. In the absence of exogenous CoS no cytotoxic response was detected in similar experimental conditions.
*This assay was carried out in the presence of $10\ \mu g\ ml^{-1}$ PHA.
† This assay was carried out in the presence of 25 mM α-methylmannoside.

Table 3 Activation of single CLPs by CoS and Con A

B6 LNLs	CoS	Con A	Expt 1	Expt 2	Expt 3
0	7 units ml^{-1}	2.5 $\mu g\ ml^{-1}$	0/24	0/24	0/24
1	7 units ml^{-1}	2.5 $\mu g\ ml^{-1}$	7/240	11/240	6/240
3	7 units ml^{-1}	2.5 $\mu g\ ml^{-1}$	14/120	6/124	12/120
10	7 units ml^{-1}	2.5 $\mu g\ ml^{-1}$	30/96	14/60	13/60
30	7 units ml^{-1}	2.5 $\mu g\ ml^{-1}$	ND	ND	15/24
100	7 units ml^{-1}	2.5 $\mu g\ ml^{-1}$	ND	ND	12/12
CLPs per 10^6 LNLs			37,074	27,644	27,911
95% confidence limits			28,216–48,711	19,672–38,846	19,659–39,625
χ^2			0.52	4.44	0.91

Culture conditions were similar to those described in Table 1 legend except that the total volume of each culture was 0.10 ml instead of 0.20 ml. The cytotoxic assays were carried out in the presence of $10\ \mu g\ ml$ PHA. The spontaneous release was determined by averaging the counts of 24 cultures that received CoS and Con A but no B6 LnLs. ND, Not determined.

CoS. Our data also support other studies showing that T-cell activation and clonal expansion require Con A and Con A-induced growth factors[19-21]. Further support for the two-signal model is provided by the recent observation of Lalande *et al.*[22] that a clone of specific cytotoxic T lymphocytes can be produced from a single CLP in the presence of alloantigen and CoS.

The other question pertinent to this discussion is whether CoS is the inductive signal in an MLR. CoS is not only produced following stimulation of spleen cells with Con A but is also a product of an MLR[8,23]. Stimulation of CoS production by Con A is dependent on a Lyt 1^+2^- T cell as well as A cells[5]; CoS production in an MLR also requires a Lyt 1^+2^- T cell[23] and metabolically active stimulator spleen cells[24]. Taken together, these observations suggest that CoS production is probably dependent on a Lyt 1^+2^- T cell, A cell(s) and metabolically active stimulator cells. These requirements are identical to those for optimal CL production in the MLR and further support the hypothesis that CoS is the inductive signal in an MLR. Factors bearing other names but with biological properties similar to those of CoS have been given the generic name interleukin 2 (ref. 25) and include the following: the 'nonspecific factor' of Waldmann and Munro[26], the 'nonspecific mediator' described by Harwell *et al.*[27], the 'thymocyte mitogenic factor' of Farrar *et al.*[28], certain 'T-cell replacing factors' (refs 29, 30) and the 'T-cell growth factor' of Gillis *et al.*[31].

1. Lafferty, K. J., Misko, I. S. & Cooley, M. A. *Nature* 249, 275–276 (1974).
2. Wagner, H., Feldmann, M., Boyle, W. & Schrader, J. W. *J. exp. Med.* 136, 331–343 (1972).
3. MacDonald, H. R., Phillips, R. A. & Miller, R. G. *J. Immun.* 111, 575–589 (1973).
4. Pilarski, L. M. *J. exp. Med.* 145, 709–725 (1977).
5. Paetkau, V. in *Molecular Mediators of Cellular Immunity* (eds Hadden, J. W. & Stewart, W. E. II) (Humana, Clifton, in the press).
6. Symington, F. W. & Teh, H.-S. *Scand. J. Immun.* (in the press).

7. Talmage, D. W., Woolnough, J. A., Hemmingsen, H., Lopez, L. & Lafferty, K. L. *Proc. natn. Acad. Sci. U.S.A.* **74**, 4610–4614 (1977).
8. Shaw, J., Monticone, V., Mills, G. & Paetkau, V. *J. Immun.* **120**, 1974–1980 (1978).
9. Plate, J. *Nature* **260**, 329–331 (1976).
10. Paetkau, V., Mills, G., Gerhart, S. & Monticone, V. *J. Immun.* **117**, 1320–1324 (1976).
11. Teh, H.-S., Harley, E., Phillips, R. A. & Miller, R. G. *J. Immun.* **118**, 1049–1056 (1977).
12. Ryser, J.-E. & MacDonald, H. R. *J. Immun.* **122**, 1691–1696 (1979).
13. Bach, F. H., Bach, M. L. & Sondel, P. M. *Nature* **259**, 273–281 (1976).
14. Lafferty, K. L. & Woolnough, J. *Immun. Rev.* **35**, 231–262 (1977).
15. Teh, H.-S., Phillips, R. A. & Miller, R. G. *J. Immun.* **118**, 1057–1062 (1977).
16. Bevan, M. J. & Cohn, M. *J. Immun.* **114**, 559–565 (1975).
17. Trowbridge, I. S., Ralph, P. & Bevan, M. J. *Proc. natn. Acad. Sci. U.S.A.* **72**, 157–161 (1975).
18. Miller, R. G., Teh, H.-S., Harley, E. & Phillips, R. A. *Immun. Rev.* **35**, 38–58 (1977).
19. Larsson, E.-L. & Coutinho, A. *Nature* **280**, 239–241 (1979).
20. Andersson, J., Grönvik, K.-O., Larsson, E.-L. & Coutinho, A. *Eur. J. Immun.* **9**, 581–586 (1979).
21. Coutinho, A., Larsson, E.-L., Grönvik, K.-O. & Andersson, J. *Eur. J. Immun.* **9**, 587–591 (1979).
22. Lalande, M. E., McCutcheon, M. J. & Miller, R. G. *J. exp. Med.* **151**, 12–19 (1980).
23. Wagner, H. & Röllinghoff, M. *J. exp. Med.* **148**, 1523–1538 (1978).
24. Okada, M., Klimpel, G. R., Kuppers, R. C. & Henney, C. S. *J. Immun.* **122**, 2527–2533 (1979).
25. *J. Immun.* **123**, 2928–2929 (1979).
26. Waldmann, H. & Munro, A. *Immunology* **27**, 53–64 (1974).
27. Harwell, L., Kappler, J. W. & Marrack, P. *J. Immun.* **116**, 1379–1384 (1976).
28. Farrar, J. J., Simon, P. L., Koopman, W. L. & Fuller-Bonar. *J. Immun.* **121**, 1353–1360 (1978).
29. Hübner, L., Müller, G., Schimpl, A. & Wecker, E. *Immunochemistry* **15**, 33–39 (1978).
30. Watson, J., Aarden, L. A. & Lefkovits, I. *J. Immun.* **122**, 209–215 (1979).
31. Gillis, S., Ferm, M. M., Ou, W. & Smith, K. A. *J. Immun.* **120**, 2027–2032 (1978).
32. Shaw, J., Monticone, V. & Paetkau, V. *J. Immun.* **120**, 1967–1973 (1978).
33. Porter, E. H. & Berry, R. J. *Br. J. Cancer* **17**, 583–595 (1964).
34. Miller, R. G. & Dunkley, M. *Cell. Immun.* **14**, 284–302 (1974).

Host-dependent evolution of three papova viruses

Eiichi Soeda*, Takeo Maruyama*, John R. Arrand† & Beverly E. Griffin†

* The National Institute of Genetics, Mishima 411, Japan
†Imperial Cancer Research Fund Laboratories, PO Box 123, Lincoln's Inn Fiels, London WC2 3PX, UK

A marked similarity has been observed in the organization of genomic information between two of the papova viruses, SV40 and polyoma virus (Py)[1], suggesting that these viruses may have diverged from a common ancestor during evolution. However, distinct differences between them and also between them and the human papova virus, BKV, are observed, for example, in their interactions with several animal cells[2], and the immunological cross-reaction between viral proteins[3,4]. Results from DNA–DNA hybridization experiments[5–8] suggest that homologies between the viral DNAs are small, although the search for homology has depended largely on the stringency of the experimental conditions. The difficulties of using hybridization (or heteroduplex) analyses for determining the extent of homology between two DNA species has been considered in detail by Yang and Wu[9]. It has also recently been pointed out that in stringent hybridization conditions, greater than 85% homology is required for the observation of double-strandedness, and that the use of less stringent conditions reveals more extensive homology between Py and SV40 than had earlier been reported[10]. Nonetheless, the above data did not seem to allow detailed discussion of the relationships between papova viruses. We therefore turned to a comparison of the nucleotide sequences of the viral genomes and found striking homologies around the DNA replication origins of these viral species[11-18]. Recently, the complete sequences of SV40[14,15] Py[19,20] and BKV DNAs[21,22] have been elucidated, providing insight into the evolutionary relationships of these viruses. We have now compared the nucleotide sequences of these viral genomes gene by gene and conclude that each of these viral species has evolved from a common ancestor and diverged with its host organism.

BKV, SV40 and Py are easily isolated from healthy human, African green monkey and mouse tissues, respectively[2,23]. They grow *in vitro* to high titres on cells from these species; therefore, we consider these to be their natural hosts. From the DNA sequence homology, we have calculated relative evolutionary distances and constructed a phylogenetic tree for the viral species. For the hosts, the evolutionary time and the relationships between species have been well documented from palaeontological studies, based on the fossil record.

According to palaeontology, the order Rodentia, which includes rats, mice and squirrels, diverged from the order Primates, to which various monkeys, the apes and man belong, about 80 Myr ago. Later in mammalian evolution, various forms of primates came into existence. In particular, the evolution of the suborder Catarrhini, a well defined group of Old World primates including the living monkeys of Asia and Africa, the

anthropoid apes and man, occurred some 35 Myr ago in the late Eocene and early Oligocene[24,25]. Therefore, applying these palaeontological facts to the evolution of the host organisms, it seems quite reasonable to suggest that the mouse separated from the African green monkey and man some 80 Myr ago and that the green monkey and man diverged from each other 35 Myr ago. Figure 1a shows the phylogenetic relationship.

For DNA sequence comparisons, data are taken from three different genes, those coding for small t antigen, large T antigen and the virus capsid proteins VP2/3. In the analysis (made by computer), the corresponding nucleotide sites of DNAs, or predicted amino acid residues of proteins, were compared and the number of identical sites or residues counted. We then calculated the ratio of the number of sites having identical nucleotides (or amino acid residues) at corresponding positions to the total number of sites (or residues) examined. We denote this ratio by P_n in the case of DNA sequence and P_a in the case of primary structure of protein. Thus, P_n is the fraction of DNA sequences which when compared have the same nucleotides, and P_a the fraction of identical amino acids. We made this calculation for parts of comparable genes for which homology was clear and for which, therefore, a meaningful comparison was possible (see Table 1). This included the entire VP2/3, small t- and large T-antigen regions of Py and SV40, a sequence of about 534 nucleotides starting from the N-terminals of VP2/3 of BKV and SV40, and others. A total of nine pairs of homologous genes from the three virus species were compared and P_n and P_a were calculated for each of them. The results are given in Table 2.

The probabilities of having identical or non-identical residues can be translated into a measure of the evolutionary distance
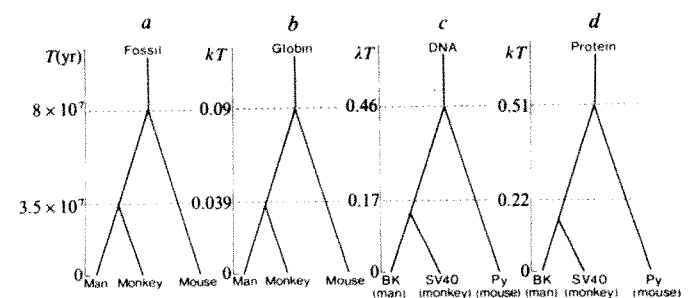
Fig. 1 Phylogenetic trees for hosts and for viruses. *a*, For the hosts, based on palaeontological evidence; each branch of the tree represents evolutionary divergence time. *b*, For the homologous globin amino acids; each branch represents the evolutionary distance measured by *kT*. *c*, For the viruses based on nucleotide sequence; each branch represents the evolutionary distance measured by λ*T*. *d*, For the viruses based on the amino acid sequence comparisons, each branch represents the evolutionary distance measured by *kT*. The dotted horizontal lines indicate the relative points where the branch should occur if the molecular evolutionary distances among the viruses agreed completely with the branchings of the hosts. As the dotted lines show only relative locations, one of the two lines can be placed at an arbitrary location. We have therefore adjusted the branchings between Py and SV40 (BKV) to the same height of the primates–rodent branching in *a*.

Table 1 Nucleotide usage in the measurement of evolutionary distance

	1	2	3	4
	Total	Compared	Gap	Unique
Small t antigen				
Py	639	519	3(0.6)	78
SV40	531		36(6.4)	
Py	636	513	3(0.6)	78
BKV	522		39(7.0)	
BKV	519	516	6(1.1)	6
SV40	525		0(0)	
Large T antigen				
Py	2,343	1,881	36(1.91)	456
SV40	2,127		6(0.3)	210
Py	1,389	1,380	21(1.5)	
BKV	1,401		9(0.6)	
BKV	1,536	1,533	3(0.2)	
SV40	1,542		0(0)	9
VP2/3				
Py	969	885	84(8.6)	
SV40	1,062		72(7.5)	81
Py	525	510	18(3.4)	
BKV	528		15(2.8)	6
SV40	534	534		
BKV	534			

Vertical column 1 shows the total number of nucleotides in the gene which codes for a particular protein that were examined. Column 2 shows the number of nucleotides compared. Column 3 shows the number of positions where gaps are left in sequence comparisons in order to maximize homology and (in parentheses) the percentage of sequence this represents. Column 4 shows the number of nucleotides that seem to be unique to an individual species and are therefore excluded from the comparison.

between the species compared. The method, originally developed by Zuckerkandl and Pauling[26], has been extensively used in molecular evolution studies[27,28]. The principle of the method is as follows. When we look at the evolution of genes at the molecular level, that is, at the primary sequence of proteins coded for by those genes, the rate at which amino acid residues become different is constant with time, and the probability of identity between corresponding homologous sites of two species declines exponentially with time. Because only a finite number of substitutions is possible for both amino acids and nucleotides, a correction factor must be, and has been, included in the calculations. If we denote the rate of amino acid substitution by k, that for nucleotides by λ and the divergence time by T, we arrive at $P_n = 0.25 + 0.75 \, (-8\lambda T/3)$ (ref. 28) for nucleotide identity and a similar formula for the amino acid sequence identity[27]. As P_n and P_a are experimentally determined quantities, substituting them into these formulae gives values for λT for the nucleotide comparison and kT for the amino acid comparison (see Table 2). If the divergence time is known, the

rates λ and k can be determined explicitly. It is important to realize that values of λT or kT, although they are the product of two quantities (rate and time), are of a linear nature and can be directly compared, whereas the values of P_n and P_a cannot.

Each comparison gives one value of the evolutionary distance and we have made a total of nine such comparisons for three species. Note that in corresponding parts of homologous genes, relative distances have not varied from one virus species to another (data not shown)[19]. This suggests that these regions might descend consistently from a common primordial gene. Although the evolutionary distances calculated from the data varied little from gene to gene, we have calculated a weight mean distance between each pair of species to construct a phylogeny. The result for the DNA sequences is presented in Fig. 1c and that for the amino acid sequences in Fig. 1d. For comparison, a calculation for the relevant globin sequences is shown (Fig 1b). A remarkable similarity is evident among the host phylogeny based on fossil record (Fig. 1a) and the two virus phylogenies constructed from the genome comparison at the molecular level. We take this agreement among the phylogenies as evidence for the co-evolution of the hosts and viruses. These data suggest that the three papova virus species diverged from each other together with the divergence of their host species.

It is necessary, however, to examine whether this hypothesis is consistent with other known facts. From data presented below, we have found no serious contradictions to our hypothesis.

A phylogeny based on the amino acid substitutions among homologous proteins of different species agrees well with relationships inferred from classical taxonomy and palaeontology. Proteins often used in constructing molecular evolutionary phylogenies are cytochrome c and globins[29,30]. The sequences of globins α and β are known for several species and, when the homologous chains are compared, identity indices (P_a) are found to be: man-monkey, 0.95; man-mouse, 0.85; monkey-mouse, 0.83. If these P_a values are converted into the linearized evolutionary distance ($2kT$), we get man-monkey, 0.74; man-mouse, 0.165; monkey-mouse, 0.189. From these, a phylogenetic tree of the host species can be constructed. The one based on these data is presented in Fig. 1b. With different proteins, although the distance values themselves change, the relative relationships remain approximately the same.

To determine explicitly the rates of evolution for the virus DNA and amino acid sequences (assuming the divergence times to be the same as their hosts), we calculated the rate for every case compared (Table 2). The rates for the virus proteins were found to be 4.0–7.8×10^{-9} per yr per amino acid site, which is relatively fast. The rates are known for several proteins and range from 1×10^{-9} for globins to an exceptionally slow rate of 6×10^{-12} for histone IV (ref. 31).

The virus nucleotide substitution rates were found to be about the same as that of their proteins. There are only a few reliable reports on DNA evolution rates, as DNA sequencing

Table 2 Comparison of nucleotide and amino acid sequences among the three virus species BKV, SV40 and polyoma virus (Py)

Virus lineage	Gene	Probability of identity		Linearized evolutionary distance*		No. of nucleotides examined	Ref.
		P_n DNA	P_a Protein	$2\lambda T$ DNA	$2kT$ Protein		
Py/SV40	Small t	0.453	0.306	0.98	1.25	513	13–16
	Large T	0.501	0.423	0.82	0.89	1,881	14–16, 32
	VP2/3	0.501	0.434	0.82	0.86	885	15, 33
Py/BKV	Small t	0.470	0.322	0.92	1.19	513†	
	Large T	0.425	0.407	1.09	0.93	1,380†	
	VP2/3	0.469	0.341	0.92	1.12	510†	
BKV/SV40	Small t	0.709	0.709	0.37	0.35	516	22
	Large T	0.721	0.753	0.35	0.29	1,533	21
	VP2/3	0.764	0.758	0.28	0.28	534	17

* This is divergence time (T) multiplied by rate (λ or k).

†The line-up of homologous peptides of BKV/Py is very similar to that observed in Py/SV40. Approximation to maximum homology of BKV/Py was mainly obtained by substitution of homologous peptides of BKV/SV40 into those found for Py/SV40.

techniques are very recent developments. Kimura[28] has examined nucleotide substitution rates by comparing homologous parts of the human and rabbit haemoglobin mRNA sequences. His data (based on 53 nucleotides from these genes) gives an estimate of the substitution rate for the haemoglobin genes of about 2.3×10^{-9} per yr per nucleotide site. The viral genes examined here seem to be evolving at rates of 4.5–6.5×10^{-9} per yr per site, which is somewhat faster than that estimated

for the haemoglobin genes. This is consistent with the virus protein data which show the viral proteins to be evolving faster than the globins. All the viral data can be accommodated by an hypothesis which suggests co-evolution of the virus and host species.

1. Fried, M. & Griffin, B. E. *Adv. Cancer Res.* **24**, 67–108 (1976).
2. Tooze, J. *Molecular Biology of Tumour Viruses*, 1–73 (Cold Spring Harbor Laboratory, New York, 1973).
3. Takemoto, K. K. & Mullarkey, M. F. *J. Virol.* **12**, 625–631 (1973).
4. Shah, K. V., Ozer, H. L., Ghazey, H. N. & Kelly, T. J. Jr *J. Virol.* **21**, 179–186 (1977).
5. Khoury, G. *et al. Proc. natn. Acad. Sci. U.S.A.* **72**, 2563–2567 (1975).
6. Ferguson, J. & Davis, R. W. *J. molec. Biol.* **94**, 135–149 (1975).
7. Newell, N., Lai, C. J., Khoury, G. & Kelly, T. J. Jr *J. Virol.* **25**, 193–201 (1978).
8. Wold, W. S. M. *et al. Proc. natn. Acad. Sci. U.S.A.* **75**, 454–458 (1978).
9. Yang, R. C. A. & Wu, R. *Proc. natn. Acad. Sci.* **76**, 1179–1183 (1979).
10. Howley, P. M., Israel, M. A., Law, M.-F. & Martin, M. A. *J. biol. Chem.* **254**, 4876-4883 (1979).
11. Soeda, E., Miura, K., Nakaso, A. & Kimura, G. *FEBS Lett.* **79**, 383–389 (1977).
12. Soeda, E., Kimura, G. & Miura, K. *Proc. natn. Acad. Sci. U.S.A.* **75**, 162–166 (1978).
13. Friedmann, T., LaPorte, P. & Esty, A. *J. biol. Chem.* **253**, 6561-6567 (1978).
14. Reddy, V. B. *et al. Science* **200**, 494–502 (1978).
15. Fiers, W. *et al. Nature* **273**, 113–120 (1978).
16. Soeda, E., Arrand, J. R., Smolar, N. & Griffin, B. E. *Cell* **17**, 357–370 (1979).
17. Yang, R. C. A. & Wu, R. *Nucleic Acids Res.* **7**, 651–668 (1979).
18. Dhar, R., Lai, C. J. & Khoury, G. *Cell* **13**, 345–358 (1978).
19. Soeda, E., Arrand, J. R., Smolar, N., Walsh, J. & Griffin, B. E. *Nature* **283**, 445–453 (1980).
20. Deininger, P., Esty, A., La Porte, P., Hsu, H. 4 Friedmann, T. *Nucleic Acids Res.* **8**, 855-860 (1980).
21. Yang, R. C. A. & Wu, R. *Science* **206**, 456–462 (1979).
22. Seif, I., Khoury, G. & Dhar, R. *Cell* **18**, 963–977 (1979).
23. Gardner, S. D., Field, A. M., Coleman, D. V. & Hulme, B. *Lancet* i, 1253–1257 (1971).
24. Romer, A. S. *Vertebrate Palaeontology* 3rd edn (University of Chicago Press, 1974).
25. Colbert, E. H. *Evolution of the Vertebrates* (Wiley, New York, 1955).
26. Zuckerkandl, E. & Pauling, L., in *Evolving Genes and Proteins* (eds. Bryson, V. & Vogel, J.) 97–166 (Academic, New York, 1965).
27. Kimura, M. *Proc. natn. Acad. Sci. U.S.A.* **63**, 1181–1188 (1969).
28. Kimura, M. *Nature* **267**, 275–276 (1977).
29. Fitch, W. M. & Margoliash, E. *Science* **155**, 279–284 (1967).
30. Fitch, W. M. & Margoliash, E. *Evolut. Biol.* **4**, 67–109 (1970).
31. Dayhoff, M. O. *Atlas of Protein Sequence and Structure* (National Biomedical Research Foundation, Washington, DC, 1972).
32. Soeda, E., Arrand, J. R. & Griffin, B. E. *Nucleic Acids Res.* **7**, 839–858 (1979).
33. Arrand, J. R., Soeda, E., Walsh, J. E., Smolar, N. & Griffin, B. E. *J. Virol* **33**, 606-618 (1980).

Avian sarcoma virus-transforming protein, pp60^{src} shows protein kinase activity specific for tyrosine

Marc S. Collett, A. F. Purchio & R. L. Erikson

Department of Pathology, University of Colorado, School of Medicine, Denver, Colorado 80262

The protein responsible for malignant transformation by avian sarcoma viruses (ASVs) has been identitifed as a phosphoprotein of molecular weight 60,000 designated pp60^{src} (refs 1–4). It has been suggested that this protein has a functional role in cellular transformation involving the phosphorylation of cellular proteins, for it was discovered that specific immunoprecipitates from ASV-transformed cells that contain pp60^{src} catalysed the transfer of phosphate from $[\gamma\text{-}^{32}\text{P}]$ATP to the heavy chain of rabbit immunoglobulin[5,6]. Additional studies involving the cell-free synthesis of the ASV src protein further demonstrated that the presence of the src polypeptide correlated with that presence of a phosphotransferase activity[7]. Our studies, involving the biochemical purification of this protein, have demonstrated that the ASV-transforming gene product, pp60^{src}, is itself a protein kinase. We have purified the pp60^{src} protein approximately 5,000-fold using either conventional ion-exchange chromatography or immunoaffinity chromatography[8,9]. The resultant partially purified preparations contain a cyclic AMP-independent protein kinase activity[8]. We report here that the soluble phosphotransferase activity of partially purified pp60^{src} results in the phosphorylation of exclusively tyrosine residues in a variety of proteins that serve as substrates.

Using partially purified pp60^{src} prepared by immunoaffinity or ion-exchange chromatography as described elsewhere[8], we have investigated the phosphorylation of a variety of proteins. Several examples are illustrated in Fig. 1. Purified pp60^{src} is able to phosphorylate the heavy chain of rabbit immunoglobulin that is immunologically directed towards pp60^{src} (TBR IgG; track 3), but not of normal rabbit IgG (track 2). Of several proteins commonly used as substrates for protein kinases, including histones, phosvitin, protamine and casein, only casein is phosphorylated by pp60^{src} (track 4). This phosphorylation of casein was largely inhibited by preincubation of the enzyme preparation with immune, but not normal IgG, demonstrating the pp60^{src}-specific nature of the

phosphotransferase activity (track 5). Using casein as the phosphate acceptor protein, we have determined the K_m for ATP to be 24 μM.

As many of the manifestations of pp60^{src} expression seem to affect cellular architecture, we have, in our initial attempts to define the molecular site(s) of action of the ASV-transforming protein, considered whether various components of the cellular cytoskeleton might serve as phosphate acceptor proteins for our partially purified pp60^{src} preparations. Figure 1 shows that actin present in microfilaments (track 6) or found in purified 10-nm filaments (track 8) served as a substrate for the pp60^{src} kinase. Desmin, the other major component of 10-nm filaments, was
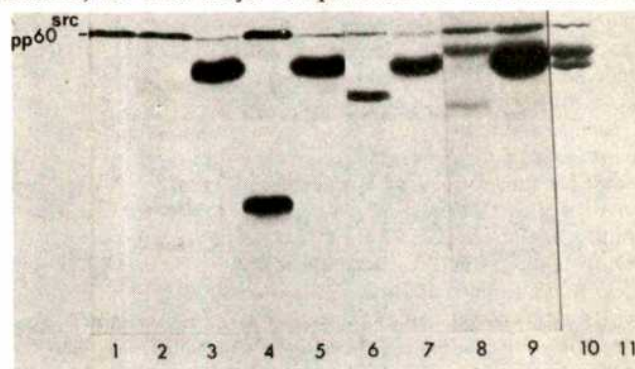
Fig. 1 Phosphorylation of various proteins by partially purified pp60^{src} protein kinase. Immunoaffinity column-purified pp60^{src} was incubated in standard protein kinase reaction mixtures[8] with a variety of exogenously added proteins. After incubation at 22 °C for 15 min, reactions were terminated and samples were subjected to SDS-10% polyacrylamide gel electrophoresis followed by autoradiography[8]. Track (1), partially purified pp60^{src} kinase alone, and with (2) normal rabbit serum IgG (1 mg ml^{-1}), (3) tumour-bearing rabbit (TBR) serum IgG (1 mg ml^{-1}), (4) casein (1 mg ml^{-1}), (5) casein plus TBR IgG, (6) rabbit skeletal muscle actin (0.5 mg ml^{-1}) purified as described[18], (7) actin plus TBR IgG, (8) dog smooth muscle 10-nm filaments (0.2 mg ml^{-1}) purified as described elsewhere[19], (9) 10-nm filaments plus TBR IgG (10) chick brain microtubules (0.5 mg ml^{-1}) purified by two cycles of polymerization–depolymerization[20], (11) microtubules with TBR serum added and the immune complexes removed by addition and subsequent pelleting of protein A-containing *S. aureus* before the phosphorylation reaction. The actin and 10-nm filament preparations showed no endogenous phosphorylation when incubated alone. Endogenous kinase activity in the microtubule preparations was completely eliminated by heating at 90 °C for 1 min before the phosphorylation reaction.
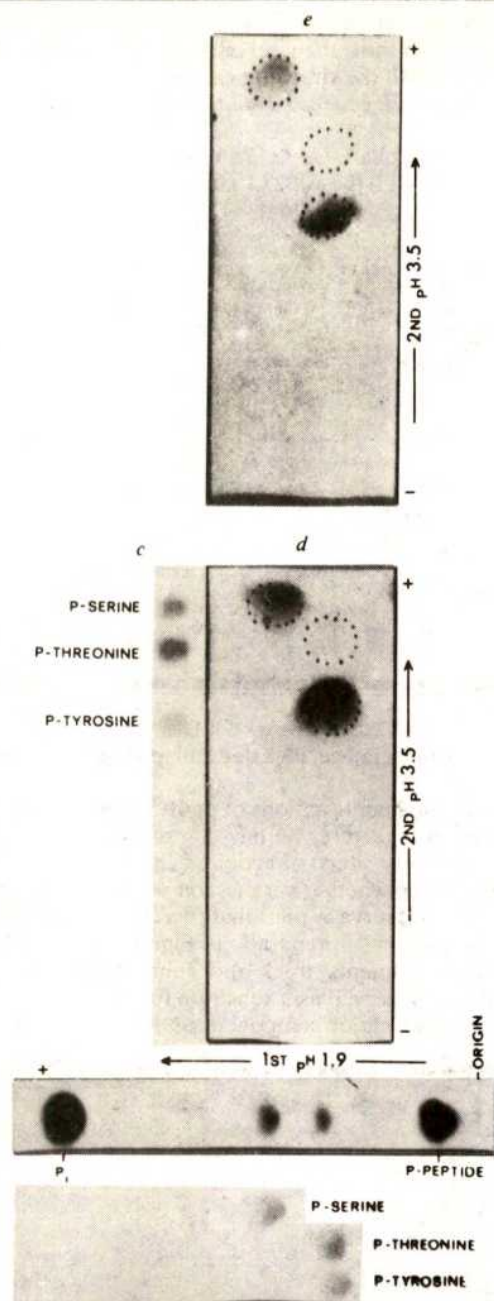
Fig. 2 Phosphoamino acid analyses of pp60[src] and pp60[sarc] isolated from ^{32}P-labelled cells in culture. ^{32}P-labelled viral pp60[src] and normal chick cell pp60[sarc] were immunoprecipitated from ASV-transformed and normal chick cells, respectively, subjected to SDS-polyacrylamide gel electrophoresis, localized by autoradiography, excised and then eluted from the gel pieces. After precipitation with 20% trichloroacetic acid, the polypeptides were subjected to acid hydrolysis in 6M HCl at 100° C for 3–4 h. Samples of the hydrolysates were spotted onto Whatman 3MM paper. Electrophoresis at pH 1.9 was as described previously[10]. Electrophoresis at pH 3.5 (pyridine/acetic acid/H_2O, 1:10:189) was carried out at 4,500 V for 0.5 h. Samples of authentic phosphoserine, phosphothreonine (both from Sigma) and phosphotyrosine (initially the gift of P. Billings and M. Blumenfeld, and subsequently synthesized by the method of Plimmer[21] as modified by Mitchell and Lunan[22]) were added to all radioactive samples analysed. Panel *a* shows the results of electrophoresis at pH 1.9 of authentic phosphoamino acids (ninhydrin stained); *b*, electrophoresis at pH 1.9 of an acid hydrolysate of ^{32}P-labelled pp60[src]; *c*, electrophoresis of authentic phosphoamino acids at pH 3.5 (ninhydrin stained); *d*, two-dimensional electrophoresis (1st at pH 1.9, 2nd at pH 3.5) of an acid hydrolysate of ^{32}P-labelled pp60[src]; *e*, two-dimensional electrophoresis of an acid hydrolysate of ^{32}P-labelled pp60[sarc]. The dotted circles show the positions of ninhydrin-stained phosphoamino acid markers.

also phosphorylated (track 8), as were the two major constituents of microtubules, α- and β-tubulin (track 10). The pp60[src]-specific nature of these phosphorylations was demonstrated by prior complexing of the kinase activity with anti-pp60[src] antibody (tracks 7, 9) or by removal of pp60[src] before the phosphorylation reaction by immune complex formation and subsequent antigen–antibody removal using protein A-containing *Staphylococcus aureus* (track 11).

Note in Fig. 1 that, even in the absence of added exogenous protein, the partially purified enzyme preparation is capable of phosphorylating pp60[src] itself. This seems to be due to pp60[src] 'self-phosphorylation' (ref. 9 and unpublished data). Structurally, the pp60[src] polypeptide contains two major sites of phosphorylation[10]. One site is a serine residue located in the amino-terminal 60% of the polypeptide, which is phosphorylated by a cyclic AMP-stimulated protein kinase activity in cell-free extracts[10]. The second major site of phosphorylation on pp60[src] we had previously reported to be a phosphothreonine residue located on the carboxy-terminal 40% of the polypeptide[10]. This residue is phosphorylated by a cyclic AMP-independent protein kinase[10], and represents the site of autophosphorylation by pp60[src] (ref. 9).

Two other tumour virus-encoded transformation proteins, the polyoma virus middle T antigen and the Abelson murine leukaemia virus p120 protein, are phosphorylated at tyrosine residues by apparent autophosphorylation reactions[11,12]. We have therefore re-examined pp60[src] for the presence of phosphotyrosine and have found that our previous analyses did not separate phosphothreonine from phosphotyrosine. On re-investigation we found that the non-serine phosphorylation in the carboxy-terminal region of the pp60[src] polypeptide involves a tyrosine residue (not threonine, as previously reported[10]) in both the phosphorylated protein isolated from transformed cells and the partially purified protein autophosphorylated *in vitro*.

We had previously carried out such phosphoamino acid studies by acid hydrolysis of the polypeptide, followed by electrophoresis at pH 1.9 (ref. 10 and Fig. 2b). However, in view of the existence of phosphotyrosine in other virus-encoded polypeptides, and the fact that phosphotyrosine and phosphothreonine are not resolved by electrophoresis at pH 1.9 (Fig. 2a), we have used electrophoresis at pH 3.5 to analyse for the presence of phosphoserine, phosphothreonine and phosphotyrosine (Fig. 2c). Figure 2d shows a two-dimensional electrophoretic separation of an acid hydrolysate of *in vivo* ^{32}P-labelled pp60[src]. The first dimension at pH 1.9 allows the separation of free phosphate, phosphoserine, phosphothreonine/phosphotyrosine and phosphopeptides (Fig. 2b). The second dimension, run at pH 3.5, clearly separates phosphothreonine and phosphotyrosine. As can be seen, pp60[src] isolated from radiolabelled cells in culture contains phosphoserine and phosphotyrosine. Thus, our previous inability to resolve phosphothreonine and phosphotyrosine led to the erroneous conclusion that the COOH-terminal phosphorylated residue in pp60[src] was phosphothreonine[10]. Similar results indicating that the viral pp60[src] protein contains a phosphotyrosine residue have recently been obtained by others[13]. Furthermore, the normal cellular protein, pp60[sarc], which is both structurally and functionally closely related to the viral pp60[src] protein[14-17], also contains a carboxy-terminal phosphotyrosine residue (not phosphothreonine as previously reported[16]) in addition to an amino-terminal phosphoserine (Fig. 2e).

For further investigation of phosphorylation by pp60[src] *in vitro*, we have analysed the phosphoamino acid residues in the various phosphate acceptor proteins for this protein kinase activity. We have found that, in addition to tyrosine being the residue of self-phosphorylation by the purified pp60[src] protein kinase activity, other soluble protein substrates of this phosphotransferase activity seem to be phosphorylated exclusively at tyrosine residues (Fig. 3). Hunter and Sefton[13] have recently reported that pp60[src] present in immunoprecipitates apparently phosphorylates a tyrosine residue in IgG. Our results confirm their report (Fig. 3, track 3); but furthermore, our more con-

ventional soluble enzymatic reactions support the validity of the original src immune complex assays for the phosphotransferase activity of pp60[src](ref.5). Note, however, that only acid-stable phosphorylated residues in the various proteins are being analysed in these studies. It is possible that other acid-labile phosphorylated amino acids may be present.

It is important to realise that caution must be exercised in the interpretation of these data concerning the various substrates of the purified pp60[src] kinase. Major structural components of microfilaments, 10-nm filaments and microtubules all seem to be substrates for pp60[src] protein kinase, and all are phosphorylated at tyrosine residues only, but no information is provided concerning the physiological significance of such phosphorylations in the transformed cell.

Studies are under way to determine whether cellular proteins which serve as efficient substrates for pp60[src] phosphorylation *in vitro* are phosphorylated at the same sites in the transformed cell. Once this is established for a protein, some functional role must then be assigned to the modification observed, which can in turn be related to the transformed phenotype. In any event, due to the uncommon presence of phosphotyrosine residues in phosphoproteins, and in view of the fact that several viral proteins associated with oncogenic disease contain these phosphorylated residues, the association of such a secondary modification of proteins with cellular transformation deserves further investigation.
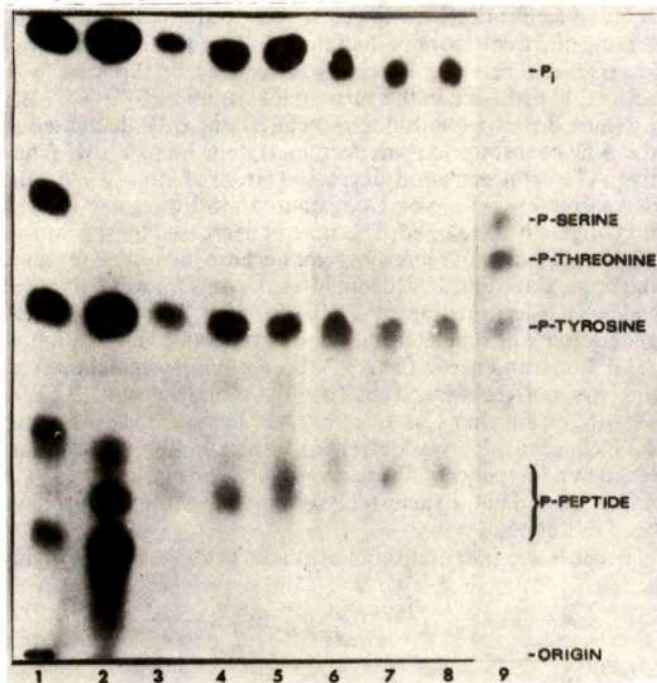
Fig. 3 Phosphoamino acid analyses of proteins phosphorylated by partially purified pp60[src] protein kinase. Various proteins phosphorylated as described in Fig. 1 legend were eluted from polyacrylamide gels and subjected to acid hydrolysis as described in Fig. 2 legend. Samples of the hydrolysates were then subjected to paper electrophoresis at *p*H 3.5. Authentic phosphoamino acid markers were included in all samples. Track (1), *in vivo* ^{32}P-labelled pp60[src], (2) *in vitro* autophosphorylated pp60[src], (3) TBR IgG, (4) casein, (5) desmin, (6) actin, (7) α-tubulin, (8) β-tubulin, (9) ninhydrin-stained authentic markers.

1. Brugge, J. S. & Erikson, R. L. *Nature* **269**, 346–348 (1977).
2. Purchio, A. F., Erikson, E. & Erikson, R. L. *Proc. natn. Acad. Sci. U.S.A.* **74**, 4661–4665 (1977).
3. Purchio, A. F., Erikson, E., Brugge, J. S. & Erikson, R. L. *Proc. natn. Acad. Sci. U.S.A.* **75**, 1567–1571 (1978).
4. Brugge, J. S., Erikson, E., Collett, M. S. & Erikson, R. L. *J. Virol.* **26**, 773–782 (1978).
5. Collett, M. S. & Erikson, R. L. *Proc. natn. Acad. Sci. U.S.A.* **75**, 2021–2024 (1978).
6. Levinson, A. D., Oppermann, H., Levintow, L., Varmus, H. E. & Bishop, J. M. *Cell* **15**, 561–572 (1978).
7. Erikson, E., Collett, M. S. & Erikson, R. L. *Nature* **274**, 919–921 (1978).
8. Erikson, R. L., Collett, M. S., Erikson, E. & Purchio, A. F. *Proc. natn. Acad. Sci. U.S.A.* **76**, 6260–6264 (1979).
9. Erikson, R. L., Collett, M. S., Erikson, E., Purchio, A. F. & Brugge, J. S. *Cold Spring Harb. Symp. quant. Biol.* **44** (in the press).
10. Collett, M. S., Erikson, E. & Erikson, R. L. *J. Virol.* **29**, 770–781 (1979).
11. Eckhart, W., Hutchinson, M. A. & Hunter, T. *Cell* **18**, 925–933 (1979).
12. Witte, O., Dasgupta, A. & Baltimore, D. *Nature* **283**, 826–831 (1980).
13. Hunter, T. & Sefton, B. W. *Proc. natn. Acad. Sci. U.S.A.* (in the press).
14. Collett, M. S., Brugge, J. S. & Erikson, R. L. *Cell* **15**, 1363–1369 (1978).
15. Brugge, J. S. *et al. J. Virol.* **29**, 1196–1203 (1979).
16. Collett, M. S., Erikson, E., Purchio, A. F., Brugge, J. S. & Erikson, R. L. *Proc. natn. Acad. Sci. U.S.A.* **76**, 3159–3163 (1979).
17. Oppermann, H., Levinson, A. D., Varmus, H. E., Levintow, L. & Bishop, J. M. *Proc. natn. Acad. Sci. U.S.A.* **76**, 1804–1808 (1979).
18. Spudich, J. A. & Watts, S. *J. biol. Chem.* **246**, 4866–4871 (1971).
19. Hubbard, B. D. & Lazarides, E. *J. Cell Biol.* **80**, 166–182 (1979).
20. Shelanski, M. L., Gaskin, F. & Cantor, C. R. *Proc. natn. Acad. Sci. U.S.A.* **70**, 765–768 (1973).
21. Plimmer, R. H. A. *Biochem. J.* **35**, 461–469 (1941).
22. Mitchell, H. K. & Lunan, K. D. *Archs Biochem. Biophys.* **106**, 219–222 (1964).

Tension generation by actomyosin thread from a non-muscle system

Fumio Matsumura, Yasuaki Yoshimoto & Noburô Kamiya

National Institute for Basic Biology, 38 Nishigonaka, Myodaijicho Okazaki, 444 Japan

A suitable motility model reconstituted from non-muscle contractile proteins should offer a powerful tool for analysing the molecular events in cell motility. Actomyosin thread has been thought to be such a model. As far as non-muscle motile systems are concerned, however, only a very limited number of experiments have been done in this direction[1,2]. No direct measurement of the tension produced by non-muscular actomyosin thread has been reported in spite of its importance for quantitative studies. We now report that a segment of actomyosin thread of *Physarum polycephalum* can generate a considerable amount of tension, which is a function of the micromolar concentration of ATP. The maximum isometric tension was as high as 10 g cm^{-2} at 10 μM ATP.

Physarum actin and myosin were purified as reported previously[3]. Actomyosin (molar ratio 1 : 1) was reconstituted by mixing actin and myosin in 20 mM imidazole buffer of *p*H 7.0, 30 mM KCl, 0.1 mM EDTA and 0.2 mM dithiothreitol (DTT). After centrifugation at 30,000*g* for 15 min, the precipitated actomyosin was dissolved in a minimum volume of 0.5 M KCl by adding 3 M KCl. Protein concentration of the actomyosin solution was 15 mg ml^{-1} as determined by the method of Lowry *et al.*[4].

To insure orderly longitudinal orientation of actomyosin, which is essential for the thread to generate tension effectively, actomyosin dissolved in the solution of high ionic strength was spun into the solution of low ionic strength as described below. The equipment for spinning consisted of three parts: (1) a syringe (Hamilton 500 μl) with a motor-driven plunger and an injection needle with a bore of 0.4 mm, (2) a shallow plastic trough filled with 20 mM imidazole buffer, *p*H 7.0, containing 30 mM KCl, 5 mM MgCl$_2$ and 0.2 mM DTT, and (3) a piece of glass tube, one end of which was fire-polished leaving a small orifice barely sufficient for the entry of the injection needle. The tube was fixed to a motor-driven sliding bench. The terminal regions of both the injection needle and the glass tube were bent and immersed in the solution in the trough facing each other with their axes in alignment with the direction of movement of the tube.

In the experiment, the actomyosin solution was loaded in the syringe and chilled in ice. The needle tip was inserted slightly

into the narrowed orifice of the glass tube. As soon as an appropriate volume of actomyosin solution had been extruded into the solution of low ionic strength in the tube, the actomyosin gelled and adhered to the tube's inner surface near the constricted orifice. The gelled actomyosin was then pulled at the rate of 2.4 mm s^{-1} by driving the glass tube away from the injection needle. At the same time, the actomyosin was extruded at the rate of 0.074 μl s^{-1} from the needle by the motor-driven shift of the plunger, with the pulling velocity four times as large as the extrusion velocity. These procedures produced flexible but strong segments of uniform actomyosin thread, 5–8 cm long and 0.2 mm in diameter. As the diameter of the gelled thread was just one-half the bore of the needle, the actomyosin gel volume did not decrease after extrusion and spinning. If the thread was formed by extrusion without pulling, it was fragile and generated only insignificant tension. Polarisation microscopic observation revealed stronger and more regular birefringence in the spun thread than in the thread formed only by spurting.

Thread segments thus obtained were mounted on a specially designed, highly sensitive horizontal-type electromagnetic tensiometer[5]. The noise level and drift were less than 0.1 mg and 0.1 mg h^{-1}, respectively. Isometric tension was measured at various ATP concentrations in the buffer solutions containing an ATP-regenerating system (20 mM imidazole buffer, pH 7.0, 30 mM KCl, 5 mM MgCl$_2$, 64 units ml^{-1} creatine phosphokinase, 4 mM phosphocreatine). Figure 1 shows the time course of tension generation in the isometric condition when 4 μM ATP was administered to the thread by perfusion. Tension increased slowly. It took 10, 6 and 4 min for the thread to reach a steady tension level after perfusion with 2, 4 and 10 μM ATP, respectively. Figure 2 shows the ATP dependence of isometric tension generation. The thread segment produced little tension below 1 μM ATP, whereas maximum tension (10 g cm^{-2}) was reached at 10 μM ATP. The half-maximum tension was observed at 2-3 μM ATP. Above 20 μM ATP, thread segments tended to break. The maximum tension of 10 g cm^{-2} is of the same order as the tension level developed by the plasmodial strand segment of *Physarum in vivo*[6]. Without the ATP-regenerating system, the sensitivity of tension generation to
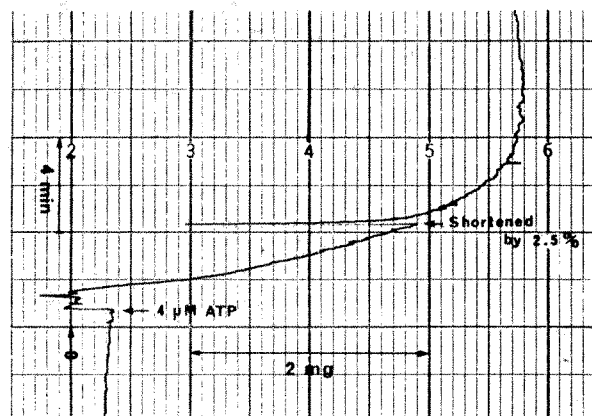
Fig. 1 Isometric tension generated by *Physarum* actomyosin thread. The thread was immersed in 20 mM imidazole buffer, pH 7.0, containing 30 mM KCl and 5 mM MgCl$_2$ in an open surface perfusion chamber set on the tensiometer. A segment of thread 20–50 mm long was looped around the thin glass hook of the tensiometer and its two free ends were attached to the other hook by drying in air for 5 min. After the double thread had been straightened by moderate stretching, it was covered with the above buffer containing the ATP-regenerating system. The thread was left in the solution for 10 min to allow complete diffusion of the ATP-regenerating system into the thread. The generation of tension was initiated by perfusion of the above solution containing ATP. Net length of the double thread, 16 mm; diameter of single thread, 0.2 mm; ATP, 4 μM. When the thread was shortened by 2.5%, the tension dropped strikingly but recovered in a short time, indicating that the thread generated active tension. Temperature, 26 °C.
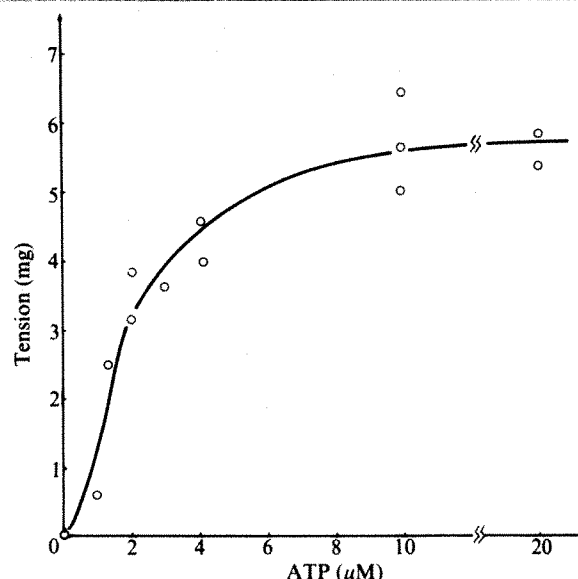
Fig. 2 Isometric tension level in relation to ATP concentration. Values of steady tension levels were plotted against ATP concentrations perfused. The data were obtained from six different segments of actomyosin thread. The maximum isometric tension (10 g cm^{-2}) was observed at 10 μM ATP, and the half-maximum tension at about 2–3 μM ATP. The generated tension was highly reproducible in the thread segments made from the same preparation of *Physarum* actomyosin.

ATP concentration was lower by one order. The maximum tension of 5 g cm^{-2}, or one-half that produced in the presence of an ATP-regenerating system, was reached in this case with about 200 μM ATP in the surrounding solution.

Figure 3 shows that full tension at 20 μM ATP decreased as the ATP concentration was decreased stepwise to 1 μM. When the ATP concentration increased from 1 to 10 μM, the decreased tension increased again to almost the same level as that originally developed. The state of decreased tension at 5 or 10 μM ATP did not represent rigor because the thread resumed the original tension 10–20 min after the tension was decreased suddenly by shortening by 2.5%. In short, isometric tension generation was regulated by the micromolar concentration of ATP. In the absence of the ATP-regenerating system, however, this was not the case. Tension once produced with ATP at 100 μM or a higher concentration was retained even when the ATP concentration was decreased. When the thread was shortened by a few per cent, the tension decreased markedly and was not recovered in the same ATP solution. The thread must have been in a state of rigor.

Because the preparation of synthetic actomyosin was highly
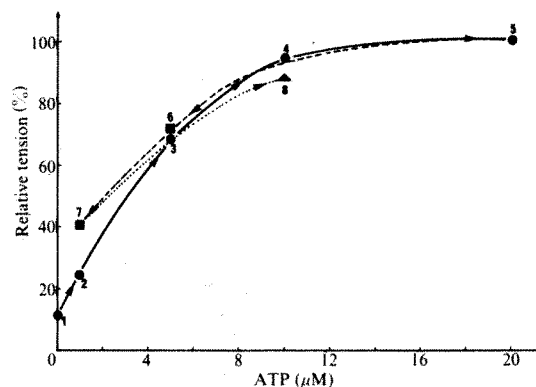
Fig. 3 Reversibility of ATP-dependent tension generation in a single thread segment. The steady tension level reached was measured when the ATP concentration was increased from 0 to 20 μM (solid line), then decreased from 20 to 1 μM (broken line), and finally increased again from 1 to 10 μM (dotted line). The number beside each symbol shows the sequence of change of the ATP concentration.

purified, the thread showed no Ca^{2+} sensitivity in tension generation at micromolar levels. Thus far we have not observed any oscillatory phenomenon, which is conspicuous in the living plasmodium of this organism, in tension production in constant ATP levels.

The actomyosin thread from *Physarum* differed from that of skeletal muscle[7] in several ways. (1) *Physarum* actomyosin thread was much more flexible, (2) the ATP concentrations sufficient to produce maximum and half-maximum tension were lower than those reported for muscle actomyosin threads, where these values were 50 and 8 μM, respectively[7], (3) tension increase in the *Physarum* actomyosin thread was slower than that in muscle actomyosin thread, where the final level of tension was reached within 2 min (ref. 7). These differences can probably be ascribed to the difference in myosin properties between *Physarum* and muscle, such as the high solubility of *Physarum* myosin at low ionic strength[8,9], a property not found in muscle myosin. Note, however, that the maximum isometric tension level reached was the same for these two different kinds of actomyosin thread with the same protein concentration[7].

A previous study on superprecipitation revealed that *Physarum* myosin formed flexible and short filaments about 0.2 μm long when it was allowed to interact with actin in the presence of ATP[3]. This suggests that such short myosin filaments may also participate in tension production by the reconstituted actomyosin thread as well as in the motility of *Physarum in vivo*.

This work was supported by grants-in-aid from the Japanese Ministry of Education, Science and Culture.

1. Beck, R., Komnick, H., Stochem, W. & Wohlfarth-Bottermann, K. E. *Cytobiologie* 2, 99–114 (1969).
2. Hinssen, H. & D'Haese, J. *Cytobiologie* 13, 132–157 (1976).
3. Matsumura, F. & Hatano, S. *Biochim. biophys. Acta* 553, 511–523 (1978).
4. Lowry, H. H., Rosebrough, N. J., Farr, A. L. & Randall, R. J. *J. biol. Chem.* 193, 265–275 (1951).
5. Kamiya, N. in *Proc. IV Int. Biophysic. Congr.*, Moscow, Symp. III, 447–465 (1973).
6. Yoshimoto, Y. & Kamiya, N. *Protoplasma* 95, 89–133 (1978).
7. Crooks, R. & Cooke, R. *J. gen. Physiol.* 69, 37–55 (1977).
8. Nachmias, V. T. *J. Cell Biol.* 62, 54–65 (1974).
9. Hatano, S. & Takahashi, K. *J. Mechanochem. Cell Motility* 1, 7–14 (1971).

Immunochemical identification of an actin-like protein from soybean seedlings

Thomas N. Metcalf III, Leslie J. Szabo, Karel R. Schubert & John L. Wang

Department of Biochemistry, Michigan State University, East Lansing, Michigan 48824

Microfilaments are recognised as ubiquitous cytoskeletal and contractile elements found in virtually all types of cells. Indeed, the major protein component of these fibrillar structures, actin, has been isolated from a variety of cells[1-5]. A number of laboratories have recently reported ultrastructural observations of microfilaments in plant cells such as *Avena sativa*, *Nicotiana tabacum*, *Nitella flexilis*, *Amaryllis belladonna*, *Haemanthus katherina*, *Mougeotia*, *Mimosa* and *Chara*[6-13]. Preliminary studies on the identification of the actin subunit of these structures have also been reported for *Nitella*, *Phaseolus vulgaris* and *Lycopesicon esculentum*[14-16]. More detailed studies have been made on actin isolated from the cellular slime mould, *Dictyostelium discoideum*[17,18]. We report here the isolation, from extracts of soybean (*Glycine max*) seedlings, of a protein that binds rabbit antibodies directed against calf thymus actin. The results suggest the presence of an actin-like polypeptide chain in soybean cells.

Soybean seeds were washed in 0.02% $HgCl_2$ and germinated at room temperature. All subsequent steps were carried out at 4 °C. Ten-day-old seedlings (350 g) were suspended in 700 ml 3 mM imidazole buffer (3 mM imidazole, 0.5 mM ATP, 0.1 mM $CaCl_2$, 0.75 mM β-mercaptoethanol, pH 7.5) containing 70 g of

polyvinylpyrrolidone (GAF Corporation) and 0.02 units ml^{-1} of the protease inhibitor, Trasylol (Sigma). This suspension was homogenised in a Waring blender for 4 min, filtered and centrifuged at 16,300g for 20 min. The supernatant was further clarified by centrifugation at 100,000g for 90 min.

When the supernatant fraction was chromatographed on a DEAE-cellulose column and eluted with a linear gradient of KCl (0–0.25 M), five major fractions (A—E, Fig.1) were obtained. SDS polyacrylamide gel electrophoresis (PAGE) of the material in these fractions showed that each consisted of highly heterogeneous populations of polypeptide chains (Fig. 2).

Fraction C (Fig. 1) was found to react with rabbit antibodies raised against purified calf thymus actin in Ouchterlony immunodiffusion tests[19]; no precipitin line was observed when the same fraction was tested against preimmune serum. The material in fraction C was labelled[20] with ^{125}I and immunoprecipitated[21] with rabbit anti-actin antibodies plus goat antibodies directed against rabbit immunoglobulin. Analysis of the precipitated radioactive protein components by SDS-PAGE[22] showed a single major polypeptide chain, with an electrophoretic mobility identical to that of calf thymus actin (Fig. 3). The molecular weight (MW) of this protein was estimated to be 45,000. No ^{125}I-labelled protein was observed when the preimmune serum was substituted for the rabbit anti-actin antibody.

When unlabelled calf thymus actin was added to the reaction mixture, the amount of ^{125}I-labelled soybean protein precipitated was reduced. Moreover, the decrease in precipitation of radioactivity was directly proportional to the amount of unlabelled actin added. These results strongly suggest that the precipitation of the 45,000-MW component (Fig. 3) was due to specific interactions with the anti-actin antibody.

Because the specificity of the antiserum is a key factor in the interpretation of our results, the following experiments were performed to ascertain that the antibodies were indeed specific for the actin polypeptide chain. First, calf thymus actin, isolated by a modification of the method used by Gordon *et al.*[23], showed a single band on polyacrylamide gels (Fig. 2a). Therefore, a highly purified protein was used for immunisation. Second, extracts of calf thymus tissue were labelled with ^{125}I and then precipitated using the rabbit anti-actin antiserum plus goat antibodies directed against rabbit IgG. Analysis of the immune precipitate by PAGE indicated that only a single ^{125}I-labelled polypeptide chain was precipitated. The electrophoretic mobility of this material was identical to that obtained with purified calf thymus actin (Fig. 3), the antigen used for immunisation. Moreover, parallel experiments using pre-immune serum showed no precipitation of any ^{125}I-labelled protein. Finally, the rabbit anti-actin antiserum produced a single precipitin line in
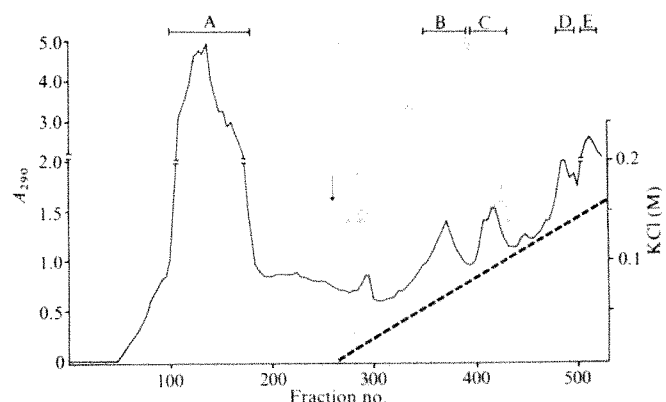
Fig. 1 Ion exchange chromatography of an extract of soybean cells on a column (4 × 25 cm) of DEAE-cellulose (Whatman DE-52) equilibrated with 10 mM imidazole, 0.5 mM ATP, 0.1 mM $CaCl_2$, 0.75 mM β-mercaptoethanol, pH 7.5. The solid line denotes the absorbance of the effluent fractions at 290 nm. At the point indicated by the arrow, a linear gradient (- - - - -) from 0 to 0.25 M KCl was initiated. The total gradient volume was 3 l. Each tube contained 10 ml of effluent.

Ouchterlony immunodiffusion tests against both the crude calf thymus extract and the purified calf thymus actin; no reaction was observed with a variety of other irrelevant proteins such as chicken muscle myosin, bovine serum albumin, fetuin and deoxyribonuclease I.

The availability of an immunochemical reagent capable of selectively binding to a single component of soybean cell extracts immediately suggested affinity chromatography as a purification step for the actin-like protein. Fraction C (Fig. 1) was chromatographed on a Sepharose column containing covalently coupled rabbit anti-actin antibodies[24]; the bound protein material was eluted with 1 M acetic acid and subjected to SDS gel electrophoresis. The gel pattern showed one predominant Coomassie blue-stained band (Fig. 2, *h*), with an electrophoretic mobility corresponding to a protein of MW 45,000. These results confirm the data from the immunoprecipitation experiments described above, obviating any interpretation problems associated with using ^{125}I-labelled proteins (such as preferential labelling of any single polypeptide chain). These results all suggest that an actin-like protein may be found in fraction C (Fig. 1) derived from extracts of soybean cells.

Actin has been isolated and characterised in a variety of animal muscle and non-muscle cells[1-5], as well as in other organisms such as *Mycoplasma pneumonia*[25], *Chlamydomonas*[26], *Physarum*[27,28], *Acanthamoeba*[23,29,30], *Saccharomyces cerevisiae*[31] and *Dictyostelium*[17,18]. In practically all cases studied to date, the various actins are remarkably similar to each other and to muscle actin, all consisting of globular subunits of approximately 45,000 MW. This identification of an actin-like protein from soybean cells with a polypeptide chain of MW 45,000 extends the list of similar proteins.

However, it remains to be demonstrated that the soybean protein shares the biological activities that have been characterised for the various actins: polymerisation into filamentous structures observable by electron microscopy, stimulation of the Mg^{2+}-ATPase activity of muscle heavy meromyosin, and stoichiometric binding of ATP. We are therefore carrying out more detailed chemical and functional analyses to compare the properties of the actin-like protein from soybean cells with the analogous proteins from other animal and plant cells.

Fig. 3 SDS–PAGE[22] of ^{125}I-labelled proteins after immunoprecipitation with rabbit antibodies directed against calf thymus actin plus goat antibodies directed against rabbit immunoglobulin. *a*, ^{125}I-labelled calf thymus actin (1.7×10^5 c.p.m. μg^{-1}); *b*, ^{125}I-labelled fraction C (Fig. 1) from soybean cells (8.3×10^3 c.p.m. μg^{-1}). ○, Radioactivity profile of immune precipitates obtained using rabbit anti-actin antiserum; ●, radioactivity profile of immune precipitates obtained using preimmune serum. The arrows indicate the positions of migration of molecular weight markers (see Fig. 2 legend).

Fig. 2 SDS–PAGE[32] of protein components obtained from soybean cell extracts after fractionation by DEAE-cellulose chromatography and by affinity chromatography using rabbit anti-actin antibodies. *a*, Calf thymus actin[23]; *b*, rabbit muscle actin[33,34]; *c–g*, fractions A–E from Fig. 1; *h*, material from fraction C (Fig. 1) purified by affinity chromatography on columns containing rabbit antibodies directed against calf thymus actin; *i*, calf thymus actin. The acrylamide composition of the gel was 7.5%. The arrows on the right indicate the positions of migration of molecular weight markers: bovine serum albumin (68,000); glutamic dehydrogenase (55,000); ovalbumin (43,000); pancreatic deoxyribonuclease I (33,000) and bromphenol blue. Approximately 10–30 μg protein was loaded in each lane of the gel.

1. Pollard, T. D. & Weihing, R. R. *Crit. Rev. Biochem.* **2**, 1-65 (1974).
2. Hepler, P. K. & Palevitz, B. A. *A. Rev. Pl. Physiol.* **25**, 309–362 (1974).
3. Clarke, M. & Spudich, J. A. *A. Rev. Biochem.* **46**, 797–822 (1977).
4. Korn, E. D. *Proc. natn. Acad. Sci. U.S.A.* **75**, 588–599 (1978).
5. Goldman, R. D., Milsted, A., Schloss, J. A., Starger, J. & Yerna, M. J. *A. Rev. Physiol.* **41**, 703–722 (1979).
6. O'Brien, T. P. & Thimann, K. V. *Proc. natn. Acad. Sci. U.S.A.* **56**, 888–894 (1966).
7. Parthasarathy, M. V. & Muhlethaler, K. J. *Ultrastruct. Res.* **38**, 46–62 (1972).
8. Palevitz, B. A., Ash, J. F. & Hepler, P. K. *Proc. natn. Acad. Sci. U.S.A.* **71**, 363–366 (1974).
9. Condeelis, J. S. *Expl Cell Res.* **88**, 435–439 (1974).
10. Forer, A. & Jackson, W. T. *Cytobiologie* **10**, 217–226 (1975).
11. Marchant, H. J. *Planta* **131**, 119–120 (1976).
12. Arraes-Hermans, M. A. & Cruz, W. B. *Revue Microbiol.* **3**, 8–9 (1976).
13. Williamson, R. E. *Nature* **248**, 801–802 (1974).
14. Kato, T. & Tonomura, Y. *J. Biochem.* **82**, 777–782 (1977).
15. Jackson, W. T. & Doyle, B. G. *J. Cell Biol.* **75**, 268a (1977).
16. Vahey, M., Trantwein, R. & Scordillis, S. P. *Biophys. J.* **21**, 23a (1978).
17. Wolley, D. E. *Archs Biochem. Biophys.* **150**, 579–530 (1972).
18. Uyemura, D. G., Brown, S. S. & Spudich, J. A. *J. biol. Chem.* **253**, 9088–9096 (1978).
19. Williams, C. A. & Chase, M. W. (eds) in *Methods in Immunology and Immunochemistry* Vol. 1 (Academic, New York, 1967).
20. Greenwood, F. C., Hunter, W. M. & Glover, J. S. *Biochem. J.* **89**, 114–123 (1963).
21. Vietta, E. S., Baur, S. & Uhr, J. W. *J. exp. Med.* **134**, 242–264 (1971).
22. Weber, K. & Osborn, M. *J. biol. Chem.* **244**, 4406–4412 (1969).
23. Gordon, D. J., Eisenberg, E. & Korn, E. D. *J. biol. Chem.* **251**, 1778–1786 (1976).
24. Cuatercasas, P. *J. biol. Chem.* **245**, 3059–3065 (1970).
25. Neimark, H. C. *Proc. natn. Acad. Sci. U.S.A.* **74**, 4041–4045 (1977).
26. Piperno, G. & Luck, D. J. L. *J. biol. Chem.* **254**, 2187–2190 (1979).
27. LeStourgeon, W.M., Forer, A., Yang, Y-Z., Betram, J.S. & Rusch, H.P. *Biochim. biophys. Acta* **379**, 529–552 (1975).
28. Jockusch, B. M., Becker, M., Hindennach, I. & Jockusch, H. *Expl Cell Res.* **89**, 241-246 (1974).
29. Weihing, R. R. & Korn, E. D. *Biochemistry* **1**, 590–600 (1971).
30. Pollard, T. D. *J. Cell Biol.* **68**, 579-601 (1976).
31. Bejanian, M. V., Surguchov, A. P. & Smirnov, V. W. *FEBS Lett.* **102**, 55–58 (1979).
32. O'Farrell, P. H. *J. biol. Chem.* **250**, 4007–4021 (1975).
33. Barany, M., Barany, K. & Guba, E. *Nature* **179**, 818–819 (1957).
34. Spudich, J. A. & Watt, S. *J. biol. Chem.* **246**, 4866–4871 (1971).

BOOK REVIEWS

Misconceptions about Malthus

Peter Laslett

THIS book boldly advertises itself as "the best exposition of Malthus to be found anywhere". While it is a pleasure to accept this statement as true — a concise, learned, penetrating and informative treatise this most decidedly is — it has to be admitted that the competition the author has faced is rather indifferent, and with one exception it seems always to have been. For the fact is that the most important of all English-speaking social scientists; as Thomas Robert Malthus may quite justifiably be called, has been ineffectively treated by posterity.

He has had to wait for a century and a half, until last year in fact, for a full length biography, *Population Malthus* by Patricia James. An ample and painstaking account of an uneventful life lived through a very eventful period (1766–1834), the book by Mrs. James in no way rivals Professor Petersen's study. Nor has he very much to fear from an enormous list of controversial works on the most refuted amongst social theorists, works which are listed accurately and usefully at the end of his book and many of which he manages to discuss individually, mostly with insight and with fairness. His one serious rival is a writer whom some might claim had a better title than Malthus himself to be first amongst English-speaking social scientists, that is to say John Maynard Keynes. Keynes' sparkling little monograph on Malthus in his famous *Essays in Biography* cannot be said to have been eclipsed by Petersen. But Keynes, like so many of the others who have written about the mild-mannered, hare-lipped cleric and professor, used the thought of Malthus to develop a position of his own.

A great deal of the text of this book has had to be devoted to the exposure and correction of the misunderstandings of Malthusian thought, and of the fallacies which have grown up about him. Outstanding amongst these of course has been the assumption that Malthus was an advocate of birth control, a misbelief which has led to contraceptive movements being christened Malthusian. The man himself classified all interference with conception as vice. For him one of the deplorable results of the pressure of popu-

Malthus. By William Petersen. Pp.336. (Harvard University Press: Cambridge, Massachusetts/Heinemann Educational: London, 1979.) £9.50.

Thomas Malthus

Courtesy National Portrait Gallery

lation on subsistence, which he was the first to delineate in quantitative, what we should be disposed to call scientific terms, was that it impelled men in the direction of these abominable practices. The control which he advocated, indeed thought inevitable, was postponement of marriage for everyone to such a time in the life of both man and wife when they could reckon to support all the children they were likely to produce. Until that point in personal experience, a point which might never be reached by a fair proportion of persons, the expedient for avoiding procreation was abstinence.

Demographic historians now know that abstinence, within and without the married state, did in fact have a great deal to do with the successful transition to a modern low-fertility regime which took place in England some time after Malthus died. They are also becoming convinced that the sense of individual responsibility for procreation, which the nuclear family brings

with it, had been a distinguishing characteristic of north-west European familial behaviour for many centuries before the time of Malthus. In this area of the world marriage had been postponed or foregone, and individualist familial and procreative life had been led for many centuries before the time of Malthus. The catastrophe associated with his name, a catastrophe which many commentators believe awaits the population of our world, when subsistence fails to keep up with increase in numbers, was in fact less likely in the region which he inhabited in his lifetime than it has been in other parts of the globe and at other times. This in spite of the evident signs of 'overpopulation' in the England of 1798, when the first, the most trenchant and most stimulating version of his *Essay on Population* was published.

The Western European principle that every marriage means a new household and can only be undertaken when two responsible individuals are in a position to found and maintain it, may be a highly effective way of keeping a population within its means over time. It is not a principle in which the West has had a monopoly of course, but it is one which certainly causes its own hardships: for the widowed and the orphaned, and those at the margin. A further circumstance which we are beginning to recognize in Western history is that these ill consequences seem to have been compensated for socially, by means of transfers from the haves to the have-nots, flowing through ecclesiastical, charitable and above all through political institutions, only to a lesser extent through the channels of kinship.

Although this mechanism seems to have been a settled feature of the England which he knew, Malthus appears to have lacked or lost confidence in its effectiveness, and this is the outstanding interest of his position. He believed that redistribution made overpopulation inevitable, because it tended to remove procreative responsibility from individuals. Transfer incomes, he felt bound to proclaim, had to be done away with, which meant that the Poor Law, the great source of welfare for the casualties of the system, had to come to an end.

This newer view of Malthus and his significance is not one of those considered by Petersen. He is rather an indifferent guide to the demography of England in Malthusian times, and somewhat insensitive, so it seems to me, to the force of the progressive and Marxist critique of Malthusian thought. He rejects the view that the ecological crisis, which we are repeatedly told stares industrial society in the face, can properly be called Malthusian, just as he is sceptical of the views of the demographic catastrophists, as are other professional demographers.

Nevertheless it is understandable that the name of Malthus should have come to bulk so large in the learned world that at the end of this month a global meeting has been arranged to take place in Paris for the exposition and celebration of what that name has come to mean. Europeans, Western and Eastern; Africans, Asians and all the rest; those from developed and developing countries, Marxists and non-Marxists, will join together in debate about the Malthusian heritage. It can be said with confidence that he is of an intellectual standing to be worthy of such an occasion, and it is fortunate indeed that a work such as Petersen's should have appeared just in time to make that point absolutely evident.

Peter Laslett is Reader in Politics and the History of Social Structure at the University of Cambridge, UK, Fellow of Trinity College and Co-director of the Cambridge Group for the History of Population and Social Structure.

Theory and practice in thermodynamics

F.L. Swinton

Chemical Thermodynamics. By M.L. McGlashan. Pp.345. (Academic Press: London and New York, 1979.) £18, $41.50.

THERE are very many bad textbooks of thermodynamics and very few that can be considered excellent. It is a not unexpected pleasure to be able to record that Professor McGlashan's new book joins such classics as Guggenheim's *Thermodynamics* (North-Holland: Amsterdam, 1967) and Prigogine and Defay's *Chemical Thermodynamics* (Longmans, Green: London, 1954) in this latter category. The present text is designed for teaching the subject up to and beyond British honours degree level and its coverage is thus more restricted than either of these two earlier works. It is more comparable in scope to books such as those by Denbigh (*Principles of Chemical Equilibrium.* Cambridge University Press: Cambridge, UK, 1966) and by Lewis, Randall, Pitzer and Brewer (*Thermodynamics.* McGraw-Hill: New York, 1961).

One original feature is the way in which, throughout the development of the subject, theory is closely wedded to experiment. There are two early chapters entitled "Practical Thermometry" and "Practical Calorimetry", and diagrams and descriptions of various pieces of apparatus used to measure thermodynamic properties are interspersed throughout the text. Whenever a new concept or function is introduced the reader is constantly being prompted to ask the question 'How do you measure it?' The author's contention is that only by asking and answering such a question can the reader build up a true appreciation of the practicalities of the subject.

While few will dispute the need to give prominence to both theory and experiment in a textbook designed to instruct readers who may have had little or no previous experience of thermodynamics, there are bound to be some who will question the wisdom of the author's strictly axiomatic theoretical development of the subject. For example, there must be very few present-day undergraduates who will accept on trust equation (5.2.1)

$$dU^a = T^a dS^a - p^a dV^a + \sum_B \mu_B^a dn_B^a$$

that defines temperature, entropy *and* chemical potential for the first time and not question its origin. Once the axiomatic foundations are accepted, the author's subsequent derivations of all the standard thermodynamic relationships proceed with great clarity and rigour, and the university teacher as well as the undergraduate will learn much from a close perusal of the text. The treatment, in Chapters 11 and 12, of systems undergoing chemical reaction is particularly noteworthy.

One criticism that can be made of the book's subject matter is that the later, more advanced, chapters are heavily biased towards Professor McGlashan's own research interests, and whereas there are three separate chapters devoted to liquid mixtures, fluid mixtures and the principle of corresponding states, there are barely that number of pages concerned with solid–liquid equilibria. This detracts from the interest the book might otherwise have had for metallurgists and, to a lesser extent, for chemical engineers.

The book is superbly printed and produced, and one notable feature is the liberal use of footnotes. Most chapters conclude with a useful collection of numerical problems.

All university teachers will want to possess a personal copy immediately and I feel that it will not be long before McGlashan's *Chemical Thermodynamics* becomes established as a (or perhaps even the) standard teaching text in the subject.

F.L. Swinton is Professor of Chemistry at the New University of Ulster, Coleraine, Northern Ireland.

Digital image processing

P.W. Hawkes

Advances in Digital Image Processing. Edited by P. Stucki. Pp.332. (Plenum: New York and London, 1979.) $23.63.

IN 1978, IBM (Germany) organized a conference on new developments in digital image processing, the proceedings of which are published here, offset from the authors' typescripts but with a number of colour plates tipped in. The book opens with two general papers, on evolution in image science by E. Klein and H.J. Metz and on trends in digital image processing research by T.S. Huang (whose volume, *Picture Processing and Digital Filtering,* has been reissued in paperback by Springer, with a short additional chapter and many new references). This chapter by Huang brings out clearly the difficulties of digital processing and indicates some of the ways in which they may be attacked. The remainder of the book is divided into theory, applications and implementations but has in fact a strongly applied flavour throughout, even the chapters on theory showing a marked engineering bias. Thus the first of these, by H.W. Schuessler, sets out from this author's *Digitale Systeme zur Signalverarbeitung* (Springer, 1973), and is addressed to readers with a background in electrical engineering. Still in the theory section, H.G. Musmann discusses digital coding of TV signals. Lastly, H. Niemann gives a formal and very well-organized account of digital image analysis, covering preprocessing, the extraction of picture constituents or primitives, including a discussion of textures, classification (in cytology, for example) and the important step of final analysis, including syntactical, graphical and relaxation methods.

The section on applications contains six chapters, on biomedical image processing (K. Preston), X-ray images (K.H. Hoehne, M. Boehm and G.C. Nicolae), Landsat (E.E. Triendl), document reproduction (P. Stucki), computer graphics (R. Williams) and industrial automation (L. Lieberman). Preston has quite recently written a very full account of digital picture analysis in cytology (in *Digital Picture Analysis,* edited by A. Rosenfeld: Springer, 1976), and the present chapter should be regarded as a supplement to that, interesting for its discussion of Golay logic. The remaining chapters in this section show why image processing is needed in the various fields considered.

The final section is devoted to implementation : distributed processing (W. Giloi), parallel processors (M. Duff), large-scale vector/array processors (G. Paul) and a low-cost system with new fast hardware (A. Peled). For many readers,

already familiar with the methods and themes of image processing, extensively reviewed in single and multi-author volumes during the past few years, these will be the most valuable chapters of this volume. The authors explain how the particular requirements of image processing may be satisfied in recent and future generations of computer hardware.

Useful though some of the material in this book is, it can hardly be regarded as indispensable in these days of rising book prices and dwindling library budgets. It is arguable that this particular volume would have been better published as a special number of a journal than in the present form. □

P.W. Hawkes is Maître de Recherches in the Laboratoire d'Optique Electronique du CNRS, Toulouse, France.

Organic chemistry

A.R. Katritzky

Physical and Mechanistic Organic Chemistry. By R.A.Y. Jones. Pp.357. (Cambridge University Press: Cambridge, UK, 1979.) Hardback £25; paperback £8.50.

THE author has attempted a synthesis of physical organic and mechanistic organic chemistry; thus the book occupies a position between those texts emphasizing the physico-chemical aspects, such as Hammett's *Physical Organic Chemistry* (McGraw-Hill: New York, 1970) and Wiberg's text of the same name (Wiley: New York, 1964), and those dealing more directly with mechanisms such as Ingold's classic (Cornell University Press: New York/Bell: London, 1969). To attempt all this within the confines of some 350 pages is a challenge indeed, yet I believe that the author has succeeded in producing a text which will be of great value.

Part I deals with the theories and techniques of physical organic chemistry in six chapters which cover structure and mechanism, kinetics, linear free-energy relationships, acids and bases, solvent effects and molecular orbital methods.

Part II (about two-thirds of the book) covers some carefully selected mechanism types. It commences with a survey of aliphatic nucleophilic substitution, proceeds to elimination and carbon–carbon double bond addition reactions and then to aromatic electrophilic substitution. This is followed by consideration of additions to the carbonyl group, the hydrolysis of esters and aromatic nucleophilic substitution. The book ends with chapters on molecular rearrangements and pericyclic reactions.

The great strength of this book lies in its clarity which is so important in a text intended for final year undergraduates or for graduate students. The sentences are short, to the point and unambiguous. Physical organic chemistry is a subject with many unresolved controversies: here the author presents both points of view with admirable detachment.

The production of the book is good (although there was a defect in the paper on p.88 of the copy examined), and there appear to be extremely few typographical errors. The book is logically put together

and most interesting to read. It has clearly been a labour of considerable magnitude but also a labour of love.

How could the next edition be improved? I would suggest that more graphs and diagrams be included. For example, at the bottom of p.255 and the top of p.256 the points dealt with could be understood even better with a suitable plot.

In summary, I consider that the stated aims have been fully achieved: "Advanced undergraduates and graduate students using this book will be able to understand the general principles on which the study of mechanism is based and to be able to apply them to most reactions of organic chemistry". □

A.R. Katritzky is Professor at the School of Chemical Sciences, University of East Anglia, Norwich, UK.

Past and future in microtubule research

H.P. Erickson

Microtubules. Edited by K. Roberts and J. Hyams. Pp.595. (Academic: London and New York, 1979.) £34, $78.50.

THE intention of the editors was to summarize those results of microtubule research that are most exciting now and that will form the basis for the next big steps forward in the field. The authors of the 11 chapters, all of whom have made important contributions in their areas, were charged to present a critical review of the important discoveries of the past and also to stand back from their field and speculate about the important future directions. The editors have made efforts to cut overlap between chapters to a minimum so that the book would read as a coherent whole. The style and depth of coverage by the different authors varies considerably, however, and I feel that the work has to be considered as a collection of individual review articles. They are all related, more or less, but each has its individual character and some are much more successful than others.

For me the most useful chapters are in the area of cell biology. "Tubulin Pools, Synthesis and Utilization" by Fulton and

Simpson is a nice example of a critical, rather than comprehensive, review. Topics discussed range from techniques for measuring tubulin to a variety of questions of cell biology. The authors avoid vague and inconclusive lists of contradictory reports and concentrate on presenting a limited number of well-established observations and conclusions. "Microtubule-associated Cytoplasmic Transport" by Hyams and Stebbings is written in a similar style and provides wide coverage of axonal flow, chromatophore movement and some other systems of particle transport. "Cell Division" by McIntosh presents a broad review of mitosis and discusses the more conclusive studies on the location and function of microtubules. Weber and Osborn present a readable review of the application of immunofluorescence microscopy to reveal microtubule arrays in cultured cells, discussing mostly their own work.

A short article by Warner reviews evidence for the sliding of microtubules as the mechanism for motility of cilia and flagella. "Microtubules and Cell Surfaces" by Berlin, Caron and Oliver is heavily weighted towards discussion of their own work and their rather speculative models. "The Spatial Organization of Microtubules" by Tucker is even more speculative and often difficult to read, perhaps reflecting the paucity of conclusive information about how the spatial organization is determined.

In "The Structure of Microtubules" Amos presents a detailed review of results from X-ray diffraction, electron microscopy and image reconstruction. Much of the discussion is technical in nature, but for those interested in this area the article is especially timely, since the recently obtained 2 nm resolution is close to the limit of specimens and techniques currently available. "The Biochemistry of Tubulin" by Lueduña should be useful as a summary of basic information and an introduction to the literature. The biochemistry of tubulin and nucleotides, an area of increasing importance in tubulin research, is expanded in a separate chapter by Jacobs.

In vitro assembly of microtubules is covered by Scheele and Borisy in a single chapter, which is devoted largely to work from their own laboratory. Their treatment of the thermodynamics and kinetics of assembly is quite useful but their lengthy discussion of tubulin rings seems out of proportion to the importance of this subject as it is currently understood. A discussion of the assembly of purified (MAP-free) tubulin and the effect of solution conditions and ligands would have been much more valuable. This important area, which could easily have merited a full chapter, is virtually ignored in the book.

This volume should be useful to people in the microtubule field, providing them with an opportunity to review the advances of the last 15 years in areas related to but outside their immediate interests. For the person unfamiliar with microtubule research it would be difficult for any publication to provide easy access to quick answers, largely because the field is now so complex. For the student who wants to consider the subject in some depth, however, this book should be useful as a fairly comprehensive summary of results and an introduction to the literature up to 1978. □

H.P. Erickson is Associate Professor in the Department of Anatomy, Duke University, Durham, North Carolina.

Solid-state spectroscopy

Derek J. Fabian

Electron Spectroscopy of Crystals. By V.V. Nemoshkslenko and V.G. Aleshin (translated from Russian by Irina Curelaru). Pp.360. (Plenum: New York and London, 1979.) £31.19.

THE major part of this monograph comprises an extensive review of published photoelectron emission data covering a range of band structure effects in solids and solid surfaces. The book includes abundant introductory theory, of assistance to the reader both in understanding the electron transition processes involved in photoemission and Auger spectroscopies and in following the interpretations offered for many of the experimental observations.

To some extent the word 'crystals' in the title should be taken to mean 'solids', for the review covers ordered and disordered metals and alloys as well as including intermetallic and non-metallic amorphous materials. On the other hand the emphasis is largely on crystalline solids, with separate chapters devoted to sphalerite-lattice compounds, alkali and alkaline-earth halides, and transition-metal compounds.

The text commences with a helpful description of commercially available electron spectrometers, which unfortunately was already dated at the time of the original Russian version of the book in 1976. An excellent chapter on background theory — misleadingly headed "Physical principles of electron spectroscopy" — provides, for the newcomer to the field, a definitive introduction to theoretical principles of photoelectron ionization and emission, together with a descriptive outline of computative methods used for calculating energy bands in solids. The chapter on metals and alloys also contains valuable descriptive theory, including the

coherent potential method in the study of disordered systems. Further chapters deal with characterization of surfaces, including some novel aspects of quantitative analysis using angularly resolved photoemission, and with multiplet and satellite structure in photoelectron core-level spectra.

A welcome theme, throughout the review of experimental data, is the comparison of band-structure information gained from X-ray photoelectron spectra with that obtained from X-ray emission and absorption studies. Photoelectron and X-ray emission spectroscopies when combined can provide a powerful tool for probing occupied energy bands in solids. This is especially well-illustrated in the chapter dealing with core-electron and valence-band energy levels in transition-metal compounds. One topic, though, not covered adequately in the book is the determination of partial densities of electron states with various symmetries from angular distributions of emitted photoelectrons.

The monograph contains an extensive bibliography, which is particularly

comprehensive in its coverage of experimental work published in the USSR; however, its usefulness would have been enhanced by the inclusion of an author index. The book has a subject index and this too could have been improved had more detail been included. These are minor criticisms that do not detract significantly from the scientific quality of the text, which also reads lucidly and smoothly with little evidence that the original was not in English. The book can be firmly recommended both as an introductory work to students and as a valuable review to established researchers in the field. The authors set out to provide a comprehensive survey of experimental energy-band data based on photoelectron spectroscopies, drawing on their own noted research at the Ukrainian Academy of Sciences in Kiev, and to fill a gap in published monographs and reviews on electron spectroscopy applied to solid-state materials. To a welcome extent they have succeeded. □

Derek J. Fabian is Reader in Metallurgy and Materials Physics at the University of Strathclyde, Glasgow, UK.

Marking tumours

A. Munro Neville

Cancer Markers. Edited by S. Sell. Pp.541. (Humana Press: Clifton, New Jersey, 1980.) $49.50.

THE past decade has witnessed a great deal of progress in the search for biochemical markers of neoplasia. In view of their potential biological, pathological and clinical importance, it is most welcome to have a book where most of the relevant data can be found. All the chapters are informative, easily read and in the main remarkably up to date.

Among the wide range of topics discussed are aspects of alphafetoprotein (AFP), the carcinoembryonic antigen

(CEA), lymphocyte markers and pregnancy proteins, all of which are discussed from a fundamental point of view as well as in clinical terms.

Most of the other currently recognized human solid tumour-associated antigens are gathered together in one chapter thereby giving a good reference source, albeit without critical comment. The chapter on teratomas in particular is a fascinating and thought-provoking account, and the section dealing with lectins and their use as probes to dissect cell surfaces is most valuable.

This is a book of great interest to all concerned with the field of tumour markers, is timely in its publication and is highly recommended. □

A. Munro Neville is a Professor at the Ludwig Institute for Cancer Research, Royal Marsden Hospital, Sutton, UK.

OBITUARY

Feodor Lynen, 1911-1979

FEODOR LYNEN died in Munich on 6 August 1979, of complications following surgery to repair an aneurysm in his aorta. It was quite typical of the man that, while in hospital preparing for surgery, he arranged that former colleagues and friends attending the Acta Endocrinologica Congress in Munich last June should receive, personally, messages of regret that he would be unable to meet them. With his death, we have lost a great biochemist, and many, the world over, have lost a good friend.

Fitzi Lynen was a Bavarian, and proud of it. He was born in Munich in 1911; he went to school and university there and then he worked there. So great was his fame, he must have had many attractive offers from other centres of learning, but his love for Bavaria kept him in Munich. He travelled widely, however, and made innumerable lasting friendships wherever he went.

At an early stage in his career, he came under the influence of the great German chemist, Heinrich Wieland. This training and the chemical skills which he developed, and encouraged in his laboratory associates, are clearly seen in all his work. He graduated PhD in 1937, became Dozent in 1942, Professor of Biochemistry in 1953, and shortly afterwards became Director of the Max-Planck Institute for Cell Chemistry. Later, he was to become Vice-President of the Max-Planck Society, President of the Alexander von Humbolt Foundation, and President of the International Union of Biophysics. At the time of his death, he was President of the International Union of Biochemistry.

Lynen's researches aimed to elucidate the chemical details of metabolic processes, and the mechanisms of their regulation. His first brilliant observation came in 1951, when he reported in *Angewandte Chemie* that acetyl-coenzyme A is "active acetate". This was something of a surprise, since at the time it was popularly believed that "active acetate" would prove to be a phosphate. However, Lynen's keen chemical insight led him to appreciate that sulphydryl groups are acidic and that thio esters would behave like anhydrides and thus as acetylating agents.

Considering the range of topics covered by Lynen's publications, one cannot fail to be impressed by his achievements. The Pasteur effect, acetic acid degradation in yeast, the isoprene unit, biotin and the fixation of CO_2, cythohaemin, the biosynthesis of cysteine, terpenes, cholesterol and fatty acids and many others, were dealt with in papers making giant strides in the advancement of knowledge.

In recognition of this magnificient work, Lynen was honoured by universities in Europe, America and Asia. In 1964, he was awarded a Nobel Prize in Physiology and Medicine, jointly with Konrad Bloch.

Despite the honours heaped upon him Lynen remained an approachable, jovial, friendly man. Students loved him, as was abundantly evident from their contributions to his 65th birthday party, an affair which was very Bavarian and far from solemn and dignified. Working in Lynen's Laboratory was an unforgettable experience. At times, he could be a strict disciplinarian, expecting long hours of work and the meeting of deadlines, but this was always tempered by good humour and no one worked harder than Fitzi. One could not fail to be enthusiastic when he was about. Difficulties were made to be overcome, and quickly. Vast quantities of mitochondria appeared overnight, a press for breaking yeast cells was made in a day or two. It was unthinkable to leave the Laboratory before Fitzi had completed his round. Then, as the slightest excuse, or none at all, everyone, Fitzi included, would finish the day in some popular "Local", drinking beer and eating sausages. Of course, work started as usual at eight the next morning.

In 1937, Lynen married Eva Wieland, and they had five children. Frau Lynen was greatly concerned about the welfare of those who worked with her husband, and visitors to the laboratory were welcomed with charming and generous hospitality at the Lynen home in Starnberg. Much of the conversation would be about music and skiing. The number of times Fitzi had broken a leg at the latter activity was legend.

We remember Fitzi Lynen the brilliant scientist, and find it difficult to forget the jovial, limping figure, with the mischievous grin, attiring himself in his office curtains to lead the biochemists at some Faschingsparty.

J. K. Grant

L. J. Wills

LONGEVITY is not unusual in geologists, but it is rare in any branch of science to record the passing of one who continued to produce highly original and outstanding work well into his nineties, whose publications span more than seventy years, some of the later ones being among the most valuable.

Leonard Johnston Wills, Sc.D., Emeritus Professor of Birmingham University, who died on 12 December 1979, shortly before his 96th birthday, graduated with a double first at King's College, Cambridge. He was awarded the Harkness Scholarship and Walsingham Medal and a Fellowship at King's College. After four years with the Geological Survey, mapping in the Llangollen area of North Wales, he took in 1913 a Senior Lectureship at Birmingham University, and succeeded to the Chair of Geology in 1932, continuing there until his retirement in 1949.

Wills' first paper (1907) described the discovery of fossils in the generally barren Keuper rocks of the Birmingham area. This led him in later years to an interest in the fauna of other continental formations, and to extensive studies of fossil scorpions and eurypterids for which he developed ingenious original methods of dissection, revealing detailed anatomical details including the respiratory and reproductive organs.

His concern with the Trias lay also in environmental aspects — a continuing thread in his work — and in the vexed problems of stratigraphic correlation which led to one of his final papers (1976) which described the Trias of the West Midlands in terms of sedimentary rhythmic units. The volume of new information in this work justified its publication by the I.G.S., but the rhythmic units are mostly of local extent. The regional problems are now being resolved by the new science of palynology.

A further realm in which Wills made major contributions was in the Pleistocene history of the Midlands, with its story of advance and retreat of continental glaciers, recognising the evidence of extensive ice-dammed lakes of which one, which he named Lake Lapworth, covered much of the northwest Midlands. This was classic work which has served as the basis for all subsequent studies of Midlands glaciation and river development.

Wills' long term interest in the Palaeozoic rocks of Wales, in the contrasting regimes represented by the Midlands Trias blanketing concealed coalfields, in the marine later Mesozoic and in the complex deposits of the glacial period led to a series of books in which environmental aspects are a major theme. The first was his *Physiographical Evolution of Great Britain* (1929), later came *The Palaeogeography of the Midlands* (1948), *A Palaeogeographical Atlas of the British Isles* (1951), and *Concealed Coalfields* (1956).

Of these publications, the Palaeogeographical Atlas has been widely used by industry as well as by academics, being particularly valuable to the petroleum industry when North Sea exploration led to the requirement for broad regional appraisals. This made "Wills" a household name for petroleum geologists. It was a notable production, including 49 maps of Britain and the adjoining areas from the Lower Palaeozoic to the Quaternary, covering tectonics, palaeogeography, sedimentary facies and glaciation. Authorities are listed for each map — often ten or eleven individuals as well as the Geological Survey — demonstrating the thoroughness of the compilation. Many of the sources provided previously unpublished information, for example from the deep boreholes made in the course of onshore exploration for oil in the 1930s and 1940s.

Wills retired from the Chair of Geology in 1949, but his thirty years in retirement were highly productive. After the work on the anatomy of fossil arthropods and publication of his text books he continued to work on problems of the Midlands Trias and to compile data on the deep geology of England and Wales. Increasing infirmity confined him to his country home near Romsley, but he was an indefatigable correspondent and kept in touch with a range of friends who could provide a flow of new information for analysis and compilation. At the age of 89, in 1973, he completed and published a palaeo-geological map of the buried pre-Permian formations of England and Wales, a map which found an immediate place on the walls of many offices and most geological departments in the country.

It was assumed that in the face of physical frailty, with only one eye useable and a serious heart condition, this would be his last production, but two years later he followed this masterpiece with a palaeo-geological map at a deeper level — the surface of the strata with Upper Devonian and later formations removed, and this led in turn to a third map of pre-Devonian formations. Each map of this series threw new light on the deep structure and stratigraphic relations of deeply buried rocks. The last two were published together with a memoir on the data and on their interpretation in 1978, and with them his scientific work finally came to an end.

Wills had been honoured by the Geological Society by the award of the Lyell Medal (1936) and the Wollaston Medal (1954) — its highest award. In recognition of his continuing prowess he was made the only British Honorary Fellow at the age of 92. The Petroleum Exploration Society elected him a life member and helped to finance his maps, and in his last few years he received medals also from the Yorkshire Geological Society and from Birmingham University.

As a lecturer Wills was difficult to follow but inspired a generation of students with his enthusiasm and interest. In his retirement he could not have accomplished so much without the support of his old university, of a wide range of correspondents, and the devotion of his daughter who looked after him for nearly thirty years after the loss of his wife. But he attracted universal affection and cooperation, and his friends felt it a pleasure and honour to be able to help him in his continuing scientific achievement.

Peter Kent

John W. Mauchly

THE DEATH occurred on 8 January 1980 at the age of 72 of John W. Mauchly who, with Dr J. P. Eckert, conceived and carried through the project for the development of the first large-scale electronic computer. This was the ENIAC (Electronic Numerical Integrator and Computer), built at the Moore School of Electrical Engineering in Philadelphia during the latter part of the war.

Mauchly was born in Cincinnati in 1907 and grew up in Chevy Chase, Maryland. After taking his PhD at Johns Hopkins University, he went to Ursinus College as head of the physics department. During several summers he worked at the department of terrestrial magnetism of the Carnegie Institution in Washington DC, where his father was employed as a physicist. In this way, Mauchly acquired an interest in weather problems that he retained throughout his life. It was while he was working on a project for the analysis of weather records that he began to appreciate the pressing need for some automatic means of computation. He early realised the role that electronics might play and he began to do some experiments in his spare time.

In 1941 Mauchly joined the faculty of the University of Pennsylvania at the Moore School and there he met J. P. Eckert. Together, in 1942, they wrote the proposal for the ENIAC. They were able to interest the US Ordnance Department — which was facing an unprecedented wartime demand for the computation of ballistic tables — in the proposal, and as a result substantial funds were made available. The ENIAC was running by the summer of 1945 and was formally dedicated on 15 February 1946.

The ENIAC contained nearly 19,000 vacuum tubes and its construction represented an outstanding example of technological courage, both on the part of its young designers and on the part of those who gave them support. Its completion was an important landmark in the development of digital computers; however, even more significant in the long term was the formulation, by Mauchly and Eckert, in association with the ENIAC group, of the principles on which modern stored program computers are constructed.

Towards the end of 1946 Mauchly left the Moore School to found, with Eckert, the Eckert-Mauchly Corporation, intended to exploit the new ideas. All went well, although the development of a stored program computer to meet commercial standards was proving a long drawn-out process, until 1950, when they suffered a severe blow by the loss of their sponsor in an air accident. This led directly to the Eckert-Mauchly Corporation being absorbed in Remington-Rand, but happily the name UNIVAC, which they gave to their computer, has survived.

Mauchly remained with Remington-Rand, which in due course, became merged with the Sperry Corporation, until 1959, when he formed a consulting company of his own. In his later years he became associated once more, on a consulting basis, with UNIVAC.

Mauchly was a member of the National Academy of Engineering and a Fellow of the IEEE. He was one of the founders of the Association for Computing Machinery and was its President during the years 1948-50. In 1966 he received the Harry Goode Memorial Award of the American Federation of Information Processing Societies. In addition, he received numerous other honours and awards.

Mauchly was twice married. His first wife, Mary, whom he married in 1930, was drowned in a tragic bathing accident in September 1946. In February 1948 he married Kay McNulty, who had worked as a programmer on the ENIAC. She survives him, along with two sons and five daughters. Mauchly was a man of great personal charm, with a gentle approach to people and affairs. His many friends will miss him greatly.

M. V. Wilkes

The future for UK university research?

SOME time ago, the British evolved the dictum that ships should not be spoiled for a ha'porth of tar. Now they seem to think that ships can be mended with the same material and at much the same cost. Such, at least, is the response so far to the mounting evidence of the 1970s that the British university system is in danger of collapse or, perhaps worse, of lapsing into mediocrity. There is to be an examination of the mechanism for supporting academic research by a committee whose chairman is Sir Alec Merrison (Vice-Chancellor of the University of Bristol) and among whose members representatives of the research councils and the University Grants Committee are conspicuous. The immediate objective is to make recommendations about the system by means of which the two sets of bodies separately provide funds for university research. The committee hopes to have something to say by the end of the year, but that is unlikely to be more than a judicious restatement of what people in university laboratories already know — that the dual support system, regarded as a monument to the British sense of fair play in earlier decades, has now quite broken down.

British universities are not of course alone in their adversity. In most industrialised countries, governments have found it necessary to call a halt to the rapid growth of public support for university teaching and research that began, in most places, in the early 1960s. Strains have, for example, been apparent for some years in the United States, where the competition for funds by university scientists has become more fierce and where the grant-making agencies themselves have been forced to make sometimes radical reappraisals of their policies. (Is peer review as equitable as it seems, and conducive the most effective use of funds? Would block-grant support for outstanding institutions yield greater benefits and, if so, would Congress ever agree?) The British problem, however, is made much more difficult because the virtual stagnation of public budgets for the past several years has been imposed on a university system so delicately balanced between conflicting interests that it cannot respond quickly to the need for change. As the ecologists were once fond of saying, everything depends on everything else.

The dual support system is such a case. The theory is simple, even admirable. The University Grants Committee provides all the universities on its books with the facilities needed to teach students, graduate students included. The UGC grant to the universities also acknowledges the requirement of the standard contract with academics that half of a person's time should be spent on research. The research councils — the Science Research Council especially — provide extra support for individual project research and for facilities which are in principle open to all universities. (Thus the Science Research Council pays the British contribution to the European Centre for Nuclear Research at Geneva.) The research councils are also the chief source of stipends for graduate students. So, the theory has it, all academics are enabled to teach well, and to conduct research. But outstanding people can compete for extra support on the merits of their proposals.

The gulf between theory and practice has quickly widened in the past few years. That part of the UGC support for universities called the Equipment Grant (now exceeding £80 million a year), which is distributed among universities separately from recurrent costs, is often too little for university departments to meet the costs of servicing essential equipment, electron microscopes or computers for example. The general shortage of funds also requires that many academics, short of technical assistance, have to work as their own repairmen. Direct support for research is at the same time increasingly under strain. Probably it is still true that outstanding projects win support from one or other of the research councils, but there is an alarming tendency towards cheeseparing that often seems (to grant recipients) calculated to ensure that even the best projects will not quite succeed. Less than outstanding but still good projects are now at risk, as are the people employed for years on soft money (from whatever source), who must be now almost as much at risk of unemployment in mid-career as are professional footballers.

All this is quickly changing the pattern and helping further to erode the spirit of much university research. The number of university departments which lack externally funded research projects is growing, further increasing the pressure on UGC funds. The supposition that students will be taught in places where research is active is too often false for comfort. The most serious threat to the future of British university research is that young men and women with outstanding projects in their minds can no longer look confidently for niches within even sympathetic university departments where a research team can grow up. The demographic log-jam among tenured university teachers, more than half of whom are still younger than forty, is largely responsible. The shadow cast by these developments on the future is long and getting darker.

Unhappily for the Merrison committee, these are problems which can be more easily described than solved. The UGC's support of university research rests on the assumption that all academics are equally free to win reputations for themselves in research. By extension, all universities are supposed equal and are thus confirmed in their proper jealousy of their independence. Support from the research councils is, on the other hand, openly and properly discriminatory; the best projects, wherever they come from, attract support. An application from the University of the Sticks has, in theory, as good a chance as one from Oxbridge. Practice is, however, somewhat different. Willy-nilly, successful researchers find their way to places where research is already strong and, once there, attract further support for their departments' research. The lists show that Oxbridge, London and the strong civic universities predominate in the hunt for funds. To ask that such concentrations should not occur is to ask that human nature should be different. The difficulty, for Merrison, is that there can be no reform of the dual-support system that avoids offending against one or other of the principles that all universities are equal and that all academics are free to work where they like (and can find a job).

The temptation, of course, will be to tinker with the system within the limits of the fixed budgets now in prospect. Transferring some of the UGC equipment grant to the research councils, so that each project grant could be accompanied by the full cost of its overheads, would help to ensure that projects were carried out in circumstances where they might succeed, but would be resented (and resisted) by most universities and their teachers. Transferring funds in the opposite direction would be equally offensive. (Constitutionalists will quickly point out that either change would require an Act of Parliament — for which there is no time.) No doubt the committee will also canvass the fashionable notion that industry should directly support more

university research — a dubious precept unlikely to be followed eagerly in the coming recession. Yet something must be done to allow such funds as there are for university research to be concentrated where they can be spent most effectively. The time, in other words, appears to have arrived when the assumption that all universities are equal will have to be openly abandoned. Some will have to draw back from in-house research.

This is where the ructions will begin. The chance is small that a committee with such narrow objectives will discover an acceptable device for working such an important change in the character of the British university system. The ideal would be that there should be incentives for helping the universities less strong in research to work out some other role for themselves, perhaps as specialised institutions or even as liberal arts colleges. The

uniformity of the British university system has been for decades its most obvious weakness. But such a change could be brought about only by a more radical reform of higher education as a whole. Before it knows where it is, the Merrison committee will find itself agonising about the selection of graduate students (now somewhat capricious), transfer of undergraduates between one university and another (still unreasonably difficult), the length of undergraduate courses (most probably too short) and the education of secondary school students (ridiculously narrow). Its problem is both the tip of an iceberg and a can of worms. It will be solved without permanent damage only if the universities themselves seize the initiative and work out a solution for themselves. Their jealously of their autonomy has been matched in recent years only by their complacency.

Inflation, interest rates and innovation

The United Kingdom in its present condition is likely to be most other nations' illustration of how not to conduct affairs. How can it be, the question will be phrased, that within a year of the election of a government dedicated to deflationary policies, the inflation rate has almost doubled (to 21.8 per cent per annum) and is certain to go still higher? Does it follow that Mrs Margaret Thatcher has misled one of the world's oldest democracies, and should promptly be replaced as Prime Minister? Or that Professor Milton Friedman has misled Mrs Thatcher, and should be stripped of his Nobel Prize? Or is it possible — this is what people elsewhere may ask — that there is some diabolic logic in the British predicament that will in due course make its influence felt elsewhere? There, but for the grace of God, so to speak, go all of us? Or is there another box in the response-frame of this implicit multiple-choice question, something labelled "Other — please specify"?

The intelligent response, of course, is none of the first. Mrs Thatcher is much like other British Prime Ministers — quick, masterful (not synonymous with "masterly") yet unwilling to give hostages to fortune by saying publicly (or even privately) what she hopes for. The innocent Professor Friedman has done nothing worse than to point to an almost arithmetical identity — that (*ceteris paribus*) governments worried about inflation have the remedy in their own hands, by their control of the supply of money, pound notes, dollar bills or what have you. If Professor Friedman were to be robbed of his Nobel Prize simply because, ten years ago, he failed to foresee the subtlety of the ways in which people would counter the stratagems of the deflationary governments they had elected by discovering new ways of raising money or, what is the same thing, buying goods, then it would be proper that other Nobel prizewinners such as Watson and Crick should be on the same plane to the medal-returning ceremony in Stockholm for having failed to guess that reverse transcriptase would be discovered. None of them will make that journey, and rightly.

The question whether we are all destined for the same fate is more tricky. Ten years ago, the Italian economy was widely regarded as a joke in poor taste. The economic miracle of the late 1950s seemed to have vanished as mysteriously as it had arrived. Inflation bobbed around at about 20 per cent a year, a then unprecedented rate for serious industrialised countries. Governments came and went with predictable irregularity. Italy has however managed to survive, largely by means of two separate devices. First, there has been a steady erosion of the strength of social institutions, both modern and ancient. The power of the central government has at the same time steadily declined, sometimes in favour of stronger regional government, sometimes urban terrorism and sometimes both. These are but the predictable consequences of inflation and do not amount to a recipe for survival. Italy has survived in spite of inflation because Italian industry has been able somehow to keep ahead, producing a range of highly saleable commodities which have sold well abroad and

at the same time building on the reputations of Italian engineering contractors for the efficient conduct of major construction projects anywhere in the world. In short, Italy has survived more than a decade of high inflation partly by paying a heavy price and partly by the ingenious exploitation of technology.

In principle the same expedient could be followed in the United Kingdom and, for that matter, by the other potentially sick men of the OECD area, the United States and possibly even Japan. Yet circumstances are now more difficult than when Italy learned how to live with inflation. The price of oil has increased ten times. The result is not merely that prices have increased and that the financial markets are flooded with unused credit, but that the populations of the countries where inflation is highest have not accustomed themselves to the notion that the increased price of oil entails a transfer of wealth to the oil suppliers. Mrs Thatcher was right to insist, last week, that British inflation will not abate until British voters acknowledge that they are individually and collectively impoverished by the increased price of oil.

Unfortunately, in the absence of such realism, even the Italian solution is less accessible. When inflation is high and unlikely quickly to abate, interest rates are bound also to rise. This is what has happened dramatically in the United Kingdom and the United States in the past twelve months. For why should people lend their money either to governments or to those wishing to start new enterprises if they have no expectation that the real value of their money will be returned to them? In principle, of course, the arithmetical rate of interest should not be an absolute brake on innovation. People confident that some new process or product will quickly dominate its rivals can simply allow for the high rate of interest in the prices which they eventually fix for what they have to sell. Reality, alas, is not quite like that. High interest rates mean proportionately greater costs for research, development and the building of new plant. In other words, the real risks of innovation are increased. The dice are loaded against those who might help to solve their countries' problems by technical innovation.

For the United Kingdom and, perhaps later, for the United States, the consequences could be calamitous. (Japan is a different case, whose problems stem not from a lack of productivity or innovation but from the financial problems of entire dependence on imported oil.) That there is a connexion between the soundness of an economy — and in particular its freedom from inflation — and the pace of technical innovation is well attested not merely by what economists say but by the economic statistics of the past ten years. Even in the United States, the rate of growth of industrial productivity has lagged well behind that of the well-founded European states. In the United Kingdom, notoriously, the pace of technical innovation has been a snail's pace. To know that these circumstances can be remedied only if there is a profound change in ordinary people's expectations of prosperity is forbidding. Too many people have a vested interest in not saying what the truth is.

Congress may threaten NIH autonomy

Washington

FEARS for the political independence of the National Institutes of Health have once again come to the surface. The cause of the trouble is a Bill now working its way through the House of Representatives that would require that the several institutes of the NIH are funded individually by Congress.

The scientific community is alarmed that the proposed arrangements would enable Congress — or individual congressmen — to attach unworkable provisions to financial legislation. Meanwhile, the administrators of the NIH have drawn the wrath of their political bosses at the Department of Health and Human Services (previously Health, Education and Welfare) by their attempts to head off the legislation in its earlier stages.

At one stage, it is widely reported, the Director of the NIH, Dr Donald Fredrickson, was told by the Secretary of DHHS, Mrs Pat Harris, to "shut up or get out". Dr Fredrickson has stayed put.

Relations between the NIH and its sponsoring department have never been easy. On this occasion, however, the House Bill may seem a lesser evil than a similar piece of legislation introduced in the Senate last year by Senator Edward Kennedy, chairman of the Senate Health and Science Subcommittee.

Kennedy's Bill would make all the institutes of the NIH separately accountable to Congress, but would also have imposed several other unpalatable conditions on the planning of medical research. One of these persists in the version of the Kennedy Bill soon to be considered by the Senate — the proposal that NIH strategy should be determined by a sixteen-member council appointed by the President.

Waxman proposes . . .
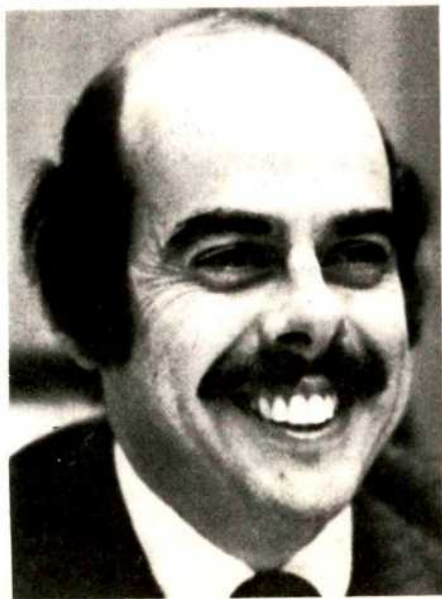
The Administration is staunchly opposed to this condition, but appears ready to accept that separate accountability will in future be required of the institutes. This position appears to have been reached only after an acrimonious dispute within the DHHS, where Mrs Harris was at first strongly opposed to some aspects of the House Bill.

The chief consequences of the Bill as it stands will be budgetary. (Two of the eleven institutes of the NIH, the National Cancer Institute and the National Heart, Lung and Blood Institute, are already dealt with separately in Congress.)

Budget strategy will be approved on a three-year basis, with a provision that

. . . Harris disposes

spending may be continued for a fourth year if Congress fails to act. Representative Henry Waxman, chairman of the Health Subcommittee, says however that there is no intention of using the new legislation as a way of cutting individual institute budgets, which will in any case be protected by separate appropriations legislation.

In spite of Mrs Harris's wrath, the NIH have won some concessions from the House of Representatives. A limit on the amount of research grant that could be approved by an individual institute council has been increased from $50,000 to $500,000. Moreover, there is a new provision for a fund of $100 million to be spent on areas considered by the Director of NIH to be especially deserving of support.

NIH officials are still unhappy, however, with the increased role of externally appointed advisory committees in the planning of research strategy, while the extent to which the Secretary of DHHS may delegate responsibilities to the Director is, it appears, to be on the Secretary's say so.

Both the Senate and House bills are likely soon to pass in their respective chambers. In the conference that follows, it should become clear in what corner Mrs Secretary Harris is fighting.

David Dickson

Marine Pollution

Clean the Med

ELEVEN Mediterranean nations signed a treaty in Athens last Saturday (17 May) which commits them to clean up their rivers and sewage discharges, to make the Mediterranean a fit place to swim and fish in again. At present 90 per cent of the sewage from the 120 largest Mediterranean cities is poured into the sea untreated; and Italy, France and Spain sweep out their industrial pollutants through the rivers Po, Rhône and Ebro. Effective control of these land-based sources — the objective of the treaty — will cost some £6 billion, it is estimated. But 100 million tourists a year and a £300 million fishing industry will benefit.

The treaty is the sweetest fruit so far of the United Nations Environment Programme's Regional Seas Programme, which is run by Yugoslav marine scientist Dr Stjepan Keckes. He takes an optimistic view. "The British began talking about cleaning up the Thames 25 years ago. Today, salmon have returned to the Thames. I believe we can make the Mediterranean a much cleaner and safer place by the end of this decade."

The foundation of the treaty is both scientific and political: a network of laboratories around the Mediterranean coasts, many of whose staff have been trained and equipped through the Regional Seas Programme. Keckes has insisted on establishing uniform measurement procedures, and has used national laboratories (rather than a single, international expert team) to ensure the respect of national governments for their data. Keckes has also aimed the programme largely towards the definition of 'water quality objectives' rather than uniform emission standards; this has the advantage that, say, the relatively undeveloped North African coast can initially accept higher-polluting factories simply because there are fewer of them — so development is not penalised. The main burden will in fact fall on Italy, France and Spain.

The treaty will have to be ratified by six nations before it comes into force. Ratification would follow the passing of the necessary national legislation.

Two classes of pollutant are defined in the treaty: 'black list' and 'grey list' substances. Black list substances will be limited to very low emissions, because of their toxicity, persistence, or accumulation

in the food chain. These include mercury, cadmium, used lubricating oils, certain carcinogens and mutagens, and radioactive materials. Grey list substances will be admitted to the Mediterranean through strict licensing agreements which will take into account the ability of the local environment to absorb them. The grey list includes zinc, copper, lead, titanium, crude oils and hydrocarbons, pathogenic micro-organisms, and non-biodegradable detergents.

Atmospheric pollution of the sea is also covered by the treaty. Measurements on the Baltic have indicated that the air, replete with exhaust fumes, may be the principal source of organic lead in surface waters far from the coasts — but the air-sea interchange is very difficult to measure. The treaty has reinstated a deep-sea, air-borne pollutants monitoring programme which had been axed, on French insistence, a year ago. "The countries recognised it was a mistake" said Keckes.

The next step, says Keckes, is to shift the £400,000 a year research programme, from one largely for training and equipping laboratories, to one of specific common research and data handling — which will be a five- or ten-year programme.

Precise environmental quality objectives, emerging from the research programmes will be defined in time for ratification. A meeting in October is expected to set the first: for bathing and shellfish growing waters (largely a matter of micro-organism levels), and for mercury in shellfish.

Robert Walgate

Research posts

Jobs for the Jugende?

WEST German post-doctoral and just pre-doctoral scientists, searching like others the world over for scarce research positions, will shortly find another 175 posts a year open to them — if the federal and regional governments approve.

The Arbeitsgemeinschaft der Gross-forschungseinrichtunungen (AGF), an association of the 12 major research centres outside the universities, has asked the governments to back a proposal to create 700 new posts over 4 years, each lasting three to five years, at a total cost of about DM90 million (£22 million). This represents little more than an annual 1% addition to the current AGF budget.

Professor Herwig Schopper, president of the AGF, said this week that the proposal was designed to cope with a national population bulge — which is beginning to swell doctoral numbers at a time when most post-doctoral posts are already filled. "We don't want to lose this

talent just because of a freak of demography" he said. The programme fitted well with another — under discussion in the Ministry of Universities — to create more junior university positions over the same period.

In making the proposal, the AGF (whose members include, for example, the high-energy physics laboratory DESY, and the German cancer research centre at Heidelberg, the DKFZ) has taken account of the age profiles of its member laboratories. An official said this week that fewer than one scientist in a hundred currently retires each year from AGF staffs, releasing fewer than 40 posts. Another 30 are freed by scientists moving to industry, but the total of 70 vacancies is far too few to retain a stable age profile in the laboratories.

However, said the official, retirement rates will begin to rise rapidly in five years. By 1992 retirements are expected to reach 7% a year, the equivalent of 280 posts. "So we just have a valley to bridge."

The proposed appointments would be made through the usual recruitment procedures of AGF members, but specified subjects will be preferred. Thus energy research would receive 175 posts; nuclear and subnuclear physics 140 posts; life sciences 140 (with appointments principally to the DKFZ, to the Gesellschaft für Biotechnologische Forschung, and the Gesellschaft für Strahlen und Umweltforschung); information technology 105; materials science 70; aerospace 35; and technology assessment 35.

The Federal science minister, Herr Volker Hauff, has approved the scheme, but it must now go to the cabinet for a decision. And as the regional (Länder) governments support AGF laboratories to 10% of their budgets, the AGF must seek their approval also. Schopper is confident of success, but he does not expect a decision before the federal elections later this year.

Robert Walgate

Innovation

Biotechnology boom at NRDC

BRITISH biotechnology may benefit from the impending change of managing directors at the National Research Development Corporation. Dr James Cain will succeed Dr William Makinson on 1 June, and is already talking of tripling the corporation's spending on biotechnology in the coming three years.

Dr Cain, a 57-year-old biochemist, is at present head of the NRDC's biosciences group, which contributes four-fifths of the corporation's £18 million licence income.

The NRDC's major earners are the cephalosporin antibiotics — developed by Professor E P Abraham of the University of Oxford — which, said Cain last week, have already earned NRDC at least £80 million through licensing agreements set up by the biosciences group since 1959. Pyrethroid insecticides are "already into millions".

Biological projects, based on patents acquired from university and government laboratories, have thus become the NRDC's bread and butter. They also appear to be good business: the cost of developing an innovation from a successful patent to the point at which it can be licensed tends to be less for biological than for hardware projects.

Investment in hardware projects still dominates the NRDC's investment. At the last count, there were 229 active projects in fields such as instrumentation and engineering, compared with only 18 in the biological sciences. The corporation's total investment in biological projects amounts to £1.5 million, a mere tenth of the NRDC's total investment. Of this £600,000 has been committed to genetic engineering. Cain hopes the £1.5 million will be doubled or tripled in the next three years.

Cain says that the corporation has been talking to industry for some time about biotechnical projects, and one involving crop plant development "is being actively followed up", with a decision possible within six months. On the academic side, "people are coming to us with projects once a month", a vast increase on say five years ago. "We've been getting experience of genetic engineering and want to increase our exposure" he said.

Most of the NRDC's projects involve collaboration with industry, but the most natural partner for many joint ventures, the pharmaceutical industry, is so used to carrying out high-risk projects on its own that experience has been disappointing. So the corporation is looking to the food industry and elsewhere in biology-based industry where indigenous research tends to be short-term.

Cain acknowledges that NRDC spending will continue to be higher in the physical sciences because such projects tend to call for the building of expensive large-scale prototypes. But the time may come when NRDC will have to build biotechnical pilot plants, which will call for larger resources. "It's quite easy to imagine a £1 million project with industry", he says, "which aimed to go commercial in three or four years."

The new interest in biotechnology does not however mean that the NRDC's traditional interests will vanish. In particular, the corporation will continue to be heavily involved in computing machinery and in computer software. But for the time being, it seems to have an edge in biological engineering.

Robert Walgate

Ariane

Getting bigger and better

THIS is yet another milestone-week for *Ariane*, the satellite launching system developed by European governments under the aegis of the European Space Agency (ESA). Tomorrow, 23 May, the second test-flight of the *Ariane* system will be carried out from the rocket base in French Guiana. Today, 22 May, the Council of the ESA is meeting to decide how the cost of the next three years' development, estimated at 175 million units of account (about £115 million) should be shared among member states.

The plan is to improve *Ariane* to carry payloads of 2,000-2,300 kg, compared with the 1,750 kg capacity of the current launcher. The new systems will be capable of placing two 1,000 kg satellites into geostationary transfer orbit and so will fulfil most of the requirements of launching heavy telecommunications satellites.

The development is planned in two phases and *Ariane* II and III should be complete by 1983. *Ariane* II will be developed first to carry payloads of up to 1,950 kg by increasing the thrust of the first and second stage engines and the propellant mass of the third stage. *Ariane* III, with a payload of 2,300 kg, will have two boosters fitted to the first stage. The volume available for carrying satellites will be increased in *Ariane* III to allow two satellites to be launched together, reducing costs.

The stimulus for the *Ariane* programme has come from the Centre National d'Etudes Spatiales in France (France has funded 55% of the 790 million accounting units of the first phase of Ariane development over the past seven years). CNES has done much of the groundwork for *Ariane* II and III and is already planning later versions. According to M Bouillard, head of advanced projects at CNES, *Ariane* IV, which would be *Ariane* II with four extra boosters and a 35% increase in first stage development and would accommodate payloads of up to 3,500 kg, could be developed by 1985. Plans for *Ariane* V, however, are more ambitious. It would be capable of putting into orbit a manned vehicle which would return to earth under its own steam. CNES is also looking at the feasibility of recovering and re-using some components of Ariane V. It hopes to develop *Ariane* V by 1990.

In the meantime, the development of *Ariane* I is coming to an end. Earlier this year ESA handed over routine production to a consortium of European industry, Arianespace. After the four test launches (the last is scheduled for early 1981) and two subsequent launches, ESA will be free
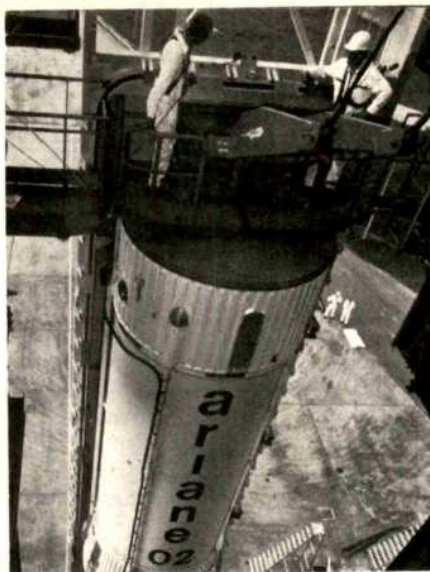
Ariane II, second stage in the development of the ESA's satellite launcher, to be launched from French Guiana tomorrow.

of financial responsibility for further production, provided that Arianespace is financially viable. ESA member states are currently signing an undertaking to help bail Arianespace out should it ever get into trouble.

ESA will, however, retain responsibility for maintenance of the *Ariane* launch pad at Kourou, French Guiana. Member states will also decide at this week's council meeting whether to fund the building of a second pad at the site. The existing pad can handle only four launches a year. When the larger versions at the rocket come into operation, ESA estimates that up to six launches will be needed each year.

Even if, as expected, the plan for *Ariane* III is approved this week, the budget will be considerably less over the next three years than it was at the height of the development of *Ariane* I. It is unlikely, however, that much of the money released will be channelled into ESA's other programmes, in particular the science programme, which desperately needs more funds. Any increase in the science budget, which is mandatory for all member states, would have to be approved by them all. Those who do not contribute to *Ariane* are unlikely to agree to spend more.

ESA's immediate concern, though, must be the success of the second Ariane test-flight, scheduled for 23 May. The two small German satellites, "Firewheel" and "Oscar 9", carried free of charge, are also dependent on the success of the mission. "Firewheel" is a small satellite built by the Max Planck Gesellschaft to release barium and lithium clouds into the magnetosphere and monitor their movement through it. "Oscar 9" is a satellite for radio hams. If the flight goes as well as the first test, ESA and the German satellite operators should have few worries. Member governments may also pay up more cheerfully.

Judy Redfearn

Grant audits

No easy riders

Washington

THE dust is refusing to settle around conflicts between research universities and government accountants over the auditing of federally-supported research grants. It is more than a year since the Office of Management and Budget (OMB) issued the final version of its revised accounting rules, a document known as Circular A-21, hoping for a temporary pause in the skirmishing around grant accountability.

But complaints continue to mount, particularly over the requirement for detailed records of how scientists and technicians spend their time. The government's obvious interest is that funds allocated to a project should not be spent on anything else.

The suggestion is now gathering momentum that tensions may be resolved only by radical changes in the basis of research grants. One possibility is a shift from the "cost-reimbursement" basis to a fixed-price, grant-in-aid system, under which, once a grant has been awarded, research workers and their universities would decide how it should be spent.

Ample evidence of continuing frustration was voiced in Washington last week at a meeting of the advisory committee to the Director of the National Institutes of Health. It was plain that financial stringency has also exacerbated tensions between scientists and their universities.

The issue is the level of overhead costs universities should be entitled to add to research-grant proposals. Overhead percentages have increased rapidly in the past decade. The proportion of NIH grants spent on indirect costs rose from 28.5 per cent in 1970 to 41 per cent in 1979, according to a survey carried out by the National Eye Institute. On the grounds that when overall budgets are static, rising overheads mean less money for research proper, the council of the Eye Institute recommended last October that the NIH should reduce all indirect-cost allowances by a third. And the University of California's faculty Senate has rejected proposals from the University President for an increase in overhead percentages.

University administrators firmly resist such reductions, insisting that indirect costs have increased dramatically, largely, they claim, because of federal regulations, for example covering affirmative action or occupational safety. They claim that most universities are able to collect only 80 per cent or less of the costs incurred in undertaking federal research commitments. At Washington University, according to Chancellor Dr. William Danforth, the total costs of carrying out federal research and training in 1978-79 was $49.6 million, but only $40.4 million was recovered from the government.
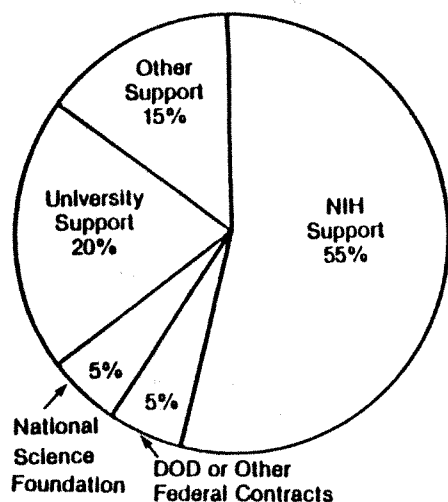
NIH estimate of the sources of income of a typical pre-clinical research laboratory in the United States (percentages of total).

More immediately troublesome for research workers is the need to give precise estimates of how much time they spend on projects.

Circular A-21 relaxed the time-and-effort demand by agreeing that faculty members need only complete such a record at the end of every term rather than every month (reports on technicians are still required monthly), and offering the alternative of "workload monitoring" where time allocation is agreed before a project is begun.

But research workers still find the system oppressive. Many claim it is unreasonable, for example, for a research scientist in a medical school to decide how time has been distributed between functions that may have been carried out simultaneously. "It is impossible to allocate one's time between research, training and patient care, and it is a sham to try to impose it," Dr David Kipnis, chairman of Washington University's School of Medicine, told last week's meeting.

Others argue about the difficulty of shifting from the rigours of scientific quantification to the "creative fictions" of the accountant. "We put a high degree of rigour on the numbers that we generate. So when we get a form asking us to put down numbers, we tend to think that they are the same type of numbers, ignoring the fact that they may not correspond to our notion of reality," said committee member Dr Howard Temin, professor of oncology at the University of Wisconsin.

Government auditors are unbowed. They insist that the revised A-21 requirements have considerably reduced the reporting load. They also point out that current auditing requirements follow directly from the way Congress has chosen to support biomedical research.

This has prompted increasing suggestions that alternative ways of supporting research should be explored. In a report on funding mechanisms soon to be published, for example, the National Commission on

Research (NCR) suggests that experiments be made with locally-managed grants-in-aid, shifting the emphasis from detailed financial accountability to scientific accountability.

Under such a system, a grant proposal would still be closely scrutinised by the funding agency using the full peer review process. But once the money had been allocated, the investigators' prime responsibility to the agency would be to report on the technical aspects of the research. Administrative details would become the responsibility of the investigator and his or her university, with the funding system becoming the main incentive for the wise management of resources.

NIH is keen to encourage experiments along these lines for certain types of grants, according to director Dr Donald Fredrickson, while OMB officials say that, in principle, such a basis would be acceptable and simpler to administer.

In a different context, the National Science Board, the governing body of the National Science Foundation, has given some thought to the merits of block-grants to universities, so far without conclusion.

Not all universities relish the prospect of having to decide how a research worker is entitled to spend a federal grant. In addition to the increased administrative load, one result could be to translate current tensions between scientists and government accountants into the university setting. And there are several procedural issues, such as the way that indirect costs are calculated (currently as a proportion of the salaries and wages included in the grant) that would need to be revised.

The NCR, a body set up two years ago to examine all aspects of research funding, considers that these changes could work. But it urges the need for experiments. The National Science Foundation is already experimenting with post-award aggregation of grants to a selected number of university chemistry departments. The NIH, which supports almost 50 per cent of federally-sponsored university research, is planning to follow suit.

David Dickson

PWR design

UK programme gathers steam

DESIGN work on modifying the Westinghouse pressurised water reactor system to meet British safety standards has begun "in earnest" following a letter of intent issued by the UK Central Electricity Generating Board to the Nuclear Power Corporation late last month.

The NPC is increasing the staff of its light water reactor team from 80 to 170 by the end of September, and plans a total of 400 by the end of 1982. Design staff, who are not nuclear experts as such, are being recruited from engineering fields associated with complicated plant design including piping engineers, quality control draftsmen, power engineers and computer specialists. In addition the NPC is transferring part of its existing staff of 1,200 to PWR work. Included in this number are engineers from the advanced gas cooled reactors located in Hartlepool, Heysham and Dungeness. Two NPC engineers will fly to Pittsburgh next month to work with a Westinghouse licensing group on the transfer of the details of PWR technology to the UK. Five Westinghouse engineers will join the NPC team next month to work on modification of the Westinghouse design to meet UK standards. Technical support from Westinghouse will grow to about 100 professionals by 1982.

NPC staff is concentrating its present efforts on computer simulations of safety procedures and on physical modelling of the layout of the 1100 MW reactor. The design of steam, water, gas and cable runs is to conform with British safety procedures developed through experience in petrochemical plant design.

In conjunction with engineers from the CEGB, the NPC will prepare its modifications of the Westinghouse system which includes a novel "double skin" consisting of two concentric concrete cylinders with the reactor hardware in the inner cylinder and the safety and standby systems in the outer cylinder to meet operator radiation dose standards and plant standby power requirements, and to "relieve burden on the human element". The design work will cost £3.5 million.

The Nuclear Installations Inspectorate says that it expects to receive the CEGB's preliminary safety report — a general outline of the standard safety procedures to ensure reactor safety — within the next few months. This will be followed by a "steady flow" of design information beginning with a safety analysis of the main design followed by fault analyses of particular areas ranging from pressure vessel integrity and the possibility of fast fracture from small cracks (*Nature*, 28 February, p804) to the reliability of used equipment and component failure records. In spite of staff shortages, the NII expects no difficulty in meeting its obligations to evaluate PWR safety.

Approval of the design modifications by the NII by 1982 will be followed by an application by the CEGB for a nuclear site license at the Magnox reactor site at Sizewell. At the same time, the promised public inquiry will also be announced and the safety documentation will be released in accordance with the government's announcement on 18 December 1979 that "principal safety documentation relevant to the initial licensing will be published and made available before the inquiry".

Jo Schwartz

Soviet psychiatry

Mock trial in London

THE second anniversary of the arrest in the Soviet Union of Alexandr Podrabinek was marked in London last week (15 May) by a "public hearing" on the alleged abuse of psychiatry in the Soviet Union. Podrabinek is the author of the *samizdat* treatise "Punitive Medicine" and a member of the organisation known by the cumbersome title of Working Commission for the Investigation of the Misuse of Psychiatry for Political Purposes.

The chief object of last week's hearing, at which Mr Louis Blom-Cooper Q.C. put the case for the prosecution, was to draw attention to the plight of the working commission, only two of whose original members remain at liberty in the Soviet Union. Other members of the commission now arrested include the mathematician Vyacheslav Bahkmin (12 February, 1980) and the physician Leonard Tarnovskii (4 April, 1980). The pharmacist Viktor

Nekipelov, who was a member of the Moscow Helsinki Monitoring Group, had worked closely with the commission until his arrest on 7 December last year.

At last week's proceedings, one of the chief witnesses was Dr Alexandr Voloshanovich, who had been forced to emigrate to Britain in February this year. He told the hearing that he had investigated a total of forty alleged victims of psychiatric abuse before his departure from the Soviet Union, but that in no case had he found "indisputable evidence of the need for hospitalization".

Interest in the West has necessarily centred on the more spectacular cases of alleged psychiatric abuse, such as the hospitalization of Petro Grigorenko for his defence of the Crimean Tartars (and whose cases was simulated in last week's mock trial). Dr Voloshanovich emphasised, however, that the cases which he had investi-

gated were varied, and that in his experience some of those sent to psychiatric hospitals had not given political offence but, rather, had simply been trouble-makers for the system.

Mr Peter Reddaway, co-author of the book "Russia's Political Hospitals", suggested that psychiatric abuse has featured "quite prominently" in recent arrests of those known to have dissident sympathies. Of 200 arrested since last autumn, he said, fifteen have ended up in psychiatric hospitals.

Even so, there are some signs that the Soviet authorities are sensitive to allegations of the misuse of psychiatry in the Soviet Union. When the Royal College of Psychiatrists (London) wrote at the beginning of the year to Dr Andrei Snezhnevskii asking for an explanation of the growing number of reports of psychiatric abuse in the Soviet Union, Snezhnevskii offered no explanation but did resign his honorary membership of the college.

Vera Rich

Antarctic ecology

Monitoring krill from land

THIS season's Polish expedition to the Antarctic returned home two weeks ago claiming that it should at some stage be possible to monitor the exploitation of Antarctic krill by observation of the land-based fauna of the Antarctic coast. This is one of the arguments that Polish ecologists will be putting to the forthcoming conference in Paris on Antarctic biomass.

The Polish Antarctic base "Henryk Arctowski" was established in 1976 on King George Island in the South Shetland Islands and can accommodate 70 people in summer, with up to twenty people over-wintering. Given the location of the station, Polish concern with the oceanic ecology of the Antarctic is understandable.

Dr Stansilaw Rakusa-Suszczewski, of the Polish Institute of Ecology and co-ordinator of the biological part of the Antarctic programme, said after the expedition had returned that Poland has no ambition to exploit Arctic krill commercially, but that for the time being at least is concerned only to understand more clearly the somewhat fragile ecology of the Antarctic.

The chief objectives of the biological part of the past season's Antarctic programme were to understand the flow of nutrients off the coast of Antarctica in such detail that marine production could be accounted for. Previous Polish expeditions to the Antarctic have drawn attention in their reports to the way in which marine production is determined jointly by off-shore upwelling and the ex-

change of material between the sea and land surfaces.

Dr Rakusa-Suszczewski now thinks that it will in due course be possible to follow the production and exploitation of oceanic krill, and of other marine animals occupying lowly positions in the food-chain — almost literally low in the oceanic pecking order — simply by maintaining regular counts of the populations of penguins and seals living on the Antarctic coastline.

Marine ecologists will no doubt await the publication of the past season's results before accepting Dr Rakusa-Suszceutski's claim. Penguins and seals are known to be in-shore feeders, and the dependence on what happens in the deep

Antarctic must be tenuous, to say the least of it.

Nevertheless, in strict compliance with the formal terms of science planning in Poland, the Antarctic programme of research is aimed at the solution of an "interdepartmental problem", defined as such because it integrates "environmental and biological research with the objective of understanding the dependence and functioning of part of the eco-system and the inflow of material in the inshore zone of Admiralty Bay".

In case all the subtleties of Antarctic ecology can be worked out only after further painstaking research, Dr Rakusa-Suszczewski is also at pains to emphasise that the past season has produced some practical benefits — the possibility that fish-bile may be a valuable source of cholic acid for the pharmaceutical industry, for example.

Vera Rich

Henryk Arctowski — no krill in sight

CORRESPONDENCE

High book prices

SIR, — It is not just a berserk economy that is to blame for the high price of books. A colleague of mine expressed horror at the price proposed for a hard-back that he had intended for students, and asked why it could not be printed as a paperback. The answer was: "If it sells well then we shall publish a cheap edition". The Russians must be laughing at our marketing.

Yours faithfully,

PHILIP J STEWART

University of Oxford, UK

SIR, — The leader entitled "Are Books too Expensive" (24 April page 649) was a wayward attempt at analysing a problem of great concern to everyone involved in publishing.

We were told that for the price of a skipped lunch we could once walk out of a bookshop with a few titles under our arm; perhaps we could be supplied with the actual year when this was possible. Let us assume it was 1962, before the boom in science publishing. I asked two colleagues who had not read the article how much a cafeteria lunch of say three courses might have cost in 1962; one said 3/-, the other said 2/6. I then checked records for the prices of monographs published in that year; a book of 256 pages cost an average 42/-. To walk out of the shop with one monograph, the author would therefore have had to skip 14 3/- lunches.

How many lunches would the author have to skip now? We have just published a monograph of 256 pages at £15.00 and a simple three course lunch seems to cost around £1.25. The author would actually have to skip two fewer lunches today!

For those who would like a more serious analysis the graph (based on figures supplies by the Publishers' Association) shows how the average price of books published in Britain has risen since 1970. In the same period the UK Retail Price Index has risen a little more, just over 300%. Average earnings have increased by more than the RPI since 1970, but perhaps what the author should be complaining about
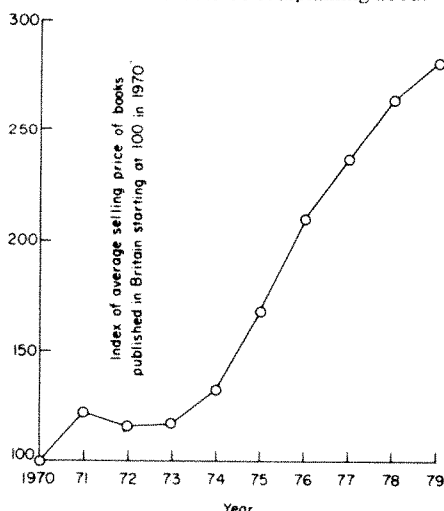
is that the average earnings of the book-buying population have probably slipped in relation to the rest of the population.

It is suggested that we should show restraint over symposia and monographs and avoid duplication. Symposia and monographs can, in fact, be published profitably if overheads are kept to a minimum as explained in the *New Scientist* (21 June 1979 page 1013) and the right number is printed, but most

publishers are leaving these to a few companies which concentrate on specialist works. The vast majority of publishers would prefer to sell more copies of fewer titles but as sales of individual titles are decreasing, the response from some publishers has been to publish more titles to maintain turnover. The Soviet Union avoids duplication by controlling publication through central committees. The members of these committees are undoubtedly exceptionally talented but as the author points out, such a system cannot always be right in predicting which book will be essential to the development of a subject.

The real problem for British-based science publishers is that, although they are trying to hold down their prices, the value of the pound abroad is hitting the export market which takes around 60-75 per cent of production. Our books are becoming too expensive in some overseas markets. Our export market has also been weakened by the rise of indigenous publishing houses moving from producing translations of successful English language texts to books written by local authors. Students are prepared to pay more for texts in their first language and aimed specially at their courses. This is a healthy development in publishing as a whole, but it means that the publishers working in the English language can no longer assume that their books are automatically international products and the first choice for students in many parts of the world.

Publishers can adapt to the problem of high selling prices resulting from the high value of the pound abroad by producing abroad; indeed many are already doing so. This however could permanently damage the UK printing industry. The curent wave of redundancies in publishing could be quickly followed by further unemployment amongst printers.

Yours faithfully,

ROBERT CAMPBELL,

Blackwell Scientific Publications
Osney Mead, Oxford, UK

No gas guzzling

SIR, — In your leading article of 17 April about energy conservation, you say that the "Gas Board . . . advertises to encourage us to use more energy".

The fact is we do precisely the opposite — and just what you advocate. Your article is headed "Conserve energy, conserve cash". One of our slogans, widely used, is: "Save Gas, Save Money". Our publicity has plugged an energy conservation line for many years now. Moreover, since early last summer, no promotion of gas or gas appliances has been pursued that would build up gas load at the peak. On the contrary, television advertising about using gas efficiently has appeared throughout the winter months and is being followed by a campaign on similar lines in the national press at present. The efficient use of gas is one of our key objectives.

Yours faithfully,

F W PLOWMAN

Public Relations Department
British Gas Corporation

Responsibility for nuclear weapons

SIR, — Despite rising international tension there is little public debate about Britain's policy on nuclear and other modern weapons, especially in comparison with the impassioned campaigns for and against nuclear energy. And yet while nuclear energy is at worst a

long-term threat to the quality of our civilisation, nuclear weapons could obliterate it in half an hour.

We have lived quietly with this peril for more than twenty years, during which the policy of deterrence has not failed. But there are several disturbing new developments that require urgent discussion, especially by scientists. First, the government's decision to consider producing chemical weapons; second, the government's decision to consider spending £5,000 million replacing Polaris nuclear submarines and missiles with the Trident system; third, the government's reaffirmation that its policy is to offer virtually no protection to civilians in the event of war; fourth, the government's decision to allow cruise missiles to be stationed in Britain; fifth, the increased accuracy of guidance systems (which could tempt the Russians or Americans into considering a first strike against each other's missiles).

The scientific community must play an important part in the extensive discussions that these ominous developments ought to provoke. In particular we should put under close scrutiny the activities of our colleagues who carry out weapons development. Lord Zuckerman has argued first, that their technical innovations have created a new situation, undermining deterrence by making all-out war a seriously-considered policy option, and, second, that the implementation of new weapons systems is often at the instigation of scientists rather than of the military. No longer should it be claimed as in the Second World War that military scientists are helping their side to win, nor, as in the 1950s that they are building up an effective deterrent. Instead, it should be recognised that the contribution of scientists to warfare has entered a third phase, in which their prolific inventive capacity is itself a powerful destabilising influence.

The consequences of the arms race continuing unchecked are so dire as to make it imperative for us to overcome the paralysing hypnosis induced by our sense of helplessness as individuals. As a small beginning we invite scientists to take the following steps:

1. To oblige those of our colleagues who devise and advocate new weapons of mass destruction to stand up and justify their work (as their counterparts in the nuclear energy industry are having to do).

2. To inform our students (and ourselves!) of the far-reaching and complex relationship between military technology and progress in 'pure' science.

3. To initiate informed discussion on weapons development in our various institutions and professional bodies and to make our own view clear. Those opposed to further weapons development might consider discouraging students from applying to enter military research establishments.

4. To support currently faltering international attempts towards arms control.

5. To promote public discussion by making MPs aware of our fears and encouraging them to play an active role in forming sane weapons policies.

Yours faithfully,

MICHAEL BERRY,
ALWYN EADES,
DAVID FIELD,
TIMOTHY POSTON,
GORDON REECE,
JOHN ZIMAN,

Bristol University, UK

JOHN CHARAP,
Queen Mary College, London, UK

NEWS AND VIEWS

The Cretaceous-Tertiary boundary event

from Finn Surlyk

SIXTY-FIVE million years ago a major crisis hit the flora and fauna of the earth. In stratigraphic terms this took place at the boundary between the Cretaceous and Tertiary systems. Evidence for the crisis lies in the more or less simultaneous extinction of major groups of animals and plants including such characteristic elements of Mesozoic life as the dinosaurs, the great marine reptiles, the flying reptiles, the ammonites and belemnites, many bivalve groups, and major groups of marine phyto- and zooplankton[1,2]. It has been estimated that as many as 75% of Cretaceous species may have been eliminated.

Searching for the cause of this event has been a favourite pastime for a large number of scientists and a great number of hypotheses have been put forward. Some observations suggest a catastrophic mechanism whilst others are indicative of more gradual processes[1-3].

In the last few years the catastrophists have dominated the scene. The main reason for this is the extremely abrupt wholesale extinction of major groups. This is well known from the type area of the lowermost Tertiary, Danian Stage in Denmark[4,5] from several sections in Spain[6], from the Italian Apennines[7], and from many holes of the Deep Sea Drilling Project[8,9].

The catastrophists of today seem to have focused on two major hypotheses. The first one is of terrestrial nature and comprises spill-over of brackish water from an isolated Arctic Ocean at the time of opening of the Greenland Sea — Norwegian Sea passage by sea-floor spreading[8,10]. Thierstein and Berger[8] supported this theory by carbon and oxygen isotope data, while Gartner and Keany[10] used nannoplankton from North Sea chalk to support the "spill-over" hypothesis. In the latter case an isolated occurrence of a 'Danian' nannoflora was

found in a core 55 m below the supposed top of the late Cretaceous, Maastrichtian stage. This was taken to suggest that 'Danian' coccolithophores and planktonic foraminifers developed during late Cretaceous times in an isolated Arctic Ocean having a greatly reduced salinity. An initial, temporary opening of the Greenland Sea thus accounts for the lowermost occurrence of "Danian" coccoliths in the late Maastrichtian.

The North Sea section was, however, reinterpreted by Perch-Nielsen *et al.*[5] and by Watts *et al.*[11] who clearly demonstrated that the Maastrichtian-Danian boundary actually occurs below the lowest 'Danian' interval and that the overlying 55 m of Maastrichtian chalk actually represents slide material redeposited in Danian time. While this work certainly invalidates the data base for the Gartner-Keany hypothesis, it does not necessarily eliminate the spill-over hypothesis.

The second major catastrophic hypothesis is of extraterrestrial nature involving the influence of a supernova, meteorite or comet. While this idea is not new it has had a considerable revival in the last few years due to the discovery by Alvarez *et al.*[5] of anomalously high levels of iridium at the Cretaceous-Tertiary boundary in several sections near Gubbio, Italy. Ir in crustal rocks is typically 10^{-3} of solar system levels, so high Ir could indicate an influx of extraterrestrial material. Ir isotope measurements show less than a 2% difference from the terrestrial Ir ratio suggesting that the Ir came from a solar system source, not a supernova.

The same anomalous trace element enrichment, especially of iridium and osmium at the time of extinction was recorded by Smit and Hertogen[5,6] (this issue of *Nature*) from an almost complete sequence across the Cretaceous-Tertiary boundary in Caravaca, SE Spain. This was

taken to support the idea of a large meteorite collision.

Hsü, also in this issue of *Nature*, has used the extinction and trace element data from Gubbio and Caravaca to advance an extreme theory[12] that suggests the extinction of the large terrestrial animals was caused by atmospheric heating during a cometary impact. Poisoning by cyanide released by the fallen comet and a catastrophic rise in the calcite compensation depth in the oceans are separately proposed as the main agents responsible for the extinction of the calcareous marine plankton. Several tests are possible for this hypothesis. First, where is the crater? Hsü assumes that the meteorite fell in the ocean, and since much of the Mesozoic ocean floor has disappeared by subduction, the crater may have vanished. The instantaneous extinction of the large terrestrial animals offers another test possibility. Where are all the accumulations of both vertebrate and invertebrate skeletons at the boundary? It may of course be argued that some of the terrestrial skeletons were destroyed by burning, but, if found, such fossel populations should have a characteristic age distribution indicating mass-mortality of the whole population.

A very recent paper on the Gubbio sequence by Wezel[13] should dampen the enthusiasm of the catastrophists.

The key geological section for the catastrophists is situated at Bottaccione near Gubbio in the Italian Apennines. It is generally interpreted as an essentially complete sequence of Middle Cretaceous to Palaeocene calcareous, pelagic sediments[14]. Palaeomagnetic studies of the Upper Cretaceous and Tertiary parts have yielded a sequence of magnetic polarity zones, which are said to correspond

Finn Surlyk is in the Geological Museum of Copenhagen University.

precisely with the marine magnetic polarity profiles. They are dated by foraminifera[7], and the section is proposed as a magnetostratigraphic type section[15]. The Bottaccione data have furthermore been used to recalibrate the existing magnetic time scale and thus to revise the oceanic spreading rates. The tectonic rotation of the Italian peninsula as an independant microplate or as part of the African plate is clearly seen in these magnetic data. Finally, trace element anomalies mentioned above have been of tremendous importance in the discussion on the late Cretaceous extinction event.

The exact nature of the sequence has thus formed the basis for the catastrophist's far reaching conclusions. Data published so far on the sedimentology of the critical strata are sparse and mainly of lithostratigraphical nature[14] and can not provide the basis for a detailed interpretation.

Wezel's recent detailed study[13] of the sedimentology of the critical sequence is thus of fundamental importance. This is particularly the case as Wezel in his introduction states that "The formation turned out not to be the product of a long and continuous 'gentle pelagic rain' and also the classical and type-biostratigraphic zones were found to contain younger reworked foraminifera" and ". . unfortunately things are not as simple as thought by previous researchers".

According to the detailed and convincing observations by Wezel a lot of the presumed 'pelagic' deposits are calciturbidites resedimented from currents flowing from the east. Stratigraphic changes of magnetic properties at Gubbio seem crudely to match local variations in bed thickness. This certainly rules out the possibility of using the section as a magnetostratigraphic type section for the Upper Cretaceous and Palaeocene. Finally, sedimentologic evidence suggests general reworking of microfossils with very few indigenous forms. This taken together with the very poor fossil preservation in the sequence and the extremely low macrofaunal diversity detracts very strongly from the stratigraphic value of the once celebrated section. Wezel's paper is so detailed that the burden of proof now rests on his opponents[7,14,15].

One feature of the Gubbio section still has to be explained; namely the anomalously high iridium and osmium contents. Since the relevant analytical

1 Hallam, A. *Nature* **281**, 430; 1979.
2 Russell, D.A. *Ann. Rev. Earth Planet. Sci.* 163; 1979.
3 Russell, D.A. *Episodes* **4**, 21; 1979.
4 Birkelund, T. & Bromley, R.G. (ed.); *Cretaceous-Tertiary boundary Events I*; 1979.
5 Christensen, W.K. & Birkelund, T. (ed.); *Cretaceous-Tertiary boundary events II*; 1979.
6 Smit, J. & Hertogen, J. *Nature* **285**, 198; 1980.
7 Premoli Silva, I., *GSA Bull.* **88**, 371-374; 1977.
8 Thierstein, H. & Berger, W.H. *Nature* **276**, 461; 1978.
9 Boersma, A., Shackleton, N., Hall, M. & Given, Q. *Init. Rep. DSDP* **42**, 695; 1978.
10 Gartner, S. & Keany, J. *Geology* **6**, 708; 1978.
11 Watts, N.L. *et al. Geology* (in press).
12 Hsü, J.K. *Nature* **285**, 201; 1980.
13 Wezel, F.C. *Ateneo Parmense, Acta Nat.* **15**, 243; 1979.
14 Arthur, M.A. & Fischer, A.G. *GSA Bull.* **88**, 367; 1977.
15 Alvarez, W. *et al. GSA Bull.* **88**, 383; 1977.

techniques are quite cumbersome, relatively few determinations of Ir and related trace elements are to be found in the literature on sedimentary rocks. The question thus arises: What do we know of the amount of iridium present in other parts of the sedimentary record? How many analyses have been undertaken and how many is it necessary to undertake before one can safely claim than an occurrence is anomalous?

It thus seems that we are back again where we started and the end-Cretaceous extinction event still presents one of the major examples of the 'Vogt-Holden Effect[5]': "New data, regardless of reliable source of high quality, have scarcely ruled out any past theory, but have fueled the promulgation of newer and even more outlandish proposals". □

Kaon-Nucleon physics

from David Miller

MESON-NUCLEON interactions are at the core of the old-fashioned strong-interaction theory of elementary particles and, although we now have a new-fangled strong-interaction theory of quarks and gluons (quantum chromodynamics 'QCD' see *Nature* **279**, 479; 1979) the structure of the meson-nucleon scattering amplitudes still has to be studied by the old techniques. The relationship between the two theories is not very direct, but one important source of data for those who try to build hadrons (strongly interacting particles) from quarks is the spectrum of meson-nucleon resonances. These resonances appear as poles in the complex scattering amplitudes and it has been the task of experimental physicists for over twenty years to measure scattering cross-sections and polarisations at a wide range of angles and energies in order to reconstruct the amplitudes. Since the data is always limited in both coverage and precision the old-fashioned theory developed a set of mathematical tools, particularly dispersion-relations, which impose strict constraints on the analyticity and continuity of the partial-wave scattering-amplitudes. Reports were presented by Koch (Karlsruhe, Helsinki) and Cutkosky (Carnegie-Mellon, Lawrence Berkeley Lab.) on the latest results of fits to the pion-nucleon data. The general mutual agreement of these fits was impressive. Unanswered questions remain. For instance, it is not clear whether the "minimum multiplets" postulated for the quark-structure of resonances can survive; only negative-parity {70} and positive-parity {56} representations in SU(6) have so far been firmly established but Cutkosky reported a number of awkward new candidates which are hard to fit in. Nevertheless, the major structures in the lower partial waves are clear and such basic dynamical quantities as the πNN coupling constant and the "sigma term" can be quoted with some precision (e.g. $g^2_{\pi NN} = 13.9 \pm 0.36$ — Samaranaika *J. Phys. G.* **5**, 657; 1979).

The structure of the kaon-nucleon and antikaon-nucleon amplitudes is by no

---

A workshop on low and intermediate energy kaon nucleon physics was held at the University of Rome, March 24-29 1980.

---

means so clear. Oades (Aarhus) reviewed the partial wave analyses and a number of speakers, especially from the host group, discussed the dispersion-relations, the zeros of the scattering amplitudes and the sigma terms. A few important features seem to be settled. The $\overline{K}N\Lambda$ coupling has been determined by a number of techniques which give different weight to different parts of the data. Queen (Birmingham) reviewed these results, which mostly give values for $g^2_{\overline{K}N\Lambda}$ between 14 and 17, in good agreement with the SU(3) prediction that $g^2_{\overline{K}N\Lambda} \simeq 1.08 \times g^2_{\pi NN}$. The ispin zero triplet p-wave in kaon-nucleon has a resonance-like behaviour in most fits, but it is generally agreed that it can be explained as a 'woolly cusp' a combination of an attractive potential and the opening up of the inelastic channels. New data were presented on K^+ neutron polarisation from groups working at KEK (the new Japanese proton-synchrotron) and at NIMROD (the retired British proton-synchrotron). Preliminary fits to the NIMROD data by the Queen Mary College — Rutherford group have shown good agreement with B. R. Martin's existing fit, but the KEK data did not seem so closely compatible with previous fits. These are preliminary results from both groups and it will be interesting to see how their presentation develops after the long corridor-discussions between their spokesmen (Takasaki from KEK and Watts from Queen Mary College). But, whatever the outcome, it seems that there is no need to strain the quark-models in order to account for an exotic (5 quark) K^+— neutron resonance.

The antikaon-nucleon resonance spectrum is still quite fluid. Different fits to the data disagree in quite low partial-waves and there is even a major puzzle, the Λ (1405), below the $\overline{K}N$ threshold. Because the mass of a K^- and a proton (1432 MeV/c^2) is considerably higher than that of a pion and a lambda-hyperon (1251 MeV/c^2) or a pion and a sigma-hyperon (1327MeV/c^2) there can be exothermic $K^-p \rightarrow (\Lambda\pi$ or $\Sigma\pi)$ transitions even from K^- interacting at rest. Experiments in which $\Sigma\pi$ states are produced in association with other final-state particles have

100 years ago

A remarkable phenomenon was observed at Kattenau, near Trakehnen (Germany), and in the surrounding district, on March 22. About half an hour before sunrise an enormous number of luminous bodies rose from the horizon and passed in a horizontal direction from east to west. Some of them seemed of the size of a walnut, others resembled the sparks flying from a chimney. They moved through space like a string of beads, and shone with a remarkably brilliant light. The belt containing them appeared about 3 metres in length and 2/3 metre in breadth.

At Paris a Society "contre l'abus du tabac" has been formed, which intends to combat the excessive indulgence in smoking which has of late become the fashion in almost the whole of Europe. The Society offers various prizes for treatises on the human health and the dangers it is subject to from excessive use of tobacco.

The Archaeological Society of Athens has purchased about half the village which stands upon the ruins of the Temple of Eleusis. The Society intends building new dwelling-house in another part, and to begin with excavations as soon as the present inmates of the village have moved.

The astronomer, Herr Rudolf Falb, well known through his theory of earthquakes, has returned from his South American exploring tour, which extended over a period of more than two years. In his researches he was led in the direction of ethnography and linguistics, and believes that he has made interesting discoveries regarding "the original language of the human race."

from *Nature* **22**; May 20, 64-66; 1880.

---

shown a clear peak in the $\Sigma\pi$ mass-spectrum at 1405 MeV/c^2. Such peaks are normally attributed to resonances, and the SU(6) theory has a place for one such resonance. But 1405 MeV/c^2 is so close to the physical $\bar{K}N$ region that the presence of a resonance should have an effect on $\bar{K}N$ scattering at the lowest energies. An elegant K matrix formalism has been developed for dealing with these processes. A. D. Martin (Durham) gave an up-date on his fit to the formalism, using dispersion relation constraints to eke out the sparse data on low energy K$^-$p collisions. Dalitz (Oxford) agreed with Martin that there was no apparent need to invoke a quark-model resonance to explain the 1405 bump. It could be produced by non-singular meson-baryon (i.e. antikaon-nucleon or pion-hyperon) interactions, complicated in this region by cross-couplings between the channels.

There is great interest in the Λ (1405) question among physicists studying strange-particles in complex nuclei. Here the binding energy brings down the effective nucleon mass, and Fermi motion adds further complications. Dover (Brookhaven) gave a review of the work that has been done on hyperfragment formation by pion and kaon beams. Little has changed since last year's hyperfragment and K$^-$ conference in Warsaw (proceedings to be published in *Nucleonika*) but he illustrated how the new generation of precision spectrometer experiments is extending nuclear structure studies into this intriguing field. Batty (Rutherford) reviewed kaonic X-ray studies. On heavy nuclei no one knows how the observed level-shifts and line-broadenings should be related to low-energy kaon-nucleon processes, but his collaboration (working at NIMROD) has set a puzzle by measuring a line which may be due to the 2p to 1s transition in antikaonic-hydrogen. The line is narrow and is not shifted significantly from the position predicted for it with a

Coulomb potential alone. This suggests a very weak antikaon nucleon coupling at threshold (1432 MeV/c^2), contrary to the results of all the fits, including A. D. Martin's. Kumar (Mc Master) claimed that he could fit the Λ (1405) as a resonance and match the weak coupling required by the kaonic-hydrogen result, but it was not clear if his model could be made consistent with all of the available low energy $\bar{K}N$ data. If the properties of the kaonic hydrogen X-ray line are confirmed by new experiments to be done at CERN, then those of us working on low energy antikaon-nucleon collisions will have to devise totally new techniques to study the scattering cross-sections at lower energies than can be reached at the moment. We had thought that our latest results (Durham, Brussels, Warsaw, UCL collaboration) were removing the remaining anomalies and agreeing well with A. D. Martin's fit, but there are still many poorly measured channels, particularly K$^-$p $\rightarrow$ $\Sigma^\circ\pi^\circ$ in which the Λ(1405) should be important, and the K matrix parametrisation remains under-constrained. $\square$

Oil geology in China

from A. Hallam

As befits a country with an impressive tally of early discoveries, there is a record of 'fire in the swamp' (evidently marsh gas or methane) in the ancient Chinese Book of Changes, written in the 11th Century BC. In the early 12th century a gas well over a kilometre deep was drilled in Sichuan Province, but the beginning of the Chinese petrolem industry dates from 1907, when a foreign crew employed by the government of the Qing Dynasty discovered Yanchang oilfield in Shanxi Province.

For most of the first half of this century oil production remained at a very modest level but since the founding of the People's Republic there has been a considerable expansion of both exploration, with the

discovery of over 160 oilfields, and production, which last year reached 106 million tons, putting China among the top dozen oil producing countries in the world. The capital city of Beijing (Peking) was thus an appropriate place for an international conference on petroleum geology.*

A measure of the importance attached to the conference by the Chinese is that the participants were granted an audience in the Great Hall of the People by Vice Premier Kang Shi En, who exhibited a considerable knowledge of the petroleum industry. He looked forward to a huge increase in production to help promote the so-called four modernisations (Agriculture, Industry, Science and Technology, and National Defence).

While the conference lectures ranged far and wide the greatest interest of the overseas participants was obviously in the Chinese contributions, because Chinese oil geology has been hitherto largely a closed book to the outside world. Three matters of especial interest may be singled out. Firstly, virtually all the oil and gas has been generated in source rocks of continental origin, and the Chinese were manifestly proud at having confounded those pundits of an earlier era who had consistently argued that significant quantities of hydrocarbons could only be generated in marine deposits. Thus the giant Daquing Oilfield in the Songliao Basin of Manchuria, which accounts for half the current production of the whole country, occurs in a region which developed as a faulted depression in Jurassic times, long after the Palaeozoic seas had retreated. By the mid Cretaceous it became established as an open lake basin, persisting into the Tertiary, in which a great thickness of organically-rich clays was deposited. Wedges of fluvial and deltaic sands in the clays, combined with anticlinal structures, provide an excellent combination of reservoir, source and cap rocks with structural traps.

A second point of major geological interest is the occurrence under the North China Plain of so-called 'buried hill' oilfields. Huge thicknesses of shallow-water carbonates of Proterozoic to Ordovician age were subjected to extensive karstification during a lengthy period of emergence from the late Palaeozoic to the early Mesozoic, with the development of numerous small and large cavities. Subsidence under tension of a zone extending SSW from Manchuria commenced in the late Mesozoic and continued into the Tertiary. The old karst landscape was deeply buried under thick Tertiary lacustrine clays and sands. The cavities in the ancient carbonates have proved to be excellent oil reservoirs, the oil having migrated laterally from Palaeogene clay source beds, as proved by the presence in the oil of spores and pollen of that age.

David J. Miller is in the Department of Physics and Astronomy, University College, London.

A. Hallam is Lapworth Professor of Geology in the University of Birmingham.

Thirdly, the Chinese exhibited a substantial knowledge of the scientific literature and technology of the West, all the more impressive bearing in mind the setbacks of the Cultural Revolution. In fields as diverse as sedimentological facies modelling and organic geochemistry they demonstrated that they had kept well abreast of modern developments. Their geophysicists, furthermore, are well ahead of the Russians in having adopted modern digital methods of seismic data processing.

Perhaps the sphere in which we in the West can offer the most help is in advice on organisation. At present the Chinese geologists and geophysicists operate independently. Efficiency could be vastly improved by integrated team efforts, for instance in the new and rapidly advancing field of seismic stratigraphy. Furthermore, it is rather strange that, while the Oil and Gas Corporation is responsible for the great bulk of the exploration and production efforts, the Ministry of Geology (effectively the Geological Survey) operates quite independently its own exploration programme both onshore and offshore.

One of the highlights of the meeting was a visit to the Renqiu Oilfield 160 km south of Beijing, which produces some 10 million tons per year from buried-hill reservoirs. This was the first-ever visit by foreigners and was accompanied not only by Chinese television camera crews and representatives of the Peoples Daily but an odd-looking assemblage of foreign pressmen, who seemed more interested in the sociology than the science or technology. The American and European

oil geologists were amazed to learn that this oilfield is quite typical in possessing its own research laboratory, equipped with the most modern petrological and geochemical apparatus. Even the microfossils are identified, as it were, on the spot. Some scepticism was expressed about how even a major oilfield could keep the laboratory workers usefully employed for long periods in more than routine monitoring.

Intensive exploration for hydrocarbons has so far been largely restricted to the eastern part of the country, although large gas discoveries in Sichuan have made the province self sufficient in that commodity. While there are some promising prospects in the vast region of Xinjiang, notably inthe Tarim Basin, the greatest hopes in the immediate future are in offshore areas. The Chinese have for some time been operating drilling rigs in the Gulf of Bohai, and extracting oil from deeply buried, tilted fault blocks created by tensional collapse in the Tertiary and reminiscent of the major oil-producing structures in the North Sea. Within the last year they have invited a number of major North American and West European companies to shoot seismic lines in the Yellow and South China Seas. The results will be analysed by Chinese specialists, who will make recommendations to the Ministry of Petroleum Industry. Representatives of the Ministry will shortly be meeting with their opposite numbers in Norway and the United Kingdom, presumably to obtain advice from those experienced in granting offshore concessions. Thus we may look forward to the possibility of companies like Exxon and B.P. drilling in Chinese water, a measure of the modern pragmatism that should cause the Gang of Four a further turn in their metaphorical grave. □

sequences of integral membrane proteins with their largely hydrophobic composition has required the development of special procedures, different from those currently used for water-soluble proteins. The complete sequence of the 247 amino acids of bacteriorhodopsin was found by Ovchinnikov and colleagues (*FEBS Letters* **100**, 219; 1979) and large portions have been confirmed by Gerber *et al. (Proc. natn. Acad. Sci U.S.A.* **76**, 227; 1979) and Walker *et al. (Nature* **287**; 1979). As expected the polypeptide chain has long tracts of hydrophobic residues that represent the transmembrane helices; these were used by Ovchinnikov in a preliminary attempt to fit sequence to structure. However the methods used by Henderson and his colleagues are somewhat more sophisticated and warrant detailed consideration.

An important preliminary to combining the sequence and the structure, was to find the molecular boundaries for a single bacteriorhodopsin molecule. This could be done because detergent treatment of the purple membrane produces *in vitro* a new two dimensional crystal form of bacteriorhodopsin. Electron diffraction analysis of this form in projection (Michel, Oesterhelt & Henderson *Proc. natn. Acad. Sci. U.S.A.* **77**, 338; 1980) shows an identical protein structure to that observed in the purple membrane, confirming the original molecular boundary.

The first step was then to locate the seven helical segments in the sequence. This was done by making use of the known points of proteolytic cleavage which must occur at surface residues, and of the similar lengths of the seven transmembrane helices, which on energetic grounds must be largely hydrophobic. In the assignment proposed by Henderson there are 27 charged residues on the membrane surfaces and 9 buried in the interior of the membrane. The neutralization of charge by pairing these 9 buried residues becomes a major determinant in the structure prediction.

The second step was to attempt to identify the seven helical segments in the sequence (labelled A to G) with the seven helical segments in the image (labelled 1 to 7). Because the orientation of the protein in relation to the inner and outer membrane surfaces had already been established, there are 7!, or 5040, ways of combining the predicted and observed helices. To reduce this number to more manageable proportions, Henderson and his colleagues filtered the models sequentially through a number of criteria, a procedure broadly similar to that currently used in predicting the tertiary structures of proteins. The first filter was concerned with minimizing the lengths of the six interhelical loops, and disallowing loops that crossed over one

Predicting a membrane protein

from Colin Blake

ONE of the most elegant and original structural studies of a biological system in the recent past has been that of Henderson and Unwin (*Nature,* 257, 28; 1975) on the 'Purple Membrane' of *Halobacterium halobium.* As the protein component of the membrane, bacteriorhodopsin, is a single molecular species organized into a two-dimensional crystalline array they were able to use electron diffraction to produce a three-dimensional low resolution image of the membrane protein *in situ.* Bacteriorhodopsin was revealed as an integral membrane protein composed of a cluster of seven almost parallel helices oriented perpendicular to the membrane surface.

This low resolution image was fascinating but to understand the general principles of membrane proteins and the

function of the purple membrane as a light-driven proton pump a model with atomic detail was required. This could be achieved either by increasing the resolution in the electron diffraction pattern, or by using the existing image as a basis for predicting the structure. The latter approach has been successfully used by Engelman, Henderson, McLachlan and Wallace (*Proc. natn. Acad. Sci. U.S.A.* 77, 2023; 1980). Although less direct than extending the resolution of the image, prediction of the bacteriorhodopsin structure brings together a number of principles of protein and membrane structure and perhaps represents the more fruitful direction for future work on membrane systems.

Knowledge of the amino-acid sequence of bacteriorhodopsin was essential to either approach. Determination of the

Colin Blake is in the Laboratory of Molecular Biophysics, Department of Zoology, University of Oxford.

another on the same side of the membrane. This reduced the number of models to 405 which were rank ordered according to the total length of the interhelical loops. These models were then subjected to the test that the nine buried charged residues should geometrically be able to form ionpairs. This reduced the number of models to 405 which were rank ordered according to the calculated electron densities of the seven predicted helices with the integrated scattering densities of the helices observed in the image of the purple membrane protein. In the image helices 1 and 5 have significantly lower scattering densities than the other five. Of the predicted helices, helix D with five glycines and no large hydrophobic residues has the lowest calculated electron density, while helix A also has much lower density than the other five. This test revealed that the model with the shortest interhelical loops and the

geometry required to neutralize the charges of the buried residues, was also one of the few to meet the helix scattering criterion.

Not only does this one model of bacteriorhodopsin emerge as by far the most probable, it also possesses a number of features that seem suitable for a proton pump. The buried charged residues form one or more networks of ion-pairs through which protons may be able to jump. The retinal group probably lies near the surface of the membrane with its ring possibly buried near an aspartic acid residue. Finally adjacent helical segments in the sequence are also adjacent in the structure suggesting a particular simple folding pathway.

Confirmation of this model will be necessary, but at present it must be regarded as easily the best view we have of the structure-function relationship in a membrane protein. □

Dual polarization radar

from Thomas A. Seliga

EVER since the development of radar in the late 1930's and early 1940's, meteorologists and hydrologists have waited for the time when radar's full capabilities could be exploited for research and field operations. Progress from remote storm detection to assessment of storm characteristics has continued to the point where we can now estimate the drop size distributions of rainfall in a scattering volume (and, therefore, water content or rainfall rate), the nature of the hydrometeors producing the radar signal (whether ice particles or rain) and the bulk motion of the hydrometeors. In this issue of *Nature* Hall *et al.*[1] clearly demonstrate the first two kinds of measurement through use of the differential reflectivity (Z_{DR}) linear polarization scheme first proposed by Seliga and Bringi[2,3] for rainfall measurements. Pulsed Doppler radar techniques have also developed rapidly over the last fifteen years,[4,5,6] producing dramatic advances in our understanding of storm dynamics. This technique has been recently reviewed[6],so here the impact that polarization radar measurements like those of Hall *et al.* might have in a number of areas of meteorology and hydrology will be examined. It should be noted that Canadian scientists have also developed the use of circular polarization techniques and that their results too, are of great potential importance[7,8,9].

Hydrology

The accuracy of the Z_{DR} technique for measuring rainfall is expected to be of the order of 30% for a single observation at a

single range gate. Since this measurement can be made within around a 200 ms time interval, and corresponds typically to an areal coverage of less than 0.5 km^2 for modest size radar antennas at S-band wavelengths, large areal surveillance (of the order of 35,000 km^2) with high spatial and temporal resolutions of rainfall will become possible.

The resultant benefits to hydrology are many: flash flood forecasting should become more reliable; study of the evolution of rainfall in different meteorological regimes and storm types will be possible, leading to improved description and classification of storms; understanding of topographical influences on rainfall should improve; watershed and stream flow modeling should progress; rainfall in semi-arid and arid lands should be more readily monitored; and, in future, hydrologic structures should be improved as a result of more accurate, detailed information on rainfall.

Cloud Physics

Possibly the most important application of Z_{DR} in meteorology will be in studies of the organization and structure of clouds and precipitation on the mesoscale and microscale.[10,11,12] The ability to measure rainfall accurately from a single radar site independent of raingauge calibration, to follow the evolution of rainfall and its drop size distribution in space and time, and to accumulate and display data in real time, should provide new insights into our understanding of precipitation processes. Quantitative data of this type, when combined with Doppler data, will test the credibility of numerical cloud models and further their development. The second very important result of Hall *et al.'s* measurements is the ability to discriminate

clearly between ice and water phase hydrometeors; this will lead to improved understanding of cloud development and precipitation formation. Important data on melting, drop breakup, and the development of raindrop size distributions, should also result from such measurements.

Climatology

The development of the Z_{DR} radar technique, which can provide accurate rainfall measurements over large areas, is very important for climatological studies, particularly within the context of the World Meteorological Organizations's World Weather Watch (WWW) and Global Atmospheric Research Programme (GARP) and their subprograms.[13,14]. For example, the recently conducted GARP Atlantic Tropical Experiment (GATE) and Monsoon Experiment (MONEX) would have benefited greatly had this radar capability been available and employed. Also, use of radar for ground truth measurements of rainfall intensity and cloud structure, particularly over the oceans, should aid in the development of reliable satellite methods of estimating rainfall over remote regions of the Earth's surface. Such data is indispensible for global weather studies and validation of general circulation and climate models. Moving to smaller scales, it is apparent that regional rainfall statistics should be largely improved as radars having polarization capability become operational.

Weather Modification

Whether human intervention can influence atmospheric conditions to enhance precipitation by significant amounts remains the foremost question in weather modification.[15] The importance of this problem is reflected by the Seventh World Meteorological Congress (1975) recent approval of a WMO Weather Modification Programme and Precipitation Enhancement Project (PEP).[16] Again, the importance of using the dual polarization radar technique in such programs becomes evident. Accurate rainfall measurements with high spatial (1 km^2) and temporal (tens of seconds)

Thomas A. Seliga is Director of the Atmospheric Sciences Program and Professor of Electrical Engineering, Ohio State University, Ohio.

1. Hall, M. P. M., Cherry, S. M., Goddard, J. W. F. & Kennedy, G. R. *Nature* **285**, 195; 1980.
2. Seliga, T. A. & Bringi, V. N. *J. Appl. Meteor.* **15**, 69; 1976.
3. Seliga, T. A., Bringi, V. N. & Al-Khatib, H. H. *IEEE Trans. Geosci. Elect.* GE-17, 240; 1979.
4. Lhermitte, R. M. *Bull. Amer. Meteorol. Soc.* **45**, 587; 1964.
5. Smith, P. L. Jr, Hardy, K. R. & Glover, K. M. *Proc. IEEE*, **62**, 724; 1974.
6. Doviak, R. J., Zrnić, D. S. & Sirmans, D. S. *Proc. IEEE*, **67**, 1522; 1979.
7. McCormick, G. C. and Hendry, A., *Radio Sci.* **10**, 421; 1975.
8. Humphries, R. G. & Barge, B. L., *IEEE Trans. Geosci. Elect.* GE-17, 190; 1979.
9. McCormick, G. C. & Hendry, A., *IEEE Trans. Geosci. Elec.* GE-17, 142; 1979.
10. Hobbs, P. V. *Revs. Geophys. and Space Phys.* **16**, 741; 1978.
11. Lilly, D. K. *Ann. Rev. Earth Planet. Sci.* **7**, 117; 1979.
12. Kreitzberg, C. W. *Revs. Geophys. and Space Phys.* **17**, 1852; 1979.
13. *Global Atmospheric Research Programme (GARP) Repts.* 1-21, World Meteorol. Org., Geneva, Switzerland.
14. *GARP Atlantic Tropical Experiment (GATE) Repts.* 1-20, World Meteorol. Org., Geneva, Switzerland.
15. Simpson, J., *Adv. Geophys.*, (ed. H. E. Landsberg; Academic Press, N.Y., 1-72, 1976.
16. *Precipitation Enhancement Project Repts. 1-17,* World Meteorol. Org., Geneva, Switzerland.

resolutions over large areas (35,000 km²) and hydrometeor phase detection, are essential ingredients to any such effort. Hall *et al.*'s RHI grey scale plots of Z_{DR} and reflectivity and drop size distribution measurements show how the Z_{DR} radar might contribute to weather modification experiments. Indeed, one can contemplate using such radar data in case studies of seeded storms as a determinant for testing weather modification techniques. Whether this approach can supplant statistical methods of evaluation deserves serious attention. Another exciting role for dual polarization measurements in weather modification might arise from using Z_{DR} signatures of tracers released with seeding agents. Possible tracers include specially designed chaff and surfactants which significantly affect raindrop shape.

Other Applications

As noted by Hall *et al.*, the polarization radar should also have important applications in communications and erosion studies. Understanding the variability and characteristics of hydrometeors along terrestrial and satellite radio propagation

paths is required for systems design while erosion, both of airborne vehicles and land surfaces, depends strongly on drop size distribution. Other possible applications might include studies of precipitation scavenging of airborne particles and pollutants, hail detection, detection and classification of severe storms, and aviation radar for detecting supercooled water droplets, a precursor to possible aeroplane icing conditions.

As more radars, modified to perform dual polariztion Z_{DR} measurements, become available, many of the above applications will be critically tested. The relative simplicity of the method and recent advances in high-power, microwave switching technology should enable many existing radar facilities to be modified at modest cost. This will offer many scientists opportunities to explore these ideas during this decade. The first measurements have produced dramatic results. Fulfilling all the hoped for applications is perhaps asking too much; being able to perform reliable, continuous and accurate measurement of rainfall would be enough! □

its effector in Ca^{2+} mobilising systems are not the protein components of the cell membrane but the phospholipids. M. J. Berridge (University of Cambridge) supported the idea that changes in a minor anionic species of phospholipid, phosphatidylinositol, might have this intermediate role. Several years ago it was pointed out that an enormous range of Ca^{2+} mobilising hormones also stimulate breakdown of phosphatidylinositol by a phospholipase C (Michell *Biochim. Biophys. Acta* **415**, 81; 1975). Berridge's experiments on fluid secretion by blowfly salivary glands demonstrate a correlation between the movement of Ca^{2+} ions into cells and the breakdown of phosphatidylinositol. However, some recent evidence in other tissues suggests that phosphatidylinositol breakdown may not have this intermediary role in Ca^{2+} mobilisation (e.g. Cockcroft *et al. FEBS Lett.* **110**, 115; 1980) although this may not preclude its having a different function — for example in the termination of the response.

A quite different phospholipid change was reported by J. Axelrod (National Institute of Health. Bethesda) in some of the cell types which are also known to show a phosphatidylinositol response. In these cells phosphatidylethanolamine can be converted by successive methylation to phosphatidylcholine, and this is degraded by a phospholipase A_2 to release fatty acids. In the systems examined a rapid response to stimulation has been seen. Unfortunately only a limited number of cell types have so far been studied, and it is likely that all of these cells synthesize prostaglandins from arachidonic acid as one consequence of cell stimulation. The observed phospholipid changes may thus be a means to generate the necessary fatty acid precursor from arachidonate-rich phosphatidylethanolamine; an effect specific to the cell types examined rather than a general process during receptor function.

There is yet another possibility. W. Trautwein (University of Saarland, Germany) described measurements of conductance changes associated with a muscarinic receptor in heart. The results showed considerable similarity to comparable experiments with the much more rapidly responding nicotinic cholinergic receptor (D. Colquhoun, University College, London,). It is generally assumed that the nicotinic receptor molecule is itself an ion channel (in this case for Na^+), although a completely convincing demonstration of that *in vitro* has still not been achieved. A possible implication is that for Ca^{2+} mobilising systems such as the muscarinic receptor there is no biochemical intermediate at all.

As yet the molecular understanding of

Drug receptors and their effectors

from Jonathan Bennett

How does hormonal information enter the cell? Are there intermediate biochemical events between binding of hormone to a cell surface receptor and the change in the cytoplasmic concentration of a second messenger? This was one of the problems pinpointed by the organising chairman (N.J.M. Birdsall, National Institute for Medical Research, London) at the recent Biological Council Symposium* on "Drug receptors and their effectors".

The best understood receptors in this respect are those whose cellular effects are mediated by the second messenger molecule, cyclic AMP. A few years ago evidence from various approaches forced the conclusion that the hormone receptor and its effector (the cyclic AMP-synthesising enzyme, adenylate cyclase) were separate molecular entities. It is now clear that a third protein component, a GTP binding protein, is involved (for a recent review, see Rodbell *Nature* **284**, 17; 1980). M. Schramm (Hebrew University of Jerusalem, Israel) described his experiments using a cell fusion technique to demonstrate that the GTP-binding protein acts as an intermediate between the hormone receptor and its effector. Binding of a hormone to the receptor causes the GTP-binding protein to change to an "active" form which in turn stimulates the

Jonathan P. Bennett is in the Department of Experimental Pathology, School of Medicine, University College, London.

enzymatic activity of adenylate cyclase.

One consequence of this intermediate step between receptor and effector in the adenylate cyclase system is that it may allow other hormones and drugs to interact to modulate adenylate cyclase activity. A. J. Blume (Roche Institute, Nutley, US) described how binding of opiates to mouse neuroblastoma cells results in an inhibition of adenylate cyclase. The binding of opiate agonists to these cell membranes is enhanced by GTP, and it is a reasonable hypothesis that the opiate receptor interacts with the adenylate cyclase system at the level of the GTP-binding protein.

There may be a similar interaction at the muscarinic cholinergic receptor (E. C. Hulme, National Institute for Medical Research, London) where GTP also interacts with agonist binding to isolated membranes. The effector molecule for this receptor is presumed to be a plasma membrane channel which allows Ca^{2+} ions to enter the cell — and certainly muscarinic responses belong to the large class of hormone effects which are mediated by an increase in intracellular Ca^{2+} as a second messenger. Does the interaction of GTP with muscarinic agonist binding imply that another GTP-binding protein acts as an intermediate in Ca^{2+} mobilising systems? This is a new possibility in a field where the molecular events following receptor activation have eluded critical analysis.

Alternative candidates for the intermediate step between the receptor and

the activation of cells by hormones which use intracellular Ca^{2+} as their second messenger lags far behind our knowledge of the adenylate cyclase system. The principal reason for this is technical — no one can yet measure changes in membrane permeability in a test tube in such a way that adenylate cyclase activities can be measured. Only when such an analysis is possible can biochemical techniques be applied. □

Platelet-activating factor

from Noel J. Cusack

WHEN IgE-sensitized rabbit leucocytes are challenged *in vitro* with antigen they secrete an extraordinarily potent, soluble, low molecular weight platelet-activating factor (PAF), which causes platelets to change shape, aggregate and release their granule contents. PAF is also released *in vivo* into rabbit plasma during the development of IgE-induced systemic anaphylactic shock and appears to be an important mediator of inflammation and allergic responses. Platelet activation by PAF is independent of arachidonic acid metabolites or released ADP. Endogenous PAF from platelets may account for that portion of thrombin and calcium ionophore induced platelet aggregation which is not prevented by blocking the ADP and arachadonic acid mechanisms, but is diminished by phospholipase A_2 inhibitors. Recent work by two independent groups (Demopoulos, Pinckard & Hanahan *J. Biol. Chem.* **254**, 9355; 1979; Benveniste *et al. C. R. Acad. Sci.* **289**, 1037; 1979) has elucidated the structure of PAF, largely by examining the effects of enzymic and simple chemical treatments on its chromatographic behaviours and its pharmacological actions on rabbit platelets.

As PAF was completely extracted into organic solvents, being found entirely in the chloroform phase of chloroform-methonol-water mixtures, it was known to be a lipid. However, its insolubility in chloroform alone, coupled with a low migration on silica gel thin layer chromatography (unaltered by acidification or basification of the chromatography solvent) pointed to a neutral, very polar lipid. Possible candidates at this stage were therefore glycosylacylglycerides, neutral phosphoglycerides and neutral sphingolipids, but the lipids with known hormone-like actions (steroids and prostaglandins) could be excluded. Glycosylacylglycerides and glycosphingolipids were eliminated because PAF was unaffected by sodium nitrite, which cleaves glycosidic linkages, and by reagents for free or vicinal hydroxyl and amino groups. PAF was unlikely to be polyunsaturated because of its stability to

prolonged storage and heating in air, or to contain an α,β unsaturated ether linkage such as occurs in plasmalogens because of its relative stability to strong acid. Rapid inactivation by strong methanolic base to a chloroform-soluble derivative was evidence for at least one ester linkage, and at least one base-stable fatty group. This, together with the insensitivity of PAF to sphingomyelinase, focused attention away from sphingomyelins and onto a phosphoglyceride derivative.

Inactivation of PAF by the specific phosphoglyceride phospholipases A_2, C and D established the presence of a 2-ester linkage and a 3-phosphate esterified to a polar head group which, since PAF was unaffected by methylating agents, was choline rather than ethanolamine. PAF was not inactivated by phospholipase A_1 (specific for 1-ester linkages) which was initially interpreted as suggesting the presence of an underivatised 1-hydroxyl group, but attempts to generate PAF-like activity by treatment of a variety of phosphoglycerides with phospholipase A_1 were unsuccessful (Benveniste *et al. Nature* **269**, 170; 1977).

Hanahan's group, exploiting the possibility that removal of the esterified group from PAF by methanolic base might provide an intermediate which could be chemically reesterified with various fatty acids to regenerate PAF activity, found that the resulting long chain fatty acid derivatives were inactive. They therefore tried esterification with short chain acids, and discovered that acetylation resulted in complete recovery of PAF activity with identical chromatographic behaviour. A 1-fatty ether structure for PAF was considered, which would remain chloroform-soluble after deesterification because of the stability of the ether linkage to methanolic base. Hydrogenation of the 1-α, β-unsaturated ether linkage of plasmalogens extracted from beef heart followed by deesterification and acetylation at the 2-position generated a compound identical in biological activity and chromatographic behaviour to PAF. Its structure was confirmed by IR and GLC as 1-0-alkyl-2-acetyl-sn-glyceryl-3-phosphorylcholine with the length of the alkyl chain mainly C_{16} and C_{18}.

Benveniste's group realised that their results with phospholipase A_1 would be equally consistent with an ether linkage at the 1-position of a glycerol phosphatidylcholine, and noticed that acetic anhydride treatment increased the PAF-like activity of crude but not purified PAF preparations. This alerted them to the possible presence of an acetyl group in the molecule. Methylation, hydrogenation and acetylation of a commercial ethanolamine plasmalogen underivatised at the 2-position yielded a compound identical to PAF, and they proposed the
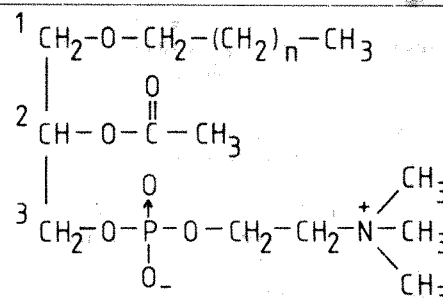
The chemical structure of platelet-activating factor.

same structure as Hanahan's group.

Synthetic PAF appears to be the most potent activator of platelets yet described, causing shape change, aggregation and the release reaction at concentrations between 10^{-11} M and 10^{-10} M. Interest in this novel compound must be further heightened by the discovery that antihypertensive polar renomedullary lipid (APRL), a lipid found in the kidney which lowers the blood pressure of artificially hypertensive animals, has an identical type of structure (Blank *et al. Biochem. Biophys. Res. Comm.* **90**, 1194; 1979). Synthetic APRL prepared from choline plasmalogens was an extremely potent antihypertensive agent that mimicked both the acute and the prolonged antihypertensive effects of APRL extracted from the kidney. The ubiquitous occurrence of phospholipids, together with increasing awareness of their functional importance, suggests that there may be other, hitherto unsuspected roles for PAF-like compounds. □

Life in the Precambrian

from Trevor D. Ford

THIRTY years ago the known Precambrian fossils could be counted on one's fingers. Today the number has increased to the point where a computer is needed to catalogue their names and literature references, with print-out an inch thick! Moreover they are now being used stratigraphically like Phanerozoic fossils, helping to map subdivisions of Precambrian rocks previously thought to be unfossiliferous. More importantly, they provide a record, albeit patchy, of the early history of life on earth. This was the theme of a recent symposium*.

Fossils in rocks of Precambrian age fall broadly into four categories: microscopic unicellular algae (nannofossils); clusters or associations of algal cells; stromatolitic structures in limestones (generally believed to have been constructed by algae); and metazoans (of coelenterate, arthropod or 'worm' affinities). There is great controversy about their assignment to one

Noel J. Cusack is in the Department of Pharmacology, Kings College, London.

*The Symposium on 'Life in the Precambrian' was held by the Palaeontological Association in Leicester from April 10-12th 1980.

or other of the traditional Phyla, about whether or not some are fossils at all, and about their chronological relationships.

Organic-walled nannofossils extracted from sediments are generally referred to as 'acritarchs' in view of the difficulty of assigning them to any known algal groups. With some hundred or so species distinguished by their shape, size, surface ornament, wall-thickness and presence or absence of openings they have provided G. Vidal (University of Lund, Sweden) with a tool for correlation of the late Precambrian in Sweden, Norway, USSR, and Greenland. Similar studies in parts of Canada, USA, and Western Europe have extended correlation sufficiently to give a reasonably good classification of these rocks into the later Riphean and Vendian stages of Precambrian time.

The classification of acritarchs has so far lent heavily on comparisons with present day algal cells, but when various states of decay or desiccation are examined it seems that some Precambrian 'species' are, in fact, the same organism in different states of preservation. C.J. Peat (Imperial College, London) proposed that we should scrap assignations to various groups of algae and classify the Precambrian fossils into purely morphological groups of Cryptarchs. C.J. Peat, W.L. Diver (Imperial College, London) and Z. Zhongying (Nanjin University, China) also suggested that acritarch studies provide no evidence for the presence of eurkaryote cells in the Precambrian; the various 'black dots' can be explained as the shrivelled inner walls of cells, or as desiccated cell contents. This argument was accepted but there must have been eukaryote algae around to allow the evolution of sex and thus of the Metazoa. When eukaryotes appeared on Earth is still a mystery and hypotheses about Precambrian atmospheric evolution cannot yet look for support from acritarchs!

That stromatolitic structures in Precambrian limestones can provide a coarse means of correlation of Proterozoic strata has been generally accepted for some years. However, being limited to shallow shelf seas, and even then with only the digitate columnar forms being useful for stratigraphy, their value is not as great as could be desired.

As shells and skeletons had not yet evolved, fossils of Metazoan life forms in the Precambrian are almost all trace-fossils or impressions; that is, they are the marks in or on sedimentary rocks made by the activities or presence of the organisms. Inevitably their interpretation can only be made by comparison with the marks made by living organisms to-day. The Precambrian Metazoan fossils include tracks, trails and burrows on the one hand and impressions of single organisms on the other. Sequences of strata below those con-

taining well-defined Cambrian trilobite body fossils have been found in various parts of the world with a host of trails, tracks and burrows. The order in which these first appear has given rise to speculation as to whether they could be used as stratigraphic markers, and whether they were representative of a fundamental evolutionary sequence. T.P. Crimes (University of Liverpool) and M. Brasier (University of Hull), A. Peréjon and M.A. de San José (University of Madrid) described the sequences of such fossils, mainly in Spain, and concluded that there was as yet no clear evolutionary sequence, but the trace type was closely related to the immediate sedimentary environment. Exact dating by radiometric methods is not yet available but it seems that no track-making animals were present in the seas before Vendian times (i.e. pre 670Ma ago).

The kind of animal that made the tracks and burrows remains a subject of speculation, but W. Gutmann (Senckenberg Institute, Frankfurt) demonstrated that penetration of sediment could only be done by animals with metameric fluid-filled hydrostatic skeletons (coelomates). Similar hydromechanical arguments supported the identification of other impression fossils as Cnidarians, some clearly of medusoid construction.

A variety of circular or oval impressions on bedding planes are now known from many parts of the world. Recent discoveries in Charnwood Forest, Leicestershire (T.D. Ford & H.E. Boynton, Leicester University), and in Carmarthenshire (J.C. Cope, University College of Wales, Swansea) include discs with few or many annular rings; are these really fossils or are they pseudofossils of the type caused by gas or water evasion from sediments? Though most agree that they are impressions made by 'medusoids' coming to rest, R.J.F. Jenkins (University of Adelaide) described scour pits remarkably like some 'medusoid' impressions on bedding surfaces but clearly penetrating the sediments when seen in section.

The abundant and varied fauna of impressions in the Conception Group of southeast Newfoundland is still undescribed in detail though found more than 10 years ago; Conway-Morris (Open University, U.K.) showed photographs indicating the presence of several frond-like 'pennatulid' *Charnia*-type coelenterates with disc-like holdfasts, as well as lobate and spindle-shaped organisms of unknown affinity. The strong lobate impressions could well represent sediment-filled gut-cavities of jellyfish, while the spindle-shaped impressions with their chevron-marked fringes could be compared with the Portuguese Man of War coelenterate.

The assemblage of medusoid, frond-like and colonial impressions has come to be known as the Ediacura fauna from the locality in South Australia where the fossils are abundant. These also include a few trails, a segmented animal (*Spriggina*) with

a crescentric head-shield, which could be either annelid or arthropod and *Dickinsonia*, probably a flat-worm. No such fossils are yet known in Newfoundland, and only one incomplete arthropod has been found in Charnwood Forest. Neither Newfoundland nor Charnwood has yielded convincing tracks, trails or burrows, so the strata there may be slightly older, signifying sequential appearance of coelenterates, followed by segmented annelid/arthropods living freely on the sediment surface, followed by those with the hydromechanics needed for burrowing. All this seems to have taken place in Vendian (or possibly very late Riphean) times, broadly within the time span of 700 to 600 Ma ago, followed of course by the explosive evolution of shelled animals in Cambrian times.

Two other long-standing problems of Precambrian palaeontology were aired: one was the true identification of the earliest known organisms in the 3 billion year old Fig Tree Formation of South Africa, where it was argued that the size distribution of the fossils did not fit normal biological patterns and that there must therefore be some doubt as to whether they were biogenic structures. The other problem was that of the Erniettomorpha, the host of Namibian phylloid, foliate and other petrifactions imaginatively reconstructed by Hans Pflüg as the common ancestors of the Plant and Animal Kingdoms. R.J.F. Jenkins (University of Adelaide) claimed them to be a single species of frond-like type in varying states of preservation; thus *Ernietta* may be no more than another pennatulid coelenterate.

The results of the symposium thus revise our knowledge of life in Precambrian times. The earliest known Fig Tree fossils are not yet proven to be biogenic; most of the acritarchs, ranging through the Precambrian, cannot yet be assigned to appropriate algal categories with confidence; the claims of eukaryote cellular nuclei as far back as 1400Ma are not substantiated; interpretation of the various medusoid impressions must proceed with caution; the sequential appearance of trace fossil types is more a matter of sedimentary facies than of evolutionary development; and the Namibian Erniettomorpha require much closer scrutiny.

On the positive side, it has emerged that there are plenty of Precambrian fossils if only they are looked for with appropriate techniques. New forms are being discovered in many parts of the world and stratigraphic correlation schemes are already workable, even if accurate radiometric dating is not fully supportive as yet. Every find needs close scrutiny before one can be sure that it is a fossil, and even then the placement of the organism within a biological category may raise many problems. Life in the Precambrian may be obscure, but it is not dull! ☐

Trevor D. Ford is in the Department of Geology, University of Leicester.

ARTICLES

Rain drop sizes and rainfall
rate measured by dual-polarization radar

M. P. M. Hall, S. M. Cherry, J. W. F. Goddard & G. R. Kennedy

Rutherford and Appleton Laboratories, Ditton Park, Slough SL3 9JX, UK

A rapidly switched dual-polarization radar technique is used for the first time to obtain two-dimensional spatial distributions of the statistical characteristics of the sizes and concentration of rain drops in rain. These have been obtained using a high-resolution 10-cm wavelength radar, and the data have been used to estimate rainfall rates within small volumes to a much greater accuracy than is available from conventional radar measurements. The technique also gives a clear distinction between ice particles and rain drops.

THIS article shows some of the potential of a new radar technique that characterizes rather than assumes the distribution of rain drop sizes within a given volume, to estimate rainfall rates with improved accuracy. Many empirical relationships have been presented to compute rainfall rate from the measured reflectivity[1], but these relationships vary widely because they are governed by the statistical distribution of drop sizes at the time of measurement. This may not be significant if averaging rainfall over large volumes or long time intervals, but the assumption of an average statistical distribution to compute rainfall rates may result in a large error for applications where data are required for a small volume (for example, the pulse volume of a high-resolution radar) and without long time averages. To overcome this, the essential characteristics of the statistical distribution at a given time and place may be determined from independent measurements of the reflectivity factors obtained using vertical and horizontal polarizations[2]. The technique relies on the fact that large falling raindrops distort to become approximately oblate spheroids, each with its axis of symmetry near vertical, and that the degree of oblateness increases with drop size[3]. Consequently, the effective radar reflectivity factor measured using horizontal polarization is greater than that measured with vertical polarization.

We report here the first measurements of the two-dimensional spatial distribution of drop size characteristics using switching between polarizations which is sufficiently rapid to be regarded as simultaneous. This technique can substantially reduce errors in radar measurements of rainfall rate in small areas. Furthermore, the technique discriminates between regions of rainfall and dry ice particles. Dual-polarization radar data are expected to be of value in research fields such as radar meteorology, hydrology, cloud physics, radio science, communications engineering and erosion by hydrometeor impact.

The dual-polarization technique

Within a certain range of rain drop sizes, the numerical distribution of rain drops may be represented by an exponential function[1]. Such a function may be characterized by two parameters, N_0 and $\bar{D}$, such that:

$$N(D) = N_0 \exp(-D/\bar{D}) \qquad (1)$$

where $N(D)$ is the number of drops per unit volume per unit interval for which D is the diameter of the spherical drop with

volume equal to the actual (distorted) drop, and $\bar{D}$ is the mean value of D. Here D and $\bar{D}$ are expressed in mm and $N(D)$ and N_0 in $mm^{-1} m^{-3}$. Because of the drop distortion, and direct measurements usually being of drop volumes rather than their diameters, D_0(mm) is normally used, the diameter of that sphere for which half the volumetric water in the distribution comes from larger drops and half from smaller drops. $D_0 = 3.67 \bar{D}$ as long as $D_0 \ll D_{max}$, the diameter of the equivolume sphere of the largest drops[4].

Theoretical relationships based on work by Seliga and Bringi[2] estimate the parameters N_0 and D_0 from the effective reflectivity factors, $Z_{H,V}$($mm^6 m^{-3}$), for horizontal and vertical polarizations and the differential reflectivity factor, Z_{DR}, which is defined as

$$Z_{DR} = 10 \log_{10}(Z_H/Z_V) \quad dB \qquad (2)$$

The effective radar reflectivity factors are defined as

$$Z_{H,V} = \frac{\lambda^4 \times 10^{18}}{\pi^5 |K|^2} \int_0^{10\,mm} \sigma_{H,V}(D) N(D) dD \qquad (3)$$

where λ(m) is the wavelength, $K = (n^2 - 1)/(n^2 + 2)$ and n is
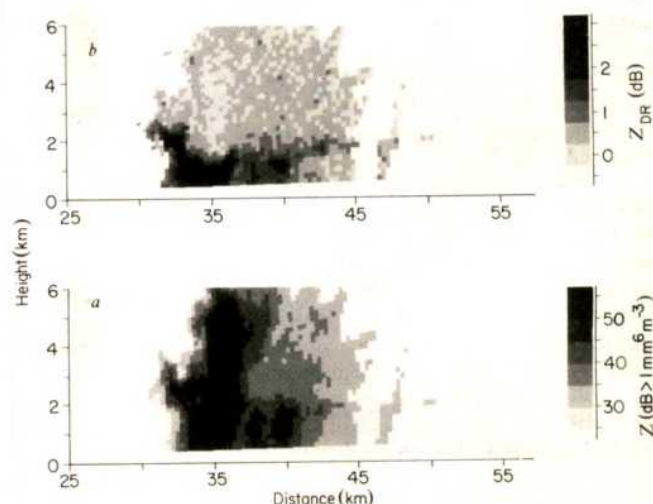
Fig. 1 Vertical scan through raincells at 13.17 UT on 15 August 1978. *a*, Absolute reflectivity factor, Z; *b*, differential reflectivity, Z_{DR}.

the complex refractive index of water. The backscatter cross-section, $\sigma_{H,V}(m^2)$, for the oblate drops at horizontal and vertical polarizations are obtained from rigorous solutions of scattering from oblate spheroids, and hence there is no assumption of the drops being small compared with the wavelength. For drops of water at the radar wavelength of 10 cm, a reflectivity factor of $1 \, mm^6 \, m^{-3}$ corresponds to a scattering cross-section of $3 \times 10^{-12} m^2$ per m^3 of cloud. Usually Z is expressed in dB relative to $1 \, mm^6 \, m^{-3}$, that is, $10 \log_{10} Z$. Unless specifically stated, Z_H is used here by convention.

The dual-polarization radar technique has been used to provide accurate measurements of Z_{DR} without excessive averaging of $Z_{H,V}$, which are time varying[5]. As with the present results, the measurements were made using a 10-cm wavelength radar mounted on the SRC's 25-m diameter paraboloidal steerable antenna at Chilbolton, UK. Alternate radar pulses were transmitted on vertical and horizontal polarizations, and examination of the time variation of the two reflectivities sampled from a single radar range gate exhibited certain points crucial to the present measurements. First, the de-correlation time of the measured reflectivity varied between 6 and 45 ms, which was considerably longer than the 1.6 ms taken to measure a pair of reflectivity values. This established that the switching was fast enough for measurement pairs to be sampled before the spatial distribution of rain drops changed significantly. Second, the cross correlation between the two reflectivity records was high, generally about 0.985. This high correlation produced a low standard error of sampling Z_{DR}, which for the system used to collect the present data was 0.1 dB. The corresponding error in Z was 0.75 dB. These random errors result in estimated standard deviations of rainfall rate, for D_0 values of 1 and 2 mm, to be 25 and 20% respectively. Limits to the errors in the calibration of Z and Z_{DR} were estimated to be 1 dB and 0.1 dB, respectively. This would result in a worst case systematic error, for D_0 values of 1 and 2 mm, of 40 and 35% respectively. By future comparison with *in situ* measurements, it is expected that bias due to the system error will be largely eliminated.

In the present study the rainfall rate has been computed using relationships between drop diameters and their fall speeds as obtained by Best[6]. These relationships assume still air, whereas there may be considerable vertical air currents in rain cells. 'Rainfall rate' is a well established characterization of the amount of rain present, and it is used here, even above ground level, without repetition of the phrase 'with respect to a frame of reference travelling at the rate of any vertical air current'.

Fig. 3 Vertical scan through raincells at 14.56 UT on 15 August 1978. *a*, Absolute reflectivity factor, Z; *b*, differential reflectivity, Z_{DR}.

Measured spatial distributions of Z and Z_{DR}

As in the system trials, the radar was operated at a frequency of 3,076 MHz and with a peak power of 500 kW. The pulse repetition frequency was 610 Hz, with alternate pulses on vertical and horizontal polarizations. Digitization of data was in 200 steps of 0.3 dB, and averaged in 128 ranges gates over 0.2 s. The sample gate width of 0.3 μs was staggered over 2 μs in 0.5-μs steps (the radar pulse width) to obtain effective range averaging over a gate width of 300 m. Spatial averaging due to dish movements amounted to one beamwidth for vertical scans (Figs 1–4) and two beamwidths for horizontal scans (Fig. 5). All averaging was of power rather than log power. The data-processing system enabled the received power at each polarization to be processed by the same logarithmic receiver and analogue-to-digital converter.

Figure 1*a* shows an example of the measured spatial distribution of Z obtained from a vertical scan through a large rain cell. There is a prominent pillar of high reflectivity at 35 km range extending to a height of 6 km, and at ranges of about 38 and 40 km there are small cells of high reflectivity that do not extend above 2 km height. Figure 1*b* shows the spatial distribution of Z_{DR} sampled at the same time as the data in Fig. 1*a*. Where the received signal level was less than 5 dB above the receiver noise level, Z_{DR} was set to a 'no data' level (as is also the case for Figs 2–4).

Fig. 2 Vertical scan through raincells at 13.55 UT on 15 August 1978. *a*, Absolute reflectivity factor, Z; *b*, differential reflectivity, Z_{DR}.

Table 1 Expected characteristics of Z and Z_{DR} at 10-cm wavelength for various hydrometeor types

Hydrometeor type	Z	Z_{DR}	Comments
Rain	High	High	Includes large oblate drops
Drizzle, cloud or fog	Low	Low	Small spherical drops of water and/or small ice particles
Dry snow flakes	Medium-low	Medium-low	Large horizontally oriented low-density aggregates
Sleet/wet snow	High	High	Large oblate horizontall oriented particles
Wet graupel	High	Negative	Large conical vertically oriented particles
Wet hail	High	Variable	Large particles: seldom spheres
Dry hail or other high-density ice particles	Medium	Low	

One of the most obvious features of Fig. 1*a, b* is that the column of high reflectivity at 35 km range has an associated high value of Z_{DR} (>2 dB) below 2 km height, but a value of Z_{DR} of only 0.13 dB (mean, with standard error 0.27 dB) between 2 and 4.5 km height. This abrupt change in Z_{DR} has been seen in many other examples. It always occurs close to the 0 °C isotherm, and marks the transition from ice particles to water drops. Unless very large asymmetries are present in low-density ice particles (snow), they will always exhibit a low value of Z_{DR} because of the low refractive index of ice and air mixtures[1]. Compact (high-density) ice particles with near-spherical shapes will intrinsically result in low values of Z_{DR}, whereas such particles with irregular shapes are likely to tumble randomly and so also have low Z_{DR}. In the absence of dual-polarization measurements, it would not be known whether the vertical column of high reflectivity in Fig. 1 were

Fig. 5 Distribution of data samples of Z, R, N_0 and D_0 in volume of rain scanned on 15 August 1978 between 13.21 and 13.26 UT—Marshall–Palmer distribution, $N_0 = 8,000 \, mm^{-1} m^{-3}$.

Subsequently, as the melting continues, the diameters would decrease (causing the observed decrease in Z), but an ice core could maintain a more oblate drop (and higher Z_{DR}) than would be possible with liquid water of the same volume. With further melting, the drop would become less oblate and the Z_{DR} would decrease. Finally, as the melting was completed, the drops would accelerate to their terminal velocity and the concentration of drops would decrease, as would the value of Z.

We shall not speculate further on the distribution of hydrometeors shown in Figs 1 and 2, but from data examined to the time of writing, the expected characteristics for various hydrometeor types are as set out in Table 1.

Fig. 4 Spatial distribution of the parameters $D_0 \, (mm)(a)$; $N_0 (mm^{-1} m^{-3})(b)$; $R (mm \, h^{-1})(c)$ computed from the data shown in Fig. 3, for heights below 1.5 km.

due to ice or water and a convective column containing rain might be assumed. When such convective columns have been observed with the dual-polarization radar, they were clearly distinguishable as having high values of both Z and Z_{DR} throughout their height.

Figure 2 shows data recorded 38 min after that of Fig. 1. There is a 'bright-band' region (of high reflectivity) at 2 km height. The cell at 33 km range has zero Z_{DR} above the bright band, whereas the cell at 22.5 km range, which has much stronger rain below the bright band, has a Z_{DR} of 0.5 dB above the bright band. It is assumed that the depression of the melting region at the centre of these cells, and that seen at 35 km range in Fig. 1, is due to the presence of compact ice particles which take longer to melt and fall faster than snow flakes. When these particles melt they scarcely change in size or fall speed, though the change to water gives the increased Z and Z_{DR} seen in Figs 1 and 2. Indeed this process probably extends to the two smaller and less intense cells to be seen between 37 and 42 km in Fig. 1. It would account for the absence of a height zone of particularly high reflectivity (bright band) near these cells.

In the range 25–30 km in Fig. 2, the largest values of Z_{DR} occur about 200 m below the bright-band height. This may be due to the following series of changes as snow flakes falling below the 0 °C isotherm melt slowly. First, water forming on the outer surface of the snow flakes would produce large effective drop diameters and the observed high Z region.

Rainfall rate and median drop sizes

Figure 3*a, b* shows data similar to those of Figs 1 and 2, but collected considerably later and in a quite different direction. There is considerable non-uniformity in the spatial distribution of Z and Z_{DR}. Figure 4*a, b, c* shows the corresponding spatial distribution of D_0 and N_0 of equation (1), and of the rainfall rate, $R (mm \, h^{-1})$, computed from Z and Z_{DR}. These are shown only for heights less than 1.5 km as we assume that the hydrometeors were water drops rather than ice particles in this region. Clearly D_0, N_0 and R all change rapidly with position. This variability may relate to many fields of study. In particular, the attenuation of radio waves due to rainfall may also be computed using N_0 and D_0 (ref. 4), and the variability of this is a current topic of study for both terrestrial and Earth-to-satellite radio paths.

Figure 5 shows values of R computed from Z_H and Z_{DR} plotted against Z (here the mean values of Z_H and Z_V), and superimposed on contours of N_0 and D_0 values. Data were collected up to a height of 1 km and up to 45 km in range whilst the radar was scanning over a width of 15°. Data for which the received signal level was within 15 dB of the receiver noise level, and samples thought to be from ground echoes, have been excluded from Fig. 5. For the lower values of Z in Fig. 5, the computed N_0 varies over the range 10^2–$3 \times 10^6 \, mm^{-1} m^{-3}$, and so some data elements have values of N_0 differing by a factor of 300 from that of the much-used distribution of Marshall and Palmer[7], for which $N_0 = 8,000 \, mm^{-1} m^{-3}$. The corresponding values of rainfall rates differ from this model by a factor of up to six. For the higher values of Z, there is apparently a much smaller spread of values of N_0, nearly all of which show lower values than that of Marshall–Palmer. However, all these samples having high Z are due to one concentrated volume of rain, and examination of data similar to those in Fig. 5, but from different rain cells, shows a quite different distribution for high Z values, with N_0 generally greater than the Marshall–Palmer value. Figure 5 also shows experimental sampling error contours at the 1 s.d.

level for D_0 of 1 and 2 mm. Evidently the data show large real differences in drop size characteristics. They also suggest that use of data from a conventional (single-polarization) radar, with an assumed drop-size distribution, may lead to large errors in computation of localized volumes of high rainfall rate.

The work described here formed part of the research programme of the Rutherford and Appleton Laboratories of the SRC.

An extraterrestrial event at the Cretaceous–Tertiary boundary

J. Smit

Geological Institute, Nieuwe Prinsengracht 130, Amsterdam, Holland

J. Hertogen

Fysico-chemical Geology, St Michielstraat 16, Leuven, Belgium

Closely spaced samples from an uninterrupted calcareous pelagic sequence across the Cretaceous–Tertiary boundary reveal that the extinction of planktonic Foraminifera and nannofossils was abrupt without any previous warning in the sedimentary record, and that the moment of extinction was coupled with anomalous trace element enrichments, especially of iridium and osmium. The rarity of these two elements in the crust of the Earth indicates that an extraterrestrial source, such as the impact of a large meteorite may have provided the required amounts of iridium and osmium.

THE Cretaceous–Tertiary boundary seems to be the only major boundary in the stratigraphic record which does not become diffuse when studied in detail[1,2]. On the contrary, all over the world the boundary can essentially be referred to one single bedding plane, even in the most complete marine sections (Gubbio, Italian Appennines[3]; Zumaya, Northern Spain[4,5]; El Kef, Northern Tunisia[6]; and many DSDP holes[7,8]). Planktonic Foraminifera occur abundantly in these sections and thus provide one of the best available ways of following the extinctions at the end of the Cretaceous[1]. This extinction and subsequent resurrection has been studied in detail in the unusually complete and thick calcareous pelagic section of Caravaca in South-east Spain[9]. Here, the topmost Maastrichtian and lowermost Palaeocene biozones (the *Micula prinsii* Zone, P. Nielsen, personal communication and the '*Globigerina' eugubina* Zone respectively) have been demonstrated. A 10-cm thick 'intermediate' bed also occurs between these zones characterized by a threefold increase of clay minerals and a peculiar indigenous fauna (J.S. in preparation). Information from the other sections mentioned above, although less complete, is compatible (Fig. 1). In the >100-m thick youngest Maastrichtian marls of the Caravaca section the rich, tropical association of planktonic Foraminifera and nannofossils[9,10] shows no significant changes up to the very last centimetre; here almost the entire association disappears within 0–5 mm. At a Maastrichtian sedimentation rate of 7 ± 3 cm kyr^{-1} (Fig. 1) this implies that the extinction took place within ~ 200 yr (ref. 1).

The impoverished association in the subsequent 10 cm intermediate bed is dominated by benthonic Foraminifera and relicts of the Cretaceous planktonic fauna, like *Hedbergella monmouthensis* (Olsson), *Globigerinelloides aspera* (Ehrenberg), *G. messinae* (Brönnimann) and *Guembelitria cretacea* (Cushman). The amazingly sharp limits of this level are apparently preserved owing to a temporarily decreased rate of burrowing, because all other sediments in the section are strongly bioturbated.

At the top of this intermediate bed the new Tertiary planktonic fauna suddenly appears in great numbers. Accompanied by the sole survivor of the terminal Cretaceous 'holocaust', *Guembelitria cretacea*, this new fauna diversifies, and shows a rapid succession of different dominant species in the lowermost 50 cm of the Palaeocene, representing the entire '*G'. eugubina* Zone[1] (Fig. 1). Hereafter the facies becomes similar to that of the Upper Cretaceous, exhibiting the same, normal, slow evolutionary changes in fauna and flora.

Analyses

To obtain more information about the extinction event (to sort out some of the current extinction models[2]), trace elements have been analysed by instrumental neutron activation (NAA) on 100 bulk samples closely spaced around the boundary: 17 elements were detected throughout the section and 10 more

Table 1   Anomalous trace element enrichments in the lowermost Tertiary of the Barranco del Gredero, Caravaca, South-east Spain

	$\bar{X}$*	Upper Cretaceous s†		$\overline{c.v.}$‡	n§	$\bar{X}$	Intermediate bed		$\overline{c.v.}$	n	$\bar{X}$	Lower Palaeocene	s	$\overline{c.v.}$	n
Ir	0.13	p.p.b.		—	?	25.5	p.p.b.		—	2	0.34	p.p.b.	—	—	1
Os	0.08	p.p.b.	—	—	2	16.1	p.p.b.		—	2	0.41	p.p.b.	—	—	1
Ni	24.2	p.p.m.	—	—	2	1065.7	p.p.m.	4	6	40.6	p.p.m.	14	13	8
Co	9.06	p.p.m.	2.8	3.4	28	270	p.p.m.	3	4	5.59	p.p.m.	2.5	4	65
Cr	56.9	p.p.m.	20	3.3	28	499	p.p.m.	2.5	4	69.6	p.p.m.	19.3	2.8	63
As	2.07	p.p.m.	1.23	12.5	16	225.8	p.p.m.	12	4	1.66	p.p.m.	1.5	13.5	31
Sb	0.35	p.p.m.	0.09	14.5	19	7.01	p.p.m.	10	4	0.23	p.p.m.	0.08	16	24
Se	0.073	p.p.m.	—	—	2	5	p.p.m.	—	2	0.138	p.p.m.	—	—	1

* Sample mean.
† Sample standard deviation.
‡ Mean coefficient of variation of the analytical error (%).
§ Number of analyses.
Analytical error for Ir, Os, Ni and Se for high values better than 2%, for low values better than 10%.

Table 2   Correlation coefficient of 17 (trace) elements analysed at IRI, Delft

	Al	Ca	Sc	V	Cr	Mn	Fe	Co	Rb	Cs	La	Ce	Sm	Eu	Yb	Hf	Th
Ca	−0.94																
Sc	0.97	−0.95															
V	0.96	−0.94	0.96														
Cr	0.86	−0.86	0.89	0.91													
Mn	−0.61	0.54	−0.59	−0.56	−0.5												
Fe	0.96	−0.94	0.97	0.94	0.85	−0.6											
Co	0.87	−0.83	0.84	0.82	0.75	−0.66	0.81										
Rb	0.82	−0.82	0.81	0.74	0.63	−0.61	0.85	0.7									
Cs	0.72	−0.73	0.73	0.63	0.51	−0.51	0.77	0.57	0.96								
La	0.6	−0.67	0.71	0.66	0.72	−0.21	0.67	0.42	0.53	0.49							
Ce	0.82	−0.84	0.89	0.8	0.74	−0.42	0.89	0.63	0.79	0.78	0.76						
Sm	0.52	−0.57	0.61	0.56	0.53	−0.16	0.58	0.39	0.43	0.35	0.86	0.58					
Eu	0.45	−0.54	0.58	0.51	0.59	−0.11	0.54	0.33	0.4	0.47	0.75	0.73	0.46				
Yb	0.14	−0.26	0.28	0.23	0.33	−0.12	0.23	0.05	0.16	0.21	0.76	0.43	0.55	0.75			
Hf	0.88	−0.86	0.87	0.82	0.77	−0.56	0.88	0.8	0.88	0.77	0.67	0.77	0.59	0.46	0.27		
Th	0.96	−0.94	0.97	0.92	0.83	−0.6	0.98	0.81	0.9	0.83	0.69	0.89	0.59	0.56	0.27	0.92	
Insoluble residue	0.88	−0.87	0.91	0.85	0.78	−0.47	0.93	0.7	0.83	0.76	0.69	0.87	0.6	0.54	0.24	0.83	0.92

93–97 pairs in correlation.

were detected in the intermediate bed only. Furthermore, we analysed five samples for iridium, osmium, selenium and nickel by radiochemical means, encouraged by a recent report of Alvarez *et al.*[12] on anomalously high levels of iridium at the boundary in the previously mentioned Gubbio section (Fig. 2, Table 1). The γ-ray countings show that the $^{184}Os/^{190}Os$ isotopic ratio in sample III (Fig. 2) is indistinguishable, within experimental error (0.1%), from the isotopic ratio in common terrestrial osmium.

Just like the planktonic fauna, none of these trace elements shows any positive or negative trend or an enrichment when approaching the extinction level. Most elements correlate nicely with the insoluble residue content (Table 2) and show a similar rise in the intermediate bed (Fig. 2). In the basal few centimetres of this bed, however, immediately above the extinction level, iridium, osmium and arsenic occur in highly anomalous quantities (450, 250 and 110 times normal, respectively) and to a lesser extent Cr, Co, Ni, Se and Sb (9, 30, 44, 40 and 20 times normal, respectively). As, Co, Ni, Cr, Se and Sb may be derived

from terrestrial source rocks. However, as Alvarez pointed out, it would be very difficult to accept a similar origin for iridium and osmium, as these elements are greatly depleted in the crust of the Earth, estimated at 0.05–0.1 parts per 10^9(p.p.b.)[11], in comparison with the average of the Solar System.

From these observations we find: (1) the extinction event was extremely abrupt, without previous warning signal whatsoever; and (2) the anomalously high amounts of iridium and osmium are clearly linked with the event.

Discussion

All the complete sections mentioned above contain almost exclusively Foraminifera and nannofossils, so any pronouncement on the syn- or diachronism of extinction with other groups or organisms remains somewhat speculative.

Attempts to achieve this correlation by palaeomagnetic means are widely debated[13–16], but irrefutable evidence for a diachronous extinction has never been produced[1]. Russell[2] has recently reviewed the current extinction models. He concluded

Fig. 1 The Cretaceous–Tertiary boundary interval in the Barranco del Gredero, Caravaca, South-east Spain. A, Micula prinsii Zone; B, 'intermediate' bed; C, *Globigerina eugubina* Zone; D, *Globigerina pseudobulloides* Zone.
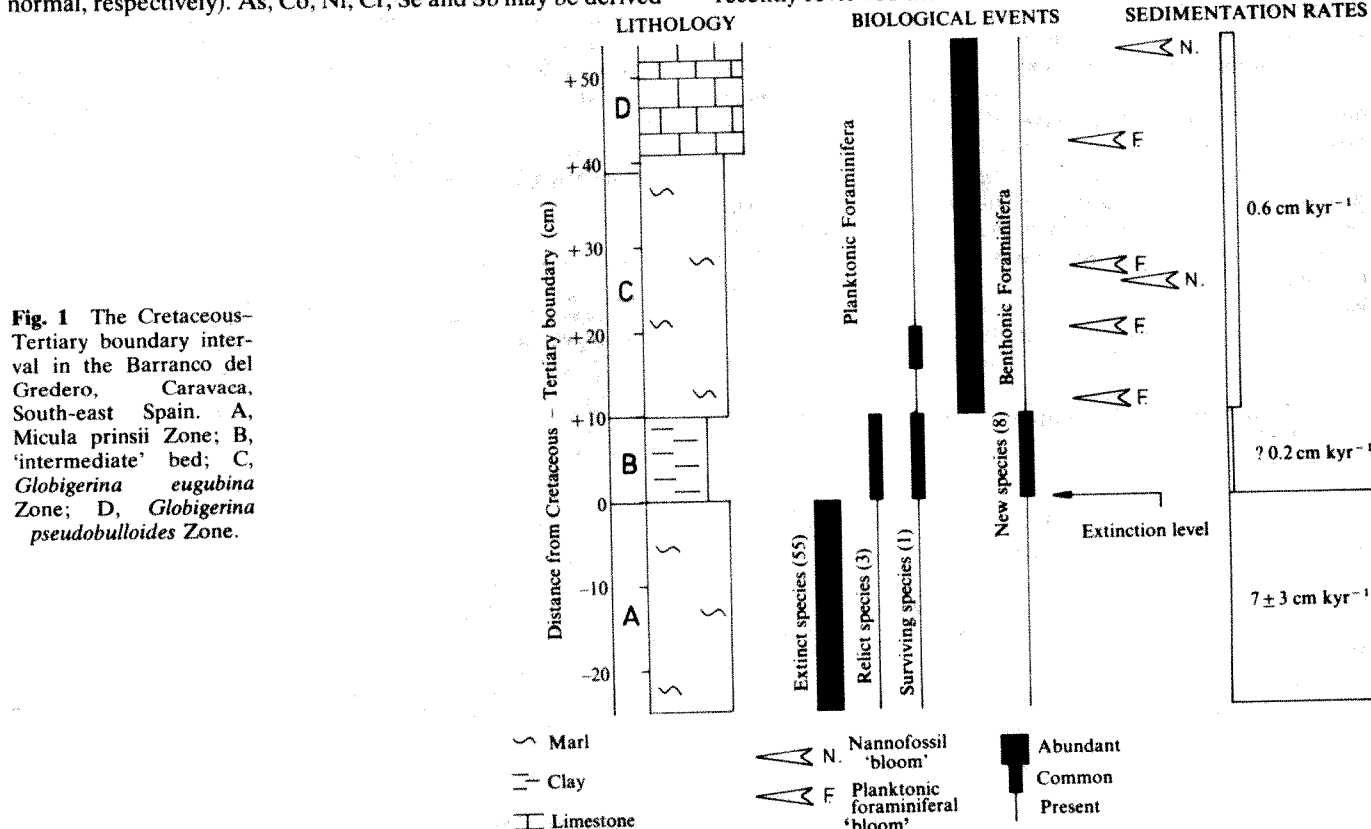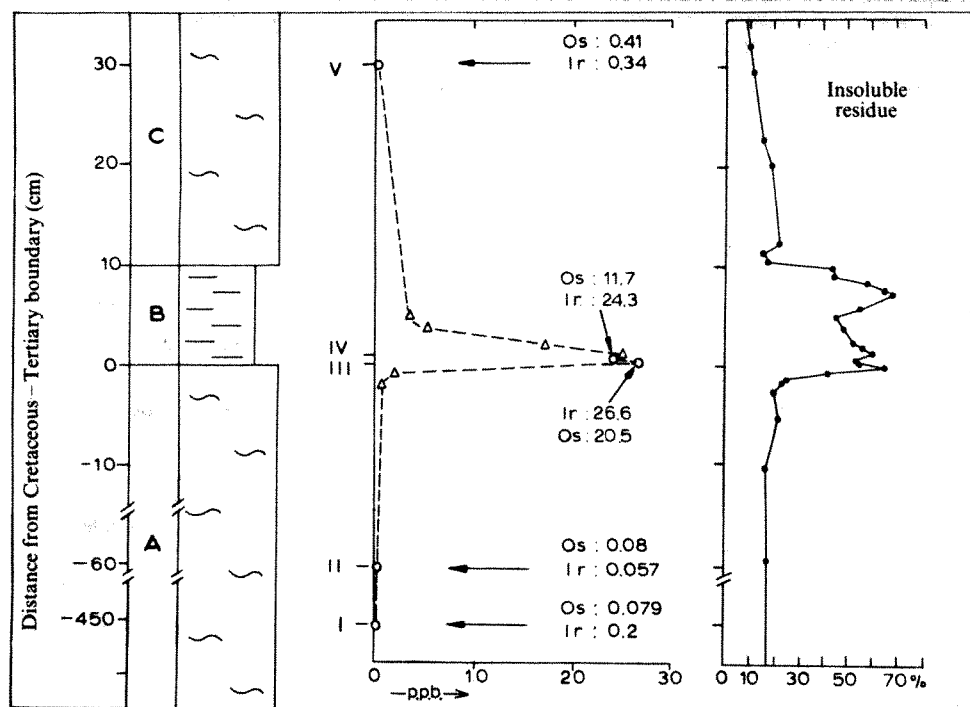
Fig. 2 Iridium, osmium and insoluble residue data from the Cretaceous–Tertiary boundary in the Barranco del Gredero. The iridium data are plotted. O, I-V Samples analysed at the Institute for Nuclear Sciences, Gent, Belgium. △, Preliminary Ir analyses, communicated by W. Alvarez. A, Micula prinsii Zone; B, 'intermediate' bed; C, '*Globigerina*' *eugubina* Zone.

that none of the existing models is entirely satisfactory, but that only a very short event, which a great part of the biosphere could not tolerate, may explain the known facts. The above mentioned points support this view.

Current extinction models may be classified in two ways; the gradual versus the catastrophic or the terrestrial as opposed to the extraterrestrial models. Most terrestrial models (nutrient depletion[17], climatic deterioration[18], rise in CCD[19], CO_2–O_2 imbalance[20], secular variations[21] and increase in volcanism[22]) are essentially gradual and should leave traces in the sediment of the imminent extinctions. None has been found yet. Reports of gradual extinction[4,19] lose their credibility on more detailed inspection[1].

There remain the catastrophic models which do not have a pre-extinction signal. One such model is the recently advocated 'Arctic flushing' of cold brackish water over the ocean surface[7,23]. In this way, however, the excess of iridium and osmium cannot be explained. Extraterrestrial influences (giant solar flare[24], supernova[2,18,25] or asteroid impact[26-28]) on the other hand are geologically speaking instantaneous and in particular the latter explains the high amounts of iridium and osmium. The frequency of disastrous impacts on the Earth or the explosion of a nearby supernova have been estimated; once every 100 Myr an impact of an asteroid or comet nucleus 10–30 km in diameter[26-28] or every 70 Myr a supernova at a distance of 50 light yr occurs[2,25]. A typical iron meteorite is $\sim 2 \times 10^4 - 4 \times 10^5$ times, and a chondrite $\sim 6 \times 10^3 - 2 \times 10^4$ times, enriched in Ir and Os relative to the crust of the Earth and when such body vaporizes on impact, or is partly broken up on entry in the atmosphere, it may deliver overdoses of Ir and Os over a large area; if we assume the Caravaca values—3 × 10⁻⁸ g cm⁻² — dispersed over the whole world and an iridium content of 5×10^{-7} g per g in a carbonaceous chondrite it may imply an impacting body of about 5 km in diameter. Geological evidence for an impact, such as a crater larger than 150 km in diameter or impact triggered sediment at the boundary have not yet been found.

The expanding shell of a supernova explosion could sweep up amounts of Ir and Os from interstellar matter.

The maximum amount that can be swept up by a supernova at 50 light yr distance is only the equivalent of the Os and Ir content of a chondrite with a diameter of 60 m. Hence it falls short by a factor of 10⁶ with respect to the required amounts (E. P. J. van den Heuvel, personal communication). Also the ratio of the stable osmium isotopes $^{184}Os/^{190}Os$ is very similar to Solar System

ratios[12]. It would be surprising if the isotopic composition in interstellar matter is within 0.1% of Solar System ratios.

Conclusions

The present evidence favours an extraterrestrial cause for the extinctions at the end of the Cretaceous. The impact of an asteroid or comet 5–15 km in diameter is the most attractive. The consequences of such an event are still poorly understood and need further investigation, as not all the facts fit this model easily.

A crucial point in the model is the near synchronous extinction of all organisms that did not cross the Cretaceous–Tertiary boundary, and the independence of the event from the known normal environmental processes going on in the latest Cretaceous.

1. Smit, J. *Proc. Cret. Tert. Bound. Events Symp.* **II**, 156–163 (1979).
2. Russell, D. A. *A. Rev. Earth planet. Sci.* **7**, 163–182 (1979).
3. Alvarez, W. *et al. Bull. geol. Soc. Am.* **88**, 367–389 (1977).
4. Herm, D. *Z. Deut. Geol. Ges.* **115**, 277–348 (1963).
5. Percival, S. F. & Fisher, A. G. *Evolut. Theory* **2**, 1–35 (1977).
6. Donze, P. *Proc. Cret. Tert. Bound. Events Symp.* **II**, 237 (1979).
7. Thierstein, H. & Berger, W. H. *Nature* **276**, 461–466 (1978).
8. Boersma, A., Shackleton, N., Hall, M. & Given, Q. *Init. Rep. DSDP* Leg **42**, 695–717 (1978).
9. Smit, J. *Proc. Kon. Ned. Akad. Wet.* **80**, 280–301 (1977).
10. Romein, A. J. T. *Proc. Kon. Ned. Akad. Wet.* **80**, 256–279 (1977).
11. Crockett, J. H. & Kuo, H. Y. *Geochim. cosmochim. Acta* **43**, 831–842 (1979).
12. Alvarez, W. *et al. Proc. Cret. Tert. Bound. Events Symp.* **II**, 69 (1979).
13. Butler, R. F. *et al. Nature* **267**, 318–323 (1977).
14. Lerbeckmo, J. F. *et al. Nature* **279**, 26–30 (1979).
15. Alvarez, W. & Vann, D. W. *Geology* **7**, 66–67 (1979).
16. Lucas, S. G. & Rigby, J. K. *Geology* **7**, 323–326 (1979).
17. Tappan, H. *Paleogeogr. Paleoclimat. Paleoecol.* **4**, 187–200 (1968).
18. Newell, N. D. *Science* **149**, 922–924 (1965).
19. Worsley, T. R. *SEPM spec. Publ.* **20**, 94–125 (1974).
20. McLean, D. M. *Science* **201**, 401–406 (1978).
21. Fisher, A. G. & Arthur, M. A. *SEPM Spec. Publ.* **25**, 19–50 (1977).
22. Vogt, P. R. *Nature* **240**, 338–342 (1972).
23. Gartner, S. & Keany, J. *Geology* **6**, 708–712 (1978).
24. Roy, J. R. *Syllogeus* **12**, 89–110 (1977).
25. Tucker, W. H. *Syllogeus* **12**, 111–124 (1977).
26. Kerr, R. A. *Science* **206**, 803–804 (1979).
27. Napier, W. M. & Clube, S. V. M. *Nature* **282**, 455–459 (1979).
28. Dachille, F. *Earth planet. Sci. Lett.* **46**, 44–52 (1977).

Terrestrial catastrophe caused by cometary impact at the end of Cretaceous

Kenneth J. Hsü

Geological Institute, Swiss Federal Institute of Technology (ETH), Zurich, Switzerland

Evidence is presented indicating that the extinction, at the end of the Cretaceous, of large terrestrial animals was caused by atmospheric heating during a cometary impact and that the extinction of calcareous marine plankton was a consequence of poisoning by cyanide released by the fallen comet and of a catastrophic rise in calcite-compensation depth in the oceans after the detoxification of the cyanide.

MASS extinction at the end of Cretaceous[1] has been related to the impact of meteorites[2], asteroids[3], or comets[4,5]. The two groups of organisms most affected are large terrestrial animals and calcareous marine plankton, especially those in tropical waters. Here it is suggested that cometary impact was the major cause of the extinction of these two groups.

Catastrophic nature of the terminal Cretaceous event

High-resolution stratigraphy indicates the very short duration of the terminal Cretaceous event[6-9]. The biological changes of the marine–planktonic world across the boundary could be separated into three phases: (1) the mass extinction of a rich marine–planktonic fauna of latest Cretaceous age; (2) the pre-dominance of small foraminifera and some special nannofossils which might be surviving species from the Cretaceous[7]; (3) the appearance and evolution of robust Tertiary species.

The first phase is recorded by an iridium-rich clay or marly layer some 1 cm thick in Italy[10], and 2–5 mm thick in Spain[9]. The second phase is recorded by the *Globigerina eugubina* zone[8,9]. The third act is represented by the higher Danian microfauna and nannofossil stages. Using sedimentation rate as a basis, the duration of the terminal Cretaceous event which caused the mass extinction was estimated to be <10,000 yr (ref. 11). In fact, the span of time could be <50 yr, if the 'iridium-spike' of Spain represents the record of that event[9]. Large terrestrial animals may have become extinct at the same time as the marine plankton[12] although this is still uncertain.

Although the terminal Cretaceous event lasted a very short time, the damage was extensive[14-16] and the destruction was selective. Evolutionary changes of terrestrial plants were gradual[17] and small animals living in freshwater were virtually unaffected by the extinction[16]. However, large terrestrial animals heavier than 25 kg did not survive the catastrophe. In the marine realms, calcareous plankton was hard hit, with some groups (for example, planktonic foraminifers and nannoplankton) being virtually wiped out[14].

The extinction seemed to have hit organisms at different stages of their evolutionary development[15]. Also there seems to have been palaeogeographical selection; virtually all Cretaceous organisms which became extinct near a major peak in their evolutionary development lived predominantly in or very near to the equatorial Tethys[18], and their vacant tropical niches were eventually occupied by new Tertiary species, which had evolved from survived stocks of euritopic temperate or cosmopolitan faunas[18]. Finally, selectivity might have been an expression of resistance to environmental stress. For example, the sparse nannofloras surviving the terminal Cretaceous event were dominated by *Braarudosphaera* and *Thorascosphaera*, both of which tolerate, or even prefer, conditions adverse for the growth of other calcareous nannoplankton in the present oceans[14].

The fossil records register a catastrophic revolution of the biosphere. The almost invariable presence of a clay layer or a hardground boundary at the Cretaceous–Tertiary is evidence of a revolutionary change in the entire hydrosphere, manifested by a rise of the CCD (calcite compensation depth), which in turn, was caused by an increase of dissolved CO_2 in seawater[13,14,19].

Studies of trace elements in the clay-rich layer just above the contact indicates an unusual concentration of iridium[9,10]. The isotopic composition of Ir indicates extra-terrestrial input from a source within the Solar System[10]. Also enriched are Co, Ni, Zn, As and Sb[9].

The clay-rich layer is absent at the Cretaceous–Tertiary boundary in some deep-sea drilling holes, for example, DSDP Holes 356, 374[20,21], where biostratigraphical analyses invariably indicate, a depositional hiatus (refs 13, 21 and K. P. Nielson, personal communication). At some localities the contact is represented by a hardground[22] indicating widespread erosion or non-deposition as a consequence of bottom-current activities[21].

The climatic changes during the late Cretaceous were gradual[17,23-27]. However, isotopic analyses of deep-sea drilling cores during the past few years indicate remarkable temperature difference across the Cretaceous–Tertiary boundary[26]. An increase of 1–5 °C of both bottom and surface temperatures has been recorded by oxygen-isotope data from widely scattered localities[26-29].

Analyses of carbon isotopes of sediments across the boundary suggest a remarkable change in the chemistry of the ocean water associated with the terminal Cretaceous event. A decrease of ^{13}C of 1–3‰ has been reported[25-30] equivalent to a change produced if the whole of the terrestrial biosphere were put into the ocean[25]!

Frequency and consequences of comet collision

Impact craters are not uncommon on the surface of the Earth[31]. Based on existing craters, Hughes[32] obtained an estimate of the rate of cratering, which can be represented by

$$\phi = \frac{1}{1,400 D^2}$$

where ϕ is the rate on Earth (yr^{-1}) and D is the diameter of the crater (km). This estimates that a small crater of 200 m may be created every 350 yr, and a large crater of 100 km every 14 Myr. Based on tektite or crater ages, Napier and Clube[5] noted that large (>50 km) impact-cratering took place during the Pleistocene (1 Myr), middle Miocene (15 Myr), late Oligocene (28 Myr), early Oligocene (35 Myr), late Eocene (38 Myr), beginning of Jurassic (183 Myr), middle Triassic (210 Myr), and late Devonian (365 Myr). Considering that almost three-quarters of the Earth's surface lie under water, one can expect oceanic craters to have largely escaped detection. Nevertheless, the statistics indicate that there should have been at least one crater bigger than 500 km during the 600 Myr of the Phanerozoic.

The energy E generated by the craters has been variously

estimated[4,5,33,34] depending on the size of the object and its collision velocity. Assuming an impact speed of 24.6 km s^{-1}, Napier and Clube[5] obtained E values ranging from 0.3 to 150×10^{30} erg, associated with 80–500 km cratering which could be produced by planetesimals 4–31 km in diameter. Urey[4] used a collision velocity of 45 km s^{-1} for a comet with a mass of 10^{18} g, which is the estimated size of the Halley's comet, and found that the impact energy is 10^{31} erg, or 250×10^6 Mton. If all energy were absorbed by the atmosphere, the air temperature would rise by 190 °C. If all energy were absorbed by the oceans, the elevation of average ocean temperature would be 0.175 °C. If all the energy were used to excavate a crater, a mass of dust 3×10^{19} g could be thrown up to encircle the Earth.

Discussing Moon cratering, Gault *et al.*[35] indicated that a third of the kinetic energy is converted to heat, which is manifested in the melting and/or vaporization of both the impacting and the impacted material. However, comets falling into the ocean may heat up both the atmosphere and hydrosphere by friction. The atmospheric heating caused by a small comet may absorb the greater share of the kinetic energy. The Tungeska explosion on 30 June 1908 may have been caused by a small comet with a mass of 5×10^{10} g, and the comet may have exploded and disintegrated in the air so that numerous craters 50–200 m in diameter, instead of one large crater, were found in the impact area[2,36]. The heat was so intense that it killed all animal life within 1,000 km² (ref. 3). Aside from the kinetic energy of 5×10^{23} erg, Hughes[36] suggested that a nuclear explosion may have been triggered by neutron production as the heated comet sped through the atmosphere; he thus offered an explanation for the ¹⁴C anomaly of 1909. For a very large comet which might generate 10^{31} erg, the fraction of kinetic energy expended to heat the atmosphere depends on the entry angles and other factors. It is unlikely that the whole atmosphere could be heated to 190 °C as Urey suggested for the extreme case of total dissipation by atmospheric heating. On the other hand, the temperature produced by a speeding comet may have been so high locally that it could produce nuclear or even thermonuclear reactions (as Hughes suggested) in addition to chemical explosions. With the possible addition of chemical and nuclear energy, it is difficult to estimate the possible heating of the atmosphere. It seems, however, that a 10–20 °C increase of air temperature is possible. The heating of a large comet falling through a 5-km deep ocean can be calculated on the basis of estimating hydrodynamic resistance. Using a resistance coefficient of 0.001 typical of motions with a very large Reynolds number[37], I obtained a value of 10^{30} erg, or about 10% of the total kinetic energy for a fallen comet with 30 km diameter, 10^{18} g mass, and 45 km s^{-1} speed. These estimates suggest that the bulk of the kinetic energy would be expended after impact, causing cratering and melting of substratum, which should become an additional source of energy to raise the temperature of the ocean further.

Chemical consequences

While the physical consequences of a large cometary collision are impressive, the chemical consequences are commonly neglected because we know little about the composition of comets. There are still debates over whether comets are dirty snowballs or dust swarms[38], although the first, also known as the icy conglomerate model first formalized by Whipple, is being favoured[38–40]. The model assumes that the nucleus of comets is an icy solid body containing chemical compounds which sublimate and dissociate to provide the radicals and simple molecules that have been observed in cometary spectra[40,41]. Optical spectra showed the presence of CN, CO⁺, CH, NH, OH, and so on[42]. When Comet Kohoutek came near the Earth in 1973, hydrogen cyanide and methyl cyanide were detected 'at a reasonable abundance'[40–42]. If the concentration were 10% the amount of cyanides dissolved from a 10^{18} g of comet, and evenly distributed in ocean water would give a concentration of 0.1 p.p.m. However, the concentration would be 3 p.p.m. if the dissolved substance was concentrated in the upper 100 m only, and even more if the poison was carried by currents and thus contained within the moving surface water mass.

CO_2 and/or CO are probably also present in the nucleus of a comet. The ocean has 130×10^{18} g of dissolved carbonates[44] mainly as HCO_3^-. Deeper ocean water is undersaturated due to its higher dissolved CO_2 and lower *p*H. However, the surface seawater is supersaturated because of the high *p*H related to disturbed buffering caused by photosynthesis. The annual CO_2 extracted from the ocean by marine plankton is $\sim 0.4 \times 10^{18}$ g, which is the same order of magnitude as the probable mass of CO_2 in a 10^{18} g comet. The sudden dissolution of CO_2 from a large fallen comet can thus greatly disturb the carbonate equilibrium, so that surface waters, at least locally, may become temporarily undersaturated.

A large input of cometary carbon should also significantly alter the isotopic composition of calcareous sediments in the ocean. The isotopic composition of carbon for meteorites and for the Earth's mantle has about the same composition of −6 to −7‰ ¹³C. However, the carbonate in meteorite and the carbon in chondrite have very heavy ¹³C, with values up to more than +50‰ (ref. 45). As the CO_2 in the nucleus of a comet may have represented a distilled fraction, it should have an isotopic composition much lighter than that of the average meteorite. Assuming a cometary $\delta^{13}C$ of −25‰, a −1.5‰ carbon-excursion in dissolved carbonate can be caused by the fall of a 10^{18} g comet of which carbon atoms constitute a quarter of its mass.

Comet impact at end of Cretaceous

Probability calculations indicate that at least one large comet with a mass of 10^{18} g and impact energy of 10^{31} erg should have hit the Earth during the Phanerozoic. The nature and severity of the terminal Cretaceous catastrophe suggest that such a comet hit the Earth at that time. The comet must have fallen into the ocean so that there would be no evidence on land of a crater of this age.

The preceding analysis showed that a cometary impact may kill by three different means: large land animals could be killed by atmospheric heating, marine organisms could be killed by cyanide poisoning, calcareous marine plankton might further suffer because of a catastrophic rise of the CCD of the oceans.

If the comet fell into the ocean, the dissolution of its nucleus should have released a large quantity of HCN, CH_3CN, CO_2, and possibly also CO. The dissolved constituents should ascend with the warm water mass heated by the fallen comet, and should find their way into a surface current system and remain relatively concentrated there. Cyanide is a powerful inhibitor, arresting cellular respiration by inactivating metallo-enzymes in the respiratory process[46]. As this process is fundamental to all living organisms, cyanide dissolved in sufficient concentration could kill all kinds of marine organisms, including nannoplankton. The cyanides could be reduced through oxidation into CO_2 (ref. 46). This CO_2 added to the extraterrestrial CO_2 brought in by the comet would increase the dissolving power of seawater. The mass-mortality of phytoplanktons would further upset the CO_2 budget with a consequent catastrophic rise of CCD, leading to a virtual extinction of the calcareous planktonic life. Furthermore, phytoplankton formed the basis of the food chain for higher organisms, so that their mass mortality should cause starvation of those marine organisms[19] that had escaped cyanide poisoning. Detoxification of cyanide also produced nitrates. Experiments with living nannoplankton indicated that they would not secrete calcareous skeletons in nitrate-rich waters (B. Funnell, personal communication). Such nannoplankton would leave no fossil record, but may have evolved into the Tertiary forms which did secrete skeletons when conditions returned to the normal.

Surface currents would converge eventually into the Equatorial Current, where the greatest contamination would occur. Consequently, the catastrophe would hit hardest those organisms which inhabited the tropics. Some organisms living in the gyres of the middle latitude would escape extinction, not

only because they were more tolerant of stress conditions, but also because the gyres were regions bypassed by polluted surface currents. Note, for example, that the nannoplankton *Braarud-osphaera* is not only a tolerant species, but its modern representatives also have a population in the gyre of the Sargasso Sea[47]. Large parts of the deep-sea bottom may also have been spared lethal contamination, so that deep marine benthic communities mostly survived the catastrophe.

On land, the large vertebrates would perish under an almost instantaneous thermal stress [2,16,24], but small or aquatic animals would largely survive. Laubenfels[2] suggested that turtles may have escaped the heat wave by diving under water for hours while holding their breath, and that crocodiles preserved their species because they had buried their eggs in mud. Because the comet fell in the oceans, temperature anywhere on land may not have been sufficiently high to cause global forest fires. In any case, land vegetations could have escaped extinction as new seeds could sprout even after a pyric catastrophe.

The palaeo-oceanography after the comet fell must have been extraordinary. The increase of dissolved CO_2, the mass extinction of phytoplanktons, and the consequent pH changes may have raised the CCD to a level near or within the photic zone. Consequently, the sediment underlying the oldest fossiliferous Tertiary beds is commonly a clay or clay-rich. The input of trace elements from the fallen comet would have contributed to the unusual concentration of Ir, As, Ni and Co in this clay-lamina[9,10]. Meanwhile, the presence of molten rock material in an impact crater under the ocean should generate thermal stress and promote active bottom-circulation in the deep sea. Consequently, a depositional hiatus other than dissolution-unconformity has been noted at many deep-sea drilling sites across the Cretaceous-Tertiary boundary. The input of converted kinetic energy, possibly supplemented by the chemical and nuclear energies, would cause the rise in ocean temperature, as manifested by the $\delta^{18}O$ shift in the oldest Tertiary sediments. The input of light extraterrestrial carbon would contribute to the accompanying carbon shift.

The climatic implication of the postulated cratering is not clear. Urey[4] as well as Napier and Clube[5] estimated that the ejectas excavated by a large fallen comet may equal, or even exceed, the mass of the comet, and much of the fine dust might reach the stratosphere to block out solar radiation, thus causing glaciation. Indeed, the timing of drastic cooling near the end of Eocene and in middle Miocene[48] coincided remarkably with that of the Popigai cratering (100 km diameter) in USSR at 38 Myr and the cratering which produced the Moldavites at 15 Myr (ref. 5). The end of the Cretaceous has been considered the beginning of a general cooling on the Earth[17]. Isotopic shift did show cooling during the first few million years of the Palaeocene following the 'heating spike' (ref. 27). However, the temperature was apparently lowered to that prevailing before the catastrophe. The emerging deep-sea record indicates that the first Tertiary cooling responsible for the initiation of Antarctic glaciation came much later, at the end of Eocene[48], or the time of Popigai cratering. The different climatic effects of cratering may be accounted for by the postulate that the terminal Cretaceous comet fell into the ocean: much of the dust-sized ejectas were trapped by the ocean and did not reach the stratosphere, in contrast with the continental landing of a comet at the end of Eocene.

Conclusions

We may never find the crater, because much of the Mesozoic ocean floor has disappeared by subduction during the past 65 Myr. However, if the crater has not yet been subducted, systematic searches should locate such a large feature. The crater should have a diameter of a few hundred kilometres. Furthermore, the cratering should have created an ejecta plume, namely rock-lava steam mixture rising vertically above the crater like a volcanic eruption[49]. Collapsing under its own potential, the mixture should have developed into a *nuée ardente* or base-surge [50,51]. The mass flow at high speed should have eroded the ocean floor and formed channels. All those geomorphic and depositional features can be detected by seismic profiling.

The cratering should have produced earthquake waves and tsunami waves which would cause subaqueous slumping and turbidite deposition. We could search for the crater through a systematic recording of the size and distribution-density of such mass-flow deposits. Likewise, we could study the palaeotemperature distribution to trace the geographical origin of the anomaly. We could study the hiatus-distribution to trace the source of the stress that induced the bottom circulations. We could refine our study of geographical patterns of mass extinction. A careful examination of the existing geological records may tell us whether the crater is still to be found or if it ever existed.

1. Russell, D. A. *Syllogeus* **12**, 11–23 (1977).
2. De Laubenfels, M. W. *J. Paleont.* **30**, 207–212 (1956).
3. Alvarez, L. *et al. LBL Rep. 9666*, UC Berkeley (1979).
4. Urey, H. C. *Nature* **242**, 32–33 (1973).
5. Napier, W. M. & Clube, S. V. M. *Nature* **282**, 455–459 (1979).
6. Birkelund, T., Bromley, R. G. & Christensen, W. K. *Cretaceous-Tertiary Boundary Events* (University of Copenhagen, 1979).
7. Perch-Nielsen, K. in *Cretaceous-Tertiary Boundary Events* Vol. 1 (eds Birkelund, T. *et al.*) 115–135 (University of Copenhagen, 1979).
8. Alvarez, W. *et al. Bull. geol. Soc. Am.* **88**, 383–389 (1977).
9. Smit, J. in *Cretaceous-Tertiary Boundary Events* Vol. 2 (eds Birkelund, T. *et al.*) 156–163 (University of Copenhagen, 1979).
10. Alvarez, W. *et al.* in *Cretaceous-Tertiary Boundary Events* Vol. 2 (eds Birkelund, T. *et al.*) 69 (University of Copenhagen, 1979).
11. Kent, D. V. *Geology* **5**, 769–771 (1977).
12. Alvarez, W. & Vann, D. W. *Geology* **7**, 66–67 (1979).
13. Lindsay, E. H. *et al. Geology* **6**, 425–429 (1978).
14. Worsley, T. in *Studies in Paleo-Oceanography* (ed. Hay, W. W.) Vol. 20, 94–125 (*SEPM Spec. Publ.*, 1974).
15. Newell, N. D. *J. Paleont.* **36**, 592–610 (1962).
16. Russell, D. A. *Am. Rev. Earth planet. Sci.* **7**, 163–182 (1979).
17. Tschudy, R. H. *Geol. Soc. Am. Spec. Pap.* **127**, 65–111 (1971).
18. Kaufman, E. G. in *Cretaceous-Tertiary Boundary Events* Vol. 2 (eds Birkelund, T. *et al.*) 29–37 (University of Copenhagen, 1979).
19. Tappan, H. & Loeblich, A. R. *Geol. Soc. Am. Spec. Pap.* **127**, 247–340 (1971).
20. Thierstein, H. R. & Okada, H. *Init. Rep. DSDP* eg **43**, 601–616 (1979).
21. Supko, P. R. & Perch-Nielsen, K. *Init. Rep. DSDP* eg **39**, 1099–1132 (1977).
22. Bromley, R. G. in *Cretaceous-Tertiary Boundary Events* Vol. 1 (eds Birkelund, T. *et al.*) 16–32 (University of Copenhagen, 1979).
23. Jerzen, D. M. *Syllogeus* **12**, 39–50 (1977).
24. McLean, D. M. *Science* **201**, 410–416 (1978).
25. Saito, T. & Van Donk, J. *Micropaleontology* **20**, 152–177 (1974).
26. Boersma, A., Shackleton, N., Hall, M. & Given, Q. *Init. Rep. DSDP* eg **43**, 695–718 (1979).
27. Thierstein, H. R. & Berger, W. H. *Nature* **276**, 461–466 (1978).
28. Buchardt, B. & Jørgensen, N. O. in *Cretaceous-Tertiary Boundary Events* Vol. 2 (eds Birkelund, T. *et al.*) 54–61 (University of Copenhagen, 1979).
29. Boersma, A. & Shackleton, N. in *Cretaceous-Tertiary Boundary Events* Vol. 2 (eds Birkelund, T. *et al.*) 50–53 (University of Copenhagen, 1979).
30. Brennecke, J. C. & Anderson, T. F. *Am. Geophys. Un Trans.* **58**, 415 (1977).
31. Weatherill, G. W. *Scient. Am.* **240**, 54–65 (1979).
32. Hughes, D. W. *Nature* **281**, 11 (1979).
33. Vortman, L. J. in *Impact and Explosion Cratering* (eds Roddy, D. J. *et al.*) 1215–1230 (Pergamon, New York, 1977).
34. Robertson, P. B. in *Impact and Explosion Cratering* (eds Roddy, D. J. *et al.*) 247–276 (Pergamon, New York, 1977).
35. Gault, D. C. *et al. J. geophys. Res.* **80**, 2444–2460 (1975).
36. Hughes, D. W. *Nature* **268**, 512–514 (1977).
37. Prandtl, L., Oswatitsch, K. & Wieghardt, K. *Führer durch Strömungslehre* (Vieweg, Braunschweig, 1969).
38. Hughes, D. W. *Nature* **270**, 558–560 (1977).
39. Whipple, F. L. *Astrophys. J.* **111**, 375 (1950).
40. Whipple, F. L. *Nature* **263**, 15–19 (1976).
41. Ulich, B. L. & Conklin, E. K. *Nature* **248**, 121–122 (1974).
42. Huebner, W. F., Snyder, L. E. & Buhl, B. *Icarus* **23**, 580–582 (1974).
43. Broecker, W. S. *Chemical Oceanography* (Harcourt Brace Jovanovich, New York, 1974).
44. Takahashi, T. in *Encyclopedia of Oceanography* (ed. Fairbridge, R.) 170–175 (Dowden, Hutchinson & Ross, Stroudsburg, 1966).
45. Hirner, A. *Schweiz. Petrol. Geol.* **45**, 47–56 (1979).
46. DeBrune, A. *Biochemical Toxicology of Environmental Agents* (Elsevier, Amsterdam, 1976).
47. Gaarder, K. R. in *North Atlantic Deep Sea Expedition 1910* Vol. 2 (ed Sars, M.) 4 (Grieg, Bergen, 1954).
48. Kennett, J. P., Burckle, L. H., Keigwin, L. D. & Woodruff, F. *Geol. Soc. Am. Abstr.* **11**, 456 (1979).
49. Andrews, R. J. in *Impact and Explosion Cratering* (eds Roddy, D. J. *et al.*) 1089–1100 (Pergamon, New York, 1977).
50. Wisotski, J. in *Impact and Explosion Cratering* (eds Roddy, D. J. *et al.*) 1101–1122 (Pergamon, New York, 1977).
51. Fisher, R. V. *Bull. geol. Soc. Am.* **88**, 1287–1297 (1977).

Bulk attenuation in the Earth and viscosity of the core

Don L. Anderson

Seismological Laboratory, California Institute of Technology, Pasadena, California 91125

Recent studies indicate that bulk absorption is required somewhere in the Earth to explain the damping of the radial modes of free oscillation. This excess absorption, if attributed to bulk viscosity in the core, requires a value of ~500 P. This is theoretically reasonable and may be due to structural or concentration fluctuations. The shear viscosity is at least several orders of magnitude smaller.

ALTHOUGH most of the seismic attenuation in the Earth can be attributed to losses in shear[1] the damping of the radial modes suggest that bulk losses occur somewhere in the mantle or core [2-4]. If all losses were in shear value the Q value of the fundamental radial mode, $_0S_0$, would be >7,000. Several recently determined values are ~4,100. The other radial modes and compressional spheroidal overtones also have high Q values but they are more sensitive to shear attenuation than $_0S_0$, the most nearly pure compressional mode. Discussions of bulk, or volume, attenuation, therefore, must rely mainly on this mode.

The mode $_0S_0$ has only been observed infrequently and the reported values for Q have a wide variation[5]. Narrow band filtering experiments indicate that its amplitude does not die off uniformly with time after an earthquake (H. Kanamori and A. Dziewonski, personal communications). During the first few days there seems to be interference[4] with adjacent, stronger excited modes, such as $_0S_5$. The decay after about 2 weeks is less rapid than the initial decay. This could be a problem of the lower signal-to-noise ratio in the later portions of the record or a re-excitation by long-period aftershocks. Some recent results are given in Table 1. Note that relatively high values are obtained if the early part or the late parts of the record are included. The first four entries in the table are consistent, within the assigned errors, and give an average value of 4,590 with an uncertainty of ~11%. This includes two multiple station analyses. An analysis by Kanamori (personal communication) for the period 1–25 days after the Indonesian event gives a Q of 5,425. The first 2 weeks of data, however, fall in the above range. For present purposes we assume that Q of $_0S_0$ is ≤4,800 and investigate the implication. If later studies establish a higher value, then the viscosities inferred in this article will be upper limits.

Sailor and Dziewonski[4] attempted to fit the radial modes by inserting a low Q_K region in the upper mantle. The radial mode $_0S_0$, however, has little energy in the upper mantle and is most sensitive to properties of the lower mantle and outer core. Anderson and Hart[3] satisfied the $_0S_0$ data by assuming a Q_K of 10^6 in the outer core; their models also have a low Q_K, 426–847, in the inner core. These values were based on body wave and inner core shear mode data, as well as on the radial modes.

The problem is not unique as there is little resolving power in the available compressional or high-Q modes. We have found that a uniform Q_K of ~10^4 throughout the Earth also satisfies these data. If only the core contributes then a slightly smaller value for this region is implied. Body wave studies[6,7] of the outer core give values for Q_P ranging from 10^2 to 10^4. This suggests that the core may contribute significantly to the observed attenuation. Furthermore, bulk attenuation is well documented in fluids and, in particular, in liquid metals. Because of the dominance of shear losses in the mantle it will be difficult to determine the bulk contribution, if any, of this region. In this article we estimate the bulk viscosity of the core from the

damping of the radial modes and then investigate if this is a reasonable number for liquid iron at core conditions.

Models

We have investigated a large number of models to learn more about possible distributions of bulk attenuation in the Earth. These included constant Q_K and frequency-dependent Q_K models, all of which satisfy the shear sensitive spheroidal and toroidal mode data. The excess absorption is attributed to bulk losses in pure compression. Some of these models and the resulting radial mode Q spectra are given in Table 2. SL8 is from Anderson and Hart[3] and is a frequency-independent Q structure. The others are a result of the present study and, at low frequencies, have $Q_K \sim \omega^{-1}$ as appropriate for a relaxation mechanism. The values given are for a period of 1,000 s. The radial mode data and results for three models are shown in Fig. 1.

The value of ~7,000 for Q $(_0S_0)$ which is obtained for Earth models exhibiting only shear losses can be reduced to a value near 4,200 by introducing a Q_K of ~10^4 distributed uniformly throughout the mantle and core. If the bulk losses occur only in the core an average Q_K of ~2×10^3 in this region is required. As

$$Q_K^{-1} = (2\pi f / \rho c^2) \eta_v \qquad (1)$$

for fluids this gives an effective bulk viscosity, η_v, for the core of ~500 P; this is an average value. ρ is the density; c, the velocity of sound; and $f = \omega/2\pi$ is the frequency. Pressure is likely to increase viscosity so that smaller values may be maintained at the top of the core. There is no detailed information about the variation of Q_K with depth but we know that the attenuation of P waves is much greater in the inner core than in the outer core. This suggests that the relaxation time in the inner core is closer to seismic periods than is the case in the outer core, and that the relaxation time increases with depth. This implies an increase in viscosity with depth. Note that previous investigators have proposed that the inner core is a highly viscous fluid rather than a crystalline solid[8].

Table 1 Q of $_0S_0$

Q	Error (%)	No. of stations	Days	Earthquake	Ref.
4,000	5	1	5–15	Alaska	4
4,100	26	5	2–24	Indonesia	22
4,589	4	7	2–16	Indonesia	*
Shorter times included					
5,663	9	1	1–17	Alaska	4
6,687	13	2	0–25	Indonesia	5
Longer times included					
5,527	2	7	2–45	Indonesia	*

* A. Dziewonski (personal communication).

Physics of attenuation in fluids

We will first consider sources of attenuation in the outer core. The absorption of sound in a liquid at low frequencies is given by

$$\alpha/f^2 = (2\pi^2/\rho c^3)\{\tfrac{4}{3}\eta_s + (c^2\beta^2\theta T/C_p^2) + \eta_v\}$$

where α is the spatial attenuation coefficient, β the thermal expansion coefficient, θ the thermal conductivity, C_p the specific heat, η_s the shear viscosity, η_v the volume viscosity, and T the absolute temperature. The first two terms on the right-hand side represent the classical Stokes–Kirchoff absorption due to shear stresses and thermal conductivity. The first term is important in the attenuation of longitudinal waves in liquid metals, but is absent for strains involving pure compression. The second term is important at laboratory frequencies but is negligible at core conditions and seismic frequencies. The remaining term is called the excess absorption and is due to bulk or volume viscosity. Both η_s and η_v contribute to damping of longitudinal waves in fluids but only η_v would contribute to the purely compressional strains which dominate the fundamental radial mode. In liquid metals at low pressure η_v is similar in magnitude to η_s (ref. 9).

Several mechanisms contribute to bulk viscosity in simple fluids. One is structural relaxation due to perturbations in the short-range order caused by the sound wave. Another is due to concentration fluctuations in alloy systems. These are comparable in magnitude in laboratory conditions but have quite different temperature, and possibly pressure dependencies. The dominant mechanism may, therefore, be different at core conditions from that in laboratory conditions. A high bulk viscosity at conditions prevailing in the core is not necessarily inconsistent with a much lower shear viscosity. The characteristic times for shear and structural relaxation are likely to be similar as they are both controlled by short range diffusion. The relaxation time due to concentration fluctuations or chemical reactions may be quite different.

Longitudinal waves in liquid metals typically are within an order of magnitude of

$$Q = 10^{11}/f$$

which in normal conditions is composed of three roughly equal parts due to shear viscosity, thermal conductivity and bulk viscosity, or excess sound absorption[9]. The attenuation in liquid metals in laboratory conditions would be quite negligible at seismic frequencies. However, the effects of pressure and alloying lengthen the characteristic relaxation times.

Bulk viscosity of molten iron

The bulk viscosity of a pure liquid metal is due to structural rearrangement as there are no internal degrees of freedom. Two-state theories have been developed to explain structural relaxation associated with pressure changes. The assumption is that a liquid is a mixture of two structural states with differing mole volumes and energies.

We use the two-state theory of Herzfeld and Litovitz[10] and Flinn et al.[9] to estimate the structural volume viscosity of iron just above the melting point, T_m, and its relation to the shear viscosity;

$$\eta_v = \frac{x_1 x_2 V}{RT_m}\left(\frac{\Delta V}{V} - \frac{\beta \Delta H}{C_p}\right)^2 \tau K^2$$

and

$$\eta_v/\eta_s = \frac{(2n-12)(12-n)}{n^2}\left(\frac{VK}{RT_m}\right)^2\left(\frac{\Delta V}{V} - \frac{\beta \Delta H}{C_p}\right)^2$$

$$x_2 = (12-n)/n = 1 - x_1$$

where x_1 and x_2 are the mole fractions of the two states which differ by ΔV and ΔH in molar volume and enthalpy, and n is the coordination number. For liquid iron at low pressure we take $n = 9$; $V = 8\ \mathrm{cm^3\ mol^{-1}}$; $\Delta V/V = 0.1$; $\Delta H/RT_m = 3$; the bulk modulus, $K = 1.3\ \mathrm{Mbar}$ (10% less than solid iron); $\beta = 70 \times 10^{-6}\ \mathrm{K^{-1}}$, $C_p = 10.2\ \mathrm{cal\ mol\ K}$; and the relaxation time, $\tau =$

5×10^{-12} s. This relaxation time is typical of liquid metals[9] (the other values are from refs 9, 11, 12, 13). $\Delta V/V$ is calculated from Fürth's relation. These parameters give

$$\eta_v = 3\ \mathrm{cP}$$

and

$$\eta_s = (5/3)\eta_v = 5\ \mathrm{cP}$$

for molten iron at low pressure. The measured value for η_s is 4.8–7.0 cP (ref. 14) and the near equality of η_s and η_v is consistent with measurements on other liquid metals[9]. Thus, the two-state theory gives satisfactory results at low pressure which leaves us to investigate the properties at core conditions.

The main effect of pressure and temperature is on the bulk modulus K and the relaxation time τ. The bulk modulus of the core is 4–10 times larger than iron at normal conditions[11,15] and relaxation times have been estimated to be of the order of 10^{-8}–10^{-9} s (ref. 16). Therefore, bulk viscosities of 4–6 orders of magnitude larger than at low pressures, or η_v of 10^2–10^4 P, are expected. The associated shear viscosities would be in the range of 10–100 P. The neglect of the effect of temperature and pressure on the other parameters would decrease these estimates slightly but probably by less than an order of magnitude. This estimate of η_s satisfies the lower limit (10 P) of Bukowinski and Knopoff[16] and the upper limit for the top of the outer core of 10^6 P based on the lack of damping of the 18.6-yr principal nutation[17].

Effect of alloying

Based on density and cosmic abundances, the core is likely to contain up to 10% Ni and other siderophiles and a similar amount of light element such as O or S. There are additional volume relaxation mechanisms associated with alloys and solutions. In particular the relaxation times can be much longer than those due to shear and structural relaxations. This might be significant in explaining the apparent frequency dependence of Q of P waves in the outer core[6,7]. There is a suggestion of a linear increase of Q_P with frequency which, if verified, indicates that the seismic band is on the high frequency side of the absorption band in the outer core. As this cannot be true for shear waves unless the unrelaxed shear modulus of the core is much lower than the rigidity of the inner core we may need a low-frequency volume relaxation mechanism. This contribution to the bulk attenuation and volume viscosity depends on concentration and may eventually shed light on the nature of alloying elements in the core.

Flinn et al.[21] found a highly temperature-dependent absorption mechanism operating in binary melts which is not present in the pure metals.
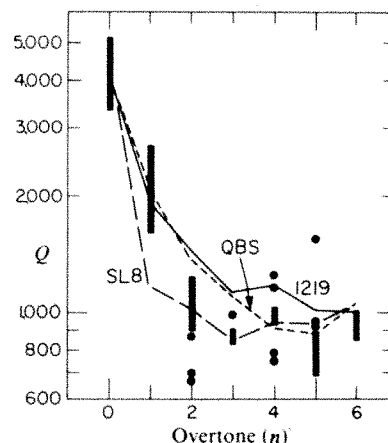
Fig. 1 Q values for the radial modes, $_nS_0$. The models SL8 and 1219 have moderate bulk attenuation in the core. Model QBS has high bulk attenuation in the upper mantle. The data are from ref. 2 and Table 1.

The extra absorption in liquid metal alloys is probably due to concentration fluctuations. Theoretically it is inversely proportional to the diffusivity or directly proportional to the shear viscosity. As with the structural viscosity it is also proportional to the square of the bulk modulus and can therefore, be expected to increase with pressure. More importantly it is a function of the curvature of the Gibbs potential versus concentration relation and, therefore, becomes very large in the vicinity of a critical point. Unfortunately, it is not possible to estimate the relaxation time of this mechanism in the core.

We conclude that structural and concentration fluctuations may be responsible for bulk viscosity in the core and contribute to the excess absorption of the radial modes.

Relaxation theory of bulk attenuation

The Q due to bulk losses in a relaxing solid or viscoelastic fluid is

$$Q_K^{-1}(\omega) = (\Delta K/K)\omega\tau_v/(1 + \omega^2\tau_v^2) \qquad (2)$$

where $\Delta K/K$ is the modulus defect and τ_v is the volume relaxation time.

$\Delta K/K$ is the fractional difference between the high frequency and low frequency moduli. This has not been measured for liquid metals but is typically ~ 0.3 for other liquids. The decrease in bulk modulus on melting of metals ranges from ~ 5 to 30%. This may be of the same order as the modulus defect for molten metals. The bulk moduli of glasses are often taken as approximately the same as the high frequency moduli of fluids. This gives a modulus defect of 0.2–0.7 for most liquid–glass systems. These estimates give Q_{min} between 10 and ~ 3 at $\omega\tau = 1$. The increase in bulk modulus at the inner core–outer core boundary is about 5% (ref. 15). If this is taken as $\Delta K/K$ we obtain an estimate of 40 for the minimum Q_K of the core at $\omega\tau = 1$. A Q_K of 2×10^3 at a period of 20 min (the period of $_0S_0$) implies, from equation (2) that $\tau \sim 4$ s or 10^4 s. The smaller value would be consistent with the solid-like behaviour of the inner core for short-period body waves. The location of the inner core–outer core boundary would then be frequency dependent and the inner core would apparently be smaller at free oscillation periods. Such a frequency dependence has, in fact, been suggested by Gutenberg[8]. A frequency-dependent inner core boundary could explain the discrepancy between free oscillation and body wave determinations of the properties of the inner core. For example, the shear velocity obtained from PKJKP[18] is ~ 20% smaller than that obtained from the free oscillation data[15,19] for a fixed inner core radius. These results can equally well be interpreted in terms of a 20% decrease in inner core radius in going from body wave to free oscillation periods. Glass-like transitions, or transitions from fluid-like to solid-like behaviour typically take place over a small range of temperature. The sharpness of the inner core boundary could be explained by such a transition occurring over a small range of pressure.

Interpreting the data in this way requires that the seismic data

Table 2 Effect of bulk dissipation (Q_K) in mantle and core on Q of radial modes

	SL8*	1219	0220†	0279
Q_K (mantle)	∞	10^4	10^4	2×10^5
Q_K (core)	10^6	8×10^4	8×10^6	7×10^3
			4×10^5	
$_0S_0$	4,374	4,310	4,803	4,062
$_1S_0$	1,180	1,939	1,797	1,902
$_2S_0$	1,024	1,459	1,351	1,381
$_3S_0$	851	1,155	1,090	1,222
$_4S_0$	945	1,206	1,072	1,136
$_5S_0$	947	1,031	863	947
$_6S_0$	1,057	1,015	834	873

* Ref. 3. Q_K (inner core) = 426–847.
† Q_K of outer core varies with depth.

for the outer core be on the low frequency side of the relaxation peak. For the outer core

$$Q_K^{-1} = \frac{\Delta K}{K}(\omega\tau_v) \qquad (3)$$

and, for the inner core

$$Q_K^{-1} = (\Delta K/K)/\omega\tau_v \qquad (4)$$

The boundary of the inner core, then, corresponds to $\omega\tau = 1$ and this is where attenuation would be a maximum. For a 1-s body wave the inferred relaxation time at the inner core–outer core boundary is $(2\pi f)^{-1}$ or ~ 0.2 s. This is close to the value deduced from Q_K in the outer core.

Bulk attenuation in solids

There are also several mechanisms that can contribute to bulk modulus or volume attenuation in solids. These include thermoelastic, magnetoelastic and phase changes. Because of the wavelength of seismic waves, thermoelastic losses would be due to heat flow between adjacent grains rather than from the compressional part to the dilatational part of the wave. Composites of anisotropic grains or grains of different compressibility should exhibit intergranular thermoelasticity[20]. This depends on grain size, d, and thermal diffusivity, D. This mechanism gives a modulus defect and relaxation time of

$$\Delta M/M = \gamma\beta TR$$

$$\tau = d^2/3/\pi^2 D$$

where R is a measure of the grain anisotropy and varies between 0 and 1.

For $\beta = 10^{-5}\,K^{-1}$, $\gamma = 1$, $T = 2,000\,K$, $d = 1\,cm$ and $D = 0.001\,cm^2\,s^{-1}$, values appropriate for the mantle,

$$\Delta M/M = 0.02R$$

or

$$Q_{min} = 100/R$$

and

$$\tau = 3\,s$$

The thermal diffusivity of iron at core conditions is $\sim 0.06\,cm^2\,s^{-1}$ (ref. 21) which shifts the characteristic thermal relaxation time to about 0.5 s for the inner core. Therefore, the intergranular thermoelastic mechanism will contribute most at body wave frequencies and for $R = 0.1$ gives a Q_K at ~ 1 s of the order of 10^3. At a period of 20 min the Q_K associated with this mechanism will be $\sim 10^6$. A distribution of grain sizes will spread out the band and reduce the peak absorption.

For grain sizes of 1 cm or smaller the intergranular thermoelastic mechanism is small at free oscillation periods. Its presence, however, makes our estimate of Q_K in the core a lower bound. The low Q_P of the inner core at body wave frequencies may be due to this mechanism or due to the proximity to the relaxation peak in a viscoelastic fluid, as discussed earlier.

Conclusion

The damping of the radial modes can be satisfied by invoking a bulk dissipation in the core equivalent to Q_K (core) of 2×10^3. This implies a bulk viscosity of 500 P. A two-state theory for bulk viscosity of liquid iron gives satisfactory results at low pressure and predicts a value at core pressures which is consistent with the radial mode data. The main uncertainty in the theoretical result is in the relaxation time. The same theory predicts a shear viscosity in the core which is several orders of magnitude lower. A relaxation theory of bulk viscosity suggests a relaxation time of the order of 1 s in the core. The same result is obtained if we assume that the inner core has relaxation times greater than body wave periods so that it seems to be a viscous fluid exhibiting unrelaxed moduli. Current estimates of the shear relaxation time in the core are highly uncertain, but are $\ll 1$ s. As structural relaxation times are expected to be the same

as shear relaxation times this may suggest that a lower frequen[c]y mechanism, such as concentration fluctuations in an alloy, is responsible for the bulk viscosity.

If appreciable bulk attenuation occurs in the mantle and inner core, for example, by intergranular thermal currents, then th[e] estimate of Q_K^{-1} in the outer core will be reduced and the estimate of the bulk viscosity will be an upper bound. The thermal relaxation time is not a strong function of temperature or pressure. It would, therefore, be a coincidence if it happened to be near the period of $_0S_0$. The viscous relaxation times, on the other hand, are strong functions of the external variables and it is not unreasonable that they sweep through the seismic band in the core.

1. Anderson, Don L., Ben-Menahem, A. & Archambeau, C. B. *J. geophys. Res.* **70**, 505 (1965).
2. Anderson, Don L. & Hart, R. S. *Phys. Earth planet. Inter.* **16**, 289 (1978).
3. Anderson, Don L. & Hart, R. S. *J. geophys. Res.* **83**, 5869 (1979).
4. Sailor, R. V. & Dziewonski, A. M. *Geophys. J. R. astr. Soc.* **53**, (1978).
5. Knopoff, L., Zürn, W., Rydelek, P. & Yogi, T. *J. Geophys.* **46**, 89 (1978).
6. Cormier, V. & Richards, P. G. *J. geophys. Res.* **81**, 3066 (1976).
7. Suzuki, Y. & Sato, R. *J. Phys. Earth* **18**, 157 (1970).
8. Gutenberg, B. *Trans. Am. geophys. Un.* **38**, 750 (1957).
9. Flinn, J., Jarzynski, J. & Litovitz, T. *J. chem. Phys.* **54**, 4331 (1971).
10. Herzfeld, K. & Litovitz, T. *Absorption and Dispersion of Ultrasonic Waves* (Academic, New York, 1959).
11. Leppaluoto, D. A. in *High Pressure Physics and Planetary Interiors*, (ed. Runcorn, S. K.) (North-Holland, Amsterdam, 1972).
12. Evans, R. & Jain, A, in *High Pressure Physics and Planetary Interiors* (ed. Runcorn, S. K.) 141-145 (North-Holland, Amsterdam, 1972).
13. Furukawa, K., *Sci. Rep. Tohoku Univ., 1st Ser.* **12**, 368 (1960).
14. Gans, R. *J. geophys. Res.* **77**, 360 (1972).
15. Jordan, T.H. & Anderson, Don L. *Geophys. J.R. astr. Soc.* **36**, 411 (1974).
16. Bukowinski, M. & Knopoff, L. *The Physics and Chemistry of Minerals and Rocks* (ed. Strens, R. G. J.) (Wiley, London, 1976).
17. Toomre, A. *Geophys. J. R. astr. Soc.* **38**, 335 (1974).
18. Julian, B. R., Davies, D. & Sheppard, R. M. *Nature* **235**, 317 (1972).
19. Dziewonski, A. M. & Gilbert, F. *Nature* **234**, 465 (1971).
20. Zener, C. *Elasticity and Anelasticity of Metals* (University of Chicago Press, 1948).
21. Flinn, J., Gupta, P. & Litovitz, T. *J. chem. Phys.* **60**, 4390 (1974).
22. Buland, R., Berger, J. & Gilbert, F. *Nature* **277**, 358 (1979).

Isolation of the chicken thymidine kinase gene by plasmid rescue

Manuel Perucho*, Douglas Hanahan*, Leah Lipsich† & Michael Wigler*

* Cold Spring Harbor Laboratory, Cold Spring Harbor, New York 11724
† Department of Biochemistry and Molecular Biology, Harvard University, Cambridge, Massachusetts 02138

We have used the bacterial plasmid pBR322 as a vehicle to isolate genes coding for selectable markers from higher eukaryotes. In this way, we have obtained the chicken thymidine kinase (tk) gene as a 2.2-kilobase EcoRI/HindIII insert in pBR322. The cloned gene transforms tk⁻ animal cells with an efficiency equal to that of the cloned herpes simplex virus-1 tk gene.

SEVERAL genes of higher eukaryotes which encode major products of at least one tissue have been isolated, chiefly by using specific hybridization probes to screen genomic DNA fragments cloned into prokaryotic vectors[1-3]. Recently, an efficient method has been developed for the stable genetic transformation of cultured animal cells[4-7]. Genomic DNA from wild-type cells has been used as donor to transfer genes coding for selectable markers, such as thymidine kinase, adenine phosphoribosyl transferase and hypoxanthine phosphoribosyl transferase, to mutant recipient cells[8-11]. These developments make possible the isolation of genes coding for selectable markers. We describe here the isolation of a chicken thymidine kinase (tk) gene by means of 'plasmid rescue'. The chicken tk gene was chosen because an excellent recipient for DNA-mediated gene transfer was available in Ltk⁻, a tk-deficient mouse cell line, which has never been known to revert spontaneously to the tk⁺ phenotype[8-12]. In addition, this gene has the advantage that both the tk⁺ and the tk⁻ phenotypes can be selected[13].

Experimental design

In our scheme, chicken DNA is first digested with a restriction endonuclease which does not cleave tk and then ligated to similarly digested *Escherichia coli* plasmid pBR322 coding for ampicillin resistance (amp)[14]. This concatenated DNA is used to transform mouse Ltk⁻ cells to tk⁺. Some transformants can be expected to contain the chicken tk gene linked to pBR322 sequences. Next, the pBR322 sequences residing in the transformant are used to 'rescue' the flanking animal host sequences containing the tk gene. For this, DNA from the transformant is cleaved with a second restriction endonuclease, ligated in cyclization conditions and then used to transform *E. coli* to ampicillin resistance. Plasmid clones resulting from transformation of *E. coli* are then tested for the ability to transfer tk back into tk⁻ animal cells. This scheme is illustrated in Fig. 1, in which the restriction endonuclease HindIII is used for the first set of cleavage/ligations and EcoRI is used for plasmid rescue.

Transformation of Ltk⁻ cells

Restriction endonuclease-cleaved chicken DNA was tested for the ability to [transf]er tk to Ltk⁻ recipients to identify the enzymes that d[o no]t cu[t th]e chicken tk gene. Among these were HindIII, BamHI and EcoRI. HindIII was chosen for initial constructions. HindIII-cleaved chicken DNA was ligated to HindIII-cleaved pBR322 at 1:1 mass ratios, and then used to transform Ltk⁻ cells by the calcium phosphate co-precipitation method[9,15]. We found that pBR322 sequences inhibited transformation in amounts exceeding 2 μg per 10^6 cells. Therefore, 1 μg of chicken DNA which was ligated to 1 μg of pBR322 was co-precipitated in calcium phosphate along with 18 μg of Ltk⁻ DNA. This mixture was added to each plate containing 10^6 cells. Cells were then selected in hypoxanthine/aminopterin/thymidine medium as reported before[7]. After 2 weeks, 12 tk⁺ colonies were cloned and cultured for further analysis.

All tk⁺ transformants were examined for the presence of pBR322 sequences by blot analysis[16,17] using ^{32}P-labelled nick-translated[18,19] plasmid as probe. Although 8 of 12 transformants contained 2–20 copies of pBR322, we could not assume that any of these was adjacent to the tk gene because far more pBR322 sequences than tk genes were present during transformation, and co-transformation with unlinked DNA fragments does occur[17].

To establish the relationship between pBR322 sequences and the chicken tk gene, a second round of transformation and
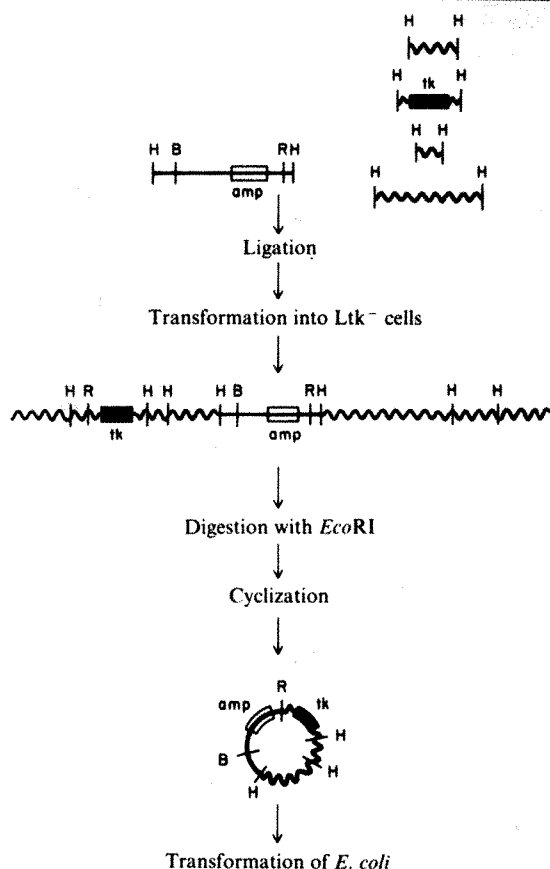
Fig. 1 A schematic illustration of the isolation of the chicken thymidine kinase gene (tk) by plasmid rescue. H, R and B refer to restriction endonuclease sites for *Hind*III, *Eco*RI and *Bam*HI, respectively (see text for details).

selection was necessary. Total DNA from each of four primary transformants containing pBR322 sequences was used to create eight secondary tk⁺ transformants. Blot analysis showed that 4 of the resulting 32 transformants (derived from 3 primary transformants) contained a single pBR322 sequence. Such sequences were not present in vast excess in the genomic DNA of primary transformants and so we concluded that the pBR322 sequences present in the secondary transformants were adjacent to the tk gene.

Rescue of pBR322 sequences

To rescue pBR322 sequences from transformed animal cells, these sequences must contain plasmid replication functions and an antibiotic resistance gene. Rtll-1a, a secondary transformant derived from the primary transformant tll, contained a *Hind*III fragment which annealed with nick-translated pBR322 and co-migrated with *Hind*III-cleaved pBR322. We concluded that no loss of pBR322 sequences occurred during transformation of this cell line. *Eco*RI and *Bam*HI were each used to rescue pBR322 from this line because they do not cleave the chicken tk gene and each cleaves pBR322 only once, on either side of the single *Hind*III site of the circular pBR322 molecule[20].

DNA from Rtll-1a was digested, ligated in cyclization conditions, and used to transform *E. coli* χ1776 (ref. 21) by a high efficiency procedure (D.H., in preparation). The efficiency of transformation of χ1776 with this cellular DNA was about 100-fold lower than expected from reconstruction experiments. Two ampicillin-resistant colonies were obtained which contained pBR322 derivatives: a 9.2-kilobase plasmid, pR-1, derived from *Eco*RI cleavage, and an 8.5-kilobase plasmid, pB-1, derived from *Bam*HI cleavage. Restriction maps of these plasmids are presented in Fig. 2.

We next verified (by hybridization) that the rescued plasmids were derived from the transformed mouse cells. Rescued

quences were nick translated and used as probes in blot analysis of restriction endonuclease-cleaved Rtll-1a DNA. Figure 3a and b show that *Bam*HI-cleaved pB-1 co-migrated with an homologous *Bam*HI fragment of Rtll-1a. Furthermore, Fig. 3c and d show that *Hind*III/*Bam*HI-cleaved pB-1 co-migrated with homologous fragments in *Hind*III/*Bam*HI-cleaved Rtll-1a. Double digestion with *Hind*III and *Bam*HI yielded two fragments not resolved in these conditions. Similarly, Fig. 4a-d show that *Eco*RI-cleaved pR-1 co-migrated with an homologous *Eco*RI fragment of Rtll-1a and that *Eco*RI/*Hind*III cleavage products of pR-1 each co-migrated with homologous fragments present in *Eco*RI/*Hind*III-cleaved Rtll-1a. The 0.6-kilobase *Hind*III/*Hind*III fragment is not visible.

We conclude that both pR-1 and pB-1 were rescued from animal cells into *E. coli*. From their respective restriction maps, a restriction map was reconstructed of pBR322 and its flanking host sequences in Rtll-1a (Fig. 2). This map was verified independently by blot analysis after cleavage of Rtll-1a DNA with a variety of restriction endonucleases.
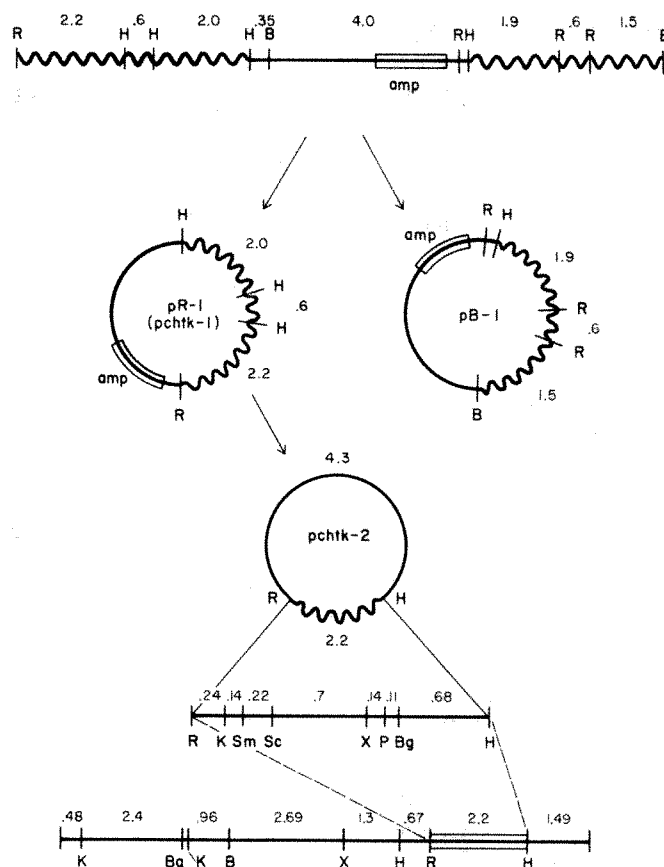
Fig. 2 Restriction maps and derivations of rescued plasmids. DNA from the secondary transformant Rtll-1a was prepared as previously described[17] and cleaved with either *Eco*RI or *Bam*HI. Digested DNA was then cyclized with T4 DNA ligase at a DNA concentration of 5 μg ml⁻¹. Cyclized DNA was used to transform *E. coli* χ1776 by a procedure to be described elsewhere (D.H., in preparation). Two plasmids, pR-1 and pB-1, were obtained from *Eco*RI-cleaved and *Bam*HI-cleaved, cyclized DNA, respectively. Restriction maps of these plasmids are shown, with pBR322 sequences denoted "▬" and inserted sequences denoted "〰". The numbers refer to kilobase pairs. From the maps of the two rescuants, a restriction map was reconstructed of the sequences flanking the pBR322 sequence resident in Rtll-1a (top line). pR-1 was found to encode tk and was renamed pchtk-1. pchtk-1 was cleaved with *Hind*III and cyclized to construct pchtk-2, which contains only the 2.2-kilobase *Eco*RI/*Hind*III insert encoding tk. Below is a restriction map (to scale) of the 2.2-kilobase insert. At the bottom is a restriction map (to scale) of the 12.5-kilobase insert of λchtk-1 isolated from a Charon 4A chicken library[22]. *Pvu*II, *Sma*I and *Sac*I sites are not mapped on the phage. Restriction enzymes are *Bam*HI (B), *Eco*RI (R), *Hind*III (H), *Kpn*I (K), *Sma*I (Sm), *Sac*I (Sc), *Xba*I (X), *Pvu*II (P) and *Bgl*II (Bg). Restriction enzyme digestions and ligations carried out in conditions described by the vendors (Bethesda Research Labs and New England Biolabs).

Table 1 Transformation data

Gene source	Restriction cleaved*	Total colonies†	Specific activity‡
pchtk-1	Uncut	1,628§	14.7
pchtk-2	Uncut	1,075§	7.6
pchtk-2	EcoRI	612§	4.3
pchtk-2	KpnI	0§	0.00
pchtk-2	SmaI	3§	0.02
pchtk-2	SacI	0§	0.00
pchtk-2	XbaI	0§	0.00
pchtk-2	PvuII	227§	1.6
pchtk-2	BglII	618§	4.4
pchtk-2	HindIII	1,863§	13.0
λchtk-1	Uncut	255‖	55.0
pTK-2 #	SalI	690‖	29.2
Chicken, genomic DNA	Uncut	51¶	63.7

* Three units of enzyme were used to digest 1 µg of DNA for 4 h at 37 °C in buffers recommended by the vendors.

† Transformations were carried out as previously described[9]. Ltk⁻ DNA was used as carrier for cloned genes at 20 µg per plate. For genomic chicken transformations, the DNA was its own carrier.

‡ Colonies per 10^8 molecules per 10^6 cells. The DNA content of chicken is taken as 2.5 pg per cell.

§ Total number of colonies in five plates, 20 ng gene per plate.

‖ Total number of colonies in five plates, 4 ng gene per plate.

¶ Total number of colonies in five plates, 20 µg per plate.

The 3.5-kilobase BamHI fragment of HSV-1 strain F (ref. 7) containing the HSV-1 tk gene was cloned into the BamHI site of pBR322. The orientation of the tk fragment is the same as the pFG5 clone of Colbere-Garapin et al.[25].

The sequences flanking pBR322 in the secondary transformant Rtll-1a could theoretically have arisen from chicken or mouse (or both), depending on events occurring during transformation. Blot analysis showed that the sequences contained in both pR- and pB-1 were derived entirely from chicken. The HindIII/BamHI insert of pB-1 co-migrated with an homologous HindIII/BamHI fragment of chicken DNA (Fig. 3c, e) whereas pB-1 showed no homology to mouse DNA in stringent hybridization conditions (Fig. 3f–j). Similarly, HindIII/EcoRI digestion of pR-1 generated one fragment of 4.3 kilobases containing only pBR322 sequences and three fragments of 2.2, 2.0 and 0.6 kilobases. These latter three fragments co-migrated with homologous fragments in chicken DNA cleaved with HindIII and EcoRI (Fig. 4c, e). Moreover, pR-1 showed no homology to mouse DNA (Fig. 4j).
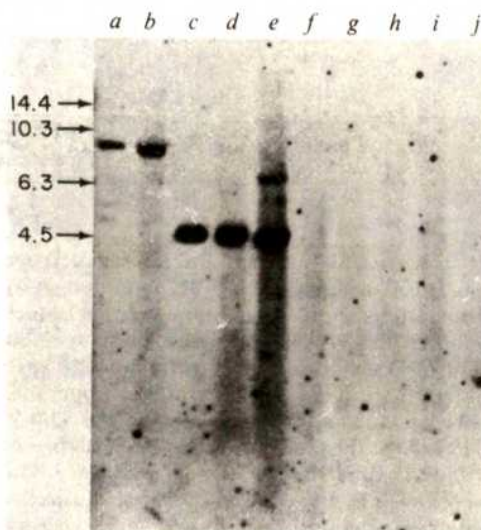
Fig. 3 Blot analysis of the pB-1 rescuant. pB-1 was ^{32}P labelled to high specific activity (2×10^8 c.p.m. per µg) by nick translation[19] and used as probe in Southern blots[17] to DNA electrophoresed in 1.0% agarose gels: a, BamHI-cleaved pB-1 (40 pg with 2 µg salmon DNA carrier); b, BamHI-cleaved Rtll-1a (10 µg); BamHI- and HindIII-cleaved DNA from: c, pB-1 (40 pg, with carrier); d, Rtll-1a (10 µg); e, chicken (10 µg); f, i, various secondary, chicken tk⁺ mouse transformants (primary transformant tll used as donor) (10 µg each); j, Ltk⁻ (10 µg). Arrows on the left are sizes (in kilobases) of restriction fragments of adenovirus-2. Digestions were in 30 µl final volume, 2 units of enzyme per µg DNA for 3 h at 37 °C.

pR-1 contains the chicken tk gene

pR-1 and pB-1 were tested in transformation assays for ability to transfer tk activity to Ltk⁻ cells. Although pB-1 gave no tk⁺ colonies, treatment of mouse cells with pR-1 yielded approximately 10 tk⁺ colonies per ng, only slightly below the frequency observed with a pBR322 clone containing the 3.5-kilobase BamHI fragment of HSV-1 which encodes the herpes simplex virus tk gene (pTK-2) (Table 1). These observations strongly suggested that pR-1 encoded the chicken tk gene, and this was confirmed by hybridization studies. As expected, pB-1 showed no homology to chicken tk⁺ mouse transformants (Fig. 3). On the other hand, pR-1 showed homology to chicken tk⁺ mouse lines but not to Ltk⁻ itself (Fig. 4f–j). Moreover, mouse cells transformed with pR-1 contained these chicken DNA sequences (Fig. 5b, c, d). No transformants contained HSV-1 tk sequences. Further confirmation was obtained by comparing the physical properties of the tk activity expressed in transformants with that of chicken, mouse and herpes tk. Isoelectric focusing of cytoplasmic extracts showed that transformants obtained using pR-1 as gene donor expressed a tk activity with the same isoelectric point (9.7) as that of 6-day-old chick embryo extracts and distinguishable from mouse (9.0) and herpes $(6.1)^{22}$. We therefore conclude that pR-1 encoded the chicken tk gene. pR-1 was renamed pchtk-1.
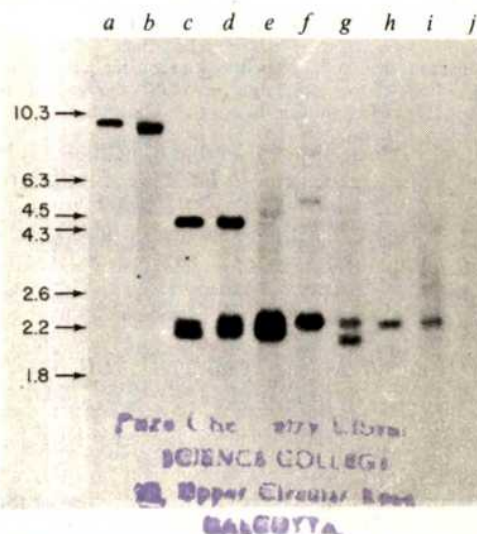
Fig. 4 Blot analysis of the pR-1 (pchtk-1) rescuant. pR-1 was used as probe in blots to DNA electrophoresed in 1.0% agarose gels: a, EcoRI-cleaved pR-1 (40 pg with 2 µg salmon carrier); b, EcoRI-cleaved Rtll-1a DNA (10 µg); EcoRI- and HindIII-cleaved DNA from: c, pR-1 (40 pg with carrier); d, Rtll-1a (10 µg); e, chicken (10 µg); f, g, h, various secondary chicken tk⁺ mouse transformants (primary transformant tll used as donor) (10 µg); i, a chicken tk⁺ primary transformant (10 µg); j, Ltk⁻ (10 µg). Arrows indicate sizes (in kilobases) of restriction fragments of adenovirus-2. Digestions were as in Fig. 3.

Localizing the chicken tk gene

pchtk-1 contains three chicken fragments bounded by EcoRI and/or HindIII sites: a 2.2-kilobase HindIII/EcoRI fragment, a 2.0-kilobase HindIII/HindIII fragment and a 0.6-kilobase HindIII/HindIII fragment. From its construction, we expected that the three chicken specific fragments of pchtk-1 were not contiguous in the chicken genome (Fig. 1). Thus, any of these fragments could have encoded the chicken tk gene. Blot analysis using nick-translated pchtk-1 as a probe showed that DNA from chicken and chicken tk⁺ mouse transformants contained in common only a 3.0-kilobase HindIII fragment. Thus, the 2.2-kilobase EcoRI/HindIII fragment contained the active gene. To test this rigorously, a second plasmid, pchtk-2, was derived from pchtk-1 by cleaving it with HindIII, cyclizing it and using it to transform E. coli. The resultant plasmid contained only the 2.2-kilobase HindIII/EcoRI fragment inserted into pBR322. This plasmid transformed Ltk⁻ to the tk⁺ phenotype with an

a b c d e f g h
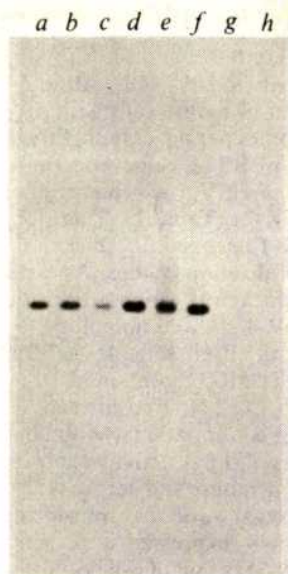
Fig. 5 Presence of the 1.4-kilobase *Eco*RI/*Pvu*II fragment in transformants, chicken, plasmid and phage DNA. DNAs from various sources were digested with *Eco*RI/*Pvu*II, electrophoresed in 1.5% agarose gels, transferred to nitrocellulose filters and hybridized *in situ* with ^{32}P-labelled, nick-translated, *Kpn*I/*Xba*I fragment of chicken tk (2×10^8 c.p.m. per µg). *a*, Charon 4A clone, λchtk-1 (200 pg); *b–d*, three different tk$^+$ mouse transformants obtained using pchtk-1 as gene donor (8 µg each); *e*, chicken (8 µg); *f*, pchtk-2 (50 pg with 2 µg salmon DNA carrier); *g*, HSV-1 tk$^+$ mouse transformant (8 µg); *h*, Ltk$^-$ (8 µg).

efficiency approximately equal to that of pchtk-1 (Table 1).

To localize the tk gene in more detail, we identified restriction sites on the 2.2-kilobase *Hin*dIII/*Eco*RI fragment using enzymes that cleave the fragment once (Fig. 2). pchtk-2 was cleaved to completion with each enzyme and the linearized plasmid was used in transformation assays (Table 1). By this procedure, we localized one end of the tk gene to the fragment bounded by the *Eco*RI and *Kpn*I sites, and the other end to the fragment bounded by the *Xba*I and *Pvu*II sites. Thus, a functional chicken tk gene is no larger than 1.4 kilobases and may be as small as 1.0 kilobase.

The plasmid carrying the biologically active chicken tk gene has had a complex history: it was passaged through mouse cells as well as through *E. coli*. To verify the structure of the tk gene independently, we have cloned it by an alternative and more familiar route. A library of chicken DNA[23,24] distributed into the bacteriophage λ vector, Charon 4A, was screened using nick-translated pchtk-2 as probe. DNA from one cloned phage (λchtk-1) contained a 12.5-kilobase chicken insert which transferred tk efficiently to Ltk$^-$ cells (Table 1). Restriction mapping and blot analysis (Figs 2, 5) confirmed the colinearity of the tk genes cloned in phage and by plasmid rescue.

The scheme we have demonstrated for the isolation of the chicken tk gene represents the first instance of the purification of a higher eukaryotic gene using essentially genetic techniques. In principle, this method is applicable to any higher eukaryotic gene coding for a selectable marker. We emphasize, however, that the isolation of tk has been greatly facilitated by its small size, a strong selection system and an excellent recipient cell used to detect its transfer.

1. Tilghman, S. M. *et al. Proc. natn. Acad. Sci. U.S.A.* **74,** 4406 (1977).
2. Tonegawa, S., Brack, C., Hozumi, N. & Scholler, R. *Proc. natn. Acad. Sci. U.S.A.* **74,** 3518 (1977).
3. Maniatis, T. *et al. Cell* **15,** 687 (1978).
4. Graham, F. L. *et al. Cold Spring Harb. Symp. quant. Biol.* **39,** 637 (1974).
5. Maitland, N. J. & McDougall, J. K. *Cell* **11,** 233 (1977).
6. Bacchetti, S. & Graham, F. L. *Proc. natn. Acad. Sci. U.S.A.* **74,** 1590 (1977).
7. Wigler, M. *et al. Cell* **11,** 223 (1977).
8. Wigler, M., Pellicer, A., Silverstein, S. & Axel, R. *Cell* **14,** 725 (1978).
9. Wigler, M. *et al. Proc. natn. Acad. Sci. U.S.A.* **76,** 1373 (1979).
10. Willecke, K., Klomfass, M., Mirau, R. & Dohmer, J. *Molec. gen. Genet.* **170,** 179 (1979).
11. Graf, L. H., Urlaub, G. & Chasin, L. *Somatic Cell Genet.* (in the press).
12. Kit, S., Dubbs, D., Piekarski, L. & Hsu, T. *Expl Cell Res.* **31,** 297 (1963).
13. Littlefield, J. *Science* **145,** 709 (1974).
14. Bolivar, F. *et al. Gene* **2,** 95 (1977).
15. Graham, F. L. & van der Eb, A. J. *Virology* **52,** 455 (1973).
16. Southern, E. M. *J. molec. Biol.* **98,** 503 (1975).
17. Wigler, M. *et al. Cell* **16,** 777 (1979).
18. Maniatis, T., Jeffrey, A. & Kleid, D. G. *Proc. natn. Acad. Sci. U.S.A.* **72,** 1184 (1975).
19. Weinstock, R., Sweet, R., Weiss, M., Cedar, H. & Axel, R. *Proc. natn. Acad. Sci. U.S.A.* **75,** 1299 (1978).
20. Sutcliffe, J. G. *Nucleic Acids Res.* **5,** 2721 (1978).
21. Curtis, R. III *et al.* in *Recombinant Molecules: Impact on Science and Society* (eds Beers, R. F. & Basset, E. G.) 45–56 (Raven, New York, 1977).
22. Kit, S., Leung, W.-C., Jorgensen, G. N., Trkula, D. & Dubbs, D. R. *Cold Spring Harb. Symp. quant. Biol.* **39,** 703 (1974).
23. Dodgson, J. B., Strommer, J. & Engel, J. D. *Cell* **17,** 879 (1979).
24. Benton, W. D. & Davis, R. W. *Science* **196,** 180 (1977).
25. Colbere-Garapin, F., Chousterman, S., Horodniceaunu, F., Kourilsky, P. & Garapin, A.-C. *Proc. natn. Acad. Sci. U.S.A.* **76,** 3755 (1979).

LETTERS

An upper limit on the EUV flux from HD192273

Don C. Barry

Department of Astronomy, University of Southern California, Los Angeles, California 90007

Bill R. Sandel, Jay B. Holberg, William T. Forrester & A. Lyle Broadfoot

Space Sciences Institute, University of Southern California, Tucson Laboratories, Tucson, Arizona 85713

Cash *et al.*[1] reported the possible detection of an extreme ultraviolet (EUV) source in the constellation Pavo. They suggested HD192273 as a possible candidate and cited a TD-1 satellite observation indicating that this star is also unexpectedly bright at 1,565 Å. Wegner[2] reported visual photometric and spectroscopic data for HD192273 and concluded that it is apparently a normal B-type star. Shipman and Wegner[3] have reviewed the available data on HD192273 and suggested that all of the observations could be explained if this object were an analogue of HZ22, an evolved, mass-exchange, binary. We report here a recent observation with the UV spectrometer (UVS) aboard the Voyager 1 spacecraft. An upper limit (2σ) of 8×10^{-3} photon cm^{-2} s^{-1} Å^{-1} is placed on the 534–776 Å flux from HD192273 at the time of observation. This is ~10% of the 500–780 Å flux reported from Pavo by Cash *et al.* The 1,565 Å flux observed by TD-1 is confirmed and is consistent with the stellar parameters determined by Wegner. Discounting the possibility that HD192273 is an EUV variable, it is probably not the potential source reported by Cash *et al.*

The Voyager 1 UVS is an objective grating instrument covering 534–1,701 Å with 126 contiguous photon counting pixels having maximum sensitivity shortward of 1,000 Å (refs 4, 5). Pre-flight laboratory calibrations were based on calibrated channeltron detectors, traceable to NBS standard photodiodes, and indicate a transfer error of ±15% from the photodiodes. The in-flight EUV sensitivity has been demonstrated in several
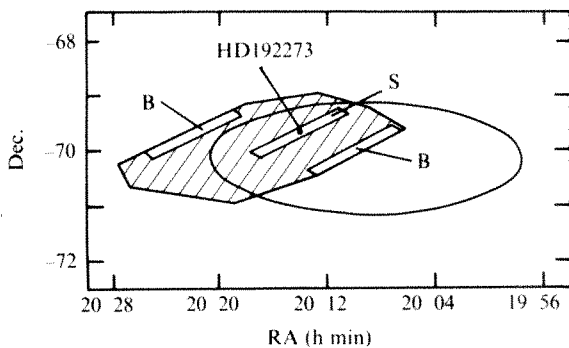
Fig. 1 The shaded area shows the portion of the sky mapped in this observation. The $0.1 \times 0.86°$ UVS field of view is shown in three positions corresponding to the spatial bins from which the stellar signal (S) and the background spectra (B) were taken. The ellipse shows the position of the 100% response contour of Cash *et al.* when a possible detection of an EUV source was made. Further mapping of this area by the Voyager UVS is planned.

ways: the Voyager 1 UVS has observed the integrated solar disk. Comparison with the published solar spectrum[6] confirms the EUV sensitivity calibration. UVS measurements of Io's ion torus[7] (534–1,000 Å) are consistent with the optical observations at other wavelengths, *in situ* measurements, and theoretical models of the torus. The recorded strength of He I 584 Å scattered by the interstellar medium confirms the EUV sensitivity of the UVS during the observation reported here.

The UVS was pointed towards HD192273 between 01.14 UT on 27 November 1979 and 21.13 UT on 28 November 1979. Spacecraft attitude control motions caused the field of view to wander over a portion of the sky shown in Fig. 1. Using pointing information, the spectra were accumulated into spatial bins. The bin (S in Fig. 1) having the strongest signal in the 912–1,701 Å range corresponds in position to HD192273. No other source was detected within the shaded area. A background spectrum was accumulated from the two areas B on Fig. 1. This background spectrum (total integration time 2,496s) was appropriately subtracted from the stellar spectrum (total integration time 2,880s) to correct for the He I 584 Å and H Lyα emission scattered by the interstellar medium plus any cosmic UV radiation.

No statistically significant signal was found in the 534–776 Å range. The measured count rate corresponds to a flux of $(2 \pm 3) \times 10^{-3}$ photon cm^{-2} s^{-1} Å^{-1} over the wavelength range. The stated 1σ uncertainty includes counting statistics and the background subtraction. The upper limit (2σ) on the EUV flux is 8×10^{-3} photon cm^{-2} s^{-1} Å^{-1} or about 10% of the flux reported by Cash *et al.* from Pavo. Of course, not all the area included in their field has been mapped in this observation, and it is possible that a source exists outside the area over which the observations over-lap. Nor can we exclude the possibility that the EUV source is variable. However, it is unlikely that HD192273 varies by more than a factor of 10 in the EUV as it is not known to vary in the visible or UV. The UVS observed a 1,396–1,701 Å flux of 1.4 ± 0.3 photon cm^{-2} s^{-1} Å^{-1} in fair agreement with the flux of 1.7 photon cm^{-2} s^{-1} Å^{-1} observed by TD-1 in the 1,400–1,730 Å band[8].

The latter (1,565 Å) flux is too bright for the Henry Draper type of B8 but not for an earlier spectral type. Wegner determined $T_e = 27,000$ K and log $g = 4.8$ from his visual observations. Using the model atmosphere results of Kurucz[9] for these parameters, the theoretical ratio of the flux in the 1,565 Å band to the flux in the V band was estimated to be ~30. The absolute calibration of α LYR (ref. 10) provides a relation between apparent magnitude and flux. The observed[3] $V = 8.83$ for HD192273 and the magnitude–flux relation imply a predicted flux of 1.2 photon cm^{-2} s^{-1} Å^{-1} at 1,565 Å which is in reasonable agreement with both the observed Voyager 1 and TD-1 fluxes.

We conclude that HD192273 is probably not the 'potential' EUV source reported by Cash *et al.* and that it is not abnormally bright at 1,565 Å for its effective temperature and gravity. However, the problem of understanding its apparently large distance from the galactic plane in terms of its small radial velocity and short life expectancy remains.

Note added in proof: Additional UVS observations of the Pavo region were obtained in February 1980. Observations of HD192273 on 6 and 18 February are consistent with the upper limit on EUV flux given above. A search of 95% of the field of Cash *et al.*[1] showed no evidence of an EUV source; a 2σ upper limit of 3.2×10^{-2} photon cm^{-2} s^{-1} Å^{-1} can be placed on any source within the area. In addition, no FUV (911 – 1,200 Å) sources other than HD192273 were found within the search area, down to a sensitivity threshold of 0.08 the brightness of HD192273. It is unlikely that HD192273 is an EUV variable, as no EUV flux has been detected in three separate observations.

1. Cash, E. *et al. Astrophys. J.* **219,** 585–588 (1978).
2. Wegner, G. *Mon. Not. R. astr. Soc.* **186,** 15p–18p (1979).
3. Shipman, H. L. & Wegner, G. A. *Nature* **281,** 126–127 (1979).
4. Broadfoot, A. L. *et al. Space Sci. Rev.* **21,** 183–205 (1977).
5. Shemansky, D. E., Sandel, B. R. & Broadfoot, A. L. *Astrophys. J.* **231,** 35–47 (1979).
6. Donnelly, R. F. & Pope, J. H. *NOAA Tech. Rep. ERL 276-SEL 25* (US Government Printing Office, Washington DC, 1973).
7. Broadfoot, A. L. *et al. Science* **204,** 979–982 (1979).
8. Thompson, G. I. *et al. Catalogue of Stellar Ultraviolet Fluxes* (Science Research Council, London 1978).
9. Kurucz, R. L. *Astrophys. J. Suppl.* **40,** 1–340 (1979).
10. Tug, H., White, N. M. & Lockwood, G. W. *Astr. Astrophys.* **61,** 679–684 (1977).

Spectra of SO₂ frost for application to emission observations of Io

L. S. Slobodkin, I. F. Buyakov & N. S. Triput

Luikov Heat and Mass Transfer Institute, Byelorussian Academy of Sciences, Minsk, 22078, USSR

R. D. Cess, J. Caldwell & T. Owen

Laboratory for Planetary Atmospheres Research, State University of New York, Stony Brook, New York 11794

We have obtained, and describe here, laboratory reflection spectra of SO₂ frost from 6 to 14 μm. For rapid deposition of the frost layer at a deposition temperature of 80 K, the frost exhibits a strong absorption band at 7.5 μm, consistent with the possible Voyager 1 identification of such a band due to suspended solid SO₂ particles within Io's atmosphere. This compatibility does not, however, exist if the frost layer is formed at 140 K or if the layer is formed slowly. Thus it may be possible to obtain information concerning the particle formation process using more detailed laboratory SO₂ frost spectra.

Although spectra of the Galilean satellites Europa, Ganymede and Callisto clearly indicate water ice absorption features representing free water in the form of surface frost[1], no water ice features have been identified in reflection spectra of Io. Instead, it has been suggested[2,3] that observed Io absorption bands in the near IR represent solid SO₂. The presence of solid SO₂ on Io's surface is compatible with the recent Voyager 1 IR experiment[4], from which gaseous SO₂ was identified on Io, with an estimated abundance consistent with a gaseous SO₂ atmosphere which is in equilibrium with solid SO₂ at the local surface temperature. As Pearl *et al.*[4] have point out, an obvious source of gaseous SO₂ consists of volcanic plumes with possible precipitation of solid

SO_2 particles from the plumes. This hypothesis would be compatible with the suggestive identification of solid SO_2 within Io's atmosphere from Voyager I emission observations over a warm region containing a volcanic feature[4]. This tentative identification refers to a possible weak absorption between 1,320 and 1,340 cm^{-1} (7.5 μm). Existing laboratory transmission spectra[5–8], for formation temperatures ranging from 20 to 93 K place the ν_3 band of solid SO_2 in this region.

But the spectra of condensed phases depends on several factors. For example, Slobodkin, et al.[9] have shown that the spectral locations of solid NH_3 bands can depend on deposition rate and deposition temperature. Moreover, they emphasize that solid particles, comprising either a cloud or a haze, are formed rapidly, and that laboratory frost-layer simulation should attempt to mimic such a rapid formation process. The point is that the polycrystalline structure of the solid is influenced by formation rate. In view of the considerable current interest concerning the composition of Io's surface and atmosphere, we have obtained new IR SO_2 frost spectra for a limited range of deposition rates and deposition temperatures. Reflection spectra have been obtained from 6 to 14 μm for 3-mm thick frost layers which were formed at 80 K, subsequently warmed to 140 K, and then cooled back to 80 K. Because, for a given formation rate, there is no distinction between warming a frost layer to a given temperature or forming it at that temperature[9], the 140 K spectra would be representative of a 140 K formation temperature. Two deposition rates were used; slow deposition at 7.5 μm min^{-1} and rapid deposition at 1,500 μm min^{-1}.

The slow deposition spectra are shown in Fig. 1. The rather minor changes in the spectra on warming from 80 to 140 K could be indicative of a polycrystalline phase transition. The 80 K (cooled from 140 K) spectrum is quite similar to the 140 K spectrum, as would be expected, as phase transitions do not occur on cooling. The 8.9-μm feature in this spectrum seems to be a blend of the 8.8-μm band and a weaker 9-μm feature, both of which appear in the other two spectra, rather than a shift in the location of the 8.8-μm band. The spectra in Fig. 1 do not agree with the transmission spectra for 20–93 K formation[5–8]. In these studies the ν_1 and ν_3 bands are located at 8.7 and 7.5 μm, respectively. Our spectra indicate a slightly shifted ν_1 band, and there are considerable differences in the 7–8 μm region. But this seems to be due to formation rate differences.

Our rapid deposition spectra are shown in Fig. 2. For 80 K formation the 7.5 and 8.7 μm band locations coincide precisely with the 20–93 K transmission spectra[5–8]. This suggests that the polycrystalline phase which was produced in obtaining the
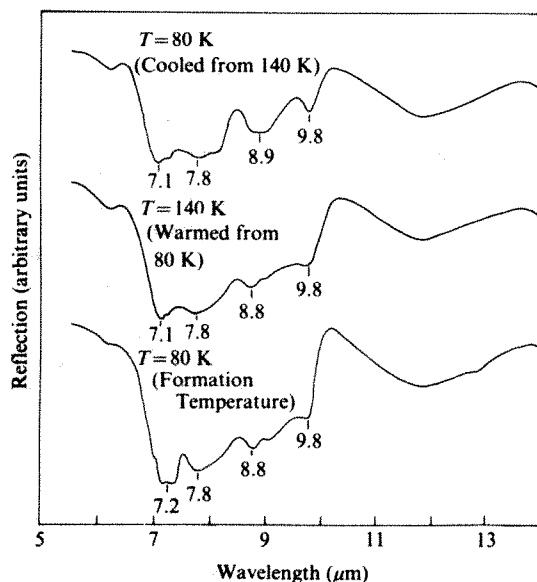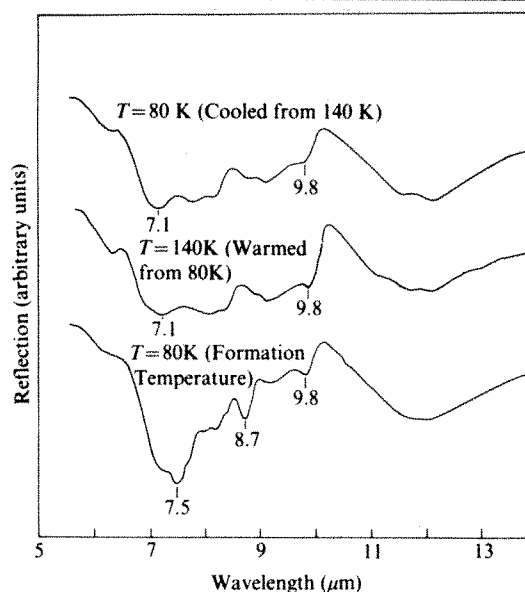
Fig. 2 Solid SO_2 reflection spectra for a frost layer formed by rapid deposition (1,500 μm min^{-1}).

transmission spectra actually coincides with our rapid-deposition frost layers. The 9.8-μm band, which appears clearly in all our spectra, is not mentioned in any of the transmission studies. But as pointed out by Herr and Pimentel[10], reflection spectra, in contrast with transmission spectra, tend to enhance weak absorption features, and thus the possibility exists that the 9.8-μm band was simply not evident within transmission spectra. Indeed Smythe et al.[2], in their near-IR reflection study, have identified several solid SO_2 bands which apparently were not evident in the most detailed of the transmission spectra[7]. The weak band at 6.2 μm, as well as the broad feature at ~11.8 μm, are most likely due to contaminant water which is also present in the near-IR reflection spectra of Smythe et al.[2], and Fanale et al.[3].

As previously discussed, we anticipate the rapid deposition frost layer to be representative of solid SO_2 particles formed within Io's atmosphere, and this is consistent with the possible identification of a solid SO_2 absorption feature at 7.5 μm from the Voyager I emission observations[4]. But this would only be compatable with the 80 K formation spectrum of Fig. 2. Evidently, at least for rapid deposition, there is a significant alteration in the structure of our frost layer on warming from 80 to 140 K, with the 140 K spectrum showing no feature which could be attributed to the possible Voyager I identification. This structural change could be partially due to changes in grain size on warming the layer, but grain-size changes should not induce a shift in band locations[11]. Instead, at least for rapid deposition, a significant polycrystalline phase transition is probably the primary cause of the alteration in our rapid-deposition spectra on warming from 80 to 140 K. The consistency of our rapid-deposition 80 K spectrum with the 93 K transmission spectra[5,6] would in turn imply that the phase transition occurs between 93 and 140 K. This further suggests that if the observed Voyager I absorption feature is due to solid SO_2 particles within Io's atmosphere, then the particles are formed at a temperature below 140 K.

If the above hypothesis is correct, it would be useful for diagnostic purposes to have laboratory spectra available covering a broad range of wavelengths and formation temperatures. We plan to obtain such spectra.

Fig. 1 Solid SO_2 reflection spectra for a frost layer formed by slow deposition (7.5 μm min^{-1}).

supported by the Byelorussian Academy of Sciences and the NSF with the latter support stemming from NSF grant no. ENG. 77-09124.

1. Clark, R. N. & McCord, T. B. *Icarus* (in the press).
2. Smythe, W. D., Nelson, R. M. & Nash, D. B. *Nature* **280**, 766 (1979).
3. Fanale, F. P., Brown, R. H., Cruikshank, D. P. & Clarke, R. N. *Nature* **280**, 761–763 (1979).
4. Pearl, J. *et al. Nature* **280**, 755–758 (1979).
5. Giguere, P. A. & Falk, M. *Can. J. Chem.* **34**, 1833–1835 (1956).
6. Wiener, R. N. & Nixon, E. R. *J. chem. Phys.* **25**, 175 (1956).
7. Barbe, A., Delahaigue, A. & Jouve, P. *Spectrochim. Acta* **27A**, 1439–1449 (1971).
8. Anderson, A., & Campbell, M. C. W. *J. chem. Phys.* **67**, 4300–4302 (1977).
9. Slobodkin, L. S., Buyakov, I. F., Cess, R. D. & Caldwell, J. *J. quant. Spectr. Radiat. Transfer* **20**, 481–490 (1978).
10. Herr, K. C. & Pimentel, G. C. *Science* **166**, 496–499 (1969).
11. Kortum, G. *Refectance Spectroscopy* (Springer, New York, 1969).

A fluid-dynamical model of differentiation and layering in magma chambers

J. Stewart Turner

Research School of Earth Sciences, The Australian National University, Box 4, Canberra 2600, Australia

Large igneous intrusions characteristically have a systematic gradation in mineral composition from top to bottom, often associated with a horizontally layered structure on several scales[1,2]. Current theories[3] invoke the settling of denser crystals as the mechanism responsible for separating the various components from the solidifying melt. However, recent laboratory experiments[4,5], using crystallization from aqueous solutions to model the essential fluid-dynamical processes, have documented another significant way in which chemical differentiation of the liquid can be caused by relative motion between crystals and the remaining melt. The growth of crystals of a denser component on a side-wall boundary leaves behind less dense fluid. (This corresponds to the behaviour of many common magmas, notably those of the calc-alkaline series. However, in tholeiitic basalt magmas, of the type which commonly form layered intrusions, crystallization leads to an increase in density of the remaining melt.) The lighter fluid rises to the top of the chamber in a boundary layer flow, which builds up a stable density gradient, by the 'filling box' mechanism[6,7] previously discussed in other contexts. In the latest experiments reported here, the process of differentiation is demonstrated explicitly: starting with a homogeneous mixture of two solutes in water, crystallization at a vertical boundary produces overall vertical composition gradients, as well as density stratification accompanied by smaller scale layering.

Previous, more extensive experiments[4] have systematically examined the additional effects due to crystallization in a 'double-diffusive' system[8] (that is, one in which the difference in molecular diffusivities of the several components has an important role). Sodium carbonate solution was chosen as the working fluid, because of its high solubility and large change in solubility with temperature, and various initial density distributions and cooling configurations were explored. Potassium carbonate has been used as the second solute in both the previous and the present experiments. The geometry adopted for the new experiments was suggested by the observations[9] of basaltic pillars on the sea floor, which are cooled by water circulating through a hollow conduit along their centres, but this analogy is immaterial for the present purpose and will not be pursued further here. The results are believed to have a more general significance, and depend only on the occurrence of crystallization at any side boundary.

There has been much recent discussion[10] about the non-newtonian behaviour of natural magmas. A finite yield strength
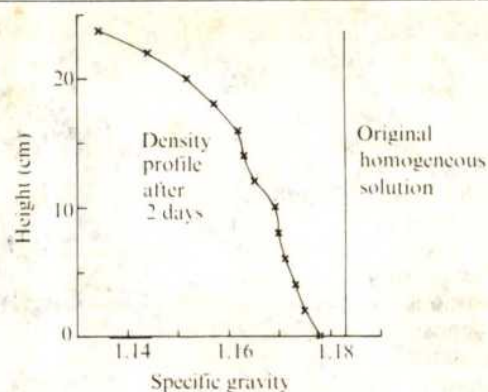
Fig. 1 The density profile produced in Na_2CO_3 solution, by the upflow accompanying crystallization at a central rod, 47.5 h after cooling began. The initial homogeneous density distribution is also shown. (The refractive index of small samples withdrawn from the tank was the property actually measured, with a calibration to relate this to density.)

can certainly inhibit the settling of small crystals, but such effects should be less important in the present case. First, crystallization at a boundary will leave the adjacent melt relatively free of crystals in suspension, so removing one likely cause of a non-newtonian viscosity. Second, a boundary layer of less dense fluid with increasing total buoyancy will eventually begin to flow upwards, whatever the nature of the viscosity. Our experiments using aqueous solutions should thus reproduce the important overall features of the prototype flows.

The experimental tank was made of Perspex, 40 cm × 20 cm in cross-section and 30 cm deep. It was fitted with a 9-mm o.d. copper tube, projecting vertically through a seal in the centre of the base and extending the whole depth of the tank. All the runs described below were started by filling the tank to a depth of ~25 cm with a homogeneous solution (or mixture of solutions), covering it with a floating, insulating lid, and then cooling it from the centre by circulating liquid coolant through the central tube from a bath held at known temperature.

Consider first an experiment using a single solute, Na_2CO_3 in an aqueous solution of specific gravity 1.183. When coolant, at 0 °C, was pumped through the central tube, a cold downflow was observed near the central rod. After a few minutes, however, crystallization began, with the crystals adhering to the cooled surface, and a strong upflow was seen instead. This upflow occurs because the formation of crystals of $Na_2CO_3 \cdot 10H_2O$, of specific gravity 1.44, leaves behind a boundary layer of depleted solution which is less dense. This layer, in which the change of concentration more than compensates for the density increase due to the decreased temperature, rises to the top of the chamber. The lightest (most depleted) solution is continually fed
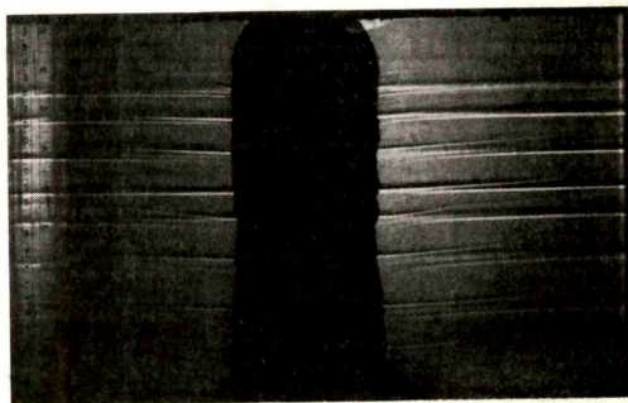
Fig. 2 Shadowgraph of the experiment described in the caption to Fig. 1. The axisymmetric crystal mass, shown in silhouette, is surrounded by 'double-diffusive' layers, produced by cooling the stable density gradient at the centre.

Fig. 3 Shadowgraph showing the layers in the fluid, and associated scallops on the crystals, formed by cooling a homogeneous solution of Na_2CO_3. (Initial specific gravity = 1.164, coolant temperature −2.5 °C. Photograph at 44 h.)

to the top of the region, and density stratification is eventually built up (see Fig. 1).

Another striking feature of this stratification is shown in Fig. 2, taken just before the density profile was measured. The shadowgraph reveals a series of layers (of which there are also some indications in the rather coarse density profile of Fig. 1). These are a consequence of the double diffusive instabilities characteristic of top and side cooling of a stable composition gradient[8]. In the present case, the side cooling probably dominates, and the layering is equivalent to that produced near a melting iceblock; this effect has recently been studied[11,12] in the context of melting icebergs.

The upflow in the boundary layer which feeds light fluid to the top of the box results in the individual layers being pushed downwards with time. Thus the crystals do not in general remain in the same relation to the interfaces as they grow, and any persistent layer structure in the crystals tends to be obliterated. At a later stage of other experiments, however, the interfaces did stay at a fixed level, and the growth (or in some cases resolution) of the sodium carbonate crystals is then clearly affected by the existence of, and circulation in, the fluid layers (see Fig. 3). Again there are close analogies to what has been observed[12] during the melting of vertical ice walls.

The behaviour to be expected when there is more than one solute can be deduced (at least in retrospect) from what has already been presented, but this case is of such importance that it is worth studying directly. The tank was filled with a homogeneous mixed solution of specific gravity 1.358, made up of Na_2CO_3 (21.45 wt %) and K_2CO_3 (11.87 wt %). In this case, the coolant was gradually brought down to 0 °C from room temperature (20.4 °C). Crystals nucleating near the central rod at first did not remain attached, but fell out to form a conical pile at the base. As the temperature dropped to about 12 °C, the crystals attached themselves, the upflow of lighter fluid began, and the chamber stratified as described previously. It was found by later analysis of the crystals that pure $Na_2CO_3 \cdot 10H_2O$ was again crystallizing out. Thus as well as being depleted in sodium, the upward flowing boundary layer was relatively enriched in potassium. Instead of recording the density distribution, it is now more instructive to plot the Na/K ratio (Fig. 4). This demonstrates directly that 'differentiation' has been produced in the experimental tank. There is a systematic variation in composition of the solution with depth which becomes more pronounced with time.

Layering is also observed in this case, as shown in Fig. 5. Several of the interfaces can be clearly identified with steps in the concentration profiles, and in the associated density profile (which was measured, but is not reproduced here). Note also the smaller steps and sharp interfaces near the top of the tank. We suspect that these are 'diffusive' interfaces produced by the
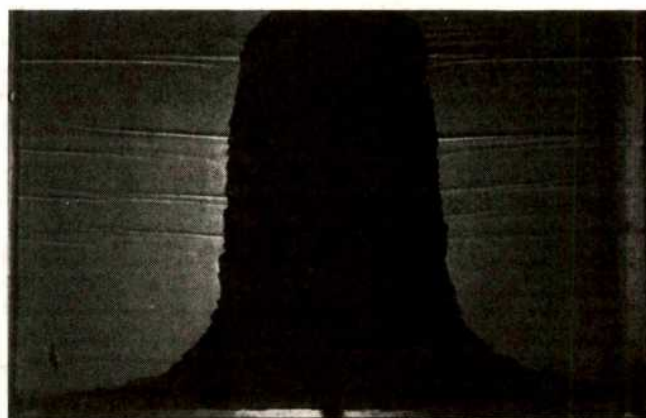
Fig. 5 Shadowgraph of the experiment described in the caption to Fig. 4, taken just before the samples were withdrawn for the concentration profile measurement. In addition to the features seen in Fig. 2, note the fine-scale 'diffusive' layers at the top.

opposing vertical composition gradients (K_2CO_3 being relatively more concentrated at the top), rather than by the horizontal temperature gradients responsible for the formation of the deeper layers. Similar structures have been observed in earlier experiments[4].

In conclusion, we re-emphasize that the deductions made above do not depend critically on the particular geometry chosen, or on the complexity of the crystallizing system. The scaling problem has been considered elsewhere[4], and it has been shown that the much larger viscosity of liquid magmas is compensated for by the larger scale, so that the laboratory and prototype flows can be dynamically similar. We have drawn attention to a previously neglected fluid process, that of upflow in the boundary layer accompanying crystallization of a heavier component at a side boundary. This is in principle capable of setting up large scale concentration and density gradients through the depth of a magma chamber, and in combination with double-diffusive processes, it can also produce smaller scale layering. It seems at least worth comparing the consequences of this model with some of the detailed petrological and geochemical data on igneous intrusions.

I thank C. F. Chen, with whom these crystallization experiments were begun, D. L. Corrigan and R. Wylde-Browne for

Fig. 4 Measurements of the ratio Na/K concentrations in solution as a function of depth, produced by crystallization of $Na_2CO_3 \cdot 10H_2O$ from an initially homogeneous mixture of sodium and potassium carbonates. ×, Spot measurements after 1 day; ●, profile after 3 days (Na and K concentrations measured using atomic absorption spectrophotometry after appropriate dilution).

technical assistance, and E. Kiss for his analysis of the samples for Na and K.

1. Wager, L. R. & Brown, G. M. *Layered Igneous Rocks* (Oliver & Boyd, Edinburgh, 1967).
2. Hess, G. B. *Geol. Soc. Am. Mem.* **132,** 503–520 (1972).
3. Yoder, H. S. Jr (ed.) *The Evolution of the Igneous Rocks: 50th Anniversary Perspectives* (Princeton University Press, 1979).
4. Chen, C. F. & Turner, J. S. *J. geophys. Res.* (in the press).
5. McBirney, A. R. *J. Volcanol. geotherm. Res.* (in the press).
6. Baines, W. D. & Turner, J. S. *J. Fluid Mech.* **37,** 51–80 (1969).
7. Turner, J. S. & Gustafson, L. B. *Econ. Geol.* **73,** 1082–1100 (1978).
8. Turner, J. S. *Buoyancy Effects in Fluids* (Cambridge University Press, 1973).
9. Francheteau, J. *et al. Nature* **281,** 209–211 (1979).
10. McBirney, A. R. & Noyes, R. M. *J. Petrol.* **20,** 487–554 (1979).
11. Huppert, H. E. & Turner, J. S. *Nature* **271,** 46–48 (1978).
12. Huppert, H. E. & Turner, J. S. *J. Fluid Mech.* (1980).

Evidence from Canada and Alaska on plate tectonic evolution of the Arctic Ocean Basin

P. B. Jones*

Dome Petroleum Ltd, Box 200, Calgary, Canada T2P 2H8

A new model for the plate tectonic evolution of the Amerasian sector of the Arctic Ocean is suggested here using data from petroleum exploration on its margin. More than 500 km of late Cretaceous dextral slip is indicated for the SW–NE trending Kaltag fault system in Alaska and northwestern Canada. Terminating against the Kaltag, an older fault system trends along the Canadian Cordillera, with dextral slip of thousands of kilometres. Its offset by the Kaltag is postulated to follow the southern margin of the Canada Basin. Restoration of the offset creates a great circle lineament from the Asian end of the Lomonosov Ridge through western North America along which Jurassic–Cretaceous transform movement could have accommodated spreading about the Alpha Ridge. Accretion of the newly-formed lithosphere to a Palaeozoic Canada Basin created the Amerasian Basin in essentially its present configuration, modified by subsequent Kaltag movement.

The Arctic Ocean is divided into the Eurasian and Amerasian basins, separated by the Lomonosov Ridge. Proponents of seafloor spreading have generally agreed that the Eurasian Basin orginated through Cenozoic spreading about the Nansen (Gakkel) Ridge[1]. The origin of the Amerasian Basin, bounded by the Lomonosov Ridge and the Arctic continental margins of North America and Siberia, is more controversial[2,3]. Petroleum exploration on the continental shelf and mainland of Alaska and northern Canada provides new data on this problem. The Richardson Mountains of Northwestern Canada are part of a broad shear zone flanked on the west by the Kaltag fault system (Fig. 1), whose principal movement was during the late Cretaceous[4]. Local and regional facies changes in Lower and Upper Cretaceous sediments occur between adjacent fault blocks[5,6], suggesting an aggregate dextral slip for the entire fault and shear zone of several hundred kilometres. The youngest strata involved in faulting are of Maastrichtian and possible Palaeocene age[7]. Offshore geophysical surveys and deep drilling have delineated an Upper Cretaceous–Tertiary sedimentary basin containing >8 km of regressive clastic sediments[6,8]. The oldest sediments drilled so far are of Palaeocene age. The sediments are deformed, but the structures are synsedimentary and do not seem to be affected by the underlying belt of strike-slip faults, implying that those movements had ceased in

* Present address: ITC Ltd, 101–4th Street SW Calgary, Canada T2P 1R9.

the early Tertiary or latest Cretaceous.

The Kaltag fault system extends from western Alaska through northwestern Canada and passes northeastward beneath the Beaufort Sea[9,10]. It separates east–west trending structures of the Brooks Range from the Interior Platform and from the eastern part of the Canadian Cordillera, represented locally by the Mackenzie Mountains. From the Beaufort Sea, it is believed to follow the linear continental margin of the Canadian Arctic Archipelago[4,6,11], with minor offset by the Wegener fault, to Greenland. The trend is continued along the southern margins of the Eurasian Basin and Barents Shelf, forming a lineament 4,500 km long.

South-west of the Richardson Mountains, the Kaltag fault intersects the Tintina fault (Fig. 2). Following the trend of the Canadian Cordillera, the Tintina fault is a major strike-slip fault whose post-Palaeozoic dextral slip, based on offsets of equivalent strata, is at least 450 km[12]. It is one of several dextral strike-slip faults, sub-parallel to one another, closely associated with ophiolite zones and areas of blueschist metamorphics, trending through the Western Cordillera of North America to the America landfall of the East Pacific Rise[13,14]. Palaeolatitudes of Palaeozoic rocks west of this zone are several thousand kilometres south of palaeolatitudes of coeval strata in the North America craton and eastern part of the Cordillera[15]. Actual displacements of the Tintina and associated faults are probably much greater than the measured offsets.

The Tintina fault terminates at its northern end against the Kaltag fault. It is postulated that it was displaced 560 km northward by the Kaltag, and that the offset continuation is represented by the sourthern margin of the Canada Basin, an abyssal plain underlain by oceanic lithosphere[8,16]. Several workers have speculated on the presence of a fault bounding the Alaskan margin of the basin [11,17]. It is suggested that such a fault, herein designated the Beaufort–Laptev fault, follows the southern margin of the Amerasian Basin from the Beaufort to the Laptev Sea, at the Asian end of the Lomonosov Ridge. Although the margin is not as linear as some fault-controlled ocean margins, the irregularity may be due to modification by volcanism and sedimentation, and by the anticlockwise rotation of the sector east of long. 180° implicit in the Kaltag fault movement.

Restored to their Mesozoic continuity (Fig. 2), the Beaufort–Laptev and Tintina faults formed part of a lineament that followed a great circle from the Asian end of the Lomonosov Ridge via the Western Cordillera of North America to the landfall of the East Pacific Rise. It is suggested that this lineament was a Mesozoic transform fault zone through which Pacific seafloor spreading was transferred to spreading about the Alpha Ridge, a Mesozoic analogue of the Cenozoic fault system connecting spreading about the Nansen Ridge with opening of the North Atlantic. Major movements along this lineament ceased when the Tintina and Beaufort-Laptev sectors became separated at the end of the early Cretaceous. Subsequent Pacific seafloor spreading was perforce accommodated by subduction beneath the Aleutian Arc.

Relative to localities in North America, the apparent polar wander (APW) path shifted abruptly at the end of the Lower Cretaceous (100 Myr)[15], the time when the offset of the Tintina–Beaufort–Laptev lineament by the Kaltag fault was initiated. Although APW paths do not indicate absolute movements of the continents relative to a magnetic north pole, it is surely more than coincidence that the angular shift of the APW path is similar to the angle between the Tintina and Kaltag faults.

Spreading about the Alpha Ridge during the Jurassic and early Cretaceous created a large trapezoidal ocean basin which, through accretion to the pre-existing Canada Basin, gave rise to the Amerasian Basin in almost its present form, modified by dextral movement of its eastern margin in the late Cretaceous.

Major discontinuities of Phanerozoic sedimentary and metamorphic facies coincide with both the Kaltag and the Tintina faults[6,18]. Maps of Mississippian through Upper Cretaceous facies can be redrawn palinspastically to relate
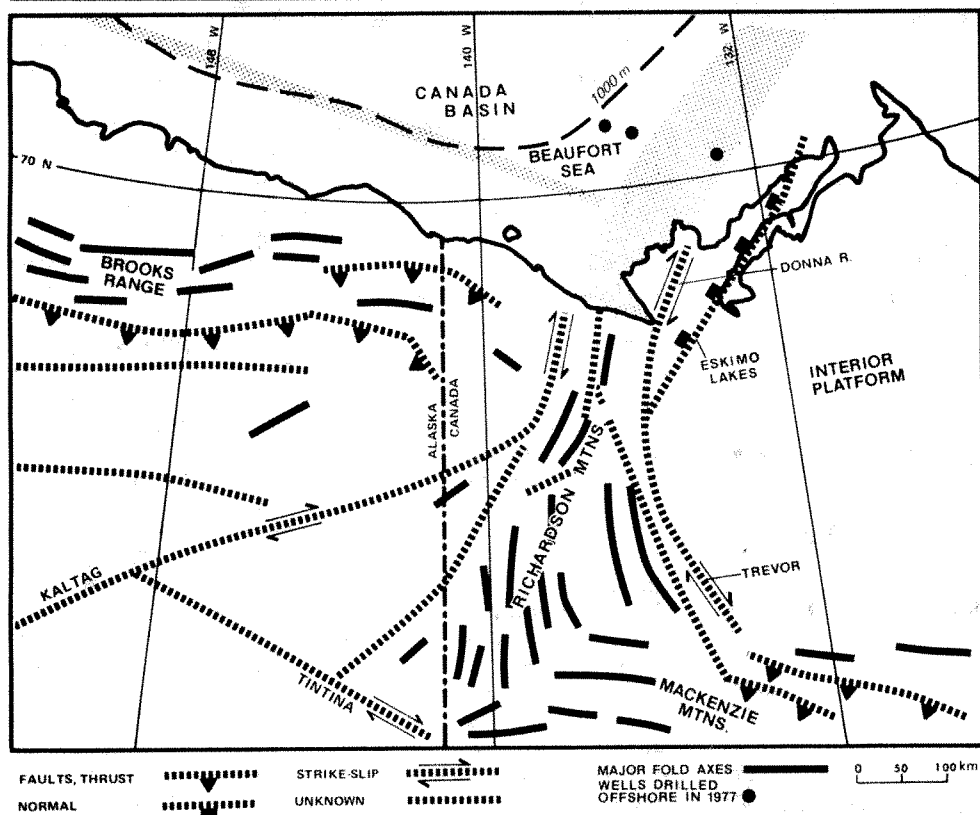
Fig. 1 Tectonic map, northwestern Canada and Alaska. Stippled areas show seaward extension of Kaltag fault and adjacent shear zone and hypothetical offset of Tintina fault. (Modified after refs 9, 24).

Fig. 2 Model for the evolution of the Amerasian Basin and associated displacements along Tintina and Kaltag faults.
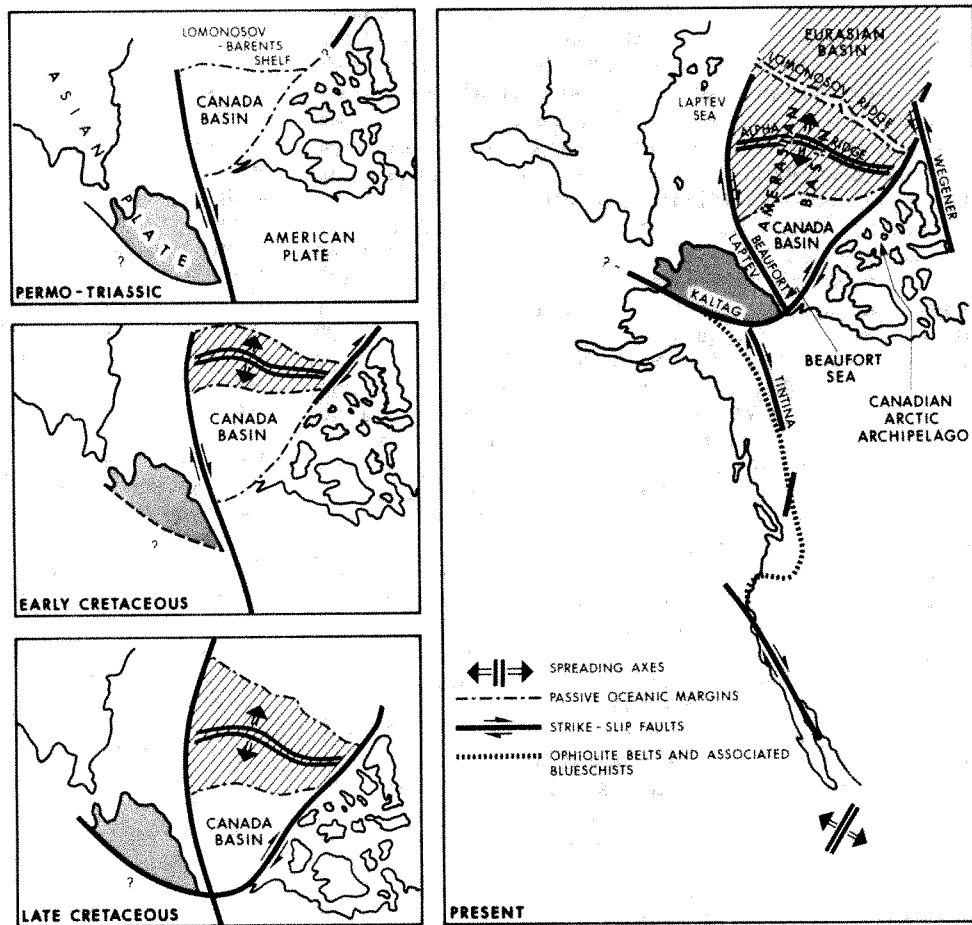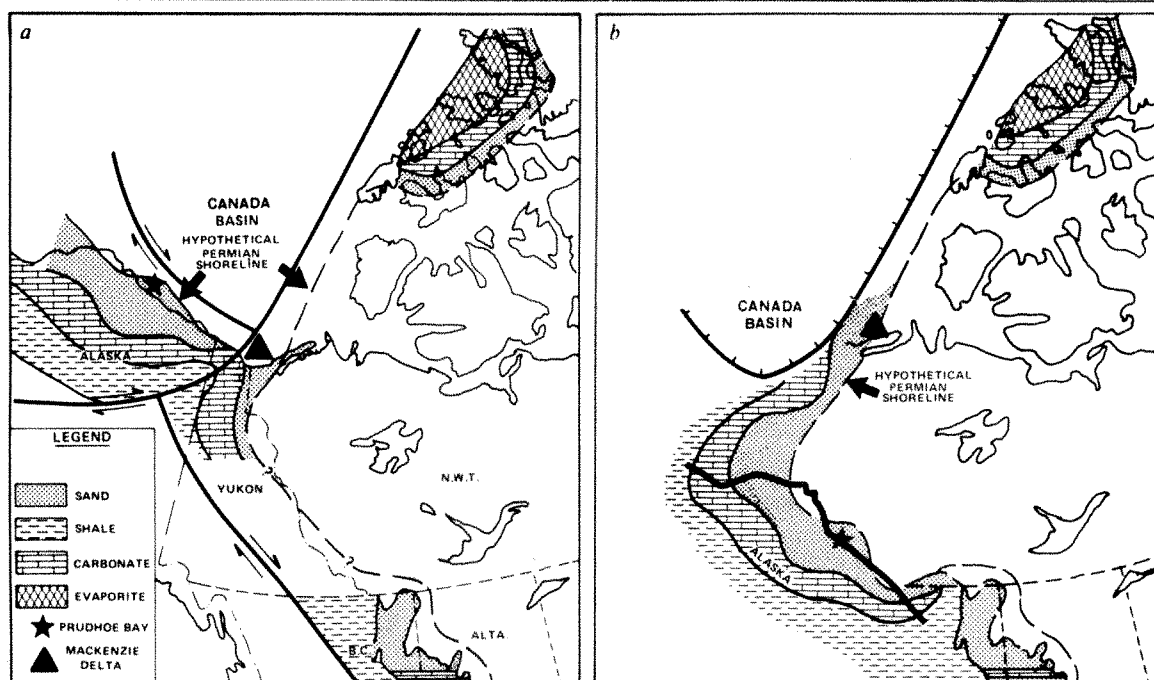
Fig. 3 *a*, Present distribution of Permian lithofacies (Modified after ref. 18). *b*, Palinspastic restoration of facies according to fault movements shown in Fig. 2.

movements of these faults to the evolution of Upper Palaeozoic and Mesozoic palaeogeography of northwestern America. The restoration of Permian facies (Fig. 3) is used as an example, since it provides a new solution to the problem of provenance of Permo-Triassic sandstones of northern Alaska, reservoir rocks in the giant Prudhoe Bay oilfield. These sediments were derived from an adjacent land mass in the area now occupied by the Canada Basin[19,20], leading many workers to conclude that their source was the Canadian Arctic Archipelago, split off from Alaska by Jurassic opening of the Canada Basin[21-23]. Figure 3 shows a common sediment source for the Permian of both northern Alaska and the Canadian Cordillera. Matching of facies across the Tintina fault entailed restoration of 1,200 km of Jurassic–Early Cretaceous dextral movement, a distance that corresponds approximately with the width of oceanic lithosphere produced by seafloor spreading about the Alpha Ridge.

This study was sponsored by the Beaufort Sea Exploration Group of Dome Petroleum Ltd. D. A. Horn, N. G. Koch, and J. K. Lentin assisted with the manuscript.

1. Vogt, P. R. & Avery, O. E. *Marine Geology and Oceanography of the Arctic Seas* (ed. Herman, V.) 84 (Springer, Berlin, 1974).
2. Churkin, M. *Arctic Geology* (ed. Pitcher, M. G.) 485–499 (American Association of Petroleum Geologists, Mem. 19, 1973).
3. Sweeney, J. F., Irvine, E. & Gever, J. W. *Arctic Geophys. Rev. Publ. Earth Phys. Branch* 45, 4, 91–99 (1978).
4. Norris, D. K. *Proc. 1973 Natn. Convention Can. Soc. Explor. Geophys.* 18—45 (1974).
5. Young, F. G. *Bull. geol. Surv. Can.* 249 (1975).
6. Lerand, M. *Future Petroleum Provinces of Canada* (ed. McCrossan, R. G.) 315–386 Canadian Society of Petroleum Geologists, Mem. 19, 1973).
7. Young, F. G., Myhr, D. W. & Yorath, C. J. *Geol. Surv. Can.* Paper 76-11 (1976).
8. Sobczak, L. W. *Bull. Can. Petrol. Geol.* 25, 698–703 (1977).
9. Yorath, C. J. & Norris, D. K., *Canada's Continental Margins* (eds Yorath, D. J. Parker, E. R. & Glass, D. J.) 589—611 (Canadian Society of Petroleum Geologists, Mem. 4, 1975).
10. Patton, W. W. & Hoare, J. M. *U.S. geol. Surv. Prof. Paper* 600-D, 147–153 (1968).
11. Herron, E. M., Dewey, J. F. & Pitman, W. C. *Geology* 2, 377–380 (1974).
12. Monger, J. W. H. *Can. J. Earth Sci.* 14, 1832–1859 (1977).
13. Monger, J. W. H. & Price, R. A. *Can. J. Earth Sci.* 16, 770–791 (1979).
14. Coleman, R. G. *J. geophys. Res.* 76, 1212–1222 (1971).
15. Irving, E. *Can. J. Earth Sci.* 16, 669–694 (1979).
16. Ostenso, N. A. & Wold, R. J. *Arctic Geology* (ed. Pitcher, M. G.) 506–516 (American Association of Petroleum Geologists, Mem. 19, 1973).
17. Grantz, A., Holmes, M. L. & Kosoki, B. A. *Canada's Continental Margins* (eds Yorath, C. J., Parker, E. R. & Glass, D. J.) 629–700 (Canadian Society of Petroleum Geologists, Mem. 4, 1975).

18. Ziegler, P. A. *The Development of Sedimentary Basins in Western and Arctic Canada* (Alberta Society of Petroleum Geologists 1969).
19. Detterman, R. L. *Pac. Sect. Am. Ass. Petrol. Geol.*, Los Angeles, 01-013 (1970).
20. Brosgé, W. P. & Dutro, J. T. *Arctic Geology* (ed. Pitcher, M. G.) 361–375 (American Association of Petroleum Geologists, Mem. 19, 1973).
21. Tailleur, I. L. *Arctic Geology* (ed. Pitcher, M. D.) 526–535 (American Association of Petroleum Geologists, Mem. 19, 1973).
22. Rickwood, F. K. *Pac. Sect. Am. Ass. Petrol. Geol.* Los Angeles, L1–L11 (1970).
23. Tailleur, I. L. & Brosgé, W. P. *Pac. Sect. Am. Ass. Petrol. Geol.* Los Angeles, E20 (1970). E10–E20 (1970).
24. King, P. B. (Compiler) *Tectonic Map of North America* (US Geolog. Survey 1969).

Large historical earthquakes and seismic risk in Northwest Syria

J. P. Poirier, B. A. Romanowicz, & M. A. Taher

Institut de Physique du Globe, Université Paris VI, 4 place Jussieu, 75230 Paris Cedex 05, France

Arabic documents and manuscripts containing detailed descriptions of material damage and ground deformation due to earthquakes in northwestern Syria have been used to establish a catalogue of local seismicity and assign epicentral intensities to the earthquakes. Large earthquakes affecting the northern Syrian fault system apparently have a recurrence interval of about 340±60 yr. Here we use this figure and a relationship between recurrence interval and seismic moment, recently proposed by Molnar, to estimate the maximum seismic moment $(0.5 \times 10^{27} \leqslant M_0^{Max} \leqslant 3.7 \times 10^{27})$ and the magnitude $(7.1 \leqslant M_w \leqslant 7.7)$ of the largest earthquakes in northwestern Syria. Such an earthquake is not expected for at least one century but an earthquake with magnitude $6 \leqslant M_w \leqslant 7$ might occur in the near future.

The great linear fault system which begins near the Dead Sea rift and continues, north of Lebanon, by the Syrian faults has exhibited only a moderate seismicity since earthquakes have been instumentally recorded (since the turn of the century).

However, archaeological and historical documents show that major earthquakes have affected Palestine and Syria in earlier times. Many biblical events can be interpreted as great earthquakes[1] affecting the Dead Sea system. Further north, Antioch, once the capital of Syria (now Antâkya in Turkey) and one of the great cities of the Mediterranean ancient world was repeatedly destroyed by terrible earthquakes[2]. Ambraseys[3] showed, and it is now generally accepted, that the instrumental record is too short to give an unbiased image of the seismicity of a given area and that historical records must be used. Thus, for large shallow earthquakes at plate boundaries, it has been possible to define recurrence intervals for large earthquakes around the Pacific and in the Caribbean[4] and forecast that shocks should occur in the near future in areas for which the recurrence interval was nearly the length of time elapsed since the last large shock. Nur and Reches[1] have recently found a recurrence interval of 200 yr for 6–7 magnitude earthquakes on the Dead Sea system.

From Arabic manuscripts and documents, Taher[5] has gathered data on historical earthquakes in the Near Middle East from the seventh up to the eighteenth century. Clearly, many earthquakes essentially affected the region of Antioch, Aleppo, the Border zone (north of Antioch along the Turkish border) and the Orontes Valley (Hama, Homs, and so on). This region corresponds to the area north of Lebanon, threaded by the Syrian fault system which comprises the straight Masyâf fault, the Gharb and Antioch grabens and the Karasu fault (Fig. 1). There is field evidence[6] that the whole system functions as left lateral strike-slip faults, thus constituting the northern part of the transform fault bounding the Arabian plate on the west, the southern part of which forms the Dead Sea system which has been shown to be the seat of a sinistral strike-slip motion[1,7]. The northern and southern parts of the fault system are separated by the compressive Lebanon region and can be considered as different rupture zones. It is, therefore, reasonable to concentrate on the seismic activity of the Syrian fault system alone. Accordingly we catalogued local seismicity (Table 1) using data from: Greek and Roman historians[2] from AD 52 to 588; Taher[5] for the period covered by arabic texts (seventh—eighteenth century); Karnik[8] for the nineteenth century and instrumental seismicity up to 1951; the ISC Bulletin (Edinburgh) from 1951 to the present.

We considered only the meizoseismal zone in the region of Antioch, Aleppo and the Orontes Valley. Epicentral intensities I_0, on the Mercalli modified scale, have been assigned to the earthquakes by using the description of damage given in the documents.

We find essentially two classes of earthquakes: the ones with $VII \leq I_0 \leq X$ and the ones with $I_0 \geq X$ for which there is evidence of ground deformation of tectonic origin and/or particularly great damage. We did not include the shocks with $I_0 < VII$ nor those with $M_L < 5$. The spectrum of epicentral intensity I_0 versus time displays a rather regular pattern with two recurrence intervals (Fig. 2): Large earthquakes ($I_0 \geq X$) occurred in AD 115, 528, 859, 1139 and 1822 with a recurrence interval:

$$T_1 = 341 \pm 62 \, yr$$

smaller earthquakes ($VII \leq I_0 < X$) occur with a recurrence interval:

$$T_2 = 71 \pm 51 \, yr$$

Quakes with $I_0 \geq VII$ reported at dates differing by <5 yr were counted as one in the average). Although the earthquake of AD 115, under Trajan was very severe, the evidence to assign it an intensity $I_0 \geq X$ is not as good as for the others; however, if the unmistakable quasi-periodicity is to have a physical meaning, the earthquake of AD 115 should be included. A gap in the spectrum for smaller earthquakes between 1408 and 1822 is attributed not to the lack of seismicity but to the lack of chroniclers in Damascus under the Ottoman rule: only the great earthquakes felt in a wide area would have been recorded.

Molnar[9] recently estimated the average recurrence interval T

of events with seismic moments $\geq M_0$ but not greater than M_0^{max} (the seismic moment of the largest earthquakes which have occurred on the fault):

$$T = \frac{(M_0^{max})^{1-\beta} M_0^{\beta}}{(1-\beta)\dot{M}_0^{\Sigma}}$$

where $\beta \simeq \frac{2}{3}$ and where $\dot{M}_0^{\Sigma}$ is the average production rate of seismic moment given by:

$$\dot{M}_0^{\Sigma} = \mu l L \bar{V}$$

where μ is the rigidity of the crust; l, the width of the fault; L, the active length of the fault system and $\bar{V}$, the average rate of motion along the fault.

We will use Molnar's formula, not to estimate the recurrence intervals from the knowledge of the seismic moments but the other way round, for the following reasons: our historical evidence refers to local earthquakes, and all reports of damage refer to the same geographical area, hence, we can compare the quakes on the basis of the importance of the damage and of the ground deformation. We therefore assume that the earthquakes to which we have assigned the maximum epicentral intensity on this basis (and which have a recurrence interval $T_1 \simeq 341$ yr) are the ones which have the maximum seismic moment M_0^{max}.

We can now estimate M_0^{max} from Molnar's formula, assuming reasonable values for the parameters β, μ, l, L and $\bar{V}$.
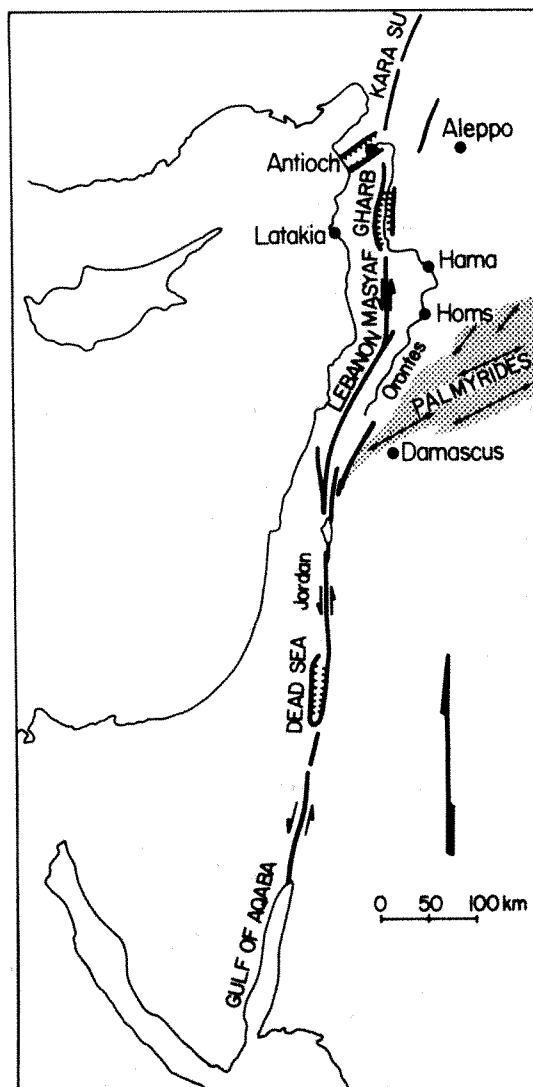
Fig. 1 Simplified map of the Dead Sea–Syrian faults system.

Table 1 Historical and instrumental seismicity

Date (AD)			I_0	M_L
52	Antioch	Destructions	VIII–IX	
115	Antioch	Heavy destructions	X–XI	
340	Antioch	Heavy destructions	IX	
394	Antioch	Heavy destructions	IX	
396	Antioch	Heavy destructions	IX	
458 September	Antioch	80,000 victims	IX	
526 May 29	Antioch	Very severe earthquake	IX–X	
528 November 29	Antioch	A mountain fell into the Euphrates at Quludhya, the Euphrates shifted its bed	X–XI	
581	Antioch	The suburb Daphne was destroyed	VIII–IX	
588 October 31	Antioch	Destroyed, 60,000 victims	IX	
634	Aleppo	Ramparts and fortress destroyed	VIII	
713 March 20	Antioch	Completely destroyed	IX	
859 December	Antioch	1,500 houses destroyed, 90 towers fell from the ramparts, Jebel al Aqra' (Bald mountain or Mons Casius 30 km SW of Antioch, close to the sea, 1,759 m high) "fell into the sea". A river disappeared into the ground; Urfa, Adana, Tarsus, Misis, Homs, Damascus destroyed	X–XI	
951 September	Aleppo	Heavy destructions, Ra'ban, Duluk (fortress between Aleppo and Antioch) destroyed	VIII–IX	
972	Antioch	Emperor Johannes Shamshik send 12,000 workers to rebuild the city	IX	
1002	Syria	Border zone, many destructions	VIII–IX	
1063 July	Antioch	Latakia, Tripolis, Acre	VIII	
1091 September 17	Antioch	70 towers fell from the ramparts	IX	
1139 November	Aleppo	Destroyed, evacuated by the inhabitants "The earth shook and the stones shook like grain in the winnowing basket"	X–XI	
1156–1159	Orontes	Aleppo, Hama, Afamya (Apamea), Shayzar (Larissa) Homs (Emessa)	IX–X	
1170 June 30	Aleppo	Totally destroyed, 80,000 victims; Damage in Orontes Valley	IX–X	
	Antioch	St Peters cathedral collapses over the patriarch		
1343 January 1	Membij	Destroyed, 5,700 victims, Aleppo fortress destroyed	IX	
1404 February 11	Aleppo	Heavy destructions, Latakia fortress destroyed	IX	
December 5	Aleppo	Three shocks	VII	
1408 December 30	Antioch	Heavy destructions, the ice fell off the top of Jebel al Aqra'	X–XI	
	Aleppo	Heavy destructions. Fissure 1 mile long in the neighbourhood (between al Qucir and Saltuhum)		
	Latakia	Sea wave		
1822 August 13	Antioch	Aleppo destroyed at 60% Sea wave at Iskenderun	X–XI	
September 5	Aleppo	Destruction of what remained, 20,000 victims		
1872 April 2	Antioch	Destroyed at 30%, 500–1,800 victims		
1936 June 14	Epicentre	near Antioch (36.5° N, 36° E)	VII	5.5
1951 April 8	Epicentre	near Antioch (36.6° N, 36°3E)	VII	5.7
1971 June 29	Epicentre	100 km of Aleppo (37.2°N, 36.8°E)		5
July 11	Epicentre	100 km of Aleppo (37.1°N, 36.9°E)		5

We take $\beta = 0.61$ from the empirical relationship found by Chinnery and North[10] for the whole world:

$$\log N = 17.47 - 0.61 \log M_0$$

where $N = 1/T$ is the frequency of the earthquakes having a seismic moment $\geq M_0$. This relationship is the same as the one on which Molnar's formula rests: $N = \alpha M_0^{-\beta}$, with $\beta = 0.61$.

We take the usual value for the rigidity of the crust: $\mu = 3.3 \times 10^{11}$ dyn cm^{-2}.

The depth l of the strike-slip faults is the depth of the brittle crust. Crustal structure studies by Ben Menahem et al.[11] in the Jordan area give $l = 20$ km. We will adopt this value.

We will take for L, the length of active fault, the total length of the fault system north of Lebanon, including the Karasu fault: $L \approx 300$ km. Although the fault system becomes more diffuse in the Antioch area this does not prevent us applying the formula[9].
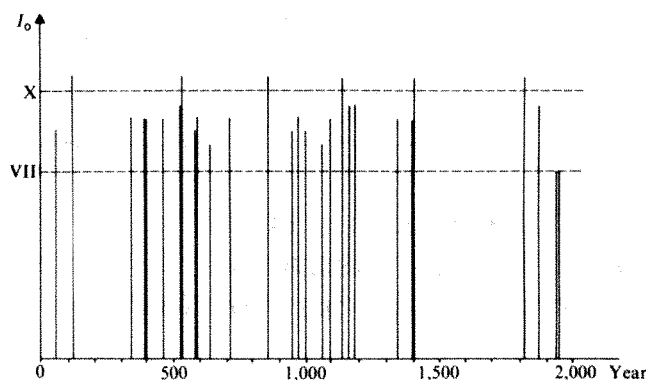
Fig. 2 Spectrum of the intensity of earthquakes in North-west Syria from the first century AD to present. The Mercalli modified intensity in the epicentral zone has been assigned from the description of damage and ground deformation (summarized in Table 1).

The value of $\bar{V}$ relative displacement velocity along the fault (rate of slip) can be calculated from the present day relative motion of the Arabic and African plate given by Minster and Jordan[12]; their results were obtained by inverting data for the whole world (among which the Red Sea and Gulf of Aden rates of expansion): the value found, $\bar{V} = 1.2$ cm yr^{-1} is probably a little high, as part of the displacement along the transform fault is absorbed by deformation of the Lebanon and the Palmyrides and by some aseismic slip[11]. We will take $\bar{V} \simeq 1$ cm yr^{-1}. (On geological evidence, Freund et al.[6] have found a value for V of the order of 0.5 cm yr^{-1} in the Dead Sea region).

The uncertainties in these parameters and in the recurrence interval make up those inherent to Molnar's formula (which we will not take into account) to make our estimate of M_0^{max} rather vague.

Assuming that the minimum value of M_0^{max} corresponds to: $T_1 = 279$ yr, $l = 10$ km, $\bar{V} = 0.5$ cm yr^{-1} and the maximum value to the choice: $T_1 = 403$ yr, $l = 20$ km, $V = 1.2$ cm yr^{-1}, we find:

$$5.4 \times 10^{26} \leq M_0^{max} \leq 3.7 \times 10^{27} \quad \text{dyn cm}$$

We can apply Kanamori's formula[13]:

$$M_w = \frac{\log M_0}{1.5} - 10.7$$

We obtain for the largest earthquakes recurring at the rate of one every 341 ± 62 yr:

$$7.1 \leq M_w \leq 7.7$$

The preferred value corresponds to $T_1 = 341$ yr, $l = 20$ km, $\bar{V} = 1$ cm yr^{-1}; it is:

$$M_0 \simeq 2.6 \times 10^{27} \quad \text{dyn cm}$$

$$M_w \simeq 7.6$$

Having an estimate for M_0^{max}, we can now estimate the seismic moment of the smaller earthquakes with a recurrence interval $T_2 = 71 \pm 51$ yr. We find:

$$2.5 \times 10^{25} \leqslant M_0 \leqslant 4.9 \times 10^{26}$$

or

$$6.2 \leqslant M_w \leqslant 7.1$$

with a preferred value:

$$M_0 \simeq 2 \times 10^{26}$$

$$M_w \simeq 6.8$$

This agrees with the figure given by Ben Menahem *et al.*[11] for the Jordan Valley where they find an average of two events per century at magnitudes from 6 to 7.

Our catalogue of local seismicity and the application of Molnar's formula suggests that there are two different recurrence interval for earthquakes in North-west Syria due to the operation of the Syrian fault system: Earthquakes with $M_w \simeq 7.6$, the largest for the region have an average recurrence interval of 341 ± 62 yr; smaller earthquakes with M_w between 6 and 7 occur with a recurrence interval of 71 ± 51 yr. The last large earthquake occured in 1822, the next one is, therefore, not due for at least one century. On the other hand, as there has been no destructive earthquake since 1872, we forecast that an earthquake with a magnitude between 6 and 7 should occur soon.

1. Nur, A. & Reches, Z. *EOS* **60**, 322 (1979).
2. Moreri, L. *Le Grand Dictionnaire Historique ou le Mélange Curieux de l'Histoire Sacrée et Profane, chez Denys Mariette à Paris* (1704).
3. Ambraseys, N. N. *Nature* **232**, 375–379 (1971); in *Geodynamics Today* 7–16, (The Royal Society, London, 1975).
4. Kelleher, J., Sykes, L. & Oliver, J. *J. geophys. Res.* **78**, 2547–2585 (1973).
5. Taher, M. A. thesis, Univ. Paris I (1979).
6. Freund, R. *et al. Phil. Trans. R Soc.* **A267**, 107—130 (1970).
7. Arthaud, F., Dubertret, L., Masson, P. & Mercier, J. L. *C. r. 6eme Réun. A. Sci. Terre* **8** (1978).
8. Karnik, V. *Seismicity of the European Area* (Reidel, Dordrecht, 1971).
9. Molnar, P. *Bull. seis. Soc. Am.* **69**, 115–133 (1979).
10. Chinnery, M. A. & North, R. G. *Science* **190**, 1197–1198 (1975).
11. Ben Menahem, A., Nur., A. & Vered, M. *Phys. Earth planet Inter.* **12**, 1–50 (1976).
12. Minster, J. B. & Jordan, T. H. *J. geophys. Res.* **83**, 5331—5354 (1978).
13. Kanamori, H. *J. geophys. Res.* **82**, 2981–2987 (1977).

Sinistral movement along the Gulf of Aqaba — its age and relation to the opening of the Red Sea

Y. Bartov & G. Steinitz

Geological Survey, Jerusalem, Israel

M. Eyal & Y. Eyal

Department of Geology & Mineralogy, Ben-Gurion University, Beer Sheva, Israel

The Red Sea forks northwards into the Suez Graben and the Dead Sea Arava Rift (Fig. 1). The southern part of the latter, about 165 km long, is occupied by the Gulf of Aqaba (Elat). A sinistral strike-slip movement of about 107 km which was suggested to have occurred along the Dead Sea–Arava Rift[1-3] is related to the opening of the Red Sea proper[1,4-6]. The opening of the Red Sea was considered to have taken place in two stages. The various dates proposed for the first movement are: from 41 to 34 Myr (ref. 5), from 29 to 24 Myr (ref. 7) and from 20 Myr onwards[6]. The second movement is generally dated from 4–5 Myr to Recent. Garfunkel and Bartov[8] claimed that the rifting in the Gulf of Suez was well under way in the span of the late Oligocene to early Miocene (30–20 Myr) and that a drastic change in the tectonic regime occurred in the middle Miocene (15—16 Myr). We suggest here, however, that the opening of the Red Sea is younger than 19–22 Myr.

Initiation of faulting within the Gulf of Aqaba[9] is assumed to predate the Neogene Raham Conglomerate which was deposited in a morphotectonic depression with structural relief exceeding 1.2 km. It was suggested that the first stage of horizontal movement began in the Mesozoic and resulted in a total displacement of about 60 km, and that a further movement of about 40–45 km was of post-Miocene age[10]. Freund and Garfunkel[11] suggested that the first stage of slip along the Dead Sea occurred in the early Miocene or earlier, and the second stage in the late Miocene or in the Pliocene. A different approach[12] suggested that the whole 107-km shear along the Dead Sea–Arava Rift may have occurred in the middle Miocene or later.

A belt of anastomosing faults was mapped by various investigators[3,13,14] in eastern Sinai, along the Gulf of Aqaba. This belt is part of the Dead Sea–Arava Rift Valley system. Small sinistral displacements, from hundreds of metres to several kilometres, were reported in this belt[3,11,13,15-17] based on offsets of lithological contacts in the Precambrian terrain or on geometric considerations pertaining to deformed strata of the sedimentary cover (Cambrian to Eocene). Freund and Garfunkel[11] suggested that these faults were active primarily, or only during the first stage of slip. Eyal[13] and Ben-Avraham *et al.*[18] noted that these faults did not participate in the youngest movements. Young faulting in this sector of the Rift is recorded only from within the Gulf and its shores[18]. In the present study we attempt to define more precisely the shear and its age along the western margin of the Gulf of Aqaba. This is a continuation of dating the movement on the Central Sinai–Negev Shear Zone[12,19].

Long basalt and olivine basalt dykes, trending SE–NW have recently been identified in southern Sinai (Fig. 1). These dykes are up to 100 m wide, tens to hundreds of kilometres long and are spaced several tens of kilometres apart. Some intrude Mesozoic sediments. They are similar to Tertiary igneous rocks which have been described in the Eastern Desert of Egypt[20-22], the Gulf of Suez[8], Central Sinai[19] and Saudi Arabia[23], all of which are considered to be of Miocene age based on field relations and K–Ar dating[12,24-26]. The dykes in southern Sinai have been dated by the K–Ar method. Results on five bodies yield ages of intrusion of 18–22 Myr which is a distinct and widespread volcanic phase in the Red Sea area.

Figure 1 presents the fault pattern along the Gulf of Aqaba. Most of the faults are in the form of lineaments within the Precambrian terrain. The general trace of the fault belt along the Gulf is of arcuate form.

The amount of sinistral movement along these faults was determined by offsets of magmatic bodies and lithological contacts in rocks of Precambrian age. These offsets were compared with offsets of the early Miocene dykes, on the same faults. In the areas where detailed mapping was undertaken identical displacements were recorded by both groups of markers.

In area A (Fig. 1) near Bir Zreir, the total cumulative displacement across the whole fault belt attains some 24 km. In most cases the amount of displacement on single faults is 0.8–4.0 km. The largest sinistral displacement recorded on a single fault in this area is 9.8 km. As the amounts of displacement measured on the Precambrian markers are in good agreement with those indicated by the early Miocene dykes, we suggest that the total 24 km of shear along this fault system postdates the early Miocene volcanic phase.

Faults showing a similar geometric pattern are recognized on the LANDSAT images of the Saudi coast of the Gulf of Aqaba
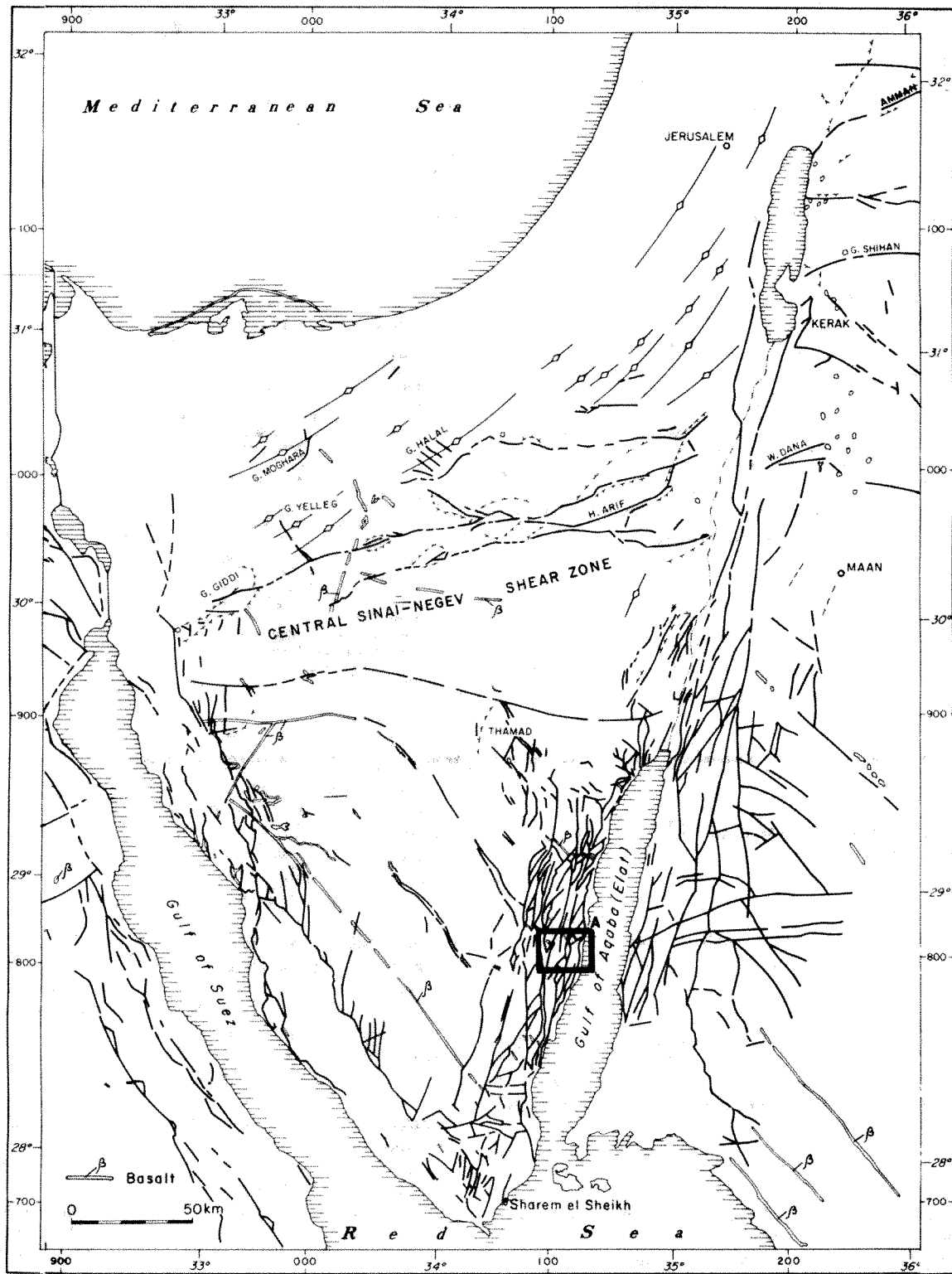
Fig. 1   Early Miocene volcanism and the Tertiary to Recent fault pattern in Sinai and adjoining areas. A, Bir Zreir area.

(Fig. 1). Some of these were mapped by Bramkamp *et al.*[27], Bender[28] and Freund *et al.*[3]. The amount of sinistral movement which is observable along these faults is at least some 18 km (based on displaced Precambrian elements that could be traced on the LANDSAT images). It is assumed that the total sinistral movement along the eastern side of the Gulf is approximately the same as that observed along the western margins of the Gulf of Aqaba. Thus only about 60 km of the total 100–105 km movement has been taken up by faults within the Gulf itself.

The analysis of the fault belt area along the Gulf of Aqaba suggests that the intrusion of very long basaltic dykes in a NW–SE direction, parallel to the coasts of the Red Sea and the Gulf of Suez, accompanied the initial stage of the development of the Red Sea. The igneous activity can probably be related to the faulting which led to the clear demarcation and subsidence of the Suez Graben[8] and the Red Sea[29]. Furthermore, some of the magnetic anomalies recorded in the Red Sea and in areas marginal to the Red Sea[30] may be related to such dyke intrusions.

A drastic change in the geotectonic regime occurs after the intrusion of the early Miocene dykes. We suggest that the large-scale horizontal movements (107 km) recorded along the Dead Sea–Arava Rift, postdate the intrusion of the early Miocene dykes, that is, are younger than 19–22 Myr. The movement along the Dead Sea–Arava reflects the seafloor spreading in the Red Sea. The age relations proved for the Dead Sea–Arava Rift imply that the opening of the Red Sea is also younger than 19–22 Myr.

Several authors have tried to relate the tectonic pattern of Israel and adjacent countries to the horizontal shear along the Gulf of Aqaba–Dead Sea Rift[4,31,32]. Considerable pre-Miocene tectonic activity is known along the Syrian Arc system[33]. Because of the age differences this activity cannot be considered as resulting from the shear along the Dead Sea–Arava Rift. This does not exclude the possibility that elements of the Syrian Arc and the Dead Sea Rift may have shown some slight initial activity as early as the Senonian [34,19].

Future work aimed at defining and correlating individual Neogene basaltic bodies on both sides of the Rift could help to establish an exact fit across the Rift.

1. Dubertret, L. *C.r. hebd. Séanc. Acad. Sci., Paris* **195**, 65–67 (1932).
2. Quennel, A. M. *Int. geol. Congr. 20th Session, Mexico, Ass. Afr. Geol. Surv.*, **385** (1956–58).
3. Freund, R. *et al. Phil. Trans. R. Soc.* A**267**, 107–130 (1970).
4. Freund, R. *Geol. Mag.* **102**, 189 (1965).
5. Girdler, R. W. & Styles, P. *Nature* **247**, 8 (1974).
6. Noy, D.J. in *Tectonics and Geophysics of Continental Rifts* (eds Ramberg, I.B. & Neumann E.R.) 279 (Reidel, Dordrecht, 1978).
7. Hall, S. A., Andreasen, G. E. & Girdler, R. W. in *Red Sea Research* 1970–1975 (F1 Directorate General of Mineral Resources, Jiddah, 1977).
8. Garfunkel, Z. & Bartov, Y., *The Tectonics of the Suez Rift. Bull. Isr. geol. Surv.* **71** (1977).
9. Garfunkel, Z., Bartov, Y., Eyal, Y. & Steinitz, G. *Geol. Mag.* **111**, 55 (1974).
10. Freund, R., Zak, I. & Garfunkel, Z. *Nature* **220**, 253 (1968).
11. Freund, R. & Garfunkel, Z. *Guidebook to Excursion Along the Dead Sea Rift* (Hebrew University, Jerusalem, 1976).
12. Steinitz, G., Bartov, Y. & Hunziker, J. C. *Geol. Mag.* **115**, 329 (1978).
13. Eyal, Y. *Isr. J. Earth Sci.* **22**, 165 (1973).
14. Bartov, Y., Eyal, M., Shimron, A. & Bentor, Y.K. *The Geological Map of Sinai 1:500.000* (Survey of Israel, 1980).
15. Garfunkel, Z. *The Tectonics of the Western Margins of the Southern Arava* (in Hebrew) (Hebrew University, Jerusalem, 1970).
16. Hildebrand, N., Shirav, M. & Freund, R. *Isr. J. Earth Sci.* **23**, 117 (1974).
17. Bentor, Y. K., Bogoch, R., Eyal, M., Garfunkel, Z. & Shimron, A. *Geological Map of Sinai, Jebel Sabbagh Sheet, 1:100,000* (Israeli National Academy of Science and Humanities, 1974).
18. Ben Avraham, Z., Garfunkel, Z., Almagor, G. & Hall, J. *Science* **206**, 214 (1979).
19. Bartov, Y. *A Structural and Paleogeographical Study of the Central Sinai Faults and Domes* (in Hebrew) (Hebrew University, Jerusalem, 1974).
20. Said, R. *The Geology of Egypt* (Elsevier, Amsterdam, 1962).
21. Garson, M.S. & Krs, M. *Bull. geol. Soc. Am.* **87**, 169 (1976).
22. Andrew, G. *Bull. Fac. Sci. Cairo Univ.* **10**, 1 (1937).
23. Blank, H. R. in *Red Sea Research 1970–1975* (G1 Directorate General of Mineral Resources, Jiddah, 1977).
24. Meneisy, M. Y. & Kreuzer, H. *Geol. Jb.* **D9**, 21 (1974).
25. Siedner, G. *Fortschr. Miner.* **50**, 129 (1973).
26. Brown, G. F. *Tectonic Map of the Arabian Peninsula* (USGS, Saudi Arabian Project Rep. 134, 1972).
27. Bramkamp, R. A., Brown, G. F., Holm, D. A. & Layne, N. M. J. *Geologic Map of the Wadi as-Sirhan Quadrangle, Kingdom of Saudi Arabia* (USGS, Misc. Geol. Invest., Map I-200A, 1963).
28. Bender, F. *Geologie Von Jordanien* (Gebrueder Borntraeger, Berlin, 1968).
29. Coleman, R. G., Hadley, D. G., Fleck, R. G., Hedge, C. T. & Donato, M. M. in *Evolution and Mineralization of the Arabian–Nubian Shield* Vol. 1 (ed. Al-Shanti, A. M.) 173 (Pergamon, Oxford, 1979).
30. Andreasen, G.E. & Petty, A.J. *Geologic Map GM-9, Kingdom of Saudi Arabia* (Ministry of Petroleum and Mineral Resources, 1974).
31. Vroman, A. J. *Bull. Isr. geol. Surv.* **43** (1967).
32. de Sitter, L. U. *Geol. En Mijnbow* **41**, 116 (1962).
33. Krenkel, E. *Centralbl. Mineral.* **9**, 274; **10**, 301 (1924).
34. Steinitz, G. *The Deformational Structures in the Senonian Bedded Cherts of Israel* (in Hebrew) (Hebrew University, Jersusalem, 1974).

Coccoliths in Pleistocene–Holocene nannofossil assemblages

W. C. Dudley*, J. C. Duplessy†, P. L. Blackwelder‡, L. E. Brand§ & R. R. L. Guillard§

* University of Hawaii at Hilo, Hilo, Hawaii 96720
† Centre des Faibles Radioactivites CNRS-CEA, 91190 Gif-sur-Yvette France
‡ Nova University Ocean Science Center, Dania, Florida 33004
§ Woods Hole Oceanographic Institution, Woods Hole, Massachusetts 02543

Marine palaeotemperature studies are increasingly using oxygen isotope analyses of the minute calcium carbonate structures produced by a group of marine phytoplankton, the coccolithophores[1–6]. To provide a sound experimental basis for palaeotemperature calculations using the isotopic data from analyses of coccoliths, we have grown coccolithophores in laboratory batch culture in controlled environmental conditions, and determined the oxygen isotopic compositions of the coccoliths produced at known temperatures. The results reported here indicate that the oxygen isotopic composition of the coccoliths of all the species studied is strongly temperature dependent. A 'vital effect' was observed in all the species, with the isotopic values of different culture samples falling into two definite groups containing separate taxa. The difference in vital effect between different species suggests that calcification processes may vary among different taxa and indicates that a re-evaluation of coccolith oxygen isotope palaeoclimatic interpretations may be in order.

Coccolithophores possess certain unique advantages for oxygen isotope palaeoclimatic studies. As phytoplankters, they are restricted to the photic zone, with maximum population densities found between 50 and 100 m depth in most oceanic areas[7]. Consequently, coccolith secretion takes place only at near-surface water temperatures. On the other hand, planktonic foraminifera may produce their tests at the various temperatures found between the surface and depths as great as 1,500–2,000 m, although depth ranges for individual taxa may be more narrowly restricted[8]. In addition, coccolithophores show a wide geographic distribution, being found in all but polar seas[7]. Finally, coccoliths are more abundant than foraminiferal tests in many Tertiary and Cretaceous marine sediments[9].

We have maintained in laboratory culture the previously isolated *Emiliania huxleyi*, and successfully isolated and cultured for the first time *Gephyrocapsa oceanica*, *Cyclococcolithus leptoporus*, and *Thoracosphaera heimii*. These four species produce coccoliths frequently encountered in many Pleistocene and Holocene sediments.

The clonal algal cultures were grown in continuous batch culture and acclimated for 2 to 3 weeks at each temperature (12, 16, 20, 24, and 28 °C) before the coccoliths of the last batch culture were collected for analysis. The cultures were grown in 33‰ seawater enriched with *f*/2 levels of nutrients as described by Guillard[10] with silicic acid omitted. Light was provided by cool white fluorescent bulbs producing 0.023 langley min⁻¹. Coccoliths were concentrated by centrifugation in buffered distilled water, then oven dried and roasted under vacuum at 400 ± 25 °C to remove residual organic matter. The carbonate samples were reacted at 50 °C according to the method developed by Shackleton[11,12] and analysed by mass spectrometry. Samples of the water of the growth medium were analysed according to the method of Epstein and Mayeda[13] and corrections made according to Craig[14,15].

Analytical data obtained from over 70 samples showed two important trends. The $\delta^{18}O$ values of the coccoliths of *G. oceanica* and *E. huxleyi* are strongly temperature dependent

(Fig. 1), but are ~1‰ positive (enriched in ^{18}O) relative to calcium carbonate precipitated at equilibrium. The $\delta^{18}O$ values obtained from coccoliths of *C. leptoporus* and from tests of *T. heimii* also show a strong temperature dependence but are ~2.5‰ depleted in ^{18}O relative to equilibrium (Fig. 1). The isotopic compositions of these latter species are similar to values reported for coccoliths of *Cricosphaera carterae*[5]. Cultures of *G. oceanica* were maintained under both 14:10 hour light/dark cycles and 24-h light regimes. The $\delta^{18}O$ data on this species (Fig. 1) indicate no significant difference in oxygen isotopic composition related to the period of illumination.

The experimental data show a temperature dependence in oxygen isotopic composition which in no case corresponds to equilibrium precipitation of calcium carbonate. This would indicate that in all the coccolithophore species studied, a not unexpected vital effect influences the fractionation of oxygen
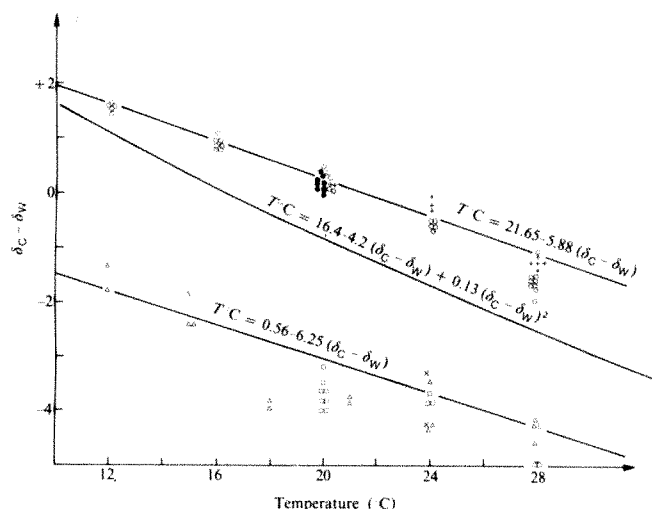
Fig. 1 The species plotted are *E. huxleyi*, 14:10 h light/dark cycle (+); *G. oceanica*, 14:10 h light/dark cycle (O), 24-h illumination (●); *C. leptoporus* 14:10 h light/dark cycle (□). *T. heimii*, 14:10 h light/dark cycle (X); and *C. carterae*[5], 12:12 h light/dark cycle (△). Each datum point represents an individual unialgal batch culture. The isotopic composition of the coccoliths are reported as $\delta_C - \delta_W$ versus temperature, where $\delta_C = \delta^{18}O$ of the coccoliths (‰ deviations from the PDB standard), and $\delta_W = \delta^{18}O$ of the water of the growth medium (‰ deviation from SMOW). The equations representing the least squares fit to the combined data of *E. huxleyi* and *G. oceanica* is $y = 3.68 - 0.17T$, ($r = 0.91$), and for *C. leptoporus*, *C. carterae*, and *T. heimii* is $y = 0.09 - 0.16T$, ($r = 0.87$).

isotopes during the secretion of the mineral. Isotopic analyses of both planktonic and benthonic foraminifera[16-19] have shown that their tests may be secreted out of isotopic equilibrium. In addition, the secretion of calcium carbonate in echinoderm tests and spines[20] and in parts of corals[21] has been found to reflect non-equilibrium conditions. Calcification in the coccolithophores is intracellular[22] in that coccoliths are produced inside each cell and extruded to the cell surface. Paasche[23] determined that bicarbonate rather than carbonate ions are used as a primary source of carbon in coccolith formation, further demonstrating that the deposition of calcium carbonate by coccolithophores is fundamentally different from any inorganic precipitation process. Therefore, comparison with products of extracellular calcification as described above can be made only with some reservation. The vital effect in the coccolithophores may reflect isotopic discrimination effects by cell membranes, as well as by the incorporation in the calcite of metabolic CO_2 or

photosynthetic O_2. Much work obviously remains to be done to understand the process of calcification in these planktonic algae. Relatively little is known about pathways, although our data do imply that calcification processes in coccolithophores may vary among different taxa. This is further suggested by the close grouping of the isotopic data for *E. huxleyi* and *G. oceanica* (Fig. 1), as these two species are thought to lie in a phylomorphogenetic lineage[24].

Recently, several investigators[3,4] have published analyses of 'bulk' carbonate samples composed of mixtures of different coccolith species and small foraminiferal tests. The isotopic signal recorded in such samples is a complex mixture of the isotopic signals of the different species comprising the bulk sample. Apparently the isotopic signal cannot be interpreted without data on the vital effect of each species included.

The presence of a vital effect in the fractionation of oxygen isotopes in coccolithophores does not preclude the use of coccoliths for oxygen isotope palaeotemperature analysis, as long as the magnitude of the effect is known over the temperature range in question. Nanofossil assemblages composed of coccoliths of *E. huxleyi* and *G. oceanica*, both of which are small, may be separated by settling and filtering techniques, and analysed for the oxygen isotopic composition. The $\delta^{18}O$ values of such an assemblage reflect the temperature and the $^{18}O/^{16}O$ ratio of the water in which these coccolithophores lived, even though the mineral was not precipitated in equilibrium. Factors such as light intensity, nutrients, and salinity may also play a role in regulating fractionation. These variables and their effect on isotopic composition are being examined in our laboratories.

Our increased understanding of the vital effect in the fractionation of oxygen isotopes by coccolithophores should increase the value of coccolith oxygen isotopic data in palaeoclimatic studies. The $\delta^{18}O$ data from coccoliths used in conjunction with oxygen isotopes data from foraminifera should allow us to determine with greater reliability variations in surface water temperature during the Pleistocene.

Note added in proof: The taxonomic position of the Thoracosphaerae, that is, whether they are coccolithophores or dinoflagellates, has been a matter for debate. Based on detailed examination of cell ultrastructure and particularly the presence of a typical dinoflagellate nucleus, we have concluded that *Thoracosphaera heimii* is a dinoflagellate and not a coccolithophore (L.E.B., P.L.B. and R.L.G., manuscript in preparation).

1. Margolis, S. V., Kroopnick, P. M., Goodney, D. E., Dudley, W. C. & Mahoney, M. E. *Science* **189**, 555 (1975).
2. Anderson, T. F. & Cole, S. A. *J. Foram. Res.* **5**, 188 (1975).
3. Berger, W. H., Killingley, J. S. & Vincent, E. *Oceanol. Acta* **1**, 203 (1978).
4. Vergnaud-Grazzini, Pierre, C. & Letolle, R. *Oceanol. Acta* **1**, 381 (1978).
5. Dudley, W. C. & Goodney, D. E. *Deep-Sea Res.* **26A**, 495 (1979).
6. Savin, S. M. *A. Rev. Earth planet. Sci. Lett.* **5**, 319 (1977).
7. Okada, H. & Honjo, S. *Deep-Sea Res.* **20**, 355 (1973).
8. Bé, A. W. H. & van Donk, J. *Science* **173**, 167 (1971).
9. Berger, W. H. in *Chemical Oceanography* (eds Riley, J. P. & Chester, R.) (Academic, New York, 1976).
10. Guillard, R. R. L. in *Culture of Marine Invertebrate Animals* (eds Smith, W. L. & Chanley, M. H.) (Plenum, New York, 1975).
11. Shackleton, N. J. in *Stable Isotopes in Oceanographic Studies and Palaeotemperatures* (ed. Tongiorgi, E.) (Spoleto, Pisa, 1965).
12. Shackleton, N. J. in *Variation du climat au cours du Pleistocene* (ed. Labeyrie, J.) (CNRS, Paris, 1974).
13. Epstein, S. & Mayeda, T. *Geochim. cosmochim. Acta* **4**, 213 (1953).
14. Craig, H. *Geochim. cosmochim. Acta* **12**, 133 (1957).
15. Craig, H. in *Stable Isotopes in Oceanographic Studies and Palaeotemperatures* (ed. Tongiorgi, E.) (Spoleto, Pisa, 1965).
16. Duplessy, J. C., Lalou, C. & Vinot, A. C. *Science* **168**, 250 (1970).
17. Vinot-Bertouille, A-C. & Duplessy, J-C. *Earth planet Sci. Lett.* **18**, 247 (1973).
18. Shackleton, N. J., Wiseman, D. H. & Buckley, H. A. *Nature* **242**, 177 (1973).
19. Vergnaud-Grazzini, C. *Palaeogeogr. Palaeoclimat. Palaeoecol.* **20**, 263 (1976).
20. Weber, J. N. & Raup, D. M. *Geochim. cosmochim. Acta* **30**, 681 (1966).
21. Weber, J. N. & Woodhead, P. M. J. *Chem. Geol.* **6**, 93 (1970).
22. Watabe, N. & Wilbur, K. M. *Limnol. Oceanogr.* **11**, 567 (1966).
23. Paasche, E. *Physiol. Pl.* Suppl. III, 1 (1964).
24. McIntyre, A. *Deep-Sea Res.* **17**, 187 (1970).

Early Jurassic plesiosaurs from Australia

Richard A. Thulborn

Department of Zoology, University of Queensland, St Lucia, Queensland, Australia 4067

Anne Warren

Department of Zoology, La Trobe University, Bundoora, Victoria, Australia 3083

Remains of plesiosaurs (aquatic reptiles of the suborder Plesiosauria, order Sauropterygia) are known from Cretaceous sediments in every continent[1], including Antarctica[2]. Jurassic plesiosaurs, by contrast, seem to have had a more restricted distribution, and are virtually unknown outside the Northern Hemisphere. We report here the discovery of two plesiosaur specimens in the Lower Jurassic of the eastern part of the Surat Basin, Queensland. These are the earliest adequate examples of plesiosaurs to be discovered in the Gondwana continents, and they greatly extend the known geographical range of early sauropterygians.

The specimens were collected from the upper part of the Evergreen Formation on Kolane property, about 60 km northeast of Wandoan, south-east Queensland. At Kolane, the Evergreen Formation is represented by ferruginous sandstones, thick seams of concretionary ironstone, and argillaceous oolites; these beds are probably an eastwards extension of the Westgrove Ironstone member, as identified towards the top of the Evergreen Formation in the western parts of the Surat Basin[3,4]. The upper part of the Evergreen Formation has been dated as Upper Liassic on the evidence of plant microfossil assemblages[3,4]. As well as plesiosaurs, the Kolane locality has yielded poorly preserved plant remains, thin-shelled lamellibranchs, and an almost complete skeleton of the last-known labyrinthodont amphibian[5].

The less complete of the two plesiosaur specimens (Queensland Museum catalogue no. F10440) is preserved in sandstone and oolite, and comprises a scattering of fragments apparently derived from a single skeleton. The bones are severely weathered, but include recognizable portions of limbs and girdles, and vertebrae bearing rib attachment scars of distinctive plesiosaurian type (Fig. 1a). The specimen is certainly a plesiosaur, but it is so incomplete that its more immediate relationships cannot be determined.

The second specimen (QM F10441) was found about 400 m north of the first, and about 10 m above the site of the Kolane labyrinthodont. It is preserved in blocks of concretionary ironstone, so that its development may present difficulties. This specimen seems to be part of an articulated skeleton, and includes vertebrae, ribs, girdle bones, limb bones and, possibly, gastralia; no cranial elements have been identified with certainty. Two of the cervical vertebrae are exposed on a broken surface and show diagnostic plesiosaurian features allowing identification down to family level (Fig. 1b). Such identification is admissible because detailed studies of vertebrae form the basis of plesiosaur classification[1,6]. Each cervical centrum is roughly cylindrical, with a fairly flat ventral surface and weakly depressed terminal faces. The floor of the neural canal forms a shallow groove in the dorsal surface of the centrum, so that the latter is slightly kidney-shaped in cross-section. On the ventral surface the large nutrient foramina are separated by a flat area. The standard height/length and width/length indices (ratios × 100) for these cervical centra are about 95 and 115, respectively. Other vertebrae show that the rear margin of each neural spine is vertically grooved—a distinctive feature noted by Welles[6] in elasmosaurid plesiosaurs, and illustrated by Owen[7] in plesiosaur vertebrae from the English Lias. A damaged cervical rib seems

originally to have been of characteristic 'hatchet shape'. Structure and proportions of these cervical vertebrae clearly indicate that specimen F10441 is a dolichodiran (or long-necked) plesiosaur, almost certainly referable to the family Plesiosauridae (part of the superfamily Plesiosauroidea).

There are few records of plesiosaurs from Jurassic or earlier rocks of Gondwanaland. The report of a 'suspected plesiosaur' in the Upper Triassic of New Zealand[8] is founded on a single fragment of limb bone; this fragment could equally well have come from some other type of reptile, or even from an amphibian (see account by W. E. Swinton in ref. 8). A single vertebra from the Upper Liassic of Argentina was originally attributed to a crocodile[9], but was identified by von Huene[10] as plesiosaurian; Welles considered[6] that this specimen was not diagnostic. Other records of plesiosaurs from the Jurassic of Argentina[11,12] are erroneous or founded on indeterminate material[1,6,13]. Isolated skull fragments of pliosaurs (plesiosaur superfamily Pliosauroidea) are known from the Upper Jurassic of India[14] and Ethiopia[15]. Fragmentary pliosaur material was also reported by Bartholomai[16] from an early Cretaceous or late Jurassic conglomerate at Mount Morgan, Queensland.
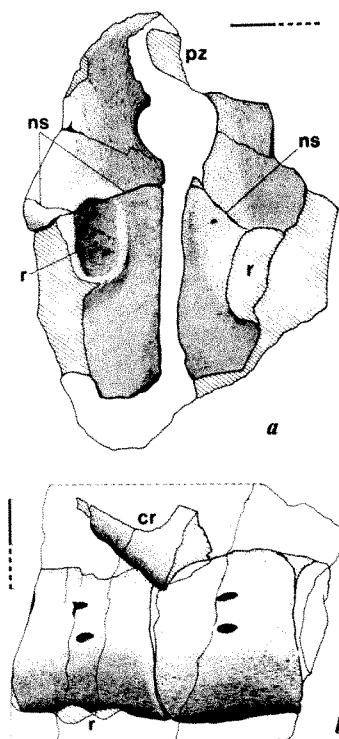
Fig. 1 Plesiosaur vertebrae from the Evergreen Formation (Upper Liassic) of south-east Queensland. *a*, Two anterior caudal vertebrae (from specimen QM F10440) in left lateral view, showing neuro-central sutures (ns), crater-like scars for rib attachment (r) and prezygapophysis of second vertebra (pz). *b*, Two cervical vertebrae (from specimen QM F10441) in ventral view, showing large nutrient foramina, detached cervical rib (cr), and damaged area of rib attachment (r). Matrix is unshaded, and badly damaged surfaces are indicated by oblique shading. Both scales represent 2 cm.

The Kolane specimens are, thus, the earliest adequate examples of plesiosaurs from Gondwanaland. Their discovery greatly extends the known geographical range of early sauropterygians and implies that the Plesiosauria might have had an almost world-wide distribution as early as the Lower Jurassic. The association of the Kolane plesiosaurs with a labyrinthodont amphibian is, at the least, surprising: plesiosaurs typically occur in marine faunas of the Jurassic and Cretaceous, whereas labyrinthodonts are mainly known from continental faunas of the late Palaeozoic and Triassic. The occurrence of a plesiosaur

referable to the Family Plesiosauridae is consistent with the Lower Jurassic age of the Evergreen Formation, and tends to confirm that the labyrinthodont is a late survivor[5]. Reiser and Williams concluded[4] that most of the Evergreen Formation was laid down in continental conditions, but that the peculiar lithology of the Westgrove Ironstone member might be suggestive of a marine origin. Either the Kolane plesiosaurs were sea-dwellers, and the associated labyrinthodont was accidentally introduced into a marine environment, or the plesiosaurs were non-marine types, ecologically comparable with those, for example, of the English Wealden.

We thank Mr and Mrs Colin Kehl, of Kolane, and Dr Mary Wade, of the Queensland Museum. Financial support came from the Australian Research Grants Committee.

1. Persson, P. O. *Acta Univ. Lund.* **59**, 1–60 (1963).
2. del Valle, R. A., Medina, F. & de Brandoni, Z. G. *Contr. Inst. Antartico Argent.* **212**, 1–13 (1977).
3. de Jersey, N. J. & Paten, R. J. *Publs geol. Surv. Qd* **322**, 1–18 (1964).
4. Reiser, R. F. & Williams, A. J. *Publs geol. Surv. Qd* **339**, 1–24 (1969).
5. Warren, A. *Nature* **265**, 436–7 (1977).
6. Welles, S. P. *Univ. Calif. Publs geol. Sci.* **44**, 1–96 (1962).
7. Owen, R. *A Monograph of the Fossil Reptilia of the Liassic Formations, Part III* (Palaeontogr. Soc., London, 1865–1881).
8. Campbell, J. D. *N.Z. Jl Geol. Geophys.* **8**, 505–9 (1965).
9. Burmeister, H. & Giebel, C. G. A. *Abh. naturforsch. Ges. Halle* **6**, 111–44 (1862).
10. von Huene, F. *Zentbl. Miner. Geol. Paläont.* Ref. B **1927**, 22–9 (1927).
11. Rusconi, C. *boln Paleont. B. Aires* **15**, 1–4 (1943).
12. Rusconi, C. *An. Soc. cien. argent.* **146**, 327–51 (1948).
13. Rusconi, C. *An. Soc. cien. argent.* **160**, 71–7 (1955).
14. Lydekker, R. *Rec. geol. Surv. India* **20**, 51–80 (1887).
15. von Huene, F. *Zentbl. Miner. Geol. Paläont.* Ret. B **1938**, 370—6 (1938).
16. Bartholomai, A. *Aust. J. Sci.* **28**, 437 (1966).

Kin preference in infant *Macaca nemestrina*

**Hannah M. H. Wu, Warren G. Holmes*,
Steven R. Medina & Gene P. Sackett**

Department of Psychology and Regional Primate Research Center, University of Washington, Seattle, Washington 98195

The ability to recognize conspecifics is a prerequisite for many types of social behaviour, including, for example, parent–offspring relations[1,2], mate selection and recognition[3,4], territorial defence[5,6] and dominance coalitions[7]. This ability is of special importance to Hamilton's kin selection hypothesis[8], which predicts that an individual's behaviour towards a conspecific will depend on the degree of genetic relatedness between them. Although recognition depends on previous experience between individuals in some species[1,2], this does not preclude the possibility that recognition could occur in its absence[12]. For example, juveniles who disperse before non-littermate siblings are born or adult males who do not participate in rearing their young might benefit from recognition abilities that are independent of prior association between the individuals. Here we show that young pigtail macaques prefer to interact with a related over an unrelated monkey in a laboratory test. Because subjects were separated from their dams at birth and reared apart from all other relatives, results suggest that kin recognition can occur in the absence of prior association with relatives.

* Present address: Department of Psychology, University of Michigan, Ann Arbor, Michigan 48109.

Subjects were 16 infant pigtail macaques (*Macaca nemestrina*) of known genealogies from a captive breeding colony (Table 1). Taken from their dams within 5 min of birth, subjects were placed in an incubator until they became homeothermic and were then transferred to a colony room (7.6 m × 11.0 m) and housed individually in wire cages. Subjects were placed in this room housing 50 other monkeys such that they had no opportunity for visual, physical or olfactory interactions with relatives or any other animals used in the experiments. To ensure normal social development, subjects interacted daily in 'play groups' with four to six similarly aged monkeys, none of whom was related to the subjects.

The Sackett self-selection circus (Fig. 1) was used to measure preference in a free-choice situation. Thus, subjects could select among three simultaneously presented stimuli by first visually orientating towards each one, and later entering the compartment to which a stimulus was attached, orientation time and entry time serving as two measures of preference. Orientation and entry time were recorded by an observer who viewed subjects from a separate room on a closed-circuit television and who knew nothing of the monkeys' genetic relationships.

Subjects were tested once in two different experiments, each using an identical testing procedure but with a different set of choice stimuli. Experiment I offered choices among a subject's paternal half-sibling, an unrelated (to both the subject and other stimulus animal) monkey, and an empty cage to examine our hypothesis that subjects would prefer their relative. Stimulus animals were matched by sex, age, weight, and general activity level and appearance (as subjectively judged by us). Both the subject's half-sibling and unrelated conspecific were delivered and reared identically to the subject. Experiment II examined the strength of the preference predicted in experiment I by providing choices among the subject's paternal half-sibling from experiment I, a 'preferred nonrelative', and an empty cage. The

Table 1 Subjects and their preference times for half-siblings, nonrelatives and an empty cage in experiment I

	Sex	Age (days)	Half-sib stimulus Age (days)	Half-sib stimulus Sex	Non-kin stimulus Age (days)	Non-kin stimulus Sex	Kin entry (s)	Non-kin entry (s)	Empty cage entry (s)	Kin orientation (s)	Non-kin orientation (s)	Empty cage orientation (s)
BS	M	344	37	F	49	F	189.1	142.3	58.7	78.6	81.2	82.4
BT	F	326	7	M	11	M	174.4	155.5	121.1	88.6	70.2	88.3
CB	M	317	7	M	11	M	400.3	28.1	124.4	87.3	82.1	83.7
DD	F	316	16	M	6	M	226.1	96.3	236.1	169.0	64.4	53.5
DW	M	276	37	F	58	F	390.4	50.7	22.5	178.8	55.6	36.4
LZ	M	206	147	F	145	F	0.8	0.0	599.2	247.9	42.3	4.2
NK	F	159	206	M	193	M	448.3	95.6	0.0	138.7	73.6	74.3
OC	M	149	159	F	160	F	216.8	84.2	66.3	133.4	97.4	37.7
OD	F	147	158	F	159	F	272.9	222.8	8.0	65.6	143.6	69.5
IV	F	91	37	M	30	M	70.2	44.9	60.5	96.5	70.3	94.5
IZ	M	86	20	M	29	M	267.3	192.8	16.2	121.5	62.6	88.6
LC	M	83	20	F	19	F	99.3	82.2	151.8	121.6	55.7	109.2
KL	F	44	92	M	85	M	46.4	0.0	9.0	90.2	70.7	89.9
LF	F	85	24	F	23	F	0.0	488.3	55.5	67.9	107.6	107.7
KK	F	61	17	M	27	M	160.6	222.2	19.4	64.0	127.3	76.8
KP	M	98	10	M	6	M	37.1	257.3	68.7	87.1	122.3	62.0

Orientation time was scored during the first 5 min and entry time during the following 10 min. See text for further details.

Lifting detail

Vacuum lifters

Vacuum lift supports

Remote TV camera

Solenoid latches

Limiting switches   Choice compartments

Start compartment

Cage mounting pin and socket

Stimulus animal cages

Orientation of subject and and stimulus monkey
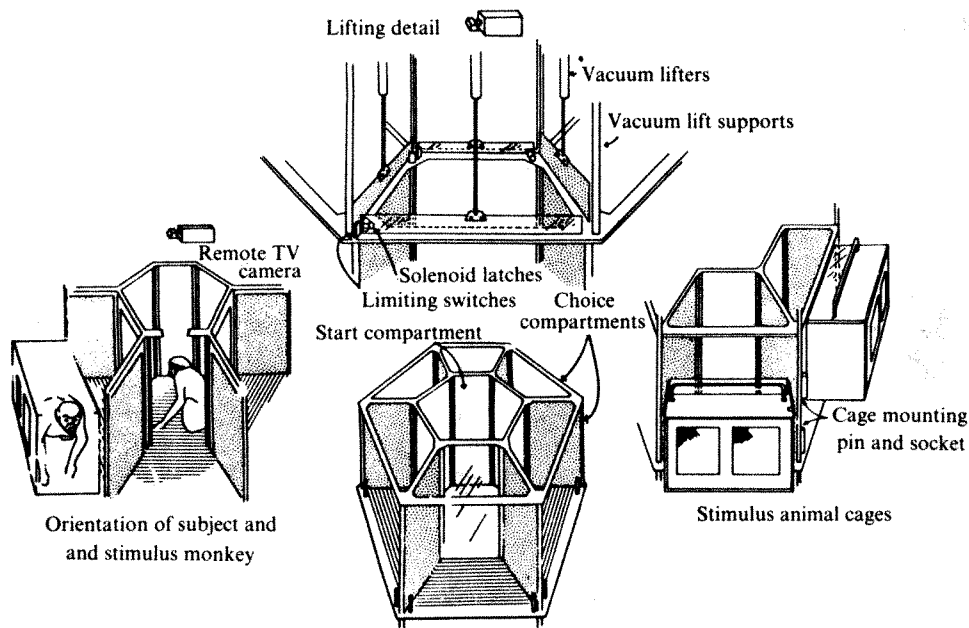
Fig. 1 The Sackett self-selection circus, used in several other studies to measure social preference in primates[9], was constructed of movable, transparent Plexiglass panels separating the apparatus into a central start compartment and six choice compartments, three of which were used. Plexiglass-carrying cages, each holding the appropriate stimulus, were attached randomly to non-adjacent choice compartments before a subject was placed in the start compartment. Subjects were adapted to the circus before testing. Each subject's preference for the three stimuli was measured during a 15-min test. During the 5-min orientation period when the subject was confined to the start compartment, its visual orientation times, scored whenever its head and body were orientated towards choice stimuli, were recorded by a trained observer (S.R.M.). The observer viewed subjects from a separate room on a closed-circuit television and knew nothing of the monkey's genetic relationships. The start compartment panels were then raised by remote control, and the subject allowed 10 min of unlimited access to the three choice compartments (and start compartment), where it could interact in all ways with the stimulus monkeys except by making physical contact. Entry time elicited by each stimulus was recorded and defined as the total time the subject spent in a particular choice compartment. Subjects typically entered each compartment more than once and also spent time in the start compartment.

preferred nonrelative was obtained for each subject in a separate choice experiment in which two matched stimulus animals, both unrelated to the subject, were presented as choice stimuli. The animal eliciting the greatest amount of entry time was defined as the preferred nonrelative.

Subjects' performances and relevant variables are summarized in Table 1 and Fig. 2. In experiment I, a significant number of subjects (13 of 16) exhibited more entry time toward half-siblings than toward unrelated animals ($P \leq 0.01$, binomial test) and a significantly greater amount of entry time towards half-siblings than towards unrelated animals ($P \leq 0.05$, Wilcoxon signed-ranks test) (Fig. 2a). Subjects' orientation time towards half-siblings was also greater than towards unrelated animals, but this difference was not significant ($P \leq 0.1$). There was no significant correlation between subjects' age and relative kin entry time (kin/total entry time), a measure that controls for developmental differences in mobility. In experiment II, half-siblings elicited more entry time and more orientation time than unrelated animals, although neither of these differences were significant ($P < 0.1$ and $P \leq 0.1$, respectively) (Fig. 2b).

Based on orientation and approach toward half-siblings in experiment I, we conclude that infant pigtail macaques prefer to interact with their half-siblings rather than nonrelatives and, therefore, can discriminate between them. Furthermore, based on rearing conditions of both subjects and stimulus animals, we conclude that this preference and discrimination ability require no previous experience with relatives. Because half-siblings were paternally related, common prenatal experience cannot explain preferences. Of course, each subject experienced itself during rearing which, in some sense, could be considered experience with a relative. And experience with one's own phenotype has been suggested as the basis for demonstrated social preferences in domestic chicks reared in isolation[10].

The data provide no evidence for the proximal basis of the discrimination ability, but results from visual orientation time imply something about the significance of visual cues. Thus, 14 of 16 stimulus animals eliciting the greatest amount of orientation time in experiment I were also favoured in entry time, suggesting that subjects had established preferences even before they were allowed into choice compartments.

Half-sib
Unrelated
Empty
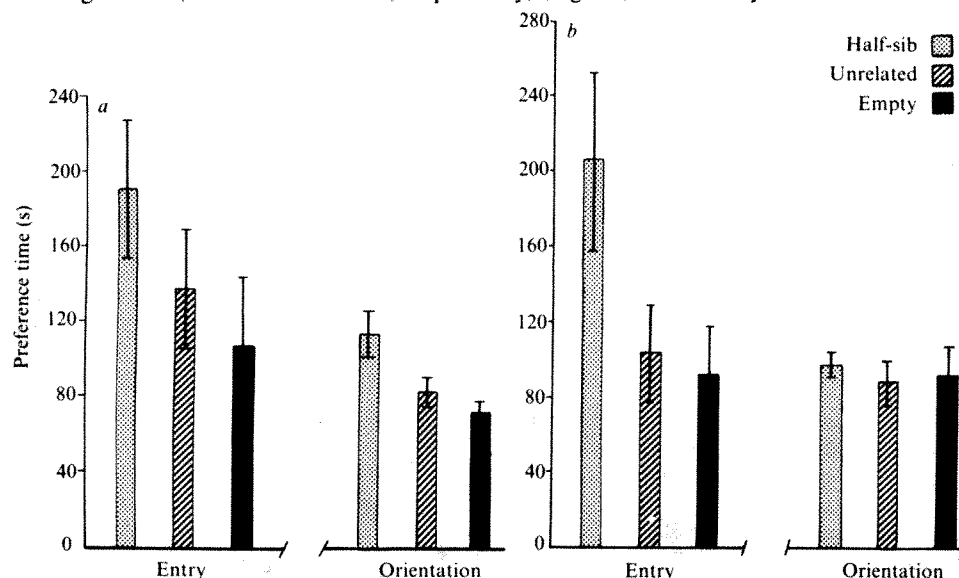
Fig. 2 Mean entry and orientation time (±s.e.) elicited by various choice stimuli in experiment I (a) and experiment II (b) ($n = 16$ for each bar). Orientation and entry times were used as two measures of subjects' preference for the choice stimuli during the initial 5-min and the following 10-min periods, respectively. Statistical comparisons (see text) were made with the Wilcoxon signed-ranks test; 1-tailed tests were used based on predicted preferences for half-siblings.

Hamilton argued that selection favours individuals assisting others in proportion to genes shared in common, other things being equal. Although a laboratory study[11] has shown that aiding is directed along lines of genetic relatedness among pigtails reared together, our data are clearly insufficient to demonstrate kin selection. Furthermore, we do not suggest that social preferences would be unaffected by experience; pigtails do prefer a familiar conspecific to an unfamiliar one[9]. Finally, although our results are based on a single age-class in one species, they do heed us to examine the frequent assumption that recognition of kin requires prior association among relatives.

We thank the members of the Animal Behavior Seminar for helpful discussions, and D. Barash, C. Crockett, W. D. Hamilton, R. Holm, J. Lewis, J. Lockard, G. Orians, G. Ruppenthal, P. Sherman, W. Sawrey and the late R. Lockard for comments. This research was supported in part by NIH grants RR00166 and HD08633.

1. Michener, G. R. Devl Psychobiol. 7, 375-384 (1974).
2. Beecher, M. D. & Beecher, I. M., in preparation.
3. Johnson, V. R. Anim. Behav. 25, 418-428 (1977).
4. Brooke, M. de L. Anim. Behav. 26, 622-629 (1978).
5. Emlen, S. T. Z. Tierpsychol. 28, 241-246 (1971).
6. Krebs, J. R. Ecology 52, 2-22 (1971).
7. Packer, C. Nature 265, 441-443 (1977).
8. Hamilton, W. D. J. theor. Biol. 7, 1-52 (1964).
9. Suomi, S. J., Sackett, G. P. & Harlow, H. F. Devl Psychol. 3, 326-336 (1970).
10. Salzen, E. A. & Cornell, J. M. Behavior 30, 44-65 (1968).
11. Massey, A. Behav. Ecol. Sociobiol. 2, 31-40 (1977).
12. Greenberg, L. Science 206, 1095-1097 (1979).

Stimulation of the cerebral cortex in the intact human subject

P. A. Merton & H. B. Morton

The National Hospital, Queen Square, London WC1N 3BG, UK

One of the most fertile methods of investigating the brain is to stimulate a part of it electrically and observe the results. So far, however, use of the method in man has been restricted by the necessity of opening the skull surgically to apply the electrodes. Much could be done, both with healthy subjects and with neurological patients, if it were feasible to stimulate through electrodes on the scalp, although the localization of the stimulus on the cortex will always be much less sharp than with electrodes on the brain surface. In an intact man, however, the brain is protected from electricity by the skull and by the scalp, both of which normally offer considerable resistance. Furthermore, the cerebral cortex does not have a particularly low electrical threshold. It is probably for these reasons (despite an occasional contrary claim[1]) that attempts to stimulate the brain by applying stimuli from conventional stimulators to the scalp have been stopped by pain or have otherwise failed. These obstacles have now begun to yield. Recently, it was found that, on stimulating muscles in the human hand[2] without any special preparation of the skin, the effective resistance fell to low values if brief but very high voltage shocks were used. Applying the same technique to the head, it has now proved possible at the first attempt to stimulate two areas of the human cortex, without undue discomfort.

The stimulating electrodes were ordinary stick-on silver-cup electroencephalogram electrodes of 1 cm diameter, filled with electrode jelly. For the motor area, one electrode was applied initially over the surface marking of the arm area of the motor cortex and the other 4 cm in front. To stimulate, a 0.1-μF condenser charged to up to ~2,000 V was discharged through the electrodes using a Morse key. The electrode over the motor area was the positive. A shunt resistance of 100 Ω ensured that the time constant of discharge was less than 10 μs.
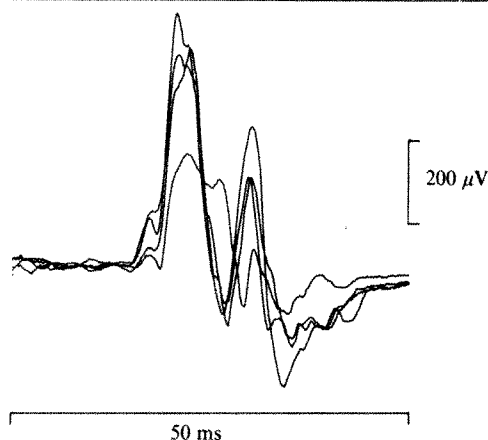
Fig. 1 Stimulation of the arm area of the motor cortex. The records shown are of action potentials from the contracting muscles in the forearm. Stimulation is at the start of the sweep. Four records are superimposed. The latency of responses was 16 ms. (Subject P.A.M.)

Stimulation showed itself by twitch-like movements of the opposite middle and index fingers, or, with the active electrode over the leg area, of the foot. In one subject (height 1.88 m), muscle action potentials recorded through surface electrodes over the active muscles showed fairly sharp latencies of 16 ms for the forearm muscles (Fig. 1) and 34 ms for the muscles in the lower leg. These values agree with those obtained by stimulating the exposed human motor cortex or the nerve fibres leaving it[3,4].

With electrodes on the back of the head, over the visual area of the cortex, illusory visual sensations ('phosphenes') were experienced. Larger voltages were necessary for the visual area than for the motor area. For each stimulus the phosphene was very brief. It appeared near the centre of the visual field as a patch, with indefinite edges, subtending some 5°, containing one or a few, sharp, bright sinuous lines. The main evidence that such phosphenes are caused by stimulation of the visual cortex is that they only occurred with electrodes over the visual area and that, within that region, the position of a phosphene in the visual field moved with the position of the stimulating electrodes in a manner that conformed with the known mapping of the visual field on the cortex (half-fields reversed and upside down, with a large area for the centre of the field on the occipital poles). Thus, with a horizontal pair of electrodes above the occipital pole (6 cm above the inion), the phosphene was below the fixation point. It moved upwards roughly to the fixation point when the electrodes were moved downwards (to 3 cm above the inion). Similarly, the phosphenes appeared mainly on the right with electrodes to the left of the mid-line, and vice versa. They disappeared altogether when the electrodes were moved away more than a few centimetres from the occiput.

Another important observation is that the phosphenes described did not disappear when the eyeballs were pressed on until sight was lost in both eyes, so they were not due to the excitation of the retina by spread of current. Such excitation occurs very readily, as the retina has a low electrical threshold; but the resulting phosphenes fill diffusely much of the visual field, are without structure, are not specially related to stimulation over the visual area, and disappear with pressure-blinding. Thus, although both may be seen simultaneously, phosphenes from current spread to the retina are readily distinguished from the phosphenes we attribute to stimulation of the visual cortex.

1. Gualtierotti, T. & Paterson, A. S. J. Physiol., Lond. 125, 278-291 (1954).
2. Hill, D. K., McDonnell, M. J. & Merton, P. A. J. Physiol., Lond. 300, 2P-3P (1980).
3. Pagni, C. A., Ettore, G., Infuso, L. & Marossero, F. Experientia 20, 691-692 (1964).
4. Milner-Brown, S. H., Girvin, J. P. & Brown, W. F. Can. J. neurol. Sci. 2, 245-253 (1975).

Slow current systems in the A-V node of the rabbit heart

A. Noma, H. Irisawa, S. Kokobun*, H. Kotake†,
M. Nishimura‡ & Y. Watanabe‡

National Institute for Physiological Sciences, Myodaiji, Okazaki,
444 Japan

Fig. 1   Voltage homogeneity in the small A-V node specimen tested by three different microelectrodes. The current feeding electrode was positioned at the centre of the endocardial side and other two recording microelectrodes were applied about 50 µm from the edge of the preparation. *a*, Simultaneous action potential discharge at three different sites. Action potential measurements are: overshoot 21 mV, maximum diastolic potential −60 mV, duration of the action potential at 50% repolarization 68 ms, maximum rate of rise $10\,V\,s^{-1}$, firing frequency $196\,min^{-1}$. *b*, Evaluation of spatial clamp during the slow inward current by monitoring the potential outside the clamp circuit (lowest voltage trace). Holding potential −40 mV, test pulse −10 mV. 1, command pulse; 2, monitor potential; 3, current trace. *c*, Spatial clamp during the delayed current. Two potential traces were displayed at the same position on the scope. 1–3, As in *b*. Note the difference in calibration between *b* and *c*.

If the heart is to function as an efficient pump, there must be an adequate time delay between the contraction of the atria and that of the ventricles. A major part of this delay is provided by the time of conduction of excitation across the atrioventricular (A-V) node, which electrically links the ventricles with the atria. When the primary pacemaker in the sinoatrial (S-A) node fails to control the cardiac rhythm, as the result of either a depressed automaticity or an impaired conduction, the A-V node can become the pacemaker of the heart[1]. In spite of these essential physiological functions of the A-V node, the precise ionic bases of conduction and the automaticity in the A-V node tissue remain unclear. Here we demonstrate the slow inward current as well as the delayed potassium current in the A-V node using the two-microelectrode voltage-clamp technique.

Recently, DeMello[2] reported the space constant of the rabbit A-V node as 0.4 mm. This clearly indicates that voltage-clamp studies on this tissue are possible using specimens smaller than 0.2 mm. In the present study, small A-V node specimens from the rabbit heart were prepared in essentially the same manner as for the S-A node[3]. The A-V node was identified by its anatomical localization and the action potential configuration[1]. Small strands of tissue 0.2 mm wide and 1–2 mm long were dissected from the A-V node in a 36 °C Tyrode solution, with their longitudinal axis roughly perpendicular to the fibrous A-V ring. This thin strand was then ligated at two sites with a fine silk fibre (prepared by unwinding commercially available silk suture). to give a final dimension of 0.2 × 0.2 × 0.1 mm.

Most of these small A-V nodal preparations spontaneously discharged action potentials (Fig. 1*a*) which were quite similar to those reported previously[4–6]. Voltage homogeneity within this small specimen was tested by using three microelectrodes. Action potentials simultaneously recorded from three different sites (50 µm apart) were closely similar (Fig. 1*a*). During the voltage clamp, the membrane potential monitored outside the feedback circuit deviated only 5 mV for about 10 ms after the onset of the test pulse (Fig. 1*b*, *c*). Therefore, no serious deviation from the command pulse occurred. Similarly good results were obtained in one out of every five specimens tested with three microelectrodes.

Figure 2 shows a family of voltage-clamp records and the current–voltage relationships. The holding potential was −40 mV, where the steady net current was about 0. The transient inward current was recorded between −40 mV and +35 mV, with its peak amplitude at around −10 mV. At −10 mV, the peak of this inward current occurred 5–10 ms after the onset of the test pulse, and the current was inactivated with a time constant of 15–30 ms (Figs 1*b*, 3*a*). This slow time course of the transient inward current is quite similar to that of the slow inward current in the S-A node[7]. To identify this current, we superfused this specimen with compound D600 (Fig. 3*a*), which abolishes the slow inward current. The transient inward current progressively decreased and finally disappeared after 3 min. In contrast, tetrodotoxin, the fast Na^+ channel blocker, caused no appreciable change in the transient inward current. These

observations agree well with previous findings that the A-V node action potential was blocked by Ca-antagonists but not by tetrodotoxin[4–6,8]. Based on these findings, the upstroke of the action potential in our small A-V node preparation is considered to depend predominantly on the slow inward current. Action potentials in the S-A node were shown to propagate at a speed of $2-3\,cm\,s^{-1}$ (ref. 9), and a similar conduction velocity was reported for the A-V node[10]. Dependency of action potentials in these two structures on the slow inward current would readily explain such a slow conduction.

Delayed current systems in these small A-V nodal specimens were also similar to those found in the S-A node. Depolarization
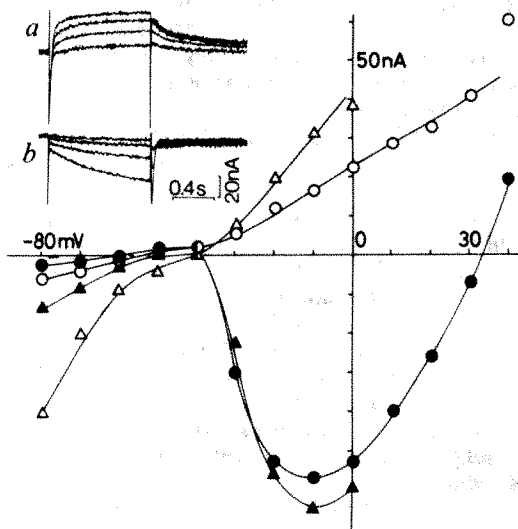
Fig. 2   Current and voltage relationships in the A-V node. Closed symbols indicate transient current, open symbols show the current at 1 s after the change in the potential. Two different experiments are shown. Inset *a* (depolarization) and *b* (hyperpolarization) represent a family of voltage-clamp records in a specimen, from which the curves with triangles were obtained. Duration of the clamp pulse is 1 s.

* Permanent addresses: Department of Physiology, Jikeikai Medical School, Toyko, Japan;
† Department of Internal Medicine, Tottori University School of Medicine, Yonago, Japan;
‡ Cardiovascular Institute, Fujita Gakuen University, Toyoake, Japan.

caused a slow increase in the outward current, whereas on repolarization, a gradual decay in this current was observed (Fig. 2). The time course of this outward current tail within 1s was well fitted by a single exponential curve, with a time constant of 189 ± 24 ms (mean $\pm$s.d., $n = 6$). The reversal potential of the outward current was measured by recording the outward current tail at various potential levels. At 10 mM K^+, the outward current tail changed its sign at around -60 mV (Fig. $3b$),
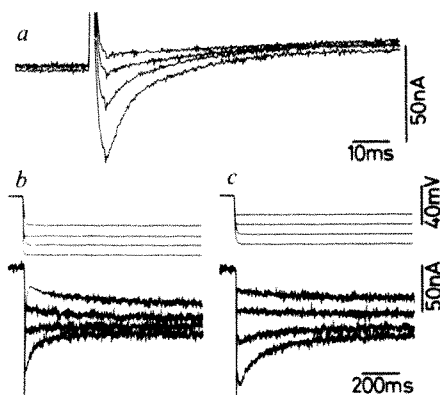
Fig. 3 a, The slow inward current and its progressive decrease induced by perfusion of D600. Current traces from bottom to top were obtained in the control solution, and 1, 2 and 3 min after perfusion of 5×10^{-7} g ml^{-1} D600, respectively. b, c. Reversal potentials of the outward current tail at 10 mM (b) and 20 mM (c) extracellular K^+ concentrations. Top, membrane potential; bottom, current trace. The membrane was depolarized to -10 mV for 1 s and then repolarized to -40, -50, -60, and -70 mV in b and to -30, -40, -50 and -60 mV in c. The time constant of the tail current was 100–240 ms at -50 to -70 mV. At the control concentration of K^+ (3 mM) the reversal of the tail current could not be recorded because of a large inward-going rectification.

whereas at 20 mM K^+, it did so between -40 and -50 mV (Fig. $3c$). From the voltage relationship of the outward current tail, the reversal potential was determined as -62 mV and -43 mV at 10 mM and 20 mM K^+, respectively. Approximately the same slope of 61 mV per 10-fold increase in K^+ concentration was also obtained in three other experiments. These results suggest that K^+ ion is responsible for this outward current. The inward-going current change noted on hyperpolarization from -40 mV to -60 mV (Fig. 2) may be attributed to deactivation of the K^+ current. On the other hand, large inward current changes recorded with further hyperpolarization may be analogous to the current induced by a strong hyperpolarization in the S-A node[11] and in the frog sinus venosus[12]. It is possible that these delayed current systems are involved in the pacemaker depolarization, as is the case for the S-A node.

The present voltage-clamp study showed that the A-V nodal cells possess transmembrane current systems quite similar to those in the S-A node. A common ionic mechanism may underlie automaticity and slow conduction in these two small but vitally important nodal structures in the heart.

1. Watanabe, Y. & Dreifus, L. S. *Circulation Res.* **22**, 717–727 (1969).
2. DeMello, W. C. *Pflügers Arch. ges. Physiol.* **371**, 135–139 (1977).
3. Noma, A. & Irisawa, H. *Pflügers Arch. ges. Physiol.* **364**, 45–52; **366**, 251–258 (1976).
4. Zipes, D. P. & Mendez, C. *Circulation Res.* **32**, 447–454 (1973).
5. Tse, W. W. *Am. J. Physiol.* **225**, 716–723 (1973).
6. Wit, A. L. & Cranefield, P. F. *Circulation Res.* **35**, 413–425 (1974).
7. Noma, A., Yanagihara, K. & Irisawa, H. *Pflügers Arch. ges. Physiol.* **372**, 43–51 (1977).
8. Akiyama, T. & Fozzard, H. A. *Am. J. Physiol.* **236**, C1–C8 (1979).
9. Brooks, C. McC. & Lu, H. H. in *The Sinoatrial Pacemaker of the Heart* (Thomas, Springfield, 1972).
10. Hoffman, B. F. & Cranefield, P. F. in *Electrophysiology of the Heart* (McGraw, New York, 1960).
11. Seyama, I. *J. Physiol., Lond.* **294**, 447–460 (1979).
12. Brown, H. F., Giles, W. & Noble, S. J. *J. Physiol., Lond.* **271**, 783–816 (1977).

α₂-Adrenergic receptors appear in rat salivary glands after reserpine treatment

David B. Bylund & J. Ricardo Martinez

Departments of Pharmacology and Child Health, University of Missouri, School of Medicine, Columbia, Missouri 65212

The regulation of central and peripheral adrenergic receptors by various chemical, physiological, pharmacological and pathological stimuli has been the subject of intense study[1,2]. For example, drug treatments can produce relatively small changes in the density of existing receptor binding sites in a variety of tissues. The α-adrenergic receptors in rat salivary gland tissue have been studied using radioligand receptor binding techniques[3]. We have recently identified and characterised α_1-adrenergic receptors in the rat submandibular gland[4], but surprisingly, α_2-adrenergic receptor binding was not detectable. We now report that a single treatment of reserpine results in the appearance of α_2-adrenergic binding sites within 12 h. Continued treatment with the drug produces further increases in the number of α_2-adrenergic receptors, such that after 7 days the levels of α_1- and α_2-adrenergic receptors are similar. This is the first example of a drug treatment resulting in the appearance of a receptor type which was not previously detectable.

α-Adrenergic receptors, which are heterogeneous in many tissues, have been divided into α_1- and α_2-subtypes on the basis of the differential potency of certain drugs[5]. The α_1-adrenergic receptors are thought to mediate postsynaptic α-adrenergic effects of noradrenaline. In contrast, the α_2-adrenergic receptors generally appear to be involved in the regulation of presynaptic function, and may be localised on the presynaptic membrane. In the appropriate conditions, ^{3}H-clonidine specifically labels α_2-adrenergic receptors in membrane fractions of various mammalian tissues[6,7]. Using this radioligand, we have characterised the α_2-adrenergic receptors in the submandibular gland of control and reserpine-treated rats.

The specific binding of ^{3}H-clonidine to α_2-adrenergic receptors in glands from control animals cannot be reliably quantified (Fig. 1). However, after seven daily injections of reserpine (0.5 mg per kg, intraperitoneally) the amount of specific binding increased dramatically. Rosenthal analysis[8] of the data from a saturation experiment indicated a single class of high-affinity receptor binding sites, having a dissociation constant (K_D) of 1.1 nM (Fig. 1). The maximal number of receptors (B_{max}) that could be labelled by ^{3}H-clonidine in these conditions was 6.1 pmol per g wet weight of tissue. In contrast to this large increase in α_2-adrenergic receptors, α_1-adrenergic receptors

Table 1   Inhibition of ^{3}H-clonidine binding in submandibular gland membranes from reserpinised rats

Drug	n	K_i (nM)
(−) Adrenaline	7	2.6 ± 0.3
(−) Noradrenaline	3	2.9 ± 0.7
(+) Noradrenaline	1	200
Phentolamine	3	3.6 ± 0.4
Prazosin	5	$5,200 \pm 900$
Yohimbine	5	63 ± 14

IC_{50} values were determined from log-probit analyses of inhibition curves using 10 concentrations of the unlabelled drug in duplicate. The concentration of ^{3}H-clonidine was 0.70 nM (13,000 c.p.m.). K_i values were calculated from the equation $K_i = IC_{50}/(1 + [^3\text{H-clonidine}] /K_D) = 0.73\ IC_{50}$.

increased only 56% (from 5.3 to 8.3 pmol per g tissue) after 7 days of reserpine treatment[4].

This time course of the appearance of α_2-adrenergic receptor binding sites is illustrated in Fig. 2. At 12 and 24 h after a single injection of reserpine, the receptor levels were approximately 2 and 3 pmol per g tissue, respectively. When daily injections were continued for 2 to 7 days, the α_2-adrenergic receptor levels continued to increase, and reached a plateau at a level about double that found after a single injection. Although not presented, an identical type of curve was obtained when the data were calculated in terms of pmol bound per mg of membrane protein. The sites labelled by ^{3}H-clonidine in glands from animals treated for 7 days with reserpine have the pharmacological specificity and characteristics of α_2-adrenergic receptors (Table 1). This induction of α_2-adrenergic receptors is also fully reversible in that 2 days after cessation of chronic reserpine treatment, the levels of α_2-adrenergic receptors decreased by about 50% and by 5 days approached the undetectable levels in control animals (unpublished data).

A major pharmacological effect of reserpine is the depletion of presynaptic stores of noradrenaline, which in turn, results in a decreased concentration of noradrenaline in the synapse[9]. There is considerable evidence in both central and peripheral systems, that changes in the density of adrenergic receptors are inversely related to changes in the amount of noradrenaline available to interact with these receptors[1,2]. Thus, it is reason-able to propose that the appearance of α_2-adrenergic receptors in the submandibular gland is a result of the decrease in noradrenaline levels. However, the mechanism of the appearance of these receptors, whether by new synthesis or by the 'unmasking' of existing receptors, is not investigated in our studies.

Fig. 2 The effect of the duration of reserpine treatment on the apparent number of α_2-adrenergic receptor binding sites. Rats were treated daily with reserpine (0.5 mg per kg, intraperitoneally) and then killed 24 h after the last injection (the 0.5 day time point was 12 h after a single injection). The submandibular glands were removed and the B_{max} for ^{3}H-clonidine binding determined as in Fig. 1. Values plotted are means ± s.e.m. and the number of experiments is given in parentheses. Although not shown, there were no significant differences in K_D among the various time points. (The mean ± s.e.m. K_D was 2.05 ± 0.14 nM.)

Fig. 1 Rosenthal analysis of ^{3}H-clonidine binding in rat submandibular gland. Glands were removed from control rats (●), and from treated rats (O) 24 h after the last of seven daily injections of reserpine (0.5 mg per kg, intraperitoneally). The glands were homogenised (Tissumizer) twice in 20 volumes of ice cold 50 mM Tris (pH 8.0 at 25°) and centrifuged at 49,000g for 10 min following each homogenisation. The pellet (a crude particulate fraction) was suspended in 90 volumes of 50 mM Tris (pH 7.4 at 25 °C). For the binding assay, 970 µl of this suspension were incubated for 25 min at 23 °C with various concentrations of ^{3}H-clonidine (22.2 Ci mmol^{-1}, NEN). The suspensions were filtered through GF/B glass-fibre filters (Whatman), washed with buffer, and the radioactivity remaining on the filter was determined. Nonspecific binding, defined by parallel incubation tubes containing 10 µM (−)noradrenaline, was subtracted from the total binding to obtain specific binding. The final concentrations of ^{3}H-clonidine were from 0.08 to 13.3 nM. For the reserpinised animal, the values calculated from a least squares linear regression analysis are, $K_D = 1.1$ nM, and $B_{max} = 68$ pM or 6.1 pmol per g tissue or 146 fmol per mg protein. The means ± s.e.m. for eight experiments are $K_D = 1.9 \pm 0.3$ nM and $B_{max} = 6.2 \pm 0.9$ pmol per g tissue. A plot of this type is often mistakenly called a Scatchard plot. The Scatchard derivation[13] assumes a single species of binding macromolecule of known molecular weight and concentration. When these values are not known, as in the present case, where binding is to membrane fragments, it is appropriate to use the Rosenthal plot[8].

The reserpinised rat has been proposed as an animal model for the human disease, cystic fibrosis[10,11]. This hypothesis is the result of studies on rats treated chronically with reserpine which have demonstrated changes in exocrine gland morphology and function similar to alterations observed in patients with cystic fibrosis. Since abnormalities in the autonomic regulation of salivary and other exocrine glands may be a contributory factor in the aetiology of this disease[12], it will be of interest to investigate α_2-adrenergic function in cystic fibrosis patients.

These data show that the levels of α_2-adrenergic receptors in the rat submandibular gland can be regulated over a far larger range than has been demonstrated for any other neurotransmitter receptor. This system thus seems ideally suited for the study of the localisation, function and mechanisms of regulation of α_2-adrenergic receptors.

1. Williams, L. T. & Lefkowitz, R. J. Receptor Binding Studies in Adrenergic Pharmacology, 127–149 (Raven, New York, 1978).
2. Bylund, D. B. in Modulators, Mediators and Specifiers of Brain Function (eds Ehrlich, Y. H. et al.) 133–162 (Plenum, New York, 1979).
3. Strittmatter, W. J., Davis, J. N. & Lefkowitz, R. J. J. biol. Chem. 252, 5472–5477; 5478–5482 (1977).
4. Bylund, D. B. & Martinez, J. R. Physiologist 22, 16 (1979).
5. Langer, S. Z. Br. J. Pharmac. 60, 481–487 (1977).
6. U'Prichard, D. C., Greenberg, D. A. & Snyder, S. H. Molec. Pharmac. 13, 454–473 (1977).
7. U'Prichard, D. C. & Snyder, S. H. Life Sci. 24, 79–88 (1979).
8. Rosenthal, H. E. Analyt. Biochem. 20, 525–532 (1967).
9. Benmiloud, M. & Von Euler, U. S. Acta physiol. scand. 59, 34–42 (1963).
10. Martinez, J. R., Adelstein, E., Quissell, D. & Barbero, G. J. Pediat. Res. 9, 463–469 (1975).
11. Martinez, J. R., Adshead, P. C., Quissell, D. & Barbero, G. J. Pediat. Res. 9, 470–475 (1975).
12. di Sant'Agnese, P. A. & Davis, P. B. New Engl. J. Med. 295, 597–602 (1976).
13. Scatchard, G. Ann. N.Y. Acad. Sci. 51, 660–672 (1949).

Changes of hippocampal Met-enkephalin content after recurrent motor seizures

J. S. Hong, P. L. Wood, J. C. Gillin*, H. Y. T. Yang & E. Costa

Laboratory of Preclinical Pharmacology and *Laboratory of Clinical Psychopharmacology, National Institute of Mental Health, Saint Elizabeths Hospital, Washington, DC 20032

Kainic acid (KA), a powerful neurotoxic analogue of glutamate, has been extensively used as a tool for selectively lesioning neuronal cell bodies; however, axons or nerve terminals are spared from damage in the area injected with kainic acid[1,2]. Injections of this neurotoxin in various brain regions were successfully used to locate cell bodies of neurones containing substance P, enkephalin and other putative neurotransmitters[3,4]. While attempting to locate the cell bodies of the enkephalin containing neurones present in hippocampus using KA injections, we found that a few days after intracerebral injections of KA a drastic increase in the Met-enkephalin (ME) content of hippocampus occurs. We now describe the delayed increase in hippocampal ME content elicited by intracerebral KA injections and examine the possible mechanism that is operative in causing this increase. Moreover, we provide some evidence suggesting that the increase in ME content elicited by intracerebral injections of KA may be related to the recurrent motor seizures elicited by intracerebral injections of KA.

Male Sprague–Dawley rats (Allison Park) weighing 180–200 g were used. The coordinates for intrahippocampal injection are: A, 3.5; L, 2.4; V, 2.5 according to the atlas of König and Klippel[5]. Unless otherwise stated, rats were anaesthetized with Equithesin (Jensen Salsbury) placed into a stereotaxic holder and injected at constant rate $(1 \ \mu l \ min^{-1})$ with KA dissolved in $1 \ \mu l$ of 0.9% NaCl. The concentration of ME in different brain regions was determined by a previously described radioimmunoassay method[6,7].

Unilateral intrahippocampal injection of KA $(1 \ \mu g$ in $1 \ \mu l$ of 0.9% NaCl) caused recurrent motor seizures lasting 4 to 6 h. ME levels in hippocampus and other brain regions were determined at various times after the injection of KA. At 6 to 12 h after the intrahippocampal injection of KA, the ME content in both injected and contralateral hippocampus was slightly lower than before the injection whereas at 24 h after injection the ME content was increased. In the side injected with KA this elevation reached a maximum after 2 to 3 days and lasted more than 2 weeks. In the hippocampus contralateral to the KA
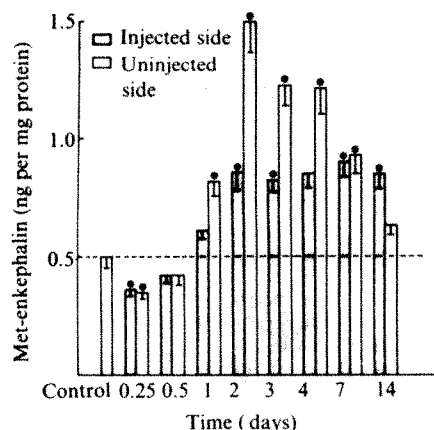
Fig. 1 Time course of change in hippocampal Met-enkephalin content after intrahippocampal injection of kainic acid $(1 \ \mu g$ in $1 \ \mu l$ of 0.9% NaCl). $n = 6$; * significantly different from control, $P < 0.05$.
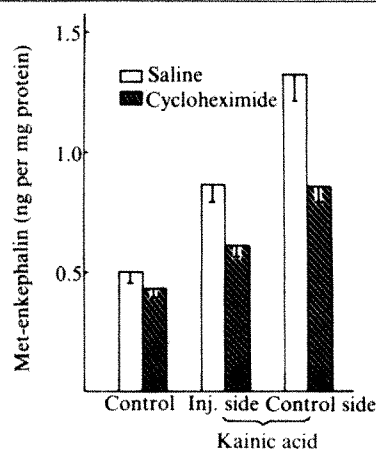
Fig. 2 Hippocampal Met-enkephalin content in control and kainic acid injected rats 24 h after intraventricular injection of cycloheximide or saline. Kainic acid $(1 \ \mu g$ in $1 \ \mu l$ of 0.9% NaCl) was infused into dorsal hippocampus. At 6 h later the rats received an intraventricular injection of either cycloheximide (500 μg in $20 \ \mu l$) or saline through a permanently implanted cannula. Rats were killed 24 h after the administration of cycloheximide or saline. $n = 6$.

injection, the increase in ME content peaked during the first 4 days after the injection and returned to control level by 2 weeks (Fig. 1). A small increase in the ME content (30–40%) was also found in the nucleus caudate and septum; in contrast, the ME content in other brain regions remained unchanged. The levels of substance P, γ-aminobutyric acid (GABA) and glutamate did not increase in either side of the hippocampus 3 days after the intrahippocampal injection of KA, suggesting that the enhancement of ME content elicited by such an injection is a specific effect. A selective increase in hippocampal ME content was also elicited by intraseptal, intrastriatal or intraventricular injections of KA (Table 1). As these injections of KA in various brain regions also caused recurrent motor seizures, it became apparent that the recurrent seizures may be related to the mechanism that triggers the increase in hippocampal ME. This hypothesis was strengthened by the finding that the increase in hippocampal ME content was also observed 2 days after the recurrent seizures induced by either isoniazid or by repeated electroconvulsive shocks (four shocks given at 30 min intervals, data not shown). Moreover, the increase in hippocampal ME content elicited by intrahippocampal KA injection was completely blocked by an injection of phenobarbital which prevents the seizure activity induced by intrahippocampal KA (Fig. 2). Muscimol (like phenobarbital) prevented the increase in hippocampal ME content and the convulsions elicited by KA (data not shown). Thus the evidence we have reported supports the view that recurrent seizures may increase the hippocampal ME content.

Table 1 Hippocampal ME content 3 days after intracerebral injections of KA

Route of injection	Dose	Met-enkephalin (ng per mg protein)	
		Control	Treated
Intrastriatal	(1 μg)	0.60 ± 0.04	1.7 ± 0.1*
Intraseptal	(0.5 μg)	0.50 ± 0.03	1.5 ± 0.12*
Intraventricular	(0.25 μg)	0.52 ± 0.03	0.52 ± 0.04
	(0.5 μg)	0.52 ± 0.03	0.60 ± 0.05
	(1.0 μg)	0.52 ± 0.03	1.0 ± 0.07*
	(2.0 μg)	0.52 ± 0.03	1.5 ± 0.12*

The coordinates, according to König and Klippel[5], for the intracerebral injections were: intraseptal (A, 7.8; L, 0; V, 1.0), intrastriatal (A,7.8; L,2.5; V,0) and intraventricular (lateral-ventricle through a permanently inplanted plastic cannula). $n = 6$–10.
 * $P < 0.05$.
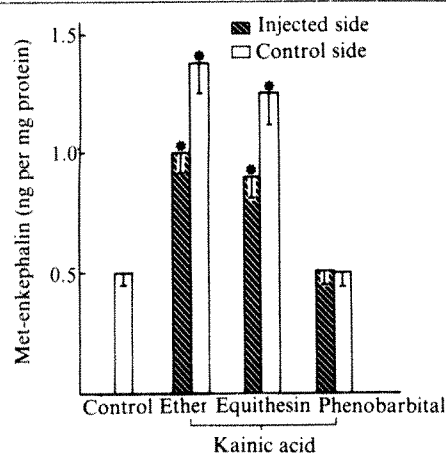
Fig. 3   Effect of pretreatment with phenobarbital (50 mg per kg, intraperitoneally) on the kainic acid induced increase in hippocampal Met-enkephalin content. Kainic acid (1 µg in 1 µl of 0.9% NaCl) was infused into dorsal hippocampus of rats under anaesthesia by either ether or equithesin (main components are chloral hydrate and pentobarbital). For the rats pretreated with phenobarbital, ether was used as anaesthetic. Phenobarbital was given 30 min before and 2 h after the injection of kainic acid. $n = 6$; * significantly different from control value, $P < 0.05$.

The mechanism of metabolic regulation of hippocampal ME is still unknown. The biphasic modification of the hippocampal ME content elicited by intrahippocampal injections of KA indicates that the metabolic state of hippocampal ME can change in response to an increase or a decrease in the rates of neuronal activity. A study of the time course of the elevation of the ME content in the hippocampus ipsilateral or contralateral to the KA injection, revealed that the extent of the increase was greater in the contralateral hippocampus but the increase was longer lasting in the ipsilateral hippocampus (Fig. 1). The persistent modification of the ME content in the injected hippocampus suggests that KA may relieve ME neurones from a tonic inhibition by GABA or other inhibitory neurones.

The hippocampus is important in the modulation of aggression[8] and memory[9], and seems to be closely associated with the pathogenesis of epilepsy[10]. This region is particularly prone to convulsions[11]. Stimulation of opioid receptors has an important role in seizures—for instance, microinjection of Leu-enkephalin into the dorsal hippocampus of cats and rats produces epileptiform patterns of electrical activity in the hippocampal EEG. This convulsant action of enkephalin was prevented by microinjection of naloxone[12]. Furthermore, naloxone curtails but morphine exacerbates the postictal behavioural depression, suggesting that opioid peptides are released during the seizure and have a role in the postictal depression of motor activity[13,14]. Although the present study does not make clear the precise mechanism whereby the biphasic change in hippocampal ME content influences seizures, it is clear that the ME content of hippocampus is decreased during recurrent seizures, and these episodes trigger a delayed, long term, rebound increase in the hippocampal ME content.

We thank Mr F. Storch for technical assistance.

1. Coyle, J. T. & Schwartz, R. *Nature* **263**, 244–246 (1976).
2. McGeer, P. L. & McGeer, E. G. *Nature* **263**, 517–519 (1976).
3. Hong, J. S., Yang, H.-Y. T., Racagni, G. & Costa, E. *Brain Res.* **122**, 541–544 (1977).
4. Hong, J. S., Yang, H.-Y. T., Fratta, W. & Costa, E. *Neuropharmacology* **16**, 451–453 (1977).
5. König, J. F. R. & Klippel, R. A. *The Rat Brain* (Krieger, Huntington, New York, 1967).
6. Yang, H.-Y. T., Hong, J. S. & Costa, E. *Neuropharmacology* **16**, 303–307 (1977).
7. Hong, J. S., Yang, H.-Y. T., Fratta, W. & Costa, E. *J. Pharmac. exp. Ther.* **205**, 141–147 (1978).
8. Gage, F. H. & Olton, D. S, *Brain Res.* **98**, 311–325 (1975).
9. Olton, D. S. *Scient. Am.* **236**, 82–84 (1977).
10. Malamud, N. *Archs Neurol.* **14**, 190–195 (1966).
11. Minckler, J. (ed.) *Pathology of the Nervous System* Vol. 2 (McGraw-Hill, New York, 1971).
12. Elazar, Z., Motles, E., Elv, Y. & Simantov, R. *Life Sci.* **24**, 541–548 (1979).
13. Frenk, H., Engel, J., Ackermann, R., Shavit, Y. & Liebeskind, J. C. *Brain Res.* **167**, 435–440 (1979).
14. Belenky, G. L. & Holaday, J. W. in *Endogenous and Exogenous Opiate Agonists and Antagonists* (ed. Way, E. L.) (Pergamon, Oxford, in the press).

Brain noradrenaline depletion prevents ECS-induced enhancement of serotonin- and dopamine-mediated behaviour

A. R. Green

MRC Clinical Pharmacology Unit, Radcliffe Infirmary, Oxford OX2 6HE, UK

J. F. W. Deakin

Division of Neurophysiology and Neuropharmacology, National Institute for Medical Research, Mill Hill, London NW7 1AA, UK

When rats are given a series of electroconvulsive shocks (ECSs) over several days, they display enhanced behavioural responses to both serotonin- and dopamine-receptor agonists [1-3]. Because these changes are seen when the ECS is given in ways closely mimicking the clinical administration of electroconvulsive therapy (ECT), it has been suggested that the changes in postsynaptic monoamine function may be involved in the antidepressant mechanisms of ECT[4,5]. Ligand-binding studies have excluded the possibility that ECS alters the characteristics of either the serotonin or dopamine receptor[6-8]; ECS may therefore be acting on neuronal systems which modulate monoamine neurotransmission. As repeated ECS has recently been reported to decrease both noradrenaline (NA)-sensitive adenylate cyclase[9] and β-adrenoreceptor binding[8,10,11], we have examined here whether changes in NA function are related to the effects of ECS on the serotonin- and dopamine-mediated behaviours. We demonstrate that although selective depletion of NA does not alter the drug-induced serotonin- and dopamine-mediated responses, it abolishes the ECS-induced enhancement of these behaviours.

Rats were anaesthetized with Nembutal (60 mg per kg), and 8 µg of 6-hydroxydopamine (6-OHDA) in 2 µl vehicle was stereotaxically injected bilaterally into the locus coeruleus and dorsal and ventral noradrenergic bundles at a level 2 mm caudal to the substantia nigra. The efficacy and specificity of the lesions were confirmed biochemically (Table 1).

Ten days after operation, sham-operated and lesioned rats were given five ECSs (130 V, 50 Hz sinusoidal for 1 s through earclip electrodes) over 10 days (days 1, 3, 5, 8 and 10). ECS-treated rats were compared with animals (sham-operated and lesioned) which had received anaesthetic only. The behavioural responses of the rats to the putative serotonin agonist quipazine (25 mg per kg) or the dopamine agonist apomorphine (2 mg per kg) were examined 24 h after the final ECS or anaesthetic treatment. These behavioural responses were quantified by placing groups of three animals in cages on Automex activity meters (PMS Instruments).

Quipazine induced several abnormal behaviours[14], and hyperactivity components were recorded by the meters. The lesion did not affect the quipazine response in non-shocked animals (Fig. 1). Furthermore, ECS enhanced the quipazine-

Table 1   Effect of the 6-OHDA lesion on whole brain monoamine concentrations

	Brain monoamine concentration (µg per g brain)		
	Noradrenaline	Dopamine	Serotonin
Sham	0.31 ± 0.01 (14)	1.01 ± 0.10 (14)	0.30 ± 0.01 (18)
Lesioned	0.04 ± 0.02 (14)*	0.85 ± 0.09 (15)†	0.31 ± 0.02 (9)

Results show mean ± s.e.m. with number of observations in parentheses. Different from sham-lesioned control values: * $P < 0.001$; † $P < 0.05$. Brain catecholamines were assayed by the method of Chang[13] and serotonin by the method of Curzon and Green[14].
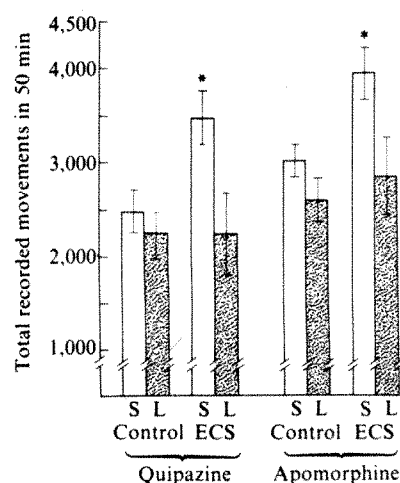
Fig. 1 Effect of 6-OHDA-induced lesions of brain noradrenergic systems on ECS-induced enhancement of quipazine- and apomorphine-mediated locomotor activity. Responses of the sham-operated (marked S and open columns) and noradrenergic-lesioned rats (marked L and stippled columns) are shown. Locomotor activity in groups of three rats following quipazine (25 mg per kg, intraperitoneally) {left hand side} or apomorphine (2 mg per kg, intraperitoneally) {right hand side} was measured in both sham and lesioned groups (control responses). Other groups were given five ECSs spread over 10 days and tested with the two drugs (ECS responses). Results show responses to both drugs in five or six experiments and are reported as the mean ± s.e.m. of the locomotor counts in the 50 min following drug administration.
* Different from appropriate control response of lesioned animals:
$P < 0.01$.

induced behaviour in the sham-operated rats, as previously reported in unoperated rats[3], but completely failed to alter the hyperactivity response in NA-depleted animals (Fig. 1).

Apomorphine produced a similar locomotor response in both the sham-operated and lesioned rats that had not received ECS (Fig. 1). Following ECF administration there was the expected potentiation of the apomorphine response[1] in the sham-operated animals, but this failed to occur in the lesioned rats (Fig. 1). The degree of enhancement in both serotonin- and dopamine-mediated responses ($\sim$30%) produced by ECS administration was very similar to that seen in other recent experiments in this laboratory[4].

These results demonstrate that destruction of brain noradrenergic systems totally abolishes the ability of ECS to potentiate quipazine- and apomorphine-induced hyperactivity. They also demonstrate that NA is not involved in the mediation of the behavioural syndromes themselves, as the lesion was without effect in non-shocked animals. This result is consistent with the finding that NA depletion with disulfiram did not alter the serotonin-mediated behaviour[15]. Our data suggest that changes occur in brain noradrenergic systems during ECS that result in enhancement of serotonin- and dopamine-mediated behaviour. Several observations indicate that ECS does affect noradrenergic systems: repeated ECS increases tyrosine hydroxylase activity[16], accelerates NA turnover[17,18] and inhibits NA re-uptake at the nerve ending[19,20]. These observations may indicate an increased release of NA from the nerve ending, which could result in the reduction in β-receptor binding observed in ECS-treated rats[8,10,11]. However, this interpretation may be challenged by the finding that ECS decreases the sensitivity of adenylate cyclase to NA in rat forebrain slices, as this occurred in 6-OHDA-lesioned rats[9]. Nevertheless, it is clear that presynaptic NA systems must be involved in the production of the enhanced monoaminergic responses we have observed following ECS. This view is supported by our recent finding that catecholamine synthesis inhibition also abolishes the ability of ECS to enhance serotonin- and dopamine-mediated behaviours[22].

Although the lesion produced a slight (16%) reduction in brain dopamine content (Table 1), this could not explain our findings, first, because apomorphine is an agonist and second, because the DA denervation would, if anything, increase the apomorphine-mediated response, by producing receptor supersensitivity.

These results demonstrate a noradrenergic mechanism of action of ECS in potentiating serotonin- and dopamine-mediated behaviours. It is tempting to speculate that the antidepressant action of ECT may involve similar mechanisms, in view of the many lines of evidence implicating monoamines in the aetiology of depression and in the mechanism of action of antidepressant drugs (reviewed in ref. 21).

1. Modigh, K. *J. neural Transmission* **36**, 19–32 (1975).
2. Evans, J. P. M., Grahame-Smith, D. G., Green, A. R. & Tordoff, A. F. C. *Br. J. Pharmac.* **56**, 193–199 (1976).
3. Green, A. R., Heal, D. J. & Grahame-Smith, D. G. *Psychopharmacology* **52**, 195–200 (1977).
4. Costain, D. W., Green, A. R. & Grahame-Smith, D. G. *Psychopharmacology* **61**, 167-170 (1979).
5. Grahame-Smith, D. G., Green, A. R. & Costain, D. W. *Lancet* **i**, 254–257 (1978).
6. Cross, A. J. *et al. Br. J. pharmac.* **66**, 111P (1979).
7. Atterwill, C. K. & Prince, A. K. *11th int. Meet. int. Soc. Neurochem.*, Jerusalem (1979).
8. Bergstrom, D. A. & Kellar, K. J. *Nature* **278**, 464–466 (1979).
9. Vetulani, J., Schwartz, R. J., Dingell, J. V. & Sulser, F. *Naunyn-Schmiedebergs Archs Pharmak.* **293**, 109–114 (1976).
10. Pandey, G. N., Heinze, W. J., Brown, B. D. & Davis, J. M. *Nature* **280**, 234–235 (1979).
11. Deakin, J. F. W., Owen, F. & Poulter, M. *Neurosci. Lett.* (in the press).
12. Curzon, G. & Green, A. R. *Br. J. Pharmac.* **39**, 653–655 (1970).
13. Chang, C. C. *Int. J. Neuropharmac.* **3**, 645–649 (1964).
14. Green, A. R., Youdim, M. B. H. & Grahame-Smith, D. G. *Neuropharmacology* **15**, 173–179 (1976).
15. Green, A. R. & Grahame-Smith, D. G. *Neuropharmacology* **13**, 949–959 (1974).
16. Mussachio, J. M., Julou, L., Kety, S. S. & Glowinski, J. *Proc. natn. Acad. Sci. U.S.A.* **63**, 1117–1119 (1969).
17. Modigh, K. *Psychopharmacology* **49**, 179–185 (1976).
18. Kety, S. S., Javoy, F., Therry, A. M., Julou, L. & Glowinski, J. *Proc. natn. Acad. Sci. U.S.A.* **58**, 1249–1254 (1967).
19. Modigh, K. in *Neuropsychopharmacology* (eds Saletu, B. & Hollister, L.) (Pergamon, Oxford, in the press).
20. Hendley, E. D. *Psychopharmac. Commun.* **2**, 17–25 (1976).
21. van Praag, H. M. *Depression and Schizophrenia* (Spectrum, Flushing, 1976).
22. Green, A. R., Costain, D. W. & Deakin, J. F. W. *Neuropharmacology* (in the press).

Partial denervation in inactive muscle affects innervated and denervated fibres equally

A. Cangiano & L. Lutzemberger

Istituto di Fisiologia, Università di Pisa,
Via S. Zeno, 31, Pisa, Italy

Possible causal factors of denervation-induced changes in muscle include inactivity, products of nerve degeneration and lack of a nerve-borne trophic agent. We now show that if the innervated fibres in a partially denervated rat muscle are rendered inactive, they undergo a reaction as intense as that of the denervated fibres. This provides further support for the view that the effects of denervation on the extrajunctional muscle membrane result from a combination of muscle inactivity and of nerve breakdown products acting diffusely throughout the muscle.

Denervation affects the properties of skeletal muscle fibres through changes which can be attributed in part to inactivity of the muscle[1,2] and in part to factors arising independently of changes in impulse activity[3-9]. Thus denervation elicits larger changes in resistance to tetrodotoxin (TTX) of the muscle action potential[5,8], fibrillatory activity[8,9] and extrajunctional acetylcholine (ACh) receptor density[6,7,9] than muscle paralysis in the absence of nerve degeneration. The difference in efficacy between denervation and paralysis *per se* could arise if cutting the nerve would interrupt the flow of neurotrophic substances to the muscle (for review, see ref. 10). Alternatively, the cut could, by causing nerve degeneration, give rise to pathological factors in the muscle which directly or indirectly affect the muscle fibres.

The latter 'products of nerve degeneration' hypothesis has recently received considerable experimental support[2,11-13]. For example, in partially denervated muscles not only the denervated but also the remaining innervated fibres develop resistance to TTX, although the innervated fibres respond less strongly[12] (but see refs 14, 15). The weaker response of the innervated fibres could be due to their activity since muscle activity is known to inhibit ACh receptor synthesis[16] and other effects of denervation[2]. In the absence of this suppressive effect

Max. rate of rise of spikes
(Vs⁻¹)

ACh sensitivity
(mV nC⁻¹)
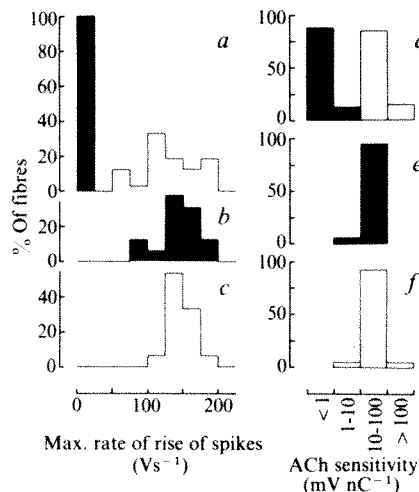
Fig. 1 Resistance of action potentials to tetrodotoxin (a, b, c) and sensitivity to microiontophoretically applied acetylcholine (d, e, f) measured in the same soleus muscle fibres at 1.5–2 mm from the endplate region. Each population is composed of 25–40 fibres from four to five muscles. a And d represent purely impulse-blocked (solid columns) and totally denervated (open columns) muscles. b, c, e And f represent partially denervated muscles (by sectioning the radicular nerve L_5) with an impulse-blocked innervation. Innervated (b and e) and denervated (c and f) fibres were distinguished on the basis of presence or absence of miniature endplate potentials (m.e.p.ps) at the endplate region. The percentage of denervated fibres found in the soleus muscles ranged from 36 to 68%. Resistance to TTX was measured at the endplate region, and, in conjunction with sensitivity to ACh, 1.5–2 mm away from it. Two intracellular micropipettes, one for recording (3 M KCl) and the other for passing currents (2 M K citrate) were used, while a third micropipette was put in a just extracellular position for ACh iontophoresis (3 M AChCl). Each fibre was followed over the indicated distance by shifting the recording electrode while applying hyperpolarizing pulses with the current electrode. An alternate pattern of exploration was followed, so that in one fibre the extrajunctional measurements were done first and those at the endplate region second, whereas in the next fibre the reverse order was followed. Resistance to TTX was determined eliciting and recording action potentials in the presence of TTX 10^{-6} M (refs 12, 24). The resting membrane potential was set at −100 mV and the strength of the depolarizing pulse adjusted to give a constant delay of 4 ms between its onset and that of the action potential. The amount of TTX resistance was measured as the maximal rate of rise of the action potential given by its electronically recorded first derivative through an RC circuit (× 10^5 Ω, 100 pF). Sensitivity to ACh was measured with conventional techniques[25]. The ACh pipettes were several hundred megohms in resistance and required less than 2 nA braking current. The RMP was set at a constant value of −80 mV with the current electrode while evoking an ACh potential. Units of ACh sensitivity represent millivolts of depolarization per 10^{-9} C of charge passed through the iontophoretic pipette. The oxygenated mammalian Ringer's solution bathing the muscles was kept at a temperature of 28 °C. The results obtained for the TTX resistance at the endplate region were similar to those shown in this figure, although all values were moderately higher than in the extrajunctional region, confirming that after denervation TTX resistance develops earlier near the endplates[24]. Thus, the maximal rate of rise of spikes in the partially denervated muscles was 128 ± 5.4 Vs⁻¹ (±s.e.m.) for the denervated fibres and 127 ± 6.7 for the innervated fibres as compared to 3.1 ± 1.5 for the paralysed control muscles with intact nerves. As far as the EDL muscles are concerned, the results obtained in three impulse-blocked, partially denervated muscles examined between 56 and 72h were similar. For example, the maximal rate of rise in TTX 10^{-6} M at the endplate region was 108 ± 10.3 for 16 denervated fibres and 122 ± 6.9 for 22 innervated fibres, while in the paralysed control muscles with intact nerves the average value was only 11 ± 2.1 (24 fibres). At the time of the acute experiment stimulation of the sciatic nerve proximal to the cuff evoked no contraction of EDL and soleus muscles in partially denervated or control preparations with intact nerves. Stimulation distal to the cuff evoked muscle twitches and transmitted action potentials could be recorded from the muscle fibres before TTX was added to the perfusion fluid. Frequency of m.e.p.ps was normal (2.3 ± 0.1 s⁻¹ in 31 innervated fibres of four partially denervated soleus and 2.1 ± 0.1 s⁻¹ in 29 fibres of three normal soleus).

of activity, the muscle fibres may become particularly sensitive to the effects of degeneration of the nerve. It is therefore possible that these effects may combine with the effects of inactivity to produce the full response to denervation. In that case one would expect innervated but inactive fibres to respond as strongly as adjacent denervated fibres to extensive partial denervation. We have tested this possibility by partially denervating muscles which in addition were paralysed by a chronic conduction block in the nerve.

The extensor digitorum longus (EDL) and the soleus muscles of adult rats were chronically inactivated by blocking impulse conduction in the sciatic nerve with TTX-impregnated cuffs[6]. At the same time the muscles were partially denervated by cutting the radicular nerve L_5 just outside the vertebral canal. Control muscles were either completely denervated or subjected to chronic nerve conduction block only. Soleus and EDL muscles were examined 56–72 h later *in vitro* for the development of extrajunctional sensitivity to ACh and of junctional and extrajunctional resistance to TTX, all essentially absent in normal soleus and EDL muscles[15,17]. The denervated control muscles were then already highly resistant to TTX and sensitive to ACh (Fig. 1a, d, open columns) while the paralysed control muscles with intact nerves were just beginning to respond (Fig. 1a, d, solid columns). As expected, the denervated fibres in the partially denervated muscles had values comparable to those in the denervated control muscles (Fig. 1c, f). The innervated fibres, on the other hand, were as resistant to TTX and as sensitive to ACh as the denervated fibres (Fig. 1b, e), which was much more than expected from the inactivity alone (Fig. 1a, d, solid columns).

Note that the fibres in the muscles with only about 50% denervation respond as strongly as the fibres in the totally denervated muscles (Fig. 1). This illustrates the efficacy of the effect of partial denervation and one possible explanation would be that at this relatively late time the muscle fibres are already responding maximally. We therefore examined the responses at an earlier time, using muscles in which we had produced different degrees of partial denervation (~10% to 90%) (Fig. 2). The results show that at 50 h there was a positive correlation between the percentage of denervated fibres and resistance to TTX for both innervated and denervated fibres (Fig. 2). Furthermore, for any degree of partial denervation there was essentially no difference between denervated and innervated fibres. Consequently, in inactive muscles, innervated and denervated fibres give equal responses to partial denerva-

% Of denervated fibres
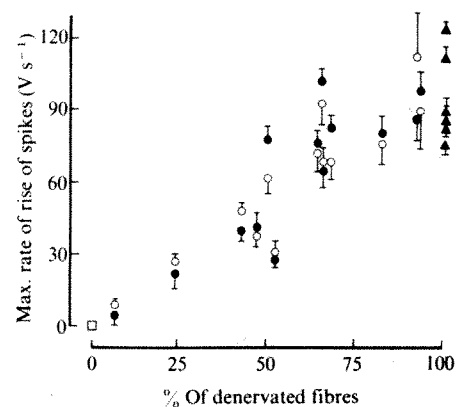
Fig. 2 TTX resistance measured in denervated (●) and innervated impulse-blocked (○) fibres, plotted as a function of the percentage of denervated fibres found in each partially denervated soleus muscle. Each point represents the average TTX resistance measured at 50 h near the endplate region in 4–15 fibres per muscle (the lowest figure applies either to the denervated or the innervated fibres of those muscles exhibiting the lowest or the highest percentage of denervation respectively). Totally denervated (▲) and purely paralysed (□) muscles are also shown for comparison. The lowest percentages of denervation were obtained by incompletely sectioning the radicular nerve L_5. To obtain a reliable value for the percentage of denervated fibres, 40–50 fibres were recorded in each muscle to observe the presence or absence of m.e.p.ps. Bars represent the standard error of the mean.
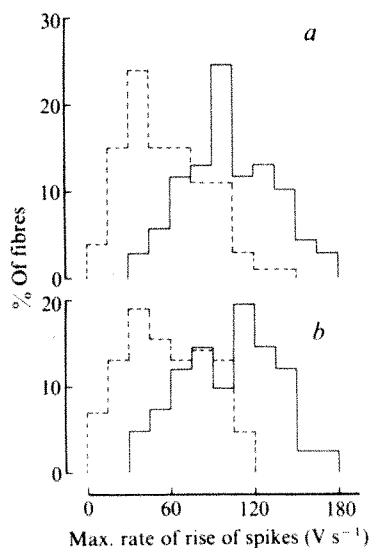
Fig. 3 Class distribution of TTX resistance measured near the endplate region in innervated impulse-blocked fibres (a) and denervated fibres (b) of 'closely' (columns with continuous lines) and 'distantly' (columns with broken lines) partially denervated soleus muscles at 50 h (about 30 fibres measured per muscle). The percentage of denervated fibres found in the muscles of the two populations was comparable: average 40% for the closely denervated (5 muscles) and 53% for the distantly denervated muscles (8 muscles). The difference in the length of the 'nerve stump' for the two populations was about 6 cm. Although no obvious trauma of the soleus occurred with 'close' partial denervation since the muscle was not exposed the possibility was considered that the greater TTX resistance at 50 h was not a nerve-length effect but a result of muscle damage, particularly because inactive muscles should be more responsive. However, this possibility was excluded because no TTX resistance was observed in the impulse-blocked soleus of three rats in which the attempted close section of the soleus nerve had failed to damage any motor axon.

tion as expected if nerve degeneration causes substances to appear in the interstitium which change the membrane properties of all fibres in that region.

The objection might be raised that nerve degeneration in the periphery is not the only consequence of partial denervation. Axotomy might have central effects which might affect the production of neurotrophic substances in adjacent intact motoneurones. In the frog, for instance, nerve section results in sprouting from contralateral intact axons apparently through changes taking place in the spinal cord[18]. To examine this possibility we partially cut the nerve supply either far from the soleus muscle by sectioning (as before) the radicular nerve L_5 or close to the muscle by incompletely sectioning the soleus nerve. The innervated fibres were rendered inactive by a TTX-containing cuff around the sciatic nerve. In agreement with previous results obtained in totally denervated muscles[4], after 50 h the TTX resistance of the denervated fibres was significantly higher in muscles with a short nerve stump than with a long nerve stump (Fig. 3b). Identical behaviour was observed in the innervated fibres of the same muscles (Fig. 3a), which indicates that the effect on the innervated fibres, as that on the denervated, is peripheral in origin and probably related to the fact that short nerve stumps degenerate more quickly than long nerve stumps[19]. Had the effect of partial denervation on the innervated fibres been of central origin, their response would have been expected to lag behind that of the denervated fibres, and to occur earlier in the experiments where the nerve was cut close to the spinal cord.

Thus the present results confirm and extend our previous study[12] by showing that partial denervation also affects the innervated fibres within the muscle. In muscles where the suppressive influence of activity on ACh receptor synthesis and other denervation-like changes[2,16] has been removed, the responses of innervated and denervated fibres become indistinguishable. This suggests that the response of the muscle fibre membrane to denervation may be accounted for as the combined result of inactivity and the effects of nerve degenera-

tion *per se*. The effect could be due to nerve breakdown products acting either directly on the muscle fibres or indirectly via Schwann cells, cells of the immune system or other tissue cells. It should be emphasized that in this work only the effects on the extrajunctional membrane have been studied and that the properties of the postjunctional membrane may be controlled by different mechanisms[20-23].

This work was supported by grants from the Muscular Dystrophy Association of America and from the Consiglio Nazionale delle Ricerche of Italy.

1. Lømo, T. & Rosenthal, J. J. Physiol., Lond. **221**, 493–513 (1972).
2. Lømo, T. & Westgaard, R. H. Cold Spring Harb. Symp. quant. Biol. **40**, 263–274 (1976).
3. Miledi, R. J. Physiol., Lond. **151**, 1–23 (1960).
4. Harris, J. B. & Thesleff, S. Nature new Biol. **236**, 60–61 (1972).
5. Cangiano, A., Lutzemberger, L. & Zorub, D. S. Neurosci. Abstr. **1**, 766 (1975).
6. Lavoie, P. A., Collier, B. & Tennenhouse, A. Nature **260**, 349–350 (1976).
7. Pestronk, A., Drachman, D. B. & Griffin, J. W. Nature **260**, 352–353 (1976).
8. Cangiano, A., Lutzemberger, L. & Nicotra, L. J. Physiol., Lond. **273**, 691–706 (1977).
9. Gilliatt, R. W., Westgaard, R. H. & Williams, J. I. J. Physiol., Lond. **280**, 499–514 (1978).
10. Purves, P. Int. Rev. Physiol. Neurophysiol. II **10**, 125–177 (1976).
11. Jones, R. & Vrbová, G. J. Physiol., Lond. **236**, 517–538 (1974).
12. Cangiano, A. & Lutzemberger, L. Science **196**, 542–545 (1977).
13. Brown, M. C., Holland, R. L. & Ironton, R. Nature **275**, 652–654 (1978).
14. Tiedt, T. N., Albuquerque, E. X. & Guth, L. Science **198**, 839–841 (1977).
15. Cangiano, A. & Lutzemberger, L. Acta. physiol. scand. (in the press).
16. Hall, Z. W. & Reiness, C. G. Nature **268**, 655–657 (1977).
17. Miledi, R. & Zelená, J. Nature **210**, 855–856 (1966).
18. Rootshenker, S. Brain Res. **155**, 354–356 (1978).
19. Miledi, R. & Slater, C. R. J. Physiol., Lond. **207**, 507–528 (1970).
20. Younkin, S. G., Brett, R. S., Davey, B. & Younkin, L. H. Science **200**, 1292–1295 (1978).
21. Jessell, T. M., Siegel, R. E. & Fishbach, G. D. Neurosci. Abstr. **4**, 369 (1978).
22. Podleski, T. R. et al. Proc. natn. Acad. Sci. U.S.A. **75**, 2035–2039 (1978).
23. Christian, C. N. et al. Proc. natn. Acad. Sci., U.S.A. **75**, 4011–4016 (1978).
24. Redfern, P. & Thesleff, S. Acta physiol. scand. **82**, 70–78 (1971).
25. Del Castillo, J. & Katz, B. J. Physiol., Lond. **128**, 157–181 (1955).

Proteinase inhibitors suppress the development of experimental allergic encephalomyelitis

Celia F. Brosnan*, Wendy Cammer†,
William T. Norton† & Barry R. Bloom‡

Department of Pathology*, Neurology† and Neuroscience‡. Microbiology and Immunology, and Cell Biology, Albert Einstein College of Medicine, 1300 Morris Park Avenue, Bronx, New York 10461

Experimental allergic encephalomyelitis (EAE) is an autoimmune inflammatory disease of the central nervous system (CNS) induced in animals by sensitization with white matter or with myelin basic protein (BP)[1,2]. EAE is dependent on cell-mediated immune (CMI) reactions requiring T-cell sensitization[2-4], and demyelination is observed in the vicinity of perivascular infiltrates of mononuclear cells[5]. However, the mechanisms by which CMI reactions initiate the clinical and pathological expression of EAE have not been well defined. Numerous mechanisms have been proposed for the degradation of myelin, including activated components of the complement system[6,7] and the action of enzymes released by inflammatory cells[8,9]. Among these enzymes, lipases, lysosomal acid proteinases and lymphocyte proteinases have been stressed[8-14]. Recent reports from this laboratory have suggested that damage to the myelin sheath may be initiated by the release of neutral proteinases, including plasminogen activator, from macrophages activated during an immune response[15]. If neutral proteinases and, particularly, plasmin, generated from plasminogen by plasminogen activator, have a key role in initiating the clinical signs and pathology of the demyelinating diseases, it might be expected that inhibitors of these enzymes would protect sensitized animals against EAE. Here we have shown that aminomethylcyclohexane carboxylic acid (AMCA), ε-amino-caproic acid (EACA) and p-nitrophenylguanidinobenzoate (NPGB), which are inhibitors of plasminogen activator and other neutral proteinases, gave significant protection against the clinical expression of EAE in Lewis rats. Other protease inhibitors gave partial or no protection.

Fig. 1 Weight loss curves for two experiments. Animals were sensitized and drugs administered as described in Table 1 legend. The mean weight for each group is expressed as per cent of the mean weight of the respective group at day 7.

inhibitors of microbial origin[17], did not prevent paralysis at a dose of 1 mg twice a day, and insufficient material was available for testing at higher doses.

AMCA is 5–10 times more effective than EACA as an inhibitor of fibrinolysis[18,19], and consistent with this is the finding that AMCA was more effective than EACA in protecting against EAE (Table 1). However, interpretation of the clinical data for NPGB, pepstatin and Trasylol is more complicated. NPGB, which also inhibits plasminogen activator and plasmin, becomes toxic at approximately 10 mg per day, is difficult to solubilize and hydrolyses readily. We suspect that the beneficial effects of NPGB in inhibiting EAE are offset by toxic effects of the hydrolysis product, p-nitrophenol[20]. Of the inhibitors used, AMCA and NPGB were most effective in decreasing the extent of weight loss which is characteristic of EAE (Fig. 1).

Pepstatin was also difficult to solubilize, and initially it was administered as a suspension in 10% ethanol. In these experiments, six out of nine animals failed to become paralysed. In the experiment shown in Fig. 1, pepstatin protected against weight loss, but this effect was not consistent. To control for the possibility that either the alcohol solvent or the particulate nature of the polypeptide, pepstatin, was protective, we treated rats with a suspension of polyvaline in 10% ethanol. Polyvaline, which is not known to inhibit proteinases, did not protect against EAE (Table 1). In animals treated with Trasylol, the onset of clinical signs was earlier and paralysis more severe than in the control animals (Table 1), and the animals lost more weight than the controls (Fig. 1).

The degree of infiltration of the CNS by inflammatory cells was evaluated histologically. Routine haematoxylin and eosin staining showed some pathological evidence of disease in animals from all the groups, but in animals successfully treated with pepstatin and NPGB (Fig. 2), both perivascular infiltration and sub-meningeal inflammation were markedly reduced. In asymptomatic animals treated with the antifibrinolytic drugs AMCA and EACA, haematoxylin and eosin sections showed perivascular infiltration to be reduced only slightly; however, it was obvious from toluidine blue-stained sections of AMCA-treated animals that the extent of invasion into the white matter and the degree of demyelination in the vicinity of the inflammatory cells were reduced considerably (Fig. 3). Histological examination of paralysed animals receiving Trasylol demonstrated a widespread diffuse cellular invasion at all levels of the spinal cord and brain, and the degrees of infiltration and demyelination were more severe than in paralysed control animals.

The findings that Trasylol exacerbated EAE and that pepstatin, an inhibitor of acid proteinases, conferred partial protection against EAE, would seem to be inconsistent with our hypothesis. Two modes of action for pepstatin can be considered. One is that

Male inbred Lewis rats weighing ~300 g were injected on day 0 in each hind footpad with 0.1 ml of an emulsion containing a freshly prepared 50% suspension in saline of guinea pig spinal cord in an equal volume of complete Freund's adjuvant containing 10 mg ml⁻¹ of heat-killed *Mycobacterium tuberculosis*, H 37 RA. Starting on day 6, proteinase inhibitors were injected intraperitoneally twice daily, and sensitized control animals were injected with sterile non-pyrogenic saline. Thereafter, rats were weighed daily and scored for clinical expression of EAE. Control animals consistently became ill on days 12–14. On day 16, animals were anaesthetized with Nembutal, killed and prepared for histology by whole body perfusion with formaldehyde for haematoxylin and eosin staining, or with glutaraldehyde for epon embedding and staining with toluidine blue[16].

Table 1 shows the proteinase targets of the respective inhibitors and summarizes the results for prevention of paralysis and pathology in the sensitized animals. AMCA was the most effective agent; EACA, NPGB and pepstatin consistently protected some of the animals. Leupeptin and antipain, which are proteinase

Table 1 Protection of sensitized rats from EAE by injection of proteinase inhibitors

Drug	Proteinase(s) vulnerable to drug *in vitro*	Daily dosage	Perivascular infiltration (spinal cord)	Clinical grade	Effect on EAE rats paralysed/total
Controls			2.9	4.0	30/35
AMCA	Neutral proteinases, incl. Plg A and plasmin[18,19]	100 mg	2.3	0.46	2/16
EACA	Neutral proteinases, incl. Plg A and plasmin[18,19]	1.6 g	2.0	1.8	4/10
NPGB	Plasmin; Plg A; trypsin; thrombin[20,34]	2 mg	1.6	1.6	7/22
Pepstatin	Acid proteinases; cathepsin D[17]	2 mg	1.5	1.5	3/9
Leupeptin	Neutral proteinases; cathepsins A and B[17]	2 mg	3.0	3.7	7/8
Antipain	Neutral proteinases; cathepsins A and B[17]	2 mg	2.5	2.2	3/5
Trasylol	Neutral proteinases[18,19]	4,000 units	3.2	4.5	9/10*
Polyvaline	None; control for pepstatin	2 mg	3.0	4.0	5/5

EACA, AMCA (both Sigma), leupeptin, antipain and Trasylol (Bayer) were administered in sterile non-pyrogenic saline, NPGB (ICN Nutritional) was administered in 1% dimethyl sulphoxide (DMSO) in saline or in 10 mM sodium acetate buffer, pH 3.6, in saline and pepstatin (Bristol Laboratories) and polyvaline (ICN Nutritional) were administered as suspensions in 10% ethyl alcohol in saline. Beginning on day 7 after sensitization, rats in the experimental groups were injected with inhibitors twice daily, and rats in the control groups were injected with saline twice daily. We also tested pepstatin in 2% DMSO. No protection was observed, but because the control animals tested with 2% DMSO alone showed marked exacerbation of the disease, the results are not included here. Clinical grades on a scale of 1–6 were evaluated by three independent investigators according to the protocol of McFarlin, Blank and Kibler[35]; and perivascular infiltration was graded on coded slides using an arbitrary scale of 1–4. Abbreviations used: Plg A, plasminogen activator; EAE, experimental allergic encephalomyelitis; AMCA, transaminomethylcyclohexane carboxylic acid; EACA, ε-aminocaproic acid; NPGB, p-nitrophenylguanidobenzoate.

* Rats became paralysed 2 days before controls.

acid proteinases, which can be secreted by macrophages[21], may be involved in the clinical and pathological expression of EAE[9-14]. Alternatively, pepstatin in suspension might be toxic for phagocytic cells. Although we cannot rule out either of these possibilities, the histological data for NPGB and pepstatin suggest that these drugs may act at stages in the activation of the cell-mediated immune system before the entry of macrophages into the CNS.

The histological picture for AMCA, where the infiltrating mononuclear cells characteristic of EAE were found but demyelination was not observed (Fig. 3), strongly suggests that AMCA protects against demyelination by inhibiting plasminogen activator, plasmin or other neutral proteinases after macrophage infiltration of the white matter.

AMCA and EACA have had limited clinical application in recent years in treating subarachnoid haemorrhage, angioneurotic oedema and chronic urticaria, with absent or moderate side effects[22-29].

Of the series of proteinase inhibitors used in the present studies on EAE, the partial efficacies of pepstatin, NPGB and EACA are consistent with the results of other investigators[30-33]. The degree of protection obtained with NPGB gives further credence to the role of serine proteinases in EAE, especially if one takes into consideration the toxicity of NPGB. The results obtained with Trasylol (aprotinin) are disturbing and difficult to explain but have been independently observed by Smith[33]. It will be possible to speculate on the mechanisms involved when more data become available regarding the effects of Trasylol on circulating and tissue levels of neutral proteinases, particularly plasmin and plasminogen activator. The results suggest caution in the possible use of any of these drugs in humans. The most significant observation is the marked protective effect of the antifibrinolytic agent, AMCA. In animals treated with AMCA the histological evidence of inhibition of demyelination in the vicinity of infiltrating mononuclear cells supports the hypothetical participation of the macrophage-secreted plasminogen activator in the pathogenesis of EAE, and, possibly, in other inflammatory demyelinating conditions.

We thank Drs Murray B. Bornstein and Cedric S. Raine for helpful discussions and for reading the manuscript, Susan Sirota, Richard De Teresa and Sion Mohaber for assistance, Violet Hantz for typing the manuscript, Drs M. E. Smith and B. Arnason for sharing with us their results of similar work, and Dr W. Troll and the
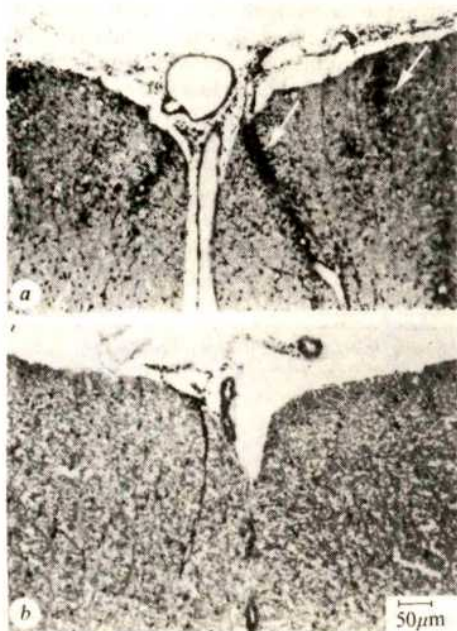
Fig. 2 Sections (7 μm) stained with haematoxylin and eosin. *a*, Paralysed rat injected twice daily with 1 ml of sterile saline. Arrows indicate perivascular cuffs in the anterior columns of the spinal cord. *b*, Asymptomatic rat injected twice daily with 1 mg of NPGB in acetate buffer. Note the absence of sub-meningeal inflammation and perivascular cuffing in the anterior columns of the spinal cord.
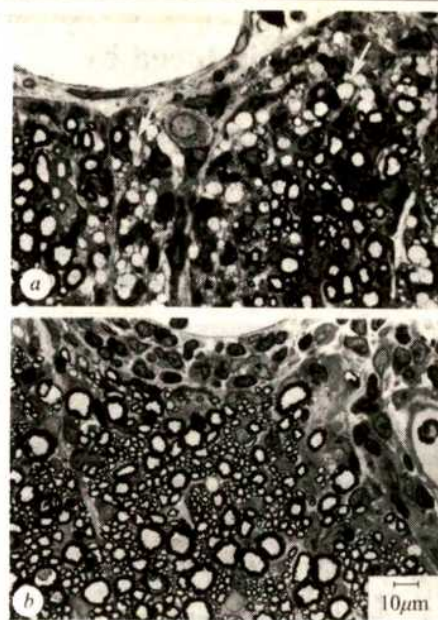
Fig. 3 Toluidine blue (1 μm) stained epon sections of spinal cords from Lewis rats perfused 16 days after sensitization with guinea pig spinal cord in CFA. *a*, Paralysed rat injected twice daily with 1 ml of sterile saline, starting on day 6. Arrows indicate demyelinated axons in the vicinity of the infiltrating cells. *b*, Representative slide of spinal cord from asymptomatic rats injected twice daily with 1ml AMCA (50 mg ml^{-1}) in saline, starting on day 6. Note the perivascular cuff of mononuclear cells, and the marked absence of demyelinated axons.

1. Kies, M. W. in *Biology of Brain Dysfunction* Vol. 2 (ed. Gaull, G. E.) 185–217 (Plenum, New York, 1973).
2. Paterson, P. Y. in *Textbook of Immunopathology* 2nd edn (eds Meischer, P. A. & Müller-Eberhard, H. J.) 179–213 (Grune & Stratton, New York, 1976); *J. exp. Med.* **111**, 119–136 (1960).
3. Gonatas, N. K. & Howard, J. C. *Science* **186**, 839–841 (1974).
4. Ortiz-Ortiz, L. & Weigle, W. O. *J. exp. Med.* **144**, 606–616 (1976).
5. Raine, C. S. *Prog. Neuropath.* **3**, 225–251 (1976).
6. Appel, S. H. & Bornstein, M. B. *J. exp. Med.* **119**, 303–312 (1964).
7. Morariu, M. A. & Dalmasso, A. P. *Ann. Neurol.* **4**, 427–430 (1978).
8. Hirsch, H. E. & Parks, M. E. *J. Neurochem.* **24**, 835–838 (1975).
9. Smith, M. E., Sedgewick, L. M. & Tagg, J. S. *J. Neurochem.* **23**, 965–971 (1974).
10. Buletza, G. F. & Smith, M. *Biochem. J.* **156**, 627–629 (1976).
11. Smith, M. E. *J. Neurochem.* **27**, 1077–1082 (1976); *Neurochem. Res.* **2**, 233–246 (1977).
12. Rauch, H. C., Einstein, E. R. & Csejtey, J. *Neurobiology* **3**, 195–205 (1973).
13. Govindavajan, K. R., Rauch, H. C., Clausen, J. & Einstein, E. R. *J. neurol. Sci.* **23**, 295–306 (1974).
14. Marks, N., Grynbaum, A. & Levine, S. *Brain Res.* **123**, 147–157 (1977).
15. Cammer, W., Bloom, B. R., Norton, W. T. & Gordon, S. *Proc. natn. Acad. Sci. U.S.A.* **75**, 1554–1558 (1978); in *Myelination and Demyelination* (ed. Palo, J.) 365–381 (Plenum, New York, 1978).
16. Stoner, G. L., Brosnan, C. F., Wisniewski, H. M. & Bloom, B. R. *J. Immun.* **118**, 2094–2102 (1977).
17. Umezawa, H. & Aoyagi, T. in *Proteinases in Mammalian Cells and Tissues* (ed. Barrett, A. J.) 637–662 (North-Holland, New York, 1977).
18. Wingender, W. in *Bayer Symp. V* (eds Fritz, H., Tschesche, H., Greene, L. J. & Truscheit, E.) 548–559 (Springer, New York, 1974).
19. Ambrus, C. M., Ambrus, J. L., Lassman, H. B. & Mink, I. B. *Ann. N. Y. Acad. Sci.* **146**, 430–437 (1968).
20. Shaw, E. in *Bayer Symp. V* (eds Fritz, H., Tschesche, H., Greene, L. J. & Truscheit, E.) 531–540 (Springer, New York, 1974).
21. Schnyder, J. & Baggiolini, J. *J. exp. Med.* **148**, 435–450 (1978).
22. Ambrus, J. L. *et al.* in *Chemical Control of Fibrinolysis-Thrombolysis* (ed. Schor, J. M.) 153–200 (Wiley-Interscience, New York, 1970).
23. Thompson, R. A. & Felix-Davies, D. D. *Br. med. J.* **ii**, 608 (1978).
24. Tant, D. *Br. med. J.* **i**, 266 (1979).
25. Maurice-Williams, R. S. *Br. med. J.* **i**, 945–947 (1978).
26. Tovi, D. *Acta neurol. scand.* **49**, 163–175 (1973).
27. Tovi, D., Nilsson, I. M. & Thulin, C.-A. *Acta neurol. scand.* **48**, 393–402 (1972).
28. Spragg, J. *J. Immun.* **120**, 592–596 (1978).
29. Agostoni, A. *et al. Allergy* **33**, 216–221 (1978).
30. Wüthrich, R., Rieder, H. P. & Ritzel, G. *Experientia* **19**, 421–422 (1978).
31. Sibley, W. A., Kiernat, J. & Laguna, J. F. *Neurology* **28**, 102–105 (1978).
32. Boehme, D. H., Umezawa, H., Hashim, G. & Marks, N. *Neurochem. Res.* **3**, 185–194 (1978).
33. Smith, M. E. in *The Suppression of Multiple Sclerosis & Experimental Allergic Encephalomyelitis* (eds Davison, A. N. & Cuzner, M. L.) (Academic, New York, in the press).
34. Dano, K. & Reich, E. *Cold Spring Harbor Conf. on Cell Proliferation* **2**, 357–366 (1975).
35. McFarlin, D. E., Blank, S. E. & Kibler, R. F. *J. Immun.* **113**, 712–715 (1974).

Myasthenia gravis induced by monoclonal antibodies to acetylcholine receptors

Vanda A. Lennon & Edward H. Lambert

Departments of Immunology, Neurology and Physiology, Mayo Clinic and Medical School, Rochester, Minnesota 55901

Autoantibodies to nicotinic acetylcholine receptors (AChRs) are demonstrable in sera of approximately 90% of patients with myasthenia gravis (MG), a disease of neuromuscular transmission[1]. The consistent abnormality in MG is a low amplitude of miniature endplate potentials (m.e.p.ps) due to decreased sensitivity of the postsynaptic membrane to the neurotransmitter, acetylcholine (ACh). This reflects a decrease in numbers of AChRs in the membrane (for review see ref. 2). The pathogenicity of anti-AChR antibodies has been documented *in vivo* by passive transfer of MG from human to mouse[3] and from rat to rat[4] and *in vitro* on cultured muscle cells[5-8]. However, titres of anti-AChR antibodies in serum do not correlate closely with severity of muscle weakness in MG patients[1]. This lack of correlation very probably reflects the heterogeneity of specificities of anti-AChR antibodies which is known to exist in MG[2]. For example, antibodies directed to determinants of AChRs which are inaccessible *in vivo* may be generated in the course of the disease without being relevant to disease pathogenesis. Identification of antigenic determinants of AChRs which are the primary target(s) of antibody attack in MG is a logical prerequisite to designing antigen-specific immunotherapy for this disease. We report here the production by hybridoma cells of monoclonal rat antibodies reactive with muscle AChR, both adult and fetal, in all of six mammalian species studied. Antibodies produced by two of these hybridoma lines bound to one or more antigenic determinant(s) exposed extracellularly, but remote from the binding site for cholinergic ligands, in the postsynaptic membrane of muscle, and caused a defect of neuromuscular transmission in mice, rats and guinea pigs. These findings establish conclusively that neuromuscular transmission can be impaired by monospecific anti-AChR antibodies which do not inhibit the binding of neurotransmitter to its receptor site.

Cells of a mutant mouse myeloma line, S194/5.XXO.BU.1, resistant to 1×10^{-4} M bromodeoxyuridine (BUdR), and a non-producer of immunoglobulin were maintained in Dulbecco's modification of Eagle's medium supplemented with 10% fetal calf serum; BUdR (1×10^{-4} M) was present for 72 h preceding fusion. AChR-primed lymphocytes were obtained from female Lewis rats inoculated at approximately monthly intervals with

AChR (purified from the electric organ of *Torpedo californica* by affinity chromatography on α-neurotoxin of *Naja naja siamensis* venom) with adjuvants[9]. At 4–5 days after final challenge with AChR, 10^8 lymphocytes from regional lymph nodes were mixed with 10^7 myeloma cells for fusion in 43% (vol/vol) polyethylene glycol 1500 (BDH) as described by Galfre *et al.*[10]. Cells were dispensed (2×10^6 lymphocytes per 2.0-ml well) in selective hypoxanthine/ aminopterin/thymidine HAT medium, with 2-mercaptoethanol, 1×10^{-4} M, into multi-well dishes (Costar no. 3524) seeded 1 day previously with rat peritoneal cells[11]. Hybrid cells producing antibodies of interest were cloned by limiting dilution in micro-well plates (0.4 cells per 0.2-ml well). To ensure monoclonality, each clone selected for study was isolated from a second cloning at this low density. Hybridomas secreting antibodies to AChR were identified by an immunoprecipitation radioimmunoassay[4] using solubilized AChR complexed with an excess of ^{125}I-α-bungarotoxin (α-BT), a cholinergic ligand which binds essentially irreversibly to the receptor's binding site for ACh. Nonspecific binding of α-BT or AChR (c.p.m. precipitated in non-immune serum) was subtracted.

Fusion of a non-secreting mouse myeloma with lymph node cells from rats primed in optimal conditions (5 days after a secondary or tertiary intradermal challenge by AChR) yielded reproducibly a high frequency of hybridomas; in five experiments, hybridoma cells appeared on initial plating in a mean of 73% of the wells; all these produced antibodies reactive with *Torpedo* AChR. In individual fusion experiments 26–100% of the hybridomas recognized determinants of *Torpedo* AChR which were shared by AChR of mammalian skeletal muscle.

The three cloned lines studied in detail here have been passaged continuously for 11–15 months without loss of specific antibody production. Their patterns of reactivity with AChR from a variety of sources are shown in Table 1. McAb-1 recognizes a determinant unique to *Torpedo*; McAb-2 and McAb-3 recognize determinants common to AChR of *Torpedo* and adult and fetal skeletal muscle from all of six mammalian species tested. Variation in the degree of binding to AChR of separate species (and to fetal and adult AChR of dog and cat) suggests differences in conformation, accessibilty and perhaps numbers of individual determinants on AChR solubilized in non-ionic detergent from membranes of muscle from different sources. To determine whether a monoclonal antibody might bind to antigenic determinants exposed extracellularly in innervated mammalian muscle *in vivo*, athymic male BALB/c nude (nu/nu) mice (ARS Sprague–Dawley), about 7 weeks old, were injected intraperitoneally with $0.2-1.0 \times 10^8$ living hybridoma cells. Mice injected with hybridomas secreting McAb-2 and McAb-3 showed no signs of weakness, weight loss or tumour in 46 days of observation. However, microelectrode studies of forearm and diaphragm muscles[12], carried out between days 7 and 46, revealed a highly significant ($\approx 50\%$) reduction in

Table 1 Specificities of three monoclonal antibodies: comparison of binding to AChRs of different species

Hybridoma Clone	Torpedo*	Relative AChR binding in % of Torpedo AChR bound										
		Rat		Human		Guinea Pig		Dog		Cat		Mouse
		A	F	A	F	A	F	A	F	A	F	A
McAb-1	100	0	0	0	0	0	0	0	0	0	0	0
McAb-2	100	57	56	40	38	15	19	34	14	36	13	39
McAb-3	100	71	69	45	48	24	19	52	22	51	20	49

Several precautions were taken to ensure valid comparison of binding specificities of the monoclonal antibodies. First, affinity-purified *Torpedo* AChR was used as a reference antigen. Preliminary assay was carried out to ensure that dilutions of antibody selected bound approximately 50% of *Torpedo* AChR (that is, in the linear range of binding). Binding of mammalian AChR was then expressed as per cent of the binding of *Torpedo*. To ensure that in each assay the same constant excess amount of mammalian muscle AChR was added, aliquots of each muscle extract were assayed for their AChR content using an excess of a polyspecific rat anti-AChR antiserum. All assays were carried out simultaneously in duplicate with a single batch of reagents. AChR was extracted in 2% Triton X-100 buffer[15]. Only in the case of *Torpedo* was AChR purified (by affinity chromatography on α-neurotoxin agarose). Adult muscle (A) was obtained from limbs of human (amputations), guinea pig, dog and cat, and from eviscerated carcasses of rat and mouse. Fetal muscle (F) was obtained from limbs of human (spontaneous abortions at 23 and 24 weeks gestation), dog (near term), cat (near term) and carcasses of fetal rat (19 d) and guinea pig (8 cm). Although the fetuses selected were at comparable stages of maturation, there is no evidence from species other than rat[22,23] that antigenic differences exist between forms of AChR found in fetal and mature adult muscle.
* Two factors may account for the consistently greater binding to *Torpedo* AChR by McAb-2 and McAb-3: first because *Torpedo* AChR was purified, its antigenic sites would be more accessible for binding; second, solubilized *Torpedo* AChR exists in a predominantly dimer form[24], in contrast to the exclusively monomeric form of mammalian muscle AChR.

Table 2 Pathogenicity of anti-AChR antibodies secreted by clonal hybridomas in nude mice

| Cells inoculated | m.e.p.p. amplitude* | | Serum antibody† titre ($\times 10^{-9}$ M ±s.e.m.) | Muscle AChR‡ | |
	Forearm (mV ± s.e.m.)	Diaphragm (mV ± s.e.m.)		Total content ($\times 10^{-11}$ moles per mouse, ± s.e.m.)	% Complexed with immunoglobulin ± s.e.m.
Nil	0.79 ± 0.042 (7)	1.41 ± 0.107 (7)	0.0 (11)	1.39 ± 0.060 (9)	0
McAb-1	0.73 ± 0.083 (6)	—	0.0 (6)	1.47 ± 0.050 (12)	0
McAb-2	0.38 ± 0.086 (4)§	0.70 ± 0.109 (4)§	8.7 ± 2.77 (4)	0.93 ± 0.143 (8)	52 ± 10
McAb-3	0.39 ± 0.027 (6)§	0.63 ± 0.086 (6)§	227.4 ± 130.51 (6)	0.49 ± 0.032 (6)	86 ± 4

* Microelectrode studies were done as described elsewhere[12]. m.e.p.p. amplitudes were corrected for non-linearity of the endplate response to ACh and to a resting potential of − 75 mV. m.e.p.p. with rise time of 0.6 ms or less were measured at 31 °C. Difference in m.e.p.p. amplitude between forearm and diaphragm is related to smaller diameter of muscle fibres in diaphragm. Diaphragms from mice inoculated with McAb-1 cells were not tested because of adherent tumour cells which were not present in McAb-2 and McAb-3. Numbers in parentheses are number of mice.

† Sera were obtained on days 31–46 and 7–27, respectively, after intraperitoneal inoculation with McAb-2 and McAb-3 hybridomas. Mouse muscle AChR, solubilized in Triton X-100 and complexed with an excess of ^{125}I-α-BT, was used as antigen[15]. Sera from mice bearing McAb-1 hybridoma cells (obtained on days 12–18) had no detectable antibody reactive with mouse muscle AChR, but titres of antibody reactive with *Torpedo* AChR were extremely high (mean 4,000 ± 289 × 10^{−9} M), reflecting the prolific intra-abdominal growth of the McAb-1 hybridoma. Binding of *Torpedo* AChR by sera of mice bearing McAb-2 and McAb-3 was similar to their binding of mouse muscle AChR (mean titres for *Torpedo* AChR, 12.0 ± 2.93 × 10^{−9} M and 247.7 ± 148.05 × 10^{−9} M, respectively).

‡ AChR was extracted in 2% Triton X-100 buffer from homogenized carcasses of individual mice and labelled with an excess of ^{125}I-α-BT. Total AChR and % complexed *in situ* with antibody were determined by immunoprecipitation[15]. Reductions in AChR content of McAb-2 and McAb-3 carcasses are highly significant ($P < 0.01$ and < 0.001, respectively).

§ Significantly different from non-inoculated group (Student's *t*-test, $P < 0.001$). Forearm m.e.p.p. amplitudes are also significantly different from those of McAb-1 group ($P = 0.02$ and < 0.01 for McAb-2 and McAb-3 groups, respectively). McAb-1 is not significantly different from control ($P = 0.5$).

Table 3 Pathogenicity of monoclonal anti-AChR antibodies passively transferred into rats and guinea pigs

| Immunoglobulin injected* | Incidence of muscle weakness | m.e.p.p. amplitude† | | Serum titre of antibody to homologous muscle‡ AChR ($\times 10^{-9}$ M ±s.e.m.) | Muscle AChR§ | |
		Forearm (mV ± s.e.m.)	Diaphragm (mV ± s.e.m.)		Total carcass ($\times 10^{-11}$ moles ± s.e.m.)	% Complexed with immunoglobulin ± s.e.m.
Rats						
Control	0/10	0.63 ± 0.021 (6)	0.89 ± 0.059 (4)	0.0	4.22 ± 0.342 (10)	0
McAb-1	0/2	—	1.05; 0.67	0.0	4.66; 4.10	0
McAb-2	10/10	—	0.36 ± 0.100 (4)	2.9 ± 0.27 (8)	1.67 ± 0.192 (8)	35 ± 1.4 (8)
McAb-3	8/8	0.10 ± 0.018 (7)	0.31 ± 0.067 (4)	11.3 ± 1.54 (8)	1.23 ± 0.103 (8)	50 ± 2.8 (8)
Guinea pigs					Forearm (moles per g × 10^{−13})	
Nil	0/3	0.80 ± 0.061 (3)	—	0.0	5.68 ± 0.324 (3)	0
McAb-3	2/2	0.38; 0.25	—	0.21; 0.63	1.56; 1.59	11; 37

* McAb-1, -2 and -3 immunoglobulins were purified from growth medium of hybridoma clones by affinity chromotography on agarose-conjugated goat anti-rat immunoglobulin[18]. Female Lewis rats and adult male guinea pigs were injected intravenously with immunoglobulin (1×10^{-10} moles in each rat and 8×10^{-10} moles in each guinea pig) and killed 2–3 days later. Control immunoglobulin was precipitated by 40% saturated ammonium sulphate from pooled serum of rats inoculated with adjuvants only, and 100 μg was injected into each rat.

† m.e.p.p. amplitudes were measured as described in Table 2 legend. McAb-2 and McAb-3 are significantly different from control ($P < 0.005$ and $P < 0.001$, respectively).

‡ Titre of antibodies in rat and guinea pig serum was determined as described in Table 2 legend but using rat and guinea pig muscle AChR, respectively. Titres of antibodies reactive with *Torpedo* AChR in sera of rats injected with McAb-1 were 4.7 and 8.2 × 10^{−9} M.

§ AChR content of muscle was measured as described in Table 2 legend. Values for McAb-2 and McAb-3 rats were significantly lower than for the control group ($P < 0.01$ and < 0.001, respectively).

amplitude of m.e.p.ps in both muscles when compared with the age-matched, non-inoculated mice (Table 2). Furthermore, McAb-2 and McAb-3 antibodies were bound extensively to AChRs of skeletal muscle in the mice and the total amount of AChRs in the muscle was reduced. These three abnormalities are characteristic of MG occurring spontaneously in humans[13] and dogs[14] and in experimental autoimmune MG (EAMG) induced by active immunization with purified AChRs in rats[15] and in mice[16]. Failure of the mice to develop weakness reflects their large safety factor of neuromuscular transmission. Although the reduction in m.e.p.p. amplitude of 50% is highly significant, it is not sufficient to cause clinical signs of weakness in mice or rats[12]. The hybridoma line secreting McAb-1 was tumorigenic in nude mice, and sera of those mice had very high titres of antibodies reactive with *Torpedo* AChR (mean = 4,000 ± 289 × 10^{−9} M). However, the immunoglobulin, which recognized only *Torpedo* AChR *in vitro*, did not bind to muscle AChR in the mice and m.e.p.p. amplitudes did not differ significantly from those of age-matched normal nude mice.

To demonstrate that the hybridomas were producing true autoantibodies, McAb-2 and McAb-3 cells (1.4 and 3.5 × 10^{8} cells) were injected intraperitoneally into 10-week-old female Lewis rats. Within 24 h profound muscle weakness occurred and

electromyographic abnormalities characteristic of the acute phase of EAMG[12] were demonstrated.

Because of the similar patterns of binding of McAb-2 and McAb-3 to AChR from different sources (Table 1), and because these hybridomas arose from a single fusion experiment, the possibility that they might be identical molecules was examined by isoelectric focusing on polyacrylamide gels using a pH 3–10 gradient[17]. Antibodies were isolated from growth medium by adsorption to agarose-bound goat anti-rat Ig[18], from which they were eluted in 1.0 M propionic acid. After adjustment to neutral pH and dialysis against phosphate-buffered saline, pH 7.4, and 0.02% NaN₃, purified McAb-2 and McAb-3 antibodies bound respectively, 1.09 and 4.37 × 10^{−9} moles of solubilized mouse muscle AChR per mg and 3.11 and 7.24 × 10^{−9} moles of purified *Torpedo* AChR per mg. Unreduced, the antibodies had very similar isoelectric points (in the range of pH 7.4–7.5). However, reduction by β-mercaptoethanol revealed that the light chain bands of McAb-2 and McAb-3 (confirmed by electrophoresis in a second dimension in a SDS-polyacrylamide slab gel) were distinctly different (p*I* values 7.2 and 6.6, respectively). This indicates that McAb-2 and McAb-3 are different molecules.

Passive transfer of purified McAb-2 and McAb-3 into rats and guinea pigs induced clinical, electrophysiological and bioche-

mical evidence of EAMG (Table 3). Thus, the determinant(s) of AChR recognized by McAb-2 and McAb-3 are exposed extracellularly at the neuromuscular junction in at least three mammalian species (mouse, rat and guinea pig) and are common to all mammalian muscle AChRs examined, including man (Table 1). The fact that both antibodies bound *in vitro* to AChR complexed with ^{125}I-α-BT (molecular weight $\sim$ 8,000) indicates that the antigenic determinant(s) recognized by these antibodies reside outside the receptor's binding site for ACh. Thus, using monoclonal antibodies produced by interspecies hybridomas we have established unequivocally that an autoimmune response to an antigenic determinant located outside the AChR's binding site for the neurotransmitter ACh can cause impairment of neuromuscular transmission *in vivo*. Idiotypic analysis may determine whether the same antigenic determinant of AChR is defined by these two different monoclonal antibodies. Analysis of the idiotypes of monoclonal anti-AChR autoantibodies should provide a means of defining antigenic determinants of AChR relevant to the pathogenesis and suppression of MG.

Two recent reports describe production of hybridomas secreting antibodies to AChR with specificities demonstrated only for *Torpedo* AChR[19,20]. We believe ours to be the first report of the production of autoantibodies by hybridomas. The hybridoma technique will have important applications in the investigation of a variety of human autoimmune diseases, particularly for obtaining pathogenic antibodies of specificities which may not be detectable in serum because of quantitative absorption to target cells[21]. Hybridization of human B lymphocytes with appropriate myelomas should enable direct investigation of those specificities.

We thank Jean Chen, Cindy Uhl, Renee McGovern and Millie Thompson for technical assistance. This work was supported by a grant from the National Institutes of Neurological and Communicative Diseases and Stroke (NS 15057) and a Research Center Grant from the Muscular Dystrophy Association.

Note added in proof: Since this article was submitted for publication it has been reported that murine myelomas hybridized with spleen cells from spontaneously autoimmune mice produced monoclonal anti-RNA[25] and anti-DNA[26] autoantibodies.

1. Lindstrom, J., Seybold, M. E. Lennon, V. A., Whittingham, S. & Duane, D. D. *Neurology* **26**, 1054–1059 (1976).
2. Lennon, V. A. in *Clinical Immunology Update: Reviews for Physicians* (ed. Franklin, E.) 259–289 (Elsevier, New York, 1979).
3. Toyka, K. V. *et al. New Engl. J. Med.* **296**, 125–131 (1977).
4. Lindstrom, J., Engel, A. G., Seybold, M. E., Lennon, V. A. & Lambert, E. H. *J. exp. Med.* **144**, 739–753 (1976).
5. Lennon, V. A. in *Cholinergic Mechanisms and Psychopharmacology. Advances in Behavioral Biology* (ed. Jenden, D. J.) 77–92 (Plenum, New York, 1977).
6. Bevan, S., Kullberg, R. W. & Heinemann, S. F. *Nature* **267**, 263–265 (1977).
7. Anwyl, R., Appel, S. M. & Narahashi, T. *Nature* **267**, 262–263 (1977).
8. Kao, I. & Drachman, D. B. *Science* **196**, 527–529 (1977).
9. Lennon, V. A., Lindstrom, J. & Seybold, M. E. *Ann. N.Y. Acad. Sci.* **274**, 283–299 (1976).
10. Galfre, G., Howe, S. C., Milstein, C., Butcher, G. W. & Howard, J. C. *Nature* **266**, 550–552 (1976).
11. Hengartner, H., Luzzati, A. L. & Schreier, M. in *Current Topics in Microbiology and Immunology* (eds Melchers, F., Potter, M. & Warner, N. L.) 92–99 (Springer, New York, 1978).
12. Lambert, E. H., Lindstrom, J. M. & Lennon, V. A. *Ann. N.Y. Acad. Sci.* **274**, 300–318 (1976).
13. Lindstrom, J. M. & Lambert, E. H. *Neurology, Minneap.* **28**, 130–138 (1978).
14. Lennon, V. A., Palmer, A. C., Pflugfelder, C. & Indrieri, R. in *Genetic Control of Autoimmune Disease* (eds Rose, N. R., Bigazzi, P. E. & Warner, N. L.) 295–306 (Elsevier, New York, 1978).
15. Lindstrom, J. M., Einarson, B., Lennon, V. A. & Seybold, M. E. *J. exp. Med.* **144**, 726–738 (1976).
16. Christadoss, P., Lennon, V. A., Lambert, E. H. & David, C. in *ICN-UCLA Symp. Molec. Cell. Biol.* Vol.16 (eds Bach, F., Bonavida, B. & Vitetta, E.) 249–256 (Academic, New York, 1979).
17. O'Farrell, P. H. *J. biol. Chem.* **250**, 4007–4021 (1975).
18. Jensenius, J. C. & Williams, A. F. *Eur. J. Immun.* **4**, 91–97 (1974).
19. Gomez, C. M. *et al. Biophys. biochem. Res. Commun.* **88**, 575–582 (1979).
20. Moshly-Rosen, D., Fuchs, S. & Eshhar, Z. *FEBS Lett.* **106**, 389 (1979).
21. Lerner, R. A., Glassock, R. J. & Dixon, F. J. *J. exp. Med.* **126**, 989–1004 (1967).
22. Almon, R. R. & Appel, S. H. *Biochim. biophys. Acta* **393**, 66 (1975).
23. Weinberg, C. P. & Hall, Z. W. *Proc. natn. Acad. Sci. U.S.A.* **76**, 504 (1979).
24. Chang, H. W. & Bock, E. *Biochemistry* **16**, 4513–4520 (1977).
25. Eilat, D., Asofsky, R. & Laskov, R. *J. Immun.* **124**, 766-768 (1980).
26. Andrzejewski, C., Stollar, B.D., Lalor, T.M. & Schwarz, R.S. *J. Immun.* **124**, 1499-1502 (1980).

Dopaminergic activation of reticulata neurones in the substantia nigra

André Ruffieux & Wolfram Schultz*

Institut de Physiologie, Université de Fribourg, Bd Pérolles, CH-1700 Fribourg, Switzerland

Dendritic release of dopamine (DA) in substantia nigra (SN) is well established in various experimental situations[1-3]. Morphological substrates for DA storage exist in dendrites[4,5], as do dendro-dendritic[6] and dendro-axonic[7] contacts. DA receptors in SN are located on both cells[8] and striato-nigral terminals[9,10]. DA is thought to regulate the activity of neighbouring dopaminergic neurones through its dendritic release by a local feedback mechanism[11,12]. However, dendrites of DA neurones also ramify close to the neuropil of non-dopaminergic reticulata neurones in SN. The question has arisen whether dendritically released DA might also influence these neurones which, to a large extent, project to ventromedial thalamus (VM) and superior colliculus[13]. A necessary condition would be that they are sensitive to DA. In the experiments reported here this was found to be the case—a considerable proportion of nigro-thalamic neurones were activated by iontophoretically applied DA. This contrasts with its known depressant effect on pars compacta DA neurones[12] which we confirmed.

Seventeen rats (210–370 g) of both sexes were anaesthetized with chloralhydrate, 350 mg per kg intraperitoneally and additional doses given when necessary. The left VM was stimulated through a stereotaxically placed bipolar electrode with 1.0–1.5 mm tip separation, using 0.1-ms pulses and currents usually of 0.1–0.5 mA (rarely up to 1.2 mA) intensity. A recording microelectrode was lowered stereotaxically into the left SN. Extracellular single cell activity was monitored with glass-coated tungsten microelectrodes (exposed tips 5–10 μm long, 2.0–3.5 μm diameter), glued alongside three- or five-barrelled glass pipettes. The tungsten electrodes protruded 12–70 μm (mean 23 μm). Tip diameters of individual pipette barrels were 2.0–2.5 μm. Iontophoresis barrels contained the following substances: dopamine hydrochloride (0.2 M, pH 4.5), γ-aminobutyric acid (GABA, 0.5 M, pH 7.2), sodium glutamate (0.5 M, pH 6.7) and fluphenazine (50 mM, pH 2.4, a gift of Squibb). Sodium chloride (2 M, pH 7.0) was used for current control and balancing current. Using standard amplification methods, cell activity was recorded with a ratemeter. All cells found to be sensitve to current alone were rejected. Antidromic excitation was established when at least two of the following criteria were fulfilled: stable latency at threshold, frequency following above 500 s^{-1}, or collision with spontaneous impulses. The positions of the stimulating electrode and of each recorded cell were reconstructed histologically after small electrolytic lesions.

DA cells of pars compacta were distinguished from reticulata cells by both their histological localization and characteristic discharge pattern. They had impulses of long duration (2.71 $\pm$ 0.77 ms, mean $\pm$s.d. compared with 1.06 $\pm$ 0.25 ms for reticulata cells; 300 Hz, $-$3dB filtering), in agreement with earlier reports[1,4,14]. Pars compacta neurones always had a low spontaneous discharge frequency (less than 8 impulses per s) whereas reticulata neurones fired with a wide range of frequencies (2–60 impulses per s).

Of 89 reticulata cells 34(39%) were activated by iontophoretically applied DA (at least 33% above the level of spontaneous activity), using currents of 25 to 200 nA (mean 97 $\pm$ 60 nA for 100% augmentation) (Fig. 1a–d). Inhibitory responses were not observed with reticulata neurones. Forty-eight

* To whom correspondence should be addressed.

reticulata neurones (55%) responded antidromically to VM thalamus stimulation with latencies of 1.75 ± 1.00 ms, in agreement with known data[13]. Of the 48 nigrothalamic neurones 16 (33%) were excited by DA. Iontophoretically applied fluphenazine, a relatively specific dopamine receptor blocker[15], prevented or greatly attenuated the response to DA in seven cells, with currents of 100 or 200 nA and onset times ranging from 4 to 60 min. A clear blocking effect was not observed with four additional cells, probably because we had not recorded long enough during fluphenazine application. The responses to glutamate or GABA remained unchanged during fluphenazine application (Fig. 1d). Fluphenazine-induced DA blockade was found to be reversible in three cases.

In contrast to reticulata neurones, the spontaneous activity of pars compacta DA neurones was depressed by iontophoretically applied DA (12 of 15 neurones) (Fig. 1e). Excitation never occurred. Currents of 25 to 100 nA (mean 48 ± 22 nA) were required for a 50% reduction of activity. The DA effect was blocked by iontophoretically applied fluphenazine in all eight cases tested, in one case reversibly.

Higher currents of DA were required to depress the activity of dopaminergic neurones than in previous studies where recording was done through one barrel of a multibarrelled pipette[12]. This may have been due to the greater distance between the recording and drug applying sites in our electrodes[16,17]. Therefore, the currents necessary for DA to activate reticulata neurones should be lower than those in our experiments when recording with multibarrelled pipettes.

The present data show a remarkable difference in the DA effects: depression of activity with pars compacta dopaminergic neurones, but activation with reticulata neurones. In striatum, DA has a predominantly depressant effect[18,19], but activations were also observed[18]. In SN, the dopaminergic neurones of pars compacta are depressed but not excited by DA[12]. Neurones histologically localized in pars reticulata are so far reported to be activated as well as depressed by DA[20]. With the additional electrophysiological criteria of this study we found that the dopaminergic and non-dopaminergic neurones of SN responded in opposite ways to iontophoretically applied DA. The mechanisms underlying these two DA effects are not yet fully understood. DA could have direct inhibitory and excitatory effects on the two types of SN cells. Alternatively, DA might activate reticulata neurones by influencing the transmitter release of afferent axonal terminals, although direct experimental evidence is as yet lacking.

Striato–nigro–thalamic connections were recently throught to function as an output of the striatum distinct from the striato-pallido–thalamic system[21]. In our study a considerable proportion of nigrothalamic neurones were found to be influenced by DA. Systemically administered amphetamine also leads to activation of reticulata neurones, and slowing of DA neurones[22]. This effect could well be mediated by its known DA releasing action from dendrites in SN[23-25]. Therefore, it may be envisaged that DA is released functionally from dendrites and influences reticulata neurones. In this way the DA system would have an output to VM thalamus directly at the level of SN without involving the striatum. VM projects to layer I of wide areas of rat cerebral cortex[26]. This pattern of terminal distribution suggests a widespread, nonspecific action of impulses ascending from VM thalamus. Through its direct action on nigrothalamic cells, as suggested by our data, the DA system would exert an influence over large areas of the cerebral cortex.

Fig. 1 Ratemeter recordings of three cells in substantia nigra. *a–c*, Recording of a cell in pars reticulata. Iontophoresis of DA$^+$ increased the discharge rate (*a*). No effect of Na$^+$-carried current alone. Iontophoretically applied fluphenazine (Flu$^+$) greatly attenuated the response to DA (*b*); and the blockade was reversible (*c*). The onset of the drug effect was delayed because the electrode used had a large longitudinal distance (70 μm) between the tips of the recording electrode and the iontophoresis barrels [16,17]. (*d*) Recordings of another reticulata cell before (left) and during (right) Flu$^+$ application. The response to DA was suppressed by fluphenazine, but the glutamate (Glu) effect remained unaltered, thus demonstrating the specificity of the response. Onset of right recording was 75 min after onset of Flu$^+$ iontophoresis. DA and Glu were ejected with current compensation. (*e*) Activity of a pars compacta DA cell was depressed by DA. The effect was blocked during fluphenazine application but the blockade was not reversible during the time studied. Fluphenazine did not block the depressing effect of GABA.

1. Korf, J., Zieleman, M. & Westerink, B. H. C. *Nature* **260**, 257–258 (1976).
2. Geffen, L. B., Jessell, T. M., Cuello, A. C. & Iversen, L. L. *Nature* **260**, 258–260 (1976).
3. Nieoullon, A., Cheramy, A. & Glowinski, J. *Nature* **266**, 375–377 (1977).
4. Björklund, A. & Lindvall, O. *Brain Res.* **83**, 531–537 (1975).
5. Hefti, F. & Lichtensteiger, W. *J. Neurochem.* **30**, 1217–1230 (1978).
6. Wilson, C. J., Groves, P. M. & Fifková, E. *Exp Brain Res.* **30**, 161–174 (1977).
7. Reubi, J. C. & Sandri, C. *Neurosci. Lett.* **13**, 183–188 (1979).
8. Nagy, J. I., Lee, T., Seemann, P. & Fibiger, H. C. *Nature* **274**, 278–281 (1978).
9. Gale, K., Guidotti, A. & Costa, E. *Science* **195**, 503–505 (1977).
10. Spano, P. F., Trabucchi, M. & DiChiara, G. *Science* **196**, 1343–1345 (1977).
11. Groves, P. M., Wilson, C. J., Young, S. J. & Rebec, G. V. *Science* **190**, 522–529 (1975).
12. Aghajanian, G. K. & Bunney, B. S. *Naunyn. Schmiedebergs Arch. Pharmac.* **297**, 1–7 (1977).
13. Deniau, J. M., Hammond, C., Riszk, A. & Feger, J. *Exp Brain Res.* **32**, 409–422 (1978).
14. Bunney, B. S., Walters, J. R., Roth, R. H. & Aghajanian, G. K. *J. Pharmac. exp. Ther.* **185**, 560–571 (1973).
15. Iversen, L. L., Horn, A. S. & Miller, R. J. in *Pre- and Postsynaptic Receptors* (eds Usdin, E. & Bunney, W. E.) 207–243 (Dekker, New York, 1975).
16. Crossman, A. R., Walker, R. J. & Woodruff, G. N. *Neuropharmacology* **13**, 547–552 (1974).
17. Tamura, Y. & Maruyama, S. *J. Neurosci. Meth.* **1**, 249–252 (1979).
18. Bloom, F. E., Costa, E. & Salmoriaghi, G. C. *J. Pharmac. exp. Ther.* **150**, 244–252 (1965).
19. Bernardi, G., Marciani, M. G., Morocutti, C., Pavone, F & Stanzione, P. *Neurosci. Lett* **8**, 235–240 (1978).
20. Dray, A., Gonye, T. J., Oakley, N. R. & Tanner, T. *Brain Res.* **113**, 45–57 (1976).
21. Garcia-Munoz, M., Nicolaou, N. M., Tulloch, I. F., Wright, A. K. & Arbuthnott, G. W. *Nature* **265**, 363–365 (1977).
22. Rebec, G. V., Groves, P. M. *Neuropharmacology* **14**, 275–282 (1975).
23. Paden, C., Wilson, C. J. & Groves, P. M. *Life Sci.* **19**, 1499–1506 (1976).
24. Hefti, F. & Lichtensteiger, W. *Neurosci. Lett.* **10**, 65–70 (1978).
25. Nieoullon, A., Cheramy, A., Leviel, V. & Glowinski, J. *Eur. J. Pharmac.* **53**, 289–296 (1979).
26. Herkenham, M. *J. comp. Neurol.* **183**, 487–518 (1979).

Selective development of tolerance without dependence in multiple opiate receptors of mouse vas deferens

Rüdiger Schulz, Michael Wüster, Heinz Krenss & Albert Herz

Department of Neuropharmacology, Max-Planck-Institut für Psychiatrie, Kraepelinstrasse 2, D-8000 München 40, FRG

Studies with isolated tissues have provided strong indications for a multiplicity of opiate receptors[1-4]. To satisfy the definition of cross-tolerance (tolerance to a specific opioid implying tolerance to all opioids), chronic exposure to an opiate agonist should cause tolerance and dependence in all opiate-sensitive systems. On the other hand, if multiplicity of opiate receptors is defined in terms of multiple recognition sites whose activation by specific opioids cause independent responses, then development of cross-tolerance is less likely. The mouse vas deferens (MVD) provides a useful model to test these considerations. This tissue contains δ-opiate receptors, for which D-Ala^2-D-Leu^5-enkephalin (DADL) represents the most selective agonist, as well as μ-receptors, for which sufentanyl appears highly selective[3,5-7]. We report here that isolated vasa deferentia of mice chronically treated with DADL are 800-fold less sensitive to this δ-receptor agonist, whereas there is no cross-tolerance to μ-receptor agonists. On the other hand, chronic exposure of mice to sufentanyl renders their vasa deferentia more than 1,000-fold less sensitive to sufentanyl, but affects their sensitivity to DADL insignificantly. Apparently, such highly tolerant preparations exhibit no detectable sign of dependence when challenged with naloxone or clonidine. These findings favour the notion that opiate tolerance and dependence dissociate in the MVD.

Mice (NMRI, 25 g) were treated chronically from osmotic minipumps with either DADL or sufentanyl. Vasa deferentia were removed from the animals and set up for electrical stimulation[4]. To prevent unmasking of opiate receptors, the bathing solution contained DADL or sufentanyl at the concentration measured in the serum. After equilibration dose–response curves were established and the drug concentrations required to inhibit electrically evoked twitches by 50% were determined (IC$_{50}$). Tests for dependence were conducted in the presence of the narcotic agonist using naloxone as antagonist.

The effect of chronic DADL infusion on vasa deferentia is shown in Fig. 1. Dose–response curves for DADL were shifted to the right, indicating development of tolerance (Fig. 1a). The degree of the shift was dependent on the amount of DADL infused—administration of 5 µg DADL per h for 6 days resulted in an 800-fold shift (IC$_{50}$ 4×10^{-7} M; naive 5×10^{-10} M). Vasa deferentia taken from DADL-treated animals, which were set up in the presence of 20 nM DADL, displayed a similar twitch tension evoked by electrical stimulation as compared to naive tissues in the absence of any drug. Washing highly tolerant preparations (5 µg DADL per h, 6 d) for 3 h with drug-free Krebs–Ringer solution increased the sensitivity to DADL slightly (IC$_{50}$ 1×10^{-7} M) and the sensitivity was not further increased by a 5-h wash procedure. In vasa deferentia taken from mice infused with 5 µg DADL per h for 24 h, only a 200-fold shift of the dose–response curve was found (IC$_{50}$ 8×10^{-8} M). Washing these preparations for 2 h with drug-free Krebs–Ringer solution resulted in a considerable loss of tolerance (IC$_{50}$ 9×10^{-10} M). Figure 1b shows dose–response curves for sufentanyl, normorphine and clonidine on vasa deferentia of naive and DADL-infused (5 µg per h, 6 d) mice. Although the vasa deferentia are highly tolerant to the δ-receptor agonist DADL, the IC$_{50}$ for normorphine was not

changed and only a fourfold increase was observed for sufentanyl. As opiate dependence is associated with subsensitivity to clonidine, additional tests were conducted with this α-adrenoreceptor agonist[8]. The IC$_{50}$ value of clonidine was not changed in tolerant preparations challenged in the presence of naloxone (200 nM).

Figure 2 shows dose–response curves for sufentanyl and DADL on vasa deferentia from untreated mice and from mice infused for 6 d with sufentanyl at a delivery rate of 10 µg per h. Again, to prevent unmasking of opiate receptors *in vitro*, the tissues of chronically treated mice were set up in the presence of 5 nM sufentanyl, the corresponding serum concentration. Sufentanyl was over 1,000-fold less potent (IC$_{50}$ 50 nM) in vasa deferentia taken from sufentanyl-treated animals as compared to naive preparations (IC$_{50}$ 0.04 nM). A high degree of cross-tolerance with normorphine was found in such preparations. In contrast, DADL showed identical activities in control and sufentanyl-tolerant vasa deferentia, as does, for example, Leu-enkephalin (details to be published elsewhere).

Highly tolerant vasa deferentia from mice chronically infused with DADL (5 µg per h, 6 d) were challenged with naloxone (50–1,000 nM) in the presence of 20 nM DADL. Neither basic tension (absence of electrical stimulation) nor electrically evoked twitch tension was affected by the narcotic antagonist. However, naloxone completely antagonized the inhibition of
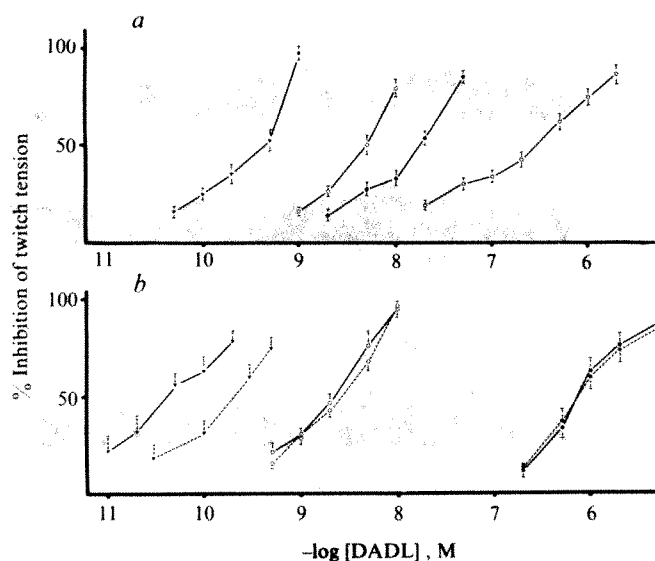
Fig. 1 *a*, Dose–response curves for D-Ala^2-D-Leu^5-enkephalin (DADL) on the electrically stimulated isolated mouse vas deferens (0.1 Hz, 0.5 ms, 40 V; basic tension 0.05 g). Data are for preparations from untreated mice (▼) and from mice infused with 0.5 µg DADL per h (○), 1.5 µg per h (●) and 5 µg per h (□) for 6 d. Infusion was from osmotic minipumps (Alza model 1701) implanted subcutaneously, which release 1 µl per h. The preparations taken from chronically DADL-treated mice were incubated *in vitro* with their corresponding serum DADL concentrations, which was 1 nM in mice receiving 0.5 µg per h, 3 nM in mice infused with 1.5 µg per h and 20 nM during infusion of 5 µg per h as determined in the isolated vas deferens. These data are the means of three to five serum samples from different mice assayed the 2nd, 4th and 6th days of the experiment. The maximal standard error of the mean serum data was <15%. *b*, Dose–response curves for sufentanyl (▽), clonidine (○) and normorphine (●) on vasa deferentia taken from non-pretreated mice and from mice infused for 6 d with 5 µg DADL. Preparations from chronically treated mice were set up for electrical stimulation in the presence of DADL (20 nM). Dotted lines represent curves obtained from vasa deferentia of infused mice. A period of 30 min was allowed for equilibration after set-up in the presence of the enkephalin derivative with changes of the bath fluid every 5–10 min. Each point on the figure is the mean of at least six tests on tissues from different animals. Vertical bars indicate standard errors.
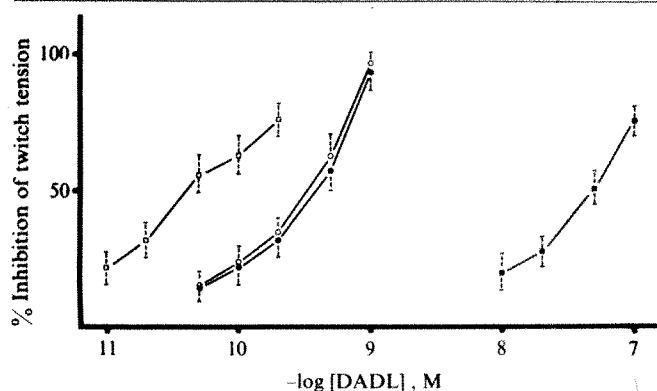
Fig. 2 Dose–response curves for sufentanyl (squares) and DADL (circles) on vasa deferentia of naive mice (open symbols), and from those infused for 6 days with 10 µg sufentanyl per h (solid symbols). The preparations of chronically treated mice were set up in the presence of 5 nM sufentanyl, the respective drug concentrations in the serum at the time of killing. Each point is the mean of at least eight determinations on tissues of different animals. Vertical bars represent s.e.m.

twitch tension produced by 10^{-6} M DADL, without an overshoot increase in tension. Similarly, no signs of withdrawal were demonstrated in sufentanyl-tolerant preparations.

The findings reported here unequivocally point to a multiplicity of opiate receptors. Selective activation of a specific population of opiate receptors, δ-receptors, for prolonged periods causes their selective desensitization (that is, tolerance), leaving the responsiveness of µ-receptors unaffected. By analogy, tolerance of the µ-receptor develops upon their chronic activation without affecting the responsiveness of δ-receptors. Thus, these data conflict with the classical notion that cross-tolerance reflects a general characteristic of opiates. The lack of cross-tolerance between δ-receptor agonists and µ-receptor agonists does not exclude, however, a mutual receptor activation at sufficiently high concentrations of these compounds.

One aspect of the present investigations relates to the phenomenon of dependence, which has been postulated to be invariably accompanied with tolerance[9,10]. Although the vasa deferentia exhibited an extremely high degree of tolerance, no signs of dependence were observed on challenge with naloxone or clonidine. The response to each of the drugs is considered a reliable test for dependence in opiate-tolerant tissues from the myenteric plexus of the guinea pig[8,11]. Although a dissociation of tolerance and dependence conflicts with the common understanding of the mechanisms underlying these phenomena[12-14], an adaptation to chronic opiate receptor activation by a reduction of opiate binding sites[15] could explain our findings. Moreover, we have some evidence that chronic DADL infusion in mice results in a reduction of the number of δ-receptors in the MVD. Such a mechanism of adaptation resembles that involved in desensitization of neurohormone receptors on chronic activation[16-18].

1. Lord, J. A. H., Waterfield, A. A., Hughes, J. & Kosterlitz, H. W. *Nature* **267**, 495–499 (1977).
2. Kosterlitz, H. W. in *Advances in Pharmacology and Therapeutics: Multiple Opiate Receptors* Vol. 1 (ed. Jacob, J.) 15–23 (Pergamon, New York, 1978).
3. Wüster, M., Schulz, R. & Herz, A. *Neurosci. Lett.* **15**, 193–198 (1979).
4. Schulz, R., Faase, E., Wüster, M. & Herz, A. *Life Sci.* **24**, 843–850 (1979).
5. Leslie, F. M. & Kosterlitz, H. W. *Eur. J. Pharmac.* **56**, 379–383 (1979).
6. Kosterlitz, H. W. *Abstr. 7th Int. Cong. Pharmac.* **2** (Paris, 1978).
7. Wüster, M. & Pfeiffer, A. *Naunyn-Schmiedebergs Arch. Pharmac. Suppl.* **311**, R64 (1980).
8. Robson, I.E., Gillan, M.G.I., Waterfield, A.A. & Kosterlitz, H.W. in *Characteristics and Function of Opioids* (eds Van Ree, J. M. & Terenius, L.) 67–68 (North-Holland, Amsterdam, 1978).
9. Shuster, L. *Nature* **189**, 314–315 (1961).
10. Goldstein, A. & Goldstein, D. B. *Proc. Ass. Res. nerv. ment. Dis.* **46**, 265–267 (1968).
11. Schulz, R. in *Developments in Opiate Research* (ed. Herz, A.) 241–277 (Dekker, New York, 1978).
12. Collier, H. O. J. & Roy, A. C. *Nature* **248**, 24–27 (1974).
13. Klee, W. A., Sharma, S. K. & Nirenberg, M. *Life Sci.* **16**, 1869–1874 (1975).
14. Hamprecht, B. in *Developments in Opiate Research* (ed. Herz, A.) 357–406 (Dekker, New York, 1978).
15. Davis, M. E., Akera, T. & Brody, T. M. *J. Pharmac. exp. Ther.* **211**, 112–119 (1979).
16. Raff, M. *Nature* **259**, 265–266 (1976).
17. Chuang, D. M. & Costa, E. *Proc. natn. Acad. Sci. U.S.A.* **76**, 3024–3028 (1979).
18. Catt, K. J., Harword, J. P., Aguilera, G. & Dufau, M. L. *Nature* **280**, 109–116 (1979).

Dopaminergic stimulation of prolactin release

Carl Denef, Danielle Manet & Raymonde Dewals

Laboratory of Cell Pharmacology, Department of Pharmacology, Leuven, School of Medicine, Campus Gasthuisberg, K.U. B-3000 Leuven, Belgium

Prolactin (PRL) secretion from anterior pituitary is believed to be under tonic inhibitory control of dopamine (DA)[1] released from the tubero-infundibular dopaminergic neurones into the hypophysial portal blood[2-4]. Inhibition of PRL release by DA seems to be mediated by stereospecific DA receptors located in PRL cells[5,6]. Apomorphine and various ergot alkaloids such as bromocryptine mimic the inhibitory effect of DA both in *vivo* and *in vitro*, presumably by a direct agonist action on these 'inhibitory' receptors[1,6,7]. We now report that PRL secretion in primary cultures of rat pituitary cells can be stimulated by DA when concentrations a thousand times lower than those required for inhibition are used. Secretion rates above basal release can also be induced by apomorphine and bromocryptine when the 'inhibitory' receptors are blocked with certain DA receptor antagonists.

Rat pituitary cells from adult male Wistar rats (300–350 g) maintained in monolayer culture[7,8] and superfused pituitary cells cultured on polystyrene beads (Biosilon, Nunc) were used. All tests were done after a period of 5 days in culture. PRL was measured using a specific rat PRL radioimmunoassay using the kits and procedures from the NIAMDD Pituitary Hormone Distribution Program, Bethesda, Maryland. Statistical analysis of the data was by multiple *t*-test.

Figure 1 shows the effect of DA in both these cell systems. In monolayer cultures picomolar concentrations of DA stimulated PRL release by more than 50% ($P < 0.001$), whereas inhibition occurred from concentrations about a thousand times higher. In superfused cells there was an 82% rise in average secretion rates during superfusion with 1–100 pM DA, compared with maintained average secretion rate during superfusion with the control medium ($P < 0.001$). Average secretion rates were 3.78 ± 0.15 ng min^{-1} and 2.08 ± 0.12 ng min^{-1}, respectively (mean ± s.e.m.). When DA was superfused together with 10 nM of the DA receptor antagonists haloperidol or (+)butaclamol, stimulation was 56% and 107% above basal release, respectively. Thus, stimulation by DA seemed to be partially antagonized by a 'low' concentration of haloperidol but not by (+)butaclamol.

Apomorphine was more potent than DA in suppressing PRL release (EC$_{50}$ 0.95 nM and 14 nM, respectively) but, as shown in Fig. 2, it had only a marginal, if any, stimulatory effect. However, when co-incubated with 10 nM of the DA receptor antagonist haloperidol, picomolar concentrations of apomorphine stimulated PRL release to ~30% above basal secretion rates ($P < 0.01$); such stimulation was not seen when haloperidol was added alone. Similar results were obtained in superfused cells. Picomolar concentrations of apomorphine also stimulated PRL release when co-incubated with 10 nM domperidone or
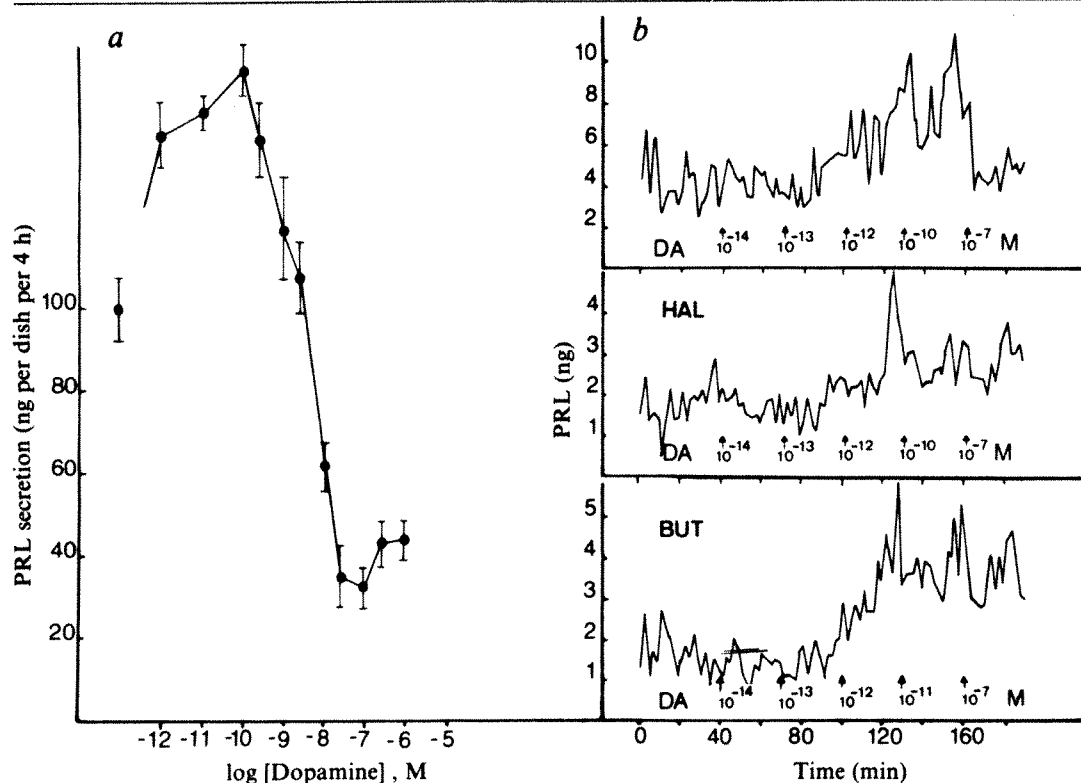
Fig. 1 Effect of dopamine (DA) alone or together with 10 nM haloperidol (HAL) or (+)butaclamol (BUT) on PRL secretion from primary cultures of dispersed rat pituitary cells (male Wistar rats, 300–350 g). The amount of PRL secreted in the medium is expressed in ng equivalents of the reference preparation NIAMDD rat-PRL-RP-1. *a, Monolayer cultures.* The culture method was as described previously[7,8]. Cells were plated in multiwell Petri plates (Falcon 308) at 2x 10^5 cells per well. Culture medium was Dulbecco's modified Eagle's medium (DMEM), supplemented as before[8] with 10% horse serum, 2.5% fetal calf serum, non-essential amino acids (all from Gibco) and antibiotics. Tests were performed on the fifth day in culture. The cultures were washed with Earle's balanced salt solution (EBSS) (Gibco), preincubated in EBSS for 1 h at 37 °C in a CO_2/air incubator, washed again and incubated for 4 h at 37°C in a CO_2/air incubator in 500 μl EBSS, pH 7.6, containing the test substances. The various concentrations of DA (Sigma), freshly dissolved and further diluted in 1% ascorbic acid and of the DA receptor antagonists (Janssen) dissolved and further diluted in ethanol were added in 5-μl aliquots. Controls received the vehicles alone. After incubation the media were collected, bovine serum albumin (BSA) added to a final concentration of 0.1%, centrifuged and the supernatants stored at −25 °C until assayed. Each value represents the mean ± s.e.m. of 6 replicate wells. *b, Superfused cell cultures.* Dispersed pituitary cells suspended in 1 ml culture medium were allowed to settle on polystyrene beads (Biosilon, Nunc average diameter 330 μm) packed in a 1-ml sterile syringe the bottom of which was closed with a 25-μm nylon mesh. Homogenous distribution was obtained by pumping the cell suspension through the column of beads at low flow rate (1 ml h⁻¹). The beads had been pretreated with poly-L-lysine[29,30] to ensure instant and irreversible attachment of the cells[8,29]. Approximately 10–15 × 10⁶ cells were loaded on 2 × 10⁵ beads. After washing with the same suspending medium the beads were gently transferred to an untreated plastic Petri dish and maintained in culture medium (see *a*). After 5 days in culture microscopic examination showed that the cells had made individual monolayers over the bead surface, although small aggregates of cells were seen on some beads. The superfusion system consisted of a small plastic column (diameter 5 mm), the bottom of which was closed with a 25-μm nylon mesh and connected to a peristaltic pump. The column and connecting tubings were mounted in a waterbath at 37 °C. To minimize adsorption of drugs, plastic containers, columns and connecting tubings were rinsed before each experiment with 1% BSA in phosphate-buffered saline. A number of beads, containing ~3–4 × 10⁶ cells, were packed on the bottom of each column and the peristaltic pump superfused the beads with DMEM at a flow rate of 1 ml min⁻¹. The volume of medium covering the beads was maintained at 1 ml. Before the control and test substances were added (dissolved and diluted as in *a*), the cells were allowed to equilibrate for 40–60 min with DMEM. Subsequently, 2-ml fractions were collected every 2 min, BSA added as in *a* and the samples stored at -25°C until assayed.

100 nM halopemide, a substituted benzamide structurally related to the butyrophenones but with a distinct pharmacological profile[9]. As expected[1,6,7], the DA receptor antagonists completely prevented inhibition by nanomolar concentrations of apomorphine. Thus, it is reasonable to assume that the DA receptor antagonists potentiate the stimulatory action of apomorphine because at the concentrations used they completely block the 'inhibitory' DA receptors but do not, or only partly, block those receptors which mediate stimulation of PRL release. Note that maximal stimulation by apomorphine was seen at concentrations similar to those of DA but that, in contrast to DA, the magnitude of the effect was less, and slightly higher concentrations even antagonized the stimulatory effect. This seems to indicate that apomorphine has a lower intrinsic activity than DA. Moreover, stimulatory concentrations of apomorphine (10–100 pM) were closer to inhibitory concentrations (0.25–10 nM) than was the case with DA (1–100 pM against 1–100 nM) and this may explain why apomorphine, when applied alone, was not capable of enhancing secretion.

As shown in Fig. 3, bromocryptine was extremely potent in suppressing PRL release. Concentrations as low as 10⁻¹⁸ M were already effective. Co-incubation with 0.1 or 1 nM haloperidol or domperidone shifted inhibition by bromocryptine towards higher concentrations but, from about 10⁻¹² M bromocryptine, PRL release again increased ($P < 0.01$ or 0.001). When incubated with 10 nM of the DA antagonists, bromocryptine stimulated PRL release above basal secretion rates

($P < 0.001$). This occurred at concentrations entirely overlapping with the inhibitory concentrations.

These experiments show that, in addition to their inhibitory effects on PRL release, DA and the DA receptor agonists apomorphine and bromocryptine have a stimulatory potency. In 5-day-old rat pituitary cell cultures, DA stimulated PRL release at concentrations as low as 1 pM, about 1,000 times lower than concentrations that cause inhibition. Picomolar concentrations of apomorphine and even lower concentrations of bromocryptine were also stimulatory, although this effect was seen only when inhibition was prevented by certain DA receptor antagonists. As apomorphine and bromocryptine are highly specific ligands of DA receptors[10,11], these findings strongly suggest that the 'stimulatory' receptors are specific DA receptors. Moreover, data indicate that these DA receptors are different from receptors that mediate inhibition. First, the relative stimulatory potencies of DA, apomorphine and bromocryptine were different from those for inhibition. DA stimulated PRL release from concentrations considerably lower than those causing inhibition, whereas apomorphine and bromocryptine stimulated release at concentrations closer to or overlapping inhibitory concentrations. Second, stimulation by DA could be antagonized, at least partially, by 10 nM haloperidol, but not by 10 nM (+)butaclamol, a DA receptor antagonist that is more potent than haloperidol in preventing the dopaminergic inhibition of PRL release[6,7]. It might be argued that stimulation is mediated by the inhibitory receptor in a different functional

Fig. 2 Effect of apomorphine alone (O) or together with 10 nM haloperidol (●), domperidone (■) or halopemide (100 nM) (▲) on PRL secretion from primary cultures of dispersed rat pituitary cells. Methods as in Fig. 1. *a*, Monolayer cultures, means ± s.e.m. of six replicate wells. *b*, Superfused cells.
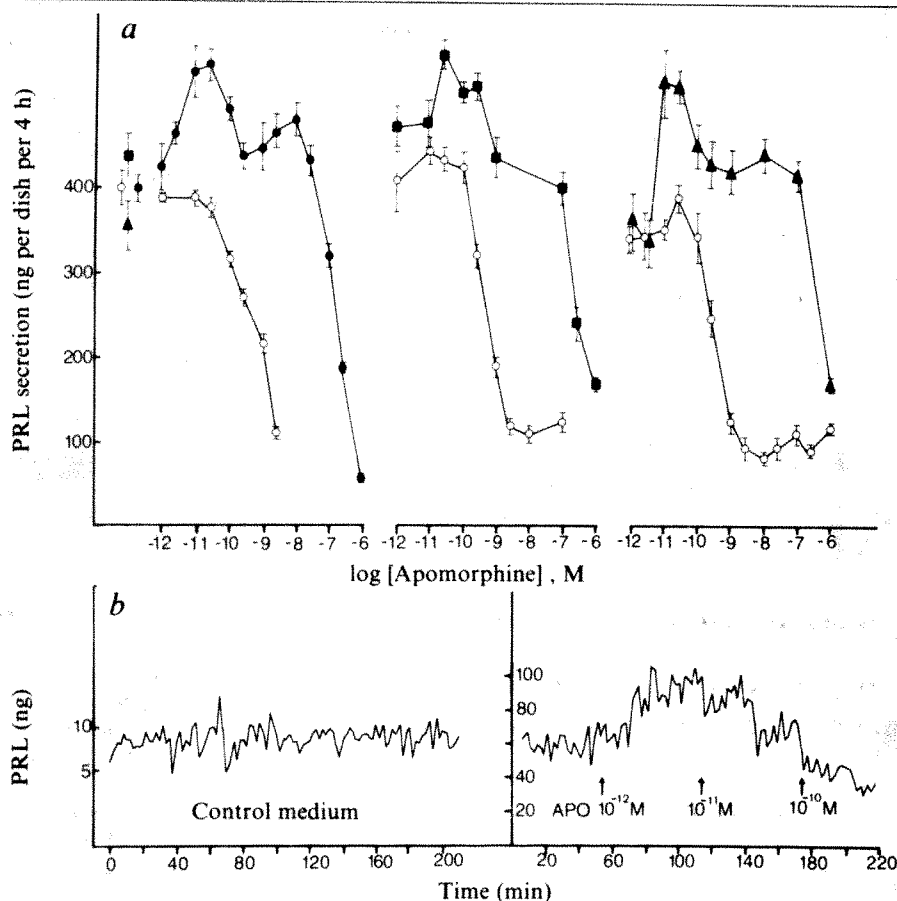
state which would exist only at low receptor occupancy. However, if this were so, it would be difficult to explain apomorphine stimulation in conditions where virtually all inhibitory receptors were occupied by a DA receptor antagonist. Thus, the action of DA on PRL release rather involves two different receptors or receptor sites.

Evidence for more than one DA receptor type has already been given for a number of tissues, particularly the brain[10,12-14].

Fig. 3 Effect of bromocryptine alone (●) or together with: *a*, 0.1 nM (O), 1 nM (△) and 10nM (▲) haloperidol; or *b*, domperidone, on PRL release from primary cultures of dispersed rat pituitary cells. Monolayer culture method as in Fig. 1. Bromocryptine (Sandoz) was dissolved and further diluted in ethanol. Means ± s.e.m. of six replicate wells.

Various receptor categories have been recognized on the basis of: their differential specificity for DA receptor agonists and antagonists[10,15-20]; differential sensitivity of behavioural[11,21,22] and electrophysiological[23] responses to DA agonists; adenyl cyclase activation[10,24]; and regulation by guanine nucleotides[25]. Recent work by Sibley and Creese has suggested that there may be a DA receptor in the anterior pituitary distinct from the receptor that mediates inhibition of PRL release[26]. This DA rereceptor seems to be regulated by guanine nucleotides and is possibly linked to adenyl cyclase. It is tempting to hypothesize that this receptor is involved in stimulation of PRL release by DA. However, the fact that DA agonist activity at this receptor is exerted at micromolar concentrations[26] is difficult to reconcile with the finding here that stimulation of PRL release is evoked at picomolar concentrations. By contrast, the receptors involved in stimulation of PRL release seem to have certain characteristics in common with the DA 'autoreceptors' on cell bodies or terminals of nigrostriatal dopaminergic neurones[23]: the latter receptors are much more sensitive to DA[23] than adenyl cyclase-linked postsynaptic DA receptors in the striatum[23]; apomorphine and bromocryptine both appear to be agonists of these receptors[11,19,22,23]; and haloperidol is a considerably more potent antagonist than (+)butaclamol[19]. Thus, certain characteristics of DA autoreceptors seem to correspond with those of pituitary receptors involved in dopaminergic stimulation of PRL release.

Thus the data presented here suggest that dopaminergic control of PRL secretion at the level of the PRL cells may involve two different receptors for DA, one being inhibitory and the other stimulatory. This is most intriguing in view of the fact that PRL release is believed to be under tonic inhibitory control by DA[1]. The average concentration of DA reported in hypophyseal portal blood of male rats is 0.25 ng ml^{-1} (about 1.3 nM)[4]. This concentration is far below that required for maximal inhibition of PRL release *in vitro* as well as *in vivo*[27] and close to the stimulatory concentrations found here. At such a concentration it is likely that the effect of DA on PRL secretion
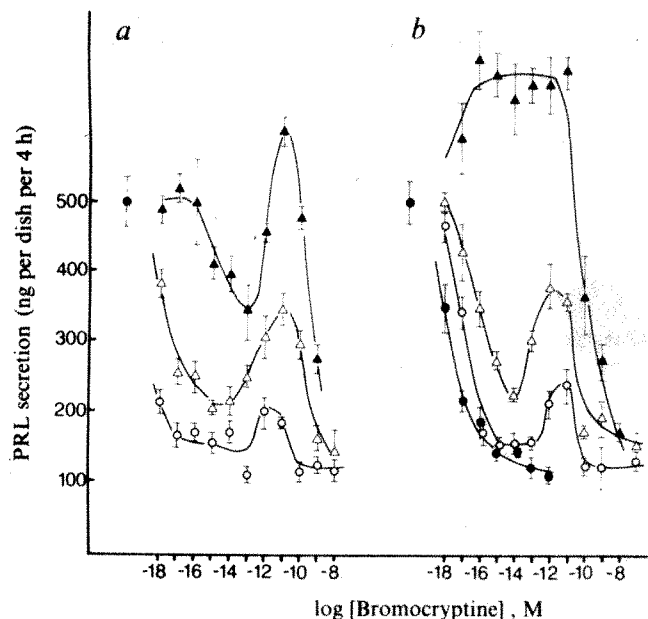
depends on the relative contribution of stimulatory and inhibitory effects. It seems, therefore, that the role of DA in control of PRL secretion is not just one of tonic inhibition. Changes in the relationship between 'stimulatory' and 'inhibitory' receptors could be one of the mechanisms underlying the dynamic regulation of PRL release by DA.

1. MacLeod, R.M. in *Frontiers in Neuroendocrinology* Vol. 4 (eds Martini, L. & Ganong. W.F.) 169–194 (Raven, New York, 1976).
2. Ben-Jonathan, N., Oliver, C., Weiner, H. J., Mical, R. S. & Porter, J. C. *Endocrinology* **100**, 452–458 (1977).
3. Plotsky, P. M., Gibbs, D. M. & Neill, J. D. *Endocrinology* **102**, 1887–1894 (1978).
4. Gudelsky, G. A. & Porter, J. C. *Endocrinology* **104**, 583–587 (1979).
5. Goldsmith, P. C., Cronin, M. J. & Weiner, R. I. *J. Histochem. Cytochem.* **27**, 1205–1207 (1979).
6. Caron, M. G. *et al. J. biol. Chem.* **253**, 2244–2253 (1978).
7. Denef, C. & Follebouckt, J. J. *Life Sci.* **23**, 431–436 (1978).
8. Denef, C., Hautekeete, E. & Dewals, R. *Endocrinology* **103**, 736–747 (1978).
9. Loonen, A. J. M., Van Wijngaarden, I., Janssen, P. A. J. & Soudijn, W. *Life Sci.* **24**, 609–614 (1979).
10. Kebabian, J. W. & Calne, D. B. *Nature* **277**, 93–96 (1979).
11. Fuxe, K. *et al. Acta endocr.* **88**, 27–56 (1978).
12. Cools, A. R. & Van Rossum, J. M. *Psychopharmacologia* **45**, 243–254 (1976).
13. Spano, P. F., Govoni, S. & Trabucchi, M. *Adv. biochem. Psychopharmac.* **19**, 155–165 (1978).
14. Titeler, M., Weinreich, P., Sinclair, D. & Seeman, P. *Proc. natn. Acad. Sci. U.S.A.* **75**, 1153–1156 (1978).
15. Creese, I., Burt, D. R. & Snyder, S. H. *Life Sci.* **17**, 993–1002 (1975).
16. Kebabian, J. W. & Kebabian, P. R. *Life Sci.* **23**, 2199–2204 (1978).
17. Jenner, P. & Marsden, C. D. *Life Sci.* **25**, 479–486 (1979).
18. Miller, R. J., Horn, A. S. & Iversen, L. L. *Molec. Pharmac.* **10**, 759–766 (1974).
19. Iversen, L. L., Rogawski, M. A. & Miller, R. J. *Molec. Pharmac.* **12**, 251–262 (1976).
20. Leysen, J. E., Gommeren, W. & Laduron, P. M. *Biochem. Pharmac.* **27**, 307–316 (1978).
21. Di Chiara, G., Porceddu, M.L., Vargiu, L., Argiolas, A. & Gessa, G.L. *Nature* **264**, 564–566 (1976).
22. Di Chiara, G., Porceddu, M. L., Vargiu, L., Stefanini, E. & Gessa, G. L. *Naunyn-Schmiedebergs Arch. Pharmac.* **300**, 239–245 (1977).
23. Skirboll, L. R., Grace, A. A. & Bunney, B. S. *Science* **206**, 80–82 (1979).
24. Quik, M. & Iversen, L. L. *Eur. J. Pharmac.* **56**, 323–330 (1979).
25. Creese, I., Usdin, T. & Snyder, S. H. *Nature* **278**, 577–578 (1979).
26. Sibley, D. R. & Creese, I. *Eur. J. Pharmac.* **55**, 341–343 (1979).
27. De Greef, W. J. & Neill, J. D. *Endocrinology* **105**, 1093–1099 (1979).
28. Denef, C. *1st Int. Symp. Neuroactive Drugs Endocr.* (September 1979).
29. Hopkins, C. R. *J. Cell Biol.* **73**, 685–695 (1977).
30. Denef, C., Hautekeete, E. & Rubin, L. *Science* **194**, 848–851 (1976).

Inhibin is absent from azoospermic semen of infertile men

R. S. Scott & H. G. Burger

Medical Research Centre, Prince Henry's Hospital, Melbourne 3004, Australia

There is ample evidence that the secretion of follicle stimulating hormone (FSH) by the pituitary gland is regulated by a nonsteroidal hormone of gonadal origin, termed inhibin[1-3]. In several species, testicular extracts[4], gonadal lymph[5] and seminal plasma[6] have been shown to contain proteins which inhibit FSH release; lack of suitable assays for inhibin has, however, prevented clear definition of its physiological significance. Men whose testes show the histological changes of germinal cell failure usually have raised FSH levels in the blood, but may have normal levels of luteinizing hormone (LH) and testosterone[7]. Such patients would thus be predicted to show reduced inhibin production. To test this, we have measured the FSH inhibitory activity of seminal plasma from azoospermic subjects with raised plasma FSH levels. We report here our confirmation of diminished inhibin levels in seminal plasma of these patients, thus providing convincing support for its physiological role as a modulator of FSH production in man.

Our subjects were eight patients with idiopathic azoospermia and raised serum FSH levels, who were attending the Infertility Clinic at Prince Henry's Hospital (Table 1). Testicular histology of three of these patients showed changes of Sertoli-cell-only syndrome, seminiferous tubule hyalinization and moderate hypospermatogenesis, respectively. Levels of LH, although higher than in eight control men with normal semen analyses, were within the laboratory normal range (0.6–3.6. IU l^{-1}). For the purpose of this study, we considered a normal semen analysis to comprise a sperm count $>20 \times 10^6$ per ml, sperm motility $>60\%$ and normal sperm morphology. FSH inhibitory activity was also measured in semen from three patients with non-functioning testicular tissue. One patient with Klinefelter's syndrome had testicles of approximately 1 cm³ (plasma FSH 30.2, LH 9.4 IU l^{-1}). The other two patients were found at operation to have small bilateral abdominal testicles. Plasma FSH levels were 17.0, 23.7 IU l^{-1} and LH levels 9.4, 4.2 IU l^{-1}. Neither was on androgen replacement treatment at the time of collection of semen samples preoperatively. Seminal plasma collected from six patients between 2 and 8 months post-vasectomy was used as an azoospermic control as vasal

obstruction does not affect the integrity of the seminiferous epithelium.

Semen samples were centrifuged twice at 3,000g for 30 min and the plasma separated. An equal volume of charcoal (Merck), 200 mg ml⁻¹ in phosphate-buffered saline (CSL, Melbourne), was added to each sample. After allowing the samples to stand for 24 h at 4 °C, the charcoal was removed by two centrifugations at 4,000g for 30 min at 4 °C. Charcoal was used to remove poorly defined small molecular weight substances that seem to interfere with the assay by causing nonspecific toxic changes.

Inhibin-like activity was measured in combined, multiple parallel line bioassays[8,9], in which the unknowns were expressed in terms of an inhibin standard derived from ovine testicular lymph (OTLP)[10], arbitrary potency 1 U per mg. The inhibin standard was added to dispersed rat anterior pituitary cell cultures over a dose range of 0.156–2.5 mg ml⁻¹ (Fig. 1). Semen samples were assayed in quadruplicate at four or five dilutions up to a maximum concentration of 50 μl seminal plasma per ml of incubation medium. At the end of the 72-h incubation period, the cells were lysed and FSH and LH were measured in the lysate (Fig. 1 legend)[9]. Lack of change of LH content was used as an index of the specificity of the inhibitory response (Fig. 1).

Table 1 Sperm counts, FSH, LH and testosterone levels* in eight normal and eight infertile patients

Group	n	FSH (IU l^{-1})	LH (IU l^{-1})	Testosterone (nmol l^{-1})	Sperm count (10^6 ml⁻¹)
Azoospermic	8	11.7 (6.8–17.0)	2.3 (1.5–3.8)	20.0 (15.0–24.0)	0
Normal	8	2.1 (1.5–2.9)	1.0 (0.7–1.8)	22.0 (13.0–42.0)	73 (22–170)

* Median (and range).

In the eight normal subjects, dose–response lines were significantly parallel to the reference standard; the samples had relative potencies of 20.8–60.0 U ml⁻¹ of inhibin activity (Fig. 2). In men with azoospermia (Fig. 2), the inhibin activity in the seminal plasma was undetectable (<2.5 U ml⁻¹ in five men) or low (<6.3 U ml⁻¹ in three men). A dose–response curve could not be obtained, because addition of seminal plasma at concentrations above 50 μl ml⁻¹ to pituitary cell cultures was often followed by morphological changes, suggesting a toxic effect, and a concomitant reduction of LH content. No FSH inhibitory activity was detectable in the semen of the three patients with testicles of small size. The six post-vasectomy samples had

measurable inhibin-like activities ranging from 4.5 to 20.2 U ml⁻¹ (mean 15.5 U ml⁻¹, s.d. 5.8 U ml⁻¹), significantly less than for normal subjects although higher than found in patients with germ cell failure.

To exclude the possibility that azoospermic seminal plasma in these patients contained a factor blocking the action of inhibin, we added inhibin derived from OTLP or human follicular fluid to azoospermic seminal plasma. In both cases, the predicted inhibition of cell content of FSH was observed, without significant change of the dose–response curve.

Although a considerable body of data suggests the existence of a non-steroidal regulator of pituitary FSH secretion[1-3], the relationship exists between the cell population of the epithelium spontaneous disorders of the seminiferous epithelium has not been studied. It has been previously shown that a reciprocal relationship exists between the cell population of the epithelium and serum FSH, and that serum FSH levels are uniformly elevated only in the presence of severe seminiferous tubule damage[11]. In the absence of a well characterized purified preparation of inhibin, physiological studies must rely on specific
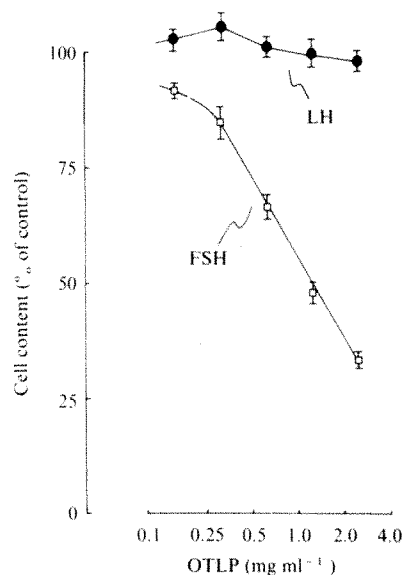
Fig. 1 FSH and LH content in 22 experiments (mean ± s.e.m.) using OTLP standard as the inhibin source. Similar dose responses of FSH, with lack of LH change, were observed after addition of treated normal human seminal plasma. Dispersed pituitary cells were prepared by enzymatic methods in sterile conditions[9,10]. Aliquots (0.5 ml) of medium containing 125,000 cells were added to each well of tissue culture plates (Coster, 3524) and incubated for 24 h at 37 °C in 5% CO_2, 95% air before adding semen samples and OTLP standard. All preparations were added in quadruplicate at four or five dilutions. After a further 72 h in culture, the medium was aspirated and discarded, and 0.5 ml of phosphate buffer containing 0.1% Triton X-100 was added to each well. This causes detachment and lysis of cells, releasing intracellular hormone into the buffer. Standards for hormones measured in the lysate were rat FSH-RP1 and rat LH-14 (NIAMDD)[9,12]. The FSH and LH concentrations were expressed as % of control (no added inhibin) and regression analysis of the FSH dose-response lines carried out by computer, calculating slope (*b*), index of precision (λ) and significance of regression (Finney's *g*)[13]. In 22 experiments using the reference standard (OTLP): −*b* = 24.0 (19.2–31.4), −λ = 0.06 (0.032–0.110) and Finney's *g* = 0.01 (0.003–0.057). Median and range are given. Interassay variation of three unknown preparations was 20.1%, 19.8% and 15.0%. Specificity is satisfactory as changes of rat LH, GH or prolactin were not significant[9]. Bioassay potency estimates of unknown preparations were similar using the more conventional methods of *in vitro* assay measuring LH-releasing hormone stimulated release[9]. From eight separate experiments, four wells per experiment, the FSH content (of control wells) at the end of 96 h culture was 636 ± 28.0 ng per 125,000 cells.

bioassay. The present results have been obtained with a reproducible assay in which the cell content of FSH, but not LH, is decreased by inhibin-containing preparations[9]. In men with severe seminiferous tubule disease, as shown by elevated levels of serum FSH and azoospermia, seminal plasma levels of inhibin are low or undetectable. These patients had normal peripheral plasma testosterone concentrations, suggesting that the elevations of serum FSH represent a release from the negative feedback influence of this inhibitor.
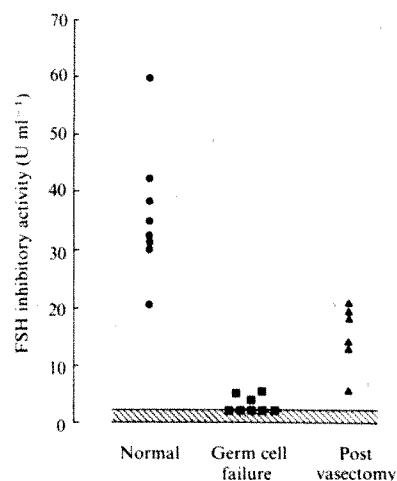
Fig. 2 FSH inhibitory activity in human seminal plasma of normal, post-vasectomized and azoospermic infertile patients. The assay limit for measurement of inhibin was 2.5 U ml⁻¹ (indicated by shading).

Seminal plasma of vasectomized patients contained FSH inhibitory activity; this suggested secretion and perhaps concentration of inhibin in the prostatic and seminal vesicular fluid. However, this does not imply extragonadal production of this inhibitor, because the levels of inhibin were low in infertile subjects despite the presence of normal concentrations of testosterone, the major factor maintaining prostatic function. Therefore, the likely source of this material is the testis, as the only difference between groups was the integrity of the germinal epithelium. Further support for the testicular production of this inhibitor is provided by the observation that no inhibin was present in the semen of the two subjects with abdominal testes or the patient with Klinefelter's syndrome. Such findings suggest a causal relationship between seminiferous tubular disease and decreased production of inhibin.

Note added in proof: A substance which diminished FSH levels in castrated male rats was found to be present in the seminal plasma of normal and oligospermic subjects, but was absent in subjects with azoospermia caused by inhibition of gametogenesis[14].

1. Lee, V. W. K. *et al.* in *Recent Advances in Reproduction and Regulation of Fertility* (ed. Talwar, G. P.) 241–252 (Elsevier, Amsterdam, 1979).
2. de Jong, F. H. *Molec cell. Endocr.* **13**, 1–10 (1979).
3. Franchimont, P., Chari, S., Hazee-Hagelstein, M. T., Debruche, M. L. & Duraiswami, S. in *The Testis in Normal and Infertile Men* (eds Troen, P. & Nankin, H. R.) 253–270 (Raven, New York, 1977).
4. Keogh, E. J. *et al. Endocrinology* **98**, 997–1004 (1976).
5. Baker, H. W. G. *et al. Int. J. Andrology* Suppl. **2**, 115–125 (1978).
6. Franchimont, P. *et al. Int. J. Andrology* Suppl. **2**, 69–80 (1978).
7. Baker, H. W. G. *et al. Recent Prog. Horm. Res.* **32**, 429–476 (1976).
8. Borth, R. in *Methods of Hormone Analysis* (eds Breuer, H., Hamel, D. & Kruskemper, H.L.) 500—513. (Thieme, Stuttgart, 1976).
9. Scott, R. S., Burger, H. G. & Quigg, H. *Endocrinology* (in the press).
10. Eddie, L. W., Baker, H. W. G., Higginson, R. E. & Hudson, B. *J. Endocr.* **81**, 49–60 (1979).
11. de Kretser, D. M., Burger, H. G. & Hudson, B. *J. clin. Endocr. Metab.* **38**, 787–793 (1974).
12. Lee, V. W. K., de Kretser, D. M., Hudson, B. & Wang, C. *J. Reprod. Fert.* **42**, 121–126 (1975).
13. Finney, D. J. *Statistical Method in Biological Assay* 2nd edn (Griffin, London, 1964).
14. Franchimont P. *J.R. Coll. Phycus, Lond* **6**, 283-298 (1972).

Renin-like effects of NGF evaluated using renin-angiotensin antagonists

D. B. Avrith, M. E. Lewis, & J. T. Fitzsimons

Physiological Laboratory, University of Cambridge, Cambridge CB2 3EG, UK

Intracranial injection of angiotensin II (AII) or activation of the cerebral isorenin–angiotensin system with intracranial renin causes an immediate thirst[1] and a delayed sodium appetite[2] in the rat. Nerve growth factor (NGF), a polypeptide trophic factor for peripheral sympathetic and sensory neurones[3], has also been reported to be a potent stimulus to thirst[4] and sodium appetite[5] when injected into the brain of the rat. Lewis et al.[5] drew attention to the marked similarity between the effects of 2.5S NGF and renin on thirst and sodium appetite and suggested that the NGF responses were mediated by the cerebral isorenin-angiotensin system. We report here that NGF-induced thirst and sodium appetite, as well as increased blood pressure and increased ornithine decarboxylase activity in the brain and liver, depend on the formation of AII (see also ref. 6).

To test the hypothesis that NGF-induced thirst and sodium appetite depend on the activation of the cerebral isorenin-angiotensin system[5], rats were pretreated with saralasin, a competitive antagonist of AII (ref. 7), or the converting enzyme inhibitors[8,9], SQ 20881 or SQ 14225. These inhibitors are effective in suppressing the thirst[10] and sodium appetite (unpublished results) elicited by intracranial administration of renin.

Intracranial injection of saralasin caused a dose-dependent inhibition of water intake induced by injection of 0.66 μg 2.5S NGF[11] through the same cannula (see Fig. 1 legend for method). In 1 h the intake of water after NGF injection was 15.3 ± 1.5 ml ($n = 18$), and this was reduced by saralasin pretreatment (1, 5 and 25 μg respectively) to 9.2 ± 2.6 ml ($n = 8$, $P < 0.05$), 6.3 ± 0.4 ml ($n = 4, P < 0.01$), and 4.4 ± 1.5 ml ($n = 6$, $P < 0.001$). The 1-h intake of 2.7% NaCl after NGF injection (2.4 ± 0.7 ml, $n = 18$) was completely abolished by 25 μg saralasin ($n = 6$, $P < 0.05$).

Intracranial injection of SQ 20881 (25 μg) or SQ 14225 (5 μg) resulted in complete inhibition of water intake during the first hour after administration of 0.66 μg 2.5S NGF through the same intracranial cannula (Fig. 1). The 18-h water and 2.7% NaCl intakes after NGF were unaffected by the single injection of 25 μg SQ 20881, but were attenuated significantly by the single injection of 5 μg of the more potent converting enzyme inhibitor, SQ 14225.

The effect of converting enzyme inhibition on the overnight intakes of water and 2.7% NaCl after NGF was further studied by infusing SQ 20881 throughout the 18 h of the experiment. Continuous infusion of the inhibitor resulted in a significant depression of the overnight water and 2.7%NaCl intakes after NGF injection (Fig. 1). The effect of NGF on thirst and sodium appetite is therefore indistinguishable from that of renin with respect to its dependence on generation of AII.

The renin-like activity of NGF preparations was further tested by measuring their pressor activity. Intravenous administration of dipsogenically active 7S NGF[12] produced a dose-dependent rise in arterial blood pressure (Fig. 2), as did 2.5S NGF (data not shown). The pressor responses to NGF were similar to those of equipotent doses of renin. The responses showed a slow onset over 1–2 min and lasted for up to 20 min. They were enhanced by nephrectomy and were completely abolished by pretreatment with 25 μg saralasin, 25 μg SQ 14225, or NGF antiserum[13]. In contrast, immunogenically

pure β NGF subunit[14] was devoid of pressor activity, and also had a smaller and more variable effect on thirst and sodium appetite compared with other preparations of NGF.

These findings raise the possiblity that other biological effects of NGF are caused by AII formed as a result of the action of the renin-like enzyme in NGF preparations. NGF has recently been reported to produce an increase in the activity of ornithine decarboxylase (ODC) in a variety of tissues[15,16], including brain[17] and liver[18]. In the present experiments intraventricular administration of either 7S NGF or renin was followed 6 h later by an increase in ODC activity in the brain and liver (Fig. 3). The enzyme induction and water intakes following intraventricular administration of either NGF or renin were reduced significantly by pretreatment with 35 μg SQ 14225. The dependence of the enzyme induction in brain and liver on AII formation is consistent with the recent finding that large doses of AII are an effective stimulus to ODC induction in these tissues[19]. Induction of ODC in the liver following NGF administration depends on activation of the pituitary-adrenal axis[18]. Furthermore, administration of NGF[20], like AII (refs 21–23), causes an increase in plasma ACTH and corticosteroids. Therefore, stimulation of ACTH by NGF preparations may depend on their content of renin-like enzymes.
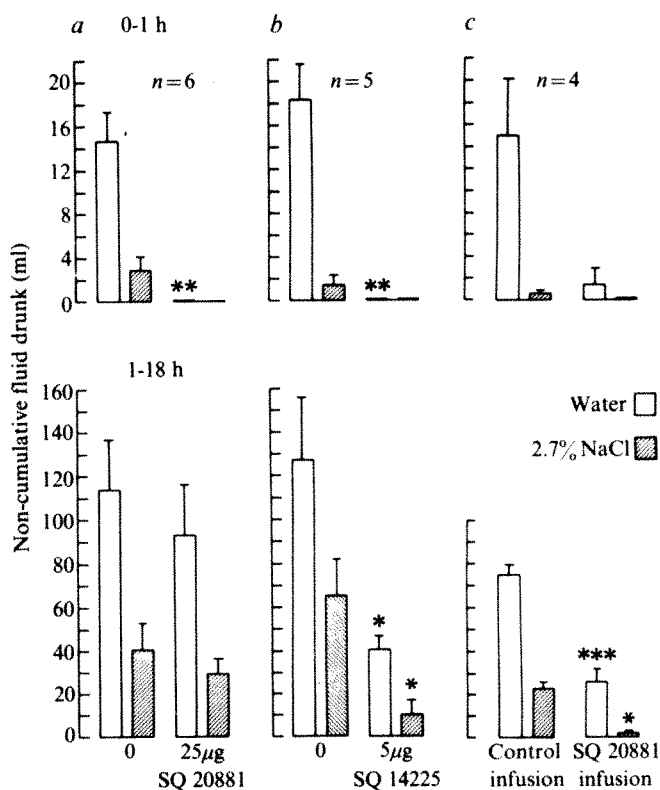
Fig. 1 The effect of angiotensin converting enzyme inhibitors on NGF-induced thirst and sodium appetite. Five min before injection of 2.5S NGF into the preoptic area or third ventricle, rats were given intracranial injections (1 μl) of 0.9% NaCl (0, vehicle), or SQ 20881 (Bachem) (a), or SQ 14225 from Dr Z. P. Horowitz, Squibb (b). For intracranial infusions into the third ventricle (c), rats were first infused with either 3 μl of 0.9% NaCl (control) or 3 μl of 0.9% NaCl containing 25 μg SQ 20881 at the rate of 1 μl every 3 min. The injector was then removed and 0.66 μg 2.5S NGF in 4 μl 0.9% NaCl was aspirated into the tubing. The injector was replaced and the rats were infused with the solution at the same rate. After 12 min the infusion rate was changed so that the rats received 25 μg SQ 20881 every hour for 18 h. Control rats received 3 μl per h of 0.9% NaCl during this period. Water and 2.7% NaCl intakes were measured at 1 and 18 h after the start of the infusion of NGF. Results are expressed as mean ± s.e.m. The statistical significance of the differences between the control and inhibitor-treated rats was evaluated using Student's *t*-test. * $P < 0.05$; ** $P < 0.01$; *** $P < 0.001$.

Fig. 2 The effect of an angiotensin converting enzyme inhibitor (SQ 14225) or an angiotensin II receptor antagonist (saralasin, P113) or NGF antiserum on NGF-induced pressor responses. Blood pressure, before and after test injections into the right jugular vien, was recorded with a strain-gauge transducer from the carotid artery of the rat anaesthetised with urethane (1 g per kg body weight intraperitoneally) and ganglion-blockaded (50 mg hexamethonium per kg body weight subcutaneously, with additional amounts as required). Inhibitors were injected 5 min before NGF administration. Responsiveness to AII was always confirmed in animals which had failed to respond to NGF after pretreatment with SQ 14225 or NGF antiserum (8.3 μl diluted to 100 μl; from Dr G. Guroff).

a Brain   *b* Liver   *c* 6-h Water intake
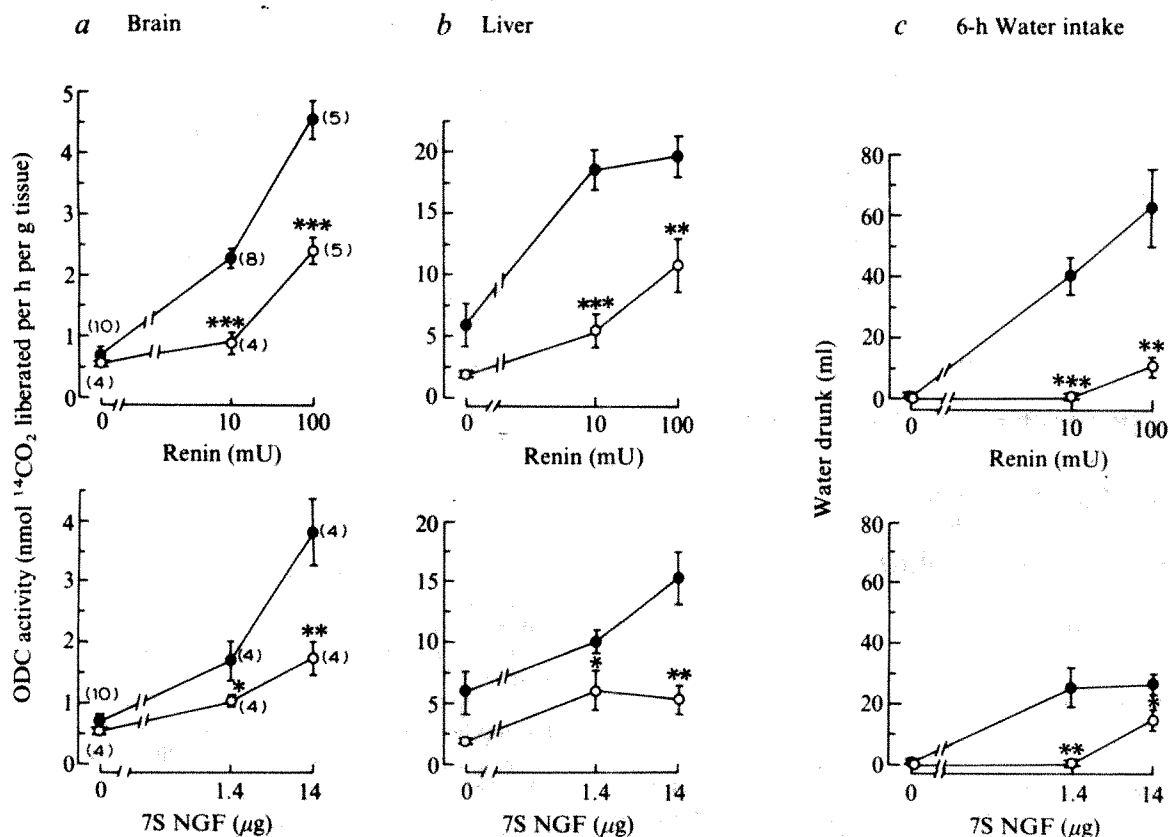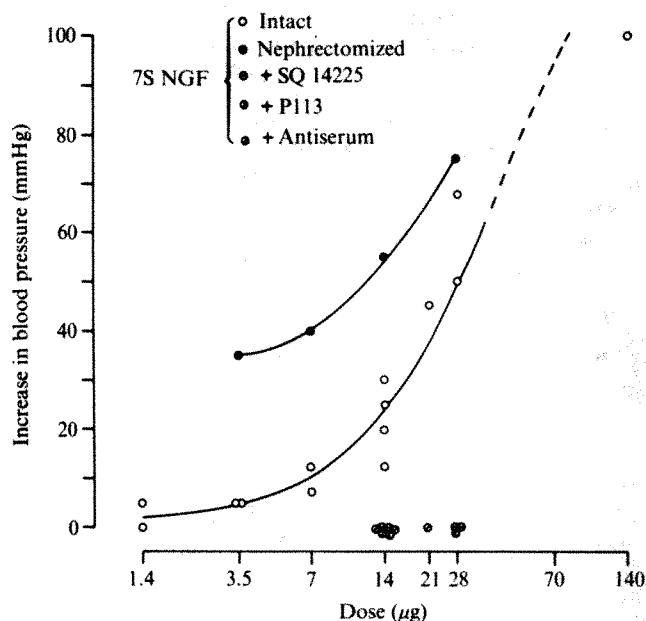
Fig. 3 The effect of a converting enzyme inhibitor (SQ 14225) on renin- and NGF-induced increases in ornithine decarboxylase activity in brain and liver and water intake in the same animals. Rats were given intraventricular injections[17] of either 7 μl or 0.9% NaCl or 7 μl 0.9% NaCl containing 35 μg SQ 14225, followed 2 min later by 5 μl injections of 0.9% NaCl, renin or 7S NGF. Six hours later, water intakes were recorded, the rats were killed and their brains and livers removed and frozen on solid CO_2. The activity of ornithine decarboxylase (ODC) in these tissues was measured essentially as described before[17,18] (mean ± s.e.m. is indicated with the number of animals in parentheses). The values for the control (●) and inhibitor-treated (○) animals were compared statistically as before. * $P < 0.05$; ** $P <$

A further question which has not been resolved is whether a renin-like enzyme should be regarded as an integral component of mouse submandibular gland NGF complexes. Isorenin and NGF are stored together in the same cells of the mouse submandibular gland[24], are closely associated physically[24], show the same sexual dimorphism and the same changes with age[25,26], and are both secreted in response to α-adrenergic stimulation[27,28].

In conclusion, experiments with inhibitors of the renin-angiotensin system demonstrate that several potent behavioural and biological effects of NGF preparations depend on the generation of AII by a renin-like enzyme in NGF. Therefore, unless renin-free preparations of NGF are used, antagonists of the renin-angiotensin system such as saralasin and SQ 14225 must be used in testing for putative NGF effects, particularly when a biological effect attributed to NGF is known to be produced by renin or AII.

We thank Miss Christine Narracott for technical assistance and the MRC for financial support. M.E.L. was supported by a Wellcome Research Fellowship from the Wellcome Trust.

1. Fitzsimons, J. T. *J. Physiol., Lond.* **214**, 295–303 (1971).
2. Avrith, D. B. & Fitzsimons; J. T. *J. Physiol., Lond.* (in the press).
3. Yu, M. Y. W., Lakshmanan, J. & Guroff, G. in *Essays in Neurochemistry and Neuropharmacology* (eds Youdim, M. B. H. *et al.*) 33–48 (Wiley, New York, 1978).
4. Perkins, M. S., Margules, D. L. & Ward, I. L. *Brain Res.* **161**, 351–355 (1979).
5. Lewis, M. E., Avrith, D. B. & Fitzsimons, J. T. *Nature* **279**, 440–442 (1979).
6. Fitzsimons, J. T., Avrith D. B. & Lewis, M. E. *Neurosci. Lett. Suppl.* **3**, S237 (1979).
7. Pals, D. T., Masucci, F. D., Denning Jr., G. S., Sipos, F. & Fessler, D. C. *Circ. Res.* **29**, 673–681 (1971).
8. Engel, S. L., Schaeffer, T. R., Gold, B. I. & Rubin, B. *Proc. Soc. exp. Biol. Med.* **140**, 240–244 (1972).
9. Rubin, B. *et al. Fedn Proc.* **36**, 1049 (1977).
10. Fitzsimons, J. T., Epstein, A. N. & Johnson, A. K. *Brain Res.* **153**, 319–331 (1978).
11. Bocchini, V. & Angeletti, P. U. *Proc. natn. Acad. Sci. U.S.A.* **64**, 787–794 (1969).
12. Varon, S., Nomura, J. & Shooter, E. M. *Biochemistry* **6**, 2202-2209 (1967).
13. Stöckel, K., Gagnon, G., Guroff, G. & Thoenen, H. *J. Neurochem.* **26**, 1207–1211 (1976).
14. Chapman, C. A., Banks, B. E. C., Carstairs, J. R., Pearce, F. L. & Vernon, C. A. *FEBS Lett.* (in the press).
15. MacDonnell, P. C., Nagaiah, K., Lakshmanan, J. & Guroff, G. *Proc. natn. Acad. Sci. U.S.A.* **74**, 4681–4684 (1977).
16. Hatanaka, H., Otten, U. & Thoenen, H. *FEBS Lett.* **92**, 313–316 (1978).
17. Lewis, M. E., Lakshmanan, J., Nagaiah, K., MacDonnell, P. C. & Guroff, G. *Proc. natn. Acad. Sci. U.S.A.* **75**, 1021–1023 (1978).
18. Nagaiah, K., Ikeno, T., Lakshmanan, J., MacDonnell, P. C. & Guroff, G. *Proc. natn. Acad. Sci. U.S.A.* **75**, 2512–2515 (1978).
19. Ikeno, T. & Guroff, G. *J. Neurochem.* **33**, 973–975 (1979).
20. Otten, U., Baumann, J. B. & Girard, J. *Nature* **282**, 413–414 (1979).
21. Daniels-Severs, A., Ogden, E. & Vernikos-Danellis, J. *Physiol. Behav.* **7**, 785–787 (1971).
22. Maran, J. W. & Yates, F. E. *Am. J. Physiol.* **233**, E273–E285 (1977).
23. Ramsay, D. J., Keil, L. C., Sharpe, M. C. & Shinsako, J. *Am. J. Physiol,* **234**, R66-R71 (1978).
24. Cozzari, C., Angeletti, P. U., Lazar, J., Orth, H. & Gross, F. *Biochem. Pharmac.* **22**, 1321–1327 (1973).
25. Bhoola, K. D., Dorey, G. & Jones, C. W. *J. Physiol., Lond.* **235**, 503-522 (1973).
26. Hendry, I. A. *Biochem. J.* **128**, 1265–1272 (1972).
27. Menzie, J. W. & Michelakis, A. M. *Fedn Proc.* **31**, 511 (1972).
28. Wallace, L. J. & Partlow, L. M. *Prc. natn. Acad. Sci. U.S.A.* **73**, 4210–4214 (1976).

Epidermal growth factor requirement for development of cultured mammary gland

Quentin J. Tonelli & Sam Sorof

The Institute for Cancer Research, Fox Chase Cancer Center, Philadelphia, Pennsylvania 19111

The mouse mammary gland in serum-free whole organ culture can be manipulated hormonally to undergo one complete physiological cycle consisting of lobuloalveolar development[1], functional differentiation and regression[2], mimicking processes that occur *in vivo*. A second cycle has not previously been achieved *in vitro*. The present study has identified a specific requirement for epidermal growth factor (EGF) in the morphological development of mammary lobuloalveoli, allowing two complete cycles of development and regression in culture.

Whole mammary glands of BALB/c mice were cultured for 9 days in serum-free development medium containing insulin (I), prolactin (P), aldosterone (A) and hydrocortisone (H) (Fig. 1 legend)[3,4]. At day 9, the glands contain fully developed lobuloalveoli[2,3] and casein[5]. When such glands are maintained in hormone-deficient regression medium (insulin as the only added hormone) for an additional 15 days (days 9–24), the lobuloalveoli involute (regress)[2,3]. Such regressed glands did not undergo a second development on return to the above IPAH medium (medium containing insulin, prolactin, aldosterone and hydrocortisone) for an additional 9 days (Fig. 1, Table 1). They were presumably depleted of necessary growth factor(s).
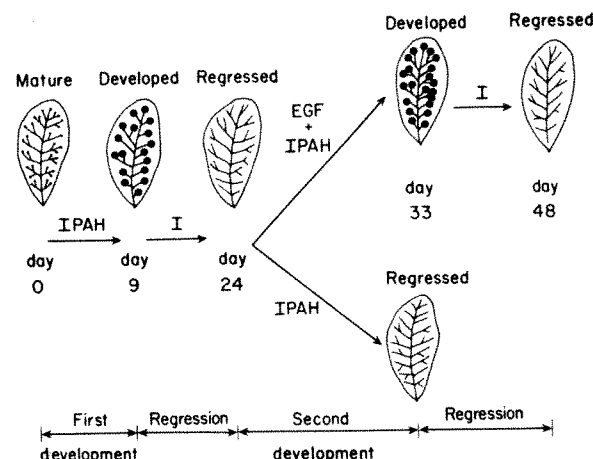
Fig. 1 Two cycles of development and regression of mouse mammary glands in whole organ culture. The serum-free culture system has been described[3,4,12]. Female BALB/c mice, 3–4 weeks old, were primed with 9 daily injections of β-oestradiol (1 μg) and progesterone (1 mg). On the day following the last injection, mice were killed and their entire second thoracic mammary glands were excised and floated on Dacron rafts. The serum-free development medium consisted of Waymouth MB752/1 medium (1 ml per gland) supplemented with $350\ \mu g\ ml^{-1}$ L-glutamine, $35\ \mu g\ ml^{-1}$ penicillin G, and $5\ \mu g\ ml^{-1}$ of each of the hormones, insulin (I), prolactin (P), aldosterone (A) and hydrocortisone (H). Medium was changed every 2 to 3 days. Glands cultured in the development medium for 9 days (days 0–9) underwent first lobuloalveolar development[1-3,12]. Exposure of these glands to regression medium containing insulin ($5\ \mu g\ ml^{-1}$) as the only added hormone for additional 15 days (days 9–24) caused first regression of the mammary lobuloalveoli[2,3,12]. Glands were then incubated in development medium with EGF for another 9 days (days 24–33), resulting in second development of the mammary glands. Second-developed mammary glands were then regressed in the regression medium for an additional 15 days (days 33-48). Glands were fixed, stained, coded[3] and evaluated as in Table 1.

We have found that the polypeptide, EGF, a purified mitogenic protein of molecular weight 6,100 (ref. 6), specifically induces a second development in previously regressed whole mammary glands. The presence of EGF in combination with IPAH for 9 days (days 24–33) elicited this effect in more than 71% of the glands in the absence of serum (Fig. 1, Table 1). The development was verified by microscopic examinations of the whole organ (Fig. 2) and at the cellular level. This positive response was in marked contrast to the refractoriness of the glands to the polypeptides, nerve growth factor, fibroblast growth factor, and multiplication stimulating activity factor, each in the presence of IPAH. Supplementations of IPAH with fetal bovine serum (FBS), growth hormone, β-oestradiol, and progesterone singly or in combinations were also ineffective. The addition of growth hormone to IPAH and EGF resulted in no additional development, and the combination of growth hormone, FBS and IPAH actually inhibited the second development-promoting activity of EGF.
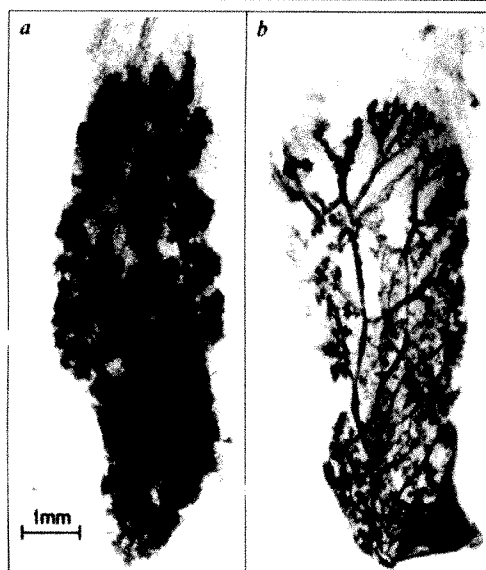
Fig. 2 Second lobuloalveolar development of mouse mammary gland in whole organ culture. Entire mammary glands were cultured for 24 days according to the protocol described in Fig. 1 legend. Glands were cultured for an additional 9 days (days 24–33) in the IPAH medium with or without 10 nM EGF. Glands were then processed as described in Fig. 1 legend and Table 1. *a*, Whole mammary gland showing second-developed lobuloalveoli after incubation in the medium containing EGF. *b*, Control gland similarly incubated in the medium without EGF. The epithelial cells are primarily ductal, and alveoli are absent.
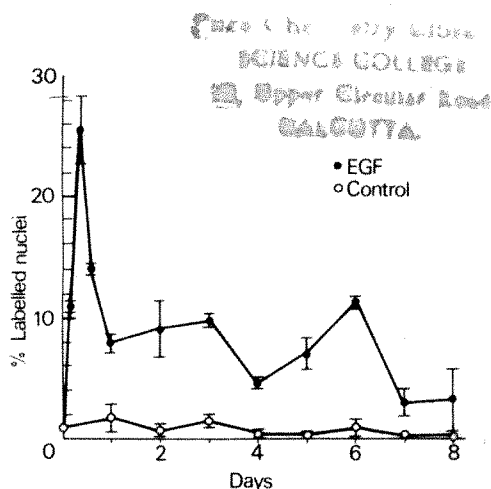
Fig. 3 ^{3}H-thymidine incorporation in mammary epithelial cell nuclei during second development of mouse mammary glands in whole organ culture. After first development (days 0–9) and regression (days 9–24), as in Fig. 1 legend, the mammary glands were placed in serum-free medium containing insulin, prolactin, aldosterone and hydrocortisone (5 μg ml⁻¹ each) in the presence (●) or absence (control, ○) of 10 nM EGF. The presence of mammary fat surrounding the epithelial cells within the fat pad apparently necessitated the uses of relatively high levels of radioactivity and long exposure time. Glands were pulsed for 1 h with 5 μCi ml⁻¹ ^{3}H-thymidine (128Ci mmol⁻¹; NEN) at the different times, and then were fixed[3]. Autoradiographs of 5-μm histological sections were prepared by dipping the slides in Kodak NTB-2 emulsion. The coated slides were placed in toluene with scintillator (4 g PPO, 0.05 g POPOP per litre), and exposed for 10 days in the dark at −60 °C. Slides were developed[21], stained with haemotoxylin and eosin, and mounted for examination. Epithelial cell nuclei with more than 5 silver grains were scored as positive. A minimum of 500 nuclei were counted from each section. Results from 4 sections are expressed as average numbers of labelled nuclei ± standard deviations (vertical limits).

The activity of EGF was concentration dependent. Significant activity was absent at 1 nM or less, but was maximal at 10 nM and 100 nM, inducing second development in 70 and 75% of the glands, respectively ($P < 0.0001$). The latter concentrations of EGF approximate those present in mammalian tissues[7].

The second development induced by EGF and IPAH apparently stimulated the mammary epithelial cells to undergo synthesis of DNA over the course of 1 week. As determined by ^{3}H-thymidine incorporated into cell nuclei, a peak of DNA synthesis occurred in 25% of the mammary epithelial cells at 8 h after addition of EGF, with perhaps a second peak at day 3, and a third at day 6 (Fig. 3). This periodicity is compatible with a cell generation of 3 days.

Glands that underwent second development in EGF (10 nM) and IPAH (each 5 μg ml⁻¹) regressed at the end of 15 days (days 33–48) in medium containing insulin as the only added hormone (regression medium) (Fig. 1). A third development was not induced in the presence of EGF and IPAH.

Table 1 Specific induction of second mammary development by epidermal growth factor in whole organ culture

Additions to IPAH	Concentration	No. of glands	>50% Alveoli developed	
			Glands	% Glands
None	—	26	2	8
EGF	10 nM	28	20	71*
NGF	10 ng ml⁻¹	28	4	14
FGF	10 ng ml⁻¹	26	1	4
MSA	10 ng ml⁻¹	28	3	11
FBS	10%	9	0	0
G	5 μg ml⁻¹	21	2	10
E + Prg	1 ng ml⁻¹, 1 μg ml⁻¹	34	2	6
EGF + G	10 nM, 5 μg ml⁻¹	16	8	50*
EGF + G + FBS	10 nM, 5 μg ml⁻¹, 10%	18	3	17

Mouse mammary glands in serum-free whole organ culture were induced to undergo first development (days 0–9) and then regression (days 9–24), as in the Fig. 1 legend. With the aim of achieving a second development, the fully regressed glands were incubated for another 9 days (days 24–33) in serum-free development medium containing IPAH (each at 5 μg ml⁻¹) and the listed additions. Epidermal growth factor (purified from male mouse submaxillary glands), nerve growth factor (NGF), fibroblast growth factor (FGF), multiplication stimulation activity factor (MSA) (all Collaborative Research), fetal bovine serum (FBS; Gibco), growth hormone (G; Miles), β-oestradiol and progesterone (E, Prg; Sigma) were present at the stated concentrations. At day 33, the organs were coded, fixed and stained[3]. The relative extents of development were scored on the basis of the percentage of developed lobuloalveoli in individual glands, 0 representing no development and 100% full development. The percents of the numbers of >50% developed glands are indicated.
* Significant second development according to Fisher's 2×2 exact test.

In contrast to its second development-promoting activity, EGF added alone or in combination with several steroid or polypeptide hormones induced little or no first development of alveoli. The hormones P, I, IA, IH, IAH, AH, each at 5 μg ml⁻¹, either alone or with EGF (10 nM), did not promote first development. However, the two combinations, IP with EGF, and PAH with EGF, did elicit moderate activities compared to IPAH without EGF (first development medium).

The polypeptide growth factor, EGF, may have a necessary and specific role in the physiological actions of the mammary gland. EGF acting with the hormones IPAH enables the mouse mammary gland to undergo a second development from the fully regressed state in serum-free culture. A stimulation of DNA synthesis seems to be involved. The requirement for EGF

is specific. The activity of EGF is maximal at physiological concentration (10 nM)[7]. Presumably endogenous stores of EGF operate in first development, as exogenous EGF does in second development. The mouse mammary gland can thus be manipulated to undergo two complete cycles of mammary gland development and regression in whole organ culture (Fig. 1).

EGF has been reported to induce mitogenesis[8-10], DNA synthesis[8-11] and RNA synthesis[8] in cultured fragments or dissociated cells of mammary glands. Starting with fragments of mammary glands already partly developed *in vivo* during pregnancy, additional development was induced in culture in response to EGF with insulin or hydrocortisone[8]. The present demonstration of the ability of EGF to promote a second development of mammary gland from the fully involuted state, permitting two cycles of development and regression *in vitro*, considerably extends knowledge of the importance of EGF in the regulation of mammary gland development.

Transformation of mouse mammary glands by chemical or carcinogens in whole organ culture is manifest as a persistance of developed lobuloalveoli in hormone-deficient medium (insulin as the only added hormone). The transformed glands, which are dysplastic, metaplastic[3,12] and oncogenic[14] have escaped from the growth controls normally imposed by prolactin and specific steroids[3,14]. The finding of an EGF role in mammary gland development and other observations[12,15-20] raise the question whether a deregulation of the EGF system may mediate the loss of controls of lobuloalveolar development that characterizes the mammary gland transformation by chemical carcinogens.

We thank Dr Wayne Ruppel for analysis of data, Dr R. Philip Custer for microscopy, Ms Gail Nussbaum for assistance and Dr Stanley Cohen for a gift of EGF. This work was supported in part by NIH grants CA-21522, CA-05945, CA-09035, CA-06927, RR-05539 and an appropriation from the Commonwealth of Pennsylvania.

1. Ichinose, R. R. & Nandi, S. *J. Endocr.* **35**, 331-340 (1966).
2. Wood, B. G., Washburn, L. L., Mukherjee, A. S. & Banerjee, M. R. *J. Endocr.* **65**, 1-6 (1975).
3. Tonelli, Q. J., Custer, R. P. & Sorof, S. *Cancer Res.* **39**, 1784-1792 (1979).
4. Banerjee, M. R., Wood, B. G., Lin, F. K. & Crump, L. R. *Tissue Culture Ass. Manual* **2**, 457-462 (1976).
5. Terry, P. M., Ball, E. M., Ganguly, R. & Banerjee, M. R. *J. Immun. Meth.* **9**, 123-134 (1975).
6. Carpenter, G. & Cohen, S. *A. Rev. Biochem.* **48**, 193-216 (1979).
7. Byyny, R. L., Orth, D. N., Cohen, S. & Doyne, E. S. *Endocrinology* **95**, 776-782 (1974).
8. Turkington, R. W. *Expl. Cell Res.* **57**, 79-85 (1969).
9. Stoker, M. G. P., Pigott, D. & Taylor-Papadimitriou, J. *Nature* **264**, 764-767 (1976).
10. Turkington, R. W. *Cancer Res.* **29**, 1457-1458 (1969).
11. Rudland, P. S., Hallowes, R. C., Durbin, H. & Lewis, D. *J. Cell Biol.* **73**, 561-577 (1977).
12. Dickens, M. S., Custer, R. P. & Sorof, S. *Proc. natn. Acad. Sci. U.S.A.* **76**, 5891-5895 (1979).
13. Telang, N. T., Banerjee, M. R., Iyer, A. P. & Kundu, A. B. *Proc. natn. Acad. Sci. U.S.A.* **76**, 5886-5890 (1979).
14. Banerjee, M. R., Wood, B. G. & Washburn, L. L. *J. natn. Cancer Inst.* **53**, 1387-1393 (1974).
15. Todaro, G. J. & De Larco, J. E. *Cancer Res.* **38**, 4147-4154 (1978).
16. Todaro, G. J., De Larco, J. E. & Sporn, M. B. *Nature* **276**, 272-274 (1978).
17. De Larco, J. E. & Todaro, G. J. *Proc. natn. Acad. Sci. U.S.A.* **75**, 4001-4005 (1978).
18. Shoyab, M., De Larco, J. E. & Todaro, G. J. *Nature* **279**, 387-391 (1979).
19. Lee, L.-S. & Weinstein, I. B. *Science* **202**, 313-315 (1978).
20. Cherington, P. V., Smith, B. L. & Pardee, A. B. *Proc. natn. Acad. Sci. U.S.A.* **76**, 3937-3941 (1979).
21. Banerjee, M. R. & Rodgers, F. M. *J. Endocr.* **49**, 39-49 (1971).

Monkey pituitary oestrogen receptors and the biphasic action of oestradiol on gonadotropin secretion

Barbara Attardi, Julane Hotchkiss & Ernst Knobil

Department of Physiology, University of Pittsburgh, School of Medicine, Pittsburgh, Pennsylvania 15261

Evidence has been advanced in favour of the hypothesis that, in the rhesus monkey, the negative feedback as well as the stimulatory or so-called 'positive feedback' action of oestrogen on gonadotropin secretion is at the level of the pituitary gland[1-3]. The cellular basis for this biphasic action of oestrogen on the gonadotroph is not understood. In oestrogen target tissues the elicitation of physiological responses is generally associated with the binding of oestrogen to cytoplasmic receptor proteins which are subsequently translocated to the nucleus. Such receptors have been characterized in the anterior pituitary of the rat[4-6]. In the ovariectomized rhesus monkey infused with ^{3}H-oestradiol, autoradiography[7] and parallel cell fractionation[8] have demonstrated the accumulation of ^{3}H-oestradiol by the nuclei of a significant number of pituitary cells. We describe here some of the properties of these putative oestrogen receptors in the anterior pituitary of the monkey and observe that their distribution between cytoplasmic and nuclear compartments is constant in response to sustained elevations in serum oestrogen concentration which produce a biphasic pattern of circulating gonadotropins.

Ten ovariectomized rhesus monkeys which had responded to a trial injection of oestradiol benzoate (30 μg kg^{-1}) by manifesting a sharp decline in circulating LH followed by an LH surge were chosen for this study. Three animals received no further treatment and were kept as controls. Silastic capsules (4 cm long, 3.35 mm internal diameter, 4.65 mm external diameter, 7-9 per

animal) filled with crystalline 17β-oestradiol[9] were implanted subcutaneously in the other seven animals under ketamine hydrochloride anaesthesia. These implants produced constant peripheral oestradiol concentrations of 300-500 pg per ml serum. The oestradiol-treated animals were killed at the following times: 12-24 h (at the time of negative feedback inhibition of gonadotropin secretion), 44-48 h (at the height of the gonadotropin surge), and 96 h (after the gonadotropin surge). Each animal was anaesthetized with sodium pentobarbital (30 mg kg^{-1} intravenously), and cannulae were inserted into the carotid arteries. The calvarium was removed, the animal was swiftly decapitated, and the head was perfused with 400 ml ice-cold 0.9% NaCl to remove all traces of blood. The anterior pituitary was dissected free from the posterior pituitary gland, weighed, and processed for measurement of cytoplasmic or nuclear oestrogen receptor content (see figure legends for details).

Oestrogen receptors labelled with ^{3}H-oestradiol in the cytosol (soluble cytoplasmic fraction) from the anterior pituitary of one untreated control animal were found to sediment at approximately 7S in low ionic strength sucrose gradients (Fig. 1). The 7S peak was completely abolished by addition of a 100-fold excess of unlabelled diethylstilboestrol (DES). There was no indication of any contamination of the cytosol fraction by sex hormone binding globulin (SHBG) from the serum[10], as the serum [3]H-

Table 1 Pituitary gonadotropin content at various times after implantation of oestradiol-containing Silastic capsules in ovariectomized rhesus monkeys

		Pituitary gonadotropin content			
		LH		FSH	
Oestradiol treatment		(μg per gland)	(ng per mg wet weight)	(μg per gland)	(ng per mg wet weight)
Untreated	(2)	55.8 ± 0.7	900 ± 128	65.6 ± 11.4	1,033 ± 20
12-24 h E_2	(3)	85.2 ± 8.2	1,370 ± 27	137.3 ± 30.8	2,166 ± 375
44-48 h E_2	(3)	78.6 ± 31.3	1,349 ± 315	59.7 ± 19.6	1,052 ± 210
96 h E_2	(1)	26.9	782	<5.5	<100

Rhesus pituitary LH and FSH were measured by specific radioimmunoassays[22,23]. Number of determinations are in parentheses. Results are expressed as mean ±s.e.m.
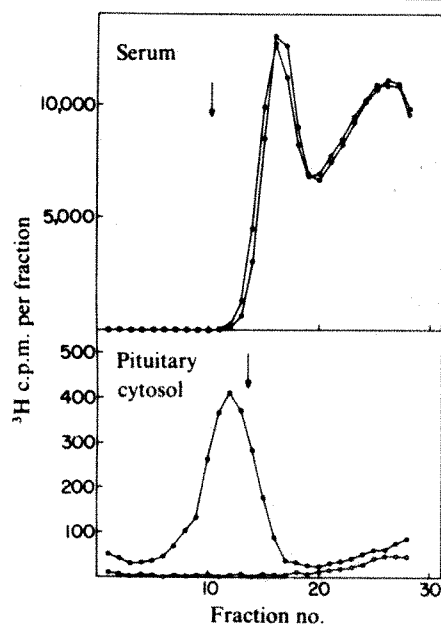
Fig. 1 Sucrose gradient centrifugation of bound ³H-oestradiol in monkey serum or anterior pituitary cytosol. The anterior pituitary (62 mg) from an untreated ovariectomized monkey was homogenized in 20 vol TED (10 mM Tris-HCl, pH 7.4 at 25 °C, 1.5 mM EDTA, 1 mM dithiothreitol) as described previously[19]. Cytosol was prepared by centrifugation of the homogenate for 1 h at 189,000 g. Blood was collected from the same animal by femoral venipuncture and allowed to clot at 4 °C overnight. Serum was separated by centrifugation and diluted 1 : 10 with TED. Cytosol or diluted serum was incubated for 2 h at 0 °C with 10 nM [2,4,6,7-³H]17β-oestradiol (NEN, 102.0 Ci mmol⁻¹) in the absence (•) or presence (O) of 1 μM diethylstilboestrol (DES). Unbound ³H-oestradiol was removed from the cytosol fraction by treatment with dextran–charcoal (1/8 vol. 1.0% Dextran T 70, 10% Norit A in TED): samples were vortexed for 10 s, kept in ice for 20 min and centrifuged at 2,075 g for 15 min. Aliquots (0.25 ml) of serum or charcoal-treated cytosol incubates were layered on 5 to 20% linear sucrose gradients in TE buffer (10 mM Tris-HCl, pH 7.4 at 25 °C, 1.5 mM EDTA) and centrifuged in an SW 50.1 rotor at 215,000 g for 14.5 h (serum) or 16 h (cytosol). Eleven-drop fractions were collected directly into scintillation vials and counted. The arrow indicates the position of bacterial alkaline phosphatase added as an internal sedimentation marker (6.2S, see ref. 18). Direction of sedimentation was from right to left.

oestradiol-SHBG complex sedimented at 4S, and binding of ³H-oestradiol was unaffected by the presence of excess unlabelled DES (Fig. 1).

Scatchard analysis[11] of equilibrium binding data obtained by incubating aliquots of pituitary cytosol from two untreated ovariectomized animals with various concentrations of ³H-oestradiol (0.2–10 nM) in the absence or presence of 1 μM DES indicated the existence of a single class of high affinity, limited capacity binding sites (see Fig. 2 for a representative Scatchard plot). The dissociation constants (K_D's) obtained from these two experiments were 0.70 and 0.73 nM, and the concentrations of binding sites were 50 and 80 fmol per mg cytosol protein. Very low levels of oestrogen receptors were localized in the nuclear fraction (<0.3 fmol per pituitary) (Fig. 3).

Implantation of Silastic capsules containing oestradiol in ovariectomized monkeys led to depletion of cytoplasmic receptors to 10–20% of the levels found in untreated controls and concomitant accumulation of oestrogen receptors in the nucleus (Fig. 3). The concentrations of cytosol and nuclear receptors were constant during the period of oestrogen treatment. The loss of receptors from the cytoplasm could be accounted for by their presence in the nucleus. The total number of oestrogen receptors in the anterior pituitary were 63.4 (0 h), 62.3 (12–24 h), 64.5 (44–48 h) and 73.1 (96 h) fmol per pituitary when 5 nM ³H-oestradiol was used for cytosol binding and 72.7 (0 h), 61.4 (12–24 h), 63.6 (44–48 h) and 71.2 (96 h) fmol per pituitary when 10 nM ³H-oestradiol was used. As a result of this oestrogen stimulus, circulating luteinizing hormone (LH) and follicle stimulating hormone (FSH) levels declined at 12–24 h, peaked at approximately 44–48 h, and decreased again to low levels at 96 h (Fig. 3).

The time course of pituitary gonadotropin concentrations from these animals is shown in Table 1. Pituitary LH and FSH content both seemed to increase during the initial 24 h of oestradiol treatment and decrease again following the gonadotropin surge (96 h). A similar pattern of pituitary gonadotropin content is observed during the menstrual cycle of the rhesus monkey with an accumulation of LH and FSH before the midcycle gonadotropin surge followed by substantial depletion several days later[12]. These results are in agreement with the changes in pituitary LH content observed during the rat oestrous cycle[13] or during a simulated preovulatory LH surge in the rat[14]. We do not know at present whether the oestrogen-induced changes in pituitary gonadotropin content in the monkey are due to effects on synthesis, packaging, and/or release of LH and FSH; however, the effectiveness of oestradiol in regulating these processes is dependent on the prior exposure of the pituitary gland to permissive amounts of the hypothalamic gonadotropin-releasing hormone (GnRH)[15]. Note that depletion of pituitary gonadotropin stores with prolonged oestradiol treatment is presumably progressive: 2 years after placement of oestradiol implants in two intact female rhesus monkeys, pituitary LH and FSH were reduced to 2–3 ng per mg wet weight (W. D. Peckham, personal communication).

We have demonstrated that the anterior pituitary gland of the ovariectomized rhesus monkey contains cytoplasmic oestrogen receptors with properties similar to those found in rodent anterior pituitary tissue[4-6]. We assume that oestrogen receptors are present in rhesus pituitary gonadotrophs because of the profound effects of oestradiol on both the morphology[16] and secretory response of these cells. The presence of oestrogen receptors in other pituitary cell types cannot be excluded, however, as ³H-oestradiol has been localized by autoradiography in the nucleus of acidophils as well as basophils in the rhesus pituitary gland[7].

A sustained increment in circulating oestradiol leads to depletion of cytoplasmic receptors and their accumulation in the nucleus where they remain as long as serum oestradiol levels remain elevated. This same oestradiol stimulus results in a decline in gonadotropin secretion followed by a massive discharge of LH and FSH. Although it may not seem surprising that the interaction of oestradiol with the monkey pituitary conforms to the general model for oestrogen action in other target cells, the dynamics of oestrogen receptor populations have not been
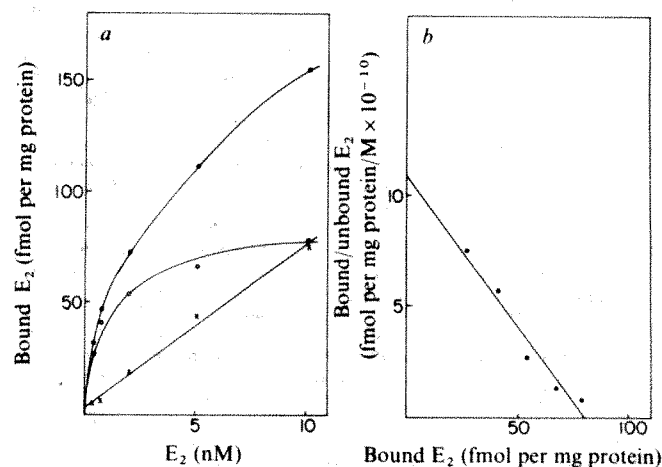
Fig. 2 Binding of ³H-oestradiol (E_2) by monkey anterior pituitary cytosol as a function of ³H-oestradiol concentration (a) or as a Scatchard plot (b). A hemi-anterior pituitary (40 mg) from an ovariectomized untreated monkey was homogenized in 40 vol TED, and cytosol was prepared as described in Fig. 1 legend. Aliquots of cytosol were incubated with various concentrations of ³H-oestradiol (0.2—4.5 nM) in the absence or presence of 1 μM DES (total vol 100 μl). Incubation times, charcoal treatment to separate bound and unbound ³H-oestradiol, and radioactivity measurements are given in Fig. 3 legend. a, Specific binding (O) represents the difference between total binding measured in the absence of excess DES (•) and nonspecific binding (×) measured in its presence. Cytosol protein was determined by the method of Lowry et al.[18] using crystallized bovine serum albumin as standard.
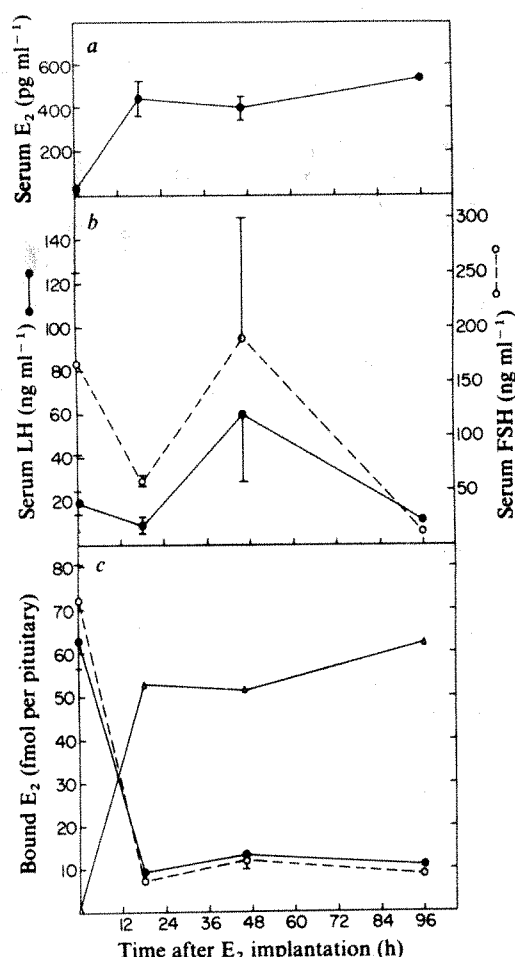
Fig. 3 Content of specific oestrogen binding sites in cytosol and nuclear fractions from the anterior pituitary of ovariectomized rhesus monkeys and circulating gonadotropin concentrations as a function of time after the implantation of Silastic capsules containing crystalline 17β-oestradiol. Placement of implants and killing of animals are described in the text. Previously reported radioimmunoassays were used to measure serum oestradiol[20,21] (*a*), LH[22] and FSH[23] (*b*) in blood samples taken immediately before killing. Specific binding of ³H-oestradiol to cytoplasmic and nuclear receptors was determined by exchange assays (*c*). Data collected at times of negative feedback (12–24 h) or of positive feedback (44–48 h) have been plotted as the means of these times, 18 h and 46 h, respectively. Cytosol was prepared as described in Fig. 1 except that anterior pituitary tissue was homogenized in 40 vol TED. Cytosol fractions, treated with dextran-charcoal to remove any possible contaminating endogenous oestradiol, were incubated with saturating concentrations of ³H-oestradiol, 5 (●) or 10 (○) nM, in the absence or presence of 1 μM DES for 2 h at 0 °C (to fill any unoccupied receptor sites) followed by 16 h at 24 °C (to allow exchange of ³H-oestradiol with receptor sites filled with endogenous oestradiol)[24,25]. Total volume of incubation mixtures was 100 μl. After incubation, samples were placed in ice for 30 min and unbound ³H-oestradiol was removed by addition of 25 μl 5% Norit A–0.5% Dextran T70 as in Fig. 1. Aliquots (50 μl) of the charcoal-treated supernatants were counted in 5 ml Econofluor in a Packard scintillation spectrometer with an efficiency of 33%. The receptor measurements illustrated represent single determinations (46 h, 5 nM ³H-oestradiol; 18 h 10 nM ³H-oestradiol; 96 h, 5 and 10 nM ³H-oestradiol) or the mean±s.e.m. of 2 (18 h, 5 nM ³H-oestradiol; 46 h, 10 nM ³H-oestradiol) or 3 (0 h, 5 or 10 nM ³H-oestradiol) determinations. For measurement of nuclear receptors, anterior pituitary tissue was homogenized and nuclei isolated by the method of Zigmond and McEwen[26]. Nuclear oestrogen receptors were assayed as described by Roy and McEwen[27]. Briefly, receptors were salt-extracted from nuclei swollen in hypotonic buffer and incubated with 10 nM ³H-oestradiol, with or without 1 μM DES, for 16 h at 25 °C in a total volume of 125 μl. Aliquots (100 μl) of the incubation mixtures were applied to 6×50 mm Sephadex LH-20 columns equilibrated with TEK-0.4 (10 mM Tris-HCl, *p*H 7.4, 1.5 mM EDTA, 0.4 M KCl) and bound 3H-oestradiol was eluted into scintillation vials with 1 ml of the same buffer. Econofluor (10) was added, and after vigorous shaking, samples were counted as above with an efficiency of 38%. Nuclei were dissolved in 0.3 M KOH, and DNA contents were measured by the procedure of Burton[28]. Each data point (Δ) represents a single determination. The corresponding values in fmol per mg DNA are 329 (18 h), 383 (46 h), and 277 (96 h).

examined previously in conditions where this steroid exerts both an inhibitory and a stimulatory effect on the same process, presumably in the same cell type. Thus, any hypothesis for the mechanism of action of oestradiol in the sequential inhibition and stimulation of glycoprotein hormone secretion must appreciate that this biphasic effect of the steroid on the anterior pituitary is manifested in the face of an unchanging distribution of cytoplasmic and nuclear oestrogen receptors.

1. Plant, T. M., Nakai, Y., Belchetz, P., Keogh, E. & Knobil, E. *Endocrinology* **102**, 1015–1018 (1978).
2. Nakai, Y., Plant, T. M., Hess, D. L., Keogh, E. J. & Knobil, E. *Endocrinology* **102**, 1008–1014 (1978).
3. Ferin, M., Rosenblatt, H., Carmetl, P. W., Antunes, J. L. & Vande Wiele, R. L. *Endocrinology* **104**, 50–52 (1979).
4. Eisenfeld, A. J. *Endocrinology* **86**, 1313–1318 (1970).
5. Notides, A. C. *Endocrinology* **87**, 987–992 (1970).
6. Korach, K. S. & Muldoon, T. G. *Biochemistry* **13**, 1932–1938 (1974).
7. Pfaff, D. W. *et al. J. comp. Neurol.* **170**, 279–294 (1976).
8. Gerlach, J. L. *et al. Brain Res.* **103**, 603–612 (1976).
9. Karsch, F. J. *et al. Endocrinology* **92**, 799–804 (1973).
10. Petra, P. H. & Schiller, H. S. *J. Steroid Biochem.* **8**, 655–661 (1977).
11. Scatchard, G. *Ann. N.Y. Acad. Sci.* **51**, 660-672 (1949).
12. Hotchkiss, J. & Butler, W. R. *Proc. Endocr. Soc.* (in the press).
13. Naftolin, F., Brown-Grant, K. & Corker, C. S. *J. Endocr.* **53**, 17–30 (1972).
14. Garner, L. L. & Blake, C. A. *Biol. Reprod.* **20**, 1055–1066 (1979).
15. Knobil, E. *Recent Prog. Horm. Res.* **36**, 53-88 (1980).
16. Tseng, M. T., Kittinger, G. W. & Spies, H. G. *Proc. Soc. exp. Biol. Med.* **147**, 412–417 (1974).
17. Attardi, B. & Ohno, S. *Endocrinology* **99**, 1279–1290 (1976).
18. Lowry, O. H., Rosebrough, N. J., Farr, A. L. & Randall, R. J. *J. biol. Chem.* **193**, 265–275 (1951).
19. Attardi, B., Geller, L. N. & Ohno, S. *Endocrinology* **98**, 864–874 (1976).
20. Hotchkiss, J., Atkinson, L. E. & Knobil, E. *Endocrinology* **89**, 177–183 (1971).
21. Korenman, S. G. *et al. J. clin. Endocr. Metab.* **38**, 718–720 (1974).
22. Karsch, F. J. *et al. Endocrinology* **92**, 1740–1747 (1973).
23. Yamaji, T., Peckham, W. D., Atkinson, L. E., Dierschke, D. J. & Knobil, E. *Endocrinology* **92**, 1652–1659 (1973).
24. Katzenellenbogen, J. A., Johnson, H. J., Jr & Carlson, K. E. *Biochemistry* **12**, 4092–4099 (1973).
25. Attardi, B. *Endocrinology* (submitted).
26. Zigmond, R. E. & McEwen, B. S. *J. Neurochem.* **17**, 889–899 (1970).
27. Roy, E. J. & McEwen, B. S. *Steroids* **30**, 657–669 (1977).
28. Burton, E. *et al. Meth. Enzym.* **12**B, 163–166 (1968).

Glucocorticoids increase osteoblast-like bone cell response to 1,25(OH)₂D₃

Glenda L. Wong, Barbara P. Lukert & John S. Adams

Division of Metabolism, Endocrinology and Genetics, Department of Internal Medicine, University of Kansas Medical Center, Kansas City, Kansas 66103

Recent reports indicate that some hormones may regulate the binding of, and subsequent response to, other hormones by their target tissue[1-6]. The adrenal glucocorticoids are prominent among these modulating hormones[3-6]. Glucocorticoids have been shown to enhance bone cell sensitivity to parathyroid hormone (PTH)[6,7] *in vitro* and this in turn has permitted PTH-induced effects to be measured at physiological doses of PTH for the first time in isolated osteoblast-like (OB) and osteoclast-like (OC) cells. It is unknown whether these findings represent a specific interaction between glucocorticoids and PTH[6] or indicate a general role for glucocorticoids in the development and/or maintenance of bone cell differentiation, of which hormonal responsiveness would be one expression. In the event of a general glucocorticoid effect on cell differentiation, increased responsiveness to other bone resorbing hormones should also be observed. We have therefore examined whether glucocorticoids enhance the sensivity of bone cells to a steroid hormone, 1,25 dihydroxycholecalciferol (1,25(OH)₂D₃), and we report here that they do.

1,25(OH)$_2$D$_3$ can induce resorption of bone *in vivo*[8-10] and *in vitro*[11]. The biochemical changes induced by 1,25(OH)$_2$D$_3$ are very similar to those initiated by PTH—in both cases bone mineral and organic matrix loss is observed. PTH also stimulates hyaluronic acid synthesis[12,13] and lysosomal enzyme release[14,15] and inhibits collagen formation[16,17], alkaline phosphatase activity[18] and citrate decarboxylation[19]. Some of these metabolic events that accompany PTH-induced bone resorption have been reproduced in OC or OB bone cells exposed to pharmacological doses of 1,25(OH)$_2$D$_3$ (ref. 20). However, physiological doses of 1,25(OH)$_2$D$_3$ were without effect in these cells.

In previous studies low doses of glucocorticoids decreased basal osteoclastic but not osteoblastic activities. As a result the major enhancement of PTH responsiveness by glucocorticoids occurred in OB cells[7]. For this reason, these studies on the relationship between glucocorticoids and 1,25(OH)$_2$D$_3$ were carried out on OB bone cells. Inhibition of OB cell citrate decarboxylation by a submaximal dose of 1,25(OH)$_2$D$_3$ (100 pg ml^{-1}) was measured alone or in combination with various doses of glucocorticoids (Fig. 1a). At prednisolone levels below 10^{-10} M the inhibition of citrate decarboxylation by 1,25(OH)$_2$D$_3$ was unchanged. However, at 10^{-9}–10^{-7} M prednisolone, the decrease in citrate decarboxylation due to 1,25(OH)$_2$D$_3$ was greater than in cells not treated with glucocorticoid. Prednisolone enhancement of the effects of 1,25(OH)$_2$D$_3$ resulted from both a decrease in the absolute amount of citrate decarboxylated in the presence of 1,25(OH)$_2$D$_3$ and a small increase in basal citrate decarboxylation. To compare the relative enhancement by different doses of prednisolone the inhibition of citrate decarboxylation by 1,25(OH)$_2$D$_3$ is further expressed as a percentage of the appropriate glucocorticoid-treated control (Fig. 1b). Maximum potentiation of 1,25(OH)$_2$D$_3$ action was seen with 10^{-9} and 10^{-8} M prednisolone.

OB cell response to various doses of 1,25(OH)$_2$D$_3$ was measured in the absence or presence of a maximally effective dose of prednisolone (Fig. 2). The dose–response curve for 1,25(OH)$_2$D$_3$ became shifted to the left in the presence of 10^{-9} M prednisolone and 2–10-fold lower doses of 1,25(OH)$_2$D$_3$ were required to bring about an established degree of inhibition of citrate decarboxylation. Addition of 10^{-9} M prednisolone to the culture medium of OB cells permitted levels of 1,25(OH)$_2$D$_3$ as low as 5–25 pg ml^{-1} (amounts well within normal circulating levels) to be assayed for the first time in this *in vitro* cell culture system. Note that although the absolute sensitivity of the isolated OB cells to
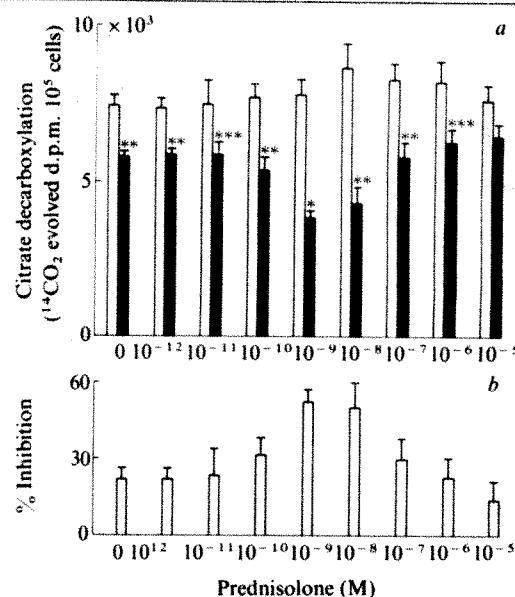
Fig. 1 Effect of various doses of glucocorticoid on OB bone cell response to 1,25(OH)$_2$D$_3$. Primary cultures of OB bone cells were prepared as previously described[24], subdivided after 5 d and inoculated into glass test tubes (1.0 × 10^5 cells per tube) containing 1.0 ml (MEM) and 10% fetal calf serum. *a*, Cells were cultured with the indicated doses of prednisolone in the absence (open bars) or presence (closed bars) of 1,25(OH)$_2$D$_3$ (100 pg ml^{-1}). After 48 h, citrate decarboxylation was measured by the addition of [6-^{14}C]citrate (0.2 μCi ml^{-1}) for 2 h. ^{14}CO$_2$ was trapped on filter paper fans saturated with Hyamine ×10 as previously described[19,25]. *b*, Results are expressed as the per cent inhibition seen when 1,25(OH)$_2$D$_3$-treated cultures were compared with the appropriate prednisolone-treated control. These values represent the average of four determinations ±s.d., and these experiments were performed five times, with similar results. *P<0.005; **P<0.002; ***P<0.05.

1,25(OH)$_2$D$_3$ varied from preparation to preparation, the relative increased sensitivity in the presence of prednisolone was always maintained.

Increased sensitivity to 1,25(OH)$_2$D$_3$ could also be demonstrated when OB cell collagen synthesis was measured in prednisolone-treated cells exposed to 1,25(OH)$_2$D$_3$ (Table 1). Inhibition of collagen synthesis by 1,25(OH)$_2$D$_3$ increased from

Table 1 Effects of prednisolone and 1,25(OH)$_2$D$_3$ on collagen synthesis by OB bone cells

	Collagen (^{3}H-proline d.p.m. per 10 cells)	Non-collagen protein	% Decrease	% Total protein*
Control	5,500 ± 300	6,200 ± 360	—	13.0
Control + 1,25(OH)$_2$D$_3$	3,885 ± 350‡	6,000 ± 450	29	10.0
10^{-4} M Prednisolone	3,930 ± 400	5,300 ± 400	—	11.0
10^{-4} M Prednisolone + 1,25(OH)$_2$D$_3$	3,310 ± 150	4,700 ± 410	16	11.0
10^{-6} M Prednisolone	5,380 ± 270	6,500 ± 350	—	12.0
10^{-6} M Prednisolone + 1,25(OH)$_2$D$_3$	3,450 ± 190†	5,850 ± 390	36	9.0
10^{-8} M Prednisolone	5,700 ± 330	6,230 ± 410	—	13.0
10^{-8} M Prednisolone + 1,25(OH)$_2$D$_3$	3,200 ± 210†	6,000 ± 380	44	8.0
10^{-10} M Prednisolone	5,000 ± 400	6,200 ± 350	—	13.0
10^{-10} M Prednisolone + 1,25(OH)$_2$D$_3$	3,800 ± 250‡	5,650 ± 430	24	10.0

OB cells were cultured in the presence of 10^{-10}–10^{-4} M prednisolone alone, or in combination with 1,25(OH)$_2$D$_3$ (125 pg ml^{-1}). After 48 h the growth medium was removed, and the cells were further cultured in minimal essential medin containing 1.0 μCi ml^{-1} L-[2,3-^{3}H]proline (50 Ci mmol^{-1}) for 24 h. The media and the cells were precipitated *in situ* with 5% trichloroacetic acid (TCA). The precipitate was centrifuged and washed 4 times over a 24-h period with 12 ml ice-cold 5% TCA. The radioactivity rendered acid soluble by heating the cell pellets at 90 °C for 45 min in 1 ml 5% TCA was used as a measure of collagen ; Alternatively, the cell layer collagen was rendered acid soluble by digestion with purified bacterial collagenase. The acid-insoluble radioactivity remaining after these procedures (non-collagenous protein) was dissolved by heating at 60 °C for 30 min in 0.5 ml 0.2 M NaOH. Each value represents the mean of triplicate determinations ±s.d.
* Corrected for relative proline enrichment in collagen by a factor of 5.8.
† P<0.005. ‡ P<0.05.

29% in the absence of glucocorticoid to 36% at 10^{-6} M prednisolone, and reached a maximum at 44% at 10^{-8} M prednisolone; no enhancement was seen at 10^{-10} M prednisolone. Glucocorticoid amplifications of the effects of $1,25(OH)_2D_3$ on collagen and citrate decarboxylation thus occurred over a similar dose range. The additional decrease in collagen formation seen with $1,25(OH)_2D_3$ acting in the presence of prednisolone was specific as there was no corresponding change induced in the synthesis of non-collagenous protein.

The molecular basis for glucocorticoid amplification of $1,25(OH)_2D_3$ effects remains to be established. $1,25(OH)_2D_3$ interacts with target cells by binding to high affinity cytosolic receptors. Such receptors have been identified in fetal rat calvaria[21] and it was recently reported that glucocorticoids retard the turnover rate of $1,25(OH)_2D_3$ receptors in bone tissue in culture[22].

In the following experiments, the ability of primary cultures of OB cells to accumulate ^{3}H-labelled $1,25(OH)_2D_3$ was measured after growth in the presence or absence of glucocorticoids. Figure 3a demonstrates that after exposure to 10^{-9} or 10^{-7} M but not to 10^{-5} M prednisolone, OB cells showed a greater uptake of ^{3}H-$1,25(OH)_2D_3$ than untreated controls, with 10^{-9} M > 10^{-7} M > 10^{-5} M. At 10^{-9} M and 10^{-7} M glucocorticoid the uptake per cell of ^{3}H-$1,25(OH)_2D_3$ was increased ~60% and 40%, respectively, whereas no increase was seen at 10^{-5} M. The increase in cellular uptake of ^{3}H-$1,25(OH)_2D_3$ thus coincided with the prednisolone dose curve for enhancement of the biological effects of $1,25(OH)_2D_3$ in OB cells.

The specificity of OB cell uptake of ^{3}H-$1,25(OH)_2D_3$ was measured by competition with unlabelled $1,25(OH)_2D_3$. The addition of unlabelled $1,25(OH)_2D_3$ to the medium at the time of exposure to ^{3}H-$1,25(OH)_2D_3$ led to a decrease in the radioactivity ultimately recovered with the cells. Addition of 0.1, 1.0 or 10.0 ng ml^{-1} unlabelled $1,25(OH)_2D_3$ resulted in a decrease of 27%, 50% and 72%, respectively (Fig. 3b). Approximately 17% of the cell-associated radioactivity could not be displaced by $1,25(OH)_2D_3$ levels as high as 1,000 ng ml^{-1}, and must, therefore, be regarded as nonspecific binding. By comparison, even 10 ng ml^{-1} $24,25(OH)_2D_3$ reduced cell-associated radioactivity by <20% (Fig. 3c). $25(OH)_2D_3$ at 10 ng ml^{-1} also reduced cell-associated radioactivity by <20% (results not shown).

These results show that OB bone cells accumulate increased amounts of ^{3}H-$1,25(OH)_2D_3$ after exposure to low physiological doses of glucocorticoids. Increased accumulation of ^{3}H-$1,25(OH)_2D_3$ by glucocorticoid-treated cells could be due to a

Fig. 3 Effects of prednisolone on the uptake of ^{3}H-$1,25(OH)_2D_3$ by OB cells. Primary cultures of $2.0-2.5 \times 10^6$ cells were exposed to 0, 10^{-5}, 10^{-7} or 10^{-9} M prednisolone for 48 h. Cell monolayers were then rinsed two times with MEM. a, Cells were further incubated with 3 ml MEM containing 30,000 pm ml^{-1} of $[23,24(n)$-^{3}H$]1\alpha,25(OH)_2D_3$ (94 Ci mmol^{-1}) (Amersham). After 60 min at 37 °C the medium was aspirated off, and the monolayers were rinsed in phosphate-buffered saline (PBS). The cells were recovered from the tissue culture flask by suspension in calcium–magnesium-free Tyrode's solution containing 0.005 M EDTA, pH 7.0 (EDTA/Tyrodes). Cells were pelleted by centrifugation at 600g for 2 min, then rinsed five times with 10 ml PBS. (At this stage the total radioactivity in the wash was <20% of that associated with the cells.) The cell pellet was then resuspended in 2 ml EDTA/Tyrodes to obtain single cells and 0.025 ml was removed for cell counting in a haemcytometer. The remaining cells were collected on a Millipore filter, which was further rinsed with 10 ml PBS, dissolved in methyl Cellosolve, mixed with aqueous scintillant, and counted in a Searle liquid scintillation counter. b, c, ^{3}H-$1,25(OH)_2D_3$ uptake (by OB cells) was measured as described above except either $1,25(OH)_2D_3$ (b) or $24,25(OH)_2D_3$ (c) was added to the cells at the same time as ^{3}H-$1,25(OH)_2D_3$. These measurements represent the average of three determinations ±s.d. and these experiments were performed four times.

Fig. 2 Amplification of bone cell response to $1,25(OH)_2D_3$ by glucocorticoid. Subcultured OB bone cells were grown in various concentrations of $1,25(OH)_2D_3$ alone (○) or further supplemented with 10^{-9} M prednisolone (●). After 48 h citrate decarboxylation was measured as the amount of $^{14}CO_2$ evolved from [6-^{14}C]citrate (0.2 μCi ml^{-1}) added to each tube for the final 2 h. Results are expressed as the per cent decrease obtained when $1,25(OH)_2D_3$-treated cultures were compared with the appropriate control and each point represents the average of four replicate samples ±s.d. These experiments were performed six times.

variety of reasons including: (1) an increase in total cell protein; (2) increased cell permeability to steroids including $1,25(OH)_2D_3$; or (3) a specific increase in the numbers or affinity of the receptors for $1,25(OH)_2D_3$. As incorporation of ^{3}H-proline (Table 1) and ^{3}H-leucine[7] into acid precipitable radioactivity was not increased in cells cultured in glucocorticoids, the first possibility seems unlikely. Furthermore, the relative inability of $24,25(OH)_2D_3$ and $25(OH)_2D_3$ to compete with ^{3}H-$1,25(OH)_2D_3$ and the ability of $1,25(OH)_2D_3$ to decrease cell-associated ^{3}H-$1,25(OH)_2D_3$ suggest that the increased accumulation of ^{3}H-$1,25(OH)_2D_3$ by glucocorticoid-treated cells was not due to a general increase in cell permeability, but rather was a phenomenon specific to $1,25(OH)_2D_3$.

The enhancement of $1,25(OH)_2D_3$ effects on OB bone cells by glucocorticoids is of interest from the molecular as well as physiological point of view. These results imply that glucocorticoids *in vivo* permit bone tissue to respond to small increases in $1,25(OH)_2D_3$. In addition, the permissive role of glucocorticoids for $1,25(OH)_2D_3$ parallels that previously described for PTH although the mechanism of action of these two hormones differ at the onset. Glucocorticoids must therefore control a complex set of cellular reactions which can result in amplification of response to at least two classes of bone resorbing hormones, one of which activates adenylate cyclase via cell surface receptors,

the other of which binds to intracellular cytosolic receptors. If hormone sensitivity can be used as a marker for cell specialisation, then glucocorticoids can be further said to enhance the expression of the differentiated phenotype in bone cells, and *in vivo* may exert some control on bone cell development and maintenance.

1. Kahn, C. R., Goldfine, I. D., Neville, D. M. Jr & DeMeyts, P. *Endocrinology* **103**, 1054–1066 (1978).
2. Rao, M. C., Richards, J. S., Midgley, A. R. Jr & Reichert, L. E. Jr *Endocrinology* **101**, 512–523 (1977).
3. Tashjian, A. H., Osborne, R., Maina, D. & Knaian, A. *Biochem. biophys. Res. Commun.* **79**, 333–340 (1977).
4. Marshall, S., Huang, H. H., Kledzik, G. S., Campbell, G. A. & Meites, J. *Endocrinology* **102**, 869–875 (1978).
5. Unsicker, K., Kirsch, B., Otten, U. & Thoenen, H. *Proc. natn. Acad. Sci. U.S.A.* **75**, 3498–3502 (1978).
6. Chen, T. L. & Feldman, D. *Endocrinology* **102**, 589–596 (1978).
7. Wong, G. L., *J. Biol. Chem.* **254**, 6337–6340 (1979).
8. Tanaka, Y. & DeLuca, H. F. *Archs Biochem. Biophys.* **146**, 574–578 (1971).
9. Reynolds, J. J., Holick, M. F. & DeLuca, H. F. *Calcified Tissue Res.* **12**, 295–301 (1973).
10. Frolik, C. A. & DeLuca, H. F. *J. clin. Invest.* **51**, 2900–2906 (1972).
11. Raisz, L. G., Trummel, C. L., Holick, M. F. & DeLuca, H. F. *Science* **175**, 768–769 (1972).
12. Johnston, C. C., Deiss, W. P. & Miner, E. B. *J. biol. Chem.* **237**, 3560–3565 (1962).
13. Luben, R. A., Goggins, J. F. & Raisz, L. G. *Endocrinology* **94**, 737–745 (1975).
14. Vaes, G. in *Parathyroid Hormone and Thyrocalcitonin (Calcitonin)* (eds Talmage, R. V. & Belanger, L. F.) 318–328 (Excerpta Medica, Amsterdam, 1967).
15. Eilon, G. & Faisz, L. G. *Endocrinology* **103**, 1969–1975 (1978).
16. Goldhaber, P., Stern, B., Glimcher, M. & Chao, J. (1968) in *Parathyroid Hormone and Thyrocalcitonin (Calcitonin)* (eds Talmage, R. V. & Belanger, L. F.) 182–195 (Excerpta Medica, Amsterdam, 1967).
17. Deitrich, J., Canalis, E., Maina, D. & Raisz, L. *Endocrinology* **98**, 943–949 (1976).
18. Hekkelman, J. W. & Moskalewski, S. *Expl Cell Res.* **58**, 283–288 (1969).
19. Chu, L. L. H., MacGregor, R. R., Hamilton, J. W. & Cohn, D. V. *Endocrinology* **89**, 1425–1431 (1971).
20. Wong, G. L., Luben, R. A. & Cohn, D. V. *Science* **197**, 663–665 (1977).
21. Kream, B. E., Jose, M., Yamada, S. & DeLuca, H. F. *Science* **197**, 1086–1088 (1977).
22. Manolagas, S. C., Anderson, D. C. & Lumb, G. A. *Nature* **277**, 314–315 (1979).
23. Meier, S. & Hay, E. *Devl Biol.* **28**, 249–270 (1974).
24. Luben, R. A., Wong, G. L. & Cohn, D. V. *Endocrinology* **99**, 526–534 (1976).
25. Wong, G. L. & Cohn, D. V. *Proc. natn. Acad. Sci. U.S.A.* **72**, 3167–3171 (1975).

Allotype-linked genetic control of a polymorphic V_H framework framework determinant on mouse T-helper cell receptors

Yinon Ben Neriah, David Givol & P. Lonai

Department of Chemical Immunology, The Weizmann Institute of Science, Rehovot, Israel

Markus M. Simon & Klaus Eichmann

Institute for Immunology and Genetics, Deutsches Krebsforschungszentrum, Heidelberg, FRG

The immune system confronts antigens through the variable domains of antigen receptors on lymphocytes. The biochemistry of these antigen receptors is fundamental to the understanding of the immune system. Whilst B cells use immunoglobulins (Ig) as antigen receptors, T cells use unknown molecules which appear to differ from Ig except for the shared variable region of the Ig heavy chain (V_H). The notion that T-cell receptors consist, at least in part, of immunoglobulin V_H regions stems largely from experiments using anti-idiotypic antibodies[1-3]. Much serological and genetic evidence has meanwhile accumulated suggesting that V_H associated idiotypic determinants are shared between Ig molecules and the antigen receptors of certain classes of T cells including helper cells, cells proliferating on mixed lymphocyte reaction delayed type hypersensitive reactive cells, and cytotoxic T cells[4-7]. This pertains to structural elements associated with hypervariable portions of V_H, but data on framework elements of V_H regions of T cells are scarce[8,9]. We have previously reported that mouse T-cell receptors react with a rabbit antibody to the V_H fragment of MOPC 315 (anti-V_H)[10-12]. The V_H framework determinants appeared polymorphic in that the T-helper cells as well as the immunoglobulin heavy (H) chains of a variety of mouse strains reacted equally well, except in the case of strain AKR[12,13]. We report here the genetic control of the V_H framework determinant whose expression through T-helper cells seems to be governed by at least one gene linked to the Igh allotype linkage group. Thus, this V_H framework determinant behaves like the rabbit V_H region allotypes which are expressed on both immunoglobulin H chains and T-cell receptors[8,9]. These data suggest the expression of entire V_H regions in T-cell antigen receptors[1-3].

The analysis of the reactivity of anti-V_H with T-helper cells involved the *in vitro* responses of spleen cells from mice previously immunized with streptococcus A (ref. 14) to trinitrophenylated group A streptococci (TNP-Strep.A). This T-helper cell-dependent response is inhibited by addition of anti-

V_H to the culture, whereas inhibition of the T-helper cell-independent response to TNP-Ficoll requires at least a 50-fold greater concentration of anti-V_H (ref. 12). Failure of anti-V_H to react with immunoglobulin molecules and B cells has been reported previously[10,12,13,15], suggesting that the inhibition of the TNP-plaque-forming cell (PFC) response to TNP-Strep. A reflects exclusively the inhibition of T-helper cells by anti-V_H (ref. 12).

Preliminary experiments showed that the responses of cells from strains A/J, DBA/2 and BALB/c were strongly inhibited by anti-V_H, whereas those from strain AKR were not (ref. 12, and unpublished data). We therefore crossed strain AKR with DBA/2 and backcrossed the F_1 to AKR. Figure 1 shows the effect of anti-V_H on the *in vitro* responses of spleen cells from mice resulting from this cross to TNP-Strep. A. It is clear that the capacity of cells to be inhibited by anti-V_H is inherited in a dominant fashion. In the backcross, no clear segregation into positive and negative groups can be seen. However, because of the gap between 31% and 38% inhibition, and because all F_1 mice were inhibited more than 38%, we divided the backcross mice into two groups: one group of 15 showed inhibition similar to that of F_1 mice; the other group of 9 were less strongly

Table 1 Association of strong and weak T-helper cell inhibition by anti-V_H and the segregation of the immunoglobulin allotype in $(ADR \times DBA/2)$ $F_1 \times AKR$ backcross mice

| (AKR×DBA/2)F_1 ×AKR total | | Total No. | Inhibition of help* by anti-V_H | | P value† |
			<31%	>38%	
		24	9	15	
H-2‡	k/k	12	4	8	0.4
	d/k	12	5	7	
Thy-1‡	1/1	10	4	6	0.3
	1/2	14	5	9	
Lyt 1‡	2/2	15	5	10	0.4
	1/2	9	4	5	
Lyt 3‡	1/1	12	4	8	0.4
	1/2	12	5	7	
Sex	♂	12	5	7	0.4
	♀	12	4	8	
C	c/c‖	9	5	4	0.2
	c/C	15	4	11	
Allotype Igh §	d/d	10	7	3	<0.005
	d/c	14	2	12	

Backcross mice are same as those of Fig. 1.
* See legend to Fig. 1.
† χ^2 Test used.
‡ Determined by microcytotoxicity assay using rabbit complement and lymphocytes from cervical lymph node.
§ Allotype was determined in Ouchterlony analysis using an A/J anti-BALB/c antiserum for Igh^c and a BALB/c anti-A/J antiserum for Igh^d allotype.
‖ C, Coat colour.

Table 2 Genetic polymorphism and dominant inheritance of helper cell inhibition by anti-V_H, using partially helper cell depleted spleen cells

Strain		TNP–PFC per 10^6 cells*		
		$-aV_H$	$+aV_H$	% Inhibition
AKR	1	223(1.10)	230(1.32)	-3
	2	196(1.12)	192(1.31)	2
	3	201(1.04)	191(1.09)	5
	4	304(1.10)	272(1.14)	12
	5	174(1.09)	166(1.42)	5
	6	94(1.22)	87(1.21)	7
	7	89(1.62)	95(1.44)	-6
	8	104(1.08)	95(1.31)	9
DBA/2	1	422(1.17)	190(1.11)	55
	2	392(1.15)	223(1.14)	43
	3	210(1.14)	92(1.31)	56
	4	312(1.14)	155(1.27)	50
	5	298(1.08)	104(1.31)	65
(AKR×DBA/2)F₁				
	1	190(1.18)	76(1.09)	60
	2	143(1.10)	63(1.24)	56
	3	198(1.30)	106(1.27)	46
	4	112(1.43)	43(1.71)	62
	5	256(1.20)	122(1.25)	56

* See legend to Fig. 2.

inhibited. These groups were then analysed with respect to seven different genetic markers—H–2, Thy 1, Lyt 1, Lyt 3, sex, coat colour, allotype—segregating in this cross. Table 1 shows that there is no association with any of these markers, except for the Igh allotype with which a significant association is observed. This suggested that this allotype had an important role in the genetic control of V_H expression in T-helper cells.

From these experiments the question arose as to whether the expression of V_H on T cells is exclusively by the Igh allotype controlled or, as would seem more likely from the data in Fig. 1 and Table 1, whether it is controlled by additional genetic factors. We investigated this by improving the quality of the T-helper cell inhibition assay using partially helper cell-depleted spleen cells as responders. This was done by mixing 20% of untreated spleen cells with 80% anti-Thy-1.1 and complement-treated spleen cells of each individual mouse. Because of the limitation of T-cell help in such cultures, smaller quantities of anti-V_H can be used for inhibition, so that the possibility of nonspecific inhibition or of B-cell inhibition is minimized[12].

An analysis of AKR, DBA/2 and (AKR×DBA/2)F₁ mice by this improved procedure again clearly reveals the genetic polymorphism and dominant inheritance of the V_H determinant

(Table 2). Analysis of an additional 20 (AKR×DBA/2)×AKR backcross mice by this typing procedure now reveals a clear segregation into a positive and a negative group and unequivocal linkage to the Igh allotype (Table 3, Fig. 2).

These data support our previous observation that T-helper cells express framework portions of immunoglobulin V_H regions[11,12]. The significance of these results is that the genetic evidence is independent of the serological data[11,12,15], and that both lines of evidence point to the same conclusion. The lack of an influence of H-2 observed in these data is not inconsistent with our previous report showing that an idiotype of alloreactive T-cells is controlled by the Igh allotype as well as by H-2 (ref. 6). One critical difference is that, whereas in the present work an antiserum to immunoglobulin V_H determinants was used, the previous report used an antiserum against T-cell receptors which presumably detects unique determinants on T-cell receptors in addition to those shared with immunoglobulin H chains. The
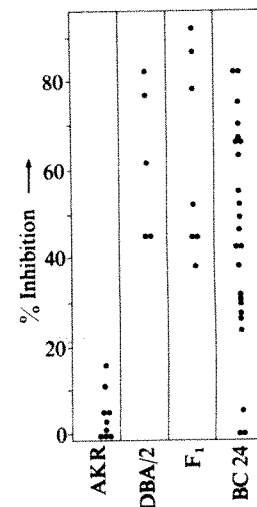
Fig. 1 Inhibition of the TNP-PFC responses of 10^6 spleen cells from individual mice immunized 3–6 weeks previously with 4×10^9 Strep.A particles, cultured for 4 days in 100 μl Click's medium in microwells together with TNP-Strep.A[12]. Sixteen identical microcultures were run of each mouse, eight of which contained 20 μg anti-V_H antibody. Each point represents the result of a single mouse and gives the inhibition of the mean PFC response of the cultures containing anti-V_H as a percentage of that of cultures without anti-V_H. Absolute PFC responses were of the order of those shown in Tables 2 and 3.

Table 3 Allotype linked segregation of helper cell inhibition by anti-V_H using partially helper cell-depleted spleen cells of (AKR×DBA/2)F₁ × AKR backcross mice

BC	Sex	Coat colour	Thy-1*	Lyt 1*	H-2*	Immunoglobulin Igh*	TNP-PFC per 10^6 cells† $-aV_H$	$+aV_H$	% Inhibition
1	♀	C/c	2/1	1/1	k/k	d/c	250(1.15)	102(1.07)	59
2	♀	C/c	2/1	2/1	k/k	d/c	344(1.31)	168(1.04)	51
3	♀	C/c	2/1	1/1	k/k	d/c	109(1.24)	46(1.24)	57
4	♀	C/c	2/1	2/1	k/k	d/d	215(1.09)	189(1.04)	12
5	♀	C/c	2/1	1/1	k/d	d/d	322(1.23)	351(1.15)	-9
6	♀	c/c	2/1	1/1	k/k	d/d	150(1.16)	140(1.24)	6
7	♀	c/c	2/1	2/1	k/d	d/d	275(1.10)	299(1.16)	-9
8	♀	c/c	1/1	1/1	k/k	d/c	320(1.21)	150(1.15)	53
9	♀	c/c	1/1	2/1	k/d	d/d	220(1.10)	202(1.10)	8
10	♀	c/c	2/1	1/1	k/d	d/d	146(1.13)	142(1.16)	3
11	♀	c/c	1/1	2/1	k/k	d/c	316(1.36)	126(1.10)	60
12	♀	c/c	2/1	1/1	k/k	d/d	93(1.30)	93(1.32)	0
13	♀	c/c	2/1	1/1	k/d	d/d	408(1.21)	412(1.12)	-1
14	♀	c/c	1/1	2/1	k/d	d/d	261(1.13)	215(1.11)	17
15	♂	c/c	2/1	1/1	k/d	d/d	334(1.27)	264(1.05)	-8
16	♂	c/c	1/1	1/1	k/d	d/d	193(1.04)	183(1.08)	5
17	♂	c/c	1/1	1/1	k/k	d/d	222(1.07)	184(1.16)	17
18	♂	c/c	2/1	2/1	k/k	d/d	195(1.08)	169(1.13)	13
19	♂	c/c	2/1	2/1	k/d	d/c	99(1.15)	36(1.35)	63
20	♂	C/c	1/1	1/1	k/k	d/d	460(1.10)	389(1.09)	15
Het/hom	6/14		6/14	13/7	8/12	9/11	6/14		

* Determined as described in Table 1 legend.
† See Fig. 2 legend.
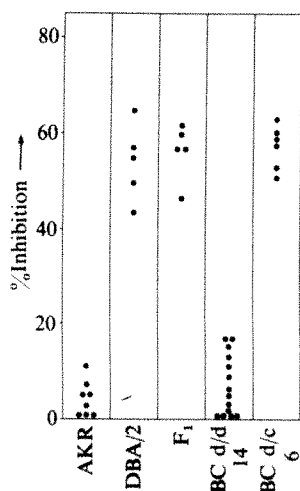
Fig. 2 Graphic representation of the data from Tables 2 and 3. The experiment was done as represented in Fig. 1, with the following modifications: cultures contained 3×10^6 cells in 300 µl medium 20% of which were spleen cells, 80% of which were previously treated with a Thy-1.1 and rabbit complement. Eight identical cultures of each mouse were run, four of which contained 5 µg anti-V_H antibody.

other difference that may be critical is that in our previous report the T-cell receptors investigated were specific for major histocompatibility complex antigens[6].

It has come to our attention that other helper cell systems are not inhibited by anti-V_H (A. Coutinho, personal communication). We conclude that anti-V_H may react with only a

proportion of T-helper cell receptors, either by masking of the V_H determinant on some T-cells by combination of V_H with other structural elements in analogy to its masking by light chains on antibodies[13], or by preference of anti-V_H for what may reflect V_H subgroups on T cells. The partial inhibition and the pronounced individual variability seen in many of our experiments[12] may be explained by subgroup preferences of the anti-V_H antibody and variability in the proportions of such V_H subgroups activated in different individuals and in response to different antigens. Taken together, we feel that antibodies to V_H framework determinants may become important in the analysis of T-cell receptors, particularly as far as their biochemical analysis is concerned.

We thank Ms I. Falk and Ms Tova Volberg for technical assistance. This work was supported by a grant for Cooperative Cancer Research between Israel and West Germany.

1. Eichmann, K. *Adv. Immun.* **26**, 195–254 (1978).
2. Binz, H. & Wigzell, H. *Contemp. Topics Immunobiol.* **7**, 113–172 (1977).
3. Rajewsky, K. & Eichmann, K. *Contemp. Topics Immunobiol.* **7**, 69–107 (1977).
4. Eichmann, K. *Immune System: Genetics and Regulation* (eds Sercarz, E., Herzenberg, L. & Fox, F.) 127–138 (Academic, New York, 1977).
5. Binz, H., Wigzell, H. & Bazin, H. *Nature* **264**, 639–640 (1977).
6. Krammer, P. & Eichmann, K. *Nature* **270**, 733 (1977).
7. Rubin, B., Hertel-Wulff, B. & Kimura, A. *J. exp. Med.* **150**, 307–321 (1979).
8. Krawinkel, U., Cramer, M., Mage, R., Kelus, A. & Rajewsky, K. *J. exp. Med.* **146**, 792–809 (1977).
9. Cazenave, P. A., Cavaillon, J. M. & Bona, C. *Immun. Rev.* **34**, 34–72 (1977).
10. Lonai, P., Ben-Neriah, Y., Steinman, L. & Givol, D. *Eur. J. Immun.* **8**, 827–834 (1978).
11. Puvi, J., Ben-Neriah, Y., Givol, D. & Lonai, P. *Eur. J. Immun.* (in the press).
12. Eichmann. K. *et al. Eur. J. Immun.* **10**, 105 (1980).
13. Ben-Neriah, Y., Wuilmart, C., Lonai, P. & Givol, D. *Eur. J. Immun.* **8**, 797–806 (1978).
14. Black, S. J., Hämmerling, G. J., Berek, C., Rajewsky, K. & Eichmann, K. *J. exp. Med.* **143**, 846–862 (1976).
15. Cramer, M. *et al. Eur. J. Immun.* **9**, 332–337 (1979).

Murine leukaemogenesis: monoclonal antibodies to T-cell determinants arrest T-lymphoma cell proliferation

Michael S. McGrath, Eric Pillemer & Irving L. Weissman

Laboratory of Experimental Oncology, Department of Pathology, Stanford University, Stanford, California 94305

We have proposed a receptor-mediated leukaemogenesis hypothesis wherein T lymphomas would be clones of T cells bearing mitogen-linked surface receptors specific for the envelope determinants of the inducing MuLV[1–3]. A prediction of the hypothesis is that T-lymphoma proliferation is dependent on continued presentation of MuLV envelope determinants to these cell-surface receptors, and that substances which interfere with receptor–virus interactions should inhibit T-lymphoma proliferation. Rat monoclonal antibodies were raised to the AKR mouse T lymphoma KKT-2, and these antibodies were screened independently for blockade of virus-binding and for cytostatic activity on KKT-2 cells. We report here that those monoclonal antibodies which block virus binding inhibit growth of KKT-2 cells in vitro, whereas monoclonal antibodies which bind to these cells but do not block virus binding are not cytostatic. Three of the four cytostatic antibodies detect determinants on the Thy-1 molecule, while none of the other (noncytostatic) antibodies detect Thy-1. Antibody inhibition of KKT-2 cell growth is precluded by saturation of KKT-2 virus receptors with the inducing leukaemia virus.

Spleen cells from Fisher rats immunized with KKT-2 lymphoma cells were fused with the hypoxanthine, aminopterin and thymidine (HAT) sensitive myeloma NS-1 (ref. 4), and antibody-forming cell hybrids were grown and cloned by limiting dilution. The antibodies used in this study and their characteristics are shown in Table 1. A complete characterization of these monoclonal antibodies, the molecules recognized, and

functions on normal cells will be described elsewhere (E. Pillemer *et al.*, in preparation).

To test the possible growth inhibitory function of these various monoclonal antibodies, we added them to logarithmically growing KKT-2 cells *in vitro*. As demonstrated in Fig. 1, exposure to dilutions of antibodies produced by clones 31-11, 31-8, 42-21 and 19XE5 resulted in greatly diminished thymidine uptake, whereas antibodies from clones 43-17, 43-13,
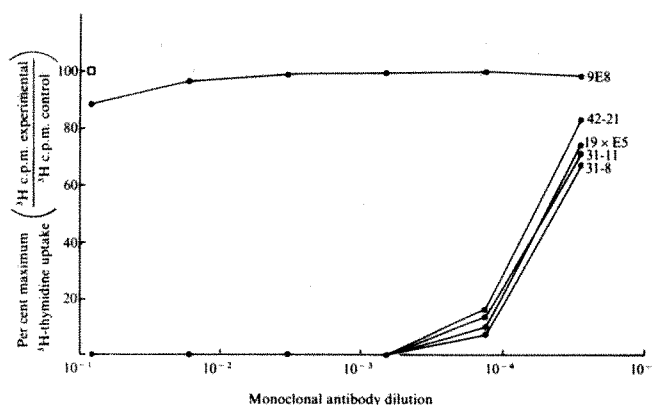
Fig. 1 Lymphoma cell growth inhibition assay. KKT-2 lymphoma cells were pelleted from subconfluent cultures and resuspended in serum-free growth medium (MEM, GIBCO) for 2 h at 37 °C at a density of 10^5 cells ml^{-1}. After repelleting, the cells were resuspended in cold tissue culture medium (MEM, 10% FCS) at a density of 2×10^4 cells ml^{-1}. 5×10^4 Cells (2.5 ml) were placed in the bottom of 25-cm^2 Corning tissue culture flasks and serial dilutions of monoclonal antibodies were added. After growing for 14 h at 37 °C, 0.1 ml of medium containing 10 µCi ^{3}H-thymidine (NEN) was added to each culture for 2 h. Labelled cells were washed, 5% TCA precipitated, and per cent growth inhibition was calculated using cells without antibody as equal to 100% growth. KKT-2 cells were tested for growth inhibition with: *a*, anti-Thy 1 (19XE5, 30-H12, 31-11, 42-21); *b*, anti-MuLV (16B7, 9E8); and *c*, anti-cell surface antibodies (31-8, 43-17, 43-13). Data represent averages of three experiments. Similar data result when 19XE5 and 16B7 antibodies purified from hybridoma supernatants (by protein A columns)[15] were utilized. □, Represents 1:12 dilutions of non-inhibitory antibodies, 43-13, 43-17, 16B7 and 30-H12.

Table 1 Analysis of monoclonal antibody specificity

		Cell-binding RIA							Virus RIA		
Antibody	Isotype	KKT-2	L691	L691/K	AKR/J NTHY	CXB/J NTHY	KKT-2 SL	MCF 247	Molecular weight	Proposed specificity	Ref.
31-8	IgG$_{2A}$	+ + +	–	–	+ + +	+ + +	–	–	80,000	T80	5
31-11	IgG$_{2A}$	+ + +	+ + +	+ + +	+ + +	+ + +	+ + +	–	27,000	Thy-1 constant	5
43-13	IgG$_{2B}$	+ +	–	+ +	–	–	+	–	{ 95,000 85,000 50,000	Cell surface	
43-17	IgG$_{2B}$	+ +	–	+ +	–	–	–	–	27,000	Thy-1 constant	
42-21	IgM	+	+	+	+	+	–	–	27,000	Thy-1.2	14
30-H12	IgG$_{2B}$	–	+ + +	+ + +	–	+ + +	–	–	15,000	p15E	15
9E8	IgG$_{2A}$	+ +	–	+ +	–	–	+ / –	–	27,000	Thy-1.1	5
19XE5	IgG$_3$	+ + +	–	–	+ + +	–	+ +	–	70,000	eco gp70	15
16XB7	IgG$_{2A}$	+ / –	–	–	–	–	–	–			

Monoclonal antibodies (31-8, 31-11, 43-13, 43-17 and 42-21) were prepared by a modification of the technique of Galfré *et al.*[4]. Briefly, Fisher rats were immunized with KKT-2 lymphoma cells; three days following the final intravenous injection, the spleen (approximately 2 × 10⁸ cells) was fused with 10⁷ NS-1 myeloma cells using 38% polyethylene glycol-1540. Hybrids were grown initially in super HAT medium[12] in 24-well plates (Falcon 3008). Supernatants were tested for binding to a panel of tumour cells, normal lymphoid cells and purified virus using a conventional radioimmunoassay (RIA) with a ¹²⁵I-labelled rabbit anti-rat second stage as the detecting reagent. MCF-247 and KKT-2-SL viruses were prepared by Sepharose 4B chromatography[13]. Molecular weight determinations were performed as previously described[5]. Specificities for most of the antibodies have been described previously; work is continuing to characterize molecules recognized by the 43-13, 43-17 and 42-21 monoclonals. Clone 31-8 has been lost. Identity of tumour cell lines: (1) KKT-2 is a spontaneous AKR/J lymphoma; (3) L691/K is the L691 lymphoma super-infected with the KKT-2-SL virus[5]. +, Relative level of binding as determined by RIA; –, indicates that binding was at the level of background obtained when using the second stage reagent alone. Rat monoclonal 30-H12 was provided by J. Ledbetter[14]. Mouse monoclonals 9E8, 19XE5 and 16B7 were provided by R. Nowinski[15].

16B7, 9E8 and 30-H12 were without effect on DNA synthesis. Growth inhibitory antibodies block DNA synthesis significantly at concentrations to 1:10,000, while cell binding, non-inhibitory antibodies are ineffective, even at concentrations approaching 1:10. This inhibition was not related to antigen mobility as the inhibitory antibodies show different patching and capping activity in the presence of second stage antibodies; 19XE5 and 42-21 caused rapid membrane capping, 31-8 intermediate capping activity, and 31-11 caps very slowly and incompletely (data not shown). The inhibition was extremely cell density dependent, and was optimal with exponentially dividing cells at less than 2 × 10⁴ cells per ml. At 2 × 10⁵ cells per ml, even 1:10 dilutions of 31-11 were not inhibitory.

Figure 2 shows that KKT-2 cell growth inhibition is directly related to the level of cell-surface antibody bound and degree of interference with murine leukaemia virus (MuLV) binding. Growth inhibitory levels of 31-11 and 42-21 (>50% saturation) significantly blocked MuLV binding whereas the non-inhibitory 43-17 antibody did not.

The effect of growth inhibitory antibodies seems to be most active in cell-cycle phase G_1. We have previously shown that after exposure to 31-11 antibody, KKT-2 cells show a linear fall to background in their ability to synthesize DNA within 8 h with a shift in DNA content from 4n towards 2n copies within 20 h. This corresponds to a shift in size from large lymphoblastic to small G_0-type lymphoid cells within 24 h, culminating in non-complement mediated cell death within 48 h[5].

If growth inhibition by particular monoclonal antibodies is mediated by steric or direct blockade of receptor–viral envelope interactions, then preincubation of lymphoma cells with their inducing retrovirus ought to fill such receptors, preventing antibody-induced growth inhibition. To test this possibility, we preincubated KKT-2 lymphoma cells with saturating concentrations of their own endogenously produced SL retroviruses, or with various viruses closely or more distantly related (as defined by host of origin[6], shared and distinct antigenic determinants[7], and cell-binding specificity[3,8]). We then added monoclonal antibodies to these mixtures at growth inhibiting concentrations. The results, shown in Table 2A, were striking: only the endogenously produced retrovirus (KKT-2-SL) prevented antibody-induced growth inhibition of KKT-2 cells. Table 2B demonstrates that this inhibition is not secondary to a direct interaction of antibody and virus, as preadsorption of limiting concentrations of antibody with a great excess of virus does not prevent growth inhibition. We have demonstrated elsewhere that prebinding of KKT-2 cells with saturating levels of virus does not alter the amount of 31-8 or 31-11 antibodies bound to these cells[5].

To test whether live viruses are necessary for continued cell growth in the presence of inhibitory antibodies, we preirradiated

KKT-2-SL virus with doses of UV known to inactivate >99.99% viral replicating and infectious activity[9] before prebinding. This radiation dose did not affect the ability of these virions to prevent growth inhibition by monoclonal antibody (Table 2C).

These experiments demonstrate that T-lymphoma cells, like T lymphocytes, are under cell-surface regulation for stimulation and cessation of DNA synthesis. It is likely, therefore, that leukaemogenic retroviral oncogene action involves stimulation of cell-surface mitogen receptors, alone or in combination with other intracellular signals. These latter signals may also be under viral genetic control, either by direct expression of viral genes or by selective activation of host genes. In this view cell-surface stimulation would be necessary, but not sufficient for lymphoma cell proliferation. As a corollary, lymphoma cell growth

Table 2 Inhibition of antibody-induced KKT-2 cell growth arrest

	Per cent control ³H-thymidine uptake	
	31-11	31-8
A Preincubated virus:		
PBS	2	2
KKT-2-SL	85	96
MCF-247	4	6
L691/G	5	3
BL/Ka[X]	7	4
BL/Ka[B]	4	3
L691/M	8	7
B Antibody preabsorbed with virus:		
PBS	5	6
KKT-2-SL	11	8
L691/M	8	7
BL/Ka[B]	8	5
C UV inactivated KKT-2-SL virus	75	105
D Control cells without inhibitory antibody addition	100	100

The standard KKT-2 cell growth inhibition assay as outlined in Fig. 1 legend was carried out with 31-11 and 31-8 antibodies at a 1:250 dilution on 5 × 10⁴ KKT-2 cells after preincubation with purified retroviruses. *A*, 0.01 A_{260} unit of Sepharose-4B purified virus[13] in 0.3 ml phosphate buffered saline (PBS) was incubated with KKT-2 cells for 60 min. at room temperature before addition of inhibitory antibodies. This amount of virus represents a receptor saturation level as previously determined[8]. The origin of each retrovirus population has also been previously described[3,8]. *B*, One A_{260} unit of Sepharose purified KKT-2-SL, L691/M and BL/Ka[B] virus in PBS was incubated with 31-11 and 31-8 antibodies at a 1:2.5 antibody dilution for 60 min at room temperature with PBS control absorbed samples. The samples were spun at 100,000g for 120 min to pellet virus, and the absorbed antibodies were tested in the standard KKT-2 cell growth inhibition assay (Fig. 1). All inhibitions were carried out at a 1:250 final antibody dilution. *C*, Sepharose-4B purified KKT-2-SL virus was UV inactivated and used to inhibit antibody induced KKT-2 cell growth inhibition as in *A*. Virus (5 ml) in PBS (1 A_{260}unit ml⁻¹) was irradiated for 145 s at 4,000 erg mm⁻² before use. *D*, Control growth inhibition of KKT-2 cells in the absence of inhibitory antibodies.
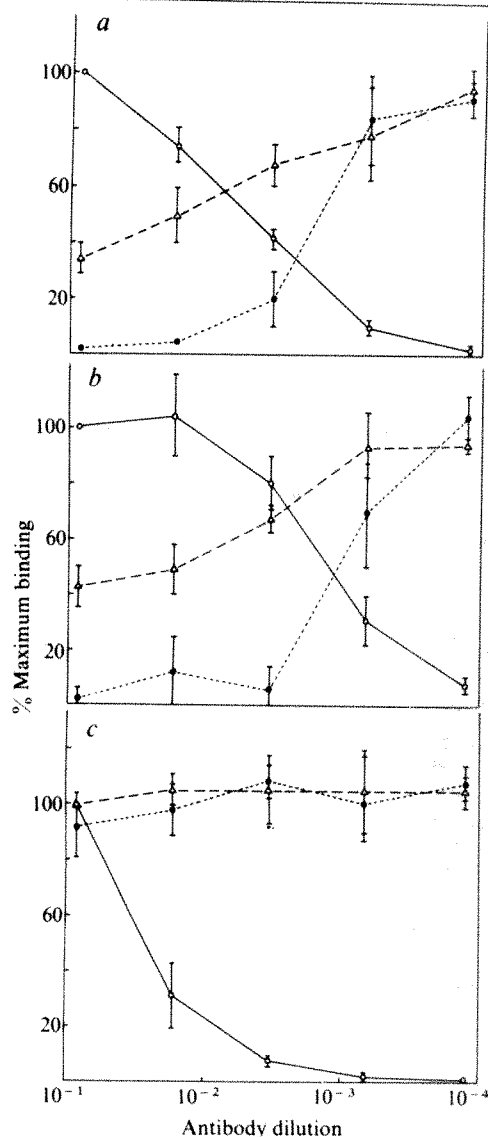
Fig. 2 Effect of serial dilutions of monoclonal antibodies prebound to KKT-2 cells on growth inhibition and MCF-247 virus binding. 10^6 KKT-2 cells were suspended at 2×10^4 cells per ml in serial dilutions of monoclonal antibody supernatants: *a*, 31-11; *b*, 42-21; *c*, 43-17, for 1 h at 0 °C before washing through neat fetal calf serum. Fluoresceinated MCF-247 binding and detection of cell-surface antibody by fluorescence-activated cell sorter analysis was carried out on 4.75×10^5 cells each as previously described[3]. 5×10^4 cells from each point were suspended in 2.5 ml of MEM/10% FCS and growth inhibition was determined as in Fig. 1 legend. 100% binding of MCF-247 was that level bound to KKT-2 cells treated in parallel without antibody. 1:1 nonfluoresceinated MCF-247 inhibition of binding showed a 43% inhibition of fluoresceinated MCF-247 binding. 100% antibody binding was that level bound to cells at the lowest dilution (1:12). Antibody binding (O————O); MCF-247 binding (△—————△); (³H-thymidine uptake experimental/³H-thymidine uptake control) × 100% (●————●). The curves represent data from three experiments ± standard deviation.

inhibitory antibodies should also inhibit antigen-induced proliferation of normal T-cell subsets. In fact, we present elsewhere evidence that the anti-Thy-1 monoclonal antibodies may inhibit concanavalin A mitogen and alloantigen induced T-cell proliferation (N. Hollander *et al.*, in preparation).

These experiments provide strong evidence that cell-surface MuLV-specific receptors on T lymphomas are involved in continued proliferation by these cells, as predicted by the receptor-mediated leukaemogenesis hypothesis[1-3]. The hypothesis, however, is not proven: for example, growth-inhibiting antibodies may affect cell proliferation by binding to molecules which generate antimitotic signals independent of viral receptors. Thus, prebound virus might inhibit antibody binding to a subset of antimitotic molecules, providing that the antimitotic subset is located near viral receptors. It is also known that some antigen-activated T cells may respond to T cell growth

factors by continued proliferation (in the presence or absence of antigen[16]). It is not yet known if KKT-2 cells belong to that category of cells, but the relative resistance of cells grown at higher density to growth inhibition by these antibodies might be due to these factors, or to higher concentrations of viral envelope determinants. Another potential difficulty with the hypothesis is the incidence of aneuploidy (trisomy 15) in AKR and RadLV-induced leukaemias[10]. While it is conceivable that this is not related to the leukaemogenic process, it seems more likely, that it is a necessary event in the progression to leukaemia[11]. Whether this is a necessary event related to cell-surface stimulation or some other aspect of unlimited cellular proliferation is still unclear.

It is interesting to speculate that other neoplastic cell types might also be regulated by stimulation of cell-surface mitogen-linked receptors by self-produced (or exogenous) complementary ligands. These cells also might be susceptible to growth inhibition by appropriate monoclonal antibodies.

1. Weissman, I. L. & Baird, S. *Life Sci. Res. Rep.* **7**, 135 (1977).
2. McGrath, M. S. & Weissman, I. L. in *Normal and Neoplastic Hematopoietic Cell Differentiation* (eds Clarkson, B., Marks, P. & Till, J.) 577–589 (Cold Spring Harbor Laboratory, 1978).
3. McGrath, M. S. & Weissman, I. L. *Cell* **17**, 65 (1979).
4. Galfré, G., Howe, S. C., Milstein, C., Butcher, G. W. & Howard, J. C. *Nature* **266**, 550 (1977).
5. McGrath, M. S. *et al. Cold Spring Harb. Symp. quant. Biol.* **44** (in the press).
6. Rowe, W. & Pincus, T. *J. exp. Med.* **135**, 429 (1972).
7. Old, L. & Stockert, E. *A. Rev. Genet.* **17**, 127 (1977).
8. McGrath, M. S., Lieberman, M., Decléve, A., Kaplan, H. S. & Weissman, I. L. *J. Virol.* **28**, 819 (1978).
9. Niwa, O., Decléve, A. & Kaplan, H. S. *Virology* **74**, 140 (1976).
10. Wiener, F., Ohno, W., Spira, J., Haran-Ghera, N. & Klein, G. *J. natn. Cancer Inst.* **61**, 227 (1978).
11. Klein, G. *Proc. natn. Acad. Sci. U.S.A.* **76**, 2442 (1979).
12. Littlefield, J. S. *Science* **145**, 709 (1964).
13. McGrath, M. S., Witte, O., Pincus, R. & Weissman, I. L. *J. Virol.* **25**, 923 (1978).
14. Ledbetter, J. & Herzenberg, L. A. *Immun. Rev.* **47**, 63 (1979).
15. Lostrom, E. *et al. Virology* **98**, 336 (1979).
16. Morgan, D.A., Ruscetti, F. & Gallo, R.C. *Science* **193**, 1007 (1976).

Lateral diffusion of lipopolysaccharide in the outer membrane of *Salmonella typhimurium*

Melvin Schindler*†, M. J. Osborn† & Dennis E. Koppel‡

† Department of Microbiology, UCONN Health Center, University of Connecticut, Farmington, Connecticut 06032
‡ Department of Biochemistry, UCONN Health Center, University of Connecticut, Farmington, Connecticut 06032

Gram-negative enteric bacteria are enveloped by two membrane systems[1]. The inner or cytoplasmic membrane is responsible for the major metabolic functions including biosynthetic activities[2], while the major known functions of the outer membrane are primarily physical: it contains receptors for bacteriophages and bacteriocins[3]; it contributes to the maintenance of cell shape[4]; and it controls access of nutrient solutes and agents such as antibiotics and detergents to the cytoplasmic membrane[5]. Several investigations have indicated that mobility of membrane components, particularly lipopolysaccharide[5,6], is essential for biogenesis of the outer membrane[7,8], and is a primary

* To whom reprint requests should be adressed.

event in phage infection[9,10]. To define more accurately the fluid dynamic properties of the outer membrane as related to function, we have now developed the capability to measure lateral diffusion coefficients *in vivo* of rhodaminated G30 lipopolysaccharide fused into *Salmonella typhimurium* G30A filamentous bacteria. The method used extends the FRAP procedure (fluorescence redistribution after photobleaching)[11,12] to bacteria and the results demonstrate rapid diffusion of lipopolysaccharide $(D = 2.0 \pm 0.9 \times 10^{-10} \text{ cm}^2 \text{ s}^{-1})$ over micrometre distances.

In the FRAP technique, lateral transport parameters are determined from the characteristic redistribution of fluorescent label after a gradient of concentration is established by a localised photobleaching pulse. Gram-negative bacteria are in general too small to be studied successfully by this approach, but mobility measurements can be performed on bacterial filaments. Nonseptate filaments 50–100 μm long, consisting of a syncytium of bacteria sharing a common, continuous inner and outer membrane, were obtained by treatment with cephalexin[13] (see Fig. 1).

Exogenous fluorescently labelled lipopolysaccharide was incorporated into the bacterial outer membrane by vesicle fusion, following methods devised by Jones and Osborn[14,15]. The lipopolysaccharide was isolated from *S. typhimurium* G30 by the method of Galanos[16], further purified by electrodialysis[17], and reacted with rhodamine isothiocyanate following the procedure of Schindler *et al.*[11]. Unilamellar phospholipid vesicles containing the lipopolysaccharide were prepared, and incubated with a preparation of bacterial filaments for 40 min, at 37 °C. Jones and Osborn[14,15] have demonstrated that this procedure transfers lipopolysaccharide to the outer membrane of the acceptor bacteria. While vesicle derived phospholipid translocates to the inner membrane, the lipopolysaccharide does not, and resides exclusively in the outer membrane[14,15].

Electron microscopy was used to examine the surface distribution of vesicle derived lipopolysaccharide (see Fig. 2). For this purpose, lipopolysaccharide was derivatised with 2,4,6-trinitrobenzene sulphonic acid (TNBS) in order to incorporate trinitrophenol hapten (TNP) groups into the molecule. Vesicles

Fig. 2 Electron microscopy of *S. typhimurium* with and without exogenously added TNP-lipopolysaccharide. Freshly prepared TNP-lipopolysaccharide-phospholipid vesicles (phospholipid/lipopolysaccharide ratio = 60:1) were prepared and incubated with cells as described elsewhere[13,14]. TNP-lipopolysaccharide G30 was prepared as follows: 5 mg G30 lipopolysaccharide was reacted with 5 mg trinitrobenzene sulphonic acid (TNBS) in 1 ml 0.2 M NaHCO₃, pH 8.5 at room temperature for 1 h; the reaction mixture was applied to a Sephadex G-25 column (1.5 × 20 cm) and eluted with water; the void volume peak was lyophilised and stored at 4 °C. Goat anti-DNP antibodies (20 μl, 1.5 mg ml⁻¹) were added to the bacteria suspended in 1 ml, 50 mM HEPES pH 7.5 and allowed to incubate at room temperature for 5 min. The cells were washed three times with 2 ml buffer and resuspended in 1 ml of the same buffer. Ferritin-labelled rabbit anti-goat IgG antibody (0.2 ml, Cappel Labs) was added to the cells for 5 min at room temperature. The cells were then washed again three times in buffer, pelleted and fixed in 2% glutaraldehyde at 4 °C for 1.5 h. Thin section preparation was performed as described previously[14]. *a* and *b* are longitudinal sections while *c* and *d* are transverse sections of *S. typhimurium* with (*a, c*) and without (*b, d*) TNP-lipopolysaccharide. Scale bars, 220 nm.

Fig. 1 Bacterial filament viewed under dark-field light microscopy. *S. typhimurium* G30A was grown in PPBE from an overnight culture at a dilution of 1/20. After one generation of normal growth cephalexin was added to the medium (10 μg ml⁻¹). The culture was shaken vigorously and allowed to grow to $A_{600} = 1.0$. The culture was then diluted 1/10 in PPBE containing cephalexin (10 μg ml⁻¹) and again allowed to grow to $A_{600} = 1.0$. The cells were collected and washed with a 10 mM HEPES/cephalexin buffer pH 7.5. Superimposed on the filament, by photographic double exposure, is a 'picture' of the incident focused laser beam produced by imaging the fluorescence excited in a thin layer of concentrated dye solution.

were prepared and fused with non-filamentous *S. typhimurium* in the usual manner. After fusion, goat anti-DNP antibodies were reacted with the bacteria followed by incubation with ferritin-labelled rabbit anti-goat IgG antibodies. The samples were fixed in glutaraldehyde and thin sectioned for examination. Figure 2 demonstrates that the vesicle derived exogenous lipopolysaccharide is incorporated in the bacterial outer membrane.

Diffusion coefficients were determined by the FRAP technique using a recently introduced 'multi-point' analysis[12]. The labelled lipopolysaccharide was photobleached with a laser beam focused to a narrow band (~1 μm wide) aligned to intercept one or more bacterial filaments (see Fig. 1). The redistribution of mobile molecules along the filaments was then followed by monitoring the fluorescence intensity excited by an attenuated beam (×5 × 10⁻⁵) sequentially positioned at each of several locations in and adjacent to the bleached area.

Recovery curves of rhodamine-labelled G30 lipopolysaccharide in the acceptor bacteria G30A are shown in Fig. 3. From the functional form of the fluorescence recovery, it is clear that all the exogenously added lipopolysaccharide is free to diffuse in the outer membrane with no immobile components (recovery is greater than 90%). From a nonlinear least squares fit of the data to the appropriate theoretical equations[12], a value of $2.0 \pm 0.9 \times 10^{-10}$ cm^2 s^{-1} was found for exogeneously added lipopolysaccharide. Following addition of anti-G30 antibody, recovery is still monophasic, but now is very much slower with a calculated diffusion constant of $2.0 \pm 0.4 \times 10^{-11}$ cm^2 s^{-1}. This clearly indicates that the majority of lipopolysaccharide is situated in the outer membrane accessible to antibody molecules.

Mühlradt et al.[6], using indirect techniques, suggested that lipopolysaccharide diffusion is much slower ($D \leqslant 3 \times 10^{-13}$ cm^2 s^{-1}). A direct comparison of our results is not possible because those experiments were performed with wild-type bacteria in which the carbohydrate side chain on the lipopolysaccharide is much longer[1]. In addition, wild-type bacteria have approximately 2.5 times more protein in the outer membrane[18]. The effect of these parameters on lipopolysaccharide mobility is now being investigated.

The relatively rapid rate of diffusion that we observe for lipopolysaccharide is in marked contrast to the immobility of matrix-porin as determined by Smit and Nikaido[19]. Very similar diffusion characteristics for lipopolysaccharide and matrix-porin were observed by us in vitro, in reconstituted outer membrane multibilayers[11].

This work further extends to the FRAP technique which has previously been used exclusively on eukaryotic cells. The use of this technique should provide new and fundamental information

on the molecular dynamics of the outer membrane and the relationship of these dynamics to biogenesis and function of the membrane. The bacterial system is readily manipulable by genetic and physiological means, and can be used as a model for exploration of causal relationships between the molecular composition and organisation of a membrane, its fluid dynamics and specific functions (including receptor function and signal transmission).

1. Osborn, M. J. A. Rev. Biochem. **38**, 501–538 (1968).
2. Osborn, M. J., Gander, J. E., Parisi, E. & Carson, J. J. biol. Chem. **247**, 3962–3972 (1972).
3. Braun, V. & Hantke, K. A. Rev. Biochem. **43**, 89–121 (1974).
4. Henning, U. A. Rev. Microbiol. **29**, 45–60 (1975).
5. Nikaido, H. Biochim. biophys. Acta **423**, 118–32 (1976).
6. Mühlradt, P. F., Menzel, J., Golecki, J. R. & Speth, V. Eur. J. Biochem. **35**, 471—481 (1973).
7. Mühlradt, P. F. Menzel, J., Golecki, J. R. & Speth, V. Eur. J. Biochem. **43**, 533—539 (1974).
8. Begg, K. J. & Donachie, W. D. Nature **245**, 38–39 (1973).
9. Ryter, A., Schuman, H. & Schwartz, M. J. Bact. **172**, 295–301 (1975).
10. Bayer, M. J. gen. Microbiol. **53**, 395–404 (1968).
11. Schindler, M., Osborn, M. J. & Koppel, D. E. Nature **283**, 346–350 (1980).
12. Koppel, D. E. Biophys. J. **28**, 281–292 (1979).
13. Spratt, B. G. Proc. natn. Acad. Sci. U.S.A. **72**, 2999–3003 (1975).
14. Jones, N. C. & Osborn, M. J. J. biol. Chem. **252**, 7398–7404 (1977).
15. Jones, N. C. & Osborn, M. J. J. biol. Chem. **252**, 7405–7412 (1977).
16. Galanos, C., Luderitz, O. & Westphal, O. Eur. J. Biochem. **9**, 245–249 (1969).
17. Galanos, C. & Luderitz, O. Eur. J. Biochem. **54**, 603–610 (1975).
18. Smit, J., Komio, Y. & Nikaido, H. J. Bact. **124**, 942–958 (1975).
19. Smit, J. & Nikaido, H. J. Bact. **135**, 687–702 (1978).
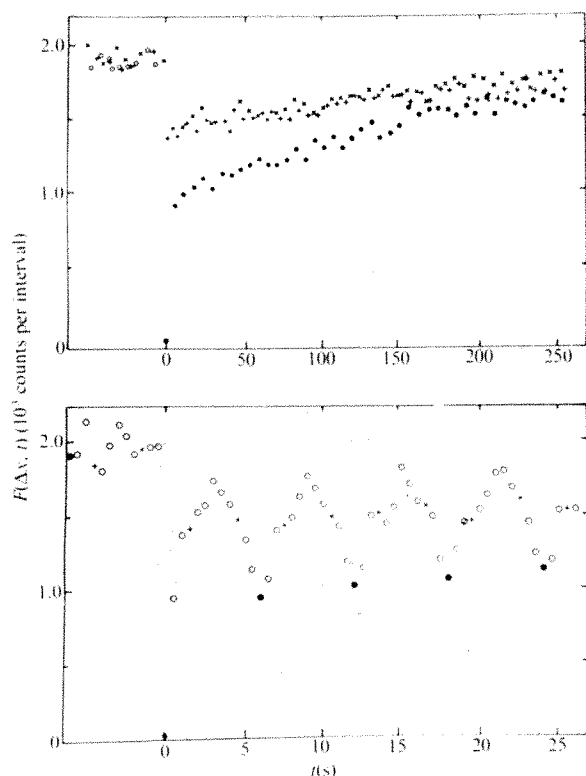
Fig. 3 Recovery curves of rhodaminated G30 lipopolysaccharide. Sample was bleached with an intense laser pulse focused to a narrow band intersecting the filament. Fluorescence intensity, $F(\Delta x, t)$, was measured as a function of position and time with an attenuated beam sequentially positioned at each of 12 equally spaced locations (0.36 μm separation) along the filament. Top: Recoveries measured at 3 of the 12 locations: coincident with the bleaching pulse (○), and 1.08 μm on either side of centre (+, ×). Bottom: Sequential scans including all 12 locations on an expanded time scale. Data were fitted to the form of equation (9) of ref. 12, assuming a 100% recovery.

A nucleosome-free region in SV40 minichromosomes

Edward B. Jakobovits, Susan Bratosin & Yosef Aloni

Department of Genetics,
The Weizmann Institute of Science, Rehovot, Israel

Simian virus 40 (SV40) DNA is found in infected cells in the form of a minichromosome[1]. It possesses a beaded structure composed of cellular histones and supercoiled viral DNA in a molecular complex which is very similar to that of cellular chromatin[2–4]. The similarity between these structures, and the fact that the major viral functions take place in cell nuclei via cellular machinery, have made SV40 an attractive model system in which to study the organization and expression of the more complex eukaryotic chromatin. Early studies on SV40 chromatin, attempting to determine the precise distribution of the histone beads (nucleosomes) along the DNA, indicated that the nucleosomes were randomly distributed relative to the viral DNA sequences[5–8]. This picture has recently been altered by a study indicating that a region close to the viral origin of replication is particularly sensitive to nuclease digestion[9–13]. Using a variety of nucleases,[10–13], the nuclease-sensitive region has been shown to map on a stretch of the genome beginning at the viral origin of replication and continuing about 400 base pairs into the 'late' side of the DNA. The simplest interpretations of the presence of a nuclease-sensitive region are that this region is either deficient in nucleosomal protein or that it contains a peculiar arrangement of these protein structures. We have analysed SV40 minichromosomes in the electron microscope in an attempt to determine whether alterations in the gross nucleoprotein structure of this region could be visualized. We report here that such an alteration does exist and that about 25% of SV40 minichromosomes observed contained a region of DNA between 0.67 and 0.75 map units which is not organized into the typical nucleosome beaded structure.
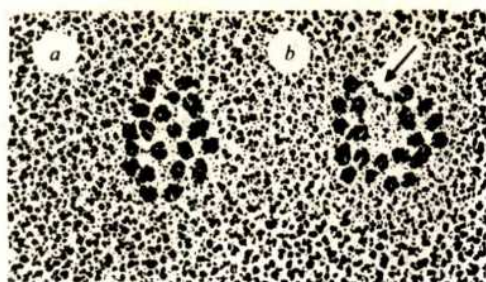
Fig. 1 Electron microscopic visualization of SV40 minichromosomes. At 48 h post-infection, SV40-infected BSC-1 cells were washed twice with 0.05 M Tris-HCl, *p*H 7.9, 0.001 M MgCl$_2$ and 0.005 M 2-mercaptoethanol (buffer H), and collected by low speed centrifugation. The cell pellet was resuspended in buffer H and centrifuged again at low speed. This procedure caused lysis of about 95% of the cells. The nuclear pellet was resuspended in 1 ml buffer H per 10^7 nuclei and incubated at 37 °C for 30 min with occasional shaking. The suspension was then centrifuged at 10,000 *g* for 1 min and the supernatant containing the SV40 chromatin was run through a 5–30% (w/w) sucrose gradient in buffer H containing 0.1 M NaCl for 2 h at 32,000 r.p.m. in the Spinco SW41 rotor at 4 °C. The 75S peak[30] (minichromosomes) was pooled, and immediately mounted on carbon membrane-coated grids activated by glow-discharge[31]. The grids were stained with 2% uranyl acetate and rotary shadowed with Pt/Pd (80:20). Molecules were visualized with a Philips 300 electron microscope, and photographs were taken at a magnification of ×42,000. *a*, Minichromosome without a gap; *b*, minichromosome with a gap, indicated by the arrow.

Figure 1 shows the appearance of representative SV40 minichromosomes with and without an exposed region ('gap') of DNA. Reproducibly we found that approximately 25% of the readable molecules contained a single gap, whereas molecules containing more than one gap comprised less than 1% of the population. We have measured the length of the 'exposed' region relative to naked SV40 DNA spread in the same sample. Figure 2 shows that the average length was 103±30 μm. Assuming the DNA to be fully extended, this gap corresponded to 320±90 base pairs of DNA. However, this length is a minimum estimate, as the spreading method used could not detect on the exposed DNA proteins that were able to cause the DNA's condensation.

To locate the gap relative to restriction sites on the physical map of SV40 DNA, minichromosomes were digested with site-specific, single-cut, restriction endonucleases. The extent of minichromosome linearization was dependent on the particular enzyme used. Digestion with either *Bam*HI or *Eco*RI converted only 20–30% of the minichromosomes to linear molecules, even in conditions of enzyme excess. Digestion with *Bgl*I produced 60–70% linear molecules. Similar proportions of linear molecules were observed when DNA extracted from minichromosomes digested by these restriction endonucleases was analysed by electrophoresis on agarose gels.
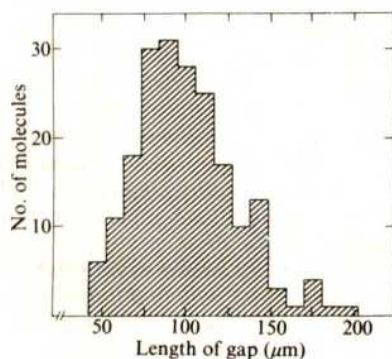
Fig. 2 Histogram of the length of the gap in the minichromosome. The length of the gap was measured in molecules as shown in Fig. 1*b*. SV40 DNA was used as internal length standard (1.7 μm).

Figure 3 shows the appearance of representative linear molecules that contain gaps, and Fig. 4 is a histogram showing the distribution of nucleosomes about the gap. When minichromosomes were cleaved with *Bam*HI, the exposed DNA stretch was located between short and long beaded arms, containing an average of 9±1 beads and 11±1 beads, respectively (Figs 3*a*, 4*a*). Similarly, when minichromosomes were treated with *Eco*RI, the gap resided between a short arm with an average of 6±1 beads and a long arm with an average of 14±1 beads (Figs 3*b*, 4*b*). Cleavage with *Bgl*I yielded a stretch of exposed DNA on the end of a string of nucleosomes averaging 19±1 beads (Figs 3*c*, 4*c*). Occasionally, we observed a solitary bead on the far end of the open stretch after treatment with *Bgl*I (see arrow, Fig. 3*c*). These results unequivocally locate the exposed stretch of DNA as starting at or very close to the *Bgl*I restriction site and extending into the late region for at least 320 base pairs. The high rate of cleavage by *Bgl*I indicated that in most molecules, the *Bgl*I cleavage site was not blocked by a nucleosome.
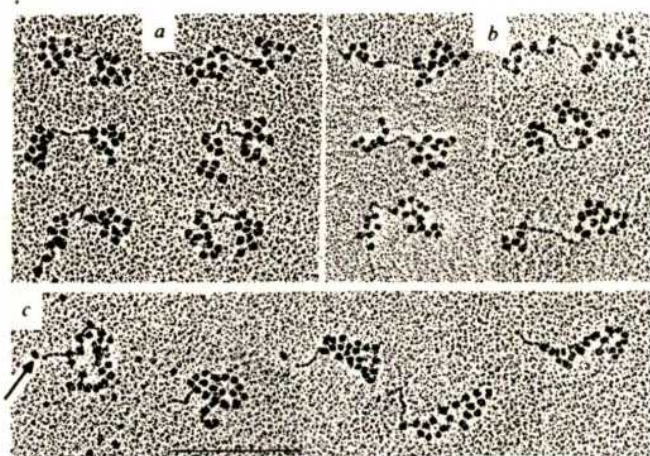
Fig. 3 Electron microscope visualization of SV40 minichromosomes cleaved with restriction endonucleases. The minichromosomes present in the 75S peak[30] of the sucrose gradient. (see Fig. 1 legend) were diluted into 1 volume of a solution containing 0.02 M MgCl$_2$ and 0.002 M dithiothreitol, and digested for 60 min at 37 °C with *Bam*HI, (*a*), *Eco*RI (*b*) and *Bgl*I (*c*), before mounting for electron microscope visualization as in Fig. 1. The cleavage sites are: *Bam*HI, 0.15 μm; *Eco*RI, 0.0 μm and *Bgl*I, 0.67 μm (see ref. 17). *Bgl*I cuts at the origin of replication[16].

Molecules without a gap possessed an average of 21±2 beads, regardless of whether or not they were linearized by restriction enzymes. Minichromosomes with a gap possessed an average of 20±2 beads, again independent of their linear or circular structure. Thus, cutting the minichromosomes with restriction endonucleases did not cause the loss of nucleosome structure due to slipping at the ends. The number of nucleosomes observed on the SV40 minichromosomes seemed to be similar in molecules with and without a gap. However, as the distribution of the number of nucleosomes is broad, we cannot distinguish between the possibility that the gap was generated during preparation by loss of one or two nucleosomes and the possibility that this site was devoid of nucleosomes *in vivo*. In the first case, the nucleosome(s) lost might be different structurally from those that remained associated with the DNA of the minichromosomes. One possibility is that they contain modified histones, which could cause the histone octamer (nucleosome) to dissociate easily from the DNA. It is also possible that in this region of the SV40 genome there is a transient binding of nucleosomes, or parts of nucleosomes, to only one strand of the DNA, as was recently proposed for eukaryotic chromatin by Palter *et al.*[14]. They suggested that this mechanism requires a major conformational change in the nucleosome, and we believe that such a change, if it occurs, may render the nucleosome unrecognizable in the electron microscope[15]. The exact mode of histone
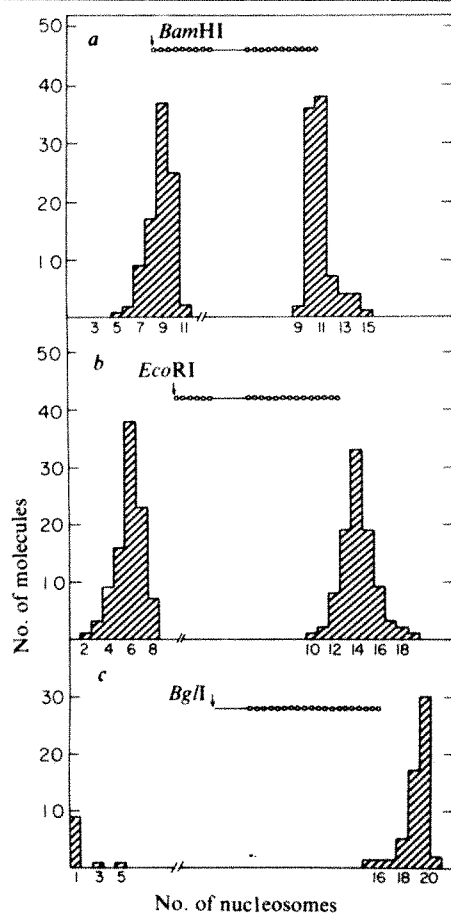
Fig. 4   Histograms of the number of nucleosomes on each side of the gap in the cleaved minichromosomes. The analysis was carried out on molecules as in Fig. 3. The inserts diagram the linearized molecules showing the nucleosomes about the exposed region relative to the enzyme cutting site.

binding to single-stranded DNA may facilitate some, or all, of the regulatory signals that have been mapped to the exposed region of the viral DNA. These include the origin of DNA replication[16], the promoters for late transcription[17], the heterogeneous 5' ends of the late mRNA[18,19], the cap structures at the 5' ends of the late mRNAs[20-22] and a major binding site for viral T antigen[23,24]. That *Escherichia coli* RNA polymerase preferentially initiates transcription *in vitro* in this region of the SV40 minichromosome and asymmetrically transcribes the late strand (E.B.J., Y.A., S. Saragosti and M. Yaniv, unpublished results) also may support this possibility. In addition, the observation that transcriptionally active regions in eukaryotic chromatin are preferentially susceptible to both DNase I[25-27] and staphylococcal nuclease digestion [28] also indicates that similar 'gapped' structures may exist in cellular chromatin[15]. It should be emphasized, however, that we have not demonstrated that SV40 minichromosomes with an exposed region are the transcriptionally active viral chromatin. Although others have concluded that only a small fraction (0.5-3%) of the SV40 minichromosomes is transcriptionally active[29], we have observed that a much larger fraction of the minichromosomes is transcribed (unpublished). We are now investigating the correlation between gapped minichromosomes and transcription.

We thank M. Yaniv and S. Saragosti for communicating unpublished results and Dr D. Roufa for critical reading of the manuscript. This research was supported by USPHS research grant CA 14995.

1. Griffith, J. D. *Science* **187**, 1202–1203 (1975).
2. Felsenfeld, G. *Nature* **271**, 115–122 (1978).
3. Kornberg, R. D. *A. Rev. Biochem.* **46**, 931–954 (1977).
4. Chambon, P. *Cold Spring Harb. Symp. quant. Biol.* **42**, 1209–1234 (1977).

5. Cremisi, C., Pignatti, P. F., Crossant, O. & Yaniv, M. *J. Virol.* **17**, 204–211 (1976).
6. Cremisi, C., Pignatti, P. F. & Yaniv, M. *Biochem. biophys. Res. Commun.* **73**, 548–554 (1976).
7. Ponder, B. A. J. & Crawford, L. V. *Cell* **11**, 35–49 (1977).
8. Polisky, B. & McCarthy, B. *Proc. natn. Acad. Sci. U.S.A.* **72**, 2895–2899 (1975).
9. Varshavsky, A. J., Sundin, O. H. & Bohn, M. J. *Nucleic Acids Res.* **5**, 3469–3478 (1978).
10. Scott, W. A. & Wigmore, D. J. *Cell* **15**, 1511–1518 (1978).
11. Sundin, O. & Varshavsky, A. *J. molec. Biol.* **132**, 535–546 (1979).
12. Waldeck, W., Föhring, B., Chowdhury, K., Bruss, P. & Sauer, G. *Proc. natn. Acad. Sci. U.S.A.* **75**, 5964–5968 (1978).
13. Varshavsky, A. J., Sundin, O. & Bohn, M. *Cell* **16**, 453–466 (1979).
14. Palter, K. B., Foe, V. E. & Alberts, B. M. *Cell* **18**, 451–467 (1979).
15. Foe, V. E., Wilkinson, L. E. & Laird, C. D. *Cell* **9**, 131–146 (1976).
16. Nathans, D. & Danna, K. J. *J. molec. Biol.* **64**, 515–518 (1972).
17. Laub, O., Bratosin, S., Horowitz, M. & Aloni, Y. *Virol.* **92**, 310–323 (1979).
18. Ghosh, P. K., Reddy, V. B., Swinscoe, J., Lebowitz, P. & Weissman, S. *J. molec. Biol.* **126**, 813–846 (1978).
19. Horowitz, M., Laub, O., Bratosin, S. & Aloni, Y. *Nature* **257**, 558–559 (1978).
20. Aloni, Y., Dhar, R., Laub, O., Horowitz, M. & Khoury, G. *Proc. natn. Acad. Sci. U.S.A.* **74**, 3686–3690 (1977).
21. Lavi, S. & Groner, Y. *Proc. natn. Acad. Sci. U.S.A.* **74**, 5323–5327 (1977).
22. Hsu, M. & Ford, J. *Proc. natn. Acad. Sci. U.S.A.* **74**, 4982–4985 (1977).
23. Tjian, R. *Cell* **13**, 165–179 (1978).
24. Jessel, D. *et al. Cell* **8**, 535–545 (1976).
25. Garel, A. & Axel, R. *Proc. natn. Acad. Sci. U.S.A.* **73**, 3966–3970 (1976).
26. Weintraub, H. & Groudine, M. *Science* **193**, 848–856 (1976).
27. Flint, S. J. & Weintraub, H. M. *Cell* **12**, 783–794 (1977).
28. Bloom, K. S. & Anderson, J. N. *Cell* **15**, 141–150 (1978).
29. Green, M. H. & Timothy, L. B. *Nucleic Acids Res.* **4**, 4279–4289 (1977).
30. Jakobovits, E. B. & Aloni, Y. *Virology* (in the press).
31. Dubochet, J., Ducommon, M., Zollinger, M. & Kellenberger, E. *J. ultrastruct. Res.* **35**, 147–167 (1971).

Decreased rate of DNA-chain growth in human basal cell carcinoma

M. Heenen & P. Galand*

Biology Unit, Institute of Interdisciplinary Research and Department of Dermatology, School of Medicine, Free University of Brussels, 2 rue Evers, 1000 Brussels, Belgium

The DNA synthetic (S) phase of cell division is about twice as long in human basal cell carcinoma (BCC) as in the normal epidermis and several non-malignant skin diseases[1-3]. A similar increase in S phase duration seems to occur in tumours of the human oesophagus[4], larynx[4] and recto-colon[5,6]. At the molecular level, the overall rate of replication in a nucleus is determined by two factors—the frequency of initiation of replication and the rate of replication fork progression along the units of replication (for review see refs 7,8). Here we present evidence (based on DNA fibre autoradiography[9-11]) that the observed increase in S phase duration may be due to a marked reduction in the rate of DNA replication along replication units, the density of simultaneously operating replication units remaining unchanged. This indicates an alteration in some biological component(s) of DNA synthesis in BCC that is of potential interest for characterizing the malignant transformation of the epidermal cell and that may perhaps be exploited therapeutically.

We used biopsy samples from five normal subjects and three patients with basal cell carcinoma, small undifferentiated tumours with a multinodular structure (nodules 50–200 cells in diameter). The tissue samples were divided into lamellae about 1 mm thick, and labelled *in vitro* with a single specific activity of ³H-thymidine. We used a previously described DNA fibre autoradiography[9-11] with pulse periods of 30 and 60 min (see Fig. 1 legend). This provides valid estimates of relative rates of DNA synthesis only, based on the length of grain tracks in the fibre autoradiograph[7,12,13]. Similarly, in these conditions, centre-to-centre distances between adjacent tracks reflect the relative density of replicating units, rather than the absolute value[7,14].

Figure 1 summarizes the results by showing the distribution histograms of grain track lengths and centre-to-centre distances for pooled data from each tissue type. Cumulated frequency curves drawn for the two parameters allow estimation of their median value. The median track length thus obtained after the 30-min and the 60-min labelling period, respectively, were

* To whom correspondence should be addressed.

Grain track lengths   Centre-centre distances
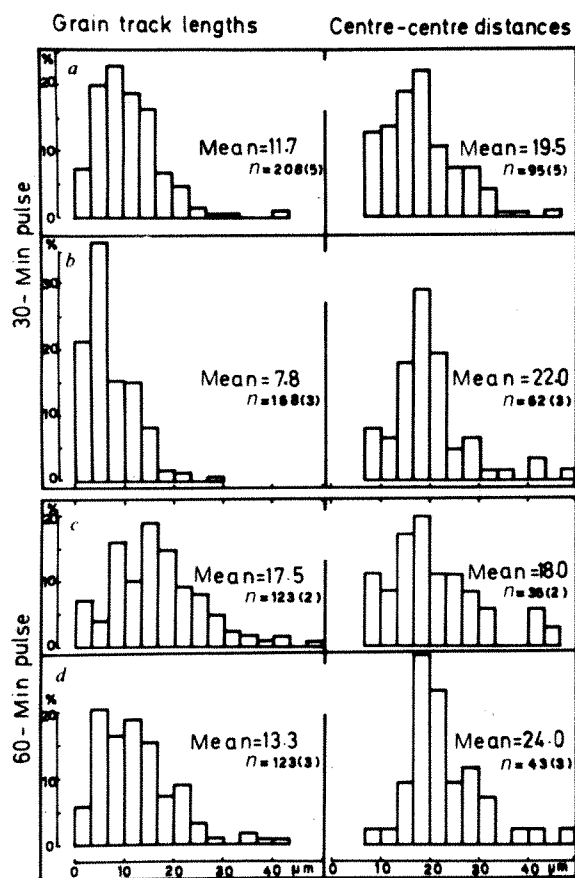
Fig. 1 Length and distance between centres of ³H-thymidine-labelled segments in DNA molecules isolated from normal cells and from basal cell carcinoma (BCC) of the human epidermis. Biopsy samples taken from the number of patients indicated in parentheses (informed consent was received from the patients) were divided into lamellae about 1 mm thick and prein-cubated in Eagle's basal minimal essential-diploid medium with 2×10^{-6}M 5-fluorodeoxyuridine (FUdR) to exhaust the endogenous thymidine nucleotide pool[25]. The tissue fragments were then incubated with 5×10^{-6} M ³H-thymidine (specific activity 40 Ci mmol⁻¹), FUdR remaining in the medium. After further incubation for 30 or 60 min, the tissue samples were rinsed and incubated at 37 °C for 30 min with 1% trypsin-0.3% dithio-erythritol (Sigma) dissolved in phosphate buffer, pH 7.8 to separate the epidermis from the dermis[26]. The process was furthered by a 10-s ultrasonic vibration at about 100 W using a Braunsonic 300 S apparatus (VWR Scientific). The dermis was removed by filtration through gauze, and the epithelial cells were further dissociated by another 10-s ultrasonic vibration (as above) (detachment of the dermis was assessed by microscopic examina-tion of histological preparations prepared at this stage). DNA fibre smears were then prepared as described by Lark et al.[27]. The smears (six slides per biopsy sample) were processed for autoradiography by dipping in K5-emulsion (Ilford) diluted at 50%. Exposure time was 45 days. Autoradio-graphs were developed for 2 min in Dektol (Kodak) and fixed. Grain track lengths and centre-to-centre distances were measured using a micrometric eyepiece and disregarding both end segments of tandem arrays on which measurements were effected. The results in each group were pooled ($n =$ total number of measurements obtained) and the mean is indicated. With both pulse durations the difference in the mean track length between BCC and normal epidermis was highly significant ($P < 0.001$, Wilcoxon's rank test), whereas there was no significant difference between distributions of centre-to-centre distances in any group and at any pulse duration. a, c, Normal epidermis; b, d, BCC.

10μm (range 8–12) and 17μm (range 15.3–17.3) for the normal epidermis and 6.3μm (range 5.2–6.7) and 12μm (range 9.7–12) for BCC. The higher track length measured in normal tissue does not seem attributable to a higher incidence of fusion between neighbouring units because the centre-to-centre dis-tance (1) was similar in both groups and (2) did not change significantly with labelling time. Also, few tracks were longer than twice the mean length, contrary to what would be expected if a high number of fused tracks were being registered[12]. Our data thus indicate that replication rate along DNA replication units is lower by a factor 1.5–1.6 in BCC than in the basal cells of the normal human epidermis.

To determine whether this might account for most of the relative lengthening (by a factor of about 1.8–1.9) of S phase duration in the cancer cells[1,2], it is necessary to consider what is known about the control of DNA replication during the S phase.

DNA replication in eukaryotic cells proceeds in a temporally and spatially regulated pattern, which seems species specific and preserved from generation to generation[7,8,11,15–18]. Coordina-tion of this programmed DNA synthesis implies that initiation is controlled by several sets of replication units sharing the same initiator (a protein, for example[18]) and/or a homologous recognition site[17,18]. It has been argued that the sequence of events that determines the duration of the S phase may cor-respond to the successive triggering of replication in sets (or 'banks') of replication units, by some event coupled to the synthesis of the preceding set in the sequence rather than by some external clock independent of DNA synthesis[19]. Accord-ing to such a model, a reduction in the rate of synthesis along replication units would result in a delayed initiation in the successive sets of units. This would result in an overall increase in S phase duration corresponding to the sum of as many delays as there are interdependent replication sets in the sequence.

For example, for an average centre-to-centre distance between tracks of 20 μm (our data), each replication fork must travel 10 μm to ensure fusion of adjacent units. A reduction by a factor of 1.5 in the rate of DNA synthesis in BCC would in that case extend the average replication time of synchronously replicating units by about 25 min (assuming a rate of fork progression of 0.2 μm min⁻¹ in the normal cell). If this were so, the observed 10-h increase in S phase duration in the tumour cells would imply that there is a sequence of 24 of the above considered sets of replication units (more, if the absolute rate of DNA synthesis in normal cells is slower), of which the initiation and the replication rate determine the S phase timing. The existence of sub-phases in S has been explicitly considered by several authors[20–22], but is difficult to prove because of the absence of markers for demarcating replication time zones[20].

However, other mechanisms, such as a change in the timing of DNA replication in a limited number of chromosomes or a difference in the process of chain termination[7,8], may also parti-cipate in the increase in S phase duration.

It is also possible that the phenomenon we have observed here is more pronounced in a particular sub-class of DNA (or of nuclei) that escaped detection. Indeed, our method probably leads to preferential scoring of the predominant class of DNA molecules present in the nucleus, and the most frequent nuclear type present in a given cell population. Again, based on higher nuclear fixation of ³H-actinomycin D in BCC (indicating a state of lower chromatin repression that would be consistent with the view that this tumour is derived from immature pluripoten-tial cells of the epidermis[23]), we previously considered[24] that an increase in the euchromatin–heterochromatin ratio might explain the longer S phase duration in the tumours.

At this stage we may only speculate on the molecular basis of the observed difference in the rates of elongation of DNA chains between normal and malignant epidermal cells. However, its potential importance for our understanding of cancer and as a possible rationale for chemotherapeutic investigation should prompt further study of this phenomenon.

1. Heenen, M., Achten, G. & Galand, P. *Cancer Res.* **33**, 123–127 (1973).
2. Heenen, M., Lambert, J. C., Achten, G. & Galand, P. *J. natn. Cancer Inst.* **54**, 825–827 (1975).
3. Frindel, E., Malaise, E. & Tubiana, M. *Cancer* **22**, 611–620 (1968).
4. Fabrikant, J. I. *Br. J. Cancer* **24**, 122–127 (1970).
5. Bleiberg, H. & Galand, P. *Cancer* **36**, 325–328 (1976).
6. Bleiberg, H., Salhadin, A. & Galand, P. *Cancer* **39**, 1190–1194 (1977).
7. Hand, R. in *Cell Biology: A Comprehensive Treatise* (eds Goldstein, L. & Prescott, D. M.) 389–431 (Academic, New York, 1979).

8. Shenin, R., Humbert, J. & Pearlman, R. E. A. *Rev. Biochem.* **47**, 277–316, 1978.
9. Cairns, J. *Cold Spring Harb. Symp. quant. Biol.* **28**, 43–46 (1963).
10. Cairns, J. *J. molec. Biol.* **15**, 372–373 (1966).
11. Huberman, J. A. & Riggs, A. D. *J. molec. Biol.* **32**, 327–341 (1968).
12. Callan, H. G. *Cold Spring Harb. Symp. quant. Biol.* **38**, 195–203 (1973).
13. Blumenthal, A. B., Kriegstein, H. J. & Hogness, D. S. *Cold Spring Harb. Symp. quant. Biol.* **38**, 205–223 (1973).
14. Leroy, F., Bogaert, C. & Van Hoeck, J. *Nature* **258**, 259–260 (1975).
15. Taylor, J. H. *J. biophys. biochem. Cytol.* **7**, 455–463 (1960).
16. Kowalski, J. & Cheevers, W. P. *J. molec. Biol.* **104**, 603–617 (1976).
17. Jansy, B. R. & Tamm, I. J. *Cell. Biol.* **81**, 692–697 (1979).
18. Hori, T-A. & Lark, K. G. *J. molec. Biol.* **77**, 391–404 (1973).
19. Hamlin, J. L. *Expl Cell Res.* **112**, 225–232 (1978).
20. Das. R. K. & Savage J. R. K. *Chromosoma* **67**,165–176 (1978).
21. Kapp, L. N. & Painter, R. B. *Expl Cell Res.* **107**, 429–431 (1977).
22. Funderud., S., Andreassen, R. & Hangli, F. *Nucleic Acids Res.* **6**, 1417–1431 (1979).
23. Pinkus, H. *Archs Derm.* **67**, 598–615 (1969).
24. Heenen, M., Preumont, A. M. & Galand, P. *Cancer Res.* **33**, 2624–2626 (1973).
25. Santi, D. V. & McHenry, C. S. *Proc. natn. Acad. Sci. U.S.A.* **69**, 1855–1860 (1972).
26. Bauer, F. W. & DeGrood, R. M. *Br. J. Derm.* **95**, 565–570 (1976).
27. Lark, K. G., Consigli, R. & Toliver, A. *J. molec. Biol.* **58**, 873–875 (1971).

Repeated folding pattern in copper–zinc superoxide dismutase

A. D. McLachlan

MRC Laboratory of Molecular Biology, Hills Road, Cambridge CB2 2QH, UK

Some globular proteins contain repeated structural patterns within the same polypeptide chain. Several enzymes[1–5] have a pseudo-symmetric two-lobed architecture: a pair of connected but well separated domains with very similar structures are grouped round an approximate 2-fold symmetry axis close to the active centre. On a smaller scale the same motif may appear inside a single protein domain: the polypeptide chain folds into two successive topologically similar subdomains which interlock symmetrically and form a compact globule[10–16]. In such a domain the two halves come into close contact round the dyad axis; as if the structural integrity of the domain depended on the interactions between its halves, while one separated subdomain could not exist as an independent folding unit. Many of these paired structures seem to have evolved from dimeric precursors by tandem gene duplication[17–19]. They contain repeated amino acid sequences or precisely repeated structural elements[3,6,13,20] in which equivalent sets of α-carbon atoms can be superimposed with root mean square deviations of the order of 1–2 Å. Here it is shown that copper–zinc superoxide dismutase[21–23] contains two paired subdomains, and the significance of the repeated folding pattern is discussed.

The copper–zinc superoxide dismutase from bovine erythrocytes has a structural core of eight antiparallel β-sheet strands which can be considered as either a flattened barrel[24,25] or a two-layered sandwich with four strands on each face (see Fig. 1A). The inter-strand connections are similar to those in the azurins[26,27] and the immunoglobin domain[28]; the β-sheet topology diagram[29] has a local dyad which relates strands d,e to g,h in the front face and c to f in the back face.

The topological dyad suggested that it might be possible to superpose the corresponding parts of the barrel. The shape comparison matrix method[10,30] was therefore used to compare every possible pair of α-carbon backbone segments which had a given fixed zone length. Segments were superposed by the rigid-body rotation and translation which minimized the sum of the mean square deviation distances.

Initial tests with zone lengths of 13,21 and 55 residues showed a local dyad on the back face relating strands b and c to e and f, with a further short repeat in the front face which related Gln 47 on strand d to Glu 119 on strand g. Further trials with α-carbon distance plots for the superposed parts revealed an extensive but interrupted structural repeat round the active centre (Fig. 1B). Here there are two long loops which extend between strands d and e on one side and between g and h on the other. When the central strands d and g which are related by the topological dyad

Table 1 Repeated structure in Cu-Zn superoxide dismutase

Atoms fitted	Results
Superoxide dismutase Cu—Zn face (d-loop-e to g-loop-h)	
37 = 109	28 atom pairs
39–51 = 111–123	R.m.s. deviation 1.58Å
53 = 125	Max. deviation 2.99Å
56–61 = 135–140	Rotation angle 177.9°
80–86 = 142–148	Shift along axis 0.32 Å
	Axis (0.984, −0.053, 0.173)
Superoxide dismutase back face (b-c to e-f)	
14–22 = 81–89	18 atom pairs
27–35 = 91–99	R.m.s. deviation 2.07 Å
	Max. deviation 3.31 Å
	Rotation angle 172.9°
	Shift along axis 0.71 Å
	Axis (0.810, −0.043, 0.584)
Both faces (c, d-loop-e) to (f, g-loop-h)	
27–35 = 91–99	37 atom pairs
37 = 109	R.m.s. deviation 3.17 Å
39–51 = 111–123	Max. deviation 5.07 Å
53 = 125	Rotation angle 177.3°
56–61 = 135–140	Shift along axis 0.28 Å
80–86 = 142–148	Axis (0.964,−0.019, 0.264)

The angles between the first two rotation axes and the third are 5.7° and 20.5°; between the first and the second, 25.8°. The Cu^{2+} ion lies within 2.1 Å of the screw axis through the Cu-Zn face. Note that although strand e is matched to strand h in the first fit and to strand b in the second, it cannot reasonably have an evolutionary relationship to both. The third fit suggests that e is related to h rather than to b. Another way of fitting both faces is to split strand e so that the first half matches half of b and the second matches half of h. The r.m.s. deviation is then considerably higher at 3.72 Å.

were superimposed large parts of the surrounding loops and strands e and h also fitted one another (Fig. 2 and Table 1) so that the front face has a high degree of spatial symmetry. In these superposition experiments no account had been taken of the active site metal ions, but the copper ion was now found to lie within 2.1 Å of the dyad axis and two of its histidine ligands, His 46 and His 118, lay in symmetrically equivalent positions. The zinc ion and its ligands lie to one side of the front face, enveloped by an irregular outlying loop (residues 62–79) which has no
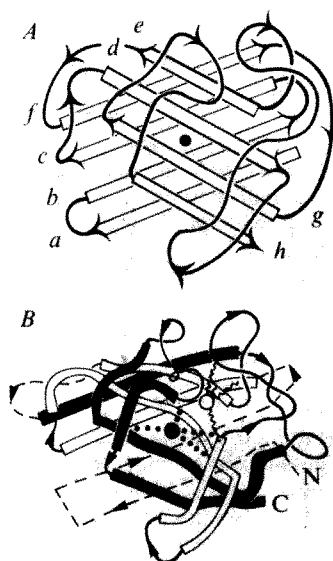
Fig. 1 β-Sheet topology. A, Connections between eight strands a–h showing front active centre face d, e, g, h with copper ion in front centre and strands a, b, c, f of back face. B, Strands c–g and loops round active centre to show the symmetry. Black and white strands are related by local dyad centred about copper ion. The open circle off-centre represents a zinc ion.
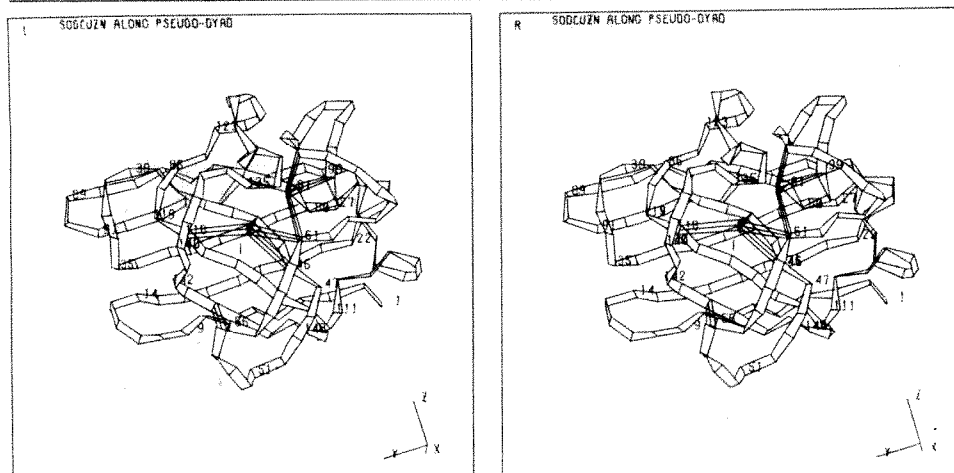
Fig. 2 Active centre face of superoxide dismutase viewed along pseudo-dyad axis (central bar). Copper ion near dyad and zinc ion to upper right are joined to ligands by triple lines. Triple line to lower left is disulphide bridge Cys 55–Cys 142. Structure repeated across pseudo-dyad includes inner floor of β-sheet 37–46, corner 47, outer cross-strand 47–51, return cross-strand 56–61 and outer floor 80–86. Back face dyad relates 27–35 to 91–99 at upper rear. Copper ligands are His46, His 118, His 44, His 61. Zinc ligands are His 61, His 69, His 78, Asp 81.

partner across the dyad and rests against an extension of the opposite loop, residues 124–134. The local pseudo-dyad in the back face centred about strands *c* and *f* does not lie along the same line as the front dyad (see Fig. 2) and the two layers of β-sheet do not fit well to a single axis (see the third fit in Table 1).

A comparison of the amino acid sequences of the structurally equivalent regions[31] also shows that the tripeptide Val-His-Gln at positions 45–47 is almost repeated across the dyad as Val-His-Glu at positions 117–119. The histidines are copper ligands, both valines are buried in the core of the barrel, while the glutamine and glutamic acid residues lie at sharp corners where the β-sheet leads into a cross-strand. There are no other sequence repeats associated with the repeated structure, although a few isolated equivalent residues match: Asp 50, Thr 56, Gly 83 to Asp 122, Thr 135, Gly 145 in the front face; Val 27, Ile 33 to Val 92, Ile 97 in the back face.

These comparisons show that the active site face of superoxide dismutase is formed by two similar paired subdomains which interlock symmetrically and enclose the catalytically essential copper ion at the centre of a shallow pit between two matching curved loops of irregular β-structure. Two of the histidine ligands occupy structurally equivalent positions in a repeated tripeptide near the dyad and 28 α-carbon atoms from each subdomain match within a root mean square distance of 1.58 Å. Approximately 14 of the related atom pairs lie in hydrogen-bonded regions of the β-sheet strands, but 14 others belong to the irregular encircling loops.

Since there is no internal homology in the amino acid sequence and only a limited structural regularity in the back face of the enzyme, all these repeated features associated with the active site might be the result of convergent evolution. However, the structural similarity between the dyad-related α-carbon backbones of the half-domains is relatively precise and compares favourably with the repeats in parvalbumin[13,20] or pepsin[14,15]. All the features may then be relics of a very early gene duplication and the enzyme could have evolved in the following way. (1) It began as a symmetrical dimer with an exact dyad axis, formed of two three-stranded β-sheet subdomains *c*, *d*, *e* and *f*, *g*, *h* which included the long *d*, *e* and *g*, *h* enveloping loops—compare the third fit in Table 1. (2) A copper ion was bound on the dyad to histidines 46 and 118, forming a primitive active site between the subunits. (3) A gene duplication united the halves of the dimer. (4) At some later time β-sheet strands *a*, *b* were added, completing the barrel and shifting the centre of the back face. (5) A zinc binding site developed at one side of the copper centre and the enveloping loops expanded between residues 61–80 and 123–135.

Although the structural evidence for this sequence of events is indirect every step has parallels in steps which have been proposed for the evolution of other symmetrical enzyme structures[1,3,5]. The scheme would be consistent with the observation that the copper ion is essential for catalytic activity, while the zinc is not[32] and can be replaced by other metals.

Richardson *et al.*[28] have pointed out a very interesting structural parallelism between the β-sheet barrels of superoxide dismutase and the immunoglobin domains, which can be superposed with considerable precision. The immunoglobins also have internal pseudo-dyad repeats (to be described elsewhere) which are considerably more regular than those in superoxide dismutase. Surprisingly the dyads do not match when the two proteins are superimposed. In superoxide dismutase the dyad passes between residues His 44 and Val 116 which lie on the outer surface of the Cu-Zn face. These correspond respectively to Tyr 42 and His 93 in the V_L domain[28] of McPC603. The dyad also passes between Gly 31 and Val 95 on the back face, which align with Met 21 and Leu 79 in V_L. But the best dyad for the immunoglobin is displaced by one residue, passing between Trp 41 and Cys 94 on one face and between Ser 22 and Thr 78 on the other. This observation shows that it would be inconsistent to assume simultaneously that the two proteins have an evolutionary relationship and that both dyads also arose by gene duplication. Instead it seems probable that both barrels are independent realisations of a very restricted number[33] of allowed β-sheet topologies.

I thank Dr Jane Richardson for helpful discussions.

1. Ploegman J. H. *et al. Nature* **273**, 124–129 (1978).
2. Anderson, C. M., Stenkamp, R. E. & Steitz, T. A. *J. molec. Biol.* **123**, 15–33 (1978).
3. Rossmann, M. G. & Argos, P. *J. molec. Biol.* **109**, 99–129 (1977).
4. McLachlan, A. D. *Eur. J. Biochem.* **100**, 181–187 (1979).
5. Tang, J., James, M. N. G., Hsu, I. N., Jenkins, J. A. & Blundell, T. L. *Nature* **271**, 618–621 (1978).
6. Rossmann, M. G., Moras, D. & Olsen, K. W. *Nature* **250**, 194–199 (1974).
7. Quiocho, F. A., Gilliland, G. L. & Phillips, G. N. *J. biol. Chem.* **252**, 5142–5149 (1977).
8. Schulz, G. E., Schirmer, R. H., Sachsenheimer, W. & Pai, E. F. *Nature* **273**, 120–124 (1978).
9. Birktoft, J. J. & Blow, D. M. *J. molec. Biol.* **68**, 187–240 (1972).
10. McLachlan, A. D. *J. molec. Biol.* **128**, 49–79 (1979).
11. Watenpaugh, K. D., Sieker, L. C., Herriott, J. R. & Jensen, L. H. *Acta crystallogr.* **B29**, 943–956 (1973).
12. Rossmann, M. G. & Argos, P. *J. molec. Biol.* **105**, 75–96 (1976).
13. Kretsinger, R. H. & Nockolds, C. E. *J. biol. Chem.* **248**, 3313–3326 (1973).
14. Andreeva, N. S. & Gutschina, A. E. *Biochem. biophys. Res. Commun.* **87**, 32–42 (1979).
15. Blundell, T. L., Sewell, B. T. & McLachlan, A. D. *Biochim. biophys. Acta* **580**, 24–31 (1979).
16. Blundell, T. L. *et al. Acta crystallogr. Suppl. B* (in the press).
17. Dixon, G. H. *Essays Biochem.* **2**, 147–204 (1966).
18. Weeds, A. G. & McLachlan, A. D. *Nature* **252**, 646–649 (1974).
19. McLachlan, A. D. *Nature new Biol.* **240**, 83–85 (1972).
20. Hendrickson, W. A. & Ward, K. B. *J. biol. Chem.* **252**, 3012–3018 (1977).
21. Richardson, J. S., Thomas, K. A., Rubin, B. H. & Richardson, D. C. *Proc. natn. Acad. Sci. U.S.A.* **72**, 1349–1353 (1975).
22. Richardson, J. S., Thomas, K. A. & Richardson, D. C. *Biochem. biophys. Res. Commun.* **63**, 986–992 (1975).
23. Beem, K. M., Rich, W. E. & Rajagopalan, K. V. *J. biol. Chem.* **249**, 7298–7305 (1974).
24. Levitt, M. & Chothia, C. *Nature* **261**, 552–558 (1976).
25. Richardson, J. S. *Nature* **268**, 495–500 (1977).
26. Adman, E. T., Stenkamp, R. E., Sieker, L. C. & Jensen, L. H. *J. molec. Biol.* **123**, 35–47 (1978).
27. Colman, P. M. *et al. Nature* **272**, 319–323 (1978).
28. Richardson, J. S., Richardson, D. C., Thomas, K. A., Silverton, E. W. & Davies, D. R. *J. molec. Biol.* **102**, 221–235 (1976).
29. Schulz, G. E. & Schirmer, R. H. *Nature* **250**, 142–164 (1974).
30. Remington, S. J. & Matthews, B. W. *Proc. natn. Acad. Sci. U.S.A.* **75**, 2180–2184 (1978).
31. Steinman, H. M., Naik, V. R., Abernethy, J. L. & Hill, R. L. *J. biol. Chem.* **249**, 7326–7338 (1974).
32. Beem, K. M., Richardson, D. C. & Rajagopalan, K. V. *Biochemistry* **16**, 1930–1966 (1977).
33. Ptitsyn, O. B., Finkelstein, A. V. & Falk, P. *FEBS Lett.* **101**, 1–5 (1979).

BOOK REVIEWS

Worlds in collision

William M. Kaula

FOR about 20 years now, A.E. Ringwood has been the most vigorous propounder of theories in two areas: the state and evolution of the Earth's mantle, and the origin of the Earth and Moon. The book reviewed here is an exposition of his ideas on the second topic. Another, heftier book of Ringwood's, *Composition and Petrology of the Earth's Mantle* (McGraw-Hill: New York, 1975) deals with the first topic; the contents thereof are recapitulated in the first two chapters of *Origin of the Earth and Moon*.

Ringwood's scenario of Earth and Moon formation is the most complete extant, which makes it a convenient entity to quote, amend or attack. This ˉrelative completeness results not only from Ringwood's energy and breadth, but also from two other factors: firstly, the explanation of as many features as possible by processes in the interiors of the Earth or Moon, the regimes with which Ringwood is most familiar; and secondly, a strong philosophical drive to adopt the simplest of hypotheses wherever possible. Baldly, the essence of Ringwood's current scenario is:

(1) The Earth, like the other terrestrial planets, formed from solid matter which had condensed in the cooling solar nebula.

(2) This solid matter came to the Earth in the form of planetesimals, the composition of which evolved moderately so that their total bulk composition is 85% a component "A" of metals and silicates condensing at temperatures above ᴧ1200°C and 15% a component "B" — "A" plus volatiles — principally alkali oxides, water, organics and sulphur compounds.

(3) Most of the volatiles were lost at planetesimal impact by being blown off by hydrogen liberated upon the interaction of iron and water.

(4) The iron core of the Earth formed early by the sinking of metal accumulations too large to attain chemical equilibrium with their silicate surroundings. One consequence was that appreciable traces of oxidized siderophiles (Ni, Co etc.) remained in the mantle.

(5) When core formation was essentially completed, a large body hit the Earth, vaporizing a lot of mantle material.

(6) An appreciable fraction of this

Origin of the Earth and Moon. By A.E. Ringwood. Pp.295. (Springer: Berlin, Heidelberg and New York, 1979.) DM45, $24.80.

material was lifted into geocentric orbit, primarily by the energy of the impact, but possibly helped by interaction of ionized material with the early geomagnetic field.

(7) The refractory component of this cloud condensed, and accreted together to form the Moon.

Most of Ringwood's text is devoted to the geochemical (primary) and cosmochemical (secondary) considerations which lead him to this chain of hypotheses: such matters as the compositional differences of the Earth and chondritic meteorites; the lighter element admixed with iron to account for the core density; the reasons for chemical disequilibrium in the Earth; accounting for density differences among the terrestrial planets; the trace elements in lunar rocks compared to terrestrial rocks and meteorites; etc. He does not attempt to develop detailed physical models of the stages outlined above (anyone who does so conscientiously will have many years of work before he can write a book). Nonetheless, Ringwood's ideas are congenial to planetary physicists and dynamicists whose minds are unable to span the dizzying leap, from the nebula dust to the present bodies, required by those who hypothesize that compositional differences among planets arose from the same processes as compositional differences among meteorites.

The key evidence pertinent to lunar origin emphasized by Ringwood is the similarity of abundances of unvolatile siderophiles between the Moon and the Earth — with one exception (always exceptions in this game) within a factor of two among the elements examined. In contrast, there are appreciable depletions of more volatile siderophiles in the Moon compared to the Earth. These unvolatile siderophile abundances are much less than in chondritic meteorites, but much more than would occur in rocks crystallizing in equilibrium with metallic iron (which one category of differentiated meteorites, the eucrites, are believed to demonstrate). The great deficiency of iron in the Moon

required by its low mean density and absence of volatiles indicates prior planetary differentiation. Primordial isotope ratios, as well as dynamical feasibility, indicate that this differentiation was either in the Earth, or in other bodies at about the same distance from the Sun. The complete absence of any evidence of these other bodies in the meteorite population is the strongest argument in favour of the Earth for the locus of the differentiation.

The persuasive (although not overwhelming) lunar siderophile evidence comes from examination of low-titanium mare basalts, which are thought to be the consequence of rather high percentage partial melts deep within the Moon. More recently, Ringwood and collaborator John Delano have presented evidence of indigenous siderophiles in lunar highland rocks and soils, an exercise requiring subtraction of a considerable meteoritic contamination, explanation of enrichment of the more volatile elements by "impact mobilization", etc. Here, Ringwood's drive to marshal all possible evidence in favour of a simple synthesizing hypothesis has again put him on the minority side of a rather technical debate. He was also, for example, about the last prominent petrologist to abandon the hypothesis that mare basalts were drawn entirely from source materials identical in composition with the bulk of the Moon.

Nonetheless, Ringwood's synthesizing drive, plus his physical intuition and sense of the issues, make this book the best introduction available to the main scientific debate generated by the Apollo project data, as well as a good target for his colleagues to snipe at. The reader coming from another scientific field will probably find much of the reasoning casual or *ad hoc*, the variety of data presented bewildering and the tone more one of strident advocacy than calm objectivity. These properties are not peculiar to Ringwood, but are rather characteristic of the field: strong intuitive biases are necessary to get anything done, and not be paralysed by indecision. The time for a Euclid is still far off. Meanwhile, a good book with much food for thought. □

William M. Kaula is Professor of Geophysics at the University of California, Los Angeles.

Of mercury and man

Roy Harrison

The Biogeochemistry of Mercury in the Environment. Edited by J.O. Nriagu. Pp.696. (Elsevier/North-Holland: Amsterdam, Oxford and New York, 1979.) $136.50, Dfl.280.

THERE are few toxic substances with a history as long as that of mercury. The metal has been known and used for at least 3,500 years and still finds wide application today. There are documented instances of inorganic mercury poisoning dating back 500 years, and alkylmercury poisoning has been known for over 100 years. Yet mercury still provides surprises. Although the first cases of Minamata disease occurred in 1953, it was not until 1959 that alkylmercury poisoning was identified as the cause with any degree of certainty. Until that time, although occupational alkylmercury poisoning was known, the possibility of poisoning of the population by environmental exposure, in this case by

consumption of fish which had absorbed alkylmercury from the effluent of a local chemical works, had not been suspected. It was not known that fish could concentrate alkylmercury from water, nor was it discovered until later that alkylation of inorganic mercury in aquatic sediments was possible.

Minamata and other incidents of mercury poisoning have stimulated more interest in mercury as a pollutant than in any other toxic agent with the possible exception of lead. Biogeochemistry, a new term to me, apparently embraces "the chemical behaviour and biological effects of mercury in the biosphere, geosphere and hydrosphere". In Nriagu's own words, it provides "the logical conceptual framework for looking holistically at the mercury cycle and the human impact upon it". These are grand ideas and to a large measure the book lives up to them. The coverage is extremely broad, including the production, uses and control of mercury, the environmental chemistry and biological effects of the metal in terms of occupational and environmental human exposure, and the effects on aquatic and

terrestrial organisms. It includes detailed analyses of the outbreaks of organomercury poisoning at Minamata and Niigata in Japan (both due to consumption of contaminated fish) and in Iraq (due to the consumption of grain seed treated with mercurial fungicides).

The book contains 24 chapters, each written by specialists in a particular area. The result is quite impressive; there is a wealth of information which should satisfy most workers in this field, with relatively little overlap between contributions. Each chapter contains a large bibliography which is in most instances fairly up to date (references up to 1978 are included). As with much review material nowadays there is rarely any attempt at critical analysis, some chapters being little more than a listing of relevant work. That criticism aside, this book represents a valuable contribution for which many workers in this broad transdisciplinary field will be grateful. □

Roy Harrison is a Lecturer in the Department of Environmental Sciences, University of Lancaster, UK.

Keeping up in physics

W. Cochran

A Perspective of Physics. Volume 3. Introduction by Sir Harrie Massey. Pp. 360. (Gordon and Breach: New York and London, 1979.) $35.50.

IN 1695 delegates from the four Scottish Universities met as a Commission "to consider methods of instruction in philosophy". Their comments on draft reports covering various parts of the subject have been preserved, and we read for instance that "One part of the delegates are of opinion that Newton's hypothesis of the ebbing and flowing of the sea should be insert, or a reason given why it is not; and the other part think that there is no need to make any mention of it. The author gives this reason why he omitted it — because neither he nor any he has conversed with on the subject do so fully understand what Newton does write thereon as they can make it intelligible to young students". Any university teacher of physics who smiles at this in 1980 should do so wryly, for we have by no means solved by specialization that problem of keeping up to date with the advances made in our subject.

Volume 3 of *A Perspective of Physics* contains a selection of the articles which appeared in *Comments on Modern Physics* during 1978. This series appears in five sections, Nuclear and Particle Physics, Solid State Physics, Astrophysics, Atomic

and Molecular Physics, and Plasma Physics. In 1978 about 100 short review articles appeared under one or other of these headings, and of these 29 are reproduced in the volume under review. The emphasis is on brevity; a typical article is 3000–4000 words in length, with 20–30 references. Topics range from "Charge Density Maps in Chemisorption" to "New Quarks and Old Ones Too", and Sir Harrie Massey is remarkably successful in putting the articles into perspective in his introduction. I must admit, however, that

while I shall continue to read *Comments on Solid State Physics* as it appears, personally I find most other reviews in this series too terse and too specialist-directed when compared with those in, for example, *Physics Today.* We are better placed than our predecessors were three centuries ago, but there will never be an easy solution to the problem of understanding advances in physics. □

W. Cochran is Professor of Natural Philosophy at the University of Edinburgh, UK.

A vitamin D encyclopaedia

D.R. Fraser

Vitamin D. The Calcium Homeostatic Steroid Hormone. By A.W. Norman. Pp.496. (Academic: New York and London, 1979.) $48, £27.

KNOWLEDGE about vitamin D, we are told, falls into eras. There was the era of ignorance before 1920, then the era of vitamin D chemistry and nutrition, followed by the 15–20-year era of vitamin D metabolism. We are now it seems in the era of vitamin D reviews, with recent books entitled *Vitamin D* being produced by D.E.M. Lawson (Academic: New York and London, 1978), H.F. DeLuca (Springer: Heidelberg and New York, 1979) and this one by A.W. Norman, plus a myriad of review articles throughout the biological literature. Truly

the subject is well publicized.

One must admire the energy and enthusiasm resulting in this latest account. The work aims and succeeds at being comprehensive. There are detailed descriptions of the chemistry, metabolism and function of vitamin D, with chapters reviewing the historical development of the topic and the medical relevance of the new knowledge. All this is supported by an extensive bibliography, the dates in which indicate a minimum delay in the publication process. It is an admirable book of reference on all aspects of the biology of vitamin D.

On the other hand it is also the vitamin D gospel very much according to Norman, and hence tends to be a catalogue of the notable achievements of the author and his colleagues. But in a curious way an opportunity has been missed here to give a lead in unravelling the complexities of vitamin D function. Rarely does the author allow his own insight to throw new light on this problem. Yet the mysteries of the mechanism of action of vitamin D are now more amen-

able to attack by imaginative intellect than they ever were in the experiments of the past.

Obviously with just one author, the significance of each finding receives very personal assessment. One might wish that more emphasis had been placed on the discovery of the 25-hydroxylation reaction which was the key finding in the identification of functional vitamin D metabolism. There is also a pervasive, conscious attribution of discovery to discoverer to the point of obsession. After noting the seventeenth century descriptions of rickets by

Whistler and by Glisson, it was concluded "only fair and reasonable to give both authors credit for first priority". With the passage of time do scientists really care who did what first?

It is helpful to have the author's special knowledge of such topics as the relationship between structure and biological activity of vitamin D and the use of filipin in studies on calcium transport. It is possible to ignore the smattering of errors which mar the text but perhaps it would be wise to correct the bizarre footnote on

aflatoxin (p.446) in any subsequent edition. There are many attractive figures and tables to illustrate the work; in some of these their artistry exceeds their comprehensibility (e.g. Fig. 6-22).

Using some of the author's favourite words, this book could be described as an exceedingly potent, dramatic, and unequivocally massive, herculean effort. It's also quite a good read. □

D.R. Fraser is at the MRC Dunn Nutritional Laboratory, University of Cambridge, UK.

Nodules in depth

Roger G. Burns

Manganese Nodules. By R. Sorem and R. Fewkes. Pp.723. (IFI/Plenum: New York and London, 1979.) £59.85.

MANGANESE nodules are intriguing marine deposits because contained in the very fine-grained matrix are accumulations of the strategic metals cobalt, nickel, copper, manganese and molybdenum. Understanding how these deep-sea ferro-manganese oxide concretions formed, and the processes by which the transition metals became enriched in the constituent manganese and iron oxide phases, requires access to very high resolution observational and analytical instrumentation. Sorem and Fewkes have catalogued data compiled at Washington State University during the past decade for several hundred marine manganese nodules using techniques of ore microscopy, X-ray diffraction, X-ray macroprobe and electron microprobe analyses. Almost half of their book consists of photographs of polished sections of manganese nodules collected from the Pacific Ocean as well as some specimens from the Atlantic and Indian Oceans. The remainder of the book documents data and describes methods used to study each of the nodules.

Five introductory chapters in Part 1 of the book (142 pages) provide detailed accounts of procedures to prepare polished mounts of manganese nodules and to photograph them in reflected light. Techniques are described for obtaining microsamples for mineral identification by X-ray diffraction, and analysing the nodules non-destructively by X-ray macroprobe and electron microprobe methods. Results of studies of internal textures, mineralogy and probe analyses of some of the nodules are given and attempts made to interpret the data. The text reads like a self-centred report to a funding agency; reference to pertinent work of other investigators is minimal.

The second part of the book (581 pages) is an encyclopaedia of data sheets and photomacrographs of almost 300 nodules

studied. The reflected light photographs of the polished sections are superb; they provide a plethora of information on the diverse internal structures and growth histories of the nodules. The data sheets painstakingly summarize the seafloor locations, physical properties and available laboratory data for each of the nodules. The features soon become repetitive, however, contradicting the authors' declared major purpose of the volume, which is "to provide the interested investigator with a factual record of the internal features of *typical* nodules".

Most of the information contained in the book is now well known to scientists studying manganese nodule geochemistry. One might question whether the frequency of occurrence of birnessite reported by the authors alone is an artifact of conditions (air drying; vacuum impregnation) used to prepare and mount their manganese nodule specimens. Current investigations indicate that delta-MnO_2 (vernadite) is as abundant as todorokite, the major host of nickel and copper, in Pacific nodules. Some of the observations and interpretations made by the authors have been superseded by results from more modern high-resolution techniques, including scanning electron microscopy and energy dispersive analysis, transmission electron microscopy and selected area diffraction, infrared and extended X-ray absorption fine structure spectroscopy. The authors do not refer to the wealth of information on synthetic mineral analogues and bacteriological studies relating to the stability and formation of manganese oxide phases hosting transition metals in manganese nodules, which drastically modify internal structures and microchemistries of manganese nodules.

The prohibitive price means that it is unlikely that individuals will buy this book. However, the magnificent photographs make the volume a showpiece for coffee tables and library display shelves. □

Roger G. Burns is Professor of Mineralogy and Geochemistry at Massachusetts Institute of Technology, and is currently a principal investigator in the Manganese Nodule Project funded by the International Decade of Oceanography Program of the National Science Foundation.

Two on physical and theoretical chemistry

J.S. Rowlinson

Statistical Thermodynamics of Simple Liquids and their Mixtures. By T. Boublik, I. Nezbeda and K. Hlavaty. Pp.145. (Elsevier: Amsterdam and New York, 1980.) $41.50, Dfl.85. *Weak Intermolecular Interactions in Chemistry and Biology.* By P. Hobza and R. Zahradnik. Pp.346. (Elsevier: Amsterdam and New York, 1980.) $48.75, Dfl.100.

THESE two monographs are the second and third in a series called "Studies in Physical and Theoretical Chemistry". Both are by Czech authors, and both are out-of-date, but there the resemblance ends. The book by Boublik and his colleagues is a compact and balanced account of the statistical mechanics of model liquids composed of spherical particles. There is a short chapter on integral equations for the molecular distribution functions and two long chapters on perturbation theory. The treatment is good on the mathematical details but cursory on the comparison of theory with the results of computer simulation, while real liquids receive but the barest mention. There are only two references later than 1974 (both Czech) and so the book is silent on the most rapidly growing part of the field in the last ten years — the extension of theories to deal with non-spherical molecules. Within these limitations it can be recommended to those who want a clear account of the authors' chosen field, and are prepared to pay the stiff price.

Weak intermolecular interactions is, perhaps, a more challenging subject since so many techniques contribute to its study: spectroscopy of many different kinds, molecular beam scattering, thermodynamic and transport properties, quantum mechanics and both equilibrium and non-equilibrium statistical mechanics. It is challenge that this badly balanced

book quite fails to meet. It starts with a pedestrian but well-referenced chapter on quantal calculations, which omits the estimation of dispersion forces from transition moments, and overlooks the existence of multibody forces in condensed systems. It starts to go badly wrong when it gets to experimental methods and their interpretation. Inversion of macroscopic properties to give intermolecular potentials

is wrongly described as "rarely successful", electronic spectroscopy of dimers is dismissed in seven lines, and molecular beams in two pages. The section on the determination of intermolecular forces from viscosity is so misjudged that it quotes equations appropriate to the theory of the viscosity of liquids whilst only gases have been used for this purpose. The final chapter, "Applications", has some more

interesting pages but it is often uncritical and repetitious. Even the useful information in the book is difficult to find without an index of systems. This disappointing book can be recommended neither to chemists nor to biologists. □

J.S. Rowlinson is Dr Lee's Professor of Chemistry in the University of Oxford, UK.

Thirst work

M.J. McKinley
and J.F. Nelson

The Physiology of Thirst and Sodium Appetite. By J.T. Fitzsimons. Pp.572. (Cambridge University Press: Cambridge, UK, 1979.) £32.50.

RENEWED interest in the study of thirst mechanisms has resulted from the experimental contributions made over the past two decades by James Fitzsimons. The last major work on this subject, *Thirst* by A.V. Wolf (Charles C. Thomas: Springfield,

Illinois, 1958), appeared more than 20 years ago and, in view of the burgeoning experimental activity in this field since then, Fitzsimons' new book is a timely and comprehensive account of knowledge on thirst.

His book is the latest of the series of monographs published by the Physiological Society. Designed primarily for readers at the level of graduate student and above, it gives a lucid analysis of the causes of drinking, discusses the comparative physiology of drinking in vertebrates, dissects the effect of cellular and extracellular dehydration, and assesses the roles of hormones and the renin-angiotensin system on drinking behaviour. A survey of the pharmacology of drinking

and clinical aspects of thirst is included as well as a chapter on sodium appetite.

It is perhaps an unfortunate necessity that, as recognized by the author, the book is no more than an interim account. Thus few of the more than 700 references cited are to results published by others during the last three years. As a consequence, for example, the importance placed by him on the renin-angiotensin system as a stimulus to thirst would now be disputed by a number of other investigators in the field.

The chapter on sodium appetite has a number of deficiencies. This is primarily a consequence of defining sodium appetite as "an innate response to sodium deficiency, that causes animals to seek and ingest sodium salts", a restrictive definition. Thus evidence which demonstrates clearly that glucocorticoids stimulate sodium appetite has been overlooked. In fact the author claims that "glucocorticoids have little if any action on sodium appetite". It also appears to be inconsistent with such a definition that he recognizes that sodium appetite increases in both rats and rabbits during pregnancy and lactation where the changes are almost certainly due to alterations in hormone secretion and not to sodium deficiency.

The synthesis of the large salt appetite of pregnancy and lactation by appropriate sequential administration of physiological amounts of steroid and peptide hormones has been shown. The experiments closely parallel those on induction of maternal behaviour by similar hormone dosage. They hardly leave any conclusions on the role of these hormones as hazardous, as the author suggests, unless quite different criteria are applied to those advanced by him for a physiological role of angiotensin in thirst. Some minor inconsistencies and errors (e.g. p.100 lists plasma K of humans as 6.3mM) in the text were also noted.

Despite these limitations the book makes a very significant contribution to the dissemination of knowledge in this rapidly advancing area of physiology, and will no doubt become a standard reference work on thirst. □

Hagfishes and lampreys

Lis Olesen Larsen

Biology of the Cyclostomes. M.W. Hardisty. Pp.428. (Chapman and Hall: London, 1979.) £20.

THOSE who wish to elucidate the early stages of vertebrate phylogeny often examine only one, or at most two, cyclostome species. Further, such studies have too often been based on a few animals, badly described as to prehistory, stage of development, sex etc. This makes much of the ample literature on cyclostomes (hagfishes and lampreys) rather superficial. Professor Hardisty, however, has spent a lifetime in devoted study of many aspects of lamprey ecology, physiology and morphology. Recently retired, he has made in this book an impressive effort to summarize what is known about lampreys and hagfishes. His main intention is to discuss the early stages of vertebrate phylogeny by comparing all aspects of the two groups. His basic assumption is that although cyclostomes are no longer considered directly ancestral to the gnathostomes, they are more likely to have retained characters of "the unknown vertebrate ancestor" than other vertebrate groups.

Each chapter compares lampreys and hagfishes, and the topics range from palaeontology, ecology, physiology and

morphology, to biochemistry and molecular biology. In a final chapter Hardisty tries to draw conclusions about evolution on the basis of an integrated view of the life of hagfishes and lampreys. Thanks to his honest discussions, this chapter made it clear to me (but not to him) that his basic assumption is not necessarily true. The probability of finding primitive characters in present-day vertebrates may be equally large in any vertebrate group. In addition our hypotheses about evolutionary pathways are always marred by the difficulties in distinguishing between primitive and specialized characters, and in knowing when changes are adaptive (that is caused by natural selection) and when they occur by chance. The latter possibility is not seriously considered by Hardisty.

Throughout the book the author lists differences, between lampreys and hagfishes and between cyclostomes and gnathostomes, in attempts to establish how these three groups relate to one another. In order to obtain knowledge about the vertebrate ancestor(s!) it may be equally useful to look for similarities among these three groups, and between each of them and the various invertebrate and protochordate groups.

The book is recommended for all who want to study cyclostomes. They will find a useful, broad and detailed basis for their studies and an updated list of references. □

Lis Olesen Larsen is an Associate Professor at the Zoophysiological Laboratory, August Krogh Institute, University of Copenhagen, Denmark.

M.J. McKinley is a C.J. Martin Research Fellow and J.F. Nelson a Senior Research Officer of the National Health and Medical Research Council of Australia. Both are employed at the Howard Florey Institute of Experimental Physiology and Medicine, University of Melbourne, Victoria, Australia.

nature

29 May 1980

Watching other people's television

THAT nations, especially new nations, equate their independence with the existence of a national airline is well-known. A separate broadcasting service has more recently also come to seem a symbol of nationhood. It is not merely that heads of state, or their chief executives, consider themselves diminished and demeaned if they cannot from time to time address messages of some kind to their people. Nobody will deny the social and political value of a national television service, potentially at least, in helping to reinforce people's sense that they belong to the same country.

Unfortunately, however, the chauvinism that argues the benefits of national broadcasting services is all too often matched by a xenophobia that amounts to downright suspicion of other people's broadcasts. So much, for example, is apparent in North America, along the forty-ninth parallel — a circumstance that fortunately does not prevent privately-owned Canadian television networks from re-distributing signals picked up from across the border. Along the frontiers within Western Europe, indifference and polite curiosity are probably the hallmarks of people's regard for such neighbouring television transmissions as they can pick up. The frontier between East and West Germay is, on the other hand, much more powerfully charged with television xenophobia. Hitherto, however, sources of strife such as these have been relatively few and far between, largely because of the limited range of ground-based television transmissions. There is now a prospect that this will be changed with the arrival of the first direct-broadcasting satellites some time in the early 1980s.

Already, in Britain, Sir Harold Wilson, the ex-Prime Minister, has talked of the way that British cultural traditions may be undermined by television transmissions (accompanied by corresponding advertising material) from mainland Europe. Elsewhere, similar fears are matched by a sense of opportunity — or even by the hope of commercial profits from novel television channels carrying a mixture of news, entertainment and advertisements to very large numbers of people. Moreover, there is no reason to suppose that the plans which have been laid for the setting-up of direct-broadcasting services are in any way defective.

Geosynchronous satelites operating at centimetre wavelengths will be able to transmit signals powerful enough for television pictures with good definition to be received on individual parabolic dishes one metre or so across. Both in Canada and France, systems such as these are intended to provide cheaper and more effective means of broadcasting existing national services than can be had with the present cumbersome system of ground-based transmitters, land-lines and relay stations. So what are the international implications of these developments? And how valid is Sir Harold Wilson's concern?

First, it must be acknowledged that the system for regulating the use of direct-broadcasting satellites internationally is, bluntly, a muddle. By international consent, the regulatory body is the International Telecommunications Union, which was a great success in the first few decades of its history, when the problems were largely those of arranging that the same countries did not use the same frequencies for long-distance radio trasmissions, long or short-wave. Since then, unfortunately, demands on the electromagnetic spectrum have increased, while novel technical developments such as the direct-broadcasting satellite have failed to conform with the precedents for international compromise worked out in the early years.

Faced, two years ago, with conflicting requests for spaces for satellites along the geosynchronous orbit, the technical committees of the ITU for all practical purposes threw up their hands in despair and chose to allocate to each member state the equivalent of five channels of television broadcasting from geosynchronous orbit. Neither need nor the likelihood that the facilities thus made available would be used was part of the calculation. The result is that in some parts of the world (North America, for example) the would-be broadcasters are unduly contrained, while elsewhere opportunities are likely to be neglected for some time to come. Moreover, while the consents which have been made by the ITU are accompanied by technical definitions of the strength of the signals from broadcasting satellites, so that the footprints on the surface of the earth will be constrained, signals from orbit will inevitably spread further across national frontiers than signals from terrestrial transmitters.

So much is clear. Technically, the first broadcasting satellites could be in service as soon as 1983, both in Europe and North America. It is much less certain what uses will be made of the new technology, and whether the international consequences will be anything like as serious as some have suggested. The fear, for example, that broadcasting satellites might be used to flood various parts of the world with propaganda from another have been to a large extent undermined by the willingness of the member governments of the ITU to accept the technical restrictions put on the footprints from "their" satellites — and by the recognition that a whole population would have to find a way of concealing a metre-dish in every attic before propaganda satellites could be effective.

The more immediate international consequences of the new technology are likely to be in Western Europe, a region divided by its Common Market. Sir Harold Wilson's instincts are to that extent correct. At least in the short-term, however, his fears are misplaced. Britain is divided from the mainland not merely by the English Channel but by the technical specification of its television signals, and from both France and Germany by language. Much the same is true elsewhere in Europe — which is not universally a cause for self-congratulation. It follows that television signals from other people's satellites will be a serious cultural problem only if and when steps are taken to devise not merely their characteristics but their content so that they will compell and hold the attention of Europe's polyglot population.

This will be no light undertaking. One of the attractions of satellite broadcasting is its cheapness. A few tens of millions of dollars will put a satellite in orbit, while the cost of servicing it from the ground with signals is unlikely to be much greater over a period of five years, say. Television broadcasters are, however, these days painfully aware that the cost of burdening the signals their transmitters put out with a content that people want to look at is very much greater. Both in Switzerland and the Low Countries, there are still unformed plans for launching (in both senses of the word) such television services, using channels allotted by the ITU to governments that will, in all probability, be unused. Given that the success of ventures such as these will depend entirely on the skill with which the content of what is broadcast is devised, can anybody make a case that they should be crabbed? Would it not, rather, be more generous and far-sighted to agree that a successful international television service must be inherently desirable and that it should therefore be encouraged? The only basis for holding to a different view must be a conviction (for which there is no evidence) that all television is bad, so that more must be worse.

If the immediate consequences of television satellites are likely to be less serious than people have been suggesting, it does not unfortunately follow that nothing should be done. Nationally, governments will have to look to the arrangements they use at

present for controlling the content of national television broadcasting. Over the years, all liberal governments have laid down rules for guiding the operations of those with a licence to broadcast electromagnetic signals — and from time to time they have prosecuted those who have chosen to violate their airspace as if they were literally pirates. If international broadcasting proves financially feasible, governments will have to reconcile themselves to having less direct control. (They may even be faced with the prospect that national politicians denied the exposure they would like on their national network would go off and hire time elsewhere, a development that might serve to put political broadcasting in perspective.) But this is a prospect that must in any case be faced. Other technical developments, cable television

for example, are similarly a threat to the traditional paternalism of governments and their regulatory bodies.

It will also be necessary to look again at the mechanism by which the ITU sets out to allocate positions along the geosynchronous orbit. For more than the coming decade, and until still higher electromagnetic frequencies are useable, the geosynchronous orbit will be a scarce resource. It is absurd that it should be shared out like a pack of cards. Means of counting need in the calculations should urgently be sought. And some thought should be given to the use of satellites as a means of making television signals internationally accessible by individuals with the wish to enjoy this luxury (and the willingness to pay for it). Television as such is valuable.

Let Finniston cool his heels awhile

THE British Government is taking its time in responding to the report of the Finniston Committee on engineering education published last year (*Nature* **279**, 352; 1979), and with good reason. The Department of Industry is planning to make public some kind of an opinion late this summer, but the Department of Education and Science will still then be taking outside opinion. It is exceedingly unlikely that the government will have hit on a policy before this year is out. Others than the impatient members of the Finniston Committee, some of whom appear to have mistaken their report for the Mosaic Tablets, will welcome a breathing space before an important part of British higher education is thrown in the melting-pot.

British governments, like their taxpayers, have been worrying about engineering education ever since the end of the Second World War. At first, the chief concern was that universities were not producing enough graduate engineers to take their places alongside those trained in more traditional ways, essentially by apprenticeship. That defect has now been remedied and the annual output of graduate engineers (from polytechnics as well as universities) approaches 20,000. Concurrently, its traditional route has been closed. More recently, interest has centred on the character and even the quality of engineering education, provoked chiefly by the reflexion that the faults of British manufacturing industry must somehow be attributable to the engineering professors up and down the country.

Few would argue that British engineering education is blameless. It is, for example, difficult to understand how British universities are confident that three years of higher education will enable a man or woman to function as an engineer (albeit under the supervision for a time of one of the engineering institution) when most other educational systems consider three years insufficient. There is also ample if anecdotal evidence to suggest that British engineering education is too much dependent on lectures, too theoretical and too much detatched from the practical problems of practising engineers. Not even the Finniston Committee has thrown light on questions such as these, however. Although it is possible to understand why it concentrated instead on the problems of how best to enhance the public prestige and the self-esteem of the engineering profession, a valuable opportunity has thus been missed. And the engineering departments, conscious as many of them are of the need for qualitative change, have no solid foundation on which to base reform.

While the Finniston Committee was sitting the initiative was stolen by the University Grants Committee, which announced two years ago a scheme under which selected universities (seven in total) would be given extra resources in order to provide four-year engineering courses for more able students differing from those of conventional pattern in that their curriculum would be "enriched" with elements of management science, industrial

relations and the law. The UGC courses were also devised so that students would spend some of their time gaining first-hand experience of what was considered two years ago to be the sector of British industry most in need of improvement — manufacturing industry. A few years from now, when the first graduates of these courses are in jobs, it may be possible to tell whether the experiment has been successful, although the chances that an objective assessment will be possible are diminished by the lack of formal criteria by which that might be done.

On the engineering curriculum, the Finniston Committee accepted that the UGC's experiment should be the model for training the most able engineering students. To that extent, the experiment is an experiment no longer. The committee's chief educational concern was to ensure that there would be funds enough to support such courses (and the student following them) wherever in Britain engineering is taught. To this end, the committee asked that its proposed Engineering Board, whose function it would be to supervise professional standards, should also have at its disposal funds with which to supplement existing ways of chanelling public money to universities and students.

This proposal is beguiling but is also a trap. Naturally it has the appearance of virtue at a time when the belief persists that a *something,* almost anything, must be done. Understandably, engineering departments are also sympathetic to the notion that more funds should come their way. But changes of the kind proposed, while helping to change the education of engineers in a direction not yet proven, would certainly change the character of British universities in a way that cannot be welcome. In their essentials, these Finniston proposals are tantamount to asking that engineering departments in British universities should be dealt with differently — and more generously, than other departments, and that engineering students should often receive higher stipends. Little imagination is needed to guess how divisive these provisions would be. And there is no evidence that their promised benefits would materialise. It is no wonder that the government's response is hesitant.

Already there are signs that British universities are more jealous of their autonomy than they are skilled at exercising it. Will their interests in the long run be served if an important part of their contribution to the national interest is controlled and financed from outside? (Although there are similarities with medical education, Finniston's proposals for engineering education go much further than the General Medical Council would dare dream.) May it not be that the universities' best course of action, in this as in other matters, would be to carry out their own more constructive examination of the problem? Nobody would be surprised if it then turned out that what is wrong with British engineers is that industry makes too little use of them.

Risk assessment by numbers

Washington

Is comparative risk assessment an idea whose time has come? Or a political attempt to short-circuit necessarily complex sets of rule-making procedures?

The answer seems to be a bit of each. Professional scientific organisations such as the American Chemical Society are now pushing for comparative risk assessment as a way of rationalising government controls on technological activity, and Congress, responding to industry's demands to lighten the burden of controls, is looking at the type of legislative backing needed to increase its role in the regulatory apparatus.

Congressman Jim Ritter of Pennsylvania, for example, has introduced a Bill that would require the Office of Science and Technology Policy to set up a government-wide mechanism for assessing the comparative risks involved in actions in "scientific, technological and related fields".

The Carter Administration is reluctant to enforce centralised risk assessment as a federal policy. But individual agencies are already giving it increasing prominence within their administrative procedures, accepting that the absolute standards of zero-risk, popular with law-makers in the mid-1970s, may be neither practicable nor scientifically sound.

The push for comparative risk assessment is part of a general drive to restructure the regulatory process by separating the scientific judgment of whether a substance or process poses a health hazard from the administrative judgement of how this hazard, once characterised, should be dealt with.

Not all agree that such a separation is desirable. "The location of a centralised entity for performing comparative risk assessment within OSTP undermines the basic consideration that risk management decisions are social policy decisions which are based only partly on hard science", Dr Nicholas Ashford of the Massachusetts Institute of Technology told the House Science and Technology Committee two weeks ago.

Others, however, including the powerful National Association of Manufacturers, see it as an essential step towards rational regulation. "Before a regulator is faced with deciding how much the public needs to be protected from a substance, he or she should be supplied with an objective assessment of the degree of risk which the substance provides", Dr William J McCarville, Director of Environmental Affairs for Monsanto, told the same committee.

Prompted by such concerns, William Wampler, senior Republican member of the House Agriculture Committee, has introduced another Bill to set up a National

Science Council. This would also operate under the auspices of OSTP, and would be responsible for deciding questions of scientific fact arising from debates on the potential harmfulness of substances involved in food production, decisions which would be binding on all federal agencies.

A similar proposal is being canvassed by the American Industrial Health Council, a body of over 100 chemical companies and trade associations, which wants the National Academy of Sciences to set up a panel of eminent scientists to evaluate the qualitative and quantitative aspects of human chronic health risks associated with all forms of industrial activity.

Neither proposal has yet provoked much enthusiasm within the Administration. But on the question of comparative risk assessment, there is a greater consensus that this should play a more prominent role in decision-making — although reluctance to impose it in a too heavy-handed way, stressing instead the need to build up the research capabilities of the regulatory agencies.

OSTP officials point out that several moves have already been taken in this direction. Two years ago, for example, in issuing an executive order on regulatory reform, President Carter directed that analyses of the costs and benefits of proposed regulation should be prepared before the regulation was introduced.

Furthermore, procedures for standardising the scientific evaluation of hazards across the federal government are being developed by the Interagency Regulatory Liason Group which has already produced a uniform regulatory policy on carcinogens.

But there remains the problem that different agencies have had their legislative mandates written at different times and in different circumstances, giving rise to what OSTP Acting Associate Director Denis Prager describes as a "crucial and necessary" pattern of diversity and pluralism in dealing with technological risks.

The US Department of Agriculture, for example, must observe meat and poultry inspection acts which state unambiguously that no substance, whatever its benefits, may be added to either food if it poses any risk to human health.

Similarly, the Occupational Safety and Health Administration has no legal requirement to take factors other than the safety of workers into account in devising exposure levels to toxic substances (although this could change as the result of an imminent Supreme Court ruling on whether cost-benefit calculations should be taken into account).

Perhaps the greatest push for comparative risk assessment has come in the nuclear field, and in particular over

arguments that base their support for nuclear power on a direct comparison with the health and environmental risks from other energy sources.

At the Environmental Protection Agency, however, which perhaps more than any other agency has had to develop different risk assessment procedures for different types of hazards, there is doubt that comparative risk analysis can be tuned sufficiently finely to meet the needs of specific regulatory situations.

"A comparison of risks within a particular regulatory context may be a useful decision-making tool, and we at EPA are ready to use it as such", Dr Richard Dowd, Chairman of the Agency's Science Advisory board, told the Congressional committee, "but I question how useful it is to go beyond the context of one statute to several statutes, or from one risk situation to a different risk situation."

David Dickson

Research animals

Two bills too many

REGULATIONS to control the use of animals in scientific experiments in Britain are likely to change within the next year or two. Before it took office in April last year, the Conservative Party pledged itself to update the existing legislation, based on the Cruelty to Animals Act of 1876. At the end of last year, Mr Timothy Raison, Minister of State at the Home Office, reaffirmed that intention when he said that the government would like to base the new legislation on the European Convention on laboratory animals, now being drawn up in Strasbourg.

Home Office officials estimate that the European Convention will not be ready until April, 1981. This means that the new UK legislation proposed by the government could not be introduced until the middle of next year at the earliest. Not everyone is prepared to wait that long. Two individual members of parliament — Lord Halsbury and Mr Peter Fry — have prepared their own bills for consideration by the Houses of Lords and Commons respectively. Debates on both bills have been proceeding throughout this session of Parliament.

Lord Halsbury's bill is further than Mr Fry's in the parliamentary process. It received its second reading last October and has just been through several months of scrutiny by a House of Lords select committee. An amended version of the bill, based on the select committee's recommendations, was published last week.

Mr Fry's bill is currently embroiled in debate in a House of Commons standing committee. The committee has so far amended the first six and three quarters of the bill's 38 clauses. At the current rate of amendment the committee will be sitting until August 1982.

Parliamentary procedure, however, will not allow Mr Fry's bill to last that long. It was introduced as a private member's bill and, as such, has to be passed into legislation this session if at all. If it fails to complete the course by late summer, it will have to go back to compete with other private members' bills in the ballot box for the next session.

The Halsbury Bill seems the more likely of the two to survive the parliamentary hurdles. It is also more likely to have the support of the scientific community because it does not advocate prior judgement of the value of scientific research with animals. Its amended form acknowledges and builds on the Protection of Animals Act 1911 but would repeal the Cruelty to Animals Act 1876. The 1911 Act prohibits general cruelty to animals, such as kicking, beating or over-working, and deals specifically with laboratory animals.

In re-drafting Lord Halsbury's Bill, the House of Lords select committee has also produced a report summarising the evidence it has taken and the need for new legislation. The report, which was made available to *Nature* last week, butit is not yet publicly available, says that new legislation is needed because of the great increase in the number of animals used in laboratories over the past century and the greater variety of procedures, not in practice in 1876, to which they may be subject.

Lord Halsbury's Bill follows the 1876 Act in requiring all experimenters with animals to obtain a licence from the Home Office. However, it differs in demanding greater specification by those applying for a licence of the number and type of animals to be used and the procedures to be done on them. Applicants for licences would also be required to state the degree of pain or suffering likely to be experienced by the animal and the measures that would be taken for relieving it.

Lord Halsbury's Bill also incorporates the 'pain' and 'anaesthesia' conditions. These are that an animal that appears to be suffering severely under any procedure must be given immediate relief or be humanely killed, and that animals undergoing procedures which may be expected to cause severe pain or suffering must be properly anaesthetised before the procedure starts,be relieved of any pain afterwards or killed humanely. If this is not feasible it should be humanely killed. The 'pain' and 'anaesthesia' conditions are not written into the 1876 Act, though they have been effectively enforced by the Home Office cruelty to animals inspectorate.

Other points of difference between the 1876 Act and the Halsbury bill concern

● the nature of the sponsors. Both require applicants for licences to have two sponsors; the 1876 Act says that one must be a professor of biology, the other a president of a learned biological society; the Halsbury Bill says that the two sponsors must be chosen from a panel nominated by the Secretary of State.
● the term of licences. The Act allows licences to run indefinitely, the Halsbury Bill for only five years.
● the constitution of an advisory committee. The 1876 Act does not provide for an advisory committee on laboratory animals, although one has been in operation since 1906. The Halsbury Bill would incorporate the advisory committee in the legislation and would give it greater powers than at present. For example, the committee would be required to monitor the extent to which animals are used in painful or stressful procedures, review the possibility of alternatives, and inform the Secretary of State on public opinion. It would also have to consider ethical matters.
● the function of a code of practice. One does exist, although it is not written into the 1876 Act. The Halsbury Bill would incorporate it, increase its status to the equivalent of othe highway code in Britain. Although infringement of the code would not constitute an offence in itself, it could be used as evidence against someone suspected of malpractice.
● batch testing of sera and vaccines. This is not included under the 1876 Act but would be under the Halsbury Bill. Under this provision, the number of procedures notified to the Home Office and the number of licences would increase considerably. Although the idea behind the Halsbury Bill is to include procedures not covered at present, most survey, field, and school work would be exempt. For example, simple injecting of animals or ringing birds would not be included.
● species of animals covered. The 1876 Act covers all vertebrates; the Halsbury Bill would extend protection to chordates and embryos or larvae capable of independent existence.

The Halsbury Bill is also broader in scope than the existing legislation. But it does not specify detail, preferring to leave that to the secretary of state. For example, he would be able to extend the bill to include other species if he chose. He would also appoint the advisory committee.

The amended Halsbury Bill will go to a committee of the whole House of Lords on 20 June. Once it has been through the report stage, it can be presented to the Commons but it is unlikely that the Commons will consider it before next session. It could then be thrown back at the Lords. Although some believe that new legislation could be passed this year, others believe that the government is likely to stick to its plan of seeing the European Convention first.

Judy Redfearn

X-rays

Selling a new source

THE European Science Foundation — normally a quiet body conducting its catalytic business behind the closed doors of committee rooms — is supporting a proposal that Europe should spend £55 million on a new, 5 GeV super-bright European Synchroton Radiation Source (ESRS). Last week at Daresbury, UK, it tried to convince the British synchrotron users that it was right. The result was cautious approval.

Britons are probably the hardest to convince of the case. Their own dedicated source, the SRS, will start producing data at Daresbury later this year, and it will be well ahead of other European sources (*see figure*). Moreover their purse-holder, the Science Research Council, is committed to other large accelerator projects (the Nuclear Structure Facility at Daresbury and the Spallation Neutron Source at the Rutherford Laboratory) up to 1984. And the cash available to run the SRS will only be enough to operate half its beam ports.

The challenge, though, comes from the US. The £12 million National Synchrotron Light Source — a two-stage source under construction at Brookhaven Laboratory, Long Island — will come on line in July 1981 (0.7 GeV) and October 1981 (2.5 GeV). The second stage should exceed the brilliance of the 2 GeV, £5 millions SRS by a factor of ten — giving the SRS just a year as world leader.

So Yves Farge, chairman of the ESF *ad hoc* committee on synchrotron radiation and director of the DCI synchrotron radiation laboratory at Orsay, France, argued last week that Europe will need a more advanced source if it is not to be in the second league. Pressure is also high from countries without access to a national synchrotron source — particularly the Scandinavians, Belgium and The Netherlands — for a European facility to be built.

According to Farge, the Scandinavians — will make the construction of the ESRF a condition of their acceptance of LEP, the next high energy physics accelerator contemplated by the European centre for nuclear research (CERN). The Scandinavian view, says Farge, is that the ESRF should be constructed in the tunnel vacated when the CERN intersecting storage rings (ISR) are shut down as a preliminary to LEP.

Farge is unhappy about that approach, however. There are no biologists at CERN, and one of the attractions of synchrotron radiation is that it is a general tool of structural analysis useful to most disciplines. Biologists, however, would feel isolated at CERN. It would be better, he

feels, to choose a different site and set up a private association to which national research councils could contribute, avoiding the need for complex international agreements. (There is a similar foundation at the Institut Laue Langevin at Grenoble.)

There is also a rapidly increasing interest in synchrotron radiation in industry, Farge believes. DCI at Orsay profited from industrial participation by £5,000 in 1979, and the figure will be £20,000 this year. Oil companies appear to be interested in the routine use of the light to seek out significant trace elements in core samples for oil prospecting; the X-ray intensity available could give them a factor of 1,000 in speed.

However the ESRF itself is a long way from a final design. A sub-group of Farge's committee, headed by Dr D J Thompson of Daresbury, has prepared a preliminary study which defines a 5 GeV, 0.5 Amp, 604 m circumference ring with the brilliance function shown in the figure. Drs B Buras and G V Marr have also defined a shopping list of instrumentation. The machine and building plus half the instruments would cost £55 million at present prices, and could be constructed within 3 to 6 years.

But a new idea has occurred to the committee: that it be an "all-wiggler" machine, a design in which the experimental radiation is taken not from the main bending magnets of the ring, but

from multipole, high field magnets which introduce local high curvature wiggles in the beam path. This would enable the machine to use lower energy and beam current for the same radiation intensity. And the overall radius, as it happens, would be "just right" for the CERN ISR tunnel.

The uses of the ESRF radiation would stretch from molecular biology to nuclear physics, the meeting was told. Using 'undulators' — wigglers with 50-100 poles that produce coherent radiation — spectral brilliances up to seven orders of magnitude greater than those obtainable at DCI are conceivable. Such increases are very rare in science, said Farge, and the consequences are unpredictable.

However Daresbury's Dr Mike Hart, who took the role of the ESRF's chief bubble-burster, claimed one thing is predictable: that such an intensity of radiation from the undulator would destroy most samples. Quick calculations by Farge and Thompson led to estimates of 33-300 Watts onto the sample. "You'll have cooling problems," says Hart.

Probably the most exciting application of the high intensity, coherent light from an undulator would be to illuminate a zone plate X-ray microscope — one that depends on diffraction effects to produce focusing and de-focusing equivalent to the lenses of an ordinary light microscope. This application is limited by the fineness

with which zone plates can be drawn, but object resolutions of 100 Angstroms are foreseeable; and with a wavelength of 25 A, tuned to detect carbon but not oxygen, the prospect opens of following ultrastructural movements in live cells.

Nevertheless the ESF has not argued the case sufficiently for the ESRF as against existing synchrotron light sources, says Hart; 70% of the arguments used in the ESF document "the scientific case" for the ESRF apply to synchrotron radiation in general, and not to the ESRF in particular. The document will have to be rewritten in two years' time, Farge admits.

Robert Walgate

Four documents on the ESRF are available from the European Science Foundation, 1 quai Lezay-Marnesia, F-67000 Strasbourg, France: 'The Feasibility Study', 'The Scientific Case', 'The Machine', and 'Instrumentation'.

Training

Thoughts from the think tank

THE British government's own think tank, known as the Central Policy Review Staff (CPRS), published last week a mildly subversive prescription for making the products of the British educational system more suited to what is called "the world of work". The CPRS report ("Education, Training and Industrial Performance", HMSO, £4.25) gives no explanation of how it came to be published or even written.

Among the points at which the recommendations of the report may seem at odds with current government policy, the following are conspicuous:

• There should be formal standards and qualifications for skills acquired by means of vocational training.

• The government should continue to provide vocational training for young unskilled workers.

• More attention should be paid, especially in the age range 16-18, to the acquisition of practical skills, preferably in colleges of further education, not schools.

The CPRS does however accord with current government policy in its advocacy of a core curriculum (consisting of English, mathematics, science, a practical subject and "possibly" a foreign language) in the age range 11-16. The report also asks that the financing of further education by public loans should be reconsidered.

The CPRS is suitably modest in its acknowledgement of how little is known of the relationship between education training of any kind and the eventual benefits to employers and the national economy. There is no single issue on which a government initiative would, in the CPRS's judgment, make training radically more effective — and, even if there were, implementation would be hampered by the

WAVELENGTH (Å)
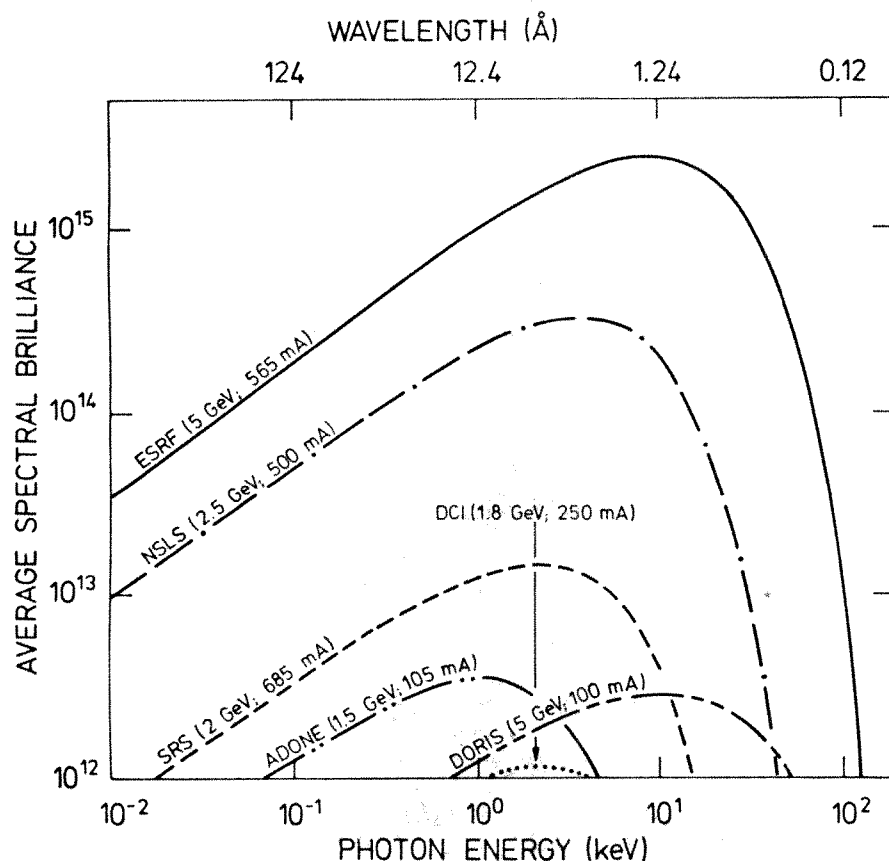
Spectral brilliance (in photons s⁻¹ mm⁻²mrad in 0.1% bandwidth) is compared for the proposed ESRF, the Brookhaven NSLS (ready October 1981), the Daresbury SRS (October 1980), and the Frascati ADONE, the Hamburg DORIS and the Orsay DCI (in operation).

decentralisation of the British educational system.

Some of the ironies of the British educational system are however neatly described by the report, which is based on an unsystematic survey of the opinions of educational and other organisations and on the CPRS's own views. One large company is quoted as holding the view that university science courses are "too academic" but nevertheless choosing to recruit graduates from the same academic courses in the belief that these would have attracted the most able students.

In its assessment of the provision of education and training, the CPRS echoes the conventional wisdom that Britain is better supplied with means of initial education and training than with facilities for continuing education and retraining.

The report has few concrete suggestions for the improvement of continuing education in Britain. It remarks that elsewhere than in the United Kingdom, and especially in the United States, continuing education flourishes because people acquiring extra qualifications are often rewarded with extra pay, and notes regretfully that "pay policy and union pressure" have prevented such incentives emerging in the United Kingdom. It therefore pins its hope for the future on part-time and evening study.

The more controversial recommendations are, predictably, those that affect the pattern of school education in the United Kingdom. The CPRS comes to the same conclusion as the Secretary of State for Education and Science, Mr Mark Carlisle, that there should be a core curriculum in the age range 11-16 but that this should be adopted voluntarily by educational authorities and not centrally imposed by Act of Parliament. (The report notes that the only present legal compulsion, the requirement that religious knowledge should be taught in schools, "has not been notably successful".)

The CPRS also wants there to be a more deliberate concern by those who design school curricula for the needs of industry (and is explicitly critical of the School Mathematics Project, now widely used in British schools, for its failure to consult with industry).

On the shortage of science and mathematics teachers in British schools, the report asks that the government should "grasp the nettle" of paying teachers with special skills more than teachers of other subjects. The report does not refer to the longstanding opposition of the teachers' unions to proposals of this kind.

The CPRS also has views about the way in which academics in British higher education should be paid. It refers in its report to the system in the United States under which some academics are paid for only nine months in each year, but are free to take paid employment elsewhere (or to carry out research) in the remaining months.

The CPRS is especially attracted by the way in which this practice may give some academics first-hand experience of industry, and asks that the Department of Education and the University Grants Committee should consider the problem and "use their influence" to get rid of existing restrictions. It hazards no guess at the salary levels that would be established after such a reorganisation. ☐

Three Mile Island

Reactor entry bid aborted

AN attempt by two Metropolitan Edison engineers to enter the contaminated containment dome of the damaged Three Mile Island reactor was abandoned last Tuesday (20 May) soon after 9.00 am when the inner door of an airlock refused to open. The engineers made three attempts to open the 3″ thick steel door leading into the containment dome by the normal procedure of giving the wheel of the door a three quarter turn and pushing. After a total of 11 minutes of the planned 15 minute "mission", the men were recalled by radio. A total of 10 millicuries of krypton-85 was vented to the atmosphere during the procedure and the engineers received a whole body radiation dose of 10 to 15 mrem.

Officials from Metropolitan Edison in Middletown, Pennsylvania, and General Public Utilities in Parsippany, New Jersey, said that further attempts to enter the dome would be postponed "indefinitely", until the situation could be analysed further. "We have only one theory" said Sandy Solon of Metropolitan Edison. "Corrosion, either around the hinges or around the door seals, is causing the door to stick". The airlock door is made to close tolerance and has not been opened for 14 months.

By noting which instruments inside the dome have not been operating, engineers have estimated that the dome is flooded to a depth of seven feet, "plus or minus one or two per cent". The airlock door is 20 feet above the floor so "there is no danger of a release of radioactive water into the airlock." Video monitors show a steady mist is falling inside the dome as heat from the reactor (which is still at 200°F) causes water on the dome floor to evaporate, rise to the ceiling and condense. "The atmosphere inside is highly corrosive, to say the least" said Bill Murray of GPU.

The presence of corrosion in the door "bodes ill" for the functioning of ventilation equipment inside required to cool the dome and maintain a negative pressure with respect to the outside to minimise the possibility of leaks. Engineers have rejected the possibility of forcing the door with hydraulic jacks for fear of tearing the polyplastic inflatable door seals. A failure of the air-lock door to reseal might necessitate the uncontrolled venting of the 57,000 curies of krypton-85 still trapped in the dome. Bill Murray of GPU said that the Nuclear Regulatory Commission may give the plant operators permission to make a controlled release of the radioactive gas to the atmosphere, thus

Three Mile Island reactor — which way back in?

permitting a forced entry. "Hundreds of thousands of curies have already been released with no ill effect. We hope the NRC will let us vent with maximum controlled dispersion and we can then reassess the situation." Non-gaseous isotopes such as Sr-90 and Cs-137 are presumed to be precipitated on the walls of the dome or trapped chemically in the ventilation filtering system.

The purpose of the attempted 15-minute entry was to monitor radiation in the dome, estimated to be 3 rem per hour of gamma radiation and 200-300 rem per hour of beta radiation. The engineers were also to check for radiation hot spots, examine the ventilation and cooling systems, check for structural damage and take "swipe samples" with gauze of radioactive residues on the walls and stairwells for detailed isotopic analysis.
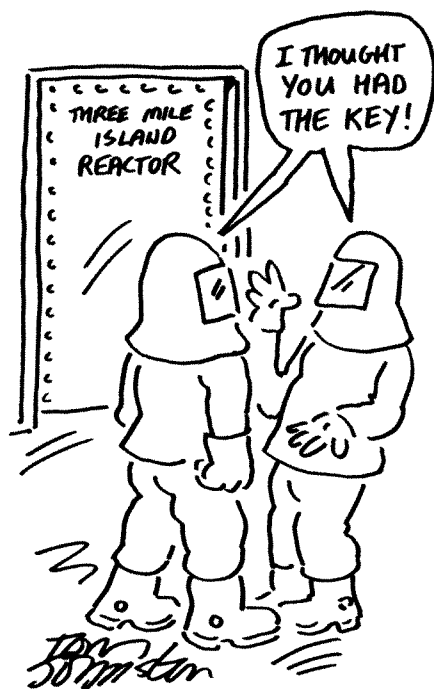
The two engineers, Michael Benson, aged 27, a nuclear engineer employed at Three Mile Island since 1974, and William H. Berhle, aged 36, a project engineer employed there since 1967, were two of several volunteers. They were fitted with Viking dry diving suits (heavy rubber suits of the type used by helmeted deep sea divers) covered by the standard yellow anti-contaminant radiation protective plastic clothing. Breathing apparatus was a Scott airpack of the type used by US firefighters with a 30-minute air supply. The men practised for two months on the identical airlock of the second Three Mile Island reactor.

Tuesday's failure was the second abortive attempt to enter the building. A previously scheduled entry on 24 April had to be cancelled when it was discovered that modifications in the breathing apparatus prepared by the Bio Marine company had not been submitted to the National Institute of Occupational Safety and Health for approval. At a press conference on 21 May, Benson and Berhle said they were "disappointed" and would volunteer again. The GPU said it would announce its next move "within a week".

Joe Schwartz

Recombinant DNA

Guidelines for scale-up

Washington

Like a man with a new pair of shoes, the US National Institutes of Health are experiencing some discomfort in administering industry's voluntary compliance with the safety guidelines covering recombinant DNA research.

Pressures on the NIH are coming from two directions. On the one hand, increasing competition from European and Japanese industry is leading US companies to complain that lengthy procedures for approving new host/vector systems and large-scale fermentation experiments are becoming a commercial handicap.

On the other, the members of the NIH's Recombinant DNA Advisory Commission are feeling their way uncertainly into the engineering and safety aspects of large-scale fermentation techniques of which few possess either detailed knowledge or expertise.

The system of voluntary compliance was proposed last year by NIH Director Dr Donald Fredrickson, largely as a way of avoiding the need for new legislation extending the guidelines to the private sector. Since the system was introduced in January, eleven companies have registered their Institutional Biohazard Committees (IBCS) with the NIH, and seven large-scale experiments have been approved.

Last year the containment guidelines were reduced for most experiments to a level requiring minimal physical safeguards, with the result that few companies now feel them to be excessively restrictive. Indeed some take comfort from the fact that Japan has recently introduced the NIH guidelines in their original, more stringent, form.

There is greater concern, however, about the time taken up by NIH's certification procedures, in particular that required to review new host/vector systems — a responsibility which many RAC members now consider to be one of the committee's most important functions.

At present, for example, the disabled bacterium strain *Escherichia coli* K-12 is the only approved host/vector system for experiments at the P1 minimum containment level (although the use of *Saccharomyces cerevisiae* strain of yeast is expected to be recommended for approval at RAC's next meeting).

The result, according to Dr Peter Farley, President of the Berkeley-based Cetus Corporation, is that European companies who can locate their operations in countries with minimal certification requirements already have a major commercial advantage through being able to exploit other host/vector systems, such as *Bacillus subtilis*.

Time is also being taken up by the need for special approval by the Director of NIH for each experiment carried out using more than 10 litres of culture — a relatively arbitrary limit set in the early days of the guidelines and apparently based on conventional laboratory practices.

Amendments to the guidelines which would accelerate the approval process for commercial developments have now been recommended to NIH by Dr Irving Johnson, Vice-President of Research for Eli Lilly and Company, which has already received permission for several scaled-up experiments in the production of human insulin.

In particular, Dr Johnson is proposing that, once approval has been given for a particular experiment to be carried out above the ten-litre limit, further volume increases using the same biological materials at the same containment levels would require merely to be approved by the local IBC.

More controversial is Dr Johnson's suggestion that, in order to make up for RAC members' lack of experience with large-scale applications, industry representatives should be added to the committee with expertise in areas such as fermentation technology and engineering.

And he is also proposing that a permanent subcommittee be set up to advise the Director of NIH on actions related to large-scale applications, with authority to recommend approval of preliminary plans for large-scale operational facilities.

The various proposals will be discussed by the RAC when it meets next week. Their reception is uncertain.

Committee members are aware that they lack expertise in either worker safety or fermentation engineering. "Many have not been entirely happy with their role" says committee member Dr David Baltimore of the Massachusetts Institute of Technology.

Yet there is disagreement over whether this lack should be made up primarily by expanding the scope of the committee, through increased use of consultants or the addition of new members. Or, alternatively, whether greater involvement should be encouraged from agencies which already have statutory responsibility for such matters, in particular the Department of Labor's Occupational Safety and Health Administration.

Either way, it seems increasingly unlikely that there will be new legislation imposing

the guidelines on the private sector. A bill seeking to do so, and requiring the registration of all industrial activities using recombinant DNA techniques, has been introduced by Senator Adla Stevenson Jr; but it has so far failed to gain any significant support, either inside Congress or without.   **David Dickson**

Comecon Science
High T, Low K

A NEW Comecon International Laboratory of High Magnetic Fields and Low Temperatures is to be built in Wroclaw during the next Five Year Plan (1971-1985) by the Academies of Science of Poland, Bulgaria, the Soviet Union and East Germany, with possible participation also by Czechoslovakia. This will replace the existing somewhat cramped premises which have served the laboratory since 1968.

According to Dr Wlodzimierz Trzebiatowski, until recently the Director of the Laboratory, and who still, in retirement, takes a keen personal interest in it, Wroclaw was originally chosen as the site of the laboratory for a number of practical reasons. First the Polish Academy of Sciences already had a flourishing Institute of Low Temperature and Structure Research in Wroclaw. Wroclaw is near the important East German science centres of Dresden and Berlin, and helium, essential for low temperature work, is available from a Polish extraction plant only 100 km away. Finally, just as the laboratory was being planned, the Lower Sjleskan electricity board, was installing new generators in the Wroclaw tramway substation and was willing to donate the old generators to the Academy of Science.

The present laboratory is concerned with such things as the properties of hard semiconductors, new magnetic materials and the measurement of specific heats below 1°K. Cooling below 4.2°K is effected by helium cooling in the field of superconducting magnets of 5T and 15T, and work is in progress on adiabatic demagnetization of nuclear and electron paramagnetics, allowing temperatures below 0.1 K to be attained.

The laboratory has a special interest in compounds of uranium with non-metals of the Vb and VIb groups — a speciality begun by Professor Trzebiatowski at the Low Temperature Institute of the Academy of Sciences in the early 1950s. (Since his initial discovery of ferromagnetic transition in uranium hydride UH_3, some fifty such uranium compounds, mostly chalcogenides, have been discovered there.) One new project, of especial interest to Dr Evgeni Leyarovski, of the Bulgarian Academy of Sciences, who was Deputy Director of the Wroclaw Laboratory from 1974-1977, is the study of superconductors
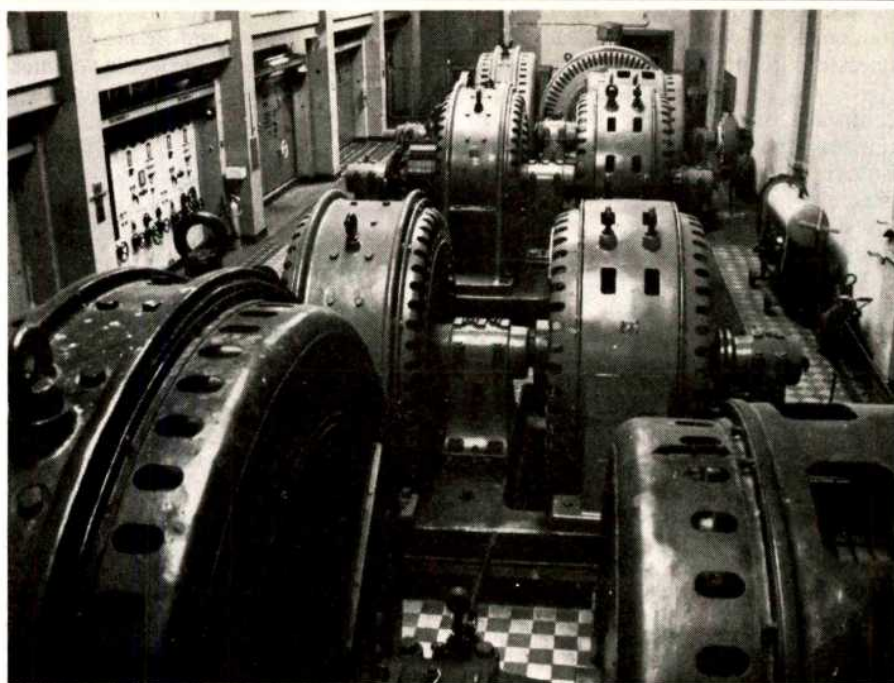
Tramway generators keep turning in Wroclaw

with magnetic impurities. Research on this phenomenon is also going forward in Sofia, but even with their new 5 tesla superconducting magnets installed this spring, the Bulgarians will still have to do much of their work in Wroclaw.

Nevertheless, even Wroclaw cannot at present offer the facilities which an international Comecon laboratory needs. Far more laboratory space is required, and, more important, the ex-tramway generators can operate only one of the three magnets at a time, so that the various teams often have to queue for "magnetic time". The new site, on the banks of the Odra, will provide space and facilities for more magnets with higher fields as well as an ample supply of water for cooling the electromagnets.   **Vera Rich**

Soviet oil
No real shortage

THE Soviet Union has initiated a major change in its method of estimating oil production costs which will result in a dramatic increase in production from proven fields, says a report* published last week by PetroStudies, a Swedish group specialising in the analysis of the Soviet oil and gas industry. The report disagrees sharply with CIA forecasts that the Soviet Union will suffer a shortfall in oil production. The CIA prediction has been used repeatedly in recent months by US oil officials to suggest that a Soviet oil shortage was leading it to have a material

"Try not to be long"

interest in controlling the Middle East.

The PetroStudies group finds that a recent 11-20 fold rise in the reference price of oil, from $0.75 — $1.50 to $17 — $20 per barrel, will correct the "systematic underexploitation of Soviet oilfields over the past thirty years". The reference price is the figure planners use to assess the cost of opening new oil fields, compared with the cost of intensively developing existing ones. The higher reference price represents a recognition by Soviet planners that development of new oil fields has created unacceptable pressures on capital, labour and material, necessitating a new economic approach to oil development. The PetroStudies report says that the new

policy means that "there is no danger whatsoever that the USSR will be forced to become a net importer of oil this decade and highly improbable that it will become so in the 1990s".

An additional feature of the new policy will be a decline in Soviet imports of American oilfield machinery, the report says. Intensive mining of existing fields by many wells will substitute for high capacity pumping from a few wells, a policy which will significantly decrease Soviet dependence on US-produced high capacity oil pumps.

According to the *International Herald Tribune*, diplomatic sources have suggested that the PetroStudies' findings

may be "part of a Soviet campaign of disinformation". M Jermol of PetroStudies explained that their analysis is based on original Soviet sources obtained though normal institutional channels. The materials include Russian texts of official oil industry documents, specialised books and journal articles, reports from Soviet research institutes, and petroleum conferences, extending back over ten years. "It would be impossible to base a report like this on a few privileged documents" said Jermol.

Joe Schwarz

"Soviet oil production reform of 1980 and its potential", PetroStudies Co., Sjoblads vag 27, S-21370 Malmo, Sweden. 260pp.

Instruments

New homes for old instruments

Is Britain's scientific heritage being ignored and forgotten by its museums? Arthur Frank, a collector of scientific instruments, believes that it is. About half of his collection of instruments dating from the early eighteenth century, which runs into thousands, has been placed in British museums — mainly central museums in London and Edinburgh. But the other half is on display only in his garage in Jersey, while Mr Frank searches for more conventional homes, so far with little success.

There are more than 1,100 museums in Great Britain and Ireland, but Mr Frank says that fewer than a dozen of them take scientific instruments seriously. But they do appear to differ in their reactions. Some have bought or borrowed instruments from Mr Frank. Others have declined to do so either on the grounds that the instruments which he has available would not fit in well with existing collections or because they would not be able to afford the prices asked. But many, mainly provincial museums, have said that they are the wrong organisation to approach because they do not have the expertise to judge scientific instruments.

One of the few provincial museums to house part of the Frank collection, however, is the Museum and Art Gallery, Doncaster, Yorkshire. Mr J Barwick, the museum's director, had to draw on outside expertise to mount the exhibition. His interest in the Frank collection stemmed from his wish to display a selection of early mining and surveying instruments appropriate to an old mining and engineering town; the public response has now persuaded him also to borrow some of Mr Frank's microscopes and astronomical instruments and he is planning to extend this section of the museum.

Doncaster Museum's special interests may be exceptional. Elsewhere, according to one official, regional and municipal museums are likely to be more interested in a display of instruments representative of different types than of a specialist sub-collection from Mr Frank's garage.

Mr Frank, nevertheless, is determined that his instruments should not be disposed of one by one. He also requires that recipients of objects from his collection should catalogue the instruments and put them all on display. He says that he is prepared to make gifts of them, lend them for twenty-one years, or sell them at two-thirds of the estimated value, dealing with learned societies as well as museums. One snag that may deter some museums is that Mr Frank's valuations seem high.

So far, the large specialist and national museums have been the chief recipients either loaning the instruments or more usually buying them under the two thirds

of value offer. The Science Museum in London has about 1,500 of his cameras and accessories, and there is a permanent exhibition of field and opera glasses and of prismatic binoculars. Inevitably, however, such a museum is primarily concerned to fill gaps in its present collection.

Elsewhere in Britain, the Royal Scottish Museum in Edinburgh has a display showing the development of the achromatic microscope in the formative years 1800-1860 (and is also negotiating for the remaining Scottish instruments in the Frank collection). There is also a collection of astronomical and terrestrial telescopes at the Royal Observatory, Edinburgh.

The parts of the Frank collection not yet disposed of are strong on spectroscopic and stereoscopic devices, as well as early spectacles. He is especially proud of his Marshall microscope (*circa* 1700) and his Ramsden astronomical instruments from the late 1700s.

Judy Redfearn
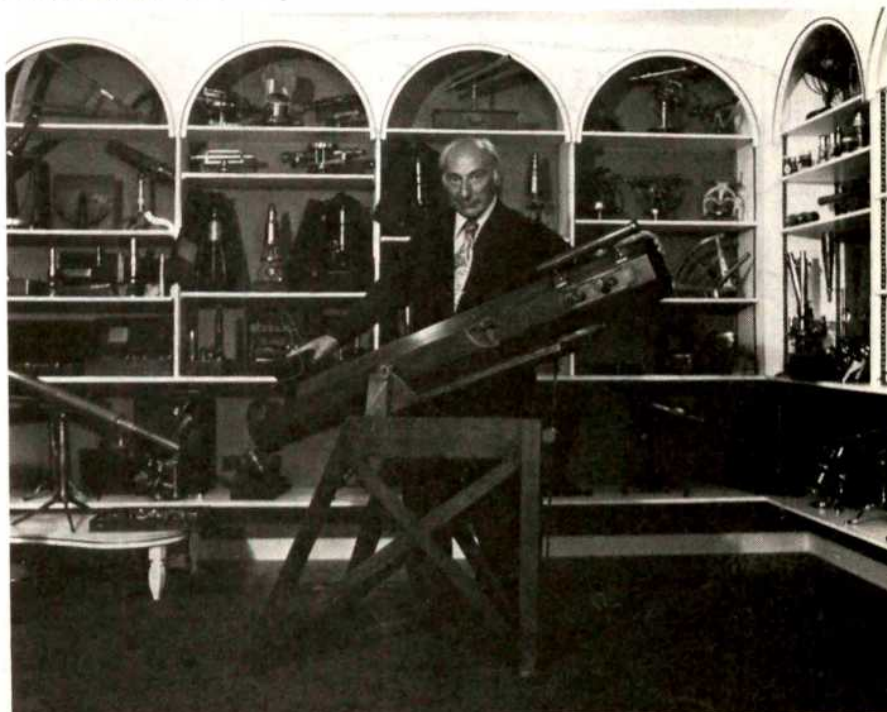
Arthur Frank with his instruments: gift horse or salesman?

CORRESPONDENCE

Parkinsonian exasperation

SIR, — Further to Robert Moss' letter (1 May, p9,) it is of interest to consider the size of a primitive group of workers when liaison begins to become less effective and an administrator is appointed. Following Parkinson's work on committees (C N Parkinson, *Parkinson's Law*, 1958), experimental evidence from both scientific and socio-political groups seems to indicate that communication remains viable for groups of between 5 to 11, with an optimum of 7 to 9. Between 12 and 14 members, a part-time administrator is usually appointed, and the stage is set for the entry of centralisation.

One of the finest examples of misgrouping to be seen in public was the three day meeting between management and union staff, shown recently on BBC 1. Possibly unaware of Parkinson's work, the two scientists who convened the meeting set up a group of approximately 21 to 23 people, with predictable results. Despite the efforts on both sides to overcome the traditional divisions between management and unions, the lack of communication due to the group size increased exasperation to the point when people began to leave. Amazed by the rising irritation, the scientists sought to alleviate it by altering the seating arrangements (*vide* Parkinson on the shape and size of committee tables). Communication was restored only when the participants spontaneously divided into two groups of 10 to 12 each, both containing managers and unionists. It was difficult to determine who generated this split, given the highly condensed version of events presented, but it was certainly not the scientists. Additional information to confirm or deny the hypothesis that smaller groups were suggested by the women trade unionists would be welcome.

Stage 3 of Parkinson's progression is considered by Moss to produce an 'intolerable' workload on the administrator, when he is burdened by 17 lines of communication

$(L_{wi} + L_{ai})$. The above empirical analysis suggests that the maximum tolerable number of $L_{wi} + L_{ai}$ will be of the order of 10 to 12.

Yours faithfully,

B M GRAY

Climatic Research Unit,
University of East Anglia,
Norwich, UK.

Feminist speculation

SIR,—The thought-provoking discussion of the reasons why increased centralization is accompanied by decreased effectiveness presented by Robert Moss was both perceptive and pertinent. I should like to comment on an aspect which Dr. Moss appears to have overlooked. He states that the results of one study showed that "the production of scientific papers per man decreased as the organization increased in size." Was the production of scientific papers by women not affected? If not, what are the most likely reasons? Can one assume that women are less likely than men to be affected by this extension of Parkinson's Law?

The administrators described by Dr. Moss were apparently male, and it would be interesting to speculate on the outcome had some or all of the administrators been female.

Yours faithfully,

C RIGBY

Aylmer,
Quebec, Canada.

Erratum

In Robert Moss's letter, "Expanding on Parkinson's Law" (1 May) there was a typographical error. In stage four of his administrators' model, the equation $l_{wi} = W$ erroneously appeared as $l_{wi} = W^2 + A$.

Editor, Nature.

Smallpox and conservation

SIR, — It has been announced by the World Health Organization that smallpox now has been eliminated. The virus responsible for smallpox, an organism formerly abundant and widespread, has been systematically, deliberately, and (as it appears) completely eradicated from all the natural systems of the world. With the exception of samples in a few laboratory 'zoos', it is extinct.

Those responsible for the demise of smallpox will be praised universally, I am sure. But what an eloquent dilemma this presents to conservationists.

Statements of the conservation ethic normally include such clauses as "the preservation of species diversity" and "the protection of endangered species". What happens to those ideals in the aftermath of smallpox? Does the conservation ethic inevitably reduce to a pragmatic formula for the protection of the human species, or to a sentimental affection for the cute and the cuddly? Would anyone care to provide a satisfactory statement of what we really do mean when we speak with solemn and genuine concern about the protection of the natural world?

Yours faithfully,

JOHN MIDDLETON,

Carleton University,
Ottawa, Canada.

Making books cheaper

SIR,—Your editorial, "Are Books Too Expensive?" (24 April) is a reasonable and most welcome voice in the discussion of rising book prices. At The University of Chicago Press we have been giving a good deal of thought to measures that would decrease the costs of book production and therefore reduce the list price. These include: the publication of more original paperback books; printing some books from camera-ready typescript rather than setting all books in type; asking authors to forego some portion or royalty on the sale of a specified number of copies of books with smaller audiences; and simply not publishing certain classes of books such as the proceedings of symposia because their relevance is commonly limited over time.

The cooperation of those who write, distribute, review, and purchase books is essential to the success of any of these measures. Many scholars prefer to purchase paper-bound books or books that are printed from typescript because they are less expensive. Yet these same scholars baulk at the prospect that their own books might be published in such a fashion, chiefly because their colleagues see such methods as characteristic of "second-rate" work or treatment. Some scholarly journals still refuse to review original paperbacks, and some libraries still refuse to buy them.

We as publishers must recognize that what is in the book must reach the intended audience and that the costs of "traditional" production may force the price of a book beyond the means of at least a fair proportion of the audience, particularly those who are students or younger faculty members, but we need and appreciate the cooperation of both authors and readers.

Yours faithfully,

SUSAN E. ABRAMS

University of Chicago Press
Chicago, UK, US.

NEWS AND VIEWS

Evolutionary genetics of snails

from J. S. Jones

MOLLUSCS are very suitable for research into evolutionary genetics. They are sluggish (and hence easy to capture and to mark), are common in a variety of habitats, and often display a striking shell polymorphism.

Many evolutionary mechanisms are now known to affect shell polymorphism in the European snail *Cepaea nemoralis*. Their importance varies greatly from population to population and the realisation that the factors influencing even this simple system are very complex is perhaps the most important point gained from the fifty years for which it has been studied.

At a recent conference* M. Lamotte (Ecole Normale Superieure, Paris) discussed the controversy between himself and A. J. Cain and the late P. M. Sheppard (University of Liverpool); this has often been misrepresented as a conflict between mutually exclusive mechanisms of visual selection by predators, of climatic selection and (in some populations) of genetic drift. However, it is now clear that to explain gene frequencies in individual populations it is usually necessary to produce complex explanations involving several evolutionary forces (for a recent review see *Ann. Rev. Ecol. Syst.* **8**, 109; 1977). This complexity probably applies also to the evolutionary biology of other polymorphisms (such as those at loci controlling soluble enzymes) but, as less information is available for most of these, there is still a tendency to search for single, unifying explanations of their existence. Climatic selection is generally accepted to affect gene frequencies in *Cepaea;* S. M. Tilling (North London Polytechnic) showed that different natural and artificial (black or white painted) morphs have behavioural differences which are related to their energy uptake in sunshine. *C. nemoralis* populations living in complex environments have more shell polymorphism than do those from habitats in which most individuals experience the same climatic stress, and experiments with snails marked with spots of dye which fade at a known rate when exposed to the sun suggest that populations exposed to a variety of climatic stresses are indeed more variable than are those with a narrower niche (J. S. Jones & R. F. Probert, University College, London).

Natural selection is also involved in the leucine amino-peptidase polymorphism of the mussel *Mytilus edulis* according to R.K. Koehn (State University of New York). In Long Island Sound a steep cline in allele frequency coincides with a salinity gradient. Each year the cline is displaced to a varying extent by the immigration of oceanic larvae, but each year selective mortality ensures that it returns to the same point.

Historical effects — whose role in the evolution of molecular polymorphism is notoriously difficult to assess — also influence the present-day distribution of shell variation in some *Cepaea* populations. Information from old records on the land use patterns of downland in southern England suggests that some local anomalies in gene frequency result from the spread of populations from woods into open habitats which become available to *Cepaea* only when sheep grazing declined (R.A.D. Cameron, Birmingham University; M. A. Carter, Portsmouth Polytechnic). Changes in gene frequency over the past 20 years in a *C. hortensis* population on the earthwork of Silbury Hill are also correlated with vegetational changes, in this case resulting from increased human usage. The intensity of selection is as much as 10% per generation (S. Wall & M.A. Carter; Portsmouth Polytechnic; B. C. Clarke, Nottingham University). These rapid evolutionary changes are a microcosm of the long-term changes in gene frequencies in English *Cepaea* shown from shells found in archaeological sites by A.J. Cain.

All theories of the origin of species depend on historical events which are by their nature not directly testable. M. J. D. White has recently put forward *(Modes of Speciation* W. H. Freeman, San Francisco; 1978) a theory of 'area effect speciation'. This arises directly from the observation by Cain and Currey *(Phil Trans. Roy. Soc. Lond. Ser. B.* **246**; 1; 1963) of 'area effects' in *Cepaea*. In many places large regions of constancy of allele frequency for shell polymorphism are separated by steep clines (which usually do not coincide with an obvious environmental discontinuity) from adjacent areas in which the *Cepaea* populations have very different allele frequencies. White suggests that each area effect is a marker for a reorganisation of the whole genome and that a slight reinforcement of this could lead to speciation within a continuous population,

without the complete geographic isolation necessary in Darwin's model. This theory adds new interest to studies of genetic differentiation in snails. One prediction might be that if adjacent area effects have diverged at many loci, some of these might be detected by enzyme electrophoresis (as is the case in incipient species of Drosophila). R. K. Selander and colleagues (University of Rochester, NY) find no evidence for parallel genetic differentiation at the morphological and the molecular level in some striking area effects in *C. nemoralis* in the Pyrenees. The pattern of distribution of species of the snail *Partula* on the Pacific island of Moorea does suggest that they have arisen as a result of the divergence of adjacent populations. B. C. Clarke and J. J. Murray showed that at some species' borders there are localised hybrid zones between populations which elsewhere act as good species, whilst in one locality there is a 'ring-species' complex with a diameter of only 3 km. Although area effect speciation might indeed be involved here, different species of *Partula* — even those from islands thousands of kilometres apart — show only slight differences in the frequencies of genes controlling molecular polymorphism. The same is true of morphologically distinct species in the freshwater genus *Elliptio* (G. M. Davis, Academy of Natural Sciences, Philadelphia). *C. nemoralis* populations do show genetic structure at the molecular level but this is independent of the area effects themselves. Pyrenean populations assort into several geographically and genetically distinct groups on a factorial analysis of enzyme and shell polymorphism, and there may also be pericentric inversion differences (which could act as isolating mechanisms) between populations of this species (C. Page, North London Polytechnic). However, area effect speciation could scarcely have occurred in the genus *Cepaea,* which has only four species but thousands of area effects.

The lack of concordance of polymorphism in the genes controlling enzyme structure with other indicators of species divergence suggests that other loci — such as regulator genes — might be involved in speciation (Wilson, Maxson & Sarich *Proc.*

J. S. Jones is in the Department of Genetics and Biometry, University College, London.

natn. Acad. Sci. U.S.A. **71**, 2843; 1974). The importance of ontogenetic and regulatory effects in molluscan population genetics is emphasised by the work of J. Heller (Hebrew University of Jerusalem) on the Israeli snail *Xeropicta,* an annual species. Adult *Xeropicta* in the mountains are dark coloured, those in the coastal plain pale. As the mean annual temperature is higher in the plain than in the mountains, this accords with the common poikilotherm pattern in which populations from hot places have a higher reflectivity of solar radiation than do those from cool. However, there are great annual fluctuations in temperature in Israel, and in the summer the snails are under extreme solar stress. They adjust their shell reflectivity to ensure that they absorb the requisite energy from the sun during the brief growing season, but are protected from excessive heat at other times; in the mountains they are born pale and become darker, while in the plain they are born pale but become paler. The structural genes controlling shell polymorphism are expressed only at the correct period of the life cycle. Ontogenetic effects are also found in the Caribbean snail *Cerion* (S. J. Gould, Harvard; D. Woodruff, University of California, San Diego). This genus shows a great variety of morphological types. Simulation of the growth process shows that simple alterations of the growth rate early in development can lead to startling differences in adult shell form. Developmental plasticity (perhaps promoted by polymorphism in the genes regulating growth rate) allows each species to attain a multiplicity of adult forms attuned to particular habitats. This may allow a single species of *Cerion* to fill the ecological niches occupied by several species of mollusc on dunes in southern Europe.

Molluscs show a range of sexual strategies from complete outcrossing to obligate parthenogenesis. They are therefore useful in research on the evolution of sex, particularly as the degree of outcrossing can be estimated from the zygotic proportions at loci controlling protein polymorphism. G. McCracken (University of Tennessee) and R. K. Selander discussed the European slugs which have colonised the US. There is great variation in the degree of outcrossing, with some species adopting a mixed strategy of sexual and asexual reproduction. Measurement of the niche breadth of several species on an ecologically well-characterised experimental plot shows that the three species with the broadest niche are present as monogenic and asexual strains. This is hard to reconcile with models which predict that sexual species have more evolutionary flexibility than do asexual.

The conference demonstrated that although the single helix of the snail's shell may be less central to modern genetics than the double helix, it continues to provide important tests of evolutionary theories. □

---

100 years ago

A proposal has been set on foot for lighting the Sheldonian Theatre, Oxford, and the Camera of the Radcliffe Library with the electric light. It has long been regretted by many members of the University that the Sheldonian Theatre is not available in the evening for any purposes of public interest, however great, for want of lighting. The neighbourhood of the Bodleian Library has, however, been a bar to any proposal for lighting by means of gas or any ordinary method. The care with which the heating apparatus of the Theatre has been inclosed within a fire-proof chamber is sufficient evidence of the importance attached by the curators of the Theatre to absolute security in this respect. The development of the electric light has now rendered it possible to illuminate public rooms by a process absolutely free from danger of fire. It has been adopted largely in the reading-rooms of our public libraries, and notably in the reading-room of the British Museum.

Herr Zehfuss has lately given (*Wied. Ann.,* 4) some personal experiences of the phenomenon of "after images of motion". These after images may be had, *e.g.,* in a train, if one look at a point on the horizon for a little, then turn to look at (say) a horizontal fibre in the wood of the carriage, or close one's eyes. Motions then seem to be still perceived; in the latter case, *e.g.,* a stream of sparks seems to be moving to the right (or if the point originally looked at have been between the observer and the horizon, there is a stream of sparks above going to the right and one below to the left). Herr Zehfuss offers a physiological explanation, in preference to the partly psychical ones proposed by Plateau and Oppel. Each individual nerve rod, he supposes, has special blood-vessels, which, when the original image of a moved object goes to the right, directs the course of the blood to that side, just as in ordinary light the decomposed blood is promptly replaced by fresh. By this preponderant direction of blood to the right a heaping up occurs in each retinal element on the right, which gives rise to return currents as soon as the outer cause has ceased to act. As the blood flows back there arise, in consequence of the specific excitability of the rods, those spark-streams, which are projected as elementary motions to the right.

from *Nature* **22**, 27 May, 87 & 90, 1880.

High-resolution imaging of laser-driven implosions

from Lynn R. Veeser

HIGH-RESOLUTION imaging of the radiation (mainly electrons, neutrons, X-rays, and alpha-particles) emitted by laser-driven DT fusion implosions is difficult because such radiation cannot easily be focused. Nevertheless, imaging could be an extremely useful diagnostic tool, especially for comparison with the extensive computer modelling now being carried out for laser-fusion compressions. Neutron imaging has not been achieved because the fluxes are small and the efficiency for detecting neutrons is low. Electrons are generally affected by the strong electric and magnetic fields in the laser plasma but X-rays and, if the fields are not too strong, alpha particles, can be imaged by pinhole cameras.

Unfortunately, to produce a high-resolution image, a pinhole camera must have a tiny aperture and this will cause low sensitivity. If additional signal strength is needed it is necessary to use more than one aperture. The resulting image, or shadowgraph, is a superposition of the images from all the apertures, and it is not useful or recognizable unless a real image of the source, similar to that seen for a single aperture, can be reconstructed from it. The two-step process by which this imaging and the subsequent reconstruction are done is known as coded-aperture imaging.

Coded-aperture imaging has been used by astronomers for a number of years to image X-ray stars, and it is employed in the field of nuclear medicine to enhance the signal-to-noise ratio and the resolution in radiographing body organs; but, because of the difficulties involved in fabricating the complicated microscopic apertures needed for ultra-high resolution, its application to laser plasma has been delayed for some time. Recently, however, groups from the US laser fusion laboratories at Livermore and Los Alamos have reported the use of coded-aperture techniques in imaging of imploding laser-driven fusion targets.

Ceglio and Larsen (*Phys. Rev. Lett.* **44**, 579; 1980) used a Fresnel zone plate (in this case a series of concentric gold rings with radially decreasing apertures and held together by thin struts) as a coded aperture to measure the X-rays from a thin glass microballoon which had been filled with DT fuel and irradiated with about 20 TW of laser power. They obtained X-ray images from the shadowgraphs by optical reconstruction; each shadowgraph was illuminated with a coherent light source, much as is done in holography, producing a magnified image of the initial source. The experiments were done at the Shiva laser facility of the Lawrence Livermore Laboratory.

When a high-power laser pulse strikes a target surface, it generates a plasma which includes a significant number of high-energy (suprathermal) electrons. The

target, consisting of fuel contained in a thin-shell microballoon known as an exploding pusher, implodes when these hot electrons heat the shell, causing it to explode both inward and outward; the inward momentum compressing the fuel. In the Shiva experiment two simultaneous short (typically < 100 ps) laser pulses, each of about equal energy, imploded the shell from opposite points (the poles). X-rays from the implosion were imaged in three energy intervals by stacking layers of X-ray film and filters. Two of the spectra were of great interest. Thermal X-rays (from 4 to 7 keV) were found near the inner part of the imploding shell and are thought to represent the hottest part of the pusher material at a time when its diameter was nearly at its minimum. Two disk-shaped regions, about 40 μm apart and clearly visible in the reconstructed radiograph, showed the pusher temperature to be hottest at the poles. Relatively few X-rays originated at the target center in the region of the compressed DT fuel. Of perhaps even greater interest was an image of the suprathermal X-rays, or bremsstrahlung, derived from interactions of the hot electrons with ions from the exploding pusher. If the hot electron distribution is assumed to be uniform, i.e., if the electron ranges are long compared to most spatial nonuniformities in their production, then a measurement of the bremsstrahlung distribution should map out the ion distribution during the early stages of the implosion. The suprathermal X-ray image (from 17 to 30 KeV) published by Ceglio and Larsen shows a hollow shell of nearly the same outer diameter, about 300μm, as the initial shell, but the X-ray density was much more intense near the poles than the equator.

The general shapes of these X-ray images, including the decrease in intensity near the equator, were matched nicely by numerical simulations. Having experimental pictures to compare with the simulations has made it possible to test the importance of various proposed energy absorption and transport mechanisms in the target. The quality of the agreement provides considerable satisfaction with the present state of numerical laser-fusion calculations.

Two features of the measurement are not found in the simulation, however. A number of ripples appear on both the inside and the outside of the X-ray shell structure, and the authors attribute the ripples to nonuniformities, or hot spots, in the laser focus. In addition, one larger protuberance, perhaps 100 μm in size, was seen on the inner side of the shell. It seems likely that this protrusion is an indication of breakup of the pusher shell occurring during the laser pulse.

In a previous experiment, Ceglio and Coleman (*Phys. Rev. Lett.* **39**, 20; 1977) used a similar zone-plate, coded-aperture

Lynn R. Veeser is in the Physics Division, University of California, Los Alamos.

technique to image alphaparticles from the thermonuclear burn region in an exploding pusher implosion at the Lawrence Livermore Laboratory Argus laser. They were able to detect burn regions smaller than 30 μm in targets which were initially about 90 μm in diameter, proving that the burn occurred near the target center, as was hoped, and not in the outer regions of the target.

A somewhat different approach to X-ray imaging of a laser fusion target was reported recently by Fenimore *et al.* (*Appl. Optics* **18**, 945; 1979). Their coded aperture was a plate with a large number of tiny pinholes. Since the signal-to-noise ratio is proportional to the square root of the number of holes, sensitivities comparable to that of the zone plate aperture were produced by choosing the appropriate aperture pattern. Fenimore was able to virtually eliminate undesired artifacts, such as "ghosts," in the reconstructed image. Furthermore, since digital (computer) reconstruction of the image was used, it was possible to avoid distortion of the image intensities relative to the source strength. Optical reconstruction tends to give an image for which isodensity contours correspond to isoemission contours of the source, but the image

density is not proportional to the source emission intensity. One drawback to using an aperture made with a large number of small holes is the difficulty of making each hole with an exactly known size, shape, and position to achieve the artifact-free images this method is capable of producing. Even though the 4×10^4 pinholes in the Fenimore aperture were 25-μm square, not as small as state-of-the-art fabrication techniques would permit, a very high-quality, linear image was obtained because of the care taken in the aperture construction. A camera aperture with 6-μm holes was recently built and should give increased resolution.

The technology for doing high-resolution imaging of particles and X-rays is advancing rapidly at present because of the need for improved diagnostics for laser-driven fusion implosions. The recently reported X-ray and alphaparticle imaging experiments have given valuable insight into the exploding-pusher implosion process, and we can expect further progress as high-resolution imaging becomes a routine diagnostic tool. It is quite likely that the imaging advances made because of laser-fusion needs will be of considerable use in other fields, particularly nuclear medicine. □

The present state of tranquility

from Leslie L. Iverson

MORE than 8000 tons of benzodiazepines were prescribed in 1977 in the United States. Some drugs in this group, such as diazepan (Valium) are used for their anti-anxiety properties, others such as flurazepam (Dalmane) and nitrazepam (Mogodon) as sleeping pills, and they have become the most widely used of all psychotropic drugs. It is only very recently, however, that progress has begun to be made in understanding how they work. This has been due to two important developments: the discovery of specific high affinity binding sites for radio-labelled benzodiazepines in brain (Squires & Braestrup *Nature* **266**, 732; 1977; Möhler & Okada *Science* **198**, 849; 1977), and the emergence of a plausible hypothesis to explain how benzodiazepines may interact with normal brain function. This hypothesis suggests that benzodiazepines act by enhancing the effectiveness of the important inhibitory chemical transmitter gamma-aminobutyric acid (GABA) in brain (for reviews see Iversen *Nature* **275**, 477; 1978; and Tallman *et al. Science* **207**, 276; 1980). With these two leads, biochemical research on benzodiazepine receptors in brain and their relation with GABA mechanisms has developed rapidly to become one of the most active areas of psychopharmacology.

A key question concerns the nature of the interaction between benzodiazepine and GABA receptors. The interaction is indirect, since the benzodiazepines do not simply mimic the actions of GABA, and

indeed do not compete directly with radioactive GABA for binding to GABA receptors in brain membrane preparations. Similarly GABA and related inhibitory compounds do not compete for the binding of radiolabelled benzodiazepine to their recognition sites. One possible clue about the nature of this interaction comes from a consideration of the mechanism by which GABA receptors control the excitability of brain cells. The effect of GABA when bound to its receptors is to trigger a specific change in the permeability of the cell membrane to chloride ions, and it is the movement of chloride which stabilises the electrical potential of the cell and reduces its excitability. The GABA receptor may thus be viewed as part of a macromolecular complex in which the GABA recognition site is associated with a chloride ionophore. Benzodiazepines might interact not with the GABA recognition sites but with the chloride channels to enhance the normal effects of GABA, as suggested by Guidotti *et al.* (*Nature* **275**, 553; 1978) and others. This view is also proposed by Simmonds (*Nature* **284**, 558; 1980) and supported by his new experimental findings. Simmonds studied the inhibitory effects of GABA in an *in vitro* preparation of small slices of rat cuneate nucleus using electrophysiological recording techniques. Addition of flurazepam to this preparation caused a small but significant potentiation of the effects of applied GABA. More importantly, flurazepam also significantly

weakened the ability of the GABA blocking drug picrotoxin to antogonise the effects of GABA, while it had no effect on the GABA-blocking actions of another antagonist drug, bicuculline. The significance of this finding is that whereas bicuculline is thought to act by competing directly at GABA receptors, picrotoxin acts at a different site, perhaps related to the chloride ionophore. Although flurazepam and picrotoxin do not appear to compete for the same site, the result points again to an interaction of the benzodiazepine receptor with the chloride channels associated with GABA receptors. Simmonds suggests that the benzodiazepines might increase the duration of channel opening for each GABA receptor activation, or improve the efficiency with which GABA receptor occupation is associated with channel opening.

A similar conclusion has been drawn from other lines of research on GABA/benzodiazepine mechanisms. A number of laboratories have observed that GABA increases the affinity of binding sites for radiolabelled benzodiazepines in brain membrane preparations *in vitro* (Tallman *et al. Nature* 274, 383; 1978; Briley & Langer *Eur. J. Pharmac.* 52, 129; 1978; Martin & Candy *Neuropharmac* 17, 993; 1978), and the latter authors also observed that this effect of GABA was considerably enhanced by chloride ions. Costa *et al.* (*Nature* 277, 315; 1978) tested a number of other anions and claimed that their effectiveness in causing increases in the affinity of benzodiazepine binding correlated with their ability to replace chloride in GABA-mediated inhibitory events, although this conclusion has been challenged by Martin and Candy (*Neuropharmac.* 19, 175; 1980).

An unexplained feature of the GABA effect on benzodiazepine binding is that a number of compounds which mimic the inhibitory actions of GABA on neuronal firing and which compete for ^{3}H-GABA binding sites fail to enhance benzodiazepine binding (Karobath *et al. Nature* 278, 748; 1979 and some of these compounds may even antagonise the effects of GABA on benzodiazepine binding (Braestrup *et al. Nature,* 280, 331; 1979). This suggests that the GABA recognition site which mediates changes in benzodiazepine receptor affinity may differ in specificity from that of the normal GABA inhibitory receptor.

Regardless of its pharmacological characteristics, however, the existence of a GABA recognition site which can influence the binding properties of the benzodiazepine receptor adds further support to the GABA/benzodiazepine interaction hypothesis, and an interesting recent observation is that GABA continues to exert a modifying action on the affinity of benzodiazepine binding even in solubilized

Leslie L. Iversen is Director of the MRC Neurochemical Pharmacology Unit, Department of Pharmacology, Medical School, Cambridge.

benzodiazepine receptor preparations (Gavish & Snyder *Life Sci.* 26, 579; 1979).

Our understanding of the complexity of GABA mechanisms in brain has been increased by the finding of an apparently novel type of GABA receptor which has a different drug specifity from the conventional post-synaptic inhibitory receptors for GABA. Bowery *et al.* (*Nature* 283, 92; 1980) have summarised the evidence for the existence of such a novel GABA receptor. GABA at micromolar concentrations inhibits the release of monoamine transmitters from nerve terminals in the brain and in the peripheral autonomic nervous system, but unlike conventional GABA responses these effects are not antagonised by bicuculline. The anti-spastic drug baclofen (ß-parachlorophenyl GABA) potently mimics these presynaptic effects of GABA, although this compound is inactive on post-synaptic GABA receptors.

Furthermore, the presynaptic GABA sites fail to recognise compounds such as 3-aminopropanesulphonic acid and muscimol, which are potent GABA-mimetics on post-synaptic GABA receptors. These observations suggest that a different type of GABA receptor may be involved, bringing GABA into line with other CNS neurotransmitters for which multiple receptor types are now thought to exist.

Research on the minor tranquilisers and brain GABA mechanisms is far from tranquil, although from this turmoil a better understanding is emerging of the cellular and molecular pharmacology of this major group of psychotropic drugs. At the same time rapid developments are now taking place in isolating and purifying benzodiazepine receptors and identifying possible naturally occurring ligands for them. □

Cataclysmic conferences show convergence

from Robert P. Harkness and Brian McMahon.

SINCE the discovery some sixteen years ago that novae and related variable stars were binary systems, theoreticians and observers have devoted a great deal of effort to understanding how the interactions between the two stellar components give rise to energetic outbursts on timescales ranging from weeks to thousands of years. Two recent informal conferences* on the nature and properties of cataclysmic variables have given a timely glimpse of the state of the art.

Our current understanding of dwarf novae was emphasised at Cambridge. These systems typically undergo irregularly spaced outbursts of some 2-4 magnitudes every few weeks, lasting for a few days at a time. It is believed that the energy required to power the outbursts comes from gravitational energy of matter which is transferred from the binary companion star to a white dwarf primary, and that this transferred matter forms a disc around the primary which is stable between outbursts. J. Pringle (Cambridge) presented a series of models due to him and G. T. Bath (Oxford) which follow the evolution of accretion discs following the injection of material from the companion star, demonstrating how the density and temperature distribution and the timescale of the resulting structural changes depend on the as yet poorly understood "viscosity" of the disc.

The existence of such accretion discs is rapidly being confirmed, particularly from combined ultraviolet and optical studies with the International Ultraviolet Explorer satellite (IUE) and ground-based optical telescopes. J. Whelan (Cambridge) showed the continuum spectra covering the wavelength region 1000 — 7500 Å of three dwarf novae taken simultaneously in the

optical and ultraviolet, and compared them with the spectral energy distribution predicted for a steady-state, optically thick accretion disc. For the two systems VW Hyi and EX Hya, no single stellar-type continuum could fit the data, but the fit was very reasonable for simple discs, and allowed disc effective temperatures to be deduced. The third system, BV Cen, showed a different flux distribution which was thought to yield information about the secondary star.

J. Papaloizou (Cambridge) discussed systems of the SU UMa type, which occasionally show more luminous "superoutbursts" lasting about a week. During these eruptions, the light curve contains periodic humps with a period differing slightly from the binary orbital period of the system. It is thought that these so-called "superhumps" may be due to a tidal process which excites toroidal modes of oscillation in the secondary and thus modulates the mass transfer flow with waves of the same period.

Such "superhumps" were observed by M. Friedjung (Paris) in the 1978 outburst of the recurrent nova WZ Sge. Spectroscopy with IUE indicates a continuum consistent with an accretion disc spectrum rather than the spectrum typical of a classical nova, but double-peaked emission lines which become narrower at outburst are interpreted as features representing an outer, slowly-rotating disc. Such a structure was suggested as an alternative cause of "superhumps".

At Austin, much new observational work on dwarf novae was presented, all of which was interpreted in terms of the now standard

Robert P. Harkness and Brian McMahon are in the Department of Astrophysics, University of Oxford.

accretion disc model. High-quality optical spectroscopy of the system SS Cyg was reported by E. Nather (Austin) and also by A. Cowley (Dominion Astrophysical Observatory), leading to a revised period of 0.275 days, but yielding no definite results for the mass ratio of the components. Abundances in the accretion disc were investigated by S. Wyckoff (Phoenix), who reported an excess of helium over hydrogen in the disc of EX Hya.

Satellites have produced much new data, and ultraviolet observations from IUE were reported from P. Szkody (Washington) and also by G. Fabbiano (Harvard-Smithsonian Centre for Astrophysics). F. Cordova (Los Alamos) presented recent X-ray results from the Einstein satellite for a number of systems, all of which had significant hard X-ray fluxes, while no ultrasoft emission at energies around 50 eV (as previously seen at outbursts of SS Cyg and U Gem) was detected. The failure of previous satellites to observe X-ray emission from most cataclysmic variables allows an upper limit to be put on the mean X-ray luminosity of 10^{31} ergs s^{-1}. Most of the ultraviolet and X-ray spectra presented were in reasonable accord with the general predictions of the accretion disc model.

Einstein and IUE observations of nova-like variables were presented by E. Sion (Villanova). These objects show a wider range of properties than ordinary dwarf novae. V471 Tau, in the Hyades cluster, has a primary which may be the hottest white dwarf known, with a temperature of over 60 000 K. High-excitation spectral lines of silicon and carbon seen in absorption are thought to arise in the photosphere of the white dwarf, and there is no evidence for an appreciable accretion disc. TT Ari and CD-42°4462 display similar features, but the latter in outburst has a very similar spectrum to that of the dwarf novae.

At Cambridge, an attempt to model the colours and eclipses of the nova-like variable RW Tri was made by J. Frank (Leicester) and co-workers. They assumed the presence of an accretion disc and a secondary on or near the main sequence. If their model is correct, it implies a mass for the white dwarf component of 1.4 times the mass of the sun, which is uncomfortably close to the Chandrasekhar maximum. This result was challenged in discussion by J. Smak (Warsaw), who claimed that radial velocity measurements on the system give a figure much closer to 0.4 solar masses.

The properties of systems related to the short-period binary AM Her were reviewed at Austin by J. Liebert (Tucson). These are characterised by strong linear and circular polarisation, and are usually X-ray sources. They exhibit no nova-like eruptions, but do have distinct "low" and "high" states. They are now usually interpreted as systems containing an accreting highly-magnetised white dwarf.

It is conjectured that the high magnetic fields disrupt or prevent a disc from forming, so that accretion columns are produced at the magnetic poles of the primary. Four of these systems are now known, the most recent discovery being the X-ray source 2A0311-227. Optical and X-ray light curves for this 81-minute eclipsing binary were presented by J. Patterson (Minnesota). The X-ray flux has a soft black body component, and a hard bremsstrahlung component with energies in excess of 11 keV. This latter component is not eclipsed at all, while the soft X-ray flux is halved at eclipse. This was interpreted as the eclipse of a hot spot in the accretion stream by the accretion column itself. This same object was discussed at Cambridge, where M. Watson (Leicester) explained the narrow spike appearing in one of the eclipse components of the optical light curve by the passage of the secondary star across the line of sight. The other eclipse features are then due to the eclipse of the magnetic poles by the body of the white dwarf itself.

While our knowledge of dwarf novae and related systems appears to be increasing steadily, less progress is being made on the problem of the classical novae, which undergo outbursts perhaps only every 30 000 years, but with ranges of 8-17 magnitudes. It is thought that these, too, are binary systems, but it is argued that the violence of their outbursts must be explained by thermonuclear ignition of hydrogen-rich material accreted by the white dwarf. It is generally agreed that the nova outburst produces an optically thick envelope around the whole binary system; as this envelope thins, one sees deeper into regions of higher temperature, so that the flux maximum moves into regions of shorter wavelength. Thus the bolometric (total) luminosity remains essentially

constant for some time, while the visual luminosity drops off rapidly. If this picture is right, one would expect to see enhanced abundances of such elements as carbon and nitrogen which are necessary to fuel the thermonuclear runaway. At Cambridge, C. Penn (London) discussed ultraviolet observations of Nova Cyg 1978 following outburst, the first time a classical nova eruption has been seen by IUE. The development of several spectral lines was followed for nearly a year, and in the early stages of the outburst many showed the P Cygni profiles expected for outflowing material. Measurements were made of carbon and nitrogen which showed them to be highly overabundant in the nebular phase.

The Austin meeting heard from M. Shara (Montreal) a theoretical paper seeking to derive the empirical relation which has long been established between the maximum magnitude of a classical nova and the speed with which it subsequently drops in luminosity by three magnitudes. This relation is of wider importance in astronomy, since a good theoretical basis for the empirically observed result would allow classical novae to be used as "standard candles" and distance indicators with greater confidence.

The Austin meeting was the fifth in an irregular series of workshops on cataclysmic variables, the Cambridge meeting the first such to be held in Britain. The range of activity demonstrated the excitement and dynamism of the subject. Now that interpretations seem to be hardening on specific theoretical models, a flurry of more detailed calculations can be anticipated, including as a major contribution models of accretion disc structure that can be compared with a large array of observational tests. □

Structural aspects of recognition and assembly in biological macromolecules

from a Correspondent

THE last decade has witnessed a dramatic increase in our understanding of the structural, thermodynamic and kinetic factors which allow recognition and assembly in molecular biology. More complex supramolecular systems have been subjected to the techniques of amino acid and nucleic acid sequencing, to high resolution X-ray analysis and spectroscopic probes, and to mechanistic and functional investigations. We can now begin to asses the role of shape, hydrophobicity, flexibility and other factors in the processes of recognition between biological molecules. This was the theme of the VIIth Aharon Katzir-

Katchalsky Conference held at Kibbutz Nof Ginossar on the shore of the Sea of Galilee, Israel, earlier this year.

Of the many biomolecular systems, enzyme substrate interactions have been most thoroughly investigated; but only recently have very high resolution (~ 1.5A) X-ray studies allowed precise definition of the molecular geometry and thermal vibrations — a measure of at least one kind of flexibility. This is proving a critical testing ground for older hypotheses of catalytic mechanism involving steric strain, charge relay systems and covalent intermediates. For instance, M.N. James and his colleagues (University of Alberta) have

cast doubt on the accepted mechanism of serine proteinases by their detailed analyses of the serine proteinase A from *Streptomyces griseus* where they find bond distances which are considerably longer than expected in the charge relay system, tetrahedral intermediate model now described in all our biochemistry text books. They also demonstrate the existence of highly ordered water in the active site which must be displaced by the solvent; the release of this water would be entropically favourable to the assembly of the complex. Another striking feature of this work is the observation that although there is high thermal motion of the "jaws" of the substrate-binding site in the native enzyme, the polypeptide in this region becomes significantly more rigid in the presence of a ligand. The flexibility may play an important role in the docking of substrate with the enzyme. Similar ordering is found by R. Huber's group (Max-Planck-Institute, Munich) in a disordered "activation domain" in trypsinogen which includes part of the specificity site when the bovine pancreatic trypsin inhibitor or other inhibitors are bound in the presence of an activator dipeptide. K. Wüthrich (ETH, Zürich) reported similar order-disorder transitions in solution using nuclear magnetic resonance studies, and it is now becoming clear that such transitions may be of general functional importance in interactions between different biological systems.

Progress is also being made in our understanding of the assembly of fibrous proteins, especially in muscle components. For instance, the amino acid sequence of tropomyosin shows a number of periodic and non-periodic features which can be correlated with its two-stranded coiled-coil structure, with its head-to-tail aggregation into long filaments, and with its interactions with F-actin and troponin (L.B. Smillie, University of Alberta). A mechanism was described whereby tropomyosin regulates muscular contraction by responding to structural changes induced in troponin in Ca^{++} ions and consequently rolling across the surface of actin, thereby uncovering the site for actin binding to myosin (D.A.D. Parry, Massey University). New results concerning the binding of myosin cross-bridges to actin suggest that these may not change their slope during contraction (K. Holmes, Max-Planck-Institute, Heidelberg) and that the contractile force may result from a helix-coil transition in the S_2 fragment of myosin (W.F. Harrington, Johns Hopkins).

Although models for the recognition of DNA by proteins have until recently assumed a dimorphic DNA consisting of only the B and A forms, it is now clear that the DNA molecule is much less rigid than previously believed. S. Arnott (Purdue University) presented evidence from fibre X-ray diffraction studies for a great variety of possible DNA double helical structures.

These structures are mostly right-handed, but specific polymers of alternating purine and pyrimidine bases were found to form left-handed duplexes similar to the Z DNA structure (*Nature* **282**, 680; 1979). Although it is generally believed that most DNA has a classical DNA double helix most of the time it is probable that such specific structures in parts of DNA may be involved in their recognition by binding proteins. H. Sobell (University of Rochester) suggested that thermally induced low-frequency-mode oscillations in a DNA duplex structure may play a central role in transitions between different structures and in the binding of other molecules to DNA.

The exact pitch of DNA in a natural environment may also differ from that in the fibres which formed the basis of the Watson-Crick double helix. A. Klug (MRC, Cambridge) described some recent experiments aimed at measuring the true pitch of DNA in solution by cleaving molecules on a very flat mica surface with DNase I. The pitch was found to be 10.6 bases; significantly different from the 10.0 bases measured in X-ray fibre studies, but quite similar to the average value of 10.4 suggested from DNase I digestion of chromatin DNA. E. Trifonov (Weizmann Institute) described a quite surprising result that the distributions of the dinucleotides CG, TG, TA and TT along DNA sequences found in chromatin are periodic. The period is about 10.5 bases which agrees within error limits with previous estimates of the pitch of DNA in chromatin.

Evidence for small variations in t-RNA structures which may be important in their recognition is also forthcoming from the structure analyses of yeast initiator t-RNA$^{Met}_f$ by J. Sussman (Weizmann Institute; see *Nature* **278**, 188; 1979) and yeast t-RNA^{Asp} by J-C. Thierry (University Louis Pasteur, Strasbourg). In contrast to the class I, chain elongation t-RNA^{Phe}, the t-RNA$^{Met}_f$ is a chain initiation t-RNA and the t-RNA^{Asp} is a class II t-RNA. Both show the canonical "L" shaped conformation of t-RNA^{Phe} but there are differences in the closing of the angle between the two long helical stems of the "L" by about 8° in t-RNA$^{Met}_f$ and the opening of this angle by about 10° in t-RNA^{Asp}. P. Sigler (Chicago University) proposed an intriguing hypothesis for the molecular basis of the unique role played by eukaryotic initiator t-RNAs in protein synthesis, suggested to him by the t-RNA$^{Met}_f$ crystal structure. The characteristic sequence features which are common and unique to eukaryotic initiator t-RNAs are clustered in a 10Å domain at the union of the D and T loops and fold in a way that preserved the backbone trace seen in other t-RNAs. However, the potential for unique interactions with cognate proteins and nucleic acids makes this region a likely focus for the specific interactions with the ribosome, that underlie the special role of t-RNA$^{Met}_f$. These

interactions stabilise a factor-mediated 80s ribosomal initiation complex which recognises the first AUG encountered from the 5'-terminus of the m-RNA as the "Start" signal.

The recently determined structure of the Southern Bean Mosaic Virus, SBMV (M. Rossmann, Purdue University) shows that there may be common features in the assembly of spherical viruses. A comparison of its structure with that of Tomato Bushy Stunt Virus, TBSV (S. Harrison, Harvard University) indicates a conformation similar to that of the shell domain of the latter. The SBMV protein also uses a similar pattern of contacts with neighbouring molecules within the viral capsid. Studying the inter-subunit contacts in the shell domain of TBSV, Harrison has found an alternating pattern of polar and hydrophobic patches, as previously found for the lateral interactions in Tobacco Mosaic Virus (A. Bloomer *et al*, MRC, Cambridge), and he suggested that this may be a general feature of interfaces which can exist in more than one quasi-equivalent state. The three types of interaction between hexons in the capsid of adenovirus (R.M. Burnett, Biocentrum, Basel) can now be understood in terms of the pseudo-hexagonal symmetry of the trimeric protein. The symmetry facilitates packing, whereas the departures from it allow the different interactions.

It is hoped that the proper understanding of recognition in self-assembling systems may provide the basis for a contribution of molecular biology to medicine. X-ray studies of fibres and crystals of deoxygenated sickle-cell haemoglobin have led to a model for the interactions specific to the mutant haemoglobin. M. Gorecki (Weizmann Institute) described the design of small peptides and esters of hydrophobic amino acids based on this model. These compounds appear to inhibit sickle cell haemoglobin aggregation, they permeate erythrocytes rapidly, and thus appear to have considerable potential for the therapeutic treatment of sickle cell anaemia. In a similar way analyses of three-dimensional models for insulin and glucagon receptor interactions (T.L. Blundell, Birckbeck College, London) have led to pharmaceutical activity in the design of insulin agonists and glucagon antagonists which may be of value in the treatment of diabetes. The recent determination of the first three-dimensional structure of a long neurotoxin by M. Walkinshaw and W. Saenger (Max-Planck-Institute, Göttingen) has suggested a refined model for the multipoint attachment of toxins to the nicotinic acetylcholine receptors which must stimulate the design of new neuromuscular blocking agents. Even greater rewards may come from studying some of the more complex structures. For instance, it will be surprising if our new knowledge of virus coat structures does not lead to the design of some useful antiviral agents. □

ARTICLES

Northward displacement of north-central British Columbia

J. W. H. Monger

Geological Survey of Canada, 100 West Pender Street, Vancouver, Canada V6B 1R8

E. Irving

Earth Physics Branch, Energy, Mines and Resources, Ottawa, Canada K1A OE4

An extensive terrain in north-central British Columbia, apparently moved ~1,300 km northwards along the western fringe of North America during the late Cretaceous or early Tertiary, perhaps in much the same fashion as Baja California is doing today. Large anticlockwise rotations occurred within this terrain.

THE western, volcanosedimentary 'eugeosyncline' of the North American Cordillera is a collage of terrains of varied origins that apparently became attached to the western continental margin of the continent at different times[1-3]. These terrains now lie to the west of the line WW in Fig. 1, which is the probable western limit of the ancient North American craton. It is delineated by the westernmost limit of Palaeozoic and Precambrian strata whose continuity with the craton can be reasonably inferred, and by the transition of the $^{87}Sr/^{86}Sr$ initial ratios from <0.704 to the west (indicating that the underlying crust is of oceanic or island arc origin) to >0.706 to the east (indicative of continental crust)[4]. EE is the eastern limit of Cordilleran deformation.

The concept of a tectonic collage derives from several lines of evidence. Each terrain has an early Mesozoic and late Palaeozoic stratigraphy which differs from that of contiguous terrains[5,6], each has early Mesozoic and late Palaeozoic faunas that differ from coeval faunas along the ancient cratonic margin[7,8], and several have yielded palaeomagnetic results indicating that they have been displaced latitudinally or rotated by large angles about local vertical axes[9-12]. The Alaskan peninsula and the Chugach Mountains (SAJ of Fig. 1), composed of Jurassic and younger rocks, have been displaced 1,500 km from the south since the Jurassic[10]. A western terrain[13], sometimes called Wrangellia[5], with distinctive Triassic stratigraphy, comprises parts of southeastern Alaska, Queen Charlotte Islands, Vancouver Island and the Hell's Canyon area of eastern Oregon the latter denoted by '?' in Fig. 1b. Wrangellia has moved at least 1,500 km, and possibly as much as 5,000 km, from the south since the late Triassic[9,11]. Much of southeastern Alaska is underlain by the Alexander terrain, with characteristic Palaeozoic and Triassic strata[14]. Recent palaeomagnetic results[15] from the Alexander terrain indicate large anticlockwise rotations and yield Triassic palaeolatitudes consistent with those for the craton. Instances of northward displacements and clockwise rotations have been reported from batholithic rocks[16,17]. The Coast Range of Oregon[18,19], and the Transverse Ranges of southern California[20] have rotated clockwise by ~60° during the Tertiary. We now present palaeomagnetic evidence from a reconnaissance survey for the northwards displacement and differential rotation of an extensive tract of country in northern British Columbia known as the Stikine terrain, together with rocks of the Cache Creek Group that lie along its eastern border.

The integrity of the Stikine terrain during the early Mesozoic is shown by the distinctive late Triassic and early to middle Jurassic rocks that extend across it. It is bordered to the east by the Cache Creek Group, which lies just west of WW. The Cache Creek Group is interpreted as late Palaeozoic–early Mesozoic ancestral Pacific Ocean crust with its overlying deposits that were thrust westwards on to the Stikine terrain in post-Oxfordian time[2,6,21]. To the east of WW there are volcanogenic terrains that may have formed along or immediately offshore from the Pacific margin of North America during the Mesozoic[2]. The displacement of terrains in the western Cordillera from the south has been suggested first to account for the juxtaposition of warmer-water western Triassic faunas and cooler-water faunas in the Rocky Mountains[7], and second to explain the peculiar distribution of Permian fusulinids whereby the Cache Creek Group, with its distinctive verbeekinid or Tethyan faunas, was inserted between schwagerinid or American faunas that occur to the west in the Stikine terrain and to the east and south in south-central British Columbia, Oregon and California[8]. Our palaeomagnetic studies were undertaken to make quantitative estimates of any displacements that might have occurred.

Palaeomagnetic results

The rocks sampled are Upper Triassic and Lower Jurassic volcanogenic strata, typical of the Stikine terrain, and a Lower Cretaceous layered intrusion cutting deformed Cache Creek rocks (Fig. 2). These three rock units were sampled at 42 sites distributed among six localities. Within each locality the sequences are continuous, with no field evidence of relative motion. Attitudes of bedding, flow layering or compositional layering were measured at each site, with the exception of some massive augite porphyries at the base of the Triassic section (Table 1, section (7)), but their continuity with overlying, compositionally similar, uniformly dipping flows suggests they have the same attitudes. Three to six oriented samples (cores or hand samples) were obtained from each site. Two cores were cut from each hand sample, making a total of 236 cores. Two specimens were cut and measured from each core.

The oldest rocks studied are from the Savage Mountain Formation of the Takla Group of late Carnian to earliest Norian age[22]. The Savage Mountain Formation consists of up to 5,000 m of dark grey-green, locally red, pillow basalt and massive subaerial flows, with associated volcanoclastics. Samples were obtained from two localities, mainly from subaerial flows. At all collecting sites, with the exception noted above, attitudes could be accurately measured. When sampling
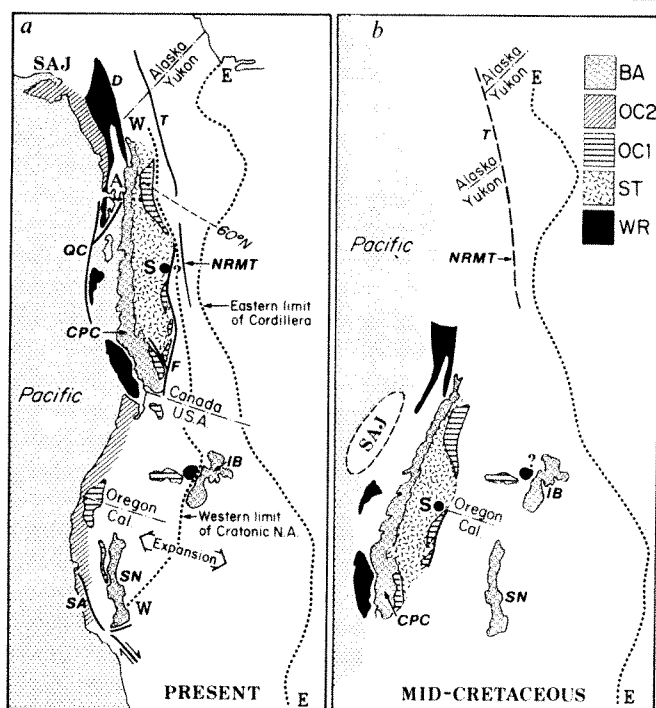
Fig. 1 *a*, A sketch-map showing some of the major tectonic elements of the Cordillera. EE is the easterly limit of deformation; WW, the westerly limit of the North American craton. BA, major plutons (CPC, Coast Plutonic Complex; IB, Idaho batholith; SN, Sierra Nevada batholith); WR, Wrangellia; ST, Stikine terrain; OC1, mid-Jurassic and older oceanic crust and rocks deposited on it; OC2, late Mesozoic and Tertiary oceanic crust and rocks deposited on it; A, the Alexander terrain is the blank area. *b*, The proposed position of the Stikine and Wrangellian terrains during the late Triassic to mid-Cretaceous. The Tertiary expansion of the Basin and Range Province is restored, and Wrangellia and the Coast Plutonic Complex are attached to the Stikine terrain in their present relative positions. These terrains are moved undistorted. We consider only gross latitudinal displacement, and no attempt is made to restore the original geometries of individual elements of the Stikine and Wrangellian terrains. Certainly large internal rotations are involved (see text). Major right-lateral strike-slip faults are marked: *D*, Denali; *F*, Frazer; *NRMT*, Northern Rocky Mountain Trench; *QC*, Queen Charlotte Island–Chatham Strait system; *SA*, San Andreas; *T*, Tintina. S is the sampling area, and SAJ is the late Jurassic displaced terrain of southern Alaska[10]. In *b* the Alaska–Yukon border is displaced on the Tintina–Northern Rocky Mountain Trench lineament to show the amount of motion that can be demonstrated geologically on one of the fault systems that might record some of the northward displacement of the Stikine terrain. The total displacement occurred by motions of comparable magnitude distributed among several such faults (see text).

Takla and Hazelton rocks, preference was given to deuterically oxidized basalts, because such rock types have been shown to be very stable magnetically[23], and our preliminary studies confirmed that this was also true for the sequences we have sampled (Fig. 3). Such oxidized rocks can usually be recognized by diagnostic minerals such as iddingsite in olivine basalts, because they are often reddish, and because they yield grey-red mud when drilled. The Takla basalts have alkaline affinities, and are generally porphyritic, with abundant clinopyroxene, feldspar, and altered olivine phenocrysts. The directions of natural remanent magnetizations (NRM) at each site are sometimes scattered, but are more commonly well grouped. During cleaning by alternating field (30–80 mT) or thermally (550–600 °C), they coalesce into good groups. The same directions persist after treatment in fields of 150 mT, and in some specimens, up to 200 mT. Blocking temperatures of this high coercive force magnetization are in the range 500–650 °C, and haematite and magnetite blocking temperatures often occur in the same specimen (Fig. 3). The directions remain unchanged between 500 and 650 °C, the haematite and magnetite magnetizations having identical directions. After cleaning, and after correction is made for the dip of the beds, the directions are westerly. This direction characterizes the

Savage Mountain Formation in the places sampled. The two localities have statistically identical inclinations, but their mean declinations differ by 19° as if they have been rotated relative to one another about vertical axes (Fig. 4, Table 1). The mean inclination of 41° yields a palaeolatitude of 23°, which is significantly lower than the late Triassic palaeolatitudes calculated from cratonic North America (Fig. 5).

Lower Jurassic rocks of the Hazelton Group were sampled at three localities spread over 100 km (Fig. 2). The Hazelton Group consist of calc-alkaline volcanics and intercalated sediments. It ranges in age from late Sinemurian to early Callovian, and extends across the eastern and southern parts of the Stikine terrain[24]. The group contains three formations: Telkwa (bottom), Nilkitkwa and Smithers (top). Late Sinemurian subaerial red basalt, and red fine-grained tuff of the Telkwa Formation were sampled from the Red Creek–Two Lake Creek area, and the Driftwood Range. Toarcian basalt and red tuff of the Nilkitkwa Formation were obtained from the Bait Range. The directions of NRM at each collecting site are usually grouped together but are occasionally scattered. Cleaning by alternating fields and heating yields well-grouped directions. The coercivity commonly exceeds 100 mT, and blocking temperatures are in the range of 500 to 700 °C, except in some tuffs in which the range is 200–600 °C (Fig. 3). The directions at the sites within a locality agree reasonably well. Moreover, the mean inclinations are statistically identical from locality to locality, but the declinations range from south-west to north-east (Fig. 4, Table 1), as if the localities have been differentially rotated by large angles about vertical axes. Alternatively, one may argue that these directions (unrotated) could be the resultants of unresolved antiparallel magnetization acquired over a substantial time interval during lithification when the geomagnetic field reversed in direction. This is improbable
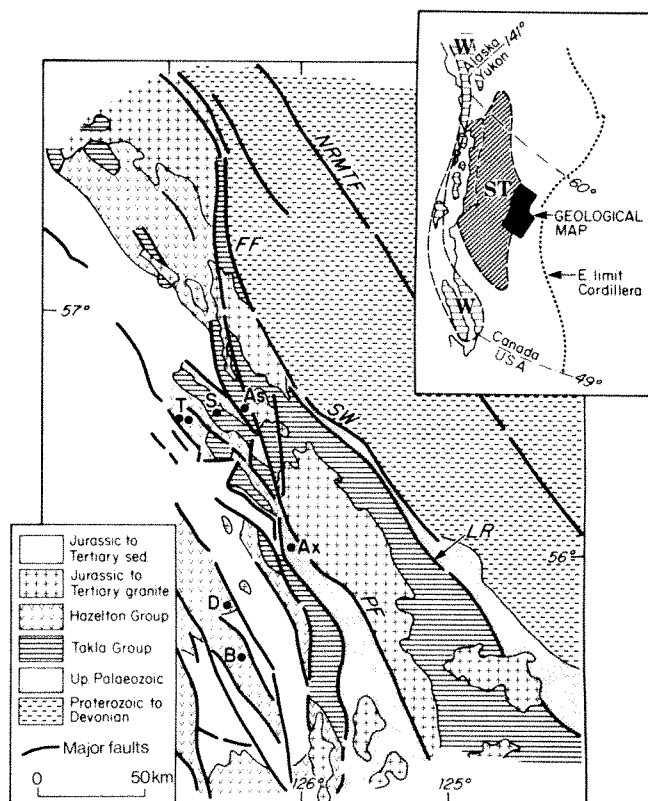
Fig. 2 Geology of the sampling region. The sampling localities are: As, Asitka Peak; Ax, Axelgold intrusion; B, Bait Range; S, Sustut Peak; and T, Two Lake Creek and Red Creek localities. The inset shows the general location and the two major displaced terrains, Wrangellia, W, and the Stikine terrain, ST. The faults marked are: FF, Findlay; LR, Lay Range; NRMT, Northern Rocky Mountain Trench; PF, Pinchi; and SW, Swannell.

Fig. 3 Demagnetization studies. Examples of thermal (TH) and alternating field (AF) demagnetization of pairs of specimens from the same oriented core. Directions are plotted on equal-area projections, the plane is the present horizontal. The numbers on the demagnetization graphs are the intensities of natural remanent magnetization (NRM) in units of 10^{-3} A m^{-1}. The Takla and Hazelton basalts are deuterically oxidized; the directions are little changed throughout the demagnetization range; remanent coercive forces are high; blocking temperatures appropriate to haematite and fine-grained magnetite occur; both minerals can be identified in polished section and both have the same magnetization direction; inclinations are positive (downward). In the Axelgold anorthosite the directions initially have negative inclination and they migrate rapidly to the characteristic direction (inclination positive) for the intrusion during removal of a soft magnetization which is randomly directed from core to core and which we attribute to lightning; there is a well-marked 'magnetite' blocking temperature; in polished section magnetite occurs as very fine rods in felspar crystals; remanent coercive forces are typical of those of fine-grained magnetite; haematite magnetizations do not occur. The red tuff from the Hazelton Group has negative inclination and the direction is little changed through the demagnetization range; the magnetization is due to very fine-grained hematite readily observed in polished section.
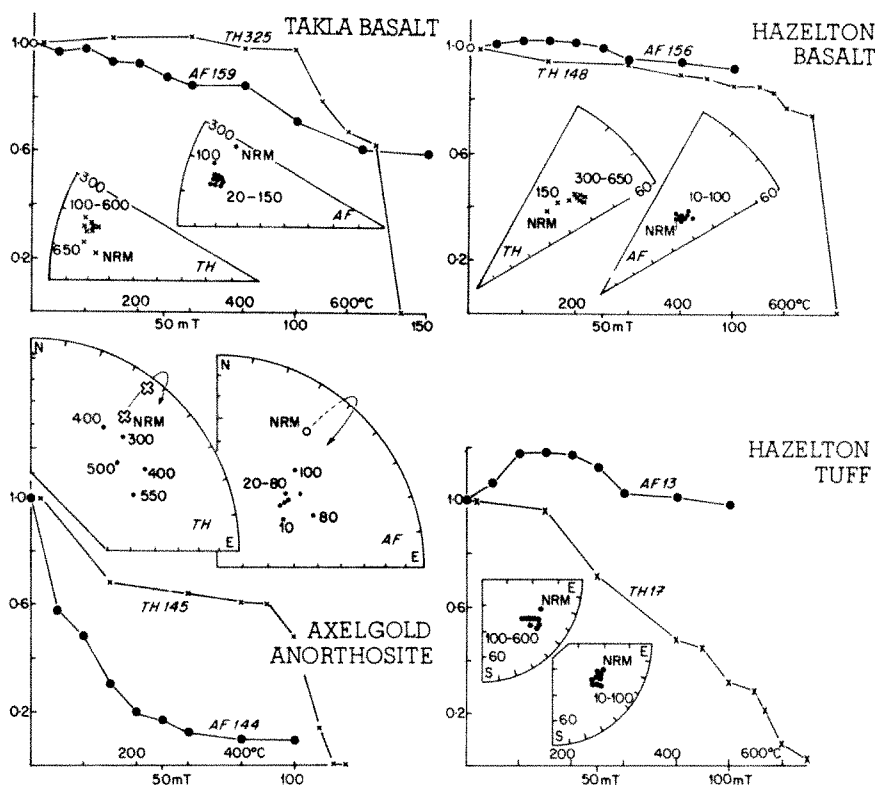
because the haematite and magnetite magnetizations that probably formed at somewhat different times always have identical directions (Fig. 3). Moreover, it is highly improbable that such a complex magnetic structure would have produced inclinations of both normal and reversed magnetizations that are consistent from locality to locality. A further possibility is that the directions (unrotated) are the resultants of primary magnetizations and stable secondary magnetizations, the latter acquired long after formation. Again, such an interpretation is highly improbable for the two reasons just given, and because we have been careful never to sample close to later igneous bodies or zones of secondary mineralization. Therefore we conclude that large relative rotations have occurred. A mean inclination (54°) is obtained by rotating all site directions so that the mean declinations at each locality agree (Hazelton rotated, Fig. 4). The mean palaeolatitude of 35° is 14° farther south than expected, but the difference is marginally significant. The large error of Fig. 5 arises from the considerable uncertainty in the early Jurassic field direction for cratonic North America as it is presently known (see below). These results from the Hazelton Group provide one of the few well-documented instances of reversals of magnetization in early Jurassic rocks.

The third unit is the Axelgold Intrusion, a layered body, 12 by 4.5 km in extent[25]. Its age is less well defined than in the previous two units. The body intrudes highly deformed rocks of the Cache Creek Group, and cuts structures that, 25 km to the north, are congruent with structures of post-Oxfordian age. The intrusion is therefore post-Oxfordian. Two biotites and one hornblende from the reaction rim of a granite xenolith in the interior of the intrusion, and from a micaceous gabbro close to the contract, yield K–Ar ages in the range 98–108 Myr (ref. 25). A second hornblende gives a K–Ar age of 155 Myr, but is considered[25] to "reflect the presence of excess argon". A mid-Cretaceous age is the most probable[25], but an early Cretaceous or late Jurassic age cannot be discounted. A mid-Cretaceous age is also consistent with the fact that we have found only normal polarities in the body, and normal polarity typifies the geomagnetic field in the interval 82–110 Myr (ref. 26). If it were late Jurassic or early Cretaceous, both normal and reversed polarity would have been expected in such a

large slowly-cooled body, because field reversals were then frequent[26].

The intrusion comprises alternating layers of anorthosite and anorthositic gabbro, ranging from ~10 to 50 cm in thickness, and dipping 10–15°. Anorthositic samples were chosen preferentially because preliminary studies showed them to be more stable magnetically. The layering was presumably produced by gravity-controlled magnetic currents and is therefore considered to be a good indicator of the palaeohorizontal. The NRM directions are usually scattered, but after cleaning in alternating magnetic fields they become well grouped, the characteristic magnetization having north-northeast declinations and steep downward inclinations (Fig. 4). The coercivity commonly exceeds 50 mT and the blocking temperatures are in the range of 500 to 600 °C. The mean inclination relative to layering is 69°, yielding a palaeolatitude of 52°, about 13° lower than expected for the mid-Cretaceous. It is possible that the layering was not formed horizontally, or that tilting occurred before the acquisition of remanence whilst the body was hot, and this estimate of palaeolatitude would then be in error. Note that the directions of magnetization relative to present horizontal (Table 1) yield a palaeolatitude of 40° which is even more aberrant. A further source of error is in the age of the intrusion. If it were late Jurassic, then the estimate of palaeolatitude would be in good agreement with that expected for North America at that time (see ref. 12, Fig. 15), implying that both the Cache Creek terrain, into which the body is intruded and the Stikine terrain were then in place relative to cratonic North America. Thus it is important to note that our preferred interpretation of Fig. 5 is uncertain because of the difficulty in determining accurately the age and the palaeohorizontal.

Discussion

The results for these three time intervals all yield mean palaeolatitudes that are close to the latitude of the California-Oregon boundary. The Stikine terrain is geologically a coherent entity so that although the observations are from a geographically restricted area they, nevertheless, indicate that from the late Triassic until sometime in the Jurassic or

Table 1 Summary of results

	Th	B	n	D, I	k	$\alpha_{95}°$	Pole λ, ϕ	$(dm°, dp°)$
(1) Axelgold, 98–108 Myr	270	13	67	025°, +69°	70	05	76°N, 033°W	(08, 07)
(2) Axelgold, uncorrected	270	13	67	032°, +60°	92	04	64°N, 012°W	(07, 05)
(3) Hazelton, mid-Toarcian	170	07	37	359°, +55°	15	16	70°N, 057°E	(22, 16)
(4) Hazelton, Sinemurian	070	04	28	242°, +56°	29	18	17°N, 175°W	(25, 18)
(5) Hazelton, Sinemurian	125	04	20	114°, −52°	14	25	40°N, 144°E	(35, 24)
(6) Takla, late Triassic	150	06	42	300°, +44°	31	06	38°N, 133°E	(15, 10)
(7) Takla, late Triassic	200	08	42	281°, +38°	18	07	24°N, 146°E	(16, 09)

(1) Axelgold layered intrusion, Axelgold Range 56.2°N, 126.1°W, cleaning 30–60 mT, normal polarity, direction relative to layering. Axelgold, directions relative to present horizontal. The precisions of (1) and (2) do not differ significantly. (3) Nilkitkwa Formation, Hazelton Group, Bait Range 55.6°N, 126.4°W, cleaning 550–600 °C, two sites reversed five sites normal polarity. (4) Telkwa Formation, Hazelton Group, Driftwood Range 55.8°N, 126.6°W, cleaning 80 mT and 550 °C, all normal polarity. (5) Telkwa Formation, Hazelton Group, Red Creek–Two Lake Creek area 56.5°N, 126.8°W, cleaning 550–600 °C and 60 mT, all reversed. (6) Savage Mountain Formation, Asitka Peak 56.7°N, 126.4°W, cleaning 60 mT and 500–550 °C, all normal polarity. (7) Savage Mountain Formation, Sustut Peak 56.6°N, 126.5°W, cleaning 60 mT and 500–550 °C, all normal. Directions in (3) to (7) are relative to bedding. Th, thickness of the section sampled in metres; B, number of sites each given unit weight in the analysis; n, number of cores (two specimens per core studied); D, I the mean direction; k, Fisher's estimate of precision; α_{95}, the 95% circle of confidence[35]. The position of the north pole is given; λ latitude, ϕ longitude. Unit weight given to each sampling site in the analysis.

Cretaceous the Stikine terrain was located ~1,300 km south of its present position relative to North America (Fig. 1).

The agreement between the mean values is excellent, better than would be expected from the associated errors (Fig. 5). The errors in palaeolatitudes of the base-maps have been obtained by giving unit weight to each rock unit when calculating the statistics of the mean polar wander path for North America[12] rather than to each determination of the geomagnetic field, that is, to each sampling site, of which there

Fig. 4 Mean directions of characteristic magnetization at each collecting site. Directions are plotted on the lower hemisphere and the perimeter is the palaeohorizontal. The magnetization have normal polarity (north-seeking directions plotted) in the Axelgold and Takla rocks. In the Hazelton both polarities occur and the reversed directions (south-seeking directions, S) are shown by open symbols. In d Hazelton results are shown unrotated, correction being made for geological dip only. In c the directions are 'corrected' for rotations about local vertical axes (see text).

may be many in an individual study. The combined error estimates of Fig. 5 may therefore be too large. To use a procedure (that of giving unit weight to each rock unit) that probably overestimates errors seems more prudent than to use a method (that of giving sites unit weight) that probably underestimates them.

We suggest that the most probable time of motion of the Stikine terrain from its more southerly position was latest Cretaceous or early Tertiary. The apparent absence of post-Triassic palaeolatitudinal motion of the Alexander terrain relative to the craton[15] indicates that the Stikine block became wedged in behind the Alexander terrain at that time. The older limit for the time of this motion is set by the Axelgold intrusion whose age uncertainty has already been discussed. An important additional argument in favour of this late motion comes from considering the palaeomagnetic evidence from the Coast Plutonic Complex (CPC of Fig. 1). The Coast Plutonic Complex is a belt of Cretaceous and early Tertiary intrusions and metamorphic bodies that has not been disrupted by later deformation. The Stikine terrain is attached to the complex because it is intruded by them. Magnetic inclinations observed in Cretaceous intrusions within the Coast Plutonic Complex (such as the Howe Sound pluton[27]) are systematically too shallow, indicating that they were emplaced 10° or more south of their present position (see ref. 17, Fig. 3). Such data suffer from the absence of accurate corrections for possible post-emplacement tilt, but the effect is systematic over 400 km, and indicate a latest Cretaceous or earlier displacement consistent with our results.

A displacement of this magnitude, so late in the history of the Cordillera, and occurring so far to the east, raises the question of where the differential movement with stable North America is located. There is no geological evidence of such a late ocean closure between the localities sampled and the craton. The Cache Creek Group is thought to be ancestral Pacific Ocean floor which was thrust westward over the eastern margin of the Stikine terrain in post-Oxfordian time. Three major faults lie east of the localities sampled, and on two of them dextral strike-slip movement has been reported. The Pinchi Fault (Fig. 2) may have been a transform fault in the late Triassic, and right-lateral slip has probably recurred along it in the late Cretaceous and/or early Tertiary[28,29]. The Swannell Fault, situated to the east of the Pinchi, juxtaposes metamorphosed Proterozoic strata against later Palaeozoic and early Mesozoic volcanogenic rocks, and may mark the ancient cratonic margin at this point. No evidence of lateral slip has been reported from it. The northern Rocky Mountain Trench is the site of the third major fault (Fig. 2). Almost certainly right-lateral slip has occurred on it, but the amount

Fig. 5 Palaeolatitudes of the Stikine terrain compared with those calculated from cratonic North America. The reference palaeopoles[12] used for North America are for 200 Myr 68°N, 093°E, for 175 Myr 78°N, 110°E, for 100 Myr 69°N, 188E. The error zones $(P=0.05)$ combine the errors in both base maps and palaeolatitude observations from the Stikine terrain. Error estimates are probably too large (see text).
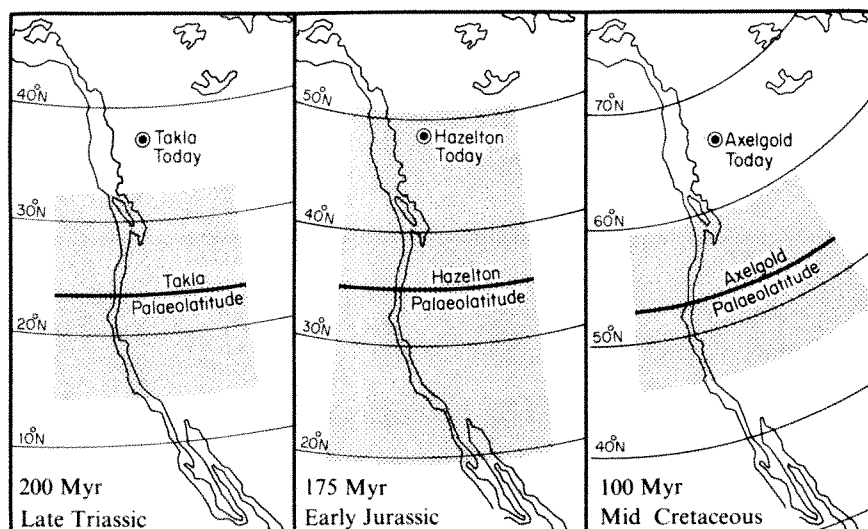
is unknown. It probably extends northwards into the Yukon Territory as the Tintina Fault (Fig. 1). Between 350 and 500 km of right-lateral movements since the mid-Cretaceous has been reported from the Tintina Fault[30,31], and the displacement may, in part, continue down the northern Rocky Mountain Trench and, in part, diverge westwards down such faults as the Pinchi and the Frazer lineaments (F, Fig. 1). The motions that can be documented geologically are much less than the 1,300 km derived from our evidence. For reasons discussed elsewhere[32] Wrangellia was very probably attached to the Stikine terrain (Fig. 1) and rode northwards with it in the late Mesozoic or early Tertiary[32].

Our interpretation conflicts with that of Symons[33] who argues that the area "has not been tectonically rotated or translated relative to stable North America". His arguments are based on his palaeomagnetic results from the Topley intrusions of the Stikine terrain. These intrusions are Jurassic in age, probably somewhat younger than the Hazelton Group. The Topley region has been intruded and partially covered by early Tertiary igneous rocks which have yielded K–Ar ages of between 50 and 63 Myr, and there was extensive hydrothermal activity and mineralization of economic importance at this time. We believe that Symons has misinterpreted his data, which are in fact consistent with our own. Symons' results (ref. 33, Fig. 3 and Table 1) fall into two distinct groups (A and B) which we believe have two separate origins. A magnetizations occur at eight sites in four of the Topley intrusions. They have a high mean stability index $(SI = 20)$ (ref. 33), normal and reversed polarity, and a mean inclination of 47°, corresponding to a palaeolatitude of 30° indistinguishable from that we find for the Hazelton (Fig. 5). The declinations are scattered and range from 294 to 348°, indicating variable anticlockwise rotations among the four Topley intrusions similar to the rotations we find for the Hazelton. The A magnetizations are, therefore, very similar to the magnetization of the Hazelton Group, and we suggest that they are primary and represent the Jurassic geomagnetic field. B magnetizations occur at seven sites in three other Topley intrusions[33]. Their polarity is always normal, they have a low mean stability index $(SI = 4)$, and are well grouped with much steeper inclinations than A $(D = 336°, I = 74°; N = 7; k = 96; \alpha_{95} = 6°)$. The corresponding pole, 75°N, 176°W, is statistically identical with the mean pole for North America at 60 Myr (77°N, 173°W; $\alpha_{95} = 7°$) (ref. 12). Hence, the less stable B magnetization was apparently acquired during the early Tertiary when igneous and hydrothermal activity was widespread in the Topley area. Symons averages all his results together and obtains a mean inclination of 63°, corresponding to a palaeolatitude of 40° $\pm 11°$, which is not significantly different from that expected

from cratonic North America. We suggest that his average result has no tectonic significance because it is derived from combining a Jurassic magnetization (A) with a Tertiary magnetization (B).

Although the continuity of rock units indicates that the Stikine terrain has behaved as a coherent entity, it has not behaved as a rigid plate, because the declinations of the magnetizations directions are highly variable (Table 1). On its eastern margin the Axelgold Intrusion has rotated 63° clockwise relative to cratonic North America (rotations were calculated using equation (9.2) ref. 18). Clockwise rotations are very common in the western Cordillera, and have been ascribed to motions of small blocks activated by right-lateral shear of the Pacific and North American plates—the so-called 'ball-bearing' hypothesis[34]. However, our palaeomagnetic declinations show large, variable and commonly anticlockwise rotations; 43° and 62° for the two Takla localities, 41° and 103° for two of the Hazelton localities and 14° clockwise for the third. Of course, the observed western declinations could be caused by much larger clockwise rotation (360° less the above angles) and so bring their sense of rotation into line with those generally found in the western Cordillera. However, the simplest explanation is that different parts of the Stikine terrain have undergone variable amounts of predominantly anticlockwise rotation relative to cratonic North America. This is inconsistent with the simple ball-bearing hypothesis[34]. The Stikine terrain at least in its eastern part seems to be an assemblage of slices of crust of continental thickness with areal dimensions comparable to or less than the thickness of the lithosphere, and which are separated by faults with high strains (Fig. 2). Within each slice the strata are only gently tilted or folded[24].

1. Hamilton, W. H. *Bull. geol. Soc. Am.* **80,** 2409–2430 (1969).
2. Davis, G. A., Monger, J. W. H. & Burchfiel, B. C. in *Mesozoic Paleogeography Western United States* (eds Howell, D. G. & McDougall, K. A.) 1–32 (Society Economics Paleography and Mineralogy, Pacific Section, 1978).
3. Monger, J. W. H. & Price, R. A. *Can. J. Earth Sci.* **16,** 770–791 (1979).
4. Armstrong, R. L. *Geol. Ass. Can. Cordilleran Sect. Prog. Abstr.* **7** (1979).
5. Jones, D. L., Silberling, N. J. & Hillhouse, J. W. *Can. J. Earth Sci.* **14,** 2565–2577 (1977).
6. Monger, J. W. H. *Can. J. Earth Sci.* **14,** 1832–1859 (1977).
7. Tozer, E. T. *Geol. Surv. Can. Econ. Geol. Rep.* **1,** 633–640 (1970).
8. Monger, J. W. H. & Ross, C. A. *Can. J. Earth Sci.* **8,** 259–278 (1971).
9. Irving, E. & Yole, R. W. *Earth Phys. Br. Publ. Energy, Mines and Resources, Can.* **42,** 87–95 (1972).
10. Packer, D. R. & Stone, D. B. *Can. J. Earth Sci.* **11,** 976–997 (1974).
11. Hillhouse, J. W. *Can. J. Earth Sci.* **14,** 2578–2592 (1977).
12. Irving, E. *Can. J. Earth Sci.* **14,** 669–694 (1979).
13. Muller, J. E. *Can. J. Earth Sci.* **14,** 2062–2085 (1977).

14. Berg, H. C., Jones, D. L. & Richter, D. H. *U.S. Geol. Surv. Prof. Pap.* **800D**, 1-24 (1972).
15. Hillhouse, J. W. *Geol. Soc. Am. Prog. Abstr. Meet.* 444 (1979).
16. Beck, M. E. & Noson, L. *Nature* **235**, 11 (1972).
17. Symons, D. T. A. *Can. J. Earth Sci.* **8**, 1388–1396 (1971).
18. Irving, E. *Paleomagnetism* 1–399 (Wiley, New York, 1964).
19. Simpson, R. W. & Cox, A. *Geology* **5**, 585–589 (1977).
20. Kamerling, M. & Luyendyk, B. P. *Bull. geol. Soc. Am.* **90**, 331–337 (1979).
21. Monger, J. W. H., Richards, T. A. & Paterson, I. A. *Can. J. Earth Sci.* **15**, 823–830 (1978).
22. Monger, J. W. H. *Geol. Surv. Can. Pap.* 76–29 (1977).
23. Wilson, R. L., Haggerty, S. E. & Watkins, N. D. *Geophys. J. R. Astr. Soc.* **16**, 79–5 (1968).
24. Tipper, H. W. & Richards, T. A. *Bull. geol. Surv. Can.* **270** (1976).
25. Irvine, T. N. *Geol. Surv. Can. Pap.* **75–1B**, 81–88 (1975).
26. Larson, R. & Pitman, W. *J. geophys. Res.* **82**, 3645–3662 (1972).
27. Symons, D. T. A. *Nature* **241**, 59–61 (1973).
28. Paterson, I. A. *Geol. Surv. Can. Paper* **74–1B**, 29–42 (1974).
29. Paterson, I. A. *Can. J. Earth Sci.* **14**, 1324–1342 (1977).
30. Roddick, J. A. *J. Geol.* **75**, 23–33 (1967).
31. Gabrielse, H. & Dodds, C. J. *Geol. Ass. Can. Prog. Abstr.* **2**, 19 (1977).
32. Irving, E., Monger, J. W. & Yole, R. W. *Geol. Ass. Can. Spec. Publ.* (in the press).
33. Symons, D. T. A. *Can. J. Earth Sci.* **10**, 1099–1108 (1973).
34. Beck, M. E. *Am. J. Sci.* **276**, 694–712 (1976).
35. Fisher, R. A. *Proc. R. Soc.* **A217**, 295–305 (1953).

Different species of messenger RNA encode receptor and secretory IgM μ chains differing at their carboxy termini

Paul A. Singer*, Helen H. Singer* & Alan R. Williamson

Department of Biochemistry, University of Glasgow, Glasgow, G12 8QQ, UK

Biosynthetic studies in the presence of an inhibitor of glycosylation indicate that individual human lymphoma-derived cell lines can synthesize both membrane receptor and presumptive secretory forms of IgM μ chains. The receptor form has a larger polypeptide chain than the secretory form and possesses a different C-terminus, but similar N-terminus, consistent with the presence of a C-terminal hydrophobic 'tail' for integral membrane binding. Messenger RNA isolated from these cells directs the synthesis of both forms of μ chain in a wheat germ translation system, indicating the presence of independent mRNAs for each form. It is proposed that the synthetic pathways for receptor and secretory IgM diverge at the post-transcriptional level, possibly by differential RNA splicing to give mRNA molecules with or without a translatable 'tail' segment.

RECEPTOR immunoglobulin molecules on the surface of B lymphocytes behave in many respects like typical integral membrane proteins. By contrast, serum immunoglobulins, which function as effector antibodies, are hydrophilic globular proteins. It is reasonable to postulate that this dichotomy of function of immunoglobulins is dictated by a duality of structure. For instance, the immunoglobulin heavy chain may be expected to possess restricted regions of hydrophobicity which would function in membrane interaction. However, serum immunoglobulins do not seem to possess such hydrophobic regions. This observation has led previous workers to postulate the presence of a hydrophobic peptide on the receptor form of immunoglobulin, which is absent from the otherwise similar secretory form[1,2]. Alternative explanations have also considered the possibility that differences in glycosylation of the receptor form could cause conformational changes which would favour membrane binding[2].

There has been a steady accumulation of indirect evidence as to the manner of membrane binding by receptor immunoglobulin. The μ chain from radioiodinated splenocyte receptor IgM has been shown to be of higher molecular weight than its secreted counterpart by SDS-polyacrylamide gel electrophoresis (SDS-PAGE)[3]. We have made a similar observation for receptor IgM and IgG μ and γ chains synthesized in several human lymphoid cell lines[4], and a similar phenomenon has been reported for receptor IgM of a mouse lymphoid cell line[5]. Buoyant density and solubility measurements in the presence of non-ionic detergents have shown a greater hydrophobicity for receptor IgM, as opposed to secretory IgM[6,7]. In spite of these findings, the basis for the observed differences in receptor and secretory immunoglobulins remained unclear. The apparent molecular weight differences could be due either to variation in the

extent of glycosylation or to a difference in polypeptide chain lengths. More recently, carboxypeptidase digestion and peptide mapping techniques have been used in several laboratories[5,8,9] to analyse membrane associated μ chains for a modified C-terminus. These studies have so far yielded conflicting results, which, in some experiments, may be due to contamination by the secretory μ-chain species.

A separate but related question to the structure of receptor immunoglobulin concerns the biosynthetic pathway which distinguishes it from secretory immunoglobulin. Previous models[10,11] have proposed that divergence of the pathways occurs just before secretion, based on the finding that intracellular transport of both forms is very similar[12,13]. However, investigations of the events preceding synthesis of the polypeptide chains have not been previously reported.

In this article we report on the structure and biosynthesis of receptor IgM chains in human lymphoid cells representing various stages of B-lymphocyte differentiation and immunoglobulin expression. We have used the drug tunicamycin as an inhibitor of glycosylation. Size comparisons of non-glycosylated μ chains indicate that the membrane form has a larger polypeptide chain than the secretory form. The larger membrane form of μ chain was isolated and shown by carboxypeptidase digestion to have a modified C-terminus (but a normal N-terminal sequence) relative to secretory μ chain, consistent with the presence on receptor μ chain of a C-terminal peptide, possibly hydrophobic in nature, capable of interaction with the plasma membrane. Unexpectedly, two forms of μ chain were detected intracellularly in Daudi and Raji nonsecretory cells, one resembling the membrane form and one resembling the secretory form with the former predominating in Daudi cells and the latter form predominating in Raji cells. This same pattern of μ-chain expression was found by cell-free translation of Daudi and Raji mRNA, indicating that the two forms of μ chain can be

---

*Present address: Max-Planck-Institut für Biologie, Corrensstrasse 42, 7400 Tübingen 1, FRG.

produced in the same cell by simultaneous translation of different mRNA molecules.

Cell lines with qualitatively and quantitatively different immunoglobulin biosynthetic capacities were chosen for examination (Table 1). Raji and Daudi cells each devote about 0.5% of their total protein synthesis to immunoglobulin production. Daudi cells deposit most of this immunoglobulin on the plasma membrane. Raji cells, by contrast, deposit very little of the immunoglobulin on the surface in a form detectable either by fluorescent antibody probes or by surface radioiodination. This comparison suggests that Raji more closely resembles a pre-B lymphocyte, while Daudi appears to be an analogue of a more mature B lymphocyte. RPMI 1788 is a high-rate IgM secreting lymphoblastoid cell line.

Our findings on the intracellular synthesis of membrane and secretory type μ chains reveal several unexpected features in the intracellular processing of μ chains by Daudi and Raji cells (Table 1). These features are discussed further below, and include the expression in characteristic ratios of two forms of μ chain by cell-free translation of isolated mRNA and in tunicamycin-treated cells, apparent lag in processing of leader sequences as revealed in the presence of tunicamycin, and probable unequal glycosylation of the two μ-chain forms.
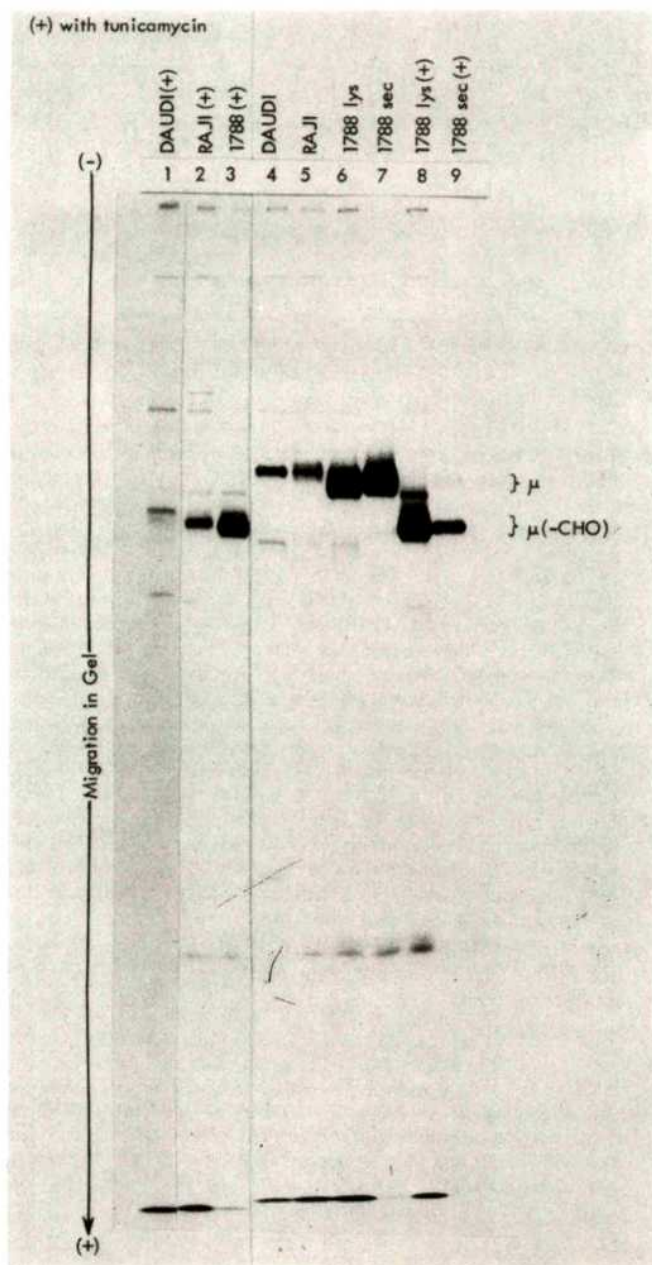
Analysis of the amino- and carboxy-terminal sequences of surface μ chains

The intracellular forms of μ chain found in nonsecretory and secretory cells can be distinguished from each other and isolated by immunoprecipitation and SDS-PAGE. Analytical characterization of the intracellular μ chains of Daudi, Raji and RPMI 1788 is shown in Fig. 1. The intracellular form of μ chain radiolabelled during a 1-h exposure of Daudi (lane 4) or Raji (lane 5) cells to ^{35}S-labelled methionine is of similar apparent molecular weight and is distinct from the lower molecular weight intracellular μ chain of the high rate secreting cell RPMI 1788 (lane 6).

The higher molecular weight of the surface μ chain could be due to either extra carbohydrate or an extra peptide at either amino-terminal or carboxy-terminal ends of the secreted μ chain. The hypothesis that surface μ chain contains an extra peptide was tested by analysis of the amino- and carboxy-terminal amino acid sequences of biosynthetically labelled μ chains. The partial amino-terminal sequences of Daudi and Raji μ chains (Fig. 2) show that each has a pattern of valine and leucine residues corresponding to the prototype $V_H III$) subgroup sequence. The period of labelling with radioactive valine and leucine was shorter than the turnover time for membrane immunoglobulin. Consequently these sequences establish that neither Raji nor Daudi μ chains retain the hydrophobic amino-terminal precursor peptide sequence, with which H chain synthesis is initiated, long enough for it to serve as a surface membrane insertion site. The μ chain of RPMI 1788 was subjected to similar analysis but proved to have a blocked amino terminus. In the absence of other sequence information, this blocked amino terminus is consistent with processing of the precursor peptide as expected for a secretory μ chain.

For comparative carboxy-terminal analysis of surface and secreted μ chains the enzyme carboxypeptidase-A was used. The carboxy-terminal residue to secretory μ chain is tyrosine[14], and carboxypeptidase-A will rapidly and completely remove a C-terminal tyrosine residue[15]. If surface μ chains possess an extra carboxy-terminal peptide they would not be expected to have a terminal tyrosine residue. This,

(+) with tunicamycin

Fig. 1 SDS-PAGE of biosynthetically labelled μ chains from tunicamycin treated and untreated cells. Log phase cultures were incubated with tunicamycin (0.5 μg ml⁻¹) for 4 h. Parallel untreated cultures were also maintained. 1×10^6 cells were collected for a 1-h pulse labelling in 0.2 ml medium containing no exogenous methionine and supplemented with 100 μCi ^{35}S-methionine (500 Ci mmol⁻¹). Complete RPMI 1640 medium (0.8 ml) supplemented with 15% fetal calf serum (growth medium) was added and incubation continued for 2 h. For the treated cultures, tunicamycin (0.5 μg ml⁻¹) was present throughout the labelling and chase periods. Cells were separated from culture medium and lysed by the addition of 0.2 ml ice cold lysis buffer (0.15 M NaCl, 1% Nonidet P-40, 1 mM phenylmethylsulphonylfluoride, pepstatin A (0.7 μg ml⁻¹), 25 mM Tris-HCl pH 8.2). Cell lysates were successively centrifuged to remove nuclei (1,000g, 10 min) and cellular debris (30,000g, 30 min) and labelled IgM was immunoprecipitated by addition of 10 μg affinity purified rabbit anti-human IgM antibody (15 min at 20°) and 25 μl of 10% solution of formalin-fixed, protein A-bearing *Staphylococcus aureus* organisms (Cowan 1 strain)[35]. The immunoprecipitates were washed three times with 0.5-ml aliquots of lysis buffer, heated to 100 °C for 2 min in SDS-PAGE sample buffer (2% SDS, 0.1 M dithiothreitol, 10% glycerol, 0.01 mg ml⁻¹ bromphenol blue dye, 0.065 M Tris-HCl pH 6.8), and electrophoresed in a 10% polyacrylamide slab gel according to the method of Laemmli[36]. Radioactive components were visualized by fluorography[37] (exposures of 2–24 h). The positions of glycosylated and non-glycosylated μ chains are indicated in the margin. Lanes 1, 2, 3, 8 and 9, tunicamycin treated; lanes 4, 5, 6 and 7, untreated cells.

Raji   -V - LV----- LV----- L-L

Daudi   -V - LV-- ----LV----- L- L

V$_H$III   EVQLVESGGGLVQPGGSLRL

Fig. 2 Partial amino-terminal amino acid sequences of μ chains. The μ chains of Raji and Daudi cell IgM were biosynthetically labelled with ³H-leucine (55 Ci mmol⁻¹) and ³H-valine (36 Ci mmol⁻¹) and isolated by immune precipitation and SDS-PAGE as described in legends to Figs 1 and 3. Amino acid sequences were determined by automated Edman degradation performed on a Beckman 890C sequenator. Repetitive yield at each cycle determined by internal standards was 88–92%. Separate sequencer runs were performed for each sample labelled with each amino acid. The V$_H$III prototype sequence is from ref. 38.

approach has already been used to investigate the carboxy terminus of μ chains from the human cell line Bri-8 and the mouse myeloma tumour McPc 1748 (ref. 8), as well as the mouse B cell line 38C-13 (ref. 5). In all three cases there was significant release of radioactive tyrosine from μ chain by carboxypeptidase-A treatment. However, in those studies there was no convincing demonstration that the μ chains investigated were of the surface form. Also there was a lack of kinetic evidence to support the proposal that the tyrosine residues released were indeed carboxy-terminal. The Bri-8 cell line studied in this laboratory is a high-rate IgM secreting line. Recently carboxypeptidase-A digestion of Daudi μ chain has been reported to release fractional molar amounts of several amino acids, including tyrosine, but kinetics suggested that valine is located closer to the carboxy terminus than tyrosine[9]. For the present studies Daudi, Raji, RPMI 1788 and Bri-8 cells were labelled for 1 h with ³H-tyrosine and the intracellular μ chains and L chains isolated by immunoprecipitation and SDS-PAGE. Patterns similar to those shown in Fig. 1 (lanes 4–6) were obtained and individual μ chains and light chains were eluted from the appropriate regions of the gel. The kinetics of carboxypeptidase-A catalysed release of ³H-tyrosine from these isolated chains is shown in Fig. 3. For the μ chains of secreted IgM of RPMI 1788 and Bri-8 approximately 1 mol of tyrosine is released per chain during 2 min of incubation. This finding is consistent with the kinetics of release of carboxy terminal tyrosine from aldolase[16]. Carboxypeptidase analysis of the ³H-tyrosine labelled light chains of RPMI 1788, Bri-8 and Raji shows no release of tyrosine. This is consistent with known sequences and established the low background in this analysis. The intracellular μ chains of characteristic surface size isolated from Daudi and Raji cells showed a partial release of tyrosine in the carboxypeptidase-A analysis (Fig. 3). Tyrosine was released from Daudi and Raji μ chains with kinetics indicating a carboxy-terminal location, but with the yield in both cases significantly lower than expected. The yields of tyrosine released correspond to approximately 0.35 mol for Daudi and 0.7 mol for Raji μ chain (based on an estimate of 20 tyrosine residues per chain). The simplest interpretation of these results is that Daudi and Raji cells contain, in different proportions, two different forms of μ chain, only one of which has a carboxy-terminal tyrosine residue.

Analysis of non-glycosylated μ chains

Human μ chains are glycosylated at five asparagine residues and the carboxydrate side chains constitute approximately 15% of the molecular weight of human IgM[17–19]. To test the hypothesis that the difference in molecular weight between

surface and secreted μ chains could be due to a difference in the extent of glycosylation, the drug tunicamycin was used to inhibit glycosylation during μ chain biosynthesis. Tunicamycin has been shown to act by inhibiting the formation of N-acetylglucosamine lipid intermediates[20], which serve as donors for the synthesis of the core regions of asparagine-linked oligosaccharides[21]. Biosynthesis of completely non-glycosylated μ chains was effected by preincubating the lymphoid cells with tunicamycin in limiting conditions[22]. SDS-PAGE analyses of the non-glycosylated μ chains are shown in Fig. 1 and in more detail in Fig. 4. The intracellular form of secretory μ chain from tunicamycin treated RPMI 1788 cells is a single band (lane 9, Fig. 4) with a considerably lower apparent molecular weight than the glycosylated intracellular μ chain of RPMI 1788 (lane 3) or the glycosylated
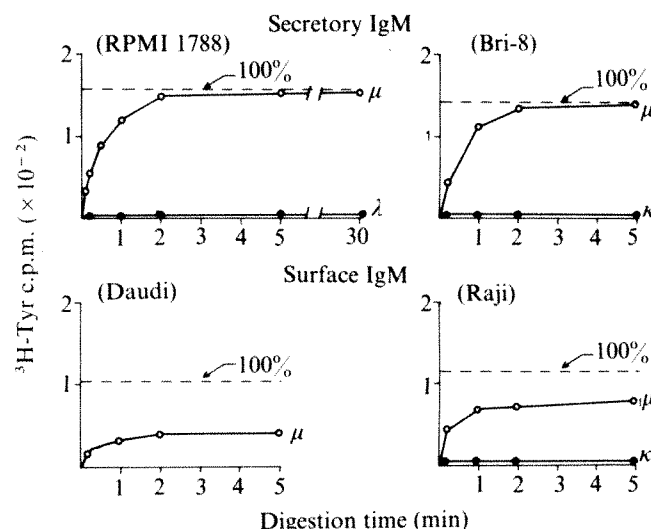
Fig. 3 Carboxy-terminal tyrosine released from intracellular μ chains of the pre-membrane and pre-secretory types. Log phase cells (5 × 10⁶ per ml) were labelled for 1 h in either 0.2 ml (Bri-8, RPMI 1788) for 0.5 ml (Daudi, Raji) RPMI 1640 lacking exogenous tyrosine and supplemented with ³H-tyrosine (500 μCi ml⁻¹; 40 Ci mmol⁻¹). Cell lysis, anti-μ immunoprecipitations, SDS-PAGE and fluorography were done as described for Fig. 1. The fluorography of the gel (not shown) revealed μ and light chain bands similar to those shown in Fig. 1, lanes 4, 5 and 6 (Bri-8 μ-chain mobility was indistinguishable from that of RPMI 1788). Bands were located by overlaying the dried gel with the fluorographic negative. Gel pieces containing the bands were sliced out and the material eluted overnight at 60 °C in 0.5 ml elution buffer (2% SDS, 20 mM dithiothreitol, 0.25 M Tris-HCl, pH 8.2). After removal of the gel slices, 0.5 mg bovine serum albumin (as carrier) and freshly recrystallized iodoacetamide (final concentration 50 mM) were added and the samples incubated in the dark at 20 °C for 30 min. The proteins were precipitated with acetone (five volumes), collected by centrifugation, and washed twice with acetone:water (5:1 v/v). The air-dried precipitates were dissolved by heating at 100 °C for 2 min in 0.9 ml digestion buffer (0.2 M LiCl, 50 mM NaHCO₃). Insoluble material (less than 10% of the radioactivity) was removed by centrifugation, and the samples adjusted to pH 8.0 with 0.5 M NaOH. Crystals of carboxypeptidase A (Worthington Biochemicals) were washed with water and dissolved in 10% LiCl at 0.2 mg ml⁻¹ ($A_{280}/2.3$ = mg ml⁻¹). Digestions (enzyme:substrate = 1:100) were initiated by addition at 20 °C of 10 μl enzyme solution with rapid mixing. Aliquots (150 μl) of reaction mixture were removed at the times indicated, immediately added to 50 μl ice cold 40% trichloroacetic acid, for determination of released ³H-tyrosine (acid-soluble) fraction. The hypothetical 100% release values are based on an estimated 20 tyrosine residues per μ chain (or 18 for RPMI 1788).

Table 1 Summary of μ-chain expression in the cell lines investigated

	IgM expression*		μ Chains detected intracellularly‡			μ chains detected by cell-free translation
	Membrane	Secretory	Level†	Glycosylated	Non-glycosylated	
Daudi	+ + +	−	0.5%	MEMBRANE / secretory } §	PREMEMBRANE presecretory	PREMEMBRANE presecretory
Raji	+	−	0.5%	membrane / SECRETORY } §	premembrane PRESECRETORY	premembrane PRESECRETORY
RPMI 1788	±	+ + +	5–10%	SECRETORY	PROCESSED SECRETORY	PRESECRETORY

CAPITALS designate the predominant or only form detected.

*Qualitative expression as determined by using fluorescent antibody, surface radioiodination and biosynthesis techniques.

†Incorporation of ^{35}S-methionine into anti-μ precipitable relative to trichloroacetic acid precipitable cellular proteins during a 60-min labelling.

‡Species labelled with ^{35}S-methionine during a 15–60-min pulse, resolved by SDS-PAGE and/or characterized by C-terminal analysis. Terminology as follows: membrane—membrane μ chain lacking C-terminal tyrosine; secretory—secretory μ chain with C-terminal tyrosine; presecretory and premembrane—respectively μ-chain forms with presumed N-terminal leader sequence; processed secretory—indicates cleavage of N-terminal leader sequence. The presence or absence of the N-terminal leader sequence (that is, yielding pre or processed μ chain respectively) can be assessed by comparison of the mobilities on SDS-PAGE of non-glycosylated μ chains with the products of cell-free translation of μ-chain mRNA.

§These are detected by SDS-PAGE as one band of membrane μ-chain size, however C-terminal analysis of glycosylated chains is consistent with the indicated composition. The processing of glycosylated chains cannot be resolved by SDS-PAGE analysis but amino-terminal sequence analysis (Fig. 2) shows that processing is complete within 6 h after synthesis.

extracellular μ chain (lane 7, Fig. 1). The non-glycosylated μ chains of Raji and Daudi intracellular IgM are resolved into two forms (lanes 7, 8, Fig. 4) differing from one another in their apparent molecular weights. The lower molecular weight μ chains of Daudi and Raji are similar in mobility to each other and have a perceptibly lower mobility than the non-glycosylated μ chain of RPMI 1788 cells (lane 9). The major difference between Daudi and Raji profiles is in the intensity of the labelling of the two forms of μ chain, with the higher molecular weight form of μ chain predominating in Daudi, and the lower molecular weight form predominating in Raji. The existence of two forms of μ chains in Daudi and Raji cells confirms the prediction made on the basis of the carboxy-terminal analysis as discussed above. Comparison of the relative proportions of the two forms of μ chain with the differential release of tyrosine from Daudi and Raji μ chains is consistent with the interpretation that the higher molecular weight form of both Daudi and Raji μ chain lacks carboxy-terminal tyrosine and the lower molecular weight form has a carboxy-terminal tyrosine residue (thus being analogous to the secreted μ chain of similar apparent molecular weight). On this hypothesis the higher molecular weight form of μ chain in Raji and Daudi cells is the precursor of surface μ chain, and the molecular weight difference relative to the secretory μ chain is due to an extra carboxy-terminal peptide attached to the secretory μ-chain sequence and preventing carboxypeptidase catalysed release of the carboxy-terminal tyrosine. Evidence consistent with this hypothesis was obtained by separation of the two forms of non-glycosylated Daudi μ chain biosynthetically labelled with tyrosine and subsequent carboxypeptidase digestion. The higher molecular weight form of μ chain has essentially no carboxypeptidase-releasable tyrosine while the lower molecular weight form of μ chain yields a mole of tyrosine and kinetics consistent with tyrosine being the carboxy-terminal residue (Fig. 5). A similar analysis of the two Raji μ chains (not shown) yielded similar results.

A comparison of the SDS-PAGE profiles of Daudi and Raji non-glycosylated μ chains with those of glycosylated μ chains (compare lanes 7 and 8, Fig. 4 with lanes 4 and 5, Fig. 1) shows that glycosylation abolishes the mobility differences observed between the membrane and secretory forms. This suggests that during a 1 h incorporation of label the secretory-type μ chains from Daudi and Raji cells have more
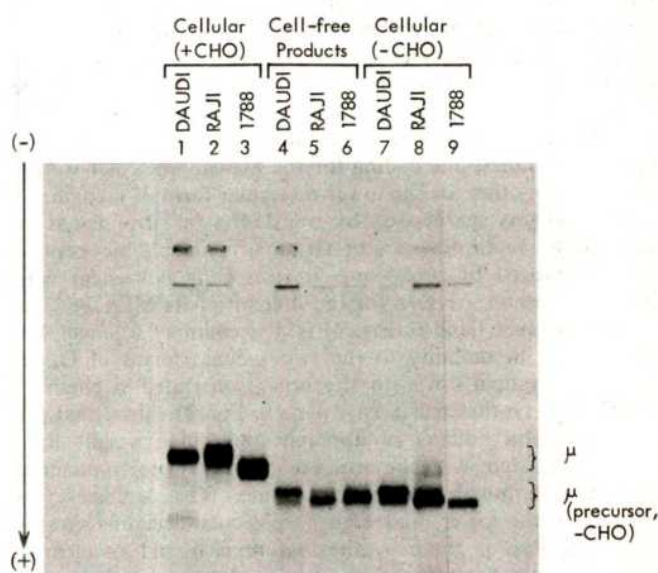
Fig. 4 SDS-PAGE comparing membrane and secretory type μ chains synthesized *in vivo* in glycosylated (+CHO) or non-glycosylated (−CHO) forms and in a wheat germ cell-free system. Cells were labelled by incorporation of ^{35}S-methionine in the presence (for 60 min) or absence (for 15 min) of tunicamycin (0.5 μg ml^{-1}) as described in the legend to Fig. 1. Wheat germ extract was prepared and assays run essentially as described previously[25]. Assays (50 μl) contained 25 μCi ^{35}S-methionine (800 Ci mmol^{-1}) and poly(A)$^+$ RNA (1 μg) prepared from each cell line by phenol extraction and oligo(dT)-cellulose chromatography of isolated polyribosomes. After incubation, assays were diluted fivefold with 3D-TKM buffer (0.1 M KCl, 5 mM MgCl$_2$, 1% Triton X-100, 1% sodium deoxycholate, 0.5% SDS, 0.1 M Tris-HCl pH 8.0). Anti-μ immunoprecipitations were carried out on cell lysates and diluted wheat-germ assays, and the immunoprecipitates analysed by SDS-PAGE on reducing 10% polyacrylamide slab gels as described in the legend to Fig. 1. The approximate mobility ranges of glycosylated, nonglycosylated and cell-free synthesized μ chains are indicated in the margin.

carbohydrate attached relative to the membrane μ chains. Mobility comparisons with the RPMI 1788 intracellular μ chain (lane 6, Fig. 1) support the idea that it is overglycosylation of the Daudi and Raji secretory-type μ chains, and not underglycosylation of the membrane forms, which is occurring. A more direct experimental approach will be required to resolve this point, however.

Cell-free biosynthesis of μ chains

The above results are consistent with, but do not prove, an independent biosynthetic origin for the two forms of μ chain in Daudi and Raji cells. A separate biosynthetic origin for these two μ chains was confirmed by their production in a cell-free protein synthesis system.

Messenger RNA capable of being efficiently translated in a wheat-germ cell-free system was isolated from Daudi, Raji and RPMI 1788 cells. Polyribosomes were prepared and polyribosomal RNA fractionated over oligo(dT)-cellulose. The poly(A) containing mRNA was translated in a wheat-germ cell-free system and the immunoglobulin chains produced were specifically immunoprecipitated and analysed by SDS-PAGE (Fig. 4). Daudi and Raji μ chains resolved into two bands (lanes 4 and 5).

These two forms of μ chains are similar in apparent molecular weight to the two non-glycosylated forms of μ chain synthesized in vivo in the presence of tunicamycin (compare lanes 4 and 5 with lanes 7 and 8, Fig. 4). It is also striking that the relative labelling intensities of the two forms of μ chain resulting from cell-free translation of Daudi and Raji messenger RNA resembles the labelling pattern seen in vivo for the non-glycosylated μ chains. The strong similarity of the patterns seen in vitro and in vivo supports the hypothesis that both Daudi and Raji cells contain two different μ-chain mRNA molecules, one coding for the higher molecular weight form and the other for the lower molecular form of μ chain.

The μ chains synthesized by translation in vitro would be expected to retain the amino-terminal hydrophobic peptide that is removed by processing in vivo. Data consistent with this phenomenon are seen for the μ chain of RPMI 1788. The cell-free product (lane 6, Fig. 4) is a μ chain of a single size intermediate in mobility to the two μ-chain forms of Daudi and Raji. Comparison with the non-glycosylated μ chain of RPMI 1788 synthesized in vivo (lane 9, Fig. 4) shows that the cell-free product differs in apparent molecular weight in a manner consistent with the presence on the cell-free μ chain of the amino-terminal precursor peptide. The similarity of mobility of the lower (and higher) molecular weight forms of Daudi nd Raji μ chain synthesized in vivo and in vitro is consistent with the retention of the precursor peptide on the Daudi and Raji μ chains synthesized in vivo in the presence of tunicamycin. This would indicate that processing takes much longer than 1 h (the pulse-labelling time) but, in the absence of tunicamycin, processing is complete within 6 h (Fig. 2). Processing of an immunoglobulin κ chain can be retarded in vivo by culturing myeloma cells with protease inhibitors[23]. The expected size difference between the precursor form of RPMI 1788 μ chain and the mature non-glycosylated form is approximately 2,000 daltons[24,25]. This allows us to estimate the molecular weight difference between the two forms of Daudi and Raji μ chain as being approximately 3,000 daltons.

The size difference between the two forms of Daudi and Raji μ chain considered together with the demonstration of the absence of carboxy-terminal tyrosine in the higher molecular weight μ chain is consistent with the presence of an extra carboxy-terminal peptide of approximately 30 residues long relative to the lower molecular weight form of μ chain. The evidence of Williams et al.[9] indicates that the carboxy-terminal peptide of Daudi surface μ chain is probably hydrophobic. It is postulated that the carboxy terminal hydrophobic peptide (tail peptide, T) serves to anchor the μ chain of surface IgM to

membrane from the point of synthesis to display of IgM on the plasma membrane. The T peptide provides a structural explanation for the difference between surface and secretory IgM and allows surface IgM to be an integral membrane protein resembling other integral membrane proteins in being attached to the membrane by a carboxy-terminal hydrophobic peptide.

Previously no direct evidence could be found for surface IgM being a transmembrane protein. The negative finding was based on the absence of iodination of μ chain on the inside of the plasma membrane[26] but those data can now be interpreted to mean that there is no tyrosine residue available in the T peptide. Two previous studies had claimed that surface μ chain has a carboxy-terminal tyrosine residue and therefore lacks a carboxy-terminal hydrophobic peptide for membrane attachment[5,8]. Those results were probably due to analysis of a mixture of secretory and surface μ chains, although it is also possible that the tyrosine released by carboxypeptidase may have been located within the T peptide since kinetic evidence for carboxy-terminal location was not supplied. The present unexpected finding that Daudi and Raji cells synthesize two forms of μ chain means that a demonstration that a given cell line does not secrete immunoglobulin can no longer be accepted as evidence that the cell line will only synthesize the surface form of heavy chain. Both Raji and Daudi cells display IgM on the surface and neither secretes any IgM; however, both lines apparently synthesize an intracellular form of μ chain lacking the T peptide. For both cell types the quantitation is consistent with the hypothesis that only the μ chain with the extra T peptide is displayed on the cell surface but this remains to be proven by a chase experiment. We suggest that the secretory-sized form of μ chain synthesized in Daudi and Raji cells is metabolized intracellularly.
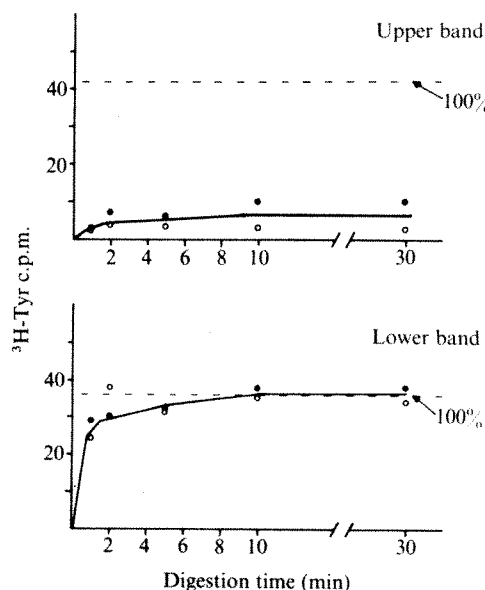
Fig.5   Carboxy-terminal analysis of the larger (top) and smaller (bottom) forms of Daudi μ chains. Daudi cells were preincubated for 4 h in growth medium containing tunicamycin (0.5 μg ml^{-1}). Cell labelling with ^{3}H-tyrosine, lysis, immunoprecipitations, SDS-PAGE, fluorography and elution of radioactive bands were done as described for Fig. 3. The gel (not shown) revealed doublet bands of μ-chain mobility similar to those in Fig. 5, lane 7. For accurate separation of μ-chain species, the bands were sliced out one at a time, and their orientation relative to the main gel preserved. Fluorographs were taken after removal of each band and used to determine the accuracy of the slicing. Gel pieces were then trimmed as necessary to minimize cross-contamination. Carboxypeptidase digestions were performed and the results are plotted as described for Fig. 3. Reproducibility of the data is indicated by the results of duplicate determinations at each time point.
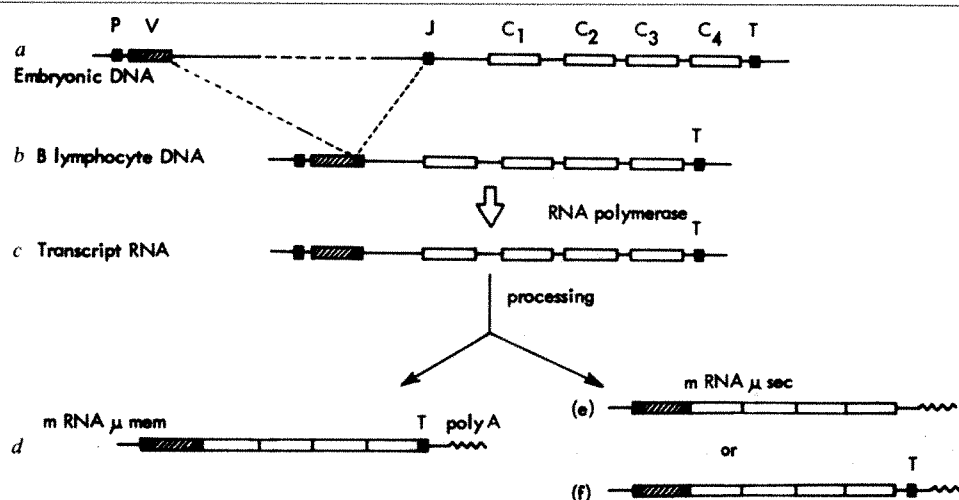
Fig. 6 Model for T-gene segment and the biogenesis of mRNAμ_{mem} and mRNAμ_{sec}. Depicted are the probable arrangements of heavy chain gene segments[39,40] in embryonic DNA (*a*) and B-lymphocyte DNA (*b*), including the postulated T segment. A DNA rearrangement bringing the P +V$_H$ segment into contiguity with the J$_H$+C$_H$ gene segments, by analogy with V$_\lambda$ rearrangement[41], is shown. A similar rearrangement of the T-gene segment from embryonic to B-lymphocyte DNA is possible, but not necessary to the model. The possibility of a later rearrangement of B-lymphocyte DNA, which would give rise to mRNAμ_{mem} or mRNAμ_{sec} is unlikely in view of the finding of simultaneous expression of both forms in individual cells. The model shows a single B-lymphocyte μ-chain transcription unit (*b*) with the T segment in its embryonic relationship to the other C-region gene segments. Expression of the heavy chain transcription unit would yield a single common nuclear precursor RNA (*c*), which would then be processed by a splicing mechanism into mature mRNAμ_{mem} (*d*, T segment joined to C$_{H4}$) and mRNAμ_{sec} (*e*, T segment spliced out or *f*, T segment in non-translated RNA). Processing would presumably require specific recognition sequences and splicing enzymes, the activity of which would determine the relative production of membrane and secretory IgM. Each immunoglobulin heavy chain class could have a unique T segment, or a single T segment could be spliced into two or more heavy chain genes during RNA processing.

Our evidence indicates that the two forms of μ chain, with and without the T peptide, are produced by translation of different mRNA molecules. These two mRNA molecules could originate either from separate genes or from a single segmented gene by differential processing of a common nuclear RNA precursor. These models must be considered in the light of our knowledge of surface immunoglobulin and the switch from surface to secretory immunoglobulin. Surface receptor antibody on B lymphocytes can apparently be of any class or subclass of immunoglobulin[27] and indeed two classes of immunoglobulin, apparently associated with the same idiotype[28–30] or antibody specificity[31], can be found on the surface of a single cell. A suitable model must therefore allow the attachment of a T peptide to the constant region of any class or subclass of immunoglobulin and embrace the simultaneous expression of the surface form of two different classes of immunoglobulin. The segmented nature of an immunoglobulin H chain gene leads to the suggestion that the T peptide is encoded by a separate DNA segment, The *T* gene segment. Each C$_H$ gene could have its own T segment or a single T segment could be shared by some or all of the C$_H$ genes with rearrangement of the T segment to allow expression. The T segments would be selected to code for a peptide with a more consistently hydrophobic nature than that of the amino-terminal precursor peptide, but as with the precursor peptides, sequence diversity of the T segment might be expected. The postulated T-gene segment would function as part of the heavy chain transcription unit.

The simultaneous production of surface and secreted forms of the same immunoglobulin molecule by monoclonal cell lines in culture[4,5] (or surface and intracellular forms as demonstrated in these studies) argues against rearrangement of DNA segments being required for the switch from surface to secreted immunoglobulin. Thus the model which best fits the present data is one in which the switch from surface to secreted H chain involves a change at the level of nuclear RNA processing (Fig. 6). It is consistent with this model that there is no evidence for different genetic markers on surface and secreted immunoglobulins of the same class. Changes in the processing of RNA transcripts have been evoked as a possible explanation for the switch from one immunoglobulin class to another during clonal expansion[32]. However, studies

on hybrid cells have so far failed to show evidence for an enzymatic mechanism involved in differential processing of μ and γ chain RNA[33]. Recently, direct evidence against this mechanism for heavy chain class switching has been obtained from the analysis of large nuclear RNA with combinations of μ, γ and α gene probes[34].

Our present finding suggests that messenger RNA molecules coding for both μ_{mem} and μ_{sec} may function in either pre-B or B lymphocytes. It is also possible that the two types of μ_{sec} messenger RNA (Fig. 6*e* and *f*) could function at different stages of B-lymphocyte differentiation.

Since this manuscript was submitted two relevant reports have appeared. (1) The murine of γ_1 heavy chain gene has been completely sequenced by Honjo *et al*.[42]. This sequence shows a putative RNA splicing site near the 3′ end of the C$_{H3}$ coding sequence. (2) Four different sizes of μ chain mRNA have been resolved in a murine lymphoma line by Perry and Kelley[43]. The translation products of these mRNA molecules have yet to be defined.

Note added in proof: Evidence supporting the mechanism illustrated in Fig. 6 has recently been obtained from sequences of a cloned DNA encoding the Cμ gene segments[44]. Evidence for two mRNA molecules differing at their 3′ ends comes from sequence of cloned cDNA corresponding to μ mRNA[45].

1. Singer, S. J. *Adv. Immun.* **19**, 1–66 (1974).
2. Vitetta, E. S. & Uhr, J. W. *Biochim. biophys. Acta* **415**, 253–271 (1975).
3. Melcher, U. & Uhr, J. W. *J. Immun.* **116**, 409–415 (1976).
4. Singer, P. A. & Williamson, A. R. *Eur. J. Immun.* (in the press).
5. Bergman, Y. & Haimovich, J. *Eur. J. Immun.* **8**, 876–880 (1978).
6. Melcher, U., Eidels, L. & Uhr, J. W. *Nature* **258**, 434–435 (1976).
7. Melcher, U. & Uhr, J. W. *Biochemistry* **16**, 145–152 (1977).
8. McIlhinney, R. A. J., Richardson, N. E. & Feinstein, A. *Nature* **272**, 555–557 (1977).
9. Williams, P. B., Kubo, R. T. & Grey, H. M. *J. Immun.* **121**, 2435–2439 (1978).
10. Uhr, J. W. *Cell Immun.* **1**, 228–244 (1970).
11. Uhr, J. W. & Vitetta, E. S. *Fedn Proc.* **32**, 35–40 (1973).
12. Sherr, C. J. & Uhr, J. W. *J. exp. Med.* **133**, 901–920 (1971).
13. Sherr, C. J., Shenkein, I. & Uhr, J. W. *Ann. N.Y. Acad. Sci.* **190**, 250–367 (1971).
14. Putnam, F. W., Florent, G., Paul, C., Shinoda, T. & Shimizu, A. *Science* **182**, 287–291 (1973).
15. Ambler, R. P. *Meth. Enzym.* **25**, 262–272 (1967).

16. Winstead, J. A. & Wold, F. *J. biol. Chem.* **239**, 4212–4216 (1964).
17. Metzger, H. *Adv. Immun.* **12**, 57–116 (1970).
18. Spragg, B. P. & Clamp, J. R. *Biochem. J.* **114**, 57–64 (1969).
19. Shimizu, A., Putnam, F. W., Paul, C., Clamp, J. R. & Johnson, I. *Nature new Biol.* **231**, 73–76 (1971).
20. Tkacz, J. S. & Lampen, J. O. *Biochem. biophys. Res. Commun.* **65**, 248–257 (1975).
21. Waechter, C. J. & Lennarz, W. J. *A. Rev. Biochem.* **45**, 95–112 (1976).
22. Williamson, A. R., Singer, H. H., Singer, P. A. & Mosmann, T. R. *Biochem. Soc. Trans.* (in the press).
23. Schmeckpeper, B. J., Adams, J. M. & Harris, A. W. *FEBS Lett.* **53**, 95–98 (1975).
24. Jilka, R. L. & Pestka, S. *Proc. natn. Acad. Sci. U.S.A.* **74**, 5692–5696 (1977).
25. Singer, H. H., Gates, F. T. III, Kindt, T. J. & Williamson, A. R. *Eur. J. Immun.* (in the press).
26. Walsh, F. S. & Crumpton, J. J. *Nature* **269**, 307–311 (1977).
27. Parkhouse, R. M. E. & Cooper, M. D. *Immun. Rev.* **37**, 105–126 (1977).
28. Salsano, F., Froland, S., Natvig, J. B. & Michaelsen, T. E. *Scand. J. Immun.* **3**, 841–846 (1974).
29. Fu, S. M., Winchester, R. J. & Kundel, H. G. *J. Immun.* **114**, 250–252 (1975).
30. Goding, J. W. & Layton, J. E. *J. exp. Med.* **144**, 852–857 (1976).

31. Pernis, B., Brouet, J. C. & Seligmann, M. *Eur. J. Immun.* **4**, 776–778 (1974).
32. Tongegawa, S., Maxam, A. M., Tizard, R., Bernard, O. & Gilbert, W. *Proc. natn. Acad. Sci. U.S.A.* **75**, 1485–1489 (1978).
33. Schulman, M. J. & Köhler, G. *Nature* **274**, 917–919 (1978).
34. Marcu, K. B., Schibler, U. & Perry, R. P. *Science* **204**, 1087–1088 (1979).
35. Kessler, S. W. *J. Immun.* **115**, 1617–1624 (1975).
36. Laemmli, U. K. *Nature* **227**, 680–685 (1970).
37. Bonner, W. M. & Laskey, R. A. *Eur. J. Biochem.* **46**, 83–88 (1974).
38. Kabat, E. A., Wu, T. T. & Bilofsky, H. *Variable Regions of Immunoglobulin Chains. Tabulation and Analyses of Amino Acid Sequences* (Bolt, Beranek and Newman, Massachusetts, 1976).
39. Sakano, H. *et al. Nature* **277**, 627–633 (1979).
40. Early, P. W., Davis, M. M., Kaback, D. B., Davidson, N. & Hood, L. *Proc. natn. Acad. Sci. U.S.A.* **75**, 857–861 (1979).
41. Brack, C., Hirama, M., Lenhard-Schuller, R. & Tonegawa, S. *Cell* **15**, 1–14 (1978).
42. Honjo, T. *et al. Cell* **18**, 559–568 (1979).
43. Perry, R. P. & Kelley, D. E. *Cell* **18**, 1333–1339 (1979).
44. Early, P. *et al. Cell* (in the press).
45. Rogers, J. *et al. Cell* (in the press).

Fidelity of DNA replication catalysed *in vitro* on a natural DNA template by the T4 bacteriophage multi-enzyme complex

Urszula Hibner* & Bruce M. Albertst

Department of Biochemistry and Biophysics, University of California, San Francisco, San Francisco, California 94143

More than 50 copies of a ΦX174 DNA template can be made in 60 min in an in vitro *DNA replication system consisting of seven purified replication proteins isolated from T4 bacteriophage-infected cells. By transfecting with the DNA products and assaying for the reversion of specific amber mutants, the high degree of base-pairing fidelity in this system is revealed; the* in vitro *system is also shown to respond to the mutagenic effect of Mn^{2+} and to display strong base-pair context effects on fidelity, as expected from* in vivo *studies.*

As a central genetic process, the synthesis of DNA proceeds with a very high fidelity in living cells. The average error frequency for base-pair substitutions has been estimated to be of the order of 10^{-8} and 10^{-10} errors per base pair replicated in T4 bacteriophage and *Escherichia coli* DNA replication, respectively[1]. This fidelity is presumably due to Watson–Crick base-pairing recognitions; however, the fidelity expected from physicochemical knowledge of the stability of non-Watson–Crick base pairs and the occurrence of alternate tautomeric forms of the bases would predict 10^{-4}–10^{-5} errors per base pair replicated[2].

DNA replication is catalysed by multi-enzyme complexes *in vivo*[3–5]. We have studied the fidelity of the replication reaction carried out *in vitro* by a multi-enzyme complex reconstituted from seven replication proteins coded for by T4 bacteriophage, each of which has been highly purified as described elsewhere[6–8]. This *in vitro* system contains the protein products of T4 genes 43 (DNA polymerase), 32 (helix destabilizing protein), 44 and 62 (a complex with DNA-dependent ATPase activity), 41 (a DNA-dependent GTPase and ATPase), 45 and 61. In general terms, the role of each of these proteins in the replication process has been defined; these results and many of the properties of the reconstituted DNA replication system have recently been reviewed[8,9]. The complete system is capable of extensive DNA synthesis on a variety of double- and single-stranded DNA templates, closely mimicking the *in vivo* reaction with respect to the rate of chain elongation, RNA priming of Okazaki fragments and general structure of the replication fork[8,13,14]. The studies presented here on the fidelity of DNA synthesis in this *in vitro* system, have been carried out using two different ΦX174

*Present address: Parasitologie Expérimentale, Institut Pasteur, 25 Rue du Dr Roux, 75015 Paris, France.

† To whom reprint requests should be addressed.

amber mutant DNAs as templates (*am3* and *am18*), and involve screening the product DNA molecules by transfection for the presence of wild-type ΦX174 revertants. The results demonstrate that remarkably few errors are made when the frequencies of specific base-pair substitutions are examined, allowing us to conclude that many of the elements of the DNA synthesis reaction that create the high fidelity observed *in vivo* also operate during the *in vitro* DNA synthesis catalysed by the reconstituted T4 system. Independent data supporting this conclusion have been obtained by Sinha and Haimes[35].

The fidelity assay

A highly sensitive measure of *in vitro* DNA replication fidelity is obtained by replicating the DNA of previously sequenced nonsense mutants of ΦX174 bacteriophage[10] and assaying for revertants to wild type in the DNA synthesized[8,11,12]. Beginning with either single-stranded or nicked double-stranded DNA circles as template, we have replicated ΦX amber mutant DNA by a 'rolling circle' mode, producing 20–100 copies in a brief incubation[13,14]. As shown schematically in Fig. 1, the long double-stranded DNA product on the rolling circle tails is then cut to genome-sized fragments by treatment with a restriction endonuclease which recognizes only one site on the ΦX genome. The resulting linear molecules with 'sticky ends' are then circularized by T4 DNA ligase, and the infectivity of these DNA circles is measured by transfection into sup^+ cells, in which the amber mutant grows [*E. coli* CQ2 (Su3$^+$)]. Wild-type ΦX revertants are scored following transfection into sup^- cells (*E. coli* C), and the fraction of revertant DNA molecules calculated. The extensive synthesis obtained in our system yields mainly a double-stranded DNA product with both strands as newly synthesized

Table 1   ΦX174 DNA synthesized *in vitro* is fully infectious

DNA synthesized *in vitro* 57.8 copies	Genome-sized DNA circles produced (% of total DNA) 29.5%	Total DNA infectivity 26.8%	Specific infectivity of DNA 0.91	Minimal estimate of specific infectivity of the newly synthesized DNA* 0.86

The reaction mixture for DNA synthesis contained 10 mM Tris-acetate *p*H 7.8, 67 mM potassium acetate, 3.8 mM magnesium acetate, 0.5 mM dithiothreitol, 2 mM dCTP, 100 μM dATP, 100 μM dGTP, 20 μM ^{3}H-dTTP (specific activity 200 c.p.m. pmol^{-1}), 500 μM rATP, 200 μM each rUTP, rCTP and rGTP, and 0.5 μg ml^{-1} ΦX174 *am3* singly-nicked, double stranded circular DNA. The replication proteins present were 43 protein (3.3 μg ml^{-1}), 32 protein (200 μg ml^{-1}) 44/62 protein (18 μg ml^{-1}), 45 protein (30 μg ml^{-1}), 41 protein (20 μg ml^{-1}) and 61 protein (0.16 μg ml^{-1}). The initial reaction volume was 10 μl. After a 45-min incubation at 37 °C, the sample was diluted to 100 μl with a reaction mixture containing all the components except the DNA. The reaction continued for 45 min at 37 °C. The DNA synthesis was assayed by trichloroacetic acid precipitation of aliquots at 22, 45, 67 and 90 min; DNA was made at an accelerating rate until the last time point. The reaction was stopped by heating (68 °C for 10 min). The DNA product was then digested with *Pst*I restriction endonuclease at 37 °C (sevenfold over digestion). The reaction was stopped by heating at 68 °C for 10 min. After cooling, rATP was added to 0.5 mM. The DNA was ligated with excess T4 DNA ligase overnight at 14 °C. To favour formation of circles over dimerization, the concentration of DNA was kept low (2 μg ml^{-1}). The DNA was extracted once with redistilled phenol equilibrated in 0.1 M Tris-HCl, *p*H 8.5 (This step is not necessary for subsequent transfection). For visualization in the electron microscope, the DNA was spread by a modification of Inman's procedure[10], shadowed with platinum and analysed in a Philips 300 microscope. One-hundred randomly chosen molecules were traced. The transfection procedure used to measure infectivity was as described in Fig. 1 legend. Specific DNA infectivity = (% total infectivity)/(% DNA circles).

*Calculated by assuming that the input DNA template retained its full infectivity.

DNA[14]. This fact eliminates possible distortions in the assay due to cellular mechanisms which discriminate against newly synthesized DNA when repairing mismatched bases[15].

Specific infectivity of DNA synthesized *in vitro*

Before studying the frequency of errors made in the *in vitro* DNA synthesis reaction on a ΦX amber mutant DNA template, we wished to establish that the product DNA is as active in infecting sup$^+$ *E. coli* cells as the original template. Such a test is facilitated by the fact that extensive amounts of DNA can be synthesized by the T4 proteins *in vitro*. By using a dilution of an initial reaction mix as template for a second reaction, we have obtained an amount of DNA product corresponding to as much as 200 copies of the input circular template. In the experiment described in Table 1, we have synthesized 58 DNA copies on a ΦX double-stranded DNA template. The product DNA was processed as described above, and the proportion of genome-sized circular DNA in the preparation was estimated by electron microscopy. One hundred randomly chosen molecules were counted, 24 of which were unit-size circles. There was one double-genome length circle. The rest of the molecules were linear and of varying lengths. The genome-sized circles constituted 29.5% of the DNA mass, whereas 26.8% of the DNA was infectious (Table 1). We conclude that the specific infectivity of the DNA synthesized *in vitro* is indistinguishable from that of the original template. As the ΦX genome is 5,375 nucleotides long[10], this result implies that less than about 2 errors are made per 10^4 base-pair replications.

Fidelity of *in vitro* DNA synthesis at the ΦX174 bacteriophage *am3* site

We initially measured the frequency of *in vitro* base-pair substitutions at the ΦX174 *am3* mutant locus. As indicated in the Fig. 1 insert, the *am3* mutation changes a C·G base pair at position 587 to a T·A base pair[16]. This base-pair

change lies in the overlap of ΦX genes *E* and *D* (ref. 16), but it affects only the amino acid sequence in the gene *E* polypeptide (Fig. 1). In theory, any one of seven different single-base changes could change the polypeptide chain-terminating amber codon in gene *E* into a codon which specifies some amino acid; however, some of these would change the amino acid specified in the gene *E* and/or gene *D* proteins in such a way as still to produce defective phage. The number of changes in the *am3* codon that could produce viable phage is not known. However, as our *in vitro* reaction conditions strongly favour reversion to the true wild type (see below), we believe that we are mainly measuring the frequency of T·A to C·G transitions at position 587 in our assays. This assumption is supported by the DNA sequencing of similarly produced *in vitro* revertant DNA molecules which has been carried out in other laboratories (ref. 35 and L. A. Loeb, personal communication).

Due to the relatively high *in vivo* reversion frequency of ΦX mutants, the population of *am3* DNA used as template in our experiments is contaminated with what seems to be wild-type revertants, at a level of about 3 × 10^{-6}. To increase the number of *in vitro* revertants above background, we have strongly biased the input concentrations of deoxyribonucleoside triphosphates (dNTPs) to favour the T·A to C·G change necessary to produce wild-type revertants. As dGTP competes with dATP to make a G·T mispair[12], a high concentration of dGTP relative to dATP will increase the probability of the G·T mispairs needed to obtain revertants to wild type when synthesizing the viral DNA strand (Fig. 1); similarly, a high concentration of dCTP relative to dTTP will increase the probability of the C·A mispairs needed to obtain revertants to wild type when synthesizing the complementary

Table 2   The frequency of an AT to GC transition depends on the mispaired intermediate

dNTP bias during the *in vitro* reaction	$\dfrac{dCTP}{dTTP} = \dfrac{100}{1}$	$\dfrac{dGTP}{dATP} = \dfrac{51}{1}$
(1) No. of infectious ΦX molecules tested	5.9 × 10^9	1.6 × 10^9
(2) No. of infective centres expected if all DNA was wild-type	5.3 × 10^5	1.25 × 10^6
(3) No. of infective centres found	7	74
(4) No. of infective centres due to wild-type contaminants in template	2	5
(5) Level of *in vitro*-produced wild-type revertants in *am3* populations	9.4 × 10^{-6}	5.5 × 10^{-5}
(6) Calculated error frequency	1.9 × 10^{-7} (C pairing with A)	2.2 × 10^{-6} (G pairing with T)

The reaction conditions were as described in Table 1 legend, except that the reaction volumes were 100 μl (dCTP/dTTP bias) or 50 μl (dGTP/dATP bias) and nicked double-stranded ΦX *am3* replicative form DNA was used as template at 4 μg ml^{-1} (wild-type revertant level of 4 × 10^{-6}). In the experiment with a dGTP/dATP bias, the concentrations of dNTPs were 1 mM dGTP, 20 μM dATP, 100 μM dCTP and 100 μM ^{3}H-dTTP (specific activity of 200 c.p.m. pmol^{-1}). The transfections were carried out with both *E. coli* CQ2 (su3) and *E. coli* C (su$^-$), as described in Fig. 1. To control for possible inhibition of expression of the small amount of wild-type revertants present by the large excess of ΦX *am3* DNA, the su$^-$ cells were also transfected with a mixture of the *in vitro* synthesized DNA with known amounts of wild-type DNA. Our results are thereby corrected for possible alterations of transfection efficiencies due to any component present in the *in vitro* DNA product. The use of dCTP/dTTP or dGTP/dATP bias in the reaction is expected to favour the AT→GC transition at position 587 (leading to wild-type revertants), as well as TA→CG transition at position 586. The latter change would result in changes in both the gene *E* (Trp→Gln) and the gene *D* (Val→Ala) proteins. It is not known whether the mutant ΦX produced from *am3* by the T·A→C·G transition at position 586 is viable. This point is, however, not crucial to our argument, because at worst we may be somewhat underestimating the replication fidelity in our *in vitro* system (that is, the reversion rate observed could possibly be a sum of reversions occurring at two neighbouring loci: positions 586 and 587). These data differ somewhat from those reported earlier[8], in that we previously underestimated the error frequencies for a G/A bias due to a technical problem.
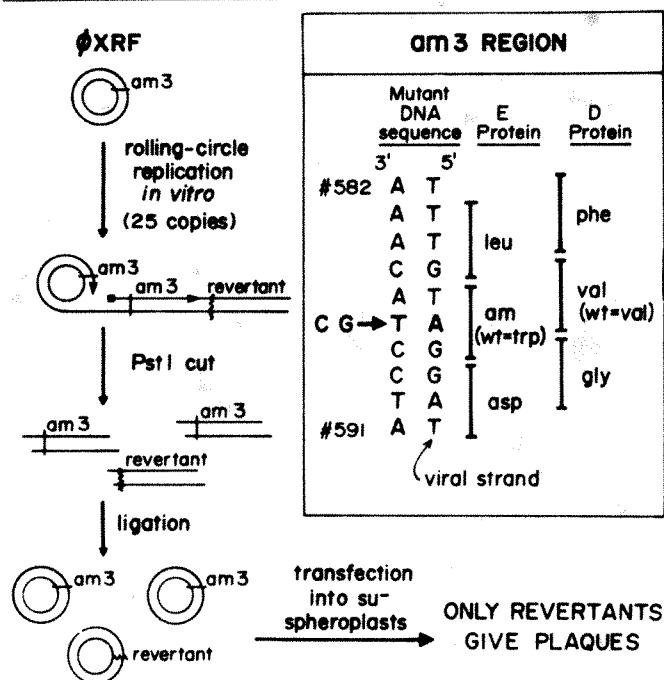
Fig. 1 Schematic summary of an infectivity assay for replication fidelity. The two arrows on the rolling circle denote the position and direction of the DNA polymerase molecule on the leading strand (intact circular template) and lagging strand (linear template displaced from circle) of the replication fork, respectively[3]. A detailed physical characterization of the products made has been reported elsewhere[13,14]. The DNA from an amber mutant of bacteriophage ΦX174 is replicated *in vitro* in a buffer containing 10 mM Tris-acetate, pH 7.8, 67 mM potassium acetate, 3.8 mM magnesium acetate (unless otherwise stated), 0.5 mM dithiothreitol, 0.5 mM rATP and 0.2 mM each of rGTP, rUTP and rGTP. The concentrations of dNTPs and ΦX DNA (double- or single-stranded) present varied, as described in each case. The concentrations of T4 replication proteins used are given in Table 1 legend. The incubations were at 37°C for 30–90 min. The time course and the extent of DNA synthesis were assayed by trichloracetic acid precipitation of aliquots. The reactions were stopped either by heating the samples at 68°C for 10 min or by phenol extraction. In all cases, contamination of dCTP by dUTP in the commercial dCTP preparations was eliminated by the use of purified dCTP or by treatment of reaction mixtures with dUTPase. The transformation procedure used is a modification of a method of Kushner[34]. A volume of 100 ml of *E. coli* CQ2 (Su3$^+$) is grown in L broth to a density of 2–3 × 10^8 cells ml^{-1}. The cells are spun and washed once at 4 °C in 50 ml of 10 mM MOPS pH 7.0, 10 mM RbCl. The washed cell pellet is resuspended in 50 ml of 0.1 M MOPS, pH 6.5, and 10 mM RbCl. A 0.5-ml volume of 5 M CaCl$_2$ is added and the cells are incubated at 0 °C for 30 min. The cells are pelleted and resuspended gently at 4 °C in 10 ml of 0.1 M MOPS pH 6.5, 10 mM RbCl and 50 mM CaCl$_2$. Aliquots of 0.2 ml are distributed to chilled glass tubes to which 3 µl dimethyl sulphoxide is added. The DNA is added to each tube in a volume of 10 µl or less. After 30 min at 0 °C the samples are heated to 45 °C for 30 s, L broth (1 ml containing 1 mM CaCl$_2$) is then added and the samples are incubated at 37 °C for 10 min. Top agar containing indicator bacteria (either *E. coli* CQ2 or *E. coli* C) is added and the mixture poured onto bottom agar plates. The ΦX174 plaques are scored after about 3 h at 37 °C. In controls with wild-type ΦX phage DNA, the transfection efficiencies for double-stranded ΦX circles were between 2 × 10^{-4} and 10^{-3} infective centres per DNA molecule for *E. coli* C and between 2 × 10^{-5} and 5 × 10^{-5} infective centres per DNA molecule for *E. coli* CQ2 cells; the true fraction of wild-type ΦX revertants is calculated by reference to calibrations with traces of wild-type DNA added as internal standards (see Table 2 legend). Single-stranded circular ΦX DNA molecules and linear double-stranded molecules do not contribute to the assay, as each is at least two orders of magnitude less infectious than double-stranded circles (data not shown).

DNA strand. Thus, in theory at least, the triphosphate bias not only makes these replication errors detectable, but also allows one to determine the types of mispair involved in creating the error.

Typical results of an experiment carried out with a high dNTP bias of each type are shown in Table 2. Comparison of the number of infective centres found (row 3) with the number expected from the level of pre-existing revertants in the template (row 4) indicates that a clearly detectable revertant

population is being produced during these *in vitro* DNA synthesis reactions. The fact that the detection of such *in vitro* revertants requires the expected triphosphate bias suggests that we are indeed observing reversion to true wild type. In row 6 of Table 2, we have assumed a linear dependence of base-pairing errors on the bias (see below) to calculate the error frequency expected for an equimolar dNTP concentration of 100 µM each. As indicated, it seems that a C pairs with A much less often than a G pairs with T at position 587. The fidelity of the multi-enzyme T4 *in vitro* DNA synthesis system is impressive; the error rates of 2 × 10^{-7} to 2 × 10^{-6} are 100–1,000-fold lower than those estimated for DNA polymerases alone on a ΦX DNA template (ref. 17).

Both single-stranded and double-stranded ΦX DNA circles can be used as a template for rolling circle DNA replication *in vitro*[13,14]. In both cases, the reaction is a highly processive one, with very few secondary replication forks established on the rolling circle tails[14]. Therefore, with a single-stranded viral DNA circle as template, all but the very first copy of the complementary DNA strand will be synthesized at the leading side of a standard replication fork, and all of the viral strand will be synthesized at the lagging side of this fork (Fig. 1; see refs 13, 14 for details). In contrast, because we rely on nonspecific nicking of a double-stranded template DNA for initiation of rolling-circle replication, there is an equal probability that either strand (viral or complementary) will be made on each side of the fork on a double-helical template. From the fact that the estimated error frequencies at *am3* for both viral (dGTP/dATP bias) and complementary (dCTP/dTTP bias) strand syntheses are the same irrespective of the type of template used (data not shown), we conclude that the fidelities of leading and lagging strand synthesis at the fork must be very similar, if not identical.

The fidelity of *in vitro* DNA synthesis is reduced in the presence of Mn^{2+}

Substitution of manganese for magnesium is known to be mutagenic both *in vivo*[18,19] and *in vitro* (for review see ref. 20). *In vivo*, the mutagenic effect of manganese on T4 DNA

Table 3 Substitution of manganese for magnesium ions during the *in vitro* DNA synthesis lowers the replication fidelity

dNTP bias during the *in vitro* reaction	$\dfrac{dCTP}{dTTP} = 20$	$\dfrac{dGTP}{dATP} = 20$
(1) No. of infectious ΦX molecules tested	3.9 × 10^8	7.5 × 10^8
(2) No. of infective centres expected if all DNA was wild type	1.8 × 10^5	1.4 × 10^5
(3) No. of infective centres found	8	98
(4) No. of infective centres due to wild-type contaminants in template	0.7	0.6
(5) Level of *in vitro*-produced wild-type revertants in *am3* populations	4.1 × 10^{-5}	7.0 × 10^{-4}
(6) Calculated error frequency	4.1 × 10^{-6}	7.0 × 10^{-5}

The reaction conditions were the same as for the experiment in Table 2, except that ΦX174 single-stranded DNA (5 µg ml^{-1}) was used as template (background wild-type revertants of 4 × 10^{-6}). The 50-µl reactions contained either 800 µM dCTP, 40 µM ^{3}H-dTTP (specific activity 200 c.p.m. pmol^{-1}) and 100 µM each of dATP and dGTP (C/T bias), or 400 µM dGTP, 20 µM dATP and 100 µM each of dCTP and ^{3}H-dTTP (G/A bias). The magnesium salt in our normal reaction mixture was substituted with MnCl$_2$ at 2.2 mM or 1.2 mM for dCTP/dTTP and dGTP/dATP biased reactions, respectively. In other experiments, the exact level of Mn^{2+} present was shown not to affect the fidelity and the different levels used here reflect an attempt always to have about 1 mM non-triphosphate-bound Mn^{2+} present. The reactions were stopped by extractions with re-distilled phenol followed by ethanol precipitation. The restriction enzyme digestion and ligation were carried out in Mg^{2+}-containing buffers.

Table 4 Site specificity of mutation rates

Type of *in vitro* reaction		Fidelity (fraction of errors)	
dNTP bias	Divalent cation	Mutant *am3* 3'AAACA⌷T⌷CCTA5' 5TTTGT⌷A⌷GGAT3'	Mutant *am18* 3'CTGC⌷A⌷TCTTC5' 5GACG⌷T⌷AGAAG3'
C>T	Mg²⁺	$3.3 \pm 0.3 \times 10^{-7}$	$2.0 \pm 0.5 \times 10^{-6}$
G>A	Mg²⁺	$2.2 \pm 0.3 \times 10^{-6}$	$9.1 \pm 2.9 \times 10^{-6}$
C>T	Mn²⁺	$4.6 \pm 1.1 \times 10^{-6}$	$5.8 \pm 2.3 \times 10^{-6}$
G>A	Mn²⁺	$5.0 \pm 0.9 \times 10^{-5}$	$1.3 \pm 0.2 \times 10^{-5}$

The reactions were carried out as described in the legends to Tables 1–3. The results of 2–10 experiments of each type are presented as the mean value plus or minus the standard error. Double-stranded ΦX174 replicative form DNA which had been singly nicked with pancreatic DNase 1, or single-stranded ΦX174 viral DNA was used as the template in duplicate reactions. The restriction enzyme used for digestion of the rolling circle tails was *PstI*, *AvaI* or *AvaII*. Either T4 DNA ligase or *E. coli* ligase was used in the presence of 0.5 mM rATP or 26 μM NAD, respectively, to create the double-stranded DNA circles used for transfections (see Fig. 1). The ΦX174 amber DNA preparations used as template contained 4×10^{-6} wild-type revertants for *am3*, and 2×10^{-6} wild-type revertants for *am18*. The sequence of each amber mutant DNA is shown, with the base pair in the box requiring a T·A→C·G transition to produce a wild-type revertant. For both mutants, the viral strand sequence is listed below the complementary strand sequence. The test for revertants at the *am18* site was carried out at 42 °C, to prevent growth of a pseudo-revertant produced by a G→C transversion at position 25 (ref. 25).

synthesis is expressed mainly as an increase in the frequency of transitions[18], both G·C→A·T and A·T→G·C transitions being enhanced by the order of 10–100-fold.

Our *in vitro* T4 DNA replication system is capable of using manganese as a divalent cation, although the range of concentrations permitting extensive synthesis is narrow. At optimal Mn²⁺ concentrations (1–2 mM), the rate of DNA synthesis is two or three times slower than in Mg²⁺ (data not shown). As shown in Table 3, the fidelity of DNA synthesis catalysed by the T4 replication proteins is lower in manganese- than in magnesium-containing buffers, as revealed by the enhanced frequency of revertants observed at the *am3* locus. The error frequencies on both the viral strand (dGTP/dATP bias) and the complementary strand (dCTP/dTTP bias) are enhanced about 20-fold in these mutagenic conditions.

The production of revertants *in vitro* increases linearly with dNTP bias

Although results obtained in the presence of Mn²⁺ ions are less relevant to the process of DNA synthesis *in vivo* than results obtained in Mg²⁺, the higher frequency of revertants observed in Mn²⁺ allowed us to test directly a crucial assumption made in the fidelity calculations presented previously in Tables 2 and 3, namely that the probability of misincorporation of an incorrect dNTP is directly proportional to the ratio of the concentration of incorrect to correct substrate. In Fig. 2, we plot the compiled results of several experiments carried out in Mn²⁺ which were designed to test the effect of triphosphate bias on the frequency of *am3* revertant production. The data points fit satisfactorily to the lines drawn with a slope of 1.0 on this log–log plot, a statistical analysis indicating actual best fit slopes of 0.91 (±0.18) and 0.89 (±0.12) for the dCTP/dTTP and the dGTP/dATP bias experiments, respectively. We conclude that both types of bias cause a simple linear increase in the appearance of revertants, as assumed.

Complications due to exonuclease 'proofreading'

Interpretation of the linear relationship between errors and triphosphate bias in Fig. 2 is complicated by the fact that misincorporated nucleotides tend to be preferentially removed by the 3'→5' proofreading exonuclease activity of DNA polymerase[21]. Because of the constant competition between polymerization and exonuclease removal, the fidelity of DNA

synthesis at each template position is strongly influenced by the rate of addition of the next dNTP normally incorporated in the DNA chain, and the error is only fixed after addition of this subsequent nucleotide[22]. For example, when synthesizing the wild-type viral strand DNA sequence on the *am3* template, any G incorporated at 587 will be 'paired' with a T on the template, and therefore be very liable to exonuclease removal. Fersht has recently shown[11] that, in a ΦX RF→SS DNA reaction, *E. coli* DNA polymerase III holoenzyme creates viral strand revertants at this sequence in proportion to [dGTP/dATP]². This is the expected result if the rate of addition of the next nucleotide, a G at position 588, increases linearly with dGTP concentration in the range tested (0.008–1.0 mM), thereby reducing the amount of time available for the exonuclease function of the polymerase to remove a misincorporated G residue at position 587 (ref. 12). However, this effect should disappear when dGTP concentrations are sufficient to give close to maximal polymerization rates.

Extrapolating to our system, the results of Goodman and co-workers with T4 DNA polymerase[22] would predict an effect of dGTP concentration on exonuclease proofreading at position 587 only when this concentration drops below ~100 μM. In fact, we obtained a [dGTP]/[dATP] dependence of error frequencies in Fig. 2 only because all our dNTP concentrations are usually kept at a high level (100 μM each); thus, all the dGTP concentrations used to create the dGTP/dATP biases in Fig. 2 are sufficient to maximize the rate of G addition at position 588.

As predicted by the data of Fersht[12] and Clayton *et al.*[22], there is a marked increase in the fidelity of synthesizing the *am3* viral strand in our system when the G to A ratio is kept at 1.0 and the dNTP concentrations are reduced from 100 μM to 20 μM. In fact, to measure the reversion frequencies on the complementary strand (T→C transitions) at low dCTP/dTTP bias in Fig. 2, it was necessary to lower the nonbiased dGTP and dATP concentrations. At higher levels of dGTP, the preferential A→G reversions on the viral strand prevent detection of the T→C transitions being tested (see Fig. 2 legend).

The fidelity of DNA synthesis *in vitro* is site dependent

The frequency of a given base-pair mutation *in vivo* is strongly dependent on the location of that base pair in the context of neighbouring DNA sequences; for the same base-pair change, mutation frequencies can differ by several orders of magnitude[23,24].

We have compared the reversion frequencies of two different ΦX174 mutants, *am3* (gene *E*) and *am18* (gene *A*), after *in vitro* DNA replication by the T4 multi-enzyme complex. The *am18* mutant is at position 23 of the ΦX DNA sequence[25], in the region of overlap of genes *A* and *B*. The DNA sequences around nucleotides 23 (*am18*) and 587 (*am3*) are compared at the top of Table 4. As indicated (boxed base pairs), reversion to wild type requires a T·A to C·G transition for both mutants.

As reported in Table 4, the *in vitro* reversion frequencies for *am3* and *am18* are quite distinct. The frequency of T→C transitions is about sevenfold higher for *am18* than for *am3*, whereas the A→G transition frequency is higher by about a factor of 4 at the *am18* site. At both sites, we obtain a higher number of ΦX revertants when using a dGTP/dATP bias (favouring G·T mispairs) than when using a dCTP/dTTP bias (favouring C·A mispairs), suggesting that the G·T mispair may more easily escape discrimination *in vitro*. This result may be related to the finding that the G·T base pair is much more stable than the A·C base pair, when tested in synthetic polynucleotide helices (J. Fresco, personal communication).

In Table 4, the substitution of manganese for magnesium during the *in vitro* DNA synthesis leads to an increase in error rate in all cases. The extent of the increase caused by Mn²⁺,
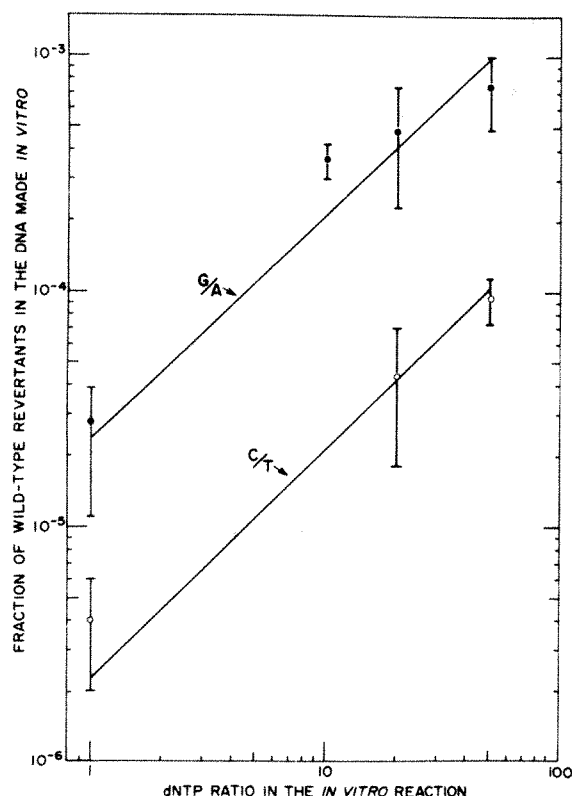
Fig. 2 Linear dependence of *in vitro* revertant frequencies on dNTP bias. The lines shown are the best fit to a slope of 1.0 on this log–log plot; an appropriately weighted statistical analysis gives actual slopes of 0.91 (±0.18) and 0.89 (±0.12) for the dCTP/dTTP and the dGTP/dATP bias experiments, respectively. The reactions were carried out on a ΦX *am3* single-stranded DNA template as described in Tables 1 and 3 legends. For the dGTP/dATP bias experiments, the dNTP concentrations were: 100 μM dCTP, 100 μM dTTP, 100 μM dGTP, 100 μM dATP (G/A = 1); 100 μM dCTP, 100 μM DTTP, 200 μM dGTP, 20 μM dATP (G/A = 10); 100 μM dCTP, 100 μM dTTP, 400 μM dGTP, 20 μM dATP (G/A = 20); 100 μM dCTP, 100 μM dTTP, 1 mM dGTP, 20 μM dATP (G/A = 50). For the dCTP/dTTP bias, the dNTP concentrations were: 100 μM dCTP, 100 μM dTTP, 20 μM dGTP, 20 μM dATP (C/T = 1); 400 μM dCTP, 20 μM dTTP, 100 μM dGTP, 100 μM dATP (C/T = 20); 1 mM dCTP, 20 μM dTTP, 100 μM dGTP, 100 μM dATP (C/T = 50). Reactions were stopped while the amount of DNA product was still increasing linearly, and we estimate that not more than half of the dNTP present in lowest concentration had been used up. Note that by changing the bias of one pair of triphosphates, we also affect the ratios of these triphosphates to the unbiased pair. However, because of the way the experiments were carried out, these other ratios did not change by the same factor. For example, changing the dGTP/dATP ratio from 1- to 50-fold changed the dGTP/dTTP and dGTP/dCTP ratios only 10-fold. These two particular changes could possibly lead to the production of pseudo-wild-type revertants at the *am3* locus by enhancing transversions; however, the linear correlation between dGTP/dATP ratio and the production of revertants *in vitro* suggests that most of the viable revertants are true wild type.

however, is very different for the different sites. The greatest effect was observed for the apparent A·G substitution at the *am3* site (about 20-fold higher errors in Mn^{2+} than in Mg^{2+}), whereas a 1.5-fold increase was found in the A→G substitutions at the *am18* site.

We find that adding increasing amounts of magnesium to manganese-containing reaction mixtures (up to a 10:1 Mg^{2+} to Mn^{2+} ratio) does not reduce the high error frequency characteristic of the manganese reaction (data not shown). As the binding constants of Mn^{2+} and Mg^{2+} for dNTPs are very similar[26], the absence of a strong Mg^{2+} competition effect in these fidelity experiments seems incompatible with the idea that manganese effects are exerted only through its complex with the dNTPs. Rather, the mutagenic activity of manganese is likely to be due largely to its interaction with the DNA polymerase or with other replication proteins.

Is *in vitro* DNA synthesis as faithful as the *in vivo* process?

The average error rate for point mutations measured for T4 bacteriophage *in vivo* is about 2×10^{-8} per base-pair replication[1]. However, when the reverse mutation rates for a number of rII loci are compared, it becomes clear that reversions occurring by exactly the same pathway (for example, a G·C→A·T transition) vary in frequency by several orders of magnitude (for example mutant uv1 gives 5×10^{-10}, mutant uv19 gives 8×10^{-8} and mutant uv102 gives 10^{-6} revertants per replication)[23]. Our estimates of overall *in vitro* frequencies for a T·A to C·G transition are about 10^{-6} and 10^{-5} revertants per base-pair replication for the ΦX174 *am3* and *am18* loci, respectively. Thus, although impressively accurate, the *in vitro* replication fidelity seems to be inferior to the *in vivo* precision observed in T4 bacteriophage-infected cells.

Several explanations for the above discrepancy should be considered. (1) It is possible, although unlikely, that the two ΦX174 mutations whose *in vitro* reversion has been studied by us represent unusually mutable sites for the T4 replication apparatus, and thus that the data in Table 4 cannot be assumed even to approximate the average of the spectrum of mutation frequencies. There is some suggestion to this effect in ref. 35. (2) The *in vivo* T4 mutation rate estimates may include contributions to fidelity from post-replication repair mechanisms which do not function in our *in vitro* system. In particular, a repair mechanism linked to DNA methylation is in principle capable of recognizing errors on newly synthesized DNA, and there is evidence that such a repair pathway increases the fidelity of *E. coli* DNA replication by a factor of 100–1,000 (ref. 15). The presence of a similar repair pathway operating in T4-infected cells could be tested for by measuring mutation frequencies for a T4 dam⁻ phage mutant[27] grown on an *E. coli* dam⁻ host[15]. (3) The conditions in which our *in vitro* DNA synthesis is carried out have not been specifically optimized to obtain maximum fidelity. Although fidelity could be increased by lowering dNTP concentrations[12,22], this would reduce the rate of *in vitro* replication fork movement far below *in vivo* levels[8]. However, it is possible that fidelity could be increased without slowing polymerization rates by altering ionic conditions, adding polyamines or increasing ATP to ADP ratios[28]. (4) The present T4 *in vitro* DNA replication system may be lacking as yet unidentified T4 or host gene products which are essential only for maintenance of maximum replication fidelity. There is good genetic evidence that such special proteins exist for the DNA replication system of uninfected *E. coli*[29], as well as indirect evidence that additional T4 proteins directly feed dNTPs into the *in vivo* T4 DNA replication complex[30,31].

Conclusions

Despite the above uncertainties, the major point of our current findings is that the rapid and extensive DNA replication observed in the present T4 *in vitro* system is highly faithful. It also responds to the mutagenic effect of Mn^{2+}, and displays the strong base-pair context effects on fidelity expected from *in vivo* studies. Genetic analyses reveal that an alteration in any one of the seven T4 DNA replication proteins used in our *in vitro* system can increase mutation rates[32,33]. Future *in vitro* studies using this system should thus allow elucidation of the detailed mechanisms of many of the fidelity-generating steps in DNA replication.

1. Drake, J. W. Nature 221, 1132 (1969).
2. Topal, M. D. & Fresco, J. R. Nature 263, 285–289 (1967).
3. Alberts, B. & Sternglanz, R. Nature 269, 655–661 (1977).
4. Wickner, S. H. A. Rev. Biochem. 47, 1163–1191 (1978).
5. Kornberg, A. Cold Spring Harb. Symp. quant. Biol. 43, 1–9 (1979).
6. Morris, C. F., Hama-Inaba, H., Mace, D., Sinha, N. K. & Alberts, B. J. biol. Chem. 254, 6787–6796 (1979).
7. Morris, C. F., Moran, L. A. & Alberts, B. M. J. biol. Chem. 254, 6797–6802 (1979).
8. Liu, C.-C., Burke, R. L., Hibner, U., Barry, J. & Alberts, B. M. Cold Spring Harb. Symp. quant. Biol. 43, 469–487 (1979).
9. Alberts, B. et al. in Proc. P & S biomed. Sci. Symp. (ed. Vogel H.J.) 31–63 (Academic, New York, 1977).
10. Sanger, F. et al. Nature 265, 687–695 (1977).
11. Weymouth, L. A. & Loeb, L. A. Proc. natn. Acad. Sci. U.S.A. 75, 1924–1928 (1978).
12. Fersht, A. Proc. natn. Acad. Sci. U.S.A. 76, 4946–4950 (1979).
13. Morris, C. F., Sinha, N. K. & Alberts, B. M. Proc. natn. Acad. Sci. U.S.A. 72, 4800–4804 (1975).
14. Sinha, N. K., Morris, C. F. & Alberts, B. M. J. biol. Chem. 255, 4290–4303 (1980).
15. Radman, M. et al. Cold Spring Harb. Symp. quant. Biol. 43, 937–946 (1979).
16. Barrell, B. G., Air, G. M. & Hutchison, C. A. III Nature 264, 34–41 (1976).
17. Loeb, L. A. et al. Cold Spring Harb. Symp. quant. Biol. 43, 921–928 (1979).
18. Orgel, A. & Orgel, L. E. J. molec. Biol. 14, 453–457 (1965).
19. Ripley, L. S. Molec. gen. genet. 141, 23–40 (1975).
20. Mildvan, A. S. & Loeb, L. A. CRC crit. Rev. Biochem. 6, 219–244 (1979).
21. Brutlag, D. & Kornberg, A. J. biol. Chem. 247, 241–248 (1972).
22. Clayton, L. K., Goodman, M. F., Branscomb, E. W. & Galas, D. J. J. biol. Chem. 254, 1902–1912 (1979).
23. Drake, J. W. The Molecular Basis of Mutation (Holden Day, San Francisco, 1970).
24. Coulondre, C. & Miller, J. M. J. molec. Biol. 117, 525–575 (1977).
25. Smith, M. et al. Nature 265, 702–705 (1977).
26. Mohan, M. S. & Rechnitz, G. A. Archs Biochem. Biophys. 162, 194–199 (1974).
27. Hattman, S., van Ormondt, H. & de Waard, A. J. molec. Biol. 119, 361–376 (1978).
28. Kurland, C. G. Biophys. J. 22, 373–392 (1978).
29. Cox, E. C. A. Rev. Genet. 10, 135–156 (1976).
30. Wovcha, M. G., Tomich, P. K., Chiu, C.-S. & Greenberg, G. R. Proc. natn. Acad. Sci. U.S.A. 70, 2196–220 (1973).
31. Reddy, G. P. V., Singh, A., Stafford, M. E. & Mathews, C. K. Proc. natn. Acad. Sci. U.S.A. 74, 3152–3156 (1977).
32. Mufti, S. Virology 94, 1 (1979).
33. Mufti, S. & Bernstein, H. J. Virol. 14, 860–871 (1974).
34. Kushner, S. R. in Proc. int. Symp. Genetic Engineering (eds Boyer, H. W. & Nicosia, S.) 17–23 (Elsevier, Amsterdam, 1978).
35. Sinha, N. K. & Haimes, M. D. in Mechanistic Studies of DNA Replication and Genetic Recombination (ICN-UCLA Symp., in the press).

LETTERS

The Centaurus I cluster of galaxies —An extreme case of contamination?

J. R. Lucey*, R. J. Dickens† & J. A. Dawe‡

*Astronomy Centre, University of Sussex, Falmer, Brighton BN1 9QH, UK
†Anglo-Australian Observatory, Private Bag, Coonabarabran, New South Wales 2857, Australia
‡UK Schmidt Telescope Unit (Royal Observatory Edinburgh), Private Bag, Coonabarabran, New South Wales 2857, Australia

Although the virial theorem is often used to calculate a system's mass from its size and velocity dispersion, there is considerable uncertainty over the result because of the problem of defining the true membership of the system. Recent analysis[1] of hypothetical galaxy systems in model universes has indicated that this local contamination can cause large errors in virial mass estimates for rich clusters. Non-member galaxies projected in the line of sight onto clusters are not easily recognized, unless they have redshifts significantly different from the cluster mean redshift. Contaminating galaxies more local to the cluster (for example, those with a small redshift difference) will be hidden in the large intrinsic motions of the cluster members. Other difficulties associated with application of the virial theorem include possible substructure within the clusters and non-virial motions (for example, infall or expansion). Such effects obscure the physical meaning of a derived virial mass. Here we emphasize the reality of these problems, as evidenced by the resolution of the Centaurus I cluster of galaxies into two distinct velocity systems, based on extensive new redshift data[2].

The Centaurus I cluster of galaxies has been studied frequently in recent years. Sandage[3] found, from 14 redshifts, $(n=14)$, a heliocentric mean cluster velocity $(\bar{V})$ of $3,360\,\text{km s}^{-1}$ and a line-of-sight velocity dispersion (σ_v) of $673\,\text{km s}^{-1}$. Dawe et al.[4], from $n=61$, found $\bar{V}=3,510\,\text{km s}^{-1}$ with $\sigma_v=870\,\text{km s}^{-1}$. Vidal and Wickramasinghe[5], from $n=25$, found $\bar{V}=3,507\,\text{km s}^{-1}$ with $\sigma_v=945\,\text{km s}^{-1}$. The brightest galaxy in the cluster, NGC4696, is the radio source[6] PKS1245 −41. This is also the centre of an extended X-ray source, in which the 7-keV Fe xxv, xxiv emission feature has been observed[7,8].

We have obtained new radial velocities with the image photon counting system on the Anglo-Australian telescope. In addition, the spectral scans obtained by Dawe et al.[4] have been remeasured with improved precision. These data have been combined with published results to yield redshifts for 164 galaxies within an UK Schmidt Telescope field centred on the cluster. The distribution of the velocities for 149 galaxies with

Heliocentric velocity ($\times 10^3$ km s^{-1})
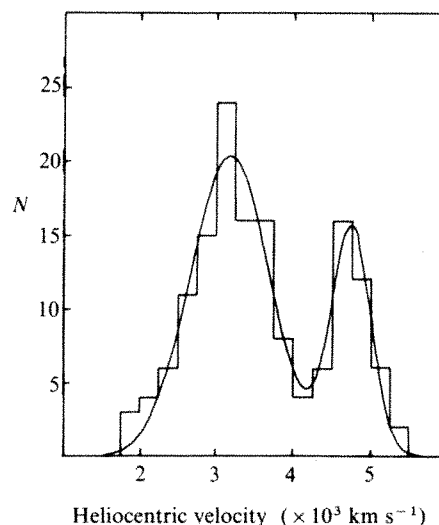
Fig. 1   Velocity distribution for galaxies on UKSTU plate, B1340 centred on NGC4696.

$V<6,000\,\text{km s}^{-1}$ is shown in Fig. 1. The histogram is clearly bimodal, with the very low probability $(P<0.001)$ of such a form originating from a single normal distribution. The 'best-fit' double normal distribution, also shown in Fig. 1, has the parameters $n_1=106$, $\bar{V}_1=3,179\,\text{km s}^{-1}$, $\sigma_v=517\,\text{km s}^{-1}$; $n_2=40$, $\bar{V}_2=4,738\,\text{km s}^{-1}$, $\sigma_v=255\,\text{km s}^{-1}$. (The dispersions are reduced to 507 and 235 km s^{-1} respectively, after correction for the measuring error of 100 km s^{-1}.) The spatial distributions of the two velocity systems are shown in Fig. 2.

If both clusters were at their respective Hubble distances, the expected difference in their distance moduli $(\Delta\mu)$ would be 0.9 mag. If this were the case, the observed number of galaxies to the same absolute magnitude limit would indicate that the clusters have equal populations (richness), a surprising result in view of the large difference in their velocity dispersions. Direct comparison of the cluster luminosity functions indicates $\Delta\mu=1.0\pm0.1$ mag, which is in good agreement with the hypothesis. Alternatively if the clusters were physically related, then their expected similar distance implies the lower velocity system to be about 2.5 times as rich as the other system. Allowing for the difference in richness, comparison of the luminosity functions indicates $\Delta\mu=0.0\pm0.2$ mag. Although the fit is poorer than the previous case, the magnitude shift is also consistent with the hypothesis. A definitive test is not possible at present because the form and variety of cluster luminosity functions makes richness and distance effects difficult to se-

7. Mitchell, R. J., Charles, P. A., Culhane, J. L. & Davison, P. J. N. *Astrophys. J.* **200**, L5-L8 (1975).
8. Mitchell, R. J. & Culhane, J. L. *Mon. Not. R. astr. Soc.* **178**, 75P-80P (1977).
9. Gregory, S. A. & Thompson, L. A. *Astrophys. J.* **222**, 784–799 (1978).
10. Tarenghi, M., Tifft, W. G., Chincarini, G., Rood, H. J. & Thompson, L. A. *Astrophys. J.* **234**, 793–801 (1979).
11. Ulrich, M. *Astrophys. J.* **221**, 422–435 (1978).
12. White, S. D. M. *Mon. Not. R. astr. Soc.* **177**, 717–733 (1976).
13. Holmberg, E. B., Lauberts, A., Schuster, H. E. & West, R. M. *Astr. Astrophys. Suppl.* **34**, 285–340 (1978).

Table 1   Galaxy groups near Centaurus I

Group name	n	v_θ (km s^{-1})	σ (km s^{-1})	r (NGC4696)
NGC4373	10	3,320	199	4.7°
NGC5011	8	3,251	160	4.7°
NGC5090	5	3.828	412	6.4°
ESO323 – G77*	5	4,817	156	3.4°

*See ref. 13.

parate. Both interpretations are quite plausible, the former because superposition of systems on galaxy clusters is not unusual[9-11] and the latter because the observed velocity difference, being less than the r.m.s. escape velocity could arise from infall of the two clusters within a bound system. The growth of clusters by the amalgamation of subunits is a characteristic phenomenon in N-body studies[13]. In either case the existence of two systems will give a substantially reduced total virial mass.

There is also evidence that other velocity systems may be present. Around the main concentrations, four distinct galaxy groups are apparent, details of which are given in Table 1. The velocities of the NGC4373 and NGC5011 groups suggest that they are associated with the lower velocity clusters whereas the ESO 323 – G77 group has a mean velocity close to that of the higher velocity cluster. Any similar groups projected on the clusters themselves would be unrecognizable. The lower velocity cluster is dominated by the galaxy NGC4696, with NGC4709 having a similar role in the other cluster. The X rays presumably originate from the lower velocity cluster, as the source[7] is coincident with NGC4696.
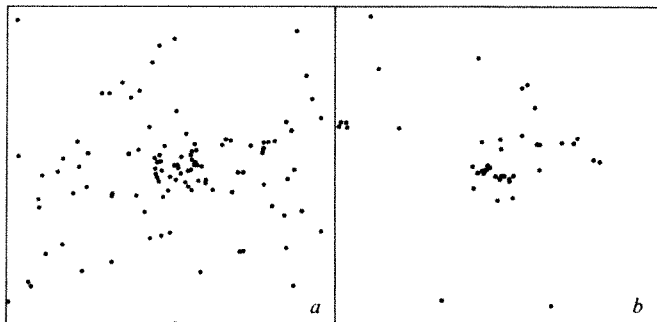
Fig. 2 *a*, The spatial distribution for galaxies with $V < 4,250$ km s^{-1} within the Schmidt field. *b*, The corresponding distribution for galaxies with $4,250 < V < 5,500$ km s^{-1}.

The resolution of Centaurus I into two clusters leads us to believe that erroneous conclusions can be drawn about even well-studied clusters. In rich concentrations of galaxies there is bound to be some degree of superposition as it is the more enhanced regions that are picked out as clusters and groups. The existence of physically related, merging subunits will enhance the probability. Clearly contamination and substructure must be accurately assessed if derived cluster parameters are to be physically meaningful.

We thank M. J. Currie for galaxy magnitudes and D. J. King for help with the data reduction. J. R. L. acknowledges the receipt of an SRC studentship.

1. Turner, E. L., Aarseth, S. J., Gott III, J. R., Blanchard, N. T. & Mathieu, R. D. *Astrophys. J.* **228**, 684–695 (1979).
2. Lucey, J. R., Dickens, R. J. & Dawe, J. A. *Mon. Not. R. astr. Soc.* (submitted).
3. Sandage, A. *Astrophys. J.* **202**, 563–582 (1975).
4. Dawe, J. A., Dickens, R. J. & Peterson, B. A. *Mon. Not. R. astr. Soc.* **178**, 675–685 (1977).
5. Vidal, N. V. & Wickramsinghe, D. T. *Mon. Not. R. astr. Soc.* **180**, 305–308 (1977).
6. Mills, B. Y., Slee, O. B. & Hill, C. *Aust. J. Phys.* **13**, 679–699 (1960).

IR photometry and polarimetry of 2A0311–227

J. Bailey & J. H. Hough

Hatfield Polytechnic Observatory, Bayfordbury House, Hertford SG13 8LD, UK

D. J. Axon

Astronomy Centre, University of Sussex, Falmer, Brighton BN1 9QH, UK
and
Department of Physics and Astronomy, University College, London WC1E 6BT, UK

The X-ray source 2A0311–227 has recently been identified with a star whose spectrum[1] and polarization properties[2] show it to be an AM Herculis type binary. These binaries are thought to consist of a synchronously rotating magnetic white dwarf, with a surface field of $\sim 10^8$ G, accreting matter from a cooler companion star[3]. The highly circularly polarized radiation emitted by these systems is thought to be due to cyclotron radiation originating in an accretion column at one or both poles of the white dwarf. We describe here IR light curves of 2A0311–227 at 1.25 and 2.2 μm, together with circular polarimetry at 1.25 μm. The light curves show a deep narrow minimum which does not have an optical counterpart, and the 1.25 μm polarimetry shows circular polarization which is much lower than that in the optical.

The observations were obtained with the 3.8 m UK IR telescope at Mauna Kea. Photometry was obtained on 10 November 1979 in the J (1.25 μm) band and on 11 November in the K (2.2 μm) band, using the $f/9$ photometer. On 13 November the Hatfield IR polarimeter[4] was used to obtain circular polarization observations at 1.25 μm. We have also obtained extensive optical photometry and polarimetry of 2A0311–227 using the 1.5 m telescope at the Cabezon Observatory, Tenerife, and the RGO Peoples photometer in its polarimetric mode[5]. These data will be described more fully elsewhere, but as well as IR results in Fig. 1 we present for comparison an optical light curve and circular polarization curve, obtained from observations in unfiltered light (extended S20 response) on 14–16 September 1979.

2A0311–227 shows a sharp linear polarization pulse repeating with its 81 min period, as first reported by Tapia[2]. Using our polarization observations between 14 and 26 September 1979 and the epoch reported by Tapia[2] the following ephemeris has been derived.

$$T_{\text{lin pol max}} = JD_\odot 2444131.6751 + 0.0562666E$$
$$\pm 0.0000006$$

Photometry in the J band by Ward *et al.*[6] showed a narrow minimum 0.8 mag deep. This feature can also be seen in our J light curve. Our K observations show that a narrow minimum is also present at this wavelength and is deeper than that at J. With our five minima (two at J and three at K) and the epoch of minimum observed by Ward *et al.*[6] we can fit several possible periods, one of which is consistent with the
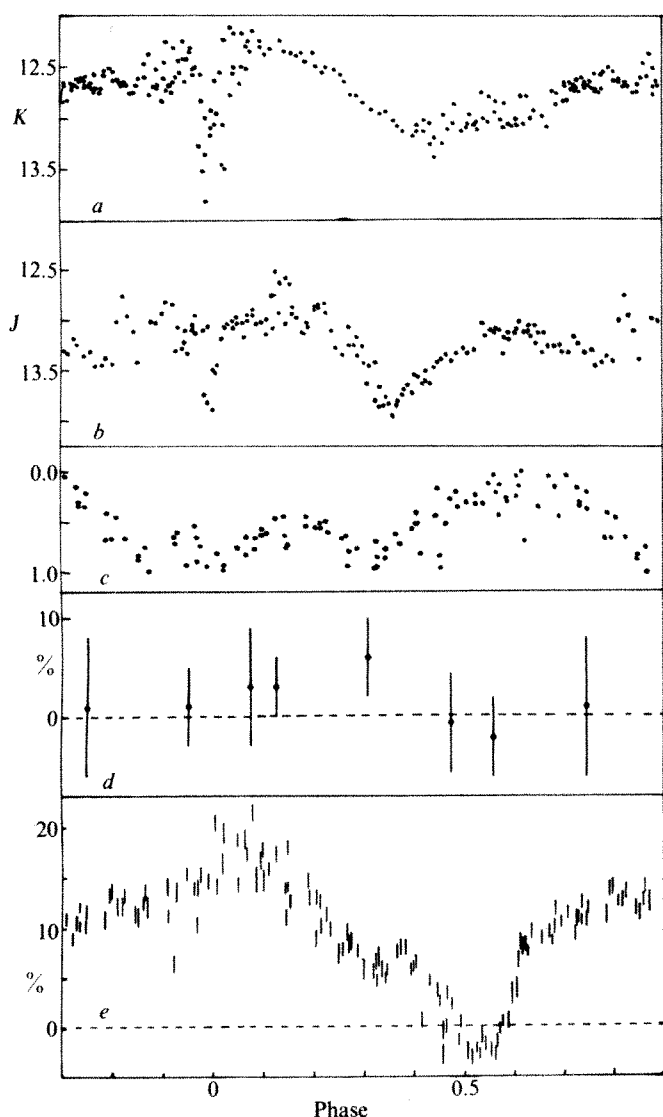
Fig. 1 *a, K* (2.2 μm) light curve obtained on 11 November 1979. Data from three cycles are plotted. Each point represents a 32-s integration. A typical point has a standard error of 0.08 mag. *b, J* (1.25 μm) light curve obtained on 10 November 1979. Data from two cycles are plotted. Each point represents a 32-s integration. A typical point has a standard error of 0.05 mag. *c* Broad band optical (0.4–0.85 μm) light curve from six cycles data obtained on 14–16 September 1979. The data are plotted on a magnitude scale with arbitrary zero point. *d* 1.25 μm circular polarization observations obtained on 13 November 1979. Each point represents a 10-min integration with standard error indicated. *e* Broad band optical (0.4–0.85 μm) circular polarization from observations of eight cycles on 14–16 and 26 September 1979.

polarization period. This corresponds to the following ephemeris:

$$T_{IR\,min} = JD_\odot 2443944.9518 + 0.0562660E$$
$$\pm 0.0000003$$

This ephemeris has been used to determine the phase for the observations plotted in Fig. 1. The narrow minimum seems to be slightly variable in phase and depth from cycle to cycle. The light curves also show flickering with amplitudes of up to 0.7 mag in *J*, and with a smaller amplitude in *K*. The flickering activity is greatest around the phase of the narrow minimum.

Observations by Tapia have been reported to show circular polarization always of the same sign[7]. However, our circular polarimetry shows a definite reversal of sign, lasting about 0.1 phase and reaching −2.5 % in unfiltered light. Observations in

narrower bands show that the reversal is largest in blue light, reaching −7 % in *B*. The linear polarization pulse occurs at phase 0.58 on the IR ephemeris, and corresponds to the change of sign in the circular polarization, as is usually the case in AM Her objects.

In contrast to the observed wavelength dependence of polarization in AM Herculis, which peaks at around 0.9 μm (refs 8, 9) our optical data show a fall off in circular polarization towards the red. The peak circular polarizations observed in September 1979 were 15 % at 0.44 μm, 29 % at 0.55 μm, 20 % at 0.68 μm and 9 % at 0.83 μm. The observed 1.25 μm circular polarization follows this downward trend and is very much lower than that in the optical. The data are consistent with zero polarization, and averaged over the whole cycle give the value 3.0 % ± 1.5 %. Unfortunately no other IR circular polarimetry of AM Her type systems exists in the literature for comparison.

Watson, Mayo and King (personal communication) claim to detect a narrow minimum in the optical light curve at the same phase as the narrow IR minimum. They naturally interpret this as being an eclipse of the cyclotron emitting region by the companion star. However, this model is not supported by our data. The narrow optical minimum is not apparent in our light curve, and of greater significance, there is no minimum in the optical polarization curve at this phase, as an eclipse of the cyclotron region requires.

It is important to consider how our optical and IR observations may be reconciled. If the IR emission is due to cyclotron radiation then the optical and IR radiations must originate in different regions. We suggest two possibilities. (1) The IR and optical radiation originate at different heights in the same accretion column. (2) The IR emission is produced at a second pole which predominantly radiates in the IR. If the accretion rates of the two columns vary then it may also be possible to account for the difference between our optical curves and those reported by Watson *et al.*

If the narrow eclipse is due to the companion star then in either of the above cases severe limitations are imposed on the inclination of the system. Additionally both these explanations require some mechanism to depolarize the IR cyclotron radiation.

Alternatively some other mechanism could be responsible for the IR radiation, and dilution by this component could then explain the low polarization at long wavelengths. In this case, however, it is not clear what other mechanism could be consistent with the observed narrow eclipse as this imposes constraints on the maximum size of the emitting region. We have investigated the possibility that free–free emission from X-ray heated gas in the accretion stream is the source of the IR radiation. Assuming an emitting region with a radius $\sim 10^9$ cm the observed K luminosity $L_K \sim 5.7 \times 10^{16}(d/100)^2$ erg s^{-1} (where d is the distance in parsecs) yields a brightness temperature $T_B \sim 3 \times 10^6 (d/100)^2$ K. The emission measure is so large that the gas will be optically thick to free–free radiation at all wavelengths considered.

With the data available we cannot offer a more complete explanation of our observations or the radial velocity data of Williams *et al.*[10] and Schneider and Young (personal communication) which depends on the detailed geometry of the accretion scheme. Clearly a detailed understanding of 2A0311−227 requires further coordinated optical and IR measurements.

1. Griffiths, R. E., Ward, M. J., Blades, J. C., Wilson, A. S. & Chaisson, L. *Astrophys. J.* **232**, L27 (1979).
2. Tapia, S. *IAU Circ.* No. 3327 (1979).
3. Chanmugam, G. & Wagner, R. L. *Astrophys. J. Lett.* **213**, L13 (1977).
4. Cox, L. J., Hough, J. H. & McCall, A. *Mon. Not. R. astr. Soc.* **185**, 199 (1978).
5. Bailey, J. thesis, Univ. Sussex (1978).
6. Ward, M. J., Allen, D. A., Smith, M. G. & Wright, A. E. *IAU Circ.* No. 3335 (1979).
7. Bond, H. E., Chanmugam, G. & Grauer, A. D. *Astrophys. J.* **234**, L113 (1979).
8. Michalsky, J. J., Stokes, G. M. & Stokes, R. A. *Astrophys. J. Lett.* **216**, L35 (1977).
9. Priedhorsky, W. C., Krzeminski, W. & Tapia, S. *Astrophys. J.* **229**, 542 (1978).
10. Williams, G. et al. *Nature* **281**, 48–49 (1979).

An upper limit to the global SO₂ abundance on Io

**P. S. Butterworth*, J. Caldwell†, V. Moore†§,
T. Owen†, A. R. Rivolo† & A. L. Lane‡**

*Department of Astronomy, University of Leicester, Leicester LE1
7RH, UK
†Department of Earth and Space Sciences, State University of New
York, Stony Brook, New York 11794
‡Jet Propulsion Laboratory, 4800 Oak Grove Drive, Pasadena,
California 91103

**Gaseous sulphur dioxide has been detected on Io by the Voyager
1 IRIS experimemt[1]. It was associated with a major volcanic
plume, and it was observable only because the local underlying
surface was warm enough (>210 K) to be detected near 7 μm,
and thereby reveal the gas in absorption. The estimated column
abundance of SO₂ was ~0.2 cm atm. At most other locations
on Io, the surface was not warm enough to be detected at this
wavelength (S. Kumar, personal communication). A refined Io
model for an SO₂ atmosphere in equilibrium with the solid at
local surface temperatures predicts a global average column
abundance of SO₂ of 0.032 cm atm (J. Pearl, personal
communication). Furthermore Smythe et al.[2] and Fanale et
al.[3] have shown the similarity between ground-based
observations of the reflectivity of Io from 1.0 to 4.2 μm and
laboratory observations of SO₂ frost. We demonstrate here that
the near UV reflectivity of Io, measured from Earth-orbit,
demands that the hemispherical average column abundance of
SO₂ at the time of our observation was very much less than the
local abundance quoted above. Our limit is also less than the
average abundance the model would predict, although we do find
the observations to be consistent with the presence of condensed
SO₂ on Io's surface. A qualitative reconciliation of these results
is presented.**

Io was observed by the long-wavelength spectrograph of the
IUE on 21 April 1979. The best Io spectrum is shown in Fig.
1, together with the solar spectrum of Broadfoot[4]. The sub-
Earth longitude on Io increased from 80 to 90° during the
period in which our best spectrum was obtained. The spectral
resolution for the Io data is 8 Å; the solar data have been
convolved with a rectangular 3 Å bandpass. This treatment of
the solar spectrum was chosen to provide a slightly better
resolution than achieved by the IUE so there would be no
doubt about the reality of any non-solar absorptions found in
the spectrum of Io. The exposure time on Io was 40 min, but
the satellite was probably outside the spectrograph aperture
for a significant fraction of this time because of guiding
uncertainties. The small motions of Io within and just outside
the aperture reduce the signal uniformly at all wavelengths and
slightly degrade the spectral resolution. However, neither effect
seriously impairs these data.

Figure 1 indicates that all the features in the spectrum of Io
from 2,900 Å to 3,100 Å are of solar rather than ionian origin.

We conservatively estimate that no absorption features occur
on Io at the 20% level. Also shown in Fig. 1 are the locations
of the strong electronic bands of SO₂ in this region[5]. We note
that SO₂ has much stronger bands near 2,100 Å, but both the
instrument's insensitivity and the intrinsic faintness of Io at
shorter wavelengths render the 3,000 Å region most suitable
for our present study.

Adopting a typical valley-to-peak absorption coefficient of
10 (cm atm)⁻¹ for SO₂ in this spectral region, assuming the
upper limit of 20% for any absorption feature, and using an
air-mass factor of 3, we calculate an upper limit of
0.008 cm atm of SO₂. Because we have been very conservative
in choosing the upper limit for undetected percentage
absorption, and because there are more than 10 candidate
bands to be sought, we believe our upper limit on the
abundance is quite firm, and must be reconciled with the IR
findings.

As a further test, we have produced the ratio spectra shown
in Fig. 2. Previous experience with IUE spectra has shown
that slight differences between the wavelength scales and slit
functions of the IUE and the convolved solar spectrum
produce high but irrelevant noise levels. The ratio spectra of
Vesta and Io illustrated in Fig. 2 were obtained by using the
same treatment of the solar spectrum that was used in Fig. 1.
Both of these ratios are tied to OAO 2 observations of the
geometric albedos of these objects[6].

The ratio spectra are indeed noisy, but their basic similarity
is easily seen. Over the wavelength range 2,500–3,000 Å, there
is no indication of any absorption in the spectrum of Io that is
not also present on Vesta. Despite the noise in these spectra,
we estimate that any broad deviation larger than 30% of the
signal would be detectable. Adopting 15 (cm atm)⁻¹ as the
average total absorption coefficient in this region and again
assuming an air-mass of 3, we again find an upper limit of
0.008 cm atm for the average SO₂ column abundance over the
visible hemisphere.

The ratio spectra of Io and Vesta in Fig. 2 diverge rapidly
at longer wavelengths, with Io becoming brighter than Vesta
as we approach 3,200 Å. Beyond 3,050 Å, the IUE calibration
is less certain than at shorter wavelengths[7]. Nevertheless, we
have found this same trend in three separate Io spectra, while
it is absent from all other spectra (several asteroids, Neptune,
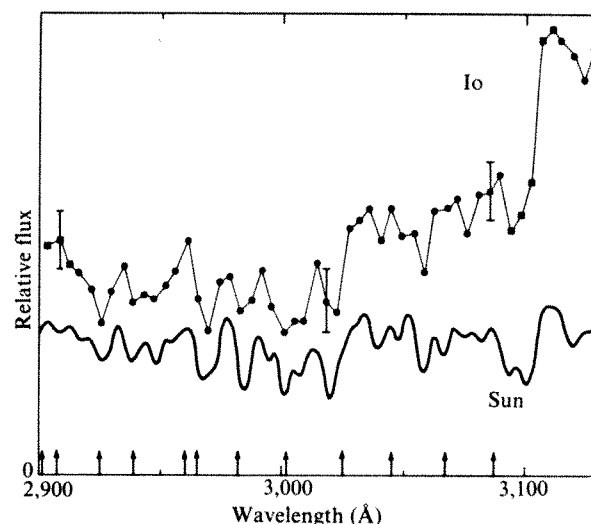
Fig. 1   UV spectra of Io, from IUE, and of the convolved Sun,
from ref. 4. The arrows along the abscissa give the locations of
strong SO₂ bands[5], the absence of which in the spectrum of Io
leads to the upper limit given in the text. The error bars on the
Io data are derived from the background measured on the
spectral image, both above and below the spectrum. Individual
Io data points are plotted as filled circles. Instrumental reseaux,
indicated by the squares near 2,900 and 3,100 Å, have no
discernible effect on this spectrum. See, however, Fig. 2.

§Permanent address: Department of Physics and Astronomy, University College London,
London WC1E 6BT, UK
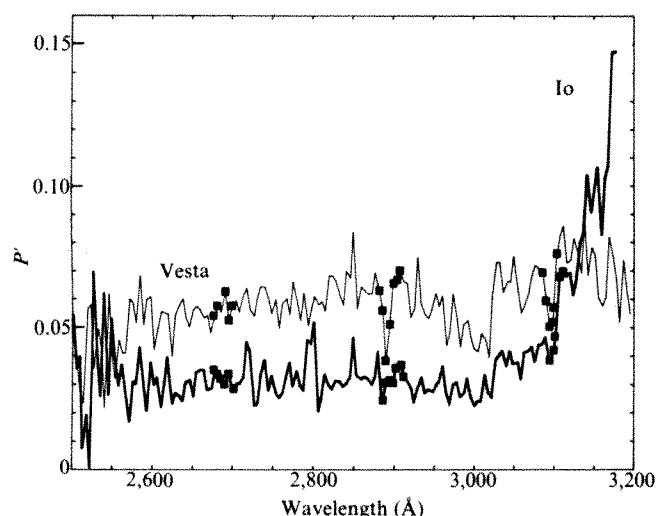
Fig. 2 Ratio spectra of Vesta and Io normalized to geomatrix albedos at 2,590 Å determined by OAO[6]. Points affected by reseaux are marked with black squares. The ordinate gives the reflectivity P' as this normalized albedo. Note that the signal is lost in the noise below 2,550 Å, and that the reflectance of Io crosses that of Vesta at 3,150 Å. Both spectra become progressively less reliable at wavelengths longer than 3,050 Å, but the relative upward trend in the Io reflectance is real.

Titan, Ganymede, Venus, Jupiter, Callisto) we have checked. This rapid rise is also consistent with ground-based observations[8], which unfortunately begin to be uncertain at just this same wavelength. We note that the reflectance of SO_2 frost deposited at 130 K is less than 3% from 2,600 to 3,000 Å, rising very steeply at slightly longer wavelengths: 47% at 3,250 Å, 68% at 3,500 Å and so on[9]. The present UV observations are thus consistent with the conclusions from IR spectra of Io[2,3] that SO_2 frost is present on the satellite's surface, but they are by no means diagnostic. For example, they are also consistent with deposits of Na_2S and K_2S (ref. 10).

There remains the apparent discrepancy between our upper limit for gaseous SO_2 and the result based on the detection by Pearl et al.[1]. One possibility is that the UV absorption coefficient could vary with temperature. While such a variation may occur from band to band, we would expect the total absorption to remain constant. In this circumstance, the calculated upper limit would be based on the stronger bands, and it would probably decrease further. (We thank E. S. Barker for calling our attention to this possibility.)

Transience on Io would also explain the discrepancy. The Voyager observations were made in early March, 1979, whereas the IUE data were obtained in mid-April. It would not be surprising for an atmospheric constituent expelled from volcanoes to be time-variable This possibility is further enhanced by the Voyager 2 finding that one major active volcanic vent from the Voyager 1 epoch had become dormant by July 1979 (ref. 11).

What seems the most probable explanation, however, is that the SO_2 'atmosphere' on Io is patchy, being confined to regions over solid deposits and sources of volcanic venting. We hypothesize that the SO_2 gas condenses locally on the surface, either as a frost or as snow, producing the white patches visible on Voyager pictures[11]. Thus the fact that our upper limit is a factor of 4 times smaller than the global average predicted by Pearl's model is simply an indication that the surface of Io is not completely covered by SO_2 frost, which is certainly consistent with the satellite's appearance. This hypothesis is also consistent with refs 1, 2 and 3, and with the upper limit on the surface pressure set by Pioneer 10 occultation experiments[12]. Our upper limit, which is a global

average, does not in any case contradict the Voyager–IRIS result for gaseous SO_2, which applies only to a very small fraction ($<1\%$) of the surface of Io. Our interpretation leaves open the possibility for small variations in global average absorption of both solid and gaseous SO_2 with time and with the sub-Earth longitude on Io, but such variations may well remain below the detection threshold of the IUE.

We thank P. Solomon for use of his graphics facilities and A. T. Sinclair for providing the ephemeris of Io. We thank J. Pearl and F. Fanale for unpublished information and B. Buratti for help with data analysis. This research was supported in part by NASA grants NSG 5250 and NGR 33-015-141 at Stony Brook. P.S.B. and V.M. were supported by the SRC.

1. Pearl, J. et al. Nature **280**, 755 (1979).
2. Smythe, W. D., Nelson, R. M. & Nash, D. B. Nature **280**, 766 (1979).
3. Fanale, F. P., Brown, R. H., Cruikshank, D. P. & Clark, R. N. Nature **280**, 761 (1979).
4. Broadfoot, A. L. Astrophys. J. **173**, 681 (1972).
5. Warneck, P., Marmo, F. and Sullivan, J. O. J. chem. Phys. **40**, 1132 (1964).
6. Caldwell, J. Icarus **25**, 384 (1975).
7. Bohlin, R. C. & Snijders, M. A. J. IUE Calibration Memo VI (September 1978).
8. Nelson, R. M. & Hapke, B. W. Icarus **36**, 304 (1978).
9. Nash, D. B., Fanale, F. P. & Nelson, R. M. Bull. Am. astr. Soc. **11**, 597 (1979).
10. Nash, D. B. & Nelson, R. M. Nature **280**, 763 (1979).
11. Smith, B. A. et al. Science **204**, 951, **206**, 927 (1979).
12. Kliore, A. et al. Icarus **24**, 407 (1975).

The terminal Eocene event: formation of a ring system around the Earth?

John A. O'Keefe

Laboratory for Astronomy and Solar Physics, Goddard Space Flight Center, Greenbelt, Maryland 20771

The most profound climatic event of the Tertiary was the terminal Eocene event at -34 Myr (ref. 1). Botanical data indicate that winters became much more severe, while summer temperatures were little affected. An explanation in terms of a change in the space direction of the Earth's axis is not dynamically acceptable. On the other hand, an ecological disaster of some kind apparently struck the Radiolaria at this time[2]; the latter event is accurately correlated (to a few tens of thousands of years) with the formation of the greatest known tektite strewn field, the so-called North American strewn field, which has recently been shown to extend at least half-way around the Earth[3]. It is suggested here that tektites and microtektites which accompanied this fall, but missed the Earth, organized themselves into a ring system like that of Saturn. The shadow of the rings fell on the winter hemisphere and so produced the observed cooling. The ring lasted between one and several million years.

Wolfe, reviewing the botanical data, found a sudden change in the relative abundance of forest plants at the end of the Eocene, at about -34 Myr which, he suggests, implies a decrease of the winter temperature by $\sim 20°C$, with little or no corresponding change of summer temperature. Wolfe attributes the event to a change in the obliquity of the ecliptic from $5°-10°$ before the event, to $25°-30°$ after it. Other calculations[4,5] have shown, however, that although changes as large as this have taken place in the obliquity, they have occurred on a time scale of billions of years; they are much too slow to control Eocene climatic changes.

Urey[6] suggested that this and other Cenozoic extinctions may have been associated with tektite strewn fields (showers of tektites). The largest known strewn field is dated at -34 Myr,

RC9 – 58

Microtektites per g
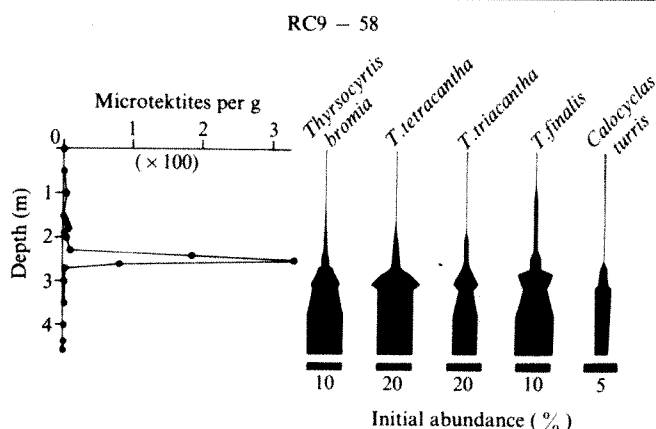
Fig. 1   Microtektites and radiolarian extinctions in a Caribbean deep-sea core. The top of the core is near the end of the Eocene. One metre of core depth corresponds to 0.1–0.2 Myr. The bar graphs display the varying abundances of five species of Radiolaria. The initial abundance of each species, relative to all Radiolaria, is marked. Burrowing animals have disturbed the sediment slightly. From Glass and Zwart[2] by permission.

close to the time of the terminal Eocene event. It has been called the North American strewn field; but Glass et al.[3] found that it extends from the Caribbean through the central Pacific to the Indian Ocean, and that its total mass is 1–10×10^9 tons. Glass and Zwart[2] have shown, from ocean-bottom cores, that five abundant species of Radiolaria, comprising two-thirds of the total radiolarian population, disappear or nearly disappear at the level at which the microtektites appear. Figure 1 compares the variations in the abundance of these species with depth in core RC 9-58, from the Caribbean. Glass estimates the sedimentation rate as 5–$10\,\mathrm{Myr^{-1}}$ in this core; he considers that the agreement between the date of the extinctions seen in Fig. 1 and that of the tektite strewn field is within a few tens of thousands of years (personal communication).

If there is a connection between tektites and climatic change, then it probably results from the screening of sunlight. The mass of even the largest strewn fields is insufficient to affect directly the dynamics of the Earth's atmosphere, not to mention the hydrosphere or the lithosphere. The screening probably also took place in space: dust in the troposphere washes out in a few weeks; in the stratosphere it falls out in a few years at most; but the evidence is for a climatic change that lasted one to several million years: dust in space can persist for that time.

The tektites are assumed here to be of cosmic origin[7]; a terrestrial origin implies the almost instantaneous production of homogeneous, non-porous, water-free glass in pieces up to several decimetres in length, out of common rocks or soil. As far as is known, glass cannot be made in this way.

Assuming a cosmic origin, it would be expected that, in addition to the tektites which reach the Earth, there would be a larger mass which would miss the Earth and be trapped in geocentric orbit. Glass et al.[3] estimate 1–10×10^9 ton for the mass of the North American strewn field; let us adopt 25×10^9 ton, or $10\,\mathrm{km^3}$, for the matter trapped in orbit. Typical diameter sizes for microtektites found in the oceanic cores are of the order of $100\,\mu\mathrm{m}$; this would imply about 2×10^{22} particles with a total area of cross-section of $1.6 \times 10^8\,\mathrm{km^2}$.

Initially the orbits of the trapped particles would form a cloud about the Earth, densest at the inner surface. The cloud would rapidly collapse to a thin ring in the plane of the Earth's equator[8]; the time scale t_1 for the collapse is given by Brahic[9] as

$$t_1 = \frac{T}{N}\left(\frac{R}{r}\right)^2$$

where T is the orbital period; N the number of particles; R a representative dimension (radius of the cloud); and r the particle radius. Then t_1 turns out to be about half a day, so that the reduction to a thin ring will be complete after a year.

An inner radius of 1.5 Earth radii is assumed, above ordinary atmospheric drag, and an outer boundary of 2.5 Earth radii is assumed, inside the Roche limit.

As the ring would lie exactly in the equatorial plane (as a result of collisional damping of north–south motion) it follows that it would cut off sunlight during the winter months, but not the summer months, as shown in Fig. 2.

Quantitatively, the total area of cross-section of the particles would be 30% of the total surface area of the rings; hence the vertical optical depth τ would be 0.30. The Sun's rays would, however, make an angle with the ring equal to the Sun's declination δ, which has a range of $\pm 23.5°$. If the particles were perfect absorbers, the fraction f of the light which would penetrate the ring would be given by

$$f = \exp(-\tau \csc \delta)$$

and f would vary from 0–0.47. Glass and Zwart[10] report three kinds of particles in the North American strewn field: transparent, opaque white, and black. The data are thus consistent with a reduction of the light by a factor of 0.75, as would be required to produce a 20° fall in temperature (grey body calculation).

Estimation of the ring lifetime requires consideration of eight effects:

(1) Gravitational clumping is not expected inside the Roche limit. (2) Tidal effects due to the attraction of the Moon will be about twice as large as the interesting but minor effects of Mimas on the rings of Saturn[11]. (3) Collisional spreading in
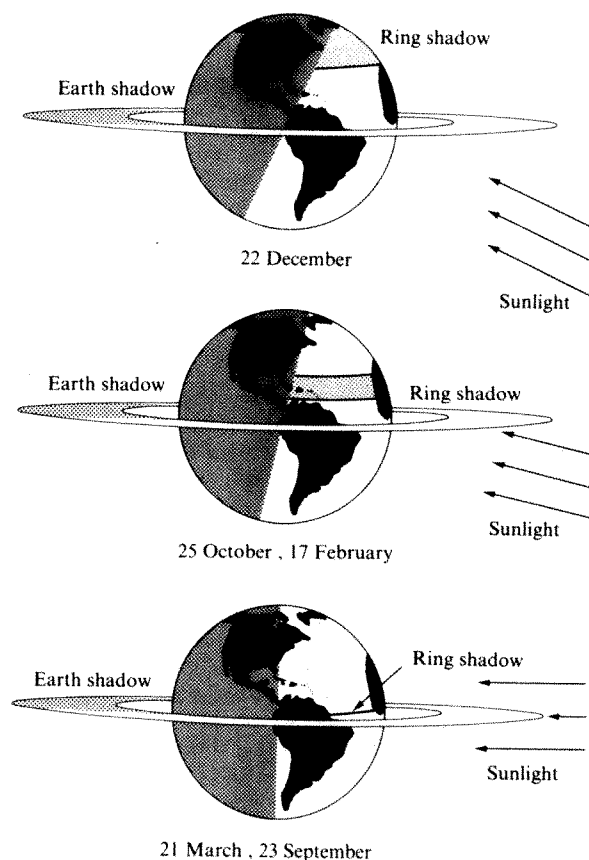
Fig. 2   The terrestrial ring, showing the movement of the shadow with the seasons. Continents shown in their present position. Dates correspond to solar declinations of $0°$, $12°$, $23.5°$. Note that the tropical zone experiences a secondary maximum of illumination around winter solstice.

the ring plane has a time scale of the order of 10^{18} yr (ref. 9); it may be neglected. (4) Atmospheric drag is eliminated because the gas molecules are mopped up by the ring[12]. (5) Micrometeorite erosion at the lunar rate (0.2–0.8 mm Myr^{-1}) would severely limit the lifetimes of the particles; but most of the erosion in the lunar case is due to craters >400 μm in diameter[13]; the small size of the ring particles has a large effect in limiting damage. (6) Rotational bursting due to windmill effects of radiation pressure[14] will be damped by collisions. (7) Thrust effects due to photon recoil[15] will also be damped by collisions. (8) The Poynting–Robertson effect would cancel out around a geocentric orbit except for the fact that part of the orbit lies in the Earth's shadow. The net effect is an outward motion (if the sense of the orbit motion is direct) which probably limits the lifetime of the ring to a few million years.

I thank A. F. Cook, B. P. Glass and M. B. Swincki for their unpublished results and D. E. Smith, J. A. Wolfe and D. P. Rubincam for helpful discussions.

Note added in proof: Ruderman and Truran[16] have similarly suggested that dust ejected from the Moon may cause sudden climatic changes on the Earth.

1. Wolfe, J. A. *Am. Scient.* **66**, 694–703 (1978).
2. Glass, B. P. & Zwart, M. J. in *Proc. Symp. Stratigraphic Micropaleontology of the Atlantic Basin and Borderlands* (ed. Swain, F. W.) 553–567 (Elsevier, New York, 1977).
3. Glass, B. P., Swincki, M. B. & Zwart, P. A. *Lunar planet. Sci.* **10**, 434–436 (1979).
4. Darwin, G. H. *Scientific Papers* Vol. **2**, 208–302 (Cambridge University Press, 1908).
5. Brosche, P. & Sündermann, J. (eds) *Tidal Friction and the Earth's Rotation* (Springer, New York, 1978).
6. Urey, H. C. *Nature* **242**, 32–33 (1973).
7. O'Keefe, J. A. *Tektites and their Origin*, 180–187 (Elsevier, New York, 1976).
8. Jeffreys, H. *Mon. Not. R. astr. Soc.* **107**, 263–267 (1947).
9. Brahic, A. *Astr. Astrophys.* **54**, 895–907 (1977).
10. Glass, B. P. & Zwart, M. J. *Bull. geol. Soc. Am.* **90**, 595–602 (1979).
11. Goldreich, P. & Tremaine, S. *Icarus* **34**, 240–253 (1978).
12. Opp, A. G. *Science* **207**, 401–403 (1980).
13. Comstock, G. M. *Lunar Science VIII*, 202–204 (Lunar Science Institute, Houston, 1977).
14. Paddack, S. J. *J. geophys. Res.* **74**, 4379–4381 (1969).
15. Jacchia, L. in *The Moon, Meteorites and Comets* (eds Middlehurst, B. M. & Kuiper, G. P.) 783–784 (University of Chicago Press, Chicago, 1963).
16. Ruderman, M. & Truran, J. W. *Nature* **284**, 328–329 (1980).

Bivalent spectator oxo bonds in metathesis and epoxidation alkenes

Anthony K. Rappé & William A. Goddard III

Arthur Amos Noyes Laboratory of Chemical Physics, California Institute of Technology, Pasadena, California 91125

Several studies suggest the importance of oxygen in the reactive intermediates for alkene metathesis,

$$M{=}CH_2 + H_2C{=}C^*H_2 \rightleftharpoons M{=}C^*H_2 + H_2C{=}CH_2 \quad (1)$$

and of additional metal–oxo bonds in epoxidations,

$$M{=}O + H_2C{=}CH_2 \rightleftharpoons M + H_2C\!\!\overset{O}{\diagup\!\!\diagdown}\!\!CH_2 \quad (2)$$

For example: (1) catalytic amounts of oxygen were found to be essential for the formation of a stable metathesis catalyst in the WCl$_6$/C$_2$H$_5$AlCl$_2$ system[1]; (2) alkene epoxidation (and general oxidation) reactants such as CrCl$_2$O$_2$, OsO$_4$, and SeO$_2$ all have at least two oxygen ligands[2]; and (3) recently Osborn (personal communication) has described an Mo–oxo carbene as an effective metathesis catalyst. From extensive *ab initio* theoretical studies of Cr and Mo complexes, we show here that the presence of spectator metal–oxo bonds drives the formation of metallocycles, thereby playing a crucial role in the chemistry.

The special role of the oxo group is illustrated by comparing the oxo bond energy of Cl$_4$Cr$=$O (343 kJ mol^{-1}) with the oxo bond energy of Cl$_2$Cr$\lesssim^O_O$ (213 kJ mol^{-1}). (Calculated numbers are based on *ab initio* calculations using valence double zeta basis sets and including electron correlation (generalized valence bond plus configuration

interaction as in ref. 3). Estimated vibrational frequencies were used to calculate ΔH (0 K) from the theoretical energy differences. Standard approaches[4] were used to estimate ΔS and the correction of ΔH to 25 °C.) The origin of this difference is that in Cl$_4$Cr$=$O there are two $d\pi$ orbitals on the Cr available for forming π bonds to the oxygen, leading to a triple bond (analogous to C$\equiv$O). However, in Cl$_2$Cr$\lesssim^O_O$ the corresponding d orbitals are each used in the π bond for different oxo bonds, leading to two double bonds (analogous to O$=$C$=$O or a ketone, R$_2$C$=$O). Thus the metal–oxo bond is dual-valent, existing in two alternative forms depending on the other ligands. The orbital character of the oxo double bond is as in a ketone[5] with a singly-occupied Opσ orbital paired with the singly-occupied metal $d\sigma$ orbital, a singly-occupied Opπ_x orbital paired with a singly-occupied $d\pi_x$ orbital and the remaining doubly-occupied Opπ_y pair nonbonding. For the oxo triple bond, the oxygen orbitals are oriented so as to have two π bonds with the pσ pair of the oxygen coordinated with an empty metal $d\sigma$ orbital. In both cases the bonding is basically covalent with a small charge on the oxygen.

Addition of an alkene to Cl$_2$CrO$_2$ to form the metallocycle oxetane from one oxo bond allows the spectator oxo bond to convert from a double bond to a triple bond, thereby providing a 130 kJ mol^{-1} push towards formation of the metallocycle (calculated $\Delta H = -113$ kJ mol^{-1}, $\Delta G(25\,°C) = -63$ kJ mol^{-1}),

$$(3)$$
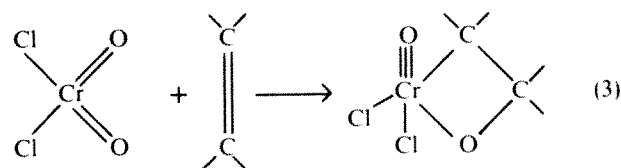
For a single oxo bond, this process is doubly bad; here there is no spectator oxo bond to drive the metallocyclization and one must also add across an oxo triple bond (calculated $\Delta G(25\,°C) = +300$ kJ mol^{-1}),

$$(4)$$
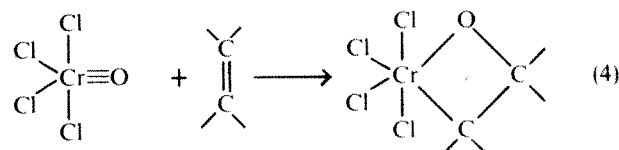
An oxo-carbene behaves similarly,

$$(5a)$$

$$(5b)$$
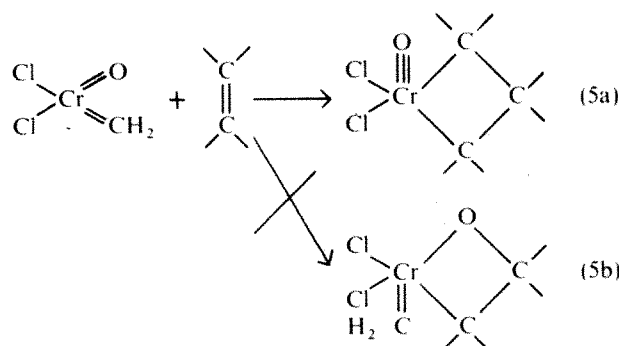
with metallocyclobutane formation favoured by conversion of the spectator oxo bond to a triple bond (calculated $\Delta G(25\,°C) = -42$ kJ mol^{-1}), whereas metallocyclooxetane formation has no such driving force and is significantly uphill (calculated $\Delta G(25\,°C) = +50$ kJ mol^{-1}).

The same effects are found from calculations on Mo [$\Delta G = -105$ kJ mol^{-1}, for reaction (3), $\Delta G = -84$ kJ mol^{-1} for reaction (5a)] and should occur also for W. The essential difference between Cr and Mo (or W) is in the decomposition products of the metallocycles and arises from the change in the

strength of metal carbon or metal oxygen bonds. For $Cl_4Mo{\equiv}O$ we find an oxo bond energy of $456\,kJ\,mol^{-1}$, whereas for $Cl_4Cr{\equiv}O$ we find $343\,kJ\,mol^{-1}$. For example, for Cr metallocycle oxetane we find that reductive elimination dominates [reaction (6a)], whereas for Mo, metal carbene formation is competitive [reaction (6b)]. Similarly, Cr metallocyclobutane reductively eliminates propane, whereas for Mo, the metathesis product is formed,
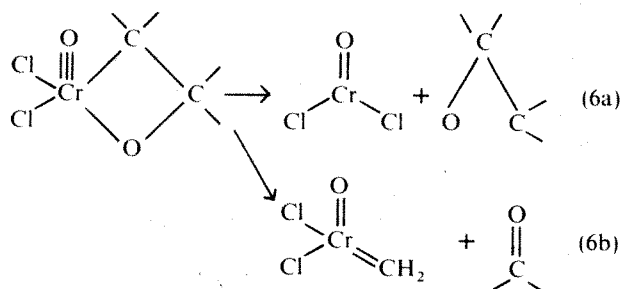
We suggest that this dual-valent character of the spectator metal–oxo bond may be generally useful for designing catalysts or substrates to promote reactions involving metallocycle formation.

This research was partially supported by the US Department of Energy Research and Development Administration grant EX-76-G-03-1305. However, any opinions, findings, conclusions, or recommendations expressed herein are those of the authors and do not necessarily reflect the view of the DOE.

1. Mocella, M. T., Rovner, R. & Muetterties, E. L. *J. Am. chem. Soc.* **98**, 4689 (1976).
2. Sharpless, K. B., Teranishi, A. Y. & Bäckvall, J. E. *J. Am. chem. Soc.* **99**, 3120 (1977).
3. Harding, L. B. & Goddard III, W. A. *J. Am. chem. Soc.* **99**, 4520 (1977).
4. Benson, S. W. *Thermochemical Kinetics* (Wiley, New York, 1976).
5. Harding, L. B. & Goddard III, W. A. *J. Am. chem. Soc.* **97**, 6293 (1975).

Observations of nitrous acid in an urban atmosphere by differential optical absorption

U. Platt*, D. Perner*, G. W. Harris†, A. M. Winer† & J. N. Pitts Jr†

*Kernforschungsanlage Jülich GmbH, Institut für Chemie 3: Atmosphärische Chemie, Postfach 1913, D-5170 Jülich, FRG
†Statewide Air Pollution Research Center and Department of Chemistry, University of California, Riverside, California 92521

In the past decade, increasing attention has been paid to the role of nitrous acid (HONO) in the polluted troposphere, primarily as an initiator of photochemical air pollution[1] through its photodissociation by solar UV radiation into hydroxyl radicals and NO. The OH radical may subsequently attack organics starting a chain photoxidation which leads to the production of O_3, peroxyacetyl nitrate and many other secondary pollutants. Measurements of the concentration of HONO, especially in the early morning, are needed to establish the initial conditions to be used in computer kinetic models of photochemical oxidant formation[2–4]. From laboratory studies, it has been suggested that nitrous acid may also be a precursor to the possible formation of nitrosamines by reaction with simple secondary and tertiary amines in urban air[5], or *in vivo* following inhalation. We report here a series of observations, at Riverside and Claremont, California, of the gradual buildup of HONO during the night and its rapid decay after sunrise. These, we believe, represent the first unequivocal measurements of HONO reported for a major urban air basin impacted by photochemical air pollution.

Nitrous acid was detected and monitored using the long path differential UV absorption technique described by Platt *et al.*[6]. The optical system in the present experiments used a 0.3 m McPherson spectrograph with a 600 grooves mm^{-1} grating blazed at 500 nm (giving a dispersion of 5.3 nm per mm). A spectral region 38 nm wide was scanned by exit slits etched in a thin metal disk, which rotated in the focal plane of the instrument.

The light signals were received by a photomultiplier (EMI 9656Q) and averaged by a DEC PDP11 MINC microcomputer. The scan rate of 105 Hz provided by the rotating disk was fast enough to eliminate unwanted signal variations. Absorption lines with optical densities as low as 10^{-4} (base 10) could be detected. We used the HONO absorption lines at 354.1 and 368.1 nm which have differential absorption cross-sections (D.P., unpublished data) of 4.7 $\times 10^{-19}$ and $3.8 \times 10^{-19}\,cm^2$ respectively. Before measuring the optical density of atmospheric HONO bands, nearby NO_2 bands were eliminated by the subtraction of a suitably weighted NO_2 reference spectrum. For the 354.1 nm band the minimum detectable optical density corresponded to 0.28 p.p.b. (parts per 10^9) HONO using a 970 m lightpath. The light source was a 500-W Xe high pressure lamp (Hanovia 959C).

The night-time buildup of HONO was measured during August and September 1979 (see Table 1) in the Los Angeles air basin at Riverside (a downwind receptor site) and at Claremont (a midbasin site). Figure 1 shows the development of HONO bands during the night of 4–5 August and their decay after sunrise. The observed bands agree well in shape and position with the reference spectrum shown. Additional broad absorption features at ~352 and 360 nm are present
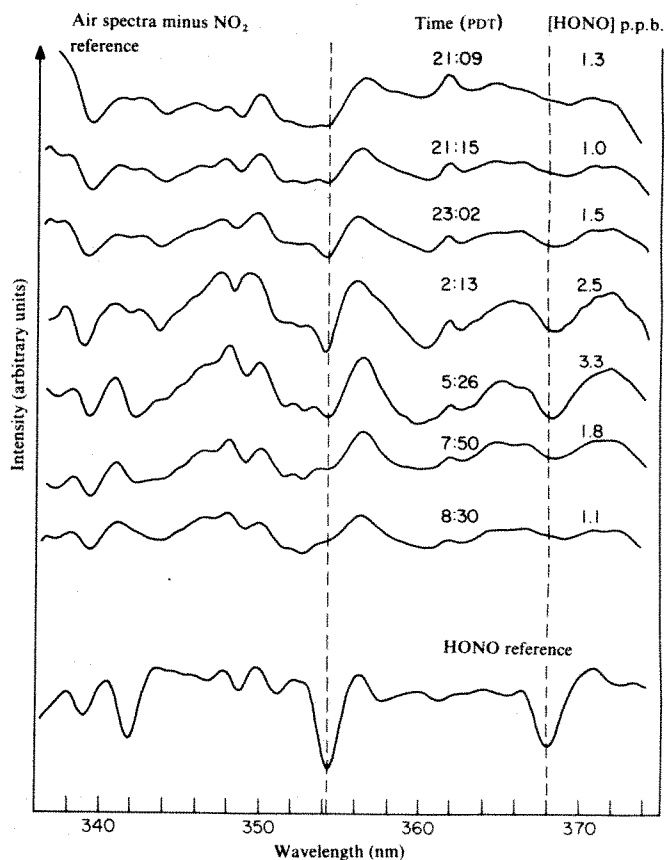
Fig. 1 Air spectra from which absorptions due to NO_2 have been substracted. 4–5 August 1979, Riverside, California. The lowest trace is a HONO reference spectrum.
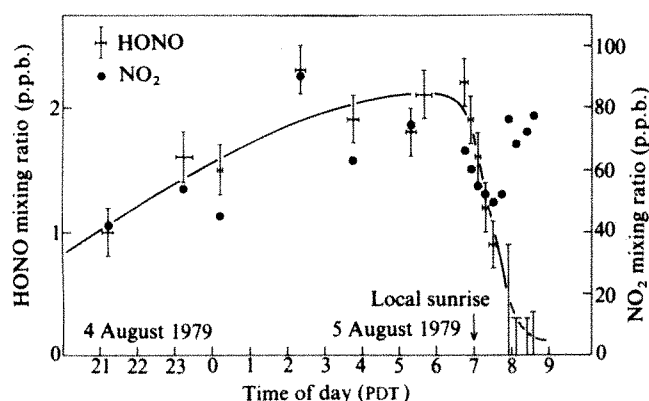
Fig. 2 Concentration–time profiles of HONO and NO_2. 4–5 August 1979, Riverside, California.

and are possibly due to hydrocarbons but are as yet unassigned; the narrow absorption near 339 nm is partly due to CH_2O. At our resolution, deconvolution of this band and the 342 nm HONO band present in the reference spectrum is difficult, leading to distortion and masking of the HONO band. This is particularly evident in the spectrum taken at 2:13 in Fig. 1. Figure 2 shows the HONO and NO_2 concentrations measured on the night of 4–5 August, and Fig. 3 shows the decay of HONO near sunrise during that and three other mornings. Table 1 gives the maximum HONO concentrations observed and the maximum rates of decay after local sunrise. These rates varied between ~ 0.3 and 2.6 p.p.b. h^{-1}, being slower and occurring longer after local sunrise, on hazy mornings as expected.

Nitrous acid was not present above our detection limit during daylight hours and hence we will confine our discussion to the night-time and early morning chemistry of HONO. Our detection limit (~ 0.28 p.p.b.) was relatively high compared to that reported for a study at Jülich, West Germany[7], as we had to use a shorter pathlength (970 m at Riverside and 750 m at Claremont) because of the poor optical transmittance of the polluted atmosphere at our observation sites. In the earlier study[7], despite a longer pathlength, HONO could only be detected on a few occasions in the morning before sunrise while during the remainder of the day concentrations were close to or below the detection limit.

Reactions which are known or have been suggested to produce HONO in the troposphere are

$$OH + NO \overset{(M)}{\rightarrow} HONO$$
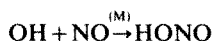
$$k_1 = 6.6 \times 10^{-12}\, cm^3\, s^{-1} \text{ (ref. 8)} \qquad (1)$$

$$HO_2 + NO_2 \overset{(M)}{\rightarrow} HO_2NO_2$$
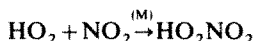
$$k_{2a} = 1.1 \times 10^{-11}\, cm^3\, s^{-1} \text{ (refs 9, 10)} \qquad (2a)$$

$$\rightarrow HONO + O_2$$
$$k_{2b} < 5 \times 10^{-16}\, cm^3\, s^{-1} \text{ (ref. 10)} \qquad (2b)$$

$$RO + NO_2 \rightarrow R'CHO + HONO$$
$$k_3 \lesssim 1.5 \times 10^{-12}\, cm^3\, s^{-1} \text{ (ref. 11)} \qquad (3)$$
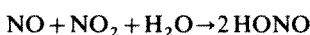
$$NO + NO_2 + H_2O \rightarrow 2 HONO$$
$$k_4 < 4.4 \times 10^{-40}\, cm^6\, s^{-1} \text{ (ref. 12)} \qquad (4)$$
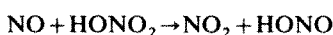
$$NO + HONO_2 \rightarrow NO_2 + HONO$$
$$k_5 = 5 \times 10^{-19}\, cm^3\, s^{-1} \text{ (ref. 13)} \qquad (5)$$

and of these, only reactions (4) and (5) can proceed at night in the absence of photolytic radical sources. During daylight HONO is destroyed rapidly by photolysis

$$HONO + h\nu(\lambda < 400\, nm) \rightarrow OH + NO \quad J = 1.7 \times 10^{-3}\, s^{-1}$$

$$\text{(solar zenith angle} = 30°)^{14} \qquad (6)$$

but at night it should accumulate at a rate reflecting the source strength. From the observed morning concentrations of 1.5 to 4.1 p.p.b., mean source strengths of 0.13 to 0.34 p.p.b. h^{-1} ($\sim 1 - 3 \times 10^6\, cm^{-3}\, s^{-1}$) can be estimated.

Kaiser and Wu[12] found that the rate of the homogeneous process reaction (4) is very slow ($k_4 < 4.4 \times 10^{-40}\, cm^6\, s^{-1}$) and for reactant concentrations typical of the night-time Riverside atmosphere ($NO_2 \sim 80$ p.p.b., NO < 1 p.p.b., $H_2O \sim 2$ vol %) the homogeneous reaction is negligible in a well-mixed air mass. The very low levels of NO also rule out reaction (5) as a major HONO source.

In motor vehicle exhaust systems only a few p.p.t. (part per 10^{12}) of HONO can be formed by the homogeneous reaction (4) during the 0.2 s residence time of the exhaust gases in the silencer of an average car with its engine running at 3000 r.p.m. (NO_x concentration ~ 100 p.p.m. and $NO/NO_2 \simeq 10$). Moreover, the homogeneous formation of HONO in plumes emanating from mobile or stationary sources, even though they provide much longer residence times, can also be neglected because the rate of HONO production decreases with the third power of the reaction partner concentrations and dilution by ambient air is rapid. Thus, if reaction (4) is important in the atmosphere, it must proceed heterogeneously, as suggested by Kaiser and Wu[12] who
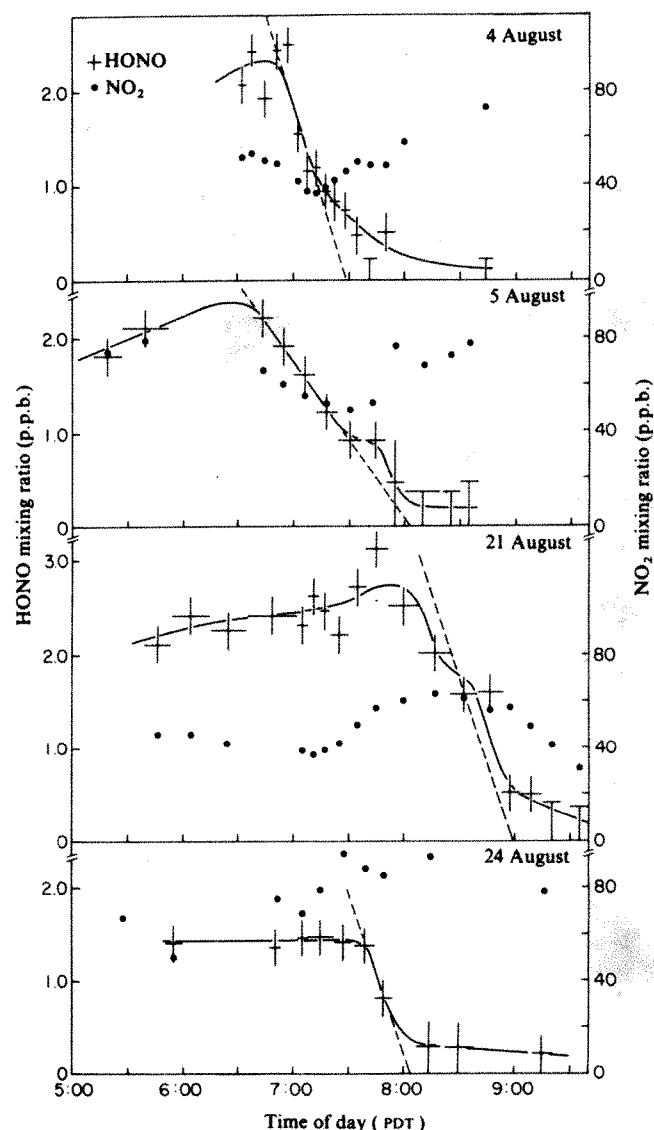
Fig. 3 Measurements of HONO and NO_2 performed near sunrise on four days during August 1979 at Riverside, California.

Table 1   Data for HONO observation at Riverside and Claremont, California

1979 date	HONO maximum (p.p.b.)	Max HONO decay rate (p.p.b. h^{-1})	HONO half-time* (PDT)	Sunrise† (PDT)
8/2	4.1	2.6	7:10	6:11
8/4	2.5	2.4	7:10	6:13
8/5	2.2	1.7	7:15	6:14
8/21	3.1	1.5	8:45	6:26
8/24	1.5	2.1	7:45	6:28
8/29‡	1.3	~0.3	~9:30	6:31
8/31‡	2.0	0.9	8:20	6:33
9/1‡	1.8	0.5	9:00	6:34
9/2‡	1.1	~0.5	~8:30	6:35

*When $[HONO] = 0.5[HONO]_{max}$.
†Local sunrise at Riverside ~45 min later because of nearby high ground.
‡Measurements at Claremont.

found that the reaction proceeded relatively rapidly on the surface of their aged Pyrex reaction vessel. The possiblity that the observed HONO may be formed directly in the combustion region of sources, should also be considered.

Whatever the source, at sunrise the HONO accumulated throughout the night is rapidly photolysed, and the HONO destruction rates given in Table 1 lead to OH production rates of up to 2×10^7 OH radicals cm^{-3} s^{-1}. By making an estimate of the lifetime of OH soon after sunrise at Riverside

of ~0.1 s (dictated largely by reaction with NO$_2$), we can conclude that up to ~2×10^6 OH radicals cm^{-3} could be produced in an approximately hour-long early morning 'pulse' from HONO photolysis, at a time when other photochemical activity is low.

While nitrosamines have not been widely detected in the atmosphere, our direct observations of p.p.b. levels of HONO in the polluted troposphere at night implies that the possibility of their formation[15], at least near sources of precursor amines, should be seriously considered. After sunrise both HONO and any nitrosamines present would be rapidly depleted by photolysis.

1. Pitts, J. N. Jr & Finlayson-Pitts, B. J. *Adv. Envir. Sci. Technol.* **7**, 75–162 (1977).
2. Falls, A. H. & Seinfeld, J. H. *Envir. Sci. Technol.* **12**, 1398–1406 (1978).
3. Hendry, D. G., Baldwin, A. L., Barker, J. R. & Golden, D. M. *Computer Modeling of Simulated Photochemical Smog* (EPA-600/3-78-059, 1978).
4. Carter, W. P. L., Lloyd, A. C., Sprung, J. L. & Pitts, J. N. Jr *Int. J. Chem. Kinet.* **11**, 45–101 (1979).
5. Pitts, J. N. Jr *Phil. Trans. R. Soc.* **A290**, 551–576 (1979).
6. Platt, U., Perner, D. & Patz, H. W. *J. geophys. Res.* **84**, 6329–6335 (1979).
7. Perner, D. & Platt, U. *Geophys. Res. Lett.* **6**, 917–920 (1979).
8. JPL Publication 79-27, *Chemical Kinetic and Photochemical Data for Use in Stratospheric Modelling* (1979).
9. Howard, C. J. *J. phys. Chem.* **67**, 5258–5263 (1977).
10. Graham, R. A., Winer, A. M. & Pitts, J. N. Jr *Chem. phys. Lett.* **51**, 215–220 (1977).
11. Batt, L. *Int. J. Chem. Kinet.* **11**, 977–993 (1979).
12. Kaiser, E. W. & Wu, C. H. *J. phys. Chem.* **81**, 1701–1706 (1977).
13. McKinnon, I. R., Mathieson, J. G. & Wilson, I. R. *J. phys. Chem.* **83**, 779–780 (1979).
14. Stockwell, W. R. & Calvert, J. G. *J. Photochem.* **8**, 193–203 (1978).
15. Tuazon, E. C., Winer, A. M., Graham, R. A., Schmid, J. P. & Pitts, J. N. Jr *Envir. Sci. Technol.* **12**, 954–958 (1978).

Correlation of 18O in precipitation with temperature and altitude

U. Siegenthaler & H. Oeschger

Physics Institute, University of Bern, Bern CH-3012, Switzerland

The 18O/16O ratio in precipitation is correlated to climatic parameters, especially temperature. However, the meteorological processes determining the stable isotope composition of precipitation are complex and only partly understood, so that a quantitative interpretation of ancient isotope ratios in precipitation, as recorded in polar ice[1] or in carbonate sediments from lakes[2], has not yet been possible. For several years we have measured 18O/16O ratios on monthly precipitation samples from Switzerland and here summarize these data.

Samples were collected at five stations (circles in Fig. 1) of the network of the Swiss Meteorological Service, so that meteorological data are at hand for correlation with $^{18}O/^{16}O$ results (Table 1). Three of the stations are situated in a valley in the Central Alps (Haslital, Eastern Bernese Oberland): Meiringen at 632 m, Guttannen at 1,055 m and Grimsel at 1,950 m above sea level. Guttannen and Grimsel are respectively 11 and 20 km away from Meiringen. The valley rises from NW to SE and is surrounded by mountains that reach altitudes between 2,000 m and 3,500 m. Bern (572 m) is situated about 70 km WNW of these three stations and away from the direct influence of the mountains. Locarno is on the southern side of the Alps, at an altitude of 366 m, and its climate is markedly different from that of the other stations.

An important factor determining $\delta^{18}O$ in precipitation is temperature. Dansgaard[3] found that on a global scale there is a good correlation for coastal and polar stations between annual means of $\delta^{18}O$ and of temperature, with an average change in $\delta^{18}O$ of 0.7‰ per degree Celsius. This global

relation between $\delta^{18}O$ and temperature can be explained semiquantitatively by considering the formation of precipitation as a Rayleigh process, whereby with continuing formation of precipitation from an air mass the remaining water vapour is progressively being depleted in ^{18}O because $H_2^{18}O$ condenses preferably to $H_2^{16}O$ (refs 3, 4). According to this simple model, $\delta^{18}O$ in precipitation on the temperature of condensation, but also on the initial conditions in the vapour source region (temperature and isotopic composition). There are further processes influencing $\delta^{18}O$ which are not taken into account by the Rayleigh model, most significantly admixture of isotopically different water vapour, and ^{18}O enrichment of the falling raindrops due to evaporation and isotope exchange with ambient vapour[3,5,6].
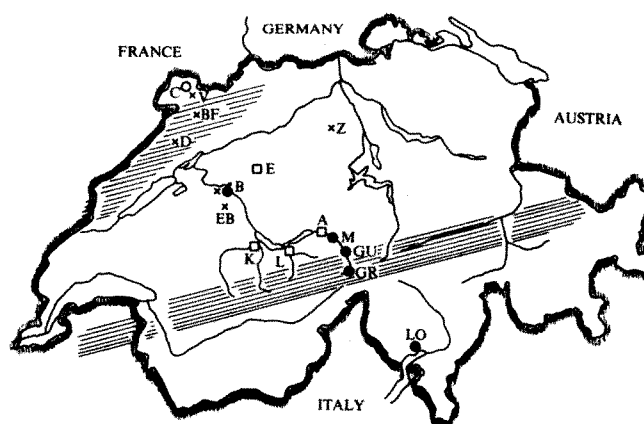
Fig. 1   Map of Switzerland with the locations mentioned in the text. ○, Precipitation sampling stations: B, Bern; M, Meiringen; Gu, Guttannen; Gr, Grimsel; Lo, Locarno; C, Coeuve. ×, springs or groundwater: V, Vendline; BF, Blanche Fontaine; D, Doux; B, Bern; Eb, Englisberg; Z, Zetzwil. □, Rivers: E, Emme; K, Kander; L, Lütschine; A, Aare. The mountain ranges of the Jura and the Alps are shown schematically as hatched areas.

Table 1 Data for the stations from which precipitation was analysed   The values are based on measurements from the period 1971–78 (1973–78 for Locarno). The temperature coefficient (last line) was obtained as the slope of a regression line of monthly $\delta^{18}O$ values as a function of temperature

	Grimsel	Guttannen	Meiringen	Bern	Locarno
Altitude above sea level (m)	1,950	1,055	632	572	366
Mean annual temperature (°C)	1.2	6.3	7.9	8.8	11.7
Mean annual precipitation (mm per yr)	2,091	1,650	1,271	964	1,945
Weighted mean $\delta^{18}O$ in precipitation (‰)	−14.4	−12.8	−11.7	−10.0	−8.8
Temperature coefficient for seasonal $\delta^{18}O$ variations (‰ per degree Celsius)	0.44	0.55	0.53	0.35	0.40

In the following we compare $\delta^{18}O$ with surface temperature at the site of precipitation sampling. According to the Rayleigh model, condensation temperature should be considered instead of surface temperature, and the initial $\delta^{18}O$ and temperature of the vapour mass should be taken into account, too. This is, however, not possible because the necessary data are not available.

Long-term mean values of $\delta^{18}O$ and temperature at different stations (Fig. 2a, large symbols) are relatively well correlated; the corresponding regression line has a slope of 0.56‰ per degree Celsius. $\delta^{18}O$ is lower at all stations than expected from the globally observed relationship (dashed line), a phenomenon known as the 'continental effect'. Possible reasons for this effect are: (1) the influence of re-evaporated continental water, already depleted in ^{18}O; (2) (in summer) a larger temperature difference between surface and condensation levels (as supported by higher temperature gradients) on the continent than on the coast.

At Meiringen and Guttannen, $\delta^{18}O$ is lower than expected from extrapolation from the temperature–$\delta^{18}O$ relation (or also from the altitude–$\delta^{18}O$ relation, Fig. 2c) obtained from the other stations. Also, the amounts of precipitation are higher at Guttannen and Meiringen than elsewhere at similar altitudes in this region north of the Alps (compare Meiringen with Bern in Table 1). Both observations can probably be explained by an orographic effect. The two stations are surrounded by high mountains which force the moist air to climb up, so that here the condensation levels are higher and condensation temperatures lower than for other stations at comparable altitudes and mean annual temperature, with the consequence of relatively low $\delta^{18}O$ and high amounts of precipitation.

In Fig. 2a, weighted mean annual $\delta^{18}O$ values of the years 1971–78 are compared with arithmetic temperature means (see also Fig. 2b). A correlation cannot be seen for any of our stations. For climatic applications this means that caution is necessary when trying to interpret, for instance, extreme $\delta^{18}O$ values in annual glacier ice layers in terms of temperature. For this comparison weighted means are taken for $\delta^{18}O$ because they are adequate for palaeoclimatic isotope records as well as for hydrologic application, while arithmetic means of temperature represent the average climate better than weighted temperature means. If looking for causal relationship, however, weighted annual mean $\delta^{18}O$ should be compared not with the arithmetic annual temperature mean, but rather with weighted mean temperature during precipitation events. Unfortunately, such weighted temperature means are not readily available. However, plots of $\delta^{18}O$ against temperature of monthly data (see below) and of daily samples collected during limited time show much scatter, which suggests that the correlation would not significantly improve when using weighted annual temperature means. Furthermore, arithmetic annual means of $\delta^{18}O$ also show no significant correlation with temperature.

Figure 2b shows the variation of $\delta^{18}O$ and of temperature (average of all stations) with time. The trends of $\delta^{18}O$ and of temperature are quite different, which again demonstrates that annual mean $\delta^{18}O$ is not determined uniquely by temperature. On the other hand, there is quite a good correlation between

different stations (Fig. 2b), with parallel trends for the stations north of the Alps as well as Locarno. From 1971 to 1975, a general decrease of 1–2‰ is observed, then an increase from 1975 to 1977, and again a decrease in 1978. This parallelism indicates that the year-to-year variations of $\delta^{18}O$ are primarily determined by the large-scale weather situation, rather than by local factors.

In Fig. 2c, the variation of mean $\delta^{18}O$ values with altitude is plotted (means over whole period of observation). Obviously, this is essentially only a different representation of
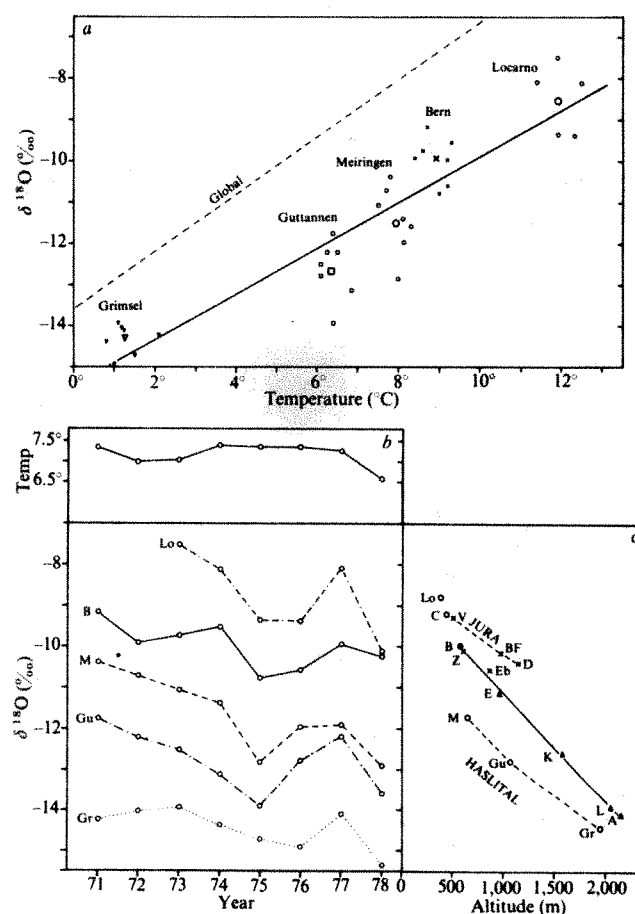
Fig. 2 Mean values of $\delta^{18}O$, weighted with amount of precipitation. a, $\delta^{18}O$ values for the years 1971–78 (1973–78 for Locarno) as a function of mean annual air temperatures. Large symbols, mean values for the entire period of observation, with corresponding regression line (solid line), $\delta^{18}O = 0.56t - 15.5$‰. Dashed line, global relationship as obtained by Dansgaard[3], $\delta^{18}O = 0.70t - 13.65$‰. b, Time trend of $\delta^{18}O$ in precipitation for Locarno, Bern, Meiringen, Guttannen and Grimsel. Top, annual mean temperature, average of all five stations. c, $\delta^{18}O$ as a function of altitude. O, Precipitation. ×, Springs or groundwater. △, Rivers (see caption to Fig. 1 for names of stations). For rivers and groundwaters, mean altitudes of the catchment basin are given, and $\delta^{18}O$ data are mean values over at least 18 months.

the $\delta^{18}O$–temperature relationship, as temperature and altitude are well correlated in our restricted area. Included are values for rivers and groundwaters from western Switzerland (see map, Fig. 1), because these reflect well the weighted mean $\delta^{18}O$ of precipitation (see Bern and stations C and V, ref. 7, in Fig. 2c). This is probably also true for the Alpine rivers (Aare, Lütschine, Kander) indicated in Fig. 2c, as evaporation is relatively unimportant at high altitudes, so that most of the annual precipitation must run off as river water.

There is a good correlation between $\delta^{18}O$ and altitude for locations on the Swiss Plateau (B, Z, Eb, E) and in the western Alps (K, L, A) except those in the Haslital. The corresponding decrease of $\delta^{18}O$ with altitude (solid line) is $-0.26\%_0$ per 100 m. This figure is in the middle of the range of values reported from studies in different regions of Europe[8–14], which are between -0.16 and $-0.4\%_0$ per 100 m (with one exception[15] where $-0.5\%_0$ per 100 m was observed). $^{18}O/^{16}O$ decreases with altitude also above 2,000 m: mean $\delta^{18}O$ in precipitation collected at Jungfraujoch (3,572 m) from August 1977 to July 1978 was $1.4\%_0$ lower than at Grimsel, corresponding to a change of $-0.09\%_0$ per 100 m between these two stations.

The stations in the Haslital, mainly Meiringen and Guttannen, show rather low isotope values compared with the general trend. This is, of course, the same phenomenon as discussed above in connection with temperature (Fig. 2a), and is presumably due to an orographic uplift of the condensation level, so that the effective altitude of formation of precipitation is higher than in the other regions considered here. Figure 2c shows a more general decrease from west (Jura) to east (Haslital) at constant altitude, comparable on a small scale with a continental effect. The decrease from Jura to Swiss Plateau reflects the rain-shadowing effect of the mountain range of the Jura. Similar phenomena, lower isotopic values on the lee side of a mountain range than on the weather side, were observed at the Sierra Nevada[16] and in Germany[9]. The fact that the elevation (or temperature, respectively) of the site of precipitation sampling is not the only parameter of influence for $\delta^{18}O$ is important for hydrological applications: stable isotope measurements may be used for estimating the mean altitude of the recharge area of springs[12,17], but only if the locally valid $\delta^{18}O$–altitude relation is known.

Finally we consider monthly data. Plotted against temperature, the monthly $\delta^{18}O$ values of a station scatter by about $\pm 3\%_0$ around a regression line, which clearly illustrates that temperature alone cannot explain the whole variability of $\delta^{18}O$. The slopes of the regression lines vary between 0.35 and $0.55\%_0$ per degree Celsius at our stations (last line of Table 1). Figure 3 shows the mean seasonal trends of $\delta^{18}O$ and temperature for Meiringen, Guttannen and Grimsel. In general, the $\delta^{18}O$ cycles are about parallel to the seasonal temperature cycles. The difference in $\delta^{18}O$ between Grimsel and the two stations at lower altitude is, however, clearly higher in summer than in winter, while the temperature difference is relatively constant. The isotopic differences between these stations (in other words, the altitude effect) can be attributed to two main factors. (1) A progressive depletion in $H_2{}^{18}O$ of the vapour, along with the raining out of a vapour mass during its orographic ascent and cooling. This corresponds to Rayleigh condensation, with progressively higher condensation levels and lower condensation temperatures. (2) ^{18}O enrichment due to evaporation of the falling raindrops. Both processes cause a positive correlation of $\delta^{18}O$ with temperature (and a negative correlation with altitude). Process (2) depends on the prevailing vapour pressure and is, therefore, more effective at higher temperatures; it is assumed to be negligible for snowflakes because probably only a very thin surface layer can be enriched in ^{18}O (refs 10, 11). Thus the evaporative altitude effect (2) is expected to be larger in summer than in winter. It therefore seems plausible that evaporation of falling raindrops is responsible for the $\delta^{18}O$ difference between Grimsel and the
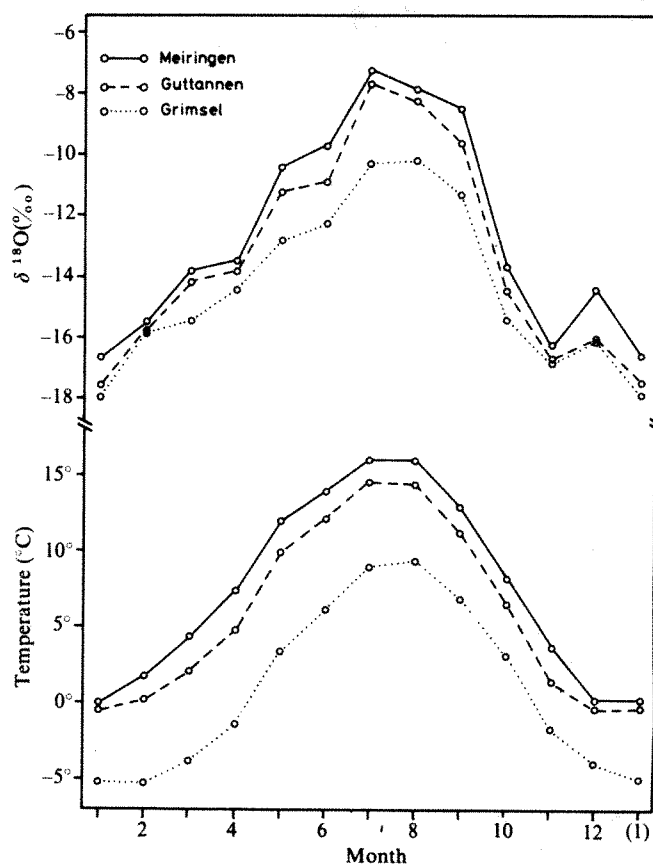
Fig. 3 Monthly $\delta^{18}O$ values in precipitation and air temperatures, mean values 1971–78. January (1) is shown twice for the sake of continuity.

two lower-altitude stations being larger in summer than in winter, and thus for the different temperature coefficients (Table 1) of these stations.

The temperature–$\delta^{18}O$ relation is of considerable interest for palaeoclimatic applications. The relation between mean values of different stations (Fig. 2a) partly reflects geographical influences and is, therefore, not directly comparable to climatic temperature and isotopic variations. On the other hand, there is a large range of 'climates' within an annual cycle. It is tempting to speculate that the temperature coefficient found for seasonal variations, $0.45 \pm 0.1\%_0$ per degree Celsius, is also valid for long-term temperature changes and therefore for the interpretation of palaeoisotope records in Central Europe. The analogy between seasonal and climatic variations is, however, incomplete, and the temperature coefficient valid for climatic changes may be quite different from that of the seasonal variation. For a better understanding of the processes affecting $\delta^{18}O$ in precipitation, additional studies covering larger geographical areas will be necessary, considering also the variations of conditions in the source regions of the water vapour.

1. Dansgaard, W., Johnsen, S. J., Møller, J. & Langway, C. C. *Science* **166**, 377–381 (1969).
2. Eicher, U. & Siegenthaler, U. *Boreas* **5**, 109–117 (1976).
3. Dansgaard, W. *Tellus* **16**, 436–468 (1964).
4. Friedman, I., Redfield, A. C., Schoen, B. & Harris, J. *Rev. Geophys. Space Phys.* **2**, 177 (1964).
5. Friedman, I., Machta, L. & Soller, R. *J. geophys. Res.* **67**, 2761–2766 (1962).
6. Ehhalt, D., Knott, K., Nagel, J. F. & Vogel, J. C. *J. geophys. Res.* **68**, 3775–3780 (1963).
7. Siegenthaler, U., Oeschger, H. & Tongiorgi, E. in *Isotope Hydrology 1970*, 373–385 (IAEA, Vienna, 1970).
8. Dansgaard, W. *Medd. Grønland* **165**, 1–120 (1961).
9. Eichler, R. *Geol. Rdsch.* **55**, 144 (1964).
10. Ambach, W., Dansgaard, W., Eisner, H. & Møller, J. *Tellus* **20**, 595–600 (1968).

11. Dinçer, T., Martinec, J., Payne, B. R. & Yen, C. K. in *Isotope Hydrology 1970*, 23–42 (IAEA, Vienna, 1970).
12. Stahl, W., Aust, H. & Dounas, A. in *Isotope Techniques in Groundwater Hydrology 1974* Vol. 1, 317–339 (IAEA, Vienna, 1974).
13. Herrmann, A., Rauert, W. & Stichler, W. *Proc. Meet. Sonderforschungsbereich* 81, Technische Universität München, 30–42 (1977).
14. Bortolami, G. C., Ricci, B., Susella, G. F. & Zuppi, G. M. in *Isotope Hydrology 1978* Vol. 1, 327–350 (IAEA, Vienna, 1978).
15. Moser, H. & Stichler, W. in *Isotope Hydrology 1970*, 43–52 (IAEA, Vienna, 1970).
16. Friedman, I. & Smith, G. I. *Science* 169, 467–470 (1970).
17. Siegenthaler, U. & Schotterer, U. *Gas Wass. Abwass.* 57, 501–506 (1977).

Accretion and episodic plutonism

Loren A. Raymond & Samuel E. Swanson*

Department of Geology, Appalachian State University, Boone, North Carolina 28608

Episodic calc-alkaline igneous activity in magmatic arcs contrasts with steady-state magmatism accompanying seafloor spreading. Gilluly[1] examined this apparent anomaly in western North America and he and Lanphere and Reed[2] concluded that igneous activity has been more or less continuous over the entire North American Cordillera since the Triassic. A similar view was held by Pitcher[3] for the coastal batholith of Peru. Numerous studies, however, support the view that episodic magmatism characterizes areas of local to regional scale along convergent plate margins[1,2,4–12]. Grow and Atwater[13] suggested that increased magmatic activity in Alaska might have been induced by subduction of a spreading ridge. If so, episodic igneous activity could be produced by successive subduction events involving spreading centres[8]. Dickinson[7] suggested a model involving frictional heating along the Benioff zone, accumulation of magma above that zone, and periodic magmatism triggered by an unknown condition or event. However, he later[8] proposed that regional episodicity is a function of the interaction between a specific site and a wavering (migrating back and forth) magmatic axis that occasionally passes through the site to produce a magmatic event. Migration of the magmatic axis results from accretion or erosion at the trench, variation in the dip of the subduction zone, and (or) reorganization of plate movements[8,14–16]. Shaw et al.[17] suggest tidal power as a source of mechanical energy which, through periodic variations in shear melting of the mantle, produces magmatic periodicity. In contrast, Gilluly[1] suggests that variations in the properties of the mantle and of the crust of the subducting plate may be responsible for magmatic episodicity. We propose an alternate explanation for local to regional plutonic episodicity. Although this 'episodic accretion plutonism model', is based on data from California, it is applicable to other segments of orogenic belts including southwestern Alaska, southern Japan and western Indonesia. We limit the discussion of igneous activity to plutonism, as geochronological data suggest that volcanism is not simply the surficial expression of plutonism. This possibility is supported by a recent re-evaluation of Andean magmatism[18]. We shall discuss the problem of volcanism and its relationship to accretion and plutonism elsewhere.

The episodic accretion–plutonism model requires that plutonic activity within segments of orogenic belts alternates with periods of accretion[19,20]. We propose that plutonism in magmatic arcs is a function of the subduction of hydrous crustal materials, especially sediments, and that plutonism is terminated by episodic accretion of these hydrous materials in the arc–trench gap adjacent to the magmatic arc. Thus, episodic plutonism is related to episodic accretion.

Episodicity may be discussed in terms of a single segment of an orogenic belt rather than the entire belt. We have chosen the California segment of the Cordilleran Mountain system as the prime example because of an excellent data base. The

study area is limited on the north by the Oregon border, on the south by the Garlock fault, on the west by the San Andreas fault, and on the east by the California–Nevada border (Fig. 1). Selection of the California–Nevada border as a boundary excludes Mesozoic–Cenozoic plutonic rocks exposed to the east[21]. However, because of the limited outcrop area of these rocks, the general lack of detailed data on discordance and resetting of dates, and the similarity in overall duration of magmatic activity between the eastern areas and California, the California data set is representative and is the only one that includes enough closely spaced, unambiguous dates and plutons to be adequately depicted on a small scale map. In the California segment of the Cordilleran Orogenic belt, some volcanic, volcanic–clastic, and sedimentary rocks of the western Sierra Nevada represent an early to middle Mesozoic accretionary wedge. The Franciscan Complex of the Coast Ranges consists of late Mesozoic and early Cenozoic accretionary wedges. The positions of the magmatic arcs of different ages, which all lie within the Sierra Nevada and Klamath Mountains, are shown in Fig. 1.

Documentation of the episodic accretion–plutonism model requires careful dating of both the accreted wedge and the magmatic arc. Figure 2 is a compilation of the data on accretion and plutonic activity for the Mesozoic and earliest Cenozoic eras in the study area. The controversial intrusive
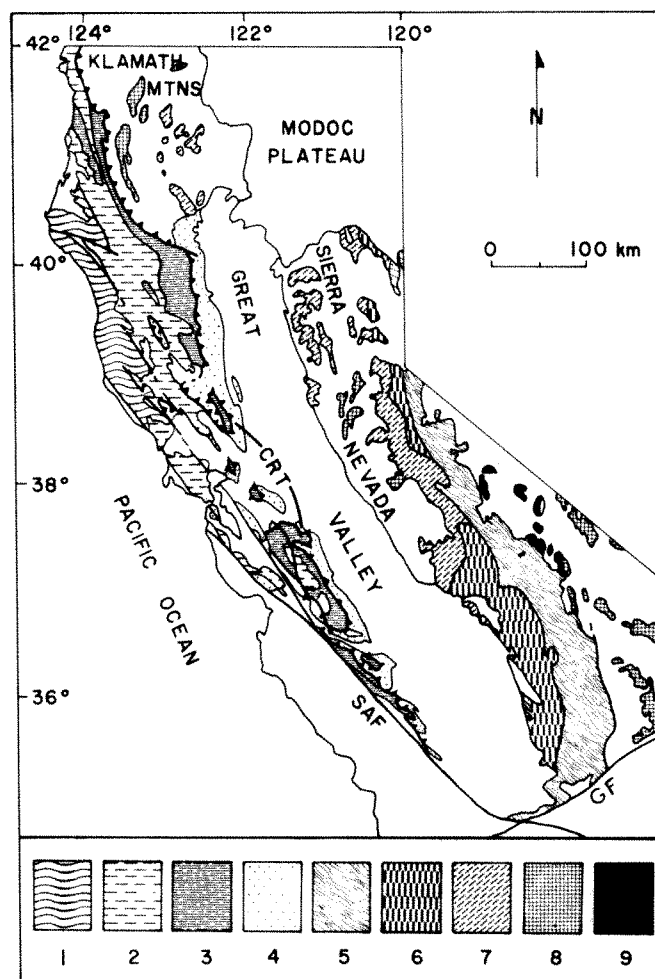
Fig. 1 Map of California showing the distribution of accreted (Franciscan) rocks and granitic rocks intruded during Sierran plutonic episodes. 1, Mid-Cenozoic accretionary wedge; 2, late Cretaceous accretionary wedge; 3, early Cretaceous accretionary wedge; 4, Great Valley sequence (arc–trench gap deposits); 5, late Cretaceous plutons; 6, early Cretaceous plutons; 7, late Jurassic plutons; 8, early Jurassic plutons; 9, late Triassic plutons. SAF, San Andreas Fault; GF, Garlock Fault; CRT, Coast Range Thrust (modified from refs 6, 25, 30).

*Present address: Division of Geoscience, Geology/Geophysics Program, University of Alaska, Fairbanks, Alaska 99701.

epochs of Evernden and Kistler[5,6,10] are used as a basis for the age of maximum pluton emplacement in the arc.

Dating episodes of accretion is more difficult than dating plutons. Mapping of accreted terrains reveals that they are composed of structurally and stratigraphically complex, generally unfossiliferous, rock assemblages. Pelagic sediments deposited on a plate moving towards a subduction zone may be succeeded by arc/continent derived clastic sediments deposited on submarine fans and by submarine landslide deposits (olistostromes) and proximal fan facies deposited in the trench. Trench slope basin deposits may cap the stratigraphic sequence before or during deformation and tectonic mélange formation in the subduction zone. As sedimentation may be continuous over the period of subduction activity, fossil dates on the entire accreted wedge will span the convergence interval. Yet, mapping and palaeontological studies reveal that accreted terrains may be subdivided into time restricted stratigraphic/structural units. Because sedimentation is terminated by the onset of accretion and/or subduction, the upper age limit given by the fossils in any stratigraphic/structural unit is considered to be the approximate age of accretion. In the Franciscan Complex, numerous studies[22-29] on fossils contained in major structural units[22,23,27,30] allow estimates of the age of accretion of these units (Fig. 2). The ages of major accreted structural units in the Sierra Nevada are less well known, but one Mesozoic mass

may be exposed[31]. Some accreted rocks may also be concealed beneath the Great Valley. To the north, in the Klamath Mountains, accreted rocks of Triassic–Jurassic age are present in the so-called 'western Palaeozoic and Triassic belt'[32] (Fig. 2).

Metamorphic dates on rocks of the accreted wedge, especially blueschist facies rocks, also mark times of accretion. That blueschist dates mark accretion events may seem to contradict the common view that blueschists are formed continuously during subduction[33]. Although blueschist facies rocks are probably formed continuously, it is only when rocks subducted to depths of <30 km are uplifted rapidly, for example during upward rotation of accreted wedges[34], that these rocks are preserved. Blueschist K/Ar dates mark the time at which accreted wedges pass upwards through the argon retention isograd. Thus, blueschist dates generally fall at the end of accretion events (Fig. 2), reflecting the time required for uplift and upward rotation of major structural/stratigraphic units.

Peak dates of metamorphism used in Fig. 2 (columns 2 and 4) are based on new dates obtained by D. Krummenacher and D. L. Martin for L. A. Raymond, plus additional dates from the literature. The meaning of metamorphic dates on accreted rocks in the Sierran foothills is equivocal, but we have used the few dates available in Behrman[35]. Dates on blueschist facies Coast Range rocks from refs 33, 36–41 were considered in constructing Fig. 2, but special attention was given to the re-evaluation of dates by Lanphere and others[41].

Coincidence of Coast Range blueschist dates and dates of termination of sedimentation in major tectono–stratigraphic units (accretion dates) with gaps in the plutonic history of the Sierra Nevada shown in Fig. 2 provides the basis for the episodic accretion–plutonism model. (Because metamorphic dates are dates of cooling, it is surprising that the coincidence is as marked as it appears in Fig. 2. The problems of dating low grade rocks and the variations expected are discussed elsewhere[40,41]. It is expected, for example, that metamorphic dates will tend to overlap the beginning of the next plutonic episode, as is the case with the 120 Myr date in the Franciscan rocks.) In addition, metamorphic dates on accreted Sierran and Klamath rocks fall in the gaps between episodes of plutonism. Together these data indicate that times of accretion in the arc–trench gap are not times of plutonism in the magmatic arc. This suggests that plutonism is controlled by subduction (and subsequent dehydration) of sediments.

Episodic accretion and plutonism are not restricted to northern California, although the timing of events in other segments of orogenic belts is generally less well known. In southwestern Alaska, accretion of a blueschist facies and lower grade terrains at ~190, 110, 50 and 20 Myr is interspersed with plutonic events dated at 195–185, 176–145, 83–58 and 28–26 Myr[42-48]. In western Indonesia, mid-Cretaceous and Miocene intrusive events were followed by late Cretaceous and Miocene accretion events[49]. Accretion events in south-west Japan during the early Cretaceous (?) and Oligocene are followed by plutonic events of mid-Cretaceous to early Tertiary age (130–60 Myr) and late Miocene to Recent age (16–0 Myr)[50].

Clearly, careful dating of events along convergent margins will be required to test the episodic accretion–plutonism model. However, available data are adequate to justify use of this model in evaluating the tectonic history of plate margins preserved in the continental geologic record.
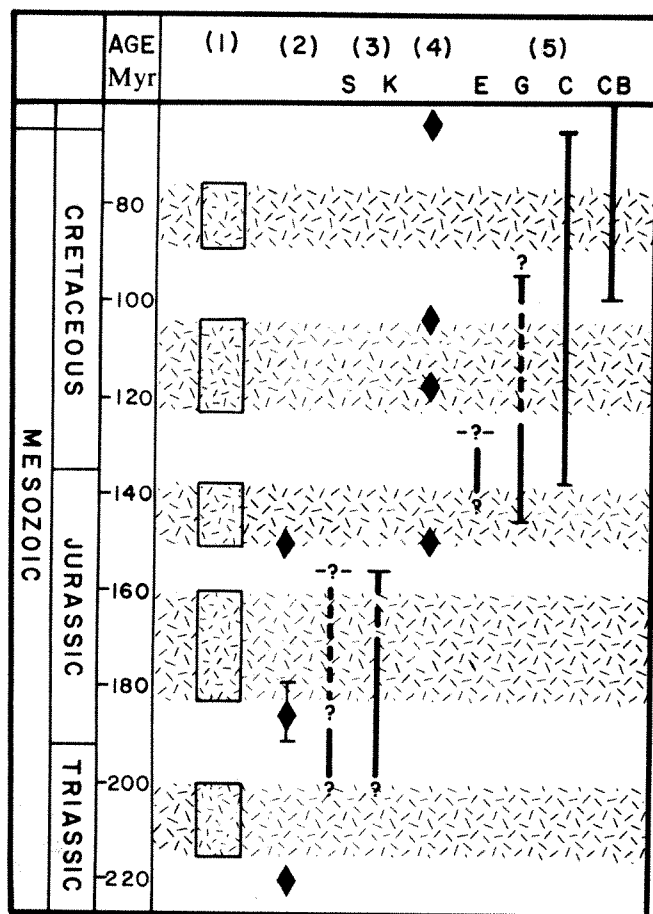
Fig. 2 Correlation chart showing: (1) Sierran intrusive episodes (after refs 5, 6, 10); (2) Sierran and Klamath metamorphic events (diamonds) (after refs 35, 41, 51); (3) Sierran (S) and Klamath (K) sedimentation episodes (after refs 31, 32); (4) peak dates of blueschist facies metamorphism in the Coast Range (Franciscan) after refs 36–41 and L.A.R., unpublished data); (5) Franciscan sedimentation episodes: E, Eastern Belt: C, Central Belt; G, the Geysers block; CB, Coastal Belt) (after refs 22, 23, 25, 26, 52–55). Time scales from ref. 56.

1. Gilluly, J. Bull. geol. Soc. Am. 84, 499–514 (1973).
2. Lanphere, M. S. & Reed, B. L. Bull. geol. Soc. Am. 84, 3773–3782 (1972).
3. Pitcher, W. S. Bull. geol. Soc. Lond. 131, 587–591 (1975).
4. Kawano, Y. & Ueda, Y. Tectonophysics 4, 523–530 (1967).
5. Evernden, J. F. & Kistler, R. W. Prof. Pap. U.S. geol. Survey 623 (1970).
6. Kistler, R. W., Evernden, J. F. & Shaw, H. R. Bull. geol. Soc. Am. 82, 853–868 (1971).
7. Dickinson, W. R. Rev. geophys. Space Phys. 8, 813–860 (1970).
8. Dickinson, W. R. Am. J. Sci. 272, 551–576 (1972).
9. Crowder, D. F., McKee, E. H., Ross, D. C. & Krauskopf, K. B. Bull. geol. Soc. Am. 84, 285–296 (1973).
10. Kistler, R. W. A Rev. Earth planet. Sci. 2, 403–418 (1974). Kistler, R. W. in Pacific Coast Paleogeography Symp. Vol. 2, 75–84 (Soc. Econ. Paleontol. Miner., Pacific Section, 1978).
11. Bussell, M. A., Pitcher, W. S. & Wilson, P. Can. J. Earth Sci. 13, 1020–1030 (1976).
12. Armstrong, R. L., Taubeneck, W. H. & Hales, P. O. Bull. geol. Soc. Am. 88, 397–411 (1977).
13. Grow, J. A. & Atwater, T. Bull. geol. Soc. Am. 81, 3715–3722 (1970).
14. Coney, P. J. Am. J. Sci. 272, 603–628 (1972).
15. Coney, P. J. & Reynolds, S. J. Nature 270, 403–406 (1977).
16. Keith, S. B. Geology 6, 516–521 (1978).
17. Shaw, H. R., Kistler, R. W. & Evernden, J. F. Bull. geol. Soc. Am. 82, 869–896 (1971).
18. Thorpe, R. S. & Francis, P. W. in Origin of Granite Batholiths, 65–75 (Shiva, Orpington, 1979).
19. Coleman, R. G. 24th int. geol. Congr. Sect 2, 19–26 (1972).
20. Prince, R. A. & Kulm, L. D. Bull. geol. Soc. Am. 86, 1639–1653 (1975).
21. Cross, T. A. & Pilger, R. H. Jr Am J. Sci. 278, 865–902 (1978).
22. Bailey, E. H., Irwin, W. P. & Jones, D. L. Bull. Calif. Div. Mines Geol. 183 (1964).
23. Blake, M. C. Jr & Jones, D. L. Spec. Pub. Soc. Econ. Paleontol. Miner. 19, 345–357 (1974).
24. Pessagno, E. A. Jr Geology 1, 153–156 (1973).
25. McLaughlin, R. J. & Pessagno, E. A. Jr J. Res. U.S. geol. Survey 6, 715–726 (1978).
26. Evitt, W. R. & Pierce, S. T. Geology 3, 433–436 (1975).
27. Berkland, J. O., Raymond, L. A., Kramer, J. C., Moores, E. M. & O'Day, M. Bull. Am. Ass. petrol. Geol. 56, 2295–2302 (1972).
28. O'Day, M. & Kramer, J. C. in Geol. Soc. Sacramento Guidebook 27, 51–56 (1972).
29. Maxwell, J. C. Bull. geol. Soc. Am. 85, 1195–1204 (1974).

30. Jones, D. L., Blake, M. C. Jr, Bailey, E. H. & McLaughlin, R. J. Tectonophysics 47, 207–222 (1978).
31. Schweickert, R. A. in Pacific Coast Paleogeography Symp. Vol. 2, 361–384 (Soc. Econ. Paleontol. Miner. Pacific Section, 1978)
32. Irwin, W. P., Jones, D. L. & Pessagno, E. A. Jr Geology 5, 557–562 (1977).
33. Suppe, J. 24th Int. geol. Congr. Sect. 3, 552–559 (1972).
34. Karig, D. E. & Sharman, G. F. Bull. geol. Soc. Am. 86, 377–389 (1975).
35. Behrman, P. S. in Pacific Coast Paleogeography Symp. Vol. 2, 337–348 (Soc. Econ. Paleontol. Miner. Pacific Section, 1978).
36. Suppe, J. Bull. geol. Soc. Am. 80, 135–142 (1969).
37. Coleman, R. G. & Lanphere, M. A. Bull. geol. Soc. Am. 82, 2397–2412 (1971).
38. Suppe, J. & Armstrong, R. L. Am. J. Sci. 272, 217–233 (1972).
39. Lehman, D. H., Gucwa, P. R., Fritz, D. & McDowell, F. W. Abstr. Prog. geol. Soc. Am. 9, 452 (1977).
40. Suppe, J. & Foland, K. A. in Pacific Coast Paleogeography Symp. Vol. 2, 431–452 (Soc. Econ. Paleontol. Miner., Pacific Section, 1978).
41. Lanphere, M. A., Blake, M. C. Jr. & Irwin, W. P. Am. J. Sci. 278, 798–815 (1978).
42. Forbes, R. B. & Lanphere, M. A. J. geophys. Res. 78, 1383–1386 (1973).
43. Reed, B. L. & Lanphere, M. A. Bull. geol. Soc. Am. 84, 2583–2610 (1973).
44. Moore, J. C. in The Geology of Continental Margins, 811–816 (Springer, Berlin, 1974).
45. Carden, J. R., Connelly, W., Forbes, R. B. & Turner, D. L. Geology 5, 529–533 (1977).
46. Plafker, G., Jones, D. L. & Pessagno, E. A. Jr. in Circular U.S. geol. Survey 751-B, 41–42 (1977).
47. Plafker, G. et al. Open-file Rept. U.S. geol. Survey 78–490 (1978).
48. Hudson, T. Geology 7, 230–234 (1979).
49. Katili, J. A. in The Western Pacific: Island Arcs, Marginal Seas, Geochemistry, 287–306 (Crane, Russak, Canberra, 1973).
50. Matsumoto, T. & Kimura, T. in Mesozoic–Cenozoic Orogenic Belts, 513–542 (Scottish Academic Press, Edinburgh, 1974).
51. Hotz, P. E., Lanphere, M. A. & Swanson, D. A. Geology 5, 659–663 (1977).
52. Wachs, D. & Hein, J. R. Geology 3, 29–33 (1975).
53. Berkland, J. O. 24th Int. geol. Congr. Sect 3, 99–105 (1972).
54. Gucwa, P. R. Geology 3, 105–108 (1975).
55. Bachman, S. B. in Pacific Coast Paleogeography Symp. Vol. 2, 419–430 (Soc. Econ. Paleontol. Miner. Pacific Section 1978).
56. van Hinte, J. E. Bull. Am. Ass. petrol. Geol. 60, 269–287 (1976); 489–497 (1976).

Caledonian Sm–Nd ages and a crustal origin for Norwegian eclogites

W. L. Griffin

Mineralogisk-Geologisk Museum, Oslo, Norway

H. K. Brueckner

Queens College of the City University of New York, Flushing, New York 11367 and Lamont-Doherty Geological Observatory, Palisades, New York 10964

Sm–Nd dating of minerals in several Norwegian country-rock eclogites reported here indicates that the rocks crystallized ~425 Myr ago. The isotopic composition of both Nd and Sr in these eclogites suggests that they formed from much older crustal rocks. The high-pressure metamorphism of which the eclogites are relics probably involved subduction of the continental Baltic plate as it was overridden by the Greenland plate during the Caledonian orogeny.

Eclogites of the Caledonian orogeny in western Norway are usually divided[1] into two types: mafic and ultramafic layers or lenses within garnet-free ultramafic bodies ('internal' or 'Type A' eclogites); and mafic boudins, layers and larger bodies enclosed directly within Precambrian gneisses ('external', 'country-rock', or 'Type B' eclogites). The origin(s) and time(s) of formation of the latter eclogites are controversial. Several workers regard them as products of progressive regional metamorphism in essentially their present stratigraphic and tectonic position. Evidence for this view[1] includes: (1) zoning in minerals, indicating growth with increasing temperature (T) and pressure (P); (2) preservation of lower-grade minerals in the cores of garnet grains; (3) field and geochemical indications that the protoliths had low-P origins; and (4) a regional gradient in maximum metamorphic P and T with highest values near the coastline. Krogh[2] proposed that the eclogites formed by metamorphism of a variety of protoliths during subduction of the continental crust. On the basis of available radiometric data[3–5] he suggested that this event was part of the Svecofennian (1,600–1,800 Myr) orogeny.

An alternative view holds that the eclogites and ultramafic rocks formed in the mantle and were later introduced into the crust as solid fragments[6,7]. Most proponents of this model favour a Caledonian origin for eclogite formation.

Neither model is necessarily time-dependent; nor does the *in situ* model preclude the incorporation of mantle fragments into the crust during subduction. However, the orogenic processes implied by the two schemes are quite different. Knowledge of the timing and mechanism of eclogite formation in this region is especially important for our understanding of the Caledonian orogeny.

We have attempted to solve these problems by Sm–Nd dating of minerals from several country-rock eclogites. The garnet–clinopyroxene pair is ideal for Sm–Nd dating, as the two phases fractionate Sm and Nd more efficiently than most rock-forming minerals. Furthermore, as Sm and Nd are nearly identical in their crystal-chemical behaviour, the isotopic system should be resistant to metamorphic effects short of total recrystallization of the host minerals. This argument, however, has not yet been rigorously tested.

Analyses were done at Lamont-Doherty Geological Observatory using methods already described[8]. The isotopic data are normalized to $^{146}Nd/^{142}Nd = 0.7219$ and $^{86}Sr/^{88}Sr = 0.1194$. The ages obtained are relatively precise, because of the large difference in the Sm/Nd ratio between garnet and clinopyroxene (Table 1), although some individual analyses are less precise than desired. The uncertainties reflect difficulties with the separation of Nd, especially from garnets. The results in Table 1 show three important features.

(1) Five out of six garnet–clinopyroxene pairs give two-point isochron ages between 407 and 447 Myr. One mineral pair is significantly older (887 Myr).

(2) A wide range in initial $^{143}Nd/^{144}Nd$ ratios (0.51162–0.51244) suggests that eclogites formed from various protoliths. If the protoliths of samples K-6, N-16 and 1428 separated from a mantle of chondritic uniform reservoir (chur) type[9], they did so long before the Caledonian orogeny. Samples 5/79A and S19 are ambiguous in this respect, as their time-integrated Sm/Nd ratios are nearly chondritic.

(3) T_{chur} model ages[9] for most individual minerals are discordant and geologically meaningless, as would be expected if metamorphism took place long after separation of the protolith from the mantle.

The ages reported here are similar to U–Pb ages on zircon from the Hareidland eclogite (400–418 Myr; compare with sample N-16)[10], to Rb–Sr whole-rock ages on late/post-tectonic granitic dykes near Kristiansund (380 Myr; compare

Table 1 Sm–Nd analytical data from Norwegian eclogites (ages in Myr)

Sample	Phase	Sm (p.p.m.)	Nd (p.p.m.)	^{147}Sm/^{144}Nd	^{143}Nd/^{144}Nd	T_{chur}	Cpx–gnt age (Myr)	^{143}Nd/^{144}Nd$_i$	^{87}Sr/^{86}Sr$_i^*$
K-6	cpx	10.49 ± 1	2.890 ± 5	0.1656	0.512065 ± 46	3081			
	gnt	1.120 ± 2	1.397 ± 4	0.7499	0.513621 ± 48	269	407 ± 24	0.511624 ± 73	
5/79	cpx	2.096 ± 5	1.126 ± 2	0.3231	0.512980 ± 40	401			
	gnt	0.7507 ± 8	1.906 ± 5	1.528	0.516316 ± 50	420	423 ± 12	0.512086 ± 65	0.71646 ± 40
U-19	cpx	4.099 ± 12	1.583 ± 3	0.2306	0.512418 ± 64	915			
	gnt	0.4717 ± 14	0.4034 ± 16	0.5146	0.514051 ± 46	671	877 ± 59	0.511092 ± 153	0.71756 ± 8†
S-19	cpx	10.13 ± 14	2.981 ± 5	0.1769	0.512560 ± 36	730			
	gnt	0.4874 ± 26	0.8423 ± 80	1.040	0.515087 ± 72	429	447 ± 20	0.512056 ± 44	0.71496 ± 14
1428	cpx	5.170 ± 16	2.652 ± 10	0.3085	0.513282 ± 34	852			
	gnt	1.570 ± 2	1.507 ± 4	0.6081	0.514102 ± 40	538	418 ± 11	0.512437 ± 110	
N-16	cpx	3.536 ± 3	1.105 ± 7	0.1879	0.512887 ± 36	<0			
	gnt	0.5485 ± 16	1.308 ± 4	1.436	0.516340 ± 150	455	423 ± 30	0.512367 ± 32	0.70589 ± 4†

K-6, Pod in gneiss, Frei, south-east of Kristiansund. Cpx + gnt + opx + biot + qtz.

5/79, Small lens in gneiss, Raudberg, north of Måløy. Cpx + gnt + qtz.

U-19, Scree sample, central Otrøy. Cpx + opx + gnt + bio + qtz. Gnt exsolution in opx.

S-19, Small pod of pegmatitic eclogite, Selje Church, north-east of Måløy. Cpx + gnt + opx.

1428, Thick layer adjoining extensive marble horizon, Tverfjell, north of Molde. Cpx + gnt + amph + qtz.

N-16, Very large body, Hareidlandet. Cpx + gnt + qtz; cpx largely symplectitized.

*Recalculated to 424 Myr BP. †Rb and Sr concentrations not measured, ^{87}Rb/^{86}Sr assumed equal to 0.0012.

with sample K-6)[4], and to Rb–Sr and K–Ar mineral ages from the gneiss region[11]. The simplest interpretation is that these ages reflect isotopic homogenization between minerals as a result of major recrystallization of the eclogite protoliths, and presumably of the enclosing Precambrian country rocks, during the Caledonian metamorphism. The Sm–Nd ages are up to 70 Myr older than most Rb–Sr and K–Ar mineral dates (380–410 Myr). This suggests that the Sm–Nd system closed sooner than the Rb–Sr and K–Ar systems, and that these ages more closely approximate the peak of Caledonian metamorphism.

It might be argued that the Caledonian Sm–Nd ages reflect a resetting of Sm–Nd systems in previously formed eclogites. This would require that the Sm–Nd systems are as easily reset as, for example, K–Ar systems, which seems unlikely on present evidence. Otherwise, this metamorphism must have taken place in conditions in which the eclogite minerals remained stable; the conclusion must still be that eclogite-facies metamorphism occurred during the Caledonian orogeny. This event, rather than a Precambrian one, thus seems to be largely responsible for the mineral assemblages of the basal gneisses of western Norway.

Clinopyroxenes from country-rock eclogites have ^{87}Sr/^{86}Sr ratios at 424 Myr that range from 0.7039 to 0.7176 (ref. 12) (see also Table 1). These ratios suggest that the eclogite protoliths, which have low Rb/Sr ratios (<0.1), had a premetamorphic crustal history during which they acquired radiogenic Sr, and Ar (ref. 5), from the enclosing gneisses. This is true even of samples (5/79A, S19) for which Sm/Nd data are ambiguous. A T_{chur} model age of ~1,600 Myr can be calculated for N-16, using available NAA analyses (Sm/Nd = 0.39) and the (^{143}Nd/^{144}Nd)$_0$ value in Table 1. The eclogite protoliths may thus have been exposed to the effects of both the Svecofennian and Sveconorwegian (~1,000 Myr) orogenies while they were in the crust.

The anomalously old age (877 Myr) of sample U-19 may reflect the effects of these earlier metamorphic events. Some eclogite garnets contain inclusions of garnet–hornblende–biotite plagioclase–quartz assemblages that formed in almandine–amphibolite facies conditions. The cores of many eclogite garnets may be relics of garnet–amphibolite assemblages formed during a Precambrian metamorphic event. The 877 Myr 'age' of sample U-19 could therefore reflect the Precambrian age of the garnet core and the Caledonian age of the garnet rim. Studies of eclogites with strongly zoned garnets should clarify this point.

The combined Nd and Sr isotopic data thus suggest that the protoliths of the eclogites studied existed as crustal rocks long before they were metamorphosed to eclogites during the Caledonian orogeny. There is no difference, in this respect, between eclogites with and without orthopyroxene or between those with fresh and symplectitized omphacite. These data are inconsistent with introduction of the eclogites as solid bodies of mantle material, during the Caledonian orogeny. They do support Krogh's[2] model of *in situ* metamorphism of various protoliths during subduction of a slab of continental crust. However, the Sm–Nd ages suggest that the actual subduction occurred in Caledonian time.

The samples studied here have all been subjected to temperatures of 700–800 °C and pressures of 14–18 k bar (ref. 2). We suggest that these conditions reflect depression of the Baltic plate as it was overridden by the Greenland (North American) plate along a Himalayan-type suture during the Caledonian orogeny. The Sm–Nd ages probably record a blocking temperature close to the peak of metamorphism. Breakdown assemblages in the eclogites reflect a nearly adiabatic decompression after the metamorphic peak[2,13]. The sequence of subduction and rapid uplift is similar to that proposed for the eclogite-bearing terrain of the western Alps[14]. The Alpine uplift was accompanied by widespread retrograde metamorphism (prasinitization); similar retrogression may have produced the present mineralogy of much of the gneiss enclosing the eclogites.

Sm–Nd dating can give very precise ages for the formation of many eclogite assemblages. Further work on these high-pressure relics will provide detailed data on the processes of subduction and obduction in the Caledonian mountain belt and in other orogenic zones that contain eclogites.

1. Bryhni, I., Krogh, E. & Griffin, W. L. *N. Jb. Miner. Abh.* **130**, 49–68 (1977).
2. Krogh, E. *Nature* **267**, 17–19 (1977).
3. Brueckner, H. K. *Norsk Geol. Tidsskr.* **59**, 141–153 (1979).
4. Pidgeon, R. T. & Råhaim, A. *Norsk Geol. Tidsskr.* **52**, 241–256 (1972).
5. McDougall, I. & Green, D. H. *Norsk Geol. Tidsskr.* **44**, 183–196 (1964).
6. O'Hara, M. J., Richardson, S. W. & Wilson, G. *Contr. Miner. Petrol.* **32**, 48–68 (1971).
7. Lappin, M. A. & Smith, D. C. *J. Petrol.* **19**, 530–584 (1978).
8. O'Nions, R. K., Hamilton, P. J. & Evensen, N. M. *Earth planet. Sci. Lett.* **34**, 13–22 (1977).

9. DePaulo, D. J. & Wasserburg, G. J. Geophys. Res. Lett. 3, 249–252 (1976); 3, 743–746 (1976).
10. Krogh, T. E., Mysen, B. O. & Davis, G. L. Carnegie Inst. Wash. Yearb. 73, 575–576 (1975).
11. Brueckner, H. K. Am. J. Sci. 267, 1195–1212 (1969).
12. Brueckner, H. K. Contr. Miner. Petrol. 60, 1–15 (1977).
13. Carswell, D. A., Krogh, E. & Griffin, W. L. (in preparation).
14. Ernst, W. G. Fortschr. Miner. 54, 192–222 (1977).

Mantle composition derived from the composition of lherzolites

S. Maaløe & R. Steel

Department of Geology, Realfagbygget, University of Bergen, 5014 Bergen, Norway

Bickle et al.[1] recently suggested that the major element composition and rare earth element (REE) content of komatiites indicate a lherzolitic composition for the mantle, and that the REE mantle/chondrite ratio must have a value of ~1.0. The $^{143}Nd/^{144}Nd$ ratios for basalts show that the mantle source for basalts has a REE distribution similar to that of chondritic meteorites[2]. The REE lherzolite/chondrite ratios display some variation, but the ratios obtained indicate an average value of about 1.0 (ref. 3), and the REE content of lherzolite is thus consistent with lherzolitic composition for the mantle. The major element composition of the mantle is very important for both geophysics and igneous petrology and we consider here the relevance of the major element composition of lherzolites to the composition of the mantle.

A recent compilation of 384 major element analyses of spinel lherzolite nodules from continental and oceanic regions defines trends for both nodules which are approximately linear and coincident[4]. Why the analyses should form such a well defined trend is unclear as the composition of a module could be controlled by various processes. However, as the nodules represent fragments of the uppermost mantle[5], the lherzolitic material of the nodules may have resulted from an ascending convection current or plume which generated basalt. If this assumption is correct then the trend of the lherzolites should be related to the process of primary magma generation. This possibility can be checked by comparing the composition of the primary magma and the trend. This comparison will only

Fig. 1 The olivine control line for primary abyssal tholeiite. The trend for abyssal tholeiite controlled by plagioclase and pyroxene fractionation is shown by a heavy line[8]. The composition 'p' is the most magnesian-rich composition on this trend. Within experimental error the control line passes through p, suggesting that the composition p may be derived from the primary abyssal tholeiite by olivine fractionation.

be possible if the composition of the primary magma generated from the mantle can be reasonably well estimated. We assume here that the primary composition should be that of primary abyssal tholeiite, because these are generated in far larger volumes than any other type of basalt[6].

The composition of primary abyssal tholeiite has been estimated in various ways. Investigators of abyssal tholeiite have suggested that the most magnesian-rich tholeiites are primary, the results being within the range 9–~20% MgO (refs 7–9). This approach does not necessarily give the correct result, and the estimates obtained from ophiolite complexes must be considered more representative. Malpas[10] and Elthon[11] have calculated the average composition of the primary abyssal magma by this method and their results are in excellent agreement, the MgO content in both cases being 18% MgO.

The composition of the primary magma estimated by Elthon, is shown in Table 1. The various ophiolite complexes have a similar structure although each displays individual features[12]. The general relevance of a primary composition based on a study of a single complex is therefore questionable. However, it is possible to check the composition proposed by Elthon[11]. The trend of abyssal tholeiites is divided into two parts, a magnesian-rich section controlled by olivine fractionation, and a low magnesian section from 9 to 4% MgO, controlled mainly by plagioclase fractionation[8]. Olivine is the dominant cumulus phase in the ultramafic part of the ophiolite complexes. The fractionation of olivine from the primary magma should therefore yield abyssal tholeiite with ~9% MgO, provided its composition is correct. Figure 1 shows that the estimated composition may be considered

Table 1 Major element compositions

	1	2	3	4	5	6
SiO_2	47.76	50.52	49.50	60.4	44.20	44.58
Al_2O_3	12.06	10.29	16.53	15.7	2.05	2.43
FeO	8.96	9.07	8.46	7.2	8.29	8.27
MgO	17.78	17.78	8.50	3.9	42.21	41.18
CaO	11.20	10.65	12.48	5.8	1.92	2.08
Na_2O	1.31	0.70	2.13	3.2	0.27	0.34
K_2O	0.03	0.00	0.11	2.5	0.06	0.11
MnO	0.12	0.17	0.08	0.1	0.13	0.13
TiO_2	0.59	0.36	1.03	1.0	0.13	0.15
P_2O_5	0.05	—	0.06	0.2	0.03	0.03
Cr_2O_3	—	—	—	—	0.42	0.41
NiO	—	—	—	—	0.26	0.25
Sum	99.81	99.54	98.88	100.0	99.95	99.96

1. Primary abyssal tholeiite[11].
2. Extrapolated composition for lherzolite trend at 17.78% MgO (ref. 4).
3. Abyssal tholeiite with 8.5% MgO (ref. 8).
4. Average for continental crust[13].
5. Average of lherzolite, upper mantle composition[4].
6. Total average for crusts and lherzolite calculated in this paper, model composition for the primitive mantle.

Fig. 2 The compositional relationship between the trend for spinel lherzolites and the primary composition for abyssal tholeiite proposed by Elthon[11]. There is overlap between the confidence intervals of the trend and the primary composition, the overlap is smallest for SiO_2. This suggests that the trend of spinel lherzolite is controlled by the generation of primary abyssal tholeiite. The olivine and enstatite compositions are in equilibrium near the solidus of a lherzolite at 20 kbar The line joining these two compositions will pass through the composition of the residuum formed at this pressure. Accepting that a residuum consists of enstatite and olivine the primary abyssal tholeiite has been formed by $\sim 20\%$ partial melting of a lherzolite with 42% MgO.

representative for primary abyssal magma (see Table 1).

Figure 2 shows the compositional relationship between the lherzolitic trend and primary abyssal tholeiite. The primary composition is more or less situated on the extrapolated trend line for most oxides, the exception being SiO_2. The silica content of the lherzolites displays the smallest relative variation of the oxides, the variation being 45.6–43.3% between 39 and 47% MgO[4]. The trend for SiO_2 is therefore, less well defined than for the other oxides. Although the deviation in the silica content is greater than desirable, because the confidence intervals overlap, the agreement is considered acceptable. The approximate position of the primary abyssal on the extrapolated trend line suggests that the trend may be related to the generation of primary abyssal tholeiite. The present evaluation does not confirm that such a relationship exists, as several tholeiitic compositions fall within the confidence interval of the extrapolated trend line. However, an origin of the lherzolitic trend by primary magma generation is consistent with the composition of primary abyssal tholeiite. The compositions of lherzolite show a variation of 39–47% MgO and this range of compositions is considered to have its origin in the accumulation processes occurring in the mantle. During the accumulation of primary magma some regions of the mantle will be depleted in magma while other regions must

be enriched, as the magma must accumulate before it is erupted. We suggest, therefore, that the trend of the spinel lherzolites originated by a partial melting process which produced primary abyssal tholeiite.

must be situated somewhere on the trend line, either within the composition range of lherzolite, or on the extrapolated trend line between the composition of primary abyssal tholeiite and lherzolite. There is no geochemical or experimental evidence to test these two possibilities. Evidence about possible changes in composition of the mantle since its formation can be obtained by considering the total amount of material it has given up to the oceanic and continental crusts. A model composition of the primitive mantle before continent formation may be approximated by adding, in correct proportions, the compositions of the crusts to the average composition of the present mantle. Assuming that the upper 700 km of the mantle is the depleted part and by using estimated volumes and appropriate densities for the oceanic and continental crusts[6] the masses are estimated as follows: continental crust, 2.249×10^{19} tons; oceanic crust, 9.223×10^{18} tons; and mantle, 1.022×10^{21} tons. The mass of the continents is thus only 2.1% of the mass of the mantle. The composition used for the mantle is the average composition of spinel lherzolite shown in Table 1. The composition of the continental crust has been estimated by Taylor[13] (see Table 1) while the composition used for the oceanic crust is that of Elthon[11]. Thus a model composition of the primitive mantle can be calculated, as shown in Table 1. This composition should be compared with the average composition of lherzolites. The two compositions are evidently very similar, and the formation of the continental crust can only marginally have affected the average composition of the mantle. There is, therefore, no reason to consider compositions outside the composition range of lherzolites as potential mantle compositions, as far as major elements are concerned. The situation for trace elements is different as isotope data for Rb/Sr and Th/U clearly show that the mantle must have been depleted in the incompatible elements[14,15], and the concentration of these elements in the lherzolite nodules must consequently differ from those of the primitive mantle. This relationship is also suggested from the present results as both Na_2O and K_2O occur in larger amounts in the calculated primitive mantle than in the average for lherzolites.

We suggest that the variation in major element composition of lherzolite is consistent with a major element composition of the mantle similar to that of lherzolite. A lherzolitic composition with 42.2% MgO is proposed for the average composition of the depleted upper mantle, while the calculated composition with 41.18% MgO is representative of the major element composition of the primitive mantle (Table 1).

1. Bickle, M. J., Hawkesworth, C. J., Martin, A., Nisbet, E. G. & O'Nions, R. K. *Nature* **263**, 577–580 (1976).
2. DePaolo, D. J. & Wasserburg, G. J. *Geophys. Res. Lett.* **3**, 249–252 (1976).
3. Frey, F. A. & Green, D. N. *Geochim. cosmochim. Acta* **38**, 1023–1059 (1974).
4. Maaløe, S. & Aoki, K. *Contr. Miner.* **63**, 161–173 (1977).
5. Yoder, H. S. *Generation of Basaltic Magma* (National Academy of Science, Washington, DC, 1976).
6. Ronov, A. B. & Yaroshevsky A. A. The Earth's Crsut and Upper Mantle (ed. Hurley, P. M.) 45–66 (MIT Press, Massachusetts, 1966).
7. Langmuir, C. H., Bender, J. F., Bence, A. E. & Hanson, G. N. *Earth. planet. Sci. Lett.* **36**, 133–156 (1977).
8. Maaløe, S. *Lithos* **12**, 59–72 (1979).
9. Flower, M. F. J., Robinson, P. T., Schmincke, H. U. & Ohnmacht, W. *Init. Rep. DSDP* **37**, 653–679 (1977).
10. Malpas, J. *Phil. Trans. R. Soc.* **A238**, 527–540 (1978).
11. Elthon, D. *Nature* **278**, 514–518 (1979).
12. Christensen, N. I. & Salisbury, M. H. *Rev. Geophys. Space Phys.* **13**, 57–86 (1975).
13. Taylor, S. R. *Geochim. cosmochim. Acta* **28**, 1273–1285 (1964).
14. Hofman, A. W. & Hart, S. R. *Earth planet. Sci. Lett.* **38**, 44–62 (1978).
15. O'Nions, R. K., Carter, S. R., Evensen, N. M. & Hamilton, P. J. *A. Rev. Earth planet. Sci.* **7**, 11–38 (1979).
16. Kushiro, I., Shimizu, N. & Nakamura, Y. *Earth planet. Sci. Lett.* **14**, 19–25 (1972).

Carbonate production by algae *Halimeda*, *Penicillus* and *Padina*

Gerold Wefer

Universität Kiel, Geologisches Institut, 2300 Kiel, FRG

The Codiacean green algae *Halimeda* and *Penicillus* and the brown alga *Padina* are important producers of both calcium carbonate and organic matter in shallow water tropical and subtropical areas[1,2]. Estimates of algal contribution to shallow water carbonate deposition range from 0 to 61%[3-5]. However, direct observations on algal carbonate production are very rare. Available data include short-term measurements of calcium and carbon uptake[6-9], observations of growth of aquarium specimens[10] and periodic observations of death rate for a year at fixed stations[11]. I report here on *in situ* measurements taken in Harrington Sound, Bermuda, a shallow subtropical lagoon. Production rates were ~50 (*Halimeda incrassata*), 30 (*Penicillus capitatus*) and 240 (*Padina sanctae-crucis*) g m^{-2} yr^{-1} calcium carbonate. The measured growth rates suggest that the algae renew their standing stock approximately once every month (*Halimeda* and *Padina*) or once every one and a half months (*Penicillus*) during their growing season.

Alizarin Red-S was used as a time marker to allow measurement of incremental growth of calcareous algae. Algae were covered by a clear plastic tent[12] into which the stain was injected as a concentrated seawater solution. The alizarin was deposited by the calcifying algae while they were thus covered. The stain remains fixed as a visible red band in the skeleton as growth continues after removal of the cover, thus defining a 'time line' in the skeleton (see Fig. 1). All skeletal carbonate deposited after staining seems to be above this time line. The *in situ* measurements were taken during August and September 1978 in the shallow sandy zone in Harrington Sound. The sediment in this zone is predominantly sand with little admixture of coarser or finer material. The coarse and medium sand fractions consist of rock and pelecypod fragments, aragonitic and calcitic algae, serpulid tubes and peneroplid Foraminifera[13].

For *Penicillus* and *Padina* the distance from the top of the alizarin band to the tip of the plant was measured (see Fig. 1). This increment divided by the number of days between staining and sampling gives the average daily growth. For *Halimeda* the number of segments after staining and the sum of all segments were counted, and a daily growth rate was calculated from the ratio of segments after staining over the sum of all segments present. Several different plant sizes were sampled at any one time, minimizing effects of any nonlinear growth with size.

Altogether, 155 individual plants of *Halimeda incrassata* were sampled 3, 5,9, 14, 21, 24 and 27 days after staining near Rabbit Island in 2-m water depth. Twelve plants did not grow during staining, 39 recommenced growth within the next 27 days after staining and the remainder continued to grow after the staining event. The daily addition of new segments was ~3% of those present (see Fig 2a). Hence, assuming a steady-state population, the plants should renew their standing stock after about 1 month. The plants can produce up to one segment per day per branch (active growing tips). Plants with several growing branches can produce several segments per day.

Seasonal observations of standing stock made by me during autumn 1977 and spring 1978 and those by other workers[14,15] indicate that in Bermuda *H. incrassata* grows almost exclusively during summer and autumn, when temperatures are above about 20 °C. Temperatures fall below 20 °C between December and April, reaching a minimum of 14 °C in January[16]. During the winter months the standing stock is very low and the plants that do remain become overgrown with other

organisms. For a growing season of 7 months a year, a turnover rate of 7 times per year is expected, if growth is steady over this period. Previous growth rate estimates range from 1 season (6 months)[17] to 1 day[18]. The findings of Colinvaux *et al.*[10] are the most similar to those presented here.

A total of 81 specimens of *P. capitatus* were sampled 1, 2, 6, 9, 13 and 20 days after staining from Old Shoals in 8-m water depth. Twelve did not grow during staining, 10 recommenced growth within the next 20 days and the remainder continued to grow after the staining event. The daily average growth was 1.04 mm per day (see Fig. 2b). An average size of 53.3 mm was determined for the *Penicillus* population within the tent. Some 50 days, therefore, would seem to be required for average size to be attained. I found no correlation between plant height and growth, although fast growth (up to 5 mm per day) was observed only in the case of young plants during initial build up of the stalk.

My observations with those of von Bodungen[15] and Bernatowicz[14] indicate that in Harrington Sound the growth period for *Penicillus*, like *Halimeda*, lasts only 7 months. Between December and April the standing stock is very low. The plants that do remain become overgrown with other organisms, especially bryozoans. The overgrowth extends to the upper tips and thus the plant seems to be dormant. If steady-state growth for the summer and autumn months is assumed the turnover rate for *P. capitatus* would be about 4 times per year. These observations agree with the suggestion of Rezak[17], that natural occurrences of *Penicillus* indicate a life span for this plant of 30–60 days. Stockmann *et al.*[11] determined an average life span of ~40 days for *Penicillus* in Florida Bay and 60 days for the inner reef tract on the South Florida Shelf. Colinvaux *et al.*[10] observed that *Penicillus* shows sporadic rapid growth lasting 1 or perhaps 2 weeks, followed by long periods of non-growth. Maturity seems to be reached within about 1 month, according to their data.

A total of 125 fronds of *P. sanctae-crucis* were sampled 1, 2, 4, 6, 8 and 11 days after staining near Rabbit Island in 1.5 m water depth. Eight of them did not grow during staining, three recommenced growth within the next 11 days and the remainder continued to grow after the staining event. The average linear growth on fronds was 0.81 mm per day (see Fig. 2c). For the whole *Padina* community inside the tent an average plant height of 20.4 mm was determined. Hence, the algal population would
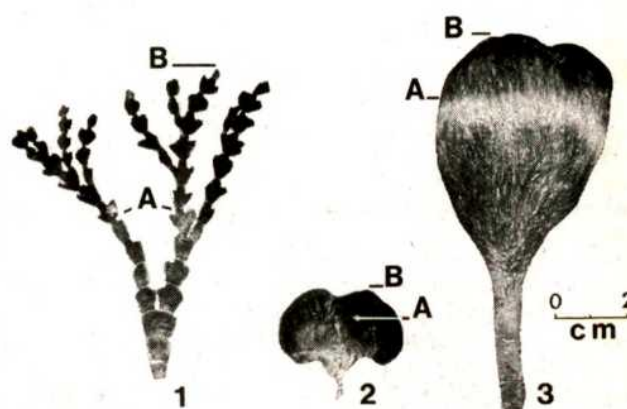
Fig. 1 *Halimeda incrassata* (1), *Padina sanctae-crucis* (2) and *Penicillus capitatus* (3). Photographs of stained plants 7 days (*Halimeda*), 11 days (*Padina*) and 15 days (*Penicillus*) after the staining event. A, Top of the Alizarin line; A–B, increment between staining and sampling. The plants were covered by a tent with a volume of ~ 2m^3. The enclosed bottom area was 3 m^2. The concentration within the tents was about 1.5 mg Alizarin Red-S per 1 seawater. Tents remained in place for 1 day. Algal colonies were sampled in 1-day to 1-week intervals.
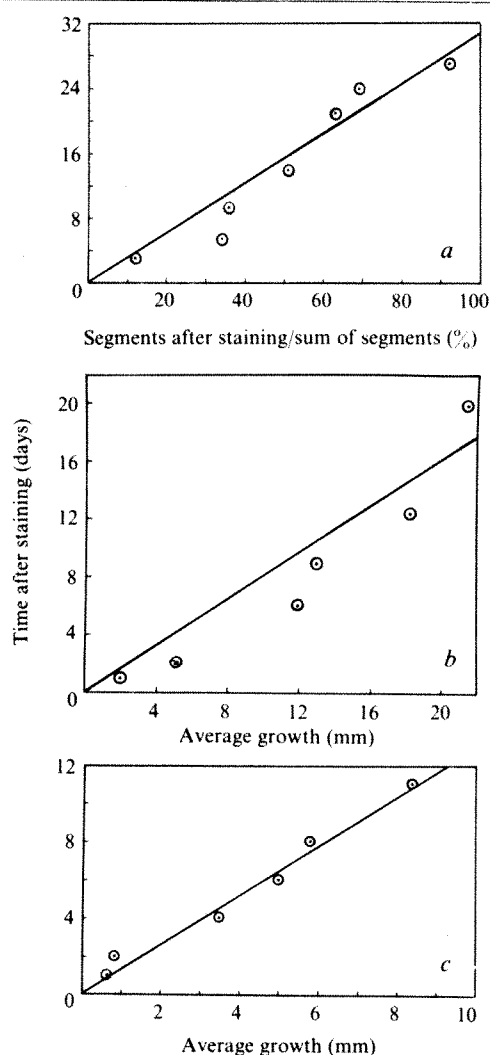
Fig. 2 *a, Halimeda incrassata.* Growth rate expressed as ratio between the new segments after staining and the total number of algal segments for the sampling dates. Each point represents the average of a representative number (10–20) of algae of the whole standing stock. The average $(\bar{s})$ of the standard deviations of the data for each point is 23. Daily average increment of the standing stock is 3%. *b, Penicillus capitatus.* Average growth rates for several sampling dates. $(\bar{s} = 6.2)$ Daily average growth for the sampled population is 1.04 mm per day. *c, Padina sanctae-crucis.* Average growth rates for several sampling dates. $(\bar{s} = 1.1)$ Daily average growth for the sample population is 0.81 mm per day.

need ~25 days to build up the standing stock sampled in the area within the tent.

During March 1978 *P. sanctae-crucis* was rare on the cliffs and rocks of the shallow area of Harrington Sound. With an increase of temperature from 18 to 20 °C in April 1978, *Padina* started to grow. Apparently, like *Halimeda* and *Penicillus*, *Padina* has its growth season during the warm period of the year. Assuming steady-state growth of the population for the summer and autumn months, the standing stock would be renewed about 8 times per year, somewhat more often than that of *Halimeda* and *Penicillus*. No data on growth are available in the literature. However, it is clear that *Padina* cannot be regarded as only a minor carbonate contributor as assumed by Millimann[2]. On the cliffs and submarine rocks of Harrington Sound (Bermuda), at a depth of 1–3 m a standing stock was measured of up to 350 g dry wt m^{-2}. With a carbonate content of 38% of dry weight[19], and at a possible turnover rate of up to 8 times per year the annual carbonate production could be as high as 1,060 g m^{-2} (the average is 240 g m^{-2} yr^{-1}). This figure is actually above the range observed for other calcareous algae in

Harrington Sound. For *Halimeda*, the carbonate production is 50 g m^{-2} yr^{-1} based on the assumed turnover rate of 7 times per year and an average standing stock of 6.7 g CaCO$_3$ per m^2 found at 31 stations arbitrarily selected in 1–4 m water depth. For *Penicillus* the carbonate production is 30 g m^{-2} yr^{-1} based on the assumed turnover rate of 4 times per year and an estimated average standing stock of 5.6 g CaCO$_3$ m^{-2} (at the 31 stations). Another important algal carbonate contributor is *Halimeda monile*, which is only common in areas equal to or shallower than 3 m and may contribute as much carbonate as *H. incrassata.* Other green algae like *Udotea, Cymopolia* and *Rhipocephalus* are mostly solitary, rare or absent in Harrington Sound and are not important as carbonate producers. The red alga *Amphiroa fragilissima* abounds on rocky substrates and may be a major carbonate producer here.

The total carbonate production by algae in the sandy area of Harrington Sound is nearly 100 g CaCO$_3$ per m^2 per yr and on the rocky substrate nearly 500 g CaCO$_3$ per m^2 per yr, which is about half of the carbonate deposition in the shallow water area of the Sound. The carbonate deposition is assessed from the bulk composition of dated sediments collected by cores. The various algal species are restricted to certain types of bottom consistency, and their relative contribution will, therefore, depend on locality. For example, *Amphiroa* and *Padina* are the dominant carbonate producers on rocky substrate and almost absent in sandy areas, while *Halimeda* and *Penicillus* are the major carbonate contributors in the sand covered regions of Harrington Sound.

I thank V. Smetacek, A. C. Neumann and W. H. Berger for helpful criticisms. Supported by Deutsche Forschungsgemeinschaft.

1. Bathurst, R. G. C. *Carbonate Sediments and their Diagenesis*, 1–620 (Elsevier, Amsterdam, 1971).
2. Milliman, J. D. *Marine Carbonates*, 1–375 (Springer, Berlin, 1974).
3. Milliman, J. D. *U.S. Geol. Surv. Profess. Pap.* 529–7 (1972).
4. Ginsburg, R. N. *Am. Ass. Petrol. Geolog. Bull.* **40**, 2384–2427 (1956).
5. Neumann, A. C. & Land, L. S. *J. Sediment. Petrol.* **45**, 763–786 (1975).
6. Goreau, T. F. *Ann. N.Y. Acad. Sci.* **109**, 127–167 (1963).
7. Stark, K. W., Ginsburg, R. N. & Shinn, E. A. *J. Sediment. Petrol.* **37**, 633–648 (1967).
8. Böhm, E. L. *Mar. Biol.* **47**, 9–14 (1978).
9. Borowitzka, M. A. & Larkum, A. W. D. *J. exp. Bot.* **27**, 864–878 (1976).
10. Colinvaux, L. H., Wilbur, K. M. & Watabe, N. *J. Phycol.* **7**, 69–78 (1965).
11. Stockmann, K. W., Ginsburg, R. N. & Shinn, E. A. *J. Sediment. Petrol.* **37**, 633–648 (1967).
12. Dustan, P. *Mar. Biol.* **33**, 101–107 (1975).
13. Neumann, A. C. *Bull. mar. Sci.* **15**, 987–1035 (1965).
14. Bernatowicz, A. J. *Pap. Mich. Acad. Sci. Arts Lett.* **36**, 3–8 (1952).
15. von Bodungen, B. *Bermuda Biological Station, Spec. Publ.* (in the press).
16. Barnes, J. A. & von Bodungen, B. *Bermuda Biological Station, Spec. Publ.* **17**, 1–190 (1978).
17. Rezak, R. in *Geology of Calcareous Algae* (eds Ginsburg, R. N., Rezak, R. & Wray, J. L.) 3.1–3.8 (The Comparative Sedimentology Laboratory, Miami, 1971).
18. Goreau, T. F. in *The Biology of Hydra*, 269–285 (University of Miami Press, 1961).
19. Böhm, E. L. & Schramm, W. in *Das Harrington Sound Projekt* (eds Wefer, G. & Hempel, G.) 20–27 (Sonderforschungsbereich 95, Kiel University, 1977).

Effects of density on monospecific stands of marine algae

David R. Schiel & J. H. Choat

Department of Zoology and Leigh Marine Research Laboratory, University of Auckland, New Zealand

Current ideas on intraspecific competition between plants in monospecific stands stem from work on terrestrial floras. The central tenet is that higher plant density exacts a price from the individuals in a stand: (1) total yield (biomass) per area reaches a constant value at high density (the law of constant final yield[1–5]); (2) the weight distribution of individuals becomes skewed, with few large and many small plants[1,5–8]; (3) survival rates may be reduced when plants are sown at higher densities[1,9].

The effects of density seem to be remarkably similar for primitive as well as higher plants[1,2,9-11] and are often summarized by the 3/2 thinning law[1,2,5-7,9-11], which indicates that if a stand of plants is sampled through time, the relationship between log weight and log density is a line of −1.5 slope. The basis of this is that mortality is density dependent, so that density is related to time through the thinning process due to crowding. We report here that these effects do not obtain for two species of subtidal marine algae. For the characters which we examined—total yield, plant length, plant dry weight and dry weight of reproductive parts— algae fared better at higher densities. We conclude that there is a difference between marine and terrestrial plants in their responses to density, and we suggest a difference in herbivory due to arthropod–plant associations in each system.

Our investigations were prompted by observations that algal plants of both stunted and lush forms, characters usually ascribed to different degrees of wave exposure[12-14], occur metres apart on the same shore in similar conditions of exposure. We hypothesized plant density to be an important factor. The questions we posed were, what effects does density have on total yield per given area, on plant size, weight, reproductive output and survival? We examined two species of algae which are quite different in form and life history. The laminarian alga, *Ecklonia radiata*, has a single erect stipe, with a primary and numerous secondary laminae; it has a life span of about 7 yr and occurs in typically dense stands in the northern New Zealand subtidal zone. The fucoid alga, *Sargassum sinclairii*, is a facultative annual bearing discrete reproductive parts and many small laminae on primary and lateral branches; it is very abundant in shallow depths. For each species, we examined monospecific, even-aged stands (1-yr old *Sargassum*, 3-yr old *Ecklonia*) from a shallow (2–6 m) open coast, tumbled boulder area. In addition to using naturally occurring populations, *Sargassum* germlings were settled at four different densities ($\bar{x} = 4.4, 12.8, 20.3, 29.7$ per cm^2) on asbestos–cement plates and transferred to the field for observations on survival. In all cases the major herbivores—sea urchins and gastropods—were excluded.

Table 1 summarizes the size frequency data. For *Sargassum*, high-density plants were normally distributed for all measures whereas at low density distributions were skewed, with most plants in the smaller size classes. *Ecklonia* at both low and high densities showed normal distributions for all measures. Few algal plants were trapped under the canopy at high density, in contrast to terrestrial systems which tend to have many smaller plants suppressed below the canopy of a few larger individuals in crowded stands[1,5-8].
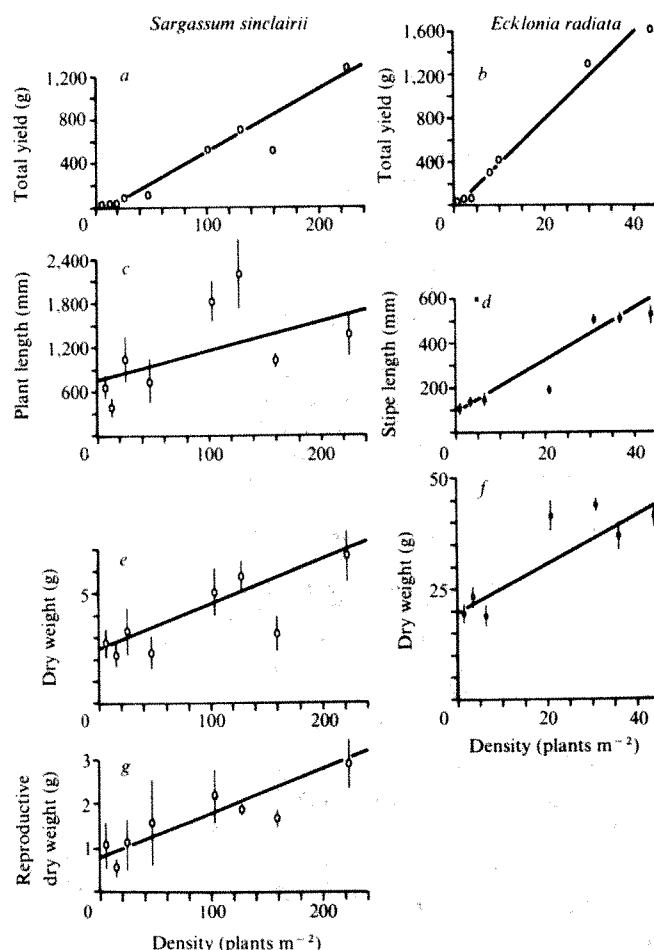
Fig. 1   Graphs relating various measures and density for *Sargassum sinclairii* and *Ecklonia radiata*. Regression equations, the probability of $\beta = 0$ and r^2 values are respectively: (*a*) $y = 5.66x - 70.34$, $P < 0.001$, $r^2 = 0.88$; (*b*) $y = 39.32x - 1.65$, $P < 0.001$, $r^2 = 0.99$; (*c*) $y = 3.80x + 757.33$, $P < 0.007$, $r^2 = 0.16$; (*d*) $y = 11.68x + 87.96$, $P < 0.001$, $r^2 = 0.66$; (*e*) $y = 0.02x + 2.46$, $P < 0.001$, $r^2 = 0.25$; (*f*) $y = 0.54x + 19.84$, $P < 0.001$, $r^2 = 0.59$; (*g*) $y = 0.01x + 0.81$, $P < 0.003$, $r^2 = 0.19$. These relationships were calculated using least squares linear regression. Each y value represents the measure of a single plant, except for the total yield against density regressions, where total dry weight per m^2 was used. For clarity of presentation, means ± 1 s.e. are plotted, but regressions were calculated using all x, y values. We realize that regression analysis may be inappropriate here and that other models may better describe these relationships. However, as the variance is high and transformations produced no significant change in r^2, we have used a simple linear model as a general description.

Table 1   Size frequency data for *Sargassum* and *Ecklonia*

Sargassum sinclairii	*Ecklonia radiata*
Low density (1–50 plants m^{-2})	Low density (1–6 plants m^{-2})
Length: $P = 0.05$, positive skew	Length: NS
Dry weight: $P = 0.01$, positive skew	Dry weight: NS
Dry weight of reproductives:	
$P = 0.01$, positive skew	
High density (160–220 m^{-2})	High density (30–45 m^{-2})
Length: NS	Length: NS
Dry weight: NS	Dry weight: NS
Dry weight of	
reproductives: NS	

G-tests for skewness of distribution[21] were used to test the frequency distributions of length, plant dry weight (*Sargassum* and *Ecklonia*) and dry weight of reproductive parts *(Sargassum)* at low and high densities. NS, Non-significant result, normal distribution.

Figure 1*a,b* shows that total yield did not reach a constant value up to the highest plant densities found. The relationship of plant length to density was a line of positive slope for both species (Fig. 1*c,d*). This is not necessarily unusual because terrestrial plants in dense stands may become etiolated[1,15]. However, the slopes were also positive for regressions of individual plant dry weight on density (Fig. 1*e,f*) and for the dry weight of reproductive parts on density for *Sargassum* (Fig. 1*g*). The largest plants by any measure generally occurred at higher densities. These relationships do not apply to all algae; a constant yield at different densities is recorded for the red alga *Porphyra*[16]. However, there is a suggestion that they may apply to at least one Japanese laminarian[17].

An examination of survival of the artificially settled *Sargassum* germlings showed that the rate of decrease in numbers through time was the same at four different initial densities (number of plants surviving regressed with time; covariance, $n = 4$, $F = 2.61$, $P = 0.10$). However, mortality of naturally occurring *Ecklonia* sporophytes was found to be density

dependent, but not markedly so (proportion of plants surviving after 1 yr regressed on initial densities: $y = -0.0054 x + 0.65$, $P(\beta=0) < 0.001$, $r^2 = 0.67$). This slightly higher proportional mortality at increased density is more than balanced, however, by greater numbers of plants per unit area and larger individual size.

Because of these density responses, the 3/2 thinning law is unlikely to apply to these marine algae. It can be argued that higher densities might produce some of the effects documented for terrestrial plants, and certainly there must be an upper limit to plant density and biomass per unit area. However, at the highest densities we found, even though thinning does occur, that there is no consequent compensation in size by other members of the stand.

We consider these density responses to be primarily the result of two factors: (1) both *Sargassum* and *Ecklonia* show faster growth for high density plants (J.H.C. and D.R.S., in preparation), and (2) there may be some protection from physical battering in the turbulent, shallow coast environment for high-density individuals which may be cushioned in their swaying by others in the stand. Our observations of a range of plant forms in the same area but at different densities suggest that the water movement intensity, which is said to influence morphological differences in some laminarians[12-14], may be altered by high density.

We also observe a noteworthy difference between terrestrial and marine systems in the nature of their plant–arthropod associations. Adult terrestrial plants often become infested with herbivorous insects, which can cause severe defoliation[18,19]; herbivore loads may be greatest in monospecific stands[20]. There is no equivalent form of herbivory on large marine plants. Although the arthropod load may be high (we have found up to 1,700 copepods, amphipods and isopods per plant), these animals do not visibly damage the algal fronds and there seems to be no high density debit due to herbivory.

Large, dense, predominantly single-species brown algal stands are a common feature of most boreal and temperate shores. Our knowledge of competition based on density stress in terrestrial plants seems to be inappropriate to deal with these patterns of algal abundance. If these density responses hold generally, they suggest two fruitful areas of comparison with terrestrial floras: (1) the relationship between plant density and herbivory, particularly plant–arthropod associations, and (2) the consequences of inter- and intraspecific competition in stands of large brown marine algae. In addition to clarifying the relationships of the dominant organisms in algal zones, there could also be useful implications for the mariculture of seaweeds.

1. Harper, J. L. *Population Biology of Plants* (Academic, London, 1977).
2. Kays, S. & Harper, J. L. *J. Ecol.* **62**, 97–105 (1974).
3. Donald, C. M. *Aust. J. agric. Res.* **2**, 355–378 (1951).
4. Kira, T., Ogawa, H. & Sakazaki, N. *J. Inst. Polytech. Osaka City Univ.* D **4**, 1–16 (1953).
5. Harper, J. L. & White, J. in *Dynamics of Populations* (eds den Boer, P. J. & Gradwell, G. R.) 41–63 (Centre for Agricultural Publications and Documentation, Wageninger, 1971).
6. Mohler, C. L., Marks, P. L. & Sprugel, D. G. *J. Ecol.* **66**, 599–614 (1978).
7. Schlesinger, W. H. & Gill, D. S. *Ecology* **59**, 1256–1263 (1978).
8. Ogden, J. *Proc. N.Z. ecol. Soc.* **17**, 1–9 (1970).
9. Yoda, K., Kira, T., Ogawa, H. & Hozumi, K. *J. Biol. Osaka City Univ.* **14**, 107–129 (1963).
10. White, J. & Harper, J. L. *J. Ecol.* **58**, 467–485 (1970).
11. Gorham, E. *Nature* **279**, 148–150 (1979).
12. Chapman, A. R. O. *Phycologia* **12**, 53–57 (1973).
13. Gerard, V. A. & Mann, K. H. *J. Phycol.* **15**, 33–41 (1979).
14. Mann, K. H. *J. Fish. Res. Bd Can.* **28**, 778–780 (1971).
15. Hodgson, G. L. & Blackman, G. E. *J. exp. Bot.* **7**, 147–165 (1956).
16. Yoshida, T. *Bull. Tohoku reg. Fish. Res. Lab.* **32**, 89–94 (1972).
17. Kawashima, S. in *Contributions to the Systematics of Benthic Marine Algae of the North Pacific* (eds Abbott, I. A. & Kurogi, M.) 93–108 (Japanese Society of Phycology, Kobe, 1972).
18. Feeny, P. *Ecology* **51**, 565–579 (1970).
19. Morrow, P. A. & La Marche, V. C. Jr *Science* **201**, 1244–1246 (1978).
20. Root, R. B. *Ecol. Monogr.* **43**, 95–120 (1973).
21. Sokal, R. R. & Rohlf, F. J. *Biometry* (Freeman, San Francisco, 1969).

Effects of methylated xanthines on mammalian cells treated with bifunctional alkylating agents

John P. Murnane, John E. Byfield, John F. Ward & Paula Calabro-Jones

Division of Radiation Oncology, University Hospital, and University of California San Diego Cancer Center, 225 Dickinson Street, San Diego, California 92103

Caffeine has been previously reported to enhance the lethal potential of many DNA-damaging agents in rodent cells[1-5]. This effect has most commonly been ascribed to the binding of caffeine to single-stranded DNA[6], and the resulting inhibition of post-replication repair[7-10], which is associated with the synthesis of abnormally small nascent DNA fragments[7,11-13]. However, certain aspects of this theory remain unclear: (1) why does the addition of caffeine to damaged cells elevate the level of DNA synthesis when it supposedly blocks post-replication repair[10,14], and (2) as pointed out by Cleaver[15], why does caffeine continue to exert its synergistic lethal effects until completion of the S phase[16,17], even though the size of newly synthesized DNA seems normal much earlier[18-20]? The present studies with nitrogen mustard (HN$_2$) fail to demonstrate any effect of non-lethal concentrations of methylated xanthines (MXs) on removal of DNA damage or post-replication repair in conditions producing synergistic lethal effects. We demonstrate an influence by MXs on initiation of DNA synthesis in damaged replicons, and propose that this effect is primarily responsible for the synergistic lethal properties of these drugs.

The effects of caffeine on damaged human cells are less consistent than those on rodent cells[16,21-24]. Figure 1 shows the survival curves obtained when human HT-29 cells (ref. 25, human karyotype confirmed by K. Benirschke) were exposed to increasing concentrations of HN$_2$ with or without a non-lethal concentration (1 mM) of caffeine. As shown by the reduction in the shoulder width of the HN$_2$ survival curve, human HT-29 cells seem to be highly sensitive to the synergistic lethal effects of caffeine in combination with HN$_2$. Similar results were obtained when mouse cells were used, melphalan or phosphoramide mustard (PM) were substituted in place of HN$_2$ or when caffeine was replaced by theobromine or pentoxyphylline.

DNA cross-links are thought to be responsible for the relatively high toxicity of bifunctional alkylating agents[26]. We have used the technique of alkaline elution developed by Kohn *et al.*[27] to estimate the appearance and removal of DNA cross-links[28,29]. As shown in Fig. 2, 1 mM caffeine has no effect on either the maximum (6 h) or residual (24 h) levels of cross-links after a 120-μM dose of PM in either human (70% lethal) or mouse cells (95% lethal). Caffeine, therefore, has no effect on either cross-link formation or removal, and, hence, its synergistic lethal effects are apparently unrelated to DNA repair.

As the synergistic lethal effects of caffeine have been reported to be associated with the inhibition of nascent DNA elongation in rodent cells, we have studied the relationship between these two phenomena in HN$_2$-treated cultures. Pulse-chase techniques have been combined with alkaline elution as done previously to demonstrate elongation of newly synthesized DNA[30]. The results shown in Fig. 3 are for mouse cells; similar results were obtained for human HT-29 cells. Figure 3a shows that ~6 h are required for newly synthesized DNA from untreated C3H-10T½ cells to elute at the rate of DNA continuously labelled for 24 h. DNA from cells pulsed 0.5 h after removal of a 99% lethal dose of HN$_2$ (Fig. 3b) requires much longer (>12 h) to reach full size, as reported previously[31]. HN$_2$-treated DNA seems initially (0 h) to elute more slowly than DNA from control

cells (Fig. 3b). A delay of 4 h after the removal of the HN₂ before pulse labelling eliminates this effect (data not shown).

Despite the increased lethality due to caffeine in HN₂-treated cells, 1 mM caffeine did not affect DNA elongation in control or HN₂-treated cultures in many experiments (Fig. 3), regardless of whether caffeine was added before or after pulse labelling. That this is true for mouse cells as well as human indicates that these results are not simply due to cell type, as alkaline elution studies in the same mouse cell lines demonstrated that caffeine inhibited DNA elongation after UV irradiation (data not shown). As reported by others[7-10], HN₂ damage, therefore, seems different from UV in that HN₂-treated rodent cells sensitized with caffeine demonstrate no inhibition of nascent DNA elongation. This failure of caffeine to inhibit elongation is not simply an artefact of the alkaline elution technique, as these results have been confirmed for HT-29 cells using alkaline sucrose gradients
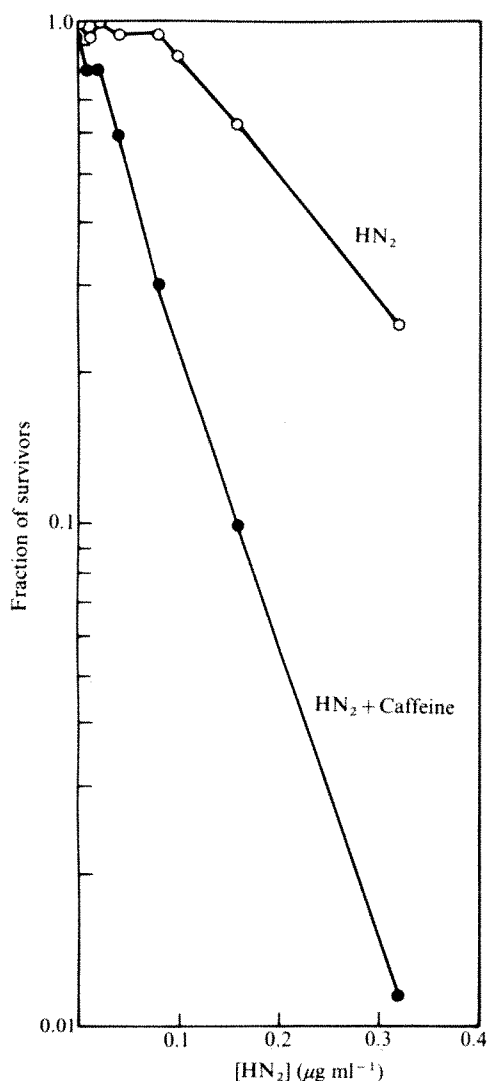
Fig. 1 Effect of HN₂ on survival of HT-29 cells with (●) and without (○) 1 mM caffeine (Sigma). Human HT-29 cells (400) were plated onto 60-mm Lux tissue culture dishes in 2 ml of Eagle's basal medium (BME, Gibco) with 10% fetal calf serum (FCS, Gibco). After 1 h at 37 °C in a humidified incubator with a 5% CO₂ atmosphere, 1 ml BME plus 10% FCS containing the various concentrations of HN₂ were added to the appropriate plates. Cells were reincubated for 2 h at 37 °C, after which the medium in all plates was removed. BME (2 ml) plus 10% FCS containing the 1 mM caffeine were then added to both HN₂-treated and untreated cells (in triplicate). After a further 72 h incubation, the medium was removed and replaced with fresh BME plus 10% FCS without caffeine. The cells were then incubated for 4 more days before fixation with methanol, Giemsa staining and counting of visible colonies.

Fraction of ³H-labelled reference DNA retained on filter
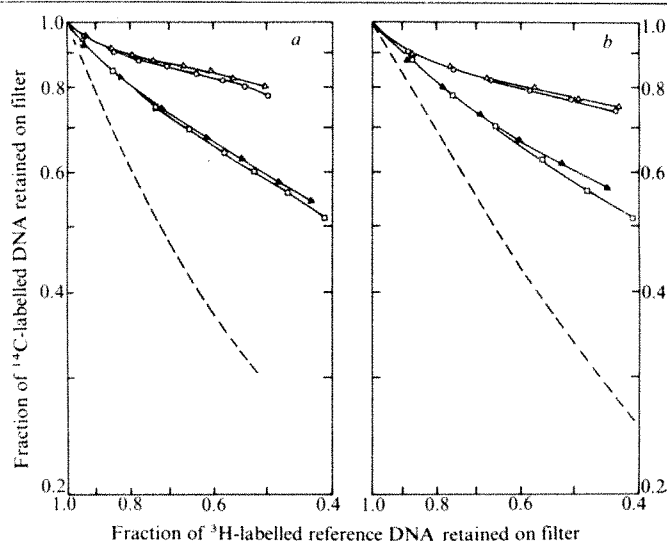
Fig. 2 Alkaline elution profiles of DNA from HT-29 (a) and C3H-10T½ (b) cells treated with 120 μM PM in BME plus 10% FCS for 2 h, rinsed and reincubated in BME plus 10% FCS for 6 (○) or 24 (□) hours; or 120 μM PM plus 1 mM caffeine in BME plus 10% FCS incubated for 2 h, rinsed and reincubated in 1 mM caffeine in BME plus 10% FCS for 6 (△) or 24 (▲) h. Alkaline elution was carried out as previously described[27,28]. Cells grown in BME plus 10% FCS were labelled for 24 h before drug treatment with 5 ml of either [6-³H]thymidine (28.5 Ci mmol⁻¹, 0.1 μCi ml⁻¹; NEN) for reference cells, or [2-¹⁴C]thymidine (52.4 mCi mmol⁻¹, 0.01 μCi ml⁻¹; NEN) for test cells. Before elution, ³H-labelled reference cells were irradiated with 300 R and test cells with 600 R of X rays (Picker orthovoltage, 280 keV, 1 mm copper filter) at 0 °C, and 5 × 10⁵ cells of each added to the elution filter. Dashed lines represent the elution profiles of control cells with or without 1 mM caffeine for 24 h. Control cells were labelled for 24 h similarly to test cells, but with a medium change 2 h before elution.

similar to those shown in Fig. 4. Thus, inhibition of DNA elongation and increased lethality do not seem to be directly related in this system, and some mechanism other than inhibition of post-replication repair is necessary to explain the effects of caffeine on cell survival.

During these experiments we found that addition of caffeine to HN₂-treated cells reversed the inhibition of DNA synthesis due to DNA damage, as previously reported by others using caffeine in combination with UV[10], cis-platinum II (ref. 14) and X rays[32]. We have since established a correlation between the synergistic lethal effects of various MX analogues and their ability to produce increased DNA synthesis in HN₂-treated cells (in preparation). We have, therefore, investigated this phenomenon further.

The decreased rate of DNA synthesis in damaged cells has been proposed to be a result of the inhibition of replicon initiation in DNA domains containing damaged sites. X rays[31,33,34], bromouracil photolysis[35] and methyl methanesulphonate[36] inhibit replicon initiation, and we have observed a similar response to HN₂ damage (Fig. 4). We have determined whether caffeine increases damaged DNA synthesis by influencing replicon initiation. Using an alkaline sucrose procedure which demonstrates replicon size distribution and elongation[33], we found that the application of 1 mM caffeine to undamaged cells reduces the size of the DNA that is normally synthesized during a short ³H-thymidine pulse (Fig. 4). This reduction in the quantity of larger DNA fragments has previously been reported to be due to an inhibition of elongation of nascent DNA[9]. However, the absence in undamaged cells of any effect of 1 mM caffeine on colony formation (Fig. 1), the rate of DNA synthesis (in preparation) or the time required for full elongation of DNA (ref. 9 and Fig.3a), lead us to concur with

Lehman[37] that an increased number of replicon initiation sites is a more likely explanation.

In contrast to the caffeine-induced reduction in the size of newly synthesized DNA in undamaged cells, the addition of 1mM caffeine to HN_2-treated cells induces the reappearance of a small-size class of DNA previously eliminated by the inhibition of replicon initiation due to DNA damage. The influence of MXs on replicon initiation is therefore capable of interfering with the regulation of DNA synthesis on damaged DNA templates. This increased initiation of DNA synthesis in damaged replicons would greatly increase the number of replication forks encountering damaged sites, and could account for the inhibitory effects of caffeine on nascent DNA elongation in rodent cells through saturation of the post-replication repair system. The variability of the effects of MXs on DNA elongation could therefore be due to differences in mechanisms used for replicative bypass of DNA damage among various cells and with various types of lesions.

The exact mechanism by which MXs influence control of replicon initiation is unclear. The inhibition of cyclic nucleotide phosphodiesterase by MXs does not seem to be involved, as drugs influencing cyclic AMP or cyclic GMP do not react similarly to caffeine[32]. Chromatin conformation has been postulated to regulate both normal DNA synthesis[39] and inhibition of damaged replicon initiation[33], suggesting that MX influences the availability of initiation sites by alteration of chromatin structure.

Reports of increased survival in cells held in a non-dividing state following treatment with various DNA-damaging agents[40,41], and of a reduced shoulder and D_0 when cells were irradiated with near-UV light during replication of DNA

Fig. 4 Alkaline sucrose gradients for HT-29 cells pulse labelled for 10 min with [6-^{3}H]thymidine (28.5 Ci mmol^{-1}, 20 μCi ml^{-1}) after HN_2 treatment (▲), HN_2 treatment plus caffeine (△), caffeine alone (○) and control cells (●). Sedimentation is from left to right. After a 2-h treatment with 0.33 μg ml^{-1} HN_2, cells were rinsed and incubated for 30 min with or without caffeine, and then given a 10-min pulse of ^{3}H-thymidine. Control cells with or without caffeine were handled similarly but without HN_2. Caffeine-treated cells also received 1mM caffeine during the ^{3}H-thymidine pulse. The treatment of cells and the alkaline sucrose procedure have been previously described[32]. After the pulse, cells were rinsed in cold PBS containing 10^{-3} M thymidine, scraped off the plates and irradiated with 1,000 R of X rays. 10^5 cells in 0.5 ml of PBS were then layered onto a 0.5-ml layer of lysis solution on top of a linear 5–20% alkaline sucrose gradient. After 15 min in the dark, the gradients were spun for 3 h at 27 K, and 25 fractions were collected from the bottom. Calf thymus DNA (100 μg) was added to each fraction, 50% trichloroacetic acid added to a final concentration of 5%, and all samples refrigerated overnight. Samples were filtered on GF/C glass fibre filters (Whatman) using cold 5% trichloroacetic acid. For determination of radioactivity, 0.4 ml of 1 M HCl was added to each filter in scintillation vials, and the vials heated at 70 °C for 1 h. After cooling, 2.5 ml of 0.4 M NaOH and 6 ml Aquasol (NEN) were added and the samples counted in gel phase.

Fig. 3 Alkaline elution profiles of C3H-10T½ cells DNA grown in BME plus 10% FCS and pulse labelled with 5 ml of [6-^{3}H]thymidine (28.5 Ci mmol^{-1}, 0.4 μCi ml^{-1}) for 20 min: *a*, without prior HN_2 treatment and chased for 0 h (●), 2 h (○), 4 h (□) and 6 h with (▲) or without (△) 1 mM caffeine; *b*, pulsed 0.5 h after changing media from a 2-h incubation with 0.33 μg ml^{-1} HN_2 and incubating further in cold media for 0 h (●), 4 h (○), 8 h (□), 12 h with (▲) or without (△) 1 mM caffeine. Untreated cells continually labelled for 24 h are shown by a dashed line in *a* and pulse-labelled cells treated with HN_2 and chased for 30 h are shown by dashed lines in *b*. Alkaline elution was carried out as previously described[30]. 10^6 cells were applied to each elution filter after being scraped into cold phosphate-buffered saline (PBS) and stored on ice. The addition of 10 μM cold thymidine in the chase media increased the apparent rate of elongation, but did not influence the absence of effect of caffeine.

regions containing bromouracil[42] indicate a correlation between damaged DNA replication and increased lethality. Thus, the inhibition of initiation of DNA synthesis due to damage may promote cell survival, and therefore damage which is 'potentially lethal' may be rendered lethal by inducing damaged replicon initiation.

1. Rauth, A. M. *Radiat. Res.* **31,** 121–138 (1967).
2. Rauth, A. M., Barton, C. & Lee, C. P. Y. *Cancer Res.* **30,** 2724–2729 (1970).
3. Walker, I. G. & Reid, B. D. *Mutat. Res.* **12,** 101–104 (1971).
4. Roberts, J. J., Sturrock, J. E. & Ward, K. N. *Mutat. Res.* **26,** 129–143 (1974).
5. Busse, P. M., Bose, S. K., Jones, R. W. & Tolmach, L. J. *Radiat. Res.* **71,** 666–677 (1977).
6. Ts'o, P. O. P. & Lu, P. *Proc. natn. Acad. Sci. U.S.A.* **51,** 17–24 (1964).
7. Cleaver, J. E. & Thomas, G. H. *Biochem. biophys. Res. Commun.* **36,** 203–208 (1969).
8. Fujiwara, Y. *Expl Cell Res.* **75,** 483–489 (1972).
9. Buhl, S. N. & Regan, J. D. *Biophys. J.* **14,** 519–527 (1974).
10. Lehmann, A. R. & Kirk-Bell, S. *Mutat. Res.* **26,** 73–82 (1974).
11. Rupp, W. D. *et al. Brookhaven natn. Lab. Publ.* No. 50203, 1–11 (1969).
12. Lehmann, A. R. *J. molec. Biol.* **66,** 319–337 (1972).
13. Buhl, S. N., Setlow, R. B. & Regan, J. D. *Int. J. Radiat. Biol.* **22,** 417–424 (1972).
14. Van Den Berg, H. W. & Roberts, J. J. *Chemico-Biol. Interact.* **12,** 375–390 (1976).

15. Cleaver, J. E. *Biochim. biophys. Acta* **516**, 489–516 (1978).
16. Roberts, J. J. & Ward, K. N. *Chemico-Biol. Interact.* **7**, 241–264 (1973).
17. Domon, J. & Rauth, A. M. *Radiat. Res.* **39**, 207–214 (1969).
18. Meyn, R. E. & Humphrey, R. M. *Biophys. J.* **11**, 295–301 (1971).
19. Lehmann, A. R. *Eur. J. Biochem.* **31**, 438–445 (1972).
20. Buhl, S. N., Setlow, R. B. & Regan, J. D. *Biophys. J.* **13**, 1265–1275 (1973).
21. Wilkinson, R., Kiefer, J. & Nias, A. H. W. *Mutat. Res.* **10**, 67–72 (1970).
22. Maher, V. M., Ouellette, L. M., Mittlestat, M. & McCormick, J. J. *Nature* **258**, 760–763 (1975).
23. Schroy, C. B. & Todd, P. *Mutat. Res.* **33**, 347–355 (1975).
24. Busse, P. M., Bose, S. K., Jones, R. W. & Tolmach, L. J. *Radiat. Res.* **76**, 292–307 (1978).
25. Fogh, J. & Trempe, G. in *Human Tumor Cells In-Vitro* (ed. Fogh, J.) 115–174 (Plenum, New York, 1975).
26. Lawley, P. D. *Prog. Nucleic Acid Res.* **5**, 89–131 (1966).
27. Kohn, K. W., Erickson, L. C., Ewig, R. A. G. & Friedman, C. A. *Biochemistry* **15**, 4629–4637 (1976).
28. Ewig, A. G. & Kohn, K. W. *Cancer Res.* **37**, 2114–2122 (1977).
29. Fornace, A. J. Jr, Little, J. B. & Weischselbaum, R. R. *Biochim. biophys. Acta* **561**, 99–109 (1979).
30. Kohn, K. W., Erickson, L. C., Ewig, R.A.G. & Iqbal, Z. M. *Biochemistry* **13**, 4134–4139 (1974).
31. Makino, F. & Okada, S. *Mutat. Res.* **23**, 387–394 (1974).
32. Tolmach, L. J., Jones, R. W. & Busse, P. M. *Radiat. Res.* **71**, 653–665 (1977).
33. Painter, R. B. & Young, B. R. *Radiat. Res.* **64**, 648–656 (1975).
34. Walters, R. A. & Hildebrand, C. E. *Biochem. biophys. Res. Commun.* **65**, 265–271 (1975).
35. Povirk, L. F. *J. molec. Biol.* **114**, 141–151 (1977).
36. Painter, R. B. *Mutat. Res.* **42**, 299–304 (1977).
37. Lehmann, A. R. *Biophys. J.* **12**, 1316–1325 (1972).
38. Ehmann, U. K., Gehring, U. & Tomkins, G. M. *Biochim. biophys. Acta* **447**, 133–138 (1976).
39. Blumenthal, A. B., Kriegstein, H. J. & Hogness, D. S. *Cold Spring Harb. Symp. quant. Biol.* **38**, 205–223 (1973).
40. Konze-Thomas, B., Levinson, J. W., Maher, M. & McCormick, J. J. *Biophys. J.* **28**, 315–325 (1979).
41. Fraval, H. N. A. & Roberts, J. J. *Cancer Res.* **39**, 1793–1797 (1979).
42. Hagan, M. P. & Elkind, M. M. *Biophys. J.* **27**, 75–85 (1979).

A herpes simplex virus type 1 function continuously required for early and late virus RNA synthesis

Roger J. Watson* & J. Barklie Clements

Institute of Virology, University of Glasgow, Church Street, Glasgow G11 5JR, UK

Controlled transcription of animal virus DNAs provides potentially useful models for elucidating the mechanisms which regulate eukaryotic gene expression. The progressive transcription of the herpes simplex virus type 1 (HSV-1) genome has been described previously[1-3]. Infection of permissive cells with HSV-1 in the presence of the protein synthesis inhibitor cycloheximide resulted in transcription of a restricted set of virus RNAs, referred to as the immediate early RNAs, which map within certain regions of the virus genome only[3-5]. Removal of cycloheximide led to the transcription of additional virus DNA sequences, which were expressed during the normal replicative cycle both at early and late times post-infection (before and after the onset of virus DNA replication, respectively) and which map throughout the virus genome[3]. Previously, we have described a temperature-sensitive mutant of HSV-1 Glasgow strain 17, *ts* K, which accumulated only the immediate early RNAs at the non-permissive temperature (NPT)[5]. Transfer of *ts* K-infected cells from NPT to the permissive temperature (PT), even in the absence of *de novo* protein synthesis, resulted in transcription of the DNA sequences expressed early and late post-infection[5]. This indicated the persistence at NPT of a non-functional immediate early polypeptide which on transfer to PT regained its function, required for progression from the immediate early to early stage of transcription. Here we demonstrate, by analysing the RNAs made in *ts* K-infected cells after transfer from PT to the NPT, that this polypeptide's function is required continuously for synthesis of HSV-1 early and late RNAs, thus identifying a control function essential for the expression of early and late HSV genetic information in eukaryotic cells.

BHK21 C13 cells were infected with *ts* K and maintained at the PT (31 °C) for either 3 or 7 h to allow accumulation of virus specified products. These incubation periods represent early and

* Present address: Laboratory of Molecular Virology, National Cancer Institute, Bethesda, Maryland 20205.

late times post-infection, as virus DNA replication initiates at approximately 4 h post-infection in these conditions (data not shown). The cells were then either maintained at the PT or transferred to the NPT (38.5 °C) and, after allowing 30 min for temperature equilibration, were labelled for 3-h periods using ^{32}P-orthophosphate. RNA isolated from these cells was hybridized to nitrocellulose blot strips containing the separated fragments of HSV-1 DNA generated by endonuclease *Bam*HI digestion, and hybridization was detected by autoradiography. The resultant hybridization patterns (Fig. 1, tracks 2–5) were compared with that of immediate early RNA isolated from *ts* K-infected cells maintained throughout at NPT (Fig. 1, track 6).

RNA samples isolated from *ts* K-infected cells labelled at the PT hybridized to virtually all the *Bam*HI DNA fragments (Fig. 1, tracks 2, 4), and these hybridization patterns were qualitatively identical to those of early and late RNA samples previously observed[3,5]. In contrast, the hybridization patterns of RNA samples labelled after transfer from the PT to the NPT, both at 3 and 7 h post-infection, were restricted. For example, there was little or no detectable hybridization of these RNA samples to *Bam*HI fragments a, c, d, f, g, h, i, m, p, r, t, uv, w, a' and b' (Fig. 1, tracks 3, 5). These restricted hybridization patterns were indistinguishable from that of *ts* K-infected cells maintained continuously at NPT (Fig. 1, track 6). The DNA regions represented in the RNA synthesized after transfer of *ts* K from the PT to the NPT (Fig. 2) correspond to the major immediate early mRNAs[6,7]. This suggests that the low abundance of immediate early mRNAs present in cycloheximide-treated cells may represent early transcripts which result from residual protein synthesis in the presence of the drug.

We conclude from the above observations that transfer of *ts* K-infected cells to the NPT resulted in the inactivation of a virus-specified activity required for early and late virus RNA synthesis. To strengthen this conclusion, further control experiments were carried out, first to ensure that the products necessary for early RNA synthesis were present at the time of the early transfer, and second to rule out the possibility that transfer inactivates a host rather than a virus function. Note that neither caveat is probable, as early RNA synthesis was already observed 1 h post-infection at 37 °C (ref. 3) and the wild-type HSV-1 control was found to be transcribed normally at 38.5 °C (ref. 8).

Cells infected with *ts* K were maintained at the PT for 3 h. Fresh medium containing 200 μg ml^{-1} cycloheximide was then added to the monolayer and, after incubating at the PT for 30 min, cells were labelled in this medium with ^{32}P-orthophosphate. This treatment thus precluded the accumulation of virus proteins following 3 h post-infection, the time of the early transfer described above.

In a further series of experiments, cells were infected at PT with a *ts*$^+$ revertant of *ts* K (*ts* K R1), and cells were labelled at 3.5 h post-infection at either the PT or NPT. RNA samples extracted from these cells were hybridized to the *Bam*H1 fragments of HSV-1 DNA, as before. The hybridization patterns obtained with these control RNA samples (Fig. 1, tracks 7–9) were in each instance qualitatively identical to those of *ts* K-infected cells maintained at the PT (Fig. 1, tracks 2, 4).

These results suggested, therefore, that the effect observed on transfer of *ts* K-infected cells from PT to the NPT was the result of cessation of early and late RNA synthesis, and resumption of immediate early RNA synthesis was due to loss of activity of a temperature-sensitive *ts* K product.

The way in which the virus transcriptional function described here acts to effect early and late RNA synthesis is unclear. No modifications of cellular RNA polymerases following HSV-1 infection have been detected by DEAE-Sephadex chromatography, nor were new polymerase activities observed[9]. It has been reported that the activity of a host cell α-amanitin-sensitive RNA polymerase is required for synthesis of all HSV-1 RNA temporal classes[10]. Thus, it seems likely that an immediate early virus-coded polypeptide interacts directly with this host cell RNA polymerase, or with the virus DNA template, to enable
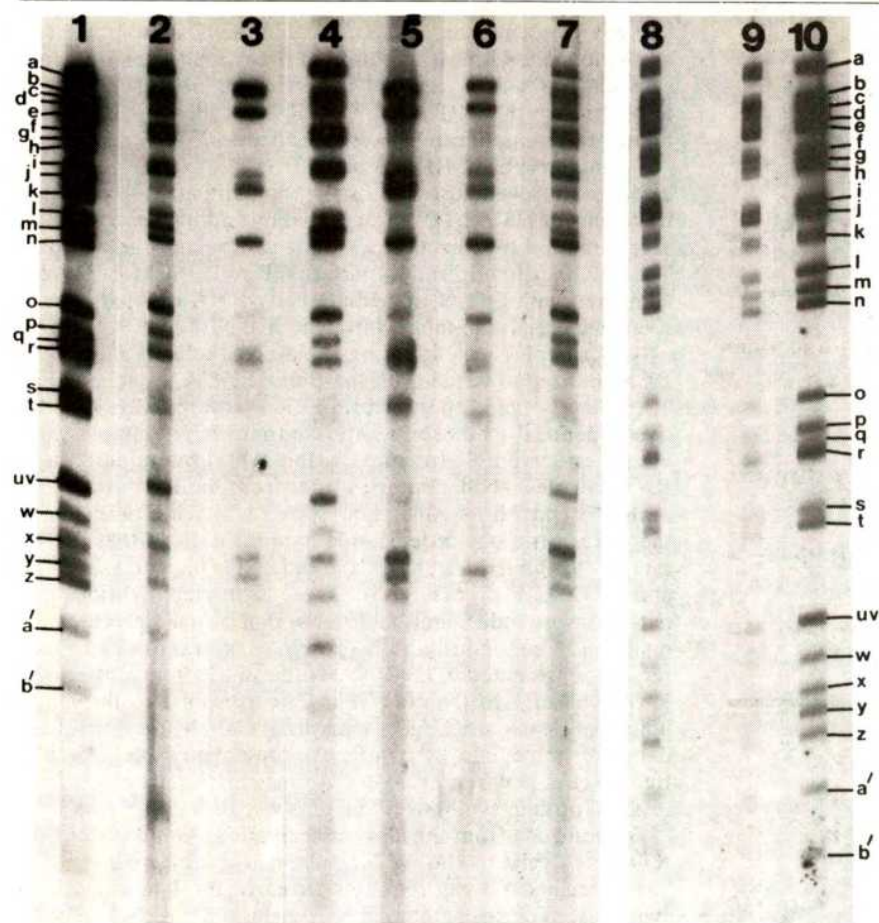
Fig. 1 Autoradiographs of ^{32}P-labelled RNA samples hybridised to the *Bam*H1 fragments of HSV-1 DNA. Samples (15 μg) of HSV-1 (Glasgow strain 17) DNA were digested to completion with endonuclease *Bam*H1 (Boehringer Mannheim), and the resultant fragments were separated by electrophoresis on a single-well 1% agarose gel[5]. The separated DNA fragments were denatured *in situ* and transferred to nitrocellulose sheets using the Southern blotting technique[14]. Strips cut from these blots were incubated with the ^{32}P-labelled nucleic acid samples described below, using hybridisation procedures published previously[3]. HSV-1 DNA, labelled *in vitro* by nick-translation[5], was hybridised to the representative blot strips to indicate the positions of the DNA fragments. Track 1 is the DNA control strip for tracks 2–7, and track 10 the DNA control for tracks 8 and 9. RNA samples were labelled in confluent BHK21 C13 cell monolayers infected at a multiplicity of 25 plaque-forming units per cell with *ts* K (isolated from wild-type Glasgow stain 17)[15] or its revertant *ts* K R1. Cells were incubated for 3 or 7 h at 31 or 38.5 °C, then either transferred from 31 to 38.5 °C or left at the temperature of infection. After allowing 30 min for temperature equilibration, pre-warmed medium containing 0.5 mCi ml^{-1} ^{32}P-orthophosphate was added, and cells were labelled for 3 h at the appropriate temperature. Total cell RNA was then isolated by proteinase K digestion and phenol extraction, and was purified by isopycnic banding in caesium sulphate gradients[5]. Cells infected with *ts* K (tracks 2–7) were pre-incubated (*a*) and labelled (*b*) in the following conditions: track 2, *a*, 31 °C for 3 h, *b*, 31 °C; track 3, *a*, 31 °C for 3 h, *b*, 38.5 °C; track 4, *a*, 31 °C for 7 h, *b*, 31 °C; track 5, *a*, 31 °C for 7 h, *b*, 38.5 °C; track 6, 38.5 °C for 3 h, *b*, 38.5 °C; track 7, *a*, 31 °C for 3 h, *b*, 31 °C in medium containing 200 μg ml^{-1} cycloheximide. Cells infected with *ts* K R1 (tracks 8, 9) were pre-incubated at 31 °C for 3 h, labelled at 31 °C (track 8); pre-incubated at 31 °C for 3 h, labelled at 38.5 °C (track 9).

transcription of early and late virus genes to occur. Such interaction must be independent of virus DNA replication, as the virus-coded transcription-modifying function is required both before and after the onset of virus DNA replication. It could be postulated that the virus function described here is required for stabilization of early and late RNAs rather than for their transcription. This explanation would require that additional transcripts are turned over extremely rapidly at NPT in *ts* K-infected cells, as early and late synthesis was not observed in the 3-h labelling periods reported here.
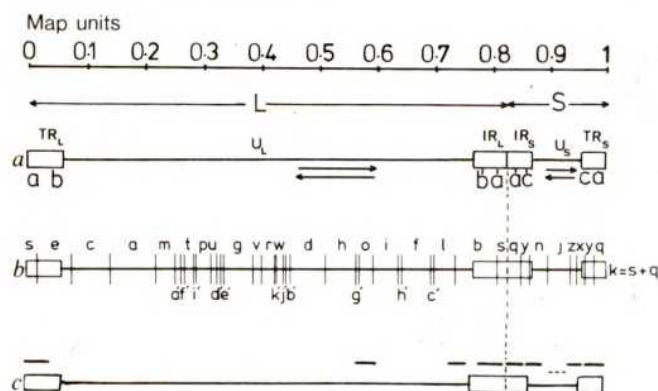
Fig. 2 *a*, HSV-1 genome organization. Two unique DNA regions U$_L$ and U$_S$ are each flanked by inverted repetitive regions (TR$_L$/IR$_L$; TR$_S$/IR$_S$) and joined at IR$_L$–IR$_S$. Virion DNA consists of four isomers arising from inversions of U$_L$ and U$_S$ (refs 16, 17) and these inversions are indicated by the directions of arrows. The sequence arrangement for a single strand is indicated, and here the non-inverted terminal redundancy is designated as a. *b*, Physical map for the HSV-1 DNA fragments generated by the *Bam*H1 restriction endonulease[5]. *c*, Genome regions represented by *ts* K RNAs labelled after transfer from PT to NPT. Regions represented by abundant RNAs are indicated by solid lines. The summary is based on hybridization to the *Bam*H1 fragments (Fig. 1, tracks 3, 5) and to virus DNA fragments generated by other restriction endonucleases[5].

The *ts* mutation of *ts* K has been mapped in the short reiterated (TR$_S$/IR$_S$) region of the virus genome[11], a region which specifies an immediate early polypeptide of apparent molecular weight 175,000 (Vmw 175)[6,12]. This polypeptide exhibited abnormal properties at NPT in *ts* K-infected cells, characterized by a failure to be fully processed and by a greater retention in the cytoplasm than in the nucleus[13]. All the abnormal properties were reversed by transfer of cells from the NPT to the PT, suggesting that they have functional significance and indicating the possibility that the temperature-sensitive *ts* K lesion is within Vmw 175.

The HSV-1 mutant *ts* K provides an attractive model for analysing the control of gene expression in infected eukaryotic cells. The development of appropriate *in vitro* transcriptional systems should enable the function required for HSV-1 transcription to be examined more readily.

1. Frenkel, N. & Roizman, B. *Proc. natn. Acad. Sci. U.S.A.* **69**, 2654–2658 (1972).
2. Swanstrom, R. I. & Wagner, E. K. *Virology* **60**, 522–533 (1974).
3. Clements, J. B., Watson, R. J. & Wilkie, N. M. *Cell* **12**, 275–285 (1977).
4. Jones, P. C., Howard, G. S. & Roizman, B. *J. Virol.* **21**, 268–276 (1977).
5. Watson, R. J. & Clements, J. B. *Virology* **91**, 364–379 (1978).
6. Watson, R. J., Preston, C. M. & Clements, J. B. *J. Virol.* **31**, 42–52 (1979).
7. Clements, J. B., McLauchlan, J. & McGeoch, D. J. *Nucleic Acids Res.* **7**, 77–91 (1979).
8. Watson, R. J. thesis, Univ. Glasgow (1979).
9. Lowe, P. A. *Virology* **86**, 577–580 (1978).
10. Costanzo, F., Campadelli-Fiume, G., Foà-Tomasi, L. & Cassai, E. *J. Virol.* **21**, 996–1001 (1977).
11. Stow, N. D., Subak-Sharpe, J. H. & Wilkie, N. M. *Virology* **90**, 1–11 (1978).
12. Preston, V. G. *et al. J. Virol.* **28**, 499–517 (1979).
13. Preston, C. M. *J. Virol.* **32**, 357–369 (1979).
14. Southern, E. M. *J. molec. Biol.* **98**, 503–533 (1975).
15. Crombie, I. K. thesis, Univ. Glasgow (1975).
16. Hayward, G. S., Frenkel, N. & Roizman, B. *Proc. natn. Acad. Sci. U.S.A.* **72**, 4243–4247 (1975).
17. Delius, H. & Clements, J. B. *J. gen. Virol.* **33**, 125–133 (1976).

Differential stimulation of capped mRNA translation *in vitro* by cap binding protein

N. Sonenberg*, H. Trachsel†, S. Hecht‡ & A. J. Shatkin

Roche Institute of Molecular Biology, Nutley, New Jersey 07110
† Friedrich Miescher-Institut, CH-4002 Basel, Switzerland
‡Departments of Chemistry and Biology, University of Virginia, Charlottesville, Virginia 22901

The cap structure, m[7]GpppN, which is present at the 5' end of most eukaryotic mRNAs, facilitates the initiation of protein synthesis[1]. Rabbit reticulocytes and mouse L and ascites cells have been shown to contain a protein (molecular weight (MW) 24,000) that specifically recognizes the cap of reovirus mRNA and several other capped mRNAs[2]. That protein partially co-purifies with eIF-3 and eIF-4B (refs 2, 3), two eukaryotic initiation factors involved in mRNA binding to ribosomes[4]. We have isolated essentially homogeneous 24,000-MW poly-peptide which stimulated translation of capped mRNAs *in vitro*[5]. Consistent with those findings, we now report that among the many protein synthesis factors tested, preparations of eIF-3 and eIF-4B that also contained the 24,000-MW cap binding protein (CBP) markedly increased translation in HeLa cell extracts of capped mRNAs but not of naturally uncapped viral messengers. Moreover, removal of the 24,000-MW protein diminished the ability of eIF-3 to stimulate translation of capped mRNA. Purified CBP, which had no effect on uncapped satellite tobacco necrosis virus (STNV) RNA, stimulated translation of this RNA after addition of a cap. The protein also relieved translational competition between capped and naturally uncapped mRNAs in favour of the capped species. These findings support the hypothesis that the CBP participates in the regulation of eukaryotic mRNA translation in normal and virus-infected cells[6].

Cap binding protein purified by affinity chromatography in m[7]GDP–Sepharose[5] stimulated translation in HeLa cell extracts of Sindbis virus mRNA which is capped[7] (Fig. 1*a*) but not encephalomyocarditis (EMC) virus RNA, an uncapped message[8] (Fig. 1*b*). The differential effect on Sindbis mRNA as well as on capped reovirus and globin mRNAs was greater at higher concentrations of CBP[5], promoting increased synthesis of Sindbis capsid and its B₁ precursor protein[9], reovirus structural proteins[10] and globin as determined by polyacrylamide gel electrophoresis of the radiolabelled products (data not shown). By contrast, there was no effect on EMC virus RNA and another uncapped message[11], STNV RNA. This was apparently not due to mRNA saturation because no stimulation was observed when low concentrations of EMC virus RNA were used (Fig. 1*d*), whereas Sindbis mRNA translation was increased at several concentrations (Fig. 1*c*).

The effect of CBP was tested in extracts directed by mixtures of capped and uncapped RNAs that presumably were in competition for components necessary for translation. Alfalfa mosaic virus (AMV)-4 RNA is a capped mRNA that codes for viral coat protein[12] (Fig. 2, lane 2). In the presence of STNV RNA, a relatively weak message in extracts of HeLa cells as compared to wheat germ[13], both STNV products (Fig. 2, lane 3) and the larger AMV coat protein were made (Fig. 2, lane 4). The yield of AMV protein was increased in response to the RNA mixture, possibly due to protection against RNase digestion by the higher total concentration of mRNA. Addition of CBP increased further the translation of AMV RNA whereas STNV RNA translation decreased slightly (Fig. 2, lanes 5–7). Similarly,
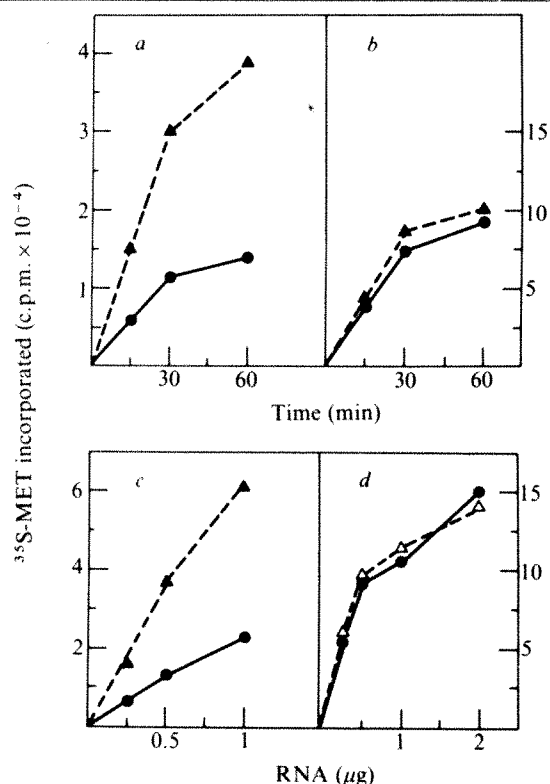
Fig. 1 Effect of CBP on translation of Sindbis virus mRNA and EMC virus RNA in HeLa cell-free extracts. Conditions of *in vitro* protein synthesis were as described previously[5]. ^{35}S-Methionine (16 µCi, specific activity 643 Ci mmol⁻¹) incorporation into acid-precipitable products was assayed in 5-µl aliquots of 25-µl incubation mixtures. Sindbis virus mRNA[25], EMC virus RNA[26] and rabbit reticulocyte 24,000-MW CBP[5] were present at ~0.5 µg, 0.5 µg and 30 ng, respectively, or at the indicated amounts. Levels of radioactivity incorporated in the absence of exogenous mRNAs (4,695 c.p.m. without and 4,970 c.p.m. with CBP) were subtracted. Panels *a*, *c*: +Sindbis virus mRNA; *b*, *d*: +EMC virus RNA. Dotted line: +CBP.

in a mixture of globin and STNV RNAs, the presence of CBP stimulated globin formation and, at the highest level, decreased the synthesis of STNV products (Fig. 2, lanes 8–11). The results suggest that the CBP discriminates against naturally uncapped mRNAs in favour of capped mRNAs in a mixture of competing molecules. Consistent with this suggestion, formation of the spectrum of EMC virus products was diminished and AMV RNA translation was increased by addition of the 24,000-MW protein (Fig. 2, lanes 12–14).

To explore the possibility that the presence of co-purified CBP accounts for some previous reports of mRNA discriminatory activity by eukaryotic initiation factors[14–18], rabbit reticulocyte factors were tested for their ability to stimulate Sindbis as compared with EMC RNA. Only eIF-4B (Table 1, expt 1) and eIF-3 (Table 1, expt 2) had discriminatory activity, increasing the translation of Sindbis mRNA 9–12-fold more than EMC virus RNA. Factor eIF-3 contains CBP unless washed with 0.5 M KCl[6]. Consequently, we also tested a preparation of salt-washed eIF-3 which had been shown to be free of the 24,000-MW polypeptide by a cap cross-linking assay[2]. This eIF-3 failed to stimulate translation of Sindbis mRNA (Table 1, expt 1) although it retained eIF-3 activity in a reconstituted mammalian cell-free protein synthesizing system[6]. Another eIF-3 that contained one-third as much CBP as the preparation used in expt 2 (Table 1) gave an intermediate ratio of 4.3 for stimulation of Sindbis compared with EMC virus RNA translation (data not shown). Thus, the presence of 24,000-MW protein is correlated with the ability of a factor preparation to stimulate differentially capped mRNA translation *in vitro*.

* Present address: McIntyre Medical Sciences Building, McGill University, Montreal, Canada.
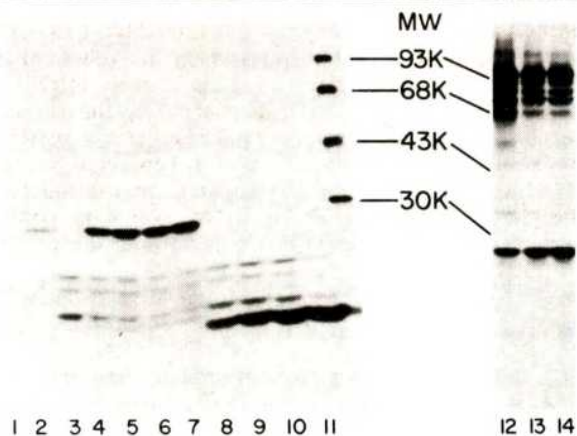
Fig. 2 The effect of CBP on translation of mixtures of capped and uncapped mRNAs by HeLa cell-free extracts. ^{35}S-Methionine-labelled products synthesized during a 60-min incubation were analysed by polyacrylamide gel electrophoresis and fluorography[27,28]. Reaction mixtures included no added RNA (lane 1) or 2 μg of each of the following RNAs: AMV-4 (lane 2), STNV (lane 3), AMV-4+STNV and 0, ~15, 30 and 45 ng CBP (lanes 4–7, respectively); globin+STNV and 0, ~15, 30 and 45 ng CBP (lanes 8–11); and, in a separate experiment, AMV-4+EMC and 0, ~15 and 30 ng CBP (lanes 12–14).

To determine if addition of a 5' cap to a naturally uncapped RNA would result in an effect of CBP, STNV RNA was translated before and after exposure to capping enzymes purified from vaccinia virus[19,20]. Because STNV RNA is a weak messenger in the HeLa system, much of the incorporated ^{35}S-methionine appeared in a prominent cellular protein (Fig. 3, lane 1). After treatment with vaccinia capping enzymes, the STNV RNA which included capped (~20%) and uncapped (~80%) molecules was less effectively translated (Fig. 3, lane 2) than untreated RNA (Fig. 3, lane 4). This was probably due to nicking of the RNA during the capping reaction, as most of the products directed by treated STNV RNA migrated slightly faster than viral capsid protein (MW ~22,000)[21]. The smaller polypeptide (MW ~18,000) which was also synthesized in response to uncapped STNV RNA but in lower amounts than capsid (Fig. 3, lane 4) presumably represents prematurely terminated capsid protein[21]. When CBP was added to an incubation mixture directed by the STNV RNA that contained

some capped molecules, it increased the synthesis of the viral polypeptide products (compare Fig. 3, lanes 2 and 3). By contrast, no stimulation occurred with untreated STNV RNA (compare Fig. 3, lanes 4 and 5).

Many investigators have reported that certain eukaryotic initiation factors can relieve translational competition between two different mRNAs in mammalian cell-free protein synthesising systems. For example, Golini *et al.*[14] reported that eIF-4B can overcome the competitive advantage of EMC virus RNA over rabbit globin mRNA and other capped cellular mRNAs. Nudel *et al.*[22] described a protein with a similar property, that is, the ability to relieve translational competition between the RNA of mengovirus, another picornavirus, and globin mRNA (and between α- and β-globin capped mRNAs). Kabat and Chappell[15] also observed that eIF-4B could overcome the preferential translation of rabbit β-globin mRNA relative to α-globin mRNA. We found that purified CBP preferentially stimulated translation of several capped mRNAs at the expense of the uncapped RNAs of EMC virus and STNV. Because we had previously observed that initiation factors eIF-4B and eIF-3 contain variable amounts of the 24,000-MW protein[2], we also tested these two initiation factors and found that both stimulated Sindbis virus capped mRNA severalfold but were without significant effect on EMC virus uncapped RNA. The differential stimulatory activity of eIF-3 for capped mRNA translation was correlated with the amount of 24,000-MW CBP in the different factor preparations. These observations agree with the report[23] that cell-free extracts of mouse L or ascites cells translate well the uncapped RNA of mengovirus, but require supplementation by reticulocyte factors for efficient translation of globin mRNA. We obtained similar results with ascites cell extracts directed by reovirus mRNA and EMC virus

Table 1 Effect of protein synthesis factors on translation of capped and uncapped RNA

		Incorporation (c.p.m.)		Fold-stimulation		Ratio of stimulation
						Sindbis RNA
		Sindbis RNA	EMC RNA	Sindbis RNA	EMC RNA	EMC RNA
	Factor added					
Expt 1*	None	1,754	8,830	—	—	—
	eIF-2 (3.5 μg)	3,952	9,527	2.2	1.1	2.0
	eIF-3	1,218	12,757	0.7	1.4	0.5
	(5 μg of 0.5 M KCl washed)					
	eIF-4A (6 μg)	9,851	19,550	5.6	2.2	2.5
	eIF-4B (1.5 μg)	23,919	12,943	13.6	1.5	9.1
	eIF-4C+D (2 μg)	1,353	4,021	0.8	0.5	1.6
	eIF-5 (0.5 μg)	1,105	14,411	0.6	1.6	0.4
	EF-2 (2 μg)	1,699	15,910	1.0	1.8	0.6
Expt 2	None	7,880	87,652	—	—	—
	EF-1 (1 μg)	9,814	81,397	1.2	0.9	1.3
	eIF-3	96,083	79,598	12.2	0.9	12.3
	(4 μg of 0.1 M KCl washed)					

RNAs (0.5 μg 25 μl⁻¹) were incubated in HeLa cell-free extracts for 60 min with ^{35}S-methionine (24 μCi, specific activity 893 Ci mmol⁻¹) as radioactive precursor. Acid-precipitable radioactivity was assayed as in Fig. 1 (refs 5, 6). Factors were estimated to be 80–90% pure by polyacrylamide gel electrophoresis[3,6], and the amounts used were above saturating levels for the reticulocyte reconstituted translation system[4].
* For expts 1 and 2 the subtracted levels of endogenous synthesis were 3,724 and 8,877 c.p.m., respectively.
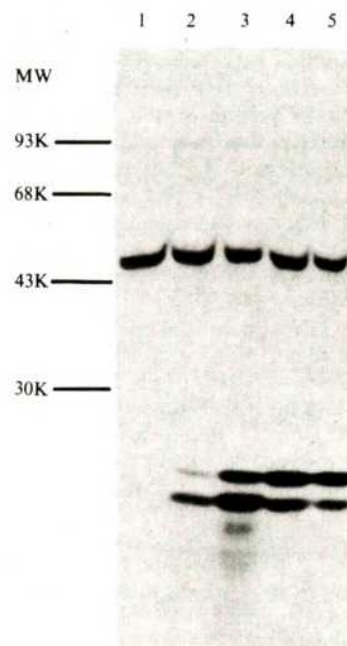
Fig. 3 Effect of CBP on the translation of capped and uncapped STNV RNA. STNV RNA was incubated for 20 min at 37 °C as described previously[19,20] in the presence of GTP, ^{3}H-methyl-*S*-adenosylmethionine and guanylyl- and methyl-transferase activities solubilized and partially purified from vaccinia virus. Analysis of a P₁ nuclease digest of the ^{3}H-labelled RNA by high voltage electrophoresis indicated that 20% of the 5' termini had been converted to the m[7]G-capped form. ^{35}S-Methionine-labelled polypeptide products directed by the RNAs were analyzed by polyacrylamide gel electrophoresis. Lane 1: no added RNA; 2: 2 μg 'capped' STNV RNA; 3: as lane 2 plus ~45 ng CBP; 4: 2 μg STNV RNA (not capped); 5: as lane 4 plus ~45 ng CBP. The yields of acid-precipitable radioactivity in c.p.m. per 5-μl aliquot of incubation mixture for lanes 1–5 were respectively, 5,528, 7,592, 11,631, 11,250 and 10,951; 20-μl aliquots were applied to the gel.

RNA (unpublished results). Furthermore, the capacity of eIF-4B to restore capped mRNA translation in poliovirus-infected HeLa cell extracts is probably due to co-purification of 24,000-MW CBP with the 80,000-MW main component in eIF-4B preparations[6]. Poliovirus apparently exerts its shut-off effect on host cell protein synthesis by inactivation of the 24,000-MW protein [6,17]. By this mechanism the uncapped viral RNA, which is presumably independent of or less dependent on CBP, redirects the translational machinery of infected cells. The *in vitro* effect of CBP on capped mRNA translation may reflect a key regulatory role in poliovirus-infected cells.

Shut-off of host protein synthesis by functional inactivation of CBP might not be restricted to picornaviruses that contain uncapped RNA but may be a more general eukaryotic control mechanism. For example, it was recently reported[24] that mouse L cell extracts prepared at late times after reovirus infection

translate uncapped, but not capped viral mRNA. This is in sharp contrast to uninfected cell extracts which, like other eukaryotic protein synthesizing systems[1], utilize capped mRNA preferentially. Thus, reovirus infection may modify the translational machinery of L cells in a way that results in a switch from translation of capped to uncapped mRNA, perhaps by inactivation of CBP with parallel development of cap-independent translation mechanisms analogous to events in poliovirus-infected HeLa cells. Other viruses may re-direct the metabolism of infected cells in similar ways.

1. Shatkin, A. J. *Cell* **9**, 645–653 (1976).
2. Sonenberg, N., Morgan, M. A., Merrick, W. C. & Shatkin, A. J. *Proc. natn. Acad. Sci. U.S.A.* **75**, 4843–4847 (1978).
3. Bergmann, J. E., Trachsel, H., Sonenberg, N., Shatkin, A. J. & Lodish, H. F. *J. biol. Chem.* **254**, 1440–1443 (1979).
4. Trachsel, H., Erni, B., Schreier, M. H. & Staehelin, T. *J. molec. Biol.* **116**, 755–767 (1977).
5. Sonenberg, N., Rupprecht, K. M., Hecht, S. M. & Shatkin, A. J. *Proc. natn. Acad. Sci. U.S.A.* **76**, 4345–4349 (1979).
6. Trachsel, H. *et al. Proc. natn. Acad. Sci. U.S.A.* **77**, 770-774 (1980).
7. Dubin, D. T., Timko, K., Gillies, S. & Stollar, V. *Virology* **98**, 131–141 (1979).
8. Frisby, D., Eaton, M. & Fellner, P. *Nucleic Acids Res.* **3**, 2771–2787 (1976).
9. Simmons, D. T. & Strauss, J. H. *J. molec. Biol.* **86**, 397–409 (1974).
10. Shatkin, A. J. & Both, G. W. *Cell* **7**, 305–313 (1976).
11. Wimmer, E., Chang, A. Y., Clark, J. M. Jr & Reichman, M. E. *J. molec. Biol.* **38**, 59–73 (1968).
12. Van Vloten-Doting, L. & Jaspars, E. M. *J. Comprehensive Virol.* **11**, 1–53 (1977).

13. Herson, D., Schmidt, A., Seal, S., Marcus, A. & Van Vloten-Doting, L. *J. biol. Chem.* **254**, 8245–8249 (1979).
14. Golini, F. *et al. Proc. natn. Acad. Sci. U.S.A.* **73**, 3040–3044 (1976).
15. Kabat, D. & Chappell, J. R. *J. biol. Chem.* **252**, 2684–2690 (1977).
16. Shafritz, D. A. *et al. Nature* **261**, 291–294 (1976).
17. Rose, J. K., Trachsel, H., Leong, K & Baltimore, D. *Proc. natn. Acad. Sci. U.S.A.* **75**, 2732–2736 (1978).
18. Gette, W. R. & Heywood, S. M. *J. biol. Chem.* **254**, 9879–9885 (1979).
19. Moss, B. *Biochem. biophys. Res. Commun.* **74**, 374–383 (1977).
20. Sonenberg, N., Shatkin, A. J., Ricciardi, R. P., Rubin, M. & Goodman, R. M. *Nucleic Acids Res.* **5**, 2501–2512 (1978).
21. Salvato, M. S. & Fraenkel-Conrat, H. *Proc. natn. Acad. Sci. U.S.A.* **74**, 2288–2292 (1977).
22. Nudel, U., Lebleu, B. & Revel, M. *Proc. natn. Acad. Sci. U.S.A.* **70**, 2139–2144 (1973).
23. Lebleu, B., Nudel, U., Falcoff, E., Prives, C. & Revel, M. *FEBS Lett.* **25**, 97–103 (1972).
24. Skup, D. & Millward, S. *Proc. natn. Acad. Sci. U.S.A.* **77**, 152-156 (1980).
25. Cancedda, R. & Shatkin, A. J. *Eur. J. Biochem.* **94**, 41–50 (1979).
26. Eggen, K. L. & Shatkin, A. J. *J. Virol.* **9**, 636–645 (1972).
27. Laemmli, U. K. & Favre, J. *J. molec. Biol.* **80**, 575–599 (1973).
28. Sonenberg, N. & Shatkin, A. J. *Proc. natn. Acad. Sci. U.S.A.* **74**, 4288–4292 (1977).

Construction *in vitro* and rescue of a thymidine kinase-deficient deletion mutation of herpes simplex virus

James R. Smiley

Pathology Department, McMaster University Medical Center, 1200 Main St W., Hamilton, Ontario, Canada L8N 3Z5

The ability to introduce defined mutations at pre-selected sites on DNA molecules *in vitro* allows one to test hypotheses about the function of specific DNA sequences. The genome of herpes simplex virus type 1 (HSV-1), consisting of 150 kilobase pairs, is probably too large to allow the direct introduction of mutations *in vitro*. Therefore, to apply these techniques to the study of HSV genes, the feasibility of a two-step procedure was examined. A defined mutation was first introduced into a small segment of HSV-1 DNA which had previously been cloned in the *Escherichia coli* plasmid pBR322; the mutation was then incorporated into the genome of infectious HSV-1 by DNA-mediated marker rescue. The approach was tested using the viral gene for thymidine kinase (TK)[1–3]. TK was chosen for several reasons. First, TK is dispensable for viral infectivity in most conditions of cell culture, and efficient selection systems are available for both the TK⁻ and TK⁺ phenotypes[1–3]. This facilitates the recovery of TK-deficient mutants and allows rapid and detailed genetic analysis[3,4]. Second, Stow *et al.*[5] have shown that TK⁻ DNA sequences are readily rescued from DNA fragments into infectious virus. Third, purified HSV-1 TK DNA is able to convert TK-deficient mammalian cells to a TK⁺ phenotype[6], so that the expression of the viral gene can be studied in both the presence and absence of other regulatory viral gene products. Thus, the TK gene provides a favourable system for an examination of the role of specific DNA sequences in the expression of genes in eukaryotic cells. The results presented here demonstrate that an 800-base pair deletion mutation at the TK locus, generated *in vitro*, was rescued at a high frequency, producing a TK-deficient deletion mutant of HSV-1.

A 3.5-kilobase *Bam*HI fragment of HSV-1 DNA, containing the TK gene[6], has been inserted at the *Bam*HI site of pBR322 (ref. 7). The resulting recombinant plasmid, pX1 (Fig. 1), was used to isolate variant plasmids bearing defined deletions which potentially inactivate the viral gene. A deletion mapping entirely within the TK coding sequence was sought, so as to minimize the probability of also inactivating any neighbouring essential HSV genes. Approximately 1.2 kilobases of DNA are required to specify the 44,000-molecular weight TK polypeptide[3]. As the TK-transforming activity of the 3.5-kilobase *Bam*HI fragment resides the largest *Pvu*II subfragment[8], and is abolished by cleaving the DNA with *Eco*RI[6], it seemed likely that a deletion of the 800-base pair *Pst*IC fragment would map entirely within TK. Accordingly, a plasmid (pd2, Fig. 1) bearing the deletion was constructed (Fig. 1 legend).

To determine whether the deletion borne by pd2 could be recovered as a viable TK-deficient mutation of HSV-1, Vero cells were transfected with a co-precipitate formed with wild-type HSV-1 43 TK⁺ (ref. 7) membrane-stripped nucleocapsids[9], 7.5 µg ml⁻¹ purified circular pd2 DNA and 10 µg ml⁻¹ carrier cell DNA, using the calcium phosphate technique of Graham and Van der Eb[10]. The virus recovered from the infected cultures was then scored for the fraction of TK-deficient mutants by plaque titration on Vero cells in the presence and absence of 6 µg ml⁻¹ 5-bromodeoxyuridine. The presence of pd2 DNA in transfections led to a fivefold increase in the frequency of recovery of TK-deficient virus (3×10^{-3} compared with 6×10^{-4} in transfections with nucleocapsids and carrier DNA alone). Seven TK-deficient plaques selected from the progeny of the mixed infection by plaque purification in the presence of 5-bromodeoxyuridine were amplified in Vero cells, then screened for deletions by examining the *Eco*RI cleavage pattern of ³²P-labelled viral DNA. Five of the seven isolates bore the expected 800-base pair deletion within the *Eco*RI N fragment[11] of viral DNA. One such isolate, HSV-1 TK d2, was plaque purified again, expanded and examined in greater detail.

Figure 2 compares the *Bam*HI and *Eco*RI cleavage patterns of the DNAs of HSV-1 43 TK⁺, HSV-1 TK d2 and the corresponding recombinant plasmids pX1 and pd2. HSV-1 TK d2 DNA differs from that of its TK⁺ parent in that the normal
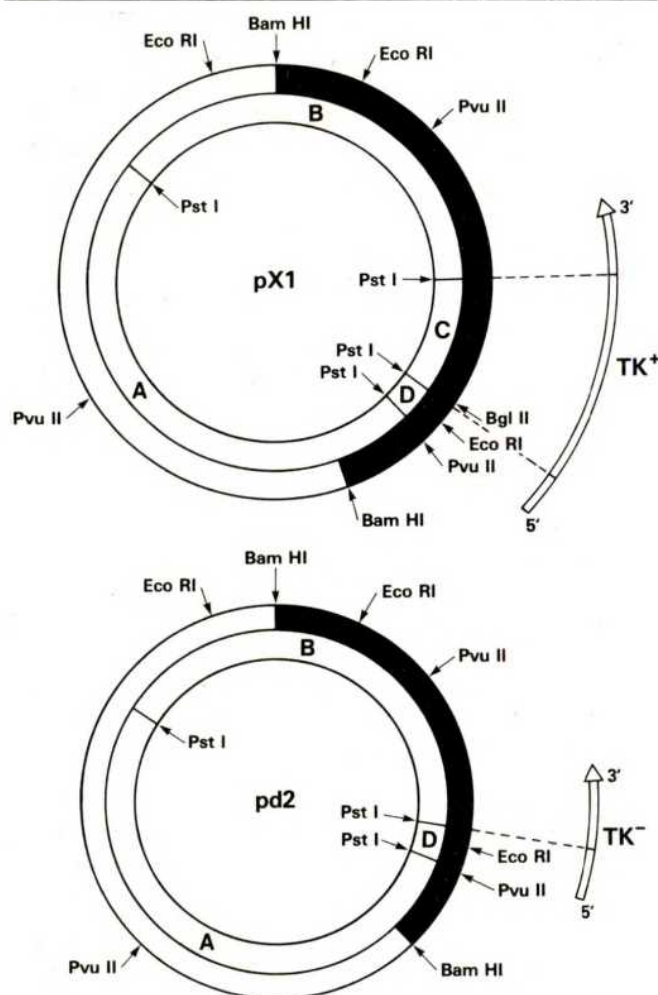
Fig. 1 Construction of pd2 from pX1. The deletion-bearing plasmid pd2 was derived from a partial *Pst*I digest of pX1 DNA. pX1 DNA (4 μg) was incubated with 0.6 units of *Pst*I (New England Biolabs) in 20 μl containing 50 mM KCl, 10 mM MgCl₂ and 10 mM Tris-HCl, pH 7.5, for 15 min at 37 °C, conditions which maximized the yield of doubly cleaved molecules. The reaction was terminated by the addition of EDTA to 20 mM, and the DNA was purified by extraction first with phenol then with ether, and concentrated by precipitation with alcohol. The partially digested DNA (100 ng) was incubated at 4 °C for 16 h in 20 μl containing 66 mM Tris-HCl, pH 7.6, 6.6 mM MgCl₂, 10 mM dithiothreitol, 0.4 mM ATP and 0.25 units of T4 DNA ligase (New England Biolabs). Following ligation, 5 units of *Bgl*II were added to the reaction mixture to inactivate any molecules retaining the *Pst*IC fragment. After a further incubation for 2 h at 37 °C, the DNA was used directly to transform CaCl₂-treated *E. coli* LE392 (ref. 7). Ampicillin-resistant transformants were obtained on LB plates containing 20 μg ml⁻¹ ampicillin. The plasmid DNA from six colonies was analysed for deletions by cleavage with *Pst*I and *Eco*RI. One plasmid (pd2), lacking only the *Pst*IC fragment, was identified. The structure of pd2 DNA was further verified by examining the fragments produced by cleavage with *Bam*HI, *Sma*I and double cleavage with *Eco*RI plus *Pvu*II. The HSV-1 DNA inserts are indicated by the filled portions of the outer circle. The locations of restriction endonuclease cleavage sites on pX1 DNA are from Enquist *et al.*[7], the approximate map location of the TK gene was inferred from the data of Colbere-Garapin *et al.*[8] and Wigler *et al.*[6], and the polarity of transcription of TK is from Smiley *et al.*[4].

3.5-kilobase *Bam*HI TK fragment is replaced by the deletion-bearing 2.7-kilobase fragment derived from pd2. This replacement of wild-type sequences by mutant DNA is partially obscured by the coincidental fixation in HSV-1 TK d2 of a smaller version of the *Bam*HI P fragment of HSV DNA, which now co-migrates with the wild-type TK fragment. The *Bam*HI P fragment, which in HSV-1 43 TK⁺ DNA runs as a broad band

just above the TK fragment, is derived from the end of the short segment of HSV DNA[12], a region of the genome known to acquire deletion and insertion mutations at a high frequency[9]. The length of this fragment varies both between HSV-1 strains[12] and between different plaque-purified stocks of the same strain (M. J. Wagner and W. C. Summers, personal communication). The replacement of wild-type TK DNA sequences by mutant DNA is more directly demonstrated by the *Eco*RI cleavage patterns: the wild-type 2.3-kilobase *Eco*RI N fragment[11] of viral DNA is replaced by the mutant 1.5-kilobase fragment derived from pd2 DNA. These data demonstrate that the deletion carried by pd2, generated *in vitro*, has been incorporated into the HSV-1 TK d2 genome. This deletion abolishes the ability of the mutant virus to induce HSV-1 TK activity following infection of TK-deficient LtA cells[13] (Fig. 3).

As neither pBR322 nor wild-type TK DNA sequences are found in HSV-1 TK d2 DNA, it follows that the mutant virus arose by two cross-over events between viral and plasmid DNA. It is not clear whether both cross-overs occurred during the
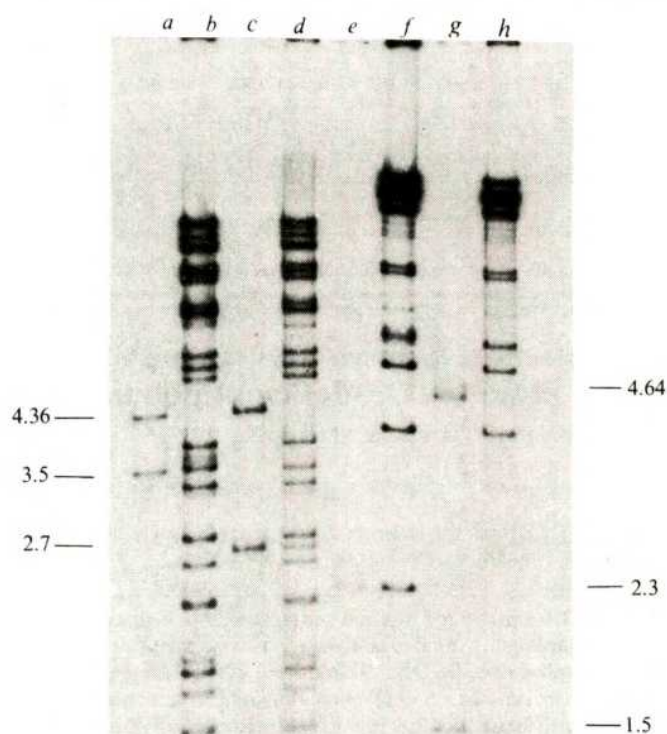
Fig. 2 Restriction endonuclease cleavage pattern of HSV-1 d2 DNA. ³²P-labelled viral DNA was extracted from viral nucleo-capsids as previously described[9]. Plasmid DNA was labelled *in vitro* by nick translation using [α-³²P]dCTP (NEN) and DNA polymerase I (Boehringer-Mannheim) according to Maniatis *et al.*[14]. No DNase I was added. The DNA was then cleaved with *Eco*RI (Boehringer-Mannheim) or *Bam*HI in a reaction volume of 10 μl, containing 50 mM KCl, 10 mM MgCl₂ and 10 mM Tris-HCl, pH 7.5. DNA fragments were resolved by electrophoresis through a 15×30-cm vertical 1.0% agarose gel as previously described[9]. *Bam*HI digests: *a*, pX1; *b*, HSV-1 43 TK⁺; *c*, pd2; *d*, HSV-1 TK d2. *Eco*RI digests: *e*, pX1; *f*, HSV-1 43 TK⁺; *g*, pd2; *h*, HSV-1 TK d2.
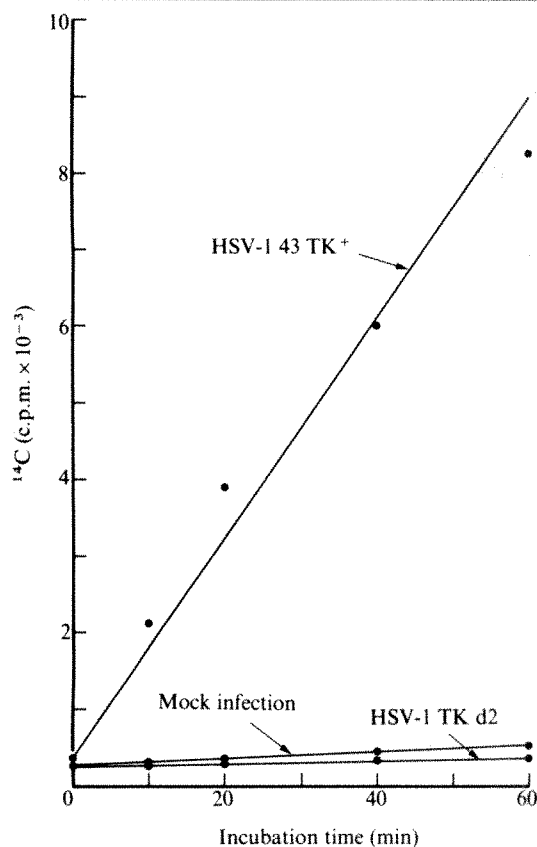
Fig. 3 TK activity induced by HSV-1 TK$^+$ and TK d2. 2×10^7 LtA cells were infected with 10^8 plaque-forming units of the indicated virus and collected 18 h post-infection. Extracts were assayed for TK activity using ^{14}C-thymidine, exactly as previously described[3].

initial interaction between the plasmid and viral DNA, or whether an initial single cross-over event between the circular plasmid and linear viral genomes gave rise to an unstable TK$^+$/TK$^-$ heterozygote which subsequently segregated TK$^-$ homozygotes by unequal crossing over between the resulting direct repeats of viral DNA. Because TK$^+$/TK$^-$ heterozygotes would score as TK$^+$, they would not have been recovered in these experiments, in which the selection was for TK-deficient virus. Experiments in which the TK$^+$ phenotype is rescued from pX1 by HSV-1 TK d2 may allow the recovery of such heterozygotes. These experiments are in progress.

The region of HSV-1 DNA encompassed by the d2 deletion is now open to exhaustive analysis by site-directed mutagenesis, as any alteration of the DNA sequences mapping within the deletion can be examined for consequent effects on the TK gene. If such an alteration inactivates TK, it can be rescued as a TK-deficient mutation; otherwise, it can be used to convert HSV-1 TK d2 to TK$^+$. The aim of this research is to extend this analysis to the DNA sequences which encode signals governing the synthesis and processing of TK mRNA. In addition, this and other deletion mutations at the TK locus of HSV-1 will be of value for correlating the physical and genetic maps of the TK gene, and for studies of the control of TK expression during lytic infection and in biochemically transformed cells. *In vitro* mutagenesis using cloned segments of HSV DNA will also be useful in the study of other viral genes.

I thank H. Swan for technical assistance, S. Bacchetti, W. E. Rawls and R. J. Redfield for critical readings of the manuscript, and W. C. Summers for *Bam*HI. This research was supported by the National Cancer Institute of Canada. Experiments with recombinant DNA were carried out in accordance with the MRC of Canada guidelines. The author is a Research Scholar of the NCI of Canada.

1. Dubbs, D. R. & Kit, S. *Virology* **22**, 493–502 (1964).
2. Klemperer, H. G., Haynes, G. R. & Watson, D. H. *Virology* **31**, 120–128 (1967).
3. Summers, W. P., Wagner, M. & Summers, W. C. *Proc. natn. Acad. Sci. U.S.A.* **72**, 4081–4084 (1975).
4. Smiley, J. R., Wagner, M. J., Summers, W. P. & Summers, W. C. *Virology* (in the press).
5. Stow, N. D., Subak-Sharpe, J. H. & Wilkie, N. M. *J. Virol.* **28**, 182–192 (1978).
6. Wigler, M. *et al. Cell* **11**, 223–232 (1977).
7. Enquist, L. W., Van de Woude, G, F., Wagner, M. J., Smiley, J. R. & Summers, W. C. *Gene* **7**, 335–342 (1979).
8. Colbere-Garapin, F., Chousterman, S., Horodniceau, F., Kourilsky, P. & Garapin, A. *Proc. natn. Acad. Sci. U.S.A.* **76**, 3755–3759 (1979).
9. Wagner, M. J. & Summers, W. C. *J. Virol.* **27**, 374–387 (1978).
10. Graham, F. L. & Van der Eb, A. J. *Virology* **52**, 456–467 (1973).
11. Skare, J. & Summers, W. C. *Virology* **76**, 581–599 (1977).
12. Locker, H. & Frenkel, N. *J. Virol.* **32**, 429–441 (1979).
13. Wigler, M., Pellicer, A., Silverstein, S. & Axel, R. *Cell* **14**, 725–731 (1978).
14. Maniatis, T., Jeffrey, A. & Kleid, D. *Proc. natn. Acad. Sci. U.S.A.* **72**, 1184–1188 (1975).

Heterogeneity in the molecular basis of hereditary persistence of fetal haemoglobin

Dorothy Tuan, Mary J. Murnane, J. K. deRiel & Bernard G. Forget

Department of Internal Medicine, Yale University School of Medicine, New Haven, Connecticut 06510

In hereditary persistence of fetal haemoglobin (HPFH), there is a uniformly high level of synthesis of fetal haemoglobin (Hb F: $\alpha_2\gamma_2$) in all red cells of affected adults. Other hereditary disorders of human haemoglobin synthesis may also be associated with persistent synthesis of Hb F into adult life, but usually at a lower level and in only a selected population of red cells. Previous studies in the common type of HPFH that occurs in blacks have demonstrated the presence of a total deletion of the linked β- and δ-globin genes of the adult haemoglobins Hb A ($\alpha_2\beta_2$) and Hb A$_2$ ($\alpha_2\delta_2$)[1-3], including approximately 4 kilobases of the DNA flanking the 5′ end of the δ gene. In contrast, $\delta\beta$-thalassaemia, in which Hb F synthesis is not as elevated or uniform as in HPFH, is associated with a partial deletion of the δ gene that leaves intact the 5′-flanking DNA of the gene[1-5]. These results provided support for previous theories[6] that regulatory sequences involved in the suppression of γ-globin gene expression might be located between the γ- and δ-globin genes, and that deletion of these sequences might be responsible for the continued expression of γ-globin genes in HPFH. To extend these observations, gene mapping studies of the non-α-globin genes have now been carried out in two additional individuals wth HPFH using restriction endonuclease digestion and gel blotting of total cellular DNA according to the method of Southern[16]. The results indicate that the molecular defects associated with HPFH are heterogeneous even in cases with similar phenotypes such as in the common variety of HPFH that occurs in blacks.

In addition to the previously studied[1,2] case of HPFH in an American black (black HPFH-1), we analysed the DNA from two other individuals with HPFH: a case of homozygous HPFH from Ghana (black HPFH-2) with the common type of black HPFH in which both $^G\gamma$- and $^A\gamma$-globin chains are synthesized, and a heterozygote for the Greek type of HPFH in which $^A\gamma$-globin chain synthesis vastly predominates[7]. The results of our restriction endonuclease mapping of these DNAs are summarized in Fig. 1.

In normal DNA, restriction endonuclease *Bcl*I cleaves outside the two γ-globin genes and generates a single 20-kilobase fragment that hybridizes to the γ-gene probe[8]. DNA from all three cases of HPFH, when cleaved by *Bcl*I, yields a single 20-kilobase fragment (Fig. 2), indicating that neither the $^G\gamma$ nor the $^A\gamma$ gene is deleted in these DNAs. This result is especially significant in the case of Greek HPFH. Because the

chromosome bearing the Greek type of HPFH is thought to direct the synthesis of predominantly $^A\gamma$-globin chains[7], it is possible that the $^G\gamma$ gene is deleted in this syndrome. If this were the case, *Bcl*I digestion of DNA from a heterozygote would be expected to generate two fragments: one 20-kilobase fragment from the normal chromosome and another fragment of a different size from the HPFH chromosome. The abnormal fragment could be either longer or shorter than the normal 20 kilobases, depending on where the next *Bcl*I site resides in relation to the endpoint of the deletion. The presence of only one normal 20-kilobase *Bcl*I fragment in DNA from the Greek HPFH heterozygote strongly suggests that the $^G\gamma$ gene is not deleted in this case. The possibility that the $^G\gamma$ gene is deleted but that the new *Bcl*I site lies exactly 20 kilobases from the preserved *Bcl*I site (to the 3' side of the non-deleted $^A\gamma$ gene) is unlikely from the results of other restriction endonuclease digestions. In particular, digestion of normal DNA with *Bgl*II yields a single 13.5-kilobase fragment containing both γ genes[1,2,9]. DNA from our three cases of HPFH also yielded only a single 13.5-kilobase fragment when hybridized to γ probe (data not shown); in the case of Greek HPFH no additional band of a different size was seen that hybridized with the γ probe. The absence of a deletion of the $^G\gamma$ gene in the Greek type of HPFH is further supported by the recent finding of small amounts of Hb F of the $^G\gamma$ type in red cells of affected individuals[10].

When *Bgl*II-digested DNA of our cases was hybridized with $\beta + \delta$ genomic DNA probes [from *Pst*I subclones of HβGl (ref. 11)], no bands were visible in the two cases of black HPFH (data not shown), confirming previous reports of total deletion of δ- and β-globin genes in these cases[1-3]; in the case of Greek HPFH, a normal pattern was obtained, indicating the presence of normal-sized fragments containing the δ- and β-globin genes. As the Greek case is only heterozygous for HPFH, these normal bands are expected from the normal chromosome, so a deletion of δ and β loci from the Greek HPFH chromosome cannot be

Fig. 2 Digestion of normal and HPFH DNAs with restriction endonuclease *Bcl*I. Digested DNA was fractionated by electrophoresis in a horizontal slab gel of 0.8% agarose as previously described[2], and the DNA was transferred to a nitrocellulose filter by the gel blotting technique of Southern[16]. The nitrocellulose filter was then hybridized in the presence of 10% dextran sulphate[17] to the indicated cloned DNA probes labelled with ^{32}P by nick-translation as described elsewhere[2]. The γ probe was a mixture of JW151 (a $^G\gamma$ cDNA clone[18]) and pRP10(an $^A\gamma$ cDNA clone[19]). The H probe was an *Eco*RI subclone of HβGl (ref. 11). Abbreviations: N, normal DNA; HPFH DNAs: 1, black HPFH-1; 2, black HPFH-2; 3, Greek HPFH.

ruled out on the basis of this result alone. However, if the δ and β loci were deleted on the affected chromosome in the Greek heterozygote, one would have expected to find an anomalous band in this DNA with one of the four enzymes and four probes that were tested (see Figs 3, 4); no anomalous bands were found and therefore a non-α-globin gene deletion could not be positively identified.

When *Bcl*I-digested DNA from our cases was hybridized to a probe from H fragment DNA [which is derived from a point 4.5 kilobases to the 5' side of the δ gene (Fig. 1 and refs 1, 11)], an 8.5 kilobase fragment was seen in all cases except for the Ghanian case of black HPFH-2, in which no band was visible (Fig. 2). Thus, DNA corresponding to the region of the H fragment, in addition to δ- and β-globin gene DNA, is deleted in this case of black HPFH but not in the other.

To map the 5' end of the deletion in black HPFH-2, the enzyme *Xba*I was used. The *Xba*I-digested DNA of black HPFH-1 and Greek HPFH, when hybridized to γ-gene, probe, exhibited a band pattern similar to that of normal DNA (Fig. 3): a 3.7-kilobase band derived from the 5' end of $^G\gamma$ gene, a 5.2-kilobase fragment spanning the $^G\gamma$ and $^A\gamma$ genes and a 7.5-kilobase fragment derived from the 3' end of the $^A\gamma$ gene[1,2,9]. In *Xba*I-digested DNA of black HPFH-2, the 3.7- and 5.2-kilobase fragments are present as expected, but the 7.5-kilobase fragment is replaced by one of 15 kilobases (Fig. 3). Thus, the *Xba*I site present at the 3' end of the 7.5-kilobase fragment in normal DNA is missing in this case of HPFH. As this *Xba*I site lies approximately 1 kilobase to the 3' side of a *Bcl*I site

Fig. 1 Map of restriction endonuclease sites in and around the human non-α-globin genes in normal DNA and DNA from three different individuals with HPFH. The solid bars represent the coding sequences of the different non-α-globin genes, each interrupted by a large intervening sequence of non-coding DNA. The cross-hatched bars represent DNA to the 3' side of the deleted segments of DNA in HPFH DNA; the open portion of the bars indicates the region of uncertainty in the precise 5' end points of the deletions. Normal DNA was from the placenta of a black infant; black HPFH-1, DNA of a lymphoblastoid cell line derived from an American black with homozygous HPFH[13]; black HPFH-2, DNA of a lymphoblastoid cell line (GM2064) derived from a Ghanaian with homozygous HPFH[3,14]; Greek HPFH, DNA of a lymphoblastoid cell line (GM2232) from a Greek HPFH heterozygote (case III-1 of family B in ref. 15). The experimental evidence for the assignment of the various restriction endonuclease sites around the γ-globin genes in normal DNA has been detailed elsewhere[1,2,8,9]. The bracket indicates the position in normal DNA of H fragment DNA of clone HβGl (ref. 11) that was used as a probe in some of the mapping experiments. Abbreviations: Bg, *Bgl*II; Bc, *Bcl*I; X, *Xba*I; B, *Bam*HI; kb, kilobases.

that is present in both normal and HPFH-2 DNA, the deletion in black HPFH-2 must start somewhere between this *Bcl*I site and the *Xba*I site to its 3′ side. Comparing the 5′ ends of the deletions in the two types of HPFH, an additional 5 kilobases of DNA is deleted in black HPFH-2 compared with black HPFH-1 (Fig. 1).

To examine whether the 3′ endpoints of the deletions in the two cases of black HPFH also differed, the enzyme *Bam*HI was used. *Bam*HI cleaves normal DNA to generate an 18-kilobase fragment which spans the $^A\gamma$ and δ genes and that hybridizes to both γ- and δ-gene probes[1,2,8,9]. *Bam*HI-digested DNA of black HPFH-1 exhibits, instead, a 14-kilobase fragment (Fig. 4 and refs 1, 2) which hybridizes to γ-gene probe but not δ-gene probe (because the δ gene has been deleted). If the 3′ endpoints of the deletions in both cases of black HPFH are the same, *Bam*HI digestion of HPFH-2 should produce a fragment 5 kilobases shorter than 14 kilobases. However, instead of a 9-kilobase fragment, a 16-kilobase fragment is generated in HPFH-2 (Fig. 4). This indicates that not only the 5′ endpoints of the deletions in HPFH-1 and HPFH-2 are different but that their 3′ endpoints also are different. The precise location of the 3′ endpoints of the deletions cannot be mapped in relation to the DNA flanking the 3′ extremity of the normal β-globin gene because of lack of appropriate probes for this region.

The above analyses demonstrate that at least two types of extensive DNA deletions differing in both their 5′ and 3′ endpoints are associated with the common $^G\gamma + {}^A\gamma$ variety of HPFH that occurs in blacks. The deletion (HPFH-1) with the lesser amount of deleted inter-γ-δ DNA has been previously reported[1,2]. The possible significance of this deletion with respect to the presence of putative γ-gene control elements situated between the γ- and δ-globin genes has also been discussed in relation to the different types of deletions detected in $\delta\beta$-thalassaemia in which the γ-globin genes are not as maximally or uniformly expressed as in HPFH[1-5,12]. The deletion of an additional 5 kilobases of inter-γ-δ-gene DNA in HPFH-2 over HPFH-1 had no significant effect on the HPFH phenotype. Despite the presence of two different types of HPFH deletion in blacks, it is remarkable that the three black phenotypic homozygotes who have thus far been studied are truly homozygous for one HPFH genotype or the other, and that neither is

γ probe   H probe   δ + β probe

Fig. 4 Digestion of normal and HPFH DNAs with restriction endonuclease *Bam*HI. Experimental procedure, probes and abbreviations are the same as in Fig. 2. The $\delta + \beta$ probe was a mixture of Hδ1 and Hβ1, *Pst*I subclones of HβGI (ref. 11). The dots in the γ probe experiment indicate the positions of the faint 18-, 16- and 14-kilobase bands.

doubly heterozygous for both genotypes. This finding suggests some initial geographical or regional segregation of the two different mutations, with little subsequent mixing of the two different gene pools.

In the Greek $^A\gamma$ type of HPFH, no DNA deletion was detected; the putative γ-gene regulatory sequences in the inter-γ-δ DNA are therefore present. It is thus likely that the phenotype of Greek type HPFH is the result of a different molecular mechanism, such as a small DNA deletion or a base mutation in the $^G\gamma$-$^A\gamma$ gene region which has escaped detection by the techniques used in the present study.

γ probe

Fig. 3 Digestion of normal and HPFH DNAs with restriction endonuclease *Xba*I. Experimental procedure, γ-cDNA probe and abbreviations are the same as in Fig. 2.

1. Fritsch, E. F., Lawn, R. M. & Maniatis, T. *Nature* **279**, 598–603 (1979).
2. Tuan, D., Biro, P. A., deRiel, J. K., Lazarus, H. & Forget, B. G. *Nucleic Acids Res.* **6**, 2519–2544 (1979).
3. Mears, J. G. *et al. Proc. nam. Acad. Sci. U.S.A.* **75**, 1222–1226 (1978).
4. Ottolenghi, S. *et al. Nature* **278**, 654–657 (1979).
5. Bernards, R., Kooter, J. M. & Flavell, R. A. *Gene* **6**, 265–280 (1979).
6. Huisman, T. H. J. *et al. Ann. N.Y. Acad. Sci.* **232**, 107–124 (1974).
7. Huisman, T. H. J. *et al. J. clin. Invest.* **49**, 1035–1040 (1970).
8. Bernards, R., Little, P. F. R., Annison, G., Williamson, R. & Flavell, R. A. *Proc. natn. Acad. Sci. U.S.A.* **76**, 4827–4831 (1979).
9. Little, P. F. R., Flavell, R. A., Kooter, J. M., Annison, G. & Williamson, R. *Nature* **278**, 227–231 (1979).
10. Clegg, J. B. *et al. Br. J. Haemat.* **43**, 521–536 (1979).
11. Lawn, R. M., Fritsch, E. F., Parker, R. C., Blake, G. & Maniatis, T. *Cell* **15**, 1157–1174 (1978).
12. Orkin, S. H., Alter, B. P. & Altay, C. *J. clin. Invest.* **64**, 866–869 (1979).
13. Forget, B. G. *et al. Cell* **7**, 323–329 (1976).
14. Ringelhann, B. *et al. Acta haemat.* **43**, 100–110 (1970).
15. Fessas, P. & Stamatoyannopoulos, G. *Blood* **24**, 223–240 (1964).
16. Southern, E. M. *J. molec. Biol.* **98**, 503–517 (1975).
17. Wahl, G. M., Stern, M. & Stark, G. R. *Proc. natn. Acad. Sci. U.S.A.* **76**, 3683–3687 (1979).
18. Wilson, J. T. *et al. Nucleic Acids Res.* **5**, 563–581 (1978).
19. Poon, R. P., Kan, Y. W. & Boyer, H. W. *Nucleic Acids Res.* **5**, 4625–4630 (1978).

Red cell sodium fluxes catalysed by the sodium pump in the absence of K⁺ and ADP

Kenneth H. Lee

Department of Biochemistry, McGill University, Montreal, Quebec, Canada H3A 2T5

Rhoda Blostein*

Division of Hematology, Department of Medicine, Royal Victoria Hospital, 687 Pine Avenue West, Montreal, Quebec, Canada H3A 1A1

In the absence of extracellular Na⁺ or K⁺, the sodium pump catalyses an ouabain-sensitive 'uncoupled' Na⁺ efflux[1-4]. With red cell ghosts Glynn and Karlish[5] showed that this Na⁺ efflux is accompanied by ATP hydrolysis and that extracellular sodium ions, at low concentrations, inhibit this efflux as well as the associated ATP hydrolysis. At higher concentrations, extracellular sodium ions restore the hydrolysis of ATP[3,6] but it is not known whether there is an associated increase in Na⁺ efflux and, perhaps, an influx. To answer this question we have used inside-out red cell membrane vesicles which are specially suitable for controlling the composition of the medium at the two membrane surfaces while measuring ²²Na⁺ fluxes in both directions. We report here that the sodium pump can operate in a mode in which influx and efflux of sodium are associated with ATP hydrolysis. This mode is different from the Na–Na exchange described by Garrahan and Glynn[7], and Glynn and Hoffman[8], which requires ADP as well as ATP[9] and is probably associated with ADP–ATP exchange rather than ATP hydrolysis[10,11].

For these experiments, we used inside-out membrane vesicles of human red cells and measured ATP-dependent ²²Na⁺ uptake and loss as described earlier[12] and detailed in Table 1. ATP-dependent ²²Na⁺ uptake was estimated from the increase in radioactivity retained in the vesicles after Millipore filtration; ATP-dependent loss of ²²Na⁺ was measured by the radioactivity appearing in the supernatant following removal of the vesicles by centrifugation, as it was not feasible to measure the decrease in vesicular ²²Na⁺ because the percentage loss was too small. Preliminary tests ascertained that the time intervals used (≤5 min for uptake and ≤15 min for loss) were sufficiently short that initial rates or near initial rates were being estimated.

We tested whether, in the absence of extracellular K⁺ and without added ADP, an increase in extracellular Na⁺ concentration is associated not only with inhibition of efflux at low extracellular Na⁺ as described above, but also stimulation of efflux at higher extracellular Na⁺ and whether this stimulation is associated with Na⁺ influx. The results show (1) both inhibition and stimulation of efflux at low and high extracellular Na⁺, respectively; (2) Na⁺ influx associated with the stimulated efflux; and (3) that these fluxes are paralleled by a decrease followed by an increase in the turnover of the phosphoenzyme intermediate of Na⁺-ATPase as the extracellular Na⁺ is increased from zero to about 50 mM.

Because the vesicles are inside-out, the terms uptake and loss are opposite to those normally used, that is uptake and loss in vesicles are equivalent to the normal efflux and influx, respectively, in cells. Similarly, intravesicular Na⁺ is equivalent to Na⁺ normally at the extracellular surface and is designated Na$_{ext}$; extravesicular Na⁺ is Na⁺ at the cytoplasmic surface and is designated Na$_{cyt}$.

The results given in Table 1 show that ATP-dependent 'uncoupled' Na⁺ uptake (equivalent to normal efflux) is inhibited by a relatively low concentration of Na$_{ext}$ (~5 mM) confirming the findings of others[1,4]. This Na⁺ flux is then increased at higher (~50 mM) Na$_{ext}$. The results show that the

increased uptake is associated with an ATP-dependent loss of ²²Na⁺ from ²²Na⁺-loaded vesicles. A quantitative comparison of uptake and loss, even when measured concurrently, has not been attempted as it has not been technically feasible to measure both fluxes by the same method (see above). Although highly reproducible results were obtained for both, uptake values probably tended to be somewhat underestimated; this may be due to the removal of a portion of ²²Na⁺ from a competent but more leaky compartment, during washing of the vesicles on the filters. As shown in Table 1, the ATP-dependent ²²Na⁺ influx and efflux occur with only micromolar levels of ATP and in the absence of added ADP. In other experiments (not shown) we have ascertained that these fluxes, in particular ²²Na⁺ efflux (equivalent to normal influx), do not require ADP as well as ATP. Thus with 4 μM ATP present, addition of ADP (5 μM) did not affect the ATP-dependent ²²Na⁺ efflux. Furthermore, ATP-dependent Na⁺ efflux is not decreased when either greater (fivefold greater) dilution of ²²Na⁺-loaded vesicles is used to reduce the concentration of ADP formed due to ATP hydrolysis to extremely low levels (≤0.1 μM at the end of the assay period, see Table 1 legend), or when creatine phosphate and creatine phosphokinase are included to regenerate ATP from ADP (not shown).

The results given in Table 2 show that ATP-dependent ²²Na⁺ loss (equivalent to normal influx) and uptake (equivalent to normal efflux) observed at relatively high Na$_{ext}$ (~50 mM) have properties consistent with the conclusion that these Na⁺ movements are manifestations of the activity of the ouabain-sensitive Na⁺ pump. Thus: (1) both are ATP-stimulated increases in unidirectional fluxes; (2) both are sensitive to inhibition by ouabain as intravesicular ouabain (equivalent to extracellular ouabain) inhibits both activities; and (3) ATP-dependent ²²Na⁺ loss (equivalent to normal influx) is absolutely
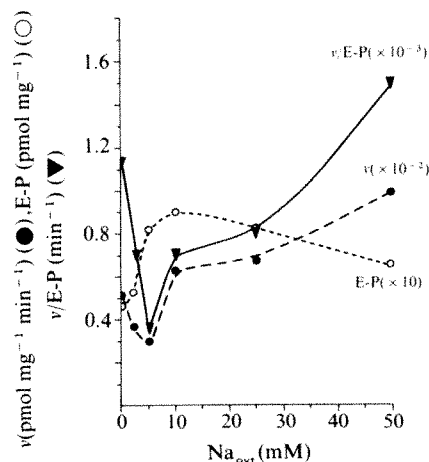
Fig. 1 Effect of Na$_{ext}$ on Na⁺-ATPase and on the steady-state level and apparent turnover of phosphoenzyme. Vesicles (2.4 mg protein ml⁻¹) were equilibrated by diluting them 1 : 1 with 100 mM KCl (baseline activity) or chloride salts of Na⁺ and choline to obtain the desired final concentration of Na$_{ext}$ as described in Table 1. The reaction was then started by adding 180 μl reaction medium containing [γ-³²P]ATP and various amounts of NaCl to 20 μl vesicles so that the final concentrations were: vesicle protein, 0.12 mg ml⁻¹, Na$_{cyt}$, 5 mM and [γ-³²P]ATP, 0.1 μM (27,000 c.p.m. pmol⁻¹). The reaction was terminated after 30 s with 2.3 ml 5% trichloroacetic acid containing 5 mM NaH₂PO₄ and 2.5 mM ATP. Aliquots (1.0ml) were taken for the measurement of ³²P$_i$ (Na⁺-ATPase, v) and 1.5 ml, for the measurement of E-³²P as described previously[12]. Values are means of triplicate determinations. The baseline values (71.4 pmol mg⁻¹ min⁻¹ for v and 0.085 pmol mg⁻¹ for E-³²P) obtained with KCl (Na⁺ omitted) were subtracted. Six similar experiments were carried out. The maximal amount of ADP formed due to ATP hydrolysis may be calculated from the maximal total activity observed (baseline plus activity at 50 mM Na$_{ext}$) as follows: (71.4+ 103.1) pmol mg⁻¹min⁻¹ × 0.12 mg ml⁻¹×0.5 min) = 10.47 pmol ml⁻¹.

Table 1 Effects of intravesicular Na^+ (Na_{ext}) on ATP-dependent Na^+ transport in the absence of ADP and K^+

Intravesicular Na^+ conc. mM Na_{ext}	^{22}Na uptake (Expt 70) (pmol min^{-1} mg^{-1})			^{22}Na loss (Expt 108) (pmol min^{-1} mg^{-1})		
	+ATP	−ATP	ATP-dependent uptake	+ATP	−ATP	ATP-dependent loss
0	868 ± 36	574 ± 30	294 ± 28	none	none	none
5	688 ± 24	516 ± 4	172 ± 14	443 ± 8	405 ± 6	38 ± 6
50	1,100 ± 38	604 ± 20	496 ± 24	7,040 ± 86	6,053 ± 96	987 ± 74

Inside-out vesicles (~ 5.5 mg protein ml^{-1}) suspended in 40 mM Tris glycylglycine, *p*H 7.4, containing 0.1 mM $MgCl_2$ were loaded by diluting 1 : 1 with 2 mM $MgCl_2$ containing 100 mM chloride salts of choline chloride and NaCl to obtain the desired concentrations (0, 5 or 50 mM Na^+). For measurements of $^{22}Na^+$ loss, $^{22}NaCl$ was included (3,385 c.p.m. μl^{-1} suspension). Equilibration was then carried out for 18 h at 0 °C followed by 30 min at 37 °C. For $^{22}Na^+$ uptake measurements, 20-μl vesicles (5.4 mg ml^{-1}) were added to 180 μl $^{22}Na^+$ medium (specific activity 558 c.p.m. nmol^{-1}) containing 5 mM NaCl with or without ATP (final concentration, 3.6 μM; Boehringer-Mannheim ATP, Na-form converted to Tris-form). After 5 min at 37 °C, $^{22}Na^+$ taken up was measured by Millipore filtration as described previously[12]. For $^{22}Na^+$ loss measurements, the $^{22}Na^+$-loaded vesicles were centrifuged at 10,000*g* for 10 min at 0 °C and the pellet was washed by resuspension and centrifugation three times in 10 ml ice-cold 5 mM NaCl in 45 mM choline chloride, 20 mM Tris-glycylglycine, *p*H 7.4, containing 1 mM $MgCl_2$ (solution A). The pellet was suspended in the same solution at the approximate original protein concentration and 10 μl (5.8 mg ml^{-1}) were then added to 90 μl solution A with and without 5.4 μM ATP. After 11 min at 37 °C, 90-μl aliquots were removed and added to 0.4 ml ice-cold solution A and within 2 min centrifuged for 10 min at 10,000*g*. Aliquots (0.4 ml) of the supernatant were taken for the determination of $^{22}Na^+$ radioactivity. Each value shown is the difference between two sets of quadruplicate determinations ±s.e.m., one without and one with ATP. The concentrations of extracellular Na^+ given are approximate, as after equilibration about 70–80% equilibration is actually achieved (other experiments, not shown). In similar experiments carried out at much higher dilution of vesicles (1/50 compared to 1/10) ATP-dependent $^{22}Na^+$ efflux was not decreased; at the higher dilution, the total ADP concentration was extremely low (0.06 μM at the end of the incubation as estimated by $^{32}P_i$ release from [γ-^{32}P]ATP).

Table 2 Some properties of ATP-dependent Na^+ transport in the absence of added ADP and K^+

	Properties tested	Addition	$^{22}Na^+$ uptake (pmol min^{-1} mg^{-1}) (ATP-dependent)	$^{22}Na^+$ loss (pmol min^{-1} mg^{-1}) (ATP-dependent)
Expt 72-3	Ouabain sensitivity	−Ouabain (control)	984 ± 17	1,391 ± 300
		+Ouabain (50 μM intravesicular)	27 ± 20	255 ± 150
Expt 106	Dependence on Na_{cyt}	−Na_{cyt}	—	38 ± 150
		+Na_{cyt}	—	1,004 ± 145

Ouabain-containing vesicles were prepared by including 50 μM ouabain during the vesiculation process. Both the control and ouabain vesicles were loaded with 25 mM NaCl and assays were performed as described in Table 1. Na_{cyt} (5 mM) was either included or omitted as indicated. The ATP concentrations were 100 μM and 6 μM and the final protein concentrations, 0.45 mg ml^{-1} and 0.65 mg ml^{-1} in experiments 72-3 and 106, respectively.

dependent on the presence of Na^+ at the opposite side of the membrane, that is, cytoplasmic Na^+. Other experiments (not shown) at varying concentrations of Na_{cyt} showed that ATP-dependent $^{22}Na^+$ loss was close to maximal with 5 mM Na_{cyt}. With ATP present (100 μM) we have detected stimulation of both $^{22}Na^+$ uptake and loss by addition of ADP, but only at ADP concentration $\geqslant 50$ μM (three experiments, not shown). This is, presumably, the Na–Na exchange associated with ADP–ATP exchange.

To gain insight to the mechanism of the effects of extracellular Na^+ on Na^+ influx at low levels of ATP, we followed the apparent turnover of the phosphoenzyme intermediate of Na^+-ATPase. For this purpose we measured the rate of Na^+-ATPase, *v*, and the steady-state level of phosphoenzyme, [E-^{32}P], using low concentrations (0.1 μM) of [γ-^{32}P]ATP as described earlier[13], to minimize nonspecific labelling. The apparent turnover of E-^{32}P was calculated as the ratio *v*/E-^{32}P. In agreement with Glynn and Karlish who used resealed red cell ghosts[3], Na^+-ATPase decreased as Na_{ext} increased from zero to about 5 mM and then increased as extracellular Na^+ was increased further to $\sim$ 50 mM (Fig. 1).

Although the decrease in hydrolytic activity was often small or not always apparent (other experiments, not shown), dramatic changes in the apparent turnover of E-^{32}P were always observed (Fig. 1). The decrease in turnover at low extracellular Na^+, from 1,143 min^{-1} to 367 min^{-1}, confirms a similar observation by Beaugé and Glynn[11] using a purified kidney preparation. They observed that Na^+, at low concentrations, slowed the rate of phosphoenzyme breakdown and suggested that this effect is at inhibitory extracellular sites. Previous studies in our laboratory[12] have shown that cytoplasmic Na^+ catalyses the phosphorylation of the enzyme; the present finding that the apparent turnover of the phosphoenzyme is increased at relatively high concentrations of Na_{ext} is consistent with the idea that, in the

same conditions, extracellular Na^+ at high concentration stimulates the rate of dephosphorylation.

From this study, we conclude that in the presence of ATP at low concentration but absence of K^+ and added ADP, extracellular Na^+ at high concentrations is transported to the cytoplasmic compartment in exchange for cytoplasmic Na^+, in a manner analogous to the exchange of K_{ext} for Na_{cyt} in normal conditions. Thus Na_{ext} at high concentrations stimulated dephosphorylation of the phosphoenzyme intermediate presumably in the reaction $E_2\text{-}P + Na_{ext} \rightarrow Na \cdot E_2 + P_i$; the resulting enzyme–Na complex may then undergo a conformational change, $Na \cdot E_2 \rightarrow Na \cdot E_1$ (compare $K \cdot E_2 \rightarrow K \cdot E_1$) before the release of Na^+ at the cytoplasmic side of the membrane. Note that in other experiments (not shown) we observed that ammonium ions, which are considered to be congeners of K^+, stimulate ATP-dependent Na^+ uptake (equivalent to normal efflux) but inhibit the loss (equivalent to normal influx) consistent with the idea that they compete for extracellular Na^+ acting at the K^+ sites involved in dephosphorylation.

1. Garrahan, P. J. & Glynn, I. M. *J. Physiol., Lond.* **192**, 159–174 (1967).
2. Garrahan, P. J. & Glynn, I. M. *J. Physiol., Lond.* **192**, 175–188 (1967).
3. Glynn, I. M. *et al. Ann. N.Y. Acad. Sci.* **242**, 357–371 (1974).
4. Lew, V. L., Hardy, M. A. & Ellory, J. C. *Biochim. biophys. Acta* **323**, 251–266 (1973).
5. Glynn, I. M. & Karlish, S. J. D. *J. Physiol., Lond.* **256**, 465–496 (1976).
6. Beaugé, L. A. & Campillo, E. D. *Biochim. biophys. Acta* **433** 547–554 (1976).
7. Garrahan, P. J. & Glynn, I. M. *J. Physiol., Lond.* **192**, 189–210 (1967).
8. Glynn, I. M. & Hoffman, J. F. *J. Physiol., Lond.* **218**, 239–256 (1971).
9. Cavieres, J. D. & Glynn, I. M. *J. Physiol., Lond.* **263**, 214–215 (1976).
10. Blostein, R. *J. biol. Chem.* **245**, 270–275 (1970).
11. Beaugé, L. A. & Glynn, I. M. *J. Physiol., Lond.* **289**, 17–31 (1979).
12. Blostein, R. *J. biol. Chem.* **254**, 6673–6677 (1979).
13. Blostein, R. & Chu, L. *J. biol. Chem.* **252**, 3035–3043 (1977).

Evidence for mutation in an *I–A* gene

Ted H. Hansen*‡, Roger W. Melvold†§, J. Scott Arn*
& David H. Sachs*

* Transplantation Biology Section, Immunology Branch, DCBD, National Cancer Institute, NIH, Bethesda, Maryland 20205
† Department of Radiation Therapy, Harvard Medical School and Shields Warren Radiation Laboratory, New England Deaconess Hospital, 50 Binney Street, Boston, Massachusetts 02115
Present addresses: ‡Department of Immunology, Merck Sharp and Dohme Research Laboratories, Rahway, New Jersey 07065; §Medical Oncology Section, Northwestern University Cancer Center, Chicago Illinois 60611

Mutant mouse strains are important tools for immunogenetic studies of the regulation, structure and function of major histocompatibility (H–2) antigens[1–3]. Several inbred strains have been established which carry *H–2*-linked mutations that cause changes in cell surface antigens as recognized by cytotoxic T cells and sometimes antibodies. Using intra-*H–2* recombinant haplotypes in skin graft complementation studies, lesions in several of these mutant strains have been genetically mapped to genes encoded in the K- or D-end of the H–2 complex[3]. More precise mapping has often not been possible as many of the available mutant strains possessed lesions in the K-end of the *H–2*[b] haplotype and a recombinant separating the K^b and *I–A*[b] regions was not previously available. The genetic locations of the lesions in some of these mutant strains could therefore only be inferred when a serological and/or structural alteration was detected (see refs 1, 2). We describe here the use of a newly established recombinant strain, B10.MBR (ref. 4), for skin graft complementation studies to map K-end mutations. These studies provide the first genetic evidence that the B6.C-H-2[bm12] mutation involves an *I–A*[b] gene and also confirm that the lesions in two other mutants can be mapped to a gene in the K^b region.

The newly discovered inbred, congeneic strain B10.MBR carries the recombinant haplotype $H-2^{bq1}$ which juxtaposes K^b and *I–A*[k] genetic markers (see ref. 4 and Table 1). Using B10.MBR mice, skin graft complementation studies were undertaken to map the mutations previously shown to involve the K^b and/or *I–A*[b] genes. Three representative mutant strains were selected for this study, B6.C-H-2[bm1], B6-H-2[bm5] and B6.C-H-2[bm12]. The first two mutations are part of an extensive allelic series of mutations (more than 15) which have been mapped into the K to *I–A* interval[5–7]. The H-2[bm12] mutation, while mapping also in K and/or *I–A*, is genetically complementary to the aforementioned allelic series, and was therefore presumed to involve a distinct second locus[3,10].

F₁ hybrids were produced by crossing mice of each of these mutant strains with B10.MBR mice. These hybrid mice then received skin grafts from B10 donors of the same sex as the recipients. As B10.MBR mice are congeneic with B10 mice, only differences associated with *H–2* should be detected in this test system. If the lesion in the mutant haplotype being tested were restricted to a gene within the K^b region, then the hybrid should not reject the skin graft since B10.MBR provides K^b antigens in the recipient. However, if the lesion in the mutant
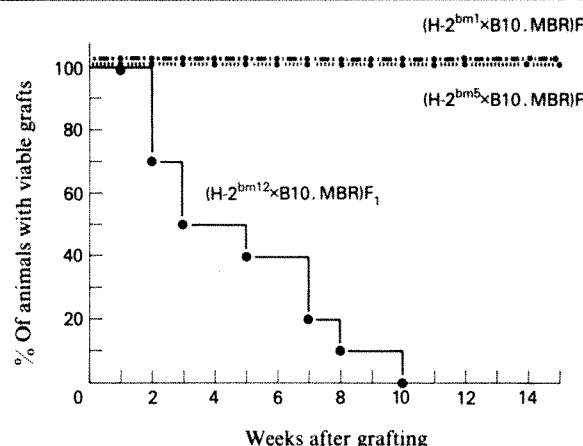
Fig. 1 Skin graft complementation study which maps the lesions in the H-2[mb1] H-2[bm5] and H-2[bm12] mutant haplotypes. Full thickness C5BL/10 tail skin grafts were trimmed to an approximate 0.5 × 1.0 cm size. Appropriately sized graft beds were prepared on the recipients' dorsal thorax by carefully removing skin with scissors without disturbing the panniculus carnosus. Five (H-2[bm1] × B10.MBR)F₁, five (H-2[bm5] × B10.MBR)F₁ and ten (H-2[bm12] × B10.MBR)F₁ hybrid mice were skin grafted in this study. All recipients were males except for two in the last category (these females had rejection times of 2 and 3 weeks). The transplanted tissues were protected with a gauze dressing and a plaster bandage for 7 days. Grafts were scored as rejected when less than 10% of the donor tissue was viable by gross inspection.

being tested involved a gene to the right of the K 4region, then the B10 skin graft would be rejected, as B10.MBR mice express H–2[k] or H–2[q] antigens in this interval.

The results of the skin graft complementation test of the H–2[bm1] and H–2[bm5] mutant strains are shown in Fig. 1. As indicated, the B10 skin grafts were not rejected by either the (H–2[bm1] × B10.MBR)F₁ or the (H–2[bm5] × B10.MBR)F₁ hybrid mice. These results provide definitive genetic evidence that the mutations in both of these strains occurred in a gene in the K^b region. In reference to the H–2[bm1] haplotype (formerly referred to as Hz–1 and H–2[ba]) the mapping to the K^b region substantiates serological[7,9] and structural[10] findings that the H–2K[b] gene product in this mutant is different from the wild-type, K[b] antigen. In addition to H–2[bm1] and H–2[bm5], several other mutant strains are members of the same complementation group. Therefore, it is reasonable to infer that all members of this allelic series have mutations in a single gene located within the K region, presumably the H–2K[b] locus which encodes a classical transplantation antigen.

In contrast to the findings with H–2[bm1] and H–2[bm5] mutations, the (H-2[bm12] × B10.MBR) F₁ mice rejected B10 skin grafts (Fig. 1). This failure of the B10.MBR antigens to complement the H–2[bm12] lesion indicated that this mutation involves a gene which maps to the right of the K^b region. Studies reported elsewhere determined that the lesion in the H–2[bm12] haplotype mapped to the left of the *I–B* region (see Table 1). Taken together with the finding reported here, it can be concluded that the H–2[bm12] mutation involves an *I–A*[b] encoded molecule. Also this *I–A*[b] encoded molecule can serve as a transplantation antigen.

Table 1 Summary of skin graft complementation data which map the lesions in the B6.C-*H–2*[bm1] and B6.C-*H–2*[bm12] strains

Donor	Recipient (mutant × recombinant)	*H—2* haplotype of recombinant strain							Fate of grafts	Conclusion regarding mapping of the mutations	Ref.
		K	A	B	J	E	C	S	D		
B10	B6.C-*H–2*[bm12] × B10.A(4R)	k	k	b	b	b	b	b	b	Rejection	Maps to the left of *I–B*[b]	8
B10	B6.C-*H–2*[bm1] × B10.A(4R)	k	k	b	b	b	b	b	b	Rejection	Maps to the left of *I–B*[b]	6
B6	B6.C-*H–2*[bm12] × D2.GD	d	d	b	b	b	b	b	b	Rejection	Maps to the left of *I–B*[b]	8
B6	B6.C-*H–2*[bm1] × D2.GD	d	d	b	b	b	b	b	b	Rejection	Maps to the left of *I–B*[b]	6
B10	B6.C-*H–2*[bm12] × B10.MBR	b	k	k	k	k	k	k	q	Rejection	Maps to *I–A*[b]	This paper
B10	B6.C-*H–2*[bm1] × B10.MBR	b	k	k	k	k	k	k	q	Survival	Maps to K^b	This paper

As this is the first mutation shown to be in an I-region encoded histocompatibility antigen, it will facilitate several functional, structural and regulatory studies of this class of cell-surface molecules. Assuming that H-2^{bm12} is a simple mutation (that is, a single affected gene) studies using this mutant strain may elucidate the relationship between I-region encoded histocompatibility antigens and the serologically detected Ia antigens. Serological studies have determined that H-2^{bm12} cells express Ia antigens distinct from those found on wild-type, H-2^b cells (ref. 8 and T.H. et al., in preparation). Functional studies of this I-region mutant are in progress to determine whether Ia antigens, Ir gene products and I-region mixed lymphocyte reaction determinants are all different manifestations of the same cell-surface antigen.

1. Klein, J. Adv. Immun. 26, 56–146 (1978).
2. McKenzie, I. F. C., Pang, T. & Blanden, R. V. Immun. Rev. 35, 181–230 (1977).
3. Kohn, H. I. et al. Immunogenetics 7, 279–294 (1978).
4. Sachs, D. H., Arn, J. S. & Hansen, T. H., J. Immun. 123, 1965–1969 (1979).
5. Bailey, D. W., Snell, G. D. & Cherry, M. in Proc. Symp. Immunogenetics of the H-2 System, 155–162 (Karger, Basle, 1971).
6. McKenzie, I. F. C., Morgan, G. M., Melvold, R. W. & Kohn, H. I. Immunogenetics 3, 241–251 (1976).
7. Apt, A. S. et al. Immunogenetics 1, 444–451 (1975).
8. McKenzie, I. F. C. et al. J. exp. Med. (in the press).
9. Klein, J., Hauptfeld, M. & Hauptfeld, V. J. exp. Med. 140, 1127–1131 (1974).
10. Brown, J. L. & Nathenson, S. G. J. Immun. 118, 98–102 (1977).

Natural killer cells mediate lysis of embryonal carcinoma cells lacking MHC

Peter Stern, Magnus Gidlund, Anders Örn & Hans Wigzell

Department of Immunology, BMC, Box 582, Uppsala University, 75123 Uppsala, Sweden

Mouse teratocarcinomas are tumours of the germ cells[1] whose tumorigenicity is a property of a pluripotent stem cell type denoted the embryonal carcinoma (EC) cell. These cells seem to be analogous to cells of the early mouse embryo and will indeed contribute to the normal development of a mouse if injected into blastocysts[2]. EC cells display an unusual transplantation behaviour and can frequently be grafted, giving tumours in several different mouse strains[3]. Thus, the protective immune mechanisms against such tumours may be less efficient than, and/or of a different nature from, those against most other tissues. Cytolytic T cells generally fail to kill EC cells[4-6], although there is one report of the apparent induction of specific anti-EC T-killer cells[7]. The failures[4-6] are easily explained as being due to the absence of major histocompatibility complex (MHC) products on the surface of ECs[3,8]. Recently, however, a new cell type, the natural killer (NK) cell, has been shown to have potent lytic activity when tested against several tumour targets[9-11]. Targets of NK cells also include normal thymocytes[12] and certain stem cells of the bone marrow[13]. As NK cells seem to display a select but distinct specificity pattern from T lymphocytes and because NK targets include normal cells at an 'immature' stage of differentiation, we considered it possible that NK cells provide an alternative to T cells in producing cell-mediated immune reactions against teratocarcinomas. Here we report that murine NK cells are highly efficient cytolytic aggressors to EC cells whereas more differentiated cell lines derived from the latter are less susceptible or completely resistant.

Figure 1 illustrates that embryonal carcinoma cells are quite susceptible targets for normal spleen cells in short-term lytic assays; for example, the EC line Nulli-SCC.1 is almost as susceptible as the 'classical' NK target, YAC, a Moloney virus-induced lymphoma[14]. However, more differentiated endodermal lines derived from ECs were significantly more resistant to this lysis or even refractory, despite the fact that spleen cells from tilorone-treated mice were used as effector cells. This

Table 1 NK nature of effector cells lysing EC cells (Nulli-SCC.1 or PC 13) or YAC cells

Treatment	Target	Effector: target ratio			
		100:1	50:1	25:1	12.5:1
Control		21.0	11.1	5.7	4.5
Nylon wool		34.2	25.3	17.3	12.6
Complement (C)	YAC	26.7	16.7	10.2	5.3
Anti-Thy. 1+C		27.9	19.3	13.2	5.9
Anti-asialo-GM$_1$+C'		3.2	1.4	0.8	0.2
Control		12.2	7.2	6.5	7.0
Nylon wool		21.0	16.2	11.7	8.6
Complement (C)	Nulli	16.8	10.2	7.5	5.1
Anti-Thy.'1 C'		15.7	9.5	6.4	6.7
Anti-asialo-GM$_1$		1.0	2.3	0.6	0.5
Control		17.1	13.9	8.1	6.9
Nylon wool		18.2	15.7	11.4	8.8
Complement (C)	PC13	14.1	10.2	6.1	3.2
Anti-Thy. 1+C'		16.8	10.1	6.7	6.7
Anti-asialo-GM$_1$+C'		3.2	2.7	2.9	2.7

Effector cells were normal spleen cells from 3-month-old CBA/H mice. The cells were treated as defined previously[16,21]. Fresh guinea pig serum absorbed with agarose served as C source.

treatment, by a mechanism involving interferon, greatly enhances the lytic ability of NK cells[15]. Two additional EC lines (PSMB and OC15S1) were also studied and found to be highly sensitive to the lytic action of normal spleen cells (data not shown). Figure 2 confirms that the lysis of the EC cells is effected by NK cells. It is well established that NK levels are under genetic control, yielding 'high' and 'low' NK strains[10]. The ability
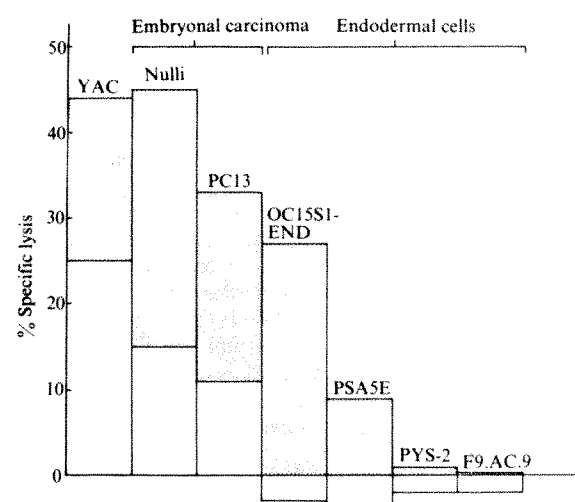
Fig. 1 NK lysis of YAC or various teratocarcinoma-derived cell lines using CBA/H spleen cells at an effector to target ratio of 100:1. Tilorone treatment and the 4-h ^{51}Cr-release assay were done as described previously[11]. The teratocarcinoma lines are as follows: PMSB is a pluripotent EC line and was grown as previously described where the stem cells do not differentiate and do not express H-2 antigens[8]. Nulli-SCC.1 is a line of homogeneous ECs which do not differentiate in vivo or in vitro and do not express H-2 (ref. 8). PC13 is a pluripotent EC line which remains undifferentiated when grown at high density in vitro; it will differentiate to endodermal cells in the presence of retinoic acid[20]. OCC15S1, when subcultured at high density daily, maintains an EC phenotype[20]; OCC15S1-END cells were obtained as the result of growth of the line at low density and there were only about 1% EC cells using anti-Forssman monoclonal antibodies in immunofluorescence tests[22]. The other EC lines were, by this criterion, as well as morphologically, homogeneous. The EC lines were routinely checked for H-2 and Ia determinants using specific antisera raised in congeneic mice in a ^{125}I-protein A test[23]. These cells do not express MHC products of the 129Sv(H-2^b) strain from which they are derived. The endodermal lines are all derivatives of 129 strain teratocarcinomas. PYS-2 is a parietal yolk sac carcinoma[24], PSA5E is an endodermal line derived from embryoid bodies grown in vitro[25], F9.AC.9 is cloned endoderm derived by retinoic acid treatment of F9 EC (ref. 26). Target cells were all grown in Dulbecco's modified Eagle's medium with 10% fetal calf serum (FCS) except YAC (Moloney lymphoma, A/Sn(H-2^a) which was kept in RPMI-1640, 10% FCS. Teratocarcinoma cells were prepared as targets by brief trypsinization at 0.1% in EDTA-phosphate-buffered saline (PBS). Specific lysis in % = (c.p.m. in test – c.p.m. in medium control)/(c.p.m. in detergent – c.p.m. in medium control) × 100. Spontaneous release was never above 20% and there was less than 5% variation in triplicates. Open blocks denote lysis as caused using normal spleen cells whereas shaded areas indicate the increment in lysis obtained using spleen cells from tilorone-treated mice.

of normal spleen cells to lyse the EC cells has the typical genetic profile of NK cells against YAC cells. The relative activities of the same panel of effector cells against the other EC cell lines are consistent with these results. In contrast, the differentiated endodermal cells (for example, PYS-2, Fig. 2) are resistant to lysis by the same effector cells.

Any analysis of claimed NK activity must exclude the role of other potential effector cells. Table 1 shows fractionation experiments attempting to eliminate in a selective manner adherent cells, B and T lymphocytes or NK cells. Removal of macrophages and B cells using nylon wool columns resulted in an increased lytic activity of the remaining cells against the EC targets. Similarly, treatment of the effector cells using anti-Thy.1 antibodies and complement (C) failed to eliminate the killer cells for EC targets. Also, spleen cells from nude mice (devoid of T cells) were highly active against EC targets (data not shown), thus further excluding T lymphocytes as the effector cells involved. Finally, anti-asialoganglioside M_1 (GM_1) antisera in the presence of C (a procedure selective for NK cells[16]) abolished the lytic ability of the anti-EC effectors. This implicates in a positive manner murine NK cells as the major effector cells against the embryonal carcinoma cells. We thus conclude that mouse natural killer cells can efficiently kill murine EC cells (PSMB, OC15S1, Nulli-SCC.1 and PC13) whereas differentiated endodermal lines are either less sensitive (OC15S1-END, PSA5E) or completely resistant (PYS-2, F9.AC.9).

The precise specificity of NK cells is unknown and there is disagreement as to their heterogeneity[10]. As teratocarcinoma cells grow as well attached monolayers *in vitro*, they can be used as possible absorbents for the NK effector cells. Figure 3 depicts two separate experiments demonstrating the ability of EC cells (the NK-susceptible targets) to remove NK activity for YAC as well as for EC targets. In contrast, the NK-resistant endodermal cells failed to remove NK cells in any significant manner. The observed effects cannot be explained by detached tumour cells in the effector populations, as less than 0.1% of the unattached spleen cells could have been tumour cells as defined by light microscopy. Thus, a sizeable proportion of NK cells with lytic ability for YAC lymphoma cells must also express binding properties to EC but not endodermal cell lines. Use of this monolayer procedure may now allow an analysis of possible murine NK subgroup heterogeneity in the same manner as previously shown to be so productive in analysis of specific killer T lymphocytes[17].

As stated above, cytotoxic T cells seem under most circumstances to be unable to kill embryonal carcinoma cells using normal chemically or virally modified cells[4-6]. There is one report of apparent T-cell killing of murine teratocarcinoma cells[7], but we have been unable to obtain any significant immunity of T-cell type against the presently tested EC cells (to be published). In contrast, they can be seen by lytic NK cells in an efficient manner. Thus, we believe that EC cells, lacking MHC products,

are suitable targets for distinguishing NK- and T-cell killing. In this respect, we consider it likely that recent attempts to map immune response genes or transplantation loci providing relative *in vivo* resistance to transplanted teratocarcinomas with suggested linkage to H-2 (refs 18, 19) were, in fact, measuring regulatory genes for NK levels which exhibit a similar linkage[10].

In conclusion, teratocarcinoma-derived cells of the most primitive type, EC, have been found to be highly susceptible to murine NK cells whereas differentiated cell lines from the same tumours are markedly more resistant. Preliminary results show that if EC cells are induced to differentiate under the influence of retinoic acid[20] there is a parallel loss of NK sensitivity. Molecular analysis of this process may result in a more refined concept of why NK cells have a specificity pattern for certain malignant cells as well as groups of relatively immature normal cell types. One attractive possibility is that NK cells recognize embryonic structures which are lost on further differentiation, but reappear during malignant transformation.

1. Martin, G. R. *Cell* **5**, 229–243 (1975).
2. Mintz, B., Illmense, K. & Gearhart, J. D. in *Roche Symp. on Teratomas and Differentiation* (eds Sherman, M. & Solter, D.) 45 (Academic, New York, 1975).
3. Artzt, K. & Jacob, F. *Transplantation* **17**, 632–634 (1974).
4. Forman, J. & Vitetta, E. S. *Proc. natn. Acad. Sci. U.S.A.* **72**, 3661–3665 (1975).
5. Zinkernagel, R. M. & Oldstone, M. B. O. *Proc. natn. Acad. Sci. U.S.A.* **73**, 3666–3670 (1976).
6. Doherty, P. C., Solter, D. & Knowles, B. B. *Nature* **266**, 361–362 (1977).
7. Wagner, H., Starzinski-Powitz, A., Rollinghoff, M., Golstein, P. & Jakob, M. J. *J. exp. Med.* **147**, 251–264 (1978).
8. Stern, P., Martin, G. R. & Evans, M. J. *Cell* **6**, 455–465 (1975).
9. Herberman, R. B., Nunn, M. E., Holden, H. T. & Lavrin, D. H. *Int. J. Cancer* **16**, 230–239 (1975).
10. Kiessling, R. & Wigzell, H. *Immun. Rev.* **44**, 165–208 (1979).
11. Kiessling, R., Klein, E. & Wigzell, H. *Eur. J. Immun.* **5**, 112–117 (1975).
12. Hansson, M., Kiessling, R., Andersson, B., Kärre, K. & Roder, J. *Nature* **278**, 174–176 (1979).
13. Kiessling, R. *et al. Eur. J. Immun.* **7**, 655–660 (1977).
14. Herberman, R. B. & Holden, H. T. *Adv. Cancer Res.* **27**, 305–377 (1978).
15. Gidlund, M., Örn, A., Wigzell, H., Senik, A. & Gresser, I. *Nature* **273**, 759–761 (1978).
16. Kasai, M., Iwamori, M., Nagai, Y., Okumura, K. & Tada, T. *J. Immun.* (in the press).
17. Brondz, B. D. *Transplantn Rev.* **10**, 112–151 (1972).
18. Avner, P. R. *et al. Immunogenetics* **7**, 103–115 (1978).
19. Siegler, E. L., Tick, N., Teresky, A. K., Rosenstraus, M. & Levine, A. J. *Immunogenetics* **9**, 207–220 (1979).
20. Adamson, E. D., Gaunt, S. J. & Graham, C. F. *Cell* **17**, 469–476 (1979).
21. Kiessling, R. *et al. J. exp. Med.* **143**, 772–780 (1976).
22. Stern, P. L. *Cell* **14**, 775–783 (1978).
23. Welsh, K. I., Dorval, G. & Wigzell, H. *Nature* **254**, 67 (1975).
24. Lehman, J. M., Speers, W. C., Swartzendruber, D. E. & Pierce, G. B. *J. cell. Physiol.* **84**, 13–28 (1974).
25. Adamson, E. D., Evans, M. J. & Magrane. G. G. *Eur. J. Biochem.* **79**, 607–615 (1977).
26. Solter, D., Shevinsky, L. Knowles, B. B. & Strickland, S. *Devl Biol.* **70**, 515–521 (1979).

Fig. 3 Selective depletion of NK cells on NK-susceptible EC monolayers. Spleen cells from tilorone-treated mice were added at 3×10^7 cells per ml in 2 ml of RPMI-1640, 10 mM HEPES 5% FCS to 9-cm Petri dishes with no cells or with confluent monolayers of PYS-2 endodermal cells or PC13 or Nulli-SCC.1 EC cells. The cells were incubated at 37 °C in a CO_2 incubator for 45 min. The unattached cells were then recovered by pouring off the medium. Cell recovery was similar on all plates and in the range of 30%. Targets used were either YAC or Nulli-SCC.1 (*a*), or YAC or PC13 (*b*). *a*: ○, Nulli-SCC.1 monolayer-depleted effector cells; △, PYS-2 monolayer-depleted effectors; ×, normal Petri dish-depleted effectors. *b*, As for *a* except using PC13 monolayer-depleted effectors ●.

Fig. 2 Comparison of genetic distribution of NK levels as measured against the 'classical' NK target YAC and the distribution profile of lytic effector cells against EC cells (Nulli-SCC.1) and the insensitive endodermal line PYS-2. Effector : target ratio 100 : 1. With or without tilorone treatment of spleen cell donors as in Fig. 1.

BOOK REVIEWS

Evolution, theology and
the Victorian scientist

Stephen Jay Gould

UNFORTUNATELY, the important issue of evolution and its historical relation with theology has been badly distorted by the stereotype of crusading, modern hero versus pompous, superannuated windbag — Huxley and Wilberforce for the British, Darrow and Bryan for Americans. Yet anyone who has ever read the leading theological scientists — from Paley whom Darwin read with pleasure in his youth, to Sedgwick who taught him geology and later branded his great work as crass materialism, to Mivart whose critique inspired the only new chapter added to later editions of the *Origin* — knows full well that the actual debates could scarcely have been further from the image of bigoted Bible-thumping versus enlightened rationalism. For these men were not miracle mongers, asserting God's continuous intervention against the lawful regularities of science; they were not, despite Lyell's words, trying "to cut rather than patiently to untie the Gordian knot". To be sure, they found God manifest in His works (nature), but their tool was science, their commitment to regularity of law and 'knowability'.

Equally unfortunately, this striking discrepancy between stereotype and actuality has engendered the equally misleading myth that there never really was any conflict between science and religion, that the theme embodied in A. D. White's famous treatise, *A History of the Warfare of Science with Theology in Christendom,* is at worst a put-on, at best a *Scheinproblem.* It is the great merit of Gillespie's book that he steers the proper path between these fallacious readings and manages to explain so well how working scientists framed the issue of conflict between science and theology in Darwin's day.

Borrowing a phrase and concept from the most fashionable intellectual of the moment, the French philosopher Michel Foucault, Gillespie recasts the debate as a

Charles Darwin and the Problem of Creation. By Neal C. Gillespie. Pp.224. (University of Chicago Press: Chicago and London, 1979.) £11.55.

contrast between two "epistemes" or world views — creationism and positivism. (Foucault, like T. S. Kuhn, tends to view intellectual history as a set of rapid switches between contrasting world views, each sufficiently encompassing to form a system necessarily excluding its rivals.) Creationism and positivism do not represent religion versus science, but two styles of doing science. (Many positivists, including Darwin at one stage of his life, believed in a personal God who may once have made the world, but declined to muck about with it thereafter.) Positivists insisted upon a fully natural and knowable system of causes, based upon unaltered laws manifest in processes now acting on Earth. The positivist, Gillespie claims, "limited scientific knowledge, which he saw as the only valid form of knowledge, to the laws of nature and to processes involving 'secondary', or natural causes exclusively". Only this kind of knowledge could be called science; indeed, only this kind of knowledge could be called valid at all. Creationists believed that an understanding of nature would reveal the working of God's mind. "The creationist", Gillespie argues, "saw the world and everything in it as being the result of direct or indirect divine activity. His science was inseparable from his theology".

Ironically, the positivist creed triumphed largely because it limited the scope of legitimate questions that science could ask about nature. No ultimate meanings, cosmic purposes or universal designs. Yet, in eschewing such grand themes, positivism gained precision and knowability — its questions could be answered and its answers could win general agreement. The

issue was not science versus God, but the range of legitimate questions within science. (The nineteenth century, after all, was not an age of rampant atheism; few positivists doubted the existence of a personal God.) Positivism held that science could do less, but could answer with agreement and authority. The victory of positivism marked the triumph of fruitfulness over interminable wrangling about the unanswerable.

Thus, the pre-Darwinian creationists — the true 'scientific creationists', in contrast with the fundamentalist imposters now parading under that banner in the United States — did believe that each new species arose *ab nihilo,* but did not use this credo to argue for God against science, miracles against law, or caprice against uniformity. Instead, they searched for regularity in the pattern of creation, hoping to specify its laws, if not its mechanism. And they held an (admittedly vague) belief in the existence of some law-like mode by which the Creator might manufacture his products. Yet, despite the brave words, their actual programme of research held out no hope for specifying or understanding such laws; they bogged down in the unanswerable. The recognition of this dead-end helps to explain why so many creationists were willing to accept Darwin's argument (but to recast it in more congenial terms as the belief that evolution represented God's mode of ordaining the history of life). As Charles Lyell wrote: "It would be more natural to suppose an ass to give rise to a striped offspring with the other characters of a zebra than that a zebra should come into being out of nothing".

But if the creationist episteme entered Darwin's age via evolution as God's mode, then positivists like Darwin and Huxley could rightly ask what creationism had added to their inquiry beyond obfuscation. How did the statement that God worked via evolution help anyone to discover the

mechanisms and processes? In this sense, God had become Laplace's unnecessary hypothesis. Worse than that. Darwin's own mechanism of natural selection seemed so purposeless and heartless to creationists that they sought God's characteristic (anthropomorphic) mode of action in such putative phenomena as variation intrinsically directed towards improvement or saltational origin of fully adapted higher forms of life. These beliefs emasculated natural selection by stripping away its essence — its creative role in building new forms by accumulating small, random, favourable variants — and relegated it to the negative role of executioner for the unfit. Again, the remnants of the creationist episteme became the source of a debate *within* science: what role did natural selection play in the origin of species?

Theology did not only invest science in the form of a lingering creationist episteme. It also influenced the outlook of positivists as well. Darwin became an agnostic in his later life and never (as a positivist) allowed his personal God any direct role in the daily operation of the Universe. But the *Origin* is studded with Darwin's theology; how could any great nineteenth-century work fail to record its influence? Gillespie argues cogently, for example, that the principle of natural selection itself can be viewed, in part, as Darwin's solution to the theological problem of evil. Buckland, and other creationists, had argued that predation was God's gift to prey because it ended their life swiftly before the pain of decrepitude set in. Darwin could not believe that a humane God would work in such a manner, especially when he considered such lingering forms of death as the living, but paralysed, caterpillar devoured by the larvae of wasps. Nature had its cruelties because God played no direct role. Darwin's concern with the problem of evil is evident in what may be the most striking, literary line of the *Origin:*

> We behold the face of nature bright with gladness . . . We do not see, or we forget, that the birds which are idly singing round us mostly live on insects or seeds, and are thus constantly destroying life; or we forget how largely these songsters, or their eggs, or their nestlings, are destroyed by birds and beasts of prey.

Gillespie writes about these matters with commendable clarity and authority but without much verve. In many places, the book is little more than a series of quotations strung together with a minimum of connecting text — as if it had been compiled in the old style from index cards, one quote to the card and properly shuffled. One shouldn't condemn a colleague for excess of scholarly zeal, and a little learning may be a dangerous thing. But judicious selection larded with incisive commentary has its place as well, and *Parsifal* might have been even better an hour or two shorter.

More importantly, though I think that the conflict of epistemes is a better model for scientific change than old myths of inductive progress, I am not sure that it always serves Gillespie well. Although he admits that aspects of both epistemes can reside in single individuals, Gillespie does have a tendency to place scientists into one or the other camp. Creationists, pursuing old and unfruitful ways, therefore achieve the unconscious status of impeder. We assume, for example, that Mivart, whom Gillespie describes as dishonest or even odious (to Darwin at least), upheld old ways as a result of his theological bent. This may be an accurate description of his psychology — of his deeper motivation for attacking Darwinism in favour of quasi-theological, directed evolution. But his specific argument still has a logic that needs to be analysed in its own terms. Often, the logic is both cogent and potent. Mivart, for example, penned a brilliant (but forgotten) chapter on homology in *The Genesis of Species*. He argued that the development of serially homologous structures in single individuals obviously cannot be attributed to natural selection, but to "laws of growth". (The laws may be a product of selection, but this is a different matter.) He then claimed that homologous structures in related species often displayed the same morphological sequences as the serially homologous structures of a single individual. How then can homologies between species be attributed only to

natural selection acting upon plastic organic matter? Selection must be strongly constrained in its potential product by the same laws of growth that produce serial homologues in individuals.

Constraint of possible directions for evolutionary change by inherited patterns of development is just now emerging as an important theme in evolutionary biology; it also runs counter to the spirit of NeoDarwinian orthodoxy which exalted the power of selection and downgraded the constraints and consequences of development. Yet, if Mivart must bear the label of "creationist episteme", we may downgrade his message because we recognize its source.

As a scientist who also doubles as an amateur historian, I do appreciate the argument of historical colleagues that present status is an utterly inappropriate category for understanding past ideas, but I also believe that many rejected thinkers of the past appreciated great truths long forgotten by modern traditions. We must separate the logic of their argument from its psychology and genesis. I doubt that Gillespie will disagree, for scientists and historians approach the past both for different reasons and (or so it should be) with a common goal of appreciation in the broadest sense. □

Stephen Jay Gould is Professor of Geology at the Museum of Comparative Zoology, Harvard University, Cambridge, Massachusetts.

Perception model

Patrick Rabbitt

Decision Processes in Visual Perception. By D. Vickers. Pp. 406. (Academic: London and New York, 1979.) £23.80, $55.

PSYCHOPHYSICISTS investigate regularities in human sensory discrimination in order to propose mathematical models for sense organs and neural structures which cannot, yet, be more directly explored in other ways. Their discipline demands a high level of ability, some mathematical sophistication, a detailed knowledge of a very large body of literature in physiology and psychology, and originality in the design and interpretation of experiments. Their work is not easily followed by most academic psychologists and is not followed at all by the public at large.

Douglas Vickers gives a novel and thoughtful account of the subject and attempts, as far as possible, to make it accessible to the general reader. The general reader must be patient and hard-working. Vickers believes that models for human brain function should be guided by what we can guess about the probable evolution of sense receptors and of their analytic backup in the central nervous

system. "Just as the ontogeny of an individual tends to recapitulate the evolution of the species . . . so the human visual system may be expected to embody a succession of progressively refined response sub-systems from [systems for] the most primitive discriminations up to the most complex and specific recognition . . ." (p. 17). This idea of the parallel, separate operation of series of separate systems of different degrees of complexity and subsuming different kinds of discrimination is a profitable one. It is not easy, otherwise, to make sense of recent results obtained from patients with occipital brain lesions who can make discriminations without, apparently, being 'aware' of the data on which they base their judgements. From the minimum perceptual requirements of a hypothetical primitive organism, Vickers attempts to deduce the various problems of discrimination and analysis of information which must arise, and to suggest the most probable mathematical and statistical techniques which the brain uses to solve them. He repeatedly returns to his main thesis that the separate component sub-systems jointly form "a kind of loose society of similar, though independent self-regulating units rather than a unified system of interdependent specialized functions such as are embodied in the

ordered sub-routines of most computer programs'' (p. 17).

Vickers is a pleasant and learned guide to the history of his subject since the publication of Fechner's *Element der Psychophysik* in 1860 and his enthusiasm for historical detail and quotation is engaging. However this would be a poorer and less coherent book if he had not also attempted to offer a unifying view of his own in terms of his (new, updated, comprehensive) ''accumulator model'' for decision processes. Earlier versions of this model have been useful guides to data analysis and interesting sources of ideas for experiments. It is instructive to follow Vickers in his attempts to stretch the new comprehensive model beyond the statistical sampling of evidence and confidence levels for decisions, beyond even discriminations between two or more stimuli, choice reaction times and signal detection, to cover adaptation levels. With less

success he interprets some issues in prolonged vigilance and inspection (pp. 230–233), as well as an extremely difficult range of problems in perceptual organization (pp. 291–341), finally covering ''Choice, Control and Consciousness'' (pp. 359–370).

Of course the model clearly fails to cope with the massive tasks which Vickers sets it. Success is not possible in the current state of the art and Vickers is to be congratulated for subjecting his model to the widest possible range of tests — including those that it is bound to fail. There is no better way to proceed since it is precisely the points at which a model fails that are of compelling interest for further work. We can know more clearly what the problems are only when we realize what we still need to know before we can begin to solve them.

Patrick Rabbitt is a Lecturer in Experimental Psychology at the University of Oxford, UK.

Nonlinear optics in gases

Peter Knight

Nonlinear Optics of Free Atoms and Molecules. By D.C. Hanna, M.A. Yuratich and D. Cotter. Pp.351. (Springer: Heidelberg and New York, 1979.) DM 79, $44.30.

THE nonlinear optical response of matter to intense radiation has been a major research field since the advent of the laser. An early spectacular demonstration of such a response was the frequency doubling of ruby laser light in a quartz crystal. Nonlinear optical processes in solids suffer from low efficiencies and damage problems. The pioneering observations of nonlinear optical processes in atomic and molecular gases by New and Ward freed the experimentalist from damage problems, and the field was further advanced by the proposal by Miles and Harris that a large enhancement in efficiency is possible when atomic or molecular resonances are exploited. Tunable frequency converters based upon nonlinear optical properties of gases are now available throughout the spectrum from the X-UV to the far infrared, using harmonic generation, stimulated electronic Raman and hyper-Raman scattering and related techniques. The authors of this book are well known for their extensive theoretical and experimental studies of nonlinear optics.

The emphasis in this much-needed book is upon the use of near-resonant nonlinear optical techniques to produce tunable radiation by frequency conversion. The first two chapters contain a careful discussion of the theory of nonlinear susceptibilities and radiation propagation. This is followed by chapters on harmonic

generation, stimulated electronic Raman scattering and hyper-Raman scattering, four-wave mixing, the nonlinear optical properties of molecules, and a final chapter on new and potentially useful developments (e.g. radiative collisions and phase conjugation). Theoretical developments are carefully integrated with experimental results, with valuable statements of what remains to be understood. Practical considerations (such as heat-pipe design) are discussed at length, as are theoretical complications of selection rules and angular momentum algebra. I particularly liked the careful attention paid by the authors to units and definitions.

There are a few things I didn't care for in this book. The idea of dressed, or 'adiabatic' atom-plus-field states is presented but is applied quite incorrectly in their discussion of optical resonant saturation. If dressed states are used to describe strong-field resonant excitation, it is quite wrong to state that such a saturating field stimulates transitions between *dressed* states as the authors do in Fig. 2.4 and elsewhere. I found their discussion of such concepts confused and misleading. It would also have added to the value of the book if an elementary derivation of the susceptibility formulae had been given from perturbation theory rather than relying on a reference to Butcher's standard but virtually unobtainable monograph.

This book is valuable despite its minor faults. I am sure it will become a standard handbook for physicists and chemists interested in the generation of tunable radiation by exploiting the nonlinear optical properties of atomic and molecular gases. □

Peter Knight is an SRC Advanced Fellow in the Optics Section, Imperial College, University of London, UK.

Russian pioneer in electricity and magnetism

I.B. Cohen

F.U.T. Aepinus: Essay on the Theory of Electricity and Magnetism. Translation by P. J. Connor. Introductory monograph and notes by R. W. Home. Pp.514. (Princeton University Press: Princeton, New Jersey, 1979.) £20.70.

FRANZ Ulrich Theodor Aepinus was an outstanding physicist of the eighteenth century. His *Tentamen Theoriae Electricitatis et Magnetismi*, published in St Petersburg in 1759, was a pioneering effort to introduce mathematical analysis into these two branches of physics. Despite its importance as an intellectual landmark, however, Aepinus's *Tentamen* was never widely read. The edition was small (650 copies); published in Russia, copies were not too easily obtained in European capitals. Furthermore, the book was not reprinted or translated until a Russian edition appeared in 1951, under the editorship of Ya. G. Dorfman. Most scientists who heard of Aepinus's work encountered it by way of a secondary source, the most important of which was the epitome of Aepinus's essay published in French in Paris in 1787 by the Abbé René-Just Haüy, the great pioneer crystallographer. The mathematician Gaspard Monge, founder of projective geometry, had earlier made a summary of the *Tentamen* for his own use. In 1801, Haüy's epitome appeared in a German translation. The first major account of Aepinus's work to be published in English was in the two-volume supplement to the third edition of the *Encyclopaedia Britannica*, where John Robinson included lengthy summaries of Aepinus's theories in his articles on electricity and on magnetism. These were given wider circulation when they were later reprinted in their entirety in Vol. 4 of Robinson's *System of Mechanical Philosophy*. Thomas Young included these theories in his *Course of Lectures on Natural Philosophy and the Mechanical Arts.*

Aepinus's theory of electricity was a development from Benjamin Franklin's theory in which ''the American's incompletely worked out ideas were for the first time rendered precise and fully consistent with each other''. Aepinus's first contribution to electricity was his discovery in 1756 that the reason a warmed tourmalin crystal attracts dust or ashes is electrical: he soon showed that this was different from the normal electrification obtained by friction, since no rubbing is required. Additionally, the warmed crystal did not simply acquire an overall charge, but rather gained ''opposite electrical charges on two opposite faces''. This

discovery was at once confirmed and applauded by others, including Benjamin Franklin.

Aepinus's work on tourmalin had been done in Rostock; soon thereafter he moved to St Petersburg and spent the remainder of his scientific life in the service of the Imperial Russian Academy of Sciences. In his book he remedied the following defects in the Franklinian theory of electricity: he got rid of Franklin's doctrine of electric "atmospheres", replacing it by the concept of electrical force acting at a distance; he explained how negatively charged bodies might attract one another by postulating that "common matter" deprived of its "normal" amount

of electrical fluid will repel similar "common matter"; finally, he attempted to reduce electrical science to a set of mathematical principles, an endeavour that fell somewhat short of the mark since Aepinus did not know the inverse-square law of electrical (and of magnetic) attraction. He also constructed a parallel theory for magnetic forces and effects.

This first translation of Aepinus's essay, by P. J. Connor of the Department of Classics of the University of Melbourne, reads well and seems to be accurate. The introductory monograph, by R. W. Home of the same university, is a mine of information concerning the life and career of Aepinus, his influence, the state of

electrical and magnetic experiment and theory in the eighteenth century, the organization of research in the Imperial Russian Academy of Sciences and much else. This monograph, it should be noted, is of book-length, just about as long as Aepinus's *Tentamen*, which it introduces.

The monograph and translation form a first-rate contribution to our knowledge of the history of science. Together they should help restore Aepinus to his proper place in the development of electricity and the use of mathematics in physical science.

I.B. Cohen is Professor in the Department of the History of Science, Harvard University, Cambridge, Massachusetts.

Birds' sense of direction

John R. Krebs

Avian Orientation and Navigation. By K. Schmidt-Koenig. Pp.180. (Academic: London and New York, 1979.) £13.80, $32.

THIS is a well-written, balanced and accurate introduction to the literature on bird navigation and orientation up to the end of 1978. The major conclusions from work on pigeons are that birds find their way by using compasses based on the Sun and the Earth's magnetic field (nocturnal migrants also use the stars) in conjunction with an unidentified map. The map might

well be based on magnetic information acquired by the pigeon during its outward journey to the release site, since pigeons transported in an altered magnetic field show less accurate homeward orientation when released. The suggestion by Italian workers that pigeons may sniff their way home by using a scent map is still controversial. One of the most convincing experiments was one in which pigeons in their home loft were exposed to clockwise or counterclockwise deflected winds. When released, these birds flew with a predicted deviation from the correct homeward direction. However, the same effect is shown by pigeons with anaesthetized olfactory epithelia, suggesting that information other than scent must be related to wind direction.

One remarkable outcome of studies of homing is that pigeons have been shown to possess unsuspected sensory capabilities. Conditioning techniques have been used to show that pigeons can detect small changes in atmospheric pressure, infrasounds as low as 0.06 Hz, ultraviolet light and the plane of polarized light. The demonstration of ultraviolet sensitivity is an interesting case history. Previous workers had noted that the sensitivity of pigeons decreased towards wavelengths of 400 nm. However, below 400 nm sensitivity suddenly increases again to a second peak at 360–325 nm. We still do not know what role these various sensory abilities play in navigation and orientation, but infrasound might be a good candidate for a large-scale auditory map, since very low frequency sounds generated by waves, wind in mountain ranges and so on may carry for several thousand kilometres. The discovery that birds, in common with many other animals, can detect the Earth's magnetic field is also the result of orientation studies. Schmidt-Koenig's book was completed just before the recent demonstration by Walcott *et al.* (*Science* **205**, 1027–1029; 1979) that pigeons have tiny crystals of magnetite in their heads which could be part of the sense organ used to detect magnetic fields.

As with homing pigeons, more is known about how natural migrants use compasses than about their maps. Even relatively complex migration routes may be followed entirely with a compass. Garden warblers (*Sylvia borin*), for example, seem to have a built-in clock and compass which tells them to fly SW for one month in the autumn, followed by SSE for another month. This takes the birds from central Europe to southern Spain and thence to west or central Africa. Whether such birds have any map sense remains uncertain.

I have summarized a small sample of the results described by Schmidt-Koenig and I recommend that anyone interested in the subject should read his book. □

John R. Krebs is a Lecturer in the Department of Zoology, University of Oxford, UK.

Multivariate biology

Robert R. Sokal

Morphometrics, The Multivariate Analysis of Biological Data. By Richard A. Pimentel. Pp.288. (Kendall/Hunt: Dubuque, Iowa, 1979.) Paperback $19.95.

PRESENTING the results of morphometric, especially multivariate morphometric research, to a scientific audience is a major challenge. How can the reader make sense of numerous matrices, vectors and bivariate plots embellished with often unfamiliar terminology and esoteric mathematical and statistical manipulations? The author has set himself the task of remedying this situation by introducing biologists in a mathematically simple manner to the various multivariate techniques. To prevent misunderstandings I must point out at the outset that Pimentel uses the term morphometrics in an unconventional sense to include the application of multivariate analysis to unravel any pattern of variation including ecology, behaviour and physiology, not just the

biometric analysis of phenotypic morphological variation in animals and plants.

The standard topics of multivariate analysis are covered in a very personal style with the author providing caveats about use of various methods and indicating quite clearly which he prefers. Multiple factor analysis is given short shrift, whereas discriminant analysis is given a very full, well-presented treatment. Although there are some examples of applications, I would have liked to see a specific section in which the methods are compared and the types of methods suitable for given biological questions are pointed out. In my judgement, multivariate morphometrics (in the narrow sense) is one of the most promising disciplines of evolutionary research. Yet so far a general discussion of this subject from a biological point of view has not appeared. Thus in addition to this useful volume we need yet another account — a discussion of the genetic, developmental and ecological implications of the multivariate assessment of morphological phenotypes. □

Robert R. Sokal is Leading Professor of Ecology and Evolution at the State University of New York at Stony Brook.

nature

5 June 1980

How to pay less for crude petroleum

WHAT is to be done about the price of petroleum? In particular, how is it to be reduced? These are unspoken questions in the backs of many minds, especially in countries (industrialised and developing) that are largely dependent on imported oil. The questions are so often unspoken because they seem dangerous questions, an impression that can only be strengthened by the continued presence of an American fleet in the Persian Gulf (even if for an unconnected purpose). The result, however, is that oil consumers have, since the meeting of the Organization of Petroleum Exporting Countries (OPEC) in Kuwait in October 1973, become catatonically accustomed to the notion that the price of oil will be a monotonically increasing function of time. This grand indifference cannot much longer persist. Something will have to be done about the price of oil. And it goes without saying that military expedients of any kind can form no part of an acceptable strategy by which the oil consumers could interrupt the apparently inexorable upward trend of prices.

The need for a break in the present pattern is now self-evident. The economic consequences of the tenfold increase of the price of oil (in real terms) since 1973 are now everywhere to be seen. Although it would be wrong to blame the increased price of oil for all the economic ills of either industrialised or developing countries, it has been for the weakest among them much more than the straw that broke the camel's back. Quite gone are the' days when optimists could calculate (as one official of the British Treasury did in 1974) that OPEC's enforced increase of the price of oil would have the beneficial (anti-inflationary) effect (because of higher consumer prices) of taking money out of circulation, and that the oil-producing governments would have no choice but to lend back their surplus and unrequited cash, so that oil-consuming governments would be able to reduce their demands on their domestic money markets, thus making capital investment easier. In reality, the trends have gone the other way. Inflation has become more rapid, especially in the weaker economies, partly because of the effect of the increased price of oil on consumer prices generally, partly because of the success with which people have persuaded their employers that they should be insulated from the OPEC prices and partly because the recycling of funds has been less effective and efficient than was originally supposed. At the same time governments, especially the weaker governments, have found it harder, not easier, to borrow money, and have found it possible to do so only by forcing up interest rates. The turbulence of the New York money market since the beginning of this year is one symptom of the malaise. Another is the absurd truth that the British government's annual borrowing (estimated at £12,000 million this year) is just about enough to pay the interest on its accumulated debt.

Especially on the eve of a recession, nobody can be sure where this will end. The conventional wisdom is to suppose that both the oil producers and consumers have a common interest in the avoidance of calamity, but that cannot be the case. Most OPEC members (but Iran and Nigeria are probably exceptions) could manage well enough if worldwide demand for oil were sharply to decline. Although the surpluses they have earned in the past years are still largely in the form of paper money, unrequited by the transfer of goods and services and continuously being eroded by the depreciation of currencies, they may well calculate, on paper correctly, that they can always make good past losses by charging even more for future production. No doubt the rash of $2 a barrel

increases in the past few months derives in part from such calculations.

Consumer resistance so far has been fitful. Several oil companies, especially Japanese oil companies, are, however, for the time being at least, declining to buy Iranian crude oil at $35 a barrel. Time will tell whether Gulf Oil and Charter Oil eventually agree to pay the $38 a barrel that Qatar is asking for contracts running from the end of April. One hapless lot of consumers will however have no choice. Customers of the British National Oil Corporation were told last week that they would have to pay $36.25 a barrel for oil from the North Sea with effect from 20 May. It is not so long since British Prime Ministers, flushed with the success of exploration in the North Sea, were making jokes about applications for OPEC membership. The formalities of membership seem not to matter where prices are concerned. The technical explanation of this curious behaviour, the effect of which will be to take even more money out of an economy now well into a recession, is that common international pricing has been written into the British government's relationship with the North Sea oil producers. British taxpayers will nevertheless with justice ask how, and in what form, they will eventually enjoy the supposed benefits of North Sea oil.

Ironically, the most recent wave of increases in the price of oil has come at a time when oil is, if anything, in good supply. Thanks to the urging of the International Energy Agency, stockpiles of petroleum in most industrialised countries are getting on for a quarter of annual consumption. Marginal oilfields outside the OPEC states are being worked harder, while there has been a cheerful pause in the previously steady decline of proved reserves in the United States. At the same time, the oil-consuming countries have made some progress — but less than it was reasonable to hope for — in limiting their consumption and import of petroleum. In the European Community, for example, oil consumption was no greater at the end of 1979 than in 1973, before the whole upheaval began. But it is too soon to think that the international market in oil has become a buyers' market.

More could however be done by the oil consumers to take advantage of the present contradiction between the plentiful supply of oil and the increasing trend of prices. For a time at least, the oil companies might be persuaded to abandon their traditional practice of buying the bulk of the oil they need (and sometimes more than they can sell) on long-term contracts from the oil producers. What the oil consumers need is a market in which some commercial balance would be struck between supply and demand. In the past few years, Rotterdam has won itself fame and fortune as the centre at which crude petroleum is traded in this way, and it is hard not to think that oil-consuming governments have an interest in strengthening this device for deciding a commercial price for oil. The oil producers at any time most in need of cash could be counted on to provide the market with something to sell. Such a way of fixing prices rationally would be made enormously more effective if industrialised countries such as the United States and Britain were to agree that some of the oil produced within their borders might also be disposed of in that way. Unfortunately, since 1973, the governments that might be able to help in such ways have moved in the opposite direction, putting self-sufficiency before self-interest.

No clever organisation of an international market in petroleum can provide more than a short-term solution to the problem of

increasing oil prices. A decision by, say, Saudi Arabia to reduce production by two million barrels a day could speedily put a crimp in the most efficient market. This is why the only long-term solution is that the oil-consuming countries should lessen their dependence on OPEC oil. So much has been clear since 1973, and is enshrined in the policies of most of the international bodies with interests in this field, the International Energy Agency and the European Community in particular. Alas, this is yet another field where declared policy and practice are far apart.

This is not to belittle what has been accomplished. In the past few years there has been a hopeful change in the pattern of energy consumption within the European Community, for example. Total energy consumption has grown less quickly than foreseen five years ago, not simply because economic activity has flagged behind the original estimates but because energy conservation has been a modest success (especially among industrial and commercial users). The supply of energy from sources other than oil has also, unfortunately, fallen behind the targets set in 1975. Both coal and nuclear energy production are unlikely, in the

coming decade, to do much to lessen dependence on OPEC oil (which will still account for nearly 50 per cent of European energy consumption in 1985). This, for Europeans, is too much for comfort. Last month, the European Commission did its best (without much success) to persuade the energy ministers of the Nine to look seriously at a series of proposals intended to make the European market in energy internally more efficient — common principles for pricing, taxation and the like.

In the United States, as always more fortunate, the benefits of President Carter's tardy and apparently reluctant freeing of the United States energy market have still to appear. As the letter from Dr Alvin Weinberg illustrates (page 382), it will be some time before even Americans acknowledge that the problem of energy prices is a serious problem. The stakes, at least for oil consumers, are high — nothing less than the perpetuation of a way of life they have grown fond of. The cost of winning the gamble may seem high — a reactor here, a strip-mine there. In reality it is not. For the only way of bringing down the price of oil is for the oil consumers to show that they could, if need be, do without it.

How not to foster new technology

The present British Government seems to be making a thorough muddle of its predecessor's plans for setting up a microcircuit industry in the United Kingdom. More than two years ago, when politicians all at once found out about micro-electronics, the then Labour Government launched a flurry of new (and expensive) programmes — schemes for helping industry at large to become familiar with the new technology, for spreading the word through the educational system, for compiling lists of consultants on information processing and the like. The most striking part of the hastily-assembled package was a decision to invest £50 million in a company called INMOS, newly formed by people with American experience, whose strategic role was to be the design, development and manufacture within the United Kingdom of an advanced range of microcircuit devices. The channel for the Government's investment was the National Enterprise Board, best known as the public shareholder in a variety of companies which successive governments have chosen to rescue from one kind of trouble or another with public funds. Sensibly enough, the NEB decided that INMOS could not have all of the promised £50 milion in one cheque — half was paid over in 1977 on the understanding that the second half would be available when the design and development phase of the enterprise had been completed.

Since then, a great deal has changed. There is a new British Government, suspicious (to say the least) of the function of the NEB. The NEB itself has changed dramatically — in November 1979, the entire board chose to quit when the Department of Industry (to which the NEB is responsible) decided to remove the aero-engine manufacturer Rolls-Royce from its field of interest. And the new government, superintending a board whose mere existence is an embarrassment, is more desperately short of taxpayers' money than it had thought possible.

INMOS, it appears, has been an unlucky victim of these changed circumstances. Last summer, when the design of two microcircuit devices had been completed (physically in the United States) the company asked the NEB for the second tranche of funds. In October, soon before the board's decision to quit *en bloc*, the plan was approved, but a formal recommendation was not passed to the Department of Industry (which keeps the cheque-book). In December, therefore, the newly-constituted NEB reconsidered INMOS's proposals, approved them formally and recommended that the Secretary of State for Industry, Sir Keith Joseph, should write a cheque. Since then, nothing has happened.

To judge from Sir Keith Joseph's exhortations to people in California last week, neither he nor the government to which he belongs has cooled on microprocessors. By all accounts, he was urging American manufacturers to establish themselves in Britain, dangling before them the attractions of tax-breaks and

low wages (on paper at least). Nothing appears to have been said about INMOS and the second £25 million.

The truth is, of course, that the British Government is morally committed to provide the second half of the investment estimated as necessary to launch INMOS and its first few products. Nobody claims that the company has failed to meet the conditions laid down when the formation of the company was encouraged by the then government. So far, two sophisticated microcircuit components have been designed and tested — a 16 K static memory and a 64 dynamic memory. Each of them is likely to interest computer manufacturers. There may be doubts about the capacity of a new and relatively small company based in Britain to sell its wares effectively in the international markets to which it must be looking. Yet having helped INMOS so far, it would be folly now not to provide it with the funds it needs to set up its manufacturing plant. To fail to do so would be disreputable. To delay is to load its dice against the company.

None of this implies that Sir Keith Joseph is not right to be agonising (as is said to be his wont) about the good sense of the mechanisms he has inherited for using public funds to sponsor technological innovations. The National Enterprise Board itself is an awkward legacy of Sir (then Mr) Harold Wilson's promise in 1963 that, if elected, he would create a second industrial revolution with "white-hot technology". The surviving marks of that period are a few aluminium smelters scattered through Britain, a number of industrial companies too big for their own comfort and the NEB, the descendant of the old Industrial Reorganisation Corporation.

Throughout this period (as before it began), governments and British governments in particular have demonstrated that they are uncommonly bad at backing technological enterprises. The reasons are simple. Civil servants are not equipped to make judgements of what will work and also sell. They and their political masters are prone to attempt too much in their sponsorship of innovation — they also seek to prop up ailing companies or to provide jobs in depressed parts of the country for reasons which have nothing to do with innovation. It would be entirely proper if the Department of Industry were to seize this opportunity for a radical re-examination of how best to foster new industry. The most important ingredient of a new policy would be to foster circumstances in which people who know what's what find it profitable to back their hunches, but there is much to be said for the British Government deliberately replacing some of its in-house research and development by contracts let to private industry. The National Enterprise Board could be abolished without much harm — and that, of course, may happen anyway if the British Government insists that it should act as an agent for going back on a promise, however unwise that may have been. □

One way ahead for British biotechnology?

BRITISH biotechnology may yet survive. A plan by three renowned molecular biology laboratories for setting up in Britain a commercial biotechnology venture is being considered by several agencies of the British government.

The laboratories concerned are the MRC Laboratory of Molecular Biology at Cambridge, the Laboratories of the Imperial Cancer Research Fund in London and the Cold Spring Harbor Laboratory on Long Island in the United States. The three principals are Dr Sydney Brenner, Dr Walter Bodmer and Dr J. D. Watson, the respective directors of the three laboratories.

The essence of the plan is to establish a small organisation in Cambridge, initially for the preparation and supply on commercial terms of monoclonal antibodies, principally for use in biomedical investigations.

This would involve exploiting a technique originally developed by Dr César Milstein of the Laboratory of Molecular Biology, Cambridge, in which lymphocytes producing antibodies of a specific kind are fused with cells of cancerous lymphoma tissue.

After suitable selection procedures, the outcome can be a line of cells with the vigour of lymphoma cells which nevertheless produce the specific antibody prolefically.

This particular plan has emerged over the past year, and thus in its origins predates the Spinks Report on biotechnology, published at the beginning of April (*Nature,* 10 April and 24 January). That urged that the research councils, public sources of venture capital in Britain, especially the National Research Development Corporation and the National Enterprise Board, should take steps to promote a British biotechnology industry. Both organizations have announced their interest in the field (*Nature,* 29 May).

The production of monoclonal antibodies has presumably been chosen as a first objective because it could be applied immediately, thus providing a new venture company with some bread and butter. The initial need of capital would be correspondingly modest.

The next steps to be taken in the setting up of a commercial venture are by no means obvious. The Medical Research Council, the obvious sponsor of such a venture, is precluded by its terms of reference from risking the loss of money. The NRDC is used to dealing with particular products and inventions, not with backing companies as such.

On the face of things, the National Enterprise Board is constitutionally better able to provide the backing a venture like this would need. One intriguing possibility is that the two private laboratories — Cold Spring Harbor and the Imperial Cancer

Research Fund — would be able to provide some of the capital if their boards of trustees agreed.

A spokesman for the National Enterprise Board declined this week to say whether his board was considering this particular proposal, but reaffirmed the organization's concern with biotechnology. It is, however, understood that

some news of the NEB's interest in the field will be forthcoming within weeks rather than months.

Much may depend on whether biotechnology is able to avoid the Catch-22 problem which has beset micro-electronics (see page 346, this issue) — if it's not good, it's not worth backing; if it is, why doesn't the market step in?

Research councils

Disquiet over NERC succession

THE appointment of Sir Hermann Bondi as full-time chairman of the UK Natural Environment Research Council (*Nature,* 15 May), although widely welcomed, is also the cause of consternation. At its meeting last week (28 May), the Council was sore that it had not been even formally consulted and concerned that the forced resignation of Mr R J H Beverton, secretary of the council for the past sixteen years, might be misinterpreted.

Members of the council agree with the chief objective of the change at the top — that NERC should be put on the same footing as the other research councils, with the responsibilities of chief executive and official accounting officer combined in the same person. Hitherto these functions have been the responsibility respectively of the Secretary and the Chairman, for the past three years Sir James Beament, head of the department of applied biology at the University of Cambridge.

What irks the council and dismays some of the directors of NERC research establishments is that when Sir Hermann's candidacy for the job became known to the Department of Education and Science early in April, both Beverton and Beament were presented with a *fait accompli* and, in effect, invited to go quietly. This, in the event, they both agreed to do.

The urgency of the decision stemmed from Sir Hermann Bondi's impending retirement as Chief Scientific Adviser to the Department of Energy with effect from

Beverton out . . .

1 October, required by Civil Service rules on age. The NERC Council was left with the impression that if the succession at NERC had not been settled quickly and to his satisfaction, Bondi would have taken his undoubted talents elsewhere.

The past few years have seen something of a change in the character of NERC's programme. Although NERC continues to spend its own funds on a programme of basic research not markedly different from in the past, funds awarded to NERC by government departments for contract research ('Rothschild money') have increasingly emphasized energy-related problems — radioactive waste disposal and physical oceanography related to the exploration of the North Sea, for example.

Although the division of the responsibil-

. . . Bondi in

ities of chief executive and accounting officer is agreed to be the long-term reason for change, the move of the NERC headquarters from London to Swindon has complicated the problems of management in the past two years. Sir James Beament, based at Cambridge, has been spending two days a week on NERC business but has been hard-pressed to divide this time between London and Swindon.

Even so, there are many who consider that some role could have been found in the new organisation for Mr Beverton, who has only two years to go to his normal retirement date.

The council was at pains to emphasise at

its meeting last week its appreciation of Beverton's service to NERC and its hope that the Civil Service would find a worthwhile job for him to do in the next few years. The council was especially at pains to emphasize that Beverton's sudden departure betokened no misconduct of NERC's affairs.

For the British research council as a whole, the incident has been a somewhat chilling reminder that their jealously guarded autonomy is, in the last resort, in the gift of the Department of Education and Science. In the week in which another government department (Energy) precipitated the resignation of the financial managing director of the British National Oil Corporation by the unwelcome appointment of a new chairman (without consultation with the board), that should not be a surprise.

Radiation

ICRP rules row

Washington

Fitting round pegs into square holes must seem childs' play compared to the political difficulties of bringing US radiation exposure regulations in line with the current state of scientific knowledge.

In an unusual reversal of roles, officials of the US Nuclear Regulatory Commission have expressed reservations about new occupational exposure guidelines being prepared by the Environmental Protection Agency, claiming that they would result in an unnecessary relaxation of certain existing restrictions.

The dispute centres on recommenda-

tions for revising occupational exposure to radiation proposed three years ago by the International Commission on Radiological Protection. These have been accepted as the basis for regulation by the Commission of the European Economic Community, but remain the centre of fierce controversy in the United States.

The method for calculating maximum exposure levels proposed by the ICRP in its report known as ICRP 26 is widely accepted as a major advance and as reflecting the best 'state of the art'. For example, it allows for joint consideration of the effects of internal and external doses of radiation, previously considered separately.

Furthermore it shifts the basis for calculating maximum exposure levels from consideration of 'critical organ' doses — using the maximum acceptable exposure to organs most susceptible to a particular radionuclide — to a method which calculates a general level of risk by integrating the weighted risks posed to various parts of the body.

The advantage of this approach is that it includes the risks to organs other than those considered the most critical. The difficulty, however, comes from the need to adjust the specific figures placed on exposure limits.

Controversy has in particular focused on the ICRP's suggestion that the maximum integrated risk should be equivalent to that represented by the existing maximum whole body exposure of 5 rems a year.

The EPA, which is reponsible for setting exposure guidelines to be followed by other agencies, has yet to issue formal proposals on revised exposure levels. But it has in-

formally sounded out the agencies on the use of the ICRP aggregated-risk methodology, based on a maximum organ dose of 30 rems a year.

Even this reduced exposure guide, however, has not been acceptable to some NRC officials. While supporting the ICRP methodology in principle, they argue that the result of meeting the overall risk requirement would be to permit an increase in permitted air concentrations for many radionuclides, in some cases by an order of magnitude.

The NRC officials, who say their arguments have been accepted as an interim position by the NRC commissioners, agree that such increased limits would not necessarily be harmful. But they argue that they would inevitably reduce the protection afforded to workers at licensed power plants and uranium mines — and that the nuclear industry apparently has little difficulty in meeting current standards.

EPA officials agree that adoption of these proposals would permit increased exposure to some radionuclides (as well as reducing exposure to others). But they insist that assessments should be based primarily on consideration of the overall risk, rather than merely the risks to separate organs.

"If someone gets cancer, it does not really make much different to them which part of the body they get it in. We are trying to limit the amount of harm to people. That is not the same as limiting the dose in an abstract sense", Dr David Rosenbaum, director of EPA's Office of Radiation Programmes, said last week.

NRC officials have proposed a hybrid scheme under which exposure limits for individual radionuclides would be calculated both by the ICRP methodology and by the 'critical organ' technique using the same methodology but old dose limits, accepting whichever is the lower. But EPA is unenthusiastic about this approach.

The situation is complicated by each agency's desire to respond to outside arguments. The EPA, for example already faces challenges by nuclear companies on its proposal that public exposure outside a nuclear facility should not exceed 25 millirem.

At the same time various public interest groups are using the uncertainties in the scientific evidence to petition the NRC to reduce the present 5 rem occupational exposure limit by an order of magnitude. Several trade unions are also planning to press the EPA not to introduce the ICRP 26 scheme without major modifications.

Given all this activity, publication of the proposed guidelines is now unlikely before the autumn, with a period for public comment to be followed by a series of public hearings next year. These promise to be lively; particularly if the Administration changes to one more concerned to minimise regulatory restraints on the growth of nuclear power. **David Dickson**

Soviet heavy neutrinos

BARELY a month after a 'Science Day' speech in which Anatolii Aleksandrov, President of the Soviet Academy of Sciences, suggested that the Soviet Union should make itself as independent as possible of western scientific results, a team of physicists led by Academician Valentin Lyubimov, has repeated the claim of Dr F. W. Reines to have established that neutrinos have mass. This has now been announced by the Russian news agency Tass. Reines, from the University of California at Irvine, described to the Spring Meeting of the American Physical Society last month the latest in a series of experiments at the Savannah River reactor in which the relative importance of the charged and neutral currents in the interaction of reactor neutrinos with deuterons was measured. The neutrino mass deduced is the equivalent to a few electron-volts.

The Russian work now referred to is based on a different method. The team concerned, from the Moscow Institute of Theoretical and Experimental

Physics, is said to have analysed the spectrum of electrons in tritium decay, deducing the mass of the neutrino from the shape of the spectrum. The discovery was announced in a report delivered to the Presidium of the Soviet Academy of Sciences.

Commenting on it, Academician Yakov Zel'dovich observed that the result could produce major changes in current cosmological concepts and possibly raise once again the question of the existence of a cosmological constant, first mooted by Einstein in 1917.

Reporting the discovery, the Tass agency said that the existence of 'heavy' neutrinos solves a number of existing paradoxes, including the question of the missing mass of galaxies and the measured deficiency of solar neutrinos from the sun. Tass claimed that it also appeared to confirm the model of solar neutrino flux proposed by Academician Bruno Pontecorvo involving the interconversion of different neutrino types.
Vera Rich

Research application

Hungary expects

Budapest, May

The Hungarian Government is hoping to reshape the balance between academic and applied research without reducing the total number of research jobs. This was the burden of a statement by Mr Joszef Marjai, one of the deputy chairmen of the Hungarian Council of Ministers, at the Investment Goods Spring Fair held here from 23 to 28 May.

Mr Marjai promised that there will be no reduction of the number of research jobs, and said that there may be even more jobs availble for scientists and technologists. "But we cannot promise that everyone will stay in the same job."

Mr Marjai's remarks, however, echo a major dilemma in Hungarian science planning. At present, science in Hungary has a top-heavy structure with, it is generally agreed, too many research institutes for a country of 10 million people to support. Last month, Janos Szentagothai, president of the Hungarian Academy of Sciences, told the General Assembly of the Academy that time and energy could no longer be wasted on 'insignificant and middle-level' basic research. Plans are now being formulated for the network of research institutes to be modified to serve 'social and economic needs'.

There is little doubt that many young scientists are reluctant to leave the academic seclusion of their research institutes. Even the show-piece Babolna collective farm has found it difficult to recruit a qualified agricultural economist. Young biology graduates joining the Plant Protection Service speak of their field-work as if it were a kind of purgatory. Hungary needs scientists to work in agriculture and industry, and while the planners so far have been unwilling to deny promising students a few years post-graduate research, the view is growing that the country simply cannot afford to give them a niche in some institute for life.

The problem can, to a certain extent, be ameliorated by directing research talents not to the needs of the Hungarian economy but to export. More than half of the Hungarian GNP comes from exports, and one pavilion at the Budapest Fair was used by the Academy of Sciences, Ministry of Education and National Committee for Technological Development to show that academic research can sometimes yield practical benefits. The goods on display ranged from a laser theodolite to a fixed-bed denitrification column and from a computer-aided electromyograph to an electronic Braille writer. "We don't want over-specialization", explained Gyoergy Paris, science organiser of the Ministry of Education. "We make what foreigners want to buy."

Nevertheless, like most Hungarian scientists, he was not over-enthusiastic about the plans to direct more scientists to industry. "It is a pragmatic solution", he said, "and not good for research. Some people simply cannot do practical work. But we are a small country — and what else can we do?"

Hungarian planners, of course, are not unique among their Comecon partners in trying to integrate science into production. The Hungarians, however, place less emphasis on the socialist virtue of the process. Nevertheless, the Hungarian problem is exacerbated by the lack of natural resources and by a long tradition of academic elitism.

As in most Comecon countries, Hungary has developed a research structure based on Academy institutes which are independent of the universities, and, perhaps, too large for the country to support. Eight years ago, Bulgaria solved this problem by integrating the staff of the institutes of the Academy of Sciences back into the teaching structure of the universities. In the next few years, it seems likely that Hungary may be forced to adopt a similar solution.

During the past year there has been a major press debate, launched in May 1979 by an article by Professor Gyoergy Adam, former Rector of Budapest University, in *Magyar Tudomany* ('Hungarian Science'). The whole role of the university and its is already under discussion. **Vera Rich**

Hungarian Academy — changing with the times?

High-energy physics

More of less money

Washington

American high-energy physicists are in a jittery mood. They are now faced with the prospect that the three main national particle accelerators may have to close down during the summer months as a result of Congressional budget cuts — and that there may be worse in store next year.

The immediate difficulty stems from a recommendation by the Appropriations Committee of the House of Representatives that $8 million would be rescinded from the $325 million already approved — and largely unspent — for the current financial year.

Half of this saving would come from delaying construction costs of the 400 GeV Isabelle Project at the Brookhaven National Laboratory, with relatively little impact expected over the full seven-year period of the project. But the remainder would include $1 million taken from physics research, $2 million from facility operations, and $1 million from high energy physics technology.

The only way such cuts could be absorbed would be to stop all experimental work at the three national accelerator laboratories until the new financial year begins in October. Dr Leon Ledermann, director of Fermilab, said last week that the decision would be disastrous.

Construction of Fermilab's new energy-saver, designed to double the accelerator's energy to 1000 GeV by the use of superconducting magnets, is already biting deeply into the laboratory's operating funds. Further reductions could mean that the operation of the accelerator was halted entirely next year, so that the construction of the Tevatron could be made the laboratory's top priority, according to Dr Ledermann.

At Brookhaven, the proposed reduction in operating funds would mean that between eight and ten weeks of experiments planned for the summer would have to be put off. And the same would be true at the Stanford Linear Accelerator (SLAC) in California, where the new PEP collider has only just come into operation, but on which experiments could not be carried out until the autumn.

In an already tight financial year, the budget axe seems to be falling particularly heavily on energy research, partly because the energy budget is considered jointly by Congress with the budget for dams and other 'pork barrel' construction projects which carry considerable appeal to legislators in an election year.

The situation for next year remains cloudy, largely because the debate over how to balance defence and social expenditures within a balanced budget means that Congress has yet to agree on its own financial guidelines. However there are

several pointers around, and none of them is promising.

Thus although the Carter Administration recommended significant increases for high energy physics both in its original budget request in January and in the revised request in April, the Senate Budget Committee has proposed reductions in the whole of the science budget to make room for extra defence spending.

The equivalent committee in the House of Representatives has not been so harsh. But, like that in the Senate, it is suggesting that first priority within the science budget be given to the space shuttle; and has pinpointed high-energy physics as one area that might accomodate a 'pause in funding'.

More specific proposals have been made by the House Science and Technology Committee, which has recommended a high-energy physics budget for next year of $6 million less then the President's revised request of $354 million.

This cut could be absorbed relatively easily. Proposals from the House Appropriations Committee are expected to be more damaging. No decision has yet been made but it is widely reported that the whole of the energy research budget — including high-energy physics — should be kept at its current level for next year, with no increase to allow for inflation.

The implication of such a proposal, if accepted by Congress, would be to wipe out the 10 per cent increase which had been expected by the high-energy physics community.

The prospect of no growth for the energy research budget has already prompted a letter from Dr Frank Press, Director of the Office of Science and Technology Policy, to the chairman of the Appropriations Committee emphasising the importance that the Administration attaches to the support of basic science.

But in a generally confused budget year, it remains unclear which direction Congress is likely to take. All that is certain is that the bleak outlook will be hanging heavily over physicists meeting this week in Woods Hole, Massachusetts, to chart a strategy for US high-energy physics over the next decade. **David Dickson**

Astronomy

Britain bids for big time

BRITISH optical and radio astronomers have decided to bid for £15.5 million-worth of new telescopes — a 4.2 m optical collector and a 15 m millimetre-wave radio dish — to be constructed at the Roque de los Muchachos Observatory site on La Palma, in the Canary Islands. The request effectively mortgages all major capital spending by the Science Research Council's Astronomy, Space and Radio Board until the middle of the decade.

The proposal is now before the Advisory Board for the Research Councils as part of the SRC's 'forward look', and is within previously agreed guidelines for SRC expenditure. However, because the cost is more than £200,000, the proposal also has to be approved separately by the Secretary of State for Education and Science. A decision is expected within a month. The

Netherlands is also involved; the National Research Council (ZWO) is considering a 20 per cent participation in the new instruments.

The 4.2 m light collector is designed to provide high resolution imaging of distant faint sources, comparable with that of the Hale telescope at Mt Palomar, but with considerably better seeing — the best, in fact, in the northern hemisphere. Combined with the UK Infrared Telescope (UKIRT) on Mauna Kea, Hawaii, and the complementary 1 m and Isaac Newton 2.5 m telescopes already destined for La Palma, the 4.2 m would double the amount of guaranteed telescope time available throughout the world to UK optical astronomers.

This estimate takes account of the Roque de los Muchachos agreement, which allocates 20 per cent of the observing time on the telescopes to Spain and 5 per cent to collaborations among other users of the observatory. These are at present Denmark and Sweden; but a site has already been reserved for a French 90 cm solar telescope, and there is a possibility that Italy will join with its own 3.5 m telescope.

The Italian move stems from its recent proposal to join the European Southern Observatory in January 1981, alongside Germany, the Netherlands and Sweden, at ESO's La Silla site in Chile. Part of the price of admission — which is still under negotiation — would be to provide a 3.5 m blank to provide a second major ESO light gatherer (a 3.6 m telescope is already in place), and Italian astronomers are considering splitting a large blank into two halves, one for La Silla and one for La Palma. However, their proposal depends on gaining Italian parliamentary support, which is often slow in coming.

The millimetre-wave radio telescope faces greater competition. The United States has had an 11m instrument reaching down to 2 mm wavelength in place at Kitt Peak for a decade; and France and Germany are constructing a similar dish, and a millimetric interferometer, within the Institut pour Radioastronomie Millimetrique (IRAM) whose headquarters are in Grenoble.

The United Kingdom rejected participation in IRAM because it involved setting up a new and expensive administration, because European salaries would have to be paid, and because it was against the SRC's policy of disengagement from large autonomous research centres.

The proposed millimetre radiotelescope would be complementary to the infrared telescope at Mauna Kea, where the seeing is as good as at La Palma. The infrared telescope, which can operate at most wavelengths between the near-visible and 1.5 mm (with the help of helium-cooled bolometers) cannot provide detailed spectral information. The proposed radiotelescope, using tuned-crystal detectors, will on the other hand be able to provide the profiles of molecular emission

Existing major international optical telescopes

Diameter (m)	nationality of operator	location
6.00	USSR	Mt Semirodriki
5.08	USA	Mt Palomar (Hale)
5.00	USA	Las Campanas, Chile
4.50 (6 × 1.8)	US (multimirror)	Mt Hopkins, Arizona
4.22	UK (infrared)	Hawaii
4.01	USA	Kitt Peak
4.01	USA	Cerro Tololo, Chile
3.94	Anglo-Australian	Siding Spring
3.66	ESO	La Silla, Chile
3.66	Franco-Canadian	Hawaii
3.05	USA	Mt Hamilton (Lick)
2.72	USA	Ford Davis, Texas (McDonald)
2.64	USSR	Crimea
2.60	USSR	Armenia
2.59	UK (Isaac Newton)	La Palma, Canaries
2.57	USA	Mt Wilson
2.54	USA	Las Campanas, Chile
2.29	USA	Kitt Peak
2.24	USA	Hawaii
2.20	W. Germany	Calar Alto, Spain
2.15	USA	Kitt Peak
2.15	Argentina	San Juan, Argentina
2.08	USA	Fort Davis, Texas (McDonald)
2.00	USSR	Chemakha

lines at wavelengths greater than 0.8 mm. It will also provide Britain's radioastronomers — whose long lead in radiointerferometry has been broken by the construction of the US Very Large Array — with access to at least one world class instrument.

Robert Walgate

Ariane

Half way to the Devil

EUROPEAN hopes of commercial competition with the delayed American space shuttle have been called into question by the failure on 23 May of the second launch test of Ariane, the European three-stage 1,750 kg payload launcher. The European Space Agency, responsible for Ariane, has always held that two successful flights in the four-flight test series (the next tests are due in November this year and February 1981) would be counted a success; but what matters is whether potential clients will take the same view. They will no doubt now be on their guard.

The rocket fell into the sea less than 10 km from its launch site in Kourou, French Guyana. It now lies in muddy waters some 7 to 10 metres deep between Kourou and the former French penal colony, Devil's Island. Two ships are searching for it, one with sonar and the other with drag-nets. If the rocket is found, it should be recoverable.

The fuel tanks were destroyed by an automatic device, but the propulsion bay — the collection of four combustion chambers where the critical fault occurred — is expected to be intact. It may prove crucial in determining the cause of the accident.

Preliminary analysis of telemetric data has revealed that one of the four first stage engines began to 'flicker' 4.4 sec after ignition, 1.1 sec after lift-off. The pressure in its combustion chamber oscillated at 1,000 Hz with an amplitude of 4 bars about its design pressure of 54 bars, and the exhaust gases turned yellow, indicating inefficient oxidation of the fuel. By 6 seconds the fault appeared to have corrected itself.

At 28 seconds the fault recurred for an instant, and then the temperature began to rise steadily in the propulsion bay from 24°C to 56°C. At 64 seconds the temperature jumped to 100°C and the combustion chamber pressure dropped to 10 bar. Ariane started to roll. By 104 sec the roll had reached 10 rpm, and two other engines lost pressure; the third followed at 108 sec. The self-destruct systems then decided that Ariane had had enough, and blew out the fuel tanks.

A similar loss of pressure was detected just after ignition of the Ariane engines on the first launch test in November 1979; but this loss was detected soon enough to abort the launch. At a subsequent attempt, lift-off and launch were successful, and the earlier fault was put down to instrument error. There may now be doubts about whether this was the case.

The Ariane first stage engines are derived from those of an earlier French rocket, 'Diamant' — and this rocket also experienced catastrophic losses of power during its development. However, 44 ground tests of the Ariane four-engine assembly showed power loss only once.

The fault probably traces back to a fluid or chemical instability in the injector, the 'carburettor' that injects fuel and oxidant into the combustion chamber; and the question arises whether the instability is triggered by a mechanical fault in the injector, or is simply an inherent instability due to a design error. If the latter, a further series of ground tests will be necessary before Ariane's third test flight, and the money available for those tests is limited.

Another possibility being considered by Ariane engineers is that the geometry of the exhaust deflectors at the launch pad led to

The Ariane launch, just as the first of the four engines began to flicker.

an acoustic effect which in turn induced the instability. The deflector geometry is completely different at Kourou from the geometry adopted in the ground-based tests.

Robert Walgate

Pesticides

EEC directive disputed

THE long-standing argument over the basis for environmental standards between some European governments and the European Commission now appears to have spread to the consumers' associations. Thus last week (27 May) the Consumers' Association, the London-based consumer group, published a criticism of the draft directive on the regulation of pesticides in foodstuffs originally promulgated in 1976.

The CA's argument is based on a comparative study carried out in the past three years in West Germany and the UK. The nub of the issue, according to the report "Pesticide Residues and Food" (Consumers' Association, 14 Buckingham Street, London WC2) is whether the regulation of pesticides in the human diet is best accomplished by fixing maximum concentrations of permissible pesticide residues in foodstuffs appearing on the domestic market.

The EEC directive proposes that there should be maximum permitted levels of certain pesticides (particularly the organocholorines) in foodstuffs, and that it should be the responsibility of national governments to sample foodstuffs regularly, analysing them for their pesticide content. This is for practical purposes the system now in operation in West Germany.

By contrast, the British system is based on a voluntary scheme for the approval (by the Ministry of Agriculture, Fisheries and Food on the recommendation of an expert Advisory Committee) of pesticides offered for sale in the United Kingdom and on estimates of what foods people eat. The CA joins with other critics of the system in urging that the approval scheme should be made statutory, but otherwise comes to the conclusion that this scheme has adequately served its purpose of keeping pesticide concentrations in human blood and tissues within acceptable limits.

One of the CA's chief arguments in favour of the British system of control is that the German system is much more expensive. But the report, while recognising that harmonisation of environmental standards is necessary in the interests of European free trade, argues that it would be inequitable that all members of the EEC should have to adopt the most stringent (and cumbersome) of the control procedures now in force.
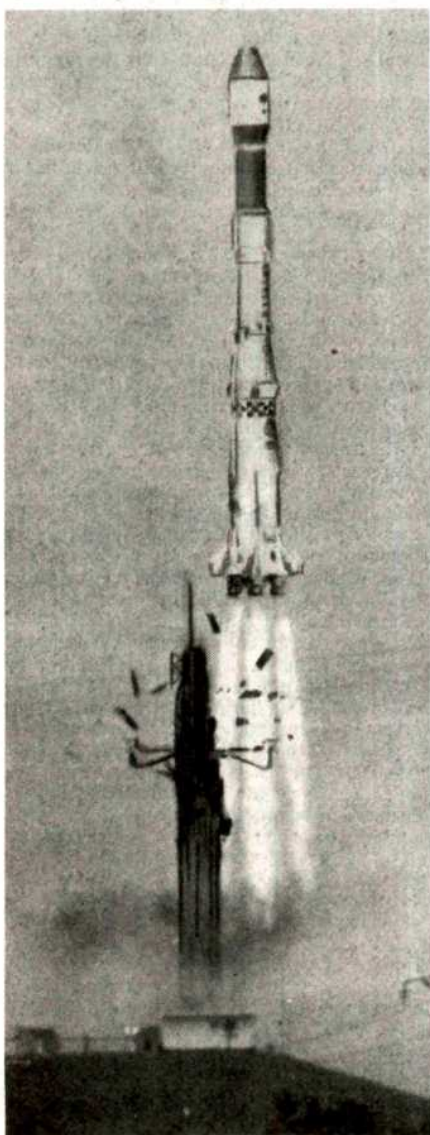
CORRESPONDENCE

Reactors away

SIR,—We nuclear technologists have plenty of reason to consider ourselves unloved and misunderstood. On 20 March in Middletown, Pennsylvania, not far from Three Mile Island, some 400 angry local residents bitterly attacked officials of the Nuclear Regulatory Commission over the proposal that the 60,000 curies of ^{85}Kr still trapped in the containment vessel should be released. This is a necessary first step in decontamination of Three Mile Island. The estimated maximum dose to any resident of Middletown caused by this release would have been 11 mr beta skin dose, 0.2 mr whole body gamma dose — the latter being of the same order as the dose received in a transatlantic flight.

The local people at the meeting were filled with bitter resentment and mistrust of NRC, as well as a deep, almost hysterical fear of low levels of radiation. I myself do not see how nuclear energy can survive in the long run — or possibly in the short run — if the public cannot distinguish between say, a millirem and a million rem.

It is for such reasons that I have urged that reactors be confined, permanently, to a relatively few and rather remote sites. C. Burwell, J. Ohanian, and J. Lane of the Institute for Energy Analysis have shown that 600 large reactors — possibly the number that will be built in the United States by the middle of the next century — could fit on about 100 large sites. Most of these could be expansions of the existing nuclear sites which, surprisingly, are already rather remote.

In heavily populated Europe, there are few remote sites — although even in Denmark such sites can be found on Zeeland. Nevertheless, even if the sites are not remote, there are many other advantages of clustered siting — better organization on site, security and internal lines of transport for example. It is significant that almost one-half of all the nuclear power to be generated outside the US by 1985 will move from sites containing four or more reactors; three sites have eight or more reactors on them.

The environmental hysteria displayed at Middletown is not confined to low levels of radiation. The litany of incidents involving toxic effluents grows longer each day — Seveso, Mississauga, Love Canal. Hardly a nightly TV news broadcast in the United States goes by without another account of people suffering maladies attributed to low levels of industrial toxicants.

I am therefore much taken by Dr Pietro Cappuro's proposal in *Clinical Toxicology* **13**, 325 (1979) "that industrial plants be concentrated in groups, at locations where natural factors such as wind, land contour, and water flow provide rapid dilution of toxic effluents". The notion of rather remote, permanent industrial enclaves is not new. It is striking that many of the same arguments that support remote, confined, and permanent siting for nuclear energy are being adduced to support a siting policy for polluting industry in general.

An important element in the proposal for nuclear siting is that each site should be committed, if not in perpetuity, then for a very long time. Low-level radioactive wastes could thereby be handled on site, as is now being done at the large Bruce site in Canada and at the seven TVA nuclear sites. This same imputation of permanence could be exploited for non-nuclear wastes as well. If the sites at which industrial activity continues are also used for disposal of low-level chemical wastes, fiascos such as that of Love Canal, where toxic wastes were nobody's responsibility,

would be dealt with rather automatically.

Like nuclear energy, the potentially dangerous chemical technologies demand long-term attention to detail and organizational integrity in return for the benefits they confer. It is striking that a recipe for living with the nuclear Faustian Bargain — to confine the enterprise to relatively few, permanent sites — is now recognized as applying to other technologies as well. Perhaps the nuclear enterprise can find some consolation in the growing realization that it is not unique in what it asks of the society in return for the benefits it confers.

Yours faithfully,
ALVIN M. WEINBERG

Institute for Energy Analysis,
Oak Ridge, Tenn., U.S.A.

Parkinson's trees

SIR,—R. Moss (*Nature*, **285**: 9) has provided a useful mathematical model to help explain the now well-established (if bureaucratically unpopular) scale effect that results in large organizations being less productive than small ones. Non-mathematical readers may find a simple ecological comparison easier to follow.

A tree may be appropriate model. The leaves represent the primary producers or scientists, the branches and trunk the support staff. The ratio of leaf to branch weight can be of the required order, averaging 12.6:10.2 in *Picea abies* (J. D. Ovington, *Advances in Ecological Research*, **1**, 103 (1962)). Trunk weight is about ten times the leaf weight but is very variable, depending perhaps on how high the tree canopy has to be elevated to reach the light.

Just what size a research group should be for maximum efficiency has been the subject of surprisingly little research, and that mainly by non-scientists. The tree analogy suggests we should consider separately the best size for a research unit (branch size), department (tree size) and national research body (forest size). The last will be directly related to the size, resources or needs of the country, but there is no reason why tree size would be related to forest size. A research department will have an optimum size and structure depending on its function, just as different species of tree will vary in size and leaf form; and a large country should establish many trees of this size, so that each can adapt to its local environment, rather than try to grow an extra large one.

If the pursuit of efficiency is desirable, useful comparisons of productivity could be made between branches of similar size on the same tree. Caution is needed to check that the branches have similar function and aspect (access to resources), while comparisons between branches on different species of tree (department or discipline) will be meaningless until some way is found of balancing their diverse aims or products. The most profitable comparisons are likely to be between branches on similar trees; for example, gamebird research units of state wildlife departments in America.

Administrators may argue that they are not dead wood but a structural device like a tree trunk to increase size, allowing successful competition with other ever-expanding trees, and enabling their research units to find a place in the sun. This, however, might be better achieved by cutting out the big trees and replacing them with smaller, more productive young ones, as any forester knows.

Before the axe falls there are the usual ecological provisos: agreement on the kinds of trees to fell and which to plant, retention of unusual trees whose genotype might be useful

in future, maintenance of variety and mixed age distributions for stability, and a reserve for such giant redwoods as the National Health Service.

Yours faithfully,
JOHN E. C. FLUX

230 Hill Road,
Belmont, Lower Hutt,
New Zealand.

Merrison's malady

SIR — That the Merrison Committee cannot resolve the malaise afflicting university research is clear enough (leading article, 22 May).

It is the readiness of our administrators to act as Healey-Joseph monetarist surgeons that has brought the malaise to this critical stage. The universities, in shedding technical and research posts, or equipment renewal and repair costs, have expected the research grant bodies to pick them up. The research councils, faced with impossible demands on static and contracting budgets, have resorted to financial limits apparently "calculated to ensure that even the best projects will not quite succeed" and to arbitrary time limits (such as the SRC's new ban on individuals holding an RA post for more than three or, exceptionally, six years).

Partly because we lack political muscle and partly because research jobs are regarded as transitory, contract researchers are being treated as optional extras — hard luck on personnel employed for years on soft money or unable to find a British university home to develop possibly outstanding projects. There are, however, some 10,000 contract workers in universities (Association of University Teachers figures) compared with 30,000 teaching staff. A proportion of university research of the order of 40 per cent might fairly be attributed to us.

Quality is relevant too. Experienced researchers are invaluable and irreplaceable for certain projects. Six or ten-year space research projects cannot be run by a succession of three-year contract researchers. To get round the SRC time limit, special dispensatins for 'project managers' are currently being sought; but such subterfuge cannot meet the need for experienced instrument designers and data analysts. Already some space projects are threatened with run-down. Expensive equipment will be unused and expensively-accumulated data will remain in store.

As you say, the Merrison joint committee between research councils and the UGC cannot be expected to discover a solution for the distribution of severely reduced funds. With only top academics and administrators, and no representatives of researchers or their trade unions, how could the seven-man (all male) working party invent an acceptable bargaining structure?

Surely the aim should instead be to analyse the malaise and conceive a holding operation; to persuade the UGC that it should not and cannot meet Government targets by cutting equipment grants, but must restore them with proper compensation for inflation, and to persuade the research councils to keep alive university laboratories and research teams.

Research itself will only suffer more from further surgery and hacking off weaker and less glamorous sectors. The holding operation should aim to maintain the successful integration of research in British universities until the government which conceives targets in monetary terms alone can be changed.

Yours faithfully,
M.K. WALLIS

University College, Cardiff, UK.

NEWS AND VIEWS

Phencyclidine

from Solomon H. Snyder

NEXT to marijuana phencyclidine, commonly known as PCP, is now the most widely abused street drug in the United States. In recent years PCP has received widespread attention because of the violent, homicidal and suicidal behavior of users. From the point of view of psychiatrists PCP is one of the most fascinating psychotropic drugs as the psychosis it elicits may provide the best available drug model of schizophrenia. For the pharmacologist PCP is a very unique psychoactive substance whose mechanism of action poses novel challenges.

Since PCP is often sold as tetrahydrocannabinol (THC), the principal psychoactive ingredient in marijuana, mescaline or LSD, it presumably mimics to a certain extent these drugs. PCP is widely sold in combination with other drugs such as barbiturates, heroin, cocaine, amphetamine, methaqualone (a barbiturate-like hypnotic), LSD and mescaline. Some of the street names for PCP include angel dust, crystal, elephant or horse tranquilizer, killer weed, super weed, monkey dust, Peace pill, goon, surfer and scuffle.

Phencyclidine is a cyclohexylamine (see figure). Large numbers of PCP analogues have been synthesized. Interestingly, at least six of these analogues are sold illicitly cn the streets of American cities, a situation which is unprecedented among drugs of abuse. Besides PCP, whose chemical structure is 1-(phenylcyclohexyl) piperidine, five other PCP analogues have been widely distributed, namely PCE (*N*-ethyl-1-phenylcyclohexylamine), TCP (1-(1-2-thienylcyclohexyl) piperidine), PHP (1-(1-phenylcyclohexyl) pyrrolidine), PCC (1-piperidinocyclohexanecarbonitrile), and ketamine (2-*o*-chorophenyl)-2-methylamine cyclohexanone).

What are the psychic effects of PCP? Its behavioural action is best understood by reviewing its history as a clinical anaesthetic and then as a drug of widespread abuse. PCP was synthesized by chemists at

the Parke Davis Drug Company at the end of the 1950s [1]. In animals it displays some stimulant effects but also affects motor coordination producing a 'drunken' state. When administered to monkeys a state of apparent tranquility appears, which in larger doses develops into general anaesthesia. Because of what seemed to be serenity in the monkeys, the brand name of 'Sernyl' was introduced. Small doses of PCP in humans produce a drunken state with numbness of the extremities reflecting analgesia and even anaesthesia. In sub-anaesthetic doses human subjects seem to be in a state of sensory isolation with their eyes wide open, but unresponsive to the environment.

The drug appeared to be a relatively safe surgical anaesthetic, because it could produce anaesthesia with profound analgesia in the presence of normal reflexes of the pharynx and larynx. Moreover, in contrast to many anaesthetics whose toxicity is associated with respiratory depression, PCP stimulated both the respiratory and cardiovascular systems. Its only drawback was that when emerging from anaesthesia patients described confusional states, vivid dreaming and hallucinations. Because of these side-effects, PCP was withdrawn from use in humans, though it is still employed commercially as an animal anaesthetic. Ketamine, a PCP derivative which is shorter acting and has somewhat fewer side-effects, has replaced PCP for human use in surgical anaesthesia, though ketamine is also widely abused.

It is unclear just what aspect of the PCP experience attracts drug abusers. Interviews with large numbers of drug users suggest that the sedation, sensory isolation, seeming "drunkenness" and hal-

---

Solomon H. Snyder is Distinguished Service Professor of Pharmacology and Psychiatry, Departments of Pharmacology and Experimental Therapeutics and Psychiatry and Behavioural Sciences, John Hopkins University School of Medicine, Baltimore.

lucinations are sought after. However, together with the apparent sensory isolation comes a feeling of depersonalization which can be terrifying to patients. Indeed it is these subjective changes which make PCP an impressive drug model of schizophrenia. Patients describe a loss of the ability to distinguish self from nonself, a dissolution of ego boundaries and a sense of unreality [2]. The disturbance in thinking has been described as "loosening of associations", "overinclusive thoughts", "concreteness", "delusional thinking", and "general disorganization", all strikingly reminiscent of the thought disorder of schizophrenics.

The most impressive evidence that PCP psychosis resembles schizophrenia is the fact that drug users have been mistaken by experienced psychiatrists for schizophrenics before obtaining the history of drug use. A particularly dramatic instance occurred in Washington, D.C. during the fall of 1973 when the admission rate for what appeared to be unusually long, severe and treatment resistant initial schizophrenic psychoses suddenly tripled in a community mental health center [3]. It was some time before the physicians recognized that these patients were suffering from PCP psychosis. Unlike the psychoses from psychelic drugs such as LSD, which generally last only about 8-16 hours, PCP psychosis lasted for periods up to two weeks. LSD psychosis can be readily distinguished from schizophrenia. Schizophrenic hallucinations are auditory, while individuals receiving LSD generally experience only distortions in visual perception. With PCP, subjects may hear voices and display autistic and delusional thinking resembling that of schizophrenics. They may display the formal thought disorder of schizophrenics with a loosening of mental associations and a "blocking" of mental processes [3]. Another link of PCP to schizophrenia comes from studies in which PCP was given to hospit-
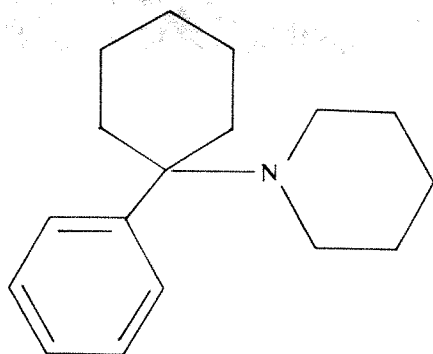
The chemical structure of phencyclidine.

alised schizophrenics [2]. LSD produces no more severe effects in schizophrenics than in normal subjects. By contrast, schizophrenic symptoms are greatly exacerbated for up to several weeks following PCP administration.

One apparently unique aspect of PCP psychosis is its frequent association with aggressive behavior. Users feel that they have superhuman strength and invulnerability. More cases of homicide and suicide are associated with PCP use than with any other drug of abuse.

How might PCP exert its remarkable psychic effects? Though PCP has anticholinergic atropine-like effects [4], these are much too weak to account for its behavioural actions. Actions at selective sites in the brain is apparent from regional metabolism studies with 2-deoxyglucose. Behaviourally active doses of PCP selectively increase 2-deoxyglucose uptake in the hippocampus, a portion of the limbic system which regulates emotional behavior[5]. A molecular locus for such an action is suggested by findings that PCP potently affects ion channels at nicotinic cholinergic receptors [6,7] which are abundant in the hippocampus. It is even possible that the seemingly great muscular strength and aggressivity of PCP users involves such effects at cholinergic receptors in the neuromuscular junction [8].

A potentially powerful new approach to characterizing PCP actions stems from two independent reports identifying PCP

1. Domino, E. F. *Int. Rev. Neurobiol.* 6, 303 (1964).
2. Luby, E. D., Cohen, B. D., Rosenbaum, G., Gottleib, J. J. & Kelly, R. *A.M.A. Arch. Neurol. Psychiat.* 81, 363 (1959).
3. Luisada, P. V. *NIDA Res. Mon.* 21, 241-253 (USPHS, Washington, DC, 1978).
4. Maayani, S., Weinstein, H., Ben-svi, N., Cohen, S. & Sokolovsky, M. *Biochem. Pharmacol.* 23, 1263 (1974).
5. Melbach, R. C., Glick, S. D., Cox, R. & Maayani, S. *Nature* 282, 625 (1979).
6. Tsai, M.-C., Aronstam, R. S., Eldefrawi, M. E., Eldefrawi, A. T. & Albuquerque, E. X. *Fed. Proc.* 38, 274 (1979).
7. Mittag, T. W. & Gross, S. P. *Int. Soc. Neurochem. Abs.* p.486 (1979).
8. Albuquerque, E. X., Adler, M., Spivak, C. E. & Aguayo, L. *Ann. N. Y. Acad. Sci.* 1980, in the press.
9. Zukin, S. R. & Zukin, R. S. *Proc. natn. Acad. Sci. U.S.A.* 75, 6372 (1979).
10. Vincent, J. P., Kartalovski, B., Geneste, P., Kemenka, J. M. & Lazdunski, M. *Proc. natn. Acad. Sci. U.S.A.*, 76, 4678 (1979).
11. Maayani, S. & Weinstein, H. *Life Science* in the press.
12. Snyder, S. H., Pasternak, G. W. & Pert, C. B. in *Handbook of Psychopharmacology* 5 (eds Iversen, L. L., Iversen, S. D. & Snyder, S. H.) 329-360 (Plenum, New York, 1975).
13. Vincent, J. P., Vignon, J., Kartalouski, B. & Lazdunski, M. in *PCP: Historical and Current Perspectives* (ed. Domino, E. F.) (NPP Publications, Ann Arbor, in the press).

binding sites in the brain which may be unique PCP 'receptors' [9,10]. PCP analogues whose affinities for the binding sites varied over a 20-100 fold range showed parallel variations in their disruption of the ability of rodents to balance themselves. Clearly the identification of specific PCP receptors would greatly assist in the understanding of how this drug and related agents act. It is possible that there are endogenous PCP-like substances analogous to the enkephalins, the normal neurotransmitters associated with opiate receptors [9,10].

Drug receptor binding studies can be deceptive because of artefactual binding sites masquerading as true 'receptors'. An artefactual binding effect was suggested by studies showing that the filters used in binding studies themselves bind radiolabeled PCP [11]. Moreover, if the brain tissue is boiled, its PCP binding properties remain essentially unaltered. Relative potencies of several PCP derivatives are the same at binding sites on intact brain membranes, boiled brain membranes or filters with no tissue. This suggests that PCP binding sites are not in

fact true receptors but merely reflect saturable binding to nonspecific sites on filters or tissue. Such saturable but artefactual binding is well known. Thus, certain filters and lipids can bind opiates in a sterospecific fashion, with optical isomers displaying the same relative potency at the opiate receptor [12].

To clarify these questions, both the French [10] and American [9] groups have performed a number of control studies. Both have shown that ^{3}H-PCP can bind saturably to tissues other than the brain. Vincent *et al.*, [13] showed that potencies of PCP derivatives vary in the different tissues. Affinities of various PCP analogues for binding sites in the brain parallel their behavioural potencies in mice, while these is no correlation between behavioural activity and drug binding in liver or kidney.

Thus, while the status of these binding studies is not yet clarified, specific quantifiable PCP receptors may exist. Whatever the final outcome of these studies, they have served to focus to attention on a drug class whose effects may hold promise in clarifying abnormal brain function in schizophrenia.

The transcription of eukaryotic genes

from R. A. Flavell

IN the past year two systems have been developed where specific transcription of eukaryotic genes can be obtained *in vitro*. Weil *et al.* (*Cell* 18, 469; 1979) showed that an S100 extract of mammalian cells conferred specificity on the transcription of adenovirus (Ad) 2 DNA by RNA polymerase II. In this case, the AD 2 specific RNAs were produced with a 5' end coincident with that of the major late AD 2 pre-mRNA. These RNAs are therefore presumably directed by the Ad 2 late promotor. Likewise, Manley *et al.* (*Proc. natn. Acad. Sci. U.S.A.* in the press) have shown that specific initiation of RNA synthesis from the same promotor occurs in a total cell extract from Hela cells.

In this issue of *Nature* Wasylyk *et al.* describe the *in vitro* transcription of the conalbumin ovalbumin genes and compare this with adenovirus late and early genes using the system of Weil *et al.* They show that the conalbumin gene and the Ad 2 late region is transcribed efficiently in this system and that the 5' ends of the *in vitro* RNAs are the same as the *in vivo* RNAs. The ovalbumin genes and the Ad 2 early 1A 'promotors' are only poorly utilized in this system. It is not clear at this stage if these differences reflect strong and weak promotors as defined in prokaryotic systems.

Sequence comparison of the 5'

extragenic regions of a number of eukaryotic genes has shown that certain DNA regions appear to be conserved in evolution. In particular, a sequence (TATAAA) similar to the Pribnow box of the prokaryotic promotor, is found around position -30 (i.e. 30 nucleotides upstream from the 1st nucleotide of the mRNA) in most eukaryotic genes (Proudfoot *Nature* 279, 376, 1979). However, some genes appear to lack a demonstrable Hogness box (notably the late regions of SV40 and polyoma). It is of great interest to determine whether these conserved DNA sequences play a role in the initiation of transcription.

Presumed promotors can also be tested by *in vitro* site-directed mutagenesis and then the deletion mutant tested for its ability to direct transcription in the assay system of choice. Using this approach, Grosschedl and Birnstiel (*Proc. natn. Acad. Sci. U.S.A.* 77, 1432; 1980) have analysed the transcription of the sea urchin H2A histone genes after injection of the DNA into the nucleus of *Xenopus laevis* oocytes. They showed that deletion of the regions immediately upstream from the H2A gene, and including the Hogness box, reduces, but does not eliminate

R. A. Flavell is in the National Institute for Medical Research, Mill Hill, London.

transcription of the H2A gene. Interestingly, this deletion appears to cause the synthesis of RNAs with heterogenous 5' ends located downstream from the normal 5' end.

A number of observations in viral systems point to the same type of phenomenon. Bending and Folk (*J. Virol.* **32**, 530; 1980; *Cell* in the press) have isolated viable deletion mutants of polyoma where both Hogness box and cap region are deleted. Likewise Benoist and Chambon (*Proc. natn. Acad. Sci. U.S.A.* in the press) have constructed the equivalent mutants in SV40, which are still able to express the early region. A large deletion removing sequences far upstream inactivates this region. Finally, Gluzman, Sambrook and Frisque (*Proc. natn. Acad. Sci. U.S.A.* in the press) have shown that a large deletion of about 200 nucleotides which eliminates the Hogness box and the upstream sequences apparently inactivates the SV40 transcription unit. It seems, therefore, that loss of the Hogness box causes the production of RNAs with heterogenous 5' ends when transcription is assayed *in vivo,* and at least in viral systems still greater deletions cause the elimination of transcription.

Clearly *in vitro* transcription assay systems offer another convenient and rapid means of mapping promotor sequences. Wasylyk *et al.* report an initial search in this direction. They show that deleting the DNA sequences upstream from position –44 has no detectable effect on the *in vitro* transcription of the conalbumin gene. However, deletion of the additional DNA sequences from this position to –8 eliminates transcription entirely.

It now seems clear therefore that at least some of the sequences required for the transcription of structural genes by RNA polymerase II are localized in the DNA immediately flanking the gene on the 5' side. This differs from the results obtained with RNA polymerase III based systems where these sequences can be deleted without affecting transcription (Sakonju *et al. Cell* **19**, 13; 1980; Bogenhagen *et al. Cell* **19**, 27; 1980; Kressmann *et al. Nucl. Acids. Res.* **7**, 1749; 1979; Thimmappaya *et al. Cell* **38**, 947; 1979)

It seems likely that the Hogness box forms part of the 'promotor' yet proof for this must await specific alteration of this region by fine structure deletions and point mutations. However, *in vivo* results point to a second DNA region, localized further upstream, that is implicated in transcription initiation. One obvious difference between the *in vivo* and *in vitro* data is that *in vivo* the DNA is packaged in some form of chromatin whereas this does not appear to be so in the *in vitro* systems, and perhaps this is involved in the functioning of this second 'region'. One thing, at any rate, is clear — the 5' ends of every gene under the sun are in for a beating with mutagens and nucleases this year in the quest for the eukaryotic promoter. ☐

---

100 years

Several papers have stated that an official commission will be appointed in France to witness the crossing of the British Channel by a balloon travelling from France to England (weather permitting). The fact is that the experiment is to be made from Boulogne by M. Javis, with his own balloon and at his own risk. But the port authorities have agreed to send M. Javis such information as will enable him to select for starting a time when the wind is blowing with some sufficient prospect of reaching England. M. Javis will keep watch from June 1 to 20. A steamer will follow as far as possible the hardy aëronaut on his adventurous trip.

The Emperor of Russia has conferred the

Grand Cross of the Order of Stanislaus upon Dr. Hermann Obst, the director of the Ethnographical Museum of Leipzig.

In a series of papers on the northern part of the continent contributed to an Australian paper the writer mentions a curious feature of the creeks and lagoons in the north of Queensland. This is what is called "floating grass." It is a tall aquatic grass, which while growing in the mud when within reach, is quite independent in that respect, and extends its creeping stems into the deepest water; and by the interweaving of these, and of the roots emitted from every joint, makes a dense mat of verdure, which, at first sight, seems to have its origin on solid ground. It is however quite possible to walk on it without risk of entanglement. The method is to keep going, lifting the feet well, and with the body in as flat a position as possible. Horse and cattle are fond of this grass, and it is said that the masses of it are sometimes so dense, although with twenty feet of water underneath, that horses have been known to cross on them.

From *Nature* **22**, 3 June, 110 & 111, 1880.

Asteroid Hektor

from Jonathan Gradie

THE asteroids are more than just the 'minor planets' of our Solar System. Their small size belies their importance to our understanding of the formation of all the planets. Today we see the asteroids not as the vestige of a disrupted planet, as was once thought, but as the remains of the process which formed the planets. They are not only a window back in time to the beginning of our solar system, but are also a record of the events as they happened in time and space.

The past decade has shown an explosion of knowledge about asteroids. Physical studies have shown the existence of at least two major types of asteroids: the low albedo ($p_v \sim 0.04$), spectrally neutral 'C' objects, and the higher albedo ($p_v \sim 0.13$), spectrally reddened 'S' objects. The 'C' objects are probably similar to if not identical to the carbonaceous chondrite meteorites; the 'S' objects appear to closely match the stony-iron meteorites. The asteroid Vesta has been found to be identical to if not the source of the basaltic achondrites.

One fascinating aspect of recent theoretical work is the study of the collisional evolution of the asteroids. Collisions appear to have dominated the history of the asteroids; collisions can range from minor erosive cratering impacts to major catastrophic events which result in the complete disruption of the body and the formation of a Hirayama family. Depending upon the circumstances of the collision, the final product can take on a most curious form, at least according to Hartmann and Cruikshank (*Science* **207**, 976; 1979). They hypothesize that under very special circumstances, some collisions

may result in the accretion of a new and larger asteroid. They cite the Trojan 624 Hektor as a possible example.

Hektor is a strange object. It orbits with the proceeding Trojan cloud at one of the Lagrangian points of Jupiter. The large amplitude (1 mag) lightcurve was originally interpreted as evidence that Hektor was a very elongated, cigar-shaped object ($b/a \sim 1{:}3$), probably a splinter from a larger asteroid destroyed by a catastrophic collision. Thermal radiometry identified Hektor as a comparatively large asteroid (long axis ~ 300 km) with a very low albedo ($p_v \sim 0.02$). As Hartmann and Cruikshank have pointed out, the combination of the 1:3 elongation and the large size is unusual among asteroids and somewhat puzzling as the other Trojans in the proceeding cloud do not appear to be splinter-like fragments of a much larger parent body destroyed by a catastrophic collision. It appears that the lightcurves may have been interpreted incorrectly, that perhaps the large amplitude lightcurve was due to albedo effects, i.e., one side light, the other dark, instead of shape effects. If the lightcurve is caused mainly by albedo variations this would remove the problem caused by the combination of elongated shape and large size. Hartmann and Cruikshank were able to prove with simultaneous observations in reflected light and emitted thermal radiation that Hektor is indeed highly elongated and that the unusual shape accounts for most of the light variation.

How did Hektor become so elongated?

Jonathan Gradie is in the Center for Radiophysics and Space Research, Cornell University.

The authors hypothesize that instead of a collision fragment, Hektor may be a compound asteroid, that is, the result of the coalescence of two Trojans of comparable size during a very gentle collision. The idea is not as far-fetched as it may seem at first. The average relative velocity of asteroids in the main belt is ~5 km/sec, which is more than enough to disrupt two equal-sized bodies, whereas the average relative velocity in the Trojan cloud is only 1-2 km/sec. Some encounters, especially on the low velocity tail of the velocity distribution, will be at a low enough velocity to leave both bodies intact and gravitationally bound.

To account for the discrepancy between the lightcurve amplitude that two spheres in contact would have and the amplitude

observed, Hartmann and Cruikshank propose that the contact zone between the two components may be photometrically brighter in a manner somewhat analogous to rays around fresh lunar craters. Whether or not this material could be detected spectrophotometrically as suggested, remains a problem, but if it is a bright neutrally colored substance, such as ice, it should show clearly.

Low velocity collisions among asteroids in the main belt have been only qualitatively explored. The current suspicion that some asteroids may have satellites or may be binary systems should provide impetus for further study in this area. It may turn out that low velocity collisions are of fundamental importance in the evolution of at least some asteroids.

□

be possible to breed in the disease resistance genes and have the best of both worlds. Two speakers testified that the mutation has no adverse effect of flavour. Although von Wettstein speculated on more sophisticated operations, such as gene transplantation to accelerate the action of brewer's yeast, advances in food (or drink) production have come in practice largely from conventional genetics. Perhaps the 1980s will see the realization in this field of the practical potential of genetic engineering with recombinant DNA.

Certainly Weissmann and his collaborators have already taken an important step towards genetically engineered drug production with the cloning of an interferon gene — or, as it now turns out, two interferon genes. Three different kinds of interferon can be distinguished on the basis of their cellular origin and activity: immune, or γ interferon, fibroblast, or θ interferon, and leukocyte, or σ inferon. Sequencing[1] of the cloned DNA for leukocyte interferon now shows that there are at least three genes for leukocyte interferon alone. The nucleotide sequences of the two genes cloned by Weissmann and his colleagues are distinctly different from one another, and neither corresponds to the amino acid sequence reported by Zoon *et al.*[2] for leukocyte interferon.

Biology in the 1980s, plus or minus a decade

From Miranda Robertson

GOOD scientists do not speculate a decade ahead of their research. So when the Friedrich Miescher-Institute invited seven good scientists to celebrate its tenth birthday by talking on biology in the 1980's it might have expected to be reminded (by C. Weissmann), that in 1970 no-one would have dreamed that eukaryotic genes were split; (by C. Blakemore) that few could have guessed the importance of peptides in brain function; and (by almost everyone) that new discoveries and conceptual revolutions are by their nature unpredictable. Weissmann put his finger on the difficulty when he quoted the last words of Gertrude Stein, which were: "What is the answer?. . ." followed after a pause by " . . . What is the question?" In science, the next question is always contingent on the answer to the last, and anyone who can see more than one or two questions ahead is probably making up stories, not doing research. Consequently most of the speakers opted to discuss the work of the past decade (or two) and raise some outstanding questions.

K. Illmensee, for example, announced a technical achievement that will make it possible to investigate some hitherto inaccessible processes in mammalian development. He has succeeded in making small clones of mice from the ectoderm and

proximal endoderm of 7-day embryos, by nuclear transplantation into fertilized eggs. Not all embryonic tissues can be used for cloning: the nuclei of trophoblast and distal endoderm are irreversibly differentiated in embryos at that stage. Because of the progressive loss of developmental potential in differentiating nuclei, this offers biologists a new system in which to look for the mechanism of gene inactivation; and it has already enabled Illmensee to investigate the reasons for the abortive parthenogenesis of LT strain mice. LT females spontaneously produce parthenogenetic embryos which sometimes implant but invariably die soon after. By transplanting the nuclei from such embryos into fertilized eggs of another strain, Illmensee has been able to produce adult mice orginating from a parthenogenetic nucleus. Since the cytoplasm of LT eggs is perfectly capable of sustaining the development of non-parthenogenetic embryos, this result is rather remarkable and implies either that fertilization provides or triggers an essential factor in the cytoplasm, or that there is a specific failure in the interaction between parthenogenetic nuclei and LT cytoplasm.

D. von Wettstein's contribution to the futuristic spirit of the occasion was a small crate of 1980s experimental lager brewed from a mutant barley with a block in the biosynthetic pathway to the proanthocyanidins, which precipitate proteins and cause lager to cloud. At present, the mutant barley lacks mildew resistance as well as proanthocyanidin, so the brewer avoids treating the beer for clouding at the expense of treating the barley for fungus: but it should eventually

The nucleotide sequence of the fibroblast interferon gene sequenced by Taniguchi *et al.*[3], on the other hand, does seem to correspond to the fibroblast interferon amino acid sequence[4]. What the functional significance of the different leukocyte interferons may be it is not possible to guess, but the question is now wide open to investigation.

The discovery of unsuspected genes (pro-opiocortin is another example) and mechanisms (RNA splicing) was no doubt what S. Brenner had in mind when he remarked that progress in science depends on new techniques, new discoveries and new ideas, probably in that order. After a decade of research on the development of the nematode nervous system, he still does not know how it is genetically programmed — possibly because, as J. D. Watson is said to have commented, the work was twenty years ahead of its time. Brenner's own reflection on the project is that the fundamental mystery of metazoan evolution and ontogeny probably cannot be solved by looking at mutations, such as those that he and others have investigated, that have obvious deleterious consequences for all mutant animals. Since each viable species is built from an earlier viable species, the informative mutations may be those with poor penetrance, or barely discernible phenotype, which could have persisted without jeopardizing survival while evolution took its leisurely course.

Miranda Robertson is an associate editor of Nature.

Such mutations are, of course, extremely difficult in investigate, but techniques for exploring them, at least in structural genes, do exist in what Weissmann chooses to call reverse genetics. The principle is, instead of selecting and manipulating phenotypes to explore the genotype, to manipulate the genotype directly and observe the effect on the phenotype. In practice, it means making discrete and specific mutations or deletions in specific regions of the DNA. By these means Weissmann has, for example, shown through deletions that the "Hogness box" upstream of the rabbit beta globin gene is necessary for the correct initiation of beta globin transcription in mouse cells. It is in principle possible to use reverse genetics to explore the phenotypic consequences, if any, of small mutations in any gene and its regulatory elements. But while that would clarify the "path from gene to phene" (to borrow Hadorn's phrase from the title of Weissmann's talk), it hardly approaches the path from genotype to phenotype which is Brenner's preoccupation.

G. Klein opened up an interesting avenue for exploring the relationship between genotype and neoplastic phenotype. He and his colleagues have shown that trisomy of chromosome 15 is associated with mouse T cell leukaemias induced by widely diverse agents, but not with non-T cell leukaemias. Klein suggests that chromosome 15 may contain genes coding for the differentiated functions of T cells, as well as for the proliferative potential of stem cells. The extra copy of chromosome 15 remains in the undifferentiated stem cell state at

1. Mantei, N. *et al. Gene* (in the press).
2. Zoon, K. C. *et al. Science* **207**, 527 (1980).
3. Taniguchi, T., Ohno, S., Fujii-Kuriyama, Y. & Maramatsu, M. *Gene* (in the press).
4. Knight, E., Hunkapillar, M. W., Korant, B. D., Hardy, W. F., & Hood, L. E. *Science* **207**, 525 (1980).
5. Leupold, U. *Nature* **263**, 811 (1980).

division and enables the leukaemic cell to express both. Another possibility is that the two chromosomes are both in the same state and the neoplastic phenotype is a gene dosage effect. It should be possible to distinguish experimentally beween these alternatives and perhaps at last shed some light on the mechanisms underlying neoplastic transformation in this and other leukaemias associated with specific abnormal karyotypes.

Two of the principal outstanding questions for the 1980s are those of the control of embryonic development, and the mechanism of plasticity in the nervous system (which is to say, learning). The answer to the first depends on techniques for identifying morphogenetic substances; and the answer to the second, at least in Blakemore's view, depends on techniques for measuring small changes in synaptic resistance. In neither field is there, or has there ever been any dearth of ideas, so perhaps Brenner is right to put technology first. Certainly recombinant DNA technology provided the means to solve the riddle of immunoglobulin diversity where his own elegant ideas and those of others on their own had failed. And yet there are cases in which the technology is trailing the ideas. Blakemore pointed out that all that the measurement of neuronal metabolic activity by 2-deoxyglucose has done so far is to confirm what was already known from more fragmentary and indirect data. The same applies to the application of recombinant DNA technology to the elucidation of the mating-type switch in baker's yeast[5].

All that advanced technology can do is to provide the tools with which to answer the questions raised by men and women of ideas; and it is perhaps just as well in these hard times that institutions such as the Friedrich-Miescher Institute exist to shelter them. □

Formation of interstellar molecules

from A. H. Cook

SINCE the first observations of microwave radiation from atomic hydrogen some thirty years ago many molecules have been detected in interstellar space. Using measurements of absorption, spontaneous emission and stimulated emission, results of general importance in astrophysics have been obtained.

Carbon monoxide is widespread in the galaxy and because it is excited above the ground state predominantly by collision with molecular hydrogen, its radiation can be used

A. H. Cook is Professor of Physics at the University of Cambridge.

to estimate the density of molecular hydrogen. This has lead to the important conclusion that the distribution of molecular hydrogen follows the spiral arms as traced out by stars and atomic hydrogen, and that the amount of molecular hydrogen in the galaxy is about the same as that of atomic hydrogen. Most molecules are not widespread but seem to occur in dense clouds of dust and gas associated with very young stars, their presence thus seems to be related to the processes by which stars are formed. It is found that the populations of the different states of molecules in such regions almost never follow the Boltzmann distribution, they are not in thermodynamic equilibrium, and

this may be a clue to the physical processes involved in the development of a star from a cloud of dust and gas.

Some idea of distributions of density, velocity, magnetic field and general level of excitation in molecular clouds can be obtained from absorption and emission data. However, as soon as one attempts to go beyond rather general statements, it becomes apparent that we have inadequate knowledge of the structure and properties of many molecules, even of the simplest and commonest. For example there is no data that would allow us to calculate possible processes by which populations of hydroxyl might be inverted. A great deal of laboratory work is required to match the astrophysical observations and some of the issues that are raised are of considerable interest for molecular physics.

A large and awkward gap in our knowledge of interstellar molecules is of the processes by which they might be formed. We know that they are destroyed by photo dissociation and the rates are sometime known; it is clear that molecules are present in dense clouds because there they are shielded from ultra-violet radiation. But the rates at which they are formed are for the most part speculative. The processes of formation are also of interest because laboratory experiments show that some molecules are formed by chemical reactions in excited states from which they can radiate stimulated emission. Molecules, it seems, may be formed from matter absorbed on the surfaces of solid grains, or they may be formed in the gas phase when the participation of ionised species is essential to obtain a sufficiently large cross section. In recent years, calculations[1] and experiment[2] have provided a rather firm basis on which to construct models of the interstellar gas in which reactions between positive ions and neutral atoms are involved and have led to a good understanding of the formation of carbon hydrogen molecules in particular[3]. There is evidence[4] that reactions of neutral atoms with molecular ions may be important and the results of a collaboration between two of the principle experimental groups in this field (those at NOAA Boulder, Colorado, and at Birmingham University) have recently been published[5]. A newly developed technique was used to enable neutral atoms to be injected into a flowing beam of molecular ions. Twenty four reactions of various molecular ions, such as

1. Black, J.H. and Dalgarno, A. *Astrophys. J. Suppl.* **34**, 405 (1977).
2. Sinnott, G. *NBS Spec. Pub.* **381**, Washington: Govt. Printing Office (1973); Ferguson, E. E. *At Data Nucl. Data Tables* **12**, 159 (1973); Huntress, W. T. *Astrophys. J. Suppl.* **33**, 495 (1977); Albritton, D. L. *At Data Nucl. Data Tables*, **22**, 1 (1978).
3. Smith, D. & Adams, N. G. *Astrophys. J.* **217**, 741 (1977); Smith, D. & Adams N. G. *Astrophys. J. Lett.* **220**, L87 (1978).
4. Fehsenfeld, F. C. & Ferguson, E. E. *J. Chem. Phys.* **56**, 3066 (1972); Fehsenfeld, F. C. *Astrophys. J.* **209**, 638 (1976); Karpus, Z., Anicich, V. & Huntress, W. T. *J. Chem. Phys.* **70**, 2877 (1979).
5. Viggians, A. A. *et al. Astrophys. J.* **236**, 492 (1980).

CH^+, CH_2^+, $C_2H_2^+$, CH_5^+, H_2O^+ and others, with N_2O and NO were studied. The rates are often relatively high, and many of the reactions are clearly likely to be important in interstellar chemistry. The reaction schemes indicate once again the importance of the HCO^+ molecular ion and of reactions with H_2.

This work not only provides much useful data but also demonstrates the importance of laboratory studies in the interpretation of interstellar chemistry and physics. ☐

	I/E	ι-ε
Harwood & Malin	0.12	8°
Yukutake & Cain	0.32	105°
Ducruix *et al.*	0.17	44°

Geomagnetic secular variation and the conductivity of the lower mantle

from David R. Barraclough

THE slow changes in the Earth's magnetic field with time provide one of the very few means to investigate the dynamics of the Earth's fluid core and the electrical conductivity of the lower mantle. Observations of the geomagnetic field changes — the secular variation — have been made ever since the seventeenth century because of their practical importance for those using magnetic charts. Nowadays, a network of 200 permanent magnetic observatories provides very accurate data free from spurious effects associated with changes of observing site.

The task of forecasting the secular variation for several years ahead is complicated by any sudden changes which may occur. Such a change appears to have taken place in about 1970. It was first noticed in the data from European observatories (Courtillot *et al. Comptes rendus* **D287**, 1095; 1978) but it has since been shown to have had world-wide effects (Ducruix *et al., Geophys. J.R. astr. Soc.* **61**, 73; 1980; Malin *et al. Ebro Obs. 75th Anniversary Volume* in the press). The phenomenon manifested itself as a sudden change in the secular acceleration, the second time-derivative of the main geomagnetic field (Barraclough & Malin, *Geophys. J.R. astr. Soc.* **58**, 785; 1979). Ducruix *et al.* found a positive change in the east component of the secular acceleration over Europe and central Russia and a negative change in this component over eastern Asia and north-western North America. Malin *et al.* examined the changes in the secular acceleration of the magnetic declination, the horizontal intensity and the vertical component. Their results for the declination are in agreement with the French results and they also find regional patterns in the other elements. Interestingly, all three elements suffered a sudden decrease in the secular acceleration over North America. Using a homogeneous set of observatory annual means covering the period from 1961 to 1978, Malin *et al.* have produced a spherical harmonic model of the phenomenon which clearly shows the details of its global distribution. There is general agreement that these sudden changes occurred on a time-scale short in comparison with that of the secular variation itself: certainly less than 4 years.

Most geomagnetic parameters vary with the sunspot cycle, which has a period of approximately 11 years. Observatory annual mean values show such a sunspot cycle variation (RV) which, although small in amplitude, can have a significant effect on secular variation estimates derived from the annual means. The source of RV is believed to lie above the Earth's surface, within the magnetosphere. Because the Earth has a finite electrical conductivity, these external magnetic field variations will induce electric currents within the Earth, together with associated magnetic fields. Thus, what is observed at the Earth's surface is a combination of the external inducing field and the internal induced field. It is possible, however, by considering the horizontal components and the vertical component of the variation field separately, to separate the internal and external parts. The ratio of the amplitudes of the two parts and their phase difference can then be used to investigate the conductivity of the regions of the Earth where the induced currents flow — the lower mantle in the case of RV. Three studies of RV have recently been published. Ducruix *et al.* (*op. cit.*) used the data from the 10 European observatories which provided the evidence for the sudden change in secular acceleration. The data spanned the interval 1947 to 1977. Yukutake and Cain (*J. Geomagn. Geoelect. Kyoto* **31**, 509; 1979) based their main conclusions on data from 21 observatories, globally distributed, and covering the period from 1900 to 1973. Harwood and Malin (*Geophys. J.R. astr. Soc.* **50**, 605, 1977) used all available data from 81 observatories with a world-wide distribution. Their earliest data were for 1842 and the most recent for 1974. The table below gives the amplitude ratios (I/E) and the phase differences (ι-ε) which result from these studies. The estimated uncertainties are approximately 0.1 for the ratios and 30° for the phase differences. Ducruix *et al.* have shown that the results

of Yukutake and Cain are not compatible with simple induction models. Considering the uncertainties, the results of the other two studies are in general agreement.

Ducruix *et al.* have used their values of I/E and ι-ε to test a series of four-layer models of mantle conductivity. The results indicate that the maximum value of the conductivity (which occurs at the bottom of the mantle) is approximately $100\Omega^{-1}m^{-1}$. The results of Harwood and Malin, which are based on a much more extensive collection of data, are also consistent with a maximum value of $100\Omega^{-1}m^{-1}$.

Runcorn (*Trans. Am. geophys. Un.* **36**, 191; 1955) showed that, for a change of the core field with a duration of 4 years to be detectable at the Earth's surface, the conductivity of the lower region of the mantle cannot exceed $100\Omega^{-1}m^{-1}$. Since the sudden change of secular acceleration about 1970 lasted for less than 4 years we are lead to the same upper limit for the conductivity as that given by the RV studies.

These two pieces of evidence thus cast considerable doubt on the higher estimates of lower mantle conductivity such as the figure of $10^4\Omega^{-1}m^{-1}$ proposed by Stacey *et al.* (*Trans. Am. geophys. Un.* **59**, 1027; 1978) and that of $10^5\Omega^{-1}m^{-1}$ favoured by Alldredge (*J. geophys. Res.* **82**, 5427; 1977).

Much work remains to be done in extending the studies of RV and the sudden changes in secular acceleration and in applying the results to determining more accurately the conductivity distribution in the lower mantle. The primary requirement is a good set of data, well distributed over the Earth's surface. The existing network of permanent magnetic observatories, which provide the most valuable data for such studies, has a very patchy distribution, very dense in Europe but very sparse throughout most of the Southern Hemisphere. Satellite surveys, such as that of the intensity and direction of the geomagnetic field currently being performed by Magsat, can only help if they are repeated at frequent intervals and even then they present their own set of problems. As far as the practical uses of the secular variation in the production of magnetic charts are concerned, we probably have sufficient knowledge of RV to attempt to correct secular variation estimates for its effects. The problem with the sudden changes is that they are, at present, completely unpredictable. Here, frequently repeated satellite surveys might help in detecting such changes as soon as possible after their occurrence. ☐

David R. Barraclough is in the Geomagnetism Unit, Institute of Geological Sciences, Edinburgh.

REVIEW ARTICLE

The Western English Channel—
an inconstant ecosystem?

A. J. Southward

Marine Biological Association, Plymouth, Devon PL1 2PB, UK

Changes in the chemistry and biology of the English Channel waters off Plymouth in the 1930s were a talking point for marine scientists 30 and 40 yr ago. The reversal of many of the changes, beginning in 1965 and continuing to 1979, may cause equal controversy about the stability of the ecosystem and the factors causing its fluctuation

THE western part of the English Channel off Plymouth has been studied for more than 75 yr, and continuous observations, interrupted only in 1940–45, are available from 1924. Between 1930 and 1936 there was a sequence of changes in abundance and species of zooplankton and pelagic fish, accompanied by a fall in the winter maximum of inorganic nutrients[1]. After 1964 these changes began to reverse, and within a few years it appeared that a cyclic change had taken place, coinciding with fluctuation in climate of the Northern Hemisphere[2]. More recent observations suggest the cycle has returned to a state close to that of the 1920s, providing an opportune moment to review the various factors, including water movements, sea temperature and nutrient chemistry, that have been suggested as causes of the cycle.

The changes

The complex series of events in the Western English Channel since the 1920s has been called the 'Russell Cycle' after its principal investigator[3]; some examples are shown in Fig. 1, and the initial phase of the cycle is mentioned in many textbooks[4]. Basically, a plankton community characterized by the chaetognath *Sagitta elegans*, was replaced over a period of about 5 yr by a community characterized by the more neritic species, *Sagitta setosa*[5]; there was a fall in the winter maximum of dissolved inorganic phosphate (Fig. 1c), one of the nutrients used by phytoplankton each spring; the standing crop of zooplankton and the numbers of planktonic stages of demersal fishes (Fig. 1c) decreased by an order of magnitude or more[6]; there were decreases in certain species of the benthos and replacement of some cold-water demersal fishes by warmer-water species[8]; the final event was the dramatic failure of the herring fishery off Plymouth in 1936 (ref. 9). At that time, the message of these changes seemed clear: a reduced flow of water into the Channel from the west led to a decline in nutrients; a lower level of nutrients would limit phytoplankton production[10]; a lower primary production would mean lower crops of copepods and other herbivores; fewer young fish would survive, and adult plankton-feeding fish would migrate elsewhere to find food; reduction in the zooplankton and pelagic fish would lead to decline of other fishes and the benthos. Research programmes were, therefore, directed to a study of natural events or processes likely to

control upwelling of 'nutrient-rich' water from the ocean and increased flow through the Channel[11,12].

After the major changes between 1930 and 1936 there was a long period, to 1961, without obvious trends; the inorganic phosphate fluctuated about a lower level, *Sagitta setosa* was the dominant chaetognath, and abundance of zooplankton and post-larval demersal fish remained low[13–15]. However, from the presence of large numbers of pilchard eggs in the plankton samples (Fig. 1b) and from echo-sounder surveys it became obvious that the numbers of adult pilchard must have greatly increased after 1935, and that this fish had replaced herring as the dominant pelagic fish[16,17]. A new hypothesis was put forward, that herring had failed in competition with pilchard[17]; the presence of large numbers of overwintering young pilchard might be sufficient to account for the lower maxima of inorganic phosphate, since they would contain, locked up in their flesh and bone, phosphorus and nitrogen that would otherwise have returned to the water each winter by death and decay of more ephemeral plankton organisms.

Search for an external cause of the increased population of pilchard was made easier by the longer series of environmental records becoming available. It was found that the waters of the Channel had warmed up between 1900 and 1950, during the general amelioration of climate of the Northern Hemisphere[18], and much of the rise had occurred in the 1920s[19,20]. Evidence had also accumulated for increased occurrences of warm-water fishes[8,21] and increases in the warm-water elements of the fauna of rocky sea-shores[22]. It was, therefore, possible to put forward a more general hypothesis to cover all the changes observed up to 1961[8]; that as a result of the climatic change there had been northward extensions of the boundaries of distribution, not only of boreal communities into the Arctic[23] but of warm temperate communities into the boreal regions. The *S. elegans* community is predominantly of cold-water origin, and herring are close to their southern limits at the entrance to the Channel. Pilchard, and many of the plankton species associated with the *S. setosa* community off Plymouth, are of warm-water origin. A shift in distribution of this nature, accompanied by slight alteration in the water circulation pattern in the Western Channel as a result of the climatic change (increased southerly influence) was regarded as sufficient to account for most of the changes in the ecosystem[8].
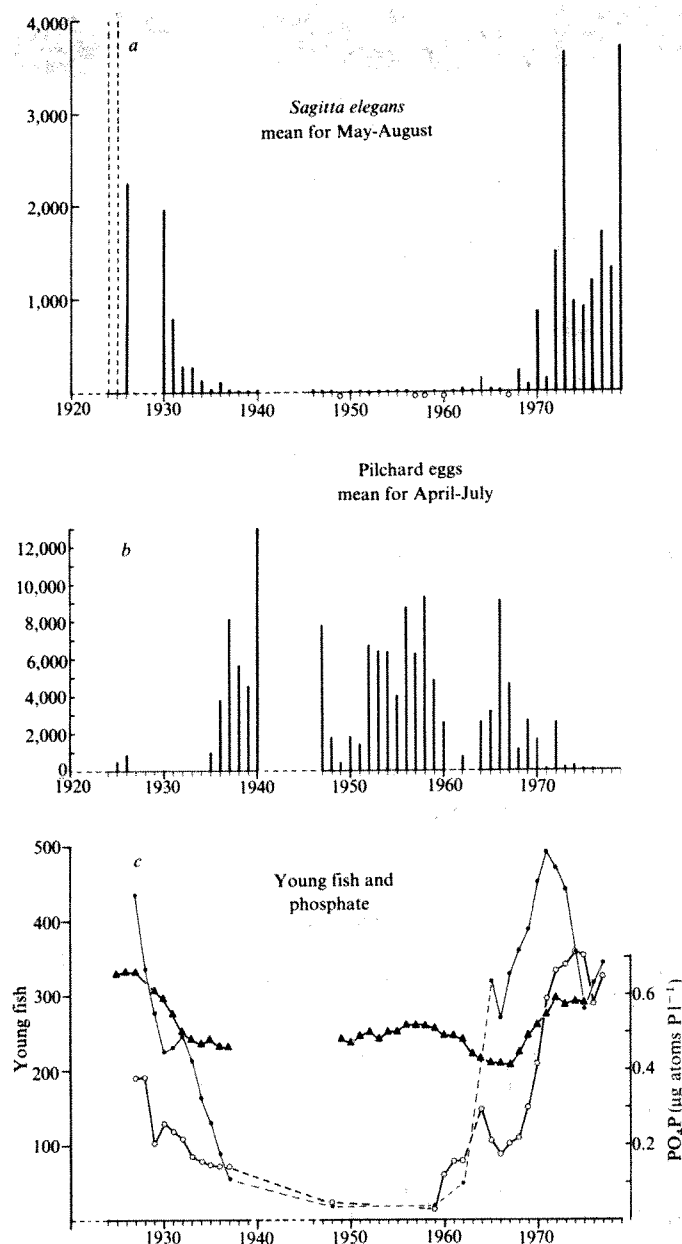
Fig. 1 Examples of some of the biological changes off Plymouth, based on weekly samples with the 2 m net at station L5 (2 miles east or 2 miles west of the Eddystone reef). The standard oblique haul filters about 5,000 m³ of water[69]. As indicated by the broken line for the ordinates, sampling was not possible in certain years; the broken columns or broken trend lines show years when sampling was incomplete. *a*, Numbers of the chaetognath *Sagitta elegans* Verrill, expressed as the average per haul for the summer months (May to August inclusive) when the offshore water is stratified. *b*, Numbers of eggs of pilchard (*Sardina pilchardus* (Walbaum)) expressed as the average per haul during the spring/summer spawning season from April to July inclusive. The number of eggs is assumed to be an index to the numbers of mature adults[16]. *c*, Comparison of smoothed values (5-yr running means) of inorganic phosphate (▲) at station E1 (50°02′N, 4°22′W), with 5 yr running means of post-larval teleosts (excluding clupeids) in the 2 m net samples at L5. The young fish are divided into spring-spawners (●), taken as the sum of the monthly means for March to June, and summer-spawners (○), taken as the sum of the monthly means for July to September. Phosphate is expressed as the 'winter maximum' of 'reactive' inorganic phosphate in μg atoms P l⁻¹. The winter maximum can be found variously from December to early March, and is allocated here to the spring of the following year if found in December.

The pilchard seemed to be associated with a more 'efficient' ecosystem[24], with a shorter food chain[25], smaller standing crops of zooplankton, and less 'wastage' to the benthos, and the fall in inorganic nutrients was seen as an index to the changed ecosystem rather than as the primary cause.

With the formulation of this hypothesis in 1963 we had reached the point where selection between the different theories could only come from new evidence, either by further changes or by a reversal or previous changes[8]. As if in answer to an ecologist's prayer the system did in fact go into reverse in the second half of the 1960s, and investigation was much stimulated. The numbers of post-larvae of demersal fishes increased from 1965, and by 1970 numbers of copepods had reached levels comparable with those of 1930[2]. The period of maximum spawning of pilchard shifted from early summer to autumn, and then both spawnings began to decline[26]; by 1975 there were virtually no pilchard eggs, and presumably no adult pilchard, off Plymouth in the first half of the year. However, herring did not return in large numbers, and mackerel became the dominant pelagic fish[27].

There was a slowing down of the rate of reversal of the cycle in the 1970s, with annual fluctuations in the ecosystem similar to those detected from 1931 to 1935 in the first phase of the cycle[28,29]. Each summer, from 1972 to 1978, there was a period with a plankton community characterized by *Sagitta elegans* and other northwestern plankton indicators[15,30] but the total dominance of *S. elegans* reported before 1930 was never achieved. However, early in 1979 changes became more noticeable. The first sign was the occurrence on poor-cod (*Trisopterus minutus*) of a parasite normally found on the gills of Norway-pout (*T. esmarkii*)[31] a northern distributed gadoid fish only once before recorded from the Western Channel[32]. It was soon confirmed that *T. esmarkii* itself had moved into the district, together with larger numbers of blue-whiting (*Micromesistius poutassou*), another small gadoid of cold-water oceanic distribution[33]. The plankton changed from February, and *S. elegans* became the dominant chaetognath, *S. setosa* being scarce or absent to the end of August. The typical associate species of pure '*elegans*' type, the trachymedusan *Aglantha digitalis* was present from April, and in July this species underwent a very big increase in abundance, with a maximum of 15 m⁻³ in August and average numbers equal to those reported in July and August 1930 (ref. 29). There was a temporary switch in the autumn of 1979 to a more typical warm-water or southwestern plankton community, with the trachymedusan *Liriope* replacing *Aglantha*, the siphonophore *Muggiaea atlantica* replacing *Nanomia* species; and the copepod *Euchaeta hebes*, some pilchard eggs and, of course, *S. setosa*, were present. A transition of this sort has occurred during the autumn of many years, marking a period of increased flow round Ushant[34] and coinciding with the breakdown of the thermocline off Plymouth, but in 1979 it was brief, and the dominance of the *elegans* community was restored in November and has continued up to the time of writing.

Figure 2*a–d* compares the distribution of *Aglantha* in the Western Channel and Celtic Sea in July of 1979, with the results of similar surveys made in previous decades during the period of dominance of *S. setosa* and pilchard off Plymouth, and with the results of a survey made in 1935, towards the end of the first period of change of the Russell cycle[35]. This species made a very big advance eastwards between 1969 and 1979, of the order of 100 nautical miles; and as shown in Fig. 2*e, f*, there was a corresponding withdrawal of the neritic chaetognath, *S. setosa*, from the entrance to the Channel. These particular changes took place well after the increase in demersal young fish and zooplankton at the Plymouth stations.

Except for return of herring, the ecosystem of the Western Channel off Plymouth has evidently returned to a stage comparable with that of the 1920s. This brief recapitulation of

Fig. 2 *a–d*, Distribution of the trachymedusan *Aglantha digitalis* O. F. Müller in the Western Channel and Celtic Sea in July, as sampled with a 1-m net (1935, 1969, 1979) or the Gulf III sampler (1959). The contours correspond to 100 and 1,000 individuals per 10 min haul of the 1 m net, filtering about 750 m^3 of water. *e, f*, Distribution of the chaetognath *Sagitta setosa* J. Muller, in July 1969 and 1979 as sampled with the 1 m net. The contours correspond to 1, 10, 100, 1,000 individuals per haul. The position of the routine sampling station (L5) is shown on *a*.
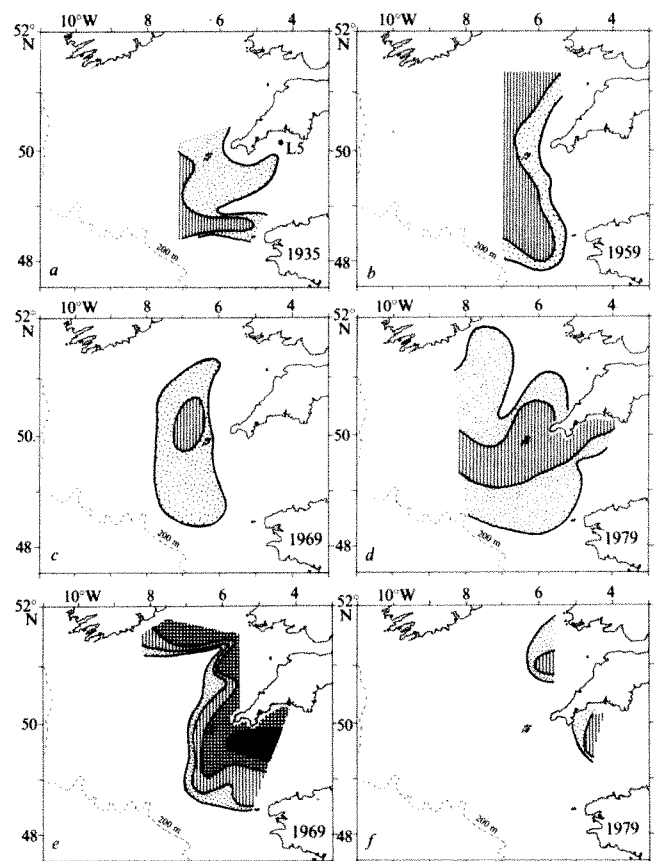
events over a 55-yr period inevitably omits much detail of the changes; describing the cycle in terms of two contrasting ecosystems (*Sagitta elegans* + herring/mackerel versus *Sagitta setosa* + pilchard) is perhaps an oversimplification, but this is the easiest way to relate the changes to causative factors and discuss the apparent competition between the two systems.

Possible causative factors

Three hypotheses concerning the causes of the change have already been mentioned: (1) nutrient control; (2) competition; (3) local effects of climate change. Other hypotheses to be considered may be called: (4) indirect effects of change in climate[36]; and (5) natural fluctuations in species equilibrium. None of these is attributed to a single author as all are essentially syntheses of several ideas.

(1) *Nutrient control*. Essentially this hypothesis assumes that many of the changes in the Russell cycle are the result of variations in the flow of water from the west into the Channel[1]. In these latitudes *Sagitta elegans* is more of an offshore species ('intermediate' or mixed coastal and oceanic water) than *S. setosa*[5,15] and a change of community from '*elegans*' to '*setosa*' such as occurred in 1930–35 implies increased coastal influence. The simplest way this could have happened is by reduction of the flow of oceanic water into the Celtic Sea and corresponding reduced flow of mixed oceanic/coastal water through the Channel. The retreat of *S. setosa* shown in Fig. 2*f* illustrates a reduction of coastal influence during the reverse phase of the cycle, and on this hypothesis implies increased flow from the west. The '*elegans*' community has been shown to be associated with increased numbers of the planktonic stages of demersal fish[37] and better survival of invertebrate larvae[38], but these qualities do not explain all the changes. A critical role is, therefore, allotted to the inorganic nutrients which are assumed to need continuous renewal if primary production is to be maintained in coastal waters[39]. On this hypothesis the change in the plankton

community is an index to a more fundamental change in hydrography, possibly linked to sinking of cold water in the Arctic, and thus indirectly influenced by climatic change[11,12,19]. Therefore the greatest changes in zooplankton abundance would be expected to accompany or follow the changes in nutrients. During the first phase of the Russell cycle the major fall in winter phosphate occurred between 1931 and 1939, accompanying the change in the more characteristic species, and preceding the period of maximum decline in zooplankton abundance. However, in 1965–75 the increase in zooplankton abundance, especially of the young stages of spring spawning demersal fish[2] preceded the rise in phosphate by several years (Fig. 3). Many of the changes in the second phase of the cycle are a mirror image of those in the first phase[3,30]; in the 1930s *S. elegans* declined first, then young of summer spawning demersal fish, then spring spawning demersal fish, while in the 1960s and 1970s the numbers of spring spawners increased first, then summer spawners, and finally *S. elegans* returned to dominance. Although some aspects of the reversal of the cycle might be expected to take place gradually, depending on the build-up of perennial populations, this is not the order that would be anticipated if water movements and inorganic nutrients were the most important environmental factors governing the cycle. Examination of some details underlines this defect; for example, the apparent correlation between winter phosphate and numbers of summer spawned fish[40]. For the period 1924–38 we have 12 pairs of values of phosphate and young fish, giving a reasonable significant relation ($n = 12$, $r = 0.77$, $P = 0.01$), but for 1964–79 the significance is less ($n = 16$, $r = 0.59$, $P = 0.02$). Taking the whole cycle there is still some significance in the figures ($n = 33$, $r = 0.49$, $P = 0.01$), but at this value for the correlation coefficient the inorganic nutrients cannot be regarded as the overriding cause of the change. The correlation between winter phosphate and numbers of *Sagitta elegans* shows a similar reduction in significance in passing from the first phase of the cycle ($n = 11$, $r = 0.82$, $P = 0.01$) to

the second ($n=16$, $r=0.55$, $P=0.05$). For the numbers of spring spawned young fish there is no relation at all, and some of the other changes are also out of phase with the phosphate values. An additional drawback of the nutrient control theory is that some of the primary production in coastal waters is related to organic nutrients (with which ammonia is classed, as distinct from nitrate)[41]. There is much current discussion on the rate of turnover of nutrients in the spring during the phytoplankton outburst and on the proportion of primary production attributable to such recycling as compared with the proportion, the 'new' production, that results from injection of nutrients into the euphotic zone from deeper water, or by runoff from the land and fixation of atmospheric N_2 (refs 42, 43). There are no direct measurements of recycling in the Channel. Using analyses for other regions[43], it can be calculated that, of the average annual primary production off Plymouth[44] (152 g carbon assimilated per m^2 per yr) over 60% might be due to recycling rather than 'new' nutrients. The average difference in the winter maximum of inorganic phosphate between the '*elegans*' period and the '*setosa*' period was 23%. If we assume that all of this represents additional nutrients replenished by increased flow
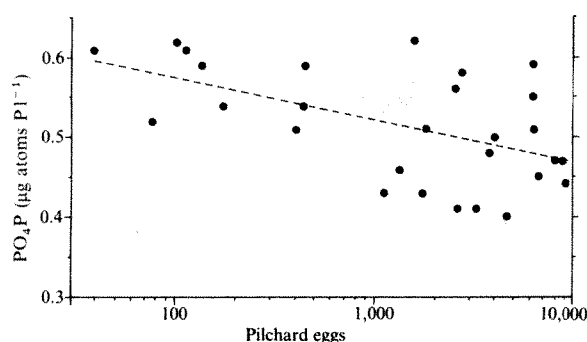
Fig. 3 Regression of winter maximum of inorganic phosphate μg atoms P l^{-1} on $\log_{10}$ numbers of pilchard eggs the previous summer, as average per haul of the 2-m net from April to July. The broken line is a least squares fit.

through the Channel, then the corresponding difference in 'new' production would be only 10% of the annual production. This difference is small compared with the changes of one or two orders of magnitude in the standing crop of zooplankton. A further argument in this direction is provided by recently developed methods for analysis of total dissolved nutrients[45]. Not much was known about the organic fractions during the earlier phase of the Russell cycle but the new data suggest that the totals of N and P undergo much less fluctuation than the inorganic components, and that it is the position of the equilibrium between the organic and inorganic fractions that has changed. This equilibrium may be related to environmental effects or to biological factors or both, but its relative position need not imply any alteration in the primary production of the system[41].

(2) *Competition.* This hypothesis assumes that the major event in the Western Channel was a competitive change of the species of pelagic fish, pilchard becoming increasingly more successful after 1925[17]. It is based on data for recruitment to the former Plymouth herring fishery[46] and the number of eggs of pilchard in the plankton, taken as an index to the adult stock of pilchards[17,25]. The increased numbers of young and adult pilchard are assumed to be responsible, through changes in the level and intensity of predation, for the other changes in the ecosystem. From the data available up to 1960 the link between herring and pilchard could be made through the winter phosphate values: there was a negative correlation between log summer pilchard eggs and phosphate the following winter, and a positive correlation between herring

recruitment (year class strength) and winter phosphate a year after hatching. The correlations were with the same value of winter phosphate, indicating a possible direct link between the two fish, irrespective of the exact role allotted to the phosphate[17]; in other words, increasing numbers of pilchard were eating up the young herring or their food.

This hypothesis has been extended to cover the effects of climatic change[3], by assuming that the degree of synchrony between the spring plankton outburst and the breeding of fish (or other animals) will critically affect the success or otherwise of the brood. Northern species tend to spawn at a fixed time in the spring, and will suffer more from a mismatch with their planktonic food if for example their rate of development is increased by rising temperatures or if phytoplankton begins to develop too early[3]. Unfortunately the data from the Channel no longer give much support to the idea of direct competition between pilchard and herring. Some missing data have been found for certain years before 1960, some of the phosphate values revised, and the series continued to 1979. The new data (Fig. 3) give an apparently significant correlation between log summer pilchard eggs and inorganic phosphate the winter after, in spite of much scatter, ($n=32$, $r=0.54$, $P=0.01$), but an almost as significant correlation can be shown between log pilchard eggs and phosphate the year before ($n=32$, $r-0.48$, $P=0.01$). Thus any direct effect of pilchard on phosphate (or herring) can be discounted, and we are left with a general similarity in long-term trends, with a tendency for less than 0.5 μg atoms of inorganic phosphate-P per litre to be associated with the period when there were more than 100 pilchard eggs per haul in summer.

An alternative version of the competition hypothesis supposes that for some reason the herring declined, allowing the pilchard to move in[8,17]. A possible cause of the decline in herring might have been increased fishing pressure, such as we know occurred in the 1920s with the introduction of new technology[8]. In spite of the well known effects of 'density-dependent' factors on year class strength of fish populations, a species which is being heavily fished may be unable to produce enough young stages to ensure their survival through mortalities caused by environmental factors[47,48], especially if the environment itself is changing[49]. However, the subsequent change from pilchard to mackerel cannot be attributed to overfishing and hence other causes of the cycle must be examined.

(3) *Local effects of change in climate.* The climate control hypothesis assumes that geographical distributions of species and communities alter in response to fluctuations in climate. It is argued that rises or falls in sea temperature, translated into north/south shifts of distribution, may be seen as fairly sudden switches of the ecosystem if observations are being made close to faunistic boundaries[8]. For example, herring is a boreal species close to its southern limits at the entrance to the Channel, whereas pilchard is a warm-temperate species close to its northern limit of regular breeding[26]. The marked rise in temperature in the 1920s is assumed to be the final stimulus that caused the herring to fail and the pilchard to extend its range north[8], and that there were corresponding shifts in species balance at other trophic levels. The disappearance of *Sagitta elegans* from the Plymouth area is regarded as an example of a retreat of a northern species. However, it was not replaced by the corresponding warm-temperate species *S. friderici*[50], which appeared only in small numbers during the warmest phase of the cycle in the 1950s and 1960s (ref. 15), but by the more neritic species *S. setosa*. The theory suggests that *S. setosa*, which has a more southern distribution than *S. elegans*, was better able to withstand the wider range of temperatures experienced[8,51]. An alternative, but not exclusive explanation was suggested, that the change in climate, especially the greater incidence of southerly and westerly weather[51], may have altered the emphasis of water movements in the Western Channel[8], bringing in a more prolonged

cyclonic phase from the south and east and reducing the anticyclonic 'spring' phase from the north and west[52]. Such an alteration of circulation pattern could have helped *S. setosa* to become dominant. It was originally implicit in the temperature control hypothesis that much of the decline in the standing crop of zooplankton resulted from increased predation by pilchard, and that the reduced level of winter phosphate was probably related to the increased numbers of pilchard[8,17]. However, the new data for the latter shown in the previous section indicate an indirect effect, through the general change in ecosystem.
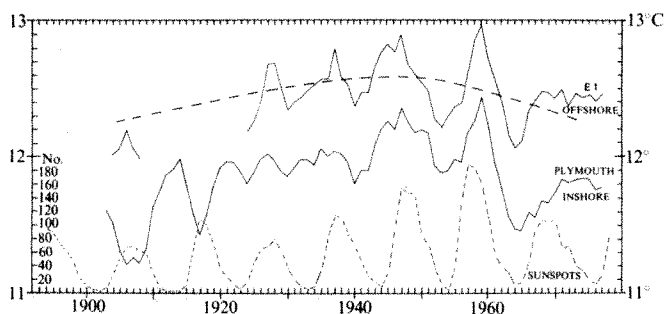
Fig. 4 Comparison of 5-yr running means of annual sea temperature offshore at station E1, 5-yr running means of annual sea temperature in Plymouth Sound, and mean annual (Zurich) sunspot numbers. The broken line is the long term trend, expressed as a polynomial regression fitted to the annual means for station E1. Note the change in phase agreement in inshore temperature and sunspots before 1930; the change in phase agreement between the E1 temperatures and sunspots since 1970; and the good agreement between E1 temperatures and sunspots from 1925 to 1965[27].

A recent re-examination of the relationship between trends in sea temperature in the Western Channel and some of the biological changes apparently supported the hypothesis of temperature control[27]. Correlations could be shown not only with the long-term secular trend, but with shorter term fluctuations of the same frequency as the 11-yr solar cycle. Similar effects of the shorter period cycle as well as longer term trends can be seen in records of sea temperature and plankton abundance for the North Atlantic[53-55]. In 1975 it was predicted[27] that there would be further gains of northern species in the Channel if the trend towards cooling continued in the Northern Hemisphere[56], and this has been borne out by events in 1979-80. However, a recent assessment of aspects of the change between 1970 and 1979 suggests a lack of synchrony between the annual mean sea temperature in the Western Channel and the short-period solar cycle (Fig. 4). This seems to be predominantly a result of higher than average temperatures during the first four months of each year from 1972. There is still a degree of correlation between the 11-yr solar cycle, sea temperatures in the latter half of the year, and some of the biological changes, but the apparent phase change during the first half of the year points to advection and weakens the argument for direct effects of temperature. There is also evidence that the current 11-yr sunspot cycle is not behaving as predicted[57,58].

(4) *Indirect effects of change in climate.* This hypothesis assumes that the balance between the '*elegans*' and '*setosa*' communities in the Western Channel depends on the rate of flow of oceanic water from the west and through the Channel into the North Sea[35]. Herring are assumed, in these latitudes, to be better adapted for survival in the ecosystem of the mixed coastal/oceanic water, pilchard in the more coastal type of plankton community. The change of climate in the Northern Hemisphere is presumed to have produced local changes in the flow of water through the Channel. During the warm period, 1920-60, the extension of the North Atlantic Drift into the high Arctic, and the wider spread of the Gulf Stream

Gyre[59,60], may have led to weaker flow in the latitude of the Channel, in spite of the increased frequency of 'westerly' weather at the time[61]. With a return of colder conditions, less penetration into the high Arctic, and a tightening of the Gulf Stream Gyre, it could be assumed that there would be greater flow into and through the Channel. Unfortunately, much of the data for flow through the Channel are incomplete or circumstantial. The measurements on the electric power cable across the Straits of Dover are for short periods only[62], and no consistent trend can be seen. The current meter readings at the Varne Light Vessel[63] were discontinued many years ago, and it was never satisfactorily shown if this site was in the main flow or an eddy[15]. The circumstantial data from biological observations indicates movement of biota from the Eastern Channel into the southern North Sea after 1970, in harmony with the period of return of *S. elegans* to the Plymouth area[64,65].

There are two principal arguments against this concept of a controlling role for climate induced changes in water flow through the Channel. One is that the sequence of events in each of the two phases of the cycle was different; in the second phase the change began in 1965, but the distribution of *Sagitta* and *Aglantha* did not alter substantially until after 1969 (Fig. 2), and *S. elegans* did not regain its former dominance until 1973-79. The second is that there is no evidence of salinity trends (ref. 55 and E. I. Butler, personal communication), such as would be expected if there had been variation in the flow of oceanic water from the west. Thus we are left with an incomplete explanation, and we have to assume some direct effects of temperature, including a shift in fish populations (F. S. Russell, personal communications).

(5) *Natural fluctuations in species equilibrium.* This hypothesis stems from recent observations on primary production in the Western Channel[44]. Although the 10-yr series began only 1-2 yr before the start of the reversal of the Russell cycle, it is clear that there was no dramatic or lasting change in primary productivity off Plymouth as measured by fixation of $^{14}CO_2$. The mean annual production at St E1 was $152 gC$ per m^2 per yr, with a standard deviation of ± 29, and the values for 1964 and 1965 do not differ significantly from later years of the fully changed ecosystem. Thus, as drastic as the change may have been from the economic point of view (in fish populations), it was hardly fundamental at the level of primary production. Note that although variations in pelagic fish populations tend to preoccupy biologists (E. I. Butler, personal communication), these fish account for less than 5% of the annual production. We may postulate that there is normally considerable fluctuation, within the confined level of primary production, of the species dominant at each trophic level. Increase of one species implies reduction of another, or changes in the food chain, so that the total balance of production and utilization is maintained. Such a state may be compared with what the economists among Eurocrats inelegantly term a 'snake in the tunnel'. The change from herring to pilchard and then to mackerel can be seen as a sequence of such 'snakes'. Each species, when it becomes dominant, will tend to stabilize the system for a while, so that the plankton community remains at the optimum structure to support the predator at the top of the ecological pyramid. A process such as this would be akin to that described as 'rectification' in the improved theory of competition[3]. It can be assumed that there is a tendency for climatic change to favour natural fluctuations more in one direction than the other, for example, rising temperatures might put an end to a period of herring dominance, but on this hypothesis such a shift would not be possible unless there was innate biological fluctuation in the system. No fundamental change in water movement is demanded, and the changes in nutrient chemistry are regarded as indices of the biological changes.

It will be seen that this hypothesis combines elements from hypotheses (2) and (3), but assumes that the ecosystem is

fundamentally unstable and that external influences are less important than supposed previously. Arguments against this hypothesis are largely geographical. There is no doubt that there have been geographical changes in species distribution: for example the east–west shifts in *Sagitta setosa* and the north–south shifts in pilchard. Once we insert a geographical component into this hypothesis there is good reason to suspect a much greater controlling role for external factors, including changes in temperature and water movements.

Conclusions

There is general agreement that the Russell cycle is broadly related to climate change[2,3,51]. Possibly the lack of satisfactory statistical correlation in detail is due to different response, at different rates of change, by the various biological and chemical components of the ecosystem, some being affected directly, others indirectly. If such is the case no single facet of the climatic change will stand out as the controlling factor, and temperature, water movements, competition and natural fluctuations may all be important. It seems likely that there is an overriding influence of climate in three ways: (i) a hemispheric shift in boundaries of distribution; (ii) direct effects of temperature on the relative competitive advantages of north–south pairs of species in regions of their overlap; and (iii) changes in the local pattern of water circulation in the western half of the Channel, between a predominantly anticyclonic pattern (as in the 1920s and recently) and a predominantly cyclonic pattern (as from 1930 to the 1960s) resulting indirectly from changes in weather and temperature. With this combination of climate related effects there is no need to assume great alteration in net transport through the Channel. The apparent detection of increased transport of Channel species into the southern North Sea[64] may merely reflect the change in communities in the Western Channel, eventually communicated to the eastern half.

We do not have a long enough series to determine the exact frequency of the Russell cycle, or to judge the suggested fit with the 180-yr solar cycle[27]. However, historic records show fluctuations in the relative fortunes of the herring and pilchard fisheries off Devon and Cornwall[16,26]. If these previous fluctuations correspond to changes in the ecosystem similar to those of the Russell cycle, then we may assume that such change is normal for the Western Channel, and that the apparent stability maintained over a period of several years is

in fact a condition of precarious equilibrium. Similar states of equilibrium may exist in other regions, especially near to faunistic boundaries, as off California and Japan[66]. However, we seem to have more detail for the English Channel system, either because it is unduly sensitive, or because it has been studied in a more effective way to reveal the fluctuations.

The degree of sensitivity of the Western Channel ecosystem is underlined by the apparent disparity between the biological fluctuations and the physical and chemical factors that have been monitored. Many species have been replaced by others, and there have been changes in abundance of one or two orders of magnitude, but no obvious trends in salinity can be found, the variation in inorganic phosphate has been less than 25% of the average, and mean annual sea temperature has changed only 0.5 °C. Variations in solar luminosity also seem to be small and difficult to relate to changes in climate[67]. A more recent solar index, sunspot umbra/penumbra ratio[68], also shows only small changes, though these apparently correspond with the secular trend in temperature of the Northern Hemisphere. Yet the economic consequences of the Russell cycle changes have been considerable. In the first phase, cold-water fish of great importance on the UK market (such as herring, cod, haddock, ling, whiting, plaice, dab, lemon-sole) became reduced in number or were replaced by warm-water species (such as pilchard, horse-mackerel and bream) of lesser market appeal[8]. Nowadays, of course, increases in pilchard and horse-mackerel, which are subjected to industrial fishing for meal, might have different economic consequences. Since the beginning of the reversal of the Russell cycle in 1965, some ports in south Devon and south-east Cornwall have seen an increase of nearly an order of magnitude in the number of vessels engaged in fishing. Part of this increase is due to market forces other than fish abundance, but the lesson is still there that almost imperceptible environmental fluctuation may be associated with biological changes of great economic impact. The need for sustained biological monitoring and development of methods of prediction is obvious.

1. Russell, F. S. *J. mar. biol. Ass. U.K.* **20**, 595–604 (1936).
2. Russell, F. S., Southward, A. J., Boalch, G. T. & Butler, E. I. *Nature* **234**, 468–470 (1971).
3. Cushing, D. H. & Dickson, R. R. *Adv. mar. Biol.* **14**, 1–122 (1976).
4. Raymont, J. E. G. *Plankton and Productivity in the Oceans* (Pergamon, Oxford, 1963).
5. Russell, F. S. *J. mar. biol. Ass. U.K.* **19**, 73–82 (1933).
6. Corbin, P. G. *J. mar. biol. Ass. U.K.* **28**, 718–722 (1948).
7. Holme, N. A. *J. mar. biol. Ass. U.K.* **32**, 1–49 (1953).
8. Southward, A. J. *J. mar. biol. Ass. U.K.* **43**, 1–29 (1963).
9. Kemp, S. *Rep. Br. Ass. Adv. Sci. 1938*, 85–101 (1938).
10. Atkins, W. R. G. *J. mar. biol. Ass. U.K.* **13**, 700–720 (1925).
11. Cooper, L. H. N. *Deep Sea Res.* **31** suppl., 212–223 (1955).
12. Cooper, L. H. N. *J. mar. Res.* **14**, 347–362 (1955).
13. Russell, F. S. *J. mar. biol. Ass. U.K.* **26**, 605–608 (1947).
14. Corbin, P. G. *J. mar. biol. Ass. U.K.* **28**, 271–275 (1949).
15. Southward, A. J. *J. mar. biol. Ass. U.K.* **42**, 275–375 (1962).
16. Cushing, D. H. *Fish. Invest., Lond.* Ser. 2 **21**, 1–27 (1957).
17. Cushing, D. H. *J. mar. biol. Ass.*, U.K. **41**, 799–816 (1961).
18. Ahlmann, H. W. *Rapp. P.-v. Reún Cons. perm. int. Explor. Mer.* **125**, 9–16 (1949).
19. Cooper, L. H. N. *J. mar. biol. Ass. U.K.* **37**, 1–3 (1958).
20. Southward, A. J. *J. mar. biol. Ass. U.K.* **39**, 449–458 (1960).
21. Russell, F. S. *Rep. Trans. Devon. Ass. Advmt Sci.* **85**, 1–17 (1953).
22. Southward, A. J. & Crisp, D. J. *J. anim. Ecol.* **23**, 163–177 (1954).
23. Blacker, R. W. *Fish. Invest., Lond.* Ser. 2 **20**(10), 1–49 (1957).
24. Dickie, L. M. *J. Fish. Res. Bd. Can.* **33**, 313–316 (1976).
25. May, R. M. *Nature* **282**, 443–444 (1979).
26. Southward, A. J. *J. mar. biol. Ass. U.K.* **54**, 641–649 (1974).
27. Southward, A. J., Butler, E. I. & Pennycuick, L. *Nature* **253**, 714–717 (1975).
28. Russell, F. S. *J. mar. biol. Ass. U.K.* **18**, 559–574 (1933).
29. Russell, F. S. *J. mar. biol. Ass. U.K.* **20**, 147–180 (1935).
30. Southward, A. J. *Nature* **249**, 180–181 (1974).
31. Llewellyn, J., Macdonald, S. & Green, J. E. *J. mar. biol. Ass. U.K.* **60**, 73–79 (1980).
32. Garstang, W. *J. mar. biol. Ass. U.K.* **6**, 274–275 (1901).
33. Southward, A. J. & Mattacola, A. D. *J. mar. biol. Ass. U.K.* **60**, 39–44 (1980).
34. Cooper, L. H. N. *J. mar. biol. Ass. U.K.* **39**, 173–208 (1960).
35. Russell, F. S. *J. mar. biol. Ass. U.K.* **20**, 507–522 (1936).
36. Russell, F. S. *J. mar. biol. Ass. U.K.* **53**, 347–355 (1973).
37. Fraser, J. H. *J. mar. biol. Ass. U.K.* **41**, 305–312 (1961).
38. Wilson, D. P. & Armstrong, F. A. J. *J. mar. biol. Ass. U.K.* **41**, 663–680 (1961).
39. Cooper, L. H. N. *J. mar. biol. Ass. U.K.* **23**, 181–195 (1938).
40. Harvey, H. W. *The Chemistry and Fertility of Sea Waters* (Cambridge University Press, 1955).
41. Butler, E. I., Knox, S. I. & Liddicoat, M. I. *J. mar. biol. Ass. U.K.* **59**, 239–250 (1979).
42. Goldman, J. C., McCarthy, J. J. & Peavey, D. G. *Nature* **279**, 210–215 (1979).
43. Eppley, R. W. & Peterson, B. J. *Nature* **282**, 677–680 (1979).
44. Boalch, G. T., Harbour, D. S. & Butler, E. I. *J. mar. biol. Ass. U.K.* **58**, 943–953 (1978).
45. Armstrong, F. A. J. & Tibbits, S. *J. mar. biol. Ass. U.K.* **48**, 143–152 (1968).
46. Ford, E., *J. mar. biol. Ass. U.K.* **19**, 305–384 (1933).
47. Dickie, L. M. *J. Fish. Res. Bd. Canada* **30**, 2496–2506 (1973).
48. Garrod, D. J. *Rapp. P.-v. Réun. Cons. perm. int. Explor. Mer.* **164**, 43–56 (1973).
49. Iles, T. D. *Rapp. P.-v. Réun. Cons. perm. int. Explor. Mer.* **164**, 228–240 (1973).
50. Furnestin, M.-L. *Rep. Trav. off. Pêches Marit.* **22**, 211–224 (1958).
51. Maddock, L. & Swann, C. L. *J. mar. biol. Ass. U.K.* **57**, 317–338 (1977).
52. Dietrich, G. *Dtsch. hydrogr. Z.* **3**, 184–201 (1950).
53. Colebrook, J. M. *Nature* **263**, 576–577 (1976).
54. Colebrook, J. M. *Oceanol. Acta* **1**, 9–23 (1978).
55. Colebrook, J. M. & Taylor, A. H. *Deep-Sea Res.* **26A**, 825–850 (1978).
56. Kukla, G. J. *et al. Nature* **270**, 573–580 (1977).
57. Lincoln, J. V. *NOAA Environm. Data Info. Serv.* **11** (1), 17–19 (1980).
58. Wood, K. D. *Nature* **240**, 91–93 (1972).
59. Martin, J. H. A. *Rapp. P.-v. Réun. Cons. perm. int. Explor. Mer.* **162**, 213–219 (1972).
60. Worthington, L. V. *Johns Hopkins Oceanogr. Stud.* **6**, 1–110 (1976).
61. Lamb, H. H. *Climate, Past, Present and Future* Vol. 1 (Methuen, London, 1972).
62. Prandle, D. *J. mar. biol. Ass. U.K.* **58**, 965–973 (1978).
63. Carruthers, J. N., Lawford, A. L. & Veley, V. F. C. *Ann. Biol., Copenhague* **6**, 115–120 (1950).
64. Reid, P. C. *Mar. Biol.* **40**, 337–339 (1977).
65. Colebrook, J. M., Reid, P. C. & Coombs, S. H. *Mar. Biol.* **45**, 209–213 (1978).
66. Birman, I. B. *Vop. Ikhtiol.* **13**, 23–37 (1973).
67. Dickie, R. H. *Nature* **280**, 24–27 (1979).
68. Hoyt, D. V. *Climatic Change* **2**, 79–92 (1979).
69. Southward, A. J. *J. mar. biol. Ass. U.K.* **50**, 689–712 (1970).

ARTICLES

Specific *in vitro* initiation of transcription on conalbumin and ovalbumin genes and comparison with adenovirus-2 early and late genes

B. Wasylyk, C. Kédinger, J. Corden, O. Brison* & P. Chambon†

Laboratoire de Génétique Moléculaire des Eucaryotes du CNRS et Unité 184 de Biologie Moléculaire et de Génie Génétique de l'INSERM, Faculté de Médecine, Strasbourg, France

Specific initiation of transcription of cloned conalbumin and ovalbumin genes has been obtained in a cell-free system in the presence of purified calf thymus RNA polymerase B. Comparison with the adenovirus-2 early (E1A) and major late genes reveals marked variations in transcriptional efficiencies. Specific fragmentation of the conalbumin gene DNA indicates that a short DNA segment 5' to the initiation site is involved in specific transcription.

IN prokaryotes, gene expression is controlled, in part, at the level of RNA transcription. The elucidation, at the molecular level, of the regulatory mechanisms which modulate the efficiency with which RNA polymerase recognizes promoter and terminator sequences has been greatly aided by the availability of appropriate mutants and of *in vitro* cell-free systems capable of synthesizing specific RNAs (see refs 1, 2 and refs therein).

In contrast, in eukaryotes, although there is evidence that the expression of at least some genes is regulated at the level of transcription (see refs 3, 4 and refs therein), little is known about the underlying molecular mechanisms. It is firmly established that cells of both higher and lower eukaryotes contain three structurally and functionally distinct classes of DNA-dependent RNA polymerase, which catalyse the synthesis of ribosomal RNA (class A or I), mRNA (class B or II) and tRNA and 5S RNA (class C or III) (reviewed in refs 5, 6). However, until recently, all attempts to demonstrate convincingly specific *in vitro* transcription of purified DNAs from viral or cellular origin with the three classes of purified RNA polymerases have failed (reviewed in refs 3, 5, 6), suggesting that additional chromatin or nuclear components are necessary.

An important advance in the identification of such components was made by Wu[7], who established a cell-free system in which the virus-associated (VA) RNA genes of purified adenovirus-2 DNA is selectively transcribed by RNA polymerase C. This has led to the demonstration of the existence of factors required for specific transcription by RNA polymerase C (ref. 8 and refs therein). More recently, using a similar system, Weil *et al.*[9] have demonstrated accurate initiation of transcription by purified RNA polymerase class B at the major late adenovirus-2 promoter. On the other hand, it has only recently become possible to make a useful search for chromatin or other cellular components necessary for purified RNA polymerase B to transcribe accurately genes encoding cellular mRNA (discussed in refs 3, 5). The main reasons for this were the complexity of eukaryotic genomes and the lack of information regarding specific transcription units. The situation has radically changed with the advent of molecular cloning and fast DNA sequencing methods. The structure of

several messenger-coding genes has been established and putative promoter regions have been positioned and sequenced (refs 10–13 and refs therein).

We report here that, using the cell-free system of Wu[7] and cloned DNA templates[11,12], purified RNA polymerase class B can accurately initiate transcription *in vitro* at the 5' ends of the transcription units of the conalbumin and ovalbumin genes [whose expressions are hormonally controlled in the chicken (see refs 11, 12 and refs therein)]. However, a comparative study of these two genes, and of early E1A and major late adenovirus-2 genes, indicates that different genes are transcribed with very different efficiencies in this system. Our experiments also demonstrate that at least part of the conalbumin DNA sequences required for specific initiation of transcription are situated in the region where presumptive promoter sequences have been previously positioned[12].

Specific initiation of transcription on the conalbumin gene

We have previously reported that the DNA sequences coding for conalbumin mRNA (con-mRNA) are contained in three *Eco*RI fragments, 'b', 'c' and 'a' (in the order of transcription)[12]. Sequence studies have shown that the cap site of con-mRNA is coded by the 5' end of exon *1*, which is contained in fragment *Eco*RI 'b' (Fig. 1B; see also Figs 1, 5 in ref. 12). Two observations suggest that the cap site could correspond to the site of initiation of transcription. First, the largest con-mRNA precursor molecule is the same size as the DNA segment containing the con-mRNA coding sequences (ref. 12, and M. LeMeur, A. Krust and S. McKnight, personal communications). Second, about 25 base pairs upstream from the cap site, there is an A+T-rich sequence which might correspond to a promoter site (refs 10–13 and refs therein). Particularly striking is the similarity between this conalbumin sequence and the corresponding sequence of the major late adenovirus-2 gene (see Fig. 7B in ref. 12). These observations prompted us to study whether the cell-free system[7] which was used by Weil *et al.*[9] to demonstrate specific *in vitro* initiation of transcription at the *in vivo* cap site of the major late adenovirus-2 genes could also be used to transcribe selectively cellular genes with purified RNA polymerase B.

To detect specific initiation of transcription on the conalbumin gene, we used the truncated template assay[9], which contains the S100 transcription cell-free system of Wu[8,14] prepared from HeLa cells, purified calf thymus RNA
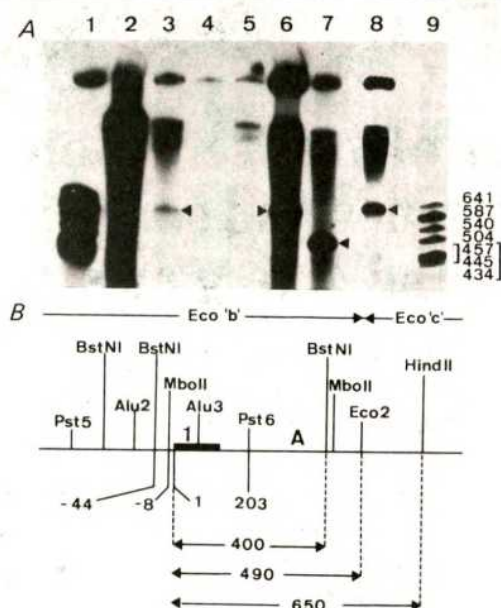
Fig. 1 Electrophoretic analysis of RNA synthesized on conalbumin 'truncated' templates. *A*, RNA was synthesized for 60 min at 30 °C in a standard reaction mixture (50 μl) containing (final concentrations) 25 μM [α-^{32}P]GTP (9,000 c.p.m. pmol^{-1}) 600 μM ATP, 600 μM CTP, 600 μM UTP, 10 mM Tris-HCl *p*H 7.9, 7.5 mM MgCl$_2$, 50 mM KCl, 0.25 mM dithiothreitol, 0.150 units of calf thymus RNA polymerase B (glycerol gradient fraction)[15], 25 μl of HeLa cell S100 extract[7-9] and conalbumin DNA (see below). After synthesis, the reaction mixture was diluted with 450 μl of a solution containing 50 mM sodium acetate *p*H 5.0, 0.5% SDS and 50 μg ml^{-1} yeast tRNA (final concentrations), extracted once with phenol, twice with chloroform, made 0.15 M in ammonium acetate and precipitated with two volumes of ethanol. The RNA pellet was dissolved in 30 μl formamide buffer, denatured for 5 min at 65 °C, chilled on ice and analysed on a 5% acrylamide-urea gel[41]. The incubations corresponding to lanes 2-6 and 8 contained 6 μg ml^{-1} of a 5,700-base pair *Hind*II fragment prepared from cloned conalbumin DNA[12] and containing 2,700 base pairs of conalbumin DNA [from the *Hind*II site in intron *A* (see below) to the *Kpn*2 site of the Eco 'b' fragment] linked to 3,000 base pairs of pBR322 [from the *Pst*I site to the *Hind*II site at position 652 (ref. 42)]. The incubations were modified as follows: lane 2: no added S100 extract; lane 3: no calf thymus polymerase B; lane 4: no DNA; lane 5: with 1 μg ml^{-1} α-amanitin; lane 6: standard reaction; lane 7; 4.2 μg ml^{-1} of purified conalbumin Eco 'b' fragment[12] instead of *Hind*II fragment. Lanes 1 and 9 contain the same amount of ^{32}P-labelled DNA size markers. Lanes 8 and 9 are the same as lanes 6 and 1, respectively, but less exposed. Arrowheads point to bands discussed in the text. *B*, Restriction enzyme map around exon *1* of the conalbumin gene. Sites *Pst*5, *Alu*2, *Alu*3, *Pst*6 and *Eco*2 have been described previously[12]. The position of the *Bst*NI, *Mbo*II and *Hind*II sites was either deduced from the DNA sequence[12] or established by restriction enzyme mapping (unpublished results). Eco 'b' and Eco 'c' refer to EcoRI conalbumin fragments 'b' and 'c' (ref. 12). The heavy line *1* and *A*, correspond to exon *1* and intron *A*, respectively[12]. The figures below the restriction map refer to the number of nucleotides from the cap site (nucleotide 1) and correspond to the restriction enzyme cutting sites on the non-coding strand (negative numbers are upstream from the cap site with respect to the direction of transcription)[12]. The distances (in base pairs) indicated by arrows are from size analysis of restriction fragments.

polymerase B (ref. 15) and either the isolated conalbumin Eco 'b' fragment or an '*Hind*II-cut' conalbumin plasmid as templates (see Fig. 1*B* and Fig. 1*A* legend). By electrophoretic analysis (Fig. 1*A*), discrete bands of 650 (lanes 6 and 8) and 500 (lane 7) nucleotides were found with the '*Hind*II' and Eco 'b' templates, respectively. These correspond to the sizes expected if transcription starts at the 5' end of exon *1* (Fig. 1*B*). Similarly, transcription of the isolated *Pst*5–*Pst*6 fragment (Fig. 1*B*) gave mainly a 200-nucleotide long RNA (not shown), confirming that transcription is occurring predominantly from the coding strand of the conalbumin gene. The comparison of lanes 6 and 7 indicates that most of the nonspecific transcription seen in lane 6 comes from the pBR322 sequences present in the '*Hind*II-truncated' template. As shown in lane 2, the S100 extract is necessary for specific transcription (no

discrete bands were observed with exposure for a shorter time), although, as previously observed in the adenovirus case[9], its addition depressed total RNA synthesis (compare Fig. 1, lanes 2 and 6, and unpublished observations). The synthesis of specific RNA is dependent on the addition of the conalbumin template (lane 4) and is catalysed by RNA polymerase B [as shown by inhibition at low concentrations of α-amanitin (lane 5)]. A small fraction of the specific synthesis is due to the RNA polymerase B which is present in the S100 extract (lane 3, also see below).

Transcription of the isolated EcoRI fragment 'b' (Fig. 1*A*, lane 7) suggests that a large fraction of the RNA synthesized on conalbumin DNA is, in fact, initiated at the 5' end of exon *1*. This is demonstrated in Fig. 2, where the RNA synthesized on EcoRI fragment 'b' hybridized much more strongly to the *Mbo*II–*Pst*6 (positions −8 to +203) (lane 2) than to the *Pst*6–*Mbo*II (lane 4) fragment (see Fig. 1*B*). In contrast, RNA randomly synthesized on denatured EcoRI fragment 'b' in the absence of S100 extract hybridized equally well to both fragments (lanes 1, 3).

The above results suggest very strongly that transcription of the conalbumin DNA is initiated on the coding strand near the 5' end of exon *1*. The modified S$_1$ mapping technique of Weaver and Weissmann[16] was used to position the 5' end of the *in vitro* synthesized RNA. Unlabelled RNA synthesized on the *Hind*II-truncated template (Fig. 3*A*, lanes 2–4) or hen oviduct poly(A)$^+$ RNA (lanes 5–7) were hybridized to the *Alu*2–*Alu*3 fragment (Fig. 1*B*) which had been labelled with ^{32}P at the 5' ends and, after S$_1$ nuclease digestion, the resistant labelled DNA was run on a sequencing gel in parallel with a G+A sequence ladder of the *Alu*3–*Mbo*II fragment (+62 to −8, Fig. 1*B*). Both *in vivo* and *in vitro* RNAs gave the same digestion patterns, of which the lowest bands (arrowheads) in each case migrate with the same mobility as the G at position −1 in the sequencing ladder. Therefore, the 5' ends of the two
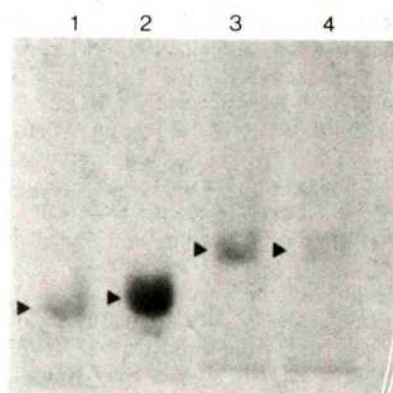
Fig. 2 Hybridization of RNA synthesized *in vitro* on conalbumin Eco 'b' fragment to conalbumin DNA fragments surrounding the cap site. The two *Mbo*II fragments from cloned *Pst*5–*Pst*6 conalbumin DNA (Fig. 1*B*) were separated on a 5% acrylamide gel, eluted, re-run on separate slots of a 3% agarose gel and transferred to diazobenzyloxymethyl (DBM) paper[43]. RNA which had been synthesized either on the native conalbumin Eco 'b' fragment (in a twofold standard reaction) as described in Fig. 1*A* legend, or on the heat-denatured fragment in the absence of S100 extract (standard reaction), was treated with D'Nase I, extracted and precipitated as described in Fig. 3*A* legend. The RNA pellet was redissolved in 75 μl of formamide-dextran buffer, rapidly cooled and hybridized to the DNA bound to the DBM paper for 12 h at 42 °C, as described by Wahl *et al.*[43]. The paper was washed with two changes of 2 × SSC for 30 min each, treated with 20 μg of pancreatic RNase (Sigma) and 10 units of T$_1$ (Sigma) in 1 ml of 2 × SSC for 1 h at 20 °C, and washed twice for 20 min at 20 °C with 2 × SSC containing 0.1% SDS and then twice for 45 min at 50 °C with 0.1 × SSC containing 0.1% SDS. Lane 1: DBM-paper-bound *Mbo*II–*Pst*6 fragment (Fig. 1*B*) and RNA synthesized on denatured DNA; lane 2: DBM-paper-bound *Mbo*II–*Pst*6 fragment and RNA synthesized on native Eco 'b' fragment; lane 3: as lane 1, but with DBM-paper-bound *Pst*5–*Mbo*II fragment; lane 4: as lane 2, but with DBM-paper-bound *Pst*5–*Mbo*II fragment. Arrowheads indicate bands discussed in the text.
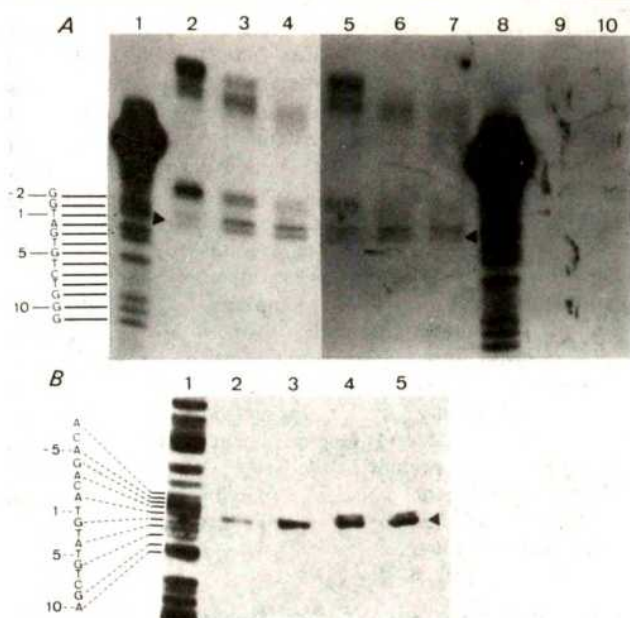
Fig. 3 Localization of the 5′ ends of RNA synthesized *in vitro* on conalbumin and ovalbumin genes by S₁ nuclease mapping. *A, Conalbumin RNA.* Lanes 1 and 8: G + A sequence ladders[41] prepared from the *Mbo*II (position −9) to *Alu*I (position 62) fragment (Fig. 1*B*) labelled at the *Alu*I site. The sequence[12] around the conalbumin cap site (position 1) is shown in the margin. Lanes 2–4: RNA was synthesized *in vitro* (2.5 times the standard reaction but with unlabelled nucleotides) on the conalbumin *Hind*II fragment (see Fig. 1*A*), purified as described in Fig. 1*A*, dissolved in 125 µl 50 mM Tris-HCl, *p*H 7.9, and 10 mM MgCl₂ and digested with 50 µg ml⁻¹ RNase-free DNase I (ref. 44) for 10 min at 37 °C. After extraction with phenol–chloroform and chloroform, the RNA was ethanol precipitated with 0.1 µg of the *Alu*2–*Alu*3 fragment (Fig. 1*B*) labelled with ³²P (specific activity ∼ 50,000 c.p.m. pmol⁻¹ of 5′ ends), redissolved in 37.5 µl of 80% formamide, 40 mM PIPES *p*H 6.5, 0.4 M NaCl and 1 mM Na-EDTA, heated to 85 °C for 5 min and incubated for 12 h at 43 °C. After cooling at −30 °C the mixture was diluted 10-fold, adjusted to 30 mM sodium acetate (*p*H 4.5), 3 mM ZnSO₄, 0.4 M NaCl and 6.7 µg ml⁻¹ sonicated calf thymus DNA and incubated with 4,000 units of S₁ nuclease (Miles) at 25 °C. After 1 h (lane 2), 4 h (lane 3) and 7 h (lane 4) Tris-HCl, *p*H 7.9, and Na-EDTA, *p*H 7.0, were added to 300 mM and 15 mM (final concentrations), and after phenol–chloroform extraction and ethanol precipitation the samples were analysed on a 12% acrylamide–urea sequencing gel[41]. Lanes 5–7: the conditions were as in lanes 2–4, except that 1.2 µg of hen oviduct poly(A⁺) RNA was hybridized with the *Alu*2–*Alu*3 probe; lanes 5–7: 1, 4 and 7 h of S₁ nuclease digestion, respectively. Lanes 9, 10: the conditions were as in lane 3 except that adenovirus major late gene DNA (see Fig. 4 legend) replaced conalbumin DNA (lane 9) or 1 µg ml⁻¹ α-amanitin was included in the incubation (lane 10). Lanes 1–4 and 5–10 are from the same sequencing gel, but were exposed for different times. *B Ovalbumin RNA.* Lane 1, G + A sequence ladder prepared from the *Pvu*II–*Hind*III (*Hind*3) site, see ref. 11) ovalbumin DNA fragment. The sequence[11] around the ovalbumin cap site (position 1) is shown in the margin. Lanes 2, 3: the conditions were as in *A*, lanes 2–4, with the following two exceptions: *Pst*4–*Eco*6 (ref. 11) ovalbumin DNA plasmid (*Pst*4–*Eco*6 inserted between the *Pst*I and *Eco*RI sites of pBR322) was linearized with *Eco*RI, and the probe was the *Pst*4–*Eco*6 ovalbumin plasmid (5 µg per hybridization) cut with *Hind*III and labelled with ³²P (specific activity ∼ 500,000 c.p.m. pmol⁻¹ of 5′ ends) (lanes 2 and 3: 6.5 h and 4 h of S₁ nuclease digestion, respectively). Lanes 4, 5: the conditions were as in *A*, lanes 2–4, except that 100 µg of hen oviduct poly(A)⁺ RNA and 1 µg of labelled probe were hybridized in 25 µl of formamide buffer. S₁ nuclease digestion was for 4 h (lane 5) and 6.5 h (lane 4) with 1,600 units of S₁. These quantities of poly(A)⁺ RNA and probe gave a similar amount of total S₁ nuclease-resistant counts as their *in vitro* counterpart (*B*, lanes 2, 3). Arrowheads indicate bands discussed in the text.

RNAs are identical and correspond to the T, numbered 1, which was previously identified as coding for the first nucleotide of con-mRNA[12]. (Two control experiments in lanes 9 and 10, described in Fig. 1 legend, show that no bands are present when the incubation was carried out in the absence of conalbumin DNA or in the presence of a low concentration of α-amanitin.) The presence of the lowest doublet bands in lanes 3, 4, 6 and 7 may be due to incomplete S₁ nuclease digestion related to capping of the RNAs (see below), whereas the upper

bands in lanes 2, 3, 5 and 6 are probably due to the secondary structure(s) of the DNA probe (see the DNA sequence in ref. 12).

All these results are compatible with specific *in vitro* initiation of transcription at the 5′ end of the conalbumin gene. This conclusion is further supported by analysis of RNase T₁ digests of the *in vitro* synthesized RNA, which shows the presence of the expected terminal T₁ oligonucleotide, both in the capped and uncapped forms (C.K. *et al.*, in preparation). Weil *et al.*[9] have also observed capping of the RNA synthesized *in vitro* from the major late adenovirus-2 gene.

Specific, but less efficient, transcription of ovalbumin and early E1A adenovirus-2 genes

As shown in Fig. 4, specific transcription was also observed with two 'truncated' templates containing the 5′ region of the ovalbumin gene and cut with either *Eco*RI or *Hind*III at the *Eco*6 or *Hind*3 sites, respectively (see Fig. 1*c* in ref. 11). The two distinct bands [400 nucleotides (lane 4) and 220 nucleotides (lane 5)] are expected if initiation of transcription is taking place at the 5′ end of the ovalbumin leader coding sequence[11]. The discrete bands which are seen above the 220-nucleotide RNA in lane 5 do not correspond to specific run-off transcripts (that is, transcription from specific sites to the end of the truncated template), as bands with identical size were observed on longer exposure of lane 4. In an experiment similar to that described above for the conalbumin transcript, S₁ nuclease mapping was used to localize more precisely the 5′ end of the *in vitro* synthesized RNA (Fig. 3*B*). *In vivo* hen oviduct poly(A)⁺ RNA or *in vitro* RNA synthesized on the truncated *Eco*6 template were hybridized to a probe 5′-labelled at the *Hind*3 site. After nuclease S₁ digestion, the resistant labelled DNA fragments were run on a sequencing gel together with a G + A sequence ladder around the 5′ end of the ovalbumin gene. The same bands were observed with *in vivo* (lanes 4, 5) and *in vitro* (lanes 2, 3) RNAs, but not in control experiments run in the absence of ovalbumin DNA or in the presence of α-amanitin (not shown). The position of the resistant bands corresponds to the A at position −1 of the ovalbumin coding strand, suggesting that the *in vitro* synthesized RNA was initiated at the T (at position 1 in the ovalbumin gene) which codes for the first nucleotide of ovalbumin mRNA[11]. Our results confirm those of LeMeur (personal communication) who, with the same *Hind*3 5′-labelled probe, showed that the 5′ ends of the ovalbumin mRNA precursor molecules map at the cap site, and found no evidence for RNA molecules initiated *in vivo* upstream from that site. It seems, therefore, that the ovalbumin gene is also specifically transcribed in the *in vitro* cell-free system. However, it is clear, from a comparison of lanes 2 and 4 in Fig. 4, that the ovalbumin gene is transcribed with a much lower efficiency than the conalbumin gene, although, for both genes, care was taken to carry out the reactions at optimum DNA concentrations. The efficiency of transcription of the ovalbumin gene was not increased by using the purified *Pst*4–*Eco*6 fragment[11] as a template (not shown).

The difference in transcriptional efficiency of conalbumin and ovalbumin genes prompted us to compare the transcription of these genes with two adenovirus genes, the major late, previously studied by Weil *et al.*[9], and the early E1A (ref. 17), whose 5′-end regions have been cloned in our laboratory (see Fig. 4 legend). The major late adenovirus gene template, truncated at the 18.2 *Sma*I site[18], gave a run-off transcript of about 560 nucleotides (lane 6), as expected from the results of Weil *et al.*[9]. Comparison with the 650-nucleotide run-off transcript of the truncated *Hind*II conalbumin template (lane 7) showed that, at optimum DNA concentrations, the major late adenovirus gene was a somewhat better template

than the conalbumin gene (variations were observed from one experiment to another, but in general the intensity of the late adenovirus band was approximately twice that of the conalbumin). Specific transcription of the adenovirus-2 early E1A gene was also observed in the cell-free system. Two truncated templates were used (see Fig. 4 legend), one cut at the *Sma*I site, which is at position 1,009 from the left end of the adenovirus genome (2.9 map units)[17], the other at an *Ava*I site, which we mapped in our adenovirus-2 DNA at position 758 (numerology of ref. 19). Because the 5' end of the E1A mRNAs maps at position 499 (see ref. 17), two run-off transcripts of 510 and 260 nucleotides, respectively, were expected, assuming that transcription starts at the cap site of E1A mRNAs. The two predicted run-off transcripts are, in fact, observed in lanes 8 and 9 of Fig. 4.

It is clear that the *in vitro* transcription of the early adenovirus E1A templates is much less efficient than that of the conalbumin and major late adenovirus genes, and in this respect is similar to that of the ovalbumin gene. Interestingly, the X gene, which evolved from the same ancestral gene as the ovalbumin gene (ref. 20, and R. Heilig and J. L. Mandel, personal communication), is transcribed *in vitro* with about the same efficiency as the ovalbumin gene (not shown). The reason that the shorter run-off transcripts of the ovalbumin (lane 5) and early EA1 adenovirus gene (lane 9) are less intense than expected from their reduced size is unknown (note in Fig. 4 legend that lanes 5 and 9 were exposed for a longer time), but similar observations were made for the short run-off transcripts of conalbumin and major late adenovirus genes.

The observed marked variation in the transcriptional efficiency of different genes raised the possibility that RNA polymerase B or the factor(s) contained in the S100 extract, or both, could have different affinities for various genes. This possibility was tested with the conalbumin and ovalbumin

genes. In the experiment shown in lane 3 of Fig. 4, the two incubation mixtures used for lanes 2 and 4 were mixed. Both the conalbumin and the ovalbumin run-off transcripts are observed in this mixed incubation (arrowheads in lane 3; although the ovalbumin band is faint it was consistently seen on the original autoradiograms). This experiment was carried out at optimum DNA concentration for both conalbumin and ovalbumin specific transcription. The same result was obtained in the presence of four times this amount of conalbumin and ovalbumin templates. These observations indicate that there is no competition between the two templates.

Several possibilities could be invoked to explain these results. First, different factors, specific for different genes, could be present in the S100 extract. Second, the same factor(s) could be used equally well for transcription of the two genes, but the rate limiting step is beyond that requiring the factor(s). Third, the factor(s) present in the S100 extract is not required by the ovalbumin gene. This last possibility is excluded, as the S100 extract was required for specific transcription of all of these genes (not shown).

Some sequences, situated 5' to the cap site, are required for specific *in vitro* transcription

The existence of related sequences (see above and refs 10–13) 5' to the *in vitro* initiation site on the conalbumin, ovalbumin and adenovirus-2 genes, led us to investigate whether these sequences are required for specific *in vitro* transcription. In this respect, the conalbumin gene is especially convenient because there is a *Bst*NI site at position −44 and an *Mbo*II site at position −8 (Fig. 1*B*). As shown in Fig. 5*A*, a *Bst*NI-digested conalbumin *Eco* 'b' fragment gave the expected run-off transcript of 400 nucleotides [lane 2; the efficiency of specific transcription was the same as on intact *Eco* 'b' fragment (not shown)], whereas this transcript was absent with a conalbumin *Eco* 'b' template cut with both *Bst*NI and *Mbo*II (lane 3). (No attempt has been made to identify the nature of the minor bands present in lanes 2 and 3 because 'non-specific' bands are seen in all these *in vitro* transcription assays.) Similarly, the isolated *Pst*5–*Pst*6 fragment (Fig. 1*B*), digested with *Bst*NI, gave a run-off band of about 200 nucleotides, whereas no distinct band was observed when the *Pst*5–*Pst*6 fragment was cut with *Mbo*II (not shown). S$_1$ mapping experiments, similar to those reported in Fig. 3*A*, showed that the 5' end of the specific transcript obtained on the '*Bst*NI-cut' template, maps at the position coding for the first nucleotide of con-mRNA (B.W., unpublished result).

To exclude the possibility that the above results could be influenced by the absence of DNA upstream from position −44 when specific synthesis is retained, and upstream from position −8 when it is lost, we have cloned the *Bst*NI (−44) to *Pst*I (+203) and the *Mbo*II (−8) to *Pst*I (+203) fragments in the *Bam*HI site of pBR322 (see Fig. 5 legend and Fig. 5*C*). The recombinant clones in the orientation shown in Fig. 5*C* (*a, b*) were cut with either *Bst*NI or *Hin*dIII and transcribed *in vitro*. As shown in Fig. 5*B*, the expected run-off transcripts are present (lanes 2, 3) when the recombinant DNA contains the conalbumin sequence up to position −44, but are absent (lanes 4, 5) when the conalbumin sequences are missing upstream from position −8. Similar results were obtained with templates where the conalbumin fragments were inserted in the opposite orientation (B.W., unpublished results).

From these results we conclude that the sequences which are situated upstream from position −44 are not required for specific *in vitro* transcription of the conalbumin gene in this cell-free system. In agreement with this conclusion, we have observed (J.C., unpublished result) that the sequences located upstream from position −48 with respect to the cap site are not required for specific *in vitro* transcription of the major late adenovirus-2 gene. On the other hand, our results demonstrate

910 —
659
655
520 —

403 —

281 —
257 —

226 —

910 —
659
655
520 —

403 —

281 —

257 —

226 —
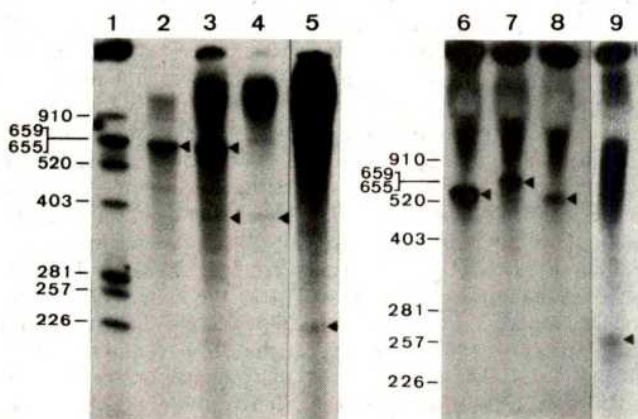
Fig. 4 Comparison of *in vitro* specific RNA transcripts synthesized on conalbumin, ovalbumin and adenovirus-2 DNA templates. RNA was synthesized and extracted as described in Fig. 1*A* legend, but using different DNA templates. DNA concentrations were chosen to give maximal incorporation into the specific RNA transcripts (see text). Lane 2: 12 μg ml⁻¹ of *Hin*dII conalbumin DNA fragment (5.7 kilobases) (see Fig. 1*A* legend); lane 4: 11 μg ml⁻¹ of ovalbumin *Pst*4–*Eco*6 plasmid (5.3 kilobases) linearized with *Eco*RI (see Fig. 3*B* legend); lane 3: reaction mixtures, equivalent to lanes 2 and 4, respectively, mixed before incubation; lane 5: 11 μg ml⁻¹ of ovalbumin *Pst*4–*Eco*6 plasmid linearized with *Hin*dIII (see Fig. 3*B* legend); lane 6: 20 μg ml⁻¹ of a *Sma*I [map position 18.2 (ref. 18)] cleaved recombinant plasmid (6.7 kilobases) consisting of the *Bal*I E fragment of adenovirus-2 DNA (map position 14.7–21.5 on the adenovirus-2 genome) integrated into the *Eco*RI site of pBR322; lane 7: 16 μg ml⁻¹ of the conalbumin *Hin*dII fragment; lane 8: 24 μg ml⁻¹ of a *Sma*I-cleaved recombinant plasmid (5.7 kilobases) consisting of the left-most *Xba*I fragment of adenovirus-2 DNA (map position 0–3.85, see ref. 17) integrated into the *Eco*RI site of pBR322 (to be published elsewhere); lane 9: 36 μg ml⁻¹ of the same recombinant DNA as in lane 8, but cleaved with *Ava*I (see text); lane 1: ³²P-labelled DNA fragment size markers. Lanes 1–5, and 6–9 correspond to two different gels. Lanes 5 and 9 were exposed for a longer time. Arrowheads indicate the bands described in the text.
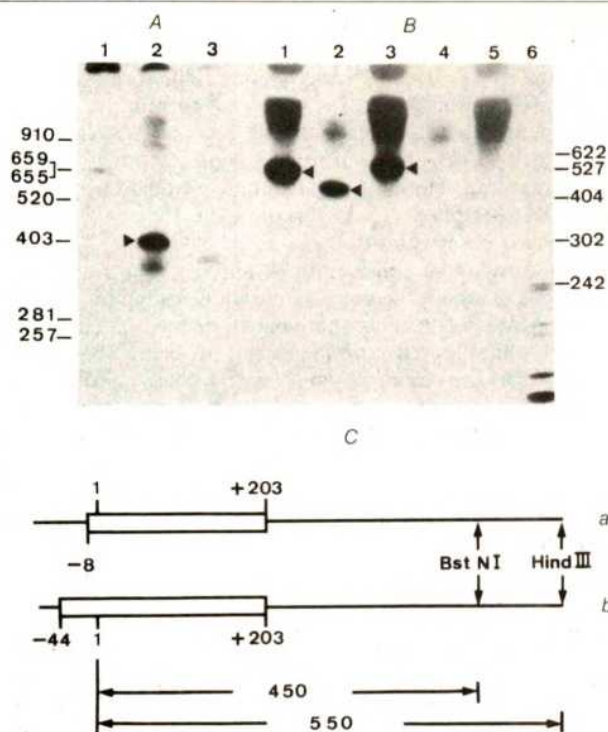
Fig. 5 Effect of deletion in the 5'-end region of the conalbumin gene on its specific transcription. *A*, The excised conalbumin *Eco* 'b' fragment was digested with *Bst*NI (lane 2) or *Bst*NI and *Mbo*II (lane 3) (see Fig. 1), purified by two phenol extractions, two ether extractions, ethanol precipitation and dialysis against 50 mM Tris-HCl, pH 7.9, and 1 mM Na-EDTA. Transcription was done at 16 μg ml^{-1} template as described in Fig. 1*A* legend. Lane 1: ^{32}P-labelled DNA fragment size markers. *B*, The conalbumin DNA fragments from *Bst*NI (−44) to *Pst*I (+203) (lanes 2 and 3) and *Mbo*II (−8) to *Pst*I (+203) (lanes 4, 5) (see Fig. 1 and part *C*) were repaired with DNA polymerase I and cloned in pBR322 which had been linearized with *Bam*HI and repaired with DNA polymerase. DNA from clones containing the conalbumin gene fragment (in the orientation shown in *C*) was digested with either *Hind*III (lanes 3, 5) or *Bst*NI (lanes 2, 4), purified as described in *A* and transcribed *in vitro* at 10 μg ml^{-1} template (Fig. 1*A*). Lane 1: transcription with 8 μg ml^{-1} purified *Eco* 'b' fragment (see Fig. 1). Lane 6: ^{32}P-labelled DNA fragment size markers. *C*, Restriction enzyme maps of the cloned *Mbo*II (−8) to *Pst*I (+203) (*a*) and *Bst*NI (−44) to *Pst*I (+203) (*b*) conalbumin gene fragments. The figures refer to the number of nucleotides from the cap site (position 1) and correspond to restriction enzyme cutting sites on the non-coding strand (negative numbers are upstream from the cap site with respect to the direction of transcription). The open lines correspond to conalbumin gene DNA and the single lines to pBR322 DNA. The lengths (in base pairs) indicated by arrows correspond to distances from the cap site to the corresponding restriction enzyme cutting site. Arrowheads in *A* and *B* correspond to bands discussed in the text.

that there is no specific transcription when the DNA located upstream from position −8 of the conalbumin gene is deleted.

Influence of the origin of RNA polymerase on specific transcription

The sequence similarities which have been observed, in both higher and lower eukaryotes, upstream from the region coding for the 5' end of mRNAs (refs 10–13 and refs therein, refs 21, 22) and the structural similarities between the eukaryotic RNA polymerases belonging to class B (refs 5, 6), raise the question of whether specific *in vitro* transcription can be achieved irrespective of the origin of the polymerase B. Figure 6 shows that the conalbumin gene was specifically transcribed with the same efficiency by both purified calf thymus[15] (lane 2) and hen oviduct[23] (lane 3) RNA polymerase B. In contrast, purified *Drosophila*[24] (lane 4), yeast[25] (lane 5) and wheat-germ[26] (lane 7) RNA polymerases B did not significantly stimulate the specific transcription above the level obtained with the endogenous polymerase B present in the S100 extract (lane 1).

This was supported by the complete disappearance of specific transcription when α-amanitin was added to the yeast incubation (lane 6) at a concentration which does not inhibit yeast RNA polymerase B (ref. 27). No specific transcription above the endogenous level was observed with *Escherichia coli* RNA polymerase (lanes 8, 9). Similar results were obtained when the ovalbumin and the late adenovirus-2 genes were transcribed with the various RNA polymerases B (the lack of specific transcription of the major late adenovirus-2 gene by the wheat-germ RNA polymerase B has been reported previously[9]). In no case did we observe specific transcription using either purified calf thymus RNA polymerase A (ref. 28) or the endogenous RNA polymerase C present in the S100 extract (see Fig. 6, lanes 6, 9, and our unpublished results).

Note that all the enzymes used in the incubations shown in Fig. 6 gave comparable amounts of RNA synthesis when incubated in identical conditions on commercial calf thymus DNA in the absence of S100 extract, and that the specific synthesis which is obtained on the most efficiently transcribed templates (major late adenovirus-2 or conalbumin genes) represents at most 1% of the synthesis which is achieved on calf thymus DNA. This low efficiency of specific transcription by the added purified RNA polymerase B raises the question of whether the endogenous enzyme B, which did not go through all the purification steps, is more efficient in promoting specific transcription. This is apparently not the case, as titration of the S100 endogenous RNA polymerase B with ^{3}H-amanitin[29] indicated that the S100 extract added to each incubation contains about one-seventh the amount of added purified polymerase B (not shown). Clearly, comparison of lanes 1 and 2 of Fig. 6 indicates that the endogenous polymerase B is not more efficient for specific transcription.

Conclusions

Our present results suggest very strongly that specific transcription of cellular genes, transcribed *in vivo* by RNA polymerase B, can be achieved *in vitro* with cloned DNA templates and purified polymerase in the presence of the S100 extract of Wu and Zubay[14]. Initiation of *in vitro* transcription seems to be accurate, taking place at the same site as *in vivo*, as there is no evidence that initiation occurs *in vivo*, on the conalbumin or the ovalbumin genes, from a site located upstream from the cap site (see above). Although we cannot
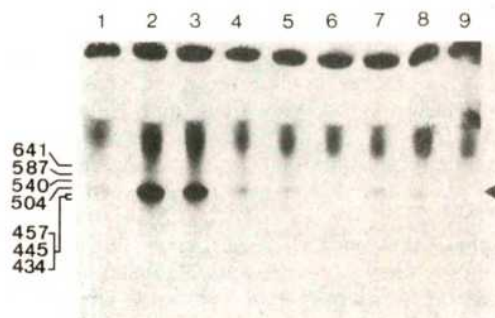
Fig. 6 Effect of different exogenous RNA polymerases on specific *in vitro* transcription of the conalbumin gene. RNA was synthesized on the conalbumin *Eco* 'b' fragment (12 μg ml^{-1}) and extracted as described in Fig. 1*A* legend, but with various RNA polymerases. Lane 1: no added RNA polymerase; lane 2: 0.102 units of purified calf thymus RNA polymerase B (see Fig. 1*A* legend); lane 3: 0.129 units of purified oviduct RNA polymerase B (fraction HA, ref. 23); lane 4: 0.110 units of purified *Drosophila* RNA polymerase B (ref. 24, and A. Krämer, personal communication); lane 5: 0.100 units of purified yeast RNA polymerase B (ref. 25); lane 6: as in lane 5, but in the presence of 0.1 μg ml^{-1} α-amanitin; lane 7: 0.130 units of purified wheat-germ RNA polymerase B (ref. 26); lane 8: 0.140 units of purified *E. coli* holoenzyme[45]; lane 9: same as lane 8, but in the presence of 1 μg ml^{-1} α-amanitin. One unit of RNA polymerase corresponds to the activity measured in the conditions described previously[15] in the presence of 3 mM Mn^{2+} and 100 mM ammonium sulphate. The arrowhead indicates the bands described in the text.

unequivocally rule out the possibility that the specific RNAs seen *in vitro* could result from processing of transcripts initiated upstream from the cap site, this seems very unlikely, at least in the case of conalbumin, where the sequences upstream from position −44 can be deleted without impairing the specific transcription, and specific 5′-terminal uncapped and capped T_1 oligonucleotides have been found.

The observation that the DNA located in the conalbumin gene between positions −8 and −44 is required for specific transcription is in agreement with the proposal that the A+T-rich 'Goldberg–Hogness box' (refs 21 and 10–13, 22, 30 and refs therein) is part of at least one class of promoter site for RNA polymerase B. In this respect, it is striking that the major late adenovirus-2 and the conalbumin genes, which have the same sequence from positions −21 to −32 (ref. 12), are transcribed *in vitro* with about the same efficiency, whereas the ovalbumin, early E1A adenovirus and X genes, which have A+T-rich regions of different sequences, were transcribed with lower efficiencies. Our results demonstrate that the sequences which are situated upstream from position −44 of the conalbumin gene are not required for specific *in vitro* initiation. Obviously, this does not exclude the possibility that some of these sequences could be required *in vivo* and involved in initiation and/or regulation of transcription by interacting with other initiation or regulatory factors. In this respect, it is interesting that homologies have been found by comparing the sequences of several genes upstream from position −44 (ref. 13).

There seem to be differences in the location (with respect to the 5′ end of the transcript) of at least some of the sequences necessary for specific initiation by RNA polymerases B and C. It has been shown that up to 50 base pairs into a 5S RNA gene can be replaced without substantially affecting initiation of transcription by RNA polymerase C (see refs 31–33, but refs 34, 35 for different results using the VA RNAI adenovirus gene or the *Xenopus* tRNA₁ Met gene as templates). Obviously, our present results do not exclude the possibility that sequences situated downstream from position −8 are also required for specific transcription by RNA polymerase B. In fact, we have found that the *Mbo*II–*Pst*5 conalbumin fragment (see Fig. 1*B*), when inserted in the *Bam*HI site of pBR322, does direct specific initiation of transcription (results not shown).

Almost nothing is known of the nature and mechanism of action of the factor(s) present in the S100 extract and responsible for the specific transcription (see also ref. 9). However, in view of the overall inefficiency of the system, other factors (either catalytic or structural) are probably required to account for the *in vivo* rates of transcription. Addition to the incubation mixtures of the RNA polymerase B stimulatory factor isolated by Stein and Hausen[36] did not increase the rate of specific transcription (H. Stein and C. Kédinger, unpublished results). It is unlikely that the overall inefficiency is related to the use of heterologous systems, as RNA polymerase B purified from hen oviduct was not more effective than the purified calf thymus polymerase B in transcribing the chicken conalbumin or ovalbumin genes (Fig. 6). In addition, transcription of the major late adenovirus-2 gene, in homologous or heterologous systems (ref. 9, and our present results), does not seem to be substantially more efficient than that of the conalbumin gene in a heterologous system. The fact that the *Drosophila*, yeast and wheat-germ polymerases B do not specifically transcribe the conalbumin, ovalbumin and adenovirus genes, in spite of the similarity between the A+T-rich presumptive promoter sequences in higher and lower eukaryotes, is perhaps not surprising in view of the low immunological cross-reactivity between the calf thymus RNA polymerase B on the one hand, and *Drosophila*[37] and yeast (A. Sentenac, personal communication) RNA polymerases B on the other, whereas immunological relatedness was observed for polymerases B of higher eukaryotes[38].

Although it is clear that cloned DNA can be transcribed specifically, the overall low efficiency of the *in vitro* system raises the question of whether some cellular post-synthetic DNA modifications (ref. 39 and refs therein) is required. Minor gene rearrangement of the ovalbumin gene during differentiation does not seem to be responsible for its low level of *in vitro* transcription, as the same results were obtained with DNA cloned from erythrocyte or oviduct cells (unpublished observation).

From all of these considerations and also the result of the experiment in which the conalbumin and ovalbumin templates were both present in the same incubation mixture (Fig. 4), we conclude that the factor(s) present in the S100 extract probably has an essential, but not exclusive, role in the initiation of transcription of most, if not all, messenger coding genes in higher eukaryotes. Several lines of evidence indicate that other important components involved in the *in vivo* regulation of transcription are missing from the present cell-free system. First, the major late adenovirus-2 gene is better transcribed *in vitro* than the early E1A gene, whereas early in the lytic cycle the major late gene is apparently not transcribed (see ref. 40 and refs therein). Second, the *in vivo* rate of transcription of the ovalbumin gene, under hormonal stimulation, can be at least as high as that of the conalbumin gene (see ref. 4 and refs therein), whereas it is obviously much lower *in vitro*. Third, the ovalbumin gene and the related X gene are similarly transcribed *in vitro*, whereas *in vivo* under hormonal stimulation the rate of transcription of the ovalbumin gene is at least 50 times higher than that of the X gene (ref. 20, and M. LeMeur and R. Palmiter, personal communications). The availability of an *in vitro* cell-free system which catalyses specific transcription of cellular genes provides a means of testing whether and how steroid hormone receptor complexes are involved in regulation of transcription, and represents the first step towards a complete elucidation of the molecular mechanisms involved in regulation of transcription in eukaryotic cells.

1. Losick, R. & Chamberlin, M. (eds) *RNA Polymerase* (Cold Spring Harbor Laboratory, New York, 1976).
2. Rosenberg, M. & Court, D. *A. Rev. Genet.* **13,** 319–353 (1979).
3. Chambon, P. *Cold Spring Harb. Symp. quant. Biol.* **42,** 1209–1234 (1978).
4. McKnight, G. S. & Palmiter, R. D. *J. biol. Chem.* **254,** 9050–9058 (1979).
5. Chambon, P. *A. Rev. Biochem.* **44,** 613–638 (1975).
6. Roeder, R. G. in *RNA Polymerase* (eds Losick, R. & Chamberlin, M.) 285–329 (Cold Spring Harbor Laboratory, New York, 1976).
7. Wu, G. J. *Proc. natn. Acad. Sci. U.S.A.* **75,** 2175–2179 (1978).
8. Weil, P. A., Segall, J., Harris, B., Ng, S. Y. & Roeder, R. G. *J. biol. Chem.* **254,** 6163–6173 (1979).
9. Weil, P. A., Luse, D. S., Segall, J. & Roeder, R. G. *Cell* **18,** 469–484 (1979).
10. Proudfoot, N. J. *Nature* **279,** 376 (1979).
11. Gannon, F. *et al. Nature* **278,** 428–434 (1979).
12. Cochet, M. *et al. Nature* **282,** 567–574 (1979).
13. Benoist, C., O'Hare, K., Breathnach, R. & Chambon, P. *Nucleic Acids Res.* **8,** 127–142 (1980).
14. Wu, G. J. & Zubay, G. *Proc. natn. Acad. Sci. U.S.A.* **71,** 1803–1807 (1974).
15. Kédinger, C. & Chambon, P. *Eur. J. Biochem.* **28,** 283–290 (1972).
16. Weaver, R. F. & Weissmann, C. *Nucleic Acids Res.* **7,** 1175–1193 (1979).
17. Perricaudet, M., Akusjärvi, G., Virtanen, A. & Pettersson, U. *Nature* **281,** 694–696 (1979).
18. Ziff, E. B. & Evans, R. M. *Cell* **15,** 1463–1475 (1978).
19. Van Ormondt, H., Maat, J., De Waard, A. & Van der Eb, A. J. *Gene* **4,** 309–328 (1978).
20. Royal, A. *et al. Nature* **279,** 125–132 (1979).
21. Goldberg, M. thesis, Stanford Univ. (1979).
22. Smith, M. *et al. Cell* **16,** 753–761 (1979).
23. Krebs, G. & Chambon, P. *Eur. J. Biochem.* **61,** 15–25 (1976).
24. Greenleaf, A. L. & Bautz, E. K. F. *Eur. J. Biochem.* **60,** 169–179 (1975).
25. Sawadogo, M., Sentenac, A. & Fromageot, P. *J. biol. Chem.* (in the press).
26. Jendrisak, J. J. & Burgess, R. R. *Biochemistry* **14,** 4639–4645 (1975).
27. Dezélée, S. & Sentenac, A. *Eur. J. Biochem.* **34,** 41–52 (1973).
28. Gissinger, F. & Chambon, P. *Eur. J. Biochem.* **28,** 277–282 (1972).

29. Cochet-Meilhac, M., Nuret, P., Courvalin, J. C. & Chambon, P. *Biochim. biophys. Acta* **353**, 185–192 (1974).
30. Baker, C. C., Herisse, J., Courtois, G., Galibert, F. & Ziff, E. *Cell* **18**, 569–580 (1979).
31. McKay, R. *Nature* **282**, 556 (1979).
32. Sakonju, S., Bogenhagen, D. F. & Brown, D. D. *Cell* **19**, 13–25 (1980).
33. Bogenhagen, D. F., Sakonju, S. & Brown, D. D. *Cell* **19**, 27–35 (1980).
34. Thimmappaya, B., Jones, N. & Shenk, T. *Cell* **18**, 947–954 (1979).
35. Kressmann, A., Hofstetter, H., Di Capua, E., Grosschedl, R. & Birnstiel, M. *Nucleic Acids Res.* **7**, 1749–1763 (1979).
36. Stein, H. & Hausen, P. *Cold Spring Harb. Symp. quant. Biol.* **35**, 709–717 (1970).
37. Greenleaf, A. L., Krämer, A. & Bautz, E. K. F. in *RNA Polymerase* (eds Losick, R. & Chamberlin, M.) 793–801 (Cold Spring Harbor Laboratory, New York, 1976).
38. Ingles, C. J. *Biochem. biophys. Res. Commun.* **55**, 364–371 (1973).
39. Mandel, J. L. & Chambon, P. *Nucleic Acids Res.* **7**, 2081–2103 (1979).
40. Flint, J. *Cell* **10**, 153–166 (1977).
41. Maxam, A. M. & Gilbert W. *Meth. Enzym.* (in the press).
42. Suttcliffe, J. G. *Nucleic Acids Res.* **5**, 2721–2728 (1978).
43. Wahl, G. M., Stern, M. & Stark, G. R. *Proc. natn. Acad. Sci. U.S.A.* **76**, 3683–3687 (1979).
44. Brison, O. & Chambon, P. *Analyt. Biochem.* **75**, 402–409 (1976).
45. Wasylyk, B., Thevinin, G., Oudet, P. & Chambon, P. *J. molec. Biol.* **128**, 411–440 (1979).

Satellite tobacco necrosis virus structure at 4.0 Å resolution

T. Unge, L. Liljas, B. Strandberg, I. Vaara, K. K. Kannan* & K. Fridborg

Department of Molecular Biology, University of Uppsala, Box 562, S-751 22 Uppsala, Sweden

C. E. Nordman & P. J. Lentz Jr†

Department of Chemistry, University of Michigan, Ann Arbor, Michigan 48109

An electron density map of satellite tobacco necrosis virus at 4.0 Å resolution was obtained using single isomorphous replacement and phase refinement by icosahedral averaging. Near the N-terminus the polypeptide chain is a three-turn helix, in contact with 3-fold related helices, extending towards the particle centre. The protein subunit has at least one twisted β-sheet.

THE satellite tobacco necrosis virus (STNV) is one of the smallest known viruses. It requires *in vivo* co-infection with tobacco necrosis virus for growth[1,2]. STNV is composed of a coat of 60 identical protein molecules (molecular weight (MW) 21,600[3,4]) and a single-stranded RNA, known to code for the coat protein[5]. The complete sequences of both STNV RNA[3] (about 1,200 nucleotides) and the STNV protein[3,4] (195 amino acids) are known. The coat protein is arranged in a $T = 1$ icosahedral surface lattice[6–8]. Thus, all 60 protein subunits have identical surroundings in the virus particle.

STNV crystallises from 1.0×10^{-3} M $MgSO_4$ in space group C2 with four particles in the monoclinic cell with $a = 318.4$ Å, $b = 305.0$ Å, $c = 185.3$ Å and $\beta = 94.37°$. The crystallographic asymmetric unit is a complete virus particle[9], with an MW of 1.7×10^6 (refs 3, 10, 11). That is, the virus particle is located in a general position in the crystallographic unit cell. Hence, the crystallographic symmetry does not exclude a determination of even the nucleic acid structure.

This article describes the structure of STNV at 4.0 Å resolution. The electron density maps were calculated with phases obtained by two procedures, in both cases using double isomorphous replacement (DIR) phases at 10 Å resolution[12] as starting phases. In one method the phases in the 10–4 Å resolution range were conventional single isomorphous replacement (SIR) phases, refined with a symmetry averaging (SA) technique, which makes use of the redundancy in the crystal data due to the 60-fold non-crystallographic symmetry of the virus protein. In the other method a combined phase extension and phase refinement was done in small steps from 10 to 4 Å resolution by the SA technique.

The preparation of STNV crystals[9], the preparation of $PtCl_4^{2-}$ and iodine derivatives used at 10 Å resolution, and the location and refinement of these heavy atom sites have been described elsewhere[12]. A modified iodine derivative with two iodine positions per subunit was prepared[13] and used for SIR at 4.0 Å resolution. The 4 Å X-ray diffraction data from native STNV crystals and STNV iodine crystals were collected using oscillation camera technique as described in Table 1. The statistics of the refinement of the two iodine atoms are given in Table 2.

Electron density calculation based on SIR and SA

The DIR-phases at 10 Å resolution were taken as the initial values for phase refinement by means of non-crystallographic symmetry[14–16]. After three cycles of refinement at 10 Å (with wF_{obs} as the structure amplitude; see Table 3) an electron density map was computed using the refined phases to 10 Å and 'best'[17] SIR phases from 10 to 4 Å resolution. This map was the starting point for eight cycles of refinement of the phases using symmetry averaging (see Table 3). No combination of SIR and SA phases was done. The electron density in each refinement cycle was calculated with a grid spacing of 1.9 Å, and 60-fold icosahedral averaging of the electron density was performed using a grid sampled at 1.7 Å intervals within a region limited by an outer, and in the four last cycles also by an inner, envelope[18]. The outer envelope was a sphere of 88 Å radius modified by addition of smaller spheres close to the 5-fold axes to account for protrusions of continuous density to a maximum radius of 96 Å. The inner envelope was a sphere of 62.5 Å radius with addition of truncated cones around the 3-fold axes penetrating to 43 Å particle radius, accounting for strong continuous density. Outside the outer envelope the electron density was levelled. Inside the inner envelope the electron density values were

*Present address: Neutron Physics Division, Bhabha Atomic Research Centre, Trombay, Bombay 400085, India.
†Present address: Department of Biology, King's College, Wilkes-Barre, Pennsylvania.
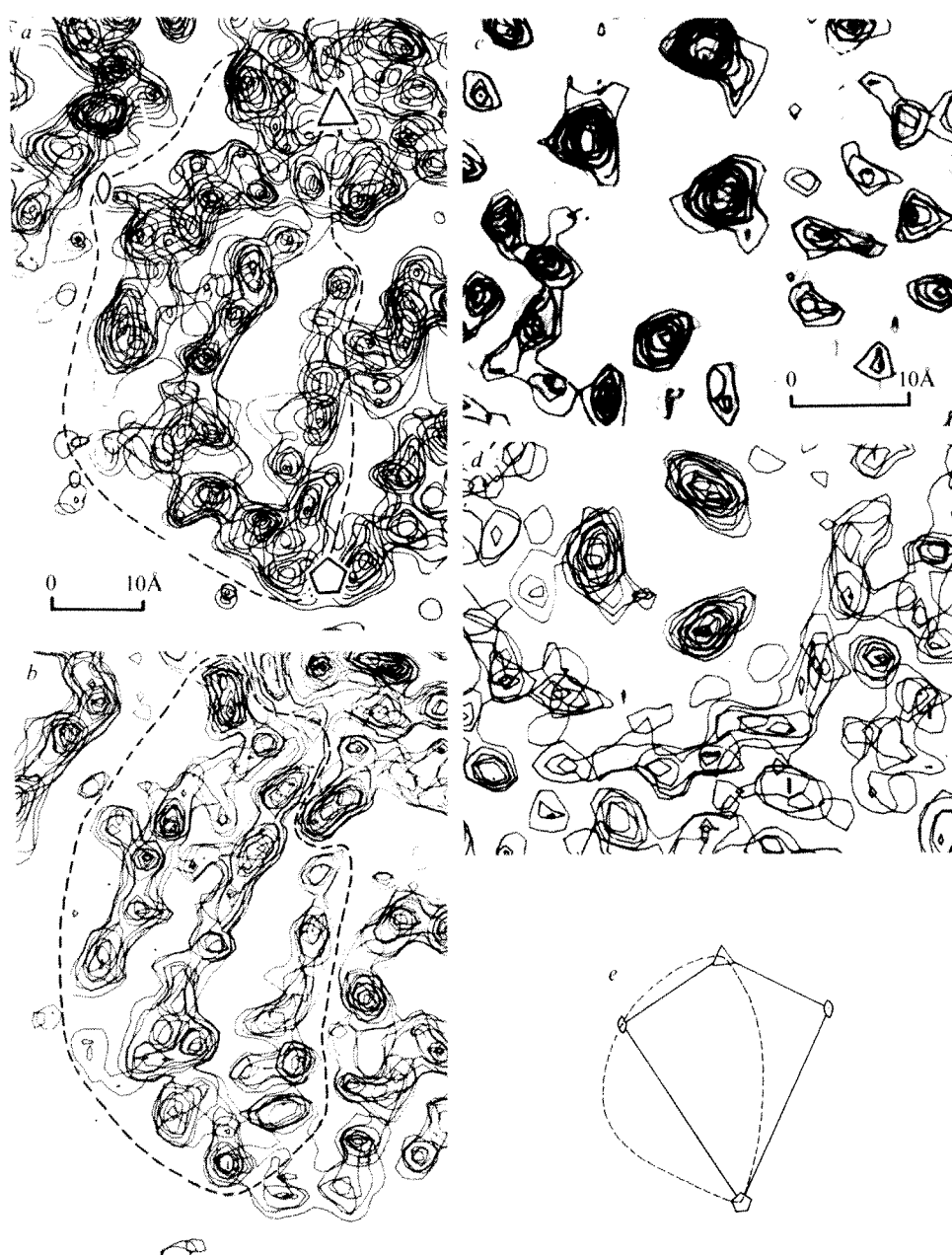
Fig. 1 Comparison of electron density maps obtained by SIR + SA (*a* and *c*) and PE + SA (*b* and *d*). All sections are plotted perpendicular to one particle 3-fold axis. Subunit boundaries are indicated. Parts *a* and *b* compare sections at 79–76 Å from the particle centre showing the protein subunit region. The densities in the PE are better resolved than the densities in the SIR maps, indicating that the SIR maps suffer from incomplete phase information. Parts *c* and *d* show the sections at 57–54 Å particle radii containing the densities interpreted as part of the 3-fold-related helices anchoring three subunits to each other. *e*, Key to Figs 1 *a–d*, 2*a*, *b* and 3*a*, *b* showing the locations of the particle 3-fold axis (perpendicular to paper), 5-fold and 2-fold axes (tilted), the boundaries of one sixtieth, that is one asymmetric unit of the virus particle (solid line), and indicating approximate subunit boundaries (broken line).

essentially left unmodified; a damping function was used to prevent build-up of noise[18]. In the phase refinement the F_{calc} values from the previously averaged map were put in for unrecorded reflections.

Electron density calculation based on phase extension (PE) and SA

The 4 Å PE calculation was based on 10 Å DIR-phases, refined with SA (three cycles). Phases in the resolution range 10–4 Å were calculated in a stepwise phase extension procedure. The resolution was increased in small increments: 2,000–3,500 reflections were added in each step. The F_{calc} values in the extended range were calculated from the latest electron density map, based on F_{obs} amplitudes and α~~~~ phases at somewhat lower resolution. The detailed procedure is explained in ref. 18. The total phase extension from 10 to 4 Å resolution included about 50 cycles of phase refinement. Grid spacing, choice of envelope and other conditions were as for the refinement of the SIR map, with the exception that no weighting factor was applied to the $|F_{obs}|$ values in the PE + SA calculation.

Argos *et al.*[19] used a phase extension procedure from 6.0 to

4.9 Å resolution in their crystallographic studies of glyceraldehyde-3-phosphate dehydrogenase (GPD) with two 2-fold non-crystallographic symmetry axes. The experience from their study was the necessity to use a rather accurate molecular envelope and the need for small increments in data resolution. Also, in the present STNV studies we have noticed the importance of good molecular envelopes (in the case of a spherical virus this is fairly simply determined) and have, in order to properly use the coupling between phase angles, also chosen small data resolution increments.

Comparison of SIR + SA and PE + SA electron density maps

Sections of the SIR + SA and PE + SA electron density maps are shown in Fig. 1. There is good agreement between the maps in the region corresponding to the protein part. In the SIR + SA map the continuity is more pronounced, while the PE map contains somewhat more resolved densities. The dissimilarities might well be explained by the rather inaccurate starting SIR phases (the main reason for this being one heavy atom derivative; other factors are incomplete data and limited

refinement of the heavy atom parameters), together with the rather limited number of refinement cycles in the SIR-SA calculation as well as differences in weighting between the methods.

Structure results

The final STNV structure, shown in Figs 2–4, is based on the PE + SA calculation at 4 Å resolution followed by several phase refinement cycles in which the Fourier and averaging grid spacings were 1.3 and 1.05 Å respectively, and the data resolution was increased to nominally 3.8 Å (about half of the F_{obs} values in the region 3.8–4.0 Å were available). A total of 135,808 reflections out of the 168,180 possible reflections were observed. The R factor for the observed reflections was 21%.

General distribution of electron density in the STNV particle

The minimum particle radius is about 86 Å in the 3-fold direction, and the maximum is 96 Å in the 5-fold direction, roughly giving the particle the shape of a regular icosahedron. The inner boundary for the main protein part has a mean radius of about 65 Å. At this radius there is a thin layer of low electron density dividing the main protein part from the interior of the particle (Fig. 3c). Also the electron density distribution of southern bean mosaic virus (SBMV)[20] contains a similar 'valley' between the protein part and the interior of the particle. The density in the interior of the particle probably reflects the distribution of the RNA. The mean radial distribution of RNA and protein is in good agreement with results from small angle neutron scattering[11]. In the vicinity of the 5-fold axes the STNV RNA density extends significantly beyond the 65 Å radius, and an apparent 'stacking' of electron density at 60–75 Å radius suggests an at least partially ordered RNA structure in these regions (Fig. 3d). The present map has not allowed a simple interpretation of the nucleic acid. Whether this is due to a statistically distributed or disordered RNA or to limitations in the phase determination remains to be settled.

Structure of the STNV protein subunit

The subunit boundaries are obvious except for a few places near the 3-fold and 5-fold axes (Fig. 2a, b). The subunit consists of one main domain, with an overall size of 25 Å × 30 Å × 50 Å, located between particle radii 60 and 96 Å and

Table 1 Statistics of data collection

*4 Å data**

	Native	STNV-iodine derivative
Fully recorded reflections measured	169,000	145,000
No. of independent reflections measured of 148,100 possible	117,000	105,000
$R_{sym} = \sum_h \left(\sum_i \left| \left|F_{hi}\right| - \left|\bar{F}_h\right| \right| \right) / \sum_{h,i} \left|F_{hi}\right|$	0.067	0.090

Reflections used in the phase calculation†

Compound	Resolution	No. of reflections in the phase calculation
STNV-PtCl$_4^{2-}$	10 Å	7,300
STNV-iodine	10 Å	7,400
STNV-iodine	4 Å	78,300

*Data were collected using a Nonius oscillation camera and an Elliott rotating anode generator equipped with a graphite monochromator or focusing mirrors. The 4-Å oscillation photographs were taken with a 1.2° oscillation range. The crystals were rotated about the c^* axis with a total oscillation range of 90°. The exposure time was 3–4 h per film set. Up to eight exposures were obtained from one position on a crystal. The films were measured with an Optronics filmscanner (50 µm raster size), and the data were processed with the film processing program of Schwager *et al.*[25]. All partical reflections and reflections with integrated intensities below background were rejected before scaling[26]. The 4-Å native data set was merged with a 5.5-Å precession camera data set giving 124,395 observed reflections out of the 148,100 possible reflections.

†A value for $B_{overall}$ of zero $[F_{Der} = KF_{Nat} \cdot \exp(-B_{overall}(\sin\theta/\lambda)^2)]$ for the 4.0 Å STNV-iodine data was obtained from three-dimensional heavy atom refinement. For the 10 Å data a value for $B_{overall} = 0$ was used without refinement. All reflections which were registered on both the native and corresponding heavy atom derivative data set were used in the phase determination.

an arm extending from the main domain into the particle at least to 47 Å radius (Fig. 4, Fig. 1d). The continuity of density is good within the whole subunit and there is one large, twisted, probably three-stranded sheet (Fig. 2a, b). In some parts of the main domain the polypeptide chain can be traced. The central portion of the arm has the approximate dimensions of a three-turn α-helix, is positioned close to the 3-

Fig. 2 Composite electron density sections (PE, 1.3-Å map grid spacing, 3.8-Å data resolution; see text) perpendicular to a particle 3-fold axis at *a*, 80–77 Å and *b*, 72–69 Å from the particle centre. Within the marked protein subunit there are ribbons of continuous electron density, whose directions show a left-handed change in going from *a* and *b* in agreement with the twist in β-sheets.

0   10Å
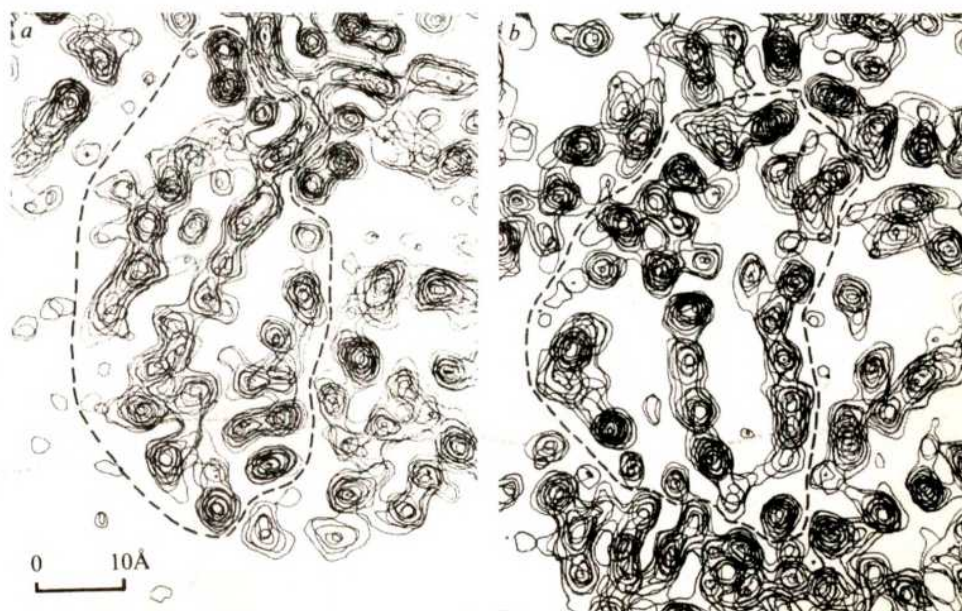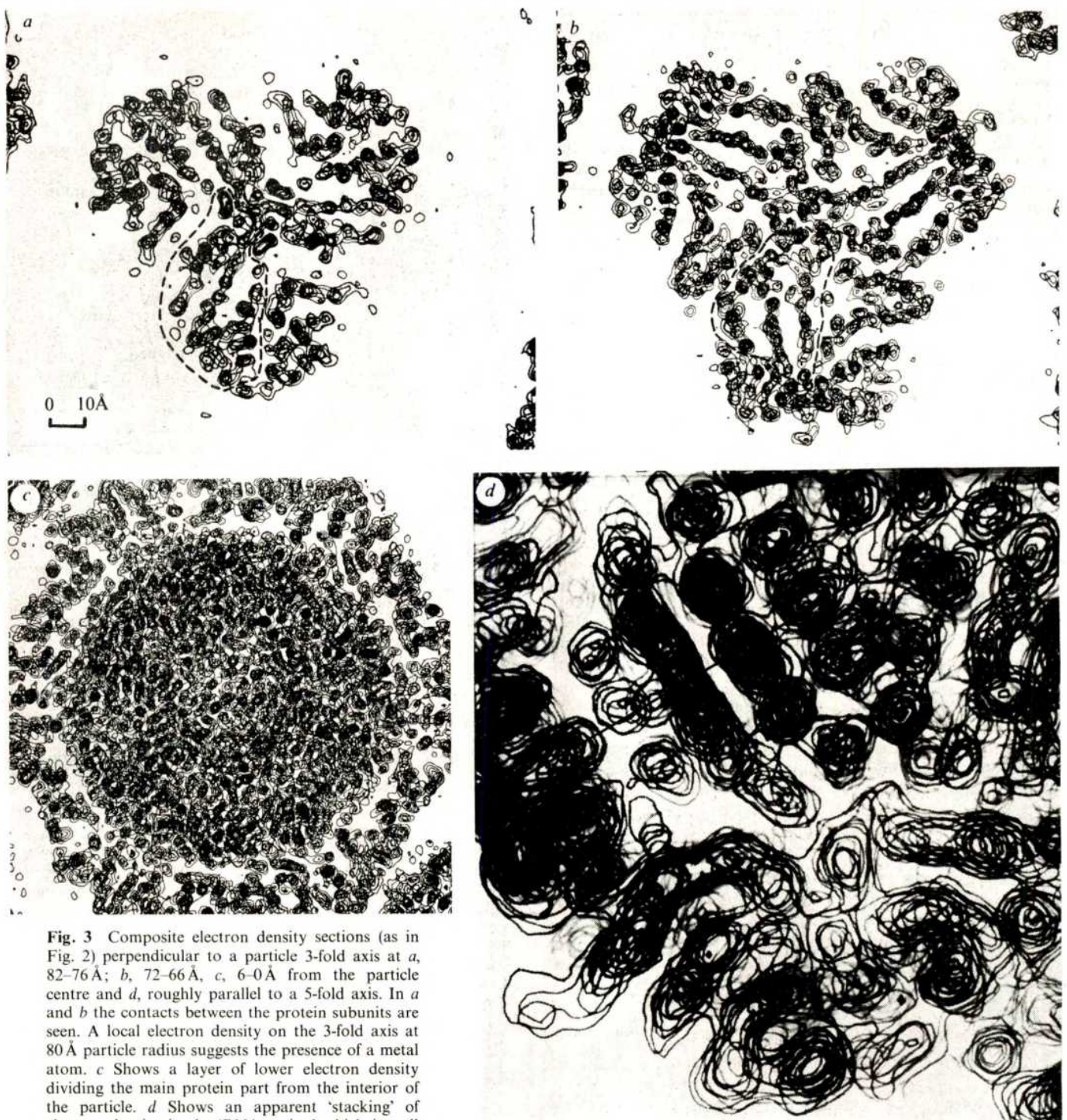
Fig. 3 Composite electron density sections (as in Fig. 2) perpendicular to a particle 3-fold axis at *a*, 82–76 Å; *b*, 72–66 Å, *c*, 6–0 Å from the particle centre and *d*, roughly parallel to a 5-fold axis. In *a* and *b* the contacts between the protein subunits are seen. A local electron density on the 3-fold axis at 80 Å particle radius suggests the presence of a metal atom. *c* Shows a layer of lower electron density dividing the main protein part from the interior of the particle. *d* Shows an apparent 'stacking' of electron density in the 'RNA region' which is well separated from the protein part (to the left in the picture). The apparent 'RNA layers' are positioned almost perpendicular to a particle 5-fold axis (arrow in the plane of the paper), at 60–75 Å particle radius and with 5.5 Å spacing between the 'RNA layers'.

fold particle axis, and is in contact with the arms of the two neighbouring 3-fold related subunits. The helices are tilted about 45° relative to each other. The figures have been drawn with a choice of hand which is based on the following observations: (1) The electron density maps shown (Fig. 2*a*, *b*) contain at least one β-pleated sheet with a left-handed twist. (2) Inspection of the electron density corresponding to the previously mentioned three-turn α-helix as well as another tentative helix indicates right-handedness. This choice of hand gives a right-handed supercoil of the three helices at a 3-fold particle axis.

The sequence of STNV RNA and the STNV protein have recently been determined[3,4]. In the iodine derivative[13] an average of 1.5 iodine atoms bind to the same histidine residue close to the N-terminus (His 23). The iodine atoms are

positioned on the long supercoiled arms, at particle radii of 56 and 59 Å respectively (Fig. 4*a*). From the knowledge of the amino acid sequence[3,4] it has been predicted that this part of the polypeptide chain is, to a high probability, in the form of an α-helix[21,22]. Of the 30 amino acids at the N-terminal (which include the arm) nine are basic residues and only one acidic[3,4], suggesting a strong interaction between this part of the protein and the nucleic acid. Model building of the α-helical region (residues 17–27), containing residue His 23 (with the marker iodine atoms), can be done placing all the four basic residues on the outside and the hydrophobic residues on the inside of the supercoil. The platinum position in the 10 Å STNV-Pt derivative is also on the outer surface of the helix at a particle radius of 51 Å. Positioning the $PtCl_4^{2-}$ group in the above mentioned model suggests attachment to amino acid

Table 2 Heavy atom parameters

Compound	Resolution	Site	Z	B	x	y	z	R_{mod}
STNV-PtCl$_4^{2-}$	10 Å	Pt	55	120	0.3131	0.4063	0.3004	0.098
r.m.s. f_c/r.m.s. $E = 2.2$, $\langle \Delta F \rangle / \langle F_{Der} \rangle = 0.10$; $R_c = 0.32$								
STNV-iodine	10 Å	I	32	85	0.3321	0.4277	0.2931	0.098
r.m.s. f_c/r.m.s. $E = 1.3$, $\langle \Delta F \rangle / \langle F_{Der} \rangle = 0.10$; $R_c = 0.60$								
STNV-iodine	4 Å	I$_1$	42	7	0.3303	0.4287	0.2913	0.174
		I$_2$	41	6	0.3247	0.4166	0.2929	
r.m.s. f_c/r.m.s. $E = 1.24$ (1.41 and 1.20 for low and high $\sin\theta/\lambda$ values, respectively)								
$\langle \Delta F \rangle / \langle F_{Der} \rangle = 0.17$; $R_c = 0.75$								

Z, occupancy in electrons on an approximate absolute scale.

B, isotropic thermal parameter for the heavy atoms.

$$R_{mod} = \frac{\sum_h \left| |F_{Der,obs}| - |F_{Der,calc}| \right|}{\sum_h |F_{Der,obs}|}$$

$$R_c = \frac{\sum_{h0l\,refl.} \left| |\Delta F_{obs}| - |F_c| \right|}{\sum_{h0l\,ref} |\Delta F_{obs}|}$$

E, lack of closure at best phase angle.

f_c, heavy atom structure factor.

Figures of merit: DIR (10 Å) = 0.62 SIR (4 Å) = 0.34.

The parameters corresponding to the 10 Å data were refined by structure factor fitting using $h0l$ reflections only[12]. The x, y, z parameters for position I$_1$ and I$_2$ were determined from a difference Fourier calculation using DIR phases (>10 Å resolution) and PE phases (10–5.5 Å resolution) refined by SA. The positional parameters were confirmed by a difference Fourier calculation using 10 Å Pt phases but not further refined. Scale factor for the 4 Å iodine-derivative and occupancies for I$_1$ and I$_2$ were refined by three-dimensional least squares technique. The occupancy for each of the 2×60 sites were refined separately and the occupancies were 60-fold averaged between each cycle.

Met 19. About the first 15 amino acids at the amino end cannot be traced in the map. The general arrangement of the subunits, showing the subunit contacts, is given in Fig. 3.

In the three spherical plant viruses which have been extensively studied by X-ray crystallography we can see similarities in the arrangement of the amino terminal end. The N-terminal part of the C subunits of tomato bushy stunt virus (TBSV)[23] and SBMV[24] as well as of STNV points into the particle close to the 3-fold axis, and is partly flexible.

We thank Dr A. Liljas for discussions, and Dr P. Argos, Professor W. Fiers, Dr D. Henriksson, Professor M. G. Rossmann, Professor R. E. Tashian and their colleagues for permission to refer to their unpublished results. We also thank Mrs M. Petef for help in data collection, Mrs A. Borell for programming assistance, Mr S. Lövgren for assistance with photography and Mrs G. Johansson for growing the virus and typing the manuscript. This was supported by grants from the

Table 3 Phase refinement of SIR phases by non-crystallographic symmetry (MR)

Cycle no. at 4 Å resolution	$\langle w \rangle$*	$\langle \Delta\alpha \rangle$†	R‡
1	0.34§	51.0	0.63
2	0.49	20.8	0.47
3	0.65	16.6	0.40
4	0.70	12.7	0.37
5	0.73	10.4	0.36
6	0.83	9.0	0.34
7	0.84	9.6	0.32
8	0.84	7.0	0.32

*Mean weighting factor; the weighting factor was a function of F_{obs}/F_{calc} for individual reflections.

†Mean phase change (in degrees) for all reflections; the total average phase change was 62°.

$$\ddagger R = \frac{\sum_h \left| |F_{obs}| - |F_{calc}| \right|}{\sum_h |F_{obs}|},$$

where F_{obs} is the measured amplitude and F_{calc} is the amplitude calculated from an icosahedrally averaged map.

§Figure of merit for the SIR phases.
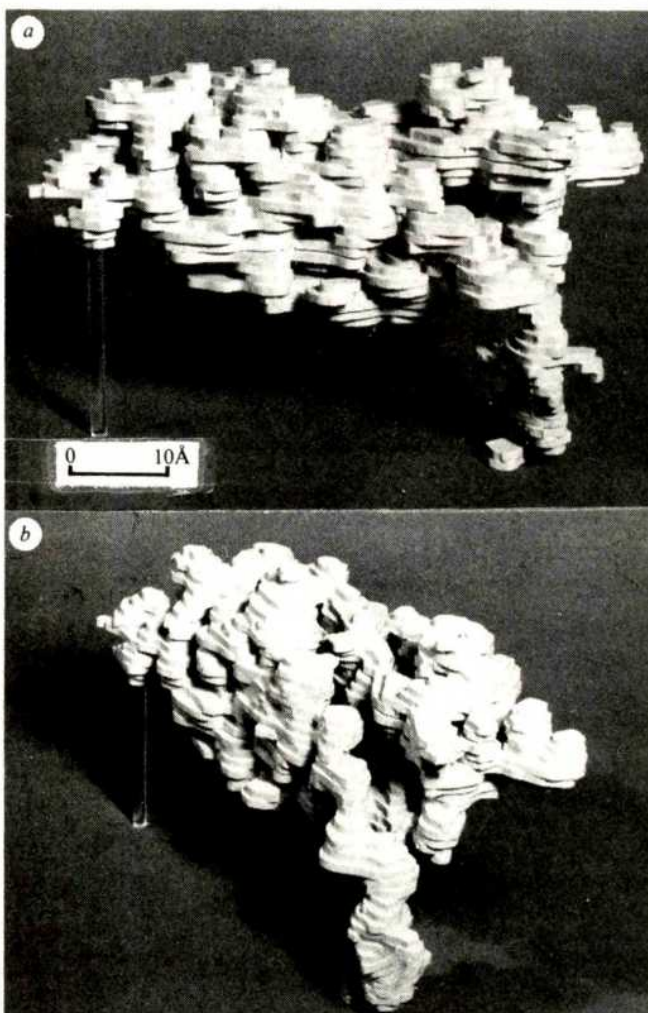
Fig. 4 Photographs of a model of the protein subunit. *a*, Viewed approximately perpendicular to the particle 3-fold axis showing the α-helical arm which extends toward the particle centre. The two iodine atoms bound to His 23 are marked. *b* View of the outer part of the protein subunit showing structural features described in Fig. 2.

1. Kassanis, B. & Nixon, H. L. *J. gen. Microbiol.* **25**, 469–471 (1961).
2. Rees, M. W., Short, M. N. & Kassanis, B. *Virology* **40**, 448–461 (1970).
3. Ysebaert, M., van Emmelo, J. & Fiers, W. *J. molec. Biol.* (submitted).
4. Henriksson, D., Tanis, R. J., Hawett-Emmett, D., Tashian, R. E. & Nyman, P. O. *J. molec. Biol.* (submitted).
5. Reichmann, M. E. *Proc. natn. Acad. Sci. U.S.A.* **52**, 1009–1017 (1964).
6. Åkervall, K. *et al. Cold Spring Harb. Symp. quant. Biol.* **36**, 469–483; 487–488 (1971).
7. Klug, A. *Cold Spring Harbor Symp. quant. Biol.* **36**, 483–487 (1971).
8. Lentz Jr., P. J. & Strandberg, B. *Acta crystallogr.* **A30**, 552–559 (1974).
9. Fridborg, K. *et al. Proc. natn. Acad. Sci. U.S.A.* **54**, 513–521 (1965).
10. Sjöberg, B. *Eur. J. Biochem.* **81**, 277–283 (1977).
11. Chauvin, C., Jacrot, B. & Witz, J. *Virology* **83**, 479–481 (1977).
12. Lentz, P.J. Jr, *et al. Acta crystallogr.* **B32**, 2979–2983 (1976).
13. Unge, T. & Strandberg, B. *Virology* **96**, 80–87 (1979).
14. Rossmann, M. G. & Blow, D. M. *Acta crystallogr.* **16**, 39–45 (1963).
15. Bricogne, G. *Acta crystallogr.* **A30**, 395–405 (1974).
16. Bricogne, G. *Acta crystallogr.* **A32**, 832–847 (1976).
17. Blow, D. M. & Crick, F. H. C. *Acta crystallogr.* **12**, 794–802 (1959).
18. Nordman, C. E. *Acta crystallogr.* (in the press).
19. Argos, P., Ford, G. C. & Rossmann, M. G. *Acta crystallogr.* **A31**, 499–506 (1975).
20. Suck, D., Rayment, I., Johnson, J. E. & Rossmann, M. G. *Virology* **85**, 187–197 (1978).
21. Unge, T. thesis (no. 523), Uppsala Univ. Faculty of Science (1979).
22. Argos, P. in *Proc. 7th Aharon Katzir-Katchalsky Conf. on Structural Aspects of Recognition and Assembly in Biological Macromolecules*, Nof Ginossor, Israel (in the press).
23. Harrison, S. C., Olson, A. J., Schutt, C. E., Winkler, F. K. & Bricogne, G. *Nature* **276**, 368–373 (1978).
24. Abad-Zapatero, C. *et al. Nature* (in the press).
25. Schwager, P., Bartels, K. & Jones, A. *J. appl. Crystallogr.* **8**, 275–280 (1975).
26. Hamilton, W. C., Rollett, J. S. & Sparks, R. A. *Acta crystallogr.* **18**, 129–130 (1965).

Analysis and prediction of protein β-sheet structures by a combinatorial approach

Fred E. Cohen, Michael J. E. Sternberg & William R. Taylor

Laboratory of Molecular Biophysics, Department of Zoology, South Parks Road, Oxford OX1 3PS, UK

Analysis of β-sheet sandwiches (for example immunoglobulin domains) suggests an algorithm that successfully predicts the tertiary fold of these proteins from their sequence and secondary structure. We propose tertiary structures for β_2-microglobulin and an HLA-B7 antigen fragment. Topological rules are presented that markedly reduce the number of folds for proteins in which a-helices pack against a parallel β-sheet.

WITH the structures of more than 60 globular proteins known to atomic resolution, it is clear that the tertiary fold is largely determined by the packing of α-helices and/or β-strands[1-7]. For many proteins[1], their fold can adequately be described by one of three motifs: a stacked pair of β-sheets (β/β); α-helices packing against a predominantly parallel β-sheet (α/β); or an assembly of α-helices (α/α). These arrangements satisfy the hydrogen-bonding requirements of buried main-chain nitrogen and oxygen atoms while shielding a substantial fraction of the nonpolar atoms from solvent[2].

From these observations we are developing a stepwise method of predicting the three-dimensional structure of a protein from its amino acid sequence (for reviews see refs 8–10). We envisage three stages: (1) predict the regular secondary structures, now possible with up to 80% accuracy; (2) pack the α-helices and β-strands into an approximate native fold, (3) use simplified energy calculations[11-13] to refine the fold into the native structure.

This approach is timely as recent work[14,15] has shown that the structures predicted solely by simplified energy calculations are not significantly better than random models for a compact globular protein. This article considers the second stage which is implemented by a combinatorial method. Initially one generates a list of trial structures by packing all combinations of the α-helices and β-strands. The native fold will be in this list and so one simply eliminates structures that violate stereochemical rules. This approach has been applied to the packing of α-helices in myoglobin[7,16,17]. Over 10^8 trial structures were generated by docking together predicted hydrophobic patches on the surfaces of the α-helices. However, only 20 folds did not violate the steric and connectivity constraints. The addition of two distance constraints obtained from experimental data on haem binding further restricted the number of allowed structures to two. The relative arrangements of α-helices in one of these structures closely resembled that in the native structure. The root mean square deviation[15,18] between this predicted structure and the native (r.m.s.d.) was 4.3 Å.

The success of this approach motivated our analyses of structures formed from β-sheet sandwiches or from α-helices packing against parallel β-sheets. This led to combinatorial algorithms to predict allowed tertiary folds.

Analysis of β-sheet sandwiches

The stability of a β-sheet sandwich results from inter-strand hydrogen bonding and the burial of hydrophobic residues both within and between the β-sheets. We estimated the contribution of the hydrophobic effect to the free energy of folding from the change in the solvent accessible contact area[7,19] of the nonpolar (C^z, side chain C and S) atoms (Φ-area) by the empirical relationship $1 \, \text{Å}^2 \equiv 80 \, \text{cal mol}^{-1}$ (ref. 7).

The structures of nine β-sheet sandwiches (Fig. 1) were

Table 1 Prediction of β-sheet sandwiches

Structure*	No. of strands†	No. of possible structures from all strands‡	No. of structures generated from strands with sites§	Position in list of strand overlap of native structure‖	r.m.s.d. predicted/ crystal structure¶ (Å)	No. of residues
FCH2	7(6)	5×10^7	6×10^5	327 (154)	2.3	34
FCH3	7(7)	5×10^7	3×10^6	36 (9)	4.9	50
FALC	7(7)	5×10^7	3×10^6	10 (5)	1.4	46
FAHC	7(7)	5×10^7	3×10^6	6 (6)	3.2	48
PRE	8(7)	2×10^8	3×10^6	12 (10)	2.0	51
FALV	8(8)	2×10^8	1×10^7	3,343 (494)	4.9	48
SDM	8(8)	2×10^8	1×10^7	1,135 (280)	5.1	51
FAHV	9(7)	6×10^8	3×10^6	509 (105)	3.5	46
REI	9(7)	6×10^8	3×10^6	988 (165)	3.6	48
B2-M	7(6)	5×10^7	6×10^5	34 (6)	—	53
AC-2	7(6)	5×10^7	6×10^5	93 (5)	—	48

*See Fig. 1 for abbreviations.

†The no. of β-strands in the sandwich with the no. of strands with sites in brackets.

‡For n strands, the number of topologies for two 3-stranded sheets is $(^nC_3)(^{n-3}C_3) \, 3!3!2^32^3/4$, where $(^nC_r) = n!/(n-r)!r!$. For each topology we estimate that there are 625 (that is, 5^4) alternative sheet structures that have a high degree of strand overlap.

§A lower estimate of the number of sheet structures generated from strands with sites placed with the 32 different phasings. In the top sheet the central residues can be phased in six ways: $-2,0,+2$; $-2,0,0$; $0,0,+2$; $0,0,0$; $+2,0,0$; $0,0,-2$. In the bottom sheet the six phasings are: $+2,0,-2$; $+2,0,0$; $0,0,-2$; $0,0,0$; $-2,0,0$; $0,0,+2$. Every pairing is allowed except for either of the last two phasings in the top sheet with the last two in the bottom sheet as both these phasings have the wrong direction.

‖The number of strand-alignment diagrams (with the number of different topologies in brackets) that have the same or higher overlap than the chosen approximation to the native.

¶The root mean square deviation between equivalenced C^z atoms in the native and predicted six-stranded core. Thus accurate prediction of the strand-alignment diagram is sufficient to yield a C^z structure close enough to the native that energy minimization could be applied.
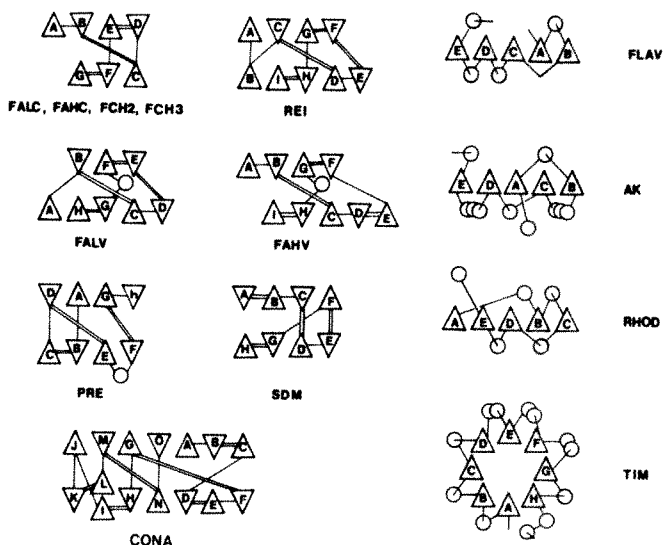
Fig. 1 The fold of β/β and α/β proteins: schematic diagrams of all the β-sheet sandwiches and some of the α-helix/β-sheet proteins considered. Each β-strand is viewed along its strand direction and is represented by a triangle whose apex points up or down according to whether the strand is viewed from the N- or the C-terminus. A circle represents an α-helix. For the β-sheet sandwiches, the connections are shown in double lines if they start at the end of the sheet close to the viewer, otherwise in single lines. FAHV, FAHC, FALV, FALC—the heavy (H) and light (L) chains of the variable (V) and constant (C) domains of Fab′ human immunoglobulin IgG(λ) new fragment[21]. FCH2, FCH3, C_H2 and C_H3 domains of human Fc (ref. 22). REI, Bence-Jones variable dimer. PRE, human prealbumin[23]. SDM, Cu;Zn superoxide dismutase. CONA, jack bean concanavalin A. FLAV, *Clostridium* flavodoxin. AK, porcine adenyl kinase. RHOD, bovine rhodanese (one domain). TIM, chicken triose phosphate isomerase. Coordinates were obtained from the Brookhaven Data Bank[29] except where a reference is given to the laboratory that supplied them.

dissected to find the patterns of changes in Φ-area in the transition from isolated secondary structure to the native conformation. Each β-strand was composed of residues that either formed intra-sheet hydrogen bonds or were in the main-chain conformation $-170° < \phi < -90°$, $100 < \psi < 170$. For each sandwich, three sets of Φ-areas were calculated from the crystallographic coordinates[20–23]:

(1) The sum of the Φ-areas of all the β-strands considered in isolation.

(2) The sum of the Φ-areas of the two β-sheets considered individually.

(3) The Φ-area of the stacked pair of β-sheets.

We can now assess the hydrophobic free energy change for the stepwise process of first condensing β-strands into two β-sheets followed by the stacking of the two sheets. For prealbumin, these values are -74 and $-24 \, \mathrm{kcal \, mol}^{-1}$. These values are the differences of set 2 from set 1, and of set 3 from set 2, respectively. Similar hydrophobic interactions occur in all the other sheet sandwiches: the values of these two area changes divided by the number of residues in the two sheets are in the ranges -0.9 to -1.2 and -0.3 to $-0.6 \, \mathrm{kcal \, mol}^{-1}$ per residue. Ancillary calculations on prealbumin demonstrate the stability of the sheet sandwich. The $-98 \, \mathrm{kcal \, mol}^{-1}$ obtained in condensing the eight strands into the sandwich represent 54% of the total change in folding a hypothetical extended polypeptide chain into the native monomeric structure. The subsequent formation of the tetramer from the monomers yields an additional $-21 \, \mathrm{kcal \, mol}^{-1}$ per subunit.

The specificity of the interactions is revealed by the Φ-area changes of the individual residues. Forming a β-sheet from isolated β-strands produces changes for most residues irrespective of their chemical nature. The effect of the twist of the β-sheet[24] is a reduction in the area change for the residues at the strand termini.

The strand alignment diagrams in Fig. 2 present the observed area changes on sheet stacking for several immunoglobulin domains. In a β-sheet sandwich, side chains in each β-strand point alternately towards and away from the other β-sheet, producing two surfaces on each sheet. Surprisingly, in these diagrams and in the other sandwiches only 2/3 of the residues in the 'buried' faces have substantial area change ($>5 \, Å^2$). This explains why, when immunoglobulin sequences are aligned[24], only some of the β-strand side chains that point towards the other sheet are always nonpolar.

The most important feature of Fig. 2 for our prediction algorithm is that the observed area changes trace a distinct pattern on the β-sheets. In the top sheet the residues with sizeable area changes progress from left to right, going down the diagram, whereas in the bottom sheet they proceed from right to left. This anti-complementary direction of the two parallelogram patterns results from the geometry of sheet packing. The twist[25] between adjacent β-strands forces the β-sheet roughly to resemble a deformed rectangle with diagonally opposite corners pointing either both up or both down (Fig. 3). Consequently the major hydrophobic interactions on sheet stacking are between the lower two corners of the top sheet and the upper corners of the bottom

Table 2 Allowed β-sheet topologies

Protein	No. of strands	No. of possible topologies	No. of topologies allowed by rule 1	No. of topologies allowed by rules 1–4
Flavodoxin	5	960	60	6
Adenyl kinase	5	960	60	6
Rhodanese first or second domain	5	960	60	6
Alcohol dehydrogenase NAD binding domain	6	11,520	360	15
Phosphoglycerate kinase catalytic domain	6	11,520	360	10
Phosphoglycerate kinase ATP domain	6	11,520	360	10
Lactate dehydrogenase NAD domain	6	11,520	360	13
Triose phosphate isomerase	8	5×10^6	40,320	21

The protein domains listed are formed from α-helices stacking against a pure parallel β-sheet. The total number of topologies for the β-strands and their connections is reduced by rule (1) and then by the use of rules (1) to (4).

sheet. This effect is enhanced by shortening some of the strands and removing residues not involved in sheet/sheet interactions[5], for example in the immunoglobulin domain designated FAHV, the carboxyl end of strands A and F.

Algorithm to predict the structure of β-sheet sandwiches

We start with the sequence and an observed (or predicted) strand assignment. Each strand is considered as a unit and we aim to predict the correct strand-alignment diagram which can then be converted to C^α coordinates. The algorithm is outlined below. The first three steps generate all possible sandwiches and the fourth step removes disallowed folds. The computer program is available on request.

(1) *Location of a hydrophobic site on each β-strand.* First, one predicts not only which surface of each β-strand will point towards the other β-sheet but also the location of the few residues that mediate the hydrophobic interaction. Each strand was scanned for a continuous site of nonpolar residues on one of its sides, for example three residues at positions $i-2$, i, $i+2$. The central residue at position i represents this site. To distinguish between alternate central residues we consider first the number of nonpolar residues in the site (4, 3 and 2) and

FCH3 OBSERVED

```
A →   arg GLU/PRO gln [VAL] tyr [THR] leu
B →   tyr PHE/GLY lys VAL leu[CYS] thr [LEU] ser VAL gln
E →   ser PHE phe LEU tyr SER lys [LEU] thr VAL
D →   asp LEU val PRO/PRO thr THR lys [TYR] asn

G →                   THR gln [LYS] ser [LEU]
F →             met [VAL] ser [CYS] ser [PHE] val
C →             ala [VAL] glu [TRP] glu
```

AC-2 PREDICTED

```
A → -2            ASP/PRO pro [LYS] thr HIS val
B → 0       tyr PHE/GLY leu ALA trp [CYS] arg [LEU] thr ALA glu
E → +2            THR phe GLU lys TRP ala [ALA] val VAL val
D →               gly ALA/PRO arg THR glu VAL leu GLU thr

G → 0                   LEU pro [LYS] pro LEU thr
F → 0             HIS gln VAL his [CYS] thr TYR
C → -2            ILE thr [LEU] thr TRP gln
```

FALC PREDICTED

```
A → 0                 ser VAL thr [LEU] phe PRO
B → 0/+2        ASP ser ILE leu [CYS] val [LEU] thr ala
E → +2      lys TYR ala ALA ser SER tyr [LEU] ser LEU thr
D →         gln LYS ser [PRO]/THR thr THR glu VAL gly

G → 0            SER thr VAL glu [LYS] thr VAL
F → 0            HIS thr VAL gln [CYS] ser TYR
C → -2           VAL thr [VAL] ala TRP lys
```

B2-M PREDICTED

```
A → -2    ile GLN arg THR/PRO lys [ILE] gln VAL tyr SER arg
B → 0          his PHE/GLY ser VAL tyr [CYS] asn LEU phe
E → 0          ser PHE tyr [LEU] leu [TYR] ser TYR thr
D →                             glu VAL lys

G → +2           LEU ser GLN pro LYS ile [VAL] lys TRP
F → 0            HIS asn VAL arg [CYS] ala TYR
C → -2           asp ILE glu [VAL] asp LEU
```

FALC OBSERVED

```
A →               ser [VAL] thr [LEU] phe [PRO]
B →         ASP ser [ILE] leu [CYS] val [LEU] thr ALA
E →    lys TYR ala ALA ser SER tyr [LEU] ser [LEU] thr
D →    gln LYS ser PRO/THR thr THR glu VAL gly

G →         SER thr VAL glu [LYS] thr [VAL]
F →         HIS thr [VAL] gln [CYS] ser [TYR]
C →         [VAL] thr [VAL] ala [TRP] lys
```

FALV OBSERVED

```
B →         GLY thr [CYS] ser [ILE] thr [VAL] arg
F →         SER ser ALA thr [LEU] ala ILE
E →               ser LYS ser [VAL] ser [PHE]

A →                         PRO ser [VAL] ser GLY
H →    LEU arg VAL phe GLY gly THR/GLY lys [LEU] thr VAL leu
G →    ASP tyr SER gln [CYS] tyr [TYR] asp ALA
C →               lys [TRP] tyr GLN gln
D →               ile LEU leu LYS
```

FAHC OBSERVED

```
A →    lys GLY/PRO ser [VAL] phe [PRO] leu
B →    phe [CYS]/ASP lys [VAL] leu [CYS] gly [LEU]
E →    leu TYR ser LEU ser SER val [VAL] thr
D →    gln LEU val ALA/PRO phe THR his VAL gly

G →         THR lys [VAL] asp [LYS] lys [VAL]
F →         [HIS] asn [VAL] asn CYS ile TYR
C →         [VAL] thr [VAL] ser [TRP] asn
```

FAHV OBSERVED

```
A →               [LEU] glu GLN ser
B →         ser [VAL] thr CYS thr [LEU] ser [LEU]
G →               [PHE] ser [LEU] arg [LEU]
F →               leu [MET] thr [VAL]

I →    CYS ile ASP/VAL trp GLY gln/gly [SER] leu [VAL] thr
H →    LEU asn ARG ala [CYS] tyr [TYR] val ALA
C →    ASP tyr [TYR] thr [TRP] val ARG gln
D →         phe [VAL] tyr GLY [ile] TRP glu LEU
E →         thr SER asp THR asp
```

Fig. 2 Strand-alignment diagrams for β-sheets. The relative positions of the strand residues are shown. β-bulges[28] are indicated as in Pro Thr in strand D of FALC. Residues with side chains pointing towards the other sheet are in capital letters. In the diagrams, observed area changes on sheet sandwiching are indicated by enclosing the residue in a rectangle if the area change is $>10\,\text{Å}^2$ and by underlining if the area change is between 5 and $10\,\text{Å}^2$. In the predicted diagrams, the central residues are in rectangles whilst the other residues that form the site are underlined. The relative phasings of the central residues are shown. For the light (B2-M) and heavy (AC-2) chains, our proposed models are described. The secondary structure prediction[31] located the β-regions in B2-M as: 1–12, 22–30, 34–39, 48–50, 61–65, 69–71, 80–89 and residues 41–47 as α-helix. The predicted β-regions in the AC-2 fragment were: 5–9, 16–24, 30–35, 46–51, 58–66, 76–81, 88–89. The potential Φ-area of a site is the sum of the available areas for the 2, 3 or 4 component nonpolar residues. The area for a nonpolar residue X is the available Φ-area of X in a model, three-stranded twisted antiparallel sheet (Cys)$_9$:(Cys$_4$XCys$_4$):(Cys)$_9$. This area agrees well with the observed change for X on sheet/sheet association. The values (Å^2) we calculated are: Ala(8), Cys(11), Ile(18), Leu(19), Met(26), Phe(24), Pro(9), Trp(34), Tyr(17), Val(13) and Lys(12) if it occurs in an edge strand. Other amino acids were designated as polar and assigned zero area.

then the magnitude of their possible hydrophobic contribution to sheet/sheet stacking from the available Φ-area (see legend to Fig. 2).

(2) Construction of all possible strand-alignment diagrams. Next strands are placed in the two β-sheets. As not all the strands contribute markedly to the sheet/sheet interaction (Fig. 2), the sandwich initially was modelled as a central hydrophobic core of two 3-stranded β-sheets. First, all possible topologies for the two sheets are generated. Each β-strand with a hydrophobic site can occupy any position and direction in either β-sheet. Next, all alignments of the β-strands are generated so as to produce the correct directionality of the anti-complementary parallelograms observed on sheet sandwiching. This was quantified by 32 allowed phasings (see legend to Table 1). For example, in FALC the relative positions of central residues in strands ABE, GFC are 0, 0, +2 and 0, 0, −2 (see Fig. 2). Between 10^6 and 10^7 different strand-alignment diagrams were considered since the information from steps 1 and 2 has reduced the number of possibilities by two orders of magnitude (Table 1). From each
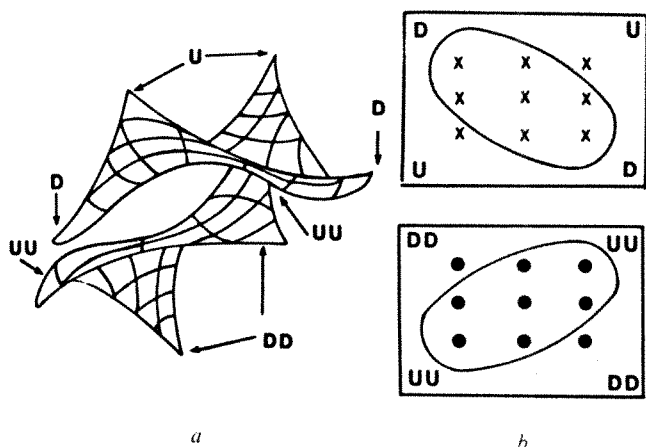
Fig. 3 The stacking of β-pleated sheets. *a*, Two twisted β-sheets with the up (U, UU) and the down (D, DD) corners of the top (one letter) and bottom (two letters) sheet. The lines on the surfaces convey curvature. *b*, The crosses and dots indicate the sheet residues that point to the other sheet. The β-strands run horizontally. The packing of the down corners of the top sheet against the up corners of the bottom sheet produces the observed anti-complementary 'parallelograms' of area changes. Note these area changes cannot be produced by simply superimposing the two ovals in the planar representation as the sheets will then pack with a positive angle rather than the observed negative angle.

central core a set of complete structures was constructed with the previously unplaced strands being located in every possible unoccupied position and with every direction. No attempt was made to phase the unplaced strands with respect to the central core. Clearly, a different approach is required for the 14 strands in CONA.

(3) *Construction of a C^α representation.* C^α coordinates can be obtained from a predicted strand-alignment diagram for the central core. Each β-sheet was built from idealized twisted β-strands[26] based on aligning the positions of the central residues. The two sheets were sandwiched by aligning the central residues of the middle strands and placing the sheets at a typical separation (10 Å) and rotation ($-30°$) suggested by analysis of the structures.

(4) *Constraints on allowed structures.* The list of generated structures is filtered by imposing the following restrictions that quantify observed topological (i, ii, iii), steric (iv, v) and hydrogen-bonding (vi, vii) features of known β-sheet sandwiches. (i) The connection between two parallel β-strands in the same sheet is right-handed[3,4]. (ii) Connections between β-strands do not cross[27]. (iii) The topology of the strands includes a generalized 'Greek-key'[6,27]. (iv) There are sufficient residues between the strands to make the required connection length. (v) Any disulphide bridge must be between residues whose C^α atoms are closer than 15 Å (a conservative estimate to allow for errors in the C^α construction). In addition, a survey of known protein structures suggests that the disulphide bridge is not allowed between cystine residues in non-adjacent β-strands in the same β-sheet (J. M. Thornton, personal communication). (vi) Given the strand composition of the sheets but not the strand positions, structures must make either all or all but one of hydrogen bonds that could be

formed. (vii) The two β-sheets in the central core must have a high degree of strand overlap. This notion was quantified as the number of main-chain hydrogen bonds formed as a fraction of the number of main-chain nitrogen (or oxygen) atoms in the sheet. Structures allowed by filters (i) to (vi) were rank ordered on strand overlap. We determined the position of the native structure in the list.

Results of the prediction of sheet sandwiches

The computer program was uniformly applied to the nine sandwiches to yield reduced lists of allowed sheet sandwiches rank ordered on strand overlap. For each sandwich, one member of the reduced list has all or most of the relative residue positions in the native strand-alignment diagram. The deviations are generally caused by β-bulges[28] that disrupt the register of some residues in a β-strand with respect to the central core. Apart from β-bulges, seven of the nine sandwiches are correctly built. The exceptions are in FCH2 where one strand is shifted by two residues, and in FAHV where one strand is one residue away from the correct alignment.

The strand-alignment diagrams contain sufficient information to construct a C^α representation that is close to the native. The r.m.s.d. between the equivalenced C^α atoms ranges from 1.4 to 4.9 Å, with 34 to 51 residues being placed. A random prediction[15] of a compact structure for pancreatic trypsin inhibitor (54 residues) would have a mean and standard deviation of the r.m.s.d. of 11.9 ± 1.5 Å.

Table 1 indicates the selectivity of the filters by giving the number of central core structures that have no less than the strand overlap of a selected approximation (see above) to the actual structure. For four of the nine sandwiches the algorithm is highly selective and <50 alternative structures (<20 different topologies) would need to be surveyed to locate the central core of the native structure. The algorithm is fairly selective ($<3,500$ structures, <500 topologies) for the other sandwiches.

Application to the prediction of unknown structures: the histocompatibility antigens

The notions quantified in the algorithm provide, for the first time, the basis for taking a secondary structure prediction and obtaining a tertiary fold for β-sheet sandwiches. Clearly further work on the overall scheme is required. (1) Secondary structure prediction algorithms must be improved to obtain a better location of the β-strands. (2) Given the predicted core, the few unplaced β-strands and all the connections have to be located. (3) The use of simplified energy calculations[11-13] must be explored first to select the correct fold from the reduced list and subsequently to refine the structure.

We will demonstrate the status of this approach by assessing the validity of predicted strand-alignment diagrams for the light chain β_2-microglobulin (B2-M) and a segment of the heavy chain (AC-2) of the HLA-B7 antigen[29,30]. Based on sequence alignments, it has been proposed that both B2-M and AC-2 will have a 4- on 3-stranded sheet sandwich structure similar to the immunoglobulin constant domains.

Fig. 4 Predicted and crystal structures of FALC. Stereo diagram of the C^α positions of the two three-stranded core of the predicted sandwich (solid lines) superimposed on the crystal structure (broken lines) for FALC.
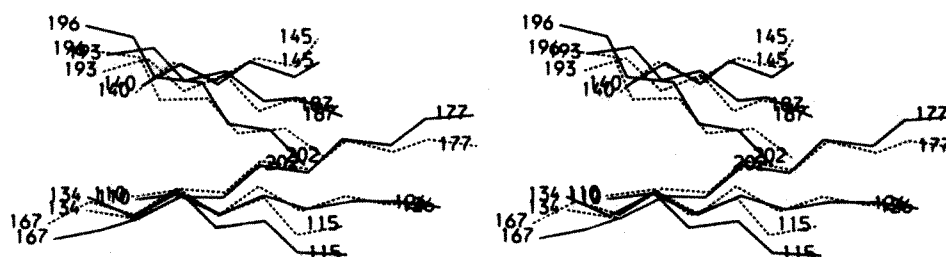
First, we predicted the secondary structure by the procedure of Robson and coworkers[31]. With suitable decision constants (more than 50% β-structure and less than 20% α-helix), trials of IgG domains localized most β-strand regions. The predicted β-strands in B2-M (see legend to Fig. 2) correspond to β-strands in IgG constant domains when the sequences are aligned as in ref. 29. From this alignment, with only slight modifications to the secondary structure, we constructed the strand-alignment diagram in Fig. 2. The predicted central residues of the hydrophobic sites have the correct anti-complementary direction. Furthermore, probable β-bulges are located in strands A and B in equivalent positions to observed bulges in FAHC and FCH3. When this approach was followed with the AC-2 sequence, we could not construct a plausible strand-alignment diagram. Trials with a sequence alignment program similar to that used for the AC-2/IgG comparisons failed to obtain the correct alignment of residues between FAHC and FAHV[21]. Accordingly, we modified the proposed sequence alignment of AC-2/IgG to obtain a strand-alignment diagram that had suitable features of hydrophobic patches and β-bulges (Fig. 2). The diagrams were taken as the 'native' structure of B2-M and AC-2, and the algorithm for predicting sheet sandwiches then established that these structures are one of a small list (<100) of allowed sandwiches compatible with the β-strand assignment (Table 1). Predicted C^{α} coordinates of the strands in B2-M and AC-2 are available upon request.

Packing of α-helices against pure parallel β-sheets

The remaining structural motif frequently observed in globular proteins involves the packing of α-helices against a predominantly parallel β-sheet. Calculations of Φ-area change are in progress. In flavodoxin, the independent docking of each α-helix against the native 5-stranded sheet yields Φ-area changes equivalent to between -10 and $-20\,\mathrm{kcal\,mol^{-1}}$. This hydrophobic effect lies between that of sheet sandwiching ($-24\,\mathrm{kcal\,mol^{-1}}$ for prealbumin) and α-helix/α-helix packing ($-13\,\mathrm{kcal\,mol^{-1}}$ for an interaction in myoglobin[7]). The α-helix/β-sheet interaction involves Φ-area changes of residues in at least three adjacent strands. This is because the van der Waals diameter of an α-helix is $10\,\text{Å}$ whilst adjacent β-strands lie about $4.25\,\text{Å}$ apart.

There are also features that reduce the number of allowed topologies. For structures with a repeating unit $(\beta x)_n$ where x is either an α-helix or an irregular coil region and where all the β-strands lie parallel, there are two known restrictions. (1) The handedness of the connection between parallel β-strands is nearly always right-handed[3,4]. (2) There is never more than one chain reversal in strand order[6]. Thus ABEDC is acceptable but ABDEC is not (letters A to E denote the sequential order of the β-strands). A survey of nine parallel β-sheets (Table 2) found two additional rules: (3) The difference in the number of α-helices on the two surfaces of the β-sheet is never more than 1. (4) The position of an α-helix trailing the last β-strand in the β-sheet can be fixed. To remove rotational symmetry the second strand is placed to the right of the first. The trailing α-helix will lie on the top of the β-sheet and to the left of the first strand; otherwise all the α-helices could not pack against the β-sheet.

In structures with n parallel strands and $(n-1)$ connections there generally are $2^{(n-1)}n!/2$ topologies[3,4,32] for the strands and connections (Table 2). In addition, the option to form a β-barrel for sheets of more than six β-strands doubles the number of topologies. The four rules drastically limit the number of allowed topologies to less than 25. Barrels with eight strands, for example triose phosphate/isomerase, must show the topology ABCDEFGH with no chain reversals (compare ref. 6). We are developing an algorithm to predict hydrophobic docking sites of α-helices and β-sheets. Thus we plan to extend the combinatorial approach to α/β structures.

Implications for protein evolution and structure prediction

We have demonstrated that there are severe restrictions on the number of allowed topologies both for sheet sandwiches and for α-helices packing against a pure parallel β-sheet (Tables 1 and 2). Therefore the similarity of structure between Cu:Zn superoxide dismutase and the immunoglobulins[33] and the related topologies of some glycolytic enzymes (see for example refs 3, 4, 32, 34) could adequately be explained as the selection of similar structures from the small list of allowed folds. Thus, in our opinion, to favour the alternative explanation of divergence from a common ancestor requires different proteins that are either β/β or α/β structures to have a very similar topology and highly significant sequence resemblances.

The combinatorial approach to structure prediction is radically different from relying solely on energy minimization. To fold a protein correctly starting from an extended structure, with possibly preset α-helices and β-strands, requires an algorithm whose radius of convergence is at least the diameter of the compact globule. Such convergence is unlikely to be achieved by energy minimization due to the problem of being trapped in a local minimum. In the combinatorial approach, all structures that obey semi-empirical rules for the tertiary fold are sampled and thereby one obtains a list of possible models that should always include the rough fold of the native. For at least the proteins that belong to one of the well-defined structural classes, further work on the lines reported might well provide a solution to the protein folding problem.

1. Levitt, M. & Chothia, C. *Nature* 261, 552–558 (1976).
2. Chothia, C. & Janin, J. *J. molec. Biol.* 105, 1–14 (1976).
3. Richardson, J. S. *Proc. natn. Acad. Sci. U.S.A.* 73, 2619–2623 (1976).
4. Sternberg, M. J. E. & Thornton, J. M. *J. molec. Biol.* 105, 367–382 (1976); 110, 269–283 (1977).
5. Chothia, C., Levitt, M. & Richardson, D. *Proc. natn. Acad. Sci. U.S.A.* 74, 4130–4134 (1977).
6. Richardson, J. S. *Nature* 268, 495–500 (1977).
7. Richmond, T. J. & Richards, F. M. *J. molec. Biol.* 119, 537–555 (1978).
8. Némethy, G. & Scheraga, H. A. *Q. Rev. Biophys.* 10, 239–352 (1977).
9. Sternberg, M. J. E. & Thornton, J. M. *Nature* 271, 15–20 (1978).
10. Schulz, G. E. & Schirmer, R. H. *Principles of Protein Structure* (Springer, New York, 1979).
11. Levitt, M. *J. molec. Biol.* 104, 59–107 (1976).
12. Kuntz, I. D., Crippen, G. M., Kollman, P. A. & Kimelman, D. *J. molec. Biol.* 106, 983–994 (1976).
13. Robson, B. & Osguthorpe, D. J. *J. molec. Biol.* 132, 19–51 (1979).
14. Hagler, A. T. & Honig, B. *Proc. natn. Acad. Sci. U.S.A.* 75, 554–558 (1978).
15. Cohen, F. E. & Sternberg, M. J. E. *J. molec. Biol.* 138, 321–333 (1980).
16. Cohen, F. E., Richmond, T. J. & Richards, F. M. *J. molec. Biol.* 132, 275–288 (1979).
17. Cohen, F. E. & Sternberg, M. J. E. *J. molec. Biol.* 137, 9–22 (1980).
18. Nyberg, S. C. *Acta crystallogr.* B30, 251–253 (1974).
19. Chothia, C. *Nature* 248, 338–339 (1974).
20. Bernstein, F. C. *et al. J. molec. Biol.* 112, 535–542 (1977).
21. Saul, F. A., Amzel, L. M. & Poljak, R. J. *J. biol. Chem.* 253, 585–597 (1978).
22. Huber, R., Deisenhofer, J., Colman, P. M., Matsushima, M. & Palm, W. *Nature* 264, 415–420 (1976).
23. Blake, C. C. F., Geisow, M. J., Oatley, S. J., Rerat, B. & Rerat, C. *J. molec. Biol.* 121, 339–356 (1978).
24. Beale, D. & Feinstein, A. *Q. Rev. Biophys.* 9, 135–180 (1976).
25. Chothia, C. *J. molec. Biol.* 75, 295–302 (1973).
26. Momany, F. A., McGuire, R. F., Burgess, A. W. & Scheraga, H. A. *J. phys. Chem.* 79, 2361–2381 (1975).
27. Ptitsyn, O. B., Finkelstein, A. V. & Falk Bendzko, P. *FEBS Lett.* 101, 1–5 (1979).
28. Richardson, J. S., Getzoff, E. D. & Richardson, D. C. *Proc. natn. Acad. Sci. U.S.A.* 75, 2574–2578 (1978).
29. Dayhoff, M. O. *Atlas of Protein Sequence and Structure* Vol. 5 Suppl. 2, 168–169 (National Biomedical Research Foundation, Washington D.C., 1976).
30. Orr, H. T., Lancet, D., Robb, R. J., Lopez de Castro, J. A. & Strominger, J. L. *Nature* 282, 266–270 (1979).
31. Garnier, J., Osguthorpe, D. J. & Robson, B. *J. molec. Biol.* 120, 97–120 (1978).
32. Schulz, G. E. & Schirmer, R. H. *Nature* 250, 142–144 (1974).
33. Richardson, J. S., Richardson, D. C., Thomas, K. A., Silverton, E. W. & Davies, D. R. *J. molec. Biol.* 102, 221–235 (1976).
34. Rossmann, M. G., Liljas, A., Branden, C.-I. & Banaszak, L. J. *Enzymes* 11, 61–102 (1974).

LETTERS

Periodicity of the γ-ray transient event of 5 March 1979

J. Terrell, W. D. Evans, R. W. Klebesadel
& J. G. Laros

University of California, Los Alamos Scientific Laboratory, Los
Alamos, New Mexico 87545

**An unusual γ-ray burst event was observed on 5 March 1979 by
nine different spacecraft[1-5]. The position of the event has been
accurately determined[1,2] as $\alpha = 5$ h 25.95 min, $\delta = -66°07.1'$
(epoch 1950.0), coincident with the location of the supernova
remnant N49 in the Large Magellanic Cloud. The burst was of
very high intensity, and if isotropic and located at the distance
(~ 55 kpc) of N49 had a peak luminosity of $> 10^{44}$ erg s^{-1}. Even
more interesting is the obvious 8-s periodicity[3-5] of the event,
following the initial very intense outburst. We report here the
time history and power spectrum of this event as determined
from the Pioneer Venus Orbiter (PVO) data.**

PVO had the best available time resolution during the
initial peak and a long usable record of clearly detectable
oscillations. The PVO γ-ray burst detector[6] is sensitive to γ
rays in the energy range 60–1,200 keV and has a rate-
dependent resolving time which can be as low as 0.244 ms. The
counts obtained during a γ burst are stored in the spacecraft
memory for later transmission.

Figure 1a shows part of the PVO record of the 5 March
event, as counts grouped into uniform 11.72-ms intervals (the
largest resolving time in memory mode) and corrected for an
effective dead time of 6 μs. The γ-ray flux rose to near its
maximum in a time ≤ 1 ms (possibly much less), a fact which
is not apparent in Fig. 1 because of the grouping of data. The
even smaller rise time of < 0.25 ms which was originally
reported[1,3] corresponds to the minimum resolving time, which
was not achieved until the peak of the outburst. The γ-ray flux
remained near the maximum level for about 30 ms, fell to a
somewhat lower level for about 70 ms, and then decayed with
an ~35-ms decay time to a level about 200 times lower. The γ
rays had energies extending above 300 keV during the initial
outburst, and a spectral distribution which can be fitted
reasonably well by an exponential in photon number with kT
$\simeq 60$ keV (E. E. Fenimore, personal communication). The
maximum counting rate, which has an uncertainty of $\sim 10\%$
due to dead-time corrections, corresponds to ~ 3
$\times 10^{-3}$ erg cm^{-2} s^{-1}. The data obtained at high time
resolution in memory mode, for 3 s before and 21 s after the
outburst, are only partially displayed in Fig. 1.

Following this outburst, which lasted about 200 ms, the γ-
ray flux oscillated with an 8-s period for at least 180 s (ref. 3),
at a level initially about 500 times less than at the peak, and
with a softer spectrum[7]. Figure 1b shows the counts grouped
in 2-s intervals (as transmitted in 'real time' mode) for 200 s,
beginning 19 s before the γ burst. There are, clearly, high peaks
in the counting rate every 8 s, beginning 4 s after the initial
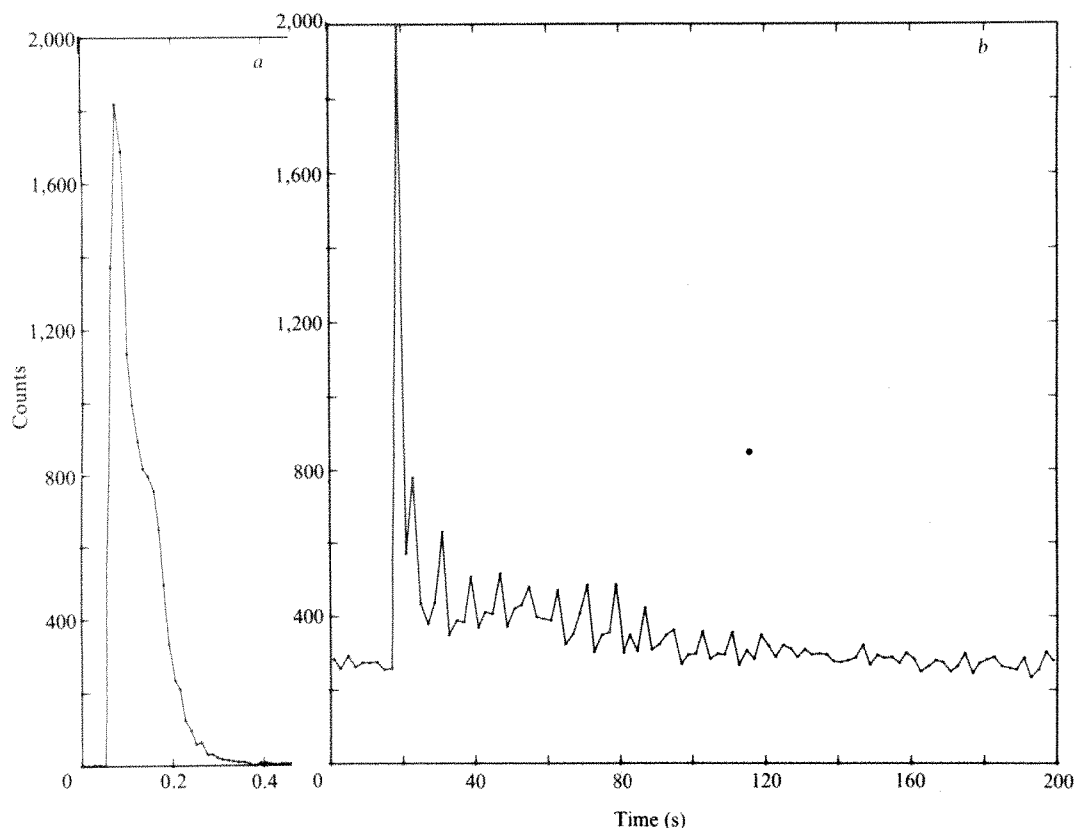
Fig. 1 Initial time history of the 5 March 1979 event (a) as seen by PVO. The counts have been grouped in uniform 11.72-ms time
intervals for Fourier analysis, so that the ≤ 1 ms rise time is not apparent here. b, PVO real-time history of the same event, with counts
grouped into 2-s bins. For clarity, the actual peak count of 13,000 is not fully shown. The energy range covered is 60–1,200 keV.
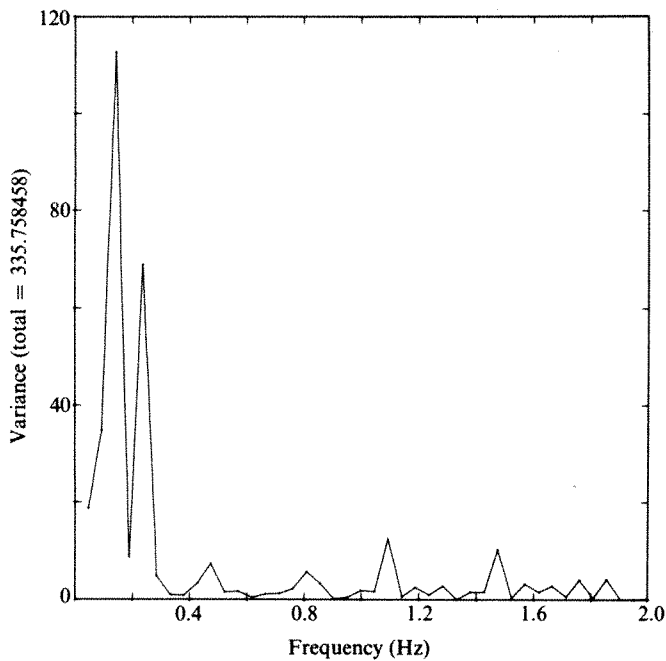
Fig. 2 Power spectrum of the 5 March 1979 event, from 21 s of high-time-resolution PVO data immediately after the peak outburst. The data have been grouped into 0.25-s bins and detrended for this analysis, but no smoothing has been used.

outburst, with lower interpulses every 8 s which evidently begin with the shoulder following the initial peak in Fig. 1.

Because of the clear evidence of periodicity, the counting data, both for memory and real-time modes, have been subjected to extensive Fourier analysis. The 21 s of high-resolution data obtained from PVO after the initial outburst yield a power spectrum, seen in Fig. 2, with clear evidence of periods of 4 and 8 s and no other periods significantly above the counting noise level. These peaks are more sharply defined in the longer time history available in real time (2-s resolution) counting mode, as seen in Fig. 3, which shows the power spectrum obtained from 120 s of data immediately following the initial outburst. The spectrum is presented as variance at each multiple of the fundamental frequency (0.00833 Hz) corresponding to the 120-s time series. No smoothing or fading have been used in these analyses; the methods used are more fully discussed elsewhere[8,9]. The data have been subjected to linear detrending before analysis to remove the very low frequency peak which would otherwise appear in the power spectrum, some trace of which can still be seen at the lowest frequencies.

The two very clearly displayed peaks in Fig. 3, at frequencies of 0.125 and 0.250 Hz, correspond to the fundamental period and its second harmonic. The peaks in this spectrum are so narrow that their width is seen only in the analyses which we have done of longer sets of the PVO data. The broad base visible around each peak is very similar to what is obtained in the analysis of decaying sine waves, performed as tests of the methods used here. Thus the shape of the peaks is essentially lorentzian, although (Fig. 1b) the decay of the oscillations is clearly not precisely exponential, nor is it the same for main pulse and interpulse; the interpulse even seems to be growing during the first few periods. The second harmonic is stronger in the long time series, undoubtedly because of the relatively higher interpulses. The second harmonic in Fig. 3 falls exactly at the Nyquist frequency of 0.250 Hz (for 2-s time resolution), above which there is no additional spectral information. However, as seen in Fig. 2, analysis of PVO data with higher time resolution shows no

significant evidence of higher frequencies. The counting noise level in Fig. 3 corresponds to an average variance of 12 (per Fourier harmonic), which is negligible compared with the peaks.

We have done numerous other power-spectrum analyses of the data of this γ-burst event, and of simulated sets of data, for varying lengths of time series and for various sub-intervals of the data. When the time series does not cover an exact multiple of the 8.0 s period, even when differing by 1 time unit out of 120, the power spectrum peaks are noticeably broadened and lowered, as would be expected for a sharp periodicity. Many such analyses of our data have made it clear that the best estimate of the period is 8.00 ± 0.05 s, in agreement with the result of Cline et al.[3] This also agrees well, of course, with the 7.9 ± 0.3 and 8.1 ± 0.1 s periods reported by Barat et al.[4] and by Mazets et al.[5], but is more precisely known because of the long time series available from the PVO and ISEE 3 spacecraft.

The power spectrum of this event is thus quite consistent with a decaying periodicity with a well defined period of 8.0 s. The strong second harmonic at 4.0 s is to be expected from the pulse shape with its obvious interpulse. There is no evidence of other harmonics in any of the data. Such a power spectrum is more likely to be produced by a rotating source than by some type of resonance. For a rotating astronomical source, centrifugal force at the surface must be less than gravitational force, leading to the equation (for a spherical source of period T)

$$\rho \geq 3\pi/GT^2 \qquad (1)$$

in which ρ is the source density and G is the gravitational constant. A rotating source with $T = 8$ s must thus have $\rho \geq 2.2 \times 10^6$, which could be consistent with a white dwarf as source. A more stringent limit is set by the ≤ 1-ms rise time of this outburst, which suggests that the radius of the source is probably $< 1,000$ km. For a source of roughly one solar mass this requires a density $\rho \gtrsim 10^9$, which is consistent only with a
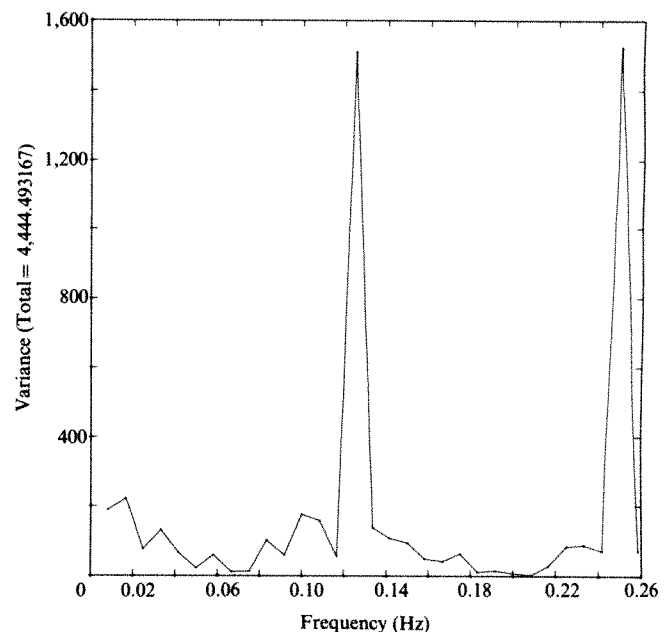
Fig. 3 Power spectrum of the 5 March 1979 event, based on 120 s of PVO data immediately following the initial outburst, with counts in 2-s groups. The data were detrended before analysis. The spectrum, presented as variance (for each Fourier harmonic), has not been smoothed.

neutron star, or with a gravitationally collapsed object of even higher density.

Thus it seems likely that the γ-ray transient event of 5 March 1979 originated in a neutron star of rotation period 8.0 s, perhaps an old pulsar. The direction of this source is coincident with the supernova remnant N49, although the distance of the source remains in some doubt[2-5,10]. It seems reasonably certain that there were two oppositely placed source regions on the rotating neutron star, perhaps at the magnetic poles. The occurrence of three additional outbursts from the same source[5,11] on 6 March, 4 April and 24 April 1979 indicates that the cause of the outbursts is related to characteristics of the neutron star itself (such as an internal restructuring[7], or a critical accumulation of accreted material) and not due to improbable recurring collisions with incoming objects.

We thank E. R. Tech and S. E. Duran for help with data processing, J. P. Glore, F. J. Wymer and R. E. Spalding for electronic design and E. E. Fenimore and R. Ramaty for useful discussions. This work was supported by the US Department of Energy and by NASA.

Note added in proof: The difficulty of radiating sufficient flux from the surface of a neutron star at the distance of the LMC[5,10,12] is avoided if the surface is at a temperature of ~ 30 keV, since the radiation pressure within the surface would be sufficient to blow off the surface layer to a depth of many optical mean free paths. The relativistically-expanding shell could readily emit the required flux, becoming optically thin before it reaches the maximum radius (40,000 km) determined[13] from the effective pulse length of 0.13 s.

1. Evans, D. *et al. IAU Circ.* No. 3356 (1979).
2. Evans, W. D. *et al. Astrophys. J. Lett.* **237**, L7–L9 (1980).
3. Cline, T. L. *et al. Astrophys. J. Lett.* **237**, L1–L5 (1980).
4. Barat, C. *et al. Astr. Astrophys.* **79**, 124–125 (1979).
5. Mazets, E. P., Golenetskii, S. V., Il'inskii, V. N., Aptekar', R. L. & Guryan, Yu. A. *Nature* **282**, 587–589 (1979).
6. Evans, W. D. *et al. Science* **205**, 119–121 (1979).
7. Fenimore, E. E., Evans, W. D., Klebesadel, R. W., Laros, J. G. & Terrell, J. *Nature* (submitted).
8. Terrell, J. & Olsen, K. H. *Astrophys. J.* **161**, 399–413 (1970).
9. Terrell, N. J. *Astrophys. J. Lett.* **174**, L35–L41 (1972).
10. Helfand, D. J. & Long, K. S. *Nature* **282**, 589–591 (1979).
11. Golenetskii, S. V., Mazets, E. P., Il'inskii, V. N. & Guryan, Yu. A. *Astr. Zh.* (submitted).
12. Petschek, A. & Colvin, J. D. Preprint.
13. Terrell, J. *Astrophys. J.* **213**, L93–L97 (1977).

The IR spectrum of the double QSO

M. J. Lebofsky*, G. H. Rieke*†, D. Walsh‡ & R. J. Weymann*

*Steward Observatory, and †Lunar and Planetary Laboratory, University of Arizona, Tucson, Arizona 85721
‡University of Manchester, Nuffield Radio Astronomy Laboratory, Jodrell Bank, Macclesfield, Cheshire, UK

The hypothesis that the double QSO, 0957 + 561A,B (separation 6 arcs s and $z = 1.4$) is formed by a gravitational lens[1] has found strong support from observations[2] suggesting the presence of an intervening giant elliptical galaxy with $z \simeq 0.4$, separated from component B by <1 arc s. According to the lens hypothesis the flux ratio of the two QSOs should be the same at all wavelengths. Any difference observed should be due only to superposition on component B of emission from the lens galaxy, which is expected to be predominantly in the IR. We report here new photometry at 1.25, 1.6 and 2.2 μm which strengthens the case for lens action and confirms that the lens galaxy is a giant elliptical.

IR photometry of the double QSO was obtained on 28 November 1979 with the 2.29-m telescope at Steward Observatory. The photometer utilized a liquid helium cooled InSb detector, 5.8 arc s diameter aperture, and interference

Table 1 IR photometry of the double QSO

	1.25 μm	1.60 μm	2.2 μm
Component A (north)	0.61 ± 0.04*	0.80 ± 0.03	0.61 ± 0.04
Component B (south)	0.71 ± 0.04	1.11 ± 0.04	1.19 ± 0.03

*All fluxes in mJy $= 10^{-29}$ W m^{-2} Hz^{-1}, errors are 1σ deviation.

filters defining the standard photometric bands J(1.25 μm), H(1.6 μm), and K(2.2 μm). The measurements were relative to reference areas 9 arc s to the east and west of the double QSO components. The seeing was ~ 1 arc s and the night was of excellent photometric quality. The flux was reduced by standard star observations[3,4]. The measurements are summarized in Table 1.

In the radio[5-7] and blue and UV[2,8] the B (southern) component of the QSO is 75 % as bright as the A component. Beginning abruptly at 5,500 Å, the B component becomes progressively redder towards longer wavelengths; for example, at 7,000 Å with 7 arc s aperture the observed ratio B/A is close to unity[2].

Our new IR observations with 5.8 arc s aperture show a striking increase in the flux ratio B/A to ~ 2 at 2.2 μm. We can test whether this is consistent with lens action by a giant elliptical galaxy as follows. We assume a constant intrinsic flux ratio B/A of 0.75. Using the published optical[2] and our IR data we subtract 0.75 of the flux of A from that of B. The excess flux from B is then expected to be the contribution from the galaxy. The derived galaxy flux is compared with the spectral energy distribution typical of nearby giant ellipticals[9,10] in Fig. 1. The standard elliptical energy distribution was redshifted by $z = 0.4$, with appropriate K corrections[11]. The galaxy near the double QSO can be seen to have an energy distribution in the J, H, K bands that is slightly redder than the typical nearby elliptical, and to have a distinct excess in the visible relative to the IR flux.

To facilitate further comparison with other galaxies at $z = 0.4$, the R colour in the Johnson system was computed from the optical data[2], and a small aperture correction was applied from our 5.8 arc s to the 7 arc s aperture used in the optical. The colours of this galaxy are given in Table 2. For comparison, a sample of four giant elliptical galaxies with z ranging from 0.38 to 0.42 (A370, 0822 + 67, 1613 + 31, and 0949.9 + 4409) have both IR and optical colours measured[11-13]. The average colours for this group of ellipticals are also given in Table 2, where the errors are indicative of the
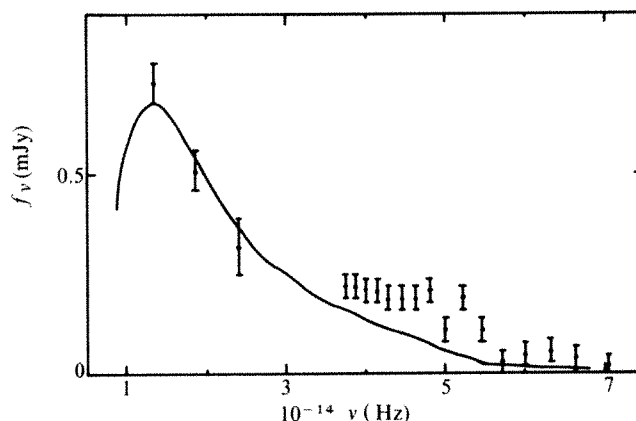
Fig. 1 The spectrum of the excess of component B of the double QSO above 75 % of the flux of component A. Data points are shown by dots, with 1-σ error bars. Errors for the data at frequencies above 3×10^{14} Hz (ref. 2) have been estimated by comparing the spectra of components A and B. The solid line shows the spectrum of a typical nearby giant elliptical galaxy, redshifted to $z = 0.4$ and normalized to fit the IR data.

Table 2   Colours of redshifted giant elliptical galaxies

	R–K	J–H	H–K
Nearby galaxy shifted to $z = 0.4$	3.55	1.07	0.75
Galaxies observed at $z = 0.4$	3.3		0.93 ± 0.06
Galaxy associated with component B	3.1	1.3 ± 0.3	0.9 ± 0.1

spread in colours and uncertainty in aperture correction between optical and IR data. Note that there are differences of up to 0.25 mag between the colours of giant ellipticals actually observed at $z = 0.4$ and those estimated from the known properties of nearby giant ellipticals. It is not appropriate to discuss this in detail here, but the effect seems to be real. However, the measured colours of galaxies at $z = 0.4$ are a very close match to the observed colours of the galaxy near component B of the double QSO. The absolute magnitude of the galaxy at K can be estimated from the observed magnitude of $K = 14.9$. Because the guiding during the observation of the southern component was done visually on the QSO, the galaxy was not centred in the beam, making an exact aperture correction difficult. A value of 0.5 mag has been adopted[14], which yields $M_K \sim -26.1$ for $q_0 = 0$, $H_0 = 100$. The values of M_K for giant ellipticals range from $M_K = -25.7$ to $M_K = -26.8$ (refs 9, 14) making this galaxy within the giant elliptical luminosity range.

The photometry of component A of the double QSO in Table 1 shows nearly equal fluxes at J and K with a larger flux at H. Hα should be shifted to 1.58 μm at $z = 1.41$. If $I(C\,IV)/I(H\alpha) = 0.5$, a typical value for QSOs[15], then the excess at H above a spectrum interpolated from J to K corresponds exactly to the expected contribution from Hα. The spectrum of the QSO from optical to IR wavelengths is remarkably flat when compared with other QSOs. For example, a power law fitted to the spectrum of component A from 0.44 to 2.2 μm has an index of $\alpha = -0.15$, compared with the normal range of $-0.5 \gtrsim \alpha \gtrsim -1.5$ (ref. 16).

A crucial test of the gravitational lens hypothesis is that the two images of the QSO should have identical spectra. At present, in the IR it is technologically feasible to test this prediction only over the 1–2.5 μm spectral region. Our measurements demonstrate that the IR spectra are consistent with the QSO images having a constant flux ratio except for contamination by a giant elliptical galaxy[2] of luminosity and colour typical for similar galaxies at the same redshift. The IR measurements therefore support the gravitational lens model of the double QSO.

This work was supported by the NSF. GHR is an Alfred P. Sloan Fellow.

1. Walsh, D., Carswell, R. F. & Weymann, R. J. *Nature* **279**, 381–384 (1979).
2. Young, P., Gunn, J. E., Kristian, J., Oke, J. B. & Westphal, J. A. *Astrophys. J.* (submitted).
3. Johnson, H. L. *Commun. Lunar Planet. Lab.* Univ. Arizona No. 53 (1965).
4. Low, F. J. & Rieke, G. H. in *Methods of Experimental Physics* Vol. 12 (ed. Carleton, N.) 415–462 (Academic, New York, 1974).
5. Pooley, G. G. *et al Nature* **280**, 461–464 (1979).
6. Roberts, D. H., Greenfield, P. E. & Burke, B. F. *Science* **205**, 894 (1979).
7. Porcas, R. W., Booth, R. S., Browne, I. W. A., Walsh, D. & Wilkinson, P. N. *Nature* **282**, 385–386 (1979).
8. Wills, B. J. & Wills, D. *Astrophys. J.* (in the press).
9. Frogel, J. A., Persson, S. E., Aaronson, M. & Matthews, K. *Astrophys. J.* **220**, 75–97 (1978).
10. O'Connell, R. W. Preprint (1980).
11. Lebofsky, M. J. in preparation.
12. Gunn, J. E. & Oke, J. B. *Astrophys. J.* **195**, 255–268 (1975).
13. Kristian, J., Sandage, A. & Westphal, J. A. *Astrophys. J.* **221**, 383–394 (1978).
14. Persson, S. E., Frogel, J. A. & Aaronson, M. Preprint (1980).
15. Baldwin, J. A. *Astrophys. J.* **214**, 679–684 (1977).
16. Neugebauer, G., Oke, J. B., Becklin, E. E. & Matthews, K. *Astrophys. J.* **230**, 79–94 (1979).

Anti-matter in the primary cosmic radiation

J. Szabelski & J. Wdowczyk

Institute of Nuclear Research, Uniwersytecka 5, Lodz, Poland

A. W. Wolfendale

Department of Physics, University of Durham, Durham DH1 3LE, UK

Anti-matter in the cosmic radiation incident on the Earth can be of two types: antiparticles from distant antigalaxies and secondary particles generated by collisions of cosmic rays with nuclei of the interstellar medium (ISM) either in our Galaxy or in other galaxies. Insofar as the 2.7 K relict radiation inhibits the former for positrons (with energy above some tens of MeV) and the expected ratio of extragalactic particles to galactic particles is very small for protons (and thus antiprotons) it is conventional to assume that collisions in the ISM are the source of the e^+ and $\bar{p}$ detected. We consider here the manner in which cosmic rays are propagated in the Galaxy by studying the fluxes of these antiparticles.

The 'leaky box' model is the simplest one for cosmic ray propagation; in it there is essentially equilibrium between the particles and their secondaries, both being lost by leakage after many collisions with the 'boundary' of the Galaxy. In this model both the primary cosmic rays and their secondaries have the same mean lifetime in the Galaxy and the amount of material traversed (the 'grammage' mean density of gas × mean lifetime × velocity) is the same for them all.

We have previously examined the positron results and concluded that there is evidence against the 'leaky box' model of propagation[1]. We showed specifically that the average
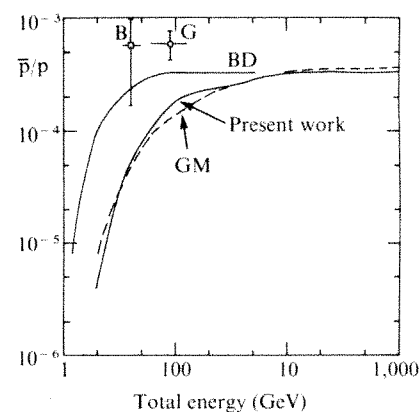
Fig. 1 Comparison of observed and expected ratios of antiprotons to protons in the primary cosmic ray beam. G denotes the measurement of Golden *et al.*[2] and B that of Bogomolov *et al.*[3]. The fomer is 15 % higher than our value because of our use of a correction for atmospheric $\bar{p}$ derived from the present calculations rather than those of Badhwar *et al.*[5]. The latter is 5 % lower than our value because they ignored an atmospheric correction. The predictions relate to the ratios expected for 5 gm^{-2} of interstellar hydrogen traversed by the cosmic rays using the leaky box model (that is the intensity of $\bar{p}$ is that generated by the locally measured cosmic ray spectrum—corrected for solar modulation—in 5 g cm^{-2} of ISM). BD denotes Badhwar *et al.*[5] (for a primary spectrum of exponent $\gamma = 2.75$). GM denotes Gaisser and Maurer[4] ($\gamma = 2.6$). In the present work the adopted primary spectrum has a variable exponent. We find it very significant that the observed ratio is much higher than our predicted ratio.

grammage traversed by positrons was significantly shorter than that traversed by nuclei, of the same rigidity, when both were calculated adopting the leaky box model.

The present analysis was prompted by the recent determination of the flux of antiprotons in the cosmic radiation by Golden et al.[2], and by Bogomolov et al.[3]. The initial objective is to take the best estimate of the primary spectra of the various cosmic ray components (p, α ...) together with nuclear physical data on p̄ production in the relevant particle collisions and to derive the expected p̄ spectrum for the traversal of $1 \, \mathrm{g \, cm}^{-2}$ of ISM (or $1 \, \mathrm{g \, cm}^{-2}$ of hydrogen-equivalent). This is compared with the observed p̄ spectrum, and the mean grammage required ($\langle \lambda \rangle_{\bar{p}}$) is determined. (In the leaky box model this is simply the observed p̄ intensity divided by the predicted p̄ intensity for $1 \, \mathrm{g \, cm}^{-2}$ traversed.) Two previous calculations have been made using modern p̄ data[4,5] but with such discordant results, that we analysed the input data rather critically.

The cross-sections were taken from the Durham–Rutherford data base and comprised all the available data on inclusive reactions $\mathrm{pp} \to \bar{p} + \mathrm{anything}$ and $\mathrm{p} - \mathrm{light \; nucleus} \to \bar{p} + \mathrm{anything}$, the latter being converted to expectation for pp. The energy range for initiating proton extended from 19.2 GeV (CERN experiments[6]) by way of 70 GeV (Serpukhov[7]) and 100–400 GeV (Fermilab[8]) to 2,096 GeV (ISR[9]) (these refs are only a selection of the many data sources used). Integration was carried out over transverse momentum and p̄ multiplicity times inelastic cross-section was derived for various proton energies and p̄ energy thresholds, as given in Table 1. The data are accurate to $\sim 15\%$ over the important energy range—which is partly confirmed by the estimation by Rossi et al.[10], who give the yield of p̄ of all energies as a function of proton energy (Table 1). The cross-section $(\sigma_{\mathrm{in}} \times \langle n \rangle (\bar{p}))$ is usually slightly more than the flux we calculated for $E_{\bar{p}} > 1.5 \, \mathrm{GeV}$. (Note that the basic data are almost the same as those used by Badhwar et al.[5], the main addition is new results from Fermilab.)

The cosmic ray proton spectrum adopted is similar to that used in our earlier work, viz: $J(E) = 2 \times 10^4 \, E^{-2.75} \, (1 + 4.26 \, E^{-0.876})^{-1} \, \mathrm{m}^{-2} \mathrm{s}^{-1} \mathrm{sr}^{-1} \mathrm{GeV}^{-1}$ where E is the kinetic energy.

For α particles a ratio of intensities of $\alpha/\mathrm{p} = 0.05$ was adopted above 20 GeV per nucleon, following the summary by Juliusson[11] (this differs slightly from our earlier assumption but not significantly so). The spectra of heavier cosmic ray nuclei have also been taken from Juliusson.

The expected energy spectrum of antiprotons from p–p collisions follows from using the data of Table 1 with $J(E)$. Assuming equal production of n̄ and p̄ the detected flux of p̄ will be higher than calculated by a factor 2 (the n̄ decay into p̄) and when allowance is made for α particles and heavier nuclei a further factor 1.25 must be applied to give the expected flux of p̄ per $\mathrm{g \, cm}^{-2}$ of H (or H-equivalent) in the ISM. (Note, the factor 1.58 adopted by Badhwar et al. relates to flux per $\mathrm{g \, cm}^{-2}$ of ISM in total and should not be compared with our factor 1.25; it does not matter which factor is used as long as the same factor is used for the grammages for the other components with which comparison is made.)

Figure 1 shows the derived p̄/p ratio from the present work for the traversal of $5 \, \mathrm{g \, cm}^{-2}$ H-equivalent together with the other predictions[4,5] for the same grammage, and the observations[2,3].

Although we have considered the predictions of the other workers referring to the same target material, hydrogen (the ratio of Badhwar et al. has been multiplied by 1.25/1.58 and that of Gaisser and Maurer by 1.25), they refer to different primary spectra, and the comparison must be made with care.

Gaisser and Maurer used a primary spectrum with constant exponent ($\gamma = 2.6$) and this is not too far from our primary spectrum over much of the energy range. Their predicted p̄/p ratio is seen to be not far from ours and this indicates that our derived cross-sections for p̄ production are similar. An accurate comparison has been made, in fact, by using the data of Table 1 with a primary spectrum having $\gamma = 2.6$; for antiprotons of energy in the range 5–10 GeV (the important range in practice) the ratio of the GM value of p̄/p to ours is 0.61. The same ratio for p̄ of all energies is 0.74. The difference in the results is greater than we would have expected from uncertainties in the cross-sections ($\sim 20\%$), but not dramatically so.

The difference in Fig. 1 between the prediction of Badhwar et al. and ours is bigger than can be explained in terms of the differing primary spectrum (they used $\gamma = 2.75$). Reworking our prediction for $\gamma = 2.75$ gives the ratio of their value of p̄/p (for 5–10 GeV) to ours of 2.7 and the ratio for all energies is 6.1. This discrepancy is hard to understand as we seem to have used the same sources of accelerator data for cross-sections for p̄ production. Their roughly constant p̄/p ratio down to a p̄ energy as low as $\sim 5 \, \mathrm{GeV}$ is particularly hard to understand; it would correspond to a plot of total number of p̄ versus proton energy at variance with accelerator data at proton energies below about 100 GeV.

Assuming that our calculations are correct, it is easy to derive the values of $\langle \lambda \rangle_{\bar{p}}$ required by the two experimental measurements of p̄/p (Fig. 1) (they are simply the measured p̄/p ratios divided by the predictions, multiplied by $5 \, \mathrm{g \, cm}^{-2}$) assuming that the leaky box model is valid.

Comparison can now be made with the mean grammages derived from the mass composition analyses ($\langle \lambda \rangle_{\mathrm{N}}$) and positron data ($\langle \lambda \rangle_{e+}$) in the same way. Although there is some spread of values of $\langle \lambda \rangle_{\mathrm{N}}$ from different workers, most lie in the range shown (see refs 12–14 for representative results). Concerning $\langle \lambda \rangle_{e+}$, we have used our analysis of the expected positron flux and its comparison with observation. The value of $\langle \lambda \rangle_{e+}$ is sensitive to the mean lifetime of electrons in the Galaxy and we have adopted a value of $\langle T \rangle = 2 \times 10^7 \, \mathrm{yr}$ for this quantity[15].

It is apparent that there is no consistency between the various values of $\langle \lambda \rangle$ such as would have been expected. Admittedly, there are uncertainties in the analysis but, what is probably the biggest—the spectrum in interstellar space of cosmic ray protons—cancels out when $\langle \lambda \rangle_{\bar{p}}$ and $\langle \lambda \rangle_{e+}$ are compared. The most likely explanation is a lack of validity of the leaky box model[1,16]. An alternative explanation is that the bulk of the antiprotons are of extragalactic origin (our evidence on the shape of the p̄ spectrum does not preclude this) but it seems rather unlikely both because of the above arguments, and because the inequality of $\langle \lambda \rangle_{e+}$ and $\langle \lambda \rangle_{\mathrm{N}}$ indicates propagation effects, and such effects can also make $\langle \lambda \rangle_{\bar{p}} \neq \langle \lambda \rangle_{\mathrm{N}}$. There may also be problems with excessive γ-ray fluxes if the postulated extragalactic flux of p̄ has high flux at low energies.

Table 1 Cross-section (mb per proton) for p̄ produced with energy above E_{p}, for proton–proton collisions, versus incident proton energy, E_{p}

$E_{\bar{p}}$ (GeV) \ E_{p} (GeV)	15	20	30	50	100	200	500	1,000
1.5	$<10^{-2}$	0.083	0.18	0.35	0.80	1.75	3.8	6.4
5	$<10^{-3}$	0.014	0.073	0.18	0.57	1.40	3.4	5.9
10		$<10^{-3}$	0.0072	0.054	0.32	0.92	2.8	5.2
σ_{in} (mb)	29.7	30.0	30.3	30.8	31.4	32.0	33.1	34.5
$\langle n \rangle$ (p̄)	2×10^{-3}	2.8×10^{-3}	5.6×10^{-3}	1.2×10^{-2}	2.8×10^{-2}	6.0×10^{-2}	1.2×10^{-1}	1.5×10^{-1}

The cross-section is $\langle n \rangle \sigma_{\mathrm{in}}$ where $\langle n \rangle$ is the mean multiplicity of p̄ above $E_{\bar{p}}$ and σ_{in} is the inelastic cross-section. The inelastic cross-section for p–p collisions, σ_{in}, is also given, as is the average number of p̄ of all energies, $\langle n \rangle (\bar{p})$. (The latter is from ref. 10.)
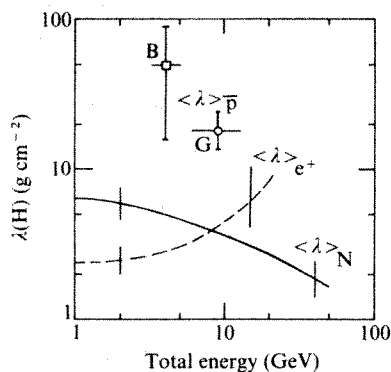
There are several ways of explaining Fig. 2 in terms of propagation effects. An attractive model is one in which protons (and probably α particles) have sources which differ in general from those of heavier nuclei. These sources could be differently distributed in space and/or time; for example, the old idea of production of protons in intermittent Galactic centre 'explosions' is attractive. This would result in protons and heavier nuclei having different distributions in the Galaxy, and the grammage 'seen' by those particles detected at the Earth would be different. A long 'tail' to the lifetime distribution would not be surprising and this would depress the positron flux and thus the $\langle\lambda\rangle_{e+}$ values shown in Fig. 2 because of the removal of positrons by synchrotron and inverse Compton losses; such losses would be quite natural if the particles spent a considerable time in the galactic halo.

Another possibility relating to propagation is the inclusion of deceleration of particles after they have accumulated the bulk of their grammage; because of the different spectral shapes of p and $\bar{p}$, and $\bar{p}/p$ ratio at low energies ($E < 10$ GeV) would be significantly enhanced by deceleration. What is quite clear is that the opposite effect is ruled out[2], viz that the bulk of the grammage is encountered before acceleration; the $\bar{p}/p$ ratio at low energies would be very small under such circumstances. Although the deceleration idea does not explain the e^+ results (for which we feel that a long lifetime 'tail' is the most likely explanation) it does have attractive features and needs further analysis.

The antiproton measurements give further evidence against the simplistic leaky box model of cosmic ray propagation and point to a more complex manner of propagation, probably involving considerable fractions of particle lifetimes spent in the galactic halo. An alternative explanation in terms of extragalactic antiprotons from antigalaxies although unlikely cannot be ruled out. A more extended measurement of the energy spectrum of $\bar{p}$ (and e^+) would probably enable a distinction to be made.

1. Giler, M., Wdowczyk, J. & Wolfendale, A. W. *J. Phys.* **A10**, 843 (1977).
2. Golden, R. L. *et al. Phys. Rev. Lett.* **43**, 1196 (1979).
3. Bogomolov, E. A. *et al. Proc. int. Cosmic Ray Conf.*, Kyoto **1**, 330 (1979).
4. Gaisser, T. K. & Maurer, R. H. *Phys. Rev. Lett.* **30**, 1264 (1973).
5. Badhwar, G. D. *et al. Astrophys. Space. Sci.* **37**, 283 (1975).
6. Allaby, J. V. *et al. Proc. 4th Int. Conf. on H.E. Collisions*, Oxford **2**, 85 (1972).
7. Antipov, Yu, M. *et al. Phys. Lett.* **34B**, 2, 164 (1971).
8. Johnson, J. R. *et al. Phys. Rev.* **D17**, 5, 1292 (1978).
9. Capiluppi, P. *et al. Nucl. Phys.* **70**, 1 (1974).
10. Rossi, A. M. *et al. Nucl. Phys.* **B84**, 269 (1975).
11. Juliusson, E. *Proc. int. Cosmic Ray Conf.*, Munich **8**, 2689 (1975).
12. Shapiro, M. M. & Silberberg, R. *Proc. R. Soc.* **277**, 319 (1974).
13. Caldwell, J. H. *Astrophys. J.* **218**, 269 (1977).
14. Garcia-Munoz, M. *et al. Proc. int. Cosmic Ray Conf.*, Kyoto **1**, 310 (1978).
15. Garcia-Munoz, M., Mason, G. M. & Simpson, J. A. *Astrophys. J. Lett.* **201**, L141 (1975).
16. Giler, M., Wdowczyk, J. & Wolfendale, A. W. *J. Phys.* **A11**, 199 (1978).

Frequency of the methane-stabilized He–Ne laser at 88 THz measured to ±3 parts in 10^11

D. J. E. Knight*, G. J. Edwards, P. R. Pearce & N. R. Cross

National Physical Laboratory, Teddington, Middlesex TW11 0LW, UK

We have measured the frequency of a methane-stabilized laser at 88 THz (3.39 μm) (ref. 1), by a method which largely eliminates the uncertainties contributed by lower-frequency lasers used as transfer oscillators. This result is primarily of interest for a proposed new definition of the metre in which the speed of light in vacuum (c_0) would be kept constant and reference would be made to the standard of time and frequency[2]. For this reason our measurement has been referred to the mean frequency of five small portable, stabilized lasers of similar design that are used as wavelength standards[3,4]. We estimate the mean frequency of the laser ensemble to have been (88,376,181,616 ± 3) kHz. The estimated standard deviation comes within about a factor of 2 of the reproducibility of the lasers themselves. This result therefore demonstrates a degree of accuracy that would permit the choice of a definition of the metre in which c_0 was kept constant, without substantial loss of accuracy compared with choosing a definition based on the wavelength of a selected stabilized laser.

The methane-stabilized helium–neon laser[1] at 3.39 μm is one of a growing group of stabilized lasers recommended for use as wavelength standards[2]. Although it lacks a visible radiation, it has a high degree of reproducibility[1,3,4], approaching 1 part in 10^{11}, and its frequency has been directly measured by comparison with the caesium standard using harmonic generation and frequency-mixing techniques[5,6]. Frequency and wavelength measurements on both this and a carbon dioxide stabilized laser[7] have established the presently accepted value of the speed of light[2]. The uncertainty in c_0, ±4 parts in 10^9, arises from the realization of the metre from the ^{86}Kr lamp[2], and is 10 times larger than was obtained for the frequency of the methane-stabilized laser. Since then wavelength-ratio determinations against other stabilized lasers have become more accurate than the methane frequency measurements[8,9].

The measurement described here was obtained using a simplified chain of comparison having only four main transfer oscillators (one a klystron) between the methane-stabilized laser and a rubidium standard. Further details appear elsewhere[10,11].

The frequencies are related by the four mixing equations

$$f_{CH_3OH} = 43 f_{99} \pm 120 \text{ MHz} \tag{1}$$

$$f_{R32} = 7 f_{CH_3OH} - 3 f_{95} \pm \Delta f_b \tag{2}$$

$$f_{He-Ne} = 3 f_{R32} - f_{55} \pm \Delta f_b' \tag{3}$$

and

$$f_{CH_4} = f_{He-Ne} \pm \Delta f_b'' \tag{4}$$

where f_{CH_4OH}, f_{R32}, f_{He-Ne} and f_{CH_4} are laser frequencies at 4.25, 29.5, 88.4 and 88.4 THz, f_{99}, f_{95} and f_{55} are klystron frequencies suffixed in GHz, and Δf_b, $\Delta f_b'$ and $\Delta f_b''$ are measured beat frequencies in the 10–100-MHz band. The mixing devices (one per equation) were (1) a Josephson junction, (2) and (3) metal–insulator–metal diodes and (4) a photodiode.

*Present address: Bureau International des Poids et Mesures, F-92310 Sèvres, France.

The beat signals were obtained sufficiently strongly to be counted with digital counters, and this in turn allowed us to make our measurements simultaneously (with a 1 s averaging time) and so eliminate the effects of frequency changes among the three transfer lasers, which were used free-running. Simultaneous counts were made on Δf_b, $\Delta f'_b$, $\Delta f''_b$ and on f_{99}, that of a klystron phase-locked to the lowest-frequency laser. The four experimenters closely monitored the beats and the state of phase lock of the klystron during the counts. f_{95} and f_{55} were controlled by quartz crystals and were measured 1 s later. A computer (Hewlett Packard 9825A) was linked to the counters and performed the arithmetic. The rubidium standard that controlled the counters was calibrated at intervals of about 2 days by carrying it to a caesium clock in another building, and the methane-stabilized laser (NPL1) was checked against another soon after the measurements and against others during the preceding 12 months.

Measurements were taken on three nights over a period of 5 days. The results of the third night are split into two groups because of an alteration made in the counting system to permit greater resolution of a critical quartz-crystal frequency controlling f_{95}. A summary of the data for the four groups, corrected for the rubidium offset and a counter offset (see below), is shown in Table 1.

Within each group the measurements were made in blocks of 10, with a quasi-random permutation between each block of the various ($\pm$) sidebands possible in the frequency chain. For each group, tests of the homogeneity of the variances and means (Bartlett's test, F-test) of the subsidiary blocks are entirely satisfactory at the 5% level. However, an F-test on the means of the four groups leads to an F-value corresponding to a probability of 5%, which indicates some inconsistency between them. Group 3b differs from the others in having a smaller standard deviation, which was the result of the change in the apparatus mentioned above, and in having an offset mean, which caused us to look for possible systematic errors in the apparatus. We found only a small error in one of the counters, shown as a 0.7-kHz correction in Table 2, but there was also evidence of a trend with time in the results, beginning in set 3a and continuing through set 3b. Parameters such as the frequency of the methane-stabilized laser or of the rubidium clock might be expected to change more between groups than within them, so, following Eisenhart[12], we take the unweighted mean of the four means of the groups. We obtain $f - f_0 = +8.8$ kHz with an estimated standard deviation of 2.0 kHz. However, as there are only four groups this value has a large uncertainty, of the order of 40%. The standard deviation corresponds to a scatter between the groups of about 2 kHz, which is rather larger than the contributions expected from the rubidium clock and stabilized laser, about 1 kHz each. However, it was not possible during these measurements to check the stabilized laser against a second

Table 1 Summary of the measurements

Group	Day (August 1979)	Time (UT)	n^*	Mean† $(f - f_0)$ (kHz)	σ_{single} (kHz)	σ_{mean} (kHz)
1	17/18	22.30–04.00	41	+12.9	32.3	5.0
2	20/21	22.30–02.30	124	+9.4	34.5	3.1
3a	22/23	21.00–02.00	110	+9.4	29.2	2.8
3b	23	03.00–0.4.30	49	+3.4	11.7‡	1.8

*About 30% of all attempted measurements were rejected at the time of measurement because of faults seen while monitoring the apparatus. A few results (about 4% in groups 1, 2 and 3a; 11% in Group 3b) were further rejected during analysis by applying a $\pm 3\sigma_{single}$ cutoff to the data.

†$f_0 = 88\,376\,181\,608$ kHz (an arbitrary reference zero). The means have been corrected for the rubidium clock offset and the error in a counter (see Table 2).

‡The counting resolution was increased for this group, see text.

Table 2 Summary of corrections* and uncertainties (kHz)

Stage of comparison	Mean correction	Uncertainty (estimated standard deviation)		
		Statistical (n)	Estimated	Total
Caesium versus rubidium	+8.5	0.7 (5)	1.1	1.3
Rubidium versus laser	+0.7†	2.0 (4)‡	0.1	2.0
Laser versus ensemble	−1.0	0.7 (5)	1.0	1.2
Total	+8.2	2.2	1.5	2.7

*The first two corrections listed have already been incorporated into Table 1. The final result is obtained by applying the third correction to the overall mean of Table 1, see text.

†Applies to groups 1, 2 and 3a only.

‡Derived from the four group means in Table 1, see text.

similar one, and further, it counts against group 3b that it spans a short period of time compared with the others.

The corrections applied to the data and the main contributions to the overall uncertainty are listed in Table 2. The uncertainty deduced from Table 1 appears in the central line; the first two corrections are already incorporated in the mean values given in Table 1. The main correction ($+8.5$ kHz, mean) is for the offset of the rubidium clock from its nominal frequency of 10 MHz. The associated statistical uncertainty comes from the scatter of the calibrations and the estimated uncertainty allows for environmental differences between use in our apparatus and being calibrated in the caesium-clock laboratory. The estimated contribution in the second line is associated with the correction and with quartz-crystal drift.

The third correction is applied to give an estimate of the mean frequency of the ensemble of five small lasers mentioned above. Frequency comparisons between these lasers[3,4], which include the laser NPL1 used in our measurement, took place over a span of about 12 months, and we restrict the data to those where the lasers were operated using sinusoidal modulation of the cavity length and third-derivative frequency lock. The statistical contribution to the uncertainty reflects the scatter shown in the comparisons, and the estimated one allows for possible offsets in NPL1 when our frequency measurements were made.

Our result for the mean frequency of the ensemble of five lasers is (88, 376, 181, 616 ± 3) kHz, where the uncertainty is derived as the root sum of squares of the components in Table 2 and approximates one standard deviation of the result.

The uncertainty is so much smaller in this measurement than in the previous ones, by more than a factor 10, that it is capable of exposing previously undetectable sources of systematic error. It agrees well with the earlier results[5,6], $+(11 \pm 50)$ kHz and $-(8 \pm 43)$ kHz, respectively, but disagrees with the recent result of Domnin et al.[13], $-(30 \pm 10)$ kHz.

The accuracy of the new methane frequency measurement can in part be transferred to the visible iodine-stabilized lasers at 0.63 μm through the wavelength ratio, determined by Layer et al.[8]. With the latter ratio accurate to ±2 parts in 10^{10}, we arrive at a situation where the frequencies of the key stabilized lasers used in length measurement are measured within about a factor three or four of their reproducibilities.

1. Barger, R. L. & Hall, J. L. *Phys. Rev. Lett.* **22**, 4–8 (1969).
2. *Com. Consult. Definition Metre (Com. Int. Poids Mesures)* 5th Session (1973); 6th Session (1979).
3. Jolliffe, B. W., Kramer, G. & Chartier, J.-M. *IEEE Trans. Instrum. Meas.* **IM-25**, 447–450 (1976).

4. Felder, R., Jolliffe, B. W. & Chartier, J.-M. *Rapport BIPM/79-7* (Bureau International des Poids et Mesures, F-92310 Sèvres, France, 1979).
5. Evenson, K. M., Wells, J. S., Petersen, F. R., Danielson, B. L. & Day, G. W. *Appl. phys. Lett.* **22**, 192–195 (1973).
6. Blaney, T. G., Edwards, G. J., Jolliffe, B. W., Knight, D. J. E. & Woods, P. T. *J. Phys.* D **9**, 1323–1330 (1976).
7. Blaney, T. G. *et al. Proc. R. Soc.* A**355**, 61–68; 89–114 (1977).
8. Layer, H. P., Deslattes, R. D. & Schweitzer, W. G. Jr *Appl. Optics* **15**, 734–743 (1976).
9. Woods, P. T., Shotton, K. C. & Rowley, W. R. C. *Appl. Opt.* **17**, 1048–1054 (1978).
10. Knight, D. J. E. *et al.* in *Proc. 6th Vavilov Conf. on Nonlinear Optics*, Akademgorodok, Novosibirsk, USSR, June 1979 (in the press).
11. Blaney, T. G., Cross, N. R., Knight, D. J. E., Edwards, G. J. & Pearce, P. R. *J. Phys.* D (in the press).
12. Eisenhart, C. *Natn. Bur. Stand.* (*U.S.*), Spec. Publ. 343, 509–518 (1971).
13. Domnin, Yu. S., Koshelyaevskii, N. B., Tatarenkov, V. M. & Shumyatskii, P. S. *Pis'ma v Zh. Eksp. Teor. Fiz.* (*USSR*) **30**, 273–5 (1979).

Soliton formation and *cis trans* isomerization in polyacetylene

James C. W. Chien, Frank E. Karasz & Gary E. Wnek

Department of Polymer Science and Engineering,
Materials Research Laboratory, University of Massachussetts, Amherst,
Massachussetts 01003

Polyacetylene can be synthesized enriched in either *cis* or *trans* structure content through varying the temperature of polymerization[1]. *Cis* rich polyacetylene is readily isomerized to the *trans* configurations by heating[2]. Such polyacetylene contains a large number of unpaired spins[3,4] and the paramagnetism has been attributed to a topological soliton[5], corresponding to a defect in a long-chain polyalkene at which point the Π-wave function amplitude vanishes. Polyacetylene prepared at a low temperature, however, and which has never been exposed to oxygen or subjected to heating and should have a nearly pure *cis* configuration, has been found to lack an EPR signal. We therefore, report here that soliton formation and configurational isomerization are intimately related, and suggest an explanation for both mechanisms.

Acetylene was polymerized as a film at 195 K using the Ti(O − n Bu)$_4$/AlEt$_3$ catalyst[1,7]. The freshly prepared film is about 85–87% *cis* as judged from the absorbances of the *cis* and *trans* IR bands at 750 cm^{-1} and 1,010 cm^{-1}, respectively (% $cis = 130\,A_{cis}/(1.3\,A_{cis} + A_{trans})^1$. The polymer film was cut into
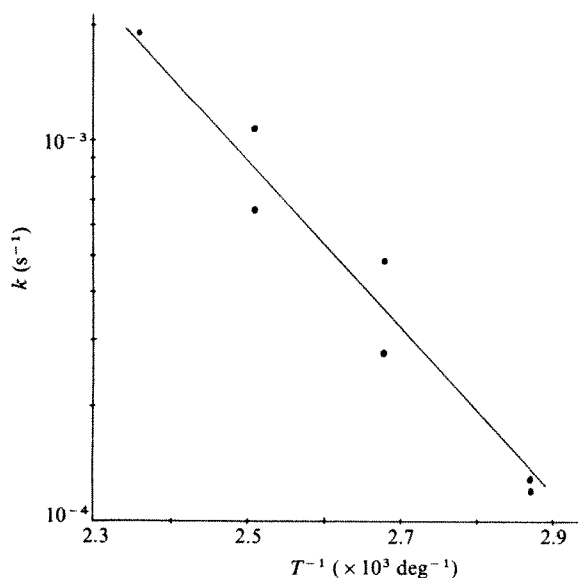
Fig. 2 Arrhenius plot for the rate constant of production of unpaired spins.

strips weighing ~8 mg and transferred to an EPR sample tube which was then capped with a serum stopper and sealed with paraffin wax, all these manipulations being performed in rigorous anaerobic conditions. The EPR signal was monitored with a Varian E-9 X-band spectrometer. By referencing to a specimen of DPPH in the dual cavity one finds a g-value of 2.0022 for the unpaired spin in polyacetylene. Three significant changes are observed on heating: an increase in EPR signal intensity, a decrease in EPR linewidth, and an increase in the *trans* content.

Heating of *cis*-rich polyacetylene resulted in a marked increase in the unpaired spin concentration, [S·], as obtained by double integration of the EPR signal. Examples at two temperatures (Fig. 1) showed that the formation of the soliton obeys first order kinetics. At any given temperature, [S·] reaches a certain steady-state value which is unchanged on standing for a reasonably long period at that temperature, and [S·] does not decrease on cooling the sample. Numerous experiments demonstrated that each incremental temperature of heating results in a new and higher plateau value of [S·]. The apparent first-order rate constants gave a reasonable Arrhenius plot (Fig. 2) and an activation energy of ~10 kcal mol^{-1}.

A mechanism of soliton formation may be proposed. *Cis* polyacetylene has a band gap, E_g, of 2.2 eV, suggesting that the molecule has weakly alternating single and double bonds. X-ray diffraction and packing analysis results[8] are consistent with the following structures:

cis-transoid   /‾_/‾_/‾\   (I)

trans-cisoid   /‾_/‾_/‾_/   (II)

The heavy lines indicate bonds having a length longer than a C=C π-double bond, and the lighter lines are shorter than a C—C σ-single bond. This partial conjugation lowers E_g.

Table 1 Soliton linewidth

Temperature (°C)	25	50	75	100	125	150
ΔH_{pp} During heating	10	7.4	4.8	3.5	1.3	0.7
ΔH_{pp} After cooled to 25°	10	7.6	5.0	4.5	2.0	1.2

Pristine polyacetylene is relatively free from defects and may be thought of having the idealized structure (I). Thermal excitation produces the soliton by bond rehybridizations as shown in Fig. 3a. The indicated shifting of adjacent long and short bonds results in a sequence of *trans*-cisoid segment of structure (II). The formation of such a neutral defect requires a much lower energy, which is estimated to be ~ 0.4 eV (ref. 5), than that required to create a conduction electron or hole, which is $E_g/2$. The lower energy is due to stabilization of the soliton bound hole. As 0.4 eV $= 9.44$ kcal mol^{-1}, the activation energy for the formation of a soliton agrees with the observed activation energy for the increase in [S·].
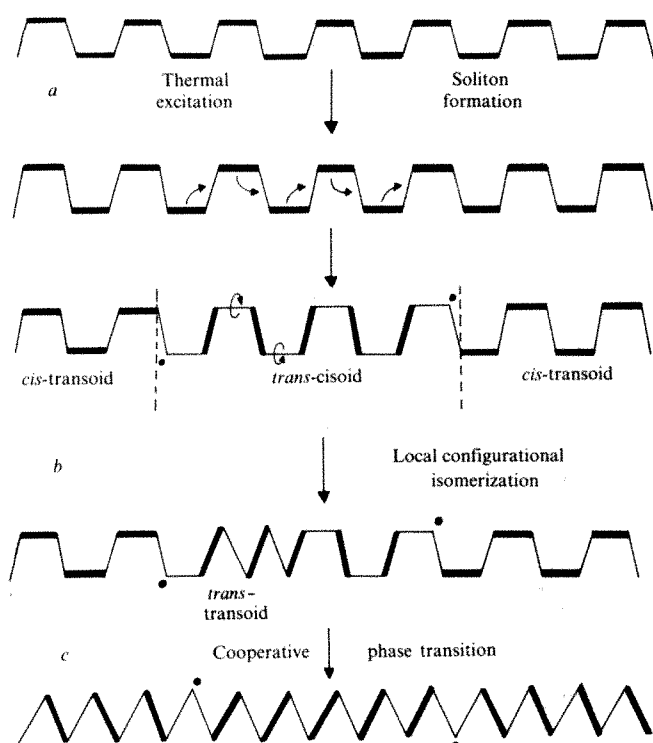
Fig. 3 Formation of neutral soliton and isomerization.

Creation of a soliton is not to be associated directly with configurational isomerization. However, as the defect has a sp^3 free radical-like structure, bond rotation is possible leading to one or more *trans*-transoid units (Fig. 3b). Thus, the *trans* content in polyacetylene should increase with [S·] but not in a linear relationship. Figure 4 shows the relationship between [S·] and the *trans* content, the latter determined by IR immediately following the EPR measurements. *Cis→trans* isomerization does not obey first order kinetics[2]; furthermore, the apparent activation energy estimated from the initial rates varied from 17 kcal mol^{-1} for polymers containing 88% *cis* configuration to 39 kcal mol^{-1} for polymers having 80% *trans* content. This may reflect the sequence lengths of *trans*-transoids being formed. Unfortunately this sequence length cannot be determined from the most intense out-of-plane CH deformation bands as the frequencies for repeat units (*trans* CH=CH$\rightarrow_m$(-cis CH=CH)$_n$ with $m, n = 2$ are estimated to be within a few per cent of long sequences of m and n (ref. 9).

Increase of temperature not only generates more solitons but also produces larger domains of *trans*-cisoid and/or *trans*-transoid units. It follows that the soliton mobility
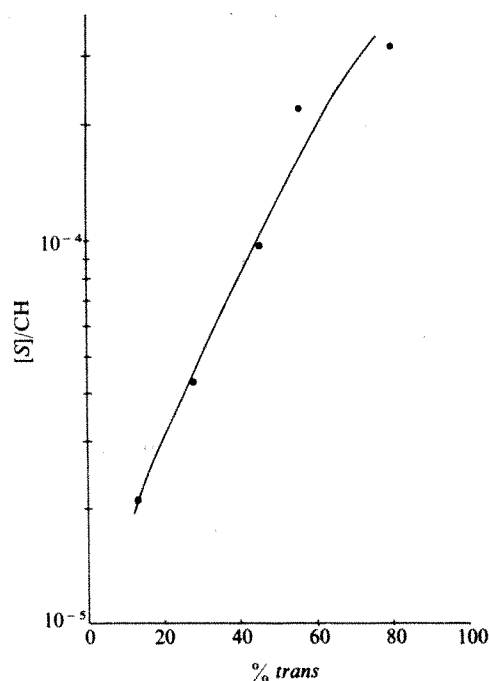
Fig. 4 Plot of unpaired spin concentration versus *trans* content.

(delocalization) is enhanced at elevated temperatures. This is supported by the EPR linewidths (ΔH_{pp} peak-to-peak in G, average of three or more experiments); the data are summarized in Table I. The greater soliton mobility corresponds to narrower linewidth.

In addition to soliton formation and configurational isomerization at intermediate temperatures, there is an irreversible phase transition with a DSC maximum for the exotherm at 145 °C. This transition is absent in those *trans* polyacetylenes synthesized at >150 °C. During this transition, the *trans*-cisoids and short sequences of *trans*-transoids are converted to the predominantly *trans* zigzag structure, probably via a cooperative crank shaft type of motion (Fig. 3c). The phase transition is accompanied by changes in the major d-spacing in X ray diffraction from $2\theta = 23.15°$ for *cis* polyacetylene to 24.0–25.0° for *trans* polyacetylene[1]. There is even a 20% increase in length of polyacetylene specimen held under tension with heating which occurs at the temperature range corresponding to the DSC exotherm (H. Skirakawa, personal communication).
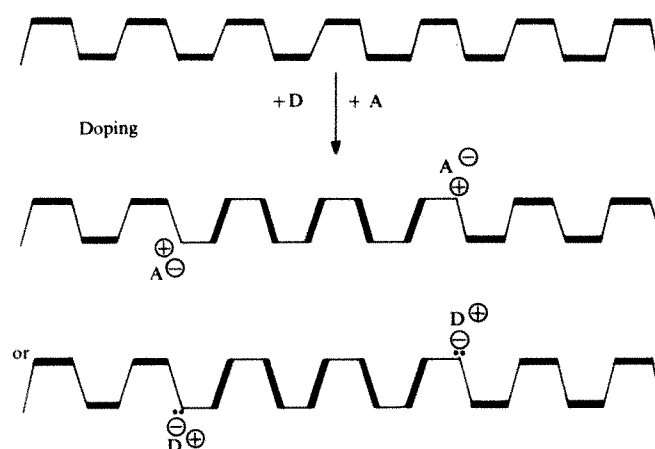
Fig. 5 Generation of charged soliton by doping.

The mechanism proposed above is also pertinent to the conversion of wide band gap semiconducting polyacetylene to highly conducting material by doping[10]. Figure 5 shows that the introduction of appropriate dopants (A for acceptor and D for donor) produces charged solitons; at low temperatures, conversion of cis-transoid to other configurations can occur as in the previous case of a neutral soliton. A semiconductor-to-meal transition occurs when the charged carrier concentration exceeds the critical value.

We thank Professor A. J. Heeger for helpful discussions, J. D. Capistran for sample preparation, and the Advanced Research Project Agency for support.

1. Ito, T., Shirakawa, H. & Ikeda, S. *J. Polym. Sci. Polym. Chem. Edn* **12**, 11 (1974).
2. Ito, T., Shirakawa, H. & Ikeda, S. *J. Polym. Sci. Polym. Chem. Edn* **13**, 1943 (1975).
3. Shirakawa, H., Ito, T. & Ikeda, S. *Makromolec. Chem.* **179**, 1565 (1978).
4. Goldberg, I. B., Crowe, H. R., Newman, P. R., Heeger, A. J. & MacDiarmid, A. G. *J. chem. Phys.* **70**, 1132 (1979).
5. Su, W. P., Schrieffer, J. R. & Heeger, A. J. *Phys. Rev. Lett.* **42**, 1698 (1979).
6. Chien, J. C. W., Karasz, F. E., Wnek, G. E., MacDiarmid, A. G. & Heeger, A. J. *J. Polym. Sci. Polym. Lett. Edn* **18**, 45 (1979).
7. Karasz, F. E. *et al. Nature* **282**, 286 (1979).
8. Baughman, R. H., Hsu, S. L., Pez, G. P. & Signorelli, A. J. *J. chem. Phys.* **68**, 5405 (1978).
9. Shirakawa, H. & Ikeda, S. *Polym. J.* **2**, 231 (1971).
10. Chiang, C. K. *et al. J. Am. chem. Soc.* **100**, 1013 (1978).

New gas phase inorganic ion cluster species and their atmospheric implications

T. D. Märk*, K. I. Peterson & A. W. Castleman Jr

Department of Chemistry and Chemical Physics Laboratory, CIRES, University of Colorado, Boulder, Colorado 80309

Recent experimental observations in our laboratory, with high pressure mass spectrometry, have revealed the existence of previously unreported species involving water clustered to sodium dimer ions, and alkali metal hydroxides clustered to alkali metal ions. We discuss here the important implications of these results concerning the existence of such species, and how from a practical aspect they confirm the stability of certain cluster species proposed by Ferguson[1] to explain masses recently detected at upper altitudes using mass spectrometric techniques.

Arnold et al.[2] reported unusual ion masses at altitudes between 37 and 56 km based on rocket-borne mass spectrometric techniques. These ions, NPH (non-proton hydrates), are listed in Table 1. The original suggestion by Arnold et al.[2] that these might be protonated formaldehyde has been discounted[3]. Later measurements[4] again led to observations of known proton hydrates (PH) as well as the NPH ions. Additional NPH ions of higher masses were also reported. These ions were proposed to have the general form $H^+X(H_2O)_n$ and to result from reactions of PH ions with an unknown stratospheric gas X. Acetonitrile (CH_3CN) was tentatively suggested by the authors[4] as being a possible candidate to explain mass X.

More recently, Ferguson[1] stated that it is difficult to accept acetonitrile as a candidate to explain the NPH ion species and speculated that they might rather be protonated sodium hydroxide cluster ions of the form $NaOH_2^+(H_2O)_n(NaOH)_m$. Values of n from 0 to 4, and m from 0 to 2 allow an interpretation of all seven of the unidentified NPH masses reported by Arnold et al.

Arijs et al. (ref. 5) have also reported positive ion

*Permanent address: Institut für Experimentalphysik, Leopold-Franzens-Universität, A-6020 Innsbruck, Austria.

Table 1 Mass spectra of NPH-ions observed in the stratosphere[2,4,5] and ion identifications given by Ferguson[1]

Observed	Proposed NaOH ion clusters[1]	Proposed KOH ion clusters[1]
$42 \pm 2\,(2)$ $43 \pm 3\,(5^*)$	$41\,NaOH_2^+$	
$60 \pm 2\,(2, 5^*)$	$59\,NaOH_2^+ \cdot H_2O$	$57\,KOH_2^+$
$78 \pm 1\,(4)$ $78 \pm 2\,(5^*)$	$77\,NaOH_2^+ \cdot 2H_2O$	$75\,KOH_2^+ \cdot H_2O$
$80 \pm 2\,(2)$ $82 \pm 2\,(5^*)$	$81\,NaOH_2^+ \cdot NaOH$	
$96 \pm 1\,(4)$ $96 \pm 2\,(5^*)$	$95\,NaOH_2^+ \cdot 3H_2O$	$93\,KOH_2^+ 2H_2O$
$99 \pm 2\,(5^*)$ $100 \pm 1\,(4)$	$99\,NaOH_2^+ \cdot NaOH \cdot H_2O$	
$114 \pm 2\,(4)$	$113\,NaOH_2^+ \cdot 4H_2O$	$111\,KOH_2^+ \cdot 3H_2O$ $113\,KOH_2^+ \cdot KOH$
$118 \pm 1\,(4)$	$117\,NaOH_2^+ \cdot NaOH \cdot 2H_2O$	$129\,KOH_2^+ \cdot 4H_2O$
$136 \pm 2\,(4)$ $140 \pm 2\,(4)$	$135\,NaOH_2^+ \cdot NaOH \cdot 3H_2O$ $139\,NaOH_2^+ \cdot 2NaOH \cdot H_2O$	$131\,KOH_2^+ \cdot KOH \cdot H_2O$

Numbers given in parentheses are references.
*E. Arijs, personal communication to E. Ferguson (see ref. 1).

measurements based on balloon-borne mass spectrometry (see Table 1). These were made at 35 km elevation after sunset. In addition to observing the normal proton hydrate ions, they reported other ions which correspond in mass to those proposed by Ferguson as being proton hydrates of sodium hydroxides and related higher-order clusters.

Although the proposed identification by Ferguson has been accepted as a likely explanation for the atmospheric observations, as far as we know no evidence of the stability of such higher order clusters involving sodium hydroxide has been given from laboratory experiments. Recent observations in our laboratory confirm not only the existence of alkali metal hydroxides clustered to alkali metal ions but also demonstrate their stability in the presence of water vapour. Proof of the latter fact is crucial in the atmospheric interpretation given by Ferguson. We report some masses which represent other types of inorganic cluster species not previously published.

A high pressure mass spectrometric technique developed[6–8] in our laboratory, with a thermionic source, was used to study the three alkali metal ions, sodium, potassium and lithium, clustered with water vapour. These studies were conducted over the temperature range 200–400 °C and at pressures of CO_2 carrier gas corresponding to 5–40 torr; the water concentrations ranged from a few hundredths to $\sim 1\%$.

Clusters observed in experiments using a sodium ion filament are shown in Table 2, along with proposed identifications. For certain masses greater than 80, an uncertainty arose in assigning their identity because of possible contamination from other species which had been previously present in the apparatus. In particular, some months ago the clustering of dimethoxyethane (DME) to sodium had been studied, and acetone had also been used in certain experiments. Although we believed that these species had been suitably removed by baking and evacuating the system for long periods of time, their presence could not be totally discounted. Therefore, to assist in the identification of these masses and to establish further their assignment as cluster species involving hydroxides, and even the dimers of the alkali metal ions, similar experiments with other alkali metal thermionic sources were made. Especially important were experiments conducted with lithium. Identification of the lower masses of lithium-containing species was unambiguous and

consequently we could make definite assignments with regard to the sodium (and the potassium) system from the results. First, lithium should bond even more strongly with acetone than would sodium. Therefore, failure to detect mass 65 ($Li^+ \cdot$ acetone) in the lithium experiments enabled mass 81 in the sodium work to be attributed to $NaOH_2^+$ (NaOH). Second, results with lithium revealed a peak at mass 31 and mass 49. Neither could arise from impurities in the apparatus and confirmed the formation of $Li^+ \cdot LiOH$ (31) and $LiOH_2^+ \cdot LiOH$ (49).

These results are especially exciting as they confirm the formation and, indeed, the stability of ions involving alkali metals co-clustered with both their corresponding hydroxides, and at the same time water. Another important finding is that the dimer ion of sodium clustered with one water molecule can form in the high pressure reaction source. As seen in Table 2, mass 64 could not be attributed to an impurity and is identified as $Na_2^+ (H_2O)$. No higher-order clusters of water about Na_2^+ exist. A related interesting aspect of the results is that no mass 32 ($Li_2^+ \cdot H_2O$) is formed; the first cluster containing two lithium atoms has an attached OH group rather than an H_2O molecule. The reaction of the alkali metal dimer ion with one water molecule is apparently exothermic for the case of lithium to form $Li^+ \cdot LiOH$, but requires the addition of a second water molecule in the case of sodium and potassium. This interpretation implies that the bond energy between an alkali metal ion and its corresponding hydroxide is relatively large. Based on thermochemical considerations, the findings indicate that the values exceed $\sim 2eV$; this is in accord with expectations considering the large dipole moments of the alkali hydroxides. Clearly, these results experimentally confirm the suggested interpretation of the atmospheric measurements[1]. Note that solely on a mass basis an alternative interpretation of the NPH ions observed in the stratosphere would be sodium chloride cluster ions of the form $Na^+ (NaCl)_x (H_2O)_y$. Values of x from 0 to 2, and y from 0 to 5 allow an assignment for all NPH ions reported. Experiments are in progress in our laboratory to investigate the possibility of the proposed switching reactions and the bond energies for the species identified in this study.

Table 2 Ion clusters observed in high pressure mass spectrometric studies* of sodium utilizing a thermionic source||

Mass	Proposed identification	Mass	Proposed identification
23	Na^+	113	$Na^+ (DME)$
41	$Na^+ (H_2O)$		$Na^+ (H_2O)_5$
59	$Na^+ (H_2O)_2$	117	$NaOH_2^+ (NaOH) \cdot (H_2O)_2$
64†	$Na_2^+ (H_2O)$	121	$Na^+ (H_2O)_3 \cdot (CO_2)$
67	$Na^+ (CO_2)$	131	$Na^+ (DME) \cdot (H_2O)$
77	$Na^+ (H_2O)_3$		$Na^+ (H_2O)_6$
81‡	$NaOH_2^+ (NaOH)$	135	$NaOH_2^+ (NaOH) \cdot (H_2O)_3$
85	$Na^+ (H_2O) \cdot (CO_2)$	139	$Na^+ (H_2O)_4 (CO_2)$
95	$Na^+ (H_2O)_4$		$[NaOH_2^+ (NaOH)_2 \cdot (H_2O)]§$
99	$NaOH_2^+ (NaOH) \cdot (H_2O)$	143	$NaOH_2^+ (NaOH) \cdot (H_2O) \cdot (CO_2)$
103	$Na^+ (H_2O)_2 \cdot (CO_2)$	149	$Na^+ (DME) \cdot (H_2O)_2$
111	$Na^+ (CO_2)_2$		$Na^+ (H_2O)_7$

*Experiments were also made with argon and nitrogen as carrier gas, and with deuterated water, to confirm the mass identifications.

†It is unlikely that the observed mass 64 is due to Na^+ attached to an impurity of mass 41 as we would then also expect to see $Na^+ (41)(H_2O)$ of mass 82.

‡Corresponds in mass to $Na^+ \cdot$ acetone. This possibility was discounted on the basis of experiments with lithium where no mass 65 ($Li^+ \cdot$ acetone) was detected.

§A possible contributor to the more predominant species involving water and carbon dioxide.

||Present studies.

1. Ferguson, E. E. *Geophys. Res. Lett.* **5**, 1035 (1978).
2. Arnold, R., Krankowsky, D. & Marien, K. H. *Nature* **267**, 30 (1977).
3. Fehsenfeld, F. C., Dotan, I., Albritton, D. L., Howard, C. J. & Ferguson, E. E. *J. geophys. Res.* **83**, 1333 (1978).
4. Arnold, R., Böhringer, H. & Henschen, G. *Geophys. Res. Lett.* **5**, 653 (1978).
5. Arijs, E., Ingels, J. & Nevejans, D. *Nature* **271**, 642 (1978).
6. Castleman, A. W. Jr, Holland, P. M., Lindsay, D. M. & Peterson, K. I. *J. Am. chem. Soc.* **100**, 6039 (1978).
7. Castleman, A. W. Jr *Kinetics of Ion Molecule Reactions* (ed. Ausloos, P.) (Plenum, New York, 1979).
8. Castleman, A. W. Jr *Advances in Colloid and Interface Science* Vol. 10 (ed. Zettlemoyer, A.) 73 (Elsevier, Oxford, 1979).

Heat flow in the Mesozoic and Cenozoic

Donald Sprague & Henry N. Pollack

Department of Geological Sciences, The University of Michigan, Ann Arbor, Michigan 48109

The present-day heat flow from the Earth has commonly been used to estimate the abundance of heat-producing isotopes within the Earth. However, if heat flow has a variability on a short time scale (compared with the isotopic decay times), then the present-day heat flow must be seen as a much coarser measure of the Earth's heat-producing isotopic content. We report here the results of an investigation into the likely variation in terrestrial heat flow over the past 180 Myr.

The empirical relationships between the terrestrial heat flux and the age of oceanic crust or the age of last tectonothermal mobilization of continental crust[1,2] (Fig. 1) can be used to estimate the global heat flux, provided the age distribution of the crust is known[3]. Various recent estimates[4-6] of the present-day mean terrestrial heat flow fall in the range 81 ± 3 mW m^{-2}. We present here a probabilistic model of crustal age distributions and heat flow from the present to the early Mesozoic. The model is based on the present-day distribution of crustal ages (see Table 1) and an estimate of the probability that crust produced or tectonothermally mobilized at an earlier time will have survived to the present day.

To determine the age distribution of the oceanic crust at a past time t, oceanic lithosphere which accreted between time t and the present must be subtracted from the present-day distribution, and lithosphere which has been subducted in the same interval must be reinstated; the age of the resurrected lithosphere is, however, uncertain, and must be estimated.

We define an age distribution at time t according to $Q_s(t,\tau)d\tau = Q_0(\tau)d\tau \cdot P_s(t,\tau)$, where $Q_s(t,\tau)d\tau$ is the area of crust of age τ surviving at time t. $Q_0(\tau)d\tau$ is the original area of crust accreted along oceanic ridges at time τ in the time interval $d\tau$, and P_s is a survival probability function giving the probability that crust accreted at time τ survives (has not been subducted) at the later time t. If the total area of oceanic crust is at all times constrained to be equal to the present-day area A_0, then production and survival can be related by

$$P_s(t,\tau) = 1 - \left[\frac{\int_t^\tau Q_0(\tau)d\tau}{\alpha A_0} \right]^{1/(\alpha - 1)}$$

in which α is the number of present-day oceanic areas produced by ocean ridge accretion during the past 180 Myr. The mean accretion rate over this period is therefore $\alpha A_0/180$. As the area of ocean accreted between times τ and t increases, the survival probability decreases, finally becoming zero. The original area accreted at time τ is estimated from the

Table 1 Percentage of global area represented by crust of indicated age

Ocean		Continent	
Age (Myr)	%	Age (Myr)	%
0–5	3.5	0–65	4.6
5–23	10.9	65–225	5.8
23–38	6.9	225–400	9.2
38–65	10.2	400–600	9.1
65–100	21.2	600–2,500	7.7
100–135	5.4	2,500–3,500	2.0
135–180	3.5		
Total	61.6		38.4

Continental shelves are included as continents of early and late Palaeozoic age.

present-day crustal distribution $Q_s(0, \tau)d\tau$ by $Q_0(\tau)d\tau$ $= Q_s(0, \tau)d\tau/P_s(0, \tau)$. As crust older than any now present (> 180 Myr) is needed to complete the ocean floor, the mean of $Q_0(\tau)$ from 180 Myr to the present is used.

The form of $P_s(t, \tau)$ is an arbitrary choice. We have tried other smooth, monotonically decreasing functions which satisfy the constraint that the accretion–subduction process yields the present-day area A_0. We find that the heat flow history is much more strongly dependent on the mean accretion rate, that is the choice of α, than on the particular functional form of P_s.

Tectonic processes affecting continents are significantly different from oceanic processes. While there is an increasing probability that old ocean crust will not survive, the same cannot be said for old continental crust. In fact, the survival of extensive areas of continental crust for more than 3,000 Myr testifies to the contrary. Old continental lithosphere is cool, thick, strong and refractory, and moreover tends to be centrally located in continental masses and is thus less frequently affected by plate margin interactions. Accordingly, we have assigned to continental areas a probability of tectonothermal remobilization that decreases exponentially with time since the previous mobilization. In contrast to old crust, recently mobilized continental crust has a high probability of being remobilized, for example in terrains above long-lived subduction zones. Another consideration is that continental mobilizations are not independent of oceanic accretion rates. Intervals of fast accretion must be accompanied by increased subduction with concomitant effects on continental margins. Formally, the calculation of area of continental crust of age τ at time t takes the form $Q_c(t, \tau)d\tau = \beta Q_0(\tau)\exp[-(\tau - t)/t_c]d\tau$, where the constants β and t_c are
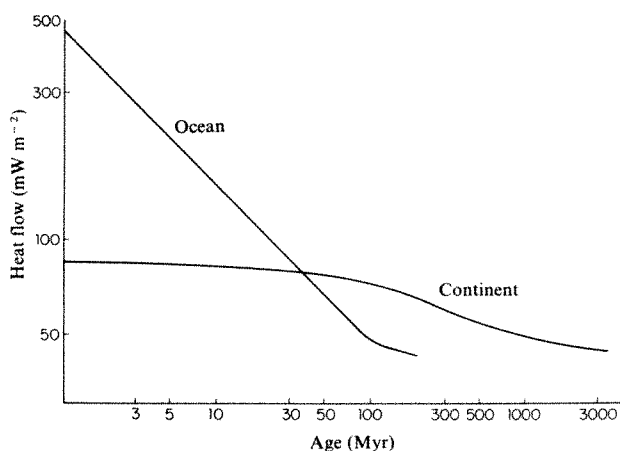
Fig. 1 Heat flow versus age relationships for oceans[1] and continents[2].

evaluated by the requirement that Q_c yield the present-day areas of Cenozoic and Mesozoic terrains. The values of β and t_c so determined are 0.15 and 100 Myr, respectively. The constant t_c is the time constant for the decay of probability of continental remobilizations.

The heat flow in both oceanic and continental regions can thus be calculated from the age distributions $Q_s(t, \tau)$ and $Q_c(t, \tau)$, and the empirical heat flow–age relationships of Fig. 1. An infinite set of possible models obtains in principle from the inherent variability allowed by the relationship between the production rate of oceanic crust and its subsequent probability of survival. All such models yield the present-day distribution of ages (Table 1) and hence the present-day distribution of oceanic heat flow. In application, however, practical constraints such as past spreading rates as deduced from marine magnetic anomalies limit the allowable models to the range $1.5 < \alpha < 3.5$. Our preferred model, shown in Fig. 2 and for which $\alpha = 2.4$, in addition correctly predicts the present-day mean age of subducting crust, 77 Myr. For the range of α cited above, the mean age of subduction ranges from 111 to 60 Myr, thus providing a moderately sensitive guide to the choice of a proper α and a preferred model.
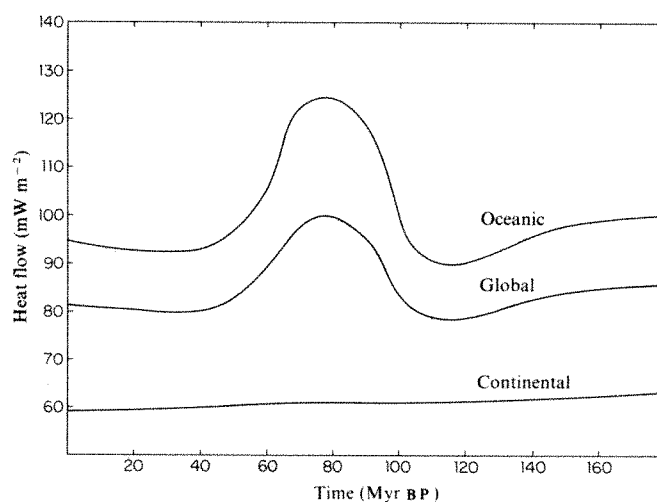
Fig. 2 Variability of mean oceanic, continental and global heat flow over the past 180 Myr.

The mean accretion rate over the past 180 Myr for this model is such that in that interval 2.4 times the present oceanic area has been produced, of which 1.4 has been subducted. Numerically this mean accretion rate is $1.33\% A_0$ Myr^{-1}, slightly above but comparable with estimates of the present-day accretion rate of 0.91–$1.14\% A_0 \mathrm{Myr}^{-1}$. (The lower value is derived from 'present-day' relative rotation vectors for the world plate system[7]; the upper value is derived from the amount of ocean floor produced in the past 5 Myr.) As shown in Fig. 2, the global heat flux varies between 78 and 101 mW m^{-2}, although for all but 40 Myr the heat flow is within ± 5 mW m^{-2} of the 81 mW m^{-2} present-day flux. The mean of the global heat flow over the 180 Myr interval is 85 mW m^{-2}, slightly above the present-day value. The principal feature of the heat flow history is the peak occurring in the late Cretaceous fast spreading episode; the minimum heat flow occurred in the early Cretaceous just before the opening of the South Atlantic Ocean. Clearly, nearly all of the variation in the global heat flux is due to the oceanic component. This results because of the greater area of ocean, the more extreme variation of heat flow with age in the oceans, and the greater impact of variations in oceanic accretion rate on oceanic heat flow than on continental heat flow.

We conclude that heat flow over the past 180 Myr has been in the range 78–101 mW m^{-2}. Throughout most of this period the heat flow was close to the present-day value of 81 mW m^{-2}; the only significant departure was the increase to the peak value of 101 mW m^{-2} during the rapid seafloor spreading of the late Cretaceous. The mean heat flow over the 180 Myr interval is 85 mW m^{-2}, somewhat in excess of the present-day vaue.

This research was supported in part by the Division of Earth Sciences, NSF, under grant EAR 78-09131.

1. Parsons, B. & Sclater, J. G. J. geophys. Res. 82, 803–827 (1977).
2. Chapman, D. S. & Furlong, K. EOS Trans. Am. geophys. Un. 58, 1240 (1977).
3. Chapman, D. S. & Pollack, H. N. Earth planet. Sci. Lett. 28, 23–32 (1975).
4. Williams, D. L. & Von Herzen, R. P. Geology 2, 327–328 (1974).
5. Sclater, J. G., Jaupart, C. & Galson, D. Rev. geophys. Space Phys. 18, 269–311 (1980).
6. Davies, G. Rev. geophys. Space Phys. (in the press).
7. Minister, J. B. & Jordan, T. H. J. geophys. Res. 83, 5331–5354 (1978).

Cambrian stromatolitic phosphorites from the Georgina Basin, Australia

P. N. Southgate

Research School of Earth Sciences, Australian National University, PO Box 4, Canberra, ACT 2600, Australia

The first details of Phanerozoic stromatolitic phosphorites are reported here. The stromatolites, from the Thorntonia Limestone in the Georgina Basin, northern Australia are of middle Cambrian age. The carbonates interfinger with and underlie the Beetle Creek Formation which contains Australia's largest known phosphate deposits. Phosphatic stromatolites had previously only been found in Proterozoic rocks, from the middle to upper Riphean Aravalli Group of Rajasthan, India and in the USSR and China[1]. It was generally considered that phosphatic stromatolites were unique to the Precambrian[2,3]. Indeed this unique association had led to hypotheses that during the Precambrian a different set of phosphogenic processes must have existed[4].

The Georgina Basin is a large epicontinental basin dominated by platform carbonates ranging in age from the early middle Cambrian to the middle Ordovician. On a regional scale the middle Cambrian sequence represents a complex facies mozaic consisting of carbonates, evaporites, phosphorites and terrigenous clastics (Fig. 1). The early middle Cambrian transgression is represented by a basal clastic interval which overlies the Precambrian basement. This interval is overlain by the Thorntonia Limestone and its lateral facies equivalents. The stromatolites occur in the Thorntonia Limestone; a carbonate unit consisting of stylolitic vuggy recrystallized dolomite and dolomitic limestone of Ordian to Templetonian age[5]. Minor diastems are common throughout the unit occurring as scalloped surfaces[6] and as phosphatized hardgrounds which were emergent for brief periods. The phosphatized stromatolites overlie minor dissolution surfaces and hardgrounds.

Although stromatolites occur at various localities within the Georgina Basin[7], phosphatic stromatolites are only known within 1–4 m thick discontinuous stromatolitic beds, ∼ 10 km south of Riversleigh Station (Fig. 1). Preservation of algal laminae and internal fabric is variable and depends on the type of replacement. Silicification and particularly dolomitization obscure the primary algal structure but where

stromatolites are phosphatic both columnar and laminar form are preserved.

Phosphatic stromatolitic columns up to 4 cm high or phosphatic cryptalgalaminite up to 5 cm thick are found overlying minor dissolution surfaces within the Thorntonia Limestone. Phosphatic laminae up to 2 mm thick occur discontinuously near the basal parts of the stromatolites and immediately overlying minor erosional surfaces within the stromatolitic bioherms. Chert-replaced laminae are not related
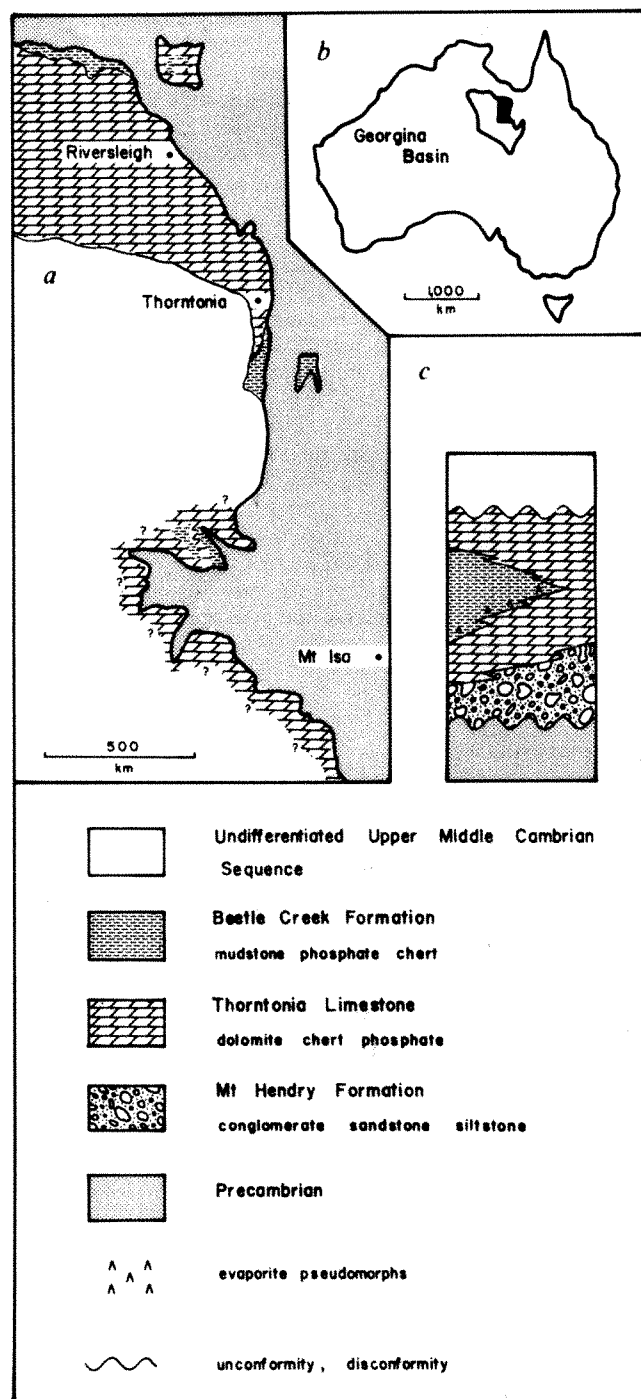
Fig. 1 *a*, map showing the northeastern margin of the Georgina Basin and the close lateral relationship between outcrop of Thorntonia Limestone and Beetle Creek Formation. *b*, Location map for the Georgina Basin, the north-east portion shown in *a*. is shaded. *c*, Generalized stratigraphic column for the lower middle Cambrian sequence of the northeastern Georgina Basin.

to minor erosional surfaces or diastems and occur randomly throughout the dolomitized parts of the stromatolites. Phosphatic stromatolites, consisting of not less than 90% collophane are generally thinnest at the base and thicken upwards. Elongate inclined columns occur as LLH-S and SH forms[8]. Columns overlie a phosphatic planar algal mat characterized by fine laminoid fenestrae (Fig. 2). The basal 0.5–2 cm of columns consist of phosphatic mat with laminae parallel to the underlying planar mat. These basal parts form low ridges which are wrapped around and overlain by a convex-upward lamination defining SH-C and V growth forms. Similar ridge and rill structures have been described from the lower intertidal zone at Shark Bay[9] and form when the planar mat is partly eroded. Ridges form where mat remains, and rills form where the mat is eroded. Later mat growth occurs preferentially on ridge tops and sides resulting in the columnar forms. Inclined and vertical stromatolites, circular in plan, occur both as single columns and laterally linked forms in the Thorntonia Limestone. Branching is present in both elongate and circular stromatolites.

Fine laminoid irregular fenestrae, now filled with dolomite occur in both columns and planar mat. Some enlarged fenestrae have several straight edges with angular relationships between the edges. As well as enlarged and fine laminoid irregular fenestrae there are slender slit-like lenticular, blocky and twinned crystal shapes and dolomite rhombs within the phosphatic columns and mat. The elongate crystal shapes are in vertical to sub-horizontal orientations. Some crystal shapes preserve remnants of a right angle cleavage and twinned crystals are characterized by re-entrant angles suggestive of former gypsum twins within the algal mats. Where angular relationships can be shown not to be due to early dolomite growth enlarged fenestrae are taken to indicate early sulphate mineral growth in fenestral voids, the displacive and/or replacive sulphate growth enlarge the fenestrae once the initial void has been filled (B. Radke, personal communication).

Whereas columnar stromatolites are phosphatic, intercolumn areas are non phosphatic, consisting of equant recrystallized dolomite with limonite present along grain boundaries. No phosphate replacement of carbonate grains or cement has been seen in intercolumn areas; the only phosphate present occurs as reworked grains of phosphatic skeletal sponge spicules and trilobite debris, as well as ovules, and internally laminate clasts of eroded phosphatic algal mat. Some skeletal grains of uncertain origin are outlined by micritic envelopes which enclose equant recrystallized dolomite. Phosphatic clasts and ovules are angular to well rounded with carbonate inclusions. Ghosted, non-phosphatic peloids are also present between columns as are sporadic glauconite grains. Ghost textures in recrystallized intercolumnar areas indicate that infills were probably either skeletal grainstone or packstone.

As shown in Fig. 1, the Thorntonia Limestone interfingers with the Beetle Creek Formation which consists of siltstone, phosphate and chert. The phosphate deposits of the Georgina Basin consist mostly of grainstone phosphate with minor microsphorite[7,10]. Consequently the locations of phosphate deposits mark sedimentary traps in which grains have accumulated. It follows that these grains may have been derived from a nearby source where phosphatization took place. The recognition of phosphatic stromatolites within the contemporaneous Thorntonia Limestone indicates that *in situ* phosphatization indeed took place in this limestone unit. Erosion of stromatolites is one possible source of phosphatic grains. Phosphatized hardgrounds (P.N.S. in preparation) have also been found in the Thorntonia Limestone further indicating the potential of this formation as a possible source for the grains of phosphate.

There are many similarities between Thorntonia Limestone phosphatic stromatolites and those reported from Rajasthan, India[2,3]. Collenia LLH, cryptozoan SH and oncolitic SS forms as well as Conophyton are documented from Indian
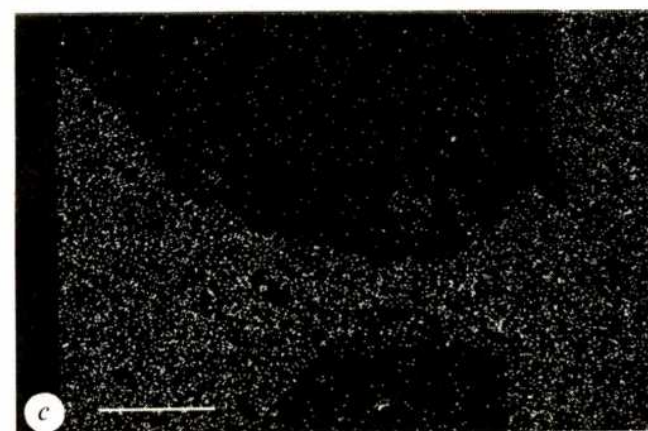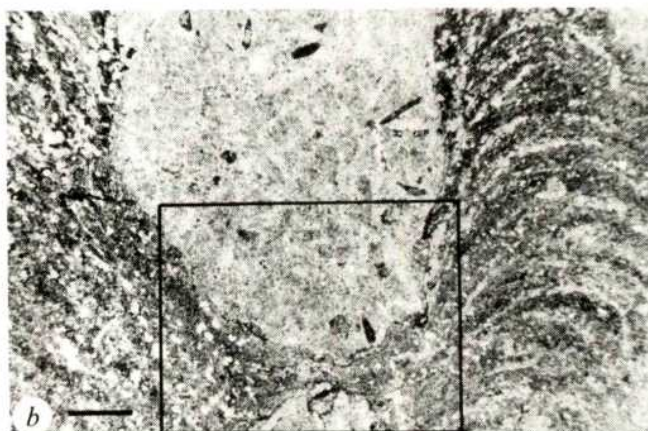
Fig. 2 *a*, Elongate, inclined LLH-S and SH columns and cryptalgalaminite. Dark areas within the phosphatic stromatolites are dolomite filled fenestrae. White specks within intercolumnar areas of dark grey dolomite are phosphate grains. Scale bar, 1 cm. *b*, Transmitted light photomicrograph of an intercolumnar area surrounded by phosphatic columnar stromatolites. Light areas outlining the algal laminations are fine laminoid fenestrae. Several phosphate grains are present in the intercolumnar area (see *c*). Scale bar, 1 mm. *c*, X-ray mapping photograph of distribution of phosphate within the area outlined in *b*. Note the concentration of phosphate (white specks) within the algal laminate parts. Also the presence of several phosphate grains within the intercolumnar area, particularly in the middle centre and middle left of the photograph. Scale bar, 1 mm.

occurrences[2,3]. Thorntonia Limestone stromatolites consist of LLH-S and SH-V and C growth forms. Phosphatic oncolites have not been found in the Thorntonia Limestone; Conophyton is not known from the Phanerozoic. The Indian and Australian examples are characterized by rapid variations in bioherm thickness along the strike; in the same bioherm completely, partially and non-phosphatic stromatolites are found only a few metres apart. Both occurrences are characterized by a marked localization of phosphate; only algal laminated rocks are phosphatic and intercolumnar areas are always non phosphatic, apart from scattered reworked phosphate grains and clasts. No reason is given for the variations in phosphate content of Indian stromatolites but those from the Georgina Basin seem to be related to underlying or adjacent dissolution surfaces or diastems.

The presence of scalloped surfaces, ridge and rill structures, inclined columns, ? sulphate pseudomorphs and enlarged fenestrae are all consistent with a shallow water to semi-emergent environment of deposition of Thorntonia Limestone phosphatic stromatolites. Furthermore the occurrence of fine laminoid fenestrae indicates that the phosphatic algal mat may be smooth mat, a mat type characteristic of the lower intertidal zone[9]. Similarly, Indian examples are thought to form in shallow water conditions, possibly in lagoons and on tidal flats[2,3].

The association between phosphatic stromatolites and features indicative of semi-emergent conditions of sedimentation are particularly significant. The reworked clasts of phosphatic cryptalgalaminite clearly show that the stromatolites were either originally phosphatic or phosphatized as a syn-sedimentary event. The close spatial association between phosphatic stromatolites and scalloped or dissolution surfaces is also important, for even though the stromatolite bioherm may be up to 4 m thick, only where algal growth is adjacent to an erosion surface are the stromatolites phosphatic. This relationship suggests that very specific physical and/or chemical conditions are necessary for the formation of phosphatic stromatolites. The nature of these conditions is still being investigated: however, the irregular relief provided by dissolution surfaces would have resulted in the formation of intertidal pools. Stromatolites growing in these pools may have been periodically subjected to unusual or stressed chemical conditions, as both the water level and temperature varied and it may have been this stressed environment which created the appropriate physicochemical conditions for the formation of phosphatic stromatolites.

I conclude that the Georgina Basin phosphatic stromatolites and associated sedimentary structures show clear evidence of having formed in very shallow to semi-emergent environments and, furthermore, indicate that phosphatic stromatolites are not a uniquely Precambrian phenomenon.

1. Bushinskii, G. I. in *Deltaic and Shallow Marine Deposits* (ed. Van Straaten, L. M. J. U.) 62–70 (Elsevier, Amsterdam, 1964).
   Bushinskii, G. I. *Old phosphorites of Asia and their Origin* (translation from *Trans. Akad. Nauk SSSR, Moskva*, No. 149) (Jerusalem, Israel Programme for Scientific Translation, 1969).
2. Banerjee, D. M. *Bull. geol. Soc. Am.* **82**, 2319–2330 (1971).
3. Sant, V. N. in *Proterozoic and Cambrian Phosphorites* Rept on 1st Int. Meeting of IGCP, Project 156 (eds Cook, P. J. & Shergold, J. H.) 39–40 (ANU, Canberra, 1979).
4. Burnett, W. C. & Sheldon, R. P. (eds) *Report on the Marine Phosphatic Sediments*, 43 (Workshop, Honolulu Hawaii, East-West Centre 1979).
5. Shergold, J. H. & Druce, E. C. *Proc. 3rd Aust. Geol. Conv.*, Townsville (1978).
6. Read, J. F. & Grover, G. A. *J. Sed. Petrol.* **47**, 956–972 (1977).
7. de Keyser, F. & Cook, P. J. *Bur. Miner. Res. Bull.* **138**, 79 (1972).
8. Logan, B. W., Rezak, R. & Ginsburg, R. N. *J. Geol.* **72**, 68–83 (1964).
9. Logan, B. W., Hoffman, P. & Gebelein, C. D. in *Evolution and Diagenesis of Quaternary Carbonate Sequences, Shark Bay, Western Australia*, 190–194 (AAPG Mem 22, 1974).
10. Russell, R. T. & Trueman, N. A. *Econ. Geol.* **66**, 1186–1214 (1971).

Late Tertiary hominoids and human origins

Henry M. McHenry
Department of Anthropology, University of California, Davis, California 95616

Robert S. Corruccini
Department of Anthropology, Southern Illinois University, Carbondale, Illinois 62901

There are two principal hypotheses about the time of the emergence of the Hominidae, the family that includes man: first, the hominid lineage emerged before 16 Myr ago[1-4]; or second, living apes and man are so similar genetically that they must have diverged later[5], perhaps as late as 5 Myr ago[6,7]. The first hypothesis is supported primarily by fossil evidence, whereas the second is championed by advocates of the molecular clock[6,7]. Hominid fossils are abundant back to 3.7 Myr (*Australopithecus afarenesis*)[8] but are rare before that. *Ramapithecus* (16–8 Myr) was once classified as a member of Hominidae, but recent discoveries and interpretations show that it should be placed in its own family, Ramapithecidae[9,10]. Two fossil specimens classified as members of Hominidae predate *A. afarensis*, however: a lower molar from Lukeino in central Kenya dating to 6.5 Myr (KNM-LN 335)[11] and a mandibular fragment from Lothagam Hill in north Kenya dated at 5–5.5 Myr (KNM-LT 329)[12]. Does their morphology justify classification as the first members of Hominidae? Their geological age is relatively secure. The Lukeino Formation which is up to 130 m thick is bracketed by K/A dates of 7–5.4 Myr[11]. The deposits from which the Lothagam Hill mandible derives are disconformably overlain by an intrusive basalt sill with a K/A date of 3.7 Myr and are associated with mammalian fauna that yields a biostratigraphical age of 5–5.5 Myr[12,13]. We report here a morphological study which indicates that the Lukeino molar has cusp proportions similar to the modern chimpanzee and the Lothagam Hill mandible is morphologically intermediate between modern pongids and *A. afarensis*.

Because taxonomic assessment is difficult with small fragments of this sort, we have sought affinities by a series of analyses using multiple measurements, including the basal diameters of the five cusps, occlusal length, cervical length and breadth, trigonid and talonid breadths, diagonal length of the crown, and crown height for both the first and second molars, plus breadth and depth of the mandible under the second molar and cervical lengths and breadths of adjacent teeth[14-18]. These measurements are defined so as to reflect features of importance as indicated by ontogenetic and functional considerations that are independent of wear. The same measurements are recorded for 50 specimens each of *Homo sapiens* (multi-ethnic), *Pan troglodytes*, *Gorilla gorilla*, and *Pongo pygmaeus*, 22 *Pan paniscus*, 17 *Ramapithecus*, 19 *Sivapithecus*, 7 *Proconsul africanus*, 15 *P. nyanzae*, 7 *P. major*, 3 *Australopithecus afarensis*, 7 *A. africanus*, 11 *A. robustus*, 7 *A. bosei*, 17 early *Homo*, and 9 *H. erectus*. We used Penrose's method[19] to calculate morphometrical distance due to size and

Table 1 Size and shape distances of hominoids from the Lukeino fossil

Taxon compared to Lukeino	Penrose distance		Mahalonobis D	
	Size	Shape	Raw	Regression-adjusted
Pan troglodytes	0.53	0.49	24.21	9.95
P. paniscus	1.35	0.70	32.02	11.83
Australopithecus afarensis	3.00	1.36	32.06	13.44
A. africanus	3.38	1.35	46.07	13.95
A. robustus	4.22	1.39	60.72	12.50
A. bosei	6.16	1.62	75.48	12.31
Homo (fossil and recent)	1.92	0.99	43.72	14.42
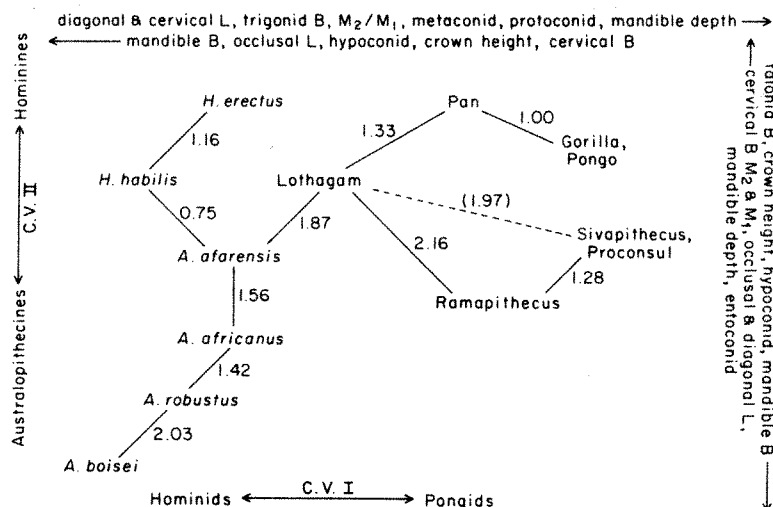
Fig. 1 Results of the canonical variates analysis of 16 size-standardized dimensions of the first molar and mandible. Traits having high correlations with canonical variate I (abscissa) and II (ordinate) are indicated in the margins with the direction of their relative increase. Taxa are indicated by their sequential arrangement when projected onto the two variates; superimposed distance between samples are direct linear shape z-score distances which are highly correlated with Mahalanobis D distances $(r = 0.88)$.

shape differences among specimens. We also performed canonical variates analyses[20] for which we used size-standardized data[21]. Size standardization was done by normalizing the measurements, forming a standard size variable which was the average normalized measurement magnitude for each case, regressing the standardized measurements against this size variable, and using the pooled within-species regression coefficient to adjust the standardized measurements to their residual from the size regression[21].

When the data are size-standardized in this way the isolated molar from Lukeino becomes metrically almost indistinguishable from modern pongids. It shares no salient hominid apomorphies (shared derived traits) or even the incipient development of such traits in the M_2 measurements. The smallest Penrose distance coefficient is with *P. troglodytes* (0.49) which is smaller than any other hominoid (Table 1). Other measures of distance give the same result. None of the results affords a basis for separation of the Lukeino molar from the genus *Pan*, but we do not advocate this classification because the close metrical similarity may reflect only shared primitive characters and there are other features of the fossil not measured by our study which differ from *Pan*[12].

The first molar and adjacent mandibular parts of the fossil from Lothagam Hill seem to have an overall morphological pattern intermediate between pongids and hominids. Figure 1 presents the results of the canonical variates analysis based on M_1 and mandibular traits. The major canonical variate separates hominids from pongids with Lothagam Hill intermediate between them. The morphological pattern characterizing hominids along this axis includes square, relatively short molars with centrally situated hyponulid, reduced trigonid breadth and protoconid and metaconid diameters, enlarged M_1 compared to M_2, shallow and thick mandibular corpus, expanded occlusal foveal length and crown breadth, large hypoconid, and high crown. The second canonical variate separates the australopithecines (with *A. boisei* at the far extreme) from the hominines. The extreme specialization of the *A. boisei* molars is reflected by the great distance separating them from other hominids. The distances shown in Fig. 1 are the direct linear z-score distances which are highly correlated with the Mahalanobis D distances[20] ($r = 0.88$). Measured in this way the Lothagam Hill specimen is intermediate between *Pan* and the earliest australopithecine, although closer to *Pan troglodytes* than to either *P. paniscus* or *A. afarensis*. It is well removed from *Ramapithecus*.

These results show that the morphology of the Lukeino molar does not necessarily justify its inclusion in the family Hominidae but the Lothagam Hill mandible does resemble later hominids in some ways. However, phylogenetic affinity depends not on a simple demonstration of degrees of similarity or difference, but on the identification of specific shared derived features independent of shared primitive traits. Among

our suite of metrical traits the Lukeino molar shows no derived features in common with *Australopithecus*. The fossil is within the sample confidence limits of *Pan troglodytes* in almost all variables, falling close to the mean for most of them. Other features such as thick enamel are not unique to Hominidae, but are present in *Gigantopithecus*, *Sivapithecus*, *Ramapithecus* and, to some extent, *Pongo*. Without further evidence it seems justifiable only to classify the Lukeino molar as Hominoidea indet. The Lothagam Hill fossil, on the other hand, does share some derived traits unique to known early members of Hominidae: relatively short occlusal length of M_1, relatively small M_1 entoconid diameter, and relatively shallow mandibular depth under M_2. It lacks several other derived features which *A. afarensis* shares with all other hominids, such as relatively large first molar cervical, and talonid breadths, relatively high crowned M_1 and relatively broad mandibular corpus under M_2.

Therefore, we recommend the Lothagam Hill specimen not be placed in *A. afarensis*, but left as Hominidae indet. It seems, therefore, that the first known member of the Hominidae is about 5 Myr old. This does not rule out the possibility of an early divergence of our evolutionary lineage, but does negate palaeontological objections to the late divergence hypothesis.

1. Simons, E. L. *Primate Evolution* (Macmillan, New York, 1972).
2. Simons, E. L. *J. Hum. Evolut.* **5**, 511–528 (1976).
3. Simons, E. L. *Scient. Am.* **236**(5), 28–35 (1977).
4. Pilbeam, D. *The Ascent of Man* (Macmillan, New York, 1972).
5. Washburn, S. L. & Moore, R. *Ape into Man* (Little & Brown, Boston, 1974).
6. Sarich, V. M. & Wilson, A. C. *Science* **158**, 1200–1203 (1967).
7. Sarich, V. M. & Cronin, J. E. in *Molecular Anthropology* (eds Goodman, M. & Tashian, R. E.) (Plenum, New York, 1977).
8. Johanson, D. C. & White, T. D. *Science* **202**, 321–330 (1979).
9. Pilbeam, D. *A. Rev. Anthropol.* **8**, 333–352 (1979).
10. Pilbeam, D. *et al. Nature* **270**, 689–695 (1977).
11. Pickford, M. *Nature* **256**, 279 (1975).
12. Patterson, B., Behrensmeyer, A. K. & Sill, W. D. *Nature* **226**, 918–921 (1970).
13. Behrensmeyer, A. K. in *Earliest Man and Environments in the Lake Rudolf Basin* (eds Coppens, Y. *et al.*) (Univ. Chicago, 1976).
14. Corruccini, R. S. thesis, Univ. California (1975).
15. Corruccini, R. S. *Z. Morph. Anthrop.* **68**, 14–25 (1977).
16. Corruccini, R. S. *J. dent. Res.* **56**, 190 (1977).
17. Corruccini, R. S. *J. dent. Res.* **56**, 1093–1096 (1977).
18. Corruccini, R. S. *Archs oral Biol.* **23**, 491–494 (1978).
19. Penrose, L. S. *Ann. Eugen.* **18**, 337–343 (1954).
20. Blackith, R. E. & Reyment, R. A. *Multivariate Morphometrics* (Academic, London, 1971).
21. Corruccini, R. S. *Homo* **28**, 222–226 (1978).

Independent effects of the pineal and a bacterial pyrogen in behavioural thermoregulation in lizards

Bruce T. Firth*†, Charles L. Ralph* & Thomas J. Boardman ‡

*Department of Zoology and Entomology, and ‡ Department of Statistics, Colorado State University, Fort Collins, Colorado 80523

The pineal complex of lizards is comprised of an extracranial photoreceptive structure known as the parietal eye, and an intracranial pineal organ which is homologous to the pineal gland of birds and mammals. Studies have shown that removing the parietal eye[1,2] or severing the parietal nerve[3] causes lizards to select higher temperatures when allowed to thermoregulate behaviourally in thermal or photothermal laboratory gradients. Although comparable studies involving removal of the lizard pineal organ have not previously been attempted, field data indicate that pinealectomy may have an antagonistic effect to parietalectomy[4]. We present evidence here which shows that (1) following pinealectomy, collared lizards (*Crotaphytus collaris*) behaviourally select or prefer lower temperatures than their controls in thermal laboratory gradients, and (2) the effect of surgical treatment is independent of the effects of a behavioural fever-inducing substance[5] which elevates by a fixed amount the environmental temperatures selected.

Eighteen collared lizards were divided into three treatment groups of six individuals each, all groups being essentially equivalent in body mass and sex ratio. One group was pinealectomised (P), one sham-pinealectomised (S) and the other group remained intact (I). Pinealectomy was accomplished by drilling through to the meninges an area with its anterior border 2 mm posterior to the interparietal scale. A small slit was made in the meninges and the pineal organ removed with watchmaker forceps. The wound was packed with Gelfoam and later sealed with dental cement. Sham-pinealectomy was achieved in the same way with the omission of the pineal removal step. Effectiveness of surgery was confirmed later by histology. In early July, 6 weeks after surgery, the animals were released randomly into individual sand-covered runways along which

† Present address: Department of Zoology, University of New England, Armidale, NSW 2351, Australia.

Fig. 1 Percentage relative frequency of temperatures selected by intact (——), sham-pinealectomised (· · · ·) and pinealectomised (- - -) *C. collaris* before pyrogen or saline injection. Temperatures on the *x* axis represent mid-points of 1 °C class intervals.

Mean percentile temperature
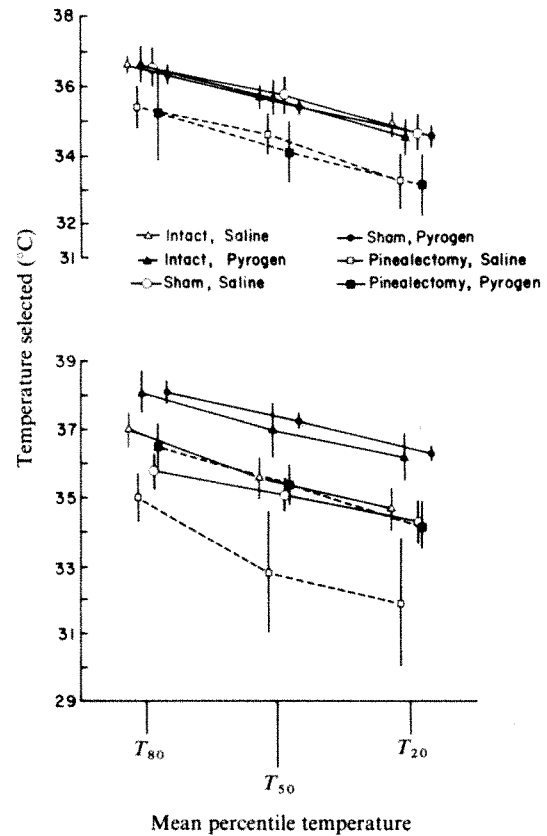
Fig. 2 Thermal selection in laboratory gradients at night by pinealectomised (P), sham-pinealectomised (S) and intact (I) *C. collaris* injected with either bacterial pyrogen or the saline vehicle. Means and standard errors (vertical lines) are compiled from two experiments carried out 5 days apart, and represent for each treatment ($n = 6$) the average of the median temperature (50th percentile or T_{50}), and temperatures around the median, that is, at the 80th percentile and 20th percentile (T_{80} and T_{20}), respectively. The temperatures at the three percentiles were obtained by ranking the 50 temperatures recorded for each animal between 1800 h and 0600 h. Thus, the temperature at T_{80} was the 10th highest temperature, that at T_{50} the 25th highest and that at T_{20} the 10th lowest. The upper plot shows thermal behaviour in the six groups of lizards the night before injection with either saline or pyrogen. The only significant factor affecting thermal selection was pinealectomy, which depressed the preferred temperature at all three ranked levels (two-way ANOVA; T_{80}, $P < 0.05$; T_{50}, $P < 0.01$; T_{20}, $P < 0.01$). A similar two-way ANOVA following the injection of saline or pyrogen (lower plot) showed a significant effect due to this factor (T_{80}, $P<0.01$; T_{50}, $P<0.02$; T_{20}, $P<0.05$), in addition to a significant effect due to surgical treatment (T_{80}, $P<0.01$; T_{50}, $P<0.05$; T_{20}, $P<0.05$). The injection of saline in the three treatment groups (P, S, I) did not significantly alter the pattern observed before injection. However, the injection of pyrogen caused a significant fever of 1–2.5 °C in the three treatment groups. Despite these independent effects, there was no significant interaction (T_{80}, $P<0.5$; T_{50}, $P<0.8$; T_{20}, $P<0.9$) between surgical and injection treatments.
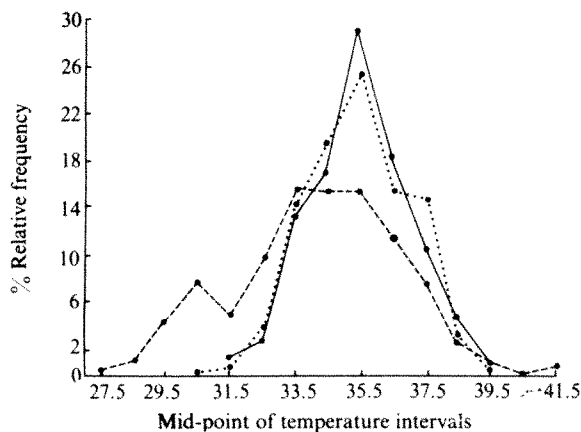
existed a thermal gradient of 12–48 °C. A 12-h light/12-h dark photoperiod (12 L:D, L 0600 h- 1800 h) was imposed by overhead fluorescent lights controlled by a timer. The hot end of the gradient was provided by incandescent lamps only during the light phase and by heat tape only during the dark phase. The cold end was maintained by cold water pumped through copper tubing. As skin temperature is thought to be an important regulated variable in lizard thermoregulation[6], only skin surface temperatures of individual lizards were recorded every 15 min from 36-gauge thermocouples taped to the base of the tail and connected to a Honeywell 112 multichannel temperature recorder.

The lizards remained in their respective runways for 10 days before the temperature measurements reported here. They were fed crickets and mealworms at the same time daily. Between 0900 h and 0930 h on day 12, half of each treatment group was injected intraperitoneally with pyrogen, a substance initiating behavioural fever[5], consisting of a 0.5 ml suspension of 2×10^9 dead *Aeromonas hydrophila* bacteria in a vehicle of 0.85% sterile saline. The remaining half was injected with the vehicle only. Because preliminary studies showed that pinealectomy had a greater effect on thermal behaviour during the scotophase, the 11th night was chosen as the pre-injection period and the 12th night as the post-injection period. The experiment was repeated 5 days later, using the same animals and the same procedure, except that the lizards previously injected with pyrogen were injected with the vehicle and vice versa.

A frequency distribution of the temperatures selected by P, S and I lizards before injection of either saline or pyrogen reveals that P animals preferred lower temperatures than controls and that temperatures were more broadly distributed than for controls (Fig. 1). These results indicate an impaired ability to thermoregulate precisely after pinealectomy. A detailed analysis of median and paramedian temperatures selected by lizards before and after injection of bacterial pyrogen (Fig. 2) shows that the preferred temperatures of all surgically treated and intact groups were elevated by a fixed amount. However, no significant interaction was observed between pinealectomy and pyrogen treatment, indicating that the pineal organ of *C. collaris* does not participate in behavioural fever.

Previous studies have shown that pinealectomy in birds and mammals can alter thermoregulatory function by inducing hyperthermia, hypothermia and disruption related to temporal and/or photic cues[7-10]. The present data indicate that behavioural thermoregulation of an ectotherm may similarly be influenced by the pineal, perhaps by altering the sensitivity or set point of a central thermostat. As it is generally regarded that this thermostat resides in the hypothalamus of both endotherms[11] and ectotherms[12,13], the thermoregulatory effects of pinealectomy may well be related to changes in hypothalamic input. Evidence for such an hypothesis is provided by (1) the anatomical and functional relationship between the pineal organ and the hypothalamus in several vertebrate groups[14], and (2) our observation that P lizards increase the range of temperatures behaviourally selected (Fig. 1), a finding similar to that shown for the thermoregulatory shuttling behaviour following preoptic hypothalamic lesions in the lizard *Dipsosaurus dorsalis*[15]. Our results further indicate that behavioural fever, which is believed to be manifested by an elevation in the set point of the central thermostat[16], is triggered by an action of pyrogen on centres other than those affected by the pineal.

1. Hutchinson, V. H. & Kosh, R. J. *Oecologia* **16**, 173-177 (1974).
2. Roth, J. J. & Ralph, C. L. *J. exp. Zool.* **198**, 17-28 (1976)
3. Engbretson, G. A. & Hutchison, V. H. *J. exp. Zool.* **198**, 29-38 (1976).
4. Stebbins, R. C. *Copeia* **1960**, 276-283 (1960).
5. Vaughn, L. K., Bernheim, H. A. & Kluger, M. J. *Nature* **252**, 473-474 (1974).
6. Barber, B. J. & Crawford, E. C. Jr *Physiol. Zool.* **52**, 250-263 (1979).
7. Binkley, S., Kluth, E. & Menaker, M. *Science* **174**, 311-314 (1971).
8. Cogburn, L. A., Harrison, P. C. & Brown, D. E. *Proc. Soc. exp. Biol. Med.* **153**, 197-201 (1976).
9. Spencer, F., Shirer, H. W. & Yochim, J. M. *Am. J. Physiol.* **231**, 355-360 (1976).
10. John, T. M., Itoh, S. & George, J. C. *Horm. Res.* **9**, 41-56 (1978).
11. Hammel, H. T. *A. Rev. Physiol.* **30**, 641-710 (1968).
12. Crawshaw, L. I. & Hammel, H. T. in *The Pharmacology of Thermoregulation* (eds Schonbaum, E. & Lomax, P.) 142-145 (Karger, Basel, 1973).
13. Hammel, H. T., Crawshaw, L. I. & Cabanac, H. P. in *The Pharmacology of Thermoregulation* (eds Schonbaum, E. & Lomax, P.) 124-141 (Karger, Basel, 1973).
14. Ralph, C. L., Firth, B. T. & Turner, J. S. *Am. Zool.* **19**, 273-293 (1979).
15. Berk, M. L. & Heath, J. E. *J. therm. Biol.* **1**, 65-78 (1975).
16. Kluger, M. *Fedn Proc.* **38**, 30-34 (1979).

Avian flocking in the presence of a predator

Thomas Caraco*, Steven Martindale & H. Ronald Pulliam†

Department of Ecology and Evolutionary Biology, University of Arizona, Tucson, Arizona 85721

Although there are several possible advantages of flocking[1-3], many authors suggest that birds forage in groups to reduce the risk of predation (see citations in ref. 4). One version of the 'many eyes' hypothesis proposes that flocking allows individuals to spend less time scanning for predators and more time feeding[5,6]. However, flocking may also cause individuals to lose time and energy in fighting one another. The way a bird divides its time among these activities, its time budget, may depend on variables governing foraging requirements and the chance of predation[7]. As one such variable is the frequency of attacks by predators[8], we flew a trained hawk over flocks of granivorous yellow-eyed juncos (*Junco phaeonotus*) to compare time budgets in the presence and absence of a predator. We found that time budgets changed after the predator was introduced and also that flock size increased in the presence of the predator.

Previous studies indicate that individual yellow-eyed juncos scan for predators less often as flock size increases, while both feeding time and aggressive behaviour increase simultaneously[7]. The proportion of time an individual spends in aggressive behaviour also varies with temperature and food availability. Dominant birds have less time to defend foraging areas when they must spend more time feeding because of low ambient temperature or low seed density. As foraging time requirements increasingly constrain aggression, lower ranking birds are not so quickly evicted from better foraging areas, and flock size increases[7]. Thus, some of the variations in foraging flock size can be explained by the relative advantages and disadvantages of flocking in terms of time budgets[9].

If the frequency of predator attacks increases, an individual might be able to increase its survivorship by scanning more often, as long as feeding time is sufficient to prevent starvation. Larger flocks might form if increased scanning entails a reduction in aggression, if grouping *per se* enhances the individual's probability of avoiding predation[4,10], or if only larger flocks allow sufficient feeding time at high attack frequencies[5].

We released a trained Harris hawk (*Parabuteo unicinctus*) in our study area for 2 h (1500-1700 h) on each of 3 days during 2 weeks in February 1978. The hawk perched in tall trees and swooped down over junco flocks to obtain a food reward from its trainer. The Harris hawk was ideal, because it did not actually catch juncos, but it did appear to 'attack'. Harris hawks seldom hunt small birds, and the juncos easily outmanoeuvred the experimental hawk (compare ref. 11).

Time budgets were sampled by observing randomly selected focal birds. At 15-s intervals we recorded the behaviour being exhibited by the bird under observation and categorized the behaviour as: (1) scanning for predators; (2) feeding (search for and handling of seeds); or (3) interference (actual aggression or movement away from nearby birds). These three categories are mutually exclusive and encompass all the activities of the birds

* Present address: Department of Biology, University of Rochester, Rochester, New York New York 14627.
† Present address: H. S. Colton Research Center, Museum of Northern Arizona, Flagstaff, Arizona 86001.

as long as they are members of foraging groups. The categories are easily distinguishable when observing juncos. For each flock size, we pooled the data from all individuals to obtain large samples and then calculated time budgets as the proportion of observations associated with each behavioural category. Data were compared with those obtained in the same area, at the same temperature, during a previous year[7].

We next recorded the rate at which individuals scanned for predators (as a function of group size) when the hawk was present. Data were computed as scans per min and compared with scanning rates observed under normal predator attack frequency. We also recorded the size of all foraging flocks observed in the study area during 2-h periods before and after the hawk was released. Temperature did not vary more than 2 °C among sampling periods, so that any flock size variation could not be attributed to a change in temperature-dependent constraints on aggression.

Table 1 Time budgets with and without hawk in the study area

Flock size		1	3-4	6-7	
Hawk absent	T_S	0.30	0.13	0.07	
	T_F	0.70	0.77	0.85	$\bar{G} = 3.93 \pm 0.86$
	T_I	0.00	0.10	0.08	
	n	159	162	149	
Hawk present	T_S	0.57	0.27	0.33	
	T_F	0.43	0.69	0.60	$\bar{G} = 7.33 \pm 1.6$
	T_I	0.00	0.04	0.07	
	n	79	52	162	

T_S, proportion of time spent scanning for predators; T_F, proportion of time spent feeding; T_I, proportion of time spent in interference. n, Sample size, and $\bar{G}$ is mean flock size ± standard error.

Table 1 summarizes the time budget data, with and without the hawk present, for flocks of 1, 3 or 4, and 6 or 7 birds. In both conditions, solitaries scanned more often than individuals foraging with other juncos. When the hawk was present, juncos spent significantly more time scanning as solitaries ($P < 0.005$, likelihood ratio test), in flocks of 3 or 4 ($P < 0.025$) and in flocks of 6 or 7 ($P < 0.005$). Feeding time was necessarily significantly less for solitaries (since scanning was greater) and also was significantly less for flocks of 6 or 7 ($P < 0.005$). The effect on feeding time alone was not significant in flocks of 3 or 4, although interference decreased as scanning increased. Mean flock size before the hawk's release was 3.93, compared with 7.33 when the hawk was present. This difference is statistically significant ($t_{46} = 2.03$, $P < 0.025$).

Whether the hawk was present or absent, the rate at which an individual scanned for predators decreased significantly with increasing flock size. If we let $y_1 = \log_{10}$ (scans per min per bird) with the hawk absent, and $y_2 = \log_{10}$ (scans per min per bird) with the hawk present, from our previous report[7] without a hawk $y_1 = 1.047 - 0.399 \log_{10}$(group size), $r = -0.92$, and with the hawk present we find that $y_2 = 1.48 - 0.38 \log_{10}$ (group size), $r = -0.72$. Analysis of covariance indicates that the slopes do not differ significantly ($F_{1,25} = 0.03$, not significant); however, the weighted means (therefore, the intercepts) do differ significantly ($F_{1,26} = 60.2$, $P < 0.005$). As flock size increased, there was a reduction in individual scanning rate under both treatments, but for any given flock size individuals scanned more often with the hawk present.

As the hawk's presence increased flock size, the relative advantages of flocking apparently increase for juncos as the frequency of predator attacks increases. The hawk's presence tended to increase scanning at the expense of feeding time more than interference. However, the feeding time of an individual foraging with others, compared to a solitary's feeding time,

showed a greater relative increase when the hawk was present. We interpret this as an indication that an individual can acquire a greater advantage with respect to feeding by joining a group when predator attacks are more frequent. As we have shown previously[7], the slope of the regression of individual scanning rate on group size suggests that an attack is more likely to be detected as flock size increases, so that larger flocks offer better protection. Furthermore, a hawk cannot capture more than one bird per attack, so an individual's probability of being the victim of successful attack decreases as flock size increases. As long as predators do not concentrate all their efforts on flocks, the relative advantages of flocking to an individual junco apparently increase with attack frequency. Predator attack frequency is then another ecological variable affecting junco flock size and its impact is mediated, at least in part, through time budgeting variation.

1. Brown, J. L. *Am. Zool.* **14,** 51-62 (1974).
2. Cody, M. L. *Theor. Popul. Biol.* **4,** 142-158 (1971).
3. Krebs, J. R. *Behaviour* **51,** 99-134 (1974).
4. Treisman, M. *Anim. Behav.* **23,** 779-800 (1975).
5. Pulliam, H. R. *J. theor. Biol.* **38,** 419-422 (1973).
6. Siegfried, W. R. & Underhill, L. R. *Anim. Behav.* **23,** 504-508 (1975).
7. Caraco, T. *Ecology* **60,** 618-627 (1979).
8. Caraco, T. *Ecology* **60,** 611-617 (1979).
9. Pulliam, H. R. in *Perspectives in Ethology* (eds Klopfer, P. H. & Bateson, P. G.) 311-332 (Plenum, New York, 1976).
10. Hamilton, W. D. *J. theor. Biol.* **31,** 295-311 (1971).
11. Kenward, R. E. *J. Anim. Ecol.* **47,** 449-460 (1978).

Anti-micrococcus antibodies recognize an antigenic marker of confluent mouse lymphoid cell lines

J. Grooten, P. De Baetselier, E. Vercauteren & R. Hamers

Instituut voor Molekulaire Biologie, Vrije Universiteit Brussel, Paardenstraat 65, 1640 St-Genesius-Rode, Belgium

In addition to the production of autoantibodies[1] and rheumatoid factors[2], other quite unique features accompany the immune response of various species to spontaneous infections or immunizations with cocci (streptococcus, pneumococcus, meningococcus, micrococcus). The immunoglobulin molecules produced are restricted in heterogeneity not only for antibodies raised against the bacteria[3], but also for those raised against other antigens to which the animal is simultaneously immunized[4,5]. In the case of micrococcus and streptococcus vaccinations where this has been investigated, dormant immunoglobulin (Ig) genes are activated and appear as new allotypes in the sera[6,7]. Serum titres against maternal Ig light-chain allotypes increase considerably after immunization with micrococcus (W. van der Loo, personal communication). Such a pleiotropic effect suggests that bacterial vaccination affects the immune response at a very fundamental level. It was suggested that this aberrant behaviour of the immune response was driven by antibodies which cross-react with glycoprotein or glycolipid membrane components of the lymphoid cell population[8]. This was supported by the finding that purified anti-micrococcus antibodies, both *in vivo* and *in vitro*, affect the response of immunocompetent cells[9]. We now report that mouse anti-micrococcus antibodies recognize a membrane marker of mouse lymphoid cell lines, and that this marker is only exhibited after transition from non-confluent to confluent culture conditions.

Rabbit and mouse antibodies raised against micrococcus and streptococcus bind or agglutinate a variety of mammalian cells[1], including a small number of autologous lymphoid cells obtained from the immunized animal (R. Hamers, personal communication). Three cloned lymphoid cell lines were selected for further investigation: WEHI 7.1, which is a BALB/c T lymphoma[10], the BALB/c myeloma Sp 2/0–Ag14, a non-producing variant of the Sp 2/HL–Ag14 line[11], and the BALB/c lymphoma S49 1/10 (ref. 12).

Binding of anti-micrococcus antibodies produced in BALB/c, CBA/Ca and C57B1 mice was analysed with a fluorescence activated cell sorter (FACS) as a function of the culture condition and of the three cell lines. Fluorescein-labelled goat anti-mouse antibody was used as the fluorescent probe. After seeding, the cultures evolve from non-confluence with exponentially growing cells, to confluence and post-confluence conditions, in which the cells ultimately stop dividing.
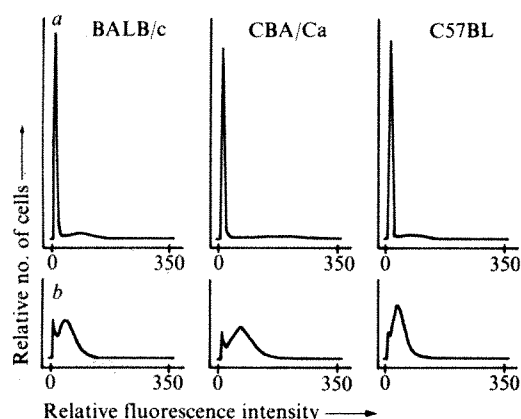
Fig. 1 Fluorescence histograms of WEHI 7.1 cells (cultured in Petri dishes) stained with anti-micrococcus antisera. The experimental protocol was as follows: 0.1 ml cells (5×10^7 cells ml^{-1}) in Dulbecco's balanced salt solution with 0.02% NaN$_3$ (DBSS) were incubated with 0.010 ml antiserum (optimal concentration) at 4 °C for 30 min followed by two washes with DBSS. After resuspension in 0.1 ml DBSS, 0.01 ml of an optimal dilution of fluorescein-labelled goat anti-mouse IgG (Nordic Immunological Laboratory) was added and the cells were incubated for 20 min at 4 °C. After two washes with DBSS the cells were fixed overnight with formaldehyde (2% formaldehyde in DBSS) and analysed on the FACS II (Becton Dickinson Electronics Laboratory). A scatter window was set to eliminate dead cells and cell debris. The anti-micrococcus antisera were obtained with the following immunisation protocol: after one initial, intravenous injection of 0.2 ml (4 mg ml^{-1} in saline) micrococcus suspension, the mice were injected 12 times intraperitoneally with the same amount over a period of 4 weeks. The animals were then given a rest period of 3 weeks, followed by a second course of nine intraperitoneal injections over 3 weeks. The sera were taken 2 weeks after the last injection. Less intense immunization protocols resulted in lower antibody titres. *a*, Early confluent culture conditions (12.5% stained cells); *b*, late confluent culture conditions (72.0% stained cells).

During the exponential growth phase no cells exhibited the membrane antigen detected by the antisera. When the cell density reached confluence, some cells began to express the marker, which in the final stage of confluence appeared on almost the entire population (Fig. 1). This phenomenon was observed on all three cell lines. Confluence cells of the Sp 2/0–Ag14 line were maintained at 37 °C after staining to study capping. In these conditions, shedding of the fluorescein-labelled antibody was complete within 1 h as measured by the FACS. Control experiments with preimmune sera show only background fluorescence. An occasional preimmune serum,

however, will exhibit a weak binding on confluent cells, probably due to spontaneous anti-bacterial antibodies present in the serum of these conventionally maintained mice.

The marker appears as soon as confluence is reached and does not seem to depend on nutrient depletion, as can be shown in experiments in round-bottom tubes, where confluence is reached much earlier and at much lower cell densities than in Petri dishes. We will designate this marker as the confluence antigen (Cag).

The apparent synchronization between the appearance of the Cag marker and the transition from non-confluent to confluent conditions suggests that only the non-dividing or slowly dividing cells express the marker. To check this, the following experiment was carried out. ^{3}H-Thymidine was added to cells at different stages of the culture and the ratio of ^{3}H-thymidine uptake of fluorescent and non-fluorescent cells was measured after separation with the FACS. It follows from these experiments that the DNA synthesis, as measured by thymidine uptake, is much lower in the fluorescent cells (Cag$^+$) than in the non-fluorescent cells (Cag$^-$) obtained from the same culture (Table 1).

We conclude that the Cag marker appears on a cell population which showed reduced DNA synthesis in the 6 h before separation. From the serology of the reaction, some clues are obtained as to the nature of Cag. Adsorption of the antibodies on micrococcus lysodeikticus results in a decrease of the binding. Conversely, antibodies purified on a micrococcus cell-wall adsorbent[13] and eluted with 0.2 M acetic acid were capable of staining the confluent cells, indicating that it is actually anti-micrococcus antibodies which bind to the Cag marker.

The confluence antigen is probably complex and several specificities and cross-reacting specificities could be involved. Antibodies from the different inbred strains do not stain the cells with the same intensities. Moreover, the binding inhibition patterns obtained using a panel of monosaccharides are qualitatively different for the three antisera (Table 2).

These results suggest that the Cag marker which is exhibited when the cell reaches confluence is a complex carbohydrate structure which comprises several different sugars. Further analysis to elucidate the carbohydrate composition of the Cag is now under way using hybridoma-produced anti-micrococcus antibodies.

Table 1 DNA synthesis of anti-micrococcus antibody-binding and non-binding cells

| Culture stage | % Cells binding antibody | ^{3}H-Thymidine incorporation (c.p.m. per 4×10^5 cells) | | | ^{3}H-Thymidine uptake $\frac{\text{non-binding cells}}{\text{binding cells}}$ |
		Total cells	Binding cells	Non-binding cells	
Early confluent	5%	118,940	14,460	122,640	8.5
Late confluent	70%	6,669	795	19,325	24.3

WEHI 7.1 cells, cultured in Petri dishes, were tested for the rate of DNA synthesis at the beginning of confluence (early confluence) and 2 days later, when confluence was generalized (late confluence). A 6-h ^{3}H-thymidine pulse was given to the cells followed by washing away the free ^{3}H-thymidine and staining the cells as described in Fig. 1 legend. A fixed number (4×10^5) of fluorescent, non-fluorescent and total cells were separated on the FACS II and the ^{3}H-thymidine incorporation of the three cell populations was estimated in a scintillation counter.

In conclusion, it seems that mouse anti-micrococcus antibodies recognize a membrane marker of murine lymphoid cell lines. This marker, which we call the confluence antigen (Cag), is only exhibited after transition from non-confluent to confluent culture conditions, and its expression is correlated with a slowing down or cessation of DNA synthesis.

Antigenic variation or heterogeneous expression of membrane antigens is not an isolated phenomenon in mammalian cells, and several authors[14-16] have described the transient expression of blood group substances in relation to the mitotic cycle. Their observations, like ours, affect membrane glycoproteins or glycolipids and must be attributed to cell cycle-associated changes in the activity of the cellular glycosylating enzymes or their substrates.

Table 2 Inhibition of antibody binding by monosaccharides

Inhibitor	Anti-micrococcus antibody source		
	BALB/c	CBA/Ca	C57BL
None	100	100	100
D(+) glucose	67	76	100
L(−) glucose	55	95	100
α−D(+) fucose	84	95	100
α−L(−) fucose	61	91	100
D-mannose	71	68	67
D-galactose	67	81	67
N-Acetylglucosamine	60	100	53

Confluent stage WEHI 7.1 cells, showing 40% antibody binding, were suspended in DBSS (5×10^7 cells ml^{-1}) containing 0.14 M inhibitory monosaccharide. The suspension was incubated with antiserum (10%) for 30 min at 4 °C, washed with DBSS and stained with fluorescein-labelled goat anti-mouse antibody as described in Fig. 1 legend. The cells were analysed on the FACS II and the decrease in fluorescence intensity estimated. Results given are values for relative fluorescence intensity at peak maximum. The position of the peak maximum is taken as 100 for the uninhibited control. The actual values for the three antisera are: BALB/c = 70, CBA/Ca = 92 and C57BL = 35 (see also Fig. 1).

The observed binding demonstrates the possibility of obtaining antibodies directed against membrane markers of neoplasms or other cells by immunization with a bacterial antigen. This is true even in the syngeneic system in which BALB/c antibodies react with cell lines of BALB/c origin. This could explain some of the suppression or enhancement effects of bacterial vaccination on tumour development[17,18]. It is more difficult to determine the relevance of our findings to the peculiar behaviour of the immune system to micrococcus vaccination and to the observed effect of anti-micrococcal antibodies on *in vitro* systems. In staining normal lymphoid cells from BALB/c, CBA and C57BL mice, considerable variation was encountered between individual animals and we do not understand the reason for this variability.

This work was supported by a grant from the ASLK Kankerfonds and by the FGWO grant 30035.76. We thank Dr Kohler for a gift of the hybridoma cell lines, Dr Luckenbach for the WEHI 7.1 line, and Dr Wikler for the micrococcus cell-wall absorbent.

1. Blue, W. T. & Lange, C. F. *Immunochemistry* **13**, 295–298 (1976).
2. Hamers, R., Hamers-Casterman, C., van der Loo, W., Strosberg, A. D. & De Baetselier, P. *Z. ImmunForsch. exp. Ther.* **149**, 187–192 (1975).
3. Braun, D. G. & Jaton, J.-C. *Curr. Topics Microbiol. Immun.* **66**, 29–76 (1974).
4. Montgomery, P. C. & Pincus, J. H. *J. Immun.* **111**, 42–51 (1973).
5. De Baetselier, P., Hamers-Casterman, C., van der Loo, W. & Hamers, R. *Immunology* **33**, 275–284 (1977).
6. van der Loo, W., De Baetselier, P., Hamers-Casterman, C. & Hamers, R. *Eur. J. Biochem.* **7**, 15–22 (1977).
7. Mage, R. G., Rejnek, J., Glendowlyn, O., Young-Cooper, G. O. & Alexander, C. *Eur. J. Immun.* **7**, 460–468 (1977).
8. De Baetselier, P., Hooghe, R., Grooten, J., Hamers-Casterman, C. & Hamers, R. *Proc. EORTC Meeting on Tumor Immunology: Clinical Tumor Immunology* (eds Wybran, J. & Staquet, M.) 253 (Pergamon, Oxford, 1976).
9. De Baetselier, P., Grooten, J., Van De Winkel, M. & Hamers, R. *Archs intern. Physiol. Biochim.* **85**, 161–163 (1977).
10. Stocker, J. W., Marchalonis, J. J. & Harris, A. W. *J. exp. Med.* **139**, 785–790 (1974).
11. Shulman, M., Wilde, C. D. & Kohler, G. *Nature* **276**, 269–270 (1978).
12. Horibata, K. & Harris, A. W. *Expl Cell Res.* **60**, 61–77 (1970).
13. Wikler, M. Z. *Immun. Forsch.* **149**, 193–200 (1975).
14. Franks, D. & Dawson, A. *Expl Cell Res.* **42**, 543–561 (1966).
15. Kuhns, W. J. & Bramson, Sh. *Nature* **219**, 938–939 (1968).
16. Thomas, D. B. *Nature* **233**, 317–321 (1971).
17. Collins, J. L. & Wust, C. J. *Cancer Res.* **34**, 932–937 (1974).
18. Verloes, R., Atassi, G., Dumont, P. & Kanarek, L. *Br. J. Cancer* **38**, 599–605 (1978).

A monoclonal antibody specific for diploid epithelial cells in *Drosophila*

Danny L. Brower, R. J. Smith & Michael Wilcox

MRC Laboratory of Molecular Biology, Hills Road, Cambridge CB2 2QH, UK

Results from various experiments suggest that the cell surface has an important role in development[1]. However, there is relatively little information on the specific surface molecules involved in developmental processes. In an effort to characterize cell-surface components that may be involved in *Drosophila* development, we have been making monoclonal antibodies against *D. melanogaster* imaginal disks[2]. The holometabolous insects are unusual in that scattered among the larval tissues are groups of undifferentiated imaginal cells which, during metamorphosis, will form most of the adult insect[3,4]. The imaginal disks, which we use as an immunogen, are hollow sacs of cells; each disk will form a specific part of the adult cuticle. Other imaginal cells are found as nests or rings in various larval organs. We describe here results indicating that one of the clones we have isolated, DA.1B6, makes an antibody against an antigen which, in larvae, is generally restricted to the undifferentiated sheets of imaginal epithelial cells. This and other results indicate that the antigen is specific for the diploid epithelia in *Drosophila*.

For the production of clone DA.1B6, a BALB/c mouse was immunized by injecting it intraperitoneally, on days 0, 5 and 12, with 200–300 sonicated imaginal disks in 0.1 ml *Drosophila* Ringer's solution (for all immunizations, and subsequent antibody binding experiments, tissues from the *D. melanogaster* Barton wild-type strain were used). On day 18 the mouse received a sonicate of 300 disks intravenously and, 2 days later, its spleen was removed. Spleen cells were fused with cells of the P3/NSI mouse myeloma line[5] using polyethylene glycol, as described in ref. 6. When large colonies of hybrid cells had grown, the culture supernatants were screened for the presence of antibodies which would bind to intact imaginal disks, using indirect immunofluorescence (see legend to Fig. 1). After its identification as an antibody-secreting line, DA.1B6 was cloned twice, serially, using the soft agar technique[7].

Table 1 catalogues the binding specificity of the antibody produced by DA.1B6. In late third instar larvae, the antibody binds to all of the imaginal disks (Fig. 1b), but it does not bind to all the cells of the disk. As shown in the section in Fig. 1c, the antibody binds to the epithelial cells of the wing disk, but not to the adepithelial cells, which are believed to be precursors of at least some of the adult muscles[8,9]. Binding is also observed to the imaginal rings in the salivary gland and gut, but there is no detectable binding to the large larval cells, either in these organs or elsewhere (Fig. 1d). In the adult, the antibody binds to the majority of the tissues which derive from these imaginal cells during metamorphosis.

The pattern of antibody binding to the larval and adult gonads is noteworthy. The ovaries of late third instar larvae show their strongest antigenic activity in a 'cap' across one end, with additional activity in a band further down the ovary (Fig. 1e). The lack of clear organization in the larval ovary makes this observation difficult to interpret, but the pattern of binding of the antibody to the adult ovary makes it likely that the larval binding is to precursors of the adult epithelia. In the adult organ, the antibody binds to the cells of the follicular epithelium surrounding the germarium and the adjacent anterior ovarioles (Fig. 1f). Small groups of cells at either end

of each follicle show especially bright fluorescence. There is no detectable binding to the germ cells in the germarium or to the developing nurse cells and oocytes. In the posterior part of each ovariole, where the follicle cells become polyploid and take an active part in vitellogenesis[10–12], the antibody fluorescence is generally much less intense than in the young follicles.

The bulk of the larval testis is antigen negative. There are, however, some localized areas of fluorescence on the surface of the testis; the most conspicuous is a small bright patch of cells at one end of the organ. In the adult gonad, the germ cells are again negative, but there is a bright fluorescent 'spot' at the distal end of the testis. These results suggest that, in both larvae and adults, there is binding to the apical cells of the germinal centre of the testis[13].

Our preliminary study of embryos demonstrates that, early in development, the antigen recognized by DA.1B6 antibody is not restricted to imaginal precursor cells. Although we have not been able to detect any antibody binding to sections of embryos at the cellular blastoderm stage, by the end of germ band shortening (stage 12 of Bownes[14]) binding is evident to virtually the entire external epithelium and to many of the internal epithelia. By hatching, the antigen is disappearing from the cells that are differentiating into larval organs such as the salivary glands and gut, finally giving rise to the larval pattern of binding described above.

In summary, DA.1B6 antibody binds to the imaginal epithelial cells in third instar larvae, but not to the large cells of the larval organs. Many of the adult epithelia retain the binding capacity of their imaginal primordia. In early embryos, the antibody binds to most if not all of the epithelial cells, but, during later embryogenesis and early larval life, this binding activity disappears from those cells which form the larval organs.

Although the antibody generally seems to be specific for epithelial cells, it does not discriminate between germ layers, for there are examples of binding to cells from ectoderm (imaginal disks), endoderm (mid-gut) and mesoderm (follicle cells). The disappearance of the antigen from the larval

Fig. 1 Fluorescence micrographs of tissues from late third instar larvae (except *f*, which is from an adult ovary) stained with antibody from clone DA.1B6. Isolated tissues were incubated directly in cell culture supernatants, or in partially purified antibody diluted in RPMI medium (Gibco), for 45 min (30 min for sectioned material) at 37 °C (similar results were obtained at 23 °C). After three washes in cold medium, the tissues were incubated in fluorescein-conjugated rabbit anti-mouse IgG (Miles), diluted in RPMI medium, for 30 min at 37 °C (15 min for sections). After three more washes, the material was mounted and viewed with a Zeiss fluorescence microscope, using trans-illumination. *a*, Control wing disk incubated in RPMI medium without DA.1B6. *b*, Wing disk incubated with DA.1B6 antibody. *c*, Wing disk fixed with formaldehyde and frozen-sectioned before treatment with antibody. DA.1B6 binds to the cells from the columnar epithelium (ep) and the peripodial membrane (pm, which is in fact a squamous epithelium). The antibody also labels the matrix cells surrounding the tracheae (tr), but fails to bind to the adjacent adepithelial cells (ad). *d*, Salivary gland; the antibody binds to the ring of imaginal cells but not to the polyploid cells of the functioning larval gland (L). *e*, Ovary; binding is confined largely to a cap across one end of the organ, although an additional faint band of fluorescence (arrowed) is visible. *f*, Anterior end of an ovariole from an adult ovary. The follicle cells fluoresce brightly but there is no binding to the germ cells of the germarium (G). There is an exceptionally bright patch of cells at either end of each follicle (arrowheads). Follicles in later stages of öogenesis show relatively little fluorescence (bottom of figure). Scale bars, 50 μm.

Table 1 Binding of antibody DA.1B6 to tissues of adults and third instar larvae

	Third instar larvae*	Adults
Epidermis†	–	
Imaginal disks: labial	+	
dorsal prothoracic	+	
eye-antennal	+	
wing	+	+‡
haltere	+	
leg	+	
genital	+	
Salivary glands	i	+
Gut†	i	+
Brain§	–	±
Thoracic muscles	–	–
Malpighian tubules	–	–
Fat body	–	–
Gonads	see text	

The binding assay is described in the legend to Fig. 1. – Little or no binding; +, binding to most or all of the cells; i, binding only to the imaginal rings of cells.

*Most of these tissues have also been examined in second instar larvae, always with identical results.

†We do not know if the imaginal histoblasts of the larval epidermis or mid-gut bind the antibody; the pupal mid-gut binds the antibody, but the activity is lost from the adult organ.

‡As judged by binding to thoracic and abdominal epithelium and to structures derived from the genital disk.

§A small region of the larval brain, sometimes seen to be associated with the eye-antennal disk, binds the antibody; binding to the adult brain is very heterogeneous.

epithelia may be related to the fact that these cells become polyploid during their differentiation[4]. This hypothesis is supported by the pattern of antibody binding to adult tissues. While most adult epithelia are recognized by the antibody, there is little or no binding to epithelia composed of polyploid cells (as indicated by Feulgen staining, our unpublished observations), such as the mid-gut. Also, in the adult ovary, there is a large reduction in the fluorescence of the follicle cells at about the time that they become polyploid during oogenesis[10]. The commitment to polyploidy by a cell entails a reduction in regulative capacity and a complete loss of proliferative potential. It seems quite possible, therefore, that the antigen is involved in these cellular processes.

Whatever the function of the antigen, the antibody can be useful as a developmental marker, particularly in organs such

as the gonads and brain, where the pattern of binding is heterogeneous. Moreover, the antibody may have biochemical applications, for example, in the purification of imaginal plasma membranes from whole larvae.

Without the unusual developmental history of the holometabolous insects, both the original identification and further characterization of DA.1B6 antibody would have been much more difficult. We believe that this and other unique features of *Drosophila* biology—for example, the elucidation of developmental compartments[15,16] and the extensive knowledge of the fate and determination of imaginal disk cells[17]—make it the ideal organism for studies of this kind.

We would like to thank Bruce Wright for supplying P3/NSI cells, and numerous colleagues for suggestions and comments. D.L.B. is a fellow of the American Cancer Society.

1. Karkinen-Jääskeläinen, M., Saxén, L. & Weiss, L. (eds) *Cell Interactions in Differentiation* (Academic, London, 1977).
2. Wilcox, M., Brower, D. & Smith, R. J. in *Development and Behaviour of D. melanogaster* (eds Siddiqi, O., Hall, L. & Babu, P.) (Plenum, New York, 1980).
3. Bodenstein, D. in *Biology of Drosophila* (ed. Demerec, M.) 275–337 (Hafner, New York, 1965).
4. Anderson, D. T. in *Developmental Systems: Insects* Vol. 1 (eds Counce, S. J. & Waddington, C. H.) 165–242 (Academic, London, 1972).
5. Köhler, G., Howe, S. G. & Milstein, C. *Eur. J. Immun.* **6**, 292–295 (1976).
6. Galfré, G., Howe, S. C., Milstein, C., Butcher, G. W. & Howard, J. C. *Nature* **266**, 550–552 (1977).
7. Cotton, R. G. H., Secher, D. S. & Milstein, C. *Eur. J. Immun.* **3**, 135–140 (1973).
8. Poodry, C. A. & Schneiderman, H. A. *Wilh. Roux' Arch.* **166**, 1–44 (1970).
9. Reed, C. T., Murphy, D. & Fristrom, D. *Wilh. Roux' Arch.* **178**, 285–302 (1975).
10. Mahowald, A. P., Caulton, J. H., Edwards, M. K. & Floyd, A. D. *Expl Cell Res.* **118**, 404–410 (1979).
11. King, R. C. *Ovarian Development in Drosophila melanogaster* (Academic, New York, 1970).
12. Mahowald, A. P. in *Developmental Systems: Insects* Vol. 1 (eds Counce, S. J. & Waddington, C. H.) 1–47 (Academic, London, 1972).
13. Hardy, R. W., Tokuyasu, K. T., Lindsley, D. L. & Garavito, M. *J. ultrastruct. Res.* **69**, 180–190 (1979).
14. Bownes, M. *J. Embryol. exp. Morph.* **33**, 709–801 (1975).
15. Garcia-Bellido, A., Ripoll, P. & Morata, G. *Devl Biol.* **48**, 132–147 (1976).
16. Crick, F. H. C. & Lawrence, P. A. *Science* **189**, 340–347 (1975).
17. Gehring, W. J. in *The Genetics and Biology of Drosophila* Vol. 2C (eds Ashburner, M. & Wright, T. R. F.) 511–554 (Academic, London, 1978).

K562 human leukaemic cells express fetal type (i) antigen on different glycoproteins from circulating erythrocytes

Minoru Fukuda

Biochemical Oncology, Fred Hutchinson Cancer Research Center, and Department of Pathobiology, School of Public Health, University of Washington, Seattle, Washington 98104

During the ontogenic change from fetal to adult human erythrocytes, as well as fetal haemoglobin being replaced by adult haemoglobin, the cell-surface antigen i is converted to I (ref. 1). Recently it has been shown that this antigenic change is the conversion of the linear repeating Galβ1→4GlcNAcβ1→3Gal structure to branched Galβ1→4GlcNAcβ1→3(Galβ1→4GlcNAcβ1→6)Gal structure[2–4]. We have shown that cell-surface labelling followed by endo-β-galactosidase digestion can distinguish these two forms on the cell surface, and that band 3 and band 4.5 are the major carriers for these antigens on mature erythrocytes[5]. Human leukaemic cell line K562, originally isolated from a patient at blast crisis of chronic myelocytic leukaemia[6], has recently been shown to synthesize glycophorin A[7], and to be capable of synthesizing haemoglobin upon induction[8,9]. I demonstrate here that K562 cells express the fetal type (i) antigen on distinctly different glycoproteins from those of erythrocytes, by the use of cell-surface labelling followed by endo-β-galactosidase digestion or followed by immunoprecipitation with specific antibodies.

Cell-surface glycoproteins were labelled using galactose oxidase/NaB[^{3}H]$_4$ (ref. 10) or by periodate/NaB[^{3}H]$_4$ (ref. 11). Labelled cells were then digested by endo-β-galactosidase[12] and the released oligosaccharides and cell pellet were separated[5]. As shown in Fig. 1, oligosaccharides of various sizes were produced from adult erythrocytes while oligosaccharides of smallest molecular weight were produced from the cord erythrocytes. The former pattern was derived from the branched polylactosaminyl structure with I-type, while the latter was derived from non-branched polylactosaminyl structure with i-type, as demonstrated previously[4,5]. Cell-surface labelled K562 cells showed the

oligosaccharide pattern essentially the same as fetal type (i) (Fig. 1c,d). The K562 cells labelled by [^{3}H]-GlcN produced disaccharide, trisaccharide and tetrasaccharide with endo-β-galactosidase digestion (Fig. 1e). If we assume the specific radioactivities of glucosamine and sialic acid in oligosaccharides derived from [^{3}H]-GlcN labelled cells are the same, the molar ratio of disaccharide to tri- plus tetrasaccharide is calculated to be 3.4:1.0, based on the radioactivities recovered from paper chromatography. This value was fairly close to that (3.2:1.0) obtained on band 3 from i variant adult[4]. These data, together with the results of immunofluorescence staining by anti-i and anti-I sera (data not shown), indicate that fetal (i) antigen with the linear polylactosaminyl structure is present on the cell surface.

Cell-surface glycoproteins were examined before and after endo-β-galactosidase digestion. As shown in Fig. 2, bands 3 and 4.5, which are major Ii antigenic carriers in mature erythrocytes[5], seemed to be absent. Instead, two bands in the band 3 region and PAS 2 were slightly affected by endo-β-galactosidase digestion. However, a glycoprotein at the position of band 3, which was heavily labelled by periodate/NaB[^{3}H]$_4$ or metabolic labelling, was scarcely affected by endo-β-galactosidase, suggesting that this glycoprotein, designated as Gp105 according to a previous report[13], is different from the band 3 glycoprotein present on matured cells. The extent of radioactivity released by endo-β-galactosidase treatment also revealed a significant difference between K562 cells and matured erythrocytes. Galactose oxidase/NaB[^{3}H]$_4$ labelled K562 cells released only 10% of incorporated radioactivity, whereas 40% was released from erythrocytes. On the other hand, 7% of incorporated radioactivity was released from periodate/NaB[^{3}H]$_4$ labelled K562 cells, whereas 5% was released from erythrocytes. The results support the above conclusion that K562 cells express a minimum amount of glycoproteins carrying polylactosaminyl structure, particularly those labelled by galactose oxidase/NaB[^{3}H]$_4$.

Cell-surface labelling followed by immunoprecipitation was then carried out. As shown in Fig. 3, anti-band 3 antiserum precipitated almost no band from cell-surface labelled K562 cells, whereas anti-glycophorin antiserum precipitated PAS 2 from the same cell line. A small amount of Gp105 also
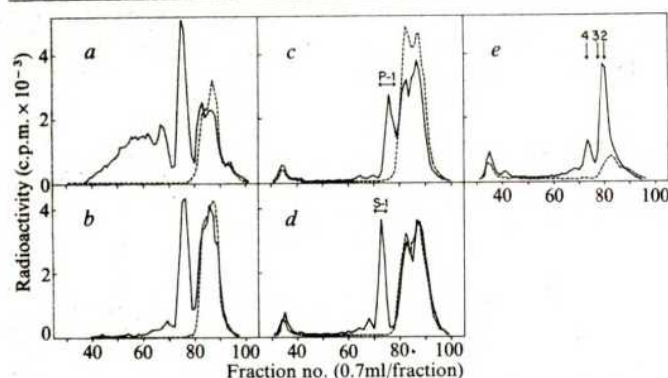
Fig. 1 Gel filtration of oligosaccharide released by endo-β-galactosidase from cell-surface labelled or metabolically labelled cells. Sephadex G-50 (1.0 × 94 cm) was equilibrated and eluted with 0.2 M NaCl. Aliquots (10 μl for *a*, *b*; 100 μl, *c*, *d*; 300 μl, *e*) of each fraction were taken for measuring radioactivity. K562 cells were cultured in RPMI 1640 medium containing 10% fetal calf serum. After washing with 0.01 M sodium phosphate buffer, *p*H 7.4 containing 0.14 M NaCl, 1 mM CaCl$_2$ and 1 mM MgCl$_2$ (PBS), the cells were labelled by galactose oxidase/NaB[^{3}H]$_4$ (ref. 10) or periodate/NaB[^{3}H]$_4$ (ref. 11). K562 cells were also metabolically labelled with [^{3}H]-GlcN as described previously[17]. Cell-surface or metabolically labelled K562 cells were digested with endo-β-galactosidase as described previously[5]. Cell supernatant after incubation with endo-β-galactosidase (———) and cell supernatant after incubation without endo-β-galactosidase (------------). Oligosaccharides from galactose oxidase-labelled adult erythrocytes (*a*) or galactose oxidase-labelled umbilical cord erythrocytes (*b*) or galactose oxidase-labelled K562 cells (*c*) or periodate labelled K562 cells (*d*) or [^{3}H]-GlcN metabolically labelled K562 cells (*e*) were applied. Oligosaccharides from periodate labelled cord erythrocytes showed a similar pattern to those from periodate labelled K562 cells[5] The radioactive peaks in Fraction 80 to 100 are inorganic tritium salt (*a–d*) or [^{3}H]-GlcN monosaccharide (*e*).
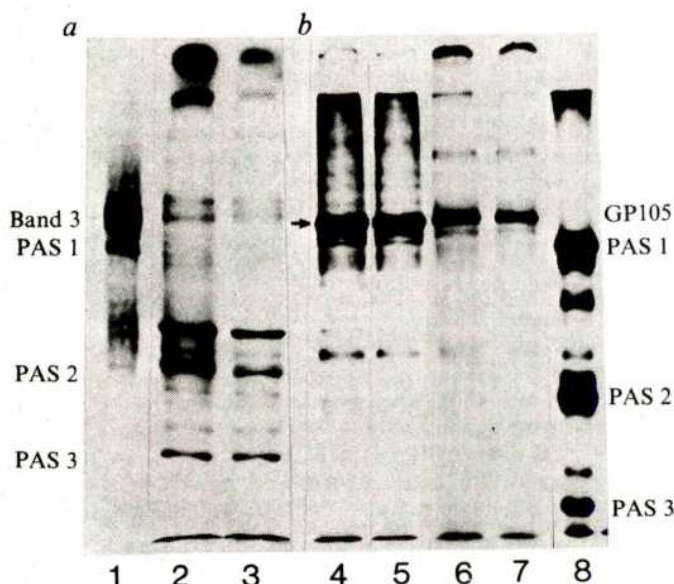
Fig. 2 Fluorograph of SDS-polyacrylamide gels of cell-surface or metabolically labelled cells. Cell pellets obtained as described in Fig. 1 legend were analysed by SDS-polyacrylamide gel electrophoresis[18], using 8% acrylamide concentration in separation gel, and gels were treated for fluorography as described previously[19]. Lane 1, galactose oxidase-labelled adult erythrocytes; Lane 8, periodate-labelled adult erythrocytes; Lanes 2, 3, galactose oxidase labelled K562 cells; Lanes 4, 5, periodate-labelled K562 cells; Lanes 6, 7, [^{3}H]-GlcN metabolically labelled K562 cells. Lanes 2, 4 and 6 are control cells incubated without endo-β-galactosidase and Lanes 3, 5 and 7 are cells incubated with endo-β-galactosidase. Electrophoresis of *a* and *b* were done on different occasions. The numerical designation for the major proteins of human erythrocyte is according to Steck[22].
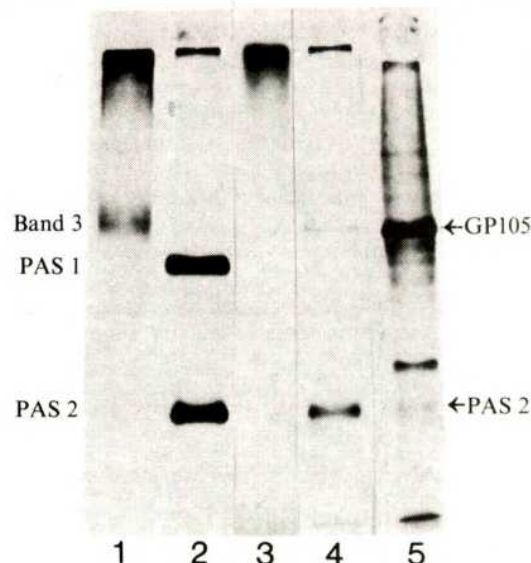
Fig. 3 Fluorograph of SDS-polyacrylamide gels of immunoprecipitates with anti-band 3 antiserum or with anti-glycophorin antiserum. Cell-surface labelled cells were lysed in 0.5% Triton X-100 in PBS containing 1 mM phenylmethylsulphonylfluoride and the extract obtained by centrifugation was treated with anti-band 3 antiserum[20] or anti-glycophorin antiserum (prepared as usual) followed by *Staphylococcus aureus*[21]. The precipitate thus obtained was analysed by SDS-polyacrylamide gel electrophoresis. Lane 1, galactose oxidase-labelled erythrocytes with anti-band 3 antiserum. Lane 2, periodate-labelled erythrocytes with anti-glycophorin antiserum. Each pre-immune serum showed negligible amounts of bands. Lane 3, periodate-labelled K562 cells with anti-band 3 antiserum; Lane 4, periodate-labelled K562 cells with anti-glycophorin antiserum. Lane 5, periodate-labelled K562 cells. The amount of membrane used in lanes 3 and 4 is about four times that of lane 5. Galactose oxidase or [^{3}H]-GlcN labelled K562 cells with anti-band 3 antiserum showed negligible amounts of bands in the same conditions.

coprecipitated with anti-glycophorin antiserum. This was probably nonspecific precipitation as the ratio of Gp105 to PAS 2 was greatly reduced after immunoprecipitation (compare gel 4 and 5 of Fig. 3). Thus Gp105 is different from band 3 or glycophorin.

It is interesting that leukaemic cell line K562 expresses fetal (i) antigen as the elevated expression of i antigen has been reported in erythrocytes of leukaemic patients[14]. This finding may be also relevant to the production of fetal and embryonic haemoglobins by K562 cells upon induction with haemin[9]. The cell-surface glycoprotein profile of this cell line is shown here to be distinctly different from that of mature erythrocytes, although both shared glycophorin as described previously[13] In addition, our recent study suggested that Gp105 was also present as a minor component on erythroblasts cultured *in vitro*[15]. It is possible that some of the unique cell-surface glycoproteins as well as its carbohydrate structure on K562 cells may provide surface markers specific to this tumour cell line or/and proerythroblasts of human cell lineage which are difficult to obtain *in situ*[16].

1. Marsh, W. L. *Br. J. Haemat.* **7**, 200–209 (1961).
2. Watanabe, K. Hakomori, S., Childs, R. A. & Feizi, T. *J. biol. Chem.* **254**, 3221–3228 (1979).
3. Feizi, T., Childs, R. A., Watanabe, K. & Hakomori, S. *J. exp. Med.* **149**, 975–980 (1979).
4. Fukuda, M., Fukuda, M. N. & Hakomori, S. *J. biol. Chem.* **254**, 3700–3703 (1979).

5. Fukuda, M. N., Fukuda, M. & Hakomori, S. *J. biol. Chem.* **254**, 5458–5465 (1979).
6. Lozzio, C. B. & Lozzio, B. B. *Blood* **45**, 321–334 (1975).
7. Jokinen, M., Gahmberg, C. G. & Andersson, L. C. *Nature* **279**, 604–607 (1979).
8. Andersson, L. C., Jokinen, M. & Gahmberg, C. G. *Nature* **278**, 364–365 (1979).
9. Rutherford, T. R., Clegg, J. B. & Weatherall, D. J. *Nature* **280**, 164–165 (1979).
10. Gahmberg, C. G. & Hakomori, S. *J. biol. Chem.* **248**, 4311–4317 (1973).
11. Gahmberg, C. G. & Andersson, L. C. *J. biol. Chem.* **252**, 5888–5894 (1977).
12. Fukuda, M. N. & Matsumura, G. *J. biol. Chem.* **251**, 6218–6225 (1976).
13. Gahmberg, C. G., Jokinen, M. & Andersson, L. C. *J. biol. Chem.* **254**, 7442–7448 (1979).
14. Giblett, E. R. & Crookston, M. C. *Nature* **201**, 1138–1139 (1964).
15. Fukuda, M., Fukuda, M. N., Papayannopoulou, Th. & Hakomori, S. *Proc. natn. Acad. Sci. U.S.A.* **77** (in the press).
16. Harrison, P. R. *Nature* **262**, 353–356 (1976).
17. Fukuda, M. & Hakomori, S. *J. biol. Chem.* **254**, 5442–5450 (1979).
18. Laemmli, U. K. *Nature* **227**, 680–685 (1970).
19. Bonner, W. M. & Laskey, R. A. *Eur. J. Biochem.* **46**, 83–88 (1974).
20. Fukuda, M., Eshdat, Y., Tarone, G. & Marchesi, V. T. *J. biol. Chem.* **253**, 2419–2428 (1978).
21. Tonegawa, Y. & Hakomori, S. *Biochem. biophys. Res. Commun.* **76**, 9–17 (1977).
22. Steck, T. L. *J. Cell Biol.* **62**, 1–19 (1974).

Fig. 1   Structural formulae of furocoumarins.

5-Methoxypsoralen, an ingredient in several suntan preparations, has lethal, mutagenic and clastogenic properties

M. J. Ashwood-Smith*, G. A. Poulton†, M. Barker* & M. Mildenberger*

*Department of Biology and †Department of Chemistry, University of Victoria, Victoria, British Columbia, Canada V8W 2Y2

Many furocoumarins found in several species of plant[1,2] **are potent photosensitizing agents known to cause lethal and mutagenic effects in a wide range of organisms, from viruses to man**[2]**. Their role in the aetiology of cancer is debatable**[3–8]**, but work has focused on the PUVA (psoralen-UVA) treatment of psoriasis with 8-methoxypsoralen (8-MOP) and near UV radiation**[9–18]**. Bergaptene (5-methoxypsoralen, 5-MOP) is a major constituent of oil of bergamot**[1,19]**, and might be expected to have qualitatively similar photosensitizing properties to 8-MOP. Although 5-MOP is widely used as a stimulus to melanin deposition in several suntan preparations surprisingly little is known about its basic photobiology**[2]**. We report here that 5-MOP has the expected properties of other biologically active furocoumarins. These properties include lethal and mutagenic photosensitization of bacteria, 'dark' induced frameshift mutagenesis in bacteria, and lethal and clastogenic effects on mammalian cells in tissue culture.**

The use of 5-MOP in a number of suntan preparations widely available in several European countries has been questioned[20]. It was suggested, in view of the evidence of the carcinogenicity of 8-MOP when combined with near UV light[3–8,15,16], that 5-MOP might have similar properties. There has been one limited study reporting lethal effects of 5-MOP on mouse tumour cells[21], and a brief report on the production of chromosome damage in onion cells[22]. However, there is some information on skin photosensitization and some biochemical effects of 5-MOP, such as binding to DNA and RNA[23–25]: studies have shown 5-MOP to be less active than 8-MOP or psoralen but more active than angelicin (see Fig. 1).

5-MOP is not available commercially but is present in expressed oil of bergamot, the essential oil of *Citrus bergamia* to the extent of 0.30–0.36% (ref. 19). Nearly all samples of bergamot oil sold in the US have been steam distilled and contain no furocoumarins, as these compounds are considered undesirable in perfumery. Pure 5-MOP was isolated[26] from oil of bergamot (Sigma), an expressed oil containing furocoumarins, as no simple method of 5-MOP synethesis has
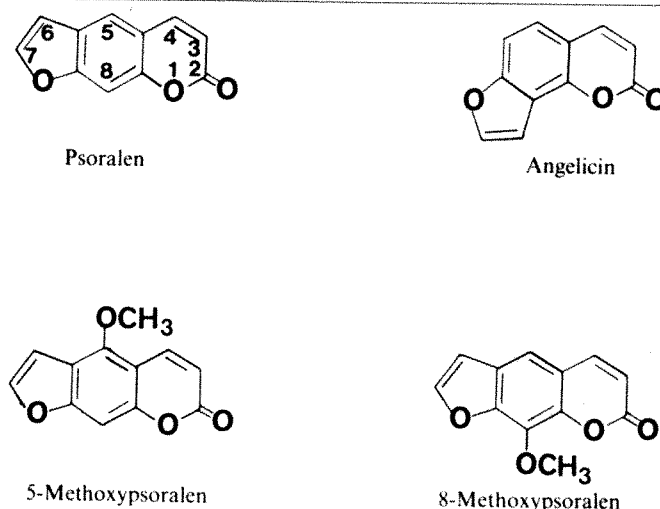
been reported. A series of photobiological studies on pure 5-MOP were compared with those of other furocoumarins.

Lethal photosensitization of *Escherichia coli* by several furocoumarins is shown in Fig. 2. Neither UV radiation alone nor any one of the test compounds was active unless combined. These results are similar to those generally seen with furocoumarins[27–29]. The effectiveness of 5-MOP in producing lethal damage relative to the most active compound, psoralen and the least active, angelicin, was essentially predictable from the early studies on photoreactivity with nucleic acids, skin photosensitization and lethal effects on tumour cells[21,24].

The mutagenic activity of 5-MOP, in the presence of near UV light, relative to three other furocoumarins is shown in Fig. 3. Base-pair substitutions were assayed in *E. coli* WP2 *try*⁻. As with the studies on lethality the order of effectiveness ranked psoralen as the most active compound and angelicin as
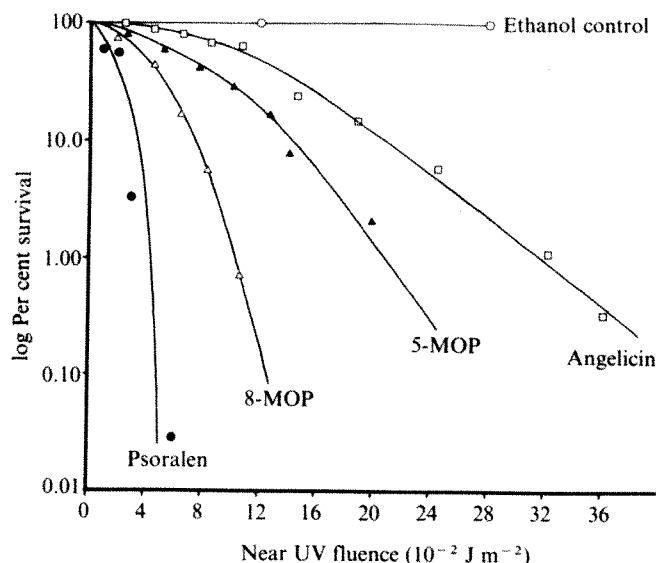
Fig. 2   Lethal photosensitization of *E. coli* with various furocoumarins (40 μg ml⁻¹ each). *E. coli* WP2 *try*⁻ was grown in nutrient broth at 22 °C and when the cells were at a density of ~5 × 10⁸ cells per ml (logarithmic growth stage) they were filtered and resuspended in 0.07 M phosphate buffer at pH 7.2 before irradiation which was 5 min after the addition of the furocoumarins. Near UV (320–380 nm) was produced by two parallel GEC black lamps (F20T12.BLB) emitting 13.4 J m⁻² as measured by chemical actinometry. Cells were plated on nutrient agar and colonies counted after 24 h of incubation at 37 °C.
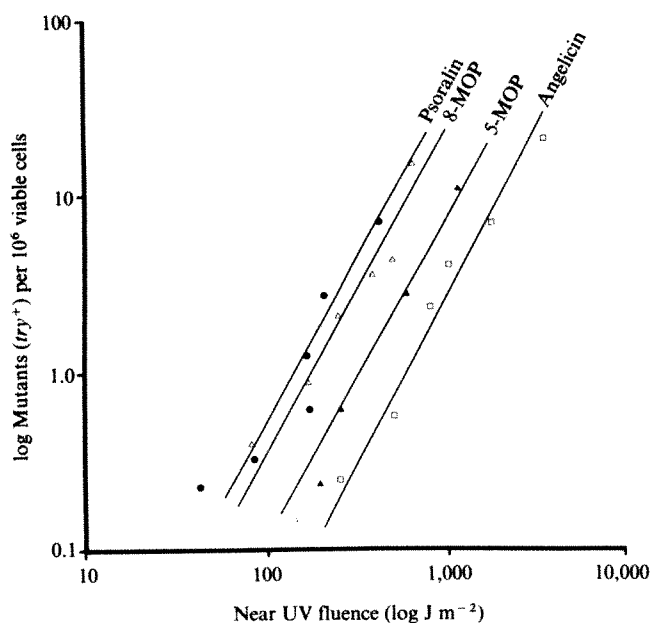
Fig. 3 Mutagenesis in *E. coli* induced by furocoumarins (40 μg ml^{-1}) and near UV light. *E. coli* WP2 *try*$^-$ was grown as described in Fig. 2 legend. Handling and irradiation conditions were identical. Mutant (*try*$^+$) cells were detected on minimal plates 48 h after incubation[27].

the least active. The slope of the log–log plot suggests a two-hit mechanism (R. C. von Borstel, personal communication) of mutagenesis, which is basically similar for all the furocoumarins.

The inability of angelicin to form DNA interstrand cross-links has been reported[28–31], and the slope of the angelicin curve is not easily explained. Interstrand DNA cross-links are implicated in death caused by photosensitizing furocoumarins[32,33]; their role in mutagenesis has only recently been studied[28,29]. The mutation system used in this experiment is well understood and is related to either true suppression of an ochre stop codon in the tryptophan synthetase pathway or reversion. Some of the original observations of mutagenesis with 8-MOP in *E. coli* were performed with this same test system[27].

Several reports have indicated that 8-MOP acts as a weak frameshift mutagen in bacteria, *per se*, in the absence of light[34,35]. Recently M.J.A.-S.[36] reported that angelicin and psoralen were frameshift mutagens in *E. coli* although surprisingly, 4,5′,8-trimethylpsoralen was inactive. Trimethylpsoralen is one of the most active photosensitizing compounds, however. Experiments with *E. coli lac*$^-$ (strain ND160) plus 5-MOP indicate that it is active as a frameshift mutagen. The rank order (relative to a standard ethanol control which gave 40 ± 23 (±s.d.) *lac*$^+$ mutants per 1 × 10⁸ viable cells and 346 ± 49 (±s.d.) *lac*$^+$ mutants with psoralen) was as follows: control, 1.0; 5-MOP, 2.4; 8-MOP, 5.1; angelicin, 5.9; and psoralen, 8.6. All compounds were tested at 40 μg ml^{-1}.

control, 1.0; 5-MOP, 2.4; 8-MOP, 5.1; angelicin, 5.9; and psoralen, 8.6. All compounds were tested at 40 μg ml^{-1}.

The lethal photosensitizing effect on Chinese hamster cells in tissue culture is illustrated in Fig. 4a. The results with psoralen are remarkably similar to those with 8-MOP and Chinese hamster cells[37]. Again, the three furocoumarins tested had the same ranked order of effectiveness in lethal photosensitization with mammalian cells as they had with bacterial cells.
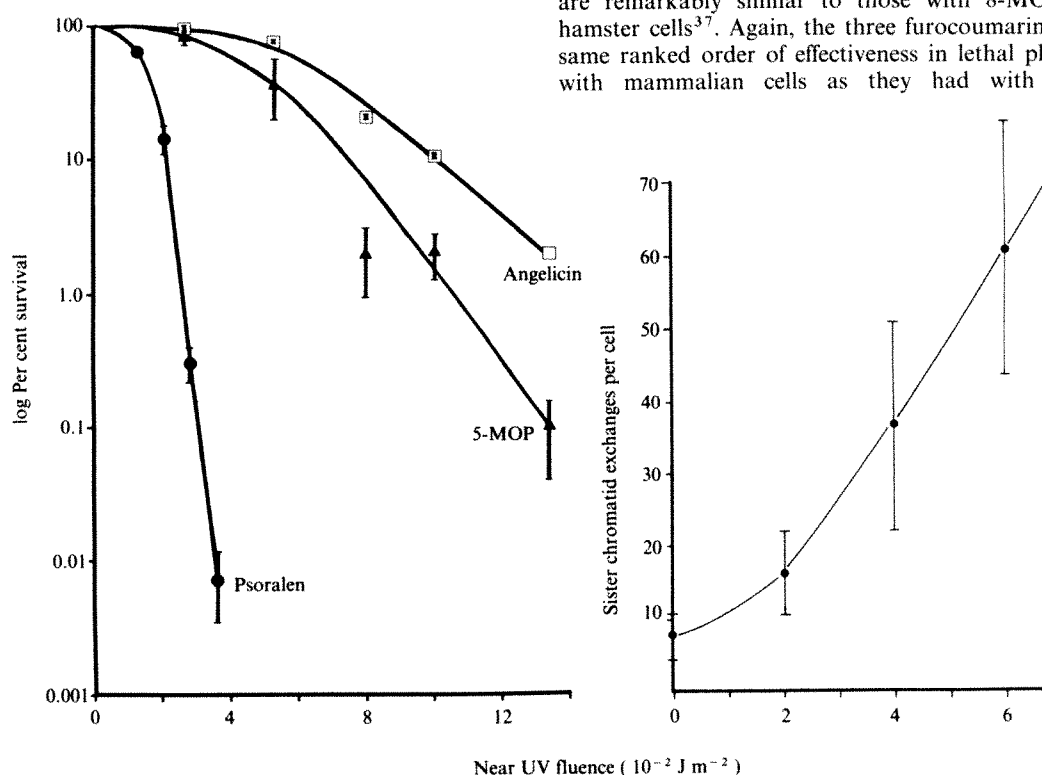
Fig. 4 *a*, Lethal photosensitization of Chinese hamster cells in tissue culture with furocoumarins (40 μg ml^{-1}). Chinese hamster cells (CHO) were grown in McCoy's medium supplemented with 15% fetal calf serum. The handling and irradiation conditions have been described[38]. Cells, attached to the surface of plastic flasks, were washed with tissue culture medium minus serum. Furocoumarins dissolved in 95% ethanol were added 10 min before irradiation. When the irradiation was completed fresh medium containing serum was added and the cells incubated for 10 days at 37 °C before colony counts were made. Results are expressed as per cent survival ± s.d. *b*, Sister chromatid exchanges in Chinese hamster cells induced by 5-MOP and near UV. Chinese hamster cells were grown and irradiated as in *a*. Standard methods for the detection of SCEs were used by growing cells for 30 h in the presence of bromodeoxyuridine after irradiation and using staining and fixation procedures essentially as described by Perry and Wolff[45]. A division delay after furocoumarin photosensitization has been observed[38] and therefore 30 h rather than 24 h (about two divisions for normal CHO cells) was chosen as the collection time. Error bars, ± s.d.

Chromosome damage in Chinese hamster cells treated with psoralen, or angelicin and near UV has been reported[38], and photosensitized cell death and mutations in surviving cells with 8-MOP has been demonstrated in several different mammalian systems[6,7,37,39], including diploid human skin fibroblasts in tissue culture[40]. The formation of sister chromatid exchanges (SCEs) when Chinese hamster cells were irradiated with near UV in the presence of $40 \mu g \, ml^{-1}$ 5-MOP is illustrated in Fig. 4b. The dose–response curve is normal and the points chosen represent lethality values induced by the treatment within a range of 5–95% kill. 8-MOP yielded SCE values similar to those obtained with 5-MOP at equivalent cell survival. The formation of SCEs in human diploid skin cells after 8-MOP and UV irradiation has recently been reported[40] and lymphocytes from patients treated with 8-MOP showed increased SCEs when irradiated *in vitro*[41]. However, after PUVA therapy there has not generally been an observable increase in SCEs[40].

Interrupted irradiation experiments similar to those described for trimethylpsoralen with tissue culture cells[42] and for bacteria with angelicin and psoralen[31] suggested that 5-MOP forms DNA interstrand cross-links. The slope of the bacterial survival curve was only slightly changed when irradiation was continued after removal of free 5-MOP from cells irradiated with UV light to a point which produced a kill of 10%. In contrast, experiments with angelicin, which cannot form cross-links, have resulted in an abrupt cessation in the lethality induced by irradiation when angelicin was removed[31]. Preliminary experiments using alkaline sucrose density gradient analysis indicate the formation of DNA interstrand cross-links, albeit perhaps less efficiently than with psoralen or 8-MOP.

We conclude that 5-MOP produces similar photobiological responses to 8-MOP, a chemical clearly possessing mutagenic, clastogenic and carcinogenic properties in conjunction with near UV radiation.

The use of 5-MOP in suntan preparations constitutes, in our judgement, a definite and unnecessary hazard. The concentrations of 5-MOP present in the most widely used preparations vary from 12 to $50 \mu g \, ml^{-1}$. Our studies with 5-MOP were conducted with $40 \mu g \, ml^{-1}$. The possible advantages derived from increased pigmentation several days after the topical application of 5-MOP are the enhanced protection against the known biological effects of sunlight. However, the problem of the molecular and chromosomal damage likely to be produced in human skin before the formation of pigment seems to us to greatly outweigh any benefits. Individuals at risk also include those bathing in swimming pools containing 'washed-off' 5-MOP.

As we learn more about the distribution of heterozygotic genes that affect DNA repair[43] the proportion of individuals at risk may be found to be much higher than anticipated. Worthy of note in this context are the unfortunate experiments where treatment of *Xeroderma pigmentosum* patients with 8-MOP and near UV resulted in skin cancers[44]. An epidemiological study of skin cancers and melanomas in which the role of these preparations is examined is clearly necessary.

Note added in proof: Studies begun in August 1978 at the Institut du Radium, Orsay, France, have shown that 5-MOP in combination with near UV is almost as potent a skin carcinogen in mice as 8-MOP (F. Zajdela, personal communication, April 1980).

1. Mitchell, J. & Rook, A. in *Botanical Dermatology* (Greengrass, Vancouver, 1979).
2. Scott, B. R., Pathak, M. A. & Mohn, G. R. *Mutat. Res.* 39, 29-74 (1976).
3. Urbach, F. *J. invest. Derm.* 32, 373-378 (1959).
4. Griffin, A. C. *J. invest. Derm.* 32, 367-372 (1959).
5. Forbes, P. D., Davies, R. E. & Urbach, F. *Fd Cosmet. Toxic.* 14, 303-306 (1976).
6. Burger, P. M. & Simons, J. W. I. M. *Bull. Cancer* 65, 281-282, 3 (1978).
7. Evans, D. L. & Morrow, K. J. *J. invest. Derm.* 72, 35-41 (1979).
8. Grube, D. D. *Proc. Am. Ass. Cancer Res.* 16, 117 (1975).
9. Epstein, J. H. & Fukuyama, K. *J. invest. Derm.* 54, 350-351 (1970).
10. Walter, J. F. & Voorhees, J. J. *Acta derm.-vener., Stockh.* 53, 469-472 (1973).
11. Weber, G. *Br. J. Derm.* 90, 317-323 (1974).
12. Parrish, J. A., Fitzpatrick, T. B. & Tanenbaum, L. *New Engl. J. Med.* 291, 1207-1211 (1974).
13. Wolf, K., Fitzpatrick, T. B. & Parrish, J. A. *Arch. Derm.* 112, 943-950 (1976).
14. Melski, T., Tanenbaum, L. & Parrish, J. A. *J. invest. Derm.* 68, 328-335 (1977).
15. Stern, R. S., Thibodeau, L. A., Kleinerman, R. A., Parrish, J. A. & Fitzpatrick, T. B. *New Engl. J. Med.* 300, 809-813 (1979).
16. Epstein, J. H. *New Engl. J. Med.* 300, 852-853 (1979).
17. Ashwood-Smith, M. J. & Grant, E. L. *Br. med. J.* i, 342 (1976).
18. Strauss, G. H. & Albertini, R. J. *J. invest. Derm.* 73, 211 (1979).
19. Cieri, U. R. *J. Ass. off. analyt. Chem.* 52, 719-728 (1969).
20. Ashwood-Smith, M. J. *Br. med. J.* ii, 1144 (1979).
21. Musajo, L., Visentini, P., Baccichetti, F. & Razzi, M. A. *Experientia* 23, 335-336 (1967).
22. Musajo, L. *Farmaco* 10, 2-7 (1955).
23. Musajo, L. & Rodighiero, G. *Prog. Biochem. Pharmac.* 1, 366-371 (1965).
24. Rodighiero, G. *et al. Experientia* 25, 479-481 (1969).
25. Rodighiero, G. *et al. Biochim. biophys. Acta* 217, 40-49 (1970).
26. Steck, W. *Phytochemistry* 9, 1145-1146 (1970).
27. Igali, S., Bridges, B. A., Ashwood-Smith, M. J. & Scott, B. R. *Mutat. Res.* 9, 289-295 (1970).
28. Averbeck, D. P., Chandra, P. & Biswas, R. F. *Radiat. envir. Biophys.* 12, 241-252 (1975).
29. Grant, E. L., von Borstel, R. C. & Ashwood-Smith, M. J. *Envir. Mutat.* 1, 55-63 (1979).
30. Rodighiero, G. *et al. Biophysik* 8, 1-8 (1971).
31. Ashwood-Smith, M. J. & Grant, E. *Experientia* 33, 384-386 (1977).
32. Cole, R. S. *Biochim. biophys. Acta* 254, 30-39 (1971).
33. Cole, R. S. *Proc. natn. Acad. Sci. U.S.A.* 70, 1064-1068 (1973).
34. Clarke, C. H. *Mutat Res.* 28, 123-125 (1975).
35. Bridges, B. A. & Mottershead, R. P. *Mutat. Res.* 44, 305-312 (1977).
36. Ashwood-Smith, M. J. *Mutat. Res.* 58, 23-27 (1978).
37. Burger, P. M. & Simons, J. W. I. M. *Mutat. Res.* 60, 381-389 (1979).
38. Ashwood-Smith, M. J., Grant, E. L., Heddle, J. A. & Friedman, G. B. *Mutat. Res.* 43, 377-385 (1977).
39. Arlett, C. F., Heddle, J. A., Broughton, B. C. & Rogers, A. M. *Clin. exp. Derm.* (in the press).
40. Burger, P. M. & Simons, J. W. I. M. *Mutat. Res.* 63, 371-380 (1979).
41. Mourelatos, D., Faed, M. J. W., Gould, P. W., Johnson, B. E. & Frain-Bell, W. *Br. J. Derm.* 97, 649-654 (1977).
42. Ben-Hur, E. & Elkind, M. M. *Biochim. biophys. Acta* 331, 181-193 (1973).
43. Paterson, M. C., Anderson, A. K., Smith, B. P. & Smith, P. J. *Cancer Res.* 39, 3725-3734 (1979).
44. Reed, B. *Acta Derm.-vener., Stockh.* 56, 315-318 (1976).
45. Perry, P. & Wolff, S. *Nature* 251, 156-158 (1974).

Selective disruption of displacement behaviour by lesions of the mesolimbic dopamine system

Trevor W. Robbins

Department of Experimental Psychology, Downing Street, Cambridge CB2 3EB, UK

George F. Koob

A. V. Davis Center for Behavioural Neurobiology, Salk Institute, San Diego, California 92138

In the wild, organisms generally allocate their time among many behavioural tendencies in response to both current and anticipated motivational requirements[1]. However, activities that are apparently 'irrelevant' often intrude, either during conflict between these behavioural tendencies, or when a strong tendency is thwarted. These 'irrelevant' activities are called displacement behaviours and are widely documented in the ethological literature[2,3]. We report here that an experimental analogue of displacement behaviour in the rat depends upon the integrity of the mesolimbic dopaminergic projection to the nucleus accumbens septi, olfactory tubercle and associated structures of the forebrain[4-6].

Hungry rats exposed to the periodic presentation of small pellets of food, with temporal delay, in an experimental chamber develop excessive drinking, which can be explained neither in terms of physiological deficit, nor as a 'superstitious' result of the adventitious pairing of drinking with the delivery

Table 1 Neurochemical effects of 6 OH-DA lesions of NAS region

Mean dopamine levels (ng per mg protein) (expt. 1)

Group	n	NAS/OT	Anterior striatum	Posterior striatum
Sham	6	13.56 ± 2.42	19.41 ± 3.95	52.00 ± 4.67
Lesion	7	2.67 ± 0.62†	6.93 ± 2.36*	53.08 ± 7.09
% Depletion		80	64	

Mean tyrosine hydroxylase activity (pm per mg L-dopa per h) (expts 2 and 3)

Group	n	NAS	OT	Corpus striatum
Sham and unoperated	12	282.2 ± 63.7	366.2 ± 66.5	442.7 ± 81.4
Lesion	12	39.6 ± 8.6†	65.5 ± 16.3†	304.1 ± 34.8
% Depletion		86	82	31

8 µg of 6 OH-DA base were infused bilaterally in 2 µl vehicle at a rate of 1 µl per min through a 30-gauge stainless steel cannula. Stereotaxic co-ordinates were; anterior to bregma +3.4; lateral ±1.7; ventral from dura −7.2 mm, using the angle of Pellegrino and Cushman[18]. Rats received pretreatment with pargyline (50 mg per kg), and (in experiments 2 and 3 only) desmethylimipramine (DMI) (15 mg per kg), 30 min prior to operation. DMI was used to protect noradrenaline (NA) from depletion by 6 OHDA[19], although NA depletion is probably not critical for these behavioural results[17]. A histological control, and details of the dissection procedure have previously been published[17]. Anterior striatum was dissected from the coronal slice containing nucleus accumbens. Nucleus accumbens (NAS) and olfactory tubercle (OT) were pooled in experiment 1. Dopamine was assayed by a radio-enzymatic technique[20,21]. Tyrosine hydroxylase activity was measured by a method modified from Hendry and Iversen[22]. Values given are means ± s.e.m.
*P < 0.05.
†P < 0.01, Student's t-test comparing lesion with control group.

of food[7]. Indeed, the incidence of other behaviours such as aggression, gnawing and wheel-running in comparable situations, for a variety of species including man, has encouraged the concept of a general category of 'adjunctive' behaviour, which is probably related to the more familiar displacement activities [1,7–9]. One possible explanation of adjunctive behaviour is that the motivational excitement or activation accompanying the delivery of a food pellet may outlast its consumption, and potentiate alternative activities evoked by available environmental stimuli[10]. These acts are performed vigorously until interruption by competing behaviour emitted in anticipation of the next food pellet[10]. The ancillary activational effect of the rewarding food pellet has been compared to that evoked by electrical stimulation of the lateral hypothalamus[11,12], which can itself engender adjunctive drinking[13]. Destruction of the lateral hypothalamus produces a reduction in adjunctive drinking[14], but this lesion also produces a profound syndrome of aphagia and adipsia[15], thus placing the specificity of the other effect in doubt. Major elements of the lateral hypothalamic syndrome have been attributed to damage of the ascending nigrostriatal dopamine (DA) projection which courses through the lateral hypothalamus[16]. A parallel dopamine projection, termed the mesolimbic DA system, originates in the ventral tegmental area (VTA) and innervates forebrain limbic areas such as the nucleus accumbens septi (NAS), olfactory tubercle (OT), and frontal cortex (FC)[4–6]. Recently, we found that destruction of the DA terminals in the NAS and OT did not produce primary motivational deficits, but did alter the apparent time-sharing among eating, drinking and locomotor activity in certain situations[17]. We now show that similar lesions attenuate adjunctive drinking, but not drinking induced by water deprivation, this report being the first of this type of dissociation. We also provide data on drinking and activity compatible with the hypothesis that the lesion attenuates adjunctive drinking by reducing activation and thus disrupting time-sharing among different activities.

In all experiments described here, destruction of DA terminals in NAS and OT was effected by stereotaxic, bilateral injections of 6-hydroxydopamine (6-OHDA) into the region of the NAS (see legend to Table 1) in anaesthetized male albino Wistar rats weighing about 300 g. Control rats received injections of vehicle (0.2 % ascorbic acid in 0.9 % saline) as sham

lesions, or in some cases, no operation at all. There were no differences in biochemical or behavioural parameters between sham-lesioned and unoperated rats, and hence their data are combined. Treatment with 6-OHDA produced reductions in activity of tyrosine hydroxylase (an enzyme involved in the biosynthesis of DA and noradrenaline), as well as regional depletion of DA in NAS/OT and the anterior striatum (Table 1).

In experiment 1, adjunctive drinking was induced by a standard procedure in lesioned and control rats[23]. Following reduction to 85 % of free-feeding weight, rats were familiarized on postoperative days 10–11, to a chamber containing a dispenser which could deliver food-pellets to a tray, and a spout connected to a graduated burette filled with water. The spout was situated 9.1 cm from the floor and 7.2 cm to the left of the food-tray. For the next 10 days, a single 45 mg food pellet (Noyes) was delivered to the tray every 60 s of the 30 min session. This schedule of delivery resulted in the gradual development of excessive drinking in 7 of 8 control rats, measured either in terms of volume of water consumed (Fig. 1), or by the number of licks recorded by a drinkometer circuit. This drinking cannot be attributed to a 'dry mouth' produced by the food pellets, since similar rats consuming about 8 times as much food of comparable nature over an identical time-period were found previously[17] to drink only about 60 % of the volume of water that these rats were ingesting by session 10. Cumulative pen-recordings of the drinking showed that it occurred predominantly in the initial portions of the period following food-delivery, the temporal locus characteristic of adjunctive behaviour[7]. In contrast to controls, rats with 6-OHDA lesions exhibited significant attenuation of adjunctive drinking, whether measured in terms of water-intake or licks recorded (Fig. 1). Dual measures were used partly because of the possibility of reduced lap volume or drinking efficiency in rats with pharmacological blockade of DA receptors in NAS[25]. Inspection of our data supports the possibility of small impairments in drinking efficiency in rats with 6-OHDA lesions, but the parallel reductions in licking and intake rule out inefficiency of licking as a simple explanation of the reduced adjunctive drinking.

Experiments 2 and 3 show that the reduction of adjunctive drinking also cannot be explained as a deficit in primary thirst, but may be correlated with reduction in motivational activation as measured by locomotor activity and changes in time-sharing among different behaviours. In experiment 2, different groups of rats with 6-OHDA lesions, and controls,
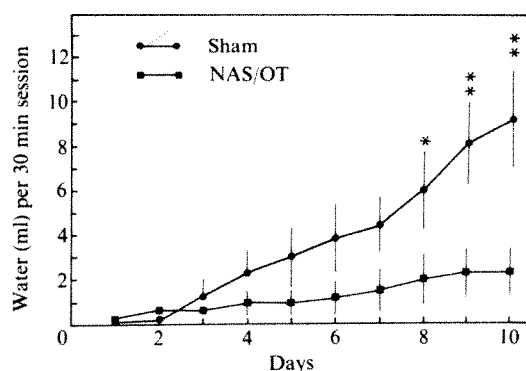
Fig. 1 Mean water intake in adjunctive drinking experiment. Asterisks indicate levels of statistical significance of difference between controls (n = 8) and rats with 6-OHDA lesions of NAS (n = 8), *P < 0.05, **P < 0.01. Following analysis of variance with repeated measures, F values for days 8, 9, and 10 were respectively: 7.17, 15.45, and 22.43 (with 1 and 33 d.f., following Satterthwaite's approximation[24]). Mean numbers of licks per 30 min of NAS and control groups for days 8, 9 and 10 were: NAS, 588.3, 642.1 and 681.9; control, 1418.9, 1835.3 and 2026.6, both respectively. These differences were significant beyond P < 0.01 for days 9 and 10, and beyond P < 0.05 for day 8.

Table 2 Behavioural results from experiment 2

Behavioural measure		n	Post-operative day			
			2	3	4	5
Locomotor activity	NAS	12	108.5 ±11.8	103.1 ± 9.2	101.6 ± 9.0	80.6 ± 8.8
(mean counts per 10 min)	Control	12	194.7 ±18.3	161.8 ±15.2	147.9 ±12.4	132.6 ±14.4
Drinking	NAS	12	1.74± 1.05	11.02± 0.72	12.27± 0.36	12.23± 0.85
(mean ml consumed per 30 min)	Control	12	0.81± 0.36	13.74± 0.76	12.06± 0.76	12.17± 0.92

Rats were not deprived on postoperative day 2, but were deprived for 23 h on days 3, 4, and 5. The NAS group was significantly less active than controls on day 2 ($F = 15.66$, d.f. = 1,22, $P < 0.001$), and on days 3, 4 and 5 ($F = 17.45$, d.f. = 1,22; $P < 0.001$). There were no overall differences in mean water intake between the two groups, either on day 2 or days 3, 4 and 5 (both $F < 1.00$, $P > 0.05$).

were familiarized 2 days after surgery for 30 min to cages each containing a single photocell beam across the long axis[17], situated 20 cm from one wall, to which were attached two burettes containing water. On 3 subsequent days, the rats were deprived of water for 23 h before testing. The rats with 6-OHDA lesions§ showed a highly significant reduction in loco-motor activity but no significant lasting attentuation of water-intake compared with controls (see Table 2).

In experiment 3, we took the same deprived rats and studied their drinking patterns and activity individually over post-operative days 7–13, in an open field (50 × 35 cm) supplied with three burettes attached to one of the shorter walls and situated at 8 cm intervals, in three 15 min trials. Again, no significant effects of the 6-OHDA lesion on water-intake were found, although there were marked changes in the pattern of drinking exhibited. For example, the rats with lesions con-sumed significantly more water from their most preferred burette on the first two trials, as measured by the preference ratio (Table 3). In addition, observations on trials 1 and 3, made via closed circuit television, revealed that the rats with 6-OHDA lesions showed significantly longer bouts of drinking (Table 3). In addition, these rats made significantly fewer crossings among the four quadrants of the open-field (Table 3) thus confirming the hypoactivity found in the photocell cages.

In explaining these results it seems unlikely that the reduced adjunctive drinking is caused by a general sensory or motor debilitation given that the lesioned rats were all capable of locating and consuming the food delivered in experiment 1 and of drinking normal amounts in experiments 2 and 3. It remains possible that the reduction in adjunctive drinking results from an inability to move the small distance from the

food tray to the water tube, although inspection of individual data revealed that all the rats with lesions at least sampled the water-tube on every session. Alternatively, the hypoactivity as well as the attenuation of adjunctive drinking results from reduced motivational excitement in the rats with 6-OHDA lesions. This reduced activation leads to fewer interruptions of behaviour made dominant by deprivation[17], or by previous training[26], thus explaining the initial 'focusing' of behaviour on a single burette and the changes in drinking pattern observed in experiment 3.

As expected, the 6-OHDA lesion produced a depletion of DA in NAS and OT. However, the demonstration of ad-ditional DA depletion in both the frontal cortex and the anterior striatum (Table 1 and ref. 17) poses the problem of defining the sufficient extent of DA depletion within the terminal areas critical for the observed behavioural effects. This problem is related to the definition of the mesolimbic DA system, itself. Recent anatomical evidence[5,6] has shown con-siderable overlap in the innervation of the forebrain DA terminal regions by the DA cell bodies of the VTA and substantia nigra thus blurring the original distinction between the ascending nigrostriatal (A9) and mesolimbic (A10) pro-jections. However, it is clear that 6-OHDA lesions of the portions of the DA terminals in the limbic forebrain produce very different effects from 6-OHDA lesions of the corpus striatum[27]. Therefore, the behavioural effects we have found may help us to understand the function of a broadly-defined mesolimbic DA system encompassing, not only the NAS and OT, but also the frontal cortex and anterior striatum.

We believe these results to be important for several reasons. First, they provide an intriguing parallel to the severe deficits

Table 3 Behavioural results from experiment 3

Behavioural measure	Group	n	Post-operative day (trials 1–3)		
			7	10	13
Mean preference ratio*	NAS	12	0.81 ±0.06	0.90 ±0.03	0.68 ±0.04
	Control	12	0.63 ±0.04	0.74 ±0.05	0.75 ±0.04
Drinking†	NAS	12	10.58 ±0.52	12.04 ±0.90	14.18 ±1.04
(mean ml consumed per 15 min)	Control	12	9.13 ±0.45	12.20 ±0.63	12.61 ±0.62
Locomotor activity‡	NAS	12	41.2 ±6.15	—	31.5 ±5.33
(quadrants crossed per 15 min)	Control	12	71.6 ±5.92	—	53.2 ±2.71
Mean duration of a bout	NAS	12	17.37 ±2.29	—	21.79 ±4.10
of drinking§ (s)	Control	12	10.19 ±1.39	—	14.47 ±1.50

*The preference ratio was calculated for each rat by dividing volume consumed from the most preferred burette by the total volume consumed from all three burettes. Values thus range from 0.33 (no preference) to 1.00 (maximum preference for a single burette). The NAS group showed significant enhancement of preference on trials 1 and 2 ($F = 8.19$, d.f. = 1,22, P, p < 0.01 and $F = 7.30$, d.f. = 1,22, $P < 0.01$, respectively), following overall analysis of variance with repeated measures[24].
†There were no significant differences in water intake between the NAS and control groups $F < 1.00$, $P > 0.05$).
‡The NAS group was significantly less active than controls ($F = 16.60$, d.f. = 1,22, $P < 0.01$).
§The NAS group exhibited significantly longer mean durations of a drinking bout ($F = 4.95$, d.f. = 1,22, $P < 0.05$). Locomotor activity and duration of drinking were measured only on trials 1 and 3. The data from one rat were excluded from trial 3 because of a technical error.

in consummatory behaviour observed in rats with nigro-striatal DA damage[16]. Our rats with lesions to the region of the NAS, while showing no regulatory impairments, exhibit instead changes in nonspecific excitement engendered by a motivational state.

Second, only one other study has demonstrated by neural means a dissociation between 'displacement' and 'deficit' drinking[28]. That experiment showed that hippocampal lesions, probably in conjunction with endocrine changes in the pituitary-adrenal axis, enhanced adjunctive drinking, while not significantly changing deprivation-induced drinking. Thus, these results support the contention that displacement behaviour may develop in part by effects of nonspecific motivational excitement, including stress.

1. McFarland, D. J. in *Advances in the Study of Animal Behaviour* Vol. 5 (eds Lehrman, D. S., Hinde, R. H. & Shaw, E.) 201–225 (Academic, London, 1974).
2. Tinbergen, N. E. *Q. Rev. Biol.* **27**, 1–32 (1952).
3. Hinde, R. A. *Animal Behaviour: a Synthesis of Ethology and Comparative Psychology* (McGraw-Hill, New York, 1966).
4. Lindvall, O. & Bjorklund, A. in *Handbook of Psychopharmacology* Vol. 9 (eds Iversen, L. L., Iversen, S. D. & Snyder, S. H.) 139–231 (Plenum, New York, 1978).
5. Fallon, J. H. & Moore, R. Y. *J. comp. Neurol.* **180**, 545–580 (1978).
6. Simon, H., Le Moal, M., Galey, D. & Cardo, B. *Brain Res.* **115**, 215–231 (1976).
7. Falk, J. L. *Physiol. Behav.* **6**, 577–588 (1971).
8. Staddon, J. E. R. & Simmelhag, V. L. *Psychol. Rev.* **78**, 3–43 (1971).
9. Kachanoff, R., Leveille, R., McClelland, J. P. & Wayner, M. J. *Physiol. Behav.* **11**, 395–398 (1973).
10. Killeen, P. R., Hanson, S. J. & Osbourne, S. R. *Psych. Rev.* **85**, 571–581 (1978).
11. Wallace, M. & Singer, G. *Pharmac. Biochem. Behav.* **5**, 483–490 (1976).
12. Wayner, M. J. *Physiol. Behav.* **5**, 1319–1325 (1970).
13. Cantor, M. B. & Wilson, J. F. *Learn Motiv.* **9**, 428–445 (1978).
14. Falk, J. L. in *Thirst* (ed. Wayner, M. J.) 95–113 (Pergamon, New York, 1964).
15. Teitelbaum, P. & Epstein, A. N. *Psych. Rev.* **69**, 74–90 (1962).
16. Ungerstedt, U. *Acta physiol. scand. Suppl.* **367**, 95–122 (1971).

17. Koob, G. F., Riley, S. J., Smith, S. C. & Robbins, T. W. *J. comp. Physiol. Psychol.* **92**, 651–660 (1978).
18. Pellegrino, L. J. & Cushman, A. J. *A Stereotaxic Atlas of Rat Brain* (Appleton-Century-Crofts, New York, 1967).
19. Breese, G. R. & Traylor, T. D. *Br. J. Pharmac.* **42**, 88–89 (1972).
20. Coyle, J. T. & Henry, D. *J. Neurochem.* **21**, 61–67 (1973).
21. Saller, C. F. & Zigmond, M. J. *Life Sci.* **23**, 1117–1130 (1978).
22. Hendry, I. A. & Iversen, L. L. *Brain Res.* **29**, 159–162 (1971).
23. Sanger, D. J. & Blackman, D. E. in *Contemporary Research in Behavioural Pharmacology* (ed. Blackman, D. E. & Sanger, D. J.) 239–287 (Plenum, New York, 1978).
24. Winer, B. J. *Statistical Principles in Experimental Design* 2nd edn (McGraw-Hill, New York, 1971).
25. Jones, D. L. & Mogenson, G. J. *Eur. J. Pharmac.* **59**, 11–21 (1979).
26. Robbins, T. W. *Neurosci. Lett.* **S58**, Suppl. 1 (1978).
27. Kelly, P. H., Seviour, P. & Iversen, S. D. *Brain Res.* **94**, 507–522 (1975).
28. Devenport, L. D., *J. comp. physiol. Psychol.* **92**, 651–660 (1978).
29. Skinner, B. F. & Morse, W. H. *J. comp. physiol. Psychol.* **50**, 279–281 (1957).
30. Holland, H. C. in *Obsessional States* (ed. Beech, H. R.) 161–173 (Methuen, London, 1974).
31. Thierry, A. M., Tassin, J. P., Blanc, G. & Glowinski, J. *Nature* **263**, 242–244 (1976).
32. Price, K. A., Farley, I. J. & Hornykiewicz, O. in *Dopamine* (eds Rogers, P. J., Woodruff, G. N. & Iversen, L. L.) 293–300 (Raven, New York, 1978).
33. Stevens, J. R. *Archs gen Psychiat.* **29**, 177–189 (1973).

Genetic retrieval of viral genome sequences from herpes simplex virus transformed cells

M. Park, D. M. Lonsdale, M. C. Timbury, J. H. Subak-Sharpe & J. C. M. Macnab

Institute of Virology, Church St, Glasgow G11 5JR, UK

Oncogenic transformation of cultured cells by inactivated herpes simplex virus (HSV) types 1 and 2 has been demonstrated[1-12]. Expression of HSV information in these transformed cells has been shown by immunofluorescence studies[2,6,8,13-15], detection of HSV neutralizing antibody in sera from tumour-bearing animals[1,4,7,11,12] and by hybridization of HSV-specific RNA[16-18]. Molecular hybridization studies of DNA from HSV-2 transformed hamster cells have detected up to 40% of the HSV genome present in several copies[16,19,20]. Complementation of three HSV-2 temperature-sensitive mutants when superinfecting the RE 1 rat embryo cell line[21] (transformed by the HSV-2 temperature-sensitive mutant *ts*1[22]) suggests that resident viral genes can be expressed. Brown *et al.*[23] used a similar approach to detect HSV information latent in human ganglia. We report here retrieval of intertypic HSV recombinants from HSV transformed cells after superinfection with *ts* mutants of the alternative serotype of HSV. Restriction enzyme analysis which clearly differentiates between HSV-1 and HSV-2 DNA[24,25] has demonstrated the isolation of recombinants spanning the genome and of virus indistinguishable from the original transforming virus.

Hooded Lister rat embryo cells transformed either by sheared DNA of HSV-1 strain α (REα)[7] or by an HSV-2 HG 52 mutant *ts*1 (RE 1) were used[5,6]. Both transformed lines express HSV antigens[26] and HSV thymidine kinase activity[27].

Recombination and complementation were studied by comparing the virus yields from control (Hooded Lister rat embryo) and transformed (REα, RE 1) cells after superinfection

with a *ts* mutant with distinct genome characteristics. Control and transformed cells of equal density were superinfected with a *ts* mutant at a multiplicity of infection of 5 plaque forming units (PFU) per cell at both the permissive (31 °C) and nonpermissive (38.5 °C) temperatures. Twenty-four hours after infection virus produced by the control and the transformed cells was harvested. The yields were then titrated in BHK 21 cells at 38.5 °C to identify putative *ts*⁺ recombinants and at 31 °C to measure total yield; where the initial incubation was at 38.5 °C this measures complementation.

ts⁺ virus (putative recombinants or revertants) was selected by picking separate plaques growing at 38.5 °C from both control and transformed cell plates and taking each isolate through three successive plaque purification steps at 38.5 °C (by picking well isolated plaques in each case). No virus picked from control cell plates survived this purification at 38.5 °C. *ts*⁺ virus isolated was then labelled with ³²P-orthophosphate. After DNA extraction and restriction enzyme digestion according to Lonsdale[28], the fragment profiles were analysed by electrophoresis on agarose gels of appropriate concentration.

Analysis of the restriction enzyme profiles unambiguously identified a number of *ts*⁺ viruses as recombinants, some generated after superinfection of the RE 1 cell line intertypically with HSV-1 17 *ts*J, and some on superinfection of the REα cell line intertypically with HSV-2 HG 52 *ts*1 or intratypically with HSV-1, 17 *ts*G syn⁺.

Restriction enzyme analysis of the intertypic recombinants from RE 1 cells × HSV-1 *ts*J and from REα cells × HSV-2 *ts*1 allows detection and mapping of HSV-1 and HSV-2 sequences present. Figure 2 (right) gives the KpnI profile of 3 recombinants (8B,6,13) selected from 11 analysed, isolated after superinfection of REα cells with HSV-2 *ts*1. Combined analysis of the BamHI, KpnI, HindIII and HpaI restriction endonuclease profiles has yielded the genome structures shown in Fig. 3. Every recombinant clearly contains DNA sequences from the genome present in the transformed cells extending
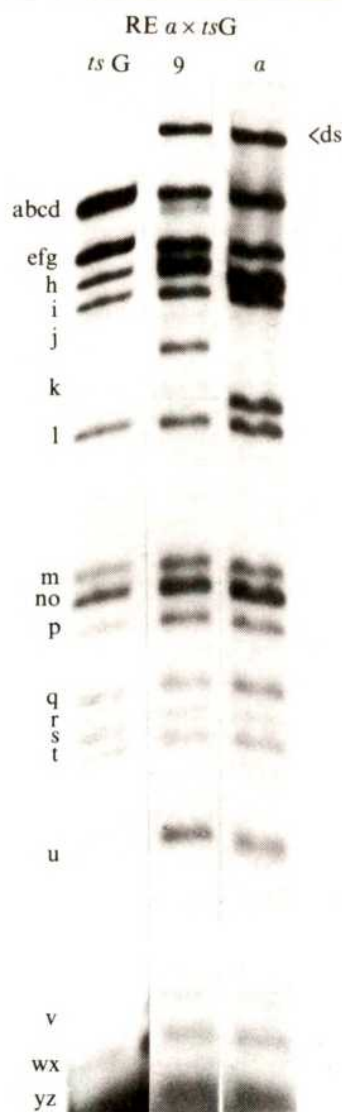
Fig. 1 Autoradiograph of ^{32}P-labelled DNA of HSV-1, HFEM α and one representative recombinant (no. 9) which were digested with restriction endonuclease *Kpn*I and subjected to electrophoresis on a 0.5% agarose gel. DNA fragments are lettered in accordance with the HSV-1 strain 17*Kpn*I restriction endonuclease map published previously[38]. Those sequences characteristic of HSV-1α at 0.54–0.65 map coordinates are detected by a *Kpn*I digest shown by the separate bands d and s of HSV-1 17 which are fused to give a new (d+s) larger molecular weight band characteristic of HSV-1α. The d+s fusion of HSV-1 HFEM α is marked ds, the molar band present in the recombinant which corresponds to neither HSV-1 strain 17 or HSV-1 HFEM α represents an intermediate band resulting from the crossover event. The restriction enzyme profiles of the nine recombinants analysed resemble one another due to the similarities between the genome structures of HSV-1 HFEM α and HSV-1 17 analysis and definition of the crossover regions in these recombinants is not possible.

Fig. 2 Autoradiograph of ^{32}P-labelled DNAs of HSV-1 *ts*J, HFEM α, HSV-2 *ts*1 and recombinants 2A, 6, 8B, 13 which were digested with restriction endonuclease *Kpn*I and subjected to electrophoresis on an 0.8% agarose gel. DNA fragments are lettered in accordance with the HSV-1 17*Kpn*I restriction endonuclease map[38] and HSV-2 HG52 *Kpn*I restriction endonuclease map[24]. Isolates 6, 8B, 13 are characteristic of recombinants analysed resemble one another, due to the HSV-2 *ts*1. The site of the *ts*1 mutation is known to map at position 0.7 from marker rescue studies[39] and all recombinants produced after superinfection with *ts*1 have a substitution of α DNA in this region, although each recombinant contains differing amounts of rescued information. Recombinant 2A isolated after superinfection of RE 1 cell line with HSV-1 *ts*J has a characteristic DNA profile of HSV-2 with an HSV-1 insertion between 0.38 and 0.50 map units. The restriction endonuclease profiles of these intertypic recombinants can clearly be related to bands originating from either the superinfecting virus or the original transforming virus. Bands which are not represented in either the superinfecting or the transforming virus are evidently intermediate bands formed as a result of the recombination event and could be identified by analysis of bands flanking the crossover region(s).

over a number of genes, some identified as coding for immediate early messages[29–31].

Recombinant 2A (Figs 2, 3) was isolated after superinfection of the RE 1 cell line with HSV-1 *ts*J and comprises ~90% HSV-2 sequences rescued from the RE 1 cell line and only a small region (~10%) of DNA originating from the superinfecting virus.

Analysis of recombinants from the RE α cell line × HSV-2 *ts*1 superinfection also produced one isolate with a restriction endonuclease profile indistinguishable from that of the original transforming virus HSV-1 α. This suggests that the sheared DNA of HSV-1 α used originally to produce the RE α

transformation may have contained some unsheared molecules and that the entire HSV-1α genome may be present in the REα transformed cell line, but apparently not in the usual infectious state. Similarly, a putative recombinant from RE 1 cell line × HSV-1 *ts*J superinfection was found to have a restriction endonuclease profile indistinguishable from HSV-2 *ts*1.

In the intratypic superinfection of the REα cell line by *ts*G syn⁺, recombinants could be selected due to their altered plaque morphology. The syncytial plaque morphology marker of the transforming virus HSV-1α and not that of the nonsyncytial superinfecting virus *ts*G syn⁺ was expressed by up to 25% of plaques grown at 38.5 °C. Linkage of the *ts*G lesion to the plaque morphology locus has been demonstrated previously[32,33]. Restriction enzyme analysis of nine separately isolated recombinants demonstrated retrieval of the HSV-1α sequence between 0.54 and 0.65 map coordinates on the HSV-1 genome (Fig. 1). The similarities of the two HSV-1 genomes, however, make further characterization of the intratypic recombinants difficult; Fig. 3 (top) diagrammatically indicates the sequences arising unambiguously from HSV-1α where recombinants have been isolated. Restriction enzyme analysis of HSV-1 strain αDNA has not shown any differences compared with HSV-1 strain HFEM from which it was derived (J. H. S.-S., unpublished). We shall, therefore, refer to HSV-1α virus as HSV-1 HFEMα.

As expected from previous results[21] several *ts* mutants are complemented by these transformed cell lines (Table 1). Intertypic and intratypic complementation is detected by elevated yields of *ts* superinfecting virus obtained at 38.5 °C from the transformed cell line compared to the control cell line. The complementation is measured by titrating this yield at 31 °C. All the *ts* mutants used are known to complement one another intratypically in standard genetic complementation tests[33].

Evidence from other laboratories suggests that up to 40% of the HSV genome is maintained in transformed hamster cells[16,19,20], although isolated restriction endonuclease fragments much smaller than this can initiate the morphological transformation of hamster cells (refs 34–36, and I. R. Cameron *et al.*, unpublished results). Heterogeneous populations of transformed cells, such as the uncloned RE 1 and REα lines, can therefore contain the HSV genetic information required not only to initiate and/or to maintain the transformed state but also for many other viral functions.

The generation of recombinants (containing a large portion or apparently all the genome of the transforming virus) may have originated through successive recombination steps, either involving initial recombinants containing various regions of the HSV genome rescued from the transformed cells, or through recombinant virus again rescuing further information from the transformed cells. It is not yet known whether the genetic material of the transforming virus is present and
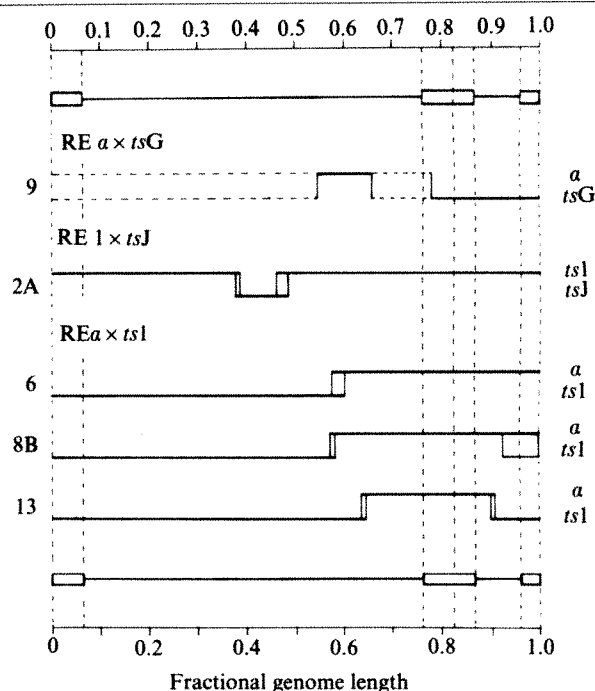
Fig. 3 Molecular model for the HSV genome[40] and analysis of crossover points in recombinants 9, 2A, 6, 8B, 13. The DNA sequences rescued from the transformed cell line form the uppermost line in each recombinant, whereas those present from the superinfecting virus compose the lower line of each structure. The box areas are those regions of uncertainty where a crossover event has occurred. The dotted lines in recombinant 9 indicate regions of uncertainty; due to similarities in restriction endonuclease profiles, HSV-1 *ts*G and HFEMα cannot be distinguished in these regions. The solid lines in this recombinant represent regions of the genome which can be identified as originating from either the superinfecting virus or the original transforming virus. Several restriction digests have revealed substantial differences between HFEMα and HSV-1 17 which show that the short unique region of these recombinants arises from the superinfecting virus HSV-1 *ts*G. Furthermore, HFEMα has a 2 × 10⁶ dalton deletion in the internal long repeat compared to HSV-1 17: this is not represented in any of the recombinants allowing characterization of these sequences as arising from HSV-1 *ts*G.

maintained in the transformed cell in plasmid form or integrated into the chromosomal material of the cell; how many copies are present; or whether all viral sequences are present in equal amounts. These problems are being investigated.

If the HSV-DNA maintained in the transformed cell contains most of the HSV genome in a non-replicating form, infection by superinfecting virus may suffice to switch on the necessary pre-extant control systems[37], or provide a missing function which enables the resident genome to undergo normal replication. Once present in the replicating pool of virus genomes, recombination of the transforming virus DNA with the superinfecting *ts* mutant DNA would eventually produce *ts*⁺ recombinants.

This novel method of genetic information retrieval by superinfection with genetic probes demonstrates not only that recombinants spanning the genome may be isolated, but also that virus with the characteristic restriction enzyme pattern of the original transforming virus can be rescued after a large number of transformed cell generations.

Table 1 Complementation of *ts* mutants by transformed cell lines

Transformed cell line	Superinfecting *ts* mutant	Complementation index
REα	HSV-1 *ts*G	39
	ts I	3.4
	ts A	13
	ts D	3.7
	HSV-2 *ts* 1	7.7
RE 1	HSV-1 *ts* J	31
	ts I	15
	ts F	6.5
	ts A	6

A complementation index ≥3 on titration of yields of *ts* superinfecting virus obtained at 38.5 °C from the transformed cell line compared to the control cell line is regarded as evidence for complementation of the mutant virus by the transformed cell line.

1. Duff, R. & Rapp, F. J. Virol. 8, 469–477 (1971).
2. Duff, R. & Rapp, F. J. Virol. 12, 209–217 (1973).
3. Kutinova, L., Vonka, V. & Broucek, J. J. natn. Cancer Inst. 50, 759–763 (1973).
4. Kimura, S., Flannery, V. L., Liez, B. & Schaffer, P. A. Int. J. Cancer 15, 786–789 (1975).
5. Macnab, J. C. M. J. gen. Virol. 24, 143–153 (1974).
6. Macnab, J. C. M. in 2nd Int. Symp. Oncogenesis and Herpesviruses Vol. 1, 227–235 (International Agency for Research on Cancer, Lyon, 1975).
7. Wilkie, N. M., Clements, J. B., Macnab, J. C. M. & Subak-Sharpe, J. H. Cold Spring Harb. Symp. quant. Biol. 39, 657–666 (1974).
8. Darai, G. & Munk, K. Int. J. Cancer 18, 469–481 (1976).
9. Darai, G., Braun, R., Flugel, R. M. & Munk, K. Nature 265, 744–746 (1977).
10. Kucera, L. S., Gudson, J. P., Edwards, I. & Herbst, G. J. gen. Virol. 35, 473–485 (1977).
11. Boyd, A., Orme, T. & Boone, C. 2nd Int. Symp. Oncogenesis and Herpesviruses Vol. 1, 429–439 (International Agency for Research on Cancer, Lyon, 1975).
12. Boyd, A. & Orme, T. W. Int. J. Cancer 16, 526–538 (1975).
13. Flannery, V. L., Courtney, R. J. & Schaffer, P. A. J. Virol. 21, 284–291 (1977).
14. Gupta, P. & Rapp, F. Proc. natn. Acad. Sci. U.S.A. 74, 372–374 (1977).
15. Reed, C. L., Cohen, G. H. & Rapp, F. J. Virol. 15, 668–670 (1975).
16. Kessous, A., Bibor-Hardy, V., Suh, M. & Simard, R. Cancer Res. 39, 3225–3234 (1979).
17. Collard, W., Thornton, H. & Green, M. Nature new biol. 243, 264–265 (1973).
18. Copple, C. D. & McDougall, J. K. Int. J. Cancer 17, 501–513 (1976).
19. Minson, A. C., Thouless, M. E., Eglin, R. O. & Darby, G. Int. J. Cancer 17, 493–500 (1976).
20. Frenkel, N., Locker, H., Cox, B., Roizman, B. & Rapp, F. J. Virol. 18, 885–893 (1976).
21. Macnab, J. C. M. & Timbury, M. C. Nature 261, 233–235 (1976).
22. Timbury, M. C. J. gen. Virol. 13, 373–376 (1971).
23. Brown, S. M., Subak-Sharpe, J. H., Warren, K. G., Wroblewska, Z. & Koprowski, H. Proc. natn. Acad. Sci. U.S.A. 76, 2364–2368 (1979).
24. Morse, L. S., Buchan, G., Roizman, B. & Schaffer, P. A. J. Virol. 24, 231–248 (1977).
25. Wilkie, N. M. et al. 3rd Int. Symp. Oncogenesis and Herpesviruses Vol. 1, 11–33 (International Agency for Research on Cancer, Lyon, 1978).
26. Macnab, J. C. M. J. gen. Virol. 43, 39–56 (1979).
27. Macnab, J. C. M., Visser, L., Jamieson, A. T. & Hay, J. Cancer Res. (in the press).
28. Lonsdale, D. M. Lancet i, 849–851 (1979).
29. Clements, J. B., Watson, R. J. & Wilkie, N. M. Cell 12, 275–285 (1977).
30. Marsden, H. S., Stow, N. D., Preston, V. G., Timbury, M. C. & Wilkie, N. M. J. Virol. 28, 624–642 (1978).
31. Clements, J. B., McLauchlan, J. & McGeoch, D. J. Nucleic Acids Res. 7, 77–91 (1979).
32. Ritchie, D. A., Brown, S. M., Subak-Sharpe, J. H. & Jamieson, A. J. Virology 82, 323–333 (1977).
33. Brown, S. M., Ritchie, D. A. & Subak-Sharpe, J. H. J. gen. Virol. 18, 329–346 (1973).
34. Camacho, A. & Spear, P. G. Cell 15, 993–1002 (1978).
35. Reyes, G. R., La Femina, R., Hayward, S. D. & Hayward, G. S. Cold Spring Harb. Symp. quant. Biol. 44 (1979).
36. Jariwalla, R. J. & Aurelian, L. Proc. Natn. Acad. Sci. U.S.A. (in the press).
37. Leiden, J. M., Buttyan, R. & Spear, P. C. J. Virol. 20, 413–424 (1976).
38. Preston, V. G. et al. J. Virol. 28, 499–517 (1978).
39. Wilkie, N. M. et al. Cold Spring Harb. Symp. quant. Biol. 43, 827–840 (1978).
40. Sheldrick, P. & Berthelot, N. Cold Spring Harb. Symp. quant. Biol. 39, 667–678 (1974).

A novel human pituitary peptide containing the γ-MSH sequence

S. Benjannet, N. G. Seidah, R. Routhier & M. Chrétien

Clinical Research Institute of Montreal, 110 Pine Avenue West, Montreal H2W 1R7, Canada

It is well established that ACTH and β-lipotropin (LPH) originate from a common precursor molecule[1-3]. Recently the complete complementary DNA sequence of the bovine precursor was reported[4], and within the cryptic sequence of this molecule is a third melanocyte stimulating hormone (MSH) region tentatively named γ-MSH[4]. The signal peptide of this molecule consists of 26 amino acids in both the rat[5] and mouse[6]. Pulse-chase experiments using both rat and mouse pituitary cells, showed the gradual maturation of this common precursor to proceed via the initial cleavage of the carboxy terminal β-LPH, followed by release of ACTH, leaving an NH_2-terminal extension of about 105 amino acids, which does not seem to undergo appreciably further maturation[1-3,7]. It is within the sequence of this NH_2-terminal extension that γ-MSH is located[4]. It is not yet clear what the biological role of this molecule is and whether γ-MSH itself is released. Recently, it was shown that a synthetic 12 amino acid bovine γ-MSH fragment possessed very little melanophore-stimulating activity as compared to α-MSH[8]. We report here the successful purification of the human NH_2 terminal cryptic peptide, its amino acid composition and present some of its tryptic fragments. The data show that human and bovine γ-MSH have identical amino acid composition.

Starting from an HCl/acetone extract of frozen human pituitaries, an initial ion-exchange fractionation on CM-cellulose was performed as previously described for the purification of human β-LPH and β-endorphin[9]. The unretained peak was further fractionated by gel chromatography on Sephadex G-75. Labelling the peptides obtained from the various fractions with ^{14}C-iodoacetamide and microsequencing allowed the identification of a fraction enriched with a peptide showing the sequence Cys 2, 8, 20 and 24. There are exactly the cysteine positions that would be expected for the bovine ACTH/LPH

Table 1 Amino acid composition of human tryptic peptides corresponding to γ-MSH

Amino acid	T1	T2	T3	T4	T5
Trp	—	0.54 (1)	—	—	—
Lys	—	—	—	0.79 (1)	1.10 (1)
His	1.02 (1)	—	—	0.97 (1)	—
Arg	1.11 (1)	1.06 (1)	1.96 (2)	1.09 (1)	—
SCM-Cys	—	—	—	—	—
Asp	—	0.98 (1)	—	—	—
Thr	—	—	—	—	—
Ser	—	—	—	—	—
Glu	—	—	—	—	—
Pro	—	—	—	—	—
Gly	1.32 (1)	—	0.84 (1)	1.39 (1)	—
Ala	—	—	—	—	—
Val	0.90 (1)	—	—	1.07 (1)	—
Met	0.78 (1)	—	—	0.80 (1)	—
Ile	—	—	—	—	—
Leu	—	—	—	—	—
Tyr	1.04 (1)	—	—	0.93 (1)	0.92 (1)
Phe	0.93 (1)	—	1.20 (1)	1.01 (1)	—

The human pituitary peptide (1 mg) was subjected to tryptic digestion. Peptides were separated in a μ-bondapak C_{18} HPLC column and purified for amino acid analysis. The data represent 24-h hydrolysates analysed on a Beckman 121M amino acid analyser. The values in parentheses represent the values expected from the bovine γ-MSH sequence reported[4].

precursor had the 26 residues signal peptide been cleaved off[5,6]. Further purification by HPLC on a Waters μ-bondapak C_{18} column[10] allowed the isolation of 5 mg of a pure polypeptide bearing identical cysteine residues sequence positions as the bovine homologue. On SDS-polyacrylamide gel electrophoresis it was homogeneous and migrated with an apparent molecular weight of 18,000. This peptide is not recognized by an $ACTH_{(1-24)}$ directed antibody[5] and hence lacks the ACTH region of the ACTH/LPH precursor.

The total amino acid composition of the purified human peptide was: Trp 2, Lys 3, His 2, Arg 8, Cys 4, Asp 11, Thr 5, Ser 12, Glu 13, Pro 8, Gly 11, Ala 6, Val 2, Met 2, Ile 1, Leu 8, Tyr 1 and Phe 4. This gives a total of 103 amino acids compared to a maximum of 105 for the bovine homologue[4]. The compositions of four major tryptic fragments (T1 to T4) and a minor chy-

Fig. 1 Comparison of the reported bovine sequence of γ-MSH[4] within the NH_2-terminal ACTH/LPH segment to that deduced from the amino acid composition of homologous human tryptic fragments. T5 is a minor chymotryptic fragment isolated.

$H_2N \text{---} Arg\text{-}Lys\text{-}Tyr\text{-}Val\text{-}Met\text{-}Gly\text{-}His\text{-}Phe\text{-}Arg\text{-}Trp\text{-}Asp\text{-}Arg\text{-}Phe\text{-}Gly\text{-}Arg\text{-}Arg \text{---} Lys\text{-}Arg\text{-}COOH$

1   50   63   105

←——————— T4 ———————→

←——————— T1 ———————→ ←——— T2 ———→ ←——— T3 ———→

←— T5 —→

motryptic one (T5) are shown in Table 1. In Fig. 1, the alignment of these human peptides with the reported bovine γ-MSH sequence is shown. The reported bovine γ-MSH sequence, Lys-Tyr-Val-Met-Gly-His-Phe-Arg-Trp-Asp-Arg-Phe-Gly - Arg-Arg fits exactly the amino acid compositions obtained from the human tryptic fragments.

An additional indication that this region of the molecule is identical in human and cattle is that peptides T1, T2 and T3 co-eluted on the HPLC chromatogram with their corresponding synthetic bovine homologues. Furthermore, an antibody raised against the bovine γ-MSH sequence, which does not recognize β-LPH, ACTH, α-MSH or β-MSH[11], showed complete cross reactivity on a molar basis for the human NH_2-terminal peptide purified as compared to the synthetic bovine γ-MSH peptide.

The finding of apparently identical structures of human and bovine γ-MSH regions emphasizes the conservation of the structure of this segment of the ACTH/LPH precursor between these species. Similar observations have been made for the species sequence homologies of the α-MSH, β-MSH and β-endorphin regions of this precursor. Although no distinct biological activity of the NH_2-terminal segment of the ACTH/LPH precursor has been found, the structural homologies suggest that this segment may have an as yet undiscovered function. The purification of a human peptide of MW 18,000 related to the NH_2-terminal segment of the ACTH/LPH precursor, in which the ACTH molecule is absent, indicates that the mode of maturation of the ACTH/LPH precursor in the human pituitary could be similar to that observed in other species such as the rat and mouse[1–3].

Since submission of this paper, Hakanson *et al.* have described the isolation of a similar peptide from pig pituitary[12].

This work was supported by grant PG-2 from the MRC of Canada.

1. Roberts, J. L. & Herbert, E. *Proc. natn. Acad. Sci. U.S.A.* **74**, 5300-5304 (1977).
2. Mains, R. E., Eipper, B. A. & Ling, N. *Proc. natn. Acad. Sci. U.S.A.* **74**, 3014-3018 (1977).
3. Crine, P. *et al. Proc. natn. Acad. Sci. U.S.A.* **75**, 4719-4723 (1978).
4. Nakanishi, S. *et al. Nature* **278**, 423-427 (1979).
5. Gossard, F., Seidah, N. G., Crine, P., Routhier, R. & Chrétien, M. *Biochem. biophys. Res. Commun.* **92**, 1042-1051 (1980).
6. Keutmann, H. T., Eipper, B. A. & Mains, R. E. *J. biol. Chem.* **254**, 9204-9208 (1979).
7. Gianoulakis, C., Seidah, N. G., Routhier, R. & Chrétien, M. *J. biol. Chem.* **23**, 11903-11906 (1979).
8. Ling, N., Ying, S., Minick, S. & Guillemin, R. *Life Sci.* **25**, 1773-1780 (1979).
9. Chrétien, M., Benjannet, S., Dragon, N., Seidah, N. G. & Lis, M. *Biochem. biophys. Res. Commun.* **72**, 472-478 (1976).
10. Seidah, N. G. *et al. J. Chromatogr.* (in the press).
11. Seidah, N. G., Benjannet, S., Lis, M. & Chrétien, M. (in preparation).
12. Håkanson, R., Eckman, R., Sundler, F. & Nilsson, R. *Nature* **283**, 789-792 (1979).

Pituitary immunoreactive γ-melanotropins are glycosylated oligopeptides

Tamotsu Shibasaki, Nicholas Ling & Roger Guillemin

Laboratories for Neuroendocrinology, The Salk Institute for Biological Studies, La Jolla, California 92037

Nakanishi *et al.*[1] have recently characterised the complete sequence of the mRNA isolated from the intermediate lobe of bovine pituitary which codes for the 31,000 molecular weight (31 K) precursor protein of corticotropin/β-lipotropin (ACTH/β-LPH). The corresponding amino acid sequence translated from this mRNA revealed in the cryptic region of the precursor protein a fragment sharing a common amino acid sequence with the α- β-melanotropins (α-MSH, β-MSH) and thus named γ-MSH[1]. To study whether this γ-MSH fragment is also processed and released as a biologically active substance and to ascertain its location in the pituitary and possibly in the brain, we have raised antibodies to the synthetic replicate of $γ_3$-MSH (ref. 2). We report here the detection of at least two γ-MSH-like peptides in the pituitary using these antibodies in a radioimmunoassay (RIA) and, furthermore, evidence that these two peptides are glycosylated.
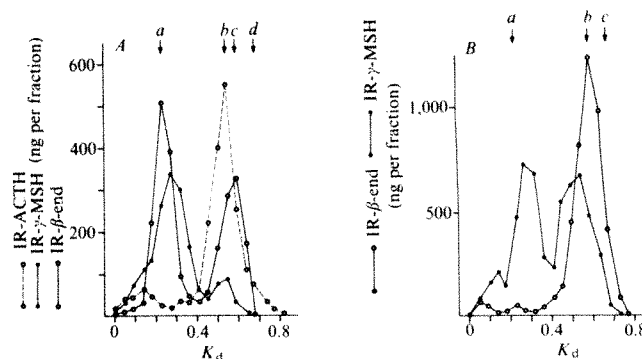
Fig. 1 Biogel P-100 gel permeation chromatography of the anterior (*A*) and intermediate (*B*) lobe extracts of bovine pituitary. For experimental conditions see text. Markers: $a = ^{125}I$-labelled β-LPH; $b = $ ACTH; $c = ^{125}I$-labelled β-endorphin; $d = ^{125}I$-labelled $γ_3$-MSH.

The antiserum raised in rabbits was obtained by injecting the synthetic replicate of $γ_3$-MSH coupled to bovine serum albumin through bis-diazotised benzidine[12]. The amino acid sequence of $γ_3$-MSH as derived from Nakanishi *et al.*[1] is Tyr-Val-Met-Gly-His-Phe-Arg-Trp-Asp-Arg-Phe-Gly-Arg-Arg-Asn-Gly-Ser-Ser-Ser-Ser-Gly-Val-Gly-Gly-Ala-Ala-Gln-OH. The peptide was prepared by solid phase synthesis and obtained in high purity using methods already described[2]. The antiserum raised against this peptide reads the portion between His 5 and Arg 14 without significant cross-reaction with α- and β-MSH, β-endorphin, β-LPH, corticotropin-like intermediate lobe peptide and ACTH.

Bovine pituitaries were obtained at a local abattoir, immediately frozen on dry ice, and kept in a freezer at −70 °C until use. After defrosting, a pituitary was carefully dissected into its three lobes. After cutting into small pieces, a 978-mg fragment of the anterior lobe and a 157-mg fragment of the intermediate lobe were extracted by Polytron in 20 ml and 8 ml, respectively, of cold 1 M acetic acid containing 20 mM HCl, 0.01 % phenylmethylsulphonyl fluoride and 130 kIU ml^{-1} Trasylol. The homogenates were centrifuged at 2,500g at 4 °C for 30 min and the supernatants lyophilized. The lyophilized materials from the anterior and intermediate lobes were reconstituted in 1.9 ml and 0.5 ml, respectively, of 4 M guanidine-HCl for gel permeation chromatography. A 0.2-ml aliquot of that solution was applied to a 0.7 × 48 cm Biogel P-100 column equilibrated in 4 M guanidine-HCl and eluted with the same solvent at 1.3 ml h^{-1} at room temperature. The column was calibrated using dextran blue, ^{125}I-labelled ovine β-LPH, ovine ACTH, ^{125}I-porcine β-endorphin, ^{125}I-labelled $γ_3$-MSH and phenol red. Fractions eluted from the column were diluted with the buffer for RIA of γ-MSH, ACTH and β-endorphin[3]. Final guanidine-HCl concentration in the RIA was 7.4 mM. An equivalent amount of guanidine-HCl was added to the tubes for preparing the RIA standard curves.

Figures 1*A* and *B* show the gel permeation chromatography of the anterior and intermediate lobe extracts as above. Two peaks with γ-MSH-like immunoreactivity in the anterior lobe extract, and two main peaks and one smaller peak with γ-MSH-like immunoreactivity in the intermediate lobe extract were detected with the γ-MSH RIA. The elution volume of the two peaks from the anterior lobe extract matches that of the latter two peaks from the intermediate lobe extract. The peak at $K_d = 0.27$ is much larger than that at $K_d = 0.55$ in the anterior lobe extract, whereas these two peaks show almost the same distribution in the intermediate lobe extract. These results suggest a difference in the post-translational processing of γ-MSH-like peptides in the anterior and intermediate lobe as is also the case in the processing of β-LPH, β-endorphin and ACTH: in the anterior lobe ACTH and β-LPH are the major products and in the intermediate lobe β-endorphin is predominant, with hardly any β-LPH or ACTH[4].

The elution profile also shows that the molecular size of the native γ-MSH-like peptides is larger than that of the iodinated synthetic γ_3-MSH with apparent molecular weights (MWs) of 13,000, 8,800 and 4,500 for the peaks at $K_d = 0.14$, 0.27 and 0.55, respectively. A possible explanation for the larger MW may be that native γ-MSH-like peptides contain more than the 27 amino acids of γ_3-MSH as derived from Nakanishi et al.[1]. Another explanation is that native γ-MSH-like peptides may contain carbohydrate; indeed, it has been reported that in mouse ACTH-secreting pituitary tumours, the 16 K fragment of the 31 K ACTH/β-LPH precursor protein, which should contain the γ-MSH region, is glycosylated[5]. Both possibilities may account for the higher molecular form of native γ-MSHs.

The fractions corresponding to the two immunoreactive γ-MSH peaks in the anterior lobe extract and the three peaks in the intermediate lobe extract of bovine pituitary were examined with affinity chromatography on concanavalin A (Con A) coupled to Sepharose 4-B. As shown in Fig. 2, all the immunoreactive (IR-) γ-MSHs from both the anterior and intermediate pituitary are glycopeptides; all were retarded on the Con A column and could only be displaced with α-methyl-D-mannopyranoside (α-MM).

In the post-translational processing of the murine ACTH/β-LPH precursor[6], glycosylation occurs in the ACTH fragment and the resulting glycopeptide is called 13 K ACTH; glycosylation also occurs in the non-ACTH/β-LPH portion of the precursor to give the 16 K fragment. In general, the asparagine residue within the amino acid sequence Asn-X-Thr (or Ser) is the site to which a carbohydrate chain is linked

Fig. 2 Affinity chromatography of γ-MSH-like peptides on Con A-coupled Sepharose 4-B. A 1-ml siliconised glass syringe was packed with 0.4 ml Con A coupled to Sepharose 4-B. After being washed with 3 ml 0.1 m acetic acid, the column was equilibrated with Con A buffer composed of 0.01 M Tris-HCl, 0.7 mM MgCl$_2$, 0.1 % bovine serum albumin, 1.0 M NaCl and 0.1 % Triton X-100 (pH 7.4)[11]. γ-MSH-like peptides for affinity chromatography were obtained by applying the anterior and intermediate lobe extracts of bovine pituitary, respectively, to a Sephadex G-75 column in 1.0 M acetic acid. The elution profiles of the two extracts were almost the same as that in the Biogel P-100 column chromatography in 4 M guanidine-HCl. The peak tubes corresponding to the elution volume at $K_d = 0.27$ and 0.55 in the anterior lobe extract and at $K_d = 0.14$, 0.27 and 0.55 in the intermediate lobe extract were lyophilised. The residue reconstituted in 0.5 ml of Con A buffer was applied to the column. After washing the column with 4.5 ml of the same buffer, 5 ml of 0.2 M α-methyl-D-mannopyranoside (α-MM) in Con A buffer was used to elute the retarded material, followed by 1.0 M α-MM and 0.1 M AcOH. Fractions (1 ml) were collected, lyophilised and the lyophilised fractions were reconstituted in buffer for RIA of γ-MSH. Recovery following elution with 0.2 M α-MM was 51–65 % of applied IR-γ-MSH. A, Synthetic γ_3-MSH; B, C, native γ-MSHs corresponding to $K_d = 0.27$ and 0.55, respectively, of the anterior lobe extract; D, E, F, native γ-MSHs corresponding to $K_d = 0.14$, 0.27 and 0.55, respectively, of the intermediate lobe extract.

through an N-acetylglucosamine[7]. However, it was proposed[6] that the aspartic acid residue at the 29th amino acid position of ACTH$_{1-39}$ is the most likely site for attachment of a carbohydrate chain in the murine 13 K ACTH fragment. In the case of the γ-MSH-like peptides, the amino acid sequence Asn-X-Ser corresponds to residues 15–17 of γ_3-MSH, and could be a likely site for glycosylation. However, native γ-MSHs may contain more than one carbohydrate chain as the Asn 15-X-Ser 17 sequence is followed by Ser 18-Ser-Ser in γ_3-MSH. This series of serine residues could also be candidates to which oligosaccharides are linked through an O-glycosidic linkage[8].

Post-translational glycosylation of the ACTH/β-LPH precursor may protect it from intracellular degradation by providing it with specific conformational stability[9]. Glycosylation of native γ-MSHs may similarly have a role in extending their biological half life. Further studies are in progress to determine the amino acid sequence of the γ-MSHs and to characterise their carbohydrate moieties.

After submission of this report, Hakanson et al.[10] described the isolation from extracts of porcine pituitaries of a large glycopeptide (103 amino acids), a partial sequence of which showed it to be the whole N-terminal region of the 31 K precursor molecule down to the starting point of ACTH. The present report shows that this large fragment is further processed to the smaller γ_3-MSH. Furthermore, we have recent evidence that an even smaller fragment corresponding to γ_1-MSH is also present in pituitary extracts and released with other fragments of the 31 K precursor.

We thank Dr S. Lavielle for helpful discussion and Mrs B. Gayer for secretarial help. The research was supported by NIH grants AM-18811-05 and HD-09690-05 and the William Randolph Heart Foundation. T.S. is a Postdoctoral fellow from the Department of Internal Medicine, Tokyo Women's Medical College, Tokyo, Japan.

1. Nakanishi, S. et al. Nature 278, 423–427 (1979).
2. Ling, N., Ying, S., Minick, S. & Guillemin, R. Life Sci. 25, 1773–1780 (1979).
3. Shibasaki, T., Deftos, L. & Guillemin, R. Biochem. biophys. Res. Commun. 90, 1266–1273 (1979).
4. Scott, A. P. et al. in Peptide Hormones (ed. Parsons, J. A.) 247–271 (University Park Press, Baltimore, 1976).
5. Eipper, B. A. & Mains, R. E. J. biol. Chem. 253, 5732–5744 (1978).
6. Eipper, B. A. & Mains, R. E. J. biol. Chem. 252, 8821–8832 (1977).
7. Sox, H. C. & Hood, L. Proc. natn. Acad. Sci. U.S.A. 66, 975–982 (1970).
8. Bhavanandan, V. P., Buddecke, E., Carabell, R. & Gottschalk, A. Biochem. biophys. Res. Commun. 16, 353–357 (1964).
9. Loh, Y. P. & Gainer, H. Endocrinology 105, 474–487 (1979).
10. Hakanson, R., Ekman, R., Sundler, F. & Nilsson, R. Nature 283, 789–792 (1980).
11. Eipper, B. A., Mains, R. E. & Guenzi, D. J. biol. Chem. 251, 4121–4126 (1976).
12. Shibasaki, T., Ling, N. & Guillemin, R. Life Sci. 26, 1781–1785 (1980).

Isolation of two novel candidate hormones using a chemical method for finding naturally occurring polypeptides

Kazuhiko Tatemoto & Viktor Mutt

Department of Biochemistry II, Karolinska Institute,
S-104 01 Stockholm 60, Sweden

Naturally occurring peptides with biological actions have in most cases been detected by observing their biological activities in crude extracts and their isolation has been followed using bioassays. As a complement to the classical biological detection systems, we have proposed a chemical detection system based on fragmentation of peptides in tissue extracts followed by identification of certain of these peptide fragments having distinct chemical features[1,2]. One such chemical feature is the C-terminal amide structure which is characteristic of many

biologically active peptides[3,4]. We have devised a chemical assay method for peptides having such a structure and have found several previously unknown peptide amides in porcine upper small intestinal tissues[1]. We report here the isolation and characterization of two of them, designated PHI and PYY. PHI is related to secretin, vasoactive intestinal polypeptide (VIP, glucagon and gastric inhibitory polypeptide (GIP); PYY is related to the pancreatic polypeptide and to neurotensin. Both peptides exhibit biological activities and appear to be present not only in the intestine but also in brain.

The presence of peptides with the amidated C-terminal structure can be detected in crude extracts using a chemical assay in which the amidated C-terminal portion of the peptide chain is cleaved off enzymatically, converted into the fluorescent dansyl derivative and then selectively isolated and identified by TLC[1]. In the present work, the levels of PHI or PYY in the tissue samples were estimated by measuring the concentration of isoleucine amide or tyrosine amide which was cleaved off from PHI or PYY, respectively, by degradation of the samples with thermolysin.

The starting material for the isolation work was a side fraction obtained during the purification of porcine secretin[5]. Boiled pig intestines (the uppermost 1 m of the small intestine) were extracted with 0.5 M acetic acid and the extracted peptides were adsorbed to alginic acid. They were then eluted from the alginic acid with 0.2 M HCl and precipitated with NaCl at saturation. The peptide concentrates were further purified by extraction with 66% ethanol, gel filtration (Sephadex G-25) and extraction with methanol[5]. The methanol-soluble fraction (after removal of the methanol) was subjected to ion-exchange chromatography on CM-cellulose (CMC) and PHI and PYY were found in a fraction eluting before secretin. This fraction was rechromatographed on CMC to separate PHI from PYY. The fractions containing PHI were further purified by gel filtration (Sephadex G-25), chromatography on DEAE-cellulose, isoelectric precipitation at pH 7.0 and finally by HPLC on the reversed phase, Bondapak C-18. The fractions containing PYY were further purified by gel filtration (Sephadex G-25), chromatography on CMC and finally by HPLC on Bondapak C-18. The final products were found to be homogenous by analysis with TLC, gel electrophoresis, HPLC, and by amino acid determinations.

The N-terminal analysis revealed the presence of histidine for PHI and tyrosine for PYY. Since the biological functions of these newly-isolated peptides are not yet established, we decided to give chemical names to them based on their N- and C-terminal amino acids (one-letter system). PHI thus designates 'the peptide (P) having N-terminal histidine (H) and C-terminal isoleucine (I) amide' and PYY designates 'the peptide (P) having N-terminal tyrosine (Y) and C-terminal tyrosine (Y) amide'.

PHI consists of 27 amino acids: 2 Ala, 1 Arg, 2 Asx, 2 Glx, 2 Gly, 1 His, 1 Ile, 5 Leu, 2 Lys, 2 Phe, 4 Ser, 1 Thr, 1 Tyr, 1 Val. A preliminary sequence analysis revealed the N-terminal sequence of His-Ala-Asp-Gly-Val-Phe-Thr-. The C-terminal sequence, -Leu-Ile-NH$_2$ was determined by the amide

Fig. 2 The partial sequence of PYY and the comparison with the pancreatic polypeptide and neurotensin. a, The carboxyl end is amidated. b, The peptide (P) with N-terminal tyrosine (Y) and C-terminal tyrosine (Y). c, The porcine pancreatic polypeptide. d, The avian pancreatic polypeptide. e, The N-terminal amino acid is pyroglutamic acid.

identification method[1]. The terminal sequences were compared with those of the secretin-glucagon family (Fig. 1) and remarkable sequence similarities were seen between PHI and secretin, VIP, glucagon and GIP, indicating that PHI probably belongs to this peptide group. PHI activated adenylate cyclase in various rat membrane systems and inhibited VIP binding to its receptors[6]. It was also found that PHI induced insulin release from an isolated rat pancreas at basal and elevated glucose levels, while it enhanced glucagon release in the presence of arginine[7].

PYY consists of 36 amino acids: 4 Ala, 4 Arg, 2 Asx, 5 Glx, 1 Gly, 1 His, 4 Leu, 1 Lys, 4 Pro, 3 Ser, 1 Thr, 5 Tyr, 1 Val. The N-terminal sequence was found to be Tyr-Pro-Ala-Lys-Pro-Glu-Ala-Pro-Gly. Treatment of PYY with trypsin yielded tyrosine amide. Since the only lysine residue in the molecule is found near the N-terminus, the C-terminal sequence should be -Arg-Tyr-NH$_2$, the same as that of the pancreatic polypeptide[8,9]. The partial sequence of PYY was therefore compared with the sequence of the porcine and avian pancreatic polypeptides (Fig. 2). In addition to the distinct sequence homology to the pancreatic polypeptide, PYY possesses sequence similarities to neurotensin[10] (Fig. 2). PYY was found to inhibit the action of secretin on the pancreas of the anaesthetized cat, the bicarbonate secretion induced by secretin in a single intravenous dose (0.2 μg per kg) being reduced to about 30% in the presence of PYY (5 μg per kg) (data not shown). In a dose range of 0.5–5 μg per kg, PYY contracted the gallbladder of the anaesthetized guinea pig in a dose-responsive fashion. Further studies on the biological properties of PYY are under way.

Preliminary studies indicate that there are unknown peptide amides in brain as well as in intestine. Judging from the chromatographic patterns, solubility properties, and the C-terminal amide determinations, it seems highly probable that both PHI and PYY are present and that PYY may constitute one of the major peptide amides of the brain.

1. Tatemoto, K. & Mutt, V. Proc. natn. Acad. Sci. U.S.A. 75, 4115–4119 (1978).
2. Tatemoto, K. & Mutt, V. Scand. J. Gastroenterol. 13, Suppl. 49, 181 (1978).
3. Dayhoff, M. O. in Atlas of Protein Sequence and Structure Vol. 5 (ed. Dayhoff, M. O.) D173-D227 (National Biochemical Research Foundation, Silver Spring, Maryland, 1972).
4. Hunt, L. T. & Dayhoff, M. O. in Atlas of Protein Sequence and Structure Vol. 5, Suppl. II (ed. Dayhoff, M. O.) 113–145 (National Biochemical Research Foundation, Silver Spring, Maryland, 1976).
5. Mutt, V. in Gut Hormones (ed. Bloom, S. R.) 21–27 (Churchill-Livingstone, Edinburgh, 1978).
6. Bataille, D. et al. Scand. J. Gastroenterol. 13, Suppl. 49, 13 (1978).
7. Szecówka, J., Tatemoto, K., Mutt, V. & Efendić, S. Life Sci. 26, 435–438 (1980).
8. Li, T-M. & Chance, R. E. Gastroenterology 67, 737–738 (1974).
9. Chance, R. E., Johnson, M. G., Hoffman, J. A. & Lin, T-M. in Proinsulin, Insulin, C-peptide (eds Baba, S., Kaneko, T. & Yanaihara, N.) 419–425 (Excerpta Medica, Amsterdam, 1979).
10. Carraway, R. & Leeman, S. E. J. biol. Chem. 250, 1907–1911 (1975).

Fig. 1 The partial sequence of PHI and the comparison with peptides of the secretin-glucagon family. a, The carboxyl end is amidated. b, The peptide (P) with N-terminal histidine (H) and C-terminal isoleucine (I). c, The vasoactive intestinal peptide (porcine). d, The gastric inhibitory peptide (porcine).

BOOK REVIEWS

Robert Boyle on science and philosophy

R.E.W. Maddison

THIS volume, prepared by Dr M.A. Stewart, Senior Lecturer in Philosophy at the University of Lancaster, is an additional title in the series of Philosophical Classics published by the Manchester University Press. It is a collection of certain writings by Robert Boyle (1627–1691) "which are of primary interest to historians of philosophy and the philosophy of science, and to those who are concerned with the interaction of philosophical, scientific and religious ideas in the period of the scientific revolution". The text of the representative writings selected for reproduction has been fully modernized so as to obviate obscurities and to give a more fluent prose for the benefit of those not acquainted with the seventeenth-century style of writing. This modernization of the original printed editions will, as the editor admits, be regarded by some as taking liberties with the text. Misprints have been corrected where necessary to restore sense to a passage; wrong references have been silently corrected; but the greatest changes have been made in punctuation. Nevertheless, a newcomer to Boyle's writings will not find them easy reading. Robert Boyle was conscious of the deficiencies of his literary style, for the quaintness of which he was twitted in his lifetime. Samuel Johnson excused it on the ground that Boyle's philosophical studies did not allow him time for the cultivation of style as he (Boyle) was more concerned in getting his thoughts down black on white.

Dr Stewart provides an introduction which comprises a short sketch of Boyle's life and work, with notes on the papers in this edition and on editorial practice.

Robert Boyle became interested in natural philosophy at an early age, and accordingly instructed himself in the Aristotelean doctrine, but found that its principles were more strongly asserted than proved, and that considerable arguments could be advanced against it. His own views on the nature of matter, supported

---

Selected Philosophical Papers of Robert Boyle. Edited by M.A. Stewart. Pp.256. (Manchester University Press: Manchester, 1980.) £12.

---

by chemical and physical experiments, were briefly expounded first of all in *Certain Physiological Essays* (1661) and then in greater detail, to "serve for an introduction into the elements of the Corpuscularian philosophy", in *The Origin of Forms and Qualities . . .* (1666) which is fully reproduced in this edition, apart from the second half of the book devoted by Boyle to "Considerations and Experiments", which is omitted. This text outlines Boyle's views on the nature of matter, which hypothesize the existence of simple corpuscles and their coalition to form complex ones, and led to a theory of simple substances.

This concept of matter is extended in "An Introduction to the History of Particular Qualities", which prefixes a volume of *Tracts* (1671) wherein the first is "The Cosmicall Qualities of Things". Boyle's "qualities" correspond to the term 'properties' in modern chemistry. The four elements of Aristotle — earth, fire, air and water — were abandoned together with their accompanying primary qualities — dry, hot, cold and wet — and their secondary qualities of causal derivatives. The qualities of bodies were then ascribed to various combinations of corpuscles and their local motion. He regarded matter and motion as the simplest physical principles.

With regard to Boyle's work on the corpuscular theory of matter, Dr Stewart names three of its significant contributions to the history of ideas.

> First, it led him . . . to important reflections on the nature of species, the determination of classes, and the basis of classification, which are the direct ancestor of Locke's discussion of nominal as against real essence, and avoid some of the psychological complications in Locke's account. Secondly, it led him into

theorizing about scientific methodology — into questions about the status of hypotheses, the role of experiment, and the criteria of a good hypothesis — about which he wrote more fully than most of his contemporaries, his views clearly crystallizing side by side with his efforts in actually promoting the corpuscularian hypothesis against its rivals; his writing as a methodologist is at least as important as his (often inconclusive) experimental work in explaining Boyle's success as an advocate of the new philosophy. Thirdly, it led him into taking a leading part in the revival of natural theology, a movement which, despite the assaults of Hume and others a century later, continued to receive powerful support until well into the nineteenth century.

The tract entitled *Of the Imperfection of the Chemists' Doctrine of Qualities* is a discourse included in *Experiments, Notes &c about the Mechanical Origine or Production of divers particular Qualities* (1675) and deals more concisely with matters treated more tediously in *The Sceptical Chymist* (1661). It is concerned with demolishing doctrines of Aristoteleans and chemists.

An important paper on the corpuscularian hypothesis entitled "About the Excellency and Grounds of the Mechanical Hypothesis" formed an appendage to *The Excellency of Theology, compared with Natural Philosophy* (1674): it is a pious defence of theology against natural philosophy, the writing of which was perhaps stimulated by claims that natural philosophy encouraged atheism. This item provides a clear exposition of the mechanical philosophy or theory of matter in motion, and Boyle's reasons for rejecting the Aristotelean elements with their associated forms and qualities.

On the whole it seems that Boyle's corpuscularian hypothesis satisfies his requirements for a good and excellent hypothesis, one manuscript version of which, being notes for a projected treatise on the philosophy of science, is reproduced on p.119. Robert Boyle wrote extensively

Robert Boyle 1627–1691

on the relation between natural science and theology, partly because he believed that study of the former is useful theologically in providing evidence for the wisdom of the Creator, and partly to combat the view held in some quarters that science tends to foster atheism. The essay entitled "A Requisite Digression concerning Those that would Exclude the Deity from intermeddling with Matter" is the fourth in *Some Considerations touching the Usefulness of Experimental Philosophy* (1663). This is one of the places in which the clock metaphor occurs, with reference to the famous astronomical clock of Strasbourg Cathedral (reproduced as the frontispiece). God not only created a mechanical world but also maintained it. Boyle did not regard theology and natural science as opposing interests; he urged a harmonious and helpful co-operation between what he probably considered as two aspects of one entity. In *The Christian Virtuoso* (1690) he wrote: "if a deep insight into nature be acquired by a man of probity and ingenuity . . . that would naturally lead him to sentiments of religion".

The whole of Section II and most of Section IV of the essay *A Free Enquiry into the Vulgarly Received Notion of Nature* (1686), have been selected for reproduction in this volume. Here, Boyle discusses the ambiguity of the term *nature*, and concludes that the vulgar notion of it is indefensible and that its use is an admission of ignorance. He discusses the main, vulgarly held views and demonstrates that they are contradicted by the facts of observation. *Ex rerum causis supremam noscere causam* was fundamental for Boyle.

In *A Discourse . . . about the Possibility of the Resurrection* (1675),

Boyle, from considerations of theology and natural philosophy, reaches the conclusion that resurrection of the body is not inconsistent with natural philosophy. Resurrection is taken as representative of a miracle, a supernatural event not capable of proof by natural philosophy, but possible through the power of God.

Finally, as a specimen of Robert Boyle's style in writing dialogue, part of *A Discourse of Things above Reason* (1681) is included, being a discussion between four characters on the question "*whether,* and, if at all, *how far,* we may employ our reasonings about things that are above our reason, as Christians grant some mysteries of their religion to be". Boyle regarded miracles as proof of things above reason, but believed that "reason, when assisted by revelation, may enable a man to discover far more excellencies in God, and perceive them, than he contemplated before, far greater and more distinctly". In this way a fuller comprehension of God's will and law is obtained. By philosophy Robert Boyle understood "a comprehension of all those truths or doctrines, which the natural reason of man, freed from prejudices and partiality, and assisted by learning, attention, exercise, experiments, &c, can manifestly make out, or, by necessary consequence deduce from clear and certain principles". The definite connection and interrelation of all parts of nature as created by God may be likened to, and mechanically explained as in the wonderful, intricate Strasbourg clock. □

R.E.W. Maddison is a Consulting Chemist, and sometime an Assistant Master at Wellington College, Berkshire, UK, and Leverhulme Research Fellow.

Relativity and Maxwell

W.B. Bonnor

Genesis of Relativity. By L.S. Swenson Jr. Pp.266. (Burt Franklin: New York, 1980.) $21.

THE sub-title of this book is *Einstein in Context*, but this is an Einstein book of an unusual kind. Indeed, Einstein hardly figures in it until p.99, and then soon after he disappears again until p.148. Only the last chapter and an epilogue concentrate on Einstein's own work. The reason is that Mr Swenson uses a great deal of space to set the scene for special relativity. He is fascinated by nineteenth-century electromagnetism and gives a detailed history of it with particular reference to the period from 1860 onwards, which was dominated by Maxwell's theory. Though the connection of some of this with relativity is somewhat tenuous, it makes very interesting reading and contains much not to be found in other books on the history of the discovery of relativity.

From our fortunate viewpoint today, electromagnetism consists of four vector Maxwell equations together with the Lorentz equation of motion and various constitutive relations, and it is not easy to comprehend the turmoil the subject was in about 1880. Maxwell had put forward his equations, but insisted that there must be a medium to carry the field. Helmholtz believed in a two-fluid theory of electricity, one fluid for charge of each sign. Kelvin, along with many scientists, felt that he could not understand the theory unless he could make a mechanical model of it, and he thought in analogues of vibrating shells and plates. Moreover, the Newtonian type of theory, based on particles and the inverse square law, still had a powerful adherent in Wilhelm Weber.

A crucial test of Maxwell's theory was the transmission of electromagnetic waves, and this was demonstrated by the experiments of Hertz, a good account of which is given. An intriguing history is also given of Michelson's famous experiment to detect the ether wind, and of his bitter disappointment at the null result.

Interesting as all this is, it gives little new information on Einstein's discovery of special relativity. Here Mr Swenson's description is similar to that in other books. The marvel, of course, was how Einstein was able to ignore the tangled skein of nineteenth-century electromagnetism and pick out the very few crucial elements which were required for his theory.

There is one chapter on general relativity. This is rather disorganized as the author is inclined to ramble somewhat aimlessly through the various parts of the

subject: for instance, although there is a section headed "Gravitation and Cosmology", a description of Hubble's law and cosmological models appear under another entitled "The Quest for a Unified Field Theory".

In an epilogue on Einstein there is an account of Einstein's social, political and religious views (and these appear here and there throughout the book). There is also, for anybody who is interested, a graph showing the numbers of papers Einstein produced during the different years of his working life!

There are some infelicitous choices of words which may prevent the reader getting the meaning the author is trying to convey. For instance on p.102 one is startled to find Oliver Lodge accused of "despicable behavior": yet it transpires that his sin consisted of nothing more than turning his interests to psychical phenomena.

The book has a good index and extensive bibliographies at the ends of the chapters. It contains practically no mathematics — but on p.124 Maxwell's equations are incorrectly given.

Those interested in the history of nineteenth-century physics and how special relativity grew out of it will enjoy this book. □

W.B. Bonnor is Professor of Mathematics at Queen Elizabeth College, University of London, UK.

Achievement in organic chemistry

Robert Ramage

Comprehensive Organic Chemistry: The Synthesis and Reactions of Organic Compounds. Overall editors Derek Barton and W. David Ollis. Six volumes. (Pergamon: Oxford and New York, 1979.) Six-volume set £687.50, $1,375. Vol. 1. *Stereochemistry, Hydrocarbons, Halo Compounds, Oxygen Compounds,* pp.1,227 (edited by J.F. Stoddart). Vol. 2. *Nitrogen Compounds, Carboxylic Acids, Phosphorus Compounds,* pp.1,329 (edited by I.O. Sutherland). Vol. 3. *Sulphur, Selenium, Silicon, Boron, Organometallic Compounds,* pp.1,323 (edited by D. Neville Jones). Vol. 4. *Heterocyclic Compounds,* pp.1,228 (edited by P. G. Sammes). Vol. 5. *Biological Compounds,* pp.1,205 (edited by E. Haslam). Vol. 6. *Author, Formula, Subject, Reagent and Reaction Indexes,* pp.1,628 (edited by C. J. Drayton).

THIS series of volumes represents a major achievement by the editors and the many authors in producing a survey of contemporary organic chemistry which is complementary to both general textbooks and the specialized works such as Houben-Weyl (George Thieme: Stuttgart). The subject of organic chemistry has developed over the last two decades to such a degree that no one book could cover the subject to the depth required to stimulate advanced students and researchers in the discipline. Selection of topics for each volume is logical and the authors are active researchers expert in the material covered in their chapters. This situation could be expected to lead to problems of imbalanced coverage of topics, and variations in style and presentation and coverage of material, leading to overlap between the individual chapters. The editors and authors should be pleased with their efforts as deficiencies of these types are minimal within the context of such a major work.

Volume 1 has a short introduction to stereochemistry which is excellent but deliberately stops short of dynamic stereochemistry in order to allow this important application to be introduced subsequently at appropriate points in the succeeding chapters and volumes. First reading of the stereochemistry section may at first sight be perplexing but on further consideration it really does set the scene for all that follows and shows that a great deal of thought has gone into the enterprise. The treatment of saturated hydrocarbons has an interesting structural and physical organic emphasis, whereas the articles on olefinic and acetylenic systems have a proper regard for the preparative organic chemistry of these reactive functional groups. Aromatic chemistry is dealt with in complementary ways by discussing first the development of aromaticity and then the chemical reactivity of arenes in impressive detail. The synthesis and properties of annulenes leads naturally from the preceding topics and is treated in an expert manner. Concluding the section on hydrocarbon chemistry are two interesting chapters on reactive intermediates. The remaining parts of the volume treat functional group chemistry in an orthodox manner placing more emphasis on synthesis. It is here that some questions may be asked about the balance of material in that the coverage of quinone chemistry is scant in comparison to that of other sections in Vol. 1.

The second volume covers organic nitrogen and phosphorus compounds with the chemistry of carboxylic acids interposed. The section on amines is dominated by discussion of non-aromatic types and assembles valuable information

> The last of the volumes of the first edition of *Research in British Universities, Polytechnics and Colleges,* Vol. 3 *Social Sciences,* has just been published by The British Library, Boston Spa, West Yorkshire, UK, price £10, $22.
>
> Volume 1 *Physical Sciences* appeared in March 1979, price £15, $32, and Vol. 2 *Biological Sciences* in December 1979, price £10, $22.
>
> The second edition of Vol. 1 will be published at the end of 1980.

concerning preparation, properties and reactions which is the typical format throughout. There is an adequate coverage of stereochemistry and spectroscopic properties followed by a detailed discussion of basicity in solution and the gas phase. In the section on reactions there is an introduction to strong base methodology, used widely throughout the volumes, and protection of amines is described briefly as a prelude to a later chapter on peptides. The chapter on polyfunctional amines concentrates on the reactions of a variety of structural types of relevance to pharmaceutical applications. Aromatic amines are dealt with in an unexceptional manner, followed by a fine section on hydroxylamine derivatives in which a good balance is struck between the preparative and reactive aspects including application of nitroxides to radical chemistry. Expert treatment of hydrazine chemistry is also in this volume and, although mechanisms are considered at appropriate points, the physical organic balance is maintained with a short contribution on nitrogen cations, anions, radicals and nitrenes. A good coverage of the extensive chemistry of nitro and nitroso compounds is followed by an exceptionally thorough article on imines, nitrones, nitriles and isocyanides. At this juncture Vol. 2 turns to carboxylic acid chemistry in the same logical and comprehensive manner. A modern treatment of carboxylic acids is developed into more complex systems with particular emphasis on preparative aspects. The treatment of oxo-carboxylic acids is excellent, covering both preparative and physical organic principles. The good cross-referencing between the volumes is exemplified by the short chapter on amino acids which allows continuity and prepares for the later section in Vol. 5. Two excellent chapters on esters and amides are well constructed and correlate well with preceding material. The conventional chemistry of the first-row elements is concluded with discussion of derivatives of carbon dioxide and peroxy acids. Finally, there is an excellent critical presentation of organophosphorus chemistry in which the important features of stereochemistry, preparation and reactions are identified for the non-specialist.

Volume 3 is impressive and is written by established experts in many of the fields covered. There is a thorough treatment of organosulphur chemistry (487 pages) which gives the professional chemist an excellent modern overview in which the main applications for synthesis are emphasized. The format is the same as in the preceding volumes, with little concern with detailed mechanism in the sections on synthesis and reactivity. Where applicable, stereochemical principles are discussed with additional reference to review literature. The volume abounds with interesting chemistry in fields of great current interest, for example organoselenium, tellurium to a lesser extent, and silicon chemistry. The chapter on silicon is beautifully constructed and will be most instructive to the readership for which this series is intended. The chapters on organoboron chemistry (254 pages) are indeed comprehensive and most useful. Due reference is given to existing monographs on the subject but this contribution is an intellectual achievement in its own right, correlating stereochemical and physical properties with chemical reactivity. The vast area of organometallic compounds is condensed into 383 pages with the emphasis being placed on transition metal chemistry where a wide sweep of this active area is discussed concisely.

The task of constructing a single volume on heterocyclic compounds is a daunting one which has largely been met in Vol. 4. The decision was obviously made to concentrate on aromatic and conjugated systems, placing strong emphasis on the preparation and reactions of the main ring-systems. Even with such constraints, the selection and organization of material is of great importance so that the fundamentals, once learned, can be applied to the many heterocyclic systems omitted from this work by necessity. With this in mind, this contribution to the series successfully surveys the field by devoting 604 pages to nitrogen heterocycles, 182 pages to oxygen heterocycles, 172 pages to sulphur and related systems, and 269 pages to mixed heteroatom systems. As expected in such a multi-author work, the presentation varies but overall is of high quality. The section on nitrogen systems is detailed and useful to non-specialists. Reference is given to naturally occurring systems throughout as examples of structural types. The pyrrole, porphyrin and indole chapters give an easy entry into these specialized themes. Treatment of the biologically important purines is expert and thorough, and will serve as a useful introduction to the chemist wishing to enter the field. The section on oxygen heterocycles gives a concise account of five- and six-membered systems, and it is interesting to compare the presentation of this section with the later chapters on organosulphur systems which contain much useful chemistry for the reader. Finally, the treatment of mixed heterocyclic systems will prove invaluable

to those entering pharmaceutical chemistry. A minor criticism could be made that with the enormous volume of chemistry to be compressed into a single volume the discussion occasionally degenerates to a cataloguing of results.

The editor of Vol. 5 had the slightly easier task of covering biological chemistry in one volume. To accomplish this meant careful selection of chapter topics and materials within individual chapters with corresponding unavoidable omissions. Again, an impressive list of experts has performed the task exceptionally well and the result of their efforts will be invaluable to specialists as well as chemists lacking biochemical training. The approach to the subject is a critical one depending heavily on experimental results with important references to vital synthetic transformations. Coverage of primary and secondary metabolites is well balanced, with an important contribution on the mechanistic aspects of enzyme catalysis. Altogether this volume makes fascinating reading.

The last volume serves to endorse the comprehensive nature of the series as it contains an impressive range of indexes which enable easy retrieval of information and cross-referencing from the previous five volumes. Direct access to specific compounds may be gained from the formula index which contains around 20,000 formulae. The subject index refers both to classes of organic compounds and reaction types, and to important specific compounds. Experienced researchers will find the excellent author index a useful and

rapid entry into the series. The reaction index has entries to material covered in Vols 1–5 together with useful supplementary lists of review articles. These entries consist of reaction types and named reactions, in addition to a listing of reagents which leads the reader to the extensive reagent index of over 25,000 compounds. This index not only serves a primary function but in addition provides access to supporting literature references.

It would be unrealistic to expect the content of the volumes to be complete in terms of the present knowledge of the subject and one has to accept the selection of material by the contributors whose judgement is of a high standard. Fortunately there are few omissions and even these can reflect the predilections of the reader. There are relatively few errors, mainly in structures, for such a large multi-author work, and these will no doubt be remedied by the publishers. I found the books to be very enjoyable and informative to read as well as extremely useful for reference in research and teaching exercises in a wide variety of topics over a realistic period of time for assessment. Thus the overall impression of *Comprehensive Organic Chemistry* is that the series is indeed comprehensive and will be an essential purchase for chemical libraries. Sadly the cost will limit the number of private purchasers of this important work.

Robert Ramage is Professor of Organic Chemistry at the University of Manchester Institute of Science and Technology, UK.

Indulging in developmental biology

D. R. Garrod

Introductory Concepts in Developmental Biology. By A. Monroy and A. A. Moscona. Pp.252. (University of Chicago Press: Chicago and London, 1980.) $16, £9.60.

THIS book claims to be (I quote from the preface) "an up-to-date introduction for beginners" and "a guidebook for graduate students and teachers to some issues, answers and challenges in developmental biology", as well as a "balanced sampling of facts, concepts and projections". As a teacher of developmental biology at elementary and advanced level for nearly a decade, my interest was aroused and I proceeded with anticipation. I was soon disappointed: the claim is too ambitious.

Chapter 1 is a brief descriptive embryology similar to, and largely derived from, previous books on the subject.

Thereafter, the book abandons any pretence at being a balanced, introductory guidebook and divides rather neatly into two sections, early development (Chapters 2 and 6 dealing with oögenesis, fertilization, cleavage and gene expression), and morphogenesis and cell aggregation (Chapters 7 and 8 respectively). No attempt is made to link these two aspects and one might be forgiven for feeling that this arrangement (and perhaps the entire book) serves no other purpose than to indulge the research interest of the authors. This is not necessarily a bad thing, but I cannot recommend the book as a students' introduction to developmental biology because many important aspects of the subject, such as organogenesis, pattern formation and differentiation, are hardly mentioned.

In some respects the book succeeds better as a review for advanced students. With the proviso that early development is not my field, I found the treatment of it comprehensive and informative. The classical work is fully outlined and many more recent developments are presented. It seems like good solid stuff — not particularly exciting, but certainly adequate.

I had more difficulty with the section on

morphogenesis and cell aggregation, perhaps because it is my field. My main objection is that it is not 'balanced'. There are many types of morphogenetic movement, yet only one class of them, long-distance cell migrations of, for example, primordial germ cells and neural crest, are considered here. Other types of morphogenetic movement — the majority in fact — such as the bending of cell sheets and the formation of tubules are not considered. The final chapter, about cell aggregation, is really little more than a review of the work of one of the authors (21 out of 28 figures in this chapter are from his own work). I would point out that cell

aggregation is not an aspect of normal development and that the significance of much of this work is questionable. Surely this is not the way to present beginners with a balanced view of developmental biology.

The figures in the book are generally of a very high standard, the bibliography is good and the index useful, though it might have been better to have separated author and subject indexes.

All in all this is a poor book, and one rather unsuitable for beginners. □

D. R. Garrod is a Lecturer in Medical Oncology at the University of Southampton, UK.

Exciting dilution analysis

Elizabeth Simpson

Limiting Dilution Analysis of Cells in the Immune System. By I. Lefkovits and H. Waldmann. Pp.262. (Cambridge University Press: Cambridge, UK, 1979.) £15, $36.

LIMITING dilution analysis is a new and very powerful way of examining cell–cell interactions in the immune response. Subpopulations of lymphocytes defined with respect to different functions and by surface markers exist, and questions of interactions between them can only be partially analysed *in vivo* or *in vitro* in bulk cultures and mixing experiments. Limiting dilution analysis allows more precise and quantitative questions to be asked. This book is an extensive treatise on the rationale of this approach. It includes both a detailed mathematical analysis and methodological descriptions so that the newcomer could set up limiting dilution experiments using the book and the examples in it as a text.

The opening chapters on the immunology of a single cell (Chapter 1) and manipulation of lymphocytes (Chapter 2) describe the immunological background clearly and well. There are minor lapses such as failure to specify whether bicarbonate- or phosphate-buffered balanced salt solutions (BSS) are used in the preculture manipulations of lymphocytes (e.g. in nylon column separations of T cells) or whether 37°C incubations in BSS

are carried out in a CO_2 incubator. Also, test tubes used in some manipulations are given a 'house' name only, e.g. Wasserman tube (p.22) or rhesus tube (p.27), and further identifying specifications are not given.

Chapter 3, "Methods of Determining B Cell Responses", is detailed and gives a comprehensive description of methods that can be adapted for use on single clones including plaquing, isoelectric focussing and radioimmunoassay.

Chapter 4, on Poisson distribution, includes a discussion of single-hit, multi-hit and multi-target events, vital for any analysis of immunological responses many of which certainly involve the interaction between two or more cell types. This is illustrated by experimental examples of titration of B precursor cells and T helper cells in Chapter 5. Further experimental data are to illustrate clone size estimation (Chapter 6). Chapter 8 describes results on the analysis of B cell responses, and Chapter 9 results on the analysis of T helper cells. These two chapters contain details of experiments performed mainly by the authors during investigations of questions they have answered uniquely by using the limiting dilution analysis.

The weakest and least developed chapter is that on analysis of other T cell functions (Chapter 10) including cytotoxic T cells. Results of frequency estimations of alloreactive cytotoxic precursors are described but from the experimental details given it would not be possible to do such experiments, and this is in contrast to the sort of experimental detail used to illustrate B cell and T helper cell function. Furthermore, no consideration is given to the presence of T helper cells for cytotoxic responses and this certainly does affect the analysis.

Nevertheless this book is an excellent one: it is timely, comprehensive, well written and transmits the authors' excitement at using limiting dilution analysis to approach questions of lymphocyte function at the single-cell level. □

Elizabeth Simpson is Senior Research Scientist at the Transplantation Biology Unit, MRC Clinical Research Centre, Harrow, UK.

In the review of *Image Analysis, Enhancement and Interpretation,* edited by D. L. Misell (*Nature* **282**, 885; 1979), the prices were incorrectly quoted, thus making the final criticisms of the reviewer unfounded. The book is available in paperback, price $31.75, Dfl. 65, or in hardback as Vol.7 of the series *Practical Methods in Electron Microscopy,* price $66, Dfl. 135.

Hard science in renewable energy

Chris Hope

Renewable Energy. By B. Sørensen. Pp.583. (Academic: London and New York, 1979.) £20, $46.

I AM always wary of a book with a title so general that it implies a great breadth of coverage. All too often the reality is a book full of the cream skimmed off the surface of a subject — tasty in mouthfuls but totally unsatisfactory as a main course. When the subject is also of intense topical interest, the suspicion that the glossy covers contain nothing that will be worth recalling next year becomes almost a certainty. This book is a reminder that the improbable does happen, for it contains a deep treatment of aspects of renewable energy that I suspect will be of lasting use.

The three chapters (460 pages) concerning the origin, diverse manifestations and means of harnessing the renewable energy flows form a comprehensive treatment of the methods and principles needed to understand what it is reasonable to expect from these sources. Techniques employed include meteorology, geology and chemistry, but with a preponderance of the various branches of physics, and it is these chapters on the hard science of the 'renewables' that will make this an enduring basic text. Succeeding chapters treat energy storage and energy supply systems in a similarly technical manner.

This central scientific core is preceded by a short scene-setting chapter that comes close to sensationalism in its comparison of Man's energy usage over the last half-million years with the enormously greater amounts of energy involved in keeping our planet in its allotted place in the heavens (approximately 8×10^{33} J, if you didn't know). The book concludes with a subjective account of socio-economic assessment. This is the only chapter in which the author's strong personal views lead him in places to write as an advocate of renewable energy rather than an impartial observer.

Of course this book will not appeal to as wide an audience as a skimmed-cream book would have done. There are no descriptions of actual devices 'as constructed by the author', no colour photographs of windmills against a blue sky, just a host of line drawings, a good deal of fairly advanced mathematics and a thorough treatment of one aspect of a small but important topic typified by the inclusion of 500 references and a 1000-item index.

I recommend this book, especially to anyone running, or thinking of setting up, a course on the physics of energy. □

Chris Hope is a member of the Energy Research Group at the University of Cambridge, UK.

BOOKS RECEIVED

Earth Sciences

LENIHAN, J. and FLETCHER, W.W. (ed.) The Biological Environment. Environment and Man Volume 9. Pp. iv + 164. ISBN-0-12-443509-2. (New York and San Francisco: Academic, 1979.) $17.50.

LOWE, J.J., GRAY, J.M. and ROBINSON, J.E. (ed.) Studies in the Lateglacial of North-West Europe. Including Papers presented at a Symposium of the Quaternary Research Association held at University College London, January, 1979. Pp. xii + 203. ISBN-0-08-024001-1. (Oxford, New York, Toronto, Sydney, Paris, Frankfurt: Pergamon, 1980.) US $38.00, £17.00.

McROSTIE, C.N. (ed.) Global Resources: Perspectives and Alternatives. XIV Nobel Conference. Pp. x + 97. ISBN-3-540-90397-6. (New York, Heidelberg, Berlin: Springer, 1979.)

SHARMA, G. D. The Alaskan Shelf; Hydrographic, Sedimentary, and Geochemical Environment. Pp. xiii + 498. ISBN-3-540-90397-6. (New York, Heidelberg. Berling: Springer-V, 1979.)

SITTIG, M. (ed.) Geophysical and Geochemical Techniques for Exploration of Hydrocarbons and Minerals. Pp. ix + 229. ISBN-0-8155-0782-8. (New Jersey: Noyes Data Corporation, 1980.) $40.00.

SMITH, R.E. Lower Devonian (Lochkovian) Biostratigraphy and Brachiopod Faunas, Canadian Arctic Islands. Geological Survey Bulletin 308. Pp. x + 155. ISBN-0-660-10221-8. (Quebec: Canadian Government Publishing Centre, 1980.) Canada $5.00 other countries $6.00.

TOKSOZ, M.N., UYEDA, S. and FRANCHETEAU, J. (ed.) Oceanic Ridges and Arcs; Geodynamic Processes. Developments in Geotectonics 14. Pp. xvi + 538. ISBN-0-444-41839-3. (Amsterdam, Oxford, New York: Elsevier Scientific, 1980.) US $29.25, Dfl. 60.00.

UNITED NATIONS ECONOMIC COMMISSION FOR EUROPE. Selected Water. Problems in Islands and Coastal Areas. With special regard to Desalination and Groundwater. Proceedings of a seminar organized by the Committee on Water Problems of the UNECE, Malta, June, 1978. Pp. xxv + 501. ISBN-0-08-024447-5. (Oxford, New York, Toronto, Sydney, Paris, Frankfurt: Pergamon, 1979.) £34.00, $68.00.

WALKER, D. and GUPPY, J.C. (ed.) Biology and Quaternary Environments. Based on the Symposium on Biological Problems in the Reconstruction of Quaternary Terrestrial Environments, held in Canberra, February, 1978. vii + 264. ISBN-0-85847-050-0. (Canberra: Australian Academy of Science, 1978.) A$11.00 flexi.

WEST, R.G. The pre-glacial Pleistocene of the Norfolk and Suffolk coasts. Pp. xi + 239. ISBN-0-521-21962-0. (Cambridge: Cambridge University Press, 1980.) £40.00.

Biology

AKINS, F. R., MACE, S.M., HUBBARD, J. W. and AKINS, D. L. Behavioral Development of Nonhuman Primates. An Abstracted Bibliography. IFI Data Base Library. Pp. ix + 304. ISBN-0-306-65189-0. (New York, Washington, London: IFI/Plenum, 1980.) $75.00.

ARBER, W. et al (ed.) Current Topics in Microbiology and Immunology. volume 88. Pp. iii + 142. ISBN-3-540-09415-6. (Berlin, Heidelberg, New York: Springer-V, 1979.) DM 64 approx. US $35.90.

ARBER, W. et al (ed.) Current Topics in Microbiology and Immunology volume 87. Pp. iii + 172. ISBN-3-540-09433-4. (Berlin, Heidelberg, New York: Springer-V, 1979.) DM 68 approx. US $38.10.

ARMSTRONG, M. A. Basic Topology. Pp. xii + 251. ISBN-0-07-084090-3. (Maidenhead: McGraw-Hill, 1979.) £7.25 flexi.

AVERS, C. J. Genetics. Pp. xi + 659. ISBN-0-442-26233-7. (New York, Cincinatti, Toronto, London, Melbourne: D. Van Nostrand and Company, 1980.) $21.95.

BARAM, P., BATTISTO, J. R. and PIERCE, C. W. (ed.) Immunologic Tolerance and Macrophage Function. Developments in Immunology Volume 4. Proceedings of the 7th Annual Mid-West Autumn Immunology Conference, Dearborn, Michigan, U.S.A., November 1978. Pp. xiii + 266. ISBN-0-444-00316-9. (New York, Amsterdam, Oxford: Elsevier/North-Holland, 1979.) $40.000.

BARRINGTON, E. J. W. (ed.) Hormones and Evolution Volume 2. Pp. xxv + 989. ISBN-0-12-079402-0. (New York, San Francisco, London: Academic, 1979.) £30.00 $69.00.

BARRINGTON, E. J. W. (ed.) Hormones and Evolution Volume 1. Pp. xxv + 491. ISBN-0-12-079401-2. (New York, San Francisco, London: Academic, 1979.) £30.00 $69.00.

BEGLEY, D. J., FIRTH, J. A. and HOULT, J. R. S. Human Reproduction and Developmental Biology. Pp. x + 250. ISBN-0-333-23423-5 hardback ISBN-0-333-2324-3 paperback. (London and Basingstoke: T. Macmillan P, Ltd. 1980.) £20.00 hardback £9.95 pbk.

BEHRESMEYER, A. K. and HILL, A. P. (ed.) Fossils in the Making. Vertebrate Taphonomy and Paleoecology. Prehistoric Archeology and Ecology. Series. Pp. xii + 338. ISBN-0-226-04168-9. (Chicago and London: The University of Chicago Press, 1980.) $7.00.

EISENBERG, J. F. (ed.) Vertebrate Ecology in the Northern Neotropics. Results from a Team research Effort sponsored by the National Zoological Park, Smithsonian Institution, March 1973 to August 1978 and a Workshop held at the National Zoological Park on December 14, 1978. Pp. 271. ISBN-0-87474-410-5 hardback ISBN-0-87474-409-1 pbk. (Washington, D.C.: Smithsonian Instition Press, 1980.) $17.50 hardback $8.95 pbk.

BOURNE, G. H. and DANIELLI, J. F. (ed.) International Review of Cytology volume 63. Pp. vii + 410. ISBN-0-12-364463-1. (New York, London, toronto, Sydney, San Francisco: Academic Press, $30.000.

BAUMEL, J. J. et al. (ed.) Nomina Anatomica Avium. An annotated Anatomical Dictionary of Birds. Pp. xxv + 637. ISBN-0-12-08150-3. (London, New York, Toronto, Sydney, San Francisco: Academic Press, 1979.) $28.00 $64.50.

CANTOR, C. R. and SCHIMMEL. P. R. Biophysical Chemistry part 1. The Conformation of Biological Macromolecules. Pp. xxvii + 341 + Appendices ISBN-0-7167-1042-0 hardback ISBN-0-7167-1188-5 pbk. (San Francisco: Freeman, 1980.) $30.00 hardback $16.95 pbk.

CLOUDSLEY-THOMPSON, J. L. Tooth and Claw. Defensive Strategies in the Animal World. Pp. 252. ISBN-0-460-04360-9. (London: J. M. Dent & Sons Ltd., 1980.)

COHEN, M. P. and FOA, P. P. (ed.) Special Topics in Endocrinology and Metabolism Volume 1. Pp. viii + 144. ISBN-0-8451-0700-3. (New York: Alan R. Liss, Inc. 1979.) np. Available in UK, Europe and Middle East through European Book Service.

COHN, W. E. (ed.) Progress in Nucleic Acid Research Molecular Biology. Volume 23. Pp. xv + 299. ISBN-0-12-540023-3. (New York, London, Toronto, Sydney, San Francisco: Academic Press, 198 $31.00.

COUGHLAN, M. P. (ed.) Molybdenum and Molybdenum-Containing Enzymes. Pp. xii + 577. ISBN-0-08-024398-3. (Oxford, New York, Toronto, Sydney, Paris, Frankfurt: Pergamon P, 1979.) $80.00 £36.00.

CREUTZFELDT, O., SCHEICH, H. and SCHREINER, Chr. (ed.) Hearing Mechanisms and Speech. EBBS-Workshop, Göttingen, April 26-28, 1979. Experimental Brain Research Supplementum 2. Pp. xxiii + 413. ISBN-3-540-09655-8. (Berlin, Heidelberg, New York: Springer-V., 1979.) DM 42 approx. US $23.10 flexi.

DE BRABANDER, M., MARREL, M. and DE RIDDER, L. (edited by.) Cell Movement and Neoplasia. Proceedings of the Annual Meeting of the Cell Tissue and Organ Culture Study Group, held at the Janssen Research Foundation, Beerse, Belgium, May, 1979. Pp. vii + 174. ISBN-0-08-025534-5. (Oxford, Pergamon, 1980.) $28.00 £13.50.

DORMER, K. J. Fundamental tissue geometry for biologists. Pp. vi + 149. ISBN-0-521-22326-1. (Cambridge, London, New York, New Rochelle, Melbourne, Sydney: Cambridge University Press, 1980.) £15.00.

EBBESON, S. O. E. (ed.) Comparative Neurology of the Telencephalon. Pp. xxi + 506. ISBN-0-306-40237-8. (New York and London: Plenum, 1980.) $45.00.

ELLENBERG, H., ESSER, K., KUBITZKI, K. SCHNEPF, E. and ZIEGLER, H. (ed.) Progress in Botany. Morphology, Physiology, Genetics, Taxonomy, Geobotany. Volume 41. Pp. xi + 356. ISBN-3-540-09769-4. (Berlin, Heidelberg, New York: Springer, 1979.) DM 119 approx. US $66.70.

FINN, C, A. (ed.) Oxford Reviews of Reproductive Biology. Volume 1, 1979. (Oxford Science Publications). Pp. viii + 485. ISBN-0-19-857534-3. (Oxford: Clarendon Press, Oxford University Press, 1980.) £30.00.

FLEGG, J. (Consultant editor.) The British Ornithologists' Guide to Bird Life. Pp. xi + 318. ISBN-0-7137-0996-0. (Poole: Blandford Press, 1980.) £10.95.

GIMENEZ, M. and SAUNIER, C. (ed.) Muscular Lung Exercise in Chronic Lung Disease. Entretiens de Physio-Pathologie Respiratoire Nancy 11e Série. Pp. v + 436. ISBN-0-08-024930-2. (Oxford, New York, Toronto, Sydney, Paris, Frankfurt: Pergamon P, 1980.) £20.00 $45.00.

GOY, R. W. and McEWEN, B. S. Sexual Differentiation of the Brain. Based on a Work Session of the Neurosciences Research Program. Pp. ix + 223. ISBN-0-262-07077-4. (Cambridge, Mass. and London: The MIT, 1980.) $17.50.

GRIDGMAN, N. T. Biological Sciences at the National Research Council of Canada: The Early Years to 1952. Pp. xxi + 153. ISBN-0-88920-082-3. (Ontario: Wilfrid Laurier University Press, 1979.) $7.50.

GROSCH, D. S. and HOPWOOD, L. E. Biological Effects of Radiations. Second edition. Pp. xv + 338. ISBN-0-12-304150-3. (New York, San Francisco, London: Academic P, 1979.) $27.50.

HARRISON, G. H. Roger Tory Peterson's Dozen Birding Hot Spots. Pp. 288. ISBN-0-671-22329-1 hardback ISBN-0-671-25405-7 paperback. (New York: Simon and Schuster, 1980.) $6.95 paperback.

HARRISON, R. J. Marine Mammals 2nd Edition. HARRISON, R. J. and KING, J. E. Marine Mammals, 2nd edition. Pp. 192. ISBN-0-09-140931-4. (London, Melbourne, Sydney, Auckland, Johannesburg: Hutchinson, 1980.) £23.95 flexi.

HECHT, M. K., STEERE, W. C. and WALLANCE, B. Evolutionary Biology volume 12. Pp. xii + 388. ISBN-0-306-40267-X. (New York and London: Plenum, 1980.) $32.50.

HENDERSON, B. E. (ed.) Second Symposium on Epidemiology and Cancer Registries in the Pacific Basin. National Cancer Institute Monograph 53. Pp. vi + 205. (Washington: UKS. Government Printing Office, 1979.) $7.50.

HERTMAN, I., SHAFFERMAN, A., COHEN, A. and SMITH, S. R. (ed.) Extrachromosomal Inheritance in Bacteria. Contributions to Microbiology and Immunology Volume 6. Pp. xiv + 238. ISBN-3-8055-2943-0. (Basel, Munchen, Paris, London, New York, Sydney: S. Karger, 1979.) Sfr. 106.00 DM 127.00 approx. US $63.50 flexi.

HOBSON, J. A. and BRAZIER, M. A. B. (ed.) The Reticular Formation Revisited: Specifying Function for a Nonspecific System. International Brain Research Organization Monograph Series volume 6. Pp. xv + 552. ISBN-0-89004-379-5. (New York: Raven P, 1980.) £9.50.

HOUCK, J. C. (ed.) Chemical Messengers of the Inflammatory Process. Handbook of Inflammation, Volume 1. Pp. xvii + 422. ISBN-0-444-80121-9. (Amsterdam and New York: Elsevier/North-Holland Biomedical Press, 1979.) US $75.00 Dfl. 164.00.

HSIE, A. W., O'NEILL, J. P. and McELHENY, V. K. (ed.) Mammalian Cell Mutagenesis: The Naturation of Test Systems. Banbury Report 2. Pp. xiv + 504. ISBN-0-87969-4. (Cold Spring Harbor: Cold Spring Harbor Laboratory, 1979.) np.

HUBEL, D. H. et al. The Brain. A Scientific American Book. Pp. viii + 149. ISBN-0-7167-1150-8 board ISBN-0-7167-1151-6 pbk. (Oxford: W. H. Freeman and Company Limited, 1980.) £9.10 board £3.30 pbk.

JAMES, V. H. T. and PASQUALINI. J. R. (ed.) Hormonal Steroids. Proceedings of the Fifth International Congress on Hormonal Steroids, New Delhi, October/November 1978. Pp. xviii + 1068. (Oxford, New York, Toronto, Paris, Frankfurt, Sydney: Pergamon P, 1979.) $120.00 £60.00.

JOHNSTON, F. E., ROCHE, A. F. and SUSANNE, C. (ed.) Human Physical Growth and Maturation; Methodologies and Factors. NATO Advanced Study Series volume 30. Pp. xii + 364. ISBN-0-306-40420-6. (New York and London: Plenum Press, 1980.) $42.50.

KANDEL, E. R., KRASNE, F. B., STRMWASSER, F. and TRUMAN, J. W. Cellular Mechanisms in the selection and modulation of behaviour. Neurosciences Research Program Bulletin Volume 17 No. 4. vi + 187. ISSN-0028-3967. (Cambridge, Massachusetts: MIT, 1979.)

KROG. H., OSTHAGEN, H AND TONSBERG, T. Lavflora. Norske busk-og bladlav. Pp. 312. ISBN-82-00-01907-1 ISBN-82-00-01988-8 (with supplement in English). (New York: Columbia University Press; London: Global Book Resources, Ltd., 1980.) Kr. 189.00 Kr. 209.00 m/eng. Bestemmelsesnokkel.

KUMAR S. (ed.) Biochemistry of Brain. Pp. vii + 625. ISBN-0-08-021345-6. (Oxford, New York, Toronto, Sydney, Paris, Frankfurt: Pergamon Press, 1979.) $100.00 £50.00.

LARSEN, K. And HOLM-NIELSEN, L. B. (ed.) tropical Botany. Proceedings of a Symposium held at University of Aarhus, August, 1978. xi + 453. ISBN-0-12-437350-X. (London, New York, San Francisco: Academic, 1979.) $66.50 £22.80.

LEE, C. P., SCHATZ, G. and ERNSTER, L. (ed.) Membrane Bioenergetics. Based on the International Workshop held at Granbrook, Michigan, 5-7 July, 1979. Pp. xxxiv + 604. ISBN-0-201-03999-0 pbk. (London, Amsterdam, Ontario, Sydney, Tokyo: Addison-Wesley Publishing Company, 1980.) US $25.50 flexi. Also available as hardback.

LEVIN, H. and ADDIS, A. B. The Eye-Voice Span. Pp. viii + 165. (Cambridge, Mass. and London: MIT, 1980.) £9.30.

LITTLE, R. J. and JONES, C. E. A Dictionary of Botany. Pp. ix + 400. ISBN-0-442-24169-0. (Wokingham: Vn Nostrand reinhold company Ltd., 1980.) £13.90.

LOFFLER, H. (ed.) Neusiedlersee: The Limnology of a shallow lake in Central Europe. Monographiae Biologicae volume 37. Pp. x + 561. ISBN-90-6193-089-8. (The Hague, Boston, London: Dr. W. Junk bv., 1980.) Dutch Guilders 195 US $102.65.

MAFAMOROSCH, K. and HIRUMI, H. (ed.) Practical Tissue Culture Applications. Proceedings of a Conference held at the International Laboratory for Research on Animal Diseases in Nairobi, Kenya August, 1978. Pp. xiii + 426. ISBN-0-12-470285-6. (New York, London, Toronto, Sydney, San Francisco: Academic, 1979.) $29.50.

MENDEL, A. Les Manipulations Génétiques. Pp. 332. ISBN-2-02-005437-X. (Paris: Editions du Seuil, 1980.) flexi.

MARCHALONIS, J. J. and COHEN, N. Contemporary Topics in Immunobiology. Volume 9. Self/Non-self Discrimination. Pp. xvi + 293. ISBN-0-306-40263-7. (New York and London: Plenum P, 1980.) $29.50.

MELNICK, M. and JORGENSON, R. (ed.) Developmental Aspects of Craniofacial Dysmorphology. The National Foundation-March of Dimes Birth Defects: Original Article Secies, Volume xv, Number 8, 1979. Pp. xi + 118. ISBN-0-8451-1033-0 (616'.043) 79-2487. (New York: Alan R. Liss, Inc., 1979.) $16.00. This title is available in Europe, the United Kingdom and the Middle East exclusively from: European book Service, Flevolaan 36-38 P.O.B. 124 1380 AC Weesp, Holland. Dfl. 48.00.

ANNOUNCEMENTS

Awards

The Council of the British Institute of Radiology have made the following awards: The Barclay Medal to **Dr R. H. Mole** (MRC Radiobiological Unit, Harwell, UK). The Barclay Prize to **Dr H. B. Meire** (Clinical Research Centre, Harrow, UK). The Röntgen Prize to **Dr S. Dische** (Mount Vernon Hospital, Middlesex, UK).

Professor R. W. Baldwin Cancer Research Campaign Laboratories at the University of Nottingham UK) has been awarded the Rabbi Shai Shacknai Memorial Prize at the Hebrew University in Jerusalem.

The 1979 ICI Diagnostic Techniques Prize of £1,000 has been awarded to **Dr M. L. Little** and **Mr R. Glanville** of the Central Electricity Generating Board (UK).

The Marconi International Fellowship invites nominations for the Seventh Marconi Fellowship Award to be presented in 1981. Nominations close the 1 October 1980. For nominations in 1980, candidates will be judged on the basis of qualifications in either: (1) Contributions to the science of technology of communications or to applications thereof, for betterment of the lives of children. (2) Contributions to fundamental knowledge or practical applications of systems that contribute to the betterment of the human condition through communications by non-verbal means. Send nominations to: Dr Walter Orr Roberts, The Marconi Fellowhip Council, Aspen Institute for Humanistic Studies, 1229 University Avenue Boulder, Colorado 80302.

Twenty Harkness Fellowships tenable for between 12 and 21 months are offered each year. The award includes return fares to the US, living and family allowances, travel in America, tuition and research expenses, a book and equipment allowance and health insurance. Candidacy is open to men and women in any profession or field of study, who are citizens of the UK and have received both secondary schooling and further education (or equivalent professional experience) wholly or mainly in the UK. Candidates must be between 21 or 30 years of age on 1 September 1981, unless qualified in medicine or employed in the Civil Service or the media, in which cases the upper age limit is 33. For application forms (available only to individual candidates) send a s.a.e. not less than 10 inches by 7 inches carrying 22p postage, to Harkness Fellowhips (UK), Harkness House, 38 Upper Brook Street, London W1, UK.

The Council of the Eugenics Society is prepared to support research in those areas for which the late Dr Marie Carmichael Stopes is best remembered: fertility control; differential fertility; eugenic aspects of reproduction and population; eugenic aspects of sex education and sexual behaviour and the impact of all these and related matters on the welfare of women and of the community, with particular emphasis (in keeping with the biosocial outlook of the Society) on interdisciplinary research. For further information contact: The Eugenics Society, 69 Eccleston Square, London SW1, UK.

Appointments

The Royal Society have elected the following foreign members: **Professor Hannes Olof Gösta Alfvén** (Royal Institute of Technology, Sweden); **Professor Philip Warren Anderson** (Bell Laboratories, USA).

The National Academy of Sciences have elected the following foreign associates: **Ignacio Bernal y Garcia Pimentel**, (National University of Mexico); **Jacques-Emile Blamont**, (CNRS, France); **John G. Bolton**, (CSIRO, Australia; **Paul Erdös**, (Hungarian Academy of Sciences); **Roger Erdös**, (Hungarian Academy of Sciences); **Roger Gautheret**, (L'Institut de France); **John B. Gurdon**, (MRC, UK); **Jean-Marie Pierre Lehn** (Université Louis Pasteur, France); **Peter Reichard**, (Medical Nobel Institute, Sweden); **Hans H. Ussing**, (University of Copenhagen, Denmark); **Leon Van Hove**, (European Organization for Nuclear Research, Switzerland); **Torsten N. Wiesel** (Sweden); **Maurice V. Wilkes**, (University of Cambridge, UK).

The Council of the Zoological Society of London have appointed **Dr. John P. Hearn** as Director of Science and Director of the Institute of Zoology from 1 August 1980, on the retirement of **Dr L. G. Goodwin**.

Meetings

10-12 June, **Developments in Power-System Protection**, London (IEE, Savoy Place, London WC2, UK).
16-18 June, **Mass Spectrometry in Biochemistry, Medicine and Environmental Research**, Milan (Dr A. Frigerio, Italian Group for Mass Spectrometry in Biochemistry and Medicine, Via Eritrea, 62, 20157 Milan, Italy).
18-19 June **NMR Spectroscopy in Solids**, London (The Royal Society, 6 Carlton House Terrace, London SW1, UK).

14-17 July, **Metallo-organics in Organic Synthesis**, Swansea (Dr John F. Gibson, The Chemical Society, Burlington House, London W1, UK).
14-17 July, **Biological Reactive Intermediates Chemical Mechanisms and Biological Effects**, Guildford (Dr G. G. Gibson, Dept of Biochemistry, University of Surrey, Guildford, Surrey, UK).
21-25 July, **Stereoelectronics Effects in Organic Chemistry**, St Andrews (Dr F. F. Gibson, The Chemical Society, Burlington House, London W1, UK).
25 July, **HPLC of Drug Metabolites**, Guildford (Dr E. Reid, Wolfson Bioanalytical Unit, IIEHS, University of Surrey, Guildford, UK).
2-9 August, **The Social Context of Energy**, Harlech (Miss J. Miller, Dept of Liberal Studies in Science, University of Manchester, Manchester, UK).
5-6 September, **Symposium Mammographicum '80**, London (The British Institute of Radiology, 32 Welbeck St, London W1, UK).
14-28 September, **Advanced Techniques in Immunological and Biochemical Approaches to Hemoparasitic Research**, Nairobi (Dr R. O Williams, ILRAD, PO Box 30709, Nairobi, Kenya).
16-19 September, **Eurotunnel '80**, Basle (The Secretary, The Institution of Mining and Metallurgy, 44 Portland Place, London W1, UK).
18 September, **Some Aspects of the Biological Basis and the Clinical Effects of Different Radiotherapeutic Practices**, Oxford (Dr C. H. Paine, Dept of Radiotherapy and Oncology, Churchill Hospital, Headington, Oxford, UK).
19 September, **Directions in Nuclear Engineering Research**, Cambridge (The Institution of Nuclear Engineers, Allan House, 1 Penerley Road, London SE6, UK).
23-25 September, **On-line Surveillance and Monitoring of Plant Reliability**, London (Conference Secretariat, Society of Chemical Industry, 14 Belgrave Square, London SW1 UK).
25-26 September, **Hard-facing materials in Nuclear Power Plants**, Avignon (SFEN, 48 rue de la Procession, F75724 Paris Cedex 15, France).
29 September-2 October, **Forestry Energy Conference**, Jonkoping (Howard Phillips Management, 7 Black ans Lane, Hadlow, Tonbridge, Kent, UK).
1 October-31 August 1981, **Training Course on Selected Topics of Modern Biology**, Szeged (Dr István Raskó Biological Research Center, Hungarian Academy of Sciences, PO Box 521, H-6701 Szeged, Hungary).
9 October, **Light Scattering Techniques**, London (Mr D. Irish , c/o Pye Unicam Ltd, York St, Cambridge, UK)

13-14 October, **New Technologies in Health Care,** Brussels (R. S. First Inc, 19a Ave Marnix, 1050 Brussels, Belg'um).

13-17 October, **2nd International Conference of Scientific Editors,** Amsterdam (Helena Tombal, Elsevier Scientific Publishing Co, PO Box 330, 1000 AH Amsterdam, The Netherlands).

14-17 October, **Water Chemistry of Nuclear Reactor Systems,** Bournemouth (British Nuclear Energy Society, 1-7 Great George St, London SW1, UK).

15-16 October, **Calcitonin 1980,** Milan (Dr M. L. Pecile, Dept of Pharmacology, School of Medicine, University of Milan, Milan, Italy).

19-22 October, **7th Canadian Symposium on Catalysis,** Edmonton (F. F. Gadallah, Alberta Research Council, 11315 -87th Ave, Edmonton, Alberta, Canada T6G 2C2).

20-23 October, **Etiology and Pathogenesis of Diabetes,** Toronto (Dr J. M. Martin, Research Institute, The Hospital for Sick Children, 555 University Ave, Toronto, Ontario, Canada M5G 1X8).

20-24 October, **International Conference on Current Nuclear Power Plant Safety Issues,** Stockholm (IAEA, Wagremestrassr 5 PO Box 100, A-1400 Vienna, Austria).

22-24 October, **HPLC Beginners Course,** Cheshire (HPLC Technology Ltd, PO Box 25, Wilmslow, Cheshire, UK).

22-24 October, **Workshop on TCDD and Related Compounds,** Rome (Prof. Dr O. Hutzinger, Laboratory of Environmental and Toxicological Chemistry, University of Amsterdam, Nieuwe Achtergracht 166, Amsterdam, The Netherlands).

21-24 October, **European Offshore Petroleum Conference and Exhibition,** London (Society for Underwater Technology, 1 Birdcage Walk, London SW1, UK).

25 October, **The Analysis of the Insect Visual System,** London (The Royal Society, 6 Carlton House Terrace, London SW1, UK).

19-23 October, **Coal Conversion and the Environment,** Washington (Patricia M. Bresina, Biology Dept, Battelle, Pacific Northwest Laboratories, Ricland, Washington 99352).

27-29 October, **Fundamental Mechanisms in Human Cancer Immunology,** Galveston (Margie Taylor, The University of Texas Medical Branch, 111-A Basic Science Building, Galveston, Texas 77550).

29-31 October, **New Trends in Antibiotics,** Milan (Fondazione Giovanni Lorenzini, Via Monte Napoleone, 23, 20121 Milan, Italy).

30 October-1 November, **New Trends in Arterial Hypertension. Cellular Pharmacology and Physiopathology,** Deauville (Dr M. Worce; Centre de Recherche, Roussel Uclaf, BP 9 93230, Romainville, France).

3-5 November, **Accelerators in Research and Industry,** Denton (J. L. Duggan, Physics Dept, North Texas State University, Denton, Texas 76203).

4-7 November, **Impact of Climate on Planning and Building,** Israel (Dr A. Bitan, International Symposium on the Impact of Climate on Planning and Building, PO Box 16271, Tel Aviv, Israel).

5-6 November, **Thermal Storage of Solar Energy,** Amsterdam (Technisch Physische Dienst TNO?TH, PO Box 155, 2600 AD Delft, The Netherlands).

10-11 November, **Gas Monitoring for the 80s,** London (Carole Meads, Sira Institute Ltd, South Hill, Chislehurst, Kent, UK).

11-13 November, **Underwater Mining Institute,** Georgia (Barbara J. Arnold, University of Wisconsin, Sea Grant Advisory Services, 1815 University Ave, Madison, Wisconsin 53706).

11-15 November, **Clinical Chemistry,** Milan (1st African and Mediterranean Congress of Clinical Chemistry, via Keplero 10, 20124 Milan, Italy).

11-14 November, **Magnetism and Magnetic Materials,** Dallas (I. S. Jacobs, General Electric CR&D, PO Box 8, Schenectady, New York 12301).

18-21 November, **Space Geodesy and its Applications,** Cannes (CNES, Dept des Affaires Universitaires, 18 Ave Edouard-Belin, 31055 Toulouse Cedex, France).

25-27 November, **Electro-Analytical Techniques,** London (Sira Institute Ltd, South Hill, Chislehurst, Kent, UK).

26 November, **Research in a Declining Industrial Environment,** London (Administrative Secretary, The Research and Development Society, 47 Belgrave Square, London SW1, UK).

1-3 December, **Prostaglandins and the Cardiovascular System,** Antwerp (Ms L. Van den Eynde, Dept of Pharmacology, University of Antwerp, Universitaitsplein 1, B-2610 Wilrijk, Belgium).

1-4 December, **Atomic and Nuclear Methods in Fossil Energy Research,** Puerto Rico (Dr R. Filby, Nuclear Radiation Center, Washington State University, Pullman, Washington 99163).

1-12 December, **7th UICC Training Course in Cancer Research,** Melbourne (Dr A. W. Burgess, UICC Course, The Walter and Eliza Hall Institute, Royal Melbourne Hospital PO, 3050, Victoria, Australia).

8-11 December, **Lipid Metabolism and its Pathology,** Lisbon (Prof. Manuel Judice Halpern, Departamento de Bioquimica, Faculdade de Ciencias Medicas da UNL, Campo dos Martires da Patria, 1100 Lisbon, Portugal).

15-17 December, **Special Ceramics,** London (P. Popper, The British Ceramic Research Association, Queens Rd, Penkhull, Stoke on Trent, UK).

16-17 December, **Chromatography, Equilibria and Kinetics,** Brighton (Mrs Y. A. Fish, The Chemical Society, Burlington House, London W1, UK).

25-26 March, **Official Methods of Analysis and Stability Testing of New Drugs,** Cambridge (Dr D. Simpson, Analysis for Industry, Factories 2/3, Bosworth House, High St, Thorpe-le-Soken, Essex, UK).

nature

12 June 1980

Nuclear proliferation and World War III

What with Iran, Afghanistan and southern Africa, most people agree that these are dangerous times. For that reason it is all the more important that there should be a cool appraisal of where the dangers lie. Unhappily, too many of us are too often tempted to look for technical solutions to what are essentially political problems. So much is apparent from the otherwise fine declarations on arms control with which Mr James Callaghan, still leader of the British Labour Party, sought to elevate the discussions of his party's special conference on 31 May. China, said Mr Callaghan, on the strength of a recent visit, is convinced that sooner or later, and probably within the next twenty-five years, there will be a major conflict between itself and the Soviet Union. In preparation, China is working hard on the development of long-range missiles and the warheads they would carry. At the same time, familiarity with nuclear technology is spreading. So efforts must be redoubled to negotiate a comprehensive test-ban, to make a start on Salt III and to do something further to inhibit the spread of nuclear weapons. Few will quarrel with the conclusions, but many will quite properly ask whether Mr Callanghan's chilling scenario of the coming quarter of a century would be substantially modified even if the current arms control agenda were miraculously to be completed overnight (which it will not be).

The trouble is that the relationship between arms control treaties and the prospects for World War III are by no means as straightforward as Mr Callaghan suggested. If, indeed, his Chinese hosts are right in their estimation of the prospects ahead of them, they will most probably simply be confirmed in their determination to stand aside from the existing instruments of arms control — the Partial Test-Ban Treaty and the Non-Proliferation Treaty in particular. If, with the passage of time, that determination persists, one consequence may be that other parties to these treaties, and the existing nuclear powers in particular, will give up their own adherence on the grounds that continued membership would put them at a disadvantage with respect to China. In short, arms control treaties in themselves are neither a sufficient nor even a necessary condition for the avoidance of World War III. Rather, progress in the negotiation of arms control treaties is a sign of governments' willingness to accommodate inevitable political tensions within the conventional framework of international relations. So much should be apparent from the way in which, in the past six months, Salt II has languished in the United States Congress and the Soviet Union has declined the American invitation to talk about tactical nuclear weapons (the intended core of Salt III).

Fortunately it does not follow that arms control treaties are merely symbolic. The Antarctic Treaty is a good illustration. No government's interest would be served by an international competition to build bigger and better military installations in this strategically irrelevant part of the world, but many of them would feel impelled to follow suit if their rivals began. The treaty serves the mutual interest of even quite strongly conflicting parties. It represents the willingness in the early 1960s of three out of the (now) five nuclear powers to give up testing nuclear weapons in the atmosphere. No doubt it has been more than a mere inconvenience for each of them, even though continued testing underground has plainly made possible new ranges of warheads. Others have benefited from the decrease of radioactive fall-out.

The Comprehensive Test-Ban Treaty would be a much more significant brake on the development of new warheads in the United States and the Soviet Union (for which reason it is ironical that the present hiatus in the negotiations centres on the British refusal to base ten monitoring stations on British territory). But a successful treaty could not last for long if it did not include China. To expect otherwise is to wish for the moon.

The benefits of the Non-Proliferation Treaty (NPT) are different again, and harder to define. Much will (or should) be heard of them in the next few months, in the run-up to the Second Review Conference due to open in Geneva on 11 August. Ostensibly, the treaty serves Mr Callaghan's goal of limiting the spread of nuclear weapons — or at least of restricting them to the existing nuclear powers. Non-nuclear powers are required to forswear nuclear arms and to accept international control and inspection provided by the International Atomic Energy Agency. Nuclear powers can keep their weapons but must work towards further measures of strategic disarmament and also help with the development of civil nuclear technology in non-nuclear states. For one reason and another, however, there has been a subtle but important change in the function of the treaty since it was negotiated in the late 1960s. It is far from clear what will happen in Geneva later in the summer.

The nuclear powers can, however, expect to be hauled over the coals (as they were at the first review conference five years ago) for backsliding on their undertaking to negotiate substantial measures of strategic disarmament. The plight of Salt II will be a black mark. So will be the hiatus in the Comprehensive Test-Ban Treaty. The nuclear powers may however escape more lightly than they feared, if only because their critics will be divided on where to put the blame. It would be a brash non-nuclear power that would in present circumstances expect that substantial agreements on strategic weapons could be made to stick.

There will be more fierce argument about the second of the undertakings originally given by the nuclear powers — that they would assist the free development of civil nuclear power elsewhere. Originally this provision was designed to sweeten the pill of the frankly discriminatory nature of the treaty. There have been two developments in the past five years which stick in the throats of the non-nuclear powers. First, a number of governments which are potential suppliers of nuclear equipment (including France, which is not a signatory of the treaty) have worked out common rules for the supply of reactors, diffusion plants and the like. Second, the United States Administration three years ago promulgated tighter rules to govern the supply and use of nuclear fuel which, by being unilateral and outside the framework of the NPT, have further injured the pride of the non-nuclear signatories (often cajoled to sign by the United States), already smarting from the sense that the NPT is unfairly discriminatory as between nuclear and non-nuclear powers. Why, some non-nuclear powers ask, if we have signed the treaty and agreed to obey the rules, should the governments that promised to help us impose still further restrictions?

Especially now that the International Fuel Cycle Evaluation Study has shown that the dangers of the diversion of plutonium to military purposes cannot be prevented by requiring that everybody should build some diversion-proof reactor, it would be seemly if the United States government were to subsume its rules

for the supply of nuclear fuel within the NPT. (It would also be sensible if the Administration were to permit again the reprocessing of nuclear fuel within the United States, if only to empty some of the reactor cooling ponds now stacked with spent uranium; the chances are, however, that that will not be possible until after the presidential election in November.) If the nuclear powers earnestly wish to use the NPT as a means of inhibiting the spread of nuclear weapons, they should see that it is the chief instrument of their common policy.

How effective would be such a strengthened treaty? The record of the past ten years is mildly encouraging. The number of signatories has grown to 120 (but states such as India and Pakistan, Israel and Egypt, France and China conspicuously remain outside). Signature of the treaty has become more and more a precondition for buying nuclear equipment and fuel (which is why it is unfortunate that the Soviet Union is proposing to supply a nuclear reactor to Cuba, a determined non-signatory). Technically, the safeguards system is working more smoothly than five years ago — and would be even more effective if the treaty required regular (say annual) publication of the inputs to

and the outputs from national fuel cycles. The absence of France from the list of signatories is not as serious as it seems (and seemed ten years ago), for the French government has openly acknowledged that it will behave as if it were a nuclear power and member of the treaty. The absence of China is more worrying. Would it not be sensible that the first three nuclear powers should swallow their pride and agree that the definition of what constitutes a nuclear power should be broadened so as to include France and. China?

Unfortunately, none of this will serve Mr Callaghan's wider purpose of postponing World War III. The most immediate danger is not that states which do not have nuclear weapons will acquire them but that states that have them will use them. Current arms control treaties, valuable though they are, have no immediate bearing on the likelihood that nuclear powers will use their nuclear weapons. Treaties in prospect, Salt II and III especially, would limit the chance of some kinds of conflicts but leave others unrestrained. As always, the immediate steps to be taken in postponement of World War III are political and not technical.

Foods, Fads and the National Academy

The National Academy of Sciences in the United States should have known it was stirring a hornet's nest by publishing last week a document unforgiveably called "Toward Healthful Diets", prepared by the Food and Nutrition Board of the National Research Council, the academy's policy-pronouncing arm. For the document dares to cast doubt on a belief now as firmly held and cherished in the United States as was the concept of motherhood in the 1950s (before everything changed) — the belief that cholesterol and saturated fats in the human diet are akin to poisons. American newspapers have been up in arms. Luckless members of the committee responsible for the document have been quizzed about their earnings as consultants for the food industry, three of them owning up to deriving up to ten per cent of their incomes from this source. On the other hand, the trade associations representing the egg and dairy industries have sprung to the Food and Nutrition Board's defence with such alacrity that its members must be wondering whether, with friends like that, they have need of enemies.

In retrospect, the Food and Nutrition Board will also acknowlege that its document was a tactless publication. Over the years the board, originally set up in 1941, has acquired a useful reputation, largely on the strength of its recommendations on the nutritional composition of the American diet. It is, for example, the source of the influential "Recommended Dietary Allowances" for the various components of the human diet. Last week's document is however not so much a measured report of scientific deliberations as an opinion. Somewhere in the cumbersome procedure within the National Academy for reviewing the publications of the National Research Council, somebody should have recognised that publication would cause a storm, if only a storm in a teacup. It is also likely that the board's objective, "to reduce the confusion in the mind of the public" stemming from the flood of contradictory recommendations on diet in the United States, would have been better served if its conclusions had been bolstered by more careful argument.

The board's impatience is, however, understandable. The past few years have indeed been marked by an over-excited flood of advice to the general public about the proper management of the human diet. Some of it has come from official sources in the United States. Some of it has been contradictory. Collectively, and by its sheer volume, this advice must have served to give at least some members of the American public the impression that eating as such is dangerous. Others have been persuaded to an over-zealous avoidance of this or that component of diet without a sufficient regard for the biological complexity of the bodies they are seeking to nourish. The argument about the role of saturated fatty acids, and of cholesterol, as contributors to cardiovascular

disease goes back twenty years — and cannot now be said to have been resolved. But the Food and Nutrition Board is also concerned, in its latest document, with the dietary habits which are evolving or being recommended for the avoidance of other degenerative diseases — obesity, hypertension, some forms of cancer and diabetes mellitus. The theme running through its opinion is that diet may indeed influence long-term health, but that it is hardly ever possible to pin down exact relationships, valid for a whole population, between the amount of some component in the diet and the risk of disease in later life. What nutritionist would quarrel with that?

The board's account of the relationship between diet and the risk of cardiovascular disease is more moderate than its critics have supposed. The board accepts that high serum concentrations of cholesterol are associated with a high risk of cardiovascular disease. It points out, however, that the three somewhat arbitrarily distinguished classes of lipoproteins in the blood appear to be differently associated with later risk. Plainly there is an urgent need for a better understanding of the underlying biochemical processes. In the meantime, the board is entitled to its opinion that it remains to be demonstrated that high concentrations of serum cholesterol are more than mere symtoms of a predisposition to cardiovascular disease. The board also points out that the presence of cholesterol in the diet is not linearly related to the concentration of cholesterol in the serum: the more cholesterol in the diet, the less efficiently it is absorbed. And natural metabolic processes account for twice as much cholesterol as that in the average diet. The board does however acknowledge, as it must, that less saturated fatty acid in the diet means less cholesterol in the blood. This, too, is beyond dispute.

The board's advice, based on this analysis and a brief consideration of the epidemiological studies which have been carried out in recent years, is that there can be no uniform rule, applying to a whole population, for regulating either the ratio of saturated to unsaturated fats in the human diet or the amount of cholesterol which it is safe to eat. Quite properly, the board says that people who lead active lives — manual workers, for example — may need to include more natural fat in their diet than other people. All this is sensible enough, and it is possible that the row which has burst about the board's head may give pause to the organisations which have been advocating the adoption of specific values for the amounts of saturated fats and of cholesterol in the diet; they have often seemed unaware that they have been playing into the hands of faddism. The board itself, however, would be well advised also to think again, and recognise that the tide of faddism will be turned back only by a much more persuasive document.

An outbreak of piracy in the literature

A rash of what appears to be piracy has turned up in the scientific literature. At least three cases are known in which either authors or editors of journals have drawn attention to the appearance elsewhere of articles which are substantially identical with articles that they have published. A common theme in these events is the appearance of the name of Dr E.A.K. Alsabti as one of the authors of the pirated articles. One illustration of the phenomenon is the appearance last year in the *Japanese Journal of Medical Science and Biology* of an article "Effect of platinum compounds on murine lymphocyte mitogenesis" which inspection shows to be a close copy of an article by Dr D. Wierda and Dr T.L. Pazdernick also published last year in the *European Journal of Cancer*. Among the three authors of the article in the Japanese journal is E.A.K. Alsabti, whose address is given as the Royal Scientific Society, Amman, Jordan.

Platinum compounds in cancer

The objectives of the research reported by Wierda and Pazdernick, and in the paper by Alsabti *et al.*, are given as the investigation of the effects of various platinum compounds of the spleen lymphocytes known as T and B cells. The issue is of practical importance because platinum compounds, like other anti-tumour drugs, kill not merely tumour cells but also the circulating lymphocytes of the immune system.

Interest in platinum compounds dates back more than a decade, when the compound DDP (*cis*-dichlorodiamine platinum) was shown by Rosenberg *et al.* (*Nature*, 222, 385; 1969) to be effective against tumours in mice. Daniel Wierda says that his own interest in the field dates back to 1975, when his then supervisor, Dr Pazdernick, at the Department of Pharmacology of the University of Kansas, suggested a library search for evidence on which to base a search for analogues of DDP whose effects on the immune system would be less marked than those of the original compound.

In the research described in the two papers now published, mice have been used to demonstrate that the analogues of DDP are more toxic to T than to B cells. From this emerges the suggestion that platinum compounds might be used in conjunction with drugs which are more toxic to B cells than to T cells. Therapeutic regimes using DDP have been introduced in the past few years, and both papers come to the conclusion that clinical trials with the analogues now studied should be carried out.

Attempts in the past few days to trace Dr Alsabti and his fellow authors have been unsuccessful. The Scientific Attaché at the Jordanian Embassy in London said on the telephone on Monday this week that he had heard of Dr Alsabti, but that he knew nothing of his present whereabouts, believing him to be in Jordan.

The attaché also said that Dr Alsabti had no present affiliation with the Royal Scientific Society in Jordan. "Some years ago", Dr Alsabti had been allowed to use the address of the Royal Scientific Society, but this arrangement had since been terminated. He had no knowledge of the two other authors.

One feature of the paper in the Japanese journal is that readers are invited to send requests for reprints to an address in Brighton, "c/o Mrs W. Aljaff, Flat No. 5, 8 Norfolk Terrace, Brighton BN1 3AD, England". No name resembling Aljaff appears in the current Brighton telephone directory. A caller at 8 Norfolk Terrace earlier this week discovered that the occupant of Flat No. 5 spoke with a pronounced English accent and that he did not know of either Aljaff or Alsabti.

The two versions of the paper differ from each other in minor but perhaps significant details. The title of the paper in the Japanese journal is given as "Effect of platinum compounds on murine lymphocyte mitogenesis". The two American authors acknowledge the help of their technical assistant, while the three Jordanian authors say that "This work was supported by His Royal Highness Crown Prince Hassan of Jordan".

The references quoted at the end of Jordanian version do not however include the reference to earlier work of Pazdernick, one of the two American authors whose joint paper with Dr Wierda in the *European Journal of Cancer* had referred to a paper by Pazdernick first published in 1978.

The dates at which the two manuscripts were processed by the respective journals are very similar. Dr H. J. Tagnon, editor of the *European Journal of Cancer,* has confirmed in writing that the American paper was received in the Brussels office on 10 October 1978 and accepted for publication on 5 January 1979. The version published in the Japanese journal carries a note "Received November 20, 1978", implying that the manuscript had been received in Tokyo before a final decision on the American paper had been made in Brussels.

The editor of the Japanese journal during the period concerned, Dr Hideo Fukumi, said in Tokyo on Monday this week that he had now retired from that post and did not know who had succeeded him. He said that he could remember nothing of the circumstances attending the publication of the paper by Alsabti *et al.*

The processing of the corresponding American paper in Brussels appears to have followed a more or less normal course. It was sent to two referees in the United states, one of whom replied (returning the manuscript and the prints of the diagrams eventually published with the article). After some delay, it turned out that the second referee had died, and that copy of the manuscript has not since been recovered.

Dr Wierda says that he is sure in his own mind that no unauthorized person would have been able to obtain a copy of his material in advance of publication, but Dr Tagnon is equally firm in his assurances that there could have been no unauthorized leakage from his office.

Whatever the circumstances, this appears not to be the first occasion on which Dr Alsabti has had the misfortune to be involved with issues of copyright to written materials.

In April this year, Professor E Frederick Wheelock of the Jefferson Medical College in Philadelphia wrote to *The Lancet* to complain that a section of a grant proposal which he had written for the US Public Health Service (and which was sub-

Two conclusions — Alsabti et al. superimposed

In conclusion, we have observed that the platinum complexes tested were more toxic to splenic T-lymphocyte function than splenic B-lymphocyte function. We have also demonstrated that DBCH and DBCP were con-

In conclusion, we have observed that the platinum complexes tested were more toxic to splenic T lymphocyte function than splenic B lymphocyte function. Collectively, the results of these experiments demonstrated that the type of immunosuppression produced by the platinum compounds is markedly different from the type of inhibition caused by such commony used immunosuppressants as cyclophosphamide (Turk and Poulter, 1972; Gale et al., 1975). Because of this unique suppression, we believe that further clinical testing of these compounds as potential antitumor agents is warranted.

one marrow nuc-sults) and spleen DP and DBP, yet inhibited T- and ectively, the re-emonstrated that ion produced by the platinum compounds is markedly different from the type of inhibition caused by such commonly used immunosuppressants as cyclophosphamide [22, 23] or X-irradiation [20]. Because of this unique suppression, we believe further clinical testing of these compounds as potential antitumor agents is warranted.

sequently funded) had appeared in a review article entitled "Tumour Dormancy" by A. E. K. Alsabti (*Journal of Cancer Research and Clinical Oncology*, **95**, 209; 1979) which had also appeared in the Czech journal *Neoplasma* (26, 351; 1979).

Professor Wheelock said earlier this week that he was hoping to persuade each of the journals to publish a correction. He said that Dr Alsabti had worked in his laboratory for a period of five months but that he had asked him to leave after a disagreement about the authenticity of some experimental data.

Another case in which Dr Alsabti's authorship is questioned is his article "Diagnosis of serum lipids in hepatoma", published in *Oncology* (36, 11 1979). This so resembles an article by Yoshida *et al.* in the *Japanese Journal of Clinical Oncology* (7, 15; 1977) that the editor of the journal has written to *Oncology* saying "I was shocked by the appearance of Dr Alsabti's article which seems a copy of that by Yoshida *et al.* . . .". A copy of this letter has been seen by Dr J. Moglivit of the Anderson Medical Center in Houston, Texas, who was for seven months the immediate supervisor of Dr Alsabti during his spell as a volunteer (unpaid) technician there at the end of 1978.

Dr A. Clarke, president of the Medical Center, said on the telephone earlier this week that Alsabti had come to work in Texas on the recommendation of a Jordanian friend of the hospital but that in the end he was dismissed as a volunteer because of reports reaching the hospital of his exaggerated claims about the work that he had been doing.

One of the referees to whom the paper by Wierda *et al.* was sent by the *European Journal of Cancer* was Dr J. A. Gottlieb of the Anderson Center at Houston. Dr Alsabti was at the center towards the end of 1978. Dr Gottlieb had died some time before.

Index Medicus records that Dr Alsabti published 13 articles in the scientific literature during 1979 and ten in the first five months of this year.

Drug regulations
Signs change

Washington

The drug industry has won a measure of support from the General Accounting Office in its complaint that the bureaucracy takes too long to license new products. In a report published last week (6 May), and based largely on comparisons with licensing practice in other industrialised countries, the GAO says that American practice is "lengthy" and that this circumstance "delays the benefits important drugs can provide to the public".

The fact that a new drug application takes on the average 20 months between the submission of test data and the receipt of licensing approval has been a hot potato in Washington for almost ten years. Without making any explicit judgement on the time needed to ensure that the scientific data is adequately reviewed, the GAO report does echo what many pharmaceutical companies have been saying for the past decade.

Excessive regulation, they claim, has not only escalated the costs of bringing a new drug to the market — now estimated at an average of $62 million — but has led to a growing proportion of their research being conducted outside the United States in countries with easier licensing regulations.

The Food and Drug Administration accepts that its licensing process is lengthy and has taken steps to accelerate the scientific review process. Two years ago, for example, it committed itself to reducing the time taken to license important new drugs by 25 per cent a year over three successive years, and claims to be on target. But the charges continue that the FDA is not doing enough. And last week congressmen keen further to speed the process quoted the GAO's conclusion that, based on a comparison of the time taken to license fourteen important drugs in six countries, the United States was slower than most in all but one case. According to the GAO, whereas it took on average five months to have a new drug approved in Great Britain and sixteen in Canada, the average time in the United States was 23 months, exceeded only by Sweden's 28 months. FDA counters with its own statistics. Analysis shows, it says, that "the few important drugs that genuinely advance medical care . . . tend to be approved today at reasonably similar times (generally within a few months) in most developed countries".

In response to the charge that its review procedures are too stringent, the agency replies that "of all new molecular entities [drugs whose active ingredient has not previously been marketed in the US] introduced into world medicine in the past decade, no country has approved more than 50 per cent of the total".

Behind the numbers game lie deeper arguments that illustrate how the time taken to approve new drugs is determined as much by the way that the United States has chosen to regulate the drug industry — with a heavy emphasis on administrative record and documented evaluation — as on the adequacy of particular regulations. Pointing to European countries, for example, where independent advisory committees can provide a buffer between a regulatory agency and the industry, the GAO suggests similar expert committees might be used more to review and approve new drugs in the United States.

The FDA disagrees. It says that the open nature of regulatory decision-making in the United States, the right of individuals to sue the government over regulatory actions and the powerful role of congressional oversight each make it difficult to go beyond the thirteen advisory committees now in place.

Another issue is that of post-marketing surveillance. The GAO report points out that in countries such as Great Britain with a national health care system, close contact between doctors and the health services encourages feedback and limits the potential dangers of premature licensing. The FDA, however, has very limited authority to take action on a drug once it has been released, and thus tends to be more cautious before giving licensing approval. There are also suggestions that physicians and hospitals may be dissuaded by the fear of increased medical liability from reporting their experiences.

Tighter provisions for post-marketing surveillance, including in particular the requirement that manufacturers should oblige doctors to notify them of any adverse side-effects, are a central feature of

Two figures — Wierda et al. bottom left

54   *ALSABTI et al.*   *Vol. 32*
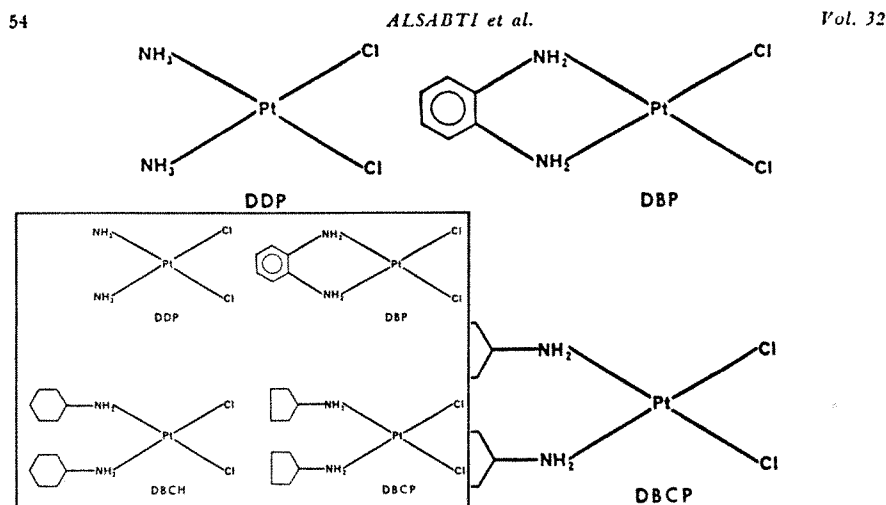
Fig. 1. Chemical structures of *cis*-dichlorodiammine platium (DDP), dichloro 1,2 benzene-diamine N,N' platinum (DBP), *cis*-dichlorobis(cyclohexylamine) platinum (DBCH), and *cis*-dichlorobis(cyclopentylamine) platinum (DBCP).

two drug regulatory reform bills currently under joint consideration in the House of Representatives.

Both bills are intended to speed up the licensing process, one introduced by the Administration, the other drawn up by Senator Edward Kennedy and passed last autumn by the Senate. For example, an arbitration process would be set up for scientific disagreements between the FDA and potential licensees.

Both bills meet the concern of the FDA that, in particular, it should be given greater flexibility in licensing. They propose, for example, that the review procedure should be speeded up for exceptionally important new drugs and that licences should be issued restricting the use of a drug to specified circumstances where general release might be undesirable.

The pharmaceutical companies are, in general, keen on such revisions. Consumer groups are less happy. "Greater licensing flexibility for so-called breakthrough drugs could provide the camel's head under the tent as far as weakening the general protection provided by the drug laws", says Ben Gordon of the Nader-affiliated Health Resources Group.

But the most important factor may prove to be a recent arrival, namely growing congressional enthusiasm for moves to stimulate industrial innovation in the face of declining productivity and increasing foreign competition, Japanese in particular.

The wish to meet this threat may prove the most potent weapon in the regulation reformers' armoury.

David Dickson

Comecon

Links with West

East-West scientific exchange, except at the Academy/Royal Society level, tends to become associated with other, not strictly academic, matters, as no fewer than three events in London during the past fortnight have demonstrated.

The first, a working visit of the Polish Minister of Metallurgy, Franciszek Kaim, resulted in the signing of two contracts between his ministry, on the one hand, and the British Steel Corporation and the British Metallurgical Producers Association respectively on the other. Although these agreements deal mainly with highly specific themes, such as new technologies for producing coke from non-coking coal, and the perennial theme of energy and raw materials saving, Mr Kaim indicated that on the Polish side at least, a great number of institutes and "other organizations which specialize in scientific research" would be involved in working out "ways and means".

At a later stage, Kaim said, there might be joint research between UK and Polish scientists, both in developing new types of steel and in basic metallurgical research.

Environment, too, he stressed, was a subject where there could be "very effective joint cooperation". (This is a sensitive issue for his ministry — only a few days before his visit, workers at the giant Lenin Steel Mills at Nowa Hut had passed a resolution that existing environmental protection measures there were insufficient.)

This was the third such UK-Polish agreement to be signed — one on mining was signed some three years ago, and one on electricity in February 1980. It comes within the framework of the Joint Commission on Trade and Technology (a linkage that arises, at least in part, from the way in which the former UK Ministry of Technology was dismantled). So did the GDR Engineering Week in Britain (2-5 June 1980).

The East Germans, however, are far less happy about the linking of technological exchange with trade, and are constantly pressing for separate international agreements to cover both. Yet for the purpose of the "Week", Dr Gerhard Beil, Secretary of State in the Ministry of Foreign Trade of the GDR, was prepared to waive these demands — the objective, he said, was "to deepen economic, scientific and technological relations".

The mighty instrument firm of VEB Zeiss-Jena makes no distinction of this kind. After a comprehensive lecture on its latest measuring instruments for the metallurgical industry, the Zeiss delegates made it quite clear that there is no distinction between the scientific and industrial instruments produced by Zeiss in the minds of the 4,000 scientists on the staff.

The third event in the past two weeks had, by contrast, little or no commercial application. Bulgaria is at present preparing for next year's celebrations of 1300 years of statehood, and, in the past few years, has been doing some quite remarkable work in molecular biology. As part of the celebrations, therefore, last week, at the Bulgarian Embassy in London, Sir John Kendrew, in recognition of his services to molecular biology, was invested with the Order of the Madara Horseman and, at the same time, made an honorary foreign member of the Bulgarian Academy of Sciences.

Vera Rich

Biotechnology

Canada stirs

Anxious not to be left behind, the Canadian government is setting up an independent working group to tell whether and how it should promote the growth of biotechnology.

The nine members of the working group are to report back within a year to the Minister of State for Science and Technology, Mr John Roberts, who announced the government's decision on Tuesday at a meeting of the Chemical Institute of Canada.

The chairman of the group is Dr Maurice Brossard, director of research at the Institut Armand Frappier in Laval, Quebec. Of the remaining eight members, three are from universities and five from industry; others, including government scientists, will be involved as consultants. Although one objective of the working group is to assess the potential of Canada to compete directly with other countries in fields such as the biological production of industrial chemicals and health care products, it is hoped that the group will pay special attention to Canada's characteristic resources and needs — in fields such as energy, mining, food, agriculture and forestry.

Accompanying Mr Roberts's announcement was the publication of a background paper prepared by Dr Louis Slotin, secretary of the committee, listing current Canadian research efforts in biotechnology, broadly defined to include genetic and cellular manipulation, enzyme technology and fermentation techniques.

The report reveals a moderate amount of effort, with total support amounting to about several million dollars a year. But it tends to be thinly spread. The 100 university research workers listed, for example, are distributed among 22 universities; and of the 33 companies indicating an interest in biotechnology research, only ten have more than one or two research workers involved.

To a certain extent Canada makes up in quality what it lacks in quantity. Scientists in the National Research Council's Division of Biological Sciences, for example, are acknowledged to be among the world's leaders in the study of the insulin gene; and several prominent Canadian biologists are already employed as advisers and consultants to US-based biotechnology companies.

The most serious difficulty ahead is a familiar one for Canada — how can an industrial sector largely dominated by foreign-based companies — often with their main research facilities in the United States or elsewhere — be encouraged to support research in Canada and to use what is already being done? There is also a gulf between university research and its potential applications. No Canadian university has a department of applied microbiology, while microbiological research is carried out almost exclusively in medical schools.

A broader issue for the working party will be that of government policy on innovation and whether it should provide direct support for broad-based industrial initiatives — as recommended in Britain's Spinks Report — or instead to follow US strategy with tax incentives and the like.

The inclination of both scientists and industrialists is towards less rather than more government involvement but with a different industrial structure and a smaller supply of individuals prepared to make

high-risk investments, some judicious mixture of private and public involvement seems the most likely recommendation.

David Dickson

Radiation limits

EEC rules soon

A new and legally binding directive on radiation protection for those occupationally at risk, based on recommendations which have provoked controversy in the United States, may be adopted by the European Community within two months. But in contrast to the situation in the United States (*Nature*, 5 June, p350),opposition to the proposed directive has been sporadic and individual.

The European Community has been preparing for a uniform treatment of radiation safety for several years. In 1976, the Community adopted a comprehensive directive on the subject which was to have come into force in 1978. But a publication of the independent International Commission on Radiation Protection (ICRP 26) caused the Community to have second thoughts.

ICRP 26 recommended a thorough revision of the principles on which radiation exposure should be limited; and the more recent ICRP 30 has derived from these principles the limits on intake of radionuclides implied by ICRP 26 in the light of up to date information on the uptake, retention and effects of radionuclides on the body. The new recommendations differ from those earlier in force by allowing for the risk from an ingested nuclide to all the organs of the body, not simply to the "critical" organs primarily at risk.

The proposed EEC directive takes the views of ICRP into account, and according to an EEC official "differs only in minor detail" from the recommendations of ICRP 26. It would become binding on member states 30 months after adoption.

One feature of the calculations of ICRP 30 is that some of the recommended limits on the rate of ingestion of particular radioactive nuclides are changed by large factors of up to 300; some limits would be more stringent, others less stringent. The US Nuclear Regulatory Commission has argued that it would be impolitic to adopt less stringent limits.

However, the chairman of the committee that prepared ICRP 30 (and its principal author), Dr Jack Vennart of the MRC Radiobiology Unit, Harwell, UK, says that it was incumbent on ICRP to take full account of up to date scientific data and of recent understanding of the physiology and metabolism of radionuclides.

In the case of airborne tritium, for example, it was now recognised that its beta emission was of too low an energy to penetrate to the epithelial tissue of the lung (the most susceptible tissue to cancer). This and other factors resulted in the recommended permitted airborne concentration rising to $2 \ 10^{10}$ Bq m^{-3}. By contrast, the recommended limits on tritiated water are more stringent because of the likelihood that it will quickly distribute itself throughout the body (whereas tritium gas is poorly absorbed). The ICRP 30 limit on gaseous tritiated water is thus $8 \ 10^5$ Bq m^{-3}.

Vennart also points out that it is not ICRP's role to set regulations; that is the business of the relevant national and international legislative bodies. ICRP in fact indicates what seems scientifically the case, and then recommends that levels be set "as low as reasonably achievable, economic and social factors being taken into account". So ICRP is strictly not recommending legislated rises in any exposure level. Vennart believes it unfortunate that "politicians simply adopt the figures wholesale".

Individual criticisms of the ICRP documents in the UK have centred mainly on ICRP 26, which sets radiation — rather than radionuclide — dose levels. Professor Joseph Rotblat, emeritus professor at St Bartholomew's Medical School, for example, says that the dose limit of 5 rems per year recommended in ICRP 26 implies that 2-3 per cent of workers would die of radiation-induced cancer if they worked continuously at that limit, on the basis of the ICRP's own figures.

Rotblat also considers that there may be frequent misuse of the concept of "dose equivalent", which sums up weighted contributions from different organs (see below). In practice, exposure will be assumed to be largely in one organ, he believes, although it may be in more; and if that organ has a low weight in the ICRP 26 scheme, unknown and dangerous high

---

ICRP standards derived

Dose equivalent in ICRP 26 is defined as follows. First, the absorbed dose after exposure to ionising readiation is given by the energy per unit mass deposited by the radiation in the tissue. It is measured in J kg^{-1}, called Grays (Gy). (In the old units, 1 Gy = 100 rad.) Because some particles are more potent than others in causing biological effects, the absorbed dose of a given radiation is multiplied by a quality factor — a function of the particle type and energy — to yield the dose equivalent. This is measured in Sieverts (in old units 1 Sv = 100 rem).

The dose equivalent limit in ICRP 26 is then defined as a weighted sum of dose equivalents over 5 'organs' of the body (gonads, breast, red bone marrow, lung, thyroid, bone surfaces and 'the remainder'), the weights taking into account the different sensitivities of these organs to given dose equivalents. (For example, for a given dose equivalent to the tissue, the breast is estimated to be five times more likely to become cancerous than the bone surfaces, so it gets a weight five times higher). The sum must be less than 0.95 Sv; and individual tissue doses must not exceed 0.5 Sv.

The limit to the sum (0-05 Sv) is chosen to control 'stochastic effects': in other words the probability of contracting cancer. Assuming all cancers are fatal, and that an average worker in the nuclear industry would receive one-tenth of the dose equivalent limit, the limit is set to produce a probability of death about the same as is already tolerated in other 'safe' industries (about 3 per thousand for a 30-year lifetime). ICRP 26 says Mat "long-continued exposure of a considerable proportion of the workers at or near the dose-equivalent limits would be only acceptable if a careful cost-benefit analysis had shown that the higher resultant risk would be justified".

The limit to individual tissue exposure (0.5 Sv, except the eye, whose limit is 0.3 Sv) is designed to eliminate 'non-stochastic effects': cumulative radiation damage which is not lethal and is undetectable below some threshold. (Cataract of the cornea and hair loss are examples.)

ICRP 30 then applies these limits to various radionuclides, taking into account (to a much greater extent than ICRP 2) their chemical form, and transmissibility from gut to bloodstream and from lung to bloodstream (which depends on particle size).

This results in an 'annual limit of intake' (ALI) which is the intake that would cause the dose equivalent limit of radiation to be reached; and the 'derived air concentration' (DAC) which is the concentration which, breathed each week for 40 hours, leads to the absorption of the ALI.

Comparisons of ICRP 30 with ICRP 2 are not direct, because the isotopes are divided into chemical classes in different ways (ICRP 2 distinguishes only 'soluble' and 'insoluble' for example) and ICRP 2 considers limits for each organ separately However, Its DACs derived from ICRP for soluble and insoluble compounds of an isotope can be compared.

Here are a few examples in Bq m^{-3}. (1 Becquerel = 1s^{-1} = 2.7 10^{-11} Ci.) In some cases only one value is quoted.

Radionuclide	DAC, ICRP 2	DAC, ICRP 30
^{3}H as ^{3}H$_2$O	$2 \ 10^5$	$8 \ 10^5$
^{3}H as ^{3}H$_2$	$8 \ 10^7$	$2 \ 10^{10}$
^{60}Co	360-12,000	50-3,000
^{90}Sr	12-200	60-300
^{131}I	360-12,000	700
^{137}Cs	400-2,400	2,000
^{226}Ra	1.2-8,000	10
^{239}Pu	0.08-0.16	0.09-0.3

Some of these figures make ICRP 2 more stringent, some ICRP 30.

Robert Walgate

---

exposures to it may be allowed while exposures of other organs may be being ignored — the exact opposite of the intention of the weighting scheme. Similar arguments have been raised in the Swedish National Institute for Radiation Protection.   **Robert Walgate**

Cosmonauts

More and merrier

ON 26 MAY, Bertalan Farkas of Hungary became the fifth non-Soviet citizen to go into orbit aboard a *Soyuz* spacecraft. With more than half the Comecon allies now accounted for, Soviet space planners are stressing that hospitality aboard their space-stations is theoretically open to countries outside the Socialist bloc. France and India are already on the waiting list. The possibility of wider participation in the Soviet space programme was advertised last February at the Hamburg Scientific Forum by Academician Nikolai Blokhim.

For the Comecon guests aboard the *Soyuz* and *Salyut* spacecraft, a certain pattern of experimental work has emerged. As well as taking part in routine biomedical and astrophysical observations, the participating country also contributes a set of experiments reflecting its own particular interests. It further contributes a crystallography experiment, in which a hermetically sealed ampoule containing a mixture of compounds that will not normally crystallize homogeneously under gravity is treated in a furnace aboard the *Salyut* station in the hope of producing new semi-conductor substances. Traditionally the experiment is given a name symbolizing the national traditions of the country concerned. For Hungary, the name chosen was *Otvos* (Goldsmith), referring to an ancient Hungarian craft, and also a tribute to Lorand Eotvos (the pronunciation is the same), the nineteenth century Hungarian physicist.

More specifically Hungarian in origin are the termoluminescent dosimetry experiments *Integral* and *Pille* (Moth). The Central Research Institute for Physics of the Hungarian Academy of Sciences has been interested in the thermoluminescent monitoring of ionizing radiations for more than 15 years, and since 1970 has contributed dosimetry instruments to the *Interkosmos* programme.

The *Integral* test measures accumulated radiation at various points of the spacecraft over several months. The first test run was inaugurated aboard *Salyut-6* in 1979, and a second set of monitors (crystalline samples of $CaSO_4$:Dy and $SaSO_4$:Tm) have now been installed. *Pille*, a miniaturized instrument by Comecon standards (1 litre volume, 1 kg mass, and with a dosage range from 10 mrad to 10 rad), is a short-term monitoring device, giving readings of accumulated dose every 2-3 days. The same type of dosimeters will ultimately be used for monitoring the personnel of the Paks nuclear power

Farkas — looking alike

station, now under construction in Hungary.

Photography and telemetry of the participating country is also now a traditional part of joint flights. For Hungary, this has meant geodesic surveying (to check existing maps and optimize land use), photographing the whole of the Hungarian section of the Danube (preparatory to monitoring environmental changes expected after construction of the hydoelectric plant at Nagymanos and the nuclear power station at Paks) and the observation of eutrophication and pollution of Lake Balaton and its tributaries.

Farkas was given charge of a series of experiments intended to throw light on the production of interferon by leucocyte cultures, but more practical considerations have not been neglected. Apparently sceptical of claims in 1978 by the Soviet-Polish mission that cosmonauts lose their sense of taste, Farkas was provided with special picnic packs by the Quartermasters' Division of the Hungarian People's Army and the Research Institute of the Cannery and Paprika Processing industry. The packs included goose-liver pate, pork-paprikas, bean salad with sausage and chicken in aspic, and were designed so that Farkas could share them with his hosts.

Vera Rich

UN assistance

No rows yet

Washington

As UN events go, last week's meeting in New York of the new Inter-Governmental Committee on Science and Technology for Development was a relatively tame affair. There were no late-night sessions, and little of the international tension that pervaded last year's UN conference on the same theme in Vienna.

But if the outcome of the meeting can be weighed more easily in terms of bureau-cratic prose than in targeted research

dollars, many third world delegates returned home confident that they had helped to steer the scientific activities of the UN system closer to their self-perceived needs.

Set up by the UN General Assembly on the recommendation of the Vienna conference, the IGC provides a forum on science policy matters for all member states of the UN — and is thus an implicit move to shift the control of such matters away from groups more heavily dominated by the developed countries (as the now-defunct Office of Science and Technology was per-ceived to be).

The committee has been created by another new creation, the Centre for Science and Technology for Development. Two days before the New York meeting, the director of the centre — who has the rank of assistant secretary–general — was named as Dr Amilcar Figueira Ferari, an engineer who was director of Brazil's National Research Council and a member of that country's delegation to UNCSTD.

Some of the developed countries made little secret of their frustration with the meeting's emphasis on administrative matters, urging that work should start on specific projects. The Canadian dele-gation, for example, put in a strong bid for the setting up of an international scientific and technological information system and were disappointed when the IGC decided that organisational and institutional arrangements should take precedence.

Most delegates from the developing countries, however, expressed the view that the coordination and control of research efforts within the UN system — as well as efforts to stimulate national and regional research programmes — may prove of more long-term significance than attempts to raise additional research funds from the industrialised nations, particularly at a time of general financial stringency.

The New York meeting faced three par-ticular issues: how to set in motion the main recommendations of the Vienna confer-ence; how to define the role of the Centre for Science and Technology with respect to the Interim Fund for Third World Science established and administered by the United Nations Development Programme; and how to approach the thorny question of 'harmonising' the scientific and tech-nological efforts of the specialised UN agencies.

On the first issue, there was little contention. A new Scientific Advisory Committee will be set up, a successor to the Advisory Committee on the Application of Science and Technology to Development (ACAST) serviced by OST. And member countries of a 27-member group of experts were named to report on the long-term pro-spects for a new science and technology financing system within the UN.

On the second issue, there was a rerun of debates in Vienna, with some Third World delegates demanding greater control by the new centre over the UNDP Fund — for

which $36 million in contributions and another $10 million in commitments was raised two months ago — while the developed countries and UNDP officials sought maximum flexibility.

In the end, a compromise was reached under which the centre will be given a role in 'reviewing' the operation of the Interim Fund. In addition new guidelines for the fund were agreed; some delegates, for example, were critical of the fact that a

large proportion of the 350 funding proposals received had originated from within UN agencies, and stipulated that all proposals for funding should come through governments. But the IGC's role remains one of direction-setting and overview rather than direct involvement.

Coordinating the scientific and technological activities of the 'organs and organisations' within the UN system will prove the hardest nut to crack. Most of the

specialised agencies, such as the United Nations Educational Scientific and Cultural Organisation, are fiercely protective of their independence, resisting any effort to subsume this independence under any centralised mechanism.

But third world delegates on the IGC remain adamant that increased coordination between the agencies is essential if the broad goals of the Vienna conference are to be met.   **David Dickson**

CORRESPONDENCE

Split syntax

SIR,—While Dr Glascock is to be congratulated on his ingeniously contrived verse on syntax (8 May, p.66), he should have been more careful in the way he worded his introductory paragraph. As the Hungarians say, "Bagoly mondja verèbnek hogy nagyfejü".*
I therefore offer the following supplementary stanza:

You are right Doctor Glascock to chide as you do
The scientist for what he has writ
But one rule of syntax eludes even you:
Infinitives should never be split!
                Yours faithfully,
                                G A GARTON,
(With but scant acknowledgements to Fowler)
Aberdeen, UK
*"The owl calls the sparrow a bighead."

No room in the ark

SIR,—Impetuosity in science is surely to be avoided in favour of caution even as exaggeration is to be eschewed in favour of understatement, but do these wise maxims excuse Mr Thomas H. Jukes for his unconscionable conservatism in his short piece "Two By Two" (*Nature* 15 May).
Commenting on the Noachian flood, Mr Jukes opines that Noah's ark would have provided less than one cubic metre, on the average, for each pair of vertebrates plus their food, a sufficient supply of which was needed to last for about a year. But why, we may wonder, did he undertake his calculations on the basis of *Genesis* 6; 19 in which Noah is directed to take aboard the ark a male and female pair of every living thing rather than *Genesis* 7; 2-3 wherein Noah is directed to take aboard seven pairs of all clean beasts and fowls of the air in addition to one pair of unclean beasts, fowls and creeping things plus food for all?
Mr Jukes would do well to read the eleventh chapter of *Leviticus* (in which clean beasts, fowls and creeping things are distinguished from unclean ones) before recommending his calculations. Whatever the results of that unenviable task may be, one cubic metre per pair of vertebrates will be excessively capacious.
Even less excusable is his calculation that 393 million cubic miles of water resulted from the flood, a figure at which he arrived on the entirely arbitrary depth of 10,000 feet. Nor was there the slightest reason for him to compare that admittedly conservative figure with 17,000 feet, the approximate elevation of Mt Ararat. *Genesis* 6; 19-20 asserts that the waters rose fifteen cubits (about twenty-two feet) above all the high hills and the mountains of the earth. That would mean that even Everest was submerged and would involve a

depth of nearer 30,000 than 10,000 feet, making 393 million cubic miles of water a mere puddle by comparison.
Is it possible that Mr Jukes, despite his air of wry scepticism, is really an apologist for scientific creationism or, perhaps, even a member of the Creation Research Society? If so, he will know how to handle the problems he raises such as the waste "disposal problem" on the ark, the "botanical problem" after the deluge, the "bacteria and protozoa" collection problem and the water dispersal problem. It is on this very point that modern profane science founders, utterly incapable, it would seem, of relying on the miraculous to solve thorny problems, theoretical or otherwise. Creation science, on the contrary, knows no such incapacity but invokes the miraculous at will, often and gladly.
                Yours faithfully,
                                DELOS B. McKOWN
Department of Philosophy
Auburn University, Ala., USA

SIR,—In Mr Jukes's article entitled "Two by Two" (*Nature*, 15 May) his most plausible argument against the biblical account of the Flood appears to lie in his last paragraph. His listing of amphibians, bacteria and protozoa as having to be gathered into the ark is open to question, and he has not mentioned the possibility that all the animals there might have been young and not mature specimens.
But his calculation of the rainfall needed to produce a universal flood, and the means of ultimate disposal of the water being held up to doubt, appear impressive only until one sees that he has overlooked the first cause of the flood. *Genesis* 7; 11 states: "The same day were all the fountains of the great deep broken up, and the windows of heaven were opened." Rain supplied only part of the flood water.
Second, Mr Jukes appears to assume that the relative heights and depths of the earth's surface before the flood were as they are now, an assumption which is in no way logical. That

great changes in the elevations and depressions of the land and seas have occurred is clear from, for instance, the burial of coal measures below thousands of feet of sedimentary rocks and the existence of submarine canyons. Radical change after the flood is suggested by another scriptural reference *Peter*, 2; 5 and 6.
It has been suggested that the statement made in *Genesis* 1; 6 about waters above the firmament indicates that there was above the earth a canopy of water vapour which was precipitated during the flood. This would account for a change in salinity of the oceans which in a recent article in *Nature* was mentioned as a possible cause of the dying out of the dinosaurs
                Yours faithfully,
                                D. CONWAY
Weymouth,
Dorset, UK

Cheaper in paper

SIR,—From the Spring Book issue of *Nature* (24 April) I have taken at random the prices of a dozen books issued in both forms. The ratio (*paperback price*)/(*hardback price*) ranges from 0.352 to 0.607 and the average for the dozen books is *0.439*. From the list of books, it can be seen that the books are not confined to books on any one subject or to books only of broad popular interest.
The books I have considered are scientific and technological. Whether there are similar difference for books in the areas of the arts and humanities, I do not know. I hope that publishers of scientific books will make paperbacks more widely available, thereby increasing sales and perhaps even profits as well.
                Yours faithfully,
                                G. W. BRINDLEY
Pennsylvania State University
University Park,
Penn., USA

| | **Prices** | | |
	Hard cover	**Paperback**	**Ratio**
Science and technology (Freeman)	£ 8.90	£ 5.40	0.607
Early diagenesis (Princeton)	£13.70	£ 5.25	0.383
Evolution of the igneous rocks (Princeton)	£19.30	£ 8.40	0.435
Evolution of North America (Princeton)	£15.20	£ 5.35	0.352
Knowledge and wonder (M.I.T.)	$15.00	$ 5.90	0.393
Mesozoic mammals (U. California)	£21.00	£ 5.75	0.274
Peano (Reidel)	$34.00	$14.95	0.440
Nuclear power and public policy (Reidel)	$19.95	$10.50	0.526
Serengeti lion (1972) (U. Chicago)	£12.25	£ 5.60	0.453
Condensed matter physics (Addison-Wesley)	$26.50	$14.50	0.547
Practical methods in electron microscopy (Elsevier)	$73.25	$27.50	0.375
Coulson's valence (Oxford)	£17.50	£ 8.50	0.485
		Average ratio	**0.439**

NEWS AND VIEWS

Chromosomal action of ecdysone

from Michael Ashburner

THE hormonal control of growth and metamorphosis in insects was discovered over 60 years ago by the Polish biologist Stefan Kopec[1] but it was not until 1965 that the chemical identity of the hormone, by then called ecdysone, was established[2]. A few years before the final chemical characterisation of ecdysone, Clever[3], in collaboration with Karlson, showed that ecdysone was able, in a period of only a few minutes, to induce puffs in the salivary gland polytene chromosome of the midge *Chironomus*. They put forward the then controversial interpretation that this represented a change in the pattern of genetic activity. It is only recently that direct evidence has shown that the puffs of polytene chromosomes are, indeed, active genes. In *Drosophila*, this has been demonstrated from the changing patterns of protein synthesis that follow changing patterns of puffs[4] and from the subsequent molecular characterisation of the genes involved[5]. Several of the genes concerned with the synthesis of the salivary gland's secretion have been mapped and shown to be coincident with puffs active at the time of the synthesis of these proteins[6].

Clever and Karlson's discovery was the first clear indication that hormones may act directly on the genes themselves, an idea that has been very fruitful for the study of the mode of action of many vertebrate steroid hormones. The induction of specific genes by ecdysone inevitably lead to interpretations of the mechanism of the hormone's action based upon the then novel ideas of the control of gene activity in *E. coli*. The reaction against this rather simplistic view was not long in coming. Kroeger[7] suggested, on the basis of the results of experiments with explanted *Chironomus* salivary glands, that what ecdysone did was to control the internal ionic mileu of the cells and their nuclei and that the genes responded to the hormone via an altered ionic environment. In particular, Kroeger suggested that ecdysone acted on the cell's membrane to effect an increase in the intracellular potassium ion concentration and that the ecdysone responsive genes were sensitive to this change.

For almost seventeen years the controversy between Kroeger and his colleagues and those who believed in a rather more direct action of ecdysone on the genes continued unabated. In the last year or so, two rather different types of experiment have yielded data that are capable of both resolving this particular conflict and, more importantly, of giving some insight as to the molecular basis of the modulation of genetic activity by ecdysteroid hormones.

Although ecdysteroids were the first hormones to be shown to have a very rapid effect on genetic activity, the study of the vertebrate steroid hormones, particularly oestrogen and progesterone, rapidly outpaced that of the ecdysteroids. This arose from the discovery that responsive cells possess specific 'receptor' proteins, that bind the hormone with high affinity and then move to the nucleus. There is good circumstantial evidence that receptor protein binding and translocation to the nucleus are obligate steps in the hormone's action and that the receptor complex binds to specific chromosomal sites, causing specific changes in gene expression.

Evidence for a similar class of receptor protein in ecdysteroid responsive tissues was difficult to find. The reasons for this were largely technical. Radiolabelled ecdysteroids of both a high enough specific activity and high enough biological activity were simply not available. It was only when Fristrom and O'Connor realised that a highly radioactive ligand, known as ponasterone A, could be prepared from a plant ecdysteroid, stachysterone C, that progress was made possible. Ponasterone A shows even greater biological activity than 20-0H ecdysone itself. Using this radiolabelled ecdysteroid Yund and Fristrom[8] and Maroy *et al.*[9] discovered ecdysteroid receptor proteins in *Drosophila* imaginal disc cells and in a permanent *Drosophila* cell line respectively.

These ecdysteroid receptors are similar to those for oestrogen or progesterone in

vertebrates; they are proteins which bind the hormone with high affinity and high specificity, the binding constants for different ecdysteroids differing just as these hormones differ in their biological activities. The hormone-receptor complex enters the cell's nucleus though, in contrast to vertebrates, this does not involve a temperature dependant activation step.

Although the ecdysteroid receptors of *Drosophila* have yet to be purified, evidence for their activity comes from the study of *Drosophila* cell lines. Many cell lines of *Drosophila* respond to low concentrations of ecdysteroid in a complex and pleiotropic manner. In derivatives of the Kc cell line, for example, this includes the induction of specific enzymes, such as acetyl cholinesterase[10] and what appears to be an inhibition of cell division. This latter effect means that any variant cells capable of resisting the hormone's effects will be selected very rapidly from a population of largely responsive cells[12,13]. Preliminary reports[18] indicate that certain ecdysteroid resistant clones of *Drosophila* cell lines lack hormone binding activity.

The eventual purification of the ecdysteroid receptor proteins will open up many avenues for research and allow direct study of the location of ecdysteroid action on the genome. However this information can be obtained in another way.

The ecdysteroids contain an α-β unsaturated ketone in the B ring of the nucleus. Gronemeyer and Pongs[11] realised that this makes it possible to photo-cross-link ecdysteroids to their cellular binding sites. Using the salivary gland polytene chromosomes of *Drosophila* they irradiated the cells with light of > 320 nm to carry out the cross-linking; the hormone was visualised by first treating the chromosome with an anti-ecdysteroid antibody and then 'staining' with a fluorescent tagged goat anti-rabbit antibody. Despite a low background fluorescence, the polytene chromosomes show specific regions which fluoresce very brightly. When these regions are analysed in detail they are found to correspond to those regions that respond to ecdysteroids by forming puffs.

The nature of the substrate to which the

Michael Ashburner is a University Lecturer in the Department of Genetics, Cambridge.

photo-cross-linked ecdysteroids are bound is unknown. It may be the ecdysteroid receptor protein itself or some other chromosomal protein. The fact that this substrate can be covalently bound to the hormone, and that the hormone can be labelled to a high specific activity suggests that this problem will not be too difficult to solve. Moreover a comparative study of, for example, hormone responsive and hormone resistant cell lines of *Drosophila* should afford a direct demonstration of the role of nuclear receptor proteins in the hormone's action. It should also be possible to isolate mutants of *Drosophila*, rather than just their cell lines, that are mutant for their receptor proteins[15].

The cloning of the ecdysteroid responsive genes of *Drosophila* is a particularly exciting prospect. Evidence from both polytene chromosomes[3,14] and tissue culture cells[13] suggests that complex

1. Kopec, S. *Bull. Acad. Sci. Cracovie, Ser. B*.**57**; 1917
2. Karlson, P. *et al. Chem. Ber.* **98**, 2394; 1965
3. Clever, U. & Karlson, P. *Exp. Cell Res.* **20**, 623; 1960
4. Tissières, A., Mitchell, H.K. & Tracy U. *J. Mol. Biol.* **84**, 389; 1974
5. Ashburner, M. & Bonner J. *Cell* **17**, 241; 1979
6. Korge, G. *Proc. natn. Acad. Sci. U.S.:A.* **72**, 4550; 1975
7. Kroeger, H. *Nature* **200**, 1234; 1964
8. Yund, M.A. *et al. Proc. natn. Acad. Sci. U.S.A.* **75**, 6039; 1978
9. Maroy, P. *et al. Proc. natn. Acad. Sci. U.S.A.* **75**,6035; 1978
10. Cherbas, P. *et al. Science* **197**, 275; 1977
11. Gronemeyer, H. & Pongs, O. *Proc. Natn. Acad. Sci. U.S.A.* **77**, 2108; 1980
12. Courgeon, A.M. *Exp. Cell Res.* **74**, 327; 1972
13. Cherbas, P. *et al. Gene Regulation by Steroid Hormones* (eds. A.K. Roy & J.H. Clark.) Springer-Verlag, 1980
14. Ashburner, M. *Chromosoma* **38**, 255; 1972
15. Kiss, J. *et al. Nature* **262**, 136; 1976
16. Clever, U. *Science*, **146**, 794; 1964
17. Ashburner *et al. Cold Spring Harb. Symp.* **38**, 655; 1974
18. Best-Belpomme, M. *et al.* In: *Progress in Ecdysone Research* (ed. J.A. Hoffmann.) Elsevier, 1980
19. Bonner, J. & Pardue, M.L. *Chromosoma* **58**, 87; 1976
20. Lepesant J.A. *et al. Proc. natn. Acad. Sci. U.S.A.* **75**, 5570; 1978

pleiotropic responses to the hormonal stimulus are mediated via a few key genes. In salivary gland polytene chromosomes, for example, only six or so genes are induced by ecdysteroids within the first half hour or so. The induction of these puffs is independent of protein synthesis. A very much larger number of puffs respond after a few hours lag and their induction requires protein synthesis, at least during the time the early puffs are active[16,17]. Analogous events occur in *Drosophila* cell lines. A very early effect of ecdysteroids is to induce the synthesis of two or three polypeptides. Cherbas[13] and his colleagues have recently isolated cDNA clones complementary to the mRNAs of these polypeptides and found that the induction of these mRNAs, like that of the early puffs, is independent of protein synthesis.

A most striking characteristic of ecdysteroid's action is its tissue specificity. The different tissues of a *Drosophila* larva respond to the hormone in many different ways. The cloning of the 'early' ecdysteroid responsive genes from different tissues, for example fat body, imaginal discs and salivary glands, will allow us to discover whether or not these different tissues use the same genes as the primary targets of the hormone[19,20]. These clones will, now the outlook for the purification of the ecdysteroid receptor protein is so bright, result in a very detailed understanding of just how this simple hormone acts to effect the changes in gene activity that eventually result in the metamorphosis of the insect. □

Such strains were first produced by D. Bailey (Jackson Laboratories, Bar Harbor, US). RI mouse strains are, in effect, permanent segregant populations that frequently eliminate the need for slow and tedious backcross linkage analyses for the mapping of genes. Two resistance genes have been mapped using RI mice. The first is a gene locus, *Lsh,* that controls the intrahepatic and intrasplenic growth of *Leishmania donovani,* the etiological agent of human visceral leishmaniasis (D. Bradley, London School of Hygiene and Tropical Medicine, London). The *Lsh* locus has been mapped to the proximal end of chromosome 1. The second locus that was mapped using RI strains, is *Ric,* a gene that controls resistance to lethal infection with *Rickettsia tsutsugamushi,* the etiological agent of human scrub typhus. The *Ric* locus has been mapped to the middle of chromosome 5, closely linked to the gene for retinal degeneration, *rd* (M. Groves, Walter Reed Army Institute of Research, Washington DC). *Ric* seems to control a very early response in infected mice, since its effects can be very clearly demonstrated within four hours of innoculation of infectious organisms.

A third resistance gene that has been mapped controls resistance to lethal infection with *S. typhimurium,* and the locus has been termed *Ity* (for immunity to *typhimurium*). It is interesting to note that *Ity* is probably identical to the gene that was first inbred by Webster. *Ity* was mapped using a more traditional linkage analysis, and is located fairly close to *Lsh* on chromosome 1 (J. Plant, St Mary's Hospital Medical School, London). Although the close linkage between *Lsh* and *Ity* suggests that these loci might be identical, several RI strains have been identified in which alleles of these loci are not concordant, indicating that the genes are closely linked but different (A. O'Brien, USUHS, Bethesda).

Genetics of resistance to infection

from David L. Rosenstreich

HUMAN populations vary markedly in their susceptibility to disease produced by infectious agents. There are abundant examples of this variability, ranging from the well documented to the anecdotal. An example of the former is the resistance of erythrocytes containing Hgb S to infection by *P. falciparum* malaria parasites. Examples of the latter would be the familiar clinical observations of the marked variation between children in the severity of disease produced by highly contagious organisms such as chicken pox. There has always been a strong feeling among medical personnel that some of this variability was genetic in origin. However, with the exception of isolated examples of traits that produce marked biochemical or immunological derangements, the only other well documented example of genetic variability in susceptibility to infectious disease in humans has been the work in the major histocompatability gene locus, HLA.

However, research with inbred mouse

populations has indicated that a large number of genes control resistance to infectious agents. Studies in this area date back to the 1930s when Webster (*J. exp. Med.* **57**, 793; 1933) developed inbred strains of mice that differed markedly in susceptibility to the etiological agent of murine typhoid, *Salmonella typhimurium,* or to arbovirus infection. Over the past four decades, reports describing variations in resistance to other microorganisms in mice have surfaced, so that patterns of variability of resistance to most classes of viral, bacterial and parasitic human pathogens are known to exist in mice. A recent workshop* showed that research in this field has greatly accelerated over the past few years.

One of the major advances discussed at the meeting was the identification of the chromosomal location of specific resistance genes. Gene mapping in mice has been greatly facilitated by the development of recombinant inbred (RI) mouse strains.

A second major theme of the meeting was the mechanism of action of various resistance genes. Although no one has as yet pinned down a specific biochemical defect, some progress in this area is evident. An unexpected findings was the role of organism specific suppression in producing susceptibility. The disease produced by *Leishmania tropica* (human cutaneous leishmaniasis) is a good example of the operation of such a suppresive mechanism (J. Howard, Wellcome Research Laboratories, Beckenham, UK). Susceptibility in this mouse strain is due to a single, autosomal co-dominant locus. In response to *L. tropica* infection, Balb/c mice develop a population of antigen — specific T suppressor cells that prevent the development of an effective cell-mediated immune response of the type that

David L. Rosenstreich is Associate Professor in the Departments of Medicine and Microbiology and Immunology, Albert Einstein College of Medicine, New York.

eliminates the organism from resistant mouse strains. Antigen -specific suppression in susceptible mouse strains was also shown to occur in response to other organisms including *Mycobacterium bovis* BCG, (R. Nakamura, NIH, Tokyo) and several viruses (E. Isael, Jewish General Hospital, Montreal) and was also found to be involved in the failure of SJL mice to develop natural killer (NK) cells (G. Cudkowicz, State University of New York).

A third important aspect of genetic control of resistance is the effect of resistance genes on the response of organisms to various therapeutic agents. Mice that are genetically susceptible to *S. typhimurium* cannot be protected from this organism by immunization with standard vaccines, in contrast to genetically resistant strains (Rohson & Vas, *J. inf. Dis.* **126**, 378; 1972). Evidence presented at the workshop by H. Perez (IVIC, Caracas) suggests that this problem may extend to responsiveness to chemotherapeutic agents as well. Mice that are genetically susceptible (Balb/c) to *L. mexicana* (mucocutaneous leishmaniasis) did not respond to treatment with the drug, glucantime, while genetically resistant mice (C57 B1/6) could be cured by similar doses.

Findings such as these may be very important in explaining the wide variations in the response of human subpopulations or individuals to vaccines or drugs that tend to be less than 100% effective.

Several other themes were brought out at the workshop. One is that that control of early resistance to many different classes of organisms appears to be expressed in macrophages. Another is that most of these early resistance genes are not linked to the mouse major histocompatibility locus, H–2, one of the major regulators of antigenic specificity. Finally, it is noteworthy that very few of the described resistance genes seem to be identical, and there is some evidence of antigen or organism specificity in the actions of these genes. While subsequent mapping studies may begin to uncover overlapping specificities for some of these genes, these findings strongly suggest that there may exist a whole class of non H–2 linked genes that also control recognition of foreign substances.

The workshop illustrated the interest and progress that is beginning in this recently rediscovered area. The application of genetic approaches to studies of complex functions such as resistance to infections offers the possibility of real breakthroughs in the future. Implications for human health and disease are profound. ☐

A year of the double quasar

from a Correspondent

IN this issue of *Nature*, Gondhalekar and Wilson show that satellite observations in the ultraviolet region verify the gravitational lens model of the twin quasars.

It is a little over a year since the discovery of the twin quasars, 0957 + 561 A and B, was reported by Walsh *et al.* (*Nature* **279**, 381; 1979). They found that the two quasars, which are only about 6 arc s apart on the sky, have nearly identical spectra, and they thus suggested that the two images are of a single quasar in a gravitational lens. Since the two images have comparable brightness, it appeared likely that the object deflecting the light would be nearly midway between them.

Since this discovery, a large number of observations have been made on the double quasar at many wavelengths, testing some of the predictions of the gravitational lens model. The remarkable similarity of the optical spectra, which was the first pointer to the model, has been further demonstrated by Weymann *et al.* (*Astrophys. J. Lett.* **233**, L43; 1979) and by Wills and Wills (*Astrophys. J.* **238**, in the press). A further stringent test has come from the radio maps obtained by Pooley *et al.* (*Nature* **280**, 461; 1979) from the Cambridge 5 km telescope in the UK, and by Greenfield *et al.* (*Science* **208**, 495; 1980) using the Very Large Array of the National Radio Astronomy Observatory in the US. The radio source was found to have a complex radio structure which extended over about 12 arc s. The brighter northern component (A) of the pair is near the centre of an extended nearly linear structure which is at a large angle to the line joining the two quasar images. This has no counterpart in the southern (B) component, which is a compact source with a weak extension pointing approximately towards the A component. The absence of any radio structure near B corresponding to that found near A is difficult to reconcile with the simple gravitational lens model as first proposed.

The other obvious approach to testing the gravitational lens model for the twin quasars is to search for the object, presumably a galaxy, which is causing the gravitational deflection of the radiation. Early attempts to do this were hampered by relatively poor seeing but showed that if a galaxy were present nearly midway between the two quasars then it would be

quite faint. However, the observation by Gunn *et al.* (*IAU Circ.* No. 3431; 1979), which showed that there is a slightly elongated galaxy at redshift $z \sim 0.4$ about 0.8 arc s north of the southern (B) quasar, and no object midway between the two images, has changed the picture considerably. If the galaxy near B is indeed the gravitational lens, calculations show that, as a point mass, it is not far enough from the light path to cause the correct light deflection, and so a more complex picture based on an extended (and perhaps non-spherical) mass distribution is required. Under these circumstances it appears that either one or three images are formed, depending on the angles of deflection required, rather than the two images produced on the simple picture. So it is now likely that B consists of two close (≤ 0.2 arc s) unresolved images, and the absence of extended radio structure around B corresponding to that found around A is no longer a problem. The apparent radio extension of B may be due to weak emission from the galaxy itself, and indeed the positional agreement between the two is very good. Asymmetries in the galaxy, or the presence of a cluster of galaxies, could easily account for the slight misalignment of the two images and the deflector.

This new picture resolves some other problems which the simple model fails to explain adequately. Another prediction of the gravitational lens model is that the flux ratio between two images of a compact object should be independent of wavelength. This has been verified at radio frequencies by Pooley *et al.* among others, in the short wavelength optical region in the original paper by Walsh *et al.*, and now in the satellite ultraviolet region, by Gondhalekar and Wilson (this issue of *Nature*). However in the red and infrared part of the spectrum, B appeared to be somewhat brighter than expected compared with A. Recent infrared measurements by Soifer *et al.* (*Nature* **285**, 91; 1980) and Lebofsky *et al.* (*Nature* **285**, 385; 1980) are, however, consistent with a constant flux ratio between the two quasar images if a giant elliptical galaxy with a redshift $z \sim 0.4$ contributes to the excess flux in B.

Thus the suggestion that 0957 + 561 A and B are two (or, now, three) images formed by a gravitational lens has been well tested, and while some of the details of the process are not as simple as first envisaged, the essential correctness of the model is no longer in serious doubt. There are a number of detailed questions which remain, many of which require further observational material that may be difficult to obtain. Comparison of the VLBI radio structure of the two compact sources should yield valuable information. Another direct check on the model is to obtain the velocity dispersion for the material in the lens galaxy to see if it is consistent with the mass and radius required to give the observed deflection of

the radiation in the two images. In principle this could be done for the starlight from the galaxy, though this is rather faint and close to one of the quasar images. Alternatively, we might expect to find redshifted MgII absorption from any gas in the galaxy to determine this quantity, but already, from the spectra given by Walsh *et al.* in the original paper, we know that such lines are fairly weak. No doubt these observations and other detailed work will be done, but it would be somewhat surprising if the overall picture were to be very different from that we have now. ☐

Transient lunar phenomena

from David W. Hughes

THREE thousand million years is a long time for the Moon to be quiet and cold, but is it completely dead? Probably not, is the most reasonable answer. For more than two centuries terrestrial observers have recorded events which have been grouped under the title of transient lunar phenomena (TLP). The possible causes of these phenomena have always been subject to considerable debate and the latest debator is Allan Mills of the Department of Astronomy, University of Leicester. His review paper is published in a recent edition of the *Journal of the British Astronomical Association* (**90**, 219; 1980).

Over 1,400 TLP's have been observed and even though a considerable number of these can be rejected as instrumental, atmospheric or physiological artefacts a sufficient residue remain to warrant a detailed physical investigation. Glows, hazes, mists, brief colour changes and temporary obscurations of lunar surface features have been reported. Events seem to be restricted to specific lunar regions, about 300 having been reported from the crater Aristarchus, 75 from Plato and 25 from Alphonsus. They also occur near the boundaries of certain regular maria and near areas rich in rills. The highlands seem to be avoided, but this apparent paucity may be an observational selection effect. Occurrency frequency is not linked with solar activity but does peak when the Moon is at the perigee of its orbit, at times when tidal activity is maximised. Phenomena have been reported from both the sunlit and dark sides of the Moon. The areal extent on the lunar surface is on average 16 km across, this containing brighter spots of between 3 and 5 km in diameter. The average duration is about 20 minutes but some have been reported as persisting intermittently for a few hours. No permanent changes have been observed on the lunar surface after a TLP, thus justifying the use of the word 'transient'. Under very favourable seeing conditions TLP's have been seen to twinkle. Colour, if mentioned at all, tends to be described as weak, unsaturated, 'reddish' or 'bluish'.

Many possible explanations have been put forward, one of the first by Sir William Herschel who reported observing bright red glows in 1783 and 1787 and wrote a paper entitled *"An account of three Volcanoes in the Moon"*. The phenomena looked like glowing charcoal thinly veiled with hot ashes and Herschel was obviously thinking of incandescence from hot lava on the lunar surface. Unfortunately, fresh lava regions have not been seen on the Moon, at Herschel's site or in other places. The visible radiation from the fresh lava would decrease rapidly although the infrared radiation would be much more persistent. No such infrared sources have been observed. The brightness is also too low. 1 km^2 of lava at 1,250 K appears as an orange-red 'star' of magnitude 5.5. Drop the temperature to 1,000 K and the magnitude becomes 10.5. This might just be visible on the dark side of the Moon but would be very hard to detect on the sunlit side.

Luminescence can be ruled out because the excitation source, the solar wind, is too weak.

Thermoluminescence can also be disregraded because even though it provides a means of storing energy the emission intensity of all known materials is still too weak to be seen from such a distance.

Triboelectric charging can occur when dust grains are rubbed together. Discharging in dust clouds above the Italian volcano Vesuvius during its 1944 eruption produced brilliant and frequent lightning strokes. The emission of light depends to an extent on the presence of gas so that a plasma can be generated. Diffuse glows occur at about 100 dyn cm^{-2} these being replaced by bright twinkling discharges as the pressure increases. The potential required to produce a discharge is related to the product of the gas pressure and the dust separation. This process will be discussed again later.

Other explanations for TLP's rely on short term modifications to the lunar surface reflectivity. One reason for the very low reflectivity of the lunar soil is the spiky 'fairy castle' structures formed by the dust grains. If these are flattened out the reflectivity increases and this flattening can be easily produced by fluidizing the upper dust layer by passing gas through it. There are two difficulties. Large quantities of gas are required to fluidize several sq. km. of lunar soil. A more pressing problem is that the enhancement in reflectivity is semi-permanent and this is ruled out by the 20 minute average duration of TLP's.

Middlehurst (*Phil. Trans. R. Soc. Lond. A* **285**, 485; 1977) compares the epicentres of deep moon quakes and high frequency teleseismic (HFT) shallow moon quakes with the areas of TLP activity. Most of the HFT sites are within 5° of at least one TLP site. The deep moon quakes originate 800 to 1,000 km below the surface, the shallow ones being much higher (the maximum depth found so far is 265 km). Middlehurst suggests that channels exist between HFT epicentres and the TLP's (the TLP's being almost vertically above the HFT's) and that gas is still escaping through these channels even though the escape rate is much smaller now than it was in the earlier days of lunar history.

Mills proposes a mechanism for TLP production which relies on gas escape but at a much lower rate than that required to fluidize the soil. The gas lifts off the very small particle fraction of lunar soil, producing a kind of moon smoke, and leaves the fairy castle structure intact. Unfortunately the scattering of light by smoke is a highly complex and incompletely modelled phenomena, which relies drastically on the particle size distribution. For particles with sizes below 0.1 λ (where λ is the light wavelength) the scattered light is highly polarised with an intensity proportional to λ^{-4}. For particles with sizes above 10 λ the scattered light is white and unpolarized. For intermediate sizes partial polarization occurs and the colours are unsaturated. As the scattering function is so complex, uniform sized dust can even produce red scattered light and volcanic dust in the stratosphere has been known to produce a blue moon.

The mass of moon smoke required to produce a TLP is of the order of 1 to 20 kg per sq. km. of lunar surface. Mills suggests that this could be blown above the moon's surface by episodic releases of gasses which have accumulated in fissures and faults in the lunar rocks. These releases are triggered by tidal forces and coincide with moon quakes. The smoke quickly falls back to the surface thus explaining the transitory nature of the phenomena.

Now this mechanism could solve the TLP problem for the sunlit regions of the lunar surface but what about the TLP's on the dark side of the moon? If they exist (and there is some doubt) Mills considers that triboelectric discharges provide the only reasonable explanation. Gases expanding from subsurface regions blow away a cloud of dust which becomes charged by interparticle friction and undergoes charge separation. This cloud discharges when the product of the pressure and the mean dust separation distance reaches about 1,000 dyn cm^{-1} and this condition is probably reached a few metres above the surface. The red colour is consistent with the gas being hydrogen.

Mills concludes that the triboelectric lightning discharges in gas-borne dust clouds can explain some TLP's especially those on the dark side of the moon. A more probable explanation requires less energy and less gas and simply relies on light being scattered by temporary clouds of moon smoke. ☐

David W. Hughes is in the Department of Physics, University of Sheffield.

100 years ago

Mr. R. L. Jack, the Government Geologist of Queensland, has been carrying out his survey operations under difficulties unknown to home geologists. While he and his party were pursuing their explorations in the north of York Peninsula they were attacked by a band of natives, Mr. Jack receiving a spear in the neck, which had to be cut out. Fortunately the wound, though troublesome, is not likely to be attended with any serious or permanent results. North of Temple Bay Mr. Jack came upon a hitherto unknown large river, which he has named the "Macmillan."

The *Daily News* gives some account of a recent lecture by Prof. Palmieri on earthquakes. Prof. Palmieri went on to say that earthquakes have no doubt shorter or longer periods of preparation. The earth is never perfectly quiet for some time before and after a great shock, but gradually sinks into repose or increases in agitation. The Professor believes that, by registering the slight preliminary tremblings and noticing their increase or decrease it would be possible to fortell an earthquake about three days in advance, just as tempests are now foretold. If a connected system of seismographic stations were to be organised — the different stations communicating with each other by telegraph — it would be quite possible, in most cases, to issue warnings to the threatened district in time. The seismographic stations should be erected by the different Governments in quiet places where the ground was not liable to be shaken by heavy railway trains.
From *Nature* 22, 17 June, 155, 1880.

Planetary nebulae

from James B. Kaler

THEORIES of the formation of planetary nebulae are supported by the important discoveries of Hazard *et al.* reported in this issue of *Nature*.

During a large portion of their lives, stars lose mass back to interstellar space. In the final episode of mass loss, a highly evolved red giant star expels most if not all of its remaining hydrogen envelope as an expanding shell of gas. As the shell expands into space, it eventually is illuminated by the remaining core of the star, which becomes very hot. We then see the phenomenon as a planetary nebula, a shell or ring of gas surrounding a hot blue nuclear star which is contracting to its ultimate state as a degenerate white dwarf.

There are about 1,000 of these beautiful objects known, and perhaps 20,000 in the Galaxy at any given time. They are ephemeral, with lifetimes of perhaps 30,000 years, and come in a startling array of varieties. The nebulae are heated by photoionization from ultraviolet light provided by the central star. The spectra of the nebulae are dominated by recombination lines of hydrogen and helium, and by collisionally excited forbidden lines of various ionization stages of oxygen, nitrogen and neon. The observed radii range from only a few hundredths of a parsec to more than 0.5 pc, with the electron densities concomitantly varying from 10^6 cm^{-3} to less than 10^2 cm^{-3}.

The central stars display an equally wide variety, with effective black-body temperatures ranging from as low as 25,000 K (the minimum required to photoionize the nebula) up to perhaps 200,000 K,

making them as a class the hottest known stars. The properties of the stars and nebulae are correlated with one another, with the largest nebulae generally having the hottest central stars. The correlation is caused by the evolution of the star during the expansion of the nebula (O'Dell *Astrophys. J.* **183**, 67; 1963; Abell *Astrophys. J.* **144**, 259; 1966; Seaton *M.N.R.A.S.* **132**, 113; 1966). However, a detailed explanation is complicated by the fact that the observed nebulae are produced by a large range in initial stellar mass (from about one to six times that of the sun), which results in a large and uncertain rage of core masses upon which the individual evolution on the log luminosity (L) — log temperature (T) plane is dependent. (Paczynski *Acta Astronomica* **21**, 417; 1971; Kaler *Astrophys. J.* **237**; in the press.)

Since the mechanisms of spectral line formation are well understood, the abundance ratios of the lighter elements can be found rather directly from the relative line fluxes. About 100 nebulae have been so analyzed by a variety of people. The compositions of the nebulae reflect the state of the interstellar gas at the time and place of the origin of the star, but they also display effects of nuclear processing of the nebular gas in the original star before the ejection of the shell (Peimbert *IAU Symposium* **76**, 215; 1977; Kaler *Astrophys. J.* **228**; 163; 1979). In particular, many nebulae are considerably enriched in helium and nitrogen. The planetaries thus provide an important probe into the inner workings of stars, and observation of them can be used to test theories of the late stages of stellar evolution.

The enrichment of He and N in the planetary shell can be explained by a series

of "dredge-up" events that carry mass processed through the nuclear burning zones of the star upwards into the hydrogen envelope before it is lifted off to produce the nebula (Iben *Astrophys. J.* **140**, 1631; 1964; **196**, 525; 1975; **208**, 165; 1976; Perinotto & Renzini *Astronomical Uses of the Space Telescope* (eds. Machetto Pacini & Tanenghi) 147, ESO, Geneva; 1978). The first of these processes occurs as the star ascends the giant branch for the first time after the exhaustion of its hydrogen core. A convection zone in the hydrogen envelope pushes into the now inactive hydrogen-burning shell that surrounds the helium core, lifting away nitrogen that has been created from carbon during CNO burning. The second episode takes place during the second ascent of the giant branch for stars larger than about 3 $M_\odot$ where the star now has an inert carbon-oxygen core which is surrounded by concentric helium and hydrogen burning shells. This time the convection zone sweeps into the helium core produced by the earlier burning of the hydrogen shell, and not only carries away more nitrogen, but large quantities of helium as well. To this point, the theoretical correlation between the He/H and N/O ratios in the hydrogen envelope agrees well with those observed for planetary nebulae (Kaler, Iben & Becker *Astrophys. J. Lett.* **224**, L63; 1978.) The final event occurs during the thermal pulsing stage on the second ascent, when convection penetrates into a region processed by the helium-burning shell, which further alters the composition of the envelope.

Renzini (*Fourth European Mtg. in Astronomy: Stars and Stellar Systems*, ed. Westerlund, 155, Reidel, Dordrecht) has placed these abundance variations within the framework of the theoretical evolution of the star on the log L-log T plane. Because of different rates of evolution, high mass stars, for which the largest helium and nitrogen enrichments should be found, are expected to appear as high temperature, low luminosity planetary nuclei. Stars of this kind are seen at the centers of the largest nebulae.

The above theories attempt to describe the conventional planetary in which processed material may be mixed into the hydrogen envelope, before it is expelled to form the nebula. But the paper by Hazard *et al.* in this issue of *Nature* adds something entirely new and of great significance. They have discovered knots of gas near the central star of the planetary Abell 30, in which the He/H ratio is at least 20 times its normal value. They thus demonstrate that not only did the formation of Abell 30 use the entire residual hydrogen envelope of the star, but that the star is in fact ejecting some of its current helium-rich envelope and that the nuclear star is extremely hot. Hazard *et al.*'s observations agree with Renzini's hypothesis, and our current notions of the development of the planetary nebulae. ☐

James B. Kaler is in the Department of Astronomy, University of Illinois at Urbana-Champaign.

Isolating colour vision mechanisms with hue substitution

*from R. W. Bowen, J. Pokorny
and V. C. Smith*

IN a review of new psychophysical techniques for isolating color-opponent neural mechanisms in human vision, J. D. Mollon[1] expresses the opinion that hue substitution[2] — a form of pure chromaticity modulation in which a chromatic field is briefly exchanged for a white of equal luminance — is not likely to activate selectively chromatic visual channels since it may generate receptoral transients detectable by 'luminance' channels. At issue is whether data obtained with hue substitution reflects functional isolation of chromatic channels or not.

Studies of visual temporal processing with hue substitution stimuli have shown that visual latency[3], two-pulse discrimination[4] and duration thresholds[5] follow a wavelength function resembling trichromatic saturation discrimination: slowest temporal response at 570nm and brisker temporal responses at the spectral extremes, suggesting that the speed of the temporal response reflects activity in red-green and blue-yellow opponent-color mechanisms.[6-8]

Mollon is among those[9-12] who have suggested that the 'violet-sensitive' receptor does not contribute to luminance channels. If we accept this postulate, receptor transients in '565-nm' and '535-nm' cones cannot explain the wavelength dependence of hue substitution data. Consider hue substitution from white to an equiluminant spectral yellow or violet where these lights are collinear on a tritanopic isochromatic line. Such stimuli have equal quantal catch for the '565-nm' and '535-nm' receptors; therefore receptor transients cannot occur at stimulus presentation. Receptor transients predict only a 'tritanopic' wave-length dependence; in fact, such dependence has been found for two-pulse discrimination of brief chromatic stimuli.[4] However, to ascribe this function to receptor transients demands the additional restraint that normalization of '565-nm' cone sensitivities is identical for both chromatic and luminance channels, a hypothesis difficult to reconcile with estimates of cone spectral sensitivities.[10,11,13,14]

The issue is addressed directly in the case of duration thresholds[5]: just-detectable hue substitution stimuli are always perceived as chromatic, a phenomenon which cannot be mediated by receptor transients in luminance channels. Further, the wavelength

R. W. Bowen is in the Department of Psychology, Loyola University of Chicago, J. Pokorny and V. C. Smith are in the Department of Psychology, University of Chicago.

dependence of temporal processing in hue substitution is identical to that observed with an independent method of measuring chromatic channel function (discriminative reaction time).[15] Finally, metacontrast masking[16] and temporal brightness enhancement[17] are abolished with hue substitution stimuli: these phenomena require physical luminance transients.

Transient receptoral responses could in principle arise from pure chromaticity modulation and might be important in some situations (e.g., high luminance levels). However, there is strong evidence that chromatic neural mechanisms dominate observed effects on visual function in the hue substitution literature cited here.   □

1.   Mollon, J. D. *Nature* **283**, 623 (1980).
2.   Weingarten, F. *Science* **176**, 692 (1972).
3.   Nissen, M. J., & Pokorny, J. *Percept. Psychophys.* **22**, 457 (1977).
4.   Bowen, R. W., Lindsey, D. T., & Smith, V. C. *J. Opt. Soc. Am.* **67**, 1501 (1977).
5.   Pokorny, J., Bowen, R. W., Lindsey, D. T., & Smith, V. C. *J. Opt. Soc. Am.* **69**, 103 (1979).
6.   Hurvich, L. & Jameson, D. *Psychol. Rev.* **64**, 384 (1957).
7.   Kaiser, P. K., Comerford, J. P., & Bodinger, D. M. *J. Opt. Soc. Am.* **66**, 818 (1976).
8.   Guth, S. L., Massof, R. W., & Benzschawel, T. *J. Opt. Soc. Am.* **70**, 197 (1980).
9.   Guth, S. L., Alexander, J. V., Chumbly, J. I., Gillman, C. B., & Patterson, M. M. *Vision Res.* **8**, 913 (1968).
10. Smith, V. C. & Pokorny, J. *Vision Res.* **15**, 161 (1975).
11. Boynton, R. M. *Human Color Vision* (Holt, Rinehart and Winston, New York, 1979).
12. Eisner, A. & MacLeod, D. I. A. *J. Opt. Soc. Am.* **70**, 121 (1980).
13. Vos, J. J. & Walraven, P. L. *Vision Res.* **11**, 799 (1971).
14. Ingling, C. R., Tsou, B. H., Gast, T. J., Burns, S. A., Emerick, J. O., & Riesenberg, L. *Vision Res.* **18**, 379 (1978).
15. Nissen, M. J., Pokorny, J., & Smith, V. C. *J. Exp. Psychol.: Human Percept. Perform.* **5**, 406 (1979).
16. Bowen, R. W., Pokorny, J., & Cacciato, D. *Vision Res.* **17**, 971 (1977).
17. Bowen, R. W. & Nissen, M. J. *J. Opt. Soc. Am.* **69**, 581 (1979).

J. D. Mollon replies

FOR validation of hue-substitution techniques, Bowen, Pokorny and Smith (their 2nd paragraph) turn primarily to the finding that measures such as reaction time vary with wavelength in hue-substitution experiments in the same way as does threshold in experiments on saturation discrimination. But this result is equally to be expected if the speed of response depends on the magnitude of transient responses generated by the 565-nm and 535-nm cones at the moment of substitution. For saturation depends ultimately on the degree to which the ratios of absorptions in different classes of cone differ from the ratios produced by white light. At a spectral locus close to 570 nm is a tritanopic neutral point (i.e. there is a yellowish monochromatic light that those who lack the short-wavelength receptors confuse with the white used in the experiment). I think we share a common theory of what this means: when this monochromatic light and the white are equated in luminance, the yellow produces exactly the same absorptions in the long- and middle-wavelength cones as

does the white. When the mono-chromatic light is substituted for the white there will be no change in the signals from these cones. Response to a substituted 570-nm field will be slow, either because it is mediated only by short-wavelength receptors or — if 570 nm does not exactly coincide with the tritanopic neutral point — because the residual transients in the long- and middle-wavelength cones are very small. As the wavelength of the substituted field increasingly diverges from 570 nm, the receptoral transients must increase, since the ratio of absorption in the long-vs. the middle-wavelength cones must significantly differ from that produced by white light. (The short-wavelength tritanopic neutral point has not been examined in hue-substitution experiments.)

This argument does not require us to know the ratio of absorption that white light produces in the long- and middle-wavelength cones and there is no need to suppose that this ratio (or the ratio of any subsequent signals) is unity; we need allow only that these ratios remain constant (or, in practice, almost constant) across the substitution to 570 nm. Bowen, Pokorny and Smith's reference to 'normalization' (their 3rd paragraph) is obscure but I would diffidently suggest that they are confounding (a) the wavelength at which the two classes of cone deliver equal signals to a putative luminance channel and (b) the wavelength (*c.* 570 nm) that delivers the same ratio of signals as does white light. If wavelength (a) is indeed remote from (b), if, say, it is 500 nm, then the ratio of signals produced by white light must be very different from unity and large transients must occur at the passage to wavelength (a).

Reference 5 does not contain formal data on perceived hue, and, being concerned only with liminal stimuli, it cannot validate the entire hue-substitution technique. To say discriminative reaction time (ref. 15) depends on saturation is to say it depends on the extent to which the absorptions produced in the several classes of cones differ from those produced by white light; the magnitudes of receptoral transients depend on these very differences. In the metacontrast experiment (ref. 16) the dependent variable was the degree of phenomenal darkening of the target; when the masking stimuli were 'equiluminant', receptoral transients would be of opposite sign for different cone classes and hence the net effect on target brightness cannot be predicted.   □

J. D. Mollon is in the Department of Experimental Psychology, University of Cambridge.

ARTICLES

Cytoplasmic free calcium and amoeboid movement

P. H. Cobbold

Department of Zoology, University of Liverpool, Brownlow Street, Liverpool L69 3BX, UK

Measurements with the Ca^{2+}-sensitive photoprotein aequorin show that locomotion in the amoeba Chaos carolinense *occurs without changes in the aequorin signal and that not more than 0.025% of the cytoplasm can exist at the micromolar threshold concentration for contraction. The results do not support the hypothesis that cytoplasmic streaming is under the control of changes in the cytoplasmic free Ca^{2+} concentration.*

IT is widely believed that the intracellular control of cell motility may involve modulation of actomyosin activity by elevated cytoplasmic free Ca^{2+} concentrations. Many non-muscle cells have been shown through insult with Ca^{2+} buffers to have a threshold for contraction of approximately micromolar free Ca^{2+}, and studies on Ca^{2+}-activation of non-muscle myosins have revealed Ca^{2+}-sensitizing factors associated with both myosin and actin. Elevated Ca^{2+} concentrations are also thought to play a part in cytoplasmic consistency (sol–gel) changes[1-6]. In view of the central controlling role attributed to Ca^{2+} it is surprising that investigations of physiological Ca^{2+} changes accompanying motile events in the normal cell have given equivocal results, with Ca^{2+} concentrations being apparently invariant or well below threshold levels[6-11]. In *Chaos* a micromolar Ca^{2+} threshold for contraction has been shown using Ca^{2+}-EGTA buffers in conjunction with naked, 'flaring' cells[12], naked cytoplasmic strands[12,13], injections into intact amoebae[14] and ultrastructural studies[15,16], providing extensive support for the concept of control by Ca^{2+}. It is shown here by means of calibrated aequorin measurements that not more than 0.025% of the cytoplasm of a locomoting amoeba can exist at the micromolar threshold for contraction and that changes in the pattern of cytoplasmic streaming are not accompanied by changes in the aequorin signal.

Calibration of the aequorin signal

Aequorin is a photoprotein which needs only to bind Ca^{2+} in order to emit light, being independent of oxygen, ATP or other cofactors[17], and which has been widely used as an indicator of cytoplasmic free Ca^{2+} concentrations[18,19]. The photomultiplier signal from an aequorin-injected amoeba, typically between 10 and 100 photoelectrons per second (background $5 \, s^{-1}$), was expressed as a fraction of the total aequorin content of the cell, as measured by recording the light emitted during killing of the cell, to give a value for the rate constant of aequorin consumption *in vivo* (Fig. 1). A value for the cytoplasmic free Ca^{2+} concentration was derived from rate constants determined *in vitro* over a range of free calcium concentrations set by Ca^{2+}-EGTA buffers (Fig. 2). Between 10^{-7} M and 10^{-6} M Ca^{2+} the rate constant rises by three orders of magnitude giving excellent sensitivity to small changes in Ca^{2+} concentration in the range of interest. Care was taken to ensure that the ionic conditions *in vitro* mimicked those in the amoeba groundplasm[20,21], since the sensitivity of aequorin to Ca^{2+} is depressed by increasing ionic

strength and free Mg^{2+} (refs 22, 23). The free Mg^{2+} concentration *in vitro* was equal to the total Mg^{2+} content of whole cells minus crystalline bodies[20,24] and is probably greater than the actual cytoplasmic free Mg^{2+}, resulting in an overestimate of free Ca^{2+}. This method of external calibration is valid only if the sensitivity of aequorin to Ca^{2+} is the same *in vivo* as *in vitro* and, although aequorin is unaffected by the presence of EGTA[25], there is some evidence that it might be inhibited by unknown cytoplasmic factors[22]. This possibility was assessed by means of 'internal calibration' experiments[22,26] in which rate constants were determined in amoebae injected with EGTA-buffers (Fig. 2 legend). There is no evidence for anomalous Ca^{2+}-sensitivity of aequorin *in vivo*. Calibration errors arising from self-absorbtion of light within the cell were not important since normal rate constants were recorded from locomoting amoebae which had previously been clarified by centrifugation and bisection. Calcium binding to EDTA injected as a contaminant of aequorin was negligible, the low cytoplasmic concentration, less than 5 μM EDTA, being entirely satisfied by Mg^{2+}. The cytoplasmic concentration of aequorin, approximately 1 μM (ref. 10) will bind approximately 16% of free 10^{-7} M Ca^{2+} (ref. 27), a small displacement which was presumably replaced from millimolar intracellular Ca^{2+} stores[20,24]. Injected amoebae recovered normal locomotion within 15 min, suggesting that the injected solution had no persistent traumatic effects. Location of aequorin in the groundplasm compartment was demonstrated by freezing an aequorin-laden cell, previously stratified by centrifugation, under an image-intensifier microscope whereupon most of the light originated from the centripetal half, most of the aequorin being excluded along with groundplasm from the organelle-rich centrifugal end. A similar approach showed that aequorin mixed throughout the groundplasm of normal cells[10]. Other precautions to satisfy the protocol proposed by Blinks *et al.*[26] are described in Fig. 1.

Aequorin signal and motility

The mean aequorin rate constant (k) *in vivo* measured on cells in various motile states, predominantly radiate (that is, a rounded and unattached cell with several radiating spindly pseudopodia), was $1.82 \times 10^{-6} \pm$ s.d. $1.58 \times 10^{-6} \, s^{-1}$ $(n=32)$. Hence log k mean was -5.74, (range $\pm$ s.d. -5.47 to -6.6), giving a mean free calcium concentration, at 5 mM free Mg^{2+}, of 8×10^{-8} M (1.5×10^{-7} M + s.d., 2×10^{-8} M − s.d.), falling to 5×10^{-8} M in 0.5 mM free Mg^{2+}. Since the actual

Fig. 1 Chart record of an experiment to determine the rate constant of aequorin consumption in an amoeba showing photomultiplier anode current expressed as photoelectrons s^{-1} against time in minutes. *Upper trace*: 0–3 min background current of 5 photoelectrons s^{-1}; 3–11 min signal from a single aequorin-injected amoeba, 10 photoelectrons s^{-1}, superimposed on background. The trace was blanked out during observation and photography. *Lower trace*: lysis of the same amoeba beginning 8 min after adding a minute quantity of solid SDS to the culture medium (1 ml), accompanied by discharge of the aequorin. An approximately 10-fold higher concentration of SDS added to aequorin in a Ca^{2+} buffer did not affect the light yield as judged by the agreement between the predicted and observed areas under the discharge curve. The peaks on this curve represent a wave of lysis spreading across the cell. The cell surface is extraordinarily resistant to lysis, probably by virtue of a thick glycocalyx, and the high extracellular Ca^{2+} upon entry into the cell at a lytic focus causes a local gelation and pinching-off of that region by a 'surface precipitation reaction'[40]; the peaks do not represent lysis of different intracellular compartments. The area under this discharge curve was equivalent to 3.3×10^7 photoelectrons so that the rate constant for aequorin consumption, k, in the intact amoeba prior to lysis was 3×10^{-7} s^{-1}. Hence $\log k$ was -6.5, corresponding to a cytoplasmic free Ca^{2+} concentration of 4×10^{-8} M (see Fig. 2). Correction of the total photoelectron count for photocathode quantum efficiency (12%) geometric counting efficiency (2.5%) and aequorin quantum yield (23%) gave a total aequorin content of 4.7×10^{10} molecules and an aequorin concentration in a cell of 40 nl volume of 2 μM. Aequorin: a saturated ammonium sulphate precipitate of aequorin purified by ion-exchange chromatography[41] was desalted by centrifugation, dialysis against Chelex (Biorad) decalcified 5 M potassium acetate followed by gel filtration on Sephadex G-25 using 10 mM ammonium formate 1 μM EDTA as eluent[25], and freeze dried. A microscopic speck of freeze-dried protein was dissolved in 100 nl of injection buffer (30 mM potassium acetate + 1 μM EDTA) held in a 3 mm length of microdialysis tube (Biofiber 50, Biorad) and dialysed for 1–3 h against several changes of buffer to remove EDTA contaminating the freeze-dried aequorin. The EDTA concentration in the dialysed solution was shown by back-titration to be less than 50 μM. Amoebae were injected to ~5% of their volume and usually recovered normal locomotion in 15 min. All experiments used aliquots from a single freeze-dried sample of aequorin to minimize errors from possible differences between preparations[26]. All *in vivo* measurements were made within 12 h of injection and all *in vitro* measurements before the signal had decayed 20% in order to minimize errors caused by significant consumption of aequorin. For equipment details see ref. 10. Temperature $20 \pm \frac{1}{2}$ °C.
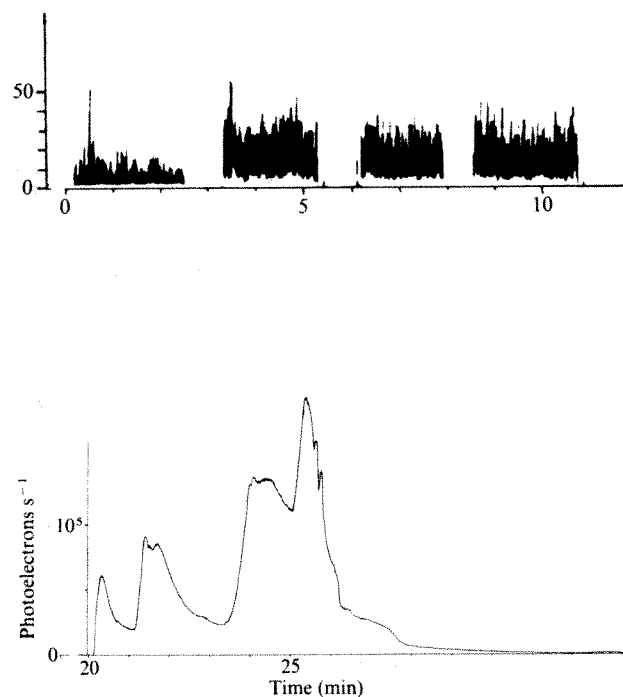
groundplasm free Mg^{2+} was probably between these limits the mean free Ca^{2+} concentration was between 50 and 80 nM. The variability in rate constant was probably due to the number of rounded, quiescent or radiate cells in the sample. Such cells often showed a slow rise and fall in the aequorin signal over a period of approximately 30 min, with Ca^{2+} rising from around 7×10^{-8} to 2×10^{-7} M, without any discernible motile activity. At their peak, these signals usually showed spiky fluctuations with a fast rise time which were not due to shot noise (compare Fig. 3b and c) and which were not abolished with external 10 mM EGTA or La^{3+}. Rounded cells (Fig. 3b) usually showed larger signals than locomoting cells and resumption of cytoplasmic streaming was accompanied by a fall in signal to levels similar to that in Fig. 3a, a change which cannot be attributed to counting geometry, which would operate in the reverse sense. The significance of these observations on rounded cells, whether quiescent or radiate, is not known, but the calcium changes did not correlate with changes in shape or streaming activity.

The aequorin signal from actively locomoting cells, whether polypodial or monopodial, showed little fluctuation above that due to shot noise and was usually lower than in quiescent cells (Fig. 3a). Signals recorded over periods of hours on more than 50 cells did not reveal any minute-to-minute changes which could be correlated with the initiation, cessation or reversal of cytoplasmic streaming or to changes in adhesion or cell shape. Even dramatic spikes such as that in Fig. 3b, which were infrequent (1 or 2 per hour) did not appear to influence shape or movement. It is impossible to escape the conclusion that changes in the pattern of cytoplasmic streaming in the pseudopodia of a locomoting cell are not accompanied by changes in the aequorin signal and therefore in the mean cytoplasmic free Ca^{2+} concentration.

It could be argued that failure to detect Ca^{2+} changes during locomotion might merely be due to inadequate sensitivity in the technique. However, it is apparent from Fig. 2 that raising 1% of a cell's volume to the 10^{-6} M Ca^{2+} threshold for contraction[14] would give log $k = -4.8$ which, for a typical cell (for example, Fig. 1) would generate a signal of 520 photoelectrons s^{-1}, considerably greater than the observed signal of 10 s^{-1}. Therefore the technique possesses excellent sensitivity, being capable of measuring sustained threshold concentrations of Ca^{2+} in small zones of the amoeba. However, it is conceivable that transient rises in free Ca^{2+}, too brief to be resolved with the present technique, might be responsible for triggering a slow-decaying Ca^{2+}-independent active state of the contractile proteins. Thus a zone of micromolar Ca^{2+} occupying 1% of cell volume and generating 520 photoelectrons s^{-1} would, if it persisted for 100 ms produce a spike in the signal which, because of limitations in the response time of the instrumentation, would be impossible to resolve amongst the Cerenkov background. In the analysis that follows it has been assumed that the elevated Ca^{2+} concentration has to be maintained in order to sustain contraction.

Zones of micromolar calcium?

The above estimate of a mean cytoplasmic free Ca^{2+} concentration of 50 to 80 nM was based on the assumption that Ca^{2+} was distributed homogeneously throughout the groundplasm, but it is conceivable that a fraction of the signal arises from local zones at the micromolar threshold for

contraction described by Taylor[14] (free Ca^{2+} values in Taylor's buffers have been recalculated; compare Fig. 2 legend). Thus, in 10^{-6} M Ca^{2+} log $k = -2.8$ (Fig. 2) so the *in vivo* mean log k (-5.8) could have been generated by a zone of micromolar Ca^{2+} influencing 0.1% of the aequorin content of the cell. However, if allowance is made for light contributed from the remaining 99.9% of the aequorin, which must generate at least 10% of the signal since even in the complete absence of Ca^{2+} log k is -6.8 due to the calcium-independent light[28], the zone falls to 0.09%. If a more realistic value for the free Ca^{2+} concentration in the bulk of the cytoplasm is used, for example 4×10^{-8} M, then the micromolar zone cannot exceed 0.07% cell volume. If the actual cytoplasmic free Mg^{2+} concentration is less than 5 mM, as it most probably is, then further restriction of the micromolar zone occurs. Thus, at 0.5 mM Mg^{2+} the *in vivo* rate constant would be generated by 5 $\times 10^{-8}$ M Ca^{2+}, probably close to the free Ca^{2+} concentration in the bulk of the cytoplasm, whereupon the possible extent of the micromolar zone falls to zero. Furthermore, active locomoting cells showed lower rate constants than the mean (for example Fig. 3a, log $k = -6.04$) and the scope for micromolar zones becomes vanishingly small, that is, 0.025% at 5 mM Mg^{2+}; 0% at 0.5 mM Mg^{2+} (bulk free Ca^{2+} assumed to be 4×10^{-8} M).

Image intensifier observations

In the more recent of their two image intensifier studies on aequorin-laden amoebae Taylor *et al.*[8,9] report luminescence arising spontaneously in the tail of the cell. Although precise calibration was not attempted, the free Ca^{2+} concentration was less than micromolar as judged by the signal from injecting 10^{-6} M Ca^{2+} buffer[9]. In an independent study using a similar intensifier[10] I failed to detect any signal from locomoting, aequorin-laden cells. This difference cannot be attributed to the amoebae since our aequorin rate constants agree [log k -5.8 and -5.6 (D. L. Taylor, personal communication)] and was probably caused by insensitive photographic recording of the intensifier output phospor, which would raise the detection limit. Figure 4 gives an estimate of the intensifier detection limit: it was possible to detect compact zones of micromolar and submicromolar Ca^{2+} in the cell. The zone of 10^{-6} M Ca^{2+} occupying 0.05% of cell volume represents the upper limit imposed by the rate constant data and would have been detectable above the randomly distributed background. Similarly the image from 1% at 4×10^{-7} M Ca^{2+}, again at the limit imposed by the rate constant data (assuming 5 mM Mg^{2+} and 40 nM Ca^{2+} in bulk of cell), would have been recognizable. The absence of a detectable signal from *Chaos* indicates that it is unlikely that micromolar zones of elevated Ca^{2+} occurred. A constraint to this argument against the existence of micromolar zones is that this analysis applies only to compact, spherical Ca^{2+} zones. An elevated Ca^{2+} zone in which the photoelectron signal is dispersed over a large image area would not be detected above background.

Does free Ca^{2+} control motility?

The most obvious interpretation of these data is that the cytoplasmic free Ca^{2+} concentration is uniformly 8×10^{-8} M (given 5 mM free Mg^{2+}). Such a conclusion would be consistent with the constant level of the aequorin signal during motility changes, the vanishingly small scope for zones of elevated Ca^{2+} and with the failure to image zones of elevated Ca^{2+} despite adequate intensifier detection limits. However, this conclusion conflicts with the requirement for micromolar calcium for contraction in EGTA buffers[14] and as the site(s) of force generation in *Chaos* is not known[29,30], arguments can be raised in support of the concept of small zones of threshold Ca^{2+}, occupying not more than 0.025% of the cell, being responsible for triggering motile activity. One such argument concerns the constant level of the aequorin signal and the
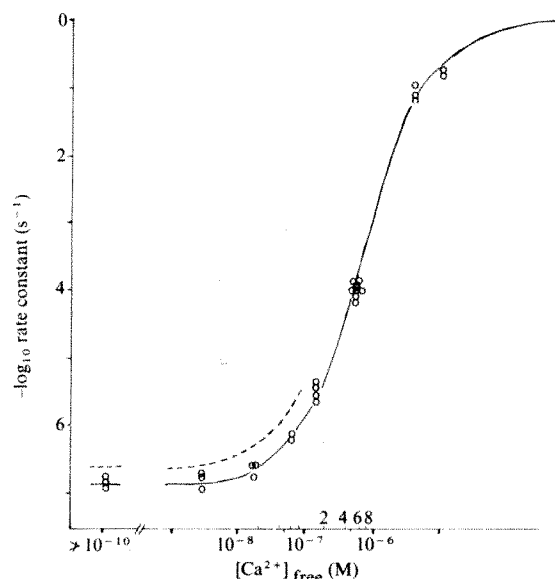
Fig. 2 Dependence of the rate constant for aequorin consumption (k) upon the free calcium concentration *in vitro*. Double log plot. Points on the curve are individual determinations using quantities of aequorin similar to those injected into single amoebae, so that instrumental errors are comparable. Rate constants were determined by expressing the light flux in the buffer as a fraction of the total light recorded during discharge of the remaining active aequorin following addition of calcium acetate. Composition of buffer (mM) KCl 30, free Mg^{2+} 5, EGTA 20, MOPS 10, KOH to pH 6.8. The broken line was extrapolated from the data of Allen *et al.*[25] for $[Mg^{2+}]_{free} = 0.5$ mM. Free calcium concentrations were calculated by successive approximation[42] allowing for Mg-EGTA using Schwarzenbach's apparent association constants appropriate for pH 6.8[43] (Ca-EGTA $k_{app} = 1.95 \times 10^6$; Mg-EGTA $k_{app} = 23.99$). For the sake of comparability the free calcium concentrations in the series of EGTA buffers used by Taylor *et al.*[12–16] have been recalculated using these association constants. As a result their 'physiological threshold for contraction' of 7×10^{-7} M becomes 1.1×10^{-6} M. The Ca^{2+}-sensitivity of aequorin in the cytoplasm was tested by internal calibration experiments in which a Ca^{2+}-buffer (mM:KCl 30, EGTA 20, MOPS 10, pH 6.8) was injected into an aequorin-laden amoeba to $\sim 5\%$ of the cell volume while recording the light signal. Injection of 10^{-5} M free Ca^{2+} gave a peak signal which decayed rapidly to a low level. Subsequent lysis of the cell with SDS then elicited a second, much larger release of light. The ratio between the areas under the first and second curves was approximately 20 suggesting that, perhaps, the injected buffer had mixed with only $\sim 5\%$ of the cytoplasm. The half life of the decay in light intensity immediately after the injection, between 2.5 and 8 s, was comparable with the half life expected from the rate constant *in vitro* (4 s). Furthermore the rate constant for aequorin consumption measured on the first peak was only 0.3 log unit less than the value obtained *in vitro*. While interpretation of these experiments is complicated by a lack of direct evidence for poor mixing (an image intensifier was not available), it seems unlikely that the explanation for the low peak light intensity following buffer injection resides in an inhibition of aequorin *in vivo* since it is then necessary to postulate a rapid sequestration of Ca^{2+} in order to explain the rapid decay in light intensity. Poor mixing of Ca^{2+}-containing solutions, which appear to elicit local gelation and a 'surface precipitation reaction'[40], is also seen in the slow-spreading discharge of aequorin in a lysing cell (Fig. 1). Exact agreement between rate constants and half-lives *in vivo* and *in vitro* should perhaps not be expected in view of the possibility of a slow spread of buffer into fresh aequorin-laden cytoplasm (prolonging half life), sequestration of Ca^{2+} (shortening half life), pH shifts affecting EGTA and uncertainty of the free Mg^{2+} *in vivo*. Light measurements following injection of 10^{-8} M Ca^{2+} buffer had to be made after withdrawal of the micropipette to eliminate the relatively large signal arising around the site of impalement[9]. Log k after injection was -6.5 compared with -6.8 *in vitro*. This difference may be due to Ca^{2+} release from stores, a lower free Mg^{2+} *in vivo*, residual micropipette injury, or perhaps to poor mixing, although low-Ca^{2+} buffers appear microscopically to mix readily with the cytoplasm.

possibility that a rising signal from a zone starting to contract might be exactly compensated by a simultaneous loss of signal from a zone undergoing relaxation, giving a false impression over the cell as a whole of a constant Ca^{2+} concentration. However, the approximately cube-law relationship between signal and free Ca^{2+} (Fig. 2) suggests that the probability of the product of the volume and Ca^{2+} concentration of both zones being so balanced as to generate a constant signal would be low. It is more likely that a constant signal indicates a constant free Ca^{2+} concentration. However, it is not possible to rule out the Ca^{2+} concentration changes with absolute certainty and, by assuming that the bulk of the cell is at 4×10^{-8} M rather than 8×10^{-8} M Ca^{2+} (5 mM Mg^{2+}), there is sufficient surplus signal to encompass a zone of 10^{-6} M Ca^{2+} occupying 0.025% of the cell volume. Two arguments suggest that it is unlikely that a volume of cytoplasm of this size could be responsible for generating the motive force. If an actively locomoting cell moves through its own length in 3 min cycling all the cytoplasm through the micromolar zone, then the mean residence time of cytoplasm in the zone would be 50 ms, and the appearance given by such brief contraction in a highly localized area of the cell would be inconsistent with the smooth-flowing appearance of normal cytoplasmic streaming. Furthermore injection of 1% of cell volume with 10^{-6} M free Ca^{2+} in an EGTA buffer influenced a volume of cytoplasm approximately ten times larger (P.H.C., unpublished), but only induced contraction in a zone ~ 50 to 100 μm in diameter[14], considerably smaller than the normal endoplasmic stream which can be 1,000 μm long. Therefore a micromolar calcium zone of 0.025% cell volume, 40 times smaller than in the injection experiment, would be quantitatively inadequate for inducing the observed cytoplasmic flows. It follows that models of cytoplasmic streaming based upon contractions or gelation changes induced by a stationary zone of micromolar Ca^{2+} through which the cytoplasm flows, such as might be envisaged in the recruitment and fountain zones, are not

tenable. In addition, such zones would be relatively compact and would have been detected by image intensification (Fig. 4 and ref. 9).

The rate constant and intensifier data are perhaps compatible with a contraction-hydraulic model involving Ca^{2+}-induced contraction of a thin sub-plasmalemmal cortex in the rear of the cell. A micromolar Ca^{2+} zone of 0.025% cell volume would be adequate to invest the internal surface of half the plasmalemmal area to a depth of 0.5 μm, comparable in extent to the layer of filamentous cytoplasm recently described in the rear of the amoeba[31,32]. Problems of residence time do not arise and the elevated Ca^{2+} could be derived from the transplasmalemmal currents described by Nuccitelli *et al.*[33], which have been implicated in the tail luminescence detected by Taylor *et al.*[9]. It is not possible on the available evidence to determine whether Ca^{2+}-induced contractile activity in the sub-plasmalemmal zone contributes to cytoplasmic streaming. However, it is conceivable that local micromorphological surface movements could be markedly influenced by Ca^{2+}-induced contraction or gelation changes in the thin felt of microfilaments. A combination of image intensification and the extracellular current probe[33] should help to resolve this question.

In smaller cells such as *Acanthamoeba* with a volume of 0.01% that of *Chaos*, or in the 'ruffling membrane' of fibroblasts, it is not difficult to envisage a role for transplasmalemmal Ca^{2+} currents in inducing contractile activity of a sub-plasmalemmal network of microfilaments. Indeed, in view of the larger surface-to-volume ratio of small cells, cortical contractile activity might make an appreciable contribution to the total locomotory effort, but experimental evidence for a direct role for Ca^{2+} in initiating sub-plasmalemmal contraction will be difficult to obtain.

Whatever the contribution of subplasmalemmal contractions to streaming in intact *Chaos* they cannot be responsible for the motile activity of naked cells held in capillaries[29,30] or
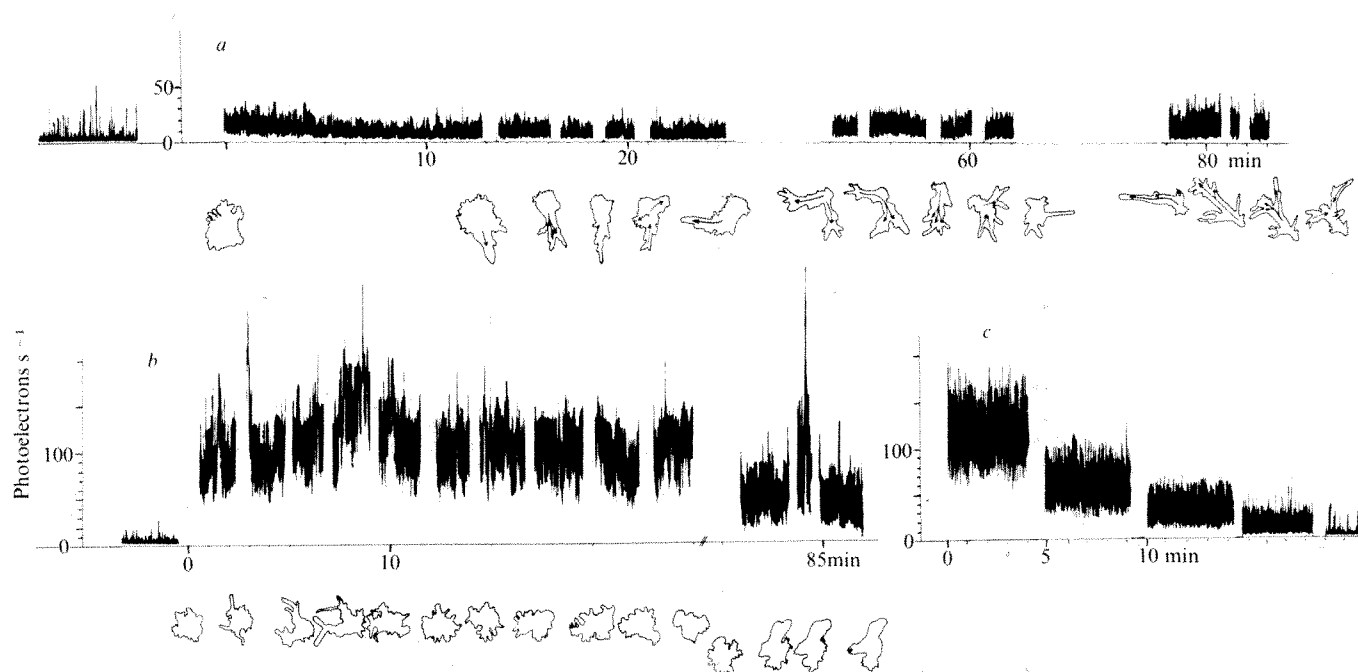
Fig. 3 Chart recordings of aequorin signals from two representative amoebae, with cell outlines traced from photographs and the direction of cytoplasmic streams arrowed. (The relative positions of the outlines are not an indication of the distance covered by the cell between photographs.) *a.* Actively locomoting, polypodial amoeba. The signal (log $k = -6.04$) remained more or less constant and showed no consistent changes with locomotory behaviour of the amoeba, a typical result. Between minutes 78 and 81 the cell moved through its own length, yet the signal was not discernibly different from the initial signal from the cell in a rounded, static condition. *b.* Rounded cell, occasionally extending spindly pseudopodia in a radiate-like fashion. No locomotion. The spikes and slower fluctuations are greater than variations due to shot noise (compare with *c*), and are found in rounded, radiate or quiescent cells but not in locomoting cells. The large spike at 84 min had no effect on cell shape or streaming. The source of the fluctuations is not known but they do not appear to correlate with the production of pseudopodia, nor are they dependent on external calcium. *c.* Shot noise at mean count rates of 130, 70, 30, 15 photoelectrons s⁻¹, followed by background (5 s⁻¹). All observations were made in Marshall's medium[21] on amoeba maintained on mixed ciliates. Recording chambers, of glass, polycarbonate or photographic film-base were kept in darkness prior to use to eliminate phosphorescent background[10]. Amoebae were illuminated in red light during observation and photography.

exposed to EGTA buffers[12]. Naked cells in capillaries continue to stream for up to an hour while naked cells bathed in EGTA buffers show motile activity which is apparently dependent on the free Ca^{2+} concentration, being immobile in 10^{-7} M, showing 'flare' streaming in 1.1×10^{-6} M and contracting radially in $\sim 3 \times 10^{-6}$ M (refs 6, 12). (The free Ca^{2+} levels have been recalculated for comparability with this study, see Fig. 2 legend). There is a serious discrepancy between these experiments and the aequorin measurements in that the concentration of free Ca^{2+} in the 'flare' solution, 1.1×10^{-6} M, is 14 times greater than the mean free Ca^{2+} in the cell, that is, 4 to 8×10^{-8} M depending on the free Mg^{2+} concentration. The cause of this discrepancy is not known, but it cannot be attributed to the absence of the plasmalemma since naked cells confined in quartz capillaries or under oil continue to stream[29,30]. One possibility is that the inhibition of motility in 10^{-7} M Ca^{2+} buffer resulted from the presence of EGTA since birefringence and ultrastructural studies have demonstrated a rapid loss of microfilaments in buffers of higher free EGTA concentrations (5 to 25 mM)[13,16]. Furthermore injection of a 5 mM EGTA buffer giving 1×10^{-7} M free Ca^{2+}, a physiological level, into intact amoebae caused a cessation of locomotion and a loss of distinction between ectoplasm and endoplasm[14]. While it is possible to explain the microfilament depolymerizing effects of high EGTA concentrations on the higher buffering capacity and hence upon the lower free Ca^{2+} levels achieved in the presence of Ca^{2+} leakage from organelles[16], this does not explain why motility is lost in physiological levels of 10^{-7} M Ca^{2+} and restored only when free Ca^{2+} is raised to 14 times normal (1.1×10^{-6} M). It may be significant that the free EGTA concentration in the 10^{-6} M buffer was ~ 0.8 mM, markedly lower than in the 10^{-7} M buffer, and the possibility has to be recognized that free EGTA at concentrations of ~ 5 mM may not be compatible with normal motile behaviour, even at physiological free Ca^{2+} levels. The question therefore arises as to whether the Ca^{2+} threshold for contraction and gelation is, in the absence of EGTA, less than micromolar. If this is so, then the control concentrations would have to be considerably less than micromolar in order to comply with the aequorin data if appreciable volumes of cytoplasm are to be influenced. Thus zones occupying 1%, 5% and 10% of the cell volume cannot exceed free Ca^{2+} concentrations of 4×10^{-7}, 2.5×10^{-7} and 2×10^{-7} M respectively. Such zones, if compact, would have been detectable with the image intensifier (Fig. 4) suggesting that the putative submicromolar threshold must be closer still to the resting Ca^{2+} level, or smaller in extent. Condeelis et al.[16] have made the interesting suggestion that microfilament depolymerization might be promoted in the normal cell by lowered Ca^{2+} concentrations. Indeed, the aequorin data would be entirely compatible with such a scheme since (see Fig. 2) if 10% of the cytoplasm were to undergo a reduction in Ca^{2+} from 8×10^{-8} M to 4×10^{-8} or 2×10^{-8} the fall in the signal would be 6% and 8% respectively, and would be undetectable in the noise. Further aequorin measurements, preferably on naked cells in capillaries where contributions to the signal from sub-plasmalemmal Ca^{2+} zones are eliminated, are obviously required to determine whether such subtle rises or falls in the free Ca^{2+} concentration are involved in motility control. At present, however, the involvement of free Ca^{2+} changes either side of the resting level must be regarded as uncertain.

The aequorin data are consistent with a constant level of cytoplasmic free Ca^{2+}, but this interpretation does not necessarily mean that the control mechanism is Ca^{2+}-independent or that Ca^{2+} binding to motile proteins is unimportant. On the contrary, the evidence of Taylor et al.[12-14] has demonstrated the sensitivity of cytoplasma to Ca^{2+} from 10^{-6} to 10^{-3} M beyond reasonable doubt. So it is conceivable that control of streaming through a constant-Ca^{2+} mechanism may involve modulation of the sensitivity of the contractile proteins to Ca^{2+}, precedents for which are seen in
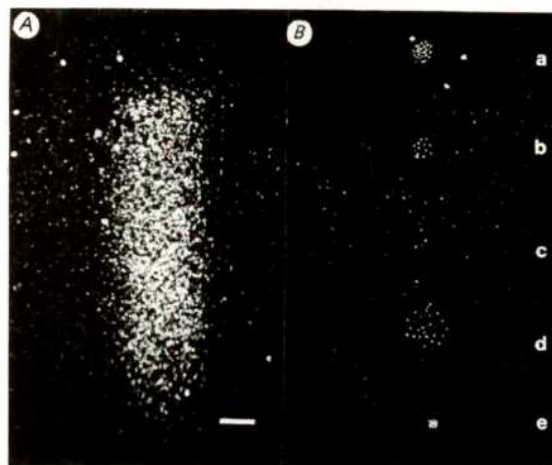
Fig. 4 Evaluation of image intensifier detection limits for small zones of sub-micromolar free calcium. *Frame A.* 10-s photograph of output phosphor of an EMI 9912 4-stage image intensifier viewing, through a microscope, an amoeba-sized (40 nl) cylindrical cuvette containing 5×10^{-7} M $[Ca^{2+}]_{free}$ buffer (see Fig. 2) injected to 5% of its volume with aequorin. Each punctate image represents one photoelectron. Scale bar, 100 μm. *Frame B*, 10-s exposure of background with five simulated images, a-e, superimposed. The photoelectron counts in these simulations were calculated from Fig. 2 using an estimate of 80 photoelectrons in a zone 91 μm diameter in frame *A*, an area which corresponds to the image of a spherical zone occupying 1% cell volume. The simulated images are; a, 1% at 5×10^{-7} M $[Ca^{2+}]$; b, 1%, 4×10^{-7} M; c, 1%, 2×10^{-7} M (not detectable above background); d, 10%, 2×10^{-7} M; e, 0.05%, 1×10^{-6} M. The detection limit for a spherical zone of 2×10^{-7} M $[Ca^{2+}]$ is between 1% and 10% cell volume. Higher $[Ca^{2+}]$ levels are detectable in zones occupying 1% of cell volume, assuming the zone is compact and quasi-spherical. Observations of amoebae under identical conditions failed to detect any signal[10]. It is therefore unlikely that persistent zones of free calcium above this detection limit occur *in vivo* in *Chaos*.

the modulation of the Ca^{2+}-sensitivity of actin-activated myosin ATP-ase by light chains[34] and in the cyclic nucleotide dependent regulation of Ca^{2+}-sensitivity of cardiac muscle[35]. In this context it is interesting to note Taylor's observation[14] that endoplasm in the rear of the cell responds more slowly to injections of threshold Ca^{2+} than anterior endoplasm. Alternatively it is possibly that the sensitivity to Ca^{2+} arises from a secondary mechanism which is not activated in the normal cell. except perhaps in the immediately sub-plasmalemmai layer[9,31,33], and that streaming is under the control of Ca^{2+}-independent processes such as myosin light chain phosphorylation[36,37] myosin heavy chain phosphorylation by cofactor protein[38] and viscosity and gelation changes induced by 5'AMP[6,39].

Before the role of Ca^{2+} in motility control can be resolved it will be necessary to improve upon the measurements in *Chaos* and to extend the technique to other motile cells for which calcium control has been proposed. The demonstration of a calcium threshold with EGTA buffers can no longer be regarded as adequate evidence for control by modulation of the cytoplasmic concentration of free calcium.

1. Pollard, T. D. & Weihing, R. R. *C.R.C. Crit. Rev. Biochem.* **2,** 1–65 (1974).
2. Hitchcock, S. E. *J. Cell Biol.* **74,** 1–15 (1977).
3. Korn, E. D. *Proc. natn. Acad. Sci. U.S.A.* **75,** 588–599 (1978).
4. Clarke, M. & Spudich, J. A. *A. Rev. Biochem.* **46,** 797–822 (1977).
5. Pollard, T. D. *J. supramolec. Struct.* **5,** 317–334 (1976).
6. Taylor, D. L. & Condeelis, J. S. *Int. Rev. Cytol.* **56,** 57–144 (1979).
7. Baker, P. F. & Warner, A. E. *J. Cell Biol.* **53,** 579–581 (1972).
8. Taylor, D. L., Reynolds, G. T. & Allen, R. D. *Biol. Bull.* **149,** 448 (1975).
9. Taylor, D. L., Blinks, J. R. & Reynolds, G. T. *Biol. Bull.* **155,** 469 (1978).
10. Cobbold, P. H. in *Detection and Measurement of Free Calcium Ions in Cells* (eds Ashley, C. C. & Campbell, A. K.) 245–256 (North-Holland, Amsterdam, 1979).
11. Ridgway, E. B. & Durham, A. C. H. *J. Cell Biol.* **69,** 223–226 (1976).

12. Taylor, D. L., Condeelis, J. S., Moore, P. L. & Allen, R. D. *J. Cell Biol.* **59**, 378–394 (1973).
13. Taylor, D. L., Moore, P. L., Condeelis, J. S. & Allen, R. D. *Expl Cell Res.* **101**, 127–133 (1976).
14. Taylor, D. L. *Expl Cell Res.* **105**, 413–426 (1977).
15. Taylor, D. L., Rhodes, J. A. & Hammond, S. A. *J. Cell Biol.* **70**, 123–143 (1976).
16. Condeelis, J. S., Taylor, D. L., Moore, P. L. & Allen, R. D. *Expl Cell Res.* **101**, 134–142 (1976).
17. Shimomura, O., Johnson, F. H. & Saiga, Y. *J. Cell comp. Physiol.* **59**, 223–239 (1962).
18. Ashley, C. C. & Ridgway, E. B. *Nature* **219**, 1168–1169 (1968).
19. Blinks, J. R. *Photochem. Photobiol.* **27**, 423–432 (1978).
20. Friz, C. T. *Comp. Biochem. Physiol.* **38A**, 477–482 (1971).
21. Bruce, D. L., Marshall, J. M. *J. gen. Physiol.* **49**, 151–178 (1965).
22. Baker, P. F., Hodgkin, A. L. & Ridgway, E. B. *J. Physiol., Lond.* **218**, 709–755 (1971).
23. Blinks, J. R. *et al. Meth. Enzym.* **57**, 292–328 (1978).
24. Greenbaum, B. W., Moller, K. M. & Thomas, R. S. *Expl Cell Res.* **18**, 385–388 (1959).
25. Allen, D. G. & Blinks, J. R. in *Detection and Measurement of Calcium in Cells* (eds Ashley, C. C. & Campbell, A. K.) 157–174 (North-Holland, Amsterdam, 1979).
26. Blinks, J. R., Prendergast, F. G. & Allen, D. G. *Pharmac. Rev.* **28**, 1–93 (1976).
27. Blinks, J. R. *Ann. N.Y. Acad. Sci.* **307**, 71–85 (1978).

28. Allen, D. G., Blinks, J. R. & Prendergast, F. G. *Science* **196**, 996–998 (1977).
29. Allen, R. D. in *Biology of Amoeba* (ed. Jeon, K. W.) 202–245 (Academic, New York, 1973).
30. Allen, R. D. & Allen, N. S. *A. Rev. Biophys. Bioengng* **7**, 469–495 (1978).
31. Hauser, M. *Cytobiologie* **18**, 19–106 (1978).
32. Wehland, J., Weber, K., Gawlitta, W. & Stockem, W. *Cell. Tissue Res.* **199**, 353–372 (1979).
33. Nucitelli, R., Poo, M-M. & Jaffe, L. *J. gen. Physiol.* **69**, 743–763 (1977).
34. Pemrick, S. in *Calcium-Binding Proteins and Calcium Function* (eds Wassermann, R. H. *et al.*) 287–289 (North-Holland, Amsterdam, 1977).
35. McClellan, G. B. & Winegrad, S. *J. gen. Physiol.* **72**, 737–764 (1978).
36. Adelstein, R. S. & Conti, M. A. in *Cold Spring Harb. Conf. Cell Proliferation* Vol. 3 725–738 (1976).
37. Adelstein, R. S. *Trends. biochem. Sci.* **4**, 27–30 (1978).
38. Maruta, H. & Korn, E. D. *J. biol. Chem.* **252**, 8329–8332 (1977).
39. Nachmias, V. T. *J. molec. Biol.* **107**, 623–629 (1976).
40. Chambers, R. & Reznikoff, P. *J. gen. Physiol.* **8**, 369–402 (1928).
41. Johnson, F. H. & Shimomura, O. *Meth. Enzym.* **57**, 271–291 (1978).
42. Portzehl, H., Caldwell, P. C. & Ruegg, J. C. *Biochim. biophys. Acta* **79**, 581–591 (1964).
43. Amos, W. B. *et al. Symp. Soc. exp. Biol.* **XXX**, 298–299 (1976).

A monoclonal antibody for large-scale purification of human leukocyte interferon

David S. Secher

MRC Laboratory of Molecular Biology, Hills Road, Cambridge CB2 2QH, UK*

Derek C. Burke

Department of Biological Sciences, University of Warwick, Coventry CV4 7AL, UK

A clone of hybrid myelomas (NK2), secreting a mouse monoclonal antibody to human leukocyte interferon, has been isolated. The antibody neutralizes the antiviral activity of the interferon and, when covalently attached to a solid support and used as an immunoadsorbent, allows interferon purification of up to 5,000-fold in a single step.

MONOCLONAL antibodies have been made by the spleen cell fusion technique of Köhler and Milstein[1] against a variety of antigens (reviewed in ref. 2). A theoretical advantage of the method is that it allows the production of specific antibodies to unpurified antigens. There is, however, no example of a monoclonal antibody that has been deliberately made to a predefined soluble antigen present at less than 1% of the immunogen. By using suitable screening methods it is possible to isolate rare hybrids producing antibody of the desired specificity, but this depends on screening with pure antigens. We describe here the properties of a monoclonal antibody to an antigen not available in pure form for screening assays and present in the immunizing material at a concentration of 0.1–1% of the total protein injected. This antigen is human leukocyte interferon, a protein (or group of proteins) that confers antiviral protection on human cells *in vitro* and *in vivo*.

There is currently considerable interest in the use of human leukocyte interferon as an antitumour and antiviral agent[3,4]. Preparation of interferon for clinical use has required the development of large-scale production facilities[5–7] coupled with extensive purification before administration to patients. Purification to homogeneity has recently been reported for two species of human interferon: fibroblast[8] (2×10^8 U per mg) and leukocyte [obtained either from leukocytes[9] ($2–4 \times 10^8$ U per mg) or from lymphoblastoid cells[10] (2.5×10^8 U per mg)] and considerable progress has been made in the characterization of human (and mouse) interferons including amino acid compositions and amino-terminal sequences[11–13]. However, the small-scale of production prevents cheap

interferon from being readily available for characterization and clinical trials. Several groups have introduced immunoadsorbent column chromatography as one step in the purification of human interferon[7,14–17], but there are several problems connected with the production of antibodies against interferon. We considered that a homogeneous, monoclonal antibody would be advantageous in purifying interferon by immunoadsorption. In addition, interest in the interaction between interferon and the immune system[18,19] has led to the need to assay low titres of leukocyte interferon in serum and other body fluids. For such purposes a radioimmunoassay, based on a monoclonal antibody, would be important. We report here the isolation of a hybrid myeloma, secreting antibody to human leukocyte interferon, and show that this antibody can be used for the purification of interferon by immunoadsorption.

The assays that have been used successfully in the production of monoclonal antibodies have been fast, reproducible, sensitive and simple. The lysis of antigen-coated red blood cells[20], binding on coated replica sheets[21], radioactive binding assays[22], haemagglutination assays (C. Milstein, personal communication) and radioimmunoassays[23], all fulfill these requirements and have been used in the isolation of monoclonal antibodies to haptens[20], cell-surface components[24], neuropeptides[23] and other antigens (see ref. 2). For interferon such assays would require large amounts of pure material or a radioimmunoassay (which is not available). Therefore, we were forced to use alternative assays based on a biological assay that is inherently complex and slow. Of the

Fig. 1 Properties of NK2 clones. Supernatants were assayed for anti-interferon activity and for the presence of secreted immunoglobulin. Hybrid cell culture supernatants were mixed with an equal volume of Dulbecco's modified Eagle's medium and 20% fetal calf serum (Gibco-Biocult) which contained 2–4 reference research units of interferon. After incubation at 37 °C for 1 h, the fluids were assayed for residual interferon by the $INAS_{50}$ assay[25,26]. Anti-interferon activity is shown by an increase in the level of viral RNA synthesis above that due to interferon alone (——). Secreted immunoglobulin was detected by a reverse plaque assay[28]. Open circles indicate that the supernatants were negative for secreted immunoglobulin, closed circles that they were positive (*a*, *b*, *c*) or untested (*d*, *e*).
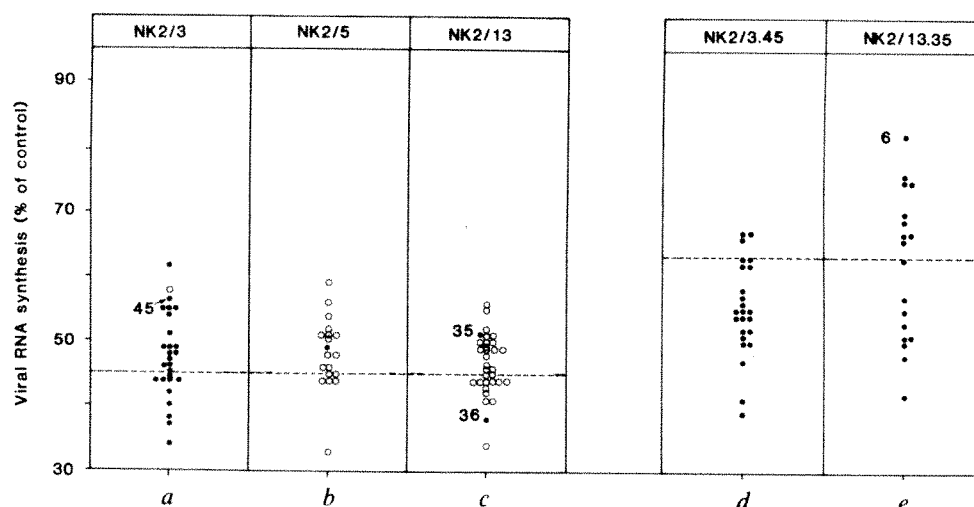
available methods we chose to use the inhibition of nucleic acid synthesis ($INAS_{50}$) assay (refs 25, 26 and J. Morser, A. Meager, D.C.B. and D.S.S., manuscript in preparation).

Production and isolation of hybrid cells making monoclonal anti-interferon

Human interferon has been shown to be immunogenic in several heterologous species, but comparative studies[14] have suggested that it is a much weaker immunogen in smaller animals (guinea pigs and rabbits) than in the large domestic animals (cows and sheep) usually used as a source of anti-interferon.

In the present study groups of mice and rats were immunized at 2-weekly intervals with lymphoblastoid interferon emulsified in complete Freund's adjuvant. A mouse with a titre (the dilution of serum that neutralized 50% of 20 U interferon) of $\log_{10}$ 3.7 was selected for the fusion. Details of the immunization and fusion, as well as the results of a previous unsuccessful fusion, will be published elsewhere (J. Morser, A. Meager, D.C.B. and D.S.S., manuscript in preparation).

Three cultures (3, 5, 13), among several showing possible anti-interferon activity, were recloned in soft agar as described[27] and 48 clones of each were picked and grown in 2-ml cultures. Culture supernatants were tested for the presence of secreted mouse immunoglobulin using a reverse plaque assay[28] (spot-test) and for anti-interferon activity in the $INAS_{50}$ assay. The results shown in Fig. 1, as well as the results of many other assays not shown, clearly demonstrated that the level of neutralization of interferon by culture supernatants was just at (and sometimes beyond) the limits of sensitivity of the assay. At the critical stage of selection of a positive clone of NK2/13, the reverse plaque assay was essential.

To confirm that the anti-interferon activity was in fact due to immunoglobulin, and to determine the immunoglobulin class, ^{14}C-lysine was incorporated into proteins secreted by selected clones and the extracellular medium analysed by SDS-polyacrylamide gel electrophoresis (PAGE) in reducing conditions[27]. Only two major bands were visible in each case; one had the mobility of immunoglobulin heavy chain (γ, NK2/13.35; μ, NK2/13.36), the other co-migrated with the immunoglobulin light chain (NSI) that was run as a marker.
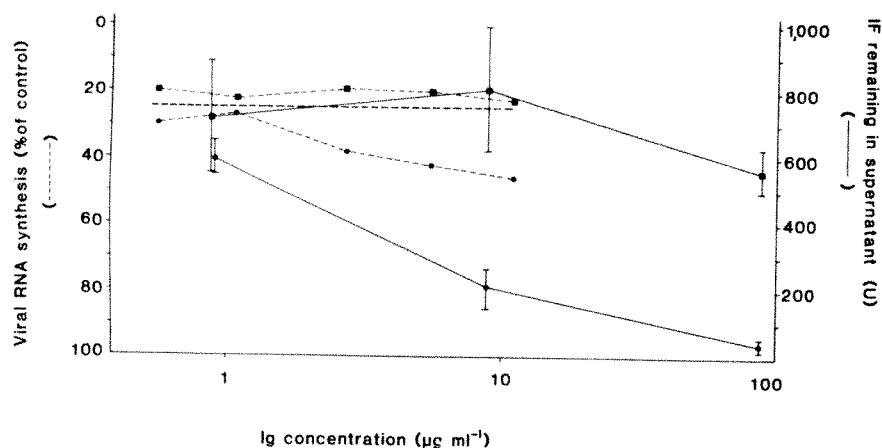
Fig. 2 Titration of anti-interferon activity of NK2 IgG. Anti-interferon activity was detected either by the standard neutralization assay or by the use of the indirect immunoprecipitation modification. Dilutions of IgG in phosphate-buffered saline (PBS) (10 µl) were incubated with about 720 U of lymphoblastoid interferon (10 µl) at 37 °C for 5 h. Antibody–antigen complexes were then precipitated by the addition of carrier mouse IgG (5 µl normal mouse serum) and 75 µl of sheep anti-mouse IgG antiserum (slight antibody excess). After incubation at 37 °C for 30 min and 4 °C for 16 h the samples were centrifuged at 8,000g for 5 min to remove the antibody–antigen precipitate and the supernatant was assayed for its residual interferon content by the $INAS_{50}$ method. IIP assays were carried out in duplicate (NK2) or triplicate (control supernatant containing irrelevant monoclonal antibody) and the mean ± 1 s.d. is indicated. ●——●, NK2, neutralization; ■——■, control, neutralization; ●——●, NK2, IIP; ■——■, control, IIP.

Clone NK2/13.35 was recloned and the most strongly positive subclone (NK2/13.35.6) in the neutralization assay (Fig. 1e) was grown to mass culture and frozen in liquid nitrogen for long-term storage. This clone was also grown in the presence of ^{14}C-lysine and the radioactive secreted proteins analysed by SDS-PAGE. Two major bands were visible; one had the mobility of immunoglobulin γ-chain, the other had a mobility slightly lower than that of the NSI light chain. No band corresponding to the NSI light chain was detectable, indicating that the clone NK2/13.35.6 produces only the antibody-specific heavy and light chains (that is, NK2/HL in the nomenclature of ref. 29).

Precipitation of immune complexes improves the anti-interferon assay

The NK2/13.35.6 culture supernatant, although usually positive, was at best only sufficient to reduce the interferon activity to 25% of its control value using the interferon neutralization assay described in Fig. 1 legend. Some modifications to the assay were therefore tested. Concentration of culture supernatants 10–20-fold by ultrafiltration (Amicon XM 50) or by ammonium sulphate precipitation increased reproducibility, but the difference between a positive and a negative supernatant was not always convincing (data not shown). However, the results did show that the anti-interferon activity was associated with a high molecular weight (MW) component which was precipitated by 50% saturated ammonium sulphate. We also looked for, but could not detect, a synergistic effect on mixing supernatants from different cultures. Such an effect might result from the mixing of two non-neutralizing monoclonal antibodies, neither of which alone would be detectable. A similar phenomenon has been observed in studies of monoclonal antibodies to cell-surface antigens[30]. A more successful modification to the assay was the introduction of an indirect immunoprecipitation (IIP) step (see Fig. 2 legend) in which interferon–anti-interferon complexes are removed (by the addition of carrier mouse immunoglobulin and anti-mouse immunoglobulin antiserum) before adding the interferon to the cells.

We also decided to use a purified IgG fraction prepared from the serum of mice bearing NK2 tumours to allow a higher concentration of immunoglobulin to be tested in the assay. (As the only clone from the NK2 fusion to be grown in mice was NK2/13.35.6 it will be abbreviated to NK2.) The

Table 1 Purification of crude interferon* by NK2-Sepharose immunoadsorbent chromatography

	Before	After
Volume (ml)	100	0.5
IF titre† (U ml^{-1})	7.2×10^4	1.4×10^7
Total U	7.2×10^6	7.0×10^6
A_{280}	2.2	0.09
Total protein‡ (mg)	220	0.04
Specific activity (U per mg)	3.3×10^4	1.8×10^8
Purification factor	1	5,300
Yield (%)	100	97

*Crude interferon was culture medium from stimulated Namalwa cells after removal of material that precipitated at pH 2.

†Error in IF assay estimated to be ±30%.

‡Estimated assuming $A^{1\%}_{1cm, 280} = 10$. Most proteins have extinction coefficients in the range 5–15.

separation of the antibody–antigen complex formation from the neutralization part of the assay allowed the use of much higher levels of interferon as the interferon was diluted for assay after removal of the antibody–antigen complex. This greatly increased the precision of the assay because, by varying the dilution of the sample for interferon assay, we could always work near the midpoint of the dose–response curve. This is impossible in the neutralization assay.

Using the IIP assay we found that at an antibody concentration of about 90 µg ml^{-1} it was possible to remove over 90% [696/720 U (reference research units as defined relative to the MRC reference standard preparation 69/19)] of input interferon. Plotting of the data from a neutralization experiment in the same figure allows a direct comparison of the two assays (Fig. 2), but note that the 45% of viral RNA synthesis obtained at 9 µg ml^{-1} NK2 IgG corresponds to the neutralization of about 80% of the interferon present (data not shown).

Towards a single-step purification of lymphoblastoid interferon

Anti-interferon antibodies have shown to be useful in the characterization of different interferons and the purification of both mouse and human interferons. Their use, however, has been limited by the fact that until recently only impure interferon preparations (such as that used in this study) were
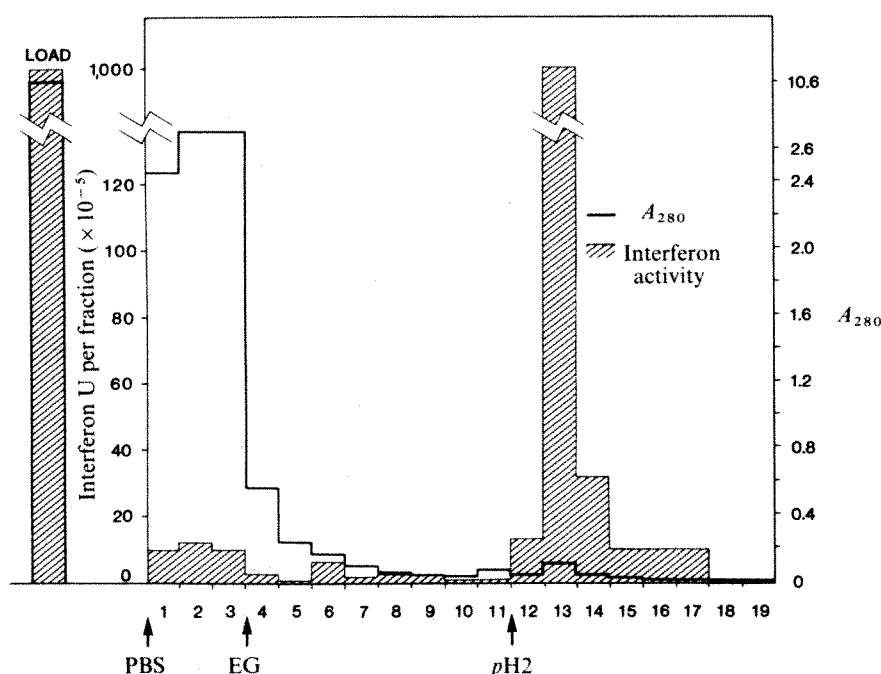
Fig. 3 Affinity chromatography of partially purified lymphoblastoid interferon. Lymphoblastoid interferon (10^8 U, 0.5 ml PBS, 1.9×10^7 U per mg) was loaded onto a 0.5 ml NK2-Sepharose column. Fractions of 0.5 ml were collected. The column was washed successively with PBS; 9 M ethane diol, 0.34 M NaCl and 0.0075 M Na phosphate buffer pH 7.4 (EG); 9 M ethane diol 0.3 M NaCl and 0.1 M citric acid (pH 2) as indicated. Fractions were assayed for interferon content and for protein content by measuring A_{280} and assuming an $A^{1\%}_{cm, 280}$ of 10 (see Table 1 legend).
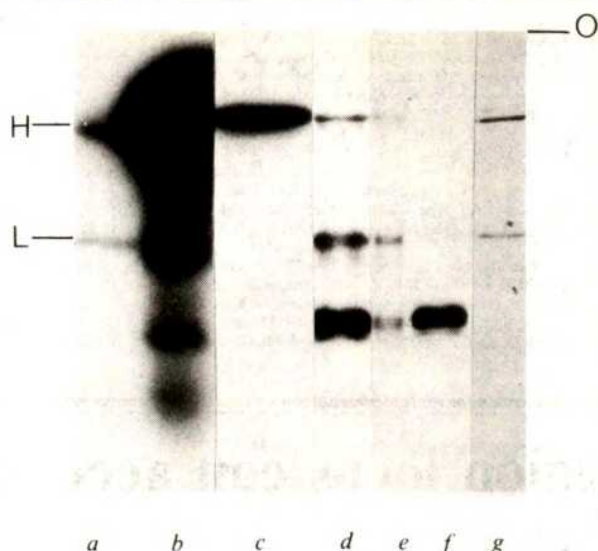
Fig. 4 Analysis of interferon samples described in the text. Interferon samples were iodinated using chloramine-T (ref. 33) (*b*, *c*) or the Bolton and Hunter reagent[34] (*d*, *e*, *f*). Aliquots were subjected to SDS-PAGE in reducing conditions[35] (14% acrylamide). The origin of migration in the separating gel is indicated (O). The mobilities of iodinated proteins (*b–f*) were compared with those of ^{14}C-labelled immunoglobulin heavy (H) and light (L) chains (MOPC 21 IgG: *a*, *g*), and unlabelled bovine serum albumin. After electrophoresis the gels were dried and autoradiographed at $-70\,^\circ$C for various times (2 h–4 days). The figure is a composite of five autoradiographs (a–b, c, d, e–f, g) of two gels (a–c, d–g) run in identical conditions (viz. mobilities of the marker proteins in tracks *a*, *g*). The iodinated samples were as follows: *c*, partially purified interferon used for immunization. The only band visible co-migrated with serum albumin; *b*, gross over-exposure of *c* to show minor bands at about 21,000, 18,000 and 16,000 MW; *d*, IF-A, that is, interferon iodinated after one passage through NK2–Sepharose column; *e*, ^{125}I-IF-A not retained on second passage through NK2–Sepharose; *f*, ^{125}I-IF-A retained on NK2–Sepharose and eluted at pH 2.

available for immunization of animals, and the antisera thus obtained were directed mainly against contaminants in the interferon preparations. Now that leukocyte and lymphoblastoid interferons have been purified to homogeneity[9,10], the purified interferon could be used as the immunogen to obtain antisera of higher specificity. However, the existing methods have not allowed the purification of sufficient interferon for immunization of domestic animals required for large-scale production of conventional antiserum. The monoclonal antibody technique should allow us to by-pass these problems, using low amounts of impure interferon to immunize small laboratory animals and, having selected a clone, to produce unlimited amounts of antibody of extremely high specificity and (presumably) high binding capacity. To prepare sufficient IgG for an immunoadsorbent column, NK2 cells were injected subcutaneously into BALB/c mice (10[7] cells per mouse) and when tumours had developed, serum samples were collected and pooled. IgG was purified from a pool of 18 ml of serum by ammonium sulphate precipitation and DEAE-ion exchange chromatography as previously described for other monoclonal mouse IgG[31]. Purified NK2 IgG (14 mg) was coupled to 1 ml of CNBr-activated Sepharose (Pharmacia) and tested as an immunoadsorbent. The results, shown in Fig. 3, demonstrate that in a single passage through a 0.5-ml column of NK2–Sepharose, a partially purified preparation of interferon (1.6×10^6 U per mg) was purified almost 100-fold further. (The activity and specific activity of the interferon used was as stated by the suppliers and was not independently measured.) Insufficient material was available for accurate

determinations of protein concentrations, and so, as an alternative approach to assessing the purity of the interferon after a single passage through the NK2–Sepharose column ('IF-A'), we radiolabelled an aliquot with ^{125}I and analysed it by SDS-PAGE (Fig. 4*d*). The autoradiograph of the gel showed a major band of MW about 18,000, with minor bands in the region of immunoglobulin heavy ($\sim 50,000$) and light ($\sim 22,000$) chains. The mobilities of the minor bands did not correspond exactly to those of the heavy and light chains of NK2 IgG and do not seem to be the result of NK2 IgG becoming detached from the Sepharose. A more likely possibility is that they are derived from the IgG produced by the lynphoblastoid (Namalwa) cells which might bind to the NK2 IgG on the column by nonspecific aggregation through the Fc. To show that the material retained on the column (IF-A) had indeed bound specifically to the NK2–Sepharose, we repurified ^{125}I-IF-A by a second passage through the same column. This time, the 18,000-MW band was specifically retained and eluted from the column, suggesting that at this stage the material was pure (Fig. 4*f*). An apparent MW of 17,500 or 18,000 for a leukocyte interferon component has been reported elsewhere[7,9,17].

As a more stringent test of the ability of the NK2–Sepharose to purify lymphoblastoid interferon, a crude sample of extracellular medium from stimulated Namalwa cells was applied to a 0.5-ml column. The results are shown in Table 1 and indicate a purification of about 5,000-fold in a single step. We have not investigated the purity of this material by SDS-PAGE but the specific activity is roughly the same as that of IF-A (1.2×10^8 U per mg).

Future prospects

The results described above clearly demonstrate that the monoclonal antibody produced by NK2 is a very useful reagent for human lymphoblastoid interferon purification. Because the antibody is the product of a transplantable tumour and can easily be purified from the serum of tumour-bearing mice, there is no limit to the amount of NK2 antibody that could be made without any further need for interferon as immunogen. Thus, the protocols described here could easily be scaled up for the large-scale purification of interferon. An important advantage of the monoclonal antibody is that this method of purification should be equally applicable to interferon from human leukocytes or indeed from any other source (such as *Escherichia coli*[32]) producing human interferon, provided it contains the NK2 antigenic determinant.

The recovery of interferon activity following iodination was quantitative and the ^{125}I-labelled interferon retained its biological activity after purification on NK2–Sepharose. Thus, it may be possible to use this material, in conjunction with the NK2 IgG, to develop a radioimmunoassay for interferon. Such an assay would greatly simplify the type of experiments described here as well as the purification of interferon and the analysis of interferon in biological fluids and in products of animal or bacterial cell cultures.

1. Köhler, G. & Milstein, C. *Nature* **256**, 495–497 (1975).
2. *Curr. Topics Microbiol. Immun.* **81** (1979).
3. Stewart, W. E. *The Interferon System* (Springer, New York, 1979).
4. Gresser, I. & Tovey, M. G. *Biochim. biophys. Acta* **516**, 231–247 (1978).
5. Cantell, K. & Hirvonen, S. *J. gen. Virol.* **39**, 541–543 (1978).
6. Cantell, K. *Interferon 1979*, 1–28 (Academic, London, 1980).
7. Bridgen, P. J. et al. *J. biol. Chem.* **252**, 6585–6587 (1977).
8. Knight, E. *Proc. natn. Acad. Sci. U.S.A.* **73**, 520–523 (1976).

9. Rubinstein, M. *et al. Proc. natn. Acad. Sci. U.S.A.* **76**, 640–644 (1979).
10. Zoon, K. C., Smith, M. E., Bridgen, P. J., Nedden, D. & Anfinsen, C. B. *Proc. natn. Acad. Sci. U.S.A.* **76**, 5601–5605 (1979).
11. Knight, E., Hunkapiller, M. W., Korant, B. D., Hardy, R. W. F. & Hood, L. E. *Science* **207**, 525–526 (1980).
12. Zoon, K. C. *et al. Science* **207**, 527–528 (1980).
13. Taira, H. *et al. Science* **207**, 528–530 (1980).
14. Mogensen, K. E., Pyhälä, L. & Cantell, K. *Acta path. microbiol. scand.* **B83**, 443–450 (1975).
15. Berg, K., Ogburn, C. A., Paucker, K., Mogensen, K. E. & Cantell, K. *J. Immun.* **114**, 640–644 (1975).
16. Berg, K. *Scand. J. Immun.* **6**, 77–86 (1977).
17. Havell, E. A., Yip, Y. K. & Vilcek, J. *J. gen. Virol.* **38**, 51–59 (1978).
18. Gresser, I. *Cell. Immun.* **34**, 406–415 (1977).
19. Johnson, H. M. & Baron, S. *Crit. Rev. Biochem.* **4**, 203–227 (1976).
20. Köhler, G. & Milstein, C. *Eur. J. Immun.* **6**, 511–519 (1976).
21. Sharon, J., Morrison, S. L. & Kabat, E. A. *Proc. natn. Acad. Sci. U.S.A.* **76**, 1420–1424 (1979).

22. Williams, A. F. in *Contemporary Topics in Molecular Immunology* Vol. 6 (eds Porter, R. R. & Ada, G. L.) 83–116 (Plenum, New York, 1977).
23. Cuello, A. C., Galfre, G. & Milstein, C. *Proc. natn. Acad. Sci. U.S.A.* **76**, 3532–3536 (1979).
24. Springer, T., Galfrè, G., Secher, D. S. & Milstein, C. *Eur. J. Immun.* **8**, 539–551 (1978).
25. Atkins, G. J., Johnston, M. D., Westmacott, L. M. & Burke, D. C. *J. gen. Virol.* **25**, 381–390 (1974).
26. Atherton, K. T. & Burke, D. C. *J. gen. Virol.* **29**, 297–304 (1975).
27. Cotton, R. G. H., Secher, D. S. & Milstein, C. *Eur. J. Immun.* **3**, 135–140 (1973).
28. Köhler, G., Howe, S. C. & Milstein, C. *Eur. J. Immun.* **6**, 292–295 (1976).
29. Herzenberg, L. A., Herzenberg, L. A. & Milstein, C. in *Handbook of Experimental Immunology* (ed. Weir, D. M.) 25.1–25.7 (Blackwell, Oxford, 1978).
30. Howard, J. C., Butcher, G. W., Galfrè, G., Milstein, C. & Milstein, C. P. *Immun. Rev.* **47**, 139–174 (1979).
31. Svasti, J. & Milstein, C. *Biochem. J.* **126**, 837–850 (1972).
32. Nagata, S. *et al. Nature* **284**, 316–320 (1980).
33. Jensenius, J. C. & Williams, A. F. *Eur. J. Immun.* **4**, 91–97 (1974).
34. Bolton, A. E. & Hunter, W. M. *Biochem. J.* **133**, 529–539 (1973).
35. Laemmli, U. K. & Favre, M. *J. molec. Biol.* **80**, 575–599 (1973).

Deletions in the constant region locus can account for switches in immunoglobulin heavy chain expression

Suzanne Cory, Jillian Jackson & Jerry M. Adams

The Walter and Eliza Hall Institute of Medical Research, Post Office, Royal Melbourne Hospital, Victoria 3050, Australia

Deletions spanning portions of the heavy chain constant region (C_H) locus in murine plasmacytomas are revealed by hybridization with cloned immunoglobulin DNA molecules. The pattern of deletions suggests that a lymphocyte clone switches expression of C_H genes by successive deletions and that the probable C_H gene order is $5'$ μ-$\gamma3$-$\gamma1$-$\gamma2b$-$\gamma2a$-$\alpha3'$.

THE immunoglobulin genes (reviewed in refs 1, 2) represent a unique system in which single polypeptide chains are encoded by more than one gene. An immunoglobulin molecule contains either κ or λ light chains and, in mice, one of eight types of heavy chain (μ, δ, α, $\gamma1$, $\gamma2a$, $\gamma2b$, $\gamma3$, ε), the heavy chain defining the immunoglobulin class (IgM, IgD, IgA, IgG1, IgG2a, IgG2b, IgG3, IgE). Chains of each type are composed of a constant (C) region and a region of variable sequence (V region) which mediates antigen binding. V and C regions are encoded separately in the germ line[3,4], and a functional immunoglobulin gene is generated within a lymphocyte clone by a recombination event[5] which associates a particular V and C gene[6]. This somatic rearrangement step, which is well documented for light chain genes[7–10], has recently been described for α and μ genes[11–13]. Rearrangement within the heavy chain locus is presumably more complex than that within the κ or λ loci, because the multiple V_H genes are shared by the different C_H genes[14], which occur in an unknown order within a tight cluster[15,16].

A fundamental puzzle posed by the immune system is that a lymphocyte clone can switch from expression of one class of immunoglobulin to another (for example, IgM to IgG1) while maintaining its V-region specificity[17–25]. This suggests that a single V_H region can associate sequentially with different C_H regions within the one cell lineage. Switching of C_H regions may be restricted to a single chromosome, because only one allele of a heavy chain gene is expressed in a given cell ('allelic exclusion')[26,27] and μ and δ chains in the same cell are derived from one chromosome[28]. Switching can be studied by comparing the DNA of different murine plasmacytomas, each of which synthesizes an immunoglobulin of a single class.

Several plausible models for heavy chain expression have been put forward (see refs 29, 30 for reviews). In one[31,32], variable splicing of a putative precursor RNA spanning the entire C_H locus generates different heavy chain mRNAs. This model now seems untenable as a general case, because the precursor RNAs seem to bear single C_H sequences[33]. In a second model[21,34], copies of a particular V_H region are inserted near each C_H gene. Evidence against this model is that two plasmacytomas have been shown not to have an increased copy number for the V_H gene they express[13]. In a third model[35], one V_H gene undergoes a series of shifts to associate it with different C_H genes. Finally, in the deletion model[36,37] (Fig. 1), the DNA between a particular V_H gene and the first C_H gene to be expressed is excised and subsequent C_H switching occurs by successive deletion of C_H genes and the intervening DNA. Deletions are not expected on any other model.

Recent evidence[9] implicates a deletion mechanism for association of the single V_λ and C_λ genes. Honjo and Kataoka[37] proposed earlier that C_H switching occurs by deletions confined to one of the two homologous chromosomes. Their kinetic hybridization $(C_0 t)$ analysis with uncloned cDNA probes suggested that the concentration of certain C_γ sequences in DNA of particular plasmacytomas was half that in DNA of non-lymphoid tissues. Their results were consistent with deletions operating on C_H genes arranged in the order (μ, $\gamma3$) $\gamma1$-$\gamma2b$-$\gamma2a$-α. Twofold differences are, however, just resolvable by kinetic hybridization and such results might be affected by probe impurities or cross-hybridization between different C_γ sequences.

We have recently used cloned μ and α cDNA probes[38] to establish that deletions are associated with rearrangement of heavy chain genes[13]. Several V_H genes were absent from one plasmacytoma, and C_μ sequences were either partially or totally deleted from seven IgG- or IgA-secreting plasmacytomas each of which retained the C_α gene. Those results stimulated us to examine different C_γ genes in the same tumours. We report here that C_γ genes undergo somatic rearrangement and that particular C_γ genes and flanking
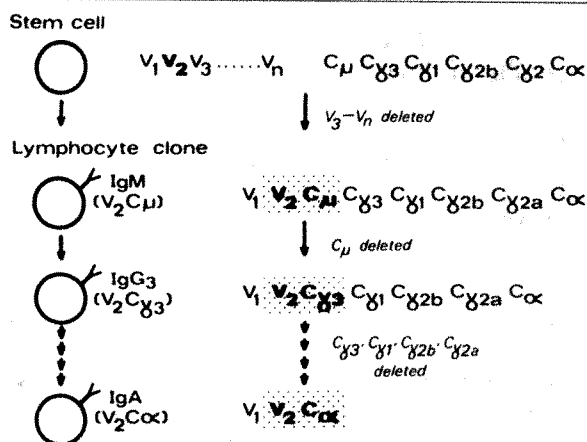
Fig. 1 Deletion model for somatic rearrangement of immunoglobulin heavy chain genes. The germ-line arrangement of V_H and C_H genes in a stem cell is compared with the corresponding arrangements postulated for a lymphocyte clone which synthesizes a μ heavy chain and then switches successively to synthesis of $\gamma 3$ and α chains, each type of heavy chain bearing the same V_H sequence (V_2). The functional $V_H C_H$ gene is shown bold. C_H genes are shown in the order favoured by the data presented in the text; the location of C_δ and C_ϵ is unknown. Embryo serves as a model of the germ line in the present study and various plasmacytomas represent lymphocytes at different stages of the switching process.

sequences have been deleted in certain plasmacytomas. The probable C_H gene order can be inferred from the deletions. The pattern of deletions is complex and cannot be accounted for by events confined to a single chromosome. Deletions extend close to rearranged, presumably active C_γ genes. The results strongly support a deletion model for switches in heavy chain expression. Immunoglobulin gene expression thus seems to be regulated by an unprecedented mechanism involving sequential excision of portions of the genetic material.

Each C_γ gene can be detected on a separate restriction fragment

We first established that we could score the four C_γ genes on restriction endonuclease fragments of mouse DNA. The probes were cloned cDNA molecules bearing $C_{\gamma 1}$, $C_{\gamma 3}$ and $C_{\gamma 2a}$ sequences[38], and for $C_{\gamma 1}$ and $C_{\gamma 3}$, cloned gene fragments (see below). We expected that the $C_{\gamma 2a}$ probe would detect the $C_{\gamma 2b}$ as well as $C_{\gamma 2a}$ gene, because the two $C_{\gamma 2}$ amino acid sequences exhibit homology[39,40] and their nucleotide sequences cross-hybridize[41]. We fractionated EcoRI endonuclease digests of embryo DNA by gel electrophoresis, blotted the fragments onto nitrocellulose filters[42] and revealed specific fragments by hybridization with ^{32}P-labelled probes. The $C_{\gamma 1}$ and $C_{\gamma 2b}$ genes lie in separate EcoRI fragments nearly 7 kilobase pairs long, neither of which contains another C_γ gene[43-46]. Figure 2A shows that, as expected, the $C_{\gamma 1}$ probe hybridized strongly to a ~7-kilobase fragment, as did the $C_{\gamma 2a}$ probe, presumably by cross-hybridization with the $C_{\gamma 2b}$ gene. The $C_{\gamma 2a}$ probe also strongly labelled a ~23-kilobase fragment and weakly labelled a ~19-kilobase fragment, whereas the $C_{\gamma 3}$ probe gave the opposite result. We conclude that the $C_{\gamma 2a}$ gene lies in the ~23-kilobase fragment and the $C_{\gamma 3}$ in the ~19-kilobase fragment. Partial cross-hybridization of $C_{\gamma 2a}$ and $C_{\gamma 3}$ sequences would be expected[41]. $C_{\gamma 2}$ and $C_{\gamma 1}$ sequences do not cross-hybridize significantly under our conditions, because the $C_{\gamma 1}$ probe did not label the ~23-kilobase $C_{\gamma 2a}$ fragment. To confirm this, we hybridized each probe to HindIII fragments of embryo DNA. The results (Fig. 2B) indicate that the $C_{\gamma 2a}$ probe barely hybridized to the fragment bearing the $C_{\gamma 1}$ gene, and that the $C_{\gamma 1}$ probe did not hybridize to fragments bearing the $C_{\gamma 2a}$ or $C_{\gamma 2b}$ genes. The pattern of cross-hybridization observed is in accord with results[41] from solution hybridization, and both the cross-hybridizations and the fragment sizes detected are entirely consistent with results from cloned C_γ sequences (refs 43–46 and J.M.A., E. Webb, S. Gerondakis and S.C., manuscript in preparation).

C_γ genes undergo somatic rearrangement

Because rearrangement of immunoglobulin genes seems to be a prerequisite for expression, we sought evidence of changes in context for C_γ genes by comparing restriction fragments bearing C_γ genes in plasmacytoma DNA with those in embryo. Figure 2C shows that $C_{\gamma 3}$ sequences in the IgG3 producer Y5606 (track b) occur in an EcoRI fragment not present in embryo (track a). This suggests that sequences surrounding the $C_{\gamma 3}$ gene have altered during development. Similarly, HindIII digests (Fig. 2D) revealed that $C_{\gamma 1}$ sequences in the IgG1 producer MOPC 21 (track c) occur in two fragments, each different in size from that in embryo (track a). The $C_{\gamma 1}$ gene is not cut by HindIII (track a and our unpublished results). Thus, there seem to be two types of rearranged $C_{\gamma 1}$ sequences in MOPC 21, as found previously for C_μ sequences in an IgM producer and for C_α in two IgA producers[13]. What the two $C_{\gamma 1}$ sequences represent is unclear; they apparently do not correspond to different alleles because our data suggest that MOPC 21 cells contain only one copy of the $C_{\gamma 1}$ gene (see below). Cellular heterogeneity could explain the two bands, if the sequence flanking the $C_{\gamma 1}$ gene underwent an additional alteration after the cloning of the
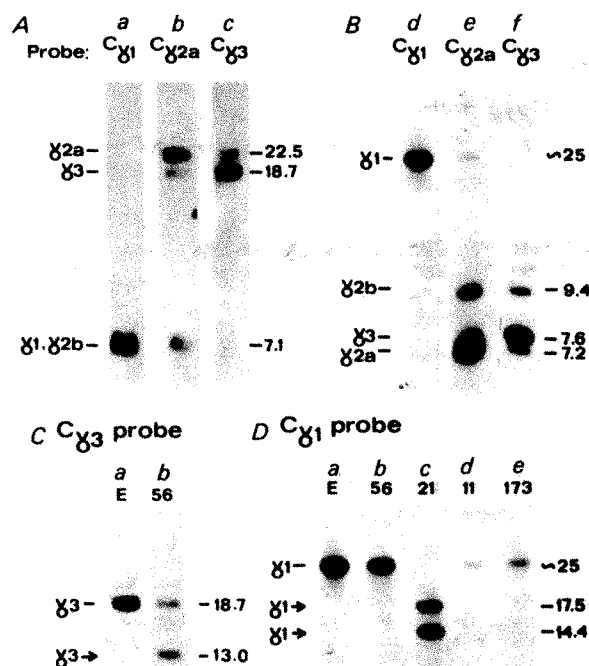
Fig. 2 Identification of restriction fragments bearing C_γ genes in germ-line context and after rearrangement. Restriction fragments (15 μg) of DNA from BALB/c embryos and plasmacytomas were fractionated by electrophoresis on 0.7 % agarose gels, blotted on to nitrocellulose filters[42] and then hybridized with ^{32}P-labelled nick-translated[57] probes as described previously[13]. Autoradiography was carried out at −70 °C with an intensifying screen[58]. A, EcoRI fragments of embryo DNA hybridized with cloned $C_{\gamma 1}$, $C_{\gamma 2a}$ and $C_{\gamma 3}$ probes as indicated. B, HindIII fragments of embryo DNA hybridized to a genomic $C_{\gamma 1}$ probe (track d) (fragment f in Fig. 4B), the $C_{\gamma 2a}$ cDNA probe (track e) and the $C_{\gamma 3}$ cDNA probe (track f). The $C_{\gamma 3}$ and $C_{\gamma 2a}$ fragments clearly resolved on a shorter exposure. C, $C_{\gamma 3}$-bearing EcoRI fragments of DNA from embryo (track a) and the IgG3 producer Y5606 (track b) detected with a genomic $C_{\gamma 3}$ probe (fragment b in Fig. 4A). The same pattern was obtained with the $C_{\gamma 3}$ cDNA probe. D, $C_{\gamma 1}$-bearing HindIII fragments of DNA from embryos (track a) and the IgG3 producer Y5606 (track b), the IgG1 producer MOPC 21 (track c) the IgG2b producer MPC 11 (track d), and the IgG2a producer MOPC 173 (track e), detected with a genomic $C_{\gamma 1}$ probe (fragment f in Fig. 4B). In C and D, fragments bearing rearranged $C_{\gamma 3}$ and $C_{\gamma 1}$ sequences are indicated by arrows. Fragment sizes are given in kilobases. The cloned cDNA sequences have been described in detail elsewhere[38]. The bottom of autoradiograms in this and subsequent figures are not shown because no smaller fragments were detected.
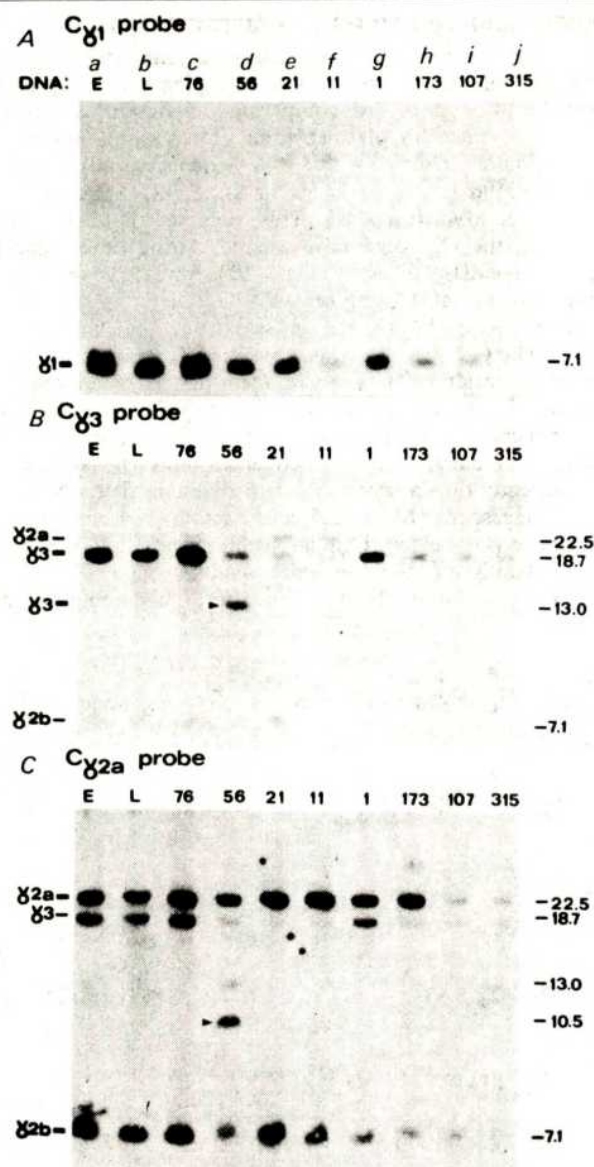
Fig. 3 Levels of C_γ sequences in embryo, liver and different plasmacytomas. The filters bore fractionated *Eco*RI digests of DNA (15 µg) from BALB/c embryos (track *a*), adult liver (track *b*) and the IgM producer HPC 76 (track *c*), the IgG3 producer Y5606 (track *d*), the IgG1 producer MOPC 21 (track *e*), the IgG2b producer MPC 11 (track *f*), the IgG2a producers HOPC 1 (track *g*) and MOPC 173 (track *h*), and the IgA producers S107 (track *i*) and MOPC 315 (track *j*). The probes were: *A*, a genomic $C_{\gamma 1}$ probe (fragment *d* in Fig. 4*B*); *B*, a genomic $C_{\gamma 3}$ probe (fragment *b* in Fig. 4*A*); *C*, a $C_{\gamma 2a}$ cDNA probe. Cloned $C_{\gamma 1}$ and $C_{\gamma 3}$ cDNA probes gave the same results as the genomic probes. Fragments bearing C_γ genes are indicated and their sizes given in kilobases. Rearranged sequences are indicated by arrows. We have not determined whether the rearranged fragment detected by the $C_{\gamma 2a}$ probe in Y5606 DNA corresponds to a $C_{\gamma 2a}$ or a $C_{\gamma 2b}$ sequence. References to the origin of the plasmacytomas are given elsewhere[13].

MOPC 21 (P3) cell line. The observation that a rearranged $C_{\gamma 1}$ gene was found only in the IgG1 producer (Fig. 2*D*) and a rearranged $C_{\gamma 3}$ gene only in the IgG$_3$ producer (see Fig. 3*B*) suggests that these changes are related to expression of those genes. We did not find evidence of a rearranged $C_{\gamma 2b}$ gene in the IgG$_{2b}$ producer MPC 11 or of a rearranged $C_{\gamma 2a}$ gene in the IgG2a producer MOPC 173, in either *Hind*III digests (not shown) or *Eco*RI digests (see Fig. 3*C*). We surmise that changes in those tumours occur beyond the nearest *Hind*III and *Eco*RI sites

C_γ genes are deleted in IgA- and IgG-producing plasmacytomas

We examined DNA from eight plasmacytomas for deletions involving C_γ genes by scoring *Eco*RI fragments with different C_γ probes (Fig. 3). Scanning across Fig. 3 reveals that the level of each C_γ gene in various plasmacytomas differs strikingly. For example, Fig. 3*A* shows that whereas $C_{\gamma 1}$ sequences are present in the IgM producer HPC 76 (track *c*) at about the same level as in embryo (track *a*) or liver (track *b*), the two IgA producers S107 and MOPC 315 (tracks *i* and *j*) contain extremely low levels and the IgG producers (tracks *d–h*) contain intermediate to very low levels. We can discount degradation as an explanation because each DNA preparation was of high molecular weight (>80 kilobases), and each digest yielded strong, well defined bands for the ~23-kilobase $C_{\gamma 2a}$ fragment (Fig. 3*C*) and/or for the C_α gene[13], as well as for V_H genes[13]. Moreover, deletions were also apparent in *Hind*III digests (Fig. 2*D*), as shown, for example, by the virtual absence of $C_{\gamma 1}$ sequences in the IgG2b producer MPC 11 (track *d*) and the IgG2a producer MOPC 173 (track *e*).

Comparing equivalent tracks in Fig. 3*A*, *B* and *C* allows assessment of the level of different C_γ genes in a particular tumour. It is clear that deletions in the IgA producers S107 (track *i*) and MOPC 315 (track *j*) involve all four C_γ genes. In contrast, only certain C_γ genes have been deleted from particular IgG producers. For example, the IgG1 producer MOPC 21 (track *e*) contains much lower levels of $C_{\gamma 3}$ sequences than of $C_{\gamma 1}$, $C_{\gamma 2a}$ or $C_{\gamma 2b}$.

We determined the copy number of each C_γ gene in the different plasmacytomas by densitometry of autoradiographs like those in Fig. 3. Because the same amount of DNA was loaded for each sample and hybridization was compared on the same filter, the autoradiographic signal is proportional to gene concentration[13,47]. Dividing the signal by that given for embryo DNA gives a measure of the copies per haploid genome, assuming a single copy per haploid genome in embryo DNA. This assumption has been validated for the C_μ gene[13] and probably also holds for each C_γ gene, because only one *Eco*RI or *Hind*III fragment of embryo DNA was detected for each C_γ gene. Table 1 presents values for the copies per haploid genome for each C_γ gene, for $C_{\gamma 1}$ and $C_{\gamma 3}$ flanking sequences described below, and for the C_α gene. We scored each C_H sequence in the different plasmacytomas at least twice and the quantitative results were reproducible. For example, scoring the $C_{\gamma 1}$ gene with a cDNA and a genomic probe gave nearly identical results (Table 1) and, in general, values from separate experiments agreed within 25%, except for very faint bands. We have shown elsewhere[13] that the very low levels of residual sequences detected in some lines probably result from a few per cent contamination of the transplanted tumours by non-lymphoid cells.

Deletions span large sequences on the 5' side of C_γ genes and extend close to active genes

It is important to establish whether the deletions include sequences between C_H genes. To permit studies with sequences flanking C_γ genes, we searched a library of clones bearing large fragments of mouse embryo DNA[48] and have identified a clone (G1.1) bearing a $C_{\gamma 1}$ sequence and another (G3.1) bearing a $C_{\gamma 3}$ gene (J.M.A., E. Webb, S. Gerondakis and S.C., manuscript in preparation). Their identity rests on the extent of hybridization with authenticated[38] $C_{\gamma 1}$, $C_{\gamma 2a}$ and $C_{\gamma 3}$ cDNA probes, on the absence of restriction sites characteristic of $C_{\gamma 2a}$ cDNA[38] and the $C_{\gamma 2b}$ gene[45,46], on an excellent correlation of the restriction map of G1.1 with those of two other $C_{\gamma 1}$-bearing clones[43,44] and on a good match between restriction sites within the $C_{\gamma 3}$ gene of G3.1 and sites[38] within γ3 cDNA. The diagrams in Fig. 4 show that G3.1 contains 8.6 kilobase of DNA on the 5' side of the $C_{\gamma 3}$ gene, with respect to its

Plasmacytoma	5' to $C_{\gamma3}$ probe a	$C_{\gamma3}$ gene cDNA	$C_{\gamma3}$ gene probe b	5' to $C_{\gamma1}$ probe c	5' to $C_{\gamma1}$ probe e	$C_{\gamma1}$ gene probe f	$C_{\gamma1}$ gene probe d	$C_{\gamma2b}$ gene cDNA	$C_{\gamma2a}$ gene cDNA	C_{α} gene cDNA
HPC 76 (IgM)	0.70	1.1	1.0	1.0	1.4	1.4	1.3	1.2	1.0	1.2 ± 0.2
Y5606 (IgG3)	0.04	0.12 *0.14‡*	0.12 *0.17‡*	0.48	0.51	0.41	0.42	0.20 *0.16¶*	0.53	0.9 ± 0.3
MOPC 21 (IgG1)	<0.01†	0.05	0.04	0.06 *0.05§* *0.01**	0.45‖	0.31	0.38	1.1	1.3	1.6 ± 0.1
MPC 11 (IgG2b)	0.02	0.03	0.02	0.05	0.04	0.03	0.05	0.25	1.1	1.2 ± 0.3
MOPC 173 (IgG2a)	0.04	0.08	0.09	0.12	0.09	0.07	0.10	0.07	0.74	1.0 ± 0.4
HOPC 1 (IgG2a)	0.15	0.31	0.39	0.42	0.39	0.32	0.32	0.11	0.52	0.8 ± 0.2
S107 (IgA)	0.03	0.05	0.05	0.09	0.09	0.06	0.08	0.07	0.08	1.0 ± 0.3
MOPC 315 (IgA)	0.02	0.04	0.06	0.08	0.06	0.05	0.04	0.04	0.06	0.8 ± 0.2

Table 1 Quantification* of C_H genes and flanking sequences in DNA from different plasmacytomas

DNA was isolated[13] from plasmacytomas (fully referenced elsewhere[13]) grown as subcutaneous tumours except where otherwise indicated. Probe a was the embryonic sequence extending 8.6 kilobases from the $C_{\gamma3}$ gene (fragment a in Fig. 4A); the results are the average of three experiments. The cDNA probe for the $C_{\gamma3}$ gene was a 0.53-kilobase *Hinf* fragment isolated by polyacrylamide gel electrophoresis from the cDNA insert of plasmid pY5606γ3.15 (ref. 38). Probe b was the 4.8-kilobase *Bam*HI/*Hind*III fragment from G3.1 (fragment b in Fig. 4A). Probe c was the 10-kilobase *Hind*III/*Eco*RI fragment from G1.1 (fragment c in Fig. 4B); the results are the average of two experiments. Probe e was the 2.8-kilobase *Eco*RI/*Bgl*II fragment from G1.1 (fragment e in Fig. 4B) obtained from the subclone pG1.1R. Probe f was the 1.4-kilobase *Bgl*II/*Eco*RI* fragment from G1.1 (fragment f in Fig. 4B), obtained from the subclone pG1.1R. Probe d was the 5-kilobase *Eco*RI/*Eco*RI* fragment from G1.1 (fragment d in Fig. 4B), which had been subcloned into pBR322 (plasmid pG1.1R). The cDNA probes for the $C_{\gamma2b}$ and $C_{\gamma2a}$ genes were 0.42- and 0.29-kilobase $C_{\gamma2a}$ fragments from the cDNA plasmid pM173γ2a.15 (ref. 38); results are the average of two experiments. The cDNA probes for the C_α gene were fragments from the cDNA plasmid pS107α.4 (ref. 38); results are the average of six experiments, including determinations made previously[13], and the standard deviation is given. Variation between experiments was greater than for C_γ fragments, perhaps due to the smaller size of the 3' C_α-bearing *Eco*RI fragment (4.7 kilobases) (ref. 13). The $C_{\gamma2b}$ gene was detected by cross-hybridization to $C_{\gamma2a}$ probes (see text).

*Results are expressed as copies per haploid mouse genome, assuming one copy of each C_H gene in the germ line. Intensities of bands on autoradiographs were measured using a Canalco model J microdensitometer. For each probe, DNAs were compared on the same filter and the values from each related to that in embryo DNA. Where more than one fragment was detected in a particular DNA, the values are listed in order of decreasing fragment size. Values for rearranged sequences are italicized.

†DNA was isolated from MOPC 21 cells (P3 clone[56]) grown in tissue culture. Equivalent experiments with DNA from the P3 line grown as subcutaneous tumours gave 0.022 ± 0.004 copies, which presumably indicates about 2% contamination of that preparation by DNA from non-lymphoid cells.

‡The 13.0-kilobase fragment in track d, Fig. 3B.

§The 7.4-kilobase fragment in track e, Fig. 4B. As this fragment contains about 5% of the label in embryo DNA, if it corresponds to one gene equivalent of the sequence in a tetraploid cell (see text), it bears $4 \times 5\% = 20\%$ of the sequences in one equivalent of the 10-kilobase fragment, or 2 kilobases of the sequences.

* A 4.6-kilobase fragment in track e, Fig. 4B, visible on longer exposures.

‖DNA was isolated from MOPC 21 cells (P3 clone[56]) grown in tissue culture.

¶The 10.5-kilobase fragment in track d, Fig. 3C, arbitrarily nominated as bearing γ2b rather than γ2a sequences.

transcription, whereas G1.1 contains 13.2 kilobases on the 5' side of the $C_{\gamma1}$ gene. Neither cloned sequence contains another C_γ gene or the C_μ or C_α genes (our unpublished results).

Using fragments from the cloned embryonic sequences as probes, we scored plasmacytoma DNAs for specific regions flanking the $C_{\gamma3}$ and $C_{\gamma1}$ genes. One probe, fragment a in Fig. 4, extends 8.6 kilobases from the $C_{\gamma3}$ gene on its 5' side. Figure 4A shows that the level of this sequence was comparable in embryo, liver and the IgM secretor HPC 76 (tracks a–c) but markedly reduced in all the other plasmacytomas, and the data in Table 1 confirm this. As the pattern of deletions was generally the same as that of the $C_{\gamma3}$ gene (Fig. 3B), we conclude that deletions involving the $C_{\gamma3}$ gene extend at least 8.6 kilobases on the 5' side of the gene. Significantly, the embryonic sequence was virtually absent from the IgG3 producer Y5606 (track d, Fig. 4A and Table 1). Hence, the deletion extends close to the $C_{\gamma3}$ gene in Y5606. Other data (S.C. and J.M.A., manuscript in preparation) suggest that the deletion stops about 2 kilobases from the $C_{\gamma3}$ gene, as indicated by the broken line at the top of Fig. 4A.

Certain deletions also involved embryonic sequences flanking the $C_{\gamma1}$ gene. Figure 4B shows that the sequences lying between 3.2 and 13.2 kilobases on the 5' side of the $C_{\gamma1}$ gene (fragment c) were deleted in several of the tumours and the deletions generally paralleled those of the $C_{\gamma1}$ gene. Deletions involving the $C_{\gamma1}$ gene must therefore extend to at least 13 kilobases on the 5' side of the gene. Significantly, very little of this sequence remained in MOPC 21 DNA, whereas the sequence lying between 0.4 and 3.2 kilobases on the 5' side of the $C_{\gamma1}$ gene (fragment e in Fig. 4B) was present in MOPC 21 at a level comparable with that of the $C_{\gamma1}$ gene (Table 1). Hence, as indicated by the broken line in Fig. 4B, the deletion in MOPC 21 must stop slightly to the left of the *Eco*RI site separating fragments c and e. If so, a new *Eco*RI fragment which hybridizes weakly with fragment c should have been generated in MOPC 21 DNA by the deletion. Such a fragment is indicated by an arrow in Fig. 4B (track e). From the extent of its labelling, we calculate that this fragment contains about

2 kilobases of the sequences in fragment c (see footnote §, Table 1). Hence, if this residual sequence lies adjacent to the *Eco*RI site, which is 3.2 kilobases from the $C_{\gamma1}$ gene, the deletion must extend to within about $3.2 + 2.0 = 5.2$ kilobases of the gene.

Although the deletion model predicts excision of sequences on the 5' side of an active C_H gene (Fig. 1), other models [21,35] postulate insertion of a V_H gene into that region. In multicopy insertion[21], for example, a V_H gene would be inserted on the 5' side of each C_H gene in every plasmacytoma. Such insertions should alter the size of fragments revealed with a flanking region probe. Except for the weakly labelled MOPC 21 fragments in Fig. 4B, no fragments of altered size were detected in any plasmacytoma DNA with fragments a, c or e as probes. Hence, the results in Fig. 4 strongly support the deletion model but not the other models.

Deletions are frequently not confined to single alleles of C_γ genes

As plasmacytomas are near tetraploid[49], we can estimate the number of copies of each C_H gene per cell by multiplying the values in Table 1 by 4. Most plasmacytomas are actually hypotetraploid, however, and the chromosome number varies somewhat in different lines[49]. The lines examined here seem to retain at least three and probably four copies of the C_H-bearing locus, because the level of C_α sequences in each line was at least 0.8 times that in embryo (Table 1). To compensate for any variation between lines in ploidy and therefore in the ratio of C_H-bearing to total chromosomes, it seems useful to relate the values for each C_H gene to that of C_α. Figure 5 thus displays the values from Table 1 for the copy numbers of C_γ genes, as well as values[13] for the C_μ gene, normalized to 4.0 copies of the C_α gene per cell. We have estimated the probable level of sequences derived from non-lymphoid cells contaminating the transplanted tumours (ref. 13 and Fig. 5 legend) and the filled portions of the bars represent our estimates for the gene copy numbers actually in plasmacytoma
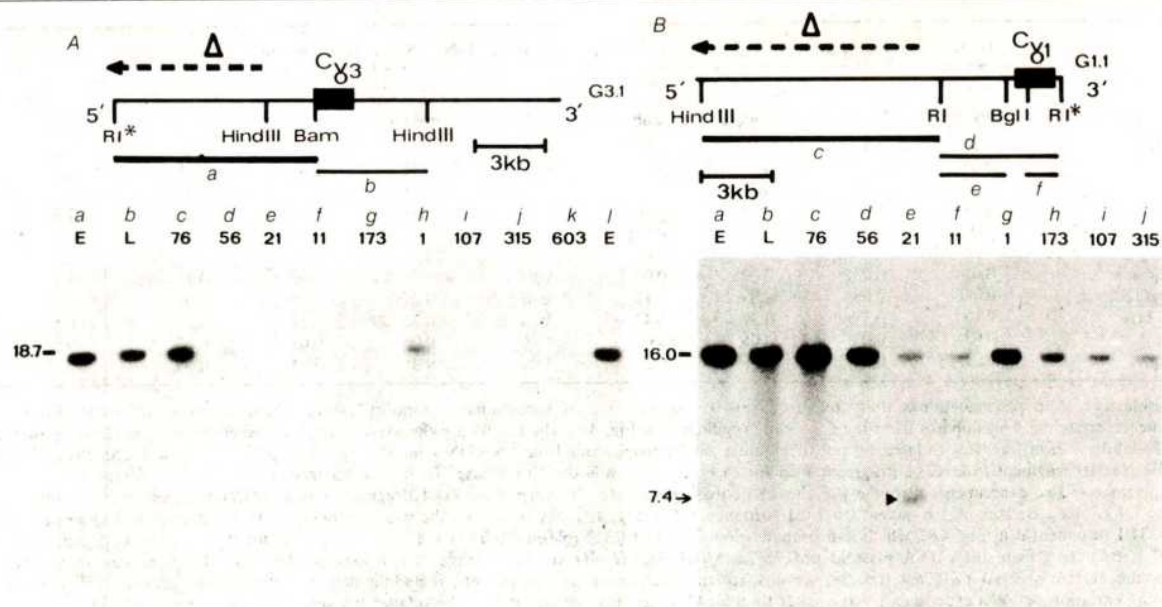
Fig. 4 Levels of embryonic sequences flanking $C_{\gamma3}$ and $C_{\gamma1}$ genes in embryo, liver and different plasmacytomas. Detailed maps of clones G3.1 and G1.1 and evidence on the position and orientation of the C_γ genes will be reported elsewhere. Only those restriction sites relevant to the isolation of fragments used in this study are indicated; 'RI' indicates an *Eco*RI site present in mouse DNA and 'RI*' an *Eco*RI site generated by the cloning technique[48]. The broken lines indicate sequences deleted ($\triangle$) in two plasmacytomas (see text). The orientation refers to the direction of transcription of the C_γ gene. *A*, Sequences detected with fragment *a* from G3.1. The filters contained fractionated *Eco*RI digests of DNA (15 µg) from BALB/c embryos (track *a* and *l*), adult liver (track *b*) and plasmacytomas HPC 76 (track *c*), Y5606 (track *d*), MOPC 21 (track *e*), MPC 11 (track *f*), MOPC 173 (track *g*), HOPC 1 (track *h*), S107 (track *i*), MOPC 315 (track *j*) and the IgA producer McPC 603 (track *k*). *B*, Sequences detected with fragment *c* from G1.1. The filter contained *Eco*RI digests of DNA from embryo (track *a*), adult liver (track *b*) and plasmacytomas HPC 76 (track *c*), Y5606 (track *d*), MOPC 21 (track *e*), MPC 11 (track *f*), HOPC 1 (track *g*), MOPC 173 (track *h*), S107 (track *i*) and MOPC 315 (track *j*). A 16-kilobase (kb) fragment is detected because that is the distance to the next *Eco*RI site to the left of that shown in the cloned sequence. A fragment (7.4 kilobases) bearing rearranged sequences is indicated by an arrow; two other weakly labelled fragments of 11.3 and 4.6 kilobases were also visible on longer exposures.

DNA. The reproducibility of different experiments leads us to conclude that our results can distinguish between 0 and 1, 1 and 2, or 2 and 4 copies of a C_H gene but probably not between 3 and 4 copies.

If deletions occurred on only one chromosome in a diploid lymphocyte, the subsequent chromosome doubling in the plasmacytomas would leave either two or four copies per cell for each C_H gene. Figure 5 shows that this is usually not the case. For example, it seems clear that all copies of the $C_{\gamma2b}$ gene must be deleted from MOPC 173, HOPC 1, S107 and MOPC 315. We conclude that deletions are frequently not confined to one allele of C_H genes. On the other hand, deletion of both alleles cannot be obligatory, as the IgG2a producer HOPC 1 retains substantial amounts of the C_μ, $C_{\gamma3}$ and $C_{\gamma1}$ genes and MPC 11 retains two copies of the C_μ gene. It seems significant that the C_μ genes remaining in both these lines have an alteration in the C_μ 5'-flanking sequence concerned with C_H switching (ref. 13 and our unpublished results).

Probable C_H gene order is μ-γ3-γ1-γ2b-γ2a-α

The deletions provide evidence on the C_H gene order, independent of any conclusions regarding switching. The rationale is that if two or more genes are deleted from the DNA of any plasmacytoma line, they are taken to be linked, the assumption being that this results from a single deletion rather than two independent ones. Thus, the virtual absence of C_μ and all C_γ sequences from the two IgA producers strongly suggests that the C_α gene lies to one side of the locus. Similarly, the absence of genes other than $C_{\gamma2a}$ and C_α in the IgG2a producer MOPC 173 strongly suggests that $C_{\gamma2a}$ and C_α are coupled, leading to the order $(\mu, \gamma3, \gamma1, \gamma2b)\gamma2a$-$\alpha$. The absence of $C_{\gamma3}$ and $C_{\gamma1}$ genes from MPC 11 DNA argues that they are coupled, and linkage of C_μ and $C_{\gamma3}$ is inferred similarly from their absence from MOPC 21, giving the order μ-γ3-γ1 and $(\mu$-γ3-γ1, γ2b)γ2a-α for the locus. Finally, the high levels of γ2b and γ2a sequences in MOPC 21 suggests that those genes are coupled, yielding the order μ-γ3-γ1-γ2b-γ2a-α.

Thus, we infer a unique, self-consistent gene order from the deletions, although physical linkage data is required to establish the order firmly. Some support for the linkage γ2b-γ2a is provided by a variant of the IgG2b producer MPC 11, which produces heavy chains bearing both γ2b and γ2a sequences[40].

This map does not indicate the orientation of the genes, that is, which strand is transcribed as mRNA. However, the deletions of the $C_{\gamma1}$ and $C_{\gamma3}$ 5'-flanking sequences in MOPC 21 and Y5606, respectively, indicate that those sequences map as follows: μ-5'γ3-γ3-5'γ1-γ1-γ2b-γ2a-α. If we assume that the other C_H genes have the same orientation, the orientation of the locus becomes 5' μ-γ3-γ1-γ2b-γ2a-α 3'.

Deletions can account for rearrangement of heavy chain genes

The deletion model postulates excision of all DNA between expressed V_H and C_H genes (Fig. 1). As heavy chain expression is confined to one allele, Honjo and Kataoka[37] postulated that deletions were confined to the chromosome(s) from which the expressed heavy chain is derived. In a tetraploid cell, two of the four homologous chromosomes could be active. Hence, the levels of C_H genes predicted in different plasmacytomas on the allelic deletion model[37] are as indicated by the dashed lines in Fig. 5. Our data clearly do not support that specific model, because many of the deletions seem to involve all four copies of the genes lying on the 5' side of the expressed gene. The results are, however, compatible with a more general model in which deletions are not necessarily confined to one allele. The critical requirement is that no C_H gene on the 5' side of the expressed C_H gene is retained on an active chromosome. The results from five lines are entirely compatible with such a model, as no deletions are predicted for the IgM producer HPC 76 and all four copies of the genes lying 5' to the expressed gene have been deleted in MOPC 21, MOPC 173, S107 and MOPC 315, and possibly also in Y5606. In MPC 11 at least two copies, and in HOPC 1 at least one copy, of each

gene on the 5' side of the expressed gene are apparently deleted, so those results are not inconsistent with the model.

The gene levels in all except two of the lines show a 'step' or 'staircase' pattern. Such patterns would be expected on the deletion model (Fig. 1), if deletions extend into the C_H locus for variable distances on different homologous chromosomes. The results for HOPC 1 and MPC 11, however, require deletions entirely within the C_H locus, because these lines retain higher levels of C_μ sequences than of subsequent genes. These complex patterns suggest that some deletions have occurred after the transition to tetraploidy, perhaps as an aberration of the normal rearrangement process.

Biological implications of the deletion model

Thus, our results provide strong support for a deletion model for C_H switching. Each IgG- and IgA-secreting plasmacytoma examined, but not an IgM producer, contained deletions involving one or more C_H genes. Loss of chromosomes bearing the C_H locus, or gross alterations of them, would not generate these effects because the deletions do not include the C_α gene and hence must be confined to a very narrow region in genetic terms. It seems unlikely that the deletions are merely a consequence of neoplasia, because a similar analysis of four T- and four B-lymphoid tumour cell lines, as well as a myeloid cell line, has revealed that neither the C_μ gene nor the C_α gene, nor a sequence 5' to the $C_{\gamma3}$ gene have been deleted (S.C., unpublished results). The deletions seem to span sizeable segments of the C_H locus, because they often include more than one C_H gene and, at least for $C_{\gamma1}$ and $C_{\gamma3}$, large sequences on the 5' side of the genes as well. An IgG1

Fig. 5 Number of C_μ, $C_{\gamma3}$, $C_{\gamma1}$, $C_{\gamma2b}$ and $C_{\gamma2a}$ genes per cell in plasmacytomas synthesizing different classes of immunoglobulin. The copy number of each C_γ gene per tetraploid cell was calculated by multiplying the mean value per haploid genome (Table 1) by 4 and then normalizing to 4.0 copies of the C_α gene per cell (see text). Values for C_μ were determined previously[13]. Because the plasmacytomas were grown as subcutaneous tumours, they are contaminated by non-lymphoid cells[13]. We estimated the levels of C_H sequences contributed by such cells as follows. In MOPC 21 DNA, C_μ and C_γ sequences were undetectable in cells grown in continuous culture[13], so the level of these sequences in MOPC 21 DNA prepared from solid tumours is a measure of C_H sequences contributed by non-lymphoid cells and was subtracted from values obtained for each of the other C_H genes. Similarly, wherever any C_H gene occurred at <0.3 copies per cell (Table 1), we took that as a measure of contamination. In the case of MPC 11, we assumed that the 0.2 copies per cell of C_μ sequences present in embryonic context[13] were derived entirely from non-lymphoid DNA. The filled portions of the bars represent the values normalized after allowing for contamination and the entire bars the normalized values ignoring contamination.

producer (MOPC 21) contains a deletion which extends relatively near the $C_{\gamma1}$ gene, and an IgG3 producer (Y5606) contains one extending close to the $C_{\gamma3}$ gene. As these lines retain only one copy of the active genes (Table 1), we suggest that the deletions constitute an integral part of the somatic rearrangement process which forms an expressed VC gene.

The evidence for simultaneous expression on the surface of B lymphocytes of more than one class of immunoglobulin, primarily IgM and IgD[28], seems to conflict with the deletion model, because the receptors are apparently synthesized continually[50] and both μ and δ chains seem to be derived from the same chromosome[28]. As B lymphocytes do not divide actively[51], however, the conflict may be resolved by longevity of immunoglobulin mRNA. More probably, μ and δ expression represents a special case in which RNA splicing[31,32] generates both μ and δ mRNAs from a single transcript. Any double producers of other types could be accounted for by a deletion bringing two C_H genes into proximity and creating a single transcriptional unit.

Our results add to the growing evidence[13,52,53] that somatic rearrangement events in plasmacytomas are frequently not confined to single alleles. This raises two interesting possibilities (see also ref. 13). First, that rearrangement on one homologous chromosome generates a correct VC join while that on the other occurs in a non-functional fashion, thereby providing a mechanism for allelic exclusion. Second, that correct VC joins are made on both chromosomes and that expression is restricted by some other means.

The deletion model makes strong predictions regarding changes in heavy chain expression during ontogeny of a lymphocyte clone. First, the switching of C_H regions would be irreversible. If a clone had switched, for example, from μ to α expression (IgM to IgA), it could not revert to μ expression, once μ mRNA had been degraded. (Conceivably, the homologous chromosome could be activated, but a special mechanism would be required to ensure activation of the equivalent V_H gene.) Second, the order of expression would be tied to the gene order. Whereas any given clone might not express the whole gamut of C_H genes, those genes that were expressed could only be expressed in the sequence defined by the C_H order.

Since submission of this article, we have learned of observations by Rabbits et al.[54], Coleclough et al.[55] and Yaoita and Honjo[59] leading to conclusions similar to those reached here.

1. Gally, J. A. in *The Antigens* Vol. 1 (ed. Sela, M.) 162–298 (Academic, New York, 1973).
2. Williamson, A. *A. Rev. Biochem.* **45,** 467–500 (1976).
3. Dreyer, W. J. & Bennett, J. L. *Proc. natn. Acad. Sci. U.S.A.* **54,** 864–869 (1965).
4. Hozumi, N. & Tonegawa, S. *Proc. natn. Acad. Sci. U.S.A.* **73,** 3628–3632 (1976).
5. Gally, J. A. & Edelman, G. M. *A. Rev. Genet.* **6,** 1–46 (1972).
6. Tonegawa, S., Hozumi, N., Matthyssens, G. & Schüller, R. *Cold Spring Harb. Symp. quant. Biol.* **41,** 877–889 (1976).
7. Bernard, O., Hozumi, N. & Tonegawa, S. *Cell* **15,** 1133–1144 (1978).
8. Max, E. E., Seidman, J. G. & Leder, P. *Proc. natn. Acad. Sci. U.S.A.* **76,** 3450–3454 (1979).
9. Sakano, H., Hüppi, K., Heinrich, G. & Tonegawa, S. *Nature* **280,** 288–294 (1979).
10. Seidman, J. G. & Leder, P. *Nature* **276,** 790–795 (1978).
11. Early, P. W., David, M. M., Kaback, D. B., Davidson, N. & Hood, L. *Proc. natn. Acad. Sci. U.S.A.* **76,** 857–861 (1979).
12. Gough, N. M., Kemp, D. J., Tyler, B. M., Adams, J. M. & Cory, S. *Proc. natn. Acad. Sci. U.S.A.* **76,** 554–558 (1980).
13. Cory, S. & Adams, J. M. *Cell* **19,** 37–51 (1980).
14. Weigert, M., Potter, M. & Sachs, D. *Immunogenetics* **1,** 511–523 (1975).
15. Herzenberg, L. A., McDevitt, H. O. & Herzenberg, L. A. *A. Rev. Genet.* **2,** 209–244 (1968).
16. Mage, R., Lieberman, R., Potter, M. & Terry, W. D. In *The Antigens* Vol. 1 (ed. Sela, M.) 299–376 (Academic, New York, 1973).
17. Nossal, G. J. V., Warner, N. & Lewis, H. *Cell. Immun.* **2,** 41–53 (1971).
18. Gearhart, P. J., Sigal, N. H. & Klinman, N. R. *Proc. natn. Acad. Sci. U.S.A.* **72,** 1707–1711 (1975).
19. Fu, S. M., Winchester, R. J. & Kunkel, H. G. *J. Immun.* **114,** 250–252 (1975).
20. Goding, J. W. & Layton, J. E. *J. exp. Med.* **144,** 852–857 (1976).
21. Sledge, C., Fair, D. S., Black, B., Krueger, R. G. & Hood, L. *Proc. natn. Acad. Sci. U.S.A.* **73,** 923–927 (1976).
22. Wang, A-C., Wang, I. Y. & Fudenberg, H. H. *J. biol. Chem.* **252,** 7192–7199 (1977).

23. Bleux, C., Ventura, M. & Liacopoulos, P. *Nature* **267**, 709–711 (1977).
24. Abney, E. R., Cooper, M. D., Kearney, J. F., Lawton, A. R. & Parkhouse, R. M. E. *J. Immun.* **120**, 2041–2049 (1978).
25. Kincade, P. W., Lawton, A. R., Bockman, D. E. & Cooper, M. D. *Proc. natn. Acad. Sci. U.S.A.* **67**, 1918–1925 (1970).
26. Pernis, B., Chiappino, G., Keus, A. S. & Gell, P. G. H. *J. exp. Med.* **122**, 853–875 (1965).
27. Cebra, J. J., Colberg, J. E. & Dray, S. *J. exp. Med.* **123**, 547–558 (1966).
28. Herzenberg, L. A. *et al. Cold Spring Harb. Symp. quant. Biol.* **16**, 33–45 (1976).
29. Hood, L., Kronenberg, M., Early, P. & Johnson, N. *ICN-UCLA Symp. molec. cell. Biol.* **6**, 1–27 (1977).
30. Williamson, A. R. & Fitzmaurice, L. C. in *The Generation of Antibody Diversity. A New Look* (ed Cunningham, A. J.) 183–211 (Academic, London, 1976).
31. Rabbitts, T. H. *Nature* **275**, 291–296 (1978).
32. Tonegawa, S., Maxam, A. M., Tizard, R., Bernard, O. & Gilbert, W. *Proc. natn. Acad. Sci. U.S.A.* **74**, 4406–4410 (1978).
33. Marcu, K. B., Schibler, U. & Perry, R. P. *Science* **204**, 1087–1088 (1979).
34. Dreyer, W. J., Gray, W. R. & Hood, L. *Cold Spring Harb. Symp. quant. Biol.* **32**, 353–368 (1967).
35. Galley, J. A. & Edelman, G. M. *Nature* **227**, 341–348 (1970).
36. Kabat, D. *Science* **175**, 134–140 (1972).
37. Honjo, T. & Kataoka, T. *Proc. natn. Acad. Sci. U.S.A.* **75**, 2140–2144 (1978).
38. Adams, J. M., Gough, N. M., Webb, E. & Cory, S. *Biochemistry* (in the press).
39. Dayhoff, M. O. (ed.) *Atlas of Protein Sequence and Structure* **5** Suppl. 3, 227 (1978).
40. Birshtein, B. K., Campbell, R. & Greenberg, M. L. *Biochemistry* (in the press).
41. Yamawaki-Kataoka, Y. *et al. Biochemistry* **18**, 490–497 (1979).
42. Southern, E. M. *J. molec. Biol.* **98**, 503–517 (1975).
43. Sakano, H. *et al. Nature* **277**, 627–632 (1979).
44. Honjo, T. *et al. Cell* **18**, 559–568 (1979).
45. Kataoka, T., Yamawaki-Kataoka, Y., Yamagishi, H. & Honjo, T. *Proc. natn. Acad. Sci. U.S.A.* **76**, 4240–4244 (1979).
46. Tucker, P. W., Marcu, K. B., Newell, M., Richards, J. & Blattner, F. R. *Science* **206**, 1303–1306.
47. Lis, J., Prestidge, L. & Hogness, D. S. *Cell* **14**, 901–919 (1978).
48. Kemp, D. J., Cory, S. & Adams, J. M. *Proc. natn. Acad. Sci. U.S.A.* **76**, 4627–4631 (1979).
49. Yoshida, T. H., Imai, H. T. & Potter, M. *J. natn. Cancer Inst.* **41**, 1083–1098 (1968).
50. Ferrarini, M., Corte, G., Viale, G., Durante, M. L. & Bargellesi, A. *Eur. J. Immun.* **6**, 372–380 (1976).
51. Sprent, J. & Miller, J. F. A. P. *Eur. J. Immun.* **2**, 384–387 (1972).
52. Lenhard-Schuller, R., Hohn, B., Brack, C., Hirama, M. & Tonegawa, S. *Proc. natn. Acad. Sci. U.S.A.* **75**, 4709–4713 (1978).
53. Steinmetz, M., Zachau, H. G. & Mach, B. *Nucleic Acids Res.* **6**, 3213–3229 (1979).
54. Rabbitts, T. H., Forster, A., Dunnick, W. & Bentley, D. L. *Nature* **283**, 351–356 (1980).
55. Coleclough, C., Cooper, D. & Perry, R. P. *Proc. natn. Acad. Sci. U.S.A.* (in the press).
56. Horibata, K. & Harris, A. *Expl Cell Res.* **60**, 61–77 (1970).
57. Rigby, P. J., Dieckmann, M., Rhodes, C. & Berg, P. *J. molec. Biol.* **113**, 237–251 (1977).
58. Laskey, R. A. & Mills, A. D. *FEBS Lett.* **82**, 314–316 (1977).

Expression of cloned β-endorphin gene sequences by *Escherichia coli*

John Shine*, Ivy Fettes†, Nancy C. Y. Lan†, James L. Roberts‡ & John D. Baxter†§

*Molecular Biology Unit, Research School of Biological Sciences, Australian National University, Canberra, Australia
†Howard Hughes Medical Institute Laboratories, Departments of Medicine and Biochemistry and Biophysics, and the Metabolic Research Unit, University of California, San Francisco, California 94143
‡Department of Biochemistry, Columbia University, College of Physicians and Surgeons, New York, New York 10032

DNA coding for the opiate peptide β-endorphin has been cloned into bacterial plasmids in such a way as to direct the synthesis of a hybrid β-galactosidase/β-endorphin protein. This hybrid protein can readily be cleaved in vitro to release biologically active β-endorphin.

THERE are two basic approaches to the programmed expression of mammalian gene sequences in bacteria. In one, the cloned mammalian coding sequences are spliced into the bacterial gene such that the bacterial initiation codon is followed directly by the codon for the first amino acid of the mammalian protein[1]. In the other, the coding sequence is inserted into an internal position in a bacterial gene so that the sequences are in phase with the bacterial coding sequences, which results in the synthesis of a hybrid bacterial–mammalian protein, from which the mammalian protein has to be released[2–8]. Although release can be a problem, there may be several advantages to the hybrid protein approach. First, it minimizes the chances of a disturbance of the mRNA secondary structure in the region of the normal ribosome binding site and initiation codon, causing a reduced rate of initiation of protein synthesis. Second, degradation of the mammalian protein in the bacterium may be reduced when it is fused. These factors may increase the yield of the mammalian protein. Third, construction of plasmids for synthesis of a hybrid protein is ordinarily simpler than for exact expression; for instance there may be less need for chemically synthesized DNA[1,3] with the hybrid protein approach. Finally, for direct expression of an exact protein, the first amino acid must be methionine which may not be cleaved.

We have, therefore, chosen the hybrid protein approach in an attempt to persuade bacteria to synthesize β-endorphin, a 31 amino acid endogenous opioid. This protein is generated by post-translational processing from a larger precursor protein

(ACTH/β-LPH precursor) which also contains the sequences of corticotropin (ACTH) and β-lipotropin (β-LPH)[9–17]. We report here the expression, in *Escherichia coli*, of cloned β-endorphin sequences as a hybrid β-galactosidase/β-endorphin protein and describe the release, from the hybrid protein, of mature, biologically active β-endorphin.

Construction of a plasmid for expression of β-endorphin gene sequences

To programme bacteria to express β-endorphin gene sequences, we used a previously cloned DNA fragment derived by reverse transcription of mRNA coding for the mouse ACTH/β-LPH precursor protein[18]. This fragment contains the coding information for amino acids 44–90 of β-LPH (Fig. 1). This portion of β-LPH is composed of the carboxy-terminal 15 amino acids of β-melanocyte stimulating hormone (MSH) and the complete β-endorphin sequence with the exception of the C-terminal glutamine. It was thus necessary to modify this cloned fragment in order to recreate the codon for the C-terminal amino acid, insert a stop codon, link the fragment in phase to a bacterial gene, and devise a method for the release of mature β-endorphin from the hybrid protein.

Our approach to these problems is outlined in Fig. 2. The cloned fragment, released from the plasmid by *Hind*III digestion, was first cleaved in the β-MSH coding region with *Hpa*II to facilitate later 'phasing' with the bacterial β-galactosidase gene. The single stranded *Hpa*II and *Hind*III termini were then partially 'filled-in' using reverse transcriptase, dATP and dCTP; this recreated the 3′-terminal glutamine codon. The remaining unpaired terminal nucleotides

§To whom correspondence should be addressed.
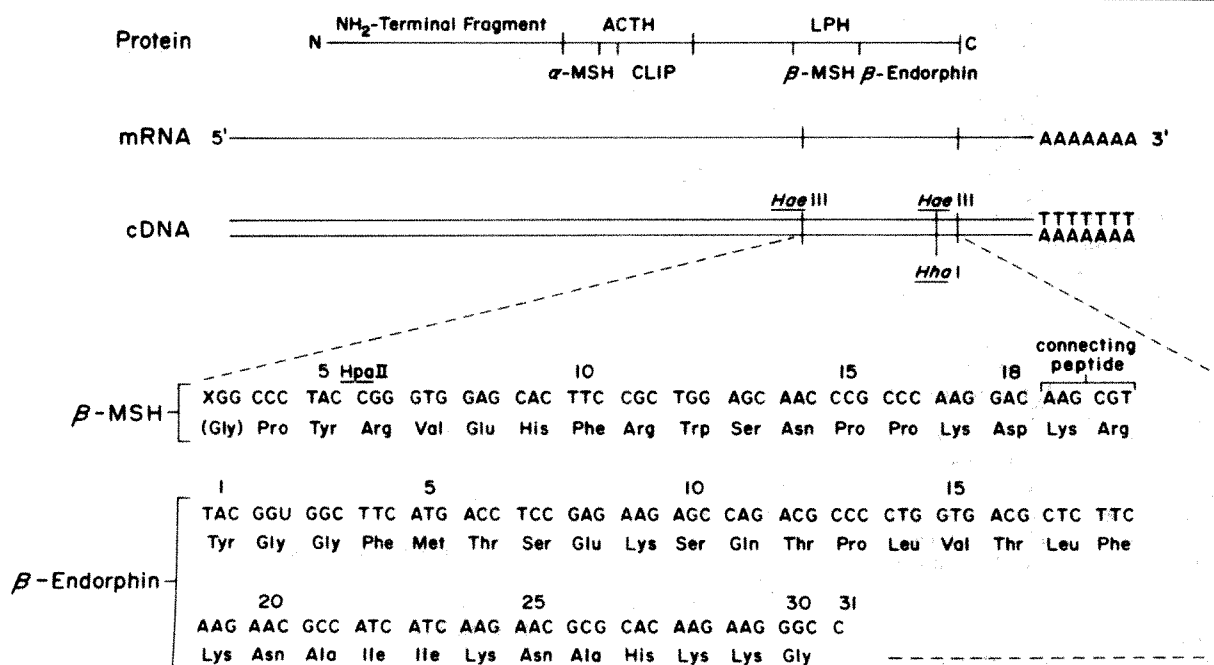
Fig. 1 Nucleotide sequence of the previously cloned fragment of cDNA to ACTH β-endorphin mRNA used to construct a plasmid for expression of β-endorphin sequences (from ref. 18). The plasmid containing this fragment (pMAE-1) had been constructed by ligating chemically synthesized decamers containing the restriction sites for endonuclease HindIII to an HaeIII digest of the cDNA. This fragment was then cloned in the HindIII site of plasmid pBR322. The HaeIII sites on either end of the cDNA are shown, but the HindIII 'linker' sequences are not indicated. The protein structure of the ACTH-β-endorphin precursor and its constituent hormones are shown and the amino acids of β-MSH and β-endorphin are numbered. The HpaII endonuclease site at which this DNA was cleaved in the construction of the expression plasmid is also indicated (see Fig. 2).

were removed by S_1 nuclease digestion and the blunt-ended fragment ligated to a synthetic octanucleotide containing the recognition site for EcoRI. Apart from providing the EcoRI termini necessary for ligation to the β-galactosidase gene, this octanucleotide provided a stop codon directly following the 3'-terminal glutamine codon. The modified fragment was then ligated into the EcoRI site of the plasmid pβ-gal (pBR322 carrying the lac control region and the coding sequence for β-galactosidase[2]). The unique EcoRI site in this plasmid occurs at the codon for amino acid 1004 of β-galactosidase. This resulted in the formation of a recombinant plasmid (pβ-gal-end) carrying a hybrid β-galactosidase-β-endorphin gene sequence.

Expression of the hybrid β-galactosidase/β-endorphin gene

E. coli RR1 cells carrying the recombinant plasmids pβ-gal or pβ-gal-end were examined for expression of polypeptides under control of the lac promoter. Polyacrylamide gel electrophoresis of extracts from stationary- or log-phase cells containing pβ-gal demonstrated the presence of large amounts of the β-galactosidase peptide, which was absent from uninduced control cells (Fig. 3). This high copy number of this plasmid (30-50 copies per cell) renders host cells mostly constitutive for β-galactosidase synthesis. Similar analysis of cells carrying pβ-gal-end demonstrated the absence of the β-galactosidase peptide and the appearance of a new band reflecting a protein approximately 30 amino acids larger than β-galactosidase-the size expected for the β-galactosidase-β-MSH-β-endorphin hybrid protein (Fig. 3e). This protein is also synthesized under the control of the lac promoter, as was demonstrated by its induction with isopropyl-β-thiogalactoside (IPTG; Fig. 3f).

Although it accounts for several per cent of the total cellular protein, the expression of the presumptive hybrid protein appears to be reduced in cells carrying the parental pβ-gal plasmid as compared to the synthesis of β-galactosidase. However, this level seems to be increased by amplification of

the plasmid DNA sequences (Fig. 3i). As was previously found with both the A and B chains of human insulin linked to the same β-galactosidase fragment[3], the hybrid protein is insoluble and can be recovered from a high speed pellet of cell extracts where it represents a substantial proportion of the total proteins (Fig. 3h).

Release and partial purification of biologically active β-endorphin

The steps used to release mature β-endorphin from the presumptive hybrid protein are shown in Fig. 4 and detailed in the legend. To do this, we made use of: (1) the arginine residue that precedes the β-endorphin sequence (Fig. 1), which can be a site for proteolytic cleavage by trypsin; (2) the absence of any internal arginines in this hormone (Fig. 1); and (3) the observation that the lysine residues in β-endorphin (Fig. 1) could be protected from attack by trypsin by reaction with citraconic anhydride in vitro[25]. Thus, after dissolving the precipitated hybrid protein and treatment with citraconic anhydride at pH 9, the β-endorphin (containing the modified lysine groups) was released from the hybrid protein by cleavage with trypsin. Native β-endorphin was subsequently produced by removal of the citraconic groups at pH 3. Cell extracts prepared in this manner were assayed for β-endorphin activity. The β-endorphin was further purified from this preparation with the use of glass extraction as described in Fig. 4 legend.

Immunological activity of partially purified bacterially synthesized β-endorphin

To test the immunological activity of the released β-endorphin, a heterologous radioimmunoassay was designed (Fig. 5). The antiserum had been raised against mouse pro-ACTH/β-LPH; radiolabelled synthetic human β-endorphin was used as the radioligand. The human hormone differs from that of mouse endorphin only at position 27 where a tyrosine is present

Fig. 2 Construction of a plasmid for the expression of β-endorphin sequences by *E. coli*. All recombinant DNA experiments were carried out in accordance with ASCORD (Australia) or NIH guidelines. Recombinant plasmids were isolated from chloramphenicol-amplified cultures as previously described[19]. The sources for restriction endonucleases, RNA-dependent DNA-nucleotidyl-transferase (reverse transcriptase), other enzymes and reagents, unless noted otherwise, are provided in previous publications[5,18,20,21]. The cloned 150-base pair fragment from pMAE-1 (Fig. 1, ref. 18) was isolated by *Hin*dIII digestion and electrophoresis in a 7% polyacrylamide gel. Digestion of 500 ng DNA with 5 U of *Hpa*II was carried out at 37 °C for 1 h in 20 µl 6 mM Tris (*p*H 7.5), 6 mM MgCl and 6 mM β-mercaptoethanol. Following phenol extraction and ethanol precipitation, the DNA was dissolved in 50 µl of a reaction mixture containing 500 µM each of dATP and dCTP. Incubation was carried out at 37 °C with 10 U of reverse transcriptase for 15 min. Unincorporated triphosphates were then removed by chromatography on Sephadex G-50 and after ethanol precipitation, the DNA was dissolved in 50 µl of 0.3 M NaCl, 30 mM Na acetate *p*H 4.5, 3 mM ZnCl$_2$ and incubated with 5 U of S$_1$ nuclease at 20 °C for 5 min followed by phenol extraction and Sephadex G-50 chromatography. The duplex DNA was then ligated to a 20-fold molar excess of octamers ('linkers') containing the restriction site for endonuclease *Eco*RI in 40 µl of 60 mM Tris (*p*H 7.5), 8 mM MgCl$_2$, 10 mM β-mercaptoethanol, 1 mM ATP, using 2 µl of bacteriophage T$_4$ DNA ligase (New England Biolabs) at 4 °C for 24 h. Following digestion with 50 units of *Eco*RI at 37 °C for 5 h, the linker fragments were removed by Sephadex G-50 chromatography and the DNA ligated to 1 µg of *Eco*RI-cleaved, and alkaline phosphatase treated[21] pβ-gal DNA[2], and transformed in *E. coli* RR1[22]. Plasmid DNA was isolated from 3-ml cultures of several independent recombinant clones and cleaved with *Hae*III to determine the orientation of the cloned fragments. One of these clones (pβ-gal-end), with the insert in the correct orientation for readthrough of β-endorphin sequences from the β-galactosidase gene, was selected for further analysis. The terminal nucleotide sequences of the inserted fragment were determined by digesting the plasmid pβ-gal-end with *Eco*RI endonuclease, isolating the inserted β-endorphin gene fragment by gel electrophoresis and electroelution, 3'- terminal labelling of the *Eco*RI termini with [α^{32}P]dATP (Amersham, 2,000 Ci mmol^{-1}) and reverse transcriptase, cleaving the fragment with *Hha*I, isolation of the two digestion products by electrophoresis in a 10% polyacrylamide gel, and subjecting these to DNA sequence analysis by the method of Maxam and Gilbert[23]. The sequences were found to be identical to those shown.

Fig. 3 Proteins synthesized from plasmids pβ-gal or pβ-gal-end. Bacteria harbouring pβ-gal or pβ-gal-end were grown at 37 °C to log phase (A_{650} of 0.25) in L-broth and collected by centrifugation. Cells were dissolved in SDS sample buffer and the equivalent of 50 µl of original culture subjected to electrophoresis in a 7% polyacrylamide gel and visualized by staining with Coomassie blue[24]. The positions of the hybrid protein β-galactosidase–β-MSH–β-endorphin and β-galactosidase are indicated by arrows. *a*, *E. coli* RR1; *b*, *E. coli* RR1 induced with 2 mM isopropyl-β-thiogalactoside (IPTG); *c*, *E. coli* RR1 carrying pβ-gal; *d*, *E. coli* carrying pβ-gal induced with IPTG; *e*, *E. coli* RR1 carrying pβ-gal-end; *f*, *E. coli* RR1 carrying pβ-gal-end induced with IPTG. Cells obtained in *e* were collected by centrifugation and the cell pellet resuspended in phosphate-buffered saline. After disruption by sonication, the cell debris and insoluble protein were pelleted by centrifugation at 15,000 r.p.m. for 30 min. *g*, Supernatant of pβ-gal-end cells after sonication; *h*, pellet from pβ-gal-end cells after sonication; *i*, proteins from pβ-gal-end cells after amplification of plasmid DNA in 50 µg per ml chloramphenicol, followed by 3 h growth in fresh L-broth.

instead of a histidine and at position 31 where a glutamic acid residue replaces a glutamine[28]. These changes do not inhibit the ability of the human hormone to react to antiserum raised against the mouse hormone. Immunological activity was examined in partially purified extracts prepared as described in the legends to Figs 3 and 4 from fully induced *E. coli* RR1 cells containing the recombinant plasmid pβ-gal-end.

The endorphin purified from *E. coli* RR1 cells carrying the recombinant plasmid pβ-gal-end competitively inhibited the binding of human [125]I β-endorphin to the mouse endorphin antibody (Fig. 5). As based on the immunological activity in the glass-purified material and the recovery from the trypsin-treated preparation (see the legends to Figs 4 and 5), it is estimated that 0.5 µg of released endorphin of molecular weight 3,900 can be obtained from 10^9 cells (8×10^4 molecules of endorphin per cell). By contrast, extracts of cells harbouring the plasmid pβ-gal which had been purified in a similar manner showed no competition for endorphin antibody binding sites. The activity demonstrated by extracts of these cells (over a series of 11 dilutions to $1:10^4$) was the same as that of the assay buffer.

To determine if the material reactive to antiserum to β-endorphin was of the anticipated size, 60 µl of the glass bead-purified preparation was filtered on a Sephadex G-50 column (Isolab 3 ml propylene column) and the column fractions were assayed for immunological activity. The column had been pre-calibrated with human β-endorphin[28]. The profile of immunological activity was included by the column and exhibited an elution pattern identical to the authentic β-endorphin. No immunological activity was found in the excluded fractions. Thus, the released peptide rather than the fusion protein appears to account for the activity.

Biological activity of bacterially synthesized β-endorphin

The opiate activity of endorphin prepared from extracts of fully induced *E. coli* RR1 cells containing the recombinant plasmid pβ-gal-end was examined by testing its ability to bind to opiate receptors of rat brain membrane preparations[31] and to elicit an opiate-like effect of inhibiting the stimulation by prostaglandin E_1 of cyclic AMP accumulation in the neuroblastoma-glioma hybrid cell line NG108-15[32].

The receptor-binding activity of the material synthesized in the bacteria was examined (Table 1) by testing its ability to inhibit the binding of a radiolabelled agonist (^{3}H-D-Ala^2-Met^5-enkephalinamide) or antagonist (^{3}H-naloxone). Endorphin prepared according to Figs 3 and 4 legends (without glass extraction) inhibited both the agonist and antagonist binding. As might be expected with this crude preparation (purified material was not available for these experiments), some nonspecific inhibition of binding was observed in the control reaction, where an extract from pβ-gal was used; however, this was substantially less than in the reaction with an extract from pβ-gal-end.

The neuroblastoma-glioma hybrid cell line NG 108-15 is richly endowed with opiate receptors[32] and possesses an adenylate cyclase which can be stimulated by prostaglandin E_1 (ref. 34). This stimulation is inhibited by morphine and the inhibitory effect of morphine can be prevented by naloxone[35]. Endorphin prepared as described in Figs 3 and 4 legends (without glass extraction) showed a significant inhibition of the stimulation by prostaglandin E_1 of adenylate cyclase activity (Table 1). This inhibition was completely reversed by addition of the opiate antagonist naloxone, and it was much greater than the activity observed in the control reaction (Table 1).

Discussion

This report demonstrates the expression of cloned β-endorphin gene sequences by bacteria in a form from which substantial amounts of biologically active β-endorphin can be obtained.

Table 1 Opiate receptor binding and opiate-like actions of extracts of pβ-gal-end

	% Inhibition	
Competition for receptor binding	pβ-gal-end	pβ-gal
^{3}H-Ala^2-Met^5-enkephalinamide		
(agonist)	84 (83–85)	65 (63–71)
^{3}H-naloxone (antagonist)	68 (67–69)	25 (17–32)
Cyclic AMP production		
No antagonist present	23.3 (21.9–24.6)	5.1 (5.0–5.2)
+ Naloxone	0	0

Rat brain membrane preparations were isolated according to the method of Snyder[31] with slight modification. Male Sprague-Dawley rats (200–220 g) were killed by decapitation and the brains minus cerebellum were homogenized in 40 volumes of 0.05 M Tris-HCl buffer pH 7.7 at 4 °C. The homogenates were first centrifuged at 600 g for 5 min to remove the nuclei. The supernatant was then centrifuged at 4 °C for 15 min at 49,000 g. The pellets were suspended in 30 ml (per rat brain) of the same Tris buffer. The resuspended pellets were then incubated at 37 °C for 30 min and centrifuged for 15 min at 49,000 g. The final pellet from each rat brain was then resuspended in 40 ml of 0.05 M Tris-HCl buffer containing 100 µg ml^{-1} of bacitracin and used for the binding assays. The binding experiments were performed, as previously described at 25 °C for 20 min, or at 0 °C for 3 h. Reaction mixtures contained 1 ml of tissue suspension and 1.5 nM of ^{3}H-D-Ala^2-Met^5-enkephalinamide (New England Nuclear, 38 Ci mmol^{-1}) or ^{3}H-naloxone (New England Nuclear, 25 Ci mmol^{-1}); 4.5 µg of bacterial extract was incubated in the reaction with ^{3}H-D-Ala^2-Met^5-enkephalinamide and 0.65 µg was used in the reaction with ^{3}H-naloxone. In each case the extracts were from a separate preparation. Non-radioactive levorphanol or naloxone[31] was used as standard competitor for each assay. The reaction was terminated by vacuum filtration over Whatman glas fibre filters (GH-B). The filters were washed with a large volume of ice-cold Tris buffer and placed in 12 ml of Hydromix scintillation fluid (Yorktown Res.). In parallel experiments 10^{-6} M of naloxone were incubated to estimate the background binding which was subtracted from the total binding to yield the specific binding. Results are reported as per cent inhibition of specific binding that was 5,613 c.p.m. per assay with ^{3}H-D-Ala^2-Met^5-enkephalinamide and 2,869 c.p.m. per assay with ^{3}H-naloxone. Mean values and ranges (in parentheses) of triplicate incubations are shown. To test for biological activity, the neuroblastoma-glioma hybrid cells (line NG108-15) were used[32]. Cells were grown in T-flasks (one T-75 flask per 60 assays) in Dulbecco's modified Eagle's medium (DMEM)[33] containing 10% fetal calf serum, 0.1 mM hypoxanthine, 10 µM aminopterin and 16 µM thymidine. At confluency, the cells were collected and homogenized in 0.32 M sucrose, 40 mM HEPES and 2 mM EDTA, pH 7.6. Incubations[34,35] were carried out at 30 °C for 15 min in a total volume of 100 µl containing 3×10^6 c.p.m. of ^{32}P-ATP, 10 units creatine phosphokinase, 50 µM prostaglandin E_1 (PGE$_1$; Upjohn), 5 µl of opiate agonist or extract (3.5 µg) of pellet material (prepared from fully induced *E. coli* RR1 as indicated in legends to Figs 3 and 4), 20 mM HEPES, 5 mM MgCl$_2$, 1 mM cyclic AMP, 20 mM creatine phosphate, 0.1 mM ATP, 0.125 mM phosphodiesterase inhibitor (ZK 62711, Schilling) and 1 mM protease inhibitor (Sigma). The reaction was stopped by the addition of 150 µl of 1M HClO$_4$ and 0.3 ml of H$_2$O containing ~30,000 c.p.m. of tritiated cyclic nucleotide per tube. After mixing and centrifuging, the supernatant solutions were poured onto Dowex 50 columns. [α-^{32}P]-cyclic AMP was then separated from other nucleotides by the two-column (Dowex 50 and alumina) method described by White and Karr[36]. The adenylate cyclase activity, which was stimulated by PGE$_1$ (level of cyclic AMP released increased from 30 to 180 pmol per mg protein per min) in the absence of opiate agonist or test material was used as control[33,34]. The activity of the bacterially synthesized endorphin preparation is expressed as the ability to inhibit this stimulation. The agonist activity of the test material was further examined by the reversibility of the effect by the opiate antagonist naloxone[34]. Mean values and ranges (in parentheses) of triplicate incubations are shown.

These data, along with those recently demonstrating the synthesis of somatostatin[2], insulin[3] and growth hormone[1,6] show the potential usefulness of bacteria to synthesize large

quantities of polypeptides of medical and economic importance. The methodology used in this report differs from and therefore complements that previously used for the other proteins. In all of these studies in which an exact hormone was produced, fairly large fragments of synthetic DNA were used. In the current study, small fragments of DNA containing restriction endonuclease sites were used to create the proper reading frame, to add the codon for one amino acid and a
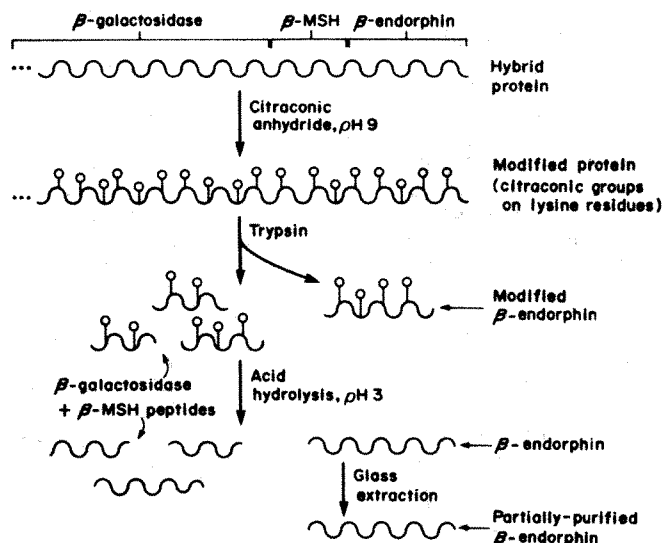
Fig. 4 Release of β-endorphin from the β-galactosidase–β-MSH–β-endorphin hybrid protein. The pellet obtained, as in Fig. 3 was dissolved in 10 ml of 6M guanidinium chloride, 1% β-mercaptoethanol and centrifuged at 20,000 r.p.m. for 1 h. Citraconic anhydride (Fisher) was added to the supernatant in three lots of 10 µl over a 15-min period, during which time the pH was maintained between 9 and 11 by the addition of 2M NaOH[25]. The solution was then dialysed overnight against 50 mM ammonium bicarbonate followed by the addition of trypsin (Worthington) to 0.5 mg ml^{-1} and incubation at 37 °C for 12 h. Trypsin was inactivated by the addition of phenylmethylsulphonyl fluoride (PMSF) to 1 mM for 1 h and the solution made 1% in formic acid before lyophilization. The dried protein was then dissolved in Tris (base) buffer pH 7.6 to yield a protein concentration[26] of 0.5–1.0 µg µl^{-1}. This preparation was tested for immunological and biological activity. To further purify β-endorphin, a modification of the technique devised for the extraction and purification of ACTH by Rees et al.[27] was used. To 0.5 ml aliquots of the crude endorphin preparation were added 0.5 ml of horse serum (Grand Island Biological) and 50 mg glass powder (140 mesh, Corning Glass Works, washed once with water, heated for 24 h at 120 °C and then stored in a desiccator until use) in a 15-ml plastic centrifuge tube. The samples were vortexed for 30 s and then centrifuged for 5 min at 3,000 r.p.m. The supernatant was discarded and the glass adsorbant washed with 3 ml of water. The endorphin was removed from the glass by addition of 1 ml of 50% acetone in 0.25–5.00 M HCl, vortexing for 30 s and then centrifuging as above. The endorphin-rich supernatant was then transferred to 10 × 75 mm polystyrene tubes (Falcon) and evaporated to dryness with a fine stream of nitrogen in a water bath at 45 °C. Dried samples were reconstituted with Tris buffer (pH 7.6) and serially diluted for radioimmunoassay. To monitor the recovery of β-endorphin in the extraction procedure, a parallel experiment was performed in which the recovery of ^{125}I-β_h-endorphin was measured. The recovery was 60%. The human β-endorphin had been synthesized by the solid phase technique by Li et al.[28] and labelled with ^{125}I by a chloramine-T procedure[29]. The iodinated peptide was then purified by adsorption to 35 mg of glass powder (Corning) in 10 ml of buffer (pH 7.4) containing 0.05 M sodium phosphate, 0.25% human albumin and 0.5% β-mercaptoethanol. After mixing for 5 min, the suspension was spun at 3,500 r.p.m. for 5 min and the pellet was washed once with water and then eluted with 2 ml of 40% acetone in 0.25 M HCl. The ^{125}I-β_h-endorphin was then diluted in the phosphate-containing buffer described above before use. Antiserum directed against mouse β-endorphin had previously been generated in rabbits by Allen et al.[30].
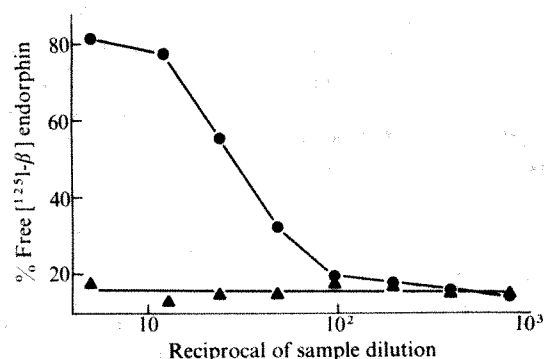
Fig. 5 Immunological activity (competitive inhibition with human ^{125}I-β_h-endorphin for antibody sites) in partially purified extracts from *E. coli* RR1 cells carrying the recombinant plasmid pβ-gal-end (●) and pβ-gal (▲). Extracts from fully induced bacteria containing these plasmids were prepared as described in Figs 3 and 4 legends. Incubations were carried out at 4 °C for 24 h in a total volume of 150 µl containing 75 µl of ^{125}I-β-endorphin (10,000 c.p.m.) (prepared as described for Fig. 4), 50 µl of endorphin antibody (final titre 1:1500 yielded 50% binding; 1:150 yielded 83% binding), 25 µl of standards or extracts (from lyophilizates at 1 µg µl^{-1} protein) at various concentrations in 0.05 M sodium phosphate (pH 7.4), 0.25% human albumin and 0.5% β-mercaptoethanol. Free radioligand was then separated from bound peptides by adding 100 µl of a dextran–charcoal suspension containing 3% charcoal (Norit A, Pfanstiehl Chemical Co), 0.75% dextran (Schwartz-Mann) and 60% horse serum (Grand Island Biological Co.) in 0.05 M sodium phosphate, pH 7.6. After a 5 min incubation the samples were centrifuged at 2,500 r.p.m. for 15 min. The supernatant was aspirated with a glass bent-tip pipette. Radioactivity was counted before incubation (total reaction mixture) and in the charcoal pellet after incubation to calculate the per cent free ^{125}I-β-endorphin (ordinate) using human β-endorphin as standard. The assay was most sensitive in the region of 10–100 pg ml^{-1}. Both inter- and intra-assay coefficients of variation were less than 5%.

'stop' codon, but larger pieces of DNA were not required. Thus, even if large pieces of synthetic DNA are not available, it is possible to construct genes to obtain an exact protein.

Bacterially expressed growth hormone[1,6], insulin[3] and somatostatin[2] have been shown to have immunological activity but their biological activity has not been reported. By contrast our β-endorphin has biological activity by several criteria. First, it competitively inhibits the binding of an opiate antagonist (naloxone) or agonist (Ala^2-Met^5-enkephalinamide) by the opiate receptors in rat brain membrane preparations. Second, like opiate agonists, the bacterially synthesized material can inhibit the prostaglandin E$_1$-induced stimulation of adenylate cyclase in cultured neuroblastoma glioma cells. That the material produced by the bacteria had the conformation of authentic β-endorphin was also demonstrated by its ability to react specifically to antiserum to β-endorphin. The immunological activity also eluted from a Sephadex G-50 column in the same region as the standard human β-endorphin, thus supporting the idea that there was cleavage of the endorphin from the hybrid protein.

Were our bacterially expressed β-endorphin to be considered for clinical use (for treatment of pain, diarrhoea or psychiatric problems, for example[37,38]), it should be noted that it differs from human β-endorphin by two amino acids. That may not affect its activity, but if it did, two plasmid codons could readily be altered to give the correct amino acids. Other codon changes could be introduced to direct the synthesis of analogues of β-endorphin which have useful or different opiate agonist or antagonist activity.

development of the radioimmunoassay, Ping-Yee Law for assistance with the adenylate cyclase assays, J. Ramachandran for the gift of the human β-endorphin and Edward Herbert for the endorphin antibody.

1. Goeddel, D. V. *et al. Nature* **281**, 544-548 (1979).
2. Itakura, K. *et al. Science* **198**, 1056-1063 (1977).
3. Goeddel, D. V. et al. *Proc. natn. Acad. Sci. U.S.A.* **76**, 106-110 (1979).
4. Chang, A. C. T. *et al. Nature* **275**, 617-624 (1978).
5. Seeburg, P. H. *et al. Nature* **276**, 795-798 (1978).
6. Martial, J. A., Hallewell, R. H., Baxter, J. D. & Goodman, H. M. *Science* **205**, 602-607 (1979).
7. Villa-Komaroff, L. *et al. Proc. natn. Acad. Sci. U.S.A.* **75**, 3727-3731 (1978).
8. Mercereau-Puijalon, O. *et al. Nature* **275**, 505-510 (1978).
9. Roberts, J. L. & Herbert, E. *Proc. natn. Acad. Sci. U.S.A.* **74**, 4826-4830 (1977).
10. Mains, R. E. & Eipper, B. A. *J. biol. Chem.* **251**, 4115-4120 (1976).
11. Nakanishi, S. *et al. Proc. natn. Acad. Sci. U.S.A.* **73**, 4319-4323 (1976).
12. Jones, R. E., Pulkrabek, P. & Grunberger, D. *Biochem. biophys. Res. Commun.* **74**, 1490-1495 (1977).
13. Nakanishi, S. *et al. Nature* **278**, 423-427 (1979).
14. Mains, R. E., Eipper, B. A. & Ling, N. *Proc. natn. Acad. Sci. U.S.A.* **74**, 3014-3018 (1977).
15. Roberts, J. W. & Herbert, E. *Proc. natn. Acad. Sci. U.S.A.* **74**, 5300-5304 (1977).
16. Roberts, J. L., Phillips, M. A., Rosa, P. A. & Herbert, E. *Biochemistry* **17**, 3609-3618 (1978).
17. Eipper, B. A. & Mains, R. E. *J. biol. Chem.* **253**, 5732-5744 (1978).
18. Roberts, J. L. *et al. Proc. natn. Acad. Sci. U.S.A.* **76**, 2153-2157 (1979).
19. Bolivar, F. *Gene* **2**, 95-119 (1977).
20. Seeburg, P. H., Shine, J., Martial, J. A., Baxter, J. D. & Goodman, H. M. *Nature* **270**, 486-494 (1977).
21. Shine, J., Seeburg, P. M., Martial, J. A., Baxter, J. D. & Goodman, H. M. *Nature* **270**, 494-499 (1977).
22. Greene, P. J. *et al. Nucleic Acids Res.* **12**, 2372-2380 (1978).
23. Maxam, A. M. & Gilbert, W. *Proc. natn. Acad. Sci. U.S.A.* **74**, 560-564 (1977).
24. Laemmli, U. K. *Nature* **227**, 680-685 (1970).
25. Dixon, H. B. F. & Perham, R. N. *Biochem. J.* **109**, 312-314 (1968).
26. Bradford, M. M. *Analyt. Biochem.* **72**, 248-254 (1976).
27. Rees, L. H. *et al. Endocrinology* **87**, 254-261 (1971).
28. Li, C. H., Lemaire, S., Yamashiro, D. & Doreen, B. A. *Biochem. biophys. Res. Commun.* **71**, 19-25 (1976).
29. Hunter, W. M. & Greenwood, F. C. *Nature* **194**, 495-496 (1962).
30. Allen, R. G., Herbert, E., Hinman, M., Schkuya, H. & Pert, C. B. *Proc. natn. Acad. Sci. U.S.A.* **75**, 4972-4976 (1978).
31. Pasternak, G. W., Wilson, H. A. & Snyder, S. H. *Molec. Pharmac.* **11**, 340-351 (1974).
32. Klee, W. A. & Nirenberg, M. *Proc. natn. Acad. Sci. U.S.A.* **71**, 3474-3477 (1974).
33. Dulbecco, R. & Freeman, G. *Virology* **12**, 185-196 (1960).
34. Hamprecht, B. & Schultz, J. *Hoppe-Seyler's Z. physiol. Chem.* **354**, 1633-1641 (1973).
35. Traber, J., Fischer, K., Latzin, S. & Hamprecht, B. *Nature* **253**, 120-122 (1975).
36. White, A. A. & Karr, D. B. *Analyt. Biochem.* **85**, 451-460 (1978).
37. Foley, K. M. *et al. Proc. natn. Acad. Sci. U.S.A.* **76**, 5377-5381 (1979).
38. Usdin, E., Burney, W. E. Jr & Kline, N. S. (eds) *Endorphins in Mental Health Research* (Oxford University Press, New York, 1979).

LETTERS

UV spectra of the twin QSOs 0957+561 A, B

P. M. Gondhalekar

SRC, Rutherford and Appleton Laboratory, Ditton Park, Slough SL3 9JX, UK

R. Wilson

Department of Physics and Astronomy, University College London, Gower Street, London WC1E 6BT, UK

Observations of the twin QSOs 0957+561 A and B by Walsh *et al.*[1] gave the same redshifts in both the emission line ($z_e = 1.41$) and absorption line ($z_a = 1.39$) systems and also showed similar spectral characteristics in the strengths of the emission lines, absorption lines and continua. This led to the proposal that they were one object, a double image of which was being formed by an intervening massive galaxy acting as a gravitational lens. More extended observations in the 6,000-6,900 Å range[2] and in the 4,000-7,000 Å region[3] confirm the similarity of the two spectra and show very close agreement (14 km s^{-1} r.m.s.) between the velocities of the absorption line systems, thus strengthening the lens hypothesis. Other data on the structure of the associated radio sources[4-6] are also consistent with the above proposition. An intervening galaxy has been looked for[7] which may act as a gravitational lens: very deep red images were taken of the field using a CCD camera on the 200-inch Palomar telescope and supplemented by multichannel spectrophotometric scans of the double system. An elliptical galaxy of red magnitude 18.5 was detected which is nearly superimposed on the south (B) component of the twin QSO and which is the brightest member of a rich cluster of galaxies. The spectrophotometric data of the system show a contribution from this intervening galaxy and from the location of the characteristic Ca II 3,950 Å break, a redshift of 0.39 is estimated. Young *et al.*[8] conclude that Q0957+561 A, B could be two images of the same object produced by this galaxy but that the lens properties are somewhat complex due to 'aberrations' induced by the rest of the cluster. We present here the first UV observations of Q0957+561 A, B and discuss them in terms of the lens hypothesis.

Two UV spectra of 0957+561 A, B were obtained with the long wavelength spectrograph (LWR) of the IUE. The images of the quasars were centred in the 10×20 arc s entrance aperture and the details of the observing programme are given in Table 1; the spectrum of HD237844, a $B3$ ($m_v = 9.4$) star was taken for comparison.

A strip of data, 20 pixels wide, along a line parallel to the spectra of 0957+561 A, B was extracted from both the RAW unprocessed image and the GPHOT image which is corrected for the intensity transfer function of the LWR camera. The RAW data and the photowrites of the images were examined to identify cosmic ray events and these signals were traced to the GPHOT images, and the enhanced data points were smoothed to the average values in the surrounding pixels. In the GPHOT data the spectra of 0957+561 A, B were confined to a strip of ~ 7 pixels wide and were blended. The data were corrected for background by smoothing the signals in 3-pixel wide strips at the edges of the 20 pixels wide band and were then averaged to obtain spectra with an improved signal-to-noise ratio. The spectra were deconvoluted by using the profile
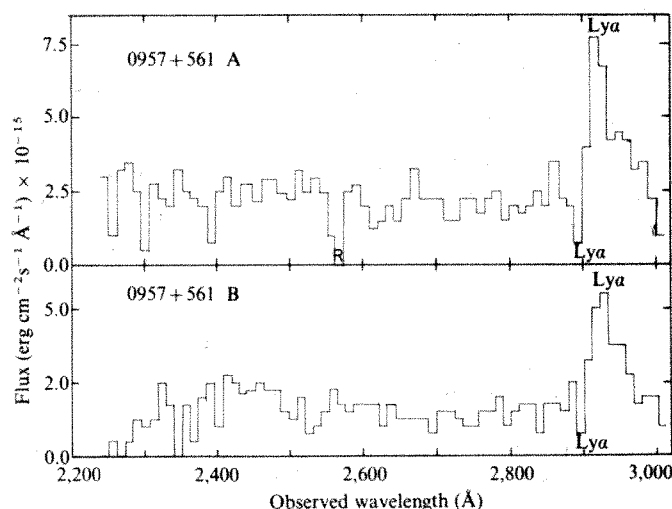
Fig. 1 The UV spectra of 0957+561 A, B binned in 10 Å bands. The Lyα line is present in emission and absorption.

Table 1 Observing log

Object	α(1950)	δ(1950)	Image	Integration time (min)	Date
0957 + 561 A, B	09 h 57 min 57.3 s	+ 56° 08′ 18″	LWR 6472	347	24 Dec 1979
0957 + 561 A, B	09 57 57.3	+ 56 08 18	LWR 6473	398	25 Dec 1979
HD 237844	09 48 31	+ 55 57 38	LWR 6471	3	24 Dec 1979

of the point-spread function perpendicular to the direction of dispersion obtained from the spectrum of HD237844. As the IUE spacecraft and the scientific instrument parameters were similar when the three spectra were obtained, this procedure seems justified. The deblended spectra of Q0957 + 561 A, B binned in 10 Å bands are shown in Fig. 1.

The UV spectrum in Fig. 1 covers the rest-frame wavelength range 950–1,250 Å. A continuum is present together with the Lyα 1,216 Å line in emission and absorption at redshifts consistent with those given by Walsh et al., that is 1.41 and 1.39 respectively. Table 2 gives the absolute intensities of the Lyα emission line in each spectrum together with its emission and absorption equivalent widths. These latter values are not unusual, lying within the range typical of QSOs. In these weakly exposed spectra, the absorption equivalent widths are the least accurate but give an equivalent hydrogen column density $N(H)$ of $\sim 4 \times 10^{19} \, cm^{-2}$. From their visible spectra, Wills and Wills[3] find the corresponding value for $N(Fe^+) \sim 3 \times 10^{14} \, cm^{-2}$. Assuming Fe is mainly in the singly ionized state and normal cosmic abundances gives $N(H) \sim 10^{19} \, cm^{-2}$. Taking the uncertainties involved into account, these two numbers are probably not inconsistent with each other.

Table 2 Observed intensities and equivalent widths of emission and absorption Lyα*

	0957 + 561 A	0957 + 561 B
Intensity of emission Lα ($erg \, cm^{-2} \, s^{-1} \times 10^{-14}$)	4.4	3.5
EW of emission Lyα (Å)	140 (58)	154 (64)
EW of absorption Lyα (Å)	13 (5)	9 (4)

*Rest-frame values in brackets.

The ratio of the UV fluxes of QSO B to A has been derived by binning the data over the range 2,750–3,000 Å where the signal-to-noise ratio is best. The result and its attendant error is given in Table 3 together with the corresponding visible and radio data taken from the references cited. The flux ratio of QSO B/A is then plotted in Fig. 2 using our UV data with the visible data of Walsh et al.[1].

The variation and structure of the flux ratio in the visible, which departs from the constant value predicted by the lens hypothesis, led Walsh et al.[1] to suggest that differential extinction in the two light paths around the lensing galaxy causes a reddening of component B relative to A with the upturn near 5,300 Å being produced by a redshifted 2,200 Å feature. This hypothesis has been investigated by Wills and Wills[3] whose data gave a best fit for a differential visual extinction $A_v = 0.65$ at a redshift $z = 1.2$. This requires QSO B

Table 3 Ratio of fluxes from 0957 + 561 B to 0957 + 561 A

Wavelength range (Å)	Ratio	Refs
2,750–3,000	0.72 ± 0.05	Present data
3,500–4,500	0.69	1
4,100–4,700	0.71	3
6,100–7,000	0.76	8
Radio	0.78 ± 0.05	4–6

to be intrinsically brighter than A by a factor of ~ 2.5 which opposes (on the lens theory) the radio value of 0.74. This may be explained by variability in the source, either due to the time delay of the order of months between the two images, or to different variability at optical and radio frequencies. However, Wills and Wills[3] do not detect any optical variability and conclude that the alternative hypothesis of two separate objects cannot be ruled out.
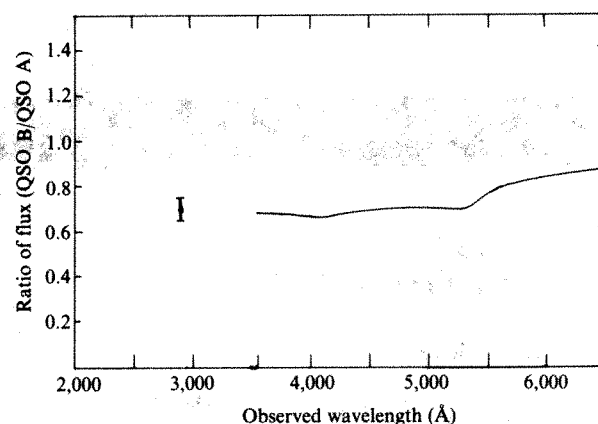
Fig. 2 The ratio of fluxes from 0957 + 561 B to fluxes from 0957 + 561 A. The visible data are from ref. 1 (solid line); I, present data.

The UV data presented here allow a far better test of any differential extinction effects, first because any extinction will be greater in the UV but, more important, any contribution to the observed UV fluxes by the intervening elliptical galaxy[7] will be negligible, unlike the visible region. Indeed, Young et al.[8] propose that the upturn near 5,300 Å is the characteristic Ca ii break caused by the contribution of the intervening galaxy and, in support of this, we propose that the less conspicuous feature near 4,000 Å (see Fig. 2) is the corresponding Mg ii break. We can therefore make a comparison between the UV and radio fluxes to derive a direct estimate of any differential extinction. The ratio of the flux ratio in the two frequency ranges is

$$\left[\frac{B}{A}\right]_{UV} \Big/ \left[\frac{B}{A}\right]_{radio} = 0.92 \pm 0.07$$

Two conclusions are drawn from this result. First, on the assumption of a galactic extinction law[9], an upper limit (3σ) can be placed on the differential reddening of $E(B - V) < 0.04$. This low value almost certainly means that the two light paths are almost extinction free, either because the intervening galaxy is dust-free or the light paths are through its dust-free halo. Second, a ratio of unity for the UV and radio flux ratios is in keeping with one of the most fundamental predictions of the gravitational lens theory, and therefore provides strong evidence in favour of that hypothesis.

1. Walsh, D., Carswell, R. F. & Weymann, R. J., *Nature* **279**, 381 (1979).
2. Weymann, R. J., Chaffee, F. H., Walsh, D. & Carswell, R. F. *Astrophys. J. Lett.* (in the press).
3. Wills, B. J. & Wills, D. Preprint (McDonald Observatory, 1979).
4. Pooley, G. G. *et al. Nature* **280**, 461, 1979.
5. Roberts, D. H., Greenfield, P. E. & Burke, B. F. *Science* **205**, 894 (1979).
6. Porcas, R. W., Booth, R. S., Browne, I. W. A., Walsh, D. & Wilkinson, P. N. *Nature* **282**, 385 (1979).
7. Gunn, J. E., Kristian, J., Oke, J. B., Westphal, J. A. & Young, P. J. *IAU Circ.* No. 3431 (1979).
8. Young, P. J., Gunn, J. E., Kristian, J., Oke, J. B. & Westphal, J. A. Preprint (Hale Observatories, 1980).
9. Nandy, K., Thompson, G. I., Jamar, C., Monfils, A. & Wilson, R. *Astr. Astrophys.* **44**, 195 (1975).

Evidence for highly processed material ejected from Abell 30

**C. Hazard*, R. Terlevich*, D. C. Morton†,
W. L. W. Sargent‡ & G. Ferland***

*Institute of Astronomy, Madingley Road, Cambridge CB3 0HA, UK
†Anglo-Australian Observatory, PO Box 296, Epping, New South Wales, Australia
‡Hale Observatories, California Institute of Technology, Carnegie Institution of Washington, Pasadena, California 91103

The discovery of compact knots of highly processed material apparently ejected from the central star of the emission nebula Abell 30 is reported here[1,2]. This emission nebula possesses other unusual features. The extended emission region, ~2 arc min in diameter has a very low surface brightness and exhibits a high degree of circular symmetry. The central star 05 fep, V = 14.3 is remarkable for its very high temperature of the order 2×10^5 K, as indicated by the strong broad O VI, He II and C IV emission lines in its spectrum and the strong [Ne V] emission in the embedding nebulosity[3]. Furthermore the star seems to be embedded in a resolved (~30 arc s) source of IR emission[4]. These new observations emphasize the peculiar nature of A30 and its importance in studies of stellar evolution.

The central star is located at 08 h 44 min 03.55 s, +18°03'48.2" (1950.0) and there is a 17.0 mag companion[5] at 5.3" and PA 142°. The compact nebulosities were discovered using a combination of a triple exposure three colour plate taken with the Palomar 48-inch Schmidt and a pair of objective prism plates taken with the UK 48-inch Schmidt with the dispersion north–south and east–west. Figure 1a shows an enlargement of the three colour plate, the images from left to right having effective wavelengths of 6,500 Å (red), 5,000 Å (green-yellow) and 3,600 Å (UV) respectively. The compact nebulosities can be seen as prominent patches of nebulosity surrounding the green-yellow image; they lie within a diameter of ~20 arc s around the central star, roughly the same size as the IR source. Of the four obvious features labelled 1 to 4, feature 1 is the galactic star probably unrelated to the planetary nebula. The nebulosities are features 2 to 4, which are absent in the red. The objective prism spectrum in Fig. 1b, which covers the wavelength range 3,400–5,300 Å, shows that the emission from these nebulosities is dominated by lines around 5,000 Å and the north–south dispersed plate shows that nebulosity 3 is similar. The natural conclusion is that the strong line is [O III]λ5,007 but the failure to detect the nebulosities in the red then suggests that the Balmer emission must be unusually weak.

Spectra of nebulosities 2 and 4 at a resolution of ~5 Å were obtained in January 1979 with a 7 × 2 arc s aperture using the image photon counting system on the Anglo-Australian telescope. The sky subtracted, in reducing these spectra was an average over several adjacent regions within the smooth extended nebulosity. This corrects the spectra not only for night sky emission but also for any contribution from the extended emission region. A spectrum of the south-east nebulosity 2 after sky subtraction and normalization is illustrated in Fig. 2. Apart from the [O III] doublet the strongest lines visible are He IIλ4,686, [Ne III]λ3,869 and [Ne V]λ3,426. The relative intensities of these lines are similar to those normally found in high excitation planetaries. However, there is no evidence of any Hβ emission although this line is usually more intense than He II 4,686. The spectrum of the north-west nebulosity is similar except that the λ4,720 line is comparable in intensity to He λ4,686. Adding together the spectra of the two nebulosities sets a limit to the He II/H He II/Hβ ratio of $I(4,686)/(Hβ) \gtrsim 20$.

As both the He λ4,686 and Hβ lines are recombination lines their ratio is directly related to the He^{2+}/H^+ ratio through a ratio of atomic constants and their observed lower limit sets the limit $He^{2+}/H^+ \gtrsim 2$ (ref. 6). After applying a small correction for singly ionized helium using the approximation $He^{2+}/H^+ = Ne^{4+}/Ne^{2+} = 0.8 I(3,426)/(3,869)$ (refs 7, 8) this sets
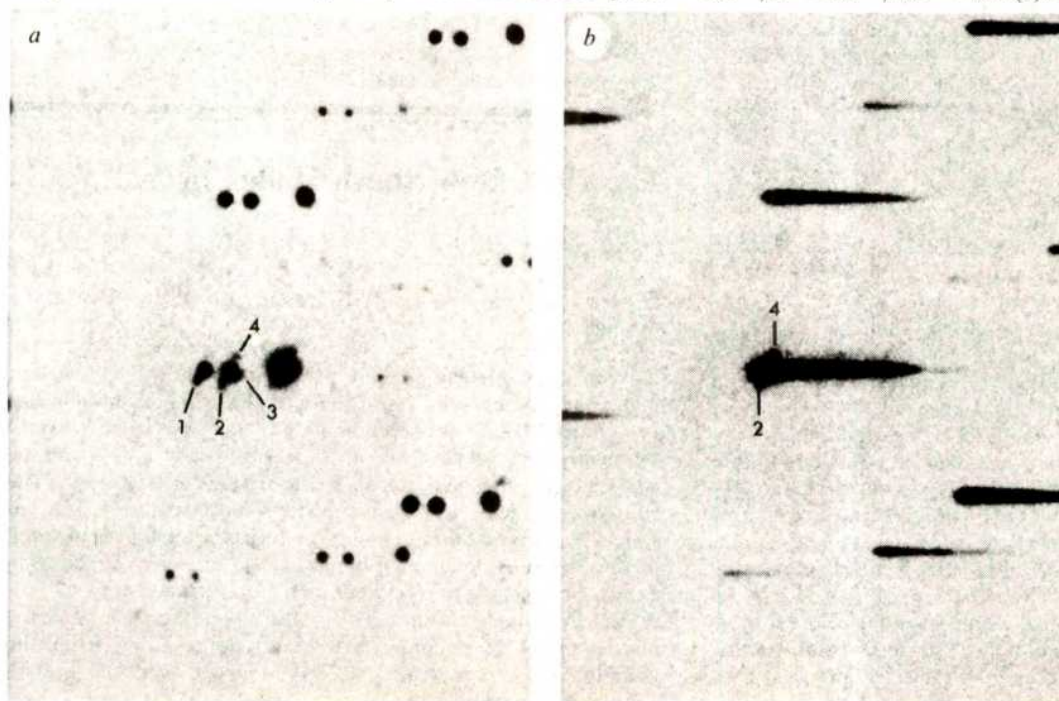
Fig. 1 *a*, An enlargement of the triple exposure three colour plate of A30 taken with the 48-inch Palomar Schmidt. The colours from left to right are, red, green-yellow and UV respectively. Object 1 is a star while features 2 to 4 are the compact nebulosities discussed in the text. The faint extended circular nebulosity is faintly visible. *b*, A reproduction of an objective prism spectron of A30 taken with the 48-inch UK Schmidt with the dispersion east–west. The emission features marked are the strong [O III] lines from the nebulosities 2 and 4. Fainter emission lines are just visible in the spectrum of the NW nebulosity.
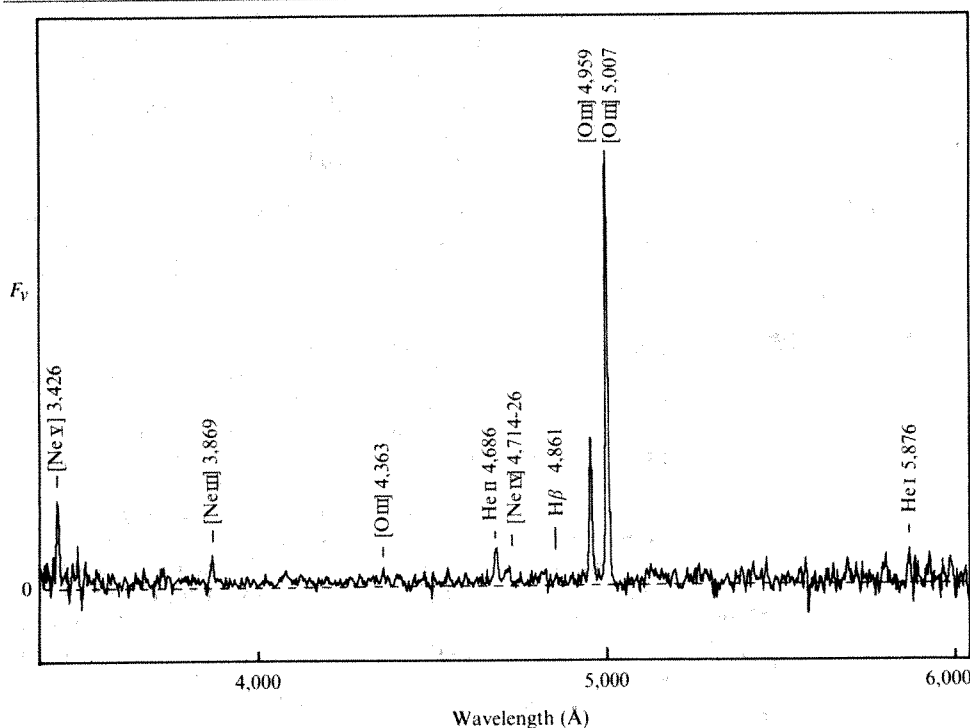
Fig. 2 A spectrum of the south-east nebulosity, feature 2 in Fig. 1, using a slit size 7×2 arcs at a resolution of ~ 5Å. Sky subtraction was performed using an average of observations in the extended emission region ~ 20 arcs from the compact nebulosity. No nebular lines apart from very weak [O III]$\lambda 5,007$ and $\lambda 4,959$ were present in these background scans.

the limit to the total helium to hydrogen ratio, He/H $\gtrsim 2.4$ which is to be compared with a value of $\simeq 0.1$ in normal planetaries. This result indicates a remarkable enhancement of helium relative to hydrogen in the nebulosities. Wide slit spectra of the extended emission show it to have a more normal composition with Hβ clearly present but the data, which have a low signal-to-noise ratio do not preclude some enhancement over the solar value.

We have made some preliminary model calculations to investigate the properties of hydrogen deficient nebulae and to study the abundances of some heavy elements: these will be discussed in detail elsewhere. Here we merely point out that the model calculations show that the observed spectrum can be reproduced reasonably well on the assumption: (1) that the filaments are photoionized by radiation from the central star; (2) that the observed He/H ratio arises through these ejecta having been through hydrogen burning which has depleted the hydrogen by a factor of $\gtrsim 20$ with a consequent increase in the helium content; and (3) that the heavy elements have normal relative abundances. The only significant discrepancy between the model and the observations is that the iron lines are predicted at about five times the observed upper limits but iron depletion has been reported in other planetary nebulae[9] which may indicate a process which selectively removes the iron nuclei from the ejected material.

As a result of both our simple estimate of the He/H ratio and the model calculations, it is established that hydrogen in the compact nebulosities has been depleted by a very large factor. A depletion of hydrogen by a factor of $\gtrsim 20$ indicates an almost complete conversion of hydrogen to helium. Evidently A30 is at a more advanced evolutionary stage than the common planetary nebulae and the central star having already shed its hydrogen envelope to expose the helium core is now shedding its helium envelope. The very tenuous nature of the hydrogen-rich extended nebulosity is consistent with a model where the previously ejected hydrogen envelope is now almost dissipated. The central star is, therefore, at a very interesting and possibly short-lived phase on evolutionary track perhaps just before collapse to a white dwarf. An alternative view is that we are dealing with a close binary system of helium stars where mass transfer is now taking place. The apparent distribution of the ejected material may give some support to this hypothesis.

Further work on this object is in progress and should help to clarify the evolutionary state of the central star. These more detailed studies should provide an important test of theories of very late stages of stellar evolution.

We thank J. Truran for helpful discussions.

Note added in proof: Since submission of this letter we have become aware that Jacoby[10] has reported an independent discovery of the nebulosites around Abell 30 from photographs taken in [O II]$\lambda 5,007$.

1. Abell, G. O. *Publ. astr. Soc. Pacif.* **67**, 258-261 (1955).
2. Abell, G. O. *Astrophys. J.* **144**, 259-279 (1966).
3. Greenstein, J. & Minkowski, R. *Astrophys. J.* **140**, 1601-1603 (1964).
4. Cohen, M., Hudson, H., O'Dell, S. & Stein, W. A. *Mon. Not. R. astr. Soc.* **181**, 233-245 (1977).
5. Cudworth, K. M. *Publ. Astr. Soc. Pacif.* **85**, 401-402 (1973).
6. Brocklehurst, M. *Mon. Not. R. astr. Soc.* **153**, 471-490 (1971); **157**, 211-227 (1972).
7. Osterbrock, D. E. *Astrophysics of Gaseous Nebulae* (W. H. Freeman, San Francisco, 1974).
8. Seaton, M. T. *Mon. Not. R. astr. Soc.* **170**, 475-486 (1975).
9. Shields, G. A. *Astrophys. J.* **195**, 475-478 (1978).
10. Jacoby, G. H. *Publ. astr. Soc. Pacif.* **91**, 754 (1979).

The 1978 New South Wales fireball

Colin S. L. Keay

Physics Department, Newcastle University, New South Wales 2308, Australia

A very large meteor fireball passed through the atmosphere above the east coast of New South Wales early in the morning of 7 April 1978. It was seen at 04.44 AEST (18.44 UT, 6 April) by hundreds of people from the cities of Sydney and Newcastle who deluged the news media with telephoned sightings. The resulting publicity led to the collection of many reports, of which 19 were useful in defining the trajectory and ground track of the fireball. I define here the ground track, which is shown in Fig. 1, and include the locations of the eye-witnesses.

An initially puzzling feature of the fireball was the consistently low estimate of the altitude resulting from the combination of observations. This indicated that the fireball should have been visible as it passed overhead at sites 300–

400 km to the south-west of Sydney. Only one newspaper report of a sighting from Mittagong, 80 km south-west from Sydney, was noted. A check with the Australian Bureau of Meteorology disclosed that the inland slopes and highlands of New South Wales at the time were shrouded by stratus cloud and/or fog: the weather station at Bowral, 90 km south-west of Sydney, reporting thick fog at 17.00 UT and continuing at 20.00 h. This was confirmed by a high-resolution IR-image transmitted by the Japanese Geostationary Satellite at 18.00 h UT (on 6 April). The coastal region and inland areas well to the north of Sydney were quite clear.

Sunrise on 7 April occurred in Newcastle at 06.12 h and Sydney at 06.15 h AEST. At the time of passage of the fireball the Moon was below the horizon.

From the reported observations, the New South Wales fireball exhibited the following characteristics:

Time,	04 h 44 ± 1 min AEST (18 h 44 min GMT 6 April)
Brightness,	−16 ± 2 mag at maximum
Heading,	65° ± 5° true
Entry angle,	8° ± 3°
End height,	15 ± 10 km
End point,	152° 10′ ± 30′ E; 32° 40′ ± 20′ S
Velocity,	between 15 and 30 km s^{-1}

At an early stage it became evident that any resulting meteorite(s) would have descended into the sea at least 50 km offshore. Many of the eye-witnesses reported that the fireball appeared to explode just after crossing the coast, ejecting several short-lived fragments.

The estimate of brightness represents a peak value around the time of the explosion. Many of the witnesses were briefly blinded by it, comparing the luminosity to that of car headlights directly ahead, while others reported the effect in

Fig. 1   Track of the New South Wales fireball. Locations of the eye-witnesses are marked.

Table 1   Comparison of two fireballs

Fireball	6 April 1978		25 April 1969
Velocity (km s^{-1})	15	20	?
True radiant RA	155°	163°	186°
True radiant dec.	−14°	−20°	−31°
Semi-major axis	1.9 AU	3.6 AU	2.6 AU
Eccentricity	0.512	0.761	0.684
Perihelion distance	0.935 AU	0.858 AU	0.823 AU
Inclination	6.71°	11.35°	12.7° ⎫
Argument of perihelion	36.5°	47.9°	56.6° ⎬ 1950.0
Longitude of ascent node	196.2°	196.2°	215.2° ⎭

terms such as: "There was a blinding flash and the place (the backyard) lit up brighter than the brightest daylight." In subsequent interviews all who witnessed the explosion insisted that the fireball luminosity was more comparable to that of the Sun rather than the full Moon. After making due allowance for the shock to dark-adapted vision, the estimated magnitude of −16 is reasonable and indicates a fireball mass of 5 tonnes or more, depending on the velocity.

As is usually the case when precise timings are not forthcoming, the estimation of velocity proved extremely difficult. In re-enactments during subsequent on-site interviews many of the eye-witnesses indicated angular speeds representing velocities of 30 km s^{-1} or higher although a few went to the other extreme. The low end-height, which can be more reliably estimated, indicates a velocity of 20 km s^{-1} or less.

Velocity is the measure to which the orbital elements are most sensitive. Accordingly, the orbit of the fireball has been computed for two reasonable velocities and is compared in Table 1 with a similar set of elements derived by Hindley and Miles[1] for another large fireball which passed over the British Isles in April 1969.

The orbit is direct and of a low inclination typical of those usually derived for metorite-producing fireballs. The similarity with the 1969 fireball is strong. Hindley and Miles drew attention to the close similarity between the 1969 fireball and a 1962 fireball over New Jersey (US) on 24 April 1962 reported by Olivier[2]. It seems probable that all three fireballs resulted from parent bodies having a common origin, either asteroidal debris or a disintegrated nucleus of a short-period comet as suggested by Hindley and Miles.

A notable feature of the 1978 fireball was the high number of witnesses reporting hissing, humming, swishing or crackling sounds simultaneous with the passage of the fireball: these were mentioned in 10 of the 22 high quality reports and 15 of the full total of 33 written reports describing the fireball. Similar sounds accompanied the 1969 fireball according to Andrews et al.[3], but the actual number is not given. Olivier did not mention anomalous sounds from the 1962 New Jersey fireball, which was only of magnitude −10.

The reports of anomalous sounds from the 1978 fireball resembled many such reports compiled in an extensive survey made by Romig and Lamar[4]. This convinced me that the sounds were physically real and led to a detailed evaluation of all of the information provided by the witnesses. Many significant clues emerged which, when interpreted in conjunction with other fireball reports, narrowed the spectrum of the electromagnetic radiation emitted by the fireball to the very low frequency (VLF) spectral range. Various generation mechanisms known to produce such radiation from nuclear weapons and the aurora were investigated and found inapplicable to meteor fireballs. Recent work by ReVelle[5] has enabled me to propose a mechanism whereby the enormous power ($\approx 10^{11}$ W) in the fireball wake is converted to electromagnetic radiation at high audio frequencies by the magnetic flux trapped in the highly turbulent wake plasma: this work will be published elsewhere, as will details of some laboratory tests just completed indicating that the E-field
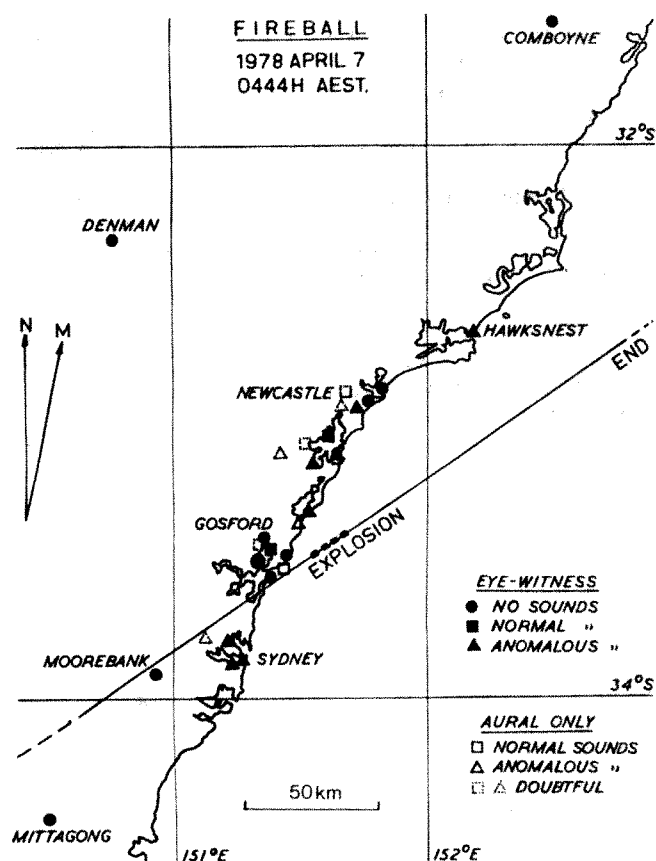
component of intense VLF radiation generates surface acoustic waves or physical vibrations which are heard by persons with sensitive high frequency hearing response. The transduction of energy from electromagnetic to acoustic, therefore, depends or the nature of the materials and objects close to the hearer, thus accounting for the sporadic distribution of reports of anomalous sounds from fireballs. Sounds emanating from brilliant auroral displays are similarly explicable.

I thank A. A. Griffin, NRC of Canada, for assistance in computing the fireball orbit.

1. Hindley, K. B. & Miles, H. G. *Nature* **225**, 255–257 (1970).
2. Olivier, C. P. *Sky Telesc.* **24**, 19 (1962).
3. Andrews, A. D., Rackham, T. W. & Wayman, P. A. *Nature* **222**, 727 (1969).
4. Romig, M. F. & Lamar, D. L. *RAND Memo.* RM-3724-ARPA (1963).
5. ReVelle, D. O. *J. atmos. terr. Phys.* **41**, 453–473 (1979).

Muon catalysis for energy production by nuclear fusion

Yu. V. Petrov

Leningrad Nuclear Physics Institute,
Gatchina, Leningrad 188350, USSR

In 1957 Jackson[1] considered the possibility of using muon-catalysed dt (deuterium–tritium)-fusion for energy production. His conclusion was negative. However, the situation has now changed and this problem should be reconsidered. The suggestion that muons would be suitable as catalysts of dt fusion was first made by A. D. Sakharov and Ya. B. Zeldovich (see ref. 2). It is shown here that the use of the muon catalysed dt fusion combined with the fissile nuclides blanket can provide a positive energy gain.

Basic reactions of muon catalysis are shown in Fig. 1. When slowing down, a negative muon forms the mesic atoms $(d\mu^-)$ or $(t\mu^-)$ with probabilities c and $(1-c)$, proportional to the relative concentration of deuterium and tritium in the dt mixture. During the time τ_{dt} the muon is transferred from deuterium to tritium. During the time $\tau_{dt\mu}$ a mesic atom $(t\mu^-)$ collides with deuterium and forms a mesic molecular ion $(dt\mu^-)^+$. It takes a short time τ_f for an exothermic nuclear fusion reaction $d+t \rightarrow {}^4He+n$ to occur. When the probability is w_s, the muon is captured by ${}^4He$ and stays there until it decays, alternatively when the probability is $1-w_s$ the muon slows down during the time τ_a and again catalyses the fusion.

The muon spends most of the cycle within mesic atoms. The fusion time [which is small because of the existence of a nuclear resonance: $\tau_f \sim 10^{-12}$ s (ref. 2)] and the time of muon slowing down and capture [$\tau_a^0 \sim 10^{-10}$ s (ref. 1)] are negligible compared with the muon lifetime $(\tau_0 = 2.2 \times 10^{-6}$ s). [The density dependent quantities τ_a, τ_{dt} and $\tau_{dt\mu}$ with superscript 0 correspond to the liquid hydrogen density 4.25×10^{22} cm^{-3}.]

The probability w_c that the muon quits the cycle is the sum of three quantities each being the product of the probability for the corresponding mesic atom formation and the probability of muon decay inside this atom $(\tau_{dt}, \tau_{dt\mu} \ll \tau_0)$:

$$w_c = c \times \frac{\tau_{dt}}{\tau_0} + \frac{\tau_{dt\mu}}{\tau_0} + w_s \qquad (1)$$

The number of cycles which a muon has time to catalyse is $x_c = 1/w_c$.

According to theoretical estimates $w_s \lesssim 10^{-2}$ (refs 1, 2) and $\tau_{dt}^0 \sim 5 \times 10^{-9}$ s (ref. 3). Recently Ponomarev *et al.*[4] have shown theoretically that $\tau_{dt\mu}^0 \lesssim 10^{-8}$ s: therefore it is also small compared with τ_0. Because of a weakly bound excited state [$\varepsilon = 0.7 \pm 0.1$ eV with respect to decay into $(t\mu^-)$ (ref. 5)] existing in the mesomolecular ion $(dt\mu^-)^+$ the big excited mesic molecule $[(dt\mu^-)^+ d\ 2e^-]^*$ is formed through resonance. [A similar mechanism for the formation of $(dd\mu^-)^+$ was considered previously on theoretical grounds by Vesman[6] and discovered experimentally by Dzelepov and his collaborators[7].]

The recent experiments confirm small theoretical values in equation (1): $\tau_{dt}^0 = (3.7 \pm 1.2) \times 10^{-9}$ s and $\tau_{dt\mu}^0 < 10^{-8}$ s (ref. 8). Thus it seems that $w_c \sim 10^{-2}$, that is, one muon can catalyse about $x_c \sim 10^2$ fusion reactions and release ~ 2 GeV of energy[4,5,16].

The muons are produced[9] during the decay of pions generated in the collisions of fast nucleons with nuclei. At moderate energies, $T_0 \sim 1$ GeV per nucleon, π^- are formed mainly in neutron–neutron collisions. The fraction of π^- produced in a single inelastic nn-collision is $w_{nn} = 0.83$; correspondingly $w_{np} = 0.23$ and $w_{pp} = 0$. For this reason, neutron-enriched nuclei should be used as target as well as projectile. Let the average number of π^- produced in a single inelastic collision of nucleons, be $\langle n_- \rangle$. It can be obtained as the average of w_{nk} over the fractions of nn- and np-collisions c_{nk}:

$$\langle n_- \rangle = c_{nn} w_{nn} + c_{np} w_{np}; \; c_{nn} + c_{np} + c_{pp} = 1 \qquad (2)$$

Because of zero total isospin of initial particles in dd-collisions π^-, π^+ and π^0 are produced with equal probabilities and $\langle n_- \rangle = 1/3$. For tt-collisions $\langle n_- \rangle$ increases up to 0.5 according to equation (2).

The yield of pions per unit energy of the incident beam is $Y_\pi = \langle n_- \rangle F\, T_0^{-1}$, where F is the number of inelastic collisions. In a thin and long cylindrical target, oriented along the beam direction only one collision will occur. For $T_0 = 1$ GeV per nucleon the fraction of inelastic collisions will be $F = 0.5$. By increasing the thickness of the target one can increase the value of F up to $F = 2/3$ without excessive absorption of the pions produced. On the other hand the maximum value of $\langle n_- \rangle$ decreases when beams (d) and targets (Li, Be, D_2O) other than tritium are used. Additional losses of mesons will take place in a converter where π^- are held by the magnetic field until their decay, and also in the walls of the mesocatalytic synthesizer. An optimistic estimate of the conversion coefficient is $\phi = 0.8\,\pi^-/\mu^-$. As a result the energy necessary to produce one μ^- is $\varepsilon_\mu = Y_\mu^{-1} = (Y_\pi \phi)^{-1} = 5$ GeV per μ^- (ref. 9).
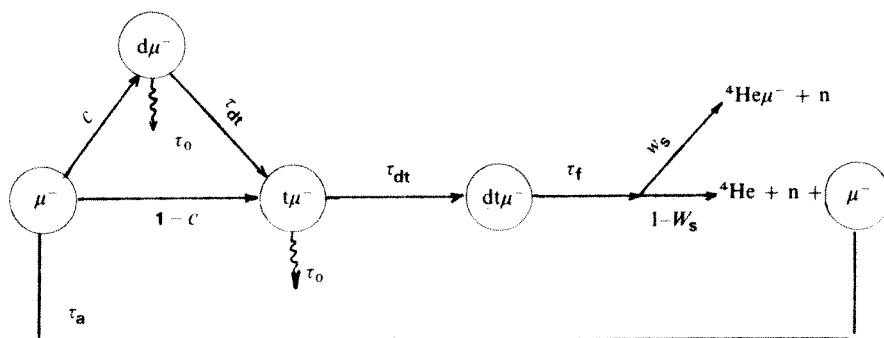
Fig. 1 Scheme of mesocatalysis.
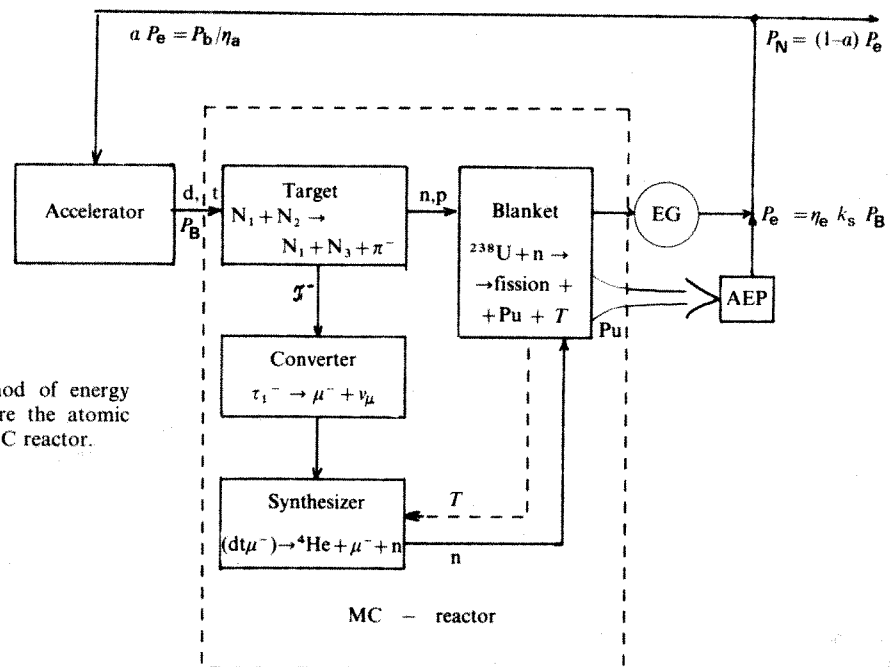
Fig. 2 Scheme of the mesocatalytic (MC) method of energy production. EG is the electric generator; AEP are the atomic energy plants, four times more powerful than the MC reactor.

Therefore in spending 5 GeV of energy we obtain less than 2 GeV. The installation efficiency (the ratio of the overall energy output to the input) is: $Q = Y_\pi \phi E_s \times x_c = 0.35 < 1$ ($E_s = 17.6$ MeV is the dt fusion energy). The total efficiency is decreased further when the energy losses in accelerator and the efficiency of transformation of heat into electricity is taken into account. Thus, the mesocatalysis alone cannot give positive energy output. Jackson[1] arrived at the same conclusion despite an overoptimistic estimate of the energy spent on μ^- production: $\varepsilon_\mu \sim 2$ GeV per μ^- for pure proton beam (without neutrons).

To increase the fusion energy in the modern projects of the hybrid thermonuclear reactors the fissile blankets are used. Fast neutrons cause the fission of the usually nonfissile isotopes ^{238}U or ^{232}Th (ref. 10) and also produce fissile isotopes. It seems reasonable to surround the MC-reactor by such a blanket[11]. The theoretical estimates[11] show that in a thick blanket made of depleted uranium the number $\delta_f = 1$ of fissions takes place and $\varepsilon_0 = 4$ slow neutrons are produced for each fusion neutron with $E_n = 14$ MeV. Direct measurements[12] give $\delta_f = 1.06 \pm 0.06$ and $\varepsilon_0 = 3.9 \pm 0.24$. Assuming the slow neutrons utilization factor to be $\vartheta = 0.85$, and spending one neutron for tritium regeneration, one can produce $\xi = (\varepsilon_0 \vartheta - 1)\delta_f^{-1} = 2.4$ commercial plutonium nuclei per fission. Additional fissions and neutrons also will be induced by the fast nucleons of the incident beam, having about 80% of their initial energy after the π-mesons production ($T_s \simeq 0.8$ GeV)[9]. From the experimental data[13] it follows that fast protons in ^{238}U cause about $z_e = 20$ fissions per GeV and produce $\xi_{e0} = 3$ neutrons per fission$^{(n/fis)}$, so that $\xi = \xi_{e0}\vartheta = 2.5$ Pu/fis[11].

The total multiplication factor of the initial beam energy is therefore

$$k = Q\delta_f \frac{E_f}{E_s} + z_e E_f \frac{T_{se}}{T_0} = Q k_B \qquad (3)$$

Here $E_f = 0.2$ GeV is the uranium fission energy. $k_B = 20$ is the energy multiplication factor caused by the nuclide blanket. The consumption of one Pu nucleus in a thermal reactor can give 1.6 fis/Pu taking into account Pu breeding. That is, one hybrid reactor can feed $\xi\Psi = 4$ cheap thermal reactors of the same power. The energy gain due to the 'blanket plus four reactors' system is $k_{BS} = k_B(1 + \xi\Psi) = 100$. The multiplication of the initial beam energy is $k_s = Q k_{BS} = 35 \gg 1$. Thus, the blanket turns a negative energy balance into a positive one, giving a considerable energy gain due to the fission of the widely spread isotope ^{238}U.

The thermal power P released in the blanket and in the reactors can be converted into electric power P_e with efficiency η_e (see Fig. 2). The part α of this electricity must be spent on the accelerator feeding. Let us denote the efficiency of the accelerator as η_a (the ratio of the beam power P_B to the input power αP_e). From the relations $P_B/\eta_a = \alpha P_e$ and $P = k_s P_B$ it follows that $\alpha = (k_s \eta_e \eta_a)^{-1}$. The net power output P_N and the total efficiency of the system η_s are

$$P_N = (1 - \alpha)P_e = (1 - \alpha)\eta_e P$$

$$\eta_s = P_N/P = (1 - \alpha)\eta_e = \eta_e - \frac{1}{\eta_a k_s} \qquad (4)$$

The beam power of the modern meson factories such as LAMPF is about $P_B \simeq 0.4$ MW for protons having $T_0 = 0.8$ GeV and $\eta_a \sim 0.1$ (ref. 14). The accelerators with $P_B = 300$ MW and $\eta_a = 0.6$ are designed now for electronuclear breeding systems[15]. (In such a system the fast protons produce energy and plutonium within uranium due to spallation.) Assuming $\eta_a = 0.6$ and $\eta_e = 0.35$ (which is the common value for nuclear power plants) we obtain $\alpha = 0.14$ and the total efficiency $\eta_s = 0.30$ which is quite acceptable.

Now let us compare the following three methods of energy production: mesocatalytic (MC), electronuclear (EN) and thermonuclear (TN) (see Table 1). To make the comparison it is convenient to take the same fission thermal power P produced in the blanket (or in uranium target) and, therefore, the same electric power. Moreover, the commercial plutonium

Table 1   Comparison of mesocatalytic (MC), electronuclear (EN) and thermonuclear energy production

Method of producing energy and Pu	TN*	EN†	MC‡
Pu production ξ (Pu/fis)	2.3	2.5	2.4
Multiplication of the beam energy by the system (k_s)	130	20	35
The fraction of energy, spent on the accelerator feeding (α)	0.03	0.24	0.13
Efficiency of the system (η_s)	0.34	0.27	0.30
Temperature of dt mixture (K)	10^8	—	10^3

*For $Q = 4$, $\delta_f = 0.6$ fis/n, $\Psi = 1.6$ fis/Pu, $\eta_a = 0.7$, $\eta_e = 0.35$ (ref. 10).
†For $z_e = 20$ fis/GeV, $\Psi = 1.6$ fis/Pu, $\eta_a = 0.6$, $\eta_e = 0.35$ (ref. 11).
‡For $Q_m = 0.6$ (taking into account the electronuclear channel), $\delta_f = 1$ fis/n, $\eta_a = 0.6$, $\eta_e = 0.35$ (ref. 11).

output should be the same, since the values of ξ are close to each other (see Table 1). The methods differ in the values of k_s and α (the fraction of the electric energy, spent on the feeding of the accelerator, or the injector for the TN reactor). The accelerator power required and the value of α for the MC hybreeder seem to be approximately half those required for EN breeders. Compared to the TN hybreeder (for example, the project[10] using the Tokamak with the magnetic confinement and with the plasma energy multiplication coefficient $Q = 4$), the value of α is four times larger for the MC reactor. However, the difference in their efficiencies is too small (η_s 0.34 and 0.30, respectively) to be considered significant. The difference in the design and the capital costs may seem more important. An evident advantage of the MC hybreeder is the absence of hot plasma.

The methods listed in Table 1 produce several times more commercial plutonium per fission than the fast-neutron breeder reactors, having $\xi < 0.5$ Pu/fis. Therefore, they are much more effective for the feeding of the cheap thermal neutrons reactors reducing the capital costs per unit energy output of the system. The thermal reactors use the slightly enriched nuclear fuel and made it possible to avoid the external fuel reprocessing cycle. This reduces the risk of nuclear weapons proliferation. However, it is important to remember that only fast-neutron reactors are in current use.

The above estimates show that the system including the MC hybreeder and usual thermal neutrons reactors provides a gain in electric power. The accuracy of the present estimates is limited, but even a considerable reduction in some of the system parameters (Q, for example) would not change this main conclusion. As to the ability of the MC hybreeder to compete with the other systems, this depends on the experimental verification of the theoretical estimate of x_c. This estimate is based on the value of w_s, which could be less than 10^{-2} (for example, due to the stripping of μ^- while slowing down $^4\mathrm{He}\mu^-$), and on the value of $\tau^0_{d t \mu} < 10^{-8}$ s which is known now only by the order of magnitude. If $x_c = 50$, then the multiplication factor K [equation (3)] is reduced from 7 to 5 and it would not be worthwhile using the MC method in preference to a more simple EN-method ($K = 4$). But it is possible that $x_c = 200$ and that conditions are more favourable; only experiments can give the answer. Another problem is to what extent can we avoid the energy losses in the actual MC reactor and in the powerful accelerator. Most serious are the losses of muons in the wall, between the converter and the synthesizer. Thus Table 1 demonstrates not the actual situation, but rather the values of parameters at which mesocatalysis becomes interesting for energy production. Only by eliminating the uncertainty in all factors mentioned above will it be shown whether the MC system can be considered as an alternative method of energy production.

I thank S. S. Gerstein for discussions and for sending the reports[16] which stimulated these estimates; also I. I. Gurevich, L. I. Ponomarev and Yu. M. Shabelsky for discussions and assistance, and D. I. Blokhintzev, G. N. Flerov, V. P. Dzelepov, V. N. Gribov, V. M. Lobashev, V. V. Orlov and O. I. Sumbayev for their interest and comments.

1. Jackson, J. D. *Phys. Rev.* **106**, 330 (1957).
2. Zel'dovich, Ya. B., Gerstein, S. S. *Usp. fiz. Nauk* **71**, 581 (1960).
3. Ponomarev, L. I. *Proc. 6th Int. Conf. Atomic Physics*, Riga (1978).
4. Vinitsky, S. I. *et al. Soviet Phys. JETP* **74**, 849 (1978).
5. Ponomarev, L. I. *Sov. Nature* **9**, 8 (1979).
6. Vesman, E. A. *Soviet Phys. JETP Lett.* **5**, 113 (1967).
7. Bystritsky, V. M. *et. al. Soviet Phys. JETP* **76**, 460 (1979).
8. Bystritsky, V. M. *et al. JINR Rep.*, D1-12696, Dubna (1979).
9. Petrov, Yu. V. & Shabelsky, Yu. M. *Soviet J. nucl. Phys.* **30**, 129 (1979).
10. Velikhov, E. P. et al. Soviet J. atom. Energy **45**, 3 (1978).
11. Petrov, Yu. V. *Proc. 14th LNPI Winter School*, Leningrad (1979).
12. Weale, J. W. *et al. J. nucl. Energy* **14**, 100 (1961).
13. Vasilkov, R. G. *et al. Soviet J. Atom. Energy* **44**, 329 (1978).
14. Michaelis, *IEEE Tr. nucl. Sci.* **22**, 1042 (1975); LASI-79-15, Los Alamos (1979).
15. Schriber, S. O. *et al. Int. Conf. High Energy Accelerators*, Protvino, (1977).
16. Gerstein, S. S. & Ponomarev, L. I. TH-2393-CERN (1977); *Phys. Lett.* **72B**, 80 (1977).

Solid phase photoreduction of methylviologen adsorbed on cellulose

M. Kaneko, J. Motoyoshi & A. Yamada

The Institute of Physical and Chemical Research, Wako-shi, Saitama, 351 Japan

There has been a growing interest in photochemical reduction of methylviologen (1,1'-dimethyl-4,4'-dipyridinium dichloride; MV^{2+}) as a means of solar energy conversion[1-4], because the cation radical (MV^+) can reduce protons to give hydrogen gas[5]. One problem in a photochemical conversion system is the effective separation of the reaction products, because a photochemical reaction in a homogeneous solution usually accompanies a spontaneous backward reaction which consumes the acquired energy. To overcome this problem, macro- or micro-heterogeneous reaction environments such as micelle[6-9] or liposome[1] have been proposed. A solid phase photochemical reaction must also be useful for constructing an effective photoenergy conversion system. We describe here how MV^{2+} adsorbed on solid cellulose could be photoreduced to give MV^+, the colour of the cellulose changing from white to deep blue. The reaction could be sensitized by tris(bipyridyl)ruthenium(II) complex ($Ru(bpy)_3$) and EDTA.

Cellulose paper was dipped into a solution of 10^{-1} M MV^{2+} in methyl alcohol for 10 min and then dried under air for 15 min. This dipping and drying procedure was repeated, and the cellulose was then dried *in vacuo* at room temperature. From the UV spectra of the solution before and after dipping, the MV^{2+} adsorbed was calculated to be 382 mg per g cellulose. When this cellulose sample was irradiated with a halogen lamp (12 V, 100 W) under vacuum at 30 °C, a blue colour appeared after several minutes. The change of the transmission visible spectra of the sample accompanying the irradiation is shown in Fig. 1. The characteristic absorptions at 402 and 620 nm induced by the irradiation indicate clearly that MV^+ is formed. The shifts of the absorptions to longer wavelengths than those in water (395 and 605 nm) or in methyl alcohol (396 and 608 nm) suggest some strong adsorption of the viologen species on cellulose. The reflection
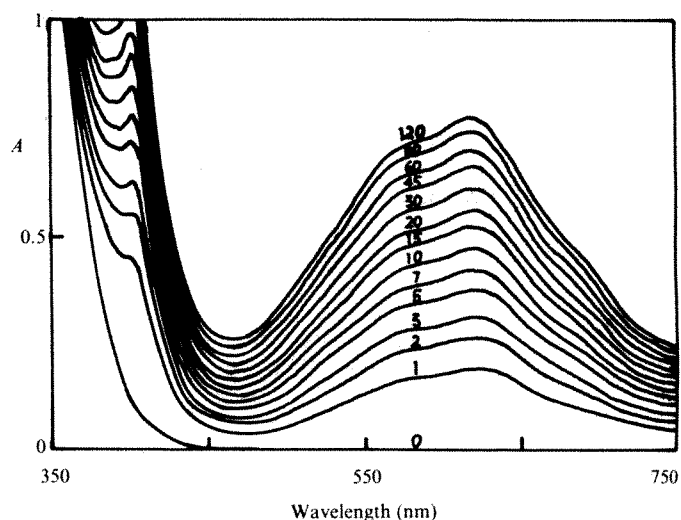
Fig. 1 Photochemical reduction of MV^{2+} adsorbed on cellulose, irradiated *in vacuo* at 30 °C. The numbers represent reaction time in min.
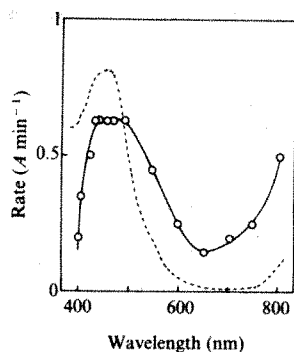
Fig. 2 Action spectrum for the formation of MV^+ in MV^{2+}–$Ru(bpy)_3$–EDTA/cellulose system, irradiated *in vacuo* at 30 °C. ――――, Absorption spectrum of the sample before irradiation.

spectrum of the sample was quite similar to that shown in Fig. 1. The electron spin resonance (ESR) spectrum also showed the formation and increase of MV^+ induced by irradiation. The ESR spectrum at room temperature was a singlet with *g*-value 1.967 and ΔH_{msl} 13.5 G. The spin concentration was determined using DPPH as a standard and related to the absorbance at 620 nm of the visible spectrum. Absorbance of 1 unit of the cellulose sample corresponds to 1.07×10^{-8} spins per cm^2 cellulose. As the absorption peak of the MV^{2+} adsorbed on cellulose lies at 267 nm, the UV irradiation is most effective for the reduction of MV^{2+}. However, the visible light obtained using a UV cut filter (>390 nm) was also effective in producing MV^+, because the adsorbed MV^{2+} shows a slight absorption up to 480 nm.

The mixture of 5×10^{-2} M MV^{2+}, 10^{-3} M $Ru(bpy)_3Cl_2 \cdot 6H_2O$ and 5×10^{-2} M EDTA·$2Na \cdot 2H_2O$ in water was adsorbed on a cellulose paper with the same procedure as the MV^{2+}/cellulose system described previously. The adsorbed MV^{2+}, $Ru(bpy)_3$ and EDTA were 64.4, 1.88 and 92.4 mg per g cellulose, respectively, which correspond to the molar ratio of 100/1/100. This cellulose sample was irradiated with a monochromatic light of 470 nm *in vacuo* at 30 °C, and the initial rate of MV^+ formation was represented by the increase of the absorbance at 620 nm. The cellulose which adsorbed MV^{2+}, $Ru(bpy)_3$ and EDTA showed much higher rate of MV^+ formation (0.360 absorbance unit min^{-1}) than the sample which adsorbed only MV^{2+} (0.010 absorbance unit min^{-1}) indicating that the photoreduction of MV^{2+} was sensitized by $Ru(bpy)_3$ and EDTA. The $Ru(bpy)_3$ alone had no effect on the photoreduction of MV^{2+}, while EDTA showed some accelerating effect without $Ru(bpy)_3$ probably because it acts as electron donor for the MV^+ formation. The presence of both $Ru(bpy)_3$ and EDTA was necessary for this remarkable photosensitization. The action spectrum for the formation of MV^+ in the MV^{2+}–$Ru(bpy)_3$–EDTA/cellulose system shown in Fig. 2 indicates clearly that the excitation of $Ru(bpy)_3$, which brings about the absorption at 460 nm due to charge transfer from metal to ligand, causes the sensitized reduction of MV^{2+}.

An interesting feature of the solid phase photoreaction system is the accumulation of MV^+ even in the presence of oxygen. In the photochemical formation of MV^+ in a homogeneous solution[2,3] or in a liposome system[1], MV^+ can be accumulated only in the absence of oxygen, and the contact of the solution with oxygen causes a rapid oxidation of the MV^+. Table 1 shows the initial rates of the photochemical accumulation of MV^+ in an MV^{2+}–$Ru(bpy)_3$–EDTA/cellulose system in the absence and presence of oxygen as well as the initial rate of MV^+ oxidation in the dark. It is surprising that the accumulation of MV^+ is very rapid even in the presence of oxygen. One reason for the low rate of MV^+ oxidation by oxygen would be the slow diffusion of oxygen into the cellulose, the MV^+ formed on cellulose was observed

to be very soluble in water, but almost insoluble in methyl alcohol which is usually a good solvent, indicating the specific adsorption of viologen on cellulose. Such strong adsorption of MV^+ may cause the remarkable stabilization against oxidation. The lower rate of MV^+ accumulation in air than in the absence of oxygen must be caused by the quenching of the excited $Ru(bpy)_3$ by oxygen, as the rate of MV^+ oxidation is low compared with the difference between the rates of MV^+ accumulation in the presence and the absence of oxygen. As MV^{2+} without cellulose did not only give MV^+ in the same irradiation condition, the cellulose molecule of the MV^{2+}/cellulose system must work as an electron donor. The MV^{2+}/cellulose irradiated with 500 W xenon lamp under air for 25 h showed the presence of carbonyl group at 1,730 cm^{-1} in the IR spectrum indicating the oxidation of cellulose to aldehyde or ketone (I). The irradiation of a

$$Cell-CH_2OH \atop Cell-C \diagdown {}^O_H \quad \xrightarrow{h\nu} \quad {2 MV^{2+} \atop 2 MV^+} \qquad (I)$$
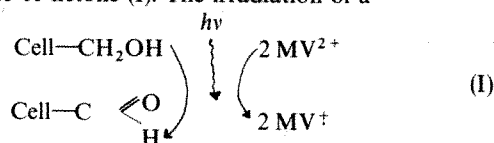
control cellulose without MV^{2+} in the same conditions did not give the absorption at 1,730 cm^{-1}.

The sensitized system composed of MV^{2+}–$Ru(bpy)_3$–EDTA/cellulose involves the irreversible oxidation of EDTA to give carbon dioxide[1,10]. The CO_2 evolved in the photochemical reaction of MV^{2+}–$Ru(bpy)_3$–EDTA/cellulose was quantitively determined by gas chromatography using a silica gel column. The amount of CO_2 evolved after irradiation with visible light under helium for 8 h corresponded to 2.09 mol% of the EDTA contained. Because the generation of one molecule CO_2 is a two-electrons process, the turnover number of the $Ru(bpy)_3$ catalyst is calculated to be 4.14 from the complex adsorbed. The photocatalytic activity of $Ru(bpy)_3$ was also indicated by the constant concentration of the bivalent $Ru(bpy)_3$ during a prolonged irradiation. The primary photoreaction is concluded to be the oxidation of the $Ru(II)$ to $Ru(III)$ complex by the MV^{2+}, as the luminescence from the $Ru(II)$ complex at 604 nm was not quenched by EDTA, but entirely quenched by MV^{2+}. The reaction mechanisms can therefore be represented by (II)

$$(II)$$
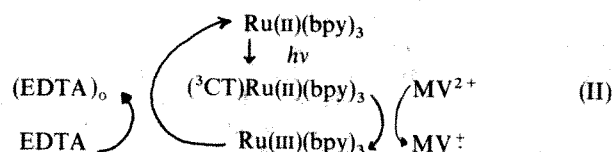
A small quantity of water adsorbed markedly retards the photoreduction of MV^{2+}. Other polysaccharides such as starch and cotton were as effective as cellulose. The effect of disaccharide (saccharose) was small, and monosaccharide (glucose) was not effective for the photochemical reaction. These experimental facts suggest that the polysaccharide structure itself plays an important part as a matrix providing some specific micro-environment for the photoreaction to occur. Considering the specific adsorption of MV^+ and the retarding effect of water, it is suggested that some hydrophobic

Table 1 Relative rate of photochemical accumulation and dark oxidation of MV^+ in a MV^{2+}–$Ru(bpy)_3$–EDTA/cellulose system

Reaction	Condition	Rate ($A\,min^{-1}$)
Photochemical accumulation of MV^+	*In vacuo*	1.15
Photochemical accumulation of MV^+	Under air	0.52
Dark oxidation of MV^+	Under air	0.0094

Irradiation was through UV and IR cutoff filters at 30 °C.

environment provided by cellulose favours the photoreaction, and also stabilizes the MV^+ against oxidation. Such aspects of the photochemical reactions on solid cellulose are quite different from those in micelle or liposomes. As the average distance between $Ru(bpy)_3$ and MV^{2+} or EDTA is calculated to be $<14\text{Å}$ on the assumption that the cellulose molecule occupies the half of the sample volume, electron transfer between the immobilized species would be possible.

Other interesting features of the solid phase photochemical reaction on cellulose are the broadening and the redshift of the absorptions of the MV^{2+} as well as of the $Ru(bpy)_3$, which leads to an utilization of wider and longer wavelengths than the corresponding solution system. The quantum yield for the production of MV^+ in the experiment *in vacuo* under 470 nm monochromatic light irradiation was estimated to be $\sim 5\%$. Natural materials containing polysaccharides were also effective as a matrix for the non-sensitized as well as sensitized photoreduction of MV^{2+}.

1. Ford, W. E., Otvos, J. W. & Calvin, M. *Nature* 274, 507–508 (1978).
2. Kalyanasundaram, K. *JCS Chem. Commun.* 628–630 (1978).
3. Takuma, K., Kajiwara, M. & Matsuo, T. *Chem. Lett.* 1199–1202 (1977).
4. Delaive, P. J., Giannotti, C. & Whitten, D. G. *J. Am. chem. Soc.* 100, 7413–7415 (1978).
5. Kawai, T., Tanimura, K. & Sakata, T. *Chem. Lett.* 137–140 (1979).
6. Wallace, S. C., Grätzel, M. & Thomas, K. *Chem. phys. Lett.* 23, 359–362 (1973).
7. Meisel, D., Matheson, M. S. & Rabani, J. *J. Am. chem. Soc.* 100, 117–122 (1978).
8. Maestri, M., Infelta, P. P. & Grätzel, M. *J. chem. Phys.* 69, 1522–1526 (1978).
9. Horsey, B. E. & Whitten, D. G. *J. Am. chem. Soc.* 100, 1293–1295 (1978).
10. Frisell, W. R., Chung, C. W. & Mackenzie, C. G. *J. biol. Chem.* 234, 1297–1302 (1959).

Major evaporite deposition from groundwater remobilized salts

J. E. Rouse* & N. Sherif†

*Geochemistry and Petrology Division, Institute of Geological Sciences, 64–78 Gray's Inn Road, London WC1X 8NG, UK
†Department of Geology, Imperial College of Science and Technology, Prince Consort Road, London SW7 2BP, UK

The coastal sabkhas of the western Gulf of Sirte, Libya developed in two stages behind a barrier-ridge complex following the penultimate and the last major sea-level rises. A strong north-to-south littoral drift led to the isolation of coastal lagoons by a seaward sand ridge following the stabilization of sea level and produced isolated basins in which evaporites have been and are depositing. A sulphur isotopic study of the groundwaters and sediments described here demonstrated that the brines mostly originated in continental groundwaters supplied from the deep aquifer by surface and sub-surface flows which carry sulphate and other ions remobilized from Cretaceous sediments.

The physiography and the sedimentary pattern of the western coastal plain of the Gulf of Sirte was formed by two major transgressive events (Fig. 1). The earlier transgression of late Pleistocene age reached a level close to that of the present sea, and a barrier-island and lagoon were formed and preserved as the inner-barrier and sabkha apparently unaffected by large scale erosion during the succeeding regressive phase. The Flandrian transgression meant that the sea reached its present level $\sim 3,700\,\text{yr BP}$ and it apparently spilled into the older lagoon behind the inner barrier. This outer barrier then developed to enclose a lagoon landwards, and carbonate sediments were deposited in both inner and outer lagoons. The inlets which allowed marine water to penetrate both lagoons ultimately closed and the lagoons developed into the present day inner and outer sabkha depressions. These are now the sites of deposition of modern evaporites covering more than $1,000\,\text{km}^2$; their sedimentology has been described by Sherif[1].

The inflow of water into these enclosed coastal sabkhas is presently almost entirely by sub-surface flow with flooding only occurring during winter when the water table rises in response to seasonal climatic change. Subsequent evaporation of the floodwater results in precipitation of surface halite. The evaporites in the sediments of these sabkhas are dominated by gypsum and halite which are produced by evaporation and simple concentration of the groundwaters, and are arranged in a roughly concentric pattern within the sabkha depressions with gypsum at the margins and halite at the centres. Dolomite and magnesite also occur and are produced by the reaction between the lagoonal carbonate sediments and the co-existing brines.

A chemical and sulphur isotopic study of the groundwaters and sediments has enabled their origin and progress during evaporation to be defined more clearly. The concentrations of the major groundwater ions are highest in the central lagoonal basins and lowest at the two extremities and this suggests that water is supplied to the sabkhas from both landward and seaward sides. Of the three possible sources of the sabkha groundwaters—terrestrial groundwaters, seawater and meteoric water—only the first two could provide the necessary volume of salts that have been and are accumulating in these basins.

Deep terrestrial groundwaters flow into the sabkha complex by sub-surface seepage from deep fissures and by sub-surface flow from spring discharge along the landward margin of the sabkhas. The most important and the only one of these springs studied in detail[2,3], is that of Tawurghah which produces some $10^8\,\text{m}^3\,\text{yr}^{-1}$ of sulphate-rich, brackish water of 2–$3\,\text{g}\,\text{l}^{-1}$ total dissolved solids. Although the sulphate content
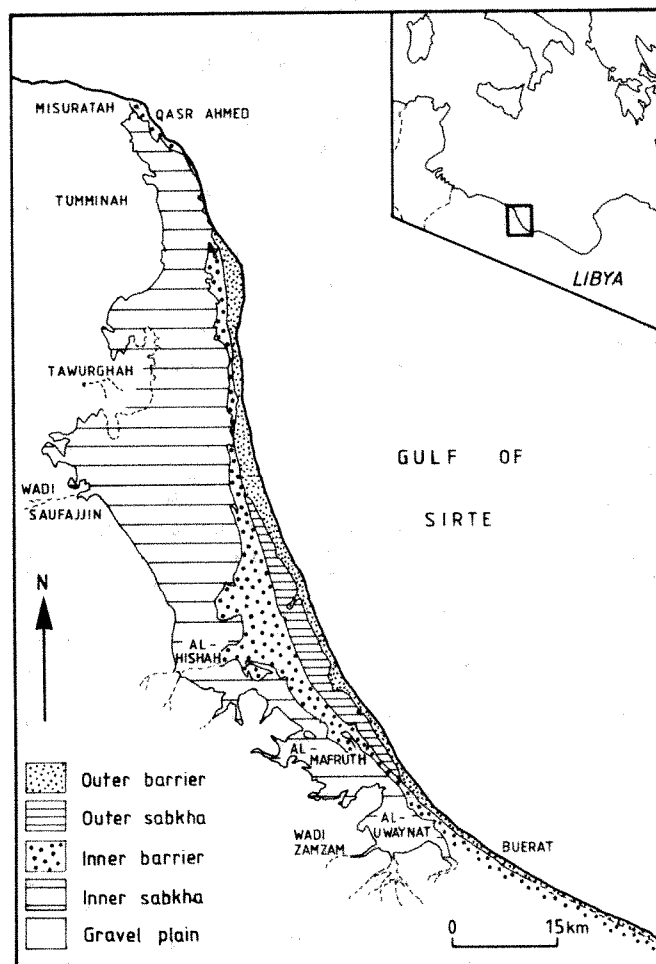
Fig. 1 The coastal plain of the western Gulf of Sirte, showing major physiographical features and sedimentary units.
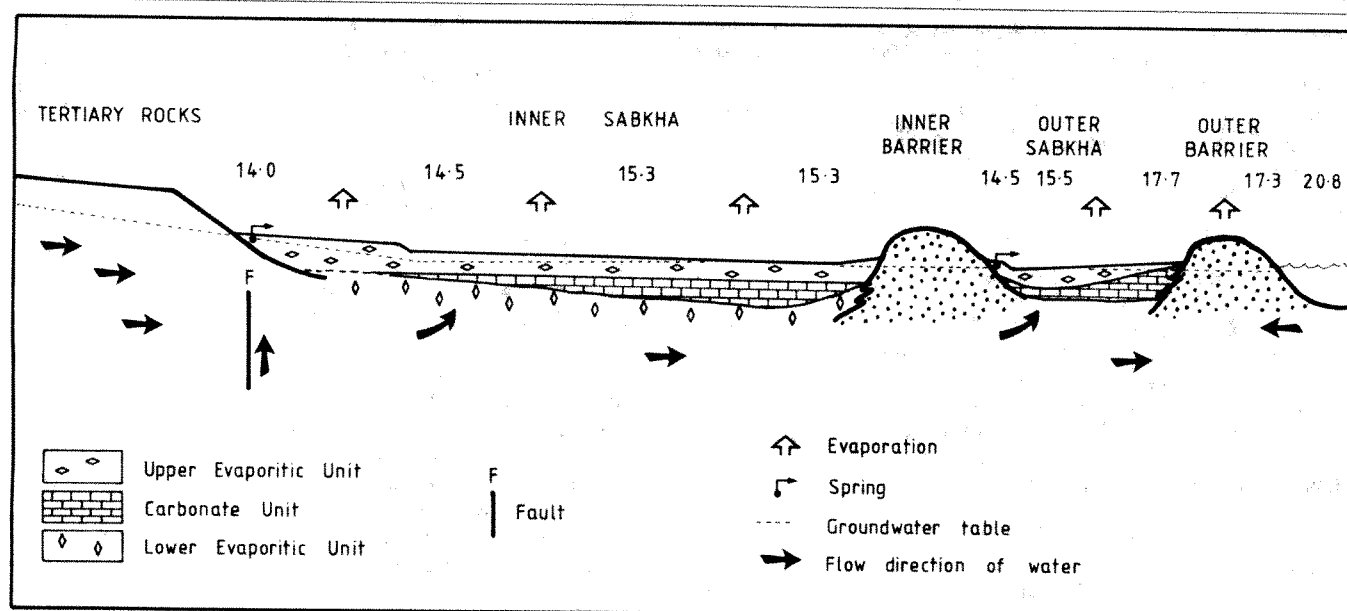
Fig. 2 The proposed hydrology of the coastal sabkha. Mean sulphur isotopic values of the groundwaters (in ‰ with respect to the Cañon Diablo meteorite standard) are superimposed above the sabkha sediment facies to which they apply.

of the various springs is very variable in the range of 0.6–5 g l^{-1}, the sulphur isotopic fractionation, δ^{34}S (with respect to the Cañon Diablo Troilite standard) is remarkably constant at +13.9±0.5‰.

Marine recharge of the sabkha groundwaters except during very exceptional storms by direct flooding over the seaward barrier-ridge is now very unlikely due to the height and extent of this feature. The most likely and probably only important mode of seawater encroachment is by sub-surface seepage through the barrier driven by a hydraulic head between mean sea level (MSL) and the sabkha groundwater table of ~3 m.

Eight samples of Mediterranean seawater were analysed to obtain a background sulphur isotopic value of the seawater source of sulphate. Four surface samples which might have been expected to show continental sulphate contamination, were not significantly different from four deep samples +20.8‰ compared with +20.4‰ respectively on average; nor were they significantly different from Atlantic surface water analysed at +20.8‰ or from the mean open ocean value of +21.0‰ of Rees et al.[4]. Salinity and sulphate content were ~10% above Atlantic levels.

Groundwater sulphur isotopic values for the inner sabkha lie in the range +14.5 to +15.5‰ and demonstrate the almost total supply of sulphate to this basin by continental waters. Only in the north, where values of +18 to +20‰ adjacent to the seaward barrier occur coincident with the maximum head between MSL and sabkha groundwater table, is there any evidence for seawater incursion. The sulphur isotopic values for the sabkha sediments, although between 1 and 2‰ heavier than the groundwaters due to the effects of water–gypsum fractionation and bacterial sulphate reduction, do not alter this conclusion. Groundwater values of the outer sabkha and the outer beach ridge grade progressively from the +15‰ value characteristic of the inner sabkha found at the inner barrier to +18‰ at the coast. One sample of coastal seawater sampled at the coast yielded an analysis of 3.8 g l^{-1} sulphate and sulphur isotopic value of +17.3‰.

Considering the low isotopic values of the outer beach ridge aquifer and locally, seawater, there is good evidence to suggest that the continental water source is supplying water, and hence light sulphate, under a significant hydraulic head to both Recent and Pleistocence sand barriers and sabkhas and to the sea possibly as sub-surface springs. Only the deeper sediments with a buried algal mat have isotopic values in the region of +20‰. Whether these higher values are the result of

an earlier more marine phase of sabkha building before the closing of the outer barrier channels, or are due to extensive bacterial reduction and hence loss of isotopically light sulphate from the sabkha sediments as sulphides, is not yet clear.

The extensive supply of sulphate to the sabkha complex of the western Gulf of Sirte clearly originates mostly from remobilized sulphate brought to the surface and distributed into the groundwater by numerous springs of sulphate or sulphate–chloride facies water. The dominant hydrogeological feature of the area is an extensive, north–south directed fault near Tawurghah which extends vertically upwards as far as the Miocene strata. This fault and its satellite fissures provide the karstic channels through which deep artesian water from the Gharyan sediments of the Upper Cretaceous reaches the Miocene[2]. Above this level, diffusion through fissures brings the water to the surface, both as springs and sub-surface flow, into the groundwaters of the sabkha (Fig. 2). The sediments of the Upper Cretaceous of the region are dominated by dolomite, anhydrite and shale beds; the latter providing the most likely source of the isotopically light sulphate, by dissolution and oxidation, to the waters of the deep aquifer.

These data can be compared with those from the sabkhas of the Trucial Coast where groundwater δ^{34}S values grade from +21‰ in the intertidal region to +17 to +19‰ at the landward edge of the Recent sedimentation[9,10]. There, seawater remains the dominant source of sulphate. Continental sabkhas, 50–80 km inland from Abu Dhabi, exhibit δ^{34}S groundwater values between +13 and +16‰ (J.E.R. unpublished data), but the brines, though sulphate saturated, produce only small amounts of anhydrite or gypsum due to the limited supply of sulphate.

Coastal sabkhas, isolated by seaward sand barriers have been reported from Egypt[5] and Sinai[6]. There is evidence for modern dissolution and redeposition of previous cycle evaporites in Egypt but in Sinai neither geochemistry[7] nor isotopic analysis[8] has demonstrated a significant continental source for the brines.

The rate of sediment production in the continental water-supplied sabkhas is dependent on the rate and salinity of water flowing from the aquifer and on the aridity of the climate to ensure a sufficiently high evaporation rate. These conditions were most likely to occur in the periods immediately following the post-glacial change to a warmer climate. Hence, according to the general variation in the regional climatography the sabkha building process may have

had a cyclic nature. An additional complication is the major variations in sea level of the past 50,000 yr, which were probably sufficiently large and rapid to prevent simple progradation of the complex, and resulted in the formation of a new sabkha barrier-ridge system as each stable point in the evolution of sea level was reached. This probably resulted in the development of a system of sabkha terraces related in height to each other by the positions of relative sea-level stability.

The present deposition rate of gypsum based on the output of the Tawurghah spring alone, is $>2 \times 10^5$ ton yr^{-1} and the total rate probably an order of magnitude greater, demonstrating the remarkably large amounts of sulphate that can be remobilized in a geologically short period and also showing that significant evaporite deposits associated with marine sediments need not be derived, as would generally be assumed, from the adjacent marine water, but can also be formed from water derived from terrestrial sources.

We thank G. Evans, P. R. Bush and M. L. Coleman for helpful discussion, M. Pugh for assistance and the Director of the Institute of Geological Sciences for permission to publish this work. N.S. thanks the Libyan government for supporting his research work.

1. Sherif, N. thesis, Univ. London (1979).
2. Eskangi, A. M. & Zogovic, D. *Relationship between the Tawurghah Spring and the Underground Water of the Area*, 14 (El Fateh Univ., Tripoli, 1970).
3. G.E.F.L.I. *Study of the Water Resources in the Zliten–Misratah–Tawurghah Area*, Appendix C, 124 Groupement D'Étude Français en Libya, Paris, 1975).
4. Rees, C. E., Jenkins, W. J. & Monster, J. *Geochim. cosmochim. Acta* **42**, 377–381 (1978).
5. West, I. M., Ali, Y. A. & Hilmy, M. E. *Geology* **7**, 354–358 (1979).
6. Levy, Y. *J. Sed. Petrol.* **47**, 451–462 (1977).
7. Levy, Y. *J. Sed. Petrol.* **47**, 463–474 (1977).
8. Gat, J. & Levy, Y. *Limnol. Oceanogr.* **23**, 841–850 (1978).
9. Butler, G., Krouse, R. H. & Mitchell, R. in *The Persian Gulf* (ed. Purser, B. H.) 453–467 (Springer, Heidelberg, 1973).
10. Olson, E. thesis, McMaster Univ. Ontario (1976).

Late Precambrian ophiolitic mélange in the eastern desert of Egypt

R. M. Shackleton*, A. C. Ries*, R. H. Graham†
& W. R. Fitches‡

*Department of Earth Sciences, The Open University, Milton Keynes MK7 6AA, UK
†Department of Geology, University College, Swansea 2AS 8PP, UK
‡Department of Geology, University College of Wales, Aberystwyth SY23 2AX, UK

Serpentinite masses in late Precambrian sediments of the eastern desert of Egypt are in a mélange with associated metagabbros and pillow lavas; they represent pieces of Precambrian oceanic crust. The mélange is of regional extent and is interpreted as a olistostrome which has been thrust northwestwards over shelf sediments and is overlain by island arc volcanics: thus the observed sequence is a structural rather than a stratigraphic one. A plate tectonic model is implied with a suture to the south-east. The interpretation of the late Precambrian (Pan-African) fold belts in Africa is controversial. It is uncertain whether, like Phanerozoic fold belts, they were formed by plate tectonic processes[1-5], or whether they are ensialic and unrelated to subduction of oceanic crust[6,7] or collision of continental plates. Here we present evidence relating to this problem from the part of the Pan-African belt exposed in the eastern desert of Egypt.

According to the literature, the sequence, in simplified form, for the late Precambrian in the eastern desert is as follows[8] (dates quoted are mostly Rb/Sr whole-rock ages, decay constants not being specified in the original publication):

(6) Younger, post-tectonic granitoids (674–506 Myr BP)[9].
(5) Hammamat Group of molasse-type conglomerates, greywackes and siltstones.
(4) Dokhan post-tectonic, calc-alkaline volcanics ($\sim$660 Myr BP)[9].
(3) Older, syn-tectonic, granitoids (987–830 Myr BP)[9].
(2) Geosynclinal metasediments (1,200–850 Myr BP)[9] interclated with Shadli Metavolcanic Group and intruded by serpentinites, possibly as sills[8].
(1) Hornblendic, psammitic and biotitic gneisses and migmatites which crop out in the Hafafit and Meatiq domes, Wadi Nugrus and east of Wadi Abu Swayel. These are thought[10] to be among the oldest rocks exposed in the eastern desert. Radiometric ages range from 1,700 Myr BP (U/Pb age on zircons, probably detrital) to 592 Myr BP (K/Ar)[9].

Mafic and ultramafic rocks, the latter mostly serpentinized or altered to talc carbonate, are abundant in the late Precambrian of the eastern desert of Egypt and north-east Sudan as shown on a recent detailed map of part of the eastern desert[11] and our own work. The relationship of these serpentinites, metagabbros and epidiorites to the associated metasediments is particularly important: if they are intrusive into the metasediments they provide no support for a plate tectonic interpretation, whereas if they are ophiolites (fragments of oceanic crust) they imply a plate tectonic model. We conclude that these ultramafic and mafic rocks are not intrusives, but are fragments of oceanic crust (ophiolites) for the following reasons:

(1) All the characteristic members of an ophiolite assemblage, including sheeted dykes, can be recognized in several localities, for example, Wadi Sodmein and along the Qena-Quseir road and also (El-Bayoumi, personal communication) in Wadi Ghadir (Fig. 1).
(2) These ophiolitic fragments are closely associated with deep-water graphitic pelites, turbidites, cherts, olistostromes and mélanges.
(3) The ultramafic bodies show no evidence of intrusion: we have found no evidence of contact metamorphism or chilling against country rocks. Instead the ultramafics form fragments mechanically incorporated in the mélange and in imbricate slices.
(4) These mafic/ultramafic rocks lie in a zone which contains well documented late Precambrian ophiolites at Jabal Al Wask[12] and at Jabal Ess[13] in Saudi Arabia and Sol Hamed[14] in north-east Sudan (Fig. 1).
(5) Analytical data so far available are compatible with an origin for these ophiolites as fragments of Proterozoic oceanic (or back-arc) lithosphere.

If it is accepted that these ultramafic and mafic assemblages are fragments of oceanic crust, it follows that they cannot be in normal superposition on the granitoid and metasedimentary gneisses which they now overlie. They must be allochthonous and the sequence given above is a structural rather than a stratigraphic sequence. All of the ophiolite contacts that we have studied in the field are tectonic. Until more detailed geochronological work is available, we regard the relative ages of the basal gneisses and migmatites, the ophiolitic mélange and the associated deep-water sediments as uncertain, and the accepted stratigraphic scheme as inapplicable.

Nowhere in the eastern desert of Egypt have we seen a complete, continuous and intact ophiolite sequence. Most of the ophiolitic rocks occur as fragments, isolated from other members of the ocean-floor sequence. These fragments vary in shape and angularity, and in size up to that of a mountain. They are embedded in a sedimentary matrix, usually a dark grey graphitic pelite. Ultramafic fragments are most common, with less frequent blocks of gabbro, epidiorite, pillow basalt and sediments (turbidites, chert, black limestone). Thus the ophiolitic rocks occur as fragments in a mélange. The field evidence suggests that this mélange is only 1 or 2 km thick, but extends over a vast area (at least 10,000 km^2) in Wadi

Mubarak, Wadi Abu Dubbab, in the Barramiya area, in Wadi Sodmein and Wadi Atalla (Fig. 1). In the Barramiya area, ophiolitic mélange and normal sediments alternate as though there are several separate mélange sheets, but the normal sediments might be large slabs within a single mélange. Some of the ophiolitic fragments are very large, although the more detailed the field mapping, the more the supposedly large masses are found to be composite, with sedimentary intercalations. An ultrabasic sheet at Barramiya which extends for about 30 km along strike, is preserved in synforms and overlies mélange and an imbricate zone with alternating thrust slices of sediment and serpentinite. The proportion of serpentinite blocks decreases downwards so that the lowest part of the sequence consists of normally bedded pelitic, turbititic and tuffaceous sediments. This Barramiya sequence, which resembles that under the Semail ophiolite in Oman[15], may suggest that the mélange could have underlain an ophiolite nappe. If so, this must have been entirely removed by erosion over most of the region before the deposition of the Hammamat Group, which seems unlikely. In Wadi Mubarak the mélange is associated with thick sequences of normal sediments (turbidites, laminated pelites) which apparently

underlie the mélange. Olistostromes, a few metres thick, occur within normal sediments in Wadi Mubarak and in Barramiya, but they only contain sedimentary, not ophiolitic fragments and their origin may therefore be different from that of the ophiolitic mélange.

The mélange was clearly formed and emplaced, sometimes in imbricated thrust slices, before the development of the earliest regional cleavage. Tight pre-cleavage folding is evident in some of the metasediments from changes in facing direction without corresponding change in bedding/cleavage sense; similar tight pre-cleavage folds affect the mélange in the Barramiya area.

The structural sections we have drawn demonstrate that the allochthonous mélange and the ophiolites are underlain by gneisses some of which are psammitic metasediments of shallow-water and presumably shelf origin (they contain 1,700 Myr BP detrital zircons which cannot have come from a late Proterozoic island arc), for example, Wadi Nugrus, while they are overlain by calc-alkaline volcanics, including basalts, andesites and ignimbrites, of island-arc affinity. These calc-alkaline volcanic rocks have nowhere been seen to be involved in the mélange. Unlike the rocks in the mélange, they occur in an orderly sequence, and are often relatively undeformed. They resemble, and are conventionally correlated with the Dokhan volcanics. We believe that they were erupted after the mélange was emplaced, but we have not seen a clear contact of volcanics unconformable on the mélange, and in Wadi Sodmein there seems to be no structural or metamorphic break between the mélange and the calc-alkaline volcanics.

There is no decisive evidence to show whether the mélange was an olistostrome (submarine slide deposit) or a tectonic mélange or both. The angular rather than lenticular shape of the fragments, lack of penetrative tectonic fabric (other than later cleavage or schistosity) in the matrix, apparently random distribution of fragments of different rock types in the matrix and small thickness of the mélange relative to its extent suggests that it is an olistostrome. It could not have been pushed and there is no evidence of an overlying thrust sheet under which it was dragged. In field characteristics it resembles the Monian mélange of Anglesey[16,17] and the argille scagliose of the Appenines[18], which are both regarded as olistostromes. However, in some localities, for example, Wadi Sodmein, tectonic deformation clearly contributed to the fragmentation of the mélange. The superposition of mélange with ocean-floor fragments on shelf sediments seems to imply extensive thrusting because it is difficult to envisage a situation where shelf sediments were at a lower bathymetric level than ocean floor. Therefore we believe that the mélange was formed as an olistostrome (itself presumably actuated by tectonic processes), which was subsequently thrust over shelf sediments.

Extensive tectonic transport is indicated by the presence, particularly in the gneisses underlying the mélange, of a regionally recumbent schistosity (folded over the Meatiq and Hafafit domes) and by a locally very intense stretching. This stretching direction, shown by the elongation of pebbles, tuff fragments, vesicles and other strain markers, trends consistently NW–SE. The direction of tectonic transport is thought to be towards the north-west, partly because of fold vergence and partly because there is no plausible source to the north-west. Because the mélange with its incorporated ophiolitic fragments is visibly underlain by metamorphosed shelf sediments at the Hafafit, Wadi Gemal and Meatiq areas, it apparently must have been transported at least 200 km northwestwards relative to the rocks beneath. Continued movement in the same direction is implied by parallel elongation of pebbles and fragments in the Hammamat Group.

We conclude that the ultramafic and associated rocks in the eastern desert of Egypt are ophiolites derived from ocean floor; that they are allochthonous, transported probably by gravity sliding, followed by thrusting onto shelf sediments from the present south-east, and that the supposed stratigraphic succession in the eastern desert is a structural, rather than a
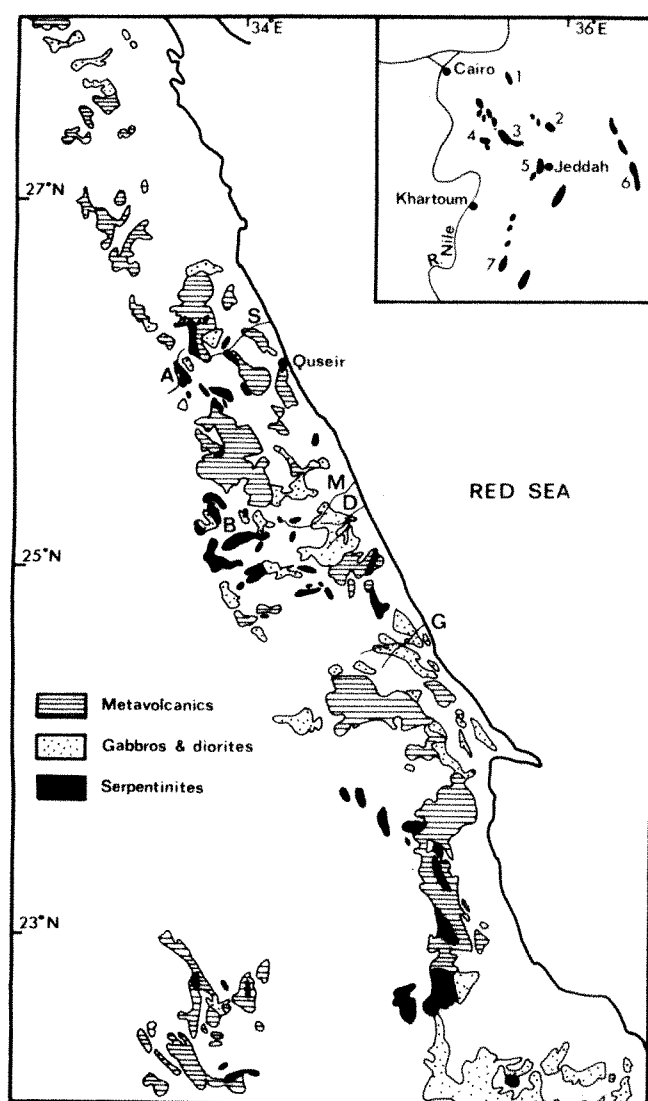
stratigraphic succession. These conclusions imply a plate tectonic model, but any suture must be to the south-east of the area we have studied.

1. Burke, K. C. & Dewey, J. F. *Afr. Geol.* 583 (1972).
2. Leblanc, M. *Nature* **261**, 34–35 (1976).
3. Gass, I. G. *J. geol. Soc.* **134**, 129–138 (1977).
4. Black, R. *et al. Nature* **278**, 223–227 (1979).
5. Shackleton, R. M. in *Evolution and Mineralisation of the Arabian–Nubian Shield* (ed. Al-Shanti, A. M. S.) (Pergamon, Oxford, 1979).
6. Kröner, A. *Precambr. Res.* **4**, 163–213 (1977).
7. Piper, J. D. A., Briden, J. C. & Lomax, K. *Nature* **245**, 244 (1973).
8. El-Ramly, M. F. *Geol. Surv. Egypt* **2**, 1–18 (1972).
9. Hashad, A. H. in *Evolution and Mineralisation of the Arabian–Nubian Shield* (ed. Al-Shanti, A. M. S.) (Pergamon, Oxford, 1979).
10. El-Ramly, M. F. & Akaad, M. K. *Geol. Surv. Egypt.* Pap. 8 (1960).
11. Sabet, A. H., Tsogoev, V. B., Bessonenko, V. V. & Babourin, L. M. *Geological Map of the Central Eastern Desert of Egypt* (Geological Survey of Egypt, 1973).
12. Bakor, A. R. & Gass, I. G. *Earth planet. Sci. Lett.* **30**, 1–9 (1976).
13. Shanti, M. & Roobol, M. J. *Nature* **279**, 488–491 (1979).
14. Hussein, I. M. thesis, Portsmouth Polytechnic (1977).
15. Glennie, K. W. *et al. Verh. Koninkl. Nederlands, Geol. Mijnbouwkundig Genootschap* **31** (1974).
16. Greenly, E. *Mem. Geol. Surv. Gr. Br.* (1919).
17. Shackleton, R. M. in *The Precambrian and Lower Phalaeozoic Rocks of Wales* (ed. Wood, A.) 1–22 (University of Wales Press, Cardiff, 1969).
18. Abbate, E., Bortolotti, V. & Passerini, P. *Sed. Geol.* **4**, 521–557 (1970).

A palaeotemperature record for the mid-Wisconsin in Vancouver Island

Melvyn Gascoyne*, Henry P. Schwarcz*
& Derek C. Ford†

Department of Geology and †Department of Geography, McMaster University, Hamilton, Ontario, Canada, L8S 4M1

Calcite speleothems are deposits of calcium carbonate (stalagmites and flowstones) found in limestone caves. They are formed by precipitation from groundwater supersaturated in Ca^{2+} and HCO_3^-. Their oxygen isotopic composition is controlled by the isotopic composition of the seepage waters from which they are deposited and by the temperature of formation. We report here the discovery of mid-Wisconsin speleothems from a cave in Vancouver Island which are significantly depleted in ¹⁸O relative to modern calcite in the same cave. We interpret the variations in ¹⁸O content over this period as an absolute palaeotemperature record for the area.

If calcium carbonate deposition is brought about by rapid loss of CO_2 from solution, or by evaporation of the seepage water (as may occur near the cave entrance or in a well ventilated passageway) kinetic effects will also influence the isotopic composition of the speleothem. Isotopic equilibrium deposition can be recognized in a fossil speleothem by the constancy of $\delta^{18}O_c$ and lack of correlation between $\delta^{18}O_c$ and $\delta^{13}C_c$ along given layers of contemporaneous calcite growth[1]. [Expressed as

$$\delta^{18}O_x = \left(\frac{^{18}O/^{16}O(x)}{^{18}O/^{16}O \text{ (PDB standard)}} - 1 \right) 10^3\%_0$$

x = sample, c = calcite, w = seepage water, sw = seawater, p = precipitation.] Variations of $\delta^{18}O_c$ in successive growth layers of equilibrium speleothem (that is, along the growth axis of the deposit) have been interpreted in terms of temperature change, by comparison with $\delta^{18}O_c$ of speleothem calcite growing in the cave at present[2,3] and also by analysis of D/H ratios of fluid inclusions in the speleothems[4–6]. Time scales

were established by ¹⁴C or U-series dating methods and the oxygen isotopic variations were correlated to late Pleistocene climatic events. In general, speleothems which grew during the past 100 kyr (the Wisconsin stage in North America) were found to be enriched in ¹⁸O relative to modern speleothems in the same caves. For these caves, therefore, $d\delta^{18}O_c/dT < 0$, where T is the temperature inside the cave. The discovery of Wisconsin speleothems, which have a lower ¹⁸O content than the modern calcite in the cave, indicates that for this area at least, $d\delta^{18}O_c/dT > 0$. The isotopic record of successive growth layers is regarded as a palaeotemperature record for the area.

The oxygen isotopic composition of cave seepage water has been shown to approximate closely to that of mean seasonal precipitation[6]. For a deep cave, well insulated from the surface, cave temperature is comparable with mean annual surface temperature. At isotopic equilibrium, the fractionation α_{c-w} between calcite and water depends only on temperature as follows[7]:

$$\Delta_{c-w} \equiv 1{,}000 \ln \alpha_{c-w} = 2.78 \times 10^6 \, T^{-2} - 2.89 \qquad (1)$$

where $\alpha_{c-w} = (1 + 10^{-3}\delta^{18}O_c)/(1 + 10^{-3}\delta^{18}O_w)$. This relationship has been found to apply for ¹⁸O exchange between modern calcite and cave seepage water[8]. For speleothems formed in isotopic equilibrium, variations in $\delta^{18}O_c$ along the growth axis (that is, over the period of deposition) are controlled by the following factors: (1) Effect of change in temperature of deposition on α_{c-w}; for example, at 10 °C, $d\Delta_{c-w}/dT = -0.24\%_0$ per °C. (2) Change in $\delta^{18}O$ of seawater; accumulation or ablation of ice on the continents causes changes in the isotopic composition of the oceans and oceanic water vapour. This causes a similar change in the isotopic composition of precipitation at the cave site. Based on changes in $\delta^{18}O$ of Foraminifera in deep sea cores, a variation of up to 1.8‰ has been suggested for a full glacial–interglacial transition[9]. (3) Effect of change in the temperature gradient between the site of evaporation and the site of precipitation on $\delta^{18}O$ of precipitation; for many oceanic and polar sites, Dansgaard[10] has shown that $d\delta^{18}O/dT = +0.7\%_0$ per °C. CLIMAP[11] has shown that the tropical ocean surface temperature changed very little between full glacial and interglacial conditions and therefore the temperature change at the cave site, ΔT, is also the change in temperature gradient between evaporation and precipitation sites.
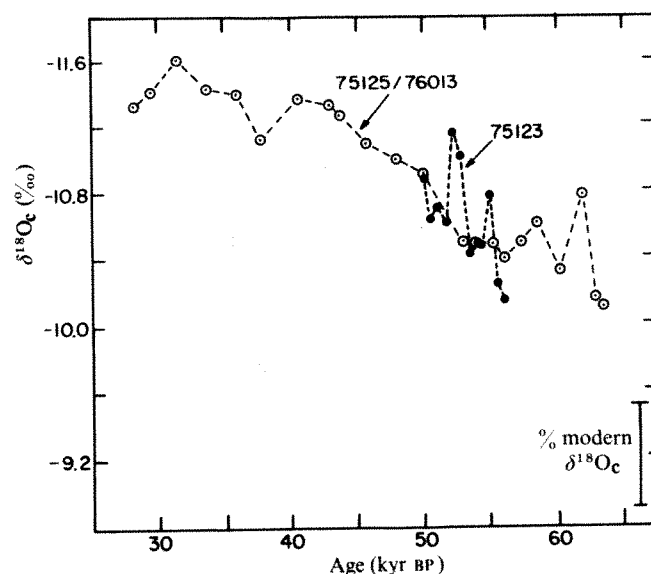
Fig. 1 Variation of $\delta^{18}O_c$ of speleothems 75125/76013 and 75123 over the dated period shown. The position of $\delta^{18}O$ of modern calcite in the same cave is shown.
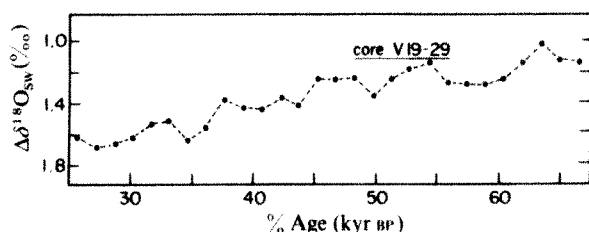
Fig. 2   Variation in $\delta^{18}O$ of seawater over mid-Wisconsin times (expressed as difference from modern values) as inferred from variations in $\delta^{18}O$ of benthonic Foraminifera[9].

The first two effects lead to increasing $\delta^{18}O_c$ with falling temperature. The precipitation effect opposes these and causes $\delta^{18}O_c$ to decrease as temperature decreases. Variation in $\delta^{18}O_c$ of speleothem can, therefore, be summarized as:

$$\Delta\delta^{18}O_c = \frac{d\Delta_{c-w}}{dT} \cdot \Delta T + \Delta\delta^{18}O_{sw} + \frac{d\delta^{18}O_p}{dT} \cdot \Delta T \qquad (2)$$

Evaluation of temperature change (ΔT) from $\delta^{18}O_c$ of ancient speleothems is hampered because the coefficient, $d\delta^{18}O_p/dT$, is commonly less than 0.7‰ per °C for precipitation at midcontinental sites and at some maritime locations[5,12,13]. This is due to meteorological effects on $\delta^{18}O_p$, such as isotopic evolution of water vapour by precipitation from clouds at varying temperatures. Also the coefficient, 0.7, determined by Dansgaard from seasonal variations in $\delta^{18}O_p$ and temperature, may not apply to secular temperature change at a site. Lower values for speleothems which grew in North America during the Wisconsin are inferred from the enrichment in ^{18}O relative to modern deposits[5] (variation in $\delta18O_c$ is predominantly due to changes in $\delta^{18}O_{sw}$ and the effect of temperature change at the cave site on α_{c-w}). Spe'eothems from some maritime locations (New Zealand[14], Bermuda[5] and North-west England[15]) show this effect even though here $d\delta18O_p/dT$ might be expected to approach the 'maritime' value of 0.7‰ per °C and so outweigh other factors.

Fossil speleothems have been collected from Cascade Cave near Port Alberni, south-central Vancouver Island. The $^{230}Th/^{234}U$ dating method has shown that many of these speleothems grew during the mid-Wisconsin interstadial 65–40 kyr BP (ref. 16). Uniformity of $\delta^{18}O_c$ along individual growth horizons of two speleothems 75123 and 76013/75125 indicates that they grew in conditions of isotopic equilibrium. Axial profiles of $\delta^{18}O_c$ are shown in Fig. 1 for the dated periods 55–50 kyr BP for 75123 and 64–28 kyr BP for 76013/75125. Analytical precision is poor for 75123 (±0.23‰) but subsequent improvements in mass spectrometer characteristics gave a precision within ±0.1‰ for 76013/75125 analyses. Good agreement between the two profiles can be seen over the period of contemporaneous growth—a further indication of isotopic equilibrium deposition.

The profile shows that $\delta^{18}O_c$ decreases steadily by ~1.3‰ from 64 to 35 kyr BP and remains fairly constant until growth ceases at 28 kyr BP. The range of five analyses of modern calcite in the cave is also shown in Fig. 1. At all times, $\delta^{18}O_c$ (fossil) is less than $\delta^{18}O_c$ (modern). These data can be interpreted in two ways: (1) if $d\delta^{18}O_c/dT$ was negative (as found in most previous work) then mid-Wisconsin temperatures were warmer than present in this area, and became even warmer towards 28 kyr when growth ceased; (2) if $d\delta^{18}O_c/dT$ was positive, then mid-Wisconsin temperatures were less than present and steadily decreased towards 28 kyr BP. However, this implies that $d\delta^{18}O_p/dT$ was larger than normally observed at cave sites.

Explanation (1) conflicts with all previous work on late Pleistocene deposits in this region[17-19] which indicates that

temperatures steadily cooled over the Olympia Interstadial (about 60–40 kyr BP) towards the maximum Fraser glaciation (~25–15 kyr BP). Explanation (2) agrees well with local evidence and permits determination of temperature change over this period if $d\delta^{18}O_p/dT$ is known. We assume here a value of 0.7‰ per °C, as the setting of this cave is very similar to maritime locations at which Dansgaard and others have observed such values.

$\Delta\delta^{18}O_{sw}$ can be readily estimated from the oxygen isotopic record of benthonic Foraminifera in deep sea cores with high sedimentation rates. Shackleton has provided analytical data for the species *Uvigerina proboscidea* in core V19-29 from the Carnegie Ridge in the eastern Pacific Ocean[9]; oxygen isotope variations in this core are thought to be almost entirely due to change in oceanic isotopic composition because present ocean water temperatures at depth in this location are near 0 °C. A time scale for the core was determined by assuming constant sedimentation rate and that isotope Stage 5e, clearly seen in the core, is dated at 125 kyr BP (ref. 20). Between 64 and 28 kyr BP these data indicate an enrichment of ~0.65‰ in $\delta^{18}O_{sw}$ (Fig. 2). From equation (2), therefore, the change in $\delta^{18}O_c$ represents a decrease of ~4.5 °C over this period at Cascade Cave.

Combining the isotopic composition of modern Foraminifera from core V19-29 (representing modern ocean water), $\delta^{18}O_c$ of modern speleothem, and modern temperature from this cave a palaeotemperature record for the mid-Wisconsin for this area can be determined. The available core top analyses and inferences about isotopic change with respect to the isotope Stage 5e and 5 kyr BP hypsithermal isotopic minima in the core, yield an estimate of $\delta^{18}O$ of modern Foraminifera of 3.35 ± 0.01‰, or, 0.9‰ less than Foraminifera laid down at 64 kyr BP. $\delta^{18}O_c$ of modern calcite in the cave is −9.2 ± 0.3‰. Mean annual cave temperature is estimated at 8.0 ± 0.5 °C, determined by the extrapolation to 300 m a.s.l. of mean monthly observational data from nearby meteorological stations, using the saturated adiabatic lapse rate (0.6 °C per 100 m for 5 °C).

Temperature differences between the mid-Wisconsin and present are determined from equation (2) for each of the $\delta^{18}O_c$ determinations in the speleothem, using an estimate of $\Delta\delta^{18}O_{sw}$ obtained from the V19-29 core record of Fig. 2. These temperature differences are shown in Fig. 3 to an estimated precision of ±1 °C.

The palaeotemperature record given by these calculations seems to be quite realistic because: first, an estimate of ~4 °C for maximum mean annual mid-Wisconsin temperature agrees with estimates from pollen spectra in sediments in southern Vancouver Island[17,19] and north-west Washington[21]; second, speleothem growth can only take place at or above 0 °C. These results generally comply with this requirement. Growth probably ceased as temperatures became continuously subzero at ~28 kyr BP. Use of a lower coefficient for the temperature dependence of $\delta^{18}O_p$ results in a larger temperature change, much of which is well below 0 °C, and therefore unacceptable.
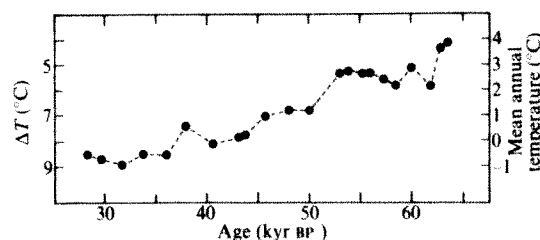
Fig. 3   Palaeotemperature curve for south-central Vancouver Island at 300 m.a.s.l. showing calculated differences between modern and ancient temperatures (ΔT), and expressed as absolute temperatures, assuming that the present cave temperature is 8 °C.

These results suggest that no strong, short-term interstadial warmings (such as may be seen in mid-continental records[22]) occurred between 64 and 28 kyr BP on Vancouver Island, probably because of the damping effect of the adjacent ocean. Furthermore, there is no evidence of a pronounced cooling due to glaciation during the interval 40–30 kyr (the late Salmon Springs glaciation) as proposed by some studies of sediment sequences in Washington[21,23].

In conclusion, these data show a gradual cooling at this site between 65 and 30 kyr BP at an almost constant rate, comparable with the uniform rate of continental ice

accumulation suggested by Fig. 1. The local setting of this cave suggests that its temperature is responding to the average sea-surface temperatures of water masses along the northern Pacific coast and that these in turn were gradually cooling through this interval.

1. Hendy, C. H. *Geochim. cosmochim. Acta* **35**, 801–824 (1971).
2. Emiliani, C. *Science* **171**, 571–573 (1971).
3. Talma, A. S., Vogel, J. C. & Partridge, T. C. *S. Afr. J. Sci.* **70**, 135–140 (1974).
4. Thompson, P., Ford, D. C. & Schwarcz, H. P. *Bull. geol. Soc. Am.* **87**, 1730–1738 (1976).
5. Harmon, R. S., Thompson, P., Schwarcz, H. P. & Ford, D. C. *Quat. Res.* **9**, 54–70 (1978).
6. Harmon, R. S., Schwarcz, H. P. & Ford, D. C. *J. Geol.* **86**, 373–384 (1978).
7. O'Neil, J. R., Clayton, R. N. & Mayeda, T. *J. chem. Phys.* **51**, 5547–5558 (1969); *U.S. geol. Surv. J. Res.* **3**, 623–624 (1975).
8. Harmon, R. S. & Schwarcz, H. P. *Nature* (submitted).
9. Ninkovitch, D. & Shackleton, N. J. *Earth planet. Sci. Lett.* **27**, 20–34 (1975).
10. Dansgaard, W. *Tellus* **16**, 436–468 (1964).
11. Gates, W. L. *Science* **191**, 1138–1144 (1976).
12. Stuiver, M. *Science* **162**, 994–997 (1968).
13. Evans, G. V., Otlet, R. L., Downing, R. A., Monkhouse, R. A. & Rae, G. *IAEA int. Symp. Hydrol.*, Neuherberg (1978).
14. Hendy, C. H. & Wilson, A. T. *Nature* **216**, 48–51 (1968).
15. Gascoyne, M. thesis, McMaster Univ. (1979).
16. Gascoyne, M., Schwarcz, H. P. & Ford, D. C. (in preparation).
17. Armstrong, J. E. & Clague, J. J. *Can. J. Earth Sci.* **14**, 1471–1480 (1977).
18. Fulton, R. F. & Smith, G. W. *Can. J. Earth Sci.* **15**, 971–980 (1978).
19. Alley, N. F. *Quat. Res.* **11**, 213–237 (1979).
20. Broecker, W. S. & van Donk, J. *Rev. geophys. Space Phys.* **8**, 169–198 (1970).
21. Heusser, C. J. *Quat. Res.* **8**, 189–201 (1977).
22. Dreimanis, A. & Goldthwait, R. P. *Geol. Soc. Am. Mem.* **136**, 71–105 (1973).
23. Hansen, B. S. & Easterbrook, D. J. *Bull. geol. Soc. Am.* **85**, 587–602 (1974).

Evidence for coexistence of dopamine and CCK in meso-limbic neurones

T. Hökfelt*, J. F. Rehfeld†, L. Skirboll*, B. Ivemark‡, M. Goldstein§ & K. Markey§

*Department of Histology, Karolinska Institutet, Stockholm, Sweden
†Institute of Medical Biochemistry, University of Aarhus, Arhus, Denmark
‡Department of Pathology, Karolinska Institutet, Stockholm, Sweden
§Department of Psychiatry, New York University Medical Center, New York, New York 10012.

Vanderhaeghen et al.[1] reported the occurrence of gastrin-like immunoreactivity in the mammalian brain. Subsequent studies have revealed that this immunoreactivity corresponded mainly to the COOH-terminal octapeptide of cholecystokinin (CCK-8), which has a COOH-terminal pentapeptide identical to gastrin[2-7]. Also, two peptides resembling the NH- and the COOH-terminal tetrapeptide fragments of CCK-8 are present in the central nervous system (CNS)[8]. Using COOH-terminal-specific antisera raised to gastrin and/or CCK, the distribution of CCK neurones has been described with immunohistochemical techniques. Although high numbers of cells and nerve terminals are found in cortical areas, the CCK systems are also present in most other parts of the brain and spinal cord[9-14]. In the CNS, true gastrin molecules, gastrin-17 and gastrin-34, have been located only in the neurohypophysis, hypothalamus[15] and occasionally in the medulla oblongata (unpublished results). We describe here the occurrence of peptides in meso-limbic dopamine neurones in the rat brain. Evidence has also been obtained that mesencephalic dopamine neurones in the human brain contain similar peptides.

Twelve male albino rats (Sprague–Dawley, 150 g) were used. Five rats received an intraventricular injection of colchicine (60 μg in 20 μl 0.9% sodium chloride) 24 h before being killed. This mitosis inhibitor is known to arrest axoplasmic transport[16,17] and to cause accumulation of peptides in cell bodies. Two rats received an intracerebral injection of 6-hydroxydopamine (6-OHDA) (8 μg in 2 μl 0.9% sodium chloride with 2% ascorbic acid added) into the posterior lateral hypothalamus. This treatment destroys ascending mesencephalic dopamine neurones[18]. The rats were perfused with ice-cold formalin as described previously[19] and, after

rinsing, the brains were processed for immunohistochemistry according to Coons' indirect technique[20]. In addition, the mesencephalon of two human post-mortem brains, fixed by immersion in formalin, were studied. Briefly, 15-μm-thick alternate sections of rat and human mesencephalon and rat forebrain were cut on a cryostat, and incubated with antiserum raised against synthetic human hexadecapeptide gastrin (antiserum 4562, specific for the C-terminus common to gastrin and CCK[21]) or against rat tyrosine hydroxylase (TH)[22], a marker for dopamine and other catecholamine neurones. After rinsing, the sections were incubated with fluorescein isothiocyanate (FITC)-conjugated sheep anti-rabbit antibodies (SBL, Stockholm), rinsed, mounted and examined in a Zeiss standard fluorescence microscope. The sections from the mesencephalon of rat and human were then treated according to the following protocol. CCK-immunoreactive (fluorescent) cells in the ventral mesencephalon were photographed and then the sections were treated with acid potassium permanganate according to Tramu et al.[23] to elute the immunostaining. The sections were then reincubated with FITC-conjugated antibodies and examined in the fluorescence microscope. If no restaining had occurred, the sections were incubated with antiserum to rat TH and FITC-conjugated antibodies and once more examined in the fluorescence microscope and photographed. Sections incubated with antiserum 4562 preincubated with CCK-8 (50 μg per ml antiserum diluted 1:10; Peninsula Laboratories) or normal rabbit serum served as controls.

After incubation with antiserum 4562, many weakly fluorescent CCK cells were observed in the ventral mesencephalon of colchicine-treated rats. The immunoreactive cells were observed mainly in the ventral tegmental area, but cells were also seen in the zona compacta, particularly at a rostral level and in its medial part. At the mid and caudal levels a small group of fluorescent cells were consistently observed in the pars lateralis of the substantia nigra. At the caudal level the cells were mostly restricted to the midline area overlying the interpeduncular nucleus. No immunoreactive cells were seen in the pars reticulata. Alternate sections incubated with TH antiserum revealed a close overlap between TH- and CCK-immunoreactive cells, although the former were much more numerous and were found also in the zona compacta and pars reticulata, in agreement with the original description of the distribution of dopamine cells of the A9 and A10 groups by Dahlström and Fuxe[24]. The elution and restaining experiments revealed that many of the CCK-immunoreactive cells also contain TH (Fig. 1a, b), although
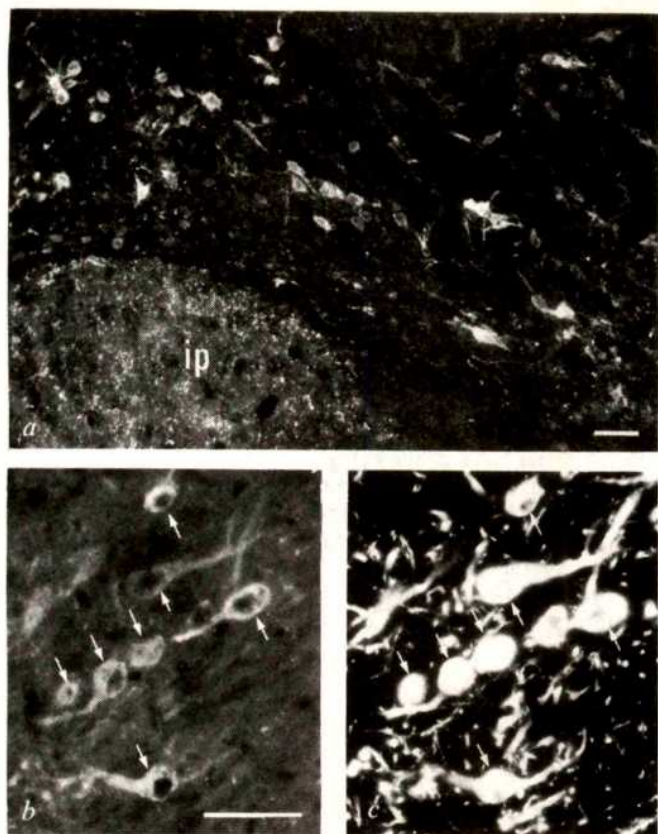
Fig. 1 *a–c*, Immunofluorescence micrographs of the ventral tegmental area of colchicine-treated rat after incubation with antisera to gastrin/CCK (*a, b*) and tyrosine hydroxylase (*c*). *b* and *c* show the same section, which, after photography (*b*) and removal of the gastrin/CCK antiserum according to Tramu *et al.*[23], has been reincubated with TH antiserum (*c*). Several fluorescent (CCK immunoreactive) cells are seen in the region overlying the interpeduncular nucleus (ip) (*a*). Note also numerous CCK-immunoreactive nerve endings in the ip (*a*). Restaining experiments show identity between CCK-immunoreactive (arrows in *b*) and dopamine (TH-immunoreactive) (arrows in *c*) containing cells. Scale bars, 50 μm.

identity could not be established in all cases. Thus, some CCK-immunoreactive cells were TH negative and vice versa.

Numerous cells containing both CCK and TH-like immunoreactivity were observed in the human mesencephalon, although, again, a large number of cells only contained the enzyme.

In the frontal brain dense networks of CCK-immunoreactive nerve fibres were observed in, among other places, the caudal, dorsomedial parts of the nucleus accumbens, in the medial parts of the tuberculum olfactorium, in the bed nucleus of the stria terminalis (caudal and dorsal parts) and in the central amygdaloid nucleus. In the alternate sections, the TH-immunoreactive fibres were present in all these areas but in higher concentrations and more widely spread within these nuclei. There were, of course, also both CCK- and TH-immunoreactive nerve fibres in many more areas of the brain stem and telencephalon but without the obvious overlap observed in the areas described above. We will not deal with such areas here but refer to previously published immunohistochemical papers[9–14].

After injection of 6-OHDA into the lateral hypothalamus, most CCK- and TH-immunoreactive fibres disappeared in the nucleus accumbens, tuberculum olfactorium and the bed nucleus of stria terminalis. After incubation with the control sera, none of the fluorescent structures described above were observed. This was also the case when the respective control serum was included in the restaining experiments.

The present findings are strong evidence that some dopamine neurones in rat and man also contain CCK peptides. Preliminary results in our laboratories indicate that, as with other brain regions, the CCK-like immunoreactivity in the dopamine neurones corresponds to CCK-8.

In the rat, only a subpopulation of the mesencephalic dopamine neurones contained CCK-like peptides. Their distribution corresponds well to the so-called A10 group located in the ventral tegmental area[2] but some neurones were also seen in the pars compacta and pars lateralis. The A10 dopamine cells are known to project mainly to certain limbic areas[25,26] and exactly in these areas we observed, on adjacent sections, overlapping dense networks of CCK- and TH-immunoreactive nerve endings. The fact that both CCK- and TH-immunoreactive fibres in these areas disappear after 6-OHDA treatment further strongly supports the coexistence hypothesis.

The present results offer a further example of coexistence of small regulatory peptides and a biogenic amine in neurones[27]. Previously, for example, somatostatin has been found in noradrenaline neurones[28] and substance P in 5-hydroxytryptamine neurones[29,30]. Such situations were early observed in endocrine cells, which according to Pearse's terminology belong to the APUD (amine precursor uptake and decarboxylation) system[31].

Evidence is accumulating that CCK-8 and/or CCK-4 may act as a neurotransmitter in the brain[32]. In addition to the morphological evidence cited above, it has recently been shown that CCK peptides can be released from synaptosome-enriched fractions of rat cerebral cortex by potassium[32,33]. Furthermore, in the hippocampus, application of CCK-8 and CCK-4 causes excitation, possibly through a direct action on pyramidal cell somata[34]. Thus, a population of meso-limbic dopamine neurones contains, in addition to dopamine, a second peptidergic putative transmitter.

The occurrence of an additional peptide transmitter and/or modulator in some dopamine neurones is interesting in view of the hypothesis of an involvement of these neurones in various nervous disorders such as Parkinson's disease[35,36] and schizophrenia[37].

1. Vanderhaeghen, J. J., Signeau, J. C. & Gepts, W. *Nature* **257**, 604 (1975).
2. Dockray, G. J. *Nature* **264**, 568 (1976).
3. Muller, J. E., Straus, E. & Yalow, R. S. *Proc. natn. Acad. Sci. U.S.A.* **74**, 3035 (1977).
4. Rehfeld, J. F. *Acta pharmac. tox.* **41**, 24 (1977).
5. Rehfeld, J. F. *J. biol. Chem.* **253**, 4022 (1978).
6. Dockray, G. J., Gregory, R. A., Hutchinson, J. B. Ieuan Harris, J. & Runswick, M. J. *Nature* **274**, 711 (1978).
7. Robberecht, P., Descholdt-Lannckman, M. & Vanderhaeghen, J. J. *Proc. natn. Acad. Sci. U.S.A.* **75**, 524 (1978).
8. Rehfeld, J. F. & Goltermann, N. R. *J. Neurochem.* **32**, 1339 (1979).
9. Straus, E., Muller, J. E., Choi, H.-S., Paronetto, F. & Yalow, R. S. *Proc. natn. Acad. Sci. U.S.A.* **74**, 3033 (1977).
10. Hökfelt, T. *et al.* in *Hypothalamus* (eds Reichlin, S., Baldessarini, R. J. & Maring, J. B.) 69–135 (Raven, New York 1978).
11. Hökfelt, T. *et al.* in *Psychopharmacology. A Generation of Progress* (eds Lipton, M. A., DiMascia, A. & Killam, K. F.) 39–66 (Raven, New York 1978).
12. Innis, R. B., Correa, F. M. A., Uhl, G. R., Schneider, B. & Snyder, S. H. *Proc. natn. Acad. Sci. U.S.A.* **76**, 521 (1979).
13. Larsson, L.-I. & Rehfeld, J. *Brain Res.* **165**, 201 (1979).
14. Lorén, I., Alumets, J., Hakanson, R. & Sundler, F. *Histochemistry* **59**, 249 (1979).
15. Rehfeld, J. F. *Nature* **271**, 771 (1978).
16. Dahlström, A. *Eur. J. Pharmac.* **5**, 111 (1968).
17. Kreutzberg, G. *Proc. natn. Acad. Sci. U.S.A.* **62**, 722 (1969).
18. Ungerstedt, U. *Eur. J. Pharmac.* **5**, 107 (1968).
19. Hökfelt, T., Fuxe, K., Goldstein, M. & Joh, T. H. *Histochemie* **33**, 231 (1968).
20. Coons, A. H. in *General Cytochemical Methods* (ed. Danielli, J. F.) 399–422 (Academic, New York 1979).
21. Rehfeld, J. F. *Clin. chim. Acta* (in the press).
22. Markey, K. A., Kondo, S., Shenkman, L. & Goldstein, M. *Molec. Pharmac.* **17**, 79 (1980).

23. Tramu, G., Pillez, A. & Leonardelli, J. *J. Histochem. Cytochem.* **26**, 322 (1978).
24. Dahlström, A. & Fuxe, K. *Acta physiol. scand.* **62**, Suppl. 232, 1 (1964).
25. Anden, N.-E. *et al. Acta physiol. scand.* **67**, 313 (1966).
26. Nauta, W. J. H., Smith, G. P., Faull, R. L. M. & Domesick, V. B. *Neuroscience* **3**, 385 (1978).
27. Hökfelt, T. *et al.* in *Regulation and Function of Neural Peptides* (eds Costa, E. & Trabucchi, M.) (Raven, New York, in the press).
28. Hökfelt, T. *et al. Proc. natn. Acad. Sci. U.S.A.* **74**, 3587 (1977).
29. Chan-Palay, V., Jonsson, G. & Palay, S. L. *Proc. natn. Acad. Sci. U.S.A.* **75**, 1582 (1978).
30. Hökfelt, T. *et al. Neuroscience* **3**, 517 (1978).
31. Pearse, A. G. E. *J. Histochem. Cytochem.* **17**, 303 (1969).
32. Rehfeld, J. F., Goltermann, N. R., Ivarsson, L.-L., Emson, P. C. & Lee, C. M. *Fedn Proc.* **278**, 2325-2329 (1979).
33. Pinget, M., Straus, E. & Yalow, R. S. *Life Sci.* **25**, 339 (1979).
34. Dood, J. & Kelly, J. S. *J. Physiol., Lond.* (in the press).
35. Carlsson, A. in *The Basal Ganglia* (ed. Yahr, M. D.) 181-189 (Raven, New York, 1976).
36. Hornykiewicz, O. in *The Basal Ganglia* (ed. Yahr, M. D.) 269-278 (Raven, New York, 1976).
37. Matthysse, S. W. & Kety, S. S. (eds) *Catecholamines and Schizophrenia* (Pergamon, Oxford, 1975).

Diurnal cycles in serotonin acetyltransferase activity and cyclic GMP content of cultured chick pineal glands

S. D. Wainwright

Biochemistry Department, Dalhousie University, Halifax, Nova Scotia, Canada B3H 4H7

Levels of serotonin N-acetyltransferase (NAT: acetyl CoA:arylamine N-acetyltransferase; EC 2.1.1.5.) activity in the chick pineal gland exhibit a marked diurnal variation in birds kept under a diurnal cycle of illumination[1-4]. Activity begins to rise rapidly at the start of the dark phase of the cycle and reaches maximum levels at mid-dark phase about 25-fold greater than the minimum basal level at mid-light phase. Thereafter, the level of activity declines to the basal level about the start of the light phase. This diurnal cycle in chick pineal NAT activity found *in vivo* has recently been reproduced *in vitro* with intact glands incubated in organ culture[4-7]. The mechanism of the 'biological clock' which regulates these variations in level of chick pineal NAT activity is unknown. However, I now report that chick pineal glands cultured under a diurnal cycle of illumination exhibit a diurnal cycle in content of cyclic GMP which roughly parallels the cycle in NAT activity. In contrast, there was no correlation between variations in pineal content of cyclic AMP and in level of NAT activity.

A very marked stimulation of the 'nocturnal' (dark phase)[4,8] increase of NAT activity occurs in chick pineal glands cultured under a diurnal cycle of illumination on treatment with the combination of theophylline with compound Ro20.1724 (4[3 - butoxy - 4 - methoxybenzyl] - 2 - imidazolidinone), which are inhibitors of cyclic nucleotide phosphodiesterase activities[9]. This combination of inhibitors also induces a marked increase of NAT activity in glands cultured under continuous illumination[8], and almost totally abolishes the inhibition of increase of NAT activity by light (unpublished data). These observations are circumstantial evidence of a possible role of cyclic nucleotides in the 'biological clock' of the chick pineal gland. Therefore, I have followed the course of variations in pineal contents of cyclic AMP and cyclic GMP in glands incubated in organ culture under a diurnal cycle of illumination.

White Leghorn male chicks were maintained under a diurnal cycle of illumination with a photoperiod of 14 h between 0100 and 1500 h at a light intensity of $\sim 1,000$ lx at the level of the birds, and a dark period of 10 h (Figs 1 and 2). Pineal glands were removed from 1-week-old chicks (7-9 days after hatching)[4] between 1030 and 1100 h and cultured under

the same standard diurnal cycle of illumination, with light at an intensity of $\sim 1,000$ lx during the photoperiod.

The pineal cyclic GMP content of glands cultured in our standard conditions[8] and the standard diurnal cycle of illumination appeared to vary in a diurnal manner (Fig. 1, curve A). It rose about fourfold during the dark phase of the cycle of illumination to a maximum at mid-dark phase, decreased rapidly in the early photoperiod to a minimum, and rose again during the dark phase of a second cycle of illumination. Decrease of pineal cyclic GMP content in the early photoperiod was not dependent on exposure to visible light, for a corresponding decrease was seen during the same interval of (clock) time in a smaller series of experiments with glands cultured in continuous darkness (curve B).

The diurnal cycle in pineal cyclic GMP content under a diurnal cycle of illumination roughly paralleled the cycle in level of pineal NAT activity (Fig. 1, curve C).

A marked difference was found between the variations in pineal cyclic GMP content and NAT activity when glands were cultured under the diurnal cycle of illumination in the presence of theophylline plus compound Ro20.1724 (Fig. 2). The cyclic GMP content (Fig. 2a) increased without apparent lag during the final hours of the photoperiod, but reached a
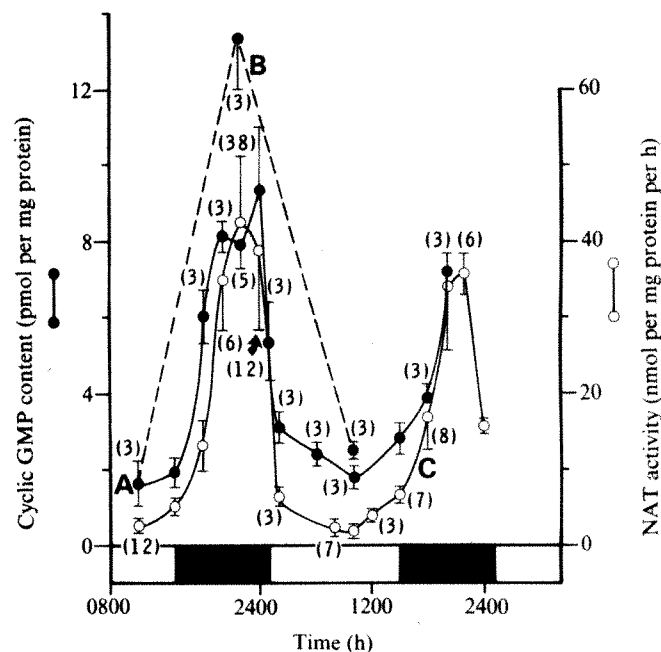
Fig. 1 Diurnal variations in chick pineal NAT activity and cyclic GMP content in culture. Groups of three pineal glands each were distributed into mini-organ cultures with 0.24 ml of medium 199 with Earle's salts[12] supplemented with antibiotics and 20% heat-inactivated fetal calf serum (Gibco)[11,13]. The cultures were incubated under 5% CO_2 in oxygen standard to the times indicated under the diurnal light cycle (bar diagram) at an intensity of $\sim 1,000$ lx, at 38 °C in a constant-environment room with forced air circulation. All glands were recovered as rapidly as possible, rinsed with saline, blotted and frozen by immersion in liquid N_2 under dim red light (~ 40 lx), regardless of lighting conditions at the end of the incubation period[4]. Cyclic GMP content (curve A) was determined on pools of six pineal glands by the radioimmunoassay method of Frandsen and Krishna[14], using commercial RIA kits (NEN). No correction was made for levels of 'apparent cyclic GMP' (< 0.05 pmol per mg protein) due to cross-reaction with cyclic AMP. Additional values for control glands incubated in constant darkness are given in curve B. NAT specific activity (curve C) was determined on pools of three glands with tryptamine as amine substrate as previously described[4]. Protein was determined by the method of Lowry *et al.*[15], with bovine serum albumin as standard. Numbers of independent determinations were either four or the value in parentheses.

peak value at mid-dark phase which was not significantly greater ($t = 1.803$, d.f. $= 7$, $P > 0.1$) than that found with control glands (curves A and B). The combination of cyclic nucleotide phosphodiesterase inhibitors markedly inhibited the subsequent decrease in pineal cyclic AMP content in the photoperiod.

When cultures were transferred to continuous darkness at mid-dark phase of the first diurnal cycle of illumination (curve C) the inhibition of subsequent decrease of cyclic GMP content was even more markedly inhibited than in glands exposed to light (curve B).

As previously reported[8], the combination of theophylline with compound Ro20.1724 markedly stimulated increase of NAT activity in the light without appreciable lag (Fig. 2a, curve B from 1100 to 1500 h on day 1 of culture). The increase of NAT activity continued in the dark to a peak level at mid-dark phase which was about four times greater than that found with control glands (curve A). The level of NAT activity decreased in the following photoperiod, but at a slower rate of net decrease than in the control glands.

This decrease of NAT activity could not be attributed to toxic effects of the drug combination. NAT activity rose again during the dark phase of a second cycle of illumination to levels at least equal to the peak level developed during the first cycle of illumination in culture (curve B). Moreover, the rate of decrease of NAT activity seen with cultures containing the inhibitors during the photoperiod (curve B) was markedly further reduced when the cultures were transferred to constant darkness shortly before start of the photoperiod (curve C).

There was no correlation between content of cyclic AMP and level of NAT activity in control pineal glands cultured under the diurnal cycle of illumination (Table 1). The cyclic AMP content after 4 h of culture was roughly half the initial content in vivo at the time of killing (1100 h) and did not change significantly during at least 15 h of further incubation. In the presence of 1 mM each of theophylline and compound Ro20.1724, the pineal cyclic AMP content increased roughly 10-fold to 223 ± 58 pmol per mg protein ($n = 3$) at 2200 h.

Assays of the pineal cyclic AMP content in vivo (Table 1) also gave no indication of any correlation between pineal cyclic AMP control and level of NAT activity.

I was unable to obtain reliable estimates of the cyclic GMP content of the chick pineal gland in vivo during the dark phase of the cycle of illumination. Observed values tended to be higher than during the photoperiod but were extremely variable. For example, nine values determined with glands removed 3 h after start of the dark phase ranged from 1.1 to 6.5 pmol per mg protein, with a modal value of 2.6. Part of this variability could possibly be attributed to differences in degree of activity exhibited by the birds, which may have reflected disturbance and attendant stress. (Noradrenaline depresses the level of NAT activity in cultured chick pineal glands[10,11].) I assume that the variability also reflects variations in length of interval between killing of the bird and freezing of the gland (average 45 s in the dark, 5 s for removal of glands from culture), and hence of duration of exposure to dim red light (legend to Fig. 1) and of postmortem metabolism.

The mechanisms of action whereby theophylline and compound Ro20.1724 elicit marked increases of NAT activity in the chick pineal gland are not known. The effects of these agents on cultured chick pineal glands have been examined for two related reasons[4,5,8,16]. First, both are known to be effective inhibitors of cyclic nucleotide phosphodiesterase activity[9]. Second, regulation of the diurnal cycle in level of NAT activity in the rat pineal gland seems to be mediated through variations in pineal content of cyclic AMP[17,18].

However, the mechanism regulating the diurnal cycle of NAT activity in the chick pineal gland differs in several important respects from that controlling the corresponding cycle in the rat pineal gland[8,19]. Therefore, increase of pineal cyclic AMP content and/or level of NAT activity in chick
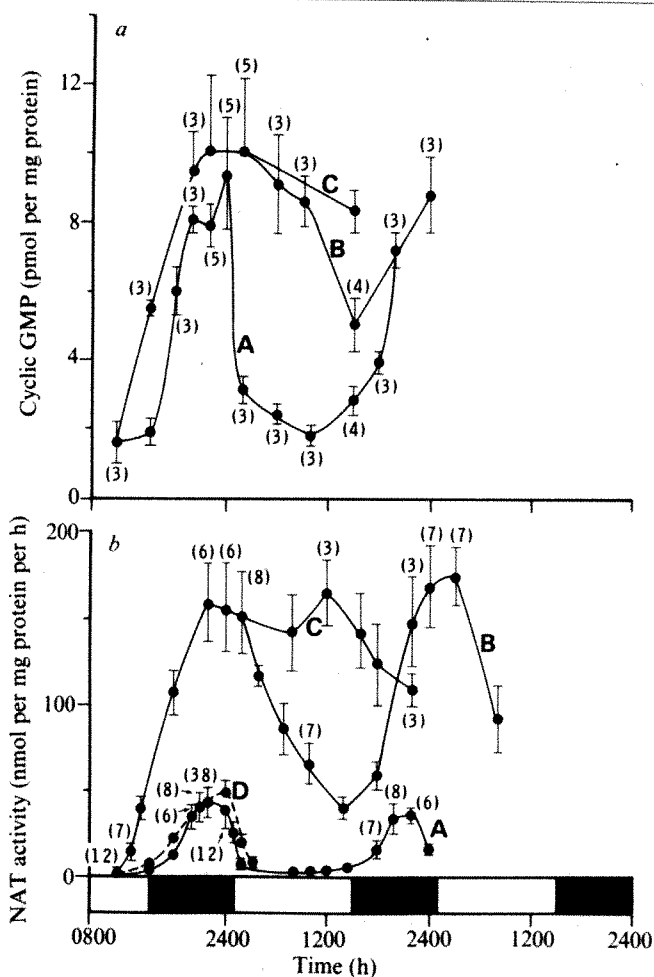
Fig. 2 Effects on the diurnal cycles in cyclic GMP content and NAT activity in culture of theophylline and Ro20.1724. Pineal glands from birds kept under the standard diurnal light cycle (bar diagram) were cultured with control medium under the standard light cycle (curve A), with 1 mM theophylline plus 1 mM Ro20.1724 under the same light cycle (curve B), and under the same light cycle to 2400 h on the first day of culture followed by continuous darkness (curve C). Levels of NAT activity in control cultures incubated in constant darkness are also given (curve D). Other details were as in the legend to Fig. 1. Levels of 'apparent cyclic AMP' due to cross-reaction of the cyclic GMP-specific antiserum with cyclic AMP were less than the s.d. of the cyclic GMP contents assayed and therefore were not corrected for. Numbers of independent determinations were either four or the value in parentheses.

pineal glands exposed to one or both of these agents is not adequate evidence that level of enzyme activity is regulated by level of cyclic GMP content.

Similarly, dibutyryl-cyclic AMP has been reported to act as an inhibitor of rat pineal cyclic phosphodiesterase activity[20]. Therefore it is imprudent to conclude that the small and variable increases of NAT activity elicited by addition of this cyclic AMP analogue to cultured chick pineal glands seen by ourselves[11] and others[5,16] strongly implicate cyclic AMP, rather than cyclic GMP, in regulation of the diurnal cycle of NAT activity in the chick pineal gland.

Indeed, the results obtained in this study (Table 1) are not readily compatible with the hypothesis that the normal diurnal cycle of NAT activity in the chick pineal gland is regulated by variations in cyclic AMP content.

In contrast, the parallel diurnal variations in both cyclic GMP content and NAT activity (Fig. 1) are compatible with the hypothesis that the variations in cyclic GMP content play an important part in regulating the normal diurnal cycle of NAT activity in the chick pineal gland.

Moreover, I assume that any effect of increased pineal cyclic GMP content on NAT activity is mediated through an increase of cyclic GMP-dependent protein kinase activity. On the other hand, reversal of that effect after a subsequent decrease of cyclic GMP content would require both a decrease of the kinase activity and the action of a protein phosphatase. Thus effects of a premature, but sustained, increase of pineal cyclic GMP content elicited by the combination of theophylline plus compound Ro20.1724 (Fig. 2a, curves A and C) could be greatly amplified in the very marked stimulation of increase of NAT activity (Fig. 2b, curves A and C).

Table 1   Variations in chick pineal cyclic AMP content

	pmol cyclic AMP per mg protein	
Time (h)	in culture	*in vivo*
1100	38.0±4.0 (7)	38.0±4.0 (7)
1500	15.6±4.9 (6)	30.7±6.8 (5)
1630	20.6±5.3 (3)	—
1700	22.1±4.3 (8)	—
1800	—	26.7±8.5 (3)
2000	25.6 (2)	21.2 (2)
2200	22.5±4.3 (12)	31.4±5.8 (5)
2400	22.8±5.3 (5)	—
0300	—	28.9 (2)
0800	19.3±4.6 (4)	—

White Leghorn chicks were kept under the standard light cycle and cyclic AMP contents *in vivo* were determined for birds killed at the times indicated. Dissections for birds in the dark were by dim red light[4]. The radioimmunoassay method for Fransden and Krishna[14] was used for determination of cyclic AMP, using commercial kits. No correction for cross-reaction with cyclic GMP was necessary. All other methods were as given in the legend to Fig. 1. Numbers of independent determinations are given in parentheses.

Nevertheless, the NAT activity elicited by the drug combination declines rapidly in the normal photoperiod (Fig. 2b, curve B), whereas decrease of pineal cyclic GMP content is markedly inhibited (Fig. 2a, curve B). Further, supplements of exogenous dibutyryl-cyclic GMP have been recently reported to depress the level of NAT activity in cultured chick pineal glands[16].

Therefore it seems that the diurnal cycle of NAT activity in the chick pineal gland is probably not determined solely by changes in pineal cyclic GMP content. Indeed, it is possible that the parallel variations of pineal cyclic GMP content and of NAT activity are the fortuitous coincidence of two unrelated cycles controlled by a single 'biological clock'.

1. Binkley, S., Macbride, S. E., Klein, D. C. & Ralph, C. L. *Science* **181**, 273–275 (1973).
2. Binkley, S. & Geller, E. B. *J. comp. Physiol.* **99A**, 67–70 (1975).
3. Fraser, I. H. & Wainwright, S. D. *Can. J. Biochem.* **54**, 103–109 (1976).
4. Wainwright, S. D. & Wainwright, L. K. *Can. J. Biochem.* **57**, 700–709.
5. Binkley, S. A., Riebman, J. B. & Reilly, K. B. *Science* **202**, 1198–1201 (1978).
6. Kasal, C. A., Menaker, M. & Perez-Polo, J. R. *Science* **203**, 656–658 (1979).
7. Deguchi, T. *Science* **203**, 1245–1247 (1979).
8. Wainwright, S. D. & Wainwright, L. K. (in preparation).
9. Zenser, T. V., Craven, P. A., de Robertis, F. R. & David, B. B. *Archs Biochem. Biophys.* **178**, 598–606 (1977).
10. Binkley, S. *Am. Zool.* **16**, 57–65 (1976).
11. Wainwright, S. D. & Wainwright, L. K. *Can. J. Biochem.* **56**, 685–690 (1978).
12. Morgan, J. F., Morton, H. J. & Parker, R. C. *Proc. Soc. exp. Biol. Med.* **73**, 1–8 (1950).
13. Wainwright, S. D. *Can. J. Biochem.* **55**, 415–423 (1977).
14. Frändsen, E. K. & Krishna, G. *Life Sci.* **18**, 529–542 (1976).
15. Lowry, O. H., Rosebrough, N. J., Farr, A. L. & Randall, R. J. *J. biol. Chem.* **193**, 265–275 (1951).
16. Deguchi, T. *J. Neurochem.* **33**, 45–51 (1979).
17. Axelrod, J. *Science* **184**, 1341–1348 (1974).
18. Klein, D. C. in *The Hypothalamus* (eds Reichlin, S., Baldessarini, R. J. & Martin, J. B.) 303–326 (Raven, New York, 1978).
19. Binkley, S. *Comp. Biochem. Physiol.* **64A**, 201–206 (1979).
20. Klein, D. C. & Berg, G. R. *Adv. biochem. psych. Pharmac.* **3**, 241–263 (1970).

Prostacyclin production by cultured smooth muscle cells from atherosclerotic rabbit aorta

Jacky Larrue*, Michel Rigaud†, Danièle Daret*, Josette Demond*, Jacqueline Durand† & Henri Bricaud*

*INSERM U8 de Recherches de Cardiologie, Avenue du Haut Lévêque, 33600 Pessac, France
†Laboratoire de Biochimie, Faculté de Médecine et de Pharmacie, 2, rue du Docteur Marcland, 87000 Limoges, France

Prostacyclin (PGI₂) synthesis seems to be one of the major physiological mechanisms involved in regulating platelet and vessel wall interactions[1]. PGI₂ is produced in large amounts by vascular endothelial cells, and vascular smooth muscle cells (SMC) also produce significant quantities[2]. The capacity of SMC to produce PGI₂, especially after endothelial injury, seems to be of importance. It is probably this type of situation that is involved in the atherosclerotic process[3]: experimental atherosclerosis in rabbits has been associated with a severe decrease in PGI₂ synthesis by arteries[4]. Lipid peroxide accumulation within the arterial wall or in the plasma may also be involved in this process[5]. Using arterial SMC in culture, we demonstrate here that, in comparison with healthy cultured cells, cells originating from atherosclerotic aorta have a decreased capacity to produce PGI₂. The results were obtained using biological and radiochemical techniques and were confirmed by GC-MS. They suggest a potential role for PGI₂ in inhibiting the atherosclerotic process.

Experiments were carried out with 1.5-yr-old rabbits. Smooth muscle cells derived from explants of the medial layer from thoracic aorta in both normal and atherosclerotic animals (cholesterol, 500 mg per day for 6 months, then maintained for 6 months on a normal diet) were grown at 37 °C in 75-cm³ plastic flasks in an atmosphere of 5% CO_2 in air essentially as described by Ross[6]. Cells were used after 5–10 trypsinizations.

At confluency cells were washed twice with serum-free culture medium, collected by scraping with a rubber policeman and suspended in Tris (0.05 M), NaCl (0.15 M) pH 7.4 buffer. Aliquots of 0.2 ml were used for protein concentration determinations according to the method of Lowry. Bovine serum albumin was used as standard. Cell counts were performed with a haemocytometer after trypsinization of cells from flasks at the same passage.

In previous studies, aliquots of cell suspensions were incubated in Tris-NaCl buffer at 22 °C. SMC incubated for 10 min released an inhibitor of ADP induced aggregation. Aliquots (100 μl) of supernatants from incubations of 10⁶ healthy and atherosclerotic cells induced an inhibition of 44% and 13%, respectively. In these experiments inhibitory activity was not detected in buffer incubated without cells or in buffer alone incubated directly with the cell layer attached to the flask. No inhibitory activity was detected in supernatants from cells pretreated with aspirin (5×10^{-2} M) for 10 min, after heating (15 min, 37 °C) or acidification.
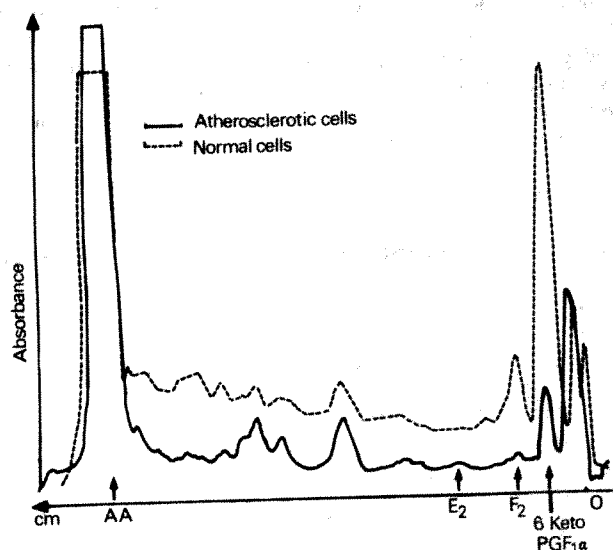
Fig. 1 Scan of autoradiogram observed after 3 days of exposure. Absorbance was measured at 550 nm. Aliquots of 20 µl ethyl acetate dissolved extracts were chromatographed on silica gel G plates previously activated for 30 min at 110 °C and developed by ascending chromatography in the organic layer of ethyl acetate, isooctane, acetic acid, water (90: 50: 20: 100 v/v). Arrows indicate the position of unlabelled standards visualized by iodine vapours. F_2, $PGF_{2\alpha}$; E_2, PGE_2; AA, arachidonic acid.

Suspensions of cells from several normal or atherosclerotic strains were incubated with ^{14}C-labelled arachidonic acid (AA). After incubation, the mixture was acidified to pH 2 and extracted with ethyl acetate. The organic phase was evaporated to dryness under nitrogen. Dried extracts were redissolved in 0.1 ml ethyl acetate and subjected to TLC. As shown in Fig. 1, a major area of radioactivity was co-chromatographed with 6 keto-$PGF_{1\alpha}$ standard (the stable breakdown product of PGI_2). In other experiments, aspirin (5 $\times 10^{-2}$ M) was added 10 min before incubation: production of 6 keto-$PGF_{1\alpha}$ was markedly reduced (Table 1).

Different cultures exhibited different rates of conversion of AA to its metabolites: limit values were 1.27 to 2.60 % for healthy cells and 0.32 to 0.85 % for atherosclerotic cells. The number of passages did not greatly influence PGI_2 synthesis between 5–10 passages, as per cent transformations ranged from 1.72 to 1.98 for L735 healthy strain cells and from 0.39 to 0.34 for L728 atherosclerotic strain cells.

Disparities occurred between different cultures from the same tissue type. This phenomenon has already been described by other authors[7]. However, it seemed obvious that in comparison with normal cells, atherosclerotic cells exhibited a strong decrease in their capacities to synthesize PGI_2 from exogenous AA (per cent transformation 0.60±0.28 and 2.00 ±0.48, respectively: $P \leqslant 0.01$).

We defined this decrease further with GC-MS determinations. Prostacyclin formed after a 30-min incubation of cells with 10 µg AA was measured as 6 keto-$PGF_{1\alpha}$, as previously described[8]. Briefly, prostaglandin $F_{2\beta}$ ($PGF_{2\beta}$) was added as internal standard before extraction with ethyl acetate at pH 3. The organic phases were pooled and evaporated to dryness under nitrogen and the biological extract subjected to silicic acid chromatography. The collected fractions were evaporated and derivated to methyl esters, methoximes and trimethylsilyl ethers. Methyl esters were prepared by treatment with anhydrous ethereal diazomethane (1.0 ml) for 1 h at room temperature. After esterification the excess reagents were evaporated at 25 °C with nitrogen. Methyl ester of 6-keto-$PGF_{1\alpha}$ was converted into methoxime by heating (60 °C, 1 h) the residue left after esterification with a saturated solution

(0.1 ml) of O-methylhydroxylamine chloride in anhydrous pyridine. Pyridine was evaporated with nitrogen. $PGF_{2\beta}$ and 6 keto-$PGF_{1\alpha}$ ester oximes were converted into trimethylsilyl ethers by heating at 60 °C for 1 h with N,O-bis(trimethylsilyl)-trifluoroacetamide (BSTFA) and trimethylchlorosilane (TMCS) (95/5, v/v).

We monitored the metabolic profiles of AA in cell preparations with glass capillary-gas chromatography and multiple ion detection (GC-MS LKB 2091). Figure 2 shows the transformation of AA incubated with normal and atherosclerotic cultured SMC. Measurements performed on different cell homogenates from L7805 healthy and L7804 atherosclerotic strains at different passages showed that 271–1,471 ng per mg protein (mean 918±574) and 185–476 ng per mg protein (mean 285±165) of 6 keto-$PGF_{1\alpha}$ was recovered from the healthy strain and the atherosclerotic strain, respectively ($P \leqslant 0.05$).

Three results demonstrate that healthy vascular smooth muscle cells in culture can synthesize PGI_2 in relatively large amounts. This finding is in agreement with values for human
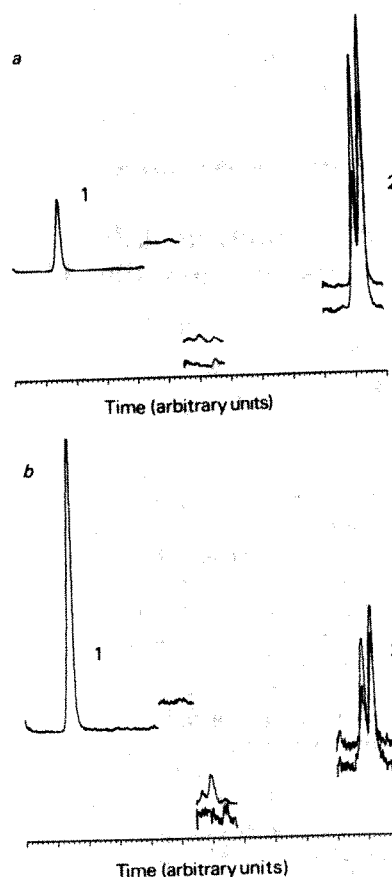
Fig. 2 Multiple ion monitoring of characteristic ions in the mass spectra of: (1) methyl ester trimethylsilyl ether $PGF_{2\beta}$, m/e =423: $M^+ -(Si-(CH_3)_3 -OH +C_5H_{11})$, $\times 25$; (2) methyl ester oxime trimethylsilyl ether 6 keto-$PGF_{1\alpha}$, $m/e = 378$, $M^+ -(Si -(CH_3)_3 -OH +C_5H_{11})$ $m/e = 418$, $M^+ -(2 \times Si -(CH_3)_3 -OH +31)$, $\times 200$. The two peaks recorded at m/e 378 and m/e 418 are the *syn* and *anti* isomers of the methoxime derivative of 6 keto-$PGF_{1\alpha}$. The recording of the two extracts, *a*, normal strain, *b*, atherosclerotic strain, use the same amplification and scale factors, therefore the area ratios, internal standard/measured product, demonstrate the difference between the two strains. Calibration curves for multiple ion detection of $PGF_{2\beta}$ and 6-keto-$PGF_{1\alpha}$ allowed quantification. GC was performed with a home-made wall coated open tubular column (length, 20 m, i.d. 0.30 mm; theoretical plates 3,500 m^{-1}, stationary phase: OV$_1$). Oven temperature ranged from 200 °C to 265 °C (2 °C min^{-1}).

Table 1 Conversion of arachidonic acid to 6-keto-PGF$_{1\alpha}$ and influence of aspirin treatment

Tissue origin	Aspirin treatment	No. of experiments	6-keto-PGF$_{1\alpha}$ (mean ± s.d.)
Healthy media	No	12	2.30 ± 0.21
L7805	Yes	6	0.46 ± 0.08
Atherosclerotic media	No	10	0.86 ± 0.17
L7804	Yes	5	0.20 ± 0.05

Results were expressed as the per cent transformation of 10 nM AA by 500 µg protein of SMC in a total volume of 0.5 ml within the 20 min direct incubation period at room temperature, or after 10 min preincubation with 5×10^{-2} M aspirin.

vascular smooth muscle cells reported by others and is similar to those obtained with fresh arterial intimal cell suspensions[2].

Atherosclerotic cells in culture synthesize PGI$_2$ at a lower rate than do normal cells. Further experiments are required to explain these differences. Several mechanisms may be involved in this process. A decrease of spontaneous generation of prostacyclin by atherosclerotic arterial rings has previously been described[4]. This phenomenon has been explained by an increase of lipid peroxidation which inhibits prostacyclin synthesis[5]. We have shown that, *in vitro*, in the same culture conditions (particularly the same lipid concentration), a decrease of prostacyclin synthetase activity occurs in cells originated from atherosclerotic aortas. Additional results (data

not shown) demonstrate that cyclooxygenase may be disturbed in the latter case but do not seem to indicate that another pathway for prostaglandin formation occurs. An increased formation of PGE$_2$ or PGD$_2$ as reported in atherosclerotic rabbit aortic rings[9], was not observed. The identification of lipoxygenase activity in vascular tissue[10,11] may be important in explaining the modifications observed, as the AA hydroperoxides may modulate PGI$_2$ production in vascular tissue by inhibiting prostacyclin synthetase[5].

Our findings suggest that the reduced capacity of atherosclerotic smooth muscle cells to produce PGI$_2$ may be significantly involved in the course of the atherosclerotic process.

We thank Dr J. Pike (Upjohn) for prostaglandins. This work was supported by the University of Bordeaux II and CHRU Dupuytren (Limoges).

1. Gryglewski, R. J., Bunting, S., Moncada, S., Flower, R. J. & Vane, J. R. *Prostaglandins* **12**, 685–713 (1976).
2. Moncada, S., Herman, A. G., Higgs, E. A. & Vane, J. R. *Thromb. Res.* **11**, 323–394 (1977).
3. Ross, R. & Glomset, J. *New Engl. J. Med.* **195**, 369–377 (1976).
4. Dembinska-Kiec, A., Gryglewska, T., Zmuda, A. & Gryglewski, R. J. *Prostaglandins* **14**, 1025–1034 (1977).
5. Moncada, S., Gryglewski, R. J., Bunting, S. & Vane, J. R. *Prostaglandins* **12**, 715–737 (1976).
6. Ross, R. *J. Cell Biol.* **50**, 172–186 (1971).
7. Beanzinger, N. L., Becherer, P. R. & Majerus, P. W. *Cell* **16**, 967–974 (1979).
8. Rigaud, M. *et al. Advances in Chromatography. Proc. 4th int. Symp.*, Houston (ed. Zlatkis, A.) 615–624 (1979).
9. Berberian, P. A., Zibou, V. A. & Hsia, J. L. *J. Lipid Res.* **17**, 40–52 (1976).
10. Greenwald, J. E., Bianchine, J. R. & Wong, L. K. *Nature* **281**, 588–589 (1979).
11. Herman, A. G., Claeys, M., Moncada, S. & Vane, J. R. *Prostaglandins* **18**, 439–452 (1979).

Pressure inhibits thermal killing of Chinese hamster ovary fibroblasts

K. W. Minton, M. A. Stevenson, J. Kendig*
& George M. Hahn

Departments of Radiology and *Anesthesiology,
Stanford University, School of Medicine, Stanford, California 94305

The increasing application of hyperthermia to cancer therapy[1-5] has resulted in intensive study of the cellular effects of small temperature elevations (from about 37 to 43 °C). The critical heat target(s) have not been identified, however, findings such as the alterations in membrane morphology, inhibition of potassium transport[6] and increased permeability to a variety of substances[7,8] implicate the plasma membrane[9]. Also, there are striking similarities between the response of cells in tissue culture to heat and various membrane fluidizing agents, including anaesthetics and alcohols[10-14]. An initial exposure of cells to non-lethal doses of heat will trigger development of subsequent resistance to both heat and ethanol, as well as to adriamycin. Similarly, an initial exposure to ethanol will result in subsequent resistance to all three of these agents[10-12]. A range of anaesthetics and alcohols also act synergistically with heat in cell killing[12-14]. As the effects of ethanol and many other anaesthetics thought to be membrane active are known to be inhibited by the simultaneous application of elevated pressure[15], we suspected that thermal cell killing would also be inhibited by high pressure, as occurs in bacterial systems[16]. There are marked differences, however, between the response of mammalian cells and bacteria to heat: mammalian cells require only very small elevations in temperatures to effect large changes in survival, and can only grow within a comparatively narrow temperature range. We demonstrate here that pressure does, nevertheless, inhibit thermal killing of mammalian cells.

The survival of cells from a sub-line of Chinese hamster ovary (CHO) fibroblasts (HA-1) was measured by their ability to form clones after exposure to elevated temperatures for varying periods. During hyperthermic exposure, cells were

pressurized up to 3,000 p.s.i. (205 ATA) under a helium atmosphere. The survival of cells heated at 42.9 °C and 43.7 °C for up to 4 h is shown in Fig. 1. The application of pressure (2,500 and 3,000 p.s.i., respectively) increased survival by up to a factor of 10^4. Control experiments showed no killing of cells incubated in identical conditions at 37 °C with or without pressure. The survival of cells heated at 44.0 °C for 90 min as a function of pressure is shown in Fig. 2. Their survival increases exponentially with increasing pressure over the range examined. Note that the degree of improved survival is actually underestimated by our technique because short periods of heating occurred before and after pressurization; also there was a small transient temperature elevation associated with the pressurization itself (see Fig. 1 legend).

We have demonstrated that the viability of heat-treated HA-1 cells, their ability to reproduce and form clones, is enhanced if pressure is applied simultaneously with the heat exposure. The most widely accepted theories of anaesthesia assert that general anaesthetics exert their effects by inducing a molecular volume expansion of cellular lipids or proteins[15,19-22]. When the cell or organism is exposed to high pressure, molecular volume is reduced and anaesthesia, therefore, abolished. If this proposed mechanism is relevant, molecular volume expansion due to temperature elevation should also be pressure-reversible. As the volume expanding and fluidizing effects of both temperature elevation and anaesthetics on lipid bilayers and biomembranes are pressure-reversible[23-25], our observation of pressure reversibility of mammalian cell thermal killing suggests the cell membrane as a thermal target. However, pressure-reversibility does not in itself implicate solely the plasma membrane: the impairment of soluble enzyme activity by heat and anaesthetics has been shown to be pressure-reversible in the luciferin–luciferase enzyme system[22,26]. An interesting question arising from this and the present findings is whether the phenotype of temperature-sensitive mutants at the restrictive temperature may be reverted to wild type by the application of high pressure.

The reversal of a temperature-induced increase in membrane fluidity by high pressure seems to have a biological analogue: when confronted by a change in environmental temperature,

cells induce compensatory alterations of membrane fluidity by changing their lipid composition[27-29]. We have recently found that CHO HA-1 cells increase their membrane cholesterol content and decrease membrane fluidity in response to elevated growth temperatures. Increased membrane cholesterol has also been associated with increased resistance to hyperthermic exposure (ref. 30 and R. Anderson et al., in preparation). It has been proposed that cells may also adapt
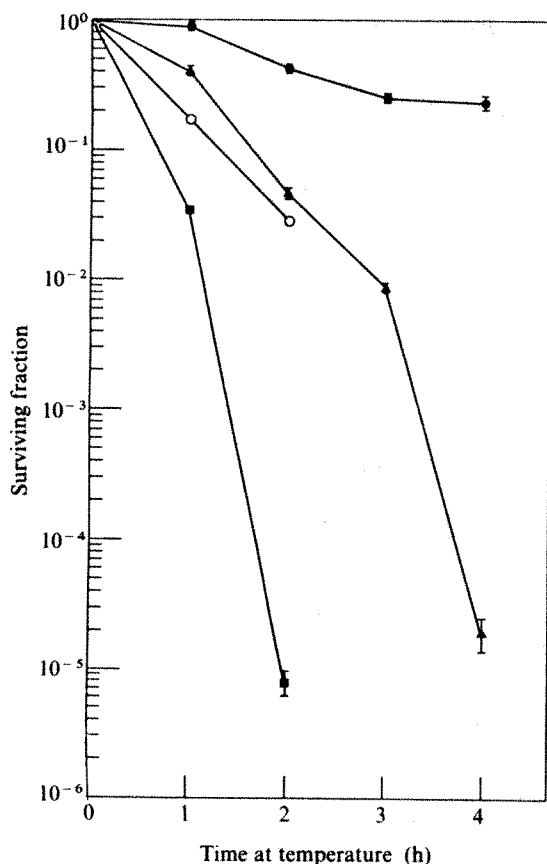
Fig. 1 The survival of HA-1 fibroblasts exposed to hyperthermia with and without pressure. HA-1 cells were grown for 3 days in 5 ml of minimal essential medium (MEM; Gibco) plus 15% fetal calf serum (FCS; Gibco) on the bottoms of gauze-plugged 50-ml volumetric flasks. Their growth was exponential with a final density of 80,000 cells cm^{-2}. Just before heating, fresh MEM plus 15% FCS was added to a total volume of 50 ml. The pressure bomb is as previously described[17]. It was filled with water and submerged in a temperature-controlled waterbath, and the system equilibrated to the desired temperature. The flask was submerged within the pressure bomb just to the end of the neck with the gauze plug above water level. Temperature equilibration of the media occurred within 5 min. The pressure bomb was equilibrated at 1 atm (14.7 p.s.i.) with 5% CO_2 and air. Helium was then added from a high pressure cylinder to achieve the desired pressure up to 3,000 p.s.i. Full pressure was achieved about 10 min after the flask was submerged. Depressurization and removal of the flask required 5 min. The pH of the medium was measured immediately before and after pressurization and remained constant at 7.6 ± 0.1; it was not affected by the degree or duration of pressurization. Temperature control was accurate to 0.1 °C except for the period during and immediately after pressurization; pressurizing resulted in an elevation of temperature within the bomb and flask of 0.3–0.5 °C which returned to baseline within 15 min. Survival was determined according to the cloning assay of Puck and Marcus[18]. ▲, 42.9 °C, unpressurized; ●, 42.9 °C, 2,500 p.s.i.; ■, 43.7 °C, unpressurized; ○, 43.7 °C, 3,000 p.s.i. Bars indicate standard error.
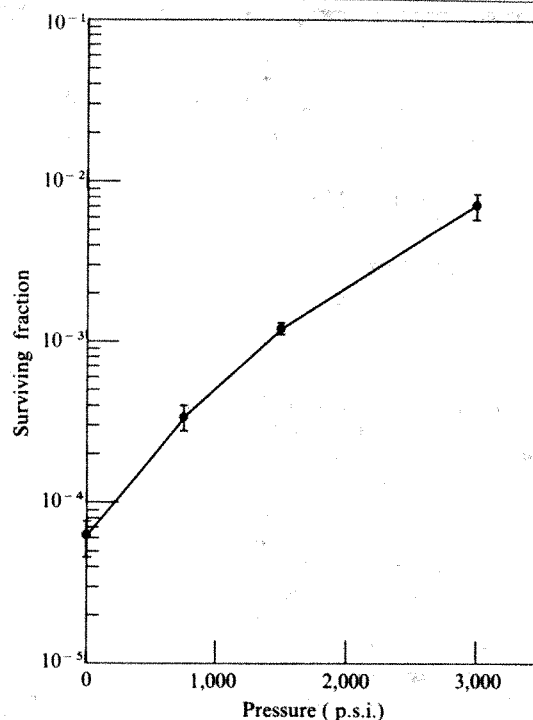
Fig. 2 The survival of HA-1 fibroblasts exposed to 44.0 °C for 90 min at pressures ranging up to 3,000 p.s.i. See Fig. 1 legend for procedure. Bars indicate standard error.

to anaesthetics by altering membrane composition[31]. This has been confirmed recently in the case of ethanol where it has been demonstrated that membranes from ethanol-tolerant mice show increased cholesterol and increased resistance to the fluidizing effect of ethanol[32,33].

1. Overgaard, K. & Overgaard, J. Eur. J. Cancer 8, 65-78 (1972).
2. Mendecki, J., Friendenthal, E. & Bolstein, C. Cancer Res. 36, 2113-2114 (1976).
3. Marmor, J. B., Hahn, N. & Hahn, G. M. Cancer Res. 37, 879-883 (1977).
4. Marmor, J. B., Pounds, D. W., Hahn, N. & Hahn, G. M. Int. J. Radiat. Oncol. Biol. Phys. 4, 967-973 (1978).
5. Marmor, J. B., Pounds, D. W., Postic, T. B. & Hahn, G. M. Cancer 43, 188-197 (1979).
6. Szmigielski, S. & Janiak, M. In Cancer Therapy by Hyperthermia and Radiation (Urban and Schwarzenberg, Baltimore, 1978).
7. Strom, R. et al. Eur. J. Cancer 9, 103-112 (1973).
8. Gerner, E. & Russell, D. Cancer Res. 37, 482-489 (1977).
9. Dewey, W. et al. in Radiation Biology in Cancer Research (Raven, New York, 1980).
10. Li, G. C. & Hahn, G. M. Nature 274, 699-701 (1978).
11. Li, G. C., Shiu, E. & Hahn, G. M. Radiat. Res. (in the press).
12. Li, G. C., Shiu, E. & Hahn, G. M. J. cell. Physiol. 93, 331-334 (1977).
13. Yatvin, M. B., Kelly, H. & Dennis, W. Science 205, 195-196 (1979).
14. Yatvin, M. B. Int. J. Radiat. Biol. 32, 513-521 (1977).
15. Miller, K. W. & Wilson, M. W. Anesthesiology 48, 104-110 (1978).
16. Johnson, F. H. & Lewin, I. J. Comp. cell. Physiol. 28, 23-45; 77-97 (1946).
17. Kendig, J. J., Trudell, J. & Cohen, E. J. pharm. exp. Ther. 195, 216-224 (1975).
18. Puck, T. & Marcus, P. J. exp. Med. 103, 653-666 (1956).
19. Halsey, M. J., Wardley-Smith, B. & Green, C. J. Br. J. Anesth. 50, 1091-1097 (1978).
20. Miller, K. W. Science 185, 867-869 (1974).
21. Eyring, H., Woodbury, J. W. & D'Arrigo, J. S. Anesthesiology 38, 415-424 (1973).
22. Johnson, F. H. & Eyring, H. in High Pressure Effects on Cellular Processes (ed. Zimmerman, A.) 1-44 (Academic, New York, 1970).
23. Kamaya, H., Ueda, I., Moore, P. & Eyring, H. Biochem. biophys. Acta 550, 131-137 (1979).
24. Mastrangelo, C., Kendig, J. J., Trudell, J. & Cohen, E. Undersea biomed. Res. 6, 47-53 (1979).
25. Chin, J. H., Trudell, J. R. & Cohen, E. Life Sci. 18, 489-498 (1976).
26. Ueda, I., Kamaya, H. & Eyring, H. Proc. natn. Acad. Sci. U.S.A. 73, 481-485 (1976).
27. Hazel, J. & Prosser, C. Physiol Rev. 54, 620-677 (1974).
28. Janoff, A., Haug, A. & McGroarty, E. Biochim. biophys. Acta 555, 56-66 (1979).
29. Martin, C. & Thompson, G. Biochim. biophys. Acta 468, 73-80 (1977).
30. Gerner, E. & Cress, A. Nature 283, 677-679 (1980).
31. Hill, M. W. & Bangham A. D. Adv. exp. Med. Biol. 59, 1-9 (1975).
32. Chin. J. H. & Goldstein, D. B. Molec. Pharmac. 13, 435-441 (1977).
33. Chin. J. H., Parson, L. & Goldstein, D. B. Biochim. biophys. Acta 513, 358-363 (1978).

Transformation of rat fibroblasts and formation of virus-induced syncytia

S. J. Kaufman & D. M. Ehrbar

Department of Microbiology and School of Basic Medical Sciences, University of Illinois, Urbana, Illinois 61801

Human KC cells[1] and rat XC cells[2] transformed by Rous sarcoma virus (RSV) fuse to form multinucleate syncytia in the presence of several retroviruses[3-11], although neither cell line itself produces virus. XC cells form syncytia on co-cultivation with cells producing murine leukaemia virus (MuLV)[3] and with purified MuLV[4]. This altered cytopathic property is readily quantified and is a useful assay both for titrating MuLV and for detecting cells producing these viruses[3,5,6]. Fusion occurs from without and does not require viral replication[7]. We recently described the fu-1 cell line of developmentally defective rat myoblasts, which can also undergo synctia formation either by co-cultivation with cells infected with Moloney MuLV (MoMuLV) or on infection with intact or UV-inactivated MoMuLV[12]. On chronic infection with MoMuLV, fu-1 cells become refractive to syncytia formation[12]; this is also true of XC and KC cells infected with their appropriate respective viruses[9,11,13]. However, in contrast with XC and KC cells, fu-1 cells do release an endogenous retrovirus[14,15]. Whereas XC, KC and fu-1 cells are transformed and can undergo virus-induced fusion, neither 118 MG cells[10] nor L$_8$ myoblasts[12] (the non-transformed parents of KC and fu-1 cells, respectively), form these virus-induced syncytia. This suggests that the capacity of cells to undergo retrovirus-induced fusion rests with their transformed status. We report here that Rat-1 cells, transformed with the temperature-sensitive transformation mutant RSV-tsLA29 (ref. 16), only form syncytia in the presence of MoMuLV when these cells are preincubated at 35 °C, the temperature permissive for transformation, and not at 40 °C, the non-permissive temperature. Rat-1 cells transformed with wild-type avian sarcoma virus form MoMuLV-induced syncytia at both temperatures. Thus, virus-induced transformation promotes changes in these cells that render them competent to undergo subsequent virus-induced fusion.

Rat-1-tsLA29 and fu-1 cells were grown for 18 h at either 35 °C or 40 °C and were then infected with MoMuLV and incubated for an additional 5 h at either temperature. MoMuLV was effective at inducing syncytia in fu-1 cells at either temperature, although the number of syncytia formed at 40 °C was slightly less than that formed at 35 °C (Table 1, expt 1). In contrast, only those Rat-1-tsLA29 cells preincubated at 35 °C fused in the presence of MoMuLV (Table 1 and Fig. 1). Although shifting the temperature from 35 to 40 °C, either at the time of infection or during the 5-h post-infection period, reduced the number of syncytia that developed, a shift from 40 to 35 °C at either of these times did not promote cell fusion. Thus, the capacity of these cells to undergo virus-induced fusion clearly depends on the expression of the temperature-sensitive transforming properties of the virus and this competence must be present during the initial interaction of the cells and virus.

Rat-1 cells not transformed by avian sarcoma virus and Rat-1 cells transformed with wild-type B77 avian sarcoma virus (Rat-1-B77 cells) were also tested for their capacity to undergo virus-induced fusion (Table 1, expt 2). MoMuLV did not induce the fusion of normal Rat-1 cells to an appreciable extent at either temperature. Rat-1-B77 cells, like fu-1 cells, fused at both 35 and 39.5 °C. Thus, fusion induced by MoMuLV is not inherent in Rat-1 cells but is dependent on the virus-induced transformation of these cells.

We have previously shown that several developmentally defective clones isolated from the L$_8$ myogenic line can undergo MoMuLV-induced fusion and that this capacity to undergo virus-induced fusion is significantly associated with several phenotypic traits characteristic of transformed cells *in vitro*[14,15]. These changes include elevated hexose transport, decreased cell-surface fibronectin, reduced serum requirements for growth and decreased adhesiveness. These are also characteristics previously reported to be associated with expression of the *src* gene of RSV. Whether any of these changes in the cell surface are causally related to the capacity of these cells to undergo retrovirus-induced fusion is of interest. Both normal and transformed cells can support productive infections by MoMuLV and this suggests that both cell types can interact with the virus. In contrast, expression of the RSV transformation gene in Rat-1, KC and XC cells, and by analogy, expression of endogenous transformation sequences in fu-1 cells, is required and mediates the competence of these cells to undergo virus-induced fusion. Whereas leukaemia virus-induced fusion has proved to be a

Table 1   MoMuLV-induced fusion of fu-1 myoblasts and avian sarcoma virus transformed Rat-1 fibroblasts

	Temperature (°C)			Syncytia per cm²	
Cells	Pre-infection (18 h)	Infection (1 h)	Post-infection (5 h)	+MoMuLV	−MoMuLV
Expt 1					
fu-1					
	35	35	35	6,376±1,185	58±115
	40	40	40	4,956±973	28±67
Rat-1-tsLA29					
	35	35	35	3,009±814	29±68
	40	40	40	14±49	0±0
	35	35	40	1,734±566	103±139
	35	40	40	1,044±283	14±49
	35	40	35	1,274±814	0±0
	40	40	35	58±60	14±49
	40	35	40	28±67	14±49
	40	35	35	14±49	44±79
Expt 2					
fu-1	35	35	35	1,120±275	0±0
	39.5	39.5	39.5	1,075±183	0±0
Rat-1	35	35	35	51±53	4±16
	39.5	39.5	39.5	43±38	0±0
Rat-1-B77	35	35	35	595±147	51±70
	39.5	39.5	39.5	564±126	16±28

Rat-1-tsLA29 cells were derived as follows: viral pseudotypes were produced by infection of chick embryo cells with subgroup D chicken leukosis virus (Carl Zilber Associated Virus) and RSV-tsLA29 (subgroup A). Rat-1 cells, a line of Fischer rat embryo cells (referred to as F2408 by Mishra and Ryan[17] and Prasad, Zouzias and Basilico[18]) were infected with the pseudotype virus; 2 weeks later foci were isolated and grown up, and the Rat-1-ts LA29 cells were cloned. At 35 °C, but not at 40 °C, these cells exhibit morphological and growth control properties of transformed cells *in vitro*, including elevated hexose transport, enhanced colony formation in soft agar, increased proteolysis and decreased adhesiveness (M. Weber, personal communication). Rat-1-B77 cells (clone B1) were derived by an analogous procedure from the 208F subclone of Rat-1 cells[19], using B77 avian sarcoma virus. Rat-1, Rat-1-tsLA29, Rat-1-B77 and fu-1 cells were grown and passaged as previously described[14,15], in Dulbecco's medium supplemented with 10% horse serum, 100 U ml⁻¹ penicillin, 100 μg ml⁻¹ streptomycin and 10 μg ml⁻¹ kanamycin. 4 × 10⁵ fu-1, 4 × 10⁵ Rat-1, 8 × 10⁵ Rat-1-B77, or 1 × 10⁶ Rat-1-tsLA29 cells were plated on 35-mm Falcon tissue culture dishes. These different numbers of cells were plated to obtain subconfluent monolayers needed for optimal fusion[12]. The cultures were incubated for 1 h at 37 °C, then for 18 h at either 35 °C or 40 °C (39.5 °C, expt 2). The medium was removed and the cells were infected with MoMuLV in 0.6 ml serum-free medium, containing 12 μg ml⁻¹ DEAE-dextran, at a multiplicity of infection of approximately 25. Control cultures were treated with the same medium, but without virus. After 1 h at 35 °C or 40 °C (39.5 °C, expt 2), the virus was removed and the cells were washed with complete medium and incubated for 5 h at the temperatures indicated. The cells were then fixed in 70% methanol for 20 min and stained with 5% Giemsa. Cells containing three or more nuclei were scored as syncytia in at least six fields on each plate, at a magnification of × 160. The mean numbers of syncytia per cm² ±s.d. in duplicate plates are given. Expts 1 and 2 were done with different lots of MoMuLV.
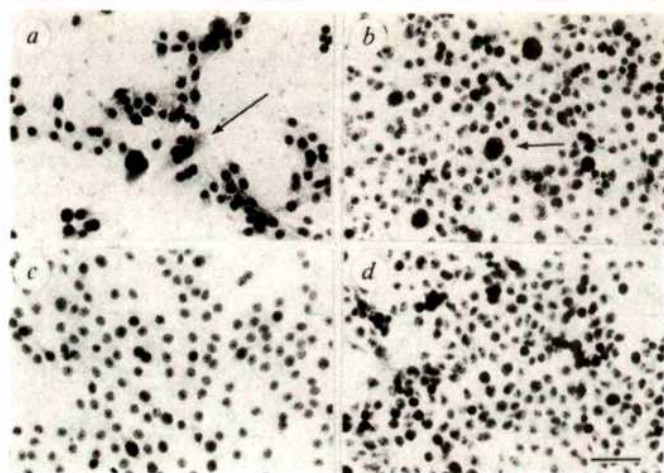
Fig. 1 Virus-induced syncytia in transformed Rat-1 cells. Syncytia were formed by infection of Rat-1-*ts*LA29 cells with MoMuLV as indicated in Table 1. Cells preincubated at 35 °C and maintained at 35 °C throughout the experiment (*a*), or transferred to 40 °C on infection and post-incubation (*b*), formed MoMuLV-induced syncytia. Cells preincubated at 40 °C and maintained at 40 °C during and after infection (*c*) did not form syncytia; similarly, cells preincubated and maintained at 35 °C did not form syncytia in the absence of MoMuLV (*d*). Scale bar, 50 µm.

useful assay for quantifying these viruses and for detecting cells producing these viruses, the results presented here suggest that MoMuLV-induced fusion may also be useful as a rapid assay for cells that have undergone virus-induced or 'spontaneous' transformation.

1. Ponten, J. & MacIntyre, F. *Acta path. microbiol. scand.* **74**, 465–486 (1968).
2. Svoboda, J. *Nature* **186**, 980–981 (1960).
3. Klement, V. *et al. Proc. natn. Acad. Sci. U.S.A.* **63**, 753–758 (1969).
4. Johnson, G. S., Friedman, R. M. & Pastan, I. *J. Virol.* **7**, 653–758 (1971).
5. Rowe, W. P., Pugh, W. E. & Hartley, J. W. *Virology* **42**, 1136–1139 (1970).
6. Rangan, S. R. S., Ueberhorst, P. J. & Wong, M. C. *Proc. Soc. exp. Biol. Med.* **142**, 1077–1082 (1973).
7. Ogura, H. *Med. Microbiol. Immun.* **162**, 175–181 (1976).
8. Rand, K. H. & Long, C. W. *Nature new Biol.* **240**, 187–190 (1972).
9. Ahmed, M. *et al. Int. J. Cancer* **16**, 747–755 (1975).
10. Rand, K. H. & Long, C. W. *J. gen. Virol.* **21**, 523–532 (1973).
11. Ogura, H. & Oda, T. *Acta med. okayama* **31**, 243–247 (1977).
12. Wong, P. K. Y., Yuen, P. H. & Kaufman, S. J. *J. Virol.* **21**, 319–327 (1977); **23**, 768–775 (1977).
13. Chan, J. C. *et al. Cancer Res.* **34**, 468–473 (1974).
14. Kaufman, S. J. & Parks, C. M. *Proc. natn. Acad. Sci. U.S.A.* **74**, 3888–3892 (1977).
15. Kaufman, S. J. *et al. Expl Cell Res.* **125**, 333–349 (1980).
16. Wyke, J. A. & Linial, M. *Virology* **53**, 152–161 (1973).
17. Mishra, N. K. & Ryan, W. L. *Int. J. Cancer* **11**, 123–130 (1973).
18. Prasad, I., Zouzias, D. & Basilico, C. *J. Virol.* **18**, 436–444 (1976).
19. Quade, K. *Virology* **98**, 461–465 (1979).

2'5'oligo(A) polymerase activity in serum of mice infected with EMC virus or treated with interferon

Indira Krishnan & Corrado Baglioni

Department of Biological Sciences, State University of New York at Albany, Albany, New York 12222

Interferon-treated cells show an increase in two double-stranded RNA (dsRNA)-dependent enzymatic activities involving an oligoadenylate polymerase and a protein kinase (ref. 1 and refs therein). The polymerase converts ATP into a series of oligonucleotides characterized by 2'5'-phosphodiester bonds, designated 2'5'-oligo(A) or 2-5A (ref. 1). These oligonucleotides activate an endoribonuclease that degrades RNA[1] in extracts of control and interferon-treated cells. These observations have been made in tissue culture cells and no information is yet available on these enzymatic activities in animals with elevated interferon levels. We report here on 2-5A synthesis in tissue homogenates and serum of mice infected with encephalomyocarditis virus (EMCV); this virus induces interferon synthesis when injected intraperitoneally into mice[2]. Significant synthesis of 2-5A was detected in extracts of spleen and lungs, but also, surprisingly, in the serum of these mice. Subsequent experiments showed synthesis of 2-5A in serum of mice treated with the interferon inducer poly(I) · poly(C) (ref. 3) or with mouse fibroblast interferon.

Male CD mice were injected intraperitoneally (i.p.) with different doses of EMCV and killed 3 days after infection. The mice were bled to obtain serum, and tissue extracts were prepared from the spleen, lungs, liver and kidney as described in Fig. 1 legend. Synthesis of 2-5A was assayed in incubations containing poly(I) · poly(C) and ³H-ATP; this assay and the separation of 2-5A from ATP by DEAE-cellulose chromatography have been previously described[4]. The assay requires at least 1% conversion of ATP into 2-5A for polymerase to be unambiguously detected. Significant synthesis of 2-5A was observed with serum, whereas lesser amounts of 2-5A were synthesized with spleen and lung extracts; no significant synthesis of 2-5A was obtained with

other tissue extracts (data not shown). The synthesis of 2-5A with serum and spleen or lung extracts was related to the dose of infecting virus, suggesting a relationship between the severity of infection and the 2-5A synthetic activity (Fig. 1a).

The failure to observe synthesis of 2-5A with liver and kidney extracts could be explained either by the absence of 2-5A synthetic activity or by the presence in these tissues of other enzymatic activities which may interfere with the activation of 2-5A polymerase or with the accumulation of 2-5A. Therefore, we assayed the extracts for degradation of poly(I) · poly(C), the activator of 2-5A polymerase, and for degradation of A2'p5'A (Table 1). An RNase which degrades dsRNA has been found in mammalian cells[5-7] and a phosphodiesterase activity that cleaves 2'-5' bonds has also been reported in extracts of tissue culture cells[8-10]. Degradation of poly(I) · poly(C) was observed with all the tissue extracts tested, but not with mouse serum.

The activation of 2-5A polymerase requires perfectly matched dsRNA more than 30 base pairs long and degradation of dsRNA by RNase may prevent synthesis of 2-5A (ref. 11). Because poly(I) · poly(C) was not degraded by mouse serum, in the following experiments we assayed synthesis of 2-5A with serum samples; we also assayed spleen extracts because of the significant accumulation of 2-5A, shown in Fig. 1. Accurate measurement of 2-5A synthesis in tissue extracts, however, requires at least partial purification of 2-5A polymerase activity, for example by adsorption to poly(I) · poly(C) bound to agarose[12] or to paper[13]. Using the paper assay Stark *et al.*[13] established the wide distribution of 2-5A polymerase in a variety of cells and tissues and demonstrated its variation with growth and changes in hormonal status. They used the much more sensitive biological assay for 2-5A to detect the polymerase[13]. We assayed liver and kidney extracts from control and infected mice after adsorption to poly(I) · poly(C)-agarose[14], but could not detect significant synthesis of 2-5A with extracts from control mice or liver of infected mice, but synthesis of 2-5A above background level was observed with extract of kidney from infected mice. It should be pointed out, however, that this assay is relatively insensitive when compared with the biological assay and that synthesis of 2-5A could possibly be detected by the paper assay in all tissues.

Phosphodiesterase activity that cleaves A2'p5'A was detected in all samples tested (Table 1). This activity, however, is inhibited by ATP present in the assay for 2-5A synthesis[10]. This was established by adding ³H-2-5A synthesized as described[10] to an incubation containing 5 mM ATP and mouse serum but not poly(I)·poly(C). Less than 5% of the 2-5A was degraded after 90 min, as determined by

Table 1 Degradation of poly(I)·poly(C) and A2'p5'A by tissue extracts and serum

Tissue	Poly(I)·³H-poly(C) (% soluble)	A2'p5'A (nmol degraded)
Spleen	92	20.4
Lungs	35	4.5
Liver	59	11.2
Kidney	43	29.2
Serum (mouse)	1	17.7
Serum (human)	86	34.5

Tissue extracts and serum were obtained from mice infected for 3 days with 1×10^7 plaque-forming-units (PFU) of EMCV as described in Fig. 1 legend; the human serum was from a healthy donor. Assays for dsRNA degradation contained: 25 μl of tissue extract or serum and 5 μg of poly(I)·³H-poly(C) (43 nCi μg⁻¹; Miles) in a final volume of 75 μl. After 60 min at 30 °C, the samples were made 5% in trichloroacetic acid and the undigested dsRNA collected on filters for counting. Per cent soluble is expressed relative to a sample not incubated. Assays for A2'p5'A degradation contained: 80 nmol of dinucleotide, 10 μl of tissue extract or serum, 0.12 m K(OAc), 20 mM Mg(OAc)₂, 1 mM dithiothreitol, 20 mM HEPES-KOH, pH 7.4, in a final volume of 50 μl. After 90 min at 30 °C the reactions were diluted to 0.5 ml with 2.5 mM Tris-HCl, pH 7.4, and passed through 0.5 × 0.5 cm columns of DEAE-cellulose equilibrated with the same buffer. Adenosine was washed from the column with another 0.5 ml of buffer. The breakthrough and wash fractions were combined and absorbance at 260 nm measured. Reactions with no added A2'p5'A were run at the same time to obtain blank values, which were subtracted to calculate nmol of adenosine formed.

Fig. 1 Synthesis of 2'5'oligo(A) with serum (●, ×) or plasma (▼), and extracts of spleen (▲) or lungs (■) of mice infected with different doses of EMC virus for 3 days (a), infected with 5 × 10⁶ PFU of EMCV for different times (b), injected with 0.1 mg of poly(I)·poly(C) complexed with 0.1 mg of DEAE-dextran (c) and injected with 10⁵ U (×) or 10⁴ U (●, ▲) of mouse fibroblast interferon (d). EMCV was grown in Ehrlich ascites tumour cells and plaque-assayed on L-cell monolayers. Virus stocks were diluted to 0.5 ml with phosphate-buffered saline, pH 7.2, and injected i.p. in CD mice. Poly(I)·poly(C) and interferon were also diluted to 0.5 ml with saline and injected in the same way. At the indicated times the mice were anaesthetized and bled from the brachial artery to obtain serum or plasma on addition of 3 mg ml⁻¹ of sodium citrate. The spleen and lungs were then excised and washed with 10 mM KCl, 1.5 mM MgCl₂, 0.5 mM dithiothreitol and 20 mM HEPES-KOH buffer, pH 7.4. Extracts were prepared by homogenization of 1 g of tissue with 2 ml of this buffer in a motor-driven Potter homogenizer and centrifugation for 5 min at 30,000g. The supernatant, serum and plasma were stored at −70 °C. Synthesis of 2-5A was assayed in 25-μl reactions incubated for 90 min at 30 °C and containing: 5 μl of extract or serum, 0.25 μg of poly(I)·poly(C), 125 nmol of ³H-ATP (about 0.2 μCi), and the other components previously described[4]. The reactions were stopped by heating to 90 °C for 3 min and applied to 0.5 × 0.5 cm DEAE-cellulose columns; ATP was eluted with 90 mM KCl and 2-5A with 0.35 M KCl, as described[4]. As a control, the nucleotides eluted with 0.35 M KCl were diluted to 90 mM KCl and reapplied to DEAE-cellulose columns; the recovery after washing and elution with 0.35 M KCl was better than 80%. The ordinate shows the concentration of ATP converted into 2-5A. Analysis of reactions without poly(I)·poly(C) or kept at 0 °C gave <700 c.p.m. eluted with 0.35 M KCl out of an input of ~125,000 c.p.m. This background was subtracted from the data shown; it corresponds to 5.6 μM ATP.

chromatographic analysis on DEAE-cellulose columns in the presence of 7 M urea (see below). Therefore, synthesis of 2-5A could be measured with mouse serum samples, since neither the activator nor the reaction product was appreciably degraded during incubations.

The synthesis of 2-5A with serum was unexpected, as 2-5A polymerase activity had previously been shown only in cell extracts[1]. Therefore, several experiments were carried out to characterize the presumptive 2-5A synthesizing activity in serum and the products of the reaction. The oligonucleotides synthesized with serum were identified as 2-5A by TLC (not shown) and DEAE-cellulose columns (Fig. 2) before and after digestion with nuclease and alkali, following previously described procedures[4,15]. The major reaction product had a net charge of about −4.6 and was eluted before a minor peak of charge about −5.6. These oligonucleotides were not digested by T2 RNase, which cleaves 3'-5' phosphodiester bonds, but were digested by snake venom phosphodiesterase to AMP, by alkali to adenosine and a nucleotide which eluted with marker p5'A2'p (Fig. 2b), and by alkaline phosphatase to products which eluted with the same charge as A2'p5'A and A2'pA2'p5'A, respectively (Fig. 2c). In this last experiment we analysed the products of a 17-h incubation with serum; a larger amount of the minor component was present in this sample.

These data and TLC results indicate that the nucleotides synthesized with serum are a di- and trinucleotide containing adenosines linked by 2'-5' phosphodiester bonds and a terminal triphosphate, as shown by the −4 charge loss on digestion with phosphatase (Fig. 2c). Furthermore, when tested for biological activity, the oligonucleotides synthesized in a 17-h incubation with serum activated an endonuclease similarly to previously characterized 2-5A (ref. 16). This was established by adding 0.2 μM presumptive 2-5A to a HeLa cell extract containing labelled viral mRNA, and measuring mRNA cleavage[16]. About 80% of the viral mRNA was cleaved in a 2-h incubation, whereas insignificant cleavage was observed with the products of a reaction containing serum of control mice (data not shown). The synthesis of these oligonucleotides was: (1) dependent on the addition of dsRNA (see Fig. 1 legend); (2) optimal with Mg²⁺ concentrations higher than 10 mM;

and (3) proportional to ATP concentration up to 7 mM. The 2-5A polymerase activity present in extracts of interferon-treated cells shows similar characteristics[4].

In subsequent experiments, synthesis of 2-5A was assayed at different times after infection with a standard dose of EMCV, and after injection of poly(I)·poly(C) or mouse fibroblast interferon (Fig. 1). Serum obtained 1 day after injection with EMCV showed significant synthesis of 2-5A; serum samples obtained later in the infection synthesized greater amounts of 2-5A (Fig. 1b). Plasma prepared with sodium citrate as anticoagulant and extracts of spleen obtained from mice infected for 2 or 3 days also synthesized 2-5A. These results indicate that during EMCV infection progressively higher levels of 2-5A polymerase activity may be present in the serum and spleen. Further experiments established that the presence of this enzymatic activity could be explained by the induction of interferon synthesis.

Mice were injected with poly(I)·poly(C) complexed with DEAE-dextran, as the latter strongly enhances the interferon[17] synthesis. Serum obtained 3–24 h after injection of the complex actively synthesized 2-5A (Fig. 1c), but serum obtained from mice 30 min, 1 h and 2 h after injection of the complex did not synthesize significant amounts of 2-5A (data not shown). Spleen extracts were most active 6 h after injection. The synthesis of 2-5A with serum obtained 3 h after poly(I)·poly(C) injection was confirmed in subsequent repeated experiments. This may be explained by the increase in circulating interferon in mice 1.5 h after injection of poly(I)·poly(C)/DEAE-dextran; the interferon titre reaches a maximum at about 3 h (ref. 17).

The serum of mice injected with mouse interferon also synthesized 2-5A (Fig. 1d). The serum of mice injected with 10[5] U interferon showed greater activity than that of mice injected with 10[4] U, but the increase in activity with time was slower than that observed in mice injected with poly(I)·poly(C) and spleen extracts were not active. It seems possible that greater levels of circulating interferon were present in mice injected with poly(I)·poly(C) than in mice receiving a single i.p. injection of fibroblast interferon; this remains to be shown, however.

In conclusion, the serum from EMCV-infected mice and from animals injected with poly(I)·poly(C) or interferon contains an enzymatic activity similar to that characterized in interferon-treated tissue culture cells. The products of incubations with serum are predominantly dimer and trimer, whereas extracts of tissue culture cells synthesize higher oligomers in optimal conditions[4]. This pattern of 2-5A synthesis may be characteristic of serum, although an overnight incubation was also necessary to obtain significant synthesis of trimer with L-cell extracts in some assay conditions[18]. Synthesis of 2-5A can also be shown in some tissues, although degradation of the activator dsRNA by tissue extracts interferes with the assay.

The presence of 2-5A polymerase activity in serum is puzzling. It cannot be due to the release of cytoplasmic enzymes from cells lysed by infecting EMCV, as a similar activity is found after interferon injection. It seems possible, however, that 2-5A polymerase activity may be released from interferon-treated cells and from cells treated with poly(I)·poly(C). The biological role of the 2-5A polymerase activity in serum, if any, is unknown. Synthesis of 2-5A with serum, however, may be indicative of a viral infection. Attempts to measure 2-5A synthesis in serum of individuals affected by viral diseases have so far failed (unpublished observations) because of the very high levels of nucleases that degrade dsRNA in human serum (Table 1 and refs 19–21). Further experiments are in progress to investigate the presence of 2-5A polymerase in human serum and the release of this enzymatic activity from cells. As Williams et al.[22] have reported the natural occurrence of 2-5A in interferon-treated mouse L cells infected with EMCV, it was of considerable
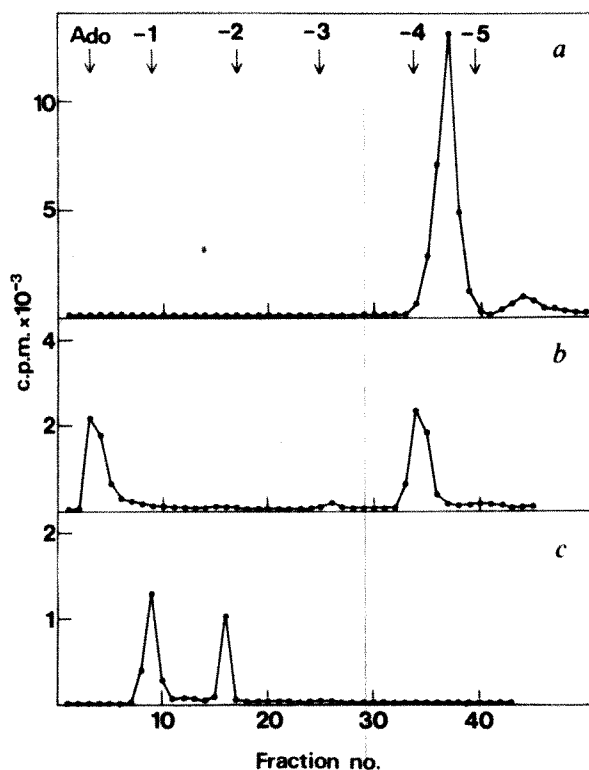
Fig. 2 Chromatographic analysis on DEAE-cellulose columns of the reaction products of serum obtained from mice either 3 days after injection with 2.5×10^7 PFU of EMCV or after injection with poly(I)·poly(C) complexed with DEAE-dextran, and incubated with poly(I)·poly(C) and 25 μCi of ^{3}H-ATP as described in Fig. 1 for 2 h (a and b) or for 17 h (c). Essentially identical results were obtained with both samples. The oligonucleotides synthesized were first adsorbed to small DEAE-cellulose columns and eluted with 0.35 M KCl[4]. a, A 10-μl sample was diluted to 1 ml with 50 mM NcCl, 7 M urea, 20 mM Tris-HCl, pH 7.6 and applied to a 0.5×25 cm column of DEAE-cellulose equilibrated with the same buffer. Unlabelled markers (Sigma) were added with the sample: adenosine (Ado), A2'p5'A (charge −1), AMP (−2), ADP (−3), p5'A2'p (−4) and p_4A (−5). The nucleotides were eluted through a recording spectrophotometer with a linear 300-ml gradient from 50 to 300 mM NaCl in the buffer described above; 3-ml fractions were collected and 1 ml counted. The position of markers is indicated by their charge, except for Ado; in separate runs ATP was eluted a few fractions before p5'A2'p. b, The sample shown in a was incubated for 17 h in 0.3 M KOH before chromatography. c, The oligonucleotides were digested with alkaline phosphatase as described[4] before chromatography. In control chromatographic analysis ATP incubated with KOH or phosphatase yielded AMP and adenosine respectively. Treatment with KOH, therefore, hydrolyses the β and γ phosphates.

interest to establish whether 2-5A itself is present in serum. Preliminary experiments were carried out with sera from control mice and from mice treated as indicated in Fig. 1. Aliquots of serum (25 μl) were heat-treated and the supernatant obtained from centrifugation was chromatographed on DEAE-cellulose to obtain a fraction eluting with 1 M NH$_4$HCO$_3$ (ref. 22); after extensive lyophilization this fraction was assayed for nuclease activation in HeLa cell extracts[16]. Nuclease activity was present in all the samples prepared in this way; therefore, these samples could not be tested in the assay for 2-5A-dependent endonuclease[16]. The presence of 2-5A in serum thus remains to be established, possibly by a more extensive purification of serum oligonucleotides[22].

1. Baglioni, C. *Cell* **17**, 255–264 (1979).
2. Baron, S., Buckler, C. E., McCloskey, R. V. & Kirschstein, R. L. *J. Immun.* **96**, 12–16 (1966).
3. Field, A. K., Tytell, A. A., Lampson, G. P. & Hilleman, M. R. *Proc. natn. Acad. Sci. U.S.A.* **58**, 1004–1010 (1967).
4. Minks, M. A., Benvin, S., Maroney, P. A. & Baglioni, C. *J. biol. Chem.* **254**, 5058–5064 (1979).
5. Busen, W. & Hansen, P. *Eur. J. Biochem.* **52**, 179–190 (1975).
6. Rech, J., Cathala, G. & Jeanteur, Ph. *Nucleic Acids Res.* **3**, 2055–2065 (1976).
7. Ohtsuki, K., Groner, Y. & Hurwitz, J. *J. biol. Chem.* **252**, 483–491 (1977).
8. Schmidt, A. *et al. FEBS Lett.* **95**, 257–264 (1978).
9. Williams, B. R. G., Kerr, I. M., Gilbert, C. S., White, C. N. & Ball, L. A. *Eur. J. Biochem.* **92**, 455–462 (1978).
10. Minks, M. A., Benvin, S., Maroney, P. A. & Baglioni, C. *Nucleic Acids Res.* **6**, 767–780 (1979).
11. Minks, M. A., West, D. K., Benvin, S. & Baglioni, C. *J. biol. Chem.* **254**, 10180–10183 (1979).
12. Hovanessian, A. G., Brown, R. E. & Kerr, I. M. *Nature* **268**, 537–540 (1977).
13. Stark, G. R., Dower, W. J., Schimke, R. T., Brown, R. E. & Kerr, I. M. *Nature* **278**, 471–473 (1979).
14. Baglioni, C., Maroney, P A. & West, D. K. *Biochemistry* **18**, 1765–1770 (1979).
15. Kerr, I. M. & Brown, R. E. *Proc. natn. Acad. Sci. U.S.A.* **273**, 684–687 (1978).
16. Baglioni, C., Minks, M. A. & Maroney, P. A. *Nature* **273**, 684–687 (1978).
17. Dianzani, F., Rita, G., Cantagalli, P. & Gagnoni, S. *J. Immun.* **102**, 24–27 (1969).
18. Kimchi, A. *et al. Proc. natn. Acad. Sci. U.S.A.* **76**, 3208–3212 (1979).
19. Sterm, R. *Biochem. biophys. Res. Commun.* **41**, 608–614 (1970).
20. Nordlund, J. J., Wolff, S. M. & Levy, H. B. *Proc. Soc. exp. Biol. Med.* **133**, 439–444 (1970).
21. De Clercq, E. *Eur. J. Biochem.* **93**, 165–172 (1979).
22. Williams, B. R. G., Golgher, R. R., Brown, R. E., Gilbert, C. S. & Kerr, I. M. *Nature* **282**, 582–586 (1979).

Antibodies to a neural cell adhesion molecule disrupt histogenesis in cultured chick retinae

Daniel R. Buskirk, Jean-Paul Thiery*, Urs Rutishauser & Gerald M. Edelman†

The Rockefeller University, 1230 York Avenue, New York, New York 10021
*CNRS et Collège de France, Institute d'Embryologie, 49 bis, av. de la Belle Gabrille, 94130 Nogent-sur-Marne, France
†To whom correspondence should be addressed

Cell-surface proteins are believed to have important roles in cell–cell interactions during brain development, particularly in such processes as cellular adhesion, neurite outgrowth and synapse formation[1–4]. The chick neural cell adhesion molecule, CAM, is a cell-surface protein specific to the nervous system and has been implicated in cell adhesion among cells and neurites of the developing retina and brain[5–8]. Previous studies have shown that F(ab′) fragments of antibodies directed against CAM inhibit the *in vitro* aggregation of cells obtained from 9-day embryonic chick retina. The specific antibody fragments also reduce the diameter of neurite fascicles that grow out from cultured dorsal root ganglia, apparently by blocking side-to-side adhesion between the neurites. In addition, anti-CAM antibodies alter the appearance of histotypic patterns in retinal cell aggregates maintained in culture for several days[7]. We now demonstrate that the antibodies can disrupt histogenesis of the developing retina in organ culture, strengthening the notion that the cell–cell adhesion properties mediated by CAM are involved in the normal development of histological layers in the chick retina.

In the chick, cell and plexiform layers of the central portion of the retina are formed between the sixth and ninth days of embryonic life[9,10]. Although many cells have left the mitotic cycle by day 6 (ref. 9), all remain in a single nuclear or 'matrix'

layer. Retinae dissected from White Leghorn embryos on day 6 and placed in organ culture for 3 days undergo histogenesis similar to that which occurs *in vivo*, as can be seen in Fig. 1. To achieve uniformity of developmental stage, all retinal fragments were dissected from the region surrounding the choroid fissure. Pigment epithelium clinging to the neural retina was largely removed; any remaining pieces of epithelium seem not to have altered the progress of development. Retinal fragments were placed with their vitreous side down on 13-mm Millipore filters, 1.2 μm pore size, that had been wetted with medium, and were cultured on the stainless steel grid of a Falcon organ culture dish. In all experiments the medium was Dulbecco's modified Eagle's medium, supplemented with 1/10 volume of heat-inactivated fetal calf serum (Microbiological Associates). The anti-CAM sera were obtained from rabbits injected with purified CAM as described earlier[5], and control antisera were obtained from unimmunized rabbits. F(ab′) fragments prepared from the antibodies were dissolved in the tissue culture medium to a concentration of 1 mg ml⁻¹. All cultures were carried out for 3 days at 37 °C in an atmosphere of 5% CO_2, and the retinae were then fixed either in Bouin's fixative for paraffin embedding or for 1 h in 2% glutaraldehyde in phosphate-buffered saline in preparation for embedding in Epon 812.

Tissues cultured in the presence of anti-CAM showed both disorder in the pattern of histological layers and an increase in the extracellular space surrounding the cell perikarya. In contrast, retinae cultured in the presence of antibodies from unimmunized rabbits developed in a manner analogous to retinae *in vivo*.

Paraffin sections of retinae cultured with non-immune serum (Fig. 1) revealed that, during the 3 days of culture, the initially rather uniform nuclear layer had developed distinct histological layers resembling the retina of a 9-day-old embryo. Inner and outer plexiform layers were clearly visible, as were the layers of photoreceptor cell bodies and cells believed to be ganglion cells. The photoreceptor cells had buds which mark the first stage in the development of the inner segments. The substantial layer of ganglion cells found in the *in vivo* 9-day retina was not observed, however, in the cultured retinae. Other workers studying the differentiation of chick retinae transplanted to the chorioallantoic membrane also observed a deficiency of ganglion cells, and attributed this to a failure to make tectal connections[11]. It is also possible that the cells observed along the vitreous edge of cultured retinae represent displaced ganglion cells which during the normal course of development are migrating back to the nuclear layer[12,13].

Retinal tissues cultured in the presence of anti-CAM displayed several additional alterations which sharply reduced the resemblance to normal retina. The ganglion cells, normally arranged in an even layer along the vitreous edge of the retina, were less organized and were found scattered throughout the inner plexiform layer. In control retinae, cells within the nuclear layer could be divided into two layers based on cell shape, the outermost consisting of bipolar and horizontal cells and the layer towards the vitreous side of the nuclear layer corresponding to the amacrine cells. In the retinae exposed to anti-CAM (Fig. 1e), these layers were not clearly distinguishable, suggesting that the distribution of specific cell types had been altered. More definitive evidence on the exact arrangement and morphological differentiation of specific cell types will require additional studies using Golgi staining techniques.

Electron microscopy of the anti-CAM-treated tissues revealed differences in the packing of cells in the nuclear layer. In the tissue cultured with anti-CAM F(ab′) fragments, large extracellular spaces surrounded the cell bodies of the nuclear layer. The extracellular spaces in the retinae cultured without anti-CAM F(ab′) were similar to those observed in sections of *in vivo* 9-day retinae. This difference was observed in all tissues

Fig. 1 *a, b* Represent *in vivo* chick retinae at 6 and 9 days of embryonic age, respectively. Retinae are from the central, most differentiated area of the retinae. The scleral side of the retinae, containing the photoreceptor cells, is shown towards the bottom in these photographs; in both photographs the pigment epithelia and scleral tissue can be seen lying below the neuroretina. In *b* the outer and inner plexiform layers are clearly visible. *c, d* Are chick retinae that have been in organ culture for 3 days following their dissection from the embryo on day 6. The retina shown in *c* was cultured in the presence of F(ab') antibody fragments from unimmunized rabbits, and that in *d* in the presence of antibodies to the cell adhesion molecule CAM. Although the cultured retinae are thinner and not as fully developed as *in vivo* 9-day retinae, the histologi-

cal layers can be clearly identified and mark a significant differentiation from the 6-day stage. The retinae cultured in the presence of anti-CAM showed identifiable but disrupted histological layers which do not have the sharp boundaries between adjacent layers characteristic of both the *in vivo* and the cultured control retinae. Ganglion cells, at the top of the photographs, form neat rows in the *in vivo* and control retinae, but are scattered in the retinae treated with anti-CAM. The light micrographs are ×650. *e, f* Are electron micrographs of cell bodies on the vitreous side of the nuclear layer of retinae cultured in the presence of non-immune and anti-CAM F(ab'), respectively. Note that the cells in the control retina show large areas of membrane apposition and small areas of extracellular space, whereas the retina cultured with antibodies to CAM shows large areas of extracellular space and few areas of cell–cell contact. Electron micrographs are ×5,800.
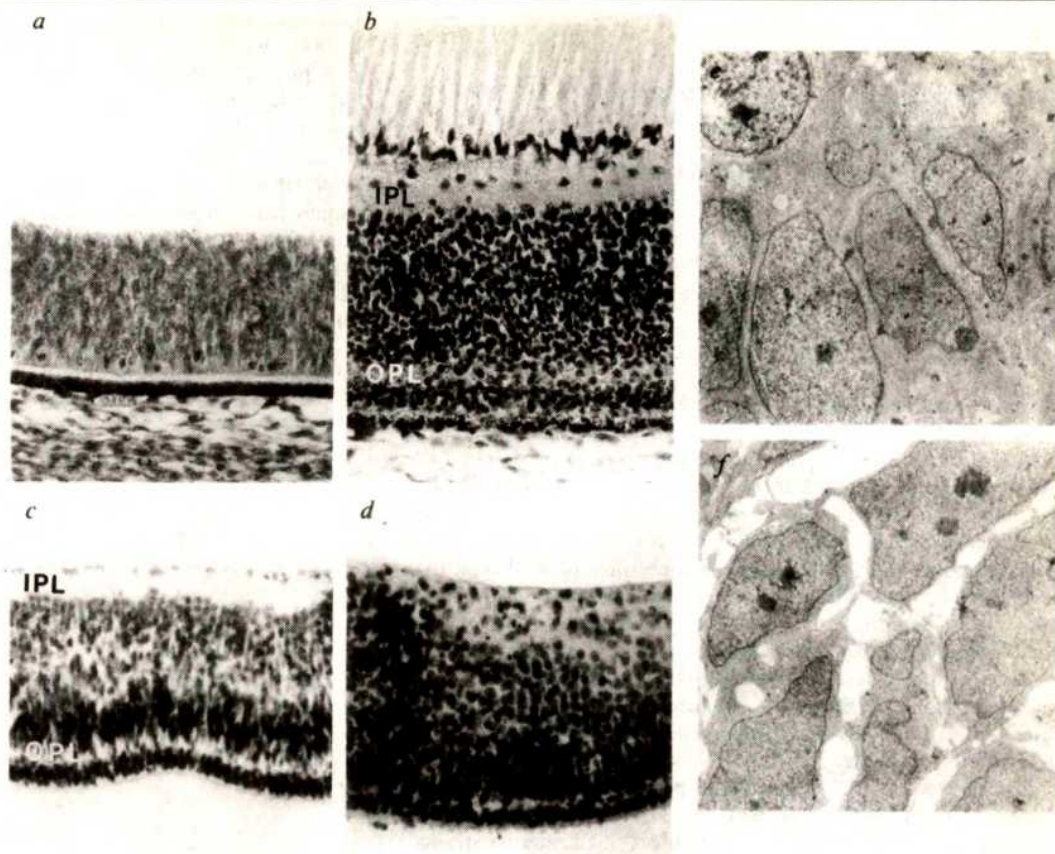
---

sectioned, including those which had differentiated poorly during the culture period. It resembles changes previously seen in histotypic aggregates that were similarly treated[7]. The possibility that this difference is a consequence of increased susceptibility of the anti-CAM-treated retinae to shrinkage during processing has not been ruled out completely, but seems unlikely in view of the normal appearance of cytoplasmic ultrastructure in the treated retinae. This question is being investigated directly through the measurement of extracellular space by horseradish peroxidase diffusion and staining techniques.

As judged by dense haematoxylin staining, necrotic cells were present in both untreated cultured retinae and those treated with anti-CAM. Approximately 1 % of the cells in the treated retinae were pycnotic at day 9, and about 0.1 % of the untreated retinal cells also seemed to be pycnotic. The amount of total cell loss during the 3-day period is not known, but both control and anti-CAM retinae were thinner than in *in vivo* 9-day retinae.

The present results extend the previous studies on CAM by demonstrating that antibodies against CAM disrupt the internal development of a tissue never subjected to mechanical dissociation. The observed increase in the extracellular space and the concomitant decrease in regions of cell–cell contact are consistent with the interpretation that CAM is a cell adhesion molecule. Because the individual cells in the anti-CAM-treated retinae were morphologically similar to those in the control tissues, it seems that the effects are not simply a consequence of changes in the developmental pathway of

individual cells. This conclusion is supported by the ability of the anti-CAM-treated retinae to form some histological layers which, although altered, could be directly identified with layers in the normal retina. It seems, then, that the processes necessary for the differentiation of cell types and the formation of plexiform layers may occur unimpeded by the presence of anti-CAM. Nonetheless, the observation of misplaced ganglion cells and the apparent mixing of cell types in the nuclear layer suggests that, during the 6–9-day period of embryonic retinal development, cell–cell interactions mediated by CAM are important in achieving the appropriate arrangement of cells in nervous tissue.

1. Brown, J. C. *Expl Cell Res.* **69**, 440–442 (1971).
2. Santala, R., Gottlieb, D. I., Littman, D. & Glaser, L. *J. biol. Chem.* **252**, 7625–7634 (1977).
3. Stallcup, W. B. *Brain Res.* **126**, 475–486 (1977).
4. Mahler, H. R. in *Complex Carbohydrates of Nervous Tissue* (eds Margolis, R. U. & Margolis, R. K.) 165–184 (Plenum, New York, 1979).
5. Brackenbury, R., Thiery, J-P., Rutishauser, U. & Edelman, G. M. *J. biol. Chem.* **252**, 6835–6840 (1977).
6. Thiery, J-P., Brackenbury, R., Rutishauser, U. & Edelman, G. M. *J. biol. Chem.* **252**, 6841–6845 (1977).
7. Rutishauser, U., Thiery, J-P., Brackenbury, R. & Edelman, G. M. *J. Cell Biol.* **79**, 371–381 (1978).
8. Rutishauser, U., Gall, W. E. & Edelman, G. M. *J. Cell Biol.* **79**, 382–393 (1978).
9. Kahn, A. J. *Devl Biol.* **38**, 30–40 (1974).
10. Mishima, H. & Fujita, H. *Albrecht v. Graefes Arch. Ophthal.* **206**, 1–16 (1978).
11. McLoon, S. C. & Hughes, W. F. *Brain Res.* **150**, 398–402 (1978).
12. Hinds, J. W. & Hinds, P. L. *J. comp. Neurol.* **197**, 277–300 (1978).
13. Heaton, M. B., Alvarez, I. M. & Crandall, J. E. *Anat. Embryol.* **155**, 161–178 (1979).

Absence of M protein in a cell-associated subacute sclerosing panencephalitis virus

Fu Hai Lin & Halldor Thormar

New York State Institute for Basic Research in Mental Retardation, Staten Island, New York 10314

Measles virus has been suggested to cause subacute sclerosing panencephalitis (SSPE), a slow central nervous system disease of children. However, several questions remain about the pathogenesis of SSPE. For example, it is not known whether alteration of the measles virus genome has a role in the initiation and persistence of the disease. Several studies have compared the RNA and protein composition of wild-type (wt) and SSPE strains of measles virus in a search for markers characteristic of the latter[1-4]. All the studies used SSPE strains that had reverted to the budding, virion-producing form, similar to wt. We have shown, however, that only cell-associated non-budding strains of SSPE virus cause an SSPE-like persistent infection in young ferrets[5]. Strong cell association and cell-fusing activity were essential for the virulence of measles virus in the brains of experimental animals and possibly humans. We have, therefore, compared the protein composition of virulent SSPE strains to that of the budding, non-virulent SSPE and wt strains. We report here that the M protein was not detectable in non-budding SSPE strains D.R., Biken and IP-3, and strain D.R. contained very little H protein.

Figure 1 shows the protein patterns in Vero cells infected with wt Edmonston virus and 3 cell-associated SSPE viruses, Biken, IP-3 and D.R. Uninfected Vero cells and purified Edmonston virions are also included. A protein of molecular weight 60,000 designated[6] NP was detected in all the infected cultures and was identical in size in all strains except for the Biken strain whose NP migrated slightly slower than that of others. Although the M protein was found in Edmonston infected cells it was not detectable in cultures infected with Biken, IP-3 and D.R. Other bands seemed to be identical in these cultures.

To determine whether M protein is synthesized in Vero cells infected with cell-associated SSPE virus strains we used strain-specific immune sera, raised in rabbits, to precipitate viral proteins. Immunoprecipitation of proteins from strain Edmonston infected cells by anti-Edmonston (E), anti-Mantooth (M), anti-D.R. (D) and anti-Biken (B) sera are shown in Fig. 2a. The antisera against Edmonston and Mantooth strains precipitated proteins H, NP, A, and M. The precipitation of H and M proteins was particularly heavy, whereas that of NP was weak. Antisera against the two non-budding SSPE strains D.R. and Biken did not show a detectable precipitation of the M protein. These two sera differed in their reaction to glycoprotein H, since the anti-D.R. serum precipitated very little H protein, whereas the anti-Biken showed appreciable precipitation of this protein. The proteins precipitated from Mantooth infected cells by these immune sera were identical to those described above for the Edmonston infected cells (data not shown). Immune precipitation of viral proteins from non-budding strain D.R. infected cells by rabbit immune sera are shown in Fig. 2b. It is seen that none of these sera precipitated M protein from the D.R. cultures even though there was a heavy precipitation of protein NP. Protein A was precipitated by all the antisera although it was weaker in lanes E and M than in lanes D and B. Proteins A and F_1 were not well separated due to the compression of the gels resulting from treatment in acetone for

fluorography. The polypeptide located about molecular weight 55,000 was not identified. Figure 2c shows proteins precipitated from cells infected with non-budding SSPE strain Biken by three immune sera. The precipitation pattern is similar to that of D.R. infected cells except that precipitation of the H protein by anti-Edmonston (lane E) and anti-Biken (lane B) sera was evident. Rabbit immune sera absorbed with uninfected Vero cells did not precipitate any proteins from control cells (Fig. 2e) except a band migrating slightly behind NP. The anti-Edmonston serum was weak in antibody against A. Figure 2d shows the protein pattern of purified measles virus (Edmonston strain) run in the same gel.

These results indicate that hyperimmune sera from rabbits immunized with non-budding SSPE strains D.R. and Biken do
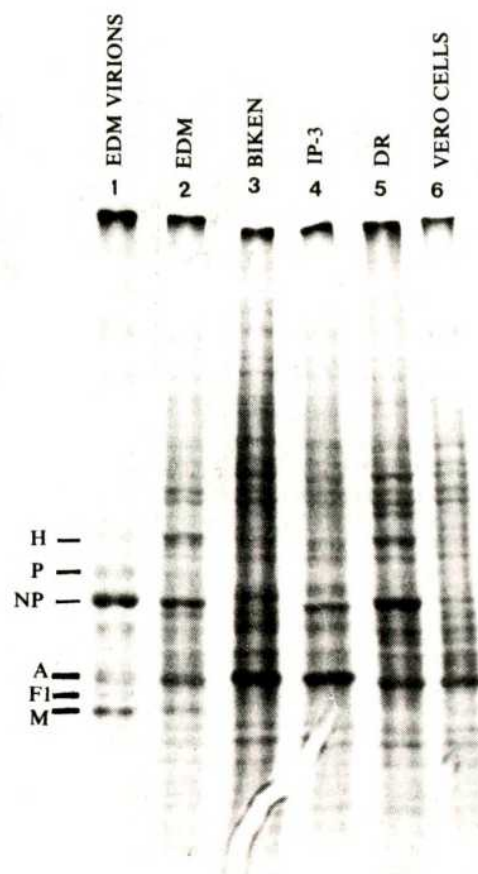
Fig. 1 Autoradiography of a slab gel containing proteins of Vero cells infected with non-budding SSPE viruses. The non-budding SSPE viruses, D.R., Biken and IP-3, were propagated by repeated trypsinization and splitting of the cell layers until the syncytia covered 50% or more of the entire monolayer, as described by Thormar *et al.*[10]. Cells were labelled with ^{35}S-methionine (100 μCi ml^{-1}, 600–1,300 Ci mmol^{-1}, Amersham), and lysed in TNE buffer (0.01 M Tris-HCl, *p*H 7.4, 0.1 M NaCl, 1 mM EDTA) containing 1% each of Nonidet P-40 and sodium deoxycholate and 1 mM TLCK[11] (*N*-α-tosyl-L-lysyl-chloromethane). Lysates were precipitated by trichloroacetic acid (10%) and the precipitate was washed twice with cold acetone. (1) Purified Edmonston virions. (2) Edmonston infected cells. (3) Biken infected cells. (4) IP-3 infected cells. (5) D.R. infected cells. (6) Uninfected cells.

E M D B   E M D B   E D B

H —

NP—

A —
M —

—H

—NP

—A
—M

a   b   c   d   e

Fig. 2 Autoradiography of a slab gel containing proteins precipitated by strain specific immune sera. Vero cells were grown in 6 cm Falcon plastic Petri dishes and labelled with ^{35}S-methionine as described in the legend to Fig. 1. Monolayers were rinsed twice with 3 ml phosphate-buffered saline (PBS), lysed in 1 ml RIPA buffer and centrifuged at 30,000 r.p.m. (Beckman 50 Ti rotor) for 30 min as described by Lamb *et al.*[11]. The supernatant was carefully recovered by pipetting and used in immunoprecipitation. To precipitate proteins, 100 μl of the extract was mixed with 20 μl of undiluted serum. The mixture was incubated at 0–4 °C for 1 h and 20 μl of *Staphylococcus aureus* protein A-Sepharose CL-4B (Pharmacia)[11] was added to the mixture and incubation continued for 1 h. The immune complex was pelleted by centrifugation at 2,000 r.p.m. (IEC PR-6) for 20 min, washed four times with 1 ml RIPA buffer, mixed with 50 μl of sample buffer, boiled for 2 min and electrophoresed in a 5–20 % gradient of polyacrylamide gel as described[9]. Fluorography was done according to the method of Bonner and Laskey[12]. Strain-specific immune sera were raised in rabbits. Infected cells were prepared as described above either disrupted by sonication or lysed by 0.1 % Nonidet P-40 in PBS. The cell lysate was mixed with equal volume of complete Freund's adjuvant and 1–2 ml of the mixture was injected intradermally into both hind footpads. Booster was done by injecting the same mixtures into hind legs (1 ml) 4–6 weeks later. Rabbits were bled 10 days after the booster. Sera were absorbed 2–3 times with lyophilized Vero cells until no precipitin line against Vero cells was observed in Ouchterlony test. *a*, Proteins precipitated by rabbit antisera from extracts of Vero cells infected with Edmonston strain of measles virus. E, anti-Edmonston; M, anti-Mantooth; D, anti-D.R.; B, anti-Biken. *b*, Proteins precipitated from extracts of Vero cells infected with D.R. strain of cell-associated SSPE virus. The amount of protein extract was 100 μl in lanes E and M and 200 μl in lanes D and B. The antisera were the same as used in *a*. *c*, Proteins precipitated from extract (200 μl) of cells infected with non-budding SSPE strain Biken by: E, anti-Edmonston; D, anti-D.R.; B, anti-Biken. *d*, Purified measles virus (Edmonston strain). *e*, Uninfected Vero cells incubated with anti-Edmonston serum. All the other immune sera showed similar results.

not have detectable antibodies against measles virus M protein. Since a serum sample was available from patient D.R. from whom the SSPE virus strain D.R. was isolated, it was of interest to test this serum against extracts of cells infected with wt strain Edmonston and strain D.R. A normal human serum with high antibody titres against measles virus was run in the same gel as a control. Figure 3*a* shows proteins precipitated by the two human sera from Edmonston infected cells. The normal human serum (N) precipitated all the proteins of strain Edmonston although the reaction with the NP protein was

very weak. The H protein antibody was extremely strong in this serum. In contrast, the H protein antibody was very weak in the serum from SSPE patient D.R. Antibodies against the other measles virus proteins were present in the D.R. serum either comparable to or stronger than in the normal human serum. When these two human sera were run against SSPE strain D.R. the results largely confirmed those obtained with the rabbit hyperimmune serum to this strain. Precipitation of the H and M proteins was extremely weak or missing with both sera, whereas the matched D.R. serum–virus pair gave a strong precipitation of the NP, A and F_1 proteins (Fig. 3*b*). The precipitation of strain Edmonston M protein by SSPE serum may be due to antibodies remaining since the initial acute measles virus infection.

The data presented in this paper strongly indicate that the matrix or M protein is not synthesized by the non-budding SSPE virus strains D.R. and Biken in Vero cells. This conclusion is based on the absence of M protein in cells infected with these strains (Fig. 1), the failure of immune sera containing strong anti-M antibody to react with protein extracts of strain D.R. and Biken-infected cells (Fig. 2*b*, *c*) and the failure of strains D.R. and Biken to elicit antibodies against the M protein in immunized rabbits (Fig. 2*a*). Finally, there is no M protein precipitation in the matched D.R. serum–virus pair, in spite of the presence of anti-M antibody in the serum (Fig. 3). Absence of M protein synthesis is also indicated in Vero cells infected with non-budding strain IP-3, although the data to support this conclusion are not as strong as for strains D.R. and Biken. A reduced antibody response to M protein in sera of SSPE patients has been reported by Hall *et al.*[7] and Wechsler *et al.*[8] indicating a lack of activity of this

N   D   N   D

H—
P—
NP—

A—
F$_1$—
M—

a   b
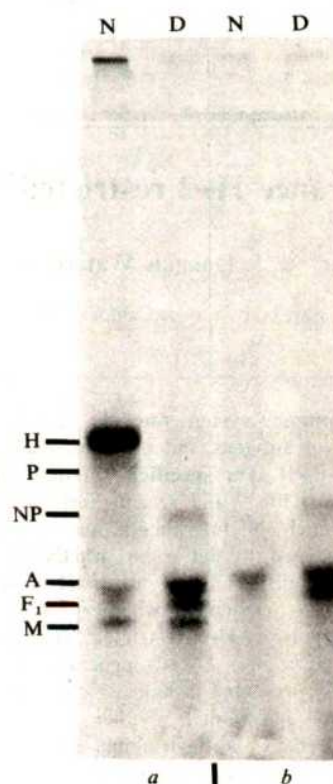
Fig. 3 Autoradiography of protein precipitates by sera from a normal person and D.R. patient. All the procedures were the same as those described in the legend to Fig. 2. *a*, Extract of Edmonston infected cells incubated with normal serum (N) or D.R. SSPE serum (D). *b*, Extract of D.R. infected cells incubated with normal serum (N) or D.R. SSPE serum (D).

protein in SSPE patients. These data are consistent with our finding that the M protein is missing in neurovirulent, non-budding SSPE virus strains. We propose that absence of M protein is an important characteristic of these strains, not only in cell cultures but also in brains of patients. Lack of M protein synthesis and the resulting loss of ability to produce infectious virions by budding may be the critical event that turns wt measles virus into neurovirulent SSPE virus and leads to this tragic disease. We hypothesise that this is caused by a defect in or alteration of the corresponding RNA genome of measles virus. However, the possibility also exists that it is suppressed under certain conditions.

We have failed to demonstrate a significant biological or biochemical difference between budding, virion producing SSPE isolates and wt measles virus. Minor differences in the size of the M protein observed by us and also reported previously by others[2-4] have not proved to be characteristic for the SSPE virus strains[7]. In view of the distinct differences between non-budding neurovirulent SSPE strains and wt measles virus, these strains rather than the budding SSPE strains may hold the clue to the unusual pathogenesis of this slow virus disease.

We thank Drs J. L. Sever and P. Albrecht (of NIH) and Dr H. Koprowski (Wistar Institute) for providing measles virus strains. The technical assistance of Mrs Ruth Lin is acknowledged.

1. Hall, W. W. & ter Meulen, V. *Nature* **264**, 474–477 (1976).
2. Hall, W. W., Kiessling, W. & ter Meulen, V. *Nature* **272**, 460–462 (1978).
3. Wechsler, S. L. & Fields, B. N. *Nature* **272**, 458–460 (1978).
4. Schluederberg, A., Chavinich, S., Lipman, N. B. & Carter, C. *Biochem. biophys. Res. Commun.* **58**, 547–551 (1974).
5. Thormar, H., Mehta, P. D. & Brown, H. R. *J. exp. Med.* **148**, 674–691 (1978).
6. Graves, M. C., Silver, S. M. & Choppin, P. W. *Virology* **86**, 254–263 (1978).
7. Hall, W. W., Lamb, R. A. & Choppin, P. W. *Proc. natn. Acad. Sci. U.S.A.* **76**, 2047–2051 (1979).
8. Wechsler, S. L., Weiner, H. L. & Fields, B. N. *J. Immun.* **123**, 884–889 (1979).
9. Lin, F. H. *J. Virol.* **25**, 207–214 (1978).
10. Thormar, H., Jervis, G. A., Karl, S. C. & Brown, H. R. *J. infect. Dis.* **127**, 678–685 (1973).
11. Lamb, R. A., Etkind, P. R. & Choppin, P. W. *Virology* **91**, 60–78 (1978).
12. Bonner, W. M. & Laskey, R. A. *Eur. J. Biochem.* **46**, 83–88 (1974).

Is self tolerance H–2 restricted?

Polly Matzinger* & J. Douglas Waterfield†

Department of Biology, University of California, San Diego, La Jolla, California 94143

An individual's immune system must be capable of responding to a wide variety of antigens, but must not react against tissues of the individual itself. The specificity of this 'self tolerance' is determined early in life[1-3] and recent work has dealt with the mechanisms by which self tolerance is maintained[4,5]. We report here a study designed to determine whether products of the major histocompatibility complex are involved in the induction of self tolerance; in particular, whether the induction of self tolerance in the mouse is H–2 restricted. H–2 restriction refers to the finding that mouse T cells generally recognize foreign antigens only when presented in association with the products of H–2 alleles[6-8]. We questioned whether T-cell precursors are made tolerant directly by antigen alone, or whether the antigen must be associated in the cell membrane with an appropriate H–2 molecule. We find that T-cell tolerance to 'self' membrane components does not seem to be H–2 restricted and discuss the possibility that this apparent lack of H–2 restriction is due to antigen processing.

*Present address: Division of Immunology, Department of Pathology, University of Cambridge, Addenbrooke's Hospital, Hills Road, Cambridge, CB2 2QQ, UK.
†Present address: Zoology Department, University College London, Gower Street, London, WC1E 6BT, UK.
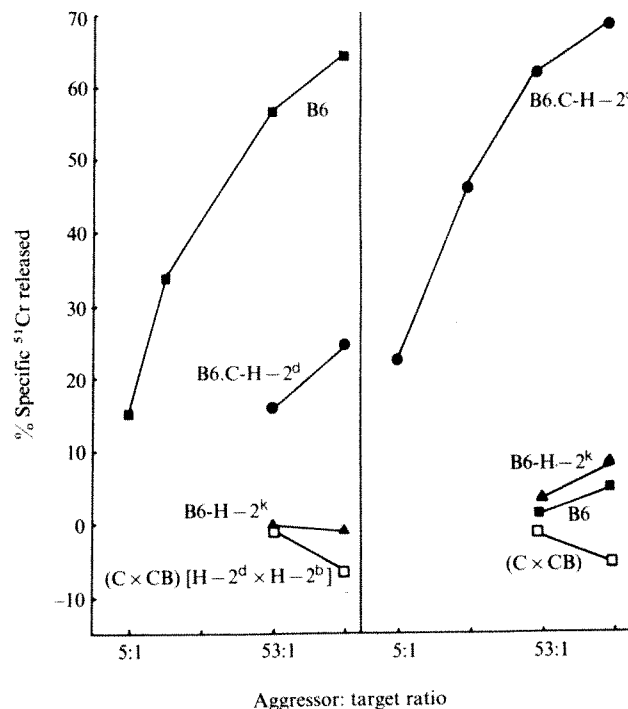
Fig. 1 Cytotoxic response of a normal $(C \times CB)F_1$ against B6 and B6.C-H-2^d. The mouse was primed with an intraperitoneal (i.p.) injection of 10^7 B6 spleen cells (and thus cross-primed for B6.C-H-2^d). After 9 months its spleen cells were boosted in a 5-day *in vitro* culture with mitomycin-C treated B6 (H-2^b)(*a*), or B6.C-H-2^d(*b*) stimulators and tested in a standard 4 h ^{51}Cr-release assay for activity on 2-day concanavalin A (Con A)-induced targets as described previously[15]. Spontaneous release was 23% (B6), 29% (B6.C-H-2^d), 27% (C $\times$ CB) and 19% (B6-H-2^k). Effector target ratio is based on the number of spleen cells originally cultured.

We investigated the specificity of tolerance in radiation chimaeras in which donor and host differed by minor histocompatibility (H) antigens. Normal (BALB/c $\times$ BALB.B) (C $\times$ C.B) [H-2^d $\times$ H-2^b] mice respond very well to minor H antigens of the C57BL/6 (B6) strain whether the minor H antigens are associated with H-2^b (as in B6 itself) or H-2^d (as in the congeneic strain B6.C-H-2^d)[9] (Fig. 1). However (C $\times$ CB)F$_1$ fetal liver cells which have matured into T cells in an irradiated B6 (H-2^b) mouse would be expected to be tolerant of B6 minor H antigens associated with H-2^b. The question is: are such chimaeras tolerant of B6 minor H antigens when presented in association with H-2^d, a combination of antigens which is not expressed by any individual cell in the chimaera?

The answer depends on whether tolerance induction is H–2 restricted. If tolerance could arise by the presentation of the minor H antigens alone[10] then the chimaeras should be tolerant of B6.C-H-2^d. However, if tolerance induction is an H–2 restricted event, then tolerance to B6.C-H-2^d should not occur since no cell in the chimaera carries the genes coding for this combination of antigens.

To test the chimaeras for tolerance to the combination of B6 minor H antigens plus H-2^d, we immunized them by intraperitoneal injection with B6.C-H-2^d cells. Between three weeks and two months later their spleens were removed, boosted in 5-day cultures with B6.C-H-2^d or fully allogeneic stimulators, and then assayed for cytotoxic activity on various targets. Figure 2 shows data from a representative experiment. It can be seen that the chimaeras respond well to allogeneic targets but have no activity against B6.C-H-2^d. Thus they appear to be unresponsive to B6 minor H antigens associated with H-2^d even though no cell in the chimaera is genetically capable of expressing this combination.

Table 1 Cytotoxic T-cell responses of (C × CB)→B6 chimaeras

Animal no.	Primed with:	Cultured with:	B6.C-H-2^d	D1.C	Third party* (D1×C)	C	(C×CB)	CB	B6	(C×B6)
1	B6.C-H-2^d	BALB.K (H-2^k)			44(BALB.K)	2			6	
		B6.C-H-2^d	1	2						−7
		D1.C(H-2^d)	3	3			1			−4
2	D1.C + B6.C-H-2^d	B1O.S(H-2^s)			39(B1O.S)	−2		5	3	
		B6.C-H-2^d	−4	−3		−2		1	5	
		D1.C(H-2^q)	−4	25		2		6	6	
3	D1.C + B6.C-H-2^d	DBA/1			65(DBA/1)		1		3	
		B6.C-H-2^d	−1				1		3	
		D1.C	−1	51		17	0		0	
4	D1.C + B6.C-H-2^d	BALB.K (H-2^k)			40(BALB.K)	4			2	
		D1.C	−1	75		−1				−5

(C × CB)→B6 chimaeras were primed, cultured and assayed as described in Fig. 2.
*Allogeneic, H–2 disparate stimulators and targets. The actual target is given in parentheses. Two chimaeras (not shown) had excellent killing activity against both D1.C and B6.C-H-2^d. Neither of these mice carried any (C × CB) cells, were therefore 100% B6 and recognized B6.C-H-2^d as a foreign H–2 type. Thus transient passage of (C × CB) fetal liver was not sufficient to tolerize.

Although tolerance is the most likely explanation for the lack of response to B6.C-H-2^d, an alternative suggested by the experiments of Bevan[11] and Zinkernagel et al.[12] needed to be ruled out. Their experiments demonstrated that F_1 T cells which had developed in a homozygous parental environment may respond poorly or not at all to an antigen when it is presented with the H–2 type of the unshared parent. Therefore, it could be argued that (C × CB)F_1→B6 chimaeras would not respond to any antigen presented with H–2^d because of this host limit on restriction. However the host-limited restriction does not seem to be absolute for anti-minor responses[11] and can be completely overcome by appropriate immunization[13]. It is therefore possible to determine experimentally whether the lack of response to B6.C-H-2^d is due to host-limited restriction or tolerance. If appropriately immunized T cells from the (C × CB)→B6 chimaeras turn out to be capable of responding to foreign minor H antigens + H–2^d, it would suggest that their unresponsiveness to B6.C-H-2^d (self minor H antigens + H–2^d) is due to tolerance induction and not host limitation.

We thus immunized several chimaeras with D1.C (H-2^d) as well as B6.C-H-2^d cells. D1.C, an H-2^d congenic of DBA/1 (D1, H–2^q) carries at least two minor H antigens which are foreign to both B6 and (C × CB)F_1 (ref. 14). As seen in Fig. 3, the chimaeras responded against D1.C (H-2^d) and fully allogeneic targets but remained completely unresponsive to B6.C-H-2^d.

There remained the possibility that the response seen against D1.C was not an H–2 restricted anti-minor response. Several investigators have recently reported the discovery of loci (Qa,Qed-1) closely linked to H–2, whose products can elicit T-cell responses which are not H–2 restricted[15,16]. Since the response to D1.C (H-2^d) was used to establish that the (C × CB)→B6 chimaeras could respond to minor H antigens in an H–2^d restricted fashion, it was necessary to demonstrate that this response was actually directed against D1 minor H antigens associated with H–2^d and not against any of the unrestricted Qed-1-like antigens known, or as yet undiscovered. We therefore tested the CTL against (D1 × C)F_1 targets. CTL directed against D1 minor H antigens + H–2^d should not lyse targets carrying the appropriate minor H antigens with the wrong H–2 (D1, H–2^q) or those carrying the appropriate H–2 without the minor H antigen (C, H–2^d). However, they should be active against an F_1 target which has received the appropriate H–2 from one parent and the right minor H antigens from the other (D1 × C) (H-2^q × H-2^d). If the anti-D1.C CTL are actually directed against non-H–2 restricted, Qed-1-like antigens, they should lyse D1. Figure 3 shows that (C × CB)F_1→B6 CTL primed and boosted with

D1.C (H-2^d) do not lyse D1(H-2^q) or (C × CB) targets, but are active against both D1.C and (D1 × C)F_1 targets. We conclude that the activity is actually directed against D1 minor H antigens + H–2^d and that this is therefore an H–2^d restricted anti-minor H antigen response rather than an unrestricted anti-Qed-1-like response.

We have shown that (C × CB)F_1 T cells which have developed in a B6 environment are capable of responding to foreign minor histocompatibility antigens in association with H–2^d and that they are nevertheless completely unresponsive
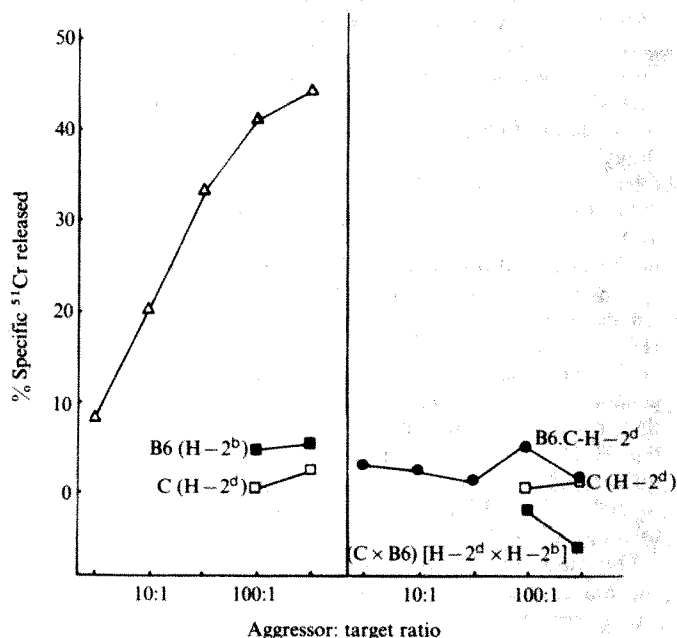
Fig. 2 Cytotoxic response of a (C × CB)→B6 radiation chimaera to B6.C-H-2^d. Chimaeras were constructed by reconstituting lethally irradiated 4 month old C57BL/6 (H-2^b) mice (925r) with 15–$40 × 10^6$ 15–17 day (C × CB) (H-2^d × H-2^b) viable fetal liver cells. Two months after reconstitution some of the chimaeras were primed by i.p. injection of 10^7 mitomycin treated B6.C-H-2^d spleen cells. Three weeks later spleen cells from a chimaera were serologically evaluated for degree of chimaerism (90% C × CB) boosted in 5-day in vitro cultures with mitomycin treated BALB/K (H-2^k) (a) or B6.C-H-2^d (b), stimulators, and assayed for cell mediated cytotoxicity on Con A blasts.
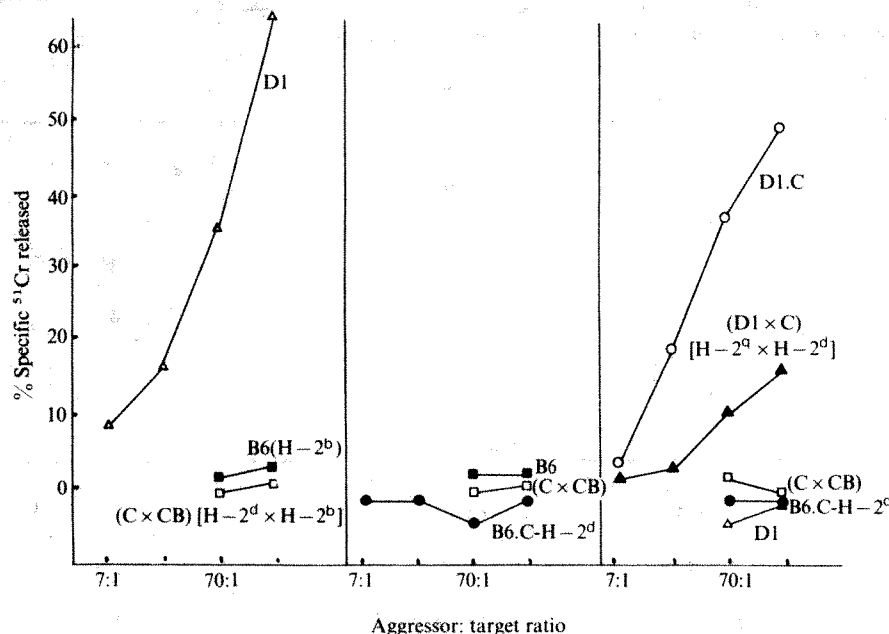
Fig. 3 Cytotoxic response of a (C × CB) → B6 radiation chimaera to D1.C (H-2^d) and B6.C-H-2^d. Two months after repopulation the chimaera was primed by i.p. injection of 10^7 each mitomycin treated D1.C (H-2^d) and B6.C-H-2^d spleen cells. Three weeks later spleen cells from the chimaeras were serologically evaluated for the degree of chimaerism (99% C × CB), boosted in 5-day *in vitro* culture with *a*, D1(H-2^q); *b*, B6.C-H-2^d; or *c*, D1.C (H-2^d) stimulators and assayed for cell mediated cytotoxicity.

to B6 minor H antigens presented in the same association (Table 1). They thus seem to be tolerant of the membrane components of the chimaera in combinations which no cell in the chimaera is genetically capable of expressing. We do not yet know whether such tolerance is mediated by suppression or deletion of the T cells which are specific for B6.C-H-2^d. In either case the induction of self tolerance does not seem to be H-2 restricted.

An early hint that tolerance induction might not be restricted came from the experiments of Billingham and coworkers using H-Y antigen[17] in which they rendered female mice tolerant of syngeneic male skin by a neonatal injection with H-2 incompatible male bone marrow. These females were subsequently found to be tolerant of syngeneic male skin even though the combination of self H-2 + H-Y was not found on the tolerizing marrow cells. Billingham and Silvers conducted their study to evaluate the degree of similarity between H-Y antigens of different strains of mice. Since H-2 restriction was not known in those days, its absence went unnoticed. Similarly von Boehmer *et al.*[18] observed that H-2^b male → (H-2^b × H-2^k) female chimaeras did not respond to H-2^k male cells. However, this may not have reflected a state of tolerance to H-2^k male cells. Von Boehmer *et al.* have shown that the generation of killer cells specific for H-2^k male cells requires the presence of helper cells specific for H-2^b male cells. Since the H-2^b male → (H-2^b × H-2^k) female chimaeras should be tolerant of H-2^b male cells at the helper cell level, their failure to respond to H-2^k male cells may not necessarily reflect tolerance of H-2^k male cells at the killer cell level.

Our study re-emphasizes the earlier findings and shows that the unresponsiveness is most likely a reflection of a state of true tolerance.

These results lead to two possible interpretations. The first is that the induction of tolerance is not really H-2 restricted. We find this unappealing. It has been shown that the apparent non-restriction of the *in vivo* induction of T killer cells against minor antigens is actually an H-2 restricted process which appears unrestricted because of host antigen processing cells[19,20]. We favour the view that tolerance induction is a similarly restricted event, also disguised by antigen processing. If so, what is the antigen processing cell? Does it function in the thymus or the periphery? And does it lead to a tolerant state mediated by suppression or deletion of the reactive T cell precursors?

We thank Drs Mike Bevan and Dick Dutton for invaluable discussions and Dr Kirsten Lindahl for suggesting the question of the Qa-like antigens. This work was supported by NIH grants AI 08795 and CA 09174-03 to R. W. Dutton, NIH postdoctoral fellowship to P.M. and Anna Fuller fellowship to J.D.W. We are grateful to R. W. Dutton for laboratory facilities.

1. Owen, R. D. *Science* **102**, 400 (1945).
2. Billingham, R. E., Brent, L. & Medawar, P. B. *Phil. Trans. R. Soc.* **239**, 357 (1956).
3. Triplett, E. L. *J. Immun.* **89**, 505 (1962).
4. Dorsch, S. & Roser, B. *J. exp. Med.* **145**, 1144 (1977).
5. Beverly, P. C. L., Brent, L., Brooks, C., Medawar, P. B. & Simpson, E. *Transplantn Proc.* **5**, 679 (1973).
6. Zinkernagel, R. M. & Doherty, P. C. *Nature* **248**, 701 (1974).
7. Shearer, G. M. *Eur. J. Immun.* **4**, 527 (1974).
8. Bevan, M. J. *J. exp. Med.* **142**, 1349 (1975).
9. Klein, J. *Transplant* **15**, 137 (1973).
10. Cohn, M. & Blomberg, B. *Scand. J. Immun.* **4**, 1 (1975).
11. Bevan, M. J. *Nature* **269**, 417 (1977).
12. Zinkernagel, R. M. *et al. J. exp. Med.* **147**, 882 (1978).
13. Matzinger, P. & Mirkwood, G. *J. exp. Med.* **148**, 84 (1978).
14. Staats, J. *Cancer Res.* **36**, 4333 (1976).
15. Flaherty, L. *Immunogenetics* **3**, 533 (1976).
16. Lindahl, K. *Immunogenetics* **8**, 71 (1979).
17. Billingham, R. E. & Silvers, W. E. *J. Immun.* **85**, 14 (1960).
18. Von Boehmer, H., Haas, W. & Helmut, P. *J. exp. Med.* **147**, 1291 (1977).
19. Korngold, R. & Sprent, J. *J. exp. Med.* **151**, 314 (1980).
20. Matzinger, P. & Dutton, R. W. (in preparation).

Inhibition of suppressor T-cell development following deoxyguanosine administration

Hans-Michael Dosch, Albert Mansour, Amos Cohen, Abraham Shore & Erwin. W. Gelfand

Division of Immunology, Research Institute, Hospital for Sick Children, Toronto, Ontario M5G 1X8

The expression of immunodeficiency in patients with specific purine enzyme defects indicates a crucial role of the purine salvage pathway in the acquisition and expression of normal immune function[1]. One current hypothesis links the failure of normal lymphocyte development in these diseases to the accumulation of deoxynucleotide triphosphates[2,3]. In our studies of human *in vitro* IgM responses[4], we observed that antigen-

induced T-suppressor cell activity was abrogated in the presence of micromolar concentrations of deoxyguanosine (dGuo)[5]. In contrast, more than 1,000-fold higher resistance to dGuo was found for both non-proliferative T-helper cell activity and the differentiation and proliferation of the precursor B lymphocytes for direct haemolytic plaque forming cells (PFC)[4,5]. To determine whether these observations could have *in vivo* relevance, we monitored the generation of murine T-suppressor cells, capable of abrogating a primary IgM response. It was found that dGuo (but not guanosine) selectively inhibited the *in vivo* development of T-suppressor cells.

Groups of 3–5 DBA/J mice (Jackson Laboratories) were immunized intraperitoneally with varying doses of the thymus-dependent, picrylated antigens ovalbumin or keyhole limpet haemocyanin (TNP-OA, TNP-KLH)[6]. After 4–6 days, direct TNP-specific PFC responses were monitored in spleen cells using fluid phase[4] and soft agar plaque assay procedures[6] with comparable results. In seven experiments bell-shaped antigen dose responses were observed with optimal numbers of PFC generated at 10 µg TNP-OA (Fig. 1) or 50 µg TNP-KLH. PFC responses declined from the optimal levels in an antigen dose-dependent fashion and background values were reached when ≥ 1 mg of either antigen was injected.

In man antigen dose-dependent suppression has been shown to reflect the activation, by antigen, of proliferating suppressor
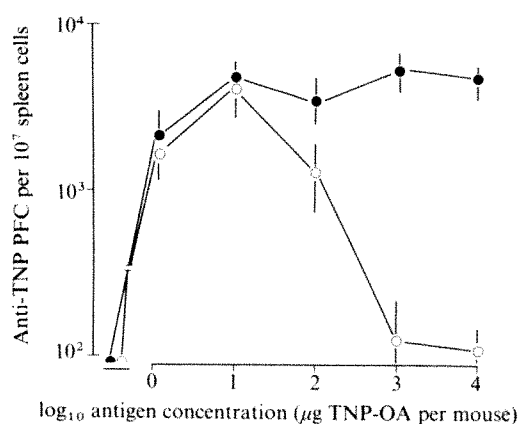
Fig. 1 Effect of dGuo on antigen dose responses of DBA/J mice to TNP-OA. Direct TNP-specific PFC were measured in Ficoll-Hypaque purified spleen cells 5 days after intraperitoneal injection of the antigen dose indicated, using picrylated sheep erythrocytes in a fluid phase haemolytic plaque assay[5]. ●, Mice receiving 1 mg per day dGuo (Sigma) throughout the immunization period. Following the injection of 1 mg dGuo serum levels of 0.2 µM were measured by HPLC for 2–4 h. ○, Pooled data from control mice, injected daily with saline or guanosine (1 mg per day, Sigma). Numbers of background PFC towards non-haptenated sheep red cells were subtracted from anti-TNP sheep red cell plaques and the results expressed as mean TNP-specific PFC ± 1 s.d. per 10[7] spleen cells. PFC responses in animals who received no antigen (−) were below the detection threshold of the assay used (< 100 PFC per 10[7] spleen cells). One of seven similar experiments is shown.

T cells[4]. As the generation of these cells was inhibited in the presence of dGuo[5], mice were injected with 0.1–10 mg dGuo per day throughout the immunization period. Controls received saline or guanosine. All mice survived the 4–6 day treatment period and body and organ weights (spleen, kidney, liver) were not significantly different in treated and control groups. Optimal PFC responses were not impaired in treated animals using TNP-OA (Fig. 1) or TNP-KLH (data not shown) as antigens. However, mice receiving 1 or 10 mg dGuo consistently failed to demonstrate any antigen dose-dependent

Table 1 Inhibition of suppressor T-cell development

Donor mice		Anti-TNP response per 10[7] recipient spleen cells Anti-Thy 1.2	
Treatment	TNP-OA	−	+
Control		$2,580 \pm 560$	$2,320 \pm 450$
Saline		$2,940 \pm 390$	$3,050 \pm 310$
Guanosine	10 µg	$2,640 \pm 330$	ND
Deoxyguanosine		$3,350 \pm 480$	$3,180 \pm 430$
Saline		320 ± 110	$2,440 \pm 520$
Guanosine	1 mg	470 ± 80	$2,190 \pm 410$
Deoxyguanosine		$2,670 \pm 440$	$2,989 \pm 360$

Groups of four donor mice were immunized with 10 µg or 1 mg TNP-OA and received a daily i.p. injection of deoxyguanosine (1 mg), guanosine (1 mg) or saline. On day 5, spleen cells were recovered and incubated with anti-Thy 1.2 plus complement (+) or with complement alone (−). Recipient mice (3–4 per group) received 10 µg TNP-OA and 10[7] treated (+ or −) donor spleen cells. Splenic PFC responses in recipient mice ($\bar{x} \pm 1$ s.d.) were assayed after 5 days. The monoclonal anti-Thy 1.2 reagent F7D5 was a gift from Dr P. Lake. ND, Not done.

suppression at supra-optimal antigen concentrations. In contrast, suppression was observed in all control groups, including those mice injected with 1 or 10 mg per day guanosine. When 0.1 mg or less dGuo was injected per day, PFC responses at high antigen doses were variable and approached the low control values.

To analyse the cellular requirements for high dose antigen-induced suppression of PFC responses, a cell transfer protocol was used. Mice received either a suppressive antigen dose of 1 mg TNP-OA, an optimal dose of 10 µg TNP-OA or no antigen. After 5 days, 1 × 10^{7} spleen cells from these 'primed' mice were transferred to recipient animals which were then immunized with an optimal antigen dose. Splenic PFC responses in recipient mice were measured after 5 days (Table 1). Spleen cells from high dose antigen-primed mice suppressed the development of optimal PFC responses in recipient mice. In contrast, cells from unprimed animals or mice who had received an optimal antigen dose were unable to do so. When suppressive spleen cells from high dose antigen-primed animals were treated with anti-Thy 1.2 plus complement before their transfer to recipient mice, their suppressive activity was eliminated.

If spleen cells were used from high dose antigen-primed mice that had been treated with dGuo (1 mg per day for 5 days), T-suppressor cell activity could not be detected in these cells transfer experiments (Table 1). These data indicated that the decline in PFC responses at supra-optimal antigen doses was mediated by antigen-induced T-suppressor cells and, since recipient animals had not been treated with dGuo, that the development but not the effect of these cells was selectively abrogated by dGuo.

The biochemical mechanism(s) involved in the dGuo-mediated abrogation of suppressor cell development remains unclear. The small population sizes of antigen-specific precursors of PFC, helper and suppressor cells precluded their direct biochemical study. Susceptibility to dGuo toxicity has been linked to the ability of a cell rapidly to accumulate and maintain high levels of intracellular deoxyguanosine triphosphate[3]. In man this capacity is typical for immature T cells and may at least partly reflect high dGuo-kinase and low 5'-nucleotidase activity[7–9]. Rodents studied seemed to be similar: DBA thymocytes expressed high dGuo-kinase activity 200 pmol per h per 10[6] cells) and low 5'-nucleotidase activity (2 nmol per h per 10[6] cells) whereas the activity profiles were inverted in splenic lymphocytes (0.07 and 16 nmol per h per 10[6] cells, respectively). Indeed, thymocytes (but not splenocytes) rapidly accumulated and maintained high levels of

deoxyGTP when incubated in the presence of low concentrations of exogenous dGuo (data not shown).

On the basis of these findings we propose that suppressor cell precursors may resemble thymocytes with respect to key purine salvage enzymes and deoxyGTP accumulation. If this property is indeed a marker of T-cell maturation[7,8] then the suppressor cell population monitored may originate from a pool of rather immature T lymphocytes. Alternatively susceptibility to dGuo toxicity may be a property expressed in the course of antigen-induced suppressor cell activation. The ability of dGuo to modulate selective aspects of an immune reaction in the absence of generalized toxicity may allow selective manipulation of immune responsiveness.

1. Seegmiller, J. E. *et al.* in *Biological Basis of Immunodeficiency* (eds Gelfand, E. W. & Dosch, H.-M.) 251 (1980).
2. Cohen, A. *et al. Proc. natn. Acad. Sci. U.S.A.* **75**, 472 (1978).
3. Cohen, A., Gudas, L. J., Amman, A. J. & Staal, G. E. J. *J. clin. Invest.* **61**, 1405 (1978).
4. Dosch, H.-M. & Gelfand, E. W. *Immun. Rev.* **45**, 242 (1979).
5. Gelfand, E. W., Lee, J. J. W. & Dosch, H.-M. *Proc. natn. Acad. Sci. U.S.A.* **76**, 1998 (1979).
6. Yamashita, U., Takami, T. & Kitagawa, M. *Cell Immun.* **18**, 396 (1975).
7. Cohen, A., Lee, J. W. W., Dosch, H.-M. & Gelfand, E. W. (submitted).
8. Edwards, N. L., Gelfand, E. W., Burk, L., Dosch, H.-M. & Fox, J. H. *Proc. natn. Acad. Sci U.S.A.* **76**, 3474 (1979).
9. Carson, D. A., Kaye, J., Matsumoto, S., Seegmiller, J. E. & Thompson, L. *Proc. natn. Acad. Sci. U.S.A.* **76**, 2430 (1979).

Alloactivated Lyt 1+2- T lymphoblasts bind syngeneic Ia antigens

Bruce E. Elliott*, Zoltan A. Nagy‡, Yinon Ben-Neriah† & David Givol†

*Cancer Research Division, Department of Pathology, Queen's University, Kingston, Ontario, Canada
†Department of Chemical Immunology, The Weizmann Institute of Science, Rehovot, Israel

A large proportion of T blasts activated in the mixed lymphocyte reaction (MLR) is capable of binding plasma membrane (PM) vesicles prepared from the stimulator strain[1,2]. The binding of vesicles is specific, and the antigens recognized are serologically detectable H–2K, D and I region products[3,4]. T blasts binding stimulator K (and D) antigens belong to the Lyt 1-2+ subclass, whereas those binding stimulator Ia antigens are Lyt 1+1- (ref. 5). We report here that antibodies against heavy chain V-region determinants (V_H)[6], and furthermore, monoclonal[7] or conventional antibodies against responder cell Ia determinants strongly inhibit the binding of radiolabelled stimulator vesicles. Anti-responder Ia inhibition is restricted to the Lyt 1+2- subset of T blasts and correlates with a weak expression of Ia determinants on these cells. The relevant Ia determinants are not resynthesized after trypsin treatment of the blasts. In these conditions anti-V_H, but not anti-Ia reagents inhibit stimulator vesicle binding. Trypsinized T blasts can, however, passively absorb Ia material from supernatants of syngeneic, lipopolysaccharide (LPS)-activated spleen cells, and thus regain their susceptibility to vesicle-binding inhibition with anti-Ia sera. Acquisition of syngeneic Ia is also blocked by the anti-V_H reagent. We conclude that Lyt 1+2- MLR blasts possess binding sites for both allogeneic (stimulator) and syngeneic Ia antigens.

‡Present address: Max-Planck-Institut für Biologie, Abteilung Immungenetik, Tübingen, FRG.

Antigen-specific T-cell receptors probably represent immunoglobulin V-gene products, which may or may not be associated with major histocompatibility complex (MHC) antigens in the T-cell membrane[8–12]. To study the possible involvement of MHC antigens in T-cell receptor function, we have attempted to inhibit the specific binding of radiolabelled stimulator PM vesicles by MLR responder T blasts using antibodies against MHC (and non-MHC) products expressed on the blasts. The representative experiment in Table 1 demonstrates that monoclonal antibodies against Ia-antigen determinants encoded by the I–A region of the responder strain MHC, strongly inhibit vesicle binding. A monoclonal antibody recognizing E/C-region products (anti-Ia 7)[7] caused less, though significant inhibition (unpublished data). The cell population susceptible to anti-Ia inhibition was depleted by anti-Lyt 1 plus rabbit complement (RC), and enriched by anti-Lyt 2 plus RC treatment. Anti-V_H as a possible probe for the receptor[13] also blocked vesicle binding, irrespective of the Lyt subclass of alloantigen-binding T blasts (Table 1). Very weak expression of both Ia and V_H by these cells was demonstrable by indirect immunofluorescence (data not shown). In contrast, antibodies against non-MHC antigens strongly expressed by the T blasts, that is, Thy 1 (Tables 1, 2) or Lyt 1, Lyt 2 and Ly 6 (B.E.E. *et al.*, in preparation), did not affect antigen binding. Thus, steric hindrance does not seem to be involved in the inhibition observed. The lack of inhibition with several antisera and our failure to detect Fc receptors on blasts generated from nylon-wool-purified lymph-node cells[3], renders the possibility of Fc-receptor mediated blocking also unlikely. The data indicate, therefore, that Ia antigens may be located very close to the binding sites for alloantigen on Lyt 1+2- MLR blasts.

To clarify further the role of self-Ia antigens in stimulator vesicle binding, we have tested whether the relevant Ia molecules are endogenous or are passively acquired. As shown in Table 2, vesicle binding was not blocked by anti-responder Ia antibodies after trypsin treatment and overnight incubation of the blasts. In contrast, anti-V_H was strongly inhibitory. These cells, however, regained susceptibility to anti-Ia inhibition after incubation with supernatant of LPS-activated cells, which contained soluble syngeneic Ia material. The reduction or complete loss of self-Ia after trypsin treatment, and the uptake of syngeneic Ia from supernatants of LPS blasts were also detected by indirect immunofluorescence (Table 3). Furthermore, the data in Table 3 demonstrate that the uptake of syngeneic Ia is inhibited by anti-V_H, but not by a conventional anti-Ig serum. Identical results were obtained with Ia-negative long-term MLR T-cell lines (B.E.E. *et al.*, in preparation). Thus, anti-responder Ia inhibition of alloantigen binding requires the presence of passively acquired self-Ia determinants which are closely associated with V-gene products on the surface of MLR T blasts.

In conclusion, Lyt 1+2- (helper) T cells proliferating in MLR apparently have binding sites for both allogeneic and syngeneic Ia determinants. Binz *et al.*[14] have recently shown that T-cell receptors isolated from rat MLR blasts exhibit similar antigen-binding specificity. We have demonstrated in independent experiments that the binding of both stimulator and responder Ia antigens is specific[3–5] (B.E.E. *et al.*, in preparation). As the uptake of both allo- and self-Ia is blocked by anti-V_H antibody, the binding sites for both antigens may consist of V_H. However, on the basis of these data we cannot determine whether identical or distinct sites recognize allo- and self-Ia, respectively. The fact that self-Ia *per se* (that is, without anti-Ia antibody) does not interfere with the uptake of stimulator vesicles, seems to support the latter possibility. Competitive binding experiments are in progress to clarify this issue.

During these experiments, we detected, as have others[13,15], some inhibition of antigen binding with antibodies against responder K and D determinants. Studies on this

Table 1 Inhibition with anti-V_H and monoclonal anti-Ia antibodies of radiolabelled PM vesicle binding by MLR blasts: Lyt phenotype of blasts susceptible to anti-Ia inhibition

MLR		Treatment	Antisera preincubation*	Binding of ^{125}I-labelled SJL vesicles	
R	S			% Labelled blasts	% Inhibition of binding
A/J	SJL	NMS + RC	—	36.4	0
			NMS	34.6	5
			Anti-Thy 1.2	32.7	10
			Anti-Ia 15 + 19	15.0	59
			Anti-V_H	6.9	81
		Anti-Lyt 1.2 + RC	—	31.2	0
			Anti-Ia 15 + 19	29.4	6
			Anti-V_H	9.0	71
		Anti-Lyt 2.2 + RC	—	44.9	0
			Anti-Ia 15 + 19	11.1	75
			Anti-V_H	9.5	79

For the MLR, responder cells were nylon-wool-passaged lymph-node cells (<2% B-cell contamination), stimulator cells were 3,300 R-irradiated spleen cells[3]. Responder/stimulator = 1:2. Day 4 blasts were purified on Ficoll/Urovison[3] (>95% Thy 1[+], FcR[−]). Treatment of blasts with anti-Lyt sera plus rabbit complement was as described elsewhere[5]. Per cent killing of blasts was as follows: normal mouse serum (NMS)+RC: 4.1; anti-Lyt 1.2 + RC: 45.2; anti-Lyt 2.2 + RC: 35.7. For antisera preincubation, cells were incubated with antibodies (diluted 1:25) for 15 min at 0 °C, followed by 30 min at 37 °C. Radiolabelled PM vesicles were added and incubation continued for 2 h at 37 °C. For the binding studies, SJL PM vesicles prepared and labelled as described previously[2,4] were used at a final concentration of 4.3 µg protein ml^{−1} (0.1 µCi per µg). Binding of vesicles was detected by autoradiography[2]. % Labelled blasts was based on scoring of 200–600 cells per group. Monoclonal anti-Thy 1.2 was from NEN. Rabbit anti-mouse V_H was purified by affinity chromatography[6], and used at 0.15 mg protein ml^{−1}.

Table 2 Loss of vesicle binding inhibition with anti-responder Ia but not with anti-V_H antibodies after trypsin treatment of MLR blasts

MLR		Antisera incubation	Binding of ^{125}I-labelled SJL vesicles by blasts preincubated with			
			Medium		AKR supernatant	
R	S		% Labelled blasts	% Inhibition of binding	% Labelled blasts	% Inhibition of binding
B10.A	SJL	—	51.6	0	53.8	0
Day 4 cells		Anti-Ia 15 + 19	50.0	3	13.9	74
after trypsin		Anti-V_H	16.3	68	22.8	58
treatment and		R anti-MIg	48.0	7	58.0	0
overnight 37 °C		Anti-Thy 1.2	46.6	10	50.0	7

MLR, antisera and vesicle binding assay were as in Table 1. Trypsin treatment of blasts was as described elsewhere[1]. AKR supernatants were produced by incubating day 3 LPS-activated spleen cells (10[7] ml^{−1}) in RPMI 1640 without serum for 6 h at 37 °C. Supernatants were recovered after centrifugation at 250g for 15 min, and 120,000g for 60 min. Soluble Ia in supernatants was demonstrated by antibody absorption. Protein concentration in the AKR supernatant used here was 50 µg ml^{−1}. Cells were incubated for 2 h at 37 °C with medium or supernatant, and washed before incubation with antisera. Rabbit anti-mouse immunoglobulin was from Behringwerke.

Table 3 Inhibition of self-Ia binding with anti-V_H antibodies

MLR		1st antiserum incubation	Ia supernatant	2nd antiserum incubation	Indirect immunofluorescence	
R	S				% Ig^{+} cells	% Inhibition
B10.A	SJL	—	—	Anti-Ia 1,2*	13.7	—
Day 4 cells		—	AKR	Anti-D[k]†	1.7	—
after trypsin		—	AKR	Anti-Ia 1,2	40.2	0
treatment and		Anti-V_H	AKR	Anti-Ia 1,2	12.8	68
overnight, 37 °C		R anti-MIg	AKR	Anti-Ia 1,2	39.0	3

MLR, 1st antiserum incubation and Ia supernatant were as in Tables 1 and 2. The 2nd antiserum incubation was for 45 min at 0 °C. For indirect immunofluorescence studies, fluorescein isothiocyanate-labelled F(ab')₂ of sheep anti-mouse IgG (H + L) (Cappel) was used as described[3,4], Ig^{+} cells were seen as a weak spotted pattern of fluorescence.

*(ABY × B10.HTT) anti-A.TL; †(B10.A(2R) × C3H.SW) anti-C3H. Antisera (100 µl) were preabsorbed as follows: anti-Ia 1,2, 4 × 10^{7} SJL spleen cells; anti-D[k], 4.5 × 10^{7} SJL LPS blasts + 1.25 × 10^{8} A/J spleen cells; R anti-MIg, 6 × 10^{7} EL4 tumour cells.

phenomenon, as well as on the possible relevance of our findings for MHC restriction[16,17] and cell–cell collaboration, are now in progress.

We thank Dr U. Hämmerling for hybridoma antibodies, Dr J. C. Ray for alloantisera, and Ms S. Mundinger, D. Evernden-Porelle and M. Florian for technical assistance. This work was supported by the NCI and the MRC of Canada.

1. Elliott, B. E., Nagy, Z., Nabholz, M. & Pernis, B. *Eur. J. Immun.* **7**, 287–291 (1977).
2. Elliott, B. E., Takacs, B. & Nagy, Z. *Eur. J. Immun.* **9**, 646–651 (1979).
3. Nagy, Z., Elliott, B. E., Nabholz, M., Krammer, P. H. & Pernis, B. *J. exp. Med.* **143**, 648–659 (1976).
4. Nagy, Z. A. & Elliott, B. E. *J. exp. Med.* **150**, 1520–1537 (1979).
5. Nagy, Z., Elliott, B. E. & Nabholz, M. *J. exp. Med.* **144**, 1545–1553 (1976).
6. Ben-Neriah, Y., Wuilmart, C., Lonai, P. & Givol, D. *Eur. J. Immun.* **8**, 797–801 (1978).
7. Hämmerling, G. J., Hämmerling, U. & Lemke, H. *Immunogenetics* **8**, 433–445 (1979).
8. Taussig, M. & Munro, M. *Nature* **256**, 103–106 (1974).
9. Taniguchi, M., Saito, T. & Tada, T. *Nature* **278**, 555–558 (1979).
10. Mozes, E. & Haimovich, J. *Nature* **278**, 56–57 (1979).
11. Binz, H. & Wigzell, H. *Scand. J. Immun.* **5**, 559–571 (1976).
12. Krawinkel, U. *et al. Cold Spring Harb. Symp. quant. Biol.* **41**, 285–294 (1976).
13. Lonai, P., Ben-Neriah, Y., Steinman, L. & Givol, D. *Eur. J. Immun.* **8**, 827–832 (1978).
14. Binz, H., Frischknecht, H., Mercolli, C., Dunst, S. & Wigzell, H. *J. exp. Med.* **150**, 1084–1097 (1979).
15. Hämmerling, G. J. & McDevitt, H. O. *J. Immun.* **112**, 1734–1740 (1974).
16. Zinkernagel, R. M. & Doherty, P. C. *Nature* **248**, 701–703 (1974).
17. Sprent, J. *J. exp. Med.* **147**, 1159–1174 (1978).

Monokine-induced synthesis of serum amyloid A protein by hepatocytes

Mitchell J. Selinger*, Keith P. W. J. McAdam†¶, Marshall M. Kaplan‡, Jean D. Sipe§, Stefanie N. Vogel‖ & David L. Rosenstreich‖

*Division of Gastroenterology, Department of Medicine, Tufts University School of Medicine, 171 Harrison Avenue, Boston, Massachusetts 02111
†Division of Experimental Medicine, Department of Medicine, Tufts University School of Medicine, Boston, Massachusetts 02111
‡Division of Gastroenterology, Department of Medicine, Tufts University School of Medicine, Boston, Massachusetts 02111
§Research Manpower Branch, National Cancer Institute, NIH, Bethesda, Maryland 20014
‖National Institute of Dental Research NIH, Bethesda, Maryland 20014

Infection or inflammation triggers the rapid appearance in the blood of a group of proteins known as acute phase reactants[1]. Serum amyloid A protein (SAA) is an acute phase protein which is believed to be the precursor for the secondary amyloid fibril protein, known previously as amyloid of unknown origin, and now as amyloid A protein (AA). The site of synthesis of SAA has been controversial, with previous evidence suggesting that AA related proteins arise in liver[2–4], connective tissues[5], polymorphonuclear neutrophil leukocytes[6] and spleen[7]. However, in none of these systems could SAA synthesis be induced *in vitro* and the evidence rested on studies of tissues or cells arising from pre-stimulated animals. Our aim in the present studies was to prove that the liver is capable of SAA production and to identify the specific cell responsible for synthesis. The experiments demonstrate that SAA is synthesized in the liver by hepatocytes. In addition, colchicine, currently used for the treatment of amyloidosis, blocks the secretion of SAA from the hepatocyte, as has been shown for another acute phase reactant, C-reactive protein[8].

Most of the acute phase SAA travels in serum in association with high density lipoprotein[9], although the physiological function of this apolipoprotein is unclear. Recent evidence suggests an immunoregulatory role for SAA when added to lymphocyte cultures *in vitro*[10], whereas SAA is thought to be

¶To whom reprint requests should be addressed.
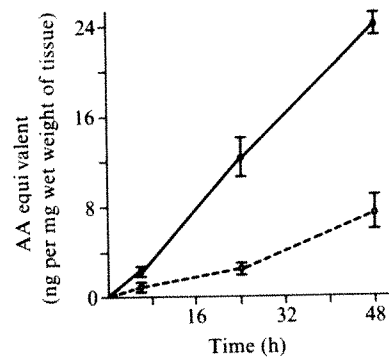
Fig. 1 Production of SAA by C57BL/10ScCR (LPS non-responder) liver organ cultures. Liver fragments $(1-2\,mm^3)$ were cultured in Falcon organ culture dishes in an atmosphere of 95 % O_2 and 5 % CO_2. Each point represents the total SAA concentration in medium and tissue at the time of collection. Dashed line, 90 % Trowell's medium and heat inactivated $(56° \times 30\,min)$, 10 % fetal calf serum (FCS). Solid line, 80 % Trowell's medium and 10 % FCS and 10 % macrophage supernatant (SAASF). This was prepared from peritoneal exudate cells (PEC) collected from C3H/HeN (LPS responder) mice which had been pretreated 6 days previously with 3 ml thioglycollate broth i.p. PEC were incubated for 3 h, the non-adherent cells were removed by vigorous washing, and the adherent cells cultured with *E. coli* K235 LPS (phenol) for 24 h. It was this culture supernatant which contained SAASF.

the precursor for the secondary amyloid fibril protein[11,12] (to be distinguished from the amyloid fibril protein of immunoglobulin origin)[13] in certain pathological situations, especially chronic inflammation. It differs in amino acid sequence and structure from another protein known as pentagonal or 'P' component, which is found in all amyloid deposits and has been shown recently to be an acute phase serum protein in mouse, though not in other species[14].

The rapid synthesis of SAA and the large amounts produced are characteristics well suited to a primary isolated cell culture system. As human SAA has the same N-terminal amino acid sequence[15,16] and shows immunological cross-reaction with AA[11,12], we have used a solid-phase radioimmunoassay to detect SAA cross-reactivity to mouse AA protein[17].

SAA was synthesized *in vitro* by isolated hepatocytes, cultured in the presence of an inducing factor which has been termed SAA inducer[18] or SAA stimulating factor (SAASF)[19]. This factor is derived from lipopolysaccharide (LPS)-stimulated macrophages. The requirement for the intermediate factor has been demonstrated by using the inbred strain of mice, C57BL/10ScCR, which exhibits an abnormal response to the lipid A moiety of LPS, similar to that found in the C3H/HeJ strain[20]. These strains have been designated LPS-non-responders, in contrast to syngeneic LPS-responder strains (C57BL/Sn and C3H/HeN, respectively). As a result of this defect, C57BL/10ScCR mice do not produce SAA when injected with lipid A or with LPS[21] from *Escherichia coli* K235, extracted by the McIntyre method[22] in hot phenol (LPS, phenol) to remove any lipid A-associated protein from the LPS[23]. SAASF was initially detected in the serum of LPS responder mice 2 h after intraperitoneal (i.p.) injection of LPS, before the appearance of SAA in the serum[18]. This 'latent phase' serum caused SAA synthesis when administered i.p. or intravenously to LPS non-responder mice, thus demonstrating that it was not LPS carry-over which was causing SAA synthesis. SAASF activity was also detected in the supernatant culture medium of LPS-responder peritoneal exudate cells stimulated *in vitro* for 24 h with LPS. This medium, containing

SAASF, caused SAA synthesis when injected into LPS non-responder mice *in vivo*[18]. In the present experiments, we have used SAASF from these supernatants to induce SAA synthesis in both liver organ cultures and hepatocyte cultures derived from LPS non-responder mice.

In initial experiments, liver fragments were cultured in plastic Petri dishes using a modification of the method of Trier[24]. Cubes of liver tissue (1–2 mm) contained a heterogeneous group of cells, including parenchymal and non-parenchymal cells, red and white blood cells, and endothelial and connective tissue cells. Supernatants from liver fragments in culture medium supplemented with serum from healthy mice contained small, but over 24 h, increasing amounts of AA antigenic activity measured by solid-phase radioimmunoassay[17]. In contrast, the addition to the culture medium of latent phase serum containing SAASF increased the SAA concentration in the supernatant (from 3 to 13 ng per mg wet weight tissue at 24 h). There was little increase in AA antigenic activity in liver tissue, suggesting rapid secretion of SAA from the fragment.

Similar results were obtained when liver fragments were cultured with macrophage supernatant containing SAASF (Fig. 1). The addition of macrophage supernatant to culture medium greatly increased SAA synthesis over spontaneous production. This effect of SAASF was abolished by cycloheximide at a dose (1 μg ml⁻¹) which inhibited protein synthesis by 90%. This dose of cycloheximide also inhibited the small amount of spontaneous production of SAA in cultures without SAASF.

Although these organ culture experiments confirmed that the liver was capable of SAA synthesis, they did not define the specific cell of origin within the liver fragments. This problem was first approached by studying colchicine-pretreated, LPS-stimulated animals *in vivo*. Pretreatment of mice with

Fig. 3 SAA production by C57BL/10ScCR hepatocyte and Kupffer cell fractions. Isolated hepatocyte and Kupffer cell-rich fractions from non-responder mice were cultured with and without macrophage supernatant (see Fig. 1). Media were collected at 72 h and assayed in the radioimmunoassay for mouse AA. □, 90% Trowell's medium and 10% FCS; ■, 80% Trowell's medium and 10% FCS and 10% macrophage supernatant (SAASF).

colchicine before LPS injection resulted in a serum response which was one-third of that in mice injected with LPS alone (Fig. 2). In contrast to this blunted serum response, the colchicine-pretreated liver contained four times higher AA concentrations than LPS-injected controls (data not shown).

Subsequent experiments relied on isolation of more homogeneous liver cell populations. The technique of collagenase perfusion of the portal vein[25] enabled cell suspensions rich in hepatocytes or Kupffer cells to be obtained. Figure 2 shows an analysis of AA levels in isolated liver cell populations from an animal pretreated with colchicine. Hepatocyte- and Kupffer cell-rich suspensions were prepared from colchicine-pretreated, LPS-stimulated and, therefore, AA-enriched, liver. Most of the AA in liver was in the hepatocyte fraction and little in the Kupffer cell fraction.

Culture of hepatocytes and Kupffer cells more directly confirmed that SAA arises from hepatocytes (Fig. 3). There was little detectable AA in culture medium collected from the Kupffer cell-rich suspension, either with or without the addition of macrophage supernatant with SAASF. In contrast, the concentration of AA in the culture medium collected from the hepatocyte suspension was 1.5 μg per 10⁶ cells and increased to 4.6 μg per 10⁶ cells when supplemented with macrophage supernatant.

In conclusion, these experiments help to clarify the controversy about the origin of SAA, and provide an explanation for the prophylactic effect of colchicine in amyloidosis related to chronic inflammation. The blunted SAA response in serum seems to be secondary to a block in hepatocyte secretion of this presumed precursor of the amyloid fibril. Our data need not imply that SAA is synthesized only in the liver. Indeed, the recent finding that human SAA exists in acute phase serum in at least six different heterogeneous forms might support the contention that SAA can also be synthesized by other tissues[26]. However, the possibility of post-translational cleavage of a common SAA precursor gene product has yet to be excluded as an explanation for this polymorphism. Of great interest is the finding that a macrophage product induces the *in vitro* synthesis of SAA, whereas the initial stimulus, LPS, does not do so directly. Thus, the many different diseases which lead to secondary amyloidosis might be expected to have in common the stimulation of macrophages which produce SAASF and thereby elevation of SAA, the putative amyloid fibril protein precursor. It seems reasonable to attribute to the resident liver macrophage, or Kupffer cell, a central role in regulating the synthesis of SAA and perhaps other acute phase proteins. Although the physiological function of SAA is unclear, we believe this to be the first report of a lipoprotein whose liver synthesis is regulated by a soluble factor derived from cells of the reticuloendothelial system.

Fig. 2 Distribution of SAA in liver cell fractions from colchicine-treated LPS responder mice. Control and colchicine-pretreated C57BL/10Sn mice were injected with 1 μg LPS (K235, phenol). Liver cell fractions were prepared by collagenase perfusion of the portal vein as described by Berry and Friend[27]. Our major modification for the smaller mouse included a reduction in pump speed to 5 ml min⁻¹ for portal vein perfusion and gentle gravity sedimentation of hepatocytes as described by Jeejeebhoy[28] to separate parenchymal from non-parenchymal cells. The final washed cell pellet was resuspended in 90% Trowell's medium (Gibco) and 10% FCS, heat inactivated at 56 °C for 30 min. Microscopy revealed a 95% pure preparation of hepatocytes. For cell culture, 4 ml of cell suspension, which contained 0.25 × 10⁶ cells ml⁻¹, was added to a 25-cm³ tissue culture flask and incubated at 37 °C in an atmosphere of 5% CO₂ and 95% air. No hepatocytes were present in the Kupffer cell-rich suspension which had been treated with pronase. Serum and cells were assayed in the radioimmunoassay for mouse AA. □, No colchicine; ■, 0.015 mg colchicine i.p. 2 h before LPS.

1. Koj, A. in *Structure and Function of Plasma Proteins* Vol. 1 (ed. Allison, A. C.) 73–131 (Plenum, New York, 1974).
2. McAdam, K. P. W. J. & Sipe, J. D. *J. exp. Med.* **144**, 1121–1127 (1976).
3. Sipe, J. D., McAdam, K. P. W. J. & Uchino, F. *Lab. Invest.* **38**, 110–114 (1978).
4. Benson, M. D. & Kliner, E. *Clin. Res.* **27**, 321 (1979).
5. Linder, E., Lehto, V. P., Virtanen, I., Stenman, S. & Natvig, J. B. *J. exp. Med.* **146**, 1158–1163 (1977).
6. Rosenthal, C. J. & Sullivan, L. *J. clin. Invest.* **62**, 1181–1186 (1978).
7. Baumal, R., Sklar, S., Wilson, B. & Laskov, R. *Lab. Invest.* **39**, 632–638 (1978).
8. Kushner, I. & Feldman, G. *J. exp. Med.* **148**, 466–477 (1978).
9. Benditt, E. P., Eriksen, N. & Hanson. R. H. *Proc. natn. Acad. Sci. U.S.A.* **76**, 4092–4096 (1979).
10. Benson, M. D. & Aldo-Benson, M. *J. Immun.* **122**, 2077–2082 (1979).
11. Husby, G. & Natvig, J. B. *J. clin. Invest.* **53**, 1054–1061 (1974).
12. Levin, M., Franklin, E. C., Frangione, B. & Pras, M. *J. exp. Med.* **138**, 373–380 (1973).
13. Glenner, G. G. & Page, D. L. *Int. Rev. exp. Path.* **15**, 1–91 (1976).
14. Pepys, M. B., Beltz, M., Gomer, K., Davies, A. J. F. & Doenhoff, M. *Nature* **278**, 259–261 (1979).
15. Rosenthal, C. J., Franklin, E. C., Frangione, B. & Greenspan, J. *J. Immun.* **116**, 1415–1418 (1978).
16. Anders, R. F., Natvig, J. B., Michaelson, T. G. & Husby, G. *Scand. J. Immun.* **4**, 397–401 (1975).
17. Sipe, J. D., McAdam, K. P. W. J., Torain, B. F. & Pollock, P. S. *Immun. Commun.* **6**, 1–12 (1977).
18. Sipe, J. D., Vogel, S. N., Ryan, J. L., McAdam, K. P. W. J. & Rosenstreich, D. L. *J. exp. Med.* **150**, 597–606 (1979).
19. Selinger, M. J. *et al. Proc. 3rd Int. Symp. on Amyloidosis*, Portugal (Excerpta Medica, Amsterdam, in the press).
20. Watson, J., Largin, M. & McAdam, K. P. W. J. *J. exp. Med.* **147**, 39–49 (1978).
21. McAdam, K. P. W. J. & Ryan, J. L. *J. Immun.* **120**, 249–253 (1978).
22. McIntyre, F. C., Sievart, H. W., Barlow, G. H., Finley, R. A. & Lee, A. Y. *Biochemistry* **6**, 2363–2372 (1967).
23. Morrison, D. C., Betz, S. J. & Jacobs, D. M. *J. exp. Med.* **144**, 821–827 (1976).
24. Trier, J. S. *New Engl. J. Med.* **295**, 150–155 (1976).
25. Miles, D. M., Zucker-Franklin, D. *Am. J. Path.* **54**, 147–166 (1969).
26. McAdam, K. P. W. J., Bausserman, L. L., Herbert, P. N. & Green, K. M. *Proc. 3rd Int. Symp. on Amyloidosis*, Portugal (Excerpta Medica, Amsterdam, in the press).
27. Berry, M. N. & Friend, P. S. *J. Cell Biol.* **43**, 506–520 (1969).
28. Jeejeebhoy, K. N., Ho, J. & Greenberg, R. G. *Biochem J.* **146**, 141–156 (1975).

Genetic heterogeneity in human neuraminidase deficiency

A. T. Hoogeveen, F. W. Verheijen, A. d'Azzo & H. Galjaard

Department of Cell Biology and Genetics, Erasmus University, Rotterdam, The Netherlands

There is a deficiency of human α-N-acetylneuraminidase in several inherited diseases. In patients with mucolipidosis I (refs 1,2) and in adults with a variant form without bony abnormalities and mental retardation[3,4], both also classified as sialidoses[4], it is the only deficient enzyme. In mucolipidosis II ('I-cell' disease) neuraminidase is one of many deficient lysosomal hydrolases[5-7] and a third manifestation combines deficiency of neuraminidase and β-galactosidase[8,9]. We have investigated the genetic background of these various neuraminidase deficiencies by somatic cell hybridization and co-cultivation. The principal conclusions from work on mutant fibroblasts, reported here, are that at least three gene mutations are involved and that the combined β-galactosidase/neuraminidase deficiency is likely to be due to defective post-translational modification of these enzymes.

Table 1 summarizes the neuraminic acid content and the activities of β-galactosidase and neuraminidase in the different mutant fibroblasts and 4 days after fusion of each cell type with itself (parental fusion). The activity of neuraminidase was measured with N-acetylneuraminosyl-D-lactose and with 4-methylumbelliferyl-α-2-N-acetylneuraminic acid (provided by Dr J. S. O'Brien), and similar results were obtained with both substrates. Because of its simplicity and high sensitivity, we

have used principally the fluorometric assay, the results of which are reported here. As Table 1 shows, the neuraminidase activity in fibroblasts from a severely mentally retarded 11-yr-old girl with the classical form of mucolipidosis I (ML I), also classified as sialidosis 2 (ref. 4), was 1% of control values. Cells from a patient with a variant form described by Durand *et al.*[3], and sometimes classified as sialidosis 1 (ref. 4), had a residual activity of 4–5%. This higher residual activity is probably responsible for the lower neuraminic acid content in these fibroblasts.

Fibroblasts from a mentally retarded adult male with myoclonus and ataxia[10] and from a 2-yr-old boy with Hurler-like features but no neurological abnormalities[11] had a profound neuraminidase deficiency in addition to a 10% residual activity of β-galactosidase (Table 1). These two patients had previously been classified as variant forms of G_{M1}-gangliosidosis[12] or β-galactosidase deficiency[13] on the basis of complementation after fusion with fibroblasts from patients with a primary defect of β-galactosidase. Fibroblasts from both parents of the patient with infantile β-galactosidase/neuraminidase deficiency (β-gal⁻/neur⁻) had normal activity of β-galactosidase but neuraminidase activity was about half the mean control value (Table 1). This makes it unlikely that β-galactosidase deficiency is the primary defect in this condition. One of our patients with β-gal⁻/neur⁻ has recently been classified as sialidosis II (ref. 4). Because the primary defect in this condition has not yet been resolved and the syndromes included in the category sialidosis 2 are so different clinically, biochemically and even genetically, such classification seems somewhat premature.

We have studied the genetic background of the various neuraminidase deficiencies by complementation analysis after somatic cell hybridization. The results of enzyme assays 4 days after fusion of each cell strain with itself (parental fusion in Table 1) indicate that the polyethylene glycol (PEG) method of hybridization[14] does not affect neuraminidase activity. The results of fusions of different mutant cell strains are summarized in the second column of Table 2. Compared with parental fusions, there was 4–15 times as much neuraminidase activity after fusion of I-cells with each of the other mutant fibroblasts. The activities after co-cultivation (third column of Table 2) were not higher than the average values for each pair of parental cells. The complementation observed after fusion of I-cells with each of the other mutant fibroblasts is most probably due to a correction of the post-translational defect in I-cell disease[7]. The rapid generation of neuraminidase activity and of other lysosomal hydrolases after fusion of I-cells with various other mutant fibroblasts[15] would agree with a normalization of the processing and/or activation of preformed glycosidases.

The fusions of classical ML I × variant ML I did not result in complementation and these conditions probably represent different mutations within one gene. The same is true for the adult type and infantile type of β-gal⁻/neur⁻ deficiency. Fusions of each of the ML I strains with each of the β-gal⁻/neur⁻ deficient fibroblasts, however, resulted in a clear increase in neuraminidase activity (3–9 times the values after parental fusion). This indicates that two different gene mutations are involved in the neuraminidase deficiency of sialidosis 1 and the combined β-gal⁻/neur⁻. The restoration of neuraminidase activity after fusion of ML I cells with β-gal⁻/neur⁻ fibroblasts might result because one cell type, most probably ML I, is deficient in the structural part of the enzyme and the other is defective in a modifying enzyme or a regulatory factor. Another explanation could be that neuraminidase is made up of different subunits which must be normal for the expression of its activity.

Neuraminidase activity also increased after co-cultivation of the different types of ML I cells with each of the β-gal⁻/neur⁻ fibroblasts (compare last column Table 2 with average values of both parental strains in Table 1). This partial restoration of

Table 1 Activities of β-galactosidase and neuraminidase, and neuraminic acid content in mutant human fibroblasts and effect of cell fusion

			Neuraminidase	
Cell type	Total neuraminic acid (10^{-9} mol per mg)	β-Galactosidase	Unfused	After parental fusion
I-Cell*	117	4	0.3	0.2
Classical ML I*	71	730	1.3	0.7
Variant ML I*	40	850	3.8	3.9
Adult β-gal⁻/neur⁻	60	45	1.3	1.5
Infantile β-gal⁻/neur⁻	59	48	0.6	0.7
Heterozygous mother	16	574	31	—
Heterozygous father	17	627	34	—
Control fibroblasts				
Mean	22	630	82	—
Range	15–31	350–1,050	43–129	—
	($n = 17$)	($n = 36$)	($n = 17$)	

Activities are expressed as nmol per h per mg protein and the values given are the means of three to six independent experiments on each mutant strain and on a large number of control fibroblasts. In all instances fibroblasts were cultured in Ham's F10 medium with 10% fetal calf serum and they were collected by trypsinization, rinsed in saline and centrifuged. Cells were disrupted by addition of bidistilled water to the pellet, and after shaking, the homogenate was used directly for biochemical analysis. Neuraminidase activity was determined with methylumbelliferyl substrate (provided by Drs T. Warner and J. S. O'Brien, see ref. 20 for synthesis). Cell homogenate (1 μl) was incubated with 2 μl 2 mM substrate in 0.25 M Na-acetate buffer, pH 4.3, for 1–2 h at 37 °C; the fluorescence of the liberated methylumbelliferone was measured after addition of 500 μl 0.5 M sodium carbonate buffer, pH 10.7, at 448 nm. The activity of β-galactosidase was also measured with methylumbelliferyl substrate as before[9]. Total neuraminic acid content was measured after hydrolysis of the cells for 1 h at 80°C in 0.1 N H_2SO_4 according to Warren[21].
*Cultured fibroblasts from a patient with mucolipidosis I were provided by Dr H. D. Bakker; those from a patient with a variant form (De PF in ref. 3) by Dr P. Durand, and those from a patient with I-cell disease by Dr A. Boué.

Table 2 Cell hybridization and co-cultivation of neuraminidase-deficient human fibroblasts

	Neuraminidase activity ($\times 10^{-9}$ mol per h per mg protein)	
Combination of cell strains	Hybridization	Co-cultivation
I-cell and class. ML I	6.2	0.5
I-cell and variant ML I	9.6	1.2
I-cell and adult β-gal⁻/neur⁻	3.5	0.6
I-cell and infantile β-gal⁻/neur⁻	5.8	0.2
Class. ML I and variant ML I	1.6	1.2
Adult β-gal⁻/neur⁻ and infant. β-gal⁻/neur⁻	0.8	1.0
Class. ML I and adult β-gal⁻/neur⁻	9.4	3.7
Class. ML I and infant. β-gal⁻/neur⁻	5.0	3.0
Variant ML I and adult β-gal⁻/neur⁻	7.0	4.0
Variant ML I and infant. β-gal⁻/neur⁻	6.8	4.9

Values are the means of three to six independent experiments. Hybridization was carried out with polyethylene glycol as before[15] adapted for human fibroblasts in monolayer. 10^6 cells of both cell strains were mixed 4 days before fusion and cultivated in Ham's F10 medium with 10% fetal calf serum. The medium was changed after 3 days and 1 day later cells were rinsed twice with medium without serum, and after removal of the medium, hybridization was carried out as follows: 1 ml of 42% polyethylene glycol (PEG) molecular weight 1,000 (Koch-Light) in Ham's F10 with 15% DMSO was added. The mixture was rocked for 2 min, 1 ml 25% PEG in Ham's F10 was added, the mixture was rocked again and 8 ml Ham's F10 was added twice. After rocking, the medium was removed, the cells rinsed with Ham's F10 and then Ham's F10 with 10% fetal calf serum was added. After 4 days of cultivation in the same medium, the heterokaryon population was collected and analysed for neuraminidase activity using 4-methylumbelliferyl as substrate. Microscopy of stained preparations after cell fusion revealed that 70–90% of the cells contained more than one nucleus, and autoradiography after incorporation of ³H-thymidine showed that nearly all multinucleate cells were heterokaryons.

neuraminidase activity was investigated further by labelling the mutant fibroblasts with fluorescent polystyrene beads, followed by co-cultivation for 3 days, separation of the two cell populations by two-colour flow sorting (FACS II) according to Jongkind et al.[16] and assay of neuraminidase. Table 3 shows a marked increase in neuraminidase activity in the combined β-gal⁻/neur⁻ fibroblasts whereas the ML I cells remain deficient. We could find no neuraminidase activity in the culture medium above the mutant cells and the labelling did not affect the enzyme activity. These experiments suggest the transfer of an unknown factor from ML I cells to fibroblasts with a combined β-gal⁻/neur⁻ deficiency, a factor which can increase the neuraminidase activity in the latter cells four- to sevenfold. Normal human fibroblasts also secrete this 'correction factor'. We found no evidence of an activator that could act in vitro, for mixing of homogenates of the two kinds of cells did not affect enzyme activity. The correction observed after hybridization (Table 2) and after co-cultivation (Table 3) may represent a normalization of the post-translational

Table 3 Co-cultivation of different neuraminidase-deficient cell strains and enzyme assays after two-colour flow sorting (FACS II)

	Neuraminidase activity ($\times 10^{-9}$ mol per h per mg protein)	
Cell type	Before co-cultivation	After 3 d co-cultivation
Classical ML I	0.7	0.7
Infantile β-gal⁻/neur⁻	0.8	5.3
Mixed cell population	0.7	2.9

Red polystyrene beads were added to the culture medium above classical ML I cells, left for 2 days, and cells were collected by trypsinization, rinsed and centrifuged (1,000 r.p.m. for 5–10 min). The same was done with green beads for β-gal⁻/neur⁻ fibroblasts. About 2 $\times 10^6$ cells of each labelled type were seeded and co-cultivated in confluency for 3 days. The two labelled cell populations were then separated and collected with a FACS II cell sorter according to Jongkind et al.[16] and neuraminidase activity was measured as described in Table 1. The values given are the mean of three independent experiments which gave very similar values.

processing of neuraminidase and β-galactosidase. It remains to be seen how neuraminidase is related to these processes, for neuraminidase deficiency can also occur without β-galactosidase deficiency. N-acetylneuraminic acid is, however, a common component of glycoproteins, certain glycosaminoglycans and gangliosides[17,18], and different neuraminidases have a role in the degradation of these compounds[8,19]. A better understanding of the nature of the neuraminidase deficiency in the various mutant cells might resolve the interrelationship with β-galactosidase deficiency. Further characterization of the correction factor is in progress; its heat lability, affinity for concanavalin A and the fact that I-cells cannot provide it (co-cultivation studies in Table 2) suggest that it is a glycoprotein.

1. Cantz, M., Gehler, J. & Spranger, J. *Biochem. biophys. Res. Commun.* **74**, 732–738 (1977).
2. Spranger, J., Gehler, J. & Cantz, M. *Am. J. med. Genet.* **1**, 21–29 (1977).
3. Durand, P. *et al. Helv. paediat. Acta* **32**, 391–400 (1977).
4. Lowden, J. A. & O'Brien, J. S. *Am. J. hum. Genet.* **31**, 1–18 (1979).
5. Thomas, G. H. *et al. Biochem. biophys. Res. Commun.* **71**, 188–195 (1976).
6. Strecker, G., Michalski, J. C., Montreuil, J. & Farriaux, J. P. *Biomedicine*, Paris **25**, 210–238 (1976).
7. Hasilik, A., Rome, L. H. & Neufeld, E. F. *Fedn. Proc.* **38**, 467 (1979).
8. Wenger, D. A., Tarby, T. J. & Wharton, C. *Biochem. biophys. Res. Commun.* **82**, 589–595 (1978).
9. Okada, S. *et al. Eur. J. Pediat.* **130**, 239–249 (1979).
10. Loonen, M. C. B., Lugt, van der, L. & Franke, C. L. *Lancet* ii, 785 (1974).
11. Andria, G., Del Guidice, E. & Reuser, A. J. J. *Clin. Genet.* **14**, 16–23 (1978).
12. Galjaard, H. *et al. Nature* **257**, 60–62 (1975).
13. Reuser, A. J. J. *et al. Hum. Genet.* **46**, 11–19 (1979).
14. Hales, A. *Somat. Cell Genet.* **3**, 227–230 (1977).
15. d'Azzo, A., Halley, D. J. J., Hoogeveen, A. & Galjaard, H. *Am. J. hum. Genet.* (in the press).
16. Jongkind, J. F., Verkerk, A. & Tanke, H. *Expl Cell Res.* **120**, 444–448 (1979).
17. Rosenberg, A. & Schengrund, C. L. *Biological Roles of Sialic Acid* (Plenum, New York, 1976).
18. Ledeen, R. W. *J. supramolec. Struct.* **8**, 1–17 (1978).
19. Cantz, M. & Messer, H. *Eur. J. Biochem.* **97**, 113–118 (1979).
20. Warner, T. G. & O'Brien, J. S. *Biochemistry* **18**, 2783–2787 (1979).
21. Warren, L. *J. biol. Chem.* **234**, 1971–1975 (1959).

Rapid response to selection for increased esterase activity on small populations of an apomictic clone of *Myzus persicae*

Steve Bunting & H. F. Van Emden

Department of Agriculture and Horticulture, University of Reading, Reading, Berkshire RG6 2AH, UK

It is generally thought that apomictic asexual reproduction produces offspring identical to the parent. In this paper we report changes that occur within a generation by selection on less than 25 offspring of an atypical strain of the aphid *Myzus persicae* starting from a single parthenogenetic mother. These changes consist of variations in the amount of a particular esterase (E_4). The amount of this enzyme has already been shown to be correlated with levels of resistance to insecticides in different strains of this aphid[1], and it has also been shown that E_4 binds and hydrolyses the activated form of the insecticide parathion[2]. Recombination between homologous chromosomes has been eliminated as the source of variation and it appears that gene amplification might be one explanation of this phenomenon. It is conceivable that this phenomenon is associated with rapid evolutionary events such as the evolution of resistance to insecticides.

Heritable changes within a clone were first noticed when we 'pressurized' a clone of *M. persicae* (Sulzer) with organophosphate insecticide, and the surviving individuals showed increased esterase activity. When examined for

Table 1 Total esterase activity of selected aphids and the mean activities of their offspring

Generation no.	Low esterase		High esterase	
	Parental activity	Mean offspring activity	Parental activity	Mean offspring activity
1	0.34 →	0.47 ± 0.04 (11)	0.34 →	0.47 ± 0.04 (11)
2	0.33 →	0.44 ± 0.9 (6)	0.70 →	0.54 ± 0.12 (9)
3	0.27 →	0.26 ± 0.03 (8)	1.37 →	1.32 ± 0.11 (12)
4	0.16 →	0.34 ± 0.05 (10)	2.06 →	1.58 ± 0.11 (12)
5	0.21 →	0.46 ± 0.07 (13)	1.81 →	1.76 ± 0.17 (11)
6	0.27 →	0.41 ± 0.08 (11)	2.54 →	1.78 ± 0.12 (12)
7	0.17 →	0.61 ± 0.13 (9)	2.46 →	1.94 ± 0.10 (9)
8	0.38 →	0.35 ± 0.05 (7)	2.30 →	2.21 ± 0.11 (12)
9	0.21 →	0.51 ± 0.04 (10)	3.14 →	2.42 ± 0.10 (25)
10			2.84 →	2.44 ± 0.23 (15)
11			4.93 →	2.77 ± 0.18 (14)
12			3.33 →	4.26 ± 0.22 (15)
13			5.75 →	4.28 ± 0.16 (17)
14			5.32 →	4.21 ± 0.25 (14)

Recloned after 8 generations of selection

$$2.21 \pm 0.11 \ (12) \xrightarrow[\text{7 generations}]{\text{No selection for}} 2.56 \pm 0.42 \ (10)$$

No. of aphids selected on in parentheses (n). Units are umol naphth-1-ol per h per mg aphid. Means given are s.e.m.
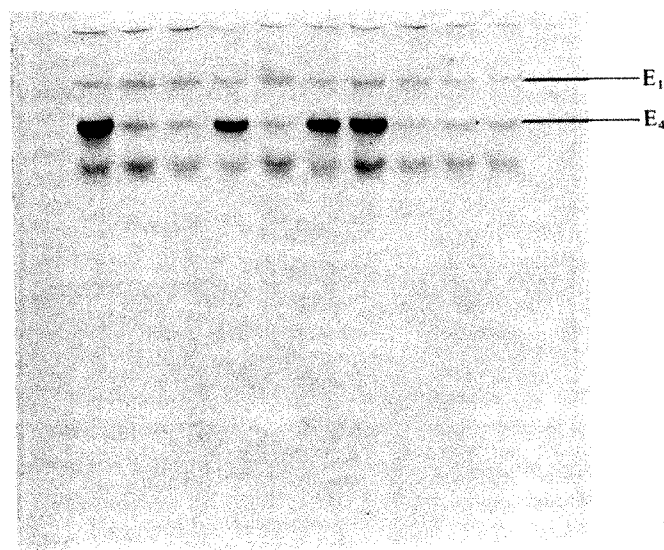
Fig. 1 Electrophoretogram of individual aphids in a culture started from a single mother of the varied clone, G_2, to show variations in E_4 activity. These variations do not occur in all clones of this species. G_2 originates from the glasshouse of the University of Reading Department of Agriculture and Horticulture. Technique was as in ref. 2, except that a continuous borate buffer system was used, and the gel was run at 80 V for 4 h and stained for 20 min.
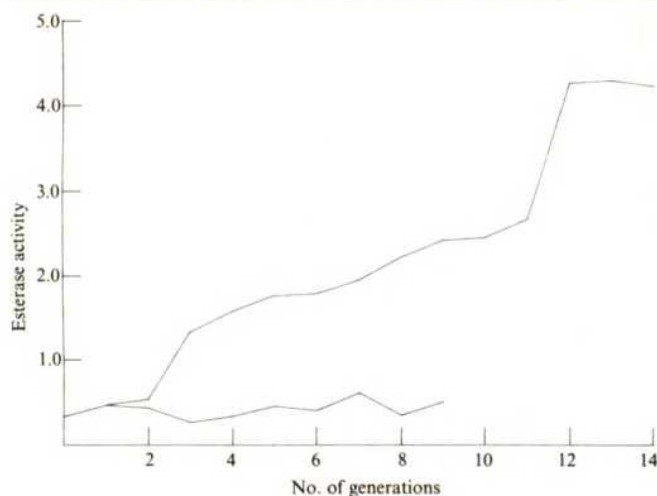
Fig. 2 Graph showing response to selection for increased and decreased esterase activity, starting from a single parthenogenetic mother. Units in μmol naphth-1-ol per h per mg aphid.

esterases by polyacrylamide gel electrophoresis[2], the survivors showed an increase in E_4, the other esterases remaining constant. This could be explained by a simple inducible system, but the problem was that the offspring had high esterase as well, despite being in an insecticide-free environment. This apparently lamarckian phenomenon is explained by the fact that a single mother is able to produce offspring varied with respect to E_4 activity (Fig. 1). This latter point was found independently by Blackman[3]. Here we are looking in detail at the results of selection on these variations. Insecticide was not used for the selection, selection being by choice, since smaller numbers can be used this way and since the interaction of organophosphate insecticides with E_4 would complicate the results. Also one cannot select for low esterase activity with insecticide. Changes in E_4 activity were quantified by total esterase assay[1]. As it is only E_4 that changes, this was a good enough index for following changes in activity at this locus.

The system of selection was as follows: A single aphid mother was taken and cultured to produce about 20 offspring. The mother was then removed and assayed for esterase activity and then, when adult, the F_1 generation were individually recloned to shed their offspring and were then individually assayed. The F_1 clones with the largest and smallest parental activities were selected by choice, and the rest were destroyed in alcohol. Selection for increased activity was continued for 14 generations. Selection for low esterase was continued for 9 generations. The kinetics of change are shown in Fig. 2 and Table 1.

The increase in E_4 activity over 14 generations was approximately 30 times that of the original mother. When left unselected for seven generations the mean activity of a high esterase clone had not changed noticeably but the variance in esterase activity had increased (Table 1), there being some very low and high esterase individuals in the culture. This clone exhibits genetic instability in terms of E_4 activity and resistance can be lost completely, but these reversions have not been studied in detail. Reversions to susceptibility have been reported in some instances[4] and it seems to be the very resistant clones with a chromosomal translocation that behave in this way[5]. The clone worked on here also possesses this translocation.

What is the basis of these changes? It has long been argued that crossing-over and segregation may occur in this species[6]. However, this dramatic response to selection occurs in a clone

which is heterozygous[7] at the E_1 locus (Fig. 3). This heterozygote has shown total stability and no homozygotes have been produced, in spite of changes at the E_4 locus. It therefore seems that the source of variation does not lie with recombination between homologous chromosomes, especially since E_1 and E_4 appear to be linked (R. L. Blackman, personal communication).

Selective gene amplification, that is the formation of multiple copies of the same gene, is one possible explanation for this variation. Selective gene amplification can occur at a very high frequency compared to normal mutations. It can be as frequent as 3×10^{-2} (R. P. Anderson, personal communication). The changes reported here can be as frequent as 3×10^{-1} (data not shown). However, it is possible that alterations in the expression of these genes are involved as well as the generation of extra gene copies.
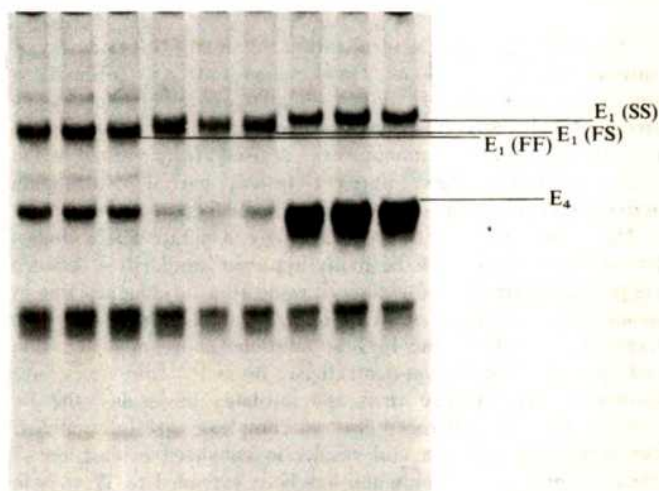
Fig. 3 Electrophoretogram showing heterozygosity of varied clone, G_2. Samples, which are in triplicate, are of clones DDTR (fast E_1), G_2 (heterozygote) and FR6 (slow E_1). For improved resolution and separation, a 0.1 M Tris-borate-EDTA buffer was used and homogenates were run at 40 μg aphid per μl sucrose solution. Gels were run at 110 V and stained for 60 min.

There is evidence for selective gene amplification in *M. persicae*[5], although the evidence suggests doublings of E_4 activity in different resistant clones, negating the possibility of a heterozygote between two clonal types. However, the circumstantial evidence for amplification is good. Genetic instability of increased enzyme levels is virtually diagnostic for gene amplification[8-11]; a translocation is associated with amplification in yeasts[8]; a stepwise response to selection for increased enzyme levels is also found in cases of amplification[10,11]; and all systems appear to be concerned with resistance or rapid evolutionary change by elevating enzyme levels.

Although the exact solution to this problem remains unknown, it is possible that the phenomenon reported here is not unique to *M. persicae* and has escaped detection in other systems because most work on selection is carried out on sexually reproducing organisms.

1. Devonshire, A. L. *Proc. 8th Br. Insecticide Fungicide Conf.* **1**, 67–73 (1975).
2. Devonshire, A. L. *Biochem. J.* **167**, 675–683 (1977).
3. Blackman, R. L., Takada, H. & Kawakami, K. *Nature* **271**, 450–452 (1978).
4. Beranek, A. P. *Entomologia exp. appl.* **17**, 381–390 (1974).
5. Devonshire, A. L. & Sawicki, R. M. *Nature* **280**, 140–141 (1979).
6. Cognetti, G. *Experientia* **17**, 168–169 (1961).
7. Blackman, R. L. *Biol. J. Linnean Soc.* **11**, 259–277 (1979).
8. Hansche, P. E., Beres, V. & Lange, P. *Genetics* **88**, 673–687 (1978).
9. Anderson, R. P. & Roth, J. R. *A. Rev. Microbiol.* **31**, 473–506 (1977).
10. Alt, F. W., Kellems, R. E., Bertino, J. R. & Schimke, R. T. *J. biol. Chem.* **253**, 1357–1370 (1978).
11. Normark, S., Edlund, T., Grundstrom, S. & Wolf-Watz, H. *J. Bact.* **132**, 912–922 (1977).

An explanation for enhanced virus plaque formation in chick embryo cells

Srisakul C. Kliks & Scott B. Halstead

Department of Tropical Medicine and Medical Microbiology, John A. Burns School of Medicine, University of Hawaii, Honolulu, Hawaii 96816

While studying virus neutralization of many togaviruses by antisera raised in chickens, Hawkes and Lafferty[1,2] observed a significant increase of plaque counts above controls when virus–antibody mixtures were assayed on chick embryo (CE) cell monolayers, or monolayers derived from other avian embryos. Among those antisera tested, partial neutralizing activity was observed at low dilutions and plaque enhancement at high dilutions above the neutralizing end point. These studies interested us because of the many apparent similarities between plaque enhancement and enhanced replication of dengue virus in mononuclear phagocytes. The latter has been shown to be mediated by anti-dengue IgG at dilutions above neutralization end points. When non-neutralized immune complexes are formed between dengue virus and antibody molecules, the Fc termini attach to cell receptors and complexes are internalized; this facilitates infection and results in enhanced production of virus[3,4]. The same phenomenon has been extended to West Nile (WN) virus demonstrated on mouse macrophage cell lines by Peiris and Porterfield[5]. Here, we have examined the infection of CE cells with virus–antibody complexes of another flavivirus, Murray Valley encephalitis (MVE) virus. Our results show that a similar mechanism operates in the antibody-mediated viral plaque enhancement of MVE virus on CE cells.

MVE virus strains 96961/53 smb-7 and BH 3479/77 smb-1 were used to propagate stock virus in suckling mouse brains. At 4 °C, infected mouse brains were homogenized to make a 10% (w/v) suspension in phosphate-buffered saline, pH 7.4, containing 20% heat-inactivated fetal calf serum and centrifuged at 12,000 g. The supernatant fluid containing virus stock used in all experiments was stored at −70 °C. Chickens were immunized with two injections of MVE virus at 3-week intervals and sera were collected at 1 and 3 weeks post-immunization. Three pools of MVE antisera were heat inactivated at 56 °C and tested for neutralizing and enhancing activities in optimal conditions for enhancement as described by Hawkes[1]. Our results confirmed those of Hawkes[1] and Hawkes and Lafferty[2]; neutralization was observed at low dilutions of antisera, followed by a two- to four-fold increase in plaque count above control values at higher dilutions. When the same virus–antibody mixtures were assayed on LLC-MK2, continuous rhesus monkey kidney cell monolayers, a greater efficiency of neutralization was observed, and there was no evidence of plaque enhancement. The same result was obtained with γ-globulins extracted from these pools of antisera as shown in Fig. 1. Viral plaque enhancement in CE cell monolayers was dependent on the Fc terminus of antibody molecules. To demonstrate this, Fc portions were cleaved from anti-MVE IgG by papain digestion[6] and the Fab fraction purified and examined for viral enhancement. The results (Fig. 2) indicate that the Fab fraction was no longer able to mediate plaque enhancement, but retained neutralizing activity.

Viral plaque enhancement was observed when avian antisera were used and virus–antibody mixtures assayed on avian embryonic cells. Mammalian antisera from rabbits and mice
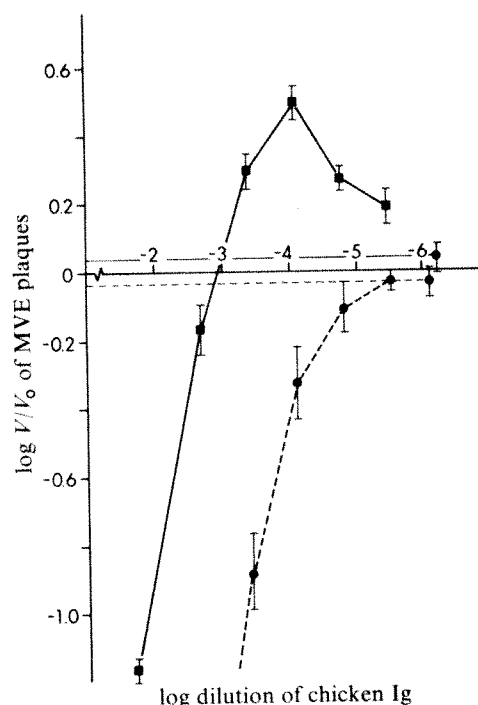
Fig. 1 Assay of mixtures of MVE–anti-MVE IgG (chicken) on CE and LLC-MK2 cell monolayers. Chicken anti-MVE γ globulin was serially diluted in Hanks' balanced salt solution containing 8% heat-inactivated normal rabbit serum, 200 µg ml^{-1} penicillin and 200 µg ml^{-1} streptomycin. Each immunoglobulin dilution was mixed with an equal volume of MVE suspension containing ~250 plaque-forming units per ml, then incubated at 0 °C for 1.5–2 h. Virus–antibody mixtures, virus–normal immunoglobulin and virus–diluent controls were inoculated onto CE and LLC-MK2 monolayers in triplicate. After 90 min at 37 °C, monolayers were covered with an agar overlay media and incubated at 37 °C for 3–4 days. V and V_0 represent numbers of plaques from virus–immunoglobulin and virus–diluent mixtures, respectively. V/V_0 values are expressed as $\log_{10}$ mean ± s.e.m. from three experiments. Symbols ■—■ and ●---● represent V/V_0 values from MVE–antibody mixtures assayed on CE and LLC-MK2 monolayers, respectively. Values from normal chicken immunoglobulin controls assayed on CE cells are shown as ——— and from LLC-MK2 assay as -----.

when tested for their antiviral activities on CE cell monolayers demonstrated only neutralization[1,2]. The dependence of viral plaque enhancement on a class homology between the vertebrates used to raise antibodies and the donors of tissues for cell monolayers suggested a requirement for complementarity between the Fc molecule and its receptor. A similar observation was noted by Ewald et al.[7], who, using erythrocyte–antibody (EA) complexes[8], found that sheep red blood cells (SRBC), coated with avian immunoglobulin, rosetted Fc receptor-bearing chicken lymphocytes, but SRBC coated with mammalian immunoglobulin did not; reptilian immunoglobulin was partially bound to chicken Fc receptors. These reports demonstrated complementary Fc and receptor structures within closely related phylogenic classes. To study this phenomenon in antibody-mediated viral plaque enhancement, normal chicken γ globulins, which had been aggregated by the method of Dickler[9], were used to treat CE monolayers at a concentration of 12.5 µg ml^{-1} for 1 h at 37 °C before use of monolayers for MVE plaque assays. This treatment ablated plaque enhancement, but did not affect the formation of virus plaques or the neutralization ability of antisera. When aggregated mammalian γ globulins[9] were

incubated with CE cells in the same manner, viral enhancement was unaffected.

We further demonstrated that plaque enhancement was associated with the presence of Fc receptors but was absent when Fc-receptor-bearing cells were removed. Antisera to SRBC raised in chickens and rabbits were used to sensitize SRBC. We tested chicken peripheral blood leukocytes (PBL), human PBL, lightly trypsinized CE and LLC-MK2 cells for EA rosette formation. Table 1 demonstrates the presence of Fc-bearing cells in chicken PBL, human PBL and CE, but their absence in LLC-MK2 cells. Again, the requirement for class homology between target cells and sensitizing antibodies for successful rosette formation was observed, confirming the observation of Ewald *et al.*[7]. Rosetted cells also exhibited immune phagocytosis. When CE-sensitized SRBC mixtures were incubated at 37 °C for 90 min instead of 4 °C, nearly all of the 1.7–2.0% cells exhibiting rosetting also phagocytosed sensitized SRBC. Normal SRBC and SRBC sensitized with rabbit antiserum were not phagocytosed.

Antibody-enhanced plaque formation, but not control virus plaque formation, was completely ablated by removal of CE

Table 1 EA rosette formation on chicken PBL, human PBL and trypsinized CE and LLC-MK2 cell suspensions

Origin of anti-SRBC	Chicken PBL	Human PBL	CE (suspension)	MK$_2$ (suspension)
Chicken	8.02 ± 0.40	0.89 ± 0.16	2.09 ± 0.13	0
Rabbit	0.04 ± 0.03	17.27 ± 2.12	0	0

Peripheral blood mononuclear leukocytes were isolated from three human donors using methods described by Halstead and O'Rourke[3] and from three chickens using the method of Lee[10]. Three batches of CE and LLC-MK2 monolayers were lightly trypsinized to remove cells from the glass surface. Cells were suspended in RPMI 1640 with 2% fetal calf serum at a concentration of 5×10^6 cells ml^{-1}; 0.2 ml of each cell type was mixed with an equal volume of a 0.5% suspension of normal SRBC or SRBC previously sensitized by chicken or rabbit anti-SRBC according to Ewald *et al.*[7]. Cell mixtures were incubated at 4 °C for 15 min, then centrifuged at 200 g for 10 min, gently resuspended and cells examined under the microscope. A rosette was defined as a cell surrounded by three or more SRBC. At least 200 cells were examined for rosettes. Means ± s.d. from three experiments are shown.

Fig. 2 Assay of MVE virus mixed with chicken anti-MVE IgG and anti-MVE Fab on CE and LLC-MK2 cell monolayers. Anti-MVE IgG at a concentration of 35 mg ml^{-1} was treated with mercuripapain at a ratio of 1:100 (ref. 6). Digestion was allowed to proceed at 37 °C for 16 h. The hydrolysates were dialysed against several changes of distilled water at 4 °C, followed by further dialysis against 1.5 M NaCl and 0.01 M phosphate buffer, pH 7.0, to promote precipitation of the Fc fraction. Fab in the supernatant fraction was purified by elution through an affinity chromatography column containing Sepharose–anti-chicken Fc to remove traces of Fc and IgG. The Fab fraction was tested for purity by the Ouchterlony technique using rabbit anti-chicken Fab, rabbit anti-chicken IgG and rabbit anti-chicken Fc. Using anti-MVE IgG and anti-MVE Fab fractions, virus–antibody mixtures were made as described in Fig. 1. Mixtures were then assayed for plaques on CE and LLC-MK2 monolayers. Symbols ■—■ and ■---■ represent V/V_0 values from virus–IgG mixtures assayed on CE and LLC-MK2 monolayers, respectively; ●—● and ●---● represent V/V_0 values from virus–Fab mixtures assayed on CE and LLC-MK2 monolayers, respectively. Each point is a log$_{10}$ mean ± s.e.m. from three experiments.

cells exhibiting EA rosetting from CE monolayers. Fc-receptor-bearing cells were removed from trypsinized chick embryonic tissue by centrifugation of EA rosettes at 400 g for 30 min through a Ficoll–Hypaque gradient with a specific gravity of 1.078. The cells at the interface were collected, washed and plated at the usual concentration for CE monolayer formation. Compared with normals, these monolayers demonstrated a 97.5% reduction in EA-rosetted cells and a 98.5% reduction of cells capable of immune phagocytosis. The assay of MVE–antibody mixtures on these depleted monolayers resulted in neutralization only; plaque enhancement was not seen.

We conclude that normal CE monolayers are composed of approximately 2% functionally active mononuclear phagocytes. These mononuclear phagocytes engulf immune complexes and are infected. The same complexes are excluded from another cell population which does not possess Fc receptors and is infected by MVE virus without the requirement for antibody. The admixture of two distinct MVE-permissive cells is responsible for the described under-neutralization and the antibody-mediated plaque enhancement phenomenon.

As shown by Hawkes and Lafferty[2], immune enhancement of viral plaque formation occurs in several virus families using a broad range of embryo-derived primary tissue cultures. The demonstration of these phenomena in CE monolayers, a cell system widely used to study neutralization and the phenomenon of non-neutralizable virus fractions, requires critical review.

1. Hawkes, R. A. *Aust. J. exp. Biol. med. Sci.* **42,** 465–482 (1964).
2. Hawkes, R. A. & Lafferty, K. J. *Virology* **33,** 250–261 (1967).
3. Halstead, S. B. & O'Rourke, E. J. *J. exp. Med.* **146,** 201–217 (1977).
4. Halstead, S. B., O'Rourke, E. J. & Allison, A. C. *J. exp. Med.* **146,** 218–229 (1977).
5. Peiris, J. S. M. & Porterfield, J. S. *Nature* **282,** 509–511 (1979).
6. Porter, R. R. *Biochem. J.* **73,** 119–126 (1959).
7. Ewald, S., Freedman, L. & Sanders, B. G. *Cell. Immun.* **31,** 847–854 (1976).
8. Ewald, S., Freedman, L. & Sanders, B. G. *Cell. Immun.* **23,** 158–170 (1976).
9. Dickler, H. B. *J. exp. Med.* **140,** 508–521 (1974).
10. Lee, L. F. *Avian Dis.* **18,** 602–609 (1974).

Is actin in eye lens a possible factor in visual accommodation?

M. A. Kibbelaar*, F. C. S. Ramaekers*,
P. J. Ringens*, A. M. E. Selten-Versteegen*,
L. G. Poels†, P. H. K. Jap†, A. L. van Rossum‡,
T. E. W. Feltkamp‡ & H. Bloemendal*§

*Departments of Biochemistry and †Cytology and Histology,
University of Nijmegen, Geert Grooteplein Noord 21, Nijmegen,
The Netherlands
‡Department of Autoimmune Diseases of the Central Laboratory of
the Netherlands Red Cross Blood Transfusion Service, Amsterdam,
The Netherlands

Actin has been purified from various non-muscle cells and characterized by its molecular weight and ability to polymerize into filaments. Although the occurrence of this protein has been postulated in the mammalian eye lens after observation of actin-like filaments in the electron microscope[1,2], definite (bio)chemical proof has been provided only recently[3]. Amino acid analysis, peptide mapping and affinity chromatography revealed the identity of lens actin with the corresponding protein in other tissues. As the filaments could be obtained by co-isolation with highly purified lens plasma membranes, we were interested to know how the actin-containing structures were located *in situ*. In the experimental approach reported here, the indirect immunofluorescence technique (IFT)[4] was applied to unfixed cryostat sections of lens tissue. The distribution of actin in calf, rat and pigeon lens is described, and evidence from this for the role of actin in visual accommodation discussed.

Sections, 4 μm thick, were obtained by cutting calf lenses in three mutually perpendicular directions, and incubated with specific antisera. A rabbit antiserum was raised against purified actin isolated from calf lens[3]. Antibodies against actin are also known to be present in the serum of patients suffering from chronic active hepatitis[5,6]. Therefore, in addition, sera from 12 patients with clinical signs of chronic active hepatitis were selected for study. All 12 sera reacted positively with smooth muscle when tested with the IFT on rat stomach.

The sections were incubated with each of these antisera. Three projections of specific immunofluorescence could then be observed, mainly in the cortical region: (1) hexagons, the shorter sides of which showed the heaviest fluorescence (Fig. 1*A*); (2) equidistant and almost parallel lines of constant fluorescence (12 μm) (Fig. 1*B*); (3) parallel lines at constant distance (4 μm) but of interrupted fluorescence (Fig. 1*C*).

For an interpretation of these patterns in terms of single fibre cell structure, the model in Fig. 2*A* is proposed. After incubation with the fluorescent antiserum the hexagonal pattern (compare Fig. 1*A*) will arise from sections parallel to plane *a* (more heavily stained at the shorter sides). Conversely, strongly fluorescent lines (compare Fig. 1*B*) will occur in sections parallel to plane *b*. These are the lines of intersection with the short planes of the hexahedral fibres. Finally, frequently non-fluorescent lines (compare Fig. 1*C*) arise from the sections cut parallel to plane *c*. These lines run at relatively short distances from one another. Immunofluorescence here is mainly observed in the areas of intersection with the short planes of the hexahedral fibres. Figure 2*B* shows schematically the expected lines of fluorescence. From Fig. 1*A–C* it can be seen that actin is concentrated in specialized regions of the cells. This typical actin localization is also visualized by immuno-electron microscopy (Fig. 3). Immunoperoxidase staining reveals that actin is concentrated close to the plasma membrane and particularly at the shorter sides of the hexagon.

Figure 3*B* suggests that microfilaments are in close contact with the plasma membranes. A similar observation has been reported by Benedetti *et al.* in isolated plasma membranes from lens fibre cells[2].

Several functions have been ascribed to lenticular actin, including accommodation[7], the process which enables the lens to change its shape so as to ensure proper diffraction of the incidental light beam. If actin has such a function, two possibilities can be envisaged. First, actin present as cytoskeletal element may enable the lens to restore its shape on accommodation. This would mean that accommodation is a passive process as far as the lens body *per se* is concerned. Second, lenticular actin may be actively involved in the process of accommodation, rendering the lens a primitive contractile organ.

Investigations on visual accommodation had shown that both extra- and intra-capsular processes are involved in lens accommodation[8]. Kleifeld *et al.*[9-11] not only confirmed these
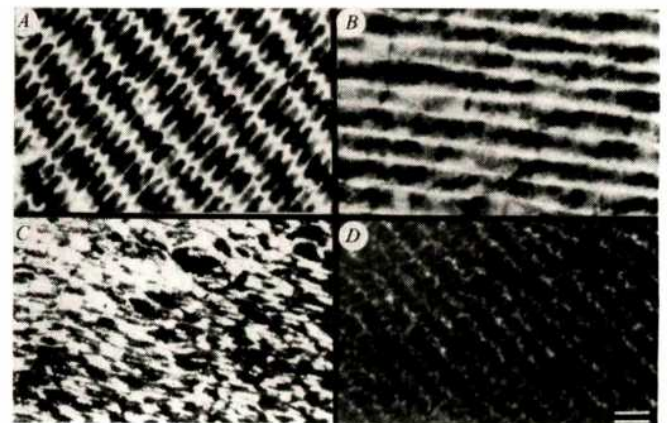
Fig. 1   Immunofluorescence of calf lens sections incubated with anti-actin serum. Unfixed cryostat sections of calf lenses (3–6-month-old animals) were used. Immediately after removal the lenses were frozen in liquid nitrogen and kept in these conditions until use. They were sectioned in three mutually perpendicular directions. The indirect immunofluorescence technique (IFT) was carried out with (1) horse anti-human immunoglobulin conjugated to fluorescein isothiocyanate (FITC) (Central Laboratory of the Netherlands Red Cross Blood Transfusion Service lot no. PH 17-4-F8; protein concentration 14.5 mg ml^{-1}, Mol F/P ratio 2.5, final dilution 1:80); (2) horse anti-rabbit immunoglobulin conjugated to FITC-labelled polyspecific anti-human immunoglobulin or anti-rabbit immunoglobulin. The sections were studied with a Leitz microscope with incident light and dichroic mirrors. Pure calf lens actin was isolated from the cortical lens fibres as described by Kibbelaar *et al.*[3]. Antiserum against this preparation was produced in a rabbit by intramuscular injection of the antigen emulsified in Freund's complete adjuvant. The animal received two booster injections with the same amount of antigen. The following antisera were also used. (1) Smooth muscle antibodies (SMA) present in blood serum of patients with chronic active hepatitis[6]. Sera from 12 patients were selected. One of the sera was shown to react specifically with muscle actin[5]. (2) Sera from a healthy blood donor and from patients with myasthenia gravis that contain antibodies only against sarcoplasmic reticulum of skeletal muscle but not against smooth muscle actin, were used as controls. *A*, Pattern obtained from a section parallel to the hexagonal structure of the fibre cell (compare Fig. 2*Aa*). The shorter side of the hexagon clearly shows heavier staining. In most instances also a small part of the longer sides of the structure shows immunofluorescence. *B*, A continuous heavy immunofluorescence from a section cutting the fibre cell as in Fig. 2*Ab*. The equidistances of the fluorescent lines are larger than those in *C*. *C*, Lines obtained from sections of the fibre cell parallel to the plane in Fig. 2*Ac*. The discontinuous immunofluorescence indicates that only part of the fibre cell is accessible to the antibodies. *D*, Pattern obtained after absorption of antiser with actin. No significant immunofluorescence is observed. Antiserum (1 ml) was diluted 10-fold in phosphate-buffered saline (PBS) at *p*H 7.4 and subsequently incubated with purified actin (1 mg ml^{-1}). To another 1 ml of the same antiserum 100 sections of rat smooth muscle were added. A blank incubation without tissue or actin was run simultaneously, as well as a control to which lens crystallins were added so as to discriminate between these major lens proteins and the specific actin antigen. The tubes were shaken at room temperature for 0.5 h and then incubated at 37 °C for a further 0.5 h. They were then kept overnight at 4 °C and centrifuged at 25,000*g* for 30 min. The supernatant was used for the IFT. All controls showed normal fluorescence. Scale bar, 20 μm.
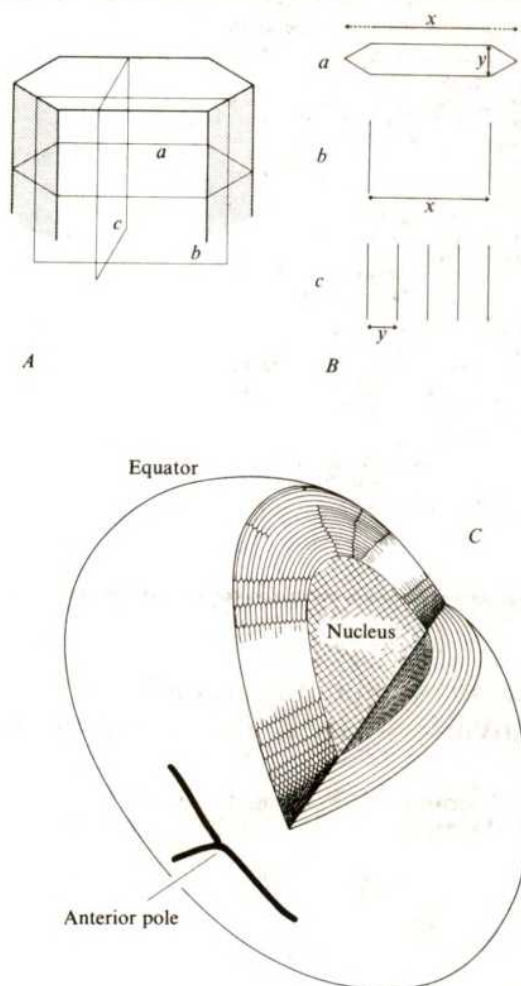
Fig. 2   A, Schematic drawing of a lens fibre with planes in three mutual perpendicular directions. Sections parallel to plane a show the hexagonal form of the fibre cells; sections parallel to plane b display the lines of intersection of the plane with the short sides of the lens fibre, and sections obtained by cutting the fibre cell parallel to plane c also show lines of intersections with the fibre cell, but with a smaller distance between one another than those obtained in plane b. B, Schematic drawing of the three main projections to be expected by sectioning the fibre cell. The distances x and y are relative to each other and do not represent real dimensions. C, Inside view of the lens illustrating the fibre cell organization. The drawing is based on a model presented by Van Heyningen[18].
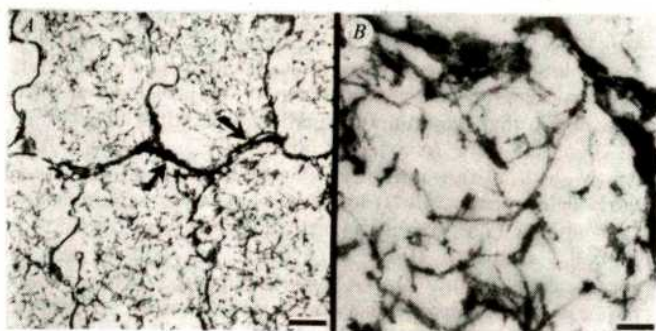
Fig. 3   Electron micrograph (immunoperoxidase staining) showing the hexagonal pattern of calf lens fibres (A). Note that the plasma membrane is covered with actin filaments (indicated by arrows, scale bar, 1 µm). These are shown at higher magnification in B (scale bar, 0.2 µm). The indirect immunoperoxidase staining for detection of actin was carried out as described by Poels et al.[19] using an antiserum directed against purified lenticular actin.

ideas, but also showed that in accommodation the intracapsular processes probably depend on active participation of the lens fibres. We wondered whether our present observations on structural features of actin in situ would fit these older theories. In three species (calf, rat and pigeon) which differ considerably in accommodative power and mechanism[12], striking differences in the immunofluorescence of actin were observed (Figs 4, 5).

The results of our study can be summarized as follows. In the calf, strong fluorescence occurs throughout the whole lens but is preferentially localized along the plasma membranes. In the rat, there is strong fluorescence, somewhat more intensive than in the calf, but less uniformly distributed. In the cortex, the hexagonal fluorescence pattern follows the plasma membranes (Fig. 4B). In the nucleus, however, the membrane regions appear dark whereas strong immunofluorescence fills the cytoplasm (Fig. 4C). In contrast to this latter observation, Mousa and Trevithick[13] were unable to detect actin in rat lens nucleus. This discrepancy can presumably be explained by the electrophoretic method used by the authors, who report that 17% of the nuclear lens protein could not be dissolved in their
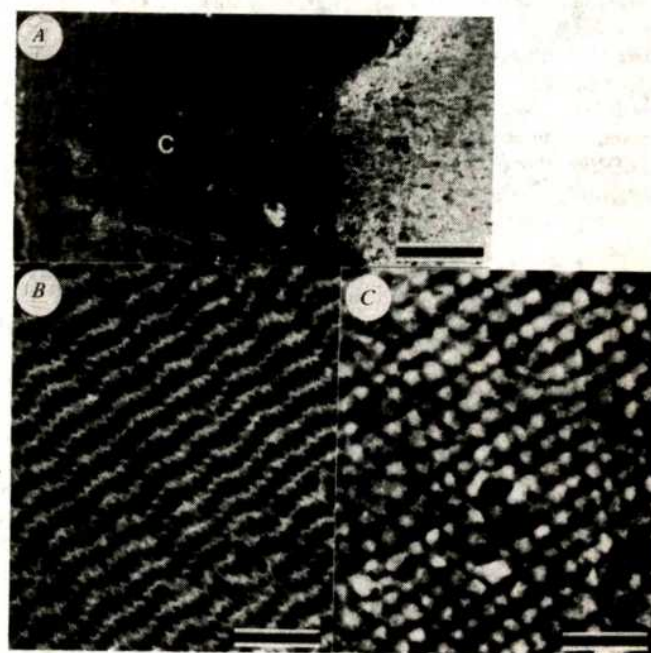
Fig. 4   Immunofluorescence of actin in rat lens sections. Sections were incubated with anti-actin serum as described in Fig. 1 legend. A, Low magnification of the rat lens showing strong fluorescence in the nucleus (N) and a weak staining in the cortical region (C) (scale bar, 100 µm). B, Cortical region showing a preferential membrane immunofluorescence (scale bar, 20 µm). C, Nuclear region showing strong cytoplasmic immunofluorescence (scale bar, 20 µm).

lysis buffer. In the pigeon, there is a lower concentration of actin than in calf and rat, with almost no fluorescence in the nucleus, and weak fluorescence mainly localized in the peripheral region of the lens and virtually restricted to the cellular membranes (Fig. 5). Furthermore, electron microscopic observations show that rat and calf lenses, in contrast to pigeon lens, are relatively abundant in filamentous structures such as microfilaments and microtubules (unpublished).

Rafferty and Goossens[14] hypothesized that cytoplasmic filaments in lens either structurally support its spherical shape or provide the contractile force involved in accommodation. Our data on calf and rat lens support the former assumption. The occurrence of actin filaments can indeed be correlated
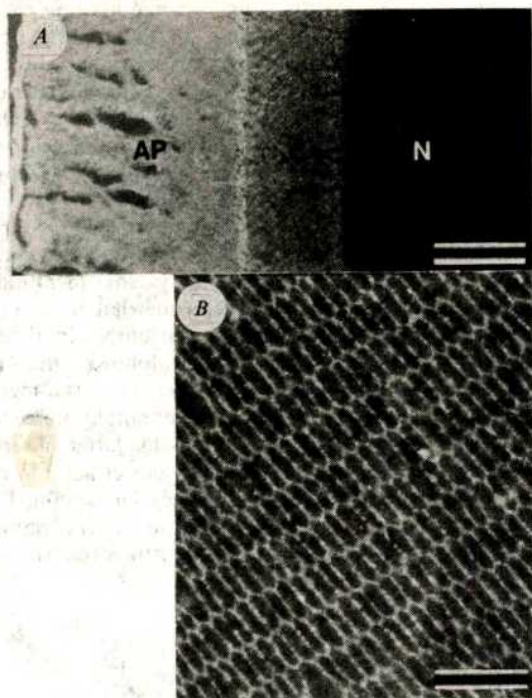
Fig. 5 Immunofluorescence of actin in pigeon lens sections. *A*, Low magnification of the pigeon lens showing moderate fluorescence in the cortical region (C) and an extremely weak fluorescence in the nucleus (N). AP, Annular pad (scale bar, 100 μm). *B*, Detail of the cortical region showing membrane immunofluorescence (scale bar, 20 μm).

1. Bloemendal, H., Zweers, A., Vermorken, F., Dunia, I. & Benedetti, E. L. *Cell Diff.* **1**, 91–106 (1972).
2. Benedetti, E. L. *et al. Biochim. biophys. Acta* **457**, 353–384 (1976).
3. Kibbelaar, M. A., Selten-Versteegen, A. M. E., Bloemendal, H., Dunia, I. & Benedetti, E. L. *Eur. J. Biochem.* **95**, 543–549 (1979).
4. Feltkamp, T. E. W. & van Rossum, A. L. *Clin. exp. Immun.* **3**, 1–16 (1968).
5. Lidman, K. *et al. Clin. exp. Immun.* **24**, 266–272 (1976).
6. Johnson, G. D., Holborrow, E. J. & Glynn, L. E. *Lancet* **ii**, 878–879 (1965).
7. Bloemendal, H. *Science* **197**, 127–138 (1977).
8. Gullstrand, A. in *Handbuch der Physiologischen Optik von v. Helmholtz* Vol. 1, 3 (Voss, Hamburg, 1911).
9. Kleifeld, O. *Documenta ophthal.* **10**, 132–173 (1965).
10. Kleifeld, O., Fuchs, R., Hockwin, O. & Arens, P. *Ber. Versamm. dt. Ophthal. Ges.* **58**, 220–231 (1953).
11. Kleifeld, O., Hockwin, O. & Arens, P. *Albrecht v. Graefes Archiv Ophthal.* **156**, 467–479 (1955).
12. Walls, G. L. *The Vertebrate Eye and its Adaptive Radiation* (Hafner, New York, 1963).
13. Mousa, G. Y. & Trevithick, J. R. *Expl Eye Res.* **29**, 71–81 (1979).
14. Rafferty, N. S. & Goossens, W. *Expl Eye Res.* **26**, 177–190 (1978).
15. Klethi, J. & Mandel, P. *Nature* **205**, 1114–1115 (1965).
16. Zapisek, W. F. & Papaconstantinou, J. *Biochim. biophys. Acta* **277**, 231–234 (1972).
17. Mandel, P. & Klethi, J. *Biochim. biophys. Acta* **28**, 199–200 (1958).
18. Van Heyningen, R. *Scient. Am.* **12**, 70–81 (1975).
19. Poels, L. G., Van Niekerk, C. C., Franken, M. A. M. & Van Elven, E. H. *Expl Parasit.* **42**, 182–193 (1977).

with lenticular rigidity. On the other hand, in species in which accommodation is achieved by considerable lens deformation (such as the pigeon), structured actin seems to be scarce. However, unstructured actin may escape detection by the immunofluorescence technique. It is possible that this form of actin is actively involved in accommodation. In this respect, data in the literature concerning lenticular ATP may also be relevant. It has been suggested that the energy (ATP) required for accommodation becomes available from a special form of metabolism (called 'labour metabolism'[8]), occurring in addition to the standard metabolism of the lens. About three times higher concentrations of ATP have been demonstrated in chick and pigeon lenses than in rat and cattle[15,16]. Moreover, in calf lens the amount of ATP differs in the various parts of the lens in that the ATP concentration in the cortex is six times higher than that in the nucleus[17].

It seems, therefore, that low accommodative power is paralleled by a low ATP content as well as by the presence of structured actin, especially along the plasma membranes. Lenses with high accommodative power (as in pigeon) reveal in their flexible part only weak and diffuse immunofluorescence, suggesting a rather random distribution of actin (see Fig. 5*A*, N). Such an arrangement would permit ATP-dependent polymerization (and depolymerization), providing the lens of some species with a primitive contractile system. On the other hand, in non-accommodating animals (for example, rat) the shape of the lens is maintained by structured actin which provides the rigidity of the organ. However, this suggested molecular basis of accommodation requires further experimental substantiation.

α-Actinin-containing branched microvilli isolated from an ascites adenocarcinoma

K. L. Carraway, J. W. Huggins, R. F. Cerra, D. R. Yeltman & C. A. Carothers Carraway

Department of Biochemistry, Oklahoma State University, Stillwater, Oklahoma 74078

Microvilli, slender projections approximately 0.1 μm in diameter which occur on the surfaces of many cell types[1], are bounded by plasma membrane except at the site of attachment to the cell body and contain microfilament bundle cores. The presence of both microfilaments and plasma membrane suggests the use of microvilli for investigations of membrane cytoskeleton interactions. Immunofluorescence studies with anti-α-actinin[2] have suggested that α-actinin is concentrated at the tips of intestinal brush border microvilli and might link actin microfilaments and the plasma membrane[3]. However, this idea was disputed by later immunofluorescence[4-7] and electrophoresis[7] studies. To investigate the components and organization of microvilli from a less highly differentiated cell type, we have used an ascites sub-line (MAT-Cl) of a rat mammary tumour, the 13762 mammary adenocarcinoma, whose microvilli are highly branched[8,9]. Because such unusual structures may provide an understanding of cell-surface assemblies important in determining cell morphology, we have developed a procedure for isolating the branched microvilli and have shown that they contain significant quantities of α-actinin.

Microvilli were removed from MAT-Cl cells (Fig. 1*a*) by gently shearing through a hypodermic needle, and observed by dark field microscopy (Fig. 1*b*). They were separated from cells and cellular debris by centrifugation on a self-forming Percoll gradient (Fig. 2). Microvilli are also shed spontaneously from MAT-Cl cells, but the 1–3 h incubation required for significant release also yields membrane fragments and vesicles. Shearing essentially eliminates those fractions, presumably by decreasing a time-dependent breakdown of the microvilli. Microvilli can be stabilized by inclusion of 20% fetal calf serum; bovine serum albumin is ineffective.

Scanning (Fig. 1*c*) and transmission (Fig. 1*d,e*) electron microscopy of isolated microvilli showed that virtually all of them were branched; the few unbranched structures were short and were presumably fragments resulting from breakage
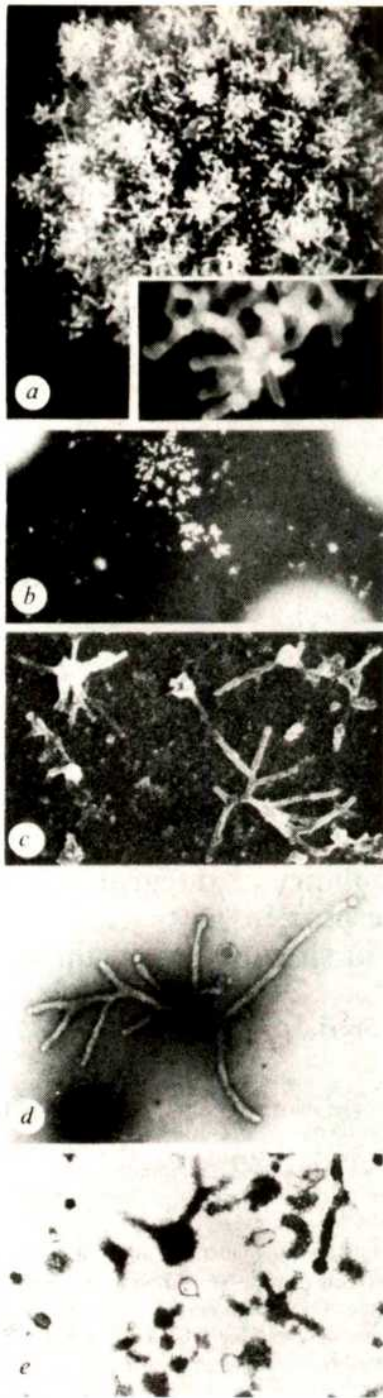
Fig. 1 Microscopic characterization of isolated microvilli prepared from MAT-Cl adenocarcinoma cells. *a*, Scanning electron micrograph of intact MAT-Cl cells (×5,400). Inset shows higher magnification of microvillus branching (×20,000), *b*, dark field microscopy of microvilli after shearing from MAT-Cl cells. The light blurs at the corners are from cells whose surfaces are out of the plane of focus; *c*, scanning electron micrograph of branched microvilli after isolation from Percoll gradient and washing (×9,400); *d*, transmission electron micrograph of branched microvillus isolated as in *c* and stained with phosphotungstic acid (×20,000); *e*, transmission electron micrograph of thin section of microvilli preparation (×17,000). For isolation of microvilli 13762 MAT-Cl cells were washed twice, suspended to 5×10^7 ml^{-1} in 20% fetal calf serum in phosphate-buffered saline (PBS) pH 7.4 and incubated at 37 °C for 15 min. Cells were drawn gently (4–5 times) through a 14-gauge needle to shear the microvilli. The process was monitored by dark field microscopy; cell viability after shearing was greater than 95% by Trypan blue exclusion. Percoll (9:1 Percoll:10 × PBS) was added to a final concentration of 30% and the mixture centrifuged at 37,000g for 45 min. Microvilli were collected from the gradient with a bent needle, diluted 1:4 with 20% fetal calf serum in PBS and centrifuged at 480g for 10 min to pellet any contaminating cells. The supernatant was centrifuged at 48,000g for 60 min to obtain a soft pellet of microvilli which was transferred to a new tube and recentrifuged at 48,000g for 15 min. Electron microscopy was performed as previously described[9,10].

intact cells and isolated microvilli. The specific activity of nucleotidase was increased from 4.0 ± 0.6 to 38 ± 5 μmol per h per mg protein (four preparations). The protein components of isolated microvilli were examined by polyacrylamide gel electrophoresis in SDS (Fig. 3). As expected, the most prominent polypeptide was a band co-migrating with actin. A second major component, with a molecular weight of about 100,000, co-migrated with turkey gizzard α-actinin. Because there has been controversy concerning the identification of α-actinin in brush border microvilli, we isolated microvilli from chicken intestine using the procedure of Bretscher and Weber[6]. Direct electrophoretic comparisons showed that the polypeptide called villin by Bretscher and Weber[6] is different from that which co-migrates with α-actinin in our preparations. Further evidence that the latter polypeptide is actually α-actinin was obtained by 'staining' polyacrylamide gels with antibody against muscle α-actinin, using the indirect

during washing to remove Percoll. There were also a few spherical structures several times larger than the diameter of the microvilli, perhaps portions of the cell body removed during the shearing process or from the 'node region' at the branch points of the microvilli which became detached during purification. Branching was also clearly evident in negatively stained samples (Fig. 1*d*). Some microvilli contained a few blebs, often associated with their tips. Blebs were also observed in stained thin sections (Fig. 1*e*), which showed branch regions, longitudinal profiles and cross-section profiles. In many thin sections it was difficult to determine the orientation, that is, whether the section was cut through the microvillus core, a node region or a piece of associated cell body. Further studies will be necessary to resolve the finer anatomical details of the branched microvillus.

For additional characterization, 5'-nucleotidase, a surface component of MAT-Cl cells (refs 9, 11), was measured in
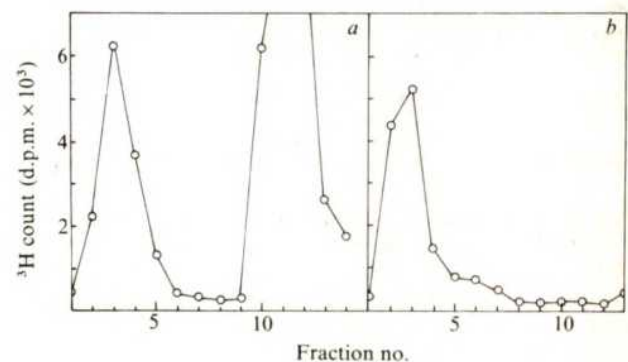
Fig. 2 *a*, Fractionation of sheared microvilli by Percoll gradient centrifugation. Cells were labelled with ^{3}H-glucosamine[10,13] and used for microvilli preparations as described in Fig. 1 legend. Microvilli band at a density of 1.02 g cm^{-3} on the Percoll gradients and are well separated from cells (fractions 10–14), which are the only other significant component after shearing. *b*, Re-centrifugation of purified microvilli on a Percoll gradient gave a single peak at the same density (1.02 g cm^{-3}). The slight peak broadening probably results from some fragmentation during isolation.
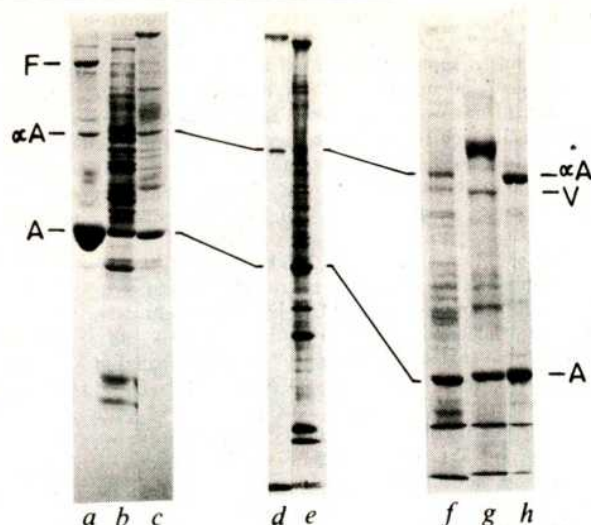
Fig. 3 Polypeptide components of isolated microvilli fractionated by polyacrylamide gel electrophoresis in SDS. Gel electrophoresis was performed as previously described[10,13]. The first panel (*a–c*, 4.5–15% acrylamide gradient, Coomassie blue stain) shows a microvillus preparation (*c*) compared with standards (*a*. A, actin; α-A, α-actinin; F, filamin[15]) and intact cells (*b*). Note the concentration of actin and α-actinin in the microvilli compared with those of other cellular proteins. The second panel (*d* and *e*) shows the identification of α-actinin in a gel of the MAT-Cl microvilli by antibody 'staining' using anti-α-actinin followed by ^{125}I-labelled anti-IgG[12,16]. *d* Is an autoradiogram of the antibody-labelled gel, and *e* is the photograph of the corresponding gel stained with Coomassie blue (gel composition 10% acrylamide, 0.13% bisacrylamide). The stains at the top and bottom of the gel are due to labelled IgG absorbed to the gel interface rather than specific staining. The antibody 'staining' was performed using an antibody preparation described and characterized previously[12,16,17]. The third panel (*f–h*, 7% acrylamide, Coomassie blue stain) shows MAT-Cl microvilli (*f*) compared with chicken intestine brush border microvilli prepared according to the method of Bretscher and Weber[6] (*g*) and a crude preparation of turkey gizzard α-actinin (α-A in *h*), which still contains a substantial amount of actin. The polypeptide of molecular weight 95,000, termed villin, was identified by comparison with published results of Bretscher and Weber[6] and is marked V. Note the absence of a band co-migrating with α-actinin in the brush border microvilli and the absence of a band co-migrating with villin in the MAT-Cl microvilli. There is a band from MAT-Cl microvilli which migrates slightly more slowly than villin, but its identity is unknown.

technique with ^{125}I-labelled anti-IgG (ref. 12). Only one band was observed, corresponding to the migration position of α-actinin (Fig. 3), indicating that α-actinin is a major component of our preparation of isolated microvilli.

The quantity of α-actinin present in the microvilli suggests that it has a structural role. There is no evidence to support its proposed role as a membrane–cytoskeleton linking agent, but its localization in the branched microvilli by immunofluorescence or immune electron microscopy should elucidate this question. Another question is why do MAT-Cl cells have such elaborate surface structures. As this sub-line is highly malignant and xenotransplantable[10,13] (that is, transplantable across the species histocompatibility barrier into mice), it is tempting to speculate that the complex surface is a protective device, for example, aiding the cells in escaping immune surveillance[14].

1. Satir, P. in *Mammalian Cell Membranes* (eds Jamieson, G. A. & Robinson, D. M.) 323–353 (Butterworth, London, 1977).
2. Schollmeyer, J. E. *et al. J. Cell Biol.* **63**, Abstr. 304 (1974).
3. Mooseker, M. in *Cell Motility: Cold Spring Harbor Conf. Cell Proliferation*, Vol. 3, Book B (eds Goldman, R., Pollard, T. & Rosenbaum, J.) 631–650 (Cold Spring Harbor Laboratory, New York, 1976).
4. Craig, S. W. & Pardo, J. V. *J. Cell Biol.* **80**, 203–210 (1979).
5. Geiger, B., Tokuyasu, K. T. & Singer, S. J. *Proc. natn. Acad. Sci. U.S.A.* **76**, 2833–2837 (1979).
6. Bretscher, A. & Weber, K. *Proc. natn. Acad. Sci. U.S.A.* **76**, 2321–2325 (1979).
7. Bretscher, A. & Weber, K. *Expl Cell Res.* **116**, 397–407 (1978).
8. Carraway, K. L. *et al.* in *Am. chem. Soc. Symp.* **80** (ed. Walborg, E. F.) 432–445 (American Chemical Society, Washington DC, 1978).
9. Carraway, K. L., Doss, R. C., Huggins, J. W., Chesnut, R. W. & Carraway, C. A. C. *J. Cell Biol.* **83**, 529–543 (1979).
10. Sherblom, A. P. *et al. Expl Cell Res.* **126**, 417–426 (1980).
11. Carraway, K. L., Fogle, D. D., Chesnut, R. W., Huggins, J. W. & Carraway, C. A. C. *J. biol. Chem.* **251**, 6173–6178 (1976).
12. Burridge, K. *Meth. Enzym.* **50**, 54–64 (1978).
13. Buck, R. L., Sherblom, A. P. & Carraway, K. L. *Biochem. Biophys.* **198**, 12–21 (1979).
14. Henney, C. S. in *Mechanisms of Tumor Immunity* (eds Green, I., Cohen, S. & McCluskey, R. T.) 55–86 (Wiley, New York, 1977).
15. Wang, K. *Biochemistry* **16**, 1857–1865 (1977).
16. Lazirides, E. & Burridge, K. *Cell* **6**, 289–298 (1975).
17. Lazirides, E. *J. Cell Biol.* **68**, 202–219 (1976).

Lateral mobility of integral membrane proteins is increased in spherocytic erythrocytes

Michael P. Sheetz*, Melvin Schindler† & Dennis E. Koppel‡

*Department of Physiology, †Department of Microbiology and ‡ Department of Biochemistry, University of Connecticut Health Center, Farmington, Connecticut 06032

Alterations of glycoprotein distribution and lateral mobility in cell membranes can provide transmembrane signals for several membrane-related phenomena[1-3]. Control of the transmembranous events has been ascribed to interaction between submembranous protein matrices (or 'cytoskeletons') and membrane glycoproteins[4-7]. A consequence of such interaction would be differential inhibition of protein lateral diffusion in biological membranes. Measurements of the lateral diffusion coefficients of membrane proteins, in fact, have generally yielded values[8-12] much less than were predicted for unhindered diffusion in a fluid bilayer[13,14]. The mouse spherocytic erythrocyte, which lacks the major components of the normal erythrocyte membrane matrix[15] (composed of spectrin, actin, bands 4.1 and 4.9 (ref. 16), in the nomenclature of Fairbanks *et al.*[17]), provides a unique system for a direct evaluation of the effect of the matrix on protein lateral mobility. After using a modification of the technique of fluorescence redistribution after photobleaching (FRAP)[18], we report here that membrane proteins diffuse about 50 times faster in spherocytic than in normal mouse erythrocytes.

Integral membrane proteins were labelled with fluorescent molecules by two methods, direct labelling and fluorescent concanavalin A (Con A) binding. Intact cells were incubated

*To whom reprint requests should be addressed.
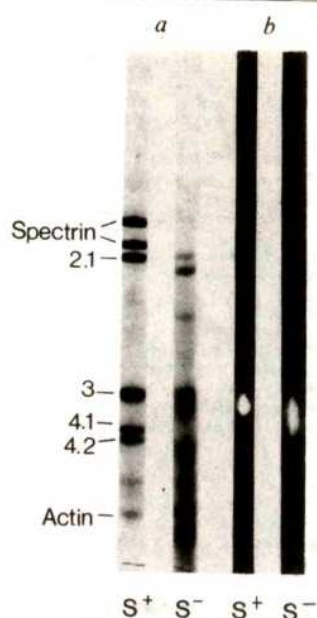
Fig. 1 SDS polyacrylamide gels (5.6% acrylamide) of DTAF labelled from S$^+$ and S$^-$ erythrocytes. In *a*, the gels were stained with Coomassie blue (30 µg of protein per gel). In *b*, unstained gels were excited with laser light at 488 nm and photographed with a 510-nm barrier filter (60 µg of protein per gel). This pattern of fluorescence did not change when acrylamide in the gel was decreased to 3.25%, which would enable resolution of glycophorin from band 3. Cells were obtained from either S$^+$ or S$^-$ (*sph/sph*) WBB6F$_1$ mice (males) by retro-orbital puncture with 2-mm internal diameter heparinized capillary tubes. Samples were washed three times with phosphate-buffered saline (PBS, 140 mM NaCl, 10 mM PO$_4$, *p*H 7.5) to remove plasma and the bulk of leukocytes and platelets. Packed washed cells were suspended in 2 volumes of PBS and mixed with 3 volumes of 1 mg ml^{-1} DTAF in 0.2 M sodium borate (*p*H 10) on ice. After 15 min, cells were washed four times with PBS. Membranes were prepared by lysis of cells 1:100 in 5 mM NaH$_2$PO$_4$ (*p*H 7.4) and centrifugation (40,000 g for 10 min). This procedure was repeated once and the membrane pellet was solubilized for SDS gel electrophoresis by the procedure of Fairbanks *et al.*[17].

with the fluorophore, dichlorotriazinylaminofluorescein (DTAF), at *p*H 10, so that a single protein was labelled in normal erythrocytes (S$^+$) and a broad protein band of similar molecular weight was labelled in the spherocytic erythrocytes (S$^-$) (Fig. 1). None of the major peripheral proteins on the cytoplasmic side of the membrane was labelled. Extraction of the labelled cells with 0.2 mM PO$_4$ (*p*H 8.0) or 0.6 M KI at 37 °C for 10 min followed by centrifugation resulted in a cell pellet containing 85% of the original fluorescence. The amount of total label that electrophoresed with lipids was less than 10% in the normal mouse cells and 25% or less in the S$^-$ mouse cells. Most of the label was found on the protein, band 3, or a variant of it in the spherocytic cells.

When labelled cells were scanned with a low-intensity focused laser beam (beam diameter ~1 µm), fluorescence was distributed as shown in Fig. 2. After two or three such scans a bleach was introduced at the edge of the cell, producing an asymmetrical distribution of fluorescence. Further scans show that the fluorescence redistributed as a function of time, the rate of redistribution being much greater in S$^-$ membranes than in S$^+$ membranes (Fig. 2). The diffusion coefficients in Table 1 were derived from the scans by a new normal mode analysis of diffusion on a spherical surface, described in detail elsewhere[19].

Additional evidence that the fast lateral mobility in S$^-$ cells was due to the diffusion of glycoproteins and not lipid was

obtained by cross-linking membrane glycoproteins with the tetravalent lectin, Con A. Con A at a concentration of 50 µg ml^{-1} or greater completely immobilized fluorescent components on spherocytic cells, but low concentrations did not cause immobilization. Accordingly, we labelled S$^-$ cells with low concentrations of rhodaminated Con A to provide another fluorescent label for FRAP. The mobility of the Con A bound to glycoproteins was as great as 1.2×10^{-9} cm^2 s^{-1} or nearly that of the components labelled directly with DTAF (Table 1). Higher concentrations of rhodaminated Con A which caused extensive cross-linking of membrane glycoproteins resulted in Con A immobility.

Previous studies have suggested that the high-intensity irradiation during the bleach may affect the diffusion of protein by inducing oxidative inter-protein cross-links, especially in the presence of spectrin[20]. Accordingly, all measurements on S$^+$ cell membranes were made in the presence of 5 mM glutathione, which prevents or rapidly reverses photo-induced cross-links in erythrocytes[20]. The diffusion coefficients thus obtained are in close agreement with values obtained for human erythrocytes in which redistribution of labelled proteins was observed after polyethylene glycol-induced fusion, without photobleaching[12].

Spherocytic erythrocytes are short-lived, and so the circulating blood cells must be predominantly reticulocytes (>90%)[15]. Geiduschek and Singer[21] have suggested that glycoproteins in reticulocyte membranes are more mobile than in adult erythrocyte membranes. To rule out the possibility that the difference in mobility between S$^+$ and S$^-$ erythrocytes was due to the presence of reticulocytes, we labelled S$^+$ reticulocytes with DTAF and found a diffusion coefficient of 1.3×10^{-10} cm^2 s^{-1}—3 times faster than that for glycoproteins in the normal mouse erythrocyte membrane, but nearly 20 times slower than in the spherocytic mouse erythrocyte membrane. These results suggest a difference in the
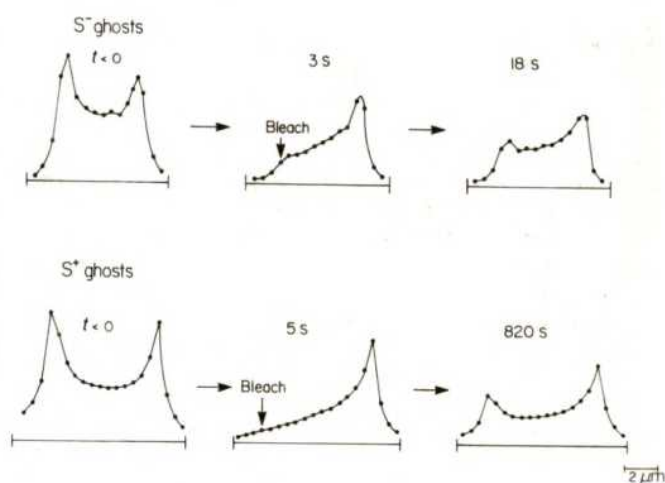
Fig. 2 Scans of the fluorescence distribution on DTAF-labelled S$^-$ and S$^+$ membranes before and after irradiation of the leading edge of the cell with a bleaching pulse for 35 ms (0.1 mJ). The apparatus used here has been described elsewhere[18]. Single scans are collected in 1 s by scanning a focused laster beam (approximately 1 µm in diameter) of 0.1 µW at 4,765Å across the membranes. Membranes of labelled S$^-$ erythrocytes were prepared by allowing spontaneous lysis to occur on the slide. Over 60% of the cells lysed within 10 min at 24 °C. Membranes of labelled S$^+$ erythrocytes were prepared by lysis (1:100 in 5 mM NaH$_2$PO$_4$, *p*H 7.5), centrifugation (40,000 g for 10 min) and resuspension in PBS with 5 mM reduced glutathione (*p*H 7.5). Similar diffusion values were obtained with membranes from S$^+$ which had spontaneously lysed during the slide preparation. Slides and coverslips were preincubated in 0.1 M NaH$_2$PO$_2$ (*p*H 7.5) and washed with distilled water before use. Samples on the slides were sealed with paraffin to prevent evaporation.

Table 1   Diffusion coefficients of erythrocyte and reticulocyte membranes

Membranes	Diffusion coefficient (s.d.) (10^{-11} cm^2 s^{-1})
S$^-$ erythrocytes	250 ± 60 (9)
S$^+$ reticulocytes	13 ± 4 (5)
S$^+$ erythrocytes	4.5 ± 0.8 (4)

Diffusion coefficients, D, were determined in a normal-mode analysis[19] from experimental estimates of $\mu_1(t)$, the normalized first moment of the concentration distribution $c(x, t)$:

$$\mu_1(t) = \int_{-1}^{1} xc(x,t)\,dx \Big/ \int_{-1}^{1} c(x,t)\,dx$$

$$\propto \exp(-2Dt/r^2)$$

where x is the cosine of equatorial angle θ on the surface of the spherical cell of radius r. In most cases, the data could fit to a single exponential within experimental error. The values of D reported were measured at 24 °C. The number of measurements made is in parentheses. S$^-$ and S$^+$ erythrocytes were prepared as in Fig. 2. For S$^+$ reticulocytes, reticulocytes were isolated from a mouse which had been bled (0.6–1.0 ml per day) for 3 days. Forty hours after the last bleeding a blood sample was obtained as in Fig. 1 and centrifuged at 15,000g for 2 min. The upper 25% of the packed cells was drawn off, washed and labelled as in Fig. 1. Reticulocyte membranes were obtained by the procedure described in Fig. 2 legend for S$^+$ membranes. For these measurements only membranes with a definite reticulum were chosen.

arrangement of reticulocyte matrices. Indeed, electron micrographs by Geiduschek and Singer document spectrin-free domains[21].

As Fig. 1 shows, S$^-$ cell membranes differ from S$^+$ cell membranes in several protein components, having less spectrin, spectrin-binding protein[22] (band 2.1) and matrix-associated protein[16] (band 4.1) and considerably more polypeptides in the low molecular weight region of the gel. There may be other differences, but additional evidence supports our contention that interactions between the membrane and the matrix control lateral mobility. Fowler and Bennett[23], using a procedure designed to weaken the association of spectrin with the membrane, observed a two-fold increase over controls in the lateral mobility of band 3. We have demonstrated that compounds normally found in erythrocytes, which specifically decrease interactions between spectrin, actin and band 4.1, increase the lateral mobility of membrane proteins[12]. Thus, decreasing interactions between the matrix and the membrane, or between matrix components, increase membrane mobility. Conversely, in preliminary experiments, the addition of spectrin to S$^-$ cell membranes inhibited glycoprotein mobility (M.P.S., M.S. and D.E.K., unpublished).

The presence of a membrane matrix could control protein mobility in either of two ways: by a direct mechanism involving attachment of mobile glycoproteins to cytoskeletal elements[6,7], or by an indirect mechanism analogous to restricted diffusion through a polymer network[6,24]. The former mechanism would be expected to slow down protein rotational as well as translational diffusion; the latter would not. It has been demonstrated that the presence of spectrin does not affect the rotational diffusion of band 3 (ref. 25). It thus seems that in conjunction with our results an indirect control must be postulated for the spectrin, actin, bands 4.1 and 4.9 matrix inhibition of lateral mobility. We suggest that matrix control mechanisms such as this are also active in other eukaryotic cells.

1. Isersky, H., Taurog, J., Poy, G. & Metzger, H. *J. Immun.* **12**, 549–555 (1978).
2. Yahara, I. & Edelman, G. M. *Proc. natn. Acad. Sci. U.S.A.* **72**, 1579–1583 (1975).
3. Orly, J. & Schramm, M. *Proc. natn. Acad. Sci. U.S.A.* **73**, 4410–4414 (1976).
4. Elgsaeter, A. & Branton, D. *J. Cell Biol.* **63**, 1018–1030 (1974).
5. Nicolson, G. & Painter, R. G. *J. Cell Biol.* **59**, 395–406 (1973).
6. Edelman, G. M. *Science* **192**, 218–226 (1976).
7. Ash, J. F., Louvard, D. & Singer, S. J. *Proc. natn. Acad. Sci. U.S.A.* **74**, 5584–5589 (1977).
8. Edidin, M., Zagyansky, Y. & Lardner, T. J. *Science* **191**, 466–468 (1976).
9. Jacobson, K., Wu, E.-S. & Poste, G. *Biochim. biophys. Acta* **433**, 215–222 (1976).
10. Schlessinger, J., Axelrod, D., Koppel, D. E., Webb, W. W. & Elson, E. L. *Science* **195**, 307–310 (1977).
11. Fowler, V. & Branton, D. *Nature* **268**, 23–26 (1977).
12. Schindler, M., Koppel, D. E. & Sheetz, M. P. *Proc. natn. Acad. Sci. U.S.A.* **77**, 1457–1461 (1980).
13. Poo, M.-M. & Cone, R. A. *Nature* **247**, 438–441 (1974).
14. Saffman, P. G. & Delbrück, M. *Proc. natn. Acad. Sci. U.S.A.* **72**, 3111–3115 (1975).
15. Greenquist, A. C., Shohet, S. G. & Bernstein, S. E. *Blood* **51**, 1149–1155 (1978).
16. Sheetz, M. P. *Biochim. biophys. Acta* **557**, 122–134 (1979).
17. Fairbanks, G., Steck, T. L. & Wallach, D. F. H. *Biochemistry* **10**, 2606–2614 (1971).
18. Koppel, D. E. *Biophys. J.* **28**, 281–292 (1979).
19. Koppel, D. E., Sheetz, M. P. & Schindler, M. *Biophys. J.* **30**, 187–192 (1980).
20. Sheetz, M. P. & Koppel, D. E. *Proc. natn. Acad. Sci. U.S.A.* **76**, 3314–3318 (1979).
21. Geiduschek, J. B. & Singer, S. J. *Cell* **16**, 149–160 (1979).
22. Bennett, V. & Stenbuck, P. J. *J. biol. Chem.* **254**, 2533–2541 (1979).
23. Fowler, V. & Bennett, V. *J. supramolec. Struct.* **8**, 215–221 (1978).
24. Schindler, M., Osborn, M. J. & Koppel, D. *Nature* **283**, 346–350 (1980).
25. Cherry, R. J., Burkli, A., Busslinger, M., Schneider, G. & Parish, G. R. *Nature* **263**, 389–393 (1976).

The conformation of subcomponent C1q of the first component of human complement

S. Gilmour*, J. T. Randall*, K. J. Willan†,
R. A. Dwek† & J. Torbet‡

*Department of Zoology, University of Edinburgh, West Mains Road, Edinburgh EH9 3JT, UK
†Department of Biochemistry, University of Oxford, South Parks Road, Oxford OX1 3QU, UK
‡Max-Planck-Institut für Festkörperforschung, 25, Avenue des Martyrs, Grenoble-Cedex, France

The complement system in the blood of vertebrates[1,2] has a vital role in the defence of the body against invading foreign material. Although it can be triggered before immunity has developed, it is usually activated following an initial intervention by antibodies, and about 20 serum proteins are involved. Some of these act as controlling inhibitors while others form nine components which, if following the classical activation pathway, all take part in bringing about membrane damage and cell lysis. The first component C1 consists of three subcomponents, C1q, C1r and C1s. C1q binds to antibody–antigen complexes as the first stage of fixation[3] and as it shows no enzymatic activity by itself, conformational changes on binding have been proposed as the driving mechanism of the subsequent reactions. Since structural investigation by electron microscopy[4–7] leaves doubt as to whether unnatural constraints were applied in the preparation and treatment of specimens, techniques such as X-ray or neutron small-angle scattering, which investigate the equilibrium state in dilute solution, provide valuable complementary evidence for both its findings and those of other physicochemical methods[8]. We have already carried out neutron work on the conformation of immunoglobulin and the influence of hapten binding (to be published) and are now studying the conformation of C1q as a preliminary to investigating the composite structures resulting from their mutual interaction. As evidence of the structure of this molecule has accumulated, the question has arisen of whether it maintains a compact closed conformation in its native state or a more open one in readiness for interaction with other proteins. The neutron small angle scattering curve is sensitive to conformational changes and although our measurements are not yet complete, model calculations suggest that the structural arrangement is indeed open.
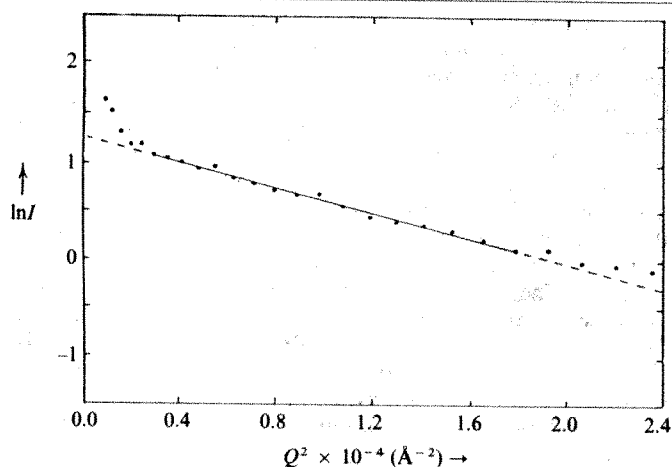
Fig. 1 Example of the $\ln I$ against Q^2 scattering curves obtained for C1q. I, corrected neutron counts on a relative scale; Q, scattering vector. The specimen solutions used were of pH 7.4 and, besides protein, contained 0.15 M sodium chloride, 0.01 M sodium phosphate and 0.01 M EDTA. They were held in high quality boron-free silica spectroscopic cells whose internal thickness was either 2 mm or, for the more highly absorbing hydrogenous sample, 1 mm. Data were collected at a specimen-detector distance of 10.5 m and a neutron wavelength of 12.1 Å ($\Delta\lambda/\lambda \approx 8\%$). Radial averaging gave intensities at annular increments of 1 cm ($\Delta(2\theta) \approx 0.03°$). Control runs of cell, solvent and buffer only were subtracted with allowance for change of transmission and the results scaled according to a water sample to correct for instrumental effects. The fit to the Guinier law for the 100% exchanged C1q sample illustrated gives an apparent radius of gyration R of 140 ± 2 Å over the range $0.75 \leqslant QR \leqslant 1.85$ with a statistical correlation coefficient of 0.996. This is close to 1 (the value for a perfect straight-line relationship) and is maintained for sets of points within the range, as is the value of R. There is therefore little evidence for the presence of aggregated particles. The deviation of the first few points in the spectrum is probably due to the proximity of the detector elements to the beam stop. The intensity measurements can only be put on an absolute scale at present by reference to spectra which are less statistically reliable, but doing so allows determination of the molecular weight of C1q as $370,000 \pm 50,000$. The accepted value from sedimentation equilibrium studies is 409,600 (ref. 9).

Human C1q was prepared as described previously[9] and made up in aqueous solutions to a concentration of 3 mg ml^{-1}. To provide a range of scattering contrast between the protein molecule and its surrounding medium[10], the solvent was 0%, 85% and 100% deuterated and, except in the case of the completely hydrogenous solution, each sample of C1q was pre-dialysed against its intended solvent to allow appropriate replacement of the exchangeable hydrogen of the protein by deuterium. Neutron small-angle scattering spectra were recorded using the multidetector D11 (refs 11, 12) at the Institut Laue-Langevin, Grenoble.

The small-angle scattering of randomly orientated identical particles in solution can be represented by the gaussian intensity curve[13]

$$I(Q) = I(0)\exp -\tfrac{1}{3}R_g^2 Q^2 \qquad (1)$$

where $Q (= 4\pi \sin \theta/\lambda)$ is the scattering vector associated with a scattering angle of 2θ at wavelength λ. Within the validity of this expression ($QR_g \lesssim 1$–1.5) the relationship between $\ln I$ and Q^2 is linear with a slope directly related to the radius of gyration R_g of each particle. Least squares fitting of the most highly correlated range of points in the plots obtained for C1q (see Fig. 1) gave apparent radii of gyration for each contrast

and the corresponding relative value of the intercept $I(0)$. After division by the measured sample transmissions, the linear variation of $I(0)^{\frac{1}{2}}$ allowed determination of the percentage deuteration at which the mean scattering density of the protein ρ is identical to that of the solvent ρ_s.

The match point found at $41.7\% \pm 0.2\%$ corresponds to a scattering density of 2.33×10^{10} cm^{-2}. As the total molecular weight of human C1q is 409,600 and the detailed composition of the 92% amino acids and 8% carbohydrate is known[9], the sum of the scattering lengths of the molecule can be calculated for any proportion of exchanged hydrogen atoms. The dry volume V was therefore deduced to be $530,000 \pm 4,000$ Å^3 and the mass density 1.28 ± 0.01 g cm^{-3}, in close agreement with the result of about 1.3 g cm^{-3} expected for a protein. As the scattering density in a particle is not in general homogeneous, the observed radius of gyration R is dependent on the contrast $\bar\rho (= \rho - \rho_s)$ and hence[14]

$$R^2 = R_o^2 + \frac{\alpha}{\bar\rho} + \frac{\beta}{\bar\rho^2} \qquad (2)$$

where α, β are constants and R_o is the mechanical radius of gyration of an object the same shape as the particle. The plot of R^2 against $1/\bar\rho$ for C1q proved to be predominantly linear and, assuming this, gave an infinite contrast result for R_o of 139.5 ± 2.5 Å. The slope α was negative rather than positive and as it is given by the second moment of the fluctuation scattering density distribution ρ_F, that is:

$$\alpha = \frac{1}{V} \int \rho_F(\mathbf{r}) r^2 d^3\mathbf{r} \qquad (3)$$

there would seem to be less than average scattering density at large distances from the centre of gravity of the molecule.

Since soluble proteins have high-scattering hydrophilic residues at their surface and low-scattering hydrophobic ones
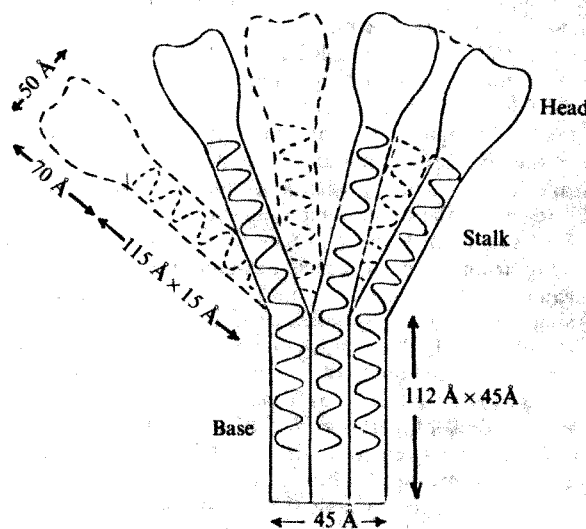
Fig. 2 Molecular structure of C1q proposed by Reid and Porter[15] (after whom the figure is taken) to account for the effects of collagenase and pepsin digestion[9,21] and the dimensions and shape of the images seen in the electron microscope[5-7]. Analysis and sequencing[9,17,24] of the three types of polypeptide chain present show clear similarities between them, notably the repeating collagen-like triplets of residues which occupy some 85 positions starting near the N-terminal end. The characteristic Gly-X-Y pattern, where the residue Y is often either hydroxyproline or hydroxylysine, is broken at position 39 of the A chain[2] and 36 of the C chain[17] allowing the bend of the triple helices (3) forming each stalk away from those in the base region.
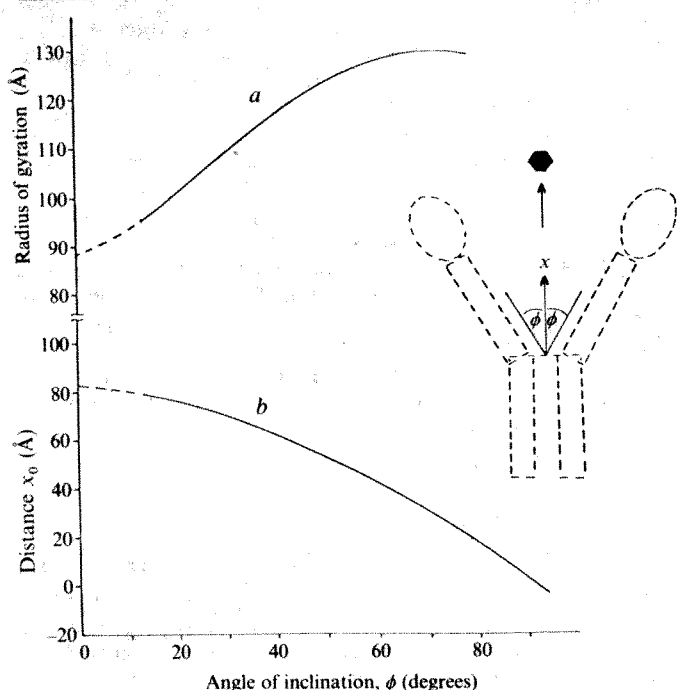
Fig. 3 Prediction of the behaviour of: *a*, the radius of gyration R_0 of a uniform object the same size and shape as the C1q molecule; and *b*, the distance x_0 of its centre of gravity above the junction of base and stalks. Both the measurement of *x* and the angle of inclination ϕ are defined in the inset which shows a cross-section of the model. The dashed portions of each curve cannot be realised as ϕ is less than the critical angle at which the globular regions touch one another.

inside, it follows that the C1q molecule does not have a simple globular form. Biochemical and electron microscopic evidence[5-7,15-17] has established that instead it has the appearance of a bunch of tulips (Fig. 2). Eighteen chains, each some 200 amino acid residues long, are linked in threes in the base and stalk regions to form collagen-like triple helices and each of the six fibres terminates in a globular head region. At least one head is held by each C_H2 domain when binding to the Fc region of the immunoglobulin molecule takes place[18,19] and it has recently been suggested[20] that sugar chains protruding from the heads act as recognition sites.

Calculations based on the dimensions shown in Fig. 2 and assuming the 6-fold symmetry seen in recent electron micrographs (K. B. M. Reid, personal communication) show that variation of the angle of inclination ϕ of the stalks to the direction of the hexad axis has a marked effect on the resulting geometric radius of gyration R_0. Right circular cylinders of radius 7.5 Å were taken to model the stalks and also the base, where six were arranged with the centres of their ends at the vertices of a hexagon of side 15 Å and the central enclosed volume was assumed to be unoccupied. The globular regions were represented by ellipsoids of revolution with semi-axes of 25 Å, 25 Å and 35 Å. Unfortunately, no estimates are available for the size and shape of the cleft which seems to divide each head into two distinct components when viewed from above[5]. For purposes of calculation a sphere of radius 17 Å was removed from the top of each ellipsoid. This reduced both the total volume to the value determined above and the proportion of it occupied by the six heads to 55 %, similar to the 57 % contribution found in weight analysis[21].

Summation of the moments of inertia of the various parts of the model about a point on the hexad axis at a height *x* above the junction of base and stalks and minimizing the resulting

expression gives $x(=x_0)$ corresponding to the centre of gravity for given ϕ. Returning this relationship to the equation for the total moment of inertia yields the dependence of the radius of gyration R_0 on ϕ. As can be seen from Fig. 3, the 14° minimum inclination corresponding to the tulip heads in contact produces a structure with an R_0 of only 95 Å, whereas the radii for angles of greater than 60° are close to the maximum of about 132 Å which occurs for $x_0 = 0$. Variation of the model to allow for differently shaped clefts seems to have a limited effect on the qualitative behaviour or the values obtained. The calculations were also repeated to assess the influence of errors in the known parameters. It is clear that the form of the R_0 versus ϕ dependence is only significantly changed by unrealistic distortions and any proportional increase in R_0 is only achieved by at least the same percentage rise in one or more dimensions of each component of the model.

As C1q is present in only very small quantities in serum and its isolation is difficult, we have not so far investigated the concentration dependence of our neutron measurements of R_0. Interparticle interference usually decreases the scattering intensities at lower Q (ref. 22) so the result of 139.5 Å would be expected to rise on extrapolation to infinite dilution. At $3\,mg\,ml^{-1}$, however, the concentration we used is already below the $5\,mg\,ml^{-1}$ recommended by Pilz[23] for negligible interference effects and, although the protein is basic ($pI \approx 10$) and therefore positively charged at pH 7.4, the ionic strength of the buffer was enhanced by the addition of 0.15 M sodium chloride. Both our own and other neutron observations of proteins indicate that unless considerable aggregation were present (which we do not believe to be the case—see legend to Fig. 1), any change in the radius of gyration would be less than 1 %. Confirmatory data from solutions at additional contrasts are also desirable but two conclusions can be drawn: first, that the dry volume of the C1q molecule determined from the neutron scattering of solutions is consistent with the structural dimensions established by electron microscopic and biochemical techniques; and second, that its conformation in solution is an open one with the angle of inclination of the tulip stalks at least the 60° corresponding to the average head-to-head bunch diameter seen in the electron micrographs of Shelton *et al.*[5]. The assumption that the conformation is unique is supported by the high statistical correlation coefficients observed in the Guinier region and by the possibility that an otherwise anomalous peak seen at $Q \approx 0.037\,Å^{-1}$ in further spectra from the same specimens is a weak subsidiary maximum.

1. Müller-Eberhard, H. J. *A. Rev. Biochem.* **44**, 697–724 (1975).
2. Porter, R. R. & Reid, K. B. M. *Nature* **275**, 699–704 (1978).
3. Müller-Eberhard, H. J. & Kunkel, H. G. *Proc. Soc. exp. Biol. Med.* **106**, 291–295 (1961).
4. Green, N. M. *Adv. Immun.* **11**, 1–30 (1969).
5. Shelton, E., Yonemasu, K. & Stroud, R. M. *Proc. natn. Acad. Sci. U.S.A.* **69**, 65–68 (1972).
6. Svehag, S.-E., Manhem, L. & Bloth, B. *Nature new Biol.* **238**, 117–118 (1972).
7. Knobel, H. R., Villager, W. & Isliker, H. *Eur. J. Immun.* **5**, 78–81 (1975).
8. Metzger, H. *Adv. Immun.* **18**, 169–207 (1974).
9. Reid, K. B. M., Lowe, D. M. & Porter, R. R. *Biochem. J.* **130**, 749–763 (1972).
10. Jacrot, B. *Rep. Prog. Phys.* **39**, 911–953 (1976).
11. Schmatz, W., Springer, T., Schelten, J. & Ibel, K. *J. appl. Crystallogr.* **7**, 96–116 (1974).
12. Ibel, K. *J. appl. Crystallogr.* **9**, 630–643 (1976).
13. Guinier, A. *Annls Phys.* **12**, 161–237 (1939).
14. Ibel, K. & Stuhrmann, H. B. *J. molec. Biol.* **93**, 255–265 (1975).
15. Reid, K. B. M. & Porter, R. R. *Biochem. J.* **155**, 19–23 (1976).
16. Brodsky-Doyle, B., Leonard, K. R. & Reid, K. B. M. *Biochem. J.* **159**, 279–286 (1976).
17. Reid, K. B. M. *Biochem. J.* **161**, 247–251 (1977).
18. Kehoe, J. M., Bourgois, A., Capra, J. D. & Fougerau, M. *Biochemistry* **13**, 2499–2504 (1974).
19. Yasmeen, D., Ellerson, T. R., Dorrington, K. J. & Painter, R. H. *J. Immun.* **116**, 518–526 (1976).
20. Mizuochi, T., Yonemasu, K., Yomashita, K. & Kobata, A. *J. biol. Chem.* **253**, 7404–7409 (1979).
21. Reid, K. B. M. *Biochem. J.* **155**, 5–17 (1976).
22. Guinier, A. & Fournet, G. in *Small-angle Scattering of X-rays* (Wiley, New York, 1955).
23. Pilz, I. in *Physical Principles and Techniques of Protein Chemistry* Part C (ed. Leach, S.) 141–243 (Academic, New York, 1973).
24. Reid, K. B. M. & Thompson, E. O. P. *Biochem. J.* **173**, 863–868 (1978).

BOOK REVIEWS

Light on the Pauli legend

John Stachel

THIS volume is the first of a series which is to include the complete scientific correspondence of Wolfgang Pauli. Pauli played a central role in the development of quantum mechanics in the 1920s, and in its interpretation and acceptance by the physics community. Among his achievements during the period covered by this volume were his writing of the classic exposition of relativity theory as a lad of twenty; his development of the Pauli or exclusion principle, for which he later won the Nobel Prize; his proof of the mathematical equivalence of matrix and wave mechanics, worked out independently of the better-known proof by Schroedinger; and his work with Jordan and Heisenberg on the foundations of quantum field theory. Weisskopf, in his Preface, tries to characterize Pauli's approach:

> Pauli had a special way of doing science. He created a unique style of thinking and research, which has deeply influenced and guided physics. It is a style that emphasizes the essential and the symmetrical in the laws of nature, and captures it in mathematical formulas without many words or empty talk. In the minds of all physicists, his mode of thinking and his whole nature stand as something ideal, clear and pure.

Something of the awe in which his intellectual powers were held may be surmised from the nickname bestowed upon him in the German-speaking physics community: 'Zweistein' (or 'two-stone'), second only to 'Einstein' (or 'one-stone').

Many stories about his formidable personality do not suggest a similar comparison with the popular saintly image of Einstein, and this volume certainly provides some documentary evidence to reinforce the Pauli legend (see the letter to Einstein quoted on p. xxxvi of the Introduction, for example), though also many examples of his helpfulness to those in difficult circumstances (see p. xxii of the Introduction, for example). In his Preface, Weisskopf gives some brief insights into Pauli's personality. On the whole, however, the annotations are rather reticent on the subject of his personal life. I could find no reference anywhere in the volume to Pauli's Jewish ancestry. The valuable chronology through 1929 on pp. 536-541 confines itself to his scientific activities and travels, avoiding such matters as the date of his marriage, with one curious exception: the date on which he

Wolfgang Pauli: Scientific Correspondence with Bohr, Einstein, Heisenberg, A.O. Volume I: *1919-1929.* Edited by A. Hermann, K. von Meyenn and V.F. Weisskopf. Pp. 577. (Springer: Heidelberg and New York, 1979.) DM 160, $88.

Wolfgang Pauli, 1900-1958

left the Roman Catholic Church is given. Perhaps this reticence befits a critical edition of his letters, which provides indispensable material for a critical biography but cannot take the place of such a biography.

In his valuable Introduction, Professor Hermann rightly stresses the importance of such collections of scientific correspondence.

> The communications system of the 'scientific community' in the twentieth century is based upon periodicals and letters. Periodicals publication is strictly regulated. Therefore the supplementary information value of letters is considerable. 'Informational value' means in the first place informational value for the recipient of the letter, therefore for contemporary physicists, but also means informational value for present-day historians of science. Historical writing which only utilizes contemporary publications can only be considered as a first beginning. Collections of letters facilitate scientific-historical work at a higher informational level.

I would add that another major source of scientific communication in this century is verbal — either the private (face-to-face

or on the telephone) or public forms (such as lectures and discussions). The former is almost always irretrievably lost, unless preserved in letters, contemporary notes or later memoirs; the latter is more often preserved in the form of conference proceedings — often altered in form by the time they reach print. Still, these are precious sources of information which should not be neglected by the historian of science.

Quotations from later letters in the course of Hermann's discussion of Pauli's role in the development of modern physics whet our appetite for future volumes. A few of Hermann's comments may raise some eyebrows, for example (p. xix): "Intellectual creation is something peculiarly human and consequently independent of time". If this were taken literally, it would be hard to see what the function of the historian of science could be.

The book proper consists of the texts of 241 letters to and from Pauli, together with running commentaries linking groups of letters and extensive annotations of the letters. Texts and commentary are in German. The letters give a fascinating picture of the interactions between Pauli and a few of the handful of physicists who were re-making theoretical physics in the 1920s. In spite of the title, only three of the letters are to (two) or from (one) Einstein; over half the letters are to or from Bohr and Heisenberg, in roughly equal number. Others with an exchange of over ten letters are Ehrenfest, Kronig and Landé. If one wants to derive the full value from their scientific content, the letters are best read in conjunction with Pauli's published papers, available in one of those facsimile collections which too often substitute for complete, critical editions of the writings of a scientist (*Collected Scientific Papers by Wolfgang Pauli.* Edited by R. Kronig and V.F. Weisskopf. Interscience: New York, 1964. 2 volumes). Fortunately, the extraordinarily rich and detailed annotations (which I understand are mainly the work of Dr von Meyenn) make reference to these papers, as well as to other contemporary writings and later historical studies, very simple. The reader will also be most grateful for the commentaries and annotations explaining the context of the letters, and various references to persons and events which otherwise would send him/her

Pauli with his wife, Francis, in Stockholm to
receive the Nobel Prize for Physics, 1946

scurrying to the reference books.

The principles of inclusion of the
material are not quite clear. In "Postscript
and Indications for the User", it is claimed
that all the scientific correspondence so far
collected is included; yet we are told that
"letters with markedly sterile content form
an exception" (p. 534). The example given,
letters from Felix Klein concerning the
editing of Pauli's famous relativity treatise,
could conceivably interest someone study-
ing scientific institutions. Still, a list of the
omitted letters can be constructed from the
"Alphabetical List of Correspondence" at
the end of the volume. Aside from seven
Klein letters, only seven others appear to

have been omitted. In the few cases where I
could compare the transcription of letters
in this volume with other transcriptions or
the originals, they seemed accurate. The
one exception, oddly enough, occurs in the
only facsimile of a Pauli letter printed in
the volume, between the Preface and the
text. Reference to the printed version of the
letter shows that a line above the salutation
has been left out. While not enough to
shake my faith in the accuracy of the texts,
this omission did give me pause.
Incidentally, one would have liked more
facsimiles and photographs. While nothing
takes the place of handling the originals, a
good facsimile can help the reader to

capture something of the flavour of the
original.

Of more concern, perhaps, is the very
concept of a division between scientific and
non-scientific letters. For example, I
understand that Pauli's correspondence
with C.G. Jung is not to be included in the
forthcoming volumes. While this may be a
gratifying confirmation for some of their
estimate of the scientific status of Jungian
psychology, it certainly will deprive us of a
great deal of insight into an important
encounter for modern intellectual history,
one which led to Pauli's study of Kepler
and influenced his later epistemology.
More generally, the division between
scientific and non-scientific aspects of a
life's work is not a simple matter. Cer-
tainly, modern approaches to the study of
the history and philosophy of science, let
alone the study of the scientific creative
process which so fascinated Pauli, do not
and cannot confine themselves to any
narrow definition of such a distinction.

But one must not cavil. In this edition we
are being given an excellently edited,
annotated and indexed collection of the
most important letters of a pivotal figure in
the development of modern physics, which
will be of interest to historians of science,
physicists concerned with their traditions,
and more generally all those fascinated by
the creative process at its highest level.
These letters will contribute immeasurably
to our understanding of Pauli the man, his
times and his achievement. □

*John Stachel is a Professor at Boston
University, currently working at the Institute for
Advanced Study, Princeton, New Jersey.*

Thinking of the mind

Stuart Sutherland

THE LAST infirmity of noble minds is the
desire to create a grand synthesis of
everything. Even such a down-to-earth
physiologist as Sherrington succumbed by
writing in his old age the impenetrable *Man
on His Nature*. At the age of 76 Gregory
Bateson, one of the pioneers of social
anthropology, has produced his own
contribution to this genre. The collocation
of words in the title, *Mind and Nature. A
Necessary Unity,* is sufficient warning of
what to expect in the contents.

The core of Dr Bateson's book is his list
of six criteria for regarding something as a
mind, as follows: (1) A mind is made up of
interacting parts — thought could not be
carried out by an entity not composed of
parts, if only because there would be no
way of representing external states of

affairs within it. (2) Mental processes are
triggered by differences or by changes —
information can only be carried by
difference. (3) Mental processes require
energy generated from within the system —
they are not simply reactions to an
externally applied force, unlike the motion
of a bullet fired from a gun. (4) They
contain circular chains of causation often
involving negative feedback. (5) In mental
processes, the effects of a difference
detected by the system are to be regarded as
a coded version of the difference itself —
Dr Bateson seems to mean by this that
mental structures represent aspects of the
external world. (6) Mental processes
involve a hierarchy of logical types — this
would appear to mean that one mental
process can serve as the input to another
and that minds are capable of reflecting on
aspects of their own activity.

Although some of the criteria are
obscurely expressed, most people would
probably be prepared to grant that they are

necessary conditions for the existence of
mind. Unfortunately, Dr Bateson does not
discuss whether they are *sufficient*
conditions. They are in fact all met by a
computer programmed to perform an
intelligent task and although one would be
happy to regard such a machine as working
in an analogous way to mind, there is little
temptation to think of it as actually
possessing a mind. Dr Bateson deliberately
ignores the problem of consciousness and
indeed appears to attribute mind to plants
and to the evolutionary process. But the
differences between the workings of the
evolutionary process and those of the mind
may be more interesting than the
similarities. He has in fact omitted from his
list of criteria for mind the one that many
would regard as the most important,
namely, the characteristic of acting by
intention, something that clearly
distinguishes the blind forces of evolution
from the human mind. One way of putting
this is that minds contain explicit
representations of their own goals in the
light of which the representation of the
external world can be manipulated in order
to formulate a suitable course of action.
The representation of future states of

affairs is at best very indirect in plants and would appear to be non-existent in the evolutionary process.

Despite its inadequacy, Dr Bateson's discussion of the nature of mind is the clearest section of his book. The remainder discusses some of the prerequisites for learning and insight and the problem of evolution, but I found it impossible to understand the general drift of the argument let alone to summarize it. He illustrates his themes with examples drawn from many different fields: few are novel and it is unclear what conclusions he draws from them. He notes, for instance, that the equation $(a + b)^2 = a^2 + 2ab + b^2$ can be represented geometrically as a square with sides of length $a + b$ and with the interior divided into four rectangles of areas a^2, ab, ab, and b^2. But he stops short at explaining why such a representation is easier for most people to grasp than the algebraic equation, and the relationship between this and other examples to his main thesis remains obscure.

In short, *Mind and Nature* is a book to be read for the incidental examples strewn through it, but anyone who wants to discover its general message will have a hard time. As Heraclitus wearily steps for very much more than the second time into yet another river, one gathers that process is important and that everything is connected to everything else — the book is indeed a grand but empty synthesis of everything. □

Stuart Sutherland is Director of the Centre for Research on Perception and Cognition at the University of Sussex, Brighton, UK.

Microelectronic technology

T.H. O'Dell

Magnetic Bubble Technology. By A.H. Eschenfelder. Pp.317. (Springer: Heidelberg and New York, 1980.) DM97, $54.40.

AT A time when microelectronic devices based upon single crystal silicon have become part of our popular culture, it is good to see a book concerned with a microelectronics based upon the far more interesting magnetic crystals, the garnets. The information-processing potential of these devices exceeds that of their silicon predecessors by at least two orders of magnitude.

While there have been two previous books on the theoretical aspects of magnetic bubbles, Eschenfelder's is the first to go into the real technical detail of devices and, like most books of this kind, a feel for the work can be obtained from a study of the index; this is good, and calls attention to Chapter 6 which is an excellent review of the available magnetic materials of bubble technology, the garnets, hexaferrites, amorphous metal films and orthoferrites. All these materials are treated very effectively using a powerful graphical technique, pioneered by Eschenfelder, in which the coordinates are chosen such that different values of exchange constant may be represented by

---

● *Statistical Mechanics* by R. H. Fowler has been reissued in paperback by Cambridge University Press, price £18.
● *Sociobiology: The Abridged Edition* by Edward O. Wilson with drawings by Sarah Landry (pp. 366; price: hardback $18.50, £11.10; paperback $9.95, £5.95) has just been published by Harvard University Press.

---

sets of parallel straight lines. The unification which this technique brings about is really striking.

Chapter 6 also contains a valuable treatment of magnetic anisotropy. In magnetic bubble garnets this is induced during the growth process for the film, one of the topics in Chapter 7 which is on device fabrication and includes a good discussion of lithography giving considerable numerical detail.

Chapter 8 deals briefly with device packaging, while Chapter 9 is on applications and is not just concerned with simple memories but also describes the fascinating information-processing possibilities of the technology. This enables data to be sorted as it is in the process of being stored or retrieved by means of the flow-steering switches pioneered by Eschenfelder's IBM colleagues Chen, Chang and Tung. The book concludes with Chapter 10 which takes a brief look at what the future may hold for this exciting and highly developed microelectronic technology.

The first five chapters of this book are not so good, however. No Appendix A, promised on p.1 to relate the Gaussian units, in which the book is unfortunately written, to SI units, exists. A conversion table is printed inside the front cover to rectify this omission. Figures 1.8 and 1.10 are repeated later as Figs 4.31 and 8.3. Page 8 sees the start of half a page of text with the most peculiar absence of capitals and punctuation.

Chapters 1–5 deal with bubble statics, dynamics and propagation structures, but give no help at points where earlier publications may have been obscure. An exception is to be found upon pp.156–158, where the elegant cross-hatch current sheet device due to Voegeli, and unpublished until now, is described. □

T.H. O'Dell is Reader in Electronics at Imperial College, University of London, UK.

Fungal ecology

John Webster

The Ecology of Fungi. By W. Bridge Cooke. Pp.274. (CRC Press: Boca Raton, Florida/Blackwell Scientific: Oxford, 1980.) $77.95, £50.75.

ABOUT 100,000 species of fungi are known. They are ubiquitous in soil, in water, on organic matter of all kinds, and occur as parasites of plants and animals, and as symbionts in association with algae in lichens, and with roots forming mycorrhizas. Their prolific reproduction and effective dispersal ensure that suitable substrata are quickly colonized, and it is uncanny how, at the right place and time, on the appropriate substratum, a particular fungus can be found, indicating precise adaptation to its niche. Fungi play important roles in ecosystems, especially as parasites and as decomposers. Some — for example, lichens, or *Rhytisma acerinum*, the cause of tar-spot of sycamore — are valuable indicators of SO_2 pollution.

To review the ecology of such a group of organisms is a daunting task and, for a single author, well-nigh impossible unless he attempts severe selection of the wealth of available material. A glance at the contents page of *The Ecology of Fungi* shows that this sets out an impressive synopsis of subject matter. Unfortunately the actual text is a great disappointment. "Basically, this book is an elaboration of an earlier review of the subject . . . ." (by W. B. Cooke in 1958). It is emphatically not a book for a beginner. Nowhere is there an attempt to set out the principles of the subject and many terms are introduced without definition. Most of the sections are annotated literature abstracts, such as might be made by compiling and arranging a collection of *Biological Abstracts*. Rarely is there any critical appraisal or synthesis. Too often, no conclusions are drawn, but merely a statement is made that a certain study has carried out. It is, of course, dangerous to make selected quotations out of context, but the following are offered, without the reference numbers, to give an impression of flavour.

> It has been shown that collections of *Schizophyllum commune* can produce turgid spores after more than a year of complete desiccation. Assuming that a turgid spore is a viable one, spores of this species can withstand considerable desiccation.

There is an obvious confusion here. The reference is to Buller (1909), and it should have been added that the *fruit-bodies* which Buller freeze-dried have been revived some 52 years later (Ainsworth in *Nature* 195, 1120; 1965).

> Transpiration was found to be a vital function in the fruit-bodies of agarics. It occurred under conditions of complete

saturation, although at a reduced rate. The rates of transpiration and translocation were similar. The behavior of fairy rings appears to bear out the theory that transpiration and translocation are closely connected.

At least one of the cellulolytic fungi, *Memnoniella echinata,* has been studied intensively, and it has been shown that spores of this fungus and of *Stachybotrys atra,* another cellulolytic fungus, may be produced on the same mycelium.

There are also, unfortunately, some serious omissions.

To date, attempts which have been made to study the succession of development of these fungi [which inhabit dung] have been weak except for the little attention which has been given to the matter in certain laboratory exercises.

There is no mention of the work of Harper, Richardson, Wicklow, Larsen, Ikediugwu, or even the reviews by Webster or Lodha.

Few studies have been made on the succession of fungi involved [in wood decay] or their contribution to the rate of decay.

The important phenomenon of fun-gistasis and Lockwood's review (*Biol. Rev.* **52;** 1977) are completely ignored. There is no mention of heterogenic incompatibility. The effects of C/N ratio on fungus growth are covered in four lines and one reference. The subject of mating behaviour in *Achlya* is discussed without reference to antheridiol and oogoniol, and that of the Mucorales without reference to trisporic acid. The illustrations are sparse, consisting mainly of graphs or histograms, with relatively few, badly reproduced half-tones. The number of misprints is high.

The most useful feature of the book is the list of 1293 references. But, as already indicated, it is seriously lacking in some subject areas, and is not very recent (116 references post-1975, 19 references dated 1977 and 1 for 1978).

With all these defects and a high price the book is not worth buying by individuals, although some well-endowed libraries may find a place for it. □

John Webster is a Professor and Head of the Department of Biological Sciences at the University of Exeter, UK.

Highways and byways of cosmology

M.J. Laird

Theoretical Cosmology. By A.K. Raychaudhuri. Pp.298. (Clarendon/ Oxford University Press: Oxford, 1979.) £10.

IN THE preface, the author expresses the hope that this book will prove both a handy reference for the professional cosmologist and a readable and informative review for the advanced graduate student and the physicist who is not a cosmologist. I should state straightaway that I am numbered among the non-cosmologists, though I was supervised by one cosmologist (H. Bondi) and did post-doctoral work under another (T. Gold).

Now for the contents of the book. After a brief introduction, the author presents the standard Newtonian and relativistic cosmologies. There are chapters on the microwave radiation background, thermal history and nucleosynthesis, singularities, perturbations, galaxy formation, and on the tricky business of analysis and inter-pretation of observational data. However, a particular feature is the inclusion of a wide range of models and theories. Some of these, such as relativistic models not satisfying the cosmological principle, varying gravitational constant and Brans–Dicke theory, and Einstein–Cartan theory, are considered in some detail. Others — two-tensor theory, the conformally invariant theory of Hoyle and Narlikar, and theories involving equal amounts of matter and antimatter — receive brief mentions. At the end of the book, the author discusses the extragalactic radio sources, and those hardy annuals, Mach's principle and Olbers' paradox.

The book is reproduced from typescript. There are some errors, including the definition of the Ricci tensor, and some places where one could be confused. For example, on one page R appears in the field equations, and on the next as the scale factor in the Robertson–Walker metric without indication that the meaning has changed. The author also writes "deuteron" for both deuterium and the deuterium nucleus.

The exposition is certainly that of the review rather than that of the monograph or treatise. Many results are presented rather than derived, though there are many references (about 800). I can vividly remember meetings of the Royal Astronomical Society at which cosmologists spoke with evangelical fervour. In contrast, the author takes a rather dispassionate view. As far as the stated objectives are concerned, I think that the non-cosmologist with no prior knowledge of the subject, or at least of general relativity, would find parts of the book fairly hard going. The cosmologist (or prospective cosmologist) might find it a useful guide to the highways and a reminder of (or introduction to) what are currently some of the byways of cosmological theory. □

M.J. Laird is Lecturer in Mathematics at King's College, University of London, UK.

One lake in great depth

Brian Moss

Neusiedlersee. Edited by H. Löffler. Pp.559. (W. Junk: The Hague, 1980.) DG195, $102.65.

SOME limnologists find their souls in the immensity of the deep glacial lakes of the Alps and Norway, others in the heat-trembling far shore of a Rift Valley salt lake. And some join Wilfred Thesiger and Majorie Stoneman Douglas in their feeling for the great marshes, where, for a time, the tall reeds still shut out the abuses, often sanctioned as acceptable water quality, now heaped on the world's fresh water.

The Neusiedlersee, a shallow, slightly saline lake linking Austria and Hungary, is half occupied by a reedswamp the beauty of which is celebrated in some colour plates at the end of this book. Like other such shallow lakes it has a fascinating history of co-existence with local peoples who exploited the reeds, sedges, fishes and wildfowl without upsetting the intricate relationships supporting the ecosystem itself. More pressure is now placed on the lake — eutrophication, tourism, tamperings with the water level — but it has fortunately yet suffered less than some comparable water bodies and hence has been an ideal subject for the many-sided investigation which is the subject of this book.

There are 30 chapters, some lengthy and of wide scope ("The Catchment Area, a Geographical Review" for example), others extremely short — one of a single page — or highly specialist (for instance on the distribution of a single species of ostracod). They contain an immense amount of information and a close reading produces as full a picture of the limnology and biota as might be expected given the man-power and financial limitations of all such studies. Particularly full are the sections on aquatic plants and birds; invertebrates are well covered as are algae from a floristic point of view, and the geological and physical information is detailed. Data on the more important inorganic nutrients are scarce. Scientists working on shallow lakes, brackish waters and swamps will find useful comparative information and the impression given is of thoroughness and precision in the listing of details.

Neusiedlersee is, however, very much a collection of separate pieces of work. Professor Löffler, the editor, has laboured hard to bring together the data of over 20 contributors, but has not seen fit to write or commission a chapter which attempts a synthesis. The orthodox separation of those who work on the open-water zooplankton or the productivity of submerged plants is hallowed. It is not easy to see how the immense production, largely ungrazed, of the reed zone may influence the organisms of the open water through, for example, export as detritus or through the cover and spawning needs of open-water fish. I am sure the authors have some sort of mental model of the integration of these and other processes and regret that they have not given some inkling of it. Projection and speculation are of equal interest to other workers as are established facts and not necessarily any less valuable if the facts are given.

The book costs no mean sum, even if book prices have not risen, relative to salaries, as rapidly as rumour would have it. It is solidly produced but will have a fairly narrow market, so I suppose the fairest way of deciding whether the £44 or so is justified is to consider the cost of obtaining the information through Inter-Library Loan were it scattered in journals. With nearly 500 pages of text, exclusive of species and general indexes and colour plates, I should think that the effort of making out all the necessary request cards plus the more obvious costs of the loan system would justify the buying of the book by libraries and by anyone closely involved with the field who has repaid his or her mortgage!   □

Brian Moss is Reader in Environmental Sciences at the University of East Anglia, Norwich, UK.

A change of climate

Graham Farmer and Jean Palutikof

Weather Force. By John Gribbin. Pp.188. (Hamlyn: London and New York, 1979.) £6.95. *Causes of Climate.* By J.G. Lockwood. Pp.260. (Edward Arnold: London, 1979.) Hardback £12.95; paperback £5.95. *World Climate.* By T.F. Gaskell and M. Morris. Pp. 144. (Thames and Hudson: London, 1979.) £7.95.

INTEREST in climatic change has grown in recent years to span almost the entire spectrum of society. The interest is in response to a number of factors: growing awareness of Man's capacity to modify the weather and climate; the recent experience of extreme conditions such as the UK drought of 1976 and the severe winter of 1978-1979; finally, perhaps, a realization that since global resources barely fulfil the demands made upon them today, any change in climate could have catastrophic consequences.

Inevitably, out of this general interest has sprung a new breed of introductory books on climatology, devoting a large proportion of the text to the subject of climatic change. This bias is shared by the three books reviewed here. And because of it, the books have in common a further structural element. To make room for the extensive treatment of climatic change, the traditional introduction to climatology through an explanation of elementary atmospheric physics is at best only cursorily treated.

The books differ greatly in level. Whereas Gribbin's book is clearly designed for the interested layman, and provides very good value for money at that level, Lockwood has produced a text for university and college introductory courses in climatology. The book by Gaskell and Morris falls between these two extremes, and as a result suffers from a problem common to all attempts at compromise, uncertainty.

Weather Force, by John Gribbin, does not set out to teach meteorology or climatology, but looks instead at the impact of climate and specific weather phenomena on Man and society. This is done through a somewhat sensationalist, but very well illustrated (there are some 200 illustrations, mostly photographs, in the 190-page text), account of extreme weather events such as hurricanes, drought, floods and record-breaking hailstones. There is heavy reliance on visual impact, with lavish photographs and items of note blocked off into boxes. The latter technique does lead to some repetition and awkwardness in following the main text.

Both Chapters 1 and 3 are devoted to the discussion of extreme weather events. These cover not only the severe winters and droughts of the 1970s, but go back in time to the Solway Firth bogburst of 1771 and beyond. Flooding and hurricanes have the greatest coverage, enlivened by numerous personal accounts. One problem, especially in Chapter 1, is that Gribbin seldom gives more than one side of an argument. For example, it is stated as fact that both the severity and the frequency of extreme events increased during the last decade, and that this trend will persist in the future. No mention is made of the extensive statistical work, such as the well-known study by Ratcliffe *et al.* (*Q.JlR. met Soc.* **104**, 243-255; 1978) which shows no such increase in variability.

Chapter 2 is a general summary of climatology. As such it is perhaps somewhat misplaced, but to have begun the book with such a summary would have led to loss of impact. It is unfortunate that some of the diagrams here are not up to the book's general high standard. For example, in the representation of a warm front the frontal line in the air does not meet the frontal line on the ground, and the diagram showing states of water in the atmosphere is confusing and lacks sufficient contrast.

Climatic change, the cause of changes in the frequency of occurrence of extreme events, is discussed in Chapters 4 and 5. There are some questionable points

Frost Fair on the Thames, 1683–1684

BBC Hulton Picture Library

regarding, for example, Scottish policy in the seventeenth and eighteenth centuries. The theory presented is disputed by many historians, but Gribbin again fails to present both sides of the argument. There are also contradictions, such as the statement that a new Ice Age would cause the Sahara to be "as bad as ever" (p.47), yet would provide "rich supplies of grain, meat and milk" (p.95).

Chapter 6, "Climate and Food", is an excellent introduction to the political and economic implications of food shortages in the developing world. Gribbin presents a well-balanced argument to show that enough food *is* available today to feed the world's population, were it not for human factors. The same theme of climate and Man is continued in the final chapter looking at weather modification, with an unusual but interesting section, "Who pays when things go wrong?".

In general, this is a professionally written and entertaining book. It would have been improved by a list of further reading beyond the two books (both by John Gribbin) mentioned in the text. There is also some danger in the one-sided presentation of views, sometimes against current scientific opinion.

John Lockwood's book, *Causes of Climate*, is intended, according to the Preface, "to provide arts and social science students with an introduction to modern climatology, and science students with a basis for further advanced study". For the non-science reader, this book assumes too much knowledge. A lecturer using it as a basic text would, for example, have to tread very carefully through the development of the Bowen ratio on pp.56–57. Terms such as specific humidity and thermal inertia are used with scant explanation. For the scientist this approach is highly satisfactory: it avoids the often laboured explanations of other standard texts trying to accommodate scientists and non-scientists alike.

Another positive attribute of *Causes of Climate* is that the standard approach of

laying a groundwork of meteorology separate from and before introducing any climatology is not used. Instead, the two are carefully woven together with the emphasis on climatology, drawing in meteorology only as and when it is necessary to elucidate a point.

The introduction is made through the general concept of systems, leading up to the climate system and the role of energy within that system. Radiation is discussed in detail and at length in the second chapter, as the prime energy source of the atmosphere. The following two chapters cover the nature of surface climates, first through the role of different types of surfaces, and second through atmospheric circulation patterns. More should have been included at this point on water in the atmosphere and in atmospheric systems such as fronts. In general, the book is inadequate in this respect.

The last two chapters are perhaps the least satisfactory. Some 12 pages in Chapter 6 entitled "The Climate Future: Climatic Models and Trends" are devoted to a detailed explanation of a hydrological model for the central Pennines devised by Lockwood and Venkatasawmy (*J. Hydrol.* **26**, 79–94; 1975). This appears to be largely irrelevant to the flow of reasoning in the chapter, and improvement would result from either discarding it or replacing it by a more appropriate example. Chapter 7, "Man and Climate", is only seven pages long, and deals with alternative climatic scenarios in the next century and their impact. Given that climate has a crucial economic role in this over-populated and under-fed world, this chapter could well have been expanded.

Overall, Lockwood's book is an excellent addition to the range of basic climatology texts, particularly for those seeking a new approach to the discipline. Although there are some omissions, these are of topics more than adequately covered elsewhere, and this is compensated for by the wealth of new material provided.

World Climate by Gaskell and Morris

attempts to approach its subject at a level somewhere between the other two books. The result is unsuccessful. The text abounds with statements which are at best unhelpful and at worst misleading: "Although there is not much air around in the stratosphere . . ." (p.100), "Part of the sun's energy is . . . trapped in the space above the atmosphere" (p.99). The book carries with it an air of haste which manifests itself in major and minor inaccuracies throughout.

After a short opening chapter, "Facts and Fluctuations", the authors attempt to condense into 12 pages the contents of an introductory meteorology textbook. For the reader this must lead to confusion, further reinforced by inaccuracy. For example, centrifugal force is mentioned in the text but not incorporated in the accompanying diagram (p.16), so that straight-line rather than curved flow would result from the balance of forces shown.

The straightforward chapters on meteorology and weather forecasting are well written and clear. The use of the six-season approach to describe the annual trend of atmospheric circulation is a useful technique. Chapter 7, "Heat from the Sun", would have been better placed amongst the earlier chapters on introductory meteorology.

Special mention must be made of the diagrams. It is disconcerting to see that acknowledgements are not given for figures taken from other works. Figure 27, showing the Russian rivers scheme, is taken without acknowledgement from p.183 of the out-of-date book by Overman (*Water: Solutions to a Problem of Supply and Demand*. Aldus: London, 1968). Figures 16 and 17 are taken from p.432 of Lamb (*Climatic History and the Future*. Methuen: London, 1977), but the caption of Gaskell and Morris is incorrect. The map is from a sixteenth (not fourteenth) century manuscript, and is drawn with a much higher degree of imaginative interpolation than Gaskell and Morris suggest. To compound these inadequacies, some of the other figures are of little use and contain inaccuracies. For example, the stylized radiation balance bears little resemblance to the correct, more intricate pattern and the caption is misleading.

The overall confusion which abounds in this book is symbolized in an example from the index: a reader searching for information on "oxygen isotopes", "cores" or "Emiliani" is directed to a photograph (p.65) of a glacial valley in Merionethshire.

Gribbin and Lockwood are to be congratulated on producing two fine and complementary books. They are recommended to all, including Gaskell and Morris. □

Graham Farmer and Jean Palutikof are Senior Research Associates in the Climatic Research Unit of the University of East Anglia, Norwich, UK.

nature

19 June 1980

What (if any) future for nuclear power?

WHAT on earth is to be done about the nuclear power industry? For the past several years, governments in the industrialised West have been perplexed to know how best to handle the domestic problems in which their own industries have become enmeshed. In most places there is a groundswell of public opposition, or at least of disquiet at the prospect that large numbers of nuclear power stations may be built. Elsewhere there are more specific problems to be resolved. In the United States, for example, the shadow of the Three Mile Island accident has not been fully dispelled by the Kemeny Report. The Nuclear Regulatory Commission has been reorganised but the 7 June deadline for the licensing of reactors built but not yet operating has been allowed to slip, postponing the time when eight reactors now ready to generate electricity can be put into commission. In the United Kingdom, the immediate problems are different but no less daunting — after a decade of optimism and two decades of hesitancy, the doubts of the public authorities (the government and the nationalised utility) about the kinds of reactors they would like to build are matched only by more general doubts about the capacity of the construction companies to do their part of the job. What (if anything) is to be done?

Perhaps the first need is to acknowledge that the present uncertainty about the future role of nuclear power is shot through with irony. First, uncertainty about nuclear power coincides with that period in recent industrial history at which a successful nuclear power industry would be as welcome as the prophets of the 1950s were fond of promising. Second, the industry itself, once fond of explaining to anybody willing to listen that its technical competence was so easily demonstrable, and its technique so innovative, that by its example it would show how the rest of industry might join the Twentieth Century, now finds itself pilloried for incompetence.

The President's Commission on the Three Mile Island accident could and should have been much more critical of the technical design of the reactor that went wrong. (It is almost beyond belief that thermocouples in the reactor core were designed to produce temperature readings within the normal range and otherwise merely question marks.) In Britain, the Advanced Gas Cooled reactors, conceived unnecessarily in the early 1960s, have been painfully and unprofitably slow in gestation. Third, public opinion of nuclear power, once approving and even applauding, has turned sour to say the least. The newspapers that were once chauvinistically full of tales of how clever their nuclear engineers had been are now full of tales, even fairy tales, of how dangerous nuclear power may turn out to be.

It is a matter of great importance, for the professional community as well as for the public at large, that these dilemmas should be quickly and sensibly got rid of. For the reputation of science and technology will be permanently tarnished if the muddle about nuclear power persists much longer. Indeed, there is a sense in which any resolution would be better than none. Not merely does the present hesitation keep large numbers of skilled people at work on plans that may never come to pass, which is a waste of resources and dispiriting for those concerned. It is also bound to seem a sign, to many intending entrants to these professions, that science and technology are much less able to change the world in welcome ways than they would have had reason, in the 1950s at least, to hope. Altruism, to be sure, is only a part of the reason why young people make careers in one field or another, and in any case there are many other fields of science and technology where people can hope to work in ways that are rewarding for others as well as themselves. It would however be mistaken to shrug off the disappointments of the nuclear power industry as entirely irrelevant.

Moreover, it is not simply bad luck that worldwide hesitancy about nuclear power should come at a time when oil is in short supply. Raking over the past, always entertaining and sometimes instructive, is also frequently dispiriting. It is however important that many of the present problems of the nuclear power industry stem from a misreading of the problems of energy supply nearly a quarter of a century ago. Thus in 1957 the OECD (then the OEEC) published a report on energy prospects by a committee under the late Sir Harold Hartley which, in essence, urged on Western governments that the most economical way of generating electricity would be by the use of cheap and plentiful oil from the Middle East. Many governments, conspicuously the then British government, took that as an opportunity for cutting back on nuclear developments. In retrospect, it is almost inexplicable that in 1970 a task force appointed by the then President Richard M Nixon assured the White House that supplies of imported oil would be reliable and free from the risk of political interruption. In reality, recent events in the oil markets of the world have been on the cards since the formation of OPEC in the early 1960s. It is too late now to know whether the course of OPEC prices would have been different if the industrialised oil importers had prosecuted the development of nuclear power more vigorously. But shortsightedness is a more plausible explanation for the coincidence of crises than bad luck.

The way in which the reputation of the nuclear power industry has been tarnished with the passage of the years is also not an accident. Again in retrospect, it is quite breathtaking that the plans hatched in the 1950s by the then new nuclear industries of the West should have been as ambitious — and as brash — as events have shown them to be. The British government's White Paper on the subject, published in 1955, will surely rank high in the archives of official wishful thinking, with its plan for embarking on a dozen nuclear power stations, involving no fewer than four different designs, in a mere decade. During the same period, nuclear people underestimated the problems such as long-term waste disposal, the risk of reactor accidents (and of the steps that should be taken to deal with them). The fact that some reactors (Three Mile Island) and some reactor types (Advanced Gas-Cooled reactors) have not lived up to what was expected of them has inevitably sharpened public uneasiness about the future of nuclear power. It must, of course, be acknowledged that opinion is also divided within the professional community.

In such circumstances, it is unreasonable and even unwise to ask that governments should not be hesitant. What else can democratic governments do but balance the conflicting wishes of their electors? To ask that they should ram disputed policies down the throats of a divided electorate is to ask that they should cease to be democratic. In Britain, if the protracted examination (now under way) of the government's new ten-year nuclear programme by the House of Commons Select Committee on Energy will help to reconcile conflicting opinions, the time spent will have been worthwhile. The promised public inquiry on the proposal to build a single pressurized water ractor may also help, at the cost of further delay. No doubt the Kemeny Commission's report will in due course also be a kind of balm. None of this, of course, excuses those occasions on which governments have timorously

postponed decisions that should have been taken (the previous British government), have over-reacted to public anxiety about some aspect of nuclear power (President Carter's pointless Non-Proliferation Act (see page 526)) and have tolerated incompetent administration (that of the US Nuclear Regulatory Commission before Three Mile Island). The consequence, however, is that it will now be several years before the industrialized nations can hope to reap whatever benefits there may be in fully integrated fission fuel cycles. In Britain, for example, it will not now be possible to commission a full-scale fast reactor before 1995.

Many professional people are deeply frustrated by this prospect. Many others, and a large section of the community at large, are fearful that even 1995 is too soon for comfort. What is to be done to reconcile these views? Given the unavoidable limitations on what elected governments can set out to do, the long-term goal must be a more or less common public understanding of what the hazards of nuclear power may be. But how, some will say, can that be attained when the technical issues are so complicated, involving the probabilistic assessment of unfamiliar risks, attempts to estimate what happens over centuries to radioactive wastes and esoteric bits and pieces of high technology? Fortunately, this is a travesty of the potential for public understanding. First, there is no reason why the public at large should not come to as useful an understanding of the niceties of nuclear power as it has, in the past decade, of the relationship between increases of salary and the rate of inflation. Second, public confusion mirrors the division of professional opinion. Only that sustains the crowds willing to turn out on public holidays for this

or that demonstration against nuclear developments of any kind, but the division is troubling also for those who stay at home. home.

The key to the future of nuclear power therefore rests where it belongs, with the professional community whose reputation is, at least in part, at stake. What must be done to bridge the gulf that now divides it? Pure reason will not by itself suffice, people's positions have become deeply entrenched. Those who hold that even fast reactors can be built without unacceptable risks have a duty to explain themselves to their colleagues (which, fortunately, they have recently been more inclined to do). Those who hold that long-lived waste can be disposed of (or stored) safely for periods of the order of 10,000 years must say how (or otherwise think of something better, like the separation of the actinides from high-level waste). Similarly, those who argue that the risks and dangers of nuclear proliferation are proportional to the amount of plutonium manufactured must be asked to justify their arithmetic. Those who hold that the risks of nuclear power are inherently greater than those of other enterprises must explain why their opinion is not cant. The trouble with the nuclear debate within the professional community is that, in spite of all the abuse that has been thrown about, it has been excessively polite. People have joined advisory committees to help write predictable reports, people have made speeches, given evidence to inquiries and talked to the newspapers and have considered their duty done. The important need is that professional people should convince each other.

More trouble about students' fees

MR Mark Carlisle, Secretary of State for Education and Science, managed only a second-rate defence of his government's policy on fees for overseas students in the House of Commons on 5 June. Although a more skillful parliamentarian might have shown his critics a cleaner pair of heels, Mr Carlisle's difficulties stem from more basic troubles. For the policies he and his colleagues are following are both inconsistent and unrelated to their other concerns, such as they may be, for the development of higher education in the United Kingdom. They will discover their defence of their position just as difficult until they are able to work out among themselves a more convincing explanation of what they are about. In the meantime, higher education and the universities in particular, not to mention their prospective students, will be subjected to needless uncertainty and, perhaps, damaging financial trouble.

Although there are many British academics who still hanker after the principle that all students at the same university should pay the same tuition fees, this was abandoned by British universities, at the government's request, more than a decade ago. And, indeed, there is something in the view that students who do not themselves or through their families contribute towards the cost of a maintained university system should pay somewhat higher tuition fees than others. This is, of course, the basis on which the state universities in the United States operate systems of tuition fees that differentiate between students from within and from outside the state concerned. That some countries, France for example, make no distinction between the fees of home and overseas students is logically irrelevant even though it may (and should) be a reminder of the value often attached to the principle of open access to higher education. The issue which has divided academics in Britain from their paymasters in the government is, however, the pragmatic question of what fees should be charged to students from overseas.

It is only charitable to suppose that when the British government announced just over a year ago that it would seek to recover the 'full economic cost' of educating overseas students, it had no more than a calculation on the back of an envelope to help. In the event, the government has interpreted that as the average cost of teaching students, implying that new students will be charged tuition fees comparable with even those in North

American universities from the beginning of the academic year. Last week, Mr Carlisle had no reply to the argument that marginal cost would have been a better basis.

For the time being, indeed, the government seems to be simply hoping for the best. All along, the universities have been concerned that the high cost of the fees now in prospect would so effectively frighten away new students that their total incomes might actually decline. (The government plans to enforce its will by reducing the recurrent grants the universities will receive in future years in proportion to their populations of overseas students.) Last week, Mr Carlisle made as much as he could in the House of Commons of the fact that the returns from the Universities' Central Council on Admissions are only 12 per cent below the corresponding figures this time last year. This, however, is an insubstantial comfort (see *Nature*, 27 March). Many students who have applied for places next year will not turn up. Others will turn up without their full fees. No amount of public speaking at this stage can discover what will be the consequences next September.

Inevitably, however, some universities and polytechnics will be more seriously affected than others. If overseas students were to show the same preferences among universities as do British students, the result might even be to take resources away from those institutions that are least able to attract students of any kind. There are grounds for hoping that in due course British universities will indeed be helped to be more competitive among themselves (*Nature*, 22 May). Unfortunately, the perturbation caused by the higher fees now in prospect is that individual universities will be affected in a more or less random fashion, according to their present intake of overseas students. If the government has seriously embarked on the encouragement of a free market in higher education, there are several constructive steps that it could take. Already, students' fees account for more than a fifth of universities' incomes, more than twice the proportion of fees obtaining before the last large increase of all students' fees in 1977. The degree of universities' dependence on the University Grants Committee's continuing support is in other words already declining. A further arbitrary push in this direction is not what the system now needs. Why not, even at this late stage, settle for marginal costing as a basis for calculating all fees?

Administration comes in from the sun

Washington

The Carter Administration's image as a strong supporter of solar energy is going into eclipse. Last June the President committed the United States to the objective that 20 per cent of its energy should come from the sun by the year 2000; but the Administration is already discussing budget figures for solar research and development which, critics say, make this goal unachievable.

The source of the controversy is a memorandum leaked from the Department of Energy last month revealing current thinking on the evolution of the energy budget over the next five years. This shows an increasing share for nuclear and fossil energy — from 37 per cent of the budget in 1981 to 43 per cent in the period 1982-86 — and a corresponding drop from 24 to 20 per cent for solar energy and conservation efforts.

Defending these figures in front of a congressional committee last week, Energy Secretary Mr Charles Duncan pointed out that they were not firm commitments, but were intended as background to preparations for the 1982 budget request, and were likely to alter from year to year.

"I believe we are on track toward achieving the nation's solar goals", Mr Duncan said. "But I believe it is unrealistic to assume, as some do, that we can lay out a detailed and precise road-map that tells us what is going to happen year by year for the next twenty years."

Given the vagaries of technological forecasting, Mr Duncan's logic is not disputed. But according to published and unpublished documents produced by committee chairman Representative Richard Ottinger, at least some DoE officials and their outside advisers feel there is a growing gulf between the political rhetoric surrounding long-term goals, and the political realities of short-term budget choices.

At the centre of the dispute is President Carter's 20 per cent target, itself based on a study carried out by White House staff and the DoE. Presented with various policy options, the President selected the "maximum practical goal" of 18.5 quads of solar energy by 2000, when total energy demand is expected to reach 95 to 100 quads. Politically, this was judged the least that the vociferous solar lobby, which had pushed for an even larger commitment, would accept, and the most that sceptics within the Administration could live with.

The President admitted that achieving the goal would require not only substantial cooperation from the private sector, but also a vigorous and sustained commitment by the federal government.

It is the desirability of this federal involvement that has since been challenged, particularly in a period of budget stringencies and of pressure to

reduce public participation in potentially commercial programmes.

Earlier this year, for example, the Committee on Nuclear and Alternative Energy Systems of the National Academy of Sciences aroused the anger of solar advocates with a report claiming that the President's goals could be approached only by federal subsidies far higher than those currently given to other energy sources. The issue has been sharpened by the tightening of budget constraints.

The detailed expenditure proposals in last year's White House review are substantially higher than those being considered by the DoE. Thus, the policy review suggested that biomass could be contributing 5.4 quads a year by the end of the century, but that an investment of at least $150 million a year over the next five years would be needed. In contrast, the DoE estimates reckon on a more modest budget of $60 million a year over this period.

What angers the critics most, however, is not so much the precise levels of proposed funding as broader evidence that the Department of Energy may not be giving adequate attention to the solar and conservation fields.

Here they are supported by two recent reports from congressional review agencies, the General Accounting Office and the Office of Technology Assessment, both of which take the DoE to task for failing to take the steps necessary to

implement the Administration's solar goals.

The OTA report, for example, published in Washington last week, concludes that solar and conservation programmes are hampered by a lack of direction and leadership.

Energy Secretary Duncan admitted at last week's hearing that such management problems had existed in the past, but listed recent steps he had taken to resolve them.

Duncan also listed the Administration's achievements in solar energy, quoting the $36 million recently awarded for the installation of solar heating and cooling systems in federal buildings, and contracts for nine major photovoltaic systems in commercial and industrial settings.

Solar advocates are not overly impressed. They point out that, although the Administration can demonstrate a spectacular rise in support for solar energy from a few million dollars in the early 1970s to a proposed budget of $1,400 million in 1981, Congress has led the way.

For two years things looked different, with positive discrimination apparently flowing from the White House in favour of solar energy as an alternative to less environmentally-acceptable options. Last month's leak may result in a small increase in the solar budget request when it comes formally to Congress next January. Otherwise, it looks as if it will be business as usual.

David Dickson

Polish chemist gets off lightly

Miroslaw Chojecki, a young Polish chemist and campaigner for academic freedom, last week went on trial in what Polish intellectual circles regard as a test case — and received as near as the authorities could come to an acquittal.

Chojecki was formerly employed at the Swierk nuclear research centre near Warsaw. In 1976, he became a member of the "Workers' Defence Committee" (an unofficial human rights group), and shortly afterwards was dismissed from his job. Since then, he said before his trial last week, he has been allowed no access to any scientific libraries or periodicals. With his own academic career at an end, Chojecki and a few friends founded, in 1977, the "Independent Publishing Enterprise, NOWA", which strives to fill the gap caused by what he described as the state monopoly of information.

In particular, NOWA has published several textbooks for the underground "Flying University" — a dissident educational self-help body which, although specialising in the social sciences and humanities, numbers among its patrons some of the most distinguished Polish natural scientists.

(Its "Dean", Professor Jan Kielanowski, is a member of the official Polish Academy of Sciences, and a world authority on animal nutrition.)

Not surprisingly, the "Flying University" came out strongly with an open letter in Chojecki's defence. Tacit support from the scientific community at large, said Chojecki, was even more widespread. On two occasions, leaflets calling for his acquittal were discharged over central Warsaw from a catapult mounted on the building of the Academy of Sciences itself.

The formal charges against Chojecki were misappropriation of a duplicator and incitement to induce two employees of a state printing concern to print a dissident work. In fact, as he stated in his 2000-word defence, everyone in court was aware that the whole issue of intellectual freedom was on trial. Chojecki made no effort to deny his publishing activities — he even submitted as evidence the catalogue of works he had produced. After an 11-hour hearing, he received an 18-months suspended sentence, and a fine which was waived in consideration of his pre-trial spell in prison.

Salaries

Physicists get on

EITHER go west, or work for the government — that seems to be the inference that young British physicists will make from the latest remuneration survey among members of the Institute of Physics published in the most recent issue of *Physics Bulletin* (May 1980).

The figures now published show that the salaries of physicists working in the Civil Service consistently exceed those of academics and industrial physicists once the age of 40 has been passed. In the age group 55-59, the peak of physicists' earnings, the median salaries of those in the institute's two most highly qualified categories of membership (fellows and members) are now £15,750 p.a. for civil servants, £13,060 for academics and £11,940 for industrial physicists. The survey has shown the same pattern of salary differentials for the institute's membership as a whole.

The results of the latest survey show that there has been no radical change in the pattern of physicists' salaries since earlier surveys in 1977 and 1974. Broadly speaking, young people do best by working in industry immediately after graduation. Fellows and members of the institute in the age group 25-29 had median salaries (in 1980) of £6,570 p.a., compared with £5,850 and £5,780 in government service and the universities respectively. For these categories of membership, the financial advantages of industrial life persist until 35, but in later age groups government physicists are ahead of those elsewhere.

Alternatively, the most highly qualified members of the institute can expect their salaries to increase during a working lifetime (between the age groups 25-30 and 55-59) from a median of £5,850 to a median of £15,750, a ratio of 2.9. The corresponding ratios for academics and those working in industry are respectively 2.26 and 1.82.

The latest survey thus bears out the suspicion of many of those leaving universities, in other fields of science as well as physics, that industrial employment, although initially somewhat more rewarding in financial terms, offers a less dynamic pattern of employment than government service and academic life.

The latest survey also shows, however, that physicists have managed to keep up with inflation reasonably well in the past few years. In all categories of membership, and in all age groups, salaries have more than doubled since 1974.

The largest increases have however gone to the younger age groups and to those in the least qualified categories of membership (associate members and associates). Indeed, the median salary of associates of the institute in the age group 25-30 (£6,720) now exceeds that of the members of the same age (£6,290 p.a.)

Proliferation

Trimming sails

Washington
More carrot, less stick. That is the message being given to President Carter by State Department officials as the US Administration reassesses its strategy for limiting the spread of nuclear weapons through unilateral controls on nuclear technology.

Staunch non-proliferationists in Congress and other parts of the Administration are demanding that the President stand firm, and in particular that he reject India's pending request for 39 tons of enriched uranium for its Tarapur power plant because of its refusal to accept international safeguards.

But elsewhere there is growing feeling that, in order to maintain credibility and effectiveness, the US must shift from the 'control and denial' aspects of non-proliferation strategy to emphasising the incentives for compliance offered by US promises of a 'reliable' supply of nuclear fuel and technology.

Such sentiments have risen to the surface following the completion in February of the International Nuclear Fuel Cycle Evaluation. Proposed by President Carter in 1977, INFCE endorsed several aspects of US policy — but fell far short of endorsing all of them.

Supporters of the nuclear industry are now using the INFCE findings to challenge key aspects of Carter's policies. For example the House of Representatives Commerce Committee last week recommended that the Nuclear Regulatory Commission proceed with licensing review procedures for a new reprocessing plant; these were suspended in 1977 at the President's request, with the promise that the order would be re-examined after the completion of INFCE.

Despite indications of a possible relaxation, the Administration has given no sign that it intends to change its basic policy in the light of INFCE. Rather it is seeking ways to enhance its image as a reliable supplier of nuclear technology, within the provisions of the Nuclear Non-Proliferation Act of 1978.

The problem is that the act poses what Dr George Rathjens, professor of political science at the Massachusetts Institute of Technology and deputy to Mr Smith, calls a 'fundamental dilemma'.

"Our policy and our law require that we condition our supply of fuel and technology on others accepting US approval rights over the use of US-origin materials", he told the congressional subcommittee. "Yet our imposition of conditions on supply necessarily reduces the confidence of others that they will have access to fuel and technology."

Various ideas on how to get round this difficulty in the light of the INFCE results are now being discussed. Drawing

on INFCE's conclusion that the economics of reprocessing appear to be marginal, for example, Mr Smith has proposed that the US agree to reprocessing by other countries wherever the demand for plutonium is dictated by the needs of fast breeder and advanced reactor research — but not where it is needed merely to manage spent fuel.

Other suggestions being pursued by the State Department are that longer-term licensing could replace current individual requests to transfer and reprocess spent fuel from states with good non-proliferation credentials, and various types of back-up fuel supply arrangements, perhaps with one country agreeing to meet commitments if another country defaults.

Whether changes in emphasis within the existing legislation will be sufficient to meet the objections of critics remains to be seen. Certainly the outcome of INFCE has done little to shift the reluctance of the member countries of Euratom to renegotiate its uranium supply agreements with the US, as required by the NNPA.

Similarly, even if Britain adopts a Westinghouse design for its next thermal reactors, the provisions of the act could lead it to reject Westinghouse as a supplier

---

Non-proliferation act

The Nuclear Non-Proliferation Act which was signed by President Carter in 1978 is an attempt to limit the proliferation of nuclear weapons by tightening restrictions on the supply of nuclear fuels and facilities by the US to foreign countries.

The act was prompted by India's explosion of a nuclear device in 1974 using nuclear fuel and technology initially provided by Canada for energy purposes. It forbids the supply of nuclear fuels, reactors or reactor components to countries not possessing nuclear weapons which explode nuclear test devices, or which otherwise violate safeguards developed by the international atomic energy authority.

A decision to refuse an export licence for such fuel or reactor components can, however, be overturned by the President if it is considered that such action would be "seriously prejudicial to the achievement of United States non-proliferation objectives or otherwise jeopardize the common defense and security." The President's action can in turn be vetoed by Congress.

In addition, the act provides that no nuclear fuel or technology exported from the US can be retransferred to the jurisdiction of any other nation or group of nations without the prior approval of the US. Nor can spent nuclear fuel either originating in the US or produced with technology from the US be reprocessed without US approval.

of major components, such as the reactor vessel and circulation pumps. Under the current terms of the act, the US would have control over any fuel once it had been irradiated using such components.

But opposition to a change in policy is firmly entrenched, particularly from those convinced of President Carter's correctness in opposing any measures that would increase the spread of plutonium. "The choice between us is not between 'leverage' and 'consensus', rather it is between sticking to our principles and abandoning them" says Dr Tom Cochran, senior staff scientist with the Natural Resources Defense Council.

Given the apparent depth of the President's previous commitment to this position, no substantial change of policy is expected, at least until after the forthcoming elections. But there are several hurdles to be met before then, in particular the Nuclear Non-Proliferation Treaty review conference which takes place in Geneva in August.

Faced with inevitable criticism for failing to secure progress towards an arms limitation agreement with the Soviet Union, the US is hoping to reply by pointing to its efforts in support of INFCE's warnings about the proliferation dangers inherent in reprocessing and fast breeders — and to the steps it is taking to enhance its image as a reliable nuclear supplier to states which sign the NPT.

But it is a long shot. US officials admit that they are faced with a no-win situation at the review conference, and that their prime tactic is likely to be 'damage limitation' rather than anything more ambitious.

David Dickson

Electric vehicles

Top speed at Lords

What will the House of Lords make of the electric car, the topic on which the Select Committee on Science and Technology appointed in January (*Nature* 20 March, page 199) chose to cut its teeth? Nobody is yet sure. But anxious, no doubt,

to fulfil its promise that the inquiry should be short and sharp, the committee has now finished taking evidence and plans to publish its report in July. Electric vehicles are in the same class as saints used to be: everybody approves provided they work. The perennial problem is whether the energy density of the batteries that drive electric vehicles can be increased substantially above that of the lead–acid battery, rated at 150 kilo-Joules kg^{-1} at full charge.

The committee has heard from the chief British battery makers, Chloride and Lucas, that the brightest prospects for increasing energy densities by a factor of between three and four lie with the sodium-sulphur battery. Unfortunately though, vehicle operators would have to put up with the inconvenience of batteries working at 350°C. So nickel-zinc batteries now seem to be the gleam in manufacturers' eyes.

Several witnesses have told the House of Lords that Britain spends little on electric vehicle research compared with the United States and Japan. About £20 million has been spend since the late 1960s, about 75% of which has been put up by private industry. The US, by contrast, has a seven-year $200 million programme which began in 1976. Yet Britain has the largest fleet of electric vehicles — 45,000 of them, mostly used for delivering milk.

The prospects for further and rapid growth of the electric vehicle fleet in the UK are not however bright. Chloride/Talbot and Lucas/Vauxhall have built small fleets of delivery vans (top speed 50 miles per hour and range 50 to 70 miles), which are now operating in several cities. They hope to achieve commercial production in the mid-1980s.

But the manufacturers are cool about the prospects for the all-electric private car. The most promising way of increasing speed and range is by mean of the hybrid vehicle running on part petrol, part battery. US manufacturers seem to be much keener on this development than their UK counterparts who are deterred by the problems of incorporating two different systems within one vehicle. A

hybrid idea which has, however, been greeted enthusiastically in the UK is the hybrid trolley-bus, which runs partly from an overhead power supply and partly on batteries.

Potential operators, the House of Lords has heard, will have little to choose between electric and conventional vehicles in terms of the efficient use of primary fuel. Operating costs will, of course, depend on the relative prices of electricity and oil. But the efficiency of the electric vehicle in terms of the load it can carry can be considerably lower than that of the conventional van because of the great weight of its batteries.

Perhaps the most important question House of Lords committee members have had at the backs of their minds is whether the level of funding in the UK is sufficient, given the current state of knowledge. The Electric Vehicle Development Group, which exists to support and advise manufacturers interested in electric vehicles, told the committee that while the level of fundamental research on battery technology is respectable, it is not matched by a comparable effort in research on motor design, control and body design. Others, however, considered that the balance is about right.

Whether further support is necessary and, if so, whether it should come from government or private forces will no doubt figure in the final report. The Department of Industry, which has put up most of the government money, points out that in allocating its resource it has to balance the potential advantages of spending more on electric vehicles research with spending more on improving the efficiency of the internal combustion engine. It is currently reviewing its priorities.

Judy Redfearn

Thalassaemia

Saudi-London plan

Saudi Arabia has signed a contract worth £1 million over 3 years for joint research on thalassaemia — a crippling genetic blood disease affecting malaria-belt countries. The contract is between two London medical schools — University College Hospital Department of Obstetrics and St Mary's Hospital Medical School Department of Biochemistry — and King Abdul Aziz University, Jeddah.

Negotiations began in 1976 — when the then Saudi Ambassador in Denmark, Sheikh Faisal al-Hegelan, took his 14-year-old thalassaemic son Khaled for treatment at UCH. Khaled was treated by Dr Bernadette Modell, and his parents wanted to know everything about his treatment. (It involved intensive blood transfusions with nightly injections of desferrioxamine to remove excess iron.)

Dr Modell — who has worked mostly with the Cypriot community in London — explained that support for clinical and fundamental research into the disease was lacking in Britain, where it is an uncommon

I THINK WE'LL STICK TO BATTERIES

DRINK MILK

Tom Johnston

condition. But in Saudi Arabia it is quite common and it is likely to emerge as a major medical burden now that adequate pre-natal and post-natal care is allowing thalassaemic babies to survive.

The Ambassador discussed the problem with Prince Sultan — Minister of Defence in Saudi Arabia — who immediately offered $100,000. He sent it to Khaled's mother in England, with the request "to build on this". He would back similar research in Saudi Arabia, he said.

Prince Sultan asked for the fund to be named after his father, King Abdul Aziz, and this may have encouraged other princes to contribute. Prince Nawaf offered $30,000; and Prince Salman bin Abdul Aziz gave £10,000 to the Thalassaemia Society, a group of parents and sufferers. The boy Khaled (who is now 18 and has a good prognosis) himself approached Sheikh Yamani, the Saudi oil minister, who chipped in £15,000 for UCH through Aramco. Dr Modell suddenly found her research — which had rubbed along on £800 a month from private patients and one Medical Research Council technician — could develop.

Meanwhile the wife of Sheikh Faisal — the Ambassador — had asked Dr Modell and her collaborators, Professor Denys Fairweather (professor of obstetrics and Gynaecology at UCH) and Professor Bob Williamson (professor of biochemistry at St Mary's preclinical school), to provide a letter explaining their research and its needs. The result was that Crown Prince Fahd encouraged a link between King Abdul Aziz University and the London schools. Saud Sejeny — the Vice Dean of the medical school — thought that research should be a major element in the contract, and so it has proved.

The £1 million will be divided roughly 50:50 between the UK and Jeddah. The British scientists and doctors will go for short visits to Jeddah, and members of the Jeddah team will travel to Britain for training.

At Jeddah departments of haematology obstetrics, paediatrics and community medicine will be involved. "We have as much to learn from them as they from us" said Dr Modell. Saudi Arabia is determined to adapt Western medicine to a form appropriate to its own culture and community needs. For example, the system of prenatal diagnosis which has been very effective in combatting thalassaemia in the London Cypriot community may not be acceptable for Saudis, as it involves sampling fetal blood at 18 weeks of pregnancy (before that the fetus is too delicate) and abortion at 20 weeks if there is a positive indication. Also there is a high rate of cousin marriage in the country, so that the question of genetic counselling would be complex.

The first step of the contract will be to export methods of clinical treatment, and help standardise techniques for diagnosing haeomoglobinopathies. Jeddah already

works in this area but London will provide "that extra tier of research thinking". The second step will be to extend research, and at Jeddah particularly to mount several surveys to help determine the genetics of thalassaemia syndromes — of which there are more than one.

Future hopes lie with developing new methods of treatment, and with earlier prenatal diagnosis (towards which Professor Williamson has had recent success — see *Nature* **285**, p144; 1980). All avenues are open in the contract and, says Modell "the Saudis will wait to see how this goes. If it goes well, they may design some other projects".　　　　**Robert Walgate**

Defence research
New customers

The British Ministry of Defence is on the way to being a substantial backer of university research. The ministry's spending on university research, amounting to £2.75 million in the financial year 1978-79, had increased to £4.2 million in 1979-80 (both figures in 1978 prices). And there is at least some hope of further growth to come.

Much of the credit goes to Professor Ron Mason, Chief Scientist at the ministry for the past two and a half years, but previously a chemist at the University of Sussex. Although his predecessors in the post have usually come from universities, he seems to have been especially keen that more defence research should be done there. Some of the topics the ministry is just now keen to foster through defence seminars for university staff and industry are operational analysis, surveillance techniques, new techniques arising from space research, applied psychology in man, machine intelligence and signal and image processing.

The stagnation of research council budgets has helped the MOD to open university doors. Mason says that researchers have begun to put aside their scruples about accepting defence money now that funds from conventional sources are scarce. But there is a snag — the general demise of the dual-support system has meant that many universities lack the basic facilities which universities used to offer. The universities have also become less attractive to external bodies seeking to place research contracts as they have become less able to offer jobs to bright young people.

Professor Mason says that the universities are now more sluggish in their response to urgent research needs than even two or three years ago. His problem is that the ministry's own research establishments (34 of them) are no better. There, too, most vacant posts go unfille^

The universities, therefore, have not lost all their appeal. There are two ways in which Professor Mason has tried to tap their resources for defence research. He is

most proud of his defence seminars intended to tell academics what the MOD is looking for and to let Mason and his colleagues know what universities have to offer. So far, there have been five seminars, most of which have led to firm research contracts. Several more are planned.

Mason also hopes for benefits from closer cooperation with the Science Research Council. Both organizations have to tread warily however because of possible conflicting interests. The MOD is oriented towards problem-solving for its own ends whereas the SRC's aim is to support research of 'timeliness and promise'. Nevertheless, says Mason, the SRC has recently become more willing to pick out topics such as polymer science and marine engineering for special attention. He sees no obstacle to future cooperation on promoting areas of mutual concern, systems analysis and space systems for example.

Talks with the SRC chairman on the former and a multi-lateral debate on the latter are already under way. Britain has wound down its national civil space programme to the extent that British scientists now have to rely on the European Space Agency for facilities. Mason, however, reckons that there is a growing interest in space among British industry which could be used to benefit both civilian and military users.

Mason's clout may be enhanced because the defence research budget does not appear to be as much under pressure as the civil research funds. The government recently announced its intention of sustaining a 3 per cent annual growth in real terms in defence until 1986. But there are problems, for defence research, involved as it is with high technology, tends to increase in cost more rapidly than inflation. Next year, Britain will spend 13 per cent of its defence budget on research and development, £1,600 million out of £10,800 million. But is the balance right, and how much should be spent on long-term as opposed to short and medium-term research? Unfortunately, says Mason, there is no way of estimating a correct balance.

The MOD research establishments have been mainly concerned with short and medium-term research, and Professor Mason believes there is a need to increase their innovative function. The MOD has recently reviewed the role of the defence research establishments so as to assess how much of their responsibility could be transferred to industry and the universities. That review is due to be brought up in Parliament before the summer recess.

In the meantime, Professor Mason says there is a need for more collaboration on research between government agencies. "The government enforces a policy of water-tight compartments. But we can't afford, given the resources, an isolated policy", he says.　　　　**Judy Redfearn**

French research

Better budgets

THE French government has proposed a 20 per cent increase in spending on research and development in 1981, as part of its plan that research and development should increase to 2.3 per cent of gross domestic product by 1985. The plan is part of the French budget and remains only to be approved by the Assembly and Senate. A total of 410 jobs would also be created, mostly at the senior postdoctoral level of 'chargés de recherche'.

French science spending, as a proportion of GDP, fell rapidly behind that of other countries in Europe during the 1970s. At present, France spends 1.8 per cent of its GDP on research and development, counting government-backed and industrial science together, compared with nearer 2.2 per cent in other large Western countries. According to figures published by the European Commission, the ratio of growth rates of government science spending and GDP in France between 1970 and 1977 was 0.79, the lowest in Europe. The highest was Ireland with 1.35; then came West Germany (1.25), The Netherlands (1.11), Denmark (1.9), the UK (1.01), Italy (0.94) and Belgium (0.92).

For this reason, Pierre Aigrain, Secretary of State for Science in the French government, has had little difficulty in convincing other ministers that the next five-year plan (1980-85) must show a substantial increase in science spending by government.

However, the recommendations of a controversial report — the Faroux report — on industrial research and development have not yet found favour. Roger Faroux, director-general of the chemical firm Saint-Gobain-Pont-à-Mousson, and his group reported to Aigrain in March that research spending in industry should increase by 65 per cent over the next five years, and that tax incentives should be used this end. The 65 per cent increase compares with the 40 per cent 'in a few years' set as the target by the Council of Ministers in August 1979; thus Faroux is recommending a substantial increase of the proportion (at present 42 per cent) of industrial research in the total research budget.

One of the principal beneficiaries of the new proposals will be the Centre National de la Recherche Scientifique (CNRS), which accounts for a large part of France's basic research. Its budget will rise 20 per cent from £874 million in 1980 to £1,040 million in 1981. (These sums include the salaries of some 20,000 scientists and staff.) Within CNRS, the biggest increase will come in 'moyens direct' — money which will be paid to laboratories without the need for approval by subject committees, and which will be used to buy and replace small to medium items of equipment (infra-red spectrometers, for example).

The CNRS has also been pressed to increase its connections with industry, and to this end has appointed a 'monsieur rayonnement' who will attempt to place departing senior CNRS scientists in industrial jobs — and also in ministries, where CNRS feels it should be better understood. There is now discussion in France as to whether to set up small scientific advisory groups in the ministries, rather on the lines of the 'chief scientist' departments in the UK; this talk is the consequence of the division of Aigrain's empire earlier this year between the Minister of Industry, M. Giraud, and himself. Giraud has taken on responsibility for the space, nuclear and other large projects that were once Aigrain's concern.

At CNRS, it has not been decided how to allocate the 240 new posts which it will receive under the new proposals; but, said a spokeswoman, 'the life sciences will be well off'. Of the other posts created by the government, 55 would go to INSERM (Institut National de la Santé et de la Recherche Medicale) and 38 to INRA (Institut National de la Recherche Agronomique).

Robert Walgate

More cosmonauts

French this time

FRANCO-SOVIET space cooperation took another step forward last week when the French National Centre for Space Studies (CNES) announced the selection of two air force fighter pilots to train for a Soyuz-Salyut orbital link-up scheduled for mid-1982. The two "spationautes", Lieutenant-Colonel Jean-Loup Chrétien, aged 40 and Commander Patrick Baudry, aged 34, will travel to the Soviet cosmonaut training grounds 40 kilometers outside Moscow on September 1 where they will undergo a year and a half of training with Soviet colleagues. The mission calls for a Soviet pilot and a French co-pilot, who will be selected from one of the two French candidates, to spend a week on board the Salyut orbital station where they will conduct a series of eight experiments. Four of the experiments are in the area of the physiology and biology of space including an investigation of the control of bacterial infections in space environments and the effects of weightlessness on the flow of blood in the human body, two are in material science with special reference to the creation of aluminium-indium alloys and two will investigate high resolution space photography. The cost of the programme is 30 million FFr.

The Franco-Soviet project is seen in France to come at a politically favourable time following the recent diplomatic meetings in Warsaw and the decision of France to participate in the Moscow Olympics. But Franco-Soviet space cooperation dates to a 1966 agreement negotiated by General de Gaulle for the purpose of "special cooperation in space research". Since then France has launched a series of satellites on Soviet rockets including the 1977 Sign-3 gamma-ray astronomy satellite and a series of three SRET satellites between 1972 and 1975 to explore cooling and radiation protection problems in space technology. Since 1977, the fields of the biology of weightlessness and space crystallography have been opened up with French and Soviet scientists collaborating on the data collected by French satellites. Future joint experiments envisaged are explorations of the planet Venus including a balloon experiment to investigate the Venusian atmosphere planned for 1984. But the main thrust of French space research, which included collaboration with Germany and the US as well as the USSR, is in applied space research. **Joe Schwartz**

Baltic oil

Moving offshore

Next month, Petrobaltyk, the consortium of Soviet, Polish and East German oil interests, will sink its first offshore bore-hole in the Baltic. This move follows four years of intensive prospecting, which, according to T. G. Vekilov, Deputy Minister of the Soviet Gas Industry, will continue in parallel with the drilling operations. Vekilov was also careful to point out, in a *Pravda* current affairs interview, that there is positively no energy crisis facing the Soviet Union, whose fossil fuel reserves are among the largest in the world. Soviet interest in possible oil or gas beneath the Baltic is, Vekilov implied, simply another aspect of the "forward thinking about future energy" urged by Mr Brezhnev at the 1979 Party Plenum.

For Petrobaltyk, this forward thinking began in November, 1975, when the three participating states signed an agreement about joint prospecting for oil and gas on the Baltic shelf. The area was, on the face of things, promising. Estonia has extensive oil shale deposits, and some small oil and gas deposits had been located in northern Poland.

The primary task of Petrobaltyk, to date, has been to carry out a major seismic survey of the Baltic — one interesting spin-off of which has been the development of a prospecting method based on anomalies of the natural electric field. By 1978, a team from Leningrad had established a set of tectonic, lithologic and hydrogeological indices for oil-bearing formations in the palaeozoic formations of the peribaltic syneclise, and had deduced that for the Cambrian and Devonian strata, prospects increased from east to west, while for the Ordovician and Silurian strata the opposite is true.

Owing to the multinational structure of Petrobaltyk, however, publication of the results of individual surveys has been restricted and geologists taking part in the

surveys have been even more than usually reticent about their preliminary findings. For a time, plans were afort to buy or hire a Vexco drilling rig, but when these had to be abondoned for lack of hard currency, the shut-down of information was total.

Petrobaltyk's own self-produced rig, capable of operating in up to 90m of water, is now moored at Gransk, waiting to go into operation. A few weeks ago, the Helsinki Convention on the Protection of the Marine Environment of the Baltic Sea Area finally became law, binding on all states of the Baltic littoral. A major point of the convention is the prohibition of oil dumping and an appeal to the contracting parties to take measures to prevent pollution resulting from the exploration and exploitation of the sea-bed and its subsoil.

Rather surprisingly, although the Soviet media paid special attention to the Baltic republics and sea in their routine annual coverage of "environment day" (June 5), the emphasis was on effluent dumping, the need for on-shore purification installations, ecology courses in universities, and the necessity for international ecology film festivals.

No mention was made of Petrobaltyk, or of what measures it proposes to take in the case of oil leakage. This may, of course, simply reflect well-placed confidence on the part of the planners. The Finns of the Asland Islands, who caught the main brunt of an oil-slick from the Gulf of Riga last year, have however expressed considerable concern; while on the south-east Baltic coast-line, the citizens of the contracting states of Petrobaltyk, though less vocal, are known to feel a similar concern.

Vera Rich

London Zoo

More falling-out

THE London Zoo has run into another spot of bother. Earlier this week, it became known that Mr Michael Hanson, the newly appointed director of administration at the Zoological Society of London, had resigned his post and would be leaving on 14 August.

Mr Hanson, whose responsibilities include the management of the establishment and the finances of the Zoo, was recruited from the British Civil Service in September 1979. It has been apparent for some time that the chief task of the administrative director is somehow to bring back to balance the Zoo's trading account, either by making sure that enough small children ride enough elephants at a sufficient price to keep all the animals (and their keepers) fed and housed or by some other means.

There is every reason to accept the statement put out by the Zoo earlier this week that Mr Hanson's resignation is unconnected with that of Dr Ronald

Zuckerman is the Zoo

Hedley, the part-time Secretary of the Zoo. Hedley, now Director of the British Museum (Natural History) is said to have been murmuring about overwork for several months.

The joint departure may however provide a chance for making a substantial appointment. The top establishment includes three directors (the other two responsible for animals and research), a secretary and a president, now Lord Zuckerman. Lord Zuckerman, by temperament and inclination, functions very much as an executive president — one council member said this week that 'Solly is the Zoo'.

Concern that he could not get on with the job for which he was hired without detailed scrutiny from above appears to have been one cause of Mr Hanson's departure. Recent meetings of the council have also dwelt on Mr Hanson's plans for re-organisation, considered to have been imaginative and yet similar in their essentials to plans out forward earlier.

When Mr Hanson first tendered his resignation, he was apparently asked by the council to reconsider it, but declined to do so. It is not known what may have passed between him and Lord Zuckerman.

Patent law

Bugs protected

By the narrowest of margins, the US Supreme Court had decided that living micro-organisms can be patented. In a verdict announced on Monday, the court ruled by five to four that there is nothing inherent in existing US patent law which prevents an invention from being patented just because it is alive. The court had been asked to decide on an appeal by the Patent and Trademarks Office against the decision of a lower court to grant a patent to Dr. Ananda M. Chakrabarty of the

General Electric Company for an artificially bred strain of the bacterium *Pseudomonas*, first developed to help clear up oil spills by degrading different chemical components.

Dr Chakrabarty's bacterium was not created with the use of recombinant DNA techniques. However it does fall within the general category of genetic engineering — and the court's verdict is seen as a welcome boost by pharmaceutical and other biotechnology companies which, together with several US university research groups, have had patent decisions on new micro-organisms held up until the Supreme Court's verdict was known.

The patent application had been rejected twice by the Patent Office, largely on the grounds that, in writing the original patent laws in the eighteenth century and in discussing their subsequent revisions, Congress had at no time indicated that living organisms were explicity included.

Wide-ranging arguments had been brought in by both sides. Those supporting the patent application argued that it should be granted because of the economic importance of micro-organisms as part of the explosion of interest in biotechnology; opponents claimed that it would legitimize interference with natural processes in general, and should also be treated with particular care because of the potential health hazards.

In the end, however, the court's ruling was based on a narrow interpretation of congressional intent in writing the patent laws. Chief Justice Warren Burger, with four of his colleagues, argued that just because living matter was not mentioned in the patent laws, this did not mean it was excluded; the minority, led by Justice Brennan, argued conversely that, because of this very ambiguity, the issue of patentability should be decided by Congress rather than the courts.

Central to the case were the implications of a special law passed by Congress in 1930 allowing for the patenting of asexually reproduced plants, with an additional act in 1970 extending protection to new plant varieties capable of sexual reproduction.

The US Patent Office had argued that, unless Congress had intended the original act to exclude living matter, this additional legislation should not have been necessary. The minority agreed.

Chief Justice Burger, however, invoked the argument of Thomas Jefferson — the original author of US patent legislation — that "ingenuity should receive a liberal encouragement" to confirm that a novel micro-organism can legitimately be considered as a 'manufacture' or 'composition of matter' under the terms of the Patent Act of 1793.

The Supreme Court's decision, which finally ends almost eight years of legal debate, brings the US in line with several European countries, such as the UK, which already allow living organisms to be patented. **David Dickson**

NEWS AND VIEWS

Eruption of Mt. St. Helens:

Seismology

from the Geophysics Program*, University of Washington

ON May 18, 1980 at 0832 local time a major geological event occurred with the cataclysmic eruption of Mt. St. Helens in Washington's Cascade Range. The eruption followed two months of intense seismic activity, surface deformation, and sporadic, but minor steam and ash eruptions. These geophysical and geological precursors signaled the reawakening of the volcano after a period of quiescence since activity was last recorded in 1856 (Crandell & Mullineaux *Science* **187**, 438; 1975; Crandell & Mullineaux, *US Geol. Survey Bull.* **1383**-c, 25p; 1978).

The cataclysmic explosions of May 18 caused an estimated $2 billion or more in damage, although the volcano lies in a relatively remote area. The cost in human life has been substantial with 22 confirmed dead and 60 to 70 still missing at the time of writing. A large sector of the north and northeast side of the mountain was devastated by pyroclastic flows, mudflows and tephra fallout. The direct blast from the explosions leveled entire forested areas on the north side; the affected area is estimated to be 400 km². Two river systems with sources near the mountain have been extensively altered by mudflows and flooding. The morphology of the volcano has drastically changed from a nearly symmetrical cone to an assymmetric edifice approximately 400 m lower in height, although much of the south and west sides of the volcano remain relatively untouched by the explosion.

Seismic activity was the first indication of the reawakening of Mt. St. Helens, beginning abruptly with an earthquake of magnitude 4 at 1547 local time on March 20, 1980. This earthquake was located just north of the summit by the regional

seismograph network which included one station 3.5 km west of the summit. Since this was the largest earthquake recorded in the southern Washington Cascade range during seven years of instrumental observations, an aftershock study was begun on March 21 in an effort to examine seismo-tectonic processes near Mt. St. Helens. To improve the seismic coverage in the area, three portable seismic recorders were installed within 15 km of the summit, and a second telemetered station was added to the permanent network 35 km northeast of the epicenter.

A rapid increase in the number of small shocks made it clear that an unusual earthquake sequence was beginning at Mt. St. Helens. The initial aftershock activity failed to follow the usual decay in the number of events with time, and on March 22 a second magnitude 4 earthquake occurred in the same region. By March 24, additional earthquakes larger than magnitude 4 had occurred and the general seismicity increased to the point that a volcanic mechanism was required to

---

The seismic monitoring of Mt. St. Helens has involved a large number of individuals, many of them students and staff of the University of Washington Geophysics Program. This preliminary, descriptive report was compiled by the following people, listed alphabetically: R.S. Crosson, E.T. Endo, S.D. Malone, L.J. Noson, and C.S. Weaver. Crosson is a Professor of Geophysics, Malone is a Senior Associate, and Noson is a network seismologist, all with the University of Washington. Endo and Weaver are geophysicists with the US Geological Survey, Menlo Park, California, and both are currently on assignment in Seattle. Significant contributions to the seismic monitoring were made by J.M. Coakley and E.E. Criley (both USGS) and by J.W. Ramey and E.H. Wildermuth (both UW).

explain the concentrated, high rates of seismicity. Additional temporary seismograph stations were installed to provide data adequate for obtaining accurate hypocenter locations in the hope that careful tracking of the hypocenters would increase our overall ability to monitor the volcanic hazard. Twenty four hour observation of the seismographic records began on March 24, and this effort has continued to the present as part of the hazard warning effort. A final, dramatic increase of seismic activity occurred on March 25, when the rate of seismicity reached its peak. Seismic stations within 8 km of the summit were continuously saturated, and individual earthquakes could no longer be distinguished from background seismic levels. More distant stations were used to resolve individual earthquakes for determining occurrence rates, magnitudes, and other earthquake parameters.

On March 27, two days after the seismicity peak, the first steam eruption occurred at 1236 local time. Moderate steam and ash eruptions continued for the next few weeks, declining in frequency until by April 23 only occasional small steam bursts were observed. On May 8 steam and ash eruptions resumed, occurring periodically for several days. Between May 14 and the cataclysmic eruption on May 18 there was only minor eruptive activity.

As the seismic energy release beneath St. Helens occurred at a high rate, count statistics for the whole episode have been kept only for earthquakes exceeding magnitude 3.2. After reaching a peak of 8 to 10 earthquakes per hour at this magnitude threshold during the evening of

March 25, the rate of activity declined irregularly until the explosive event of May 18. Figure 1 shows a smoothed curve of the rate of occurrence against time. The rate of seismic energy release generally follows the count curve although the decrease is not as great. This reflects the fact that large earthquakes continued at a slightly increasing rate during April and May, while the smaller events declined in frequency. Earthquakes larger than magnitude 4 occurred at an average rate of 5 per day in early April and 8 per day during the week preceding May 18, while the number of events larger than magnitude 3 went from 77 per day to 28 per day during the same period. The largest earthquakes recorded were approximately magnitude 5 and occurred late in the sequence. We estimate the total seismic energy release to date to be equivalent to a single magnitude 6.7 earthquake.

Several periods of harmonic tremor were observed. Normally, a nearly monochromatic 1 Hz signal, lasting from a few minutes to half an hour, was observed on stations within 30 km of the mountain. In several cases these signals were large enough to be observed on seismic stations 250 km distant. There was no apparent correlation of these monochromatic tremor periods and eruptions or unusual earthquake activity. During the intense earthquake activity of March 25-26 harmonic tremor would have been completely masked by the earthquake signals.

By May 1, a total of 15 seismograph stations were operating within a radius of 32 km of the summit. The station distribution is excellent for control of hypocenter coordinates though the velocity model is still poorly known for the immediate area. Virtually all of the earthquakes occurred in an area of 5 km radius centered approximately 2 km directly north of the summit crater (Figure 2). Depths ranged from 0 to about 5 km with a few events possibly as deep as 10 km beneath the average topographic surface.
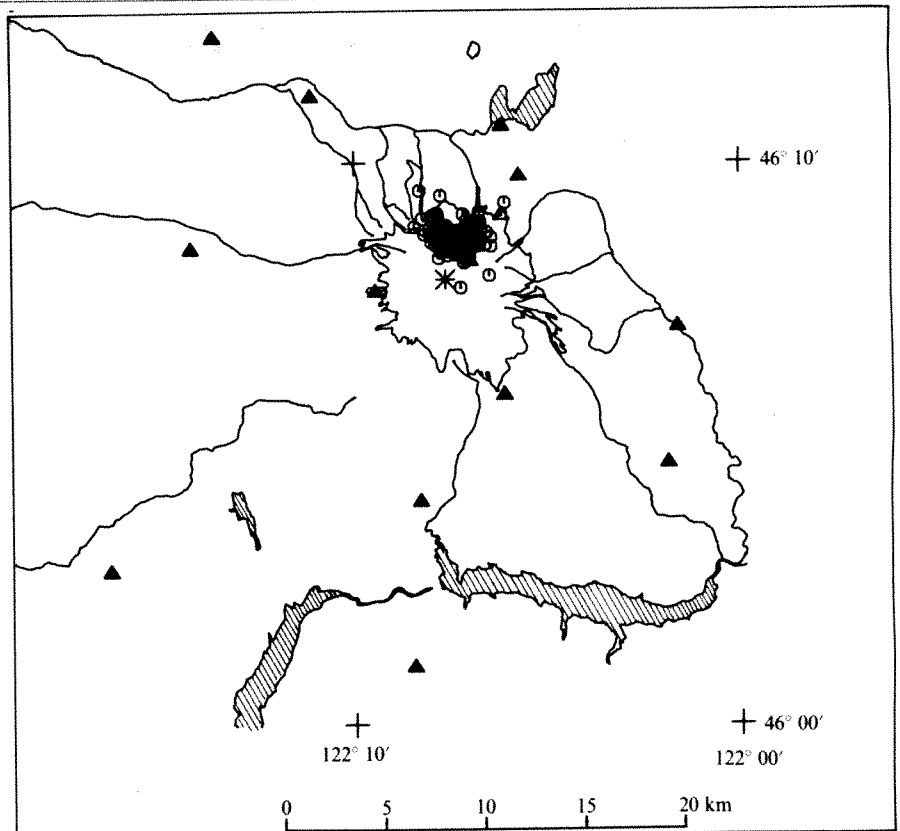
Map of epicenters above approximately 3.2 for period May 1, 1980 to May 18, 1980. Epicenters are open circles, seismograph stations are solid triangles, and bodies of water are shaded. Tree-lines and rivers are drawn. Dark area is epicenter cluster centered 2 km north of the summit.

At this preliminary stage of investigation, we have not been able to obtain good depth measurements of very shallow earthquakes, but it seems probable that many moderate earthquakes (magnitudes 3 to 4) occurred at shallow depths near the base of the volcanic edifice or up in the cone itself.

The blast of May 18 was not preceded by any anomalous seismic activity on a time scale of hours to days. At 0832 local time, an earthquake occurred at a depth of 3 km beneath the volcano. This event may have triggered a landslide off the north side of the mountain which led immediately to the explosion. The details of the explosion and its relation to the earthquake and landslide have not yet been worked out. A standard Wood-Anderson seismograph in Seattle recorded a magnitude 5.1 event at this time though the signals are more complicated than expected for a single earthquake. After the initial seismic event was over (it lasted for over 8 minutes) the earthquake activity dropped back to a level of only one or two discrete events per minute. This period of relative quiesence lasted for over three hours when both the earthquake activity and volcanic tremor increased. There was a steady increase in the level of seismic activity from 1140 PDT until 1530

Earthquake occurrence rate against time for the Mt. St. Helens eruptive sequence.
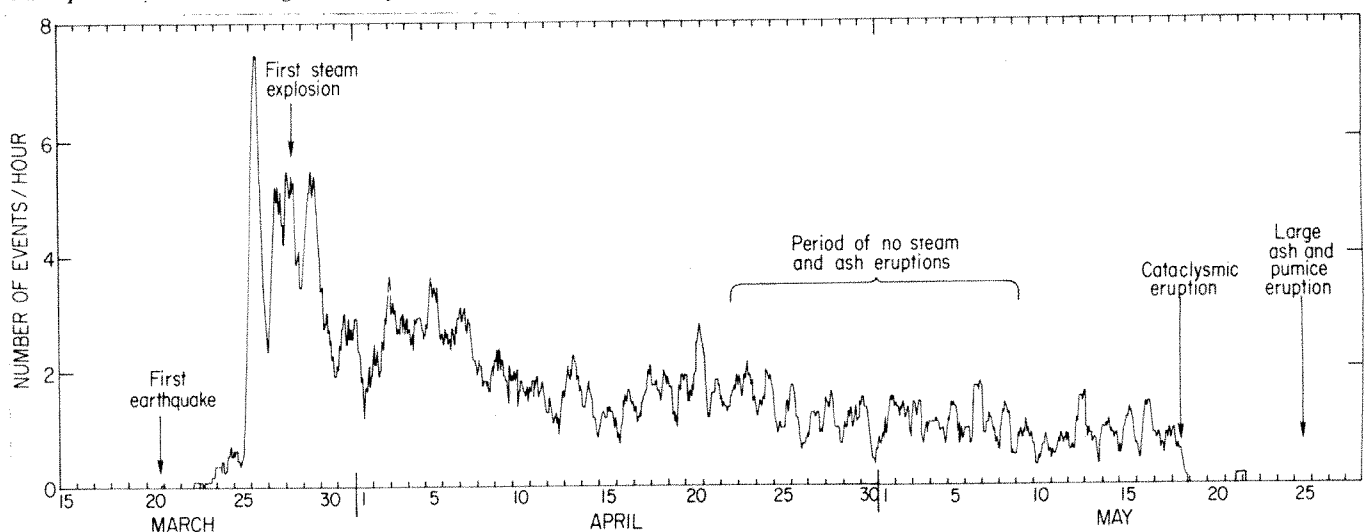
PDT when all seismic stations within 100 km were completely saturated and strong tremor was recorded 250 km away. Around 1730 PDT the tremor and earthquake activity abruptly diminished.

Since May 18 the earthquake activity dramatically declined until by the end of May there were only a few small earthquakes per day in the vicinity of the mountain. There was a moderate earthquake swarm coincident with an ash eruption on May 25. Low amplitude seismic noise, often with tremor-like characteristics, has been recorded nearly continuously since the May 18 eruption; although the noise is usually only monitored on the two stations still operating on the flanks of the mountain.

Comparison of the St. Helens sequence with the eruptive behaviour of other volcanoes may yield clues to the physical processes involved and to the predictable aspects of these processes. A particularly interesting example is the eruption of the Kamchatka volcano Bezymianny in 1956 (Gorshkov *Bull. Volcan.* **20**, 77; 1959). This volcano went through a cycle remarkably similar to that of Mt. St. Helens: a) a period of almost one month of volcanic earthquakes, b) strong ash eruptions lasting over one month, c) a stage of moderately declining activity lasting nearly 3 months, d) a gigantic explosion approximately six months after initial activity, and e) a post-eruptive stage of about six months of declining but sporadic activity. Except for the time table which is longer and the fact that earthquakes were estimated to be of greater depth (up to 50 km) in the case of Bezymianny, these two volcanic histories are sufficiently similar to suggest the possibility that a moderately predictable process is involved. The explosion of Bezymianny was in fact accompanied by a strong earthquake although the exact time sequence is not as well known as at Mt. St. Helens. The resultant craters of the two volcanoes are also very similar in size and shape.

Our preliminary conclusions are that seismicity provides an intermediate term warning of explosive volcanic hazard (scale of weeks to months) but no apparent short term warning (hours to days). The rate processes which may be extracted from the seismic data such as the strain energy release rate may be valuable in establishing the overall magma injection characteristics and other variables in the volcanic cycle when a sufficiently good understanding of the physical processes is available. Other measurements such as ground deformation must be made to provide basic information upon which to model the entire process. Unfortunately, it is still not clear that reliable short term prediction is feasible. Considering the wealth of seismic data that we have obtained, along with the variety of other observations made on Mt. St. Helens, a unique opportunity exists to probe the inner workings of an explosive volcano. □

Volcanology

from Robert L. Christiansen*

THE explosive eruption of Mount St. Helens completely destroyed its north flank, opening a crater 1.5 km wide, and producing an eruption cloud that deposited a blanket of ash over a large area of the northwestern United States. The eruption, the culmination of a series of seismic and eruptive events that began in late March, was notable for the rapidity with which activity began and progressed and for the magnitude of energy released, both seismically and eruptively. Although further eruptions (including the eruption of lava into the volcano's crater) are likely, it seems probable that the greatest energy release occurred within two months of the initial earthquake of the sequence.

Activity began with a single shock of magnitude 4 on March 20 and grew within 5 days to a swarm in which magnitude 4 + earthquakes occurred at a rate of more than 8 per hour. An interesting decrease in seismicity (although to rates including more than 5 earthquakes of magnitudes 4 + per day — high by any ordinary standard) occurred during the day and a half before the first eruption, which was a crater-forming burst beginning at 1238 on March 27.

After a pause until about 0300 the following morning, the volcano erupted again, this time for a sustained period of nearly two hours. Similar eruptions continued for the following four days, with both short, essentially single-burst eruptions and sustained longer eruptions. The eruptions were all probably steam-generated and produced only lithic-crystal ash that apparently was derived by shallow explosions within a 350-year old summit dome. A moderate amount of this ash was distributed 50 km away and some was reported as far as 100 km to the east, but most of it fell within 5-20 km of the volcano's summit.

Phreatic eruptions continued after April 1 but were mainly of short duration and occurred at successively longer intervals. They ceased temporarily after a small eruption that produced ash on the volcano's upper flank on the morning of April 22. Up to that time the summit crater,

The new crater formed by the explosive eruption.
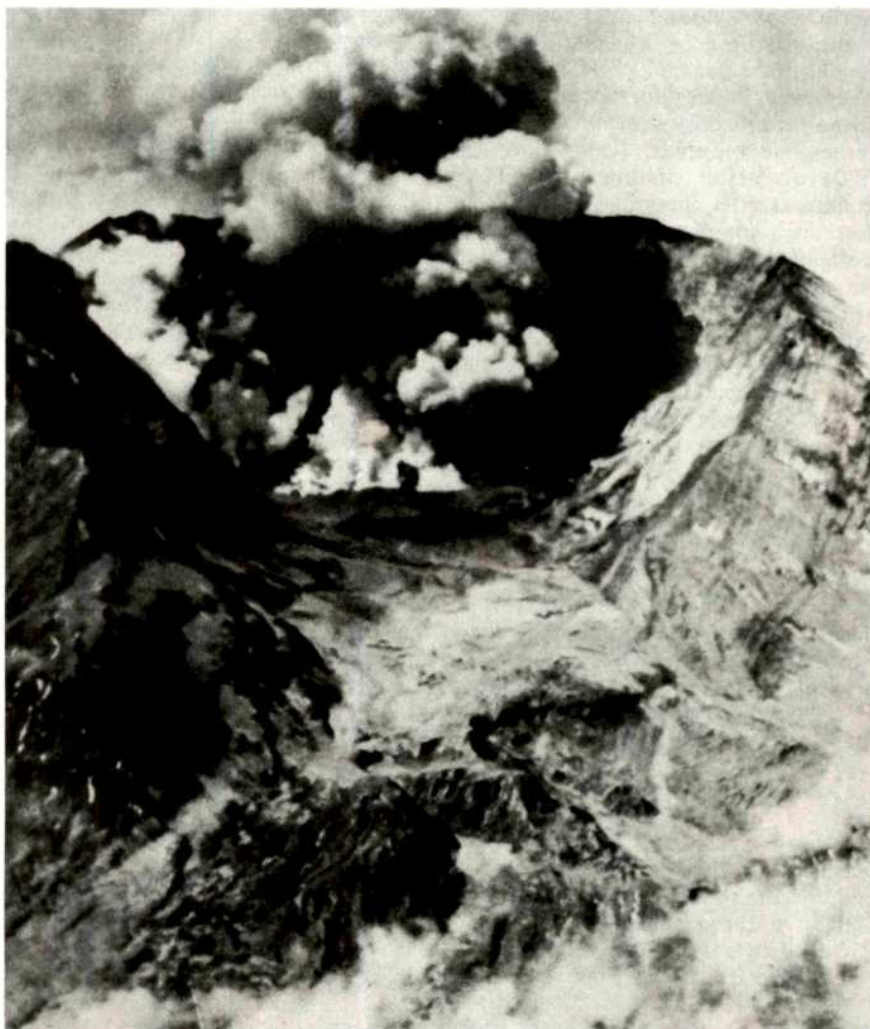
from which all of the eruptions had occurred, was nearly free of steam between eruptions except for areas of diffusely steaming ground. By contrast, during the late April to early May pause in eruptions, fumaroles vented continuously from several points within the crater. Weak to moderate phreatic eruptions occurred again for a few days in early May but once again ceased while fumarolic steaming continued in the crater.

The typical spring weather of Mount St. Helens made observational conditions poor for most of the time. The mountain was not visible by air from late morning of March 25 until a few hours after the eruption began on March 27. When the view cleared that afternoon, a remarkable series of changes was apparent at the volcano's summit and on its upper north flank. During the period of peak seismicity and initial eruption, a nearly continuous east-trending fracture system 5,000 m long had formed across the summit, nearly bisecting the old snow-and-ice filled summit crater. Another somewhat less continuous system of fractures paralleled the major one along the old north crater rim and bounded a block of the volcano's north flank that was conspicuously displaced above the former elevations of the flank. Later photogrammetric measurements showed this block of the north flank to stand more than 100 m higher than the corresponding previous points on the flank; much of the apparent discrepancy in elevation was, however, due to northward displacement of the flank rather than true uplift.

Deformation of the north flank continued after the initial displacement, forming a conspicuously visible bulge of both the glaciers and the rock edifice of the volcano. Continued photogrammetric re-contouring of this north flank was coupled with frequently repeated geodetic measurements and tilt monitoring to study a remarkable rate of deformation on the north flank. A total northward displacement of over 100 m occurred during the nearly two months from the time of initial formation of this bulge until the climactic eruption of May 18. The rate of deformation at each surveyed point remained quite constant throughout the period of intensive observation, which lasted from April 25 until the morning of the major eruption. Rates in the fastest-growing parts of the bulge were 1.5 to 2 m per day; the displacement vectors were nearly horizontal toward the north-northwest.

Although it was hoped that changes in seismicity and in the rate of deformation on the north flank, as well as other precursors, might give warning of a major slope failure, the possibility that such a failure might occur resulted in the closing of the area north of the volcano by civil authorities. That such a slope failure might trigger an eruption was also considered a distinct possibility. The event finally

occurred, however, essentially without warning at 0832 on the morning of May 18. It appears to have been triggered by a large earthquake, which probably had a Richter magnitude of 5 (unusual wave characteristics preclude a simple evaluation of the magnitude of the event). The earthquake shook the walls of the summit crater, causing numerous avalanches, and the entire north slope of the volcano began to separate from the main edifice along a crack that opened across the upper part of the bulge. A small dark ash-rich eruption cloud emerged from this crack as the slope failed in a catastrophic avalanche below.

Within seconds, the avalanche was overtaken by a large laterally directed blast (see cover pictures) that carried lithic ash and lapilli in a devastating hurricane over a northward sector of nearly 180 degrees, 30 km across from west to east and extending outward more than 20 km from the volcano's summit. In an inner zone of nearly 10 km width virtually everything in the path of this blast was destroyed, and no trees remain in that formerly densely forested area. Beyond, to nearly the limit of the blast, all the trees were blown down to the ground, and at the blast's outer limit the trees were thoroughly seared.

The avalanching north flank raced down the slope of the volcano, slammed into a ridge about 8 km to the north, displaced the water of Spirit Lake, raising its bed by more than 60 m, and formed a hummocky debris flow that locally crossed the ridge to the north but mainly turned and flowed down the valley of the North Toutle river for 18 km. The displaced water of Spirit Lake, melting blocks of ice from former glaciers of the volcano's north flank, water from the displaced river bed, and melting snow and ice on the volcano's remaining slopes produced mudflows that flooded the debris flow and generated floods all the way down the Toutle River, the Cowlitz river below it, and into the Columbia River.

The initial events of the eruption — the avalache-debris flow and the lateral blast — caused most of the casualties and destruction in the region of the volcano. However, before the lateral blast had reached its full proportions a vertical eruption column began to rise from the position of the former summit crater and

within less than 10 minutes had risen to a height of more than 20 km. Ash from this eruption cloud was rapidly blown northeastward, producing lightning and starting hundreds of small forest fires, causing darkness as far east as 100 km, and depositing lithic-vitric ash for many hundreds of kilometers. Major ash falls occurred as far east as central Montana, and ash fell visibly even in the Great Plains of the central United States. As this plinian eruption column formed, it reamed out the volcanic conduit, forming a central crater more than 1.5 km in diameter. This crater, along with the north flank that was entirely removed by the initial avalanche and blast formed a great amphitheater 1.5 × 3 km across, enclosed by the volcano's former east, south, and west flanks.

As the plinian column continued to erupt vigorously for more than 9 hours before gradually decreasing in height and intensity, it produced numerous ash flows. The first of these were thin flows that spread out over the entire upper surface of the volcano and were generated by both the initial blast cloud as it expanded in the vicinity of the summit and by the plinian eruption column. Later, the ash flows were all directed out through the large northward breach of the crater to form a fan of pumiceous ash flows over the debris flows, extending past Spirit Lake and part way down the former drainage of the Toutle River. These ash flows continued to be observed until dark on the 18th. The hot blast deposits, the debris flow, and these ash flows were frequently disrupted in the vicinity of Spirit Lake and the former Toutle river by large phreatic eruptions that blew through them to form craters as large as 20 m across and drove columns of ash to heights as great as 2000 m above the surface (see picture opposite).

The magma produced during and since the major eruption of May 18 has been dacite. The principal juvenile material is light-colored hypersthene-hornblende dacite having a range of silica content from 64% to 68% (chemical analyses by K. Wozniak, S. Hughes, E. M. Taylor of Oregon State University). In addition, there is a darker, denser dacite whose composition has not yet been determined but that appears also to be juvenile. The eruption had already begun to decrease in intensity by about 1700 on Sunday May 18th, but continued intermittently for the rest of the week. On the following Saturday night a series of increasingly energetic ash eruptions led to the second largest eruptive event on Sunday May 25. That eruption began at about 0230 during a period when winds were erratic, having greatly different directions at different elevations. Although the eruption was an order of magnitude less voluminous than that of the 18th, it scattered ash over wide areas of western Washington and Oregon.

Since the end of the eruption of May 25, late in the day, the volcano has continued to emit large quantities of steam that

Robert L. Christiansen is a geologist with the US Geological Survey in Menlo Park, California. He is writing on behalf of about 40 geologists and geophysicists with the USGS, too many to acknowledge individually, operating out of Vancouver, Washington. A number of other organizations and individuals have also contributed to this effort.

One of them Dave Johnston, a geologist with the USGS, was killed in the cataclysmic blast that began the May 18 eruption while manning an observation post 8 km north-northwest of the mountain. Dave had been involved in the monitoring of Mt. St. Helens from the beginning of the seismic sequence, and had hoped to be able to issue a short term warning of the impending eruption.
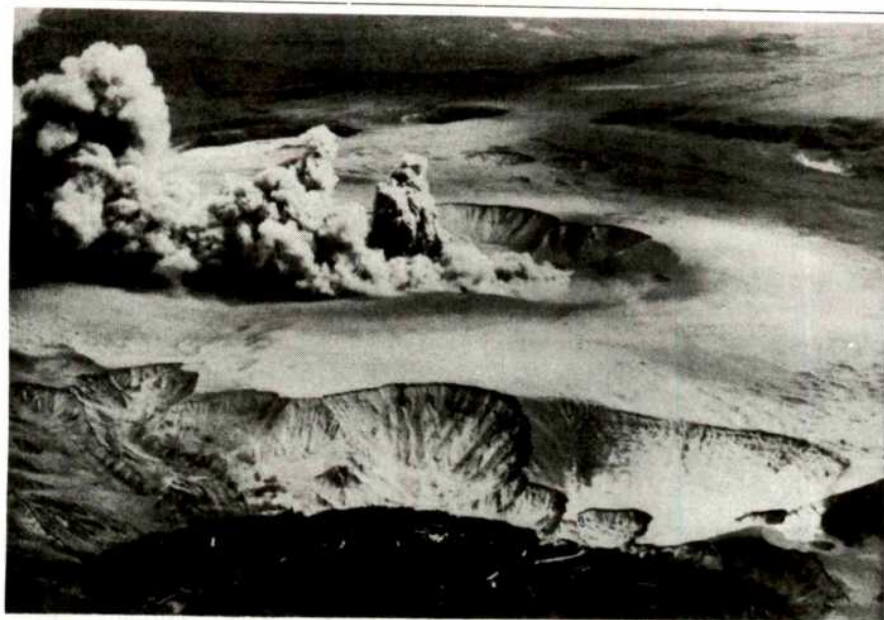
Spirit Lake on May 29, 1980

condense in the air to form plumes that rise to altitudes of 3 to 5 km above sea level. The odor of sulfur gases is prominent in these plumes, but relatively little ash has been carried by them, and almost none has fallen more than a few kilometers beyond the volcano.

No lava has yet appeared at the surface. There have, however, been several night observations of incandescent rock, probably caused by hot gases streaming through the vents from a magma body not far below. The rapid pace and high rates of energy release to date, from the initial earthquakes, through the early phreatic eruption phases, to the explosive magmatic eruptions of the last few weeks are noteworthy. That magma will yet reach the surface to form a volcanic dome, whose emplacement would possibly be accompanied by further explosive eruptions, seems distinctly probable. Further disruption and rebuilding of such a dome could continue for weeks, months, or years to come, but it seems likely that the volcanic edifice will be rebuilt by the outpouring of both dacitic and andesitic lavas, as has happened so many times before in the brief but eventful history of Mount St. Helens. □

Effects on climate

from C.B. Sear and P.M. Kelly

Now that the dust has settled over the United States after the explosive eruptions of Mount St. Helens, attention will turn to the longer term effects of these events on world weather and climate. There has been much concern in recent years over the possibility that anthropogenic increases in atmospheric carbon dioxide will produce a major climatic change over the next fifty to one hundred years. Natural mechanisms, such as the level of dust thrown into the stratosphere by explosive volcanic activity, have, however, been held responsible for significant climatic fluctuations in the past, and must also be considered in any attempt to predict the world's future climate. Benjamin Frankling, whilst sojourning in Paris, proposed that the severe European winter of 1783-84 was caused by the eruptions of Icelandic volcanoes in May and June of 1783.

Volcanic aerosols injected through the tropopause into the stratosphere can remain there for several years. After a few months, under the influence of the stratospheric wind systems, they form a veil which can cover most of a hemisphere and occasionally, after very large eruptions, the whole globe. The spread of a dust veil is dependent on the latitude of injection, the height reached by the dust, the size of the dust particles and the state of the stratospheric circulation during the development of the veil. In general, this circulation tends to restrict veils resulting from northern hemisphere middle and high latitude eruptions to regions north of 30°N, whereas dust from low latitude eruptions, such as those of Krakatau (1883) and Agung (Bali, 1963), tends to spread over the whole globe. In the case of Mount St. Helens, there is a good chance that the dust, although injected into middle latitudes, will spread over a greater latitudinal range than usual. This is because May is the month with the greatest equatorward component of flow in the lower stratosphere.

The amount of solar energy reaching the Earth's surface is reduced by a dust veil, as the radiation balance is altered by back scattering, forward scattering and absorption within the dust veil. The relative importance of these processes varies considerably with the height of the veil and the size and chemical composition of the dust particles and aerosols. Indeed, very often, several distinct layers occur and calculation of the net effect on the radiation balance is complex. The reduction in the direct solar radiation at the surface is offset to some extent by an increase in diffuse radiation.

In the case of large explosive eruptions, these alterations in the energy budget are believed to be sufficient to produce changes in the atmospheric circulation and climate. Absorption within the dust veil results in stratospheric warming and the reduction in energy received at the Earth's surface leads to cooling in the lower atmosphere. Lamb, in an exhaustive work (*Phil. Trans. Roy. Soc., A.* **266**, 425; 1970), has discussed the effects of these dust veils and has produced a chronology of major explosive volcanic events for the period since AD 1500

Recently, theoretical modelling has been undertaken in order to provide estimates of the magnitude of the effects of major eruptions on the temperature and circulation of the lower atmosphere. Hunt, (*Mon. Wea. Rev.* **105**, 3, 247; 1977) has estimated the climatic effects of a dust input of Krakataun magnitude using a nine level general circulation model. The maximum depression of hemispheric mean surface temperature was around 0.3°C, occurring about three months after the initial input. Pollack *et al* (*J. geophys. Res.* **81**, 1071; 1976) modelled surface temperature changes during periods of high volcanic activity, such as occurred during the 1880s. They found a resultant cooling of the order of 1°C and stressed the importance of the contribution of sulphuric acid aerosols to the energy balance changes in the stratosphere. On the other hand, Deirmendjian (*Adv. Geophys* **16**, 267, 1973) has concluded that there is little solid evidence for climatological effects of major eruptions in the conventional meteorological parameters.

A number of empirical and statistical studies have revealed evidence of volcanic effects on climate and the atmospheric circulation. Mass and Schneider (*J. Atmos. Sci.* **34**, 1995; 1977) have found a short term volcanic signal in air temperature records. Kelly (*Nature* **268**, 616; 1977) has noted the correspondence between long term trends in central England temperature, the North Atlantic westerly winds and the degree of explosive volcanic activity. Bryson and Goodman (*Science* **207**, 1041; 1980) have recently suggested that climate prediction for more than two years ahead will require forecasts

100 years ago

A LACUSTRINE VOLCANO

In a recent number of *La Nature* further details, furnished by the French Consul of San Salvador, M. J. Laferrière, are given concerning the recent volcanic phenomenon in Lake Ilopango in that State. The accompanying illustration, from a photograph, will show the nature of the crater which has risen in the midst of the lake. Earthquakes were felt in San Salvador in the first half of January of this year; there were three strong shocks, less violent, however, than those of 1876. These earthquakes had their centre in the vicinity of Lake Ilopango, in the midst of which rose three volcanic openings connected with each other. This new crater, which, seen from a distance as in the illustration, appears a small islet, rises above the surface of the water, however, about twenty metres. An attempt was made to approach it in a boat, but the waters were all in a state of ebullition from contact with the burning rock, and gave off torrents of steam. An abundant column of smoke rose in the air, assuming the aspect of an immense cloud, which was seen from a great distance, and formed an imposing spectacle. The phenomenon was preceded by an exceptional rising of the lake, increased by the abundant winter rains. According to an old tradition the Spaniards maintain that when the lake rises earthquakes are to be feared. Formerly, also, it was the custom to dig trenches to facilitate the escape of the
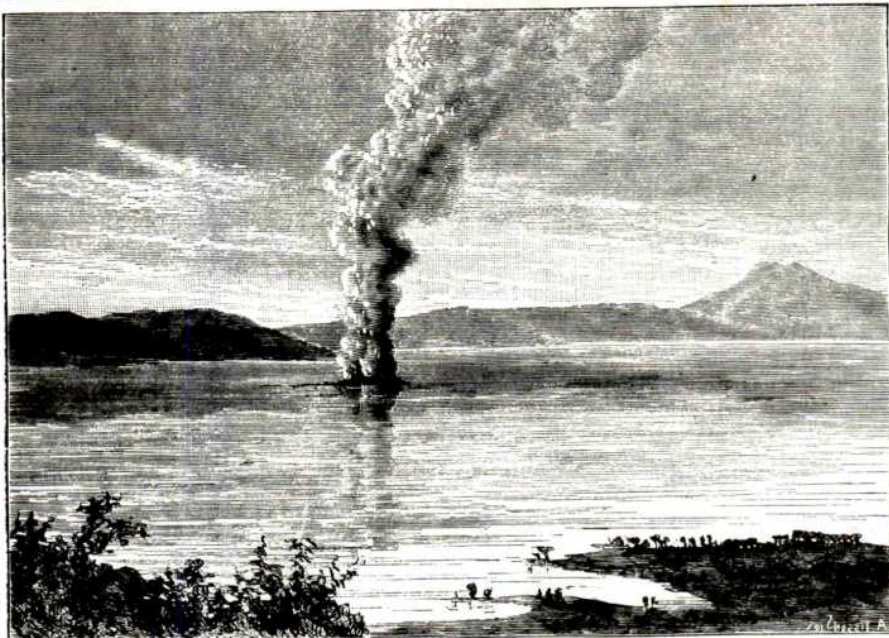
Aspect of the Volcano in Lake Ilopango

waters. This practice was followed without intermission for a century, and volcanic phenomena did not appear during all that time. The present phenomena seem to justify this tradition.

If it is difficult to explain the fact it is still interesting to remember that a great number of volcanoes are submarine, that others are found for the most part in islands or in maritime regions, and that water may be one of the feeders of volcanic fires. Lake Ilopango, also known as Lake Conjutepec, is, according to M. Laferrière, a sunk crater. It is in the volcanic line, and it is a general fact in Central America that lakes alternate with volcanic cones. The water of this lake is

brackish, very bitter, and almost viscous. It gives off sometimes, here and there, bubbles of sulphohydric acid gas. The lake is about 12 kilometres long by 16 broad; the depth is unknown. It is about 12 kilometres from the city of San Salvador. The Consul of France in Guatemala, M. de Thiersant, states that Lake Ilopango has now a temperature of $38°C$ on its shore, and is in complete ebullition round the volcano. All the fishes are cooked and float upon the surface, with a great number of shellfish and other aquatic animals. The volcano continues to rise, and the level of the lake is being gradually lowered.

From *Nature* **22**, 10 June, 129, 1880.

---

of the general level of global volcanic activity. It has been suggested that the high frequency of explosive eruptions during the 17th century and early 19th century may have been a major cause of the most severe phases of the Little Ice Age and that the general warming of the early 20th century was a result of the reduced level of volcanic activity at that time. Miles and Gildersleaves (*Nature* **271**, 735; 1978) do not, however, believe that this reduction was sufficient to produce the observed temperature trends. Finally, many authors have attributed the rapid drop in tropospheric temperatures during the middle 1960s to the eruption of Agung in 1963.

These theoretical and empirical studies have only dealt with the most general aspects of the problem and many questions remain unanswered. How do the effects of eruptions occurring at different latitudes and at different times of the year differ? What are the spatial patterns of climatic change following individual eruptions and accompanying longer term fluctuations in the frequency of explosive volcanic activity? Finally, how can the effects of an individual eruption be distinguished in the

'noisy' climatic record? The year-to-year variability of climate is such that the effects of any one eruption, unless it is of a very great magnitude, are unlikely to be readily apparent.

It is therefore difficult to be precise about the climatological significance of the Mount St. Helens events. Reliable estimates of the volume of material ejected are not yet available. First estimates suggest that from 3 to 7 km^3 of material was removed from the mountain in the eruptions that occurred in May 1980, but it is not clear how much of this material reached the stratosphere. It is believed, however, that a significant amount did penetrate the tropopause. On the basis of present evidence, it appears that of the major middle and high latitude eruptions this century probably only that of Katmai (Alaska, 1912) was much larger, although estimates of the volume of material ejected by that event vary widely. The first Mount St. Helens eruption of the 18th May appears to have been of the same order of

C.B. Sear and P.M. Kelly are in the Climatic Research Unit, University of East Anglia, Norwich.

magnitude as that of Ksudatch (Kamchatka, 1907) and Bezymianny (Kamchatka, 1956). The eruption of Agung was of the same magnitude, but was probably more significant climatologically because of its equatorial position. Thus the eruption of Mount St. Helens could well prove to be among the most powerful of this century. After the explosive eruption of Mount St. Helens in 1842, three other eruptions occurred in the Cascade Mountains during the following thirteen years; Mount Rainier (1843), Mount Baker (1854) and Mount Hood (1854).

While we cannot predict the climatic effects of the recent eruptions with any certainty, it is likely that the dust veil will have noticeable optical effects over coming months. A brilliant red glow may be observed lingering near the horizon for some time after sunset, and a corona, or Biship's ring, may be seen surrounding the sun. These effects were last widely seen after the eruption of Mount Fuego (Guatemala, 1974). In the past, extensive dust veils have given the sky a milky-white appearance for many months over large areas of the globe. It has even been suggested that similar optical effects

influenced the painting of the English artist, Turner.

One of the major problems in determining the climatic impact of past eruptions has been a lack of firm data. There is insufficient information concerning the amount and composition of the material injected into the stratosphere by previous major eruptions. It is also only in recent years that reliable observations of the atmosphere, and particularly the upper layers, have become readily available. The catastrophic eruption of Mount St. Helens affords an important, first opportunity to study in detail the physics, chemistry, meteorology and climatology of the impact of a major middle latitude explosive event.

□

The advantages of being evergreen

from Peter Moore

THE evergreen habit in plants has a number of obvious advantages, such as the conservation of energy and the capacity to indulge in photosynthesis over a considerable surface area whenever conditions are suitable. But there are some, rather contrasting, habitats in which the advantages may be more subtle. Take, for example, bogs and Mediterranean type heaths (chaparral or maquis). These two habitats are at opposite ends of the water supply spectrum, yet both are characterized by a flora in which evergreens are particularly prominent.

Since many evergreen plants are also xeromorphic, their association with wetlands is particularly intriguing. It is possible that the low temperatures and anaerobic conditions associated with bog peats results in a physiological drought even where water is apparently abundant, but an alternative and attractive explanation was put forward by Small (*Can. J. Bot.* **50**, 2227; 1972). He approached the problem from the point of view of the efficiency of nutrient utilization, for this is often a limitation to plant growth on bog peats As a measure of efficiency in nutrient use, he took the length of time a unit of nitrogen remains in the plant before being lost by leaf fall. On this basis he found that deciduous bog plants perfomed about 60% more photosynthesis per unit nitrogen residence time than non-bog deciduous species, but that values for bog evergreens were 235% higher than for the bog deciduous species. Here, in the realm of nutrient conservation, could be the secret of the bog evergreen's success.

Small's Canadian study site had a very limited growing season, and this could have

Peter Moore is in the Department of Botany, King's College, London.

affected the conclusions, but this does not apply to a study conducted in a swamp in Georgia by Schlesinger and Chabot (*Bot Gaz* **138**, 490; 1977). They compared the mineral nutrition and water relations of selected evergreen and deciduous swamp plant species and they found no evidence of water stresses developing, (the lowest leaf water potentials observed were – 12.5 bars), thus eliminating the physiological drought hypothesis for this site. Leaf longevity on the part of the evergreen, however, could once again form the basis of a higher efficiency in the utilization of the limited nutrient resource. Although the nutrient and carbon costs in producing a leaf were greater for the evergreen, this was more than compensated for by its longer working life.

It is possible that evergreens also make better use of the available nutrients in chaparral habitats. Here the normal climate consists of cool, wet winters and hot, dry summers, and the bulk of plant growth occurs in spring. Litter falling in the dry season is thus subjected to leaching by the winter rains prior to the demand imposed by the spring flush of growth. Mooney and Rundel (*Bot Gaz* **140**, 109; 1979) have examined the pattern of nutrient uptake in the evergreen shrub, *Adenostoma fasciculatum* in the chaparral of California, and they find that there is an increase in the content of nitrogen and phosphorus as well as in the biomass of old

leaves during the winter period. This occurs prior to any new leaf production in the spring and it suggests that the old leaves are being used as a nutrient reservoir in which a nutrient capital can be accumulated during the winter dormancy. This is an efficient nutrient conservation technique since it avoids the winter leaching losses and it places the plant in a strong position for rapid growth when nutrient demand rises in the spring.

The long-lived, evergreen leaf may thus play an important role in the annual movement and storage of nutrients in the plant. Indeed, this value of the evergreen leaf may be prolonged beyond annual events. Rundel and Parsons (*Amer. J. Bot* **67**, 1980) have conducted long term analyses of the foliage of *Adenostoma* and of *Ceanothus leucodermis* in California, and they find that the highest observed leaf concentrations of nitrogen, phosphorus and potassium in these species are in the years immediately after a fire, when there is a surplus of these elements in the soil. After about six years the foliar concentrations have fallen by up to 30% and they continue to decline very slowly over the next 60 years. The evergreen leaf, therefore, can provide a storage organ for excess nutrient elements which act as a reservoir for rapid further foliage growth over the four years following a fire. It seems that the longevity of the leaf is the essential feature which allows it to assume this function. □

Human babesiosis

from F.E.G. Cox

THE babesias are small intraerythrocytic protozoa, common in many mammals, some of which are important pathogens of cattle, horses, sheep and dogs. Several species occur in rodents and two, *Babesia microti* and *rodhaini*, are easily transmitted to mice and rats and have been extensively studied in the laboratory. From time to time, babesia-like parasites have been seen in smears of human blood but, because of their morphological similarity to malaria parasites, their significance has not been appreciated. Over recent years, however, human cases have become increasingly well documented and it is now possible to assess the importance of these parasites in man.

The first human cases were all in splenectomised individuals in Europe and, because cattle babesias are well known, it was assumed, and later shown to be correct, that these were the sources of the human infections. This assumption coloured attempts to identify the parasites involved in later cases and the rodent babesia, *B. microti,* was ignored. *Babesia microti* is practically universally found in rodents and insectivores throughout the northern hemisphere and easily infects laboratory rodents and splenectomized

monkeys (Shortt & Blackie *J. Trop. Med. Hyg.* **68**, 37; 1965) which the cattle species do not. *Babesia microti* was implicated as a cause of human babesiosis in the 1970s when a number of cases were recognized in the Nantucket Island area of the US and the parasite was isolated and transmitted to laboratory rodents.

The current status of human babesiosis has now been clarified and it seems that there are two quite distinct forms, the European, in splenectomised individuals and the American, in people with spleens. In the United States, there have been a number of serologically positive cases and 21 parasitological diagnoses, 19 of which definitely harboured *B. microti.* (Ruebush *Trans. R. Soc. Trop. Med. Hyg.* **74**, 149; 1980) and none of which had been splenectomised. This infection is mainly limited to the islands off the New England coast where the wild reservoirs of *B. microti* are the deer mouse, *Peromyscus leucopus,* and the meadow vole, *Microtus pennsylvanicus.* The vector is a deer tick, *Ixodes dammini* (Spielman *et al. J. Med. Ent.* **15**, 218; 1979) which feeds in its larval and nymphal stages on the deer mouse and meadow vole. No babesias have been

found in the deer on which the ticks also feed (Piersman *et al. J. Med. Ent.* **15**, 573; 1979) and the fact that isolates of *Babesia* from wild mice and voles resemble the human isolates using immunological criteria (Benach *et al. Amer. J. Trop. Med. Hyg.* **28**, 643; 1979) confirms that these rodents are the sources of the human infections. In Mexico, an unidentified babesia that infects hamsters has been isolated from three asymptomatic individuals (Osorno *et al. Vet. Parasit.* **2**, 111; 1976).

In Europe, the human cases now total 6; 2 from Yugoslavia, 2 from France and one from each of Ireland, Scotland and the USSR. In all cases the infected individuals had been splenectonised and all but the two from France died. The parasites implicated are *B. bovis* and *B. divergens* in Yugoslavia, *B. divergens* in Ireland and Scotland and one of the French cases, *B. bovis* in the USSR and the identity of the parasite in the remaining French case is unknown (Garnham *Trans. R. Soc. Trop. Med. Hyg.* **74**, 153; 1980). In the Scottish case the parasite has been returned to cattle and also passaged into gerbils, the first time

F.E.G. Cox is Professor of Zoology at King's College, London.

a rodent has been successfully infected with a cattle piroplasm. (Lewis & Williams *Nature* **278**, 170; 1979). The vector of human babesiosis in Europe has not yet been identified but *Ixodes ricinis* must be a possibility (Donnelly *Trans. R. Soc. Trop Med. Hyg.* **74**, 158; 1980). It is unlikely that *B. microti* will infect man in Britain where the vector is *I. trianguliceps* which seldom, if ever, feeds on man.

Human babesiosis, then, occurs in two distinct forms. The American form, which is relatively avirulent, occurs in intact individuals and is caused by *B. microti* from rodents and the European form, which is usually fatal, occurs in splenectomised individuals and is caused by *B. divergens* or *B. bovis* from cattle. All these cases can be regarded as accidental infections of man acquired by farmers, campers and others likely to be bitten by ticks. The infection is characterised by fevers and anaemia with small rings resembling malaria parasites in the blood but the parasites are not killed by chloroquine.

This is a rare but interesting disease and is the latest addition to the growing list of zoonoses, those parasites transmissible from wild or domesticated animals to man. □

at least some recognition of the eukaryote signal sequence by the appropriate bacterial membrane receptors and possibly, processing enzymes.

A comparison of the gene and amino acid sequences of F-IF and Le-IF (T. Taniguchi *et al.* Nature, this issue, p547) reveals a number of interesting features. First, although there is an average homology of about 45% between the nucleotide sequences coding for amino acids, the longest common stretch is only 13 nucleotides indicating that the interferons are the products of two closely related genes and not the result of a differential splicing process on the pre-mRNA product of one common gene. Second, three (or four) main domains of homology can be discerned between the coding nucleotide sequences of the two interferons, a feature which is even more pronouned upon comparing the amino acid structures, having lined up the presumed initiator methionine codons. Clearly, it is possible to speculate that these domains are responsible for important common functions of the two proteins such as the binding to common cellular receptors (Wiranowska-Stewart *et al. J. Gen. Virol.* **37**, 629; 1977) and the anti-viral and anti-tumour activities. Third, the overall data clearly suggest that there was a common ancestral gene for these two interferons.

It is also revealing to compare the amino-terminal sequence and amino acid composition of a human lymphoblastoid interferon (Zoon *et al. Science* **207**, 527; 1980) with the corresponding Le-IF data. While the former is probably of the leukocyte type (see Paucker *The Interferon System. Texas Reports on Biology and Medicine* (eds. Baron & Dianzani) **35**, 23; 1977), it seems as if it is the product of a distinct, non-allelic gene. Indeed, a second Le-IF cDNA clone has been observed by Mantei *et al.* which appears different from the first in terms of its restriction enzyme map. However, its degree of relatedness to the latter and the human lymphoblastoid interferon remains to be seen.

We can now look forward to further results from cloning experiments (both cDNA and genomic cloning) to provide more valuable information on the number and arrangement of genes coding for a particular type of interferon and their relatedness to each other and other types of interferon genes. It may now also be possible to modify and re-arrange these genes using standard genetic engineering techniques and other methods (e.g. Muller *et al. J. Mol. Biol.* **124**, 343; 1978) to produce new interferons with some particular advantages in specificity and activity. Such studies could also help in the detailed assignation of structure to function. Clearly, the work discussed here signifies the start of an era from which the molecular mechanism of interferon action will hopefully be elucidated □

Human interferon gene sequences

from Michael Houghton

THE excitement that has been generated recently by human interferon studies is continuing with the elucidation of the gene sequences (and hence polypeptide structures) of human fibroblast (F-IF) and Leukocyte (Le-IF) interferons. The two molecules are currently receiving much attention over their potential as *in vivo* anti-viral and antitumour agents (Stewart *The interferon system* Springer, Berlin, 1979).

Although both molecules seem to induce similar biological effects, the target cell specificities differ and antibodies raised against one type do not neutralise the other (Stewart *op cit.*). Also, there is some evidence that the two proteins are encoded by different mRNA molecules (Cavalieri *et al. Proc. natn. Acad. Sci. U.S.A.* **74**, 3287; 1977). The origins of these differences have become clearer now that sequences are available from both F-IF (Taniguchi *et al. Gene* **10**, 11; 1980; Houghton et al. *Nucl. Acids Res.* **8**, 1913; 1980; Derynck *et al. Nature* this issue, p542) and Le-IF (Mantei *et al. Gene* **10**, 1; 1980).

The F-IF mRNA contains 836 nucleotides (excluding the 3' poly A tail and the possible 5' cap structure) consisting of 72 and 203 nucleotides in the presumed 5' and 3' untranslated regions respectively, 63 nucleotides coding for a hydrophobic pre-peptide signal sequence that is responsible for protein secretion, and 498 nucleotides coding for a further 166 amino acids. If the latter are all present in the mature protein,

then a polypeptide molecular weight of 20,000 daltons can be predicted, a value which is significantly higher than the 16,500 dalton species that is thought to represent the cleaved, but unglycosylated protein observed in a reconstituted cell-free system (Derynck *et al.*). Also, the native glycosylated form of F-IF has itself been estimated to be 20,000 daltons (Havell *et al. J. Biol. Chem.* **252**, 4425; 1977) and so at this stage, one cannot completely rule out the possibility of additional processing of F-IF besides the cleavage of the N-terminal signal sequence.

Le-IF mRNA contains around 865 nucleotides (excluding the 3' poly A tail and probably a small number of nucleotides at the 5' terminus that have been removed during cDNA preparation) of which 242 are located in the presumed 3' untranslated region. As in the case of F-IF mRNA, there seems to be a region coding for a pre-peptide signal sequence of either 15 or, more probably, 23 amino acids again followed by a coding sequence of 498 nucleotides corresponding to 166 amino acids in the mature protein, assuming no further processing. Interestingly, in view of the fact that the biologically active product of Le-IF genes cloned in bacteria seems to be sequestered into the periplasmic space (Mantei *et al.*), it would seem there is

Michael Houghton is in the Biochemistry Department, Searle Research and Development, G.D. Searle & Co. Ltd., High Wycombe, U.K.

ARTICLES

Late Quaternary water exchange between the eastern Mediterranean and the Black Sea

Daniel Jean Stanley & Christian Blanpied

Divison of Sedimentology, Smithsonian Institution, Washington DC 20560

Sea of Marmara sediments provide an almost complete record of major palaeo-oceanographic events affecting the Aegean and Black Seas between the late Pleistocene and the Recent. Fluctuating patterns of water mass exchange, resulting from regionally important climatic oscillations, produced the marked differences in lithofacies mapped between the Sea of Marmara and the eastern Mediterranean and Black Seas.

THE Sea of Marmara in northern Turkey is an elongate, east-west trending, almost totally enclosed depression between Thrace to the north and Anatolia to the south. It lies between the Black Sea to the north-east and the Aegean Sea to the south-west (Fig. 1). Connections with the Black and Aegean Seas are restricted, involving two narrow and shallow straits: the NNE-SSW trending Bosporus, 30 km long and locally as shallow as 35 m, at the north-east Marmara sector, and the longer (60 km) and somewhat deeper (50-60 m), NE-SW trending Dardanelles to the west. The 210-km long Sea of Marmara contains three relatively deep basins, respectively 1,097, 1,389 and 1,238 m from west to east, and is bordered to the south by a broad shelf [1].

The lithofacies of radiocarbon-dated cores (latest Pleistocene to Holocene) collected in the easternmost basin, called the Eastern Marmara Basin [2], are described here for the first time, and are compared with recently detailed lithostratigraphic sections of comparable age from the Black Sea [3] and the eastern Mediterranean [4]. Marked differences in the facies sequences and particularly in the age of the dark, organic-rich Holocene sapropel layers are recorded: those in the Aegean accumulated at ~ 9,000-7,000 yr BP (ref. 5); those in the Black Sea at ~ 7,000-3,000 yr BP (ref. 3). The origin of the Mediterranean sapropels remains controversial and has been attributed to changes of evaporation relative to precipitation [6,7], marked increase of freshwater outflow from the Black Sea [8-10], and an increase in discharge from rivers surrounding the eastern Mediterranean, particularly the Nile [4]. All hypotheses applicable to both Mediterranean and Black Sea sapropels imply broad-scale climatic changes that induced marked regional density stratification of water masses, progressive depletion of dissolved oxygen, and formation of hydrogen sulphide [11,12]; development of euxinic conditions led to preclusion of higher forms of life on the sea floor. The most recent Holocene sapropel in the Mediterranean formed during what most workers believe to be a warming trend [13]; its appearance throughout the Levantine and Ionian basins has been directly related to the depth of the shallow Bosporus sill which controlled the westward overflow of fresh water from the Black Sea [8-10]. In contrast, the age and stratigraphic position of the youngest Black Sea sapropel are apparently not as closely related to sill depth and eustacism. The difference in sill depth between the Bosporus and Dardanelles, only ~ 10-15 m, is too small to explain satisfactorily the much younger age of the Black Sea Holocene sapropel.

We interpret here the sequence of events that probably induced differences in the timing of sapropel accumulation in Aegean and Black Seas, and also evaluate differences between Late Quaternary lithofacies sequences deposited in the two regions. Four University of Miami gravity cores recovered in

1965 (RV Pillsbury cruise P6507) in the eastern Sea of Marmara (Table 1) were used in this study. The investigation of these cores included X-radiography, radiocarbon dating and petrological examination of 44 core sample splits: grain-size analyses, total organic matter and calcium carbonate content, scanning electron microscopy (SEM) of silt-size fraction, X-ray diffraction of clay and silt-size fractions, and petrographic identification of both terrigenous and biogenic components of the sand (> 63 μm) fraction. All data are summarized in tables available from the National Physical and Solar-terrestrial Data Center, NOAA, Code 621, Boulder, Colorado (Accession no. MGG-21025001). Simplified, dated core logs of the Marmara units based on these results, and well established stratigraphic sections from the Aegean and Black Seas, are shown in Fig. 2.

Marmara sequences and palaeo-oceanographic implications

The base of one core, P6507-G6, on the southwestern slope of the Eastern Marmara Basin, is dated at ~ 14,000 yr BP. This core was supplemented by two others (G7, G8) from the basin plain in which recovered sections were dated at ~ 5,000 and 5,500 yr BP; the base of a fourth core, G9, from the eastern slope of this basin, is dated at about 6,800 yr BP (Table 1). Although this region lies along the presently active North Anatolian Fault [14,15], it has been shown that structural displacement has been relatively minor during the short time span considered [16]. We thus assume that the major late Pleistocene to Holocene eustatic rise depicted on the sea-level curves [17,18], rather than tectonics, is responsible for the sequence of palaeo-oceanographic events observed in the sedimentary record in this region. Five major late Quaternary to Recent events are identified (Fig. 3).

The basal section of the Sea of Marmara core G6, nearly 14,000 yr BP (Fig. 2), consists of olive, generally structureless, clayey silts with minor amounts (< 5%) of sand. Substantial amounts of iron sulphide occur in the sand fraction, some filling a few, poorly preserved and probably reworked planktonic and benthonic foraminiferal tests. Moderate proportions of disseminated gypsum crystals of coarse silt and sand size also occur; although an authigenic origin is not precluded, the distribution pattern of gypsum as viewed in X-radiographs is comparable with that found in some natural saline lakes [19], but may also have resulted from the effects of later groundwater brines (L. A. Hardie, personal communication). Total organic matter ranges to 15%, and calcium carbonate content to 6%. This facies suggests deposition in anaerobic conditions in a lake, possibly saline, that was bordered to the south by a broad, subaerially
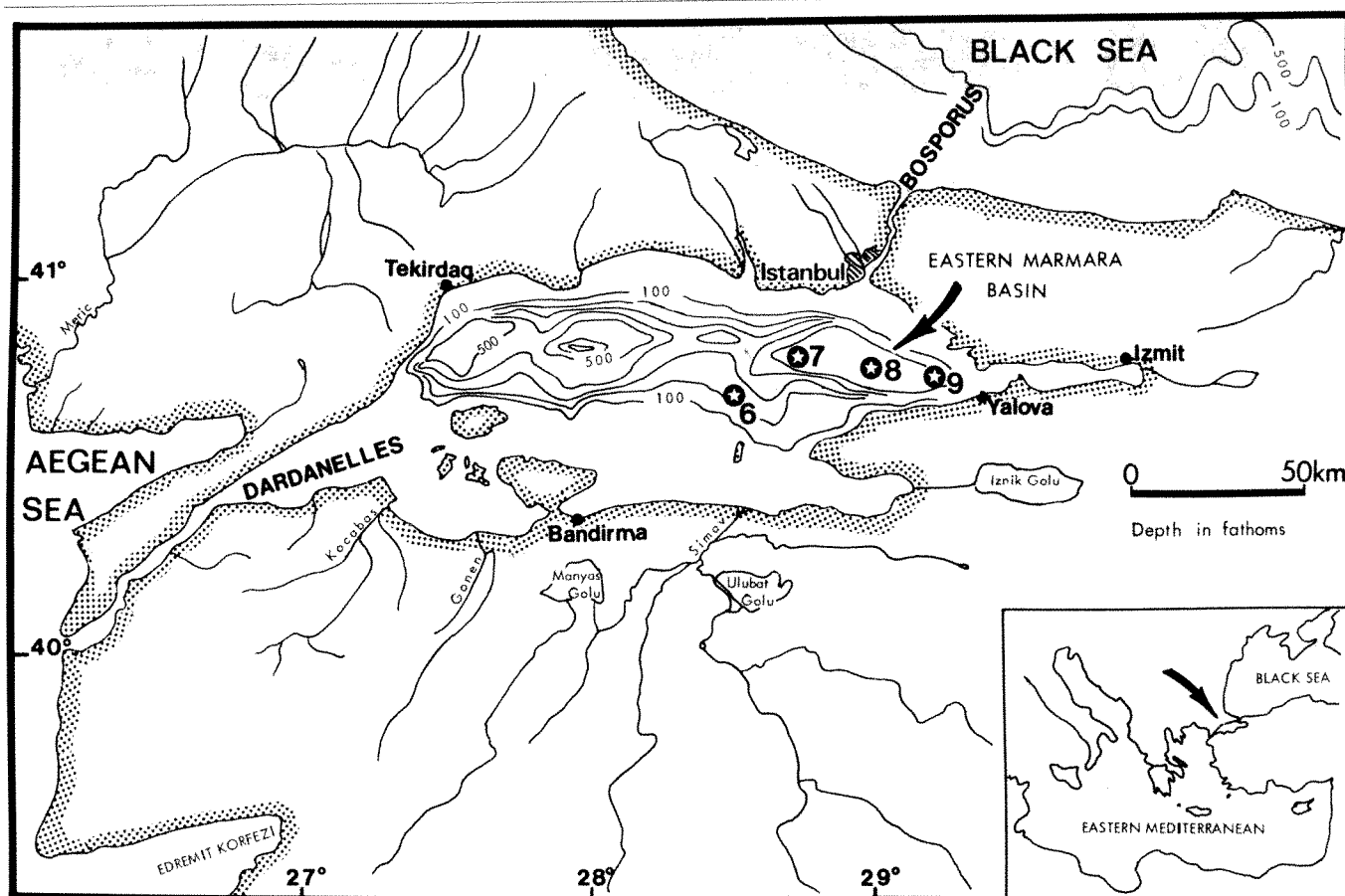
Fig. 1 Chart of the Sea of Marmara showing position of the cores discussed in the study.

exposed shelf. At this time of very rapid eustatic rise, Aegean sea level was at least 60 m below the present stand according to widely used eustatic curves[17,18], and thus the Sea of Marmara was effectively blocked to the west by the Dardanelles. In contrast to the Marmara sequence, the typical Aegean Sea–eastern Mediterranean facies during this period records deposition under open marine, vertically mixed and oxygenated conditions (Fig. 3 in ref. 5; Fig. 2 in ref. 4). At this time, the Bosporus was probably a fluvial valley that separated the Marmara lake from the Black Sea[16]. The latter, in a lake phase, received meltwater from the receding Eurasian ice caps[13], and thus displays freshwater characteristics; the Black Sea cores indicate that deposition occurred in conditions that intermittently involved sulphide formation and temporary anoxic settings[3]. Between the time of maximum eustatic low stand and ∼12,000 yr BP, we postulate three totally separated seas, each with its distinct water mass configuration (Fig. 3a).

A marked change is noted in the core G6 section dated at ∼12,000 yr BP (Fig. 2): the fine-grained sediment becomes dark olive-grey, contains an increased proportion of coarse silt, and displays poorly defined laminae. There is a sharp increase in large (1–2.5 mm), euhedral, well crystallized gypsum dominated by hemipyramidal faces (L. A. Hardie, personal communication); some crystals are coated with what is probably a bassanite-type $(CaSO_4 \cdot \frac{1}{2}H_2O)$ dehydrate gypsum[20]. Further change occurs in the overlying, somewhat younger sections (12,000–9,500 yr BP): gypsum crystals are translucent, and there is a sharp decrease in iron sulphide. A few planktonic tests include small forms of *Globigerina* cf. *G. atlantisae* Cifelli and Smith (R. Cifelli, personal communication), and rare coccoliths noted in SEM photographs. Total organic matter remains high (to 16%), but calcium carbonate content is reduced (to 3%). These characteristics suggest continuation of isolated lacustrian conditions with depleted dissolved oxygen and reduction

prevailing at the sampling site. Observed changes, however, signal an early, yet limited, introduction of water from basins adjacent to the Sea of Marmara. Aegean sea level at this time had risen to ∼50 m below the present stand, sufficient to allow minor overflow of marine waters into the Sea of Marmara (Fig. 3b). Evidence is provided by the presence of low, but increased proportions of planktonic Foraminifera and nannofossils that could only have been transported from the west. The iron sulphide casts of some of these tests, associated with the dark colour of sediments, reflect continued anoxic bottom conditions resulting from maintenance of stratification at depth of Marmara water conditions. The Black Sea during the period from ∼12,000 to 10,000 yr BP, still in its freshwater lake phase[3], was receiving by way of major rivers (Danube, Dnestr, Dnepr and others) and also the Caspian Basin overflow[13] a maximum quantity of meltwater from the receding European ice sheet. It has been suggested that this period was one of increased widespread wetness[21,22]. These regionally important climatic influences resulted in a substantial rise of the Black Sea level and westerly-directed overflow of large volumes of water across both the Bosporus and Dardanelles straits. Evidence of important Black Sea freshwater input to the eastern Mediterranean, coincident with possible changes in precipitation relative to evaporation, is recorded by the widespread presence of a grey, protosapropelic layer, usually 2–12 cm thick, that normally underlies the youngest (Holocene) sapropel in the eastern Mediterranean[23]. Such protosapropels record the beginning of marked stratification and oxygen depletion in the Aegean and adjacent Mediterranean basins. The eustatic factor *per se* played only a minor role during this event of almost one-way flow from the Black Sea, across the Sea of Marmara, to the Aegean Sea (Fig. 3b).

The G6 core section corresponding to ∼10,000–9,000 yr BP (Fig. 2) is lighter in colour, displays fine laminae and contains

Table 1 Sea of Marmara RV Pillsbury cores examined in study (dates from Smithsonian Institution Radiation Biology Laboratory)

Core	Latitude	Longitude	Depth	Core length (cm)	Depth from core top (cm)	Age (yr BP)
P6507-G6	40°40.8′N	28°33′E	384 m (210 fm)	120	15–25	5,900 ± 130
					100–110	13,530 ± 160
P6507-G7	40°45.5′N	28°46.5′E	1,193 m (650 fm)	117	50–60	Recent
					100–110	4,970 ± 110
P6507-G8	40°44.5′N	29°01.8′E	1,209 m (660 fm)	110	50–60	4,755 ± 130
					100–110	5,470 ± 125
P6507-G9	40°44′N	29°15.4′E	795 m (435 fm)	70	25–37	5,660 ± 130
					60–70	6,800 ± 130

lower percentages of iron sulphide and total organic matter (to 15%) and slightly higher carbonate content (to about 4%). Although the proportion of microfauna (planktonic Foraminifera, nannofossils) remains low, a few open-marine benthonic Foraminifera (primarily *Bolivina* sp., *Fursenkoina* sp.) appear for the first time. The tests are well preserved without obvious dissolution features. Pyramidal gypsum crystals, larger than those in underlying sections, dominate the core section, and what is interpreted as a bassanite-type gypsum form reappears at ∼9,000 yr BP, but is absent in younger overlying sections. Between 9,500 and 7,000 yr BP sediments are darker, richer in organic matter (to 18%), and show a decrease in iron sulphide, while benthonic

Foraminifera temporarily disappear. The continued eastward overflow of saline Mediterranean water across the Dardanelles spread along density interfaces in the eastern Marmara Basin, and water above the bottom remained partially, and at times completely, euxinic. The continued rapid eustatic sea-level rise during this period also enabled minor amounts of Mediterranean waters to cross the Bosporus and overflow into the Black Sea[3]. The period between ∼9,500 and 7,000 yr BP experienced a two-way flow regime above the Sea of Marmara, but the westward movement of fresh water into the Aegean and beyond clearly predominated (Fig. 3c). This resulted from continued, but reduced, influx of meltwater and fluvial discharge from the Danube and Russian rivers into the Black
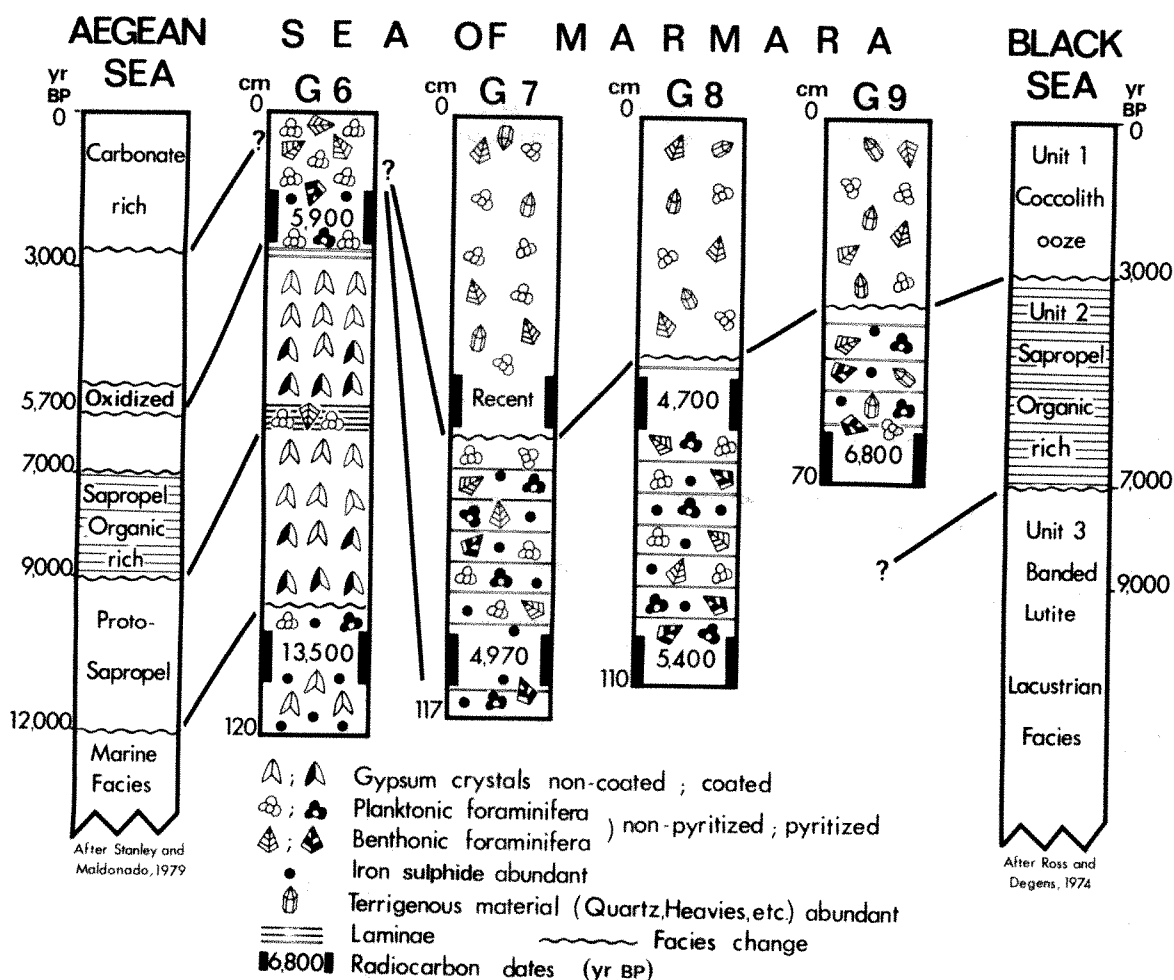
Fig. 2 Simplified logs of the Sea of Marmara (RV Pillsbury cruise P6507) core sequences, and correlation with stratigraphic sections in the Aegean[4] and Black Seas[3].
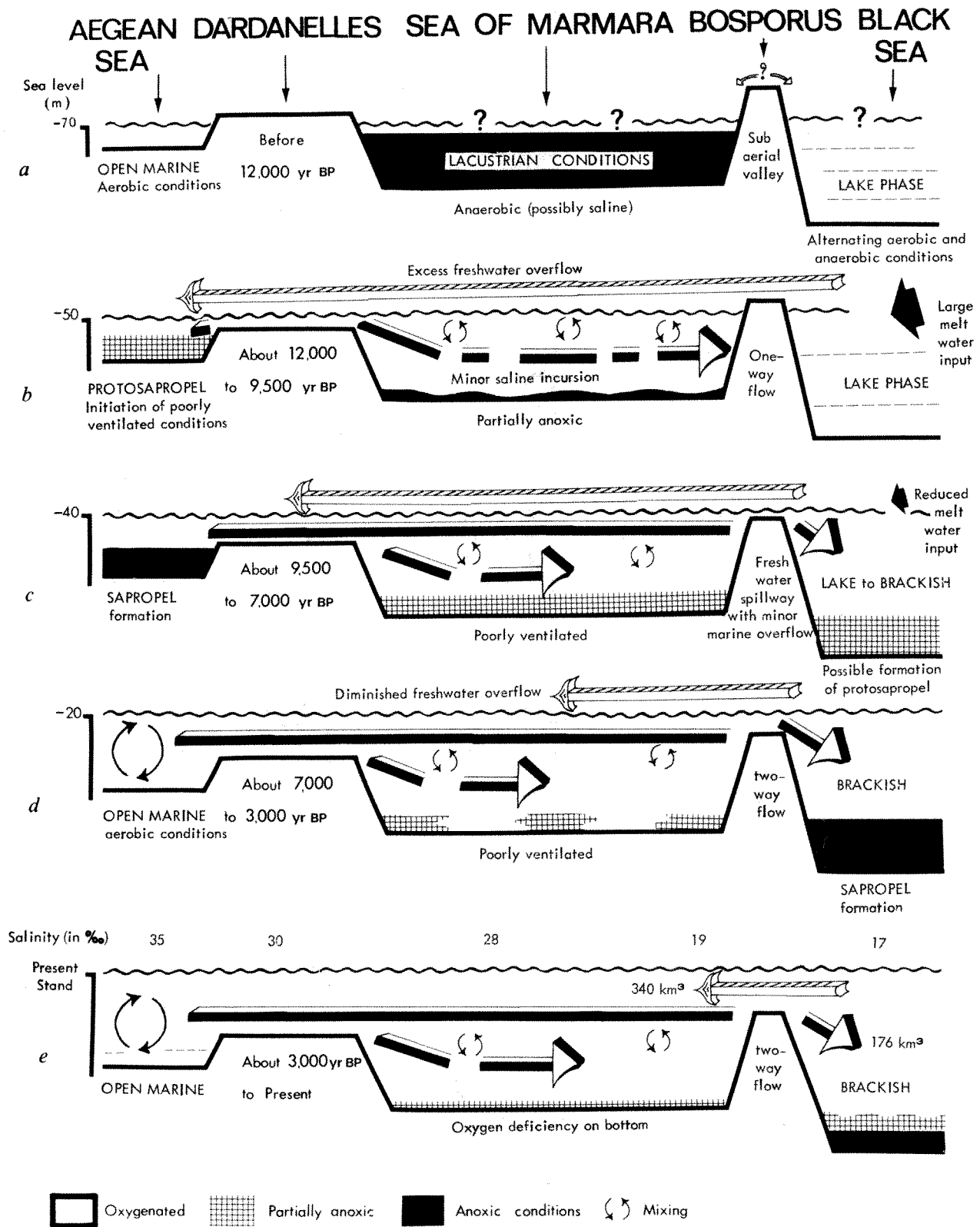
Fig. 3 Schematic depiction of oceanographic conditions in the Sea of Marmara region showing changes with time and the sequence of water exchange patterns between the Aegean and Black Seas. The shallower depth of the Bosporus still is exaggerated, and the Marmara morphology much simplified, see text.

Sea, and apparently coincides with another short period of widespread wetness[21]. The powerful westward flow of Black Sea freshwater has been cited as a major factor in the formation of the most recent sapropel (9,500–7,000 yr BP) throughout most of the eastern Mediterranean Sea[8-10]. Moreover, this discharge probably induced temporary current reversals and also the formation of grey reduced layers in the western Mediterranean[9,24].

A facies change occurs in core G6 at ~7,000–6,000 yr BP (Fig. 2). Sediments are lighter olive, coarser grained, include both well defined and vague laminae, and are characterized by the disappearance of gypsum crystals and slight diminution of total organic matter (to ~16%). Both planktonic and benthonic foraminiferal tests increase markedly (to ~30% of the sand fraction) and this is reflected by the higher percentage of carbonate content (to 6%). The planktonic foraminiferal population comprises only small tests of *Globigerina*, many of which are filled with iron sulphide. An essentially marine regime prevailed in the Sea of Marmara (Fig. 3*d*), and although not euxinic, the deeper parts of the basin remained oxygen-deficient. As a result of the, continued but slower rise of sea level, increased amounts of Mediterranean water entered and influenced the formation of Black Sea sapropels during the period from ~7,000 to 3,000 yr BP (ref. 3) (Fig. 3). The reduced fluvial discharge into the Black Sea diminished the westwardly outflow of fresh water across the straits and the Sea of Marmara, allowing a return to vertical water mass circulation and oxygenated bottom water conditions as presently observed in the Aegean[25]. A well defined oxidized layer, dated at ~5,700 yr BP and widely distributed throughout the eastern Mediterranean[4] (Fig. 2), may be related to the proposed increased evaporation regime at 6,500–5,500 yr BP (ref. 21).

There is a good correlation among core G7, G8 and G9 lithofacies dated between ~6,000 yr BP and the present (Fig. 2). Sediments from ~5,000 to 3,000 yr BP are olive grey, laminated clayey silts with a high iron sulphide content. The sand fraction, ~5% of the total sediment, includes pelagic (dominant) and benthonic foraminiferal species similar to those of underlying sections. Small pelecypods and echinoderm fragments appear for the first time; these and sand-size terrigenous components, including light and heavy minerals, lithic fragments and plant matter, were probably displaced basinward from the Marmara shelf by turbidity currents. Some iron-stained quartz may also have a windblown origin (core G9). About 30% of the fauna displays an iron sulphide filling. Total organic matter ranges from 11 to 19%, and the calcium carbonate content does not exceed 5%. Radiocarbon dating of basin cores G7 and G8 reveals high sediment accumulation rates (to at least 70 cm per 1,000 yr) between 5,500 and 4,500 yr BP, indicating periodically intensified precipitation and increased discharge from rivers, primarily from the south, flowing into the Sea of Marmara.

At ~3,000 yr BP, Marmara sediments are darker olive and coarser grained (Fig. 2). Total organic matter remains high and calcium carbonate content low. Those layers in basin cores containing high proportions of terrigenous material of sand and silt-size were probably emplaced by turbidity currents. The marked increase in sediment accumulation rates at this time may be related to regionally important climatic fluctuations recognized in the eastern Mediterranean[26], or intensified tectonic activity[15]. This period coincides with the end of sapropel formation and the first major coccolithophore invasion in what had now become the brackish Black Sea[3], and with carbonate-rich deposition that prevailed in the eastern Mediterranean[4] (Fig. 2).

Conclusions

We postulate that the physical oceanographic conditions presently measured in the Sea of Marmara, including the two-way exchange of water masses through the Bosporus and Dardanelles[16,25,27], were established at ~3,000 yr BP. The Sea of Marmara is presently characterized by salinity, temperature and chemical nutrient distribution patterns between those of the vertically circulated, well oxygenated marine Aegean (>35‰ salinity) and the brackish (<20‰ salinity) Black Sea (Fig. 3*e*). The low dissolved oxygen content in the Sea of Marmara (1.5 ml l^{-1}) and the high (to 14%) total organic content in surficial sediments result from continued stratification of water in this quasi-enclosed depression[27]. The present environmental conditions are largely responsible for the restricted planktonic foraminiferal population (scarcity and small size of tests, few species).

We identify the Sea of Marmara as the easternmost branch of the Mediterranean, with the Bosporus Strait serving as the major boundary with the Black Sea. Lithostratigraphic sequences deposited in the Sea of Marmara during the latest Pleistocene to the present include facies which typify deposition in almost continuously restricted circulation regimes. These sequences provide an almost complete record of palaeo-oceanographic events because of the quasi-enclosed physiographic configuration and intermediate position of this catchment basin between the larger seas. The dated Sea of Marmara facies offer a means to correlate more precisely sequences between the eastern Mediterranean and the Black Sea, and to explain lithologic differences in terms of fluctuating water mass exchange patterns resulting from regionally important climatic oscillations.

1. Carter, T. G. *et al.* in *The Mediterranean Sea—A Natural Sedimentation Laboratory* (ed. Stanley, D. J.) 1–24 (Dowden, Hutchinson & Ross, Stroudsburg, 1972).
2. Gunnerson, G. G. & Ozturgut, E. in *The Black Sea—Geology, Chemistry and Biology* (eds Degens, E. T. & Ross, D. A.) Mem. **20**, 99–114 (American Association of Petroleum Geologists, Tulsa, 1974).
3. Ross, D. A. & Degens, E. T. in *The Black Sea—Geology, Chemistry and Biology* Mem. **20**, 183–199 (American Association of Petroleum Geologist, Tulsa, 1974).
4. Stanley, D. J. & Maldonado, A. *Sed. Geol.* **23**, 37–65 (1979).
5. Pastouret, L. *Tethys* **2**, 227–266 (1970).
6. Letolle, R. & Vergnaud-Grazzini, C. in *Les Méthodes Quantitatives d'étude des Variations du Climat au Cours du Pleistocène* Vol. 219, 231–238 (CNRS, Paris, 1973).
7. Shackleton, N. J. in *Abstracts with Programs 1979 Annual Meetings*, 514 (Geological Society of America, Boulder, 1979).
8. Ryan, W. B. F. in *The Mediterranean Sea—A Natural Sedimentation Laboratory* (ed. Stanley, D. J.) 149–169 (Dowden, Hutchinson & Ross, Stroudsburg, 1972).
9. Stanley, D. J. *Nature* **274**, 149–152 (1978).
10. Thunell, R. C. & Lohmann, G. P. *Nature* **281**, 2111–2113 (1979).
11. Deuser, W. G. in *The Black Sea—Geology, Chemistry and Biology* (eds Degens, E. T. & Ross, D. A.) Mem. **20**, 133–136 (American Association of Petroleum Geologists, Tulsa, 1974).
12. Degens, E. T. & Stoffers, R. *Nature* **263**, 22–27 (1976).
13. Grosswald, M. G. *Quat. Res.* **13**, 1–32 (1980).
14. McKenzie, D. P. *Geophys. J. R. astr. Soc.* **30**, 109–185 (1972).
15. Sengör, A. M. C. *J. geol. Soc.* **136**, 269–282 (1979).
16. Scholten, R. in *The Black Sea—Geology, Chemistry and Biology* (eds Degens, E. T. & Ross, D. A.) Mem. **20**, 115–116 (American Association of Petroleum Geologists, Tulsa, 1974).
17. Curray, J. A. in *The Quaternary of the United States* (eds Wright, H. F. Jr & Frey, D. J.) 723–726 (Princeton University Press, Princeton, New Jersey, 1965).
18. Mörner, N. A. *Paleogeogr. Paleoclimatol. Paleoecol.* **9**, 153–181 (1969).
19. Siesser, W. G. & Rogers, J. *Sedimentology* **23**, 567–577 (1976).
20. Haar, S. V. in *The Encyclopedia of Sedimentology* (eds Fairbridge, R. W. & Bourgeois, J.) 391–394 (Dowden, Hutchinson & Ross, Stroudsburg, 1978).
21. Sarnthein, M. *Nature* **272**, 43–46 (1978).
22. Street, F. A. & Grove, A. T. *Quat. Res.* **12**, 83–118 (1979).
23. Maldonado, A. & Stanley, D. J. *Mar. Geol.* **20**, 27–40 (1976).
24. Stanley, D. J., Maldonado, A. & Stuckenrath, R. *Paleogeogr. Paleoclimatol. Paleoecol.* **18**, 279–291 (1975).
25. Miller, A. R., Tchernia, P. & Charnock, H. *Mediterranean Sea Atlas of Temperature Salinity, Oxygen, Distribution of Nutrient Chemical Properties* Atlas Series Vol. 3 (Woods Hole Oceanographic Institution, Woods Hole, 1970).
26. Magaritz, M. & Kaufman, A. *Nature* **243**, 462–464 (1973).
27. Anderson, J. J. & Carmack, E. C. *Deep-Sea Res.* **21**, 877–886 (1974).

Isolation and structure of a human fibroblast interferon gene

Rik Derynck*, Jean Content†, Erik DeClercq‡, Guido Volckaert*, Jan Tavernier*, René Devos* & Walter Fiers*

*Laboratory of Molecular Biology, State University of Ghent, Ledeganckstraat 35, B-9000 Ghent, Belgium
†Institut Pasteur du Brabant, rue du Remorqueur 28, B-1040 Brussels, Belgium
‡Rega Institute for Medical Research, Katholieke Universiteit Leuven, Minderbroedersstraat 10, B-3000 Leuven, Belgium

Chimaeric plasmids containing double-stranded cDNA copies of mRNA induced in human fibroblasts by poly I · C were screened by an RNA selection method. A series of clones to which human fibroblast interferon mRNA selectively hybridized was identified. From the nucleotide sequence of the gene, the complete amino acid sequence of human fibroblast interferon was deduced. The protein is 166 amino acids long and is preceded by a 21-amino acid signal sequence.

AT least three interferons with different antigenic specificity have so far been recognized. Leukocyte interferon, lymphoblastoid interferon and fibroblast interferon represent the type I interferons, whereas mitogen-induced immune interferon is a type II interferon (see ref. 1 for review). Although the structure of leukocyte and fibroblast interferons may be sufficiently similar for them to be recognized by the same receptor[2], there is evidence that they are encoded by different genes[3]. Biologically, they have a different host-cell range[1], different dose–response curves when assayed for antiviral activity on cell culture[4,5] and a varying degree of cytostatic action in several types of cells[6,7]. Both interferons have immunomodulating activities, both are able to activate 'natural killer' cells[8-10] and both have promising clinical antiviral and antitumour activities[11-15].

The differences and similarities in activity of the two interferons will be better understood when their structures are known. All that is known so far of the structure of HF-IF (human fibroblast interferon) is the sequence of the 13 NH_2-terminal amino acids[16] and the fact that it is a glycoprotein of about 20,000 molecular weight (MW)[17-20].

Two laboratories have recently used recombinant DNA technology to clone interferon cDNA[21,22]. We have been working along similar lines, and here describe the construction and isolation of hybrid plasmids containing cDNA of HF-IF. The nucleotide sequence of the mature mRNA is derived from the analysis of the cloned DNA. On the basis of this information, the total amino acid sequence of HF-IF is deduced.

Isolation of RNA and construction of chimaera plasmids

Total RNA was isolated from VGS cells, a human diploid fibroblast cell line[23]. The cells were primed with homologous human fibroblast interferon, induced for interferon production with poly I · C and superinduced with the antibiotic cycloheximide. Induction by poly I · C has been shown to induce only HF-IF in human fibroblasts, in contrast to viral induction, which results in a certain level of leukocyte interferon production[24]. Confluent VGS fibroblasts passage 23–26 (usually 20 roller bottles, 670 cm^2 each) were primed with 100 units ml^{-1} HF-IF for 16 h (ref. 23), and induced with 100 µg ml^{-1} poly I · C in the presence of 50 µg ml^{-1} cycloheximide for 4 h (ref. 25). The cells were scraped off, lysed with NP40, and the total cytoplasmic RNA was extracted with phenol. Usually 60–80 µg of total RNA was obtained from a confluent roller bottle. Purification over oligo(dT)-cellulose yielded polyadenylated mRNA representing 3–5% of the total RNA. This mRNA fraction was further enriched for interferon

mRNA by sedimentation in a 5–20% sucrose gradient in 50% formamide[26]. Alternatively, the mRNA fraction was separated on a polyacrylamide gel and the fractionated RNA eluted from 2-mm gel slices[27] (the average decrease in mRNA length per successive gel slice was about 45 nucleotides). In all cases, the presence and amount of interferon mRNA were monitored by translation in *Xenopus laevis* oocytes[28], followed by assaying of interferon activity, based on reduction of the cytopathogenic effect caused by vesicular stomatitis virus (VSV). The use of human fibroblasts trisomic for chromosome 21 gave a 5–10-fold enhanced sensitivity to HF-IF in comparison with the diploid human fibroblasts[29]. The peak fractions of these gradients were further used for the synthesis of double-stranded cDNA and cloning. The *in vitro* synthesis of cDNA was carried out by sequential treatment with avian myeloblastosis virus (AMV) reverse transcriptase, RNases T1 and A, *Escherichia coli* DNA polymerase I and S_1 nuclease, essentially as described elsewhere[30]. This double-stranded cDNA was fractionated by polyacrylamide gel electrophoresis. The full-size interferon double-stranded cDNA was considered to be about 850 base pairs long on the basis of a prominent band on polyacrylamide gel with cDNA synthesized from the active mRNA, which was itself narrowly sized by gel fractionation (see above). This size estimate agrees with the sedimentation value of interferon mRNA in sucrose gradients[31]. The eluted double-stranded cDNA was elongated with homopolymeric (dT)-tails by terminal deoxynucleotidyl transferase. This tailed insert DNA was annealed to a double molar concentration of pBR322 plasmid DNA that had been cleaved in the β-lactamase gene by *Pst*I restriction endonuclease and treated with terminal transferase to add homopolymeric (dA)-tails at the cleavage sites[30]. The annealed hybrid plasmids were introduced into competent *E. coli* K12 HB101 cells[32]. About 97% of the tetracycline-resistant transformants were sensitive to carbenicillin, suggesting the presence of an insert cDNA in the *Pst*I site of the β-lactamase gene. In this way, a library of about 17,000 transformants was constructed using 270 fmol (128 ng) of tailed insert DNA.

Identification of clones containing human interferon cDNA

An RNA selection method was used to identify clones with an HF-IF cDNA insert. Plasmid DNA from the clones was coupled to diazobenzyloxymethyl (DBM)-cellulose powder[33]. Total RNA from induced VGS cells was hybridized to the DNA and the hybridized mRNA was eluted in 99% formamide[34]. The plasmid pSTNV-1 DNA, a pBR322

derivative containing the double-stranded cDNA from satellite tobacco necrosis virus (STNV) RNA[35], was added to the plasmid DNAs to be coupled; as the hybridization reaction was carried out in the presence of STNV RNA, we could evaluate the efficiency of hybridization, the extent of RNA degradation throughout the procedure and the possible presence of translational inhibitors. Half of the recovered RNA fractions were translated in the nuclease-treated rabbit reticulocyte lysate[36], followed by immunoprecipitation of the *in vitro* synthesized STNV coat protein and analysis on polyacrylamide gel (data not shown). The other half of the non-hybridized or hybridized RNA was assayed for the

presence of interferon mRNA by translation in *Xenopus* oocytes followed by the antiviral interferon assay.

Twelve groups of 46 clones from the library were screened for the presence of an interferon cDNA-containing plasmid (Table 1). One of the two which showed a positive response was subdivided into eight groups. One of these showed a clear positive interferon response after translation of the hybridized RNA. The individual clone containing the interferon cDNA was finally detected using DBM–cellulose paper disks, allowing elution with water at 80 °C and thus reducing the RNA degradation. The bacterial clone identified in this way is designated G-HB101-pHFIF-1, the plasmid being referred to as pHFIF-1.

Other clones containing double-stranded interferon cDNA were detected using the colony hybridization technique originally described by Grünstein and Hogness[37], as modified by Hanahan and Meselson (personal communication). Restriction enzyme analysis of pHFIF-1 revealed an internal *Hin*fI fragment of about 170 base pairs. This fragment was ^{32}P-labelled by nick translation[38] and the probe was used for screening part of the library for clones related to pHFIF-1. In this way, several additional clones were selected, their plasmids being designated pHFIF-2 to pHFIF-13. In our collection an average of 1% of the clones hybridized to the 170-base pair fragment of pHFIF-1. As the mRNA used for the cloning was 20–40-fold enriched by formamide–sucrose gradient centrifugation, one may estimate that approximately 1 out of 2,000–4,000 mRNAs is HF-IF mRNA under the induction regimen used for the VGS fibroblasts. That the secondary clones, detected by colony hybridization, actually contained interferon-specific sequences was further supported by the observation that plasmid DNA of one of these clones, pHFIF-2, was equally effective in selecting interferon mRNA (data not shown). Furthermore, the mRNA hybridized to either pHFIF-1 or pHFIF-2 gave rise to the same polypeptide of about 18,500 MW after translation in the rabbit reticulocyte lysate and immunoprecipitation with antiserum against partially purified HF-IF (Fig. 1). Addition of a microsomal fraction of dog pancreas to the reticulocyte lysate[39] produced two modified forms of this polypeptide, one with an apparent MW of ~20,500 and the other ~16,500, the former corresponding in size to HF-IF secreted from induced culture cells[17–19]. The protein of lower MW suggests maturation by cleavage of a signal peptide, as will be discussed below.

Fig. 1 Polyacrylamide gel electrophoresis of cell-free translation products from HF-IF mRNA after hybridization on different plasmid DNAs. Samples (30 µg) of total induced VGS-RNA were hybridized[34] to DBM–cellulose filters containing 3 µg DNA from pHFIF-1 or pHFIF-2. All RNA samples were divided into two equal parts and translated for 45 min at 31 °C in 25-µl reaction mixtures containing 1.7×10^7 c.p.m. ^{35}S-methionine (~1,000 Ci mmol^{-1}) and 150 µg ml^{-1} calf liver tRNA in a micrococcal nuclease-treated rabbit reticulocyte lysate[36] in the absence (lanes 2–9) or presence (lanes 10–13) of 6 A_{280} ml^{-1} dog pancreas microsomes[39]. The reaction products were precipitated by addition of 2 µl of goat anti-HF-IF (200,000 HF-IF neutralizing units ml^{-1}) in the presence of 1% sodium deoxycholate and 1% NP40 for 1 h at 37 °C and 30 µl of a 10% suspension of *Staphylococcus aureus* Cowan I for 30 min at 20 °C. After extensive washing, the bacterial pellet was resuspended and boiled for 2 min in electrophoresis sample buffer, clarified for 2 min at 9,000g and applied to a 13% polyacrylamide gel. After electrophoresis, the gel was treated with En[3]hance (NEN) and fluorographed for 5 days at −70 °C. Lane 1, ^{14}C-protein markers (Radiochemical Centre); the MW of the proteins are indicated at the left; lanes 2 and 10, pHFIF-1, non-hybridized RNA; lanes 3 and 11, pHFIF-1, hybridized RNA; lanes 4 and 12, pHFIF-2, non-hybridized RNA; lanes 5 and 13, pHFIF-2, hybridized RNA; lane 6, endogenous activity of the reticulocyte lysate; lane 7, total RNA from non-induced VGS cells (2 µg); lanes 8 and 9, total RNA from induced VGS cells (2 µg). The estimated MWs of the HF-IF precursor (lanes 3, 5) and of its putative processed, non-glycosylated and glycosylated derivatives (lanes 11, 13) are indicated at the right.

Physical characterization and sequence analysis of the cDNA insert

The plasmid DNAs of a series of clones containing an interferon cDNA insert as detected by hybridization were further characterized using restriction enzymes. Most attention was given to pHFIF-1, 2, 3, 6 and 7. Using the detailed physical map of pBR322 (ref. 40), the insert length could be estimated, either by using enzymes which do not cleave the insert, such as *Msp*I (= *Hpa*II) and *Hha*I, or by summation of the length of different restriction fragments. The insert cDNA of pHFIF-1 was, on the basis of its length, considered to be incomplete. Three other plasmids, pHFIF-3, 6 and 7, all had an insert of more than 850 base pairs, approximately the expected size of a full-length cDNA. Although most restriction enzymes tested had the same number of cleavage sites in these DNAs, clear differences could be observed in the patterns of restriction fragments obtained. Detailed analysis revealed that some awkward inversions had occurred. The arrangement of these inversions all had a similar appearance (Fig. 2). In all three cases, only a single segment was transposed, for example, in pHFIF-3, the *Pst*I–*Hind*II segment is inverted. The arrangement was confirmed and shown by nucleotide sequence analysis always to involve a cross-over point in the 5′-untranslated leader sequence. A second cross-over could conceivably have occurred in the tail region but it is also

Table 1 Outline of the screening strategy used for detecting plasmids containing interferon-specific DNA

Library (17,000 clones)	→	Group (46 clones)	→	Subgroup (7 or 8 clones)	→	Individual clone

Plasmid DNA source	Plasmid DNA bound on DBM–cellulose	Interferon activity ($\log_{10}$ units ml^{-1})*	
		Non-hybridized RNA	Hybridized RNA
Group 0 (46 clones)	1 µg DNA per clone	0.2	0.5
Subgroup 0$_1$ (8 clones)	3 µg DNA per clone	0	1.2
		0	1.5
		0	0.5
Individual clone 0$_1$/8 (subsequently referred to as pHFIF-1)	3 µg DNA per clone	0	1.0
		0	1.7
		0	1.2

Two groups of 46 clones were chosen arbitrarily from a total library of 17,000 clones (see scheme at top of table). As an example, the results of a positive group (group 0), subgroup (three experiments) and individual clone (also three experiments) are given. Total cytoplasmic RNA (15 µg) from induced VGS cells was used for hybridization. The non-hybridized and hybridized mRNA fractions[34] were precipitated twice with ethanol, dissolved in 2 µl water and assayed for the presence of interferon mRNA as follows. Five *X. laevis* oocytes were injected with 50 nl per oocyte[28]. After incubation, a homogenate was obtained by crushing the oocytes in 40 µl incubation medium and cleared by centrifugation at 9,000*g* for 2 min. Human fibroblast interferon was assayed by a CPE (cytopathic effect)-inhibition technique in human fibroblasts trisomic for chromosome 21 in microtitre trays. The cells were challenged with VSV (Indiana strain) and the CPE was recorded at 24 h. All assays included an internal standard of HF-IF which was itself calibrated against the NIH human fibroblast reference G023-902-527.

* The limit of detection is 0.1 $\log_{10}$ units ml^{-1}.

possible that only a single cross-over was necessary to generate the inversion. The actual reason for this phenomenon is unclear; presumably it is a cloning artefact, although we have never seen this in our other work.

Restriction fragments labelled at the 5′ end were prepared and sequenced, essentially according to Maxam and Gilbert[41]. The procedure used for *in vitro* DNA synthesis and cloning enabled us to determine the orientation of the coding strand. Indeed, the cDNA synthesis on the mRNA was initiated by a p(dT)$_{10}$ primer hybridized to the poly(A)-tail at the 3′ end of the mRNA. This results in a (dA)$_{10}$ stretch at the 3′ end of the (+)strand (the second DNA strand), followed by a dT-tract due to the elongation with terminal deoxynucleotidyl transferase. This feature allowed us to identify the 3′ end of the coding strand in several plasmids examined.

Figure 3 shows the strategy for the sequencing analysis. All sequences were read several times, either on the same strand but from different restriction sites, or on the opposite strand. These results obtained on the series of clones allowed us to deduce the total nucleotide sequence of HF-IF cDNA.

The deduced primary structure of human fibroblast interferon mRNA and protein

The primary structure of the mRNA was determined on the basis of the DNA sequence and is shown in Fig. 4. The sequence we have deduced is 828 nucleotides long, excluding the poly(A) tail at the 3′ end. One continuous reading frame was established, starting from the AUG codon at position 65 (immediately preceded by the *Hin*dII site) and ending with the stop codon UGA at position 626, followed almost immediately by the single *Bgl*II restriction site. This region is 561 nucleotides long and thus is coding for 187 amino acids. The untranslated 5′ end is 64 nucleotides long, but is presumably incomplete considering the method of *in vitro* synthesis of double-stranded cDNA. Although the total mRNA has an A + U content of 58% and the coding region an A + U content of 55% (normal values for a eukaryotic mRNA), the 5′-untranslated sequence is rather low in these bases—48% A + U. The 3′-untranslated region, excluding the poly(A) tail, is 203 nucleotides long and can be divided into two segments.
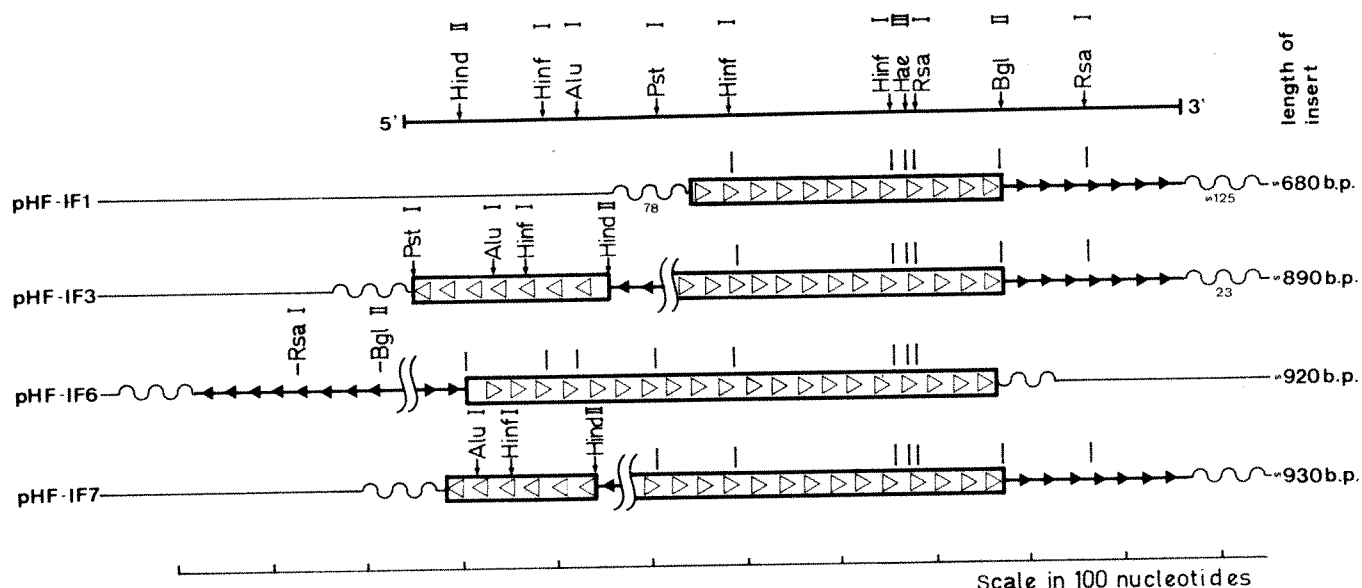
Fig. 2 Schematic representation of the organization of the cDNA inserts in pHFIF-1, 3, 6 and 7. The upper line represents a complete cDNA copy of interferon mRNA, with some reference restriction sites, and can be aligned with the more detailed map in Fig. 3. The dA·dT tails are indicated by a wavy line (the length, when known, is given underneath). The boxed segments indicate the translated sequence of the mRNA and the triangles indicate the 5′→3′ direction of the coding strand of the insert DNA, in the translated region as well as in the 5′ and 3′ untranslated regions. An interruption in the base line of the maps indicates the cross-over regions of the inversion. b.p., Base pairs.

Fig. 3 Restriction map and sequencing strategy for the HF-IF cDNA gene. The central diagram shows the organization of the mRNA for human fibroblast interferon, with the 5′-untranslated region, the boxed translated sequence with the presumed signal peptide and the 3′-untranslated segment, the number of amino acids (aa) and nucleotides being indicated for each region. At the top, the regions covered by sequencing are indicated; the open dots correspond to the ^{32}P-labelled 5′ ends. The numbers above the arrows refer to the different clones analysed. Using 0.5-mm gels, it was occasionally possible to read over 300 nucleotides from the labelled site. Below is a restriction endonuclease map of the double-stranded cDNA, constructed by computer search on the basis of the complete nucleotide sequence, many of these sites being experimentally verified. Enzymes cutting the double-stranded cDNA only once are indicated on the top line and enzymes cleaving at multiple sites are indicated individually below. Recognition sequences of restriction enzymes are listed by Roberts[56].

Fig. 4 Nucleotide sequence of the human fibroblast interferon mRNA and corresponding amino acid sequence. The nucleotide sequence is presented as the mRNA sequence, derived from analysis of the double-stranded cDNA in several plasmids; the actual mRNA may be longer at the 5′ end. The initiation and termination codons are shown in heavily outlined boxes. The AAUAAA sequence, presumably present near the 3′ end in all polyadenylated eukaryotic cellular mRNAs, is shown in a dashed box. The nucleotide numbering is given at the right. The nucleotide sequence is translated into an amino acid sequence consisting of a 21-amino acid signal peptide, from the initiation codon up to the vertical arrow, and the mature polypeptide. The boxed amino acid sequence, starting from the vertical arrow, indicates the NH₂-terminal sequence derived from direct analysis of the protein[16].

	U	C	A	G	
U	Phe $\{^4_5$ Leu $\{_3$	Ser $\{^1_1$	Tyr $\{^4_6$ Ochre Amber	Cys $\{^2_1$ Opal ⊙ Trp 3	U C A G
C	Leu $\{^3_6\ ^2_{10}$	Pro $\{^1$	His $\{^3_2$ Gln $\{^3_8$	Arg $\{_1$	U C A G
A	Ile $\{^5_4\ _2$ Met 4	Thr $\{^2_3\ _2$	Asn $\{^4_8$ Lys $\{^4_7$	Ser $\{^2_5$ Arg $\{^5_5$	U C A G
G	Val $\{^1_3\ _1$	Ala $\{^2_3\ _1$	Asp $\{^2_3$ Glu $\{^5_8$	Gly $\{^1_1\ ^2_2$	U C A G

Fig. 5 Codons used in human fibroblast interferon mRNA. The numbers refer to the frequency with which each triplet is used.

The region proximal to the UGA termination codon has a normal A + U content, whereas the distal portion is extremely A + U rich, a feature also observed, although not to this extent, in the mRNA of rat growth hormone[42]. Indeed, starting from position 744, only two C and eight G residues are present in a total of 84 nucleotides. A striking feature of this same region is the presence of many $A(U)_{2-5}$ stretches. The AAUAAA sequence presumably present in all polyadenylated eukaryotic cellular mRNAs and thought to be involved in processing or polyadenylation of the mRNA[43], is found some 20 nucleotides before the often observed C residue immediately preceding the poly(A) tail.

As in other vertebrate DNA and RNA sequences characterized so far, the dinucleotide CG is very rare in the mRNA for HF-IF. Only one of the six occurring CG dinucleotides is used within a codon (Fig. 5). This deficiency is reflected in the strong preference for AGG and AGA as codons for arginine, a preference which has also been observed in the genome of SV40 (ref. 44) and polyoma[45] and the haemagglutinin gene of a human influenza strain[46], but not, however, in the mRNA for rat growth hormone[42] or human chorionic somatomammotropin[47]. The apparently strong preference for CUG as codon for leucine, which seems to be a general phenomenon in eukaryotic cellular mRNAs but not in the mRNAs of SV40 (ref. 44) or polyoma[45] virus, is also found in HF-IF mRNA. There is also preference for AGU and AGC as codons for serine.

The amino acid sequence of HF-IF, deduced from the nucleotide sequence of the coding region, is also presented in Fig. 4. The 13 NH_2-terminal amino acids of mature HF-IF were recently directly determined by protein microsequencing techniques[16]. A corresponding nucleotide sequence begins at nucleotide 128; therefore, we conclude that this represents the NH_2-terminus of the mature HF-IF. It is preceded by a segment of 21 amino acids starting with an AUG at position 65. As interferons are secretory proteins, we postulate that this region is a signal peptide, cleaved off during or after transport of the nascent protein across the membrane. Indeed, it has been well established that the majority of secretory proteins start with a hydrophobic signal peptide which is subsequently removed[48]. The hydrophobicity of this segment, mainly of the central part, and its length of 21 amino acids are consistent with the known properties of a signal peptide[48,49]. Also, as generally observed[48,49], this signal peptide ends with an amino acid (serine in this case) of lower MW than the first NH_2-terminal amino acid of the cleaved protein. Direct evidence for this signal peptide has been obtained experimentally: addition of the microsomal fraction of dog pancreas to the *in vitro* translation mix, followed by immunoprecipitation with anti-interferon antiserum, results in a protein with an apparently lower MW than the unprocessed protein, indicating that a segment has been cleaved off (Fig. 1).

The mature HF-IF contains 166 amino acids on the basis of the deduced protein sequence. The amino acid composition is

in reasonable agreement with the composition as determined by direct analysis[16,19]. It has a remarkably low content of proline and is very rich in the hydrophobic amino acids leucine and isoleucine, and also in tyrosine. The intrinsic hydrophobicity of HF-IF is well known and is also revealed by its interaction with several ligands[50]. Three cysteines are present in HF-IF, which means that there must be at least one free thiol group.

The mature fibroblast interferon has been shown to be a glycoprotein[17-19]. However, direct localization and characterization of the carbohydrate moieties on the polypeptide have not been described. Attachment of carbohydrate through N-glycosidic linkage is known to occur on the asparagine in the triplets Asp-X-Ser or -Thr, the presence of this sequence being a necessary but not a sufficient condition for glycosylation[51]. Only one asparagine allowing this type of glycosylation is found in fibroblast interferon, at position 80 of the amino acid sequence. Alternatively, or additionally, O-glycosidically linked oligosaccharides could be attached to serine and/or threonine residues, a good example of this being the human erythrocyte glycophorin[52].

We are now in a position to reconstruct a plasmid with the total HF-IF genetic information under a prokaryotic transcription signal and to test for its expression in a bacterial system.

After submission of this manuscript, we identified a clone, pHFIF-21, having a full-length insert without rearrangements. Also we learned that Taniguchi *et al.*[53] have also determined the nucleotide sequence of a cloned HF-IF gene. The deduced amino acid sequence is identical to that reported here and shows the homology (see accompanying paper[54]) with the sequence of human leukocyte interferon[55].

1. Stewart, W. E. II *The Interferon System* (Springer, Berlin, 1979).
2. Wiranovska-Stewart, M. & Stewart, W. E. II *J. gen. Virol.* **37**, 629–634 (1977).
3. Cavalieri, R. L., Havell, G. A., Vilcek, J. & Pestka, S. *Proc. natn. Acad. Sci. U.S.A.* **74**, 3287–3291 (1977).
4. Vilcek, J., Havell, G. A. & Yamazaki, S. *Ann. N.Y. Acad. Sci.* **284**, 703–710 (1977).
5. Edy, V.-G., Billiau, A. & De Somer, P. *J. gen. Virol.* **31**, 251–255 (1976).
6. Einhorn, S. & Strander, H. *J. gen. Virol.* **35**, 573–577 (1977).
7. Kuwata, T., Fuse, A., Suzuki, N. & Morinaga, N. *J. gen. Virol.* **43**, 435–439 (1979).
8. Herberman, R. R., Ortaldo, J. R. & Bonnard, G. D. *Nature* **277**, 221–223 (1979).
9. Zarling, J. M., Eskra, L., Borden, E. C., Horoszewicz, J. & Carter, W. A. *J. Immun.* **123**, 63–70 (1979).
10. Huddlestone, J. R., Merigan, T. C. Jr & Oldstone, M. B. A. *Nature* **282**, 417–419 (1979).
11. De Smyter, J. *et al. Lancet* **ii**, 645–647 (1976).
12. Horoszewicz, J. S. *et al. Cancer Treat. Rep.* **62**, 1899–1906 (1978).
13. Sundmacher, R., Cantell, K., Skoda, K., Hallermann, C. & Neumann-Haefelin, D. *Albrecht v. Graefes Arch. Opthal.* **208**, 229–233 (1978).
14. Dolen, J. G. *et al. Am. J. Med.* **67**, 127–131 (1979).
15. Treuner, J. *et al. Lancet* (in the press).
16. Knight, E. Jr, Hunkapiller, M. W., Korant, B. D., Hardy, R. W. F. & Hood, L. E. *Science* **207**, 525–526 (1980).
17. Knight, E. Jr *Proc. natn. Acad. Sci. U.S.A.* **73**, 520–523 (1976).
18. Havell, E. A., Yamazaki, S. & Vilcek, J. *J. biol. Chem.* **252**, 4425–4427 (1977).
19. Tan, Y. H., Barakat, F., Berthold, W., Smith-Johannsen, H. & Tan, C. *J. biol. Chem.* **254**, 8067–8073 (1979).
20. Heine, J. W., De Ley, M., Van Damme, J., Billiau, A. & De Somer, P. *Ann. N.Y. Acad. Sci.* (in the press).
21. Nagata, S. *et al. Nature* **284**, 316–320 (1980).
22. Taniguchi, T. *et al. Proc. Jap. Acad.* **B55**, 464–469 (1979).
23. Billiau, A., Joniau, M. & De Somer, P. *J. gen. Virol.* **19**, 1–8 (1973).
24. Hayes, T. G., Yip, Y. K. & Vilcek, J. *Virology* **98**, 351–363 (1979).
25. Reynolds, F. H. Jr, Premkumar, E. & Pitha, P. M. *Proc. natn. Acad. Sci. U.S.A.* **72**, 4881–4885 (1975).
26. Pawson, T., Harvey, R. & Smith, A. E. *Nature* **268**, 416–420 (1977).
27. Cleveland, D. W., Kirschner, M. W. & Cowan, N. J. *Cell* **15**, 1021–1031 (1978).
28. Lebleu, B. *et al. Biochem. biophys. Res. Commun.* **82**, 665–673 (1978).
29. Tan, Y. H., Schneider, E. L., Tischfield, J., Epstein, C. J. & Ruddle, F. H. *Science* **186**, 61–63 (1974).
30. Devos, R., van Emmelo, J., Contreras, R. & Fiers, W. *J. molec. Biol.* **128**, 595–619 (1979).
31. Sehgal, D., Lyles, D. & Tamm, I. *Virology* **89**, 186–198 (1978).
32. Lederberg, E. M. & Cohen, S. N. *J. Bact.* **119**, 1072–1074 (1974).
33. Goldberg, M. L., Lifton, R. P., Stark, G. R. & Williams, J. G. *Meth. Enzym.* **68**, 206–219 (1980).
34. Paucha, E. & Smith, A. E. *Cell* **15**, 1011–1020 (1978).
35. Van Emmelo, J., Devos, R., Ysebaert, M. & Fiers, W. *J. molec. Biol.* (in the press).
36. Pelham, R. B. & Jackson, R. J. *Eur. J. Biochem.* **67**, 247–256 (1976).
37. Grünstein, M. & Hogness, D. S. *Proc. natn. Acad. Sci. U.S.A.* **72**, 3961–3965 (1975).
38. Rigby, P. W. J., Dieckmann, M., Rhodes, C. & Berg, P. *J. molec. Biol.* **13**, 237–251 (1977).
39. Shields, D. & Blöbel, G. *J. biol. Chem.* **253**, 3753–3756 (1978).

40. Sutcliffe, J. G. Nucleic Acids Res. 5, 2721–2728 (1978).
41. Maxam, A. M. & Gilbert, W. Proc. natn. Acad. Sci. U.S.A. 74, 560–564 (1977).
42. Seeburg, P. H., Shine, J., Martial, J. A., Baxter, J. D. & Goodman, H. M. Nature 270, 486–494 (1977).
43. Proudfoot, N. J. & Brownlee, G. G. Nature 263, 211–214 (1976).
44. Fiers, W. et al. Nature 273, 113–120 (1978).
45. Soeda, E., Arrand, J. R., Smolar, N., Walsh, J. E. & Griffin, B. E. Nature 283, 445–453 (1980).
46. Min Jou, W. et al. Cell 19, 683–696 (1980).
47. Shine, J., Seeburg, P. H., Martial, J. A., Baxter, J. D. & Goodman, H. M. Nature 270, 494–499 (1977).

48. Blobel, G. et al. Soc. exp. Biol. Symp. 33, 9–36 (1979).
49. Habener, J. F. et al. Proc. natn. Acad. Sci. U.S.A. 75, 2616–2620 (1978).
50. Davey, M. W., Sulkowski, E. & Carter, W. A. J. biol. Chem. 251, 7620–7625 (1976).
51. Neuberger, A., Gottschalk, A., Marshall, R. D. & Spiro, R. G. in The Glycoproteins: Their Composition, Structure and Function (ed. Gottschalk, A.) 450–490 (Elsevier, Amsterdam, 1972).
52. Tomita, M. & Marchesi, V. Proc. natn. Acad. Sci. U.S.A. 72, 2964–2968 (1975).
53. Taniguchi, T. et al. Gene 10, 11–15 (1980).
54. Taniguchi, T. et al. Nature, 285, 547–549 (1980).
55. Mantei, N. et al. Gene 10, 1–10 (1980).
56. Roberts, R. J. Gene 8, 329–343 (1980).

Human leukocyte and fibroblast interferons are structurally related

Tadatsugu Taniguchi*, Ned Mantei†, Marco Schwarzstein†, Shigekazu Nagata†, Masami Muramatsu* & Charles Weissmann†

*Department of Biochemistry, Cancer Institute, Japanese Foundation for Cancer Research, Tokyo 170, Japan

†Institut für Molekularbiologie I, Universität Zürich, 8093 Zürich, Switzerland

The coding sequences of the cDNAs of cloned human leukocyte interferon 1 and human fibroblast interferon show homologies of 45% at the nucleotide and 29% at the amino acid level. We conclude that the two genes were derived from a common ancestor.

THE acid-stable human interferons are subdivided into two major groups, fibroblast interferons (F-IF) and leukocyte interferons (Le-IF); these are the major components of the interferons produced by induced fibroblasts and leukocytes, respectively. Some cells, such as the lymphoblastoid Namalva cell line, produce a mixture of 90% Le-IF and 10% F-IF[1,2]. The two interferon types have several features in common: both are glycoproteins with molecular weights ranging from 16,000 to 26,000 (refs 3–9), the induction and shut-off of their synthesis seem to be under similar control[6], and at least some of the responses elicited in target cells are similar, such as induction of an antiviral state, which is accompanied by increased synthesis of several proteins[10–13]. Nonetheless, the two kinds of interferon differ in many respects. Antibodies directed against Le-IF do not neutralize F-IF and vice versa[14], the target cell specificities of the two interferons differ[15], and the sequences of the 13 amino-terminal amino acids of F-IF and Le-IF (from lymphoblastoid cells) show no homology[16,17]. Although Le-IF and F-IF are encoded by different mRNA species[18], it is not known whether these mRNAs are transcribed from distinct genes or whether they arise from the same gene through a common precursor which is processed or spliced in different modes.

We have recently cloned and sequenced one species each of Le-IF (Le-IF I)[19,20] and F-IF cDNA[21,22]. A second species of Le-IF (Le-IF II) cDNA has recently been identified (M. Streuli, S.N. and C.W., unpublished results).

Comparison of the amino acid sequences of Le-IF and F-IF

In Fig. 1 the nucleotide sequences of Le-IF I and F-IF cDNA were aligned so that the AUGs closest to their 5' termini coincided. From the amino-terminal sequence published for F-IF[16] and lymphoblastoid Le-IF[17], one can determine that for F-IF and Le-IF, respectively, the 21st and 23rd codons following the initiation triplet represent the first amino acid of the interferon polypeptide. Presumably, the stretch in between encodes a signal peptide. As the respective putative signal peptides of Le-IF and F-IF comprise 23 and 21 amino acids, the IF polypeptides, as aligned in Fig. 1, are shifted by two residues relative to their termini. In this alignment, 48 of 166 positions (29%) of the interferon polypeptides have identical amino acids. By introducing appropriate gaps, better homology could be achieved, particularly in the region of the

signal sequence; in the present comparison this has not been done.

To plot the degree of homology between the F-IF and Le-IF as a function of the map distance, the sequence was subdivided into segments of 8 amino acids (or 24 nucleotides), each overlapping by 4 amino acids (or 12 nucleotides) with the neighbouring segments, and the per cent coincidence of amino acids (and nucleotides) for each segment was determined (see ref. 23). As seen in Fig. 2, amino acid sequences show three domains of homology. The first one, with the least degree of homology, corresponds to the putative signal sequence, which is rich in hydrophobic residues and has 4 identical amino acid positions out of 21; the second domain, between amino acids 28 and 80 (counted on the Le-IF sequence), has 21 identical residues out of 51 (41% homology), and the third, between positions 115 and 151 (Le-IF sequence), has 19 out of 35 identical residues (54%). The longest stretches of contiguous conserved amino acids are Gln-Phe-Gln-Lys (positions 47–50 of Le-IF and 49–52 of F-IF) and Cys-Ala-Trp (positions 139–141 and 141–143, respectively); the latter sequence is notable because it comprises Cys and Trp, which are preferentially conserved in related proteins[24]. Table 1 shows that conservation was highest between the interferon polypeptides (not considering the signal sequences) for Trp, Phe, Arg, Cys and Tyr residues, in agreement with the general experience that the amino acids most likely to be conserved between related proteins are Trp > Cys > Tyr > Arg > Phe, His (ref. 24). Even where amino acids are conserved, the codons show one or more nucleotide changes in half the instances. The codons of three out of seven conserved Leu residues are unrelated, as are two of four codons pertaining to conserved Ser residues. This suggests that there is a strong selective pressure favouring the conservation of several amino acids. It is quite likely that at least some of the conserved amino acids are essential for a function common to Le-IF and F-IF, perhaps the induction of the virus-resistant state in the target cell. These findings may provide guidelines for the tailoring of modified[25], possibly shorter polypeptides possessing certain activities of interferon.

Comparison of the nucleotide sequences of Le-IF and F-IF

The nucleic acid sequences show an average homology of 43% in the domain of the signal sequence and of 45% in the interferon polypeptide sequence. On a random basis, about

G   CT CTA GGT TCA GAG TCA CCC ATC TCA GCA AGC CCA GAA GTA TCT GCA ATA TCT ACG ATG GCC TCG CCC TTT GCT TTA CTG ATG GTC CTG GTG GTG CTC AGC
23

S1 ... S10

MET ALA SER PRO PHE ALA LEU LEU MET VAL LEU VAL VAL LEU SER

MET THR ASN LYS CYS LEU LEU GLN ILE ALA LEU LEU LEU CYS PHE

GTC AAC ATG ACC AAC AAG TGT CTC CTC CAA ATT GCT CTC CTG TTG TGC TTC

S20   1   10   20

TGC AAG TCA AGC TGC TCT CTG GGC TGT GAT CTC CCT GAG ACC CAC AGC CTG GAT AAC AGG AGG ACC TTG ATG CTC CTG GCA CAA ATG AGC AGA ATC TCT CCT TC

CYS LYS SER SER CYS SER LEU GLY CYS ASP LEU PRO GLU THR HIS SER LEU ASP ASN ARG ARG THR LEU MET LEU LEU ALA GLN MET SER ARG ILE SER PRO SE

SER THR THR ALA LEU SER MET SER TYR ASN LEU LEU GLY PHE LEU GLN ARG SER SER ASN PHE GLN CYS GLN LYS LEU LEU TRP GLN LEU ASN GLY ARG LEU GL

TCC ACT ACA GCT CTT TCC ATG AGC TAC AAC TTG CTT GGA TTC CTA CAA AGA AGC AGC AAT TTT CAG TGT CAG AAG CTC CTG TGG CAA TTG AAT GGG AGG CTT GA
1   10   20

30   40   50   60

TCC TGT CTG ATG GAC AGA CAT GAC TTT GGA TTT CCC CAG GAG GAG TTT GAT GGC AAC CAG TTC CAG AAG GCT CCA GCC ATC TCT GTC CTC CAT GAG CTG ATC CAG

SER CYS LEU MET ASP ARG HIS ASP PHE GLY PHE PRO GLN GLU GLU PHE ASP GLY ASN GLN PHE GLN LYS ALA PRO ALA ILE SER VAL LEU HIS GLU LEU ILE GLN

TYR CYS LEU LYS ASP ARG MET ASN PHE ASP ILE PRO GLU GLU ILE LYS GLN LEU GLN GLN PHE GLN LYS GLU ASP ALA ALA LEU THR ILE TYR GLU MET LEU GLN

TAT TGC CTC AAG GAC AGG ATG AAC TTT GAC ATC CCT GAG GAG ATT AAG CAG CTG CAG CAG TTC CAG AAG GAG GAC GCC GCA TTG ACC ATC TAT GAG ATG CTC CAG
30   40   50   60

70   80   90

CAG ATC TTC AAC CTC TTT ACC ACA AAA GAT TCA TCT GCT GCT TGG GAT GAG GAC CTC CTA GAC AAA TTC TGC ACC GAA CTC TAC CAG CAG CTG AAT GAC TTG

GLN ILE PHE ASN LEU PHE THR THR LYS ASP SER SER ALA ALA TRP ASP GLU ASP LEU LEU ASP LYS PHE CYS THR GLU LEU TYR GLN GLN LEU ASN ASP LEU

ASN ILE PHE ALA ILE PHE ARG GLN ASP SER SER THR GLY TRP ASN GLU THR ILE VAL GLU ASN LEU LEU ALA ASN VAL TYR HIS GLN ILE ASN HIS LEU

AAC ATC TTT GCT ATT TTC AGA CAA GAT TCA TCT AGC ACT GGC TGG AAT GAG ACT ATT GTT GAG AAC CTC CTG GCT AAT GTC TAT CAT CAG ATA AAC CAT CTG
70   80   90

100   110   120

GAA GCC TGT GTG ATG CAG GAG GAG AGG GTG GGA GAA ACT CCC CTG ATG AAT GCG GAC TCC ATC TTG GCT GTG AAG AAA TAC TTC CGA AGA ATC ACT CTC

GLU ALA CYS VAL MET GLN GLU GLU ARG VAL GLY GLU THR PRO LEU MET ASN ALA ASP SER ILE LEU ALA VAL LYS LYS TYR PHE ARG ARG ILE THR LEU

LYS THR VAL LEU GLU GLU LYS LEU GLU LYS GLU ASP PHE THR ARG GLY LYS LEU MET SER SER LEU HIS LEU LYS ARG TYR TYR GLY ARG ILE LEU HIS

AAG ACA GTC CTG GAA GAA AAA CTG GAG AAA GAA GAT TTC ACC AGG GGA AAA CTC ATG AGC AGT CTG CAC CTG AAA AGA TAT TAT GGG AGG ATT CTG CAT
100   110   120   130

130   140   150   160

TAT CTG ACA GAG AAG AAA TAC AGC CCT TGT GCC TGG GAG GTT GTC AGA GCA GAA ATC ATG AGA TCC CTC TCT TTA TCA ACA AAC TTG CAA GAA AGA TTA AGG

TYR LEU THR GLU LYS LYS TYR SER PRO CYS ALA TRP GLU VAL VAL ARG ALA GLU ILE MET ARG SER LEU SER LEU SER THR ASN LEU GLN GLU ARG LEU ARG

TYR LEU LYS ALA LYS GLU TYR SER HIS CYS ALA TRP THR ILE VAL ARG VAL GLU ILE LEU ARG ASN PHE TYR PHE ILE ASN ARG LEU THR GLY TYR LEU ARG

TAC CTG AAG GCC AAG GAG TAC AGT CAC TGT GCC TGG ACC ATA GTC AGA GTG GAA ATC CTA AGG AAC TTT TAC TTC ATT AAC AGA CTT ACA GGT TAC CTC CGA
140   150   160

166

AGG AAG GAA TAA CAT CTG GTC CAA CAT GAA AAC AAT TCT TAT TGA CTC ATA CAC CAG GTC ACG CTT TCA TGA ATT CTG TCA TTT CAA AGA CTC TCA CCC CTG

ARG LYS GLU

ASN

AAC TGA AGA TCT CCT AGC CTG TGC CTC TGG GAC ————————T GGA CAA TTG CTT CAA GCA TTC TTC AAC CAG CAG ATG CTG TTT AAG TGA CTG ATG GCT AAT
166

CTA -TA ACT ATG ACC ATG CTG ATA AAC TGA TTT ATC TAT TTA AAT ATT TAT TTA ACT ATT CAT AAG ATT TAA ATT ATT TTT GTT CAT ATA ACG TCA TGT GCA

GTA CTG CAT ATG AAA GGA CAC TAG AAG ATT TTG AAA TTT TTA TTA AAT TAT GAG TTA TTT TTA TTT ATT TAA ATT

CCT TTA CAC TGT GGT TAG TGT AAT AAA ACA TGT TCC TTA TAT TTA CTC AAA AAA A

———————————TT ATT TTG GAA AAT AAA TTA TTT TTG GTG CAA A-A GTC AAA A

Fig. 1 Comparison of the nucleotide sequences of human leukocyte interferon I (Le-IF I) and human fibroblast interferon cDNA and of the derived amino acid sequences. The sequences are from Mantei *et al.*[20] and T.T. *et al.*[22]. They were aligned to give maximal homology without introducing gaps in the coding sequence. Identical amino acids are framed, identical nucleotides are marked by a dot. S1–S23 indicate the amino acids of the putative signal sequence and 1–166 the amino acids of the interferon polypeptides.

25% of the nucleotide positions should coincide. Within the interferon ,coding sequence, the nucleotide homologies are more evenly distributed than the amino acid homologies. However, one may distinguish, albeit to a less pronounced degree, the same three blocks of similarity noted for the amino acids. The longest region without mismatches extends for 13 nucleotides (compare 47th to 51st codon of Le-IF with 49th to 53rd codon of F-IF). There are, in addition, sequences of 17, 18 and 20 nucleotides with 3, 3 and 4 mismatches, respectively. The heteropolymeric 3′-terminal noncoding region of Le-IF cDNA has 242 nucleotides, and is longer by 39 residues than its counterpart in F-IF cDNA. In aligning the two sequences, four gaps were introduced to maximize homology, as described by van Ooyen et al.[23]. In this way, several segments were matched with 29–41% homology. The introduction of gaps in the alignment may be justified in view of the arguments presented previously, that intervening sequences and noncoding regions of reduplicated genes diverge as a consequence of block insertions and/or deletions in the course of evolution[23,26]. It is unlikely that the extent of homology between Le-IF and F-IF cDNA would allow significant cross-hybridization between the two species.

A common ancestral gene for Le-IF and F-IF

On the basis of our findings, there is no doubt that Le-IF and F-IF genes are derived from a common ancestral sequence. When did the separation of these genes occur? Human α- and β-globin show 57% amino acid mismatches, and human β-globin and myoglobin, as well as α-globin and myoglobin, 76% mismatches. If the rate of divergence of interferons and globins is comparable (however, this is quite uncertain, see ref. 24, p. 50, for proteins showing both higher and lower rates), the separation of interferon genes occurred after that of myoglobin and haemoglobins but before that of α- and β-globins, that is between 500 and 1,000 Myr ago[24], which is about the time vertebrates arose[27]. This would mean that both types of interferon gene should occur in all vertebrates, unless one and/or the other was lost by deletion. Indeed, as shown by the sequencing of 13–24 amino-terminal residues[16,17,28], mouse interferons A and B show significant homology with human fibroblast interferon, and mouse interferon C with human
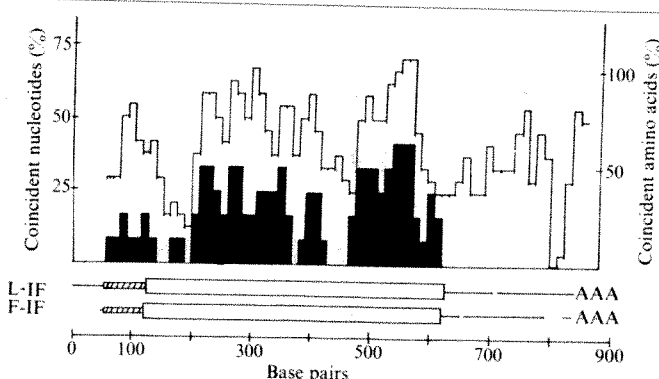
Fig. 2 Similarity of the nucleotide and amino acid sequences of human leukocyte interferon I and fibroblast interferon. The sequences shown in Fig. 1 were subdivided into segments of 8 amino acids or 24 nucleotides, each overlapping by 4 and 12 residues, respectively, with the neighbouring segments. The percentage of concident residues was plotted as a function of map position. Open vertical blocks, nucelotides; filled vertical blocks, amino acids. L-IF, leukocyte interferon cDNA; F-IF, fibroblast interferon cDNA; lines, noncoding sequences; hatched bars, putative signal peptide; open bars, interferon polypeptide.

lymphoblastoid interferon, whereas the mouse species A and B on the one hand, and the species C on the other show no significant homology within the short segment sequenced. Thus, at least in the mouse, representatives of both interferon families exist. It will be of interest to determine the evolutionary relationship of these to the third type of interferon, immune or γ-interferon.

After submission of this article, we learnt that Derynck et al. had cloned and sequenced fibroblast interferon (see accompanying article[29]), confirming the deduced amino acid sequence of T.T et al.[22].

Table 1 Conservation of amino acids in leukocyte and fibroblast interferon

	F-IF	Le-IF	Conserved amino acids	No. of changes in codon of conserved amino acids			
				0	1	2	3
Leu	25	22	8	1	4	3	
Cys	3	5	2	1	1		
Asn	12	6	1	1			
Arg	11	12	5	1	3	1	
Phe	9	8	4	2	2		
Pro	1	6	1		1		
Gln	11	10	3	3			
Lys	11	8	3	2	1		
Ala	6	10	2	2			
Glu	13	15	4	4			
Ile	11	7	3	2	1		
Ser	9	13	4		2	1	1
Trp	3	2	2	2			
Tyr	10	4	4	1	3		
Val	5	6	1	1			
Asp	5	11	1	1			
Thr	6	9	0				
Gly	6	3	0				
Met	4	6	0				
His	5	3	0				
Total	166	166	48	24	18	5	1

The data are from T.T. et al.[22] and Mantei et al.[20].

1. Havell, E. A., Yip, Y. K. & Vilček, J. J. gen. Virol. **38**, 51–59 (1977).
2. Paucker, K. Tex. Rep. Biol. Med. **35**, 23–28 (1977).
3. Bridgen, P. J. et al. J. biol. Chem. **252**, 6585–6587 (1977).
4. Knight, E. Jr Proc. natn. Acad. Sci. U.S.A. **73**, 520–523 (1976).
5. Tan, Y. H. et al. J. biol. Chem. **254**, 8067–8073 (1979).
6. Hayes, T. G., Yip, Y. K. & Vilček, J. Virology **98**, 351–363 (1979).
7. Rubinstein, M. et al. Proc. natn. Acad. Sci. U.S.A. **76**, 640–644 (1979).
8. Stewart, W. E. II & Wiranowska-Stewart, M. Virology **97**, 473–476 (1979).
9. Havell, E. A., Yamazaki, S. & Vilček, J. J. biol. Chem. **252**, 4425–4427 (1977).
10. Lebleu, B., Sen, G. C., Shaila, S., Cabrer, B. & Lengyel, P. Proc. natn. Acad. Sci. U.S.A. **73**, 3107–3111 (1976).
11. Hovanessian, A. G., Brown, R. E. & Kerr, I. M. Nature **268**, 537–540 (1977).
12. Hovanessian, A. G. & Kerr, I. M. Eur. J. Biochem. **93**, 515–526 (1979).
13. Schmidt, A. et al. Proc. natn. Acad. Sci. U.S.A. **76**, 4788–4792 (1979).
14. Havell, E. A. et al. Proc. natn. Acad. Sci. U.S.A. **72**, 2185–2187 (1975).
15. Stewart, W. E. II in The Interferon System, 134–145 (Springer, New York, 1979).
16. Knight, E. Jr., Hunkapiller, M. W., Korant, B. D., Hardy, R. W. F. & Hood, L. E. Science **207**, 525–526 (1980).
17. Zoon, K. C. et al. Science **207**, 527–528 (1980).
18. Cavalieri, R. L., Havell, E. A., Vilček, J. & Pestka, S. Proc. natn. Acad. Sci. U.S.A. **74**, 3287–3291 (1977).
19. Nagata, S. et al. Nature **284**, 316–320 (1980).
20. Mantei, N. et al. Gene **10**, 1–10 (1980).
21. Taniguchi, T. et al. Proc. Jap. Acad. **B55**, 464–469 (1979).
22. Taniguchi, T., Ohno, S., Fujii-Kuriyama, Y. & Muramatsu, M. Gene **10**, 11–15 (1980).
23. van Ooyen, A., van den Berg, J., Mantei, N. & Weissmann, C. Science **206**, 337–344 (1979).
24. Dayhoff, M. O. in Atlas of Protein Sequence and Structure Vol. V (Natn. Biomed. Res. Fdn. Washington, 1972).
25. Müller, W., Weber, H., Meyer, F. & Weissmann, C. J. molec. Biol. **124**, 343–358 (1978).
26. Konkel, D. A., Maizel, J. V. Jr & Leder, P. Cell **18**, 865–873 (1979).
27. Kurten, B. in Proc. XVI int. Congr. Zool. Vol. 6 (ed. Moore, J. A.) 327–354 (Natural History Press, New York, 1965).
28. Taira, H. et al. Science **207**, 528–530 (1980).
29. Derynck, R. et al. Nature **285**, 542–547 (1980).

Sequence of retrovirus provirus resembles that of bacterial transposable elements

Kunitada Shimotohno, Satoshi Mizutani & Howard M. Temin

McArdle Laboratory for Cancer Research, University of Wisconsin-Madison, Madison, Wisconsin 53706

The nucleotide sequences of the terminal regions of an infectious integrated retrovirus cloned in the modified λ phage cloning vector Charon 4A have been elucidated. There is a 569-base pair direct repeat at both ends of the viral DNA. The cell–virus junctions at each end consist of a 5-base pair direct repeat of cell DNA next to a 3-base pair inverted repeat of viral DNA. This structure resembles that of a transposable element and is consistent with the protovirus hypothesis that retroviruses evolved from the cell genome.

RETROVIRUSES are a family of RNA viruses that infect animals and replicate through a DNA intermediate, the provirus[1]. The protovirus hypothesis suggests that retroviruses evolved from the cell genome, in particular from a portion of the cell genome involved in normal transfer of genetic information in and between cells[2].

The recent availability of recombinant DNA techniques for cloning eukaryotic genes and of rapid DNA sequencing techniques has enabled us to isolate several infectious proviruses of spleen necrosis virus and their surrounding cellular sequences[3] and to sequence several hundred bases including the cell–virus junctions of one of these proviruses. (Spleen necrosis virus is an avian retrovirus that has genus-specific relationships to mammalian type C retroviruses[4-6].) The regions sequenced include the two cell–virus junctions, the complete terminal repeats, the positions of origin and terminus of viral RNA, and a binding site for a putative primer tRNA. In particular, the cell–virus junction sequences seem to have a 5-base pair direct repeat of cellular DNA next to an inverted repeat of viral DNA. This structure resembles that of bacterial transposable elements[7-12] and is consistent with the protovirus hypothesis that retroviruses have evolved from part of the normal cell genome.

Sequencing of terminal regions of an integrated spleen necrosis virus

14-44 is a recombinant clone of the modified phage λ cloning vector, Charon 4A, containing chicken DNA with an infectious provirus of spleen necrosis virus (SNV)[3]. 14-44 was selected from phage packaged with Charon 4A arms ligated to *Eco*RI-digested DNA isolated from chicken cells 4 days after infection (acute infection). Restriction endonuclease cleavage sites in 14-44 have been mapped previously, as indicated in Figs 1 (top) and 2a (see ref. 3). In particular, the virus–cell junctions were located just left of the 5′ *Sac*I site, and approximately 600 base pairs right of the 3′ *Sac*I site and 200 base pairs left of the 3′ *Eco*RI site by comparison with restriction enzyme digests of 10 cloned proviruses and of unintegrated viral DNA, and also by electron microscopic heteroduplexing[3].

Subclones containing the junction regions were isolated as described in Fig. 1 legend. Fine structure restriction enzyme maps (Fig. 2b) were prepared for the subclones containing each end of the provirus using the method of Smith and Birnstiel[13] with labelling of the *Sal*I end or the *Eco*RI end, respectively. Starting from the left end of both subclones, after

Fig. 1 Construction of subclones of 14-44 DNA in pBR322. DNA (100 μg) of clone 14-44 was digested with *Hind*III and *Eco*RI, and the fragments separated by gel electrophoresis in 1% agarose. The DNA bands of 14-44 were visualized with the aid of ethidium bromide, were cut out, and the agarose removed by soaking the crushed gel in 1 M NaCl, 1 mM EDTA, 0.1% SDS, 20 mM Tris-HCl (pH 8.0) at 37 °C for 20 h followed by ethanol precipitation. Each DNA fragment was then separately ligated with T4 DNA ligase at 4 °C for 20 h to the large fragment of *Eco*RI-*Hind*III-digested pBR322 DNA. Calcium chloride-treated competent *Escherichia coli* cells were transformed with the ligated DNA and the cells plated on medium containing 70 μg each of tetracycline and ampicillin. The colonies which appeared were transferred to nitrocellulose filters for colony hybridization[49]. The filter was treated with 0.1 M NaOH for 1 min, neutralized with 1 M Tris-HCl (pH 7.2), 0.6 M NaCl, and dried at 80 °C under vacuum to immobilize the DNA on it. The filter was hybridized with ^{32}P-labelled SNV cDNA (specific activity about 10[8] c.p.m. per μg) at 63 °C for 20 h and washed to remove unhybridized cDNA. Autoradiographs were made after drying. The subcloned DNA which carried the 5′ half *Eco*RI-*Hind*III fragment of 14-44 DNA was further digested with *Sal*I and self-ligated with T4 DNA ligase as described above. Calcium-treated competent *E. coli* cells were transformed, and cells were plated on Petri dishes containing 50 μg ampicillin. An aliquot of each colony which appeared was transferred to agar-medium containing 50 μg tetracycline, and plates were kept at 37 °C for 24 h. Colonies which could not grow on the medium containing tetracycline contained the 5′ *Eco*RI-*Sal*I DNA fragment of 14-44. Plasmid DNA was purified from chloramphenicol-treated bacteria which contained the subcloned plasmids as follows: The bacteria which contained the plasmids were grown to late log phase. Chloramphenicol was added to a final concentration of 20 μg per ml of culture medium. Incubation was continued another 5 h. Cells were collected by centrifugation and lysed with EDTA, lysozyme and Briji 58 (ref. 50). Cellular DNA was pelleted by centrifugation at 27,000 r.p.m. for 60 min. The supernatant was taken, CsCl added, and the refractive index adjusted to 1.395. Ethidium bromide was also added to a final concentration of 50 μg per ml of solution. The lysates were centrifuged at 35,000 r.p.m. for 72 h using a Beckman 50 Ti rotor. The lower DNA band was collected and centrifuged at the same speed for 48 h. The DNA band was taken out, the ethidium bromide was removed by extraction with isobutyl alcohol, and the DNA was dialysed and ethanol precipitated.
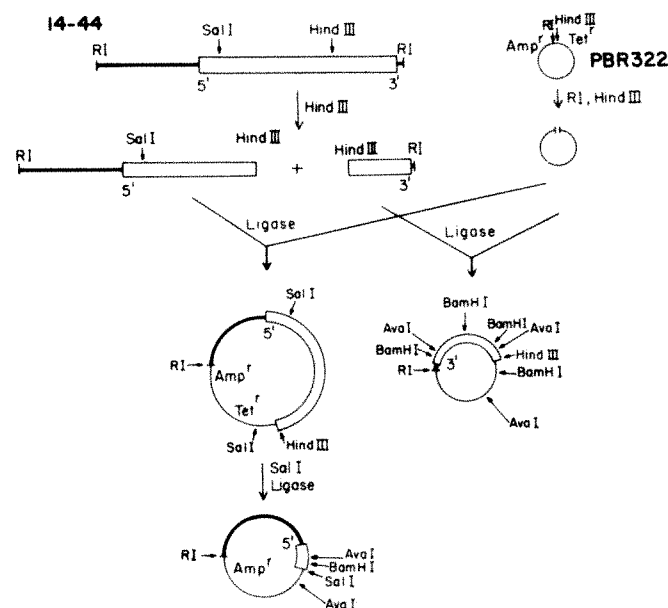
Fig. 2 Structure of recombinant clone 14-44 and subclones containing 5′ and 3′ ends of SNV. *a*, Restriction map of the inserted DNA of clone 14-44, containing an infectious provirus of SNV[3]. 5′ And 3′ are defined in terms of the ends of viral RNA[14]. The formation of subclones containing the 5′ and 3′ junction sequences is described in Fig. 1 legend. Mapping of the cleavage sites of restriction endonucleases in the subclones (*b*) was done as follows: The purified subcloned DNAs in pBR322 were digested with *Sal*I or *Eco*RI. After removal of phosphate residues from the 5′ end of the fragments with alkaline phosphatase, the 5′ ends were labelled using polynucleotide kinase in the presence of [γ-^{32}P]ATP. Labelled DNAs were further digested with *Eco*RI or *Hind*III, respectively, and were separated by agarose gel electrophoresis. The DNAs were extracted from the agarose as described in Fig. 1 legend and purified by ethanol precipitation. Labelled DNAs were partially digested with restriction endonuclease (2 min, 4 min, 8 min and 15 min incubation at 37 °C in 50 μl of reaction mixture containing 1 μg DNA and 1 unit restriction enzyme), and fragments were separated by gel electrophoresis in 1.5% agarose at 1.5 V cm^{-1} for 8 h. Gels were dried and autoradiographs made. The molecular weight of each fragment was calculated from the extent of migration of labelled restriction fragments. End-labelled *Hind*II and *Taq*I fragments of pBR322 DNA were used as markers in the agarose gel electrophoresis. *c, d* The extent of sequence determined from restriction enzyme fragments labelled at their 5′ ends with ^{32}P as described by

Maxam and Gilbert[51]. Labelled termini are indicated by (—) and the direction and extent of sequencing with arrows. Fragments for sequencing were isolated using agarose or polyacrylamide gel electrophoresis. In each case, after 5′ labelling, molecules were digested with another restriction enzyme as indicated below. (Numbering is from the beginning of the terminal repeat (see Fig. 4).) *3′ end. Eco*RI: digested with *Hind*III and the 2.6-kilobase-pair fragment was isolated. *Bam*HI: The 4-kilobase pair fragment was isolated and digested with *Eco*RI and the 160-pair fragment was isolated. The 1.7-kilobase-pair fragment was isolated and digested with *Ava*II and the 570-base pair fragment was isolated. *Ava*I: The 3.6-kilobase-pair fragment was isolated and digested with *Eco*RI and the 300-base pair fragment isolated. The 2.5-kilobase pair fragment was isolated and digested with *Ava*II and the 420-base pair fragment was isolated. *Avr*II: digested with *Eco*RI and the 700-base pair and 6.7-kilobase pair fragments were isolated. *Avr*II to *Eco*RI 750-base pair fragment was digested with *Taq*I. The 260-base pair fragment was digested with *Bam*HI and the 170-base pair fragment was isolated. Half the 250-base pair fragment was digested with *Ava*I and the 200-base pair fragment was isolated. The other half of the 250-base pair fragment was digested with *Hha*I and the 210-base-pair fragment was isolated. *5′ end. Sal*I: digested with *Eco*RI and the 6-kilobase pair fragment was isolated. *Bam*HI: digested with *Eco*RI and both fragments were isolated. *Ava*I: digested with *Eco*RI and both fragments were isolated. *Sac*I: digested with *Eco*RI and *Ava*I and the 4.2-kilobase-pair and 400-base-pair fragments were isolated.
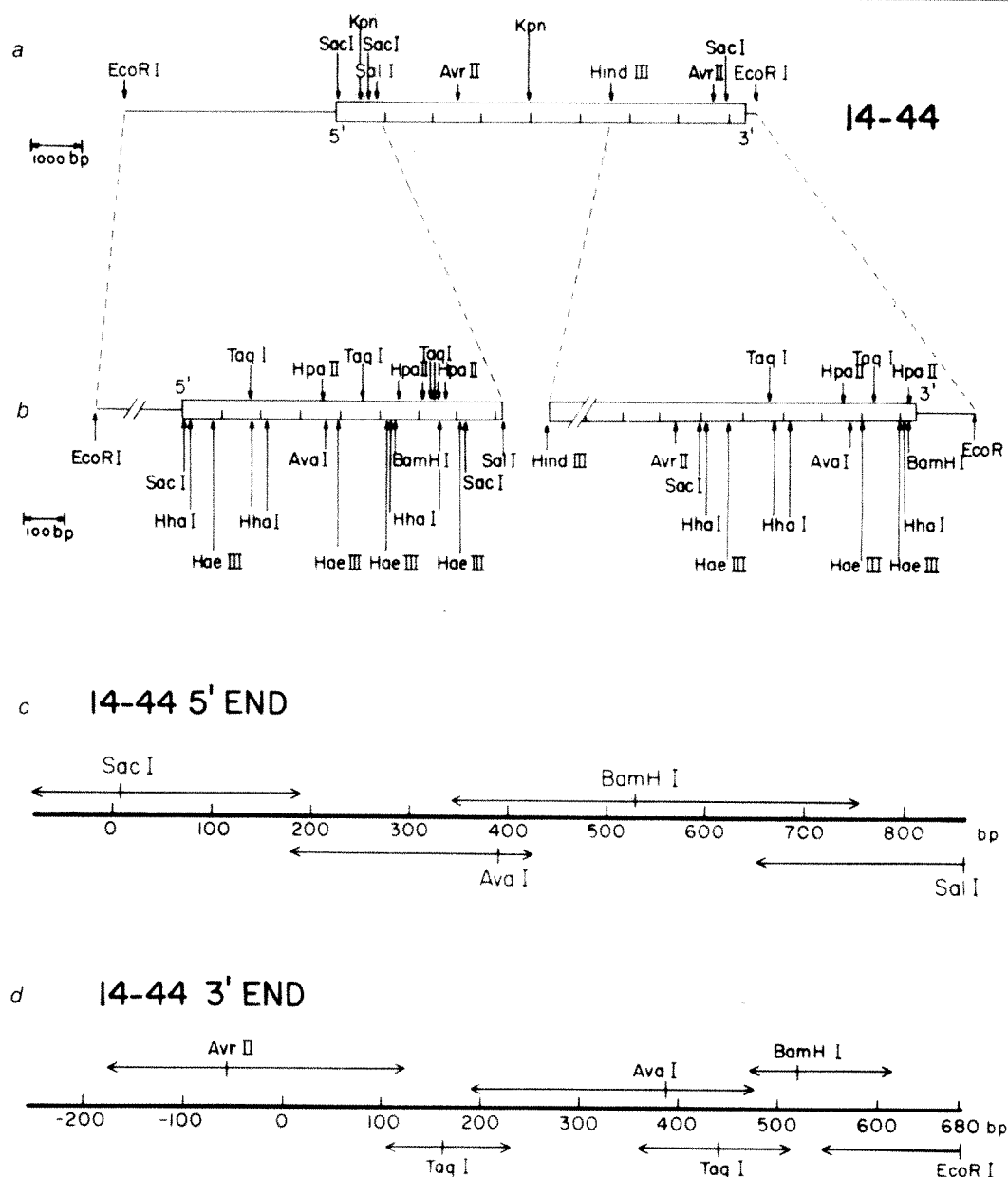
the *Avr*II site present only in the subclone with the 3′ end of SNV, the same cleavage sites are seen: *Sac*I, *Hha*I, *Hae*III, . . . up to the *Hae*III, *Hha*I, *Bam*HI and *Hpa*II sites. Then the maps diverge. These data indicate that the terminal regions in the SNV provirus are repeated, as they are in the unintegrated SNV DNA[14], and that the terminal repeats are near to or at the ends of the viral DNA, as defined by comparison with the restriction cleavage sites in 10 cloned proviruses and in unintegrated DNA and by electron microscopic heteroduplexing of several of the cloned proviruses[3].

DNAs of the pBR322 subclones containing the 5′ and the 3′ cell–virus junctions were digested with different restriction endonucleases, and the fragments were isolated, labelled, and further digested by restriction enzymes as described in Fig. 2c, *d*. The fragments were then sequenced as illustrated in Fig. 3.

Nucleotide sequences of terminal regions of provirus in 14-44

The sequences of the 890 bases at the 5′ end of SNV in 14-44 and the 850 bases at the 3′ end of 14-44 are given in Fig. 4. These sequences contain all of the restriction endonuclease sites mapped at the ends of the virus DNA (Fig. 2*b*), as well as the *Alu*I and *Hinf*I restriction endonuclease sites which were also mapped in the plasmid DNA (data not shown).

Comparing the sequences of the 5′ and 3′ ends directly, one sees that a 569-base pair sequence from nucleotides 1 to 569 at the 5′ end is the same as the nucleotide sequence from nucleotides 1 to 569 at the 3′ end. The sequences to either side diverge. Therefore, the terminal repeat in viral DNA is 569 base pairs. This is similar in size to that of the terminal repeat
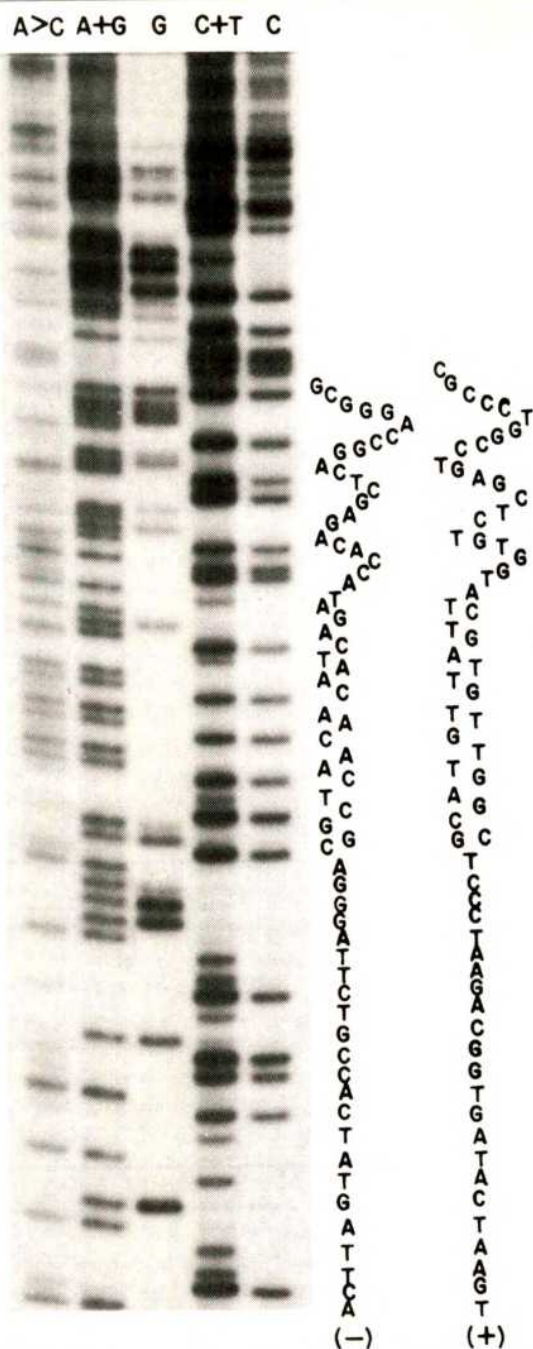
Fig. 3 Example of a sequencing gel. The 5' end of 14-44 was sequenced from the *Sal*I site (Fig. 2*d*) using the Maxam–Gilbert method[51]. Five base-specific cleavages were used (A>C, A+G, G, C+T, and C). Electrophoresis was carried out in thin 20%, 10%, 8% polyacrylamide–7 M urea gels[52]. The bases marked are from nucleotides 815 to 750 of 14-44 5' end (see Fig. 4). (−) Represents strand which is complementary to sense of viral RNA (+).

of unintegrated SNV DNA (J. J. O'Rear, personal communication), and considerably larger than the 300-base pair repeat reported for avian sarcoma virus DNA[15,16]. There are no ATG codons in the only reading frame open for a large distance, nucleotides 344 to 664 of the 14-44 5' end. Therefore, apparently no polypeptide is coded by the terminal repeat.

We have also sequenced portions of the ends of SNV RNA (manuscript in preparation). The RNA sequence starting approximately 10 bases from the 5' cap of viral RNA is the same as the proviral DNA sequence from nucleotides 405 to 425 of the 14-44 5' end (Fig. 4). The RNA sequence for 150 bases from the 3'-polyadenylated end is the same as the proviral DNA sequence from nucleotides 470 to 320 of the 14-44 3' end (Fig. 4).

Therefore, viral RNA begins at about nucleotide 394 of the

14-44 5' end, approximately 25 nucleotides after the sequence TATAAG and after the sequence TTGCT (boxed in Fig. 4). These sequences have been found in other animal DNAs 5' to the beginning of RNAs[17–20]. Viral RNA ends at approximately nucelotide 473 of the 14-44 3' end, 20 nucleotides after the sequence AATAAA (AAUAAA in viral RNA) (boxed in Fig. 4). This sequence has been found near the 3' end of mRNAs 5' to the poly(A)[17,21–24].

The terminal repetition in the RNA, called R (ref. 25), is about 80 nucleotides long. As was the case with the DNA repeat, R is larger than the 21 base-pair repeat in avian leukosis/sarcoma virus RNA, and the approximately 60-base pair repeat in murine leukaemia virus RNA[26–31].

One consequence of the proviral nucleotide sequence is that viral RNA synthesis starting at the 5' end of viral DNA progresses through a stop sequence at the 5' end of viral DNA. In addition, there is a second start signal at the 3' end of viral DNA. Thus, RNA synthesis might begin also at the 3' end of viral DNA.

tRNA^Pro has been reported to be the primer for REV-A, a member of the same retrovirus species as SNV[54]. A sequence complementary to the 18 3' nucleotides of tRNA^Pro (ref. 32) is found from nucelotides 572 to 589 of the 14-44 5' end (Fig. 4). This sequence includes the complement to the tRNA terminal CCA. Presumably this sequence represents the primer binding site (PBS) in viral RNA. The size of 'strong stop' DNA (from PBS to the 5' end of viral RNA) and of U5 (from PBS to R)[25] can then be calculated as 180 and 100 base pairs, respectively. These are also somewhat larger than for avian sarcoma and murine leukaemia viruses[26,28,29,33].

We have previously shown that some sequences from the 3' end of SNV RNA are present at the 5' end of SNV DNA[14], called U3 (ref. 25). Therefore, we compared the sequence at the 5' end of viral DNA, as defined above, with the homologous sequence at the 3' end of viral RNA (or DNA) (found in the 14-44 3' end, Fig. 4) (Fig. 5). From 5' (reading backwards) to TGT (nucleotides 1 to 3 in the 14-44 5' and 3' ends) the sequences diverge. We propose that this divergence marks the 5' junction of cellular and viral sequences.

Similarly, we compared the sequence at the 3' end of viral DNA, as defined above, to the homologous sequence at the 5' end of viral RNA (or DNA) (Fig. 5). From 3' (reading forwards) to ACA (nucleotides 567–569 in the 14-44 5' and 3' ends) the sequences diverge. We propose that this divergence marks the 3' junction of viral and cellular sequences. It is 2 base pairs 5' to the primer binding site and the start of viral DNA synthesis[54].

Resemblances to transposable elements

The sequence of AAAAT in cellular DNA is repeated at both proposed junctions of the viral sequences (Fig. 5). A 5-base pair repeat of cellular DNA has been found at the end of several transposable elements, IS*2*, Tn*3*, phage Mu, a 200-base pair sequence in pSC101, and δγ (refs 34–39). Although our data do not permit the unambiguous conclusion that the cell DNA is repeated as a result of the integration process, we suggest that it is. (Further clones containing proviruses are being sequenced to check this hypothesis.) Furthermore, the 3-base pair sequence of viral DNA next to the 5-base pair repeat of cellular DNA is an inverted repeat, TGT and ACA. However, the sequence of the provirus, especially the location of the putative primer binding site, leads us to propose that the structure of the precursor to integration is that shown in Fig. 6, that is a 5-base pair inverted repeat at the ends of linear unintegrated viral DNA with integration occurring 2 bases from the terminus. (This hypothesis is being checked by sequencing cloned unintegrated linear viral DNA.) The putative 'insertion sequence' ACATT probably has to be terminal, as the sequence ACATT is also found in the terminal repeat starting at nucleotide 409. Note that the analogous sequence, next to the primer binding site, in avian sarcoma and murine leukaemia virus RNAs is TCATT[26,29,33].

14-44 5' End

_-20_Chicken cell
AAGCA AAATAAAAGA TACAAAAAAT̆

U3-SNV
TGTGGGAGGG AGCTCTGGGG GAAATAGCGC TGGCTCGCAA CTGCTATATT AGCTTCTGTA CTCATGCTTG CTTGCCTGGC CACTAACCGC
         Sac I   HhaI   HaeⅢ
CATATTAGCT TCTGTACACA TGCTTGCTTG CCGTAGCCGC CATTGTACTT GATATGCCAT TTCTCGGAAT CGGCATCAAG TTTCGCTTCT

CGAGAGCAAG CCCACAAACC ACAAAAGGAA ACGCGCACCG AAGGCAAGCA TCAGACCACT TGCGCCATCC AATCATGAAC GGACACGAGA
TaqI   Hha I   Hha I
TCGGACTATC ATACTGGAGC CAATGGTTGT AAAGGGCAGA TGCTACTCTC CAATGAGGGA AAATGTCATG TAACACCTG TAAGCTGTAA
                                    U3-R
GCGGCTATAT AAGCCGGGTA CATCTCTTGC TCGGGGTCGC CGTCCTGCAC ATTGTTGTTG TGACGTGCGG CCCAGATTCG AATCTGTAAT
          HpaⅡ   AvaI   HaeⅢ   TaqI
AAAACTTTTT CTTCTGAATC CTCAGATTGG CAGTGAGAGG AGATTTTGTT CGTGGTGTTG GCTGGCCTAC TGGGTGGGCG CAGGGATCCG
          R-U5   U5 PBS   PBS   HaeⅢ   HhaI BamHI Hpa
GACTGAATCC GTAGTACTTC GGTACAACAT TTGGGGGCTC GTCCGGGATA CCCTCCCCAT CGGCAGAGGT GCCAACTGCT TCTTCGAACT)
Ⅱ   HpaⅡ   TaqI
(TTCTTCGAAC TCCGGCGCCG GTGAGTTAAG TACTTGATTT TGGTACCTCG CGAGGGTTTG GGAGGATCGG AGTGGTGGCG GGACGCTGCC
       TaqI HpaⅡ HhaI HpaⅡ   KpnI   Hpa
GGGAAGCTCC ACCTCCGCTC AGCAGGGGAC GCCCTGGCCT GAGCTCTGTG GTATCTGATT GTTGTTGAGC CGTCCCTAAG ACGGTGATAC
Ⅱ   HaeⅢ Sac I
TAAGTCGTGG (CTTGTGTGTT TGTTTGT)TGC (CTTGTGTTTG TTCGT)CGTTT GTCGAC
                                                             Sal I

14-44 3' End

_-160_
G AAGGCCCTTG ACTCTGCATT ATCCATTGAC AAAATGCAGG CAGTAAAAAT CCTAGCACTA GTCCCACAAT
ACAAGCCACT CCCACAATAC AAGCCACTCC CAACAGAGAT GGATACCCTA GGTCAATGAT TTGACCAGAA TGTACAAGAG CAGTGGGGAA
U3   AvrⅡ
TGTGGGAGGG AGCTCTGGGG GAAATAGCGC TGGCTCGCAA CTGCTATATT AGCTTCTGTA CTCATGCTTG CTTGCCTGGC CACTAACCGC
         Sac I   HhaI   HaeⅢ
CATATTAGCT TCTGTACACA TGCTTGCTTG CCGTAGCCGC CATTGTACTT GATATGCCAT TTCTCGGAAT CGGCATCAAG TTTCGCTTCT
CGAGAGCAAG CCCACAAACC ACAAAAGGAA ACGCGCACCG AAGGCAAGCA TCAGACCACT TGCGCCATCC AATCATGAAC GGACACGAGA
TaqI   Hha I   Hha I
TCGGACTATC ATACTGGAGC CAATGGTTGT AAAGGGCAGA TGCTACTCTC CAATGAGGGA AAATGTCATG TAACACCTG TAAGCTGTAA
                                    U3-R
GCGGCTATAT AAGCCGGGTA CATCTCTTGC TCGGGGTCGC CGTCCTGCAC ATTGTTGTTG TGACGTGCGG CCCAGATTCG AATCTGTAAT
          HpaⅡ   AvaI   HaeⅢ   TaqI
AAAACTTTTT CTTCTGAATC CTCAGATTGG CAGTGAGAGG AGATTTTGTT CGTGGTGTTG GCTGGCCTAC TGGGTGGGCG CAGGGATCCG
          R-U5   U5-SNV CHICKEN CELL   HaeⅢ   HhaI BamHI Hpa
GACTGAATCC GTAGTACTTC GGTACAACAA AAATCCGATT TACCCAGGCA ATTCTCCAAA AAAGTTTAAA AAAGAGGGGG TGGGAAGTGG
Ⅱ
ATTTTATGAA GGTACTATGG AGGCTGGCGA AAGCAAGGAA TGAATGCCTA GAAGAAAAGA AAGAATTC
                                                                     EcoRI

Fig. 4 Nucleotide sequences of 14-44 5' and 3' ends. The sequence of the (+) strand (same sense as viral RNA) only is presented. Numbering is from the beginning of the terminal repeat. Restriction enzyme cleavage sites shown in Figs 1 and 2 are overlined and the name of the enzyme is written below. Regions of interest are marked: U3 is the sequence from the 3' end of viral RNA also present at the 5' end of viral DNA; R is the sequence repeated at both ends of viral RNA; U5 is the sequence from the 5' end of viral RNA between R and PBS and also present at the 3' end of viral DNA; and PBS and also present, minus 2 base pairs, at the 3' end of viral DNA; and PBS (primer binding site) is the sequence complementary to the 3' end of tRNA^Pro, the putative primer[54]. Possible regulatory sequences are boxed. Neighbouring repeats are indicated by parentheses. Bases in these parentheses not perfectly repeated are marked. (We are unsure of nucleotides 179 and 184.) The sequences were analysed by the computer program of Korn et al.[53].
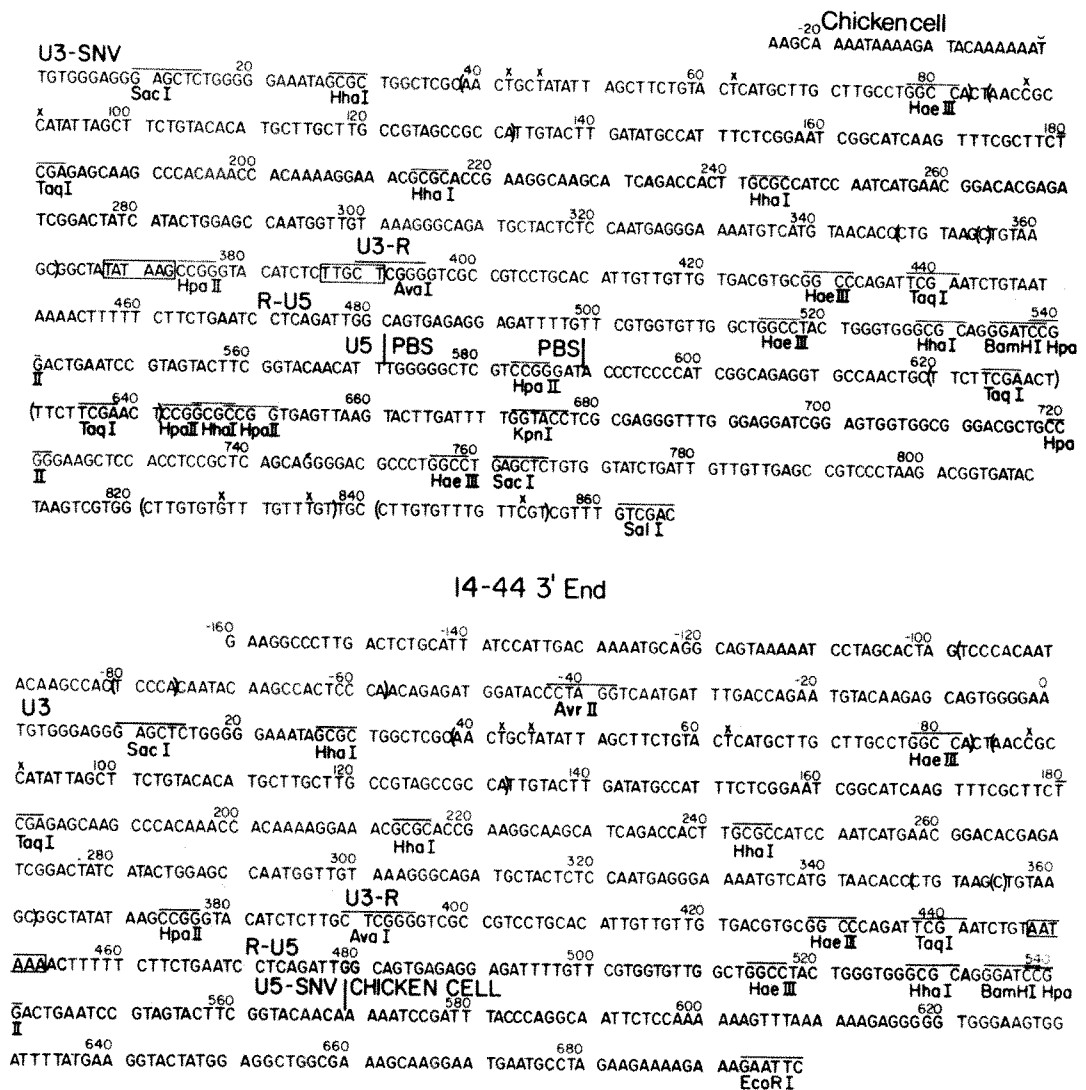
Fig. 5 Portions of sequencing gels with the ends of the terminal repeats of viral DNA. Portions of the sequencing gels used to secure the sequences shown in Figs 4 and 6 are presented. NT, nucleotides. 14-44 3' end NT −11 to 25 is from a gel labelled at the AvrII cleavage site; 14-44 5' end NT 4 to −17 is from a gel labelled at the SacI cleavage site; and 14-44 5' end NT 564 to 584 and 14-44 3' end 548 to 574 are from gels labelled at the BamHI cleavage site. Arrows mark the last nucleotide in common in the analogous sequences (gels placed next to each other). (14-44 5' end NT 4 to −17 is read in the opposite direction (3' to 5') to the other gels (5' to 3').) (−) Represents strand which is complementary to sense of viral RNA (+).

14-44 5' END   NT. 4 to -17   14-44 3' END   NT. -11 to 25   14-44 3' END   NT. 548 to 575   14-44 5' END   NT. 564 to 584
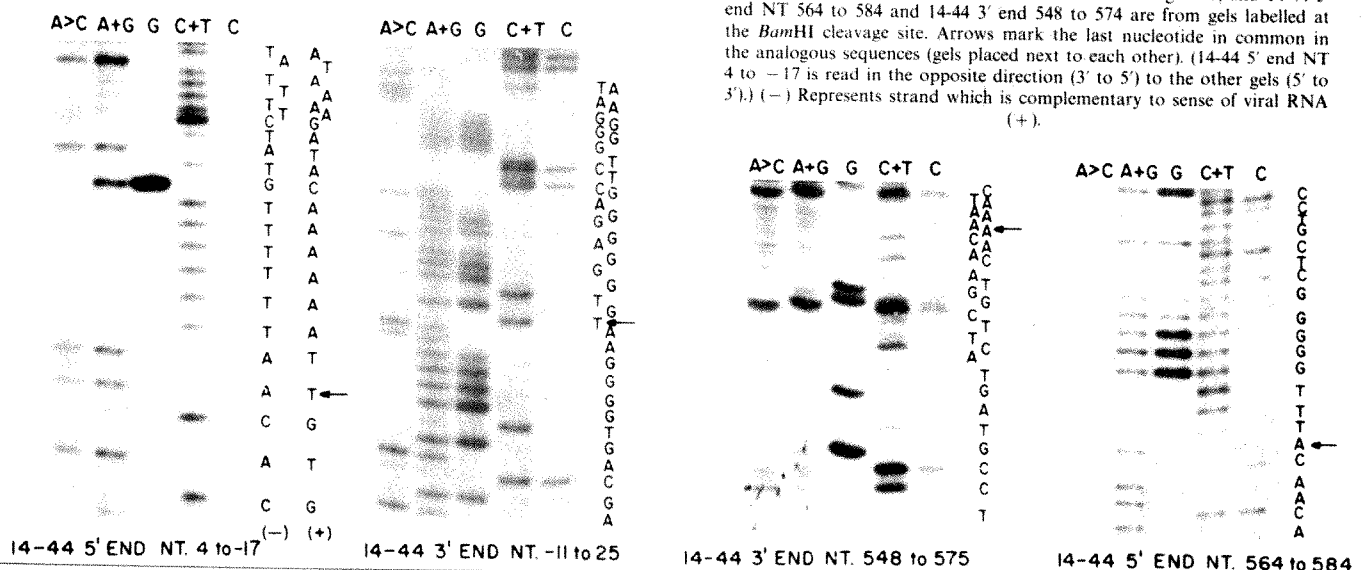
Fig. 6 Proposed sequences of viral and cell precursors to provirus. The viral genome is that of a linear unintegrated DNA with terminal repeats at both ends starting at the end of the primer binding site and the analogous nucleotide on the 5′ (U3) end. Integration occurs two bases from each end in the centre of a 5-base pair inverted terminal repeat. The cell DNA is nucleotides −24 to 0 of 14-44 5′ end (Fig. 4) and nucleotides 570 to 698 of 14-44 3′ end (Fig. 4) with an overlap of five bases. Nucleotide 1 corresponds to nucleotide −24 of 14-44 5′ end; and nucleotide 30 corresponds to nucleotide 579 of 14-44 3′ end. Arrows in the cell DNA represent possible cleavage sites of a putative nuclease. Alternatively, a 5′ overhang could be formed.
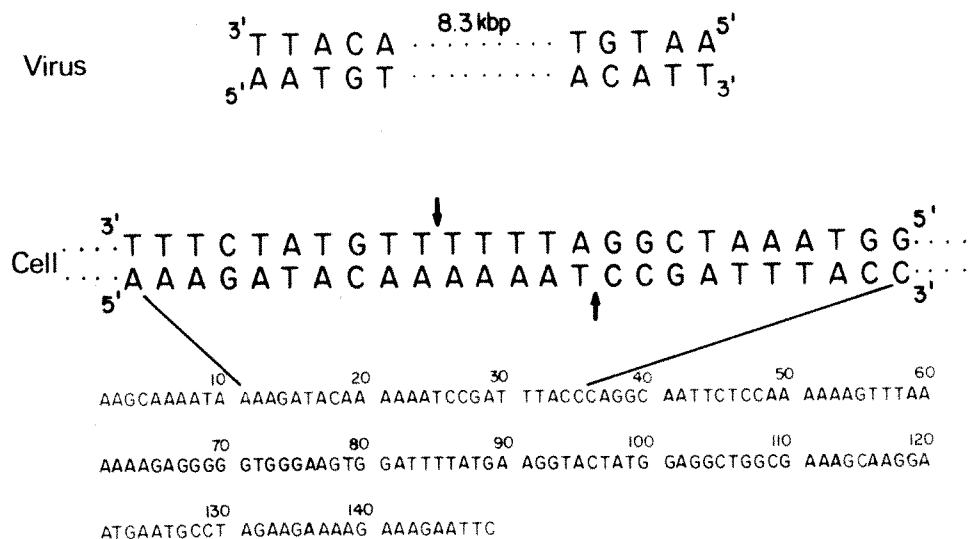
Transposable elements also end with inverted repeats, although usually they are over 20 base pairs long[7–12,35–42].

The integration of viral DNA may require only one or two specific nucleases and a ligase. The presence of DNase and DNA ligase activities in purified virions of avian retroviruses has been reported[43–45]. These findings support the hypothesis that retrovirus virions contain all the proteins necessary for provirus synthesis[44].

The sequences in the provirus next to the 5′ end and near the 3′ end are G+C rich. This base composition may be significant.

The sequence of cell DNA around the site of insertion may be reconstructed (Fig. 6). It is very A+T rich (73% A+T; chicken DNA is 58% A+T) and has no stop codons in one reading frame. Further sequencing of proviral clones will be required to determine if these characteristics or the exact sequence at the integration site have any specificity or if they are correlated with proviral infectivity[14,46]. The sites of insertion of Tn3 seem to be A+T rich[47].

The resemblance of the provirus to transposable elements indicates that retroviruses may have evolved from such elements. Evolution might possibly have involved the appearance of start and stop sequences for RNA synthesis in an insertion element[48]; appearance of a sequence that could bind a tRNA in the insertion element proximal to the site of the start sequence for RNA; the presence of a DNA polymerase in cells that could use this tRNA as a primer and the RNA as a template; formation of a transposon by integration of two of these insertion sequences around the coding sequences for this polymerase; and addition of nucleotide sequences for the rest of the present virion proteins. As the transposon transposed through an RNA intermediate, a long inverted repeat would not be needed to mark its end, as the end would also be the end of a molecule. Therefore, the size of the inverted terminal repeat would have decreased.

Since submission of this article, the same pattern of a 5-base pair repeat of cellular DNA, different in every case, next to the 3-base pair inverted repeat of viral DNA, the same in every case, has been found in five other clones of SNV proviruses.

1. Temin, H. M. *Science* **192**, 1075–1080 (1976).
2. Temin, H. M. *J. natn. Cancer Inst.* **46**, III–VII (1971).
3. O.Rear, J. J., Mizutani, S., Hoffman, G., Fiandt, M. & Temin, H. M. *Cell* **20**, 423–430 (1980).
4. Hunter, E., Bhown, A. S. & Bennet, J. C. *Proc. natn. Acad. Sci. U.S.A.* **75**, 2708–2712 (1978).
5. Barbacid, M., Hunter, E. & Aaronson, S. A. *J. Virol.* **30**, 508–514 (1979).
6. Bauer, G. & Temin, H. M. *J. Virol.* **34**, 168–177 (1980).
7. Bukhari, A.-I. *A. Rev. Genet.* **10**, 389–412 (1976).
8. Cohen, S. *Nature* **263**, 731–738 (1976).
9. Starlinger, P. & Saedler, H. *Curr. Topics Microbiol. Immun.* **75**, 111–152 (1976).
10. Nevers, P. & Saedler, H. *Nature* **206**, 109–115 (1977).
11. Kleckner, N. *Cell* **11**, 11–23 (1977).
12. Bukhari, A. I., Shapiro, J. A. & Adhya, S. (eds) *DNA Insertion Elements, Plasmids and Episomes* (Cold Spring Harbor Laboratory, New York, 1977).
13. Smith, H. O. & Birnstiel, M. L. *Nucleic Acids Res.* **3**, 2387–2398 (1976).
14. Keshet, E., O'Rear, J. J. & Temin, H. M. *Cell* **16**, 51–61 (1979).
15. Shank, P. R. *et al. Cell* **15**, 1383–1395 (1978).
16. Sabran, J. L. *et al. J. Virol.* **29**, 170–178 (1979).
17. Konkel, D. A., Tilghman, S. M. & Leder, P. *Cell* **15**, 1124–1132 (1978).
18. Goldberg, M. thesis, Stanford Univ. (1979).
19. Ziff, E. B. & Evans, R. M. *Cell* **15**, 1463–1475 (1978).
20. Nishioka, Y. & Leder, P. *Cell* **18**, 875–882 (1979).
21. Proudfoot, N. J. *J. molec. Biol.* **197**, 491–525 (1976).
22. Hamlyn, P. H., Brownlee, G. G., Cheng, C. C., Gait, M. J. & Milstein, C. *Cell* **15**, 1067–1075 (1978).
23. Seeburg, P. H., Shine, J., Martial, J. A., Baxter, J. D. & Goodman, H. *Nature* **270**, 486–494 (1977).
24. Tucker, P. W., Marcu, K. B., Slightom, J. L. & Blattner, F. R. *Science* **206**, 1299–1303 (1979).
25. Coffin, J. M. *J. gen. Virol.* **42**, 1–26 (1979).
26. Haseltine, W. A., Maxam, A. M. & Gilbert, W. *Proc. natn. Acad. Sci. U.S.A.* **74**, 989–993 (1977).
27. Schwartz, D. W., Zamecnik, P. C. & Weith, H. L. *Proc. natn. Acad. Sci. U.S.A.* **74**, 994–998 (1977).
28. Stoll, E., Billeter, M. A., Palmenberg, A. & Weissmann, C. *Cell* **12**, 57–72 (1977).
29. Shine, J., Czeinilofsky, A. P., Friederick, R., Bishop, J. M. & Goodman, H. M. *Proc. natn. Acad. Sci. U.S.A.* **74**, 1473–1477 (1977).
30. Coffin, J. M. & Haseltine, W. A. *Proc. natn. Acad. Sci. U.S.A.* **74**, 1908–1912 (1977).
31. Coffin, J. M., Hageman, T. C., Maxam, A. M. & Haseltine, W. A. *Cell* **13**, 761–773 (1978).
32. Harada, F., Peters, G. & Dahlberg, J. G. *J. biol. Chem.* **254**, 10979–10985 (1979).
33. Haseltine, W. A., Kleid, D. G., Panet, A., Rothenberg, E. & Baltimore, D. *J. molec. Biol.* **106**, 109–131 (1976).
34. Rosenberg, M., Court, D., Shimatake, H., Brady, C. & Wulff, D. L. *Nature* **272**, 414–423 (1978).
35. Ghosal, D., Sommer, H. & Saedler, H. *Nucleic Acids. Res.* **6**, 1111–1122 (1979).
36. Ohtsubo, H., Ohmori, H. & Ohtsubo, E. *Cold Spring Harb. Symp. quant. Biol.* **43**, 1269–1277 (1978).
37. Allet, B. *Cell* **16**, 123–129 (1979).
38. Ravetich, J. V. *et al. Proc. natn. Acad. Sci. U.S.A.* **76**, 2195–2198 (1979).
39. Reed, R. R., Young, R. A., Steitz, J. A., Grindley, N. D. F. & Guyer, M. S. *Proc. natn. Acad. Sci. U.S.A.* **76**, 4882–4885 (1979).
40. Grindley, N. D. F. *Cell* **13**, 419–426 (1978).
41. Calos, M., Johnsnud, L. & Miller, J. H. *Cell* **13**, 411–418 (1978).
42. Ohtsubo, A. & Ohtsubo, E. in *DNA Insertion Elements, Plasmids and Episomes* (eds Bukhari, A. I., Shapiro, J. A. & Adhya, S.) 591–593 (Cold Spring Harbor Laboratory, New York, 1977).
43. Mizutani, S., Boettiger, D. & Temin, H. M. *Nature* **228**, 424–427 (1970).
44. Mizutani, S., Temin, H. M., Kodama, M. & Wells, R. D. *Nature new Biol.* **230**, 232–235 (1971).
45. Golomb, M. & Grandgenett, D. P. *J. biol. Chem.* **254**, 1606–1613 (1979).
46. Keshet, E. & Temin, H. M. *Proc. natn. Acad. Sci. U.S.A.* **75**, 3372–3376 (1978).
47. Tu, C.-P. D. & Cohen, S. N. *Cell* **19**, 151–160 (1980).
48. Saedler, H., Reif, J. H., Hu, S. & Davidson, N. *Molec. gen. Genet.* **132**, 265–289 (1974).
49. Benton, W. D. & Davis, R. W. *Science* **196**, 180–182 (1977).
50. Clewell, D. B. & Helinski, D. R. *Proc. natn. Acad. Sci. U.S.A.* **62**, 1159–1166 (1969).
51. Maxam, A. M. & Gilbert, W. *Proc. natn. Acad. Sci. U.S.A.* **74**, 560–565 (1977).
52. Sanger, F. & Coulson, A. R. *FEBS Lett.* **87**, 197–110 (1978).
53. Korn, L. J., Queen, C. L. & Wegman, M. N. *Proc. natn. Acad. Sci. U.S.A.* **74**, 4401–4405 (1977).
54. Peters, G. G. & Glover, C. *J. Virol.* **33**, 708–716 (1980).

LETTERS

Far UV observations of PKS2155–304

L. Maraschi*†, E. G. Tanzi*, M. Tarenghi‡ &
A. Treves*†

*Laboratorio di Fisica Cosmica del C.N.R. Milano, Italy
†Istituto di Fisica dell'Università, Milano, Italy
‡European Southern Observatory, Geneva, Switzerland

In BL Lac objects the absence of broad emission lines may be due either to a lack of ionizing continuum or to a lack of cool gas $(T \lesssim 10^4 K)$[1]. UV observations of BL Lac objects are interesting in that they provide a measurement of the continuum, and they include the wavelength range of Lyα, which is in principle the most favourable line for detection. We report here several spectra of the BL Lac object PKS2155 – 304 in the 1,150–3,200 Å band taken with the IUE when the object was in a bright phase. The UV flux connects smoothly with the optical and IR observations of the source in its brightest state and its extrapolation matches the soft X-ray flux, implying a change in spectral slope around 10^{15}Hz.

This object was discovered as a result of X-ray observations by HEAO I of a region of the sky where the source 2A2151 – 316 was reported by the Ariel 5 Catalogue[2]. The precise positioning identified it with a 14 mag star-like object and with the radio source PKS2155-304 (refs 3–5). The observation in the optical range of a blue featureless continuum with polarization of ~5% (refs 6, 7) indicated its BL Lac nature. A weak emission feature subsequently detected by Charles et al.[8] was confirmed by further observations by one of us (M.T.). If the feature is identified with the O III doublet (λλ4,959, 5,007) as proposed by Charles[8], the corresponding redshift is 0.17, which makes this the most intrinsically luminous BL Lac object known thus far. In the past 40 years its visual magnitude has ranged from 12.8 to 14.2 (ref. 7). Recent optical observations show variability in flux and spectral shape on time scales of about one month. Variability in X rays

seems to be more rapid, on a day scale. No data on variability at radio and IR frequencies have yet been obtained.

IUE observations were performed using a blind offset technique with coordinates:

$$\alpha(1950) = 21\,\text{h}\,35\,\text{min}\,58\,\text{s}\,0.33\,\text{s} \quad \delta(1950) = -30°27'53.7''$$

as measured on the glass copy of the ESO quick blue sky survey. Five spectra were taken with the short wavelength camera (SWP: range 1,100–2,000 Å) and three with the long wavelength camera (LWR: range 2,000–3,000 Å). The large aperture (10 × 20 arc s) and the low resolution mode were used for each observation. Observations are listed in Table 1: the data were reduced to absolute fluxes using the calibration curves of Bohlin et al.[9]. The spectrum SWP 6855 is heavily saturated in extended wavelength regions; the other spectra taken each day, summed and combined to cover the entire wavelength interval, are shown in Fig. 1 together with the portion of the long-exposed spectrum where saturation is incomplete. No correction has been applied for reddening. The absence of a broad absorption feature around 2,200 Å infers an upper limit $E(B - V) \sim 0.02$ (ref. 10).

In the region around 1,900 Å, where the range of the two cameras joins, a mismatch is apparent, probably due to inadequacies of the LWR calibration. The spectra are affected by microphonic noise, which makes identification of the weak features difficult. However, several dips visible in all individual spectra can be tentatively identified with galactic absorptions (see Table 2). In particular C IV (λ1,550) and Al II (λ1,670) show up clearly in the region of the long exposed spectrum (see inset in Fig. 1). The absorptions compare well with those observed by Savage and de Boer[11] and by Ulrich et al.[12], except for Mg II at 2,800 Å, which is not detectable in our spectra.

The emission expected to be strongest is Lyα, which, for a redshift of 0.17, should be at 1,420 Å. A small feature is present at this wavelength in the long exposed spectrum, which is not completely saturated in this region. In the short exposures, however, the feature is absent, and an upper limit of about 1 Å can be placed on its equivalent width, assuming a FWHM of
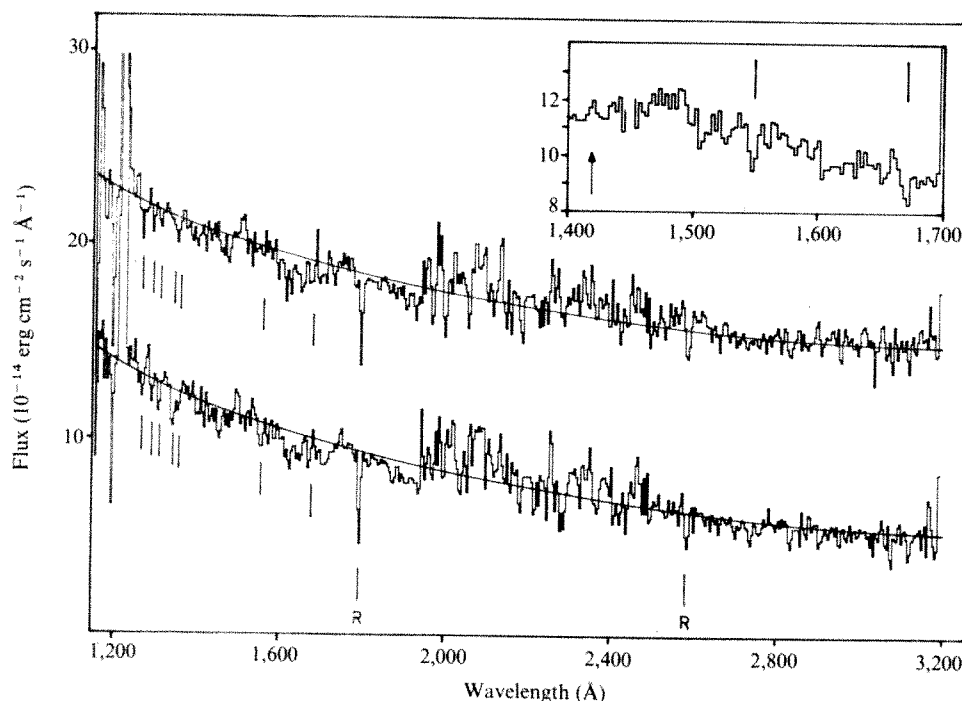
Fig. 1 Combined spectra of 13 and 14 October 1979 shown with a λ^{-1} fit for the continuum. The upper spectrum (14 October) has been displaced by 10^{-13} erg cm^{-2} s^{-1} Å^{-1}. The inset shows the overexposed spectrum of 13 October in the region where saturation is not complete. Vertical lines correspond to the absorption features reported in Table 2. The position of the expected Lyα emission is indicated by an arrow.

Table 1   Integral fluxes in units of 10^{-12} erg cm^{-2} s^{-1}

Image no.	SWP 6855	LWR 5828	SWP 6856	LWR 5829	SWP 6857	SWP 6867	LWR 5839	SWP 6868
Epoch October 1979 (UT)	13.700	13.797	13.823	13.846	13.872	14.642	14.674	14.706
Exposure time (min)	240	30	40	21.5	48	48	30	48
$F_{1,250-1,450}$	Heavily saturated		24.9		24.5	22.5		22.1
$F_{1,450-1,650}$	21.5		20.9		21.8	18.9		18.8
$F_{1,650-1,850}$	Heavily saturated		18.3		18.6	17.1		16.8
$F_{2,000-2,220}$		19.0		19.6			16.3	
$F_{2,200-2,400}$		15.8		16.8			14.8	
$F_{2,400-2,600}$		13.9		14.7			13.1	
$F_{2,600-2,800}$		12.2		12.8			11.5	
$F_{2,800-3,000}$		11.9		12.1			10.6	

10 Å. Given this upper limit other emissions should be undetectable. Note, however, that the two features at 1,390 and 1,495 Å which are present in all the spectra, if real, may correspond to C I ($\lambda 1,164$) and ($\lambda 1,277$). The second of these lines has been observed in emission in M31 (ref. 13).

If, as indicated by the overall spectrum, the continuum can be extrapolated beyond the Lyman limit the absence of strong emission lines cannot be ascribed to a deficiency of exciting UV photons, but rather to physical conditions of the gas surrounding the central source different from those of Seyferts and QSOs. This is also true for the two other BL Lac objects observed in the UV, Markarian 421 and 501 (refs. 14, 15).

Apart from the region 2,000–2,200 Å, a good fit is obtained with a power law of spectral index -1, with $F_\lambda = 1.70 \times 10^{-10} \lambda^{-1}$ and $1.55 \times 10^{-10} \lambda^{-1}$ erg cm^{-2} s^{-1} Å^{-1} for 13 and 14 October, respectively. Taking into account the possible reddening correction, the spectral index would change at most up to -1.1. According to the performance characteristics of IUE[9] the flux variation between 13 and 14 October over the entire wavelength range is significant, and appears, in fact, between each of the spectra taken on different days (see Table 1), while spectra taken within few hours do not show significant variations.
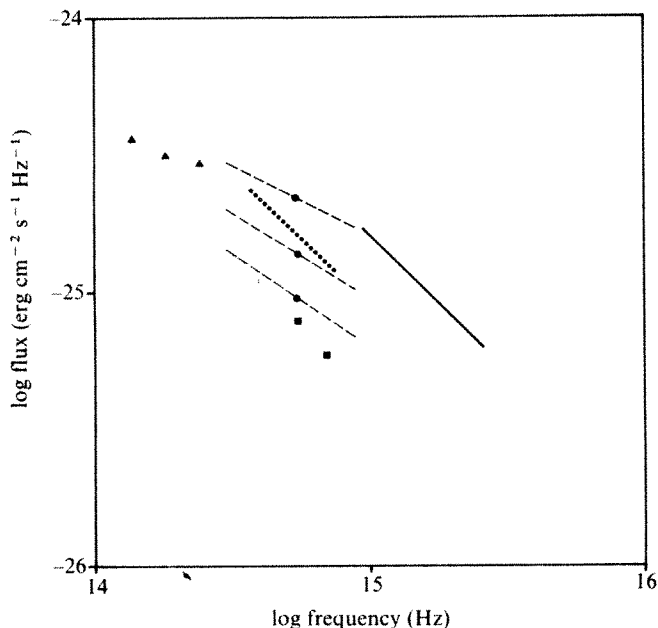
Fig. 2   Variability of PKS2155–304. ———, 14 October 1979, from this paper; — ● —, 23 October 1978 (lower), 2 November 1978 (medium), 24 December 1978 (upper) from ref. 19; ·······, 2–3 December 1978, from ref. 18; ■, 24–27 October 1978 from ref. 8; ▲, 24 December 1978, from ref. 17.

The UV spectrum is compared with the optical data in Fig. 2, which summarizes the available information on the variability in this band. At the epoch of the UV observations the B magnitude, as given by the onboard optical monitor (FES), was between 12.8 and 13.1. The spectral index in the optical band, measured by Greenstein *et al.*[17] when the source was at the same intensity level, was $\alpha = 0.5 \pm 0.1$, indicating a signficant difference with respect to that in the UV band. This conclusion is, however, tentative, because the spectral index in the optical is variable and the observations were not simultaneous: for example a spectral index in the optical, $\alpha = 0.95 \pm 0.15$, is reported by Griffiths *et al.*[7], on 2 December 1979, when the intensity (as derived from Fig. 4 of ref. 7) was lower by 40%.

For the other two BL Lac objects observed in UV, MK421 and MK501 (refs 14, 15) the slope of the continuum is 1.2 and 0.57 respectively, in agreement with the extrapolation of their optical spectra. Comparison of the optical and UV data with radio, IR and X-ray observations for these objects, indicates a spectral 'break' at $\nu_B \simeq 10^{13}$ Hz and $\nu_B \simeq 10^{16}$ Hz in the two cases[13,14].

The overall spectrum of PKS2155–304 is shown in Fig. 3 which only includes optical data for the brightest state. The X-ray data, taken 40 days before the optical ones, lie on the extrapolation of the UV continuum thus supporting the spectral steepening around $\nu_B = 10^{15}$ Hz. The slope variation in the optical band, suggests that ν_B may be variable with a higher value in the brightest state.

For the three BL Lac objects observed in the UV in the radio to soft X-ray spectrum seems to be a two component spectrum with a rather abrupt break at a frequency ν_B, which for different objects varies between 10^{13} and 10^{16} Hz.

An interpretation in terms of radiative losses of relativistic electrons yields a relationship between the magnetic field and the lifetime t_c of the particles radiating at ν_B:

$$\nu_B = 3.5 \times 10^{23} \frac{B}{(B^2 + 8\pi W_{ph})^2 t_c^2} \ \text{Hz}$$

where W_{ph} is the photon energy density in erg cm^{-3}. For PKS2155–304 the optical variability time scale, $t_v \sim 1$ month,

Table 2   Absorption lines of galactic origin

Observed wavelength (Å)	Proposed identification
1,261	Si II (1,263)
1,284	C I (1,281)
1,304	O I (1,305) + Si II (1,304)
1,335–1,350	C II (1,336) + not identified
1,550	C IV (1,584, 1,551)
1,669	Al II (1,671)

and the known distance allow a direct evaluation of W_{ph} $\simeq 1\,\mathrm{erg\,cm^{-3}}$. The maximum lifetime is obtained for $B^2/8\pi$ $\simeq W_{ph}$ ($B \simeq 5\,\mathrm{G}$) and $\nu_B \sim 10^{15}\mathrm{Hz}$ implies that $t_e \simeq 10^3 s$. As $t_e \ll t_v$ a continuous acceleration mechanism is required with a time scale $\sim t_e$. The synchrotron self absorption frequency for these parameters is $10^{11}\mathrm{Hz}$, implying that the radio emission comes from a larger region.

Another interpretation of the spectral steepening is that the flat part is due to synchrotron radiation from a mildly relativistic gas ($T \simeq 10^{10}\,\mathrm{K}$) in a high magnetic field $B \sim 10^6\mathrm{G}$, while the steeper part is due to multiple Compton scattering of the synchrotron photons in the hot gas[20].
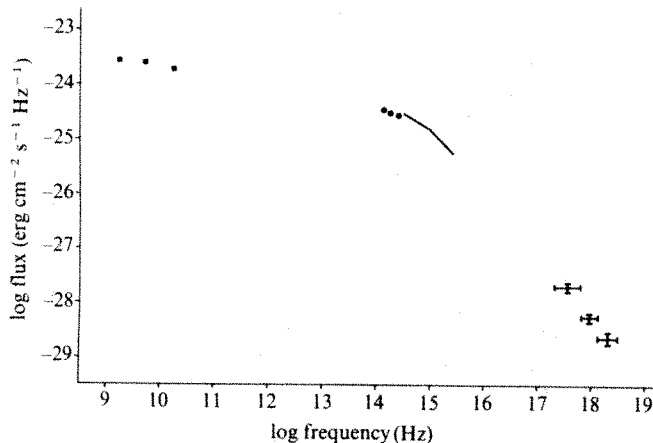
Fig. 3 Overall spectrum of PKS2155–304 near maximum brightness. Radio data are from ref. 16, IR data from ref. 17, optical data (24 December 1978) from ref. 19, UV data (13–14 October 1979) from this paper, X-ray data (8 November 1978) from ref. 5.

The main difference between the two hypotheses is that in the second the mean electron energy is lower and the dimension of the source is smaller. Discriminating features would therefore be variability on short time scale and a cutoff in the spectrum in the MeV region due to the low effective electron energy and high opacity.

Our observations of PKS2155–304 show that as in MK421 and MK501 the absence of emission lines is not due to the absence of a UV continuum. The break between the optical and UV bands is an important constraint on the emission mechanism. Further observations would be useful for studying the variability of this feature.

1. Stein, W. A., O'Dell, S. L. & Strittmatter, P. A. *A. Rev. Astr. Astrophys.* **14**, 173 (1976).
2. Cooke, B. A. *et al. Mon. Not. R. astr. Soc.* **182**, 489 (1978).
3. Schwartz, D. A., Doxsey, R. E., Griffiths, R. E., Johnston, M. D. & Schwartz, J. *Astrophys. J. Lett.* **229**, L53 (1979).
4. Agrawal, P. C. & Riegler, G. R. *Astrophys. J. Lett.* **231**, L25 (1979).
5. Griffiths, R. E. & Briel, U. *IAU Circ.* No. 3279 (1979).
6. Wade, R. A., Szkody, P. & Cordova, F. *IAU Circ.* No. 3279 (1979).
7. Griffiths, R. E., Tapia, S., Briel, U. & Chaisson, L. *Astrophys. J.* **234**, 810 (1979).
8. Charles, P., Thorstensen, J. & Bowyer, S. *Nature* **281**, 285 (1979).
9. Bohlin, R. C., Holm, A. V., Savage, B. D., Snijders, M. A. J. & Sparks, W. M. *Astr. Astrophys. J.* (submitted).
10. Nandy, H., Thompson, G. I., Carnochan, D. S. & Wilson, R. *Mon.Not. R. astr. Soc.* **184**, 733 (1979).
11. Savage, B. D. & de Boer, K. S. *Astrophys. J. Lett.* **230**, L77 (1979).
12. Ulrich, M. H. *et al. The First Year of IUE* (ed. Willis, A. J.) (NASA-ESA-SRC, 1979).
13. Johnston, H. M. *Astrophys. J. Lett.* **230**, L137 (1979).
14. Boksenberg, A. *et al. Nature* **275**, 34 (1978).
15. Snijders, M. A. J. *et al. Mon. Not. R. astr. Soc.* **189**, 873 (1979).
16. Hjellming, R. M., Schnopper, H. W. & Moran, J. M. *IAU Circ.* No. 3309 (1978).
17. Persson, S. E. *IAU Circ.* No. 3324 (1979).
18. Wilson, A. S., Ward, M. J. & Griffiths, R. E. *IAU Circ.* No. 3279 (1979).
19. Greenstein, J. L., Oke, J. B. & Wade, R. A. *IAU Circ.* No. 3324 (1979).
20. Maraschi, L., Perola, G. C., Reina, C. & Treves, A. *Astrophys. J.* **230**, 243 (1979).

Electromagnetic scattering lifetimes for dust in Jupiter's ring

Guy J. Consolmagno

Harvard/Smithsonian Center for Astrophysics, 60 Garden Street, Cambridge, Massachusetts 02138

Dust particles of $4\,\mu m$ radius which are reported to lie in a ring at 1.8 jovian radii around Jupiter may be charged to $-10\,V$, but any larger charge would lead to non-circular orbits, due to interactions with Jupiter's dipole magnetic field. Such dust will be scattered randomly in eccentricity and inclination by variations in Jupiter's magnetic field strength as seen by the dust particles. We report here that this scattering will effectively dissipate the ring in a time scale less than 100 yr; and that the ring must, therefore, be constantly replenished, as suggested by Burns[1], or else it is a short-lived phenomenon.

The discovery of a ring of micrometre-sized particles orbiting Jupiter at a distance of 1.8 jovian radii[2] has raised speculations as to the lifetime of such particles against perturbing forces. Burns[1] pointed out that such particles will be subject to a Poynting–Robertson drag (with a lifetime of 10^5 yr) and will be eroded by sputtering with magnetospheric particles over a time scale of 10^2–10^5 yr. He suggests such particles originate from the regolith of one or more small (1–10 km) satellites; they may be fragmented and eroded by sputtering, electrostatic bursting, or meteoric collisions and self-collisions to their characteristic size of $4\,\mu m$ (refs 3, 4).

Such particles existing in the circum-jovian plasma will certainly have a surface charge and interact with the jovian magnetic field, as pointed out by Hill and Mendis[4]. In the case of Jupiter, the field in the region of the rings is still essentially a dipole[5] of $4.25\,G$ and the plasma around Jupiter at this radius can be considered co-rotating with Jupiter at $1.74 \times 10^{-4}\,\mathrm{s^{-1}}$ (ref. 6). This co-rotation leads to an electric field of $\mathbf{E}_c = -(\omega/c \times \mathbf{r}) \times \mathbf{B}$ where ω and $\mathbf{B}$ are Jupiter's spin frequency and magnetic field vectors, and $\mathbf{r}$ the radius vector from the spin axis. In addition, particles orbiting with a velocity $\mathbf{v}$ will also see an electric field equal to $\mathbf{E}_0 = (\mathbf{v}/c \times \mathbf{B})$. Defining a term $\gamma = qr_0^3/mc$, where q is the charge on particles of mass m, and given B_0, the strength of the magnetic field at radius r_0, we can calculate the equations of motion in r and θ directions:

$$\ddot{r} - r\dot{\theta}^2 = -\frac{\mu}{r^2} + \frac{\omega\gamma B_0}{r^2} - \frac{\dot{\theta}\gamma B_0}{r} \tag{1}$$

$$\frac{1}{r}\frac{d}{dt}(r^2\dot{\theta}) = \frac{\dot{r}\gamma B_0}{r^3} \tag{2}$$

where μ is the keplerian constant (here equal to the gravitational constant G times the mass of Jupiter). Equation (2) can be integrated directly to yield

$$r^2\dot{\theta} = -\gamma B_0/r + h$$

where h, the constant of integration, is the angular momentum of the orbiting particle per unit mass. From this, one can solve for $\dot{\theta}$ and substitute directly into equation (1) to yield

$$\ddot{r} = -\frac{\mu}{r^2} + \frac{h^2}{r^3} - \frac{3\gamma B_0 h}{r^4} + \frac{\omega\gamma B_0}{r^2} + \frac{2(\gamma B_0)^2}{r^5} \tag{3}$$

In a circular orbit with $\gamma = 0$, one sees the expected result that $h^2 = \mu r$; magnetic field effects will become important only when the last three terms are of comparable magnitude to the first two.

For spherical particles it can be shown that $\gamma = 9.7 \times 10^{15} V/b^2\rho$ where V is the electrostatic voltage on the dust particles, and ρ and b the dust mass density and radius. For ring particles with $\rho = 2\,\mathrm{g\,cm}^{-3}$ and $b = 4\,\mu\mathrm{m}$, equation (3) can be integrated numerically to find the range of r traversed by ring particles.

The results of such an integration show that particles charged to $-10\,\mathrm{V}$ will produce a ring as wide as the observed bright outer ring ($0.05\,R_J$). A charge of $-100\,\mathrm{V}$ would spread particle orbits out to a much greater extent than is observed. One can thus conclude that $-10\,\mathrm{V}$ is an upper limit on the charge.

Theoretical estimates for the charge on the dust in Jupiter's plasma depend on a better knowledge of the typical plasma energies than are currently available. Intriligator and Wolfe[7] suggested that a 100 eV plasma may exist close to Jupiter, which would produce dust voltages of $-200\,\mathrm{V}$ if the charge on the dust were in thermal equilibrium with the plasma. Hill and Mendis[4] also calculated that dust 1 μm or larger in Jupiter's magnetosphere should bear potentials of many hundreds of volts. However, as we have just seen, such high voltages for ring particles are incompatible with the observed width of the ring. More recently, work by Johnson *et al.*[8] using Voyager data estimate the voltage on dust inside Io's orbit to be $-10\,\mathrm{V}$, which is compatible with the ring width.

This dust will travel in slightly eccentric orbits, but these orbits will no longer be closed. The smaller the dust, the more eccentric the orbit and the wider the range of r traversed. Because γ varies as b^2, particles of 1 μm will be an order of magnitude more strongly affected than the 4 μm ring particles, and will quickly spread away from the rings, while 10 μm particles will be virtually unaffected.

The effect of this extra force is outward, as the rings are within the synchronous orbit point; thus if the ring dust is produced by the eroding of larger particles in originally circular orbits, these particles will immediately spread away from Jupiter in orbits whose perijoves are at the orbit of the source material. This argues against the observed small satellite at the outer edge of the rings being the direct source of the ring particles; the sources ought to be at the inner edge of the ring, if the ring width is determined by electromagnetic forces.

In addition to the extra force terms which the magnetic field adds to the equation of motion of the dust particles, fluctuations within the field can cause a scattering of particle orbital elements in a manner similar to that outlined for interplanetary dust[9]. For brevity, let us consider the case where the eccentricity $e = 0$ and i is small (here, i will be the tilt of the dipole, or $10°$).

The perturbing accelerations R, N and T in the directions radial, normal to the orbit plane, and in the direction of the orbit arise from the cross product of a B field whose strength varies as a dipole but whose direction is varying randomly in all coordinates, crossed with the orbital velocity of the dust and the co-rotating velocity of the plasma.

For $e = 0$, the change in semimajor axis, a, depends only on T; but T must be zero, as all accelerations must be normal to the particle or plasma velocity vector. Thus no change in a is expected.

The acceleration $R = \gamma[v_\theta B_\phi - v_\phi B_\theta] \simeq \gamma[(h/a)(-\sin i \cos \eta\, B_{0\phi} - (\cos i - r\omega)B_{0\theta})]$. If $T = 0$, the change in e depends entirely on R and can be written

$$\frac{de}{dt} = \gamma \sin \eta\, [\sin i \cos \eta\, B_{0\phi} + (\cos i - a^2\omega \cos i/h)B_{0\theta}]$$

Following the procedure outlined by Consolmagno[9], this equation is squared, averaged over one orbit, and integrated over time intervals which are long compared with the correlation time for changes in the magnetic field, arriving at

$$\langle \Delta e^2 \rangle = (\gamma/a^3)^2 [\sin^2 i P_{\phi\phi}/8 + (\cos^2 i + a^3\omega^2/\mu - 2a\omega \cos i/(a\mu)^{\frac{1}{2}})P_{\theta\theta}/2]\Delta t \tag{4}$$

where $P_{\phi\phi}$ and $P_{\theta\theta}$ are the power spectral densities of the magnetic fields.

Likewise the N component can be calculated, and a mean square change in inclination derived, to be

$$\langle \Delta i^2 \rangle = \gamma^2 \sin^2 i (1 + a^3\omega^2 \cos^2 i/\mu - 2a\omega \cos i/(a\mu)^{\frac{1}{2}})P_{rr}\Delta t/(8a^6) \tag{5}$$

Finally, we must derive values for P_{rr}, $P_{\phi\phi}$ and $P_{\theta\theta}$. In each case we will assume these are equal to some portion of the mean square dipole field strength times some correlation time.

The ϕ component arises only from fluctuations of the θ direction field. We can assume these fluctuations to be sinusoidal with an amplitude of 0.1 times the field strength (matching observed B_ϕ strengths[10]) and a period of roughly 10 min (matching observed fluctuations in the B field[11]). Although the θ component field itself does not reverse, we can assume that fluctuations within the field will exist and produce a $P_{\theta\theta}$ component of the same magnitude as $P_{\phi\phi}$.

For P_{rr} we note that the B_r field will appear to reverse itself as the particle passes above and below the magnetic equator. Furthermore this field is offset from the centre of Jupiter by $0.1\,R_J$. The period of oscillations is roughly the synodic period of the particles and the rotating dipole ($\sim 25\,\mathrm{h}$ for ring grains). Recall that the strength of the dipole falls as the cube of the radial distance; due to the offset dipole and the eccentricities produced by the non-keplerian forces discussed above, the grains will not see equal field strengths above and below the equator, so the average effect will not cancel out. The net effect will depend on the initial orientation of the dust and on variations in its eccentricity, both of which depend on the history of the dust which cannot be predicted. Thus we will assume that an order of magnitude estimate for the mean square change in inclination can be made by treating the fluctuations as random changes of the B_r field with a correlation time of 10^5 s.

Substituting these values and taking square roots, we find that a root mean square change in eccentricity of 0.05 will occur over 10^3 yr for 4 μm grains. This produces a spread greater than the observed width of the ring. Again, 1 μm particles would be spread an order of magnitude more.

The change in inclinations is more dramatic, spreading by $0.6°$ in 1 yr, or $6°$ in 100 yr, resulting in a ring thickness of 14,000 km. Again, smaller particles will be even more drastically affected.

We conclude that Jupiter ring particles will be strongly perturbed and scattered by electromagnetic forces on short time scale (100 yr) if they are charged to $-10\,\mathrm{V}$. Larger voltages are incompatible with the observed width of the ring. Given $-10\,\mathrm{V}$ potentials, the ring must be constantly replenished, or else it is a temporary phenomenon. Alternatively, voltages may be much lower than those predicted previously.

The electromagnetic forces will be very effective in scattering particles smaller than the ring particles. Thus these forces are probably the cause of the dust cloud observed to extend above, below and beyond the jovian ring itself[12].

1. Burns, J. A. *Bull. Am. astr. Soc.* (in the press).
2. Owen, T. C. *et al. Nature* **281**, 442 (1979).
3. Pilcher, C. *Icarus* **37**, 559–574 (1979).
4. Hill, J. R. & Mendis, D. A. *Moon and Planets* **21**, 3–16 (1979).
5. Goertz, C. K. in *Jupiter* (ed. Gehrels, T.) 32–58 (University of Arizona Press, Tucson, 1976).
6. Hill, T. W. *J. geophys. Res.* **84**, 6554–6558 (1979).
7. Intriligator, D. S. & Wolfe, J. H. in *Jupiter* (ed. Gehrels, T.) 848–869 (University of Arizona Press, Tucson, 1976).
8. Johnson, T. V., Morfill, G. & Grün, E. *Geophys. Res. Lett.* (in the press).
9. Consolmagno, G. J. *Icarus* **38**, 398–410 (1979).
10. Acuna, M. H. & Ness, N. F. in *Jupiter* (ed. Gehrels, T.) 830–847 (University of Arizona Press, Tucson, 1976).
11. Smith, E. J., Davis, L. Jr & Jones, D. E. in *Jupiter* (ed. Gehrels, T.) 788–829 (University of Arizona Press, Tucson, 1976).
12. Cook, A. F., Danielson, G. E. & Owen, T. *COSPAR* (submitted).

Photocatalytic hydrogen production from water on Pt-free SrTiO₃ in alkali hydroxide solutions

F. T. Wagner & G. A. Somorjai

Materials and Molecular Research Division, Lawrence Berkeley Laboratory and Department of Chemistry, University of California, Berkeley, California 94720

Semiconductor surfaces can act as photosensitizers for small molecules which on their own do not absorb solar photons. Such sensitizers can be used for the photoassisted decomposition of water to hydrogen and oxygen. Most previous work on this process has concentrated on photoelectrochemical cells using oxide semiconductor photoanodes for oxygen evolution and platinum cathodes for the evolution of hydrogen[1-3]. We report here the sustained photogeneration of hydrogen on SrTiO₃ single crystal surfaces by a different mechanism, when no platinum coating or platinum counterelectrode is present. Hydrogen yields far exceed the monolayer amounts ($\sim 10^{15}$ molecules cm⁻²) expected from a surface stoichiometric reaction. The reaction takes place on illumination of the crystal with band gap radiation ($hv \geq 3.2$ eV) in aqueous alkaline solution. The rate of hydrogen evolution increased with increasing hydroxide concentration in the solution. We also report the use of water vapour as a reactant through saturation of a layer of a basic deliquescent compound, such as NaOH, which coated the crystal. The photocatalytic generation of hydrogen on the illuminated surface of metal-free SrTiO₃ crystals shows that strongly reductive as well as oxidative reactions can be carried out and sustained on illuminated oxide semiconductors. A wide range of photocatalytic reactions may possibly be carried out in conditions not amenable to the operation of photoelectrochemical cells by using this new mechanism.

Single crystal wafers of SrTiO₃ cut within 1° of the (111) plane were dipped in a saturated NaOH solution, dried to leave $\sim 30\,\mu$m of NaOH on the surfaces, and inserted into a stainless steel vacuum cell equipped with a sapphire window. The crystal was held in a quartz glass basket; no metal was in
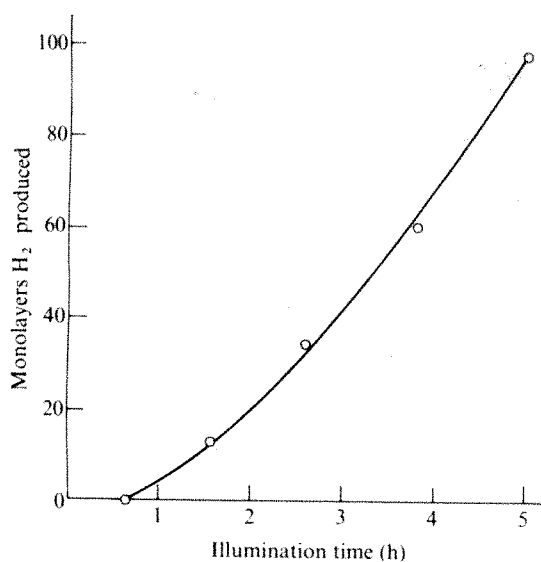
Fig. 1 Hydrogen photogeneration on a metal-free stoichiometric SrTiO₃ crystal on illumination in 20 M aqueous NaOH at 44 °C.
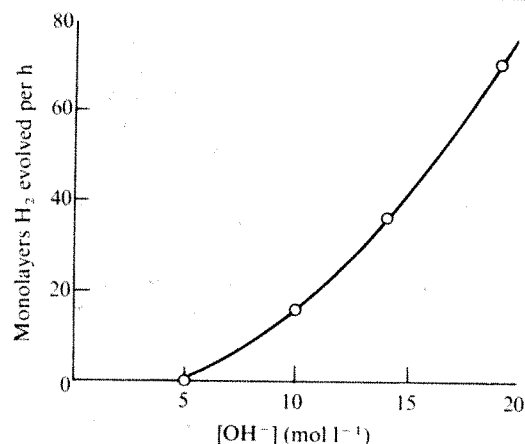
Fig. 2 Hydrogen photoproduction on a metal-free stoichiometric SrTiO₃(111) crystal as a function of aqueous NaOH concentration at 44 °C.

contact with it or the NaOH layer. The cell was evacuated and then backfilled with a saturation pressure of water vapour (~ 20 torr). A stainless steel bellows pump circulated the vapour and product gases around a closed loop which included a gas sampling valve. A gas chromatograph equipped with a thermal conductivity detector and a molecular sieve 5 A column and operated with an argon carrier gas allowed the hydrogen concentration in the loop to be periodically measured. The crystal was illuminated with the focused, water-filtered output of a 500 W high pressure mercury lamp which provided a flux of bandgap ($hv \geq 3.2$ eV) photons of $\sim 10^{16}$ cm⁻²s⁻¹. The use of coloured glass filters enabled the band gap and sub-band gap ($hv < 3.2$ eV) radiation to be separated.

Metal-free crystals coated with NaOH and illuminated in water vapour yielded hydrogen at rates of 20–100 monolayers (1 monolayer $= 1 \times 10^{15}$ molecules per cm² illuminated surface) per hour. This range of rates was obtained on both stoichiometric (insulating) and prereduced (n-type) crystals. No hydrogen production was obtained when any of the following were absent: band gap light, saturation pressure of water vapour, SrTiO₃, or a coating of a basic deliquescent compound such as NaOH, Cs₂CO₃, or KOH greater than 2 μm thick. Similar results were obtained when metal-free crystals were immersed in 10 ml of thoroughly outgassed aqueous solution in a Pyrex vacuum cell and then illuminated (Fig. 1). Metal-free crystals yielded up to 50 monolayers h⁻¹ of hydrogen when illuminated in 20 M NaOH at 41 °C. This rate could be maintained for tens of hours. Hydrogen production was observed only in basic solutions, and the rate of hydrogen photogeneration increased with the concentration of NaOH solutions, as shown in Fig. 2. Sealing off the non-illuminated surfaces of a metal-free SrTiO₃ crystal with ultrahigh vacuum compatible epoxy caused no decrease in the rate of hydrogen photogeneration, indicating that hydrogen was produced on the illuminated surface. The epoxy was shown not to be a source of hydrogen.

For comparison, experiments were also performed with platinized crystals. The backs of such crystals were coated with platinum through the thermal reduction of chloroplatinic acid. Platinized, prereduced crystals yielded hydrogen at rates up to 1,600 monolayers h⁻¹ when coated with NaOH and illuminated in water vapour. Rates up to 4,500 monolayers h⁻¹ were observed in 20 M NaOH electrolyte. Hydrogen photogeneration on platinized crystals showed a hydroxide concentration dependence similar to that observed on metal-free crystals. Covering the platinized surfaces with epoxy decreased the hydrogen evolution rates to those observed on metal-free crystals. A standard SrTiO₃/Pt photoelectrochemical cell[2] with discrete electrodes was also

operated in the vacuum cell and gave hydrogen generation rates about five times those observed on platinized crystals, probably due to the provision of a true ohmic contact between the $SrTiO_3$ and platinum by use of a Ga–In eutectic.

In photoelectrochemical cells or platinized crystals of n-type semiconductors, photogenerated electrons and holes are separated by the electric field within the semiconductor depletion layer. Holes rise to the semiconductor surface where they can oxidize solution species. Electrons are driven into the semiconductor bulk and then to the platinum surfaces where reductive chemistry occurs. Hydrogen production on metal-free crystals occurs at the illuminated semiconductor surface, presumably through the generation of local reduced and oxidized centres on the crystal surface. Photoemission studies of $SrTiO_3$ (111) surfaces in our laboratory[4] have shown that a reduced Ti^{3+} surface species can be regenerated by shining band gap light upon the oxygen-covered surface. The regeneration of Ti^{3+} is accompanied by oxygen photodesorption. Such reduced centres may be involved in the photocatalytic hydrogen production reported here.

High hydroxide concentrations were required for hydrogen production from metal-free crystals and also greatly increased the rates obtained on platinized crystals. Hydroxide ions at or near the surface may serve as facile hole acceptors, decreasing the probability of electron hole recombination and increasing the mean lifetime of electrons at the surface. Hydroxyl groups can be monitored on $SrTiO_3(111)$ surfaces by photoelectron spectroscopy[4] and their effects on the photochemistry are being further investigated.

This work was supported by the Division of Chemical Sciences, Office of Basic Energy Sciences, US Department of Energy.

1. Fujishima, A. & Honda, K. *Nature* **238**, 37–38 (1972).
2. Wrighton, M. S. *et al. J. Am chem. Soc.* **98**, 2774–2779 (1976).
3. Wrighton, M. S., Wolczanski, P. T. & Ellis, A. B. *J. Solid State Chem.* **22**, 17–29 (1977).
4. Ferrer, S. & Somorjai, G. A. *Surface Sci.* (in the press).

Structural characteristics of fulvic acids from Continental Shelf sediments

Patrick G. Hatcher*†, Irving A. Breger*† &
Mark A. Mattingly‡

*US Geological Survey, Reston, Virginia 22092
†Department of Chemistry, University of Maryland, College Park, Maryland 20742
‡Bruker Instruments, Bellerica, Massachusetts 01821

Fulvic acids are those components of soil organic matter that remain soluble after a dilute alkaline extract of the soil is acidified to *p*H 2 (refs 1, 2). This extraction procedure has been applied to marine sediments, and the organic compounds so recovered have been called marine sedimentary fulvic acids. These fulvic acids are thought to form more complex humic substances in marine sediments by condensation reactions[3]. However, the chemical structural compositions of marine fulvic acids have not been defined sufficiently to allow this precursor relationship to be made. Here NMR spectroscopy is used to identify more clearly the chemical structural components of some marine sedimentary fulvic acids, thus enabling a more useful examination of their relationship to more complex humic substances.

Fulvic acids of soils are thought to be composed primarily of benzenecarboxylic acid structures condensed by hydrogen bonds[2,4,5]. Substances such as carbohydrates, proteins and lipids have been reported as components of fulvic acid

preparations[6-8]. The presence of carbohydrates in fulvic acid preparations is not surprising considering that polysaccharides, free sugars and uronic acids are extracted from sediments by similar methods to those used for fulvic acids (by weak alkali and acid)[7,9].

Although the composition and structural components of marine fulvic acids have not been as extensively studied as those of soil fulvic acids, several major differences and similarities between them have been noted[10-12]. Although the nature and amounts of various oxygen functional groups in these two types of fulvic acids are believed to be similar, there is a large difference in degree of aromaticity[12]. Like soils, a significant polysaccharide content is expected for marine fulvic acids, but no definitive studies have been made to establish this fact, although Ishiwatari[13] pointed out that fulvic acids of marine sediments are rich in total carbohydrates as determined by colorimetry.

IR spectroscopy provided some early evidence for the presence of certain functional groups of fulvic acids[14,15] but the lack of resolution and uncertainties in peak assignments have limited its usefulness. Chemical degradations by hydrolysis, saponification, oxidation, reduction and methylation have provided valuable clues as to the structural composition of fulvic acids[2]. The relationships between degradation products and the unaltered structures of fulvic acids, however, have always been questioned.

As non-destructive NMR techniques have recently shown promise in providing structural information on humic substances[12,16-20] we have used this technique, as well as IR spectometry, to examine the structural components of fulvic

K6.77.12b

MN.4

25

8 6 4 2 0 δ(TMS)   200 150 100 50 0 δ(TMS)

¹H   ¹³C
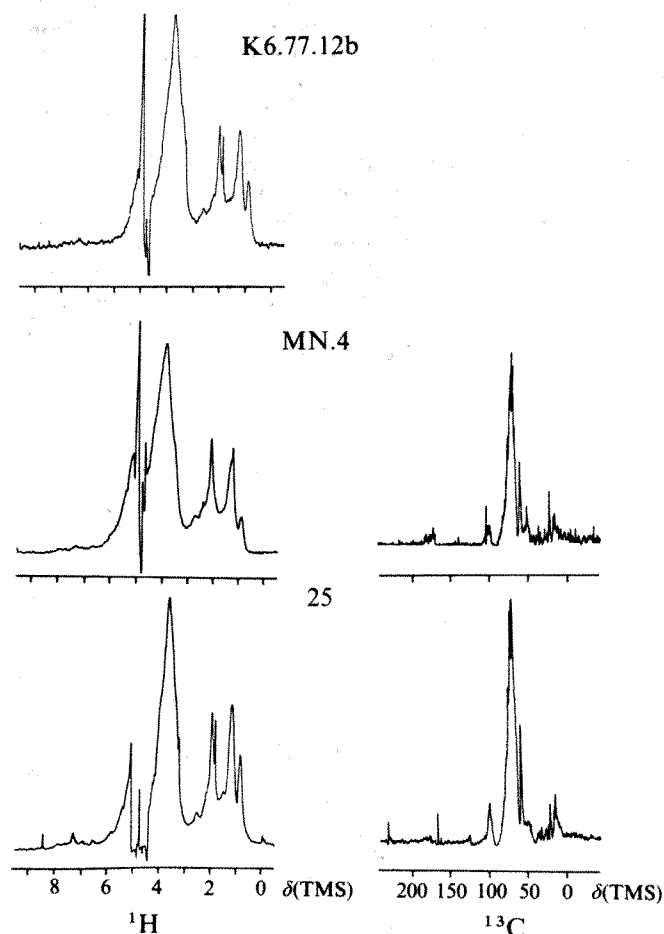
Fig. 1 The ¹H and ¹³C spectra of fulvic acids from Continental Shelf sediments of the New York Bight. In the ¹H spectra the OH protons were decoupled. The ¹³C spectra are spectra of approximately 10,000 transients. Chemical shifts are in p.p.m. downfield of tetramethylsilane (TMS).

acids isolated from a few samples of marine sediments. Carbohydrate analyses were also performed in an attempt to establish the polysaccharide contents of these fulvic acids.

Bottom sediments were collected from locations off the Continental Shelf of the New York Bight by a Shipek grab sampler. Samples 25 (a medium-grained sand) and MN-4 (a silty sediment) were collected ~25 nautical miles from the New York Harbor. Two other samples were collected further offshore in the New York Bight; sample K6-77-12b is a sand that was located near the shelf break, and HuG'R' is an olive-grey mud from a 270-m water depth in the Hudson Canyon.

Fulvic acids were extracted from sediments by the usual procedure[2] (0.5 M NaOH under N_2 overnight at room temperature). They were separated from humic acids by acidification on Dowex 50W X 8 (H^+)[20]. The raw isolates were dialysed by ultrafiltration through an Amicon PM 10 membrane. Retentates were then lyophilized and redissolved in 4 ml of 0.5 M NaOD in D_2O. Pulsed Fourier transform ^1H and ^{13}C spectra were obtained with a Varianf XL 100 FT NMR spectrometer operating at 100 and 25.2 MHz, respectively. ^1H spectra were obtained on a 90° pulse with 2-s acquisition times and no delay. The number of transients required for an adequate signal-to-noise ratio were generally more than 1,000. ^{13}C spectra were recorded following a 90° pulse and 0.4-s acquisition time with no delay. More than 10,000 transients were usually required on ~100 mg of sample for a good signal-to-noise ratio. Because of doubts about the quantitative nature of ^{13}C signals in solution spectra[20], we also examined a marine fulvic acid using solid-state ^{13}C NMR with the cross polarization and magic-angle sample spinning (CPMASS). In these conditions, VanderHart and Retcofsky[21] have indicated that ^{13}C NMR signals are quantitative.

IR spectra were recorded on samples (~1 mg) pelletized with KBr (~300 mg) by a Perkin-Elmer model 621 spectrophotometer. Total carbohydrate content of fulvic acids were analysed by the phenol–sulphuric acid method[22]. Total uronic acids were determined by the carbazole method[23].

For component sugar analyses, a fulvic acid was hydrolysed in 2 M H_2SO_4 at 100 °C for 2 h to release free sugars which were analysed as trimethylsilyl ethers by gas chromatography[24].

The ^1H and ^{13}C spectra for samples 25 and MN-4 are shown in Fig. 1. The organic matter in these two samples is believed to be relatively free of significant terrestrial input because the humic acids are essentially marine in origin[20], and hence their fulvic acids should be of a marine continental shelf or marine origin. Because of insufficient sample size, only a ^1H spectrum was obtained for fulvic acids of sample K6-77-12b. The CPMASS ^{13}C spectrum of fulvic acids from sample Hug'R' is shown in Fig. 2.

The complexity and broadness of the NMR peaks show that fulvic acids are complex macromolecular compounds. Several intense signals are observed in both ^1H and ^{13}C spectra: the most notable being the cluster of peaks between 3 and 4.2 p.p.m. in the ^1H spectra and 60–110 p.p.m. in the ^{13}C spectra. These peaks are, respectively, characteristic of protons β to, and carbons α to an oxygen atom and are identical to those peaks obtained from carbohydrates or polysaccharides[25]. In the ^{13}C spectra, the peak at 65 p.p.m. represents the resonance of the no. 6 carbon of hexoses. Ring carbon resonances centre at 72 p.p.m. where a strong band is observed. Anomeric carbons of polysaccharides yield a signal at ~105 p.p.m. where another major peak is discernible in the fulvic acid spectra.

In the solid-state ^{13}C spectrum (Fig. 2) a similar set of peaks to those in the solution ^{13}C spectra is observed indicating the domination of polysaccharides. By integration, polysaccharide carbon accounts for ~52% of the total carbon. As carbon signals obtained by this cross-polarization with magic-angle spinning technique are quantitative, this confirms that polysaccharides compose more than 50% of the organic matter of marine sedimentary fulvic acids.
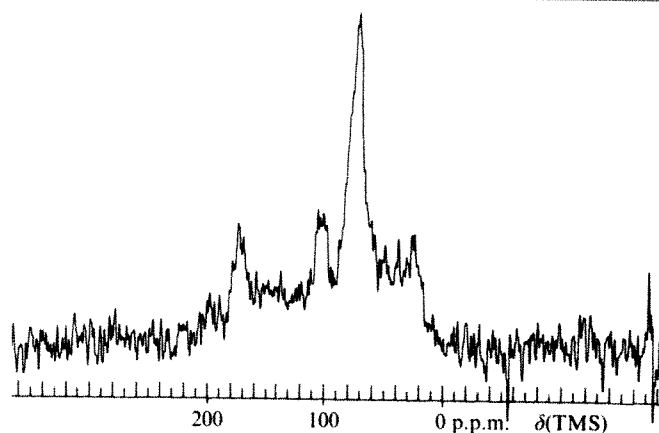
Fig. 2 The ^{13}C NMR spectrum of fulvic acids from marine sediment sample HuG'R'. The spectrum represents 71,000 scans accumulated by the CPMASS technique (contact time, 2 ms; sweep width, 10 kHz; 62 kHz proton decoupling; 1,024 data points on FID; 50 s dwell time; 4 s repetition).

Although other peaks are observed in the ^1H and ^{13}C spectra of fulvic acids, their contributions to the total signal in other p.p.m. regions are small. Unsubstituted aliphatic carbons and associated protons have resonance bands in the 0–50 p.p.m. and 0.6–1.5 p.p.m. regions, respectively. Methyl protons (0.9 p.p.m.) and carbons (15 p.p.m.) make significant contributions to the unsubstituted aliphatic bands. Methene protons and carbons account for peaks at 1.2 p.p.m. and 18–40 p.p.m. respectively. The relatively high proportion of methyl protons suggests that the unsubstituted aliphatic structures are of a highly branched nature.

Protons α to a carboxyl or amide functional group have chemical shifts in the 1.8–2.2 p.p.m. region. The peak at 2.0 p.p.m. indicates the presence of these protons. The presence of carboxyl or amide carbons is confirmed by the peak at ~175 p.p.m. in the ^{13}C spectra (Figs 1 and 2). Quantitatively, these carbons account for ~15% of all carbons as measured in the CPMASS ^{13}C spectrum (Fig. 2). Carboxyl groups in marine fulvic acids could be partly derived from uronic acid moieties associated with polysaccharides (polyuronic acids).

Although the NMR data are conclusive, IR spectroscopic and colorimetric tests have been used to confirm that polysaccharides containing uronic acids are dominant components of marine sedimentary fulvic acids. IR spectra of fulvic acids are shown in Fig. 3: these are not significantly different from published spectra of marine and terrestrial sedimentary fulvic acids[15]. An important band that may have been overlooked previously is the 1,050 cm^{-1} band of polysaccharides, which is a strong absorber in these and other spectra of fulvic acids. Even soil fulvic acids (Fig. 3c) have a sizeable band in this region suggesting the presence of polysaccharides. This 1,050 cm^{-1} band has, however, been variously interpreted: Whitby and Schnitzer[11] attributed Si–O stretching vibrations to this band, whereas Stevenson and Goh[15] identified this band as the C–O stretch of polysaccharides. This is not surprising because ash contents of fulvic acids are not easily lowered, and silica can be tenaciously associated with fulvic acids[26]. In fact, this may be a major reason why the high polysaccharide content of marine sedimentary fulvic acids has been overlooked.

A strong band is observed for carbonyl vibrations at 1,720 cm^{-1} in all IR spectra, which can be attributed to carboxyl groups in fulvic acids. This band may also be attributed to the carboxyl group of uronic acids. Hence, the IR data tend to confirm the presence of polyuronic acids.

Colorimetric tests were used to calculate the total carbohydrate and total uronic acid contents of these fulvic acids. The results are presented in Table 1. In all samples, carbohydrates compose a large fraction of the fulvic acids which could be expected on the basis of the NMR data, but

Table 1   Total carbohydrate analysis of fulvic acids

Sample	% Total carbohydrate*	% Total uronic acids†
HuG'R'	38	NA
Mn-4	47	17
25	57	20

*Calculated as glucose weight relative to moisture and ash-free weights of fulvic acids.

†Calculated as glucuronic acid weight relative to moisture and ash-free weights of fulvic acids.

NA, Not analysed.

we must consider that the colorimetric technique may be biased by incomplete hydrolysis and the presence of interfering substances. The total uronic acid contents of fulvic acids (Table 1), as determined by the colorimetric carbazole method, also indicate that uronic acid moieties compose a large fraction of the fulvic acids examined. This confirms that polyuronic acids are important components of marine fulvic acids.

Component sugar determinations were made for sample 25: glucose, galactose, arabinose, mannose, xylose and rhamnose appear as the major sugars resulting from hydrolysis of this fulvic acid. Although glucose and galactose are ubiquitous components of plant and sedimentary polysaccharides[27,28], rhamnose, mannose, ribose and arabinose, seem to be components of microbial polysaccharides[6,9].

Of the studies on the nature of marine sedimentary fulvic acids, few have unambiguously identified the major structural components. Ishiwatari[13] observed that polysaccharides composed a large fraction of sedimentary fulvic acids. Steelink[29], and Rashid and King[10], suggested that polysaccharides or polyuronic acids could be isolated from sediments as fulvic acids or humic acids. Ernst[30] isolated uronic acids from fulvic acids in sediments of the North Sea. The present evidence indicates that polysaccharides containing uronic acid moieties are, by far, the most abundant components of the marine sedimentary fulvic acids examined. The solubility of polysaccharides and polyuronides in weak acidic and basic solutions has long been known[31] and hence, in most sedimentary environments containing plant and microbial residues, these polysaccharides will be extracted. In soils where large quantities of dark aromatic humic substances are also extracted as fulvic acids, polysaccharides will probably be present in small amounts. In marine sediments, where dark aromatic substances may not be present in large amounts, polysaccharides can be the dominant components of fulvic acids, as is observed in this study. Therefore, we suggest that
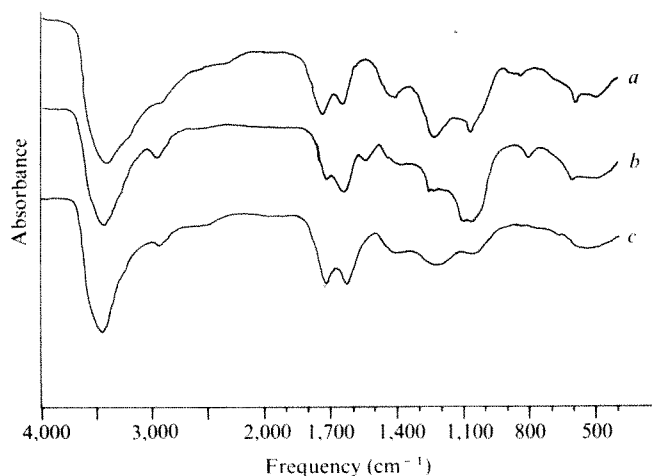
polysaccharides are always extracted from sediments in low yields and that the low concentrations of dark aromatic substances determines their predominance in the fulvic acid extract.

Marine sedimentary fulvic acids are thought to be precursors of marine humic acids and kerogen[3,32,33]. Hatcher et al.[20] have shown by ^{1}H and ^{13}C NMR that marine sedimentary humic acids from these same samples are composed predominantly of highly branched unsubstituted aliphatic structures. Polysaccharides in marine fulvic acids would have to undergo substantial transformations to produce structures such as those found in humic acids. Although these transformations may occur, it is more likely that if fulvic acids do condense to form humic acids, polysaccharides are probably eliminated by hydrolysis and decomposition, and the minor components of fulvic acids (those observed as minor peaks in the NMR spectra) enter into this condensation process. The aliphatic and aromatic components may play an increasingly important part in this process as polysaccharides disappear.

The decreasing ratio of fulvic acids to humic acids in sediment cores from both Continental Shelf and deep-sea sediments has been attributed to the condensation of humic acids from fulvic acids[32], and the ratio has been used to estimate the diagenetic maturity of humic substances in sediments. The same data sets can be explained if the fulvic acids had contained significant quantities of polysaccharides in their early depositional states and if these polysaccharides were eventually destroyed or hydrolysed. Therefore, no condensation mechanisms are needed to explain this change in ratio. Obviously, the diagenetic pathway proposed by Welte[3] needs further study, and we suggest NMR as a means by which the diagenetic changes of fulvic acids and humic acids might be examined in sediment cores.

1. Oden, S. *Kolloidechem. Beihefte* **11**, 75 (1919).
2. Schnitzer, M. & Khan, S. U. *Humic Substances in the Environment* (Marcel-Dekker, New York, 1972).
3. Welte, D. in *Advances in Organic Geochemistry* (eds Tissot, B. & Bienner, F.) (Editions Technip, Paris, 1973).
4. Ogner, G. & Schnitzer, M. *Can. J. Chem.* **49**, 1053–1063 (1971).
5. Neyroud, J. A. & Schnitzer, M. *Can. J. Chem.* **52**, 4123–4132 (1974).
6. Swincer, G. D., Oades, J. M. & Greenland, D. J. *Aust. J. Soil Res.* **6**, 225–235 (1968).
7. Martin, J. P. *Soil Biol. Biochem.* **3**, 33–41 (1971).
8. Sequi, P., Guidi, G. & Petruzzelli, G. *Can. J. Soil Sci.* **55**, 439–445 (1975).
9. Swincer, G. D., Oades, J. M. & Greenland, D. J. *Aust. J. Soil Sci.* **6**, 211–224 (1968).
10. Rashid, M. A. & King, L. H. *Geochim. cosmochim Acta* **34**, 193–201 (1970).
11. Whitby, L. M. & Schnitzer, M. *Can. J. Soil Sci.* **58**, 167–178 (1978).
12. Stuermer, D. H. & Payne, J. R. *Geochim. cosmochim. Acta* **40**, 1109–1114 (1976).
13. Ishiwatari, R. in *Proc. int. Meet. Humic Substances*, Nienrsluis (1972).
14. Schnitzer, M. *Can. Spectrosc.* **10**, 121–127 (1965).
15. Stevenson, F. J. & Goh, K. M. *Geochim. cosmochim. Acta* **35**, 471–483 (1971).
16. Vila, F. J. G., Lentz, H. & Ludemann, H. D. *Biochem. biophys. Res. Commun.* **72**, 1063–1069 (1976).
17. Lentz, H., Ludemann, H. D. & Zeichmann, W. *Geoderma* **18**, 325–328 (1977).
18. Sposito, G., Schaumberg, G. D., Perkins, T. G. & Holtzclaw, K. M. *Envir. Sci. Technol.* **12**, 931–934 (1978).
19. Wilson, M. A., Jones, A. J. & Williamson, B. *Nature* **276**, 487–489 (1978).
20. Hatcher, P. G., Rowan, R. & Mattingly, M. A. *Org. Geochem.* **2**, 77–85 (1980).
21. VanderHart, D. L. & Retcofsky, H. L. *Proc. Coal Chem. Symp.* (Stanford Research Institute, 1976).
22. Gerchakov, S. M. & Hatcher, P. G. *Limnol. Oceanogr.* **17**, 938–943 (1972).
23. Stark, S. M. Jr *Analyt. Chem.* **22**, 1158–1160 (1950).
24. Sweeley, C. C., Bentley, R., Makita, M. & Wells, W. W. *J. Am. chem. Soc.* **85**, 2497–2507 (1963).
25. Voelter, W. & Breitmaier, E. *Org. Magn. Reson.* **5**, 311–319 (1973).
26. Schnitzer, M. & Kodama, H. *Proc. Soil Sci. Soc. Am.* **31**, 632–636 (1967).
27. Vallentyne, J. R. in *Organic Geochemistry* (ed. Breger, I. A.) (Pergamon, London, 1963).
28. Prashnowsky, A., Degens, E. T., Emery, K. O. & Pimenta, J. N. *Jb. Geol. paläont. Mh.* **8**, 400–413 (1961).
29. Steelink, C. *J. chem. Educ.* **40**, 379–384 (1963).
30. Ernst, W. *Veröff. Inst. Meeresforsch., Bremerh.* **10**, 81–92 (1966).
31. Wise, L. E. & Jahn, E. C. *Wood Chemistry* (Reinhold, New York, 1952).
32. Huc, A. Y. & Durand, B. in *Advances in Organic Geochemistry* (eds Tissot, B. & Bienner, F.) (Editions Technip, Paris, 1973).
33. Nissenbaum, A., Baedecker, M. J. & Kaplan, I. R. in *Advances in Organic Geochemistry* (eds V. Gaerther, H. R. & Wehner, H.) (Pergamon, Oxford, 1972).

Fig. 3   IR spectra of fulvic acids from marine sediments sample K6-77-12b(*a*) and sample HuG'R'(*b*) and from a podzol soil in Prince Edward Island (*c*).

Metamorphism in the Troodos ophiolite: implications for marine magnetic anomalies

Suzanne Beske-Diehl* & Subir K. Banerjee

Geology and Geophysics Department, University of Minnesota, Minneapolis, Minnesota 55455

The magnetic mineralogy and Koenigsberger ratio (the ratio of the remanent to induced magnetization) of basaltic rocks from the Troodos ophiolite undergo critical transformations at the zeolite–greenschist facies boundary. At this boundary the magnetic mineralogy changes abruptly from titanomaghaemite to magnetite and the Koenigsberger ratio decreases to less than 1. If similar metamorphism is occurring near the active oceanic ridges today, then the application of the two-layer model to marine magnetic anomalies may be primarily due to the degree of metamorphism and not to the mode of emplacement, intrusive versus extrusive. We show here that apparently in the Troodos ophiolite and, therefore, probably in oceanic rocks formed at spreading centres, the presence of magnetite at depth is a function of the pressure and temperature regime seen at the spreading centre.

Despite extensive efforts, deep-sea drilling has not yet reached beyond 580 m into the oceanic crust (basement). Thus scientists have had to study ophiolites, thought to be fragments of subaerially exposed oceanic crust[1–4], to obtain data for working models of the basic physical properties, origin and subsequent alteration of the oceanic crust. Research at the University of Minnesota palaeomagnetics laboratory has concentrated on defining the magnetic properties of ophiolites to establish boundary conditions for deeper sources of sea-floor magnetic anomalies. However, recent data also indicate that magnetic parameters can be sensitive indicators of chemical and thermal alteration[5,6].

The Troodos ophiolite was generally considered a fragment of Cretaceous (85 Myr) oceanic lithosphere formed at a spreading centre[2,3,7,8], until Miyashiro[9] suggested that the major element chemistry was more compatible with its origin as a young island arc. The ensuing discussion emphasized that no single piece of evidence can unequivocally establish the origin of an ophiolite. Subsequent evaluation of the geological evidence combined with numerous isotopic, rare earth, major and minor element analyses suggests that the Troodos ophiolite formed within a small marginal ocean basin[10,11].

The basaltic rocks in Troodos have been divided into the Upper Pillow Lavas, thought to be an off-axis sequence of alkalic extrusives, and the Axis Sequence of saturated pillow lavas and sheeted dykes[10]. The ophiolite has undergone metamorphism from zeolite to amphibolite facies with the deeper lithologies showing the higher grade metamorphism. The transition between zeolite and greenschist facies fluctuates near the depth where the pillow lavas between dykes become scarce. This facies transition is entirely endependent of the intrusive–extrusive ratio[8]. Strontium and oxygen isotope analyses indicate that this alteration involved large amounts of oceanic water and was probably produced at an oceanic ridge[12,13].

Vine and Matthews[3] measured susceptibility and natural remanent magnetization of the Troodos ophiolite lithologies; their magnetic data were categorized according to lithology.

The dykes were found to have a much lower ratio of induced to remanent magnetization (Koenigsberger ratio) than the pillow lavas and, therefore, were considered poorer contributors to magnetic anomalies. However, in the pillow lavas from the Macquarie Island ophiolite, the Koenigsberger ratio was seen to vary closely with metamorphic facies[14]. There the unmetamorphosed pillows exhibited high Koenigsberger ratios which contrasted with the low ratios of the greenschist facies pillows. More importantly, magnetite was discovered in the greenschist facies, while the unmetamorphosed pillows contained titanomaghaemite similar to that in oceanic pillows. These results generated speculation that magnetite may be found at depth in the basaltic rocks of the oceanic lithosphere. Our study of the Troodos ophiolite further defines the magnetic changes involved in differing basaltic lithologies and metamorphic facies, and also indicates that the greatest magnetic contrast is not between basaltic lithologies as originally suggested by Vine and Matthews[3] but that it occurs between zeolite and greenschist metamorphic facies rocks.
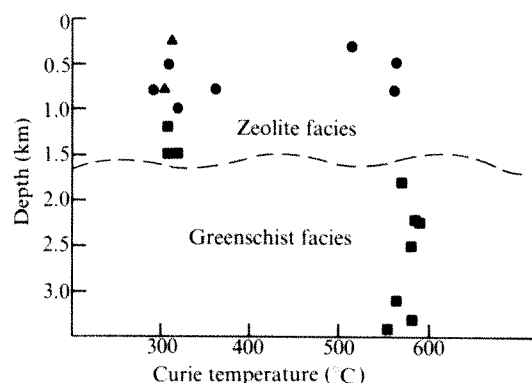
Fig. 1 The relationship between the Curie temperature of basalt samples and depth below the top of the Troodos ophiolite. The Curie temperatures near 300 °C in the zeolite facies rocks represent the onset of unmixing before the actual Curie point (probably between 350 and 450 °C) was reached.

Preliminary thermomagnetic curves of Troodos ophiolite samples from the top portion of the basaltic layer were irreversible, similar to those from oceanic pillows that have undergone low temperature oxidation[15,16]. The titanomaghaemite in these rocks had not inverted to magnetite and an associated titanium-rich mineral and, therefore, had not undergone heating greater than 200–250 °C (refs 17, 18). Thermomagnetic curves from deeper lithologies indicated the presence of magnetite. To obtain more precise information of the location and character of these magnetic changes, further samples were obtained from J. Smewing and were carefully selected to represent increasing depths into the ophiolite. Remanent intensity and susceptibility were measured, and the Koenigsberger ratio calculated. Thermomagnetic analyses were performed on representative samples. Additional magnetic properties such as the behaviour of the natural, anhysteretic and viscous remanences during alternating field demagnetization were obtained and are reported elsewhere[15,16]. Here we describe the drastic changes in magnetic mineralogy and decrease in Koenigsberger ratio observed in the basaltic rocks at the zeolite–greenschist facies boundary.

Figure 1 shows the sharp contrast between the character of the thermomagnetic curves above and below the zeolite–greenschist facies boundary. In the zeolite facies pillow basalts,

sills and dykes, most of the saturation magnetization versus temperature curves were irreversible, whereas below the metamorphic boundary all were reversible with Curie points between 560 and 580 °C. However, note that the points plotted (Fig. 1) as 'Curie temperatures' near 300 °C in the zeolite facies rocks actually refer to temperatures at which unmixing occurred. More realistic Curie temperature estimates are probably between 350 and 450 °C. The thermomagnetic behaviour of samples from the zeolite facies rocks suggest titanomaghaemite whereas those in the greenschist facies are typical of low titanium magnetite.

To substantiate these conclusions, precise X-ray diffraction patterns were obtained for two dyke samples on either side of the metamorphic facies boundary. The magnetic separate from dyke rock above the boundary gave a cell edge of 8.418 ± 0.002 Å similar to highly oxidized titanomagnetite. Electron microprobe analyses also indicated an ülvospinel content of 51% ($\chi = 0.51$). High titanium phases were not found. In contrast, the sample from below the boundary had a cell edge of 8.397 ± 0.003 Å similar to that of magnetite. Thus, the X-ray and electron microprobe analyses verify the thermomagnetic studies.

The presence or absence of characteristic metamorphic minerals in each facies places the zeolite–greenschist boundary at about 200 °C (ref. 8). This temperature is sufficient to cause the inversion of titanomaghaemite to magnetite. If metamorphism is occurring near the present oceanic ridges, then magnetite is present at or near the depth of greenschist facies metamorphism. Thus no additional heating is required during obduction to produce the magnetite in these rocks.
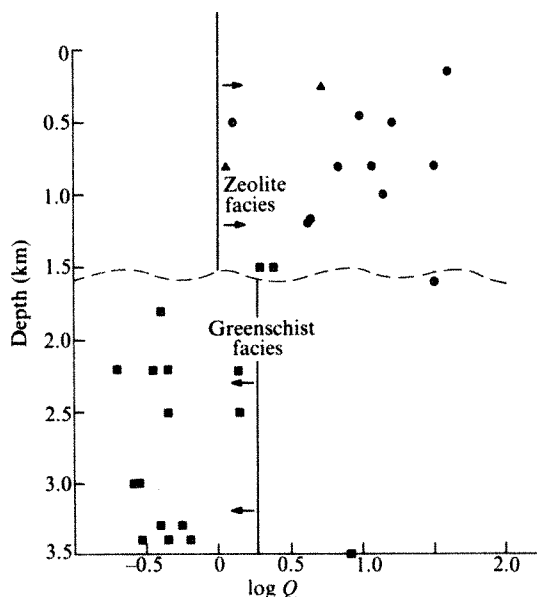
Fig. 2 Semi-log plot showing the relationship between the Koenigsberger ratio (Q) and the depth below the top of the Troodos ophiolite.

Figure 2 shows the marked change of Koenigsberger ratio at the zeolite–greenschist facies boundary. The dykes and pillows of zeolite facies all display Koenigsberger ratios greater than 1, whereas most of the greenschist facies rocks exhibit values less than 1. Among the exceptions to the latter observation is a greenschist pillow which shows an exceptionally high ratio of 31.6. The thermomagnetic curve indicates the presence of maghaemite which may be of post-obduction origin[5]. Therefore, the high Koenigsberger ratio and

thermomagnetic curve of this sample are not considered as characteristic of greenschist facies oceanic crust. The decrease of the Koenigsberger ratio generally reflects the behaviour of the remanent intensity near the zeolite–greeschist metamorphic boundary, whereas the susceptibility remains relatively constant. In addition, the stability, defined by the alternating field at which half of the remanent magnetization is destroyed, showed little variation. However, the greenschist facies basalts did acquire a large amount of viscous remanence, as did these same rocks from the Smartville and Othris ophiolites[5,6,15]

Figure 2 indicates that the magnetic signature of the Troodos basalts depends greatly on the extent of metamorphism. Although the Koenigsberger ratio also seems to be slightly affected by the mode of emplacement, that is, pillow versus sheeted dykes, the change of values is not as distinct as that seen at the metamorphic facies boundary. More compelling is the sudden change in magnetic mineralogy at this same facies boundary, suggesting that it may influence the Koenigsberger ratio.

The importance of the zeolite–greenschist metamorphic boundary indicated by the magnetic data from Troodos suggests that grouping magnetic data according to basaltic lithology as is currently practised[3], may be inappropriate in many cases and may mask important trends. More importantly, the boundary between the zeolite and greenschist metamorphic facies should be of primary consideration when modelling marine magnetic anomalies. The actual amount which the greenschist facies basalts contribute to the magnetic anomaly pattern may not be insignificant but would depend on their thickness relative to the zeolite basalts.

The remarkable transition in magnetic properties from the zeolite to greenschist facies rocks is paralleled by a substantial increase of 1.7 km s^{-1} in seismic velocities measured at the outcrop[19]. This increase is attributed to an increase in rigidity caused by the presence of quartz in the greenschist facies rocks[8]. However, the direct application of these seismic results to the oceanic crust is hindered by the velocity changes caused by the subaerial exposure of the Troodos ophiolites, the accompanying release of hydrostatic pressure, and the onset of weathering. Thus, velocities measured in the laboratory under hydrostatic pressures are as much as 1.0 km s^{-1} faster, but the great difference in velocities between the metamorphic facies still seem to be present[20]. Multiple layers in oceanic layer 2 are now detectable by sonobuoy techniques. If this seismic method should succeed in detecting metamorphic boundaries, then this data, plus the Troodos results regarding magnetic contrasts across this boundary, would offer important constraints for magnetic anomaly modelling of the ocean floor.

1. Hess, H. H. *A Study of Serpentinite* (ed. Burke, C. A.) 169 (National Academy of Science, National Research Council Publ. 1188, 1964).
2. Moores, E. M. & Vine, F. J. *Phil. Trans. R. Soc.* A**268**, 443 (1971).
3. Vine, F. J. & Moores, E. M. *Geol. Soc. Am. Mem.* **132**, 195 (1972).
4. Dewey, J. F. & Bird, J. M. *J. geophys. Res.* **76**, 3179 (1971).
5. Beske-Diehl, S. J. & Banerjee, S. K. *Earth planet. Sci. Lett.* **44**, 451 (1979).
6. Banerjee, S. K. *J. geophys. Res.* (in the press).
7. Gass, I. G. & Masson-Smith, D. *Phil. Trans. R. Soc.* A**255**, 417 (1963).
8. Gass, I. G. & Smewing, J. S. *Nature* **242**, 26 (1973).
9. Miyashiro, A. *Earth planet. Sci. Lett.* **19**, 218 (1973).
10. Smewing, J. D., Simonian, K. O. & Gass, I. G. *Contr. Miner. Petrol.* **51**, 49 (1975).
11. Kay, R. & Senechal, R. G. *J. geophys. Res.* **81**, 964 (1976).
12. Spooner, E. T. C. & Fyfe, W. S. *Contr. Miner. Petrol.* **42**, 287 (1973).
13. Spooner, E. T. C., Beckinsale, R. D., Fife, W. S. & Smewing, J. D. *Contr. Miner. Petrol.* **47**, 41 (1974).
14. Butler, R. F., Banerjee, S. K. & Stout, J. H. *Geophys. J.* **47**, 179 (1976).
15. Levi, S. & Banerjee, S. K. *J. Geomagn. Geoelectr.* **29**, 421 (1977).
16. Levi, S., Banerjee, S. K., Beske-Diehl, S. & Moskowitz, B. *Geophys. Res. Lett.* **5**, 473 (1978).
17. O'Reilly, W. & Readman, P. W. *Z. Geophys.* **34**, 321 (1971).
18. Johnson, H. P. & Merrill, R. T. *J. geophys. Res.* **78**, 4938 (1973).
19. Lort, J. M. & Matthews, D. H. *Geophys. J.* **27**, 383 (1972).
20. Poster, C. K. *Nature phys. Sci.* **243**, 2 (1973).
21. Blakely, R. J. *Geophys. Monogr.* **19**, 227 (1976).

Antlers, body size and breeding group size in the Cervidae

T. H. Clutton-Brock & S. D. Albon

King's College Research Centre, King's College, Cambridge CB2 1ST, UK

Paul H. Harvey

Museum of Comparative Zoology, Harvard University and School of Biological Sciences, University of Sussex, Brighton, UK

The tendency for large deer species to have relatively big antlers for their body size has been explained as the result of an inevitable evolutionary trend leading to increased antler size[1-4], of linkage between genetic factors influencing body size and relative antler size[5], of the increased need for larger deer to lose heat[6] and of an increased reliance of larger deer species on displays to avoid fighting[7]. Here we test an alternative hypothesis: that large deer species tend to be more polygynous than smaller ones and that intense inter-male competition in large species has led to the development of relatively large antlers. Analysis of comparative data[8-42] confirms two predictions based on this hypothesis: (1) that large deer species form bigger breeding groups than small ones; and (2) that deer which form large breeding groups have relatively larger antlers for their body size than those that form smaller ones. However, antler size is not proportional to body size among species that form breeding groups of similar size, indicating that other factors must also be involved.

The distribution of antler size across deer species poses a problem to evolutionary explanation. Small deer species, such as muntjac or brocket, have small antlers relative to their body size while larger species, like red deer or reindeer, have relatively large ones[5,7]. In the early part of this century, the large antlers of the deer was usually explained as the result of a directional evolutionary trend[1-4]. Huxley[5] contested this view, arguing that the trend occurred because the genetic factors responsible for large body size were linked to those responsible for relatively large antler size and that selection for increased body size automatically increased the relative size of antlers. More recently, two functional explanations have been suggested. First, Gould[7] has argued that large deer species seldom fight—settling disputes instead by antler displays—and that this has caused selection to favour large antlers. However, the available information indicates that fights between competing males are not uncommon[43,44] and there is no firm evidence that individuals assess their opponents by the size of their antlers or that individual differences in antler size are closely related to fighting ability or dominance when differences in age and body size are taken into account: none of the studies relating antler size to dominance or fighting ability[45-47] have controlled adequately for the effects of age and body size, which are commonly correlated with social rank[43,48]. Moreover, as stags rarely fight outside the rut, and during the rut their fighting ability declines as their body condition deteriorates[43], it would be an inefficient assessor that judged its opponent principally on traits that were insensitive to short-term changes in condition[49].

Second, Stonehouse[6] has argued that large deer may have relatively large antlers for thermoregulatory reasons: during their period of growth, antlers may assist heat loss and larger species may have developed relatively large antlers on account of their reduced surface to volume ratios. But this explanation is unsatisfactory because of the obvious integration of antler growth with the sexual cycle[50,51], the lack of a close

Table 1 Measures of mean shoulder height and mean record antler length used in the analysis

Cervidae		Shoulder height (cm)	Antler length (cm)	Breeding group size	Refs
Muntiacinae					
Muntiacus muntjak	Indian muntjac	56.7	17.6	A	10
M. reevesi	Reeve's muntjac	44.5	8.9	A	11
Cervinae					
Dama dama	Fallow	91.0	72.9	C	12
Axis axis	Chital, Spotted	93.5	93.0	C	13
A. porcinus	Hog	68.6	49.2	C	13,14
A. kuhlii	Bawean, Kuhl's	68.6	24.8	A	15
Cervus duvauceli	Swamp	120.0	95.2	C	13,16
C. elaphus	Red	121.9	93.6	C	17,18
C. canadensis	Wapiti	160.0	147.4	C	19,20,21,40
C. eldi	Eld's, Thamin	124.4	94.3	C	22,23
C. nippon	Sika	80.9	56.7	C	24,25
C. unicolor	Sambar	150.7	109.8	B	14
Elaphurus davidianus	Père David's	116.8	73.7	C	26
Odocoileinae					
Odocoileus hemionus	Mule, Black-tailed	101.2	71.0	B	27,28
O. virginianus	White-tailed	98.2	65.6	B	29,41
Capreolus capreolus	Roe	69.4	28.3	B	30,31,42
Alces alces	Moose	205.7	108.0	B	32,33,34
Rangifer tarandus	Reindeer, Caribou	120.0	117.2	C	35,36
Hippocamelus bisulcus	Huemul, Guemal	96.9	24.8	B	37
H. antisensis	Huemul, Guemal	86.4	26.4	C	38
Mazama americana	Red brocket	69.8	11.5	A	9
M. gouazoubira	Brown brocket	56.0	11.5	A	9
M. rufina	Little red brocket	43.6	9.4	A	9
Pudu pudu	Pudu	35.5	7.5	A	39

Species were classified into three groups on breeding group size: A ≤ 2; B, 3–5; C ≥ 6 animals. Refs 8 and 9 were also used for each species.

association between seasonal variation in temperature and the period for which the antler is in velvet, and because of the tendency for species with sub-arctic ranges to have the largest antlers[44,46,52].

This paper tests a third functional explanation of the relationship between body size and relative antler size: that inter-male competition is more intense among large deer species than among small ones because large deer tend to form bigger breeding groups[53], and that sexual selection has consequently favoured the greater development of fighting apparatus in larger species. This argument rests on three assumptions: that antlers are regularly used in fighting; that gross increases in antler size improve their effectiveness in defence or attack; and that the size of breeding groups is related to the intensity of inter-male competition. There is now much evidence that fights between breeding males are common in polygynous deer species and that antlers are important in these fights, enabling animals to grip their opponents during pushing contests and protecting their heads and shoulders[43,44]. Studies of fighting tactics indicate that the large, complex antlers of the bigger deer species probably form a safer guard against injury than the smaller and simpler ones typical of smaller species[54,55]. Evidence from other groups of vertebrates suggests that inter-male competition increases with the size of breeding groups[56,57] and that male weaponry and other characteristics which improve combative ability (including increased body size) are more developed where inter-male competition is strong[57,58].

If this explanation accounts for the interspecific allometry in antler size among deer, two predictions should be fulfilled: (1) larger deer species should form bigger breeding groups than smaller ones and relative antler size should consequently be greatest among species forming large breeding groups; and
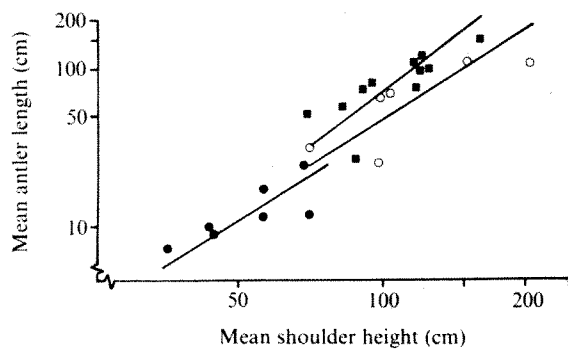
Fig. 1 Mean (record) antler length plotted on mean shoulder height for different deer species (see Table 1). ●, group A; ○, group B; ■, group C. Lines show major axes (see text).

(2) among species forming breeding groups of similar size, antler size should be directly proportional to body size.

To test these predictions, data on body size, antler size and breeding group size, were taken from the literature (Table 1). Our measure of body size was mean shoulder height and, of antler size, the mean length from coronet to top point of all heads, for which measurements are provided by Ward[8]. The latter measure had two important disadvantages: although gross differences in antler length among cervids reflect variation in antler volume and complexity, some genera (for example *Alces*) have antlers that are relatively short for their volume; and there is a danger that the use of estimates of average shoulder height and record antler lengths will increase the slope of antler size on body size (though previous analyses indicate that this effect is probably unimportant[7]). Species were allocated to three categories according to the reported size of groups during the breeding season: A, group size ≤ 2; B, group size 3–5; C, group size ≥ 6.

Group sizes used to categorize species included both males and females. However, sex ratios in breeding groups are typically female-biased and, in the sample of species for which estimates of the average number of females in breeding groups were available, this measure correlated well with total group size ($r_s = 0.991$, $n = 7$, $P < 0.001$). The three categories we have used disguise many differences in behaviour between species, but the available information on breeding systems of cervids does not permit finer classification. To investigate relationships between antler length and shoulder height in different groups, we used major axis analysis[59] on the logarithmically transformed data. To compare relationships between groups, we used the maximum likelihood method for testing heterogeneity of slopes[60].

Within all three groups, as well as across the sample as a whole, there is a close relationship between antler length and shoulder height (see Table 2). The analysis confirms that, as our hypothesis predicts, breeding group size is positively correlated with shoulder height ($r = 0.433$, $t = 2.15$, d.f. = 22, $P < 0.05$). As no heterogeneity of slopes was revealed by the maximum likelihood analysis ($\chi_2^2 = 0.201$) we have imposed the common slope (2.082) through the mean for both variables and sought differences in weighting on the minor axis (a process analogous to testing for differences in elevation using

regression analysis). Significant differences exist between groups A and C ($t = 2.140$, d.f. = 16, $P < 0.05$) and B and C ($t = 2.200$, d.f. = 15, $P < 0.05$), but not between groups A and B ($t = 0.304$, d.f. = 11, not significant). As predicted, antler size is larger in group C than in groups A or B and within-group slopes tend to be shallower than the overall slope (see Table 2).

Contrary to prediction, the allometric relationship between shoulder height and antler length remains within all three groups (Table 2). This may be because of the coarseness of our categorization of breeding systems, but it seems more likely that other factors are involved. However, before we need have recourse to non-adaptive explanations, there are three functional hypotheses which should be considered: (1) Larger deer can deal heavier blows than smaller ones, their attacks are likely to be more damaging and males may consequently be selected to develop a more effective guard[55]. (2) If larger deer species have longer lifespans than small ones[61], males may engage in a greater number of fights during their lifetimes and may have a higher overall risk of being injured. For this reason, they may invest in larger and more effective antlers. (3) Larger species tend to occur in northern countries where the energetic costs of antler production may be reduced by seasonal superabundance of food supplies[62,63].

We thank Professor J. Felsenstein, Dr G. Mace, J. Seger, B. Smuts, Professor V. Geist, Dr C. Packer, Professor R. V. Short and Professor S. J. Gould for advice, criticism or assistance with techniques of analysis. The research is supported by King's College Research Centre, Cambridge.

1. Johnston, H. *British Mammals* (Hutchinson, London, 1903).
2. Reynolds, S. H. *The Giant Deer: a Monograph of the British Pleistocene Mammalia* Vol. 3, part 3 (Palaeontographical Society, London, 1929).
3. Lull, R. S. *Organic Evolution* (Macmillan, New York, 1924).
4. Common, R. H. *Irish Nat. J.* **4**, 187–188 (1933).
5. Huxley, J. S. *Problems of Relative Growth* (MacVeagh, London, 1932).
6. Stonehouse, B. *Nature* **218**, 870–872 (1968).
7. Gould, S. J. *Evolution* **28**, 191–220 (1974).
8. Ward, D. *Records of Big Game* 9th edn (Roland Ward, London, 1969).
9. Whitehead, G. H. *Deer of the World* (Constable, London, 1972).
10. Barette, C. *Mammalia* **41**, 1–29 (1977).
11. McCullough, D. R. *Status of Larger Mammals in Taiwan* (Tourism Bureau, Taipai, Taiwan, 1974).
12. Chapman, D. & Chapman, N. *Fallow Deer: their History, Distribution and Biology* (Dalton, Lavenham, 1975).
13. Schaller, G. B. *The Deer and the Tiger* (University of Chicago Press, 1967).
14. Boonsong, L. & McNeely, D. *Mammals of Thailand* (Association Conservation of Wildlife, Bangkok, 1977).
15. Blouch, R. A. & Atmosoedirdjo, S. in *Threatened Deer*, 129–142 (Int. Un. Conserv. Nat., Morges, 1978).
16. Panwar, H. S. in *Threatened Deer*, 143–158 (Int. Un. Conserv. Nat., Morges, 1978).
17. Darling, F. F. *A Herd of Red Deer* (Oxford University Press, London, 1937).
18. Gibson, R. M. & Guinness, F. E. *Anim. Behav.* (in the press).
19. de Vos, A., Brokx, P. & Geist, V. *Am. Midl. Nat. Monogr.* **77**, 390–417 (1967).
20. Struhsaker, T. T. *Z. Tierpsychol.* **24**, 80–114 (1967).
21. McCullough, D. R. *The Tule Elk: its History, Behavior and Ecology* (University of California Press, Berkeley, 1969).
22. Sinh, Ranjit *J. Bombay nat. Hist. Soc.* **72**, 243–255 (1975).
23. Long-hui, H. & Chan-ho, L. *Zool. Mag.* **3**, 39–40 (1974).
24. Horwood, M. T. & Masters, E. H. *Sika Deer* (British Deer Soc. Publ. No. 3, Broadwater Press, Welwyn Garden City, 1970).
25. Lowe, V. P. W. in *The Handbook of British Mammals* 2nd edn (eds Corbet, G. B. & Southern, H. N.) 423–428 (Blackwell, Oxford, 1977).
26. Schaller, G. B. & Harmer, A. *Zool. Gart., N.F.* **48**, 1–15 (1978).
27. Dasmann, R. F. & Taber, R. D. *J. Mammal.* **37**, 143–164 (1956).
28. Cowan, I. McT. in *The Deer of North America* (ed. Taylor, W. P.) (Stackpole, Harrisburg, 1956).
29. Hirth, D. H. *Wildl. Monogr.* **53**, 1–55 (1977).
30. Prior, R. *The Roe Deer of Cranborne Chase: An Ecological Survey* (Oxford University Press, London, 1968).
31. Bramley, P. S. *J. Reprod. Fert.* Suppl. **11**, 43–70 (1970).
32. Peterson, R. L. *North American Moose* (University of Toronto Press, Toronto, 1955).
33. Geist, V. *Behaviour* **20**, 378–416 (1963).
34. Houston, D. B. in *The Behaviour of Ungulates and its Relation to Management* (eds Geist, V. & Walther, F.) (Int. Un. Conserv. Nat., Morges, 1974).
35. Henshaw, J. *Anim. Behav.* **18**, 256–258 (1970).
36. Bergerud, A. T. in *The Behaviour of Ungulates and its Relation to Management* (eds Geist, V. & Walther, F.) (Int. Un. Conserv. Nat., Morges, 1974).
37. Povilitis, A. in *Threatened Deer*, 109–128 (Int. Un. Conserv. Nat., Morges, 1978).
38. Roe, N. A. & Rees, W. E. *J. Mammal.* **57**, 722–730 (1976).
39. Rose, N. A. *Red Data Book* Mimeograph Report (Int. Un. Conserv. Nat., Red Data Book, Cambridge, 1975).
40. Flook, D. R. *Can. Wildl. Serv. Rep. Ser.* No. 11 (1970).
41. Wood, A. J., Cowan, I. McT. & Nordan, H. C. *Can. J. Zool.* **40**, 593–603 (1962).
42. Andersen, J. *Dan. Rev. Game Biol.* **2**, 127–155 (1975).

Table 2 Analysis of relationships between $\log_e$ (antler length) and $\log_e$ (shoulder height) in cervids (see Table 1).

Group	A	B	C	Overall
Sample size	7	6	11	24
Correlation between $\log_e$ (antler length) and $\log_e$ (shoulder height)	0.776	0.805	0.769	0.903
b (slope)	1.907	1.888	2.265	2.356

567

43. Clutton-Brock, T. H., Albon, S. D., Gibson, R. M. & Guinness, F. E. *Anim. Behav.* **27**, 211–225 (1979).
44. Geist, V. *Mountain Sheep* (University of Chicago Press, 1971).
45. Topinski, P. *Acta theriologica* **19**, 509–511 (1974).
46. Henshaw, J. *Nature* **224**, 1036–1037 (1969).
47. Bubenik, A. B. *Deer* **8**, 208–214 (1968).
48. Suttie, J. M. *J. Zool.* **190**, 217–224 (1980).
49. Clutton-Brock, T. H. & Albon, S. D. *Behaviour* **69**, 145–170 (1979).
50. Lincoln, G. A. *J. Zool.* **163**, 105–123 (1971).
51. Lincoln, G. A. *J. exp. Zool.* **182**, 233–250 (1972).
52. Geist, V. *J. Quat. Res.* **1**, 283–315 (1971).
53. Clutton-Brock, T. H. & Harvey, P. H. *Nature* **273**, 191–195 (1978).
54. Geist, V. *Behaviour* **27**, 175–214 (1966).
55. Geist, V. in *Aggression, Dominance and Individual Spacing* (eds Kramer, L., Pliner, P. & Alloway, T.) (Plenum, New York, 1978).
56. Emlen, S. T. & Oring, L. W. *Science* **197**, 215–223 (1977).
57. Alexander, R. D., Hoogland, J. L., Howard, R. D., Noonan, K. M. & Sherman, P. W. in *Evolutionary Biology and Human Social Behavior* (eds Chagnon, N. A. & Irons, W.) (Duxbury, Massachusetts, 1979).
58. Harvey, P. H., Kavanagh, M. & Clutton-Brock, T. H. *J. Zool.* **186**, 475–486 (1978).
59. Jolicoeur, P. & Mosiman, J. E. *Biometrie-Praximotrie* **9**, 121–140 (1968).
60. Morrison, D. F. *Multivariate Statistical Methods* (McGraw-Hill, New York, 1967).
61. Western, D. *Afr. J. Ecol.* **17**, 185–204 (1979).
62. Geist, V. in *Behaviour of Ungulates in Relation to Management* (eds Geist, V. & Walther, F.) (Int. Un. Conserv. Nat., Morges, 1974).
63. Geist, V. *Am. Zool.* **14**, 205–220 (1974).

Subdivision of nature reserves and the maintenance of species diversity

Michael E. Gilpin

Department of Biology, University of California, San Diego, La Jolla, California 92093

Jared M. Diamond

Department of Physiology, University of California, Los Angeles, Los Angeles, California 90024

The roles of area—its size, shape and possible subdivision—in the conservation of species is an important but controversial topic[1-5]. The fundamental assumption is that nature reserves act as habitat islands in an inhospitable sea of environment that has been modified by man, and thus that the empirical and theoretical findings of island biogeography are pertinent. Empirical studies of oceanic islands and continental habitat islands show that larger areas hold more species. The relationship between these two variables is such that a 100% increase in area produces roughly a 25% increase in species. Thus, two small habitat islands which have more than this 25% difference in their species composition, hold more species than a single habitat island of the same total area. This is probably due to microhabitat differences between these two smaller habitat islands. Yet, even against a constant ecological background, stochastic fluctuations ('turnover') of species due to random colonization and extinction[6] will cause inter-island variation in species composition.

In the preceding article Higgs and Usher[7] have shown that three, presumed homogeneous and similarly-sized quarry reserves have sufficient differences in species composition to overcome the area effect and to favour subdivision as the best strategy for maximization of diversity. We have found the same effect in 13 New Hebrides islands. This trend is consistent with equilibrium island biogeographic theory.

We choose for our empirical study 13 central New Hebridian islands with very much the same lowland rainforest habitat for the 52 bird species that occur on the archipelago. From the species lists of the 13 islands[8-9], we can determine the number of distinct species on each of the 78 possible island pairings and relate this to the corresponding total area of each pair. The regression line for this relationship can be compared to the species–area regression for single islands (Fig. 1): two paired islands hold just slightly (about 5–10%) more species than are expected to be contained on a single island of the same total area, in qualitative agreement with Higgs and Usher.
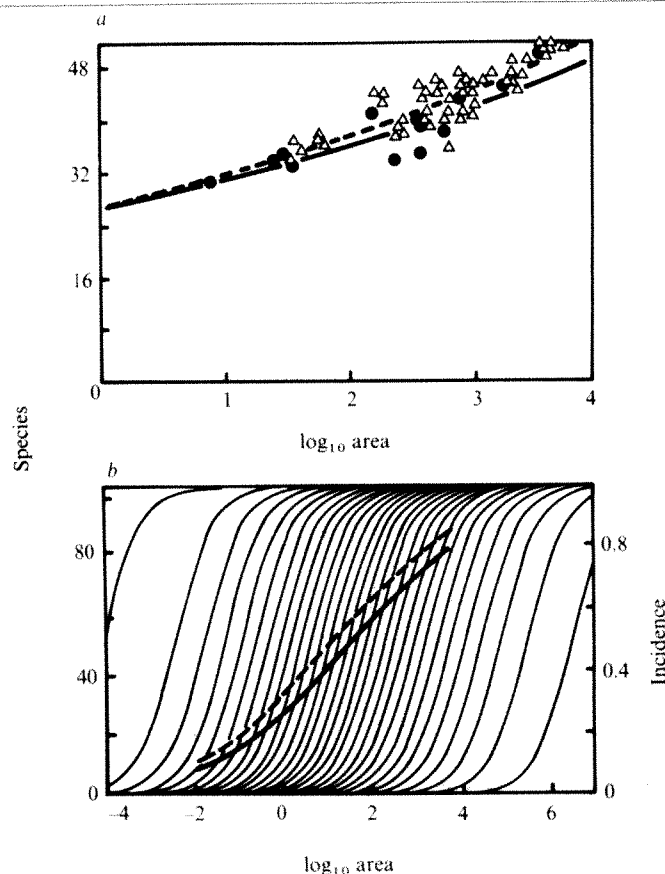
Fig. 1 *a*, New Hebrides species–area relationships. ●, individual species number versus area for 13 central islands, the regression line for which (solid line) is $S = 26.6A^{0.0666}$. △, the total number of distinct species on pairs of islands versus their total area; the regression for this (dashed line) is $S = 26.9A^{0.072}$. *b*, the light lines are an example of a set of area-dependent incidence functions (on the right-hand abscissa) whose parameter b_i is distributed log-normally with a mean and variance chosen to maximize the fit of $\Sigma J_i(A)$, given by the solid line, to the empirical Solomon Island S–A relationship. The dashed line is expected number of species on a pair of identical islands whose total area is A.

Our analysis of this result is based on the classical equilibrium theory[6] and on the additional patterns revealed in Diamond's extensive study of the Pacific avifauna[10]. By analysing the area requirements of individual species, he found that the probability of a species' occurrence on an island, which he called its incidence, increases sigmoidally with increasing logarithm of island area. We[11] have since demonstrated that such incidence curves should have the form $J_i(A) = 1/(1 + a_i/A)$, where J_i is the incidence of the ith species, A is island area and a_i is a species-specific ratio of extinction rate to colonization rate. A log normal distribution of the values of a_i for the T possible mainland pool species can be fitted by regression analysis to explain the observed distribution of the Solomon Island avifauna (Fig. 1). The number of species expected for any given area is the sum of all the incidence functions evaluated at that area: $S = \Sigma J_i(A)$. The number of species expected on two islands of half the area is: $S' = \Sigma(2J_i(A/2) - J_i(A/2)^2)$, where the $J_i(A/2)^2$ term subtracts out the species expected to occur on both islands. With this theoretical treatment, which is based on the data for the Solomon Islands, we can show that S' is ~10% greater than S over the entire range of relevant areas, which closely agrees with the New Hebrides pattern (Fig. 1).

There are thus two compensatory effects dependent on island size: lumping of areas produces more species per island, but subdivision of area produces a more complete sampling of the possible colonist species for islands of that size. Our

analysis shows that division in twos produces increased species diversity. But the even more thorough sampling of still smaller but more numerous islands quickly proves suboptimal: 10 islands of a tenth the total area have fewer species than a single whole island of the same area.

Different species will tend to be preserved by these different strategies. More species with intermediate incidence curves (relatively moderate area requirements) will be picked up with subdivision, while the species with high incidence functions (large area requirements) will only be found with lumping. Thus, truly enlightened conservation practice depends not only on knowledge of the ecology of individual species, but some particular evaluation, whether based on aesthetics or economics, of the value of each species.

1. May, R. M. *Nature* **254**, 177–178 (1975).
2. Diamond, J. M. *Biol. Conserv.* **7**, 129–146 (1975).
3. Simberloff, L. S. & Abel, L. G. *Science* **191**, 285–286 (1976); *Science* **193**, 1027–1032 (1976).
4. Terborgh, J. *Bioscience* **24**, 715–722 (1974).
5. Terborgh, J. *Tropical Ecological Systems: Trends in Terrestrial and Aquatic Research* (Springer, Berlin, 1974).
6. MacArthur, R. H. & Wilson, E. O. *The Theory of Island Biogeography* (Princeton University Press, 1967).
7. Higgs, A. J. & Usher, M. B. *Nature* **285**, 568–569 (1980).
8. Diamond, J. M. & Marshall, A. G. *J. anim. Ecol.* **46**, 703–727 (1977).
9. Diamond, J. M. & Marshall, A. G. *Emu* **76**, 187–200 (1976).
10. Diamond, J. M. *Ecology and Evolution of Communities* (Harvard University Press, Cambridge, 1975).
11. Gilpin, M. E. & Diamond, J. M. *Proc. natn. Acad. Sci. U.S.A.* **73**, 4130–4134 (1976).

Should nature reserves be large or small?

A. J. Higgs & M. B. Usher

Department of Biology, University of York, York YO1 5DD, UK

Conservation of wildlife is one form of land use that competes with agriculture, forestry, urban development and outdoor recreation for an extremely limited supply of land. Conservationists are often faced with having to make decisions of priority, and the question arises as to whether it is better to have the area allocated for conservation in one large unit or in several smaller units. The scale of these units will vary both with different habitats and with different species being conserved: thus, in the tropics the area being considered is likely to be of the order of thousands of hectares, whereas in the industrialized world the areas may be only a few hectares in extent. The problem of how best to use limited resources becomes critical both to amateur conservation organizations (whose 'shopping lists' for reserves are long, but whose financial resources are limited by the extent of their charitable status) and to national organizations such as, in the UK, the Nature Conservancy Council (whose ability to support management agreements under Section 15 of the 1968 Countryside Act is limited by an overall budget). The question is: should such limited resources be devoted to the conservation of a few large sites or to two or three times as many smaller sites? The following argument shows that the proportional overlap of species is the critical factor, and data indicate that a number of small reserves have more species than a single large reserve.

Theoretical studies on nature reserves[1-3] all indicate that size is an important design consideration. These studies advocate larger preserves, although some of the disadvantages of large size have been raised[4,5]. In studies on conservation evaluation, size is often listed with diversity or species richness[6]. Both these criteria seem to be given equal weight in the final assessment of conservation value, even though the theoretical studies indicate that such criteria may be closely correlated. Such a correlation arises from the species–area relationship, which has been used to

justify conserving larger areas. It has, however, been pointed out[4,5], although not formalized, that the species–area relationship may favour the setting up of several smaller reserves. The predictions that can be made from the species–area curve on the total number of species conserved on two reserves depend on the proportion of species that occur on both reserves. Such predictions consider only the total number of species and not the possibility of future trends due to extinction or immigration (often associated with successional processes).

Suppose that the limited financial resources allow for the conservation of only A units of area. The option facing the designer of a reserve system may be between one 'large' area, of A units, or two 'small' areas of pA and $(1-p)A$ units $(0 < p < 1)$. Assuming a species–area relationship $(S = CA^z)$ for organisms on nature reserves[7,8], the number of species occurring on one large block, S_1, is given by

$$S_1 = CA^z \tag{1}$$

where C and z are positive constants. The total number of species on the two smaller pieces is given by

$$S_2 = C(pA)^z + C\{(1-p)A\}^z - V \tag{2}$$

where V is the number of species common to the two smaller areas, that is, the overlap. If the same number of species are conserved in either situation, then $S_1 = S_2$ and

$$V = \{p^z + (1-p)^z - 1\}CA^z \tag{3}$$

If V exceeds this value, more species will be conserved on one large reserve, whereas if V is smaller the two smaller reserves conserve more species (ignoring possible future extinctions). Defining the proportional overlap on the two smaller reserves as

$$P_v = V/S_2 \tag{4}$$

which is the same as the Jaccard coefficient used in classificatory studies, and substituting equations (2) and (3) in equation (4), we obtain

$$P_v = p^z + (1-p)^z - 1 \tag{5}$$

a function which is shown in Fig. 1. It will be seen that the value
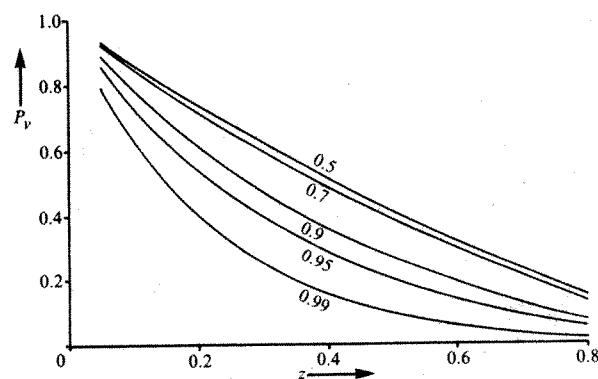
Fig. 1   Isoclines of the function relating P_v to z, equation (5). Values of p are given on each isocline.

of p has relatively little effect on the relationship between P_v and z. Thus, for z of about 0.3 (ref. 8) and with the two areas not differing by more than about half an order of magnitude in size, there will be more species on two reserves if the proportional overlap between them is less than approximately 0.6.

Studies on three quarry nature reserves (Table 1) indicate that, to maximize the number of higher plant species on nature reserves of a similar geological type, there is a benefit to having a number of smaller areas, although some of these benefits are extremely small (the estimated P_v values from field sampling are all less than the values calculated by equation (5)). There is thus no evidence, purely to house numbers of species on reserves, to suggest that one large chalk quarry is the optimal strategy.

Table 1 A comparison of three quarry nature reserves in the chalk (Cretaceous) of the Yorkshire Wolds (KCP, Kiplingcotes Chalk Pit; RBQ Rifie Butts Quarry; WQ, Wharram Quarry)

Reserves compared	p	P_v estimated field lists	P_v calculated from equation (5)
RBQ, WQ	0.94	0.40	0.44
WQ, KCP	0.59	0.43	0.65
RBQ, KCP	0.92	0.45	0.48

A value of $z = 0.276$ (ref. 7) has been used. If P_v from field lists is less than the calculated P_v, then two smaller reserves are favoured.

Limestone pavements in the Yorkshire Dales National Park show a low, but statistically significant, value of $z = 0.086$ (ref. 9), although similarly low values of z have been obtained with New Hebridean island birds[10]. Comparisons of 16 limestone pavements, with areas between 2 and 5 hectares, gave the values of P_v shown in Fig. 2. In all 120 comparisons, a greater number
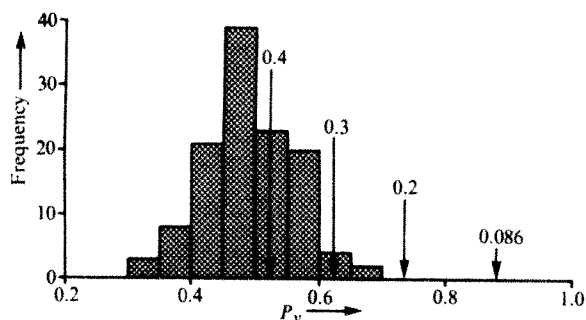
Fig. 2 A histogram of 120 P_v values in the comparison of 16 limestone pavements with areas of between 2 and 5 hectares. Two smaller pavements contain more species if P_v is less than the value indicated for an appropriate z value ($z = 0.086$ for these pavements. Values of z are indicated on arrows.

of species would be conserved if two small pavements were preserved rather than one larger pavement equal in area to that of the two smaller pavements. Even if a more typical z value between 0.2 and 0.4 was selected, there would still be a balance in favour of conserving, for the diversity of their species, several small pavements rather than a few large pavements. Qualitatively similar conclusions seem to hold for other habitats which are the focus of nature conservation management: these include soft coastal habitats in Scotland and lowland heaths in Yorkshire.

However, the number of species at one time is only one factor to be considered when designing a system of nature reserves. Higgs[11] discusses the limitations of applying the ideas of island biogeography to nature reserve design. Although these ideas are useful in considering the diversity of species, and possibly also in suggesting future trends in numbers of species with possible extinctions, the aims of managing the reserve, the biological attributes of the organisms being conserved and the practicalities of management, are also important considerations.

1. May, R. M. *Nature* **254**, 177-178 (1975).
2. Diamond, J. M. *Biological Conservation* **7**, 129-146 (1975).
3. Wilson, E. O. & Willis, E. O. in *Ecology and Evolution of Communities* (eds Cody, M. L. & Diamond, J. M.) (Belknap Press, Cambridge, Massachusetts, 1975).
4. Simberloff, D. S. & Abele, L. G. *Science* **191**, 285-286 (1976); **193**, 1027-1032 (1976).
5. Abele, L. G. & Connor, E. F. in *Proc. 1st Conf. Sci. Res. in National Parks* Vol. 1, 89-94 (ed. Linn, R. M.) (US Department of the Interior, Washington, DC).
6. Ratcliffe, D. A. *A Nature Conservation Review* Vol. 1 (Cambridge University Press, 1977).
7. Usher, M. B. *Biological Management and Conservation* (Chapman & Hall, 1973).
8. Usher, M. B. *J. appl. Ecol.* **16**, 213-215 (1979).
9. Usher, M. B. *Field Studies* (in the press).
10. Diamond, J. M. & Marshall, A. G. *J. Anim. Ecol.* **46**, 703-727 (1977).
11. Higgs, A. J. *J. Biogeogr.* (submitted).

Increased pulmonary α-adrenergic and reduced β-adrenergic receptors in experimental asthma

Peter J. Barnes, Colin T. Dollery & J. MacDermot

Department of Clinical Pharmacology, Royal Postgraduate Medical School,
Ducane Road, London W12 0HS, UK

The role of adrenergic mechanisms in the pathogenesis of asthma is controversial. Increased airways resistance in asthmatics is reversed by β-adrenergic receptor agonists such as isoprenaline, and it has been suggested that β-adrenergic activity is diminished in this condition[1]. This is supported by studies showing reduced metabolic responses to β-adrenergic agonists[2,3] and fewer lymphocyte β-adrenergic receptors in asthmatics than in normal subjects[4]. However, the main contributory factor to diminished β-receptor responsiveness is probably a history of treatment with β-adrenergic agonists, resulting in tachyphylaxis[5,6]. Nevertheless, similar but less pronounced changes have been observed in untreated asthmatic patients[7]. α-Adrenergic agonists produce bronchoconstriction in asthmatic patients, but not in normal subjects[8,9]. Similarly, in vitro studies show α-adrenergic receptor-mediated constriction of bronchial smooth muscle from patients with increased airways resistance, but not from normal controls[10,11]. In addition increased α-adrenergic receptor-mediated responses in vascular and pupillary smooth muscle have been reported in asthmatics[12]. Using radioligand binding techniques, we have investigated the possibility that changes in numbers of α- and β-adrenergic receptors or their affinity are associated with the changes in adrenergic responsiveness observed in asthma. We report here that increased α- and fewer β-adrenergic receptors were observed in pulmonary homogenates of an animal model of chronic asthma than in those from controls.

In this model of experimental asthma, affected animals have many characteristic symptoms, including wheezing, dyspnoea and airway hypersensitivity[13]. Guinea pigs were sensitized to ovalbumin by intraperitoneal injection, and then exposed daily to an ovalbumin aerosol for 4 weeks. They developed dyspnoea, coughing and cyanosis during and after each 45-s exposure. Control animals were exposed to saline aerosol only. A lung membrane homogenate was prepared, and a radioligand binding assay was performed as before[14]. β-Adrenergic receptors were identified with ^{3}H-dihydroalprenolol (^{3}H-DHA), and specific binding (>90% of total) was defined as that displaced by 1 μM (±)propranolol. Stereospecificity of binding of β-adrenergic receptors was confirmed with (−)propranolol ($K_i = 2.3$ nM) which was 200 times more potent than (+)propranolol as an inhibitor of ^{3}H-DHA binding. Butoxamine, a selective β_2-adrenergic antagonist, was more potent ($K_i = 620$ nM) than the selective β_1-adrenergic antagonist atenolol ($K_i = 86$ μM) as an inhibitor of ^{3}H-DHA binding to β-adrenergic receptors in this pulmonary homogenate. α-Adrenergic receptors were identified with ^{3}H-prazosin, and specific binding (60-70% of total) was taken as that displaced by 10 μM phentolamine. The specificity of binding indicated that α_1-adrenergic receptors (postjunctional) were identified with ^{3}H-prazosin[14].

There was a significant ($P < 0.001$) difference in binding to α-adrenergic receptors (Fig. 1), with maximum binding (B_{max}) of ^{3}H-prazosin of 47.3 ± 3.7 fmol per mg protein (mean ± s.e.m.; $n = 6$) in controls and 99.5 ± 8.5 fmol per mg protein in sensitized animals ($n = 6$). There was no difference in binding affinity with equilibrium dissociation constant (K_D) values of

0.51 ± 0.04 nM in controls, and 0.59 ± 0.05 nM in sensitized guinea pigs. There was a small, but significant $(P < 0.05)$, difference in ^{3}H-DHA binding to β-adrenergic receptors (Fig. 2), with B_{max} values of $1,482 \pm 96$ fmol per mg protein in controls, compared with $1,185 \pm 51$ fmol per mg protein in sensitized animals. The K_D values for ^{3}H-DHA binding were not significantly different between the two groups $(0.75 \pm 0.07$ nM in controls and 0.73 ± 0.08 nM in sensitized guinea pigs). Activation of adenylate cyclase mediated by β-adrenergic receptors was measured in pulmonary homogenates of control and sensitized guinea pigs (Fig. 3). There was no significant difference in maximum activation by isoprenaline $(73 \pm 7\%$ in controls compared with $67 \pm 4\%$ in sensitized animals), or in the concentration of isoprenaline producing half-maximum activation in control $(110 \pm 8$ nM) and sensitized animals $(100 \pm 6$ nM).

Lung homogenates of sensitized animals that had been exposed chronically to antigen aerosol had twice the

Fig. 2 Scatchard analysis of ^{3}H-DHA binding to lung membranes in typical control (●) and sensitized (○) guinea pigs. $K_D = 0.58$ nM and $B_{max} = 1,453$ fmol per mg protein for one of the control animals; 0.64 nM and $1,135$ fmol per mg protein for one of the sensitized animals. Specific binding was defined as that displaced by 1 μM ($\pm$)propranolol. Methodology was as described in the legend to Fig. 1. The ^{3}H-DHA (specific activity 59 Ci mmol^{-1}) was supplied by the Radiochemical Centre.

concentration of α_1-adrenergic receptors, and a marginally lower concentration of β-adrenergic receptors than controls. No significant difference was observed in β-adrenergic regulation of cyclic AMP synthesis, suggesting that in this

Fig. 1 Scatchard plot of specific ^{3}H-prazosin binding to lung membranes of typical control (●) and sensitized (○) animals. $K_D = 0.48$ nM and $B_{max} = 44$ fmol per mg protein for one of the control animals; 0.49 nM and 88 fmol per mg protein for one of the sensitized animals. The slope was determined by linear regression analysis. The abscissa intercept gives the maximum binding capacity (B_{max}), and $1/$slope gives the dissociation constant (K_D). Male Dunkin-Hartley guinea pigs were sensitized by intraperitoneal injection of 1 mg ovalbumin in 1 ml saline. Two weeks later animals were exposed daily to an aerosol containing 1% ovalbumin, delivered by a Wright nebulizer into a specially designed box. Each animal was exposed for 30–60 s, 5 days each week for 4 weeks. In some cases the resultant dyspnoea necessitated revival with 100% oxygen. Control animals were injected with the saline carrier, and exposed to a saline aerosol only. The lungs were removed after cervical dislocation, homogenized in 0.32 M sucrose, and centrifuged at 500g at 4 °C to remove undisrupted cells and nuclei. The supernatant was centrifuged at 50,000g at 4 °C for 15 min, and the resulting pellet was washed by resuspension in 50 mM Tris-HCl buffer, pH 7.4 (assay buffer). After a second centrifugation at 50,000g, the pellet was suspended in assay buffer with a concentration of approximately 1 mg protein per ml. This membrane preparation was incubated with increasing concentrations of ^{3}H-prazosin (specific activity 33 Ci mmol^{-1}; a gift from Dr P. Greengrass, Pfizer, Sandwich) at 25 °C for 15 min. Nonspecific binding was determined by incubation in the presence of 10 μM phentolamine. Incubations were terminated by filtration under reduced pressure, and the membranes were isolated on Whatman GF/B glass fibre filters. The filters were washed three times with 6 ml of the assay buffer at 0 °C. Filters were counted in a Packard liquid scintillation spectrometer with an efficiency of 40%.

Fig. 3 a, Activation of adenylate cyclase (ATP pyrophosphate-lyase (cyclizing); EC 4.6.1.1) by increasing concentrations of $(-)$isoprenaline in lung homogenates of typical control (●) and sensitized (○) guinea pigs. b, Eadie-Hofstee plots of these results where Δv is the increase in adenylate cyclase activity at any particular $(-)$isoprenaline concentration. Lung homogenates were taken from experiments described in the legend to Fig. 1, after the 500g centrifugation. Adenylate cyclase activity was determined by a modification[16] of the method C of Salomon *et al.*[17]. Incubations of 100 μl contained 50 mM Tris-HCl buffer, pH 7.4:5 mM MgCl$_2$; 85 mM sucrose; 20 mM creatine phosphate, disodium salt (Sigma); 10 IU creatine kinase, 150 IU per mg protein (ATP creatine N-phosphotransferase; EC 2.7.3.2, Sigma); 1 mM cyclic AMP, sodium salt (Sigma); 0.25 mM Ro20-1724 (phosphodiesterase inhibitor, Roche); 0.5% ethanol; 1 mM [α-^{32}P]ATP (3 μCi, Radiochemical Centre); 0.1% ascorbate; 10 μM pargyline (Sigma); and 280–350 μg homogenate protein. Reaction mixtures were incubated at 37 °C for 12 min. The concentration of ^{32}P-cyclic AMP in each incubation was determined by liquid scintillation spectrometry, with correction for recovery of ^{3}H-cyclic AMP after the chromatographic separation of ATP and cyclic AMP. The production of ^{32}P-cyclic AMP was proportional to protein concentration within the range 50–460 μg of homogenate protein per reaction mixture; similarly ^{32}P-cyclic AMP synthesis increased linearly for 15 min.

animal model altered sensitivity to β-adrenergic agonists is not important. However, the ratio of $\alpha:\beta$-adrenergic receptor binding sites was 1:12 in sensitized animals and 1:30 in controls, which provides a possible explanation for altered sensitivity to adrenergic agents in asthma, and suggests a mechanism of airway obstruction in this experimental model involving responses mediated by α-adrenergic receptors.

The cellular location of the receptors identified remains obscure because we used homogenates of whole lung which included airways, blood vessels and parenchyma. Increased numbers of α-adrenergic receptors might be localized to bronchial smooth muscle, and mediate muscle contraction and increased airway resistance. Increased sensitivity to α-adrenergic agonists has been demonstrated previously *in vitro* in human bronchial smooth muscle after exposure to histamine[11]. An alternative site for increased α-adrenergic receptors is the mast cell, where α-adrenergic agonists facilitate release of histamine[15]. Increased release of histamine might then result in a secondary hypersensitivity of bronchial smooth muscle to α-adrenergic agonists, as suggested above. These results are preliminary, but support the hypothesis that altered adrenergic responses in asthma may be mediated by changes in numbers of receptors.

1. Szentivanyi, A. *J. Allergy* **42**, 203 232 (1968).
2. Inove, S. *J. Allergy* **40**, 337 347 (1967).
3. Middleton, E. & Finke, S. R. *J. Allergy* **42**, 288 299 (1968).
4. Kariman, K. & Lefkowitz, R. *J. Clin. Res.* **25**, 503A (1977).
5. Conolly, M. E. & Greenacre, J. K. *J. clin. Invest.* **58**, 1307 1316 (1976).
6. Galant, S. P., Duriseti, L., Underwood, S. & Insel, P. A. *New Engl. J. Med.* **299**, 933 936 (1978).
7. Brooks, S. M., McGowan, K., Bernstein, L., Altenau, P. & Peagler, J. *J. Allergy clin. Immun.* **63**, 401 406 (1979).
8. Anthracite, R. F., Vachon, L. & Knapp, P. H. *Psychosom. Med.* **33**, 481 488 (1977).
9. Snashall, P. D., Boother, F. A. & Sterling, G. M. *Clin. Sci. molec. Med.* **54**, 283 289 (1978).
10. Simonsson, B. G., Svedmyr, N. & Skoogh, B. E. *Scand. J. resp. Dis.* **53**, 227 231 (1972).
11. Kneussl, M. P. & Richardson, J. B. *J. appl. Physiol.* **45**, 307 311 (1978).
12. Henderson, W. R. *et al. New Engl. J. Med.* **300**, 642 647 (1979).
13. Souhrada, J. F. & Dickey, D. W. *Respirat. Physiol.* **27**, 241 251 (1976).
14. Barnes, P., Karliner, J., Hamilton, C. & Dollery, C. *Life Sci.* **25**, 1206 1214 (1979).
15. Kaliner, M., Orange, R. P. & Austen, K. F. *J. exp. Med.* **136**, 556 567 (1972).
16. Sharma, S. K., Nirenberg, M. & Klee, W. A. *Proc. natn. Acad. Sci. U.S.A.* **72**, 590 594 (1975).
17. Salomon, Y., Londos, C. & Rodbell, M. *Analyt. Biochem.* **58**, 541 548 (1974).

(−)N-(Chloroethyl)norapomorphine inhibits striatal dopamine function via irreversible receptor binding

B. Costall*, D. H. Fortune*, S.-J. Law†,
R. J. Naylor*, J. L. Neumeyer† & V. Nohria*

*Postgraduate School of Studies in Pharmacology, University of Bradford, Bradford, BD7 1DP, UK
†Department of Medicinal Chemistry, Northeastern University, Boston, Massachusetts

β-Haloalkylamine derivatives such as phenoxybenzamine are thought to irreversibly inactivate noradrenaline receptors by a process involving the formation of a reactive ethyleneimmonium cation which is followed by ring scission yielding the reactive carbonium ion which can then react further with a nucleophilic centre located on the receptor. Further study of catecholamine function has awaited the development of similar agents which can alkylate the dopamine receptor. We report here on the structure (Fig. 1) and evaluation of one agent with such potential, (−)N-(chloroethyl)norapomorphine [(−)NCA], and that this compound may be of significant value as a pharmacological and biochemical probe of the dopamine receptor.

Fig. 1 The structures of apomorphine (APO), (−)N-n-propylnorapomorphine (NPA) and (−)N-(chloroethyl)norapomorphine (NCA). See ref. 8 for the synthesis of NCA.

(−)NCA was shown to prevent the action of a reference dopamine agonist, either apomorphine or (−)N-n-propylnorapomorphine [(−)NPA], or to cause effects characteristic of dopamine receptor blockade, in both behavioural and biochemical assessments of action in the

Fig. 2 *a*, Prevention by peripherally administered (−)NCA of apomorphine induced ipsilateral circling behaviour in mice with unilateral striatal electrolesions. *b*, Induction of ipsilateral circling in rats by apomorphine following unilateral intrastriatal (−)NCA. Circling is indicated in revs per 2 min measured in an open field and the effects of (−)NCA within 3 h to 7 days after injection are shown. Effects on day 14 were indistinguishable from those reported for day 7. Standard stereotaxic techniques were used for the induction of striatal electrolesions in mice (male B.K.W., 25–30 g) and for implantation of guides for intracerebral injection in rats (male, Sprague-Dawley, 275–300 g) (see refs 9, 10). Control values in *a* (stippled shadings) are indicative of the circling caused in mice by 0.5 mg per kg apomorphine-HCl, (Macfarlan Smith, prepared in distilled water containing 0.1% sodium metabisulphite) given subcutaneously (s.c.) within 3 h to 7 days after treatment with vehicle for (−)NCA.HCl (minimum quantity of N,N-dimethylformamide made up to volume with distilled water). In electrolesioned mice circling to apomorphine was dose-dependent, the threshold dose was 0.25 mg per kg s.c. (1–3 revs per 2 min) and the maximum was 1.0 mg per kg s.c. (10–12 revs per 2 min) (circling was not observed following appropriate solvent administration). The circling to 0.5 mg per kg s.c. apomorphine was submaximal both in electrolesioned mice receiving no further treatment or given the solvent for (−)NCA (6–9 revs per 2 min). Circling of rats shown in *b* was caused by 0.5 mg per kg apomorphine following the unilateral intrastriatal administration of (−)NCA, 10 and 40 µg in 4 µl. Control unlesioned untreated rats and mice showed no circling behaviour at all. $n = 6$–20. Vertical bars indicate the s.e.m. values. The reduction in circling in *a* is significant to *P < 0.001 (Student's *t*-test).

dopamine-rich striatal area of the rodent brain. Thus, the ipsilateral circling behaviour induced in unilateral striatectomized mice by apomorphine, one of the most valuable models for indicating change in striatal dopamine function[1,2], could be abolished by the peripheral administration of (−)NCA, presumably by an action on striatal dopamine receptors in the 'intact' hemisphere (Fig. 2a). Further, it appeared that the intrastriatal injection of (−)NCA in the rat caused a blockade of dopamine receptors at the site of injection since, if the injection was made into one hemisphere only, peripherally administered apomorphine caused rats to circle ipsilateral to that side, which would again indicate a limitation of action to the 'intact' hemisphere (Fig. 2b). An important observation from each experimental situation was the persistence of the apparent dopamine inhibitory actions of (−)NCA for 2–4 days (recovery of the behavioural response possibly reflecting the resynthesis of receptors).

Confirmation that (−)NCA could indeed interact at dopamine receptors was obtained from receptor binding
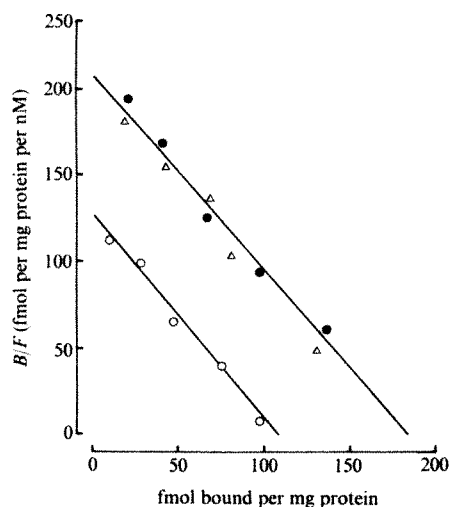
Fig. 3 Effect of intrastriatal (−)NCA on the binding of ³H-NPA to striatal tissue. Three types of striatal tissue were examined (1) that taken from control, untreated rats (●), (2) that taken from animals receiving (−)NCA (40 μg 4 μl, 1 μl per min) (○) in the left hemisphere and (3) that taken from the contralateral hemisphere to (2) and which had been subject to administration of the vehicle for (−)NCA (4 μl, 1 μl per min) (△). Binding to striatal tissue was determined on days 2, 7 and 14–16 after intracerebral injection. Only data obtained on day 2 are presented, values obtained on days 7 and 14–16 for vehicle and (−)NCA being indistinguishable from control values. Values given in the Scatchard analysis are the means of three experiments involving triplicate determinations using ³H-NPA (61 Ci mmol⁻¹, NEN) in a range of 0.0625–2.0 nM. The K_D and B_{max} values were 0.88 nM, 184 fmol per mg protein, 0.89 nM, 179 fmol per mg protein and 0.88 nM, 108 fmol per mg protein respectively for control, vehicle and (−)NCA treatments. Striata were dissected out over ice and homogenized (100 vol, w/v) in 50 mM ice cold Tris–HCl buffer (pH 7.4 at 25 °C) with a Polytron homogenizer. The homogenate was centrifuged twice (10 min, 50,000g) at 4 °C with resuspension in fresh buffer. Final resuspension (100 vol w/v) was in Tris–HCl buffer (pH 7.4 at 37 °C) containing 0.1 % ascorbic acid, 12.5 μM nialamide and 5 mM Na₂EDTA. Each assay tube contained 5 mg wet weight striatal tissue (equivalent to approximately 275 μg protein, measured by the method of Lowry *et al.*[11]) in a total volume of 1.1 ml. After incubation (15 min, 37 °C) with ³H-NPA samples were rapidly filtered under vacuum over Whatman GF/B filters and rinsed rapidly with 2 × 5 ml ice cold Tris–HCl buffer: the bound radioactivity was determined. Specific binding was defined as the difference between ³H-NPA binding in the absence and presence of 10 μM ADTN and under optimal conditions accounted for approximately 75 % of ³H-NPA binding.
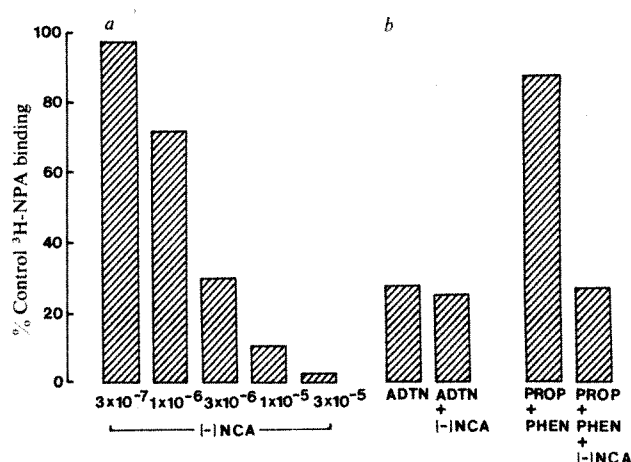
Fig. 4 Effect of (−)NCA on the binding of ³H-NPA to rat striatal homogenates. Binding is expressed in *a* as per cent of the specific binding, and in *b* as per cent of the total binding of 0.5 nM ³H-NPA (fmol per mg protein). Each point represents the mean of three experiments involving triplicate determinations. The s.e.m. values were less than 16 % (calculated on original data, before conversion to percentages, for *a*, specific binding and *b*, total binding). Incubation tubes containing homogenate were preincubated for 2.5 min at 37 °C with (−)NCA (3 × 10⁻⁵–3 × 10⁻⁷ M), ADTN (1 × 10⁻⁵ M), ADTN + (−)NCA (3 × 10⁻⁵ M), propranolol (PROP) (1 × 10⁻⁶ M) + phentolamine (PHEN) (1 × 10⁻⁶ M) and propranolol + phentolamine + (−)NCA (3 × 10⁻⁵) prior to the addition of 0.5 nM ³H-NPA for incubation at 37 °C for 15 min (an increase in pre-incubation times up to 30 min did not modify the effects of drug treatments). Membranes were collected by filtration as indicated in Fig. 3 legend.

studies using ³H-NPA as ligand. Subsequent to establishing the value of this ligand for the characterization of dopamine receptors, as indicated by other workers[3,4], it was shown that intrastriatal (−)NCA could significantly reduce ³H-NPA binding and that this biochemical change followed the behavioural effects which essentially reflected 'striatectomy' by (−)NCA. Thus, on day 2, when animals showed not only an active ipsilateral circling when challenged with apomorphine but also exhibited a resting ipsilateral asymmetry, each identical to effects one would expect from striatectomy or striatal dopamine receptor blockade, the number of binding sites for the dopamine agonist ³H-NPA was reduced by approximately 50%. As the behavioural effects of (−)NCA disappeared on days 7 and 14, so the number of sites available for the binding of ³H-NPA returned to control values (Fig. 3). That the reduction in ³H-NPA binding reflects a change in receptor numbers rather than a change in affinity for the receptor sites is indicated by the constancy of K_D values (0.88–1.12 nM) for binding to striatal tissue both from control animals and those treated for various times with (−)NCA.

The ability of (−)NCA to inhibit the binding of ³H-NPA was further established in *in vitro* experiments which facilitated an examination of the doses and conditions under which (−)NCA could inhibit dopamine mechanisms. It was shown that (−)NCA caused a 50% inhibition of ³H-NPA binding at 1.8 × 10⁻⁶ M (Fig. 4), and that this inhibition was also apparent in the presence of high concentrations of phentolamine and propranolol which could be expected to hinder occupancy of other catecholamine receptors by either ³H-NPA (see also ref. 4) or (−)NCA (it is accepted that although this indicates a dopamine involvement with the (−)NCA/³H-NPA interaction, the use of further ligands would be required to establish specificity). Further, the inhibition of 'specific' ³H-NPA binding by 2-amino-6,7-dihydroxytetralin (ADTN, for suitability of use see refs 5–7) could not be increased further by (−)NCA, indicating that the ability of (−)NCA to prevent ³H-NPA binding does not occur at

'nonspecific' sites. Finally, the prevention of ^{3}H-NPA binding by $(-)$NCA $(10^{-5}$ M) was not reversed by repeated washing.

Thus our results indicate that $(-)$NCA, when administered peripherally or intrastriatally, can cause behavioural change and concomitant change at the receptor level to indicate a persistent dopamine receptor blockade.

The persistence of the blockade, and the structure of $(-)$NCA, preclude an analogy with the dopamine receptor blockade caused by typical neuroleptic agents such as haloperidol. We propose that the process by which $(-)$NCA can inhibit dopamine receptor function may involve covalent bonding of the receptor more analogous to the action of phenoxybenzamine on the noradrenaline receptor.

This work was supported by grants from the MRC and the Wellcome Trust (University of Bradford), from the NIH and NCI (Northeastern University).

1. Ungerstedt, U. Acta physiol. scand. Suppl. 367, 49–68 (1971).
2. Costall, B., Marsden, C. D. Naylor, R. J. & Pycock, C. J. Brain Res. 118, 87–113 (1976).
3. Titeler, M. & Seeman, P. Eur. J. Pharmac. 56, 291–292 (1979).
4. Creese, I., Padgett, L., Fazzini, E. & Lopez, F. Eur. J. Pharmac. 56, 411–412 (1979).
5. Quik, M. & Iversen, L. L. Naunyn-Schmiedeberg's Arch. Pharmac. 304, 141–145 (1978).
6. Seeman, P., Woodruff, G. N. & Poat, J. A. Eur. J. Pharmac. 55, 137–142 (1979).
7. Fuxe, K., Hall, H. & Kohler, C. Eur. J. Pharmac. 58, 515–517 (1979).
8. Law, S.-J., Neumeyer, J. L., Kula, N. & Baldessarini, R. J. J. med. Chem. (in the press).
9. Costall, B., Fortune, D. H., Naylor, R. J. & Nohria, V. Eur. J. Pharmac. 56, 207–216 (1979).
10. Costall, B., Naylor, R. J. & Pinder, R. M. J. Pharm. Pharmac. 26, 753–762 (1974).
11. Lowry, O. H., Rosebrough, N. J., Farr, A. L. & Randall, R. J. J. biol. Chem. 193, 265–275 (1951).

Control of X chromosome transcription by the maleless gene in Drosophila

John M. Belote* & John C. Lucchesi

Department of Zoology and Curriculum in Genetics, University of North Carolina, Chapel Hill, North Carolina 27514

In Drosophila, a large group of structural genes exhibit coordinate regulation, not because they function in a common developmental pathway but because they happen to reside on the X chromosome. These genes are subjected to the regulatory mechanism of dosage compensation which insures that their phenotypic products are identical in the sex with one and in the sex with two X chromosomes. This equalization of gene products is achieved by regulating the level of transcription of both X chromosomes in females and of the single X chromosome in males[1]. We report here that, reasoning that sex-specific lethal mutations may represent lesions in the processes controlling the transcription of X-linked loci, we sought and recovered several male-specific lethal mutations and noted that they affect the levels of X-linked enzyme activities in crude extracts of homozygous male larvae. Autoradiographic monitoring of RNA synthesis in larval polytene chromosomes of males homozygous for one of these mutations, mle^{ts}, reveals a significant reduction in the rate of X chromosome transcription.

A screen of ethyl methane sulphonate-treated major autosomes resulted in the isolation of four new male-specific lethal mutations representing three complementation groups on chromosome 2. No female-specific lethals were recovered[2]. The mutants male-specific lethal-1 (msl-1) and lethal-1b (msl-1^b) are alleles of a gene located at position 2-53.3; male-specific lethal-2 (msl-2) is at position 2-9.0; the mutant maleless-temperature-sensitive (mle^{ts}) is a conditional allele of mle, a mutant previously described[3,4] and located at 2-56.8. In homozygotes (at 25 °C or at higher ambient temperatures for

*Present address: Department of Biology, University of California, San Diego, La Jolla, California 92093.

Table 1 Nucleic acid synthesis in homozygous mle^{ts} males and females

	Sex	No. of nuclei	No. of glands	Average [X]	Average [2R]	r	b ± s.d.
RNA	Females	39	6	103	101	0.997	0.948 ± 0.034
	Males	48	9	135	188	0.995	0.761 ± 0.028
DNA	Females	31	6	417	391	0.979	1.099 ± 0.077
	Males	38	6	180	301	0.990	0.675 ± 0.029

Average [X] and average [2R] = overall average of grain counts over the X and 2R, respectively. r, Correlation coefficient of the mean grain counts for individual glands, [X] and [2R]. b, Regression coefficient of [X] on [2R].

mle^{ts}) each of these recessive mutations kills males but has no detectable effect in females.

The activities of eight enzymes were measured in crude extracts of third instar male larvae homozygous for each of the male-specific lethal mutants; controls were heterozygous male sibs and a mixture of heterozygous and homozygous mutant female sibs. Four of the enzyme activities are X-linked: glucose-6-phosphate dehydrogenase (G6PD), 6-phosphogluconate dehydrogenase (6PGD), fumarase (FUM) and β-hydroxy acid dehydrogenase (β-HAD); four are autosomal: α-glycerophosphate dehydrogenase (α-GPDH) and alcohol dehydrogenase (ADH) on chromosome 2, NADP-dependent isocitrate dehydrogenase (IDH-NADP) and aldehyde oxidase (AO) on chromosome 3. The results, presented in Fig. 1, show a significant reduction in G6PD, 6PGD and FUM activity in males homozygous for any one of the four mutants to about 60% of that found in controls. In contrast, the levels of all autosomal enzymes measured are not affected by the male-specific lethals. The failure of β-HAD to fit into this pattern may be attributable to several factors. This enzyme shows a peak of activity in mid-larval stages and a rapid decline as larvae approach pupation[5]. If homozygous mutant males were selected at an earlier developmental stage than control larvae, real differences in activity between these types may have been masked. β-HAD is present mainly in malphighian tubules and is almost completely absent in the fat body[6]. Extracts from homozygous mutant males in which the fat body is smaller than in controls would yield a relatively higher specific activity for the enzyme. The validity of such explanations is suggested by measurements of enzyme levels in adult male escapers homozygous for mle^{ts} (data not shown). These males exhibit a reduction in β-HAD activity comparable with that of other X-linked enzymes. Once again, autosomal enzyme activities are not affected by the presence of the mutant.

In Drosophila, the polytenic X chromosome in the salivary glands of male larvae contains half the amount of DNA[7,8] but is as wide as the two paired X chromosomes of females. The bloated appearance of the male X is thought to result from the accumulation of some products of gene activity and to represent, therefore, a cytologically visible manifestation of dosage compensation[9]. Examination of polytene chromosome preparations revealed that the X of homozygous mle^{ts} male larvae was narrower and more intensely stained than the X of heterozygous males, suggesting a reduction in X chromosome function by the mle^{ts} mutation (Fig. 2a, b). The chromosomes of mle^{ts} homozygous females seem to be normal (Fig. 2c). This analysis could not be extended to males homozygous for the other male-lethal mutations as they do not have good salivary gland chromosomes.

To corroborate that the mle^{ts} mutation reduces the transcription of X-linked genes, we used autoradiography to monitor RNA synthesis by the polytene chromosomes of salivary glands. The results, presented in Table 1 and Fig. 3a, indicate that the rate of incorporation of ^{3}H-uridine by the X in mle^{ts} males is 80% of that in mutant females. These measurements must be corrected for the fact that a chromosome which is synapsed with a homologue emits fewer β particles capable of producing silver grains than does an
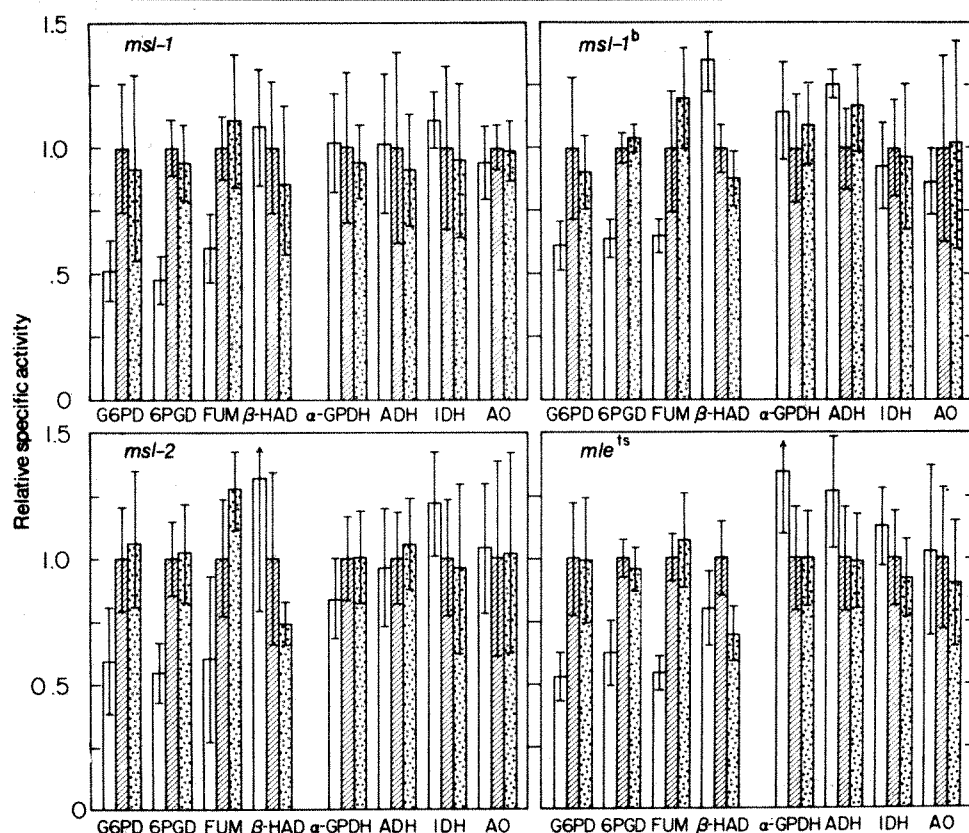
Fig. 1 Enzyme activities in mutant and control larvae. The various strains were cultured on standard cornmeal–agar–molasses–yeast medium supplemented with active dry yeast and maintained at 25 °C. Large third instar larvae were selected when they left the food and began to crawl on the side of the culture bottles. Males and females could be easily separated on the basis of gonad size. Homozygous mutant male larvae developed very slowly and crawled out of the food long after control larvae had pupated (up to 12–14 days post-hatching, as opposed to 4–5 days for control males and females[2]). Extracts were prepared by homogenizing third instar larvae which had crawled out of the medium at a concentration of eight individuals per ml of 0.1 M Tris, 0.27 mM EDTA and 1 mM phenylthiourea (to inhibit phenol oxidase activity) at pH 8.0. The extracts were allowed to stand on ice for 15 min and were centrifuged at 10,000g in a refrigerated centrifuge for 30 min. The clear supernatant was used as a source of enzyme in the assays. The assays for G6PD[11], 6PGD[12], β-HAD[5], FUM[13], ADH[14], α-GPDH[12], IDH-NADP[15] and AO[16] have been published previously. Extract protein concentrations were determined using bovine serum albumin as a standard[17]. Enzyme activities were expressed as change in absorbance per min per mg of protein. The heterozygous males are given relative specific activity values of 1.0, and the 95% confidence limits of the means are indicated. Open columns, homozygous mutant males; hatched columns, heterozygous males; stippled columns, homozygous and heterozygous females.

Fig. 2 Phase contrast photomicrographs of larval salivary gland chromosomes. Glands were dissected in buffered Ringer's, fixed for 5 min in 45% acetic acid and squashed. Following removal of the coverslip, they were post-fixed in ethanol:glacial acetic acid (3:1), stained with acetic carmine, dehydrated and mounted in Euparol. *a*, Homozygous *mle*[ts] male; *b*, heterozygous male; *c*, homozygous *mle*[ts] female.

unpaired chromosome[10]. This correction can be achieved by expressing RNA synthesis data in terms of the DNA content of the chromosomes determined by the same technique, that is, by autoradiography. Measurements of ^{3}H-thymidine incorporation following chronic exposure to this labelled DNA precursor are presented in Table 1 and Fig. 3b. The slope of the *mle*[ts] female measurements is not twice that of the *mle*[ts] males, but only 1.63 times greater, a difference in magnitude consistent with our expectations based on the absorption of β particles in wild-type larvae[8]. Figure 3c repeats the data presented in Fig. 3a but with the female values corrected for the differential self-absorption of β particles by the X chromosomes in the two sexes. The slope of the line of X against autosomal activity in *mle*[ts] females is now 1.17 (95% confidence interval: 1.12–1.21); in mutant males the slope of X against autosomal activity is 0.76 (95% confidence interval: 0.74–0.78). These results show that the rate of X chromosome RNA synthesis in *mle*[ts] males is only 65% of that in *mle*[ts] females. This is in striking contrast to wild type, where the rate of RNA synthesis by the single X chromosomes in males is equivalent to that of the two X chromosomes in females[8,10]

Our data provide complementary lines of evidence that the *mle*[ts] mutation produces a 35–45% reduction in the transcription of X chromosome loci in mutant males. Because mutations at two other loci studied (*msl-1* and *msl-2*) similarly reduce the specific activity of X-linked enzymes but not of autosomal enzymes, it seems likely that the wild-type alleles of these loci also specify products necessary for normal levels of X chromosome transcription in males. We believe this to be the first demonstration of single mutations with a conspicuous regulatory effect on the transcription of a large segment of the *Drosophila* genome.

Of considerable interest is the particular sex-related mechanism in which these regulatory genes function. Dosage compensation is a mechanism which modulates X chromosome transcription so as to equalize, in males and females, the products of X-linked genes not involved in sex differentiation. Because dosage compensation seems to be functioning in all X chromosomes/sets of autosomes classes

1. Lucchesi, J. C. *Science* **202**, 711–716 (1978).
2. Belote, J. M. & Lucchesi, J. C. *Genetics* (submitted).
3. Fukunaga, A., Tanaka, A. & Oishi, K. *Genetics* **81**, 135–141 (1975).
4. Tanaka, A., Fukunaga, A. & Oishi, K. *Genetics* **84**, 257–266 (1976).
5. Tobler, J. & Grell, E. H. *Biochem. Genet.* **16**, 333–342 (1978).
6. Borack, L. I. *Experientia* **30**, 31 (1974).
7. Aronson, J. F., Rudkin, G. T. & Schultz, J. J. *Histochem. Cytochem.* **2**, 458–459 (1954).
8. Maroni, G., Kaplan, R. & Plaut, W. *Chromosoma* **47**, 203–212 (1974).
9. Dobzhansky, T. *Chromosoma* **8**, 691–698 (1957).
10. Mukherjee, A. S. & Beermann, W. *Nature* **207**, 785–786 (1965).
11. Steele, M. W., Young, W. J. & Childs, B. *Biochem. Genet.* **3**, 359–370 (1969).
12. Lucchesi, J. C. & Rawls, J. M. Jr *Biochem. Genet.* **9**, 41–51 (1973).
13. Whitney, J. B. & Lucchesi, J. C. *Insect Biochem.* **2**, 367–370 (1972).
14. Jacobson, K. B., Murphy, J. B. & Hartman, F. C. *J. biol. Chem.* **245**, 1075–1083 (1970).
15. Fox, D. J. *Biochem. Genet.* **5**, 69–80 (1971).
16. Courtwright, J. B. *Genetics* **57**, 25–39 (1967).
17. Lowry, O. H. *et al. J. biol. Chem.* **193**, 265–275 (1951).
18. Maroni, G. & Plaut, W. *Chromosoma* **40**, 361–377 (1973).

Binding of adenovirus VA RNA to mRNA: a possible role in splicing?

Michael B. Mathews

Cold Spring Harbor Laboratory, PO Box 100, Cold Spring Harbor, New York 11724

Fig. 3 Autoradiographic analysis of *mle*[ts] male and female larval salivary gland chromosomes. For RNA synthesis measurements, mature third instar larval salivary glands were excised and incubated in buffered Ringer's solution containing [5,6-^{3}H]uridine (NEN, 40 Ci mmol^{-1}) at a concentration of 10 μCi ml^{-1}. Incorporation was stopped after 5 min by transferring the glands to 45% acetic acid. Salivary gland chromosome squashes were prepared for autoradiography by a standard procedure[18]. Autoradiographs were exposed for 17 days. Grains were counted over the entire euchromatic portion of the X and 2R. For chronic labelling of the DNA, first instar larvae were placed on standard *Drosophila* medium containing [5,6-^{3}H]thymidine (NEN, 6.7 Ci mmol^{-1}) at a concentration of 20 μCi ml^{-1}. Mature third instar larvae were dissected in buffered Ringer's solution and salivary gland chromosomes prepared for autoradiography as above. Autoradiographs were exposed for 3 days. Grains were counted over the X and 2R. For all autoradiographs mean grains counts over the X chromosome [X̄] and the autosome [2R̄] were computed for every gland in which there were three or more scorable nuclei. The slope of the regression line of [X̄] on [2R̄] is a measure of the average increment in the number of grains over the X which accompanies a unitary increment in the number of grains over the autosome. This slope, represented by the regression coefficient *b*, is a measure of the rate of RNA synthesis by the X, or of its DNA content, relative to these parameters in the autosome. ○, *mle*[ts]/*mle*[ts] females; ●, *mle*[ts]/*mle*[ts] males. The large symbols represent the overall means. *a*, ^{3}H-uridine incorporation; *b*, ^{3}H-thymidine incorporation; *c*, ^{3}H-uridine incorporation, corrected for differential self-absorption of β particles by the X chromosomes in the two sexes; female values were multiplied by 2 × 0.675, 1.099 = 1.23.

and because male-specific lethal genes have no effect in females, these genes must act at a control level other than that determined by the X:A ratio. This ratio may affect the preconditions for X chromosome transcription, for example, by altering the accessibility of its chromatin. The wild-type products of male-specific lethal genes may, in turn, permit the higher levels of X chromosome transcription to occur (perhaps by modifying RNA polymerase molecules to make them more specific for X chromosome binding sites). In females, where each X is transcribed at a relatively low rate, the X:A balance would dictate the rate of transcription and the male-specific lethal gene products would not be required. In males, the X:A balance would allow high levels of X transcription which, for it to occur, would require the products of the male-lethal loci.

Most, though not all[1,2], of the messenger RNAs of higher cells are composed of transcripts from two or more non-contiguous DNA segments that are 'spliced' together by mechanisms which are poorly understood. There has been recent speculation that small RNA molecules may play a part in the splicing reaction, acting as templates or adaptors to stabilize the appropriate conformation of a precursor RNA[3-6]. Adenovirus-2 codes for two low molecular weight RNAs, the virus-associated (VA) RNAs I and II, major and minor species, respectively[7]. These RNAs are about 160 nucleotides long and have both been sequenced[8]. They originate from closely spaced genes which are transcribed by RNA polymerase III[9], but have not been definitively associated with any function. We have shown previously[7] that a fraction of the VA RNA of infected cells is complexed with high molecular weight RNA in a denaturation-sensitive fashion. Results presented here show that the VA RNAs bind to unfractionated late virus mRNA and to a cloned copy of a single mRNA species, but not to corresponding cloned segments of viral genomic DNA. It is suggested that VA RNA may act as a template in the splicing reaction.

To assay the binding, ^{32}P-labelled VA RNA is incubated in conditions used for R-loop formation[10] with unfractionated RNA isolated from the cytoplasm of adenovirus-2-infected HeLa cells. The RNA is precipitated from the reaction, redissolved and passed over a column of oligo(dT)-cellulose to trap polyadenylated RNA together with any associated molecules. The column is washed and the poly(A)[+] RNA is eluted with a buffer of low ionic strength. Formation of complex is detectable after 1 min of incubation, reaches a maximum at 30 min and remains stable for at least 5 h. Elution profiles obtained with a reaction that was cycled three times over oligo(dT)-cellulose are shown in Fig.1*a–c*. About 70% of the radioactivity in the poly(A)[+] fraction chromatographs with the poly(A)[+] fraction through second and third cycles of chromatography. Only trace amounts of VA RNA that had been incubated in the absence of cytoplasmic RNA appeared in the poly(A)[+] fraction, and none of this nonspecifically bound and eluted ^{32}P-VA RNA stuck to the column when reapplied, validating the assay and verifying that adherence to the column requires an interaction between the VA RNA and component(s) of the infected cell RNA. Other control experiments showed that preselected poly(A[+]) RNA can bind
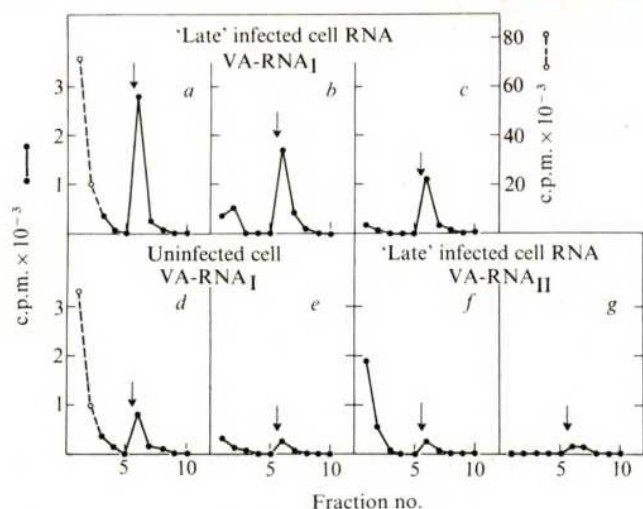
Fig. 1 Binding of VA RNA to polyadenylated RNA. ^{32}P-labelled VA RNA, isolated by two-dimensional gel electrophoresis[7], was incubated with cytoplasmic RNA[14] at 50 °C for 3 h in 100-μl reactions containing 70% formamide, 0.4 M NaCl and 0.01 M PIPES buffer (pH 6.8). Reactions were terminated by chilling and dilution. The RNA was precipitated, dissolved in TE (10 mM Tris-HCl, pH 7.4, 1 mM EDTA), and applied to a 0.3-ml column of oligo(dT)-cellulose in 1 ml of TE containing 0.5 M NaCl. The flow through was re-applied three or four times to obtain maximal binding of poly(A)$^+$ RNA and the column was washed with four 1-ml aliquots of the loading buffer. Polyadenylated RNA was eluted with five 1-ml aliquots of TE buffer. The radioactivity in each fraction was determined by Cerenkov counting. For recycling of the poly(A)$^+$ material (b, c, e, g), appropriate fractions were pooled from the experiments of a, b, d and f, respectively, made 0.5 M with NaCl, and re-applied to the column as described above. Reaction a contained 100 μg of cytoplasmic RNA isolated 27 h after adenovirus-2 infection of HeLa cells and 95,000 c.p.m. of VA RNA$_I$; fractions 6 and 7 were recycled (b), and fractions 6 and 7 were recycled again (c). Reaction d contained 56 μg uninfected HeLa cell cytoplasmic RNA and 86,000 c.p.m. of VA RNA$_1$; fractions 6–8 were recycled (e). Reaction f contained 100 μg infected cell RNA and 3,000 c.p.m. of VA RNA$_{II}$; fractions 6 and 7 were recycled (g). The arrows mark the beginning of the elution of polyadenylated RNA.

VA RNA, and that the product is sensitive to ribonuclease; these experiments strongly indicate that the VA RNA is indeed binding to mRNA.

The specificity of the reaction is the subject of Fig. 1d–g. A small amount of radioactive VA RNA bound to and eluted from the column with the poly(A)$^+$ fraction of uninfected cell RNA, but little of this re-bound in a second cycle (Fig. 1d,e). Bearing in mind that the radioactivity of the VA RNA is heavily diluted by the presence of VA RNA in the infected cell RNA but not in the uninfected cell RNA, it seems that the latter binds VA RNA very much less effectively than does the infected cell RNA. Figure 1f,g shows the only experiment described here which used the minor VA RNA$_{II}$ species. Although only limited amounts of radioactivity were available, it is apparent that this RNA was also bound to and eluted from the column with late poly(A)$^+$ RNA and that most of the counts in this fraction chromatographed with the poly(A)$^+$ fraction when re-cycled. Thus, the interaction between poly(A)$^+$ RNA and VA RNA is specific for infected cell RNA but not for the species of VA RNA.

To explore the nature of the complex, material isolated after one passage over oligo(dT)-cellulose was subjected to electrophoresis in an agarose gel in non-denaturing conditions. Figure 2, lane c, shows that most of the radioactivity contained in the complex penetrated the gel only slightly and that a small fraction ran with the mobility of free VA RNA (lane a). Much (if not all) of the free VA RNA in lane c presumably represents the portion which fails to

chromatograph with the poly(A)$^+$ fraction on re-cycling over oligo(dT)-cellulose. Heating to 100 °C released all the VA RNA to run with the mobility of the marker (Fig. 2, lane e), showing that it is present in a substantially intact form as part of a thermally unstable complex. Moreover, the complex was resistant to the detergent SDS (Fig. 2, lane d), suggesting that protein contaminants are probably not involved in its stabilization. These data indicate that the complex is likely to be held together by base pairing forces but yields no information on the nature of the other component because the mobility of the complex, being much less than that of known adenovirus mRNAs, implies either an outspread conformation or a multimeric nature, and in any case does not permit identification of the other protagonist.

To study the viral RNA involvement, a cloned DNA copy[11] of a late viral mRNA, coding for the fibre protein, has been used. In the plasmid pJAW43, the DNA sequences inserted into the pBR322 vector include the first, second and third segments of the tripartite leader common to most late adenovirus mRNAs[12,13], the fourth leader specific for some forms of fibre mRNA[13,14], and about half of the sequences corresponding to the main body of the fibre mRNA and representing the N-terminal portion of the protein. The results in Table 1, expt 1, indicate that VA RNA hybridizes to nitrocellulose filters carrying this recombinant plasmid but not to filters carrying pBR322 DNA alone. Ribonuclease T$_1$ fingerprints[7] of the material thermally eluted from the filter, or indeed from the complex with poly(A)$^+$ RNA, confirmed that the bound material is indeed VA RNA$_I$ and not a contaminant. Experiment 2 (Table 1) shows that VA RNA does not bind to unrelated viral DNA sequences, such as a cloned cDNA copy of the unspliced polypeptide IX mRNA[2], even if they are inserted by the same A-T tailing method used in constructing pJAW43 (as is the case with pJAW1).
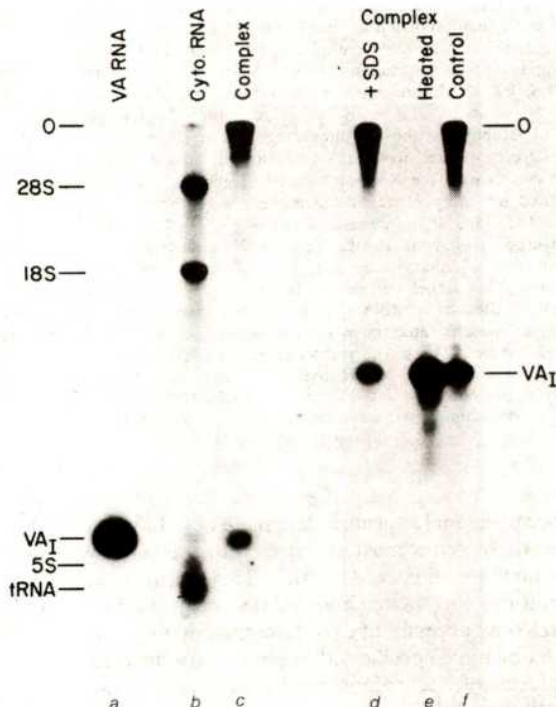
Fig. 2 Analysis of VA RNA:mRNA complex by agarose gel electrophoresis. Complex between ^{32}P-labelled VA RNA$_I$ and polyadenylated late infected cell RNA was isolated as in Fig. 1b,c, precipitated, and dissolved in TE buffer. Aliquots were subjected to electrophoresis through 2% agarose gels in TBE buffer (89 mM Tris, 89 mM boric acid, 1 mM EDTA), and the gels were dried on DEAE-paper before autoradiography. Lane c, untreated complex; lane d, complex incubated for 15 min at room temperature with 0.1% SDS; lane e, complex heated to 100 °C for 1 min; lanes a, b, marker tracks with ^{32}P-labelled VA RNA$_I$ and cytoplasmic RNA from infected cells, respectively.

Table 1 Hybridization of VA RNA with immobilized fragments of adenovirus DNA

		^{32}P-VA RNA bound (c.p.m.)		
Plasmid	Viral sequences	Expt 1	Expt 2	Expt 3
None	—	114	396	113
pBR322		177	—	—
pJAW43	Fibre mRNA–cDNA	45,321	55,698	22,611
pJAW1	Protein IX mRNA–cDNA	—	361	—
pAd21	31.5–37.3 m.u.	—	117	—
pAd5	73.6–79.9 m.u.	—	71	—
pAd33	80.6–89.5 m.u.	—	108	—
pAd20	89.5–97.3 m.u.	—	619	—
pBa1E	14.7–21.5 m.u.	—	—	80
pBa1D	21.5–28.5 m.u.	—	—	60

Plasmid DNA was linearized by cleavage with a restriction enzyme, extracted with phenol and with chloroform, alcohol precipitated, denatured by boiling in water and applied to 3-mm squares of nitrocellulose paper[17]. Pairs of filters were incubated with ^{32}P-VA RNA[1] for 3 h at 50 °C in 50 µl of solution containing 70 % formamide, 0.4 NaCl, 0.01 M PIPES buffer (pH 6.8) and 0.1 mg ml^{-1} calf liver tRNA. The free liquid was removed and the filters were washed 15 times in 1 ml of 1 × SSC (0.15 M NaCl, 0.015 M Na citrate) with 0.5 % SDS by vigorous vortexing followed by aspiration. Filters were then washed three times with 1 ml of TE (10 mM Tris-HCl pH 7.4, 1 mM EDTA) containing 0.15 M NaCl, and three times with 1 ml of TE. Radioactivity was determined by Cerenkov counting. Incubations contained 1.4, 0.5 and 0.3 × 10^6 c.p.m. of VA RNA in expts 1, 2 and 3, respectively. In expt 1, each filter carried 10 µg pJAW43 DNA or 4 µg pBR322 DNA; in expts 2 and 3, each filter carried recombinant DNA equivalent to 10 µg of adenovirus-2 DNA. m.u., Map units.

Furthermore, VA RNA fails to anneal with cloned segments of the virus genome containing various portions of the fibre mRNA sequence—the first and second leaders (16.5–16.6 and 19.5–19.7 map units), the third leader (26.5–26.8 map units), the fourth leader (78.6–79.1 map units) and the mRNA body (86.3–91.2 map units)[13]. Thus, the binding must depend on a cooperative interaction between VA RNA and non-contiguous segments of viral DNA which are brought together in the pJAW43 plasmid. Presumably, when the individual components of the sequence which binds VA RNA are separated, the binding is too weak to be detected by the assay used: the low melting temperature of the hybrid, 55 °C in 0.3 M salt, is consistent with a structure composed of one or more short or imperfect duplexes. Experiments to pinpoint the interactions are in progress.

These results are open to more than one interpretation. One possibility is that VA RNA binds to spliced mRNA(s) and is involved in some subsequent process, such as transport from the nucleus into the cytoplasm or protein synthesis (although no effect of VA RNA binding on cell-free translation of viral mRNA has been detected). An alternative and attractive hypothesis is that VA RNA plays the part of a template in the splicing reaction, bridging two conserved regions which flank intervening sequences within a precursor RNA. In this way, the 5′ and 3′ borders of the impending splice point could be juxtaposed in preparation for the cleavage and ligation reactions. The existence of two VA RNA species, synthesized at different rates during the course of the infections[9], might allow temporal regulation of the production of late viral mRNAs from their common precursor[15]. One can also speculate that small nuclear RNAs of uninfected cells could serve a similar function in the generation of cellular mRNAs[6,16].

1. Crick, F. H. C. *Science* **204**, 264–271 (1979).
2. Aleström, P. *et al. Cell* **19**, 671–681 (1980).
3. Reanney, D. *Nature* **277**, 598–600 (1979).
4. Murray, V. & Holliday, R. *FEBS Lett.* **106**, 5–7 (1979).
5. Zain, S., Gingeras, T. R., Bullock, P., Wong, G. & Gelinas, R. E. *J. molec. Biol.* **135**, 413–433 (1979).
6. Lerner, M. R. & Steitz, M. A. *Proc. natn. Acad. Sci. U.S.A.* **76**, 5495–5499 (1979).
7. Mathews, M. B. & Pettersson, U. *J. molec. Biol.* **119**, 293–328 (1978).
8. Akusjärvi, G., Mathews, M. B., Andersson, P., Vennström, B. & Pettersson, U. *Proc. natn. Acad. Sci. U.S.A.* **77**, 2424–2428 (1980).
9. Söderland, H., Pettersson, U., Vennström, B., Philipson, L. & Mathews, M. B. *Cell* **7**, 585–593 (1976).
10. Casey, J. & Davidson, N. *Nucleic Acids Res.* **4**, 1539–1552 (1977).
11. Zain, S. *et al. Cell* **16**, 851–861 (1979).
12. Berget, S., Moore, C. & Sharp, P. A. *Proc. natn. Acad. Sci. U.S.A.* **74**, 3171–3175 (1977).
13. Chow, L. T. & Broker, T. R. *Cell* **15**, 497–510 (1978).
14. Dunn, A. R., Mathews, M. B., Chow, L. T., Sambrook, J. & Keller, W. *Cell* **15**, 511–526 (1978).
15. Nevins, J. R. & Darnell, J. E. Jr *Cell* **15**, 1477–1493 (1978).
16. Jelinek, W. & Leinwand, L. *Cell* **15**, 205–214 (1978).
17. Ricciardi, R. P., Miller, J. S. & Roberts, B. E. *Proc. natn. Acad. Sci. U.S.A.* **76**, 4927–4931 (1979).

F plasmid provides a function that promotes *recA*-independent site-specific fusions of pSC101 replicon

Christine A. Miller & Stanley N. Cohen

Departments of Genetics and Medicine, Stanford University School of Medicine, Stanford, California 94305

Recently, it has been reported that the tetracycline (Tc) resistance plasmid pSC101 (ref. 1) can undergo integrative recombination (that is, fusion) with a plasmid or bacteriophage genome that lacks extensive DNA sequence homology with pSC101. Such fusion of pSC101 with a second replicon can occur in the absence of the bacterial *recA* gene function, and seems to involve DNA sequences on pSC101 that closely resemble the inverted repeat termini of the transposable genetic element, Tn3 (refs 2, 3). In both of the observed instances of replicon fusion involving pSC101, the fertility plasmid F was present in the bacterial cell; in one case an autonomously replicating F plasmid was used to support the infection of the male-specific bacteriophage fl (ref. 2), whereas in the other F was integrated into the chromosome of an Hfr bacterial strain being used to study mobilization of a non-conjugative plasmid[4]. However, in many studies with the pSC101 plasmid carried out in the absence of F in our laboratory and elsewhere, pSC101 has not been observed to undergo fusion to a second concurrently present replicon. These observations suggested to us that the F plasmid might carry a function that enables pSC101 to undergo replicon fusion. We report here results indicating that the F plasmid does, in fact, provide a *trans*-acting function that promotes *recA*-independent site-specific recombination by pSC101, and that the function carried by F is located in the segment of the plasmid that includes the *tra* genes and the *γδ* sequence.

The pPM103 plasmid[5], which is a temperature-sensitive (*ts*) mutant of pSC101, and the ColE1 plasmid were introduced independently by transformation into a *recA56* derivative of *Escherichia coli* strain C600 (PM191, constructed in our laboratory by P. Meacock). F′Km, an F plasmid derivative carrying a kanamycin (Km) resistance gene (from R. Curtiss III), was introduced by conjugation[6] into a clone carrying the other two plasmids. F′Km and F$^-$ strains were grown overnight at 30 °C in the absence of Tc and then plated at 42 °C in the presence of Tc (see Table 1). A variation of the selected translocation procedure[7] was used to identify clones in which fusion of pPM103 to another replicon had occurred; as replication of pPM103 does not take place at 42 °C (ref. 5), isolation of Tc-resistant cells following growth at this temperature implies that either recombination of pPM103 with a non-*ts* replication system or reversion of its *ts* mutation has occurred.
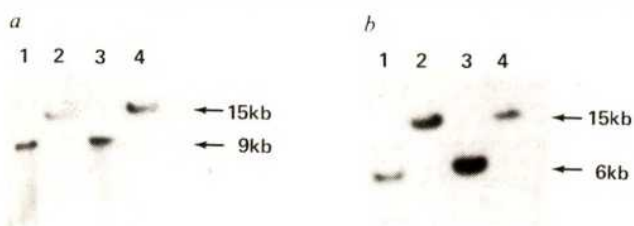
Fig. 1 Plasmid DNA isolated from an F⁺ or F⁻ clone carrying the pPM103 and ColE1 plasmids was treated with *Bam*HI (or *Eco*RI) endonuclease, subjected to electrophoresis on agarose gels[25] and analysed by hybridization on nitrocellulose filters[16]. The ³²P-labelled probes were: *a*, pSC101; *b*, ColE1. A molecular size standard consisting of *Eco*RI-cleaved pRR12[9] was used to indicate fragment length. *a*, Lane 1, pSC101; lane 2, pSC134 (an *in vitro* recombinant of ColE1 and pSC101 linked at the *Eco*RI site of each plasmid[26]); lane 3, plasmid DNA from a Tc^R colony of PM191 (pPM103, ColE1) grown at 42 °C; lane 4, plasmid DNA from a Tc^R similarly grown colony of PM191 (F'Km, pPM103, ColE1). All DNAs were digested with endonuclease *Bam*HI. *b*, Lane 1, ColE1: lanes 2, 3, 4 are the same as *a*. Lanes 1 and 3, DNA digested with endonuclease *Eco*RI; lanes 2 and 4, DNA digested with endonuclease *Bam*HI.

Table 1 shows the effect of the F'Km plasmid in promoting fusion of pPM103 to a concurrently present replicon. As can be seen, the presence of an F'Km resulted in an 80-fold increase in the fraction of cells that retain Tc resistance after growth at 42 °C (expts 1 and 2); all but two of 21 F'Km clones examined contained a 15-kilobase plasmid equal in size to the sum of pPM103 (9 kilobases) and ColE1 (6 kilobases). The remaining two colonies growing at 42 °C in the presence of Tc contained two small plasmids the size of ColE1 and pPM103 and presumably represent instances of reversion of the temperature-sensitive mutation of pPM103. No instance of fusion of pPM103 to F itself or to the bacterial chromosome was observed when the multicopy ColE1 plasmid was also present. However, insertion of pPM103 into F in Tc-resistant clones occurred at approximately the same frequency as reversion of the *ts* mutation following growth at 42 °C in the absence of ColE1 (our unpublished data). In bacteria lacking F, no co-integrate plasmid was observed in 17 colonies examined (expt 1); 16 of the 17 colonies contained two small plasmids the size of pPM103 and ColE1; the remaining colony had a single plasmid the size of pPM103. When ColE1 was replaced by the pACYC177 (ref. 4) (Km^R, Ap^R) or pTU4 (ref. 8) (Cm^R) plasmids (both of which use the p15A plasmid replicon) or the pDPT234 plasmid[9] (an Sp^R plasmid carrying replication functions of an NR1 plasmid copy number mutant), in the above experiments, analogous results were observed (expts 4 and 5 and unpublished data). However, the increased frequency of rescue of pPM103 with pDPT234 (expts 4, 5) was 10–30-fold higher than with ColE1 (expts 1, 2).

The R6-5 antibiotic-resistance plasmid[10], which is largely homologous with F in the fertility region[11] but carries repressed *tra* genes, does not promote fusion of the pPM103 plasmid (expt 3); however, a closely related plasmid (R100.1)[12], which is de-repressed and thus expresses *tra* functions at a high level, does promote replicon fusion (expt 6), and this occurred at a frequency two orders of magnitude higher than was seen with F. In contrast to the results with F, R100.1-promoted fusion involved insertion of pPM103 into the R100.1 plasmid itself even in the presence of ColE1; preliminary evidence indicates that such insertion occurs preferentially at a specific location within R100.1. An F-plasmid mutant deleted for almost half of the molecule including the *tra* gene segment (JC7247, FΔ446 (ref. 13), expt 10) fails to promote replicon fusion. Plasmids containing individually cloned *Eco*RI fragments from the *tra* gene region[14] of the F plasmid also do not promote replicon fusion (expt 7); such fusion is accomplished, however, by F-plasmid derivatives that contain single mutations in *tra* genes A, C, D, E, J of I (ref. 15 and unpublished data). Thus the *tra* genes

themselves may not be involved in 5 promoted replicon fusion. The γδ sequence, a transposable element known to have Tn3 light termini similar to those on the pSC101 plasmid[27] is present on the F plasmid seqments that promote replicon fusion, and may very well be implicated in the process.

Plasmid DNA was isolated from representative F'Km or F⁻ ColE1-containing Tc-resistant clones grown at 42 °C and digested with the *Bam*HI endonuclease, which cleaves pPM103 (that is, pSC101) DNA but not ColE1, or *Eco*RI endonuclease which cleaves ColE1 once. The DNA was then subjected to electrophoresis on agarose gel and analysed by hybridization[16] with ³²P-labelled pSC101 or ColE1 DNA (Fig. 1). As shown in Fig. 1, the 15-kilobase DNA species present in F'Km cells is a composite plasmid that hybridizes with both pSC101 and ColE1 DNA. In contrast, the two plasmids remain as separate replicons in bacteria that lack F.

Restriction endonuclease/agarose gel analysis of fusion plasmids from a series of F'Km clones indicates that the site of recombination is unique with respect to the pPM103 plasmid, but that it seems to be nonspecific with regard to the second small plasmid replicon (in this instance, three randomly selected clones of pDPT234; Fig. 2). Analysis of DNA digested by the *Hinc*II endonuclease, which cleaves pPM103 several times but the pDPT234 plasmid only once, shows that the same *Hinc*II fragment (fragment C) of pPM103 is lacking in all the recombinants, indicating that the junction site on pPM103 occurs within this fragment in each of these fusions. Digestion of the 15-kilobase co-integrate plasmid with the *Mbo*II endonuclease resulted in analogous findings (*Mbo*II fragment 'F' was missing), and permitted more precise localization of the pPM103 recombination site on a pSC101 endonuclease fragmentation map constructed in our laboratory by C.-P.D. Tu (unpublished data). That map shows that the *Mbo*II F fragment and the *Hinc*II C fragment overlap at a position that corresponds, within the limits of resolution by such analysis, to the site at which pSC101 was shown previously to integrate into bacteriophage fl DNA[2]. In contrast to the unique position of the junction with respect to
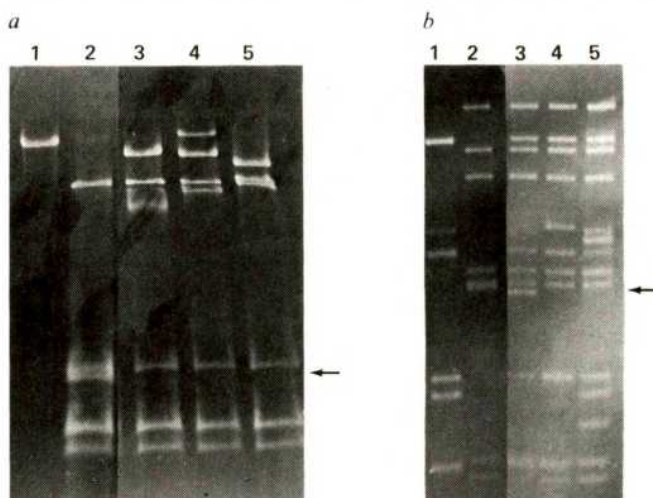
Fig. 2 *a*, Agarose gel analysis of pPM103/pDPT234 fusion plasmids. DNA samples from three separate fusion plasmids and DNA of pSC101 and pDPT234 was isolated as described[22], cleaved with endonuclease *Hinc*II and analysed by gel electrophoresis[25]. Samples were run in 1% agarose gels, Tris-borate buffer, *p*H 8.3, for 3 h at 150 V. pCM431, 432, 433 are 14-kilobase (kb) pPM103/pDPT234 fusion plasmids obtained in separate experiments. The pDPT234 plasmid is cleaved once by *Hinc*II endonulease; the C band of pPM103 (arrow) is absent in all the fusion plasmids and new bands are formed. Lane 1, pDPT234; lane 2, pSC101; lane 3, pCM431; lane 4, pCM 432; lane 5, pCM433. *b*, The same DNA samples were analysed in 1.2% agarose gels run in Tris-borate for 2.5 h following digestion with endonuclease *Mbo*II. *Mbo*II band F of pPM103 (arrow) is missing in all of the independently isolated recombinants, indicating that the pPM103/pDPT234 joint is located at the same site in each of these plasmids. A different pDPT234 band is missing in each fusion plasmid, indicating that the junction with pPM103 occurs at different pDPT234 locations.

Table 1 Effect of F′Km plasmid in promoting fusion of pPM103

Bacterial strain and plasmids	Tc^R Colonies at 42 C/Total colonies at 42 C	Plasmid DNA isolated from Tc^R colonies grown at 42 C
PM191 (pPM103, ColE1)	1.5×10^{-5}	16/17 two plasmids (9, 6) 1/17 one plasmid (9)
PM191 (F′Km, pPM103, ColE1)	1.2×10^{-3}	19/21 one plasmid (15) 2/21 two plasmids (9, 6)
PM191 (R6-5, pPM103, ColE1)	1.5×10^{-6}	10/11 two plasmids (9, 6) 1/11 one plasmid (9)
PM191 (pPM103, pDPT234)	2.5×10^{-8}	3/3 two plasmids (9, 5)
PM191 (F′Km, pPM103, pDPT234)	3.0×10^{-5}	3/3 one plasmid (14)
PM191 (R100.1, pPM103, ColE1)	1.0×10^{-1}	4/4 two plasmids (89, 6†)
PM191 (pCM1891*, pPM103, ColE1)	2.5×10^{-7}	2/2 two plasmids (9, 6)
JC1569 (pPM103, pDPT234)	9.0×10^{-8}	4/4 two plasmids (9, 5)
JC1569 (F′Km, pPM103, pDPT234)	5.0×10^{-5}	4/4 one plasmid (14)
JC1569 (F 446, pPM103, pDPT234	4.0×10^{-7}	4/4 two plasmids (9, 5)

Single colony isolates of the recA56 E. coli strain PM191 carrying the plasmids shown were grown overnight in L-broth at 30 C in the absence of selection. The cells were diluted appropriately and plated at 42 C with or without Tc. The ratio of Tc-resistant to total colonies after overnight growth at 42 °C is shown. Plasmid DNA isolated from cultures[22] was examined by agarose electrophoresis to determine the nature and size of plasmids present. The pPM103 plasmid, a temperature-sensitive replication mutant of pSC101[5], the ColE1 plasmid and R6-5 were introduced into bacteria by transformation[23]. The F′Km plasmid was transferred by conjugation from E. coli strain χ916 into PM191 (pPM103, ColE1), as was R100.1. The FΔ446 plasmid, which has a deletion of the tra region of F leaving the sequence between 16 and 58 min (ref. 14), was introduced into the recA⁻ strain JC1569[24] by conjugation. The plasmid pDPT234[9] was also introduced by transformation and used as the recipient in some cases. Numbers in parentheses indicate the size of the plasmids in kilobases.
*pCM1891 = pACYC189[4] with EcoRI fragment 1[14] cloned into the EcoRI site. Similar results were obtained with EcoRI fragments 2, 3, 5, 6, 15.
†The very large plasmid, a composite of the R100.1 and pPM103, was found to have the pPM103 inserted into the same region in each of the isolates as determined by digestion of plasmid DNA with endonucleases EcoRI, BamHI or SalI.

pSC101, the fragment of pDPT234 that was involved in the recombinational event differed for each fusion plasmid.

Recently, it has been shown that the Tn3 transposon, which has inverted repeat termini similar to the sequences involved in site-specific recombination of the pSC101 plasmid[2], encodes a protein of molecular weight 100,000 essential for transposition of this element[17,18]. We therefore tested the ability of the Tn3 transposon located on the bacterial chromosome to promote fusion of pPM103 with ColE1 or with a ColE1:Tn3 plasmid (that is, pACYC199) as a recipient for the pPM103. Our results indicate that the Tn3 transposon does not promote simple replicon fusion of the type promoted by F, but suggest that a more complex interaction of the Tn3-like sequence on pPM103 with the Tn3 termini may occur, resulting in replicon fusions involving the Tn3 transposon.

The findings reported here indicate that the trans-acting function provided by F and mapping in the region of the tra genes enables the pSC101 plasmid derivative pPM103 to undergo site-specific replicon fusion at a location where Tn3-like inverted repeat sequences have been identified previously. Current models for transposition[19-21] propose that replicon fusion is an intermediate step in the transposition process. If this proposal is correct, it seems that the function provided by F is at least capable of carrying transposition through the intermediate step by accomplishing replicon fusions of pSC101 and its pPM103 derivative.

The ability of F to promote fusion of a replicon that carries inverted repeat sequences but is unable by itself to undergo site-specific recombination may be of some importance in the structural evolution of extrachromosomal genetic elements. As Tn3-like inverted repeat sequences have also been identified on at least one other small plasmid replicon (pTU4)[8], these

findings suggest that the phenomenon we have observed may be an example of a more widespread occurrence.

1. Cohen, S. N. & Chang, A. C. Y. Proc. natn. Acad. Sci. U.S.A. 70, 1293–1297 (1973).
2. Ravetch, S. V. et al. Proc. natn. Acad. Sci. U.S.A. 76, 2195–2198 (1979).
3. Ohsumi, M., Vovis, G. F. & Zinder, N. D. Virology 89, 438–449 (1978).
4. Chang, A. C. Y. & Cohen, S. N. J. Bact. 134, 1141–1156 (1978).
5. Meacock, P. A. & Cohen, S. N. Molec. gen. Genet. 174, 135–147 (1979).
6. Lederberg, J., Cavalli, L. L. & Lederberg, E. M. Genetics 37, 720–730 (1952).
7. Kretschmer, P. J., Chang, A. C. Y. & Cohen, S. N. J. Bact. 124, 225–231 (1975).
8. Tu, C.-P.D. & Cohen, S. N. Cell 19, 151–160 (1980).
9. Taylor, D. P. & Cohen, S. N. J. Bact. 137, 92–104 (1979).
10. Silver, R. P. & Cohen, S. N. J. Bact. 110, 1082–1088 (1972).
11. Sharp, P. A., Cohen, S. N. & Davidson, N. J. molec. Biol. 75, 235–255 (1973).
12. Sugino, Y. & Hirota, Y. J. Bact. 84, 902–910 (1962).
13. Guyer, M. S. & Clark, A. J. J. Bact. 125, 233–247 (1976).
14. Skurray, R. A., Clark, A. J., Uhlin, B. E., Nagaishi, H. & Hya, S. Microbiology 192–196 (1978).
15. Achtman, M., Willetts, N. & Clark, A. J. J. Bact. 110, 831–842 (1972).
16. Southern, E. M. J. molec. Biol. 98, 503–517 (1975).
17. Chou, J., Lemaux, P. G., Casadaban, M. J. & Cohen, S. N. Proc. natn. Acad. Sci. U.S.A. 76, 4020–4024 (1979); Nature 282, 801–806 (1979).
18. Gill, R. E., Heffron, F. & Falkow, S. Nature 282, 799–801 (1979).
19. Grindley, N. D. F. & Sherratt, D. J. Cold Spring Harb. Symp. quant. Biol. 43, 1257–1261 (1979).
20. Shapiro, J. A. Proc. natn. Acad. Sci. U.S.A. 76, 1933–1937 (1979).
21. Arthur, A. & Sherratt, D. Molec. gen. Genet. 175, 267–274 (1979).
22. Kupersztoch, Y. M. & Helinski, D. R. Biochem. biophys. Res. Commun. 54, 1451–1459 (1973).
23. Cohen, S. N., Chang, A. C. Y. & Hsu, L. Proc. natn. Acad. Sci. U.S.A. 51, 2110–2114 (1972).
24. Clark, A. J., Chamberlin, M., Boyce, R. P. & Howard-Flanders, P. J. molec. Biol. 19, 442–453 (1966).
25. Sharp, P. A., Sugden, B. & Sambrook, S. Biochemistry 12, 3055–3063 (1973).
26. Timmis, K., Cabello, F. & Cohen, S. N. Proc. natn. Acad. Sci. U.S.A. 71, 4556–4560 (1974).
27. Reed, R. R., Young, R. A., Steitz, J. A., Grindley, N. D. F. & Guyer, M. S. Proc. natn. Acad. Sci. U.S.A. 76, 482–486 (1979).

Yeast mitochondrial tRNA^Trp can recognize the nonsense codon UGA

Nancy C. Martin, Hung D. Pham & Karen Underbrink-Lyon

Department of Biochemistry, University of Texas Health Science Center at Dallas, Texas 75235

Dennis L. Miller & John E. Donelson

Department of Biochemistry, University of Iowa, Iowa City, Iowa 52242

DNA sequence analysis of mitochondrial genes that code for some mitochondrial proteins has suggested that the opal terminator, UGA, is used as a sense codon in mitochondria[1-4]. The complete sequences of both the yeast[2,4] and human[3] genes coding for cytochrome oxidase subunit II contain UGA codons in the reading frame. When the protein sequences predicted by these DNA sequences are compared with the known protein sequence of bovine mitochondrial cytochrome oxidase subunit II, there are regions of homology, in which UGA codons correspond to tryptophan residues. Therefore it has been suggested that UGA specifies tryptophan in the mitochondrial code. We have isolated a yeast mitochondrial tRNA^Trp and used it to locate the mitochondrial tRNA^Trp gene in pBR322-mitochondrial DNA recombinants. DNA sequence analysis of this gene revealed that the mitochondrial tRNA^Trp anticodon is 5′UCA3′. Because there is a U in the wobble position, this tRNA can recognize and insert tryptophan into a growing polypeptide chain in response to the nonsense codon UGA.

To determine if the mitochondrial tryptophan tRNA of yeast has a structure compatible with the hypothesis that UGA specifies tryptophan it is necessary to determine the primary sequence of the tRNA itself or of the tRNA gene.

Only one species of yeast mitochondrial tRNA[Trp] has been identified[5] and the gene coding for it has been mapped[6]. We isolated mitochondrial tRNA from a mitochondrial DNA deletion mutant known to retain several tRNA genes, including the tRNA[Trp] gene, and separated the tRNAs on a two dimensional polyacrylamide gel. Six individual mitochondrial tRNAs were recovered and tested for their ability to accept ^{3}H-tryptophan in an *in vitro* assay using mitochondrial synthetase. As Table 1 shows, only one tRNA was charged with tryptophan.

The tRNA[Trp] was labelled with ^{32}P and used as a probe to locate the tRNA[Trp] gene in a bank of pBR322 plasmids containing cloned mitochondrial DNA, and DNA was isolated from a clone containing sequences homologous to the tRNA. This plasmid, pYm132, contains a mitochondrial DNA insert of 3,600 base pairs. Hybridization of the tRNA[Trp] to Southern transfers of restriction endonuclease digests of pYm132 DNA enabled us to identify a *Hae*III fragment of approximately 500 base pairs that contained the tRNA[Trp] gene. This fragment is cut once with *Taq*I to yield two fragments of approximately 100 base pairs and 400 base pairs. These fragments were labelled at the *Taq*I site using α^{32}P-dCTP and DNA polymerase and sequenced by the procedure of Maxam and Gilbert[7]. We adopted this strategy because preliminary sequence data of the RNA itself, while ambiguous in the anticodon loop, showed there was a *Taq*I site in the TΨ loop (H. D. Pham, unpublished).

Figure 1 shows an autoradiogram of a 20% gel on which the cleavage products of the 400-bp fragment are displayed. The sequence, read from the bottom up, corresponds to the tRNA sequence from the TΨ loop to the 5′ end of the tRNA. The anticodon predicted from this sequence is 5′UCA3′. A cloverleaf model based on the DNA sequence obtained from this fragment and from the 100-bp fragment (data not shown) is shown in Fig. 2.

Other wild-type tRNAs[Trp] that have been sequenced have the anticodon 5′CCA3′ (ref. 8) and, according to wobble rules, can translate only the single codon UGG[9]. In the

Fig. 1 Autoradiogram of the cleavage products obtained from the 400-bp fragment containing a portion of the tRNA[Trp] structural gene. In this particular set of cleavage reactions the A cleavage was not monospecific but also caused cleavage at C. As are identified by the absence of cleavage products in the C and C +T lanes while Cs are identified by the presence of cleavage products in C, C+T and A lanes.

Fig. 2 Cloverleaf model of yeast mitochondrial tRNA[Trp]. The sequence is based on DNA sequencing data so that the identity or positions of any modified nucleotides are not known. The 3′ CCA sequence, which is not encoded in the gene, has also been added.

Table 1 Charging of individual tRNAs with ^{3}H-tryptophan

tRNA	C.p.m. incorporated
I	735
II	44,057
III	0
IV	489
V	0
VI	0

tRNAs were charged with mitochondrial synthetase in a reaction containing 100 mM Tris, 15 mM $MgCl_2$, 6 mM ATP, 0.2 mM dithiothreitol and 5 µCi ^{3}H-tryptophan (11.7 Ci mmol^{-1}). Trichloroacetic acid-precipitable counts were determined and blank values have been subtracted.

absence of sequence data, one can consider several possibilities that might alter the codon recognition pattern of a single mitochondrial tRNA^{Trp} so that both UGA and UGG can be read. First, if the anticodon is CCA, one or more modified bases either in the anticodon loop or elsewhere might alter codon recognition to include UGA. We are not aware of a specific precedent for this possibility. Second, a primary sequence which dictates an unusual tertiary structure for the yeast mitochondrial tRNA^{Trp} might enable it to read both

UGG and UGA. The UGA suppressor strain of *E. coli* that inserts tryptophan in response to UGA does retain a CCA anticodon but differs from the wild-type in a single base change in the D stem[10]. Finally, the anticodon of the mitochondrial tRNA^{Trp} might be different from other wild-type tRNAs^{Trp} so that following wobble rules, both UGA and UGG can be read. Our sequencing data are consistent with that last possibility, so that the presence of UGA in the reading frame of mitochondrial protein genes is accommodated by a tRNA^{Trp} that can recognize UGA. Unless there is a modification in the anticodon that prevents G-U wobble, this tRNA^{Trp} should also recognize the tryptophan codon UGG.

1. Macino, G., Corruzzi, G., Nobrega, F., Li, M. & Tzagoloff, A. *Proc. natn. Acad. Sci. U.S.A.* **76**, 3784–3785 (1979).
2. Corruzzi, G. & Tzagoloff, A. *J. biol. Chem.* **254**, 9324–9329 (1979).
3. Barrell, B. G., Banker, A. T. & Drouin, J. *Nature* **282**, 189–194 (1979).
4. Fox, T. *Proc. natn. Acad. Sci. U.S.A.* **76**, 6534–6538 (1979).
5. Martin, N. C. & Rabinowitz, M. *Biochemistry* **7**, 1628–1634 (1978).
6. Martin, N. C., Rabinowitz, M. & Fukuhara, H. *Biochemistry* **16**, 4672–4677 (1977).
7. Maxam, A. & Gilbert, W. *Proc. natn. Acad. Sci. U.S.A.* **74**, 560–564 (1977).
8. Gauss, D. H., Gruter, F. & Sprinzl, M. *Nucleic Acids Res.* **6**, r1–r19 (1979).
9. Crick, F. H. C. *J. molec. Biol.* **19**, 548–555 (1966).
10. Hirsh, D. *Nature* **228**, 57 (1970).

Retinoid prevents transformation of cultured mammary glands by procarcinogens but not by many activated carcinogens

Michael S. Dickens & Sam Sorof

The Institute for Cancer Research, Fox Chase Cancer Center, Philadelphia, Pennsylvania 19111

Specific hormones[1,2] in concert with epidermal growth factor[3] induce the mouse mammary gland in serum-free whole organ culture to undergo two physiological cycles[3], each consisting of lobuloalveolar development, differentiation and involution (regression). In addition, chemical carcinogens cause an epithelial transformation, which is operationally defined by the presence of nodule-like alveolar lesions that have escaped the hormonal controls of lobuloalveolar development[4-9]. The transformed mammary glands are also dysplastic, metaplastic[4,5] and oncogenic[6]. Chemically analogous non-carcinogens have little or no transforming activity[4,8]. Furthermore, transformation by the carcinogen 7,12-dimethylbenz[a]anthracene (DMBA) is prevented, suppressed and apparently reversed by retinoid[5] (chemical related to vitamin A). The retinoid acts anti-promotionally, that is, it apparently blocks the transformation process at a stage after the interaction of carcinogen with critical cellular target(s). We report here that the ability of retinoid to prevent mammary gland transformation anti-promotionally is largely limited to carcinogens (procarcinogens) that require metabolic activation to become reactive. Mammary gland transformations caused by low concentrations of procarcinogens are blocked by the retinoid 2-retinylidene-5,5-dimethyl-1,3-cyclohexanedione (retinylidene dimedone). In contrast, transformations by five activated carcinogens and by high concentrations of procarcinogens are not prevented. The present findings suggest important limitations of retinoids in the prevention of epithelial transformation by chemical carcinogens.

Whole mammary glands of BALB/c mice were cultured for 10 days in serum-free development medium containing insulin, prolactin, aldosterone and hydrocortisone (Fig. 1 legend)[4,5,10]. By day 10, the glands possess fully developed lobuloalveoli[2,4] and casein[11]. During days 3–4 only, the cultured glands were treated with solvent containing or lacking carcinogen, and after development were maintained for 14 days (days 10–24) in

serum-free regression medium (insulin being the only added hormone). The lobuloalveoli of untransformed glands regressed completely. Transformed glands (defined in Table 1) were dysplastic, metaplastic[4,5], and contained one or more morphologically developed lobuloalveoli (nodule-like alveolar lesions)[4-9]. The ability of retinoids to prevent transformation was examined by their inclusion in the development medium at different periods (Fig. 1).

Retinylidene dimedone failed to prevent transformation when administered before (days 0–3) the carcinogens (days 3–4) (Fig. 1, protocol I). This failure occurred with all the tested procarcinogens, benzo[a]pyrene (BP) and N-2-fluorenylacetamide (FAA), and activated carcinogens, benzo[a]pyrene trans-7,8-dihydrodiol,9,10 epoxy (anti) (BP-diol epoxide) and N-acetoxy-N-2-fluorenylacetamide (N-AcO-FAA) (Table 1). These findings agree with our results with the procarcinogen, DMBA[5]. The retinoid thus did not pre-adapt the mammary glands to block transformation by the procarcinogens or activated carcinogens. Retinylidene dimedone also failed to prevent transformation when present concurrently (days 3–4) with the above procarcinogens and activated carcinogens (Fig. 1, protocol II, and Table 1), as with DMBA[5]. The retinoid thus did not act as an anti-initiator.

Retinylidene dimedone did anti-promotionally inhibit transformations by the procarcinogens (Fig. 1, protocol IIIa). Treatment with the retinoid during days 4–10, following exposure to procarcinogens at days 3–4, blocked transformation by BP up to 100% ($P < 0.03$), and by FAA up to 61% ($P = 0.02$) (Table 2). The procarcinogen, DMBA, acted similarly[5]. The retinoid at 10^{-7} M was effective against 10-fold molar excesses of BP and FAA. However, 100-fold excesses of these procarcinogens overcame the retinoid, resulting in no significant prevention ($P \geq 0.09$) (Table 2).

In contrast, transformations by low levels of five of the six activated carcinogens were not prevented by retinoid (Fig. 1, protocol IIIb). All tested concentrations of activated carcinogens, benzo[a]pyrene-trans-7,8-dihydrodiol (BP-diol), BP-diol epoxide, N-hydroxy-N-2-fluorenylacetamide (N-OH-FAA), N-AcO-FAA and 1-methyl-1-nitrosourea (MNU), significantly transformed the cultured glands, except BP-diol epoxide at 10^{-9} M (Table 2). The presence of retinylidene dimedone ($\leq 10^{-5}$ M) during days 4–10 did not significantly inhibit these transformations. N-(4-hydroxyphenyl)-all-trans-retinamide (HO-phe-ret) at 10^{-6} M and retinyl acetate (10^{-7} M) were also ineffective against transformation by MNU

Table 1 Lack of prevention by early additions of retinylidene dimedone in chemical transformations of cultured mammary glands of mice

Days of treatment	Dimedone (M)	Carcinogen, M		No. of glands	Toxicity (%)†	No.	Incidence (%)	Prevented (%)
0–3	0	None		49	39	1	2	—
	0	BP	10^{-6}	31	45	12	39	—
	10^{-7}	BP	10^{-6}	32	41	11	34	13
	0	BP-diol epoxide	10^{-7}	31	58	6	19	—
	10^{-7}	BP-diol epoxide	10^{-7}	32	50	9	28	(0)
	0	FAA	10^{-6}	14	21	3	21	—
	10^{-7}	FAA	10^{-6}	27	48	8	30	(0)
	0	N-AcO-FAA	10^{-6}	14	71	5	36	—
	10^{-7}	N-AcO-FAA	10^{-6}	15	40	5	33	8
3–4	0	None		46	22	1	2	—
	0	BP	10^{-6}	32	31	10	31	—
	10^{-7}	BP	10^{-6}	32	25	10	31	0
	0	BP-diol epoxide	10^{-7}	32	22	6	19	—
	10^{-7}	BP-diol epoxide	10^{-7}	32	28	11	34	(0)
	0	FAA	10^{-6}	28	57	6	21	—
	10^{-7}	FAA	10^{-6}	28	54	7	25	(0)
	0	N-AcO-FAA	10^{-6}	28	54	4	14	—
	10^{-7}	N-AcO-FAA	10^{-6}	29	55	5	17	(0)

Mammary glands were treated with retinoid before (days 0–3), or concurrently (days 3–4) with carcinogen. Glands were in development medium during days 0–10, and in regression medium during days 10–24.

*Transformed mammary glands contained nodule-like alveolar lesions, which are the product of the escape from the hormonal controls of alveolar development in whole organ culture. This change to hormone independence, which is brought about by chemical carcinogens, constitutes the operational definition of the chemical transformation[4,5]. See text for definition of carcinogen abbreviations.

†Per cent of glands with paucity of alveolar buds[4], resulting in part from uses of the solvents of carcinogens and of retinoid.

(Table 2). Even the presence of retinylidene dimedone (10^{-7} M) throughout the entire period of mammary gland development (days 0–10) failed to prevent transformation by equimolar BP-diol epoxide ($P > 0.1$) (not shown).

The nitrosamide, N-methyl-N'-nitro-N-nitrosoguanidine (MNNG), was the only reactive carcinogen whose transformation was blocked by retinylidene dimedone. Without retinoid, MNNG had significant transforming activity ($P < 0.02$; Table 2). Acting anti-promotionally in protocol IIIa (Fig. 1), the retinoid at 10^{-7} M significantly inhibited transformation by 10-fold and 100-fold molar excesses of MNNG ($P \leq 0.04$).

Thus, mammary gland transformations caused by three procarcinogens, DMBA, BP and FAA, were prevented anti-

promotionally by retinylidene dimedone (Fig. 1). In contrast, transformations by five of six activated carcinogens were not prevented (BP-diol, BP-diol epoxide, N-OH-FAA, N-AcO-FAA and MNU). Further, 100-fold molar excesses of the procarcinogens overwhelmed the preventive actions of the retinoid. The ability of retinoid to block mammary gland transformations after, but not during or before, the period of treatment with the procarcinogens argues against a mechanism of chemoprevention involving anti-initiation, that is, inhibition of activation of carcinogens or interference at the level of activated carcinogens per se. The present findings suggest that the retinoid prevented only those transformations that resulted from very low concentrations of activated carcinogens that were generated endogenously. It is difficult to test this

Fig. 1 Protocols of the transformations of mouse mammary glands by chemical carcinogens, and of the prevention of transformations by retinylidene dimedone (retinoid). The serum-free culture system has been described elsewhere[4,5,10]. Female BALB/c mice, 3–4 weeks old, were primed with injections of β-oestradiol (1 μg) and progesterone (1 mg) for 9 consecutive days. On the day after the last injection, mice were killed and their entire second thoracic mammary glands excised and floated on Dacron rafts. The serum-free development medium consisted of Waymouth MB752/1 medium (1 ml per gland) supplemented with 350 μg ml⁻¹ L-glutamine, 35 μg ml⁻¹ penicillin G, and 5 μg ml⁻¹ of each of insulin (I), prolactin (P), aldosterone (A) and hydrocortisone (H). On day 3, the medium was replaced with development medium containing 0.1% (v/v, final) dimethylsulphoxide with or without a listed carcinogen. The medium was renewed without carcinogen 24 h later, and every 2–3 days thereafter as required. Retinylidene dimedone (retinoid) in up to 0.5% ethanol (v/v, final) was present in the development medium during the intervals shown. Control cultures contained matching amounts of dimethyl sulphoxide and/or ethanol. All glands were cultured in the development medium during days 0–10, resulting in full morphological lobuloalveolar development[2,4], and then in regression medium containing I (5 μg ml⁻¹) as the only added hormone for an additional 14 days (days 10–24). Glands were fixed, stained, coded and evluated[4,5]. In untransformed glands, all the lobuloalveoli underwent involution (regression). Transformed glands contained one or more nodule-like alveolar lesions that had not regressed. Statistical significance was determined by Fisher's 2 × 2 exact test.
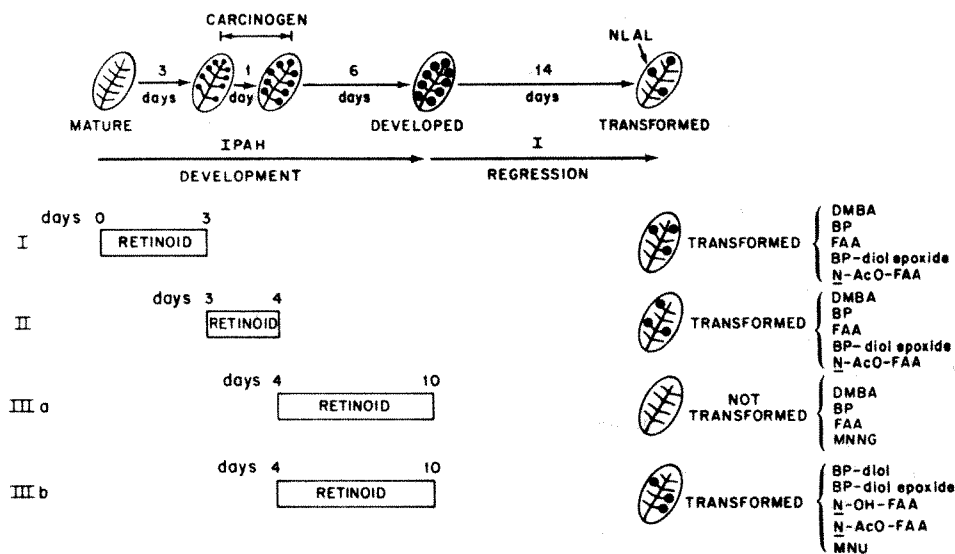
Table 2 Effects of late additions of retinoids on chemical transformations of cultured mammary glands of mice

Carcinogen	M	Dimedone (M)	HO-phe ret (M)	Retinyl acetate (M)	No. of glands	Toxicity (%)*	No.	Incidence (%)	Prevented (%)
None	0	0			234	21	1	0.4	—
	0	10^{-5}			58	31	0	0	—
	0	10^{-7}			131	15	1	0.8	—
	0	0	10^{-6}		48	40	0	0	—
	0	0	0	10^{-7}	32	31	0	0	—
BP	10^{-5}	0			29	34	7	24	—
	10^{-5}	10^{-7}			30	30	5	17	29
	10^{-6}	0			32	22	11	34	—
	10^{-6}	10^{-7}			32	19	2	6	82†
	10^{-7}	0			26	23	5	19	—
	10^{-7}	10^{-7}			23	9	0	0	100†
BP-diol	10^{-7}	0			77	38	23	30	—
	10^{-7}	10^{-5}			32	34	8	25	17
	10^{-7}	10^{-7}			35	23	6	17	43
	10^{-8}	0			24	29	6	25	—
	10^{-8}	10^{-7}			26	23	5	19	24†
	10^{-9}	0			26	15	4	15	—
	10^{-9}	10^{-7}			26	23	2	8	47
BP-diol epoxide	10^{-7}	0			56	50	18	32	—
	10^{-7}	10^{-5}			20	40	7	35	(0)
	10^{-7}	10^{-7}			36	44	12	33	(0)
	10^{-8}	0			27	26	3	11	—
	10^{-8}	10^{-7}			26	19	2	8	27
	10^{-9}	0			23	22	2	9	—
	10^{-9}	10^{-7}			23	26	3	13	(0)
FAA	10^{-5}	0			18	67	10	56	—
	10^{-5}	10^{-7}			18	28	5	28	50
	10^{-6}	0			25	40	14	56	—
	10^{-6}	10^{-7}			23	22	5	22	61†
N-OH-FAA	10^{-6}	0			56	39	18	32	—
	10^{-6}	10^{-5}			28	46	6	21	34
	10^{-6}	10^{-7}			28	39	5	18	44
N-AcO-FAA	10^{-6}	0			57	33	18	32	—
	10^{-6}	10^{-5}			27	37	7	26	19
	10^{-6}	10^{-7}			30	30	7	23	28
MNU	10^{-6}	0	0		72	49	15	21	—
	10^{-6}	10^{-7}	0		42	26	9	21	0
	10^{-6}	0	10^{-6}		28	57	10	36	(0)
	10^{-7}	0	0		74	45	13	18	—
	10^{-7}	10^{-7}	0		46	37	10	22	(0)
	10^{-7}	0	10^{-6}		27	44	5	19	(0)
	10^{-6}	0	0	0	32	56	13	41	—
	10^{-6}	0	0	10^{-7}	31	55	10	32	22
	10^{-7}	0	0	0	32	50	14	44	—
	10^{-7}	0	0	10^{-7}	31	65	11	35	20
MNNG	10^{-5}	0			42	48	16	38	—
	10^{-5}	10^{-7}			42	31	6	14	63†
	10^{-6}	0			40	40	14	35	—
	10^{-6}	10^{-7}			44	34	7	16	54†

Glands were treated with carcinogens during days 3–4, and with retinoid during days 4–10. Mammary glands were in development medium during days 0–10, and in regression medium during days 10–24. The definition of transformed mammary glands is given in Table 1. See text for definition of carcinogen abbreviations.

*Per cent of glands with paucity of alveolar buds[4], resulting in part from uses of solvents of carcinogen and of retinoid.

†Significant prevention according to Fisher's 2 × 2 exact test.

suggestion directly as addition of very low concentrations of activated carcinogens to cultured glands would not result in significant transforming activity due to their consumption in nonspecific interactions with nucleophiles in the medium and mammary gland. Similarly, such low concentration of MNNG presumably survived to cause transformation that was prevented by the retinylidene dimedone, whereas the remainder of the carcinogen was consumed in the nonspecific interactions. The same effect may explain why the feeding of retinyl acetate and HO-phe-ret to rats significantly delayed the appearance of mammary tumours arising from intravenous injections of MNU[12–14], whereas these retinoids did not prevent transformation by MNU in the present *in vitro* study.

Two hypotheses may explain the inability of retinoid to prevent mammary gland transformations by most of the activated carcinogens and by high concentrations of procarcinogens. First, the relatively high levels of activated carcinogens from either source may interact with and render

inoperative sensitive elements—such as genes—in the retinoid-action system itself. Second, retinoid may inhibit the early stages of transformation arising from low concentrations of procarcinogens, but fail to block subsequent stages that may result from multiple hits on cellular targets by relatively high concentrations of activated carcinogens.

Retinoids are under intensive study as possible agents for preventing cancer in man[15–16]. The inability of retinoids to prevent epithelial transformation by activated or direct-acting carcinogens and by high levels of procarcinogens in this system may reflect important limitations of certain anti-promoters in chemoprevention of chemical oncogenesis.

We acknowledge microscopic examinations of cultured mammary glands by Dr R. Philip Custer, helpful discussions with Dr Quentin J. Tonelli and statistical analyses of data by Dr Wayne Ruppel, and we thank Dr Michael B. Sporn for gifts of retinylidene dimedone and retinyl acetate. The dimedone was synthesized by Drs Nancy Acton and Arnold

Brossi. N-(4-hydroxyphenyl)-all-*trans*-retinamide was provided by Dr Robert J. Gander of Johnson and Johnson Co. This work was supported in part by NIH grants CA-21522, CA-05945, CA-06927, and RR-05539, and an appropriation from the Commonwealth of Pennsylvania.

1. Ichinose, R. R. & Nandi, S. *J. Endocr.* **35**, 331–340 (1966).
2. Wood, B. G., Washburn, L. L., Mukerjee, A. S. & Banerjee, M. R. *J. Endocr.* **65**, 1–6 (1975).
3. Tonelli, Q. J. & Sorof, S. *J. Cell Biol.* **83**, 29a (1979); *Nature* (in the press).
4. Tonelli, Q. J., Custer, R. P. & Sorof, S. *Cancer Res.* **39**, 1784–1792 (1979).
5. Dickens, M. S., Custer, R. P. & Sorof, S. *Proc. natn. Acad. Sci. U.S.A.* **76**, 5891–5895 (1979).
6. Telang, N. T., Banerjee, M. R., Iyer, A. P. & Kundu, A. B. *Proc natn. Acad. Sci. U.S.A.* **76**, 5886–5890 (1979).
7. Banerjee, M. R., Wood, B. G. & Washburn, L. L. *J. natn. Cancer Inst.* **53**, 1387–1393 (1974).
8. Kundu, A. B., Telang, N. T. & Banerjee, M. R. *J. natn. Cancer Inst.* **61**, 465–469 (1978).
9. Lin, F. K., Banerjee, M. R. & Crump, L. R. *Cancer Res.* **36**, 1607–1614 (1976).
10. Banerjee, M. R., Wood, B. G., Lin, F. K. & Crump, L. R. *Tissue Culture Ass. Manual* **2**, 457–462 (1976).
11. Terry, P. M., Ball, E. M., Ganguly, R. & Banerjee, M. R. *J. immun. Meth.* **9**, 123–134 (1975).
12. Moon, R. C., Grubbs, C. J., Sporn, M. B. & Goodman, D. G. *Nature* **267**, 620–621 (1977).
13. Moon, R. C. *et al. Cancer Res.* **39**, 1339–1346 (1979).
14. Thompson, H. J., Becci, P. J., Brown, C. C. & Moon, R. C. *Cancer Res.* **39**, 3977–3980 (1979).
15. Sporn, M. B., Dunlop, N. M., Newton, D. L. & Smith, J. M. *Fedn Proc.* **35**, 1332–1338 (1976).
16. Sporn, M. B. & Newton, D. L. *Fedn. Proc.* **38**, 2528–2534 (1979).

Histone exchange in chromatin of hydroxyurea-blocked Ehrlich ascites tumour cells

G. Russev, L. Vassilev & R. Tsanev

Institute of Molecular Biology, Bulgarian Academy of Sciences, 1113 Sofia, Bulgaria

It is well established that DNA and histone synthesis are tightly coupled[1,2]. Nevertheless, these two processes can be partially uncoupled by drugs specifically inhibiting protein[3,4] or DNA[5,6] synthesis, and also during *n*-butyrate-induced differentiation of Friend cells[7]. The fate of the histones synthesized in the absence of DNA synthesis is unknown; they could be: (1) degraded without joining chromatin; (2) deposited on chromatin as extra histones; or (3) replace original chromatin histones. The only data concerning this problem are a recent report[5] supporting the second possibility. We present evidence here in favour of the third possibility by showing that the histones synthesized in the absence of DNA synthesis enter chromatin and become organized in nucleosomes.

Exponentially growing Ehrlich ascites tumour (EAT) cells were incubated *in vitro* with 5 mM hydroxyurea (HU). At different intervals, samples from control and HU-treated cells were taken, incubated for 30 min with ^{3}H-thymidine and ^{14}C-protein hydrolysate and the specific radioactivities of the histones and DNA in the isolated chromatin[8] were determined. In full agreement with the reported effect of HU on other cell lines[5], DNA synthesis was almost completely inhibited within an hour of HU treatment and remained low for several further hours (Fig. 1). At the same time the incorporation of ^{14}C-labelled amino acids continued in all five histones of chromatin, although at a reduced rate amounting to 30–40% of the corresponding controls (Fig. 1). This result shows that the histones synthesized during the HU block (HU-histones) have joined chromatin. It was reported that these histones were deposited as extra histones onto certain chromatin fractions which could be separated from the rest of chromatin on the basis of their higher protein-to-DNA ratio[5]. To check this possibility chromatin from control and HU-treated cells was extensively fragmented by sonication and run on shallow metrizamide density gradients. Both chromatins showed certain heterogeneity with respect to the protein-to-DNA ratio of the fragments (Fig. 2), reflecting the presence in total chromatin of fractions with different non-histone protein
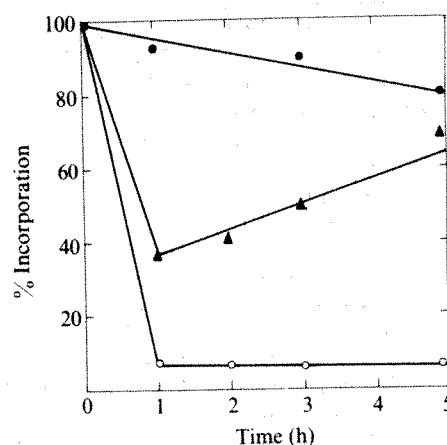
Fig. 1 Effect of HU on the synthesis of DNA and histones in EAT cells. On day 7 after intraperitoneal inoculation of EAT cells to Agnes-Blum white mice, the ascites liquid was obtained in sterile conditions and 5-ml aliquots were mixed with 50 ml of Gibco carbonate-free 199 medium containing 50 mM HEPES buffer (BDH), pH 7.1. The mixture was incubated at 37 °C under gentle shaking. Hydroxyurea (Serva) was added to a final concentration of 5 mM and at the specified time intervals 5-ml aliquots were taken and incubated with 2 μCi ^{3}H-thymidine (11 Ci per mg) and 10 μCi of ^{14}C-protein hydrolysate (1.5 mCi per mg) per ml for 30 min. The samples were cooled on ice and immediately used for isolation of chromatin by extraction of Nonidet P40 nuclei with increasing salt concentrations up to 0.35 M NaCl (ref. 8). The final pellet was dissolved in deionized water and DNA determined spectrophotometrically assuming $1 A_{260} = 50 \mu g$ of DNA. For radioactivity measurement 0.5-ml samples were mixed with 5 ml of a toluene–Triton X-100 (2:1) scintillation mixture[20] and differentially counted for ^{3}H and ^{14}C in a LKB Ultrobeta 1210 liquid scintillation counter. Histones were extracted from chromatin with 0.5 M H_2SO_4 in the cold and precipitated with ethanol. They were resolved by electrophoresis in 15% polyacrylamide gels containing 0.9 M acetic acid–2.5 M urea[10]. The gels were stained with Amidoblack, scanned at 580 nm with a gel scanner (ISCO 1310) and cut into 2-mm slices. The slices were dissolved in 0.5 ml of 25% NH$_4$OH–30% H_2O_2 (1:4) mixture at 60 °C and counted as above. The histone fractions were pooled together and the specific radioactivity of the total histone was determined in arbitrary units as the ratio between the total counts and the area under the peaks. ●, Specific radioactivity of DNA from control cells; ○—○, specific radioactivity of DNA from HU-treated cells; ▲, specific radioactivity of total histone from HU-treated cells.

content. However, the sedimentation profile of the HU-treated chromatin was identical to that of control chromatin and showed no additional fraction comprising predominantly the labelled proteins. This disputes the theory that HU-histones are deposited as extra histones.

The fate of the HU-histones was further studied using micrococcal nuclease. Isolated nuclei[9] from HU-treated cells labelled for 90 min with ^{14}C-protein hydrolysate were digested with micrococcal nuclease to give about 15% acid-soluble DNA and the digest was run on linear 5–30% sucrose density gradient. Histones were isolated from different fractions of the gradient and from the undigested pellet and their specific radioactivities were determined. They were the same in all fractions and in the pellet, which suggested that the HU-histones were organized in nucleosomes indistinguishable from the normal chromatin nucleosomes.

To confirm this point we studied isolated nucleosomes from HU-treated and control chromatin. They had the same total protein-to-DNA ratio of 1.15:1.00, histone-to-DNA ratio of 1:1, and a full complement of nucleosomal histones as judged by acetic acid–urea polyacrylamide gel electrophoresis[10] (not shown). These nucleosomes were analysed by sucrose density gradient and by equilibrium metrizamide density gradient centrifugation. In both gradients HU-treated nucleosomes co-sedimented with the control nucleosomes (Fig. 3).

The metrizamide density gradient is more sensitive to changes in the protein-to-DNA ratio. It has been shown (and confirmed in our experiments) that there is a linear relationship between this ratio and the buoyant density of the deoxyribonucleoprotein[11]. This relationship shows that the addition of one histone per nucleosome (which would increase the protein-to-DNA ratio of our particles by 10%) will increase their buoyant density by 0.01 g cm^{-3}. To see how this increase would affect the ^{3}H- and ^{14}C-labelled peaks in the density gradient, the following points should be taken into consideration: (1) The ^{3}H peak represents a small fraction of DNA pulse-labelled before the HU block; (2) the ^{14}C peak also corresponds to a small fraction of histones synthesized after the HU block; and (3) if this histone fraction is additionally adsorbed it would be distributed at random among nucleosomes containing labelled and nonlabelled DNA. Thus it can be deduced that if the ^{14}C-histones bind to the nucleosomes as extra protein the whole ^{14}C-labelled peak in Fig. 3d would be shifted to the left, while the ^{3}H-labelled peak would remain practically unaffected due to the small percentage of (^{14}C, ^{3}H)-labelled heavy particles.

This shows that in our conditions of labelling the addition of new histone molecules to the nucleosomes would cause a shift of the ^{14}C peak relative to the ^{3}H peak. Such a relative

Fig. 3 a, b, Sucrose density gradient, c, d, equilibrium metrizamide density gradient centrifugation of nucleosomes from control (a, c) and HU-treated (b, d) chromatin. EAT cells were incubated with ^{3}H-thymidine for 30 min to prelabel DNA, treated with HU for 1 h and labelled with ^{14}C-protein hydrolysate for 90 min as described for Fig. 1. Control cells were labelled according to the same protocol, omitting the HU treatment. Nuclei were isolated by treating the cells with Nonidet P40 at low ionic strength[9] in the presence of 1 mM phenylmethyl sulphonyl fluoride (PMSF) (Serva). They were suspended in 1 mM $CaCl_2$, 10 mM Tris–HCl, pH 8 to make 40–50 A_{260} ml^{-1} and were digested with 2 EU of micrococcal nuclease (Boehringer) per A_{260} unit at 37 °C for 10 min. The reaction was stopped by adding EDTA to a final concentration of 2 mM EDTA, pH 8. Samples (4 ml) were layered on 5–30% linear sucrose density gradients containing 1 mM EDTA, 5 mM Tris–HCl, pH 8. The gradients were centrifuged in the Beckman SW 27 rotor at 26,000 r.p.m. at 4 °C for 18 h and unloaded from the bottom with a LKB peristaltic pump. Aliquots from each fraction were diluted and differentially counted as described in Fig. 1 legend. The fractions containing the mononucleosome peak were pooled together and precipitated with 5 mM $CaCl_2$ (ref. 21). After 2 h in the cold, the precipitated nucleosomes, which represented about 80–90% of the total A_{260} of the fractions, were collected by centrifugation and resuspended in 2 mM EDTA, pH 8 containing 1 mM PMSF. Samples (0.5 ml) were layered on 5–20% linear sucrose density gradients prepared as above and were run in the Beckman SW40 rotor at 38,000 r.p.m. at 4 °C for 20 h. The homogeneous material from the middle of the sucrose gradients was used for the equilibrium centrifugation which was performed exactly as described in Fig. 2 legend, with the only difference that the final concentration of metrizamide was 35%. The gradients were fractionated and counted as described for Figs 1 and 2 and the buoyant densities of the metrizamide gradient fractions were calculated from the corresponding refractive indices[22]. ●—●, ^{3}H-DNA; ○–○, ^{14}C-protein; ...., calculated position of the ^{14}C-peak if the protein-to-DNA ratio increased by 10% (one extra histone per nucleosome).

Fig. 2 Equilibrium metrizamide density gradient centrifugation of control (a) and HU-treated (b) EAT cells. EAT cells were grown *in vitro* in the presence of 5 mM HU for 5 h and then labelled with ^{3}H-thymidine and ^{14}C-protein hydrolysate as described for Fig. 1. Control and HU-chromatins were fragmented by sonication with a MSE ultrasonic unit at setting 1A for 5 min (5 × 1 min in an ice bath) to give fragments containing 200–1,000 base pairs of DNA. Aliquots (0.5-ml) were mixed with 4 ml of 45% metrizamide (Nyegaard) in 1 mM EDTA, 5 mM Tris–HCl, pH 8 to a final concentration of 40% metrizamide. The tubes were filled up with liquid paraffin and spun in the Beckman Ti 50 rotor at 33,000 r.p.m. at 4 °C for 65 h. The gradients were unloaded with a LKB peristaltic pump from the bottom and after 1:4 dilution with distilled water were counted for ^{3}H and ^{14}C as described for Fig. 1. ●—●, ^{3}H-DNA; ○–○, ^{14}C-protein.

shift would be easily detected because ^{3}H and ^{14}C counts are measured in the same double-labelled fraction of the density gradient and the ^{14}C/^{3}H ratio would change significantly. If a nucleosome binds one extra histone per molecule the shift of the ^{14}C peak relative to the ^{3}H peak could be detected as shown in Fig. 3d and the ^{14}C/^{3}H ratio of the fractions will change significantly (a decrease of 20–40% in the right shoulder of the peak).

Note that these changes in the position of the ^{14}C peak and ^{14}C/^{3}H ratio should be regarded as minimal estimates, for adsorption of single histone molecules on the nucleosomes would hardly occur *in vivo*. It has been shown that histones can form dimers[12], tetramers[13] and octamers[14],[15] and that they join chromatin as such preformed stoichiometric complexes. This is demonstrated by the fact that during chromatin replication, old and new histones do not mix[16] and that both *in vitro*[17,18] and *in vivo*[19], H3/H4 tetramers and H2A/H2B dimers sequentially enter chromatin. All these data strongly indicate that it is unlikely that individual newly synthesized histone molecules would be found in the nucleus and if new histones in HU-chromatin join nucleosomes as additional protein they would be adsorbed as dimers and tetramers which will shift the ^{14}C peak in Fig. 3*d* still further to the left. However, as can be seen, this peak coincides exactly with the peak of ^{3}H-DNA, and the ^{14}C/^{3}H ratio of all fractions is the same as in the corresponding control nucleosomes. This eliminates the hypothetical situation of even one extra histone per nucleosome.

Our results show that the HU-histones are not additionally bound to already existing nucleosomes, but are present in chromatin as components of octamers associated with the old (prelabelled) DNA. This result can be explained by assuming that the newly synthesized histones in HU-arrested cells have replaced some of the old histones, which in the conditions of HU-block have dissociated from DNA. It contradicts the current concept that, once incorporated in chromatin, histones cannot be replaced, which seems to be true for normal situations only.

1. Borun, T. W. in *Results and Problems of Cell Differentiation* Vol. 7 (eds Reinert, J. & Holtzer, H.) 249–290 (Springer, New York, 1975).
2. Elgin, S. C. R. & Weintraub, H. *A. Rev. Biochem.* **44,** 725–774 (1975).
3. Weintraub, H. *Cold Spring Harb. Symp. quant. Biol.* **38,** 247–256 (1973).
4. Wolf, H., Raydt, G., Puschendorf, B. & Grunicke. H. *FEBS Lett.* **35,** 336–340 (1973).
5. Nadeau, P., Oliver, D. & Chalkley, R. *Biochemistry* **17,** 4885–4893 (1978).
6. Balhorn, R., Tanphaichitz, N., Chalkley, R. & Granner, D. K. *Biochemistry* **12,** 5146–5150 (1973).
7. Zlatanova, J. & Swetly, P. *Nature* **276,** 276–277 (1978).
8. Tsanev, R. & Russev. G. *Eur. J. Biochem.* **43,** 257–263 (1974).
9. Hancock, R. *J. molec. Biol.* **86,** 649–663 (1974).
10. Panyim, S. & Chalkley, R. *Archs Biochem. Biophys.* **130,** 337–346 (1969).
11. Rickwood, D., Birnie, G. D. & MacGillivray, A. J. *Nucleic Acids Res.* **2,** 723–733 (1975).
12. Sperling, R. & Bustin, M. *Nucleic Acids Res.* **13,** 1263–1275 (1976).
13. Weintraub, H., Palter, K. & Van Lente, F. *Cell* **6,** 85–110 (1975).
14. Thomas, J. O. & Kornberg, R. D. *Proc. natn. Acad. Sci. U.S.A.* **72,** 2626–2630 (1975).
15. Ruiz-Carrillo, A. & Jorcano, J. L. *Biochemistry* **18,** 760–768 (1979).
16. Leffak, I. M., Grainer, R. & Weintraub, H. *Cell* **12,** 837–845 (1977).
17. Ruiz-Carrillo, A. & Jorcano, J. L. *Cold Spring Harb. Symp. quant. Biol.* **42,** 165–170 (1978).
18. Wilhelm, F. X., Wilhelm, M. L., Erard, M. & Daune, M. P. *Nucleic Acids Res.* **5,** 505–521 (1978).
19. Worcel, A., Han, S. & Wong, M. L. *Cell* **15,** 969–977 (1978).
20. Anderson, L. A. & McClure, W. O. *Analyt. Biochem.* **51,** 170–173 (1973).
21. Honda, B. M., Baillie, D. L. & Candido, P. M. *J. biol. Chem.* **250,** 4643–4647 (1975).
22. Rickwood, D. & Birnie, G. D. *FEBS Lett.* **50,** 102–110 (1975).

Spectrin tetramer–dimer equilibrium and the stability of erythrocyte membrane skeletons

Shih-Chun Liu & Jiri Palek

Department of Research, St Elizabeth's Hospital, Boston, Massachusetts 02315, and the Department of Medicine, Tufts Medical School, Boston, Massachusetts 02135

The inner side of the red-cell membrane is laminated by a two-dimensional network of membrane proteins which include spectrin, actin and some other components[1–4]. After extraction of lipids and integral proteins from the membrane, this membrane skeleton can be visualized as a ball-shaped network consisting of twisted fibres[1–4] and globular protrusions[4]; however, the assembly of the individual proteins in the membrane skeleton is not well understood. Spectrin can be eluted from the membrane in the form of dimers and tetramers[5–8]. Electron microscopic study with low-angle shadowing technique shows that spectrin dimers are two parallel strands of twisted fibres presumably representing bands 1 and 2 of spectrin[9]. Spectrin tetramers presumably formed by head-to-head associations of two dimers are twice as long[9]. In solution, the spectrin dimer–tetramer equilibrium depends on temperature and salt concentration[7,8]; however, it is not known whether the same equilibrium exists in the membrane and whether it affects the physical properties of the membrane, such as its structural stability and deformability. We now demonstrate that spectrin dimers and tetramers are in a reversible equilibrium in the membrane and that in physiological conditions this equilibrium favours spectrin tetramers. Furthermore, we show that transformation of spectrin tetramers to dimers, as induced by ghost incubation in hypotonic conditions, diminishes the structural stability of the Triton-insoluble membrane skeletons.

We have altered the equilibrium between spectrin tetramers and dimers in the membrane by exposing ghosts to changes in temperature and ionic strength which alter spectrin dimer–tetramer equilibrium in solution. After stabilization of the equilibrium by cooling of ghosts to 0 °C, spectrin was extracted from the red-cell ghosts by overnight dialysis in the cold against a low ionic strength buffer. The amount of spectrin dimers and tetramers was measured by gel filtration on a 4% agarose column[5]. The spectrin tetramers and dimers could also be resolved by electrophoresis at 4 °C on agarose/acrylamide composite gels in a buffer containing 40 mM Tris-HCl pH 7.4, 20 mM Na acetate, 2 mM mercaptoethanol and 2 mM EDTA.

About 80% of the spectrin was extracted from freshly isolated red-cell ghosts by overnight dialysis in the cold against low ionic strength buffer. The extracted spectrin was mostly in the form of tetramers (Fig. 1, peak II), and a high molecular weight void volume complex (Fig. 1, peak I) as previously observed by others[7,8]. After a subsequent incubation of this extract at 37 °C for 15 min in isotonic conditions, about 60% of the void volume complex and 70% of spectrin tetramers were dissociated and recovered mostly as spectrin dimers (Fig. 1, peak III). In contrast, incubation of intact ghosts rather than spectrin extracts in identical conditions (37 °C, 15 min) in isotonic buffer failed to transform spectrin tetramers to dimers as indicated by the elution profile of crude spectrin extracted from such ghosts (Fig. 2*a*).

In contrast to a relative stability of spectrin tetramers in ghosts incubated in isotonic conditions, ghost incubation at 37 °C for 15 min at low salt concentrations (5 mM sodium phosphate pH 7.4, 10–30 mM NaCl), resulted in a dissociation of spectrin tetramers to dimers; this transformation was stimulated by a decrease in salt concentration (Fig. 2*b–e*). At 37 °C, an equilibrium between the two species was reached in minutes, as is observed in solution[7,8].

The supernatants of ghosts incubated either at isotonic or hypotonic conditions (37 °C, 15 min) contained only very small amounts of spectrin (1–3%) indicating that during such short incubation spectrin was not released from the membrane. Furthermore, the total amount of spectrin extracted from the membrane (80%) was the same in fresh ghosts containing mostly spectrin tetramers and in hypotonically pretreated ghosts (5 mM Na phosphate pH 7.4, 10 mM NaCl, 1 mM mercaptoethanol, 37 °C, 15 min) in which spectrin tetramers were converted to dimers. After preincubation in isotonic conditions spectrin extractability decreased from 80% to about 65%. However, this 15% difference in spectrin extractability cannot account for the fact that in hypotonic conditions over 40% of spectrin was present in a dimer form. Thus, the
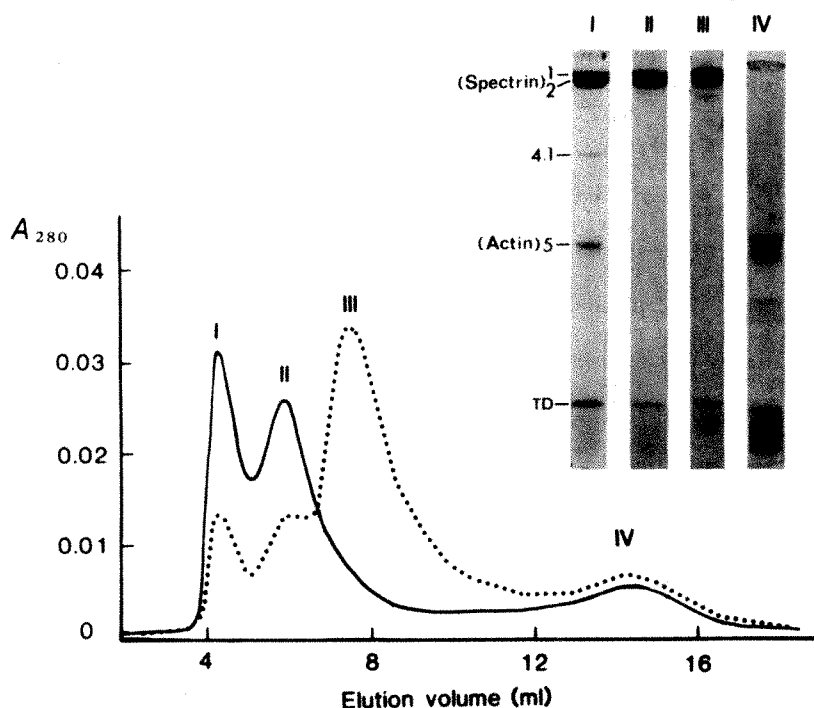
Fig. 1 Demonstration of spectrin transformation in solution by gel filtration analysis of crude spectrin incubated at 37 °C in isotonic conditions. Crude spectrin from fresh human erythrocytes was prepared by dialysis of ghosts[31] against 0.1 mM Na phosphate, 0.1 mM EDTA pH 8.0, at 0–4 °C for 20–30 h. The fragmented ghosts were pelleted by centrifugation at 250,000g for 30 min at 4 °C. Crude spectrin supernatants (0.7 ml, $A_{280} = 0.6$) with (-----) and without (———) further incubation in isotonic conditions (5 mM Na phosphate, 150 mM NaCl, 5 mM mercaptoethanol, 5 mM EDTA pH 7.5, 37 °C, 15 min) were eluted in the cold from the Bio-Gel A-15 m (200–400 mesh) agarose column (1 cm × 40 cm) with 10 mM Na phosphate, 150 mM NaCl, 5 mM mercaptoethanol, 5 mM EDTA pH 7.5 (ref. 5). Protein in the effluent was monitored by absorbance at 280 nm. Gel electrophoresis of proteins in fraction I (the void volume fraction containing polymerized complexes of spectrin, actin, and band 4.1), II (spectrin tetramers[5,7]), III (spectrin dimers[5,7]), and IV (mostly actin) was carried out in the system of Laemmli[32].

changes in the amount of spectrin tetramers and dimers in ghosts pretreated in various conditions are likely to reflect alterations in the equilibrium between the two spectrin species in the membrane *in situ* rather than a selective extraction of one of the two spectrin species from the membrane.

The transformation is readily reversible: spectrin dimers reassociate into tetramers in the membrane after restoration of isotonicity at 37 °C (Fig. 2f). Such reversibility indicates that spectrin tetramers are the physiological species and that the transformation of spectrin tetramers to dimers in the membrane in hypotonic conditions is a consequence of thermodynamic equilibrium but not a result of proteolytic degradation.

It is not surprising that at physiological ionic strength and temperature, spectrin tetramers are the predominant species in the membrane (Fig. 2a), whereas spectrin dimers predominate in identical conditions in solution (Fig. 1). Spectrin at the membrane surface is highly concentrated [probably about 230 mg ml^{-1} (ref. 10), that is about 100 to 1,000 times more than the concentration typically used in the *in vitro* studies of spectrin dimer–tetramer equilibrium]. Furthermore, membrane-associated spectrin is confined to two dimensions thus having a lower entropy than spectrin in solution.

The absence of higher self-association states of spectrin (such as hexamers or octamers) in the membrane and the presence of high molecular weight complexes (mw > 1.5×10^7) containing spectrin, actin and band 4.1 (Fig. 1) further suggest that spectrin tetramers are cross-linked non-covalently by other skeletal components such as actin and band 4.1 in the membrane, as recently also suggested by others[11–15].

To test the role of spectrin tetramer–dimer equilibrium in maintaining membrane structural integrity, we varied the ratio of spectrin dimers to tetramers in ghosts by incubating them at 37 °C in hypotonic conditions and subsequently examined the susceptibility of such ghosts or their Triton-insoluble membrane skeletons to fragmentation by mechanical shaking. Ghosts exposed to hypotonic conditions at 37 °C were not fragmented after a vigorous shaking (40 min, 1,550 oscillations per min). However, membrane skeletons prepared from such ghosts were more easily fragmented by shaking (Fig. 3f) than the skeletons from untreated ghosts (Fig. 3c). The instability of membrane skeletons exhibited a similar dependence on salt concentration in the medium as did the spectrin dimer–tetramer equilibrium in the native membranes. The decrease of

skeleton stability was noted in Triton-extracted samples prepared at both 25 °C and 0 °C.

Membrane skeletons and skeleton fragments in suspension were best visualized after staining with uranyl acetate.
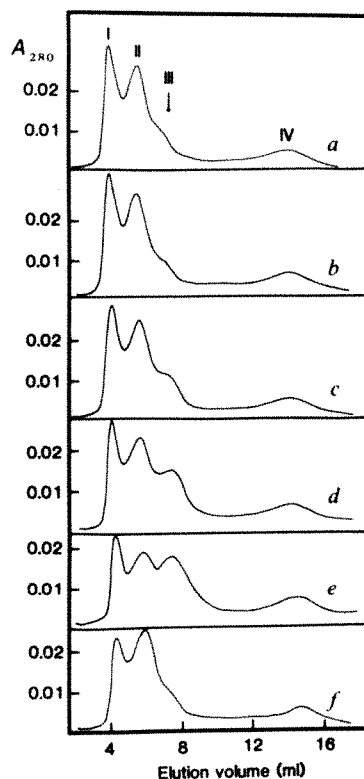
Fig. 2 Demonstration of spectrin transformation in the erythrocyte membrane by gel filtration analysis of crude spectrin extracts from ghosts incubated in hypotonic conditions. Before low ionic strength extraction and fractionation in the cold, as described in Fig. 1, ghost cells were incubated at 37 °C for 15 min in a buffer containing NaCl at 150 mM (a), 40 mM (b), 30 mM (c), 20 mM (d) and 10 mM (e). f Is the elution profile of crude spectrin derived from isotonic-buffer-reincubated ghosts (5 mM Na phosphate, 150 mM NaCl, 1 mM mercaptoethanol 37 °C, 15 min) which were previously hypotonic-buffer-incubated as in e.

RBC ghosts   Membrane skeletons Mechanically shaken
                                  membrane skeletons
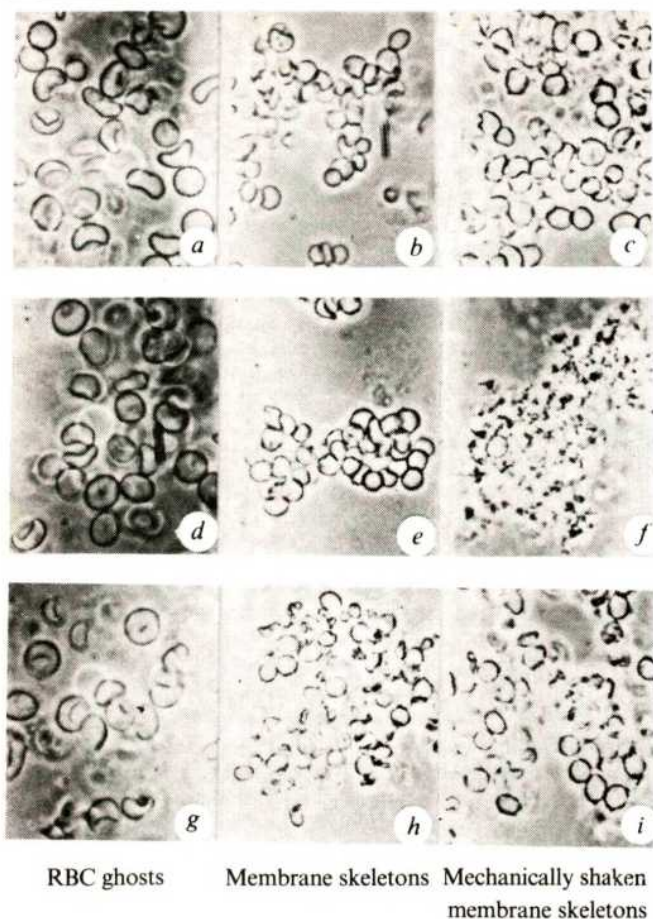
Fig. 3 Diminished stability of membrane skeletons from ghosts incubated at 37 °C in hypotonic conditions. *a*, Untreated; *d*, hypotonic-buffer-incubated (as in Fig. 2*e*); and *g*, isotonic-buffer-reincubated (as in Fig. 2*f*) ghosts were incubated at 25 °C for 15 min with two volumes of Triton X-100 solution[1] (3 % Triton X-100 in 5 mM Na phosphate, 1 mM mercaptoethanol *p*H 7.4) to remove most lipids and integral proteins from the ghosts. Aliquots (200 μl) of skeleton suspensions from these three samples were transferred to small test tubes (0.7 cm × 7 cm), mounted horizontally on a pipette shaker (Clay Adams, 1,550 oscillations per min) and examined morphologically before (*b*, *e*, and *h*, respectively), and after (*c*, *f*, and *i*, respectively) shaking (linear travel of 4 mm per oscillation) for 40 min at 4–6 °C. The membrane skeleton suspension (5 μl) was taken out of the tube, applied onto a siliconized glass slide, gently mixed with 1 % uranyl acetate (5 μl), covered with a siliconized cover slip, and examined under the phase contrast light microscope. A gross disintegration (>90 %) of membrane skeletons derived from ghosts incubated in hypotonic conditions was usually noted after shaking for about 30–50 min (40 min in Fig. 3*f*), whereas those derived from untreated or isotonic-buffer-reincubated ghosts usually remained intact (>90 %).

Although uranyl acetate artefactually induces a clumping and shrinking of membrane skeletons (Fig. 3*b*, *e*), the disintegration of skeletons into fragments can be easily recognized (Fig. 3*f*). A low concentration of uranyl acetate was used to avoid the precipitation of integral proteins from the suspension. Similar changes in stability of membrane skeletons were also observed in unstained skeletons after addition of >30 mM NaCl. NaCl did not induce skeleton clumping but it produced much less contrast for examination by phase contrast light microscopy.

Reincubation of the spectrin dimer enriched ghosts in isotonic conditions, which resulted in a reassociation of spectrin dimers to tetramers in the membrane (Fig. 2*f*), restored the skeletal stability to normal (Fig. 3*i*). Since no more than 1–3 % of spectrin is released into the supernatant in such conditions, we conclude that the transformation of

spectrin itself rather than the reattachment of spectrin to the membrane was responsible for the restoration of membrane skeleton stability.

Previous work suggests that the stability of membrane skeletons depends on the state of spectrin phosphorylation[16]. We have therefore explored the effect of red cell metabolic depletion on the spectrin tetramer–dimer equilibrium in the membrane. We have incubated intact red cells under nitrogen at 37 °C without metabolic substrates for 16 h to deplete red-cell ATP levels to less than 10 % of preincubation values. ATP depletion in such cells did not alter the proportion of spectrin tetramers and dimers in freshly prepared ghosts or in ghosts subsequently subjected to incubation at 37 °C in isotonic or hypotonic conditions (data not shown). Thus, the spectrin tetramer–dimer equilibrium is probably not influenced by spectrin phosphorylation–dephosphorylation[8].

A decrease in membrane skeleton stability has recently been reported after treatment of skeletons with DNase-I[15], which is associated with a depolymerization of actin oligomers in the membrane skeleton. Thus, it seems that both spectrin tetramers and actin oligomers may serve as important structural links in the membrane skeleton. This is consistent with the recent membrane skeleton model[10,17,18], which postulates flexible spectrin tetramer fibres connected into a two-dimensional network by oligomeric complexes of actin and band 4.1. Recent evidence further indicates that this skeletal network is linked to the erythrocyte membrane through interaction of spectrin with ankyrin or syndein[19-22] (band 2.1, which anchors spectrin to the major transmembrane protein, band 3), interaction of spectrin with negatively charged phospholipids[23], and binding of oligomeric actin to unidentified membrane binding sites[24]. Cross-linking studies also suggest a proximity of band 1 of spectrin and band 3 in the membrane[25]. It is possible that these interactions may strengthen skeleton stability *in situ* and hence, account for a normal mechanical stability of spectrin dimer enriched ghosts. It remains to be determined whether the altered spectrin dimer–tetramer equilibrium further affects other membrane phenomena such as the distribution and mobility of intramembrane particles[26-29] and glycoproteins[30], or membrane deformability.

1. Yu, J., Fischman, D. A. & Steck, T. L. *J. supramolec. Struct.* **1**, 233–248 (1973).
2. Lux, S. E., Joh, K. M. & Karnovsky, M. J. *J. clin. Invest.* **58**, 955–963 (1976).
3. Sheetz, M. P. & Sawyer, D. *J. supramolec. Struct.* **8**, 399–412 (1978).
4. Liu, S. C. & Palek, J. in *Erythrocyte Mechanics and Blood Flow* (eds Cokelet, G. R. *et al.*) 15–29 (Liss, New York, 1980).
5. Ralston, G. B. *Aust. J. biol. Sci.* **28**, 259–266 (1975).
6. Kam, Z., Josephs, R., Eisenberg, H. & Gratzer, W. B. *Biochemistry* **16**, 5568–5572 (1977).
7. Ralston, G. B., Dunbar, J. & White, M. *Biochim. biophys. Acta* **491**, 345–348 (1977).
8. Ungewickell, E. & Gratzer, W. *Eur. J. Biochem.* **88**, 379–385 (1978).
9. Shotton, D., Burke, B. & Branton, D. *Biochim. biophys. Acta* **536**, 313–317 (1979).
10. Lux, S. E. *Semin. Hemat.* **16**, 21–51 (1979).
11. Dunbar, J. C. & Ralston, G. B. *Biochim. biophys. Acta* **510**, 283–291 (1978).
12. Brenner, S. L. & Korn, E. D. *J. biol. Chem.* **254**, 8620–8627 (1979).
13. Cohen, C. M. *J. Cell Biol.* **83**, 308a (1979).
14. Ungewickell, E., Bennett, P. M., Calvert, R., Ohanian, V. & Gratzer, W. B. *Nature* **280**, 811–814 (1979).
15. Sheetz, M. P. *J. Cell Biol.* **81**, 266–270 (1979).
16. Pinder, J. C., Bray, D. & Gratzer, W. B. *Nature* **270**, 752–754 (1977).
17. Palek, J. & Liu, S. C. *Semin. Hemat.* **16**, 75–93 (1979).
18. Palek, J. & Liu, S. C. in *Immunobiology of the Erythrocyte* (eds Sandler, S. G. *et al.*) 21–44 (Liss, New York, 1980).
19. Bennett, V. & Stenbuck, P. J. *J. biol. Chem.* **254**, 2533–2541 (1979).
20. Luna, E., Kidd, G. K. & Branton, D. *J. biol. Chem.* **254**, 2526–2532 (1979).
21. Yu, J. & Goodman, S. R. *Proc. natn. Acad. Sci. U.S.A.* **76**, 2340–2344 (1979).
22. Bennett, V. & Stenbuck, P. J. *Nature* **280**, 468–473 (1979).
23. Marinetti, G. V. & Crain, R. C. *J. supramolec. Struct.* **8**, 191–213 (1978).
24. Cohen, C. M. & Branton, D. *Nature* **279**, 163–165 (1979).
25. Liu, S. C. & Palek, J. *J. supramolec. Struct.* **10**, 97–109 (1979).
26. Elgsaeter, A. & Branton, D. *J. Cell Biol.* **63**, 1018–1036 (1974).
27. Peters, R., Peters, J., Tews, K. H. & Bahr, W. *Biochim. biophys. Acta* **367**, 282–294 (1974).
28. Fowler, V. & Branton, D. *Nature* **268**, 23–26 (1977).
29. Cherry, R. J., Burkli, A., Busslinger, M., Schneider, G. & Parish, G. R. *Nature* **263**, 389–393 (1976).
30. Nicolson, G. I. & Painter, R. G. *J. Cell Biol.* **59**, 395–406 (1973).
31. Fairbanks, G., Steck, T. L. & Wallach, D. F. H. *Biochemistry* **10**, 2606–2616 (1971).
32. Laemmli, U. K. *Nature* **227**, 680–685 (1970).

Is resistance of a muscle to fatigue controlled by its motoneurones?

V. R. Edgerton, G. E. Goslow Jr, S. A. Rasmussen & S. A. Spector

Departments of Kinesiology, Brain Research Institute, University of California, Los Angeles, California 90024 and Departments of Biological Sciences and Physical Education, Northern Arizona University, Flagstaff, Arizona 86011

The original experiment of Buller et al.[1] and the many subsequent confirmatory reports clearly show that the time-to-peak tension and many other speed-related parameters of slow and fast muscle fibres are dictated by the motoneurone[2]. It has been concluded that the motoneurone exerts this control of the physiological and associated biochemical properties by the frequency at which it excites the muscle fibre[3]. However, no studies have been reported on the fatigue properties and the associated biochemical characteristics after cross-reinnervation. Based on the 'size principle' of motoneurones[4], it would be reasonable to assume that a muscle fibre reinnervated by a small motoneurone would be active often and that this would be manifested biochemically as an elevated oxidative capacity[5]. Also, it has been shown repeatedly that the mitochondrial content of a muscle fibre can be modified by daily endurance type exercise[6]. Thus, it would seem that the motoneurone at least indirectly also controls the mitochondrial content of a muscle fibre by controlling the degree of activity. We have now tested this hypothesis using self- and cross-reinnervated muscles in cats. We found that fast- and slow-twitch muscles retained their characteristic fatigue resistance properties regardless of whether the nerve to which they had become connected had originally innervated a fatigue-resistant or relatively fatiguable muscle.

The soleus and flexor hallucis longus (FHL) muscles of nine cats were denervated and reinnervated with their own nerve or with the nerve which had formerly innervated the other muscle. One leg was always self-reinnervated while the contralateral limb was cross-reinnervated. After 12–14 months, 70 single motor units were isolated through ventral root dissection and studied as described by Goslow et al.[7]. Histochemical analyses were carried out as reported by Edgerton et al.[8].

Six of the nine animals produced muscles which had been reinnervated by both the contralateral and original nerves. Such a preparation was seen for six soleus muscles and two FHL muscles. Careful dissection distally from the point of original nerve transection facilitated the placement of stimulating electrodes on each of the two muscle nerves. Thus, confirmation of the isolation of an α axon belonging to either a self- or cross-reinnervated motor unit was provided by a record of an all-or-none action potential from the spinal nerve filament following stimulation of the distal whole muscle nerve.

The fatigue test, carried out at the end of the experiment, consisted of a 330-ms train of impulses delivered every second. The impulse frequency within each train was 40 Hz (ref. 9). These trains were continued for 4 min. The fatigue index chosen was the ratio, expressed as a percentage, of the accumulated peak tension during the first 2 min divided by the accumulated peak tension during the entire 4-min[10,11] test. This ratio ranges from 100% in a completely fatiguing muscle to 50% in one which is completely resistant to fatigue. Values below 50% indicate potentiation of the unit's response during the 4-min period.

The relationship between the distribution of times to peak tension of the isolated motor units and their fatigue indices is shown in Fig. 1. Based on the proportion of muscle
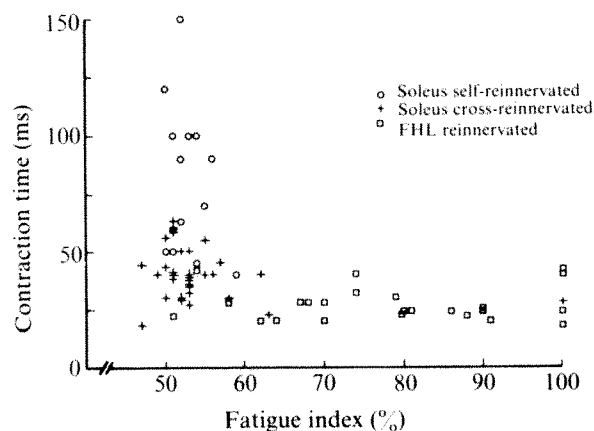
Fig. 1 The relationship between contraction time and the fatigue index (%, see text) for the soleus self-reinnervated ($n = 13$), soleus cross-reinnervated ($n = 33$) and FHL self-reinnervated ($n = 24$) motor units. Note that, with the exception of one cross-reinnervated soleus unit, all soleus units, either self-reinnervated or crossed with the nerve of the FHL, exhibit a similar resistance to fatigue.

histochemical fibre types[12] and motor unit types[13] in the normal FHL muscle, if the motoneurone was responsible for the endurance properties of the innervated fibres, approximately 65–70% of the cross-reinnervated motor units in the soleus would have been expected to have demonstrated considerable fatigue. However, of the 33 soleus cross-reinnervated motor units studied, only one unit became severely fatigued. The profile of fatigue indices for all other cross-reinnervated units (mean of 52%) was almost identical ($P > 0.05$) to that for the self-reinnervated soleus units (mean of 53%): all of these units were highly resistant to fatigue. In contrast, the 24 motor units from the self-reinnervated flexor muscles exhibited a wide spectrum (51–100%) of fatigue indices (mean 78%), which tallies well with histochemical[12] and physiological[13] findings for normal FHL muscle.

The tension and electromyographic potential from the stimulation pulses from a soleus motor unit reinnervated by a foreign flexor nerve are shown in Fig. 2. Note that the first and last trains of impulses induced similar peak forces in the cross-reinnervated soleus motor unit. Additionally, this unit showed no sag property[14] when stimulated at a sub-fusion frequency.

Consistent with the high resistance to fatigue in the cross-reinnervated soleus units, the histochemical population of these units consisted solely of slow-oxidative- and fast-oxdiative-type fibres[15] as shown in Fig. 3. Also, for those soleus cross-reinnervated fibres that stained lightly with myofibrillar ATPase, pH 10.4, the staining profile for the glycolytic enzyme α-glycerophosphate dehydrogenase (Fig. 3c)
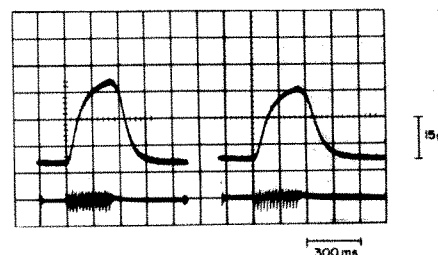
Fig. 2 The fatigue response of a soleus motor unit cross-reinnervated with an FHL nerve. The contraction on the left represents the initial tetanic tension developed (20 g) in response to a 40-Hz train of impulses lasting 330 ms, and the contraction on the right illustrates the tension developed at the end of the 4-min fatigue test (see text). The fatigue index of this unit was 50%. The time to peak tension was 40 ms, and its twitch tension was 1.2 g. The twitch was potentiated by 50% with a tetanus; no 'sag' of the tetanus was evident.

was completely transformed to that expected for fast-oxidative-glycolytic fibres[15]. This type of enzyme profile is rare in the normal soleus muscle[12]. Interestingly, the soleus muscle in which the fatiguable unit was found did not differ histochemically from the other soleus cross-reinnervated muscles. In no instance did a cross-reinnervated fibre that stained darkly for myofibrillar ATPase not stain darkly also for α-glycerophosphate dehydrogenase. The reverse was not always true. The remaining cross-reinnervated fibres maintained the enzyme profile typical of a normal cat soleus muscle. No fibres could be classified as fast twitch glycolytic in self- or cross-reinnervated soleus muscle. Fibres in the self-reinnervated soleus and FHL (Fig. 4) muscles rarely contained any enzyme profile different from those observed in the normally innervated muscles[12].

There are several possible explanations for the maintenance of the fatigue resistance properties of the soleus muscle cross-reinnervated by a nerve that normally innervates a relatively fatiguable muscle. Based on normal data[12], one would expect that approximately 70% of the motor units would be very fatiguable assuming that the reinnervation process was random. The possibility that the motor units that innervate the fatigue-resistant muscle fibres may have reinnervated more effectively is not supported by the normal ratio of motor unit and histochemical types seen after self-reinnervation in the FHL muscle (Fig. 4). A second plausible explanation is that whatever the variable associated with excitation of the muscle (pattern or degree of activity) that one might assume to have changed was not actually modified by the cross-reinnervation. However, if this were the case, the major underlying assumption of the cross-reinnervation study by Salmons and Sreter[3] and many others who conclude that impulse pattern was the factor regulating the physiological and contractile properties would require re-evaluation. A third and perhaps

Fig. 4 A high percentage of low NADH-D-staining fibres are seen in the self-reinnervated FHL muscle (*a*), consistent with the concept that many of the FHL axons that reach the soleus would be expected to result in a high proportion of easily fatigued units. Figure 4*b* illustrates the ATPase, *p*H 10.4 preincubation, and *c*, the ATPase, *p*H 4.6 preincubation, for the same muscle. These staining profiles are consistent with normal muscle. Scale bar in upper right corner indicates 100 μm.

more plausible interpretation is that the basic genetic programme which regulates mitochondrial content in a muscle fibre is determined to a major extent by factors within the fibre. Although the quantity of mitochondria can be readily modified by stimulation[16] or by introducing an exercise training programme[6], this does not justify the assumption that activity level is the sole or even basic mechanism dictating mitochondrial concentration in a muscle fibre. This interpretation is supported by the finding that the normal array of fatigue properties and histochemical profiles in soleus and gastrocnemius motor units still exists 3 months after a low thoracic complete transverse section of the spinal cord[17].

1. Buller, A. J., Eccles, J. C. & Eccles, R. M. *J. Physiol., Lond.* **150**, 417–439 (1960).
2. Close, R. *Nature* **206**, 831–832 (1965).
3. Salmons, S. & Sreter, F. A. *Nature* **263**, 30–34 (1976).
4. Henneman, E., Somjen, G. G. & Carpenter, D. D. *J. Neurophysiol.* **38**, 560–580 (1965).
5. Burke, R. E. & Edgerton, V. R. in *Exercise and Sports Science Reviews* Vol. 3 (eds Wilmore, J. H. & Keogh, J. F.) 31–81 (Academic, New York, 1975).
6. Baldwin, K., Klinkerfuss, G. H., Terjung, R. L., Mole, P. A. & Holloszy, J. O. *Am. J. Physiol.* **222**, 373–378 (1972).
7. Goslow, G. E. Jr, Stauffer, E. K., Nemeth, W. C. & Stuart, D. G. *J. Morph.* **137**, 335–352 (1972).
8. Edgerton, V. R., Barnard, R. J., Peter, J. B., Maier, A. & Simpson, D. R. *Expl Neurol.* **46**, 115–131 (1975).
9. Burke, R. E., Levine, D. N., Zajac, F. E. III, Tsairis, P. & Engel, W. K. *Science* **174**, 709–712 (1971).
10. Stephens, J. A., Gerlach, R. L., Reinking, R. M. & Stuart, D. G. *Control of Posture and Locomotion* (eds Stein, R. B., Pearson, K. G., Smith, R. S. & Redford, J. B.) 179–185 (Plenum, New York, 1973).
11. Reinking, R. M., Stephens, J. A. & Stuart, D. G. *Expl Brain Res.* **23**, 301–313 (1975).
12. Ariano, M., Armstrong, R. B. & Edgerton, V. R. *J. Histochem. Cytochem.* **21**, 51–55 (1973).
13. Westerman, R. A. *Studies in Neurophysiology* (ed. Porter, R.) 313–337 (Cambridge University Press, 1978).
14. Peter, J. B., Barnard, R. J., Edgerton, V. R., Gillespie, C. A. & Stempel, K. E. *Biochemistry* **11**, 2627–2633 (1972).
15. Burke, R. E. & Tsairis, P. *J. Physiol., Lond.* **234**, 749–765 (1973).
16. Pette, D. *et al. Pflügers Arch. ges. Physiol.* **361**, 1–7 (1975).
17. Edgerton, V. R., Smith, L. A. & Eldred, E. *Neurosci. Abstr.* **5**, 369 (1979).

Fig. 3 Serial cross-sections of a cross-reinnervated soleus muscle stained for NADH-D (*a*), myofibrillar ATPase, *p*H 4.35 preincubation (*b*), α-glycerophosphate dehydrogenase (*c*) and myofibrillar ATPase, *p*H 10.4 preincubation (*d*). Note the scattered array of a relatively few fibres staining intensely for ATPase (*p*H 10.4) and a rather high and homogeneous staining for NADH-D. Note also that all the darkest-staining fibres in *c* correspond to the dark fibres in *d* and the light ones in *b*, whereas moderately stained fibres in *c* cannot be identified in *d*. Fibre type grouping was the exception rather than the rule in all self-reinnervated and cross-reinnervated muscles. Scale bar in upper right corner indicates 100 μm.

MATTERS ARISING

Bounds on food web connectance

REJMÁNEK AND STARÝ[1] have shown that the product of the number of species in a community (*m*) and the proportion of possible interactions (*C*) is a constant; that is, their relationship is hyperbolic. Though the authors present this as only an empirical result it is consistent with May's[2] result derived from considerations of model stability. However, an alternative, perhaps simpler explanation suffices. Suppose that each species in a community has a number of predator and prey species independent of the number of species in the community. The number of interactions in the system scales in proportion to the number of species in the system. However, the potential number of interactions scales as $m(m-1)$, if we exclude intraspecific effects. Thus, the connectance scales as $1/(m-1)$ which, for large *m* will be indistinguishable from the result predicted by May[2]. Such hyperbolic relationships between species number and connectance are apparent in a number of collections of food webs[3,4] though Rejámanek and Starý's data are unique in being collected by the same authors on comparable systems.

Although I agree that stability constraints make interesting predictions about food web design[5-7], many of which are supported by data in the real world[4,7], hyperbolic relationships between *C* and *m* must be considered ambiguous: a constant number of predators and prey per species might be caused by various factors other than system stability.

The webs shown in Fig. 1 of ref. 1 are quite remarkable in that they lack species that feed on more than one trophic level (omnivores). Omnivores average one per top predator in food webs dominated by vertebrates and considerably more in webs composed of insects, their parasitoids and hyperparasitoids[4]. The absence of omnivores may be a result of omitting hyperparasitoids (which are highly omnivorous), and (or) placing emphasis on the prey's predators, rather than all the prey of a particular predator. Considering only a species' predators gives source webs, in Cohen's[3] terminology, considering all the prey gives sink webs. Cohen's single source web is also unusually simple[4,7]. If omissions have been made they will reduce the connectance of the webs.

Counting interactions directly between species that share the same food supply implies competition over and above that for these shared resources. Even intraspecific interference appears unusual in insects, though data are few[8]. Adding connections in this way will increase the apparent connectance.

Finally, I must caution the use of May's inequality for the kind of data discussed here. May's result that *mC* should be less than one divided by the squared interaction strength comes from the application of the semicircular law[9,10]. Assuming a number of features which, at best, are only approximated by insect population dynamics, one obtains this result: a semicircle describes the frequency distribution of the real parts of all the eigenvalues. The semicircle is centred on the average of the self-limiting terms in the system. May assumed all the self-limiting terms to be unity and so unity appears in the numerator of the inequality. This is probably appropriate for communities composed entirely of resource limited competitors, but does not seem reasonable for food webs. Here, only species at the base of the web are likely to suffer external resource limitation[11], though the phenomenon of 'pseudo-interference' in insect–parasitoid systems will add more self-limiting terms[12,13]. In short, if connectance were to be restricted by stability considerations, one might expect the limit to be related to the number of externally resource limited species, and for this number to vary between systems. I thank Post *et al.*[14] for a discussion on this last point.

STUART L. PIMM

Department of Biological Sciences,
Texas Tech University,
Lubbock, Texas 79409

1. Rejmanek, M. & Starý, P. *Nature* **280**, 311–313 (1979).
2. May, R. M. *Nature* **238**, 413–414 (1972).
3. Cohen, J. E. *Food Webs and Niche Space* (Princeton University Press, 1978).
4. Pimm, S. L. *Ecology* (in the press).
5. Pimm, S. L. *Theor. Pop. Biol.* **16**, 144–158 (1979).
6. Pimm, S. L. & Lawton, J. H. *Nature* **268**, 329–331 (1977).
7. Pimm, S. L. & Lawton, J. H. *Nature* **275**, 542–544 (1978).
8. Whitham, T. G. *Nature* **279**, 324–325 (1979).
9. Mehta, M. L. *Random Matrices* (Academic, New York, 1967).
10. Wigner, E. O. *Proc. fourth Can. Math. Congr.*, Toronto, 174–184 (1959).
11. Lawton, J. H. & Pimm, S. L. *Nature* **272**, 189–190 (1978).
12. Free, C. A., Beddington, J. R. & Lawton, J. H. *J. Anim. Ecol.* **46**, 543–554 (1977).
13. Hassell, M. P. *Arthropod Predator-Prey Systems* (Princeton University Press, 1979).
14. Post, W. M., Shugart, H. H. & DeAngelis, D. L. *Oak Ridge natn. Lab. Tech. Mem.* 6475 (1978).

REJMÁNEK AND STARÝ REPLY—Pimm is right to suppose that the number of predators and prey per species may be independent of the number of species in the community (or, more precisely, there is a constant mean number of edges per vertex in diagrams of food webs). Unfortunately, this fact can hardly be viewed as an attribute of species *per se*. At the moment, dynamical community constraints seem to provide a more plausible explanation of why *mC* is constant.

In his discussion Pimm repeats in more words what we said in our last sentence[1], and we agree with him. Only the introduction of hyperparasitoids of the genus *Dendrocerus* (Hymenopteria, Ceraphronoidea) and predators of the family Syrphidae (Diptera) into our[1] plant–aphid–parasitoid food webs raises the value of *mC* to a figure comparable to the mean for Cohen's web collection. On the basis of data available to us[2], the *mC* product for Cohen's 'community' and 'sink' food webs exhibited mean values of 4.21 and 5.29, respectively.

Incidentally, hyperparasitoids of aphids are rarely omnivorous[3-7]. A high proportion of omnivorous species seems to be typical of inherently unstable communities such as inhabitants of oak galls[8].

Pimm's most important point is the question of the number of self-limited species in real food webs. According to him, diagonal elements of interaction matrices should be zero for all consumer species. The importance of the number of externally resource limited species for stability of such matrices has been stressed by Saunders[9]. We agree that self-regulation of consumer species is rather rare in nature and only scattered evidence[10-13] supports May's[14] assumption of self-regulation at all trophic levels. The constant value $a_{ii} = -1$ is, of course, artificial and has been chosen by May to set a time scale for damping time. Some increasing probability density function on the interval $\langle -1,0 \rangle$ seems to be more realistic. This implies shifting the critical values for stability in May's model to lower 'tolerable' connectance. But most of the links in food web diagrams are in no way density dependent or controlling[15]. Then, an increasing number of species does not necessarily cause a decrease in the probability that the interaction matrix will be stable (resilent in the sense of Harrison[16]): the main point of our[1] letter.

M. REJMÁNEK
P. STARÝ

Institute of Entomology,
Czechoslovak Academy of Sciences,
Viničná 7, 128 00 Praha 2,
Czechoslovakia

1. Rejmánek, M. & Starý, P. *Nature* **280**, 311–313 (1979).
2. MacDonald, N. J. *J. theor. Biol.* (in the press).
3. Evenhuis, H. H. *Entomophaga* **9**, 227–231 (1964).
4. Takada, H. *Insecta Matsum.* N.S. **2**, 1–76 (1973).
5. Starý, P. *Acta ent. bohemoslov.* **74**, 1–9 (1974).
6. Askew, R. R. *Parasitic Insects* (Heinemann, London, 1971).
7. Clausen, C. P. *Entomophagous Insects* (Hafner, New York, 1962).
8. Askew, R. R. *Trans. Soc. Br. Ent.* **14**, 237–268 (1961).
9. Saunders, P. T. *Nature* **272**, 189 (1978).
10. Way, M. J. & Cammel, M. E. *Animal Populations in Relation to their Food Resources* (ed. Watson, A.) 229–247 (Blackwell, Oxford, 1970).
11. Kluijver, H. H. *Ardea* **39**, 1–135 (1951).

12. Brown, G. C., Berryman, A. A. & Bogyo, T. P. *Envir. Ent.* **7**, 222 (1978).
13. Menšutkin, V. V., Žakov, L. A. & Umnov, A. A. *Vopr. Icht.* **8**, 881–891 (1968).
14. May, R. M. *Stability and Complexity in Model Ecosystems* (Princeton University Press, 1973).
15. Beddington, J. R. & Lawton, J. H. *J. Phys.* **39**, Colloque

Bombesin—satiety or malaise?

IT has recently been claimed by Gibbs et al.[1] that bombesin (BBS), like cholecystokinin (CCK), produces satiety in rats. However, their report ignores crucial evidence and lacks critical controls.

First, there is good evidence that CCK suppresses feeding because it produces malaise. This has been shown by appropriate conditioned taste aversion tests[2]. Reports of aversive symptoms in human subjects injected with small doses of CCK corroborate the evidence from rats[3]. Further, doses of CCK that produce food intake suppression produce abnormal patterns of duodenal activity, quite different from the patterns observed during normally induced satiety, from which it is concluded that the amounts of CCK injected to produce intake suppression are much larger than those that are normally secreted[4].

Second, Gibbs et al.[1] present no relevant evidence to show that BBS in the dose injected is not an aversive agent. It is well known[5,6] that even quite powerful doses of some agents producing conditioned taste aversion produce no observable symptoms of distress. Moreover, only a very small dose of one such agent (LiCl) is necessary to suppress food intake to the extent reported for BBS[7]. Gibbs et al.[1] did not use the conditioned taste aversion test to screen for aversive effects. (In such a test a taste is followed by a dose of the agent being tested for aversive properties. If the taste is avoided in a subsequent test, this shows that the agent is indeed aversive.) It has been argued that the results of such a test are ambiguous: conditioned satiation[8] could lead to a reduction of intake in the same way as conditioned aversion; or, satiation and mild discomfort or malaise may in fact be identical. Both such arguments are contradicted by the experimental evidence. Conditioned satiation would resemble conditioned aversion in a situation where the rat is presented only with the conditioned taste in the test (the so-called single bottle test). However, in a two bottle test where the rat chooses between a neutral solution and the conditioned solution, experiments have shown that when the proper nutrient solutions[9,10] as well as other reinforcers[11] are paired with a taste then that taste is preferred over a neutral taste in a subsequent test. On the other hand, when aversive agents are paired with a taste, that taste is avoided[12,13].

Clearly, conditioned satiation leads to the opposite result that conditioned aversion does. Such results also dispose of the second argument. If satiation was aversive, stimuli conditioned to it would not be preferred. Even tastes paired with very weakly aversive stimuli produce an aversion[7]. Without evidence from proper behavioural screening tests, the claim that bombesin is a satiety agent cannot be taken seriously. At present it seems most probable that BBS, like CCK, is being administered in unphysiological doses and is therefore suppressing food intake by producing malaise.

J. A. DEUTSCH

Department of Psychology,
University of California,
San Diego, La Jolla,
California 92093

1. Gibbs, J. *et al. Nature* **282**, 208–210 (1979).
2. Deutsch, J. A. & Hardy, W. T. *Nature* **266**, 196 (1977).
3. Sturdevant, R. A. L. & Goetz, H. *Nature* **261**, 713–715 (1976).
4. Deutsch, J. A., Thiel, T. R. & Greenberg, L. H. *Behav. Biol.* **24**, 393–399 (1978).
5. Gamzu, E. in *Learning Mechanisms in Food Selection* ch. 19 (eds Barker, L. M., Best, M. R. & Domjan, M.) 477–509 (Baylor Univ. Press, 1977).
6. Barker, L. M., Smith, J. C. & Suarez, E. M. in *Learning Mechanisms in Food Selection* ch. 21 (eds Barker, L. M., Best, M. R. & Domjan, M.) 533–553 (Baylor Univ. Press, 1977).
7. Deutsch, J. A. & Gonzalez, M. *Behav. Biol.* **24**, 317–326 (1978).
8. Booth, D. A. *J. comp. Physiol. Psychol.* **81**, 457–471 (1972).
9. Holman, G. L. *J. comp. Physiol. Psychol.* **69**, 432–441 (1968).
10. Puerto, A., Deutsch, J. A., Molina, F. & Roll, P. *Behav. Biol.* **18**, 123–134 (1976).
11. Zahorik, D. M. in *Learning Mechanisms in Food Selection* ch. 8 (eds Barker, L. M., Best, M. R. & Domjan, M.) 181–199 (Baylor Univ. Press, 1977).
12. Grote, F. W. Jr & Brown, R. T. *Behav. Res. Meth. Instrum.* **3**, 311–312 (1971).
13. Dragoin, W., McCleary, G. E. & McCleary, P. *Behav. Res. Meth. Instrum.* **3**, 309–310 (1971).

GIBBS AND SMITH REPLY—We did not use a conditioned taste aversion paradigm in our study of the effect of bombesin (BBS) on feeding[1] because this paradigm can no longer be considered a critical test of the presence or absence of malaise[2]. As a variety of agents (including isotonic saline and chlorpromazine, a drug with anti-nausea action) which serve as effective unconditioned stimuli for the formation of conditioned taste aversions[3,4] do not produce sickness, the conditioned taste aversion test cannot be used as evidence of sickness. Conversely, as some rapidly acting rodenticides (including strychnine and cyanide) do not produce a conditioned taste aversion[5], the failure to produce a taste aversion is not evidence that rats are not sick[6]. Thus, sickness is neither necessary nor sufficient for the formation of a conditioned taste aversion.

We rely instead on our demonstrations that BBS fails to affect the initial rate of feeding, fails to affect body temperature, fails to affect water ingestion in the range

of doses that reduce food intake, and selectively affects feeding[1]. These results are good evidence that the effect we report on feeding is not due to sickness; none of these results would have been predicted if BBS were acting simply by producing illness. We have previously reported very similar observations[7] as indications that the action of cholecystokinin (CCK) on food intake is not due to malaise, and it is important that these observations have proved to be excellent predictors of the results of human studies.

The satiety effect of CCK in humans has been dissociated from subjective reports of discomfort in three studies to date. The first report was that of Sturdevant and Goetz[8], which Deutsch misquotes. These authors demonstrated that, while an intravenous (i.v.) injection of impure CCK at a high dose produced side effects, an i.v. injection of a lower dose significantly reduced food intake without causing any side effects or discomfort. This critical dissociation has now been reproduced twice in humans: pure or highly purified preparations of CCK reduce food intake[9] and ratings of appetite[10] without producing reports of illness.

Deutsch concludes by assuming that CCK and BBS are producing malaise because the doses are unphysiological. We have previously shown that intraperitoneal injections of impure CCK as small as 2.5 Ivy units kg^{-1} will reduce food intake in rats[7] and that a slow i.v. infusion of a pure preparation of CCK as small as 30 ng kg^{-1} will reduce food intake in humans[9]. Both doses are within the ranges required to achieve the classic visceral effects of the hormone in each species, and are therefore likely to be physiological.

The evidence does not support Deutsch's dismissal of the actions of CCK and BBS on food intake. The possibility that these peptides have a role in satiety can be taken seriously.

J. GIBBS
G. P. SMITH

Department of Psychiatry,
Cornell University Medical College,
Bourne Laboratory,
The New York Hospital,
White Plains, New York 10605

1. Gibbs, J. *et al. Nature* **282**, 208–210 (1979).
2. Smith, G. P. & Gibbs, J. in *Progress in Psychobiology and Physiological Psychology* Vol. 8 (eds Sprague, J. M. & Epstein, A. N.) 179–242 (Academic, New York, 1979).
3. Berger, B. D. *J. comp. Physiol. Psychol.* **81**, 21–26 (1972).
4. Revusky, S. H., Smith, Jr, M. H. & Chalmers, D. V. *Physiol. Behav.* **6**, 341–343 (1971).
5. Nachman, M. & Hartley, P. L. *J. comp. Physiol. Psychol.* **89**, 1010–1018 (1975).
6. Deutsch, J. A. & Gonzalez, M. F. *Behav. Biol.* **24**, 317–326 (1978).
7. Gibbs, J., Young, R. C. & Smith, G. P. *J. comp. Physiol. Psychol.* **84**, 488–495 (1973).
8. Sturdevant, R. A. L. & Goetz, H. *Nature* **261**, 713–715 (1976).
9. Kissileff, H. R., Pi-Sunyer, F. X., Thornton, J. & Smith, G. P. *Clin. Res.* **27**, 552A (1979).
10. Stacher, G., Bauer, H. & Steinringer, H. *Physiol. Behav.* **23**, 325–331 (1979).

Mélange in Trondheim Nappe, central Norwegian Caledonides

THE speculative conclusions of Horne[1] following his contention that mélange is present in the Trondheim Nappe of central Norway are untenable in the light of our current knowledge of this region. Three main objections may be raised.

(1) The crude 'fanning of structural surfaces' across regional strike, which is central to Horne's model, is documented in several tectonic structural studies of the central Scandinavian Caledonides as a product of the Silurian evorogenic deformation, and can in no way be construed as representing a subduction-related accretionary fan-structure.

(2) Accretionary prisms of arc–trench subduction complexes are composed principally of offscraped oceanic sediments, igneous rocks and trench-fill deposits. In Horne's[1] hypothetical model (his Fig. 5) the prism embraces four tectonostratigraphic units ranging from low-grade, Ordo-Silurian volcanites and flyschoid (Köli) metasediments in the east, through high-grade Gula (Seve) migmatites and gneisses of probable Sveconorwegian or older age, and into the low-grade 'Selbusjøen mélange' in the west. An accretionary prism of such extreme age range and embracing long-transported nappes of varying origin[4,5] is incompatible with the composition and derivation of forearc subduction complexes.

(3) Continuing studies of volcanite geochemistry (major, trace and rare earth elements) confirm earlier results[4,6] showing that the Støren Group metabasalts are ocean-floor tholeiites. With the discovery of associated sheeted dolerite dykes and gabbro in one area[7], the interpretation of the Støren as an ophiolite fragment[8] is even more secure. In contrast, the Fundsjø Group contains a greater proportion of acidic extrusives, and basalt geochemistry reveals that both island arc and ocean-floor tholeiites are represented[9]. Horne's[1] diagram, showing the Støren as a magmatic arc and the Fundsjø as an 'oceanic remnant'—with the Støren and Fundsjø transposed—is, therefore, misleading.

Despite these criticisms, the presence of a mélange of latest Cambrian oceanic and trench sediments, with pre-Arenig fan-thrusting and folding, would not be out of place in this ophiolite setting, but detailed mapping would be required to ascertain its true character.

A final point, and one of major importance in a consideration of Horne's hypothesis, is that the concept of Silurian, pre-F_1 obduction[4] has been discarded. Based on analysis of new data from mapping and structural studies, the Støren–Fundsjø obduction, eastward on Gula rocks, is now considered to date to pre-Middle Arenig time[8,10], of Finnmarkian/Grampian age[11], with the

Lower Hovin deposited on the folded and uplifted ophiolite fragment[8,12,13]. This situation is comparable with that in the Lower Palaeozoic of western Norway[8,10,11]. Continuing southeastward subduction during Ordovician time, although perhaps located further to the west, produced an Arenig–Llanvirn volcanic arc and marginal basin spreading[12-14]. Horne's[1] interpretations, therefore, conflict with the results of other recent research in the Trondheim region Caledonides[7-14].

D. ROBERTS
Norges geologiske undersøkelse,
Post Box 3006,
7001 Trondheim,
Norway

1. Horne, G. S. *Nature* **281**, 267–270 (1979).
2. Dickinson, W. R. in *Island Arcs, Deep Sea Trenches and Back-arc Basins* (eds Talwani, M. & Pitman, W. C.) 33–40 (American Geophysical Union, 1977).
3. Scholl, D. W., Marlow, M. S. & Cooper, A. K. in *Island Arcs, Deep Sea Trenches and Back-arc Basins* (eds Talwani, M. & Pitman, W. C.) 199–210 (American Geophysical Union, 1977).
4. Gale, G. H. & Roberts, D. *Earth planet. Sci. Lett.* **22**, 380–390 (1974).
5. Gee, D. G. *Am. J. Sci.* **275-A**, 468–515 (1975).
6. Roberts, D. & Gale, G. H. *Geol. Soc. Lond. Misc. Pap.* **2**, 11–13 (1974).
7. Grenne, T., Grammeltvedt, D. & Vokes, F. M. *Proc. int. Ophiolite Symp.* Cyprus (in the press).
8. Furnes, H., Roberts, D., Sturt, B. A., Thon, A. & Gale, G. H. *Proc. int. Ophiolite Symp.* Cyprus (in the press).
9. Vokes, F. M. & Grenne, T. *Caledonian Orogen 1977*, Årsrapport, 54–59 (IGCP, 1978).
10. Furnes, H. *Proc. IGCP Symp.* Blacksburg (U.S. Geological Survey, 1979).
11. Sturt, B. A., Thon, A. & Furnes, H. *Geology* **7**, 316–320 (1979).
12. Ryan, P. D., Williams, D. M. & Skevington, D. *Proc. IGCP Symp.* Blacksburg (U.S. Geological Survey, 1979).
13. Bruton, D. L. & Bockelie, J. F. *Proc. IGCP Symp.* Blacksburg (U.S. Geological Survey, 1979).
14. Roberts, D. & Gale, G. H. in *Evolution of the Earth's Crust* (ed. Tarling, D. H.) 255–324 (Academic, New York, 1978).

HORNE REPLIES—Roberts' objections to my speculative model for the early development of the Trondheim Nappe do not bear directly on the tenability or applicability of my hypothesis. My brief response to each criticism follows.

(1) Roberts' structural arguments are debatable, yet he offers no evidence to support his contention. Clearly, an inherited fan structure would have been reactivated during and after obduction as the Trondheim Nappe was translated eastward during the Silurian. The problem involves dating the initial deformation and identifying the cause of earliest thrusting. I interpret Roberts' F_1 deformation[1] as occurring synchronously with the accretion process.

(2) Roberts' second criticism contains several inaccuracies. My Fig. 5 (ref. 2) shows that, although I presumed that the Seve and Köli sequences had been bulldozed in front of and obducted with the Trondheim Nappe, I did not consider them to have been incorporated into the forearc region by sea-floor accretion.

Comprehensive and comparative studies of forearc regions[3] show that subduction complexes are indeed characterized by heterogeneous stratal assemblages that include various igneous rocks, metamorphic tectonites, chaotic mélanges, and isoclinally folded sequences of bedded sediments that "represent a wide range of oceanic environments" (p. 19, ref. 3). Roberts' supposition that the Gula Group is Precambrian is based on a tenuous correlation with tectonites exposed to the west of the main Trondheim succession that have only been indirectly implicated to be Precambrian[4].

(3) The statement that Støren metavolcanics are ocean-floor tholeiites is misleading. They are spillitic greenstones that have suffered both regional metamorphism and local metasomatic alteration. The presence of associated bedded pyroclastics, including lappili tuff and limestone, certainly argues against a deep marine environment. Notwithstanding recent evidence[5] from modern sea-floor basalts that warns strongly against using trace element composition for tectonic labelling, Roberts has used the trace element distribution within Støren greenstones to ascribe the Støren to either ocean floor or arc settings[6]. Intra-ocean arcs clearly must be built on and from the oceanic lithosphere, and many ensimatic arcs tend to nucleate along transform faults with attendant ophiolite emplacement[7]. The infrastructure of such arcs should indeed comprise ophiolite fragments[8], as Roberts testifies.

Roberts' final point concerning the Hovin having been deposited unconformably on folded Støren metavolcanics contradicts well codumented field evidence from many areas in the Trondheim region. I agree that the age evidence bearing on time of obduction is crucial, and that it demands critical analysis.

Note added in proof: Very recent evidence from Troms[9] casts doubt on the concept of pre-Arenig Sinnmarkian abduction.

GREGORY S. HORNE
Wesleyan University,
Middletown, Connecticut 06457

1. Roberts, D., Springer, J. & Wolff, F. C. *Geol. Mag.* **107**, 133–145 (1970).
2. Horne, G. S. *Nature* **281**, 267–270 (1979).
3. Dickensen, W. R. & Seely, D. R. *Bull. Am. Ass. Petrol.* **63**, 2–31 (1979).
4. Råheim, A. *Norsk geol. Tidsskr.* **57**, 193–204 (1977).
5. Kay, R. W. *Earth planet. Sci. Lett.* **38**, 95–116 (1978).
6. Gale, G. H. & Roberts, D. *Earth planet. Sci. Lett.* **22**, 380–390 (1974).
7. Dewey, J. F. & Casey, J. F. *Geol. Soc. Am. Abstr.* **11**, 413 (1979).
8. Upadhyay, H. D. & Neale, E. R. W. *Earth planet. Sci. Lett.* **43**, 93–102 (1979).
9. Binns, R. E. & Gayer, R. A. *Nature* **284**, 53–55 (1980).

Exploring pictures by hand

RECENTLY, Magee and Kennedy[1] have found that blindfolded sighted people can identify a raised-line drawing more readily when the index finger of one hand is guided along its outline than when the finger is allowed to trace the figure without guidance. This finding could evidently be used in perfecting methods of teaching the blind how to use and interpret raised-line drawings.

However, three difficulties render the conclusions of this study inapplicable to the teaching of blind persons. First, the blindfolded condition is in no sense equivalent to, or a model for, blindness. The study should have been conducted both with blind children and with recently blinded adults, who may differ from each other and from the sighted population in the extent of their first-hand experience with objects whose two-dimensional representations they are asked to identify tactually.

Second, and much more important, a blind person does not perceive a raised-line drawing by tracing its outline with the tip of one index finger; instead, the drawing is first scanned by several fingers of both hands, and later traced in segments and in various directions by the index fingers of each hand. This method is analogous to visual inspection of pictures. If a raised-line illustration consists of more than just an outline, the single-finger tracing method would be inefficient, confusing and uninformative.

Finally, the results that Magee and Kennedy obtained probably depend on the size of the drawing. From their data I calculate that it took an observer about 30 s to be guided around the perimeter of a swan whose representation fits in a 10-cm square. I suspect that single-finger tracing without guidance is far more efficient on a small drawing than on one as large as that used by Magee and Kennedy. In fact, moderately small-scale drawings are probably easier to interpret than large-scale illustrations, as was clearly recognized by those who developed and perfected the Braille alphabet.

In conclusion, the work of Magee and Kennedy is one of many examples of the tendency for research on blindness to be conducted with little understanding of blindness itself. Despite this ignorance, conclusions from such studies have great impact on the education of the blind.

GEERAT J. VERMEIJ
Department of Zoology,
University of Maryland,
College Park, Maryland 20742

1. Magee, L. A. & Kennedy, J. M. *Nature* **283**, 287 (1980).

MAGEE AND KENNEDY REPLY—Vermeij's response to our report[1] is concerned with the practical application of our findings to the use of raised-line drawings by the blind. This is a fruitful approach to research in this area. Yet, one should not confuse an empirical method used to test a theory with an extrapolation to the pedagogy of the blind.

We tested the generality of a well established claim in haptic form perception—namely that unaided exploration is superior to aided exploration. Contrary to popular opinion, we found that self-guided exploration of raised-line drawings is inferior to aided exploration. We then used this result to evaluate the relative contribution of cutaneous and kinaesthetic sensitivity to identification and found that kinaesthetic information is predominant.

Vermeij does not question these basic findings but does ask whether they are applicable to the blind. It should be noted that traditionally (see, for example, ref. 2) the blindfolded, not the blind, have been used as subjects in experiments on haptic form perception. To the extent that the blind and blindfolded have that same physiological mechanisms underlying the receptive functions of the hand, we believe our results to be generally applicable. Indeed, Kennedy and Fox[3] have found very little difference among the blindfolded, adventitiously blind and congenitally blind in their ability to identify raised-line drawings.

Vermeij says—and we agree—that a blind person generally uses more than one finger when exploring a raised-line drawing. However, the crucial point is that a technique focusing on a single finger allows one to manipulate exploration and make comparisons in performance which would be exceedingly difficult, if not impossible, if 10 fingers had to be controlled simultaneously. Moreover, the blind are able to identify drawings with a single finger. Note, we are not proposing that single-finger tracing is optimal or establishing the efficacy of this mode of exploration compared to other strategies.

Vermeij speculates that our results probably depend on the size and complexity of the drawing. Our pilot studies have not found any interactions of this type.

In sum, our major theoretical findings are quite clear. Guidance can be useful in haptic form perception and the source of information subserving identification of raised lines is predominantly kinaesthetic. The practical implications are that a teacher need not refrain from helping a blind student explore raised-line figures and that an emphasis on movement variables may be beneficial when displays of this type are made.

LOCHLAN E. MAGEE
JOHN M. KENNEDY
Division of Life Science,
Scarborough College, West Hill,
Ontario, Canada M1C 1A4

1. Magee, L. E. & Kennedy, J. M. *Nature* **283**, 287 (1980).
2. Gibson, J. J. *Psychol. Rev.* **69**, 477 (1962).
3. Kennedy, J. M. & Fox, N. in *The Arts and Cognition* (eds Perkins, D. & Leondar, B.) (Johns Hopkins University Press, Baltimore, 1977).

BOOK REVIEWS

The ethological approach to human behaviour

Stuart Sutherland

THERE are two distinct ways of explaining behaviour. One is to show what function it serves, the other is to specify the mechanisms that produce it. Ethologists have concentrated on the former kind of explanation, psychologists on the latter. If one is interested in function, it is essential to observe the animal's responses in its natural environment; only by recording the occasions on which a given kind of behaviour occurs and taking note of the context can its likely function be assessed. Ethologists have therefore concentrated on observations of naturalistic behaviour, whereas psychologists have tried to arrive at the underlying mechanisms by experimentally manipulating behaviour in the laboratory. The dichotomy between the two disciplines has of course never been complete: Niko Tinbergen, one of the doyens of ethology, has performed many ingenious experiments, and from J.B. Watson onwards psychologists have increasingly come to apply ethological methods to the study of human beings, particularly to ontogenetic development and to social interactions. *Human Ethology* is based on the proceedings of a conference the aim of which was to assess both the merits and the difficulties of this approach.

As so often happens, most of the contributors have failed to keep their eye on the ball and have merely provided detailed accounts of their own researches. No general message emerges, though some striking if unsystematized new findings are described. For example, it would appear that the behaviour of mothers towards their infants is nicely adjusted to the infant's stage of development. A mother tends to hold her new-born baby about 25 cm in front of her face: this distance is that at which objects are brought into sharpest focus for the baby, though not necessarily for the mother. Again, the repetitive nature of the baby-talk in which infants are addressed may be suited to the limited rate at which they can learn and its high pitch may match that of their own voices. Yet it is not known whether making

Human Ethology: Claims and Limits of a New Discipline. Edited by M. von Cranach, K. Foppa, W. Lepenies and D. Ploog. Pp.764. (Cambridge University Press: Cambridge, UK, 1980.) Hardback £35; paperback £12.50.

baby-talk is an inborn skill or whether it is culturally determined, and without experimental manipulation we can only speculate about how necessary it is for the baby to be exposed to this form of talk. Very young babies have a remarkable capacity for imitation: they can even respond in kind to seeing their mother stick her tongue out. It seems possible that the capacity for this sort of imitation is inborn, but what sort of genetically determined mechanism is needed for the baby to match up its mother's tongue to its own which it has never seen?

The virtue of the ethological approach is that it provides many new data that are a challenge to explanation. Nevertheless, as several contributors to this volume, and in particular William Mason, point out, it has its dangers. Ascribing a function to behaviour is often a perilous undertaking: Freud relied wholly on functional explanations and many of them are virtually untestable. Mason reports a study of infant monkeys reared by canine mothers: their development was sufficiently normal for him to conclude that "the relevant dimensions of the early social environment for the development of coping strategies are not closely tied to the species-specific structure of the mother-infant relationship". Moreover, there are well-attested cases of infants reared under conditions of appalling deprivation who on being transferred to a better environment developed into normal adults. Despite the volume of research currently being conducted on the subject, we can hardly begin to specify the range of experience that is necessary for normal development.

Not all of *Human Ethology* is devoted to

ontogeny; amongst the other topics considered are rituals, attitudes to property and territory, aggression, and other aspects of social relationships. The fallacious argument that if there is an analogy between an aspect of human behaviour and that of other animals, the behaviour must be genetically determined, appears repeatedly. To the extent that learning itself depends on genetically determined structures, all behaviour has a genetic component, but to say of a given behaviour that it is genetically determined is an empty statement unless the range of environmental experiences necessary for its occurrence can be specified. We still know remarkably little about the malleability of human behaviour or human emotions, notwithstanding the pronouncements of the sociobiologists.

Human Ethology contains contributions by ethologists, social psychologists, psycholinguists, anthropologists and sociologists. The debates between them have an air of unreality largely because, despite the interest of the observations recorded, few contributors put forward properly articulated theories. Unfortunately verbiage is catching and the sociologists appear to have infected the other contributors with their own brand of pompous obscurity. One chapter begins: "In this paper I claim evidence that human infants are *intentional, conscious and personal*; that above all they have a faculty of *intersubjectivity*" (p.530). Who could argue with that? Or again, what is one to make of the claim that "privacy operates as a dialectic, optimizing, multilevel boundary process" (p.101)? Even the author of this rebarbative phrase has doubts, since he goes on "The question arises: So what?" It is a question that might well be asked of the whole book. □

Stuart Sutherland is Director of the Centre for Research on Perception and Cognition at the University of Sussex, Brighton, UK.

Earth science

Don L. Anderson

The Earth: Its Origin, Structure and Evolution. Edited by M.W. McElhinny. Pp.597. (Academic: London and New York, 1979.) £36, $83.

THIS volume is a collection of 17 review papers written to honour the two outstanding geophysicists who were responsible for the development of earth sciences at the Australian National University in Canberra. Under the direction of John C. Jaeger and Anton Hales, the ANU has become a world centre of earth-science research. This book, written exclusively by present and past members of the Research School of Earth Sciences, is one of the most significant collections of papers on this vast subject to appear in some years. The 'subject' is the Earth, and the material is about equally divided between chemistry and physics. There are sections on the crust, the mantle and the dynamics of the core.

The crustal chapters include petrogenesis of oceanic crust, evolution of granitoids, and the relation of porphyry copper deposits to calc-alkaline volcanism. The power of isotopes and incompatible trace elements is fully exploited in chapters by Taylor, Compston and Chappell. The chapter by Green, Hibberson and Jaques withdraws the previous Canberra model for the origin of mid-ocean ridge basalts, the basis of the pyrolite model, in favour of the O'Hara model which had formerly been bitterly contested. Green *et al.* now prefer a picritic parent magma and conclude that there cannot be a simple direct genetic relationship between the mafic and ultramafic rocks of ophiolite complexes. This important conclusion, if verified, will make it necessary to reconsider the composition of the upper mantle.

There are four chapters covering the areas of geomagnetism, palaeogeomagnetism, polarity time-scales and apparent polar wandering, and one on the history of the Earth's rotation. Altogether there are 11 chapters with primary emphasis on geophysics.

The mantle receives a great deal of attention, but much of the discussion of composition and evolution is based on concepts developed before the constraints provided by isotopes, the incompatible trace elements and anelasticity were fully appreciated. Subjects covered include composition, structure, phase changes and elasticity. The chapter on mantle convection by Stevenson and Turner is one of the best of several recent reviews of the subject.

The chapter by Liu summarizes the large amount of information he has obtained in

diamond anvils on phase changes in mantle silicates. This productive, but exploratory, field of research has verified many of Ringwood's predictions about the crystal structure of various regions of the mantle. It is still uncertain at what depth these phase changes occur and what the physical properties, other than density, will be. For this, a large amount of *in situ* data and better controlled temperatures will be required. Liu has made a preliminary attempt to estimate density as a function of depth in various mantle mineral assemblages. One interesting point is that eclogite is denser than garnet-peridotite to a depth of about 500 km but is less dense between 500 km and 800 km. This seems to preclude subduction of oceanic lithosphere into the lower mantle. If verified, this will have enormous implications for the composition and evolution of the mantle and convection therein. Ringwood's chapter on the composition and evolution of the Earth develops the viewpoint that

the mantle is basically chondritic and homogeneous.

The book is rounded out with chapters on rock mechanics, earthquakes and plate tectonics.

The breadth of coverage from the faculty and alumni of a single institution is tribute to the wisdom and foresight of Jaeger and Hales who always managed to keep ANU at the forefront of earth science by picking the areas and people that would contribute most to the understanding of our planet. This volume is an important contribution to that end. It is probably the most comprehensive single volume on the subject of the origin, evolution and dynamics of the Earth presently available. It is unfortunate that its price will make it unavailable to students and many libraries.

Don L. Anderson is Director of the Seismological Laboratory and Professor of Geophysics at the California Institute of Technology, Pasadena.

Archaeological dating

Georges Valladas

Thermoluminescence Techniques in Archaeology. By Stuart Fleming. Pp.233. (Clarendon/Oxford University Press: Oxford, 1980.) £15.50.

THE technique of dating by thermoluminescence (TL), a method which has been well established now for some dozen years, is discussed in articles scattered among many specialized journals. This book will therefore be welcome to physicists in that it gathers together the principles of the subject in one place.

The fundamentals of TL were developed in the Research Laboratory for Archaeology and History of Art at Oxford under the leadership of Martin Aitken. The author of this volume, Stuart Fleming, is one of the team of physicists trained in the laboratory at Oxford, and is thus well placed to have written this work, the fruit of experience acquired in the course of the investigations which were to provide the first absolute ages of ancient pottery.

Certain minerals making up a piece of pottery emit light when they are heated, and the older the pottery the more intense the light. The phenomenon is essentially due to the action of the radioactivity contained in the minerals. This action can be represented as the dose of radiation received by the minerals in question over the time elapsed since the original baking of the pottery, an act which destroys its initial (potential) TL. Thus the age of a piece of pottery can be deduced if the dose received in a single year is known. The book treats the following three, more or less

interdependent, subjects: (1) the preparation of the mineral after its extraction from the pottery; (2) the use of thermoluminescence to define the radiation dose received by the mineral — the archaeological dose; (3) the analysis of the radioactivity of the pottery and of the surrounding earth in order to deduce the annual radiation dose to which the mineral has been subject.

The preliminary pages are dedicated to crystalline TL and its measurement, and the properties of natural radioelements (uranium, thorium, potassium-40) and the dosimetry of α-, β- and γ-rays are the objects of a detailed analysis. The author examines the consequences of the structure of ceramics on the distribution of the radiation dose among its constituents. The radioelements are concentrated in the clay phase of the pottery and are practically absent from the crystalline inclusions. Among the latter, those which are of a certain size and occur frequently in ancient pottery, such as quartz grains, therefore receive a weaker dose than the clay fraction. Hence, α-rays penetrate to few of these grains which thus receive doses of nothing but β- and γ-radiation. This is not the case for micro-inclusions, for which the α-dose is important. Now, the TL induced in each circumstance has distinct properties. These facts lie at the root of the two principal methods of dating: the 'quartz-inclusion technique' (S. Fleming) and the 'fine-grain technique' (D.W. Zimmerman).

In Chapter 3, the quartz inclusion technique is discussed. Fleming analyses the properties of the TL of quartz and defines that interval of temperature best adapted to the determination of the archaeological dose. This is a method of great importance due to the reliability of

quartz as a dosimeter and the relative simplicity of the calculation of the annual dose. Fleming is primarily interested in pottery and does not consider the natural extension of this technique to the heated stones of prehistoric hearths (flint, quartzites, sandstone etc.), a method still in its infancy when the book was written.

Also in Chapter 3 there is a résumé of the elegant method which uses a very sensitive thermoluminescence dosimeter (fluorine) to measure directly the annual dose deposited by β-radiation in pottery. This method is also applicable to the measurement of the γ-dose coming from the soil. Here the problem of radon (radium emanation) must be considered, the active deposit of which is responsible for about 50% of the γ-dose, which therefore depends on the movement of radon in the soil. Chapters 2 and 6 give a very complete analysis of this problem.

The pre-dose technique (Chapter 5), which also involves quartz inclusions, has a use limited to those ceramics which have received a relatively low archaeological dose and are thus relatively young (< 1000 years old). On the other hand this permits it to be used instead of carbon-14 techniques which are practically useless for any period more recent than the fourteenth century.

Despite the difficulties which are inherent in it and which concern in particular the contribution of α-radiation

to the annual dose, the fine-grain technique has been brought up to the level of a routine measurement at Oxford. It is the subject of a detailed exposition in Chapter 4 which begins with the art of making the deposits of fine grains on aluminium discs which forms the basis of the whole method.

The last third of the book and Appendix E constitute an anthology of dates and of applications of TL to the authentification of ceramic artworks and of those bronzes which contain kernels of baked clay. Results bearing on the neolithic ceramics of Central Europe and Africa, relative to the Nok culture among others, are examples showing the great importance of TL for the dating of sites which in the absence of organic remains are not datable by the carbon-14 method. When the two methods have been applied simultaneously, the ages they have yielded are in agreement.

In conclusion, the methodological exposition is as complete as can reasonably be wished, given the present state of TL dating. Moreover, the book is rich in examples. Novices will find encouragement here to face up to problems which are still insufficiently resolved and archaeologists (particularly those strong in maths!) will discover the lucid explanations of the technique they have lacked until now. □

Georges Valladas is a Physicist at the Centre d'Etudes Nucléaires, Saclay, France.

A range of lattice path problems

Michael Berry

Lattice Path Counting and Applications. By Sri Gopal Mohanty. Pp.185.(Academic: New York and London, 1980.) $24, £13.60.

CONSIDER the unit square lattice whose points have integer coordinates x,y, and let a 'path' be a sequence of steps between neighbouring points. How many paths run from the origin to the point with coordinates mn, $(m \neq n)$ without touching the line $x=y$? It is with such problems, and their applications, that this book is concerned.

In the general case, where the lattice has more than two dimensions, where the paths are subject to more complicated restrictions (such as not touching boundaries of general form), and where diagonal steps are permitted, the enumeration of paths is very difficult. In many cases, however, recently developed combinational techniques make it possible to obtain solutions in closed form.

It is remarkable what a wide range of problems can be put into correspondence with the enumeration of lattice paths. The classical example, due to Bertrand, is to calculate the probability that the victor in

an election had more votes than the loser at every stage of counting. Another case is random walks on a line, for example the probability distribution of times when the walk (starting from the origin) first passes a given point. Other problems considered in the book are the lengths of queues, the enumeration of Cayley trees and the convolution identities (of binomial type) that can be proved by considering combinations of lattice paths.

For all problems treated, the exact solutions are given, involving for the most part binomial coefficients. In many cases, however, what are required are asymptotic approximations (for example as the number of steps tends to infinity), which are simpler and might be derived directly; but no such results are given here.

This is not an easy book to read. The author's style is terse, and the non-experts for whom the book is presumably intended will have to work hard to follow the argument. Such phrases as "one can easily show that" or "a little reflection will show" are unhelpful, and an argument alleged to provide "pictorial insight" would have been clearer if accompanied by an illustration. However, the book is greatly improved by the provision of extensive lists of references and challenging problems at the end of each chapter. □

Michael Berry is Professor of Physics at the University of Bristol, UK.

Large African wildlife

Brian Bertram

The Ecology and Conservation of Large African Mammals. By S.K. Eltringham. Pp.268. (Macmillan: London, 1980.) £15.

WE have waited a long time for this book — not only because Dr Eltringham has taken a long time writing it but also because there has been a conspicuous and lamentable absence of a book which spanned the wide and fascinating area of field studies of large African mammals. The author is thoroughly well qualified to fill the void. He was Director of the Nuffield Unit of Tropical Animal Ecology in Uganda, and has for years been Associate Editor of the *East African Wildlife Journal* (now the *African Journal of Ecology*). It is this journal which has published many of the results of the large mammal field studies conducted at the Nuffield Unit, the Serengeti Research Institute, the Tsavo Research Project and East African universities.

So Keith Eltringham knows his facts. What has he done with them that is new? Essentially he brings them together in one place, and he discusses in general terms not the various mammal species themselves but the differences between those species, the interactions among them, and human interaction with and influence upon them. The book thus complements the many excellent and detailed accounts, at both popular and scientific levels, of field studies of single species or groups. It is not a review of those accounts — rather it provides the background to them, plus a much needed dose of general knowledge, experience and common sense, which may be widely shared but is too rarely written down.

The book starts with a brief summary of the African regions, and a description of some of the techniques used in wildlife research, principally counting, marking and immobilizing methods. Each of the following six chapters takes a particular theme and considers the range of ways in which large African mammals behave in that respect. These themes are social structure and social behaviour, followed by territorial behaviour, then population ecology, reproduction, herbivore feeding and carnivore feeding. Three chapters on conservation, wildlife management, and Man and national parks complete the text. To my mind the last six chapters are much better than the four preceding ones. There is a valuable bibliography of over 400 references, maps of African national parks and reserves, and a useful list of scientific names of mammals each with its authority and date. There are 27 informative black and white photographs, about 20 tables and as many diagrams.

What are the merits and limitations of the book? Most importantly it fills a glaring gap. It gives a range of useful information on a range of interesting species, and it makes it palatable — the text is free of jargon yet does not underestimate the reader's intelligence, and the reader is certainly going to need intelligence. The arrangement allows, indeed causes, abundant discussion of general topics such as social hierarchies, functions of territoriality, population regulation, sociobiology, plants' defences against being eaten and their use of animals in seed dispersal, the range of herbivores' antipredator techniques, 'the elephant problem' (to cull or not to cull), fire, disease and tourism. Evolutionary and functional questions abound.

It is extremely difficult when dealing with diverse, often 'hot', subjects to trace a satisfactory route which avoids oversimplifying, confusing, pontificating or taking sides, but in most cases Dr Eltringham manages to do so. Of course, he says things which to my mind are highly contentious, such as (p.231) that "If disease is identified in a national park attempts should be made to eliminate it" (this also conflicts with p.228 which states that "Disease is a natural factor in wild animals and rarely requires management attention"). I also disagree with his statement (p.210) that "It is questionable whether reintroduction will ever become a practical proposition, although much play is made by zoos and other animal collectors on their important conservation role in preserving species for eventual release". After all, it is not "questionable" that reintroduction of the European bison has already proved to be a practical proposition, and indeed a success. Zoos recognize better than most people the variety of problems involved, but we do not accept that they are insuperable.

I would do more than disagree with statements such as (p.41) "a pack of wild dogs, a herd of buffaloes and a troop of baboons are all essentially similar in social structure and should be given the same collective name", since wild dogs, unlike the others, have a most unusual system involving female transfer and usually only one reproductive female per pack. Similarly (p. 109) "in the llama the process [of copulation] occurs with both partners lying down"; the mind boggles — in fact the male squats on top of the female who rests on her brisket. But who could produce a stimulating book without the occasional contentious or fallacious statement? And who could fail to agree with so lovely a sentence as (p.122) "Fortunately for the mother [rhino] the baby is born without its horns"?

The book is largely intended for biology students in universities, as an introductory textbook to more detailed studies. It will inform the non-biological visitor to Africa, but he or she will have to work hard at it. And it provides a useful source of references, nearly a third of them from the *East African Wildlife Journal*.

Despite its title, the book is mainly about the large mammals of the East African grasslands only, but is none the worse for that. It ignores, for example, species such as the okapi, pigmy hippo, sable, greater kudu and chimpanzee, on some of which a considerable amount of field research has been carried out. But it is right, I think, to emphasize the East African side, because East Africa has on the whole produced the most, as well as the best, field research on large mammals. Directly or indirectly Keith Eltringham has been associated with a great deal of it. And directly or indirectly his fine book will stimulate and help much more of it. ☐

Brian Bertram is Curator of Mammals at the Zoological Society of London, Regent's Park.

Plasma phenomena and the Solar System

S.-I. Akasofu

Solar System Plasma Physics. Edited by Charles F. Kennel, Louis J. Lanzerotti and Eugene N. Parker. Three volumes. (North-Holland: Amsterdam and New York, 1979.) Vol. I. *Solar and Solar Wind Plasma Physics*, pp.340. Vol. II. *Magnetospheres*, pp.396. Vol. III. *Solar System Plasma Processes*, pp.373. Each volume Dfl.150, $73.25; three-volume set Dfl.382, $186.25.

IONIZED gases have been a focus of intense study in several subject areas — plasma physics, controlled nuclear fusion and gaseous discharge research, astrophysics and geophysics. From several subdisciplines in astrophysics and geophysics, such as solar physics, geomagnetism, magnetospheric physics, cosmic ray physics and ionospheric physics, has emerged a new discipline, solar system plasma physics. This is defined by the three editors of the book as "the study of plasma phenomena throughout the solar system, extending from the solar photosphere to the outer boundary of the heliosphere (the cavity formed in the interstellar medium by the solar wind)".

The beginning of this new discipline can be traced back to the pioneering work by Sydney Chapman, Hannes Alfvén and others on geomagnetic storms. It is, however, only in the last two decades that it has been developed explosively, stimulated by the availability of *in situ* spacecraft observations. In fact, the book "celebrates the twentieth anniversary of space research", providing ample evidence of spectacular progress and establishing an important milestone in this particular field of science.

The first volume deals mainly with solar activity, the solar wind and cosmic rays. The second volume is concerned with the Earth's magnetosphere and ionosphere and the planetary magnetosphere. The third volume singles out several specific plasma processes which may be seen throughout the Solar System, such as collisionless shock waves, magnetic field reconnection, hydromagnetic waves, plasma waves and plasma instabilities. These subjects are reviewed in 24 papers, contributed by 28 authors. Obviously, this book is a historic undertaking.

Although the level of the papers varies somewhat, new graduate students should be able to grasp the general scope of this area of research since many of the articles are written in a textbook style, and there should not be any difficulty for plasma physicists to review the progress which has been made in space plasma physics. Astrophysicists, too, should find the book very useful, since many papers are based on *in situ* measurements of plasma quantities and of magnetic fields. Similar conditions may be present in some stellar atmospheres and interstellar space. This is likely to be the case because a magnetosphere appears to be a rather common feature in various astrophysical phenomena (the head–tail galaxies, pulsars, magnetic stars etc.).

Above all, specialists in the discipline will, undoubtedly, find the three volumes most valuable. In the ever-increasing trend towards specialization, it is worthwhile to read such a series of reviews which covers practically the entire field. It provides a unique opportunity for the specialist to familiarize himself with major progress and the current ideas in each subdiscipline. Such a comprehensive edition of review papers covering the entire discipline will not appear too often. All the papers are extensively and properly referenced, and the readers should not have any difficulty in expanding their knowledge. It appears that all of the contributors made a special effort to provide a good reference list.

Each author attempted to describe unsolved problems and difficulties which are facing his particular subdiscipline: for example, T.E. Holzer presents a "Timetable for Solar Wind Research"; B.U.Ö. Sonnerup gives a useful list of recommendations for future study of reconnection processes; and astrophysicists may particularly be interested in "Recommendations for Continued Plasma Wave Research" by S.D. Shawhan. I feel that more emphasis along these lines would have made most of the articles more stimulating. In most papers discussion of current ideas predominates, although some of the problems in the field appear to be insur-

mountable without new approaches.

In his review of the modulation theory of cosmic rays, L.A. Fisk describes the present situation as "in a state of wary optimism". Although this may indeed be the case in certain areas, it remains to be seen how many of the ideas will survive another decade. It is useful to note in this connection that one of the most important events in solar system plasma physics in the last few years was the finding of a very interesting electric potential structure above the aurora (described in Vol. III, 1.5 and 1.6). The possibility of the presence of an electric field along magnetic field lines in a collisionless plasma should receive wide attention by astrophysicists in general. In this connection it may be recalled that various exotic acceleration mechanisms of energetic particles have been described in the past by assuming that such a parallel electric field cannot exist. This unexpected finding of the potential structure has already considerably changed the course of our thinking and will continue to do so during the next decade. New findings by deep space probes may also drastically alter our ideas on the heliosphere. In this respect, the authors could have been a little more bold by injecting new ideas as it is rather difficult to do so in a paper for a regular journal these days, given the conservative attitude of many referees.

As stressed earlier, however, there is no other up-to-date and comprehensive review available which covers the entire scope of solar system plasma physics. It is hoped that the book will be widely read by everyone who is interested in plasma physics in general. □

S.-I. Akasofu is Professor of Geophysics at the Geophysical Institute of the University of Alaska, Fairbanks, Alaska.

Photoresearch for physical chemists

D.W. Turner

Photoabsorption, Photoionization and Photoelectron Spectroscopy. By J. Berkowitz. Pp. 469. (Academic: New York and London, 1979.) $61, £39.80.

THE story of the exploration of that area of the electromagnetic spectrum which falls between the optical and the X-ray regions is an extremely exciting one, partly in terms of the succession of new theoretical and interpretative problems that have arisen, but most especially because of the elegant, painstaking and sometimes heroic experimental techniques which have been called for. From the earliest pioneering work of Schumann and Lyman to the present day, advance has always been associated with new techniques in the hands of gifted experimenters. Some major leaps forward and acceleration in activity in the area can be identified in retrospect — the observation of molecular Rydberg series in the 1930s, the application of photoionization threshold measurements in the 1950s and photoelectron spectroscopy in the following decade. The latter gave, for the first time, access to the inner valence shells of complex molecules and at this stage a unification with parallel developments in the soft X-ray region established an area of work which had become essentially chemical in its applications, though the methods were those of the physics laboratory. The present text is the first which has made a serious attempt to draw all of these threads together and show the application of these and other related techniques to the understanding of the structure of some quite complex molecules and their ions.

After a survey of some fundamental principles and an outline of physical processes underlying the absorption of high-energy radiation and ionization processes generally, the author devotes three chapters to describing photo-absorption below the first ionization limit, quasi-discrete states above the first ionization limit and the physics of the ionization continua. There then follows a discussion of photoabsorption and photo-ionization cross-sections for selected molecules in which all the information available for each case is brought together for critical evaluation, and then a similar critical discussion of partial cross-sections of a range of molecules in which extensive use is made of photoelectron spectral data. A separate chapter considers the problem of the angular distribution of photoelectrons.

This is essentially theoretical with a rather small number of applications to simple molecules being described. The book ends with a survey on instruments and methods which is particularly well done.

This is a text produced to an extremely high standard and the author speaks with authority and clarity. It is to be recommended particularly to research workers in the field. Chemical physicists generally will find it a valuable reference text. □

D.W. Turner is Reader in Physical Chemistry at the University of Oxford, UK.

Principles of gel permeation

J.V. Dawkins

Modern Size-exclusion Liquid Chromatography: Practice of Gel Permeation and Gel Filtration Chromatography. By W.W. Yau, J.J. Kirkland and D.D. Bly. Pp.476. (Wiley: New York and Chichester, UK, 1979.) $36.60, £17.45.

STUDIES of the chromatographic fractionation of macromolecules by a size-exclusion mechanism have progressed along two parallel paths. Gel filtration, which is widely used for analytical and preparative separations of biological macromolecules in aqueous media, resulted from the preparation of soft porous gels, as described by Porath and Flodin in *Nature* (**183**, 1657–1659; 1959). Rigid porous packings such as cross-linked polystyrene, silica and glass particles for fractionations of synthetic polymers in organic media by the technique known as gel permeation chromatography were reported in 1964-1967. The theme bringing the two techniques together in this book is the use of rigid microparticulate packings for performing fast (minutes) high-resolution separations. The decrease in the separation time from several hours in the classical size exclusion techniques has followed from the amazing advances, to which Kirkland has made important contributions, that have occurred in liquid chromatography during the past decade. Whilst high-speed separations of many synthetic polymers may be performed with porous cross-linked polystyrene microspheres, suitable microspherical rigid packings for widespread routine use in gel filtration are still in an active state of development.

Following a brief introductory chapter, there are three chapters on retention mechanisms, band-broadening and resolution. The authors have concentrated on principles rather than detailed theoretical treatments, so the practitioner can clearly identify the important variables which determine separation power and column performance. Chapters 5-11 are the most valuable sections of the book with comprehensive accounts of equipment and detectors, column packings and technology, operating variables, laboratory techniques, calibration, data handling and special techniques. The experimental aspects are well illustrated with figures and detailed tables, with more examples taken from gel permeation than from gel filtration, but the bibliography is very selective with the total number of cited references for these seven chapters below 200. Thus, it is surprising that the

important calibration method proposed by Frank, Ward and Williams in 1968 (*J. Polymer Sci.* Part A-2; *Polymer Phys.* **6**, 1357–1369) is not mentioned. Chapter 12 covers gel permeation applications and it is not possible in 37 pages to give a representative survey from the extensive published literature. The examples chosen are only covered briefly and the treatments of branched polymers and copolymers are

disappointing. The final chapter reviews the advances made in the last five years in high-performance separations of biopolymers with microparticulate packings.

In summary, this book is highly recommended. It will be welcomed by practitioners of gel permeation separations who have never had access to a suitable reference book. For those interested in separations of biopolymers, the authors

clearly demonstrate the advantages of rigid microspheres over soft gels for fast analytical separations. The high-performance technique is likely to be increasingly used by biochemists during the next few years as column packings are improved. □

J. V. Dawkins is Lecturer in Polymer Science in the Department of Chemistry, Loughborough University of Technology, Loughborough, UK.

Attraction to viroid research

William McClements

Viroids and Viroid Diseases. By T.O. Diener. Pp. 252. (Wiley: New York and Chichester, UK, 1979.) $30.55, £14.55.

Viroids and Viroid Diseases is a comprehensive review of these smallest of known pathogens. It begins in 1922 with the first report of the potato spindle tuber disease and moves, in the author's words, "from the field through the greenhouse and into the laboratory". Thus, we are introduced to such plant maladies as chrysanthemum stunt disease and the exotic sounding cadang-cadang disease of coconuts. However, once out of the field, potato spindle tuber viroid (PSTV) receives greatest attention and serves as a model for viroids in general. Many of the author's early experiments with PSTV are reiterated here and provide the reader with the requisite background to appreciate the critical moment in this research: the recognition, by the author, of the novel character of viroids. It was the demonstration that the causative agent in potato spindle tuber disease was an unencapsidated RNA of remarkably low molecular weight (~ 100,000 daltons) that led Diener, in 1971, to propose the term 'viroid' for this new class of pathogen. Subsequent work by several groups showed viroids to be extensively base-paired, single-stranded RNA existing in both circular and linear forms. This work culminated with the report of the complete sequence of the 359 nucleotide circular form of PSTV. Some studies on other viroids are also included, mainly as confirmation of PSTV results.

In light of this unusual structure, the initial confusion about the size and shape of viroids is understandable: a confusion compounded by the reluctance of some to accept a totally new form of pathogen. Much of what is known about viroid structure today is a direct result of Diener's persistence during the early stages of viroid research. This persistence is reflected in the initial PSTV studies included in this volume. Also reflected in the language of the text is the sometimes contentious competition in this field.

The biology of viroids is far less well known than their structure. They do not appear to encode polypeptides; replication probably occurs in the nucleus and is host dependent. Evidence supporting both RNA- and DNA-directed replication is presented along with speculative models. It also appears that some viroid-related sequences occur in uninfected plant genomes. Even less is known about the mechanism of pathogenicity, as is illustrated by the fact that this section occupies less than one page of text. In the absence of

any demonstrated viral functions other than replication, it is speculated that viroids act at a regulatory level; however, there is no direct evidence for this. Perhaps it is this very ignorance which will fulfil the desire expressed in the preface, that this book might attract additional investigators to viroid research. Certainly, *Viroids and Viroid Diseases* is a fine starting point for newcomers. □

William McClements is a Senior Staff Fellow in the Laboratory of Molecular Virology at the National Cancer Institute, Bethesda, Maryland.

Cycling bacteria

John Postgate

Bacteria and Mineral Cycling. By T. Fenchel and T.H. Blackburn. Pp.225. (Academic: London and New York, 1979.) £14.60, $34.

MICROBES are of fundamental importance for the persistence of living things on this planet. Their transcendent role in the biosphere becomes clear when scientists consider the natural cycles of the biological elements and examine the roles of microbes at each step: the cycles of carbon, hydrogen, oxygen, nitrogen and sulphur are utterly dependent on the chemical activities of microbes. This truism, well known to microbiologists, is at last penetrating to non-microbiological ecologists and environmentalists and is indeed being recognized in the activities of international agencies such as SCOPE. So a text that provides a background in terms of the ecology and chemistry of microorganisms is very timely. The authors have made distinguished contributions to microbial ecology and their expertise is well displayed in the central chapters of the book, which concern bacteria in detritus food chains (Chapter 3), the carbon cycle (Chapter 4), the nitrogen cycle (Chapter 5), and the sulphur cycle (Chapter 6); cycles of other elements are dealt with in Chapter 7 and a global view of the major cycles is presented in the final article, Chapter 9. They have deliberately chosen to exclude eukaryotic microbes from their presentation, as well as most industrial and

economic aspects of their topic, so some imbalance must be accepted.

The authors' subject (unrelated to mineralogy, by the way) is vast so their treatment of it in what amounts to about 130 pages of core text is amazingly condensed. While brevity is a virtue, it can also be misleading if authors make categorical statements over issues which many would consider controversial or unsettled: examples of questionable items here include the evolutionary age of biological nitrogen, the unimportance of nitrification in the nitrogen cycle, the ability of Desulfovibrio to oxidize hydrocarbons, the reliability of S-isotope fractionation in geomicrobiology. Brevity may also have led to some factual errors and use of curiosities of nomenclature, but in compensation there are excellent sections dealing with areas familiar to the authors, such as the exposition of the rumen associations in Chapter 8 (which deals with symbioses in general).

A short book of such broad scope in so newly developing a scientific area cannot fail to generate disagreement, but the final paragraph of the authors' preface disarms criticism: "Readers may find . . . that it is biased in some places and that some topics are over-emphasized whereas others are treated superficially, or even contain misunderstandings". Amen. But the authors have certainly achieved the aim expressed in the sentence that follows: "We hope that the general principles of the subject will be understood". □

John Postgate is Professor of Microbiology and Director of the Unit of Nitrogen Fixation at the University of Sussex, Brighton, UK.

BOOKS RECEIVED

Technology

SCHACH, R., GARSHOL, K. and HELTZEN, A. N. (ed.) Rock Bolting A Practical Handbook. Pergamon International Library of Science, Technology, Engineering and Social Studies. Pp. vii + 84. ISBN-0-08-022503-9. (Oxford, New York, Toronto, Sydney, Paris, Frankfurt: Pergamon, 1980.) $11.75 £5.25.

SORENSEN, B. Renewable Energy. Energy Science anz Engineering: Resources, Technology, Management. An International Series. Pp. xvii + 683. ISBN-0-12-656150-8. (London, New York, Toronto, Sydney, San Francisco: Academic, 1979.) £20.00 $46.00.

STARR, C. and RITTERBUSH, P.C. (eds) Science, Technology and the Human Prospect. Pergamon Policy Studies on Science and Technology. Pp. xiv + 228. ISBN-0-08-025595-7. (New York, Oxford Toronto, Sydney, Frankfurt, Paris: Pergamon, 1980.) £15.00.

UHLMANN, D. Hydrobiology; A text for engineers and scientists. Pp. 313. ISBN-0-471-99557-6. (Chichester, New York, Brisbane, Toronto: John Wiley & Sons, 1980.) £15.00.

UPPER, D. and CAUTELA, J.R. (eds) Covert Conditioning. Pergamon International Library of Science, Technology, Engineering and Social Studies. Pp. ix + 386. ISBN-0-08-023346-5. (New York, Oxford, Toronto, Sydney, Frankfurt, Paris: Pergamon, 1980.)

VOIGHT, B. (ed.) Rickslides and avalanches, 2 Engineering Sites. Developments in Geotechnical Engineering, 14B. Pp. xviii + 850. ISBN-0-444-41508-4. (Amsterdam and New York: Elsevier Scientific Publishing Company, 1980.) US $117.00 Dfl. 240.00.

WALKER, G. Stirling Engines. Pp. xxii + 531. ISBN-0-19-856209-8. (Oxford: Clarendon Press: Oxford University Press, 1980.

WILLIAMS, F.C. and DEESE, D.A. (eds) Nuclear Nonproliferation: The Spent Fuel Problem. Pergamon Policy Studies-32. Pp. xi + 221. ISBN-0-08-023887-4. (New York, Oxford, Toronto, Sydney, Frankfurt, Paris: Pergamon, 1980.) £15.00 $30.00.

WILD, R. Operations Management; A Policy Framework. Pergamon International Library of Science, Technology, Engineering and Social Studies. Pp. ix + 217. ISBN-0-08-022504-7 hardback ISBN-0-08-022505-5 flexi. (Oxford, New York, Toronto, Sydney, Paris, Frankfurt: Pergamon Press, 1980.) $30.00 £13.00 hardback $15.00 £6.25 flexi.

Biology

MILLER, T. A. Insect Neurophysiological Techniques. Springer Series in Experimental Entomology. Pp. xiii + 308. ISBN-3-540-90407-7. (Berlin, Heidelberg, New York: Springer-V, 1979.) DM 54 US $29.70.

MORGANE, P. J. And PANKSEPP, J. (ed.) Anatomy of the Hypothalamus. Handbook of the Hypothalamus Volume 1. Pp. xv + 726. (New York and Basel: Marcel Dekker, Inc., 1979.) SFr. 288.

MOISKALENKO, Y. E. et al. biophysical Aspects of Cerebral Circulation. Pp. ix + 164. ISBN-0-08-022672-8. (Oxford, New York, Toronto, Sydney, Paris, Frankfurt: Pergamon, 1980.) £18.00 $41.00.

MOSS, R. W. The Cancer Syndrome. Pp. 347. ISBN-0-394-50859-9. (New York: Grove Press, Inc., 1980.).

PARISH, J. H. (ed.) Developmental Biology of Prokaryotes. Studies in Microbiology Volume 1. Pp. xii + 297. ISBN-0-632-00423-1. (Oxford, London, edinburgh, Melbourne: Blackwell Scientific, 1979.) £19.00.

PARISH, J. H. (ed.) Developmental Biology of Prokaryotes. Studies in Microbiology Volume 1. Pp. xii + 297. ISBN-0-520-04016-3. (Berkely and Los Angeles: University of California Press, 1980.) $48.50.

PEDLEY, T. J. The Fluid Mechanics of Large Blood Vessels. Cambridge Monographs on Mechanics and Applied Mathematics. Pp. xv. ISBN-0-521-22626-0. (Cambridge, London, New York, New Rochelle, Melbrourne, Sydney: Cambridge University Press, 1980.)

PERLMAN, D. (ed.) Annual Reports or Fermentation Processes Volume 3. Pp. xiv + 346. ISBN-0-12-040303-X. (New York, London, Toronto, Sydney, San Francisco: Academic, 1979.) $22.00.

RAINSFORD, K. D. and FORD-HUTCHINSON, A. W. (ed) Prostaglandins and Inflammation: Conference, London, 1979. Pp. iv + 240. ISBN-3-7643-1132-0. (Basel, Boston, Stuttgart: Birkhäuser Verlag, 1979.) SFr. 44.00.

RATAZZI, M. C., SCANDALIOS, J.-G. WHITT, G. S. (ed) Isozymes; Current Topics in Biological and Medical Research volume 3. Pp. xii + 215. ISBN-0-8451-0252-4. (New York: Alan R. Liss, Inc., 1979.) $22.00.

ROSE, A. H. (ed) Secondary Products of Metabolism. Economic Microbiology Volume 3. Pp. xvi + 595. ISBN-0-12-596553-2. (London, New York, San Francisco: Academic, 1979.) $78.50 £34.00.

ROSE, A. H. and MORRIS, J. G. (ed) Advances in Microbial Physiology. Volume 19. Pp. ix + 375. ISBN-0-12-027719-9. (London, New York, San Francisco: Academic Press, 1979.) £17.80 $41.00.

ROSE, A.H. and MORRIS, J.G. (ed) Advances in Microbial Physiology. Volume 20. Pp. x + 367. (London, New York, Toronto, Sydney, San Francisco: Academic, 1979.) £19.60 $45.50.

ROSE, A. H. (ed) Microbial Biomass. Economic Microbiology Volume 4. Pp. xv + 459. ISBN-0-12-596554. (London, New York, San Francisco: Academic, 1979.) £27.80 $64.00.

ROSENBLATT, J. S., HINDE, R. A., BEER, C., and BUSNEL, M.-C. (ed) Advances in the Study of Behaviour Volume 10. Pp. xv + 314. ISBN-0-12-004510-9. (New York, London, Toronto, Sydney, San Francisco: Academic, 1979.) $26.50.

SHEETS, P. D. And GRAYSON, D. K. (ed.) Volcanic Activity and Human Ecology. Pp. xvi + 644. ISBN-0-12-639120-3. (New York, Londin, Toronto, Sydney San Francisco: Academic, 1979.) $49.50.

SKINNER, F. A. and LOVELOCK, D. W. (ed.) Identification Methods for Microbiologists, Second Edition. The Society for Applied Bacteriology Technical Series No. 14. xii + 315. ISBN-0-12-647750-7. (New York, London, Toronto, Sydney and San Francisco: Academic, 1980.) £14.80; $34.50.

SMITH, K. M. and RITCHIE, D. A. Introduction to Virology. Pp. vii + 212. ISBN-0-412-21960-3 hardback ISBN-0-412-21970-0 paperback. (Andover: Chapman & Hall, 1980.) £12.00 hardback £5.95.

SMYTHIES, J. R. and BRADLEY, R. J. (ed) International Review of Neurobiology. Volume 21. Pp. vii + 417. ISBN-0-12-366821-2. (New York, Londin, toronto, Sydney, San Francisco: Academic, 1979.) $39.00.

SUDA, M., HAYAISHI, O. and NAKAGAWA, H. (ed) Biological Rhythms and their Central Mechanism. A NATO Foundation Symposoum. Pp. xv + 453. ISBN-0-444-80136-7. (Amsterdam, New York, Oxford: Elsevier/North-Holland Biomedical Press, 1979.) US $83.00 Dfl. 170.00.

TAMIR, L. M. Communication and the Aging Process. Interaction throughout the Life Cycle. Pergamon General Psychology Series volume 86. Pp. xix + 195. ISBN-0-08-024621-4. (New York, Oxford, Toronto, Sydney, Frankfurt, Paris: Pergamon, 1980.) £11.25 $22.50.

TER HAAR, M. B. (ed.) Trends in Neuro Sciences. Reference Edition Volume 2. Pp. vii + 323. ISBN (Amsterdam: Elsevier/North-Holland Biomedical Press, 1979.) Dfl. 165.

TULCHINSKY, D. and RYAN, K. J. Maternal-fetal Endocrinology. Pp. xi + 418. ISBN-7216-9811-6. (Philapelphia, London, Toronto: W. B. Saunders Company, 1980.) £22.00.

WINTROBE, M. M. BLOOD, PURE And Eloquent. A Story of Discovery of Poeple, and of Ideas. Pp. xxiii + 771. ISBN-0-07-071134-6. (New York: McGraw-Hill, 1980.)

WOLMAN, B. B. (ed.) Handbook of Human Sexuality. Pp. xii + 365. ISBN-0-13-378422-3. (Hemel Hempstead: Prentice/Hall International, 1980.) £22.70. $47.20.

YATES, A. J. biofeedback and the Modification of Behavior. Pp. xii + 512. 0-306-40226-2. (New York and London: Plenum, 1980.)

YOUNG, R. S. Cobalt in Biology and Biochemistry. Pp. ix + 147. ISBN-0-12-772750-7. (London, New York, San Francisco: Academic, 1979.) £11.80 $25.00.

Applied biology

ALQHOUSE, R. et al (prepared by.) WORLD HEALTH ORGANIZATION. Chemicals and Industrial Processes associated with Cancer in Humans. IARC Monographs, Volumes 1 to 20. xi + 71. ISBN-92-832-1402-1. (Lyon: International Agency for Research on Cancer, 1979.) S fr. 10.00.

ARNO, J. Atlas of Lymph Node Pathology. Current Histopathology Volume 1. Pp. 96. ISBN-0-85200-228-9. (Lancaster: MTP Press Limited, 1980.) £16.98.

BAILAR III, J. C. (ed.) Aspects of Cancer Research 1971-1978. Editorials from The Journal of the National Cancer Institute. Pp. x + 531. (Maryland: National Cancer Institute, 1979.) $13.00.

BARENDSEN, G. W., BROERSE, J. J. And BREUR, K. (ed) High-Let Radiations in Clinical Radiotherapy. Proceedings of the 3rd Meeting on Fundamental and Practical Aspects of the Application of Fast Neutrons and other High-LET Particles in Clinical Radiotherapy, The Hague, September, 1978. Published as a supplement to the European Journal of Cancer. Pp. = 287. ISBN-0-08-024383-5. (Oxford, New York, Toronto, Sydney, Paris, Frankfurt: Pergamon, 1980.) £63.00 $142.00.

BASU, R. N., JEZEK, Z. and WARD, N. A. The Eradication of Smallpox from India. Who History of International Public Health Series No. 2. Pp. xv + 346. ISBN-92-9022-105-4. (New Delhi: World Health Organization South-East Asia Regional Office, 1979.) Sw. fr. 30.

BOUCHET, P., DANRIGAL, F. and HUYGHENS, C. Living Seashells. Molluscs of the English Channel and Atlantic Coasts. Pp. 144. ISBN-0-7137-1031-4. (Poole: Blandford, 1980.) £4.95.

BRUNE, K. and BAGGIOLINI, M. (eds) Arachidonic Acid Metabolism in Inflammation and Thrombosis. Proceedings of the First European Workshop on Inflammation held in Basel in March, 1979. Pp. 301. ISBN-3-7643-1095-2. (Basel, Boston, Stuttgart: Birkhäuser Verlag, 1979.) SFr. 55.00.

COLLINS, J. A. and LUNDSGAARD-HANSEN, P. Surgical Hemotherapy. Bibliotheca Haematologica No. 46. Pp. viii + 252. ISBN-3-8055-0361-X. (Basel, Munchen, Paris, London, New York, Sydney: S. Kargel, 1980.) SFr. 90 DM 108 approx. US $54.00. flexi.

COOKE, R. C. Fungi, man and his environment. Pp. xiv + 144. ISBN-0-582-44262-1. (Harlow: Longman Group Limited, 1980.) £2.95 pbk.

COUSINS, N. Anatomy of an Illness as Perceived by the Patient. Reflections on Healing and Regeneration. Pp.173. ISBN-0-393-01252-2. (New York, London: W. W. Norton, 1980.) £5.75.

COX, P. H. (ed.) Progress in Radiopharmacology. Selected Topics. Progress in Radiopharmacology, Volume 1. Pp. x + 250. ISBN-0-444-80178-2. (Amsterdam, New York, Oxford: Elsevier/North-Holland Biomedical Press, 1979.) US $41.50. Dfl. 85.00.

CUMMINGS, D. J. et al. (ed.) Extrachromosomal DNA. ICNUCLA Symposia on Molecular and Cellular Biology Volume XV, 1979. Pp. xvi + 564. ISBN-0-12-198780-9. (New York, London, Toronto, Sydney, San Francisco: Academic Press, 1979.) $29.50.

DJERASSI, C. The Politics of Contraception. Pp. xii + 274. ISBN-0-393-01264-6. (London: W. W. Norton & Company Ltd., 1980.) £6.50.

DUMONT, R. and COHEN, N. The Growth of Hunger. A new Politics of Agriculture. Ideas in Progress series. Pp. x + 229. ISBN-0-7145-2641-X hardback ISBN-0-7145-2642-8 pbk. (London, Boston: Marion Boyars, 1980.) £6.95 hardback £3.50 pbk.

EBBELS, D. L. and KING, J. E. (ed.) Plant Health. The Scientific Basis for Administrative Control of Plant Diseases and Pests. Pp. xii + 322. ISBN-0-632-00294-8. (Oxford, London, Edinburgh, Melbourne: Blackwell Scientific Publications, 1979.) £14.50.

FENCHEL, T. and BLACKBURN, T. H. Bacteria and Mineral Cycling. Pp. xi + 225. ISBN-0-12-252750-X. (London, New York, San Francisco: Academic, 1979.) £14.40 $34.00.

FOSTER, R. (ed.) Molecular Association Including Molecular Complexes. Volume 2. Pp. xvi + 497. ISBN-0-12-262702-4. (London, New York, San Francisco: Academic, 1979.) £38.50 $89.00.

GUPTA, I. C. Use of Saline Water in Agriculture in Arid and Semiarid Zones of India. vi + 210. (New Delhi, Bombay, Calcutta: Oxford & IBH Publishing Co., 1979.) Rs. 50.00.

HAUGHTON, P. M. Physical Principles of Audiology. Medical Physics Handbooks 3. Pp. x + 183. ISBN-0-85274-502-8. (Bristol: Adam Hilger Ltd., 1980.) £12.95.

HALL, A. E., CANNELL, G. H. and LAWTON, H. W. (ed.) Agriculture in Semi-Arid Environments. Ecological Studies Vol. 34. Pp. xvi + 340. ISBN-3-540-09414-8. (Berlin, Heidelberg, New York: Springer-Verlag, 1979.) DM 89 US $49.00.

HALL, T. C. and DAVIES, J. W. (ed.) Nucleic Acids in Plants. Volume 1. Pp. vii + 261. ISBN-0-8493-5291-6. (Oxford: Blackwell Scientific Publications, 1979.) £44.75.

HERRON, J. (ed.) Neuropsychology of Left-Handedness. Pp. xii + 357. ISBN-0-12-343150-6. (New York, London, Toronto, Sydney, San Francisco: Academic, 1979.) $24.50.

INTERNATIONAL AGENCY FOR RESEARCH ON CANCER. IARC Monographs on the Evaluation of the Carcinogenic Risk of Chemicals to Humans. Some Halogenated Hydrocarbons. Volume 20. Pp. iv + 609. ISBN-92-832-1220-7. (Lyons: International Agency for Research on Cancer, 1979.) S. fr. 60.00.

LAING, J. A. (ed.) Fertility and Fertility in Domestic Animals. 3rd Edition. Pp. ix + 262. ISBN-0-7020-0699-8. (London: Bailliere Tindall, 1980.) £8.75 flexi.

LEHNER, T. and BARNES, C. G. (eds) Bechet's Syndrome. Clinical and Immunological Features. Proceedings of a Conference sponsored by the Royal Society of Medicine, February, 1979. Pp. xii + 323. ISBN-0-12-442680-8. (London, New York, Toronto, Sydney, San Francisco: Academic, 1979.) £16.40 $38.00.

LETT, J. T. and ADLER, H. (eds) Advances in Radiation Biology Volume 8. xvi + 462. (New York, London, Toronto, Sydney, San Francisco: Academic Press, 1979.) $45.00.

LIENER, I. E. (ed.) Toxic Constituents of Plant Foodstuffs. Second edition. Food Science and Technology series of Monographs. Pp. xiv + 502. ISBN-0-12-449960-0. (New York, London, Toronto, Sydney, San Francisco: Academic, 1979.) $39.50.

KAYE, A. M. and KAYE, M. (ed) Development of Responsiveness to Steroid Hormones. Advances in the Biosciences volume 25. Pp. x + 483. ISBN-0-08-024940-X. (Oxford, New York, Toronto, Sydney, Paris, Frankfurt: Pergamon, 1980.) $66.00 £30.00.

MARTINI, L. and GANONG, W. F. (ed) Frontiers in Neuro-endocrinology volume 6. Pp. x + 418. ISBN-0-89004-404-X. (New York: Raven, 1980.) $39.00.

MELNICK, M. and MYRIANTHOPOULOS, N. C. External Ear Malformations: Epidemiology, Genetics and Natural History, Birth Defects: Original Article Series 1979 Volume xv Number 9. Pp. ix + 140. ISBN-0-8451-1034-9. (New York: Alan R. Liss, Inc., 1979.) $18.00. Available in Europe, UK, and Middle East from European Book Service, 1380 AC Weesp, Holland Dfl. 54.00.

MILGROM, F. and ALBINI, B. Immunopathology. Sixth International Convocation on Immunology, Niagara Falls, N. Y. June 1978. Pp. x + 350. ISBN-3-8055-2971-6. (Basel, München, Paris, London, New York, Sydney: S. Karger, 1979.) SFr. 149 DM 178 approx. US $89.25.

MILJAN, T. (ed.) Food and Agricultured in Global Perspective. Discussions in the Committee of the Whole of the United Nations. A volume in the NIEO Library. xviii + 289. ISBN-0-08-025550-7. £12.50 $25.00.

McGREEVY, T. Inflation can be cured. A Definite Plan. Pp. 308, ISBN-0-9506655-1-7. pbk. ISBN-0-9506655-0-9 hardback. (Emsworth, Hants. Tomlines Ltd. m 1980. £7.95 hardback £4.50 pbk.

McLAUGHLIN, P. A. Comparative Morphology of Recent Crustacea. Pp. xiv + 177. ISBN-0-7167-1121-4. (San Francisco: Freeman, 1980.) $21.50.

NORMAN, W. H. and SCARAMELLA, T. J. (ed.) Mid-Life: Developmental and Clinical Issues. Pp. xviii + 189. ISBN-87630-221-5. (New York: Brunner/Mazel, 1980.) $15.00.

OSBURN, B. I. and SCHULTZ, R. D. (Guest Editors.) Basic and Clinical Aspects of Veterinary Immunology. Advances in Veterinary Science and Comparative Medicine. Volume 23. Pp. xii + 309. ISBN-0-12-039223-2. (New York, London, Toronto, Sydney, San Francisco: Academic, 1979.) $33.50.

PAVONE-MACALUSO, M., SMITH, P.H. and EDSMYR, F. (ed) Bladder Tumors and Other Topics in Urological Oncology. Ettore Majoran International Science Series Volume 1. Pp. xvi + 528. ISBN-0-306-40308-0. (New York and London: Plenum, 1980.) $59.50.

PIMENTAL, D. and PERKINS, J. H. (ed.) Pest Control: Cultural and Environmental aspects. AAAS Selected symposium 43. Pp. xix + 243. ISBN-0-89158-753-5. (Boulder, Colorado: Westview Press, 1980.) $20.00.

RANGANATHAN, D. and RANGANATHAN, S. Challenging Problems in Organic Reaction Mechanisms. Pp. xi + 160. ISBN-0-12-580050-9. (New York and London: Academic, 1972.) $15.50.

ROWAN, A.N. and STRATMANN, C.J. (ed) The Use of Alternatives in Drug Research. Pp. xii + 190. (ISBN-0-333-27014-2. (London and Basingstoke: Macmillan, 1980.) £8.50 flexi.

SCHIPPERS, B. and GAMS, W. (ed) Soil-Borne Pathogens. Proceedings of the Fourth International Symposium on factors determining the behaviour of plant pathogens in soil, held at Munchen, August, 1978. Pp. xv + 685. ISBN-0-12-624850-8. (London, New York, San Francisco: Academic, 1979.) £27.00 $62.50.

SCHNEPF, M. (ed.) Farmland, Food and the Future. Pp. x + 214. ISBN-0-935734-03-1. (Iowa: Soil Conservation of America, 1980.) $8.00.

SELL, S. (ed.) Cancer Markers; Diagnostic and Developmental Significance. Pp. xxvii + 541. ISBN-0-89063-009-1. (New Jersey: The Humana Press, Inc., 1980.) $49.50.

SHAPCOTT, D. and HUBERT, J. (ed.) Chromium in Nutrition and Metabolism. Proceedings of the Symposium on Chromium in Nutrition held Sherbrooke, June 1979. Developments in Nutrition and Metabolism Volume 2. Pp. viii + 264. ISBN-0-444-80188-X. (Amsterdam, New York, Oxford: Elsevier/North-Holland Biomedical Press, 1979.) US $44.00 Dfl. 90.00.

SLEIN, M. W. and SANSONE, E. B. Degradation of Chemical Carcinogens. An Annotated Bibliography. Pp. xi + 172. ISBN-0-442-24489-4. (New York, Cincinnati, Atlanta, Dallas, San Francisco, London, Toronto, Melbourne: Van Nostrand Reinhold Company, £16.90.

SMARDA. J. The Effects of Colicins. Pp.213. ISBN-55-954-79. (Brno: J. E. Purkyne University, Medical Faculty, 1978.)

SOCIETY OF CHEMICAL INDUSTRY. Insect neurobiology and pesticide action (Neurotox 79.) Pp. vi + 517. ISBN-090100-161-9. (London: Society of Chemical Industry, 1980.) £35.00 $80.00 flexi.

TALLARIDA, R. J. and JACOB, L. S. The Dose-Response Relation in Pharmacology. Pp. xiii + 207. ISBN-3-540-90415-8. (Berlin, Heidelberg, New York: Springer-Verlag, 1979.) DM 48 approx. US $26.40.

TEXON, M. Hemodynamic Basis of Atherosclerosis. Pp. xxi + 95. ISBN-0-89116-146-5. (Washington, New York, London: Hemisphere Publishing Corporation, 1980.)

THE MARINE POLLUTION SUBCOMMITTEE OF THE BRITISH NATIONAL COMMITTEE ON OCEANIC RESEARCH. The Effects of Marine Pollution: Some Research Needs. A Memorandum. Pp. 78. ISBN-0-85403-135-9. (London: The Royal Society, 1979.) £2.25 UK £2.45 overseas.

THIENPONT, D., ROCHETTE, F and VANPARIJS, O. F. J. Diagnosing Helminthiasis through Coprological Examination. Pp. 187. ISBN-361-52-1401. (Beerse, Belgium: Janseen Pharmaceutica, 1979.) BF 220.

THOMPSON, J.P. and SKERMAN, V.B.D. Azotobacteraceae: The Toxonomy and Ecology of the Aerobic Nitrogen-Fixing Bacteria. Pp. xxi + 417. ISBN-0-12-689050-1. (London, New York, Toronto, Sydney, San Francisco: Academic, 1980.) £32.00, $74.00.

WORTH, H.G.J. and CURNOW, D.H. Metabolic Pathways in Medicine. Pp. ix + 182. ISBN-0-7131-4336-3. (London: Edward Arnold Ltd., 1980.) £13.95.

KEZDI, A. Handbook of Soil Mechanics Volume 2: Soil Testing. Pp. 258. ISBN-0-444-99778-4. (Amsterdam, Oxford, New York: Elsevier Scientific, 1980.) US $70.75, Dfl. 145.00.

Psychology

AL-ISSA, I. The Psychopathology of Women. Pp. ix + 390. ISBN-0-13-736827-5 hardback ISBN-0-13-736819-4 pbk. (Hemel Hempstead: Prentice/Hall International, 1980.) £10.35 hardback, £5.15 pbk.

BAUERLE, R., EGLI, U. and STECHOW, A. von (ed.) Semantics from Different Points of View. Springer Series in Language and Communication volume 6. Pp. viii + 419. ISBN-3-540-09676-0. (Berlin, Heidelberg, New York: Springer, 1979) DM 49 approx. US $27.00.

DiCAPRIO, N.S. Adjustment; fulfilling human potentials. Pp. x + 501. ISBN-0-13-994101-7. (Hemel Hempstead: Prentice/Hall International, 1980.) £8.40, $16.85 flexi.

FREYBERGER, H. (ed.) Advances in Psychosomatic Medicine. Vol. 10: Psychotherapeutic Interventions in Life-Threatening Illness. Pp. xvii + 206. ISBN-3-8055-3066-8. (Basel, München, Paris, London, New York, Sydney: S. Karger, 1980.) SFr. 95.00 DM 114.00 approx. US $57.00.

KAPLAN, O.J. (ed.) Psychopathology of Aging. xiv + 316. ISBN-0-12-396950-6. (New York, London, Toronto, Sydney, San Francisco: Academic Press, 1979.) $24.50.

KLATEZKY, R.L. Human Memory: Structures and Processes. Second edition. Pp. x + 358. ISBN-0-7167-1113-3 hardback ISBN-0-7167-1114-1 pbk. (San Francisco: Freeman, 1980.) $17.00 hardback.

KRASNER, L. (ed.) Environmental Design and Human Behavior. A Psychology of the Individual in Society. Pergamon General Psychology Series-85. Pp. xiv + 514. ISBN-0-08-023858-0. (New York, Oxford, Toronto, Sydney, Frankfurt, Paris: Pergamon, 1980.) £14.25, $28.50.

LANGER, J. The Origins of Logic. Six to Twelve Months. Developmental Psychology Series. Pp. ix + 437. ISBN-0-12-436250-1. (New York, London, Toronto, Sydney, San Francisco: Academic, 1979.) $26.50.

LAYTON, J.R. The Psychology of Learning to Read. Educational Psychology Series. Pp. xv + 356. ISBN-0-12-438850-7. (New York, London, Toronto, Sydney, San Francisco: Academic, 1979.) $21.50.

LEE, R.B. The Kung San. Men, Women, and Work in a Foraging Society. Pp. xxv + 526. ISBN-0-521-22578-7 hardback ISBN-0-521-29561-0. pbk. (Cambridge, London, New York, New Rochelle, Melbourne, Sydney: Cambridge University Press, 1980.) £22.00 hardback £7.95 pbk.

MAHONEY, M.J. (ed.) Psychotherapy Process. Current Issues and Future Directions. Pp. xvi + 403. ISBN-0-306-40244-0. (New York and London: Plenum, 1980.) $22.50.

MILLER, M. The Logic of Language Development in Early Childhood. Springer Series in Language and Communication volume 3. Pp. xvi + 478. ISBN-3-540-09606-X. (Berlin, Heidelberg, New York: Springer, 1979.) DM 49 approx. US $27.00.

MONJAN, S.V. and GASSNER, S.M. Critical Issues in Competency Based Education. Pergamon General Psychology Series-Volume 84. Pp. xi + 218. ISBN-0-08-024623-0. (New York, Oxford, Toronto, Sydney, Frankfurt, Paris: Pergamon, 1980.) $25.00, £12.50.

RACHMAN, S.J. and HODGSON, R.J. Obsessions and Compulsions. The Century Psychology Series. Pp. ix + 437. ISBN-0-13-629139-2. (Hemel Hempstead: Prentice-Hall International, 1980.) £12.95, $26.95.

REESE, H.W. and LIPSITT, L.P. (ed.) Advances in Child Development and Behaviour. Volume 14. Pp. ix + 343. ISBN-0-12-009714-1. (New York, San Francisco, London: Academic Press, 1979.) $27.50.

ROSENTHAL, R. (ed.) Skill in Nonverbal Communication; Individual Differences. Pp. xviii + 270. ISBN-0-89946-000-3, Cambridge, Mass.: Gunn & Hain, Inc., 1979.) np.

SCHAFFER, K.F. Sex-Role Issues in Mental Health. Addison-Wesley series in Clinical and Professional Psychology. Pp. xii + 227. ISBN-0-201-06762-5. (Reading, Mass., Menlo Park, Cal. London, Amsterdam, Ontario: Addison-Wesley, 1980.) £4.90.

SCHEIN, E.H. Organizational Psychology 3rd edition. Prentice-Hall Foundations of Modern Psychology Series. Pp. xiv + 274. ISBN-0-13-641340-4 hardback ISBN-0-13-641332-3 pbk. (Hemel Hempstead: Prentice-Hall International, 1980.) £7.75, $15.55 hardback £4.50, $9.05 pbk.

SKOU, J.C. and NORBY, J.G. (ed.) Na, K-ATPase Structure and Kinetics. Proceedings of the 2nd International Conference on the Properties and Functions of Na, K-ATPase, held at Sandbjerg Castle, Sonderberg, Denmark, September 1978. Pp. xii + 549. ISBN-0-12-647650.0. (London, New York, San Francisco: Academic, 1979.) £22.50, $52.00.

THOMAS, A. M.D. and CHESS, S. M.D. The Dynamics of Psychological Development. Pp. xxiii + 287. ISBN-87630-232-0. (New York: Brunner/Mazel, 1980.) $15.00.

Sociology

CARTER, C. Higher Education for the Future. Mainstream series. Pp. ix + 149. ISBN-0-631-11331-2. (Oxford: Basil Blackwell, 1980.) £7.50.

FELD, W.J. Multinational Corporations and U.N. Politics. The Questr for Codes of Conduct. Pergamon Policy Studies on U.S. and International Business. Pp. ix + 173. ISBN-0-08-022488-1. (New York, Oxford, Toronto, Sydney, Frankfurt, Paris: Pergamon, 1980.) £12.50, $25.00.

GUILFOYLE, A. The Family of Animals. Peaceable Kingdom. Pp. 151. ISBN-0-04-591016-2. (London, Boston, Sydney: George Allen & Unwin, 1980.) £9.95.

LILLEGRAVEN, J.A., KIELAN-JAWOROWSKA, Z. and CLEMENS, W.A. (ed.) Mesozoic Mammals. The First Two-Thirds of Mammalian History. Pp. x + 311. ISBN-0-520-03582-8. (Berkeley, Los Angeles, New York, London: University of California Press, 1980.) $35.00 hardback, $9.75 pbk.

MILLER, A.V. (compiled by) The Genetic Imperative: Fact and Fantasy in Sociobiology. A Bibliography. Pp.x107. ISBN-0-920430-X. (Toronto: Canadian Gay Archives, 1979.) $6.00.

NEWBY, H. Green and Pleasant Land? Social Change in Rural England. Environment Sociology & Anthropology. Pp. 301. ISBN-0-14-02-2252-9. (London: Penguin Books Ltd., 1980.) £2.50 flexi.

ROBBINS, LORD L. Higher Education Revisited. Pp. viii + 117. ISBN-0-333-28606-5. (London and Basingstoke: Macmillan Ltd., 1980. £12.00.

ROTENSTREICH, N. Practice and Realization Studies in Kant's Moral Philosophy. Pp. x + 153. ISBN-90-247-2112-1. (The Hague, Boston, London: Martinus Nijhoff, 1979.) Guilders 57.

SAUGSTAD, P. A Theory of Language and Understanding. Pp. 107. ISBN-82-00-01952-7. (Oslo: Universitetsforlaget P.O. Box 2977., London: Global Book Resources Ltd., United States and Canada: Columbia University Press, 1979.) Nkr. 69.00, US $14.00. flexi.

STEWART, M.A. (ed.) Selected Philosophical Papers of Robert Boyle. Pp. xxxi + 256. ISBN-0-7190-0681-3. (Manchester: Manchester University Press, 1980.) £12.00.

General

BARBAULT, R., BLANDIN, P. and MEYER, J.A. Recherches D'Ecologie Théorique. Les stratégies adaptatives. Recherches Interdisciplinaires Collection dirigée par Pierre Delattre. Pp. viii + 298. ISBN-2-224-00602-0. (Paris: Maloine s.a., 1980.) flexi.

BARWELL, F.T. Bearing Systems; Principles and Practice. Pp. xxiv + 565. ISBN-0-19-856319. (Oxford: Oxford University Press, 1979.) £25.00.

BEALE, J.G. The Manager and the Environment. General Theory and Practice of Environmental Management. Environmental Sciences and Applications. Pp. xvi + 211. ISNB-0-08-024043-7. (Oxford, New York, Pergamon, 1980.) £12.50, $28.00.

BÉCHERVAISE, J. Antarctica — The Last Horizon. Pp. xi + 138. ISBN-0-7269-0474-0. (London: Cassell Ltd., 1980.) £8.95.

BOOKER, C. The Seventies; Portrait of a Decade. Pp. xii + 349. ISBN-0-7139-1329-0. (London: Allen Lane, 1980.) £7.50.

BREZHNEV, L. Virgin Lands. Two years in Razakhstan, 1954-5. Pp.vii + 100. ISBN-0-08-023584-0 hardback ISBN-0-08-023583-2 flexi. (Oxford, New York, Toronto, Sydney, Paris, Frankfurt: Pergamon Press, 1979.) $13.00, £6.00 hardback $5.50, £2.50 flexi.

BROCKWAY, L.H. Science and Colonial Expansion. The Role of the British Royal Botanic Gardens. Studies in Social Discontinuity Series. Pp. xiv + 215. ISBN-0-12-134150-X. (New York, London, Toronto, Sydney, San Francisco: Academic, 1979.) $21.00.

BROWER, K. The Starship and the Canoe. Pp. v + 270. ISBN-0-233-97240-4. (London: Whizard Press/André Deutsch, 1980.) £5.50.

BRUMFIT, C. Problems and Principles in English Teaching. Language Teaching Methodology Series. Pp. xii + 156. ISBN-0-08-024559 hardback ISBN-0-08-024558 flexi. (Oxford, New York, Toronto, Sydney, Paris, Frankfurt: Pergamon, 1979.) $11.95, £5.95 hardback $4.95, £2.95.

BLAZYNSKI, G. Flashpoint Poland. Pergamon Policy Studies-52. Pp. xix + 416. ISBN-0-08-024638-9. (New York, Oxford, Pergamon Press, 1980.) $39.50, £19.75.

CAIRNCROSS, S. et al. Evaluation for Village Water Supply Planning. Pp. xviii + 179. ISBN-0-471-27662-6. (Chichester, New York, Brisbane, Toronto: John Wiley & Sons, 1980.) Published in association with international Reference Centre for Community Water Supply) £7.00.

CHATTERJEE, G. P. Fundamentals of Units and Dimensions with Special Reference to SI Units. Pp. xxiv + 375. ISBN-33390-093-6. Delhi, Bombay, Calcutta, Madras (The Macmillan Company of India Limited, 1975). Rs. 18 flexi.

COMMITTEE ON INTERNATIONAL DISASTER ASSISTANCE. Assessing International Disaster Needs. xiii + 146. ISBN-0-309-02893-0. (Washington: National Academy of Sciences, 1979.) $6.00.

CONOMOS, T. J. (ed.) San Francisco Bay: The Urbanized Estuary. Investigations into the Natural History of San Francisco Bay and Delta with Reference to the Influence of Man. Fifty-eighth Annual Meeting of the Pacific Division/American Association for the Advancement of Science held at San Francisco State University, June 1977. Pp. 493. ISBN-0-93494-01-6. (San Francisco: California Academy of Sciences, 1979.) $16.95 flexi.

DOMINOWSKI, R.L. Research Methods. Pp. viii + 390. ISBN-0-13-774315-7. (Hemel Hempstead: Prentice/Hall International, 1980.) £10.35 $20.75.

D'DOUZA F. (ed.) Refugees. A special issue devoted to viewpoints, case studies and theoretical considerations on the care and management of refugees. The International Journal of Disaster Studies and Practice, Pp. ii + 134. ISBN-0-08-025460-8. (Oxford, New York, Toronto, Sydney, Paris, Frankfurt: Pergamon Press, 1980.) $15.25 £6.75.

nature

26 June 1980

What not to say about interferon

PHYSICIANS on both sides of the Atlantic appear to be worried at the lively public interest in the possibility that interferon may at some stage have a part to play in the treatment of cancer. Two weeks ago, for example, the Glasgow Health Board appealed for what sounded very much like a moratorium on publicity about the clinical trials being carried out with the meagre quantities of interferon now available. Last week, a number of distinguished physicians in the United States made a very similar appeal. Everybody will sympathize with the dilemma of those working in the treatment of cancer when they are confronted by patients and their relatives pleading for the better chance of survival which they are frequently persuaded interferon might provide. The physicians are not concerned to shuffle off their professional responsibilities; rather, they are anxious to protect their patients and their relatives from such needless distress as there is bound to be when it is believed that a potentially beneficial drug is being withheld. It is no comfort to those concerned to know that the quantities of interferon now available are sufficient only to sustain a handful of clinical trials here and there, or that they are excluded by the protocols laid down from such clinical trials as are being conducted. But alas, a moratorium on publicity will not suffice. The need is rather for more but better publicity.

For the truth is that the professional community can no longer hope to conceal from the wider public its own motives and excitements. That this should have become the case is not a misfortune but the opposite — a sign that after many decades in which the professional community has wrung its hands at the poverty of the public understanding of what science is about, the point may now have been reached at which people in general are beginning to appreciate what is happening in the laboratories. Who would turn that clock back? Moreover, it can take very little ingenuity for the general public to discover that many professional people are indeed excited about interferon because of the possibility that it may have a role to play in the treatment of at least some kinds of cancer. Thus a correspondent writing in last week's *Nature* about the structure of a human fibroblast interferon gene, and about the structural relationship between leukocyte and fibroblast interferons, explained in passing that part of the interest in these two molecules stemmed from "their potential as *in vivo* anti-viral and anti-tumour agents". So it does, and it would be dishonest even of simple biochemists (if there are such) to pretend otherwise. The questions for the professional community, physicians included, is therefore not that of avoiding publicity but of making sure that the harmful consequences of publicity are avoided.

How should that be accomplished? The short answer, paradoxically, is to say more, not less. Perhaps the most urgent need is for a wider understanding of the reasons why the pace of research with interferon has recently so rapidly accelerated. After all, there will be many who recall that the first mention of interferon dates back for more than twenty years, when in Britain the Medical Research Council of the day held a widely reported press conference to announce the discovery of what seemed to be a universal anti-viral agent. What, people will rightly ask, has been happening in the interval? The answer is, of course, instructive. After the initial excitement, it quickly emerged that the problems of isolating interferon in any but the smallest quantities were such that people would quickly have become disheartened at the prospect of setting up industrial production lines to make interferon. In any case, several years went by in

which people almost lost their patience in their attempts to characterize the material properly (which is not surprising in the light of the more recent discoveries of several different but related types of interferon, apparently produced by different genes). In reality, it is only within the past decade that techniques have been worked out for setting up and stimulating cell cultures that will yield measurable quantities of pure interferon. It is remarkable how much the techniques of molecular biology — nucleic acid hybridization and the like — have contributed already to the characterization and purification of interferon. It goes without saying that there must be great excitement at the possibility that genetic manipulation may be applicable to the production of interferon on a commercial scale — a prospect that remains to be substantiated.

Thus even as things are, interferon is not a drug in the sense in which that word applies to aspirin or cyclophosphamide. It remains a name for a group of materials, only some of which have been fully characterized and none of which can be manufactured in the ordinary sense of that word. Moreover, the natural role of interferon in or outside the cells in which it is produced remains obscure. What has emerged, after more than twenty years, is that interferon plays a part still to be fully defined in the regulation of viral replication within eukaryotic cells, and in some way yet to be defined, with cell replication as a whole. The possibility that interferon may be an anti-tumour agent springs more from clinical studies than theoretical understanding. By the same test, however, interferon used as a drug must be expected to have side-effects — even though there may be theoretical reasons for hoping that these may turn out in some cases to be less damaging than those which accompany (and sometimes limit) some of the cancer therapies now in use.

No physician would of course be rash enough to base his treatment of real patients on what he or she would no doubt call fairy stories such as these. Physicians are right to ask that the hints and nudges provided by laboratory experiments should not guide the design of methods of treatment until their efficacy and their safety have been demonstrated by means of clinical trials. (Increasingly, patients and potential patients insist on nothing less.) And there is a host of practical questions to be answered — what doses should physicians think of using against which kinds of cancers, what precisely are the side-effects and how might they be mitigated? Even if the supply of interferon were not limited (as it will be for some time to come), and even if the highest hopes for interferon are borne out by the trials now under way — and they may not be — it would be some time, say a couple of years, before interferon could be widely used in hospitals. As things are, the time-lag is likely to be longer before interferon could be made generally available. That is another essential element in what needs to be widely understood.

But how does one set about telling a patient suffering from cancer that there may at some stage be a more effective treatment than at present, but that it cannot be generally available for some years, by which time he or she may be dead? Nobody will envy physicians such tasks. It is however in the public interest that they should be tackled, and tackled energetically. In other less spectacular fields of pharmaceutical innovation, the lack of a general appreciation of what is involved in the development of new drugs is a serious brake on the pace of innovation. The steps now being taken to tell whether interferon has any substantial therapeutic value are a splendid illustration of what must be done

to bring a new drug into therapeutic use. The very fact that interferon has become such a powerful focus of public interest provides the professional community with a valuable opportunity for public enlightenment.

To be sure, the enlightenment will not be comfortable news for all those who receive it. Some will learn that they may be denied the chance to benefit from some innovation. It is however entirely consistent with the temper of the times that people should have to learn to live with the painful knowledge that what happens to them, literally their fate, may be intrinsically determined by chance. Curiously enough, people were more ready to accept this hard truth in mediaeval times, no doubt because of their common conviction that heaven was, in any case, a better place. Now that circumstances have changed, more robust philosophies are needed. It would be unfair to ask that physicians alone should shoulder the whole burden of helping their patients to come to terms with unlucky chance — but it would be wrong of them, and a disservice to their craft, if they were to fudge the issue.
As it happens, recent professional practice leaves very little to be asked for. The Medical Research Council, commenting last week

on the report by Dr David Sacher and Professor D.C. Burke (*Nature*, 12 June) that it has been possible to prepare monoclonal antibodies against human interferon which may be of service in the preparation of pure material, did not flinch from using the phrase "possible anti-tumour activity" but went on to refer to the urgent need "to test whether interferon really is useful in the treatment of any or all cancers". The Imperial Cancer Research Fund, which announced last week the allocation of £1 million to a clinical trial with interferon in the next two years, made very similar noises. In the past few weeks, most newspapers have similarly behaved sensibly and properly, mentioning the "possible anti-tumour activity" of interferon only with a warning that the case has not been established. That is how it should be. In this day and age, it would be ridiculous to conceal the promise simply because the promise has not yet been substantiated, just as it would be irresponsible to pretend that interferon has already been shown to be beneficial. It is also essential that everybody should understand that interferon may yet turn out to have no role in the treatment of cancer of any kind. Or it may simply be another anti-tumour agent.

Can DNA properly be called selfish?

The response to the articles which appeared earlier this year on the theme of "selfish DNA" (Doolittle and Sapienza, Orgel and Crick, *Nature*, 17 April) has understandably been voluminous; the notion is, after all, midly shocking. In essence, the authors are concerned to account for the presence in eukaryotic cells of much DNA that appears to have no function — the so-called "junk" DNA. They note that DNA sequences — any DNA sequences — are above all capable of replication; that the environment of the cell nucleus is well-suited to such replication; and that once a DNA sequence has been incorporated into the eukaryotic genome, there is no particular mechanism by means of which it can be got rid of. So, the argument goes, if there are DNA sequences which, because of their structure, are incorporated into the genome more easily than other sequences, they will tend not merely to stay there but to multiply, at least until the metabolic burden of replicating all this functionless DNA at every cell division becomes too great. This is selfish DNA — and the batch of comments on the subject which appears on pages 617-620, mostly approving of the notion as a stimulating idea, shows that not everybody accepts that something like this goes on in molecular evolution. Indeed, both the comments now published, and the general gossip about selfish DNA that there has been, suggest that people are uneasy about the concept.

Part of the trouble is undoubtedly semantic. Implicitly at least, people appear to be asking (among other questions) whether, and if so in what circumstances, it can be proper to attribute to a class of molecules the property of selfishness. For are we not told, from a quite tender age, that we should avoid anthropomorphism like the plague? And while it may be proper to extend the notion of selfishness, originally intended as an attribute of individual human beings that distinguished them from others, to animate species as a whole, is it not misleading to call a class of mere molecules "selfish"? Certainly the usage goes against the grain. No doubt if somebody could think of a better word, everybody would use it. Yet the image is defensible.

First, if it is at all acceptable that the word "selfish" should be applied to the behaviour of a species in, say, its competition with another, who is to say that it should not also apply to the competition of one species of DNA molecule with another? Nobody, of course, pretends that DNA molecules are in themselves living things; in present circumstances, DNA molecules cannot replicate unless they are made up into intact organisms of some kind, virus particles at the simplest. But it would be excessively pedantic to ignore the sources of the concept now advanced, and in particular the way in which it has emerged from the studies intended to throw light on the origin of life (in which Orgel is one of the outstanding exponents), and which have

plausibly suggested that in the primaeval soup, as it is called, the course of molecular evolution may have been determined by competition between different species of RNA molecules. The authors of the concept of selfish DNA might fairly ask how, in such circumstances, the concept of life as such is to be defined? And if the word "selfish" can be applied to a contemporary species in competitive evolution with others, why should it not also be applied to molecules in competitive molecular evolution? If there is an error, it is in the use of "selfish" in any but its original meaning.

The second justification of the use of "selfish" applied to DNA is the prior use of the word in relation to a gene. Thus Dawkins, in 1976, used the title "The Selfish Gene" for his account of how it appears that the effect of natural selection is to favour favourable genes and not strictly the organisms which carry them. This is, of course, a contentious field. The familiar aphorism that "the organism is DNA's way of making more DNA" may turn out to be more than a mere joke, but whole-organism biologists find it offensive. In the present argument about selfish DNA, however, the use of "selfish" is justified on literary grounds: in a field in which many people are familiar with at least the title of Dawkins's book, to apply the same word to DNA suggests graphically what the authors are driving at. Is that not how the language itself evolves?

None of this constitutes a licence for the use of anthropomorphic words wherever and whenever they have some suggestive or figurative value. It is, indeed, to be hoped that the word "selfish" will wither away once people have grasped the point that Doolittle and Sapienza and Crick and Orgel are trying to make. On present form, that may take some time. The question of whether they are right or wrong is clouded by other semantic issues. Is it, for example, proper to use the term "natural selection" to refer to the preferential emergence of some species of nucleic acid molecule either in the primaeval soup or in the environment of the eukaryotic nucleus? Part of the trouble is that natural selection is synonymous with Darwinian selection but selfish DNA has Lamarckian tendencies. Unfortunately the neutral word "selection" is not a sufficient substitute, implying as it does that the selection is undertaken by some unspecified agent; "to be selected", on the other hand, is clumsy and only strengthens the habit of writing in the passive. This, however, is a minor issue compared with the way in which "selfish" appears to have provoked in many people's minds, almost by free association, the belief that the selfish DNA must be the antonym of "altruistic DNA" and that the questions now raised are somehow linked with those which keep sociobiologists busy at public speaking. That is a cruel misfortune.

Nairobi centre's director to quit

THE World Bank's network of international agricultural research centres has been dealt a serious blow with the departure of Dr A C Allison as director of the International Laboratory for Research on Animal Diseases in Nairobi.

Dr Allison, a distinguished immunologist, was appointed director at Nairobi just over a year ago. He said on the telephone from Nairobi last week that the decision that he should leave his post was taken at the meeting of the governing council in April. Dr Allison says that he intends to stay in Nairobi until the review of the laboratory's five-year plan is completed in October, and possibly until the next council meeting in the spring of 1981.

Allison is the third director of ILRAD to leave in the six short years of its existence. The first died and the second, like Allison, resigned. It is an open secret that Allison and some members of the scientific and administrative staff at Nairobi have been at loggerheads almost since the beginning. Last week, Allison said that he had not been given the support he had reason to expect from the council itself.

ILRAD is one of the more recently created of the international centres now run by the Consultative Group on International Agricultural Research, a consortium
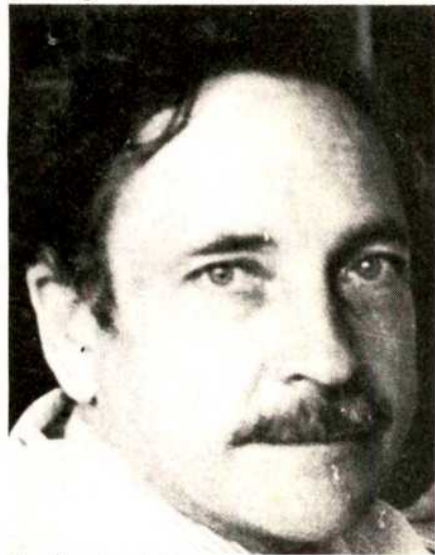
Ex-director designate?

of donor organizations among which the World Bank is the chief contributor. The founder members of the network of nine centres were the wheat and rice research centres in Mexico and the Philippines respectively.

Unlike other centres in the CGIAR network, ILRAD was set up to carry out a somewhat specific task — the protection of animals against trypanosomiasis and theileriosis (or East Coast Fever), a tick-borne disease fatal to large proportions of susceptible cattle.

ILRAD's first big success came soon after the foundation of the laboratory in

1974, when a technique for the *in vitro* culture of trypanosomes was developed. Since then it has seemed that the development of a vaccine against trypanosomiasis, African sleeping sickness, may be complicated by the antigenic variability of the infective organisms as recovered from infected animals.

Still more recently, however, it has appeared that genetic variability is by no means as apparent in the tsetse fly vectors of the disease, which appears to suggest ways in which the disease may be tackled. The prospects of vaccines against theileriosis are, by contrast, bright — some say that another two years may be sufficient.

The laboratory has a permanent staff of some 40 scientists, together with students and visiting fellows. The annual budget is now approaching $10 million which has provoked some criticism of the laboratory on the grounds of extravagance. In practice, the costs are not much out of line with those of other laboratories in the World Bank network, and are held to reflect the costs of supporting a largely expatriate staff in developing countries such as Kenya.

The chief anxiety of the laboratory management now appears to be the problem of recruiting their fourth director in six years in circumstances that may appear to potential candidates to be unpropitious.

Short commons for nuclear physics

Washington

ONE of the most disruptive effects of the budget battles currently being fought in Washington has been the defeat of several attempts to map out medium-term strategies for the support of basic research. A prominent victim is nuclear physics.

Earlier this year, physicists advising the Department of Energy and the National Science Foundation had proposed — and the Administration had accepted — that stability should be brought to nuclear physics funding by planning for a constant real growth of about three per cent over the next five years (just as three years ago agreement was reached to keep funding level in real terms for high-energy physics).

In particular, about $20 million a year would be allocated for the construction or upgrading of research facilities. This would be about one-sixth of the total, and a considerable increase on the average equivalent of $1.3 million a year spent over the past two decades.

A list of priorities was agreed with the department and was headed by the superconducting cyclotron now under construction at Michigan State University and a tandem linac accelerator system (Atlas) at the Argonne National Laboratory, for which funds had already been requested in the 1981 budget. Following these were plans for an electrostatic accelerator at Washington University and the upgrading of a tandem accelerator at Yale, with other projects climaxing in a national continuous beam high-energy electron accelerator.

Now the whole scheme is threatening to collapse like a house of cards. In revising its budget request in March, the Administration decided that construction at Atlas should be deferred. And last week the House of Representatives Appropriations Committee, taking a broad swipe at the whole energy research budget, recommended that rather than increase the Department of Energy's budget for nuclear

physics by seven per cent as had originally been proposed, it should be reduced by five per cent below its current 1980 level in 1981, in real terms a contraction of about 15 per cent. Operating funds would fall to their lowest level since the early 1960s, and construction costs would be cut from $13.3 million to $9.3 million by delaying construction of the Michigan machine.

Before the latest cuts, nuclear physicists had been optimistic that they were seeing the end of a decade's decline. Central to this optimism had been the DoE's apparent acceptance of a report prepared by its Nuclear Science Advisory Committee, chaired by Professor Herman Feshbach of the Massachusetts Institute of Technology.

The report sets out a detailed rationale for a slow but steady increase in funding over the next five years. Particular attention is paid to the need for increased funding for new medium-sized and large facilities, as well as the upgrading of existing facilities. But the report also emphasizes that these should not be funded unless "a clear plan of action is developed that shows that the required balance in (national) capability can be retained".

In a normal budget year, this is the type of language that appeals to congressional committees. This year, it has cut little ice, and the promises of the January budget request seem unlikely to materialize.

At the National Science Foundation, for example, the Administration had suggested that the physics budget should be increased by 16 per cent to compensate for the relative growth of the biological sciences during the 1970s. This figure has been successively cut back, and is unlikely to end up as more than an eight or nine per cent increase.

It is the DoE's budget, however, which is threatened with the most damage. Here the House Appropriations Committee, shifting funds into politically popular dam construction projects, has proposed that the whole of the energy research budget should be kept at roughly the 1980 level, a

real contraction of about ten per cent.

The cuts would be shared across the board. The high-energy physics budget, for example, would have a proposed growth of 11 per cent cut to three per cent, with a $20 million cut in operating funds for the major accelerator laboratories and in particular a $5 million cut in funds for the construction of Fermilab's energy saver/doubler.

Administration officials have been working hard behind the scenes, hoping the Senate can be persuaded to mitigate some of the worst effects. Unless the funding prospect improves, there will "really be some sort of chaos and disaster", warns Dr Edward Frieman, director of DoE's Office of Energy Research, predicting in particular that up to 1,500 scientific and technical jobs could be lost at the national laboratories.

So far, nuclear physicists seem to be accepting what is in store for them phlegmatically. Almost two-thirds of the 76 university-based accelerators operating in 1970 have since had to close, many for lack of operating funds.

There is also widespread concern that these developments are putting off potential research students, while the supply of postgraduate research workers is also beginning to dry up. One estimate is that there are currently several hundred vacant teaching and research assistantships.

DoE officials still hope that a reasonable programme can be salvaged. Internal figures being used in planning next year's budget include an increase in nuclear physics funding from $115 million to $130 million between 1982 and 1986 (in 1980 dollars) — in contrast to level-pegging for high-energy physics.

But nobody pretends that this year's tide can easily be turned. Mr Robert N Giaimo, chairman of the House Budget Committee, told a meeting of the American Association for the Advancement of Science last week that in the near future "there has to be more discrimination between basic research which is likely to be useful and basic research which is not likely to be" — and that faced with the prospect of a non-expanding pie, the competition for funds will get increasingly fierce.

David Dickson

Heidelberg lab

Danes drag feet

A GROUP of Danish scientists who advise the government on the scale and division of Denmark's basic research budget has recommended that Denmark should no longer contribute to the costs of the European Molecular Biology Laboratory, based in Heidelberg. If the Danish government were to accept the advice, it would be a severe blow to the morale — if not the pocket — of the £10 million a year laboratory, which was launched by an

agreement of ten nations in July 1974 and opened in May 1978.

Denmark was obliged to make a decision on EMBL this year. So far, its Natural Science Research Council and its Agricultural and Veterinary Research Councils have been supporting EMBL (to the tune of some £120,000 a year) out of their own budgets; but it had been agreed in July 1974 that this arrangement should last for only seven years. The source in Denmark of the EMBL contribution for 1981 thus came into question.

Normally in Denmark, subscriptions to international bodies are paid out of government rather than research council funds — that is to say, the sums are allocated from the total research budget before it is divided among the various research councils. So when a committee of scientists from the Natural and Agricultural Research Councils considered who should pay for EMBL in 1981, it attempted to transfer the burden to what it considered to be the rightful place — at government level, but effectively shared among all the other research councils.

None of this need have caused a stir in Heidelberg. In making its administrative recommendation, however, the joint committee chose also to criticise Danish participation in EMBL. For example, the committee pointed out that there is no Dane at the laboratory, and that its programme of research seemed to be rather disjoint from Denmark's.

When this rather qualified recommendation went to the government's science advisory body, the body decided against further participation in EMBL, in the light of tight financial constraints imposed upon it by government.

Denmark thus finds itself in a difficult position. The agreement establishing EMBL was reached as a treaty by West Germany, Austria, Denmark, France, Israel, Italy, the Netherlands, the UK, Sweden and Switzerland, and abrogating it would be a diplomatic matter, as it would be for a nation leaving the high-energy physics laboratory, CERN (on which the EMBL constitution was modelled). However, Danish scientists believe the money will be found somehow, probably by a small group of research councils footing the bill independently, somewhat as before. The new arrangements will have to be complete by mid-October, in time for the Finance Committee of the Danish parliament to consider them in November.

Robert Walgate

Helsinki agreement

West looks East

Brussels
The whole system of West-East technology transfer needs re-examination, according to Charles Levinson, secretary-general of the International Federation of Workers in the Chemical Industry. This

was one of the few clear ideas to emerge this week from the review by the European Parliament's Political Affairs Committee's of the Helsinki agreements.

Levinson described West-East technology transfer as an inevitably expanding process without any political control of interdependence between Western enterprises and Eastern state trading corporations. The Western entrepreneurs, he said, were providing credits for transfer of capital technology which could then only result in the flooding back of joint production onto Western markets. However, Levinson's grasp of the situation was not echoed by many of his colleagues.

At an international hearing of this kind, it might be supposed that apparent naivety was intended simply to stress a point on the record. However, Dr Guido Carli, former director of the Bank of Italy and now president of UNICE, seemed unaware of several contradictions. Speaking on what the Helsinki agreements call Basket II (economic, scientific, technological and environmental exchange) he accepted unquestioned the CIA estimates that the Soviet Union would become a net importer of energy in 1985 (a forecast which the Soviets emphatically deny).

On the other hand, he failed to rise to a question from the floor on the possible economic threat of increasing West German dependence on gas imports from the Soviet Union. Carli proposed a joint research project into energy saving between the major energy importers, including the Soviet Union, as a future counter to OPEC, yet showed no firm grasp of the statistics and parameters involved.

Professor Stefano Silvestri, of the Institute of International Affairs in Rome, suggested that the EEC's lack of a common "or even serious" energy policy and its consequent dependence on Middle Eastern oil was essentially another aspect of the political and military instability of the Mediterranean area. In general the Mediterranean featured largely in discussions, perhaps because of the presence of Willy Brandt, initiator of the North-South Report on sharing of world resources.

Linkage of the three Helsinki baskets — defence, trade and human rights — is a fundamental of Western policy. Max van der Stoel, former minister of foreign affairs of the Netherlands, stressed that dialogue does not have to be "music in the ears of the Eastern states".

The problem of Sakharov, other Soviet dissidents and Charter 77 signatories must, he said, be raised at Madrid. Linkage between Basket II, trade and technology, and Basket I, defence, normally comes to the fore in connection with the transfer of militarily sensitive and strategic technology.

However, Colonel Jonathan Alford of the International Institute for Strategic Studies in London illustrated another

aspect of that problem. The Western observers at Warsaw Pact manoeuvres, present under the terms of the Helsinki accords, had, he said, been virtually incapacitated by maps drawn to an inappropriate scale and binoculars which somehow failed to work.

Vera Rich

Biotechnology

Products work

Another hurdle has been cleared in the pursuit of profitable products from genetically manipulated bacteria. Evidence presented to the Food and Drug Administration in Washington at the beginning of June makes it clear that at least one bacterially produced human hormone has the biological activity of the natural product.

It was no coincidence that the evidence emerged when and where it did, for the aim was for the FDA to decide whether there is a need for special requirements before the licensing of bacterially derived hormones and other peptides or proteins, particularly for clinical use. Clearly the more evidence there is for the identity, not only in structure but also in activity, of bacterial and natural products, the less necessary will be additional requirements for bacterial products.

Not surprisingly, it was the San Francisco company Genetech Inc., one of the first and most voluble of the biotechnology companies, which produced the crucial evidence. Genetech's evidence centred on human growth hormone (hGH), which has been produced by Genetech bacteria for at least the past year.

When Genetech published its first account of expression of the gene for hGH in *Escherichia coli* (*Nature*, **281**, 544; 1979) there was no evidence that the hormone had the biological activity of natural hGH. Now Genetech has at least a solid foundation for that evidence.

The mainstay of their new claim is a comparative study of the stimulation of the growth of rats without pituitary glands by hGH from bacteria and from human pituitaries. The overall weight gains and the tibia growth with either hormone or with a mixture of them were virtually indistinguishable. In a further test, the bacterial hGH appeared, if anything, more potent than the pituitary hGH — an observation which Genetech attempted to relate to analytical evidence that the bacterial hGH is the purer of the two.

Genetech has also explored the possibility that its hGH-producing bacteria would stimulate the growth of rats without pituitary glands when simply present in the gut. A positive result might have rekindled the debate about the hazards of recombinant DNA. In the event, the result was negative. The rats put on no weight even though some of the bacteria survived for several days within the intestinal tract.

Genetech also revealed to the FDA that, in collaboration with Hoffman-La Roche Inc., it had successful carried out a preliminary test of the biological activity of bacterially produced interferon. Because of the limited quantities of bacterial interferon available, the test was confined to showing that three animals survived infection by a potentially fatal virus when given the drug.

The importance of this test, if confirmed, is that it would establish the activity of bacterially produced interferon even though the carbohydrate groups of the natural product are missing.

Workers from the European company Biogen, in their own paper on the construction of interferon-producing bacteria earlier this year (*Nature*, **284**, 316; 1980) expressed concern about the possible inactivity of the bacterial interferon. "If a lack of appropriate glycosylation diminishes the activity of the molecule, we shall have a problem on our hands". Their rivals at Genetech seem now to have provided a measure of reassurance on that score.

Peter Newmark

Soft money jobs

Policy rebels

The UK Science Research Council Astronomy II committee decided last week to ignore the SRC's six-year limit on short-term contracts in its future consideration of grant applications. The 25 members of the committee, which deals with infra-red, optical and ultra-violet astronomy, decided that they would advise senior researchers to "appoint the best person for the job" even if the potential researcher has been supported for more than six years on soft money.

The committee intends to consider applications for projects employing researchers whose time would run out before completion as well as applications involving the employment of a researcher who has already exceeded the SRC's upper limit of two three-year contracts.

The committee is taking its action "as a temporary measure" until a formal policy is evolved. Applications will be dealt with case by case, and the committee will fight for its recommendations, expected to be positive in all but borderline cases, on the Astronomy, Space and Radio Board, the next step up in the SRC hierarchy. The committee also empowered the Royal Astronomical Society to act on its behalf in a "big" meeting with the council to take place some time in November.

The committee's action comes at a time when the lack of university openings and requirements of modern astronomical research for specialized technology are placing a premium on retaining experienced researchers in temperary jobs. The SRC's policy, enacted in 1975, had been loosely applied until last November when

the SRC circulated a memorandum instructing its research directors to apply "rigidly" all rules on postdoctoral employment (*Nature*, 7 February). Since then, senior researchers have had their research programmes disrupted and a number of physicists have been forced out of work or have left the country. "It is a major cock-up all along the line. We are sure it is going to be reversed eventually" said committee member Professor Mike Disney of University College, Cardiff.

The case of Paul Gough, a physicist at the University of Sussex, is cited as one example of how the restriction is preventing good experiments from being carried out. Gough, whose final contract will expire in 1982, responded to an emergency call for experiments issued by the SRC on 16 April to fill vacant space created by US withdrawal from the Swedish Viking satellite. Gough proposed a novel experimental technique to study magnetospheric particle bunching by onboard data analysis of information collected from other magnetosphere experiments. Data on particle correlations, normally lost because of telemetric limitations, can be sent in analysed form through existing telemetering systems. The experiment is intended to provide information on links in the magnetosphere. Gough has been told by the SRC that the project was acceptable and would be proposed to the Swedish experimenters but that he would not be permitted to work on it because the work would carry him past his 1982 limit. The SRC has no alternative candidate to do the work. Other proposals that have received similar treatment recently include a cometary probe, a study of moon rocks and a proposal to study incoherent radio scatterring from the aurora.

The SRC admits that the policy is presenting difficulties. Brian Oakley, Secretary of the SRC, says "it is a choice of evils, but we believe the restriction is best for science as a whole. The young man is important because of his freshness in comparison to the experience of the older man." Oakley also points out that SRC has created a small number of advanced fellowships (60) to assist the estimated 3,000 researchers affected by its decision and has begun to investigate the situation in an attempt to "free the log jam" caused by the lack of university openings.

Underlying the SRC's policy is the widespread assumption that the major contributions are made by younger physicists. The glamorous figures of quantum physics — Pauli, Heisenberg, Dirac — add fuel to the belief that the newcomer just around the corner is somehow going to change the course of an investigation overnight. As Brian Oakley says, "it stands to reason doesn't it? Once mental images get fixed they are extremely difficult to break."

The problems of people on short-term contracts are increasingly recognized to be

a symptom of the strains on the UK's dual support system for the support of research, exacerbated by the lack of tenured jobs in university faculties. The SRC said however last week that it had had an encouraging response to its advertisement to university vice-chancellors of a scheme whose effect' would be to help older faculty members to be replaced by younger scientists.

Joe Schwartz

Nuclear Iraq

Plan set back?

The murder of an Egyptian nuclear physicist in his Paris hotel on 14 June has raised questions about the implications of a nuclear pact between France and Iraq, signed in 1975.

The Egyptian, 48-yr-old Dr Yahia el Mashad, was, according to Israeli radio, "one of the rare Arabs commanding authority in matters of nuclear energy". Trained in Alexandria, the United States and Moscow, he was playing a central role in the construction of two research reactors, based on French know-how, a short distance from Baghdad.

The reactors are designed to use, 93%-enriched uranium, a bomb-grade material. The project is under International Atomic Energy Agency safeguards but, said Israeli radio, the death of Mashad will make it "very difficult for Iraq to continue its efforts towards the production of an atomic bomb".

Iraq is the second largest supplier of oil to France, furnishing 18% of her needs; and when the Vice-President of Iraq's Revolutionary Council, Mr Sadam Hussein, requested access to nuclear technology during a visit to Paris in 1975, it was rapidly granted.

The agreement is worth £145 million to France, and involves the construction in the desert of a large thermal "swimming pool" research reactor (similar to Osiris at the French research centre Saclay). Called Tamuz I, it was due to be charged with 13 kg of highly enriched uranium at the end of 1981, and is already under construction. A second much smaller reactor (0.8 MW) is also to be supplied, creating a research centre for some 600 engineers and scientists.

This is the second time that the project has been threatened. Last April, explosions at the naval construction yard of Seyne-sur-Mer damaged metal casings destined for the reactors, and Iraq accused the Israeli Secret Service and the Central Intelligence Agency of complicity in the incident. Israel has certainly been concerned about the deal; a few days before Mesha's murder, General Yeoshoua Saguy declared that Iraq would probably have an atomic weapon by the mid-1980s "which will create a totally new situation in the region'''. Certainly the motive does not seem to have been criminal. Meshad was left with 1400 French francs in his wallet.

Robert Walgate

Harvard finances

Half power-plant

Washington

What started as an attempt to save money by cogenerating steam and electricity for the Harvard Medical School complex is threatening to turn into one of the biggest white elephants in the history of the university.

Construction delays, cost over-runs and disagreements about the dangers to the local community from nitrous oxide emissions have more than quadrupled the original cost of $50 million. The university has had to dig deeply into its capital reserves; and this in turn could squeeze support for other projects more directly related to teaching and research.

The university first proposed in the early 1970s to build a Medical Area Total Energy Plant (MATEP) to replace its 74-year-old steam and chilled water generator. The plant has been designed not only to provide hot water and air conditioning to a dozen medical and educational institutions in Boston's Longwood medical area, but also to produce electricity for these institutions with six 7000 kilowatt diesel-powered generators.

Once construction costs had been paid for, argued the university, the 30 per cent extra energy that cogeneration provides from a gallon of oil would save more than $2 million a year. But it reckoned without the rapid increase of oil prices, the effects of inflation on construction costs and community opposition to a new power plant in a heavily-populated area of Boston.

Public opposition has come to focus on the potential dangers of short-term exposure to nitrous oxides. This had been of little concern when the plant was planned, but was raised in a 1976 report from the World Health Organization as a

possible health hazard from diesel-powered automobile exhausts.

The Massachusetts Department of Environmental Quality and Engineering ruled in 1978 that the steam/chilled water part of the plant could proceed. But in the absence of federal standards covering short-term nitrous oxide exposure (still awaited from the Environmental Protection Agency), refused to grant a permit for the diesel engines.

Critics of the plan claim that short-term exposure to as little as 200 micrograms per cubic metre can be harmful. While not accepting this figure, the DEQE ruled that emissions should not exceed 320 micrograms (based on a hearing officer's conclusion that harmful effects have been observed in laboratory animals at exposures of 940 micrograms per cubic metre and his use of a safety factor of three).

Though disputing the scientific evidence, Harvard has accepted this figure and has drawn up a plan showing ways in which it can comply for more than 99 per cent of the time.

Following further hearings, the DEQE has now accepted most of the university's arguments about the plant's safety and rejected protesters' claims that carcinogenic hazards require further investigation.

However, the state's Deputy Commissioner, Mr David Fierra, two weeks ago again refused an operating permit on what Mr Edward Lashman, Director of Special Projects at Harvard, calls a "single, highly technical issue". This is whether, under certain operating conditions, the plant will endanger public health by contributing further to already high concentrations of nitrous oxides arising from traffic exhaust at a number of congested "hot spots" in the area.

The university is now seeking a further hearing, claiming that the 320 microgram limit will be exceeded at these locations for only 20 out of 8,760 hours in the year, and

No power for the patients?

raising the question of "whether the frequency of adverse diesel impact will be significant enough to justify disproving the diesels".

University officials are confident that they will win their case. But even if the plant is given permission to operate — and local community groups are keeping up strong opposition — the university already faces a large bill resulting from the delays so far.

The latest cost is estimated at about $215 million. Attempts to borrow this money have failed, largely because potential investors have been scared off by the regulatory uncertainties and the unwillingness of potential customers to sign long-term contracts into which the extra costs have been absorbed.

Furthermore, the university is unlikely to be allowed to raise its charges for electricity to hospital facilities to a rate higher than that charged by the local utility company, Boston Edison, therefore having to subsidize the power it provides for some time to come.

With a total endowment of $1,400 million, there is no danger of bankruptcy. However, university officials emphasize that they have no intention of using existing endowment funds — or the extra $250 million in capital reserves being sought in a fund-raising campaign — to cover the costs of MATEP.

Unless the money can be borrowed from elsewhere, the result will be intense pressure on the university's general operating account, which has already had to cover $170 million in construction costs.

David Dickson

European space

Meeting Halley

In spite of worries about two of its most highly-prized projects, the European Space Agency is giving some attention to the more cheerful prospect of a fly-by mission to Halley's comet in the mid-1980s. This has the support of solar system physicists throughout Europe, although approval would rob high-energy astrophysicists (increasingly sensing neglect by ESA) of a mission to meet their needs.

The agency's scientific advisory committee, which gives advice on the scientific merits of proposals and which includes high-energy astrophysicists among others, came out strongly in favour of the cometary mission last week. This is, after all, the only opportunity for 76 years to investigate the physics of the solar system's most notable comet. Before the final go-ahead can be given, the mission will have to be approved by the committee of official delegates of ESA's eleven member stages at their meeting early in July.

The chief objective of the mission would be to investigate the materials in the tail region. To this end, the spacecraft would be equipped with mass spectrometers for the measurement of neutral and charged atoms and simple molecules.

Most probably the project will be approved, although some delegates from countries with strong astrophysics communities (for example the Netherlands) and France may take some persuading. The Soviet Union and Japan are also considering Halley missions but the ESA is now the only hope of a Western mission to the comet; the US National Aeronautics and Space Administration abandoned its plans for such a mission some months ago, after budget cuts by Congress. In the circumstances, US scientists and NASA are understandably keen on cooperating with the Europeans. In the past few weeks, this prospect has been dimmed by the uncertainty about the joint ESA-NASA solar polar mission, one of the projects threatened by Congress.

Last week, however, Congress agreed that the international solar polar orbiter should remain as part of the NASA budget after the personal intervention of Dr Frank Press, the President's Science Advisor, and under pressure from the State Department.

ESA's current plan is less ambitious than that widely discussed last year to send one ESA and one NASA spacecraft to both the Halley and Tempel 2 comets. That would have cost about 500 million accounting units (about £315 million). The new plan will cost substantially less, chiefly through the use of the Geos 3 technology.

The European spacecraft would be launched by the Ariane rocket, probably with another satellite heading for a geosynchronous transfer orbit. Confidence in Ariane, however, has ebbed slightly since the failure of the second test flight last month and the option of using a US TD launcher is being considered. (Geos 3 is incompatible with the space shuttle.) The future of the TD launcher, however, is in many ways even more uncertain than that of Ariane. If NASA sorts out its problems with the space shuttle soon, it might have ceased to operate TD launchers by 1986, the latest date for the Halley launch.

With so many uncertainties, ESA is unlikely to decide on collaboration with NASA until the end of this year. Part of the deal would be that NASA should supply a deep space network to track the spacecraft and to relay data.

Sending a spacecraft to a comet is a risky business. Launching it on Ariane with a satellite to be put into a geosynchronous transfer orbit would reduce the launch window to only two weeks. The timing would be even finer when the spacecraft reached the comet: the most valuable data would have to be collected in a matter of minutes. The encounter would be brief — relative velocities between the comet nucleus and spacecraft would be about 60 km/sec — while positioning and tracking would have to be accurate enough to avoid collision with the cometary nucleus.

The planned flight path approaches within 1000 km of the nucleus on the tail side, so there would be also be a fairly high risk of damage from dust particles or micro-meteorites. Nevertheless, both space scientists and technologists believe there is a reasonable chance of success. A decision to go ahead would affect the pattern of other ESA missions. Within the budget limits, ESA would have to wait until the beginning of 1982 before starting on its next project — possibly a mission to observe transient phenomena in X-ray sources or POLO, the Polar Orbiting Lunar Observatory. Hipparcos, the astrometry mission approved earlier this year, would also have to be postponed for six months.

Judy Redfearn

Orbit of comet Halley with planned track of spacecraft
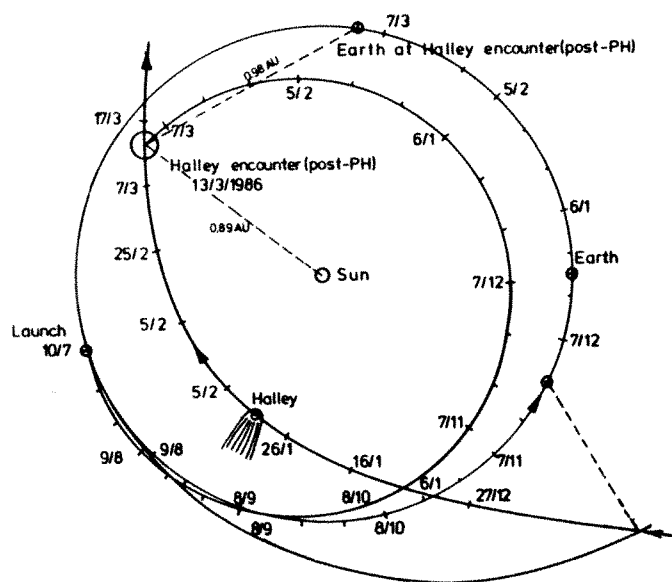
CORRESPONDENCE

Plan denied

SIR, — In your issue of 5 June you describe under "One way ahead for British biotechnology" a plan by the directors of "three renowned molecular biology laboratories" including the Medical Research Council's Laboratory at Cambridge. To set the record straight there is and has been no plan of the sort you describe, although the three scientists you name have, in common with many other experts, been consulted by the National Enterprise Board as part of that body's concern with biotechnology.

If the NEB were to set up a company to help exploit British skills in biotechnology — and the Medical Research Council has already warmly endorsed the recommendation in the Spinks' Report for such an initiative — any role the Council might play in it would involve far more than the work in the Cambridge Laboratory (distinguished though that is) and will, of course, be negotiated by the Council in consultation with all its relevant Unit directors.

<div align="right">

Yours faithfully
J. L. GOWANS
Secretary, Medical Research Council
London, UK

</div>

Controversy buried

SIR, — The adversarial approach to resolving matters of public importance has its uses, but where those matters turn upon facts, which must be acquired and interpreted, it can be counter-productive. The attempt to clarify issues by oversimplifying them polarizes the arguments and the truth appears as the opinion of the dominant faction. It becomes difficult and sometimes impossible to express an alternative view. In recent years we have seen the controversies over cyclamate sweeteners and pesticides polarized in this way and today the media presentation of the "debate" over nuclear power amounts to little more than a statement of the anti-nuclear case.

While journalists are much to blame, scientists themselves may contribute to the confusion either by retreating into a splendid isolation while the information they have obtained is used responsibly or irresponsibly by propagandists, or by joining the fray, perhaps unwittingly, and seeking data to support the cause of their choice. In itself this is harmless enough, and science often proceeds by accumulating evidence to support an attractive hypothesis, while contradictory evidence, which eventually destroys the hypothesis, is obtained more slowly. Where a polarized argument creates a false sense of urgency, however, so that important decisions are made on the basis of partial information, the public interest is not served. The history of the US Environmental Protection Agency contains many examples of such hasty decisions and recommendations.

The latest victim of adversarial skirmishing is the debate over the effects of chlorofluorocarbon (CFC) compounds on the ozone layer. As a writer and a scientist we have tried to suggest that the ban on most aerosol propellant uses for CFCs cannot be justified by the evidence that is available. We have a case, or so we believe. While we do not quarrel with the general proposition advanced by Rowland and Molina, that CFCs can destroy ozone, we note that two-dimensional atmospheric models suggest that much of the resultant depletion will occur over the arctic during winter, when lost ozone is not replaced. We are not convinced that CFCs could

endure indefinitely in the troposphere, yet a CFC sink here would reduce the ozone depletion substantially. Nor do we regard it as certain that a small increase in UV radiation at the surface would be malign. The basis of the view that UV radiation is highly dangerous — and hence of our concern over the ozone layer — is that advanced organisms could not evolve, and dry land could not be colonized, until sufficient oxygen had been released by photosynthesizing organisms in the seas to allow an ozone layer to form. There is no evidence to support this view and it is challenged strongly by many biologists. Probably there is a causal relationship between exposure to UV and nonmelanoma skin cancer in humans, but the link between UV and melanoma is too weak to be convincing. Finally, we would point out that if CFCs are so dangerous as to warrant banning, pressure will soon build to extend the aerosol ban to other uses of CFCs in refrigeration, insulation and foams, for which we may incur an energy penalty as well as an economic one.

Our views are hardly revolutionary, but we have had difficulty in expressing them in public. An article has been commissioned from us, so we have no grounds for personal complaint, but an earlier article that had been commissioned was rejected on the advice of American referees and another offer of an article was politely declined. We know of other writers who have experienced similar difficulties in criticising the CFC ban, and we believe that contrary views are being suppressed while truth is dictated by fashion.

If we are committed to decision by combat it is rather important that those who make the decision be exposed equally to all arguments and that we find some way to give weight to the view that the information available justifies no decision at all. We fear that by crying "Wolf!" repeatedly over supposed environmental threats, one day we may not be heard when the threat is real. Indeed, it is a curious fact that amid all the quite genuine threats to the global environment about which we do possess information, the purely theoretical CFC threat to the ozone layer is the one that has resulted in legislation. We may embrace the adversarial method or we may reject it, but we must not distort it in this way. If we are to embrace it, scientists must be prepared to participate and journalists and their editors must assist them to do so.

<div align="right">

Yours faithfully,
MICHAEL ALLABY
Wadebridge, UK

J.E. LOVELOCK
Launceston, UK

</div>

Discussion stilled

SIR, — As the author of one of the reports "which have become the centre of fierce controversy in the climate research community" (*Nature*, 8 May), I feel compelled to respond briefly to your short piece on the possibility that increased atmospheric CO_2 concentrations could lead to increased tensions between those nations of the world classified as rich and poor. It comes as no surprise to me that the special committee of the National Academy of Sciences that issued the report with this conclusion agrees with the experts consulted that our dissenting reports are "based on incomplete assessments that unrealistically omit important feedback processes".

Our findings that the greenhouse effects of atmospheric CO_2 are a full order of magnitude less than the previous scientific consensus are so much at odds with the thinking of the past

several decades that it will be some time before they receive a dispassionate and objective evaluation. This is particularly so because they are based essentially on experiment, whereas most earlier work in this area has been of a theoretical nature. It is therefore doubly curious that the experts claim we have omitted important feedback processes for we have dealt with the real atmosphere, measuring the effects of whatever feedback processes of a significant nature are occurring in real time.

I would thus like to encourage those experts that disagree so violently with our findings to submit their judicious appraisals of our work[1] for publication, where they can be answered in a public forum.

<div align="right">

Yours faithfully
SHERWOOD B. IDSO
Tempe, Arizona, USA
[1]Idso, S.B., *Science*, 280, 1462; (1980).

</div>

Engine exhausts

SIR, — David R.L. Davies (17 April), points out that automobile combustion chamber deposits accumulating as a result of the use of leaded petrol cause an increase in octane requirement. Unfortunately, he implies incorrectly that deposits from unleaded petrol do not have such effects. In fact, combustion chamber deposits from unleaded petrol generally cause greater increases in octane requirements than those from leaded fuel.

Of the several investigations of this subject, the work of the US Coordinating Research Council (CRC), which involved contributions from 15 major US laboratories (auto manufacturers, fuel suppliers, etc.) is the most extensive. They reported that their data "indicate that cars operated on fully leaded fuels have less Octane Requirement Increase (ORI) than those cars operated on unleaded or low lead fuels". A summary of the work by the CRC was presented before the US Society of Automotive Engineers in 1973 by Bigley and Benson (SAE Paper 730013) who reported the average ORI effect was 2.0 to 2.5 research octane numbers *higher* for unleaded than for leaded petrol.

To avoid knocking complaints for a given percentage of vehicles, the octane quality of unleaded fuel must be increased above that of the leaded petrol which it replaces. This increases the cost and crude oil consumption penalties associated with unleaded petrol.

<div align="right">

Yours faithfully
WILFRED E. BETTONEY
E.I. du Pont de Nemours & Co., Inc.,
Wilmington, Del., USA

</div>

SIR, — In response to my earlier correspondence (17 April) on lead based petrol additives, combustion chamber deposits and fuel efficiency, Wilfred E. Bettoney points to tests conducted by the US Coordinating Research Council in 1972. My understanding of the tests by the US CRC is that they compared leaded petrol containing additives to reduce and modify deposits of lead compounds with unleaded petrol where no effective effort was made to reduce carbonaceous deposits.

In any case, tests carried out on the 1971 US vehicle fleet are not directly relevant to European or Japanese vehicles designed since 1973. To be more specific, recent developments such as electronic ignition control and a shift to lean fuel mixtures have reduced both the need for high octane fuel and the rate of carbon deposition.

<div align="right">

Yours faithfully
DAVID R.L. DAVIES
Centre for Resource and Environmental
Studies, Australian National University,
Canberra, Australia

</div>

NEWS AND VIEWS

Heat flow and the deep structure of the continents

from Philip England

SOME seismologists now believe that the plates which form the mobile outer skin of the earth differ strongly in their thermal and mechanical properties between continent and ocean, these differences extending to depths of 400 km or more[9]. If this is true, the implications for the chemical evolution and mechanical stability of the continents are profound. Unfortunately, the seismic data are scanty and the interpretations controversial, so constraints from an independent set of data would be valuable. Recently, Vitorello and Pollack[7] have argued that measurements of surface heat flow on the continents provide just such an independent constraint, and that it too requires that continents have 'roots' more than 300 km thick.

It has been recognised for some fifteen years that conductive heat flow from the surface of the continents is related to the geologic age of the crust. Developing from the observation that heat flow from Precambrian (more than 600 Myr old) provinces is generally lower than it is from younger regions[1], it has now become generally accepted that there is a monotonic decrease in the surface heat flow with increasing age of the crust, on a timescale of 200–500 Myr[2-5].

The study of heat flow from the ocean floor, and of ocean bathymetric data which are closely linked to heat flow, has provided crucial insights into the origin and development of the oceanic portions of the plates. The surface heat flow and the elevation of the oceanic crust both decrease with age and approach steady state values when the crust is 70–100 Myr old. These observations can be explained in terms of the cooling of the upper mantle from a condition of partial melting at the mid-ocean ridges to one of near thermal equilibrium in the old oceans, where a cool, and therefore rigid, mechanical boundary layer some 100 km thick overlies a convecting upper mantle. The dominant mode of heat transport in this layer — the lithosphere — is by conduction.

The directness with which interpretations of oceanic heat flow led to improved understanding of the thermal and mechanical nature of the oceanic lithosphere has naturally resulted in similar attempts to analyse continental heat flow.

However, the determination of heat flow on land — and of its relation to the age of the crust — is far more difficult than the corresponding tasks at sea. Continental temperature measurements are confused by such effects as topography, groundwater flows and conductivity contrasts. Whereas the age of the oceanic lithosphere is clearly given by the date of solidification of its basaltic crust (a process occurring over a few million years at most), the tectonic process affecting continental crust take considerably longer (100 Myr is not an unusual duration for an episode of mountain building) and may strike the same piece of crust more than once in its history.

Nevertheless, the overall picture we have of heat flow decay on the continents, although originally derived from less than 150 observations[2], has changed little now it is based on 1,700 observations[5]. When the heat flow measurements are grouped according to the time elapsed since the last major tectonic event to affect the crust they show a decay of continental surface heat flow from an average of around 80 mWm^{-2} in terrains less than 200 Myr old to an average 60 mWm^{-2} in terrains 300–400 Myr old with an approximately steady average heat flow of 45–50 mWm^{-2} for terrains in the range 600–2,500 Myr old. It must be emphasized that these data exhibit great scatter, much of which results from the uncertainties mentioned above. In addition, a significant proportion arises from a complexity not present in the oceanic case.

In the oceanic crust the proportion of radioactive isotopes present is very small, and they contribute less than 5% to the surface heat flow, but on the continents, the decay of radio-active isotopes is responsible for around 50% of the surface heat flow. These radiogenic elements are unevenly distributed within the crust and thus the surface heat flow in a province of a given age can vary considerably, just because of changes in the intensity of near-surface heat production, without in anyway indicating variation in the deep thermal structure of the region.

Philip England is IBM Research Fellow in the Department of Earth Sciences, Bullard Laboratories, Cambridge University.

The scatter of heat flows measured within provinces of given age spans are greater than the range of the means from provinces of all the different age spans. It is thus natural to ask whether the variation in continental heat flow is the result solely of the variation of conditions within the crust, or whether the slow decline in heat flow with age reflects some deeper seated thermal process within the continental lithosphere.

In the past, the latter class of explanation has been favoured and the thermal development of the continental lithosphere has been explained in terms of cooling from an initial high temperature regime, with erosion playing a comparatively minor part by removing near surface radiogenic heat sources.

The most recent and most thorough explanation of this type has been given by Vitorello and Pollack[7]. They propose a three component model for the continental heat flow decay: **I** a component due to radiogenic isotopes within the crust, this is in part removed by erosion on a timescale of 300–400 Myr; **II** a component due to the decay of a temperature perturbuation caused by the 'tectonothermal' event (e.g. mountain building, plate boundary volcanism, etc.) that now defines the age of the crust; **III** a constant background contribution from the upper mantle. To fit the surface heat flow observations, a decay of some 40mWm^{-2} over 300–400 Myr is required. Relying on an empirical relation[8] suggesting that 40% of continental surface heat flow is generated within the crust (i.e. by component I.) Vitorello and Pollack suggest that 40% of the heat flow decay comes from the removal by erosion of an approximately 10km thick layer of crust rich in radiogenic elements.

The remainder of the secular decay must now come from component II of their model — the conductive decay of the temperature perturbation produced by the 'tectonothermal' event. It is here that the major implication of Vitorello and Pollack's model becomes apparent, for they require this decay of around 30mWm^{-2} to take place over 400–500 Myr and show that this requires the conducting boundary layer beneath the continents to be over 300 km thick — three

times the thickness of the corresponding layer in the oceans. For this layer to remain stable, and not become involved in mantle convection, and to explain the absence of the large thermal subsidence (analogous to, but larger than the 4 km difference in elevation between ocean ridges and the abyssal plains) which the cooling of such a thick layer would involve, Vitorello and Pollack suggest that the 'tectonothermal' events which perturb the continental mass result in partial melting of the upper mantle to give basaltic volcanism, leaving behind a cold viscous residue which is reduced in density owing to the extraction from it of the denser fractions which go to make up the basalt.

This model has considerable geochemical and geophysical implications. First, it implies that every 'tectonothermal' event which affects the crust involves considerable partial melting of the mantle, with the transport of mantle-derived melt into the crust and the depletion of some 300 km of upper mantle in iron and a number of other elements — notably the heat producing ones. This bears closely on the argument raging among geochemists as to whether the differentiation of the earth is a continuing process — with new crust constantly being created — or whether the bulk of continental crust was created in intense activity 2,000 to 3,000 Myr ago while the earth was much hotter.

Second, Vitorello and Pollack's requirement of deep, stable continent roots lends support to the claims by a small but vociferous band of seismologists that differences in seismic velocity between continents and oceans extend at least as deep as 400 km (for a recent review see ref. 9). Among other things, this model would also imply that it should be harder to move plates that have large continents on them, because the drag on their 'keels' is much greater than that on the 100 km thick oceanic plates.

This model, then, has intriguing possibilities, and the success of similar interpretations of the oceanic data, makes it tempting to accept Vitorello and Pollack's conclusions. However, the conclusions are model-dependent and in view of their weighty geophysical and geochemical implications it is disappointing that the authors do not suggest a mechanism to account for the far greater depth extent

which they propose for partial melting beneath the continents than beneath the mid-ocean ridges; nor do they give any indication of whether the quantity of partial melting they invoke is consistent with the volumes of basic volcanics associated with present or past zones of activity in the continental crust.

In addition, many geologists familiar with young mountain belts will be surprised at the small length scale and long timescale that Vitorello and Pollack assign to the erosion in their model, 10 km of erosion over 400 Myr is quite small when compared, for example, with the 20 km or so of erosion from the axial zone of the Alps in the last 30 Myr, or the widespread inference, from mineral assemblages, of burial depths of 20 to 30 km experienced by crustal rocks during mountain building episodes throughout geologic time. Richardson[10] has shown that the entire variation of continental surface heat flow can be explained by the removal by erosion of the radiogenic elements contained in 20 km of continental crust. The geological

record suggests that thickening of the crust by 20 km and subsequent erosion by this amount is a common occurrence in zones of continental collision like the present day Alpine-Himalayan chain.

So, there are at least two explanations of the continental heat flow relations, one in terms of a deep-seated thermal 'root' to the continents and the other in terms of purely crustal processes.

While Vitorello and Pollack have produced some persuasive reasons for interpreting continental heat flow in terms of the cooling of a boundary layer 300 km thick, they have not shown that this model is required by the data; other models with lithosphere no thicker than the oceanic one are also consistent with the data[10,11], and are in better agreement with our understanding of the evolution of mountain belts.

In conclusion, the controversial seismic observations which seem to suggest that continents have deep roots must await support from some other source than surface heat flow data. □

1. Kraskovski, S.A. *Izv. Akad. Nauk. Arm. SSR Geol. Geogr. Nauki. Eng. Tran.* 247 (1961).
2. Lee, W.H.K. & Uyeda, S. *Geophys. Monogr. Series* 8, 87 (ed. Lee W.H.K. AGU, Washington 1965).
3. Polyak, B.G. & Smirnov Ya. B. *Geotectonics Eng. Trans.* 4, 205 (1968).
4. Sclater, J.G. & Franchetau, J. *Geophys. J. Roy. Astr. Soc.* 20, 509 (1970).
5. Chapman, D.S. & Furlong, K. *EOS Trans AGU* 58, 1240 (1977).
6. Parsons, B. & McKenzie, D.P. *J. Geophys. Res.* 83, 4485 (1978).
7. Vitorello, I. & Pollack, H.N. *J. Geophys. Res.* 85, 983 (1980).
8. Pollack, H.N. & Chapman, D.S. *Tectonophys.* 38, 279 (1977).
9. Jordan, T.H. *Nature* 274, 544 (1978).
10. Richardson, S.W. in *Geodynamics Today — a review of the Earth's Dynamic Processes.* 123 (Royal Society, London, 1975).
11. England, P.C. & Richardson, S.W. *Geophys. J. Roy. Astr. Soc.* 62 in the press.

Cereal yields and drought resistance

from S.A. Quarrie

CEREAL yields in the UK have been increasing by 50-70 kg/ha each year for the past 30 years. They are now about 80% higher than they were in 1950. Improvements in agronomic practices, particularly the increased use of nitrogen fertiliser and crop protection chemicals, account for part of this increase. How successful, then, have the breeders been in improving the yields of cereal varieties and what are the prospects for the future?

Answers to these questions for winter wheat have now been provided by Austin *et al.* (*J. agric. Sci.* 94, 675; 1980). They compared the yields of old varieties dating back to 1908 with those of modern ones in an experiment in which lodging (bending at or near the soil surface) and severe infections of disease were prevented. On two sites of differing fertility the best of the new varieties consistently outyielded the old varieties by about 40%. At each site the total dry matter production of the varieties was similar. The new varieties, which were much shorter, had lower stem weights than the older ones. So the breeders, in seeking to achieve resistance to lodging by selecting for dwarf habit, have gained a bonus. Because the total dry matter has not changed, reductions in stem weight have been accompanied by exactly balancing increases in grain weight. The modern varieties flower earlier and grain filling occurs over a longer period.

The authors suggest that there is a limit to which stem weights can be reduced with a concomitant increase in grain yield and this would give at most a further 25% yield

increase. Thus, to continue increasing grain yields into the 21st century will require varieties capable of giving a greater biomass yield. Unfortunately, even if the genetic resources are available to do this, an increase in biomass yield is likely to increase water use. But shortage of water is already a factor limiting yields of wheat and barley in the UK. Using data from various irrigation experiments in recent years, Austin (*ADAS Quart. Rev.* 29, 76; 1978) has estimated that drought causes an average yield reduction of 17% in the UK. The beneficial effect of irrigation was most marked on light soils, but, since irrigation would not be economic for cereals in Britain, it seems clear that in the future greater emphasis needs to be placed on more efficient use of available rainfall and stored water. Although it may be possible to reduce yield losses due to drought by cultural treatments, recent research has suggested ways by which the drought resistance of new varieties may be improved by breeding.

For many years physiologists and breeders have been looking for characters which reliably predict drought resistance, but with relatively little success. The problem is twofold. First, drought itself is often variable both in its severity and timing, and this determines the way and extent to which yield may be reduced. Second, few scientists studying the problem have had adequate genetic material for testing the effects of variation in a single character in a uniform genetic background. Physiologists are now

working with breeders to create the genetic diversity necessary for this work.

There are some recent examples of this. Jones (*J. exp. Bot* **28**, 162; 1977) looked at the effect on transpiration of stomatal frequency in related lines of barley bred by Rasmusson. Contrary to expectation a reduction in stomatal frequency did not cause a reduction in transpiration. Instead, the lines with a low stomatal frequency had larger stomata and larger leaves and these differences totally compensated for the reduced stomatal frequency; to decrease transpiration selection for small stomata or small leaves would also have to be carried out.

The development of the root system is obviously of vital importance to the water economy of the plant. In two recent papers (O'Brien, *Aust. J. Agric. Res.* **30**, 587; 1979; Robertson *et al. Crop Sci.* **19**, 843; 1980) the authors have looked at genetic variability in the length and number of wheat roots. Their ultimate objectives were to improve our understanding of the requirements for optimising water uptake in different environments. They found that potentially useful genetic variability exists in the length and number of seminal and lateral wheat roots, and O'Brien is already preparing experimental lines by hybridisation and selection. From studies with these lines it will be possible to elucidate the interrelationships between root growth, moisture uptake and crop yield. Optimum root development patterns can then be defined for various kinds of drought.

The biochemistry of stress is also being studied. The concentration of the amino acid proline often increases several-fold in response to water stress. Work in the early 70s suggested that proline may have a role to play in determining drought resistance in barley. However, Hanson *et al.* (*Crop Sci.* **19**, 489; 1979) have recently studied proline accumulation in related barley lines selected on the basis of their high or low drought-induced proline accumulation. They found no evidence that accumulation of free proline was of survival value during severe drought and concluded that proline accumulation was essentially a symptom of the development of severe plant water deficit.

The plant hormone abscisic acid (ABA), the concentration of which also increases during drought, may be more directly related to drought responses. Applied ABA has effects on the development and physiology of plants similar to those of water stress. An additional effect of ABA in droughted plants has been suggested by Morgan (*Nature,* this issue p655). Water stress at meiosis reduces seed set and Morgan has shown that applied ABA can also do this. When plants were droughted, ABA concentration in the flag leaves increased and ABA was also transported to

the ears, although these did not develop stress. Several cereal species have now been examined for differences in drought-induced ABA accumulation. Larqué-Saavedra and Wain (*Ann. appl. Biol.* **83**, 291; 1976) looked at related lines of maize known to differ in drought resistance and found that the more resistant lines had a greater capacity to accumulate ABA when droughted.

Many physiological and morphological characters are significant for water economy, though for a given character the useful variation within a cereal species may be limited. Once the characters which can be exploited to improve drought resistance in cereals have been identified it might be possible for plant breeders to maintain the rates of yield improvement they have achieved in recent decades.   □

S.A. Quarrie is in the Plant Breeding Institute, Trumpington, Cambridge.

Flares without acceleration, or acceleration without flares?

from John C. Brown

A basic problem associated with solar flares, after the difficulty of producing sufficiently rapid primary energy dissipation, is that of particle acceleration, a process also observed to occur under other cosmic conditions. Any acceleration problem involves explanation of generating sufficiently high individual particle energies and of acceleration of sufficiently many particles (total particle energy). In principle the former is readily achieved for flares by the electric fields of up to 10^{10} V, which could be induced by the rapid reduction in flare magnetic field, sufficient to account for the most energetic (GeV) ions observed. On the other hand, the bulk of the total energy of flare particles resides in the non-relativistic ($\simeq 1\text{--}100$ keV) electrons detected directly in space and by the hard X-ray (bremsstrahlung) and radio (gyrosynchroton microwave and Type III plasma oscillation metre wave) bursts they emit in the flare plasma.

Till now most interplanetary electron event observations have been confined to energies $E \geq 10$ keV. At such energies it has been found (Lin *Space Sci. Rev.* **16**, 189; 1974) that while electron events are closely associated with flares, the converse is not true i.e. many flares produce no (detectable) electron event. This is consistent with the notion that particle acceleration is a process which is secondary to a basically thermal dissipation of magnetic energy in flares and is only initiated by a sufficiently large or transient primary release. On the other hand in those flares where acceleration does get under way the ≥ 10 keV electrons often acquire a fraction of the total flare energy sufficiently large to demand a substantial acceleration efficiency, and perhaps to play an important role in transporting energy through the flaring solar atmosphere.

Potter, Lin and Anderson (*Astrophys. J. Let.* **236**, L97; 1980) have now extended the survey of interplanetary electron events down to 2 keV energies using data collected by the International Sun-Earth Explorer (ISEE) 3. They have found that the acceleration of 2–10 keV electrons is a very

frequent event, apparently occurring without a detectable electron event at higher energies and in the absence of any reported flare activity as measured by chromospheric (Hα) events and by radio and X-ray bursts. These low energy electron events, however, seem closely associated (as are more energetic electron events) with low frequency (< 1MHz) type III radio bursts (also observed by ISEE–3) believed to be due to plasma wave excitation in the low density outer solar atmosphere by the electron stream passage. Potter *et al* regard these observations as direct evidence for non-flare associated electron acceleration in the corona. While the possibility is not yet excluded that Hα and X-ray bursts did occur in these electron events, but below the threshold for detection (or reporting), the data certainly indicate the frequent operation of a dissipation process whose primary product (energetically) is accelerated electrons rather than hot plasma. The possibility that this can also sometimes occur at higher electron energies was suggested earlier on the basis of a survey of indirect electron data by Kane *et al* (*Solar Physics* **38**, 438; 1974).

The best venues for production of non-thermal effects are theoretically those where the thermalisation time is as long as possible compared to the duration of energy release — in this case high in the corona where the plasma density is low and collision times long so that electrons escape before they can thermalise. Potter *et al* argue that this is indeed the acceleration site from which the 2–10 keV electron events emanate, and specifically suggest an altitude of at least 0.5 solar radii ($R_\odot$) above the photosphere. Their conclusion is based essentially on the observation that the electron events have spectra extending smoothly down to about 2 keV with no turn-over (though the power-law index does decrease at the lowest energies). It is then argued that if the electrons started out with a power-law spectrum E^{-4} at an

John C. Brown is in the Department of Astronomy, University of Glasgow.

altitude $\lesssim 0.5$ R . (density n $\lesssim 10^7$ –10^8 cm^3) collisions with the intervening plasma would turn over the low energy end of the event spectrum seen near the earth. This argument, though attractive, is not watertight. In particular if the acceleration spectra were steeper at low energies then collisions would flatten them toward the observed form. Second, any tendency for collisions to turn over an initially power-law spectrum would be offset by the spectral redistribution due to plasma waves generated by the bump in the electron velocity distribution itself, Nevertheless it seems likely that the argument used by Potter *et al* does indicate the density of the acceleration region correct to order of magnitude and it is of interest to pursue further its physical implications.

First, there arises the question of stability of the electron stream in a plasma of such low density. In particular, the electron flux over an assumed area of $(10^{-2} R_\odot)^2 \simeq 5 \times 10^{17}$ cm^2 would be about 5×10^{13} cm^{-2}s^{-1}, which, in an ambient plasma density of $\gtrsim 10^7$ cm^{-3} will drive a return current with drift velocity $v_D \lesssim 5 \times 10^6$ cm s^{-1}. This is below the ion-sound speed for any reasonable coronal temperature, so that the return current should be ion-sound stable. For these same parameters, Ohmic losses to the beam in driving the return current should also be small compared to the direct collisional losses, as tacitly assumed in the Potter *et al* analysis. Second, the magnetic field strength at these high altitudes will be low but, as Potter *et al* point out, still adequate to supply the total electron energy by annihilation of a 1 gauss field in a volume of $(10^{-2} R_\odot)^3$. Third, at a density of 10^7 cm^{-3} and temperature around 10^6 K, the electron collisional relaxation time is several seconds for thermal electrons and several tens of seconds for 2 keV electrons. As indicated above such time scale conditions are favourable for release of energy primarily into nonthermal forms.

It appears then that pure acceleration of (low energy) electrons in the corona without chromospheric flare effects may be a common occurrence and as potentially important an acceleration diagnostic as flares themselves. For higher energy electrons to be accelerated, magnetic fields and gradients must presumably be stronger, so that lower altitudes and correspondingly higher densities will be involved. The shorter thermalization times would then lead to substantial heating of the coronal plasma (soft X-ray flare) and the combined effects of downstreaming electrons and of thermal conduction would also produce chromospheric flaring. Further elucidation of the relative importance of heating effects associated with acceleration of electrons of different energies and fluxes, should emerge from the current Solar Maximum Mission with its wide spectral coverage and coordination with other space, and also ground based, experiments. □

Early steps in excision repair

from A.R. Lehmann

WHEN excision-repair of DNA damage was discovered by Setlow and Carrier in 1964, they suggested that it could be carried out by four enzymatic steps: an endonucleolytic nick was made in the vicinity of the damage, the damaged section was removed by an exonuclease, the resulting gap filled in by a DNA polymerase, and the new stretch of DNA joined to pre-existing DNA by ligase. Though this model remains correct in outline, the details of excision repair have turned out to be much more complex in detail, the whole process being under the control of numerous gene products both in *Escherichia coli* and in eukaryotic systems. A variation of the classical scheme of 'nucleotide excision-repair' was discovered some years ago, when it was found that a number of altered bases in DNA such as uracil, hypoxanthine and 3-methyladenine were excised in a different manner, termed 'base excision-repair'. The first step in the removal of these bases was not the scission of the phosphodiester backbone, but the rupture of the glycosylic bond between the altered base and the deoxyribose sugar. The resulting AP (apurinic or apyrimidinic) site in the DNA could then be removed by sequential action of an AP endonuclease (found ubiquitously) and exonuclease.

The major type of damage produced in DNA by UV light is the pyrimidine dimer, resulting from the formation of a cyclobutane ring joining two adjacent pyrimidine bases. This lesion causes a large distortion of the DNA helix, and it has been studied more extensively than any other type of DNA damage. Until very recently the pyrimidine dimer was thought to be removed by nucleotide excision repair rather than base excision repair because pyrimidine dimer-specific endonucleases, purified from either *Micrococcus luteus* or T4-infected *E.coli* seemed to make endonucleolytic nicks on the 5′ side of pyrimidine dimers. This mechanism now seems to be incorrect, as shown by work published in this issue of *Nature* (Haseltine *et al.* p634) and by several papers presented at the recent NATO-EMBO Advanced Study Institute on Chromosome Damage and Repair (Godøysund, Norway, 27 May-5 June, 1980). Haseltine and coworkers were investigating the specificity of the endonuclease from *M. luteus* by using a sequenced piece of DNA, and comparing the cleavage sites after UV-irradiation and treatment with endonuclease, with those produced by specific chemical digestion. The results of these experiments showed that if the starting DNA was labelled at the 5′-end, the enzyme-digested fragments were one nucleotide longer than would be anticipated if the enzyme cleaved the DNA on the 5′ side of the pyrimidine dimers. In other words the cleavage site appeared to be on the phosphodiester backbone between the two dimerized pyrimidines. Such a cleavage would in itself be of no obvious advantage in removing the pyrimidine dimer, and the authors went on to demonstrate that this was in fact the second step of the reaction, the first step being the rupture of the glycosylic bond between the 5′-pyrimidine of the dimer and the deoxyribose sugar, leaving an apyrimidinic site. This was then cleaved by AP endonuclease activity as shown in the figure below.

In support of this mechanism they first provided chemical evidence for the apyrimidinic site at the 3′ end of the 5′-labelled fragments. They then purified the enzyme further and were able to separate the glycosylase activity from most (but not all) of the AP endonuclease activity. The glycosylase was specific for DNA containing pyrimidine dimers and the product of the reaction did indeed contain AP sites. Finally, treatment of the product with DNA photolyase or with further exposure to UV (treatments which cleave the cyclobutane ring between the two pyrimidines of the dimer, returning them to their original conformation), resulted in release of free thymine. This could only have arisen from the 'dangling' 5′-pyrimidine of the dimer, formed by the action of the glycosylase.

Similar conclusions have been reached by three groups working with the pyrimidine-dimer specific endonuclease from T-4 infected *E.coli*, the product of the T4 *v* (or *den V*) gene. Linn and co-workers (University of California, Berkeley; *Nature* in the press) showed that the product of the reaction of this enzyme with UV-irradiated DNA contained an AP site at the 3′-end of the cleavage site, and Radany and Friedberg (Stanford University; *Nature*, in the press), like Haseltine *et al.* demonstrated that subsequent to enzymatic action by the T4 endonuclease thymine could be released by photoreversal. This release of free thymine was correlated with loss of pyrimidine dimers from the DNA, and could not be effected with extracts of cells infected with *v*-gene mutants of T4.

(B = base, T̂T = thymine dimer)
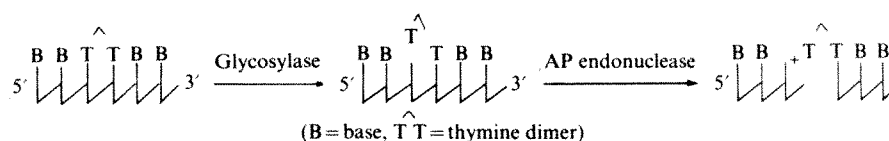
Seawell, Smith and Ganesan have also studied the action of the T4 UV-endonuclease (*J. Virol.* in the press). Their enzyme preparation contained both glycosylase and AP endonuclease activity, but only the former was active at 0°C. Thus the product of the reaction at 0°C, using colEl-DNA as substrate, contained AP sites, which were only converted into nicks if the temperature was subsequently raised to 37°C. Attempts to separate the two activities by physical procedures were unsuccessful. On the other hand assays of extracts of *E.coli* infected with T4 containing temperature-sensitive mutations in the *v* gene revealed that the glycosylase, but not the AP endonuclease activity, was thermolabile. This shows that the *v* gene codes for the dimer-specific glycosylase activity.

These studies provide convincing evidence that the *M.luteus* and T4 'UV-endonucleases' first rupture the glycosylic bond of the 5'-pyrimidine of the dimer and then cleave the phosphodiester backbone between the resulting apyrimidinic site and the 3' pyrimidine of the dimer. What is not yet established is whether the glycosylase has intrinsic AP-endonuclease activity or whether the two activities can be separated.

With these two enzymes the distinction between base and nucleotide excision repair has become less clear-cut. We now await results with enzymes from *E.coli* and human cells. In *E.coli* the incision step is controlled by three genes (*uvr A, B* and *C*) which code for high molecular weight proteins. Unlike the enzymes from *M.luteus* and T4, the *uvr* gene products recognise other bulky adducts as well as pyrimidine dimers, and the incision step is carried out by a complex of the three gene products in an ATP-dependent reaction (Seeberg, *Proc. natn. Acad. Sci. U.S.A.* **75**, 2569; 1978). Neither the *uvrA* nor the *uvrB* gene product contains glycosylase activity (Seeberg, Norweigan Defense Research Establishment, Kjeller, Norway) and

A.R. Lehmann is in the MRC Cell Mutation Unit, University of Sussex, Brighton.

preliminary results from several groups suggest that the *uvr* gene products do not act via a glycosylase-AP endonuclease sequence, but rather via a classical endonuclease action.

The *uvr* genes have been cloned in several laboratories (Seeberg, Norway; Rupp, Yale University; van Sluis, Leiden); and the properties of the gene products are under intensive study. We can thus expect the elucidation of the mechanism of 'UV-endonuclease' action in *E. coli* within a short space of time.

In human cells the incision step is controlled by at least seven gene products, the seven complementation groups of the genetic disorder xeroderma pigmentosum, all of which are deficient in effecting incision of their DNA after UV-irradiation of the cells. Studies on the enzymes from mammalian cells are, however, fraught with all the worst problems of enzymology (small quantities and extremely labile enzymes), and it may be some years yet before we can explain the mysteries of excision-repair in human cells. □

Prothoracicotropic hormone-secreting cells in the insect brain

from Lynn M. Riddiford

THE specific cells that produce prothoracicotropic hormone (PTTH) have been identified in the insect brain (Agui *et al. Proc. natn. Acad. Sci. U.S.A.* **76**, 5694; 1979) and this has been followed by identification of the neurohaemal storage organs (see *Nature* this issue, p669). The hormone causes the prothoracic glands to secrete ecdysone which controls the growth and metamorphosis of the insect.

Ablation studies in a variety of insects had attributed PTTH activity to neurosecretory cells in the dorsum of the brain but it was a new, very sensitive assay, developed in Gilbert's laboratory (Bollenbacher *et al. Proc. natn. Acad. Sci. U.S.A.* **76**, 5148; 1979) that allowed the identification of the specific cells.

Using isolated prothoracic glands of freshly ecdysed *Manduca sexta* (the tobacco hornworm) pupae and a radioimmunoassay for the secreted ecdysone, they showed that homogenates of larval brains would stimulate the basal rate of ecdysone secretion fourfold. Moreover, half-maximal activation of the glands required only 0.16 brain equivalents. Pupal brains showed similar activity and had the additional advantage that both groups of neurosecretory cells (the medial and the lateral) were visible in the living brain due to iridescence caused by the Tyndall effect. Agui *et al.* first showed that the region of the pupal brain containing the lateral neurosecretory cells had the major portion of the PTTH activity, thus confirming the earlier bioassay results of Gibbs & Riddiford (*J. Exp. Biol.* **66**, 255; 1978). By

an extremely delicate dissection using an eyebrow hair, Agui *et al.* separated the two histologically distinct groups of lateral neurosecretory cells, then isolated the two cells (each about 20 μm diameter) of the most lateral group that had contained the PTTH activity. Although these two cells could not be distinguished morphologically or topographically, only one of them contained the activity of the whole cluster. Thus in the *Manduca* pupal brain only two cells seem to produce PTTH — one in either hemisphere.

The absence of significant PTTH activity in the medial neurosecretory cell cluster was unexpected. In the blood-sucking bug *Rhodnius prolixus* both electrical and secretory activity of the medial neurosecretory cells has been correlated with the time of PTTH release (Steel in *Comparative Endocrinology* (eds. P. J. Gaillard & H. H. Boer) Elsevier, North Holland, 1978). Moreover, in another moth species *Hyalophora cecropia* both groups of cells seem to be necessary for the initiation of the molt from the pupa to the adult (Williams *Symp. Soc. Devel. Biol,* **8**, 61; 1948; Van der Kloot *Amer. Zool.* **1**, 3; 1961). The role of each of these cell groups can now be resolved using the new PTTH assay.

Agui *et al.* also showed that the corpora allata (the endocrine glands that produce juvenile hormone in the larva and in the adult) are the neurohaemal storage organs

Lynn M. Riddiford is Professor of Zoology, University of Washington, Seattle.

for PTTH. Classically the insect corpora cardiaca have been considered to be the respository for the neurosecretory products from the brain. The axon of the PTTH-secreting cell crosses over and exits from the contralateral side of the brain, then passes through the corpus cardiacum to the corpus allatum (Nijhout *Int. J. Insect Morphol. Embryol.* **4**, 529; 1975). Both the pupal and the larval corpora allata contain 4-5 times the PTTH activity of the corpora cardiaca (Agui *et al., Nature* this issue p669). Extraction of the corpora allatal homogenates with hexane to remove the juvenile hormone showed that the stimulation of ecdysone secretion was not due to this hormone. These data strongly support the conclusion that the corpora allata of Lepidoptera are the neurohaemal organs for PTTH, a suggestion first made by Ichikawa and Nishiitsutsuji-Uwo (*Biol. Bull.* **116**, 89; 1959). Whether the corpora allata play a similar role in other insects remains to be seen.

The identification of the cell producing PTTH as well of the neurohaemal storage organ and release site for the hormone paves the way for the isolation and identification of this all-important hormone for insect growth and development. Studies to date suggest that it is a peptide of 5,000 daltons although larger sizes have also been reported (reviewed in Gilbert *et al. Ann. Rev. Physiol.* **42**, 493; 1980). These past studies have used brains as a source of PTTH, but in light of these recent results the pupal corpora allata which seem to store PTTH but are devoid

of allatotropin should be a better source. Small amounts of released hormone for confirmatory studies can probably be obtained from these glands by stimulation of the nerve leading to them or by high K$^+$ depolarization as has been done with the diuretic hormone of *Rhodnius* (Maddrell &

Gee, *J. Exp. Biol.* **61**, 115; 1974). Also the identification of the PTTH-secreting cell makes possible a detailed neurophysiological study of the control of the release of this hormone by various internal and external signals such as larval size, photoperiod, and temperature. □

Dielectric relaxation spectroscopy

from J. H. Calderwood

IF the permittivity (or refractive index) of a dielectric material is measured over a frequency range extending from very low values up to the infrared, a number of abosorptions will be observed. Frequencies at which these absorptions occur, and their strengths, may be a decisive factor in determining the practical use to which the materials can be put. Study of the spectra can yield information about the structure of the molecules of the material, and of the molecular dynamics of the system which the molecules, and in some case aggregates of molecules, comprise. These studies and their applications in science and industry were the theme of a recent conference.*

The interpretation of the dielectric measurements presents further problems. H.A. Price of the University College of Wales, Aberystwyth, pointed out that although isotropic liquids usually show only one absorption maximum in their relaxation spectrum, it may be broader than the absorption which would be predicted by the Debye equation. In some cases, the broadening is sufficient to allow the relaxation to be resolved into multiple processes corresponding to whole molecule rotation and the internal rotation of a flexible group within the molecule. Debye considered spherical molecules, but if his treatment is generalised to ellipsoidal molecules as was done by Perrin, then separate relaxation processes are predicted corresponding to rotation about the different molecular axes. Price gave details of the observation of multiple relaxation processes for some liquid crystals, and the particular cases of p-methoxy-benzylidene -p-n-butylaniline (MBBA) and n-heptyl-cyanobiphenyl (7CB).

R. Toomer from the University College of North Wales, Bangor, was concerned with the separation of conduction and relaxation processes as energy loss in a dielectric can be caused by either of them. Metal electrodes are normally used for dielectric measurements, but as they are capable of injecting charge into dielectric solids, thus initiating a conduction process, it is necessary to separate that conduction from the dielectric relaxation phenomena. Toomer described an experimental technique whereby a material could be polarized by

induction, without any direct metallic contact, and the surface scanned by a sensitive induction probe, again without contact being made, to determine the time decay of the surface potential, and so determine the relaxation time of the specimen.

Another technique, especially suitable for the investigation of charge storage mechanisms, is that of field-induced thermally stimulated currents (FITSC). It involves raising of the temperature of a specimen at a known rate while the current is measured. Vanderschueren of the University of Liège gave a critical account of how such measurements should be interpreted and paid particular attention to the tests that should be carried out to ensure that spurious effects are absent. In particular, a systematic variation of experimental parameters which might affect the results should be carried out: these include such factors as electrode material, specimen thickness and field intensity. Other techniques involving thermal relaxation should also be used to confirm the results of FITSC.

The more traditional method of the examination of the frequency spectrum can be used to investigate the behaviour of aggregates of melecules of the micelle type. R. Pottel of the University of Göttingen described measurements in the frequency range 0.1MHz to 60GHz on liquid crystalline aqueous systems and showed how the dynamical behaviour could be influenced by the molecules of the solvent, and by the solute concentration. Molecular dynamics can also be studied by the rather unusual technique of non-linear dielectric spectroscopy, when materials are polarized by fields of high strength. If the polarization is expressed by a power series, the second and higher order of coefficients characterise the non-linear properties. Helleman of the University of Leuven described how the non-linear effects observed for reactive systems are an indication of the extent to which the field has perturbed the chemical composition of the sample. Thus from the relaxation of the non-linear effect, information on chemical rates can be collected. This is a very unusual tool to be employed for the investigation of chemical rate processes.

A portion of the frequency spectrum which is more difficult than most is the

millimetre wave region. At longer wavelengths, waveguides, lines, closed cavities, and bridges are available, while at shorter wavelengths optical techniques become applicable. A. Gebbie and P. R. Mason of Imperial College, London, described how over-moded cavities could be used in the millimetre region. The over-moding is produced by means of a rotating paddle in the cavity which scatters the radiation in all directions, thus ensuring that the specimen will be subjected to its influence, without the possibility of its being affected by a special wave pattern. The open resonator provides another very useful means of measurement in the microwave region, and its advantages become particularly significant as the wavelength decreases. A. L. Cullen of University College, London, described the construction of an open resonator suitable for measuring the permittivity of a material in the form of a sheet. In order to assess the error which might result from some small departure from the ideal in a design feature, the interesting technique was adopted of deliberately making the departure large, and making measurements as it was progressively reduced. A. C. Lynch, also of University College, discussed the limitation in the accuracy of permittivity measurements and showed how some of the difficulties might be overcome. For example, in a microwave resonator it is possible to arrange that the surface of the sheet specimen are in a field which is nearly zero, thus reducing the effect of any error in making the most difficult measurement associated with the experiment. Surprisingly, that is the measurement of the thickness of the specimen!

Even when we know how to obtain good results, and how to interpret them, the problem remains of how to predict them. Prediction is made possible by the construction of models which corresponded in some analogous way with the physical reality. Although in principle the construction of such models might be fairly straight forward the analysis of the model to determine the behaviour which it predicts is usually a matter of considerable technical complexity. The problems associated with modelling dielectric behaviour were discussed by M. W. Evans of the University College of Wales, Aberystwyth, P. Bordewijk of Leiden University, and C. Brot of the University of Nice. Computer simulation is liable to be very expensive in computer time, but Brot showed how reliable values of complex permittivity of highly polar fluids could be obtained by a two-dimensional simulation involving only a few hundred molecules, despite the long-range character of dipolar interaction. This is an encouraging advance in a field in which progress is not easy. □

How selfish is DNA?

In the 17 April issue, Doolittle and Sapienza and Orgel and Crick separately used the term 'Selfish DNA' to describe certain DNA sequences in eukaryotic organisms. They argued that the process of DNA replication allows the accumulation within the replicating genome of DNA sequences which have no functional (phenotypic) significance but whose presence stimulates the further accumulation of sequences of the same kind. This 'selfish' DNA is supposed, in particular, to account for some of the apparently functionless DNA in the genomes of higher organisms. The two articles have stimulated a great deal of comment, some of which appears below. The original authors will reply at a later stage.

from T. Cavalier-Smith

WHILE it may be futile to look for a 'special function for every piece of DNA', it is a mistake to imply[1,2] that selection within the genome for 'selfish DNA' (intragenomic selection) explains the C-value paradox[3]. One should also not neglect existing evidence for the idea that the overall amount of DNA in the genome has definite (nucleotypic[3,5–7]), effects on cellular and organismal phenotypes, which are of profound adaptive significance[3,7]. Orgel and Crick[1] imply and Doolittle and Sapienza[2] explicitly suggest that the strong and widespread correlations between C-values, cell and nuclear volumes and cell cycle length[3,5] can be explained simply in terms of an evolutionary equilibrium between a universal, constant, tendency for C-values to be increased by the multiplication of selfish DNA sequences, and selection against such increases, which would be more intense in smaller and more rapidly reproducing cells.

There are two objections to their treatment of the problem. First, even on their theory the decisive factor accounting for the unexpectedly great variation in C-values is variation in the selective force against high C-values. This selective force acts not within the genome, but between genomes differing in C-value i.e. different nucleotypes[5] (nucleotypic selection). Second, their assumption that nucleotypic selection is always for smaller genomes would only be reasonable if there was no evidence that the overall amount of DNA exerts a causal nucleotypic control on cell and nuclear volume and cell cycle length.

In some circumstances nucleotypic selection for larger genomes is also to be expected[3] if causal nucleotypic effects genuinely exist. Two phenomena strongly argue that they do: (1) the increased cell volumes and cell cycle lengths caused by increased numbers of B-chromosomes[8], (2) the reduction in cell volume caused by chromosome elimination and chromatin diminution[3], which occurs in certain invertebrates. These effects are of key importance for our understanding of the C-value paradox, for they provide positive evidence for a differential selective

advantage for different C-values at different stages of the life cycle. As very large amounts of DNA are eliminated in somatic cells, but retained in the germ line, not only must a low C-value be positively advantageous in somatic cells, but also a markedly higher C-value must be of positive selective advantage to the animal in the germ line. The idea that the extra DNA is retained merely because it cannot be got rid of[1,2] is completely untenable in this case, for a mechanism of elimination clearly exists.

A "relatively small proportion" of extra DNA would not be strongly selected against, but the extra non-coding DNA whose presence we have to explain is often not merely "a relatively small proportion" of the total DNA. In single-celled eukaryote algae, C-values vary at least several thousand-fold[3], so the amount of non-coding DNA in the highest C-value species is probably many thousands of times that of the coding DNA. Even by Orgel and Crick's own criterion this makes an explanation of the C-value paradox in terms of selfish DNA highly implausible. It seems more reasonable to suppose that large cells actually require more DNA than do small ones.

Whatever the mechanism of evolution of larger cell size, larger cells require more rRNA transport to the cytoplasm per cell cycle than do smaller cells. One would therefore expect selection to increase the rate of RNA transport in larger cells, lest it become rate limiting to cell growth and unduly lengthen the cell cycle. This could be done by increasing the amount of skeletal DNA (S-DNA)[3] so as to increase the nuclear surface area and the number of nuclear pores. The suggestion is therefore that excess DNA is used, not, as has been incorrectly stated[1], to slow development but rather to prevent the excessive slowing of development which would otherwise be caused by large increases in cell size[3].

It is entirely beside the point that cells can[1] slow their growth without increasing

their genome size, for only if growth is slowed as a secondary consequence of increased cell size (which in practice is invariably associated with increased C-values) does one expect slow growth to be associated with a high C-value[3]. It is well known that some slow growing organisms have small cells and low C-values. But what should never occur on my theory[3] — and has not been observed — is that high C-value organisms have small cells and short life cycles.

Though there are undoubtedly several ways of evolving larger cells[3,7], a simple and direct way would be by increasing the number of replicon origins involved in the volume-dependent control of DNA replication[3,7]. This cannot provide the fundamental explanation of the C-value paradox, since it does not necessitate a larger genome (as it involves only a small fraction of the genome), but it would facilitate the coordinated evolution of cell and nuclear volumes, which the nucleotypic theory[3] postulates. It also explains the variation in cell size caused by B-chromosomes and chromatin elimination. On this theory[3,7] it is the extra replicon origins not the larger nucleus, or the larger genome as such, which increases cell size: what the C-value controls more directly is nuclear volume.

It also seems premature to dismiss all middle repetitive DNA as selfish DNA[2]. Where C-values have greatly increased relatively recently much of it may be selfish in the restricted sense of having no sequence-specific function (but not in the wider sense[1] of lacking nucleotypic effects on the phenotype), as suggested[3] for *Plethodon* and *Lathyrus;* but in organisms like mammals with evolutionarily stable C-values it seems to be strongly conserved[10], and there is recent evidence that it may form replicon origins[11], as proposed earlier[3]. Even in *Plethodon* a fraction of middle repetitive DNA is strongly conserved[12] which suggests that there are in general two quite distinct categories of middle repetitive DNA, one with sequence specific functions (and therefore G-DNA[3]), and the other being a

T. Cavalier-Smith is in the Department of Biophysics, King's College, London.

form of S-DNA having only nucleotypic functions and whose related sequences merely reflect their relatively recent common origin by duplication and transposition and which will eventually by mutation and random drift become unique DNA.

Unless the idea that genome size has a directly causal nucleotypic effect on cell and nuclear volumes and cell cycle length is refuted, it is merely begging the question to speak of the extra DNA in high C-value organisms as 'junk' or having 'no specific function, or 'useless', or having 'no phenotypic expression'. Quantitative scaling[6] of cell or nuclear volumes and developmental rates is a very specific function, even if it is mediated by DNA the bulk of whose sequences (but not amount) could be changed without changing the phenotype. The idea that nuclear surface area and the number of nuclear pores are functionally important aspects of the phenotype[3] is supported by the fact that they are developmentally adjusted (for example in oocytes) to varying cell volumes and rates of transcription: one should not simply ignore evidence that the total amount of DNA, as well as its degree of folding or unfolding, causally influences nuclear surface area.

Intragenomic selection is clearly important for understanding evolution within genomes and for understanding the significance of certain DNA sequences[1-4], but it does not in itself clarify the evolutionary forces determining genome size; the situation is analogous to that in animal populations where the selective forces acting between competitors tell us little or nothing about what determines the overall population size. Present evidence for direct nucleotypic effects of genome size on cell and nuclear volume and cell cycle lengths suggests that selection acting on these important evolutionary parameters[3,7] would greatly outweigh selfish-DNA-like effects in determining genome size. But the relevant level of selection here is that acting between genomes of different sizes (i.e. nucleotypic selection), rather than the lower-level intragenomic selection.

As far as evolution of genome size is concerned, the activities of 'selfish' DNA

1. Orgel, L.E. & Crick, F.H.C. *Nature* **284**, 604 (1980).
2. Doolittle, W.F. & Sapienza, C. *Nature* **284**, 601 (1980).
3. Cavalier-Smith, T. *J. Cell Sci.* **34**, 247 (1978).
4. Cavalier-Smith, T. *Nature* **270**, 10 (1978).
5. Bennett, M.D. *Proc. R. Soc. B.* **178**, 277 (1971); *Proc. R. Soc. B.* **181**, 109 (1972).
6. Bachmann, K., Chambers, K.L. & Price, H.J. *Pl. Syst. Evol. Suppl.* **2**, 41 (1979).
7. Cavalier-Smith, T. *BioSystems* **12**, 43 (1980).
8. Rees, H. & Jones, R.N. *Chromosome Genetics* (Edward Arnold, London, 1977).
9. Östergren, G. *Bot. Notiser* **2**, 157 (1945).
10. Rubin, C.M. *et al. Nature* **284**, 372 (1980).
11. Jelinek, W.R., *et al. Proc. natn. Acad. Sci. U.S.A.* **77**, 1398 (1980).
12. Mizuno, S. & MacGregor, H.C., *Chromosoma* **48**, 239 (1974).
13. Williams, G.C. *Adaptation and Natural Selection* (Princeton University Press, 1966).
14. Dawkins, R. *The Selfish Gene* (Oxford University Press, 1976).
15. Whitehouse, H.L.K. *Towards an Understanding of the Mechanism of Heredity.* (Arnold, London 1965).
16. Watson, J.D. *Molecular Biology of the Gene 3rd edn* (Benjamin, Menlo Park, California, 1976).
17. Sinnott, E.W., Dunn, L.C. & Dobzhansky, T. *Principles of Genetics*, 4th edn (McGraw-Hill, New York, 1952).

sequences are best regarded as mutational processes serving to provide the variation in genome size on which nucleotypic selection then acts.

Intragenomic selection may often lead to a slight upward 'mutation pressure' on genome size, but the implication[1,2] that such pressures are always upwards is unfounded for this would prevent evolutionary reductions in genome size, which seem often to have occurred[3]. Using the analogy mentioned above, one may say that nucleotypic selection sets the 'population size' of the DNA sequences (i.e. the genome size) within which 'selfish DNA' sequences may compete with each other by intragenomic selection. It is important when discussing genome evolution to distinguish these two levels of selection, both from each other and from the more usual form of selection between alternative alleles, which has been the stock in trade of population geneticists and which it would be better to call allelic selection instead of genic[13] selection.

This distinction between allelic, intragenomic, and nucleotypic selection enables one to discuss the C-value paradox more precisely than the superficially seductive phrases 'selfish gene' (which in Dawkins' use[14] conflated all three types of selection) or 'selfish DNA' which conflates intragenomic and nucleotypic selection. The term 'intragenomic selection' is clearer than 'non-phenotypic selection'[2] because it directs attention to the fundamental phenomenon in question — intragenomic competition between different sequences — without begging the question as to the phenotypic effects of the competing sequences, or misleadingly implying that there is a well-defined contrasting concept of phenotypic selection or 'phenotypic benefit'.

The term 'phenotype' as used in the definition of selfish DNA[1], in 'non-phenotypic' selection[2], and in my earlier discussion of intragenomic selection[3], departs radically from the traditional meaning of phenotype[15-17] as embracing all observable traits including such things as transposability of DNA sequences, the renaturation rates of middle repetitive DNA, nuclear volumes or C-values. Since this new restricted use of 'phenotype' to exclude certain traits (but which?) associated very directly with DNA has never been clearly defined, the concepts of 'non-phenotypic selection' and 'selfish DNA' themselves lack precision. It might be better to redefine selfish DNA as DNA whose presence makes no positive contribution to the fitness of the cell or whole organism, and which spreads by intragenomic selection.

Finally, one should emphasise that, though the phrases 'selfish DNA' and 'intragenomic selection' are both new, the concepts they stand for were very clearly formulated 35 years ago by Östergren[7], who speculated that B-chromosomes were useless parasites.

Ignorant DNA?

from Gabriel Dover

IT has recently been suggested that the more the organisation of the eukaryote genome is unravelled the more it can be taken as a depository of many inconsequential acts of DNA replication and transposition. Selfish DNA that has 'subverted the mechanism of duplication'[1] and 'evolved a strategy for survival'[2] has entered the ordered house of the genes and created mayhem: a state of disorganisation that is of no concern to the organism. Or has it? It is in answer to this question that two recent articles[1,2] have attempted to review the evidence. Both emphasize, with some qualification, that the majority of the DNA of the eukaryotic genome may indeed be selfish. In doing this they have rightly underscored the molecular and populational pitfalls inherent in all naive attempts to define functions for an heterogeneous assemblage of non-coding DNA, which is excessive in mass, and which is organised mainly into families of multiple copies that intervene between and within the genes. This is a refreshing approach and one that has not been over-stressed in the past. However, it is one thing to brush aside the naive functionalist looking for precise molecular interactions and another inadvertently to throw out the baby (that small amount of suggestive evidence) with the bathwater and to replace it with genetically awkward concepts concerning the process of accumulation of 'junk'.

Recent studies of fluctuations in size and position of shared families of sequences in carefully compared genomes of related species[3-6] and of alterations in genomic position of sequences in recently separated populations[7-9], have shown that the composition of the higher genome is constantly changing and often mobile[25]. These changes are occurring both on an evolutionary timescale and within the space of a few generations. The underlying mechanisms are not known but the present-day distribution of sequences between species and patterns of arrangements of sequences within a species can be ascribed to quirks of DNA replication that recurrently amplify and intersperse (or transpose) the new with the old families,[10-12]. Although not all investigators would agree on the details, the consensus view would be that DNA is rather an ignorant molecule that frequently gets out of hand and is quite capable of generating a multitude of sequence arrangements. In what ways can we expect the results of this sort of flux to affect the biology of organisms? Doolittle and Sapienza, and Orgel and Crick expect it to have very little obvious molecular influence on the phenotype and consequently they focus their attention on the sociobiology of the change itself. It is at

Gabriel Dover is a lecturer in the Department of Genetics, University of Cambridge and a Fellow of King's College, Cambridge, UK.

this point that they construct a process of selfishness[1,2] and non-phenotypic selection[2] that in its assumptions overlooks some of the details of genome organisation and activity which reveal a somewhat different process of evolution.

The idea of selfishness was originally used by Dawkins[13] to highlight the increase in frequency of one gene (allele) in a population at the expense of another. As a caricature of evolutionary processes that appear to endow single genes with 'motivation' it is harmless. As a description of the process of natural selection and adaptation operating on collections of interacting genes locked within genomes, and that may contribute only in part to the selected phenotype, it is inadequate and misleading. Nevertheless, selfish increase in numbers at another's expense could be used to describe the outcome (but not necessarily the process) of any self-replicating unit. If we ignore the unfortunate teleological implications of selfishness we can predict that extant families of DNA would represent a limited range of accumulated sequences that contained within them a high content of highly efficient and mobile replicators. However, with respect to this, there is no obvious molecular commonality in the internal sequence organisation of the many families that have been examined. These families are complex and are of every possible size (number of copies), periodicity ('kinetic complexity'), sequence composition, internal organisation and interspersion. Examples are too numerous to list but recent reports of sequence organisation in rye, cow and fruit-fly reveal the very different intricate patchworks of sequences that have evolved[4,14,15].

Considering the data *in toto*, we cannot escape the notion that the genome is subjected to a range of random processes that are capable of generating any conceivable pattern of organisation. Thus there is a clear predictive distinction of the outcome between selfish and stochastic processes. In addition, if the majority of the families have no effect on the phenotype and are also not 'parasitic' (*sensu* Orgel and Crick) then they are simply neutral and spread (or not), according to statistical processes of drift, similar to neutral alleles. It could be that dispersal throughout a sexually reproducing population is accelerated, as Orgel and Crick have rightly suggested, by the fact that copies of a sequence become distributed throughout a karyotype (parasitic DNA) and it is to this particular property, although seemingly common to most of the randomly produced families, that the appellation of selfish could be used if we so wished. There is also the interesting suggestion that diminution and loss of a family are occurring at a much slower rate. However, there would probably be more thrust to the central and important argument that much of the genome makes no direct molecular sense if Doolittle,

Sapienza, Orgel and Crick had clearly underlined the limitless ways of creating and disseminating 'junk' by random processes rather than appearing to rely on the more limited idea of the genome as an arena for selfish replicators under 'non-phenotypic selection'. This is a small but necessary quibble, for in making this distinction a second point of clarification can be raised concerning the biological consequences of these processes.

Selfish DNA, by definition, makes no specific contribution to the phenotype[1] and no phenotypic explanation is required for its continued existence[2]. The attribution of selfishness to the sequences appears to prejudge the issue of their biological effects, whereas judgement of the biological consequences of randomly accumulated sequences is a separate consideration.

Indeed it could be argued that the present levels of accumulation of sequences are due to phenotypic selection for tolerance to extant families rather than to their selfishness. If this were not so one highly efficient replicator might be expected eventually to replace the whole genome. However setting this aside, are we yet in a position, in our ignorance of the mechanisms of so many fundamental biological processes, to strip the bulk of these sequences (whether random or selfish) of all biological activity? To answer this, we need to turn to several diverse and suggestive observations.

First, the overall growth of the genome is not a completely haphazard phenomenon in that it is known from several species groups that chromosome arms increase proportionately in length as species accumulate more DNA, e.g. in salamanders[16]. This might be a reflection of some process, perhaps involved in primary transcription or the meiotic behaviour of chromosomes, that requires that certain regions of the genome should be kept as separable and unique entities. If this is so, then there would be a high premium for straightforward selection for a balanced

interspersion of new families of DNA as an aspect of chromosome phenotype.

Second, there are interesting experiments of Davidson and Britten and their colleagues on the activity of sea urchin genomes. They have shown that up to 30% of the genome is transcribed into heterogeneous nuclear RNA, some of which is composed of contiguous stretches of repetitive and structural gene sequences. Very recently they have shown that there are developmental and tissue-specific differences in the abundance of nuclear transcripts of different repetitive families, but not of the structural genes, and that the nuclear RNA falls into many sets, each of which can be characterized by a particular pattern of repetitive sequences[12]. Repetitive sequences have been found to be intimately interspersed within developmentally regulated globin gene clusters in rabbit[17] and man[18] which in the latter are homologous to several nuclear RNAs[19]. If the splicing and transport of short coding transcripts are affected by differences in organization of the longer transcripts then phenotypic selection might arbitrate between some patterns of dispersion based on this activity. It is also interesting to hear that the very abundant (satellite) DNAs are transcribed during meiosis in new oocytes[20].

Third, there is an intriguing correlation, discussed by Orgel and Crick, between total DNA amount (C-value) and the durations of cell cycles and generation time of a species[21]; critical adaptive parameters through which selection might influence the size of a genome.

Fourth, some families of DNA, because of their presence and position, rather than their precise sequence, affect the state of chromatin condensation which in turn can alter both the frequency and localisation of recombination[22], and the expression of nearby genes, (position effect variegation). Recently, a correlation has been found between the transposition of sequences and viability[23] and gene activation[24] in *Drosophila* and several other species[25].

Finally there is evidence that in primates, Gramineae and rodents, specific and quite intricate patterns are shared between chromosomes and between species[4,5,6,26]. In species of rodents in particular the sharing extends to 'segmental sequence variants' (minor patterns) and their proportions within a family of repeats, despite the evidence that within each species and within each chromosome there are recurrent rounds of amplification[6,26]. The reasons for the detailed preservation of such patterns are not known and it might be interpreted in terms of selfish sequences. However, we have recently obtained evidence (Dover & Ribbert) that in the blow-fly, all genomic sequences co-replicate during the polytenisation of chromosomes in germline cells but not in polytene somatic cells in which satellite DNA families suffer a preferential under-replication. There

1. Orgel & Crick *Nature* **284**, 604 (1980).
2. Doolittle & Sapiens *Nature* **284**, 601 (1980).
3. Moore *et al. Cell* **15**, 189 (1978).
4. Bedbrook *et al. Cell* **19**, 545 (1980).
5. Donehower & Gillespie *J. Mol. Biol.* **134**, 805 (1979).
6. Brown & Dover *Nature* **285**, 47 (1980).
7. Young *Proc. natn. Acad. Sci. U.S.A.* **76**, 6274 (1979).
8. Strobel *et al. Cell* **17**, 424 (1979).
9. Cameron *et al. Cell* **16**, 739 (1979).
10. Dover *Nature* **272**, 123 (1978).
11. Flavell *et al.* in *Genome Organisation & Expression in Plants.* (Plenum, 1980).
12. Davidson & Britten *Science* **204**, 1052 (1979).
13. Dawkins *The Selfish gene* (Oxford Up, 1976).
14. Pech *et al. Cell* **18**, 883 (1979).
15. Wensink et al. *Cell* **18**, 883 (1979).
16. Mizuno *et al. Chromosoma* **88**, 239 (1974).
17. Shen & Maniatis *Cell* **19**, 379 (1980).
18. Fritsch *et al. Cell* **19**, 939 (1980).
19. Jelinek *et al. Proc. natn. Acad. Sci. U.S.A.* **77**, 1398 (1980).
20. Varley *et al. Nature* **283**, 686 (1980).
21. Bennett *Proc. Boy. Soc. B* **181**, 109 (1972).
22. Yamamoto & Miklos *Chromosoma* **66**, 71 (1978).
23. Gvozdev *et al. Cold Spring Harbor Symp.* **XLV** (1980).
24. Gehring & Green *Cold Sping Harbor Symp.* **XLV** (1980).
25. Movable genetic elements *Cold Spring Harbor Symp.* **XLV** (1980).
26. Brown & Dover *Nucleic Res.* **8**, 781 (1980).
27. Goldschmidt *Material Basis of Evolution.* (Yale UP, 1940).
28. Dover in *Insect Cytogenetics. Roy. Ent. Soc. Symp.* **10**, (Blackwell, 1980).
29. Stanley *Macroevolution* (Freeman, 1980).

might be a specific need for the retention of all sequence patterns during germ-line differentiation and meiosis.

These varied aspects of organisation and activity suggest, albeit tenuously, that there is some overall selective marshalling of arbitrary sets of sequences which give some specific and common form to closely related genomes. Although the sequences concerned may not intrinsically define a specific function, selection may act on the phenotypic effects arising from the mere presence or position of the sequences within a genome.

When we enter the depths of the higher genome we should not abandon all hope of arriving at an understanding of the manner in which some sequences might affect the biology of organisms in completely novel and somewhat unconventional ways. It was imaginatively suggested by Goldschmidt in 1940[27] that saltatory steps in chromosome repatterning lead to abrupt changes in phenotype, some of which ('hopeful monsters') might have a degree of success in particular environments. It may be that the rapid changes in sequence organisation (in particular of the germ-line) can give rise to interesting discontinuities in morphology or developmental timing in such a process of speciation[28]. Evidence is accumulating that speciation is rarely the result of a gradual and large accumulation of adaptive allelic differences, but that it is episodic and rapid followed by long periods of morphological and genetic constancy, (aptly reviewed in detail by Stanley.[29]) The accidental and sudden accumulation of extraneous DNA sequences might lead to the inception of a process whose subsequent constancy reflects the much slower rate of diminution and loss of these elements, (among other things). □

Occam's razor

from Temple F. Smith

DOOLITTLE and Sapienza argue that since the evolution of properties such as transposability ensure sequence survival, no other selective or functional properties are required to explain the existence of much of this 'extra DNA'. Orgel and Crick argue, in addition, that for the eukaryote no phenotypic selective pressures of sufficient strength are known to forbid the internal genomic evolution of these nonviral parasitic DNAs. These arguments are at their base a variant on Occam's razor, and have an analogue in the axiom of high energy physics: what (state transition) is not forbidden is mandatory. These apparent solid arguments are supported by considerable data: the large variation in total DNA content among organisms of equal complexity, if not always of close

taxonomic association; and, the recent work on the yeast Ty-1 element (Cameron, Loh & Davis *Cell* **16**, 739; 1979) which is strongly suggestive of just such a parasitic sequence.

No rigorous calculations, however, have been made of phenotypic selections on such extra DNAs. The coordinate evolution required between parasitic sequences and the enzymes manipulating nucleic acids, particularly those with sequence specificity, requires more detailed analysis. There is a need for careful statistical analysis on transposables as to their probability of disrupting functional sequences or on the stability of non-functional repeats generated via such mechanisms as consecutive uneven cross-overs. There are also other curious statistics which must be investigated in connection with these ideas. For example, the entire GC content of the vertebrates appears constrained by the genetic code (Smith *Math. Biosci.* **4**, 1979; 1969) to a very narrow region about 42% while invertebrates are less constrained and prokaryotes not at all. This, at first glance, seems in direct contradiction to the expectation of the 'Selfish DNA' hypothesis.

For many evolutionary biologists, there is another problem inherent in these discussions on selfish DNA. It is epistemological in nature, as the presented theory appears nearly irrefutable. If a phenotypic constraint or function is found for any given sequence, it is either removed from consideration under the theory or it is argued that its function was a later adaptation exploiting the already existing parasitic sequence. Similar considerations have, of course, plagued the theory of evolution from its inception. Yet the important question is not to prove the potential for neutral parasitic sequences (of that there seems little doubt) but rather to predict by the 'selfish hypothesis', under known phenotypic gene level selection pressures, the distribution and other statistical characteristics of particular genetic sequences. The more constraining the predictions, the more seriously we must take the theory. □

Selfish DNA in 'Petite' mutants

from R. A. Reid

DIRECT experimental evidence of DNA arising in eukaryotes by non-phenotypic selection is furnished by 'petite' mutations of the mitochondrial DNA of *Saccharomyces cerevisiae*. These mutants are promising systems for investigating the questions raised by Orgel and Crick[1] on the molecular mechanisms involved in the appearance and maintenance of seemingly

superfluous DNA and the selective disadvantages of carrying such DNA. In brief, suppressive 'petite' mutants have defective mitochondria that cannot respire because of the deletion of large segments of mit DNA. Typically, these deletions, which probably arise through site-specific illegitimate recombination events[2], are accompanied by amplification of the non-deleted DNA so that the total amount of DNA in defective mitochondria is very similar to that of the wild type[3]. This amplification confers no obvious advantages; the resulting mit genome appears to be irrelevant to the immediate needs of the cell which, being deprived of functional mitochondria, uses energy from sugar glycolysis for growth. In other words spontaneous or artificially induced 'petite' mutations constitute systems where selfish DNA is created before our eyes and confirm that strategies exist for increasing the probability of survival of DNA that does not contribute to organismic phenotypic fitness.

Yeast mit DNA is probably more closely allied to eukaryotic nuclear DNA than to prokaryotic DNA as it contains highly reiterated short sequences and introns[4,5]. Therefore its small genome size (26 μ) and the ease with which amplification can be induced and identified make it an attractive system for testing models of how middle repetitive and highly reiterated sequences can arise in eukaryotes without phenotypic selection. Progress has already been made in defining the nucleotide sequences that delimit the repeat units of recently arisen and old petite mutants relative to their wild type parental strains[6]. The mit DNA of 'petites' can amount to over 10% of the total cell DNA. Far from contributing to fitness this implies a selective disadvantage of about 10^{-2} if some reasonable assumptions are made about the energy costs, and suggests that under substrate limiting conditions the redundant mit DNA could be substantially eliminated within some thousands of generations. Theoretically it would seem easier for a yeast strain under metabolic stress to rid itself of irrelevant DNA in redundant mitochondria than to carve out selfish DNA already integrated into the nuclear genome, and quite different mechanisms may apply. Nevertheless, detailed long-term studies of the evolution of the mit DNA of new 'petites' grown under defined selective pressures should at least illuminate the proposition that the DNA loads of extant cells represent compromises between the expansionist tendencies of selfish DNA and the restraining forces of selective disadvantage. □

Temple F. Smith is Professor of Physics in the Biophysics Laboratory, Northern Michigan University.

R. A. Reid is in the Department of Biology, University of York, York.

1. Orgel, L.E. & Crick, F.H.C. *Nature* **284**, 604 (1980).
2. Bernardi, G., Prunell, A. & Kopecka, H. In *Molecular Biology of Nucleocytoplasmic Relationships* p85 (ed. Puiseux-Dao, S.) Elsevier (1975).
3. Locker, J., Rabinowitz, M. & Getz, G.S. *Proc. natn. Acad. Sci. U.S.A.* **71**, 1366 (1974).
4. Slonimski, P.P. *et al.* in *Biochemistry and Genetics of Yeasts* p.339 (eds. Bacila, M., Horecker, B.L. & Stoppani, A.O.M.) Elsevier-North Holland. (1978).
5. Bos, J.L. *et al. Nature* **275**, 336 (1978).
6. Faugeron-Fonty, G. *et al. J. Mol. Biol.* **134**, 493 (1979).

ARTICLES

Th and U in sedimentary rocks: crustal evolution and sedimentary recycling

Scott M. McLennan & S. R. Taylor

Research School of Earth Sciences, Australian National University, Canberra, ACT 2600, Australia

Thorium and uranium abundances in sedimentary rocks increase at the Archean–Proterozoic boundary, in response to an episodic change in the composition of the upper continental crust. Uranium decreases and Th/U increases during post-Archean time due to significant recycling of sedimentary rocks.

SECULAR variations in sedimentary rock compositions are of major importance because they constrain models of crustal evolution and the amount of sedimentary recycling through geological time. (For reviews of major element trends see refs 1–5). Of the important trends noted for the rare earth elements (REE)[6–11] the most significant is the sharp change in sedimentary REE patterns associated with the Archean–Proterozoic boundary about 2,500 Myr ago. This has been interpreted as being the result of a major episodic change in the composition of the exposed crust at the end of the Archean Era[9–11].

Such changes in crustal composition through time (mafic to felsic) should be reflected by a change in Th and U abundances in sedimentary rocks. The possible role of sedimentary recycling can also be assessed from such data. During rock weathering, U^{4+} is readily oxidized to U^{6+} and forms the highly soluble species $[UO_2]^{2-}$; on the other hand, Th^{4+} does not change oxidation state during weathering and remains relatively very insoluble. Hence, if recycling of material is important in the chemical evolution of sedimentary rocks, it should be accompanied by a steady increase in Th/U ratios, as U would be continually lost during successive cycles of weathering and redeposition, providing oxygen is available in the atmosphere–hydrosphere system.

Ronov and Migdisov[12] have examined Th and U distributions as a function of age for sedimentary rocks of the North American and Russian Platforms. Using those data, Veizer[2,13] noted a general increase, for Th/Al and U/Al, in progressively younger rocks. This has been interpreted as support for a gradual change in the composition of the exposed crust from mafic to felsic[12,13]. However, the quality of the analytical data, as measured by analyses of international inter-laboratory rock standards, has not been well established in these studies. The trends noted have not been confirmed on other continents. Finally, the Th/Al and U/Al trends could be an artefact of possible decreases in Al in sedimentary rocks[4].

For several years, this laboratory has been accumulating high quality trace element data, including Th and U, for clastic sedimentary rocks, primarily from Australia, of all ages[6–8,14–17]. Some 90 samples covering an age range of >3,700 Myr to the present have been analysed. The distribution of Th and U in these rocks, the implications for the evolution of the continental crust, and the possible role of sedimentary recycling are discussed here.

Samples and results

For this type of investigation, the use of fine-grained clastic sedimentary and metasedimentary rock is most appropriate, as these represent the end product of sedimentary processes. In the present work, we have relied mainly on such rocks, including shales and mudstones of approximately uniform major element composition. In a few places (such as Henbury) where suitable samples were not available, sub-greywackes and siltstones of similar major element composition were used. This is acceptable as these rocks also represent an effective sampling of the upper crust. No significant differences were seen in major element or trace element distributions that could be attributed to the difference in lithology.

Most samples were obtained from drill core material, to minimize trace element mobility due to weathering. Composite samples were avoided because of the possibility of inclusion of aberrant material. Sedimentary rocks which obviously were derived from a first cycle of sedimentation, such as the Devonian · volcanogenic greywackes of the Baldwin Formation[7], were excluded. Samples showing visible or geochemical indications of alteration were also excluded.

All samples were analysed for Th and U by spark source mass spectrography. The details of the method were recently discussed by Taylor and Gorton[18]. This technique is sensitive for both Th and U (detection limit 0.02 p.p.m.) and both elements can be accurately determined. Accuracy and precision are better than ±5%.

The concentrations of Th and U at the time the rocks were deposited would not be the same as those measured in the rocks today, as both Th and U undergo radioactive decay. Thus the original U concentration would have been more than twice the present measured concentration for a rock deposited 3,800 Myr ago. The Th/U ratio is also affected as the half lives of Th and various uranium isotopes are different. However, the trends noted in the present study are not controlled by such processes as all possible source regions, as well as the samples themselves, have undergone such decay.

The results of this study have been tabulated in two ways. Table 1 summarizes the raw data for Th, U and Th/U, on the basis of location and approximate age. To help identify major trends the data were also grouped into 500-Myr intervals (Table 2). The period 2,000–1,000 Myr was included in one interval due to the lack of samples.

Thorium. The variation of Th in sedimentary rocks with geological time is shown in Fig. 1. During the early Archean (>3,000 Myr) the average abundance of Th was very low, at ~1.5±0.8 p.p.m. (errors indicate the 95% confidence interval on the mean). The significance of the very early Archean Th and U data is questionable because of possible metamorphic effects. The other Archean samples have higher Th abundances at 4.5±1.0 p.p.m. There seems to be a sharp increase in Th

Table 1 Summary of Th and U data for sedimentary rocks

Location	Samples (*n*)	Approximate age (Gyr)	Th*	U*	Th/U*†	Ref.
Godthåb (Akilia association; Greenland)	7	>3.7	1.4± 1.4	0.38±0.24	3.1±1.3	17; This study
Godthåb (Malene supracrustals; Greenland)	5	>3.0	1.6± 1.5	0.73±0.76	2.4±1.5	This study
Kambalda (Australia)	14	2.8	4.3± 1.4	1.3 ±0.4	3.4±0.3	14
Kalgoorlie (Australia)	7	2.8	4.8± 1.4	1.4 ±0.3	3.4±0.8	7
Hamersley Basin (Australia)	7	2.47	18.1± 4.3	3.5 ±1.2	5.7±2.4	This study
Pine Creek Geosyncline (Australia)	9	2.2	12.8± 2.2	3.6 ±1.2	3.9±0.9	10
Mount Isa (Australia)	5	1.5	11.4± 2.9	3.9 ±3.0	3.5±1.5	6
Henbury (Australia)	3	1.1	14.7± 3.4	3.1 ±1.1	4.8±0.8	15
Amadeus Basin (Pertatataka Formation; Australia)	6	0.85	14.4± 2.5	2.6 ±0.3	5.6±0.7	6
Amadeus Basin (Arumbera Formation; Australia)	3	0.50	9.1± 2.8	1.5 ±0.4	5.9±0.9	6
State Circle (Australia)	7	0.45	14.3± 1.1	2.6 ±0.3	5.5±0.7	6
Perth and Canning Basins (Australia)	5	0.30	16.0± 3.3	2.8 ±0.8	5.8±0.7	6
Perth Basin (Australia)	4	0.22	14.7±13.3	3.1 ±2.4	4.7±1.8	6
Carnarvon Basin	2	0.15	23.5	3.2	7.6	16

*Uncertainties represent 95% confidence limits on the means.
†Th/U values are the averages of individual Th/U for each sample.

abundances associated with the Archean–Proterozoic boundary (which for these samples is at ~2,500 Myr). Linear regression of the post-Archean Th ungrouped data (Fig. 1) indicates no change through time although this correlation is not statistically significant. The means of the data in the intervals 2,500–2,000 Myr and 500–0 Myr are statistically indistinguishable. We conclude that there is no significant trend in the Th concentrations during the post-Archean. The average concentration of Th in post-Archean samples is 14.6 ±1.2 p.p.m.

Uranium. Figure 2 displays the grouped U data plotted against geological time. There is a sharp increase in U concentrations similar to that for thorium, associated with the Archean–Proterozoic boundary. The abundance of U seems to decrease during post-Archean times. Linear regression of the U ungrouped data (Fig. 2) seems to confirm such a trend with the correlation significant at ~98% confidence level. A decrease in U during the post-Archean is also indicated by the fact that samples deposited beyween 2.5 and 1.0 Gyr are statistically distinct from these samples deposited after 1.0 Gyr. The average U concentration in the post-Archean samples is 3.1 ±0.4.
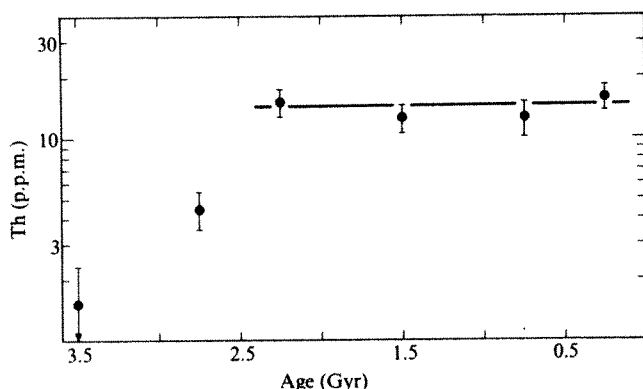
Fig. 1 Plot of Th abundances in sedimentary rocks against geological time. The points and error bars represent the mean and 95% confidence interval, respectively, of the grouped Th data (Table 2). The heavy solid line is based on a linear regression of the post-Archean ungrouped Th data (summarized in Table 1). It is unlikely that Th abundances have changed during post-Archean times.

Th/U ratios. Th/U data are plotted against geological time in Fig. 3. There is a clear trend of increasing Th/U with time for the grouped data. Linear regression of the post-Archean Th/U data illustrates the trend but the correlation is significant only at ~98% confidence level. Inclusion of the Archean data in the regression generates a similar trend (dashed line in Fig. 3) of increasing Th/U with geological time. This correlation is significant at a greater than 99.9% confidence level.

Discussion

The early Archean samples have very much lower Th, U and Th/U ratios than all other samples. If these values are representative of the original concentrations in these rocks, then a progressive increase in Th and U throughout the Archean is suggested. The increasing Th/U ratio through the Archean could imply that sedimentary recycling in an oxidizing environment was an important phenomenon back to >3,700 Myr (see below). Samples used in this study were taken from the Akilia association (>3,700 Myr) and Malene supracrustals (>3,000 Myr) of the Godthåb district in West Greenland. All these rocks have been metamorphosed to amphibolite grade and some may have reached granulite grade metamorphism[17,19–22]. Recent study of U in metamorphic rocks[23] indicates that this element (and presumably Th as well) is essentially immobile up to amphibolite grade, but is lost, through migrating fluid phases, during granulite metamorphism. Heier[24] has also noted the depletion of Th and U in granulites. Studies of early Archean high grade terrains[24,25] clearly suggest widespread loss of Th and U during high grade metamorphism. The cause of changes in the Th/U ratio during granulite metamorphism is not clear. Although many of the samples used in this study did not reach granulite grade, their proximity to such environments makes the Th and U data suspect and conclusions derived from these data equivocal. Much more work is needed to understand the significance of the low Th, U and Th/U in early Archean sedimentary rocks.

Several recent lines of evidence indicate that the chemical evolution of the upper continental crust is sharply episodic. This was demonstrated by Veizer[26] and Veizer and Compston[27], who estimated from carbonate rocks, the Sr isotopic evolution of seawater following on the early work of Gast[28]. The $^{87}Sr/^{86}Sr$ ratio of Archean oceans was similar to upper mantle values, but an extremely sharp increase of the radiogenic component ($\Delta^{87}Sr/^{86}Sr$ ~0.0025) was found at about the Archean–Proterozoic boundary. This would

correspond to a major addition of a felsic component to the exposed crust at that time. Studies of REE in sedimentary rocks have also documented a dramatic change in REE patterns associated with the Archean–Proterozoic boundary[8–12]. This was interpreted as a major change in the composition of the upper crust related to the intrusion of large quantities of K-rich granites at the end of the Archean[9,12]. In addition, the uniform REE pattern in post-Archean sedimentary rocks[6] indicates that there has been no substantial compositional change during that time.

The Th and U data agree with these models of crustal evolution. Both Th and U abundances show steep increases associated with the Archean–Proterozoic boundary, coinciding with changes shown by Sr-isotopes in carbonates and REE in sedimentary rocks. The intrusion of late Archean K-rich granites into the upper crust could account for this change. Such rocks contain high Th and U concentrations (for example, two late Archean K-rich granites from the Pine Creek Geosyncline have U contents of 3.5 and 5.3 p.p.m. and Th contents of 17 and 21 p.p.m. respectively[10]). The lack of any secular variation in Th abundances would also support the contention that there have been no significant changes in upper continental crustal composition during post-Archean times. Plots of Th abundances against time for fine-grained rocks of the North American and Russian Platforms[12] also show no significant change for this element during the post-Archean. Trends noted for U and Th/U ratios are probably a secondary feature and will be discussed below.

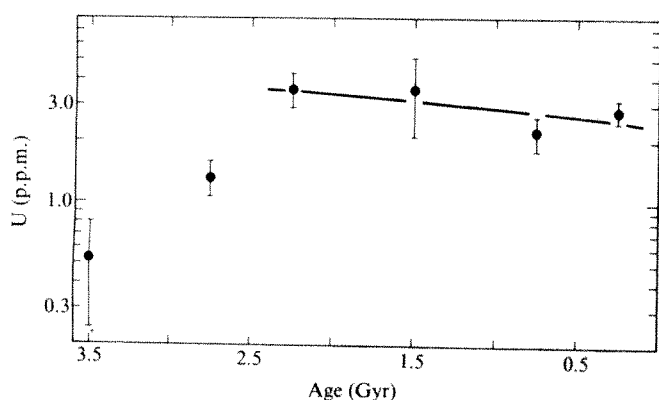

Fig. 2 Plot of U abundances in sedimentary rocks against geological time. The heavy solid line represents a linear regression of the post-Archean ungrouped U data.

It has been pointed out that a suitable test for these models could be made on sedimentary rocks from the late Archean of South Africa (Pongola, Dominion, Witwatersrand Systems)[29]. These rocks, though clearly Archean in age (>2,700 Myr), closely resemble typical lower Proterozoic sequences. These rocks were deposited after the major crust-forming (intrusive) event in that area. If the models of episodic crustal evolution suggested above are correct, these rocks should show post-Archean geochemical signatures. Five sedimentary samples from the Pongola succession (∼3,000 Myr) have been analysed. The results show: Th = 8.9 ± 3.3 p.p.m.; U = 2.7 ± 1.8 p.p.m.; and Th/U = 3.8 ± 1.5. The Th and U values are significantly higher than those typical of Archean samples and approach values typical for the post-Archean. The Th/U ratio is somewhat low but within the range found for Lower Proterozoic (2.5–2.0 Gyr) sedimentary rocks (average Th/U = 4.7 ± 1.0).

The role of large scale recycling of sedimentary rocks has been discussed by several authors[1–3,5]. Recently, Veizer and Jansen[5] have provided detailed models, invoking large-scale sedimentary recycling throughout time, to explain many physical, chemical and isotopic features of the sedimentary record. They proposed that the sedimentary cycle is about 65% cannibalistic.

Table 2 Summary of Th and U data, grouped by age, for sedimentary rocks

Time interval (Gyr)	Samples (n)	Th*	U*	Th/U*†
3.0	12	1.5 ± 0.8	0.53 ± 0.29	2.8 ± 0.8
3.0–2.5	21	4.5 ± 1.0	1.3 ± 0.3	3.4 ± 0.3
2.5–2.0	16	15.2 ± 2.4	3.6 ± 0.7	4.7 ± 1.0
2.0–1.0	8	12.6 ± 2.2	3.6 ± 1.6	4.0 ± 0.9
1.0–0.5	9	12.6 ± 2.6	2.2 ± 0.4	5.7 ± 0.5
0.5–0.0	18	15.9 ± 2.3	2.8 ± 0.4	5.6 ± 0.5

*Uncertainties represent 95% confidence limits on the means.
†Th/U values are the averages of the individual Th/U for each sample.

The Th and U data also suggest an important role for sedimentary recycling in controlling the chemical composition of sedimentary rocks, at least as far back as the Archean–Proterozoic boundary. Th and U data should show an increase in Th/U ratio with time if sedimentary recycling is a dominant process. Such a feature is noted in Fig. 3 and seems to be mainly controlled by a decrease in U (Fig. 2), at least during the post-Archean.

The increases in Th/U (and possible decrease in U) in sedimentary rocks, through geological time, is best explained by separation of U from Th due to U loss from repeated cycles of weathering and resedimentation. The sharp changes in the concentrations of Th and U at the Archean–Proterozoic boundary do not easily allow direct extrapolation of this conclusion back into Archean times. However, the average Th/U ratio for Archean samples falls on a trend similar to that delineated by the post-Archean and could suggest that sedimentary recycling in an oxidizing environment has been important well back into the Archean (see further discussion below).

If U is lost selectively from the sedimentary sequences, what is the ultimate fate of this element? Uranium has a much longer residence time than Th and the Th/U ratio of seawater is of the order of 3×10^{-3} (ref. 30). However, the mass of U in the oceans is much lower than in the exposed crust and it is unlikely the oceans themselves could be a major sink. The most likely sink for U is in altered oceanic basalt. Aumento et al.[31] have recorded enrichments of up to a factor of 40 in such rocks. Bloch[32] has estimated that between a half and two-thirds of the U delivered to the oceans finds its way into oceanic basalts through hydrothermal alteration or submarine weathering.

The addition of U to oceanic basalt would decrease the Th/U ratios of such rocks. This phenomenon would also result in the subduction of uranium which was derived from the continental crust. The implications of uranium subduction have
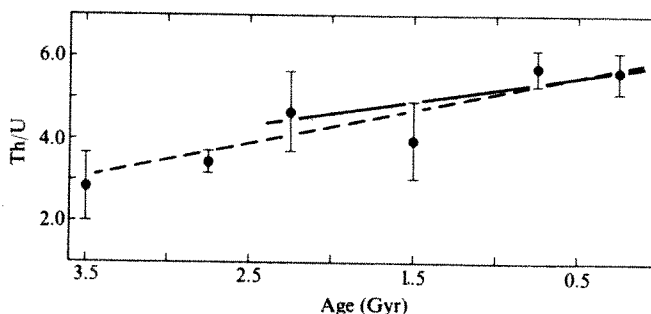

Fig. 3 Plot of Th/U ratios in sedimentary rocks against geological time. The heavy solid line represents a linear regression of the post-Archean ungrouped Th/U data (r is significant at ∼98% confidence level). The heavy dashed line represents a linear regression which includes the Archean Th/U data (see Table 3) (r is significant at >99.9% confidence level).

recently been extensively discussed by Fyfe[33]. Note that both mid-ocean ridge basalts and island-arc tholeiites have low Th/U. Whether this is due to crustal recycling or to the derivation of both magma types from a mantle depleted in Th relative to U remains questionable.

At least three other controls on the Th and U distributions are possible. Work on Pb-isotope systematics indicates that substantial amounts of U have been lost from many rocks, probably due to weathering[34,35]. As the Pb-isotopes were not affected in these studies, the weathering must have occurred fairly recently. Samples used in this study were taken mostly from drill core to minimize this effect. We see no reason that a recent episode of weathering should preferentially affect younger rocks, thus producing the U and Th/U trends observed here. On the other hand, the effects of a recent period of weathering, which removes a more or less constant proportion of uranium from all samples, will not affect any of the noted trends.

Many workers have argued that the early Precambrian atmosphere had too little free oxygen to allow efficient solution and mobilization of U during weathering (see, for example, refs 2, 29, 36–39). The best estimate when free O_2 was abundant enough to cause oxidation of uranium is · ∼2,300 Myr (refs 29, 37). The increase in Th and U abundances at the Archean–Proterozoic boundary cannot be attributed to this feature, as an influx of O_2 would not affect Th and would decrease U in sedimentary rocks. On the other hand, the lack of abundant O_2 during Archean times certainly affects the interpretation of Th/U ratios during this period. The trend of Th/U ratios during post-Archean time demands an oxidizing environment. If the Archean atmosphere was deficient in free O_2, Th/U would not be affected by weathering processes and should remain essentially constant throughout the Archean.

Thus, two models can explain the observed data. First, the Th/U ratio in sedimentary rocks may have steadily increased throughout geological time indicating an oxidizing atmosphere and hydrosphere as far back as about 3,800 Myr. Alternatively, the Th/U ratios of sedimentary rocks may have remained essentially constant throughout the Archean with a substantial change near the Archean–Proterozoic boundary, when Th and U were added to the upper crust (see above and Figs 1 and 2). The Th/U ratio would then steadily increase during the post-Archean due to recycling of sedimentary rocks in an oxidizing environment. Determining the correct model could provide crucial evidence on the nature of the early atmosphere and hydrosphere. Various statistical tests have been performed on the data but are unable to reject either model unequivocally. The question is complicated by the possible metamorphic effects on the early Archean samples (see above). We are initiating a project on early Archean, low

grade metamorphic sedimentary rocks from Western Australia to illuminate this important problem.

Another possible influence on U abundances is the amount of organic carbon in sedimentary rocks. If carbon content has increased with time, this could cause the decreasing U content and increasing Th/U ratio, as U is strongly concentrated in carbon-bearing sedimentary rocks[40]. However, recent studies[41] indicate no clear trends with time for organic productivity and preservation as far back as ∼3,400 Myr. Hence it seems unlikely the trends noted in this study are primarily related to secular variations in organic productivity and preservation.

Lower Proterozoic conglomerate-type and unconformity-type U ore deposits are among the largest uranium deposits in the world[13,42]. These occurrences coincide with the large volumes of U introduced into the upper crust in relation to the intrusion of late Archean K-rich granites. Early dispersion of this material would contribute significantly to the formation of large U-deposits in the Lower Proterozoic.

Conclusions

Th, U and Th/U are very low in early Archean sedimentary rocks compared with sedimentary rocks of all other ages. Whether this is a primary feature or one imposed by metamorphic redistribution is uncertain. A sharp increase in Th and U abundances is associated with the Archean–Proterozoic boundary. This seems to be in response to a dramatic, episodic change in the composition of the upper continental crust related to widespread granitic intrusions at the end of the Archean Era. No evidence for a major change in upper crustal composition during post-Archean times is observed in these data. A secular increase in Th/U and a secular decrease in U is observed in sedimentary rocks during post-Archean time. These features are best explained by sedimentary recycling in the presence of an oxygen-rich atmosphere and hydrosphere, which results in a distinct fractionation of Th and U during successive weathering cycles. Extrapolation of the Th/U trend into Archean times is equivocal. With the present data, models involving gradual changes in the Th/U throughout time or an episodic change in Th/U at the Archean–Proterozoic boundary cannot be distinguished. Rapid dispersion of uranium introduced into the upper crust during the late Archean is probably closely related to the large uranium ore deposits of the Lower Proterozoic.

1. Garrels, R. M. & Mackenzie, F. T. *Evolution of Sedimentary Rocks* (Norton, New York, 1971).
2. Veizer, J. *Contr. Miner. Petrol.* **38**, 261–278 (1973); *Precamb. Res.* **6**, 381–413; *The Origin and Evolution of the Elements* (ed. Ahrens, L. H.) 269–278 (Pergamon, London, 1979).
3. Veizer, J. & Garret, D. E. *Precamb. Res.* **6**, 367–380.
4. Schwab, F. L. *Geology* **6**, 532–536 (1978).
5. Veizer, J. & Jansen, S. L. *J. Geol.* **87**, 341–370 (1979).
6. Nance, W. B. & Taylor, S. R. *Geochim. cosmochim. Acta* **40**, 1539–1551 (1976).
7. Nance, W. B. & Taylor, S. R. *Geochim. cosmochim. Acta* **41**, 225–231 (1977).
8. Taylor, S. R. *The Earth: Its Origin, Structure and Evolution* (ed. McElhinny, M. W.) 353–376 (Academic, New York, 1979).
9. McLennan, S. M., Fryer, B. J. & Young, G. M. *Geochim. cosmochim. Acta* **43**, 375–388 (1979).
10. McLennan, S. M. & Taylor, S. R. *Int. Uranium Symp. Pine Creek Geosyncline* (IAEA, Vienna, in the press).
11. Taylor, S. R. & McLennan, S. M. *Precambrian Plate Tectonics* (ed. Kröner, A.) (Elsevier, Amsterdam, in the press); *Phil. Trans. R. Soc. A* (in the press).
12. Ronov, A. B. & Migdisov, A. A. *Sedimentology* **16**, 137–185 (1971).
13. Veizer, J. *Handbook of Strata-bound and Stratiform Ore Deposits* (ed. Wolf, K. H.) 1–41 (Elsevier, Amsterdam, 1976).
14. Bavinton, O. A. & Taylor, S. R. *Geochim. cosmochim. Acta* **44**, 639–648 (1980).
15. Taylor, S. R. & McLennan, S. M. *Geochim. cosmochim. Acta* **43**, 1551–1565 (1979).
16. Nance, W. B. thesis, Australian National Univ. (1975).
17. McGregor, V. R. & Mason, B. H. *Am. Miner.* **62**, 887–904 (1977).
18. Taylor, S. R. & Gorton, M. P. *Geochim. cosmochim. Acta* **41**, 1375–1380 (1977).
19. McGregor, V. R. *Phil. Trans. R. Soc. A* **273**, 343–358 (1973).
20. Bridgwater, D., McGregor, V. R. & Myers, J. S. *Precamb. Res.* **1**, 179–197 (1974).
21. Wells, P. R. A. *Contr. Miner. Petrol.* **56**, 229–242 (1976).
22. Bridgwater, D. & McGregor, V. R. *Grønl. Geol. Unders. Rapp.* **65**, 49–54 (1974).
23. Dostal, J. & Capedri, S. *Contr. Miner. Petrol.* **66**, 409–414 (1978).
24. Heier, K. S. *Phil. Trans. R. Soc.* A**273**, 429–442 (1973); *Fortschr. Miner.* **50**, 174–187 (1973).
25. Collerson, K. D. & Fryer, B. J. *Contr. Miner. Petrol.* **67**, 151–167 (1978).
26. Veizer, J. *The Early History of the Earth* (ed. Windley, B. F.) 569–578 (Wiley, London, 1976).
27. Veizer, J. & Compston, W. *Geochim. cosmochim. Acta* **40**, 905–914 (1976).
28. Gast, P. W. *Bull. geol. Soc. Am.* **66**, 1449–1454 (1955).
29. McLennan, S. M. *Biogeochemistry of Ancient and Modern Environments* (eds Trudinger, P. A. & Walter, M. R.) (Australian Academy of Science and Springer, Berlin, in the press).
30. Brewer, P. G. *Chemical Oceanography* Vol. 1, 2nd edn (eds Riley, J. P. & Skirrow, G.) 415–496 (Academic, London, 1975).
31. Aumento, F., Mitchell, W. S. & Fratta, M. *Can. Min.* **14**, 269–290 (1976).
32. Bloch, S. *Geochim. cosmochim. Acta* **44**, 373–377 (1980).
33. Fyfe, W. S. *Chem. Geol.* **23**, 89–114 (1978); *Phil. Trans. R. Soc.* A**291**, 433–445 (1979).
34. Rosholt, J. N., Zartman, R. E. & Nkoma, I. T. *Bull. geol. Soc. Am.* **84**, 989–1002 (1973).
35. Oversby, V. M. *Geochim. cosmochim. Acta* **39**, 1107–1125 (1975).
36. Cloud, P. *Am. J. Sci.* **272**, 537–548 (1972); *Trans. geol. Soc. S. Afr.* **79** (Annexure) 1–32 (1976).
37. Roscoe, S. M. *Huronian Stratigraphy and Sedimentation* (ed. Young, G. M.) 31–47 (Geological Association Canada Special Paper 12, 1973).
38. Holland, H. D. *The Early History of the Earth* (ed. Windley, B. F.) 559–567 (Wiley, London, 1976).
39. Grandstaff, D. E. *Trans. Geol. Soc. S. Afr.* **77**, 291–294 (1974); *Eos* **55**, 457 (1974).
40. Adams, J. S., Osmond, J. K. & Rogers, J. J. W. *Phys. chem. Earth* **3**, 298–348 (1959).
41. Reimer, T. O., Barghoorn, E. S. & Margulis, L. *Precamb. Res.* **9**, 93–104 (1979).
42. Dahlkamp, F. J. *Miner. Depos.* **13**, 83–104 (1978).

Energy-dependent uptake of cytoplasmically synthesized polypeptides by chloroplasts

Arthur Grossman, Sue Bartlett & Nam-Hai Chua

The Rockefeller University, New York, New York 10021

Light stimulates the uptake of polypeptides synthesized in vitro *into intact chloroplasts. The light-stimulated uptake is inhibited by uncouplers, but not by the electron transport inhibitor dichlorophenyldimethylurea (DCMU) or the protein synthesis inhibitor chloramphenicol(CAP). Addition of ATP to the uptake mixture in the dark mimics the light stimulation of transport, and it reverses the uncoupler inhibition of transport in the light. These data demonstrate that cytoplasmically synthesized polypeptides are imported into the chloroplast by an energy-dependent process.*

MANY proteins localized within chloroplasts are synthesized on cytoplasmic ribosomes[1]. Such proteins must be transported across the two chloroplast envelope membranes to reach their final destinations in the stroma or thylakoids. Although the precise mechanism of transport is still unknown, recent reconstitution experiments *in vitro* demonstrate convincingly that protein synthesis and transport are independent events[2] in contrast with co-translational transfer of secretory proteins across the endoplasmic reticulum[3].

Synthesis and transport of three major chloroplast proteins have been studied extensively. The small subunit (S) of ribulose-1,5-bisphosphate carboxylase is synthesized *in vitro* as a larger precursor (pS) with an amino terminal chain extension of molecular weight between 4,000 and 5,000 (refs 4–9). If the products of cell-free translation are incubated with intact chloroplasts, pS is taken up, processed to S (refs 6–8) and assembled with endogenous large subunit in the stroma to form the holoenzyme[6,7]. In addition to pS, larger precursors of two polypeptide constituents, designated 15 and 16, of the light-harvesting chlorophyll *a/b* protein complex have been identified in cell-free translation systems[10,11]. These precursors (p15 and p16) are also taken up post-translationally by chloroplasts, processed to their mature sizes, and assembled correctly into thylakoid membranes[11].

In an attempt to define the mechanism(s) by which cytoplasmically synthesized polypeptides traverse the envelope, we determined experimental conditions for optimal polypeptide transport into intact chloroplasts. In previous studies using suboptimal conditions, light failed to stimulate uptake of pS (refs 6, 7). However, during the present study, we noted that polypeptide uptake by pea chloroplasts is greatly stimulated by light. Here we provide evidence that the light stimulation is due to the production of ATP within the organelle.

Light stimulation of polypeptide uptake by intact chloroplasts

Uptake of many pea poly(A) RNA translation products by intact pea chloroplasts *in vitro* is stimulated by light (Fig. 1). This light stimulation applies to the uptake of stromal proteins as well as polypeptides associated with the thylakoid membranes. Although the extent of the light response varies among experiments, a 2- to 10-fold enhancement of uptake of most proteins is obtained consistently (Fig. 1, Table 1).

Effects of specific inhibitors on polypeptide uptake

Several processes within chloroplasts are stimulated by light including: (1) chloroplast protein synthesis; (2) noncyclic electron flow, cyclic electron flow and the concomitant

production of NADPH and ATP; and (3) the generation of chemical and electrical gradients across the thylakoid membranes and the chloroplast envelope. We used specific inhibitors to determine which of these processes is responsible for the light stimulation of polypeptide uptake. CAP is a specific inhibitor of chloroplast protein synthesis[16]. DCMU prevents the formation of NADPH by blocking electron flow between the two photosystems[17]. Neither inhibitor alters the light-stimulated uptake of stromal (Fig. 2) or thylakoid membrane polypeptides (results not shown). We conclude from these results that polypeptide uptake by chloroplasts depends neither on concomitant protein synthesis nor on non-cyclic photosynthetic electron flow. As dithiothreitol (DTT) is present in the incubation medium with DCMU, photosystem I would probably be reduced. This would allow for continued cyclic electron flow in the presence of DCMU[18], the generation of chemical and electrical gradients across the thylakoid membranes, the generation of similar gradients across the chloroplast envelope, and the production of ATP. Indeed, protein synthesis in isolated intact chloroplasts is stimulated by DCMU if the incubation medium contains 0.7 mM DTT (unpublished results). Therefore, we examined the effects of uncouplers on polypeptide uptake. Uncoupler effects were assessed quantitatively by excising gel bands

Table 1 Effects of uncouplers and ATP on the uptake of polypeptide A, the small subunit of ribulose-1,5-bisphosphate carboxylase, and polypeptides 15 and 16

| Treatment | Radioactivity in excised gel bands (c.p.m.) | | |
	Polypeptide A	Small subunit	Polypeptides 15 and 16
Dark	192	2,495	229
Light	2,619	10,882	1,603
Dark + ATP	2,151	10,178	856
Light + ATP	2,361	10,105	875
Dark + Sal	329	3,165	266
Light + Sal	229	2,167	239
Dark + Sal + ATP	2,890	12,188	964
Light + Sal + ATP	1,906	7,082	504
Dark + SF6847	213	2,364	320
Light + SF6847	376	4,389	242
Dark + SF6847 + ATP	1,768	11,477	736
Light + SF6847 + ATP	1,502	10,054	729

Polypeptide bands were excised from the dried gel and the radioactivity in each band was released by incubation with 20% H_2O_2 (0.5 ml per band) at 50 °C for 24 h. The samples were counted in a Beckman LS 8000 after the addition of 10 ml of Aquasol II.

corresponding to four polypeptides and assaying their radioactivity. Salicylanilide XIII (Sal, ref. 19) completely abrogates the light-stimulated uptake and processing of pS, p16 and p15, and an unidentified polypeptide whose mature product is designated A (molecular weight ~45,000). Similarly, 3,5-di-tert-butyl-4-hydroxybenzylidenemalononitrile (SF6847), another uncoupler[19], suppresses the enhanced level of polypeptide uptake in the light but inhibition of uptake of pS is not as complete as that of the other polypeptides (Table 1).

Effects of ATP on polypeptide uptake

Results obtained with the uncouplers indicate that the light stimulation is due either to ATP production directly or to a *p*H gradient or membrane potential across the thylakoid membrane and/or the chloroplast envelope. As chloroplasts prepared from young pea plants can translocate ATP from the medium into the stroma[20], we examined the effects of exogenous ATP on polypeptide uptake. Addition of 10 mM ATP to the incubation medium substantially increases transport of chloroplast polypeptides in the dark (Fig. 3, Table 1). The extent of ATP stimulation differs for stromal and thylakoid membrane polypeptides. While ATP in the dark elevates the transport of stromal polypeptides to the light level (Fig. 3), ATP-stimulated uptake of most thylakoid-membrane polypeptides never achieves the light level (see Table 1 for polypeptides 15 and 16; entire profile not shown). Direct measurements of radioactivity reveal that ATP is as effective as light in stimulating uptake of the precursors to S and
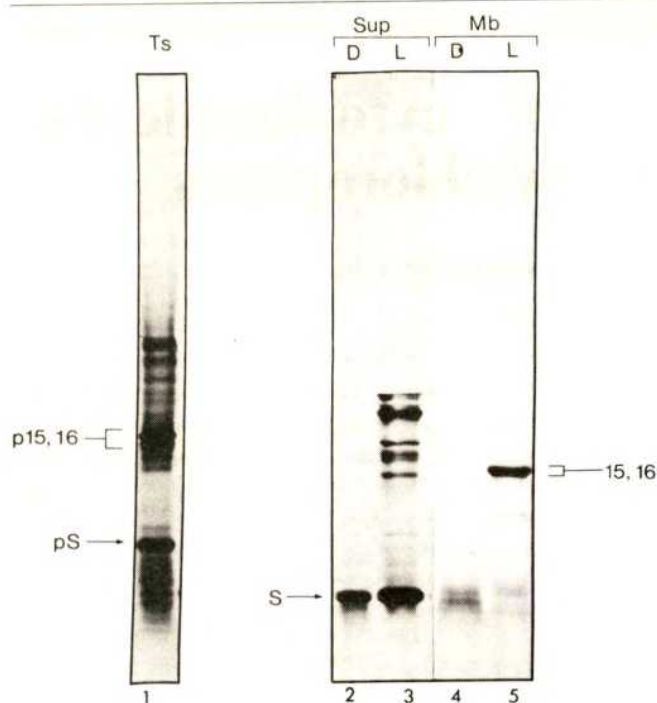
Fig. 1 Effects of light on the uptake of polypeptides translated from pea poly(A) RNA into intact pea chloroplasts. Pea poly(A) RNA was translated in a wheat-germ cell-free system which contained 130 mM K acetate, 1.2 mM Mg acetate, 0.4 mM Tris acetate (*p*H 7.6), 20 mM HEPES–KOH (*p*H 7.5), 2 mM DTT, 0.25 mM spermine (neutralized to *p*H 7.0), 750 μCi ml^{-1} ^{35}S-methionine (>600 Ci mmol^{-1}), 0.5 mM ATP (neutralized to *p*H 7.5), 16 μM GTP, 8.4 mM creatine phosphate, 40 μg ml^{-1} phosphocreatine kinase, 24 μM each of the 19 amino acids (minus methionine), 1 absorbance unit per ml of poly(A) RNA, and 0.4 volume of wheat-germ extract[12]. After incubation at 27°C for 1.5 h, ribosomes were pelleted (140,000g for 1 h) from the translation mixture and the resulting post-ribosomal supernatant was incubated with intact pea chloroplasts which had been purified on silica sol gradients[13]. The incubation mixture (300 μl) for polypeptide uptake contained 100 μl post-ribosomal supernatant, 200 μg chlorophyll of intact pea chloroplasts, 50 mM HEPES–KOH (*p*H 8.0), 8.3 mM methionine and 0.33 M sorbitol. After incubation at 25°C for 1 h, the chloroplasts were diluted with 5 ml of 50 mM HEPES–KOH (*p*H 8.0), 0.33 M sorbitol, pelleted by centrifugation to 4,000g and brake, resuspended in 0.5 ml of HEPES–KOH (*p*H 8.0), 0.33 M sorbitol and treated with trypsin and chymotrypsin (160 μg ml^{-1} of each) for 30 min at 4°C. Following proteolysis, the chloroplasts were diluted with 5 ml of 50 mM HEPES–KOH (*p*H 8.0), 0.33 M sorbitol, 1 mM phenylmethylsulphonylfluoride (PMSF), 1 mM Benzamidine–HCl, and 5 mM ε-amino-*n*-caproic acid, pelleted, resuspended in 2.0 ml of dilution buffer, and reisolated by centrifugation through a layer of 40% Percoll (3,000g for 3 min; ref. 14). The reisolated chloroplasts were washed with the dilution buffer and lysed in distilled H$_2$O containing 1 mM PMSF, 1 mM benzamidine–HCl and 5 mM ε-amino-*n*-caproic acid. The thylakoid membranes were separated from the stromal proteins by centrifugation at 12,300g for 15 min and both fractions were prepared for electrophoresis. Samples were run on SDS gels containing a 7.5–15% acrylamide concentration gradient[6,7]. The gels were stained, destained and fluorographed[15]. 1, *In vitro* translation products (Ts) of pea poly(A) RNA; 2 and 3, polypeptides imported into chloroplast stroma (Sup) in the dark (D) and light (L) (9,000 lux), respectively; 4 and 5, polypeptides imported into chloroplast thylakoid membranes (Mb) in the dark (D) and light (L) (9,000 lux), respectively. Polypeptides 15 and 16, the constituent polypeptides of the light-harvesting chlorophyll *a/b*-protein complex; p15 and p16, precursors to 15 and 16; S, the small subunit of ribulose-1,5-bisphosphate carboxylase; pS, precursor to S.

Fig. 2 Effects of DCMU and CAP on the uptake of polypeptides into the chloroplast stroma. *In vitro* reconstitution of polypeptide uptake was performed as described in the legend to Fig. 1. Samples were analysed on SDS gels containing a 12–18% acrylamide gradient and 8 M urea (Matlin and N.-H.C., unpublished method). 1 and 2, Stromal polypeptides imported in the dark (D) and light (L), respectively; 3 and 4, stromal polypeptides imported in the presence of DCMU (2 μM) in the dark and light, respectively; 5 and 6, stromal polypeptides imported in the presence of CAP (100 μg ml^{-1}) in the dark and light, respectively. S, the small subunit of ribulose-1,5-bisphosphate carboxylase; A, an unidentified stromal polypeptide of molecular weight ~45,000.
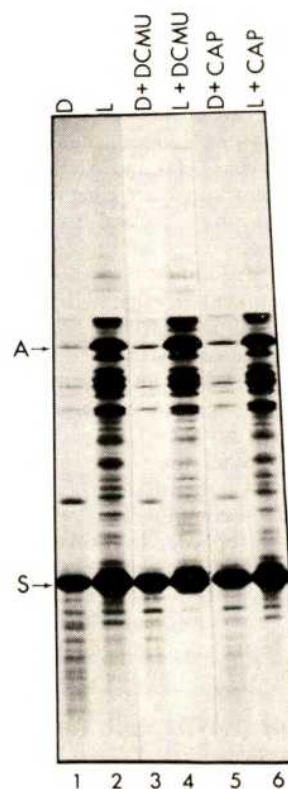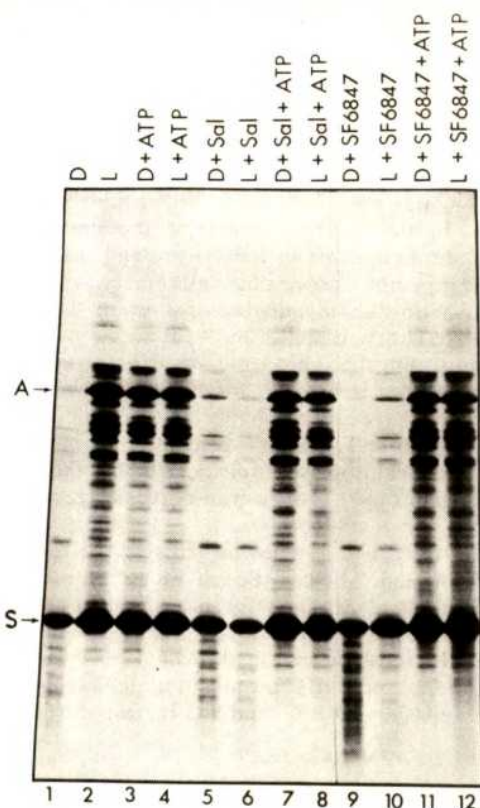
Fig. 3 Effects of uncouplers and ATP on the uptake of polypeptides into the chloroplast stroma. *In vitro* reconstitution of polypeptide uptake was performed as in Fig. 1 and samples were analysed as in Fig. 2. 1 and 2, stromal polypeptides imported in the dark (D) and light (L), respectively. 3 and 4, stromal polypeptides imported in the presence of 10 mM ATP in the dark and light, respectively; 5 and 6, same as 1 and 2, respectively, except with the addition of 2 µM Sal; 7 and 8, same as 3 and 4, respectively, except with the addition of 2 µM Sal; 9 and 10, same as 1 and 2, respectively, except with the addition of 2 µM SF6847; 11 and 12, same as 3 and 4, respectively, except with the addition of SF6847 (2 µM). S, small subunit of ribulose 1,5-bisphosphate carboxylase; A, unidentified stromal polypeptide.

polypeptide A (Table 1). ATP-stimulated transport of p15 and p16 is approximately fivefold over the dark control; however, the level attained is only 55% of the light level (Table 1). Illumination of chloroplasts in the presence of ATP has little effect on polypeptide uptake, indicating that light and ATP do not act synergistically (Fig. 3, Table 1). Perhaps uptake is limited by some factor other than energy. In these conditions, uptake of p15 and p16 in the light is consistently greater when ATP is not present (Table 1). The reason for this is unclear at present.

While the present results suggest that light-stimulated polypeptide uptake is due to the photoproduction of ATP we could not rule out the possibility that the exogenously added ATP is used inside the chloroplast to generate both chemical and electrical gradients. Because such gradients are collapsed by uncouplers, we examined the effects of Sal and SF6847 on polypeptide uptake sustained by ATP. Sal has no inhibitory effect on the ATP-stimulated polypeptide uptake in the dark, but is slightly inhibitory in the light (Figs 3 and 4; Table 1). The latter effect may be due to increased ATP hydrolysis in the presence of the uncoupler. Similar results were obtained with SF6847, another uncoupler (Fig. 3, Table 1). These results provide conclusive evidence that the stimulation of polypeptide transport by ATP is independent of its ability to generate a chemical or electrical gradient.

Conclusions

We have shown that transport of pea poly(A) RNA translation products into pea chloroplasts *in vitro* is increased severalfold by light. Three lines of evidence demonstrate that the light stimulation is due to the production of ATP by photosynthetic phosphorylation: (1) exogenous ATP mimics light in elevating dark polypeptide transport; (2) light stimulation is inhibited by uncouplers of photosynthetic phosphorylation and (3) the inhibitory effects of uncouplers are reversed by ATP. Taken together, these results also demonstrate that energy in the form of ATP is required to move polypeptides across the chloroplast envelope. Previous studies purporting to show no effect of illumination on uptake of polypeptides by pea chloroplasts were performed in suboptimal conditions[6,7] in which ATP was probably not the limiting factor.

Barley and Romaine lettuce chloroplasts exhibit light-stimulated uptake similar to that reported here for the pea, while little or no light stimulation is observed with spinach chloroplasts (unpublished results). Spinach chloroplasts contain high levels of endogenous chloroplast ATP even in the dark[22]. Accordingly, the energy requirement for polypeptide transport into all chloroplasts is probably absolute. The level of dark uptake in our *in vitro* system probably reflects the concentration of endogenous ATP in the organelle plus ATP added exogenously with the translation mix.

This conclusion may seem to be in conflict with data from other studies. For instance, etioplasts and developing plastids which cannot yet synthesize ATP in the light contain polypeptides of cytosolic origin[23]. Moreover, mutants of
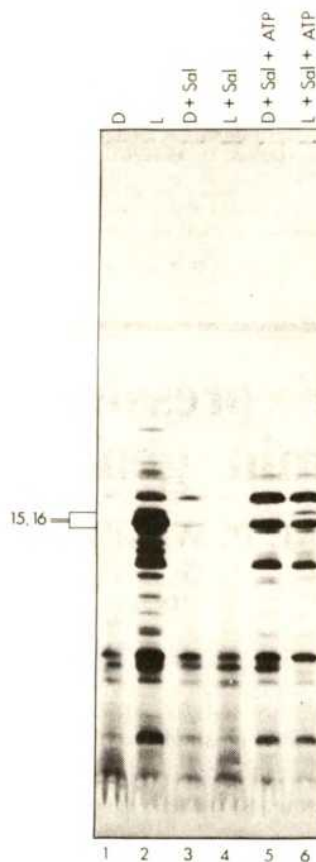
Fig. 4 Effects of Sal and ATP on the uptake of thylakoid membrane polypeptides. The experiments were performed as in Fig. 3. The thylakoid membranes were separated from the chloroplast envelope according to the method of Poincelot and Day[21]. 1 and 2, thylakoid membrane polypeptides imported in the dark (D) and light (L), respectively; 3 and 4, thylakoid membrane polypeptides imported in the presence of 2 µM Sal in the dark and light, respectively; 5 and 6, same as 3 and 4, respectively, except with the addition of 10 mM ATP.

Chlamydomonas reinhardtii defective in photosynthetic phosphorylation contain thylakoid membrane polypeptides synthesized on cytoplasmic ribosomes[24]. However, plastids incapable of photosynthetic phosphorylation can recruit ATP in at least three different ways: (1) ATP might be imported directly from the cytosol via the envelope adenine nucleotide translocator[25]. (2) Indirect energy transfer from the cytosol can be accomplished by the uptake of dihydroxyacetone phosphate, a glycolytic intermediate, through the envelope phosphate carrier[26]; oxidation of dihydroxyacetone phosphate in the chloroplast stroma would generate ATP; (3) dihydroxyacetone phosphate is also produced within the organelle by phosphorolysis of starch, which occurs commonly in etioplasts and developing chloroplasts[26].

Previous studies have established that pS (refs 6–8) and precursors to membrane polypeptides 15 and 16 (ref. 11) are imported into chloroplasts after their synthesis is complete. This post-translational mode of transport has now been confirmed for many as yet unidentified chloroplast proteins localized in the stroma or associated with the thylakoid membranes[11,12]. The results presented here show that the transport of these chloroplast proteins requires ATP. In contrast, synthesis and transport of secretory proteins are concomitant events. The driving force for membrane traversal is presumably provided by elongation of the growing polypeptide chain and the folding of the nascent chain on the cisternal side of the endoplasmic reticulum membrane.

However, because high energy compounds are required for translation, the exact energy requirement for co-translational transport cannot be resolved.

Nelson and Schatz[27] reported that yeast cells depleted of mitochondrial ATP accumulate precursors to certain mitochondrial proteins, demonstrating that energy is required for processing these precursors. As the subcellular location of these precursors was not established, ATP could be required for transport. In the absence of energy, the untransported precursors would accumulate in the cytosol and therefore not be accessible to the processing machinery within the mitochondria. With the *in vitro* reconstitution experiments reported here we clearly establish an ATP requirement at the level of transport. On the other hand, we cannot rule out the possibility that energy is required for precursor processing as well because we have been unable to separate the two phenomena. Joyard and Douce[28] characterized an ATPase associated with the chloroplast envelope. Whether this ATPase plays a role in chloroplast protein transport is currently under investigation.

1. Gillham, N. W., Boynton, J. E. & Chua, N.-H., *Curr. Topics Bioenerg.* **8**, 211–260 (1978).
2. Chua, N.-H. & Schmidt, G. W. *J. Cell Biol.* **81**, 461–483 (1979).
3. Blobel, G. & Dobberstein, B. *J. Cell Biol.* **67**, 835–851 (1975).
4. Dobberstein, B., Blobel, G. & Chua, N.-H. *Proc. natn. Acad. Sci. U.S.A.* **74**, 1082–1085 (1977).
5. Cashmore, A. R., Broadhurst, M. K. & Gray, R. E. *Proc. natn. Acad. Sci. U.S.A.* **75**, 655–659 (1978).
6. Chua, N.-H. & Schmidt, G. W. in *Photosynthetic Carbon Assimilation* (eds Siegelman, H. W. & Hind, G.) 325–347 (Plenum, New York, 1978).
7. Chua, N.-H. & Schmidt, G. W. *Proc. natn. Acad. Sci. U.S.A.* **75**, 6110–6114 (1978).
8. Highfield, P. E. & Ellis, R. J. *Nature* **271**, 420–424 (1978).
9. Schmidt, G. W., Devillers-Thiery, A., Desruisseaux, H., Blobel, G. & Chua, N.-H. *J. Cell Biol.* **83**, 615–622 (1979).
10. Apel, K. & Kloppstech, K. *Eur. J. Biochem.* **85**, 581–588 (1978).
11. Schmidt, G. W., Bartlett, S., Grossman, A. R., Cashmore, A. R. & Chua, N.-H. in *Genome Organization and Expression in Plants* (ed. Leaver, C. J.) 337–351 (Plenum, New York, 1980).
12. Grossman, A. R., Bartlett, S., Schmidt, G. W. & Chua, N.-H. *Ann. N.Y. Acad. Sci.* (in the press).
13. Morgenthaler, J.-J., Marden, M. P. F. & Price, C. A. *Archs Biochem. Biophys.* **168**, 289–301 (1975).
14. Mills, W. R. & Joy, K. W. *Planta* **148**, 75–83 (1980).
15. Bonner, W. M. & Laskey, R. A. *Eur. J. Biochem.* **46**, 83–88 (1974).
16. Ellis, R. J. *Biochim. biophys. Acta* **463**, 185–215 (1977).
17. Izawa, S. & Good, N. E. *Meth. Enzym.* **24**, 355–377 (1972).
18. Crowther, D., Mills, J. D. & Hind, G. *FEBS Lett.* **98**, 386–390 (1979).
19. Heytler, P. G. *Meth. Enzym.* **55**, 462–472 (1979).
20. Robinson, S. P. & Wiskich, J. T. *Biochim. biophys. Acta* **461**, 313–340 (1977).
21. Poincelot, R. P. & Day, P. *Pl. Physiol.* **54**, 780–783 (1974).
22. Inoue, Y., Kobayashi, Y., Shibata, K. & Heber, U. *Biochim. biophys. Acta* **504**, 142–152 (1978).
23. Bradbeer, J. W. in *Biosynthesis and its Control in Plants* (ed. Milborrow, B. V.) 279–302 (Academic, London, 1973).
24. Bennoun, P., Masson, A., Piccioni, R. & Chua, N.-H. in *Chloroplast Development* (ed. Akoyunaglou, G.) 721–726 (Elsevier, Amsterdam, 1978).
25. Heldt, H. W. *Horiz. Biochem. Biophys.* **2**, 199–229 (1976).
26. Heber, U. & Walker, D. A. *Trends biochem. Sci.* **4**, 252–256 (1979).
27. Nelson, N. & Schatz, G. *Proc. natn. Acad. Sci. U.S.A.* **76**, 4365–4369 (1979).
28. Joyard, J. & Douce, R. *FEBS Lett.* **51**, 335–340 (1975).

Expression of a chicken chromosomal ovalbumin gene injected into frog oocyte nuclei

M. P. Wickens*, S. Woo†, B. W. O'Malley† & J. B. Gurdon*

*MRC Laboratory of Molecular Biology, Hills Road, Cambridge CB2 2QH, UK
†Department of Cell Biology, Baylor College of Medicine, Houston, Texas 77030

Ovalbumin is synthesized by Xenopus oocytes injected with a plasmid containing either the chicken chromosomal ovalbumin gene or a plasmid from which the 5' region of the chromosomal gene has been deleted. However, oocytes injected with a plasmid containing full-length ovalbumin cDNA do not synthesize ovalbumin, despite the fact that at least as much stable, ovalbumin-specific RNA is transcribed from the cDNA as from the chromosomal gene.

THE production of functional mRNA from a eukaryotic gene involves many steps, including transcription, RNA splicing and base modification, transport from the nucleus and assembly into polyribosomes. Previous work has shown that *Xenopus* oocytes can carry out these steps from injected genes[1–6]. Oocytes injected with cloned sea urchin histone genes synthesize functional messengers for histones H2A and H2B (ref. 6). Because the coding sequences of these genes are not interrupted by an intervening sequence, no RNA splicing is

necessary. Oocytes injected with SV40 DNA synthesize the virion proteins VP1, VP3 (ref. 4) and the tumour antigens small t and large T (ref. 5); the production of functional mRNA for the T tumour antigen requires the precise excision of a single intervening sequence[7–9].

In the study reported here, we have examined the expression of a cloned chicken ovalbumin gene injected into *Xenopus* oocytes. Our criterion for expression was the synthesis of ovalbumin protein. This assay provides a particularly stringent

test of the RNA processing activities involved in messenger production, because at least six intervening sequences must be removed from the primary transcripts before the RNA can serve as a template for ovalbumin synthesis[10,11].

We considered the following problems. (1) Do oocytes injected with the chromosomal ovalbumin gene synthesize ovalbumin? (2) How does the amount of ovalbumin synthesized (after at least six splicing events) compare with the amount of SV40 VP1 synthesis (after not more than one splice)? (3) The cap site and TATATAT sequence at the 5' terminus of the chromosomal gene have been implicated in transcription initiation in chicken oviduct cells; are these regions essential for the production of functional ovalbumin mRNA in oocytes injected with the chromosomal gene? (4) Are any non-structural sequences present in the chromosomal clones necessary for expression; that is, do oocytes injected with a full-length cDNA clone synthesize ovalbumin? We have extended previous experience with injected oocytes by analysing in some detail the expression of a gene which is strikingly regulated in development and whose transcription depends on RNA polymerase II activity.

Ovalbumin DNA templates

The following published information[10,11] concerning the structure of the chicken ovalbumin gene is relevant. Seven intervening sequences (introns) interrupt the ovalbumin messenger sequence in the chromosomal gene; six of these lie within the protein-coding region. The seventh lies within the 5'-untranslated region of the mRNA sequence, separating the first 45 untranslated nucleotides by 1.6 kilobases from the translation initiation codon at position 65. These first 45 residues have been termed a leader sequence by analogy with eukaryotic viral gene structure[10,11].

We examined the expression of three recombinant plasmids containing ovalbumin DNA (Fig. 1). pOv230 is a cDNA clone in which all but the 5'-terminal 12 nucleotides of the
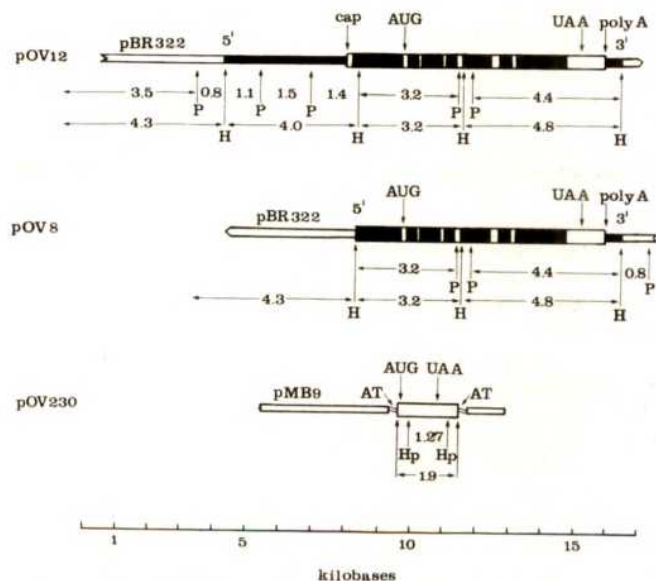

Fig. 1 Structure of cloned chicken ovalbumin genes injected into oocytes. pOv12 and pOv8 are clones of the chromosomal ovalbumin gene; pOv230 is a full-length ovalbumin cDNA clone. Their construction has been described elsewhere[10,12–14] (detailed structural information in refs 10, 12). pOv12 and pOv8 were constructed by ligation into the *Hind*III site of pBR322; pOv230 was constructed by dA:dT tailing into the *Eco*RI site of pMB9. Note that the chicken DNA in pOv8 and pOv12 is inserted in opposite orientations. Unshaded, thinner regions represent vector sequences; shaded thinner regions, chicken DNA outside the ovalbumin gene (not between the cap site and the polyadenylation site); unshaded thicker regions, exons (coding); shaded, thicker regions, introns (spliced out of the primary transcript); ≈, dA:dT tails. The position of the cap site, polyadenylation site, and translation initiation (AUG) and termination (UAA) sites are indicated. All *Hind*III (H) and *Pst*I(P) sites in pOv12 and pOv8 are indicated. The only *Hph*I (Hp) sites shown are those in pOv230 which are relevant to Fig. 5b.

messenger sequence have been copied and inserted into the plasmid pMB9[12]. Both pOv8 and pOv12 are clones of the ovalbumin chromosomal gene in pBR322[13]. pOv12 contains 12 kilobases of chicken DNA, including all ovalbumin exons and introns, plus 3.78 kilobases to the 5' side of the cap site and 0.66 kilobases to the 3' side of the polyadenylation site. It contains that A-T-rich region, 32 bases before the cap site, which has been suggested to be involved in transcription
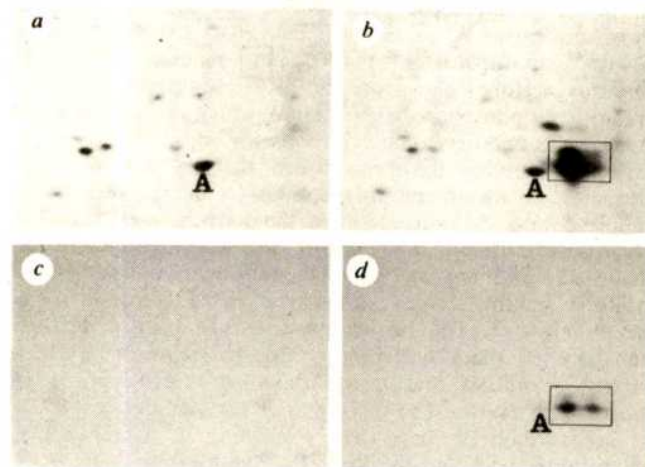

Fig. 2 Position of ovalbumin in two-dimensional polyacrylamide gels of unfractionated oocyte extract and anti-ovalbumin immunoprecipitates. The same central region of each gel is shown. A designates actin; a rectangle surrounds the four ovalbumin spots. The gel is in the same orientation as the gel in Fig. 3. The dark spot to, the upper left of ovalbumin in *b* is probably conalbumin, based on its intensity relative to ovalbumin and apparent molecular weight[33]. *a, c*, Oocytes injected with buffer only; *b,d*, oocytes injected with 40 ng of chick oviduct poly(A)-containing RNA; *a* and *b*, unfractionated homogenates; *c* and *d*, anti-ovalbumin antibody immunoprecipitates. Polysomal poly(A)-containing RNA from oestrogen-stimulated chicken oviduct was prepared as before[33]. Ovalbumin mRNA was about 20% of the total nucleic acid in the sample as judged by denaturing gel electrophoresis[34]. Oocytes were injected either with injection buffer[35] or with 40 ng chicken oviduct poly(A)-containing RNA, aiming at the equatorial band. After injection, they were transferred directly into a small volume of MBS culture medium[36] (5 μl per oocyte) containing ³⁵S-methionine (1–2 mCi per oocyte, 1,000–2,000 Ci mmol⁻¹) and incubated for 16–24 h. Oocytes plus their labelling medium were homogenized in 15 mM Tris, pH 6.8, and 150 μg phenyl methyl sulphonyl fluoride PMSF per ml[37], with a final volume of 10–20 μl per oocyte. Oocyte homogenates were then extracted with an equal volume of trichlorofluoroethane (freon) and centrifuged for 15 min at 13,000 g to remove yolk protein. No ovalbumin is lost into the organic phase at this step, as judged by gel electrophoresis of extracted and unextracted samples. Extracted homogenates were re-centrifuged to remove residual cell debris. When necessary, homogenates were stored at −20 °C. An immunoprecipitation reaction mixture of 150–250 μl was prepared which contained the following: 10⁵–10⁷ acid-insoluble c.p.m. of the ³⁵S-methionine-labelled extract (1–20 oocytes), 10 mM sodium phosphate, 150 mM NaCl, 1% Triton X-100, and 1% sodium deoxycholate[38]. Anti-ovalbumin antibody was added, and the mixture was incubated for 30 min at room temperature. Unlabelled purified chick ovalbumin (5 μg) was then added. Incubations were continued at room temperature for 4 h, then transferred to 30 °C for 30 min. Immunoprecipitation reactions were then overlayered onto discontinuous sucrose gradients in soft Brinkmann microfuge tubes, and precipitates were pelleted by centrifugation[38]. In these conditions, the antibody quantitatively precipitates the 5 μg ovalbumin carrier (data not shown). Ovalbumin cross-reacting material present in the extract should have bound to the antibody in the first incubation, before the addition of exogenous ovalbumin. Quantitative recovery of cross-reacting material in the extract is ensured by the addition of carrier ovalbumin. To verify experimentally that most ovalbumin in the extracts was recovered, aliquots of an mRNA-injected homogenate were electrophoresed either directly or after immunoprecipitation. As judged by the relative intensities of the ovalbumin spots, recovery was extremely high. Unfractionated extracts were prepared for electrophoresis as described by O'Farrell[16]. Immunoprecipitates were prepared as follows. After centrifugation of immunoprecipitation reactions, tubes were frozen on dry ice and cut with a razor blade so as to retain the pellet and a small amount of the sucrose gradient. The sucrose was removed, 30 μl of 0.1 M NaOH was added and the tubes were incubated at 60 °C for 15 min. The base was then neutralized with 0.1 M HCl, adjusted to 0.1 M Tris, pH 6.8, and brought to 1 × A buffer concentrations[16]. Solid urea was then added to a final concentration of 9 M. Two-dimensional electrophoresis was carried out as before[16], using a 12.5% polyacrylamide–SDS gel in the second dimension[39]. Gels were fluorographed[40], dried and exposed to hypersensitized film.
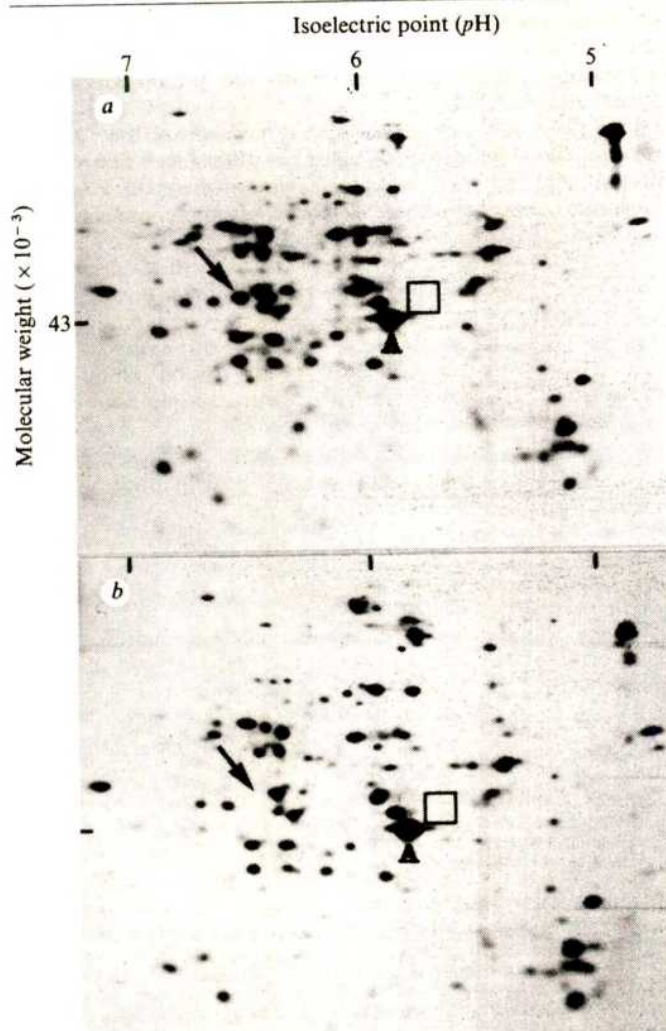
Fig. 3 Two-dimensional gel electrophoresis of unfractionated homogenates of oocytes injected with pOv12 or SV40 DNA. *a*, Oocytes injected with SV40 DNA; *b*, oocytes injected with pOv12. The arrow indicates the position of VP1; the square indicates the position of ovalbumin; A designates actin. 10 ng DNA was injected per oocyte, aiming for the nucleus[1]. Groups of about 20 injected oocytes were incubated in a large volume of MBS-H for 36 h, then transferred to fresh MBS-H (5–10 µl per oocyte) containing ^{35}S-methionine (10 µCi per oocyte, 1,000–2,000 Ci mmol^{-1}) for a further 36 h. In these conditions all isotope is taken up by the oocytes; 25–50% is incorporated into acid-insoluble material. All other procedures were as described in Fig. 2 legend, except that a 10% polyacrylamide-SDS gel[39] was used in the second dimension.

initiation *in vivo*[11,14,15]. pOv8 may be regarded as a deletion of pOv12 in which the 5′ 4-kilobase *Hind*III fragment has been removed. The chicken DNA is reversed in orientation relative to pBR322.

Ovalbumin is synthesized by oocytes injected with chromosomal gene

In this section we describe a sensitive assay for ovalbumin and demonstrate that injection of the 'complete' chromosomal gene, in pOv12, results in the synthesis of ovalbumin. This expression requires transcription of the chicken DNA, splicing of at least six introns, transport of the mRNA to the cytoplasm, and translation.

In all these studies we assayed ovalbumin production by two-dimensional gel electrophoresis[16] of either unfractionated oocyte homogenates or anti-ovalbumin antibody immunoprecipitates. The second, more sensitive method shows clearly that ovalbumin is produced, while the first aids in quantification.

We determined the location of ovalbumin in these two-dimensional gel assays by using oocytes injected with crude chicken ovalbumin mRNA (Fig. 2). Unfractionated

homogenates of mRNA-injected oocytes display a cluster of four ovalbumin spots absent in saline-injected controls (Fig. 2*a*, *b*, in rectangle). These lie in the correct molecular weight region for ovalbumin (43,500) and are specifically precipitated by anti-ovalbumin antibody, as demonstrated in Fig. 2*c*, *d*. (The presence of four prominent spots may in part result from modifications which ovalbumin is known to undergo in chicken cells *in vitro*[17,18]. The heterogeneity in isoelectric point could reflect the presence and absence of phosphorylation, because oocytes accurately modify proteins they normally do not contain[19,20]. Oocytes are known to glycosylate ovalbumin[21], but this probably is not responsible for heterogeneity in the SDS-polyacrylamide dimension (A. Colman, personal communication). Heterogeneity in molecular weight may reflect errors in translation termination in which termination does not occur at the normal UAA codon, but at the in-phase UGA codon 12 bases downstream[30].) In these mRNA-injected oocytes, ovalbumin constituted 15% of the total labelled protein; immunoprecipitates from saline-injected controls contained a background of 0.5% of the total. Because the level of ovalbumin is high, no background spots are seen in the gels of immunoprecipitates (Fig. 2*c*, *d*). If the level of ovalbumin is reduced 100-fold, as we anticipated it might be in oocytes injected with pOv12, the 0.5% background appears as a complex array of spots representing proteins nonspecifically trapped in the immunoprecipitate (data not shown).

The analysis of unfractionated extracts of pOv12-injected oocytes is shown in Fig. 3. The position of ovalbumin is indicated by a square and contains no detectable new spots when pOv12-injected and control SV40-injected oocytes are compared. Virion protein 1 (VP1 position indicated by arrows) is among the most highly labelled spots obtained from oocytes injected with SV40 DNA, in agreement with previous results[4]. We conclude that any ovalbumin made in pOv12-injected oocytes is present at a level considerably less than that of VP1 in SV40-injected oocytes.

The analysis of anti-ovalbumin antibody immunoprecipitates by two-dimensional gel electrophoresis demonstrates that ovalbumin is indeed synthesized in oocytes injected with pOv12 (Fig. 4*a*–*c*). The background of spots is similar in immunoprecipitates from pBR322 (Fig. 4*b*) and pOv12 (Fig. 4*a*) injected oocytes. Those injected with pOv12, however, produce the four characteristic ovalbumin spots, whereas those injected with pBR322 do not. Moreover, the most basic pair precisely co-migrate with exogenous ovalbumin added to a control immunoprecipitate (Fig. 4*c*).

pOv12-directed synthesis of ovalbumin is eliminated by co-injection of α-amanitin at a concentration (1 µg ml^{-1}) which inhibits RNA polymerase II but not III (data not shown)[2,22]. The correct polymerase—polymerase II—therefore is responsible for generating the transcripts which are ultimately translated into ovalbumin.

We quantified the level of ovalbumin in pOv12-injected oocytes by comparison with the level of VP1 in oocytes injected with SV40 DNA. That ovalbumin is present at a relatively lower level is clear from our analysis of unfractionated homogenates (Fig. 3) and from the intensity of the ovalbumin spots compared to those in the background of immunoprecipitates (Fig. 4*a*). We compared by microdensitometry the summed intensity of the four ovalbumin spots in Fig. 4*a* with that of the single prominent VP1 spot (Fig. 3*a*). Ovalbumin is present at 2.1% of the VP1 level by this analysis. (A correction has been made for the relative methionine contents of ovalbumin and VP1 (Fig. 4 legend).) This figure relies on the quantitative recovery of ovalbumin from oocyte homogenates as is apparently achieved by our immunoprecipitation procedure (Fig. 2 legend). VP1 is roughly 0.5% of the total labelled protein in oocytes injected with SV40 DNA[5]; ovalbumin is therefore about 0.01% of the total.

In summary our analysis of oocytes injected with pOv12 demonstrates that ovalbumin is synthesized. We identified the

protein by three independent criteria: isoelectric point, molecular weight and antigenic specificity. Although it is present at only about 2% of the level of VP1 in SV40 DNA-injected oocytes, it is remarkable that any is produced, in view of the number of processing steps required to generate functional ovalbumin messenger. We conclude that frog oocytes can carry out all those steps with a primary transcript of the 'complete' chicken ovalbumin gene.

Ovalbumin synthesis does not require 5' end of chromosomal gene

We next analysed oocytes injected with pOv8 to determine whether the 5' region of the ovalbumin gene, present in pOv12, is essential for expression. As discussed earlier, pOv8 is similar to pOv12 except that the 5' 4 kilobases of the chicken DNA insert have been deleted. It therefore lacks both the cap

site and the TATATAT sequence implicated in transcription initiation *in vivo*[11,14,15]. pOv8 does, however, retain the second exon intact, and therefore still has the chicken AUG translation initiation codon.

Injection of pOv8 results in the synthesis of ovalbumin at a level similar to that of pOv12 (Fig. 4d). The same characteristic four spots are seen in the proper position, with intensities comparable to those found in immunoprecipitates from pOv12-injected oocytes. The 5' flanking sequence, cap site, leader sequence and first intron can all be deleted without affecting the level of ovalbumin production. We conclude that in *Xenopus* oocytes, none of the steps required to generate functional messenger from a primary transcript of the ovalbumin gene is contingent upon transcription initiation at the sequence thought to be involved in transcription initiation in chicken cells *in vivo*. The expression of pOv8 also suggests that ovalbumin synthesis in pOv12-injected oocytes does not require initiation at or near the cap site in the cloned chicken DNA.

Oocytes injected with full-length cDNA clone synthesize no ovalbumin

Homogenates prepared from oocytes injected with the full-length cDNA clone, pOv230, contain no detectable ovalbumin as assayed by two-dimensional gel electrophoresis of anti-ovalbumin immunoprecipitates (Fig. 4e). This suggests that pOv230 lacks sequences present in the genomic clones that are required for expression, particularly because the amounts of ovalbumin-specific transcripts in oocytes injected with pOv230 and pOv12 are comparable (see below).

Taken together, the expression of pOv8 and non-expression of pOv230 suggests that some genomic sequences are required for the production of functional messenger in injected oocytes, but that they do not lie near the cap site. Studies of SV40 mutants[23,24] and β-globin: SV40 recombinants[25,26] have indicated that the splicing of transcripts is critical for their stability and subsequent expression. We suggest that the defect in pOv230 expression relative to the genomic clones also may reflect the absence of intervening sequences.

Level of ovalbumin transcripts in DNA-injected oocytes

The following experiments establish that the lack of ovalbumin synthesis in pOv230-injected oocytes is not due to a lack of transcripts containing ovalbumin messenger sequences. In addition, the data indicate that most stable transcripts from the chromosomal clones are not transcribed exclusively from
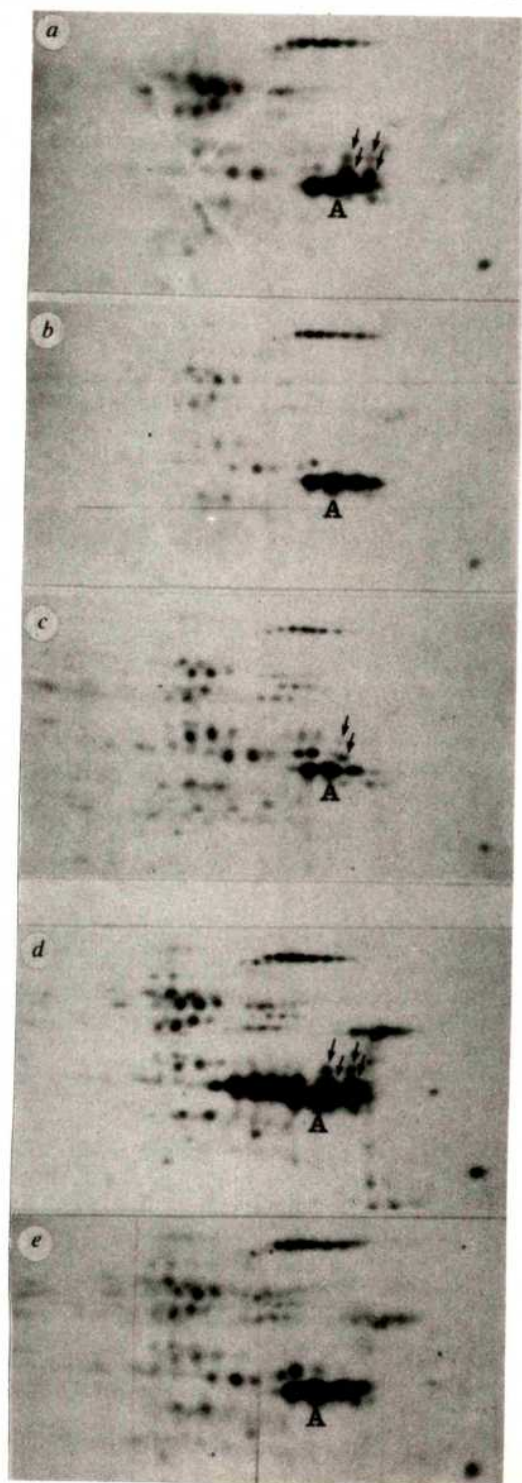

Fig. 4 Anti-ovalbumin immunoprecipitates of DNA-injected oocytes analysed by two-dimensional gel electrophoresis. All manipulations were carried out as described in Fig. 3 legend. The same central region of each gel is shown. Arrows indicate the position of ovalbumin spots; A designates actin. The gel is in the same orientation as the gel in Fig. 3. a, Oocytes injected with pOv12; b, oocytes injected with pBR322; c, same as b, but with the addition of a trace amount of ovalbumin mRNA-injected oocyte homogenate (same sample as in Fig. 2b, hence only two of four spots seen); d, oocytes injected with pOv8; e, oocytes injected with pOv230. In e the spot just above and slightly to the right of actin is not ovalbumin but a background spot of variable intensity; it sometimes is obscured by large amounts of ovalbumin (a and d), but is just visible in b and c as well as in e. In c it can be distinguished from the nearest (lower left) ovalbumin spot. The heterogeneity of background spots, in which rows of several tightly packed spots seem to have been derived from a single protein, is ascribed to artefactual charge heterogeneity (see ref. 16). The base treatment involved in sample preparation is likely to destroy certain amino acid residues[41], and result in charge heterogeneity. To quantify ovalbumin expression relative to VP1, the total optical density of the four spots shown in a was compared to that of the single VP1 spot shown in Fig. 3a. Fluorograms of shorter exposure were used. Twenty-five times more homogenate was used for the ovalbumin immunoprecipitation than for the VP1 analysis, in order to produce spots of comparable intensity with similar exposures. Optical density was measured using a Joyce–Loebl microdensitometer. Entire spots were scanned. The conditions of film exposure used yield a linear relationship of optical density to radioactivity[40]. Corrections were made for the relative amounts of radioactivity analysed, relative exposure times, and the relative methionine contents of VP1 (2.2%, ref. 9) and ovalbumin (4.4%, ref. 30).

Table 1   Level of stable transcripts synthesized from various injected DNA templates

DNA injected	% Oocyte ^{32}P-RNA hybridized (d.p.m.)*	% ^{3}H-cRNA hybridized (d.p.m.)†	% Oocyte ^{32}P-RNA complementary to injected DNA‡
pBR322	5.3 (9,850)	17.0 (85,000)	31.1%
pMB9	16.7 (31.050)	78.8 (181,000)	21.2
pOv230	6.1 (11,280)	32.3 (80,700)	18.8
pOv8	2.5 (3,520)	23.9 (59,900)	10.6
pOv12	3.6 (4,970)	19.5 (77,900)	18.4
SV40	6.9 (9,770)	32.3 (129,500)	21.6

Oocytes were injected with 10 ng supercoiled DNA and 0.5 µCi α-^{32}P-rGTP, then incubated at 19 °C for 48 h. Oocyte ^{32}P-labelled RNA was prepared by homogenizing 20–30 oocytes in 1 ml of 40 mM Tris, pH 7.5, 4 mM EDTA, 0.3 M NaCl, 2.0% SDS and 2 mg proteinase K per ml, extracting the homogenate with an equal volume of phenol:chloroform (1:1), and precipitating with ethanol[6,42]. ^{3}H-cRNA was synthesized from each template DNA using *E. coli* RNA polymerase with sigma factor (given by A. Travers) and ^{3}H-UTP (52 Ci per mmol, Amersham). A mixture of oocyte ^{32}P-RNA and ^{3}H-cRNA was redissolved in formamide-PIPES buffer and hybridized to 11-mm diameter DBM-filters on which 50 µg of DNA had been immobilized[27]. Hybridizations were incubated for 30 h at 42 °C, the filters were washed, and the hybrids were eluted with 0.4 N NaOH as described[27]. All hybridizations were performed in duplicate.

*Total ^{32}P radioactivity in each hybridization ranged from 1.4 × 10⁵ d.p.m. to 2 × 10⁵ d.p.m. Less than 0.2% of each ^{32}P-labelled or ^{3}H-labelled RNA hybridized to filters bearing calf thymus DNA. These low backgrounds have been subtracted.

†The total ^{3}H radioactivity in each hybridization ranged from 1.5 × 10⁵ c.p.m. to 5 × 10⁵ c.p.m.

‡Per cent of oocyte ^{32}P-RNA complementary to injected DNA = (% ^{32}P-RNA hybridized)/(% ^{3}H-RNA hybridized) × 100. This calculation assumes that the hybridization efficiencies of oocyte ^{32}P-RNA and ^{3}H-cRNA are identical.

the inserted chicken DNA; rather, most transcription of the chromosomal gene seems likely to result from readthrough from the vector (see discussion).

First, the total amount of stable RNA transcribed from each DNA template was determined. ^{32}P-labelled RNA prepared from DNA-injected oocytes was hybridized to DBM-paper filters on which large amounts of the injected type of DNA had been immobilized[27]. Hybridization efficiency was internally monitored in each assay by the addition of ^{3}H-cRNA. Table 1 shows that transcripts from the templates examined constitute from 10 to 30% of the total acid-insoluble radioactivity incorporated by the oocytes, a value consistent with previously reported results[1]. Because total acid-insoluble incorporation does not change substantially in oocytes injected with any of these DNAs (data not shown), we conclude that each template produces approximately the same amount of stable RNA. In particular, the quantities of stable RNA transcribed from pOv12 and pOv230 do not differ significantly.

Second, the relative amounts of stable RNA transcribed from the chicken and vector regions of the ovalbumin plasmids were determined. ^{32}P-labelled RNA prepared from oocytes injected with a cloned ovalbumin DNA template was hybridized to filters to which DNA restriction fragments had been transferred from an agarose gel and immobilized[28]. (For relevant restriction map data, see Fig. 1.) After hybridization, filters were treated with ribonuclease, and the radioactivity hybridized to each fragment was determined by microdensitometry or scintillation counting.

Transcripts from pOv12: ^{32}P-labelled RNA prepared from oocytes injected with pOv12 or pOv8 yields similar results when hybridized to the *Hind*III restriction fragments of pOv12 (Fig. 5*a*1,2). In both cases, three to five times more RNA hybridizes (per kilobase of DNA) to the pBR322 fragment (4.3 kilobases) than to the chicken DNA fragments (3.2, 4.0 and 4.8 kilobases). Hybridization of pOv12 RNA to the *Hind*III–*Pst*I fragments of pOv12 presents the same general pattern, in that the 3.5-kilobase fragment which contains only pBR322 sequences is most highly labelled (Fig. 5*a*4). Moreover, transcripts of the 1.1- and 1.5-kilobase fragments which flank the gene on the 5′ side are present at approximately the same level per kilobase of DNA as transcripts from the 1.4-kilobase fragment which contains the cap site and first exon. These data indicate that most stable transcripts of pOv12 are derived from pBR322, not from the ovalbumin gene.

Transcription of both chicken and vector DNA is strongly inhibited by a concentration of α-amanitin previously

shown[2,22] to inhibit SV40 and plasmid transcription in oocytes without affecting the transcription of tRNA or 5S RNA genes (Fig. 5*a*3). Therefore RNA polymerase II is responsible not only for the transcription of those RNAs which are translated into ovalbumin (see above), but also for most of the total RNA complementary to pOv12.

Transcripts from pOv230: Comparison of the levels of ovalbumin-specific RNA in pOv230- and pOv12-injected oocytes is complicated by the fact that pOv230 was constructed by A-T-tailing into the *Eco*RI site of pMB9[12] whereas pOv12 was constructed by ligation into the *Hind*III site of pBR322[13]. To compare the level of transcripts from ovalbumin structural sequences directly, ^{32}P-labelled RNA from pOv230- and pOv12-injected oocytes was hybridized to filters bearing immobilized *Hph*I fragments of pOv230 (Fig. 5*b*). The 1.27-kilobase fragment is composed exclusively of sequences found in ovalbumin mRNA (from position 336 to 1,605)[30]. The 0.85-kilobase fragment is exclusively vector DNA (part of the tetracycline resistance gene common to pMB9 and pBR322 (position 453 to 1,306 in pBR322))[43]. In pOv230-injected oocytes, the abundance of stable transcripts from the 1.27-kilobase fragment is roughly equal (per kilobase of DNA) to the abundance of stable transcripts from the 0.85-kilobase pMB9 fragment (Fig. 5*b* 1; see Fig. 5*b* legend). Moreover, about five times more labelled RNA homologous to the 1.27-kilobase fragment is found in oocytes injected with pOv230 than in oocytes injected with pOv12 (Fig. 5*b*2; for comparison of pOv230 and pOv12, levels of hybridization to the 1.27-kilobase fragment were standardized relative to the 0.85-kilobase fragment, as detailed in Fig. 5*b* legend). Although these data suggest that the lack of ovalbumin synthesis in pOv230-injected oocytes is not due to a lack of ovalbumin-specific transcripts, the possibility remained that the dA:dT homopolymeric tracts used to insert the cDNA might act as transcription terminators such that only the nonsense strand of the ovalbumin cDNA insert in pOv230 was transcribed. This was not the case, however, because slightly more pOv230 RNA hybridizes to the sense strand than to the nonsense strand of the 1.27-kilobase *Hph*I pOv230 fragment (Fig. 5*c*). Because transcripts of the ovalbumin region of pOv230 require no splicing events to juxtapose adjacent exons, it seems likely that the concentration of RNA molecules possessing the contiguous messenger sequence is, in fact, higher in pOv230-injected oocytes than in those injected with pOv12. Thus the lack of ovalbumin synthesis in oocytes injected with pOv230 is not correlated with a lack of transcripts containing the necessary structural information.

Discussion

The ability of oocytes injected with the 'complete' chromosomal ovalbumin gene, pOv12, to synthesize ovalbumin, clearly demonstrates that frog oocytes can perform all the steps necessary to generate functional mRNA from initial transcripts of this gene. In particular, the production of functional ovalbumin messenger requires that at least six introns present in a precursor RNA be accurately removed by RNA splicing.

An 'incomplete' ovalbumin gene that lacks the leader sequence, cap site, TATATAT region and 5′ flanking sequence, directs ovalbumin synthesis with about the same efficiency as the intact gene. Therefore, at least when the ovalbumin gene is present as part of a recombinant plasmid, none of these regions is absolutely required for transcription, accurate RNA processing, transport or translation. These results do not necessarily show that the same regions have no function in normal ovalbumin gene expression in the chicken oviduct.

Our data demonstrate that a functional mRNA can be generated from a primary transcript lacking the proper 5′ terminus. This raises an intriguing possibility, particularly because we suspect that most ovalbumin transcripts are derived from transcription which 'reads through' from the vector (see below). Perhaps the normal production of functional mRNA from some genes does not require initiation of transcription at a precise sequence.

Oocytes injected with a full-length cDNA clone synthesize no detectable ovalbumin, yet accumulate more stable RNA containing ovalbumin messenger sequences than do oocytes injected with the chromosomal gene. The deficiency of functional mRNA among pOv230 transcripts may be due to the absence of introns. It has been suggested from work in other systems that RNA splicing has a critical role in the production of functional mRNA[23–26]. Our results with pOv230 are consistent with this proposal. In these other systems, however, splicing seems to be necessary for the stabilization of primary transcripts[21,22,26]; apparently this is not the case with transcripts from the ovalbumin region of the cDNA clone, because they are, in fact, somewhat more abundant than those from the ovalbumin region of the chromosomal clone.

There are several possible explanations for our finding that the amount of ovalbumin produced by oocytes injected with the chromosomal gene is roughly 2% of the amount of VP1 produced by oocytes injected with SV40. One concerns the difference in the number of processing steps required to generate VP1 and ovalbumin messengers. The ovalbumin gene contains seven introns and the VP1 gene only one. If splicing occurs with 50% efficiency for each intron, then ovalbumin
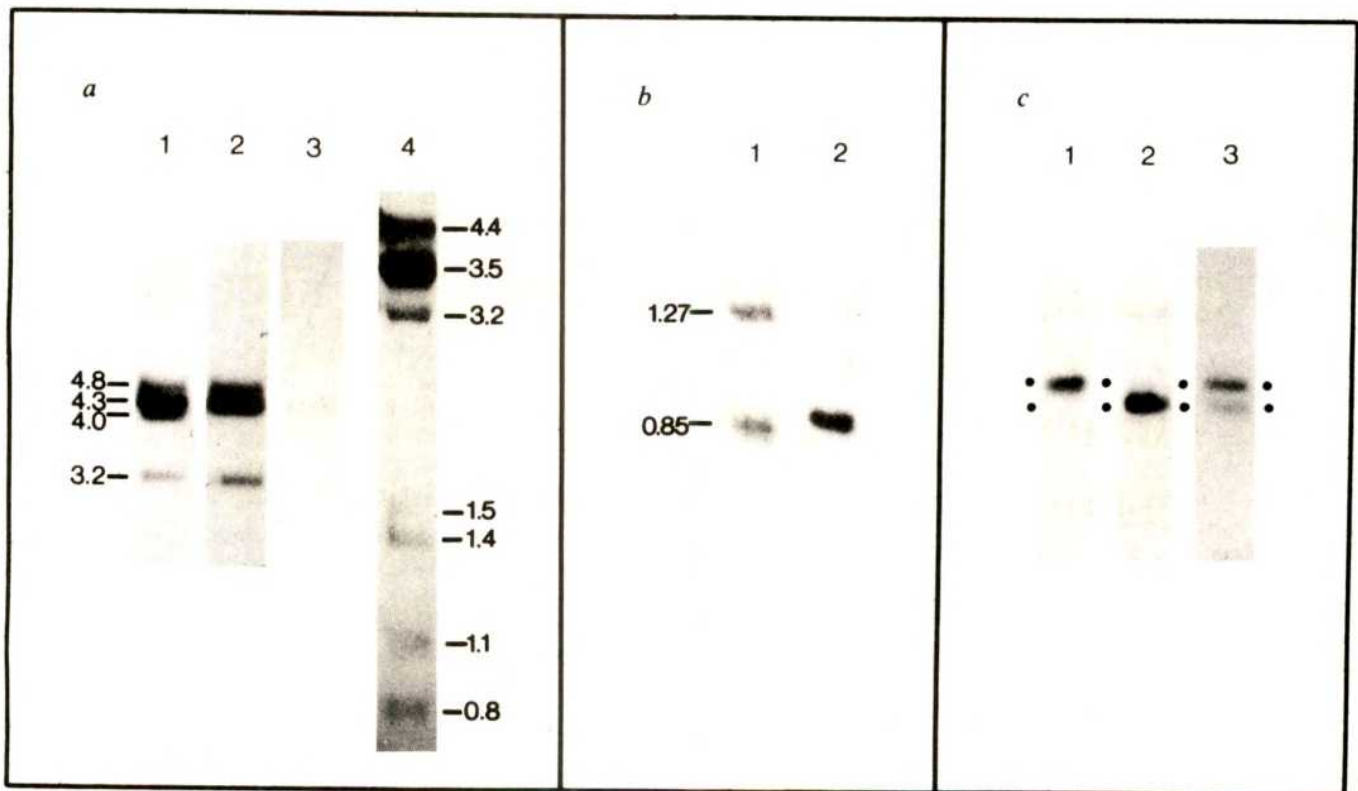

Fig. 5 Relative abundance of RNA transcribed from various regions of the ovalbumin clones. Each experiment follows a similar protocol. After digestion with restriction enzymes, 1–2 µg of DNA was electrophoresed through an agarose gel and transferred to nitrocellulose[28] (*a*) or DBM-paper[29] (*b* and *c*). Filters were then hybridized to ^{32}P-labelled RNA prepared from DNA-injected oocytes as described for Table 1. Between 2×10^5 and 10×10^5 acid-insoluble d.p.m. were used in each hybridization. For each fragment, bound DNA was in excess over complementary ^{32}P-labelled RNA. After hybridization for 1.5 to 3 d, filters were washed extensively, treated with DNase-free RNase (25 µg per ml) for 1 h at 37 °C, and exposed to hypersensitized film[40]. To quantify hybridized radioactivity, two techniques were used. Either bands were cut out of the filter and bound radioactivity was determined in a scintillation counter (*a*), or autoradiograms were scanned with a Joyce–Loebl microdensitometer (*a*–*c*). Each hybridization was performed in duplicate. *a*, Transcripts from pOv12 and pOv8. ^{32}P-labelled RNA prepared from oocytes injected with pOv12 (tracks 1 and 4), pOv8 (track 2), or pOv12 plus α-amanitin (1 µg per ml, track 3) was hybridized to the *Hind*III fragments of pOv12 (tracks 1, 2 and 3) or the *Hind*III-*Pst*I fragments of pOv12 (track 4), *b*, Transcripts from pOv230 and pOv12. ^{32}P-labelled RNA prepared from oocytes injected with pOv230 (track 1) or pOv12 (track 2) was hybridized to the *Hph*I fragments of pOv230. Only the relevant region of the fel is shown. The amount of ^{32}P-RNA hybridized per kilobase of DNA was determined by microdensitometry. The values oftained for the 0.85-kilobase fragment were set to 100% in both hybridizations. Relative hybridization to the 1.27-kilobase fragment was: track 1, 85%; track 2, 18%. Thus the level of stable RNA derived from the 1.27-kilobase fragment is 4.7-fold higher in pOv230-injected oocytes. *c*, Transcription of both the sense and non-sense strands of pOv230. Separated strands of the 1.27-kilobase *Hph*I pOv230 fragment were prepared by electrophoresis of the purified, alkali-denatured fragment through a cold 1.4% agarose gel as described[42]. The two strands (present in equal amounts in the same gel) were then transferred to DBM-paper[29]. Black dots indicate the position of the two strands on the filter. Filters were hybridized to the following radioactive probes. Track 1: ^{32}P-labelled ovalbumin mRNA (prepared by terminal labelling of mRNA fragments generated by boiling for 15 min in formamide), track 2: single-stranded ovalbumin cDNA synthesized *in vitro* from ovalbumin mRNA using a 20-min reverse transcriptase reaction in the presence of 4 mM sodium pyrophosphate; track 3: ^{32}P-labelled RNA prepared from oocytes injected with pOv230.

mRNA would be present at $(0.5)^6$, or 1.6% of the VP1 mRNA level. A second explanation is that the transcription initiation and termination signals in the late region of SV40 might be more efficiently recognized by *Xenopus* oocytes than are those in the ovalbumin gene, resulting in greater translational efficiency of SV40 transcripts.

Most pOv12 transcripts do not both initiate at the cap site and terminate at the polyadenylation site. Rather, we suspect for the following reasons that most are produced either by random transcription initiation and termination throughout the template, or by transcription initiated within the vector which reads through into the inserted ovalbumin gene. (1) The level of transcripts from the vector is higher than the level of transcripts from the ovalbumin gene in the same plasmid; (2) transcripts from all regions of the inserted chicken DNA, including those lying outside the ovalbumin gene, are present in similar amounts; (3) no more stable RNA is synthesized

from pOv12 than from pBR322, and (4) electron microscopy of pBR322 transcription complexes by the Miller technique often reveals transcripts much longer than pBR322 itself (M. Trendelenburg and J.B.G., unpublished results). Although these data are all consistent with readthrough transcription, none provides compelling proof of it, and one observation could be taken to argue against it: the ovalbumin gene is inserted in opposite orientations in pOv8 and pOv12, yet the two templates direct ovalbumin synthesis with comparable efficiencies. If transcription of the chromosomal gene is due solely to readthrough transcription from the vector, then it must occur in both directions.

1. Mertz, J. E. & Gurdon, J. B. *Proc. natn. Acad. Sci. U.S.A.* **74**, 1502–1506 (1977).
2. Melton, D. A. & Cortese, R. *Cell* **18**, 1165–1172 (1979).
3. De Robertis, E. M. & Olson, M. V. *Nature* **278**, 137–143 (1979).
4. De Robertis, E. M. & Mertz, J. E. *Cell* **12**, 175–182 (1977).
5. Rungger, D. & Turler, H. *Proc. natn. Acad. Sci. U.S.A.* **75**, 6073–6077 (1978).
6. Probst, E., Kressmann, A. & Birnstiel, M. L. *J. molec. Biol.* **135**, 709–732 (1979).
7. Crawford, L. V. *et al. Proc. natn. Acad. Sci. U.S.A.* **75**, 117–121 (1978).
8. Reddy, V. B. *et al. Science* **200**, 494–502 (1978).
9. Fiers, W. *et al. Nature* **273**, 113–120 (1978).
10. Dugaiczyk, A. *et al. Proc. natn. Acad. Sci. U.S.A.* **78**, 2253–2257 (1979).
11. Gannon, F. *et al. Nature* **278**, 428–434 (1979).
12. McReynolds, L., Catterall, J. & O'Malley, B. W. *Gene* **2**, 217–231 (1977).
13. Lai, E. C., Woo, S. L. C., Bordelon-Riser, M. E., Fraser, T. H. & O. Malley, B. W. *Proc. natn. Acad. Sci. U.S.A.* **77**, 244–248 (1980).
14. Lai, E. *et al. Cell* **18**, 829–842 (1979).
15. Roop, D. R., Tsai, M. J. & O'Malley, B. W. *Cell* **19**, 63–68 (1980).
16. O'Farrell, P. *J. biol. Chem.* **250**, 4007–4021 (1975).
17. Lee, Y. & Montgomery, R. *Archs Biochem. Biophys.* **97**, 9–17 (1962).
18. Milstein, C. *Biochem. J.* **110**, 127–134 (1968).
19. Lane, C. D. & Knowland, J. S. in *The Biochemistry of Animal Development* IV (ed. Weber, R. A.) (Academic, New York, 1975).
20. Lane, C., Shannon, S. & Craig, R. *Eur. J. Biochem.* **101**, 485–495 (1979).
21. Deacon, N. & Ebringer, A. *FEBS Lett.* **79**, 191–194 (1977).
22. Gurdon, J. B. & Brown, D. D. *Devl Biol.* **67**, 346–356 (1978).
23. Lai, C. & Khoury, G. *Proc. natn. Acad. Sci. U.S.A.* **76**, 71–75 (1979).
24. Gruss, P., Lai, C., Dhar, R. & Khoury, G. *Proc. natn. Acad. Sci. U.S.A.* **76**, 4317–4321 (1979).
25. Hamer, D., Smith, K., Boyer, S. & Leder, P. *Cell* **17**, 725–735 (1979).
26. Hamer, D. H. & Leder, P. *Cell* **18**, 1299–1302 (1979).
27. Stark, G. R. & Williams, J. G. *Nucleic Acids Res.* **6**, 195–203 (1979).
28. Southern, E. M. *J. molec. Biol.* **98**, 503–518 (1975).
29. Wahl, G. M., Stern, M., & Stark, G. R. *Proc. natn. Acad. Sci. U.S.A.* **76**, 3683–3687 (1979).
30. McReynolds, L. *et al. Nature* **273**, 723–728 (1978).
31. Miller, O. & Bakken, A. in *5th Karolinska Symp.*, 155–157 (Karolinska Institutet, Stockholm, 1972).
32. Trendelenburg, M. & Gurdon, J. B. *Nature* **276**, 292–294 (1978).
33. Buell, G., Wickens, M., Payvar, F. & Schimke, R. *J. biol. Chem.* **253**, 2471–2482 (1978).
34. Bailey, J. & Davidson, N. *Analyt. Biochem.* **70**, 75–85 (1976).
35. Gurdon, J. B., Lane, C. D., Woodland, H. R. & Marbaix, G. *Nature* **233**, 177–182 (1971).
36. Gurdon, J. B. *J. Embryol. exp. Morph.* **36**, 523–540 (1976).
37. Laskey, R. A., Mills, A. D., Gurdon, J. B. & Partington, G. A. *Cell* **11**, 345–351 (1977).
38. Rhoads, R., McKnight, G., & Schimke, R. *J. biol. Chem.* **248**, 2031–2039 (1973).
39. Laemmli, U. *Nature* **227**, 680–685 (1970).
40. Laskey, R. & Mills, A. D. *Eur. J. Biochem.* **56**, 335–341 (1975).
41. Hirs, C. *Meth. Enzym.* **11**, 325 (1967).
42. Perlman, D. & Huberman, J. A. *Analyt. Biochem.* **83**, 666–677 (1977).
43. Sutcliffe, J. G. *Cold Spring Harbor Symp. quant. Biol.* **43**, 77–90 (1978).

Cleavage of pyrimidine dimers in specific DNA sequences by a pyrimidine dimer DNA-glycosylase of *M. luteus*

William A. Haseltine, Lynn K. Gordon & Christina P. Lindan

Sidney Farber Cancer Institute, Harvard University, Boston, Massachusetts 21205

Robert H. Grafstrom, Nancy L. Shaper & Lawrence Grossman

Biochemistry Department, The Johns Hopkins University School of Hygiene and Public Health, Baltimore, Maryland 21205

Pyrimidine dimer formation in response to UV radiation is governed by the thymine content of the potential dimer and the two flanking nucleotides. An enzymatic activity can be purified from Micrococcus luteus that cleaves the N-glycosyl bond between the 5' pyrimidine of a dimer and the corresponding sugar without rupture of a phosphodiester bond. We propose that strand scission at a dimer site by the M. luteus enzyme requires two activities, a pyrimidine dimer DNA-glycosylase and an apyrimidinic/apurinic endonuclease.

ULTRAVIOLET light creates potentially lethal and mutagenic damage in the DNA of exposed organisms. The principal photoproduct is the pyrimidine cyclobutane dimer formed between adjacent pyrimidines, producing thymine-thymine (T<>T), thymine-cytosine (T<>C), and cytosine-cytosine (C<>C) dimers. Cells can recover from damage induced by UV light through various mechanisms including excision repair, enzymatic photoreversal, and post-replication repair[1,2]. One process of excision repair proceeds via endonucleolytic strand scission in the vicinity of the photoproducts with subsequent

excision of dimers[1,3]. Endonucleases that specifically cleave DNA near the site of pyrimidine dimers have been identified in several bacterial species[4–7] in slime moulds[8], rat liver[9], and in mammalian tissue[10]. In most organisms repair of UV damage is multigenic[2].

We have investigated the effect of local sequence on the distribution of UV light induced photodamage in DNA. The effect of neighbouring sequences in the formation of such damage is important to an understanding of the mutagenic effect of UV radiation. Since previous studies have indicated

that local sequence may affect the formation of pyrimidine dimers[12-15], it seemed likely that DNA sequencing methods could be used to measure the effect of neighbouring sequence on the distribution of photodimers. Accordingly, a UV endonuclease prepared from *Micrococcus luteus* was used to cleave DNA substrates of defined sequence that had been irradiated with UV light, and the products were analysed on high resolution polyacrylamide gels.

During these experiments we observed that the dimer-specific *M. luteus* endonuclease activity did not cleave the DNA 5′ to the site of the dimer as originally suggested by other methods. Rather, we found that strand scission occurs at the site of a pyrimidine dimer by the combined action of two enzymatic activities, a pyrimidine dimer DNA-glycosylase that cleaves the glycosylic bond between the 5′ pyrimidine of the dimer and its sugar, and an apyrimidinic/apurinic (AP) endonuclease.

Distribution of dimer damage within a defined sequence

DNA fragments of defined sequence were used as substrates for UV radiation and endonuclease cleavage. The DNA restriction fragments of defined sequence were obtained from a plasmid, pLJ3 (refs 16, 17). The DNA substrates were terminally labelled with ^{32}P at either the 5′ or 3′ end. Labelled DNA was first irradiated and then cleaved with the dimer-dependent endonuclease, partially purified as the Sephadex G-75 fraction from *M. luteus*[7]. Fragments resulting from endonucleolytic cleavage were layered onto denaturing, high-resolution polyacrylamide gels of the type used for DNA sequencing. To determine the length of the reaction products and, therefore, the precise site of enzymatic strand scission, the electrophoretic mobility of the cleavage products was compared to the migration rate of fragments produced by chemically sequencing the same strand[18].

In an initial experiment, a DNA fragment labelled at the 5′ terminus was irradiated with increasing doses (from 500 to 10,000 J m^{-2} of 254-nm light (UV-DNA) from a germicidal lamp. High doses of UV radiation were used because the target size was small. The irradiated DNA was treated with concentrations of the endonuclease that had previously been shown to be saturating for the cleavage reactions. The products of these reactions were analysed by polyacrylamide gel electrophoresis and the resulting migration patterns were analysed by autoradiography (Fig. 1). Inspection of the gel reveals that the UV-DNA was cleaved by the endonuclease at specific sites and only in the vicinity of possible pyrimidine dimers. The endonuclease did not cleave unirradiated DNA (Fig. 1, lanes 1 and 2), and breaks were not apparent in the DNA irradiated with 10,000 J m^{-2} and not exposed to enzyme (Fig. 1, lane 13). With increasing doses of UV radiation up to 3,500 J m^{-2}, the yield of cleavage products also increased.

In order to determine if the extent of dimer formation is sequence specific, similar experiments were performed using doses between 75 and 7,500 J m^{-2}. Quantitative data were obtained from experiments in which the DNA was irradiated, treated with the Sephadex G-75 fraction and layered onto denaturing gels. The amount of each product was determined by measuring the amount of radioactivity in each band. This calculation assumed that the enzyme cleaved quantitatively at all dimers. This assumption is justified, since previous experiments demonstrated that the dimer-dependent endonuclease of *M. luteus* cleaved DNA in response to all possible dimers, T⬦T, C⬦T, and C⬦C; also, the combined action of the UV endonuclease preparation and added exonucleases resulted in the complete removal of all dimers from the DNA[3,19]. Furthermore, in the reaction conditions utilized in these experiments, increased amounts of enzyme did not lead to an increased number of breaks. The incision frequencies at each dimer do not reflect a property of the *M. luteus* enzyme alone, since the same distribution of
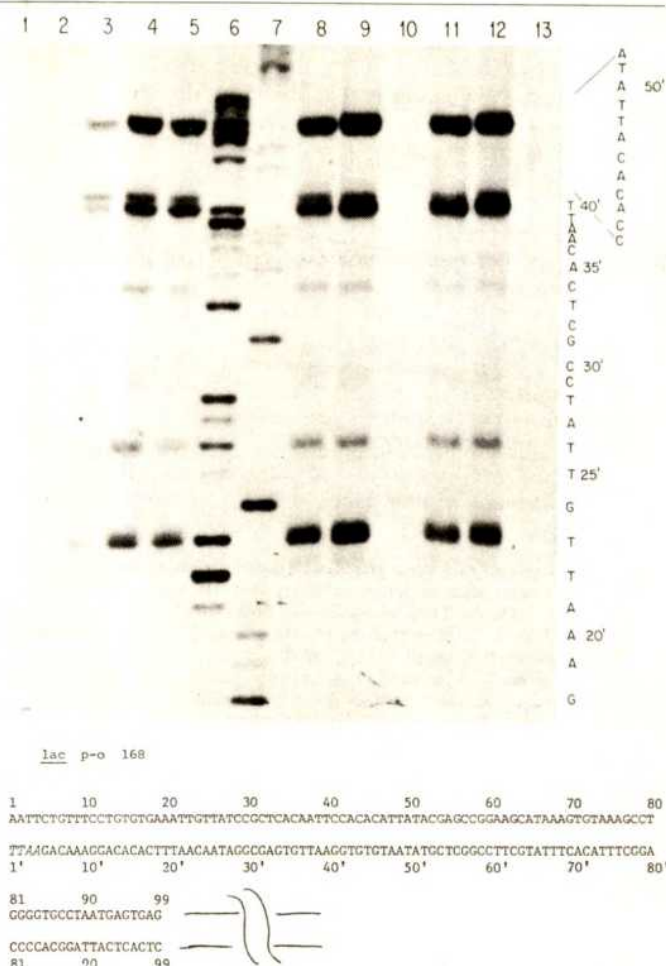

lac p–o 168

```
1        10        20        30        40        50        60        70        80
AATTCTGTTTCCTGTGTGAAATTGTTATCCGCTCACAATTCCACACATTATACGAGCCGGAAGCATAAAGTGTAAAGCCT
TTAAGACAAAGGACACACTTTAACAATAGGCGAGTGTTAAGGTGTGTAATATGCTCGGCCTTCGTATTTCACATTTCGGA
1'       10'       20'       30'       40'       50'       60'       70'       80'

81       90        99
GGGGTGCCTAATGAGTGAG
CCCCACGGATTACTCACTC
81       90        99
```

Fig. 1 Site-specific cleavage by the dimer dependent endonuclease on DNA irradiated with various doses of UV light. 168 base pair ^{32}P-5′ end-labelled *lac p–o* DNA[16,17] was irradiated with the indicated amounts of 254-nm light and incubated with saturating amounts of the Sephadex G-75 fraction of the *M. luteus* enzyme. (Sephadex G-75 fraction: dimer-specific endonuclease containing both the pyrimidine dimer DNA-glycosylase and the AP endonuclease.) Samples were layered onto a urea-containing polyacrylamide gel. The DNA was heated for 2 min in 0.01 M Na$_2$H PO$_4$ *p*H 7.0 and 10% glycerol before loading the sample. The amount of endonuclease necessary to carry the reaction to completion was determined in separate experiments in which the extent of cleavage of the DNA fragment irradiated at 500 J m^{-2} was determined as a function of enzyme concentration. These experiments showed that an increase in the concentration of the enzyme above 1 unit per 50 µl of reaction mix did not cause further scission. The reaction buffer contained 0.01 M Tris-HCl *p*H 7.4, 0.05 M NaCl, 0.001 M Na$_2$EDTA. Incubation was for 60 min at 37 °C. Reaction mixtures contained: unirradiated DNA treated with 3 units (lane 1) and 9 units (lane 2) of the Sephadex G-75 enzyme; DNA irradiated with 120 J m^{-2} (lane 3), 480 J m^{-2} (lane 4), 960 J m^{-2} (lane 5), 1,440 J m^{-2} (lane 8), 4,320 J m^{-2} (lane 9), lane 10 is blank, 7,200 J m^{-2} (lane 11), 10,000 J m^{-2} (lane 12). Three units of enzyme were added to these reactions. DNA of lane 13 was exposed to 10,000 J m^{-2} but no enzyme was added to the reaction. Lane 6 contains products of neocarzinostatin sequencing reactions producing cleavage at T's and A's[21]. Lane 7 contains products of dimethyl sulphate modification with cleavage at G's and A's[18]. Only the central portion of the gel is pictured here. The DNA sequence of the substrate is given above for the first 99 nucleotides. For this experiment the DNA was labelled at the 5′ terminus in reactions that contained [γ-^{32}P]ATP and polynucleotide kinase in an exchange reaction[32]. In subsequent experiments the substrate was also labelled at the 3′ terminus using [α-^{32}P]dATP and [α-^{32}P]dTTP in reactions that contained the Klenow fragment of *E. coli* DNA polymerase I[33]. The unprimed numbers indicate the DNA strand labelled at the 5′ terminus; the primed numbers DNA labelled at the 3′ terminus. The italicized letters indicate the positions of the 3′ labelled nucleotides.

enzyme sites was obtained in similar experiments using the dimer-dependent endonuclease V (ref. 6) purified from T4 infected *Escherichia coli* (data not shown).

The per cent incision at potential dimer sites as a function of the irradiation dose is plotted in Fig. 2*a* for representative sequences. Several conclusions can be drawn from this data.
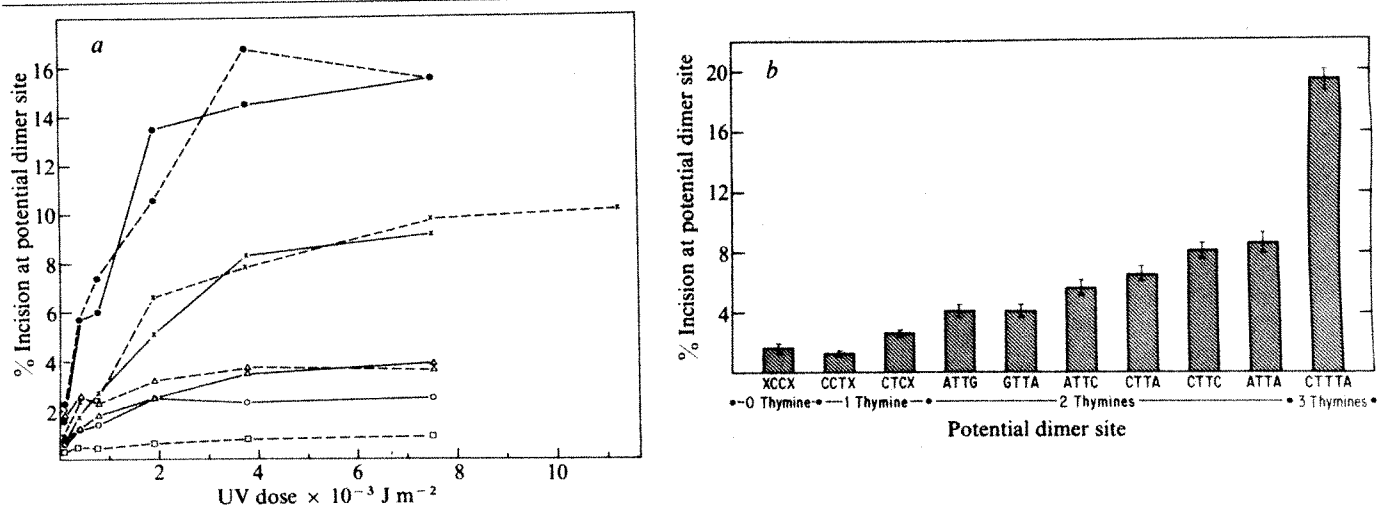
Fig. 2 Frequency of scission at potential dimer sites as a function of UV dose and sequence. *a, Dose–response: lac p–o* 117 (see below) and *lac p–o* 168 DNA (see Fig. 1) were used for this experiment. The DNA was irradiated with 254-nm light from a germicidal lamp at the indicated dose at a dose rate of 7.5 J m^{-2}s^{-1}. The *M. luteus* endonuclease (Sephadex G-75 fraction)[7] was used at a saturating dose such that the addition of more enzyme did not produce additional breaks. Three units of the enzyme were used in a 50-μl reaction mixture that contained 0.01 M Tris-HCl pH 7.4, 0.05 M NaCl, 0.001 M Na$_2$EDTA and the reactions were incubated at 37 °C for 60 min. The DNA was precipitated and the fragments separated on 8%, 12% or 20% polyacrylamide gels that included 7 M urea; products of the same DNA fragments subject to the DNA sequencing reactions described by Maxam and Gilbert[18] or treated with neocarzinostatin[21] were layered on adjacent lanes of the gel to permit determination of the length of each scission product. The labelled DNA products were visualized by autoradiography. Because of the possibility that a single DNA molecule might contain more than one dimer, the values for per cent incision were determined using a correction factor. This empirical factor accounts for products that were removed from a band that corresponded to breakage at dimer site X by breakage of the molecules between site X and the labelled terminus. Thus,

$$\text{per cent incision} = 100 \left[\frac{\text{c.p.m. site X}}{\text{c.p.m. total}} + \frac{\text{c.p.m. faster than site X}}{\text{c.p.m. total}} \times \frac{\text{c.p.m. site X}}{\text{c.p.m. total}} \right]$$

The c.p.m. total was determined by Cherenkov counting of the total material in each lane of the gel. The time of the electrophoresis was such that all the radioactive material of each lane was present on the gel. The location within the DNA substrates of the potential dimers that were used to construct this figure are indicated below. The values are those deduced from the amount of radioactivity in the band that corresponds to a scission event at the central dimer only, except in the case of the sequence CTTTA. This value is a summation of the total incision frequency at the two possible central dimers. The relative rate of incision was approximately equal at each of the two possible thymine dimers of this sequence.

● ———————— ●	CTTTA:	lac p–o	168	3′	73′–77′
● – – – – – – ●	CTTTA:	lac p–o	168	3′	66′–70′
× ———————— ×	ATTA:	lac p–o	117	3′	54′–57′
× – – – – – – ×	ATTA:	lac p–o	117	5′	12–15
△ ———————— △	ATTG:	lac p–o	117	3′	80′–83′
△ – – – – – – △	ATTG	lac p–o	117	5′	65–68
○ ———————— ○	TTCA:	lac p–o	168	3′	17′–20′
□ – – – – – – □	CCCC:	lac p–o	117	5′	20–24

b, Sequence dependence: Three DNA fragments labelled at either the 5′ or 3′ end were used for this experiment. The DNA was irradiated with 254 nm light from a germicidal lamp at 7,500 J m^{-2} at a dose rate of 7.5 J m^{-2}s^{-1}. UV-irradiated DNA was cleaved with the endonuclease (Sephadex G-75 fraction) and analysed as in *a*. The error bars indicate ±s.e.m. as calculated from the number of independent measurements at each site as indicated in parentheses. The following numbers indicate the location of the dimer within the sequences. Sequences are listed in the 5′ to 3′ direction.

XCCX (13):	117: 20–23 (7)	**ATTC** (12):	117: 63′–66′ (4)			
	168: 28–31 (2)		168: 38–41 (5)			
	168: 56–59 (2)		S–2: 73–76 (1)			
	S–2 53′–56′ (2)		S–2: 24′–27′ (2)			
CCTX (8):	117: 14′–17′ (2)	**CTTA** (9):.	S–2: 31–34 (7)			
	117: 23′–26′ (2)		S–2: 21′–24′ (2)			
	168: 78–81 (2)					
	168: 87–90 (2)					
CTCX (12):	117: 9–12 (2)	**CTTC** (10):	117: 41–44 (9)			
	117: 48–51 (2)		168: 60′–63′ (1)			
	117: 69′–72′ (2)					
	168: 32–35 (3)					
	168: 53′–56′ (3)					
ATTG (24):	117: 65–68 (8)	**ATTA** (20):	117: 12–15 (4)			
	117: 80′–83′ (2)		117: 54′–57′ (4)			
	168: 21–24 (6)		168: 47–50 (6)			
	168: 36–39′ (3)		S–2: 58–61 (2)			
	S–2: 16–19 (5)		S–2: 70–73 (2)			
			S–2: 33′–36′ (2)			
GTTA (8):	117: 77′–80′ (2)	**CTTTA** (31):	117: 27–31 (14)			
	168: 24–27 (6)		117: 34–38 (11)			
			168: 66′–70′ (3)			
			168: 73′–77′ (3)			

```
c
1        10        20        30        40        50        60        70        80
AATTCTCACTCATTAGGCACCCCAGGCTTTACACTTTATGCTTCCGGCTCGTATAATGTGTGGAATTGTGAGCGGATAA

TTAAGAGTGAGTAATCCGTGGGGTCCGAAATGTGAAATACGAAGGCCGAGCATATTACACACCTTAACACTCGCCTATT
1'       10'       20'       30'       40'       50'       60'       70'
81       90        99
CAATTTCACACAGGAAACAG    ─┐   ┐
                         ├┐  ├─      lac  p-o  117
GTTAAAGTGTGTCCTTTGTC    ─┘   ┘
81'      90'       99'

1        10        20        30        40        50        60        70        80
AATTCATGCTCCTATATTCGATAAGAATAAACTTAATACGGTAAACGGGAAATGGGGTATTAGGGGATTTAATTATTCTTT

TTAAXTACGAGGATATAACTATTCTTATTTGAATTATGCCATTTGCCCTTTACCCCATAATCCCTAAATTAATAAGAAA
81       90        99
ATGATATAAAAAGTCCTAG    ─┐   ┐
                        ├┐  ├─          S2
TACTATATTTTCAGGATC     ─┘   ┘
81       90'       99'
```

Up to six sites were used to calculate each value in panel *b* and the value of each sequence was determined in at least eight independent measurements. At some sequences the values were obtained using DNA that had been labelled at either the 5′ or the 3′ terminus, and in either case the calculated incision frequency was the same. The s.e.m. was within ±10% of the values indicated for each sequence regardless of its location within the DNA fragments. The sequences used for this work were the *lac p–o* 168 DNA fragment (see legend to Fig. 1) the *lac p–o* 117 fragment[16,17] and DNA fragment designated S2. The sequence of these substrates is indicated in panel *c*. S2 is derived from the pLJ3 plasmid[16,17] by terminal labelling of the *Eco*RI digested plasmid followed by cleavage with *Hae*III. S2 is a DNA fragment approximately 350 nucelotides long. The sequence shown was determined by B. Royer-Pokora and R. Martin (unpublished observations).

For some potential dimer sites, the extent of dimer formation increased with increasing doses between 75 and 3,500 J m^{-2}. At doses greater than 3,500 J m^{-2}, a plateau level for the extent of dimer formation was reached at every potential dimer site. The per cent incision observed at the plateau level probably reflects the photo-steady state level that is governed by the relative rates of dimer formation and photoreversal.

Figure 2a also demonstrates that there are measurable differences in the extent of dimer formation at different sites. To investigate the effect of neighbouring sequences, the extent of dimer formation was determined for 38 different possible dimer sites at a dose of 7,500 J m^{-2}, at which a photo-steady state was reached. The results are presented in Fig. 2b.

The primary determinant of the extent of dimer formation at adjacent pyrimidines is the thymine content of the sequence. Less than 3% of the sequences that contain cytosines form dimers even at the highest doses of radiation. This low level may reflect both the slow forward rate of cytosine-cytosine dimer formation and the rapid reversal rate or photolysis of these dimers[20]. It is noteworthy that in these conditions the photosteady state level was reached when only a small fraction of the pyrimidines were dimerized. For example, thymine-cytosine dimers reached a steady state when 1 to 3% of the potential sites were dimerized. The actual value for dimer production is affected by the two nucleotides that flank the dimer with the extent of dimerization varying from 4% at the sequence ATTG to almost 9% at the sequence ATTA. There is no major effect of sequence composition other than that produced by the nucleotides that immediately flank the dimer.

For example, the extent of dimer formation in the underlined dimers is the same for the sequence TGGAA_TT_GTGAG (lac p–o 117, 61–72) and CCTATA_TT_GATTAA (S2, 11–24). Figure 2a also shows that the dose–response curves as well as the plateau levels are similar for identical sequences, regardless of their location within the DNA substrate.

The site of enzymatic cleavage

The electrophoretic mobilities of products resulting from endonuclease cleavage of UV-DNA were unexpected. Previous biochemical experiments indicated that the site of endonucleolytic breakage of UV-DNA places the photoproduct at the 5' end of the phosphodiester bond break[7,19]. According to Fig. 1, however, scission of the DNA at a pyrimidine dimer results in DNA fragments that had electrophoretic mobilities similar to those of DNA sequencing reactions in which a 3' pyrimidine would have been eliminated. The sequencing reactions with 5' end-labelled DNA fragments result in species that are phosphorylated at the 3' terminus[18,21]. Therefore, comparable mobility of the enzyme-treated DNA might imply that the endonuclease had cleaved the UV-DNA between the two thymines of a dimer. However, the cyclobutane bond of the dimer remains intact after incision of the DNA by the M. luteus enzyme[22]. It seemed unlikely that the enzymatic and chemical sequencing products were identical, even though they displayed similar electrophoretic mobilities.

One explanation for the anomalous mobility of the enzymatic cleavage products was that the 3' termini of these
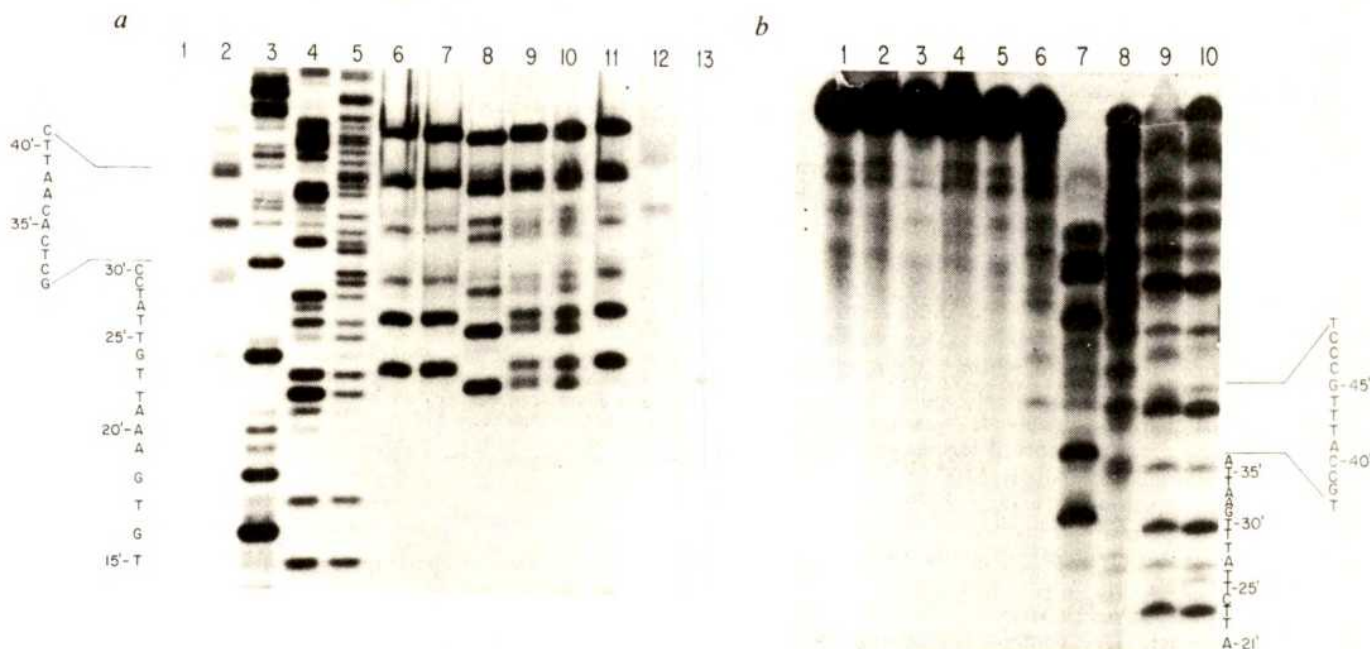

Fig. 3 Effect of alkaline hydrolysis on the electrophoretic mobility of 5' and 3' end-labelled DNA scission products. a, 5' End-labelled lac p–o 168 DNA was used for these experiments. Where indicated, DNA was irradiated with 480 J m^{-2} (UV-DNA). Lane 1, unirradiated DNA was heated in 0.1 M NaOH at 90 °C for 30 min (heat/alkali treatment) and layered on the gel in a buffer that contained 0.05 M NaOH 7 M urea. Lane 2, UV-DNA treated as in lane 1. Lanes 3, 4 and 5, unirradiated DNA treated with either dimethyl sulphate (DMS)[18] to generate cleavage at positions of G's and to a lesser extent at A's (lane 3), neocarzinostatin to produce cleavage at T's and to a lesser extent at positions of A's[21] (lane 4), and hydrazine[18] to cleave at positions of C's and T's (lane 5). Lanes 6–11 contain UV-DNA treated with 3 units of the Sephadex G-75 fraction of the M. luteus endonuclease as described in Fig. 1. The loading buffer was 0.01 M Na$_2$HPO$_4$, pH 7.0, 10% glycerol (lane 6) or 0.05 M NaOH, 7 M urea (lane 7). The DNA in lane 8 was heated in 0.1 M NaOH at 90 °C for 30 min before loading in a solution of 0.1 M NaOH, 10% glycerol. Lane 9 contains DNA products which were heated at 37 °C for 30 min in 0.1 M NaOH before loading in a solution of 0.1 M NaOH, 10% glycerol. Lane 10 contains DNA products heated at 90 °C for 30 min in 0.1 M Na$_2$HPO$_4$ pH 7.0 and loaded in that buffer plus 10% glycerol. Lane 11 contains the reaction products heated at 37 °C for 30 min in 0.01 M Na$_2$HPO$_4$ pH 7.0 and layered directly in a buffer that contained 0.01 M Na$_2$HPO$_4$ 10% glycerol. (Note that this lane demonstrates that cleavage of the phosphodiester bonds occurs in DNA treated with the Sephadex G-75 enzyme fractions alone. Heat or alkaline treatment of the product are not required for DNA breakage with this preparation.) Lane 12, UV-DNA treated in 0.01 M Na$_2$HPO$_4$ pH 7.0 at 90 °C for 30 min and loaded in 0.01 M Na$_2$HPO$_4$, 10% glycerol. Lane 13, unirradiated DNA incubated with the Sephadex G-75 fraction and loaded in a solution that contained 0.05 M NaOH, 7 M urea. Note that the 5' to 3' orientation of the DNA fragments on polyacrylamide gels of a and b are different due to labelling the fragments at the 5' or 3' ends. b, 3' End-labelled S2 DNA was used for this experiment. Unirradiated DNA was layered onto the gel without (lane 1) and with (lane 2) treatment at 90 °C for 30 min in 0.1 M NaOH (heat/alkali). Unirradiated DNA treated with 3 units of the Sephadex G-75 fraction of the M. luteus enzyme was also layered on the gel before (lane 3) and after (lane 4) the heat/alkali treatment. DNA irradiated with 7,500 J m^{-2} of UV light was layered onto the gel before (lane 5) and after (lane 6) heat/alkali treatment. UV-irradiated DNA (7,500 J m^{-2}) was treated with 3 units of the enzyme and layered directly onto the gel (lane 9) or after heat/alkali treatment (lane 10). Unirradiated DNA was treated with DMS (lane 7) or with neocarzinostatin (lane 8). All samples were loaded in 0.05 M Tris-HCl pH 7.5, 0.05 M boric acid, 0.001 M Na$_2$EDTA pH 8.3 and 7 M urea.

Table 1 Sodium borohydride reduction of apyrimidinic site produced by pyrimidine dimer DNA-glycosylase

Sample		Per cent breakage after treatment	
		−Alkaline hydrolysis	+Alkaline hydrolysis
Native DNA + PyDNG	Control	15	18
	NaBH₄ Reduced	15	15
Apurinic DNA	Control	25	90
	NaBH₄ Reduced	17	16
UV DNA	Control	18	22
	NaBH₄ Reduced	16	17
UV DNA + PyDNG	Control	29	86
	NaBH₄ Reduced	23	24

^{3}H-Labelled ΦX174 RFI DNA was either untreated, UV-irradiated at 30 J m^{-2} or made apurinic as described in the legend to Fig. 4. Assays contained 4.0 nmol of the appropriate DNA, and 14 units of the pyrmidine dimer DNA-glycosylase (PyDNG, the CM-cellulose fraction) in 400 μl of buffer A. Incubations were performed at 37 °C for 20 min and stopped by heating at 70 °C for 15 min. The pH was adjusted to 6.5 with 1 M acetic acid. 2 M K$_2$HPO$_4$ (pH 6.5) was added to 0.5 M. Samples were split into two equal portions and one was reduced with 0.3 M NaBH$_4$. Samples were then assayed for alkaline sensitive sites by treating with 2 ml of alkaline denaturation buffer for 5 min at room temperature or for 90 min at 37 °C. They were then neutralized with 0.4 ml of 2.0 M Tris-HCl (pH 4.0) and the conversion of RFI to RFII measured as described in Fig. 4. The numbers indicate the per cent of the substrate molecules that sustained at least one single-stranded break after the indicated treatments.

DNA fragments were neither phosphoryl groups, such as those produced in the DNA sequencing reactions, nor hydroxyl groups. An apyrimidinic deoxyribose at the 3′ terminus could result in the observed electrophoretic mobility of the cleavage product. To test the possibility that the cleavage product had a 3′-apyrimidinic terminus, a group sensitive to β-elimination conditions, UV-DNA was first incubated with the enzyme preparation and subsequently treated in 0.1 M NaOH at 90 °C for 30 min. The DNA was then analysed on polyacrylamide gels as before. Figure 3a demonstrates that the heat/alkali treatment alters the electrophoretic mobility of the cleavage products so that they migrate as if they were one nucleotide shorter (compare Fig. 3a, lanes 7 and 8). Identical results were also obtained when enzyme-treated DNA was heated with 0.5 M piperidine at 90 °C for 30 min (another agent that promotes β-elimination, data not shown). A mixture of both slow- and fast-migrating fragments was observed at each isolated thymine dimer sequence if less stringent post-enzyme hydrolysis conditions were used (37 °C in 0.1 M NaOH for 30 min) before suspension in loading buffer (Fig. 3a, lane 9). Both fragments were also obtained on heating of enzyme-treated DNA at neutral pH (Fig. 3a, lane 10), whereas incubation at 37 °C at neutral pH produced no shift in migration (Fig. 3a, lane 11). These experiments suggested that the 3′ terminus might be composed of an apyrimidinic site which would have been associated originally with the 5′ thymine moiety of the dimer.

Similar experiments were performed using DNA fragments labelled at the 3′ terminus. The electrophoretic mobility of these cleavage products was unaffected by the heat and alkaline hydrolysis conditions, which resulted in altered mobilities of the 5′ end-labelled DNA products (Fig. 3b). These experiments demonstrate that the 5′ terminus of the break does not have a structure that is labile to conditions that promote β-elimination. Furthermore, these experiments also show that the increased electrophoretic mobility of the 5′ end-labelled DNA upon alkaline hydrolysis is not an artefact of either UV radiation of DNA or of general β-elimination conditions.

Figure 3a (lane 2) shows that heavily irradiated DNA sustains damage that results in strand scission only upon treatment of the DNA with 0.1 M NaOH at 90 °C. The length

of these cleavage products suggests that such breaks occur predominantly at positions of cytosine and to a lesser extent at adenosine. The nature of these lesions is currently under investigation.

Purification of a pyrimidine dimer DNA-glycosylase

It had been previously reported that the *M. luteus* endonuclease cleaves DNA such that the pyrimidine dimer is at the 5′ terminus of a phosphodiester bond break generating 3′-hydroxyl and 5′-phosphoryl groups. Analysis of the electrophoretic mobilities before and after alkaline hydrolysis
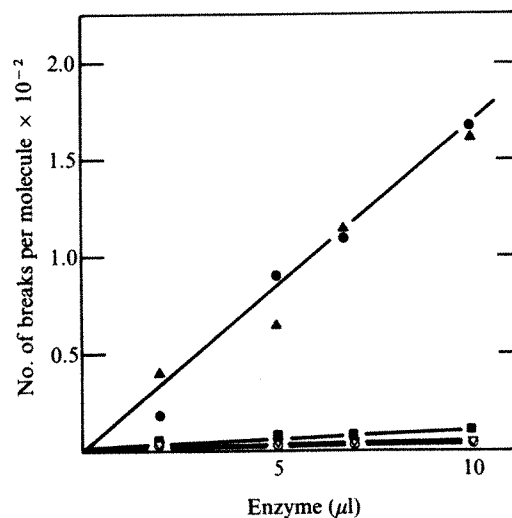

Fig. 4 Activity of pyrimidine dimer DNA-glycosylase for UV-irradiated DNA. The purification of the activity used in these experiments is given below. One unit is the amount of enzyme necessary to produce 1 break per nmol of UV-damaged ^{3}H-labelled-ΦX174 RFI DNA for 20 min at 37 °C in 100 μl of buffer A which is 0.05 M Na-HEPES (pH 7.6), 0.001 M Na$_2$EDTA, 0.005 M MgCl$_2$ when coupled to alkaline hydrolysis or addition of an excess of human AP endonucleases. Assay conditions for these activities are described below.

	Protein (mg ml^{-1})	Activity (Units ml × 10^{-3})	
		DNA-glycosylase	AP endo
Phosphocellulose	8	360	—
Sephadex G-75	0.05	46.4	3.1
Hydroxylapatite	0.002	13.9	0.53
CM-cellulose	—	17.0	0.18

	Specific activity (Units μg^{-1})		Ratio of DNA-glycosylase to AP endonuclease
	DNA-glycosylase	AP endo	
Phosphocellulose	45	—	—
Sephadex G-75	928	62	15
Hydroxylapatite	6,950	265	26
CM-cellulose	—	—	94

ΦX174 RFI DNA was: untreated; heated at 70 °C for 15 min in 0.1 M NaCl, 0.01 M Na acetate (pH 5.0) to make apurinic DNA^{34}; or UV-irradiated at a dose of 30 J m^{-2}. Assays containing 1.0 nmol of the appropriate DNA in 100 μl of buffer A with the indicated volume of enzyme were incubated for 20 min at 37 °C and stopped by the addition of 2.0 ml of alkaline denaturation buffer (0.1 M Na$_2$HPO$_4$, 0.3 M NaCl, 0.025 M Na$_2$EDTA, pH 11.7). After 5 min at room temperature, the samples were neutralized in 0.4 ml of 2 M Tris-HCl (pH 4.0). In these conditions RFII and linear molecules are irreversibly denatured while RFI renatures. The conversion of RFI to RFII is then measured by filtering through nitrocellulose filters (Schleicher and Schuell BA85) which bind the denatured single strands of RFII DNA^{7,19}. The numbers of breaks per molecule were calculated from the Poisson distribution $N = -\ln\alpha$, where α is the fraction of molecules with no breaks. △, Untreated DNA + DNA glycosylase + AP endonuclease; ○ apurinic DNA + DNA glycosylase; ■ UV-DNA + DNA glycosylase; ▲ UV-DNA + DNA glycosylase + AP endonuclease; ● UV-DNA + DNA glycosylase + alkaline hydrolysis (37 °C, 90 min in alkaline denaturation buffer).

suggested a different mechanism of enzymatic cleavage. The electrophoretic gel patterns of the cleavage products could be produced by cleavage of the N-glycosylic bond between the 5' pyrimidine moiety of the dimer and the corresponding deoxyribose, as well as cleavage of the phosphodiester bond 3' to the apyrimidinic sugar moiety. The dimer would still be located at the extreme 5' end of the broken chain in this suggested mechanism. Therefore, our data implied that two different enzymatic activities were involved in the strand scission event, a DNA-glycosylase and an apurinic/apyrimidinic (AP) endonuclease.

The possibility that the Sephadex G-75 fraction of the M. luteus enzyme used for these experiments contained an AP endonuclease activity was investigated using ΦX174 RFI (a double-stranded covalently closed circular DNA molecule) that contained apurinic sites as a substrate. The Sephadex G-75 fraction contained such an activity when judged by conversion of RFI to nicked cirular (RFII) and linear forms (see legend to Fig. 4). The Sephadex G-75 fraction was further purified to resolve the AP endonuclease from the DNA-glycosylase activity. Since treatment of UV irradiated DNA with enzyme fractions lacking the endogenous AP endonuclease would not result in direct breakage of phosphodiester bonds, DNA treated with the purified enzyme fractions was assayed for strand scission of ΦX174 UV irradiated RFI DNA by including an excess of the homogeneous AP endonuclease from human placenta[23]. Using this assay, an enzymatic activity was purified from the Sephadex G-75 fraction by sequential column chromatography on hydroxylapatite and CM-cellulose. The relative level of AP endonuclease activity was substantially diminished in the CM-cellulose fraction which contained as a major component the pyrimidine dimer DNA-glycosylase activity. (Py-DNG) (see legend to Fig. 4).

The CM-cellulose fraction exhibited an optimum activity for alkaline-dependent breakage of UV-irradiated DNA between pH 6.5 and 8.0 which was stimulated by the presence of 50 to 100 mM salt. The catalytic activity was seven times greater in the presence of $MgCl_2$ than in the presence of EDTA but was not stimulated by $CaCl_2$, $ZnCl_2$ or $MnCl_2$. The dimer DNA-glycosylase activity was unaffected by the presence of ATP in the range 0.2 to 5.0 mM and no detectable exonuclease or RNase activity could be demonstrated in this fraction. Previously, it had been reported[7,19] that the Sephadex G-75 fraction could be separated into two distinct 'UV endonucleases' by chromatography on DNA-cellulose. It has since been found that, during elution of the protein from a DNA-cellulose column, the DNA-glycosylase activity was preceded by a Mg^{2+}-dependent AP endonuclease and was followed by an AP endonuclease that was active in the absence of magnesium and in the presence of EDTA. In examining gross endonucleolytic activities specific for pyrimidine dimers, this phenomenon resulted in what appeared to be two chromatographically separable and unique 'UV endonucleases'[7].

To determine if the more highly purified activity recognized photodimers rather than other types of UV damage, DNA exposed to low doses of UV radiation was treated with the DNA-glycosylase in the presence of an excess of human AP endonuclease[23]. The number of DNA breaks was found to be directly proportional to the dose of UV light and hence to the number of dimers present. Pretreatment of the UV-irradiated DNA with photolyase purified from yeast and with long wavelength UV light, a treatment that specifically reverses pyrimidine dimers[24], produced DNA which no longer acted as a substrate for the enzyme. DNA irradiated with long-wavelength UV light in the presence of acetophenone, a photosensitizer that produces predominantly thymine dimers[25,26], was able to act as a substrate for the enzyme.

To determine the amount of phosphodiester bond cleavage of UV-irradiated DNA in the presence and absence of excess

AP endonuclease activity, UV-irradiated ΦX174 RFI was incubated with increasing concentrations of the DNA glycosylase. Figure 4 shows that the conversion of RFI to RFII and linear forms was much less in the absence of added AP endonuclease. The low but detectable level of strand scission still observed may be attributed to the low level of AP endonuclease still present in this preparation (legend to Fig. 4). Treatment of UV-irradiated RFI with the DNA-glycosylase modified the DNA such that it was converted to RFII and linear forms on alkaline hydrolysis (Fig. 4).

The above experiments suggested that the enzyme created an intermediate that contained an AP site. To test this possibility further, UV-irradiated DNA incubated with the CM-cellulose fraction was treated with sodium borohydride. Such treatment should reduce the potential aldehyde of the deoxyribose to the corresponding alcohol and thus stabilize the AP DNA to mild alkaline hydrolysis as was observed (Table 1). Reduction with sodium borohydride also stabilized[23] the UV-irradiated DNA that had been treated with the CM-cellulose enzyme (Table 1). Therefore, we conclude that treatment of UV-irradiated DNA with the CM-cellulose fraction creates an apyrimidinic site in the absence of phosphodiester bond hydrolysis.

Sites of DNA strand scission produced by the more purified CM-cellulose fraction were compared to those produced by the Sephadex G-75 fraction. 5' End-labelled UV-irradiated DNA was incubated with either enzyme fraction and then treated with 0.1 M NaOH for 30 min at 90 °C. In these
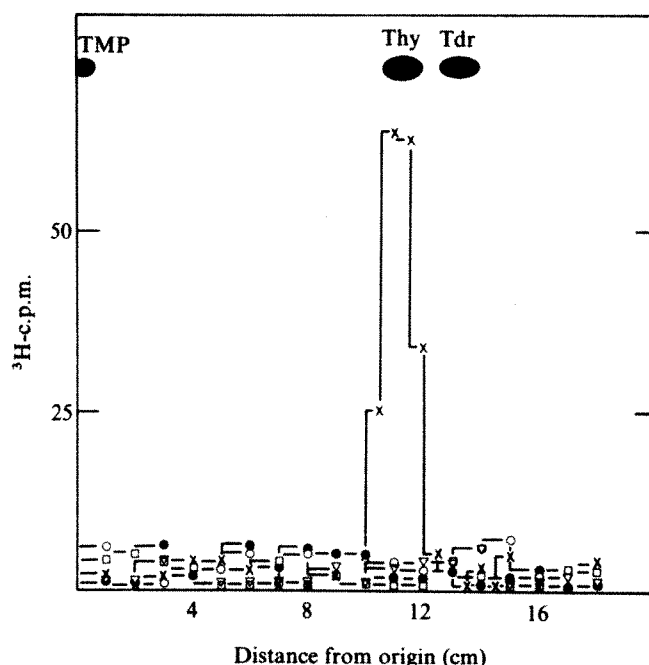

Fig. 5 Release of thymine by the pyrimidine dimer DNA-glycosylase and yeast photolyase. Assays containing 11 nmol of ³H-labelled ΦX174 RFI DNA (11,000 c.p.m. per nmole of nucleotide equivalent) that was either untreated or exposed to 600 J m⁻² of UV irradiation were incubated at 37 °C for 15 min in the presence of 400 units of the dimer DNA-glycosylase (hydroxylapatite fraction) in 500 μl of buffer A (see Fig. 4). Samples were adjusted to 6 mM Na₂EDTA, 10 mM mercaptoethanol, and 150 mM NaCl. 800 Units of photolyase were added and samples were incubated at 30 °C for 90 min in the presence of a black light. Samples were analysed for the release of ³H-thymine by diluting with 2 ml of H₂O and passing over a 0.5 ml QAE Sephadex (Cl) column equilibrated with H₂O, washed twice with 1 ml aliquots of 10 mM Na-HEPES, 2 mM Na₂EDTA buffer (pH 7.6). The flow through and washes were pooled and the samples were desalted over charcoal, analysed for thymine on PEI-cellulose plates in H₂O. This procedure separates thymine from thymidine, TMP, and thymine dimers. □, UV-DNA + photolyase + black light; ○, UV-DNA + DNA-glycosylase + black light; ▽, UV-DNA + DNA-glycosylase + photolyase; ×, UV-DNA + DNA-glycosylase + photolyase + black light; ●, untreated DNA + DNA-glycosylase + photolyase + black light.
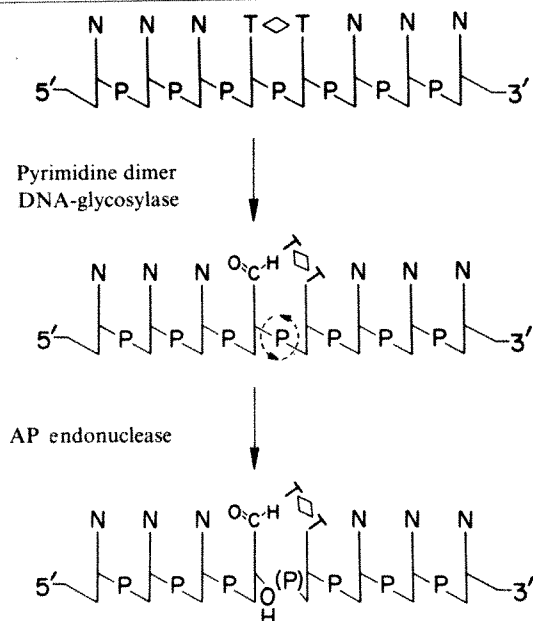
Fig. 6   A two-step model for incision at sites of pyrimidine dimers.

conditions, both enzyme preparations cleaved the irradiated DNA at the same sites and with the same relative frequency (data not shown).

The production of an AP site in UV-DNA treated with the dimer DNA-glycosylase proves that the enzyme cleaves an N-glycosylic bond. The electrophoretic mobility of the labelled cleavage products suggests that the bond broken is only that of the 5' pyrimidine moiety of the dimer. If this mechanism is correct, then the structure of the photoproduct should be that of a mixed thymine-thymidylate dimer that is still attached to the DNA. Photoreversal of such a structure should release free thymine. To test this possibility, UV-DNA that had been treated with the DNA-glycosylase was subsequently treated with yeast photolyase in the presence of visible light. Free thymine was released in the reactions that contained the yeast photolyase but only on exposure to visible light (Fig. 5). The amount of free thymine released by the enzymatic photolysis was approximately 70% of that expected if only one of the thymines of every dimer were released. Treatment of UV-DNA labelled with ^{3}H-thymine with the glycosylase alone did not release any labelled thymine. Had ^{3}H-thymine dimers been released, they would have remained at the origin in this chromatographic system. Similar results were obtained by UV photolysis with a second irradiation of the DNA-glycosylase treated DNA with 254-nm light (data not shown). Again, in these experiments thymine was only released from the UV-irradiated DNA by photoreversal after pre-treatment of the UV-irradiated DNA with the DNA-glycosylase. Moreover, thymine was not released from unirradiated DNA treated with the DNA-glycosylase followed by photoreversal. From these experiments we conclude that the CM-cellulose fraction contains an activity that cleaves the N-glycosylic bond between the 5' pyrimidine of the dimer and its sugar.

Discussion

The experiments presented here demonstrate that dimer formation is governed by (1) the number of adjacent thymines and (2) the nature of the nucleotides that flank the dimer. Thus the sequence of a potential target site can influence the frequency of mutation induced by UV light at the site.

The experiments also demonstrate that cleavage of the UV-irradiated DNA with the *M. luteus* enzyme occurs at the site of the dimer itself rather than 5' to the dimer as proposed

previously. As a result, it has been possible to purify a 'pyrimidine dimer DNA-glycosylase' activity from the *M. luteus* UV endonuclease preparation. This activity creates an AP site in the UV-irradiated DNA but does not rupture the phosphodiester backbone. After treatment of UV-DNA with the pyrimidine dimer DNA-glycosylase, free thymine can be released from UV-irradiated DNA upon photoreversal of the mixed thymine thymidylate dimer with either yeast photolyase or photolysis. Based on this evidence, we propose that the cleavage activity of UV-irradiated DNA observed in the less purified Sephadex G-75 fraction of the *M. luteus* endonuclease fraction occurs via the combined action of two enzymatic activities as shown in Fig. 6. The pyrimidine dimer DNA-glycosylase breaks the N-glycosylic bond between the 5' pyrimidine of the dimer and the corresponding sugar. The resulting AP site is then cleaved by an AP endonuclease. The selective loss of the AP endonuclease activity of the *M. luteus* enzyme relative to that of the pyrimidine dimer DNA-glycosylase on purification suggests that the two activities may be separable.

Inherently, cleavage by a DNA-glycosylase at a pyrimidine dimer requires an additional catalytic step to produce strand scission which presumably is directed by an AP endonuclease. Analysis of the mobility of the cleavage products on high resolution polyacrylamide gels suggest that *M. luteus* contains an endonuclease which acts 3' to the AP site generated by the pyrimidine dimer DNA-glycosylase. We infer that the product of cleavage by the *M. luteus* endonuclease (G-75 fraction) is a 3' AP site and a 5' thymine-thymidylate dimer, since a change in mobility of the incised fragments in β-eliminating conditions was only observed after cleavage of the 5' end-labelled and not the 3' end-labelled fragments.

The removal of the site of UV damage by excision processes in *M. luteus* must be bidirectional, both to remove a 3' sugar to provide a 3'-hydroxyl site for DNA polymerization and to excise the dimer allowing reinsertion to occur. It is of interest to note that those exonuclease activities which have been implicated in the excision process share bidirectional exonucleolytic capabilities. DNA polymerase I of *M. luteus* and *E. coli*[3,28], the *M. luteus* UV exonuclease[29], and the *E. coli* exonuclease VII[30], are able to initiate hydrolysis at both the 3' and 5' termini. As a consequence of this dual capability, excision is potentially a two-step process. Cleavage at AP sites may occur either 3' to the sugar as shown here, or 5' to the sugar as the result of cleavage by 5'-AP endonucleases. If cleavage occurs 5' to the sugar, then only a 5' unidirectional excision process is required for damaged nucleotide removal. It is apparent, therefore, that control of AP site incision may have a pivotal role in determining the enzymatic pathway of excision repair.

1. Hanawalt, P. C. *Genetics* **79**, 179–197 (1975).
2. Grossman, L., Braun, A., Feldberg, R. & Mahler, I. *A. Rev. Biochem.* **44**, 19–43 (1975).
3. Hamilton, L. D. G., Mahler, I. & Grossman, L. *Biochemistry* **13**, 1886–1896 (1974).
4. Braun, A. G., Radman, M. & Grossman, L. *Biochemistry* **15**, 4006–4120 (1976).
5. Yasuda, S. & Sekiguchi, M. *Proc. natn. Acad. Sci. U.S.A.* **67**, 1839–1845 (1970).
6. Friedberg, E. & King, J. J. *Bact.* **106**, 500–507 (1971).
7. Riazuddin, S. & Grossman, L. *J. biol. Chem.* **252**, 6280–6286 (1977).
8. Deering, R. A. & Hense, D. S. *J. Bact.* **121**, 1211–1213 (1975).
9. Van Lancker, J. A. & Tomura, T. *Biochim. biophys. Acta* **353**, 99–114 (1974).
10. Waldstein, E. A., Peller S. & Setlow, R. B. *Proc. natn. Acad. Sci. U.S.A.* **76**, 3746–3751 (1979).
11. Kushner, S. R., Kaplan, J. C., Ono, H. L. & Grossman, L. *Biochemistry* **10**, 3325–3334 (1971).

12. Brunk, C. F. *Nature new Biol.* **241**, 74–76 (1973).
13. Birnboim, H. C. *Photochem. Photobiol.* **22**, 71–73 (1975).
14. Setlow, R. B. & Carrier, W. L. *J. molec. Biol.* **17**, 237–254 (1966).
15. DeBoer, G., Pearson, M. L. & Johns, H. E. *J. molec. Biol.* **27**, 131–144 (1967).
16. Haseltine, W. A., Lindan, C., D'Andrea, A. & Johnsrud, L. *Meth. Enzym.* **65**, 235–248 (1980).
17. Johnsrud, L. *Proc. natn. Acad. Sci. U.S.A.* **75**, 5314–5318 (1978).
18. Maxam, A. & Gilbert, W. *Proc. natn. Acad. Sci.* **74**, 560–564 (1977).
19. Riazuddin, S. & Grossman, L. *J. biol. Chem.* **252**, 6287–6293 (1977).
20. Wang, S. Y. in *Photochemistry and Photobiology of Nucleic Acids, Pyrimidine Biomolecular Products,* 296–356 (Academic, New York, 1976).
21. D'Andrea, A. D. & Haseltine, W. A. *Proc. natn. Acad. Sci. U.S.A.* **75**, 3608–3612 (1978).
22. Carrier, W. L. & Setlow, R. B. *J. Bact.* **102**, 178–186 (1970).
23. Shaper, N. L. & Grossman, L. *Meth. Enzym.* **65**, 216–224 (1980).
24. Herriott, R. M. *Analyt. Biochem.* **95**, 77–81 (1979).
25. Rahn, R. O., Setlow, J. K. & Landry, L. C. *Photochem. Photobiol.* **18**, 39–41 (1973).
26. Lamola, A. A. *Photochem. Photobiol.* **9**, 291 (1969).
27. Kotchetkov, N. K. & Budovskii, E. I. *Organic Chemistry of Nucleic Acids,* 542–612 (Plenum, New York, 1972).
28. Kelly, R. B., Cozzarelli, L. R., Deutscher, M. P., Lehman, I. R. & Kornberg, A. *J. biol. Chem.* **245**, 39–45 (1970).
29. Kaplan, J. C., Kushner S. R. & Grossman, L. *Biochemistry* **10**, 3315–3324 (1971).
30. Chase, J. & Richardson, C. C. *J. biol. Chem.* **249**, 4553–4561 (1974).
31. Grossman, L., Riazzudin, S., Haseltine, W. A. & Lindan, C. P. *Cold Spring Harb. Symp. quant. Biol.* **43**, 947–955 (1978).
32. Birkner, K. L. & Folk, W. R. *J. biol. Chem.* **252**, 3176–3184 (1977).
33. Jacobsen, H., Klenow, H. & Overgaard-Hansen, F. *Eur. J. Biochem.* **45**, 623–627 (1974).
34. Lindahl, T. & Anderson, A. *Biochemistry* **11**, 3618–3622 (1972).

LETTERS

The triple QSO PG1115+08: another probable gravitational lens

Ray J. Weymann*, David Latham†, J. Roger P. Angel*, Richard F. Green*, James W. Liebert*, David A. Turnshek*, Diane E. Turnshek* & J. Anthony Tyson‡

*Steward Observatory, University of Arizona, Tucson, Arizona 85721
†Smithsonian Astrophysical Observatory, Cambridge, Massachusetts 02138
‡Bell Telephone Laboratories, Murray Hill, New Jersey 07974

Recently, Walsh, Carswell and Weymann[1] reported the discovery of two objects (0957+56A,B) with identical spectra and separated by 6 arc min. They suggested that a gravitational lens was responsible. The cumulative result of subsequent work on this object (see refs 2–9) corroborates this interpretation. The example of 0957+56A,B and the data presented here suggest a similar phenomenon is involved in the case of PG1115+08.

PG1115+08 was selected on the basis of its UV excess and identified spectroscopically as a QSO in survey work by Green and Schmidt (see ref. 10). It has a visual magnitude of 15.8 and an emission redshift of 1.722. Its 1950 coordinates are RA = 11 h 15 min 41.5 s and dec = +08° 02' 24". A finding chart is published by Green *et al.*[11] who report on IUE spectra showing a featureless continuum extending down to a rest wavelength of 432 Å.

In the course of an image tube spectroscopic survey at high resolution of some of the PG objects now underway at Steward Observatory by three of us (R.F.G., D.A.T. and R.J.W.), PG1115+08 was observed. The spectrum shows C IV and N V absorption at a redshift of 1.7309, slightly redward of the emission lines. Also present in absorption is a possible triplet at wavelengths of 3,923.2, 3,929.4 and 3,935.2 Å. This can be interpreted as overlapping C IV doublets at redshifts of 1.5339 and 1.5378; however, the blue member is not definitely present. Additional absorption lines occur at wavelengths of 3,968.9 Å and 4,338.4 Å. The former is possibly due to galactic H at 3,968.5 Å and the latter is unidentified. If the H line is present, the K line at 3,933.6 Å might be confusing our interpretation of the absorption 'triplet'. Although the image appears stellar on the POSS plates, observation of the object with the TV guiding monitor during a brief period of good seeing revealed two other stellar objects about 2.5 mag fainter within 3 arc s of the QSO itself.

Our next opportunity of good seeing and transparency was on 12 and 16 May, during the first trial of the MMT spectrograph. We were able to obtain spectra of the more distant of the two companions (denoted 'C') as well as the bright QSO itself (denoted 'A'). Data on the nearer companion ('B') was obtained at the Steward Observatory's 2.3-m telescope on 16 May. Figure 1 shows a polaroid print of the 2.3-m television monitor with the bright object A placed in the 2.5 arc s round aperture. Figure 2*a,*

b show the MMT spectra of C and A, along with the divided spectra, C/A. Figure 3 shows the corresponding data for objects A and B taken with the 2.3-m telescope. The relevant data are summarized in Table 1.

These figures and Table 1 show that to within the accuracy of the data all three spectra are identical.

However, there is a significant observational difference between 0957+56A,B and PG1115+08A,B,C: the much closer separation of the objects in PG1115+08 and the large flux ratio of A/C and A/B make the question of contamination of the spectra of C and especially B by A serious. We attempted to deal with this problem during the observations by making separate observations of blank sky with A located symmetrically opposite the slit with respect to its location during the B and C observations. The contamination is variable due to variations in the image quality. The last column of Table 1 estimates the fraction of the signal measured for B and C due to contamination by A, based on the blank sky measures. For the 2.3-m observations, the amount of scattered light was found to be direction- and colour-dependent, which produced the non-zero slope in the divided spectrum B/A as shown in Fig. 3. Observations of a
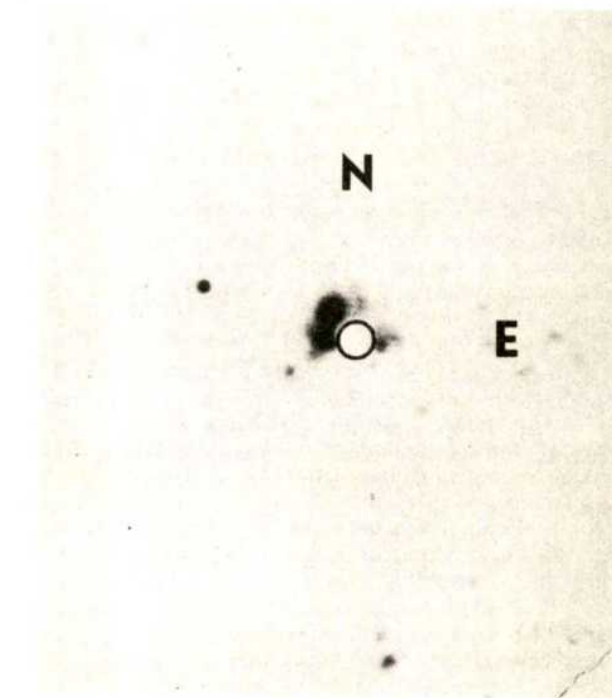

Fig. 1 Reproduction of a Polaroid photograph of the 2.3-m TV guiding screen. The brighter of the three objects, PG1115+08A was placed in the 2.5 arc s aperture (○) and the other two images, B and C, are readily visible to the west and north-west outside the aperture.
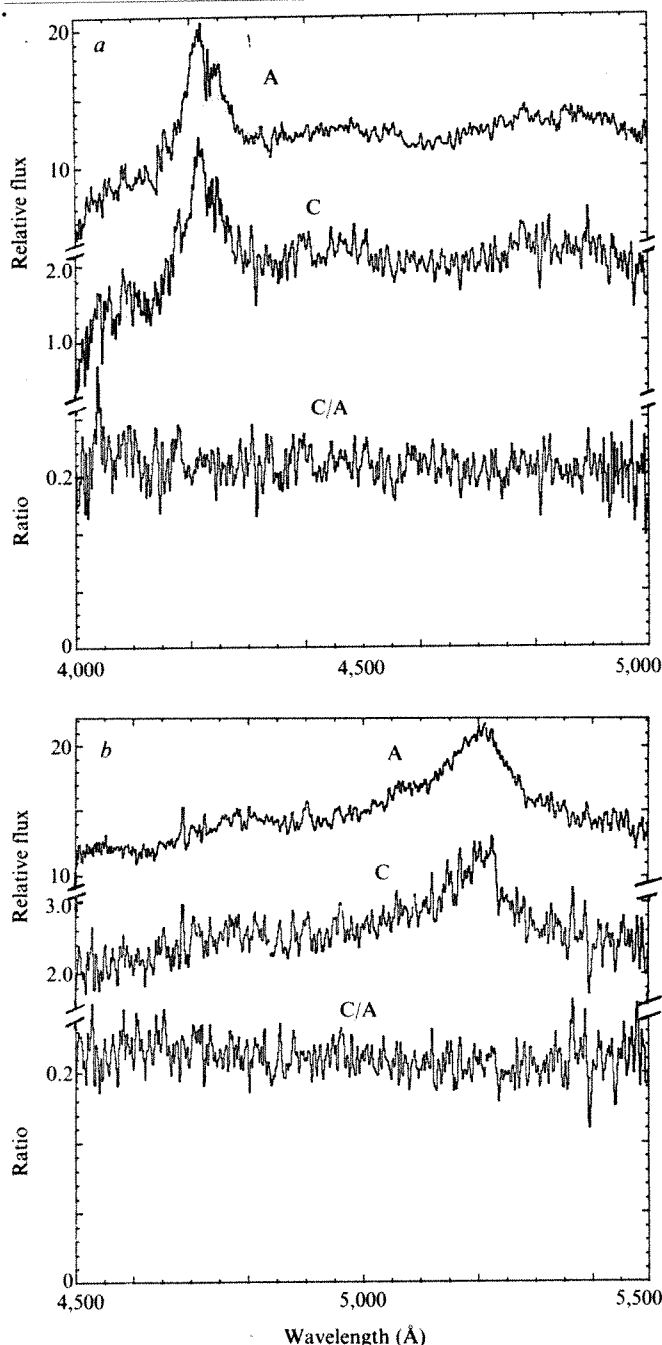
Fig. 2 Spectra of PG1115 + 08A and C obtained with the MMT spectrograph/intensified Reticon system. The C IV absorption features mentioned in the text are visible in both A and C just to the red of the C IV emission peak. C/A represents the result of dividing C by A.

Table 1 Spectroscopic data for PG1115 + 08

Telescope	Object	C IV λ1,549 Observed EW(Å)	C IV λ1,549 λ_OBS(Å)	C III] λ1,909 Observed EW(Å)	C III] λ1,909 λ_OBS(Å)	Contamination*
MMT†	A	60 ± 6	4,225 ± 5	72 ± 6	5,210 ± 5	
MMT†	C	‡	4,225 ± 5	‡	5,202 ± 10	0.10 ± 0.10
2.3 m§	A	—	—	67 ± 10	5,205 ± 10	
2.3 m	B	—	—	‡	5,200 ± 10	0.35 ± 0.10

* The contamination is the estimate of the fraction of the signal at B or C due to scattered light from A.

† The MMT spectrograph used a 3.0 by 1.5 arc min rectangular slit; the spectral resolution was 3 Å FWHM.

‡ Equivalent widths in B, C are estimated to be equal to those in A to within 10% on the basis of the divided spectra B/A, C/A.

§The 2.3 m spectrograph used a 2.5 arc s round aperture; the spectral resolution was ∼ 10 Å.

Note that error estimates are subjective estimates of probable errors.

(Table 1) show that the contamination from A is probably not more than 10% and certainly not more than 20%. For object B the blank sky measures show that ∼35% of the red light is contributed by scattering, and when corrected for colour dependence, the same ratio applies to the region of C III] emission. The possibility of B being intrinsically much redder than A and hence implying a large fraction of the signal at C III] arising from scattering seems excluded by visual observation with the TV monitor: the flux ratio of the three components seems identical through both the unfiltered camera and through an intermediate bandpass filter centred on the C III] emission line.

The data are inconsistent with B, and especially C not having significant C IV and C III] emission with wavelengths identical to A and probably identical equivalent widths as well. We thus
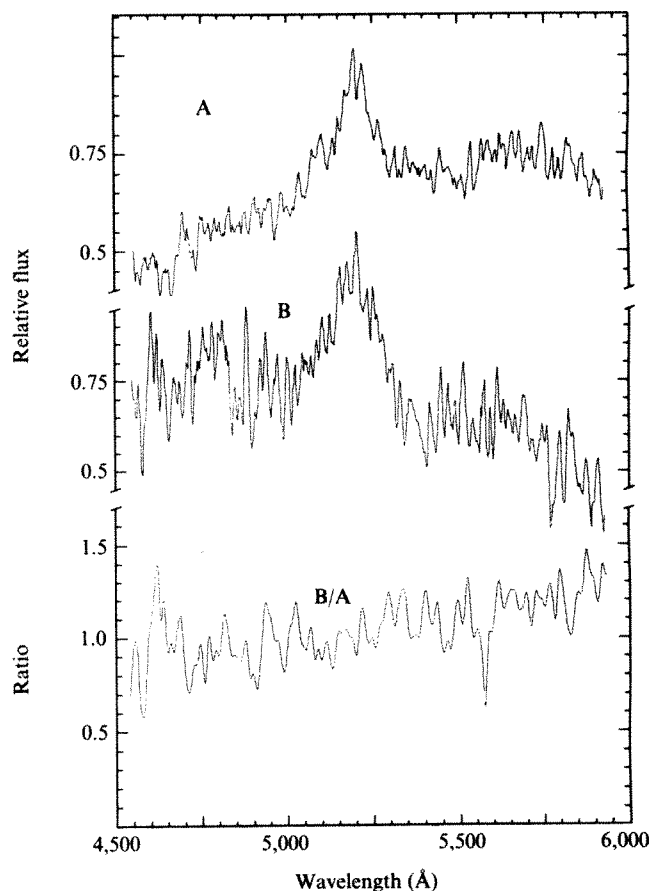
nearby star with colours similar to the QSO provide a basis for correcting the colour of the scattered light from the blank sky measurements and also indicate that instrumental effect rather than atmospheric dispersion is the main factor in this dependence. After making this correction, the ratio B/A becomes flat to within the uncertainty.

From the divided spectra shown in Figs 2 and 3 we estimate that the difference in equivalent width of the C III] and C IV emission lines between the signal in either aperture B or C and A is < 10%. This fact implies that the spectra of B and C are the same as A in the region of the emission lines to within an error of $10 (1 + S/F)\%$, where S is the scattered flux from A and F is the flux from B or C. Only if 90% or more of the flux of observations B and C were scattered from A would the data be consistent with B and C not having emission lines at the same wavelengths as the C III] and C IV emission lines in A. For C the blank sky measures

Fig. 3 Spectra of PG1115 + 08A and B obtained with the Steward Observatory 2.3-m telescope and Reticon spectrograph. As described in the text, colour-dependent scattering of A into the aperture during the B observation causes the divided spectra B/A not to be flat.

Fig. 4 A 20-min exposure of PG1115 + 08 with the Bell Labs CCD camera on the 2.3-m telescope, with seeing 2.5 arc s. The brightest of the QSO triplet, object A, has been subtracted, leaving B and C to the west and northwest and the object S 23 arc s to the south. In spite of the relatively poor seeing, relative fluxes of the three objects may be obtained by subtraction of comparison star profiles.
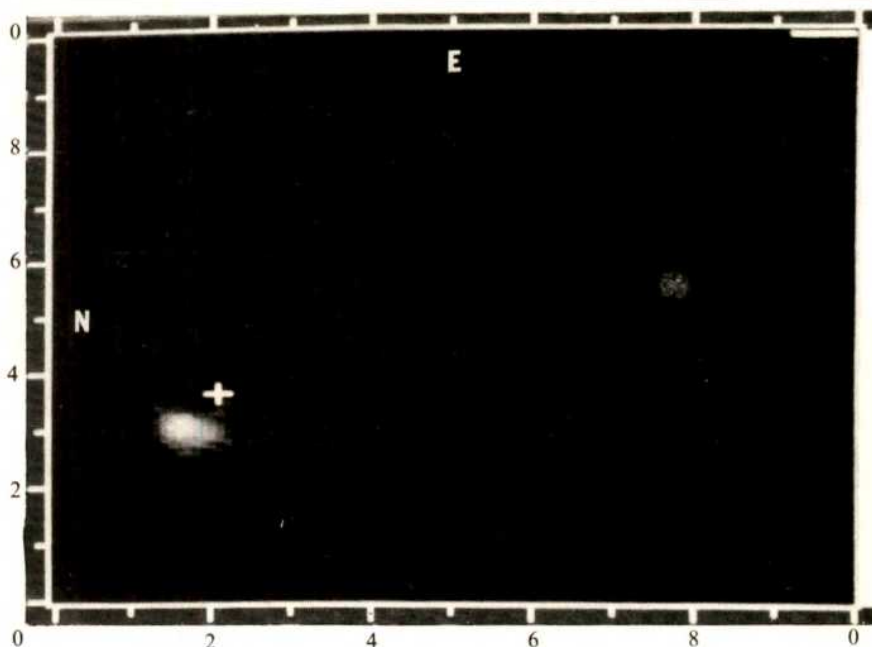
infer that PG1115 + 08 is another example of a gravitational lens.

Direct deep images of this field are of obvious interest. A CCD camera developed by one of us (J.A.T.) was attached to the 2.3-m telescope to image a 30 by 40 arc min field. The average seeing during the 20-min exposure was ~2.5 arc s. Figure 4 shows the result of the processed image in which the bright component A has been subtracted. This was done by combining images of nearby stars before and after the QSO exposures, scaling, moving recursively nearer the peak of the triple QSO image and subtracting. Taking A + B + C = 15.8 mag (ref. 11), we find B + C = 18.1 mag. The object denoted 'S' is 23 arc s to the south of the triple QSO and has a CCD magnitude about 19. Table 2 summarizes relevant data on these four images.

A second major difference between 0957 + 56A,B and PG1115 + 08A,B,C concerns the geometry of the images. There are three distinct (apparently stellar) objects readily visible and separated from each other by comparable distances. Young *et al.*[4] and Bourassa and Kantowski[12] have shown that a rich variety of image displacements and brightness ratios are possible when there is more than one mass concentration responsible for the deflection and when realistic density distributions of matter in the deflector are taken into account. We think it premature to speculate on what combination of parameters would produce the observed image configuration until better direct images are available. We note, however, that PG1115 + 08 is among the most luminous QSOs and it is possible that its flux has been enhanced by the lens. Note also that the radiation from A does not pass through any clouds that are optically thick in the Lyman continuum.

Finally, we note with regret that PG1115 + 08 is not detectable to the 1.5-mJ flux level with VLA (see ref. 13) and hence this tool is not readily available to help in the interpretation of this fascinating object.

We thank T. Bauer, J. Geary, R. Hilliard, C. Hughes, S. Mileski, R. Miller, D. Mitchell, J. T. Williams, W. Wyatt and R. Young for exceptional efforts in completing the MMT spectrograph and detector system in time for our run and M.

Chabin and C. Heller for their assistance at the 2.3-m telescope. We also thank the MMT telescope operators P. Evans, W. Kindred and W. Light for making the MMT observations possible. J.R.P.A. and R.J.W. acknowledge support from the NSF. Part of the research reported here used the Multiple Mirror Telescope Observatory, a joint facility of the University of Arizona and the Smithsonian Institution. J.A.T. thanks R. Lee for help with the CCD software.

1. Walsh, D., Carswell, R. F. & Weymann, R. J. *Nature* **279**, 381 (1979).
2. Weymann, R. J. *et al. Astrophys. J. Lett.* **233**, L43 (1980).
3. Wills, B. & Wills, D. *Astrophys. J.* (in the press).
4. Young, P., Gunn, J. E., Christian, J., Oke, J. B. & Westphal, J. A. *Astrophys. J.* (in the press).
5. Stockton, A. (in preparation).
6. Soifer, B. T. *et al. Nature* **285**, 91 (1980).
7. Lebofsky, M., Rieke, G. H., Weymann, R. & Walsh, D. *Nature* **285**, 385–388 (1980).
8. Greenfield, E. P., Roberts, D. H. & Burke, B. F. *Science* **208**, 495 (1980).
9. Porcas, R. W., Booth, R. S., Browne, I. W. A., Walsh, D. & Wilkinson, P. N. *Nature* **282**, 385 (1980).
10. Green, R. F. *Publ. A.S.P.* **88**, 665 (1980).
11. Green, R.F. *et al. Astrophys. J.* (in the press).
12. Bourassa, R. & Kantowski, R. *Astrophys. J.* **195**, 13 (1975).
13. Shaffer, D. B., Green, R. F. & Schmidt, M. (in preparation).

Giant shells around normal elliptical galaxies

David F. Malin & David Carter

Anglo-Australian Observatory, Box 296, Epping, New South Wales 2121, Australia

Photographic enhancement of deep IIIaJ and IIIaF plates taken with the UK Schmidt and Anglo-Australian telescopes reveals the existence of giant ellipsoidal shells within and around the envelopes of several normal elliptical galaxies. The dimensions of these features are vast; they occur at radii of up to 180 kpc (assuming $H_0 = 50 \, km \, s^{-1} \, Mpc^{-1}$). We report here that these features probably consist of stars and are either the result of a burst of star formation initiated by a powerful shock wave in an intergalactic medium, perhaps during the formation of the galaxies, or are old stars displaced from the nucleus by an explosive event.

The existence of very low surface brightness shells or loops around some peculiar elliptical galaxies has been reported for M89 (ref. 1), and for NGC1316 (ref. 2). We have examined apparently normal elliptical galaxies for similar features at extremely low surface brightnesses. High contrast positives of
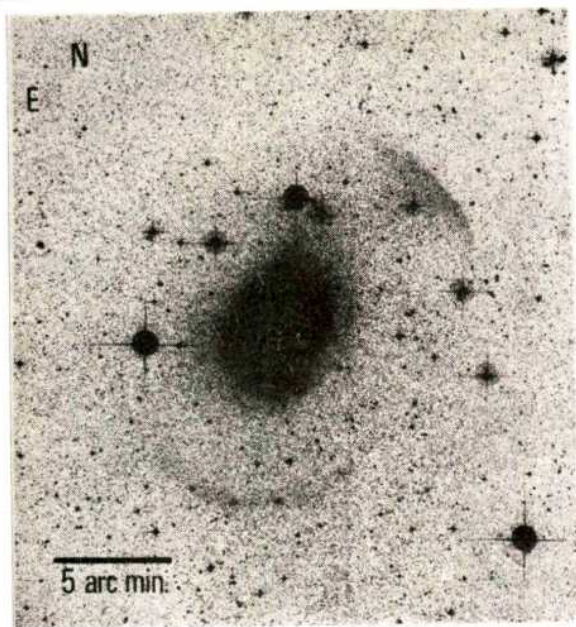
Table 2 Image properties of PG1115 + 08A, B, C

Object	Visual Magnitude	Position angle (deg)	Separation from A (arc s)
A	15.9	—	—
B	19:	270	2.1
C	18.6	320	2.7
S	19:	161	23.0

Fig. 1 Outer shells associated with NGC1344. Print made from UK Schmidt IIIaJ plate.

UK Schmidt plates were made using a contact copying process[3], and low contrast features within the envelopes of the galaxies were brought out using an unsharp masking technique[4]. We found that a surprisingly high proportion of normal ellipticals showed well defined shells, or fragments of shells, at a wide range of distances from the centre of the galaxy. The shells were most clearly visible on derivatives of IIIaJ plates, which is probably an indication of the fainter limiting magnitude of this emulsion rather than of any intrinsic blueness of the shells. Shells have not previously been revealed by digital surface photometry (refs 5–8 and refs therein) owing largely to the small areas processed in these digital studies and the large angular size of the shells.

The original plates were closely examined for ghost images or internal reflections from bright stars diametrically opposite the program galaxies which might produce spurious images. None were found. Our photographic techniques have been shown[1] to be free from distracting artefacts. In one case the same shells were seen on both blue and red plates taken on different field centres. We conclude, therefore, that the features are real.

Forty-three isolated elliptical galaxies south of −18°, brighter than apparent magnitude 13 were selected from the Second Reference Catalogue[10]. Of this sample we examined high contrast derivatives of 12, the sole selection criterion being the ready availability of plate material from the UK Schmidt telescope. Internal or external concentric shells were found around NGC1344, NGC1395 and NGC3923 and a similar feature was seen near IC4797 but not concentric with the main body of the galaxy. A series of shells has also been noted around an SO galaxy found on direct 3.9 m AAT plates taken for another purpose. This uncatalogued object is at RA 01 h 33 min 59.0 s, dec. −12° 53″03′ (1950).

The most spectacular features we have found occur around the isolated elliptical galaxies NGC1344 and NGC3923, shown in Figs 1–3. A high contrast derivative of NGC1344 (Fig. 1) shows two sharp fragments of a large shell at a radius of 9 arc min (∼56 kpc assuming $H_0 = 50 \, \text{km s}^{-1} \, \text{Mpc}^{-1}$) from the centre of the galaxy. On the southern and western sides of the main image fragments of an inner shell (radius 2 arc min) can be seen, although this is not as well defined as the outer shell. We estimate the surface brightness of these outer shells to be about 27 mag arc s^{-2}, based on the appearance of the jet in M89 which has been found to have a surface brightness of

26.9 mag arc s^{-2} (Elliott and D.F.M., unpublished). Both features are just visible on examination of the original deep IIIaJ plates.

A similar print of NGC3923 shows a fragment of a giant shell in the north-east quadrant at a radius of 20 arc min (∼180 kpc assuming $H_0 = 50 \, \text{km s}^{-1} \, \text{Mpc}^{-1}$) and a suggestion of another fragment of the same shell in the south-west quadrant (along the major axis). Figure 2, a masked high contrast print of the inner regions of NGC3923, shows three additional distinct inner shells, lying within the envelope of the galaxy at radii of 2.2, 3.3 and 5.9 arc min. All shells are more prominent on the north or north-east sides of the galaxy and, in common with NGC1344, lie largely on the major axis. Figure 3 shows the positions of all four shells associated with this galaxy.

The shell-type galaxy found on the AAT plates is a lenticular or possibly an Sa galaxy with a high bulge-to-disk ratio, seen very nearly edge on. The major axis diameter is some 12 arc s. Two fragments of a faint shell are just visible on a normal copy, and clearly visible on a high contrast derivative; they are at a radius of ∼25 arc s and lie near the apparent minor axis of the main body of the galaxy. On the high contrast derivatives an even fainter shell feature is visible; it lies at a radius of 54 arc s and near the minor axis of the galaxy.

In view of the extremely low contrast and surface brightness of the shells, their interpretation presents some difficulties, particularly in the absence of spectral data. We must consider the possibility that the faint shells result from reflection nebulosity, caused by dust shells. Sandage[9] gives the surface brightness (SB) of a dust reflection nebula illuminated by a galaxy as

$$SB = m - 2.5 \log \left[\alpha \tau / 4\pi Q (206265)^2 \right] \, \text{mag arc s}^{-2}$$

where m is the apparent magnitude of the galaxy as seen from the reflection nebula; α is the albedo of the grains, Q is the 'efficiency factor' of the grains and τ is the optical depth of the nebula. The NGC1344 outer shell is at a radius of 540 arc s; the apparent magnitude of NGC1344 is $B_t = 11.25$ (ref. 10): this gives $m = -1.66$. To cause a reflection nebula of surface brightness 27 mag arc s^{-2} we would need $\alpha\tau/Q \simeq 1.85$. Sandage adopts $\alpha = 0.5$; $Q = 2$ for high latitude reflection nebulosity around our galaxy. If the scattering material around elliptical galaxies were assumed similar these values would imply $\tau \simeq 7.4$.
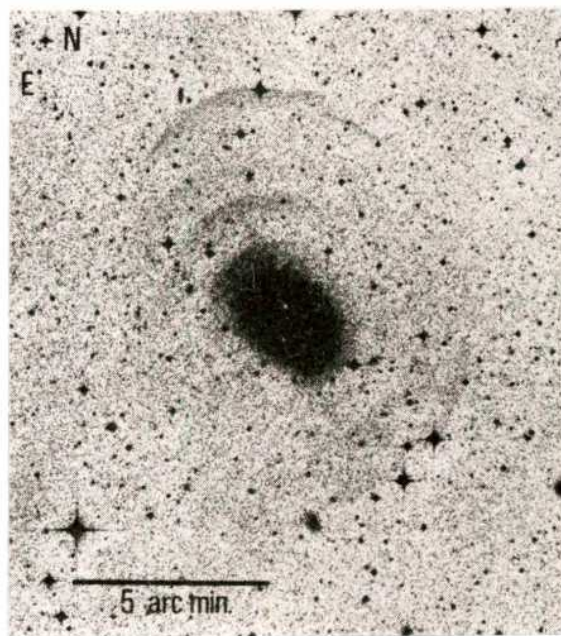

Fig. 2 Inner shells of NGC3923 print made by masking/high contrast technique from UK Schmidt IIIaJ plate.
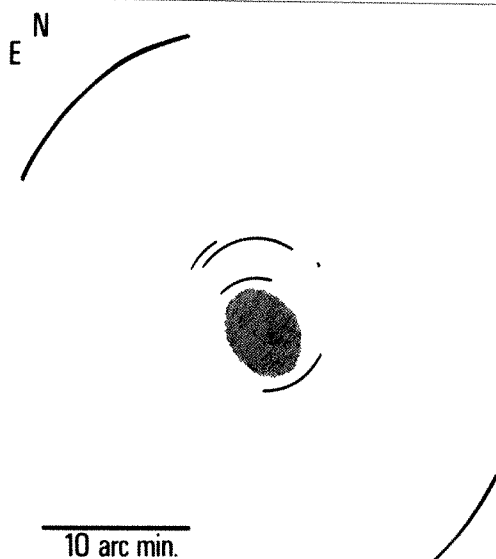
Fig. 3 Combined data from two derivatives of UK Schmidt plate of NGC3923 showing location of inner and outer shells.

We estimate a lower limit for the surface brightness of the outer (20 arc min) shell around NGC3923 to be 30 mag arc s^{-2}; this would imply $\alpha\tau/Q=0.5$, $\tau\simeq2$. Normal colours of these ellipticals rule out this kind of optical depth in a dust shell; but there remains the remote possibility that we are seeing reflection from a thick dust ring, which somehow contrives to resemble a thin shell. The efficiency of scattering by dust varies as λ^{-1} at optical wavelengths[11]; therefore, one would not expect bright reflection nebulosity around a source whose light is dominated by K and M stars.

Reproductions of IIIaJ and IIIaF pairs show that the colours of the features are not much different from those of the envelopes of the galaxies. Although we cannot eliminate the possibility that they consist of emission line nebulosity the simplest interpretation is that they are stars. Although the features give the impression of being shells seen in projection we must also consider the possibility that they are weak large-scale arms—features in a plane. We believe this unlikely in NGC1344, 1395, 3923 and M89. The features around IC4797 appear more like arms, and could be tidal in origin, as there is an apparently close, disturbed, companion.

If, as seems the simplest interpretation, the features are shells of stars, then the next consideration is whether they were formed in their present location or displaced by some explosive event from the inner regions of the galaxy. It is probably significant that most examples of this phenomenon occur in isolated galaxies. The crossing time of a galaxy in a rich cluster is of the order of 10^9 yr. It would seem inevitable that a single passage through the core of a rich cluster would disrupt the observed structure. Thus the absence of such structures in rich clusters implies an age greater than 10^9 yr for the shells. Assuming a mass of $10^{12} M_\odot$ for NGC3923 the free fall time of the shell or ring at 180-kpc radius is 2.3×10^9 yr. This would seem to set a lower limit on the survival time of such a structure in the absence of interactions with other galaxies, and is short enough to dismiss the possibility that the shells consist of infalling primordial material.

If the shells were formed in situ some violent shock must have triggered a burst of star formation in an intergalactic medium which is not, or was not, as tenuous as we believe the intergalactic medium to be. Large scale shocks could be caused either by collapse, or by an explosive event in the nucleus of the galaxy. Russian cosmologists (see refs 12–14) have discussed the possibility of galaxy formation through adiabatic instabilities in the early Universe. Large scale shocks are a natural consequence of this hypothesis, but it is unclear what the present appearance of the remnants of such shocks

would be. However, if these shells are such remnants then the shocks must have contrived to place stars in stable and fairly eccentric orbits, which give rise to a surprisingly thin shell. Others (see refs 15–17) have discussed a theory of galaxy formation in which ellipticals form from mergers of spirals. M89, NGC1344 and NGC3923 exhibit no peculiarities in their colours which would lead one to suspect that they have formed from mergers of blue galaxies. Colours are not available for NGC1395. Additionally the galaxies display no irregularities in their nuclei which could be taken as an indication of cannibalism[18].

We are left with the possibility that shocks, perhaps caused by an explosive event in the nucleus, formed the outer expanding shells, and that successive eruptions formed the inner structures. It is likely that the shells have existed for a substantial part of the life of the galaxy. This is supported by the fact that, apart from M89, none of the four galaxies mentioned above have active nuclei to the detection limit (12 mJy) of the 5 GHz survey of Disney and Wall[19]. M89, which is a compact, variable radio object has other optical peculiarities[1] which may be younger than the outer shell, 47 kpc from the nucleus. The radio properties and optical spectra of these galaxies merit further investigation.

1. Malin, D. F. Nature 277, 279–280 (1979).
2. Schweizer, F. Astrophys. J. 237, 303–318 (1980).
3. Malin, D. F. Nature 276, 591–593 (1978).
4. Malin, D. F. Am. astr. Soc. Phot. Bull. No. 16, 14–17 (1977).
5. King, I. R. Astrophys. J. 222, 1–13 (1978).
6. Fraser, C. W. Astr. Astrophys. Suppl. 29, 161–194 (1977).
7. Carter, D. & Dixon, K. L. Astr. J. 83, 574–582 (1978).
8. Kormendy, J. Astrophys. J. 214, 359–382 (1977).
9. Sandage, A. R. Astr. J. 81, 954–957 (1976).
10. de Vaucouleurs, G., de Vaucouleurs, A. & Corwin, H. G. Second Reference Catalogue of Bright Galaxies (Texas Press, 1976).
11. Martin, P. G. in Cosmic Dust, 38 (Oxford University Press, 1978).
12. Zeldovich, Ya. B. Proc. IAU Symp. No. 79, 409–421 (1978).
13. Doroshkevich, A. G., Saar, E. M. & Shandarin, S. F. Proc. IAU Symp. No. 79, 423–425 (1978).
14. Doroshkevich, A. G., Shandarin, S. F. & Saar, E. M. Mon. Not. R. astr. Soc. 184, 643–660 (1978).
15. Toomre, A. The Evolution of Galaxies and Stellar Populations (eds Tinsley, B. M. & Larson, R. M.) 401–416 (Yale University Press, 1977).
16. White, S. D. M. Mon. Not. R. astr. Soc. 184, 185–203 (1978).
17. Aarseth, S. J. & Fall, S. M. Astrophys. J. 236, 43–57 (1980).
18. Hausman, M. A. & Astriker, J. P. Astrophys. J. 224, 320–336 (1978).
19. Disney, M. J. & Wall, J. V. Mon. Not. R. astr. Soc. 179, 235–254 (1977).

Upper limit to any 59.35-s periodic radio emission at 18 cm from CG195.5+4.5

M. Emin Özel

Physics Department, Middle East Technical University, Ankara, Turkey

John R. Dickel & John C. Webber

Astronomy Department, University of Illinois, Urbana, Illinois 61801

To understand the true nature of the 100-MeV cosmic γ-ray source CG195.5+4.5 (also known as γ195+5, or Geminga), its identification at other wavelengths seems essential. Unfortunately, its positional uncertainty is large and several attempts to establish a counterpart at radio wavelengths (ref. 1 and H. A. Mayer-Hesselwander, personal communication), optically[2], in X-rays[3–5], and in very high energy ($>10^{11}$eV) γ rays[6], have produced no conclusive identification. In most cases, the reported 59-s γ-ray periodicity[7,8] was used as a basis for a search. We report here an intensive radio search for this object at a wavelength of 18 cm using the 37-m telescope at the Vermilion River Observatory of the University of Illinois, which has a 22-arc min half-power beamwidth at this wavelength. The radiometer consisted of a parametric amplifier with a 10 MHz bandwidth operating in a noise-adding mode to give a system noise temperature of 100 K. The output was sampled and recorded at 184 ms intervals.

Observing consisted of a point-by-point search at 15-arc min intervals over a $2° \times 2°$ error box surrounding the γ-ray position (see Fig. 1). Each of the 99 positions was sampled for 12 min. At several positions for which there were possible signals or suggested objects from other reports, multiple observations were made. The data at each position were then binned and folded to look for a periodicity at 59.35 s, the value calculated from the P and $\dot{P}$ derived from COS B observations[8] extrapolated to the epoch of the present observations (April–May 1979). If the adopted period is in error then, as the data are accumulated over the 12-min interval, any repeating feature will slide through the folded period and smear the apparent amplitude variation. We have divided the folded data into 25 bins which allows us to cover an unsmeared range in a period of 200 ms, well within the published uncertainty. After folding, the resultant pulse amplitude was evaluated for a random occurrence probability by a χ^2 analysis. The average r.m.s. noise per bin in this analysis was:

$$\sigma = 0.015\,K(T_A) = 0.075\,\text{Jy} \qquad (1)$$

In the distribution of the largest deviation from the mean at each position no deviations greater than 5σ were found and none are statistically significant. We can, therefore, place an upper limit on any 59.35-s periodic emission with a duration of $(59.35/25 =)$ 2.37 s at this 5σ level of

$$F(18\text{cm}) < 0.375\,\text{Jy} \qquad (2)$$

Any periodic signal with a duration longer than one bin will be correlated in adjacent bins increasing the effective integration time to allow detection to a smaller limit by a factor of $(2.37/\text{duration})^{1/2}$. Shorter pulses will apparently be spread over the whole 2.37-s interval and would, therefore, have correspondingly higher detection limits.

A compilation of measurements as well as upper limits to the flux density of CG195.5+4.5 at different photon energies, including the present results, is given as Fig. 2. By comparison with the spectrum of the Crab pulsar, one might conclude that the object could be a weak old pulsar; however, it is difficult to reconcile a 59-s period with the spin of a standard pulsar. If the period difficulty can be overcome, the reported γ-ray pulse profile[7,8] with multiple (probably four) peaks is suggestive of pulsar emission models with two pulses per pole[9]. Such objects

have not been observed, but they may be a subclass of the γ-ray sources reported by the COS B group[10,11]. A search for periodic emission from such γ-ray sources would prove very useful in this respect.

The reported γ-ray periodicity may possibly be false, because in each of the γ-ray reports[7,8] the amplitude of the pulse profile is less than 4σ. If the emission is not pulsed, other source models such as a dark cloud complex excited by a nearby supernova[12]; a system containing a compact object (a close binary or black hole), or a special kind of supernova remnant (SNOB)[13] could be considered as possible explanations for the γ-ray emission from this region of space.
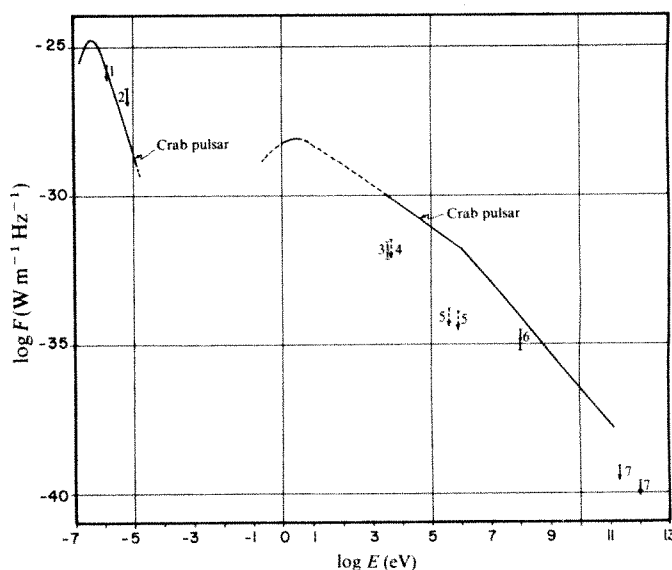

Fig. 2 An energy spectrum of CG195.5+4.5 compiled from all reported observations. Points with broken lines represent data for which no periodicity search at the γ-ray period was made. For comparison, the energy spectrum of the Crab pulsar[19] is shown. 1, Ref. 1, 325 MHz; 2, present study, 1,666 MHz; 3, ref. 3, 2–10 keV, Uhuru; 4, ref. 4, 2–6 keV, HEAO 1; 5, Coe *et al.* (1978), ~500 keV, Ariel 5; 6, Hermsen *et al.* (1977), ~100 MeV, COS B; 7, ref. 6, >200 GeV.
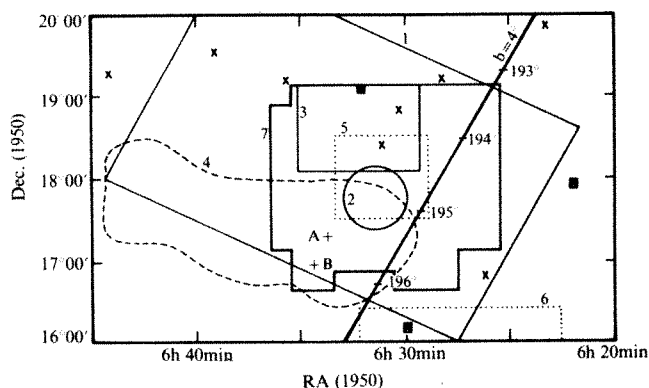

Fig. 1 The region of the sky covered by the present survey together with other reported observations for CG195.5+4.5. The numbers on the various boundaries are for: 1, the SAS 2 error box[7]; 2, the reduced COS B error box (R. Lamb, personal communication); 3, the HEAO 1 90% error box[4]; 4, the Uhuru 2σ X-ray contour where A and B are the most probable source positions[3]; 5, Bonn 18-cm survey (H. A. Mayer–Hesselwander, personal communication; 6, Westerbork 49-cm survey[18]; 7, the present survey at 18 cm. Continuum radio sources previously catalogued in refs[14–18] are indicated by X. Those found in the present survey are enclosed in boxes.

Several continuum surveys at long radio wavelengths have covered all or part of this area[14–17] and 13 point sources have been catalogued within the boundaries of Fig. 1. No source lies particularly near the best position for the γ-ray source and all appear to have 'normal' spectra. To check for continuous radio emission we have mapped a large area around the source at 18 cm using the same telescope system described above. This is the shortest wavelength at which the region has been surveyed. Scans in right ascension have been combined to provide a 20-s integration time for each half-beamwidth interval. A slight additional noise was added to the system by the scanning procedure to give an r.m.s. noise of 0.15 Jy on the map. Only three previously catalogued sources were expected to have large enough flux densities to be seen at our flux density limit at the frequency of the present survey. These three were found as expected but no other sources brighter than our 5σ limit of 0.75 Jy were detected. Thus any source with a peculiar spectrum must be weak and no strong candidate for the γ-ray source is apparent.

1. Mandolesi, N., Morigi, C. & Sironi, G. *Astr. Astrophys.* **67**, L5 (1978).
2. van den Bergh, S., *Astr. J.* **84**, 71 (1979).
3. Julien, P. F. & Helmken, H. F. *Nature* **272**, 699 (1978).
4. Lamb, R. & Worral, D. *Astrophys. J. Lett.* **231**, L121 (1979).
5. Haymes, C., Meegan, C. A. & Fishman, G. J. *Astro. Astrophys.* **79**, 88 (1979).
6. Helmken, H. F. & Weeks, T. C. *Astrophys. J.* **228**, 531 (1979).
7. Thompson, D. J., Fichtel, C. E., Hartman, R. C., Kniffen, D. A. & Lamb, R. C. *Astrophys. J.* **213**, 252 (1977).
8. Masnou, J. L. *et al., 12th ESLAB Symp.*, ESA-SP-124, 33 (1978).
9. Cheng, A. & Ruderman, M. Preprint Rutgers Univ. (1979).
10. Swanenburg, B. N. *Europhys. Study Conf. γ-ray Astronomy after COS B*, Erice (1979).
11. Pinkau, K. *Nature* **277** 17 (1979).
12. Abdulvahap, M. & Morrison, P. *Astrophys. J. Lett.* **221**, L33 (1978).
13. Montmerle, T. *Astrophys. J.* **231**, 95 (1979).
14. Pauliny-Toth, I. I. K., Wade, C. M. & Heeschen, D. S. *Astrophys. J. Suppl.* **13**, 65, (1966).
15. Dickel, J. R., Yang, K. S., McVittie, G. C. & Swenson, G. W. *Astrophys. J.* **72**, 757 (1967).
16. Hoglund, B. *Astrophys. J. Suppl.* **15**, 61 (1967).
17. Gower, J., Scott, P. F. & Wills, D. *Mon. Not. R. astr. Soc.* **71**, 49, (1967).
18. Bignami, G. F., Gavazzi, G. & Harten, R. H. *Astr. Astrophys.* **54**, 951 (1977).
19. Manchester, R. N., Taylor, J. H. *Pulsars*, 59 (W. H. Freeman, San Francisco, 1978).

Does feroxyhyte occur on the surface of Mars?

Roger G. Burns

Department of Earth and Planetary Sciences, Massachusetts Institute of Technology, Cambridge, Massachusetts 02139

The red colour of Mars has long been attributed to the occurrence of ferric oxides on its surface and in atmospheric dust storms. Such a belief has been accentuated by results of Viking Lander experiments on the surface of Mars, which suggested the presence of maghaemite, γ-Fe_2O_3 (refs 1, 2). This dark brown, ferromagnetic iron (III) oxide phase not only conforms with the colour and magnetic properties of dust on the martian surface, but suggests that maghaemite acted as a catalyst in some of the biological experiments performed *in situ* on Mars[3]. Many of the physical properties and chemical reactions attributed to maghaemite, however, are also displayed by δ-FeOOH, an oxide hydroxide polymorph of ferric iron[4,5]. On Earth, δ-FeOOH occurs as the mineral feroxyhyte in gleyed soils and in submarine manganese nodule deposits[6]. Some of the properties and paragenetic relationships of feroxyhyte are described here and it is suggested that δ-FeOOH is a prime candidate for the red-brown ferromagnetic phase coating the surface of Mars.
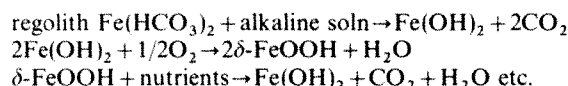
Synthetic δ-FeOOH is formed as a deep-brown precipitate during the oxidation of $Fe(OH)_2$ in partially deoxygenated, slightly alkaline solutions[7,8]. It is generally poorly crystalline and may contain up to 3 wt % excess H_2O (ref. 7). Significantly, δ-FeOOH differs from other FeOOH polymorphs by being ferromagnetic ($T_c \approx 450$ K), and therefore resembles γ-Fe_2O_3. Depending on its particle size, the saturation magnetization of δ-FeOOH is 30–50% the value of γ-Fe_2O_3 at ambient martian temperatures (200 K)[7,9], so that δ-FeOOH, too, will adhere to magnets such as those attached to the Viking Lander spacecraft[1]. The IR spectrum of δ-FeOOH contains three maxima in the range 2.95–3.4 m (refs 7, 10); similar spectral features are observed in remote-sensed spectra of Mars[11]. The catalytic efficiency of δ-FeOOH in the decomposition of H_2O_2, for example, is 10-fold higher than α-FeOOH (geothite) and α-Fe_2O_3 (haematite)[12], and is comparable to γ-Fe_2O_3 (maghaemite) which was postulated to interfere with the biological experiments on the Viking Landers[3].

In the marine environment on Earth, the formation of feroxyhyte is believed to involve redox reactions in buried sediments[6,13]. The $Fe(HCO_3)_2$ generated there migrates in

pore waters to the surface of the sediments. At the sediment–seawater interface, where the temperature and *p*H are typically 275 K and 8.1, respectively, $Fe(OH)_2$ is formed initially, but is oxidized by the oxygenated seawater to feroxyhyte. This poorly crystalline δ-FeOOH phase coats debris and authigenic silicates such as zeolites, and forms a substrate for the deposition of manganese (IV) oxides in ferromanganese crust and nodule deposits[14]. The δ-FeOOH phase is also susceptible to secondary redox reactions inside manganese nodules, where it catalyses the decomposition of enclosed biogenic debris and organically chelated Ni(II) and Cu(II) species[15], leading to the enrichment of these transition metals in manganese nodules on the sea floor beneath equatorial high biological productivity zones.

Such processes in the terrestrial marine environment enables us to postulate on the reactions on Mars which might lead to the formation of feroxyhyte in the martian regolith. Ferrous ions, derived from disintegration of basalt by chemical weathering, mechanical abrasion (ablation and freeze-thaw) and photochemical[16] processes, form stable $Fe(HCO_3)_2$ in the choride–sulphate-rich, CO_2-saturated, O_2-depleted brines in the permafrost on Mars. When the $Fe(HCO_3)_2$ is slowly oxidized, poorly crystalline feroxyhyte is produced which forms a thin red-brown veneer on the fractured rock surfaces. The fine-grained feroxyhyte particles are easily transported during dust storms and become major components in the bright areas of the martian surface. The large specific surface of the feroxyhyte particles also makes them effective substrates for the reversible chemisorption of water vapour from the martian atmosphere.

The synthesis and chemical properties of δ-FeOOH might also explain some of the results obtained during the Viking biological experiments on Mars[3,17]. Metal peroxides or superoxides on the martian surface when moistened would liberate oxygen and produce alkaline solutions, thereby initiating the following reactions:

$$\text{regolith } Fe(HCO_3)_2 + \text{alkaline soln} \rightarrow Fe(OH)_2 + 2CO_2$$
$$2Fe(OH)_2 + 1/2 O_2 \rightarrow 2\delta\text{-FeOOH} + H_2O$$
$$\delta\text{-FeOOH} + \text{nutrients} \rightarrow Fe(OH)_2 + CO_2 + H_2O \text{ etc.}$$

The biological experiments on Mars thus promoted the conversion of $Fe(HCO_3)_2$ in the regolith to feroxyhyte, the catalytic properties of which led to the breakdown of nutrients supplied during the Viking Lander experiments.

Feroxyhyte, therefore, has suitable colour, magnetic, chemisorption, spectral, redox and paragenetic properties to make it a constitutent of the surface of Mars.

1. Hargraves, R. B., Collinson, D. W., Arvidson, R. E. & Spitzer, C. R. *J. geophys. Res.* **82**, 4547 (1977).
2. Toulmin, P. III *et al. J. geophys. Res.* **82**, 4625 (1977).
3. Oyama, V. I. & Berdahl, B. J. *J. geophys. Res.* **82**, 4669 (1977).
4. Burns, R. G. & Burns, V. M. in *Marine Manganese Deposits* (ed. Glasby, G. P.) 212 (Elsevier, Amsterdam, 1977).
5. Murray, J. W. in *Marine Minerals* Ch. 2 (ed. Burns, R. G.) 47 (Mineralogy Society of America Monograph 6, 1979).
6. Chukhrov, F. V., Zvyagin, B. B., Yermilova, L. P. & Gorshkov, A. I. *Miner. Deposita* **11**, 24 (1976).
7. Okamoto, S. *J. Am. ceram. Soc.* **51**, 594 (1968).
8. Atkinson, R. J. *Aust. J. Chem.* **29**, 2149 (1976).
9. Coey, J. M. D. & Khalafalla, D. *Phys. Stat. Sol.* A **11**, 229 (1972).
10. Feitknecht, W., Haeni, H. & Dvorak, V. in *Proc. 6th int. Symp. Reactivity of Solids*, 237 (1969).
11. Houck, J. R., Pollack, J. B., Sagan, C., Schaack, D. & Decker, J. A. Jr *Icarus* **18**, 470 (1973).
12. Sara, J. *Chem. Listy.* **63**, 112 (1969).
13. Burns, R. G. & Burns, V. M. in *The Sea* Vol. 7 (ed. Emiliani, C.) (Wiley, New York, in the press).
14. Burns, R. G. & Burns, V. M. *Nature* **255**, 130 (1975).
15. Burns, V. M. & Burns, R. G. *Earth planet. Sci. Lett.* **39**, 341 (1978).
16. Huguenin, R. L., Prinn, R. G. & Maderazzo, M. *Icarus* **32**, 270 (1977).
17. Klein, H. P. *Icarus* **34**, 666 (1978).

Instantaneous structure of an MgSiO₃ melt simulated by molecular dynamics

Yoshito Matsui

Institute for Thermal Spring Research, Okayama University, Misasa, Tottori-ken 682–02, Japan

Katsuyuki Kawamura

Geological Institute, Faculty of Science, The University of Tokyo, Hongo, Tokyo 113, Japan

A series of molecular dynamics (MD) calculations[1] has been carried out to visualize the atomic configuration in MgSiO₃ melt and glass. The 'computer-generated' configuration seemed to be realistic. At zero pressure the Si–O–Si angle distribution gave a clear peak at ~145° in agreement with the result of ordinary X-ray study on vitreous SiO₂ (ref. 2). Coordination of O around Mg was irregular, because the whole structure is dominated by packing of the rather regular SiO₄ tetrahedra which are linked together by sharing O atoms at corners. The 'melt' also showed a partial conversion from a 4- to 6-coordination state on 'compression' within a reasonable density range, accompanied by a steady decrease in the Si–O–Si angles. The MD calculation, which is simply the numerical integration of the classical newtonian equations of motion for many particles in a hypothetical periodic space, has been successfully applied to various molten ionic salt systems[1]. Following Woodcock et al's[3] first application of MD to vitreous SiO₂, we decided to extend the MD calculation to systems of geochemical importance and report our results here.

To carry out the MD calculation, a set of potential parameters is needed to evaluate the force acting on every ion. Recently, Miyamoto and Takeda (personal communication) estimated the parameters for Si^{4+} and O^{2-} in the following pair potential expression assuming a purely ionic nature of the system:

$$\phi_{ij} = \frac{z_i z_j e^2}{r_{ij}} + f(b_i + b_j) \exp\left(\frac{a_i + a_j - r_{ij}}{b_i + b_j}\right)$$

where ϕ_{ij} is the pair potential between ions i and j, z denotes the formal charge number, e is the unit charge, r_{ij} is distance between i and j, a_i and b_i are crystal radius and softness parameter of ion i, and f is an arbitrary constant. Miyamoto and Takeda refined the relevant parameters using the WMIN program written by Busing[4], to minimise the lattice energy of Mg_2SiO_4 (forsterite) with structural parameters given by Smyth and Hazen[5], taking $a_{Mg} = 0.97$ Å (1 Å = 100 pm) and $b_{Mg} = 0.065$ Å given by Busing[4] and $f = 1$ kcal mol⁻¹ Å⁻¹ ($= 6.9478 \times 10^{-6}$ dyn) as fixed values.

The 215 ions (43 MgSiO₃) were placed into a cubic basic cell (edge length, L) with randomly generated coordinates and an assumed zero pressure density 2.49 g cm⁻³ ($L = 14.225$ Å), which corresponds to a 20% increase in volume over MgSiO₃ orthopyroxene (31.4 cm³ mol⁻¹) (ref. 6). In the following calculation the summation of repulsive force and the first (direct lattice) series in the Ewald sum of electrostatic force were terminated at $0.5L$, and the second (reciprocal lattice) series in the Ewald sum was terminated within 61 adjacent unit cells. The relative error due to the termination was estimated to be within 1%.

The MD calculation was started at constant temperature (8,000 K) with a time increment 10^{-16} s. On approaching thermal equilibrium the calculation was switched to a constant energy mode with a time increment 1.25×10^{-15} s. After disappearance of systematic drift in temperature, additional 750 steps were calculated at constant energy. The 'product' was then 'cooled' at a rate of 100 K per 10 steps down to 2,000 K, and annealed at ~2,000 K for more than 1,000 steps and further quenched to 500 K when necessary.

The 'compression experiments' were carried out starting from the configuration obtained above, decreasing interatomic distances uniformly to give $0.8V_0$ (3.11 g cm⁻³), $0.7V_0$ (3.56 g cm⁻³) and $0.6V_0$ (4.15 g cm⁻³). The same procedure was applied in subsequent computation as outlined above.

The calculated structures for V_0 and $0.8V_0$ were similar with each other. A typical instantaneous configuration of ions for $0.8V_0$ at ~500 K is shown in Fig. 1 as a stereoscopic pair. The important features are as following. First, regular SiO₄ tetrahedra show an extensive polymerization by sharing O ions at corners: out of four O ions per one tetrahedron 2.2–2.3 O ions are shared by adjacent tetrahedra on average. As Fig. 1 shows, however, this does not imply the existence of the infinite SiO₃ chains as those in pyroxenes. Second, the distribution of Si–O(bridging)–O angle shows a clear peak at ~145° as stated earlier. Third, coordination of O ions around Mg is irregular, the number of the nearest O ions ranging from three to four.

A striking change in configuration is observed at $0.6V_0$ as can be seen in Fig. 2. At least one-third of Si atoms are more or less regularly coordinated by six O ions. Edge sharing among the adjacent SiO₆ octahedra, which is common in the crystals containing Si in 6 coordination, is extensive although this is not
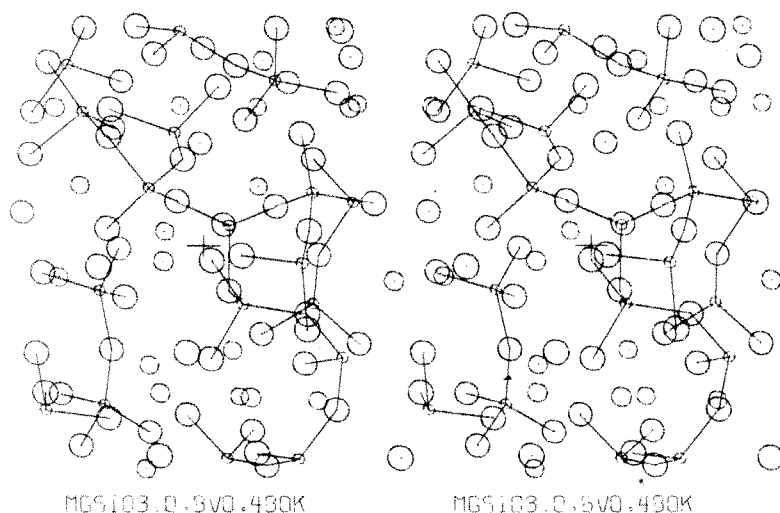

Fig. 1 Stereoscopic pair drawing of the instantaneous structure of MgSiO₃ at 3.11 g cm⁻³ and 480 K. The Si–O pairs with distances less than 179 pm are connected by solid lines. Circles represent Si, Mg and O atoms in the increasing order in sizes.

MGSIO3.0.5V0.480K   MGSIO3.0.5V0.480K

Fig. 2 Stereoscopic pair drawing of the instantaneous structure of MgSiO₃ at 4.15 g cm⁻³ and 510 K. The Si–O pairs with distances less than 175 pm are connected by solid lines. Regular SiO₆ octahedra are seen at centre and lower right.
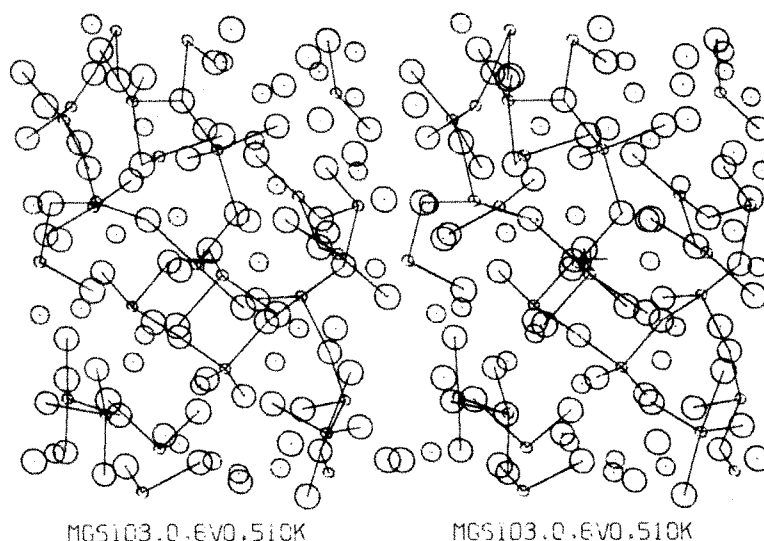
clear in Fig. 2 because of the overcrowded population of ions. The coordination number of Mg, too, increases on 'compression': Most of Mg ions are in 4–6 coordination with respect to the nearest O ions.

In contrast to the remarkable change in configuration, calculated radial distribution functions (RDF) displayed rather little variation: The first maxima for Si–O, Mg–O and O–O distances shifted from 1.62 to 1.66 Å, 1.96 to 1.92 Å (a decrease) and from 2.65 to 2.51 Å, respectively, on compression. In view of the broadening of peaks in RDF on compression, however, this does not necessarily mean a decrease in the mean Mg–O distance. The small change in RDF might have been a reason for the pessimistic conclusion by Woodcock *et al.*[3] that most Si atoms remain in 4 coordination even under a heavy 'compaction'.

The crystalline MgSiO₃ is known to assume the ilmenite structure under pressures above 24 GPa at 1,000 °C where Si atoms are in 6 coordination with a density 3.795 g cm⁻³ (at ambient conditions)[7] and further transforms to the orthorhombic perovskite structure (4.108 g cm⁻³ at ambient conditions) at 27 GPa and 1,000 °C (refs 8, 9). Note that the simulated melt or glass undergoes a similar mode of coordination change in a comparable density range with the solid–solid transitions, although in the molten or vitreous state the change seems to be gradual.

The MD calculation provide a very promising way of obtaining information of both the structural and physical properties even in the not-so-perfectly ionic systems as silicate melts, of which knowledge in the atomistic level has been recognized to be vital in recent years[10,11].

We thank Dr I. Okada for instruction and computer programs, Dr H. Takeda and Mr M. Miyamoto for permission to use potential parameters before publication, and Professor W. S. MacKenzie and Dr M. J. Dempsey for valuable comments.

1. Woodcock, L. V. *Advances in Molten Salt Chemistry* (eds Braunstein, J. *et al.*) 1–74 (Plenum, New York, 1975).
2. Mozzi, R. L. & Warren, B. E. *J. appl. Crystallogr.* **2**, 164–172 (1969).
3. Woodcock, L. V., Angell, C. A. & Cheeseman, P. *J. chem. Phys.* **65**, 1565–1577 (1976).
4. Busing, W. R. *Trans. Am. Crystallogr. Ass.* **6**, 57–72 (1970); *J. chem. Phys.* **57**, 3008–3009 (1972).
5. Smyth, J. R. & Hazen, R. M. *Am. Miner.* **58**, 588–593 (1973).
6. Stephenson, D. A., Sclar, C. B. & Smith, J. V. *Miner. Mag.* **35**, 838–846 (1966).
7. Ito, E. & Matsui, Y. *High-Pressure Research—Applications in Geophysics* (eds Manghnani, H. & Akimoto, S.) 439–461. (Academic, New York, 1977).
8. Ito, E. & Matsui, Y. *Earth planet. Sci. Lett.* **38**, 443–450 (1978).
9. Yagi, T., Mao, H. & Bell, P. M. *Phys. Chem. Miner.* **3**, 97–100 (1978).
10. Henderson, P. *Miner. Mag.* **43**, 399–404 (1979).
11. Kushiro, I. *Earth planet. Sci. Lett.* **41**, 87–90 (1978).

Oceanic bathymetry profiles flattened by radiogenic heating in a convecting mantle

Gary T. Jarvis & W. R. Peltier

Department of Physics, University of Toronto, Toronto, Ontario, Canada M5S 1A7

Reliable measurements of both ocean floor topography and heat flow indicate a linear dependence on the square root of the age, *t*, of the ocean floor for $t \lesssim 90$ Myr (ref. 1) or about half the age of the large oceanic plates. Consequently, major topographic and heat flow variations perpendicular to mid-ocean ridge axes are generally believed to be thermally induced and associated with contraction of the lithosphere as it moves away from the ridges[1-4]. For $t > 90$ Myr, measurements of bathymetry (but not of heat flow) indicate a systematic departure from a $t^{\frac{1}{2}}$ relationship reaching almost 20% at the oldest ages. We present here numerical calculations of thermally induced topography above two-dimensional convection cells which are heated partially from within and partially from below. These exhibit the same general features as oceanic bathymetry and we suggest that departures of the latter from a $t^{\frac{1}{2}}$ dependence may be due to radiogenic heating within the mantle.

Ignoring horizontal conduction and assuming isostatic compensation at the base of the lithospheric plate, Parsons and McKenzie[2] derived the following energy balance equation for a column through the plate:

$$-(\rho_m - \rho_w)\frac{C_p}{\alpha}\frac{\partial D}{\partial t} + q_u = q_b + \int_z H'(z)\mathrm{d}z \qquad (1)$$

where ρ_m is the mantle density (below the plate), ρ_w is the density of water, α is the coefficient of thermal expansion, C_p is the specific heat, D is the depth of the ocean floor beneath the sea surface, t is the time, q_u is the heat flux across the upper surface of the plate, q_b is the heat flux into the base of the plate, H' is the rate of radioactive heating per unit volume in the column and the integral is taken over the height, z, of the column. Note that any thermal models with the same total heat sources given by the right-hand side of equation (1) will predict the same temporal variations of D and q_u. If there are no heat sources on the right-hand side, equation (1) reduces to

that governing the boundary layer behaviour for high Rayleigh number viscous fluids heated entirely from below[5-9]. Away from the vertical plumes, the surface heat flow is primarily due to conductive cooling of the initially hot plume material moving horizontally across the upper surface. Balancing the horizontal advection and vertical diffusion, Turcotte and Oxburgh[5] first predicted that $q_u \propto t^{-1/2}$; hence from equation (1) $D \propto t^{1/2}$. Although this prediction is borne out for $t \lesssim 90$ Myr, at later times D increases more slowly than predicted and a non-zero heat source term can be inferred for $t > 90$ Myr.
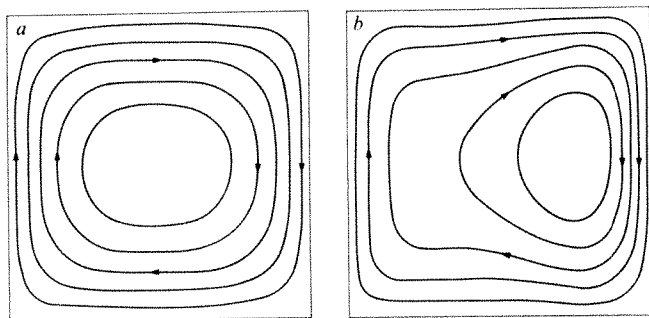
Fig. 1 Numerically determined streamlines of the flow in convection cells which are: a, heated entirely from below; and b, heated 20% from within and 80% from below. Both solutions shown here were obtained on a 96 × 96 finite-difference grid at $R = 1.25 \times 10^7$. The main feature is the different orientation of near-surface streamlines in the two cases. The asymmetry of the flow structure in b results in advective heat transport towards the upper surface for a major portion of the cell.

Parsons and McKenzie[2] have reviewed several models which include a variety of heat sources in an attempt to account for this 'flattening' of the bathymetry profile with respect to the $t^{\frac{1}{2}}$ behaviour predicted by boundary layer theory. We consider here another source of basal heating, q_b, which in the case of whole mantle convection may account for the observed ocean floor flattening. This is the vertical advection of heat into the upper thermal boundary layer which occurs continuously across convection cells which are heated partially from within and partially from below. We assess this mechanism quantitatively using high Rayleigh number model solutions obtained numerically on two-dimensional finite-difference grids. Although direct application to the Earth's mantle is somewhat speculative, the basic physics is not and has apparently been overlooked previously.

The numerical scheme used is essentially the same as that used by McKenzie et al.[10] and Jarvis and McKenzie[11] except that the program package for solving Poisson's equation has been replaced by a more flexible (though less efficient) package available from NCAR (National Centre for Atmospheric Research). The solutions discussed below were obtained on finite-difference grids of various dimensions ranging from 24 × 24 to 96 × 96 mesh points. Free-slip boundary conditions were imposed together with a constant temperature at the upper surface and a constant heat flux at the base. Solutions were obtained in square boxes with vertical boundaries being planes of mirror symmetry with respect to the temperature and velocity fields. The Boussinesq approximation was assumed and thermodynamic variables were assumed constant.

The two dimensionless parameters which are relevant to the following discussion are the Rayleigh number

$$R = \frac{g \alpha d^4 E}{C_p \kappa^2 \eta} \qquad (2)$$

and the ratio of internal heating to total heat flow across the upper surface of the box

$$\mu = Hd/(F + Hd) \qquad (3)$$

where g is the acceleration due to gravity, d is the depth of the convection cell, E is the heat flux across the top of the box, κ is thermal diffusivity, η is the viscosity, F is the heat flux into the base of the box, H is the rate of radioactive heating per unit volume, and other parameters are as defined above (note that $E = F + Hd$).

Several numerical models were run varying both R and μ to study the dependence of the bathymetry D on these parameters. We find that flattening of the bathymetry occurs as a consequence of the shift of the centre of circulation towards the descending plume in partially internally heated flows (Fig. 1). The broad zone of upwelling produced by this shift can result in advective heat transport to the base of the thermal boundary layer well beyond the mid-point of the box.

The bathymetry was computed using a simple boundary layer expression[12] which is consistent with equation (1),

$$D(x) = \frac{\alpha \rho_m}{\rho_m - \rho_w} \int_0^{z_1} (T_m - T(x, z)) \, dz \qquad (4)$$

where ρ_m is the mantle density, ρ_w is the density of water, T_m is the temperature in the central core, z is the vertical coordinate measured positively downward and z_1 is the depth of isostatic compensation (taken to be immediately below the thermal boundary layer). Although $D(x)$ can be expressed more accurately in terms of the dynamic forces associated with the fluid flow[10,14], the conclusions presented below are not
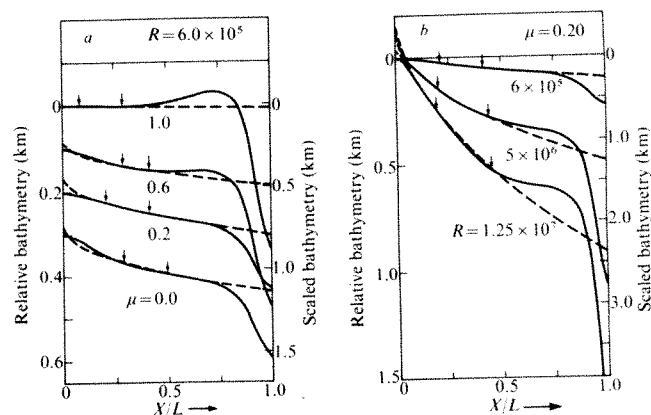

Fig. 2 Plots of thermally induced bathymetric variation across the top of convection cells of width L. Bathymetry computed from the model solutions is indicated by the solid lines. Reference curves, proportional to $x^{\frac{1}{2}}$ and constrained to fit the model curves at the points indicated by the small arrows, are shown as broken lines. Bathymetry is plotted relative to the highest point. In a, $R = 6.0 \times 10^5$ and μ varies from 0.0 to 1.0. Successive curves have been offset by 0.1 km of relative bathymetry at $x = 0$ for the sake of clarity. All model solutions for a were obtained on a 24 × 24 finite-difference grid. In b, $\mu = 0.20$ and R varies. For $R = 6 \times 10^5$, 5×10^6 and 1.25×10^7, the respective finite-difference grids had dimensions of 24 × 24, 64 × 64, and 96 × 96. The left-hand vertical axes indicate the bathymetry as computed using mean mantle values for ρ_m and α (as given in the text). The right-hand vertical axes indicate the bathymetry corrected for near surface values of these parameters (3.33 g cm^{-3} and 3.2 × 10^{-5} K^{-1} respectively[1]).

very sensitive to which equation is used (this point will be discussed in more detail elsewhere).

The dependence of $D(x)$ on both μ and R is illustrated in Fig. 2. The sequence of bathymetry profiles at $R = 6 \times 10^5$ (Fig. 2a) shows that $D(x)$ departs from the reference $x^{\frac{1}{2}}$ curves increasingly as μ increases. We define the percentage flattening, P, as the maximum difference between the model curve and the reference $x^{\frac{1}{2}}$ curve expressed as a percentage of the value on the reference curve; P increases with μ. The sequence of bathymetry profiles at $\mu = 0.20$ (Fig. 2b) shows that P is also an increasing function of R (for $R = 6 \times 10^5, 5 \times 10^6$ and 1.25×10^7, $P = 1, 12$ and 19% respectively).
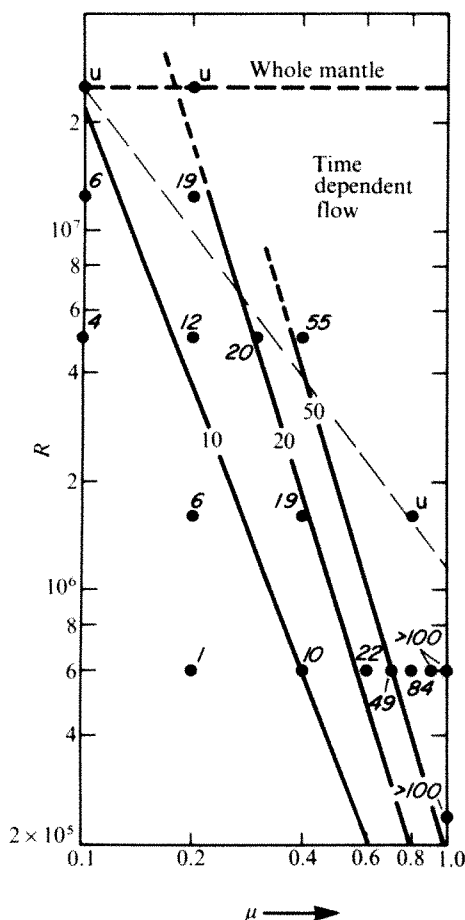
Fig. 3 Domain diagram on which the percentage flattening P is plotted as a function of R and μ. Solid circles indicate the (R, μ) coordinates for which values of P were obtained and the adjacent numbers give the values of P ($\%$). Contours of constant P are shown for $P = 10, 20$ and 50%. The broken diagonal line roughly divides domains of steady and non-steady single cell flows: Steady single-cell solutions can be obtained at all points below the line, time-dependent (or multi-cell) solutions above. Points for which solutions were too unsteady to compute meaningful values for P are indicated by Us. The horizontal broken line at $R = 2.5 \times 10^7$ indicates our estimate of R for whole mantle convection. The model solutions were obtained on finite-difference grids with dimensions of 24×24 for $R \leq 6 \times 10^5$, 48×48 for $R = 1.6 \times 10^6$, 64×64 for $R = 5 \times 10^6$ and 96×96 for $R \geq 1.25 \times 10^7$.

The joint dependence of P on both μ and R is summarized in Fig. 3. Here P is plotted as a function of μ and R. Values of P are indicated for the states examined and manually drawn contours for constant P indicate the trends. For a given amount of flattening, the value of μ required is a decreasing function of R.

If convection involving the ocean floor is confined to the upper 700 km of the mantle[2,5,6,10] the aspect ratio of the flow is much greater than 1 and the results presented here (for an aspect ratio of 1) cannot be applied directly. The most direct application to the Earth is in the context of whole mantle convection, as originally envisaged by Hess[13], in which it is assumed that the oceanic lithosphere forms the thermal boundary layer of the convective circulation[15]. In this case a cell with an aspect ratio of 1 (width $= 2,900$ km at mid-depth) would have a linear surface dimension of 3,752 km, comparable to the mean plate size. Allowing for the geometrical effects of curvature in the spherical Earth we estimate a value for the heat flux E at mid-mantle depths of 9.34×10^{-2} W m^{-2}. Substituting this value for E into equation (2), together with the following parameter values

$$g = 10^3 \, \text{cm s}^{-2}$$

$$\alpha = 1.4 \times 10^{-5} \, \text{K}^{-1}$$

$$\rho_m = 4.9 \, \text{g cm}^{-3}$$

$$d = 2.9 \times 10^3 \, \text{km}$$

$$\eta = 5 \times 10^{22} \, \text{P}$$

$$\kappa = 2.5 \times 10^{-2} \, \text{cm}^2 \text{s}^{-1}$$

$$C_p = 1.2 \, \text{J g}^{-1} \text{K}^{-1}$$

(assumed to be representative of the whole mantle), gives an estimated value of $R = 2.5 \times 10^7$ for mantle-wide circulation. The extrapolated contours on Fig. 3 suggest that, at $R = 2.5 \times 10^7$, 10–20% flattening can be expected provided $0.1 \leq \mu \leq 0.2$; the data from the ocean floor[1] indicate a value of $P = 18\%$. Thus in the context of the present constant property model, if radiogenic heat sources are uniformly distributed throughout the mantle, they must contribute less than 20% to the total heat flow at the Earth's surface. (A larger contribution would result in flattening in excess of the observations.) Consequently, the large scale convective circulation must be driven substantially by the flow of heat across the core–mantle boundary.

Other processes not included in the simple convection models studied here (notably the rigid behaviour of the lithosphere) undoubtedly will alter, quantitatively, the results presented here. In particular the amount of internal heating compatible with the observations may well exceed 20%. Moreover, application to the Earth is complicated by the presence of continents on many of the large plates. The main result to which we wish to draw attention here is that the topography deduced from the thermal structure at the upper surface of a convection cell is significantly flattened by partial internal heating.

1. Parsons, B. & Sclater, J. G. J. geophys. Res. 82, 803–827 (1977).
2. Parsons, B. & McKenzie, D. P. J. geophys. Res. 83, 4485–4496 (1978).
3. McKenzie, D. P. J. geophys. Res. 72, 6261–6273 (1967).
4. Sclater, J. G. & Francheteau, J. Geophys. J. R. astr. Soc. 20, 509–542 (1970).
5. Turcotte, D. L. & Oxburgh, E. R. J. Fluid Mech. 28, 29–42 (1967).
6. Turcotte, D. L. & Oxburgh, E. R. Ann. Rev. Fluid Mech. 4, 33–68 (1972).
7. Robinson, J. L. J. Fluid Mech. 30, 577–600 (1967).
8. Roberts, G. O. Geophys. Astrophys. Fluid Dynamics 12, 235–272 (1979).
9. Olson, P. & Corcos, G. M. Geophys. J. R. astr. Soc. (in the press).
10. McKenzie, D. P., Roberts, J. M. & Weiss, N. O. J. Fluid Mech. 62, 465–538 (1974).
11. Jarvis, G. T. & McKenzie, D. P. J. Fluid Mech. 96, 515–583 (1980).
12. Oxburgh, E. R. & Turcotte, D. L. Rep. Prog. Phys. 41, 1249–1312 (1978).
13. Hess, H. H. in Petrologic Studies: A Volume in Honor of A. F. Buddington (eds Engel, A. E. J., James, H. L. & Leonard, B. F., 599–620 (Geological Society of America, 1962).
14. McKenzie, D. P. Geophys. J. R. astr. Soc. 48, 211–238 (1977).
15. Peltier, W. R. in Physics of the Earth's Interior (eds Dziewonski, A. & Boschi, E.) (Academic, New York, 1980).

Asymmetric spreading in back-arc basins

Peter F. Barker

Department of Geological Sciences, University of Birmingham, PO Box 363, Birmingham B15 2TT, UK

Ian A. Hill

Department of Geology, University of Leicester, University Road, Leicester LE1 7RH, UK

Lineated magnetic anomalies indistinguishable from those generated at mid-oceanic ridges have been found behind many subduction zones. They show that back-arc spreading, like its mid-oceanic counterpart, is to a first approximation symmetric. Nevertheless, consistently asymmetric spreading has been found in some ocean basins, and in both actively spreading and extinct back-arc basins. We argue here that the sense of asymmetry found in active back-arc basins strongly supports a mechanism for the origin of asymmetric spreading which is dominated by the thermal effects of migration of the ridge crest over the sub-asthenospheric mantle. Conversely, it provides no support for the simple fluid mechanical models, nor for models in which back-arc extension is driven directly by the subduction process. If the thermal effect also dominated asymmetric spreading in extinct back-arc basins, the sense of asymmetry would provide information about 'absolute' plate motions at the time of opening.

Divergent plate boundaries accrete asymmetrically by the action of ridge jumps, or by a kind of smoothly asymmetric spreading in which the discontinuities, if any, are too small to be detected using magnetic anomalies[1-4]. Although the two modes can co-exist their origin is probably essentially different. Unlike all but the smallest ridge jumps, asymmetric spreading is a ridge crest phenomenon, produced in the central rift zone in conditions perhaps only marginally different from those giving rise to the more usual symmetric spreading. We consider here only the smooth asymmetry, despite obvious resemblances between the larger ridge jumps in the main ocean basins and episodic back-arc extension, in which (as in the Philippine Sea[5,6]) an old centre is abandoned in favour of new spreading directly behind the magmatic arc.

Certain detection of smoothly asymmetric spreading requires detailed examination of long and well-formed magnetic anomaly sequences, to rule out the spurious effects of undetected ridge jumps, fracture zones and changes in ridge obliquity. Hence the validity of some, particularly older, claims of asymmetric spreading in the main ocean basins must be debatable. Reasonably well-documented examples, however, often with one sense of asymmetry persisting over several million years, are found south of Australia[1,2], in the South Atlantic[3] and Panama Basin[7-10] and, inferentially[11], on the East Pacific Rise.
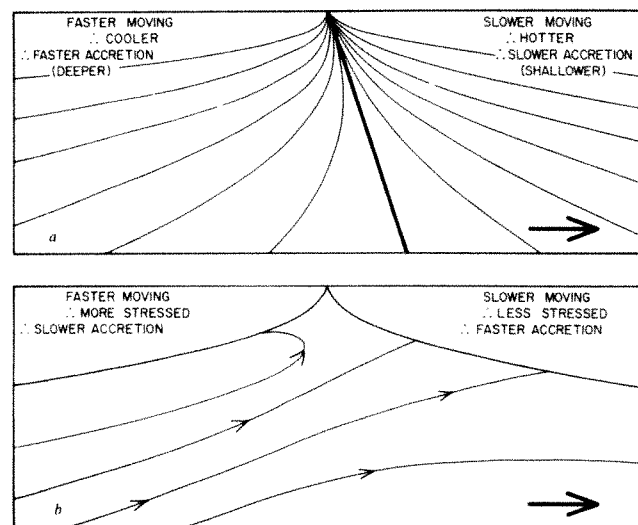

Fig. 1 Simple schematic models relating asymmetric spreading to ridge crest migration over the underlying mantle. Both cases are shown in a ridge crest reference frame with mantle moving to the right (thick arrow). Thus, with respect to the mantle, the left flank of the spreading centre is actually the faster moving. *a*, Thermal model[1,3]. Migration is represented by sloping the central injection boundary (thick line) of the conventional numerical models of oceanic lithosphere formation[12], which skews the isotherms so that the slower moving (right) flank is hotter for any given depth and age and, therefore, accretes less and rides higher. This elevation asymmetry should decay with age of the ocean floor. *b*, Fluid mechanical model[13], in which the greater viscous shear stress beneath the faster moving (left) flank hinders accretion. Solid arrowed lines are schematic contours of stream function.

Smoothly asymmetric spreading has been associated with migration of the ridge crest across the underlying mantle in two models (Fig. 1), one invoking the thermal asymmetry produced by ridge migration[1,3], the other[13] the asymmetric shear stresses beneath the diverging plates. The models predict asymmetric accretion in opposite senses; accretion favours the cooler flank, which is the faster-moving, but also the less stressed flank, which is the slower moving.

Using recent versions[14,15] of the mean hotspot reference frame (MHRF) to compute absolute motions, for the better documented examples (south of Australia, the South Atlantic and, with much greater complexity, the Panama Basin) the sense of asymmetry suggests the dominance of the thermal effect. However, the entire data set from the main ocean basins does not provide overwhelming support to either model and it is not clear why, when almost all mid-oceanic ridges are migrating to some extent[16], asymmetric spreading is not much more widespread. An additional enabling or decoupling mechanism may exist, perhaps within processes in the upper (magma chamber, sheeted dyke) levels of new oceanic lithosphere[1,3] where the mode of operation of either model in the simplistic form described here is in any case unclear.

The existence of asymmetric spreading in back-arc basins provides the opportunity to examine in a different environment the models discussed so far, and to compare their predictions with those of the subduction-specific class of model for back-arc extension, notably the 'forced convection' model of Toksoz and Bird[17]. To test the ridge migration models, the back-arc basins must be actively extending so that absolute motions may be derived, and must possess well-formed, unambiguously identified Vine–Matthews magnetic lineations. Only the South Sandwich[18] and Bismarck Sea[19] basins meet these criteria at present. The Lau[20] and Marianas[21] basins are also active, and show lineated magnetic anomalies, but present data are inadequate for unambiguous identification of the anomalies and the location and orientation of fracture zones. Both the South

Table 1 Absolute plate motion vectors in areas with asymmetric spreading

Area	Position	Plate	Motion (mm yr⁻¹)	Vector[15] (°)	Motion (mm yr⁻¹)	Vector[14] (°)
Australia–	50°S 130°E	IND	76	009	65	015
Antarctic Ridge		ANT	6	041	13	132
South Atlantic	49°S 15°W	SAM	21	258	20	292
		AFR	14	083	22	052
Panama Basin	2°N 90°W	NAZ	47	086	54	084
		COC	84	041	90	041
Sandwich Plate	60°S 30°W	SAM	17	256	16	302
		ANT	5	182	9	026
Bismarck Sea	4°S 150°E	IND	72	019	66	031
		PAC	101	294	91	288
Shikoku Basin	30° N 137°E	EUR	3	055	12	151
		PAC	107	288	97	282

Sandwich and the Bismarck Sea basins show asymmetric spreading, the sense of which is compatible with the dominance of a thermal effect. In the South Sandwich system (Fig. 2a and Table 1) the trench and arc (Sandwich plate) migrate rapidly eastwards in absolute terms (60–80 mm yr^{-1}), while the remnant arc moves only slowly westwards (0–20 mm yr^{-1}). (The range of speeds results from the unknown apportionment of the slow east–west SAM–ANT motion between the North and South Scotia Ridge[22]). The ridge crest migrates eastwards at 15–35 mm yr^{-1} and the asymmetry, ~10% of the total spreading rate, favours accretion to the eastern, trench flank, in agreement with the prediction of a thermal model.

The back-arc spreading centre in the Bismarck Sea[19] is shown in Fig. 2b as part of the Pacific–Bismarck plate boundary. The Pacific (PAC) plate is here moving rapidly to the west-northwest (Table 1), but even more rapid back-arc extension (~130 mm yr^{-1}) permits the New Britain arc-trench system to advance to the east-southeast. The ridge crest migrates slowly to the west-northwest, so that the observed 10% asymmetry, which here favours the remnant arc (western, PAC) flank, is again compatible with a thermal model. The existence of a Caroline plate, with the slow movement relative to the Pacific plate suggested by Weissel and Anderson[23], would not affect this conclusion.

The value of these two examples extends beyond their support for a dominantly thermal model. The sense of the asymmetry, although consistent with respect to the 'absolute' migration of the ridge crest, is not consistent in terms of the polarity of the arc and trench. That is, in one case the asymmetry favours accretion to the trench side, in the other to the remnant arc. We regard this as strong evidence against those models, such as the 'forced convection' model[17], which drive back-arc extension directly from the subduction process, and for which (whether generated thermally or by stress) a consistent sense of asymmetry with respect to the trench would be expected. Rather, these results emphasize the sensitivity of back-arc extension to absolute plate motions, and to this extent support the suggestion by Chase[24], that back-arc extension is induced so that the trench may 'advance' over the sub-asthenospheric mantle. Note that the recently reported Bismarck Sea spreading also supports Chase's hypothesis more directly; without it, the trench would be 'retreating' extremely rapidly.

Unfortunately, no other active back-arc basins with well-formed, unambiguously identified magnetic anomalies are known at present: the two cited provide more emphatic support for a thermal model than do the main ocean basins. If further

support were to become available from other examples, it would be reasonable to assume that the association of asymmetric spreading with ridge crest migration could be applied also to extinct back-arc basins. Provided that the regional tectonic situation was fairly simple while extension was taking place, then the observed sense of asymmetry might be used to deduce the polarity of ridge crest migration in the direction perpendicular to the crest itself. We choose two examples, the central Scotia Sea and the Shikoku basin, where such information would contribute towards an understanding of regional tectonic evolution.

East–west magnetic lineations[25] in the central Scotia Sea (Fig. 2c) reveal a spreading episode extending from 21 to 6 Myr, with an asymmetry of 5–10% favouring accretion to the southern flank. During this period, major plate (SAM–ANT) motion was probably slow, sinistral and east–west, as it is today[14,15]. South Sandwich back-arc extension[18] had not yet begun, but extension in the 120–300° direction was taking place in Drake Passage to the west[26]. Recently dredged Miocene low-K arc tholeiites from the eastern South Scotia Ridge[27] suggest that the central Scotia Sea formed by back-arc extension behind a southeast-facing intra-oceanic arc, the Discovery Arc, as shown in Fig. 2c. However, the nature of the coupling between the various spreading systems is uncertain, so that, although about two-thirds of the Scotia Sea floor is now dated, its tectonic evolution is not yet fully understood. In particular, subduction at the Falkland trough, beneath a northward-migrating North Scotia Ridge[28] (shown unshaded in Fig. 2c) may conceivably have been responsible for central Scotia Sea opening, in different coupling conditions. The sense of the asymmetric spreading, if compatible with a thermal model, would suggest that the ridge crest was migrating to the south, and therefore that most if not all of the subduction was taking place at the Discovery Arc, as shown in Fig. 2c.

The Shikoku Basin lies at present on the Philippine plate, which is itself being subducted slowly in the north-west beneath the Eurasian plate, while its eastern margin is the site of fast subduction of Pacific plate. A recent re-evaluation of all available Shikoku Basin magnetic data by Shih[29] shows that the basin opened between ~24 and 15 Myr ago, with an asymmetry of 5–7% favouring accretion to the western, remnant arc side. The thermal model predicts from this a component of ridge crest migration along 250°, and therefore a migration of the western flank of the ridge crest in the same direction at a rate at least as fast as the half spreading rate (17–24 mm yr^{-1}). If the absolute motions of the Pacific and Eurasian plates were then similar to those of today (Fig. 2d and Table 1), this migration alone would require subduction of the western flank beneath the Eurasian plate, independently of any northward movement implied by palaeomagnetic evidence[5].

This raises another point of interest. The direction of back-arc basin opening within the Cenozoic, with respect to the island arcs and also probably in absolute terms, has been largely east–west, a motion not amenable to detection by palaeomagnetic means. If a consistent ridge migration/asymmetry relationship were to be established, it would be possible to detect at least the polarity of such palaeomotion. If, in addition, Chase's subduction imperative[24] that trenches advance were accepted, the motions of some island arcs could be deduced within quite narrow limits. At the time of Shikoku Basin opening, for example, the palaeo-Mariana/Bonin arc would have been advancing eastward more slowly than the half-spreading rate (15 to 22 mm yr^{-1}). Such data would be of value in studies of the global distribution of plate motions at times in the past, aimed at modelling the driving forces[30], but it should be remembered that the MHRF, with all its assumptions, would have been involved in their production.

As in the active back-arc examples, the sense of asymmetric spreading in one of the extinct basins described above favours accretion to the remnant arc side, and in the other to the side carrying the island arc and trench; this adds to the argument against 'forced convection' models of back-arc extension. Thus, although some of the foregoing discussion is undoubtedly pre-
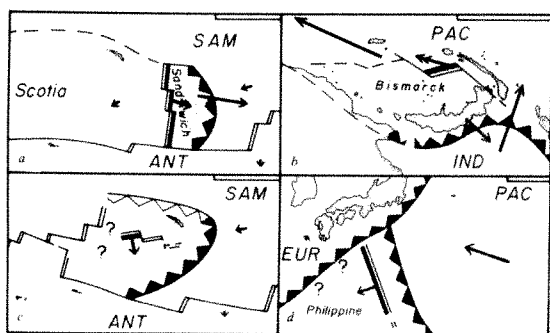

Fig. 2 Asymmetric spreading in presently active East Scotia Sea[18] (a) and Bismarck Sea[19] (b), and extinct central Scotia Sea[25] (c) and Shikoku[5] (d) back-arc basins. Spreading ridges are double lines, the thicker indicating the faster-spreading flank. Single-headed thick arrows are 'absolute' plate motions, from ref. 15 (Table 1) or as derived in the text. Double-headed arrow (a and b) is absolute motion of ridge crest. Length of line in upper right of each diagram shows 500 km distance and 100 mm yr^{-1} arrow length. Extinct back-arc basins (c and d) both shown as at ~15 Myr ago, but with present-day major plate motions; spreading centre arrows show ridge crest migration component compatible with thermal effect.

mature, being based on so few examples, it is clear that asymmetric spreading is of some interest both as a means of understanding active margin processes and for its possible use in estimating components of absolute plate motions in the past.

1. Hayes, D. E. *Bull. geol. Soc. Am.* **87**, 994–1002 (1976).
2. Weissel, J. K. & Hayes, D. E. in *Antarctic Research Series* Vol. 19, 165–196 (American Geophysical Union, Washington, DC, 1972).
3. Barker, P. F. *Geophys. J. R. astr. Soc.* **59**, 131–145 (1979).
4. Macdonald, K. C. *Bull. geol. Soc. Am.* **88**, 541–555 (1977).
5. Karig, D. E. in *Init. Rep. DSDP* Leg **31**, 857–879 (1975).
6. Watts, A. B. Weissel, J. K. & Larson, R. L. *Tectonophysics* **37**, 167–181 (1977).
7. Hey, R., Johnson, G. L. & Lowrie, A. *Bull. geol. Soc. Am.* **88**, 1385–1403 (1977).
8. Hey, R. *Bull. geol. Soc. Am.* **88**, 1404–1420 (1977).
9. Lonsdale, P. & Klitgord, K. D. *Bull. geol. Soc. Am.* **89**, 981–999 (1978).
10. Hey, R. *Geology* **7**, 504–506 (1979).
11. Elvers, D., Srivastava, S. P., Potter, K., Morley, J. & Seidel, D. *Earth planet. Sci. Lett.* **20**, 211–219 (1973).
12. Sclater, J. G. & Francheteau, J. *Geophys. J.R. astr. Soc.* **20**, 509–542 (1970).
13. Stein, S., Melosh, H. J. & Minster, J. B. *Earth planet. Sci. Lett.* **36**, 51–62 (1977).
14. Chase, C. G. *Earth planet. Sci. Lett.* **37**, 355–368 (1978).
15. Minster, J. B. & Jordan, T. H. *J. geophys. Res.* **83**, 5351–5354 (1978).
16. Solomon, S. C., Sleep, N. H. & Richardson, R. M. *Geophys. J.R. astr. Soc.* **42**, 769–801 (1975).
17. Toksoz, M. N. & Bird, P. in *Maurice Ewing Series* Vol. 1, 379–393 (American Geophysical Union, Washington DC, 1977).
18. Barker, P. F. *Earth planet. Sci. Lett.* **15**, 123–132 (1972).
19. Taylor, B. *Geology.* **7**, 171–174 (1979).
20. Weissel, J. K. in *Maurice Ewing Series* Vol. 1, 429–436 (American Geophysical Union, Washington DC, 1977).
21. Karig, D. E., Anderson, R. N. & Bibee, L. D. *J. geophys. Res.* **83**, 1213–1226 (1978).
22. Forsyth, D. W. *J. geophys. Res.* **80**, 1429–1443 (1975).
23. Weissel, J. K. & Anderson, R. N. *Earth planet. Sci. Lett.* **41**, 143–158 (1978).
24. Chase, C. G. *J. geophys. Res.* **83**, 5385–5387 (1978).
25. Hill, I. A. & Barker, P. F. *Geophys. J.R. astr. Soc.* (in the press).
26. Barker, P. F. & Burrell, J. *Mar. Geol.* **25**, 15–34 (1977).
27. Barker, P. F., Hill, I. A., Weaver, S. D. & Pankhurst, R. J. in *Antarctic Geoscience* (University of Wisconsin Press, Madison, in the press).
28. Ludwig, W. J., Windisch, C. C., Houtz, R. E. & Ewing, J. I. in *Am. Ass. petrol. Geol. Mem.* **29**, 125–137 (1979).
29. Shih, T. *Init. Rep. DSDP* (in the press).
30. Solomon, S. C., Sleep, N. H. & Jurdy, D. M. *J. geophys. Res.* **82**, 203–212 (1977).

Solution of the continuity equation for the Karnak area

T. C. Billard & George Burns

Department of Chemistry, University of Toronto, Toronto, Ontario, Canada M5S 1A1

Concern has long been expressed that ancient Egyptian temples alongside the Nile deteriorate with time. Deteriorations were usually associated with annual inundations. When flood waters receded, salt deposits attacked the porous sandstone, reducing it to sand, and thus destroying the foundations. With the construction of the first dam, and of the High Dam near Aswan (in 1965), the annual inundations were eliminated. However, monitoring of the deterioration continued, especially in the Thebes–Karnak area[1], where the temples are particularly numerous and important. The dam's construction was generally considered beneficial[2] mostly because earlier causes of land salinization were eliminated. But this consensus was based on hydrological, climatological and chemical data[1] and was only qualitative, and it has not been possible to answer this question even semi-quantitatively. However, visual observation indicates that some form of deterioration, due to salts appearing at the foundation of some monuments in Egypt, still takes place. Consequently, a deeper understanding of salinization processes is needed. We describe here a computer simulation of the flow of saline water in the area of the Great Temple of Karnak, to determine whether salinization in the post-dam, that is, present time, is a serious threat to the antiquities there.

The Karnak Temple is situated on the east bank of the Nile ~ 450 m from the river. It is ~ 500 m wide, and together with adjacent temple complexes, stretches along the Nile for about 1 km. It was constructed over a period of $\sim 2,000$ yr from the
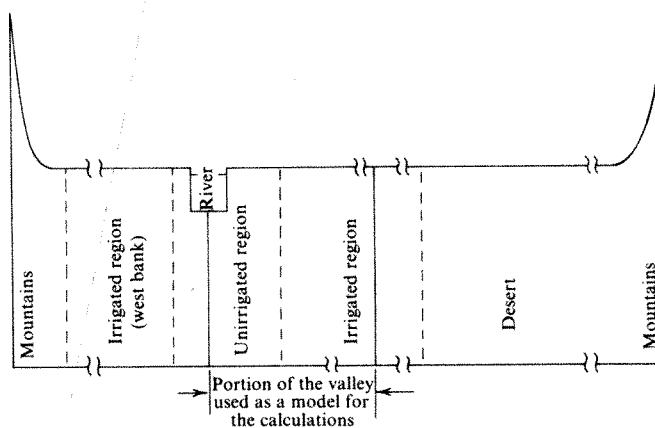

Fig. 1 Cross-sectional diagram of Nile Valley in Karnak Temple area (not drawn to scale).

time of the Middle Kingdom until Ptolomean time, and consists of smaller temples, shrines, courts, halls and chapels. It fell into disrepair in Roman times, $\sim 2,000$ yr ago.

The physical system considered in this simulation is shown in Fig. 1 and is represented by a river valley between two rows of mountains impermeable to water. A large area of the valley is irrigated but between this area and the river is an unirrigated region where the temples are situated. Mathematically, this is a two-dimensional system, because the system is approximately uniform in the y direction which is parallel to the river. The dimensions are defined by the direction, x, normal to the river towards the irrigated land, and the direction, z, normal to the ground surface, that is, the depth. We considered a portion of the physical system, as shown in Fig. 1 for our calculations. As we are interested in the average processes occurring in the valley, and because the climate and hydrology of the valley are relatively stable[1], the system was assumed to be in a steady state.

The difference in the levels of the Nile and the water table under the irrigated fields constitutes a driving force that moves the water and soluble salts from the fields into the river. As there is no irrigation in the temple area, the evaporation of moisture at the surface of the ground constitutes another driving force that moves saline water from the water table to the surface, where salts, which had been in solution, are deposited. The relative importance and the approximate rates of these processes were determined here for the water saturated region by solving the steady-state continuity equation, with Darcy's law

$$J = K\nabla P$$

defining the flux, where K is the hydraulic conductivity, and P the gravitational potential plus hydrostatic pressure potential.

The steady-state continuity equation is

$$\nabla J = K\nabla^2 P = 0$$

therefore

$$\nabla^2 P = 0$$

The solution to this equation for the Karnak area is most easily done numerically due to the nonlinearity of the boundaries of the system.

Initially the IBM 370-65 and 3300 computers were used for these calculations; however, the final work was done using a SEL 55 mini-computer which was approximately 16 times slower than the IBM 3300. The computer program developed yielded a solution for the equation which was stable, consistent and convergent, and required typically 5 h of the mini-computer time. The effort in this work was in obtaining

significant data, rather than in developing an efficient computer program. Therefore, further improvement in computer time used may be anticipated.

The hydraulic conductivity of the soil was chosen to be 0.003 cm min^{-1}. This value is in the low range of alluvial soil hydraulic conductivities, and it was selected to obtain a conservative estimate of water flow. The flow results, including the amount of salts deposited in unirrigated areas, are directly proportional to the hydraulic conductivity. Although the soil of the system is not uniform, for calculating average water flow in and out of the system, it is reasonable to assume soil uniformity (constant K).

Figure 2 shows the movement of the underground water in the Karnak area. These results were obtained from solutions of the continuity equation with boundary conditions deduced from the geological survey map of the Luxor–Karnak area, from geological surveys[3][5] and from previously published data[1]. The boundary conditions are: (1) no flow, $(\partial P/\partial x) = 0$, at the water divide in the irrigated fields, and at the bedrock, $(\partial P/\partial z) = 0$, which is the lower boundary; (2) no flow below the river from one bank to the other, $(\partial P/\partial x) = 0$; (3) zero-potential, $(P = 0)$, at the river/soil boundary; (4) the potential at the upper boundary is equal to the height of the water table, above the river height.

The key boundary condition is the height of the water table. At Karnak, it is an experimentally known quantity[1] and implicitly includes the effect of the evaporation at the ground surface, because the position of the water table is determined by the extent of irrigation and evaporation.

The flows of water across the boundaries were calculated and are given in Table 1. These results for the underground water flow for the Karnak regions show that $\sim 92\%$ of the water, which drains from the irrigated land, is evaporated on or near the surface of the unirrigated land, including the Karnak Temple site. The concentration of salts in the underground water in the Karnak area was determined to be on average 15 m Equiv. l^{-1} (ref. 1) which is in good agreement with our own measurements. This yields the average rate of salt deposition in the immediate area of the Karnak Temple area as 0.04 Equiv. yr^{-1} m^{-2}. As the soil conductivity was chosen conservatively, the average salt deposition calculated above is also a conservative number.

Although pre-Aswan Dam deterioration of the Karnak Temples has been eliminated, we conclude that new physicochemical processes operate since the Aswan Dam was built, causing salinization of land and ancient monuments.

Salinization occurs because irrigation raises the water table and causes a flow of saline underground water, which evaporates over dry unirrigated land. As archaeological monuments in the Nile Valley were commonly situated on dry
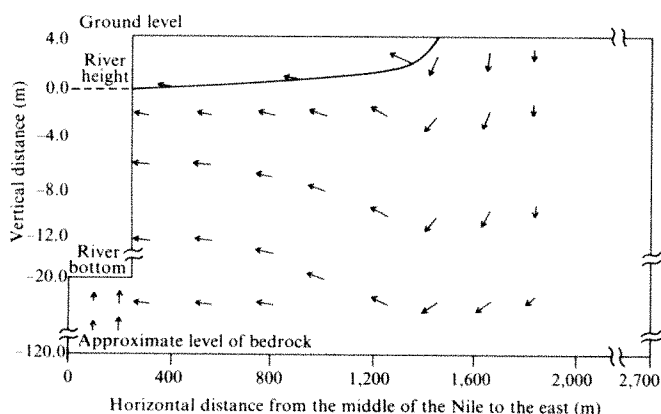
Table 1 Flows in the water saturated system per metre parallel to the river

Flow into the system through the irrigated fields (m^2 min^{-1})	6.1×10^{-5}
Flow out of the system into the river (m^2 min^{-1})	0.3×10^{-5}
Flow out of the system through the water table (m^2 min^{-1})	5.8×10^{-5}

land in the vicinity of irrigated fields, one would expect that processes of salinization, as described in the present model, occur not only in the Karnak area, but also elsewhere in Egypt. Such salinization endangers the foundations of the temples and unexcavated antiquities. As these processes are continuous and cumulative, over a long period of time, they threaten the very existence of the great monuments.

These calculations are being refined and the method will be applied to other regions, where hydrological data[1] are available.

1. Traunecker, C. *Kémi* **20**, 195 (1970); **20**, 213 (1970); **21**, 177 (1971); **21**, 197 (1971); *Karnak* **5**, 119 (1975); **5**, 131 (1975).
2. Lauffray, J. *Le Courrier du CNRS* **9**, 28 (1973).
3. Attia, M. L. *Geological Survey of Egypt-Deposits in the Nile Valley and the Delta* (Government Press, Cairo, 1954).
4. Hume, W. F. *Survey of Egypt-Geology of Egypt* (Government Press, Cairo, 1925).
5. Lyons, H. G. *The Physiography of the Nile River and its Basins* (Finance Department of Egyptian Government, Cairo, 1906).
6. *Conservation Problems in Egypt* (UNESCO Consultant Report, Contract No. 33.591, 1970).

Possible role of abscisic acid in reducing seed set in water-stressed wheat plants

J. M. Morgan

Agricultural Research Centre, RMB 944, Tamworth 2340, Australia

One of the primary effects of water stress on grain yield in wheat is the reduction of the number of seeds set per spikelet through an increase in male sterility[1][2]. However, little is known of the relationship between loss of pollen viability and the water relations of the developing spikelets, so that it is not known whether the effect of water deficit occurs as direct dehydration of the anther or by some other means. We report here that seed set may be reduced by water deficits which cause leaf wilting but have no effect on spikelet turgor or relative water content. This raises the possibility that abscisic acid (ABA), which is known to increase substantially when the leaf wilts[3][4] and to modify developmental processes in plants[5], is involved in the processes causing floret infertility. In support of this hypothesis we show that reductions in seed set due to water stress are accompanied by increases in endogenous ABA in both leaf and spikelet, and that foliar application of synthetic ABA at the stage of meiosis also reduces seed set and causes malformation of pollen grains and anthers.

The relationship between leaf turgor and seed set was derived from studies on wheat plants (*Triticum aestivum* L. cultivar Condor) which were grown in pots containing equal volumes of sand and peat moss in a glasshouse. The plants
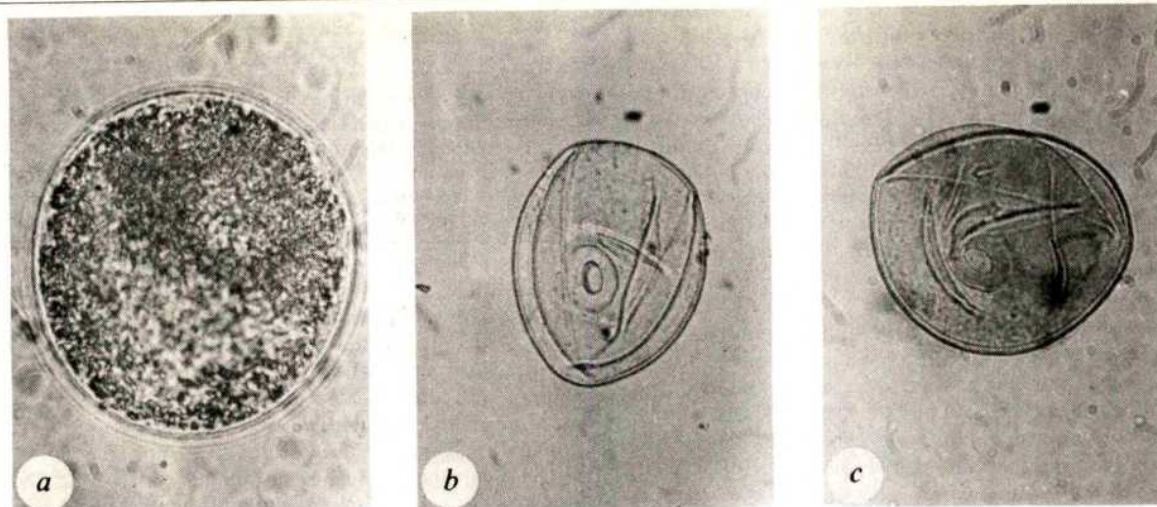
Fig. 2 Water flux on the east bank of the Nile River at Karnak. The water table level is indicated by a curve which extrapolates into the river height. (Relative magnitude of flux is on a log$_e$ scale.)

Fig. 1 Mature pollen grains from well watered (*a*), water stressed (*b*) and ABA-treated (*c*) plants (×1,250).

were watered daily and received standard nutrient solution twice weekly in sufficient quantity to saturate the soil and provide a small amount of drainage. Water stress was produced by withholding water when the anthers of basal florets in the centre of the ears of the primary tillers were near to the stage of meiosis. This stage was reached when the flag leaf ligule was ~4 cm above the ligule of the enclosing leaf. Pilot experiments and published results[2] have indicated that male sterility results from water stress at this stage. Tillers which were 2–4 d more advanced (early booting) were also sampled. Measurements of water (ψ), and osmotic (π) potentials (using Spanner-type thermocouple psychrometers[6]) and relative water contents (ζ) (using the technique of Slatyer and Barrs[7]) were made on tillers with leaves which had just wilted or were at higher water potentials; samples were also taken from unstressed plants. (Turgor potential, *P*, was taken as $\psi - \pi$). The first signs of wilting occurred within about 6 d of withholding water. Each sampled tiller was matched with a labelled tiller at the same stage of development and the pots were rewatered. After maturity, seeds and florets were counted on ears of tagged tillers.

and without reduced seed set (Table 1) because reductions in spikelet water potentials were fully matched by reductions in osmotic potential. Because the onset of water stress was rapid, the leaves did not show osmotic adjustment, and the turgor declined to zero. Observations of pollen morphology and fertilization tests confirmed that affected florets were male sterile.

The reduction in seed set in the absence of water deficits in the spikelets suggests that the effect is indirect, possibly involving plant growth regulators. Indeed, the coincidence of reduced seed set with loss of leaf turgor suggests the involvement of ABA because the amount of this substance is known to increase substantially when the leaft wilts[3,4].

This was confirmed in a second experiment, similar to the first except that levels of ABA were measured in the spikelets and leaves. Endogenous ABA was determined by gas chromatography (electron capture detector) after purification of the samples by solvent partitioning as described by King[8], except that purification of the methylated samples was achieved using a high pressure liquid chromatograph instead of a thin-layer chromatograph. Recovery was greater than 60%. The concentration of ABA in wilted leaves ($P = 0.0$ MPa) was 143 ng g^{-1} fresh weight compared with 23.5 ng g^{-1} in turgid leaves ($P = 0.6$ MPa). Furthermore, the levels of ABA in the spikelets of plants with wilted and turgid leaves were 111.0 ng g^{-1} and 35.2 ng g^{-1}, respectively, even though there was no difference in spikelet turgor potential (mean *P* = 0.6 MPa). The seed set, however, was reduced from 55% in turgid plants to 4% in wilted plants.

On the basis of these results and published data[3,4], it seemed possible that a reduction in seed set due to water stress could be linked with an increase in the level of ABA due to leaf wilt. To test this hypothesis, synthetic ABA was applied to the flag leaves of tillers when the basal florets of spikelets in the centre of the ear were between meiosis and second mitosis, and after second mitosis (boot swell stage). The plants were grown in the same way as described above. Aqueous solutions of ABA of 1, 10 and 30 mg l^{-1} were made up by dissolving the ABA in ~10 ml of 1M KOH, diluting with water and adjusting the final solution to *p*H 5.8. The control solution was the same but contained no ABA. The solutions were applied by immersing the leaves for 2 min. Each treatment was replicated five times. Tillers were tagged and observations were made of pollen morphology just before anthesis by squashing the anther in water or acetocarmine and photographing through a microscope. Several weeks after anthesis numbers of florets and seeds of tagged tillers were recorded.

Applications of ABA of 10 and 30 mg l^{-1} at meiosis reduced seed set by 43 and 27% (significant at 0.1% level) below

Table 1 Seed set and water relations of spikelets of plants with wilted and turgid leaves

Stage of development when stress applied	Range of leaf turgor (MPa)	Spikelet Mean P (MPa)	Mean ζ	% fertile florets
Meiosis	0.1–1.2	0.6 ± 0.1	0.93 ± 0.06	67.8 ± 1.5
	−0.1–0.1	0.6 ± 0.1	0.95 ± 0.01	44.0 ± 2.6
Early booting	0.2–1.0	0.6 ± 0.1	0.94 ± 0.04	67.8 ± 1.9
	−0.1–0.0	0.6 ± 0.1	0.94 ± 0.02	43.0 ± 2.0

The most significant result is that there was no change in seed set until the leaf had reached approximately zero turgor (Table 1). Thus, at meiosis, the data could be formed into two groups, depending on whether seed set had been reduced or not; one covering the range of *P* from 0.1 to 1.2 MPa in which there was no change in seed set and the other for the range of *P* from −0.1 to 0.1 MPa in which there were 36% fewer seeds per floret. Tillers at the early booting stage showed the same response. This reduction in seed set was not related to either spikelet turgor or spikelet relative water content. There was no difference in either of these parameters between plants with

control values respectively, but 1 mg ABA l⁻¹ had no effect (Table 2). At the later stage there was a reduction of 8 % (non significant) when 30 mg ABA l⁻¹ was used, but no effect when lower levels of ABA were used. The reductions in seed set due to applications at meiosis were associated with distorted pollen grains devoid of starch granules; these were identical to pollen grains affected by water stress (Fig. 1). Also the anthers, which were reduced in size, pale yellow and often shrivelled, were identical to those affected by water stress. Furthermore, both water stress and treatment with ABA produced a few tillers which failed to develop beyond the early boot swell stage.

Table 2 Effects of ABA on seed set

Stage of development when ABA applied	ABA concentration (mg l⁻¹)			
	0	1	10	30
Meiosis	65.6	64.6	37.3	48.2
Booting	61.0	65.1	60.5	56.3

Effects were measured as per cent fertile florets.

From these results it is not possible to determine the precise stage of microsporogenesis at which ABA acts. Although seed set was reduced by applications of ABA when basal florets were between pre-meiosis and second mitosis, other florets, particularly the central ones in the spikelets and those near the tip and base of the ear, would have been at an earlier stage of development. It was usually those that failed to develop grain. It is possible that the effects of ABA are mitigated through the production of ethylene[9], in which case the ABA could be affecting pollen development in the same way as Ethrel, which is known to break down to produce ethylene in plant cells at low pH. Ethrel causes male sterility only when applied before meiosis[10].

The fact that an increase in the amount of ABA in the leaf through application causes a reduction in seed set and alteration of pollen morphology identical to that caused by water stress supports the hypothesis that water stress affects seed set through an increase in endogenous ABA,' though further studies are needed to clarify the mode of action. If this hypothesis is correct, it implies that ABA has a role in regulating grain number in anticipation of further periods of water stress, thereby reducing the number of 'sinks' for carbohydrates, the supply of which would be reduced by stress. The results also highlight the importance of mechanisms which maintain leaf turgor during periods of declining water potential, such as osmotic adjustment[11], as a means of reducing yield losses in crop plants growing in semi-arid environments.

1. Salter, P. J. & Goode, J. E. *Crop Responses to Water at Different Stages of Growth* (Commonwealth Agricultural Bureau, Farnham Royal, 1967).
2. Bingham, J. *Ann. appl. Biol.* **57**, 365–377 (1966).
3. Harrison, M. A. & Walton, D. C. *Plant Physiol.* **56**, 250–254 (1975).
4. Zabadal, T. J. *Plant Physiol.* **53**, 125–127 (1974).
5. Quarrie, S. A. & Jones, H. G. *J. exp. Bot.* **28**, 192–203 (1977).
6. Waister, P. D. *Nature* **205**, 922–923 (1965).
7. Slatyer, R. O. & Barrs, H. D. *UNESCO Arid Zone Res.* **25**, 331–342 (1965).
8. King, R. W. *Planta, Berl.* **132**, 43–51 (1976).
9. Goren, R., Altman, A. & Giladi, I. *Plant Physiol.* **63**, 280–282 (1979).
10. Bennett, M. D. & Hughes, G. W. *Nature* **240**, 566–568 (1972).
11. Morgan, J. M. *Nature* **270**, 234–235 (1977).

Morphogenesis of branching tubules in cultures of cloned mammary epithelial cells

D. C. Bennett

The Salk Institute, PO Box 85800, San Diego, California 92138

Morphogenesis (the development of biological form, usually of multicellular organisms or their parts) is generally studied in simple organisms like the slime mould *Dictyostelium*[1], for in mammals even single tissues like the mammary epithelium discussed here appear complex. Mammary epithelium, supported by mesenchymal tissue, forms a system of branching, tubular ducts. During phases of rapid growth these ducts end in solid, swollen 'end-buds', and when mature in globular 'alveoli'[2]. The mesenchyme influences the morphogenesis of the epithelium and may be essential for this process[3,4]. An unknown number of cell types are present in both the epithelium and the mesenchyme. One step towards a better-defined 'model gland' was taken by Yang et al.[5], who recently described three-dimensional, solid, tumour-like outgrowths from clumps of mouse mammary tumour cells cultured in floating 'collagen gel'[6] instead of on a plastic surface. I now describe behaviour retaining some elements of natural morphogenesis, in a cloned line of epithelial cells and thus in the unequivocal absence of mammary mesenchyme—unless mesenchyme can arise from epithelium. On floating collagen gel Rama 25 cells (derived from a rat mammary tumour[7]) could generate three-dimensional structures which, although often disorganized and tumour-like, included branching, hollow tubules, sometimes with bulbous ends. Thus all the information to specify such organization resided in a single cell type and survived cloning. This raises the possibility of a simple mammalian system in which morphogenetic mechanisms, and their relation to cell differentiation, can be studied as readily as in *Dictyostelium*.

Cultures of Rama 25 'cuboidal' cells were maintained as described previously[7]. These cells behave in culture as 'stem cells': despite repeated cloning they form other types of cells including 'elongated' cells, believed to be mammary myoepithelial cells[7–9]. Elongated cells show epithelial behaviour during early passages, forming cohesive colonies and resisting detachment by trypsin, but they share some structural and antigenic features with mesenchymal cells[7,9]. Studies of Rama 25 cells on floating collagen gel were undertaken when Emerman et al.[10] reported exceptional functional differentiation in normal, mouse mammary epithelial cells maintained on this substrate. 'Fixed' collagen gels were prepared as described in Fig. 1 legend, or with minor differences in protocol whose effects are analysed below. Rama 25 cells were plated on top. The cells attached and proliferated less quickly than on plastic, but formed a confluent cell layer in 4–9 days. The layer was very dense but predominantly one cell thick[7]. Occasional foci of elongated cells were present beneath the monolayer, but usually no other departures from the monolayer were present at this stage.

The gels were now released to float[6]. Over the subsequent 3–4 weeks, three-dimensional structures of several types appeared, with marked variation between different gels (see below). The most striking type, often observed, consisted of blunt projections into the gel. These were seen from about day 3–7 after floating and were usually in clusters, of which between 5 and 30 generally developed per gel. Branching of these outgrowths was observed (Fig. 1), sometimes up to five times in succession. Sometimes the tips of the branches were bulbous (Fig. 1a), like mammary 'end-buds'[2]. Some such outgrowths resembled early mammary rudiments[3]. Histological studies showed that these structures were
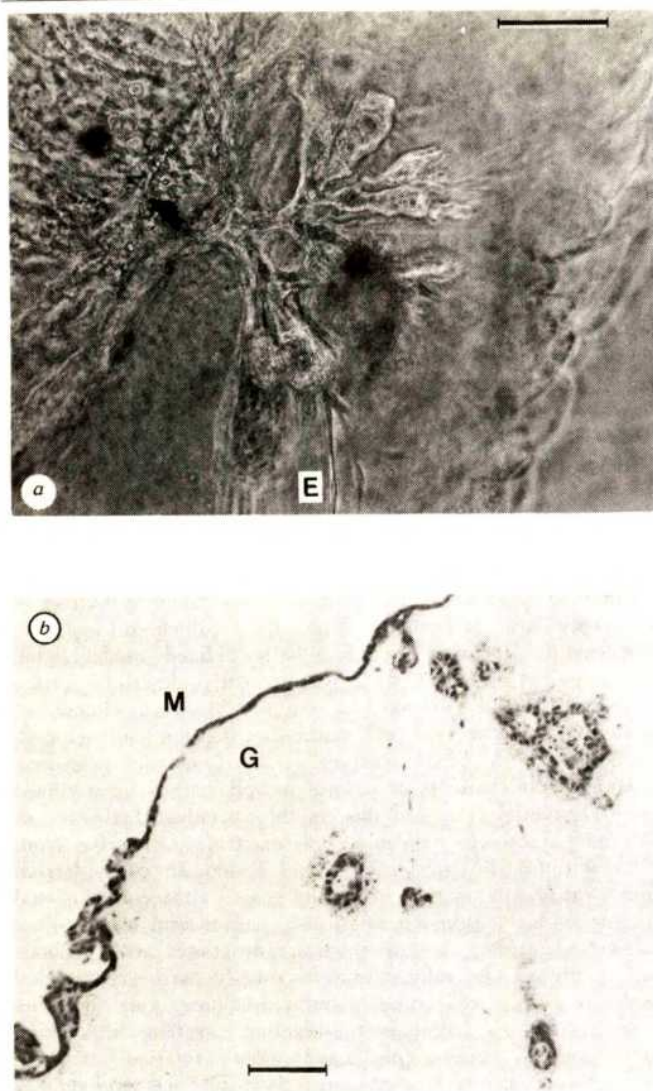
generally hollow tubules (Fig. 1*b*). These tubules resembled tubular carcinoma more closely than normal mammary epithelium: their walls were usually one cell thick (sometimes up to three); the cells were small and somewhat pleomorphic; mitotic figures were seen quite frequently; pyknotic cells were scattered both in and outside some tubules, and the outer layer of myoepithelial cells present in normal mammary ducts[2] was not observed in these.

Elongated (myoepithelial-like) cells were present focally in all cultures, but they usually migrated into the gel in densely branching chains and spikes instead of forming a second cell layer. Cloned elongated cells of the line Rama 29 (ref. 7) produced similar formations, although these cells also grew preferentially on the gel surface. Mammary cells invading collagen gel have previously been assumed to be mesenchymal[5,10]. However, these elongated cells arose from cloned epithelial cells and so are probably myoepithelial (see above). Perhaps this behaviour was associated with the failure of Rama 25 cells on collagen gel to produce a continuous basal lamina, as shown by electron microscopy[7]. Some otherwise similar spiky outgrowths had thicker, apparently solid branches and were reminiscent of the predominant structures described by Yang *et al.*[5]. Many small, apparently solid 'lumps' a few cells in diameter appeared from days 1–4. Broader areas with a convoluted surface like that of brain coral arose later, probably by coalescence of the lumps. In section these areas resembled papillary hyperplasia (Fig. 1*b*). Finally, groups of globules or spheres arose from days 16–22, in a few cultures only, either directly from the monolayer or from the tubular outgrowths (Fig. 2). Preliminary histological sections showed, among scattered elongated cells, circular cavities lined by one layer of small, flat cells. Some mitoses were seen, while pyknotic cells were again present, Thus, despite a superficial resemblance to mammary alveoli, these outgrowths were again more like some form of dysplasia.

The variation in the numbers and types of structures produced, between gels and between experiments, seemed largely due to small variations in the preparation of the gel. For example, sterilization of the gels under UV light as generally used[6,10] proved to cause drying of the gels. When gels were deliberately dried at 37 °C for different times (16–48 h) before use, the longer-dried gels were thin and flaccid when released. Cells initially attached and proliferated very well on these dehydrated gels, but after floating tended to form
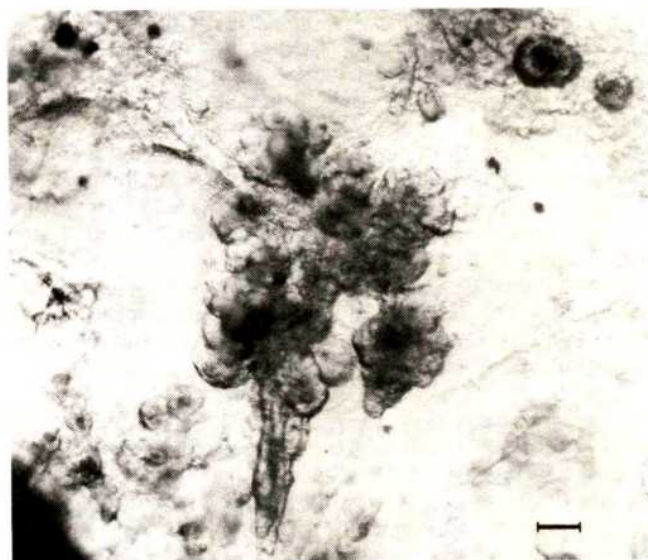
Fig. 1 Gland-like outgrowths from Rama 25 cells on floating collagen gels. Collagen solution was prepared by acetic acid extraction of rat-tail tendons[6] in sterile conditions then centrifuged for 1 h at 10,000*g* and the pellet discarded. 1 M NaOH solution was mixed with 2× concentrated DEM (Dulbecco's modification of Eagle's medium) to give 0.11 M NaOH, and the precipitate removed using a 0.22 μm filter (Nalge). This medium and the collagen solution were kept at 4 °C. To make each of four gels, 1.5 ml of the alkaline medium were mixed at 4 °C with 5 ml of collagen solution and 1.5 ml were dispensed quickly to each 33-mm culture dish (Falcon). When set, each gel was overlaid with 2 ml of culture medium (DEM with 7% or 10% fetal calf serum), and left for 1 day or more in a humid incubator at 37 °C, gassed with 10% v/v CO_2 in air. A suspension of Rama 25 cells was prepared[7] and plated on the gels in a fresh 2 ml of the same medium at 2×10^5 cells per dish. Incubation was resumed and the medium was renewed every 2–3 days until the cultures were confluent. Each gel was now released to float[6] and transferred to an 85-mm, bacteriological grade dish (Falcon) with 10 ml of medium to support the many cells now present. Incubation was resumed, with fresh medium every 5 days or less. *a*, Living culture seen by phase contrast microscopy, 2 weeks after floating, showing outgrowth from cell layer at left, branching about four times and with bulbous ends. E denotes chain of elongated cells. *b*, 5 μm paraffin section of similar culture, fixed in neutrally buffered formalin (haematoxylin and eosin stain; transmission optics). G denotes gel; M, surface of cell sheet which faced culture medium. Several tubules are sectioned, showing branch-points and mostly single-layered epithelium; at left cell layer forms papillae. Scale bars represent 100 μm.

Fig. 2 Later form of outgrowth from Rama 25 cells. The figure shows living culture, prepared as for Fig. 1 and photographed on day 17. Duct-like outgrowths present in this gel up to day 14 had given place to clusters of spheres as shown (only part of cluster in focus). Transmission optics. Scale bar, 100 μm.
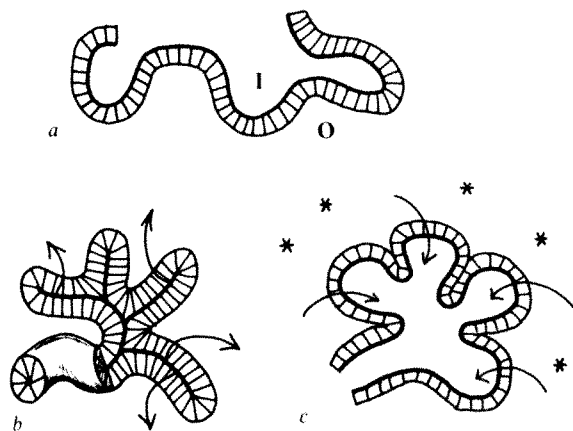
Fig. 3 Hypothetical set of properties allowing cells of a single type to form tubules and alveoli. *a*: (1) Cells cohere to form a membrane. (2) The membrane has limited thickness, for example, a single cell layer with an upper limit to cell height. (3) Cell volume has a lower limit. (4) Cells are readily distorted. (5) The membrane remains continuous (cannot fragment). (6) 'Inside' (I) and 'outside' (O) surfaces are different. *b*: (7) Processes exist which keep the inside surface area at a minimum (zero). The interior is thus one-dimensional: a point for very small membranes or a line, which can branch. The membrane then forms an occluded sphere or (branching) tube respectively. It can grow while maintaining this form. (7a) (optional) if the membrane is relatively impermeable and separates two fluid compartments, a strong force contributing to (7) can be the net outward transport of fluid by cells (arrows). The resulting pressure difference tends to collapse the interior. *c*: (8) Cells respond to an environmental signal (*) by transporting fluid inwards, causing inflation into an alveolar form.

only lumps and 'brain coral' instead of the more penetrating structures. The depth of the gel was significant, as was the mixing procedure. The initiation of tubular outgrowths seemed in general to be promoted by irregularities in the cell monolayer, including lumps and especially foci of elongated cells.

It is the formation of hollow, branching tubules in these cultures which seems particularly interesting. Mesenchyme may control the initial determination of epithelium as mammary tissue, and can certainly modulate the epithelial branching pattern[3,4], but this study shows that the basic 'glandular' form of branching tubes can be generated by isolated, cloned epithelial cells. (The same form is seen in developing salivary gland, pancreas and lung.) This is not too surprising, for Gierer has shown that in theory only one cell type is needed to form tubes, among other structures[11]. Figure 3 illustrates this with a combination of properties which could plausibly be possessed by the lining epithelial cells of the breast, and also by Rama 25 cuboidal cells. Property (7) may be the least plausible, but glandular epithelial cells contain at their apical or inner face a 'terminal web' of microfilaments which contain myosin-like protein[12] and which may thus be contractile. Mammary ducts and ductules are not always occluded[13], but morphogenesis can depend on transient processes[11]. Property (7a) would explain the production of 'domes' or multicellular blisters in cultured sheets of mammary epithelial cells[7,14], for domes seem to result from transport of ions and water from the apical to the basal ('outer') cell surface[14,15]. Milk secretion could provide property (8). The example in Fig. 3 is not meant as a claim that glands contain only one cell type, nor to account for all of mammary morphogenesis. For example it does not explain the branching of ducts. The essential point is that both ducts and alveoli have simple, easily defined forms: forms which do not require multiple cell types.

In conclusion, either the morphogenesis of branching tubules can be achieved by a single epithelial cell population, or

1. Kay, R. R., Town, C. D. & Gross, J. D. *Differentiation* **13**, 7–14 (1979).
2. Mayer, G. & Klein, M. in *Milk: the Mammary Gland and its Secretion* 1 (eds Kon, S. K. & Cowie, A. T.) 47–126 (Academic, New York, 1961).
3. Kratochwil, K. *Devl Biol.* **20**, 46–71 (1969).
4. Sakakura, T., Nishizuka, Y. & Dawe, C. J. *Science* **194**, 1439–1441 (1976).
5. Yang, J. *et al. Proc. natn. Acad. Sci. U.S.A.* **76**, 3401–3405 (1979).
6. Michalopoulos, G. & Pitot, H. C. *Expl Cell Res.* **94**, 70–78 (1975).
7. Bennett, D. C., Peachey, L. A., Durbin, H. & Rudland, P. S. *Cell* **15**, 283–298 (1978).
8. Lennon, V. A., Unger, M. & Dulbecco, R. *Proc. natn. Acad. Sci. U.S.A.* **75**, 6093–6097 (1978).
9. Rudland, P. S., Bennett, D. C. & Warburton, M. J. *Cold Spring Harb. Symp. Cell Proliferation* **6**, 677–699 (1979).
10. Emerman, J. T., Enami, J., Pitelka, D. R. & Nandi, S. *Proc. natn. Acad. Sci. U.S.A.* **74**, 4466–4470 (1977).
11. Gierer, A. *Q. Rev. Biophys.* **10**, 529–593 (1977).
12. Puchtler, H., Waldrop, F. S., Carter, M. G. & Valentine, L. S. *Histochemistry* **40**, 281–289 (1974).
13. Hollman, K. H. in *Lactation: A Comprehensive Treatise* 1 (eds Larson, B. L. & Smith, V. R.) 3–95 (Academic, New York, 1974).
14. McGrath, C. M. *Am. Zool.* **15**, 231–236 (1975).
15. Cereijido, M., Robbins, E. S., Dolan, W. J., Rotunno, C. A. & Sabatini, D. D. *J. Cell Biol.* **77**, 853–880 (1978).

Selective killing of mycoplasmas from contaminated mammalian cells in cell cultures

Menashe Marcus*, Uri Lavi*‡, Alona Nattenberg*, Shlomo Rottem† & Ora Markowitz†

*Department of Genetics, The Hebrew University of Jerusalem, Jerusalem, Israel

†Department of Clinical Microbiology, The Hebrew University–Hadassah Medical School, Jerusalem, Israel

Mycoplasmas are common contaminants of animal cells in cell cultures[1-3]. About 25 *Mycoplasma* and *Acholeplasma* species have been identified as cell culture contaminants but the most frequent are *Mycoplasma hyorhinis*, *Mycoplasma orale*, *Mycoplasma arginini* and *Acholeplasma laidlawii*[3]. These species are responsible for almost 85% of the contaminations in cell cultures[3]. We have devised a method for the selective killing of mycoplasmas in contaminated cell cultures, based on the differential nucleic acid metabolism of mycoplasma and mammalian cells. Mycoplasmas are unusual in that they have a nutritional requirement for nucleic acid precursors which can be met by purines and pyrimidine bases or by nucleosides[4-6]. Mammalian cells, on the other hand, incorporate very little free pyrimidines[7,8] and for that reason incorporation of free bases such as uracil has been used to detect mycoplasmas in contaminated cell cultures[9]. One of the free base analogues which can be incorporated selectively into nucleic acids of mycoplasmas is 5-bromouracil (5-BrUra). Visible light induces breaks in 5-BrUra-containing DNA[10] and this photosensitivity can be greatly increased by binding of the fluorochrome 33258-Hoechst to DNA[11]. Its unusually high content of A + T makes the mycoplasma DNA[3] an excellent candidate for the induction of breakage by the combined action of 5-BrUra, 33258-H and light because 33258-H has a high affinity for A–T base pairs and an even higher affinity for A–BrUra base pairs[12]. We report here that treating them in this way provides a practical and simple method for the selective killing of contaminating mycoplasmas; they are probably killed by the breakage of their DNA.

‡Permanent address: Agriculture Research Organization, Volcani Center, Bet Dagan, Israel.

Table 1 Incorporation of pyrimidine bases into nucleic acids of uncontaminated and mycoplasma-contaminated mouse RAG cells

	Radioactivity (c.p.m. per 10^4 RAG cells)	
^{3}H-Pyrimidine	Uncontaminated	Contaminated
Uracil	340	78,000
Thymine	630	550
5-Bromouracil	190	6,800

Uncontaminated or contaminated cells (5×10^4) were inoculated into 3-cm Petri dishes in Dulbecco's modified minimal essential medium (DMEM) enriched with 10% fetal calf serum (FCS). After 20 h of incubation at 37 °C the medium was replaced with fresh DMEM containing 1 μCi ml^{-1} (20 Ci mmol^{-1}) of ^{3}H-uracil, ^{3}H-thymine or ^{3}H-5-BrUra. After 60 min of pulse, the cells were trypsinized, washed in cold DMEM and 10^4 cells precipitated in 5% cold trichloroacetic acid (TCA). The precipitate was collected on glass fibre GF/C filters, washed, dried and counted in a Packard Tricarb liquid scintillation spectrometer.

Cells of the Chinese hamster cell line E-36, in small culture flasks containing about 2×10^6 cells, were inoculated with about 10^6 colony-forming units (CFU) of *M. hyorhinis* or *A. laidlawii*. After several weeks of growth, the cell cultures reached a stable state of contamination. Cytological observation by the method of Chen[13] showed that every cell was contaminated with at least 100 mycoplasma cells. We also used two other cell lines contaminated with unknown mycoplasma strains: one, BHK-21 (ref. 14) originated from the Syrian hamster and the other, RAG (ref. 15) originated from the mouse. Because the mouse cells were very heavily contaminated, we used them to examine the differential incorporation of pyrimidine bases into nucleic acids in both mycoplasma-free and contaminated cells.

Table 1 shows that the incorporation of uracil and 5-BrUra was high in the contaminated cells and very low in mycoplasma-free cells. However, as McIvor and Kenny have shown[6], thymine incorporation was always low. Similar results were obtained with E-36 cells contaminated with either *M. hyorhinis* or *A. laidlawii*.

The high and selective incorporation of 5-BrUra into contaminated cells encouraged us to treat the cells with the combination of 5-BrUra, 33258-H and light. Treated cells were diluted and clones from single or 100 cells were grown and tested for the presence of mycoplasma. The results of the treatment of E-36 cells contaminated with *M. hyorhinis* are given in Table 2. They show that after 5 days of treatment, E-36 clones grown from 100 cells were cured whereas clones from single cells were cured in 2–3 days (data not shown). Cold thymine (10^{-5} M) was always added to the cloned cultures to prevent incorporation into cellular DNA of any 5-bromo-2-deoxyuridine (5-BUdR) released from dead mycoplasma cells. 2-Deoxycytidine (10^{-5} M) was also added to the cloned cultures to prevent possible toxic effects of 5-BUdR on the growth of cells[16].

The remaining viable mycoplasma contaminants in the growing clones were detected by selective ^{3}H-uracil incorporation[9] which is a simple and fast method, by cytological observation[13] and by the viability counting of CFU[5]. As reported[17], the first two approaches detect only heavy contamination, whereas the CFU technique detects much lower levels of contamination and that was always used as the critical test. We obtained equally good selective killing of mycoplasma from E-36 cells contaminated with *A. laidlawii*. We also eliminated the unknown strains of mycoplasma from RAG cells and BHK-21 cells. The results in Fig. 1 show the effectiveness of our treatment on heavily contaminated RAG cells.

Our findings show that *M. hyorhinis* and *A. laidlawii* contaminating Chinese hamster cells can be selectively killed by our technique and cured clones of cells can be easily obtained from the treated cell culture. The same selective killing technique proved efficient in curing RAG and BHK-21
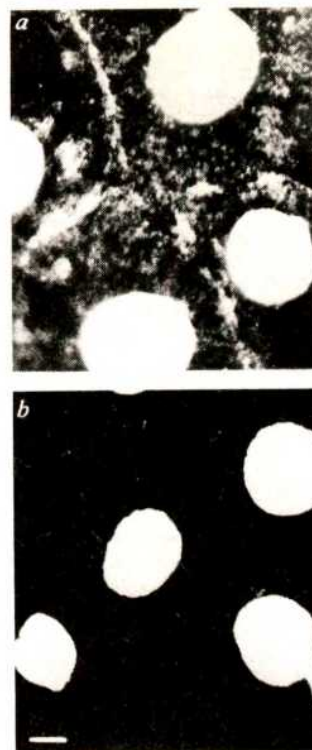
Fig. 1 *a*, RAG cells heavily contaminated with mycoplasmas. The cell nuclei have been stained according to Chen[13]. They fluoresce brightly. *b*, Cured RAG cells. No mycoplasma cells are seen. Only brightly fluorescing cell nuclei are seen.

Table 2 Elimination of *M. hyorhinis* from E-36 cells by combined 5-BrUra, 33258-Hoechst and light treatment

5-BrUra treatments (d)	^{3}H-Uracil incorporation (c.p.m. per 10^4 E-36 cells)	Cytological determination of contaminants	Viability count (CFU ml^{-1})
0	31,000	+ + + +	2×10^7
2	700	+ +	1.8×10^5
3	190	+	4×10^3
4	220	−	1×10^2
5	70	−	0

Contaminated cells were grown at 37 °C in DMEM + FCS. 5-BrUra (30 μg ml^{-1}) was added to the cultures. After 24 h 33258-Hoechst (1 μg ml^{-1}) was added for 60 min and the cultures were then illuminated by a 400-W cold bright fluorescence lamp at a distance of 5 cm for 30 min. The medium was then replaced with a fresh DMEM + FCS containing 5-BrUra and the Hoechst treatment was repeated at 24-h intervals. After two to five treatments the cells were trypsinized, washed and diluted in fresh DMEM + FCS containing 10^{-5} M thymine and 10^{-5} M 2-deoxycytidine. The cells were cloned in Microtest plates. In each well, clones from 100 cells were started. The growing clones were transferred to 3-cm Petri dishes and screened for mycoplasma contamination by the DNA fluorochrome staining procedure[13] and the CFU counting technique[5]. ^{3}H-Uracil incorporation into acid-insoluble material was determined 24 h after the end of each combined 5-BrUra–33258–Hoechst–light treatment. E-36 cells (5×10^4) were inoculated into a 3-cm Petri dish in DMEM + FCS. After 24 h of incubation at 37 °C the medium was replaced with fresh DMEM containing ^{3}H-uracil (1 μg ml^{-1}, 20 Ci mmol^{-1}). After 60 min the cells were trypsinized, washed in cold DMEM and 10^4 cells were precipitated in 5% cold TCA. The precipitate was collected by filtration, washed, dried and counted as in Table 1. Cytological determinations were carried out according to Chen[13] using the DNA fluorochrome staining procedure. The results are expressed as follows: 4+, all cells are contaminated with at least 100 mycoplasmas per cell; 2+, only some of the cells are contaminated with 5–50 mycoplasmas per cell; +, only a few cells are contaminated with 1–20 mycoplasmas per cell; −, no mycoplasma cells observed in at least 50 screened E-36 cells.

cells from unknown contaminating mycoplasma strains. Our cured RAG and BHK-21 clones have already been grown continuously for several months and no contaminating mycoplasma has been found. These results suggest that our technique could be applied generally in the elimination of contaminating mycoplasma strains from mammalian cell cultures.

1. Stanbridge, E. *Bact. Rev.* **35**, 206–227 (1971).
2. Barile, M. F. in *Contamination in Tissue Culture*, 131–172 (Academic, New York, 1973).
3. Barile, M. F. in *The Mycoplasmas* (eds Tully, J. G. & Whitcomb, R. F.) 425–474 (Academic, New York, 1979).
4. Rodwell, A. W. *J. gen. Microbiol.* **58**, 39–47 (1969).
5. Stanbridge, E. J., Hayflick, L. & Perkins, F. T. *Nature new Biol.* **232**, 242–244 (1971).
6. McIvor, R. S. & Kenny, G. E. *J. Bact.* **135**, 483–489 (1978).
7. Prusoff, W. H. *Cancer Res.* **23**, 1246–1259 (1963).
8. Levine, E. M. & Becker, B. G. in *Mycoplasma Infection of Cell Cultures* (eds McGarrity, G. J., Murphy, D. G. & Nichols, W. W.) 87–104 (Plenum, New York, 1978).
9. Kenny, G. E. in *Microbiology* (ed. Schlesinger, D.) 32–36 (American Society for Microbiology, Washington, 1975).
10. Puck, T. T. & Kao, F. T. *Proc. natn. Acad. Sci. U.S.A.* **58**, 1227–1234 (1967).
11. Stetten, G., Latt, S. A. & Davidson, R. L. *Somatic Cell Genet.* **2**, 285–290 (1976).
12. Latt, S. A. & Wohlleb, J. C. *Chromosoma* **52**, 297–316 (1975).
13. Chen, T. R. *Expl Cell Res.* **104**, 255–262 (1977).
14. MacPherson, T. & Stoker, M. *Virology* **16**, 147–151 (1962).
15. Klebe, R. J., Chen, T. R. & Ruddle, F. H. *J. Cell Biol.* **45**, 74–82 (1970).
16. Meuth, M. & Green, H. *Cell* **2**, 109–112 (1974).
17. Thangavelu, M., Ernø, H. & Therkelsen, A. J. *Hum. Genet.* **47**, 199–202 (1979).

Macrophages overcome mycoplasma infections of cells *in vitro*

L. Schimmelpfeng, U. Langenberg & J. Hinrich Peters

Institut für Genetik, Universität Köln, Weyertal 121, D-5000 Köln 41, FRG

Mycoplasmal infections still cause severe problems in cell cultures, particularly permanent lines, and although rapid detection is possible[1,2] the only methods proposed for the elimination of the mycoplasma are either laborious or unsatisfactory. Treatment with antibiotics often leads to the development of resistance[3] and we have found it more successful to passage contaminated cells in nude (thymusless) mice[4] although the cells cannot always be recovered. But when the resulting subcutaneous tumours can be collected, the cells are both free of mycoplasma and accompanied by a large number of macrophages. Because nude mice have no T cell-dependent immune response, it seemed possible that the macrophages could be responsible for the elimination of the mycoplasma. The experiments reported here support this hypothesis, and have led to a rapid and reproducible technique for eliminating mycoplasma *in vitro* by a brief co-cultivation of contaminated cells with mouse macrophages, in the presence of antibiotics.

Three different preparations of mouse macrophages were used with identical success: peritoneal macrophages actuated by thioglycollate, the same preparation kept as frozen stock before use (frozen in 90% serum plus 10% dimethyl sulphoxide), and macrophages grown *in vitro* from bone marrow precursors stimulated with conditioned medium containing macrophage growth factor[5]. Eradication of mycoplasma was most efficient when contaminated cells were applied to a macrophage monolayer in a ratio of about 1:100, together with antibiotics (Table 1). If the ratio of cells to macrophages was greater or if either antibiotics or macrophages were omitted, results were less reliable, although

in the absence of antibiotics macrophages sometimes eliminated the mycoplasma. Antibiotics alone, as expected, were variably effective. Conditioned medium obtained from thioglycollate-activated macrophages did not affect contamination nor markedly alter the effect of antibiotics.

To confirm these results, we co-cultivated 10 permanent cell lines (BHK, RBH, NRK, 3T3, L6TG, L929, A9, A9HT, D-98AH2, and KB) heavily infected with mycoplasma, with macrophage monolayers (infected cells/macrophages 1:100), in the presence of antibiotics. When cells grew particularly rapidly on the macrophage monolayer (probably due to a feeder layer effect), we reduced the serum concentration to 2% in order to slow down the proliferation and not to exceed the optimal cell number. Following this protocol, we purified all cell lines. Most of them have been examined repeatedly for

Table 1   Effect of macrophages, macrophage-conditioned medium and antibiotics on mycoplasma elimination from two cell lines

Treatment	Cell type	No. of cells inoculated ($\times 10^{-3}$)					
		1	2	4	8	10	14
Antibiotics	A9	–	–	+	+	+	+
		+	+	+	+	+	+
	BHK	–	–	–	–	–	–
		–	–	–	–	–	–
Conditioned medium	A9	+	+	+	+	+	+
		+	+	+	+	+	+
	BHK	+	+	+	+	+	+
		+	+	+	+	+	+
Conditioned medium plus antibiotics	A9	+	+	+	+	+	+
		–	–	–	–	–	–
	BHK	–	–	–	+	+	+
		–	–	–	+	+	+
Macrophages (3.5 × 10^5 per well)	A9	+	+	+	+	+	+
		+	+	+	+	+	+
	BHK	–	–	+	+	+	+
		–	–	–	–	+	+
Antibiotics plus macrophages	A9	–	–	–	–	+	+
		–	–	–	–	+	+
	BHK	–	–	–	–	–	–
		–	–	–	–	–	–

Mouse peritoneal macrophages were elicited by intraperitoneal injection of 1 ml 10% thioglycollate medium (Difco 0256-01) into BALB/c mice. Four days later the cells were collected by rinsing of the peritoneal cavity and cultured at 3.5×10^5 cells per 1.5-cm well in Dulbecco's modified Eagle's minimal essential medium, supplemented with 10% heat inactivated fetal calf serum, penicillin ($10,000\,\text{U ml}^{-1}$) and streptomycin ($10,000\,\mu\text{g ml}^{-1}$). After 1 day of culture, the cells had formed a confluent monolayer. Non-adherent cells were removed by rinsing with growth medium. Mycoplasma-infected cells, either mouse A9 fibroblasts (a derivative of mouse L cells), or baby hamster kidney (BHK) cells were seeded at various numbers onto the macrophage monolayers. Control cultures contained no macrophages. Some of the cultures received mycoplasma-specific antibiotics ($100\,\mu\text{g ml}^{-1}$ lincomycin plus $100\,\mu\text{g ml}^{-1}$ tylosin), and/or 50% conditioned medium from 2 days cultures of thioglycollate elicited macrophages. After 3 days, A9 or BHK cells were separated from macrophages by treatment with trypsin (0.2%), a dose which does not detach macrophages. After another 3 days of culture, recovered cells were tested for the presence of mycoplasma by staining with the DNA-specific fluorescent dye, Hoechst 33258, previously described as a mycoplasma test[1]. After another 2–4 weeks of culture, the cells were examined by autoradiography of incorporated tritiated thymidine (1 µCi per ml per 24 h; 25 Ci mmol^{-1}, exposure time 4 days). In uninfected cells labelling was restricted to the nucleus, whereas mycoplasma-infected cells showed a marked peripheral labelling[6]. The results are expressed as presence (+) or absence (−) of mycoplasma. Double symbols indicate the results of two independent experiments.

more than 6 months and no mycoplasmal recrudescence has been observed.

Because macrophage-conditioned medium did not affect the mycoplasma, we do not regard secreted macrophage products (such as lysozyme) as the principal factors acting against mycoplasma. Instead, macrophages seem to act directly on the mycoplasma, particularly by phagocytosis. The combined action of phagocytic macrophages and antibiotics may reduce the probability that antibiotic resistance will develop, for macrophages rapidly clear the cultures of contaminants. However, we cannot rule out the possibility that co-cultivation may carry the risk of infecting the cells with endogenous murine viruses from the macrophages, as is equally true for cells injected into nude mice.

The observed synergism of macrophages and antibiotics may be useful for the *in vitro* study of defence mechanisms that are influenced by antibiotics *in vivo*. Indeed, we have observed the complete elimination of yeast and bacteria from tissue culture cells through the combined action of macrophages and antibiotics (kanamycin, gentamycin, or nystatin) when antibiotic treatment in the absence of macrophages is of limited efficacy.

This work was supported by the Deutsche Forschungsgemeinschaft (SFB 74).

1. Russel, W. C., Newman, C. & Williams, D. H. *Nature* **253**, 461–462 (1975).
2. McGarrity, G. J., Vanaman, V. & Sarama, J. *Expl Cell Res.* **121**, 159–165 (1979).
3. Kenney, G. E. *In Vitro* **14**, 338 (1978).
4. Van Diggelen, O. P., Shin, S. & Phillipps, D. M. *Cancer Res.* **37**, 2680–2687 (1977).
5. Meerpohl, H. G., Lohmann-Matthes, M. L. & Fischer, H. *Eur. J. Immun.* **6**, 213–217 (1976).
6. Perez, A. G., Kim, J. H., Gelbard, A. S. & Djordjevic, B. *Expl Cell Res.* **70**, 301–310 (1972).

In vivo cyclic change in B-lymphocyte susceptibility to T-cell control

R. A. Calderon & D. B. Thomas

Division of Immunology, National Institute for Medical Research, The Ridgeway, Mill Hill, London NW7 1AA, UK

The humoral response to hapten–protein conjugates is an invaluable model for dissecting the cellular elements of lymphocyte cooperation, and the Mitchison secondary adoptive transfer system provides convincing evidence of cooperation between hapten-specific B cells and carrier-specific T cells in the production of anti-hapten antibody[1-3]. Recently, attention has focused on the role of suppressor T cells in the regulation of antibody production[4]. Several workers have shown that carrier-priming may, in some instances, suppress a subsequent hapten antibody response, both *in vivo* and *in vitro*[5-9]. This effect is attributed to a suppressor T-cell population, generated during the initial phase of the immune response[8,9]. Gershon and co-workers have postulated that such suppressor T cells function in a feedback regulatory loop to limit the duration of an immune response[10]. We have examined the suppressive effect of carrier immunization in a secondary anti-hapten response *in vivo* and demonstrate a cyclic change in susceptibility of memory B cells to T-help and suppression. Such variation presents a severe restriction to any model of feedback control by suppressor T cells.

Spleen cells from CBA mice, primed 2–4 months earlier to dinitrophenyl keyhole-limpet haemocyanin (DNP-KLH), were adoptively transferred to lethally irradiated syngeneic recipients and assayed for indirect, anti-hapten plaque forming

cells (IPFC) at day 6 (Table 1). Treatment of the donor population with anti-Thy-1 and complement eliminated the IPFC response and this could be restored to almost normal values by the supplementary transfer of KLH-primed spleen cells (Table 1, expt 1*b*, *c*). There was no detectable anti-hapten response, however, if the carrier-primed population was boosted with KLH 3 days before cell transfer (expt 1*d*). This was unlikely to be a trivial artefact, such as failure of 'activated' helper cells to localize in recipient spleens, as boosting of hapten-primed donors with DNP-KLH (expt 2*a*) or KLH alone (expt 2*b*) did not diminish a subsequent anti-hapten response. Lack of cell cooperation was also observed in a heterologous system using DNP-KLH-primed spleen cells and human γ-globulin (HGG)-primed, or boosted, helper cells (expt 3) and the control experiment (expt 4) ruled out any nonspecific effect of immunization: HGG-boosted spleen cells did not suppress a secondary response to DNP-KLH.

There was a brisk decline in helper activity of carrier-primed donors after re-challenge with KLH (Fig. 1*a*), reaching a baseline value at 3 days followed by a gradual recovery to the pre-boost level. A comparison was also included of the effects of carrier-boosting in adult-thymectomized donors (as thymectomy is claimed to diminish suppressor T-cell activity[11-13]). Here, the effects of carrier immunization were marginal.
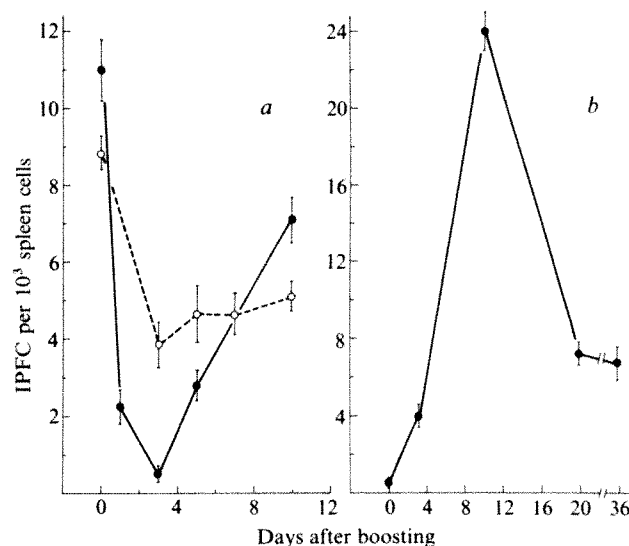

Fig. 1   *a*, Effect of carrier-boosting at various times before adoptive transfer. Groups of five normal, or adult-thymectomized CBA mice, primed to KLH, were injected i.v. with aqueous antigen 10 μg at the times indicated, before adoptive transfer. Spleen cells (10⁷) were combined with DNP-KLH-primed B cells (10⁷, previously treated with anti-Thy-1 and C′), 10 μg DNP-KLH and transferred to irradiated recipients. Adult thymectomy was carried out at 4 weeks and mice were primed with KLH alum-pertussis 1 week later. ●, Normal, KLH-primed mice; ○, adult thymectomized, KLH-primed mice. *b*, Effect of hapten-carrier boosting at various times before adoptive transfer. Groups of five CBA mice, primed to DNP-KLH, were injected i.v. with aqueous DNP-KLH (10 μg), at the times indicated, before adoptive transfer. Spleen cells were treated with anti-Thy-1 and C′, and combined with KLH-primed spleen cells (10⁷), boosted 3 days earlier with KLH (10 μg).

It could be argued from the above, and earlier reports of carrier-specific suppression in primary anti-hapten responses[7-9], that carrier immunization recruits a population of suppressor cells during the initial phase (Fig. 1*a*; 3 days) of the immune response. However, a strikingly different picture emerged when helper activity was assayed against memory B cells which had also been re-challenged with antigen before adoptive transfer (Fig. 1*b*): KLH-primed spleen cells, boosted

Table 1 Effect of carrier boosting on a secondary anti-hapten response *in vivo*

Hapten-primed donor	Carrier-primed donor	Antigen	IPFC per 10^6 spleen cells*
Expt 1			
a DNP-KLH	—	DNP-KLH	$11,089 \pm 750$
b DNP-KLH(anti-Thy-1+C')†	—		<150
c DNP-KLH(anti-Thy-1+C')†	KLH		$3,770 \pm 253$
d DNP-KLH(anti-Thy-1+C')†	KLH(−3d)‡		<150
Expt 2			
a DNP-KLH+hapten carrier(−3d)‡	—	DNP-KLH	$8,443 \pm 770$
b DNP-KLH+carrier(−3d)‡	—		$2,721 \pm 330$
c DNP-KLH+carrier(−3d)‡(anti-Thy-1+C')	KLH(−3d)‡		178 ± 30
Expt 3			
a DNP-KLH	—	DNP-HGG	$2,915 \pm 216$
b DNP-KLH	HGG		$21,008$
c DNP-KLH(anti-Thy-1+C')	HGG		$24,022 \pm 2,129$
d DNP-KLH	HGG(−3d)‡		340 ± 64
e DNP-KLH(anti-Thy-1+C')	HGG(−3d)‡		$1,393 \pm 177$
Expt 4			
a DNP-KLH	—	DNP-KLH	$59,400 \pm 5,400$
b DNP-KLH(anti-Thy-1+C')	KLH(−3d)‡		750 ± 105
c DNP-KLH	HGG(−3d)‡		$57,383 \pm 7,779$

CBA/Ca mice were immunized at 6–8 weeks with 100 μg alum-precipitated antigen (DNP$_{270}$-KLH; KLH; DNP$_{16}$-HGG; HGG) and 10^9 *Bordetella pertussis* and used 2–4 months later. Secondary challenges (boosting) of aqueous antigen (10 μg) were injected intravenously (i.v.). Recipients were irradiated with 850 rad from a ^{60}Co source and injected i.v. a few hours later with 10^7 hapten-primed spleen cells, and/or 10^7 carrier-primed spleen cells, and aqueous antigen (10 μg).

*Indirect plaque-forming cells (PFC) were assayed by the slide method[17], using DNP-Fab-anti-sheep red blood cells to coat erythrocytes, and developed with a polyspecific rabbit anti-Ig in the presence of a specific goat anti-μ serum (to suppress direct PFC). Values for IPFC per 10^6 spleen cells are the arithmetic mean ± s.e.m. for three or more spleens, assayed individually at two or more cell dilutions.

†Spleen cells (4 × 10^8, 2 ml) were incubated for 30 min at 3 °C with an equal volume of anti-Thy-1-2 serum (¼ dilution; AKR anti-C3H, cytotoxic titre > 1/200), washed and reincubated for 30 min at 37 °C with guinea pig complement (agarose absorbed; ⅓ dilution).

‡DNP-KLH or KLH or HGG-primed mice were boosted with 10 μg antigen 3 days before adoptive transfer.

3 days before adoptive transfer, suppressed a secondary anti-DNP response yet gave adequate help to memory B cells, re-challenged with antigen, 3–36 days before transfer.

There were several likely reasons for these cyclic changes in the anti-hapten response after boosting of the carrier (Fig. 1a) or hapten-primed donors (Fig. 1b). For instance, a secondary response to carrier might alter a pre-existing homeostatic balance between helper cells and suppressor cells in favour of the latter and/or produce a quantitative reduction in effective T-cell help. Alternatively, cell cooperation might require synchronous recognition of antigen by B and T cells, and subsequent cell proliferation leading to a parallel decline in the help provided (Fig. 1a) and help required (Fig. 1b) on adoptive transfer. The following cell titration experiments show that carrier immunization generates a population of suppressor T cells, whereas boosting of memory cells does not alter their requirement for carrier-specific help.

Optimum anti-DNP responses (5–15 × 10^5 IPFC per spleen) were regularly obtained on adoptive transfer to irradiated recipients of 10^7 DNP-KLH-primed B cells and 0.6–0.8 × 10^7 KLH-primed spleen cells. Addition of increasing numbers of KLH-primed and boosted (−3 days) spleen cells led to a progressive decline in IPFC, with optimum suppression (>90%) at cell ratios >1.5 for carrier-boosted to carried-primed cells (Fig. 2). Suppression was reduced by pretreatment of the carrier-boosted population with anti-Thy-1 and complement. In a reciprocal titration, optimum help was obtained at cell ratios >1.5 for carrier-primed to carrier-boosted donor cells. These results suggest that help or suppression in a secondary anti-hapten response is determined by the numerical balance between two populations of carrier-specific T cells; in which case there is the immediate paradox that memory B cells, re-challenged with antigen, cooperate superbly with a carrier-primed (and boosted, −3 days) population containing an apparent excess of suppressor cells (Fig. 1b). This suggests that memory cells become refractory to T-cell suppression, and/or require less 'available' help after
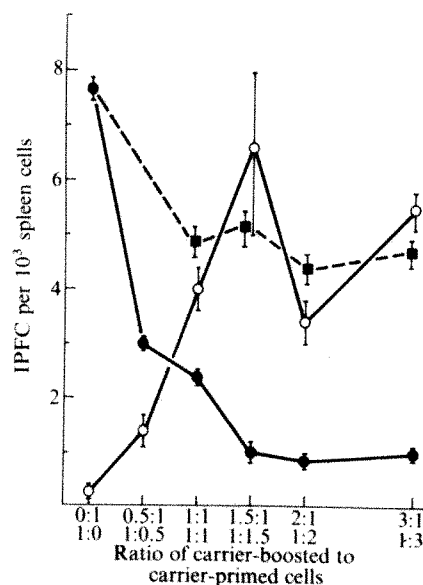

Fig. 2 Suppression of a secondary anti-DNP response by various proportions of carrier-primed to carrier-boosted spleen cells. ●, 10^7 DNP-KLH-primed B cells, 6 × 10^6 KLH-primed spleen cells and increasing proportions (6–18 × 10^6) of KLH-boosted (3 days previous) spleen cells. ○, 10^7 DNP-KLH-primed B cells, 6 × 10^6 KLH-boosted (3 days previous) spleen cells and increasing proportions (6–18 × 10^6) of KLH-primed spleen cells. ■, 10^7 DNP-KLH-primed B cells, 6 × 10^6 KLH-primed spleen cells and increasing proportions of KLH-boosted (3 days previous) spleen cells, pretreated with anti-Thy-1 and C'. Cell numbers were adjusted to equivalence before cell transfer (3.4 × 10^7 per recipient) by the appropriate addition of normal spleen cells.
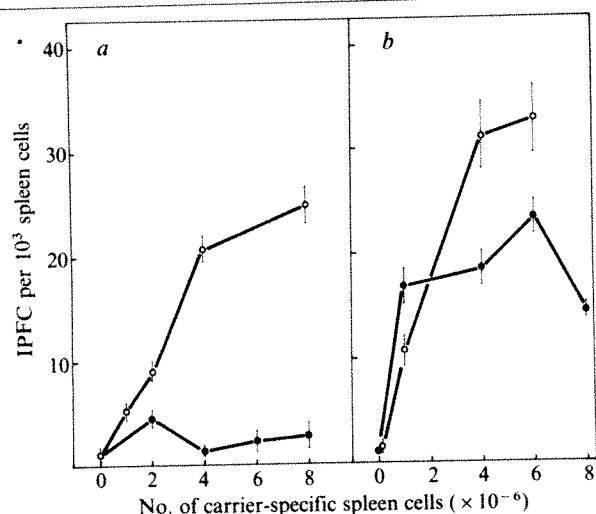
Fig. 3 Titration of carrier-specific help for: *a*, DNP-KLH primed B cells; *b*, DNP-KLH primed and boosted (10 days previous) B cells. ○, KLH-primed spleen cells; ●, KLH-primed and boosted (3 days previous) spleen cells. Cell numbers were adjusted to equivalence before cell transfer (18×10^6 per recipient) by the appropriate addition of normal spleen cells.

here is that the suppressor cells, generated by carrier immunization, exert no effect on an ongoing anti-hapten response, but rather may prevent its initiation. This raises an immediate question: how do suppressor T cells function in the postulated feedback regulatory loop[10] to curtail an immune response? The paradox is still to be resolved.

1. Ovary, Z. & Benacerraf, B. *Proc. Soc. exp. Biol. Med.* **114**, 72–76 (1963).
2. Mitchison, N. A. *Eur. J. Immun.* **1**, 18–27 (1971).
3. Raff, M. C. *Nature* **226**, 1257–1258 (1970).
4. Gershon, R. K. *Transplantn Rev.* **26**, 170–185 (1975).
5. Katz, D. A., Paul, W. E. & Benacerraf, B. *J. Immun.* **110**, 107–117 (1973).
6. Tada, T. & Takemori, T. *J. exp. Med.* **140**, 239–252 (1974).
7. Elson, C. J. & Taylor, R. B. *Eur. J. Immun.* **4**, 682–687 (1974).
8. Eardley, D. D. & Sercarz, E. E. *J. Immun.* **116**, 600–605 (1976).
9. Eardley, D. D. & Sercarz, E. E. *J. Immun.* **118**, 1306–1310 (1977).
10. Eardley, D. D. *et al. J. exp. Med.* **147**, 1106–1115 (1978).
11. Baker, P. J., Stashak, P. W., Ansbaugh, D. F., Prescott, B. & Barth, R. F. *J. Immun.* **105**, 1581–1583 (1970).
12. Okumura, K. & Tada, T. *J. Immun.* **106**, 1019–1025 (1971).
13. Basten, A., Miller, J. F. A. P. & Johnson, P. *Transplantn Rev.* **26**, 130–169 (1975).
14. Janeway, C. A. *J. Immun.* **114**, 1394–1401 (1975).
15. Cantor, H. & Boyse, E. A. *J. exp. Med.* **141**, 1376–1389 (1975).
16. North, J. R. & Askonas, B. A. *Eur. J. Immun.* **6**, 8–15 (1976).
17. Dresser, D. W. in *Handbook of Experimental Immunology* 3rd edn (ed. Weir, D. M.) (Blackwell, Oxford, 1978).

secondary challenge. To solve this problem, a limiting dilution analysis was made of the helper requirements for memory cells before, and after, a secondary antigenic challenge.

Constant numbers of DNP-KLH-primed B cells (10^7) were transferred to lethally irradiated recipients together with limiting numbers of KLH-primed, or boosted (-3 days), spleen cells (1–8×10^6) and assayed for an anti-DNP response. Increasing the number of carrier-primed cells produced a linear increase in the IPFC response to a discrete plateau (6–8×10^6, slope of 1 for log dose–response curve), whereas a background plaque response was obtained at all cell dilutions for the carrier-boosted donors. (Janeway[14] has claimed a 'premium effect' in this assay system with increasing numbers of helper cells, indicative of 2-hit kinetics, but we have consistently failed to confirm that finding.)

In a parallel experiment, B cells were re-challenged with DNP-KLH 10 days before adoptive transfer. There was no significant reduction in the requirement for help from carrier-primed donors (Fig. 3*b*), but surprisingly the carrier-boosted populations cooperated optimally at much lower cell dilutions (1–4×10^6). Once again, the paradox is emphasized: a carrier-specific population, containing an apparent excess of suppressor cells (Figs 1*a*, 3*a*) provided adequate help for memory B cells also re-challenged before adoptive transfer (Figs 1*b*, 3*b*).

If carrier-specific help and suppression (Table 1) are indeed mediated by distinct T-cell subsets[15], an abrupt and qualitative change occurs in the B-cell memory compartment after antigenic challenge, rendering the population refractory to T-cell suppression (Figs 1*b*, 3*b*). North and Askonas have reported a qualitative change in memory B cells after secondary challenge, as measured by their ability to sustain an IgG anti-DNP response *in vitro*[16]. Elson and Taylor have already proposed that in a hapten-carrier system "help or suppression depends on the stage of progression of T-cells in relation to the stage of progression of B-cells in their respective responses" (ref. 7).

A temporal restriction of T-cell help and suppression, imposed by the B cell, would provide a first order control to the immune response, ensuring selective and synchronous recruitment of memory B cells. Cyclic changes in the susceptibility of a B cell to T-cell help and suppression affords a mechanism, albeit in a hapten-carrier secondary adoptive transfer system. Perhaps the most significant finding presented

Carrier-priming leads to hapten-specific suppression

Leonore A. Herzenberg, Takeshi Tokuhisa & Leonard A. Herzenberg

Department of Genetics, Stanford University School of Medicine, Stanford, California 94305

Studies over the past two decades have established[1,2] that 'helper' T lymphocytes primed to a 'carrier' protein increase B-lymphocyte antibody responses to 'haptenic' determinants on the carrier protein. T cells from donors primed with one commonly used carrier protein, keyhole limpet haemocyanin (KLH), have been shown by many workers to augment B-cell IgG anti-dinitrophenyl (DNP) responses in adoptive recipients stimulated with DNP-KLH. Therefore, we were surprised recently to find that the KLH-primed mice we normally use as donors for carrier-specific helper T cells in adoptive transfers[3] show reduced rather than augmented IgG *in situ* anti-DNP antibody production when stimulated with DNP-KLH. Here we show that hapten-specific regulation of antibody production is responsible for this response failure. That is, that KLH-priming before DNP-KLH exposure reduces the production of IgG anti-DNP antibody without interfering with the anti-KLH response or with the development of anti-DNP memory B cells, and that IgG anti-DNP production remains low after further stimulation with DNP on KLH or an unrelated carrier. Thus initial stimulation with a carrier-protein creates an oddly compromised animal in which IgG antibody production to a 'new' haptenic determinant on the carrier is kept minimal despite the presence of normal anti-hapten memory and carrier-specific help capable of supporting other responses to the hapten–carrier conjugate.

Figure 1 shows that very little IgG anti-DNP antibody is produced in KLH-primed mice stimulated with 100 μg DNP-KLH on alum and stimulated again 6 weeks later with 1 μg of aqueous DNP-KLH. The average affinity of this minimal anti-DNP response is 10–100-fold lower than the anti-DNP affinities obtained in mice not previously exposed to KLH (Table 1). The Igh-1a (IgG2a) anti-DNP responses from

Table 1 Carrier-priming reduces the amount and affinity of anti-hapten responses stimulated by the hapten–carrier conjugate but does not interfere with anti-carrier response

| | | | *In situ* IgG2a antibody responses | | |
| | Antigenic stimulation | Time | Anti-KLH | Anti-DNP | |
Group	Protocol	(weeks)	units	units	Mean K_a $(\times 10^6)$
I	Hapten-carrier first				
	DNP-KLH (100 µg on alum) →	0			
		2	15	35	(5)
		6	15	30	(8)
	DNP-KLH (1 µg aqueous) →	6			
		7	130	140	(100)
		8	120	120	(500)
II	Carrier first				
	KLH (100 µg on alum) →	−6			
		−4	20	<1	(<0.3)
	DNP-KLH (100 µg on alum) →	0			
		2	170	5	(<0.3)
		6	ND	5	(<0.3)
	DNP-KLH (1 µg aqueous) →	6			
		7	370	9	(0.5)
III	Hapten-carrier first				
	DNP-KLH (100 µg aqueous) →	0			
		2	4	3	(<0.3)
IV	Carrier first				
	KLH (100 µg on alum) →	−6			
	DNP-KLH (100 µg aqueous) →	0			
		2	140	5	(<0.3)

(BALB/c × SJL)F$_1$ hybrid mice (Igh^a/Igh^b), approximately 10 weeks old at the beginning of the stimulation protocols, were used. All antigens were injected intraperitoneally (i.p.). Mice were bled from the tail at indicated times and serum assayed for anti-KLH and anti-DNP activities by solid phase radioimmunoassay (RIA). Data for the Igh-1a (IgG2a) allotype response are shown here; Igh-1b allotype responses were similar. IgG1 responses were somewhat higher (see text). Units of antibody are equal to the percentage of allotype anti-DNP antibody in a standard serum pool of BALB/c × SJL adoptive secondary response sera[12]; 1 units ≈ 1 µg ml^{-1} of anti-DNP antibody. Mean K_a(M^{-1}) values are estimated from the ratio of RIA binding obtained on DNP$_{12}$ bovine serum albumin (BSA) and DNP$_{42}$BSA. Studies with monoclonal anti-DNP antibodies have shown that this ratio is proportional to log K_a determined by fluorescence quenching with ε-DNP-lysine[3]. ND, not determined.

Igh^a/Igh^b (BALB/c × SJL)F$_1$ hybrids shown are similar to Igh-1b responses in the same mice. Production of IgG$_1$ anti-DNP is also reduced in carrier-primed mice but often increases with repeated DNP-KLH stimulation. IgM responses, in contrast, are not reduced (data not shown). These findings are representative of results obtained using a variety of protocols in which DNP-KLH was injected 1–6 weeks after KLH and at different doses either on alum or in aqueous form (see Table 1).

Table 1 also shows that although the anti-DNP response is severely reduced in the KLH-primed mice exposed repeatedly to DNP-KLH, the anti-KLH response in these mice proceeds normally (that is, increases with each subsequent exposure to KLH determinants). As both these responses require help from carrier-primed T cells, the specific and continued failure of the anti-DNP response cannot be ascribed simply to the lack of such help. Nor can this failure be ascribed to deficiencies in anti-DNP memory B-cell development. Adoptive transfer data in Table 2 show that splenic memory B cells generated by DNP-KLH in KLH-primed mice (groups I and III) are indistinguishable from memory populations generated by our usual protocol for priming anti-DNP memory B cells (group II)[3]. Both the magnitude and the affinity of B-cell memory in each of these three groups are essentially the same. Thus functional memory B cells are clearly present but generally remain silent in mice primed first with KLH (on alum) and then exposed repeatedly to DNP-KLH.

In situ and memory responses from mice primed with aqueous DNP-KLH (group III, Tables 1 and 2) show that inadequate priming reduces all responses to the hapten–carrier conjugate rather than specifically reducing anti-DNP antibody production. These results therefore indicate that alum priming
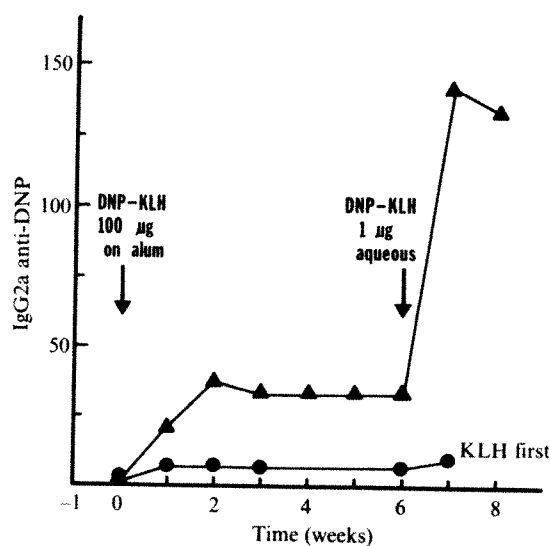

Fig. 1 Carrier-priming prevents hapten–carrier stimulation of anti-hapten antibody responses. (BALB/c × SJL)F$_1$ hybrids were used for these experiments. BALB/c and BAB/14 mice showed similar results. Data for Igh-1a (IgG2a) allotype anti-DNP responses are shown here. Protocol and assay details are as described in Table 1 legend. ●, Primed with 100 µg KLH at −6 weeks; ▲, no prior antigenic exposure.

with KLH (free or hapten-conjugated) is required to induce adequate carrier-specific help for optimal *in situ* antibody production and memory B-cell development. Furthermore, since anti-DNP memory development occurs normally in KLH (on alum)-primed mice exposed to DNP-KLH, these results confirm that adequate carrier-specific help is present and operative with respect to DNP-KLH in these mice, even though the anti-DNP antibody production is minimal.

Finally, data in Fig. 2 show that exposure of KLH-primed mice to DNP-KLH renders these mice incapable of responding to DNP conjugated to an unrelated carrier protein but does not interfere with response to the carrier protein itself, that is chicken γ-globulin (CGG). Figure 2 also shows that mice not exposed to DNP-KLH respond normally to DNP-CGG. Therefore, we conclude first that the induction of non-responsiveness to DNP requires exposure to hapten on the carrier used initially for priming, and second that the effector mechanism responsible for preventing production of the anti-DNP antibody is hapten-specific and does not depend on specific interaction with the carrier protein.

Since the effector mechanism prevents production of antibodies with particular variable region structures (that is the majority of those capable of combining with DNP) and since it 'actively' suppresses anti-DNP responses by co-transferred DNP-primed populations in adoptive transfer recipients (data not shown), we tentatively regard the non-responsiveness for DNP demonstrated here as due to the induction of a broad idiotype suppression[4,5] occasioned by exposure of carrier-primed animals to DNP conjugated to the carrier used for priming.

The characteristics of *in situ* antibody responses in a number of other immunization systems indicate that the inability of carrier-primed mice to produce IgG antibody to 'new' haptenic determinants on the carrier is a general regulatory phenomenon which applies even to haptenic determinants presented with the carrier when these initially fail to stimulate an antibody response. For example, we have observed that repeated stimulation of individual mice producing antibodies to IgG2a allotypic determinants elicits production of very little antibody to determinants not detected
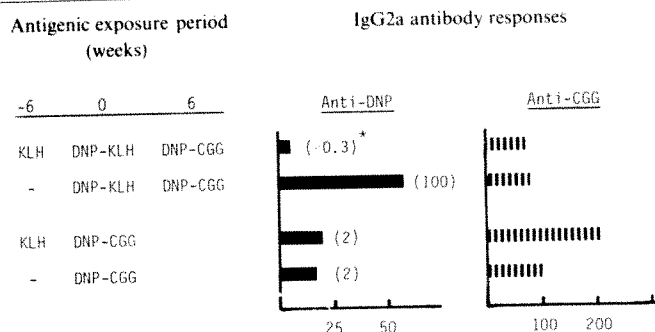

Table 2 Hapten–carrier stimulation of anti-hapten memory B cells is normal in carrier-primed mice

Memory B-cell donors form of antigenic stimulation			Adoptive IgG anti-DNP response	
Group	KLH	DNP-KLH	Units	Mean K_a ($\times 10^6$)
I	*	Alum	73	10
II	Alum	Alum	73	8
III	*	Aqueous	18	0.7
IV	Alum	Aqueous	50	8

Donors (BALB/c × SJL) from groups listed in Table 1 were killed 3 weeks after the first indicated stimulation with DNP-KLH. Splenic B cells were prepared by cytotoxic depletion of T cells using monoclonal anti-Thy-1.2 (30-H12, J. Ledbetter). Cells obtained from 10^7 spleen cells were co-transferred with 2×10^6 nylon-passed syngeneic T cells from KLH-primed donors (100 μg on alum plus 10^9 *Bordatella pertussis* at least 6 weeks before transfer). Recipients (650 rad irradiated BALB/c) were stimulated with 1 μg aqueous DNP-KLH (intravenous) at time of transfer and bled 1 week later for assay. Assay details are as described in Table 1 legend. Igh-1b (IgG2a) response data are shown here. Igh-1a (IgG2a) and IgG1 response data were similar. Responses in mice receiving nylon T (no donor B) were three units of very low affinity antibody. The proportion of IgD^+ memory (also an index of memory population maturity[3] was similar in groups I, II and IV and higher in group III, indicating less maturation (to IgD^-) in mice primed with aqueous antigen. Anti-KLH memory was similar in groups I, II and IV and lower in group III.

*No KLH injection.

Fig. 2 Homologous hapten–carrier conjugate induces hapten-specific suppression in carrier-primed mice. Each indicated antigenic stimulation was given as 100 μg of antigen on alum, i.p. Responses were measured 1 week after last indicated stimulation; RIA units shown are relative to 'standard' antiserum pools for each antigen. Mean K_a (in parentheses, $\times 10^6$) was determined from RIA binding. Assay details are as described in Table 1 legend.

---

in the early antibody populations. "Original antigenic sin" studies[6] with viral antigens also suggest that initial reactivity defines the scope of subsequent antibody production. Finally, although we (and some of our colleagues) were surprised that carrier-primed mice respond poorly *in situ* to a 'new' hapten on a hapten–carrier conjugate, the basic elements of this finding have already been described[1,2,7].

In fact, extensive evidence (albeit otherwise interpreted) has been presented demonstrating that suppression for anti-hapten responses develops when carrier-priming precedes exposure to hapten–carrier conjugates. 'Carrier-specific' suppression, for example[8], is usually defined by the ability of carrier-primed mice to suppress the response to a hapten conjugated to the priming carrier but not to the same hapten on a non-related carrier. Our demonstration that hapten–carrier conjugates induce specific anti-hapten suppression in similarly primed mice suggests (but does not prove) that in some cases this so-called carrier-specific suppression may really be hapten-specific. A similar argument applies to studies of feedback suppression[9].

Evidence[1,2,7] demonstrating that carrier-priming reduces subsequent responses to hapten–carrier conjugates has been largely ignored because hapten and carrier immunization protocols were developed that yielded the expected *in situ* secondary anti-hapten responses in carrier-primed animals (for example, ref. 10). Once these studies showed that carrier-primed T cells help hapten-primed B cells *in situ*, the matter of the anomalous response failures faded into the background and investigations shifted to exploring the mechanism of T–B interactions in adoptive transfer systems that avoid problems associated with *in situ* responses.

The conditions required to demonstrate carrier-specific help *in situ*, however, are of interest: before challenge with carrier and hapten–carrier conjugate, animals must be primed with the hapten (on an unrelated carrier)[10]. This suggests that the induction of hapten-specific suppression fails when cell populations that normally arise during hapten priming (that is, anti-hapten memory B cells and their idiotype-specific helper T cells) are present before the carrier/hapten–carrier exposure sequence. Which, if either, population prevents suppression induction is unclear; however, the participation of idiotype-induction is unclear; however, the participation of idiotype-specific help would be consistent with the idea that antibody-specific help would be consistent with the idea that antibody-specific help responses are controlled by idiotype-specific "core regulatory circuits"[11] configured such that they tend to stabilize in either a suppression or a help mode (depending on whether more suppressor or more helper T cells are induced by the initial priming conditions).

In any event, the dramatic reduction of the high affinity IgG anti-DNP response that we have shown to occur in KLH-primed mice subsequently exposed to DNP-KLH now brings hapten-specific regulatory processes into the arena of commonly studied heterogeneous antibody responses. Furthermore, it suggests an even closer functional interrelationship between carrier-specific and haptern (idiotype?)-specific regulation than previously supposed, as it indicates that carrier-specific priming contributes to the induction of hapten-specific suppression. This offers some entirely new perspectives on the mechanisms involved in response regulation and possibly on mechanisms of tolerance induction and prevention of autoantibody production.

1. Mitchison, N. A. Eur. J. Immun. 1, 10–17 (1971).
2. Rajewsky, K., Schirrmacher, V., Nase, S. & Jerne, N. K. J. exp. Med. 129, 1131–1143 (1969).
3. Herzenberg, L. A., Black, S. J., Tokuhisa, T. & Herzenberg, L. A. J. exp. Med. (in the press).
4. Hetzelberger, D. & Eichmann, E. Eur. J. Immun. 8, 839–846 (1978).
5. Woodland, R. & Cantor, H. Eur. J. Immun. 8, 600–606 (1978).
6. Fazekas de St. Groth, S. Cold Spring Harb. Symp. quant. Biol. 32, 525–536 (1967).
7. Sarvas, H., Mäkelä, O., Toivanen, P. & Toivanen, A. Scand. J. Immun. 3, 455–460 (1974).
8. Tada, T. in Immunological Tolerance (eds Katz, D. H. & Benacerraf, B.) 471–492 (Academic, New York, 1974).
9. Eardley, D. & Gershon, R. K. J. exp. Med. 142, 524–529 (1975).
10. Katz, D., Paul, W. E., Goidl, E. A. & Benacerraf, B. J. exp. Med. 132, 261–282 (1970).
11. Herzenberg, L. A., Black, S. J. & Herzenberg, L. A. Eur. J. Immun. 10, 1–11 (1980).
12. Tsu, T. T. & Herzenberg, L. A. in Selected Methods in Cellular Immunology ch. 18, 373–397 (eds Mishell, B. B. & Shiigi, S. M.) (W. H. Freeman, San Francisco, 1980).

Lack of M-MuSV tumour regression associated with T lymphocyte tolerance

Luigi Chieco-Bianchi, Dino Collavo,
Paola Zanovell & Anita De Rossi

Laboratory of Oncology, University of Padova, Padova, Italy

Anthony J. S. Davies

Division of Biology, Chester Beatty Research Institute, Fulham Road, London SW3 6JB, UK

Moloney murine leukaemia virus (M-MuLV) and Moloney murine sarcoma virus (M-MuSV) are competent and replication defective forms, respectively, of a type C retrovirus which is oncogenic in some inbred mouse strains[1]. M-MuLV induces lymphomas, mostly of T lymphocyte origin, following injection into newborn animals. M-MuSV together with M-MuLV, its natural helper, and in the absence of an appropriate immune response can elicit the formation of an unusual sarcoma which may grow and kill. This sarcoma is unusual in that, at least initially, it is a polyclonal entity within which continual recruitment of previously uninvolved mesenchymal cells occurs[2]. Resistance to the induction of tumours by M-MuSV is thought to depend on activation of appropriate T lymphocytes. The main evidence for this is the finding that animals numerically deficient in T lymphocytes are highly susceptible to sarcoma induction[3–5] and that normal mice and previously challenged animals can generate T lymphocytes specifically cytotoxic in vitro for tumour cells carrying viral antigens[6]. Animals injected with M-MuLV at birth are susceptible to M-MuSV challenge and incapable of generating cytotoxic T lymphocytes active against virus-infected cells in vitro[7,8]. On the other hand, the M-MuLV

neonatally injected animals immunized as adults against allogeneic leukaemic cells are fully competent in generating alloreactive cytotoxic T lymphocytes[8]. T-cell deficient mice can in addition be reconstituted in their capacity to resist challenge by M-MuSV by implantation of syngeneic thymus grafts or injection of normal T lymphocytes[4,5]. The exact role of T lymphocytes in the control of the acute phase of the infection with M-MuSV is not certain but it probably involves a cytotoxic capacity of T cells comparable with that seen in vitro. The role of antibody in bringing about resistance is not clear, as passive immunization per se is relatively ineffective in preventing tumour growth in T-cell deficient mice[5], as was transfer of specifically primed B cells (our unpublished data). We present here evidence that neither thymuses nor peripheral lymphocytes removed from mice injected with M-MuLV at birth are capable of reconstituting T-cell deficient mice in such a manner as to promote resistance to challenge with M-MuSV.

CBA/Ca (CBA) male mice, 4 to 6 weeks old, were rendered numerically deficient in T cells by a sequence of adult thymectomy, 850 rad total-body irradiation and injection with syngeneic bone marrow cells, as detailed elsewhere[5]. The mice were transplanted with one thymus lobe under the kidney capsule or were given an intraperitoneal (i.p.) injection of lymph node cells in suspension[5]. Thymuses to be grafted and lymph node cells for injection were obtained from donor syngeneic mice which had been injected subcutaneously (s.c.), within 48 h after birth, with 0.05 ml of 0.1 gEq cell-free extracts of primary leukaemias induced by M-MuLV, passage A Gross-(G-) MuLV in BALB/c or CBA mice, respectively.

Table 1 Growth of M-MuSV tumours in T-cell deprived mice receiving thymus graft from syngeneic donors neonatally injected with MuLV

Group	Total no. of mice	No. of mice with tumour	No. of mice with regressed tumour	No. of mice dead with tumours
Deprived	35	33	1	32
Deprived + thy graft from normal donors	11	11	10	1
Deprived + thy graft from M-MuLV injected donors	22	21	1	20
Deprived + thy graft from passage A G-MuLV injected donors	5	4	4	0

Four- to six-day old mice were used as thymus donors; thymus graft was performed 5 days before M-MuSV injection in recipient mice.

Normal syngeneic mice of comparable age and sex served as alternative thymus or lymph node cell donors. Mice of the various groups were challenged intramuscularly (i.m.) in the thigh region with 0.05 ml of pooled M-MuSV extract, a virus dose which was equivalent to 5 to 8×10^4 focus-forming units (FFU) when titrated on 3T3/FL cells. The time sequence of the various operations is indicated in Tables 1 and 2.

Table 1 reports the evolution of tumours induced by M-MuSV in deprived mice grafted with a thymus lobe obtained from normal or M-MuLV-injected donors. Most of the deprived mice bearing M-MuSV tumours eventually died with progressive tumour growth, although only a few of those reconstituted with a normal thymus graft were killed. The protective effect conferred by thymus grafting was not seen when the mice were transplanted with a thymus lobe from donors that had been neonatally injected with M-MuLV. All

these mice, with one exception, developed tumours which did not regress. Deprived mice were also transplanted with a thymus lobe derived from donors neonatally injected with passage A G-MuLV, known to induce type-specific tumour associated antigens distinct from those determined by M-MuLV. Protection was achieved in this group, suggesting that unresponsiveness in mice implanted with thymuses from 'tolerized' mice was specific. (Note that, at autopsy, the grafted thymic tissue was always detected macroscopically and appeared histologically normal.)

Table 2 Growth of M-MuSV tumours in T-cell deprived mice receiving lymph node cells from donors neonatally injected with MuLV

Group	Total no. of mice	No. of mice with tumour	No. of mice with regressed tumour	No. of mice dead with tumours
Deprived	15	15	0	15
Deprived + LN cells from normal donors	10	6	4	2
Deprived + LN cells from M-MuLV injected donors	16	14	0	14
Deprived + LN cells from passage A G-MuLV injected donors	7	5	3	2

Deprived mice, 10 days before M-MuSV inoculation, were given intraperitoneally 10×10^6 lymph node cells from 6 to 8-week old donors.

As shown in Table 2, 10×10^6 lymph node cells, from normal or passage A G-MuLV neonatally injected mice, transferred i.p. 10 days before M-MuSV inoculation were effective in preventing tumour development as well as in reducing mortality in the recipients. No protection was afforded by lymph node cells from M-MuLV neonatally infected donors since all the 14 mice developing tumours eventually died with extensive neoplastic involvement of thigh and pelvic tissues.

The diversity in tumour behaviour cannot easily be imputed to differences in the degree of T-cell reconstitution because both passage A G-MuLV neonatally injected, M-MuSV tumour regressors and M-MuLV neonatally injected mice bearing progressing tumours possessed comparable T cell levels—about 20–25% of the total peripheral blood lymphocyte population. These values (assessed 5 weeks after lymph node cell transfer, in a cytotoxic assay with anti Thy 1.2 serum and guinea pig serum as a complement source) were comparable with those observed in deprived mice reconstituted with normal lymph node cells. Less than 5% of T cells were found in the blood of tumour bearing T-cell deficient mice which had received no reconstituting lymphocytes.

In our experiments the latency period for tumours after the challenging injection of M-MuSV was about 16 days in all groups of mice except those which received lymph node cells from neonatally injected mice, in which the latency period was about 30 days, with death within 2 months. No explanation can be offered for this finding at present.

Tests were carried out for the presence of virus in some of the lymph node donor animals. M-MuLV titre was determined on tail tissue extracts using the SC-1/XC cell plaque assay as previously reported[9]. Mice injected at birth with M-MuLV had a titre of 10^4 plaque-forming units (PFU) per ml of 2% tail extract, whereas normal control mice showed negligible M-MuLV production ($<10^1$ PFU). Further, aliquots of the

lymph node cell suspensions used to reconstitute T-cell deprived mice were tested for M-MuLV production by co-cultivation with SC-1 cells and after 4 days the cultures were UV irradiated and tested for XC plaques as detailed elsewhere[10]. Lymph node cell suspensions from neonatally M-MuLV injected mice had a titre of $1–5 \times 10^4$ PFU per 10×10^6 lymph node cells, whereas lymph node cell suspensions from control mice showed $<10^1$ PFU per 10×10^6 lymph node cells.

The experimental results obtained are in line with the general phenomenon of immunological tolerance which can follow introduction of foreign antigens at an early stage of development. The indications are also that the tolerance observed is along the T-cell axis.

In line with this, it has been shown[8] that mice neonatally injected with M-MuLV produce antibodies specific for the virus components despite their incapacity to generate cytotoxic T cells against virally infected cells. However, it cannot be assumed that the tolerance involved is entirely T-cell rather than B-lymphocyte orientated. This conclusion would require a more rigorous assessment of the quantities and quality of anti-viral antibodies produced, particularly in view of the possibility that type C retroviruses other than the injected M-MuLV (that is, endogenous eco- and xeno-tropic, as well as 'recombinant' new viruses) may be expressed in the tolerized hosts.

It is intriguing that the viral yield was high in the tolerized mice and in the lymphocytes transferred from them. Furthermore, our preliminary experiments indicate that thymus, spleen and lymph node cells a few days after neonatal injection of animals with M-MuLV already possess surface antigenic components which are recognized as targets by M-MuSV immune spleen cells in a short-term incubation ^{51}Cr-release assay. The lymphoid cells from M-MuLV infected mice, when used as stimulators, are also able to elicit the generation of cytotoxic T cells *in vitro* (data not shown). Thus it could be argued that the tolerized cells were unable to distinguish, as foreign, virus-associated antigens that they lived with and accepted as self. Note also the additional possibility that the thymic epithelium of thymus grafts from tolerized mice had the capacity to imprint on those lymphocytes that it processed, subsequent to tolerogenesis, the ability to recognize viral antigens as self. To determine whether such a process is distinguishable from infection would require further study. Finally, we have obtained no evidence to show that suppressor T cells exert an active role in the tolerance phenomenon (manuscript in preparation): such a role has been suggested to explain the results of some experiments in which rats were injected with G-MuLV[11].

1. Levy, J. P. & Leclerc, J. C. *Adv. Cancer Res.* **24**, 1–66 (1977).
2. Chieco-Bianchi, L. & Collavo, D. in *Scientific Foundations of Oncology* (eds Symington, T. & Carter, R. L.) 388–393 (Heinemann, London 1976).
3. Stutman, O. in *The Nude Mouse in Experimental and Clinical Research* (eds Fogg, J. & Giovanella, B.) 411–435 (Academic, New York, 1978).
4. Collavo, D., Colombatti, A., Biasi, G., Chieco-Bianchi, L. & Davies, A. J. S. *Nature* **249**, 169–170 (1974).
5. Collavo, D., Colombatti, A., Biasi, G., Chieco-Bianchi, L. & Davies, A. J. S. *J. natn. Cancer Inst.* **56**, 603–608 (1976).
6. Collavo, D., Parenti, A., Biasi, G., Chieco-Bianchi, L. & Colombatti, A. *J. natn. Cancer Inst.* **61**, 885–890 (1978).
7. Chieco-Bianchi, L. *et al.* in *Tumour-associated Antigens and their Specific Immune Response* (eds Spreafico, F. & Arnon, R.) 71–84 (Academic, New York, 1979).
8. Chieco-Bianchi, L., Sendo, F., Aoki, T. & Barrera, O. L. *J. natn. Cancer Inst.* **52**, 1345–1350 (1974).
9. Colombatti, A., De Rossi, A., Taylor, B. A., Chieco-Bianchi, L. & Meier, H. *Int. J. Cancer* **21**, 179–185 (1978).
10. Colombatti, A., De Rossi, A., Hilkens, J., Collavo, D. & Chieco-Bianchi, L. *J. natn. Cancer Inst.* **62**, 1451–1457 (1979).
11. Myburgh, J. A. & Mitchison, N. A. *Transplantation* **22**, 236–244 (1976).

Corpus allatum is release site for insect prothoracicotropic hormone

N. Agui

Department of Entomology, The National Institute of Health,
Kamiosaki, Shenagawa-ku, Tokyo 141, Japan

W. E. Bollenbacher, N. A. Granger & L. I. Gilbert

Department of Biological Sciences, Northwestern University,
Evanston, Illinois 60201

The primary effector of insect postembryonic development is a
peptide neurohormone, the prothoracicotropic hormone
(PTTH)[1,2]. PTTH is the product of a single neurosecretory cell
(NSC) in each hemisphere of the protocerebrum of the tobacco
hornworm, Manduca sexta[3]. Its neurohaemal organ, however,
has not previously been identified. Determination of the site of
release would complete the identification of the neuroendocrine
axis of PTTH and establish the boundaries of an intracellular
system within which factors controlling the synthesis, transport,
storage and release of an identified neurohormone could be
investigated. The neurohaemal organ for PTTH has been
assumed to be the corpus cardiacum (CC), a structure located
between the brain and corpus allatum (CA)[1,2], but alternative
sites of release have been suggested, including the CA[4-7] and the
brain itself[8,9]. In this study, a novel in vitro assay for PTTH[10,11]
has been used to identify the CA as the neurohaemal organ for
PTTH in Manduca.

Establishment of the neurohaemal organ for PTTH required
the identification of the cerebral NSC responsible for its
synthesis and their axonal distribution, as well as a titre of
PTTH in the brain and retrocerebral complex (CC plus CA)
during metamorphosis. The PTTH NSC in freshly ecdysed
pupae of Manduca have recently been identified[3,11] and a
previous cobalt backfill study of NSC in the pupal brain
demonstrated that the axons of the PTTH NSC terminate in
the CA[12]. These data suggest that the CA may be the site of
release, but do not preclude the CC as the neurohaemal site
(because of the limitations of the backfill technique, such as
interneuronal migration[13]). However, in conjunction with the
cell localization and backfill data, a titre of PTTH in the CC
and CA during larval-pupal metamorphosis could directly
establish the neurohaemal site for this hormone.

To establish the CA as the neurohaemal site, it had to be
demonstrated that the CA contained most of the PTTH
activity in the retrocerebral complex at critical stages of
development and that the levels approximated those for the
brain. Since the PTTH NSC axons destined to terminate in
the CA must traverse the CC, the CC would presumably
possess only a low level of PTTH activity. To quantify PTTH
activity, a dose-response protocol for in vitro activation of the
prothoracic glands (PG) by the neurohormone was
used[3,10,11]. Before assaying PTTH, it was necessary to prove
that the activity being assayed was due to PTTH. This
was accomplished by demonstrating the heat stability of the
PTTH activity in the CC and CA and a dose-related response
for activation of the PG by supernatants of homogenates of
the brain, CC and CA from day 0-1 pupae (Fig. 1). In
addition, the sum of the reciprocals of the A_{50} tissue
equivalents (see Fig. 1 legend) for each component closely
approximated the reciprocal of the A_{50} tissue equivalents for
the brain plus retrocerebral complex, thus demonstrating that
the PTTH activity was quantifiable. The possibility of juvenile
hormone (JH) involvement in PG activation[2] by CA
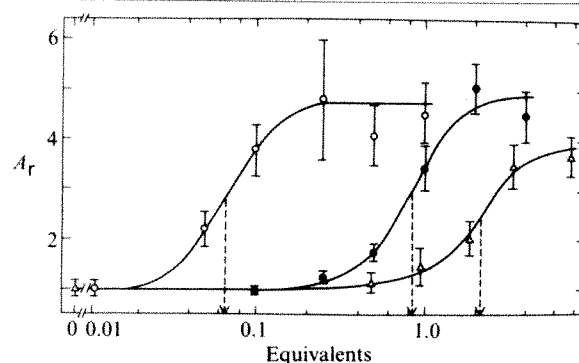homogenates was eliminated by showing that endogenous

Fig. 1 Dose response of PG activation by brain (○), CA (●)
and CC (△) from day 0-1 Manduca pupae. The PTTH assays
were performed on supernatants of heat-treated (100 °C, 2 min)
tissue extracts[10]. The abscissa represents the tissue equivalents
assayed with one equivalent equal to 1 brain, 2 CA (1 pair) or 2
CC (1 pair). Activation is expressed as an activation ratio (A_r)
obtained by dividing the amount of ecdysone synthesized by the
experimental gland by that synthesized by the control gland.
Ecdysone was quantified by radioimmunoassay. The total PTTH
activity present in the brain plus retrocerebral complex could be
quantified by summing the reciprocals of the equivalents for each
tissue (brain, CC, CA) necessary to elicit half maximal activation
(A_{50}) of ecdysone synthesis by the PG[3,11]. Thus, the reciprocals
of the A_{50} values (dashed vertical lines) for the brain (0.066), CA
(0.84) and CC (2.15) were 15.1, 1.2 and 0.5, respectively. Their
sum equals 16.8, which is 107% that of the reciprocal value
obtained with the A_{50} tissue equivalent for the brain plu
retrocerebral complex assayed together (15.7). Each datum poin.
represents the average ± s.e.m. of three separate assays, each run
in triplicate.

levels of JH in the CA are very low[14] and that the supernatant
of a CA homogenate following a hexane partition to remove
JH elicited the same dose response of PG activation as an
untreated supernatant.

The PTTH titre of the CC and CA was then determined for
the last larval instar and early pupal development (Fig. 2). The
data revealed that PTTH activity in the CA was always
significantly greater than that in the CC. Early in the last
instar (day 1-3), an increase in activity was observed for the
CA in contrast to a decrease in CC activity. An increase in
PTTH activity in the CA at this time would be expected if this
gland were the neurohaemal organ since presumably PTTH is
released at ~day 4 (ref. 15) to elicit the small ecdysteroid
peak[16] responsible for a change in commitment from larval to
pupal development[17]. The slight decrease in activity in the CA
between days 3 and 5 may reflect this release. Although
dramatic changes in the level of PTTH activity in the CA did
not occur until pupation, there was another slight increase
between days 5 and 7, possibly in preparation for PG
activation at ~day 8 (ref. 15); the resulting second ecdysteroid
peak elicits apolysis and pupal ecdysis[15,16]. Again, a very
slight decrease in CA activity was noted between days 7 and 9,
possibly indicating that release had occurred. A large de-
crease in PTTH activity occurred just at pupation, the
endocrinological significance of which is not known. During
the first 24 h after the pupal moult, the PTTH activity in the
CA reached its maximum titre, presumably in preparation for
release at approximately day 2 of pupal life (L. M. Riddiford,
personal communication). The slight decrease in CA activity
expected after PTTH release was again observed (day 1-3). An
increase in PTTH activity also occurred in the CC during
pharate pupal development and again at pupation, probably
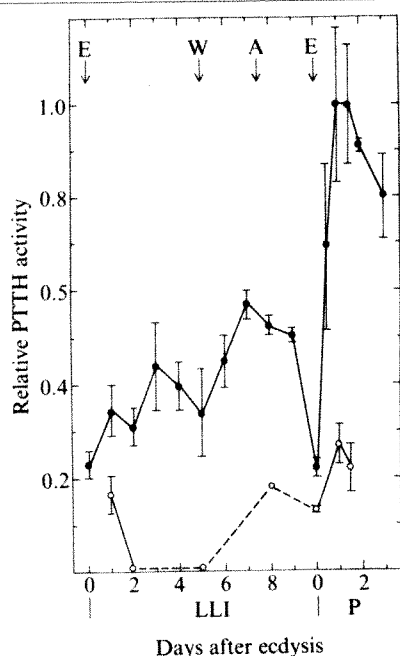due to a higher level of this hormone in the traversing NSC
axons.

Fig. 2 Titre of PTTH activity in the CA (●) and CC (○) during the last larval instar (LLI) and early pupal stage (P) of *Manduca*. PTTH activity was quantified using a dose-response protocol and is expressed relative to the hormone activity of one pair of day 1 pupal CA. E, W and A signify the times of ecdysis, wandering and apolysis, respectively. Each datum point represents an average ± s.e.m. of three to four separate assays, each run in triplicate (see Fig. 1). The s.e.m. values for CC at days 2 and 5 were smaller than the data points, while the day 8 value represents one determination run in triplicate. Dashed lines signify that daily determinations were not made during that period.

These data reveal that during larval–pupal development, the CA contains far greater PTTH activity than the CC. In addition, since hormonal activity in a neurohaemal organ would probably reflect activity at the site of synthesis, it is significant that changes in the titre of PTTH in the CA are similar to those noted for the brain of *Manduca* during the same developmental period (unpublished). Thus, based on the identification of the PTTH NSC in the brain, the axonal distribution pattern of these NSC, and the titre of PTTH activity in the CA during larval–pupal development, it is concluded that the CA is the neurohaemal organ for PTTH in *Manduca sexta*.

We thank Nancy Grousnick for clerical assistance. This research was supported by grants from NIH and NSF.

1. Wigglesworth, V. B. *Insect Hormones* (Freeman, San Francisco, 1970).
2. Gilbert, L. I. & King, D. S. in *The Physiology of Insecta I* (ed. Rockstein, M.) 249–370 (Academic, New York, 1973).
3. Agui, N., Granger, N. A., Gilbert, L. I. & Bollenbacher, W. E. *Proc. natn. Acad. Sci. U.S.A.* **76**, 5694–5698 (1979).
4. Ichikawa, M. & Nishiitsutsuji-Uwo, J. *Biol. Bull. Woods Hole* **116**, 88–94 (1959).
5. Ishizaki, H. *Devl Growth, Diff.* **11**, 1–7 (1969).
6. Gibbs, D. & Riddiford, L. M. *J. exp. Biol.* **66**, 255–266 (1977).
7. Morohoshi, S. & Shimada, J. *Proc. Japan Acad.* **51**, 744–748 (1975).
8. Nishiitsutsuji-Uwo, J. *Z. Zellforsch.* **54**, 613–630 (1961).
9. Takeda, N. *Appl. Ent. Zool.* **11**, 143–153 (1976).
10. Bollenbacher, W. E., Agui, N., Granger, N. & Gilbert, L. I. *Proc. natn. Acad. Sci. U.S.A.* **76**, 5148–5152 (1979).
11. Bollenbacher, W. E., Agui, N., Granger, N. & Gilbert, L. I. in *Invertebrate Systems In Vitro* (eds Kurstak, E., Maramorosch, K. & Dübendorder, A.) (Elsevier, Amsterdam, in the press).
12. Nijhout, H. F. *Int. J. Insect Morph. Embryol.* **4**, 529–538 (1975).
13. Strausfeld, N. F. & Obermayer, M. *J. comp. Physiol.* **110**, 1–12 (1976).
14. Granger, N. A. *et al. Molec. cell. Endocr.* **16**, 1–17 (1979).
15. Truman, J. W. & Riddiford, L. M. *J. exp. Biol.* **60**, 371–382 (1974).
16. Bollenbacher, W. E., Vedeckis, W. V., Gilbert, L. I. & O'Connor, J. D. *Devl Biol.* **44**, 46–53 (1975).
17. Riddiford, L. M. *Nature* **259**, 115–117 (1976).

Presence of a low molecular weight endogenous inhibitor on 3H-muscimol binding in synaptic membranes

Yukio Yoneda & Kinya Kuriyama

Department of Pharmacology, Kyoto Prefectural University of Medicine, Kamikyo-Ku, Kyoto 602, Japan

The specific binding of 3H-muscimol to synaptic membrane preparations obtained from the rat brain has been thought to reflect the association of γ-aminobutyric acid (GABA), a potential candidate as an inhibitory neurotransmitter in the mammalian central nervous system (CNS), with its synaptic receptors[1,2]. Treatment of synaptic membranes with Triton X-100 significantly increases the specific binding of 3H-muscimol[2]. Several reports also indicate the presence of endogenous substances, such as GABA[3], acidic protein[4] and phosphatidylethanolamine[5], which inhibit Na-independent binding of 3H-GABA in the synaptic membranous fractions from the rat brain. We report here that in the supernatant obtained from Triton-treated synaptic membranes there exists a new type of endogenous inhibitor of 3H-muscimol binding which is apparently different from the inhibitory substances described previously[3–5]. The new inhibitor has a low molecular weight (MW) and probably originated from neurones rather than glial cells. We have termed this endogenous inhibitor the GABA receptor binding inhibitory factor (GRIF).

Treatment of crude synaptic membrane fractions obtained from the rat brain with Triton X-100 significantly increased the specific binding of 3H-muscimol[2]. One explanation for this increase in binding is that an endogenous binding inhibitory substance may be present in synaptic membranes and that this inhibitor is removed by the Triton treatment. In fact, it has been reported that an endogenous inhibitor of the Na-independent binding of 3H-GABA is present in the particulate[3] as well as the crude synaptic membrane fractions[4,5] of the rat brain.

The supernatant (Sup T) obtained from Triton-treated synaptic membranes, when added to the assay mixture for 3H-muscimol binding, produced a drastic reduction of specific 3H-muscimol binding to Triton-treated as well as to untreated normal membranes (Fig. 1a). Addition of a large amount (0.9 ml) of Sup T almost completely inhibited the specific binding without affecting nonspecific binding. These results strongly suggest that an endogenous inhibitor of 3H-muscimol binding is present in synaptic membrane fractions and is removed from the membranes by the Triton treatment.

It has been shown that synaptic membrane preparations contain low- and high-affinity binding sites for 3H-muscimol and the former site is easily converted into the latter form by Triton X-100 treatment[2]. This phenomenon has also been confirmed in the present study. Therefore, we examined the effect of Sup T on high-affinity 3H-muscimol binding to Triton-treated synaptic membranes. Scatchard analysis of the data from experiments on Sup T-induced inhibition of high-affinity 3H-muscimol binding to Triton-treated membranes revealed that the apparent affinity (K_d) of 3H-muscimol for GABA receptor binding sites is reduced, whereas the number of maximal binding sites (B_{max}) is not affected by the addition of Sup T (Fig. 1b). These results coupled with our recent findings that Triton treatment makes the high-affinity binding sites more sensitive to alterations of external pH and temperature (unpublished data), suggest that the inhibitor in Sup T may exhibit its action by reducing the affinity and inducing conformational changes in the binding sites.
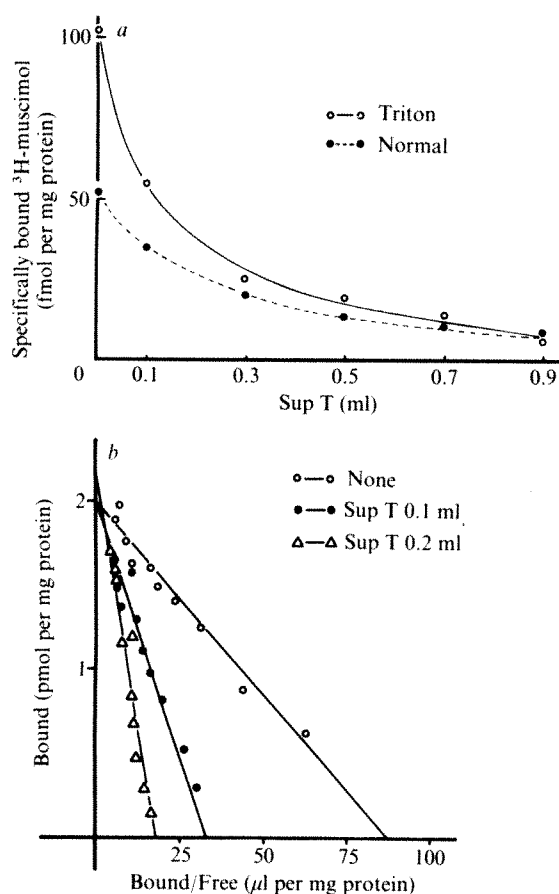
Fig. 1 Effect of *in vitro* addition of Sup T on specific ^{3}H-muscimol binding. *a*, Inhibition with increasing concentration of Sup T; *b*, Scatchard analysis of Sup T-induced inhibition of the binding to Triton-treated synaptic membranes. Crude synaptic membrane fractions were obtained from the whole brain (including cerebellum) of male Wistar rats (200–250 g) as previously reported[13]. After repeating the washing procedures three times using 50 ml of 50 mM Tris-citrate buffer (*p*H 7.1) to remove endogenous GABA, the pellet finally obtained was frozen at −20 °C for 1–7 days. These frozen pellets were thawed and washed once with 50 ml of Tris-citrate buffer before each use. For preparing the Triton-treated membranes, suspensions of the frozen-thawed pellets were preincubated with 0.01 % of Triton X-100 at 25 °C for 30 min instead of washing by buffer. The preincubation with Triton X-100 was terminated by the centrifugation at 48,000 g for 20 min. The supernatant (Sup T) obtained from the Triton-treated membranes was directly added to the assay system for ^{3}H-muscimol binding as needed. The assay system for ^{3}H-muscimol binding was as follows. The membranous suspensions treated or not treated with Triton X-100 were incubated with 1 nM of ^{3}H-muscimol ([*Me*-^{3}H]3-hydroxy-5-aminomethyl isoxazole, 12.9 Ci mmol^{-1}, NEN) in 1 ml of 50 mM Tris-citrate buffer (*p*H 7.1) at 2 °C for 30 min. The incubation was terminated by the addition of 2 ml of ice-cold buffer and subsequent filtration with membrane filter (pore size: 0.45 μm, Toyo Roshi) under vacuum[10]. After washing the filter twice with 2 ml of ice-cold buffer, the radioactivity trapped on the filter was measured as described previously[10]. The radioactivity found in the presence of 1 mM nonradioactive GABA was considered to be due to nonspecifically bound ^{3}H-muscimol and subtracted from each experimental value to obtain the specific binding of ^{3}H-muscimol. The specific binding of ^{3}H-muscimol was saturable with increasing concentration of ^{3}H-muscimol and indicated the presence of two different types of binding site: a high-affinity site with a K_d of 4.7 nM and a low-affinity site having a K_d of 90 nM. The maximal binding to the high- and low-affinity sites is 0.6 and 1.7 pmol per mg protein, respectively. These values are essentially in agreement with the previously reported values[2]. The protein concentration usually used was 400 μg protein per assay. Protein content in Sup T was 150 ± 30.8 μg protein per ml. For Scatchard analysis (*b*), the membranous preparations were incubated with 10 nM of ^{3}H-muscimol in the absence and presence of various concentrations of nonradioactive muscimol which was synthesized in our laboratory according to the method of Nakamura[14]. Triton treatment only: $B_{max} = 2.0$ pmol per mg protein, $K_d = 22$ nM; Sup T 0.1 ml added: $B_{max} = 2.0$ pmol per mg protein, $K_d = 52$ nM; Sup T 0.2 ml added: $B_{max} = 2.2$ pmol per mg protein, $K_d = 163$ nM. Each determination was always carried out in triplicate and each varied less than 10 %. Values given represent the mean of at least two separate experiments. Protein was determined by the method of Lowry *et al.*[15].

Column chromatographic analysis of Sup T using Dowex 50 W × 8 resin revealed that this inhibitor co-eluted with ^{3}H-GABA (Fig. 2*a*). The peak of inhibitory activity of Sup T was, however, completely separated from that of ^{3}H-GABA when the Sup T was applied to a Sephadex G-10 column (16 × 180 mm) (Fig. 2*b*). These results clearly indicate that the inhibitory activity of Sup T on the binding is not derived from GABA itself. As *in vitro* addition of Triton X-100 did not cause significant inhibition as Sup T (Table 1; maximal concentration of Triton X-100 derived from Sup T is calculated to be less than 0.005 %), we conclude that the endogenous inhibitor, which we term the GABA receptor binding inhibitory factor (GRIF), is indeed present in the synaptic membrane fractions.

The inhibitory action of GRIF was greatly attenuated following the dialysis of Sup T, whereas boiling and enzymatic treatments of Sup T with trypsin, collagenase, peroxidase and phospholipase C had no significant effect (Table 1). GABA-induced inhibition of ^{3}H-muscimol binding was diminished by the addition of fluorescamine, but the inhibition by GRIF was not affected by this primary amine reactive reagent (Table 1). These results suggest that GRIF may be a thermostable substance with a low MW and that no primary amine structure is involved in its activity. In fact, the apparent MW of GRIF was estimated to be less than 500 according to the filtration experiments using the Amicon Diaflo membrane UM05 (Table 1).

Table 1 Some characteristics of GRIF in Sup T

Addition	Specifically bound ^{3}H-muscimol (fmol per mg protein)
None	104.3 ± 5.8 (10)
Triton X-100	
0.01 %	94.0 ± 2.4 (5)
0.05 %	70.3 ± 4.5 (5)
Sup T (0.5 ml)	
Untreated	31.5 ± 4.3 (5)
Dialysis (2 h)	82.7 ± 3.6 (5)
Ether extraction	27.2 ± 2.0 (5)
Boiling (95 °C, 10 min)	30.9 ± 4.7 (5)
Trypsin (500 μg ml^{-1})	33.7 ± 5.5 (5)
Collagenase (500 μg ml^{-1})	32.8 ± 3.0 (5)
Peroxidase (500 μg ml^{-1})	32.4 ± 4.7 (5)
Phospholipase C (500 μU ml^{-1})	29.7 ± 2.9 (5)
Sup T (0.1 ml)	59.6 ± 2.1 (5)
Sup T (0.1 ml) + fluorescamine	61.2 ± 3.8 (5)
Fraction 14 (GRIF) (0.1 ml)	23.6 ± 2.7 (4)
Fraction 14 (0.1 ml) + fluorescamine	22.1 ± 2.5 (4)
GABA 10^{-7} M	40.2 ± 3.4 (5)
GABA 10^{-7} M + fluorescamine	72.9 ± 1.7 (5)
GABA 10^{-6} M	5.3 ± 1.2 (5)
GABA 10^{-6} M + fluorescamine	13.7 ± 2.2 (5)
GABA 10^{-5} M	0.5 ± 0.1 (5)
GABA 10^{-5} M + fluorescamine	3.8 ± 0.6 (5)

Filtration by Diaflo membrane UM05

Filtrate	0.1 ml	33.6 ± 1.2 (4)
	0.5 ml	13.2 ± 0.9 (4)
Residue	0.1 ml	89.3 ± 6.9 (4)
	0.5 ml	70.5 ± 12.0 (4)

Treatments: Dialysis: 10 ml Sup T was dialysed against 300 ml of H_2O at 4 °C for 2 h. Ether extraction: 5 ml Sup T was added to 20 ml ether and the mixture was vigorously shaken for 10 min. Following the centrifugation of this mixture at 3,000 g for 10 min, the upper layer thus obtained was removed by suction. These procedures were repeated four times. Enzyme treatments: following the incubation of Sup T with trypsin, collagenase, peroxidase or phospholipase C at 37 °C for 2 h, the reaction was terminated by boiling the incubation mixture for 10 min. Fluorescamine reaction: 50 μl of 0.1 % fluorescamine (w/v, in acetone) was rapidly added with stirring[12] to 1 ml GABA solution, Sup T or fraction 14 (see Fig. 2*a*) obtained following cation exchange chromatography. After taking away the acetone by a N_2-gas stream, each sample was subjected to the binding assay. Filtration experiments: 5 ml of concentrated Sup T was filtrated on the Amicon Diaflo membrane UM05 under N_2-gas pressure (5 kg cm^{-2}). The solution (0.6 ml) remaining on the filter was diluted by H_2O into 5 ml. The diluted residue and the filtrate were subjected to the binding assay, respectively. Each value represents the mean ± s.e.m. obtained from various numbers of separate experiments as indicated in parentheses.

To determine whether or not GRIF indeed originates from neurones, we examined the effect o selective neuronal degeneration by kainic acid[6,7] on the endogenous level of GRIF. Unilateral microinjection of kainic acid $(2 \mu g \mu l^{-1})$ into the corpus striatum produced a significant degeneration of neurones at the injected side without affecting the non-injected side, as described elsewhere[8]. The inhibitory activity of Sup T obtained from the injected side of the corpus striatum is significantly lower than that from the non-injected side (Fig. 3a, b). As the neuronal degeneration induced by kainic acid significantly diminished the level of GRIF, it is reasonable to consider that GRIF may be present in neurones rather than in other CNS components such as glial cells.

Thus, we have demonstrated that in crude synaptic membrane fractions from the rat brain there is an endogenous inhibitor of GABA receptor binding (GRIF) which has a relatively low MW. GRIF is apparently different from the protein type of inhibitor of GABA receptor binding reported previously[4,9]. The protein type of inhibitor showed an anionic property[4], whereas GRIF was adsorbed to the cation exchange resin (Fig. 2a). The interrelationship between the protein type of inhibitor and GRIF, however, remains to be elucidated. It is conceivable that GRIF. is one of the main active constituents of the protein type of inhibitor.

Fig. 3 Effect of neuronal degeneration by kainic acid on GRIF in Sup T. Animals were fixed with a stereotaxic apparatus under pentobarbital anaesthesia (50 mg per kg, intraperitoneally) and kainic acid $(2 \mu g \mu l^{-1})$ dissolved in the artificial cerebrospinal fluid was injected slowly (over 3 min) into the left corpus striatum using a Hamilton microsyringe. The needle was carefully removed 3 min after the end of injection. The stereotaxic coordinates were made according to Pellegrino and Cushman[15] (A: 7.8, L: 3.0, V: 4.5 mm) and the exact location of the injected site was confirmed histologically. Seven days after the injection, animals were killed by decapitation and the corpus striatum was dissected out on a chilled glass. Samples from each unilateral side (injected side and non-injected side, respectively) obtained from 30 animals were combined and frozen at $-20\,^\circ C$ for 1–7 days. These frozen samples were sonicated in 50 ml of ice-cold H_2O with a Polytron (setting no. 6 for 30 s) and the homogenates were centrifuged at 48,000 g for 20 min. The resultant precipitates were resuspended in 50 ml of 50 mM Tris-citrate buffer (pH 7.1) and recentrifuged in the same conditions. After repeating these washing procedures twice to remove endogenous GABA, the pellets obtained were suspended in H_2O using a polytron. The suspensions obtained from each unilateral side of the corpus striatum were preincubated with 0.05% of Triton X-100 at $25\,^\circ C$ for 30 min. Following termination of the preincubation by centrifuging at 48,000 g for 20 min, the supernatant thus obtained (Sup T) was subjected to the binding assay. In these experimental conditions, there were significant reductions (50–60%) in GABA content, activities of L-glutamic acid decarboxylase and GABA transaminase succinic semialdehyde dehydrogenase and the uptake and release of ^3H-GABA in the corpus striatum[8]. Similar tissue masses were dissected out from injected and non-injected sides of the corpus striatum, respectively $(31.4 \pm 2.1 \, mg$ for the injected corpus striatum and $31.9 \pm 1.5 \, mg$ for the non-injected corpus striatum). GABA contents in the final membranous preparations obtained from the injected and non-injected sides of the corpus striatum were 218 ± 53 and $276 \pm 88 \, pmol$ GABA per mg protein, respectively. It was also found that the specific binding of ^3H-muscimol is significantly increased at the injected side of the corpus striatum over that of non-injected side $(68.9 \pm 6.9$ compared with $35.6 \pm 5.1 \, fmol$ per mg protein). Each value given represents the mean obtained from two separate experiments. a, Inhibitory activity is expressed as a function of the protein content in Sup T. b, Inhibitory activity is expressed as a function of the protein content in original striatal particulate preparation.

Fig. 2 Elution profiles of GRIF and ^3H-GABA. a, Dowex 50 W × 8, 200–400 mesh, H^+ form; b, Sephadex G-10. Sup T was obtained as described in Fig. 1 legend and heated at $95\,^\circ C$ for 10 min. Following the centrifugation of this boiled Sup T at 10,000 g for 20 min, the supernatant was evaporated to dryness using a rotary evaporator at $40\,^\circ C$. The resultant residue was suspended with H_2O and the suspension was applied to the glass column packed with cation exchange resin Dowex 50 W × 8 (200–400 mesh, H^+ form, 6 × 120 mm). The column was eluted with H_2O and subsequently with 2 M NH_4OH. The eluate (2 ml) was collected successively and evaporated to dryness to remove eluted NH_4OH. After suspending the residue with a similar volume (2 ml) of H_2O, 0.2-ml portions of each fraction were added to the assay mixture for ^3H-muscimol binding to examine the effect on the binding. The activity of GRIF was eluted in consistency with the elution of NH_4OH. ^3H-GABA (0.5 μCi; 34.5 Ci mmol^{-1}, NEN) was also applied to the column and similarly eluted. For experiments on Sephadex G-10 (b), the supernatant obtained from boiled Sup T was evaporated to dryness and suspended with 0.3 ml of H_2O. The suspension was applied to the Sephadex G-10 column (16 × 180 mm) and the column was eluted with H_2O. The eluate (3 ml) was collected successively and 0.1-ml portions of each fraction were subjected to the binding assay.

Recently, it has also been reported that the incubation of Triton-treated synaptic membrane with phosphatidyl-ethanolamine, a phospholipid, significantly reduces the specific binding of ^3H-GABA without affecting the non-specific binding[5]. The concentration of the phospholipid required to induce half-maximal inhibition of the binding, however, seems to be relatively high (0.1 mM) as compared with the small amount of Sup T required to induce half-maximal inhibition of the ^3H-muscimol binding. In addition, there are some property differences between phosphatidylethanolamine and GRIF such as solubility in ether, permeability to Diaflo membrane UM05 and participation of primary amine structure in its inhibitory activity. Considering these facts with the finding that GRIF completely inhibits the specific binding to untreated normal membrane as well as Triton-treated membrane, it is unlikely that GRIF is phosphatidylethanolamine itself.

We have also demonstrated that neuronal degeneration of the left striatum by kainic acid injection significantly increases the specific binding of ^{3}H-muscimol at the injection side and that this increase seems to result from the decrease of the endogenous level of GRIF[10]. Considering these previous findings with the results obtained in this study, it seems reasonable to conclude that the denervation supersensitivity phenomenon at the GABA receptor occurs as the result of removal of the endogenous inhibitor of receptor binding as suggested by Andrews and Johnston[11]. Although we consider that GRIF may originate from neurones rather than glial cells, the exact location of this inhibitor is unclear. If GRIF is present in presynaptic terminals, it is possible that GRIF is released from presynaptic nerve endings together with GABA during neuronal excitation and modulates synaptic transmission at GABAergic synapses. Studies on biochemical characteristics and the exact physiological roles of GRIF are under way in our laboratory.

1. Snodgrass, S. R. *Nature* **273**, 392–394 (1978).
2. Beaumont, K., Chilton, W., Yamamura, H. I. & Enna, S. J. *Brain Res.* **148**, 153–162 (1978).
3. Greenlee, D. V., Van Ness, P. G. & Olsen, R. W. *Life Sci.* **22**, 1653–1662 (1978).
4. Toffano, G., Guidotti, A. & Costa, E. *Proc. natn. Acad. Sci. U.S.A.* **75**, 4024–4028 (1978).
5. Johnston, G. A. R. & Kennedy, S. M. E. in *Amino Acids as Chemical Transmitters* (ed. Fonnum, F.) 507–516 (Plenum, New York, 1978).
6. Coyle, J. T. & Schwarcz, R. *Nature* **263**, 244–246 (1976).
7. Schwarcz, R. & Coyle, J. T. *Life Sci.* **20**, 431–436 (1977).
8. Kurihara, E., Kuriyama, K. & Yoneda, Y. *Expl Neurol.* **68**, 12–26 (1980).
9. Guidotti, A., Toffano, G. & Costa, E. *Nature* **275**, 553–555 (1978).
10. Kuriyama, K., Kurihara, E., Ito, Y. & Yoneda, Y. *J. Neurochem.* (in the press).
11. Andrews, P. R. & Johnston, G. A. R. *Biochem. Pharmac.* **28**, 2697–2702 (1979).
12. Yoneda, Y. *et al. Jap. J. Pharmac.* **27**, 881–888 (1977).
13. Enna, S. J. & Snyder, S. H. *Molec. Pharmac.* **13**, 442–453 (1977).
14. Nakamura, N. *Chem. Pharm. Bull.* **19**, 46–51 (1971).
15. Lowry, O. H., Rosebrough, N. J., Farr, A. L. & Randall, R. J. *J. biol. Chem.* **193**, 265–275 (1951).
16. Pellegrino, L. J. & Cushman, A. J. in *A Stereotaxic Atlas of the Rat Brain* (Appleton-Crofts, New York, 1967).

Electrochemical, photoelectrochemical, electrocatalytic and catalytic reduction of redox proteins

A. E. G. Cass, M. J. Eddowes, H. A. O. Hill & K. Uosaki

Department of Inorganic Chemistry, University of Oxford, South Parks Road, Oxford OX1 3QR, UK

R. C. Hammond, I. J. Higgins & E. Plotkin

Biological Laboratories, University of Kent, Canterbury, UK

Redox proteins catalyse[1] the reactions of a wide variety of otherwise intractable substrates, such as dinitrogen, alkanes, arenes, terpenes and steroids. Two major factors impede the utilization of these enzymes—the inefficient electron transfer between the enzyme and electrode, and the properties often, but not inevitably, associated with enzymes, such as instability, complexity, and expense. We have now shown that the former can be overcome and that proteins can be coupled, via electrodes, to a number of energy sources; the latter is[2] the subject of much effort elsewhere. We demonstrated previously[3-6] that certain redox proteins can be reduced very efficiently electrochemically (Fig. 1a). Light and hydrogen are the two other convenient energy sources that could be used for such reductions, and we now report the reduction of cytochrome c by these means.

When ferricytochrome c is reduced to ferrocytochrome c photochemically, an amino acid residue in close proximity of the haem of the cytochrome is oxidized[7]. This is avoided by using the configuration shown in Fig. 1b, which illustrates photoelectrochemical reduction. The system consisted of TiO$_2$ (1 cm^2 polycrystalline)/potassium phosphate buffer (pH 7), 0.1 M NaClO$_4$//potassium phosphate buffer (pH 7), 0.1 M NaClO$_4$, 10 mM 4,4′-bipyridyl and 100 μM ferricytochrome c/Au; it gave an open circuit potential of 350 mV and short circuit current of ~40 μA when TiO$_2$ was illuminated by a 350 W xenon lamp. Water is oxidized to oxygen at a TiO$_2$ surface[8] and cytochrome c is reduced at the gold surface, the 4,4′-bipyridyl acting[3-6] as a promotor of electron transfer. After 150 min 30% of the cytochrome c is reduced as monitored by spectroscopy. Two methods with dihydrogen as a reducing agent were used; electrocatalytic and catalytic reduction. The experimental arrangement for electrocatalytic reduction is shown in Fig. 1c. A Pt-based fuel cell electrode (donated by Johnson & Matthew Ltd) was used as an anode. Other configurations are the same as those used in the photoelectrochemical experiments. When H$_2$ gas was passed over the fuel cell electrode, an open circuit potential of 600 mV was observed, which is that expected from the relevant redox potentials. A short circuit current of 60 μA was obtained. After 1 h, 30% of cytochrome was reduced. Catalytic reduction was effected as shown in Fig. 1d. Hydrogen gas was passed through 1 ml of potassium phosphate buffer (pH 7) containing 10 mM bipyridyl and 100 μM ferricytochrome c. No significant change in the spectrum of the solution was observed until Au gauze (8 cm^2) was placed into it. As shown in Fig. 2, the ferricytochrome c was reduced, the reduction following first order kinetics with a rate constant of 6.67×10^{-5} s^{-1}.

Although cytochrome c was used in these experiments there are many redox proteins which could be reduced by these methods and the possible applications of such redox reactions are wide. For example, the methods could be used in the synthesis of organic compounds. This has already been exploited[9,10] in electroenzymological syntheses utilizing monooxygenases which catalyse the reaction, $AH + O_2 + 2e \xrightarrow{2H^+} AOH + H_2O$, the reducing equivalents being supplied electrochemically. For example camphor can be oxidized to *exo*-5-hydroxycamphor using the configuration shown in Fig. 1a and a wide variety of hydrocarbon substrates can be oxidized electroenzymologically using the methane monooxygenases present in extracts of methanotropic bacteria[9,10]. When the enzymes concerned can be reduced at relatively positive potentials, one can use light or dihydrogen as a reducing agent and synthesize compounds with electricity as a by-product compare (Fig. 1b and c) or efficiently drive the reaction catalytically (Fig. 1d).
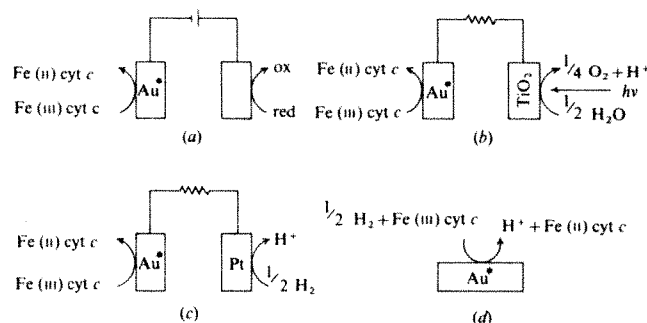

Fig. 1 Reduction of cytochrome c by various methods *a*, Electrochemical: reduction by external source. *b*, Photoelectrochemical: illumination of TiO$_2$ excites electron which reduces cytochrome c at a gold electrode. *c*, Electrocatalytic: H$_2$ gas passed over Pt fuel cell electrode is ionized and supplies electron which reduces cytochrome c at a gold electrode. *d*, Catalytic: H$_2$ gas is passed over gold at which cytochrome c is reduced. In all cases, Au* is gold modified by 4,4′-bipyridyl.
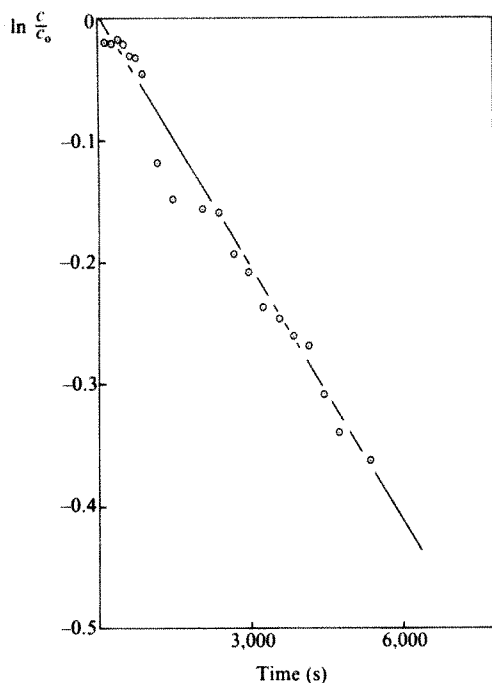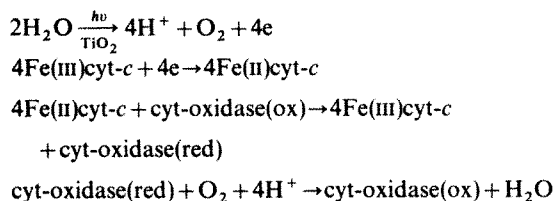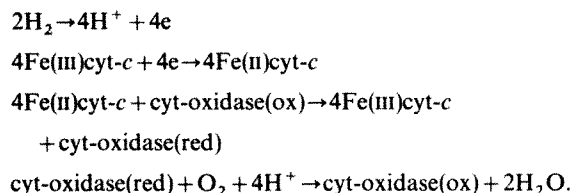
Fig. 2   Time dependence of the concentration of reduced and oxidized form of cytochrome c in the case of catalytic reduction of cytochrome c by hydrogen on gold. c_0 and c are the concentration of Fe(III)cytochrome c at time 0 and at time t.

When the generation of electricity is the main concern, one can apply these systems as photoelectricity generators or bio-fuel cells. For example, the TiO_2/cytochrome c, cytochrome oxidase/Au system will give electricity by illuminating TiO_2 as in the reactions shown below with no net chemical reaction except for the conversion of light to electricity:—

$$2H_2O \xrightarrow[TiO_2]{h\upsilon} 4H^+ + O_2 + 4e$$

$$4Fe(III)cyt\text{-}c + 4e \rightarrow 4Fe(II)cyt\text{-}c$$

$$4Fe(II)cyt\text{-}c + cyt\text{-}oxidase(ox) \rightarrow 4Fe(III)cyt\text{-}c$$

$$+ cyt\text{-}oxidase(red)$$

$$cyt\text{-}oxidase(red) + O_2 + 4H^+ \rightarrow cyt\text{-}oxidase(ox) + H_2O$$

Also the (H_2) Pt/buffer solution//cyt-c, cyt-oxidase/Au(O_2) system will give electricity with the net chemical reaction of $2H_2 + O_2 \rightarrow 2H_2O$. This is a bio-fuel cell resulting from the reactions given below:

$$2H_2 \rightarrow 4H^+ + 4e$$

$$4Fe(III)cyt\text{-}c + 4e \rightarrow 4Fe(II)cyt\text{-}c$$

$$4Fe(II)cyt\text{-}c + cyt\text{-}oxidase(ox) \rightarrow 4Fe(III)cyt\text{-}c$$

$$+ cyt\text{-}oxidase(red)$$

$$cyt\text{-}oxidase(red) + O_2 + 4H^+ \rightarrow cyt\text{-}oxidase(ox) + 2H_2O.$$

In view of the fact that the oxygen reduction reaction has not yet been perfected this latter application could be useful.

1. Boyer, P. D. (ed.) *The Enzymes* Vols XII, XIII (Academic, New York, 1975, 1976).
2. Chibate, I. *Immobilized Enzymes; Recent Developments* (Wiley, New York, 1978).
3. Eddowes, M. J. & Hill, H. A. O. *Chem. Commun.* 771–772 (1977).
4. Eddowes, M. J. & Hill, H. A. O. *J. Am. chem. Soc.* **101**, 4461–4464 (1979).
5. Eddowes, M. J., Hill, H. A. O. & Uosaki, K. *J. Am. chem. Soc.* **101**, 7113 (1979).
6. Eddowes, M. J., Hill, H. A. O. & Uosaki, K. *Bioelectrochem. Bioenergetics* (in the press).
7. Vorkink, W. P. & Cusanovich, M. A. *Photochem. Photobiol.* **19**, 205–215 (1974).
8. Honda, K. & Fujishima, J. *Nature* **238**, 37–38 (1972).
9. Higgins, I. J. & Hill, H. A. O. U.K. Patent application 33388178.
10. Higgins, I. J. *et al.* in *Hydrocarbons in Biotechnology* (Harrison, D. E. F., Higgins, I. J. & Watkinson, R. J.) (Institute of Petroleum, London, in the press).

Isolation and mapping of a cloned ribosomal protein gene of *Drosophila melanogaster*

Charles A. Vaslet, Peter O'Connell, Marta Izquierdo* & Michael Rosbash

Department of Biology and Rosenstiel Basic Medical Sciences Research Center, Brandeis University, Waltham, Massachusetts 02254

Molecular cloning techniques are particularly well suited to the study of gene organization in *Drosophila melanogaster* because recombinant DNA can easily be localized in the genome by *in situ* hybridization to salivary gland polytene chromosomes. We report here the isolation and preliminary characterization of a recombinant phage, designated C25, containing a *bona fide D. melanogaster* ribosomal protein gene. *In situ* hybridization demonstrates that this sequence maps to region 99D on chromosome 3.

To isolate segments of *D. melanogaster* DNA containing ribosomal protein (r-protein) genes we purified a probe enriched for r-protein mRNA and hybridized a cDNA copy of it to a *D. melanogaster* genomic library contained in the λ-derived cloning vector Charon 4. Previous work has demonstrated that many yeast r-proteins are encoded by low molecular weight poly(A)$^+$ mRNA[1,2]. Because the number and molecular weight range of r-proteins from yeast[3] and *Drosophila*[4] are similar, we purified a 6S–12S poly(A)$^+$ mRNA probe for screening. Electrophoretic analysis of the wheat-germ translation products obtained from this small mRNA revealed that the probe was highly enriched for mRNAs coding for proteins of molecular weight less than 20,000, among which were many ribosomal proteins (data not shown).

The 6S–12S poly(A)$^+$ mRNA was labelled to a high specific activity (10^8 c.p.m. per µg) with AMV reverse transcriptase[5] and used to screen a *D. melanogaster* DNA library in Charon 4 (ref. 6). After plaque purification, candidate phage were analysed for the presence of r-protein genes. We identified these phage by a method devised for the purpose and also used to identify r-protein genes from yeast[7]. Briefly, it consists of incubation of cloned DNA and RNA in the presence of high formamide concentrations to generate R-loops, separation of the R-loops from unhybridized RNA by gel filtration chromatography, and *in vitro* translation of the RNA able to form R-loops. The *in vitro* translation product resulting from one of the first 10 clones examined, designated C25, is shown in Fig. 1b and will be the subject of the remainder of this report. The evidence that this protein is a *D. melanogaster* r-protein is as follows. First, this *in vitro* translation product co-migrates on a two dimensional gel with a known *D. melanogaster* r-protein of approximately 20,000 daltons, designated r-protein 49 (Fig. 1). Second, a peptide map analysis of protein 49 and this *in vitro* product verifies that the C25 gene product is indeed identical to the known 20,000-dalton r-protein. To do this, both the *in vitro* and *in vivo* labelled proteins were purified on two-dimensional gels and subjected to proteolysis with *Staphylococcus aureus* V8 protease[8]. The digests produced by this enzyme were composed of several peptide fragments whose molecular weights were sufficiently different to facilitate their separation on an SDS slab gel; the two proteins gave identical peptide patterns in a side-by-side comparison (Fig. 2). These results are consistent with the notion that C25 contains a DNA sequence homologous to an mRNA which directs the synthesis of a *D. melanogaster* ribosomal protein.

*Present address: Centro de Biología Molecular, Universidad Autónoma de Madrid, Canto Blanco, Madrid 34.

Fig. 1 Two-dimensional fluorogram of total *D. melanogaster* ribosomal proteins labelled *in vivo* with ^{35}S-methionine (*a*) and clone C25 gene product similarly labelled *in vitro* (*b*). An arrow indicates r-protein 49 encoded by C25. Two-dimensional gel electrophoresis was done by the method of Mets and Bogorad[19]. After electrophoresis, gels were subjected to fluorography according to Bonner and Laskey[20]. The procedure for labelling and purifying r-proteins was as reported by Berger[21]. C25 gene product was obtained by cell-free translation of mRNA complementary to phage DNA as reported by Woolford *et al.*[7]. Poly(A)[+] containing 3S–14S mRNA prepared as before[22] was subfractionated on a 15–30% continuous sucrose density gradient made up in SDS buffer (0.5% SDS, 0.1 M NaCl, 0.01 M Tris, *p*H 7.5, 0.001 M EDTA) in order to isolate the 6S–12S material used in screening the *Drosophila* library. All other polysomal RNA was prepared by a modification of the method of Lis *et al.*[23]. Embryos 6–18 h old were homogenized at 4 °C in a buffer containing 0.25 M KCl, 0.025 M MgCl, 0.05 M Tris, *p*H 7.4, 0.5% NP-40 and cycloheximide (200 µg ml^{-1}). The homogenate was centrifuged in a Sorvall SS34 rotor at 17,000 r.p.m. for 30 min at 4 °C to remove debris. Polysomes were collected as a pellet prepared by centrifuging the low speed supernatant through a 10-ml cushion of 50% sucrose in homogenization buffer lacking NP-40 and cycloheximide for 8 h at 25,000 r.p.m. in a Beckman SW25.2 rotor at 4 °C. The polysomal pellet was resuspended in 1% SDS, 50 mM Tris, *p*H 9, 1 mM EDTA, 15 mM Na acetate and was extracted 3 times with phenol–chloroform–isoamyl alcohol. The RNA was pelleted and dissolved in 0.1 M Tris, *p*H 8.3, 0.03 M EDTA, 0.1 M NaCl, 1% SDS containing proteinase K (300 µg ml^{-1}). After a 30-min incubation at 37 °C, the preparation was extracted with phenol as above and the RNA was alcohol-precipitated. Poly(A)[+] mRNA was obtained by hybridization to oligo(dT)-cellulose columns[24].

Fig. 2 Fluorogram of peptide mapping by limited proteolysis with *S. aureus* V8 enzyme[8]. The patterns represent only ^{35}S-methionine-labelled peptides from digests of clone C25 gene product (*a*), and the known 20,000 dalton r-protein with which it co-migrates on a two-dimensional gel (*b*). Proteins were isolated by punching out spots from preparative two-dimensional gels run as described previously. Care was taken to insure that each plug cut from the gel contained only one electrophoretic mobility class. Protein isolates were digested without prior elution by placing the gel plugs in the sample wells of a second SDS gel containing 20% acrylamide and overlaying with 10 µg *S. aureus* V8 protease in 10 µl of 0.125 M Tris-HCl, *p*H 6.8, 0.17% SDS, 1 mM EDTA and 10% glycerol. Electrophoresis was performed as usual, except that the current was turned off for 30 min when the bromphenol blue tracking dye neared the bottom of the stacking gel.

a   *b*

To determine the size of the *Drosophila* DNA insert in clone C25 an *Eco*RI restriction digest was performed and the fragments were separated on an agarose gel. In addition to the 19.5- and 10.2-kilobase arms of the Charon vector, fragments of 7.2, 5.5, 2.6 and 2.4 kilobases indicated a total insert size of 17.7 kilobases (Fig. 3). These fragments were ordered by subjecting C25 DNA to single and double digestion with the restriction enzymes *Eco*RI, *Xba*I and *Hin*dIII. The arrangement of these fragments is supported by an analysis of three C25 *Hin*dIII fragments subcloned into the plasmid vector pBR322 (data not shown).

To investigate the arrangement of this 17.7 kilobase segment of cloned DNA within the *Drosophila* genome, hybridizations to *Drosophila* genomic DNA were carried out with labelled C25 as a probe[9] (Fig. 3). The bands detected in the genomic DNA lane are identical to C25 DNA with respect to molecular weight and similar with respect to intensity. This suggests that the 17.7 kilobase insert which includes an r-protein structural gene is therefore largely, if not entirely, single copy. The number and location of the coding regions present in this sequence remain to be defined although several distinct R-loops have been visualized in preliminary electron microscopic studies (unpublished observations).

Having determined that clone C25 contains a structural gene for a *D. melanogaster* r-protein, we mapped its genomic position by *in situ* hybridization[10,11]. An ^{3}H-nick translated[12]
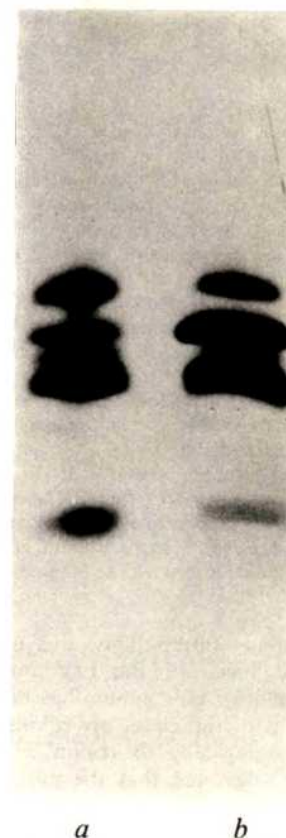
probe was prepared from total C25 DNA and hybridized to squashes of salivary gland polytene chromosomes. As Fig. 4 shows, labelled DNA from C25 hybridized exclusively to chromosome 3R at region 99D. This result was found in several preparations and in no instance were grains observed over any other chromosome arm. This location is interesting because some data had suggested the X-chromosome linkage of r-protein genes in *D. melanogaster*[13,14]. Although our findings do not refute this possibility for some ribosomal proteins, they demonstrate that at least one r-protein structural
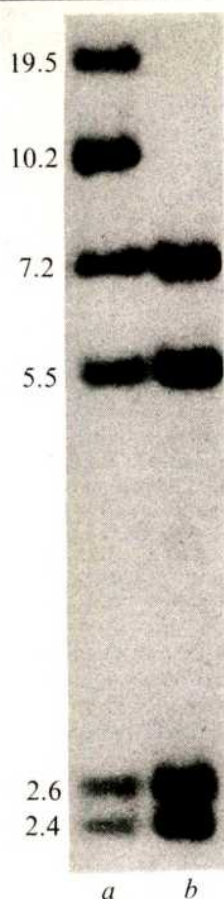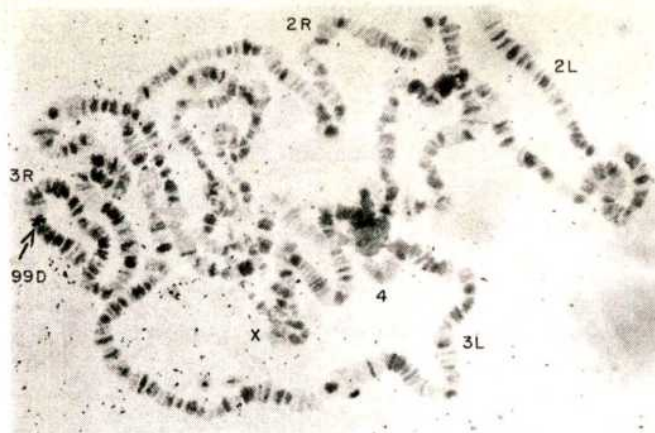
Fig. 4 Salivary gland chromosome squashes were prepared for hybridization by a modification of the procedures of Atherton and Gall[10] and Pardue and Gall[11]. Before hybridization slides were treated with pancreatic RNase at $1 \mu g \, ml^{-1}$ in $2 \times SSC$ for 2 h at 37 °C. The RNase was washed from the slides with several rinses in $2 \times SSC$ for 10 min, followed by an overnight wash with gentle swirling in $2 \times SSC$ containing 1 mM EDTA. The slides were then dehydrated through a series of ethanol baths (70%, 70% 95%, and 95%) and air dried. Chromosomal DNA was denatured in 0.07 M NaOH for 1.5 min at room temperature and then the slides were again passed through an ethanol series and air dried. *In situ* hybridization of ³H-labelled nick-translated clone DNA was done under 22-mm² coverslips in a total incubation volume of 20–30 μl (approximately 2×10^5 c.p.m. per slide and 10^6 c.p.m. per μg DNA). The hybridization buffer contained $2 \times SSC$, 2.5 mM Tris, *p*H 7.5, and 50% formamide. Reactions were carried out at 37 °C for 16 h in a buffer-saturated chamber. After hybridization, the slides were washed in hybridization buffer at 37 °C for 60 min, then in several changes of $2 \times SSC$ for 3 h at room temperature. The slides were finally dehydrated through an ethanol series, air dried, dipped in Kodak NTB-2 liquid emulsion and stored at 4 °C for 2 weeks. The slides were developed for 2.5 min in Kodak D-19 and the chromosomes were stained with Giemsa stain diluted 1:20 in 0.01 M NaPO₄ buffer, *p*H 7.0. The chromosome position of high grain densities was determined by using Bridge's polytene chromosome maps[26] as interpreted by Lefevre[27]. The arrow points to grains found over region 99D of chromosome 3.

Fig. 3 Autoradiograph of ³²P-labelled C25 hybridized to *Eco*RI-digested C25 (*a*), and *Eco*RI-digested *D. melanogaster* genomic DNA (*b*). In *a* 0.6 ng of *Eco*RI-digested C25 was mixed with 2 μg of *Eco*RI-digested yeast carrier DNA to approximate the mass of a C25 single length copy sequence within 2.0 μg of the 165,000-kilobase *D. melanogaster* genome. In *b* 2.0 μg of *Eco*RI-digested *D. melanogaster* DNA was loaded. These samples were electrophoresed on 1% agarose gels. The 19.5- and 10.2-kilobase fragments seen in *a* correspond to the Charon 4 vector DNA. High molecular weight *D. melanogaster* DNA was prepared from 6–18-h old embryos (a gift of S. Elgin) as described by Schachat and Hogness[25]. The DNAs were denatured and transferred to nitrocellulose paper in $10 \times SSC$. Hybridizations were carried out in 50% formamide, $5 \times SSC$, 1 ×Denhardt's solution, 20 mM NaPO₄, and sonicated salmon sperm DNA $(100 \mu g \, ml^{-1})$ at 42 °C. *In vitro* labelled C25 DNA was prepared utilizing the nick-translation technique described by Maniatis *et al.*[12], except that a small amount of DNase I was added to stimulate incorporation of nucleotides.

gene is on an autosome. Interestingly, this map position is close to the genetic locus of the first minute mutation discovered, *M(3)l* (ref. 15). This minute has been mapped 0.3 map units to the right of the claret eye-coloured gene which has been mapped cytologically to region 99 C-E (ref. 16). Ritossa *et al.*[17] have suggested that the positions of minute loci represent tRNA genes although this hypothesis seems no longer viable[18]. Their prediction had been based on the similarity in number of minute loci and tRNAs and the phenotypic abnormalities associated with the minutes (bristle deformities, delayed development and small size) suggesting a reduction in general protein synthesis. We are intrigued by the possibility that the 60 or more minute mutations may be ribosomal protein mutants. This possibility and some of its implications are under investigation.

1. Mager, W. H. & Planta, R. *Eur. J. Biochem.* **62**, 193–197 (1976).
2. Warner, J. R. & Gorenstein, C. *Meth. Cell Biol.* **20**, 45–60 (1979).
3. Otaka, E. & Kobata, K. *Molec. gen. Genet.* **162**, 259–268 (1978).
4. Berger, E. *Molec. gen. Genet.* **128**, 1–9 (1974).
5. Hereford, L. M. & Rosbash, M. *Cell* **10**, 453–462 (1977).
6. Benton, W. D. & Davis, R. W. *Science* **196**, 180–182 (1977).
7. Woolford, J., Hereford, L. & Rosbash, M. *Cell* **18**, 1247–1259 (1979).
8. Cleveland, D. W. *et al. J. biol. Chem.* **252**, 1102–1106 (1977).
9. Southern, E. M. *J. molec. Biol.* **98**, 503–517 (1975).
10. Atherton, D. & Gall, J. *Drosoph. Inf. Serv.* **49**, 131–133 (1972).
11. Pardue, M. L. & Gall, J. *Meth. Cell Biol.* **10**, 1–16 (1975).
12. Maniatis, T., Jeffrey, A. & Kleid, D. G. *Proc. natn. Acad. Sci. U.S.A.* **72**, 1184–1188 (1975).
13. Steffensen, D. M. *Nature new Biol.* **244**, 231–234 (1973).
14. Falke, E. V. & Wright, T. R. *Genetics* **81**, 655–682 (1975).
15. Lindsley, D. L. & Grell, E. H. in *Genetic Variations of Drosophila melanogaster* (Carnegie Institution of Washington, 1971).
16. Bridges, C. B. & Morgan, T. H. in *The Third Chromosome Group of Mutant Characters of Drosophila melanogaster* (Carnegie Institution of Washington, 1923).
17. Ritossa, F. M., Atwood, K. C. & Spiegelman, S. *Genetics* **54**, 663–676 (1966).
18. Elder, R., Szabo, P. & Uhlenbeck, O. in *Transfer RNA: Biological Aspect* (Cold Spring Harbor Laboratory, New York, 1980).
19. Mets, L. J. & Bogorad, L. *Analyt. Biochem.* **57**, 200–210 (1974).
20. Bonner, W. H. & Laskey, R. A. *Eur. J. Biochem.* **46**, 83–88 (1974).
21. Berger, E. *Molec. gen. Genet.* **155**, 35–40 (1977).
22. Izquierdo, M. & Bishop, J. O. *Biochem. Genet.* **17**, 473–497 (1979).
23. Lis, J. T., Prestidge, L. & Hogness, D. S. *Cell* **14**, 901–919 (1978).
24. Rosbash, M., Ford, P. J. & Bishop, J. O. *Proc. natn. Acad. Sci. U.S.A.* **71**, 3746–3750 (1974).
25. Schachat, F. S. & Hogness, D. S. *Cold Spring Harb. Symp. quant. Biol.* **38**, 371–381 (1974).
26. Bridges, C. P. *J. Hered.* **26**, 60–64 (1935).
27. Lefevre, G. in *The Genetics and Biology of Drosophila* 1a (eds Ashburner, M. & Novitski, E.) (Academic, New York, 1976).

BOOK REVIEWS

Hearing voices: the public planning process after Windscale

Frederick Warner

THESE books have a common origin in the Windscale Public Inquiry (WPI). That from the Town and Country Planning Association in association with the Political Ecology Research Group summarizes evidence given and usefully supplements the bibliography in Vol. 3 of the Windscale Report. The other is a report by Professor D. Pearce on a project for which he received a grant from the Social Science Research Council Energy Panel, of which he is a member. It expresses his concern at the way in which opposition groups were treated and on the efficiency of public planning inquiries in general and Windscale in particular.

Professor Pearce heads a department of political economy and his book emphasizes the political nature of the planning process. He uses the Windscale Inquiry as an illustration of one element in a system for planning which he sees as dominated by official thinking and insufficiently open. This hampers objectors who have insufficient access to information and lack the resources to prepare for the compressed time-scale of a public inquiry. The system also prevents the questioning of values — for example that the development would be unnecessary with a simpler life-style or with a stricter examination of needs. It also obscures substantial disagreement on the risks involved and the benefits to be obtained.

The remedy, according to Professor Pearce, lies in new procedures and institutions which will become more efficient through a Freedom of Information Act: "The public can also improve decision-making by raising issues that decision-makers may have overlooked or under-played". They would be helped in this by an Energy Policy Commission reviewing decisions on investment and R&D programmes. The Commission would monitor local planning applications and, where wider issues were involved, recommend review by a Planning Inquiry Commission (PIC), reporting to Parliament through a Select Committee; it would provide funds for objectors to make representations to the PIC and the local

The Nuclear Controversy: A Guide to the Issues of the Windscale Inquiry. By M. Stott and P. Taylor. Pp.204. (Town and Country Planning Association: London, 1980.) £6.95. *Decision Making for Energy Futures.* By D. Pearce, L. Edwards and G. Beuret. Pp.296. (Macmillan: London and Basingstoke, 1979.) £10.

planning inquiry; it would be full-time and high-powered, in contrast with the existing Commission on Energy and the Environment chaired by Lord Flowers.

These criticisms are said to arise in part from the time-table for the Windscale Inquiry (shown on p.135 of the book) as announced on 22 December 1976, opening on 14 June, closing on 4 November 1977, and reporting on 26 January 1978. However, Professor Pearce's discussion of the issues begins in 1974 when the plan for re-processing oxide fuel was announced, and carries through the Church House debate in January 1976 between opposition groups and British Nuclear Fuels Ltd to the Flowers Report of the Royal Commission in September 1976. Given the scope of the Flowers Report it is not easy to see how the debate was hampered for lack of information and would have been bettered by an Energy Policy Commission.

There is a difficulty in assessing Professor Pearce's argument. He disclaims particular intentions and then reinstates them: "Criticism of a process is not therefore a criticism of the individuals who find themselves part of that process. Clearly, a disagreement can exist if they defend that process as Mr Justice Parker has done publicly" (p.132). In reviewing these books, I have to face this possibility, but more readily as the independence of the Inquiry has in any case been questioned.

Professor Pearce is critical of the lack of examination at WPI of economics or the engineering aspects of scaling-up. The evidence on costs was made difficult because the commercial secrecy of the contract with the Japanese, with its payments in advance, led to erroneous discounted cash flow forecasts by the

objectors. The evidence on the need for a pilot plant reflected old-fashioned chemical engineering practice and was irrelevant to the actual scale of the Windscale operations which are more the size of pilot plants themselves.

He begins with the effects of low-level radiation and on p.146 states that "The history seems important because, whatever the format of an inquiry, personalities intervene and what Professor Radford, and other witnesses, did was to question the very role of ICRP and the validity of its work as a basis for setting standards. Yet one of the assessors, Sir Edward Pochin, was, and is, a prominent member of ICRP". ICRP is the International Commission on Radiological Protection and Professor Radford chairman of the US National Academy of Sciences Committee on Biological Effects of Ionizing Radiation (BEIR). This is due to publish a report which will show Professor Radford in disagreement with his committee. One member, Dr Fabrikant, in a March 1980 paper (Jerusalem) says: ". . . such disagreement centres not on the scientific facts or the epidemiological data, but rather on the assumptions and interpretations of the available facts and data. However, based on the radiation risk estimates derived . . . such risks are extremely small when compared with those available from alternative options".

The ICRP publications, in particular 26 and 27, give guidance for the comparison of risks and some economists have attempted to make comparisons, the most recent being Siddall in Canada (Chalk River, 12–14 September, 1979) with CSX, the cost of saving one life. Professor Pearce has lost time between writing and publication so that his study suffers from being overtaken by events. This is shown by the references to the International Fuel Cycle Evaluation Programme (INFCEP) announced in April 1977 by President Carter. Its report in March 1980 has now cleared up many of the questions. It states that proliferation cannot be prevented by technical fixes such as spiking nuclear fuel, that there is an urgent need to meet world

Mr. Justice Parker (centre) who headed the Windscale enquiry, with Sir Frederick Warner (left) and Sir Edward Pochin.

energy requirements with nuclear power, especially for developing countries, and that some countries need to build and operate fast reactors and hence to reprocess nuclear fuel. Professor Pearce criticizes Mr Justice Parker for not referring in the Windscale Report to the letter to the Foreign Office from Joseph Nye, Presidential Adviser, dated 19 December 1977, yet makes clear on p.90 that the Report could only refer to evidence given to the Inquiry.

The march of time is also shown by the section on energy futures. This compares the scenario of the Department of Energy in 1977 with those put forward by Leach and Chapman during WPI. Since then the 1979 figures of the Department, which show reduced estimates of supply and demand, have been put to the Belvoir Inquiry. The nuclear component is only slightly less than the 1977 estimate, but coal comes down from the 170 million tons for the year 2000 to 135, and oil from 150 to 100 Mtce. The Leach demand analysis was discussed in the last report of the Advisory Council for Energy Conservation with the conclusion that with his assumptions the figures are not in basic disagreement with the Department's. Professor Pearce does not accept that official views need be given greater credence than unofficial and (p.155) criticizes "references to some of the forecasts (that of Arthur Scargill of the Yorkshire Area Mineworkers Union) as 'fanciful'. It is presumably not possible to know what is 'fanciful' without having a prior view of what is reasonable". This is the place to use the TCPA/PERG guide (p.57) "Silsoe questioned Scargill's figures for new investment required, and the rate of new pit openings in order to achieve this projected target of 250 million tons by 1992".

Throughout Professor Pearce's book, the Windscale Inquiry receives grudging tributes for doing the job at all, in contrast with the regard in other countries, especially France, for the openness and seriousness of its attempts to hear every voice. It achieved in fact what his new bureaucratic apparatus (p.205) could never do in providing information and guidance which is sought by the public. □

Sir Frederick Warner is a Consulting Chemical Engineer and Visiting Professor at University College, University of London, UK.

Reactors from Russia

Jeffery Lewins

Fast Pulsed and Burst Reactors. By E.P. Shabalin. Pp.260. (Pergamon: Oxford, 1979.) £26, $59.

THIS monograph is translated from the Russian, by W.E. Jones, in the Pergamon tradition of scientific translation. And a good job he has made of it. Generally the translation reads very well with occasional confusion between Russian letters and Roman or Greek letters.

Russian translations do have a minor defect in regard to the double translation of English or American names quoted in references to Russian and back again. Keepin for example will be interested to read of his sea change to Kipin and Paul Gribler for Greebler is in for a similar surprise. More seriously — and a defect avoidable in these days of automated library science — the return translation does not always identify the text the original was (in many cases) pirated from before Russia joined the copyright protocol. I speak as an author pirated without knowing, let alone agreeing, and as an editor of a series left here with only its Russian edition for reference.

But to the book. It is a detailed exposition of the physics of fast reactors used in pulse and burst mode, that is applied as dynamic research tools. Additional material is given on certain engineering aspects such as thermal elastic effects, dynamic control etc., as well as to combined boosters (neutron sources and subcritical multipliers). The text is completed with a chapter on the peculiar aspects of safety and a look ahead to current and future applications of these devices for physics research.

The text reads well. The first five chapters were, it seemed to me, reasonably clear of misprints but the standard (in a readable typescript production) fell off in Chapters 6 to 10, however. Most of the errors I caught were trivial. Occasionally there were muddles between the el and one so tedious to get correct on a typewriter (for example eqn 6.12), and also eqn 6.3 would benefit from a couple of extra primes.

The book is a valuable summary of the special theory of dynamic fast reactors and a comparative source of their leading characteristics, both Eastern and Western, which I have not met elsewhere. □

Jeffery Lewins is a Lecturer in Nuclear Engineering at the University of Cambridge, UK, and is a Past President of the Institution of Nuclear Engineers.

Gel chromatography

Torvard C. Laurent

Gel Chromatography: Theory, Methodology and Applications. By T. Kremmer and L. Boross. Pp.300. (Wiley: Chichester, UK, and New York, 1979.) £16.50, $45.

ALTHOUGH earlier reports appeared on the separation of substances according to molecular size when chromatographed on granulated gels, the introduction of gel chromatography as a preparative and analytical method can be dated to 1959, to a paper by Porath and Flodin in *Nature* (**183**, 1657-1659). The following decade saw a rapid development of the practical and theoretical aspects of the technique, to a large extent due to the collaborative investigations of scientists at the University of Uppsala and Pharmacia Fine Chemicals. During the last 20 years, gel chromatography has become one of the major tools in many fields of research and manufacturing. Many names have been used for the procedure (gel filtration, exclusion chromatography, molecular sieving, gel permeation chromatography etc.) but gel chromatography has now been adopted by most reviewers of the field.

Several books or articles have been

written about the technique, and this volume, by Tibor Kremmer and László Boross, is the most recent. It has been translated from an original Hungarian version and contains three main chapters: "Theory", "Methods and Techniques", and "Applications". The first two chapters were written by Kremmer and the last by Boross. The authors have cited a large amount of the earlier work in the field but their description is not very lucid and contains numerous errors. Furthermore, a

number of ambiguities have been introduced in the translation. The chapter on methods and techniques relies heavily on literature produced by the manufacturers of gels and chromatographic equipment; manufacturers' handbooks do, however, usually present the material in a clearer fashion.

The value of the book could have been that of a reference volume on the applications of gel chromatography in various fields; unfortunately, however, it is

not up to date. The last reference cited is from 1976 and of the references only one out of six is from the five-year period 1972–76.

Given the lack of clarity and the dated section of references, this book is not an important addition to the literature on gel chromatography. □

Torvard C. Laurent is Professor of Medical and Physiological Chemistry at the University of Uppsala, Sweden.

Authority and politics on iron metabolism

William H. Crosby

Iron Metabolism in Man. By T. H. Bothwell, R. W. Charlton, J. D. Cook and C. A. Finch. Pp.576. (Blackwell Scientific: Oxford, 1980.) £33.50.

THIS superb review and analysis is the product of four scientists, two South African, two American, whose long careers have been engrossed with iron nutrition and iron metabolism. It is a comfortably written book, authoritative and completely documented (more than 2,600 references) up to 1978. It is a book that I shall use and treasure for the rest of my life.

The organization of the material departs from the ordinary in that a 240-page section on nutritional and clinical aspects comes first, followed by discussions of the basic physiology of iron metabolism. A third section (100 pages) describes in detail the laboratory methods that are used to study iron metabolism. Think of some aspect of iron in man and — except for 'spleen' — you'll find it listed in the index and discussed in the text in satisfactory detail.

All this is not to imply that there's no worm in the bud. During the past 20 years, the authors have been activists in the politics of nutrition, committed to universal fortification of foods with iron. Such programmes are intended to prevent mild iron deficiency. (It has yet to be demonstrated that fortification improves mildly iron-deficient people or injures those with undiagnosed iron-storage diseases, such as haemochromatosis.) The book is marked by a bias that favours fortification even at the expense of objectivity. Mild iron deficiency is treated with a concern worthy of a dread disease while the potentially lethal haemochromatosis is brushed across because it is rare, as though the improvement of a laboratory result in many could offset deadly damage done to only a few.

However rare haemochromatosis is, it

would seem to be not rare enough. In a discussion of the evidence that haemochromatosis may develop only in homozygotes comes this observation: "Sheinberg has estimated the incidence of homozygous births as not more than 1 in 10,000 and heterozygous 1 in 50; the latter figure in particular seems at this time to be much too high". That the latter figure derives from the other is a matter of genetics and arithmetic, not opinion.

At one place in the book, the authors compute that a woman with normal iron stores would, during a normal pregnancy, have a requirement for an additional 740mg of iron. In another place, it is recommended that such women should receive 30mg per day of "supplemental

iron". In yet a third place, we find this polemic: "The presence of medicinal iron in the homes of pregnant women is responsible for the deaths of small children from acute iron poisoning, and nutritional deficiency must be held responsible for this too".

Nutritional anaemia, in this setting, refers to the iron deficiency that results from copious menstrual blood loss.

There are other statements as unfortunate as these. Yet, in balance, the book is the best of its class; that it is also a vehicle for propaganda is sad. □

William H. Crosby is at the Walter Reed Army Institute of Research, Washington DC.

Periglacial processes six years on

R. J. E. Brown

Geocryology: A Survey of Periglacial Processes and Environments. By A. L. Washburn. Pp.416. (Edward Arnold: London/Halsted Press: New York, 1979.) £27.50, $64.95.

INCREASING recognition of the importance of resource developments in the cold areas of the Earth has focused continuing and growing concern on environmental conditions and physical processes in these regions. In 1973, A. L. Washburn published *Periglacial Processes and Environments* (Edward Arnold: London), which brought together the knowledge and ideas on this topic to that time. The present book is a revised and updated edition of that volume.

The author is one of the world's foremost authorities on processes taking place in cold regions, with more than 30 years' experience of the subject. He states that his book " . . . is intended as a rather comprehensive overview of periglacial processes and their effects, present and past . . .. The book is neither a formal text nor a reference manual but something of both and a guide to the enormous

literature. Geocryology is included in the title to emphasize the pervasive influence of ice and its phase changes in these processes. . . The term is in fact used in the restricted sense as applying to frozen ground (seasonally frozen ground as well as permafrost) but not to glaciers."

The 1973 edition was an impressive and most useful text; this volume is equally so, being monumental in its coverage of the field. No one involved in periglacial investigations can afford to be without it. The format of the new book with hard cover, 7½" × 10" page size and a full page of text in two columns is an improvement on the earlier work with its horizontal 8" × 10" page size, smaller amount of text per page and single columns. The tremendous volume of literature that has appeared since 1973 and the author's thorough treatment of it are demonstrated by a comparison of the two editions. The 1973 edition has 262 pages, the 1979 publication 320 pages. However, the total text of the latter is nearly twice that of the former. The larger print of the earlier work is slightly easier to read but the smaller typeface used in the new work is no drawback. One of the most impressive aspects, and certainly an indication of the phenomenal increase of literature over six years, is the current bibliography. From about 1,000 references in 1973, the list has grown to about 2,700. This is reflected in the text by the presence of one or more citations on virtually every line. I experienced some difficulty at first in

literally wading through a sea of parentheses, but one quickly becomes accustomed to it. This encyclopaedic format is in fact very successful in quickly acquainting the reader with the literature. The index items have been increased in number from about 800 to 1,000. There are also more illustrations, about 200 instead of 150. Finally, the tables number 23 as compared with 10 in the earlier version. It will be interesting to see how much more periglacial literature is produced by 1985.

For such an impressive publication I have only a few criticisms, generally of a minor nature. The title of the earlier work seems more suitable to the contents of both books. The inclusion of "Geocryology" does not seem necessary especially in the more restricted sense specified by the author. Soviet permafrost workers use the term to refer to the study of the frozen zones of the Earth's crust. The author restricts its use to emphasizing the pervasive influence of ice in frozen ground. Somehow it seems redundant to include it in the title. "Periglacial" says it all because it includes frozen ground together with all its associated features.

The material on palsas and peat plateaux is somewhat thin, but I should admit to a bias because of my own particular interest in such landforms. There is now a large body of literature on investigations into the origin and development of these controversial features. Some photographs and diagrams would have suitably filled out this section. Russion terms for palsas are confusing. Actually the Russian word 'bugor' means only 'mound' and does not refer specifically to palsas. They could use the term 'palsa' but do not choose to do so. The closest approximation is 'torfyaniy bugor' or 'peat mound'. The Russian (Yakutian) word 'bulgunnyakh' actually is used for 'pingo' or 'hydrolaccolith' and is not used to refer to palsas.

Chapters 7 to 12 inclusive are each very short and produce an imbalance in the text. Perhaps some sort of grouping of these short chapters might have been possible. Chapters 6, 7 and 8 could have possibly been integrated into a single section.

Finally, it is regrettable that the new book is so expensive, putting it completely out of the reach of students. Nevertheless, every library should have at least one copy. Serious research workers of the periglacial will welcome it as a prime source of information. The painstaking effort that has gone into this work is truly remarkable and a great tribute to the experience of the author. I very much hope that he will be able to do a repeat performance in 1985 — he is certainly the one for this immense task. □

R. J. E. Brown is a Senior Research Officer at the National Research Council of Canada, Ottawa, Ontario.

Island botany

F.R. Fosberg

Plants and Islands. Edited by D. Bramwell. Pp.442. (Academic: London and New York, 1979.) £24, $55.50.

THIS SUBSTANTIAL volume comprises the papers given at an international symposium on plants and islands, held in April 1977 in Las Palmas, Canary Islands.

The papers cover a wide spectrum of knowledge of island botany, both in subject matter and geography, though mention of the vast island areas of Polynesia and Micronesia is conspicuously absent from the list of titles. Tahiti and Fiji are discussed only incidentally, the Marquesas as the home of remarkable endemics, and Hawaii as an example of the results of destruction of flora and vegetation by human agency. Understandably, five of the chapters are specifically on Macronesian floras.

The contribution are arranged in four sections, titled "Origins", "Endemism and Evolution", "Special Topics" and "Conservation".

The papers, generally, are interesting, mostly well prepared and give, for the subjects covered, a summary of the present state of knowledge and of the unfortunate present condition of the floras of most islands. Much of our knowledge must be pieced together from accounts of nineteenth-century visitors, fragmentary herbarium records and relicts of the vegetation as it was when European visitors first saw the islands.

The fascination that islands and their floras hold for so many biologists is well conveyed by most of the chapters. Effective dispelling of some of the exaggeration of the peculiarities of island floras is to be found in the provocative papers by Mabberley and Guédès. A masterly overview, such as we have come to expect from Ehrendorfer, is presented on reproductive biology in island plants and on several related topics. This chapter should be read, particularly by those who are concerned with the difficult problem of the preservation of the numerous endangered species on islands. Endemism is treated intensively in three chapters and less so in most others, but some of the discussions are marred by the use of largely undefined polysyllabic terminology.

Ideas involving plate tectonics and continental drift pervade many of the chapters, and provide explanations for many otherwise intractable problems. These ideas, long propounded by some biologists, have now become respectable and accepted by the formerly sceptical geological profession. However, one sometimes has the feeling that the time-frame in which the crustal movements took

place seems to stretch unduly the age of some of the Angiosperm taxa concerned.

It is a pity that the discussions of these papers that must have taken place were not recorded and published in appropriate places in the volume. Some fascinating marks must have been exchanged.

Mabberley's concluding paragraph (.274) points out one of the handicaps of searching into plant geography: the piecemeal approach fostered by the circumstances of modern research support and the difficulty of undertaking long-term work on large taxonomic groups. The poor understanding that flaws our knowledge of large and complicated genera is reflected in unsound plant geographic hypotheses. "Who has time to use his intellect to unravel the stories of *Cassia, Eugenia,*

Euphorbia, Piper, Solanum or *Vernonia* and their pachycauls?'' Corner, in a secure position without too great a burden of teaching, was able to point the way in his studies of *Ficus.*

The editing is generally good, though a few errors slipped by such as the indication in Table 1 (p.173), of a total native flora of 65 species for the Cape Verde Islands. Several of the diagrams are rather hard to follow. The quality of reproduction of the half-tones (e.g. Figs 1–4, pp. 264–265) leaves much to be desired.

One gets the impression that the selection of topics, or perhaps the selection of speakers, was somewhat hit or miss, and that the only basic organization was that the papers must be on plants and islands. Here and there, there seems to be some

relation between the topics, but the section on conservation is the only one that tends to come into focus as a whole, and even there it seems that perhaps each author did not know that the others were writing. However, the conservation prospects on islands are so uniformly dismal that perhaps a consistent impression in this section was unavoidable.

The price of the book will keep it out of reach for most of those who will want it. However, it is a boon to all students of island floras and biogeography that this symposium was published and is available.

F. R. Fosberg is a Botanist Emeritus at the Smithsonian Institution, Washington DC, with an interest in the geography and ecology of island floras.

The great British drought

Timothy O'Riordan

Atlas of Drought in Britain 1975–76. Edited by J.C. Doornkamp, K.J. Gregory and A.S. Burn. Pp.82. (Institute of British Geographers: London, 1980.) £27.50.

For a natural hazard that has no recorded parallel since at least 1698, and may have a probability of occurrence of 0.001, the great British drought of 1975–76 left remarkably little impact. For most of the public it has become lost in faded memory, while groundwater supplies, surface water resources, agricultural production and even most nature reserves are restored to normality. Yet the event was an important one in many ways, so this impressive production by the British Geomorphological Research Group in collaboration with the talented cartographic unit at the University of Southampton provides a valuable service.

The objective of the Research Group was to present a pictorial image of both the physical and the economic–administrative aspects of a major natural hazard. This is a worthy motive, but it necessarily involves a lot of collaboration amongst people who are already geared up to study the event and, if all the relevant researchers are not available at the right time, the result can be patchy and incomplete. The first section on the climatological characteristics of the drought is well done with excellent analyses of rainfall, sunshine and evaporation statistics for Britain and continental Europe. The blocking anticyclone that was responsible for the drought of 1976 was really the Mediterranean high pressure transferred some 1,000 km to the north — a shift probably caused by an unusually cold North Pacific which in turn moved the North Atlantic jet stream well to the north. As a result some depressions moved into the Mediterranean where, over the 18-month period, higher than average

rainfalls were recorded. Surprisingly in this section there is no record of temperature.

The second section covers the hydrological impacts of the drought in

The reservoir at Pitsford, 5th May 1976, 20 ft below normal for the time of year.

Britain. The national reviews of rainfall, evaporation, groundwater levels and soil moisture are well documented, but the rest of this section is rather uneven for the editors were dependent on workers who happened to be in the field at the time, writing up their case studies. The result is an interesting set of cameos but little in the way of a national perspective.

In economic terms the drought seems to have been remarkably friendly. The editors wisely avoid calculating a specific figure, but apart from a 40% loss of root and horticultural crops in the south-east, much of British agriculture was not savagely affected and apparently recovered quickly in the heavy rains that followed. The insurance companies certainly paid out a lot on claims for property damage due to clay shrinkage but will doubtless have raised their premiums since. The water authorities are now wiser about how far the public can be persuaded to cut consumption (up to 25% in the worst-hit areas following a sustained campaign) and are armed with much more specific powers to withhold water from non-essential customers (mainly domestic properties) during times of drought.

The large page format (30mm × 42mm), while making the book a little unwieldy, does mean that many diagrams can be presented on one page and that the text of each contribution can be fitted in without requiring the turning of a page. The diagrams are beautifully drawn in a uniform style. A lot of work has gone into this production and the editors are to be congratulated for their efforts. But the task of recording the varied dimensions of such an event is a formidable one, and even this stalwart effort falls a little short of what would be desirable. It is a particular pity that the scale and nature of recovery were not also recorded for this would have helped greatly to place the drought in proper perspective. □

Timothy O'Riordan is Professor of Environmental Sciences at the University of East Anglia, Norwich, UK.

BOOKS RECEIVED

General

CURRAN, S. C. and CURRAN, J. S. Energy and Human Needs. Pp. xix + 330. ISBN-0-7073-0237-4. (Edinburgh: Scottish Academic Press, 1979.) £8.50.

GRIBBIN, J. Future Worlds. Pp.225. London: Sphere Books Limited, 1979.)

FAST, Herausgegeben von G. Orchideen kultur. Botanische Grundlagen, Pflanzenbeschreibungen. Pp. 460.) DM 98.

FEUERSTEIN, R. *et al.* Instrumental Enrichment. An Intervent Program for Cognitive Modifiability. Pp. xxiii + 436. ISBN-0-8391-1 (Lancaster: MTP Press, Ltd. 1980.) £12.95.

FRITZ, C. Combating Nutritional Blindness in Chilren. A Case Study of Technical Assistance in Indonesia. Pergamon Policy Studies-57. Pp. x + 205. ISBN-0-08-024636-2. (New York, Oxford, Toronto, Sydney, Frankfurt, Paris: Pergamon, 1980.) £7.50.

FREUDENSTEIN, R. (ed.) Teaching Foreign Languages to the very young. Papers from seven countries on work with 4-to-8-year olds. Pp. xii + 97. ISBN-0-08-024576-5. (Oxford, New York, Toronto, Sydney, Paris, Frankfurt: Pergamon Press, 1979.) £2.95 $5.95.

GARFIELD, E. (ed.) Transliterated Dictionary of the Russian Language. An abridged dictionary consisting of Russian-to-English and English-to-Russian sections. Pp. xi + 382. ISBN-0-89494-003-7 hardback ISBN-0-8945-011-8 flexi. (Philadelphia: ISI, 1980.) $25.00 hardback $14.95 flexi.

GIBSON, W. B. SRI the Founding Years. A significant step at the golden time. Pp. x + 212. ISBN-0-913232-80-7. (California: William Kaufmann, Inc., 1980.) $20.50 (domestic) $25.00 (foreign).

GOLDSTEIN-JACKSON, K. Activities with Everyday Objects. Pp. ISBN-0-285-62439-3. (London: Souvenir Press, 1980.) £4.95.

GORDON, M. J., MILNER, A. J. and WADSWORTH, C. P. Edinburgh LCF. A Mechanised Logic of Computation. Lecture Notes in Computer Science. 78. Pp. viii + 159. ISBN-3-540-09724-4. (Berlin, Heidelberg, New York: Springer-Verlag, 1979.) DM 21.50 approx. US $12.10 flexi.

HARTLEY, W. C. F. An Introduction to Business Accounting for Managers. Third edition. Pergamon International Library of Science, Technology, Engineering and Social Studies. Pp. xiv + 221. ISBN-0-08-024062-3 flexi ISBN-0-08-024061-5 hardback. (Oxford, New York, Toronto, Sydney, Paris, Frankfurt: Pergamon, 1980.) $11.25 £4.95 flexi $24.00 £10.50 hardback.

HEATHCOTE, R. L. and THOM, B. G. (ed.) Natural Hazards in Australia. Proceedings of a Symposium sponsored by Australian Academy of Science, Institute of Australian Geographers, Academy of the Social Sciences in Australia. Pp. xii + 531. ISBN-0-85847-056-X. (Canberra: Australian Academy of Science, 1979.) A$20.00.

INMAN, W. H. W. (ed.) Monitoring for Drug Safety. Pp. xxv + 673. ISBN-0-85200-234-3. (London: MTP Press, Limited, 1980.) £24.95 $24.95.

I.R.S.I.A. Institut pour l'Encouragement de la Recherche Scientifique dans l'Industrie et l'Agriculture. Rapport Annuel 1978. Pp. 343. (Bruxelles: Institut pour l'Encouragement de la Recherche Scientifique dans l'Industrie et l'Agriculture.) flexi.

JOYNER, N. T. Jr. Joyner's Guide to Official Washington for Doing Business Overseas. Pergamon Policy Studies on U.S. and International Business. Pp. xxi + 364. ISBN-0-08-025108-0. (New York, Oxford, Toronto, Sydney, Frankfurt, Paris: Pergamon, 1980.) £47.50 $95.00.

Psychology

FORGUS, Ronald, and SHULMAN, Bernard, H. Personality: a Cognitive Vew Pp.xiii + 434. ISBN-0-13-657882-9. (Englewood Cliffs, NJ., and Hemel Hempstead: Prentice Hall, Inc., 1979.) £11.

GROTH, A.N. Men Who Rape; The Psychology of the Offender. Pp.xviii + 22 ISBN-0-306-40268-8. (New York and Lonon: Plenum, 1979.) $15.00.

GURKAYNAK, M.R. and LeCOMPTE, W.A. (ed.) Human Consequences of Crowdir Pp.ix + 331. ISBN-0-306-40298-X. (New York and London: Plenum Press, 1979.) $32.50.

HAINES, Richard F. (ed.) UFO Phenomena and the Behavioral Scientist. Pp.xiv + 4 ISBN-0-8108-1228-2. (Metuchen, N.J. Scarecrow, Inc., 1979.) $18.50.

HARDY, Alister. The Spiritual Nature of Man. Pp.viii + 162. ISBN-0-19-824618-3. (Oxfor Oxford University Press, 1979.) £6.95.

IBRAHIM, M.A. The Case-Control Study Consensus and Controversy Pp.iv + 144.ISBN-0-08-024907-8. (Oxford, New York, Paris, Frankfurt: Pergamon Press, 1979 $25.00, £12.50.

LEWIS, M. and BROOKS-GUNN, J. Social Cognition and the Aquisition of Sel Pp.xix + 296. ISBN-0-306-40232-7. (New York and London: Plenum, 1979.) $19.50.

SMILANSKY, M. and NEVO, D. The Gifted Disadvantaged; A Ten Year Longitudinal Stud of Compensatory Education in Israel. Pp.x + 245. ISBN-0-677-04400-0. (New York, Londor Paris: Gordon & Breach, 1979.) £12.50.

Applied Biology

McNAMARA, J.R. (ed.) Behavioural Approaches to Mediċine. Application and Analysis Pp.xxiii + 311. ISBN-0-306-40238-6. (New York and London: Plenum Press, 1979.) $25.00.

MEJIA, A., PIZURKI, H. ROYSTON, E. (reported by.) Physician and Nurse Migration Analysis and Policy Implications. Report of a WHO Study. Pp.xiv + 476. ISBN-92-4-156059- (Geneva: World Health Organisation, 1979.) Sfr.64.

MILAN, F. A. (ed.) The Human Biology of circumpolar populations. International Biologic Programme 21. Pp. xv + 381. ISBN-0-521-22213-3. (Cambridge, London, New York, Ne Rochelle, Melbourne, Sydney: Cambridge University Press, 1980.) £35.00.

NETH, R., GALLO, R.C. HOFSCHNEIDER, P.-H. and MANNWEILER, K. (ed.) Mod Trends in Human Leukemia III. Newest Results in Clinical and Biological Research. 9th Scienti Meeting of "Gesellschaft Deutscher Naturforscher und Arzte", June 19-23, 1978. Pp.xxi + 5 ISBN-3-540-08999-3. (Berlin, Heidelberg, New York: Springer, 1979.) Flexi.

PHILLIPS, G.O. TALLENTIRE, A. and TRIANTAFYLLOU, N. (ed.). Radiat Sterilization: Irradiated Tissues and their potential Clinical use. Papers presented at an Advis Group Meeting. Pp.x + 242. (Clwyd: The North Wales Institute, 1978.)

SUTHERLAND, I. (ed.). Health Education; Perspectives and Choices. Pp.xi + 27 ISBN-0-04-371069-7. (Hemel Hempstead: George Allen & Unwin, 1979.) £10.00.

WORLD HEALTH ORGANIZATION. Specifications for Pesticides used in Public Hea Insecticides, Molluscicides, Repellents, Methods. Fifth Edition. Pp.327. ISBN-92-415410 (Geneva: World Health Organization, 1979.) SFR. 48.00.

WORLD HEALTH ORGANIZATION. The International Pharmacopoeia Third editi Volume 2. General Methods of Analysis. Pp.223. ISBN-92-4-154150-4. (Geneva: World Hea Organization, 1979.) SFr.24.00.